U.S. Department of Transportation
Federal Highway Administration

Publication No. FHWA-NHI-15-047
April 2007
Revised July 2015

NHI Course No. 130081, 130081A, and 130081B

Load and Resistance Factor Design (LRFD) for Highway Bridge Superstructures

REFERENCE MANUAL

NATIONAL HIGHWAY INSTITUTE

ACCREDITED IACET PROVIDER

This page intentionally left blank.

LRFD for Highway Bridge Superstructures

REFERENCE MANUAL

LRFD for Highway Bridge Superstructures

REFERENCE MANUAL

LRFD for Highway Bridge Superstructures

REFERENCE MANUAL

This page intentionally left blank.

Technical Report Documentation Page

1. Report No. FHWA-NHI-15-047	**2. Government Accession No.**	**3. Recipient's Catalog No.** FHWA-NHI-15-047
4. Title and Subtitle Load and Resistance Factor Design (LRFD) For Highway Bridge Superstructures - Reference Manual		**5. Report Date** July 2015 **6. Performing Organization Code** FHWA/DTS-NHI-1
7. Author (s) Michael A. Grubb, P.E., Kenneth E. Wilson, P.E., S.E., Christopher D. White, P.E., William N. Nickas, P.E.		**8. Performing Organization Report No.** MBRM137804
9. Performing Organization Name and Address Michael Baker International Airside Business Park, 100 Airside Drive Moon Township, PA 15108		**10. Work Unit No. (TRAIS)** **11. Contract or Grant No.** DTFH61-11-D-00046
12. Sponsoring Agency Name and Address Federal Highway Administration National Highway Institute (HNHI-10) 1310 North Courthouse Road Arlington, VA 22201		**13. Type of Report and Period Covered** Final Submission September 2013 – July 2015 **14. Sponsoring Agency Code** FHWA
15. Supplementary Notes Baker Principle Investigator: Mary P. Rosick, P.E. Baker Project Manager: Scott D. Vannoy, P.E. FHWA Contracting Officer's Representative: Louisa M. Ward FHWA Technical Team Leader: Brian M. Kozy, Ph.D., P.E.		

16. Abstract

This document presents the theory, methodology, and application for the design and analysis of both steel and concrete highway bridge superstructures. The manual is based on the *AASHTO LRFD Bridge Design Specifications*, Seventh Edition, 2014, with Interim Revisions through 2015. Design examples and commentary throughout the manual are intended to serve as a guide to aid bridge engineers with the implementation of the *AASHTO LRFD Bridge Design Specifications*.

This Reference Manual consists of eight chapters. Chapter 1 provides an introduction to LRFD, including an overview of the LRFD design philosophy and a description of the various LRFD limit states. Chapter 2 provides general information about location features and design objectives, as well as a brief overview of Accelerated Bridge Construction. Chapter 3 presents loads and load factors, including design criteria for common bridge loads, as well as load factors used for various LRFD load combinations. Chapter 4 provides a general summary of structural analysis, including general analysis considerations, dead load analysis, live load analysis, and various methods of analysis. Chapter 5 provides valuable information for the design of concrete girder superstructures, including preliminary design decisions, flexural design of prestressed I-girders, design for shear and torsion, prestressing, and reinforcement details. Similarly, Chapter 6 provides valuable information for the design of steel girder superstructures, including LRFD girder verifications for constructibility, service, fatigue and fracture, flexure, and shear, as well as design provisions for various steel superstructure details. Chapter 7 describes decks and deck systems, covering such topics as traditional design method, empirical design method, deck overhang design, precast deck slabs, and bridge railings. Chapter 8 provides general information about bearings and joints, including design requirements for elastomeric bearings and pot bearings. Finally, a glossary of common terms related to bridge superstructures and LRFD is provided.

17. Key Words Bridge Design, Load and Resistance Factor Design, LRFD, Superstructure, Deck, Girder, Structural Steel, Reinforced Concrete, Prestressed Concrete, Bearing, Limit State, Load Combination, Analysis	**18. Distribution Statement** This report is available to the public from the NHI Bookstore at http://www.nhi.fhwa.dot.gov/training/nhistore.aspx

19. Security Classif. (of this report) Unclassified	**20. Security Classif. (of this page)** Unclassified	**21. No. of Pages** 1698	**22. Price**

ACKNOWLEDGEMENTS

We would like to express appreciation to the following individuals who served on the Technical Review Team:

Reggie Holt, P.E.
Federal Highway Administration

Derek Constable, P.E.
Federal Highway Administration

Jeffrey J. Ger, Ph.D., P.E.
Federal Highway Administration

Bijan Khaleghi, Ph.D., P.E., S.E.
Washington State DOT

Thomas K. Saad, P.E.
Federal Highway Administration

Gerald B. Lacosta
Sevatec, Inc.

Dennis R. Mertz, Ph.D., P.E.
University of Delaware

Brandon W. Chavel, Ph.D., P.E.
HDR Engineering, Inc.

We would also like to acknowledge the contributions of the following staff members at Michael Baker International:

Francesco M. Russo, Ph.D., P.E.
Bryan T. Ott
Sandra L. Fitzgerald
Maureen Kanfoush
Thomas W. Ryan, P.E.
Lori E. Schnaider
John A. Wattick
Gregory M. Willenkin

Finally, we would like to acknowledge the contributions of the following individuals to the original edition of this document:

Staff members of Michael Baker Jr., Inc.:
Justin W. Bouscher, P.E.
Jeffrey J. Campbell, P.E.
Leslie J. Danovich
Sean J. Hart, P.E.
Raymond A. Hartle, P.E.
Ronald J. Ladyka, P.E.
Eric L. Martz, P.E.
Linda Montagna
Brett Schock
Rachel A. Sharp, P.E.
William R. Sobieray
Laura E. Volle, P.E.
Roy R. Weil
Roberta L. Wilson

Technical Review Committee:
John M. Kulicki, Ph.D., P.E.
Thomas P. Macioce, P.E.
Edward Wasserman
Robert Cisneros

Other technical support:
John A. Corven, P.E.
Dann H. Hall
Reid W. Castrodale, Ph.D., P.E.
Alan Moreton
Shrinivas B. Bhide, S.E., P.E., Ph.D.
Michelle Roddenberry
Alan Shoemaker
William F. McEleney
Heather Gilmer

Table of Contents

Chapter 1 – Introduction to LRFD

Chapter 2 – General Design and Location Features

Chapter 3 – Loads and Load Factors

Chapter 4 – Structural Analysis

Chapter 5 – Concrete Girder Superstructures

Chapter 6 – Steel Girder Superstructures

Chapter 7 – Decks and Deck Systems

Chapter 1
Introduction to LRFD

Section 1.1 Introduction

Bridges have helped shape our nation and its people. Bridge design and construction methods have advanced significantly in America and have helped advance the nation's transportation, commerce, and economy, as well as the well-being of its people.

Bridges in the United States are designed in accordance with specifications published by the American Association of State Highway and Transportation Officials (AASHTO). These specifications are entitled *AASHTO LRFD Bridge Design Specifications* (hereafter referred to as *AASHTO LRFD*), and they provide the minimum standards for highway bridge design according to the Code of Federal Regulations. By Federal Highway Administration (FHWA) policy, all bridges designed after 2007 were required to be designed based on the Load and Resistance Factor Design (LRFD) method.

This chapter describes the design philosophy of LRFD, including the evolution of design specifications and LRFD calibration. It describes the primary design philosophies and codes, including Allowable Stress Design (ASD), Load Factor Design (LFD), and LRFD. A design example is included for each of these three design philosophies. It also describes the original LRFD calibration work, more recent calibration work, and the development of site-specific load factors.

This chapter also presents the general principles of limit states in bridge design, and it describes the primary limit states used in LRFD – service, fatigue and fracture, strength, and extreme event. For each limit state, the various load combinations, load factors, and primary applications are presented. Finally, the load modifier, η, used in LRFD is described, including its three components.

Section 1.2 LRFD Design Philosophy

1.2.1 General

The LRFD design philosophy accounts for variability in both resistance and loads, it achieves relatively uniform levels of safety within the superstructure and substructure (excluding foundations) and their various members, and it is based on risk assessment founded on reliability theory.

As an example, for the earlier design philosophies (ASD and LFD), the level of safety varied as a function of the span length, span arrangement, and member type (such as girder, floorbeam, pier cap, or column). This variability existed because, at a given limit state, the design loads and their application were not calibrated to result in a force effect with the same level of safety for all span and member types. Similarly, the material and member resistances were not calibrated as well.

Simply stated, safety in any engineering design is assumed when the demands placed on components and materials are less than what is supplied, so that the following basic equation is satisfied:

$$\text{Demand} < \text{Supply}$$

Another way of stating this same principle with respect to structural engineering is that the effect of the loads must be less than the resistance of the materials, so that the following requirement is met:

$$\text{Load} < \text{Resistance}$$

When a particular loading or combination of loadings reaches the component or material resistance, safety margins approach zero and the potential for failure exists. The goal of the basic design equation is to limit the potential for failure to the lowest probability practical for a given situation.

When applying this principle to design, it is essential that both sides of the inequality be evaluated for the same conditions. For example, if the effect of applied loads produces tension in a concrete member, the load should be compared to the tensile resistance of the concrete and not some other aspect of the material such as the compressive resistance.

For bridge design, the left side of the inequality representing the loads is constantly changing due to live loads and other environmental loads. Under some circumstances, due to deterioration of the structure over time, the right side of the inequality representing the resistance might also change. These uncertainties

throughout the life of the structure are very difficult to predict but must be accounted for.

1.2.2 Evolution of Design Specifications

1.2.2.1 General

The manner in which the uncertainties of bridge design are considered is what separates different design philosophies. In recent decades, three design philosophies (or codes) for bridge design have been in general use in the United States. In order of age, they are Allowable (or Working) Stress Design (ASD), Load Factor Design (LFD), and Load and Resistance Factor Design (LRFD).

For ASD, a single factor of safety on the resistance side of the inequality accounts for the uncertainty. The use of LFD, on the other hand, applies load factors to each type of load depending on the combination, and the material resistance is also modified by reduction factors. Hence, LFD accounts for uncertainty on both sides of the inequality.

LRFD is similar to LFD in the fact that the uncertainty is accounted for on both sides of the inequality. However, the major advantage of LRFD over LFD is that LRFD is probability-based. LRFD was developed based on a specific reliability index that targets a specific probability of failure. Each design philosophy is discussed in more detail in the following sections.

1.2.2.2 Allowable Stress Design

Allowable Stress Design (ASD), also known as Working Stress Design (or WSD), is the oldest of the three design codes commonly used for bridges in the United States in recent decades. Of the three philosophies, ASD is the most simplistic.

The ASD method of design utilizes unfactored loads which are combined to produce a maximum effect in a member. The maximum load or combination of loads cannot exceed the allowable (or working) stress of the material. The allowable or working stress is found by taking the strength of the material and applying an appropriate factor of safety that is greater than unity.

The basic equation for Allowable Stress Design is the following:

$$\sum DL + \sum LL = R_u / FS \qquad \text{Equation 1.2.2.2-1}$$

where:

DL = dead loads applied to the component under consideration
LL = live loads applied to the component under consideration
R_u = ultimate capacity of the component under consideration
FS = factor of safety > 1.0

Note that loads other than dead load and live load have been excluded from the above equation for simplicity. However, they are also included in ASD, as applicable.

A graphical representation of the ASD philosophy is presented in Figure 1.2.2.2-1. As can be seen in the figure, the assumption of ASD is that loads and resistances both have a probability of occurrence of 1.0. The load types include dead loads, live loads, and environmental loads, all of which in reality have different occurrence probabilities and different effects.

Therefore, it is evident that the factor of safety applied to the resistance side of the inequality dictates the width of the safety margin in the graphical representation and is the only aspect of ASD that accounts for uncertainty.

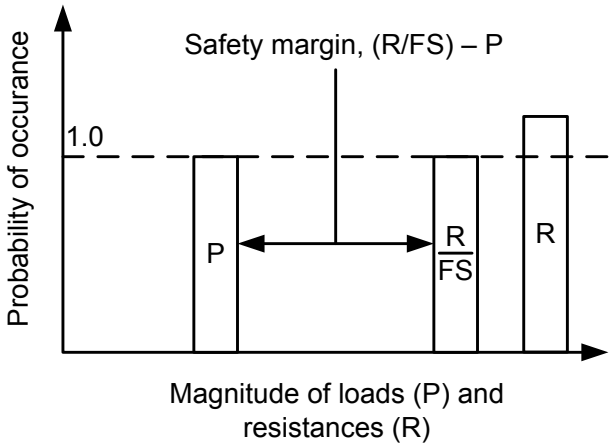

Figure 1.2.2.2-1 Graphical Representation of Allowable Stress Design

The primary advantage of ASD is the following:

- ASD has an inherent simplicity. Because it does not involve the use of load factors or resistance factors, the computations are relatively simple.

The primary limitations of ASD are the following:

- In ASD, no consideration is given to the fact that various types of loads have different levels of uncertainty. For example, the dead load of a bridge can be estimated with a high degree of accuracy. However, earthquake loads acting on bridges cannot be estimated with the same degree of accuracy and confidence. Nevertheless, dead loads, live loads, and environmental loads are all treated equally in ASD.

- Because the factor of safety applied to the resistance side of the inequality is based on experience and judgment, consistent measures of risk cannot be determined for ASD.

1.2.2.2.1 Allowable Stress Design Example

For this example, assume a dead load of 50 kips, a live load of 25 kips and an ultimate capacity of 150 kips. Use a minimum factor of safety of 1.5 for this example.

$\Sigma DL + \Sigma LL = 50 \text{ kips} + 25 \text{ kips} = 75 \text{ kips}$

$FS = R_u / (\Sigma DL + \Sigma LL) = 150 \text{ kips} / 75 \text{ kips} = 2.0$

Since the calculated factor of safety (2.0) is greater than the minimum factor of safety (1.5), the fundamental equation for ASD is satisfied and the design is acceptable for the given loadings.

1.2.2.3 Load Factor Design

Load Factor Design (LFD) was introduced several decades ago in an effort to refine the ASD philosophy. LFD utilizes loads multiplied by load factors and load combination coefficients, which are generally greater than unity. The factored loads are combined to produce a maximum effect in a member. Load factors vary by type of load and reflect the uncertainty in estimating magnitudes of different load types.

In LFD, uncertainty is also accounted for in the resistance side of the inequality. The resistance side is multiplied by a reduction factor, phi (ϕ), which is generally less than unity in order to account for variability of material properties, structural dimensions, and workmanship. The combination of the factored loads cannot exceed the strength of the material multiplied by a reduction factor less than unity.

The following relationship represents LFD design. Note that loads other than dead load and live load have been excluded from the equation for simplicity, but they must be included when designing with LFD, as applicable.

$$\gamma(\Sigma \beta_{DL} DL + \Sigma \beta_{LL} LL) = \phi R_u \qquad \text{Equation 1.2.2.3-1}$$

where:

DL = dead loads applied to the component under consideration
LL = live loads applied to the component under consideration
R_u = ultimate capacity of the component under consideration
γ = load factor applied to all loads
β_{DL} = load combination coefficient for dead loads

β_{LL} = load combination coefficient for live loads
ϕ = reduction factor

The primary advantages of LFD are the following:

- In LFD, a load factor is applied to each load combination to account for the relative likelihood that a specific combination of loads would occur simultaneously.
- In LFD, consideration is given to the fact that various types of loads have different levels of uncertainty. For example, the dead load of a bridge can be estimated with a higher degree of accuracy than the live loads. Therefore, the load combination coefficient for live load is greater than that for dead load.

The primary limitations of LFD are the following:

- LFD is not as simple to use as ASD.
- LFD does not achieve relatively uniform levels of safety.

1.2.2.3.1 Load Factor Design Example

Using the same loads and ultimate structural resistance from the ASD example in Section 1.2.2.2.1, the design inequality for LFD Strength Load Combination I is presented below. Note that a reduction factor of 0.9 has been assumed.

γ = 1.3
β_{DL} = 1.0
β_{LL} = 1.67
ϕ = 0.9

$\gamma (\Sigma \beta_{DL} DL + \Sigma \beta_{LL} LL) = 1.3 [(1.0 * 50 \text{ kips}) + (1.67 * 25 \text{ kips})] = 119.3 \text{ kips}$

$\phi R_u = 0.9 * 150 \text{ kips} = 135 \text{ kips}$

Since the factored load (119.3 kips) is less than the factored capacity (135 kips), the fundamental equation for LFD is satisfied and the design is acceptable for this particular strength combination.

1.2.2.4 Load and Resistance Factor Design

The Load and Resistance Factor Design (LRFD) method is the latest advancement in transportation structures design practice. In the year 2000, AASHTO, in concurrence with FHWA, set a transition date of October 1, 2007, after which all new bridges on which states initiate preliminary engineering shall be designed in accordance with the requirements of *AASHTO LRFD*.

The LRFD design methodology is similar to LFD design. On the load side of the inequality, LRFD utilizes load factors but not load combination coefficients. The combination of the factored loads, termed "limit states" in LRFD, cannot exceed the resistance of the material multiplied by a resistance factor less than or equal to unity. Several load combinations are included for service, fatigue and fracture, strength, and extreme event considerations.

The resistance side of the LRFD inequality is similar to that of LFD, although resistance factors differ from those used in LFD. The following relationship represents LRFD design. Note that loads other than dead load and live load have been excluded from the equation for simplicity, but they must be included when designing with LRFD, as applicable.

$$(\sum \gamma_{DL} DL + \sum \gamma_{LL} LL) = \phi R_n \qquad \text{Equation 1.2.2.4-1}$$

where:

DL = dead loads applied to the component under consideration
LL = live loads applied to the component under consideration
R_n = nominal resistance or strength of the component under consideration
γ_{DL} = load factor for dead loads
γ_{LL} = load factor for live loads
ϕ = resistance factor

The general LRFD design equation used by AASHTO is presented and described in Section 1.3.1. The *AASHTO LRFD* design equation includes a load modifier, eta (η), which is applied to all loads equally.

A graphical representation of the LRFD philosophy is presented in Figure 1.2.2.4-1. As can be seen in the figure, the factored safety margin is small, but when the theoretical actual loads and nominal resistances are observed, the actual safety margin is actually much wider. LRFD also takes into account the different probabilities of occurrence for loads and resistances.

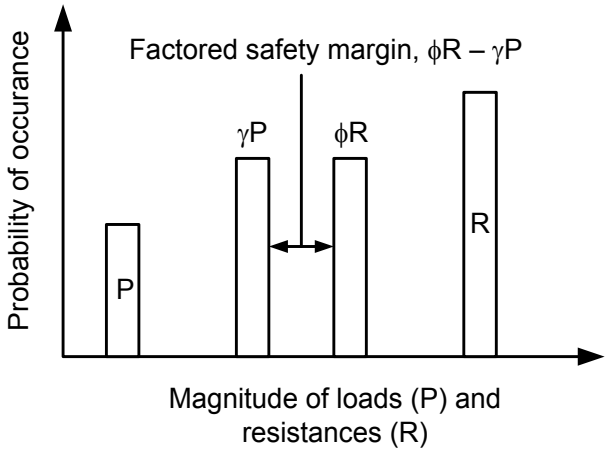

Figure 1.2.2.4-1 Graphical Representation of Load and Resistance Factor Design

The primary advantages of LRFD are the following:

- LRFD accounts for variability and uncertainty in both resistance and loads.
- LRFD achieves relatively uniform levels of safety for different limit states and material types to the extent possible.
- LRFD provides more consistent levels of safety in the superstructure and substructure (excluding foundations) as both are designed using the same loads for predicted or target probabilities of failure.

The primary limitation of LRFD is the following:

- The most rigorous method for developing and adjusting resistance factors to meet individual situations requires availability of statistical data and probabilistic design algorithms.

Bridge designers who are accustomed to using the LFD design code generally recognize many similarities when learning the LRFD design code. While load and resistance factors differ for LRFD as compared to LFD, many procedures for determining design loads and material strengths are the same.

1.2.2.4.1 Load and Resistance Factor Design Example

For LRFD, load factors are determined from *AASHTO LRFD* Article 3.4.1 and resistance factors are determined from *AASHTO LRFD* Articles 5.5.4.2 and 6.5.4.2 for concrete and steel, respectively.

Using the same loads and ultimate resistance from the ASD example in Section 1.2.2.2.1 and using the following factors corresponding to a strength limit state, the design is as follows:

η = 1.05 (η_D = 1.00, η_R = 1.00, and η_I = 1.05)
γ_{DL} = 1.25
γ_{LL} = 1.75
ϕ = 0.9

Although there is only one load modifier, η, for each bridge, η is applied to each load individually in accordance with *AASHTO LRFD* Equation 1.3.2.1-1. This is illustrated in the following equation:

$(\Sigma\eta\gamma_{DL}DL + \Sigma\eta\gamma_{LL}LL) = [(1.05*1.25*50 \text{ kips}) + (1.05*1.75*25 \text{ kips})] = 111.6 \text{ kips}$

The factored resistance is computed as follows:

$\phi R_n = 0.9 * 150 \text{ kips} = 135 \text{ kips}$

Since the factored load (111.6 kips) is less than the factored resistance (135 kips), the fundamental equation for LRFD is satisfied and the design is acceptable for this particular load combination of the strength limit state.

1.2.3 LRFD Calibration

The differences in how load factors are applied in LFD and in LRFD are significant, but perhaps the greatest difference between LFD and LRFD is that reliability theory was used in LRFD to derive the load and resistance factors. The load and resistance factors were statistically "calibrated" in an effort to obtain a more uniform level of safety for different limit states and types of material.

Research into the safety of bridges generally includes calculations of a safety or reliability index, often denoted as β (beta). The reliability index quantifies the structural reliability or, conversely, the risk that a design component has insufficient resistance and that a specific limit state will be reached. Higher betas denote higher reliability.

The reliability index is illustrated by the bell curves presented in Figure 1.2.3-1 and Figure 1.2.3-2. Figure 1.2.3-1 illustrates the normal distribution of loads and resistances in the shape of bell curves. The application of load factors and resistance factors is also illustrated in Figure 1.2.3-1. The overlap of the two bell curves represents the region for which the limit state has been exceeded. Figure 1.2.3-2 provides a graphical representation of the reliability index, β.

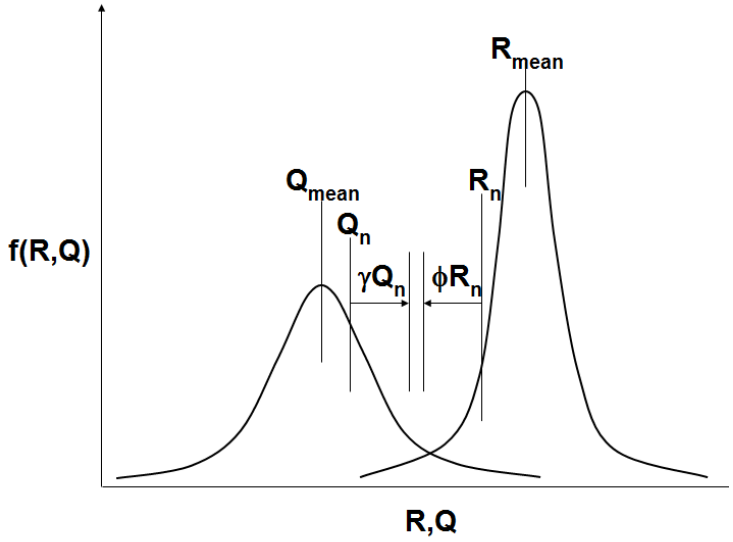

Figure 1.2.3-1 Bell Curves Illustrating Distribution of Load and Resistance

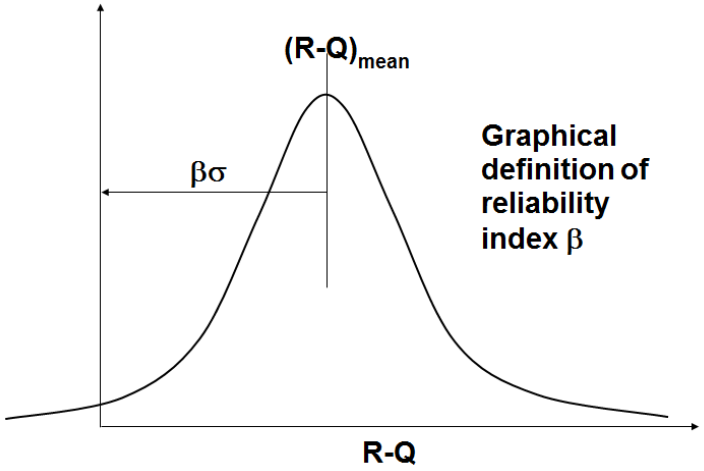

Figure 1.2.3-2 Graphical Definition of Reliability Index, β

The reliability index, β, is computed as follows:

$$\beta = \frac{\text{Mean value of g}}{\text{Standard deviation of g}} \qquad \text{Equation 1.2.3-1}$$

$$g = R - DL - LL \qquad \text{Equation 1.2.3-2}$$

where:

g = safety margin

R = resistance
DL = dead load effect
LL = live load effect, including dynamic load allowance

Based on these calibrations and reliability indices, a higher load factor or lesser resistance factor is applied to loads and materials whose behavior is less-well known and cannot be as accurately predicted. In this manner, greater knowledge of some resistances and loadings can be accounted for, allowing more efficient designs while still applying appropriate levels of safety to those resistances and loads which are more ambiguous. As research is conducted and the knowledge base increases, load and resistance factors can be altered to account for the greater certainty, or in some cases, greater uncertainty of loads or resistances.

1.2.3.1 Original Calibration Work

In 1999, the original calibration work by Dr. Andrzej S. Nowak was published in NCHRP Report 368 (Nowak, 1999). Much of the work for this report was actually completed prior to 1991, prior to the final selection of load and resistance factors used in *AASHTO LRFD*. NCHRP Report 368 provides the background information and the calibration procedure for *AASHTO LRFD*. The original calibration was for the strength limit state, and calculations were carried out for beam- and slab-type bridges. For the original calibration work, it was assumed that resistance would not change over time (assuming that maintenance would be adequate to preserve the original strength) and that the weight of legal loads would not increase over time.

For the original calibration work that served as the basis for the 1994 *AASHTO LRFD*, the reliability index, β, was set at a target of 3.5. The inherent reliability indices of previous specifications ranged from as low as 2.0 to as high as 4.5. A target reliability index of 3.5 was considered appropriate, as it was slightly higher than an average of previous specifications and design philosophies (Nowak, 1999; Kulicki, et al., 2007).

1.2.3.2 Latest Calibration Work from SHRP 2

In December 2013, new calibration work specific to the service limit state was completed as part of the second Strategic Highway Research Program (SHRP 2), administered by the Transportation Research Board. A project team consisting of Modjeski and Masters, University of Nebraska at Lincoln, University of Delaware, and NCS Consultants documented their work in a final report entitled “Bridges for Service Life Beyond 100 Years: Service Limit State Design” (Modjeski and Masters, et al., 2013). The primary objectives of this project (SHRP 2 Project R-19B) were to develop design and detailing guidance to provide 100-year bridge life, to develop calibrated service limit states to provide 100-year bridge life, and to develop a framework for further development of calibrated service limit states.

1.2.3.3 Development of Site-specific Load Factors

In addition to the load factors specified by AASHTO, transportation agencies can also calibrate site-specific load factors, which can be derived using local traffic conditions. The generalized load factors presented in AASHTO are representative of bridges throughout the nation with similar traffic volumes. However, site-specific load factors can be computed using truck weight data collected from weigh-in-motion (WIM) sites that follow the same procedures used to derive the LRFD live load factors.

Based on structural reliability principles, uniform target safety levels can be attained by reducing uncertainty. This is achieved by collecting site-specific information from WIM sites to determine and quantify the local uncertainty in the live loads, rather than relying on generalized information regarding uncertainty throughout the nation. Site-specific load factors are more refined than the generalized AASHTO load factors, because they are based on a specific bridge site, route, or region. They reflect the actual truck traffic in that specific region, and they generally capture the maximum loadings over the exposure period.

Such site-specific load factors are computed and used primarily for design of signature bridges using LRFD and for evaluation of existing bridges using Load and Resistance Factor Rating (LRFR) methodology. The requirements for computing site-specific load factors generally preclude their use for common workhorse bridges, but they can provide significant benefit for signature bridge design and for LRFR load ratings.

Additional information about development of site-specific load factors is available in NCHRP Report 683, *Protocols for Collecting and Using Traffic Data in Bridge Design* (Sivakumar, et al., 2011).

Section 1.3 Limit States

Load and Resistance Factor Design utilizes load combinations called limit states. As defined by AASHTO, a limit state is a condition beyond which the bridge or component ceases to satisfy the provisions for which it was designed. LRFD limit states are generally classified into four major categories – service, fatigue and fracture, strength, and extreme event. Different load combinations are intended to analyze a structure for certain responses, such as deflections, permanent deformations, ultimate capacity, and inelastic responses without failure.

It should be noted that, in the context of LRFD design of bridges, the term “failure” does not necessarily mean collapse of the bridge or catastrophic damage. Rather it

means no longer satisfying the provisions for which it was designed. This is unique for each limit state and is described further in the following sections.

Not all limit states need to be checked for all structures, and the design engineer should determine the applicable limit states for a specific bridge. When all applicable limit states and combinations are satisfied, a structure is deemed acceptable under the LRFD design philosophy.

Each limit state contains several load combinations, numbered with Roman numerals. These combinations reflect different load types and different load factors, based on the intended loading condition and the probability of simultaneous occurrence of loadings.

For reference, the load factors table presented in *AASHTO LRFD* Table 3.4.1-1 is presented in Section 3.9.1.1. In addition, for strength and extreme event limit states, permanent loads are factored individually as presented in *AASHTO LRFD* Table 3.4.1-2, which is also presented in Section 3.9.1.1.

1.3.1 General AASHTO LRFD Design Equation

In Section 1.2.2.4, a limited description of the LRFD design equation is presented for the purpose of comparison with ASD and LFD. Only dead load and live load were included in the example equation presented in Section 1.2.2.4.

However, this section describes the general AASHTO LRFD design equation, as presented in *AASHTO LRFD* and as applicable for all limit states and all load combinations. The general AASHTO LRFD design equation is expressed as follows:

$$\sum \eta_i \gamma_i Q_i \le \phi R_n = R_r \qquad \text{Equation 1.3.1-1}$$

AASHTO LRFD Equation 1.3.2.1-1

where:

- η_i = load modifier, relating to ductility, redundancy, and operational importance
- γ_i = load factor; a statistically based multiplier applied to force effects
- Q_i = force effect
- ϕ = resistance factor; a statistically based multiplier applied to nominal resistance
- R_n = nominal resistance
- R_r = factored resistance

Load factors are statistically-based multipliers applied to the force effects, and they are usually greater than 1.0. Load factors account primarily for the variability of

loads, the lack of accuracy in analysis, and the probability of different loads occurring simultaneously. However, they are also related to the statistics of the resistance through the calibration process.

Resistance factors are also statistically-based multipliers, but they are applied to the nominal resistance. Their values are less than or equal to 1.0. Resistance factors account primarily for variability of material properties, structural dimensions, and workmanship, as well as uncertainty in the prediction of resistance. However, they are also related to the statistics of the loads through the calibration process.

Both load factors and resistance factors are selected to yield reliability factors close to the target reliability index, β_T. For each load component (such as dead load, live load, and wind load), the load factor, γ_i, is computed as a function of the bias factor (which is defined as the ratio of the mean value to the nominal value) and the coefficient of variation (which is defined as the standard deviation divided by the average value).

Some general principles in selecting load factors are presented in Table 1.3.1-1.

Table 1.3.1-1 Selection of Load Factors

General Principle	Example
Lower load factors are assigned to loads with a low degree of variability.	The weight of water has very low variability (0.0624 kcf), and therefore the load factor assigned to water load is 1.00 for all load combinations.
Similarly, higher load factors are assigned to loads with a high degree of variability.	Live load weight and configuration has relatively high variability, and therefore the load factor for live load is as high as 1.75 (for Strength I).
The likelihood of simultaneous loads affects the selected load factor.	For Extreme Event II, the load factor for live load is 0.50, because it is likely that reduced live load will be present on the bridge during an extreme event.
The number of simultaneous loads affects the selected load factor.	For Strength I (without wind on structure or on live load), the load factor for live load is 1.75. However, for Strength V (with wind on structure and on live load), the load factor for live load is 1.35.

It should be noted that the bridge engineer generally does not select load factors but rather uses the load factors that have been selected by AASHTO, as presented in *AASHTO LRFD* Tables 3.4.1-1 and 3.4.1-2. The AASHTO load factors were selected based on extensive research and calibration.

The load modifier is computed as described in Section 1.3.6, and it applies to all force effects acting on the entire bridge. However, different load factors are used for different force effects, as presented in Section 3.9.1.1.

All limit states are considered to be of equal importance, and the general LRFD design equation must be satisfied for all limit states that are applicable to the specific bridge.

1.3.2 Service Limit State

The service limit state provides restrictions on stress, deformation, and crack width under regular service conditions. It provides experience-related provisions that cannot necessarily be derived solely from statistical or strength considerations. Within the service limit state, there are four load combinations that are designed to test various aspects of the structure being analyzed. These load combinations are designated Service I through Service IV. These load combinations represent loading conditions which could easily be expected during normal operation and will occur many times during the design life of the structure. The service limit state is intended to control deflections in superstructures and cracks in prestressed concrete structures. For the service limit state, failure means that stresses, deformations, or crack widths exceed the limitations established by AASHTO. However, it does not necessarily mean collapse or inability of the component to resist the applied loads.

1.3.3 Fatigue and Fracture Limit State

The fatigue and fracture limit state provides restrictions on stress range as a result of a single design truck occurring at the number of expected stress range cycles. It also provides material toughness requirements as set forth in the AASHTO Material Specifications. The fatigue and fracture limit state consists of two load combinations intended to produce the greatest effect of a stress range on a structural component which controls the possibility for cracking in steel members from a single truck loading, as specified in *AASHTO LRFD* Article 3.6.1.4. These two load combinations are designated Fatigue I and Fatigue II, and they relate to infinite load-induced fatigue life and finite load-induced fatigue life, respectively. This limit state is not applicable to all bridge designs, and the design engineer must determine whether the effects of fatigue and fracture could be a problem for each specific bridge. For example, AASHTO does not require fatigue limit state checks for concrete decks or wood decks, as specified in *AASHTO LRFD* Article 9.5.3. For the fatigue and fracture limit state, failure means that crack growth under repetitive loads exceeds the limitations established by AASHTO to prevent fracture during the design life of the bridge.

1.3.4 Strength Limit State

The strength limit state assures that strength and stability requirements, both local and global, are satisfied to resist the specified statistically significant load combinations that a bridge is expected to experience during its design life. All members must satisfy ultimate capacity requirements under various live load and wind load conditions. These load combinations would not generally occur during normal daily operation of the structure, but they could occur during the design life of the structure. There are five strength load combinations, designated Strength I through Strength V. For the strength limit state, failure means that the bridge resistance has been exceeded. Extensive distress and structural damage may occur under the strength limit state, but overall structural integrity is expected to be maintained.

1.3.5 Extreme Event Limit State

The extreme event limit state assures the structural survival of a bridge during a major earthquake, flood, collision by a vessel, collision by a vehicle, or ice flow. The extreme event limit state represents unique loadings whose return period may be significantly greater than the design life of the bridge. Specific loads which apply only to the extreme event limit state are earthquake load, blast loading, ice load, vehicular collision force, and vessel collision force. Each of these five loadings is analyzed separately and is not combined with any of the other four extreme event loadings. The two load combinations for this limit state are designated Extreme Event I and Extreme Event II, each possessing different load factors for live load. For the extreme event limit state, failure does not mean complete loss of structural integrity or collapse under these extreme loading conditions. However, the effects of an extreme event load combination are allowed to cause damage to a structure. Stresses and deformations well into the inelastic range are permitted and, in some cases, expected for the extreme event limit state.

1.3.6 Load Modifier, η

As described in Section 1.3.1, *AASHTO LRFD* introduces a new term in the design equation. This new term is called a load modifier. *AASHTO LRFD* Article 1.3.2.1 defines the load modifier, η (eta), as a combination of factors due to the effects of ductility, redundancy, and operational importance. These three terms are designated as η_D, η_R, and η_I, respectively.

The original intent of the load modifier was to encourage enhanced ductility and redundancy. Operational importance was included to provide additional reliability for more important bridges.

The placement of the load modifier on the load side of the basic LRFD equation may seem counterintuitive since ductility and redundancy are generally considered to be characteristics of resistance rather than load. However, the load modifier was placed on the load side since the final combination of η factors depends on the desired loading condition. For maximum values of γ_i:

$$\eta_i = \eta_D \eta_R \eta_I \geq 0.95 \qquad \text{Equation 1.3.6-1}$$

AASHTO LRFD Equation 1.3.2.1-2

However, for minimum values of γ_i:

$$\eta_i = \frac{1}{\eta_D \eta_R \eta_I} \leq 1.0 \qquad \text{Equation 1.3.6-2}$$

AASHTO LRFD Equation 1.3.2.1-3

1.3.6.1 Ductility

The ductility factor, η_D, can be modified for the strength limit state to reflect a bridge's ductility characteristics. A higher value of 1.05 is used for nonductile components and connections. A value of 1.00 is used for conventional designs and details that comply with *AASHTO LRFD*. A lower value of 0.95 is used for components and connections for which measures have been taken beyond those required in *AASHTO LRFD* to enhance ductility in the bridge. For all non-strength limit states, a factor of 1.00 is used.

1.3.6.2 Redundancy

The redundancy factor, η_R, as the name implies, accounts for the redundant nature of the bridge or component. The preference is to design bridge members with a suitable level of redundancy unless there is a specific reason not to do so. For the strength limit state, a value of 1.05 is used for nonredundant members, and a value of 0.95 is used for exceptional levels of redundancy beyond girder continuity and a torsionally-closed cross section. For bridges with conventional levels of redundancy, and for all limit states other than strength, a value of 1.00 should be used.

The value of η_R used for design is based largely on subjective judgment. However, NCHRP Project No. 12-86 entitled "Bridge System Reliability for Redundancy" quantifies the structural system redundancy (that is, the system factor). The current AASHTO *Manual for Bridge Evaluation* has already adopted the system factor on the resistance side of the basic equation. It is anticipated that future editions of *AASHTO LRFD* will adopt the system factor to quantify the redundancy of the structure.

1.3.6.3 Operational Importance

The use of the operational importance factor, η_I, is somewhat more subjective than the ductility and redundancy factors. The operational importance of a bridge is the decision of the Owner, although *AASHTO LRFD* Article C1.3.5 provides some guidance. For the strength limit state, operational importance can range from 1.05 for critical or essential bridges to 0.95 for relatively less important bridges. For typical bridges, and for all limit states other than strength, a factor of 1.00 should be used.

Section 1.4 References

Kulicki, J. M., Z. Prucz, C. M. Clancy, D. R. Mertz, and A. S. Nowak. 2007. *Updating the Calibration Report for AASHTO LRFD Code, Final Report*. National Cooperative Highway Research Program, Project No. NCHRP 20-7/186.

Modjeski and Masters, University of Nebraska at Lincoln, University of Delaware, and NCS Consultants. 2013. *Bridges for Service Life Beyond 100 Years: Service Limit State Design*. Second Strategic Highway Research Program (SHRP 2), Transportation Research Board, Washington, DC.

Nowak, A. S. 1999. *Calibration of LRFD Bridge Design Code*. National Cooperative Highway Research Program, Report 368. Transportation Research Board, National Research Council, Washington, DC.

Sivakumar, Bala, Michael Ghosn, and Fred Moses. 2011. *Protocols for Collecting and Using Traffic Data in Bridge Design*. National Cooperative Highway Research Program, Report 683. Transportation Research Board, National Research Council, Washington, DC.

Chapter 2
General Design and Location Features

Section 2.1 Introduction

During the preliminary phase of a bridge design, several critical decisions must be made which set the course for the final design phase. These decisions relate to general design requirements and location features, and they directly influence whether the bridge design and construction will be successful or burdened with problems.

Ill-conceived preliminary designs cannot be made efficient during final design, regardless of how well the individual bridge components are designed. Therefore, general design considerations and location features must be carefully addressed early in the design process.

This chapter describes several important location features. It also describes fundamental design objectives, including safety, serviceability, constructibility, economy, aesthetics, security, and roadway drainage. Finally, a section describing Accelerated Bridge Construction (ABC) is provided in this chapter as well.

Section 2.2 Location Features

Location features that must be addressed during preliminary design include the route location, the bridge site arrangement, and clearances and geometry considerations.

To assist in these design decisions, AASHTO publishes *A Policy on Geometric Design of Highways and Streets*, commonly referred to as the "Green Book." This document contains the current design research and practices for highway and street geometric design. It provides guidance to highway engineers and designers who strive to make unique design solutions that meet the needs of highway users while maintaining the integrity of the environment. It is intended to serve as a comprehensive reference manual to assist in administrative, planning, and educational efforts pertaining to design formulation. Design guidelines are included for freeways, arterials, collectors, and local roads, in both urban and rural locations, paralleling the functional classification used in highway planning.

2.2.1 Route Location

2.2.1.1 General

The location and alignment of the bridge must satisfy both the on-bridge and under-bridge requirements. The bridge must be designed for the alignment of the roadway or railway it is supporting. This can result in a tangent bridge if the alignment is straight or slightly curved, a curved bridge if the alignment has a significant curve, or a flared bridge to allow for a varying roadway width. A curved bridge, supporting a roadway with an alignment of significant horizontal curvature, is shown in Figure 2.2.1.1-1.

Figure 2.2.1.1-1 Bridge with Curved Alignment

The preliminary design must also consider the need for skewed substructure units. A skew may be necessary if the feature that is being crossed (such as a roadway, railway, or waterway) is not oriented perpendicular to the bridge.

The route location for bridges must be established to facilitate a cost-effective design, construction, operation, inspection, and maintenance. It must also provide the desired level of traffic service and safety, and it must minimize adverse highway impacts.

2.2.1.2 Waterway and Floodplain Crossings

For bridges over waterways or in floodplains, it is best to avoid hydraulic problems by carefully selecting the bridge location rather than to minimize hydraulic problems later in the design process caused by an unfavorable bridge location.

Bridges over waterways must be aligned and located based on the following considerations:

- Hydrologic and hydraulic characteristics of the waterway, including flood history, channel stability, and any tidal ranges and cycles
- Effect of the proposed bridge on flood flow patterns
- Scour potential at the bridge foundations
- Potential for creating new flood hazards or worsening existing flood hazards, both upstream and downstream
- Various environmental impacts on the waterway

In addition, bridges over floodplains must be aligned and located based on the following considerations:

- Consistency with the standards and criteria of the National Flood Insurance Program, where applicable
- Long-term aggradation or degradation
- Any environmental approval requirements, including environmental restrictions during construction (which may affect construction methods and therefore also affect bridge type and span arrangement)

2.2.2 Bridge Site Arrangement

2.2.2.1 General

When defining the bridge site arrangement, any possible future variations in the alignment or width of the bridge or of the waterway, highway, or railway spanned by the bridge must be considered. For example, if the roadway being crossed may be widened in the future, then consideration should be given to locating the bridge's substructure units to facilitate the future roadway width. In addition, the bridge width should be determined with consideration to future widening of the roadway supported by the bridge.

2.2.2.2 Traffic Safety

When establishing the bridge site arrangement, careful attention must be given to traffic safety. *AASHTO LRFD* Article 2.3.2.2 provides guidance for the protection of portions of the bridge, protection of people or vehicles on the bridge, geometric requirements, roadway surface requirements, and vessel collision protection requirements.

Some of these traffic safety requirements include the following:

- Unless a rigid barrier is provided, barriers protecting substructure units should be located such that the roadway face of the barrier is at least 2 feet from the face of the substructure unit (to prevent transmission of force effects from the barrier to the substructure unit being protected).
- Similarly, the face of guardrails or other devices should be at least 2 feet outside the normal shoulder line.
- Movable bridges must satisfy unique requirements in the *Manual on Uniform Traffic Control Devices.*
- The width of shoulders and the geometry and crash test level of traffic barriers must satisfy the requirements of AASHTO and of the Owner.
- Road surfaces must satisfy design requirements for anti-skid characteristics, roadway crown, drainage, and superelevation.
- Bridge structures that may be subject to vessel collision must be protected using fenders, dikes, or dolphins, or they must be designed to resist the collision force effects specified in *AASHTO LRFD.*

2.2.3 Clearances and Geometry Considerations

In addition to route location and bridge site arrangement considerations, bridges must also be designed to satisfy all clearance and geometry requirements. The two basic types of clearance requirements are vertical clearance and horizontal clearance. Clearances must be considered for navigational, highway, railroad, and environmental requirements.

2.2.3.1 Navigational Clearances

For bridges over navigable waterways, required navigational clearances, both vertical and horizontal, must be established and satisfied in cooperation with the U.S. Coast Guard. In addition, permits for construction must be obtained from the Coast Guard, as well as from any other agencies having jurisdiction over the waterway.

2.2.3.2 Highway Vertical Clearances

Vertical clearance requirements are established to prevent collision damage to the superstructure, such as that shown in Figure 2.2.3.2-1. Requirements for vertical clearance are defined in AASHTO's *A Policy on Geometric Design of Highways and Streets*. Vertical clearance is measured from the top of the roadway surface to the bottom of the lowest superstructure component. For complex structures, it may be necessary to investigate the vertical clearance at several locations to ensure that the controlling value has been determined.

Figure 2.2.3.2-1 Violation of Vertical Clearance Requirement

Minimum vertical clearance is dependent on the roadway classification. For local roads and collector roads (and for roads with AASHTO functional classifications of local roads or collector roads), minimum vertical clearance is generally 14 feet. However, for arterials and freeways, minimum vertical clearance is generally 16 feet. In addition, for all four roadway classifications, an extra 6 inches of vertical clearance should be provided as additional consideration for future resurfacing.

The vertical clearance requirement for sign supports and pedestrian overpasses is generally 1 foot greater than for highway structures due to their reduced resistance to traffic impact.

When evaluating whether or not to utilize wider girder spacings, a number of issues should be considered. Girder depth limitations based on vertical clearance requirements may limit how many girders can be removed from a cross section. Maintaining the required vertical clearance by raising the bridge profile is generally not economical.

2.2.3.3 Highway Horizontal Clearances

No object on or under the bridge should be closer than 4 feet from the edge of a traffic lane, with the exception of a barrier, whose inside face should not be closer than 2 feet from the edge of the traffic lane or from any nearby object. The purpose of this requirement is to prevent collisions from errant vehicles or from vehicles carrying wide loads.

The roadway width on the bridge should not be less than the width of the approach roadways, including shoulders, curbs, gutters, and sidewalks.

Horizontal clearance requirements under the bridge are established to prevent collision damage to the substructure. Horizontal clearance requirements can be used to determine the type of abutment selected. For example, stub abutments are often used when a wide opening is required under the superstructure, and they provide a larger scope of view for the driver. Full-height abutments restrict the opening under the superstructure, but they also facilitate shorter span lengths.

2.2.3.4 Railroad Overpass Clearances

Railway bridges have clearance requirements that are set forth in American Railway Engineering and Maintenance-of-Way Association (AREMA), *Manual for Railway Engineering*. Clearances for railroad bridges must also satisfy design standards of the Association of American Railroads, AASHTO, local laws, and any additional requirements of the railroad owner.

2.2.3.5 Environmental Considerations

During the preliminary stages of a bridge design, any environmental considerations unique to the bridge site and bridge type must also be addressed. For example, the impact of the bridge and its approaches on local communities, historic sites, wetlands, and any other aesthetically or environmentally sensitive regions must be considered.

The Engineer must ensure that all laws and regulations are satisfied, including any state water laws, provisions of the National Flood Insurance Program, and any federal and state regulations concerning encroachment on floodplains and wetlands, fish, and wildlife habitats.

For bridges crossing waterways, the stream forces, consequences of riverbed scour, removal of embankment stabilizing vegetation, and impacts to tidal dynamics must also be considered.

Section 2.3 Design Objectives

During the design of a bridge, there are many different objectives that must all be satisfied and balanced by the Engineer. These design objectives include safety, serviceability, constructibility, economy, aesthetics, security, and roadway drainage.

2.3.1 Safety

The primary responsibility of a bridge engineer is to ensure the safety of the traveling public. This objective is fulfilled primarily by designing the bridge such that it fully satisfies the design requirements of *AASHTO LRFD*, as well as any other governing design requirements.

To ensure that this responsibility is fulfilled, bridge design projects should include a comprehensive check of all calculations and drawings, as well as an independent Quality Control review after the work is completed by an Engineer not associated with the specific work.

2.3.2 Serviceability

Another design objective is serviceability of the bridge, or its ability to provide service to the traveling public as intended.

Serviceability includes many different criteria, such as durability, maintainability, rideability, and deformations. These criteria are generally based on past practices, but they are not necessarily based on scientific evidence or research. However, in December 2013, new calibration work specific to serviceability was completed as part of the second Strategic Highway Research Program (SHRP 2), administered by the Transportation Research Board. Serviceability criteria are intended to ensure that the bridge can provide 75 years of service life.

2.3.2.1 Durability

The single most significant design decision that can enhance bridge durability is the elimination or reduction of the number of deck joints. When road de-icing agents are used on bridges with deck joints, deterioration is common for the structural components immediately below and in the vicinity of the joint. Experience has shown that the best way to prevent this deterioration is to eliminate deck joints as much as possible.

Where deck joints cannot be eliminated, careful attention should be given to making the joint as leak-proof as possible, as well as providing for the protection of bridge components beneath the joint. As shown in Figure 2.3.2.1-1, damage from snow plows, traffic, and debris can cause joint seals to be torn, pulled out of the anchorage, or removed altogether.

Figure 2.3.2.1-1 Damaged Compression Seal Resulting in Leakage

Another way to enhance bridge durability is to protect the post-tensioning system tendons. *Grouted Post-Tensioning Specifications*, a document developed by the Post-Tensioning Institute (PTI) and the American Segmental Bridge Institute (ASBI), provides Protection Levels (PL) for post-tensioning system tendons. PL1 is defined as a duct with grout providing durable corrosion protection, and PL2 is defined as PL1 plus a watertight, impermeable envelope providing a leak tight barrier. PL2 is generally accepted as the appropriate protection level for a bridge structure.

There are several other steps that can be taken to enhance durability for various bridge materials, as presented in Table 2.3.2.1-1:

Table 2.3.2.1-1 Durability of Bridge Materials

Material	Practices to Enhance Durability
Structural steel	• Self-protecting, long-life coating system, or cathodic protection
Reinforcing bars	• Epoxy or galvanized coating • Proper concrete cover
Concrete	• Proper density and chemical composition of concrete • Air-entrainment • Non-porous painting of concrete surface or cathodic protection
Prestressing strands	• Practices similar to those for reinforcing bars • Grout or other protection for strands in cable ducts
Attachments and fasteners used in wood construction	• Stainless steel, malleable iron, aluminum, or steel that is galvanized, cadmium-coated, or otherwise coated
Wood components	• Treated with preservatives
Aluminum components	• Electrically insulated from steel and concrete components

In addition, *AASHTO LRFD* Article 2.5.2.1.2 specifies the following measures to enhance bridge durability:

- Provide continuous drip grooves along the underside of the concrete deck near the fascia edge
- Provide slope on bearing seats to enable rain to wash away debris and salt
- Protect bearings against contact with salt and debris near open deck joints
- Interrupt wearing surfaces at deck joints and provide a smooth transition to the joint
- Protect steel formwork against corrosion

2.3.2.2 Inspectibility

Another serviceability consideration is to facilitate future inspection of the bridge. Such features as catwalks, walkways, inspection ladders, covered access holes, lighting provisions, and permanent hand rails for lanyard hooks should be considered, depending on the bridge type and size. Catwalks are frequently provided on large bridges to facilitate inspection of the superstructure from beneath the deck, as shown in Figure 2.3.2.2-1.

Figure 2.3.2.2-1 Catwalk to Facilitate Bridge Inspection

Fracture critical bridges often have features to facilitate future inspection as well. Fracture critical members should be sized and detailed to facilitate hands-on inspection. For example, fracture critical box members should be sized to facilitate interior inspection of the box, when feasible.

The *Guide Specifications for Design and Construction of Segmental Concrete Bridges* (AASHTO, 2003) provides requirements for external access hatches, openings at interior diaphragms, and venting intervals. These requirements also apply to similar bridges designed based on *AASHTO LRFD*.

2.3.2.3 Maintainability

Bridges must also be designed to facilitate preventive maintenance during the service life of the bridge. According to the AASHTO Subcommittee on Maintenance, preventive maintenance is defined as a planned strategy of cost-effective treatments to an existing roadway system and its appurtenances that preserves the system,

retards future deterioration, and maintains or improves the functional condition of the system without substantially increasing structural capacity (FHWA, 2011).

Since maintenance often requires jacking the bridge, jacking points should be clearly identified on the bridge drawings. The bridge should be designed for the anticipated jacking forces, and jacking stiffeners adjacent to the bearing stiffeners are often provided with steel girders.

Bridge Owners generally apply preventive maintenance to bridges that are in fair to good condition and to components that still have a significant remaining service life. Preventive maintenance applied in a cost-effective manner can keep bridges in good condition throughout their service life, reduce significant deterioration, and prevent large expenditures for bridge repair or replacement.

Preventive maintenance can be either cyclical or condition-based. Cyclical preventive maintenance includes activities that are performed at a pre-determined interval to preserve existing conditions. Cyclical maintenance does not necessarily improve bridge conditions, but it generally delays the onset of deterioration. Some examples of cyclical maintenance activities include the following:

- Wash and clean bridge decks or entire bridge
- Install deck overlay on concrete decks
- Seal concrete decks with waterproofing penetrating sealant
- Zone coat the ends of steel beam and girders
- Lubricate bearing devices
- Clean deck joints and troughs

On the other hand, condition-based preventive maintenance includes activities that are performed as-needed based on bridge inspection findings. Some examples of condition-based maintenance activities include the following:

- Sealing or replacement of leaking joints
- Installation of deck overlays
- Installation of cathodic protection systems
- Spot painting or coating of steel structural elements
- Installation of scour countermeasures

2.3.2.3.1 Design Considerations for Future Redecking

Since bridge decks frequently have a shorter service life than other bridge components, redecking is a fairly common maintenance activity. Therefore, it is important that bridges are designed to facilitate future redecking.

Half-width construction is often used for redecking. In half-width construction, one half of the bridge width is redecked while all traffic is diverted to the other half, and then the other half of the bridge width is redecked while all traffic is diverted to the new portion. Redecking using half-width construction is illustrated in Figure 2.3.2.3.1-1.

Figure 2.3.2.3.1-1 Redecking Using Half-Width Construction

A primary design consideration for future redecking is ensuring both strength and stability of the bridge during all anticipated conditions of redecking. Changes in live load distribution must be considered to account for the reduction in the number of girders carrying load. Some Owners require the use of five girder lines for new bridge designs since it enables future redecking using half-width construction, with each half of the bridge supported by three girder lines. An example of such a girder configuration is shown in Figure 2.3.2.3.1-2. The use of four girder lines, although it might be satisfactory for the final condition, might preclude the use of half-width construction for future redecking.

Figure 2.3.2.3.1-2 Half-Width Redecking with Each Half on Three Girder Lines

An alternative to half-width construction is the use of an adjacent parallel structure. The method of future redecking should be considered during the initial design process, and design provisions should be made to facilitate future redecking.

2.3.2.4 Rideability

Another serviceability consideration is rideability for the travelling public. The deck must be designed to allow the smooth movement of traffic over the bridge. There are several steps that can be taken to improve rideability, as presented in Table 2.3.2.4-1:

Table 2.3.2.4-1 Improving Rideability

Feature	Practices to Improve Rideability
Approaches to bridge	• Use approach slabs between the approach roadway and the bridge abutments
Construction tolerances	• Specify on the plans, in the specifications, or in the special provisions the required construction tolerances for the profile of the finished deck
Deck joints	• Minimize the number of deck joints • Protect edges of joints in concrete decks from spalling and abrasion • Specify on the plans that prefabricated joint assemblies must be erected as a single unit
Deck overlay	• Provide an additional thickness of ½ inch to permit corrections of the deck profile by grinding and to compensate for abrasion of the concrete deck

2.3.2.5 Utilities

Another serviceability consideration during design is to support and maintain the conveyance of utilities. Utilities crossing a bridge are often supported underneath the bridge deck in one of the girder bays. Supports are provided that span between adjacent girders at regular intervals to support the utilities. The design of such supports must account for the weight of the utility itself (such as a pipe), any additional weight (such as the weight of the water within the pipe), and the weight of the support itself.

Ducts are sometimes provided within concrete parapets to facilitate the passage of utilities.

Even if no utilities are required on the bridge at the time of the initial bridge design, consideration should be given to designing provisions for potential future utilities.

2.3.2.6 Deformations

2.3.2.6.1 General

Deformations on a bridge must also be considered during the design process. Deformation criteria are presented in *AASHTO LRFD* Article 2.5.2.6, and they are sometimes linked more with human psychological response than with bridge structural response.

Many deflection limitations and girder depth limitations are optional in *AASHTO LRFD*, although these limitations have a long history dating back to the first half of the 1900's. They are intended to restrict excessive deformations, excessive bridge vibrations or motion, and the appearance of sagging in the girders.

For horizontally curved and/or skewed bridges, additional deformation investigations are required since they are subjected to torsion, which results in larger deflections and twisting than in tangent bridges. These additional investigations include the following:

- Check of bearings, joints, integral abutments, and piers under elastic deformations
- Check of the end girder rotation and bearing rotation, accounting for the assumed construction sequence
- Computation of camber, accounting for the assumed construction sequence

2.3.2.6.2 Deflection Criteria

AASHTO LRFD Article 2.5.2.6.2 provides both optional and required deflection criteria. Optional deflection criteria are summarized in Table 2.3.2.6.2-1, and required deflection criteria are summarized in Table 2.3.2.6.2-2.

Table 2.3.2.6.2-1 Optional Deflection Criteria

Loading	Optional Deflection Limit
Steel, aluminum, or concrete bridges: Vehicular load, general	Span/800
Steel, aluminum, or concrete bridges: Vehicular and pedestrian loads	Span/1000
Steel, aluminum, or concrete bridges: Vehicular load on cantilever arms	Span/300
Steel, aluminum, or concrete bridges: Vehicular and pedestrian loads on cantilever arms	Span/375
Timber bridges: Vehicular and pedestrian loads	Span/425
Timber bridges: Vehicular load on wood planks and panels (extreme relative deflection between adjacent edges)	0.10 Inch

Table 2.3.2.6.2-2 Required Deflection Criteria

Loading	Required Deflection Limit
Orthotropic plate decks: Vehicular load on plate deck	Span/300
Orthotropic plate decks: Vehicular load on ribs of orthotropic metal decks	Span/1000
Orthotropic plate decks: Vehicular load on ribs of orthotropic metal decks (extreme relative deflection between adjacent ribs)	0.10 Inch
Precast reinforced concrete three-sided structures	Note: Deflection criteria for concrete structures are required for this structure type
Metal grid decks and other lightweight metal and concrete bridge decks: No pedestrian traffic	Span/800
Metal grid decks and other lightweight metal and concrete bridge decks: Limited pedestrian traffic	Span/1000
Metal grid decks and other lightweight metal and concrete bridge decks: Significant pedestrian traffic	Span/1200

When checking the deflection limit, live load should be applied as follows:

- The larger of design truck alone or 25 percent of the design truck taken together with the design lane load (see *AASHTO LRFD* Article 3.6.1.3.2)
- All design lanes loaded
- Include dynamic load allowance
- Include multiple presence factor
- Use Service I load combination
- The number and position of loaded lanes should be selected to produce the maximum effect

For composite design, the deflections should be computed using a stiffness which includes the entire roadway width as well as any structurally continuous portions of the sidewalks, median barriers, and railings.

For straight, non-skewed girder systems, all supporting components are assumed to deflect equally. The composite bending stiffness for each girder may be taken as the total stiffness for all girders divided by the number of girders.

However, for curved girder systems, the deflection of each girder should be computed individually based on an analysis of the entire girder system. The entire girder system is generally considered for sharply skewed bridges as well.

2.3.2.6.3 Optional Criteria for Span-to-Depth Ratio

AASHTO LRFD Table 2.5.2.6.3-1 provides optional criteria for span-to-depth ratios for a variety of structural materials, types, and span configurations. Ratios are provided for various types of reinforced concrete, prestressed concrete, and steel bridges, and they are provided for both simple spans and continuous spans. Since deflections are generally less in continuous spans than in simple spans, the recommended depth for continuous spans is less than or equal to the recommended depth for simple spans. The ratio is based on the minimum depth of the entire section, including both the girder and the deck.

For curved steel girder systems, *AASHTO LRFD* Article 2.5.2.6.3 specifies a preferred minimum depth, *D*, as follows:

$$D \geq \frac{L_{as}}{25} = 0.04L_{as} \qquad \text{Equation 2.3.2.6.3-1}$$

where L_{as} is the arc girder length defined as follows:

- Arc span for simple spans
- 0.9 times the arc span for continuous end spans
- 0.8 times the arc span for continuous interior spans

The recommended limit is to be applied to the I-beam portion only of curved steel girders when F_y in regions of positive flexure is less than or equal to 50 ksi, and when one of the following two conditions applies:

- F_y in regions of negative flexure is less than or equal to 70 ksi
- A hybrid section is used in regions of negative flexure

This preferred minimum depth is larger than the traditional values. This reflects the fact that the outermost steel girder receives a disproportionate share of the load and should be stiffer. *D* is defined in *AASHTO LRFD* as the overall depth of the steel girder, but it is recommended that *D* instead be taken as the web depth for simplicity.

In curved skewed bridges in particular, cross-frame forces are directly related to the relative girder deflections. Therefore, increasing the depth and stiffness of all the girders in a curved skewed bridge leads to smaller relative differences in the deflections and smaller cross-frame forces. Deeper girders also result in reduced out-of-plane rotations, which tend to make the bridge easier to erect. Sections deeper than the suggested minimum depth may be desired to provide greater stiffness during erection.

Whenever steels having yield stresses greater than 50 ksi are used for curved girders in regions of positive flexure, an increased minimum girder depth is recommended using the following equation:

$$D \geq \frac{L_{as}}{25}\sqrt{\frac{F_{yt}}{50}} = 0.04\,L_{as}\sqrt{\frac{F_{yt}}{50}} \qquad \text{Equation 2.3.2.6.3-2}$$

where:

F_{yt} = specified minimum yield strength of the bottom (tension) flange

Deeper girders with higher yield steel may be somewhat counterintuitive since stronger steels lead to smaller flanges and stockier webs. The use of higher strength steels results in the tendency to use shallower girders with larger flanges than would be required with a deeper web. The recommended relationship for this case is intended to ensure approximately the same dead and live load deflection as would be obtained at an L_{as}/D ratio of 25 when 50 ksi steel is used. In some cases, a hybrid girder using a 50 ksi top flange and web with a 70 ksi bottom flange is more

efficient in positive flexure. For this reason, the specified minimum yield strength of the bottom (tension) flange, F_{yt}, is used in Equation 2.3.2.6.3-2.

2.3.2.7 Future Widening

Since traffic volumes generally increase during the service life of a bridge, the need for additional lanes of traffic often requires a widening of the bridge at some point in the future. If there is any possibility that the bridge might be widened in the future, it should be designed to easily accommodate such a future widening.

Specifically, the exterior girders should be designed such that their load-carrying capacity is at least equal to that of an interior girder. In addition, consideration should be given to designing the piers and abutments for both the original condition and the widened condition.

2.3.3 Constructibility

Another essential design objective is to design the bridge such that it can be constructed. Constructibility requires consideration of such issues as site access, bearing installation, girder lifting and placing, deck forming systems, reinforcement bar placement, construction of the deck, and deck curing.

To assist the bridge engineer, FHWA has developed several design and analysis tools, including the *Manual on Engineering Stability in Construction of Bridge Superstructures*.

2.3.3.1 Site Access

The means of access to the site will determine the method of delivering the girders and other bridge components, whether by road, rail, or water. It will also influence the type, size, and capacity of cranes for lifting and placing girders. Accessibility for delivery and crane capacity will influence the choice of girders and other bridge components.

If a site is remote, such as in rugged terrain where access is difficult, it would be appropriate to adopt the lightest possible section size for the necessary span. For small span structures, small steel sections or precast concrete planks can be sufficiently light-weight for lifting and placing by a single crane suitably located on a stable platform.

Occasionally a crane may rest upon parts of the structure already completed, and components may be delivered along a portion already built. This can be useful for building long, simple trestles across low lying wetlands or similar areas where delivery and erection cannot be made over the ground.

The use of a crane located at each pier or abutment to pick up a girder at each end helps minimize crane size but requires two cranes. Larger sized, heavier girders typically require two medium to heavy-duty cranes. On land, cranes require firm temporary surfaces, support platforms, or access (see Figure 2.3.3.1-1). Also, at land sites, it may be necessary to construct special accesses or roads for delivery. All of these access requirements rapidly drive up construction costs. In such cases, it may be cheaper to use shorter spans and smaller girders, even if it requires additional piers.

Figure 2.3.3.1-1 Erection using Two Cranes

Large girders are often more suited to marine sites where water delivery is possible and heavier cranes can be conveniently placed on barges (see Figure 2.3.3.1-2). Not only are costs of marine construction generally greater than on land, but environmental controls must be considered if temporary channels must be dredged.

Figure 2.3.3.1-2 Crane on Barge

2.3.3.2 Bearing Installation

For many bridge construction projects, simple elastomeric pads can be used for the bearings. For short span bridges in which the deck effectively acts as a solid slab, a continuous elastomeric strip may be placed under the ends of the slab. For larger girders and spans, laminated elastomeric bearings are often required.

For stability and prevention of walking or rolling, elastomeric bearings are often set horizontal regardless of longitudinal grade. In turn, this requires the top of bearing seats to be constructed horizontally.

When there is little or no longitudinal gradient, girders can usually be placed directly on the elastomeric pad or bearing. The bearing design (that is, the plan dimensions, thickness, durometer hardness, laminations, and elastic properties) should take into account the need to accommodate longitudinal gradient, initial camber, and changes in rotation as the deck slab is cast.

For prestressed concrete girders, when there is a significant longitudinal gradient, it may be accommodated by a suitable varying thickness of a durable mortar, cement-based or sand-filled epoxy grout placed atop the bearings (see Figure 2.3.3.2-1). In some cases, it may be convenient and expedient to carefully place the girder while the mortar or grout is still wet but stiff, using the weight of the girder to automatically form the required variable thickness. In other cases, the mortar or grout may be dry-packed or injected under pressure while the girder is held on temporary blocks. In

all cases, the initial camber and subsequent change in end rotation as the deck is constructed should be taken into account in the design of the bearings.

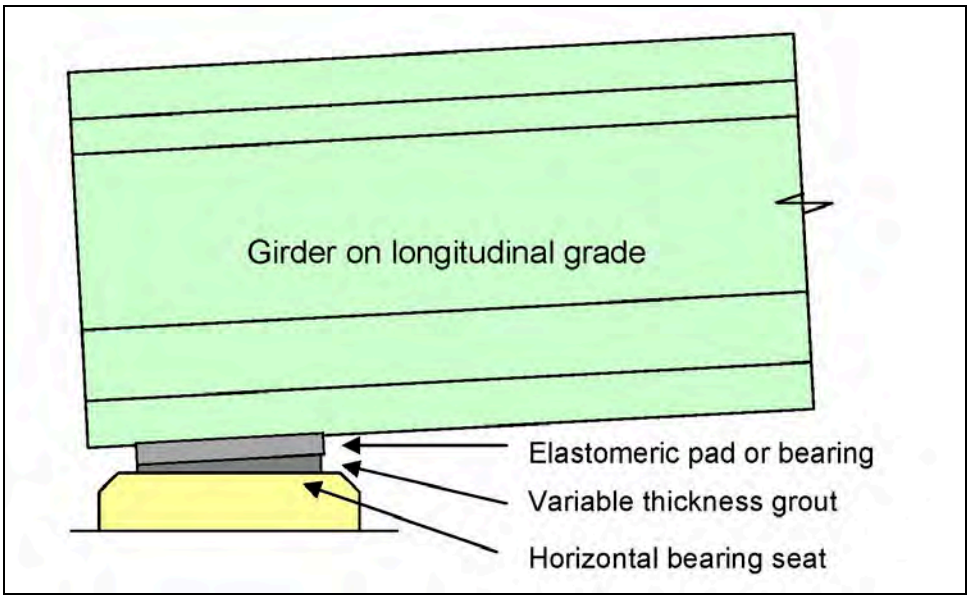

Figure 2.3.3.2-1 Elastomeric Bearing Detail for Longitudinal Gradient

Care is required with skewed structures (see Figure 2.3.3.2-2). Bearing pads should be oriented perpendicular to the in-plan axis of the girder and not parallel with the pier cap or abutment face (except perhaps for relatively low skews). For higher skews, if the pad is not perpendicular to the girder, the combination of camber, skewed-bearing, and longitudinal gradient will cause uneven load distribution which is concentrated more to one corner of the bearing than to the others. This may lead to undesirable consequences, such as local overstress of the bearing and temporary instability of the girder during erection. If this condition is unavoidable, then a suitable allowance should be made in the design, fabrication, and installation of the bearings, and measures should be taken to temporarily brace girders during erection.

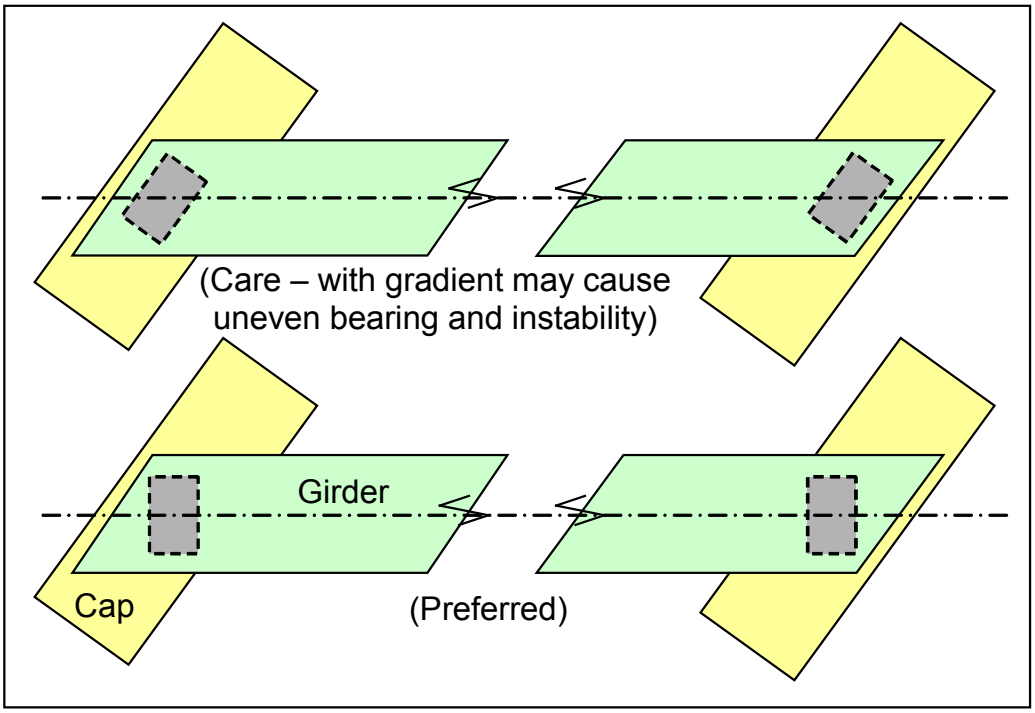

Figure 2.3.3.2-2 Bearing Orientation for High Skew

2.3.3.3 Girder Lifting and Placing

Short span components and girders may be sufficiently light to be transported using a single crane. Long girders usually require simultaneous lifting by a crane at each end.

For prestressed concrete girders, lifting attachments, such as loops of strand or other devices, are usually cast into the component at the precasting yard. Structurally, lateral stability of most precast concrete sections is assured by the width of the compression flange. However, during lifting and placing, care must be exercised to keep the girder vertical to ensure that it will set evenly on bearings or temporary supports. Tilt, along with excessive sweep, can lead to instability, especially with some long “top-heavy” sections. Temporary lateral bracing may be necessary when erecting some sections, particularly long girders, until permanent diaphragms have been installed. Temporary steel diaphragms have been used in some concrete girder structures to provide construction stability until the deck slab has been cast (see Figure 2.3.3.3-1). The cost of temporary intermediate steel diaphragm frames, including their installation and removal, should be considered in relation to the cost and benefits of alternative, permanent intermediate reinforced concrete diaphragms.

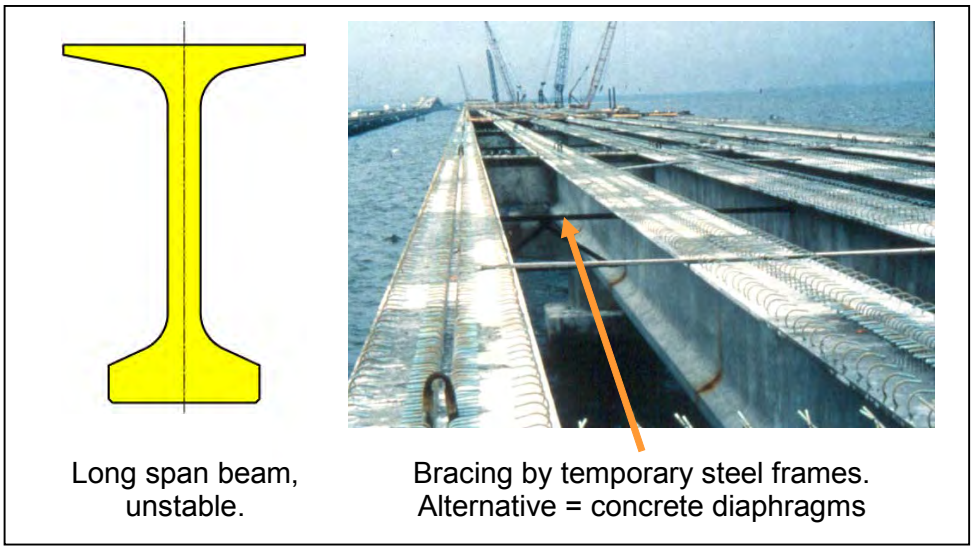

Figure 2.3.3.3-1 Temporary Bracing for Construction Stability

2.3.3.4 Deck Forming Systems

For many years, formwork for bridge deck slabs traditionally consisted of transverse timber joists supporting plywood soffit forms. Joists are suspended by hangers from the edges of the top flange of the girders. The lumber is temporary and is removed upon completion of the deck slab construction (see Figure 2.3.3.4-1). Temporary lumber formwork remains an economical and preferred choice in some regions and may be necessary in some cases for technical or environmental considerations.

Figure 2.3.3.4-1 Lumber Joists to Support Plywood Formwork

Many bridge construction projects use permanent, "stay-in-place," metal forms. These are generally made of galvanized steel folded to a section of multiple trapezoidal-shaped flutes (see Figure 2.3.3.4-2). The minimum required slab depth is typically measured to the top of the metal flutes, so that the weight of the metal form and concrete filling the flutes must be added to the dead load of the slab. A disadvantage of this system is that the support angles might eventually corrode or come loose, creating a risk to anything beneath the structure. Even though such instances are rare, the use of removable formwork may be preferred for certain spans.

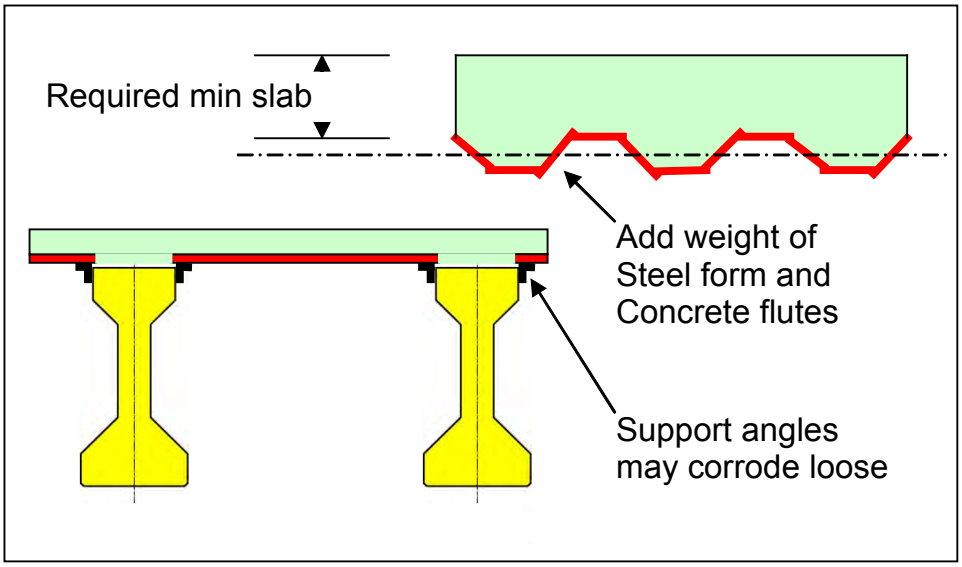

Figure 2.3.3.4-2 Stay-in-Place Metal Forms

Another alternative is to use permanent precast concrete panels as formwork. These are usually designed to be about half the depth of the slab. They must be securely set on a stiff mortar bed or other firm material on the top edge of the girder flange. Care must be taken in the design, fabrication, and construction to ensure that there is sufficient width of edge support and that the top flange does not crack or spall. Also, to ensure composite action between the girder and deck slab, reinforcement bars project from the top of girders and a designed width of cast-in-place slab must be in direct contact with the top of the girder. Therefore, panels cannot extend more than a few inches onto the flange (see Figure 2.3.3.4-3). Sometimes precast concrete deck panels may comprise the full slab thickness, leaving a gap along the top of each girder for a cast-in-place joint to develop composite action.

Because concrete shrinks and because different concretes of different maturity shrink by differing amounts, there is a tendency for shrinkage cracks to develop around the edges of precast deck panels. These cracks are aggravated by impact

and stress from local wheel loads and so, as a deck ages, shrinkage and reflective stress cracks tend to propagate. Great care must be taken with design, detailing, fabrication, installation, and casting of the deck slab and any concrete joints in order to minimize or eliminate such disadvantages.

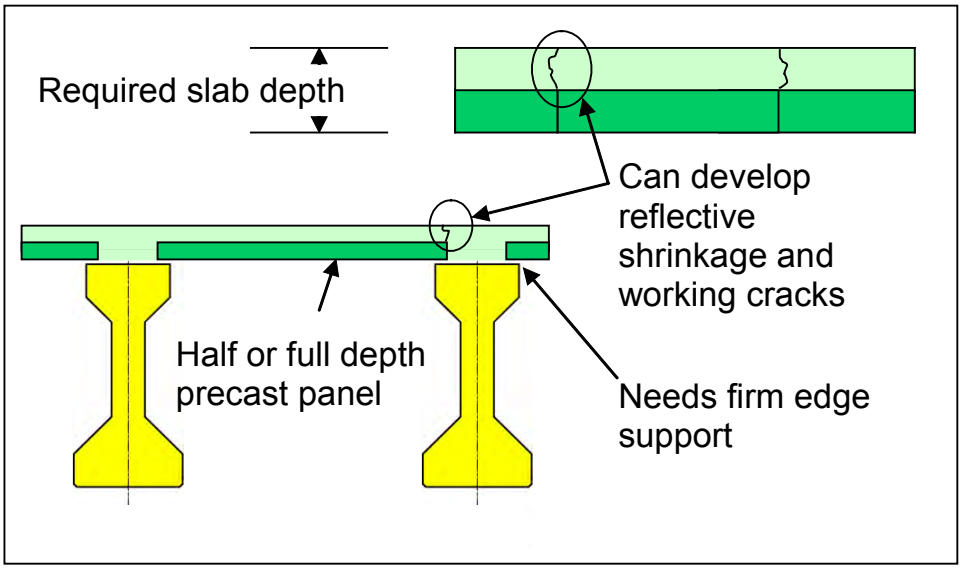

Figure 2.3.3.4-3 Precast Concrete Deck Slab Panels

In terms of on-site construction activity, the use of precast panels and stay-in-place metal forms is typically faster than the use of lumber formwork, but time is not the only factor. Consideration should be given to the particular needs of the project, the site, environment, advantages, disadvantages, maintenance, and relative costs of one system versus another. Figure 2.3.3.4-4 shows a lumber form system for widely spaced U-beams.

Figure 2.3.3.4-4 Lumber Form System for Widely Spaced U-Beams

2.3.3.5 Reinforcement Bar Placement

Once the formwork is in place, reinforcing steel for the deck slab may be prepared. However, prior to installing rebar, it is usually practical to first install any scuppers, hardware for expansion joint devices, and anchor devices for lights, signs, barriers, and similar embedded items. Reinforcing steel is usually assembled and placed on the forms using chairs of an approved (non-corrosive) material to provide the correct cover to the soffit. Chairs may be of different heights in order to support the top and bottom mat at the correct elevation (see Figure 2.3.3.5-1).

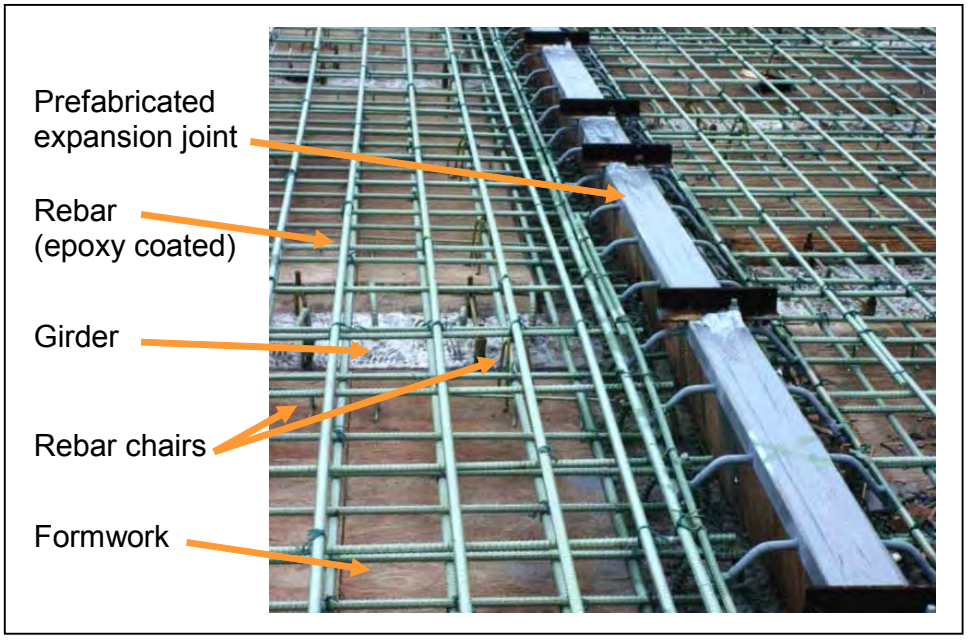

Figure 2.3.3.5-1 Installation of Deck Slab Reinforcing Steel

2.3.3.6 Construction of Deck

When the position and cleanliness of formwork, reinforcing steel, and embedded items have been checked, concrete placement may begin. Concrete is placed by different techniques, such as direct discharge from a truck mixer where access is feasible, or by chute, conveyor belt, or pump (see Figure 2.3.3.6-1).

Concrete is consolidated by vibrators and struck off to level by hand or by a mechanical screed. The mechanical screed rides on rails on each side of the deck. The rails are adjusted to line and level to provide the correct surface geometry. After screeding, the surface is usually worked a little more by hand floats or by additional passes of the screed to attain the desired accuracy and finish. Hand screeding and float finishing is rarely used for bridge construction today; rather, most decks are finished by machine.

Pump discharge

Vibration and Screeding

Figure 2.3.3.6-1 Placing, Consolidating, and Screeding a Concrete Slab

2.3.3.7 Deck Curing

To attain the required concrete strength, the heat of hydration must be slowly dissipated. To prevent undesirable effects of excessive shrinkage due to rapid water loss, deck slabs must be properly cured.

In most cases, a curing membrane is required for all exposed surfaces that have not been formed. Curing membranes are spray-applied compounds that form surface films to help minimize moisture loss.

Once the concrete has taken an initial set, curing blankets are placed to cover exposed surfaces. Curing blankets are usually a composite burlap-polyethylene sheet and may be quilted for added thermal protection. An alternative, often used in the past, is simply wet burlap. Polyethylene sheet is also sometimes used. Curing blankets are normally kept wet during the curing period, which may range from three days to over a week. In cold regions, it may be necessary to use steam or fog curing applied under covers or enclosures to help maintain air temperature at an acceptable level.

When the deck slab concrete has attained a certain required minimum strength, formwork may be released and removed. This is not normally done until the end of the curing period.

Project specifications should include a requirement that decks not be used for traffic or storage of construction material for a minimum period, usually 14 days, after placing concrete. Likewise, a deck is not normally opened to traffic until the curing is complete and the concrete attains its specified 28-day strength.

If access from the deck is necessary for continued construction activity, then special procedures may be considered, such as a higher strength concrete, a mix designed for rapid hardening, or special curing techniques such as steam or controlled heat and insulation, as appropriate or as necessary for the site.

2.3.4 Economy

Another objective for bridge design is economy. Cost comparisons are often an important element in preliminary design, facilitating selection between various alternative types of bridge structures. Although cost can be the most obvious comparison method, many other factors go into the selection of the appropriate bridge type, span length and arrangement, superstructure type, substructure type, and all other design elements of a bridge. For example, aesthetics, local environmental concerns, and Owner preferences can also factor into the final bridge selection. Public involvement can also help to determine the outcome, which may or may not be the least cost alternative under consideration.

2.3.4.1 Alternative Bridge Types

When performing a cost comparison, several alternative bridge types are usually considered. Each bridge type has a typical associated cost, which is based on previous design experience and is usually expressed in dollars per square foot.

These costs can be used for preliminary cost estimates, although they represent a cost only at a single point in time, at a specific location, and under specific economic conditions. These costs can vary greatly depending on the cost of materials at the time of construction, local labor rates in the vicinity of the construction site, proximity to access routes, fabricators, and raw materials. Before using these costs as a guide for selecting a low-cost alternative, local conditions should be analyzed and the costs per square foot adjusted to reflect the local conditions at the time of the construction of the bridge.

2.3.4.2 Span Length

One of the primary drivers of cost and a valuable comparison method for alternative bridge types is the consideration of the effects of span length on the cost of a structure. This comparison involves the cost of both the superstructure and substructure, as varying span length affects the cost of both components. As can be seen in Figure 2.3.4.2-1, an increased span length will cost more in superstructure but less in substructure, and the opposite is true of short span lengths over the same length of bridge.

For example, a single-span 800-foot steel superstructure will require massive beams with very high superstructure costs but with minimal substructure costs. On the

other hand, 40 20-foot spans over the same length of structure will require a much smaller superstructure, significantly decreasing the superstructure costs. However, it will also require 39 piers, greatly increasing the substructure costs.

To select the most appropriate span arrangement to achieve a low-cost alternative, plotting number of spans versus cost will generally produce a parabolic curve, with the low point being the optimum span configuration. As with other cost comparison methods, using the least-cost span arrangement may not be the most appropriate method due to aesthetic, environmental, and Owner considerations.

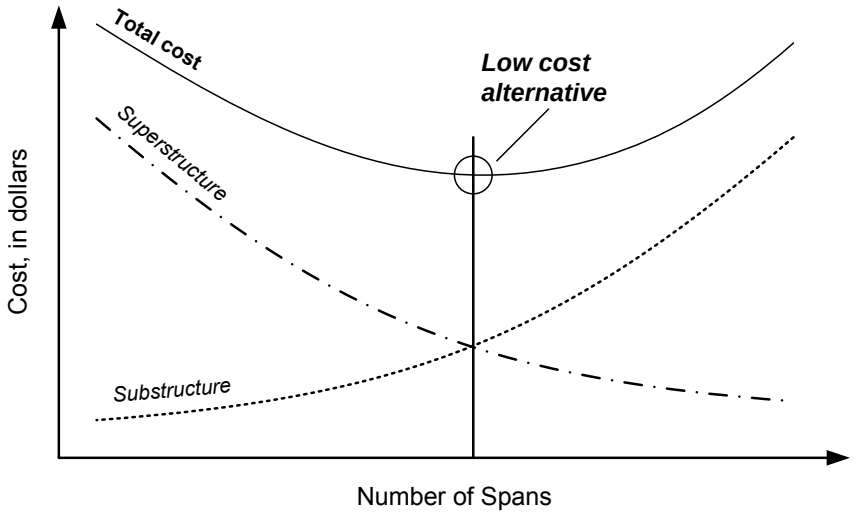

Figure 2.3.4.2-1 Number of Spans versus Cost

A curve similar to Figure 2.3.4.2-1 can be generated for each material type. If the axes are lined up, cost comparisons considering not only span arrangement but also structural material and any other differences in alternatives can also be considered. Again with an overlapping comparison, selection of the lowest point of the total cost parabolic curves will be the most cost-effective span arrangement and superstructure type. An example of this type of comparison is shown in Figure 2.3.4.2-2.

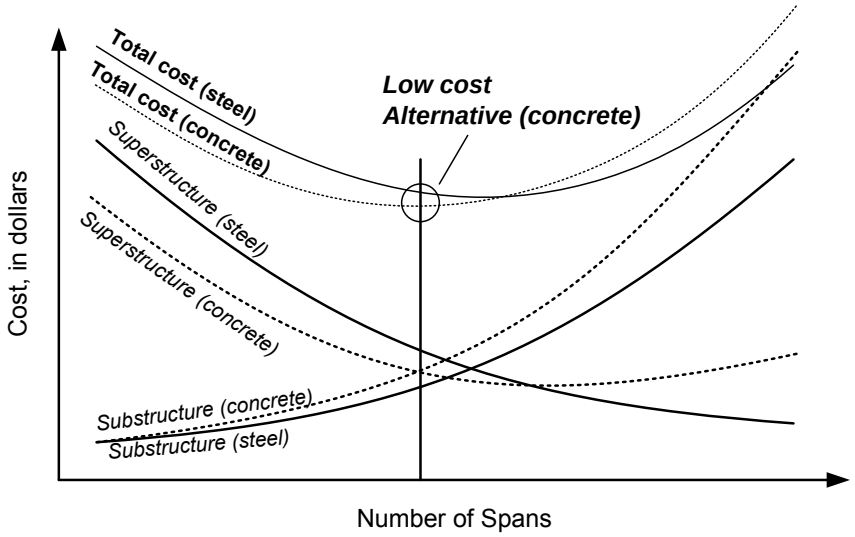

Figure 2.3.4.2-2 Spans and Materials versus Cost

2.3.4.3 Alternative Superstructure Materials

While Owner preference, aesthetics, and environmental concerns may govern the selection of superstructure materials, cost comparison is often a primary deciding factor. Prestressed concrete beam costs typically include all of the materials that go into the girders. Reinforcing steel, prestressing steel, and concrete all contribute to the cost of prestressed concrete beams, which are usually expressed in a unit cost of dollars per beam. Steel girder costs include the manufacturing and fabrication of plate, rolled, and box girders and are typically expressed in a unit cost of dollars per pound of steel.

When selecting alternatives, the best options can be selected before any design is performed based on typical costs of superstructure materials and the expected span length. In shorter span bridges, prestressed concrete girders often provide the least cost option, while in longer span bridges, steel beams are typically the less costly option. Prestressed concrete girders generally have a maximum permissible span length, which can limit their use in longer span bridges. Other considerations for alternative superstructure materials should include long-term effects of maintenance costs and other complete life-cycle costs.

2.3.4.4 Preliminary Cost Estimates

Cost comparison of bridge alternatives in the preliminary design stage typically involves the creation of an itemized cost estimate for each different superstructure type, span arrangement, and any other major differentiating factors between alternatives. These cost estimates are variable based on the final construction location of the bridge structure; therefore, using previous cost estimates for future

jobs should be done with caution to ensure that the proper material categories, unit costs, and contingencies are included.

Itemized cost estimates involve the creation of a material take-off. The material take-off is created using the preliminary bridge structure plans by estimating the amount of various construction materials for the bridge. Typical categories include girders, deck concrete, pier concrete, abutment concrete, guiderails, lighting structures, concrete coatings and sealers, and structural paint. However, these categories can vary from state to state. Once the material take-off has been tabulated, each category of construction material has an associated cost per unit. These unit costs are also tied to local conditions and will vary greatly from state to state, even within states. The measurement units can also vary, and designers need to be sure that the right amounts of material are being associated with the proper unit cost. The unit cost includes provisions for material and labor. Unit costs can be obtained from many sources, including previous jobs in similar areas, ASCE, AASHTO, and state DOTs. The application of the correct unit cost is imperative to providing a quality cost comparison and should be as exact as possible in the preliminary stages.

Finally, itemized cost estimates are summed and a contingency factor is applied. This contingency factor can range from 10 percent to 35 percent, depending on the design engineer's confidence in the bridge design, the variability of unit costs, and local typical practices. The contingency is intended to account for changes in the bridge design which may occur between preliminary and final design, changes in unit costs between preliminary and final design, and the cost of minor items that may not have been included in the preliminary cost estimate.

Another method of generating the preliminary cost estimate for comparison purposes is to apply a typical cost per square foot for that bridge type based on the area of the deck surface. The actual cost per square foot for a bridge structure will vary greatly depending on location, time of construction, distance from fabrication facilities, access to main roads, span length, substructure height, and many other factors. Because of all of the variables in a cost estimate, the cost per square foot, which is typically based solely on previous construction projects which may or may not match the conditions of the project being evaluated, will give a less accurate estimate than an itemized material take-off.

In conclusion, preliminary cost comparisons can provide a useful tool in the selection of the optimum bridge alternative for a specific location, but the design engineer should work with the Owner to consider other factors, such as aesthetics, environmental concerns, and Owner preferences. There should also be a distinction made between the initial cost of a bridge project and the life-cycle cost. In some cases, due to maintenance, expected rehabilitation, and other long-term factors, life-cycle costs of a bridge alternative could be higher for a structure with a lower initial

cost. Selection based on initial cost alone could prove to be more costly in long-term maintenance of the structure. Therefore, life-cycle cost analysis and comparison should be carried out before making a final decision of the most favorable bridge alternative.

2.3.5 Aesthetics

Every bridge makes a visual impact within its unique setting, some favorable and others unfavorable. Although beauty can sometimes be in the eyes of the beholder, there are several qualities of beauty to which most people can attest. Just as people can generally agree on what makes a painting or a symphony a work of beauty, so it is with bridges. There are several guiding principles that generally lead to the design of an aesthetically pleasing bridge.

Some of the most basic characteristics of aesthetically pleasing bridges include the following:

- They are generally simple – that is, they have few individual elements, and their elements are similar in function, size, and shape.
- They have relatively slender girders.
- The lines of the bridge are continuous, or they appear to be continuous.
- The shapes of the bridge's members reflect the forces acting on them – that is, they are largest where the forces are greatest and smallest where the forces are least.

Since bridge engineering is a profession that serves the general public, Engineers must take responsibility for the aesthetic impact of their bridges. Bridges generally last for a very long time, some for several centuries. The bridge engineer's responsibility to the public is not limited to designing safe, serviceable, and economical bridges. They are also obligated to design bridges that are pleasing for people to look at on a daily basis for many decades to come. The ability to design aesthetically pleasing bridges is a skill that can be developed by Engineers by following a series of aesthetic principles. It is the Engineer's responsibility to the traveling public to learn and master these skills.

Some of the most important determinants of a bridge's appearance are described below (Gottemoeller, 2004). These ten determinants are listed in order of importance to the aesthetic quality of the bridge.

2.3.5.1 Vertical and Horizontal Geometry

This first and most important determinant involves the basic geometry of the bridge relative to its surrounding topography and other nearby structures. While the bridge engineer usually is not able to define the vertical or horizontal geometry of the

bridge, small adjustments in the bridge's alignment can lead to significant improvements to its appearance. Some of these adjustments include the following:

- Locate the bridge along an alignment that appears to be the shortest distance between points.
- Provide a vertical and horizontal alignment that consists of long and continuous curves and tangents rather than a series of short and dissimilar segments.
- Whenever possible, provide curve lengths that are longer than the minimums set by AASHTO.
- Curve lengths should be as long as possible, preferably longer than the bridge itself.
- Whenever possible, provide a crest vertical curve on overpasses.
- Adjust the horizontal alignment if needed to simplify column placement and to provide consistent pier types.

2.3.5.2 Superstructure Type

The superstructure type is the second most important determinant of bridge appearance. Superstructure type is generally a function of structural requirements and economic considerations. It is often governed by the unique bridge site and the corresponding span lengths. Some of the primary factors influencing the choice of superstructure type are the following:

- If the bridge is curved or tapered, then the girders must be well suited to the required curve or taper.
- The span requirements and the required vertical clearances will affect the superstructure type and proportions.
- The nature of the bridge site and its surrounding topography may limit the choice of superstructure type (such as the unique bridge site requirements for arches, rigid frames, and cable-supported bridges).
- The superstructure type plays a major role in the establishment of a signature bridge.
- Relative slenderness is desirable in the selection of the superstructure type. An example of this is given in Figure 2.3.5.2-1.
- Continuity of structural form, material, and depth should be maintained as much as possible, as well as continuity between adjoining bridge types.

For girder bridges, several considerations can enhance the aesthetic quality of the bridge. Curved girders should be used for roadways with a significant horizontal curve. If the underside view of the bridge is especially important, box girders can provide an attractive solution. Integrally framed cross frames emphasize the visual continuity of the superstructure and can minimize the pier size. If girders must be

added to accommodate a flared bridge width, the girders should be added in a systematic and logical manner.

For arches and frames, the aesthetic quality of the bridge is enhanced by providing a visual thrust for the arch, either by the surrounding topography or by visual thrust blocks. For rigid frames, the legs should be approximately one-quarter to one-half of the span length.

For trusses, the design should incorporate a graceful and simple shape, a minimum number of members, a consistency of the angles, and small connection details.

Figure 2.3.5.2-1 Slenderness Improves the Aesthetic Quality of a Bridge

2.3.5.3 Pier Placement

The next most important determinant of a bridge's appearance is the pier placement. The placement of the piers is affected by several factors, including the under-bridge clearance requirements, hydraulic requirements, navigational channels, foundation conditions, and span length requirements. In addition to satisfying each of these pier placement criteria, there are also several aesthetic principles for pier placement:

- For most bridges, there should be an odd number of spans. An example of this is given in Figure 2.3.5.3-2.
- Piers should not be placed in the deepest part of a valley or cut.
- Whenever possible, piers should be placed on natural points of high ground.

- Piers should be placed as symmetrically as possible relative to shorelines.
- The span length should generally exceed the pier height.
- The ratio of the pier height to the span length should be similar from span to span.

Figure 2.3.5.3-1 Providing an Odd Number of Spans Enhances Bridge Aesthetics

2.3.5.4 Abutment Placement and Height

The visual function of an abutment is to get the bridge started and to connect the bridge with the earth. The placement, height, and appearance of the abutment can play a significant role in improving or detracting from the beauty of a bridge. As a general rule of thumb, the abutments should be placed to open up the view to the people traveling under the bridge. An example of this is given in Figure 2.3.5.4-1. The following are some general guidelines for abutment placement and height:

- The abutment height should not be less than one-half of the girder depth.
- For three- or four-span bridges, use minimum height pedestal abutments.
- If both abutments are visible at the same time, provide the same height-to-clearance ratio at both ends of the bridge.
- Use abutment wingwalls that are parallel to the roadway crossing the bridge (U-wings).

For skewed bridges, it can be beneficial to place the abutment near the top of the embankment and to place it at right angles to the roadway crossing the bridge. This improves the aesthetics of the bridge, reduces the amount of required fill, and simplifies analysis and construction. While it may increase span lengths, it also

reduces the required length and height of the abutments, which may provide a compensating savings.

Figure 2.3.5.4-1 Abutment Placement Providing an Open View

2.3.5.5 Superstructure Shape, Including Parapet and Railing Details

After the superstructure type has been selected and the abutments and piers have been located, there are additional choices that can be made to enhance the superstructure shape and the parapet and railing details. As previously described, it is desirable to design the superstructure such that it appears to be slender, light, and continuous. In addition, the superstructure shape should accentuate the function of the superstructure and the flow of forces through the superstructure to the substructure. Slenderness, lightness, and continuity can be achieved using some of the following techniques:

- Maximize the girder spacing, and maximize the girder overhang.
- Make the overhang no less than the girder depth.
- Provide a structural depth that is either constant or that varies smoothly over the length of the bridge.
- Consider haunched girders where feasible. An example of this is given in Figure 2.3.5.5-1.
- Make haunches long enough to be in proportion to the span length.
- Use pointed haunches at the piers to accentuate the flow of forces.
- Provide a haunched girder depth that is approximately 1.3 to 2.0 times the shallowest girder depth.

Figure 2.3.5.5-1 Haunched Girders Can Improve the Aesthetics of the Bridge

Railings and parapets also affect the aesthetic statement of a bridge. The height of the parapets should be between one-quarter and one-half of the exposed girder depth. In addition, it should also be no less than 1/80th of the span length. Incisions, recesses, and sloped planes can break up the face of the parapet horizontally, enhancing the aesthetics of the superstructure.

2.3.5.6 Pier Shape

Pier shape can play an important role in the visual impact of a bridge, especially for girder bridges. There is no single correct pier shape for all bridges, but it is important that a clear visual relationship is maintained for all substructure units.

For short piers, it is desirable to use piers which eliminate or minimize the pier cap. The taper of V-shaped and A-shaped piers should be limited, and hammerhead piers should have logical shapes. The pier width should be proportional to the superstructure depth, the span lengths, and the visible pier heights.

For tall piers, no more than two columns should be used at each pier line, if possible. The vertical members should be tapered or flared such that they are wider at the base of the pier. In addition, the pier shaft and cap should be integrated as much as

possible, rather than giving the appearance of two distinct elements. An example of this is given in Figure 2.3.5.6-1.

For groups of piers, each pier should have the same basic shape, and the shapes and curves of adjoining piers should be consistent.

Figure 2.3.5.6-1 Aesthetically-pleasing Tall Piers

2.3.5.7 Abutment Shape

The abutment shape can also play a significant role in the aesthetic quality of a bridge, especially for bridges of four spans or less. The shapes and details of the abutments should be selected to complement and enhance the shapes and details of other bridge components.

To frame the opening and to create a sense of transition between the abutment and the superstructure, the face of the abutment can be sloped inward. However, to make the superstructure appear longer or to emphasize the separation between the abutment and the girders, the face of the abutment can also be sloped outward. Abutments should be designed such that the adjoining retaining walls blend into the abutment without an abrupt change in appearance.

2.3.5.8 Colors

Although the shapes and patterns of the superstructure and substructure play the most significant role in creating the visual statement of a bridge, the surfaces of

those shapes can also add to that visual statement. The two most prominent qualities of the surface are its color and its textures and ornamentation.

The application of a specific color to a bridge is not necessary for the creation of an aesthetically-pleasing bridge. At the same time, however, the application of color cannot compensate for poor decisions elsewhere in the aesthetics of the bridge.

2.3.5.9 Surface Textures and Ornamentation

Similar to color, surface textures and ornamentation can also enhance the shapes and patterns for the bridge, but they cannot undo the visual impact of poor decisions concerning those shapes and patterns.

Concrete provides many opportunities for surface textures through the use of form liners and custom formwork. However, it is important to ensure that the pattern contributes to the overall design features and patterns of the structure itself. In addition, the pattern should be large enough to be recognizable to travelers on or beneath the bridge.

2.3.5.10 Signing, Lighting, and Landscaping

Finally, signing, lighting, and landscaping also influence the aesthetics of the bridge. Bridge-mounted signs should fit into the overall design of the bridge, and overhead sign structures on bridges should be kept as simple as possible.

Light should be avoided on short bridges, if possible. However, if they are necessary on the bridge, they should be placed in some consistent relationship to the geometry of the bridge, and their poles should be mounted on a widened area in the parapet.

Landscaping can be used to emphasize continuity of the space throughout the bridge and to soften the hard edges of the bridge. The colors and shapes of the landscaping should complement those of the bridge itself.

After studying these ten determinants of the bridge's appearance, it is important to note that the most important determinants are those which affect the geometry and appearance of the entire bridge, and the least important determinants are those which affect smaller details of the bridge. It is also important to note that many of these ten determinants can be fully implemented at no additional cost to the Owner.

2.3.6 Security

Assessing the need for bridge security measures has become increasingly important in recent years for both Engineers and Owners alike. Such a security assessment should include the following considerations:

- Social and economic impact of the loss of the bridge
- Availability of alternate routes
- Effect of closing the bridge on the security, defense, and emergency response of the region

For bridges that are considered critical or essential, a formal vulnerability study should be conducted and bridge security measures to mitigate against vulnerabilities should be considered and included during the design of the bridge.

Progress continues to be made in establishing procedures for vulnerability studies and effective bridge security measures. Recent developments and additional information can be found in the following references (see Section 2.5):

- Science Applications International Corporation, 2002
- The Blue Ribbon Panel on Bridge and Tunnel Security, 2003
- Winget, 2003
- Jenkins, 2001
- Abramson, 1999
- Williamson, 2006

2.3.7 Roadway Drainage

A final design objective for bridges is the effective drainage of water from the bridge roadway. Both the bridge and its approaches must be designed to provide conveyance of surface water such that the safety of the travelling public using the bridge is maximized. Roadway drainage can be facilitated in several ways.

First, drainage in the transverse direction on a bridge is provided through the use of a transverse cross slope or superelevation. This prevents water from ponding and ensures that it will flow away from the travel lanes towards the fascias. For bridges with more than three lanes in each direction, special rough surfaces or other special drainage measures should be considered to help prevent hydroplaning.

Second, drainage in the longitudinal direction is provided by using a longitudinal gradient on the bridge. Zero gradients and sag vertical curves should be avoided on bridges.

Third, deck drains should be provided on the bridge to satisfy the hydraulic requirements for bridges (AASHTO, 2005). In addition, water flowing downgrade towards the bridge should be intercepted into drains before reaching the bridge. Deck drains on the bridge are generally designed based on the design storm used for the pavement drainage system design of the adjacent roadway. If the design speed is less than 45 mph, then the deck drain design should ensure that the spread does not encroach on more than half of any traffic lane. If the design speed is greater than or equal to 45 mph, then the deck drain design should ensure that the spread does not encroach on any portion of the traffic lanes. Deck drains must be designed for hydraulic efficiency and accessibility for cleaning.

Finally, other bridge features that may be prone to water build-up should be designed for proper drainage. For example, sufficient deck drains should be provided to prevent water ponding at or near deck joints. In addition, weep holes in concrete decks and drain holes in stay-in-place forms can be used to prevent accumulation of water at the interface of decks with non-integral wearing surfaces or stay-in-place forms.

Roadway drainage must be provided in a manner that is consistent with other design objectives, including safety and aesthetics.

Section 2.4 Accelerated Bridge Construction

2.4.1 General

Accelerated Bridge Construction (ABC) provides a faster way than conventional construction to build new bridges or replace existing bridges through a variety of innovative methodologies. Using ABC technologies, State DOTs can replace bridges within as little as 24 to 72 hours, which results in significantly reduced traffic delays and road closures, as well as the potential for reduced project costs.

With conventional construction, the bridge is constructed in its final location using conventional construction methods, thereby interrupting traffic for an extended period of time. With ABC, however, the bridge is often assembled at a different location, usually immediately adjacent to the bridge site, and is then moved into its final location, interrupting traffic for a very limited period of time. Another ABC method involves assembly with prefabricated elements and systems, which also reduces interruption to traffic. With ABC, the need to minimize construction impacts and interruption time to the travelling public is given a significantly higher priority than with conventional construction. At a time when approximately 25 percent of our Nation's aging bridges need repair or replacement and when our highways are already congested, ABC significantly reduces the strain on the public due to road closures or extended traffic control.

Three particular ABC technologies are being promoted through FHWA's Every Day Counts initiative:

- Prefabricated bridge elements and systems (PBES)
- Slide-In Bridge Construction
- Geosynthetic Reinforced Soil – Integrated Bridge System (GRS-IBS)

PBES are structural components of a bridge that are built either offsite or adjacent to the alignment. PBES is best suited to features that reduce the onsite construction time and mobility impact time that occurs if conventional construction methods were used. Additional information about PBES is provided in Section 2.4.3 of this chapter.

Slide-In Bridge Construction is a cost-effective technique for deploying PBES or quickly replacing an existing bridge. Slide-In Bridge Construction involves building a new bridge on temporary supports parallel to an existing bridge. After construction of the new bridge is completed, the road is temporarily closed and the existing bridge structure is demolished or slid out of the way. The new bridge is then slid into place, tied into the approaches, and paved, usually all within about 24 to 72 hours. A Slide-In Bridge Construction project in Mesquite, Nevada is shown in Figure 2.4.1-1.

Figure 2.4.1-1 Overhead View of a Slide-In Bridge Construction Project (Source: Nevada DOT)

FHWA and Utah DOT published a *Slide-In Bridge Construction Implementation Guide* in December 2013. This guide includes information from the perspective of bridge ownership, design, and construction, and it includes case studies, sample plans, and sample special provisions. The *Slide-In Bridge Construction Implementation Guide* can be found at the following:
http://www.fhwa.dot.gov/construction/sibc/pubs/sibc_guide.pdf

GRS-IBS is a construction method that combines closely spaced geosynthetic reinforcement and granular soils into a composite material. The primary benefit of GRS-IBS is that it is easier and faster to construct, as well as easier to maintain, than conventional reinforced concrete abutment construction. Conventional construction requires forming, rebar installation, concrete placement, and concrete curing. These conventional steps require additional time, heavier equipment, and larger costs than GRS-IBS abutment construction. GRS-IBS has been found to be 25 to 60 percent more cost effective than conventional construction methods. GRS-IBS is a suitable application to construct abutments and approach embankments where settlement problems that could create a bump at the end of the bridge are not anticipated. Two reports are available from FHWA related to GRS-IBS design and implementation. The first, "Geosynthetic Reinforced Soil Integrated Bridge System Interim Implementation Guide" (FHWA-HRT-11-026), can be found at the following:
http://www.fhwa.dot.gov/publications/research/infrastructure/structures/11026/

In addition, "Geosynthetic Reinforced Soil Integrated Bridge System, Synthesis Report" (FHWA-HRT-11-027) can be found at the following:
http://www.fhwa.dot.gov/publications/research/infrastructure/structures/11027/11027.pdf

ABC methodologies currently used in the United States are based, at least in part, on an international scanning study conducted in Belgium, France, Germany, Japan, and the Netherlands during April 2004. The scanning study was sponsored by FHWA and AASHTO, and the 11-member team included three representatives from FHWA, four representatives from State DOTs, one representative from the National Association of County Engineers, one university representative, and two industry representatives. The countries were selected based of their known use of prefabricated systems. The objectives of the scanning study were to identify international uses of prefabricated bridge elements and systems, and to identify decision processes, design methodologies, construction techniques, costs, and maintenance and inspection issues related to the use of this technology. The study focused on prefabricated bridge systems that provide the following benefits:

- Minimize traffic disruption
- Improve work zone safety
- Minimize environmental impact
- Improve constructibility

- Increase quality
- Lower life-cycle costs

The report from the 2004 scanning study, entitled "Prefabricated Bridge Elements and Systems in Japan and Europe," can be found at the following: http://international.fhwa.dot.gov/prefab_bridges/pl05003.pdf

Since that study, ABC methodologies have taken root in many parts of the United States. To evaluate the effectiveness of ABC, two time metrics are often used – onsite construction time and mobility impact time.

Onsite construction time is the time period beginning when a contractor first alters the project site location and ending when all construction-related activity is removed. This includes the maintenance of traffic, materials, equipment, and personnel.

Mobility impact time is any period of time in which the traffic flow of the transportation network is reduced due to onsite construction activities. Traffic impacts on ABC projects are often categorized in the following five tiers:

- Tier 1 – traffic impacts within 1 to 24 hours
- Tier 2 – traffic impacts within 3 days
- Tier 3 – traffic impacts within 2 weeks
- Tier 4 – traffic impacts within 3 months
- Tier 5 – overall project schedule is significantly reduced by months to years

There are many ongoing NCHRP projects related to ABC, including development of design specifications, tolerances, and quality assurance and quality control guidelines. In addition, FHWA provides a wealth of references and documents related to ABC at the following: http://www.fhwa.dot.gov/construction/sibc/resources.cfm

2.4.2 Benefits and Applicability

ABC provides several benefits during construction, and it can be used for a broad range of applications. Some of the primary benefits of ABC include improvements in the following areas:

- Safety
- Quality
- Social costs
- Environmental impacts

ABC improves safety for both construction workers and the traveling public, since bridge construction generally does not take place in the vicinity of traffic.

ABC improves site constructibility, total project delivery time, and work-zone safety for the traveling public. At the same time, it reduces traffic impacts, onsite construction time, and weather-related time delays.

A common application for ABC is projects on which traffic impacts must be minimized to safeguard the traveling public and to maintain the flow of the transportation network during onsite construction-related activities. Other common applications for ABC relate to site constructibility issues. For example, where conventional construction methods would require long detours or costly temporary structures, ABC can provide a more practical and economic solution. ABC also provides benefits where the construction site is remote or where construction periods are limited.

With approximately one-fourth of the Nation's bridges requiring rehabilitation, repair, or total replacement, ABC will likely become increasingly important with each passing year. Using conventional construction, the work that occurs from on-site construction can have significant social impacts to mobility and safety and, in some cases, the direct and indirect costs of traffic detours resulting from bridge closure during construction can exceed the actual cost of the bridge itself. For example, full-lane closures in large urban centers or on highways with heavy traffic volumes can have a significant economic impact on commercial and industrial activities in the immediate region. In addition, partial lane closures and other bridge activities that occur alongside adjacent traffic can result in safety concerns.

ABC elevates minimizing traffic disruptions during bridge construction to a higher priority, and it provides a construction methodology that significantly reduces these undesirable economic and safety impacts.

2.4.3 Prefabricated Bridge Elements and Systems

The use of prefabricated bridge elements and systems (PBES) is a common ABC methodology. PBES are structural components of a bridge that are built offsite or near the site. They reduce the onsite construction time and mobility impact time, as compared with conventional construction methods, and they can also include innovations in design and high-performance materials. Because PBES are built offsite and under controlled environmental conditions, improvements in safety, quality, and long-term durability can be achieved. Some examples of PBES are presented in Table 2.4.3-1.

Table 2.4.3-1 Examples of Prefabricated Bridge Elements and Systems

Element	Examples
Deck elements	• Partial-depth precast deck panels • Full-depth precast deck panels with and without longitudinal post-tensioning • Lightweight precast deck panels • FRP deck panels • Steel grid (open or filled with concrete) • Orthotropic deck • Other prefabricated deck panels made with different materials or processes
Deck beam elements	• Adjacent deck bulb tee beams • Adjacent double tee beams • Adjacent inverted tee beams • Adjacent box beams • Modular beams with decks • Post-tensioned concrete thru beams • Other prefabricated adjacent beam elements
Full-width beam elements	• Truss span without deck • Arch span without deck • Other prefabricated full-width beam element without deck
Miscellaneous elements	• Precast approach slabs • Prefabricated parapets • Deck closure joints • Overlays • Other prefabricated miscellaneous elements

Connection details for PBES components must be carefully considered. Extensive information about PBES connection details can be found at the following: http://www.fhwa.dot.gov/bridge/prefab/if09010/

2.4.4 Structural Placement Methods

Some common structural placement methods used in ABC include the following:

- Self-Propelled Modular Transporters (SPMTs)
- Slide-in Bridge Construction
- Longitudinal launching
- Conventional and heavy-lifting equipment and methods

The first method, Self-Propelled Modular Transporters (SPMTs), involves a motorized vehicle that moves at walking speed and is capable of carrying a bridge from offsite locations and positioning it precisely into its final position. SPMTs are a combination of multi-axle platforms, they are operated by computer, and they are able to pivot 360 degrees to lift, carry, and set the bridge load as required. After the bridge has been positioned precisely in its final position, the SPMT is removed from the site, opening the bridge to traffic within a matter of a few minutes to a few hours. The use of SPMT technology provides Owners and contractors with considerable flexibility and speed in removing and installing bridges. An SPMT is shown in Figure 2.4.4-1.

Figure 2.4.4-1 Self-Propelled Modular Transporters

In addition, a report by the FHWA, entitled "Manual on Use of Self-Propelled Modular Transporters to Move Bridges," can be found at the following:
http://www.fhwa.dot.gov/bridge/pubs/07022/hif07022.pdf

Slide-In Bridge Construction is often referred to as a lateral slide. For a Slide-In Bridge Construction project, the new bridge is built on temporary supports parallel to the existing bridge while traffic continues uninterrupted on the existing bridge. When construction of the new bridge is completed, the road is temporarily closed and the existing structure is demolished or removed. The new bridge is then slid into place and attached to the approaches, usually within about one to three days. An alternative is to slide the existing bridge to a location immediately parallel to its original alignment and use it as a temporary detour bridge while the new bridge is constructed on the original alignment.

Longitudinal launching can be used for bridge construction over deep valleys, water crossings with steep slopes, or environmentally protected regions. It can also be used for bridge construction over roadways to minimize impacts to the roadway below. Longitudinal launching is similar to lateral slides, except that the slide is in the longitudinal direction rather than the lateral direction. It involves assembling the bridge superstructure on one side of an obstacle to be crossed and then moving, or launching, the superstructure longitudinally into its final position. Some advantages of this method include creating minimal disturbance to the surroundings, providing a concentrated work area for superstructure assembly, and possibly increased worker safety due to the improved erection environment.

Conventional and heavy-lifting equipment and methods can be used to move large prefabricated bridge elements and systems into place. When PBESs are being used on ABC projects, conventional cranes are often required to lift the prefabricated elements, move them to their required location, and facilitate their proper integration into the bridge. Such equipment and methods are similar to those used for conventional construction.

Section 2.5 References

AASHTO. 2003. *Guide Specifications for Design and Construction of Segmental Concrete Bridges*, Second Edition, 2003 Interim Revisions. American Association of State Highway and Transportation Officials, Washington, DC.

AASHTO. 2005. *Model Drainage Manual*, Third Edition, MDM-3. American Association of State Highway and Transportation Officials, Washington, DC.

Abramson, H. N., et al. 1999. *Improving Surface Transportation Security: A Research and Development Strategy*. Committee on R&D Strategies to Improve Surface Transportation Security, National Research Council, National Academy Press, Washington, DC.

The Blue Ribbon Panel on Bridge and Tunnel Security. 2003. *Recommendations for Bridge and Tunnel Security*. Special report prepared for FHWA and AASHTO, Washington, DC.

Culmo, M. P. 2009. *Connection Details for Prefabricated Bridge Elements and Systems*. Report No. FHWA-IF-09-010, Federal Highway Administration, Washington, DC.

FHWA. 2011. *Bridge Preservation Guide*. Publication No. FHWA-HIF-11-042, Federal Highway Administration, Washington, DC.

Gottemoeller, F. 2004. *Bridgescape: The Art of Designing Bridges*, Second Edition, John Wiley & Sons, Inc., New York, NY.

Jenkins, B. M. 2001. *Protecting Public Surface Transportation Against Terrorism and Serious Crime: An Executive Overview*. MTI Report 01-14. Mineta Transportation Institute, San Jose, CA.

Science Applications International Corporation (SAIC), Transportation Policy and Analysis Center. 2002. *A Guide to Highway Vulnerability Assessment for Critical Asset Identification and Protection*. Report prepared for The American Association of State Highway and Transportation Officials' Security Task Force, Washington, DC.

Williamson, E. B., D. G. Winget, J. C. Gannon, and K. A. Marchand. 2006. *Design of Critical Bridges for Security Against Terrorist Attacks: Phase II*. Pooled Fund Project TPF-5(056) Final Report. University of Texas, Austin, TX.

Winget, D. G., and E. B. Williamson. 2003. *Design of Critical Bridges for Security Against Terrorist Attacks*. TXDOT Project No. 0-4569, Phase 1 Report. University of Texas, Austin, TX.

This page intentionally left blank.

Chapter 3
Loads and Load Factors

Section 3.1 Introduction

The limit state design which characterizes the *AASHTO LRFD* specifications utilizes specific load types. These load types include dead loads, live loads, accumulated locked-in force effects, construction loads, wind loads, force effects due to superimposed deformations, friction forces, and blast loading. Each of these loads is described in this chapter.

The load types presented in this chapter apply primarily to the design of bridge superstructures, and additional loads must be considered in the design of bridge substructures. In addition, the load types presented in this chapter do not include those associated with extreme events, nor do they include those which apply exclusively to less common signature bridges.

Section 3.2 Permanent Loads

Permanent loads acting on a bridge superstructure include dead loads, as well as accumulated locked-in force effects. Each of these two load types is described in the following sections.

3.2.1 Dead Loads

3.2.1.1 General

Dead loads include all loads that are relatively constant over time, including the weight of the bridge itself. In LRFD bridge design, there are two primary types of dead load:

- Dead load of structural components and nonstructural attachments, designated as *DC*
- Dead load of wearing surfaces and utilities, designated as *DW*

For strength and extreme event limit states, the maximum load factors for *DW* dead loads are generally greater than the maximum load factors for *DC* dead loads due to the greater uncertainty of the presence and the exact value of *DW* dead loads.

Other dead loads are specified by the *AASHTO LRFD* specifications and are included specifically in some load combinations. These loads are due to the effects of earth pressure (both vertical and horizontal), earth pressure surcharge, and other geotechnical effects. These loads are not discussed in this section, as they influence the design of substructures and rarely, if ever, influence the design of a bridge superstructure.

3.2.1.2 Component Dead Loads, *DC*

AASHTO LRFD defines *DC* loads as "dead load of structural components and nonstructural attachments." Most dead loads that consist of the self-weight of the superstructure are considered to be *DC* loads, with the exception of wearing surfaces and utilities, which are *DW* loads.

DC dead loads are typically divided into two categories, frequently designated as *DC1* and *DC2*. *DC1* loads are *DC* dead loads that are resisted by the non-composite section, and they typically include the self-weight of girders, deck sections, and cross-frames. *DC2* loads are *DC* dead loads that are resisted by the composite section. *DC2* loads are typically placed later in the erection procedure, and they include raised sidewalks, roadway barriers, lighting structures, and other attachments to the structure. Although *DC1* loads and *DC2* loads are applied to different section properties, both *DC1* and *DC2* loads are considered one load type, *DC*, for purposes of determining a load factor for load combinations.

In the service limit state, *DC* loads are assigned a load factor of 1.00 to reflect normal operating conditions for the service limit state. In the strength limit state, the *DC* load factor has a minimum value and a maximum value. The maximum value is used in most cases. However, the minimum value is used when a minimum value of dead load is being computed, such as in computations for uplift at a support. Dead loads for the extreme event limit state are evaluated similar to dead loads for the strength limit state to account for possible variability of these permanent loads under abnormal, and possibly extreme, loading conditions. Fatigue limit state evaluation does not account for the effects of dead loads.

When computing component dead loads, the geometric properties of the various bridge components are used to calculate the expected gravitational effects. The design engineer is encouraged to investigate local conditions, specific bridge construction specifications or methods, and advances in materials technology to obtain the most appropriate unit weights for determination of dead loads. In the absence of more specific information, *AASHTO LRFD* provides guidance for typical unit weights in Table 3.5.1-1. An excerpt of that table for some of the most common structural materials is presented in Table 3.2.1.2-1.

Table 3.2.1.2-1 Unit Weights

Material	Unit Weight (kcf)
Concrete, Lightweight	0.110
Concrete, Sand-lightweight	0.120
Concrete, Normal weight with $f'_c \le 5.0$ ksi	0.145
Concrete, Normal weight with 5.0 ksi < $f'_c \le 15.0$ ksi	$0.140 + 0.001f'_c$
Steel	0.490
Wood, Hard	0.060
Wood, Soft	0.050

(excerpt from *AASHTO LRFD* Table 3.5.1-1)

3.2.1.2.1 Component Dead Loads Design Example

Both prestressed concrete girders and steel girders are commonly used in bridge design. For prestressed concrete girders, common shapes are available, and a weight per linear foot is generally provided for each shape. Therefore, prestressed girder weight computations are generally not required. However, for steel plate girders, the weight of the steel girder must be computed. Therefore, for illustrative purposes, a steel girder is used in the following design example.

Calculate the component dead load that is applied to the steel-only section for the steel girder and tributary area of normal weight concrete (f'_c = 4.0 ksi) as shown in Figure 3.2.1.2.1-1.

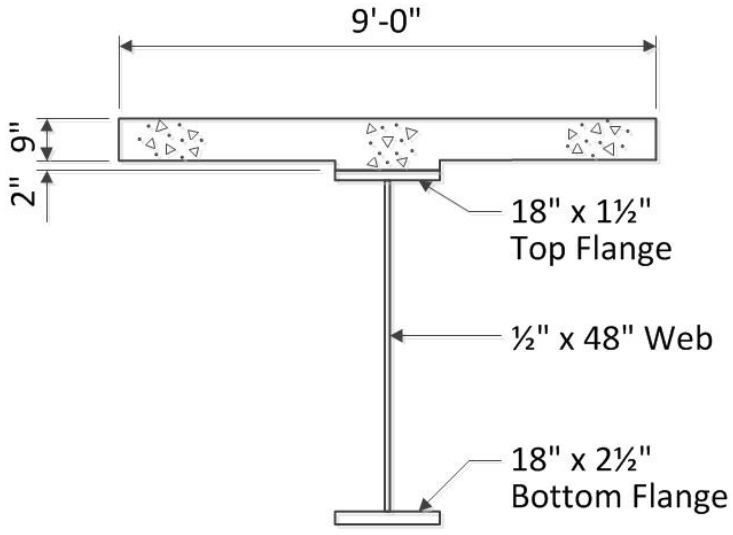

Figure 3.2.1.2.1-1 Steel Girder and Tributary Area

First, the area of concrete contributing to the *DC1* load must be computed. Since sidewalks and barriers are placed after the deck and girders and act on the

composite section, they are considered *DC2* loads and are not applied to the steel-only section. Therefore, sidewalk and barrier dead load is not included in this calculation.

Deck width = 9'-0" = 108"
Deck thickness = 9"
Haunch width = 18"
Haunch thickness = 2"
Deck and haunch area (concrete) = (108" x 9") + (18" x 2") = 1008 in^2

The area of the girder is calculated as follows:

Flange width = 18"
Top flange thickness = 1.5"
Bottom flange thickness = 2.5"
Web thickness = 0.5"
Web depth = 48"
Girder area (steel) = (18" x 1.5") + (18" x 2.5") + (48" x 0.5") = 96 in^2

The unit weight of normal weight concrete (f'_c = 4.0 ksi) from Table 3.2.1.2-1 is 0.145 kips per cubic foot. The unit weight of steel from Table 3.2.1.2-1 is 0.490 kips per cubic foot. Applying these unit weights to the areas already calculated gives the following linear weights:

$$(1008\ in^2 / 144\ in^2/ft^2) \times 0.145\ kcf = 1.015\ kips/ft$$
$$(96\ in^2 / 144\ in^2/ft^2) \times 0.490\ kcf = 0.327\ kips/ft$$

These two loads are then added together to compute the total *DC1* load per foot acting on the girder, as follows:

$$1.015\ kips/ft + 0.327\ kips/ft = 1.342\ kips/ft$$

3.2.1.3 Wearing Surface and Utility Loads, *DW*

Dead loads due to wearing surfaces and utilities are grouped together within the *DW* load type. Wearing surfaces can be those applied at initial construction or anticipated future wearing surfaces for maintenance of the bridge. Utility loads include the weight of conduits and attachments for not only bridge components but also those using the bridge as a method of crossing. Similar to wearing surfaces, utility loads can also be those applied at initial construction or anticipated future utilities.

DW dead loads are slightly more variable than *DC* dead loads described in the previous section. The wearing surface that is used in the future may have a different

thickness than what is anticipated during design. Similarly, utilities may be added or removed, and the weight of conduits and connectors in the future may change. To reflect this variability, in strength and extreme event limit states, the load factors for wearing surface and utility dead loads are 0.65 for minimum effects and 1.50 for maximum effects.

3.2.2 Accumulated Locked-In Force Effects, *EL*

Another loading condition that must be considered in bridge design is accumulated locked-in force effects. Similar to dead loads, these are considered to be permanent loads, and they are designated as *EL* in *AASHTO LRFD*. These force effects can result from the construction process, and they include such effects as secondary forces from post-tensioning and jacking apart of cantilevers in segmental construction. Accumulated locked-in force effects vary both in magnitude and in nature, depending on the bridge type and the erection method. *EL* loading is the only permanent load for which AASHTO assigns a maximum load factor of 1.00 and a minimum load factor of 1.00.

Section 3.3 Construction Loads

Construction loads are those loads which are applied to the structure during the erection process, including casting of deck sections and other sequential activities, and which introduce additional forces outside the normal range of service forces applied to the bridge during its design life. Some construction loads remain a consideration for the structure after construction is completed, such as in cable-stayed bridges. Other construction loads represent equipment and pedestrian loads which will not be present after the structure opens for service.

It is recommended that design engineers consult with contractors experienced in the erection procedure that is being recommended to obtain the most accurate construction loading information. Bridges should be checked for construction loads to ensure that structural damage will not occur during the construction process.

The construction loads considered during design should be noted on the contract drawings and documents to inform the Owner and bidding contractors of the maximum construction loads for which the structure has been evaluated. Construction loads for bridges can include the following:

- Erection loads
- Temporary supports and restraints
- Closure forces due to misalignment
- Residual forces and deformations from removal of temporary loads and supports

- Residual strain-induced effects from removal of temporary loads and supports

When constructing a reinforced concrete deck, either temporary formwork or stay-in-place formwork can be used. For bridges utilizing stay-in-place formwork, the formwork should be designed as specified in *AASHTO LRFD* Article 9.7.4, and its weight should be included as a *DC* dead load.

Section 3.10.2 of this chapter provides information about load factors for construction loads, including both strength limit state and service limit state.

Section 3.4 Live Loads

3.4.1 General

In addition to dead loads, which are continually acting on a bridge, and construction loads, which generally act on a bridge only during its construction, a bridge must also be designed to resist live loads. The primary difference between dead loads and live loads is that dead loads are permanent but live loads are transient. That is, dead loads act on the bridge at all times, but live loads are not necessarily present at all times. In addition, dead loads are stationary loads, but live loads are moving loads. Two common forms of live loads are vehicular loads and pedestrian loads.

3.4.1.1 Number of Design Lanes

When designing a bridge for live load, the bridge engineer must determine the number of design lanes acting on the bridge. The number of design lanes is directly related to the roadway width.

There are two terms used when considering the placement of live load across the width of the bridge:

- Design lane
- Loaded width within the design lane

A design lane generally has a width of 12 feet. The number of design lanes is simply computed as the roadway width divided by the 12-foot design lane width, rounded down to the nearest integer. For example, if the distance between the curbs is 70 feet, then the number of design lanes is five. When computing the number of design lanes, possible future adjustments to the roadway should be considered. For example, if a median is currently present on the bridge but may be removed in the future, then the number of design lanes should be computed assuming that the median is not present.

There are a few exceptions to the 12-foot design lane width. First, if the actual traffic lanes on a bridge have a width of less than 12 feet, then the design lane width should equal the actual traffic lane width. Second, for a roadway width between 20 and 24 feet, the bridge should be designed for two lanes, with the design lane width equal to one-half the roadway width.

The design lanes can be positioned anywhere across the width of the roadway, but they cannot overlap one another. In designing a bridge, the design lanes should be positioned such that the effect being considered is maximized. For example, when computing the maximum moment in an exterior girder, the lanes should be positioned as close as possible to that exterior girder. This is illustrated in Figure 3.4.1.1-1.

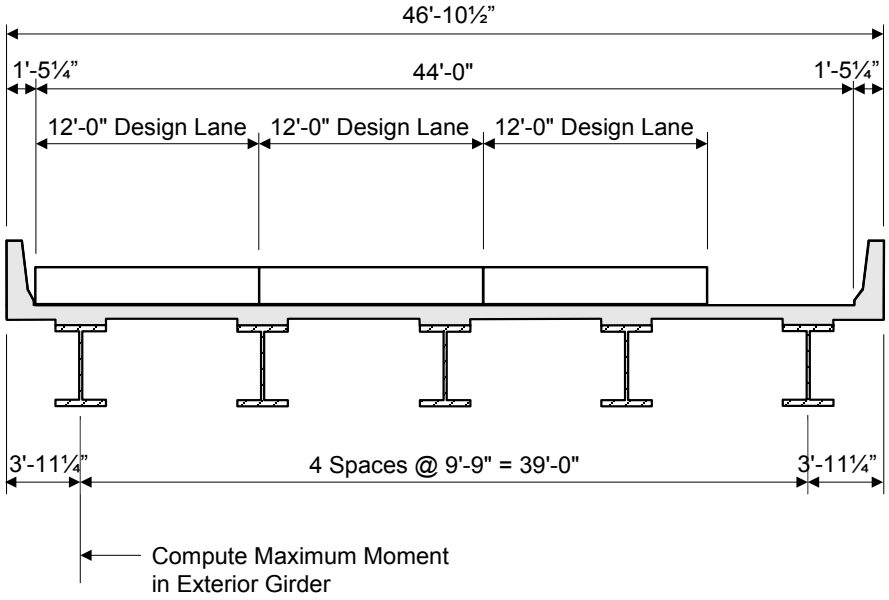

Figure 3.4.1.1-1 Position of Design Lanes

While the design lane generally has a width of 12 feet, the loaded width within the design lane is only 10 feet. The design truck, the design tandem, and the design lane load must be located entirely within the 10-foot loaded width. The 10-foot loaded width can be located anywhere within the 12-foot design lane, as long as the entire 10-foot loaded width is entirely within the 12-foot design lane. Similar to the placement of the design lane, the loaded width within the design lane is positioned such that the effect being considered is maximized. For example, for the exterior girder from the previous example, the loaded widths would be positioned as illustrated in Figure 3.4.1.1-2.

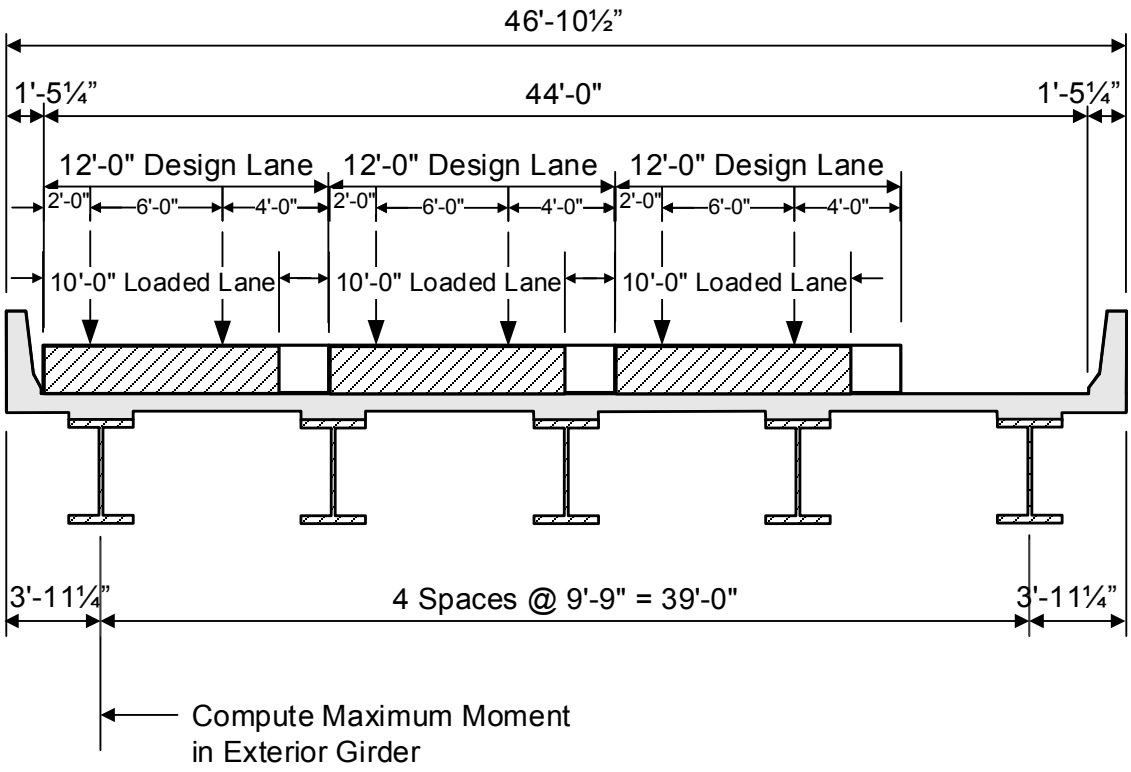

Figure 3.4.1.1-2 Position of Loaded Width within Design Lanes

As another example, if the maximum moment in the second girder from the left were being computed, then the 10-foot loaded width within the leftmost design lane should be shifted to the right side of that design lane.

3.4.1.2 Multiple Presence Factors

As previously described, a bridge must be designed for the number of design lanes that can be placed on the roadway. In addition, it must be designed for the HL-93 live load (described in Section 3.4.2.1), which conservatively represents the maximum load effects of vehicles that may legally act on the bridge. For a bridge design with more than one design lane, the controlling HL-93 live load configuration must be placed in each design lane simultaneously.

However, for a bridge with several design lanes, it is unlikely that each lane will be fully loaded with trucks simultaneously. To account for this improbability, AASHTO applies multiple presence factors. The bridge engineer must consider each possible combination of number of loaded lanes. For each number of loaded lanes, the Engineer must compute the force effect, then multiply that force effect by the corresponding multiple presence factor, and then use the loading condition for which

the effect being considered is maximized. Multiple presence factors are presented in Table 3.4.1.2-1.

Table 3.4.1.2-1 Multiple Presence Factors
(Based on *AASHTO LRFD* Table 3.6.1.1.2-1)

Number of Loaded Lanes	Multiple Presence Factor, *m*
1	1.20
2	1.00
3	0.85
>3	0.65

As presented in Table 3.4.1.2-1, the multiple presence factor, *m*, for one loaded lane is 1.20 rather than 1.00. This is because LRFD was calibrated based on the presence of two loaded lanes. Since the probability that all lanes will be fully loaded decreases as the number of loaded lanes increases, the multiple presence factor also decreases as the number of loaded lanes increases. Therefore, if the number of loaded lanes is greater than two, the multiple presence factor is less than 1.00. Similarly, if the number of loaded lanes is less than two, the multiple presence factor must be greater than 1.00.

For the purposes of determining the number of loaded lanes, pedestrian loads may be taken to be one loaded lane. It is important to note the applications for which multiple presence factors should and should not be used. Multiple presence factors should be applied in the following cases:

- For use with refined analysis methods
- For use with the lever rule
- For use whenever a sketch is required to compute the live load distribution
- For use with braking forces

However, multiple presence factors should not be applied in the following cases:

- For the approximate live load distribution factors computed as specified in *AASHTO LRFD* Article 4.6.2
- For the fatigue limit state in which one design truck is used

The multiple presence factors have already been included in the approximate live load distribution factor equations presented in *AASHTO LRFD* Article 4.6.2. Therefore, for the fatigue limit state, the force effects must be divided by the multiple presence factor for a single lane, which is 1.20.

3.4.2 Design Vehicular Live Load, LL

Vehicles crossing a bridge come in various shapes, sizes, and weights, such as cars, motorcycles, tractors, buses, and trucks. A bridge must be designed to resist all of the live loads that may legally pass across the bridge. However, the vehicles that most significantly affect a bridge are trucks. When compared with the effects of trucks on a bridge, the effects of cars and other vehicles are negligible. Therefore, the live loads used to design a bridge are based on truck loads.

There are many different types of trucks acting on our bridges today. Trucks come in many different configurations, varying in the following ways:

- Number of axles
- Spacing of axles
- Weight on each axle
- Total truck length
- Total truck weight

Since today's bridges must be able to resist a wide variety of trucks, bridges must be designed to resist all of those trucks. However, for the bridge engineer to consider every possible truck configuration that may act on a bridge would be excessively time consuming and unfeasible. Therefore, bridge engineers have developed what is called a notional vehicular load. A notional vehicular load is a theoretical or imaginary load that does not actually exist but that conservatively represents the load effects of vehicles that may legally act on the bridge. The design vehicular loads currently used by AASHTO are notional vehicular loads.

3.4.2.1 General

The design vehicular load currently used by AASHTO is designated as HL-93, in which "HL" is an abbreviation for highway loading and "93" represents the year of 1993 in which the loading was adopted by AASHTO. The HL-93 live load is based on a 1990 study by the Transportation Research Board (Cohen, 1990), and it consists of three different load types:

- Design truck
- Design tandem
- Design lane load

The following sections describe how these three different load types are configured in the longitudinal direction, how they are configured in the transverse direction, and how they are combined to form the HL-93 loading.

3.4.2.2 Design Truck

In the longitudinal direction, the design truck has three axles. The first axle has a loading of 8 kips, and the second and third axles have loadings of 32 kips each. The spacing between the first and second axles is 14 feet, but the spacing between the second and third axles varies between 14 and 30 feet. The axle spacing is selected such that the maximum effect is achieved. The minimum axle spacing of 14 feet usually controls. However, a situation in which an axle spacing greater than 14 feet may control is for a continuous short-span bridge in which the maximum negative moment at the pier is being computed and the second and third axles are positioned in different spans. The design truck is illustrated in Figure 3.4.2.2-1.

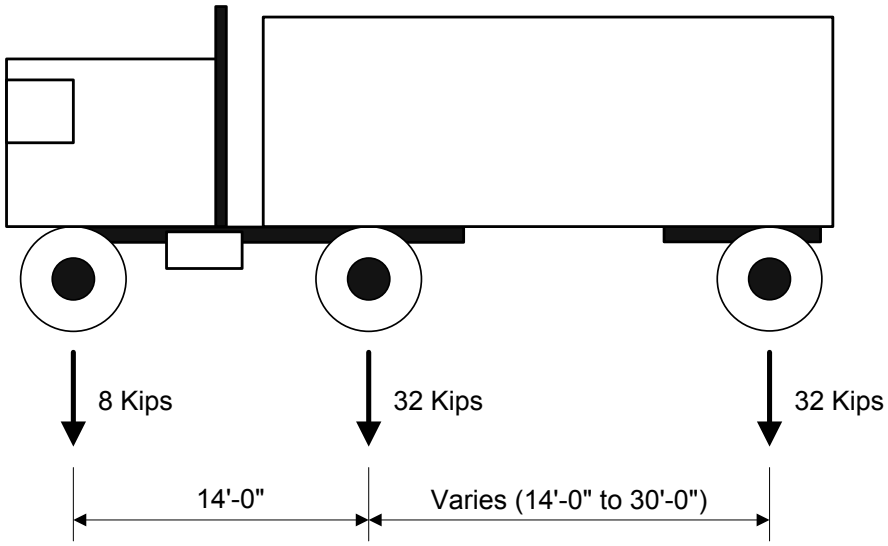

Figure 3.4.2.2-1 Design Truck

3.4.2.3 Design Tandem

The design tandem has two axles, each with a loading of 25 kips. The axle spacing for the design tandem is 4 feet. The design tandem is illustrated in Figure 3.4.2.3-1.

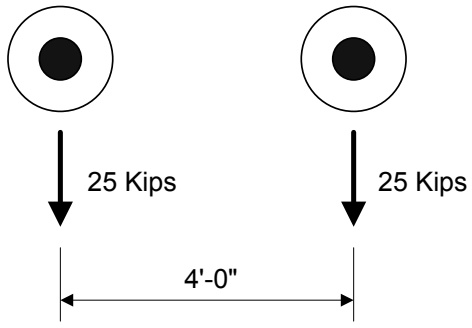

Figure 3.4.2.3-1 Design Tandem

3.4.2.4 Design Lane Load

The design lane load has a uniform load of 0.64 kips per linear foot, distributed in the longitudinal direction. The design lane load is applied only to that portion of the bridge that adds to the force effect being investigated. For example, if maximum positive moment is being computed in the center span of a three-span bridge, then the design lane load would be applied to the center span since that loading would result in positive moment in the center span. However, the design lane load would not be applied to the two end spans since that loading would reduce the maximum positive moment in the center span.

The design lane load is illustrated in Figure 3.4.2.4-1.

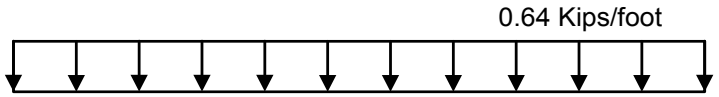

Figure 3.4.2.4-1 Design Lane Load

3.4.2.5 Tire Contact Area

While the above live load types were described in terms of axles and uniform load, the actual point of contact between vehicular traffic and bridges is the tire. The tire contract area of a wheel consisting of one or two tires is assumed to be a single rectangle measuring 20 inches wide and 10 inches long. The tire pressure is assumed to act uniformly within the tire contact area. For the design of orthotropic decks and wearing surfaces on orthotropic decks, the tire contact area for the front wheels is assumed to be a single rectangle measuring 10 inches wide and 10 inches long.

Tire contact area applies only to the design truck and tandem. In addition, its use is limited only to specific bridge elements, such as some decks and other members on which the vehicular tire directly bears. For the design of other superstructure members, such as girders and beams, wheel loads are considered to be concentrated point loads.

3.4.3 Application of Design Vehicular Live Loads

The design truck, design tandem, and design lane load are the building blocks for the design vehicular live load. They must be applied and combined in accordance with *AASHTO LRFD* and in such a way that results in the maximum value of the force effect being considered.

3.4.3.1 Longitudinal Application

The HL-93 loading consists of various combinations of the design truck, design tandem, and design lane load. Specifically, the HL-93 loading is taken as the maximum of the following two conditions:

- The effect of the design tandem plus the design lane load (see Figure 3.4.3.1-1)
- The effect of the design truck plus the design lane load (see Figure 3.4.3.1-2)

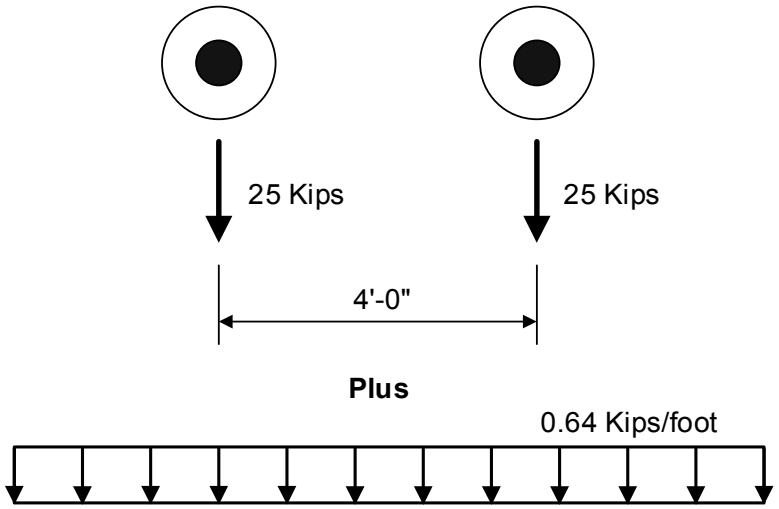

Figure 3.4.3.1-1 Effect of Design Tandem Plus Design Lane Load

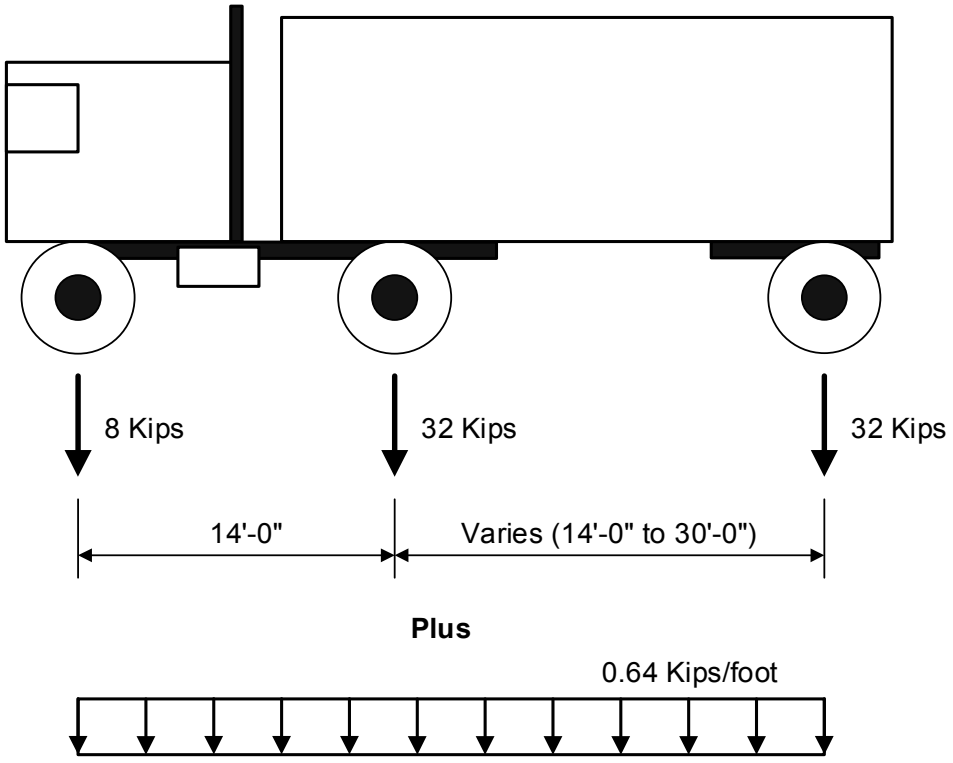

Figure 3.4.3.1-2 Effect of Design Truck Plus Design Lane Load

In addition, for negative moment between points of contraflexure based on a uniform load on all spans and for reaction at interior piers, a third condition is also considered. A second truck is added with a minimum headway between the front and rear axles of the two trucks equal to 50 feet. In addition, the distance between the two 32.0-kip axles of each truck is taken as 14 feet, and all loads are reduced by 10 percent. The two trucks are placed in adjacent spans to produce the maximum force effect being considered.

The design truck and the design lane load are similar to those used in the AASHTO *Standard Specifications for Highway Bridges* (AASHTO, 2002), which preceded the *AASHTO LRFD Bridge Design Specifications*. However, in the AASHTO *Standard Specifications for Highway Bridges* (AASHTO, 2002), the design truck and design lane load are considered separately and are not combined, whereas they are combined for the HL-93 live load in the *AASHTO LRFD Bridge Design Specifications*.

For design trucks and design tandems, axles that do not contribute to the force effect being considered are ignored. Similarly, for design lane load, longitudinal portions of the bridge that do not contribute to the force effect being considered are not loaded with design lane load.

The HL-93 loading was developed as a "notional" loading. That is, it does not represent a loading that is actually applied to bridges, but rather it was developed as a representation of the shears and moments produced by a group of vehicles routinely permitted on highways of various states under "grandfather" exclusions to weight laws. The vehicles considered to be representative of these exclusions (known as exclusion vehicles) were based on a study conducted by the Transportation Research Board (Cohen, 1990). The HL-93 load model is "notional" because it is not intended to represent any particular truck.

3.4.3.2 Transverse Application

In the transverse direction, the design truck and design tandem should be located in such a way that the effect being considered is maximized. However, the center of any wheel load must not be closer than 2 feet from the edge of the design lane. The single exception is for the design of a deck overhang, in which case the center of the wheel load can be as close as 1 foot from the face of the curb or railing.

The transverse live load configuration for a design truck or design tandem is illustrated in Figure 3.4.3.2-1.

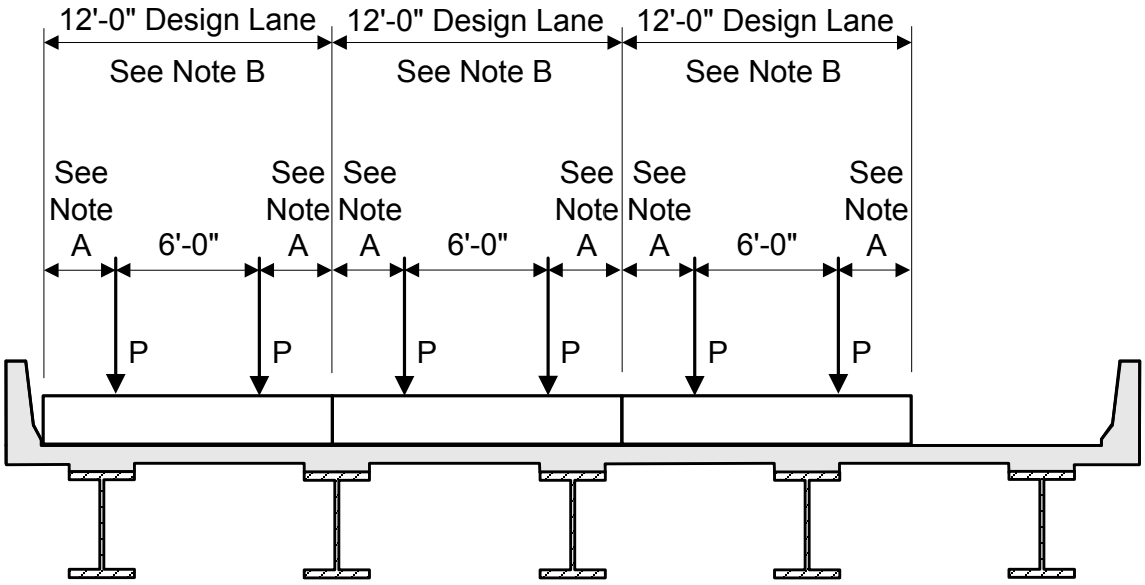

P = Wheel Load

Note A: Position wheel loads within the design lane such that the effect being considered is maximized; minimum = 2'-0".

Note B: Position design lanes across the roadway such that the effect being considered is maximized.

Figure 3.4.3.2-1 Transverse Configuration for a Design Truck or Design Tandem

Similarly, the design lane load is distributed uniformly over the 10-foot loaded width. Since the design lane load is 0.64 kips per linear foot in the longitudinal direction and it acts over a 10-foot width, the design lane load is equivalent to 64 pounds per square foot. The transverse live load configuration for a design lane load is illustrated in Figure 3.4.3.2-2.

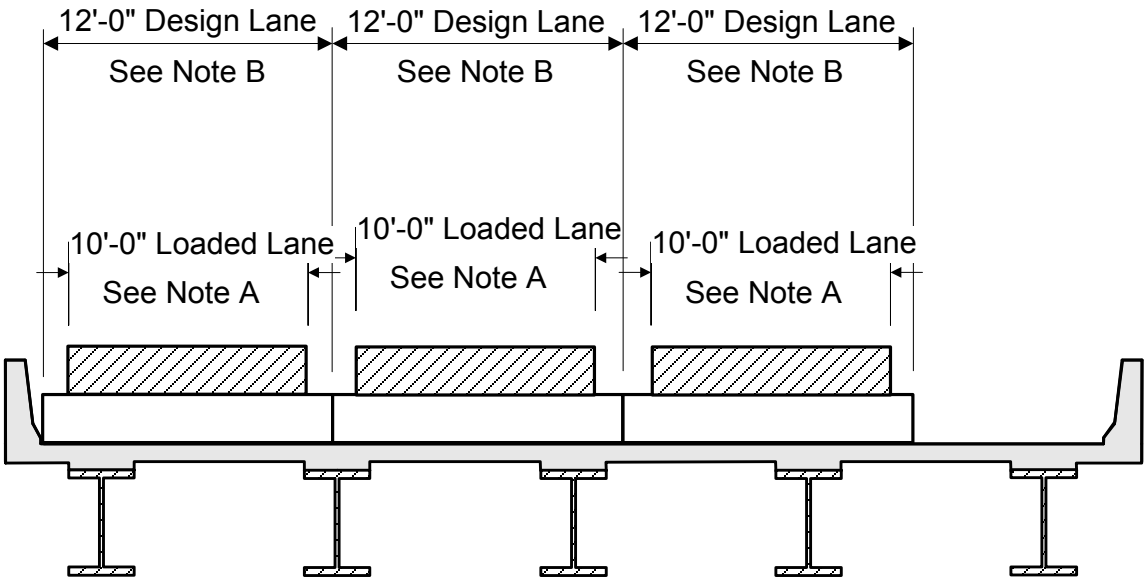

Note A: Position loaded lane within the design lane such that the effect being considered is maximized.

Note B: Position design lanes across the roadway such that the effect being considered is maximized.

Figure 3.4.3.2-2 Transverse Configuration for a Design Lane Load

3.4.3.3 Loading for Optional Live Load Deflection Evaluation

In *AASHTO LRFD* Article 2.5.2.6.2, optional criteria for deflection control are provided. If an Owner chooses to invoke these optional criteria for deflection control, then the live load used for this evaluation should be the larger of the following:

- Design truck only
- Design lane load applied with 25 percent of the design truck

The optional criteria for deflection control are based on requirements from the AASHTO *Standard Specifications for Highway Bridges* (AASHTO, 2002), which preceded *AASHTO LRFD*. These live load deflection control criteria were developed based on the HS20 live loading specified in the AASHTO *Standard Specifications for Highway Bridges* (AASHTO, 2002), and they are now optional in *AASHTO LRFD*. The loading for the optional live load deflection evaluation described above is intended to approximate the HS20 loading upon which these criteria were originally based.

3.4.3.4 Design Loads for Decks and Deck Systems

For the design of bridge decks and slab bridges using the approximate strip method, the design load is an axle load rather than a single wheel load. For slabs that span primarily in the transverse direction, only the axles of the design truck or design tandem should be applied to the deck slab. Similarly, for slabs that span primarily in the longitudinal direction with a span length not exceeding 15 feet, only the axles of the design truck or design tandem should be applied. However, for slabs that span primarily in the longitudinal direction with a span length exceeding 15 feet, the live load requirements normally used for bridge elements (as previously described in Section 3.4.3.1) should be applied.

When refined methods are used to analyze the bridge deck, the live load requirements normally used for bridge elements (as previously described in Section 3.4.3.1) should be applied to slabs that span primarily in the longitudinal direction, regardless of the span length.

Each wheel load is assumed to equal one-half of the axle load. Centrifugal forces and braking forces need not be considered in the design of bridge decks. According to *AASHTO LRFD* Article C3.6.1.3.3, Owners may choose to develop other axle weights and configurations to capture the load effects of the actual loads within their jurisdiction for decks and deck systems.

3.4.3.5 Design Loads for Deck Overhangs

For the design of deck overhangs, the outside row of wheel loads may be replaced with a uniform load of 1.0 kip per linear foot, applied 1 foot from the face of the railing. This provision applies if the deck overhang cantilever is less than or equal to 6 feet from the centerline of the exterior girder to the face of a structurally continuous concrete railing. This provision does not apply if the concrete railing is not structurally continuous.

The loading of 1.0 kip per linear foot is based on the assumption that the 25-kip half-weight of a design tandem is uniformly distributed over a longitudinal length of 25 feet. Structurally continuous concrete railings have been found to be effective in distributing the 25-kip load in the overhang over a 25-foot length.

3.4.4 Fatigue Load

In addition to the live loading described above, fatigue live load must also be considered. Fatigue is a phenomenon of material failure caused by repeated applications of a load. When applied infrequently, these loads would cause no undesirable effects, but when applied repeatedly, they can lead to failure. When the load is cyclic, the stress level that leads to failure can be significantly less than the

material yield stress. The effects of fatigue are based on the following considerations:

- The type and quality of the structural detail
- The magnitude of the stress range
- The number of applications (or cycles) of this stress range

3.4.4.1 Magnitude and Configuration

Since most trucks have a weight less than the design vehicular load, it would be excessively conservative to use the HL-93 loading previously described for fatigue load. Therefore for fatigue load, AASHTO uses the design truck with the following adjustments:

- The axle spacing between the two 32-kip axles is a constant 30 feet.
- The fatigue truck is placed in only one lane.

The fatigue load is illustrated in Figure 3.4.4.1-1.

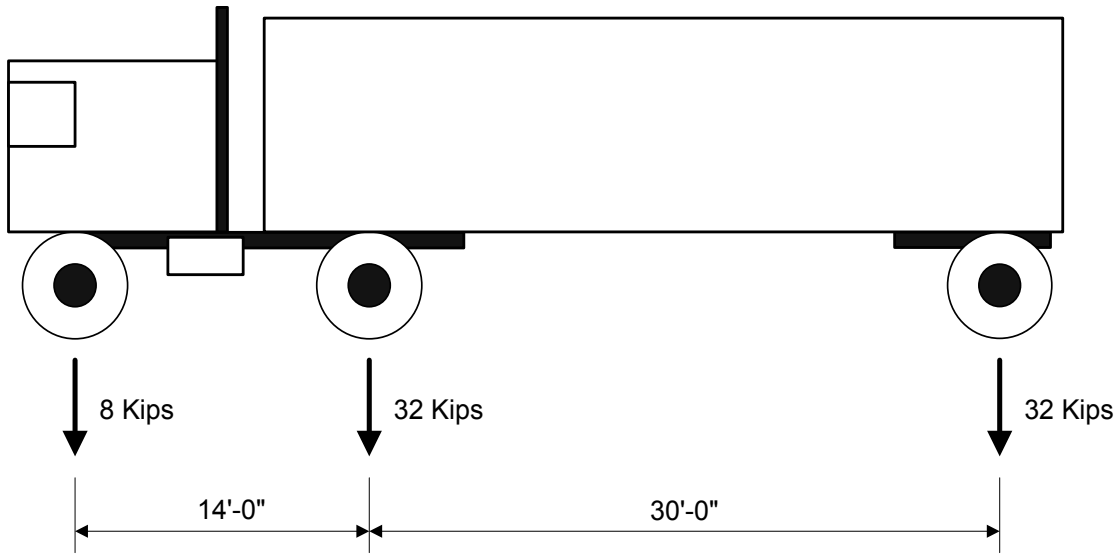

Figure 3.4.4.1-1 Fatigue Load

3.4.4.2 Frequency

In addition to the actual loading, the number of cycles also influences the fatigue design of a bridge. In the absence of more accurate traffic data, the average daily truck traffic (*ADTT*) for a single lane may be computed as follows:

$$ADTT_{SL} = p(ADTT)$$ Equation 3.4.4.2-1

AASHTO LRFD Equation 3.6.1.4.2-1

where:

$ADTT_{SL}$ = number of trucks per day in a single lane averaged over the design life

p = fraction of traffic in a single lane (see Table 3.4.4.2-1)

$ADTT$ = number of trucks per day in one direction averaged over the design life

Table 3.4.4.2-1 Fraction of Truck Traffic in a Single Lane, *p*
(Based on *AASHTO LRFD* Table 3.6.1.4.2-1)

Number of Lanes Available to Trucks	*P*
1	1.00
2	0.85
3 or more	0.80

In the above equation, the *ADTT* can usually be obtained from the Owner. However, if *ADTT* data is not available, then the *ADTT* can be estimated based on the average daily traffic (*ADT*) and the fraction of truck traffic to total traffic. This fraction can vary widely, depending on the type of roadway crossing the bridge and the location of the bridge. If more accurate data is not available, the fractions presented in Table 3.4.4.2-2 can be used. The *ADTT* can be estimated by multiplying the *ADT* by the fraction presented in Table 3.4.4.2-2. It should be noted that the number of stress cycles does not affect the fatigue load but rather the fatigue resistance.

Table 3.4.4.2-2 Fraction of Trucks in Traffic
(Based on *AASHTO LRFD* Table C3.6.1.4.2-1)

Class of Highway	Fraction of Trucks in Traffic
Rural Interstate	0.20
Urban Interstate	0.15
Other Rural	0.15
Other Urban	0.10

3.4.4.3 Load Distribution for Fatigue

For bridges analyzed by any refined method, a single fatigue truck is placed on the bridge deck, both longitudinally and transversely, without regard to the location of the striped lanes or design lanes on the deck, such that the maximum fatigue stress range or deflection is obtained.

For bridges analyzed by approximate methods, the distribution factor for one traffic lane should be used.

3.4.4.4 Refined Design Truck for Fatigue Design of Orthotropic Decks

For orthotropic decks and wearing surfaces on orthotropic decks, the 16-kip wheel loads are modeled as two 8-kip loads spaced 4 feet apart. This more accurately models a modern tractor-trailer with tandem rear axles. In addition, the wheel loads are distributed over a specified contact area of 20 inches wide by 10 inches long for the rear wheels and 10 inches wide by 10 inches long for the front wheels. This model better approximates the actual pressures applied from a dual tire unit. This loading is positioned on the bridge to create the worst effect, ignoring the striped lanes on the bridge. The design load for orthotropic decks and wearing surfaces on orthotropic decks is presented in Figure 3.4.4.4-1.

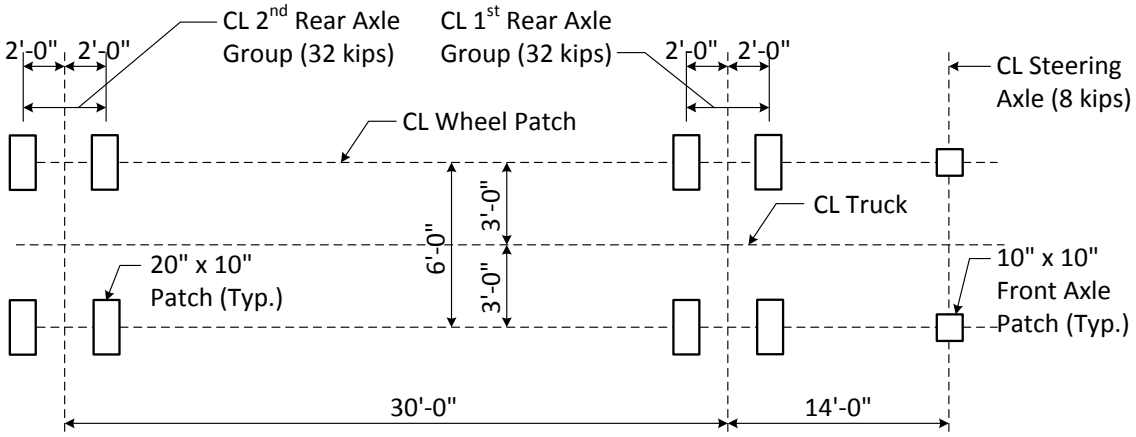

Figure 3.4.4.4-1 Refined Design Truck Footprint for Fatigue Design of Orthotropic Decks

3.4.5 Design Permit Loads

In addition to the HL-93 design vehicular live load described in Section 3.4.2.1, some bridges are also designed for permit loads. Permit loads are generally based on oversize or overweight vehicular loads which may be applied to the bridge at some time during the design life of the bridge. Permit loads generally result in greater force effects than the HL-93 live load.

The federal government does not issue permits for oversize or overweight vehicles. Instead, issuing permits is a state option. Most states require load ratings based on permit loads to ensure that the bridge can resist the permit loads. In addition, some states require that permit loads be considered during the design of the bridge to ensure that the load ratings for permit loads will be sufficient.

Each state generally has its own permit loads and permit policies. More detailed information can be found at each state's permitting web site or by contacting the state permitting office by telephone.

3.4.6 Rail Transit Loads

For bridges carrying rail transit loads, or which may carry rail transit loads at some time during its design life, the Owner must specify the characteristics of the transit load, as well as the anticipated interaction between highway traffic and rail transit traffic. Transit load characteristics that must be specified include the following:

- Loads
- Load distribution
- Load frequency
- Dynamic allowance
- Dimensional requirements

Regardless of the rail transit characteristics, the bridge should also be designed as a highway bridge of the same bridge width, anticipating the potential for the exclusive presence of highway traffic on the bridge at some time during its design life.

Railroad bridges are designed to meet the requirements of the *Manual for Railway Engineering*, published by the American Railway Engineering and Maintenance-of-Way Association (AREMA). Similarly, light rail systems are designed per other specifications.

3.4.7 Pedestrian Loads, *PL*

For bridges designed for both vehicular and pedestrian load and with a sidewalk width exceeding 2 feet, a pedestrian load, *PL*, of 75 pounds per square foot should be applied to the sidewalk during design. If vehicles can mount the sidewalk, or if the sidewalk may be removed during the design life of the bridge, then vehicular live load should be considered on that portion of the bridge. However, vehicular live load should not be considered concurrently with pedestrian loads on that portion of the bridge.

If a sidewalk may be removed during the design life of the bridge, then the vehicular live load should be applied at 1 foot from the edge of the deck for the design of the overhang and at 2 feet from the edge of the deck for the design of all other bridge elements, as described in Section 3.4.3.2. For such vehicular live load, dynamic load allowance need not be considered.

Bridges intended exclusively for pedestrian, equestrian, light maintenance vehicle, and/or bicycle traffic should be designed in accordance with AASHTO's *LRFD Guide Specifications for Design of Pedestrian Bridges* (AASHTO, 2009). A pedestrian loading, *PL*, of 90 pounds per square foot is specified. However, pedestrian loading is not applied to portions of the bridge that do not contribute to the force effect being considered. In addition, dynamic load allowance should not be considered with pedestrian loading.

3.4.8 Dynamic Load Allowance, *IM*

The HL-93 loading is based on a static live load applied to the bridge. However, in reality, the live load is not static but is moving across the bridge. Since the roadway surface on a bridge is usually not perfectly smooth and the suspension systems of most trucks react to roadway roughness with oscillations, a dynamic load is applied to the bridge and must also be considered with the live load. AASHTO refers to this dynamic effect as *dynamic load allowance* (although it was previously referred to as *impact*).

Dynamic load allowance is defined in *AASHTO LRFD* Article 3.2 as "an increase in the applied static force effects to account for the dynamic interaction between the bridge and moving vehicles." This additional dynamic force effect is illustrated in the generic live load response curve presented in Figure 3.4.8-1.

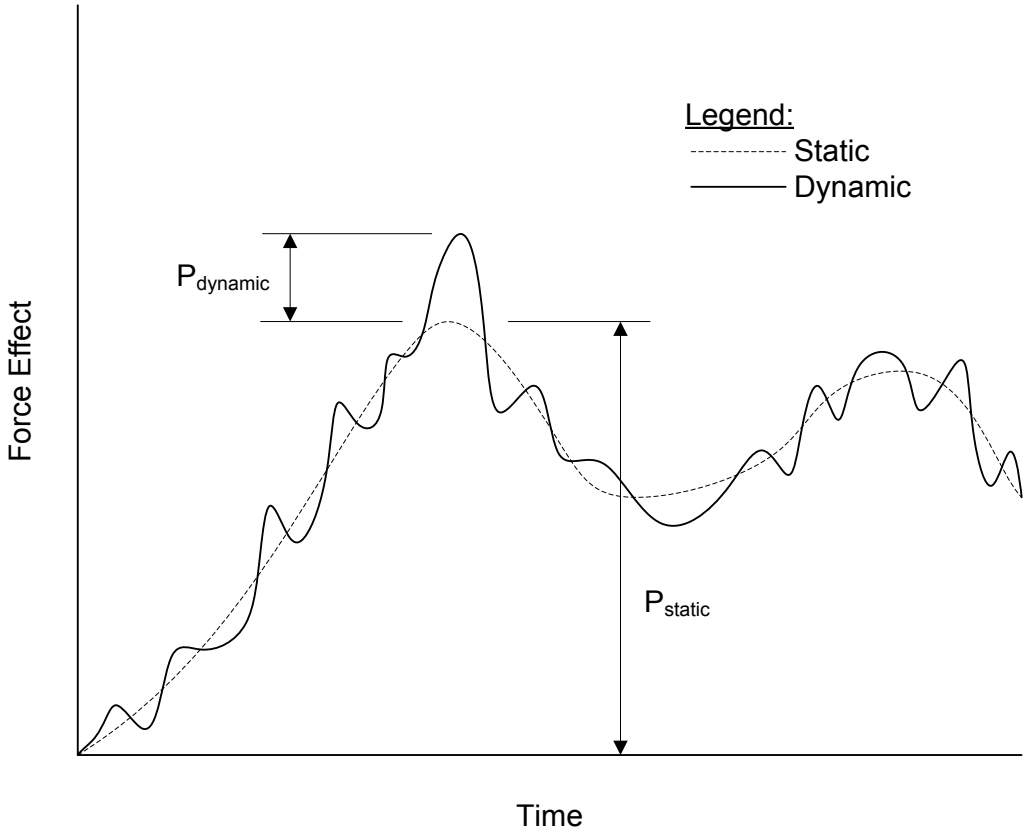

P_{static} = Maximum static force effect

$P_{dynamic}$ = Maximum additional dynamic force effect

Figure 3.4.8-1 Static and Dynamic Live Load Response

Referring to Figure 3.4.8-1, the dynamic load allowance is equal to:

$$IM = \frac{P_{dynamic}}{P_{static}} \qquad \text{Equation 3.4.8-1}$$

To compute the total live load effect, including both static and dynamic effects, the following equation is used:

$$P_{LL+I} = P_{LL}(1 + IM) \qquad \text{Equation 3.4.8-2}$$

where:

P_{LL+I} = force effect due to both live load and dynamic load allowance
P_{LL} = force effect due to live load only (without dynamic load allowance)
IM = dynamic load allowance (previously referred to as impact)

In previous specifications, AASHTO defined impact such that its value increased to a maximum value of 30% as the span length decreased. However, in the *AASHTO LRFD Bridge Design Specifications*, dynamic load allowance is not a function of span length, and its value depends only on the component and the limit state. AASHTO currently assigns values to dynamic load allowance as presented in Table 3.4.8-1.

Table 3.4.8-1 Dynamic Load Allowance, *IM*
(Based on *AASHTO LRFD* Table 3.6.2.1-1)

Limit State	Dynamic Load Allowance, *IM*
Deck Joints: All Limit States	75%
All Other Components: Fatigue and Fracture Limit State	15%
All Other Components: All Other Limit States	33%

Deck joints have a greater dynamic load allowance because the hammering effect of the passing vehicles is more significant for deck joints than for other components, such as girders, beams, bearings, and columns.

Dynamic load allowance should not be applied to the following loads:

- Centrifugal force
- Braking force
- Pedestrian load
- Design lane load (dynamic load allowance is applied to the design truck and design tandem but not to the design lane load)

In addition, there are several bridge components for which dynamic load allowance should not be applied, including the following:

- Retaining walls not subject to vertical reactions from the superstructure
- Foundation components that are entirely below ground level
- Wood components
- Any other components identified by the specific agency governing the bridge design

3.4.9 Centrifugal Force, *CE*

3.4.9.1 General

Vehicular centrifugal force is defined as a lateral force resulting from a change in the direction of a vehicle's movement (*AASHTO LRFD* Article 3.6.3). Centrifugal forces are to be applied horizontally at a distance 6.0 feet above the roadway surface. A load path to carry the radial forces to the substructure must be provided.

Centrifugal force is applied to the design truck or tandem and to the fatigue live load. However, centrifugal force is not required to be applied to the design lane load, since the spacing of the vehicles in the design lane load at high speed is assumed to be large, resulting in a low density of vehicles preceding and/or following the design truck or tandem. At the strength and service limit states, the design lane load is still considered even though centrifugal force effects are not applied. Permit loads may also not be expected to reach design speeds, so centrifugal force effects may not need to be considered for these loads, at the Owner's discretion.

Force effects with centrifugal force included should be compared to force effects without centrifugal force included, and the worst case should be selected.

Vehicular centrifugal force is computed using the following equation:

$$C = f\frac{v^2}{gR}$$ Equation 3.4.9.1-1

AASHTO LRFD Equation 3.6.3-1

where:

f = 4/3 for load combinations other than fatigue, and 1.0 for fatigue
v = highway design speed in ft/sec (1.0 ft/sec = 0.682 mph)
g = gravitational acceleration (= 32.2 ft/sec^2)
R = radius of curvature of traffic lane in feet

The factor, *C*, is multiplied by the total of the axle weights of the design truck, design tandem, or fatigue live load, as applicable.

The HL-93 design vehicular live load specified as a combination of the design truck and design lane load represents a group of exclusion vehicles that produce force effects of at least 4/3 of those caused by the design truck alone on short-span or medium-span bridges. Therefore, this ratio is introduced in *AASHTO LRFD* at the strength and service limit states through the use of the factor, *f*, in the equation for *C*.

The factor, *f*, is set to 1.0 at the fatigue limit state, consistent with cumulative damage analysis.

The highway design speed, *v*, is to be taken not less than the value specified in the most current edition of the AASHTO publication, *A Policy on Geometric Design of Highways and Streets* (AASHTO, 2011).

Centrifugal force causes an overturning effect on the wheel loads because the radial force is applied 6.0 feet above the top of the deck. Therefore, the centrifugal force tends to increase the vertical wheel loads toward the outside of the bridge and decrease the wheel loads toward the inside of the bridge. The net result is that the outermost girder will receive slightly greater load and the innermost girder will receive slightly less load. This effect is illustrated in Figure 3.4.9.1-1.

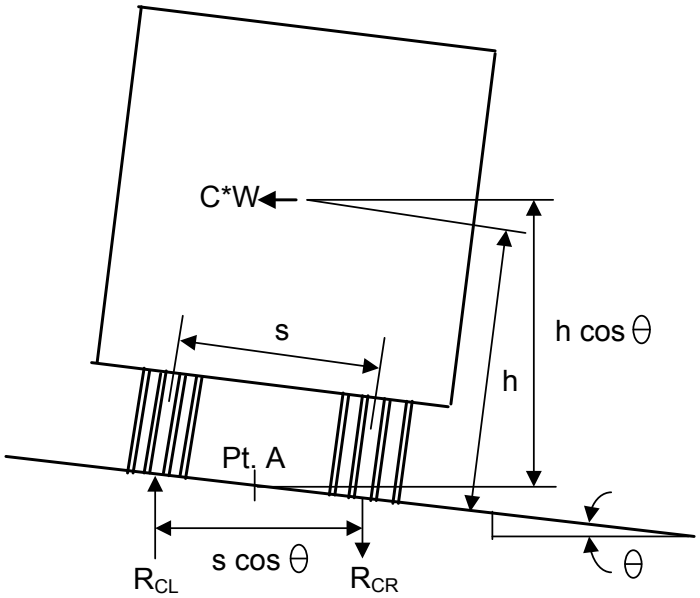

Figure 3.4.9.1-1 Vehicular Centrifugal Force Wheel-Load Reactions

The wheel-load reactions, R_{CL} and R_{CR}, due to centrifugal force are computed by summing moments about Point A, as follows:

$$R_{CL} = -R_{CR} = (C * W)\frac{h\cos\theta}{2\left[\frac{s}{2}\cos\theta\right]} \qquad \text{Equation 3.4.9.1-2}$$

where *W* is equal to the axle weight. Whenever the wheel spacing, *s*, is equal to the height at which the radial force is applied above the deck, *h* (which is typically the case), the equal and opposite wheel-load reactions, R_{CL} and $-R_{CR}$, are simply equal to *C* multiplied by *W*. That is, the superelevation has no effect.

However, superelevation helps to balance the effects of the overturning moment due to the centrifugal force. *AASHTO LRFD* Article 3.6.3 permits this beneficial effect to be considered in the computation of the wheel-load reactions due to centrifugal force, as shown in Figure 3.4.9.1-2.

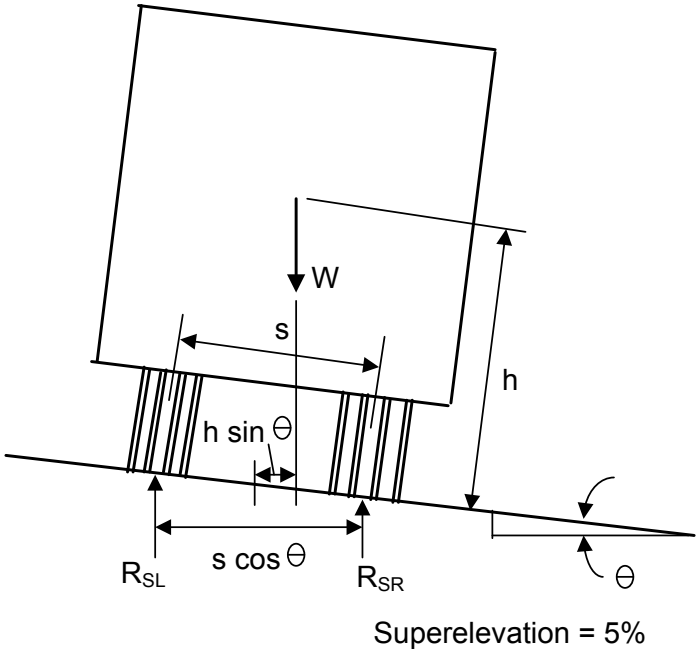

Figure 3.4.9.1-2 Effects of Superelevation on Wheel-Load Reactions

The wheel-load reactions, R_{SL} and R_{SR}, due to superelevation are computed by summing moments about the left wheel, as follows:

$$R_{SR} = \frac{\left[\frac{s}{2}\cos\theta + h\sin\theta\right] * W}{s\cos\theta} \qquad \text{Equation 3.4.9.1-3}$$

$$R_{SL} = 1.0W - R_{SR} \qquad \text{Equation 3.4.9.1-4}$$

If the superelevation is significant, the design engineer may wish to consider its effect for the case with no centrifugal force effects included (that is, a stationary

vehicle), since the superelevation will cause an increase in the vertical wheel loads toward the inside of the bridge and an unloading of the vertical wheel loads toward the outside of the bridge, which may potentially be a more critical case for the interior girders. However, since the vehicle is assumed to be stationary, the dynamic load allowance should not be included in this case.

3.4.9.2 Unit Wheel-Load Factors

For refined analyses, unit wheel-load factors can be computed based on the sum of the wheel-load reactions due to the centrifugal force and superelevation effects, as shown in Figure 3.4.9.2-1.

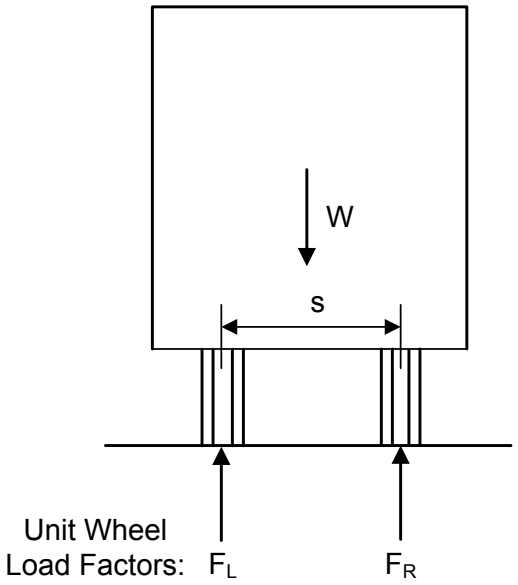

Figure 3.4.9.2-1 Unit Wheel-Load Factors due to the Combined Effects of Centrifugal Force and Superelevation

The left and right unit wheel-load factors, F_L and F_R, are computed as follows:

$$F_L = 2.0\frac{R_{CL} + R_{SL}}{W} \qquad \text{Equation 3.4.9.2-1}$$

$$F_R = 2.0\frac{R_{CR} + R_{SR}}{W} \qquad \text{Equation 3.4.9.2-2}$$

The sum of F_L and F_R must equal 2.0. The factors can be used to increase and decrease accordingly the wheel loads that are applied in the analysis.

For approximate analyses in which a line girder methodology is used, it is recommended that a "pile-group analogy" be used to determine the vertical loads acting on each girder resulting from the overturning moment due to centrifugal force effects. The moment that can be balanced by any superelevation may be considered in this approach. This methodology is illustrated in Section 3.4.9.4.

The entire horizontal centrifugal force, *C*W*, is assumed to be carried to the bridge bearings though transverse bending of the deck slab and transverse shear in the support cross-frames. No particular account need be taken of the horizontal effect of centrifugal force on the bridge superstructure, except that the support cross-frame diagonals should be adequately proportioned to deliver the load to the bearings.

Dynamic load allowance is not to be applied to the force effects due to vehicular centrifugal force. The load factor to be applied to the force effects due to centrifugal force in the various strength, service, and fatigue load combinations is the same as for the design vehicular live load.

3.4.9.3 Centrifugal Force Design Example

A curved I-girder bridge has a horizontal curve with a radius of 700 feet along the centerline of the bridge. The highway design speed, *v*, is 35 mph, and the deck cross slope (superelevation) is 5%. Compute the unit wheel-load factors for the combined effects of centrifugal force and superelevation to apply in a refined analysis to determine the vehicular live load force effects at the strength and service limit states.

The first step in this design example is to compute the value of *C*, as follows:

$$C = f\frac{v^2}{gR} = \left(\frac{4}{3}\right)\frac{(35/0.682)^2}{(32.2)(700)} = 0.156$$

Note that to compute the unit wheel-load factors for the fatigue limit state, the 4/3 factor should be changed to 1.0 in the preceding equation. This results in a *C* value of 0.117.

The next step is to compute the wheel-load reactions, R_{CL} and R_{CR}, due to centrifugal force effects. Since the wheel spacing, *s*, and the height at which the radial force is applied above the deck, *h*, are both equal to 6.0 feet, the equal and opposite wheel-load reactions, R_{CL} and $-R_{CR}$, are simply equal to *C* multiplied by *W*, as illustrated below.

$$R_{CL} = -R_{CR} = (C * W)\frac{h\cos\theta}{2\left[\frac{s}{2}\cos\theta\right]} = C * W = 0.156W$$

This is an upward reaction for the left wheel and an equal and opposite downward reaction for the right wheel.

Next, the effect of superelevation on the individual wheel-load reactions is computed as follows:

$$\theta = \tan^{-1}(0.05) = 2.86°$$

$$R_{SR} = \frac{\left[\frac{s}{2}\cos\theta + h\sin\theta\right] * W}{s\cos\theta} = \frac{\left[\left(\frac{6\text{ ft}}{2}\right)\cos(2.86°) + (6\text{ ft})\sin(2.86°)\right] * W}{(6\text{ ft})\cos(2.86°)} = 0.550\,W$$

$$R_{SL} = 1.0\,W - R_{SR} = 1.0\,W - 0.550\,W = 0.450\,W$$

Unit wheel-load factors due to the combined effects of centrifugal force and superelevation are then computed as follows:

$$F_L = 2.0\frac{R_{CL} + R_{SL}}{W} = 2.0\frac{0.156\,W + 0.450\,W}{W} = 1.212$$

$$F_R = 2.0\frac{R_{CR} + R_{SR}}{W} = 2.0\frac{-0.156\,W + 0.550\,W}{W} = 0.788$$

F_L and F_R represent the factors that must be multiplied by the left wheel load and the right wheel load, respectively, in the analysis to take into account the combined effects of both centrifugal force and superelevation. F_L and F_R are unitless, and their sum is always equal to 2.0.

If no centrifugal force and no superelevation are present, then both F_L and F_R equal 1.0. That is, both the left wheel load and the right wheel load are simply 1.0 times the weight of the wheel. The sum of F_L and F_R is again 2.0.

Force effects from the analysis due to cases with centrifugal force effects included (i.e., utilizing unit wheel-load factors F_L equal to 1.212 and F_R equal to 0.788) are compared to force effects due to cases with no centrifugal force included (i.e., utilizing unit wheel-load factors F_L and F_R equal to 1.0), and the worst case is selected.

From separate computations similar to the above, the unit wheel-load factors, F_L and F_R, for the example bridge at the fatigue limit state are 1.134 and 0.866, respectively.

3.4.9.4 Pile-group Analogy Design Example

For the same example I-girder bridge, compute the vertical loads on the girders due to the overturning moment caused by centrifugal force and superelevation utilizing a pile-group analogy. The computation will be done for the determination of the live load force effects at the strength and service limit states. The bridge cross section is shown in Figure 3.4.9.4-1.

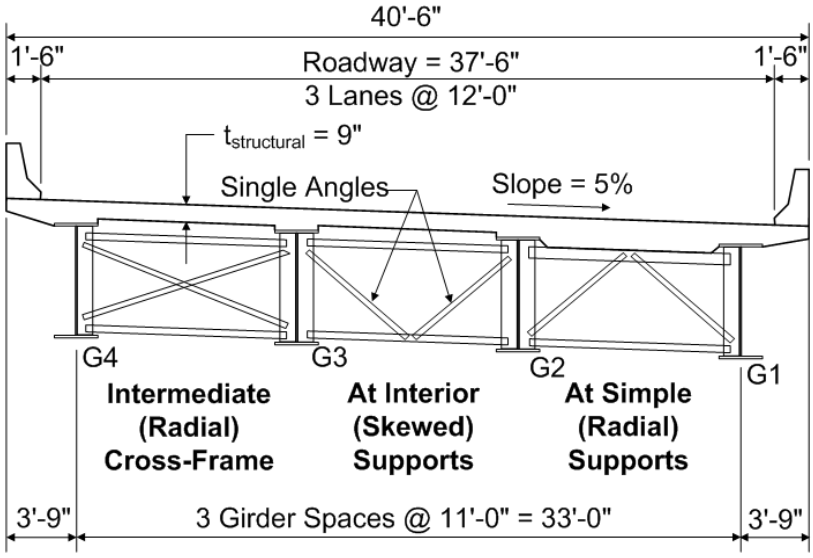

Figure 3.4.9.4-1 Example I-Girder Bridge Cross Section

As previously computed, the value of *C* at the strength and service limit states is 15.6% (0.156*100). However, the value of *C* is balanced by the superelevation, as illustrated in Figure 3.4.9.4-2. If *K* is defined as the fraction of *W* that is balanced by superelevation (that is, producing equal wheel reactions), then *K* can be computed by summing moments about Point A, as follows. (By inspection, the moments at Point A due to the reactions at the two wheels cancel one another.)

$$W(h\sin\theta) - K * W(h\cos\theta) = \text{Moment}_{\text{Point A}} = 0$$

$$W(h\sin\theta) = K * W(h\cos\theta)$$

$$K = \frac{W h \sin\theta}{W h \cos\theta} = \frac{\sin\theta}{\cos\theta} = \tan\theta = \text{Superelevation}$$

Therefore, it can be seen that the fraction of *W* that can be balanced by superelevation is equal numerically to the superelevation rate.

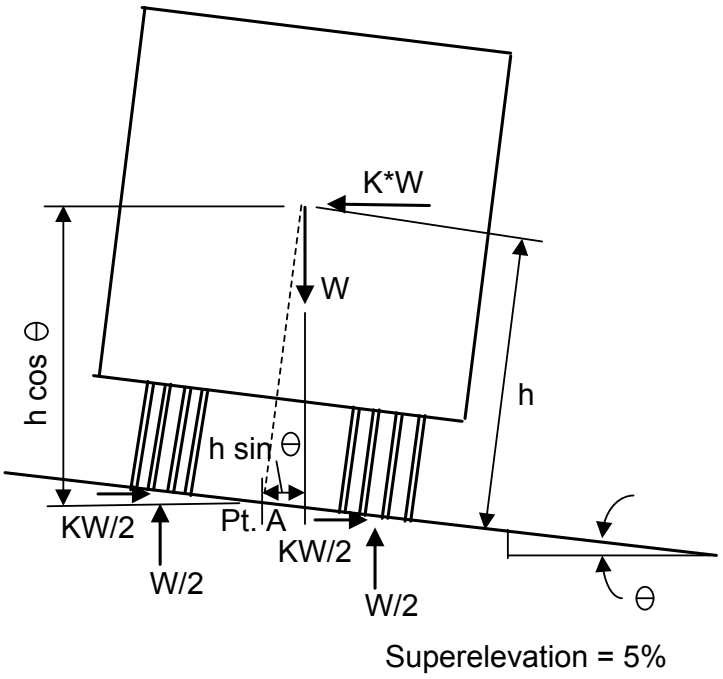

Figure 3.4.9.4-2 Centrifugal Force Balanced by Superelevation

Therefore, for this design example, the value of centrifugal force (15.6%) is balanced by the superelevation (5.0%), as follows:

$$C = C_{\text{centrifugal force}} - C_{\text{superelevation}} = 15.6\% - 5.0\% = 10.6\%$$

Thus, 10.6 percent of the centrifugal force remains to produce an overturning moment about the mid-depth of the slab. With three design lanes of live load permissible on the bridge, the centrifugal force in terms of lanes is computed as:

$$CF = (0.106)(3\,\text{lanes}) = 0.318\,\text{lanes}$$

A "pile-group analogy" can then be used to determine the vertical loads acting on each girder resulting from the overturning moment due to centrifugal force and superelevation effects. The "moment of inertia" of the four girders treated as piles is computed as follows:

$$I_{\text{pile group}} = 2\left\{[(0.5)(11.0\,\text{feet})]^2 + [(1.5)(11.0\,\text{feet})]^2\right\} = 605\,\text{feet}^2$$

The moment arm for the centrifugal force is computed from the location of the centrifugal force, 6.0 feet above the top of the deck, to the deck mid-depth, as follows:

$$\text{Moment arm} = \frac{6.0 \text{ feet}}{\cos(2.86^\circ)} + \frac{0.75 \text{ feet}}{2} = 6.38 \text{ feet}$$

The computation of the moment arm is illustrated in Figure 3.4.9.4-3.

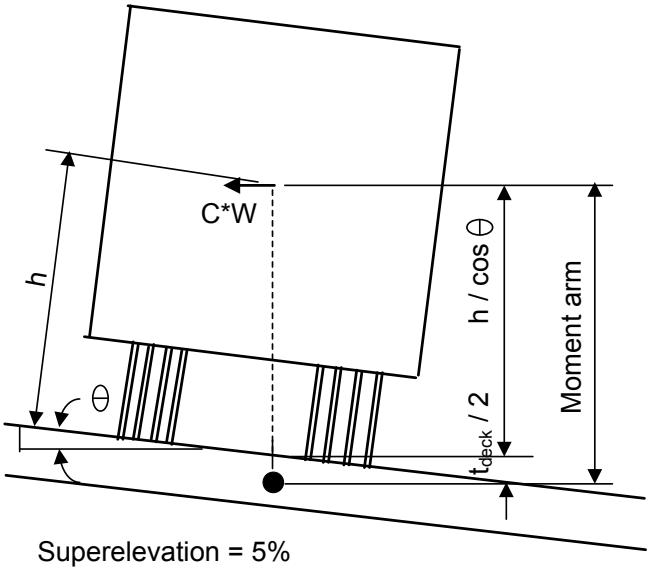

Figure 3.4.9.4-3 Computation of Moment Arm

The vertical load on the left exterior girder, G4, is then computed as follows, similar to the computation of a pile load in a pile group:

$$CF_{\text{Load on G4}} = \frac{(0.318 \text{ lanes})(6.38 \text{ feet})(1.5)(11.0 \text{ feet})}{605 \text{ feet}^2} = 0.055 \text{ lanes}$$

Similarly, the vertical load on the left interior girder, G3, is computed as follows:

$$CF_{\text{Load on G3}} = \frac{(0.318 \text{ lanes})(6.38 \text{ feet})(0.5)(11.0 \text{ feet})}{605 \text{ feet}^2} = 0.018 \text{ lanes}$$

The *CF* vertical loads on the two right girders, G1 and G2, can conservatively be assumed to be zero since the *CF* vertical loads would be upward and would be subtracted from all other vertical loads. This is equivalent to the case in which live load is present on the bridge but is not moving.

3.4.10 Braking Force, *BR*

When a truck decelerates or stops on a bridge, a longitudinal force is transmitted to the bridge deck, which is also transmitted to the substructure units with fixed bearings. This longitudinal force is known as the braking force.

The braking force is specified by AASHTO as the greater of either:

- 25 percent of the axle weights of the design truck or design tandem
- 5 percent of the design truck plus lane load, or 5 percent of the design tandem plus lane load

The 25% factor is derived using the following kinetic energy formula:

$$F_B = \left(\frac{v^2}{2ga}\right)W = bW \qquad \text{Equation 3.4.10-1}$$

where:

F_B = braking force
v = initial truck velocity (assumed to be 55 mph)
g = gravitational acceleration (= 32.2 ft/sec^2)
a = length of uniform deceleration (assumed to be 400 feet)
W = truck weight
b = braking value

Substituting the assumed values into the above equation leads to a value for b of approximately 25%.

AASHTO specifies that the braking force is to be based on all lanes which are considered to be loaded and which are carrying traffic in the same direction. For bridges which may become one-directional in the future, all lanes should be loaded. In addition, the appropriate multiple presence factor should be applied in the braking force computations.

The braking force is applied 6.0 feet above the roadway surface, and it acts longitudinally in whichever direction causes the maximum force effects.

3.4.11 Vehicular Collision Force, *CT*

In the design of decks and overhangs, a vehicular collision force must be considered. Vehicular collision force is described in *AASHTO LRFD* Article 3.6.5, and deck and overhang design is described in Chapter 7 of this Reference Manual.

For crash tests on barriers, AASHTO specifies six different test levels. These six test levels are based on NCHRP Report 350, "Recommended Procedures for the Safety Performance Evaluation of Highway Features" (Ross, 1993). They are summarized in Table 3.4.11-1.

Table 3.4.11-1 Bridge Railing Test Levels
(Adapted from *AASHTO LRFD* Article 13.7.2)

Name	Abbreviation	Description
Test Level One	TL-1	Generally acceptable for work zones with low posted speeds and very low volume, low speed local streets
Test Level Two	TL-2	Generally acceptable for work zones and most local and collector roads with favorable site conditions as well as where a small number of heavy vehicles is expected and posted speeds are reduced
Test Level Three	TL-3	Generally acceptable for a wide range of high-speed arterial highways with very low mixtures of heavy vehicles and with favorable site conditions
Test Level Four	TL-4	Generally acceptable for the majority of applications on high speed highways, freeways, expressways, and interstate highways with a mixture of trucks and heavy vehicles
Test Level Five	TL-5	Generally acceptable for the same applications as TL-4 and where large trucks make up a significant portion of the average daily traffic or when unfavorable site conditions justify a higher level of rail resistance
Test Level Six	TL-6	Generally acceptable for applications where tanker-type trucks or similar high center-of-gravity vehicles are anticipated, particularly along with unfavorable site conditions

For each test level, barriers are available that have been tested to verify their conformance with specific performance requirements. Additional information about vehicular collision forces and bridge railings is presented in *AASHTO LRFD* Section 13. The crash test criteria for the various bridge railing test levels are presented in *AASHTO LRFD* Article 13.7.2.

The user agency is responsible to determine which of the above test levels is most appropriate for the bridge site. For most interstates, TL-4 generally satisfies the design requirements. For each test level, AASHTO specifies vehicular collision force

requirements that the bridge railing must satisfy. These vehicular collision force requirements include the following:

- Weight of vehicle, *W*
- Out-to-out wheel spacing on an axle, *B*
- Height of vehicle center of gravity above the bridge deck, *G*
- Angle of vehicular impact (as measured from the face of the railing), θ

The first three variables are illustrated in Figure 3.4.11-1.

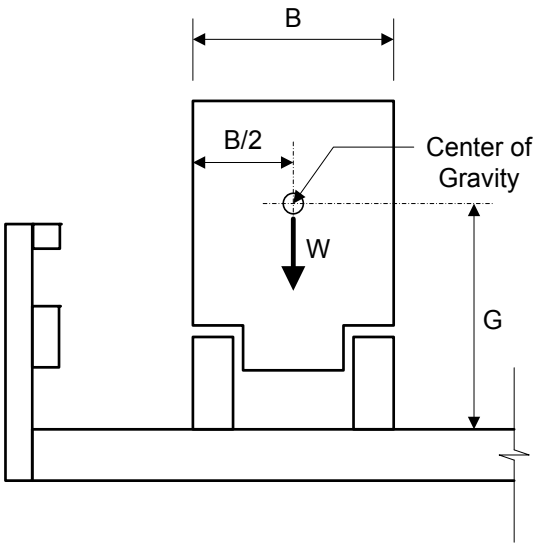

Figure 3.4.11-1 Vehicular Collision Force

The AASHTO *Manual for Assessing Safety Hardware* (MASH) is the new state of the practice for the crash testing of safety hardware devices for use on the National Highway System (NHS). MASH updates and replaces NCHRP Report 350. All new testing will be done following MASH evaluation techniques. However, hardware accepted under NCHRP Report 350 is appropriate for replacement and new installation, and retesting is not required. Effective January 1, 2011, all new products must be tested using MASH crash test criteria for use on the NHS. The need for updated crash test criteria was based primarily on changes in the vehicle fleet. Vehicles have increased in size and light truck bumper heights have risen since the NCHRP Report 350 criteria were adopted in 1993.

Section 3.5 Wind Loads

Wind loads represent the typical wind conditions of the local area where the bridge is being constructed. Only exposed surfaces are subject to direct application of wind loads, and different wind load cases exist for wind on structure, wind on live load,

wind on construction equipment, and wind in the vertical direction. Load combinations vary in their load factors for application of wind loads, the desired wind speed, and its effects on live load. In general, smaller structures are not controlled by wind effects, but larger structures with more exposed surfaces can be controlled by wind load.

3.5.1 Horizontal Wind Pressure

3.5.1.1 General

The base design wind velocity, V_B, as specified by AASHTO is 100 miles per hour. This represents a conservative estimate of the highest wind speeds that a structure will experience over the design life of the structure. The wind pressure load from this horizontal wind is applied to all exposed surfaces when the structure is viewed in elevation, perpendicular to the direction of the wind. All girders, decks, attachments, and other structural components which are exposed in elevation are subject to the same uniform wind pressure. Any analysis of wind loads should include multiple attack angles to determine from which direction wind causes the greatest force effect.

For bridges or parts of bridges more than 30.0 feet above low ground or water level, the base wind velocity is modified using the following equation from *AASHTO LRFD* Article 3.8.1.1.

$$V_{DZ} = 2.5V_0\left(\frac{V_{30}}{V_B}\right)\ln\left(\frac{Z}{Z_0}\right) \qquad \text{Equation 3.5.1.1-1}$$

AASHTO LRFD Equation 3.8.1.1-1

where:

V_{DZ} = design wind velocity at design elevation, Z (mph)
V_0 = friction velocity, see Table 3.5.1.1-1
V_{30} = wind velocity at 30.0 feet above low ground or design water level (mph)
V_B = base wind velocity, 100 mph
Z = height of structure above low ground or water level at which wind loads are being calculated, > 30.0 (feet)
Z_0 = friction length, see Table 3.5.1.1-1

The values of V_0 and Z_0 are determined based on meteorological effects corresponding with the surrounding land conditions of the bridge. The descriptions of these land features are paraphrased from *ASCE 7-93* in *AASHTO LRFD* and are as follows:

- Open country – Open terrain with scattered obstructions with heights generally less than 30.0 feet. This category includes flat, open plains and grasslands.
- Suburban – Urban and suburban areas, wooded areas, or other terrain with many closely spaced obstructions with the size of a single-family dwelling or larger dwellings. The suburban category is used only if the terrain type extends for 1,500 feet or greater in the prevailing upwind direction from the bridge structure.
- City – Large city centers with at least half the buildings having a height in excess of 70.0 feet. The city category is used only if the terrain type extends for one-half mile or greater in the prevailing upwind direction from the bridge structure. In addition to typical wind loads, possible channeling effects and increased wind velocities due to the bridge being located in the wake of larger structures should be considered in the analysis of wind loads.

Once the terrain type is determined, V_0 and Z_0 are selected from *AASHTO LRFD* Table 3.8.1.1-1, shown here as Table 3.5.1.1-1.

Table 3.5.1.1-1 Values of V_0 and Z_0 for Various Upstream Surface Conditions

Condition	Open Country	Suburban	City
V_0 (mph)	8.20	10.90	12.00
Z_0 (feet)	0.23	3.28	8.20

The value of V_{30} may be established by the following criteria, as presented in *AASHTO LRFD* Article 3.8.1.1:

- Fastest-mile-of-wind charts available in *ASCE 7-88* (ASCE, 1988) for various recurrence intervals
- Site-specific wind surveys
- In the absence of better criterion, the assumption that $V_{30} = V_B = 100$ mph

3.5.1.1.1 Calculation of Design Wind Velocity Design Example

For this example, assume a bridge structure 40.0 feet in height above the design water level. The structure is located in an area where wooded terrain prevails for at least two miles in all directions. From *ASCE 7-88* (ASCE, 1988), the fastest-mile-of-wind is 115 mph for the area in which the bridge is located.

Based on the definitions and principles presented in Section 3.5.1.1, the bridge is located in a suburban environment, and the design wind velocity is computed as follows:

$$V_{DZ} = 2.5(10.90)\left(\frac{115}{100}\right)\ln\left(\frac{40.0}{3.28}\right) = 78.4 \text{ mph}$$

3.5.1.2 Wind Pressure on Structures, *WS*

The load case for horizontal wind on structures, *WS*, is based on the design wind speed and given base wind pressures, in the absence of more precise local information. The information shown in Table 3.5.1.2-1 is taken from *AASHTO LRFD* Table 3.8.1.2.1-1 and is used to determine the horizontal wind pressure force.

Table 3.5.1.2-1 Base Pressures, P_B, Corresponding to V_B = 100 mph

Superstructure Component	Windward Load, ksf	Leeward Load, ksf
Trusses, Columns, and Arches	0.050	0.025
Beams	0.050	N/A
Large Flat Surfaces	0.040	N/A

The wind pressure can then be calculated using the following equation:

$$P_D = P_B\left(\frac{V_{DZ}}{V_B}\right)^2 = P_B\frac{{V_{DZ}}^2}{10{,}000} \qquad \text{Equation 3.5.1.2-1}$$

AASHTO LRFD Equation 3.8.1.2.1-1

As a limit, the total wind load on windward chords of trusses and arches, and on beams and girders, cannot be less than 0.30 klf. The total wind load on leeward chords of trusses and arches cannot be less than 0.15 klf.

Various angles of attack for wind direction should be investigated to determine which produces the worst case response in the bridge structure. The angle of attack should be determined as the skew angle from a perpendicular to the longitudinal axis of the member in question. For various standard angles of attack, the value of base pressure, P_B, will vary as shown in Table 3.5.1.2-2, taken from *AASHTO LRFD* Table 3.8.1.2.2-1.

Table 3.5.1.2-2 Base Wind Pressures, P_B, for Various Angles of Attack and V_B = 100 mph

Skew Angle of Wind (Degrees)	Trusses, Columns, and Arches		Girders	
	Lateral Load (ksf)	Longitudinal Load (ksf)	Lateral Load (ksf)	Longitudinal Load (ksf)
0	0.075	0.000	0.050	0.000
15	0.070	0.012	0.044	0.006
30	0.065	0.028	0.041	0.012
45	0.047	0.041	0.033	0.016
60	0.024	0.050	0.017	0.019

For both lateral loads and longitudinal loads, the wind pressure should be applied to the centroid of a single plane of exposed area (generally based on the elevation view of the bridge). As shown in Table 3.5.1.2-2, the lateral load has a maximum value and the longitudinal load is zero for a skew angle of 0 degrees (perpendicular to the longitudinal axis of the bridge). As the skew angle increases, the longitudinal load increases and the lateral load decreases. The pressures for lateral loads and longitudinal loads are to be applied simultaneously.

For girder and slab bridges with an individual span length of 125 feet or less and a maximum height of 30.0 feet above low ground or water level, a wind loading of 0.050 ksf in the transverse direction and 0.012 ksf in the longitudinal direction can be applied simultaneously.

3.5.1.3 Wind Pressure on Vehicles, *WL*

In addition to the wind loads that are applied to all exposed surfaces of bridge superstructures, wind also affects the exposed surfaces of live load traffic passing over the bridge. Wind pressure on vehicles is designated as *WL*. The pressure exerted on a superstructure due to the wind on live load is consistent with the assumptions made in the determination of limit states and load combinations. Specifically, at wind speeds in excess of 55 miles per hour, the amount of traffic that would be present on the structure at one time is significantly reduced.

The *WL* load consists of an uninterruptible, moving force of 0.10 klf acting normal to the roadway, located 6.0 feet above the roadway. For any situation in which an attack angle other than normal to the lane has been found to be the controlling wind direction, *WL* should be taken as shown in Table 3.5.1.3-1, which is taken from *AASHTO LRFD* Table 3.8.1.3-1.

Table 3.5.1.3-1 Wind Components on Live Load

Skew Angle (Degrees)	Normal Component (klf)	Parallel Component (klf)
0	0.100	0.000
15	0.088	0.012
30	0.082	0.024
45	0.066	0.032
60	0.034	0.038

For girder and slab bridges with an individual span length of 125 feet or less and a maximum height of 30.0 feet above low ground or water level, a wind on live load of 0.10 klf in the transverse direction and 0.04 klf in the longitudinal direction can be applied simultaneously.

3.5.2 Vertical Wind Pressure

For load combinations in which wind on live load is not considered, and uplift of the structure is potentially a problem, vertical wind pressure may generate loads that need to be considered. This load type is considered to be a 0.020 ksf upward force for all wind speeds, but only when the wind direction is taken to be perpendicular to the bridge structure. The area of effect for vertical wind pressure includes the width of all deck surfaces, parapets, and sidewalks. Vertical wind pressure is considered to be a longitudinal line load, and it is applied at the windward quarterpoint of the deck width in conjunction with the horizontal wind loads specified in Section 3.5.1.

Section 3.6 Seismic Loads

Bridges are designed for seismic loads such that they have a low probability of collapse or total failure due to a seismic event. However, they may suffer significant damage or disruption due to earthquake ground motions. Partial or complete replacement may be required following a seismic event.

AASHTO LRFD Article 3.10 specifies the design requirements for seismic loads. The design earthquake motions and forces are based on a low probability of being exceeded during the normal design life of a bridge. The *AASHTO LRFD* requirements for seismic design specify seismic resistance within the elastic range of the structural components without significant damage from small to moderate earthquakes. In addition, large earthquakes should not cause collapse of all or part of the bridge, and damage should be easily detectable and accessible for inspection and repair.

The general procedure for seismic design uses the peak ground acceleration coefficient (*PGA*) and the short-period and long-period spectral acceleration coefficients (S_s and S_1, respectively). These values can be obtained using a series of maps with contour lines presented in *AASHTO LRFD* Figures 3.10.2.1-1 through 3.10.2.1-21.

The calculation of seismic design forces is dependent on the seismic zone in which the bridge is located. Seismic Zone 1 represents the zone with the least potential for significant seismic loads, and seismic analysis for bridges in Zone 1 is generally not required. Default values for minimum design forces are specified in *AASHTO LRFD* Article 3.10.9 in lieu of rigorous analysis. At the other extreme, Seismic Zone 4 represents the zone with the greatest potential for significant seismic loads. Bridges located in Zone 4 require seismic analysis.

More detailed information about seismic loads is presented in *AASHTO LRFD* Article 3.10.

In addition to *AASHTO LRFD*, *AASHTO Guide Specifications for LRFD Seismic Bridge Design* covers seismic design for typical bridge types. It applies to non-critical and non-essential bridges. It is approved as an alternate to the seismic provisions in *AASHTO LRFD*, and it differs from the current procedures in *AASHTO LRFD* in the use of displacement-based design procedures instead of the traditional force-based R-Factor method. It includes detailed guidance and commentary on earthquake-resisting elements and systems, global design strategies, demand modeling, resistance calculation, and liquefaction effects. It also includes prescriptive detailing for plastic hinging regions and design requirements for protection of those elements that should not experience damage.

Section 3.7 Force Effects Due to Superimposed Deformations

3.7.1 General

In addition to forces caused by applied loads, bridges must also be designed to resist forces due to superimposed deformations. The following force effects must be considered during bridge design where appropriate:

- Uniform temperature, *TU*
- Temperature gradient, *TG*
- Creep, *CR*
- Differential shrinkage, *SH*
- Settlement, *SE*
- Secondary forces from post-tensioning, *PS*

3.7.2 Uniform Temperature, *TU*

The first force effect due to superimposed deformations that must be considered in bridge design is uniform temperature change, in which the entire superstructure changes temperature by a constant amount. Uniform temperature change causes the entire superstructure to lengthen due to temperature rise or shorten due to temperature fall. In addition, if the supports are constrained, uniform temperature change induces reactions at the bearings and forces in the corresponding substructure units. Uniform temperature change is illustrated in Figure 3.7.2-1.

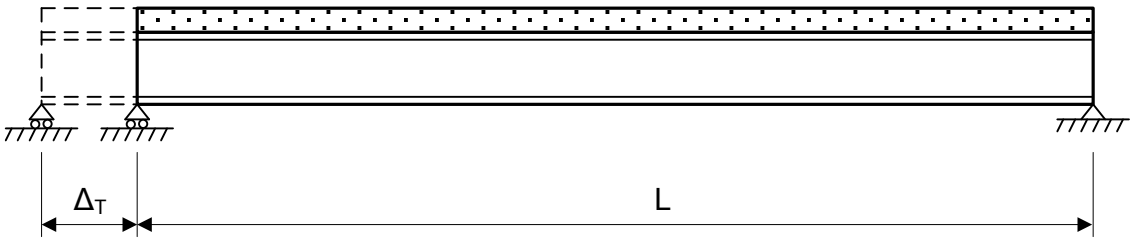

Figure 3.7.2-1 Uniform Temperature Change

As depicted in Figure 3.7.2-1, the entire superstructure changes in length when subjected to a uniform temperature change. The magnitude of the change in length, Δ_T, is a function of:

- Material properties
- Temperature change
- Expansion length

This relationship is expressed mathematically as follows:

$$\Delta_T = \alpha L \left(T_{MaxDesign} - T_{MinDesign}\right) \qquad \text{Equation 3.7.2-1}$$

AASHTO LRFD Equation 3.12.2.3-1

where:

Δ_T = design thermal movement range
α = coefficient of thermal expansion
L = expansion length
$T_{MaxDesign}$ = maximum design temperature
$T_{MinDesign}$ = minimum design temperature

It is important to note that the expansion length is measured to a point of fixity. The coefficient of thermal expansion is approximately 0.0000065/˚F for steel, 0.0000060/˚F for normal weight concrete, and 0.0000050/˚F for lightweight concrete.

AASHTO provides two methods for determining the minimum and maximum design temperatures. These two methods are called Procedure A and Procedure B. Either Procedure A or Procedure B may be used for concrete deck bridges having concrete or steel girders. Procedure A must be used for all other bridge types.

Procedure A, which has traditionally been used by AASHTO, is based on the temperature ranges presented in Table 3.7.2-1.

Table 3.7.2-1 Temperature Ranges
(Based on *AASHTO LRFD* Table 3.12.2.1-1)

Climate	Steel or Aluminum	Concrete	Wood
Moderate	0˚F to 120˚F	10˚F to 80˚F	10˚F to 75˚F
Cold	-30˚F to 120˚F	0˚F to 80˚F	0˚F to 75˚F

As used in Table 3.7.2-1, moderate climate is defined as climate in which less than 14 days have an average temperature of less than 32˚F, and cold climate is defined as climate in which 14 or more days have an average temperature of less than 32˚F. The temperature range for concrete is less than that for steel or aluminum, because concrete generally has more thermal inertia than does steel or aluminum, which makes concrete more resistant to changes in temperature.

To illustrate the application of the above table, for a steel girder in cold climate which was constructed at 68˚F, the total design temperature range is 120˚F – (-30˚F) = 150˚F, the design temperature rise is 120˚F – 68˚F = 52˚F, and the design temperature fall is 68˚F – (-30˚F) = 98˚F.

Procedure B was developed in 2002 and is based on contour maps which present contour lines for the maximum and minimum design temperatures for both concrete girder bridges and steel girder bridges. The bridge engineer can locate the bridge site on the contour maps and determine the maximum and minimum design temperatures to within about 10˚F, either by interpolating between contour lines or by using the most conservative adjacent contour line.

Uniform temperature change must be considered in the design of many bridge components, including the following:

- Deck joints
- Bearings
- Piers at which the bearings are constrained against thermal movement

For curved or skewed bridges, the bridge engineer must carefully consider the orientation of the bearing guides and the freedom of bearing movement. Sharp

curvature and sharply skewed supports can cause significant lateral thermal forces at supports if only tangential movement is permitted. In addition, for wide bridges, lateral thermal forces must be considered in addition to longitudinal thermal forces.

3.7.3 Temperature Gradient, *TG*

Another type of thermal load that may need to be considered in bridge design is temperature gradient. Past experience, Owner input, and bridge type are all factors that should be used in determining whether temperature gradient should be considered. When subjected to heat from the sun, the bridge deck usually heats more than the underlying girders. Since heat causes expansion, this causes the deck to expand more than the girders, which results in upward bending. Temperature gradient is illustrated in Figure 3.7.3-1.

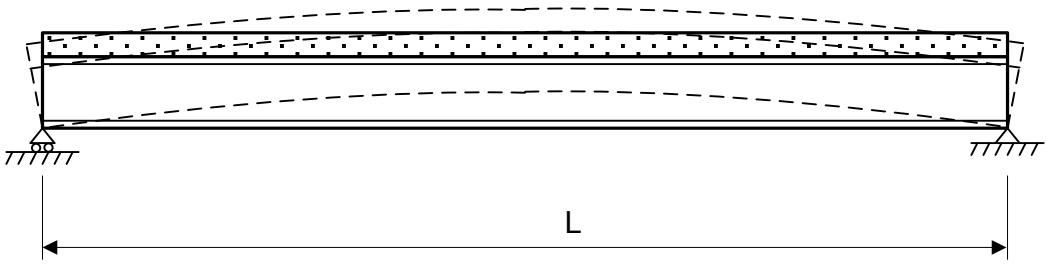

Figure 3.7.3-1 Temperature Gradient

Bridge location plays a more significant role in temperature gradient than in uniform temperature change. Bridges located in western states are generally more sensitive to temperature gradient than bridges located in eastern states. To assist the bridge engineer in computing temperature gradient, AASHTO has divided the nation into four solar radiation zones, identified as Zones 1, 2, 3, and 4. Zone 1 has the highest gradient temperatures.

The variation in temperature throughout the depth of the superstructure is illustrated in Figure 3.7.3-2.

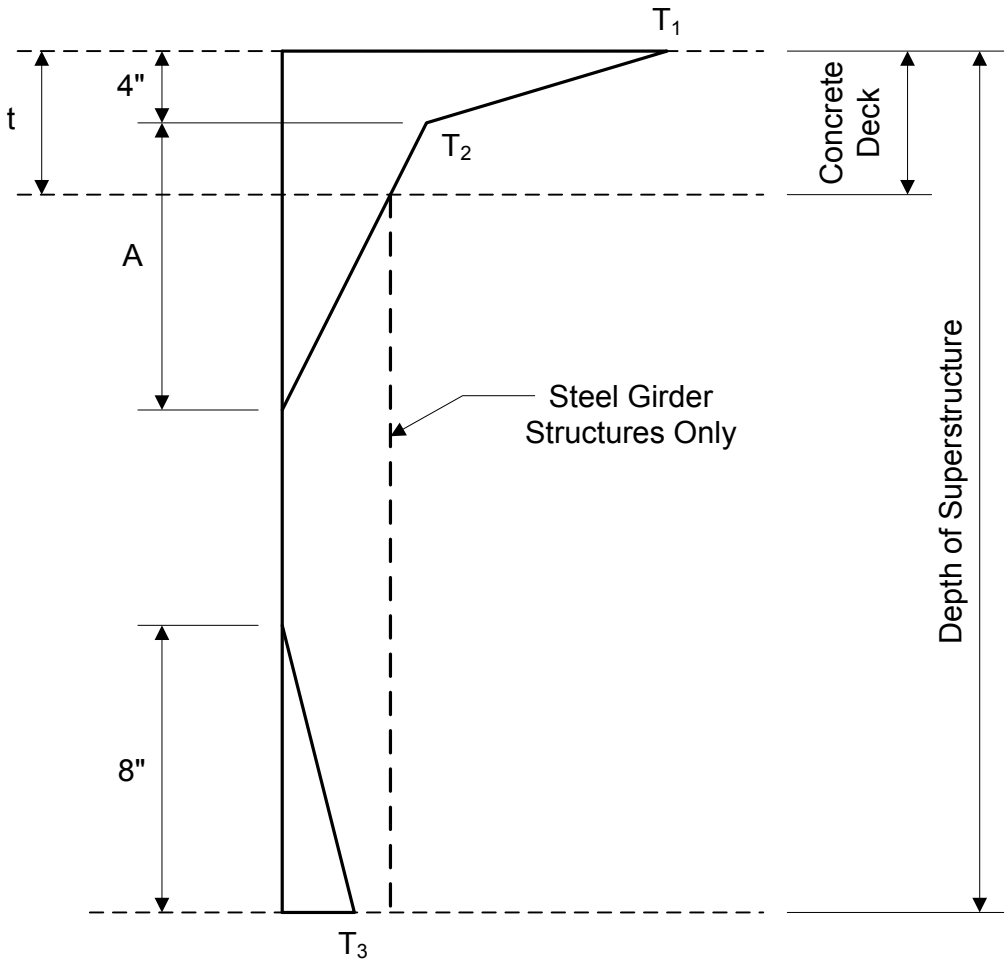

Figure 3.7.3-2 Positive Vertical Temperature Gradient

The value for *A*, as shown in Figure 3.7.3-2, depends on the superstructure material and depth. The values for the temperatures (T_1, T_2, and T_3) are a function of the solar radiation zone in which the bridge is located.

When analyzing a bridge for temperature gradient, internal stresses and structure deformations due to both positive and negative temperature gradients must be considered.

3.7.4 Creep, *CR*, and Differential Shrinkage, *SH*

The force effects due to superimposed deformations are creep and shrinkage. Creep is a material property in which the member continues to deform with time under sustained loads at unit stresses within the elastic range. Shrinkage is a material property in which the volume changes independently of the loads it

sustains. Both creep and shrinkage are time-dependent deformations. They may occur concurrently, and they generally cannot be separated from each other.

Creep is generally considered only for concrete, but it can also apply to prestressed wood decks. For shrinkage, the Engineer may specify construction requirements to minimize stresses due to differential shrinkage between components. For both creep and shrinkage, the load factor may be reduced to 1.0 if physical testing is performed to establish material properties and if upper bound values are used in the analysis.

For concrete bridges, some of the parameters that most significantly influence creep and shrinkage are the following:

- Water-cement ratio
- Curing method
- Ambient humidity
- Aggregates
- Air content
- Age at load application

Creep and shrinkage influences both the internal stresses and the deformations of a bridge.

3.7.4.1 Stresses

In segmental bridges, the creep and shrinkage effects on the internal stresses can be significant, and their contribution to the final stresses must be included in the design process. As an illustration, consider a three-span segmental bridge constructed by the cantilever method. Moment diagrams for various conditions are presented in Figure 3.7.4.1-1.

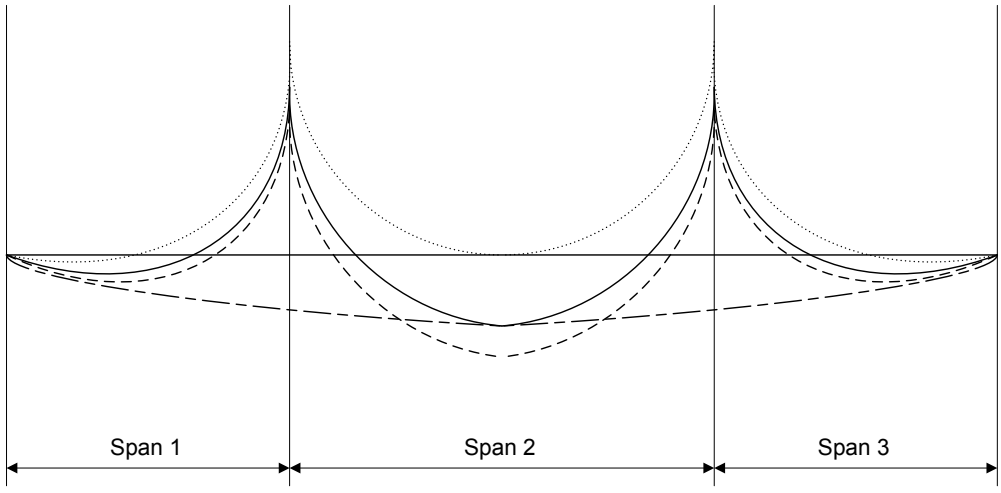

Moment Diagram

Legend:

Moment diagram as constructed by the cantilever method (without creep and shrinkage effects)

Moment diagram at time infinity (with creep and shrinkage effects)

Moment diagram as constructed on falsework (without creep and shrinkage effects)

Approximate representation of creep and shrinkage effects

Figure 3.7.4.1-1 Moment Diagrams for Three-span Segmental Bridge

It can be seen from Figure 3.7.4.1-1 that the forces induced by applied loads are affected not only by the construction method but also by creep and shrinkage. The moment diagram with forces at time infinity (with creep and shrinkage effects) is somewhere between the moment diagrams as constructed by the cantilever method (without creep and shrinkage effects) and as constructed on falsework (also without creep and shrinkage effects). In other words, the final forces in the structure are somewhere between the "cantilever-method" constructed forces and the "falsework" constructed forces.

3.7.4.2 Deflections

In segmental bridges, the creep and shrinkage effects on the deflections can also be significant. Their contribution to deformations must be considered when computing:

- Deformations
- Casting curves
- Camber data
- Internal stresses due to deformations

Creep and shrinkage effects induce both stresses and deformations that affect the internal forces on the structural system. For prestressed concrete bridges, cable-stayed bridges, composite structures, and many other indeterminate structures, creep and shrinkage effects can govern the design of the structural members.

3.7.5 Settlement, *SE*

Another force effect due to superimposed deformations is settlement. Extreme values of differential settlements among substructure units throughout the bridge, as well as within individual substructure units, must be considered where appropriate.

Force effects due to settlement may be reduced by considering creep. The Engineer should consider various combinations of differential settlement, and the bridge should be designed for the combination creating the critical force effects in the structure.

3.7.6 Secondary Forces from Post-Tensioning, *PS*

Secondary forces from post-tensioning must also be considered during the design of continuous post-tensioned bridges. For such bridges, post-tensioned forces produce reactions at the supports and internal forces that are collectively called secondary forces. In frame analysis software, the secondary forces are often computed by subtracting the primary prestress forces from the total prestressing.

Section 3.8 Friction Forces, *FR*

Another load that must be considered in bridge design is friction forces. Friction forces result when two elements move in relation to one another. Friction forces are most significant in the design of bearings.

Friction forces are included in all strength, service, and extreme event load combinations, and they are assigned a load factor of 1.00 for all load combinations.

The value of friction forces, *FR*, is directly related to the coefficient of friction between the sliding surfaces and the applied force normal to the sliding surface. In computing *FR*, extreme values of the coefficient of friction should be used. High and low values of the coefficient of friction can generally be obtained from standard textbooks. In addition, values can be determined by physical tests, especially if the surfaces are expected to be roughened during the service life of the bridge.

The effect of moisture, possible degradation of sliding or rotating surfaces, or possible contamination of sliding or rotating surfaces upon the coefficient of friction should be considered where appropriate.

Section 3.9 Blast Loading, *BL*

Although most bridges are not designed for blast loading, some bridges may be vulnerable to either intentional or unintentional blast force and must be designed to resist such a force. The value of the blast force, *BL*, is a function of the following considerations:

- Size of explosive charge
- Shape of explosive charge
- Type of explosive charge
- Location of explosive charge
- Stand-off distance
- Capacities of potential modes of delivery
- Fragmentation associated with explosives delivered by vehicle

The first four considerations listed above determine the intensity of the blast force produced by the explosive charge. Explosive charges are generally expressed in units of equivalent TNT charge weights.

The stand-off distance is the distance from the center of the explosive charge to the bridge element being considered. The peak pressure on the bridge element due to an explosive charge is inversely proportional to the cube of the stand-off distance. For example, if Location A has half the stand-off distance of Location B, then the peak pressure at Location A from a given explosive charge will be 8 times greater than the peak pressure at Location B.

The specific location of the explosive charge determines the amplifying effects of the blast wave. For example, a blast wave reflecting from the ground surface may have a different effect than a blast wave reflecting from the surfaces of surrounding structural elements. In addition, the specific location of the charge also determines the severity of damage caused by fragments from other components near the blast traveling away from the blast center.

For bridges which must be designed for blast loading, the specific design requirements are generally defined by the Owner or the contracting agency.

Section 3.10 Load Factors and Load Combinations

Load and Resistance Factor Design utilizes limit states which represent the various loading conditions which structural elements must be able to resist. The following four limit states are considered in LRFD bridge design:

- Strength – design to ensure that strength and stability are provided to resist increased load combinations that a bridge may experience during its design life
- Service – design to restrict stresses, deformations, and cracks under regular service conditions
- Extreme event – design to ensure structural survival of a bridge during events of large loading which have a recurrence period longer than the design life of the bridge
- Fatigue and fracture – design to limit crack growth under repetitive loads to prevent fracture during the design life of the bridge

These limit states involve a number of load factors and resistance factors which are applied to the basic LRFD equation:

$$\sum \eta_i \gamma_i Q_i \leq \phi R_n = R_r \qquad \text{Equation 3.10-1}$$

AASHTO LRFD Equation 1.3.2.1-1

where:

η_i = load modifier, relating to ductility, redundancy, and operational importance
γ_i = load factor; a statistically based multiplier applied to force effects
Q_i = force effect
ϕ = resistance factor; a statistically based multiplier applied to nominal resistance
R_n = nominal resistance
R_r = factored resistance

For the case in which only dead loads and live loads are applied, the basic LRFD equation takes the following form:

$$\eta(\sum \gamma_{DL} DL + \sum \gamma_{LL} LL) \leq \phi R_n = R_r \qquad \text{Equation 3.10-2}$$

where:

DL = dead load force effects applied to the element under consideration
LL = live load force effects applied to the element under consideration
η = load modifier applied to all loads
γ_{DL} = load factor for dead loads
γ_{LL} = load factor for live loads

Each limit state contains several load combinations, numbered with Roman numerals. Some load combinations reflect instances of normal operating conditions. Some reflect instances of high wind, in which live load would not typically be present on a bridge but wind loads are very high. Still others represent earthquake

conditions or vehicular collisions with bridge structures. Resistance factors affecting the resistance of structural materials also vary based on the limit state being investigated.

Not all limit states or load combinations need to be checked for all structures, and the design engineer should determine which are applicable for a specific bridge. When all applicable limit states and load combinations are satisfied, a structure is deemed acceptable under the LRFD design philosophy.

3.10.1 Base Load Factors and Combinations

3.10.1.1 General

AASHTO LRFD Article 3.4.1 defines the base load factors and load combinations used in LRFD bridge design. For each of the four limit states introduced in Section 3.10, there are several load combinations. In addition, for each load combination, a unique set of load factors is assigned based on the intended loading condition, the probability of simultaneous loadings, the uncertainty of the value of the associated loads, and the purpose of the limit state.

Load factors for each load combination are defined in *AASHTO LRFD* Tables 3.4.1-1, 3.4.1-2, and 3.4.1-3. For reference, the load factors table presented in *AASHTO LRFD* Table 3.4.1-1 is presented below in Table 3.10.1.1-1.

Table 3.10.1.1-1 *AASHTO LRFD* Load Combinations and Load Factors

Load Combination / Limit State	*DC DD DW EH EV ES EL PS CR SH*	*LL IM CE BR PL LS*	*WA*	*WS*	*WL*	*FR*	*TU*	*TG*	*SE*	*EQ**	*BL**	*IC**	*CT**	*CV**
Strength I (unless noted)	γ_p	1.75	1.00	--	--	1.00	0.50/1.20	γ_{TG}	γ_{SE}	--	--	--	--	--
Strength II	γ_p	1.35	1.00	--	--	1.00	0.50/1.20	γ_{TG}	γ_{SE}	--	--	--	--	--
Strength III	γ_p	--	1.00	1.40	--	1.00	0.50/1.20	γ_{TG}	γ_{SE}	--	--	--	--	--
Strength IV	γ_p	--	1.00	--	--	1.00	0.50/1.20	--	--	--	--	--	--	--
Strength V	γ_p	1.35	1.00	0.40	1.00	1.00	0.50/1.20	γ_{TG}	γ_{SE}	--	--	--	--	--
Extreme Event I	γ_p	γ_{EQ}	1.00	--	--	1.00	--	--	--	1.00	--	--	--	--
Extreme Event II	γ_p	0.50	1.00	--	--	1.00	--	--	--	--	1.00	1.00	1.00	1.00
Service I	1.00	1.00	1.00	0.30	1.00	1.00	1.00/1.20	γ_{TG}	γ_{SE}	--	--	--	--	--
Service II	1.00	1.30	1.00	--	--	1.00	1.00/1.20	--	--	--	--	--	--	--
Service III	1.00	0.80	1.00	--	--	1.00	1.00/1.20	γ_{TG}	γ_{SE}	--	--	--	--	--
Service IV	1.00	--	1.00	0.70	--	1.00	1.00/1.20	--	1.00	--	--	--	--	--
Fatigue I *LL, IM, CE only*	--	1.50	--	--	--	--	--	--	--	--	--	--	--	--
Fatigue II *LL, IM, CE only*	--	0.75	--	--	--	--	--	--	--	--	--	--	--	--

Legend:

* Use one of these at a time

As presented in Table 3.10.1.1-1, for strength and extreme event limit states, permanent loads are factored individually as presented in *AASHTO LRFD* Table 3.4.1-2, and as shown in Table 3.10.1.1-2.

Table 3.10.1.1-2 Load Factors for Permanent Loads, γ_p

Type of Load, Foundation Type, and Method Used to Calculate Downdrag	Maximum Load Factor	Minimum Load Factor
DC: Component and Attachments	1.25	0.90
DC: Strength IV only	1.50	0.90
DD: Downdrag, Piles, α Tomlinson Method	1.40	0.25
DD: Downdrag, Piles, λ Method	1.05	0.30
DD: Downdrag, Drilled shafts, O'Neill and Reese (1999) Method	1.25	0.35
DW: Wearing Surfaces and Utilities	1.50	0.65
EH: Horizontal Earth Pressure, Active	1.50	0.90
EH: Horizontal Earth Pressure, At-Rest	1.35	0.90
EH: Horizontal Earth Pressure, *AEP* for anchored walls	1.35	N/A
EL: Locked-in Construction Stresses	1.00	1.00
EV: Vertical Earth Pressure, Overall Stability	1.00	N/A
EV: Vertical Earth Pressure, Retaining Walls and Abutments	1.35	1.00
EV: Vertical Earth Pressure, Rigid Buried Structure	1.30	0.90
EV: Vertical Earth Pressure, Rigid Frames	1.35	0.90
EV: Vertical Earth Pressure, Flexible Buried Structures, Metal Box Culverts and Structural Plate Culverts with Deep Corrugations	1.50	0.90
EV: Vertical Earth Pressure, Flexible Buried Structures, Thermoplastic culverts	1.30	0.90
EV: Vertical Earth Pressure, Flexible Buried Structures, All others	1.95	0.90
ES: Earth Surcharge	1.50	0.75

As shown in Table 3.10.1.1-2, several loads have a minimum value and a maximum value for the strength and extreme event limit states. The maximum value is used in most cases. However, the minimum value is used when a minimum value of that particular loading is being computed. For example, the minimum load factor for DC and DW dead loads would be used for computations of uplift at a support.

AASHTO LRFD Table 3.4.1-3 provides load factors for permanent loads due to superimposed deflections, γ_p. Load factors are provided for secondary forces from post-tensioning, as well as for force effects due to creep and shrinkage.

3.10.1.2 Strength Limit State Load Combinations

3.10.1.2.1 General

Strength limit state combinations are intended to create conditions of maximum loading on a bridge structure. These combinations bring the structure under considerable loading which may cause overstresses and structural deformations, but the structural integrity of the bridge must be maintained.

The strength limit state ensures that strength and stability requirements, both local and global, are satisfied to resist the load combinations that a bridge is expected to experience during its design life. These load combinations would not generally occur during normal operation of the structure, but they could occur during the design life of the structure. Overall structural integrity is ensured for the strength load combinations. Not all strength load combinations apply to all bridge structures, and the designer must use engineering judgment to decide which load combinations must be included for their specific design.

3.10.1.2.2 Strength I

The Strength I load combination is the primary load combination for evaluating the resistance of structural members under full live load conditions without wind effects. A load factor of 1.75 is applied to live load for this load combination, and neither wind load on the structure nor wind on live load is applied. Most checks against failure will occur with this load combination. The Strength I load combination applies to almost all bridge designs.

3.10.1.2.3 Strength II

This load combination can be tailored to each specific bridge project to allow Owners to specify special design vehicles, evaluation permit vehicles, or both. Permit vehicles are oversize or overweight vehicles that are allowed on the bridge only under specific circumstances. Wind loads are not included in this load combination, similar to the Strength I load combination.

3.10.1.2.4 Strength III

This load combination reflects a high wind condition, with a wind velocity exceeding 55 miles per hour. This would normally prevent the presence of significant live load on the bridge. While some live load may be present, it would be considered statistically insignificant, and therefore the load factor for live load is zero for this load combination. The wind loads on the structure are increased through higher load factors to account for the focus of this load combination.

3.10.1.2.5 Strength IV

The Strength IV load combination emphasizes dead load force effects in bridge superstructures. It also produces a more uniform reliability across the full range of spans and dead load to live load ratios. The level of reliability produced by this load combination is similar to that produced by other strength load combinations. The maximum load factor for DC dead load for Strength IV is greater than the maximum load factor for DC dead load for the other strength load combinations.

3.10.1.2.6 Strength V

The Strength V load combination is a blending of the Strength I and Strength III conditions, in which high winds and significant live load both affect the bridge. Live loads are reduced somewhat from the Strength I load combination to reflect the fact that high winds will discourage some live load, and wind loads are not increased as much as in the Strength III load combination. For the strength limit state, wind on live load is applied only to this load combination.

3.10.1.2.7 Design Applications

The specific design applications of the various strength load combinations are summarized in Table 3.10.1.2.7-1.

Table 3.10.1.2.7-1 Design Applications of Strength Load Combinations

Strength Load Combination	Design Applications
Strength I	• Basic load combination • Normal vehicular use of the bridge • No wind load
Strength II	• Related to Owner-specified special design vehicles, permit vehicles, or both • No wind load
Strength III	• Bridge is exposed to wind velocity exceeding 55 mph • No live load or wind on live load
Strength IV	• Emphasizes dead load force effects in bridge superstructures • Increased maximum load factor for DC dead loads • No wind load • Generally applies to long span bridges • Not applicable to the investigation of construction stages
Strength V	• Normal vehicular use of bridge • Includes wind load • Only strength load combination with wind on live load

For a typical multi-girder highway overpass, the Strength I load combination will usually control the design of the superstructure.

3.10.1.3 Service Limit State Load Combinations

3.10.1.3.1 General

The service limit state contains load combinations which reflect loadings intended to control stresses, deformations, and crack widths in structural elements. Loads in service limit states are taken at regular service conditions, and most of the service load factors are equal to or close to 1.00.

Within the service limit state, there are four load combinations that are designed to test various aspects of the structure being analyzed. Unlike the strength load combinations, the service load combinations are generally material specific. They are intended to control deflections in superstructures and cracks in prestressed concrete structures, and they represent nominal loading conditions which could easily be expected during normal operation of the structure. The basic function of each service load combination is described in the following sections.

3.10.1.3.2 Service I

This load combination includes loads that could be expected under normal operating conditions with a 55 mile-per-hour wind. Most loads are assigned a load factor of 1.00, although some wind loads and temperature loads are factored by other values. The results of this load combination can be used to control deflections in a superstructure and to control crack widths in reinforced concrete members. For prestressed concrete, the Service I load combination should be used to investigate compression, while tension should be investigated with the Service III load combination.

3.10.1.3.3 Service II

The Service II load combination applies only to steel structures, and it contains load factors combined to produce maximum effects for yielding of steel structures, as well as slip of slip-critical connections within the structure. Vehicular live load is the focus of this service load combination, as the load factor for live load is 1.30 rather than 1.00. The Service II load combination corresponds to the overload provisions for steel structures that appeared in past AASHTO specifications for ASD and LFD designs.

3.10.1.3.4 Service III

Within the Service III load combination, loads are factored and combined to produce the greatest effect on prestressed concrete superstructure elements. Investigating tensile stresses and crack control are primary objectives of this load combination, and it uses a load factor for live load of 0.80 rather than 1.00. This load combination also applies to principal tension in the webs of segmental concrete girders.

3.10.1.3.5 Service IV

The Service IV load combination is intended to control cracking due to tension in prestressed concrete columns. For this load combination, a load factor of 0.70 is applied to wind load, and no live load is applied. This load combination is based on a wind speed of 84 miles per hour. This load combination is generally applicable for substructures only.

3.10.1.3.6 Design Applications

The specific design applications of the various service load combinations are summarized in Table 3.10.1.3.6-1.

Table 3.10.1.3.6-1 Design Applications of Service Load Combinations

Service Load Combination	Design Applications
Service I	• Control deflections in a superstructure • Control crack widths in reinforced concrete members • Investigate compression in prestressed concrete
Service II	• Applies only to steel structures • Control yielding of steel structures • Control slip of slip-critical connections
Service III	• Investigate tension and crack control in prestressed concrete • Investigate principal tension in webs of segmental concrete girders
Service IV	• Does not apply to superstructures

3.10.1.4 Extreme Event Limit State Load Combinations

3.10.1.4.1 General

The extreme event limit state analyzes the ability of the bridge to withstand an event of extreme loading with a recurrence period that is greater than the design life of the structure. Such events include earthquakes, blast loading, ice flow impact, vehicular collisions, or vessel collisions. Not all extreme event load combinations apply to all areas of the country or to all types of bridge construction. Therefore, it is the design engineer's responsibility to choose which extreme event load combinations apply to a specific bridge. All five load types that are included as extreme events are analyzed separately.

The effects of an extreme event load combination are allowed to cause damage to a structure. Stresses and deformations well into the inelastic range are permitted and, in some cases, expected. However, full loss of structural integrity or collapse must be prevented for the extreme event limit state.

Two extreme event load combinations are presented in *AASHTO LRFD*. These load combinations differentiate between the live loads that would most likely be present during the different extreme events, as well as the extreme event which is being considered in each load combination.

3.10.1.4.2 Extreme Event I

The Extreme Event I load combination is used to analyze a bridge for earthquake loading. For this load combination, the load factor value for live load is not yet fully

resolved. Previous AASHTO specifications have set this value, γ_{EQ}, equal to zero. However, according to *AASHTO LRFD* Article C3.4.1, current research shows that setting this value to $\gamma_{EQ} < 1.0$, or more specifically to 0.50, may be applicable for most average daily truck traffic (ADTT) conditions.

3.10.1.4.3 Extreme Event II

This load combination includes the effects of blast loading, ice flow impact, vehicular collisions, and vessel collisions. The effects of these four loadings are not to be combined such that they are assumed to act simultaneously. Instead, each of the applicable loadings is to be checked individually without the presence of the other extreme event loads. The load factor for live load for this load combination is 0.50, reflecting the fact that if one of the extreme events occurs, the likelihood of full live load being present on the bridge is small.

3.10.1.4.4 Design Applications

The specific design applications of the two extreme event load combinations are summarized in Table 3.10.1.4.4-1.

Table 3.10.1.4.4-1 Design Applications of Extreme Event Load Combinations

Extreme Event Load Combination	Design Applications
Extreme Event I	• Earthquake
Extreme Event II	• Blast loading • Ice flow impact • Vehicular collisions • Vessel collisions

3.10.1.5 Fatigue and Fracture Limit State Load Combinations

3.10.1.5.1 General

The fatigue and fracture limit state is intended to control the stress range of a structural element to limit the possibility of cracking. The loading conditions represent a single fatigue truck, occurring over a specific number of cycles. The material toughness requirements are based on the AASHTO Material Specifications. This limit state is not applicable to all bridge design checks, such as concrete decks and wood decks, and the design engineer must determine whether the effects of fatigue and fracture could be a problem for each specific bridge. The basic function of each fatigue load combination is described in the following sections.

3.10.1.5.2 Fatigue I

The Fatigue I load combination relates to infinite load-induced fatigue life. For this load combination, a load factor of 1.50 is applied to live load effects, and no other loads are applied. The load factor for this load combination reflects load levels that represent the maximum stress range of trucks for infinite fatigue life design. The load factor was selected assuming that the maximum stress range is twice the effective stress range caused by the Fatigue II load combination.

It should be noted that for orthotropic decks, when evaluating fatigue at the welded rib-to-floorbeam cut-out detail or at the rib-to-deck weld, the live load factor, γ_{LL}, for the Fatigue I load combination should be increased from 1.5 to 2.25. This increase is based on studies indicating that the ratio of maximum stress range to effective stress range is greater in orthotropic decks by a factor of approximately 1.5 as compared to standard bridge girders. This increase is due to several factors, including the occasional presence of heavy wheels and a reduction in local load distribution in orthotropic decks as compared with standard bridge decks.

3.10.1.5.3 Fatigue II

The Fatigue II load combination relates to finite load-induced fatigue life. For this load combination, a load factor of 0.75 is applied to live load effects, and no other loads are applied. The load factor for this load combination reflects load levels that represent the effective stress range of trucks with respect to a small number of stress range cycles and to their effects in steel elements, components, and connections for finite fatigue life design.

3.10.1.5.4 Design Applications

The specific design applications of the two fatigue load combinations are summarized in Table 3.10.1.5.4-1.

Table 3.10.1.5.4-1 Design Applications of Fatigue Load Combinations

Fatigue Load Combination	Design Applications
Fatigue I	• Related to infinite load-induced fatigue life • Only controls the design of steel elements, components, and connections for a limited number of steel superstructures
Fatigue II	• Related to finite load-induced fatigue life • Only controls the design of steel elements, components, and connections for a limited number of steel superstructures

3.10.2 Load Factors for Construction Loads

3.10.2.1 General

In addition to the base load factors and combinations described in Section 3.10.1, bridges should also be checked for construction loads to ensure that structural damage will not occur throughout the entire construction process. Load factors for construction loads are described in *AASHTO LRFD* Article 3.4.2.

3.10.2.2 Strength Limit State

Construction loads should be checked for the strength limit state using the same load combinations as presented in *AASHTO LRFD* Table 3.4.1-1.

However, for Strength I and III load combinations, the weight of the structure and appurtenances, including both *DC* and *DW* dead loads, should be assigned a load factor of 1.25 or greater.

For the Strength I load combination, unless otherwise specified by the Owner, the load factor for the construction loads and for any associated dynamic effects should be 1.50 or greater. Since the actual construction loads can vary from contractor to contractor, state to state, and even with the time of year and location of construction, the estimation of the loads due to mounted equipment, mobile equipment, and construction workers is less certain than the load due to the gravitational self-weight of bridge structural components.

Wind forces can greatly affect a bridge under construction, as the surfaces on which wind acts can be greater and more random than those for a completed bridge structure. Therefore, for the Strength III load combination, a factor of 1.25 or greater should be applied to all wind loads in combination with construction loads.

In addition to the strength load combinations described above, an additional strength load combination should be considered when accounting for construction conditions, unless otherwise specified by the Owner. This additional load combination should include maximum force effects of primary steel superstructure components during construction, including the applicable *DC* loads and any construction loads that are applied to the fully erected steelwork. For this additional load combination, the load factor for *DC* and construction loads, including dynamic effects (if applicable), should not be less than 1.4.

3.10.2.3 Service Limit State

In the absence of other directives in the project special provisions, any deflection requirements should be checked using the Service I load combination for the various

construction stages. Any deflection requirements during construction should be defined in the contract documents. Construction dead loads should be included with the permanent loads, and construction transient loads should be included with the live loads.

3.10.3 Load Factors for Jacking and Post-Tensioning Forces

3.10.3.1 Jacking Forces

The design forces for jacking in the service limit state should be at least 1.3 times the permanent load reaction at the bearings adjacent to the point of jacking, or as directed by the Owner.

If the bridge will be open to traffic during the jacking operation, the jacking load should also include a live load reaction based on the maintenance of traffic plan. The load factor for live load should be applied to that jacking load.

3.10.3.2 Post-Tensioning Anchorage Zones

For post-tensioning anchorage zones, the design force should be 1.2 times the maximum jacking force.

Section 3.11 References

AASHTO. 2002. *Standard Specifications for Highway Bridges*, 17th Edition, HB-17. American Association of State Highway and Transportation Officials, Washington, DC.

AASHTO. 2009. *LRFD Guide Specifications for Design of Pedestrian Bridges*, Second Edition, GSDPB-2. American Association of State Highway and Transportation Officials, Washington, DC.

AASHTO. 2011. *A Policy on Geometric Design of Highways and Streets*, GDHS-6. American Association of State Highway and Transportation Officials, Washington, DC.

ASCE. 1988. *Minimum Design Loads for Building and Other Structures*, ASCE 7-88. American Society of Civil Engineers, New York, NY.

Cohen, H. 1990. *Truck Weight Limits: Issues and Options*, Special Report 225. Transportation Research Board, National Research Council, Washington, DC.

Ross, H. E., D. L. Sicking, R. A. Zimmer, and J. D. Michie. 1993. *NCHRP Report 350: Recommended Procedures for the Safety Performance Evaluation of Highway*

Features. Transportation Research Board, National Research Council, Washington, DC.

Chapter 4 Structural Analysis

Section 4.1 Introduction

Structural theories that have evolved from statics and strength of materials have been used in the analysis of girder bridges and have been taught in structural analysis courses for decades. These concepts, melded with bridge design codes, are used in the design of girder bridges today. Powerful digital computers and modern software have enabled the Design Engineer to better apply these concepts to anticipate the behavior of bridges during design. When properly employed, this technology leads to bolder, better and more efficient bridges that are safe during construction and will dependably serve the public for decades to come.

This chapter first describes general LRFD requirements for structural analysis, the effective width of the concrete deck, uplift, requirements that allow for the neglect of curvature effects in the determination of major-axis bending moments and shears, the effective length factor for compression-member design, and moment redistribution.

The chapter next discusses structural analysis for dead load and structural analysis for live load, including the computation of approximate live load distribution factors. The use of influence lines and influence surfaces for live load analysis is also discussed.

The chapter concludes with a general discussion on the various methods of analysis, including approximate 1D methods of analysis, and more refined 2D and 3D methods of analysis.

Section 4.2 General

4.2.1 General LRFD Analysis Requirements

This section reviews some of the general *AASHTO LRFD* specification requirements for structural analysis. Methods of structural analysis are discussed in Section 4.5.

As specified in *AASHTO LRFD* Article 4.5, mathematical models are to include loads, geometry and material behavior of the structure, and where appropriate, the response characteristics of the foundation. The choice of the model is to be based

on the limit states investigated, the force effect being quantified, the complexity of the structure and the accuracy required of the analysis.

Linear elastic behavior of materials is assumed so specification of material properties is rather straightforward. An elastic modulus (Young's Modulus) and a Poisson's Ratio is specified for each material. From these properties the shear modulus can be computed. The density of the material is required to address the weight or mass of each element. This property may be specified as the mass density with a gravitational constant or as a gravitational density with a gravitational constant of 1.0 if no dynamic analyses are to be performed. If dynamic analyses are employed, the mass density is appropriate. In these cases, a gravitational constant other than unity is required. Specification of a weight density is generally preferred since it is more common. In these cases, a gravitational constant of 1.0 is specified. A fourth optional property is the thermal coefficient of expansion, which is necessary if a thermal analysis is required.

A second basic assumption made is that deflections are small. This means that it is assumed that the structure does not deflect enough to cause the point of application of the loads to be displaced enough to affect the analysis results. For example, a catenary cable changes shape under load and generally would not satisfy this assumption.

By assuming first-order small deflection theory and elastic behavior, influence lines and influence surfaces can be employed for live load analysis (Section 4.4.3).

Another requirement related to linear behavior is that changes in structure stiffness during loading are not permitted. For example, lift-off at a bearing as load is applied would change the structure stiffness and cause the model to behave in a non-linear fashion. Such behavior is not considered in the analyses discussed in this manual. Inelastic analysis is also not covered herein, although it can be used to better evaluate moment redistribution and seismic behavior.

According to *AASHTO LRFD* Article 4.6.1.2.1, for structures curved in plan, the moments, shears and other force effects required to proportion the superstructure components are to be based on a rational analysis of the entire superstructure. Equilibrium of curved girder bridges is developed by transfer of load between the girders (more so in curved I-girder bridges than in curved box-girder bridges). Thus, the analysis must recognize the integrated behavior of all the structural components. Bracing members are considered to be primary members in these bridges since their action is necessary to provide equilibrium. The concrete deck acts in transverse flexure, longitudinal flexure, vertical and horizontal shear. Torsion increases the horizontal deck shear in curved and/or skewed box-girder bridges.

In such cases, the entire superstructure, including bearings (Figure 4.2.1-1), is to be considered as integral with the structural unit. An analysis should consider the bearing orientation and the restraint of the bearings afforded by the substructure, including the stiffness of the substructure. The resulting lateral reactions are considered in designing the bearings, cross-frames/diaphragms, lateral bracing, deck and substructure. The lateral restraint offered by integral abutments or piers can be recognized in a proper analysis.

Figure 4.2.1-1 Bearings

When girder sections are subjected to significant torsion, as they are in curved bridges and in bridges with skewed supports, the girder sections do not remain plane. Experience has shown that distortion of I-shaped cross-sections need not be considered in the structural analysis of a properly braced bridge. Cross-section distortion can have a significant effect on the torsional behavior of steel box girders and its effect is typically attenuated by the provision of sufficient internal cross bracing. Although the section is allowed to distort, the position of the loads is assumed not to change in linear elastic analyses. Classical methods of analysis are usually based on strength of materials assumptions that do not recognize the effects of cross-section distortion. Refined analyses (e.g. 3D finite element analyses) in which the actual cross-section shape of the I- or box girder is rigorously modeled can recognize cross-section distortion and its effect on structural behavior (Section 4.5.3).

Centrifugal force effects are considered in the analysis of horizontally curved bridges, as discussed further in Section 3.4.9.

4.2.2 Effective Width of Deck

4.2.2.1 General

The concrete deck of concrete and steel composite girders subject to vertical bending is loaded through horizontal shear via the shear connectors. When the shear first is introduced, the effective width of concrete is very small. However, the shear stiffness of the deck soon distributes the force from the shear connectors to the rest of the deck. It takes some length of girder before the force in the concrete reaches equilibrium. At this point, the force in the deck near the shear connectors is somewhat higher than at the extreme edges. This shear-lag phenomenon is evident in Part A of Figure 4.2.2.1-1. Since the concrete deck is wider and less efficient than the girder in distributing the shear, there can be significant distortion of the concrete deck; that is, plane sections do not remain plane as illustrated in Part A of Figure 4.2.2.1-1. Of course with this distortion there is a non-uniform longitudinal stress distribution across the concrete slab, as shown in Part B of Figure 4.2.2.1-1.

Theoretical solutions for the true longitudinal stress distribution across the section can be determined from the theory of elasticity as applied to plates, but the solutions are not amenable for design use as they are complex and depend on the relative dimensions and stiffness of the system, as well as on the applied loading. Concentrated loads and reactions introduce a sharp discontinuity in shear, which creates a most significant shear lag effect. For example, the effective width of the composite deck near a reaction is less than in the center of a long span with a uniform load applied. It is rather intuitive that the full width of the deck would not be effective at an interior support of a continuous span. It becomes effective over some distance away from the reaction.

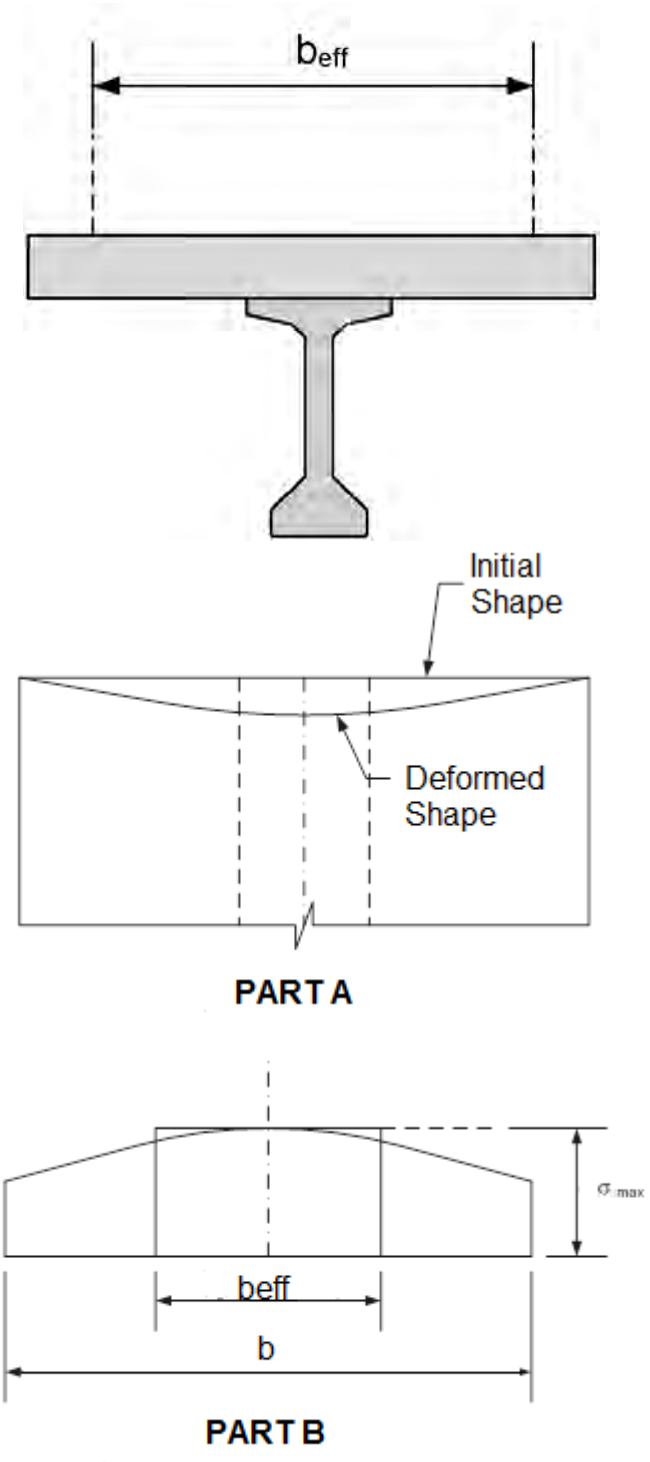

Figure 4.2.2.1-1 Shear Lag in a Composite Girder

The question arises as to how much of the deck can be safely assumed in the design of composite girders. To address this question in a simple manner the

concept of an effective width was introduced. The effective width (b_{eff} in Part B of Figure 4.2.2.1-1) is the width of concrete deck which can be assumed to be uniformly stressed. This width is the width of deck over which the assumed uniformly distributed longitudinal stresses result in approximately the same deck force and member moments calculated from elementary beam theory (i.e. assuming plane sections remain plane) as would be produced by the actual non-uniform stress distribution. The effective width of the deck used in the computation of the composite section properties accounts for the shear-lag effect. The thickness of the deck is tacitly assumed constant and equal to the full structural deck thickness.

The effective width for conventional composite-girder bridges (i.e. beam-slab bridges) is specified in *AASHTO LRFD* Article 4.6.2.6.1. In general, unless noted otherwise in *AASHTO LRFD* Article 4.6.2.6.1, the effective width of the concrete deck slab for determining cross-section stiffnesses for analysis and for determining flexural resistances may be taken as the tributary width perpendicular to the axis of the member. That is, referring to Figure 4.2.2.1-2:

- For interior girders (or interior webs of box sections), the effective width may be taken as the sum of one-half the distances to the adjacent girders (or webs) on each side of the girder (or web) under consideration; and
- For exterior girders (or exterior webs of box sections), the effective width may be taken as one-half the distance to the adjacent interior girder (or web) plus the full deck overhang width.

For box sections, the total effective width of the deck would then be taken as the sum of the effective widths over the interior and exterior webs of the box.

The article lists cases where the slab effective width should instead be determined by a refined analysis, including when the largest skew angle in the bridge system is greater than 75°, where the skew angle is measured relative to a normal to the longitudinal centerline of the bridge system. The reader is referred to *AASHTO LRFD* Article C4.6.2.6.1 for a more detailed discussion of the effective width provisions, and the research that justified the removal of the previous provisions for effective width, in which the effective width was dependent on the slab thickness, span length or girder spacing (Chen et al., 2005). Previous theoretical solutions proposed for the effective concrete width, which ignored the effect of any transverse deck cracking and inelastic behavior, generally tended to give a smaller effective width than experimentally determined values (Chapman and Teraskiewicz, 1968).

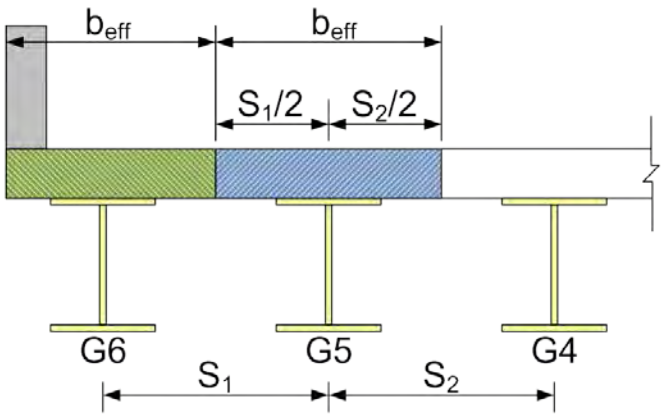

Figure 4.2.2.1-2 Effective Deck Width Based on Tributary Width of Deck over Each Girder

The effective flange width, determined as specified above, is generally to be used to determine the resistance of the composite section at all limit states. *AASHTO LRFD* Article 4.6.2.6.1 further recommends that for the calculation of live load deflections, the provisions of *AASHTO LRFD* Article 2.5.2.6.2 are to apply, where it is stated that the entire roadway width be included in determining the composite stiffness of the design cross-section for the computation of live load deflections at the service limit state.

AASHTO LRFD Article 2.5.2.6.2 also recommends that the structurally continuous portion of barriers, sidewalks and railings be included in determining the composite stiffness when a structurally continuous concrete barrier is present and included in the models used for the analysis as permitted. Although there is currently no specific requirement given in the specification for attachment of the barrier or its reinforcement to the deck, such attachment is understood to satisfy barrier crash testing requirements and may be satisfactory to ensure composite behavior with the deck. Further discussion of this requirement may be found in Section 2.3.2.6.2. *AASHTO LRFD* Article 4.6.2.6.1 permits the width of the deck overhang for this analysis, and for checking the composite girder resistance, to be extended by the following amount:

$$\Delta w = \frac{A_b}{2t_s}$$ Equation 4.2.2.1-1

AASHTO LRFD Equation 4.6.2.6.1-1

where:

A_b = cross-sectional area of the barrier (in.^{2})
t_s = structural thickness of the concrete deck (in.)

For straight girder systems in which a line-girder analysis is employed, the composite bending stiffness of an individual girder for the calculation of live-load deflections may be taken as the total composite stiffness, determined as outlined above, divided by the number of girders.

4.2.2.2 Orthotropic Steel Decks

Tests have shown that for most practical cases, shear lag may be ignored in calculating the ultimate compressive strength of stiffened or unstiffened girder flanges (Dowling et al., 1977). As a result, an orthotropic deck plate acting as the top flange of a longitudinal superstructure component or a transverse beam may normally be considered to be loaded uniformly across its width. According to *AASHTO LRFD* Article 4.6.2.6.4, consideration of the effective width of an orthotropic steel deck plate can be avoided by the application of refined analysis methods, as specified in *AASHTO LRFD* Article 4.6.3.2.4.

For simplified analysis, the width of the deck, including the deck plate and ribs, may be considered fully effective at the strength limit state for both positive and negative flexure when *L*/*B* is greater than or equal to 5 (*AASHTO LRFD* Article 4.6.2.6.4). *L* is the span length of the orthotropic girder or transverse beam, and *B* is the spacing between orthotropic girder web plates or transverse beams. The procedures given in AISC (1963) are considered an acceptable means of simplified analysis for orthotropic decks; however, it has been demonstrated that the simplified analysis procedures given in AISC (1963) may result in rib effective widths exceeding the rib spacing, which may be unconservative.

For the case of *L*/*B* less than 5, the effective width of the deck is to be taken as *L*/5 according to *AASHTO LRFD* Article 4.6.2.6.4. The flange effectiveness should be considered in greater detail for cases with particularly slender edge panels or stiffeners (Burgan and Dowling, 1985; Hindi, 1991). The effective width is increased as compared to elastic analysis when inelastic behavior of the deck panel is considered. At ultimate loading, the region of the flange plate above the web yields and distributes the stress outward if local stability of the plate is maintained (Lamas and Dowling, 1980). Similar behavior was observed in studies by Chen et al. (2005) on composite steel girders when inelastic behavior was considered; as a result, the

full deck slab width may be considered effective in both positive and negative moment regions in the majority of cases (Section 4.2.2.1).

For service and fatigue limit states in regions of high shear, a special investigation into shear lag should be done to determine the effective width using a refined analysis or other accepted approximate methods. Further information on orthotropic decks may be found in FHWA (2012).

4.2.2.3 Transverse Floorbeams and Integral Bent Caps

The effective width overhanging each side of a transverse floorbeam web or the web of an integral bent cap designed with a composite concrete deck slab is not to exceed six times the least slab thickness or one-tenth of the span length (*AASHTO LRFD* Article 4.6.2.6.5). The span length is to be taken as two times the length of the cantilever span for cantilevered transverse floorbeams or integral bent caps. These provisions are based on past successful practice.

4.2.3 Uplift

Uplift is an important consideration in the safe design and proper performance of girder bridges. Uplift is assumed to occur any time the factored reactions causing uplift exceed the factored permanent load reactions available to resist uplift. Uplift can occur due to gravity loads in the completed bridge or at any stage of construction of the bridge. Uplift may also occur due to thermal forces. An example of uplift on a bearing is shown in Figure 4.2.3-1.

Uplift is a non-linear phenomenon that may require changing the boundary conditions and cannot be treated properly with software that uses influence surfaces. Typically, the analysis reflects the assumption that the bearing is tied down, which is incorrect.

Figure 4.2.3-1 Uplift on a Bearing

Redecking of bridges under traffic can lead to uplift that does not occur under normal operating conditions. In checking for uplift during redecking with part of the deck intact for traffic, relocated barriers and removed deck loads are considered. The presence or absence of any future wearing surface should also be recognized in these investigations.

Thermal effects should be considered when checking uplift, particularly for skewed and curved structures, because these bridges can experience significant vertical reactions due to thermal forces. These reactions are properly computed by recognizing the bearing vertical offsets from the neutral axis of the superstructure girders. Both uniform temperature and thermal gradient conditions need to be considered. It should be noted that a 2D grid analysis will not recognize thermally induced uplift or any other vertical reaction since all forces are in-plane.

Potential uplift at bearings must be investigated at each critical construction stage, in particular during erection and deck casting.

Although it is desirable to avoid uplift, there are cases where reverse reactions are identified and countermeasures must be taken. Uplift can sometimes be addressed by modification of the framing to alter the transverse stiffness of the bridge, though the provision of tie-down devices or counterweight(s), or by removal of the bearing. Where a decision is made to permit uplift, the analysis should be modified to recognize the absence of vertical restraint at the support experiencing lift-off, which may result in uplift at other locations.

When checking for uplift at the strength limit state, the appropriate minimum load factor, γ_p, specified in *AASHTO LRFD* Table 3.4.1-2 (Section 3.9.1.6) should be

applied to any upward permanent load reactions resisting uplift. Potential uplift of the superstructure at any support under the combination of permanent load and other specified load types (including uniform temperature change, thermal gradient and/or wind load) may be investigated according to the following suggested load combinations, as applicable, subject to the approval of the Owner.

Uplift may simply lead to in-service or maintenance problems, such as reduced bearing life or unanticipated bending in the deck. In such cases, potential instability of the bridge due to uplift is typically not a concern and the inequality given by Equation 4.2.3-3 may be applied. However, narrow bridges (e.g. single box girders) can become unstable under certain conditions due to uplift. When uplift occurs in such bridges, it can lead to unloading of supports that in some cases can cause instability leading to structural failure. Where potential instability due to uplift is deemed to be of concern, the inequalities given by Equation 4.2.3-1 and Equation 4.2.3-2 may be employed instead.

On the left-hand side of the inequalities given by Equation 4.2.3-1 through Equation 4.2.3-3, the appropriate minimum load factors specified in *AASHTO LRFD* Table 3.4.1-2 are applied to the vertical reactions due to dead loads resisting uplift, including any wearing surface and/or utility loads. Reactions due to a future wearing surface load resisting uplift should conservatively be ignored. On the right-hand side of the inequalities are any uplift reactions that may be caused by various loads; reactions due to loads not causing uplift or not considered are ignored in checking the inequality.

- Where potential uplift may cause instability of the bridge:

$$0.9R_{DC} + 0.65R_{DW} > 1.25R_{(DC)u} + 1.50R_{(DW)u} + 1.75R_{LL+IM} + 0.5R_{TG} + 0.5R_{TU} + 0.5R_{WS} + 0.5R_{WL}$$

Equation 4.2.3-1

and:

$$0.9R_{DC} + 0.65R_{DW} > 1.25R_{(DC)u} + 1.50R_{(DW)u} + 1.75R_{LL+IM} + 1.0R_{TG} + 1.0R_{TU}$$

Equation 4.2.3-2

- Where potential uplift does not cause instability of the bridge:

$$0.9R_{DC} + 0.65R_{DW} > 1.0R_{(DC)u} + 1.0R_{(DW)u} + 1.0R_{LL+IM} + 0.5R_{TG} + 1.0R_{TU}$$

Equation 4.2.3-3

where:

R_{DC} = vertical reaction due to component dead loads resisting uplift (kips)
R_{DW} = vertical reaction due to wearing surface and/or utility loads resisting uplift (kips)
$R_{(DC)u}$ = uplift reaction due to component dead loads; zero if no uplift or not considered (kips)

$R_{(DW)u}$ = uplift reaction due to wearing surface and/or utility loads; zero if no uplift or not considered (kips)

R_{LL+IM} = uplift reaction due to the design vehicular live load specified in *AASHTO LRFD* Article 3.6.1.2 (Section 3.4.2) plus the corresponding dynamic load allowance specified in *AASHTO LRFD* Article 3.6.2.1 (Section 3.4.8); zero if no uplift or not considered (kips)

R_{TG} = uplift reaction due to the temperature gradient specified in *AASHTO LRFD* Article 3.12.3 (Section 3.6.3); zero if no uplift or not considered (kips)

R_{TU} = uplift reaction due to the uniform temperature change specified in *AASHTO LRFD* Article 3.12.2 (Section 3.6.2); zero if no uplift or not considered (kips)

R_{WS} = uplift reaction due to the wind pressure on the structure specified in *AASHTO LRFD* Article 3.8.1.2 (Section 3.5.1.2); zero if no uplift or not considered (kips)

R_{WL} = uplift reaction due to the wind pressure on vehicles specified in *AASHTO LRFD* Article 3.8.1.3 (Section 3.5.1.3); zero if no uplift or not considered (kips)

Where the applicable inequality is not satisfied, uplift is assumed to occur at the support under consideration. Where uplift occurs and is to be countered with a tie-down device or counterweight, the suggested factored design uplift reaction, R_u, for the design of any countermeasure may be computed as follows subject to the approval of the Owner:

$$R_u = 0.9R_{DC} + 0.65R_{DW} + 1.25R_{(DC)u} + 1.50R_{(DW)u} + 1.75R_{LL+IM} + 0.5R_{TG} + 0.5R_{TU}$$

Equation 4.2.3-4

The signs of the various reactions must be considered in applying Equation 4.2.3-4. Reactions due to loads not causing uplift or not considered should be ignored. The effects of thermal movements of the superstructure should be considered when designing tie-down devices or counterweights.

Design checks for potential uplift under any extreme event limit state force effects should be handled separately according to the appropriate design provisions for those situations. Potential uplift due to water loads, WA, acting on the superstructure in an extreme event may also need to be considered at the discretion of the Owner.

4.2.4 Neglect of Curvature Effects

4.2.4.1 General

This section reviews the *AASHTO LRFD* specification requirements and conditions as to when certain effects of horizontal curvature may be neglected in the analysis of horizontally curved steel I-girder bridges and horizontally curved closed steel box or tub girder bridges. For curved I-girder bridges, these conditions are listed in *AASHTO LRFD* Article 4.6.1.2.4b. For curved closed box or tub girder bridges, these conditions are listed in *AASHTO LRFD* Article 4.6.1.2.4c.

The conditions under which the effects of horizontal curvature may be ignored in the analysis for determining the vertical bending moments and bending shears are reviewed. When the bridge under consideration satisfies all the applicable listed conditions, an individual I-girder or an individual closed box or tub girder in a steel or concrete bridge may be analyzed as an isolated straight girder with a span length(s) equal to the girder arc length(s) for the determination of the vertical bending moments and bending shears. The effect of curvature on the torsional behavior of the girder must still be considered regardless of the amount of curvature since strength and stability of curved girders is different from that of straight girders (Hall and Yoo, 1996).

4.2.4.2 I-Girders

AASHTO LRFD Article 4.6.1.2.4b specifies that I-girder bridges satisfying the following four conditions may be analyzed neglecting the effects of curvature in determining the vertical bending moments and bending shears:

- All girders must be concentric;
- Bearing lines must not be skewed more than 10° from radial;
- The stiffnesses of the girders must be similar. Similar girder stiffnesses are required to avoid large and irregular changes in stiffness that could alter the transverse distribution of load; under such conditions, a refined analysis is more appropriate;
- For all spans, the arc span, L_{as}, divided by the girder radius, R, in feet must be less than 0.06 radians, where L_{as} is to be taken as follows:

  For simple spans:
  L_{as} = arc length of the girder
  For end spans of continuous members:
  L_{as} = 0.9 times the arc length of the span
  For interior spans of continuous members:
  L_{as} = 0.8 times the arc length of the span

Lateral flange bending effects due to torsion in steel girders should still be determined from an appropriate approximation and considered in the design (refer to *AASHTO LRFD* Eq. C4.6.1.2.4b-1). The derivation of *AASHTO LRFD* Eq. C4.6.1.2.4b-1 is discussed further in NHI (2011). Cross-frame spacing should be set to limit lateral flange bending in the girders. Cross-frames should be designed for forces computed by a rational means.

4.2.4.3 Closed Box and Tub Girders

AASHTO LRFD Article 4.6.1.2.4c specifies that closed box or tub girder bridges satisfying the following four conditions may be analyzed neglecting the effects of curvature in determining the vertical bending moments and bending shears:

- All girders must be concentric;
- Bearing lines must not be skewed;
- For all spans, the arc span, L_{as}, divided by the girder radius, R, in feet must be less than 0.3 radians, where L_{as} is to be taken as follows:

  For simple spans:
  L_{as} = arc length of the girder
  For end spans of continuous members:
  L_{as} = 0.9 times the arc length of the span
  For interior spans of continuous members:
  L_{as} = 0.8 times the arc length of the span

- The girder depth must be less than the width of the box at mid-depth of the box. If the box is haunched or tapered, the shallowest girder depth is to be used on conjunction with the narrowest width of the box at mid-depth.

Where the bridge satisfies the preceding conditions and the approximate live load distribution factor for box sections specified in *AASHTO LRFD* Article 4.6.2.2.2b is used to determine the live load vertical bending moments and bending shears, the bridge should also satisfy the special geometric restrictions for the use of the distribution factor given in *AASHTO LRFD* Article 6.11.2.3.

Torsion is often more significant in box sections than in open I-sections. Torsional shears are typically large and the box web shears are particularly affected by the torsional shears. Double bearings also resist significant torque compared to a box-centered single bearing. Thus, the torsional effects should be evaluated by a rational means that recognizes the specific location of loads, as well as the torsional stiffness of the entire cross-section. The approximate M/R Method (Tung and Fountain, 1970) addresses the torsional effect of the geometry of the section and the application of loads to a degree.

Closed concrete curved girder bridges resolve torsional stresses into diaphragms at the supports. Typically, strut-and-tie models are developed for diaphragms at these supports.

4.2.5 Effective Length Factor, K

Equations for the compressive resistance of columns and moment magnification factors for beam-columns include an effective length factor, *K*, which is used to modify the physical length of the column according to the restraint at the ends of the column against translation and rotation. *K* is applied to the actual member unbraced length, ℓ, to compensate for translational and rotational boundary conditions other than pinned ends. *K* represents the ratio of the idealized pinned-end compression member length to the actual length of a member with other than pinned ends.

In many cases, some degree of end restraint exists causing an effective length factor other than 1.0. *AASHTO LRFD* Table C4.6.2.5-1 provides a table of theoretical *K* values taken from SSRC (1998) for idealized end conditions in which translational and/or rotational end conditions are either fully restrained or free. Because actual member end conditions are seldom perfectly fixed or perfectly unrestrained as represented by the ideal conditions, *AASHTO LRFD* Table C4.6.2.5-1 also provides recommended design values as suggested by the Structural Stability Research Council (SSRC). These simple modifications of the ideal values lead to either equal or somewhat higher *K* values.

In the absence of refined inelastic analysis, *AASHTO LRFD* Article 4.6.2.5 provides recommended *K* values in the braced plane of triangulated trusses, trusses and frames where lateral stability is provided by diagonal bracing or other suitable means. The recommended values are as follows:

- For bolted or welded end connections at both ends: $K = 0.750$
- For pinned connections at both ends: $K = 0.875$
- For single angles, regardless of end connection: $K = 1.0$

The recommended values for *K* do not account for any relative translation or rotation of the ends of the member. These relative motions are not usually present in building columns. They more closely resemble the actions found in transmission towers. Caution should be exercised in applying these recommended values to cases with larger unbraced lengths where elastic buckling may control.

A conservative *K* value of 1.0 is suggested for single angles since these members are often loaded through only one leg and are subject to eccentric loading as well as twist. These effects may not be properly recognized in design. The recommended value of $K = 1.0$ for single angles also closely matches that provided in ASCE (2000)

(the design of single-angle compression members is discussed in more detail in Section 6.6.3.4.5).

SSRC (1998) gives more specific recommendations of *K* values to use for in-plane buckling of various truss members. In some cases, the *K* values are higher than the recommended values given above. This reference also gives recommendations for buckling of truss members in the out-of-plane direction. Suggested *K* values for in-plane buckling of arch members are provided in *AASHTO LRFD* Article 4.5.3.2.2c. The reader is referred to White (2012) for additional discussion of *K* values.

Where non-rigid rotational restraint exists, *K* may be determined from traditional alignment charts for sidesway-inhibited or sidesway-uninhibited cases that are provided in *AASHTO LRFD* Article C4.6.2.5. Closed-form equations are also provided. The assumptions made in the alignment charts and equations are discussed in detail in the commentary to Chapter C of AISC (2005). Modifications are also presented there that extend the range of applicability of the alignment charts. The reader is urged to review these assumptions and modifications prior to using the alignment charts and/or equations.

4.2.6 Moment Redistribution

AASHTO LRFD Article 4.6.4 discusses the redistribution of negative moments in continuous beam bridges. Redistribution of force effects in multi-span, multi-beam girder superstructures may be permitted at the discretion of the Owner. Inelastic behavior is to be restricted to the flexure of the beams or girders; inelastic behavior due to shear and/or uncontrolled buckling is not permitted. Redistribution of force effects is only to be considered in the longitudinal direction, and is not to be considered in the transverse direction. The reduction of the negative moments over interior supports is to be accompanied by a commensurate increase in the positive moments in the spans (Figure 4.2.6-1).

The negative moments over the supports, determined from a linear elastic analysis, may be decreased by more refined methods, such as a redistribution process considering the moment-rotation characteristics of the cross-section, or by a recognized mechanism method. Or in lieu of a more refined analysis, simplified approximate redistribution procedures may be employed.

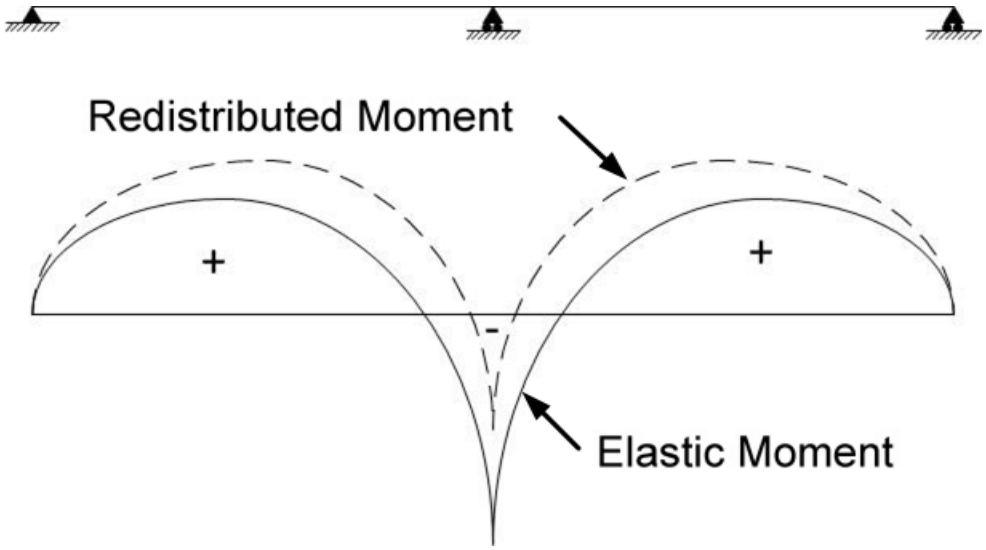

Figure 4.2.6-1 Redistribution of Bending Moment in a Multi-Span Girder Superstructure

AASHTO LRFD Appendix B6 to Section 6 of the *AASHTO LRFD* Specifications provides optional provisions for the calculation of redistribution moments from the interior-pier sections of straight continuous-span steel I-girder bridges at the service and/or strength limit states (Section 6.5.6.6). Several restrictions are specified on the use of these approaches in order to ensure adequate ductility and robustness at interior-pier sections (Section 6.5.6.6.3). According to the provisions, the redistribution moments may be calculated using either a simplified effective plastic moment method that intrinsically accounts for the interior-pier section moment-rotation characteristics (Section 6.5.6.3.3), or a more refined method in which a direct shakedown analysis is conducted to ensure the simultaneous satisfaction of continuity and moment-rotation relationships at all interior-pier sections from which moments are redistributed (Section 6.5.6.6.4).

AASHTO LRFD Article 5.7.3.5 discussed a simplified approach that may be employed to redistribute negative moments over the interior supports of continuous reinforced concrete beams with bonded reinforcement that may be used in lieu of a refined analysis.

Section 4.3 Dead Load

4.3.1 Self-Weight of Superstructure Members

Self-weight of superstructure members is easily modeled in the analysis using the body weight of the modeled members based on the input density of the material. In line-girder analyses, typically only the weight of the main longitudinal superstructure members is considered in this fashion. The self-weight of transverse members, such

as cross-frames or diaphragms, is usually input separately. The weight of details, such as stiffeners, splices, shear connectors, etc., is not typically included unless specifically included in the analysis model. It can be easily accounted for by increasing the density of the material, or by including the detail weight as a separate input load. If structural steel is to be painted, an additional three percent can be added to the steel density to account for the weight of the paint.

4.3.2 Concrete Deck

Weight of the concrete deck may be applied as a uniform load that will typically be converted in the analysis to a series of concentrated loads applied at the nodes and perhaps with some nominal end moments. Alternatively, the deck weight may be applied to the model with concentrated loads at the nodes representing the tops of the girders. Wet concrete is usually assumed to have no stiffness. The deck may be modeled using the self-weight of the deck in this case, but that has the disadvantage of dealing with some assigned stiffness. It would be incorrect to use the concrete stiffness, which would distribute the weight differently than if it were wet with no stiffness. The weight of any concrete deck haunches over the girders may also be considered in the analysis in a similar fashion. The weight of the concrete deck and deck haunches is applied to the non-composite section in the analysis of steel bridges.

The concentrated load applied to each girder top node is determined by the tributary area of deck associated with the distance between girder nodes and the girder spacings. Where concentrated loads are used to apply the deck weight, the discretization of the model must be sufficient to ensure that the series of concentrated loads applied to the girder nodes will be refined enough to represent the uniform load. This issue can be seen in the following example shown in Figure 4.3.2-1. The maximum moment due to a uniform load on a simple beam is $1/8w\ell^2$; the maximum shear is $w\ell/2$.

Representing a span with two beam elements with half of the load applied in the center and a quarter of the load applied at each end gives a maximum moment of

$$M_{max} = \left(\frac{w\ell}{2} * \frac{\ell}{2}\right) - \left(\frac{w\ell}{2} * \frac{\ell}{4}\right) = \frac{w\ell^2}{8} \qquad \text{Equation 4.3.2-1}$$

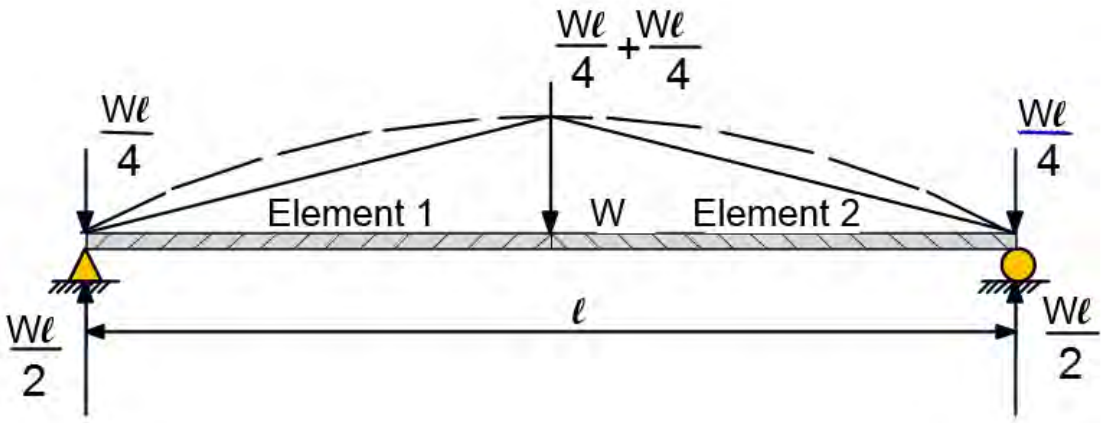

Figure 4.3.2-1 Discretization of Model for Deck Weight Using Two Elements – Bending Moment

However, the moment diagram is parabolic for the uniform load and triangular for the single concentrated load, as is evident in Figure 4.3.2-1. The moment along the span at locations other than at the center of the span can be significantly in error depending on the length of the two elements.

As illustrated in Figure 4.3.2-2, the maximum shear is in error by 50 percent in this case since the loads at the ends of the span are applied to the nodes and not to the beam. Obviously, a more refined model is required.

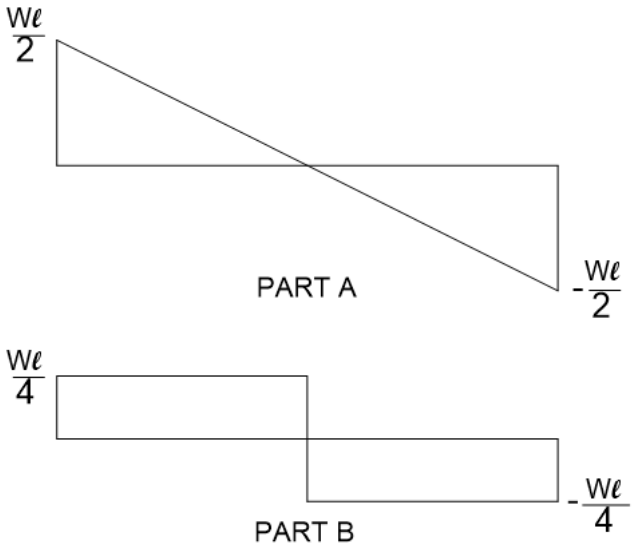

Figure 4.3.2-2 Shear Diagram for Deck Weight

A) Uniform Load; B) Concentrated Loads Using Two Elements

In steel bridges, the action of the cross-frames tends to distribute the weight of the wet concrete deck so that the girders deflect nearly equally on a straight bridge with right supports (Section 6.3.2.5.5.1). If all the girders are of equal or nearly equal stiffness in these bridges, the deck weight will be carried nearly equally by all the girders via the restoring forces in the cross-frames. *AASHTO LRFD* Article 4.6.2.2.1 recognizes this fact by stating that for multi-girder bridges satisfying certain conditions (e.g. width of the deck is constant, girders are parallel and have approximately the same stiffness, number of girders is not less than four, conditions for neglect of curvature discussed in Section 4.2.4 are met, etc.), the permanent load of the wet concrete deck may be distributed equally to each of the girders in the cross-section for approximate line-girder analyses (in lieu of the traditional tributary area assumption). In the case of most skewed and/or curved steel-girder bridges, however, the distribution of the deck weight is rather complex and must be ascertained by analysis. However, it is always distributed in a manner consistent with the restoring forces in the cross-frames. This is one of the important functions of the cross-frames.

Deck placement or phased construction situations, in which the deck is placed in sequential stages longitudinally along the girder, and/or the deck weight is placed on only one side of a girder creating significant torsion on the girder, should be recognized not only in deflection calculations, but also stress determinations.

4.3.3 Other Component Dead Loads

The weight of permanent deck forms should be considered in the analysis if the forms are to be permanent. This weight can be applied directly to the girders as a uniform load or as concentrated loads as done for the deck. Alternatively, the load may be considered by specifying an increase in the non-structural deck thickness to be used to compute the deck loads. Recall that these forms typically exist only between flange edges in the interior bays. Like the deck, the weight of deck forms is applied to the non-composite section in the analysis of steel bridges.

If temporary forms are planned and it is desired to consider their weight in the analysis, their weight can be introduced in a similar manner as for the permanent type. However, in this case, it is necessary to apply a reverse load to the composite section to represent removal of the forms. This consideration is usually not made except in extreme cases.

AASHTO LRFD Article 4.6.2.2.1 also indicates that for bridges satisfying the previously stated conditions (Section 4.3.2), permanent loads applied to the deck after the deck is made composite may also be distributed equally to each girder. Heavier superimposed dead loads such as parapets, barriers, sidewalks or sound walls should not be distributed equally to all the girders for the analysis. The traditional approach has been to distribute these loads uniformly to all the girders.

However, previous specifications never condoned this practice. The provisions called only for curb and railing loads to be uniformly distributed. They did not permit barriers or sound walls, which are much heavier than curbs, to be uniformly distributed. Proper consideration of the location of these loads usually results in the loads causing larger moments in the exterior girders and smaller moments in the interior girders.

Whenever refined methods of analysis are employed, these loads may be applied at their true location. However, engineering judgment should be applied in distributing these loads for approximate line-girder analyses. Usually the largest portion of the parapet load on an overhang is assigned to the fascia girder, or to the fascia girder and the first interior girder. In fact, in some cases, the exterior girder may receive more than the weight of a heavy parapet, sound wall, etc. on the extreme deck overhang due to the cantilever effect, with resulting uplift of one or more interior girders.

Estimating the distribution of these superimposed dead loads to the individual girders for line-girder analyses is particularly difficult in skewed bridges because the loads (e.g. parapets) may only be on one side of the bridge over significant portions of the span. Skew produces torsion in girders, which should be dealt with by other analytical means that generally involve a more refined analysis. In steel bridges, these superimposed dead loads are applied to the long-term composite section for the analysis to account in an approximate fashion for long-term creep effects.

4.3.4 Wearing Surface and Utilities

For wearing surface loads and deck overlays, the assumption of an equal distribution of the load to each girder for approximate line-girder analyses is reasonable and has been the customary practice. Engineering judgment may be employed for the distribution of utility loads to the individual girders. These loads are typically applied to the composite section, with the loads applied to the long-term composite section in steel bridges to account for long-term creep effects.

For refined analysis, wearing surfaces and deck overlays may be applied to the analysis model as uniform loads acting over the roadway deck area, as a series of concentrated loads, or by inputting an artificial density of the hardened concrete deck. Utility loads may be applied at their proper locations in the model.

Section 4.4 Live Load

4.4.1 General

This section discusses structural analysis considerations for live load. Approximate assignment of live-load effects to the individual girders in beam-slab bridges caused by one or more lanes of load is typically accomplished through the use of the live load distribution factors specified in *AASHTO LRFD* Article 4.6.2.2, and described further in Section 4.4.2. The determination of the base moving live load force effects (e.g. moments, shears, and reactions) is accomplished through the use of either influence lines or influence surfaces, as described further in Sections 4.4.3.1 and 4.4.3.2, respectively.

4.4.2 Live Load Distribution Factors

4.4.2.1 General

AASHTO specifications have favored the use of live load distribution factors (LLDFs) for decades over other methods commonly used in Europe and elsewhere. LLDFs were originally developed assuming non-composite girders with nominal cross-frames. The original factors assumed two lanes loaded. They were developed for narrowly-spaced straight girders with no skew, which were commonly used in the 1930s and 1940s. Typical in those days were very small overhangs so the exterior girders were less critical than the interior girders. Because the factors were simple, the accuracy varied quite a bit between bridges.

Investigations in the 1980s and 1990s resulted in the development of more complex LLDFs found in the *AASHTO LRFD* specifications at present (Zokaie et al., 1991). These factors addressed more parameters than girder spacing in the computation of the LLDFs. Of particular importance in this development was the recognition that the exterior girder in modern bridges is often the critical girder. Shear and moment were separated with their own sets of factors. A set of correction factors to be applied to the LLDFs was also created to account in an approximate fashion for the effects of skew.

The LLDFs found in the *AASHTO LRFD* specifications are modified from those in Zokaie et al. (1991) to account for the different multiple presence factors that are used in the AASHTO LRFD specifications, and are expressed in units of lanes rather than wheels.

These advances provided an improvement in the accuracy of LLDFs. However, they were not able to address curved-girder bridges at all; other methods are typically required. The digital computer with appropriate software rescued the Design

Engineer in such cases by providing the ability to analyze the superstructure and, in some cases, the entire bridge as a system (Section 4.5.3).

The LLDFs in the *AASHTO LRFD* Specification were determined by randomly compiling more than 800 actual bridges from various states to achieve a national representation. For each beam-slab bridge category within this larger data set, average bridges were obtained, and then refined analyses were conducted on selected bridges from each group (Zokaie et al., 1991).

Approximate formulas were then developed to capture the variation in the LLDFs with each of the critical geometric and material parameters. The effect of each parameter was assumed modeled by an exponential function, with the final LLDFs determined based on a multiple regression analyses. Cross-frames/diaphragms were disregarded in the analyses of multi-girder bridges, effectively increasing the moments in the interior girders and decreasing the moments in the exterior girders. The width of the concrete parapets was also often neglected increasing the load in the outer two girders. The effect of bottom lateral bracing in steel I-girder bridges was not considered, and is not comprehended by the LLDF equations. To assure conservative results, the constants in the LLDF formulas were adjusted so that the ratio of the value computed using the approximate LLDF to the more accurate distribution factor would in most cases be greater than 1.0.

As specified in *AASHTO LRFD* Article 4.6.2.2.1, the LLDF equations may be used for girders, beams, and stringers (other than multiple steel box girders – see instead *AASHTO LRFD* Article 6.11.2.3) with concrete decks that satisfy the following conditions (and the ranges of applicability that are identified in the tables of LLDFs that are provided):

- Width of the deck is constant;
- Unless otherwise specified, the number of girders/beams/stringers is not less than four;
- The girders/beams/stringers are parallel and have approximately the same stiffness;
- Unless otherwise specified, roadway part of the deck overhang, d_e, does not exceed 3.0 ft;
- Curvature in plan is less than the limit specified in *AASHTO LRFD* Article 4.6.1.2.4 (Section 4.2.4), or where distribution factors are required in order to implement an acceptable approximate or refined method of analysis for bridges of any degree of curvature in plan; and
- The cross-section is consistent with one of the representative cross-sections shown in *AASHTO LRFD* Table 4.6.2.2.1-1.

For bridges that satisfy the preceding conditions, the self-weight of the deck and any permanent loads on the deck may be distributed uniformly to the girders/beams/ stringers.

Where moderate deviations from a constant deck width or parallel beams exist, the distribution factor may either be varied at selected locations along the span, or else a single distribution factor may be used in conjunction with a suitable value for the girder/beam/stringer spacing. *AASHTO LRFD* Article C4.6.2.2.1 contains suggested rational approaches that may be used to extend the use of LLDFs to bridges with splayed girders.

AASHTO LRFD Table 4.6.2.2.1-1 contains 12 different representative bridge types, eight of which utilize precast concrete. Longitudinal joints connecting adjacent members are shown for five of the structure types in the table (Types "f", "g", "h", "i", and "j"). If the adjacent beams for these types are sufficiently interconnected by transverse post-tensioning of at least 0.25 ksi, or by a reinforced structural overlay, or both (see also *AASHTO LRFD* Article 5.14.4.3.3f), they may be considered to act monolithically. For concrete beams, other than box beams, used in multi-beam decks with shear keys, deep rigid end diaphragms are required. If the stem spacing of stemmed beams is less than 4.0 ft or more than 10 ft, a refined analysis method must be used.

Where the girder/beam/stringer spacing exceeds the range of applicability for the LLDF equations specified in *AASHTO LRFD* Articles 4.6.2.2.2 and 4.6.2.2.3, the live load on each girder/beam/stringer is to be determined as the reaction of the loaded lanes based on the lever rule, unless otherwise specified. The lever rule involves summing moments about one support (girder) to find the reaction at another support (girder) assuming that the supported component (deck) is hinged at interior supports. In applying the level rule, the AASHTO rules for live-load placement must be followed (Section 4.4.3.2.2). When other ranges of applicability in the table are exceeded, or one or more of the above conditions is not satisfied, engineering judgment should be employed in extending the application of the LLDF equations to cases slightly beyond the limits, or else the bridge is to be analyzed using a refined method of analysis (Section 4.5.3).

Multiple presence factors specified in *AASHTO LRFD* Article 3.6.1.1.2 (Section 3.4.1.2) are not to be used with any of the LLDF equations specified in *AASHTO LRFD* Articles 4.6.2.2.2 and 4.6.2.2.3 because these factors are already incorporated in the equations. However, multiple presence factors are to be applied whenever the lever rule or statical method (Sections 4.4.2.2.2.2 and 4.4.2.3.2.2) is employed, or whenever refined analysis methods are used in lieu of LLDFs.

As specified in *AASHTO LRFD* Article 3.6.1.1.2, multiple presence factors are not to be applied at the fatigue limit state for which one design truck is used. For

determining the force effects due to the single fatigue design truck, LLDFs for one-lane loaded must be used. Therefore, whenever the single-lane LLDF equations specified in *AASHTO LRFD* Articles 4.6.2.2.2 and 4.6.2.2.3 are used, the force effects are to be divided by 1.2 (or the multiple presence factor for one-lane loaded). Whenever the lever rule, or statical method (Section 4.4.2.2.2), or a refined analysis method is employed, the force effects due to the single fatigue design truck should not be multiplied by 1.2.

The LLDFs may also be used for permit and rating vehicles whose overall width is comparable to the width of the design truck. If one lane is loaded with a special vehicle or evaluation permit vehicle in combination with routine traffic, the design force effect per girder resulting from the mixed traffic may be approximately determined as specified in *AASHTO LRFD* Article 4.6.2.2.5 (Section 4.4.2.5), or else determined from a refined analysis.

The value of *L* (length) to be used in the LLDF equations specified in *AASHTO LRFD* Articles 4.6.2.2.2 and 4.6.2.2.3 for positive and negative moment LLDFs will differ within spans of continuous girder bridges, as will the LLDFs for positive and negative flexure. The value of *L* to be used in the LLDF equations is given in *AASHTO LRFD* Table 4.6.2.2.1-2 (Table 4.4.2.1-1) as follows:

Table 4.4.2.1-1 *L* for Use in LLDF Equations

Force Effect	*L* (ft)
Positive Moment	Length of the span for which moment is being calculated
Negative Moment – near interior supports of continuous spans between points of contraflexure under a uniform load on all spans	Average length of the two adjacent spans
Negative Moment – other than near interior supports of continuous spans	Length of the span for which moment is being calculated
Shear	Length of the span for which shear is being calculated
Exterior Reaction	Length of the exterior span
Interior Reaction of Continuous Span	Average length of the two adjacent spans

In the rare case where a continuous-span arrangement is such that an interior span does not have any positive uniform load moment (i.e. no uniform load points of contraflexure), *AASHTO LRFD* Article C4.6.2.2.1 indicates that the region of negative moment near the interior supports is to be increased to the centerline of the

span, and the *L* to be used in determining the LLDFs is to be taken as the average length of the two adjacent spans.

The longitudinal stiffness parameter, K_g, given in the LLDF equations is to be taken as:

$$K_g = n\left(I + Ae_g^2\right) \qquad \text{Equation 4.4.2.1-1}$$

AASHTO LRFD Equation 4.6.2.2.1-1

where:

A = area of the girder/beam/stringer (in.^{2})
e_g = distance between the centers of gravity of the girder/beam/stringer and deck (in.)
I = moment of inertia of the girder/beam/stringer (in.^{4})
n = E_B/E_D Equation 4.4.2.1-2

AASHTO LRFD Equation 4.6.2.2.1-2

E_B = modulus of elasticity of the girder/beam/stringer material (ksi)
E_D = modulus of elasticity of the deck material (ksi)

For steel girders/beams/stringers, the parameters, *A* and *I*, in Equation 4.4.2.1-1 are to be taken as those of the non-composite girder/beam/stringer. For girders/beams/stringers with variable moments of inertia, K_g may be based on average properties. Simplifications of the terms in the LLDF equations involving the longitudinal stiffness parameter, K_g, along with the term, *I*/*J*, are given in *AASHTO LRFD* Table 4.6.2.2.1-3, but may only be used with the concurrence of the Owner.

Unless future widening of the bridge is virtually inconceivable, regardless of the method of analysis that is used, exterior girders/beam/stringers of multi-beam bridges are not to have less resistance than interior girders/beams/stringers.

The following discussion of the LLDF equations for beam-slab bridges is for bridges with concrete decks only. For bridges with other types of decks (e.g. timber, open grids, etc.), the reader is referred to *AASHTO LRFD* Articles 4.6.2.2.2 and 4.6.2.2.3. The results from all the equations are given in terms of lanes rather than wheels.

The notation below is used in the LLDF equations summarized in the following sections:

b = width of beam (in.)
C = stiffness parameter = $K(W/L) \le K$
d = depth of beam (in.)

d_e = horizontal distance between the centerline of the exterior web of the exterior girder/beam/stringer at the deck level and the interior edge of the curb or traffic barrier (ft)
D = width of distribution per lane (ft)
e = correction factor for exterior girder LLDFs
g = live load distribution factor (lanes)
I = moment of inertia of girder/beam/stringer (in.^{4})
J = St. Venant torsional constant (in.^{4})
k = a non-dimensional constant = $2.5(N_b)^{-0.2} \geq 1.5$
K = a non-dimensional constant = $[(1 + \mu)(I/J)]^{0.5}$
K_g = longitudinal stiffness parameter given by Equation 4.4.2.1-1 (in.^{4})
L = length of girder/beam/stringer (Table 4.4.2.1-1) (ft)
N_b = number of girders/beams/stringers
N_c = number of cells in a concrete box girder
N_L = number of design lanes
S = spacing of girders/beams/stringers or webs (ft)
t_s = depth of concrete slab (in.)
W = edge-to-edge width of bridge (ft)
W_e = half the web spacing, plus the total overhang (ft)
θ = skew angle measured with respect to a normal to the girder tangent (degrees)
μ = Poisson's ratio for concrete, usually taken equal to 0.2

4.4.2.2 Girder Distribution Factors for Moment

4.4.2.2.1 Interior Girders

4.4.2.2.1.1 General

The equations giving the LLDF, *g*, for bending moment in interior girders/beams/stringers with concrete decks are given in *AASHTO LRFD* Table 4.6.2.2.2b-1 (subject to the ranges of applicability listed for each bridge type), and are summarized as follows:

4.4.2.2.1.2 Steel I-Girders (Type "a")

One Design Lane Loaded

$$g = 0.06 + \left(\frac{S}{14}\right)^{0.4}\left(\frac{S}{L}\right)^{0.3}\left(\frac{K_g}{12.0Lt_s^3}\right)^{0.1} \quad \text{Equation 4.4.2.2.1.2-1}$$

Two or More Design Lanes Loaded

$$g = 0.075 + \left(\frac{S}{9.5}\right)^{0.6}\left(\frac{S}{L}\right)^{0.2}\left(\frac{K_g}{12.0Lt_s^3}\right)^{0.1} \qquad \text{Equation 4.4.2.2.1.2-2}$$

When N_b is equal to 3, use the lesser of the values obtained from the equations above with N_b equal to 3, or the lever rule, for both of the preceding cases.

EXAMPLE

For a steel I-girder bridge cross-section shown in Figure 4.4.2.2.2.2-1 for a three-span continuous bridge, calculate the LLDFs for bending moment in the interior girders in regions of positive flexure in the end spans for the case of one design lane loaded, and for the case of two or more design lanes loaded. The 40′-0" roadway width can accommodate up to three 12′-0"-wide design lanes (*AASHTO LRFD* Article 3.6.1.1.1 – Section 3.4.1.1). The supports are not skewed.

According to Table 4.4.2.2.2.2-1, in regions of positive flexure, the length of the span for which the moment is being calculated is to be used for *L* in the above equations. The end span is 140′-0" in length. The moment of inertia of the non-composite steel girder at the point of maximum positive moment is 62,658 in.^{4} The cross-sectional area of the steel girder at that point is 75.25 in.^{2} The structural deck thickness is 9.0 in. The distance from the center of gravity of the non-composite steel girder to the center of gravity of the structural concrete deck, e_g, is 46.63 in. The modular ratio, n, is equal to 8. Therefore, the longitudinal stiffness parameter, K_g, is computed as (Equation 4.4.2.1-1):

$$K_g = n\left(I + Ae_g^2\right) = 8\left(62{,}658 + 75.25(46.63)^2\right) = 1.81 \times 10^6 \text{ in.}^4$$

Although the K_g term varies slightly along the span, the value at the maximum positive moment section in the end spans is used in this example to compute the distribution factor to be used in all regions of positive flexure in the end spans. Other options are to compute a separate K_g based on the average or a weighted average of the properties along the span in the positive-flexure region, or to compute K_g based on the actual values of the section properties at each change of section resulting in a variable distribution factor along the span within the positive-flexure region. However, the distribution factor is typically not overly sensitive to the value of K_g that is assumed.

One Design Lane Loaded (Equation 4.4.2.2.1.2-1):

$$g = 0.06 + \left(\frac{S}{14}\right)^{0.4}\left(\frac{S}{L}\right)^{0.3}\left(\frac{K_g}{12.0Lt_s^{\,3}}\right)^{0.1}$$

$$g = 0.06 + \left(\frac{12.0}{14}\right)^{0.4}\left(\frac{12.0}{140}\right)^{0.3}\left(\frac{1.81 \times 10^6}{12.0(140)(9.0)^3}\right)^{0.1} = 0.528 \text{ lanes}$$

Two or More Design Lanes Loaded (Equation 4.4.2.2.1.2-2):

$$g = 0.075 + \left(\frac{S}{9.5}\right)^{0.6}\left(\frac{S}{L}\right)^{0.2}\left(\frac{K_g}{12.0Lt_s^{\,3}}\right)^{0.1}$$

$$g = 0.075 + \left(\frac{12.0}{9.5}\right)^{0.6}\left(\frac{12.0}{140}\right)^{0.2}\left(\frac{1.81 \times 10^6}{12.0(140)(9.0)^3}\right)^{0.1} = 0.807 \text{ lanes (governs)}$$

The LLDF for the interior girder in regions of positive flexure in the end spans for the case of one design lane loaded for strength and service limit state investigations is 0.528 lanes. For fatigue investigations, this factor must be divided by the multiple presence factor of 1.20 for one design lane loaded, or 0.528/1.2 = 0.440 lanes. The LLDF for the interior girder in regions of positive flexure in the end spans for the case of two or more design lanes loaded for strength and service limit state investigations is 0.807 lanes (which controls over the case of one design lane loaded).

4.4.2.2.1.3 Concrete I-Beams, Bulb-Tees, or Single or Double Tee Beams with Transverse Post-Tensioning (Types “i”, “j”, and “k”)

One Design Lane Loaded

$$g = 0.06 + \left(\frac{S}{14}\right)^{0.4}\left(\frac{S}{L}\right)^{0.3}\left(\frac{K_g}{12.0Lt_s^3}\right)^{0.1} \quad \text{Equation 4.4.2.2.1.3-1}$$

Two or More Design Lanes Loaded

$$g = 0.075 + \left(\frac{S}{9.5}\right)^{0.6}\left(\frac{S}{L}\right)^{0.2}\left(\frac{K_g}{12.0Lt_s^3}\right)^{0.1} \quad \text{Equation 4.4.2.2.1.3-2}$$

When N_b is equal to 3, use the lesser of the values obtained from the equations above with N_b equal to 3, or the lever rule, for both of the preceding cases. Example calculations of the above LLDFs are given in PCI (2011) Design Examples 9.1a, 9.2, 9.7, and 9.8.

4.4.2.2.1.4 Open or Closed Precast Concrete Spread Box Beams (Types "b" and "c")

One Design Lane Loaded

$$g = \left(\frac{S}{3.0}\right)^{0.35}\left(\frac{Sd}{12.0L^2}\right)^{0.25} \qquad \text{Equation 4.4.2.2.1.4-1}$$

Two or More Design Lanes Loaded

$$g = \left(\frac{S}{6.3}\right)^{0.6}\left(\frac{Sd}{12.0L^2}\right)^{0.125} \qquad \text{Equation 4.4.2.2.1.4-2}$$

If S exceeds 18.0 ft, the lever rule is to be used for both of the preceding cases. Example calculations of the above LLDFs are given in PCI (2011) Design Example 9.6.

4.4.2.2.1.5 Adjacent Concrete Box Beams Used in Multibeam Decks with Cast-in-Place Overlay or Transverse Post-Tensioning (Types "f" and "g")

One Design Lane Loaded

$$g = k\left(\frac{b}{33.3L}\right)^{0.5}\left(\frac{I}{J}\right)^{0.25} \qquad \text{Equation 4.4.2.2.1.5-1}$$

Two or More Design Lanes Loaded

$$g = k\left(\frac{b}{305}\right)^{0.6}\left(\frac{b}{12.0L}\right)^{0.2}\left(\frac{I}{J}\right)^{0.06} \qquad \text{Equation 4.4.2.2.1.5-2}$$

In a preliminary design situation, $(I/J)^{0.06}$ may be assumed equal to 1.0 (PCI, 2011). Example calculations of the above LLDFs are given in PCI (2011) Design Examples 9.4 and 9.5.

4.4.2.2.1.6 Concrete Channel Sections, or Box, or Tee Sections Connected by "Hinges" at the Interface (Types "g", "h", "i", and "j")

Regardless of Number of Loaded Lanes

$$g = \frac{S}{D} \qquad \text{Equation 4.4.2.2.1.6-1}$$

where:

- If $C \leq 5$, then

$$D = 11.5 - N_L + 1.4N_L(1 - 0.2C)^2 \qquad \text{Equation 4.4.2.2.1.6-2}$$

- If $C > 5$, then

$$D = 11.5 - N_L \qquad \text{Equation 4.4.2.2.1.6-3}$$

Values of *K* for use in preliminary design are suggested in *AASHTO LRFD* Table 4.6.2.2.2b-1. Example calculations of the above LLDFs are given in PCI (2011) Design Example 9.3.

4.4.2.2.1.7 Cast-in-Place Concrete Multicell Box Girders (Type "d")

One Design Lane Loaded

$$g = \left(1.75 + \frac{S}{3.6}\right)\left(\frac{1}{L}\right)^{0.35}\left(\frac{1}{N_c}\right)^{0.45} \qquad \text{Equation 4.4.2.2.1.7-1}$$

Two or More Design Lanes Loaded

$$g = \left(\frac{13}{N_c}\right)^{0.3}\left(\frac{S}{5.8}\right)\left(\frac{1}{L}\right)^{0.25} \qquad \text{Equation 4.4.2.2.1.7-2}$$

Cast-in-place concrete multicell box girders may be designed as whole-width structures, which is appropriate for torsionally stiff cross-sections where load-sharing between girders is extremely high. Such cross-sections are to be conservatively

designed for the LLDFs given for interior girders multiplied by the number of girders (i.e. webs). The prestressing force should be evenly distributed between girders. Cell width-to-height ratios should be approximately 2:1.

4.4.2.2.1.8 Multiple Steel Box Girders (Types "b" and "c")

Regardless of Number of Loaded Lanes

$$g = 0.05 + 0.85\frac{N_L}{N_b} + \frac{0.425}{N_L} \qquad \text{Equation 4.4.2.2.1.8-1}$$

As discussed further in Section 6.3.2.5.6, the preceding live load distribution factor is only applicable for multiple steel box-girder bridges satisfying the special restrictions specified in *AASHTO LRFD* Article 6.11.2.3. For bridges not satisfying one or more of the specified restrictions, a refined analysis is required to determine the live load effects. Section 6.3.2.5.6 also discusses the application of the preceding equation to cases where the spacing of the box girders varies along the length of the bridge. An example calculation of the above LLDF is given in Chavel and Carnahan (2012).

As discussed in Section 4.4.2.1, multiple presence factors specified in *AASHTO LRFD* Article 3.6.1.1.2 (Section 3.4.1.2) are not to be used with the preceding equation because these factors are already incorporated in the equation. However, for the case of N_L = 1.0, a multiple presence factor of 1.0 (rather than the specified value of 1.2) was incorporated in Equation 4.4.2.2.1.8-1 in the original development. Thus, for fatigue limit state investigations, for which N_L is to be taken as 1.0 in computing the LLDF from Equation 4.4.2.2.1.8-1, the resulting LLDF should not be divided by the multiple presence factor of 1.2.

4.4.2.2.2 Exterior Girders

4.4.2.2.2.1 General

The equations giving the LLDF, *g*, for bending moment in exterior girders/beams/stringers with concrete decks are given in *AASHTO LRFD* Table 4.6.2.2.2d-1 (subject to the ranges of applicability listed for each bridge type), and are summarized in the following. If the girders are not equally spaced, and *g* for the exterior girder is a function of $g_{interior}$, $g_{interior}$ should be based on the spacing between the exterior girder and the first interior girder.

In the following, the distance, d_e, is to be taken as positive if the exterior web is inboard of the interior face of the parapet, and negative if it is outboard of the parapet. However, if a negative value of d_e falls outside its range of applicability as

shown in *AASHTO LRFD* Table 4.6.2.2.2d-1, d_e should be limited to -1.0 ft as specified in *AASHTO LRFD* Article 4.6.2.2.2d.

4.4.2.2.2.2 Steel I-Girders (Type "a")

One Design Lane Loaded

Use the Lever Rule

Two or More Design Lanes Loaded

$$g = eg_{interior} \qquad \text{Equation 4.4.2.2.2.2-1}$$

where:

$$e = 0.77 + \frac{d_e}{9.1} \qquad \text{Equation 4.4.2.2.2.2-2}$$

When N_b is equal to 3, use the lesser of the values obtained from the equation above with N_b equal to 3, or the lever rule, for the case of two or more design lanes loaded.

In addition, as specified in *AASHTO LRFD* Article 4.6.2.2.2d, in steel beam-slab bridge cross-sections with cross-frames/diaphragms, the LLDF for the exterior girder/beam/stringer is not to be taken to be less than that which would be obtained by assuming the cross-section deflects and rotates as a rigid cross-section. This additional investigation is required because the LLDF equations for multi-girder bridges were developed without consideration of the effect of cross-frames/diaphragms and their effect on the distribution of load to the exterior girders of steel I-girder bridges. These members cause a larger portion of the load to be transferred to the exterior girders than if they were not present. A statical approach to determine the reaction, *R*, on an exterior girder/beam/stringer (in terms of lanes) under one or more lanes of loading based on the above assumption is provided in *AASHTO LRFD* Article C4.6.2.2.2d; the procedure is equivalent to the conventional procedure used to approximate loads on pile groups. The equation is given as follows:

Regardless of Number of Loaded Lanes

$$R = \frac{N_L}{N_b} + \frac{X_{ext} \sum^{N_L} e}{\sum x^2} \qquad \text{Equation 4.4.2.2.2.2-3}$$

AASHTO LRFD Equation C4.6.2.2.2d-1

where:

e = eccentricity of a design truck or a design lane load from the center of gravity of the pattern of girder (ft)

x = horizontal distance from the center of gravity of the pattern of girders to each girder (ft)

X_{ext} = horizontal distance from the center of gravity of the pattern of girders to the exterior girder (ft)

EXAMPLE

For a steel I-girder bridge cross-section shown in Figure 4.4.2.2.2.2-1, calculate the LLDFs for bending moment in the exterior girders for the case of one design lane loaded, and for the case of two or more design lanes loaded. The 40′-0" roadway width can accommodate up to three 12′-0"-wide design lanes (*AASHTO LRFD* Article 3.6.1.1.1 – Section 3.4.1.1). The supports are not skewed.

One Design Lane Loaded: Use the Lever Rule

The lever rule involves the use of statics to determine the lateral distribution to the exterior girder by summing moments about the adjacent interior girder to find the wheel-load reaction at the exterior girder assuming the concrete deck is hinged at the interior girder (Figure 4.4.2.2.2.2-2). A wheel cannot be closer than 2'-0" to the base of the curb (*AASHTO LRFD* Article 3.6.1.3.1). For the specified transverse wheel spacing of 6'-0", the wheel-load distribution to the exterior girder is computed as:

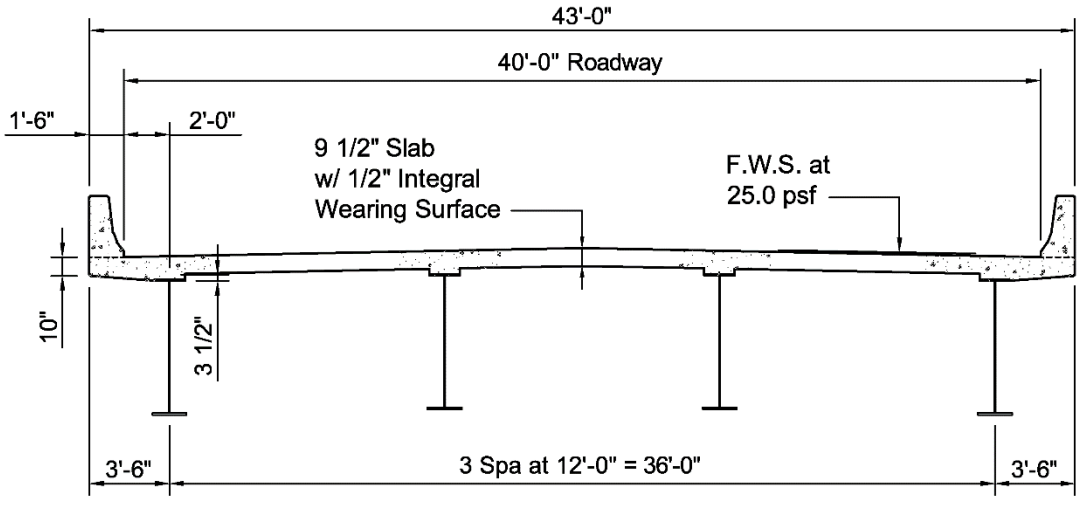

Figure 4.4.2.2.2.2-1 Example Steel I-Girder Bridge Cross-Section

$$\frac{9.0}{12.0} = 0.750$$

Multiple presence factor $m = 1.2$ (AASHTO LRFD Table 3.6.1.1.2 - 1)

$$1.2(0.750) = 0.900 \text{ lanes}$$

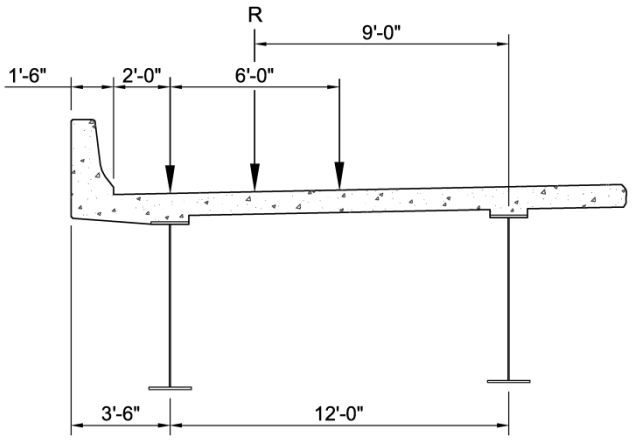

Figure 4.4.2.2.2.2-2 Exterior Girder LLDF – Lever Rule

Two or More Design Lanes Loaded:

Modify Interior-Girder LLDF (Equation 4.4.2.2.2.2-1)

The factor, *e*, in Equation 4.4.2.2.2.2-1 is computed from Equation 4.4.2.2.2.2-2 using the distance, d_e, where d_e is the distance from the exterior girder to the edge of the curb or traffic barrier (must be less than or equal to 5.5 ft). d_e is negative if the girder web is outboard of the curb or traffic barrier (must be greater than or equal to -1.0 ft). The multiple presence factor is not applied.

$$e = 0.77 + \frac{d_e}{9.1}$$

$$e = 0.77 + \frac{2.0}{9.1} = 0.990$$

$$0.990(0.807) = 0.799 \text{ lanes}$$

Special Rigid Cross-Section Analysis (Equation 4.4.2.2.2.2-3)

Assuming the entire cross-section rotates as a rigid body about the longitudinal centerline of the bridge, LLDFs for the exterior girder are also computed for one, two and three lanes loaded using the following equation (Equation 4.4.2.2.2.2-3):

$$R = \frac{N_L}{N_b} + \frac{X_{ext} \sum^{N_L} e}{\sum^{N_b} x^2}$$

where the terms in the equation are as defined above.

The lanes are positioned on the bridge according to the AASHTO rules for live load placement (Section 4.4.3.2.2), as shown in Figure 4.4.2.2.2.2-3.

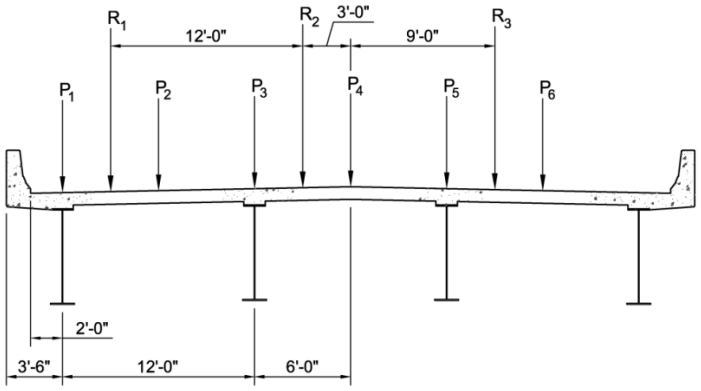

Figure 4.4.2.2.2.2-3 Exterior Girder LLDF – Special Rigid Cross-Section Analysis

The multiple presence factors are given in *AASHTO LRFD* Table 3.6.1.1.2-1 (Table 4.4.2.2.2.2-1) as follows (Section 3.4.1.2):

Table 4.4.2.2.2.2-1 Multiple Presence Factors, m

Number of Lane	*m*
1 lane	$m_1 = 1.2$
2 lanes	$m_2 = 1.0$
3 lanes	$m_3 = 0.85$

Referring to Figure 4.4.2.2.2.2-3:

- For one design lane loaded:

$$R = \frac{1}{4} + \frac{(12.0 + 6.0)(12.0 + 3.0)}{2\left(18.0^2 + 6.0^2\right)} = 0.625$$

$$m_1 R = 1.2(0.625) = 0.750 \text{ lanes}$$

- For two design lanes loaded:

$$R = \frac{2}{4} + \frac{(12.0 + 6.0)(12.0 + 3.0 + 3.0)}{2(18.0^2 + 6.0^2)} = 0.950$$

$$m_2R = 1.0(0.950) = 0.950 \text{ lanes (governs)}$$

- For three design lanes loaded:

$$R = \frac{3}{4} + \frac{(12.0 + 6.0)(12.0 + 3.0 + 3.0 - 9.0)}{2(18.0^2 + 6.0^2)} = 0.975$$

$$m_3R = 0.85(0.975) = 0.829 \text{ lanes}$$

The governing LLDF for the exterior girder for the case of one design lane loaded for strength and service limit state investigations is given by the lever rule as 0.900 lanes. For fatigue investigations, this factor must be divided by the multiple presence factor of 1.20 for one design lane loaded, or 0.900/1.2 = 0.750 lanes. The governing LLDF for the exterior girder for the case of two or more design lanes loaded is given by the special rigid cross-section analysis as 0.950 lanes (as controlled in this instance by the specific case of two design lanes loaded). The LLDF of 0.950 lanes controls over the case of one design lane loaded (i.e. 0.900 lanes) for strength and service limit state investigations.

4.4.2.2.2.3 Concrete I-Beams, Bulb-Tees, or Single or Double Tee Beams with Transverse Post-Tensioning (Types “i”, “j”, and “k”)

One Design Lane Loaded

Use the Lever Rule

Two or More Design Lanes Loaded

$$g = eg_{interior} \qquad \text{Equation 4.4.2.2.2.3-1}$$

where:

$$e = 0.77 + \frac{d_e}{9.1} \qquad \text{Equation 4.4.2.2.2.3-2}$$

When N_b is equal to 3, use the lesser of the values obtained from the equation above with N_b equal to 3, or the lever rule, for the case of two or more design lanes loaded.

4.4.2.2.2.4 Open or Closed Precast Concrete Spread Box Beams (Types "b" and "c")

One Design Lane Loaded

Use the Lever Rule

Two or More Design Lanes Loaded

$$g = eg_{interior} \qquad \text{Equation 4.4.2.2.2.4-1}$$

where:

$$e = 0.97 + \frac{d_e}{28.5} \qquad \text{Equation 4.4.2.2.2.4-2}$$

If *S* exceeds 18.0 ft, the lever rule is to be used for the case of two or more design lanes loaded.

4.4.2.2.2.5 Adjacent Concrete Box Beams Used in Multibeam Decks with Cast-in-Place Overlay or Transverse Post-Tensioning (Types "f" and "g")

One Design Lane Loaded

$$g = eg_{interior} \qquad \text{Equation 4.4.2.2.2.5-1}$$

where:

$$e = 1.125 + \frac{d_e}{30} \geq 1.0 \qquad \text{Equation 4.4.2.2.2.5-2}$$

Two or More Design Lanes Loaded

$$g = eg_{interior} \qquad \text{Equation 4.4.2.2.2.5-3}$$

where:

$$e = 1.04 + \frac{d_e}{25} \geq 1.0 \qquad \text{Equation 4.4.2.2.2.5-4}$$

4.4.2.2.2.6 Concrete Channel Sections or Tee Sections Connected by "Hinges" at the Interface (Types "h", "i", and "j")

One Design Lane Loaded

Use the Lever Rule

Two or More Design Lanes Loaded

Use the Lever Rule

Application of the lever rule to this case presents some interpretation problems regarding how many lanes should be loaded (e.g. 2, 3, or 4 lanes if the roadway width is 48 ft or more). Until this question is resolved, PCI (2011) recommends using the same LLDF for exterior beams as for interior beams.

4.4.2.2.2.7 Cast-in-Place Concrete Multicell Box Girders (Type "d")

Regardless of Number of Loaded Lanes

$$g = \frac{W_e}{14} \qquad \text{Equation 4.4.2.2.2.7-1}$$

Alternatively, the provisions for a whole-width design described previously in Section 4.4.2.2.1.7 may be used.

4.4.2.2.2.8 Multiple Steel Box Girders (Types "b" and "c")

Regardless of Number of Loaded Lanes

$$g = 0.05 + 0.85\frac{N_L}{N_b} + \frac{0.425}{N_L} \qquad \text{Equation 4.4.2.2.2.8-1}$$

Refer to Section 4.4.2.2.1.8 for further discussion regarding the preceding equation.

4.4.2.2.3 Skewed Bridges

4.4.2.2.3.1 General

Correction factors to some of the individual LLDFs for bending moment are provided in *AASHTO LRFD* Table 4.6.2.2.2e-1 to account in a limited fashion for the effects of skewed supports on the live-load effects (not all the bridge types are currently covered). The correction factor for bending moment is optional, and reduces the bending moment LLDF for larger skew angles. The correction factors given below

are only valid in cases where the difference between the skew angles of two adjacent lines of supports does not exceed 10 degrees. Ranges of applicability for the factors are also specified in the table. A correction factor is not provided for the dead load bending moments in skewed bridges.

4.4.2.2.3.2 Steel I-Girders (Type "a")

$$\text{Correction Factor} = 1 - c_1(\tan\theta)^{1.5} \qquad \text{Equation 4.4.2.2.3.2-1}$$

where:

$$c_1 = 0.25\left(\frac{K_g}{12.0Lt_s^3}\right)^{0.25}\left(\frac{S}{L}\right)^{0.5} \qquad \text{Equation 4.4.2.2.3.2-2}$$

- If θ < 30°, then c_1 = 0.0
- If θ > 60°, use θ = 60°

Correction factors are not available for cases involving large skews and/or skews in combination with curved alignments. In such cases, where torsional effects become more significant, the use of LLDFs is inappropriate and refined methods of analysis (Section 4.5.3) should be employed. Also, the correction factor should only be applied if the cross-frames are contiguous; the factor was not developed for cases where cross-frames are discontinuous.

4.4.2.2.3.3 Concrete I-Beams, Bulb-Tees, or Single or Double Tee Beams with Transverse Post-Tensioning (Types "i", "j", and "k")

$$\text{Correction Factor} = 1 - c_1(\tan\theta)^{1.5} \qquad \text{Equation 4.4.2.2.3.3-1}$$

where:

$$c_1 = 0.25\left(\frac{K_g}{12.0Lt_s^3}\right)^{0.25}\left(\frac{S}{L}\right)^{0.5} \qquad \text{Equation 4.4.2.2.3.3-2}$$

- If θ < 30°, then c_1 = 0.0
- If θ > 60°, use θ = 60°

4.4.2.2.3.4 Precast Concrete Spread Box Beams, Adjacent Box Beams with Concrete Overlays or Transverse Post-Tensioning, Double Tees in Multibeam Decks, and Cast-in-Place Multicell Box Girders (Types "b", "c", "d", "f", and "g")

$$\text{Correction Factor} = 1.05 - 0.25\tan\theta \le 1.0 \qquad \text{Equation 4.4.2.2.3.4-1}$$

If $\theta > 60°$, use $\theta = 60°$

4.4.2.3 Girder Distribution Factors for Shear

4.4.2.3.1 Interior Girders

4.4.2.3.1.1 General

Shear LLDFs are normally higher than the moment LLDFs for the same cross-section and span. The equations giving the LLDF, *g*, for shear in interior girders/beams/stringers with concrete decks are given in *AASHTO LRFD* Table 4.6.2.2.3a-1 (subject to the ranges of applicability listed for each bridge type), and are summarized as follows:

4.4.2.3.1.2 Steel I-Girders (Type "a")

One Design Lane Loaded

$$g = 0.36 + \frac{S}{25.0} \qquad \text{Equation 4.4.2.3.1.2-1}$$

Two or More Design Lanes Loaded

$$g = 0.2 + \frac{S}{12} - \left(\frac{S}{35}\right)^{2.0} \qquad \text{Equation 4.4.2.3.1.2-2}$$

When N_b is equal to 3, use the lever rule for both of the preceding cases.

4.4.2.3.1.3 Concrete I-Beam, Bulb-Tee, or Single or Double Tee Beams with Transverse Post-Tensioning (Types "i", "j", and "k")

One Design Lane Loaded

$$g = 0.36 + \frac{S}{25.0} \qquad \text{Equation 4.4.2.3.1.3-1}$$

Two or More Design Lanes Loaded

$$g = 0.2 + \frac{S}{12} - \left(\frac{S}{35}\right)^{2.0} \qquad \text{Equation 4.4.2.3.1.3-2}$$

When N_b is equal to 3, use the lever rule for both of the preceding cases.

4.4.2.3.1.4 Open or Closed Precast Concrete Spread Box Beams (Types "b" and "c")

One Design Lane Loaded

$$g = \left(\frac{S}{10}\right)^{0.6}\left(\frac{d}{12.0L}\right)^{0.1} \qquad \text{Equation 4.4.2.3.1.4-1}$$

Two or More Design Lanes Loaded

$$g = \left(\frac{S}{7.4}\right)^{0.8}\left(\frac{d}{12.0L}\right)^{0.1} \qquad \text{Equation 4.4.2.3.1.4-2}$$

If S exceeds 18.0 ft, the lever rule is to be used for both of the preceding cases.

4.4.2.3.1.5 Adjacent Concrete Box Beams Used in Multibeam Decks with Cast-in-Place Overlay or Transverse Post-Tensioning (Types "f" and "g")

One Design Lane Loaded

$$g = \left(\frac{b}{130L}\right)^{0.15}\left(\frac{I}{J}\right)^{0.05}$$ Equation 4.4.2.3.1.5-1

Two or More Design Lanes Loaded

$$g = \left(\frac{b}{156}\right)^{0.4}\left(\frac{b}{12.0L}\right)^{0.1}\left(\frac{I}{J}\right)^{0.05}\left(\frac{b}{48}\right)$$ Equation 4.4.2.3.1.5-2

where *b*/48 must be greater than or equal to 1.0.

4.4.2.3.1.6 Concrete Channel Sections or Tee Sections Connected by "Hinges" at the Interface (Types "h", "i", and "j")

One Design Lane Loaded

Use the Lever Rule

Two or More Design Lanes Loaded

Use the Lever Rule

4.4.2.3.1.7 Cast-in-Place Concrete Multicell Box Girders (Type "d")

One Design Lane Loaded

$$g = \left(\frac{S}{9.5}\right)^{0.6}\left(\frac{d}{12.0L}\right)^{0.1}$$ Equation 4.4.2.3.1.7-1

Two or More Design Lanes Loaded

$$g = \left(\frac{S}{7.3}\right)^{0.9}\left(\frac{d}{12.0L}\right)^{0.1}$$ Equation 4.4.2.3.1.7-2

4.4.2.3.1.8 Multiple Steel Box Girders (Types "b" and "c")

Regardless of Number of Loaded Lanes

$$g = 0.05 + 0.85\frac{N_L}{N_b} + \frac{0.425}{N_L}$$ Equation 4.4.2.3.1.8-1

Refer to Section 4.4.2.2.1.8 for further discussion regarding the preceding equation.

4.4.2.3.2 Exterior Girders

4.4.2.3.2.1 General

The equations giving the LLDF, *g*, for shear in exterior girders/beams/stringers with concrete decks are given in *AASHTO LRFD* Table 4.6.2.2.3b-1 (subject to the ranges of applicability listed for each bridge type), and are summarized in the following.

In the following, the distance, d_e, is to be taken as positive if the exterior web is inboard of the interior face of the parapet, and negative if it is outboard of the parapet. However, if a negative value of d_e falls outside its range of applicability as shown in *AASHTO LRFD* Table 4.6.2.2.2d-1, d_e should be limited to -1.0 ft as specified in *AASHTO LRFD* Article 4.6.2.2.2d.

4.4.2.3.2.2 Steel I-Girders (Type "a")

One Design Lane Loaded

Use the Lever Rule

Two or More Design Lanes Loaded

$$g = e g_{interior}$$ Equation 4.4.2.3.2.2-1

where:

$$e = 0.6 + \frac{d_e}{10}$$ Equation 4.4.2.3.2.2-2

When N_b is equal to 3, use the lever rule for the case of two or more design lanes loaded.

In addition, as specified in *AASHTO LRFD* Article 4.6.2.2.2d, in steel beam-slab bridge cross-sections with cross-frames/diaphragms, the LLDF for the exterior girder/beam/stringer is not to be taken to be less than that which would be obtained by assuming the cross-section deflects and rotates as a rigid cross-section. The following equation, provided in *AASHTO LRFD* Article C4.6.2.2.2d, satisfies this assumption and may be used (refer to Section 4.4.2.2.2.2 for further discussion, and for the definitions of the terms in the equation):

Regardless of Number of Loaded Lanes

$$R = \frac{N_L}{N_b} + \frac{X_{ext} \sum^{N_L} e}{\sum x^2 N_b}$$ Equation 4.4.2.3.2.2-3

AASHTO LRFD Equation C4.6.2.2.2d-1

4.4.2.3.2.3 Concrete I-Beam, Bulb-Tee, or Single or Double Tee Beams with Transverse Post-Tensioning (Types "i", "j", and "k")

One Design Lane Loaded

Use the Lever Rule

Two or More Design Lanes Loaded

$$g = eg_{interior}$$ Equation 4.4.2.3.2.3-1

where:

$$e = 0.6 + \frac{d_e}{10}$$ Equation 4.4.2.3.2.3-2

When N_b is equal to 3, use the lever rule for the case of two or more design lanes loaded.

4.4.2.3.2.4 Open or Closed Precast Concrete Spread Box Beams (Types "b" and "c")

One Design Lane Loaded

Use the Lever Rule

Two or More Design Lanes Loaded

$$g = eg_{interior}$$ Equation 4.4.2.3.2.4-1

where:

$$e = 0.8 + \frac{d_e}{10}$$ Equation 4.4.2.3.2.4-2

If *S* exceeds 18.0 ft, the lever rule is to be used for the case of two or more design lanes loaded.

4.4.2.3.2.5 Adjacent Concrete Box Beams Used in Multibeam Decks with Cast-in-Place Overlay or Transverse Post-Tensioning (Types "f" and "g")

One Design Lane Loaded

$$g = eg_{interior} \qquad \text{Equation 4.4.2.3.2.5-1}$$

where:

$$e = 1.25 + \frac{d_e}{20} \geq 1.0 \qquad \text{Equation 4.4.2.3.2.5-2}$$

Two or More Design Lanes Loaded

$$g = eg_{interior}\left(\frac{48}{b}\right) \qquad \text{Equation 4.4.2.3.2.5-3}$$

where:

$$e = 1 + \left(\frac{d_e + \frac{b}{12} - 2.0}{40}\right)^{0.5} \geq 1.0 \qquad \text{Equation 4.4.2.3.2.5-4}$$

where *(*48/*b)* must be less than or equal to 1.0.

4.4.2.3.2.6 Concrete Channel Sections or Tee Sections Connected by "Hinges" at the Interface (Types "h", "i", and "j")

One Design Lane Loaded

Use the Lever Rule

Two or More Design Lanes Loaded

Use the Lever Rule

4.4.2.3.2.7 Cast-in-Place Concrete Multicell Box Girders (Type "d")

One Design Lane Loaded

Use the Lever Rule

Two or More Design Lanes Loaded

$$g = eg_{interior} \qquad \text{Equation 4.4.2.3.2.7-1}$$

where:

$$e = 0.64 + \frac{d_e}{12.5} \qquad \text{Equation 4.4.2.3.2.7-2}$$

4.4.2.3.2.8 Multiple Steel Box Girders (Types "b" and "c")

Regardless of Number of Loaded Lanes

$$g = 0.05 + 0.85\frac{N_L}{N_b} + \frac{0.425}{N_L} \qquad \text{Equation 4.4.2.3.2.8-1}$$

Refer to Section 4.4.2.2.1.8 for further discussion regarding the preceding equation.

4.4.2.3.3 Skewed Bridges

4.4.2.3.3.1 General

Correction factors to some of the individual LLDFs for shear are provided in *AASHTO LRFD* Table 4.6.2.2.3c-1 to account in a limited fashion for the effects of skewed supports on the live-load effects (not all the bridge types are currently covered). The correction factor for shear is required when LLDFs are used and one or more supports are skewed, and increases the girder shears. Ranges of applicability for the factors are also specified in the table. The factors are valid up to and including a skew angle, θ, of 60 degrees. A correction factor is not provided for the dead load shears in skewed bridges.

The correction factors are to be applied to the shear LLDFs for the exterior girder/beam/stringer at the obtuse corner of the span (Section 4.4.2.3.2), and if the beams are well connected and behave as a unit, to the shear LLDFs for the first interior girder/beam/stringer adjacent to that exterior girder (Section 4.4.2.3.1). If the girders are not deemed well connected (i.e. do not deflect in a rigid manner), the correction factors are to be applied to the corresponding LLDFs for all the girders.

The effectiveness of connectivity is dependent on the geometry and details that are used, and is left to the judgment of the Engineer.

The factors are to be applied at all skewed supports (i.e. at both end and intermediate skewed supports). As specified in *AASHTO LRFD* Article 4.6.2.2.3c, the factors should also be applied between the point of support at the obtuse corner and mid-span, and may be decreased linearly to a value of 1.0 at mid-span regardless of the end condition.

In cases of large skew and/or short exterior spans in continuous beams, *AASHTO LRFD* Article C4.6.2.2.3c recommends that a supplementary investigation of uplift be considered using the terms other than 1.0 in the correction factors given below, taken as negative for the exterior girder/beam/stringer on the acute corner. However, it should be noted that uplift is also possible in the obtuse corners in some cases.

4.4.2.3.3.2 Steel I-Girders (Type "a")

$$\text{Correction Factor} = 1.0 + 0.20\left(\frac{12.0Lt_s^3}{K_g}\right)^{0.3}\tan\theta \qquad \text{Equation 4.4.2.3.3.2-1}$$

Correction factors are not available for cases involving large skews and/or skews in combination with curved alignments. In such cases, where torsional effects become more significant, the use of LLDFs is inappropriate and refined methods of analysis (Section 4.5.3) should be employed. Also, the correction factor should only be applied if the cross-frames are contiguous; the factor was not developed for cases where cross-frames are discontinuous.

4.4.2.3.3.3 Concrete I-Beams, Bulb-Tees, or Single or Double Tee Beams with Transverse Post-Tensioning (Types "i", "j", and "k")

$$\text{Correction Factor} = 1.0 + 0.20\left(\frac{12.0Lt_s^3}{K_g}\right)^{0.3}\tan\theta \qquad \text{Equation 4.4.2.3.3.3-1}$$

4.4.2.3.3.4 Open or Closed Precast Concrete Spread Box Beams (Types "b" and "c")

$$\text{Correction Factor} = 1.0 + \frac{\sqrt{\frac{Ld}{12.0}}}{6S}\tan\theta \qquad \text{Equation 4.4.2.3.3.4-1}$$

4.4.2.3.3.5 Adjacent Concrete Box Beams Used in Multibeam Decks with Cast-in-Place Overlay or Transverse Post-Tensioning (Types "f" and "g")

$$\text{Correction Factor} = 1.0 + \frac{12.0L}{90d}\sqrt{\tan\theta} \qquad \text{Equation 4.4.2.3.3.5-1}$$

4.4.2.3.3.6 Cast-in-Place Concrete Multicell Box Girders (Type "d")

For the Exterior Girder

$$\text{Correction Factor} = 1.0 + \left(0.25 + \frac{12.0L}{70d}\right)\tan\theta \qquad \text{Equation 4.4.2.3.3.6-1}$$

For the First Interior Girder

$$\text{Correction Factor} = 1.0 + \left(0.042 + \frac{12.0L}{420d}\right)\tan\theta \qquad \text{Equation 4.4.2.3.3.6-2}$$

4.4.2.4 Transverse Floorbeam Distribution Factors for Moments and Shear

As specified in *AASHTO LRFD* Article 4.6.2.2.2f, if a concrete deck is supported directly by floorbeams with a spacing, *S*, not exceeding 6.0 ft, the individual floorbeams may be designed for moment and shear for a fraction of the wheel load equal to *S*/6. Wheel-load fractions for other types of decks are provided in *AASHTO LRFD* Table 4.6.2.2.2f-1.

The specified wheel-load fractions are to be used in conjunction with the 32.0 kip axle load alone. For spacings of floorbeams exceeding the indicated range of applicability (e.g. S exceeding 6.0 ft for a concrete deck supported by floorbeams), all of the design live loads are to be considered, and the lever rule may be used.

4.4.2.5 Special Loads with Other Traffic

For cases where one lane is loaded with a special vehicle or evaluation permit vehicle in combination with routine traffic, such as might be considered in the Strength II load combination (Section 3.9.1.2.3), *AASHTO LRFD* Article 4.6.2.2.5 indicates that the final girder force effect, *G*, may be determined as:

$$G = G_p\left(\frac{g_1}{Z}\right) + G_D\left(g_m - \frac{g_1}{Z}\right) \qquad \text{Equation 4.4.2.5-1}$$

AASHTO LRFD Equation 4.6.2.2.5-1

where:

- G_p = force effect due to the special vehicle or evaluation permit vehicle (kips or kip-ft)
- g_1 = LLDF for one design lane loaded (lanes)
- G_D = force effect due to the design live loads (kips or kip-ft)
- g_m = LLDF for two or more design lanes loaded (lanes)
- Z = a factor taken as 1.20 where the lever rule is not utilized, and taken as 1.0 when the lever rule is used to determine the LLDF for one design lane loaded

The preceding equation is not to be applied where either it is specified that the lever rule must be used for both single lane and multiple lane loadings, or where the special rigid cross-section requirement for exterior girders of steel beam-slab bridges is applied (Sections 4.4.2.2.2.2 and 4.4.2.3.2.2). Both of these methods may utilize a multiple presence factor other than 1.0 (see below), and could potentially be used to compute the distribution factor directly in lieu of using Equation 4.4.2.5-1.

The factor, *Z*, in Equation 4.4.2.5-1 is used to distinguish between situations where the LLDF for one design lane loaded must be determined from a specified algebraic equation and situations where the lever rule must be used to determine the LLDF for one design lane loaded. The specified multiple presence factor of 1.20 for one design lane loaded (Section 3.4.1.2) is included in the algebraic equation, and must be removed by using Z = 1.20 in Equation 4.4.2.5-1 **s**o that the LLDF for one design lane loaded can be utilized in Equation 4.4.2.5-1 to determine the force effect resulting from a multiple lane loading.

Because the number and location of the loaded lanes used to determine the multiple-lane LLDF, g_m, is not known, the multiple presence factor for the combined multiple-lane LLDF is implicitly set to 1.0 in Equation 4.4.2.5-1. Equation 4.4.2.5-1 assumes that only two lanes are loaded, which results in conservative final force effects versus the force effects computed using the multiple presence factors for three or more lanes loaded.

The development of Equation 4.4.2.5-1 is discussed in Modjeski and Masters (1994). The equation is used with the appropriate multiple-lane distribution factor taken from the AASHTO table (which assumes that all trucks are the same) and tries to split the factor between the heavy truck and the other standard trucks in the surrounding lanes. It assumes that the heavy truck is placed at the location that maximizes the distribution factor for this truck, i.e. will be equal to the single lane distribution factor,

and the remaining portion of the multiple lane distribution factor is caused by the other standard trucks in the surrounding lanes.

The equation assumes that the multiple-lane LLDF is larger than the single-lane LLDF after removing the 1.20 multiple presence factor. The equation also assumes that when multiple lanes are loaded with mixed traffic, one lane is located at the same location that produces the single lane maximum effects, and therefore, the contribution of this lane to the combined multiple-lane LLDF is equal to the-single lane LLDF (i.e. g_1/Z). The remaining portion of the combined multiple-lane LLDF (i.e. $g_m - g_1/Z$) is produced by the other loaded lane.

Since it is assumed that the heavier special vehicle or evaluation permit vehicle is positioned where the load from a single lane is maximized, positioning lighter loads (e.g. sidewalk loads) where the equation assumes a heavier load is applied will result in an unconservative result; the lever rule or a refined analysis method should be used instead in such cases.

4.4.3 Influence Lines and Influence Surfaces

4.4.3.1 Influence Lines

The influence line was first used by Professor E. Winkler of Berlin in 1867 (Kinney, 1957). The influence line shows graphically how the movement of a unit load across a beam-type structure influences some force effect in the structure. Influence lines and influence surfaces (Section 4.4.3.2) are commonly used to determine the maximum and minimum force effects at a specific point due to moving live loads, which can be located anywhere on the structure. Most line-girder analysis programs use influence lines to generate their live load envelopes. Refined 2D and 3D analysis programs typically use influence surfaces.

Application of influence lines is limited to linear elastic structures and supports with load applied directly to a single line girder. If a support deflects under load, it must deflect elastically in order for the influence line to be considered correct. For example, if a bearing lifts off its support as a unit load transverses the beam, the influence line method is inappropriate because the stiffness of the support is non-linear. Likewise, if permanent set occurs at a support, or if the analysis includes non-linear deformation of a member, the influence line method is also not applicable.

James Clerk Maxwell first published his law of reciprocal deflections in 1864, which states that for an elastic structure “the deflection at point A in a structure due to a load applied at another point B is exactly the same as the deflection at B if the same load is applied at A” (McCormac, 1975). Maxwell’s presentation of his theorem was so brief that its value was not fully appreciated until 1886 when German professor, Henrich Müller-Breslau, showed its true worth in creating influence lines for statically

indeterminate structures. Breslau used Maxwell's law and the principle of virtual displacements to establish the Müller-Breslau Principle (McCormac, 1975). The Principle states that the ordinate values of an influence line for a force effect at a point are proportional to the ordinates of the deflected shape obtained by removing the restraint at that point corresponding to the force effect, and introducing a force effect that causes a unit displacement (or rotation) in the proper sense of the desired action at that point. That is, the deflected structure draws its own influence line when the proper displacement is applied.

The Müller-Breslau Principle can be used on other than beam structures, such as frames; this review will only address beams. The principle is used to determine qualitative influence lines, which are useful to quickly obtain the correct shape of the influence line and to obtain a better understanding of a particular action. The Müller-Breslau Principle can also be used to obtain the influence line ordinates for statically determinate and indeterminate structures. The principle as stated above is applied in Figure 4.4.3.1-1.

Determination of the end reaction in a simple-span beam illustrates the application of the Müller-Breslau Principle. Remove the reaction and displace that point by a unit displacement in the direction of the reaction, as shown in Figure 4.4.3.1-1 Part A. In this case (as is the case in all determinate structures), the force is zero. The resulting deflected shape is proportional to the true influence line for the end reaction. Since no force was required to cause the deflection, the deflected shape is linear.

The qualitative influence line for shear at a section is found by removing the shear resistance at the section by inserting a roller, as shown in Figure 4.4.3.1-1 Part B. Introducing a unit deflection between the free ends at the roller provides the influence line for shear at the point if the deflections properly reflect the sign convention. The magnitude of the displacement of the two ends is proportional to the location of the section in relation to the span. Note that for a statically determinate beam, the resulting influence line is linear because no actual force was required to deflect the structure with the roller installed.

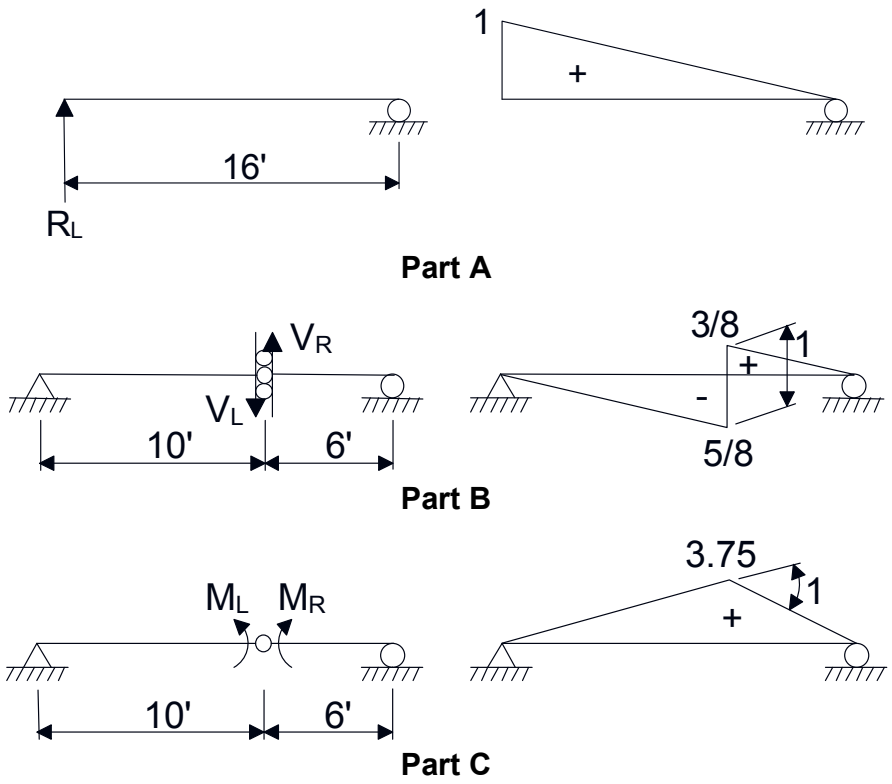

Figure 4.4.3.1-1 Application of the Müller-Breslau Principle

A) End Reaction in a Simple-Span Beam; B) Shear at a Section in a Simple-Span Beam; C) Vertical Bending Moment at a Section in a Simple-Span Beam

To obtain a qualitative influence line for vertical bending moment at a section (Figure 4.4.3.1-1 Part C), remove the moment resistance (i.e. introduce a hinge) at that section while maintaining axial and shear force resistance. Next, apply equal and opposite moments in the proper sense on the left and right sides of the hinge. These moments introduce a unit relative rotation between the two tangents of the deflected shape at the hinge. The corresponding elastic curve is the influence line for bending moment at that section.

For statically determinate structures (e.g. simple-span structures), an influence line is determined by introducing unit deflections; no force is required. Influence lines are linear for statically determinate structures.

Influence lines for statically indeterminate structures (e.g. continuous-span structures) are typically determined from an indeterminate analysis. Theoretically, the same result would be obtained using the Müller-Breslau Principle, which introduces a unit deflection or rotation at the point of interest after the proper release is introduced.

The ordinates of influence lines are typically determined by applying a series of vertical unit loads at increments along the girder. Figure 4.4.3.1-2 shows a typical influence line for a three-span continuous beam (with equal 100-foot spans) for vertical bending moment at $0.4L_1$ = 40 feet from the abutment in an end span. Influence lines in statically indeterminate structures are curved.

In Figure 4.4.3.1-2 Part A, the influence line ordinate of +20.4 kip-ft/kip at $0.4L_1$ is determined by applying a vertical unit load to the beam at $0.4L_1$. The ordinate represents the vertical bending moment at $0.4L_1$ when a vertical unit concentrated load is applied at $0.4L_1$. In Figure 4.4.3.1-2 Part B, the influence line ordinate of -3.0 kip-ft/kip at $0.5L_2$ is determined by applying a vertical unit load to the beam at $0.5L_2$. This ordinate represents the vertical bending moment at $0.4L_1$ when a vertical unit concentrated load is applied at $0.5L_2$. Finally, in Figure 4.4.3.1-2 Part C, the influence line ordinate of +1.0 kip-ft/kip at $0.5L_3$ is determined by applying a vertical unit load to the beam at $0.5L_3$. This ordinate represents the vertical bending moment at $0.4L_1$ when a vertical unit concentrated load is applied at $0.5L_3$.

For live load, the objective is to determine maximum and minimum responses of critical actions in the bridge to the specific live load(s) that the bridge is being designed to carry. This is accomplished by systematically applying the live load(s) to the influence line.

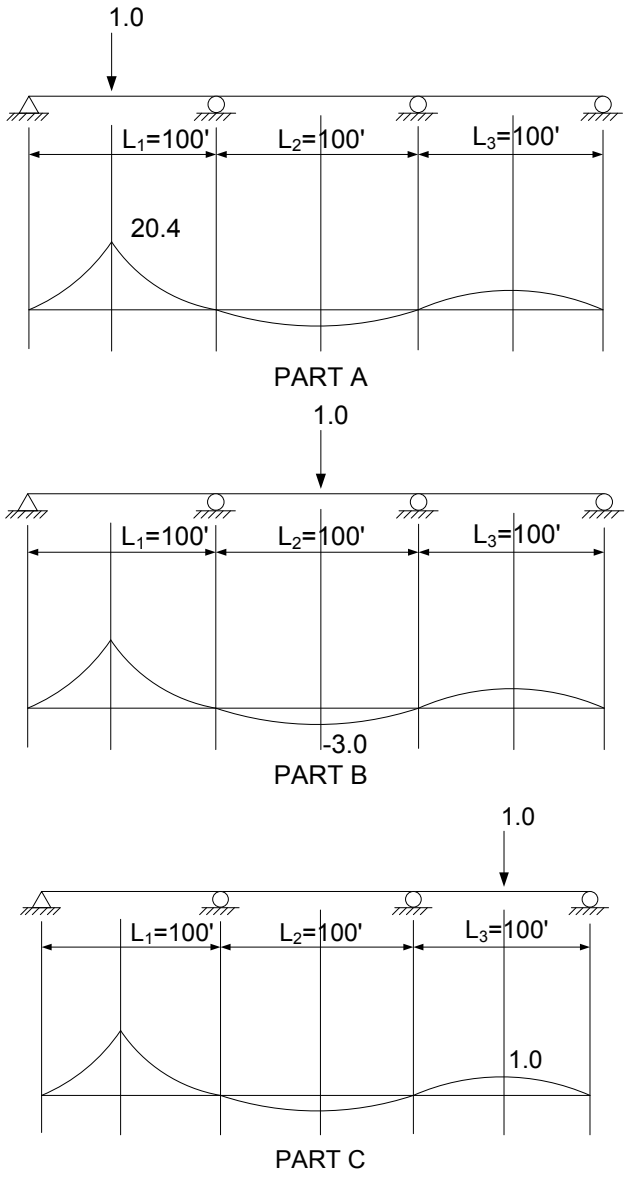

Figure 4.4.3.1-2 Development of Influence Line Ordinates for Vertical Bending Moment at 0.4L_1 in a Three-Span Continuous Beam by Application of Unit Loads

A) Unit Load Applied at 0.4L_1 to Obtain Ordinate for Moment at 0.4L_1;

B) Unit Load Applied at 0.5L_2 to Obtain Ordinate for Moment at 0.4L_1;

C) Unit Load Applied at 0.5L_3 to Obtain Ordinate for Moment at 0.4L_1

The ordinate of the influence line is the response at a specific location to a load of one unit applied at the point of the specific ordinate. Hence, when a concentrated live load (e.g. a wheel load) is applied at that point; the magnitude of the wheel load

is multiplied by the ordinate of the influence line to find the response to that wheel load at the specific location of interest.

This is illustrated in Figure 4.4.3.1-3 for the *AASHTO LRFD* HL-93 design live load (Section 3.4.2), which is placed in position for the maximum positive vertical bending moment at $0.4L_1$ in the same three-span continuous beam examined above. The lane load is placed in the first and last spans where the influence line ordinates are positive. The design truck load is placed in the direction shown so that the larger rear-axle load is placed over the larger influence line ordinate adjacent to the critical section at $0.4L_1$.

For the concentrated load portion of the HL-93 loading, represented by the design truck load, the live load force effect is determined by multiplying the magnitude of each concentrated load by the corresponding influence line ordinate opposite each load (Figure 4.4.3.1-3 Part A). The resulting force effect due to the truck load is then multiplied by the dynamic load allowance of 33 percent. For the uniform load portion of the HL-93 loading, represented by the design lane load, the live load force effect is determined by multiplying the magnitude of the uniform load by the area of the influence line opposite the section covered by the load (Figure 4.4.3.1-3 Part B). No dynamic load allowance is applied to the resulting force effect from the design lane load.

The total force effect (i.e. the vertical bending moment at $0.4L_1$ in this case) is taken as the sum of the force effects due to the design truck and design lane load. The resulting live load force effect is then multiplied by an appropriate live load distribution factor (LLDF) to account for the transverse load effects (Section 4.4.2). Because influence lines are applied to one-dimensional line-girder configurations, transverse live load effects must be accounted for by applying LLDFs that are applicable to the force effect in the girder under consideration.

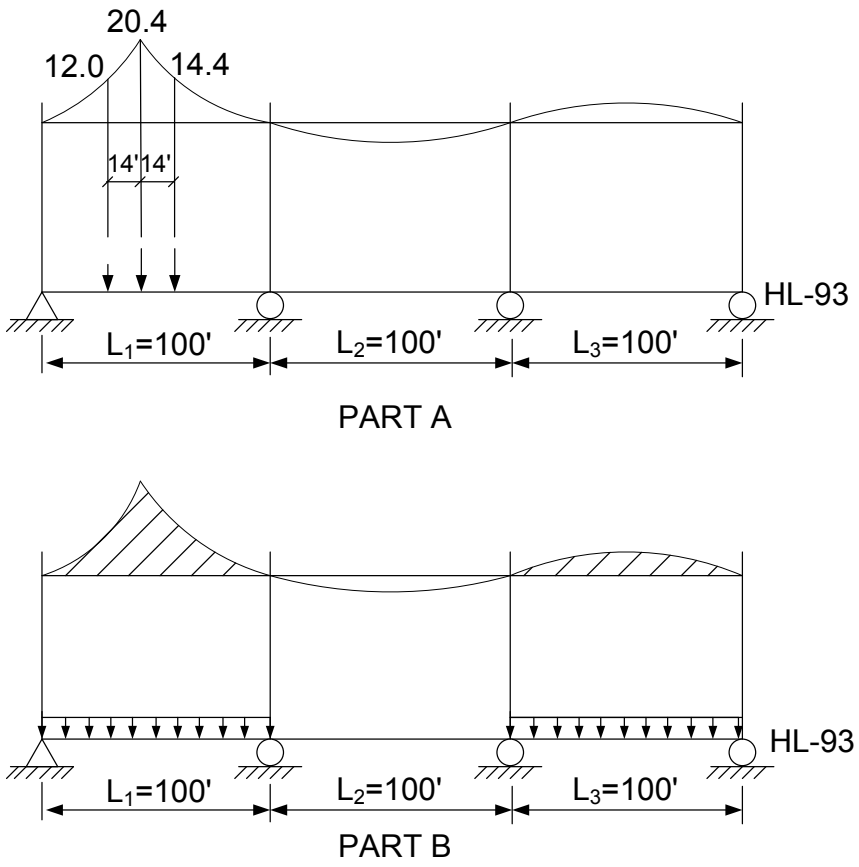

Figure 4.4.3.1-3 Application of HL-93 Live Load to an Influence Line for a Three-Span Continuous Beam to Determine the Vertical Bending Moment at $0.4L_1$

A) HL-93 Design Truck Load; B) HL-93 Design Lane Load

LLDFs that are computed using the equations presented in the tables given in *AASHTO LRFD* Article 4.6.2.2 are not to be multiplied by multiple presence factors. The effects of multiple presence have already been accounted for in the derivation of the equations. Multiple presence factors are to be applied, however, whenever the lever rule or the special rigid cross-section requirement for exterior beams is applied to compute the distribution factor. Multiple presence factors are discussed in further detail in Section 3.4.1.2.

Since skewed and curved bridges are best analyzed as systems, the use of LLDFs is typically not appropriate; thus, influence surfaces rather than influence lines are most often utilized to more accurately determine the necessary live load force effects for these bridge systems. Influence surfaces are examined in more detail in Section 4.4.3.2.

EXAMPLE

A two-span continuous example bridge is shown in Figure 4.4.3.1-4.

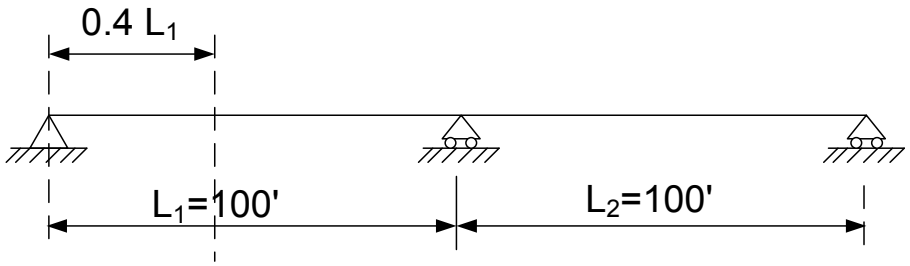

Figure 4.4.3.1-4 Example Two-Span Continuous Bridge

Calculate the approximate critical unfactored positive live load plus impact moment at $0.4L_1$ due to the HL-93 live load. HL-93 includes a truck load and a lane (uniform) load, as illustrated in Figure 4.4.3.1-5.

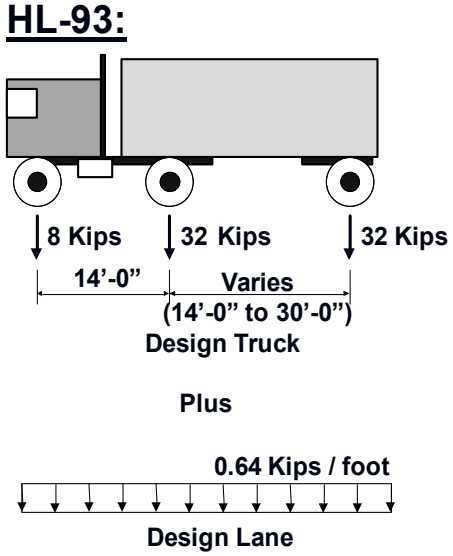

IM = 1.33
LLDF = 0.813 Lanes for Moment

Figure 4.4.3.1-5 HL-93 Live Load plus IM and Multi-Lane Moment LLDF for the Example Two-Span Bridge

The figure also gives the dynamic load allowance (impact) value applied only to the truck load, and the multi-lane live load distribution factor (LLDF) for vertical bending moment in units of lanes.

This load is applied to the influence line for vertical bending moment at $0.4L_1$ given in Figure 4.4.3.1-6. The ordinates of the influence line are given at tenth points of the

two spans, or in 10-foot increments in this case. Note that the design lane load is applied only to the positive region of the influence line. The design truck is applied with the center wheel applied at the cusp of the influence line.

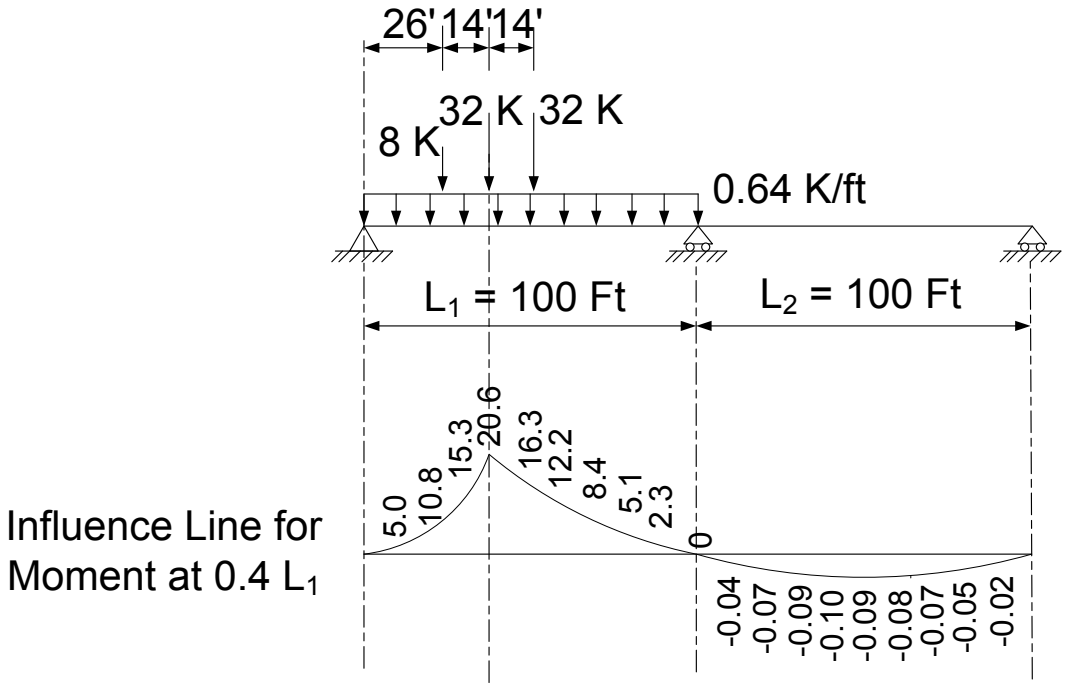

Figure 4.4.3.1-6 HL-93 Live Load Applied to Influence Line for Vertical Bending Moment at 0.4L_1 in the Example Two-Span Bridge

The positions of the truck and the lane load are so as to determine the maximum positive HL-93 vertical bending moment at 0.4L_1. Note that the truck could be pointed in either direction, but the right-to-left direction places the heavy rear axle on the larger ordinate in this case.

Interpolation between influence ordinates is necessary. The influence ordinate (Ordinate A) for the leftmost 8-kip axle load is computed as follows:

$$\text{Ordinate A} = 10.8 + \left(\frac{6'}{10'}\right)(15.3 - 10.8) = +13.5 \text{ kip} - \text{ft/kip}$$

The Ordinate B for the middle 32-kip axle load is +20.6 kip-ft/kip. By linear interpolation, the influence ordinate (Ordinate C) for the rear 32-kip axle load is computed as follows:

$$\text{Ordinate } C = 16.3 - \left(\frac{4'}{10'}\right)(16.3 - 12.2) = +14.7 \text{ kip} - \text{ft/kip}$$

The effect of the lane load is found by integrating the area under the positive portion of the plot times the load intensity. Using a linear approximation, the total area under the positive portion of the influence line shown in Figure 4.4.3.1-6 is estimated as follows:

$$A = 10\left[\left(\frac{0+5.0}{2}\right)+\left(\frac{5.0+10.8}{2}\right)+\left(\frac{10.8+15.3}{2}\right)+\left(\frac{15.3+20.6}{2}\right)+\left(\frac{20.6+16.3}{2}\right)+\left(\frac{16.3+12.2}{2}\right)+\left(\frac{12.2+8.4}{2}\right)+\left(\frac{8.4+5.1}{2}\right)+\left(\frac{5.1+2.3}{2}\right)+\left(\frac{2.3+0}{2}\right)\right]$$

$$= 960 \text{ ft}^2$$

Accounting for impact (dynamic load allowance), and the live load distribution factor, the approximate critical unfactored positive live load plus impact moment at $0.4L_1$ due to the HL-93 loading is computed as follows:

$$\text{Moment} = (\text{LLDF})(\text{Impact})\left[\sum(\text{Axle Load})(\text{Ordinate})\right] + (\text{LLDF})\left[(\text{Uniform Load})(\text{Area})\right]$$

$$\text{Moment} = (0.813)(1.33)\left[\sum(8 \text{ kips})(13.5) + (32 \text{ kips})(20.6) + (32 \text{ kips})(14.7)\right] + (0.813)\left[(0.64 \text{ kips/ft})(960)\right]$$
$$= 1{,}838 \text{ kip} - \text{ft}$$

Calculate the approximate critical unfactored range of live load plus impact shear at $0.4L_1$ due to the fatigue live load for the same bridge shown in Figure 4.4.3.1-4. The fatigue live load is shown in Figure 4.4.3.1-7; the rear-axle spacing is fixed at 30 feet. The figure also gives the dynamic load allowance (impact) value applied only to the fatigue live load, and the single-lane live load distribution factor (LLDF) for shear in units of lanes.

By inspection, the location of the fatigue truck to produce the maximum positive live load plus impact shear due to fatigue is as shown below in Figure 4.4.3.1-8. Similarly, the location of the fatigue truck to produce the maximum negative live load plus impact shear due to fatigue is also shown in Figure 4.4.3.1-8. These locations give the maximum shear values at $0.4L_1$; they are not loaded simultaneously. In fact, they are based on the truck headed in opposite directions, which is not realistic for the shear range for the single passage of a truck. However, it is only slightly conservative. The algebraic difference between these values is the critical unfactored range for fatigue live load plus impact shear.

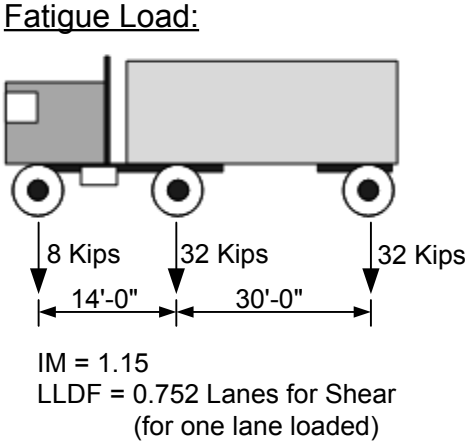

Figure 4.4.3.1-7 Fatigue Live Load plus IM and Single-Lane Shear LLDF for the Example Two-Span Bridge

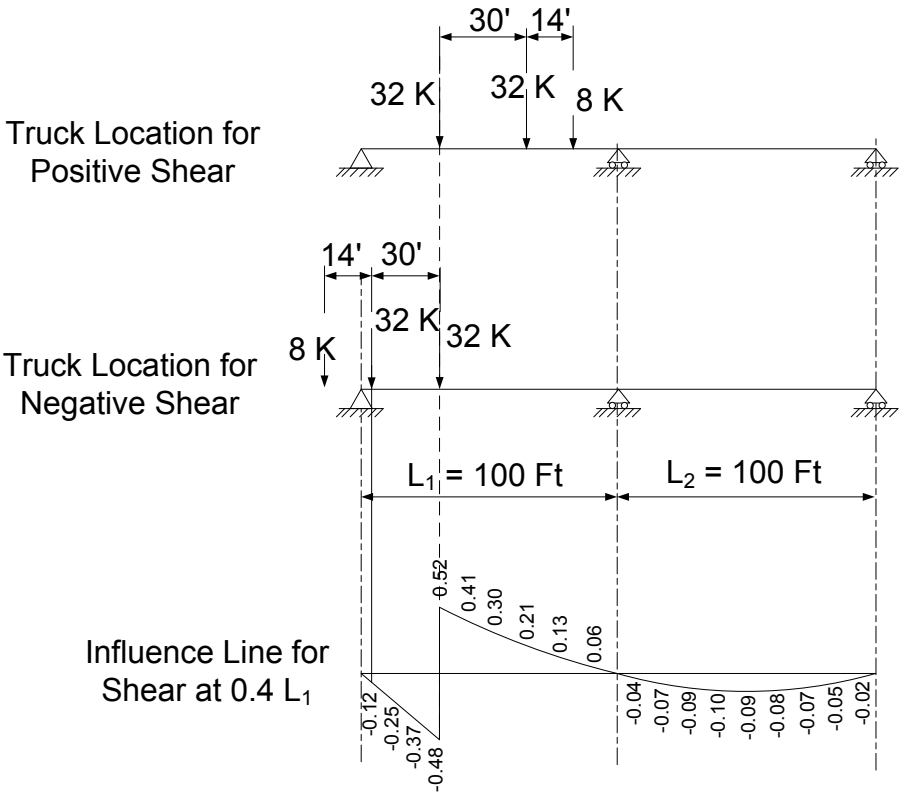

Figure 4.4.3.1-8 Fatigue Live Load Applied to Influence Line for Shear at 0.4L_1 in the Example Two-Span Bridge

The maximum unfactored positive live load plus impact shear at 0.4L_1 due to the fatigue live load is computed as follows:

The Ordinate A for the rear 32-kip axle load is +0.52. The Ordinate B for the middle 32-kip axle load is +0.21. The influence ordinate (Ordinate C) for the rightmost 8-kip axle load is computed as follows:

$$\text{Ordinate C} = 0.13 - \left(\frac{4'}{10'}\right)(0.13 - 0.06) = +0.10$$

$$\text{Shear} = (\text{LLDF})(\text{Impact}[\sum(\text{Axle Load})(\text{Ordinate})]$$

$$\text{Shear} = (0.752)(1.15)\left[(32\ \text{kips})(0.52) + (32\ \text{kips})(0.21) + (8\ \text{kips})(0.10)\right] = +20.9\ \text{kips}$$

Similarly, the maximum unfactored negative live load plus impact shear at $0.4L_1$ due to the fatigue live load is computed as follows:

The Ordinate A for the rear 32-kip axle load is -0.48. The Ordinate B for the middle 32-kip axle load is -0.12. The leftmost 8-kip axle load is off the bridge. Therefore:

$$\text{Shear} = (0.752)(1.15)\left[(32\ \text{kips})(-0.48) + (32\ \text{kips})(-0.12)\right] = -16.6\ \text{kips}$$

Therefore, the approximate critical unfactored range of live load plus impact shear at $0.4L_1$ due to the fatigue live load is computed as the difference of these two values, as follows:

$$\text{Shear Range} = +20.9\ \text{kips} - (-16.6\ \text{kips}) = 37.5\ \text{kips}$$

4.4.3.2 Influence Surfaces

4.4.3.2.1 General

Influence lines are applicable to one-dimensional configurations. Thus, transverse live load effects must be accounted for by applying live load distribution factors to the resulting force effects. Since the use of live load distribution factors is typically not appropriate for skewed and curved bridges, which are best analyzed as systems, influence surfaces are most often utilized to more accurately determine the live load force effects in these bridge systems.

The same basic principles discussed previously for influence lines are applicable to influence surfaces. The difference is that influence surfaces consider the transverse position of the live loads as well as the longitudinal position.

There is no need for live load distribution factors to account for transverse effects. Influence surfaces provide influence ordinates over the entire deck. Typically, these

ordinates are determined by applying a vertical unit load at selected longitudinal and transverse positions. Live loads are then placed on the surface at critical positions permitted by specification (Section 4.4.3.2.2). The load effect that the influence surface was developed for is determined by multiplying the intensity of the load times the corresponding ordinate. Influence surfaces are applicable to all linearly elastic responsive structures.

In skewed and curved bridges, influence surfaces are generally needed for other actions in addition to major-axis bending moment, shear, reactions and deflections. For example, additional surfaces are typically needed for live load cross-frame forces and lateral flange bending moments.

Figure 4.4.3.2.1-1 shows an influence surface for the vertical bending moment in Span 1 of the outside fascia girder of a three-span continuous skewed and curved I-girder bridge. The orange represents the deck surface and the zero values of the surface. The framing plan for the bridge is shown in the figure to indicate (with a circle) the location for which the influence surface is developed. A typical bridge design requires several hundred such influence surfaces that must then be loaded.

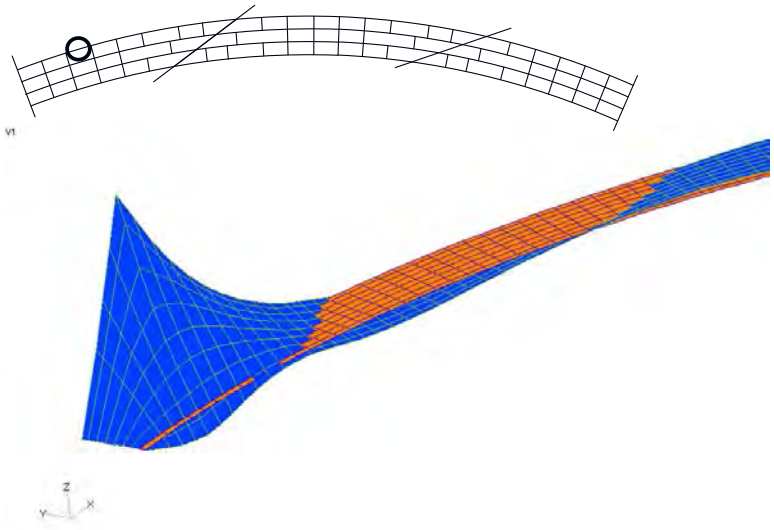

Figure 4.4.3.2.1-1 Influence Surface for Vertical Bending Moment in Span 1 of G4 of the Example I-Girder Bridge

Figure 4.4.3.2.1-2 shows an influence surface for the vertical bending moment at an interior pier in the inside fascia girder of the same bridge. The yellow represents the deck surface and the zero values of the surface. Regions of the surface above the yellow represent a positive response. Note that positive moment is introduced at the pier by loading in portions of Span 1. This is due partially to the skew and curvature.

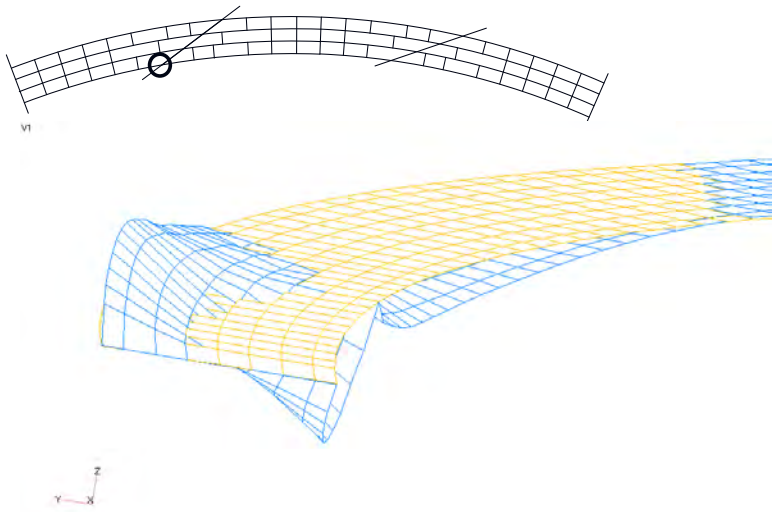

Figure 4.4.3.2.1-2 Influence Surface for Vertical Bending Moment at Pier 1 of G1 in the Example I-Girder Bridge

Figure 4.4.3.2.1-3 shows the influence surface for vertical shear in the inside fascia girder in Span 1 at the location identified (approximately 75 feet from the abutment).

.

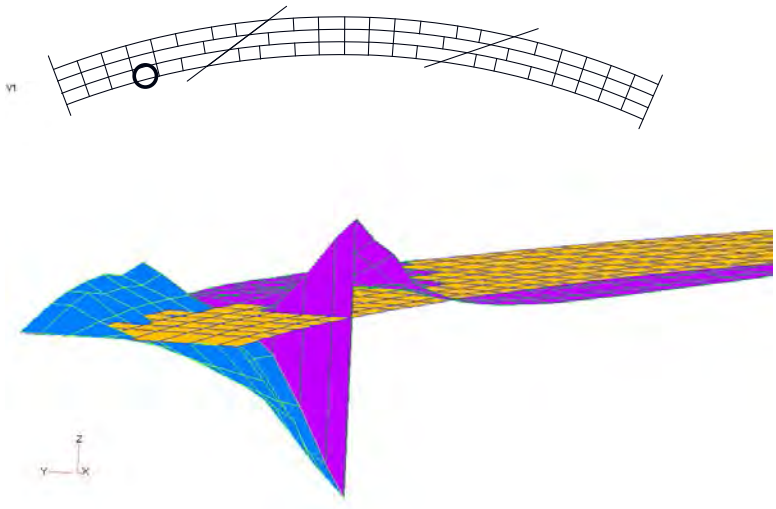

Figure 4.4.3.2.1-3 Influence Surface for Vertical Shear in Span 1 of G1 of the Example I-Girder Bridge

Another category of influence surface is for cross-frame forces, as shown in Figure 4.4.3.2.1-4.

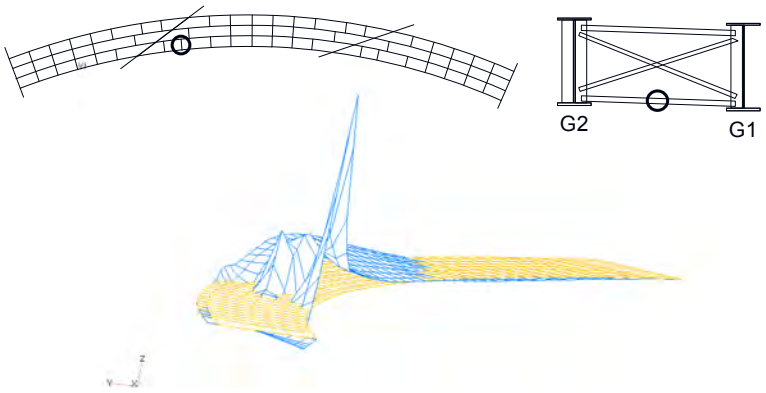

Figure 4.4.3.2.1-4 Influence Surface for Cross-Frame Force in the Bottom Chord of a Cross-Frame in Span 2 of the Example I-Girder Bridge

Additional actions must be considered in the design of skewed and curved girder bridges. Cross-frames are treated as primary members in such bridges, so they should be modeled in system analyses. Obviously, it is important to consider the live-load effects for strength and fatigue.

The live load is typically placed in a longitudinal path. The range of force in transverse members (for fatigue design) often occurs when the live load is permitted to roam transversely on the surface. This is evident from viewing the surface shown in Figure 4.4.3.2.1-4. Observe the local peaks in the surface and the non-linear behavior between girders.

Obviously, vehicles rarely if ever, move transversely. Also, there is an extremely low probability of trucks being located in two critical relative transverse positions over millions of cycles. Therefore, in order to compute more representative ranges of stress or torque for checking fatigue in transverse members whenever refined analysis methods are employed, *AASHTO LRFD* Article C6.6.1.2.1 recommends that the fatigue truck be positioned to determine the maximum range of stress or torque, as applicable, in these members as specified in *AASHTO LRFD* Article 3.6.1.4.3a, with the truck confined to one critical transverse position per each longitudinal position throughout the length of the bridge in the analysis.

Figure 4.4.3.2.1-5 shows an influence surface for the bottom flange lateral bending moment in G2 of the same bridge at a cross-frame located in Span 2. Note that the cross-frames are staggered at this location; this causes larger flange lateral moments.

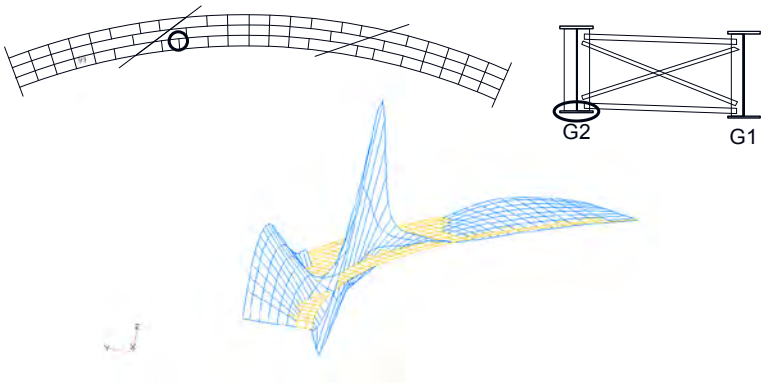

Figure 4.4.3.2.1-5 Influence Surface for Bottom Flange Lateral Bending Moment in G2 of the Example I-Girder Bridge at a Cross-Frame in Span 2

The maximum bottom flange lateral moment at this location is 41 kip-ft for HL-93 loading. The design truck and design lane each produce approximately 20 kip-ft. Design of the flange requires that the stresses due to the lateral moment and the vertical moment be combined. Typically, the two cases are combined although the two actions are not caused by the live load placed in the same position. It is not practical to find the critical combined cases. There are an infinite number of possible live load locations to check. Each case would have to be carried to the final stages and recorded to find where the critical case is located.

The influence surfaces extend to the edges of the deck to ensure that loads beyond the exterior girder will be treated properly. The live load is only permitted to roam on the deck within the realms defined by *AASHTO* (Section 4.4.3.2.2) and controlled by the Design Engineer.

4.4.3.2.2 Live Load Placement

The term “design lanes” is generally defined as the number of 12-foot-wide lanes loaded with live load. Design lanes are taken as the integer part of the ratio *w*/12.0, where *w* is the clear roadway width in feet between curbs and/or barriers (*AASHTO LRFD* Article 3.6.1.1.1).

Each design lane is a segment of the deck that may have the specified live load applied within its boundaries. On straight bridges with no skewed supports, design lanes generally may run in a straight line at a specified distance from a curb or barrier. However, when the bridge is curved or has skewed supports, the design lanes may wander in order to produce a critical response. The need to assume this is evident from examination of the influence surfaces. The specifications are silent on the subject of lanes wandering.

The design truck is assumed to be six-feet wide and is permitted to be no closer than two feet from the edges of the design lane in which it is placed. The design lane (uniform) load is assumed to be 10-feet wide. The loaded lanes are positioned on the influence surface within the roadway width to produce the extreme force effects in the component under consideration. Live load force effects due to concentrated and uniform loads are determined in the same fashion as discussed previously for influence lines.

An example of lane positioning is shown in Figure 4.4.3.2.2-1. In this case, three design lanes are shown to produce the maximum effect in the left-most girder. Note that this positioning is only certain for the position over the point investigated. At other points on the bridge, the design lanes may have wandered on the deck. Usually, it is assumed that lanes may not cross each other.

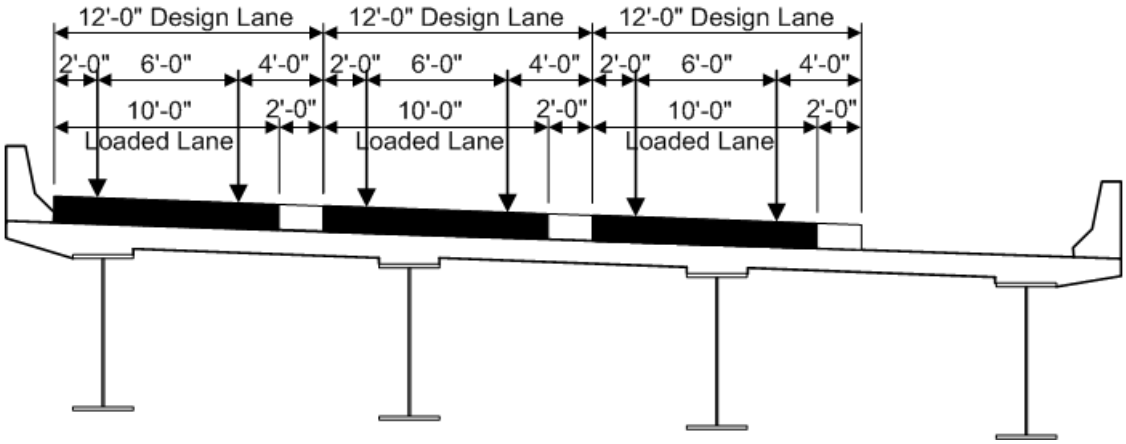

Figure 4.4.3.2.2-1 Positioning of Design Lanes and Loaded Widths within Lanes

Roadway widths from 20.0 to 24.0 feet are to have two design lanes, with each taken equal to one-half the roadway width. In cases where traffic lanes are less than 12.0 feet in width, the number of design lanes is to be taken equal to the number of traffic lanes, with the width of each design lane taken as the width of the traffic lane (*AASHTO LRFD* Article 3.6.1.1.1). Design lanes may be assumed to be 10 feet wide rather than 12. Some Owners prefer this option as a standard.

Design vehicle wheel loads are to be positioned transversely such that the center of a wheel load is not closer than 2.0 feet from the edge of the design lane, as mentioned above. For design of the deck overhangs, wheel loads are to be positioned not closer than 1.0 foot.

Loads need not be positioned side-by-side within their lanes on the surface. Typically, for skewed and curved bridges, the loads will need to be placed in staggered positions (or possibly even in different spans) within adjacent lanes in order to determine the critical responses. Wheel loads may be adjusted by the unit wheel-load factors to account for centrifugal force effects (Section 3.4.9.2).

The appropriate multiple presence factors (Section 3.4.1.2) are applied to the live load force effects whenever refined analyses are employed. For example, they are applied to the force effects determined from influence surfaces. Suggested multiple-presence factors to be applied to live load force effects when influence surfaces are loaded with design permit loads, or where one design permit load is considered in combination with the full HL-93 design live load in one or more of the remaining design lanes, are given in NHI (2011).

EXAMPLE

For the example bridge shown in Figure 4.4.3.2.2-2 and Figure 4.4.3.2.2-3, and the influence surface shown Figure 4.4.3.2.2-4, the following will be computed by positioning the wheels of the single *AASHTO LRFD* fatigue truck at least 2.0 feet from the curb line, and by including the effects of centrifugal force:

- The approximate critical unfactored positive live load plus impact vertical bending moment at Node 24 (Figure 4.4.3.2.2-3).

- The approximate critical unfactored negative live load plus impact vertical bending moment at Node 24 (Figure 4.4.3.2.2-3).

Figure 4.4.3.2.2-2 shows a cross-section of the example I-girder bridge, which is used in this illustration.

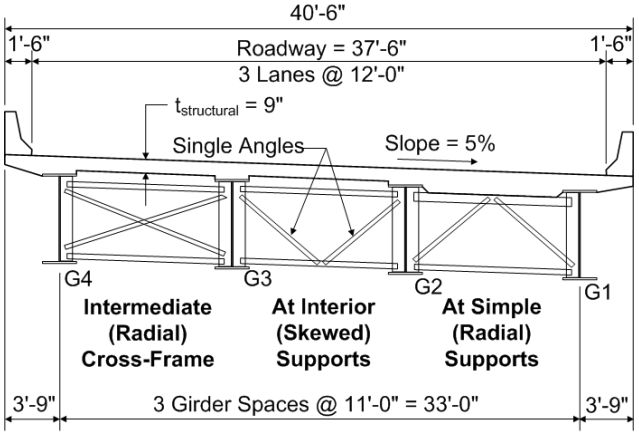

Figure 4.4.3.2.2-2 Example I-Girder Bridge Cross-Section

Figure 4.4.3.2.2-3 is a plan view of the example bridge with a contiguous cross-frame arrangement, which is also assumed in this illustration.

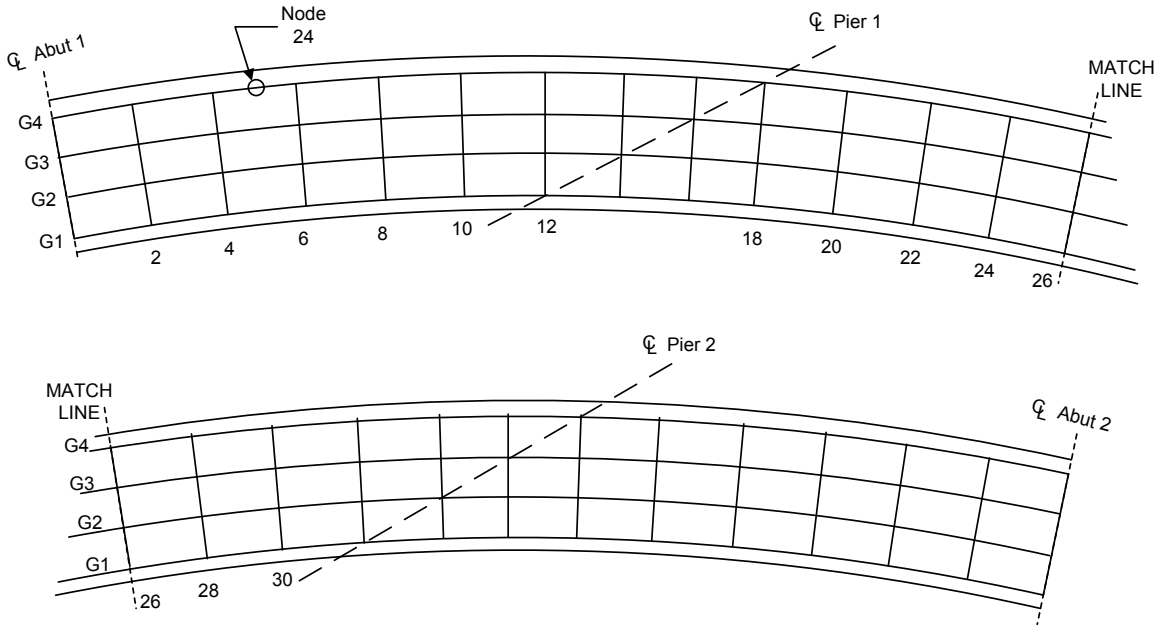

Figure 4.4.3.2.2-3 Plan View of the Example I-Girder Bridge with a Contiguous Cross-Frame Arrangement

Node 24 is shown in Figure 4.4.3.2.2-3. This example is based on the influence surface for vertical bending moment at Node 24. The girder lines and the edge of the deck are included in this plan view as well.

The influence surface shown in Figure 4.4.3.2.2-4 is for the vertical bending moment at Node 24, which is in the outside fascia girder, G4, in Span 1 of the example bridge. The influence surface ordinates are provided in subsequent figures.

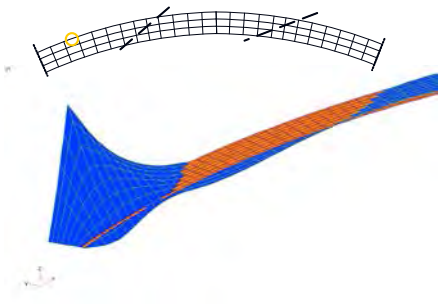

Figure 4.4.3.2.2-4 Influence Surface for Vertical Bending Moment at Node 24 in Span 1 of G4 of the Example I-Girder Bridge

Figure 4.4.3.2.2-5 presents the fatigue live load (Section 3.4.4) used in this example. The fatigue live load is a single truck, without the lane load, with a dynamic load allowance of 15 percent applied.

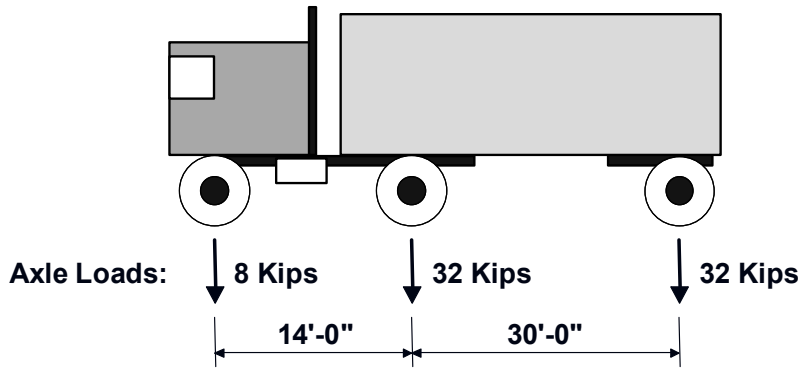

IM = 1.15

Figure 4.4.3.2.2-5 Fatigue Live Load

The rear-axle spacing of the fatigue live load is a constant 30'-0". The constant rear-axle spacing approximates that for the 4- and 5-axle semi-trailers that do most of the fatigue damage to bridges. The fatigue live load occupies a single lane on the bridge; it does not occupy multiple lanes. The multiple presence factor of 1.2 is not to be applied for fatigue investigations (Section 3.4.1.2).

The unit wheel load factors to be applied to the fatigue live load to account for the effects of centrifugal force (Section 3.4.9.2) are given as:

Outside wheels = 1.134
Inside wheels = 0.866

Figure 4.4.3.2.2-6 illustrates a schematic of the wheels of the fatigue live load (drawn to scale) that will be placed on the influence surface in subsequent figures.

Figure 4.4.3.2.2-6 Schematic of the Wheels of the Fatigue Live Load (drawn to scale)

The approximate critical unfactored positive live load plus impact vertical bending moment at Node 24 due to the fatigue live load will be calculated first.

Figure 4.4.3.2.2-7 presents the influence surface ordinates in Span 1 for the vertical bending moment at Node 24, which are required to accomplish this computation.

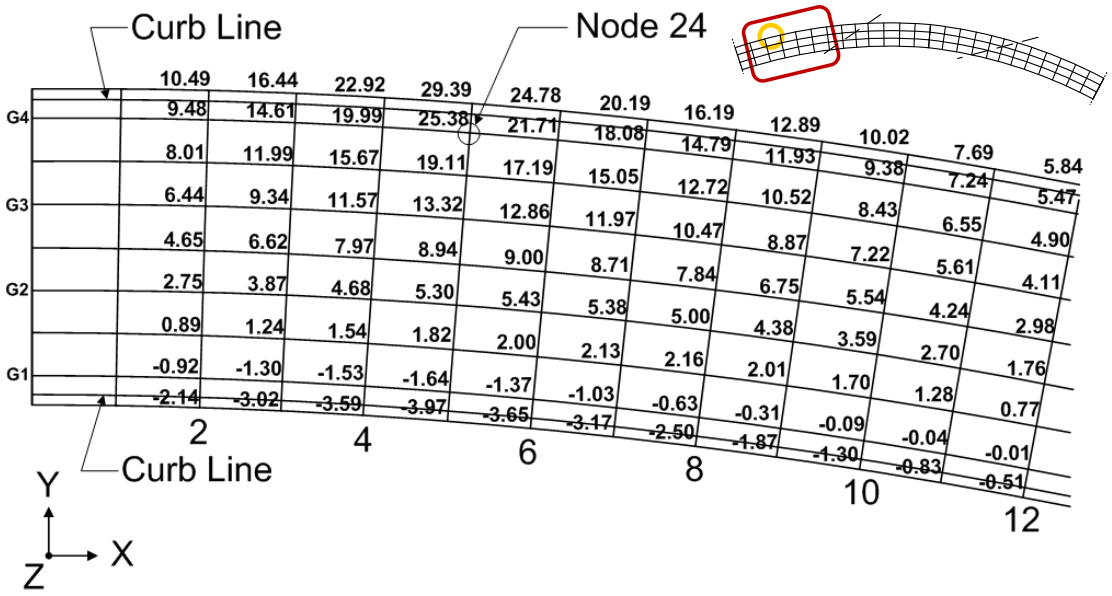

Figure 4.4.3.2.2-7 Influence Surface Ordinates in Span 1 for Vertical Bending Moment at Node 24

The schematic wheel-load model of the fatigue live load (Figure 4.4.3.2.2-6) is positioned on the influence surface in Figure 4.4.3.2.2-8 so as to maximize the positive vertical bending moment at Node 24 based on the influence ordinates shown. The wheel loads must be least two feet from the curb line.

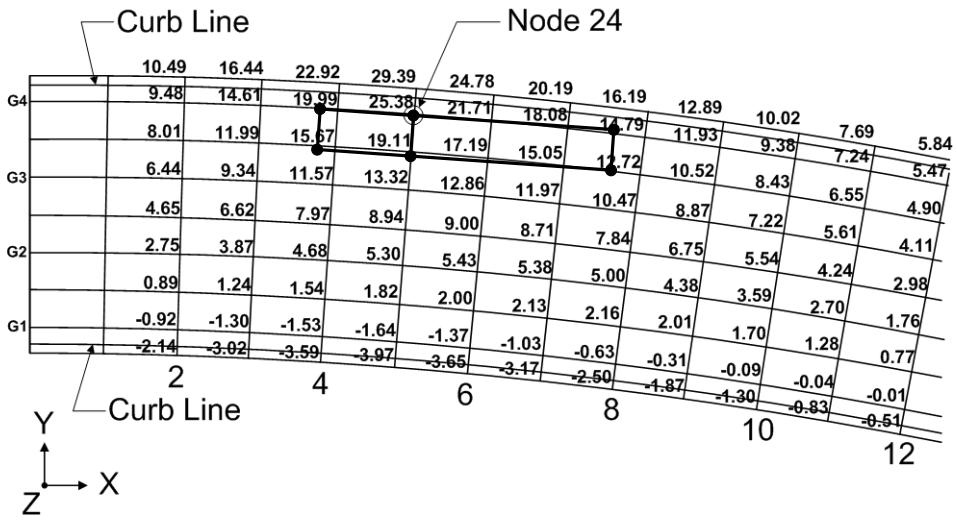

Figure 4.4.3.2.2-8 Wheel-Load Model of the Fatigue Live Load Positioned on Influence Surface to Maximum the Positive Vertical Bending Moment at Node 24

Figure 4.4.3.2.2-9 illustrates in general how the influence surface ordinates shown in Figure 4.4.3.2.2-7 are obtained. An influence surface ordinate corresponds to a specific force effect at a specific location.

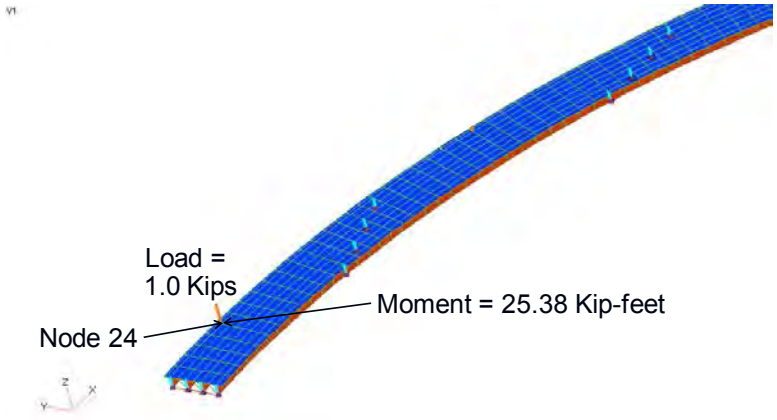

Figure 4.4.3.2.2-9 Determination of the Influence Surface Ordinate for Vertical Bending Moment at Node 24 for a Load Applied at Node 24

For example, to determine the influence surface ordinate for the vertical bending moment at Node 24 caused by a load applied directly to Node 24, the 3D model of the bridge (in this case) is analyzed for a vertical unit load applied at Node 24 (Figure 4.4.3.2.2-9). The corresponding influence surface ordinate has a value equal to the vertical bending moment at Node 24 caused by that unit load (or 25.38 kip-feet/kip in this case). The ordinates at other nodes in that span shown in Figure 4.4.3.2.2-7 are determined in a similar fashion.

The following equation is used to compute the approximate critical unfactored positive live load plus impact vertical bending moment at Node 24 due to the fatigue live load:

$$\text{Moment} = \sum\left[(\text{WheelLoad})(\text{Impact})(\text{Effect of Centrifugal Force})(\text{Influence Surface Ordinate})\right]$$

For this illustration, influence surface ordinates not directly under a wheel load are determined using linear interpolation. The solution is the sum of the six components from each of the six individual wheel loads.

The columns in the following computations are as follows:

First column – wheel load (kips)
Second column – dynamic load allowance (impact) (unitless)
Third column – unit wheel-load factor to account for effects of centrifugal force (unitless)
Fourth column – estimated influence surface ordinate from Figure 4.4.3.2.2-8 (kip-ft/kip)
Fifth column – positive live load plus impact moment due to the wheel load under consideration (kip-ft)

In the third column, the larger unit wheel-load factor for centrifugal force is applied to the outside wheels (i.e. the wheel loads closest to the edge of deck), and the smaller unit wheel-load factor is applied to the inside wheels.

1	2	3	4	5
4.0 x	1.15 x	1.134 x	18.8 =	98
16.0 x	1.15 x	1.134 x	25.4 =	530
16.0 x	1.15 x	1.134 x	16.0 =	334
4.0 x	1.15 x	0.866 x	14.5 =	58
16.0 x	1.15 x	0.866 x	18.8 =	300
16.0 x	1.15 x	0.866 x	13.0 =	207

$\sum = 1{,}527$ kip-ft

Therefore, the approximate critical unfactored positive live load plus impact vertical bending moment at Node 24 due to the fatigue live load is 1,527 kip-feet.

The critical unfactored negative live load plus impact vertical bending moment at Node 24 due to the fatigue live load is computed next.

Figure 4.4.3.2.2-10 presents the influence surface ordinates in Span 2 for the vertical bending moment at Node 24 in Span 1 that are required to accomplish this computation. Note that the ordinates are all negative in Span 2.

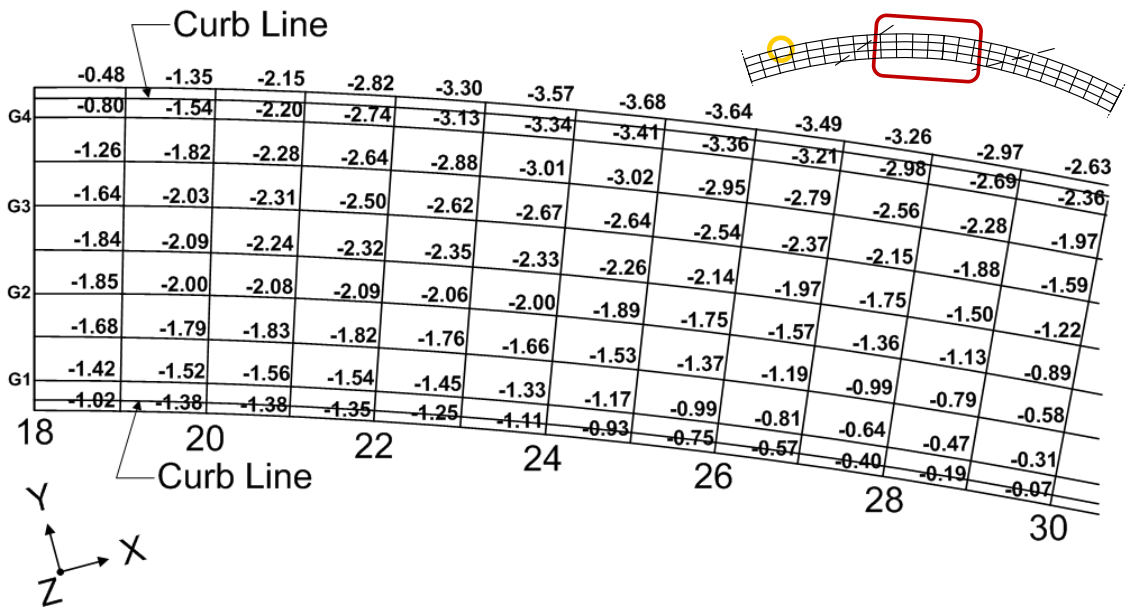

Figure 4.4.3.2.2-10 Influence Surface Ordinates in Span 2 for Vertical Bending Moment at Node 24

In this case, to determine the influence surface ordinate for the vertical bending moment at Node 24 in Span 1 caused by a load applied at a specific location over G4 in Span 2, the 3D model of the bridge (in this case) is analyzed for a vertical unit load applied at that location in Span 2 (Figure 4.4.3.2.2-11). The corresponding influence surface ordinate has a value equal to the vertical bending moment at Node 24 caused by that unit load (or -3.41 kip-feet/kip in this case). Again, the ordinates at the other nodes in that span shown in Figure 4.4.3.2.2-10 are determined in a similar fashion.

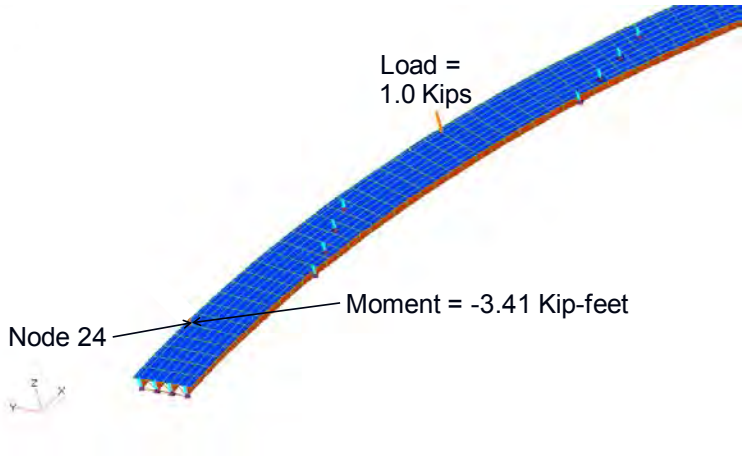

Figure 4.4.3.2.2-11 Determination of the Influence Surface Ordinate for Vertical Bending Moment at Node 24 for a Load Applied Over G4 in Span 2

The schematic wheel-load model of the fatigue live load (Figure 4.4.3.2.2-6) is positioned on the influence surface in Figure 4.4.3.2.2-12 (in Span 2) so as to maximize the negative vertical bending moment at Node 24 in Span 1 based on the influence ordinates shown. Once again the wheel loads must be least two feet from the curb line.

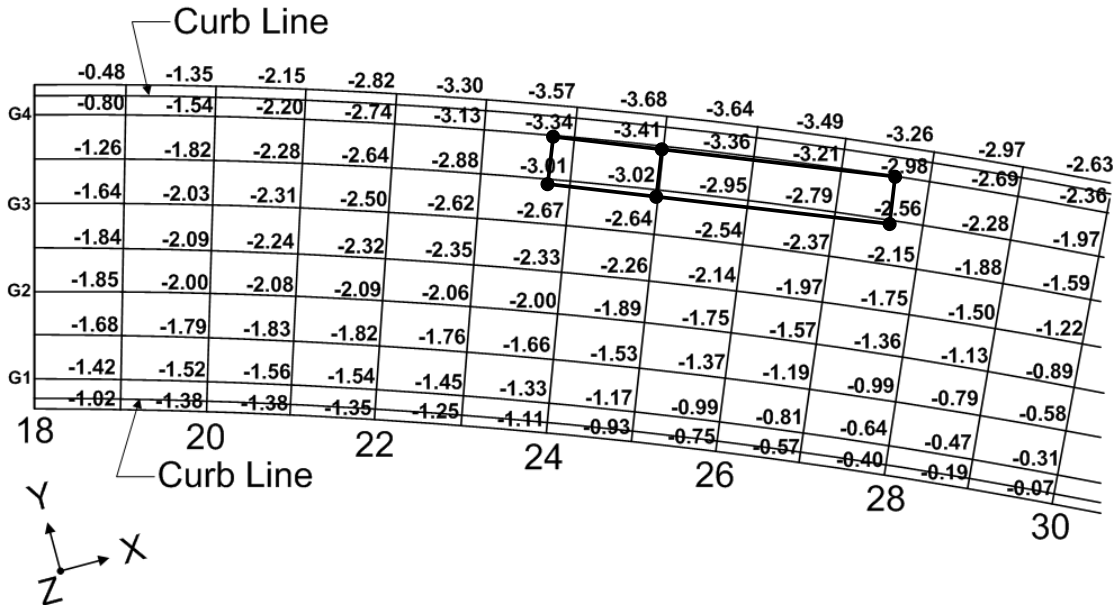

Figure 4.4.3.2.2-12 Wheel-Load Model of the Fatigue Live Load Positioned on Influence Surface to Maximum the Negative Vertical Bending Moment at Node 24

The equation shown previously is used to compute the approximate critical unfactored negative live load plus impact vertical bending moment at Node 24 due to

the fatigue live load. Influence surface ordinates not directly under a wheel load are once again determined using linear interpolation. The solution is the sum of the six components from each of the six individual wheel loads. The data in the columns below are the same as defined previously:

1	2	3	4	5
4.0 x	1.15 x	1.134 x	-3.3 =	-17
16.0 x	1.15 x	1.134 x	-3.4 =	-71
16.0 x	1.15 x	1.134 x	-3.1 =	-65
4.0 x	1.15 x	0.866 x	-3.0 =	-12
16.0 x	1.15 x	0.866 x	-3.0 =	-48
16.0 x	1.15 x	0.866 x	-2.6 =	-41

$\sum = -254$ kip-ft

Therefore, the approximate critical unfactored negative live load plus impact vertical bending moment at Node 24 due to the fatigue live load is -254 kip-feet.

Section 4.5 Methods of Analysis

4.5.1 General

This section describes the various methods of analysis that are typically applied in the design of girder-bridge superstructures. These methods include approximate methods of analysis (Section 4.5.2), and refined methods of analysis (Section 4.5.3). Refined methods of analysis include 2D methods of analysis (Section 4.5.3.2), and 3D methods of analysis (Section 4.5.3.3).

4.5.2 Approximate Methods of Analysis

Even with the ever-increasing use of refined analysis techniques as discussed in Section 4.5.3, the use of approximate methods of analysis is appropriate for several reasons. First, they provide some historical perspective on the evolution of analysis approaches; second, the techniques are relatively simple to employ and may be useful in the preparation of preliminary designs, or perhaps as some measure of validation for more complex analysis techniques; and third, the methods are useful in aiding in the basic understanding of the distribution of forces and the overall behavior of bridges.

Permissible approximate methods of analysis are described in *AASHTO LRFD* Article 4.6.2.

4.5.2.1 Beam Bridges

A one-dimensional (1D) analysis is a type of approximate method of analysis. A 1D analysis is one in which the resultant quantities (moments, shears, axial loads, deflections, etc.) are a function of only one spatial dimension. One-dimensional analysis replaces the structure with a single series of line elements that follow the geometry of the structure as seen in plan view. For a curving structure, that dimension may be measured along the curved axis; that is, the reference dimension does not have to be straight. Examples of a 1D analysis include a line girder analysis of a straight bridge or a spine beam model of a curved concrete box structure.

The application of live load distribution factors to beam-slab bridges (Section 4.4.2) is categorized as an approximate method of analysis, and is covered in *AASHTO LRFD* Article 4.6.2.2. According to this article, distribution factors may be applied to straight-girder bridges, horizontally curved concrete bridges, and horizontally curved steel bridges complying with the provisions of *AASHTO LRFD* Article 4.6.1.2.4 (Section 4.2.4). Distribution factors may also be used as a starting point for some more refined methods of analysis to determine force effects in curved girders of any degree of curvature in plan.

AASHTO LRFD Article 4.6.2.2.4 specifies that approximate methods may be used for the analysis of curved steel bridges. The Design Engineer must ascertain that the approximate analysis method used is appropriate by confirming that it satisfies the requirements for acceptable methods of structural analysis given in *AASHTO LRFD* Article 4.4. An approximate method of analysis for curved steel I-girder bridges known as the V-load method (Richardson, Gordon and Associates, 1963) is discussed in detail in NHI (2011). A method to approximate the lateral bending stresses in steel I-girder flanges (and the top flanges of steel tub girders) due to curvature, based on V-load theory, is also described (refer to *AASHTO LRFD* Eq. C4.6.1.2.4b-1). An approximate method of analysis for curved steel box-girder bridges known as the M/R method (Tung and Fountain, 1970) is also discussed in NHI (2011). Further guidance on the applicability of approximate methods of analysis to curved steel bridges may be found in NCHRP (2012).

4.5.2.2 Other Structure Types

Approximate analysis methods for decks are discussed in *AASHTO LRFD* Article 4.6.2.1. Included is equivalent strip method of analysis for concrete decks (except for top slabs of segmental concrete box girders for which the provisions of *AASHTO LRFD* Article 4.6.2.9.4 apply), in which the deck is subdivided into strips perpendicular to the supporting components (Section 7.3.2.2). Equivalent strip widths for slab-type bridges are provided in *AASHTO LRFD* Article 4.6.2.3, and equivalent strip widths for box culverts are provided in *AASHTO LRFD* Article

4.6.2.10. Equations to estimate the live load force effects for fully and partially filled grid decks, or unfilled grid decks composite with reinforced concrete slabs, are provided in *AASHTO LRFD* Article 4.6.2.1.8.

Approximate analysis of truss and arch bridges is covered in *AASHTO LRFD* Article 4.6.2.4. The effective length factor, *K*, used in the design of compression members (Section 4.2.5) is discussed in *AASHTO LRFD* Article 4.6.2.5. The effective flange width (Section 4.2.2) is discussed in *AASHTO LRFD* Article 4.6.2.6. *AASHTO LRFD* Article 4.6.2.7 discusses lateral wind load distribution in multi-beam bridges (Section 6.5.6.5). *AASHTO LRFD* Articles 4.6.2.8 and 4.6.2.9 discuss seismic lateral load distribution, and the analysis of segmental concrete bridges, respectively.

4.5.3 Refined Methods of Analysis

4.5.3.1 General

The use of refined methods of analysis has come to bridge design in the U. S. slower than in many other areas of structural design, such as buildings, transmission towers and dams. Even today, many bridge superstructure girders are designed as single-dimension lines. Loads are assigned to the line by various assumptions, some rather complex; all have their limitations. The enabling technologies of computers and finite element software permit the confident analysis of complex bridges that permit unique and more cost-effective designs constrained only by the laws of physics and the Design Engineer's imagination and skill. PCI (2011) recommends that refined analysis be used for the design of concrete bridges with high span-to-depth ratios because these methods allow for a significant reduction in the required release strength, or alternatively, an increase in the span capability. This section discusses some of the basics of 2D and 3D methods of analysis as applied to bridge superstructures.

4.5.3.2 2D Methods of Analysis

4.5.3.2.1 General

A two-dimensional (2D) analysis is one in which the resultant quantities (moments, shears, axial loads, deflections, etc.) are a function of two spatial dimensions. Two-dimensional finite element analysis models have been used in design since the early 1960s, and were developed during a time when much less computational capacity was available. This section discusses the types of 2D analysis models that are most commonly used for the design of bridge superstructures; suggested improvements to these conventional 2D models to improve the accuracy of the results; the modeling of truss-type cross-frames in 2D models; the determination of flange lateral bending moments in 2D analysis models; and the advantages, disadvantages, and limitations of 2D analysis models.

4.5.3.2.2 Types

4.5.3.2.2.1 General

2D finite element modeling actually encompasses a broad category of analysis models. There are two main types of grid analysis models generally available in design office practice; 1) traditional 2D grid models (Section 4.5.3.2.2.2); and 2) Plate and Eccentric Beam models (Section 4.5.3.2.2.3).

For practical 2D modeling, designers have the choice of using either bridge-specific software packages, or building their own 2D model in a structural finite-element software package. Differences between using a bridge-specific 2D bridge analysis design package and building a 2D model in a structural finite-element method (FEM) package are summarized in Table 4.5.3.2.2.1-1.

Table 4.5.3.2.2.1-1 2D Modeling: Bridge-Specific vs. Structural FEM Packages

Issue	Bridge Specific	Structural FEM
Automated model generation	Readily available	Becoming more available in some packages
Live load modeling	Generally fully automated	Significant user input
Extracting results	Generally mostly or fully automated	Significant user effort
Design code checks	Generally fully automated for girder design, not so much for cross-frames/diaphragms	Generally must be performed outside of the FEM model, using tools such as spreadsheets
Transparency	Can be somewhat of a “black box”	Generally fairly transparent, since model is built by the user

With most bridge-specific 2D bridge analysis packages, it is generally quick and easy to build a model, run the analysis, and obtain results, including girder code checks. However, these programs can be somewhat of a “black box,” and the user is at the mercy of the software vendor with regard to the design assumptions that are made, and the flexibility of the analysis package.

Building the model in a structural FEM analysis package gives the user a great deal of control over modeling assumptions and significant flexibility in modeling any feature of the structure. However, in exchange for this freedom and power, the user typically has to expend a significant amount of effort in building the model (e.g., building the nodal geometry, building the member connectivity, and establishing section properties), running live loads on the model (which can be a significant effort), post-processing the results, extracting key design loading information and performing detailed design checks.

It is particularly important for the Design Engineer to understand the nature of the software that is used (i.e., what type of analysis is the software performing and what

assumptions are being made), as these aspects can dramatically affect the analysis results.

4.5.3.2.2.2 Traditional Grid Models

Traditional 2D grid models consist of a purely two-dimensional array of nodes and beam elements. An example of a typical traditional grid model is shown in Figure 4.5.3.2.2.2-1.

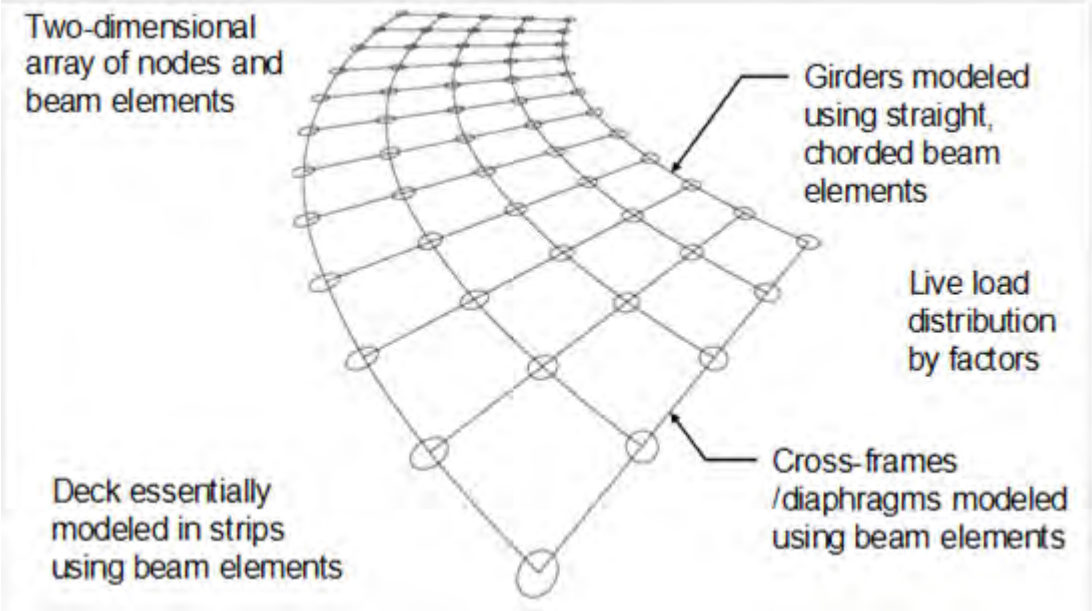

Figure 4.5.3.2.2.2-1 Traditional 2D Grid Model

The vertical depth of the superstructure is not considered in traditional 2D Grid models. The girders and their cross-frames or diaphragms are connected together in a single common plane, implicitly taken at the centroidal axis of the girders. All of the bearings are located at this same elevation in the model (Section 4.5.3.2.2.4). General modeling parameters should follow the guidelines provided in *AASHTO LRFD* Articles 4.6.3.3.1 and C4.6.3.3.1. Hambly (1991) also offers an excellent and comprehensive reference on modeling with grids. Further general guidance regarding node layout is provided in Section 4.5.3.3.2.2.

Girders and cross-frames/diaphragms are modeled using beam elements (Figure 4.5.3.2.2.2-2). In a traditional 2D grid analysis model, this element models both the girder and the composite girder and deck. The elements used are fairly conventional beam-type elements modeling six degrees of freedom (6 DoFs) at each end representing the flexure, axial and shear stiffness of the girder (refer to Section 4.5.3.3.2.3.1 for additional information on beam elements). A DoF is a direction of movement associated with axial, flexural and shear deformations. St. Venant

torsional stiffness, *J*, is also typically modeled, but most beam elements do not have the ability to model warping stiffness, C_w. Instead, warping stiffness is usually neglected, and flange lateral bending stresses are approximated (Section 4.5.3.2.3). Section 4.5.3.2.2.5.2 discusses one possible approach for considering the warping stiffness. The beam elements used to model the girders are straight elements, chorded between nodes in the model.

For thin-walled, hollow precast box sections, the torsional constant, *J*, may be computed as follows:

$$J = \frac{4A_o^2}{\sum(s/t)} \qquad \text{Equation 4.5.3.2.2.2-1}$$

where:

A_o = area enclosed by the centerlines of the elements (walls), in.^{2}
s = length of a side element (in.)
t = thickness of that element (in.)

For precast concrete I-beams, rational methods should be used to compute *J* (Eby et al., 1973). The use of formulas for open thin-walled sections is not appropriate. Values of *J* for AASHTO I-beams are tabulated in Section 7.5.3 of PCI (2011).

For composite load cases, the deck is effectively modeled in strips in the longitudinal direction by adjusting the girder element cross-section properties to reflect composite section properties of the gross or uncracked section computed using the tributary width of the deck (Section 4.2.2). The distribution of applied live load effects to individual girders is accomplished by means of the *AASHTO LRFD* empirical live load distribution factors (Section 4.4.2).

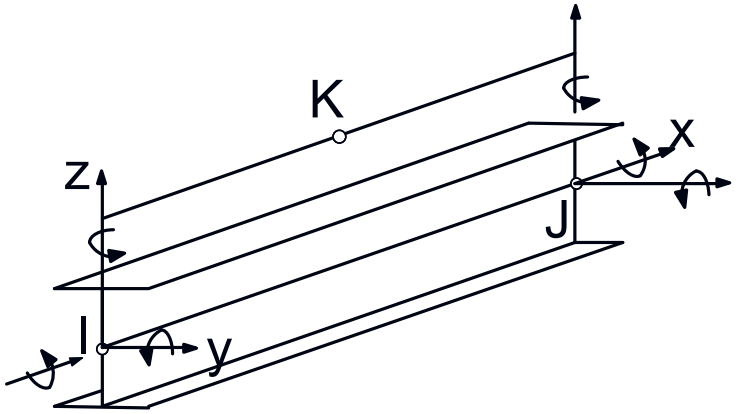

Figure 4.5.3.2.2.2-2 Beam Element

In the transverse direction, the deck serves primarily to help distribute live loads and composite dead loads to the girders and to tie the girders together (in conjunction with the cross-frames/diaphragms) so they act together as a system. Assumptions must be made to distribute the composite dead loads to the girders (e.g., barriers and wearing surface). The deck stiffness in the transverse direction is either not modeled directly, or else attempts may possibly be made to model the stiffness in strips tributary to the cross-frames/diaphragms.

A suggested procedure to determine section properties for truss-type cross-frames modeled using single beam elements is discussed in Section 4.5.3.2.2.5.3.

4.5.3.2.2.3 Plate and Eccentric Beam Models

In Plate and Eccentric Beam models (Figure 4.5.3.2.2.3-1), the deck is typically explicitly modeled using plate (shell) elements, and is offset from the grid of beam elements used to model the girders and the cross-frames/diaphragms to represent the offset of the neutral axis of the girders and cross-frames/diaphragms from the neutral axis of the deck (and thus, better account for the depth of the structure). The offset length between the deck and girder elements is typically equal to the distance between the centroids of the girder and deck sections. A rigid link is typically employed to connect the nodes of the beam element representing the girder to the deck nodes above.

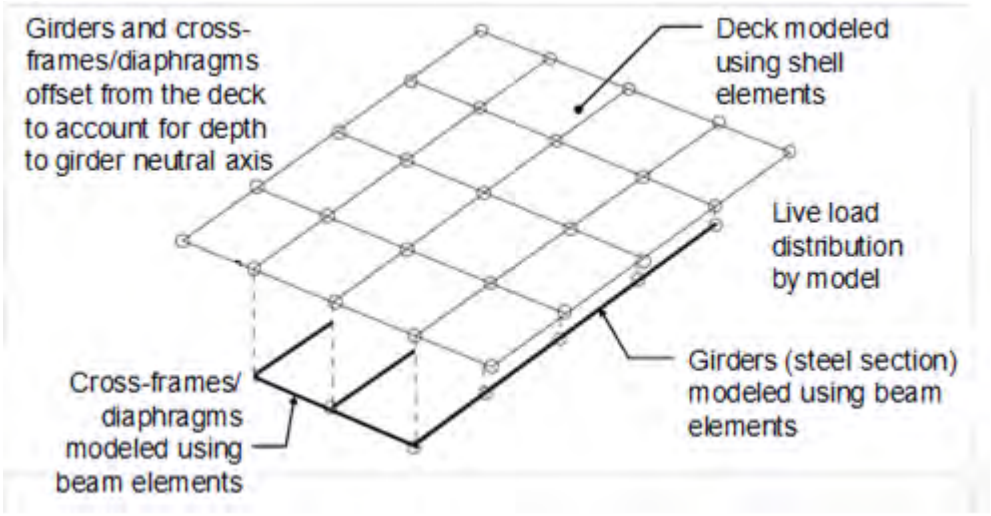

Figure 4.5.3.2.2.3-1 Plate and Eccentric Beam Model

This allows for the model to distribute live load based on relative stiffness rather than through the use of empirical live load distribution factors. Live load forces effects are usually determined through the use of an influence surface analysis (Section

4.4.3.2). Similarly, this avoids having to use simplified assumptions regarding composite dead load distribution to the girders.

For this modeling approach, beam and plate element internal forces need to be eccentrically transformed to obtain the composite girder internal forces (bending moment and shear) used in the bridge design. Warping stiffness in the beam elements is again usually neglected (see Section 4.5.3.2.2.5.2 for one possible approach to consider the warping stiffness), and flange lateral bending effects must still be approximated (Section 4.5.3.2.3). Section properties for truss-type cross-frames, which are modeled using single beam elements, should be determined as discussed in Section 4.5.3.2.2.5.3.

4.5.3.2.2.4 Boundary Conditions

For traditional 2D grid models, the boundary conditions are relatively simple; in most cases, pin supports may be assumed at all support locations (Figure 4.5.3.2.2.4-1). There is no theoretical error introduced in modeling either fixed or expansion bearings as pin supports in a 2D grid model. Longitudinal (tangential) reactions do not develop because the depth of the superstructure is not modeled.

Proper modeling of integral substructures (e.g., integral abutments, integral piers and straddle bents) is difficult with a traditional grid model since there is a strong transverse interaction between the reactions, and the superstructure depth is not explicitly modeled.

In a Plate and Eccentric Beam model, the depth of the structure is included in the model. For this reason, greater care must be taken in modeling the boundary conditions. It is important in Plate and Eccentric Beam models to choose boundary conditions that match the actual bearing configurations of the bridge. Otherwise, the model may improperly reflect conditions of moment restraint, which affects the determination of girder moments and deflections.

Care must be taken in these models to release the longitudinal (tangential) translation DoFs at bearings that are free in that direction; otherwise, moment restraint will develop at the bearings from the longitudinal reactions that result. For example, the last case shown on the right in Figure 4.5.3.2.2.4-1 indicates the moment restraint effect that can occur in a Plate and Eccentric Beam model if pins are provided at both ends of the beam (with the supports located at the bottom flange) such that the longitudinal (tangential) translational DoF is restrained.

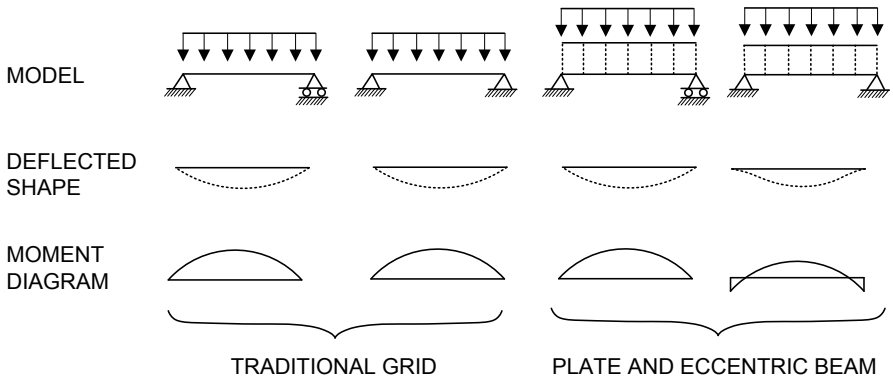

Figure 4.5.3.2.2.4-1 Effects of Different Boundary Condition Assumptions on Traditional Grid and Plate and Eccentric Beam Models

In a Plate and Eccentric Beam model, if all boundary conditions are modeled as pins, then the model will produce results which show some level of moment restraint. If all bearings on the bridge are fixed, perhaps this would be the correct way to model the bridge. However, the more likely case is that the bridge has some fixed, some guided, and some free bearings. Thus, the boundary conditions for a Plate and Eccentric Beam model of that bridge should be chosen to match the actual bearing conditions. Some commercial software may set their default boundary conditions to restrain the longitudinal (tangential) translation DoFs.

Modeling of the boundary conditions for thermal analyses requires special consideration. Bearing constraints can cause significant forces even with a uniform temperature change since the supports are not located at the neutral axis of the girders. If thermal effects are to be considered, the boundary conditions must be carefully modeled considering both the bearing fixity and also the specific orientation (direction) of guided bearings.

Care should be exercised when modeling thermal effects in a 2D model. Some commercial 2D modeling packages cannot model a bearing orientation other than locally tangent to the girder at the point of support. Traditional grid models do not permit different temperatures to be introduced through the depth of the structure in order to represent a thermal gradient.

4.5.3.2.2.5 Improved 2D Models

4.5.3.2.2.5.1 General

Enhancements that can improve the overall accuracy of 2D analysis results have evolved based on research work completed as part of NCHRP Project 12-79, and described in NCHRP (2012). Revisions to *AASHTO LRFD* Article 4.6.3.3 have been

made to incorporate these enhancements. These enhancements include the following:

- Improved modeling of cross-frame stiffness by developing the equivalent beam stiffness using a shear-deformable beam (Timoshenko Beam) approach, as discussed in Section 4.5.3.2.2.5.3. This approach involves the calculation of an equivalent moment of inertia as well as an equivalent shear area for a shear-deformable (Timoshenko) beam element representation of the cross-frame, including consideration of the influence of end-connection eccentricities in single-angle and flange-connected tee cross-section members, as discussed in Section 4.5.3.2.2.5.3; the axial rigidity of these members is reduced due to end connection eccentricities.

- Consideration of both the St. Venant torsion constant and the warping stiffness of the girder through the J equivalent term (J_{eq}), which provides a reasonable estimate of warping stiffness, as discussed in Section 4.5.3.2.2.5.2.

4.5.3.2.2.5.2 Improved Modeling of the Torsional Stiffness of I-Girders

General

In a 2D traditional grid analysis or a Plate and Eccentric Beam analysis of an I-girder bridge subject to significant torsional effects, the use of only the St. Venant torsional stiffness, GJ/L_b, where L_b is the unbraced length between the cross-frames, can result in a substantial underestimation of the girder torsional stiffness. This is due to the neglect of the contribution from girder cross-section warping, or the corresponding lateral flange bending, to the torsional response. For I-girders, the torsional contribution from the girder warping rigidity, EC_w, is often substantial compared to the contribution from the St. Venant torsional rigidity, GJ.

A 3D refined finite element analysis of an I-girder bridge, in which the girder webs are modeled using shell elements, and the girder flanges are modeled separately using beam, shell or solid elements, is capable of directly capturing the contribution of the girder warping rigidity to the torsional stiffness. Such is not the case in a 2D analysis, unless the beam elements used to model the girders include an additional warping degree of freedom, which is often not the case.

For steel I-girder bridges under non-composite loading conditions, the behavior of 2D grid models and Plate and Eccentric Beam models can be particularly sensitive to the contribution from the warping rigidity to the girder torsional stiffness. The use of an improved 2D model that includes the contribution of the warping rigidity can lead to significantly improved predictions of the girder displacements and cross-frame forces, particularly in cases where torsion is significant (NCHRP, 2012). The

behavior tends to be a bit less sensitive to the girder warping rigidity under composite loading conditions.

An area where the neglect of the warping rigidity can have a significant effect on the accuracy of the analysis results is the case where an additional node is placed in-between the cross-frames in a 2D analysis model, particularly in the case of a horizontally curved girder (Figure 4.5.3.2.2.5.2-1).

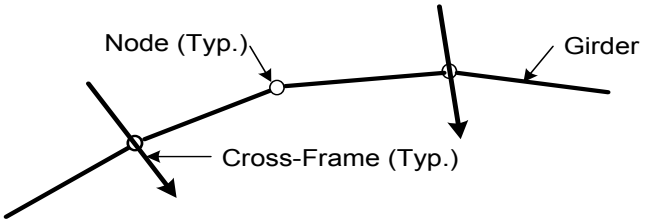

Figure 4.5.3.2.2.5.2-1 Additional Node Placed in-between the Cross-Frames in a 2D Model of a Horizontally Curved Girder

Because there is less resistance to the internal girder torsion due to curvature at the additional node due to the neglect of the warping rigidity, and the absence of a cross-frame at that node, the girder vertical displacements will be affected and will tend to be significantly overestimated (depending on the degree of curvature) as a result of the coupling that exists between the torsional and flexural response.

As a result of these concerns, AASHTO LRFD Article 4.6.3.3.2 now states that for the analysis of curved and/or skewed steel I-girder bridges where either $I_c > 1$ or $I_s > 0.3$, the warping rigidity of the I-girders must be considered in 2D grid, and in 2D Plate and Eccentric Beam methods of structural analysis, where:

I_c = I-girder bridge connectivity index

$$= \frac{15{,}000}{R(n_{cf}+1)} \qquad \text{Equation 4.5.3.2.2.5.2-1}$$

AASHTO LRFD Equation 4.6.3.3.2-1

I_s = bridge skew index, taken as the maximum of the values of Equation 4.5.3.2.2.5.2-2 determined for each span of the bridge

$$= \frac{w_g \tan\theta}{L_s} \qquad \text{Equation 4.5.3.2.2.5.2-2}$$

AASHTO LRFD Equation 4.6.3.3.2-2

m = bridge type constant, equal to 1 for simple-span bridges or bridge units, and equal to 2 for continuous-span bridges or bridge units, determined at the construction stage and/or loading condition being evaluated

n_{cf} = minimum number of intermediate cross-frames or diaphragms within the individual spans of the bridge or bridge unit at the construction stage and/or loading condition being evaluated

R = minimum radius of curvature at the centerline of the bridge cross-section throughout the length of the bridge or bridge unit at the construction stage and/or loading condition being evaluated (ft)

w_g = maximum width between the girders on the outside of the bridge cross-section at the completion of the construction or at an intermediate stage of the steel erection

L_s = span length at the centerline

θ = maximum skew angle of the bearing lines at the end of a given span, measured from a line taken perpendicular to the span centerline

Equivalent Torsion Constant, J_{eq}

An approximate method of considering the girder warping rigidity, applicable for I-girder bridges or bridge units in their final constructed condition, as well as for intermediate non-composite conditions during steel erection, is described in NCHRP (2012), and is also presented in (AASHTO/NSBA, 2014). A so-called equivalent torsional constant, *Jeq*, is determined by equating the stiffness, GJ_{eq}/L_b, to the analytical torsional stiffness associated with assuming warping fixity at the intermediate cross-frame locations, and warping free conditions at the simply-supported ends of a bridge girder. The use of J_{eq} results in significant improvements in the accuracy of 2D analyses for I-girder bridges.

By equating GJ_{eq}/L_b to the torsional stiffness, T/ϕ, for an open-section thin-walled beam associated with warping fixity at each end of a given unbraced length, L_b, where T is the applied end torque and ϕ is corresponding relative end rotation, J_{eq} for unbraced lengths in-between intermediate cross-frames is obtained as:

$$J_{eq(fx-fx)} = J\left[1 - \frac{\sinh(pL_b)}{pL_b} + \frac{[\cosh(pL_b)-1]^2}{pL_b \sinh(pL_b)}\right]^{-1} \qquad \text{Equation 4.5.3.2.2.5.2-3}$$

where:

$$p = \sqrt{\frac{GJ}{EC_w}} \qquad \text{Equation 4.5.3.2.2.5.2-4}$$

C_w = warping torsional constant given by *AASHTO LRFD* Equation C6.9.4.1.3-1 (in.^{6})

E = modulus of elasticity (ksi)

G = elastic shear modulus (ksi)
J = St. Venant torsional constant given by *AASHTO LRFD* Equation A6.3.3-9 ($in.^4$)

For the analysis of composite loading conditions using 2D plate and eccentric beam analysis models, it is sufficient to calculate the warping rigidity of the I-girders, EC_w, using solely the girder cross-section and without the consideration of any composite torsional interaction with the composite deck.

Similarly, by equating GJ_{eq}/L_b to the torsional stiffness, T/ϕ, for an open-section thin-walled beam associated with warping fixity at one end, and warping free boundary conditions at the opposite end of a given unbraced length, J_{eq} for unbraced lengths adjacent to simply-supported girder ends where the warping of the flanges is unrestrained at one end is obtained as:

$$J_{eq(s-fx)} = J\left[1-\frac{\sinh(pL_b)}{pL_b\cosh(pL_b)}\right]^{-1} \qquad \text{Equation 4.5.3.2.2.5.2-5}$$

Appendix C, Section 6.1.2 of NCHRP (2012) shows a complete derivation of these equivalent torsion constants. NCHRP (2012) also provides examples showing the implementation of this methodology.

When implementing this approach, a different value of J_{eq} must be calculated for each unbraced length having a different value of L_b, or with any difference in the girder cross-sectional properties within that unbraced length. Furthermore, it is important to recognize that the use of a length less than L_b typically will result in a substantial overestimation of the torsional stiffness. Therefore, when a given unbraced length is modeled using multiple elements, it is essential that the unbraced length, L_b, be used in the equations for J_{eq}, and not the individual element lengths.

With the equivalent torsion constant, *Jeq*(*fx-fx*), it is possible to simulate the torsional stiffness of an I-girder with warping-fixed ends. It is recommended that *Jeq*(*fx-fx*) be used to model the torsional rigidity of the interior girder segments, which are the segments defined between two intermediate cross-frames. The assumption of warping fixity at all of the intermediate cross-frame locations is certainly an approximation. 3D-frame analysis generally shows that some flange warping rotations occur at the cross-frame locations. Nevertheless, at least some degree of warping restraint to the flanges is provided by the adjacent girder segments. The assumption of warping fixity at the intermediate cross-frame locations leads to a reasonably accurate characterization of the girder torsional stiffness pertaining to the overall deformations of a bridge unit as long as:

- There are at least two I-girders connected together, and
- The girders are connected by enough cross-frames such that $I_C < 20$.

At the girder ends, the flanges typically are free to warp. For the girder end segments, defined as the segments between the discontinuous end of a girder and the first intermediate cross-frame, the equivalent torsion constant, *Jeq*(*s-fx*), derived assuming that the warping boundary conditions are fixed-free at the segment ends, should be used.

In summary, Equation 4.5.3.2.2.5.2-3 should be used to model the torsional rigidity of interior girder segments, or the segments between two intermediate cross-frames/diaphragms, and Equation 4.5.3.2.2.5.2-5 should be used to model girder end segments, or the segments between the discontinuous end of a girder where the girder flanges are free to warp and the first intermediate cross-frame/diaphragm adjacent to the girder end.

4.5.3.2.2.5.3 Modeling of Truss-Type Cross-Frames

General

Cross-frames generally exhibit substantial beam shear deformations when modeled using equivalent beam elements in a 2D structural analysis due to their predominant action as trusses. The modeling of cross-frames using Euler-Bernoulli beam elements, which neglect the effect of beam shear deformations, typically results in a substantial misrepresentation of their physical stiffness properties. Timoshenko beam elements, or other types of beam elements that include explicit modeling of beam shear deformations, provide a significantly improved approximation of the cross-frame stiffnesses (NCHRP, 2012).

As a result, *AASHTO LRFD* Article 4.6.3.3.4 now states that when modeling a cross-frame with a single line of equivalent beam elements, both the cross-frame flexure and shear deformation must be considered in determining the equivalent beam element stiffness.

Timoshenko Beam Approach

The more accurate shear-deformable (Timoshenko) beam approach for the calculation of an equivalent beam stiffness simply involves the calculation of an equivalent moment of inertia, I_{eq}, as well as an equivalent shear area, A_{seq}, for the beam element representation of a truss-type cross-frame.

Figure 4.5.3.2.2.5.3-1 illustrates the first step of the approach (AASHTO/NSBA, 2014). In this step, the equivalent moment of inertia, I_{eq}, is determined by assuming a pure flexural deformation of the cross-frame (i.e. zero shear). The cross-frame

model is supported as a cantilever at one end, and is subjected to a unit force couple applied at the corner joints at the other end, thus producing a constant bending moment. The associated horizontal displacements are determined at the free end of the cantilever from the analysis of this cross-frame model, and the corresponding end rotation is equated to the value of the rotation calculated from the beam pure flexure solution, $M/(EI_{eq}/L)$. The resulting EI_{eq} represents the "true" flexural rigidity of the cross-frame.

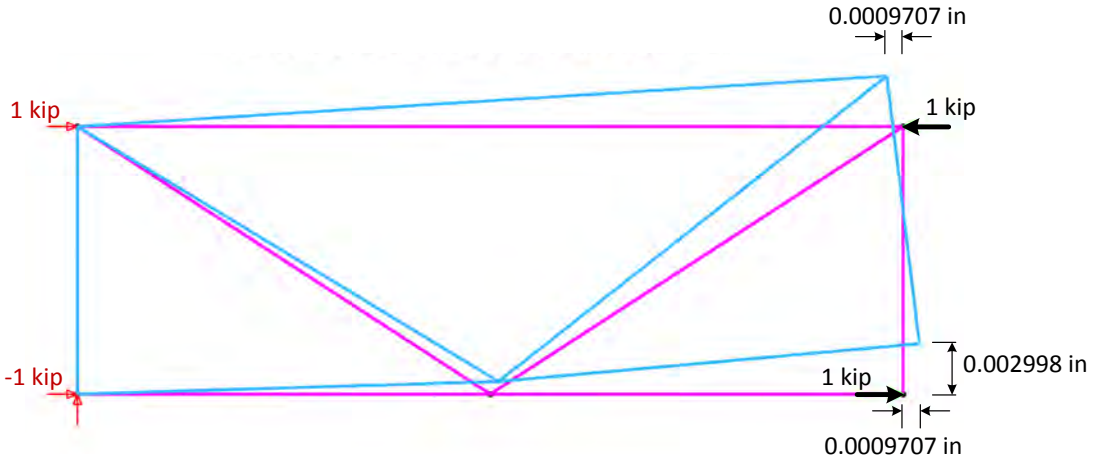

Figure 4.5.3.2.2.5.3-1 Timoshenko Beam Approach: Calculation of I_{eq} Based on Pure Bending

For the example case shown in Figure 4.5.3.2.2.5.3-1, assuming a cross-frame height of 34 inches and a cross-frame length of 105 inches:

$$2(0.0009707)/34 = 0.0000571 = ML/EI_{eq} = 34(105)/29000I_{eq}$$
$$I_{eq} = 2156 \text{ in.}^4$$

Figure 4.5.3.2.2.5.3-2 illustrates the second step of the approach (AASHTO/NSBA, 2014). In this step, the equivalent shear area, A_{seq}, is determined. The cross-frame is still supported as a cantilever, but is subjected to a unit transverse shear at the right-hand corner. Figure 4.5.3.2.2.5.3-2 shows the corresponding displacements and reactions from the analysis of this cross-frame model.

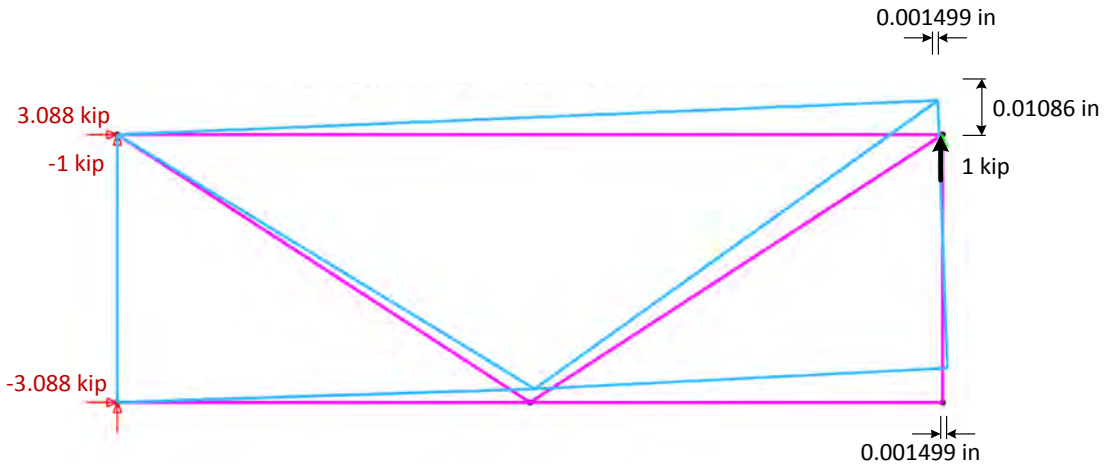

Figure 4.5.3.2.2.5.3-2 Timoshenko Beam Approach: Calculation of A_{seq} Based on a Unit Transverse Shear

For the example case shown in Figure 4.5.3.2.2.5.3-2, again assuming a cross-frame height of 34 inches and a cross-frame length of 105 inches:

$$\Delta = 0.01086 \text{ in.} = VL^3/3EI_{eq} + VL/GA_{seq}$$
$$= 1(105)^3/3(29000)(2156) + (1)(105)(2.6)/29000A_{seq}$$
$$A_{seq} = 2.008 \text{ in.}^2$$

The end rotation of the equivalent beam shown in Figure 4.5.3.2.2.5.3-2 is computed as:

$$\theta = VL^2/2EI_{eq} - V/GA_{seq}$$
$$= 1(105)^2/2(29000)(2156) - (1)(2.6)/(29000)(2.008) = 0.00004352 \text{ radians}$$

However, from the deflected shape in Figure 4.5.3.2.2.5.3-2, θ = 2(0.001499)/34 = 0.00008818 radians. Therefore, the shear-deformable Timoshenko beam element is not able to match the "exact" kinematics of the cross-frame.

Figure 4.5.3.2.2.5.3-3 compares the cross-frame end shears and moments from an exact physical model to the nodal shears and moments from the equivalent Timoshenko beam for the case of a propped cantilever subjected to an end moment. The Timoshenko beam comes reasonably close to fitting the force response of the cross-frame, compared to similar results from the flexure stiffness approach using an Euler-Bernoulli beam element (Figure 4.5.3.2.2.5.3-4), for which the left-end moment is significantly larger than the moment from the exact physical model, and is not even in the correct direction (NCHRP, 2012).

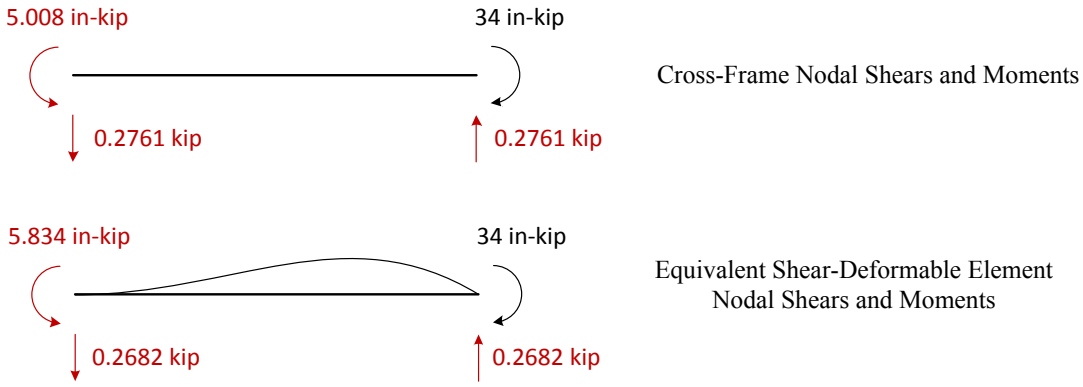

Figure 4.5.3.2.2.5.3-3 Comparison of Cross-Frame Nodal Shears and Moments and Equivalent Shear-Deformable (Timoshenko) Beam Shears and Moments

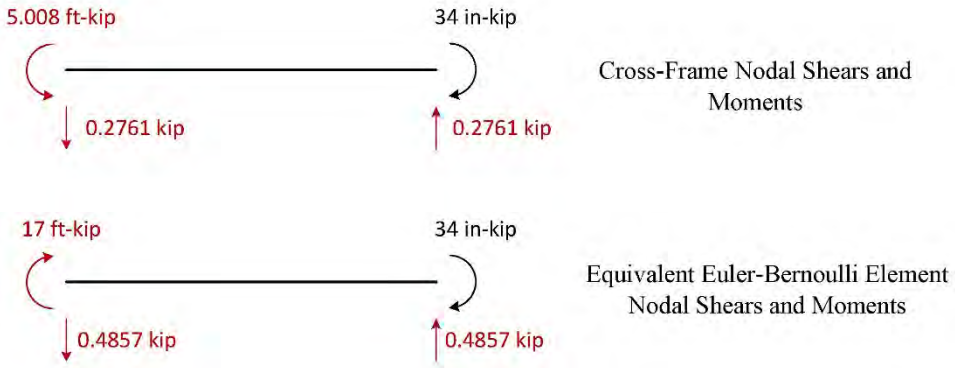

Figure 4.5.3.2.2.5.3-4 Comparison of Cross-Frame Nodal Shears and Moments and Equivalent Euler- Bernoulli Beam Shears and Moments (Flexure Stiffness Approach)

The Timoshenko beam element provides a closer approximation of the physical model cross-frame behavior compared to the Euler-Bernoulli beam element for all other types of cross-frames typically used in I-girder bridges as well, including X-type and inverted K-type cross-frames with top and bottom chords, as well as X-type and K-type cross-frames without top chords. However, the Timoshenko beam model is unable to provide an exact match for all cases (NCHRP, 2012).

Influence of End Connection Eccentricities

The axial rigidity, *EA*, of single-angle and flange-connected tee-section cross-frame members is reduced due to end connection eccentricities. Battistini, et al. (2013) performed a range of experimental and analytical studies of different X, K, and Z-type cross-frames composed of single-angle members. Their experimental studies indicated physical cross-frame stiffness values ranging from 0.55 to 0.75 of the

calculated stiffness values based on the analytical modeling of the cross-frames using truss elements.

These reduced stiffnesses were due to the bending eccentricities at the connections of the single-angle cross-frame members. The behavior of flange-connected tee sections is similar, again due to the effect of the significant end connection eccentricities. Solid plate diaphragms were not examined as part of this study and are not typically subject to significant end connection eccentricities.

As a result, *AASHTO LRFD* Article 4.6.3.3.4 now states that the influence of end connection eccentricities is to be considered in the calculation of the equivalent axial stiffness, $(AE)_{eq}$, of single-angle and flange-connected tee-section cross-frame members. *AASHTO LRFD* Article C4.6.3.3.4 recommends that in lieu of a more accurate analysis, $(AE)_{eq}$ of equal leg single angles, unequal leg single angles connected to the long leg, and flange-connected tee-section cross-frame members may be taken as $0.65AE$. More accurate values of $(AE)_{eq}$ may be computed from equations given in Battistini, et al. (2014). In many bridges, the response is relatively insensitive to the specific value selected for $(AE)_{eq}$.

Therefore, in the application of the Timoshenko beam approach for the calculation of the equivalent beam stiffness of truss-type cross-frames in 2D analysis models, the area of any single-angle or flange-connected tee-section members in the applicable separate cross-frame model(s) should be reduced by a factor of 0.65 (or a more accurate value if desired) for the analysis of the separate cross-frame model(s) used to determine I_{eq} and A_{seq}. The resulting A_{seq} for the equivalent beam should not be reduced further by this factor; the effect of the end connection eccentricities is already comprehended in the computation of both I_{eq} and A_{seq}. In 3D refined analysis models (Section 4.5.3.3), the area of such cross-frame members should be reduced directly by the 0.65 factor (or a more accurate value if desired).

Internal Cross-Frame Member Forces

The beam element in the 2D model represents the actual cross-frame in the model. Therefore, the loads calculated from the 2D analysis model for that beam element represent the loads on the actual truss cross-frame.

However, the form of the loads on the beam element is not directly applicable to the truss cross-frame; that is, the 2D model does not directly calculate the forces in the truss cross-frame top chord, bottom chord and diagonals. The forces calculated by the 2D model are the global forces acting on the entire cross-frame. Shears and bending moments are the primary force effects in the beam element representation of the cross-frame, as shown at the top of Figure 4.5.3.2.2.5.3-5. One more step must be taken to convert those global forces into the specific internal forces in the cross-frame members.

Another way to think of this is to consider the forces on the beam element as external forces acting on the overall cross-frame truss structure, as shown at the bottom of Figure 4.5.3.2.2.5.3-5. In order to design the individual truss cross-frame members and connections, the internal forces, or the forces in each specific internal member of the truss structure, are needed.

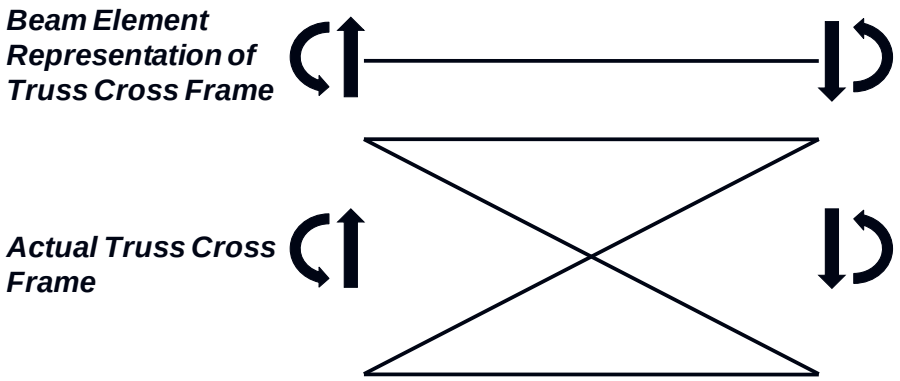

Figure 4.5.3.2.2.5.3-5 Global Forces Acting on the Beam Element Representation of the Truss-Type Cross-Frame and the Actual Truss-Type Cross-Frame

Most 2D models consider the self-weight of the structure, and therefore, consider the self-weight of the beam element modeling the cross-frame. For this reason, the shear at the left and right ends of the cross-frame element, as reported in the 2D analysis, may be slightly different. This effect is typically negligible. Design Engineers can simply use the higher of the two shear values.

The moments, M_1 and M_2, at each end of the beam element modeling the cross-frame, however, are usually significantly different, with the difference representing the fact that shear is being transferred across the length, S, of the cross-frame (Figure 4.5.3.2.2.5.3-6).

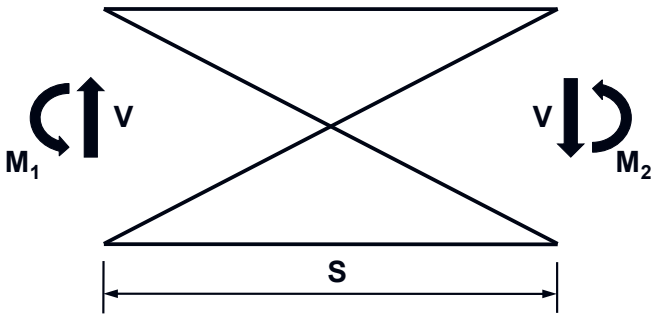

Figure 4.5.3.2.2.5.3-6 Global Shear and Moment on the Truss-Type Cross-Frame

By simple statics (i.e. the sum of the moments about any given point must equal zero), the difference in the moments can be verified. By statics, the moment at one end of the cross-frame must equal the product of the shear times the length of the cross-frame, minus the moment at the other end of the cross-frame. Thus:

$$M_2 = VS - M_1 \qquad \text{Equation 4.5.3.2.2.5.3-1}$$

Keep in mind that consistent sign conventions must be used to perform this calculation.

Depending on the type of cross-frame, different assumptions should be used to proportion the shear to each joint in the cross-frame.

For a K-type cross-frame, all of the shear should be assumed to act at the joint where the diagonal frames into the chord at each end of the cross-frame. The diagonal is the primary load path for the shear force. This can be demonstrated whether the connections in the cross-frame are considered pinned or not. By the principles of relative stiffness, all of the shear will act at the point where there is a very stiff shear load path; i.e., at the joint into which the diagonal frames.

For an X-type cross-frame (Figure 4.5.3.2.2.5.3-7), the shear can be assumed proportioned equally to the top and bottom joints at each end of the cross-frame since there is a diagonal framing into each one of those joints.

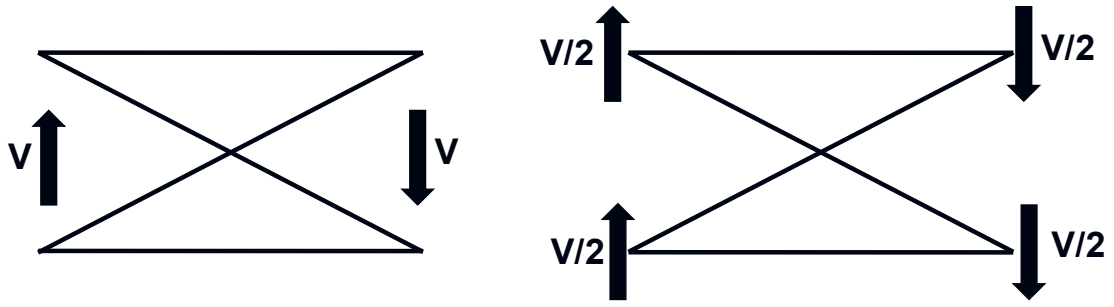

Figure 4.5.3.2.2.5.3-7 Assumed Distribution of Shear Forces for an X-Type Cross-Frame

Statics can be used to resolve the moment at each end of the cross-frame into a force couple at each end of the cross-frame by dividing the end moments by the vertical distance, *h*, between the top and bottom chords (Figure 4.5.3.2.2.5.3-8).

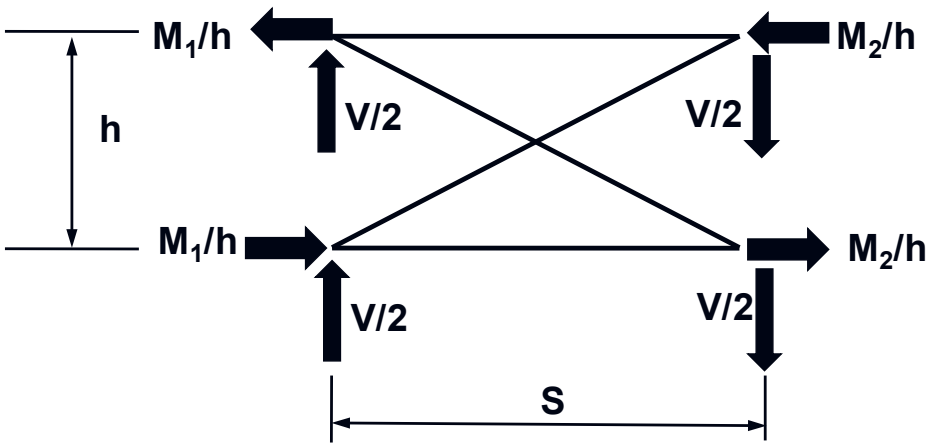

Figure 4.5.3.2.2.5.3-8 Resolution of the End Moments into Force Couples (X-Type Cross-Frame)

With the global external forces now resolved into specific external forces at the nodes of the truss, statics (i.e. the method of joints) can further be employed to calculate the specific internal forces in the truss, or the forces in the top chord, bottom chord and diagonals.

Live load moments and shears at each end of the cross-frame are typically not concurrent due to the various positions of the live load required to cause maximum effects in the individual grid elements. Because the live load forces are not concurrent, equilibrium of the cross-frame cannot be attained from the envelope actions typically reported at each end. Thus, for live load, by considering each end of the cross-frame separately and enforcing statics locally at the joints, the critical live load member forces can be deduced.

EXAMPLE

Given the truss-type cross-frame and the global force results in the beam element representing the cross-frame from the 2D analysis model (Figure 4.5.3.2.2.5.3-9), calculate the chord and diagonal forces in the cross-frame.

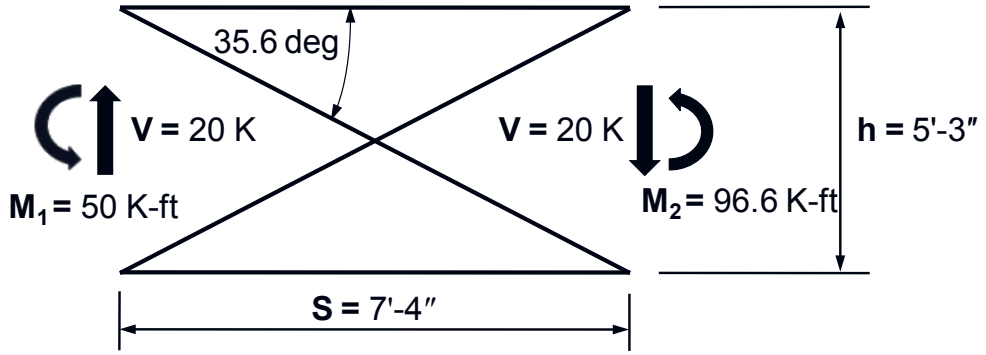

Figure 4.5.3.2.2.5.3-9 Global Forces on Example Cross-Frame from 2D Analysis Model

For the case of an X-type cross-frame, the shear is assumed divided equally between the top and bottom node at each end of the cross-frame, as shown in Figure 4.5.3.2.2.5.3-10.

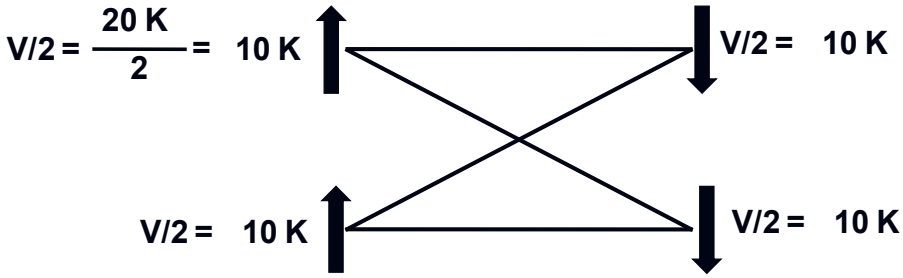

Figure 4.5.3.2.2.5.3-10 Assumed Distribution of Shears in the Example Cross-Frame

Statics can be used to resolve the moment at each end of the cross-frame into a force couple at each end of the cross-frame by dividing the end moments by the vertical distance, *h*, between the cross-frame chords (Figure 4.5.3.2.2.5.3-11).

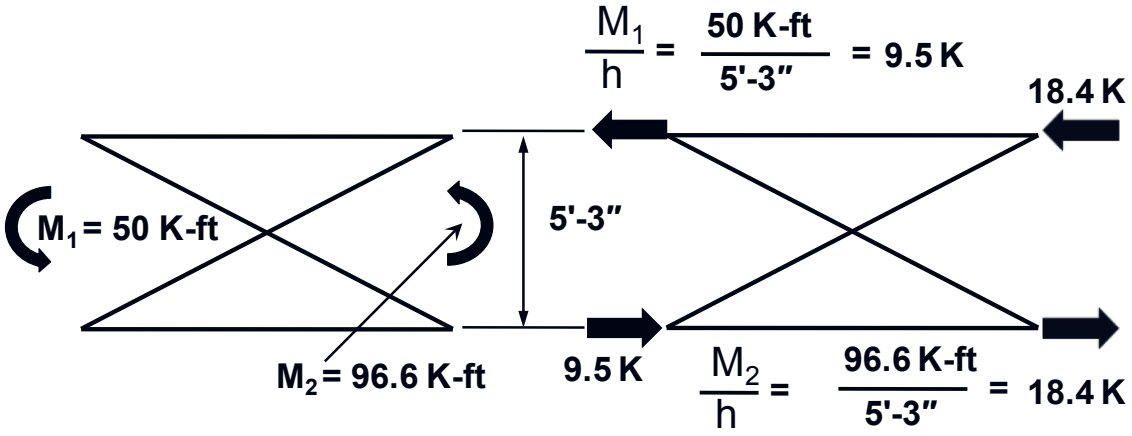

Figure 4.5.3.2.2.5.3-11 Resolution of End Moments into Force Couples for the Example Cross-Frame

With the global external forces now resolved into specific external forces at the nodes of the truss, statics (i.e. the method of joints) can be used to calculate the specific internal forces in the truss members. The resulting internal member forces are shown in Figure 4.5.3.2.2.5.3-12.

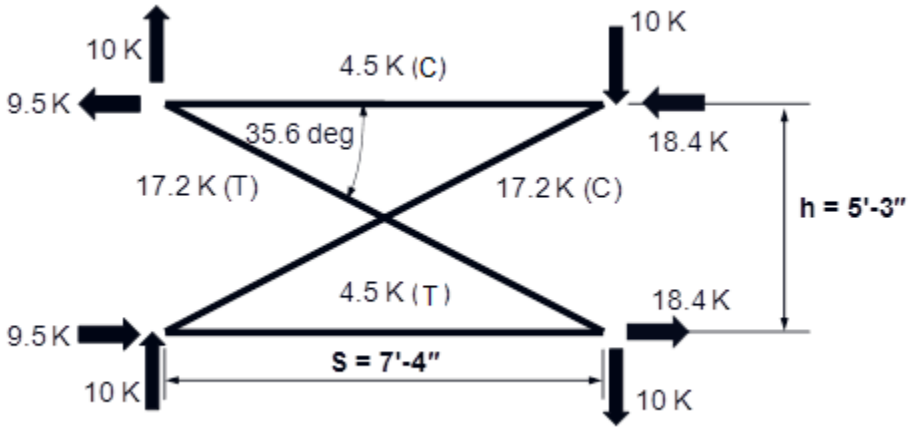

Figure 4.5.3.2.2.5.3-12 Example Cross-Frame Internal Member Forces Calculated Using the Method of Joints

4.5.3.2.3 Flange Lateral Bending Stresses

As discussed previously, the beam elements used to model the girders in 2D analysis models typically do not include a warping stiffness parameter. The elements are also straight elements, chorded between nodes in the model. Thus, flange lateral bending moments and stresses due to curvature and skew effects cannot be obtained directly from 2D analysis models.

In both traditional grid and Plate and Eccentric Beam 2D analysis models, the flange lateral bending moment due to curvature resulting from warping torsion, M_{lat}, at a cross-frame/diaphragm may instead be approximated using the V-load formulation (Richardson, Gordon, and Associates, 1963) given as:

$$M_{lat} = \frac{M\ell^2}{NRd}$$ Equation 4.5.3.2.3-1

AASHTO LRFD Equation C4.6.1.2.4b-1

where:

M = major-axis bending moment at the cross-frame/diaphragm (kip-ft)
ℓ = unbraced length (ft)
R = girder radius (ft)
D = web depth (ft)
N = a constant taken as 10 or 12 in past practice

Flange lateral bending stresses at the cross-frame due to curvature can then be computed by dividing the flange lateral bending moment from Equation 4.5.3.2.3-1 by the lateral section modulus of the flange under consideration. A similar approximate closed-form expression is not available for estimating the flange lateral bending moments and stresses due to skew effects. Approximate values of the flange lateral bending stresses due to skew effects, in the absence of results from a refined analysis, are suggested in *AASHTO LRFD* Article C6.10.1.

Section 3.2.4 of NCHRP (2012) presents one suggested improved method of rationally estimating I-girder flange lateral bending moments and stresses in straight-skewed I-girder bridges and curved I-girder bridges with or without skew resulting from a grid or Plate and Eccentric Beam analysis. The method utilizes statically equivalent lateral loads transferred at the flange level from the cross-frames using the cross-frame forces determined from the analysis results. The reader is referred to NCHRP (2012) for further details on this improved approach.

4.5.3.2.4 Advantages, Disadvantages and Limitations

The primary advantage of 2D refined methods of analysis is that they are generally less expensive than 3D refined analysis.

Disadvantages of 2D refined methods of analysis include, but are not limited to, the following:

- Warping stiffness for direct modeling of flange lateral bending is typically not included;

- Girders and cross-frames/diaphragms are modeled as single beam elements with no depth;
- Cross-frame/diaphragm actions cannot be obtained directly;
- Horizontal reactions are sometimes not available and/or may not be oriented properly (e.g., for thermal analyses);
- The horizontal shear stiffness of the deck is not properly represented in traditional 2D grid models;
- Questionable accuracy of wind load analysis results, particularly when lateral bracing is present;
- Assumptions usually must be made to distribute dead and live loads to the individual girders in traditional 2D grid models, and;
- Twist and layover of girders during construction cannot be reported directly.

There are exceptions to the above shortcomings that are addressed to a degree through the use of Plate and Eccentric Beam models (Section 4.5.3.2.2.3), and the improvements discussed in Section 4.5.3.2.2.5.

There are currently no specific limitations related to the application of 2D refined analysis methods. However, diligence should probably be exercised in situations involving the following:

- Significant curvature and/or skew;
- Longer spans involving the use of deeper girders;
- Irregular span arrangements and/or where uplift might be a concern;
- Variable depth girders;
- The use of lateral bracing;
- Complex framing (i.e., bifurcations or splayed girders, discontinuous girders or staggered cross-frames), and;
- The use of integral abutments, integral piers or straddle bents.

4.5.3.3 3D Methods of Analysis

4.5.3.3.1 General

A three-dimensional (3D) analysis is one in which the resultant quantities (moments, shears, axial loads, deflections, etc.) are a function of all three spatial dimensions. Often, a 3D analysis uses a model in which all the major components of the superstructure are mathematically modeled. The superstructure is modeled, including the structural depth and including explicit modeling of the girder flanges and webs, the cross-frames or diaphragms, and the deck.

Typically, girder flanges are modeled with beam elements, girder webs are modeled with shell elements, cross-frame members are explicitly modeled with truss

elements, and the deck is modeled with shell or solid elements. Live load influence surface analyses (Section 4.4.3.2) are typically employed to find the maximum and minimum live load force effects in the various bridge components. Although not clearly defined, spine models for curved bridges are often considered to be 3D analysis models.

In the linear elastic finite-element method, which is based on strength-of-materials and statics, a mathematical model of the bridge is arranged in a matrix formulation that is amenable to solution by a digital computer. The structure is divided into a finite set of so-called elements. Second, the spring stiffness of the individual elements is computed. For each direction that each element is capable of resisting translation or rotation, a stiffness resisting each motion must be computed. Assembly of these stiffnesses in matrix form is called the element stiffness. Other properties, including the element's mass and material properties, are also included. The element stiffness matrices are defined by the local axes of the element.

The topology of the model defines the orientation and connection of the elements forming the model. The assembled model is defined in a set of so-called global axes. The element connecting points are referred to as nodes. Models of bridge and most other structures require a foundation. The points of foundation are called boundaries that support the model, as do the bearings of a bridge.

The final step in setting up the problem is to resolve the stiffnesses, using transformations, to get the stiffnesses oriented in the global axes at each node. This information is assembled into the global matrix of the structure. There are potentially three translations and three rotations at each node. Each direction of movement is called a degree of freedom (DoF). The DoFs are directions of movement associated with axial, flexural, torsional and shear deformations (the torsional warping degree of freedom, which is typically not available in most finite element software packages, is ignored). All of the DoFs at each node have unknown displacements that must match with all deformations of the neighboring elements connected at that node. In actual solver packages, the node equations are shuffled to minimize the number of active terms, or terms in any equation. Fortunately, the software develops the information in an optimum matrix, and solves the matrix with little assistance from the Design Engineer.

This section reviews some of the basics of 3D finite element modeling of bridge superstructures, including node layout, elements and the application of loads to 3D analysis models. Also discussed are the advantages, disadvantages, and limitations of 3D analysis models. Further information on 3D methods of analysis may be found in NHI (2011).

4.5.3.3.2 3D Finite Element Modeling

4.5.3.3.2.1 General

3D finite element modeling permits the most realistic representation of the structure with few simplifying assumptions. The refinement of the mesh or the elements determines the accuracy of the results. This discussion is limited to 3D models that represent the gross structure. It does not discuss buckling of members or the eccentricity of cross-frame members, etc. although the method is capable of addressing these items. Instead, it addresses modeling the structure to obtain reasonably correct results at the macro level that can be solved by employing a mathematically rigorous solution algorithm. This provides a tool that enables a knowledgeable Design Engineer to analyze bridge designs so he/she can confidently prepare designs that are unique, efficient, durable and economical.

This discussion will examine the typical components of a finite element model of a girder-bridge superstructure, and discuss the types of structural elements most commonly used for 3D modeling of those components. Construction of a reasonable 3D finite element model of the bridge superstructure from these elements to provide the desired results on a macro level will also be discussed. Discretization of the model and issues related to node layout will be included as part of this discussion. Also to be discussed are the boundary conditions and loads applied to the analysis model. Proper boundary conditions and proper releases of degrees of freedom are absolutely necessary to obtain correct results. These issues are beyond the scope of this discussion, but should be well understood by any user of finite element modeling techniques.

4.5.3.3.2.2 Node Layout

Generally, nodal locations are specified in the global coordinate system, while element properties are local in nature. Cartesian coordinates are typically used to define global coordinates, although other systems such as cylindrical may be used to simplify the model. Local axes are local with respect to each element and are used to define the individual elements. The local axes are used to specify the sequence of element node numbering, which in turn is used to define the output such as moments, shears, axial force and stresses. For example, a beam element is a straight element between two nodes, but typically requires a third node to define the orientation of its local axes.

The Design Engineer should keep in mind the objective of the analyses to be performed when determining the degree of discretization required in the model. Laying out the nodes is important because as long as the framing does not change, member properties can be changed and new analyses made rather efficiently. A

relatively coarse mesh is generally satisfactory for determining girder moments and stresses, shears, reactions and cross-frame/diaphragm actions at the macro level. The stress state around a diaphragm access hole might require a more refined mesh than would a beam containing no large holes, or a beam in which stress concentrations around bolt holes or weld discontinuities are of no interest. Such issues may be important, but are beyond the scope of this discussion.

Discretization, or determining the number of elements, is somewhat subjective and requires some level of experience and judgment, but there are some basic concepts that are important to keep in mind. For example, looking at the moment diagram of a continuous beam gives some clues as to how to discretize its elements. In order to obtain a reasonable continuum of moment, shear, etc. along the span, the beam needs to be discretized such that the curvature of the beam is properly represented. Typically, a beam element has the characteristic of being isoparametric, meaning that the element can represent only one curvature. The element is loaded only at its ends. Concentrated loads or moments may be applied. However, the element can only recognize a singular curvature. If the applied loads require that the element have two curvatures to represent the behavior, an error is introduced. If the element is discretized into two elements, each with a single curvature, the two curvatures can be represented and the solution will be more correct. It is the modeler's responsibility to understand these limitations and to compensate for them in laying out the model. The more interrupted the continuum, the greater the number of elements required to properly represent the behavior. A minimum of nine (9) nodes per girder span is typically preferred.

The first step in creating a 3D finite element model of a girder-bridge superstructure is to describe the node layout for the bridge. Each finite-element package has its own preprocessor that assists in the layout. This discussion does not address the specifics of these operations, but only addresses the issues that the Design Engineer should consider in determining the proper nodal grid.

The model must have nodes that match the layout, or alignment, of the deck and the girders. There are four types of horizontal alignments commonly found on bridges:

- Straight (Figure 4.5.3.3.2.2-1 Part A)
- Constant radius curved upward or curved downward (Figure 4.5.3.3.2.2-1 Part B)
- Spiral from straight to curved (Figure 4.5.3.3.2.2-1 Part C)
- Spiral from curved to straight.

A node is required at each change in alignment.

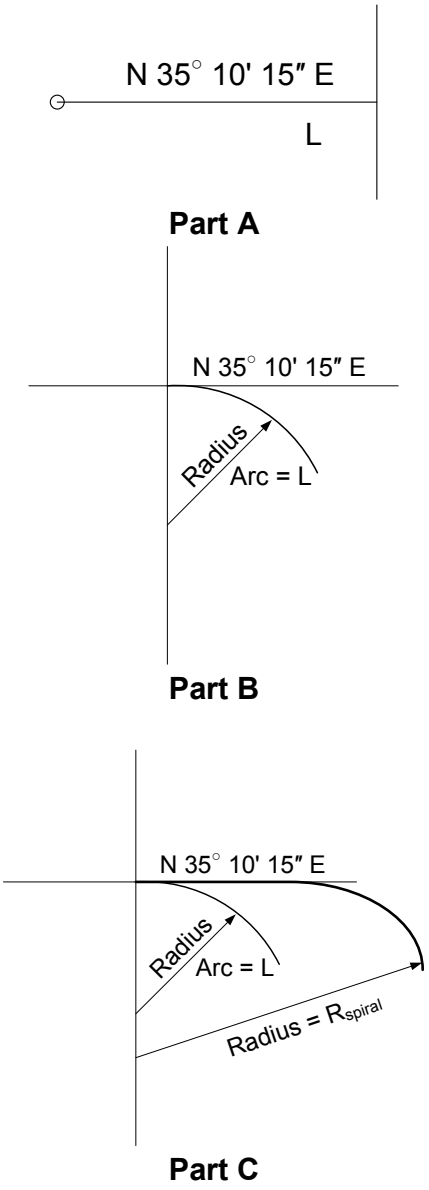

Figure 4.5.3.3.2.2-1 Horizontal Node Layout for Different Alignments
A) Straight; B) Curved with Constant Radius; C) Spiral from Straight to Curved

Starting with the horizontal roadway alignment is usually the ideal way to commence the layout of the node geometry. The length and shape of each alignment segment must be specified, and its location in space defined. This is often done with the control line, or baseline. A straight segment has only one parameter (length) in addition to its bearing and point of initiation. A constant curve segment has an additional parameter; radius. A means of specifying whether the radius curves right or left is also required. A spiral is defined as a line commencing with a straight

alignment that increases in curvature linearly over its length to a specified radius at its end.

Nodes must be also specified at each bearing and cross-frame location. Additional nodes may also be required to accommodate discontinuous girders. Nodes at field-section locations are needed if an erection study is to be undertaken. There are other reasons for placement of nodes that will be examined subsequently.

With skewed supports, it often becomes necessary to compute offset lengths at the supports in order to locate the support nodes along the skew. These lengths are used to determine the proper lengths along the baseline adjacent to the supports that are necessary to project radially from the baseline the correct coordinates for the girder support nodes. Figure 4.5.3.3.2.2-2 illustrates one possible approach to compute these offset lengths at skewed supports on horizontally curved bridges. Alternatively, node locations may be created from software, such as COGO, that may have been used to layout the bridge for drawing.

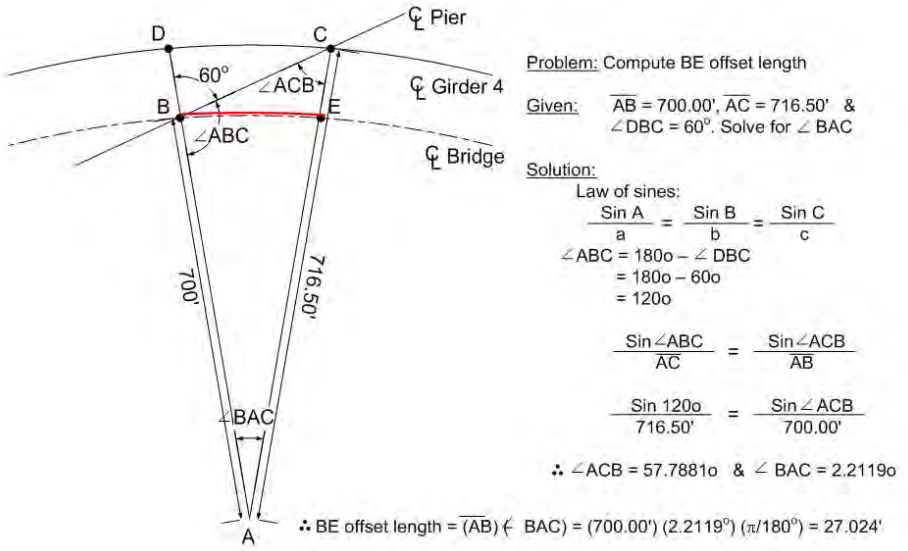

Figure 4.5.3.3.2.2-2 Calculation of Offset Length for Skewed Support Nodes

Accurate stresses at solid and shell element nodes are difficult to obtain, and are generally not used. Stresses at mid-element length are used instead. This is an important concept to understand when dealing with a 3D model. The bending moment can be reported directly at a node from the analysis in a traditional grid model or a line model, but this is not true in a 3D model. For example, the cross-section is composed of flange, web and deck elements. A collection of the stresses must be made and the moment calculated from the stresses. However, stresses are determined at mid-element length so the moment is computable only at mid-length of

the element; not at a node. Moments at the nodes must be determined by fitting the moment data computed at mid-length of the element. The curvature of the moment curve at interior supports is increasing as the moment approaches the support. Shorter elements near the support provide a better estimate of the maximum moment at the support.

Nodes are required at flange and web size changes in grid analyses if moments are to be used to check sizes. This is not necessary with a 3D analysis since curve fitting is required to get the moment at a node, unless the software can only check stresses at nodes. Flange plate changes located within a few feet of a node do not introduce significant error in the analyses, unless there are too few elements in a span to properly curve fit.

Flange lateral moments are computed at nodes if flanges are modeled using beam elements. In the case of a curved flange, a single straight beam element between cross-frames gives negligible lateral moments because equilibrium at the nodes is established by the restoring forces in the cross-frame members attached at the flange nodes and the lateral moment effect of curvature is negated. Part A of Figure 4.5.3.3.2.2-3 shows a single flange element between cross-frame nodes. Lateral bending is caused by the non-collinearity of the axial force in the flange. Hence, at least one additional girder node is required along the arc between cross-frames in curved flanges to activate the non-collinearity effect and generate the flange lateral moments. Figure 4.5.3.3.2.2-3 Part B shows the two-element flange arrangement needed to create lateral bending.

Two nodes along the arc between cross-frame nodes have been found to give slightly larger, more realistic lateral flange moments. The lateral moments at interior nodes tend to have the opposite sign of those at the cross-frames.

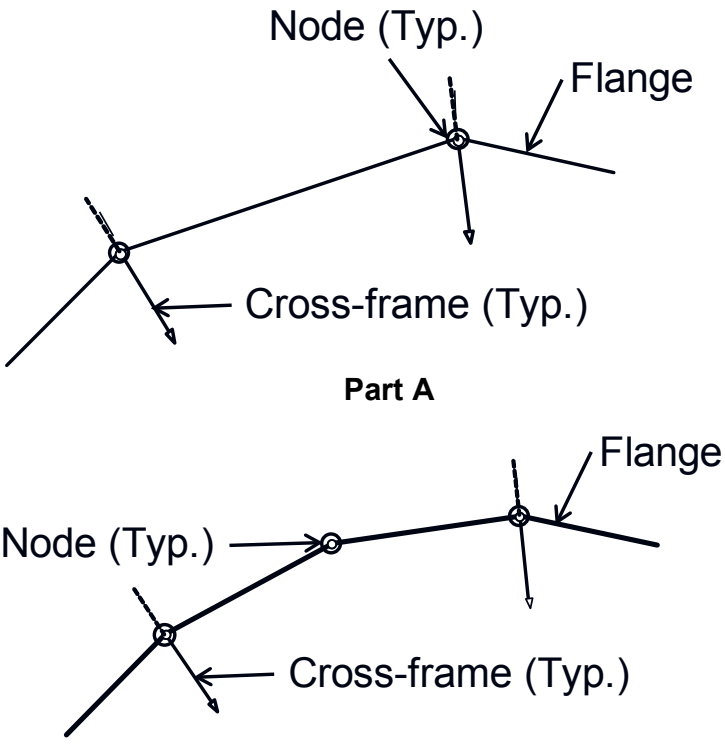

Figure 4.5.3.3.2.2-3 Cross-Frame Nodes

A) Node at End of Straight Beam Element; B) Additional Node between Cross-Frames Necessary to Create Lateral Bending

Additional layers of nodes are required for a 3D model. Other layers of nodes can be built off the basic nodes defining the girders (Figure 4.5.3.3.2.2-4). The deck may be defined with a single layer of nodes if shell elements are used for the deck. Alternatively, two layers of nodes are required if solid elements are used to model the deck. Vaulted (i.e. variable thickness) decks may be properly modeled by varying the elevation of the bottom layer of deck nodes if solid elements are used. The original girder layout nodes may be used to represent the tops of the girders. A fourth layer of nodes is defined under that layer to represent the bottoms of the girders.

A variable depth girder can be correctly modeled by varying the vertical location of the bottom layer. Superelevation or grade may be modeled by applying a transformation to the model nodes.

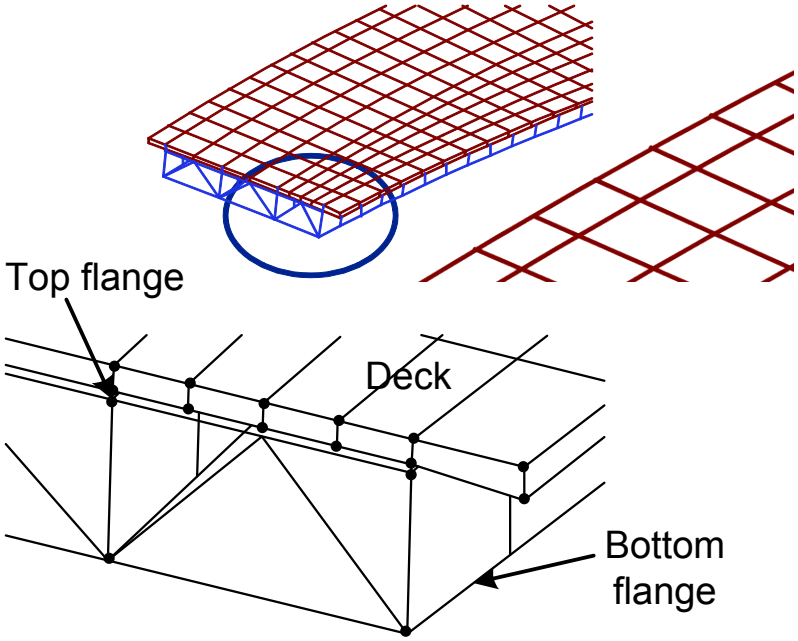

Figure 4.5.3.3.2.2-4 Node Layers

4.5.3.3.2.3 Elements

4.5.3.3.2.3.1 Beam Elements

The beam element (Figure 4.5.3.3.2.3.1-1) typically has six DoFs at each node: bending about two of the local axes; torsion about its third (longitudinal) axis; shears in two planes; and axial force along its longitudinal axis. The typical beam element does not accommodate warping (commonly referred to as the seventh DoF). However, the warping DoF is not needed in a 3D model to model a girder since the girder is typically modeled with a web (shell element) and individual flanges (beam elements). A third node is assigned to orient the two local axes.

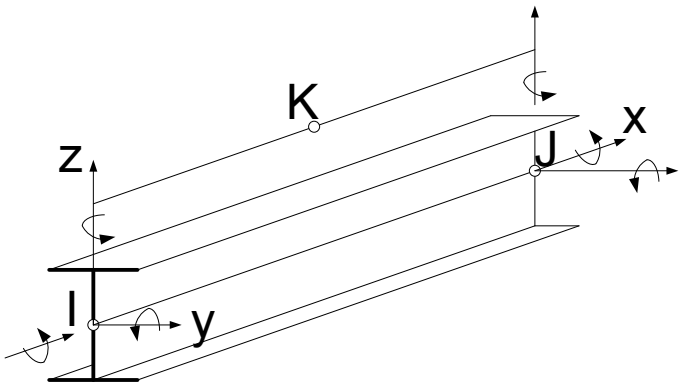

Figure 4.5.3.3.2.3.1-1 Beam Element

The properties required for a beam element are: cross-sectional area, bending stiffness about two local axes, torsional stiffness, and two shear areas. The mass or weight of the element is specified and temperatures can be input at each node. Lateral pressures can be applied to a beam element. If a load or pressure is applied to a beam element, the element properties are used to transform loads or pressures to end moments and forces applied at its two nodes.

Typically, a beam element recognizes only single curvature bending. As discussed previously (Section 4.5.3.3.2.2), this type of element is referred to as an isoparametric element. If a beam in the true structure is anticipated to undergo reverse bending (reverse curvature), more than one isoparametric beam element is required to properly recognize its behavior. Of course, there are more elaborate types of beam elements available with more capability.

Girder flanges are typically modeled with beam elements attached to the top and bottom of the web elements (Figure 4.5.3.3.2.3.1-2). Deck elements may be connected to the girders with beam elements acting as rigid links to model the shear connectors. These members also define the location of the deck with respect to the girders (Figure 4.5.3.3.2.3.1-2). The element length represents the deck haunch. These elements should be modeled to ensure that the deck does not rotate independently at the nodes in order to ensure that plane sections remain plane. Thus, an additional beam element spanning the nodes defining the top and bottom of the deck elements over each girder (assuming solid elements are used) is usually required.

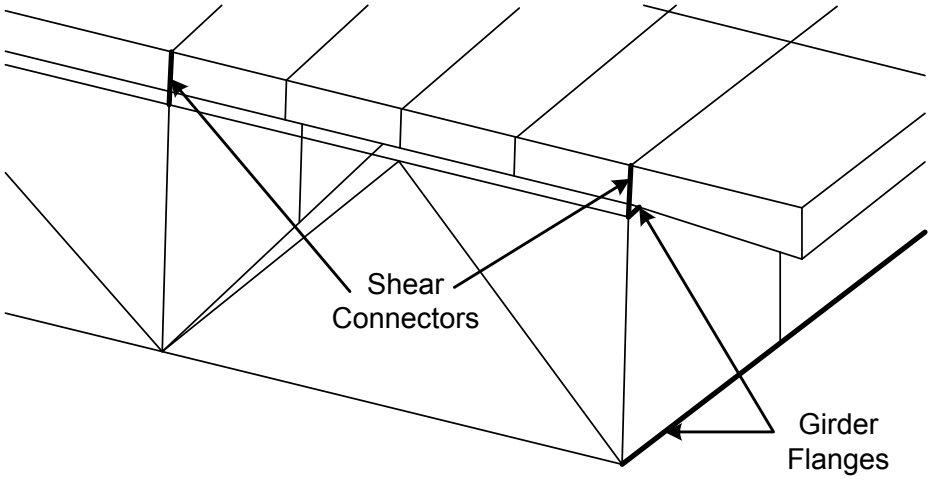

Figure 4.5.3.3.2.3.1-2 Beam Elements Used to Model Girder Flanges & Shear Connectors

4.5.3.3.2.3.2 Shell Elements

A shell element, typically used to model a girder web, has four nodes (quadrilateral element) with six DoFs at each node -- the three translations and three bending DoFs about the local x, y, and z axes -- for a total of 24 DoFs per element. A shell element is shown in Figure 4.5.3.3.2.3.2-1. All six DoFs at each node must be accounted for in the analysis. For example, if only a truss element is connected at a shell element, the three DoFs associated with bending of the shell element at that node cannot be resisted by the truss element and are accounted for by specifying that they are released (or free). If the truss element is oriented such that it cannot resist all three translations, a further modification of DoFs is required. Thicknesses and temperatures may be assigned to each node of a shell element. Pressures may also be applied to the element. The aspect ratio of the element preferably should not exceed about 5.0.

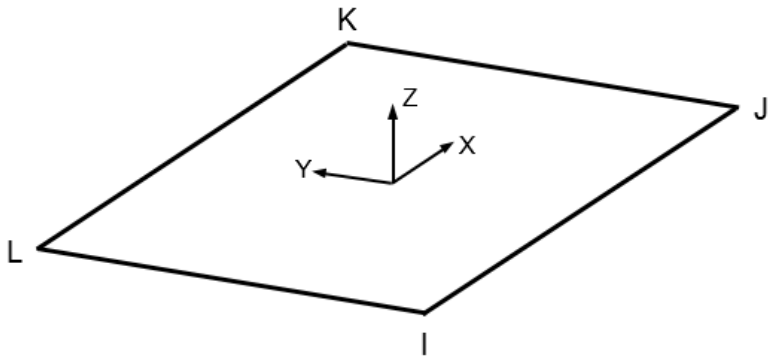

Figure 4.5.3.3.2.3.2-1 Shell Element

The nodes of a shell element are typically identified in the counterclockwise direction. The local z-axis is normal to the plane of the element. The reason for a specific pattern is so the output stresses can be identified.

Figure 4.5.3.3.2.3.2-2 shows a girder web modeled with a shell element.

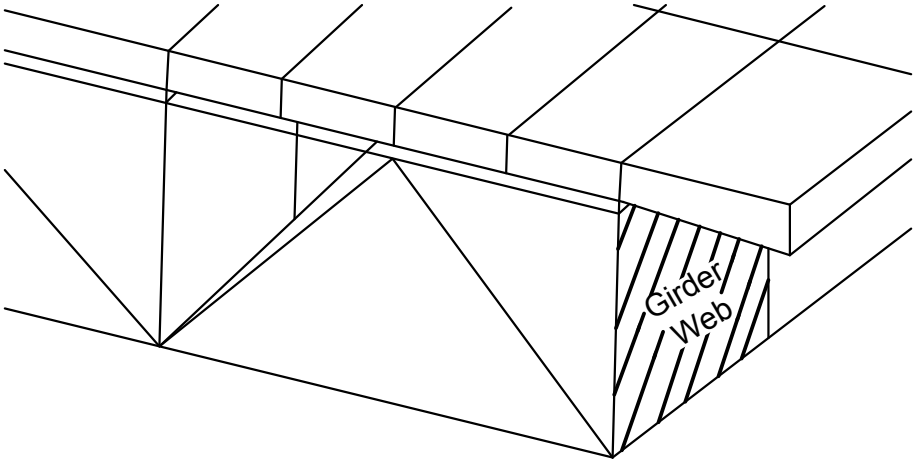

Figure 4.5.3.3.2.3.2-2 Shell Element Used to Model a Girder Web

4.5.3.3.2.3.3 Solid Elements

Eight-node 3D solid elements are the simplest of all solid elements. This element typically has three translation DoFs at each of the 8 nodes for a total of 24 DoFs. Eight-node solid elements can be collapsed to form triangular solid elements having six nodes. In Figure 4.5.3.3.2.3.3-1, the face defined by nodes I, J, K and L in clockwise fashion can be any face. The other face is defined by nodes M, N, O and P, but node M must be behind node I. The order defines the local coordinate system. The thickness of solid elements is not input explicitly, but is instead implicitly defined through the specification of the proper nodal coordinates. Thus, no geometric properties are required; only a material identification is required for these elements. Again, the aspect ratio of the element preferably should not exceed about 5.0.

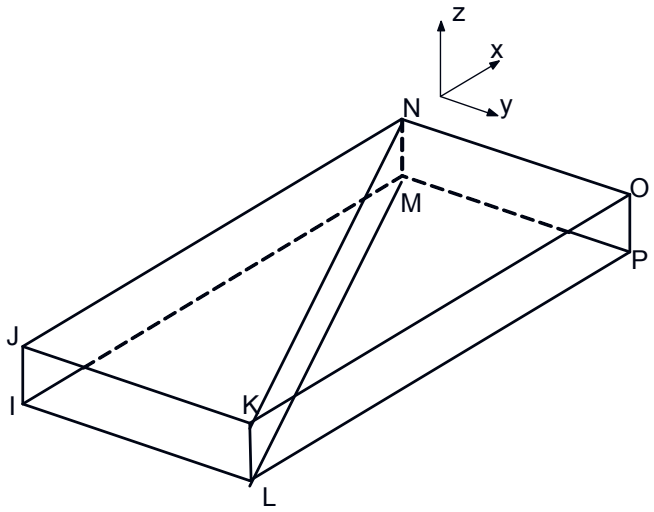

Figure 4.5.3.3.2.3.3-1 Solid Element

If a beam element is attached to a solid element and to no other element that takes bending, the two bending and one torsional DoF in the beam element at the connecting node must be specified “free” since the solid element has no ability to react to the bending DoFs of the beam element.

Figure 4.5.3.3.2.3.3-2 shows a portion of a composite deck modeled with 8-node solid elements.

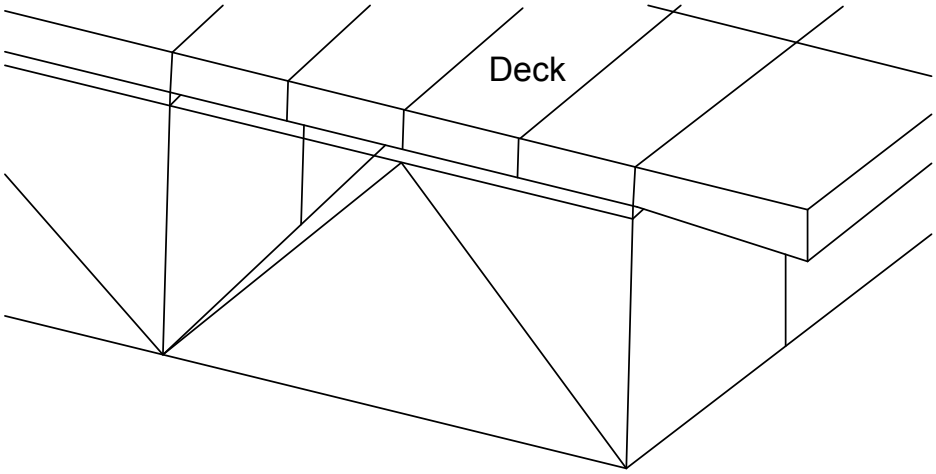

Figure 4.5.3.3.2.3.3-2 Solid Elements Used to Model the Concrete Deck

4.5.3.3.2.3.4 Truss Elements

The simplest finite element is the truss element shown in Figure 4.5.3.3.2.3.4-1. This straight two-node element resists only axial force. The element length is defined by the coordinates of the nodes at its ends. The element is assigned a cross-sectional area, and material properties; Young’s modulus, density and thermal coefficient of expansion. The truss element reacts to force by changes in its length. The length of the element changes according to force and its stiffness, or an amount equal to *PL*/*AE*. Hence, the truss element has one degree of freedom (DoF). Temperatures can be input at each node of a truss element.

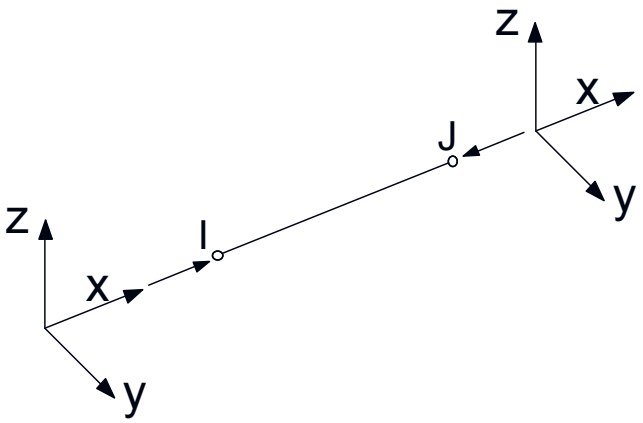

Figure 4.5.3.3.2.3.4-1 Truss Element

Cross-frames are typically modeled with truss elements connected to the top and bottom of the web (Figure 4.5.3.3.2.3.4-2). Lateral bracing members may also be modeled with truss elements. Lateral bracing can also be approximately modeled with an equivalent shell element.

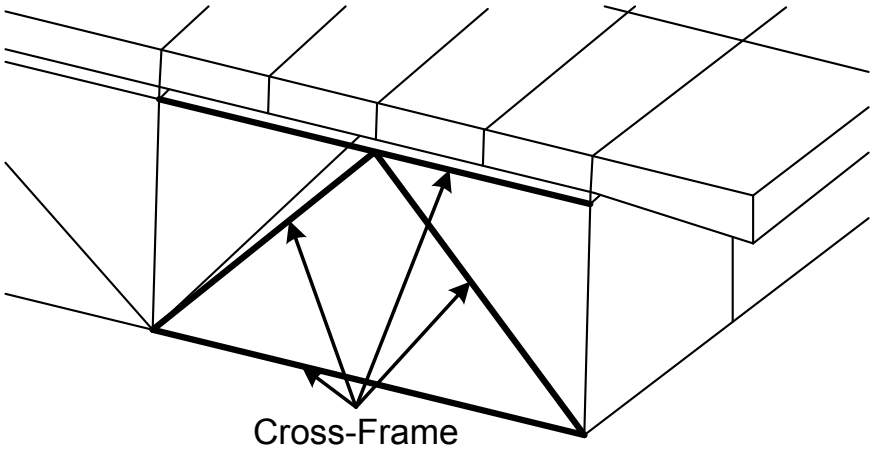

Figure 4.5.3.3.2.3.4-2 Truss Elements Used to Model a Cross-Frame

4.5.3.3.2.3.5 Foundation Elements

Bridges supported on rigid bearings can be modeled by specifying that the node at the support point be restrained against selected translations and free to rotate (the support would usually be free to rotate). More typically, bearings are modeled with so-called “foundation elements”. These dimensionless elements provide for six stiffnesses; three translations and three rotations. The local axes of these elements must be carefully specified.

A foundation element is shown in Figure 4.5.3.3.2.3.5-1. The “I” node identifies the element location of action, the “L” node identifies the local y-axis, the “J” node identifies the orientation of the element along the local z-axis, and the “K” node identifies the orientation of the element along the local x-axis. Typically, the z-axis of the foundation element would be the global vertical axis. The x-axis may, for example, be oriented along the girder with the y-axis orthogonal to the girder line. If the bearing is guided, the x-axis of the foundation element may be assigned zero stiffness. The stiffness of the bearing resisting lateral movement would be input as the stiffness along the y-axis. Pier stiffnesses may be included in these stiffnesses if the pier is not modeled. If the substructure is explicitly modeled, the foundation element would rest on the pier, and would allow the pier stiffness to act on it as well as the superstructure.

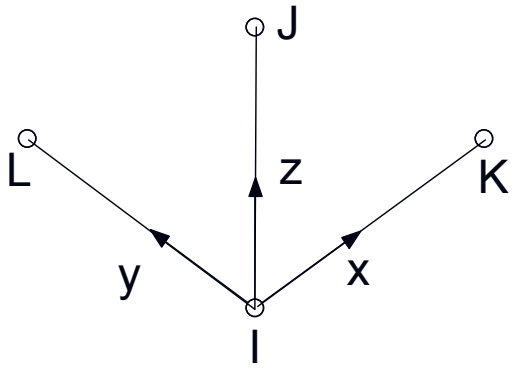

Figure 4.5.3.3.2.3.5-1 Foundation Element

4.5.3.3.2.3.6 Element Connectivity

The depth of each girder is typically identified by the nodes defining the web elements. A girder can be adequately modeled with one or more shell elements representing the depth of the web. The web thickness is input as the thickness of the shell element(s).

The stiffness of very shallow girders may be underestimated if the flange beam elements are common with the top and bottom nodes of the web elements placed at the elevation of the web itself. In girders less than roughly 50 inches deep, it may be desirable to overstate the web depth in order the define the distances between the centers of gravity of the flanges properly (Figure 4.5.3.3.2.3.6-1). In the figure, *D* is the assigned web depth.

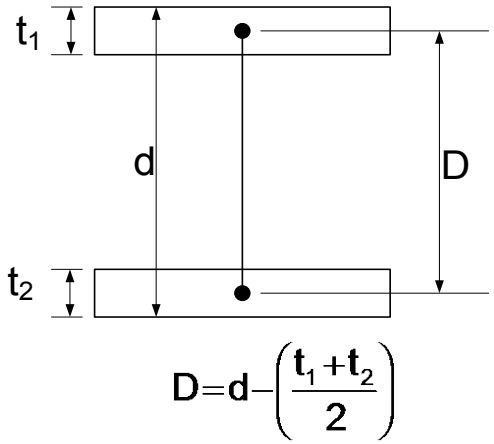

Figure 4.5.3.3.2.3.6-1 Overstating of the Web Depth in Shallow Girders

The deck elements are discretized to account for shear lag due to horizontal shear; thus, the deck should be separated into at least two or more isoparametric elements in-between girder lines.

Deck elements must be connected to the girders as discussed in Section 4.5.3.3.2.3.1.

Cross-frames are usually used to connect adjacent girders. Since the depth of the webs has been properly represented, the cross-frames can be reasonably represented by attaching them to the top and bottom web nodes. Individual members of the cross-frames may be modeled with either truss or beam elements.

Alternatively, the girders may be connected with diaphragms, which transfer load through bending and shear. Diaphragms may be modeled similar to the girder with a series of shell elements for the web and beam elements for the flanges (Figure 4.5.3.3.2.3.6-2). It is important to remember that the diaphragm needs to be divided into enough elements (at least three) along its length to properly represent its deflected shape; often moments in diaphragms reverse sign.

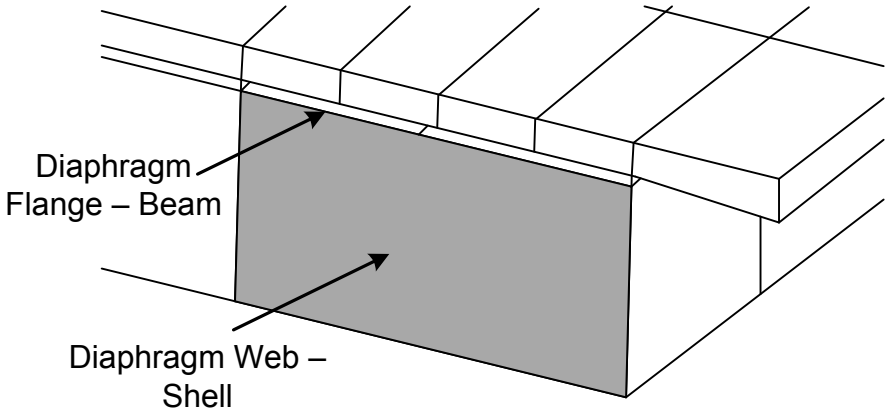

Figure 4.5.3.3.2.3.6-2 Shell Elements Used to Model Diaphragm Webs and Beam Elements Used to Model Diaphragm Flanges

4.5.3.3.2.4 Boundary Conditions

Bearings can be represented in the 3D model as described in Section 4.5.3.3.2.3.5. A bearing with lateral restraint(s) can introduce longitudinal force into the girder and attached diaphragm or cross-frame. Such restraints introduce bending and shear into the girder as well as axial force into the cross-frames. Clearly, it is important that the proper orientation and stiffness of the bearings be modeled.

Recognizing the proper bearing arrangement is particularly important for skewed bridges. Skewed supports can lead to large horizontal forces in the bearings due to gravity as well as thermal loads. These forces can be computed reliably with 3D models. Modeling of a fixed bearing on a pier must recognize the stiffness of the pier.

There is an interaction between restrained bearings on a pier. It is possible the bearings on opposite sides of a skewed pier will have longitudinal thermal forces in opposite directions when the bearings are fixed. In such cases, the longitudinal stiffness of a bearing in the model would be related to the torsional as well as the flexural stiffness of the pier.

Girders may be supported with several types of integral piers. The girders may penetrate an integral pier cap (Figure 4.5.3.3.2.4-1 Part A), or an articulated pier cap on a pier column. Another type of support is the straddle beam which has two or more supports, with the girders integral with the straddle beam or resting on top of it. The straddle beam may be either simply supported, or if the beam is concrete, it may be integral with the columns forming a bent (Figure 4.5.3.3.2.4-1 Part B). However, it is nearly impossible to properly model these arrangements with bearing stiffnesses alone since there is an interaction between the girder reactions. Stiffnesses of a

single bearing cannot properly represent the interactive behavior of the bearings of a multi-girder bridge on a flexible support. The proper way to model these conditions is to explicitly model the straddle beam or entire pier. Modeling the combined girder superstructure and the substructure is beyond the scope of this discussion, but is an important consideration for this type of bridge.

Part A

Part B

Figure 4.5.3.3.2.4-1 Alternative Supports

A) Concrete Straddle Beam; B) Integral Concrete Pier Cap

4.5.3.3.2.5 Loads

4.5.3.3.2.5.1 Dead Loads

Self-Weight

Self-weight is easily modeled using body weight of the modeled members. Thus, the self-weight includes the cross-frames as well as the girders. The weight of detail items such as stiffeners and splices is not included, unless specifically included in the model. It can be easily accounted for by changing the material density.

Concrete Deck Weight

Weight of the wet concrete of the deck may be applied to the model with concentrated loads at the nodes representing the tops of the girders. The concrete is usually assumed to have no stiffness. Alternatively, deck weight may be specified as a uniform load, but that will be converted to a series of concentrated loads applied at the nodes and perhaps with some nominal end moments. The deck may be modeled using the self-weight of the deck, but that has the disadvantage of dealing with some assigned stiffness. It would be incorrect to use the concrete stiffness, which would distribute the weight differently than if it were wet with no stiffness.

The concentrated load applied to each girder top node is determined by the tributary area of deck associated with the distance between girder nodes and the girder spacings. Where concentrated loads are used to apply the deck weight, the discretization of the model must be sufficient to ensure that the series of concentrated loads applied to the girder nodes will be refined enough to represent the uniform load, as discussed further in Section 4.3.2.

The weight of deck forms needs to be considered if the forms are to be permanent. This weight can be applied directly to the girders as concentrated loads as done for the deck. Alternatively, this can be accomplished by specifying an increase in the non-structural deck thickness to be used to compute the deck loads applied to the top girder nodes. Recall that these forms exist only between flange edges in the interior bays.

If temporary forms are planned and it is desired to consider their weight in the analysis, their weight can be introduced in a similar manner as for the permanent type. However, in this case, it may be necessary to apply a reverse load to the composite section to represent removal of the forms. This consideration is usually not made except in extreme cases.

Deck overhang bracket loads may be addressed more rigorously by the addition of overhang brackets to the 3D model. These additional members receive the weight of the overhang forms, a portion of the deck overhang weight, the weight of the screed rail, the weight of any walkway and railings, and perhaps the weight of the deck-finishing machine. These loads subject the outside girders to a vertical load and a lateral couple or torque. The cross-frames also act with these loads. The 3D model is able to not only provide the resulting actions in the girder and cross-frames, but is also able to provide vertical and lateral deflections. It is not required to model each overhang bracket; some judgment is required to ensure that adequate nodes are provided to allow for a reasonable number of brackets between cross-frames.

Figure 4.5.3.3.2.5.1-1 shows overhang brackets added to a model of a simple span with skewed supports and staggered cross-frames. This extra investigation was undertaken because the Contractor's Engineer was concerned about the effect of the rather large overhang, over four feet, on the fascia girders. The first analysis included a portion of the overhang concrete, the walkway and railing and screed rail. The effect of the finishing machine was also investigated. Small additional diaphragms were added in the exterior bays when the Contractor's Engineer decided that the fascia girders would rotate excessively, and that the lateral flange bending caused by the overhang bracket loads would cause excessive lateral flange bending stresses unless the additional diaphragms were used.

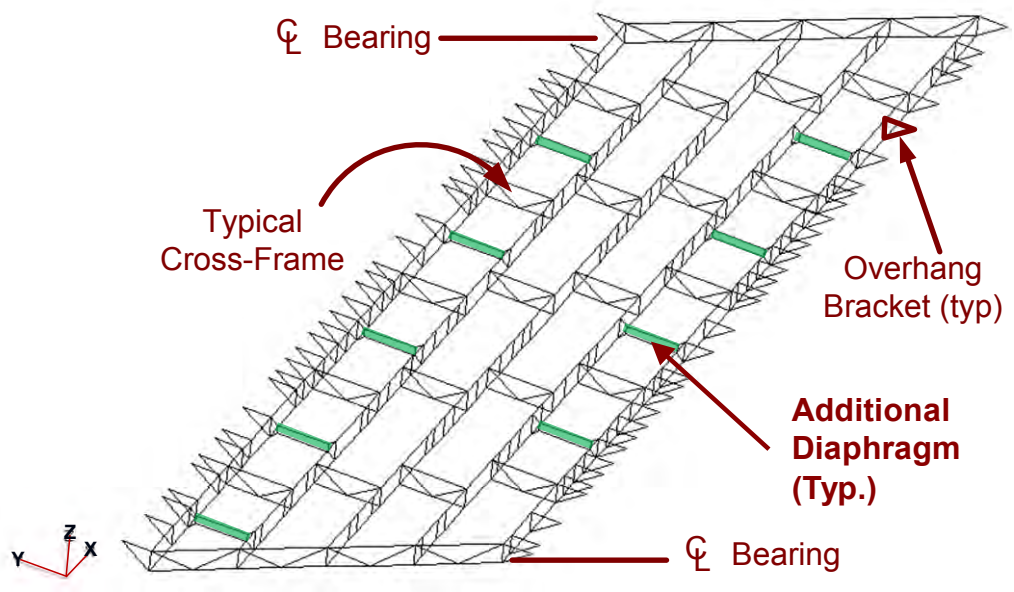

Figure 4.5.3.3.2.5.1-1 Overhang Brackets in a 3D Model

Superimposed Dead Loads

Superimposed dead loads applied to the composite section can be properly located on the deck of a 3D model. For example, barrier loads may be placed at the edges of the deck where they are actually located. The traditional approach has been to distribute these loads uniformly to all the girders. Previous specifications never condoned this practice. The provisions called only for curb and railing loads to be uniformly distributed. They did not permit barriers or sound walls, which are much heavier than curbs, to be uniformly distributed. Proper consideration of the location of these loads usually results in the loads causing larger moments in the exterior girders and smaller moments in the interior girders. Barriers or sound walls on large overhangs have even been found to cause reverse loads on the interior girders. The computed reacting forces in the cross-frames are also increased when the barriers are properly located on the edge of the deck. Similarly, utility loads may also be applied at their proper locations.

Future wearing surfaces and deck overlays can be applied to the model as uniform loads acting over the roadway deck area, as a series of concentrated loads, or by inputting an artificial density of the hardened concrete deck.

4.5.3.3.2.5.2 Live Loads

Live loads may be applied on the deck of the model, or to influence surfaces built from analyses of the model (Section 4.4.3.2). The influence surface is a more efficient approach. Special software may be used to accomplish this, or loads may be placed by hand—a tedious assignment. The construction of influence surfaces is accomplished by applying a unit load to selected deck nodes. Generally vertical loads are used for gravity loads, although influence surfaces in other than the vertical directions may also be developed. From the individual analysis for each of these loads, responses are found for the actions of interest. Then, the responses are assembled into sets of data; each forming an influence surface.

Loading the influence surface is typically performed with software separate from the finite element solver. Wheel loads are positioned according to the specification rules for live load placement in order to compute the maximum and minimum magnitudes of the desired effect (Section 4.4.3.2.2). Lanes of live loads need not necessarily be placed side-by-side within their lanes. This powerful analytical tool can replace live load distribution factors (and associated correction factors).

As discussed further in Section 3.4.9.2, individual wheel loads can be modified to account for the vertical effects of centrifugal force and superelevation. These modified wheel loads increase or decrease accordingly the wheel loads that are applied to the influence surfaces of curved alignments to account for vertical centrifugal force effects.

4.5.3.3.2.5.3 Wind Loads

The application of wind loading to a 3D model of a bridge superstructure is similar in principle to the application of the deck load. Typically, it is assumed that the wind is unidirectional. This means that it is applied at differing angles to horizontally curved bridges as a series of concentrated loads applied in a single uniform direction to the projected area of the bridge. The projected area of the bridge includes the sum of the projected girder areas taken perpendicular to the assumed wind direction. Superelevation and curvature are considered in determining the exposed area and wind load. Areas of the deck and barrier are, of course, included. The overturning wind can be applied in a similar manner. The critical direction of wind is usually not obvious and several angles of attack are often required to determine the critical condition.

The 3D model recognizes the girder depth, which permits wind loads to be applied to the top and bottom of the girder. These loads are typically applied as concentrated loads to the exterior windward girder at the top and bottom nodes along the girder. Each individual load, computed from the wind pressure and distance between nodes and structure height, is typically resolved into global x and y components.

The 3D model provides proper recognition of the horizontal diaphragm shear action of the concrete deck in resisting wind loads applied to the bridge in its final condition. Investigation of the forces due to wind in cross-frames and lateral bracing is also possible.

Wind on live load creates an overturning force on the vehicle similar to the effect of centrifugal force on vehicles and may be handled in a similar to that for centrifugal force, except it is also applied to the lane load instead of only to the truck loading in the case of centrifugal force. Of course, there is also a lateral force that must be considered. The calculation of wind load on the structure (WS) and wind load on the live load (WL) is discussed further in Section 3.5.1.

4.5.3.3.2.5.4 Thermal Loads

Temperature changes usually cause thermal forces in the superstructure and substructure. Thermal forces are often larger in curved bridges and bridges with skewed supports. These forces are a function of the bearing orientation and the stiffness of the substructure, as well as the magnitude of the temperature change. A uniform temperature change is usually assumed. The different specified coefficients of thermal expansion for concrete and steel can be taken into account. For normal-weight concrete, the coefficient of thermal expansion, α, is $6.0 \times 10^{-6}/^{\circ}F$ and for steel, α is $6.5 \times 10^{-6}/^{\circ}F$. The 3D model permits a different temperature to be applied to the deck. Most 3D packages also allow a thermal gradient to be investigated. Uniform

temperature change and thermal gradient are discussed in Sections 3.7.3 and 3.7.4, respectively.

4.5.3.3.3 Advantages, Disadvantages and Limitations

Advantages of 3D finite element methods of analysis include, but are not limited to, the following:

- Permits recognition of the proper location of the deck with respect to the girder neutral axis. This permits consideration of the contribution of the horizontal shear stiffness of the deck, which is the stiffest element in a girder bridge. Deck shear stresses can be determined. This is particularly important in skewed bridges.
- Permits recognition of the proper location of bearings. This permits consideration of lateral and longitudinal bearing constraints. This is critical in computing end cross-frame or diaphragm forces in bridges with skewed supports.
- Permits recognition of lateral bracing. These members greatly affect the distribution of load in structures. The lateral bracing can be very advantageous in curved-girder bridges in many instances when these members are properly modeled.
- Provides the proper modeling of cross-frame members. This assures that the behavior of these members is properly handled in the analysis and that the forces in them can be ascertained directly. It also reduces the effort required to compute and input cross-frame equivalents in a 2D model.
- Permits various substructures to be included integrally with the superstructure for analysis. This improves the accuracy of the analysis of both parts of the bridge.
- Permits proper recognition of the torsional stiffness of I-girders, including direct determination of flange lateral moments and girder twist.
- Permits proper loading of box girders by providing two webs. Hence, torque is properly introduced into the model.
- Transverse deck stresses can be computed that recognize the effect of relative girder deflections. This is important when designing post-tensioned deck slabs.
- Provide proper torsional stiffness of box members by recognizing St. Venant and warping torsional shear simultaneously.
- Variable depth (haunched) girders can be more accurately modeled. The shear component in bottom flanges of haunched girders is recognized.
- Allows for more efficient and detailed modeling of erection sequences.
- 3D finite-element analysis permits much bolder bridges that are not dependent on rules-of-thumb, but on the solid principles of structural analysis.

The following is a non-exhausted list of disadvantages of the 3D finite element method of analysis:

- Requires a greater level of knowledge. Experience with finite element analysis is required to properly construct the models and to compile, interpret and use the results; it should not be used without experienced guidance and assistance.
- Plethora of results to deal with unless a special package is employed.
- Greater modeling effort required unless a pre-processing software for bridges is used.

There are virtually no limitations on the type or complexity of models that can be constructed and analyzed using 3D finite element methods. Limitations that may exist are related to the limitations of the software package, the experience level of the modeler and Design Engineer, and of course, time and cost factors relative to the benefits that would accrue from employing a more sophisticated and complex analysis for the specific application under consideration. The effort required to build the model and process the results is also very dependent on the pre- and post-processing software available.

Section 4.6 Acknowledgments

The past contributions of Mr. Dann H. Hall and Mr. A. Richard Lawin of Bridge Software Development International, Ltd., Domenic A. Coletti of HDR Engineering, Inc., and Prof. Donald W. White of the Georgia Institute of Technology to significant portions of the material provided within this chapter are acknowledged.

Section 4.7 References

AASHTO/NSBA Steel Bridge Collaboration. 2014. *Guidelines for Steel Girder Bridge Analysis, G13.1*, 2nd edition, NSBASGBA-2, American Association of State Highway and Transportation Officials, Washington, DC.

AISC. 1963. *Design Manual for Orthotropic Steel Plate Deck Bridges*. American Institute of Steel Construction, Chicago, IL.

AISC. 2005. *Specification for Structural Steel Buildings*. ANSI/ASCE 360-05, American Institute of Steel Construction, Chicago, IL, March 9.

ASCE. 2000. *Design of Latticed Steel Transmission Structures*. ASCE 10-97, American Society of Civil Engineers, Reston, VA.

Battistini, A.D., S.M. Donahue, W.H. Wang, T.A. Helwig, M.D. Englehardt, K.H. Frank. 2013. “Brace Stiffness and Forces of X-Type, K-Type, and Z-Type Cross

Frames in Steel I-Girder Bridge Systems," *Proceedings of the Annual Stability Conference, Structural Stability Research Council*, April 16-20, 2013.

Battistini, A., W. Wang, S. Donahue, T. Helwig, M. Engelhardt, and K. Frank. 2014. "Improved Cross Frame Details for Steel Bridges." Report No. FHWA/TX-13/0-6564-1, Center for Transportation Research, University of Texas at Austin, Austin, TX, May, pp. 306-307.

Burgan, B.A., and P.J. Dowling. 1985. "The Collapse Behavior of Box Girder Compression Flanges – Numerical Modeling of Experimental Results." CESLIC Report BG 83, Imperial College, University of London, U.K.

Chapman, J.C., and J.S. Teraskiewicz. 1968. "Research on Composite Construction at Imperial College", *Proc. Conf. On Steel Bridges*, British Constructional Steelwork Association, London, England.

Chavel, B., and J. Carnahan. 2012. "Steel Bridge Design Handbook Design Example 4: Three-Span Continuous Straight Composite Steel Tub Girder Bridge". Publication No. FHWA-IF-12-052 – Vol. 24, U.S. Department of Transportation, Federal Highway Administration, Washington, DC, November.

Chen, S.S., A.J. Aref, I.-S. Ahn, M. Chiewanichakorn, J.A. Carpenter, A. Nottis, and I. Kalpakidis. 2005. *Effective Slab Width for Composite Steel Bridge Members*. NCHRP Report 543, Transportation Research Board, National Research Council, Washington, DC.

Dowling, P.J., J.E. Harding, and P.A. Frieze, eds. 1977. *Steel Plated Structures*. In Proc., Inperial College, Crosby Lockwood, London, U.K.

Eby, C.C., J.M. Kulicki, and C.N. Kostem. 1973. "The Evaluation of St. Venant Torsional Constants for Prestressed Concrete I-Beams." Report No. 400.12, Fritz Engineering Laboratory, Lehigh University, Bethlehem, PA.

FHWA. 2012. *Manual for Design, Construction, and Maintenance of Orthotropic Steel Bridges*. Federal Highway Administration, Washington, D.C.

Hall, D.H., and C.H. Yoo. 1996. "I-Girder Curvature Study". Appendix A of NCHRP Report 424: Improved Design Specifications for Horizontally Curved Steel Highway Bridges, Transportation Research Board, National Research Council, Washington, D.C., pp. 49-74.

Hambly, E.C. 1991. *Bridge Deck Behaviour*. Second Edition, Taylor & Francis Group, Boca Raton, FL, July 25.

Hindi, W.A. 1991. "Behavior and Design of Stiffened Compression Flanges of Steel Box Girder Bridges." Ph.D. Thesis, University of Surrey, Guilford, U.K.

Kinney, J.S. 1957. *Indeterminate Structural Analysis*. Chapter 1, Addison-Wesley, Reading, MA.

Lamas, A.R.G., and P.J. Dowling. 1980. "Effect of Shear Lag on the Inelastic Buckling Behavior of Thin-Walled Structures." *Thin-Walled Structures*, J. Rhodes & A.C. Walker, eds., Granada, London, P. 100.

McCormac, J.C. 1975. *Structural Analysis*. Third Edition, Intext Educational Publishers, New York, NY.

Modjeski and Masters. 1994. *Report to Pennsylvania Department of Transportation*, Harrisburg, PA.

NCHRP. 2012. "Guidelines for Analytical Methods and Construction Engineering of Curved and Skewed Steel Girder Bridges," NCHRP Report 725, Transportation Research Board, National Research Council, Washington, DC.

NHI. 2011. "Analysis and Design of Skewed and Curved Steel Bridges with LRFD – Reference Manual." FHWA NHI Report No. 10-087, Federal Highway Administration National Highway Institute, Arlington, VA, December.

PCI. 2011. "Bridge Design Manual – 3rd Edition." Precast/Prestressed Concrete Institute, Chicago, IL.

Richardson, Gordon and Associates. 1963. "Analysis and Design of Horizontally Curved Steel Bridge Girders." United States Steel Structural Report, ASUSS 88-6003-01, United States Steel Corporation, Pittsburgh, PA.

SSRC (Structural Stability Research Council). 1998. *Guide to Stability Design for Metal Structures*. Fifth Edition, Galambos, T.V., ed., John Wiley and Sons, Inc., New York, NY.

Tung, D.H.H., and R.S. Fountain. 1970. "Approximate Torsional Analysis of Curved Box Girders by the M/R Method." *AISC Engineering Journal*, Vol. 7, No. 3, Chicago, IL.

White, D.W. 2012. "Steel Bridge Design Handbook: Structural Behavior of Steel," Publication No. FHWA-IF-12-052 – Vol. 4, U.S. Department of Transportation, Federal Highway Administration, Washington, DC, November.

Zokaie, T., T.A. Osterkamp, and R.A. Imbsen. 1991. "Distribution of Wheel Loads on Highway Bridges." NCHRP Project 12-16, Transportation Research Board, Washington, D.C.

Chapter 5
Concrete Girder Superstructures

Section 5.1 Introduction

Concrete girders are commonly used as the primary supporting elements for bridge superstructures throughout the nation. The presence of prestressing steel greatly increases the applicability of concrete girders, including the potential for significantly increased span lengths. Therefore, concrete girders used for bridge superstructures are generally prestressed.

This chapter introduces the fundamentals of prestressed concrete girder design. It describes the fundamental properties of materials used in concrete girder design, it introduces general design considerations for prestressed concrete girders, and it presents preliminary design decisions such as girder type selection and sizing. This chapter also describes flexural design of prestressed concrete I-girders, design for shear and torsion, fundamental principles of prestressing such as stress limitations and prestress losses, details of reinforcement, and development and splices of reinforcement. Finally, it presents some unique provisions for various concrete girder structure types, including slab superstructures, precast deck bridges, beams and girders, post-tensioned spliced precast girders, cast-in-place box girders and T-beams, segmental box girders, and arches.

It should be noted that this chapter is not intended to be a comprehensive guide to the design of concrete girder superstructures. Rather, it is intended to provide valuable information that complements the specifications provided in *AASHTO LRFD*. For a more comprehensive treatment of this subject, refer to *Bridge Design Manual*, MNL-133-14, 3rd Edition, Second Release, August 2014, Precast/Prestressed Concrete Institute, Chicago, IL.

Section 5.2 Materials

This section provides a general overview of materials commonly used in concrete girder design, including material properties and behavior and their influence upon bridge design and construction.

Variations in material characteristics carry significant implications for design and construction, and they must be properly estimated and carefully addressed in the design drawings, specifications, and procedures. This is especially true for time-dependent properties such as concrete creep, concrete shrinkage, and relaxation of prestressing steel.

The materials described in this section include concrete, reinforcing steel, prestressing steel, and post-tensioning hardware.

5.2.1 Concrete

For bridge construction, concrete can either be precast or cast-in-place. Concrete can be produced in a batch plant at a precast production facility, on site, or at a ready-mix concrete plant. Generally, concrete plants and precast production facilities are qualified or certified to ensure quality. For the Owner and designer, the essential qualities of concrete are strength and durability, assured by appropriate project specifications. For the contractor, cost, equipment, and schedule drive decisions to adopt precast or cast-in-place construction.

When selecting the bridge type, the advantages of using precast concrete must be weighed against those of using cast-in-place construction. For example, for a concrete deck slab supported by precast concrete girders, resources for delivering, placing, consolidating, and finishing the slab must be considered, as well as allowing sufficient time for the deck to cure before applying live load. By contrast, other types of construction, such as precast segmental (in which the deck is complete after the segments have been erected), require no additional time to cure before applying live load. Such considerations influence overall construction schedules and costs.

At the preliminary design stage, concrete types and special requirements should be considered, including both strength and long-term durability. For example, consideration should be given to available resources of indigenous aggregates versus the need to import materials. The benefits, costs, and uses of various materials should be considered during preliminary design and appropriately incorporated into the final project specifications, as necessary. Such materials include fly-ash, blast furnace slag, micro-silica, and additives such as air-entraining agents and high-range water reducers to enhance durability. In general, concrete mixes, specifications, and uses of concrete should be adapted to normal practices for the project location.

5.2.1.1 Strength Characteristics

The strength characteristics of concrete directly affect the behavior of concrete, and these must be understood and carefully considered during bridge design. The

primary strength characteristics of concrete, which are described in the following sections, are compressive strength, tensile strength, and shear strength.

5.2.1.1.1 Compressive Strength

The fundamental property of concrete is its compressive strength, conventionally denoted by the symbol f'_c. Compressive strength, f'_c, is determined at an age of 28 days by standardized compression tests of sample cylinders measuring 6 inches in diameter by 12 inches long, in accordance with ASTM C42. Concrete matures and gains strength with age, as illustrated in Figure 5.2.1.1.1-1. Strength gain is rapid during the first several days, but it then slows, eventually becoming very gradual in the long term. The conventional time for defining the strength of concrete is at 28 days, as shown in Figure 5.2.1.1.1-1.

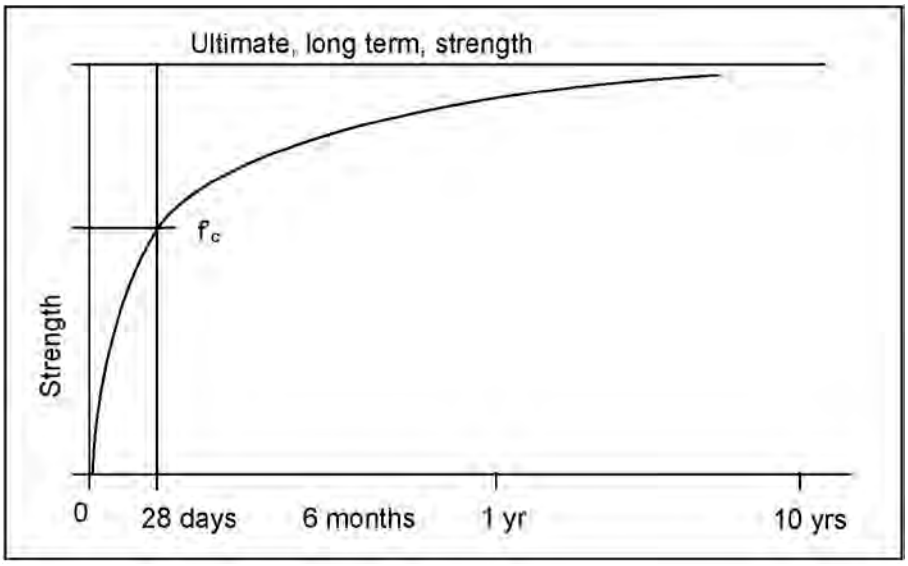

Figure 5.2.1.1.1-1 Gain of Concrete Strength with Time

Other properties, such as stress-strain relationship, tensile strength, shear strength, bond strength, creep, and shrinkage, are often defined in terms of strength. Such relationships are empirical, having been established by experiment and experience.

Compressive strength is primarily governed by the strength of the cement paste, by the bond between the cement paste and aggregate particles, and by the strength of the aggregate itself. These are influenced by the following concrete characteristics:

- Ratio of water to cementitious material
- Ratio of cementitious material to aggregate
- Grading, surface texture, shape, and strength of aggregate
- Maximum size of aggregate

In general, a lower ratio of water to cementitious material produces a higher strength. Consequently, in addition to compressive strength, concrete is further conventionally defined by the maximum “water-cementitious ratio” and/or “aggregate size.”

Other mix factors, either partially or wholly independent of water-cementitious ratio, that affect concrete strength include the following:

- Type and brand of cement
- Amount and type of admixture, such as air-entraining agent or super-plasticizer
- Type and amount of other pozzolanic materials (e.g., fly-ash and micro-silica)
- Mineral composition, gradation, and shape of aggregate

Factors such as the brand of cement and mineral composition of aggregate are clearly regionally dependent. A controlled percentage (such as 4% to 8%) of well dispersed, microscopic air bubbles introduced by air-entraining agents enhances durability against freeze-thaw and improves workability for placement and consolidation. Super-plasticizers improve workability, which facilitates reduced water content and enhanced strength. Cement replacement by a certain percentage of fly-ash and/or the use of micro-silica improves durability.

Concrete sets and gains strength as a consequence of a chemical reaction, or hydration, between the cementitious material and water. This forms chemical bonds and gradual crystal growth in the cement matrix. Too much water will react prematurely with the cement, preventing the growth of bonds and crystals and resulting in a weak matrix. However, too little water will result in an incomplete reaction, low strength, and an unworkable mix. The mix must be correct. Also, to ensure complete hydration, not only must the mix be correct, but the concrete must be properly cured. The primary purpose of curing is to prevent unnecessary moisture loss, especially during the first few days of the initial hydration and strength development. Hydration is an exothermic reaction, so heat builds up, particularly in the interior of a component. This heat must be gradually dissipated in a controlled manner. Curing processes involve covering the concrete, keeping covers and exposed surfaces damp to prevent moisture loss, and allowing heat to slowly dissipate. Controlled steam or fog curing is also widely used, especially at precast concrete production yards, where concrete mixes are designed for relatively rapid strength gain in the first few hours or days to facilitate turnover.

Concrete mix design is clearly very important, not only to the inherent strength of the structure but also to long-term performance and durability. Therefore, project specifications should comprehensively address concrete mix requirements,

production, handling, placing, consolidation, finishing, curing, and appropriate quality control.

Guidance regarding the class of concrete for various applications is provided in *AASHTO LRFD* Article 5.4.2.1. Concrete mix characteristics, including 28-day compressive strength, minimum cement content, maximum water-to-cement ratio, air content range, and coarse aggregate, are presented for each class of concrete in *AASHTO LRFD* Table C5.4.2.1-1.

For example, for bridge construction, reinforced concrete for abutments, piers, and deck slabs is typically Class A, which has a minimum 28-day compressive strength, f'_c, of 4.0 ksi. For prestressed concrete, Class P is generally required, which has an f'_c normally in the range of approximately 5.0 to 8.5 ksi. However, compressive strengths as high as 10.0 ksi have been used for special cases of prestressed concrete.

For a given project and location, an appropriate 28-day compressive strength, f'_c, should be established for each concrete component as one of the first steps in the design process.

5.2.1.1.2 Tensile Strength

Concrete has significantly greater compressive strength than tensile strength. Therefore, because of the limited tensile strength of concrete, reinforcing steel is used in virtually all concrete applications for bridges to resist tensile stresses. In addition, prestressing steel is used in most concrete girder applications for bridges to limit tensile stresses.

The direct tensile strength of concrete should be determined using either ASTM C900 or ASTM C496 (AASHTO T 198). Based on *AASHTO LRFD* Article C5.4.2.7, for normal weight concrete with f'_c up to 10.0 ksi, the direct tensile strength may be estimated as follows:

$$f_r = 0.23\sqrt{f'_c} \qquad \text{Equation 5.2.1.1.2-1}$$

When using the above equation, it is important to note that both f'_c and f_r are in units of ksi.

5.2.1.1.3 Shear Strength

In a manner similar to tensile strength, the shear strength, or diagonal tension strength, of concrete can also be expressed as a function of compressive strength. Although requirements are not specified in *AASHTO LRFD*, guidance is offered in

the AASHTO *Guide Specifications for Design and Construction of Segmental Concrete Bridges*. In addition, some authorities have adopted criteria to limit service cracking.

5.2.1.2 Strain Characteristics

In addition to the strength characteristics of concrete, it is also important to understand and consider the strain characteristics of concrete when designing a bridge. The primary strain characteristics of concrete, which are described in the following sections, are modulus of elasticity, Poisson's ratio, and volume changes due to such effects as shrinkage and creep.

5.2.1.2.1 Modulus of Elasticity

The modulus of elasticity, E_c, is the ratio of normal stress to corresponding strain in compression or tension. For concrete, the stress-strain curve is non-linear, as illustrated in Figure 5.2.1.2.1-1. The value of E_c is illustrated in Figure 5.2.1.2.1-1 as the slope of the stress-strain curve.

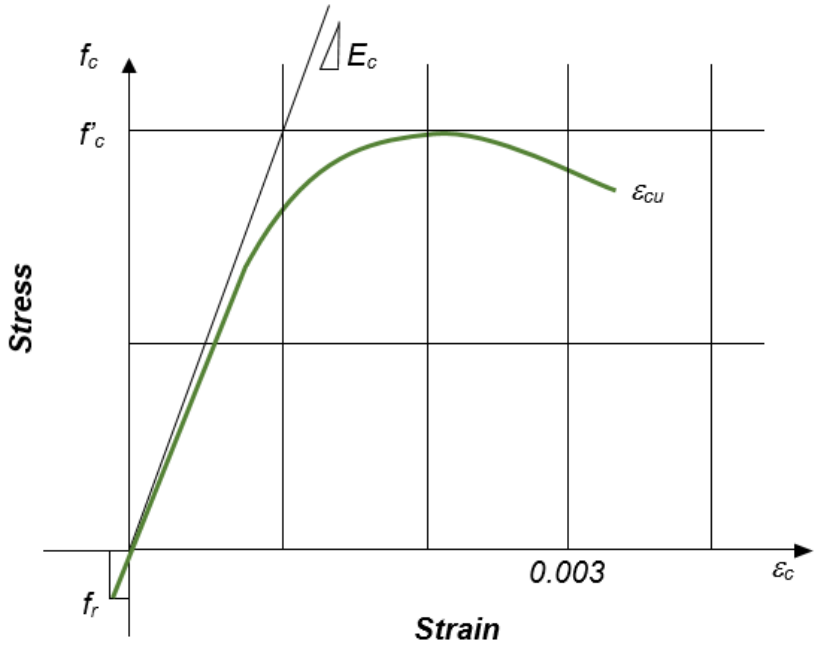

Figure 5.2.1.2.1-1 Stress-Strain Curve for Concrete

The modulus of elasticity is required for the calculation of deflections, axial shortening, and buckling. Since concrete is composed of different materials with different characteristics, the modulus of elasticity is not easily formulated. However, from empirical results, the modulus of elasticity can be expressed with sufficient

accuracy as a function of concrete density, concrete strength, and aggregate stiffness.

For concretes with unit weights between 0.090 and 0.155 kcf and with specified compressive strengths up to 15.0 ksi, *AASHTO LRFD* Article 5.4.2.4 specifies the value of E_c as follows:

$$E_c = 33{,}000\, K_1\, w_c^{1.5}\, \sqrt{f'_c} \qquad \text{Equation 5.2.1.2.1-1}$$

AASHTO LRFD Equation 5.4.2.4-1

where:

- K_1 = correction factor for source of aggregate; taken as 1.0 unless determined by physical test, and as approved by the authority of jurisdiction
- w_c = unit weight of concrete (kcf)
- f'_c = specified compressive strength of concrete (ksi)

5.2.1.2.2 Poisson's Ratio

Poisson's ratio is defined as the ratio of lateral strain to axial strain for an axially and/or flexurally loaded structural element. For concrete, *AASHTO LRFD* Article 5.4.2.5 prescribes a value of 0.2. Poisson's ratio has little importance in the longitudinal analysis of concrete superstructures. However, it is an important characteristic in the analysis of complex details using finite element techniques or in predicting the degree of confinement developed in laterally reinforced concrete members.

5.2.1.2.3 Volume Changes

Volume changes in concrete arise from variations in temperature, shrinkage due to air-drying, and creep caused by sustained stress. These are influenced by environmental conditions such as temperature and humidity, as well as the time and duration of loading. They are also affected by the maturity of the concrete, which is influenced by whether it is cast-in-place or precast. Volume changes affect structural performance and must be properly accounted for when determining long-term deflections and loss of prestress.

AASHTO LRFD Article 5.4.2.2 defines the coefficient of thermal expansion. For normal weight concrete, the coefficient of thermal expansion is 0.000006 per degree Fahrenheit. However, for lightweight concrete, the value is 0.000005 per degree Fahrenheit.

5.2.1.2.3.1 Shrinkage

Volume changes can occur due to shrinkage, which is primarily a result of sustained air-drying. Shrinkage occurs rapidly in the first few days but gradually slows as time passes, approaching but never quite reaching an ultimate limit (see Figure 5.2.1.2.3.1-1). The rate of shrinkage and the shape of the shrinkage curve vary with the concrete type, maturity, exposure, and environment.

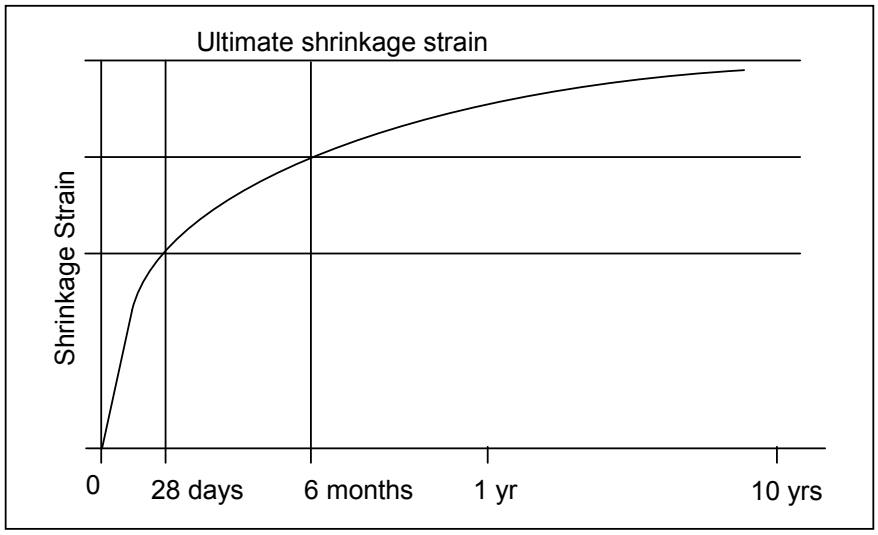

Figure 5.2.1.2.3.1-1 Shrinkage

5.2.1.2.3.2 Creep

Volume changes can also occur due to creep, which is the prolonged deformation of concrete under sustained stress. When loaded, concrete undergoes an initial "instantaneous" elastic strain which is a function of the modulus of elasticity at the time of loading. When the stress is sustained, a delayed strain occurs over time. If the stress is held indefinitely, the strain approaches an ultimate limit which is typically in the range of 2 to 2.5 times the instantaneous strain. If at some point the stress is released, there is an instantaneous recovery, proportional to the effective modulus of elasticity for the age of the concrete. A delayed recovery of strain follows. However, the recovery is never 100%, and a residual permanent strain remains. This is illustrated in Figure 5.2.1.2.3.2-1.

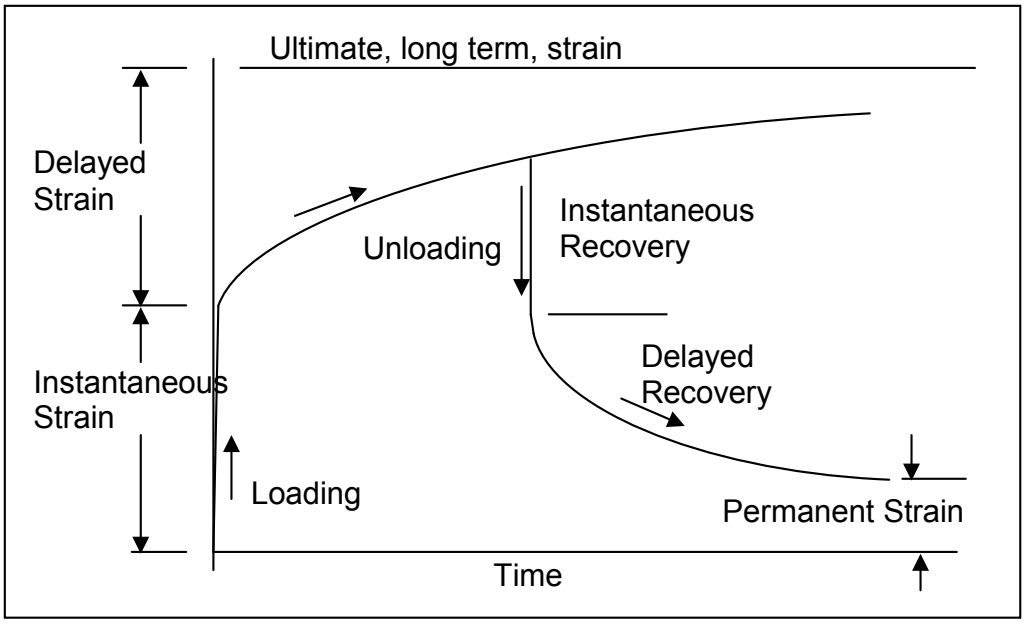

Figure 5.2.1.2.3.2-1 Creep and Concrete's Response to Sustained Stress

AASHTO LRFD Article 5.4.2.3 offers basic formulae and guidance for shrinkage and creep. It also allows shrinkage and creep to be determined by the provisions of CEB-FIP (European Code) and ACI 209. The approach of each code takes into account the same key factors using similar but slightly different formulations. The key factors include the following:

- Maturity of concrete
- Strength of concrete
- Time and duration of sustained stress
- Exposed perimeter (volume to surface ratio)
- Average relative humidity
- Water-cementitious ratio
- Aggregate characteristics
- Type of curing

Experience and comparison of results of different codes for different projects and locations might sometimes reveal different proportions of shrinkage and creep. Figure 5.2.1.2.3.2-2 and Figure 5.2.1.2.3.2-3 show relative values of creep and shrinkage predicted by four codes. These results are the average of values computed for four segmental bridges and one bulb tee girder bridge. Although the individual components of creep and shrinkage predicted by the different codes may vary, the sums of the two volumetric changes are sufficiently close to warrant the use of any of the codes in design.

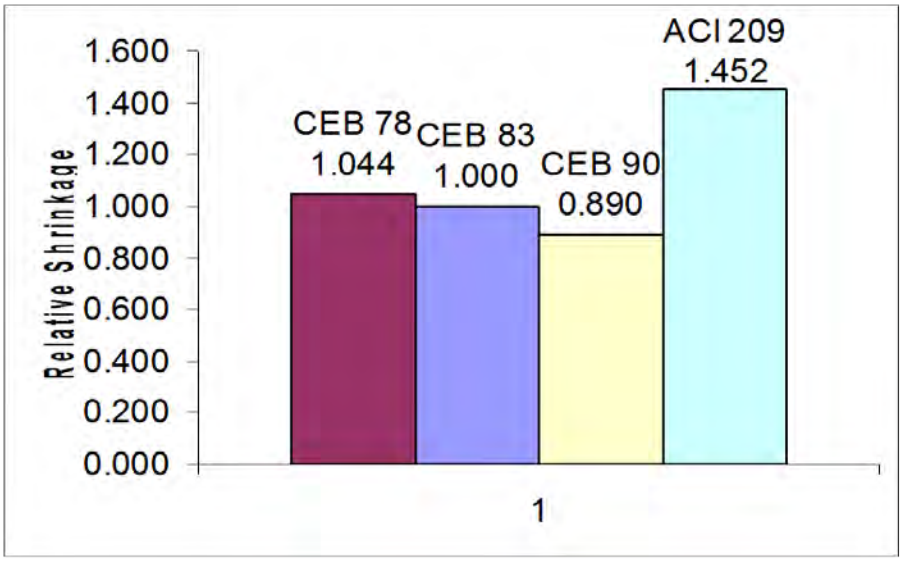

Figure 5.2.1.2.3.2-2 Relative Shrinkage by Different Codes

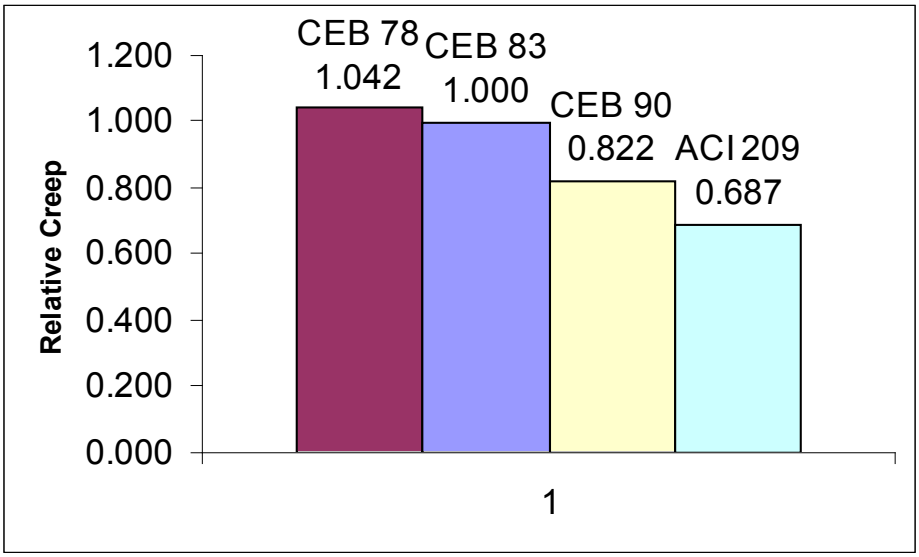

Figure 5.2.1.2.3.2-3 Relative Creep by Different Codes

5.2.1.3 Density

Some concrete design provisions in *AASHTO LRFD* are different for normal weight concrete than for lightweight concrete. Specific concrete design provisions that depend on the concrete density include the following:

- Coefficient of thermal expansion (see *AASHTO LRFD* Article 5.4.2.2)
- Modulus of rupture (see *AASHTO LRFD* Article 5.4.2.6)
- Resistance factors (see *AASHTO LRFD* Article 5.5.4.2)

- Torsion and shear resistance (see *AASHTO LRFD* Article 5.8.2.2)
- Cohesion and friction factors (see *AASHTO LRFD* Article 5.8.4.3)
- Nominal shear resistance for design of shear-friction reinforcement (see *AASHTO LRFD* Article 5.13.2.4.2)

5.2.1.3.1 Normal Weight Concrete

AASHTO LRFD defines normal weight concrete as concrete having a weight between 0.135 and 0.155 kcf.

For purposes of dead load computations, *AASHTO LRFD* assigns a unit weight of 0.145 kcf for normal weight concrete with f'_c less than or equal to 5.0 ksi, and 0.140 + 0.001 f'_c (in units of ksi for f'_c and kcf for unit weight) for normal weight concrete with f'_c between 5.0 ksi and 15.0 ksi.

5.2.1.3.2 Lightweight Concrete

AASHTO LRFD defines lightweight concrete as concrete containing lightweight aggregate and having an air-dry unit weight not exceeding 0.120 kcf, as determined by ASTM C567. Lightweight concrete without natural sand is termed "all-lightweight concrete," and lightweight concrete in which all of the fine aggregate consists of normal weight sand is termed "sand-lightweight concrete."

For purposes of dead load computations, *AASHTO LRFD* assigns a unit weight of 0.110 kcf for lightweight concrete and 0.120 kcf for sand-lightweight concrete.

For lightweight concrete, the air-dry unit weight, strength, and any other unique properties should be specified in the contract documents.

5.2.1.4 Curing

Concrete is cured by different methods according to local conditions and procedures. These may involve steam curing, covering with wet burlap, fogging, or application of curing compounds to exposed top surfaces. After several days, when the concrete attains a required minimum strength determined by control cylinders, side forms are removed and strands are released by carefully cutting at the end of each girder, transferring their force to the girders. This is referred to as the "transfer" or "initial" condition. The corresponding concrete strength is the initial strength, denoted as f'_{ci}.

Girders are then transported to a storage area in the casting yard (Figure 5.2.1.4-1). In storage, girders must be carefully supported on temporary blocks at the locations of the bearings or as otherwise approved by the Engineer. Because the prestressing effect is greater than the effect of self-weight, most I-girders have a positive, upward camber, as seen in Figure 5.2.1.4-1. If girders are in storage for a long time, the

initial camber can grow due to creep of the concrete under sustained stress. Camber growth can encroach into the build-up above the top flange that is permitted by design. In such cases, it may be necessary to adjust the bearing elevations in the field prior to setting the girders so that the deck slab can be built to the correct elevation.

Figure 5.2.1.4-1 Handling and Storage of Girders in Casting Yard

Occasionally while in storage, girders might develop a lateral bow, often referred to as “sweep.” The cause of sweep can be orientation of the girder to direct radiant sunlight. Normally, such sweep is relatively small and inconsequential. However, if sweep grows or persistently exceeds a couple of inches in about 100 feet, the source should be more thoroughly examined. It might indicate a problem with the stressing operation that somehow applies more force to one side of the girder than the other, or it may be due to a misalignment or lateral eccentricity of strands in the casting bed. Sweep and temporary support blocks should be checked during storage to make sure the girders are stable and are not likely to topple over.

During the time in storage, girders are inspected and any defects are remedied. Minor defects, such as small, superficial air bubbles or “bug-holes,” may need to be filled. However, more significant defects, such as cracks or spalls, should be reported to the Engineer for further examination. In addition to dimensions, tolerances, material certifications, cylinder strengths, and stressing forces, project specifications should also contain requirements and guidance regarding the acceptability of finished products, as well as when such products are likely to be unacceptable and possibly subject to rejection. Such standards help not only the Owner but also the Producer, because they lead to early identification and rectification of potential production problems before components are shipped.

For additional information about curing and storage of concrete girders, refer to the following documents:

- *Manual for Quality Control for Plants and Production of Structural Precast Concrete Products*, MNL-116, Precast/Prestressed Concrete Institute, Chicago, IL
- *Manual for the Evaluation and Repair of Precast, Prestressed Concrete Bridge Products*, MNL-137-06, Precast/Prestressed Concrete Institute, Chicago, IL

5.2.2 Reinforcing Steel

The use of reinforcing steel is common and routine practice in the construction industry. Its quality and installation are addressed by normal construction specifications.

Today, ordinary mild steel reinforcement typically has a yield strength of 60 ksi or greater, although *AASHTO LRFD* places a limit of 75 ksi for design calculations regardless of actual strength (*AASHTO LRFD* Article 5.4.3.1). The modulus of elasticity is assumed to be 29,000 ksi (*AASHTO LRFD* Article 5.4.3.2).

Other types of mild reinforcement, such as stainless steel or stainless clad reinforcement, have also been used effectively. While producing increased resistance to corrosion, these steels originally did not have yield strengths or moduli of elasticity consistent with code requirements. However, since their introduction, producers of these types of reinforcing steel bars have altered their formulation to produce acceptable characteristics.

5.2.3 Prestressing Steel

Prestressing strand is available in nominal diameters ranging from ¼ inch to 0.6 inches, depending on the strand grade or type. However, it is most commonly provided in nominal diameters of 0.5 inches or 0.6 inches. A nominal diameter of 0.5 inches is more widely used for the production of pretensioned girders, piles, and similar components at precast concrete production factories. Both strand sizes are used in post-tensioning, but the choice depends upon the particular supplier (manufacturer) of the post-tensioning system hardware (i.e., anchorages, wedges, wedge-plates, and jacks). The use of a particular system depends upon the Contractor and his selection of a sub-contract supplier. For this important commercial reason, project specifications, plans, and documents should allow for variations in the selection of a post-tensioning system. This is normally and routinely accommodated through an appropriate “Shop Drawing” submission and review process.

Prestressing bars are most commonly used for relatively short permanent or temporary tendons. Temporary prestressing bars are frequently used to erect

precast segments in order to secure, tightly close, and compress match-cast joints until an applied epoxy seal has set.

Prestressing strand is very high strength steel with a specified tensile strength, f_{pu}, much greater than the yield point, f_y, of ordinary mild steel reinforcing (Figure 5.2.3-1). Typical seven-wire prestressing strand (for pre-tensioning or post-tensioning) typically has an ultimate strength of 270 ksi, or 4.5 times the yield point of 60 ksi for most mild steel reinforcing. Bars for post-tensioning typically have a specified tensile strength of 150 ksi.

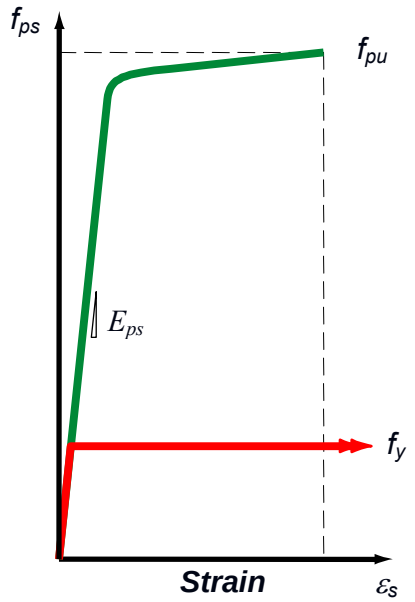

Figure 5.2.3-1 Stress-Strain Curves for Prestressing Strand and Mild Steel

Unlike mild steel, prestressing steel does not have a definite yield point, although its behavior is linear-elastic to approximately $0.75f_{pu}$. Thereafter, it is non-linear but exhibits a significant strain to failure. The yield strength is taken as the point at which the strain reaches 1% or the point where a line parallel to the initial modulus at a 0.2% offset meets the stress-strain curve. Both techniques produce similar results.

The modulus of elasticity for prestressing strand is usually assumed to be 28,500 ksi for elongation calculations during stressing operations (*AASHTO LRFD* Article 5.4.4.2). This value is less than that for prestressing bar (i.e., 30,000 ksi) or that of an individual wire of a strand. This is attributed to the helically wound outer six wires being slightly longer than the central king wire, resulting in a very slightly longer actual test gauge length than theoretical. Along with the tightening or straightening effect of the outer wires under load, this leads to a slightly lower modulus of elasticity.

Prestressing makes use of the full elastic range to impart a sustained force on the concrete. The stress in the prestressing steel at tensioning is typically $0.75f_{pu}$. After initial and long-term losses, which must be accounted for in the design, the final stress is usually in the range of $0.55f_{pu}$ to $0.65f_{pu}$, depending upon the application. This final stress level (typically at least 150 ksi for strand and 83 ksi for bar) is greater than the yield strength of mild steel (60 ksi) and is only possible by the availability of high strength steel.

Under sustained stress, prestressing steel creeps and relieves itself of stress in a process referred to as relaxation. Two types of strand are available – stress-relieved (normal relaxation) and low relaxation. The latter has undergone an additional treatment and has a final relaxation of about 3.5%, one quarter that of stress-relieved strand. Since losses are detrimental to prestressed concrete, low-relaxation strand is most commonly used.

The yield strength, f_{py}, of prestressing strand is taken as $0.90f_{pu}$ for low-relaxation strand and $0.85f_{pu}$ for all other strands.

The significant difference between the modulus of elasticity of steel and the modulus of elasticity of concrete is the primary reason it is possible to make prestressed concrete function structurally.

5.2.4 Post-Tensioning Hardware

For strand tendons, post-tensioning hardware consists of an anchorage, wedges to grip each individual strand, and a wedge-plate that houses all of the wedges and that bears upon the anchorage. The anchorage itself is usually a high strength casting that comprises one or more (multi-plane) bearing plates and forms a cone-shape taper from the wedge plate to the post-tensioning duct (Figure 5.2.4-1). The cone connects to the post-tensioning duct. The duct itself is usually an approved plastic or steel material, depending on whether the tendon is internal (within the concrete) or external (exterior to the concrete). Different sizes and types of anchorage devices are available from most suppliers according to the number of strands in the tendon.

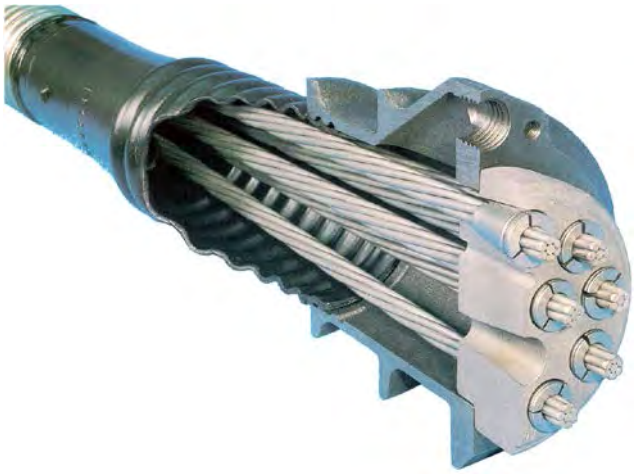

Figure 5.2.4-1 Post-Tensioning Anchor

Bar tendons are secured by a threaded anchor nut that bears against an anchor plate. The anchor plate may be a square or rectangular steel plate or a special embedded casting, depending upon the system.

Various types and sizes of components are commercially available for post-tensioning. For bridges, post-tensioning bars are most often used for temporary construction uses, such as for erecting precast segments, as well as for permanent applications. Bar anchorages are either rectangular plates, usually for surface mounts, or special embedded components. Couplers are available for post-tensioning bars. Post-tensioning bar anchors and couplers are illustrated in Figure 5.2.4-2.

For additional information about post-tensioning, including the installation and grouting of post-tensioning, recommendations for the location of grout injection ports, vents, laboratory and field tests, quality control, and records, refer to *Post-Tensioning Tendon Installation and Grouting Manual*, available from the Federal Highway Administration. Additional information is also available from the Post-Tensioning Institute.

Figure 5.2.4-2 Post-tensioning Bar Anchors and Couplers

5.2.5 Other Materials and Components

Any other miscellaneous materials or components should be addressed in appropriate project specifications or plan notes. For example, occasionally in pre-tensioned girders, strands in the web may be deflected upwards to a draped (depressed) profile. This requires embedding special hold-down devices in the bottom flange. A widely used alternative is to debond several strands in the bottom flange near the ends of the girder using a suitable plastic shield (pipe) around each strand. These components must be of an approved material and must be properly installed.

In post-tensioned construction, tendons pass through ducts and enter anchorages. Ducts may be made of plastic or metal. Anchorages must be sealed and protected to prevent intrusion of deleterious elements. In addition, ducts are usually filled with a cementitious grout after installation and stressing of the tendons. All components and materials should be of approved materials and should be properly installed.

Section 5.3 General Design Considerations and Fundamentals

5.3.1 Concrete Behavior

Concrete is strong in compression but relatively weak in tension. Tensile stresses, whether due to external loads or to internal deformation and restraint during initial strength gain, can cause cracks to develop at low load levels. The resistance of a

plain concrete beam in flexure is limited by the flexural tensile strength of the extreme fiber or "modulus of rupture". *AASHTO LRFD* Article 5.4.2.6 provides two different equations (one upper bound and one lower bound) for the modulus of rupture depending on the usage of the value.

When used to calculate the cracking moment of a member in *AASHTO LRFD* Articles 5.7.3.4, 5.7.3.6.2, and 5.7.3.3.2, the modulus of rupture to be used is computed as follows:

$$f_r = 0.24\sqrt{f'_c} \qquad \text{(upper bound)}$$

When used to calculate the cracking moment of a member in *AASHTO LRFD* Article 5.8.3.4.3, the modulus of rupture to be used is:

$$f_r = 0.20\sqrt{f'_c} \qquad \text{(lower bound)}$$

The equations above are for normal-weight concretes (density between 0.135 and 0.155 kcf.) with strengths up to 15.0 ksi. For sand-lightweight concrete and all-lightweight concrete single expressions are used:

$$f_r = 0.20\sqrt{f'_c} \qquad \text{(Sand-lightweight concrete)}$$

$$f_r = 0.17\sqrt{f'_c} \qquad \text{(All-lightweight concrete)}$$

Considering a concrete with a 28-day compressive strength (f'_c) of 5.5 ksi, the predicted upper bound modulus of rupture (f_r) would be 0.56 ksi, or about 10% of the compressive strength. This low tensile strength means that a plain concrete beam has very little flexural resistance (Figure 5.3.1-1) and fails easily under load.

The flexural resistance of concrete beams is improved greatly by placing reinforcing steel to resist the tension that the concrete cannot carry (Figure 5.3.1-2). Under load the concrete cracks as the tensile strength is exceeded. The reinforcing steel crossing the cracks resists the tensile stresses, providing internal equilibrium and increased load-carrying resistance.

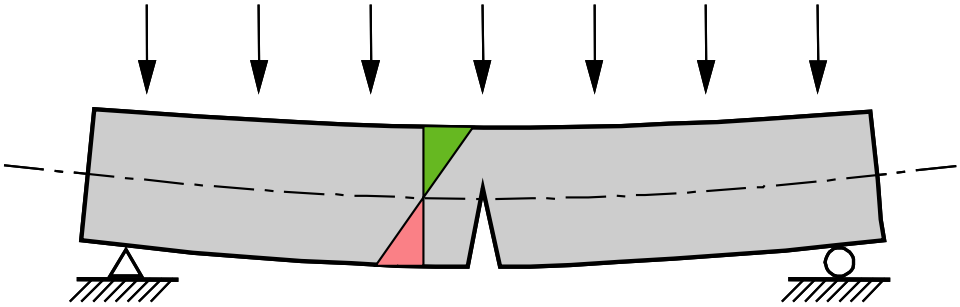

Figure 5.3.1-1 Plain, Unreinforced Concrete Beam in Flexure

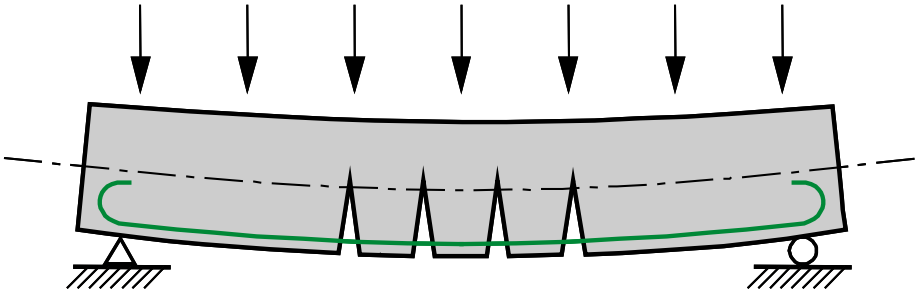

Figure 5.3.1-2 Reinforced Concrete Beam in Flexure

Reinforced concrete construction has been satisfactorily used for flat slab bridges and bridge beams with relatively short spans. Span length limitations for these bridges are approximately 25 to 30 feet based on typical concrete strengths used in such applications. As span lengths increase above these limits, the quantity of reinforcing steel and concrete dimensions required to effectively resist self-weight and applied loads increase significantly. The results are heavy members that are not cost-effective.

Although cracks in reinforced concrete bridges can be controlled by reinforcing steel to be relatively narrow and well distributed, the cracking that occurs prior to engaging the steel can be undesirable. Even small cracks afford pathways for corrosive agents to attack reinforcing steel. In addition, bridges in regions subjected to cyclical freeze-thaw action can experience undesired deterioration of the concrete and reduced long-term durability.

Introducing a means of pre-compressing the tensile zones of concrete to offset anticipated tensile stresses makes efficient use of the compressive strength of the concrete and reduces or eliminates cracking, producing more durable concrete bridges.

5.3.2 Prestressing

Prestressing involves the introduction of a predetermined compressive force into the concrete. Tension stress caused by load must first overcome this initial compression before it can crack the concrete. Prestressing is applied by means of high-strength steel strands or bars tensioned so as to react against the concrete. The effect of prestressing is illustrated in Figure 5.3.2-1. Placing the prestressing low in the simple-span beam induces uniform compression over the cross-section depth (axial force) plus additional compression in the tension zone at the bottom of the beam (load eccentricity.) This latter effect creates an upward camber which opposes the deflection caused by load.

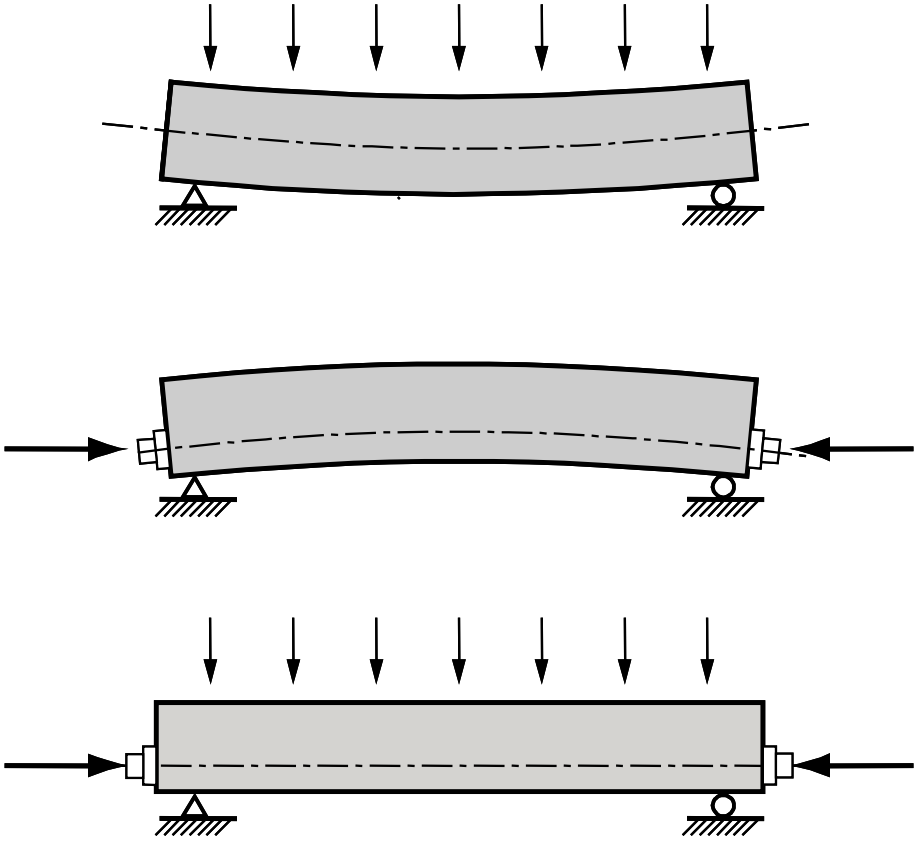

Figure 5.3.2-1 Effect of Prestressing in Simple-Span Beam

The design of prestressed concrete members involves balancing the effects of loads and prestressing to eliminate or minimize tension, eliminate cracks, and optimize materials leading to structural efficiency and reduced construction cost.

Prestressing can be applied in two ways, by pretensioning or post-tensioning.

Pretensioning – In pretensioned members strands are installed along the length of a casting bed and tensioned against restraining bulkheads before the concrete is

cast (Figure 5.3.2-2). After the concrete has been placed, allowed to harden and gain sufficient strength, the strands are released and their force is transferred to the concrete member by bond. The resulting tensile stress in the steel (and compressive stress in the concrete section) increases from a value of zero at the end of the member to a maximum value over a distance known as the "transfer length" determined by bond strength and friction between the steel strand and concrete. At the end of the transfer length it is assumed that the prestressing in the cross-section is fully effective.

Figure 5.3.2-2 Casting Bed for Pretensioned Girders

Post-Tensioning – Post-tensioned construction involves installing and stressing strand or bar tendons after the concrete has been placed, cured and hardened. Ducts are placed inside the concrete so that the tendons can be threaded through the member after the concrete hardens. Once in place, the tendons are tensioned by jacks and anchored against the hardened member using anchorage devices cast into the concrete.

At the anchor, strands are gripped by hardened steel wedges housed in a wedge-plate (Figure 5.2.4-1). The wedge plate bears against an anchor plate, or in this figure a special steel cast anchor device that bears upon the concrete. The tendon force is then transferred from the anchor plate or device to the concrete by bearing. Figure 5.3.2-3 shows a typical application of post-tensioning during the erection of a precast concrete segmental box girder bridge.

Figure 5.3.2-3 Jacking of Post-Tensioning Tendon

Whether pretensioning or post-tensioning is used, the objective is to introduce precompression into the concrete member to increase the level at which self-weight and applied loads cause tensile stresses, cracking and ultimately failure of the member.

5.3.3 Beam (B-Region) Flexural Design

A reinforced or prestressed concrete bridge superstructure can and should be divided into semi-discrete regions for the purposes of selecting design methods that appropriately represent member behavior within the regions. To this end it is useful to classify portions of the structure as either B- (Beam or Bernoulli) Regions or D- (Disturbed or Discontinuity) Regions.

B-Regions occur in members whose length is significantly greater than their depth. They represent portions of the member away from the supports where stress is linearly proportional to strain and plane sections remain plane in bending.

Determination of Flexural Design Stresses – Prestressed concrete beams are designed by *AASHTO LRFD* for flexure using stress limits at the service limit state, then checked at ultimate for flexure and shear using factored loads at the strength limit state. In order to demonstrate the effect of prestressing, consider first the flexure of a simply-supported concrete beam section under the action of its own self weight as shown in Figure 5.3.3-1. Top and bottom stresses are determined according to normal beam theory. The top of the beam is in compression; the bottom is in tension. For plain concrete without reinforcing steel the tensile stress will likely exceed the modulus of rupture – the beam will crack and fail.

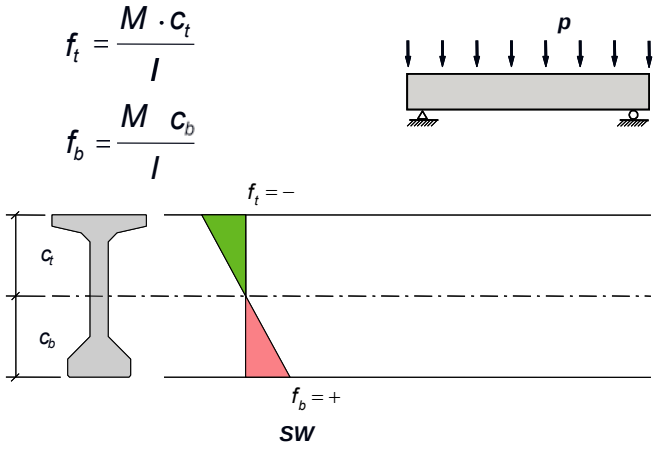

Figure 5.3.3-1 Self Weight Flexure Stress in Simply-Supported Beam

If a purely axial compressive stress is applied to the beam (Figure 5.3.3-2), more compression will be induced in the top and the tension in the bottom will be reduced. However, unless a sufficient level of compression is applied, the bottom fiber will remain in tension and the beam might still crack under its own weight. Even if the structure remains uncracked under self-weight, it will be incapable of carrying any appreciable level of externally applied load.

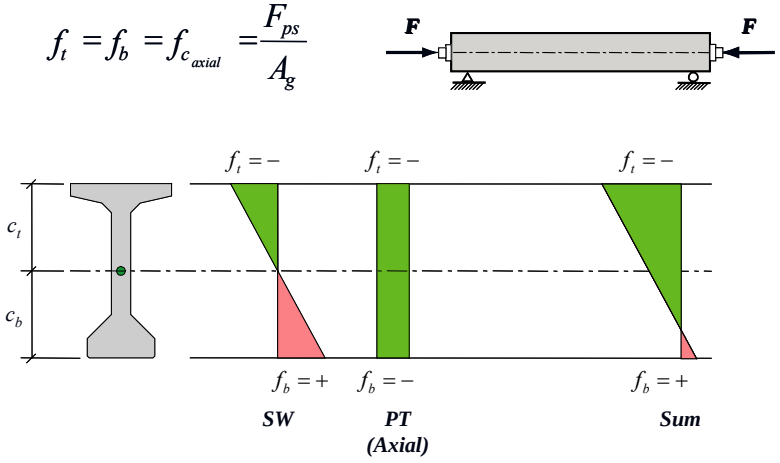

Figure 5.3.3-2 Self Weight Plus Axial Compression

In order to increase the compression in the bottom fiber significantly without overstressing the top fiber in compression, the prestressing force should be applied eccentrically (Figure 5.3.3-3) In addition to the self-weight stress and the axial prestress effect, the eccentricity causes an upward flexural moment which induces compression in the bottom of the beam and tension in the top.

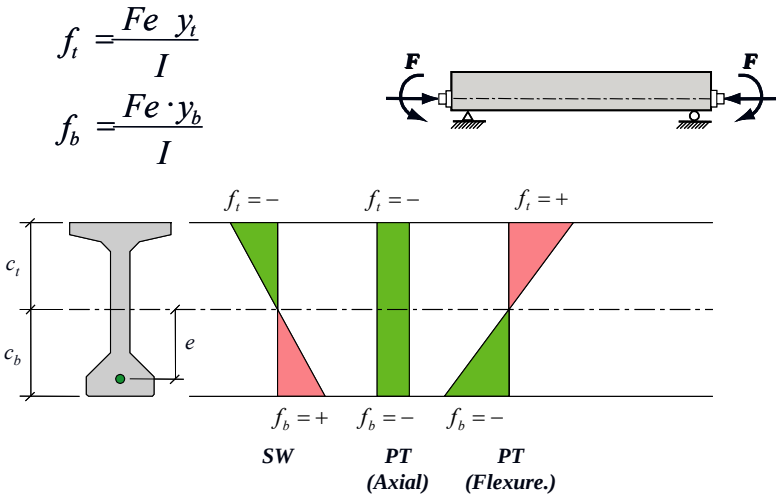

Figure 5.3.3-3 Self Weight, Axial and Eccentric Prestress Stresses

The summation of these three effects (i.e., self-weight, axial prestress and eccentric prestress) is shown in Figure 5.3.3-4. The result is compressive stress throughout the depth of the beam with more compression in the bottom than the top. Henceforth, additional load applied to the beam must overcome the compression at the bottom fiber and the tensile strength of the concrete before the beam can crack. Eccentric prestressing utilizes the advantages of concrete (good in compression) and prestressing steel (good in tension) to the greatest benefit while overcoming concrete's inherent weakness in tension.

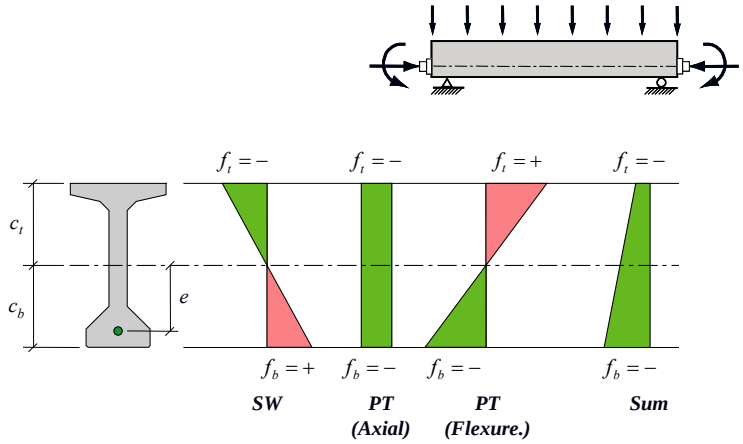

Figure 5.3.3-4 Summation of Self Weight, Axial and Eccentric Prestress Stresses

The incremental summation (superposition) of stresses illustrated in Figure 5.3.3-1, Figure 5.3.3-2, Figure 5.3.3-3, and Figure 5.3.3-4 for mid-span flexural stress in a simple beam can be applied at other locations over the cross section and along the beam length, not only for flexure but also for web shear stress. The resulting flexural,

axial and shear stresses at any point can then be combined using Mohr's circle analysis to determine the principal tensile stress in the beam. In a prestressed concrete structure the incremental summation of stresses is fundamental to determining the final state of stress – particularly if the cross section properties change during construction, as is the case for composite behavior with a deck slab cast atop a precast girder. The incremental summation of stresses is also necessary when post-tensioning is applied in stages, as sections or beam segments become composite, or as a structure's statical scheme changes (e.g. simply-supported to continuous) during construction.

Determination of Shear Design Stresses – The shear stresses in a composite, prestressed concrete bridge beam can be determined at critical locations within the cross section (generally the center of gravity or the interface between precast beam and cast-in-place deck) using conventional methods described in mechanics of materials textbooks – i.e., (V x Q) / (I x t). However, the shear design of such members by *AASHTO LRFD* is performed at the strength limit state after selection of the cross section and determination of prestressing steel based on flexural design at the service limit state.

Though designed for shear forces at the strength limit state, the maximum shear stresses (or more appropriately, the principal tension stresses) of certain types of prestressed concrete bridge beams should be checked to prevent diagonal cracking of the webs. This topic is addressed in Section 5.6 of the manual.

Summary of Benefits of Prestressing – Prestressing offers many benefits to concrete bridge structures:

- Compared to reinforced concrete members, it reduces the cross section size and girder depth, reducing both the volume and weight of concrete
- The weight reduction afforded by prestressing facilitates longer spans and greater structural efficiency than reinforced concrete alone
- Precompression of otherwise tensile zones in the concrete minimizes cracking and increases durability
- Greater structural efficiency and durability reduces both initial costs and maintenance costs

5.3.4 Disturbed (D-) Region Design

D-Regions are portions of the structure that exhibit complex variations in strain. D-Regions include segments near abrupt changes in geometry (geometrical discontinuities) or concentrated forces (statical discontinuities). They may comprise entire structural members whose length is short relative to their depth (e.g., deep beams, ledges, corbels). For prestressed beams or other long members, D-Region

behavior extends approximately one section depth of the region on either side of the discontinuity (St. Venant's principle).

Design considerations for D-regions can be carried out using a variety of tools and methods, including strut-and-tie, finite element, or force flow diagrams. The design of post-tensioned anchor zones using strut-and-tie modeling is presented in Section 5.7.5.2.

Section 5.4 Preliminary Design Decisions

5.4.1 Layout Considerations for Preliminary Design

Key considerations for selecting a preliminary bridge type and layout include:

- Site-specific and roadway geometric constraints
- Access and traffic maintenance
- Shipping and handling
- Constructibility and specialized erection equipment
- Aesthetics

Although these items are generally applicable to all bridge types and materials, the discussion in this section will focus on those aspects specifically related to precast concrete superstructures.

Site-Specific and Roadway Geometric Constraints – The bridge layout process is largely influenced by site-specific constraints. Span lengths and pier locations are established based on the features to be crossed. These may include existing or new highways, railroads, navigation channels or locations where it is not possible to place piers and foundations for geotechnical reasons. Span lengths and other considerations may dictate the type of bridge cross section and construction methods.

Roadway geometric constraints include: horizontal alignments and lateral clearances; vertical profile and permanent or temporary vertical clearances; width of the superstructure (deck); and width and skew of individual substructure units. Horizontal curvature of a superstructure may dictate, for example, the maximum practical span for a straight precast girder in order to restrict the width of deck slab overhang. A tight curvature radius or skewed abutment may require precast girders of varying length within a span. The varying length girders may in turn require more prestress (pre- or post-tensioning) in the longer girders. Alternatively, curvature may require the use of a completely different superstructure type, such as a continuous, trapezoidal box section designed to better follow the radius. Figure 5.4.1-1 shows a typical layout for a straight girder bridge on a curved horizontal alignment.

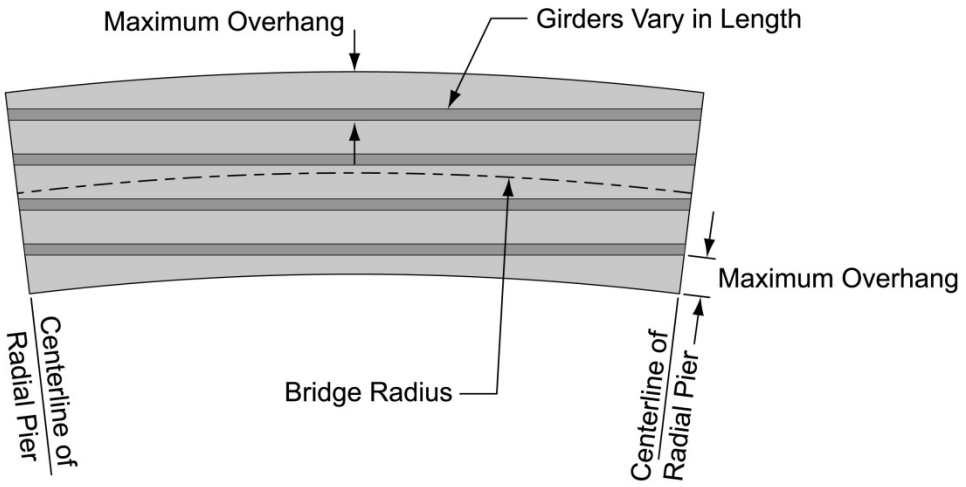

Figure 5.4.1-1 Typical Span of a Curved Girder Bridge

Vertical profile and minimum clearance requirements often restrict the depth of a superstructure. This in turn limits the maximum span length achievable with a particular girder type which may require more piers at closer spacing, more girders in a deck or both.

Skewed substructures may require longer spans and a deeper superstructure. This may result in more girders in the cross section, more prestress force or both. Skewed substructure units also require special attention to details for diaphragms and the positioning of bridge bearings for girder superstructures. Figure 5.4.1-2 shows two configurations of bearings for a girder bridge resting on skewed substructure caps. In Figure 5.4.1-2(a) the bearings are placed parallel to the pier caps. This minimizes the width of bent cap required, but for extreme skews it can also lead to bearing instability and/or increased design requirements for the end diaphragms. Figure 5.4.1-2(b) aligns the bearings along the axis of the girders. In this case the bearing performance is improved but the width of the pier cap may need to be increased to accommodate the bearing placement.

One additional consideration affecting superstructure cross section type and the layout of span lengths and pier locations is the relative cost of bridge superstructure to substructure. In general as the cost of substructure construction increases due to factors such as water depth or foundation size and depth, the span length must increase in order to reduce the number of substructure units. Such span length increases may dictate the use of a different superstructure type altogether in order to meet increased load demands.

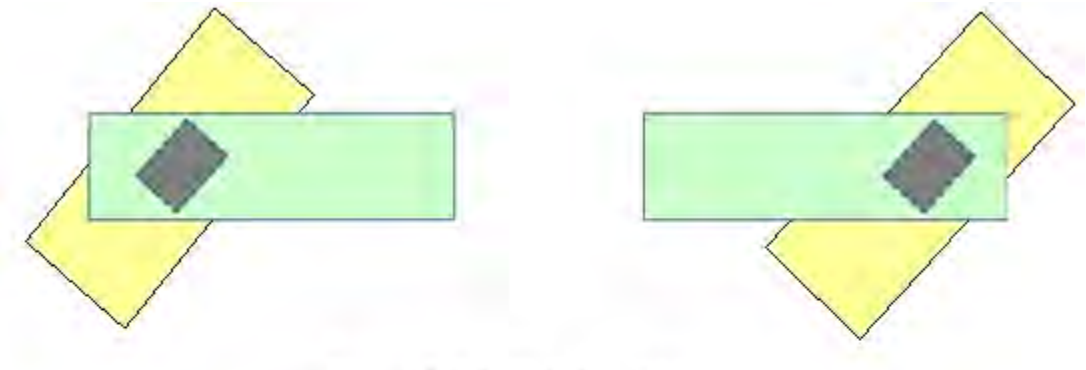

Figure 5.4.1-2(a) Bearings oriented parallel with pier caps.

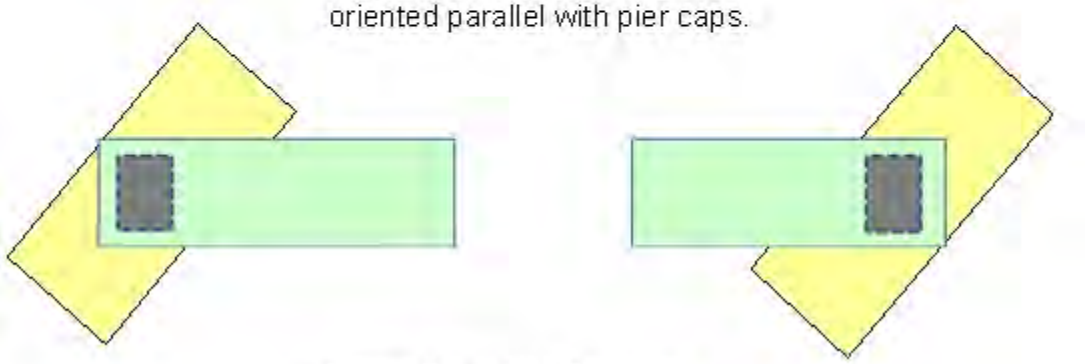

Figure 5.4.1-2(b) Bearings oriented normal to girders.

Figure 5.4.1-2 Bearing Placement for Skewed Structures

Access and Traffic Maintenance – Constructibility considerations that influence the bridge development process include accessibility to the site for the delivery of materials, equipment and prefabricated components and the means of that delivery – whether by road, rail or water. The number, capacity, and reach of cranes should be considered for lifting and placing precast components when circumstances dictate. Although it is the Contractor's responsibility to safely operate cranes from a barge or static foundation, it is prudent to allow for reasonable accessibility, clearances and possible crane locations during layout of the design. In general the size of precast components, such as girders and girder segments, should be selected with access and delivery limitations in mind. The need to construct temporary access roads or dredge channels should be considered when appropriate. In some cases special erection techniques, such as overhead gantries, the use of temporary supports or allowances for placing smaller equipment on existing or new bridge decks, may avoid the need for special access or heavy cranes.

For many sites the erection of precast components (girders or segments) or the delivery of supplies such as ready-mixed concrete requires local traffic diversions or temporary road or lane closures with attendant traffic signs, safety and control

measures. In some cases it might influence the location of permanent or temporary piers. Such anticipated needs should be considered in the planning and layout of the bridge. It is therefore imperative that the structure designer work closely with the roadway designer during the bridge development process. It is also prudent to consider incorporating construction phasing schemes with sequences and plans for possible “maintenance of traffic” (traffic control) in the final construction documents.

Shipping and Handling – The shipping of prefabricated components, especially heavy precast girders or girder segments, may require special routing or permits for weight limitations. Intermediate handling and transfer from one mode of transport to another, such as from roadway trailer to water barge, may necessitate the use of intermediate cranes or temporary storage which could increase costs or cause inadvertent delays. The shipping of long, slender girders also requires appropriate precautions for lateral stability.

Most precast concrete girders and components are conveniently shipped by road transport. However, longer and heavier girders may require heavy transporters and special permits (Figure 5.4.1-3). Under certain circumstances it may be more convenient to ship by rail or water, depending upon access to the production facility and jobsite and providing that intermediate trans-shipment (i.e. off-loading, temporary storage and re-loading) costs are reasonable. Accessibility can control, not only transport and girder size, but also the size of cranes capable of lifting and placing girders in the structure. Refer to *Bridge Design Manual*, MNL-133-14, 3rd Edition, Second Release, August 2014, Precast/Prestressed Concrete Institute, Chicago, IL for further information regarding transportation of precast, prestressed concrete members.

Figure 5.4.1-3 Roadway Transport of Prestressed Concrete U-beams

Constructibility and Specialized Erection Equipment – For most conventional precast girder superstructures (e.g. I-girders, bulb-tees, u-beams, box beams and slab beams), constructibility considerations will be limited primarily to the items noted previously. These include: availability of local materials; ability to transport prefabricated members to the jobsite; maintenance of traffic; and construction access for member erection and foundation drilling equipment. Although these items are ultimately the contractor's responsibility as part of his "means and methods," it is prudent to ensure that they do not require special treatment for the proposed structure.

Aspects of constructibility for more complex structures, such as the use of formwork, falsework, special lifting equipment, launching gantries, trusses, form-travelers and the like, are beyond the scope of this manual. In general, the greater the span length the more complex the structure type, construction methods and equipment needed. Structure types required to accommodate specific span ranges are identified in Section 5.4.2.

Figure 5.4.1-4 shows typical special falsework required for the construction of a three span, post-tensioned spliced girder bridge. Figure 5.4.1-5 shows a typical truss configuration for span-by-span segmental box girder construction.

Figure 5.4.1-4 Temporary Falsework for Spliced Girder Construction

Figure 5.4.1-5 Span-by-Span Construction using Erection Trusses

Aesthetics – Appealing aesthetics can be very affordable when incorporated into the bridge type selection and design processes early in the bridge development phase. Layout considerations involving aesthetics may include: span arrangements;

pier locations; girder soffit and fascia lines; the use of end slopes or end walls; and long-term maintainability of bridge materials and member surfaces. Some general principles to follow are:

- Adopt clean, uninterrupted lines to present a natural unobstructed feature for the eye to follow
- Aim for the shallowest superstructure
- Provide uniformity/compatibility in span lengths and deck overhangs
- Avoid the unresolved duality of a middle pier or obstruction when appropriate by adopting an odd number of spans (i.e. 1, 3, 5)
- Adopt and adapt slender and interesting pier shapes
- Adapt textures and colors to the local terrain
- Consider the entire structure within its local context

In general, bridges are large bold, intrusive and exist for a lifetime or more. Appearance is important. There is only one opportunity - it is worthwhile pursuing a pleasing but practical and cost-effective engineering solution.

Refer to Chapter 5 of *Bridge Design Manual*, MNL-133-14, 3rd Edition, Second Release, August 2014, Precast/Prestressed Concrete Institute, Chicago, IL for further information regarding aesthetics for precast concrete bridges.

5.4.2 Cross-Section and Span Length

Deck Cross-Section – Cross section types for concrete girder bridges can be categorized as follows for design purposes (in order of increasing span length):

- **CIP Slab / Precast Deck Bridges** include precast units placed adjacent to each other in the longitudinal direction and joined together transversely to form a deck system. Examples of this type of cross section include: solid or voided planks; adjacent box beams; T- and double-T beams. Figure 5.4.2-1 and Figure 5.4.2-2 show solid precast deck beam (plank) and adjacent box beam superstructures, respectively.

- **Beam / Girder Bridges** consist of spread precast beams (girders) joined by a composite concrete deck (Figure 5.4.2-3 thru Figure 5.4.2-5.) Precast members for this type of cross section range in depth from relatively shallow (≤ 36 in. – e.g. spread box beams; inverted-T beams; Type I or II AASHTO girders) to depths of 96 in. or more. However, these types of bridges most commonly use girders in the 45 in. to 72 in. range (AASHTO I-girders, bulb-tees, U-beams.) For efficiency reasons bulb-tee shapes are generally favored over the older AASHTO I-girder shapes, and many DOTs have developed their own standardized bulb-tee shapes. A number of states use standardized

U-beam shapes as an aesthetic improvement over the lighter I-girder and bulb-tee shapes.

- **Cast-in-Place Box Girder** & **T-Girder Bridges** represent another cross section addressed in *AASHTO LRFD*, however, the latter type is rarely used any more. Post-tensioned CIP box girders (Figure 5.4.2-6) are used frequently in a handful of states where falsework construction is common.

- **Precast and Cast-in-Place Segmental Box Girder Bridges** (Figure 5.4.2-7) represent a type of superstructure construction where the individual precast (or CIP) elements are short box-shaped units with a monolithic deck extending the full (or nearly full) width of the deck. The spans are made of multiple units erected incrementally and joined together by longitudinal post-tensioning.

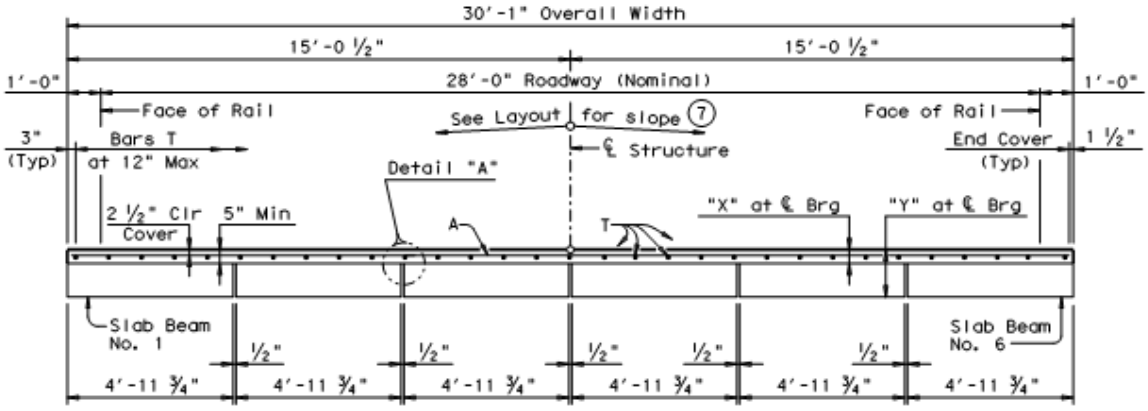

Figure 5.4.2-1 Precast Solid Slab Beam (Plank) Bridge

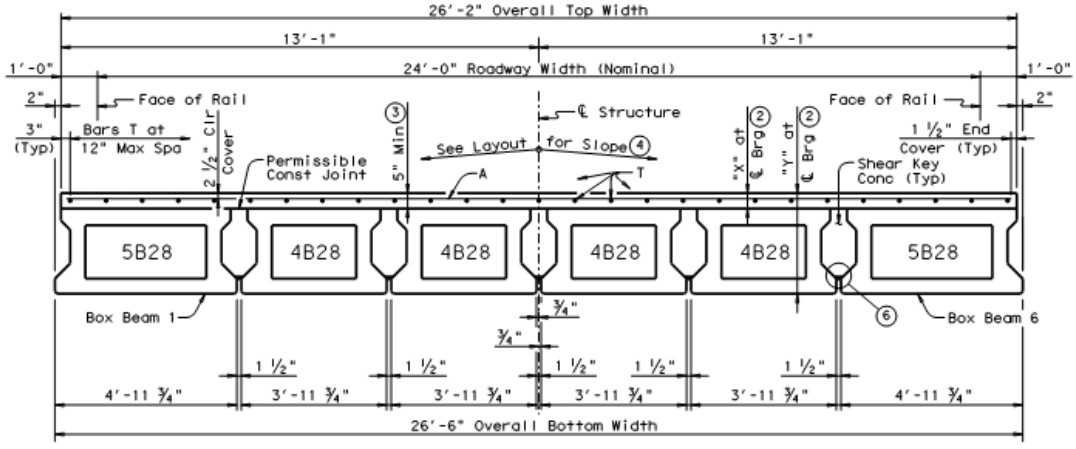

Figure 5.4.2-2 Adjacent Precast Box Beam Bridge

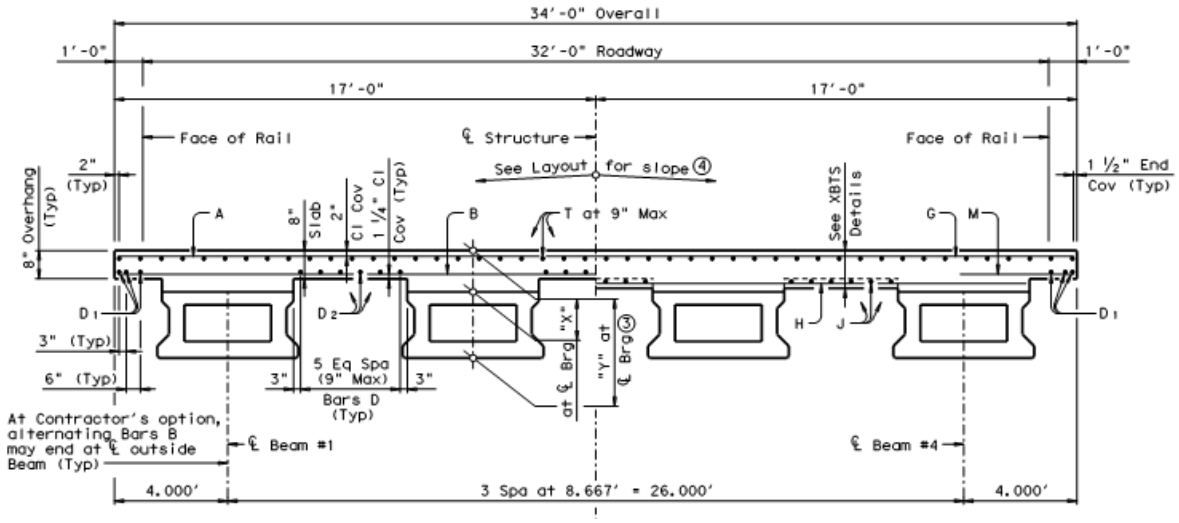

Figure 5.4.2-3 Spread Precast Box Beam Bridge

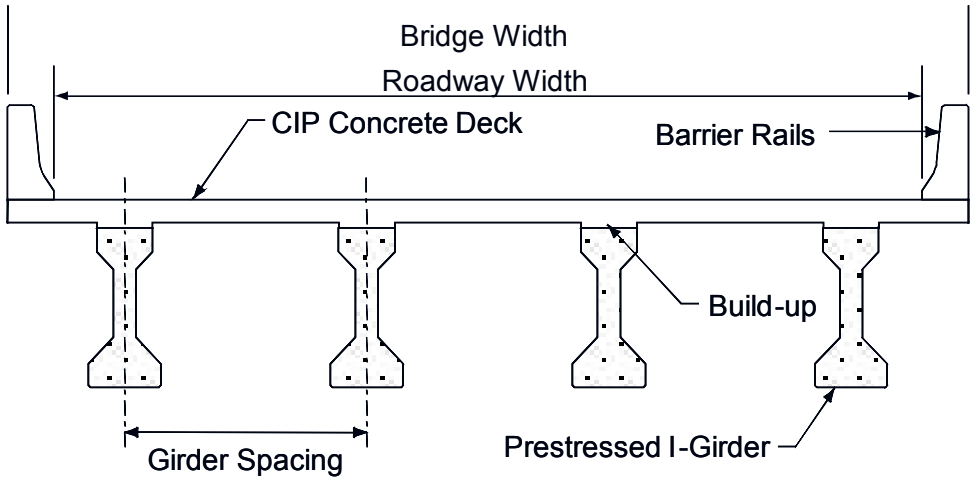

Figure 5.4.2-4 Typical AASHTO I-Girder Bridge

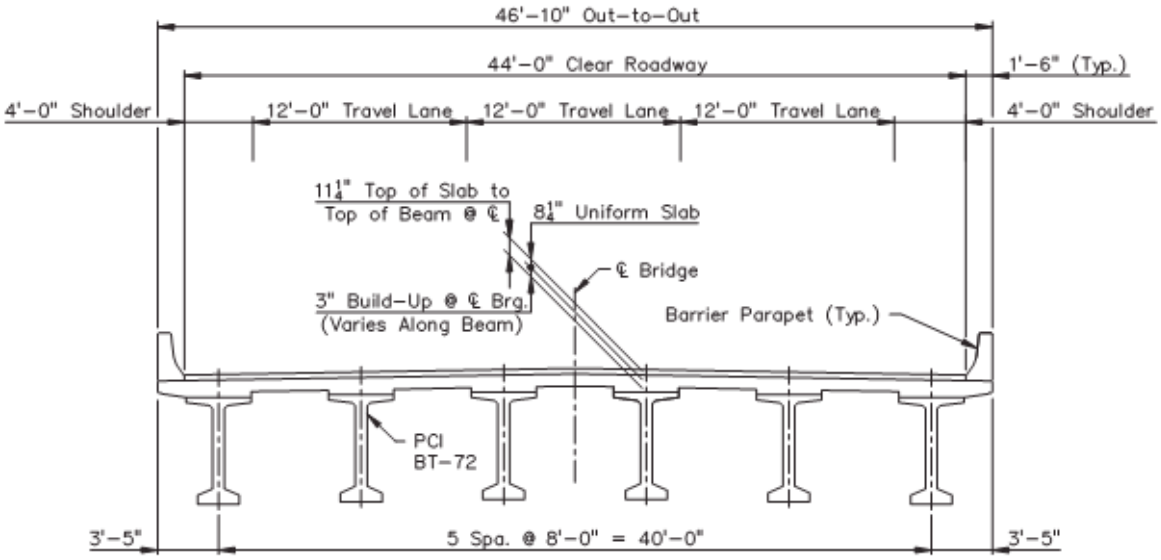

Figure 5.4.2-5 Typical AASHTO Bulb-Tee Girder Bridge

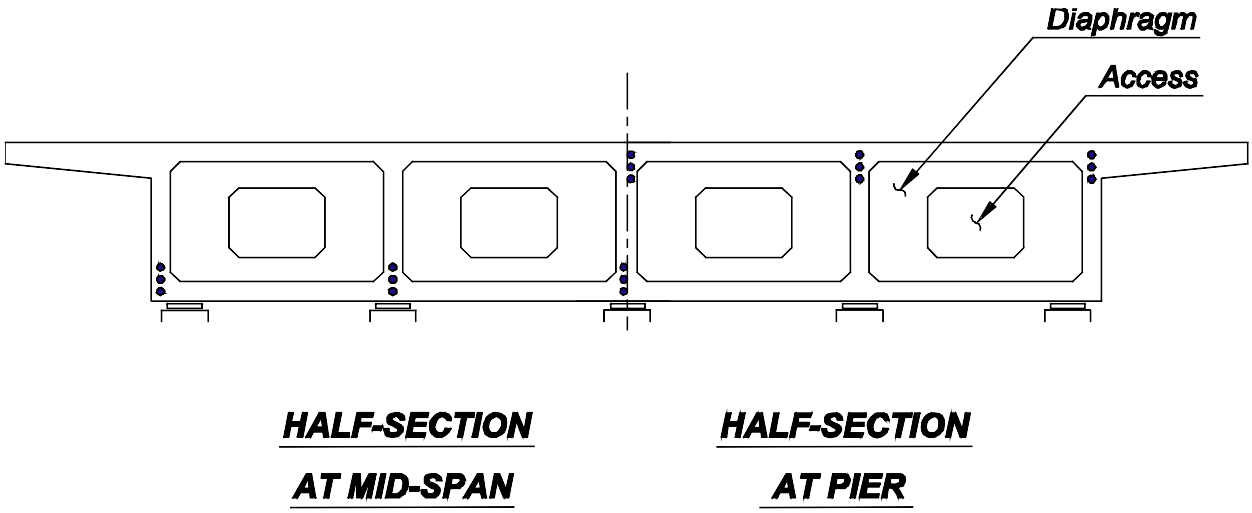

Figure 5.4.2-6 Four-Cell CIP Box Girder Bridge

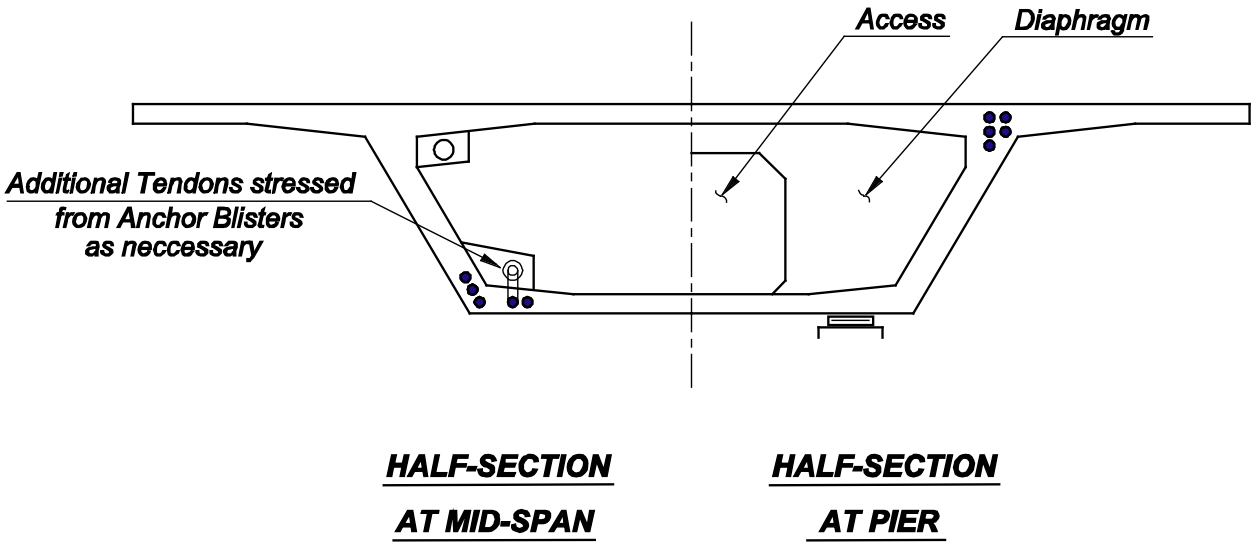

Figure 5.4.2-7 Single-Cell Precast Segmental Box Girder Bridge

Span Length Considerations – Within the basic cross section types previously identified, the maximum achievable span length may depend on variations that are influenced by constructibility, contractor familiarity or local DOT preferences. For example, I-girder or bulb-tee girder superstructures may utilize simple-span girders, girders continuous for live load or fully continuous girders. They may also be used in conjunction with post-tensioning and longitudinal splicing of girder segments to greatly increase span lengths beyond those achievable by prestressing alone (see NCHRP Report 517, "Extending Span Ranges of Precast Prestressed Concrete Girders," Transportation Research Board, Washington, DC, 2004. Segmental box girder bridge superstructures may be built using different construction methods (e.g. precast vs. cast-in-place, span-by-span, balanced cantilever or incremental launch) depending on span length, site constraints, size of project and construction schedule. For a particular type of bridge construction (e.g. precast girders, cast-in-place boxes, etc.) increasing the span length increases the cost of the structure. As a result, as spans increase beyond a certain limit, it becomes more economical to switch to an alternative, usually more complex, type of construction better suited to the circumstances. See Figure 5.4.2-8 for a chart showing bridge span capabilities for various types of concrete superstructure systems.

Although relative superstructure cost data as shown in Figure 5.4.2-8 is useful for preliminary design, it should never be assumed that the comparison of bridge type and cost can be based solely upon span length and superstructure cost. Optimizing the layout and design of a bridge involves a complex interaction between different variables – span length; superstructure depth and cross-section; number of piers; size of piers and foundations; and constructibility considerations. The goal of the optimization is to develop the lowest total cost solution that meets all the owner's preferences and objectives.

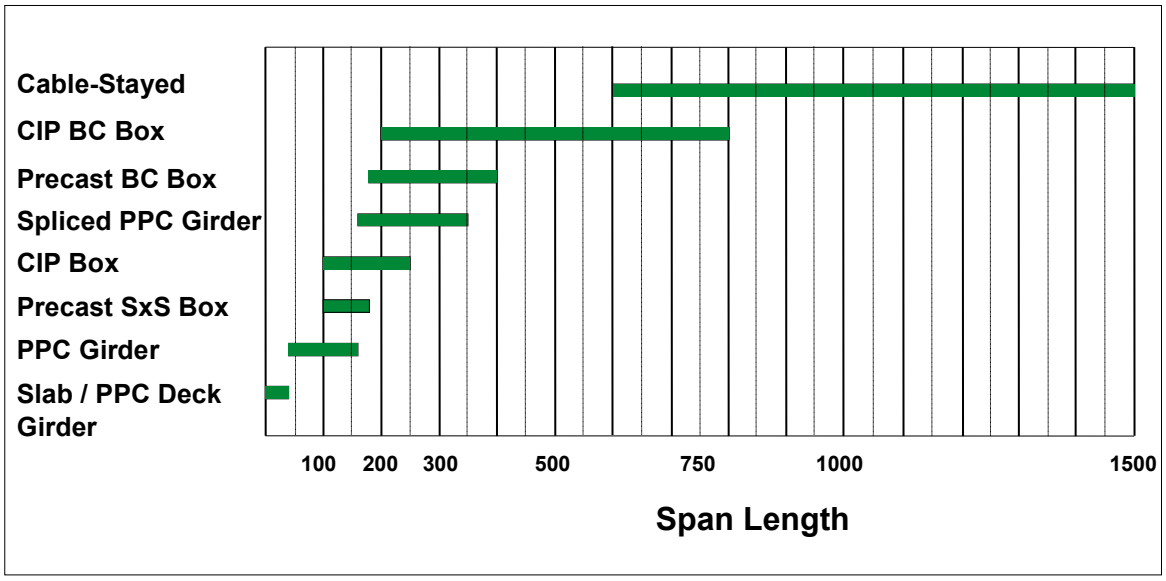

Figure 5.4.2-8 Bridge Type vs. Applicable Span Range

where:

CIP BC Box = Cast-in-place, post-tensioned box girder superstructures built using the balanced cantilever method of construction

Precast BC Box = Precast, post-tensioned box girder superstructures built using the balanced cantilever method of construction,

CIP Box = Cast-in-place, post-tensioned box girder superstructures typically cast on falsework

Precast SxS Box = Precast, post-tensioned box girder superstructures built using the span-by-span method of construction

PPC Girder = Precast, prestressed concrete girder superstructures with cast-in-place deck slabs (e.g. I-girder, bulb-tee, U-beam)

Slab / PPC Deck Girder = Cast-in-place slab or precast, prestressed concrete girder superstructures with cast-in-place deck slab (e.g. slab beam, adjacent box beam, double-tee)

Many preliminary design situations lend themselves to consideration of just a single bridge type or perhaps a narrow comparison between two or three “viable” options. For example, a grade separation structure crossing a four- or six-lane divided highway will likely favor a multi-girder superstructure solution. Near the other end of the scale a 3000 ft. long bridge over a deep-water river with heavy barge traffic will necessitate a longer span solution, such as a cast-in-place balanced cantilever segmental or cable-stayed structure. Therefore, within a given bridge type it is just

as important to optimize span lengths as when comparing two or more different potential bridge types – for example, the choice of using various depth standard AASHTO I-girders or PCI bulb-tee shapes with different span lengths, numbers of piers, and girder spacings. For longer spans where the choice may lie, for instance, between precast or cast-in-place balanced cantilever, the span optimization exercise should consider the difference in construction techniques, schedules and times, in addition to the locations and numbers of piers for different span lengths.

It is more complex and sometimes can be misleading to compare span lengths and costs across different bridge types – for example, I-girders versus precast segmental. In such cases, a comprehensive examination of all relevant considerations may include factors such as aesthetics, owner or local contractor familiarity with a certain bridge type, bridge element fabrication lead times and overall schedule.

In cases where bridge piers may be subjected to significant lateral loads (e.g. vessel impact or earthquake), span lengths and foundation sizes should be chosen to balance demand between sustained loads over the service life of the structure and larger but less probable load effects from extreme events. It may be more cost effective to adopt a longer span to take advantage of the large foundations required for the infrequent high lateral loads or to locate piers within a lower vessel impact zone.

Optimization of preliminary concepts and alternative bridge types taking into account the various constraints, constructibility and engineering requirements noted above will lead to a matrix of possible bridge configurations and construction costs for selection, further development or refinement during final design. For preliminary design and cost-estimating purposes, it is usually sufficient to base estimates upon previous unit prices or contract history, suitably adjusted for inflation, market conditions and geographic region.

5.4.3 I-Girder Design and Sizing

Because of their versatility and wide-spread use around the country, much of this chapter is devoted to the design of prestressed I-girder or bulb-tee girder superstructures. AASHTO I-girders (Types I through VI) were developed primarily in the late 1950s and early 1960s in an effort to standardize a family of prestressed girders shapes that could be used anywhere in the country. The various girder depths accommodated the most common highway bridge span configurations in use during that era. However, by the early 1970s some state DOTs, in conjunction with the local precast industry, were developing more efficient “bulb-tee” shapes, which featured wider top flanges to accommodate longer spans with reduced self-weight. Although standard AASHTO girder shapes are still in common use around the country, the number of states using bulb-tee shapes has increased rapidly over the

past twenty years to meet demands for greater clear spans and increased safety. This growth has been facilitated by advancements in concrete and high-strength steel materials. Besides permitting greater span lengths due to reduced girder weights and more prestressing for a particular depth, the wider top flanges of bulb-tee shapes afford greater lateral stability for transport and handling during construction.

Throughout this chapter the terms “I-girder” and “bulb-tee girder” are used interchangeably since the design principles involved for the various shapes are interchangeable. Also, the terms “girder” and “beam” are considered equivalent.

Applicable simply-supported span ranges for the most common prestressed I-/bulb-tee girders are shown in Figure 5.4.3-1. The chart is based on standard practice and parametric analysis results from the PCI *Bridge Design Manual* for AASHTO I-girder and PCI bulb-tee standard sections. Considerable overlap of span ranges for different sizes of girders offers flexibility to best suit the circumstances of an individual project – such as site layout, geometric constraints, accessibility, etc. The absolute maximum span length attainable by a particular girder type in a particular application is dependent on a number of factors, which may include: locally available concrete materials (i.e., concrete strength); beam spacing; temporary tensile stress limits and release strength restrictions; final tensile stress limits; size and number of strands; draping and/or shielding of strands; deck thickness; assumed distribution of barrier rail loads; and requirements for a concrete wearing surface.

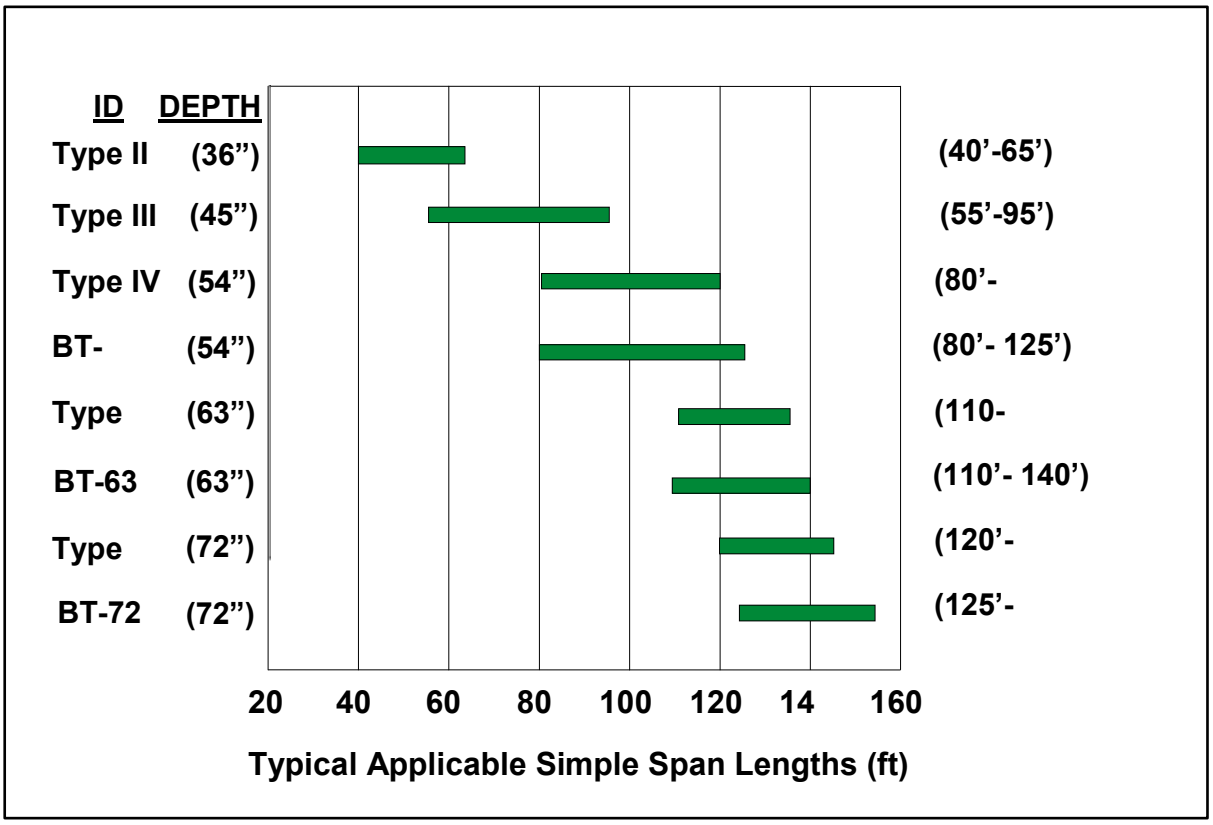

Figure 5.4.3-1 Simple-Span Precast Girder Types and Typical Span Ranges (AASHTO I-Girders; PCI Bulb-Tees)

By making girders fully structurally continuous with spliced joints and post-tensioning, it is possible to increase spans by 10% to 20% as indicated in Figure 5.4.3-2.

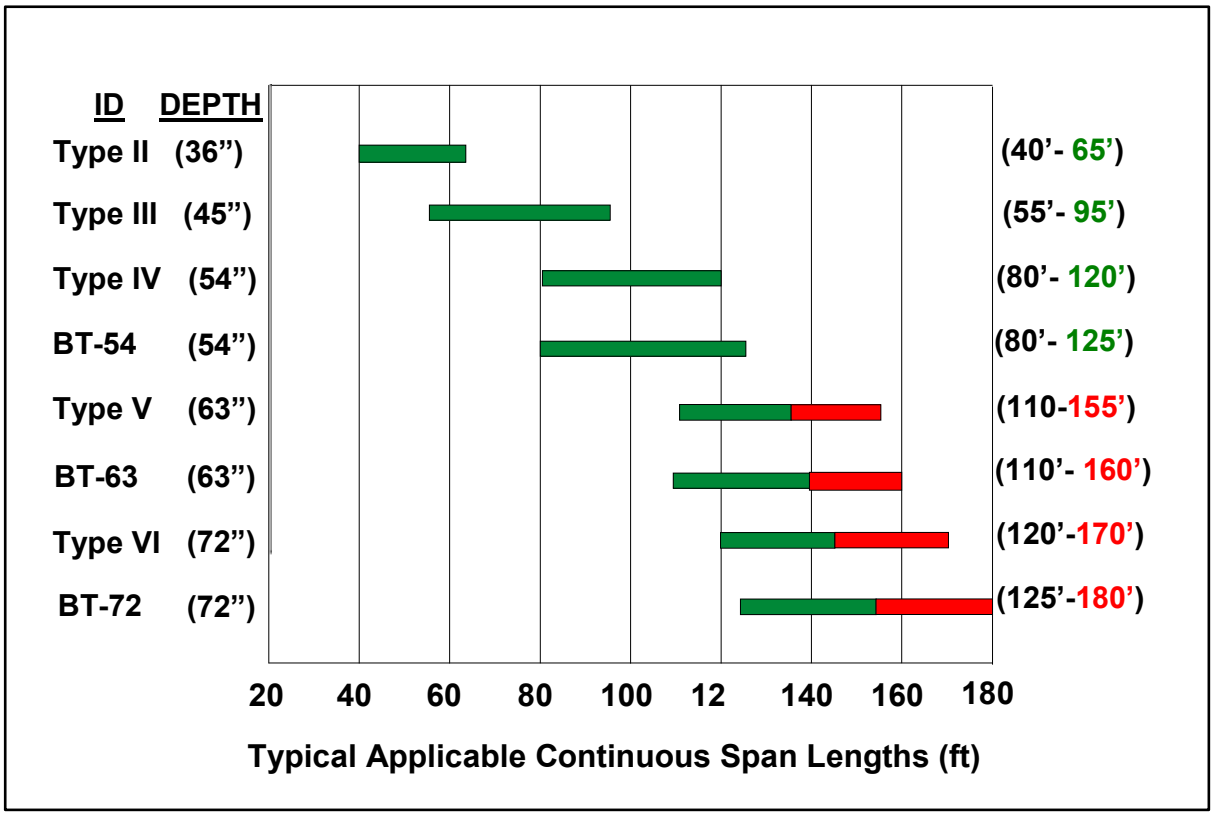

Figure 5.4.3-2 Increase in Span Length from Structural Continuity

A span is generally 16 to 24 times the depth of a girder (*span/depth ratio*) but this may also depend upon girder spacing and stiffness (or thickness) and weight of the deck slab. Girder spacing may range from 4 to 12 feet – but is more usually between 6 and 10 feet. – and is chosen to suit the required overall width of the highway deck

All precast girder sections developed over the years are able to accommodate a sufficient number of pre-tensioning strands to provide the necessary flexural resistance for the span range of each type of girder. Longitudinal pre-tensioning strands are most often 0.5" nominal diameter, although 0.6" dia. strand may be used in some cases. The number of strands can be varied, but must be arranged to a specific pattern and spacing within the section. The strand size and pattern depends upon the manufacturing facility and, in particular, the size and capacity of the stressing bulkheads. Before commencing a design, check with industry concerning local availability.

The calculation process for starting a new design usually begins with a selected girder section and an initial estimate of the strand-layout, force and eccentricity.

5.4.4 Box Girder Design and Sizing

5.4.4.1 Typical Superstructure Sections

The most common types of cross-section are multiple cell (multiple webs - Figure 5.4.4.1-1) or single cell (two-web) boxes, or similar variations. Variations include vertical or sloping outer webs, deck slabs with multiple T-section ribs, with or without bottom flanges, voided slabs or similar sections. The key feature is that the whole cross-section is “non-composite” and is subject to all loads and longitudinal post-tensioning force; i.e. there is no separately cast, “composite” deck-slab as considered in foregoing sections of this manual.

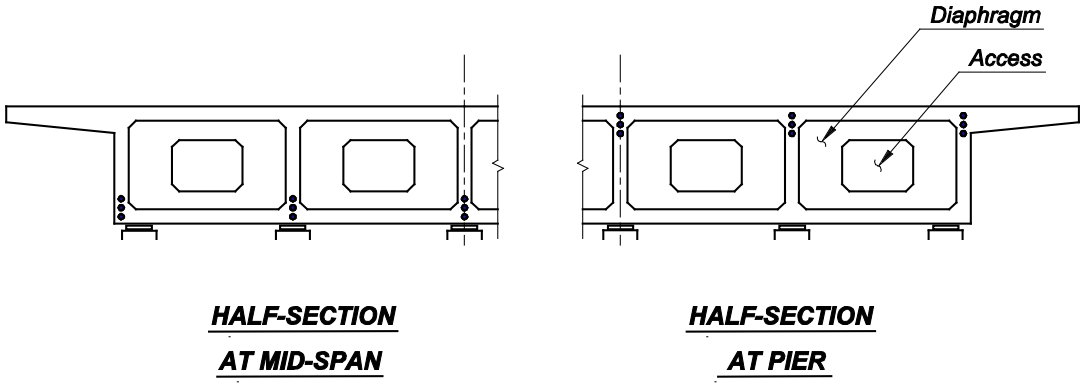

Figure 5.4.4.1-1Typical Multi-Cell Cast-in-Place Superstructure

5.4.4.2 Effective Cross-Section and Preliminary Sizes

Although the whole cross-section contributes to dead load, it does not necessarily participate structurally in resisting loads and prestress. In some cases, only portions of the top and bottom slabs may be considered effective, depending upon various proportions. For design purposes, the effective width of slabs is given in *AASHTO LRFD* Article 4.6.2.6.

AASHTO LRFD Article 5.14.1.5.1 gives minimum thicknesses for top flange, bottom flange and webs, but existing design plans for structures of a similar type and size probably provide better guidance for practical member thicknesses. Attention should be paid to thicknesses necessary to accommodate cover, reinforcement, longitudinal and transverse post-tensioning, construction tolerances, maximum size of aggregate and clearance for effectively placing and consolidating concrete.

As a general guide the following are offered for estimating initial concrete thicknesses:

- The minimum depth of a top slab should be 7 inches - to which would be added any necessary depth for grinding and grooving (*AASHTO LRFD* Article 9.7.1.1). Durability considerations (e.g. additional cover at riding surface for future resurfacing or deck steel and post-tensioning corrosion resistance) favor an 8 in. minimum thickness.

- If the deck slab (top flange) at coping edges needs to accommodate transverse post-tensioning anchors, it should be ≥ 9 inches to allow for the height of the anchor plate, local anchor reinforcement, top and bottom rebar and cover. The thickness of a top slab at the root of the cantilever wing should be about the edge thickness plus 0.5" to 0.75" for each foot of total overhang.

- The minimum depth of a bottom flange should be ≥ 5.5 inch (*AASHTO LRFD* Article 5.14.1.5). However, 7 in. is a preferable minimum to facilitate steel placement and casting and to ensure durability.

- The total (sum of all) web thickness may be estimated at approximately 0.6 to 1.0 inches per foot of overall deck width (i.e., correlation to dead loads and number of lanes.)

- The minimum individual web width should be sufficient to accommodate post-tensioning ducts, rebar, cover, tolerances, maximum aggregate size, and concrete placement and consolidation.

- For a structure of constant depth the overall structural depth is usually in the range of L/24 to L/18, where L = span length.

- For a structure of variable depth the overall depth at an interior pier is usually about L/20 and at mid-span a minimum of L/40.

- In longer spans of box girders (usually > 160 feet) the bottom slab may need to be thickened near interior piers to provide increased concrete compression area for negative moment resistance.

The above recommendations are for initial guidance only. Local commercial conditions will govern the availability of concrete of a particular strength and size of aggregate. Local environmental conditions usually govern minimum cover requirements.

Section 5.5 Flexural Design of Prestressed I-Girders

5.5.1 Service and Fatigue Limit States

The flexural design of precast, prestressed concrete girders is typically governed by stress control at the service limit state. The girder must be verified under these service conditions from initial prestress transfer through final service conditions.

Fatigue of reinforcement is typically not a concern for prestressed concrete girder superstructures. Fully prestressed components designed for the Service III Load Combination (*AASHTO LRFD* Table 3.4.1-1) to meet the tensile stress limits of *AASHTO LRFD* Table 5.9.4.4.2-1 need not be checked for fatigue.

5.5.2 Strength and Extreme Event Limit States

Once the girder has been designed to satisfy flexural service stress limits, the girder is designed for both flexure and shear at the strength limit state to ensure overall resistance of the structure to safely resist factored design loads.

For conventional precast pretensioned girder bridges, extreme event limit states (earthquake, vessel collision, and vehicle collision) often will not govern superstructure design per se. However, this depends on the specific seismic zone in which the bridge is built. For more complex bridges like continuous, post-tensioned spliced girder or segmental box girder superstructures, the transfer of earthquake or vessel collision forces from the substructure to the superstructure may need to be considered.

5.5.3 Service Design

5.5.3.1 Loads and Bending Moments for Composite Construction

Bridges with precast concrete girders and cast-in-place deck slabs utilize composite construction in which loads and moments are applied first to a non-composite girder section and then, after hardening of the deck slab, to the composite girder/slab section.

The different loads and bending moments acting on the non-composite and composite sections are summarized in Figure 5.5.3.1-1. This figure also illustrates that stresses are calculated separately, according to the section acting at the time of application of the load or moment. Final stresses must be determined by accumulating the individual stresses (i.e., not by accumulating moments.)

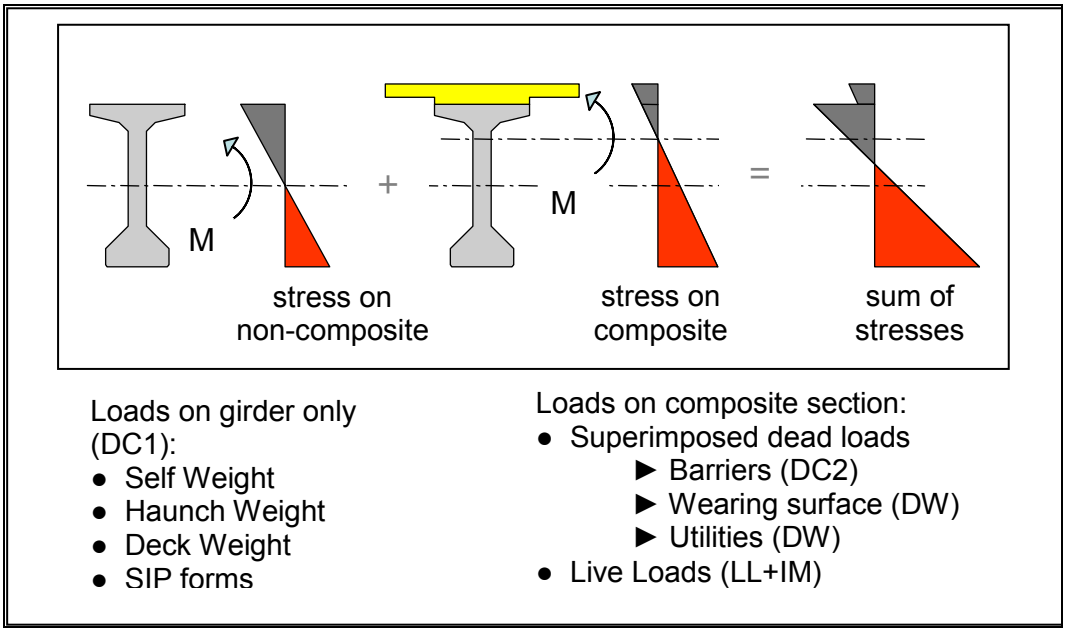

Figure 5.5.3.1-1 Loads and Stresses in Composite Construction

The permanent load factor of 1.0 at service limit state simplifies the incremental summation of stresses, particularly since this process depends upon the change from non-composite to composite section properties.

For convenience a designer may prefer to calculate the individual stress from each of the applied load conditions in Figure 5.5.3.1-1 at sections and elevations of interest along the girder before attempting to establish a necessary level of prestress. The calculation of stresses depends upon the appropriate section properties. These are defined and determined as follows.

5.5.3.2 Composite and Transformed Section Properties

5.5.3.2.1 Non-Composite and Composite Properties

Prior to hardening of the deck slab, all load (i.e., self-weight of girder and the weight of the deck slab, temporary or permanent forms) is applied only to the non-composite girder section, and stresses are determined for the girder's section properties alone (or the properties using the transformed area of prestressing steel.) After the slab has been cast and hardens, subsequent loads are applied to the composite section of the girder and slab so stresses are calculated using the composite section.

5.5.3.2.2 Effective Flange Widths

Composite section properties are calculated for effective slab widths according to *AASHTO LRFD* Article 4.6.2.6. The effective flange width of a composite pretensioned girder bridge may be taken as one-half the distance to the adjacent girder on each side of the component (Figure 5.5.3.2.2-1), or one-half the distance to the adjacent girder plus the full overhang width (Figure 5.5.3.2.2-2). These provisions apply in most situations involving pretensioned composite girders with the exception of an overhang greater than one-half the girder spacing or skew angle θ greater than 75 degrees, where θ is the angle between the bent centerline and a line normal to the centerline of girder.

The top slab is of concrete different than the girder (different strength and maturity). It is therefore necessary to transform the slab concrete area to an equivalent area of girder concrete by multiplying the effective width of the slab by the modular ratio (n) of the modulus of elasticity for the slab concrete divided by that for the girder concrete (i.e., $n = E_{slab}/E_{girder}$) – see Figure 5.5.3.2.2-3.

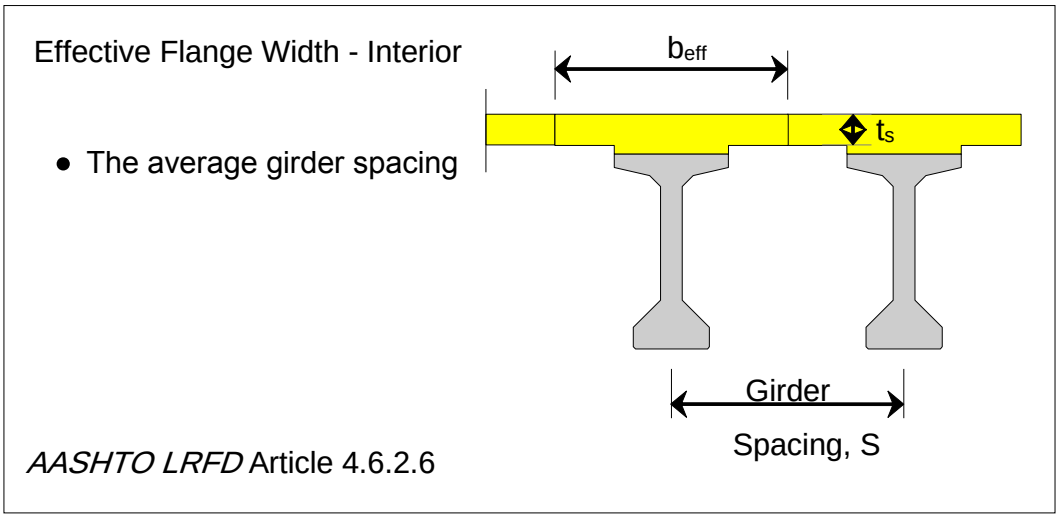

Figure 5.5.3.2.2-1 Effective Flange Width of Interior Girder

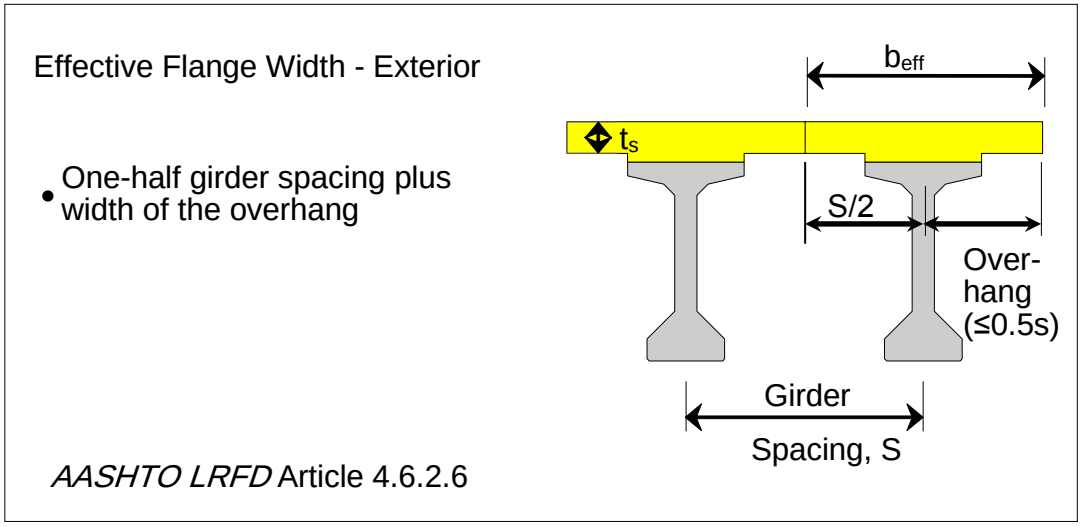

Figure 5.5.3.2.2-2 Effective Flange Width of Exterior Girder

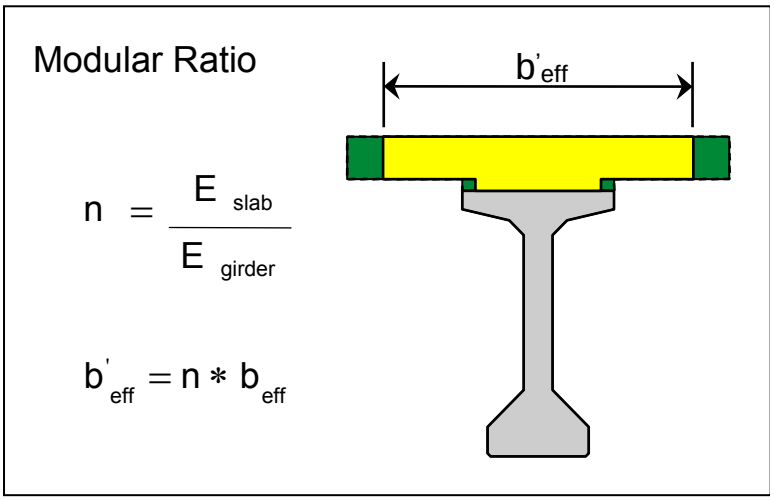

Figure 5.5.3.2.2-3 Modular Ratio (n) of Slab to Girder Concrete

Gross composite section properties are calculated using formulae illustrated in Figure 5.5.3.2.2-4.

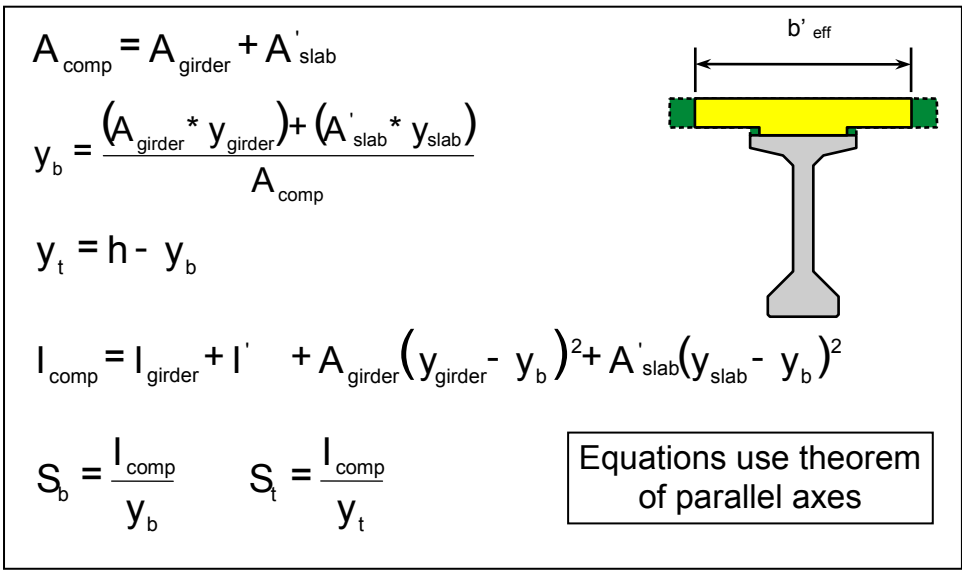

Figure 5.5.3.2.2-4 Calculation for Composite Section Properties

5.5.3.2.3 Transformation of Prestressing Steel

Some jurisdictions allow the transformation of the prestressing steel to an equivalent area of concrete section equal to $(n'-1)A_{ps}$ (where n' = modular ratio of elastic modulus of prestress steel to that of the girder concrete) located at the average eccentricity, e, when determining section properties for the girder alone. In which case, the above composite section properties are calculated using the transformed non-composite properties (Figure 5.5.3.2.3-1).

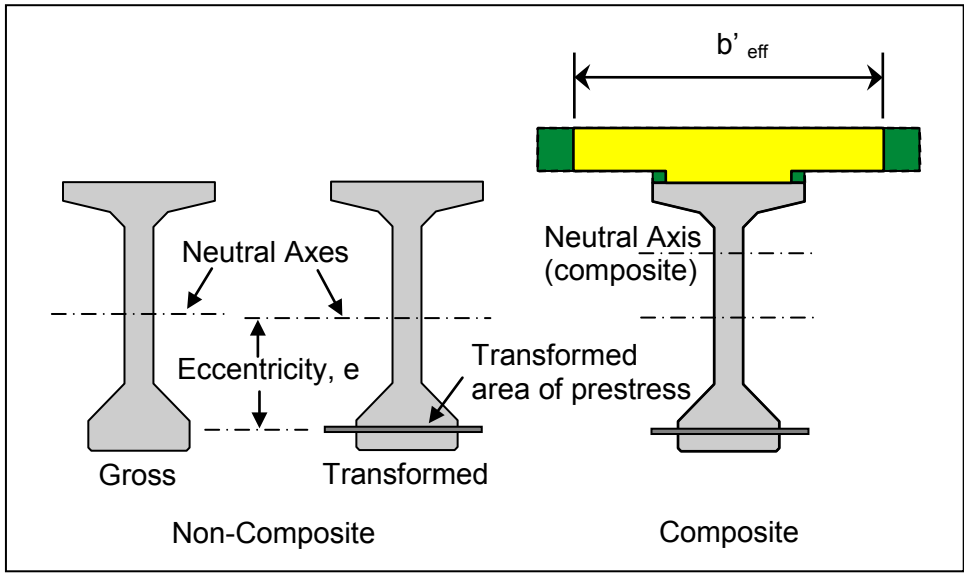

Figure 5.5.3.2.3-1 Transformed Area of Prestress

When using the transformed prestress area, in accordance with *AASHTO LRFD* Article C5.9.5.2.3a elastic shortening loss Δf_{pES} should not be applied at transfer as it is automatically accounted for by using the transformed steel area.

5.5.3.3 Accumulation of Stress in Non-Composite and Composite Sections

Calculation of stress is made by classical beam theory. Flexural stresses are determined at the top of the deck and at the top and bottom of the girder by dividing the applied moment by the applicable section modulus at each of these elevations. The resulting flexural stresses at the top and bottom of the girder are the actual stresses the girder experiences under the applied moment. However, the stress at the top of the slab is given as a stress in terms of girder concrete. To convert it to one of magnitude appropriate to the strength of the slab concrete, it is multiplied by the modular ratio of the elastic modulus of the slab to that of the beam (n).

Final stresses are determined by summation of all individual stresses applied to the non-composite and composite section in turn, from the time of transfer to final (long-term) service conditions after all loss of prestress due to elastic shortening, shrinkage, creep and relaxation of the prestressing steel has occurred. (For calculation of losses see Section 5.7.3)

5.5.3.4 Typical Design Sequence

This section illustrates the typical design process for a pretensioned concrete bridge girder with a composite deck.

5.5.3.4.1 Prestress Force and Eccentricity, Begin a Design

Calculation of the eccentricity of a group of prestressing strands from the neutral axis of the non-composite section is made using the technique illustrated in Figure 5.5.3.4.1-1.

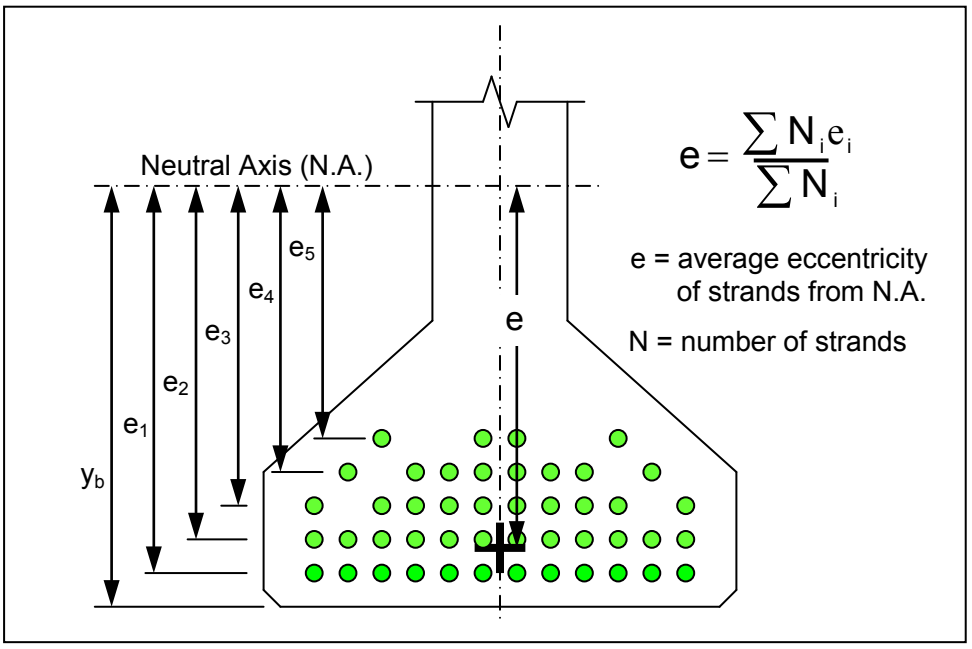

Figure 5.5.3.4.1-1 Eccentricity of Prestress Strands

Strands are set out in the pattern of available bulkhead stressing locations. The prestressing force depends upon the number of strands and their eccentricity at various sections along the girder. Key sections are mid-span, at each end of the girder, and at locations where strands are deflected or the number is reduced by debonding with plastic shielding. The design process involves iteration and repetitive calculation to arrive at the optimum solution. It is helpful to have a simple spreadsheet or program to facilitate calculation of strand eccentricity.

A new design generally begins by making an estimate of the required magnitude of the final prestress force and eccentricity at mid-span, after all losses, to satisfy final service conditions for the bottom fiber tensile stress limit. This requires first knowing the bottom fiber tensile stress induced by all accumulated dead and live loads on the non-composite and composite section and the appropriate tensile stress limit.

A convenient starting point for a new design is to assume that the final prestress after all losses is in the range of 58 to 62% of f_{pu} – say, 60% of f_{pu}. An assumed final prestress force at an assumed eccentricity is applied to the non-composite section (Figure 5.5.3.4.1-2). The effect of the self-weight of the deck slab, forms and diaphragms are applied on the non-composite section and the stresses are added to those from the assumed final prestress (Figure 5.5.3.4.1-3).

Superimposed dead loads are applied to the composite section and the stresses at each elevation are added to the previous ones (Figure 5.5.3.4.1-4). Finally, service live load is applied to the composite section and the stresses are added to the

previous ones giving the final conditions (Figure 5.5.3.4.1-5) for the assumed final prestress.

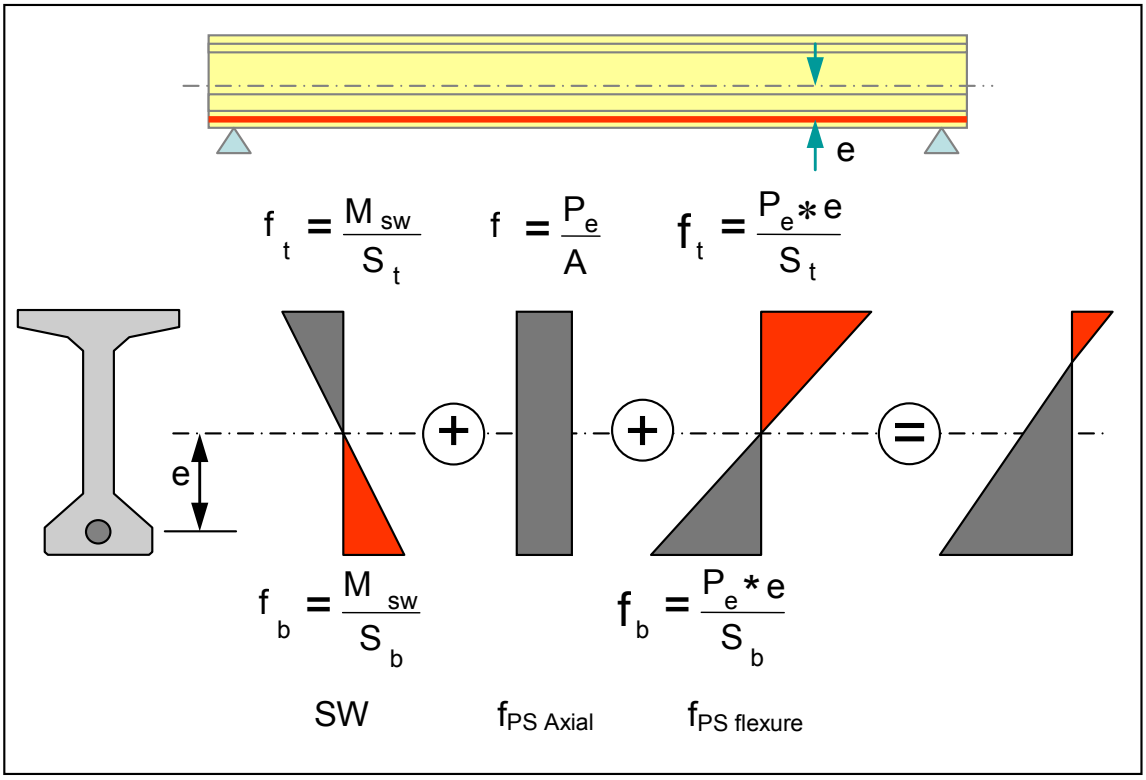

Figure 5.5.3.4.1-2 Non-Composite Section under an Assumed Final Prestress

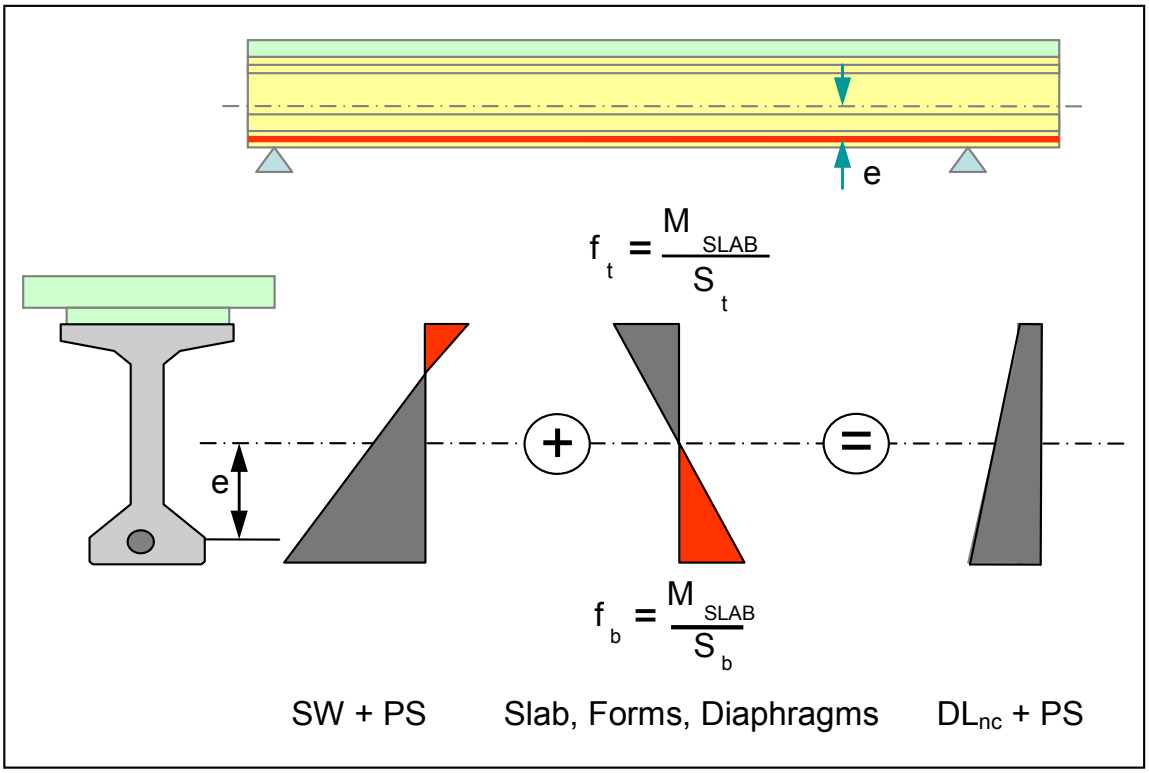

Figure 5.5.3.4.1-3 Loads of Slab, Forms and Diaphragms Applied to Non-Composite Section

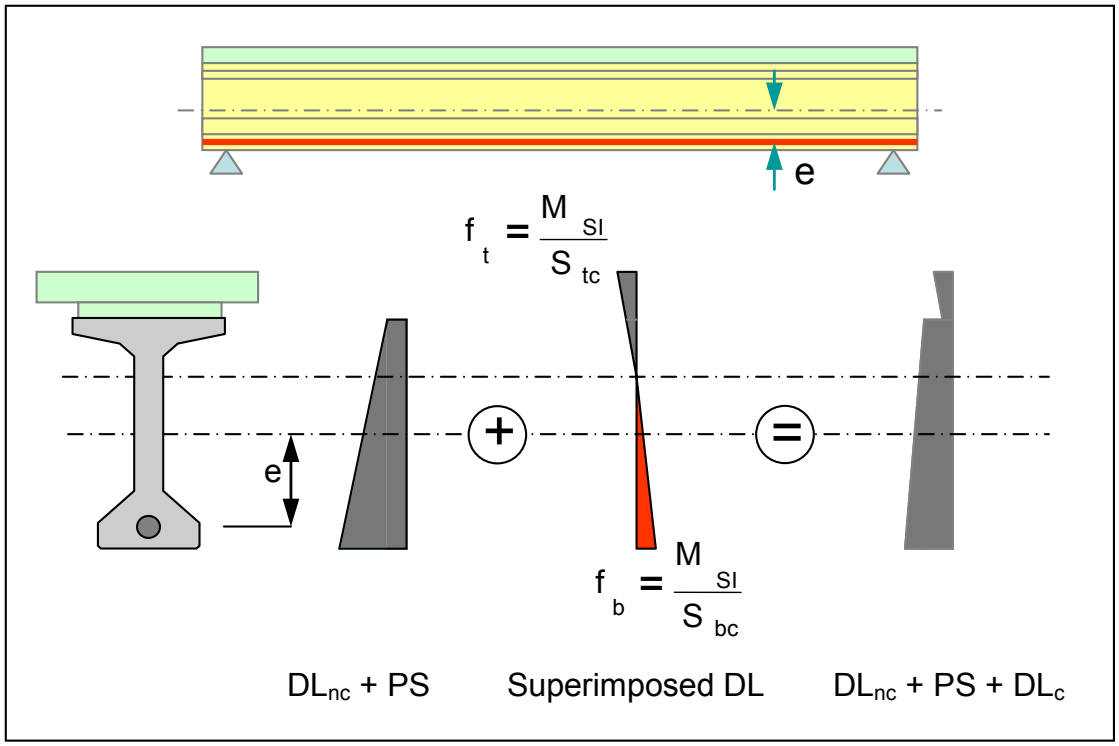

Figure 5.5.3.4.1-4 Application of Superimposed Dead Load on Composite Section

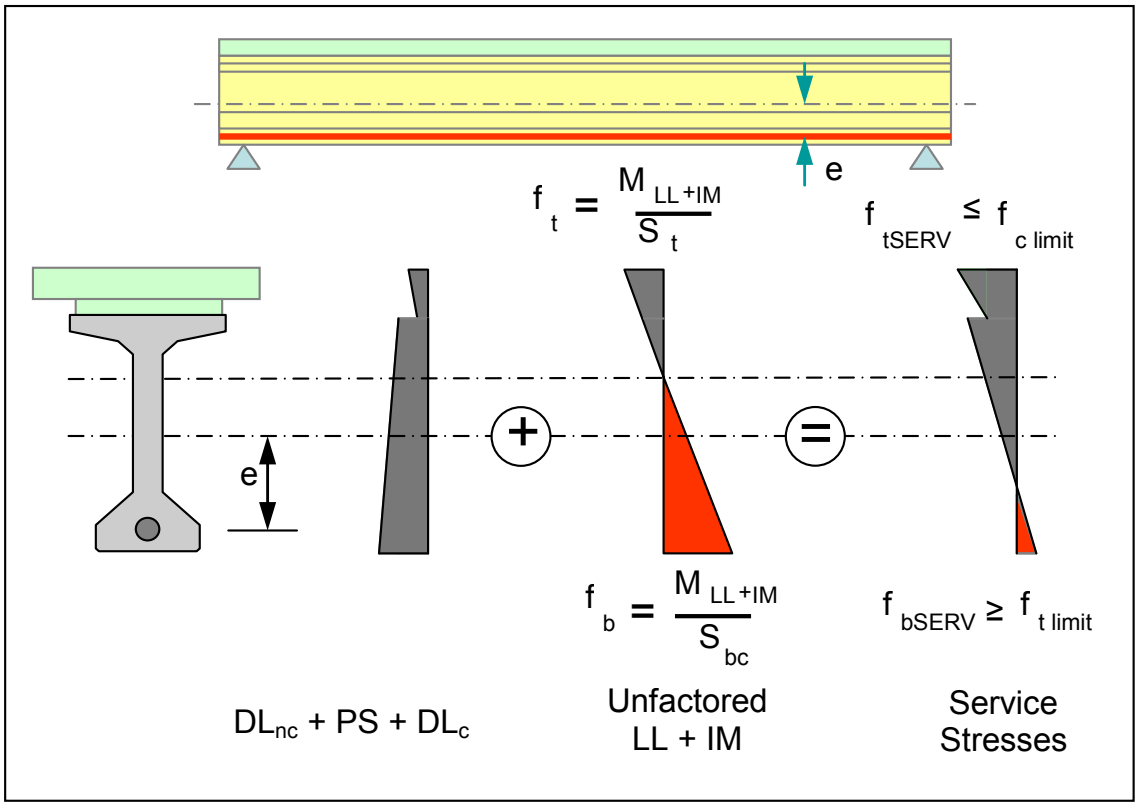

Figure 5.5.3.4.1-5 Application of Live Load on Composite Section

The assumed final force and eccentricity is adjusted until the bottom fiber tensile stress satisfies the service tensile stress limit. This gives a revised estimate of the required final prestress force, area of prestress, A_{ps}, number of strands and eccentricity at mid-span.

The number of strands is laid out to the available bulkhead pattern and the actual eccentricity at mid-span, e_m, is calculated (Figure 5.5.3.4.3-1). Initially, section properties may be based on gross sections with or without the transformed area of the prestressing steel, as appropriate.

Also, for the purpose of beginning a new design, the top fiber tension may be checked at this point for the initial condition at transfer assuming a transfer stress of 0.70 or 0.75f_{pu} for stress relieved or low relaxation strands, respectively. Appropriate checks should be made at mid-span, with the self-weight bending moment of the girder acting, and at the ends where there is no self-weight moment. The prestress force and eccentricity should be revised, as necessary. This calculation is refined as iterations improve estimates for the actual number of strands and eccentricity at various sections.

5.5.3.4.2 Flexural Conditions that Control the Required Prestress Force

For a simply-supported precast pretensioned girder two conditions generally control:

1. Tensile stress in the bottom fiber at mid-span when the girder is in long-term service carrying all dead and live loads after all loss of prestress force has occurred.

2. Tensile stress in the top fiber at transfer when the initial force in the strands is released from the stressing bulkheads and transferred to the newly cast section. This is particularly critical at the ends where there is little or no top fiber flexural compression from self-weight to offset tensile stress from eccentric prestress force. Similarly, it is also important to check the mid-range of the span where both prestress force and eccentricity are usually at a maximum and induce significant top tension.

Limits on tensile stress in concrete are given in *AASHTO LRFD* Article 5.9.4.

The above two conditions occur not only at different times and maturity (strength) of the girder concrete, but apply to structurally different cross sections – the second applies to the non-composite girder section alone at transfer; the first applies to the non-composite girder section for most dead load and to the composite section of the deck slab plus girder for superimposed dead and live load.

The objective is to make sure that the final prestressing force is sufficiently large to avoid excessive tensile stress in the bottom fiber in service after all losses, yet not so large as to induce cracking in the top at transfer.

5.5.3.4.3 Incremental Summation of Stress and Final Prestress Strand Selection

The need and technique for properly summing stresses was demonstrated in the foregoing paragraphs and figures. Once the beginning estimate has been made for the final prestress force and eccentricity at mid-span, detailed calculations may commence with the initial transfer conditions, through all intermediate steps, including prestress losses, to conclude with revised final stresses and the actual effective prestress force at each section and elevation of interest. If necessary, revisions are made and the process repeated to attain an optimum solution.

Although iteration may appear tedious, much of the information remains the same (for instance, accumulated applied load stresses). It leads to the required strand pattern and eccentricity after only a few iterations. This can be facilitated by a

spreadsheet or computer program. The final controlling bottom fiber tensile limit conditions at mid-span are shown in Figure 5.5.3.4.3-1.

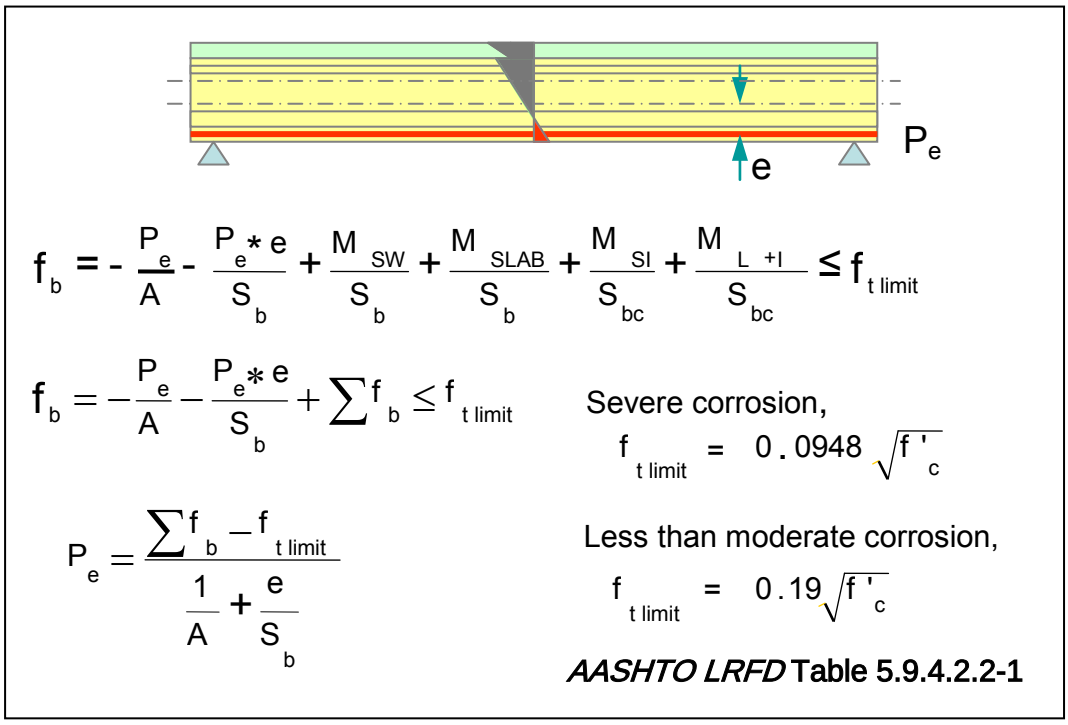

Figure 5.5.3.4.3-1 Final Effective Prestress Force for Bottom Fiber Tensile Limit

The final bottom fiber service stress must be less than the tensile stress limit – if not, increase the prestress force (i.e., number of strands). If the final bottom fiber stress is significantly less than the tensile stress limit, it may be feasible to decrease the number of strands. It is a relatively simple task to adjust the magnitude of the final effective prestressing force and eccentricity until the bottom fiber tension is satisfied.

Because the two main variables are the assumed magnitude and eccentricity of the final prestress force, iteration involves only the first two terms of the equations in Figure 5.5.3.4.3-1. All other stresses in the summation remain unaffected. Summarizing, the required final prestressing force, P_e, and thus the number of strands, may be determined from:

$$P_e = \frac{\sum f_b - f_{tAllow}}{\frac{1}{A} + \frac{e}{S_b}}$$

where:

Σf_b = sum of stresses due to permanent gravity loads and the maximum live load in the bottom fiber, calculated and summed for the applicable section properties

So far, the magnitude of the final prestress force has been set by the first of the controlling criteria, the bottom fiber tensile limit. It is now necessary to reconsider conditions at transfer; properly account for prestress loss at transfer, and if necessary, revise the prestress to satisfy the second controlling condition – that of the initial top fiber tension (*AASHTO LRFD* Table 5.9.4.1.2-1).

Loss of prestress occurs due to shrinkage and creep of the concrete and relaxation of the prestressing steel during the time from transfer until the girder is erected and the deck slab cast. Further time-dependent losses occur under permanent loads as the deck slab and girder continue to shrink and creep and the prestressing steel relaxes, until these effects gradually diminish, finally reaching a long-term level at which no further loss occurs.

When the calculated prestress loss is incorporated into the incremental summation process (previous figures), it leads to the final stresses in Figure 5.5.3.4.3-2 at each section and elevation of interest. Compression stress in the top of the girder and deck slab should be checked against the maximum limit allowed for the service limit state (*AASHTO LRFD* Article 5.9.4).

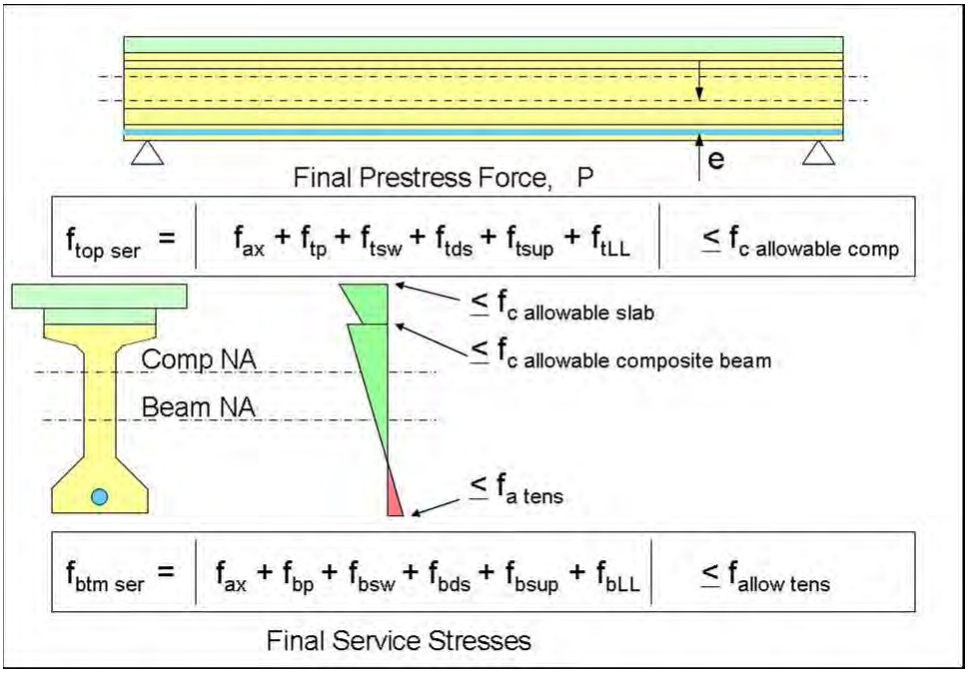

Figure 5.5.3.4.3-2 Final Stresses in Service After All Prestress Losses

The iterative calculation process is illustrated by the flowcharts in Figure 5.5.3.4.3-3, Figure 5.5.3.4.3-4, and Figure 5.5.3.4.3-5. However, before the calculation of prestress loss is considered, it is necessary to examine conditions at transfer and the use of de-bonded or deflected strands to improve the end conditions.

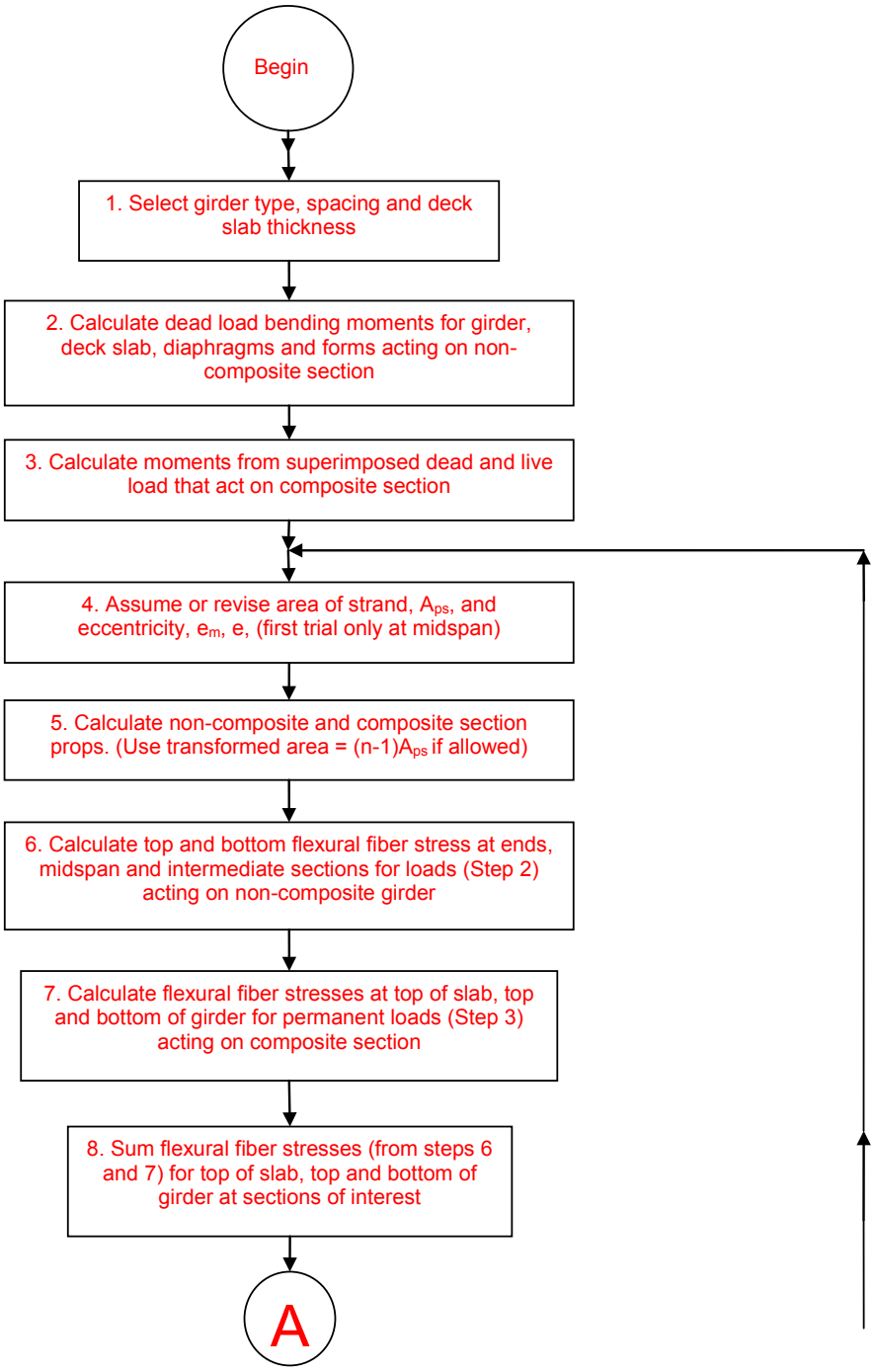

Figure 5.5.3.4.3-3 Flowchart for Determination of Prestress Force and Strand Pattern, Part (a)

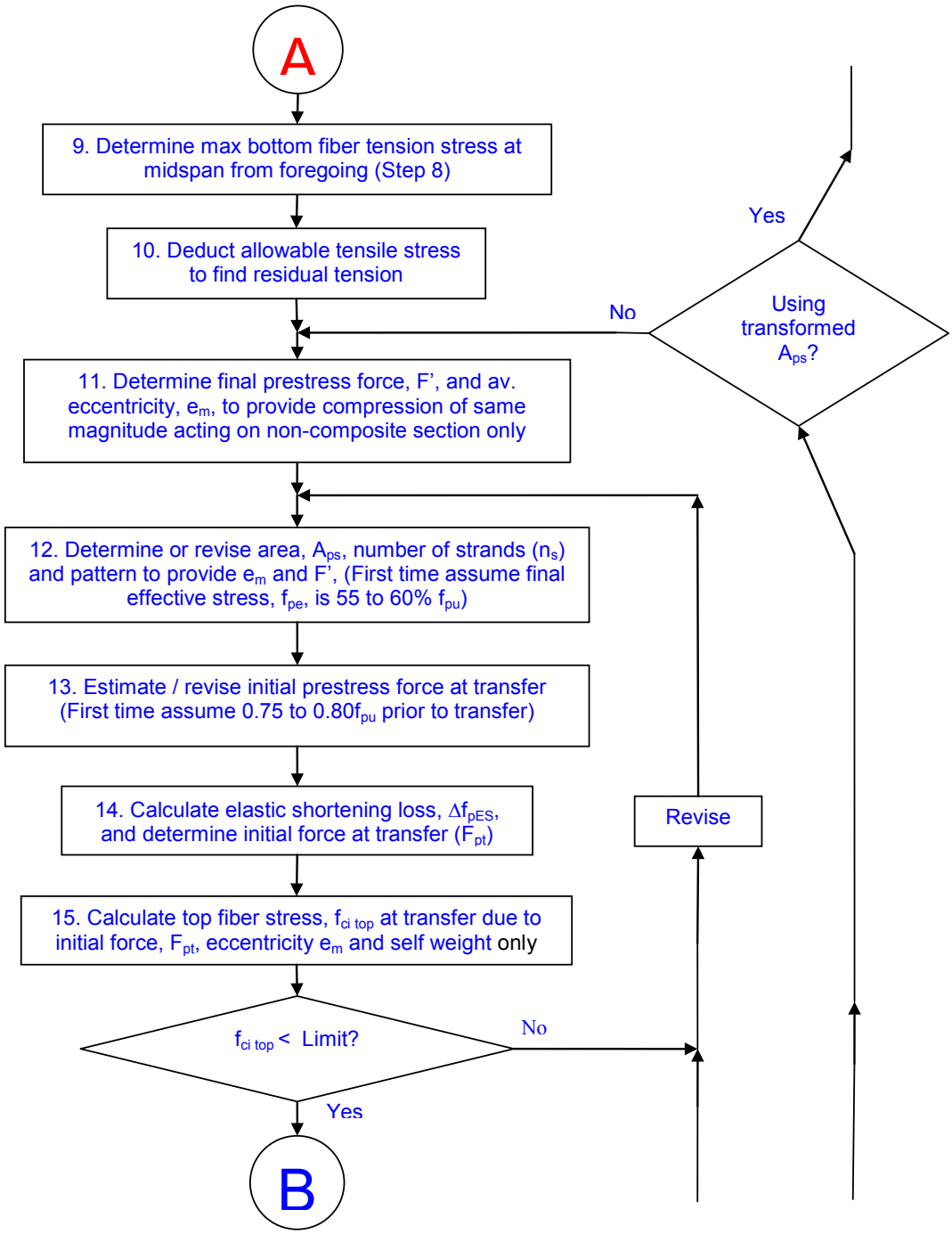

Figure 5.5.3.4.3-4 Flowchart for Determination of Prestress Force and Strand Pattern, Part (b)

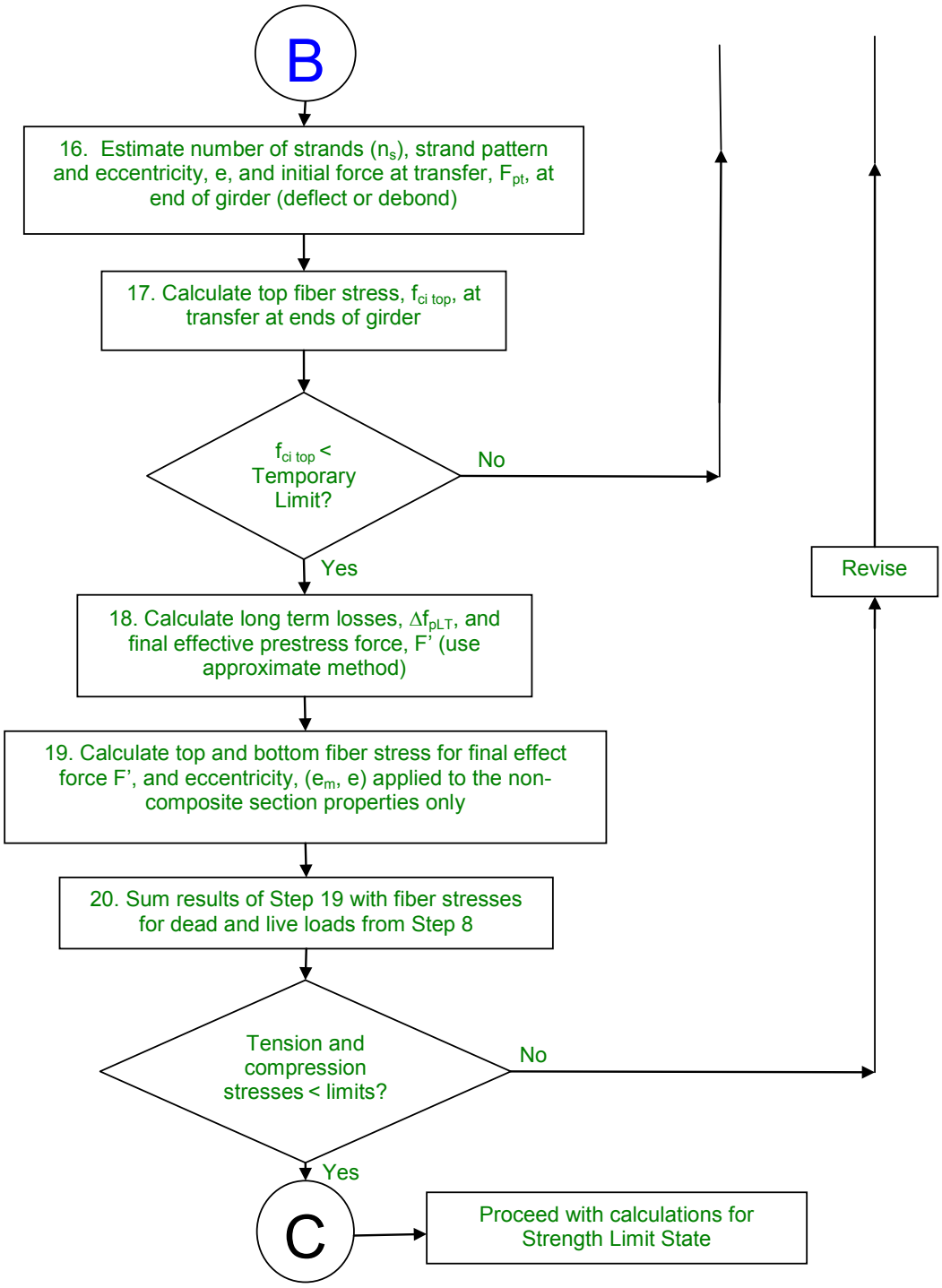

Figure 5.5.3.4.3-5 Flowchart for Determination of Prestress Force and Strand Pattern, Part (c)

5.5.3.4.4 Stress at Other Locations of Interest

For flexure, at any given cross-section, e.g. mid-span, the final state of stress requires the summation of stress (not moment) from loads and prestress applied first to the non-composite section alone and then to the composite section. Stress is calculated at each elevation at each section of interest for each stage of construction through final conditions. Elevations of interest are usually: top and bottom of non-composite girder and then top of deck slab and top and bottom of girder for the composite section. Sections of interest are mid-span, the girder ends, location of deflection points for deflected strands and locations of debonded strands.

In addition, stresses can be calculated or interpolated for intermediate elevations, such as, for example, the elevation of the prestress (for losses), and the neutral axes of the non-composite and composite sections, as necessary. The reason or interest for doing this is that, although not required by the specifications, a designer may consider it prudent to determine the residual flexural tensile stress. Alternatively, it may be necessary to combine flexural stress with a shear stress to provide principal tensile stresses at the neutral axes or other locations of interest. This is facilitated by keeping a detailed stress accumulation in a program or spreadsheet.

5.5.3.4.5 Conditions at Transfer

It is essential to check temporary stresses in the girder at transfer (second controlling condition.) Under the initial release of the strand force in the casting bed, the only load is the self-weight of the girder. At transfer there is far more prestress than necessary to support the girder itself (Figure 5.5.3.4.5-1) The result is that the girder flexes upwards and the top experiences flexural tension (Figure 5.5.3.4.5-2)

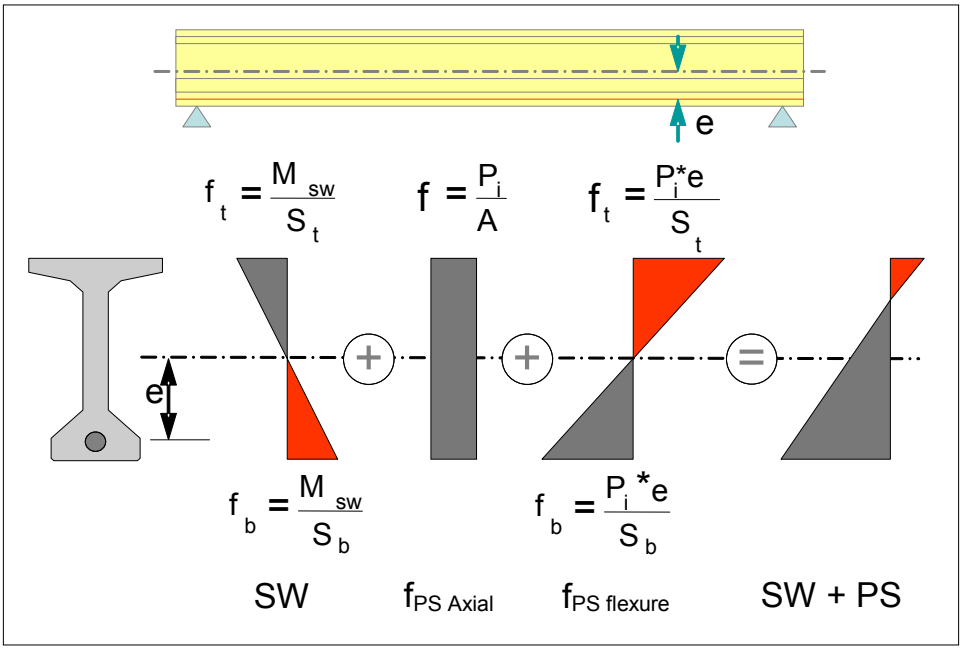

Figure 5.5.3.4.5-1 Girder Self-Weight and Prestress Only, at Transfer

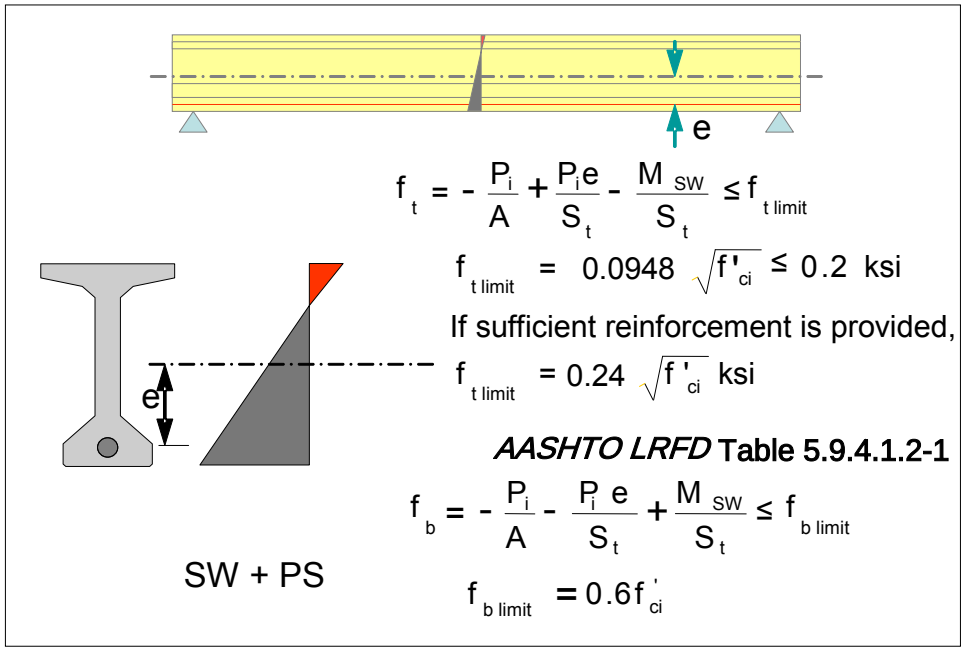

Figure 5.5.3.4.5-2 Stress Limits at Transfer

Top tension can be significant, particularly at the ends where the self-weight moment and compression stress reduces to zero (Figure 5.5.3.4.5-3). If the net resultant of the line of prestress is below the kern (the "middle-third") of girder section, top tension is induced. If precautions are not taken to reduce the force and/or eccentricity, the top of the girder may crack. In addition, this tension can make local conditions worse, especially when combined with shear stress in the web or splitting effects from the local, concentrated transfer of prestress. For this reason, even though it is not required in most situations by *AASHTO LRFD*, sometimes it is prudent to check the principal tensile stress (Mohr's circle stress) in the web from combined flexural and shear stress. (See Section 5.7.2.3 of this manual for guidance of when this check is required.)

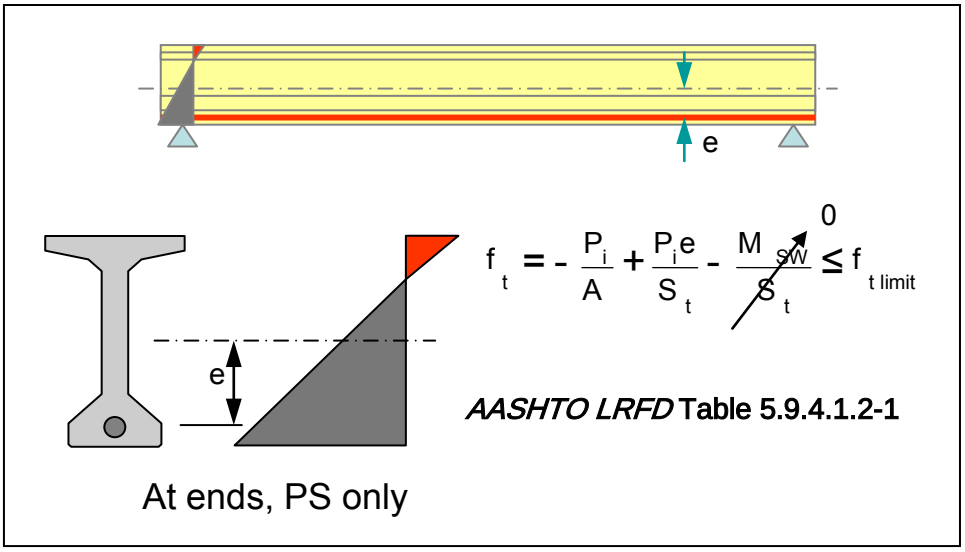

Figure 5.5.3.4.5-3 End Conditions at Transfer

5.5.3.4.6 Debonded Strands

One method of reducing the effective prestress force is to de-bond a number of strands near the ends of the girder using shielding. This reduces the effective force and slightly changes the eccentricity. By shielding a number of strands by different lengths from each end, it is possible to reduce the prestress force in a few steps to best suit the necessary stress conditions both at transfer and under final service loads (Figure 5.5.3.4.6-1).

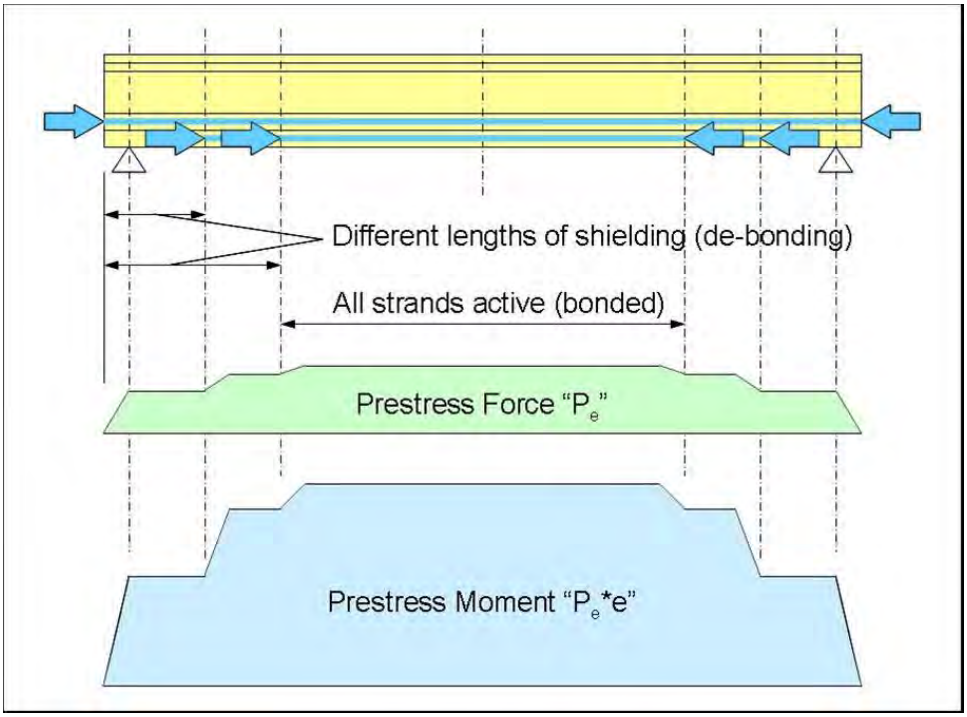

Figure 5.5.3.4.6-1 Reduction of Prestress Force by Shielding Strands (Debonding)

The force does not immediate develop at each step because a short distance is needed to effectively transfer the force in each individual strand through bond with the concrete. This is referred to as the transfer length and is typically about 2'-6" for ½" strand. Shielding of strands reduces prestressing force but may not be sufficient to eliminate top tensile stress altogether, while at the same time retaining sufficient prestress for bottom flexure and other local conditions near the ends of the girders. Consequently, if the top tensile stress exceeds $0.0948\sqrt{f'_c}$ (*AASHTO LRFD* Table 5.9.4.1.2-1), it is necessary to provide local longitudinal mild steel reinforcement to carry the total estimated tensile force. (Note: Concrete under any level of tension is prone to cracking. Although such cracking is often minor and inconsequential, Owners are reluctant to accept cracked members coming from the Fabricator. On the other hand, Fabricators are reluctant to add mild reinforcement as required for tension in excess of $0.0948\sqrt{f'_c}$. Therefore, it is best to stay under this limit if at all possible.) Under no circumstances should the tensile stress exceed $0.24\sqrt{f'_c}$ (*AASHTO LRFD* Table 5.9.4.1.2-1) – should it do so, then the prestressing force should be modified or a new girder section chosen.

5.5.3.4.7 Deflected Strands

An alternative to debonding is to deflect some of the pretensioning strands upward in the web, from about the one-quarter to one-third points of the span to the ends of the girder. This significantly reduces the eccentricity but does not significantly change

the force. It leads to a more ideal, axial prestress condition at the girder ends. Deflected strands can eliminate all top tension at the ends and enhance the shear resistance of the girder at the same time by virtue of the vertical component of the prestressing force. The technique is illustrated in Figure 5.5.3.4.7-1. It requires the use of special hold-down devices passing through the soffit form and special frames to elevate the deflected strands in the casting bed. As deflection forces can be quite large, care and attention to equipment and procedures is necessary. As used in the context of prestressed concrete, the term “deflected strand” is synonymous with the terms “draped strand” and “harped strand.”

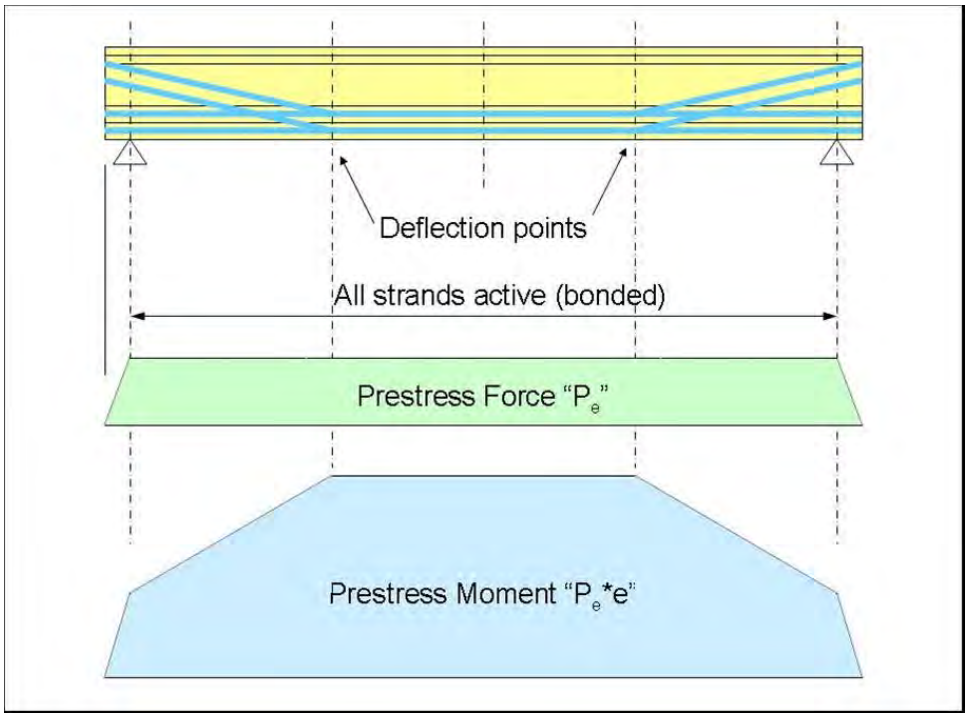

Figure 5.5.3.4.7-1 Deflected Pre-Tensioning Strands

5.5.3.4.8 Service Limit Verification (Flexure)

Once the loss in prestressing force has been determined in accordance with Section 5.7.3.2 of this manual, using either the refined or approximate method, the final prestressing force is known. It is a simple matter then to return to the summation of stress (shown previously) and recalculate the final conditions. This process is repeated at as many sections of interest as necessary along the length of the girder. These should also include the locations at which shielding (debonding) of strands terminates.

If it is not possible to satisfy the stress limits in *AASHTO LRFD* Article 5.9.4 – for both tension and compression at transfer and final conditions – then the prestressing force and/or eccentricity should be revised and/or a new girder section chosen.

Alternatively, using the same section, adding a girder line might solve the problem by reducing moments and forces on the critical member.

For the prestressing steel, the initial stress at transfer and final stress after all losses should not exceed the limits in *AASHTO LRFD* Table 5.9.3-1. To illustrate, consider for example: For Grade 270 ksi low relaxation strand at transfer the stress should not exceed $0.75f_{pu}$ = 0.75*270 = 203 ksi. After all losses, the stress should not exceed $0.80f_{py}$. If it is assumed that the yield stress is, say, 90% of the ultimate strength, then the final stress should be less than 0.80*0.90*270 = 194 ksi. In general, for pretensioned girders, the final stress after losses is rarely greater than $0.65f_{pu}$ = 0.65*270 = 175 ksi – so this latter condition is usually satisfied.

5.5.4 Strength Check

This section presents the approach by which the girders, having been designed for flexural service conditions, are verified at the strength limit state. Figure 5.5.4-1 depicts a simple-span girder subjected to a loading beyond its flexural tension resistance. As the flexural tension resistance is exceeded, the girder cracks. As the load is increased further, the cracks increase in both length and opening size potentially leading to failure of the girder. To offset the inability of the concrete to resist significant tension, reinforcing bars are added in the tension regions. As load is applied, the girder deflects, the reinforcing strains, and force is produced in the steel (in accordance with Hooke's Law.) This tensile force in the steel is counter-balanced by compression in the concrete on the opposite face of the girder. These balancing tensile and compressive forces multiplied by the lever arm between the centroids of action produce an internal bending moment resisting the moments caused by the applied loads. The bottom portion of Figure 5.5.4-1 shows the relationship between girder cross section, strains produced by loads, forces in the steel and concrete, and the resisting moment.

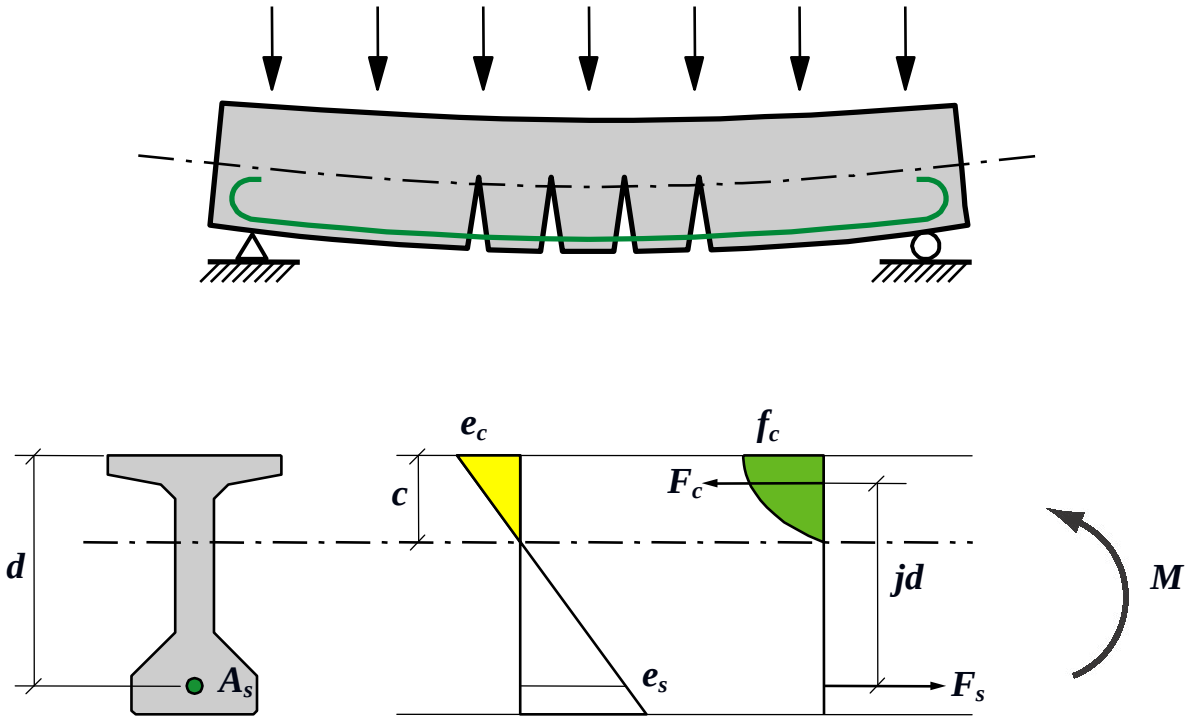

Figure 5.5.4-1 Ultimate Flexural Resistance in Girders

The internal resistance described above is fundamentally the same whether a girder is reinforced with mild reinforcing or prestressing strands. Results differ, however, as a result of material differences between mild reinforcing and prestressing steel, and the state of stress in the steel at the onset of loading. With regard to the state of stress at loading, there is no initial strain in the reinforcing steel of a reinforced concrete girder when first subjected to loading. Prestressed girders, on the other hand, have a significant precompression stress as a result of the jacking operation.

The strain produced by external loads at the strength limit state is in addition to the initial strains.

5.5.4.1 Load Factors

Load factors for the strength limit state are addressed in *AASHTO LRFD* Table 3.4.1-1.

5.5.4.2 Strain Compatibility Approach

AASHTO LRFD provides equations for determining the nominal resistance of typical prestressed girders with composite deck slabs. These equations, presented in detail subsequently, were developed from the more generalized approach of considering

strain compatibility between the materials at a cross-section of a girder subjected to load. Figure 5.5.4.2-1 shows the relationships between strain, stress and force for this more generalized approach.

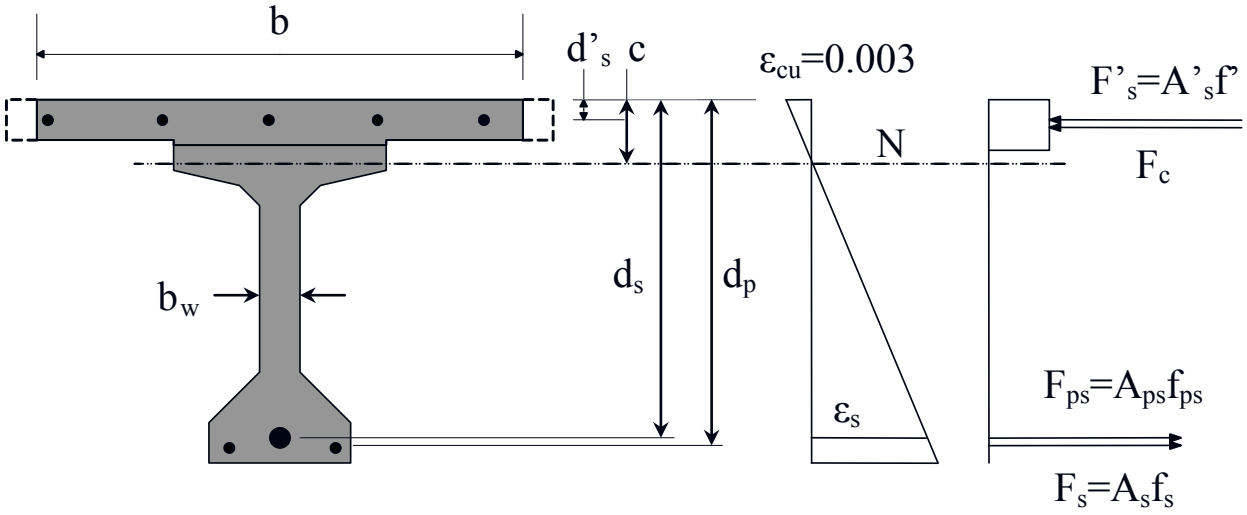

Figure 5.5.4.2-1 Strain Compatibility for a Composite Concrete Girder

where:

b	=	effective width of the slab
b_w	=	width of the web of the prestressed girder
c	=	distance to the neutral axis
d_s	=	distance from the extreme compression fiber to the centroid of mild tension reinforcing
d_p	=	distance from the extreme compression fiber to the centroid of prestressing steel
d'_s	=	distance from the extreme compression fiber to the centroid of mild compression reinforcing
ε_{cu}	=	ultimate strain in the concrete
ε_s	=	strain in a layer of reinforcing or prestressing steel
A_s	=	area of flexural tension reinforcing
A_{ps}	=	area of prestressing steel
A'_s	=	area of compression reinforcing
f_s	=	stress in the flexural tension reinforcing
f_{ps}	=	stress in the prestressing steel
f'_s	=	stress in the compression reinforcing
F_s	=	force in the flexural tension reinforcing
F_{ps}	=	force in the prestressing steel
F'_s	=	force in the compression reinforcing
F_c	=	force in the concrete

Application of strain compatibility in *AASHTO LRFD* is based on assumptions that must be considered in order to know when its use is appropriate. These assumptions are:

- Plane sections remain plane during loading. The implication is that for a girder whose length is significantly greater than its depth strains will be linearly distributed over the depth of the cross section at locations (B-regions) away from the support and can be found by simple geometry. The use of strain compatibility to justify member sections whose behavior is contrary to this assumption, such as deep beams (D-regions), should be avoided.

- The section is said to fail when the extreme concrete compression fiber reaches a strain of ε_{cu} = -0.003 (compression shown as negative). Another assumption is that plane faces remain plane or that the member will displace with linear strain over the cross-section.

- A couple of simplifications are allowed: (1) to neglect the tensile strength of the concrete; and (2) to model the compressive stress-strain distribution as either rectangular or parabolic.

- The first step in applying the principles of strain compatibility using *AASHTO LRFD* is to understand the Whitney stress block, or the equivalent rectangular stress block as it is sometimes called, illustrated in Figure 5.5.4.2-2. The equation reads $a=\beta_1 c$. This is a well-known approximation that the compressive stress can be modeled as a uniform stress with a depth a. The value β_1 is based on experimental studies by Whitney. The β_1 value varies linearly from 0.85 for concrete with a 28-day compressive strength of 4.0 ksi or less to 0.65 for concrete with a 28-day compressive strength of 8.0 ksi or more.

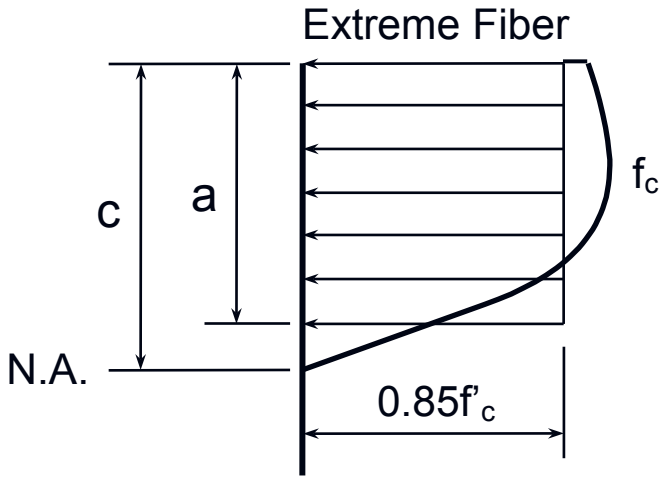

Figure 5.5.4.2-2 Concrete Stress Block Assumption

5.5.4.3 Flexural Resistance

AASHTO LRFD allows the use of an approximate method for determination of flexural resistance in a prestressed concrete girder, which is derived from the strain compatibility approach with a few simplifications. The set of equations beginning with *AASHTO LRFD* Equation 5.7.3.1.1-3 involve the internal balance of forces for a prestressed concrete beam member at nominal resistance. For example, the compressive force in a cross-section must be equal in magnitude to the tensile force in the same cross-section. Using this property and knowing the tensile force in the prestress and the mild reinforcing, the depth of the compressive stress block can be determined.

If the tension in concrete is neglected as small, then tensile forces come from two sources, the prestressing and the mild steel. For example, if it is assumed that the prestress is comprised of bonded and grouted tendons, then the total tensile force is given by:

$$F_T = A_{ps} \cdot f_{ps} + A_s \cdot f_y$$

Then *AASHTO LRFD* Equation 5.7.3.1.1-1 can be substituted into the above equation to reveal:

$$F_T = A_{ps} \cdot f_{pu} \cdot (1 - k \cdot \frac{c}{d_p}) + A_s \cdot f_y$$

Expanding this equation gives:

$$F_T = A_{ps} \cdot f_{pu} - k \cdot A_{ps} \cdot c \cdot \frac{f_{pu}}{d_p} + A_s \cdot f_y$$

Expressions for compressive forces are a little more complicated due to the changes in compressive area as the neutral axis deepens. The basic equation for the compressive force is:

$$F_C = 0.85 \cdot f'_c \cdot area_C + A'_s \cdot f'_s$$

5.5.4.3.1 Flanged Sections

The term "*area*$_c$" (previous section) for pretensioned composite girder cross-sections in positive bending can be either rectangular (if the compression block remains within the slab – i.e., $c \le h_f$ in Figure 5.5.4.3.1-1) opr T-shaped (if the compression blocks extends deeper than the slab – i.e., $c > h_f$.)

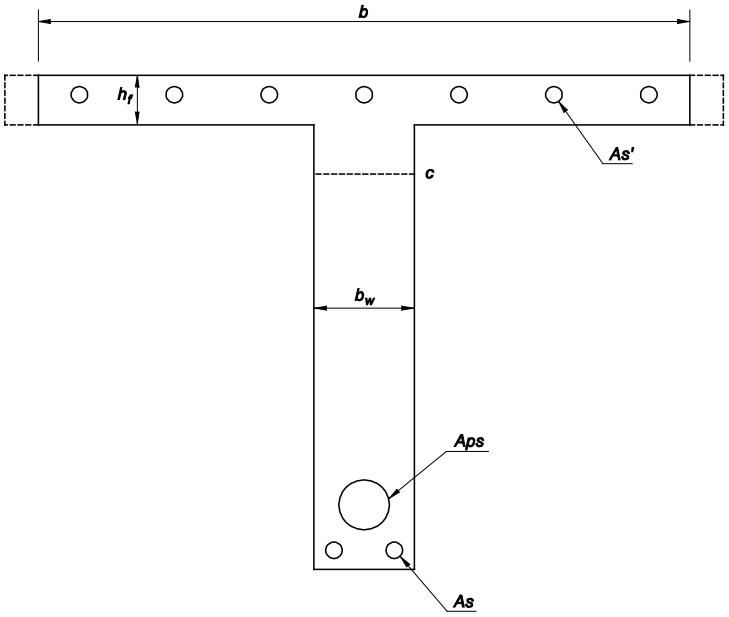

Figure 5.5.4.3.1-1 Schematic Drawing of T-Section

Although composite I- or bulb-tee girders generally have a variable width top flange due to the slab width and girder flange/build-up width being different, *AASHTO LRFD* treats the section as a true T with only one abrupt change in width.

Also, as described in *AASHTO LRFD* Article 5.7.2.1, it is generally acceptable to assume that $f'_s = f'_y$ when using the approximate flexural resistance equations in *AASHTO LRFD* Article 5.7.3.

Using these simplifications and assuming that the compression block extends beyond the theoretical flange depth, h_f, the T-Section compressive force could be written as:

$$F_C = 0.85 \cdot f'_c \cdot [a \cdot b - (a - h_f) \cdot (b - b_w)] + A'_s \cdot f'_y$$

By substituting $\beta_1 c$ for "a," this equation becomes:

$$F_C = 0.85 \cdot f'_c \cdot [\beta_1 \cdot c \cdot b - (\beta_1 \cdot c - h_f) \cdot (b - b_w)] + A'_s \cdot f'_y$$

Expanding the terms in the brackets gives:

$$F_C = 0.85 \cdot f'_c \cdot [\beta_1 \cdot c \cdot b - \beta_1 \cdot c \cdot (b - b_w) + h_f \cdot (b - b_w)] + A'_s \cdot f'_y$$

The next step is to simplify this, giving:

$$F_C = 0.85 \cdot f'_c \cdot [\beta_1 \cdot c \cdot b_w + (b - b_w) \cdot h_f] + A'_s \cdot f'_y$$

Expanding this by terms that are multiplied by $0.85 f'_c \beta_1$ provides:

$$F_C = 0.85 \cdot f'_c \cdot \beta_1 \cdot c \cdot b_w + 0.85 \cdot f'_c \cdot (b - b_w) \cdot h_f + A'_s \cdot f'_y$$

All that remains is to set the compressive force, F_C, equal to the tensile force, F_T, and to solve for "*c*". Equating forces gives:

$$0.85 \cdot f'_c \cdot \beta_1 \cdot c \cdot b_w + 0.85 \cdot f'_c \cdot (b - b_w) \cdot h_f + A'_s \cdot f'_y = A_{ps} \cdot f_{pu} - k \cdot A_{ps} \cdot c \cdot \frac{f_{pu}}{d_p} + A_s \cdot f_y$$

Collecting together on the left side of this equation all terms containing the unknown quantity "*c*", gives:

$$0.85 \cdot f'_c \cdot \beta_1 \cdot c \cdot b_w + k \cdot A_{ps} \cdot c \cdot \frac{f_{pu}}{d_p} = A_{ps} \cdot f_{pu} + A_s \cdot f_y - A'_s \cdot f'_y - 0.85 \cdot f'_c \cdot (b - b_w) \cdot h_f$$

From which it is found that:

$$c = \frac{A_{ps} \cdot f_{pu} + A_s \cdot f_y - A'_s \cdot f'_y - 0.85 \cdot f'_c \cdot (b - b_w) \cdot h_f}{0.85 \cdot f'_c \cdot \beta_1 \cdot b_w + k \cdot A_{ps} \cdot \frac{f_{pu}}{d_p}}$$

This expression is identical to *AASHTO LRFD* Equation 5.7.3.1.1-3. As a final verification, the neutral axis must be compared to the initial assumption of T-beam behavior. If the assumption is not correct, then a new assumption must be made and the process repeated for rectangular section behavior (assuming $b_w = b$.)

5.5.4.4 Stress in Prestressing Steel at Nominal Flexural Resistance

5.5.4.4.1 Components with Bonded Tendons

There are two commonly used methods of obtaining the stress in pretensioning steel at locations where the strand is bonded (i.e., not locally debonded or shielded):

The *AASHTO LRFD* equation, which can be used for bonded and closely grouped strands (i.e., all steel can be assumed lumped at the location defined by d_p), states:

$$f_{ps} = f_{pu}\left(1 - k \cdot \frac{c}{d_p}\right) \qquad \textit{AASHTO LRFD} \text{ Equation 5.7.3.1.1-1}$$

where all terms are as defined in *AASHTO LRFD* Article 5.7.3.1.1.

This equation uses the ultimate strength of the steel and makes adjustments for the type of tendon and the ratio of the neutral axis depth to the depth of the post-tensioning. Since it assumes all prestressing steel has yielded, this equation is only appropriate for prestressing concentrated at a singular level (Figure 5.5.4.4.1-1).

For bonded prestressing which is spread throughout a section, the stress in the prestressing steel must be derived from the fundamentals of strain compatibility. Due to the nonlinear nature of steel after yielding, strain compatibility is an iterative process. An initial assumption as to the depth of the neutral axis must be made. Using the neutral axis depth, along with an assumption that the extreme compression fiber is at a strain of -0.003, the linear nature of strain compatibility will reveal a strain at every elevation throughout the member under strength conditions. From a stress-strain curve for the prestressing steel (Figure 5.5.4.4.1-2), the stress at each strand location can be extracted and used to determine the steel force there. Next the forces are summed to verify the neutral axis depth assumption. The neutral axis depth is modified, and the process repeats itself until the depth assumption is confirmed by the sum of forces. It is important to remember that, unlike mild reinforcing steel, the strain in the prestressing steel is not equal to the strain in the surrounding concrete. Allowance must be made for the difference in strain between the steel and the concrete when they are bonded together. Once this strain is known, the pretensioning stress can be determined by using equations such as those in Chapter 8 of the PCI *Bridge Design Manual*, MNL-133-14, 3rd Edition, Second Release, August 2014, Precast/Prestressed Concrete Institute, Chicago, IL.

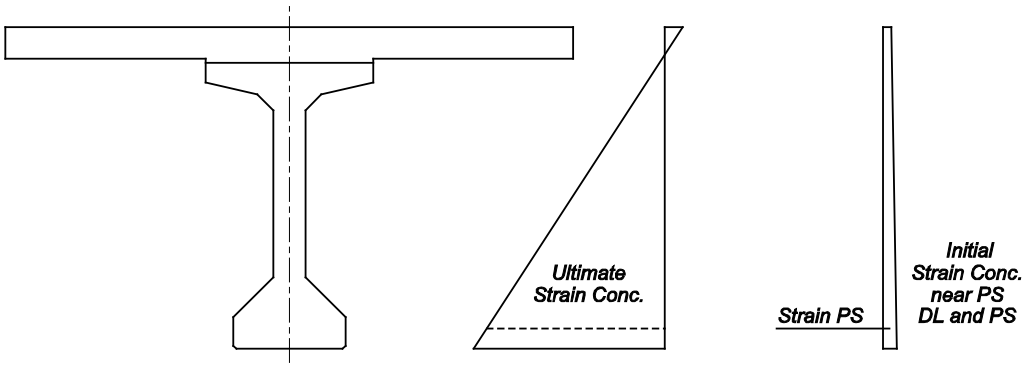

Figure 5.5.4.4.1-1 Total Strain in Prestressing at Strength Limit State

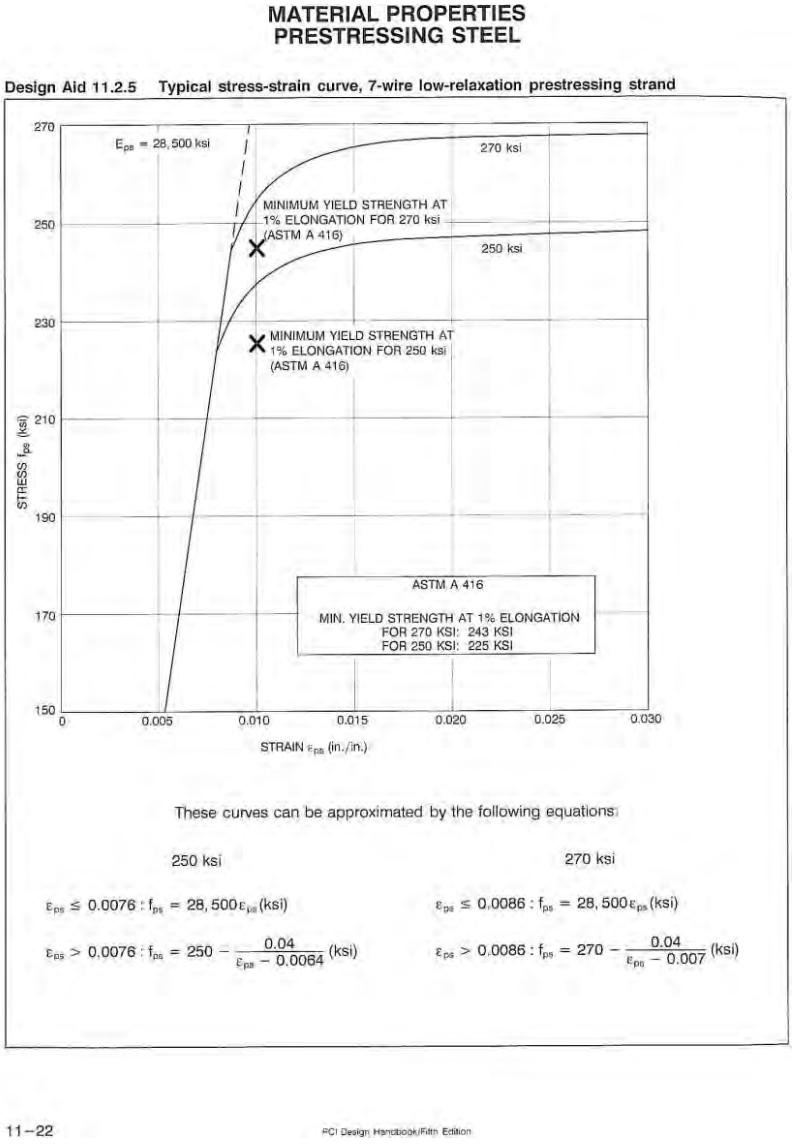

Figure 5.5.4.4.1-2 Material Properties of Prestressing Steel

5.5.4.4.2 Components with Unbonded Tendons

In components with fully unbonded or partially unbonded prestressing tendons (i.e., external tendons, locally debonded or shielded strands), the difference in strain between the tendons and the concrete section and the effect of deflections on tendon geometry are included in the determination of the stress in the tendons, which is given as:

$$f_{ps} = f_{pe} + 900 \cdot (d_p - c)/l_e \leq f_{py} \quad \textit{AASHTO LRFD} \text{ Equation 5.7.3.1.2-1}$$

where all terms are as defined in *AASHTO LRFD* Article 5.7.3.1.2.

The location of the neutral axis can then be determined from *AASHTO LRFD* Equation 5.7.3.1.2-3 as:

$$c = \frac{A_{ps} \cdot f_{ps} + A_s \cdot f_y - A'_s \cdot f'_y - 0.85 \cdot f'_c \cdot (b - b_w) \cdot h_f}{0.85 \cdot f'_c \cdot \beta_1 \cdot b_w}$$

As with bonded tendons, the above equation is valid for T-section behavior or rectangular section behavior ($b_w = b$.)

5.5.4.4.3 Components with Both Bonded and Unbonded Tendons

In general, for components with both bonded and unbonded tendons a detailed analysis needs to be performed in accordance with *AASHTO LRFD* Article 5.7.3.1.3a. However, in certain situations it may be possible to use a simplified analysis in accordance with *AASHTO LRFD* Article 5.7.3.1.3b.

5.5.4.5 Resistance Factors for Flexure

AASHTO LRFD relates the resistance factor (ϕ) for combined flexure/axial force loadings to whether a cross section is compression controlled or tension controlled. *AASHTO LRFD* Article 5.7.2.1 offers the following definitions for these behaviors:

- Sections are compression-controlled when the net tensile strain in the extreme tension steel is equal to or less than the compression-controlled strain limit at the time the concrete in compression reaches its assumed strain limit of 0.003. The compression-controlled strain limit is the net strain in the reinforcement at balanced strain conditions. For Grade 60 reinforcement, and for all prestressed reinforcement, the compression-controlled strain limit may be set equal to 0.002.

- Sections are tension-controlled when the net tensile strain in the extreme tension steel is equal to or greater than 0.005 just as the concrete in compression reaches its assumed strain limit of 0.003. Sections with net tensile strain in the extreme tension steel between the compression-controlled strain limit and 0.005 constitute a transition region between compression-controlled and tension controlled sections.

Using these definitions, *AASHTO LRFD* Article 5.5.4.2 provides the following resistance factors:

- For tension-controlled prestressed concrete sections as defined in *AASHTO LRFD* Article 5.7.2.1, ϕ =1.00.

- For compression-controlled sections with spirals or ties, as defined in *AASHTO LRFD* Article 5.7.2.1, except as specified in *AASHTO LRFD* Articles 5.10.11.3 and 5.10.11.4.1b for Seismic Zones 2, 3 and 4 at the extreme event limit state, ϕ =0.75.

- For sections with net tensile strain ε_t in the extreme tension steel at nominal strength between the above tension- and compression-controlled limits, the value of ϕ will be between 1.00 and 0.75 as determined by linear interpolation in *AASHTO LRFD* Figure C5.5.4.2.1-1.

5.5.5 Limits for Reinforcement

5.5.5.1 Maximum Reinforcement

The current provisions of *AASHTO LRFD* eliminate traditional maximum steel reinforcement limits and unify the design of prestressed and non-prestressed tension- and compression-controlled members. Below a net tensile strain in the extreme tension steel of 0.005 as the tension reinforcement quantity increases, the increase in ϕ-factor (as described previously) effectively compensates for decreasing ductility with increasing overstrength. See *AASHTO LRFD* Article C5.7.3.3.1 for further explanation.

5.5.5.2 Minimum Reinforcement

The minimum reinforcement limit is defined in *AASHTO LRFD* Article 5.7.3.3.2. The requirement is that the flexural resistance (ϕM_n) should be greater than γ_3 times the cracking moment or 1.33 times the controlling strength limit state. γ_3 times the cracking moment is defined by *AASHTO LRFD* Equation 5.7.3.3.2-1 as:

$$M_{cr} = \gamma_3 \left[\ (\gamma_1 f_r + \gamma_2 f_{cpe}) \cdot S_c - M_{dnc} \left(\frac{S_c}{S_{nc}} - 1 \right) \ \right] \leq S_c f_r$$

where:

f_{cpe} = compressive stress in concrete due to effective prestress forces only (after allowance for all prestress losses) at extreme fiber of section where tensile stress is caused by externally applied loads (ksi)

M_{dnc} = total unfactored dead load moment acting on the monolithic or noncomposite section (kip-in.)

S_c = section modulus for the extreme fiber of the composite section where tensile stress is caused by externally applied loads (in^3)

S_{nc} = section modulus for the extreme fiber of the monolithic or noncomposite section where tensile stress is caused by externally applied loads ($in.^3$)

γ_1 = flexural variability cracking factor (= 1.2 for precast segmental structures; = 1.6 for all other concrete structures.)

γ_2 = prestress variability factor (= 1.1 for bonded tendons; = 1.0 for unbonded tendons.)

γ_3 = ratio of specified minimum yield strength to ultimate tensile strength of the reinforcement (=0.67 for A615, Grade 60; = 0.75 for A706, Grade 60; =1.00 for prestressed concrete structures.)

Mathematically this works out to the extra moment that, when added to the moment from dead load and prestressing, will create a stress that will cause a crack in the member.

5.5.6 Control of Cracking by Distribution of Reinforcement

All reinforced concrete members are subject to cracking under any load combination, including thermal effects and restraint of deformations, which produces tension in the gross section in excess of the cracking strength of the concrete. As a general rule, the use of smaller diameter bars with smaller spacing is preferable to large bars at large spacing. However, there are other factors to consider including member type, member geometry, materials and environmental conditions. The provisions of *AASHTO LRFD* Article 5.7.3.4 address distribution of reinforcement to control cracking in concrete members.

5.5.7 Moment Redistribution

AASHTO LRFD Article 5.7.3.5 allows for redistribution of negative moment at the strength limit state. If the strain in the tensile steel in the negative moment region yields and the net tensile strain (ε_t) exceeds 0.0075, the moment determined by

elastic theory at the strength limit state may be reduced by a percentage not greater than $1000\varepsilon_t$% or 20% at that section. In order to maintain equilibrium, positive moments should be adjusted to account for the change in negative moments. Positive moment resistance should be checked for the redistributed amounts.

5.5.8 Deformations

5.5.8.1 Deflection and Camber

All girders deflect under load. The amount of deflection depends upon the magnitude of the load and the flexural stiffness of the girder, as represented by the product "EI" of the modulus of elasticity of the concrete, E, and the inertia of the section, I. A simply-supported girder deflects downward under the action of gravity loads and deflects upwards as a result of internal prestress forces. For example, consider an axial prestress force, F, at an eccentricity, e_m, below the neutral axis. This creates a mostly constant negative moment, $M = -(F)(e_m)$, that flexes the girder upward. At transfer in the casting bed, this upward prestress deflection is only partially countered by the self-weight deflection of the girder alone. The net effect at transfer is a residual upward deflection. The girder lifts off the bed, being supported at its ends. This is clearly noticeable in the Type 4 girders in casting yard storage in Figure 5.5.8.1-1.

After erection, under the weight of the deck slab and forms, a girder will again deflect downward. Finally, after construction a girder will continue to deflect due to creep under the total effect of all permanent loads (prestress and dead load).

To compensate for deflections it is necessary to determine the elevations to which the bearings should be set and those to which the deck should be cast. It is also necessary to determine the variable depth of the haunch (build-up) over the girders to which the deck forms should be set at the time of construction so that deck elevations will be correct in the long-term configuration. Making such adjustments to compensate for deflections is referred to as "camber". It is basically the difference between the vertical profile to which the deck should be cast and the desired highway geometry vertical profile grade. Deriving correct "camber" requires calculation of deflections for various load conditions.

Figure 5.5.8.1-1 Residual, Upward Deflection from Prestress and Self-weight

For a simply-supported structure, deflections are determined for:

1. The self-weight of the girder at transfer (downward.)
2. The prestress in girder at transfer (upward but greater than magnitude of (a.))
3. The growth of the net deflection of the above due to creep during the time from transfer to casting the deck slab (upward.)
4. The deflection of the girder under the weight of the wet concrete deck slab, diaphragms and deck forms (downward.)
5. The recovery of deflection of the now composite section when forms are removed (usually slight and sometimes disregarded.)
6. The deflection of the composite section under the weight of superimposed dead load.
7. The growth of deflection of the composite section due to creep under all sustained permanent effects (including prestress) from the time of casting the slab to final long-term conditions. This includes the creep of the non-composite girder itself due to the locked in forces at the time of casting the slab. This may also include the effect of the differential shrinkage of the deck slab relative to the girder, if it is significant.

Deflections may be calculated at intervals along the span. Some of the deflections may be relatively small and inconsequential as far as making adjustments in the field. However, it should be evident that there is an important need to calculate deflections in order to establish bearing and girder elevations and the depths of haunches (build-ups).

5.5.8.2 Calculation of Deflection

Calculation of deflection is based upon routine Euler-Bernoulli Beam Theory. Using Euler-Bernoulli beam behavior requires the following assumptions:

- The girder length is much greater than its width or depth
- Load is applied in the vertical plane and symmetric to the section
- Deflections are small
- Plane sections remain plane
- The material has linear-elastic behavior
- Materials are isotropic

Under these conditions, the classic Euler-Bernoulli equations for deflection and rotation of a portion of a beam given a constant value of *EI*, are given in Figure 5.5.8.2-1.

$p = \text{load}$
$V = \text{shear}$
$M = \text{moment}$
$\phi = \text{curvature}$
$\theta = \text{rotation}$
$w = \text{deflection}$

$$\frac{dV}{dx} = p$$

$$\frac{dM}{dx} = V$$

$$\frac{d\theta}{dx} = \phi = \frac{M}{EI}$$

$$\frac{dw}{dx} = \theta$$

$$EI\frac{d^4w}{dx^4} = p$$

(EI = constant)

Figure 5.5.8.2-1 Euler-Bernoulli Equations for Deflection and Rotation

Solution and application of the above equations is possible using different methods, such as rigorous mathematics, numerical integration, area-moment, slope-deflection, McCauley's method, virtual work (Castigliano), published design aids or stiffness solution by matrix inversion. The classical solution for a uniform load on a simply-supported beam is given in Figure 5.5.8.2-2.

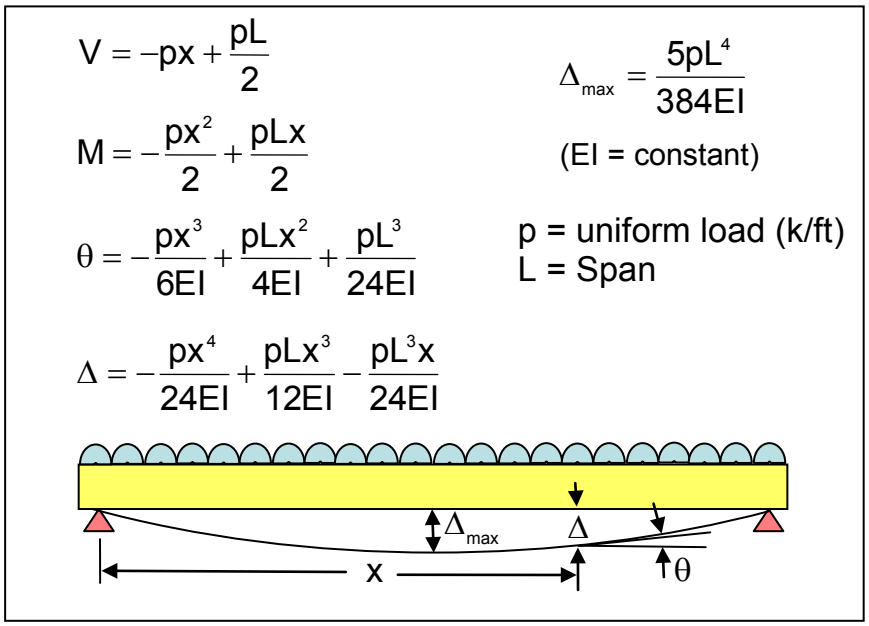

Figure 5.5.8.2-2 Deflection of a Beam under Uniform Load

Many design aids are available for calculating deflections for the more commonplace types of load found in bridge applications; namely, uniformly distributed loads, partial distributed loads and point loads. Eight solutions for external load on a simply supported beam are provided in Figure 5.5.8.2-3 and Figure 5.5.8.2-4.

In addition to applied (gravity) loads, the same approach is used to calculate upward girder deflections from the effects of prestress. A practical approach is to reduce prestress effects to a set of equivalent loads that can be applied “externally”. Deflections are then calculated for these equivalent loads using any of the above methods. Figure 5.5.8.2-5 illustrates equivalent loads and deflections for the most commonly encountered prestress patterns.

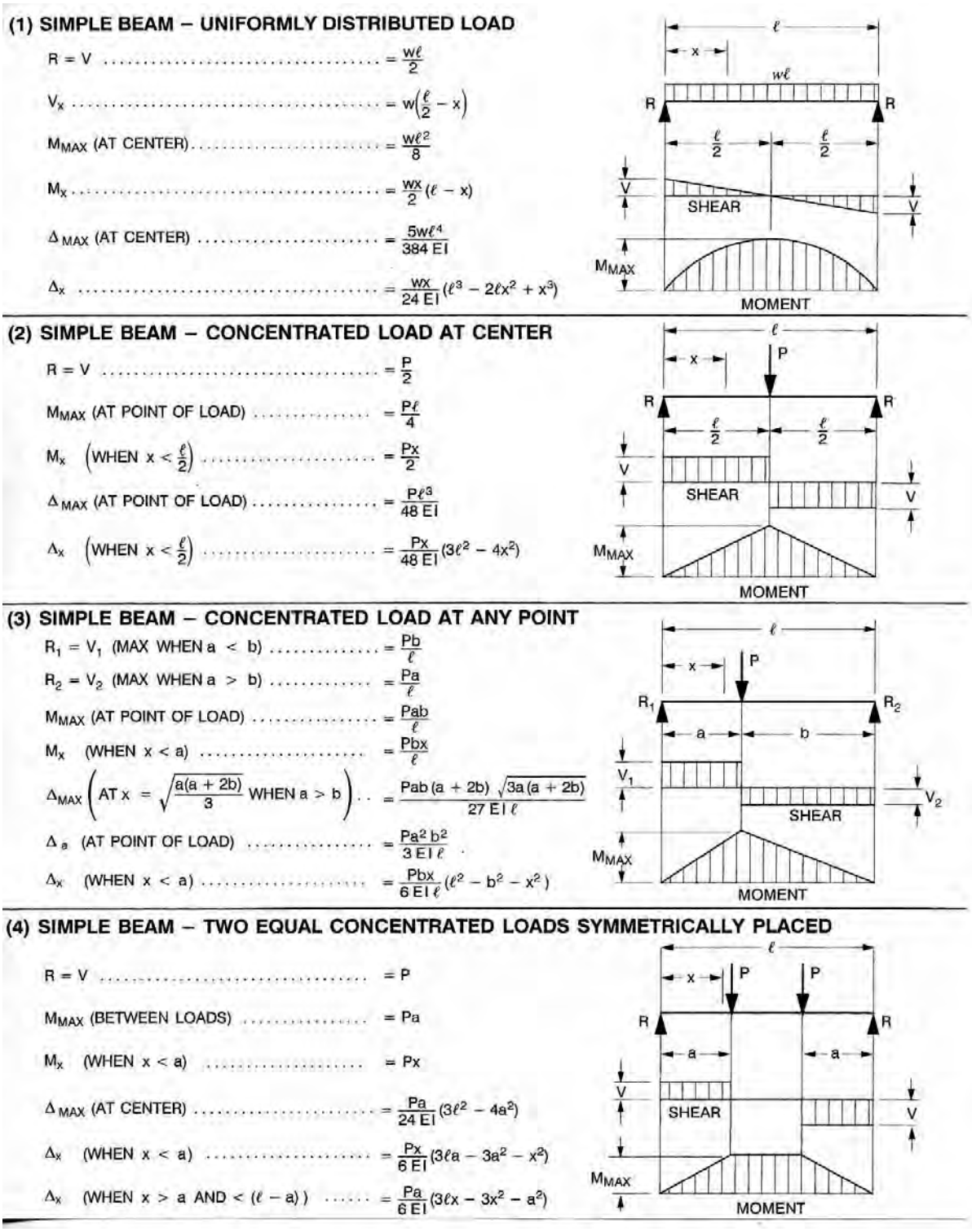

Figure 5.5.8.2-3 Deflection of Simply-Supported Beam under External Load

(Source: AISC *Steel Construction Manual*)

(5) SIMPLE BEAM – TWO UNEQUAL CONCENTRATED LOADS UNSYMMETRICALLY PLACED

$R_1 = V_1 = \frac{P_1 (\ell - a) + P_2 b}{\ell}$

$R_2 = V_2 = \frac{P_1 a + P_2 (\ell - b)}{\ell}$

V_x (WHEN $x > a$ AND $< (\ell - b)$) $= R_1 - P_1$

M_1 (MAX WHEN $R_1 < P_1$) $= R_1 a$

M_2 (MAX WHEN $R_2 < P_2$) $= R_2 b$

M_x (WHEN $x < a$) $= R_1 x$

M_x (WHEN $x > a$ AND $< (\ell - b)$) $= R_1 x - P_1 (x - a)$

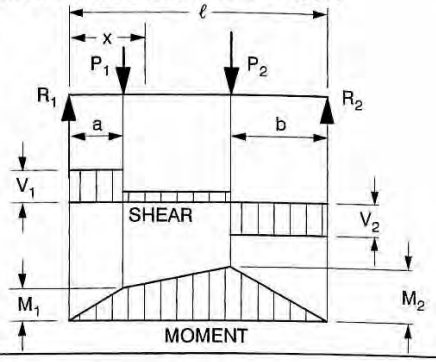

(6) SIMPLE BEAM – UNIFORM LOAD PARTIALLY DISTRIBUTED

$R_1 = V_1$ (MAX WHEN $a < c$) $= \frac{wb}{2\ell}(2c + b)$

$R_2 = V_2$ (MAX WHEN $a > c$) $= \frac{wb}{2\ell}(2a + b)$

V_x (WHEN $x > a$ AND $< (a + b)$) $= R_1 - w(x - a)$

M_{MAX} $\left(\text{AT } x = a + \frac{R_1}{w}\right) = R_1 \left(a + \frac{R_1}{2w}\right)$

M_x (WHEN $x < a$) $= R_1 x$

M_x (WHEN $x > a$ AND $< (a + b)$) $= R_1 x - \frac{w}{2}(x - a)^2$

M_x (WHEN $x > (a + b)$) $= R_2 (\ell - x)$

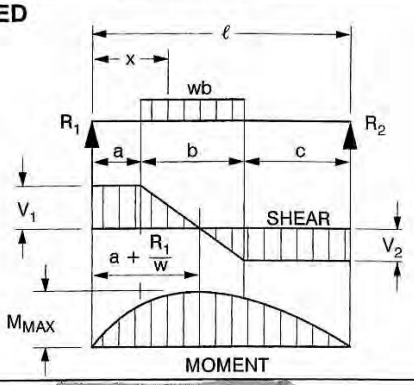

(7) SIMPLE BEAM – LOAD INCREASING UNIFORMLY TO ONE END (W IS TOTAL LOAD)

$R_1 = V_1 = \frac{W}{3}$

$R_2 = V_2$ MAX $= \frac{2W}{3}$

$V_x = \frac{W}{3} - \frac{Wx^2}{\ell^2}$

M_{MAX} $\left(\text{AT } x = \frac{\ell}{\sqrt{3}} = .5774\ell\right) = \frac{2W\ell}{9\sqrt{3}} = .1283\,W\ell$

$M_x = \frac{Wx}{3\ell^2}(\ell^2 - x^2)$

Δ_{MAX} $\left(\text{AT } x = \ell\sqrt{1 - \sqrt{\frac{8}{15}}} = .5193\,\ell\right) = .01304\,\frac{W\ell^3}{EI}$

$\Delta_x = \frac{Wx}{180\,E\,I\,\ell^2}(3x^4 - 10\ell^2x^2 + 7\ell^4)$

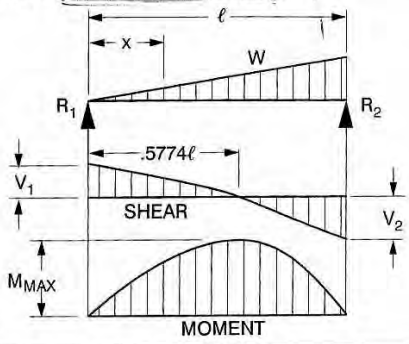

(8) SIMPLE BEAM – LOAD INCREASING UNIFORMLY TO CENTER (W IS TOTAL LOAD)

$R = V = \frac{W}{2}$

V_x $\left(\text{WHEN } x < \frac{\ell}{2}\right) = \frac{W}{2\ell^2}(\ell^2 - 4x^2)$

M_{MAX} (AT CENTER) $= \frac{W\ell}{6}$

M_x $\left(\text{WHEN } x < \frac{\ell}{2}\right) = Wx\left(\frac{1}{2} - \frac{2x^2}{3\ell^2}\right)$

Δ_{MAX} (AT CENTER) $= \frac{W\ell^3}{60\,E\,I}$

Δ_x $\left(\text{WHEN } x < \frac{\ell}{2}\right) = \frac{Wx}{480\,E\,I\,\ell^2}(5\ell^2 - 4x^2)^2$

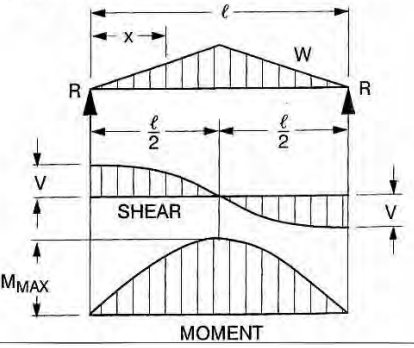

Figure 5.5.8.2-4 Deflection of Simply-Supported Beam under External Load

(Source: AISC *Steel Construction Manual*)

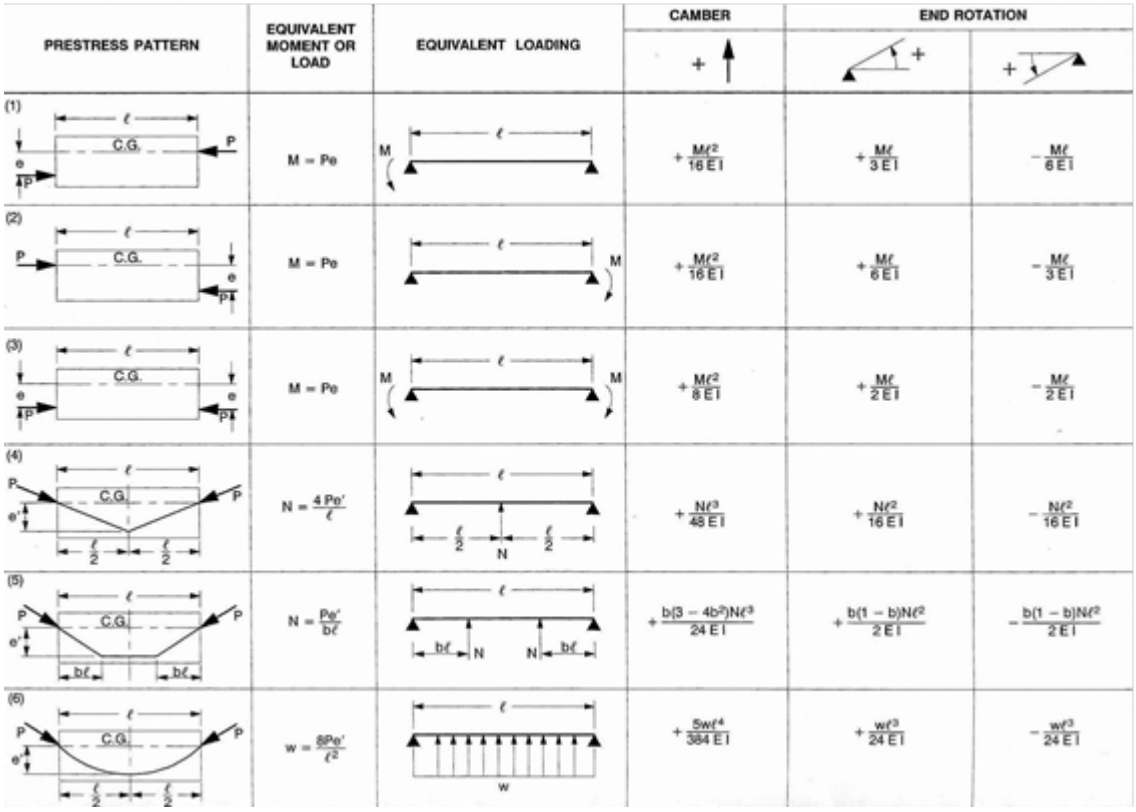

Figure 5.5.8.2-5 Deflection of a Girder under Common Prestress Patterns

(Source: *PCI Design Handbook*)

In lieu of using rigorous classical methods, other techniques are available to the engineer for the computation of deflections of prestressed concrete girders. These techniques include: numerical integration, area-moment, slope-deflection, virtual work, published design aids, and computer based stiffness solutions.

Newmark's Method of Numerical Analysis (Figure 5.5.8.2-6) divides a girder into segments of convenient length. Bending moments are determined by statics, and curvatures are found along the girder by dividing the bending moment by the modulus of elasticity and the girder inertia (EI). The distributed curvatures are concentrated to nodes at the ends of the segments using concentration formulas. The concentrated curvatures are summed across the girder to give the slopes of the individual segments. The chord slopes are then multiplied by the segment length to give deflection increments, which in turn are summed to find girder deflections. This solution begins with a boundary condition of no rotation or deflection at the first node. Corrections may need to be applied in order to satisfy actual boundary conditions.

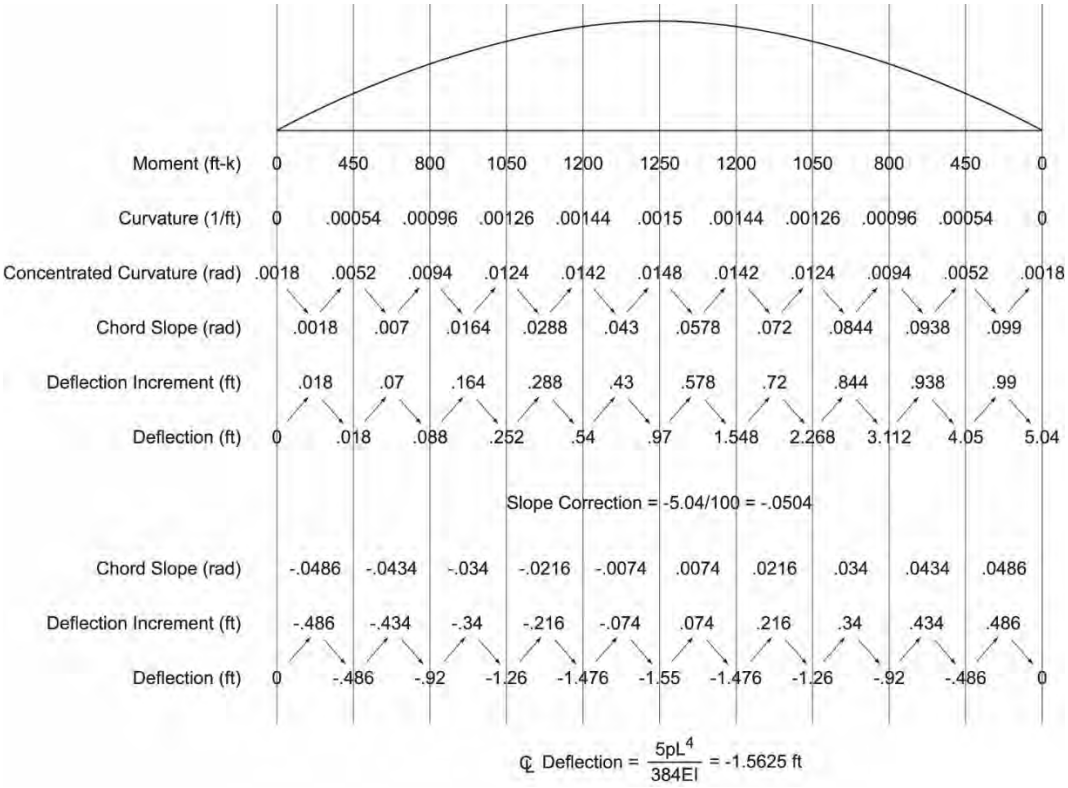

Figure 5.5.8.2-6 Numerical Integration for Slopes and Deflections (Newmark)

For comparison, the maximum deflection for the simply-supported girder using numerical integration is found to be 1.55 feet units; whereas classical (rigorous) formulae gives 1.5625 feet units – i.e., sufficiently good agreement for practical purposes.

Using a greater number of intervals will improve the accuracy of the numerical integration. Numerical integration methods are readily adaptable to spreadsheet computation and may, in principle, be extended to spans of variable depth and continuous structures.

Section 5.6 Design for Shear and Torsion

AASHTO LRFD allows several options for shear and torsion design (see *AASHTO LRFD* Article 5.8). These options are divided into two categories, those that address a single transverse section through the member ("sectional design") and those that consider the behavior of the entire member. For the sectional method there are several approaches, as follows:

1. Simplified sectional model for non-prestressed members using $\beta = 2.0$ and $\theta = 45°$ (*AASHTO LRFD* Article 5.8.3.4.1)

2. General sectional model using equations for β and θ (*AASHTO LRFD* Article 5.8.3.4.2) (see Hawkins, Neil M., Daniel A. Kuchma, Robert F. Mast, M. Lee Marsh, and Karl-Heinz Reineck, *Simplified Shear Design of Structural Concrete Members,* NCHRP Report 549, Transportation Research Board, Washington, DC, 2005)
3. General sectional model using the tabulated and iterative methods in *AASHTO LRFD* Appendix B5 - General Procedure for Shear Design with Tables
4. Optional shear method for segmental bridges (*AASHTO LRFD* Article 5.8.6)
5. Service check limiting the principal tension stress in segmental concrete box girder webs to 0.110 $\sqrt{f'_c}$ (ksi) (*AASHTO LRFD* Article 5.8.5) (Note: This provision will soon be extended to webs in all post-tensioned girders and to pretensioned girders with concrete design strengths in excess of 10 ksi)

Shear methods that require consideration of the entire member are generally applicable to disturbed ("D") regions (*AASHTO LRFD* Article 5.6.3, Strut and Tie Model) or seismic behavior (AASHTO *Guide Specifications for LRFD Seismic Bridge Design*).

5.6.1 Nominal-Resistance Design (Strength Limit State)

In simply-supported precast pretensioned girders, shear force is at a maximum at or near supports and reduces to zero at mid-span. The applied shear force is made up of a combination of dead load, superimposed dead load and live load. The contribution of live load is determined according to acceptable live load distribution techniques of *AASHTO LRFD* Section 4. The vertical component of prestress, V_p, arising from deflected pretensioned strands (or draped post-tensioning) is taken as an unfactored contribution to the overall shear resistance.

AASHTO LRFD Article 5.8.2.9 defines the shear stress on concrete as:

$$v_u = \frac{V_u - \phi V_p}{\phi b_v d_v}$$

A*ASHTO LRFD* requires only that the strength limit state be satisfied to safely resist factored shear forces for traditional pretensioned girders with concrete strengths below 10 ksi.

The illustration in Figure 5.6.1-1 defines the terms traditionally used in sectional analysis.

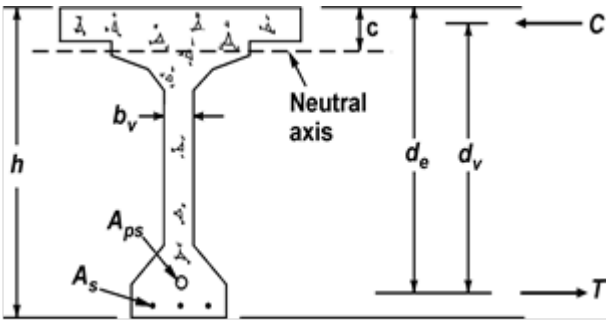

Figure 5.6.1-1 Terms Used in Sectional Analysis

As discussed earlier, *AASHTO LRFD* specifies multiple methods for shear design at the strength limit state. This manual will focus on the sectional model and its use in "flexural regions" where plane sections remain plane after loading. Flexural ("beam," "bending" or "B") regions are defined in *AASHTO LRFD* as portions of members where the response at a section depends only upon the forces – i.e., moment, shear, axial load and torsion – at that section, and not upon how the force effects are introduced into the member. Sectional design can be used for concrete members containing reinforcing steel and/or prestressing tendons.

In contrast to sectional design, strut-and-tie is used primarily for:

- Regions near discontinuities, such as regions adjacent to abrupt changes in cross-section, openings and dapped ends, deep beams and corbels, where the assumption that plane sections remain plane is not valid
- Components in which the distance from the point of zero shear to the face of the support is less than 2d, or components in which a load causing more than ½ of the shear at a support is closer than 2d from the face of the support

5.6.1.1 Sectional Design Model

5.6.1.1.1 Introduction

Shear design using modified compression field theory (MCFT), as first introduced into *AASHTO LRFD*, required an iterative process to determine β and θ (similar to the current *AASHTO LRFD* Section 5, Appendix B method). This was regarded by some engineers as time-consuming. The Canadian Standards Association adopted a direct solution, and in 2008, AASHTO moved the β and θ tables to Appendix B for use as an alternative solution method. Some states still use these tables for prestressed concrete design. Either method is allowed by the code for precast, pretensioned girders. Shear design for continuous, post-tensioned members is similar with a few refinements or additional considerations.

In a simply-supported girder, or any statically determinate structure, internal forces from the prestressing do not cause reactions at the supports. However, when girders are continuous, the structure becomes statically indeterminate. Prestressing then causes secondary reactions due to the profile of the tendon. This is sometimes called the "continuity effect". The "secondary reactions" induce corresponding shear forces and secondary moments. This directly modifies the summation of shear forces from all loads. Secondary effects have been discussed in the context of prestressed girders made continuous with reinforced joints (see Section 5.10.3.3 of this manual).

Although common practice for simply-supported pretensioned girders is to use straight strands, they can be draped upwards at the ends. Continuous or post-tensioned girders usually have draped prestressing at the ends of the girders and over the supports to counteract negative moments arising from dead and live loads. The force in the strands can be resolved to give a vertical component - typically being opposite the shear force from dead and live loads. Essentially, the effect is a reduction in shear demand. However, *AASHTO LRFD* includes this effect as a component of resistance rather than a reduction in demand. In this case, the vertical component of the effective prestressing force, V_p, is added to the strength of the concrete, V_c, and vertical reinforcement, V_s. The total shear strength is then:

$$V_n = V_c + V_s + V_p$$

If V_p is in the same direction as the dead and live load demand, then V_p should be taken as negative in this equation for total shear strength. Whether positive or negative, since V_p is considered to be a component of "strength", then shear effects from prestressing must *not* be included as a load "demand."

5.6.1.1.2 Background

It is important to understand the "traditional approach" to shear design, which is part of the AASHTO *Standard Specifications*. In the past a fixed-angle truss model was used to predict shear strength. This type of approach incorporates diagonal compression struts to direct the applied loads to the supports, longitudinal tension ties at the bottom, compression ties at the top, and vertical steel ties to connect the diagonals. The result is a system of members that resembles a truss, which can be solved using equilibrium.

In the traditional approach the shear strength comes from the vertical stirrups and from an empirically-derived concrete strength. Prior to the formation of cracks, the vertical stirrups have no noticeable effect on strength. After cracking, however, the vertical stirrups that cross the crack are engaged and, therefore, contribute to the strength. The diagonal compression struts are assumed to have the same orientation as the cracks. Details of the development of the traditional equation for

shear strength will not be covered in this section since it will be discussed with other components of the shear resisting mechanism in the following section on MCFT. However, equilibrium of the truss model would lead to the following well-known expression for the vertical stirrup component of shear strength:

$$V_s = \frac{A_v f_y}{s} d_v \cot\theta$$

where:

A_v	=	area of transverse reinforcement within distance s (in^2)
f_y	=	minimum yield strength of reinforcing bars (ksi)
d_v	=	effective shear depth, taken as the distance between the resultants of the tensile and compressive forces due to flexure; it need not be taken less than the greater of $0.9d_e$ or $0.72h$, where d_e is the distance from the extreme compression fiber to the centroid of the tensile force in the tensile reinforcement, and where h is the overall depth of the member (in)
s	=	spacing of reinforcing bars (in)
θ	=	angle of inclination of diagonal compressive stresses (degrees) (with θ = 45 degrees in the fixed-angle truss model of the *Standard Specifications*)

The simplified approach for nonprestressed concrete in *AASHTO LRFD* Article 5.8.3.4.1 assumes that the crack angle is 45 degrees (similar to AASHTO *Standard Specifications*), simplifying the expression to the following:

$$V_s = \frac{A_v f_y d_v}{s}$$

The expression can be modified to take into account inclined stirrups if necessary.

AASHTO LRFD includes an additional component of shear strength, V_c, loosely referred to as the "contribution of the concrete". The equation, not repeated here, was determined from experimental results. The total shear strength is then equal to the following:

$$V_n = V_c + V_s$$

The above approach can be "significantly unconservative" for large members (see *AASHTO LRFD* Article C5.8.3.4.1). The traditional shear approach also did not require longitudinal reinforcement checks at each section (see *AASHTO LRFD* Article 5.8.3.5).

In *AASHTO LRFD*, shear design is based upon the MCFT, also known as the sectional model. The rationale was developed by Vecchio and Collins (1986 and 1988) and Collins and Mitchell (1991). It is based on the following rules of mechanics:

- Constitutive laws (stress-strain)
- Equilibrium
- Strain compatibility

Experimental tests have shown that a beam has more shear resistance than that provided by stirrup reinforcement, by an amount about equal to the cracking strength. The MCFT theoretically analyzes, based on the rules of mechanics listed above, the principal stresses in a beam, with the principal compression, f_2, being parallel to the cracks and the principal tension, f_1, being the average tension that the concrete can carry in between the cracks. The angle of orientation of the principal stresses is also derived from the theory.

5.6.1.1.3 Constitutive (Stress-Strain) Laws

The material behavior of concrete leads to relationships between the components of stress and strain at the principal tension limits. Experimental tests on concrete specimens containing bonded reinforcement show that, after concrete in tension cracks, tensile strains still exist, due to aggregate interlock. This strain drops gradually after cracking, and can be expressed as follows:

$$f_{c1} = \frac{f_{cr}}{1+\sqrt{500\varepsilon_1}} \qquad \text{Equation 5.6.1.1.3-1}$$

where:

f_{c1} = average principal tensile stress in concrete
f_{cr} = cracking stress of concrete
ε_1 = average principal tensile strain

This is illustrated in Figure 5.6.1.1.3-1.

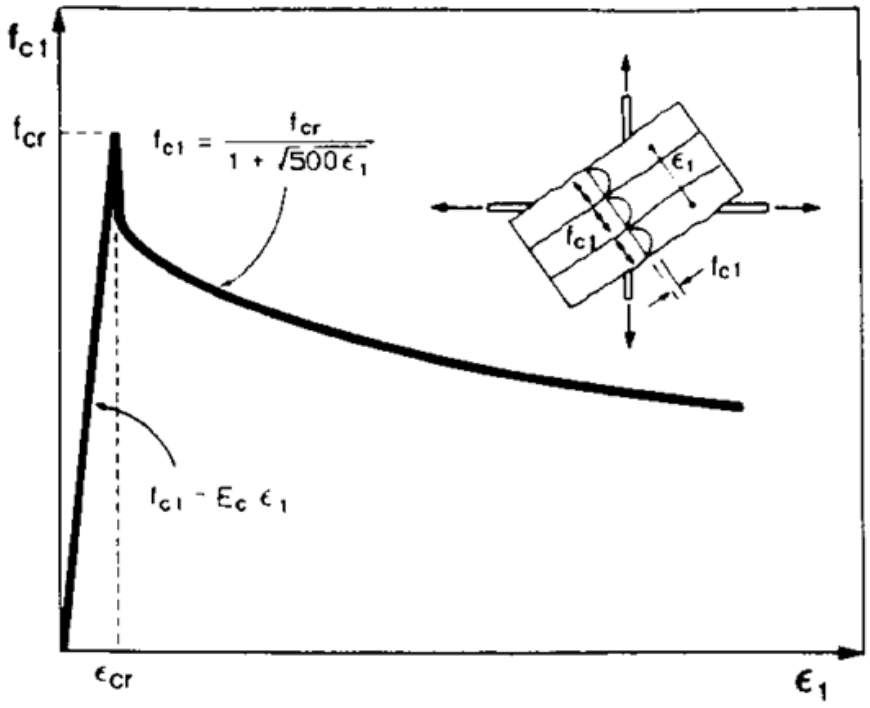

Figure 5.6.1.1.3-1 Average Tensile Stress-Strain Relationship in Reinforced Concrete Section Before and After Cracking

The compressive strength of concrete, f'_c, is usually obtained from cylinder tests, in which uniaxial compression is applied to the specimen. However, in a beam element, stresses in two directions, i.e., biaxial stresses, exist. In concrete, when tensile strains exist perpendicular to the compression, the compressive strength decreases, known as “softening”. The stress-strain relationship diagram in Figure 5.6.1.1.3-2 compares uniaxially loaded to biaxially loaded concrete in compression.

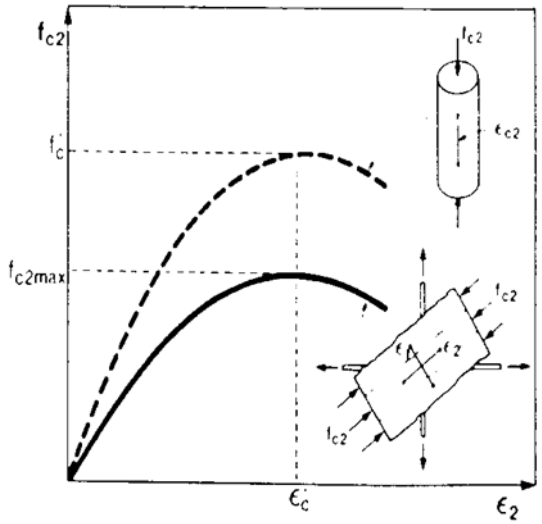

Figure 5.6.1.1.3-2 Comparison of Concrete Compressive Strength between Cylinder in Uniaxial Compression (Dashed Line) and Beam Subjected to Combined Flexure and Shear (Solid Line)

A relationship between the compressive strain, the compressive stress, and the tensile strain has been derived experimentally, giving the following expressions:

$$f_{c2} = f_{c2max}\left[2\left(\frac{\varepsilon_2}{\varepsilon'_c}\right) - \left(\frac{\varepsilon_2}{\varepsilon'_c}\right)^2\right] \qquad \text{Equation 5.6.1.1.3-2}$$

$$\frac{f_{c2max}}{f'_c} = \frac{1}{0.8 + 170\varepsilon_1} \le 1.0 \qquad \text{Equation 5.6.1.1.3-3}$$

where:

f_{c2}	=	principal compressive stress
f_{c2max}	=	reduced peak compressive stress
ε_2	=	principal compressive strain
ε_1	=	principal tensile strain
ε'_c	=	maximum strain corresponding to f'_c
f'_c	=	28-day compressive strength of the concrete

Setting ε'_c = -0.002 and substituting the expression for f_{2max} from Equation 3 into Equation 2, and solving for ε_2 leads to the following expression:

$$\varepsilon_2 = -0.002\left(1-\sqrt{1-\frac{f_{c2}}{f_c'}\left(0.8+170\varepsilon_1\right)}\right) \qquad \text{Equation 5.6.1.1.3-4}$$

5.6.1.1.4 Equilibrium of Vertical Section

The basic expression for shear strength that includes the contribution of the concrete and stirrup steel is found from equilibrium. Equilibrium forces in a diagonally cracked beam, cut vertically, is shown in Figure 5.6.1.1.4-1.

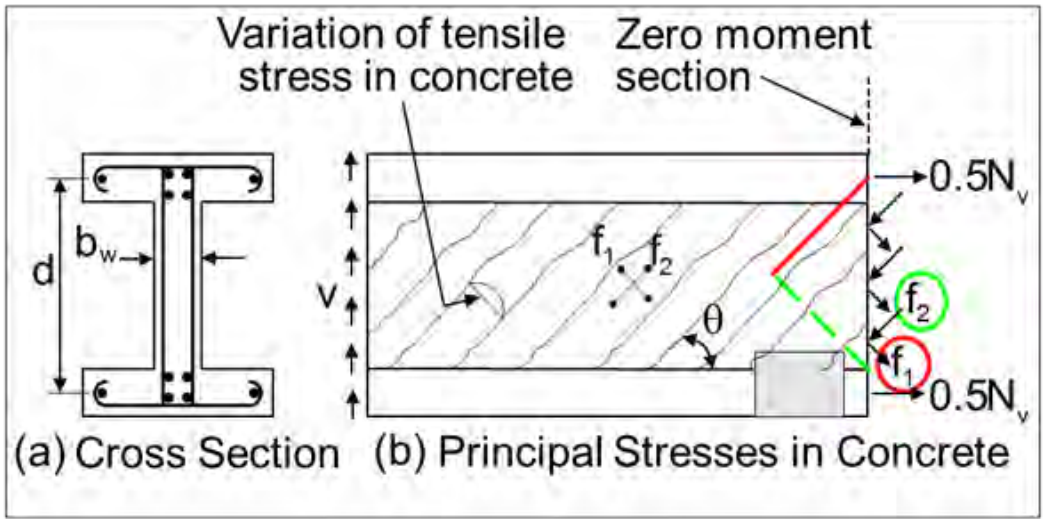

Figure 5.6.1.1.4-1 Equilibrium Conditions by Modified Compression Field Theory in Diagonally Cracked Beam

The compressive stress, f_2, is projected onto the dashed line, which has a length $d(\cos\theta)$, while the tensile stress, f_1, is projected onto the solid line, which has a length $d(\sin\theta)$. The stresses are then resolved into their vertical components and added together, giving:

$$V = f_2\left(b_w d\ \cos\theta\right)\sin\theta + f_1\left(b_w d\ \sin\theta\right)\cos\theta$$

where:

b_w = width of web
d = d_v

which reduces to:

$$f_1 + f_2 = v / \sin\theta\cos\theta \qquad \text{Equation 5.6.1.1.4-1}$$

where:

ν = shear stress = $V/b_w d$

Equilibrium can also be taken from a portion that is cut from the bottom of the beam as illustrated in Figure 5.6.1.1.4-2.

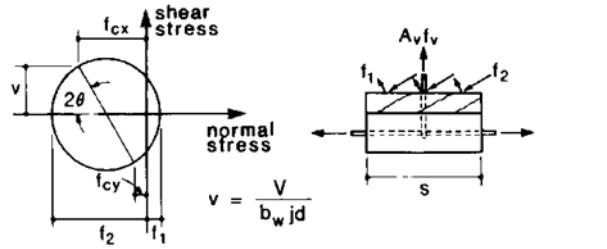

(c) Average concrete stresses (d) Tension in web reinforcement

Figure 5.6.1.1.4-2 Equilibrium Conditions by Modified Compression Field Theory in Diagonally Cracked Beam

Using the same procedure as above, the force in the stirrup steel is found to be:

$$A_v f_v = f_2(b_w s \sin\theta)\sin\theta - f_1(b_w s\cos\theta)\cos\theta$$

where:

f_v = stress in the transverse reinforcement

which reduces to:

$$(f_2 \sin^2\theta - f_1\cos^2\theta)b_w s = A_v f_v \qquad \text{Equation 5.6.1.1.4-2}$$

Combining Equations 1 and 2 and setting $f_v = f_y$, where f_y = yield strength of the reinforcement, gives:

$$V = f_1 b_w d\cot\theta + \frac{A_v f_y}{s} d\cot\theta \qquad \text{Equation 5.6.1.1.4-3}$$

where the first part of the equation is referred to as the concrete contribution to the shear strength, V_c, and the second part is the steel reinforcement contribution, V_s:

$$V_n = \text{"}V_c\text{"} + \text{"}V_s\text{"}$$

5.6.1.1.5 Shear Transfer at a Crack

Because of aggregate interlock, concrete has the ability to transfer shear along a crack. Experimental tests show that this ability is limited by the crack width, *w*, and the maximum aggregate size, a_{max}. The crack width will be put in terms of the principal tensile strain later. In the final formulation, a_{max} is assumed. Crack slipping may be prevented if the following limit is placed on the shear stress along the crack:

$$v_{ci} \le \frac{12\sqrt{f'_c}}{0.31 + 24w/(a_{max} + 0.63)} \qquad \text{Equation 5.6.1.1.5-1}$$

The shear stress along a crack can be related to the tensile stress by taking vertical equilibrium at a crack and also between cracks.

The stress flow at a crack is illustrated in Figure 5.6.1.1.5-1. The forces that counteract shear are the concrete shear along the crack, v_{ci}, and the stirrup reinforcement.

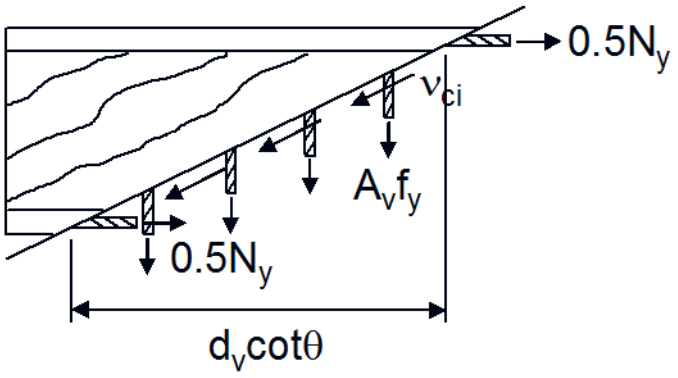

Figure 5.6.1.1.5-1 Force Transfer Across a Crack (Local Stresses)

Note that the concrete tension stress, f_1, discussed previously is not included because it is an average between the cracks; directly at a crack, the concrete does not carry tension. The number of bars engaged along the crack is essentially *d*(cot θ)/*s*, giving a force in the stirrups equal to $A_v f_y d \cot\theta / s$. Note that the stirrups are assumed to be yielding because the concrete has cracked and the stirrups are fully engaged. The concrete shear acts along an inclined length of d/sinθ; taking the vertical component of this shear results in $v_{ci}(b_w d / \sin\theta)\sin\theta$. Adding the two components results in:

$$V = A_v f_y \frac{d\cot\theta}{s} + v_{ci} b_w d \qquad \text{Equation 5.6.1.1.5-2}$$

Taking a section between two cracks the stress flow is as illustrated in Figure 5.6.1.1.5-2. The forces that counteract shear are the tensile stress in the concrete and the stirrup reinforcement.

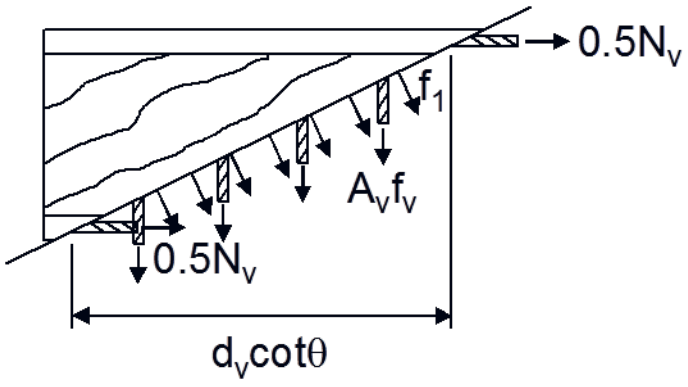

Figure 5.6.1.1.5-2 Force Transfer in Uncracked Concrete Between Two Cracks (Calculated Average Stresses)

The force in the stirrups at a section between the cracks is the same as that derived at a crack except that the stirrups are not yielding (i.e., $A_v f_v d\cot\theta / s$.) The concrete tension acts along an inclined length of $d/\sin\theta$; taking the vertical component of this shear results in $f_i(b_w d/\sin\theta)\cos\theta$. Adding the two components results in:

$$V = A_v f_v \frac{d\cot\theta}{s} + f_1 \frac{b_w d}{\sin\theta}\cos\theta \qquad \text{Equation 5.6.1.1.5-3}$$

Equating the shear given by Equations 2 and 3 gives:

$$f_1 \le v_{ci}\tan\theta \qquad \text{Equation 5.6.1.1.5-4}$$

with the inequality added to set an upper limit for f_1 in order to prevent crack slipping, as defined by the parameter v_{ci}. Substituting Equation 1 for v_{ci} gives:

$$f_1 \le \frac{12}{0.31 + 24w/(a_{max} + 0.63)}\sqrt{f_c'}\tan\theta \qquad \text{Equation 5.6.1.1.5-5}$$

The equation above can be simplified by defining a new parameter β, with the upper limit imposed to limit crack slipping, as:

$$\beta \le \frac{12}{0.31 + 24w/(a_{max} + 0.63)}$$ Equation 5.6.1.1.5-6

The crack width w can be expressed in terms of the tensile strain as:

$$w = \varepsilon_1 s_{m\theta}$$ Equation 5.6.1.1.5-7

where:

$s_{m\theta}$ = mean crack spacing

In the final formulation, a crack spacing is assumed, so β becomes a function of the tensile strain, ε_1, and aggregate size. Substitution of β into Equation 5 results in:

$$\beta = \frac{f_1}{\sqrt{f'_c}} \cot\theta \text{, or alternatively, } \beta\sqrt{f'_c} = f_1 \cot\theta$$ Equation 5.6.1.1.5-8

which can be substituted into Equation 3 to give the final expression:

$$V_n = \beta\sqrt{f'_c} b_w d + \frac{A_v f_y}{s} d \cot\theta$$ Equation 5.6.1.1.5-9

Equation 5 (dropping the subscript "*c*" from "f_{ci}") is combined with Equation 8, and using $f_{cr} = 0.33\sqrt{f'_c}$ gives:

$$\beta = \frac{0.33 \cot\theta}{1 + \sqrt{500\varepsilon_1}}$$ Equation 5.6.1.1.5-10

To calculate β, a final expression is needed for the tensile strain ε_1. This can be found from strain compatibility.

5.6.1.1.6 Strain Compatibility

One assumption of the MCFT is that the angle of orientation of the principal stresses is equal to the angle of the principal strains. From the transformation equations for plane strain from mechanics, the principal strains are related to the longitudinal strain, ε_x, and θ in the formula:

$$\varepsilon_1 = \varepsilon_x + (\varepsilon_x - \varepsilon_2)\cot^2\theta \qquad \text{Equation 5.6.1.1.6-1}$$

Combining this expression with Equation 6 and Equation 1, and considering f_1 in Equation 1 to be small in comparison to f_2, would give:

$$\varepsilon_1 = \varepsilon_x + \left[\varepsilon_x + 0.002\left(1 - \sqrt{1 - \frac{\nu}{f_c'}\frac{0.8 + 170\varepsilon_1}{\sin\theta\cos\theta}}\right)\right]\cot^2\theta \qquad \text{Equation 5.6.1.1.6-2}$$

5.6.1.1.7 *AASHTO LRFD* Procedure

As seen from the previous derivation, the equations used in the MCFT contain variables that cannot be isolated for a closed end solution; therefore, calculating the most efficient shear steel arrangement can be time consuming because an iterative method is required. The basic procedure is as follows. First, the shear stress, ν, is calculated. After estimating θ, ε_x and ε_1 are calculated. Next β is calculated, from which the shear strength can be determined. The procedure can be repeated for different values of θ until the shear steel requirement is minimized. Alternately, one may use the *AASHTO LRFD* design aid tables found in *AASHTO LRFD* Appendix B5, which were originally presented (in a slightly different format) by Collins and Mitchell (1991). To eliminate the iterative process the 2008 *AASHTO LRFD Bridge Design Specifications* adopted a direct method for determining β and θ as an allowable alternative procedure. Both the iterative method and direct method used in *AASHTO LRFD* are discussed as follows.

5.6.1.1.8 Basic Equations for Shear Strength

The equations for shear strength in *AASHTO LRFD* Article 5.8.3.3 are similar to those derived above, where the concrete contribution is:

$$V_c = 0.0316\beta\sqrt{f_c'}\,b_v d_v \qquad \textit{AASHTO LRFD} \text{ Equation 5.8.2.5-1}$$

The constant of 0.0316 is added so that f'_c can be entered in ksi instead of psi.

The strength from the steel stirrups is:

$$V_s = \frac{A_v f_y d_v (\cot\theta + \cot\alpha)\sin\alpha}{s}$$ *AASHTO LRFD* Equation 5.8.3.3-4

The angle α allows for the case of inclined stirrups, where α is 90 degrees for vertical stirrups (i.e., cot θ = 0.) The total shear strength, including the effect of prestressing, V_p, is:

$$V_n = V_c + V_s + V_p$$ *AASHTO LRFD* Equation 5.8.3.3-1

To ensure that the concrete in the web does not crush prior to yield of the transverse reinforcement, the strength is limited by:

$$V_n = 0.25 f'_c b_v d_v + V_p$$ *AASHTO LRFD* Equation 5.8.3.3-2

To use the method in *AASHTO LRFD*, the values for the shear stress on the concrete, v_u, and the longitudinal strain, ε_x, are needed. The shear stress is calculated from:

$$v_u = \frac{V_u - \phi V_p}{\phi b_v d_v}$$ *AASHTO LRFD* Equation 5.8.2.9-1

where:

v_u = average factored shear stress on the concrete
V_u = factored shear force at section
ϕ = resistance factor

The longitudinal strain, ε_x, caused by the applied loads and the prestressing is illustrated in the diagram shown in Figure 5.6.1.1.8-1 for flexural, axial and shear regions.

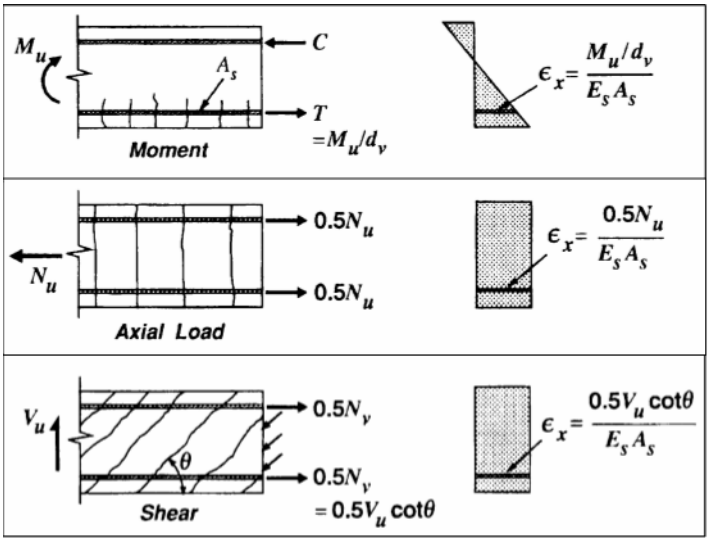

Figure 5.6.1.1.8-1 Longitudinal Strain Caused by Applied Loads and Prestressing

In the *AASHTO LRFD* Appendix B5 approach, the longitudinal strain can be found from one of three equations. If the section contains at least the minimum transverse reinforcement given elsewhere in the specifications, the section has the capacity to redistribute shear stresses. Thus, the maximum strain within the web can be calculated as follows:

$$\frac{\left(M_u/d_v\right) + 0.5N_u + 0.5\left(V_u - V_p\right)\cot\theta - A_{ps}f_{po}}{2\left(E_sA_s + E_pA_{ps}\right)} \le 0.001$$

AASHTO LRFD Equation B5.2-1

where:

M_u = factored moment at the section

N_u = applied factored axial force, taken as positive if tensile

A_{ps} = area of prestressing steel

f_{po} = a parameter taken as modulus of elasticity of prestressing tendons multiplied by the locked-in difference in strain between the prestressing tendons and the surrounding concrete (for the usual levels of prestressing, a value of $0.7f_{pu}$ is appropriate for both pretensioned and post-tensioned members

E_s = modulus of elasticity of nonprestressed tension reinforcement

A_s = area of nonprestressed tension reinforcement

E_p = modulus of elasticity of prestressing tendons

If the section contains less than the minimum transverse reinforcement, the strain is calculated by:

$$\varepsilon_x = \frac{\left(M_u / d_v\right) + 0.5N_u + 0.5\left(V_u - V_p\right)\cot\theta - A_{ps}f_{po}}{E_sA_s + E_pA_{ps}} \le 0.002$$

AASHTO LRFD Equation B5.2-2

If a negative value of ε_x results from either of the two equations above, there is compression at that location. The concrete stiffness will contribute and should be added in the denominator, for:

$$\varepsilon_x = \frac{\left(M_u / d_v\right) + 0.5N_u + 0.5\left(V_u - V_p\right)\cot\theta - A_{ps}f_{po}}{2\left(E_cA_c + E_sA_s + E_pA_{ps}\right)}$$

AASHTO LRFD Equation B5.2-3

If the above approach is used the crack spacing parameter shall be taken as *AASHTO LRFD* Equation B5.2-4.

Essentially, both transverse and longitudinal reinforcement contribute to shear strength. The horizontal component of the compression strut in the web has to be resisted by longitudinal tension reinforcement. The longitudinal reinforcement can be checked for adequacy with the following *AASHTO LRFD* Equation:

$$A_sf_y + A_{ps}f_{ps} \ge \frac{|M_u|}{d_v\phi_f} + 0.5\frac{N_u}{\phi_c} + \left(\left|\frac{V_u}{\phi_v} - V_p\right| - 0.5V_s\right)\cot\theta$$

AASHTO LRFD Equation 5.8.3.5-1

where:

f_{ps} = average stress in prestressing steel at the time for which the nominal resistance of member is required

If this inequality is not met, either the transverse or the longitudinal reinforcement must be increased.

5.6.1.1.9 Procedure for Reinforcement Selection Using *AASHTO LRFD* Appendix B5

Rather than presenting all of the equations that are needed to calculate β, *AASHTO LRFD* Tables B5.2-1 and 5.8.2-2 give θ and β values for sections with and without

the minimum amount of transverse reinforcement. This simplifies the procedure to just a few steps, which are outlined by a flow chart in *AASHTO LRFD* Figure CB5.2-5, and are summarized below:

1. Calculate factored load effects. Assume a value for θ.
2. Determine d_v. Calculate V_p. Check that b_v satisfies *AASHTO LRFD* Equation 5.8.3.3-2.
3. Calculate shear stress ratio v_u/f'_c.
4. Calculate the effective value of f_{po} if the section is within the transfer length of any strands. Otherwise, assume $f_{po}=0.7f_{pu}$.
5. Calculate ε_x using *AASHTO LRFD* Equations B5.2-1, -2 or -3.
6. Determine θ from *AASHTO LRFD* Tables B5.2-1 and B5.2-2, choosing the next-larger ε_x. Alternatively, interpolate the tables to find θ.
7. Recalculate ε_x in Step 5, and reselect new θ from the tables. Repeat until θ converges.
8. Select β from the tables.
9. Calculate V_c. Then calculate V_s required. The required stirrup spacing can then be found by assuming a bar size.
10. Check that the longitudinal reinforcement can resist the resulting tension using *AASHTO LRFD* Equation 5.8.3.5-1.
11. If there is not enough longitudinal reinforcement, either provide more longitudinal reinforcement or more transverse reinforcement. If the designer chooses to provide more transverse reinforcement, the strength V_s should be recalculated, and Step 10 should be repeated to obtain the reduced requirement for longitudinal reinforcement.

5.6.1.1.10 Procedure for Reinforcement Selection using the *AASHTO LRFD* Section 5.8.3.4.2

Rather than using the θ and β values for sections with and without the minimum amount of transverse reinforcement the code allows the direct calculation of β and θ. This simplifies the procedure by eliminating the iterative process. The steps are summarized below:

1. Calculate factored load effects.
2. Determine d_v. Calculate V_p. Check that b_v satisfies the requirement in *AASHTO LRFD* Equation 5.8.3.3-2.
3. Calculate $\varepsilon_s = \dfrac{|Mu|/dv + 0.5N_u + |V_u - V_p| - A_{ps}f_{po}}{E_sA_s + E_pA_{ps}}$ (*AASHTO LRFD* Equation 5.8.3.4.2-4) if ε_s is negative use 0.
4. Assuming section contains at least the minimum amount of transverse reinforcement, use *AASHTO LRFD* Equation 5.8.3.4.2-1 and determine β. If

there is not enough transverse reinforcement use *AASHTO LRFD* Equation 5.8.3.4.2-2.
5. Determine the angle of diagonal compression using *AASHTO LRFD* Equation 5.8.3.4.2-3.
6. Compute the concrete contribution using *AASHTO LRFD* Equation 5.8.3.3-3.
7. Check whether reinforcement is required using *AASHTO LRFD* Equation 5.8.2.4-1.
8. If V_u is greater than resistance of V_p+V_c, provide reinforcement in accordance with *AASHTO LRFD* Equation 5.8.3.3-1.
9. Determine V_s using *AASHTO LRFD* Equation 5.8.3.3-4.
10. Calculate v_u with *AASHTO LRFD* Equation 5.8.2.9-1.
11. Determine Maximum Spacing of reinforcement using *AASHTO LRFD* Article 5.8.2.7.
12. Check that the longitudinal reinforcement can resist the resulting tension using *AASHTO LRFD* Equation 5.8.3.5-1.
13. If there is not enough longitudinal reinforcement, either provide more longitudinal reinforcement or more transverse reinforcement. If the designer chooses to provide more transverse reinforcement, the strength V_s should be recalculated, and Step 12 should be repeated to obtain the reduced requirement for longitudinal reinforcement.

5.6.1.2 Alternate Method for Post-Tensioned Box Girders

Previous AASHTO LRFD and LFD methods for calculating shear strength resistance generally followed the basic principles contained in the above and, in particular, took account of the strength provided by the three key components namely; concrete, reinforcement and prestress, including not only the vertical component of prestress but also the magnitude of the axial prestress itself towards enhancing overall behavior. An alternative approach based upon the traditional shear and torsion design for plane sections, has been retained in the AASHTO *Guide Specification for Segmental Bridges*. It sets a limit on the overall resistance for shear and for the combination of both torsion and shear effects in relatively large boxes. The procedure is subject to certain constraints; for instance, that there are no significant discontinuities such as abrupt changes in cross section or openings, that there are limits on the contribution from concentrated loads near supports and that certain requirements for reinforcement detailing are met. The overall approach is straightforward, yet appropriate to the circumstances of large box sections. It is a conservative approach since the effective angle of the tension crack is implicitly assumed to be 45°, which is the assumption used in the LRFD simplified shear procedure for reinforced (non-prestressed) concrete. Slightly modified versions that account for the beneficial reduction in the potential shear crack angle as a result of axial or longitudinal compression stress, have been studied and used occasionally for enhanced load rating under increased loads or permit conditions.

5.6.1.3 Regions Near Discontinuities (D-Regions)

AASHTO LRFD Article C5.6.3.1 explains that strut-and-tie modeling is a convenient way of determining force effects where a traditional strength of materials approach is not applicable because of nonlinear strain distribution. The proportioning of the model is defined in *AASHTO LRFD* Articles 5.6.3.3 through 5.6.3.6 for compressive struts, tension ties, node regions, and crack control, respectively.

This tool is particularly valuable for analyzing simultaneous flexure and shear when the distance between the face-of-support and the location where shear is zero is located less than twice the member depth away. Another region of applicability is where the applied load is less than two member depths away from the support. In other words, use when plane-sections do not remain plane. Common substructure applications include integral bent caps, C-bent caps, footings and outrigger bents.

Common superstructure uses are diaphragm/bearing areas as illustrated in Figure 5.6.1.3-1. This technique has been used in the end regions of pretensioned girders but is generally most applicable to post-tensioned structures.

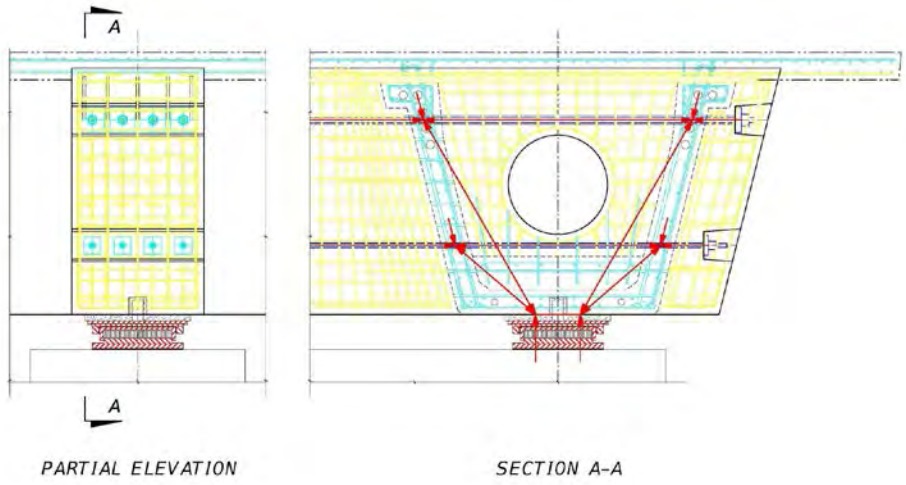

Figure 5.6.1.3-1 Pier Segment Diaphragm in a Post-Tensioned Segmental Box Girder Bridge

For additional guidance concerning the use of strut-and-tie methods for bridge design, see NCHRP Report 20-07/Task 217 “Verification and Implementation of Strut-and-Tie Model in LRFD Bridge Design Specifications.” In 2010 additional requirements were placed on the crack control section

Dr. Dennis Mertz states in his AASHTO LRFD Column in the Winter 2011 issue of *ASPIRE*, “The strut-and-tie model is a powerful tool for strength load cases when

conventional methods of strength of materials are no longer valid. It harkens back to when the structural engineer first learns to analyze a simple truss. By visualizing the members of the truss, the struts and ties, the designer achieves a better understanding of the mechanisms that allow complex structures to safely carry loads."

5.6.2 Serviceability Check (Service Limit State)

With the focus on longer service life, the need to check principal tensile stress at the service limit state has gathered more attention in post-tensioned concrete box structures. In general, the control of service level cracking in prestressed concrete is good practice.

Design for shear is a strength limit state function. Verifying there is adequate concrete in the web section to resist service load cracking is a requirement for post-tensioned box sections in *AASHTO LRFD*. However, to be mindful of the need for durability, a designer may choose to assure himself that the structure will not experience shear cracking at the service level. High shear forces can cause diagonal cracking in webs as the result of large principal tensile stresses. The magnitude of the effect can be determined by applying classical theory using Mohr's circle for stress. Limiting the principal tensile stress to 3 or $4\sqrt{f'c}$ (psi) at the elevation of the neutral axis has traditionally and conveniently been used to establish an approximate web thickness for durability and detailing purposes.

Limits on the magnitude of pure "shear stress" itself cannot be defined in the context of a prestressed member where longitudinal axial compression, in addition to flexural tension or compression stress, is present at a section of interest. Rather, it is necessary to consider shear stress in the context of the associated principal tensile stress. The latter is the resultant tensile stress on a small element, usually taken as a portion of the web, subject to shear stress due to vertical shear force, longitudinal compression or tension and any concomitant vertical compression or tension – as illustrated in Figure 5.6.2-1. Stresses are determined according to classical beam theory and Mohr's circle (Figure 5.6.2-2) provides the magnitude and direction of the principal tensile stress.

Near the end of a plain or reinforced concrete beam, the direction of principal tension lies at 45° below the neutral axis. Under sufficient shear force, it gives rise to classical diagonal shear cracks rising at 45° from the soffit. The influence of longitudinal compressive prestress near the end of a girder is to reduce the angle of the diagonal shear crack – the higher the local axial prestress, the shallower the crack. The result is to lengthen the potential crack, prior to the onset of cracking. This increases the effective length of web that can potentially be mobilized to resist shear. In turn this increase the magnitude of shear force needed to induce cracking.

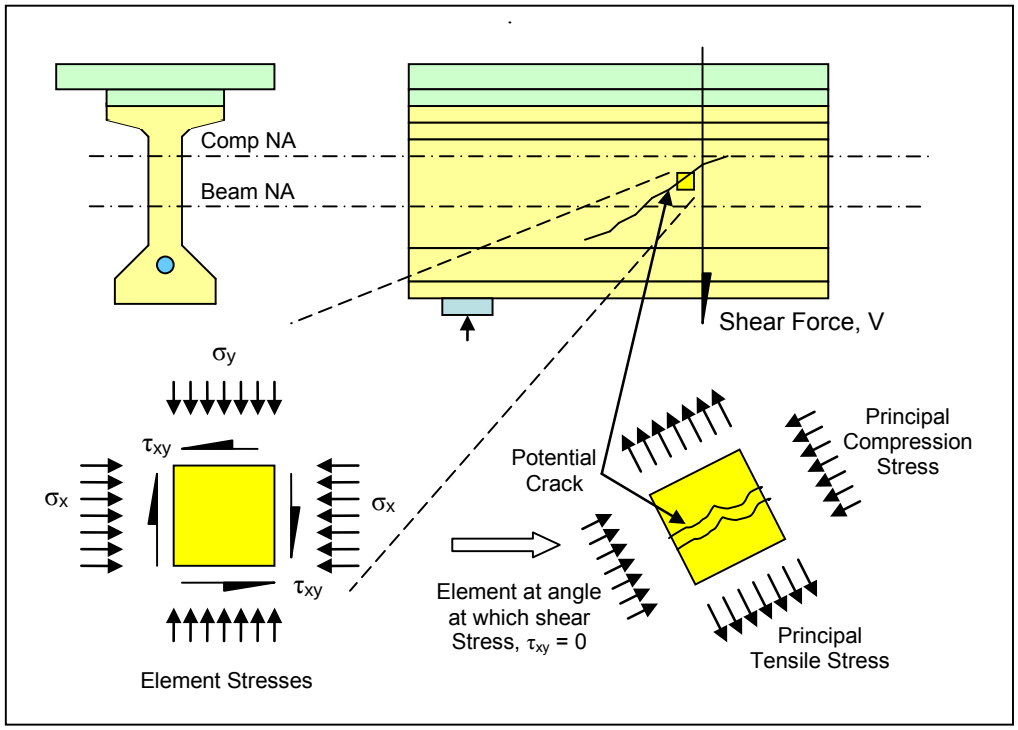

Figure 5.6.2-1 State of Stress in Web Element near the End of a Beam

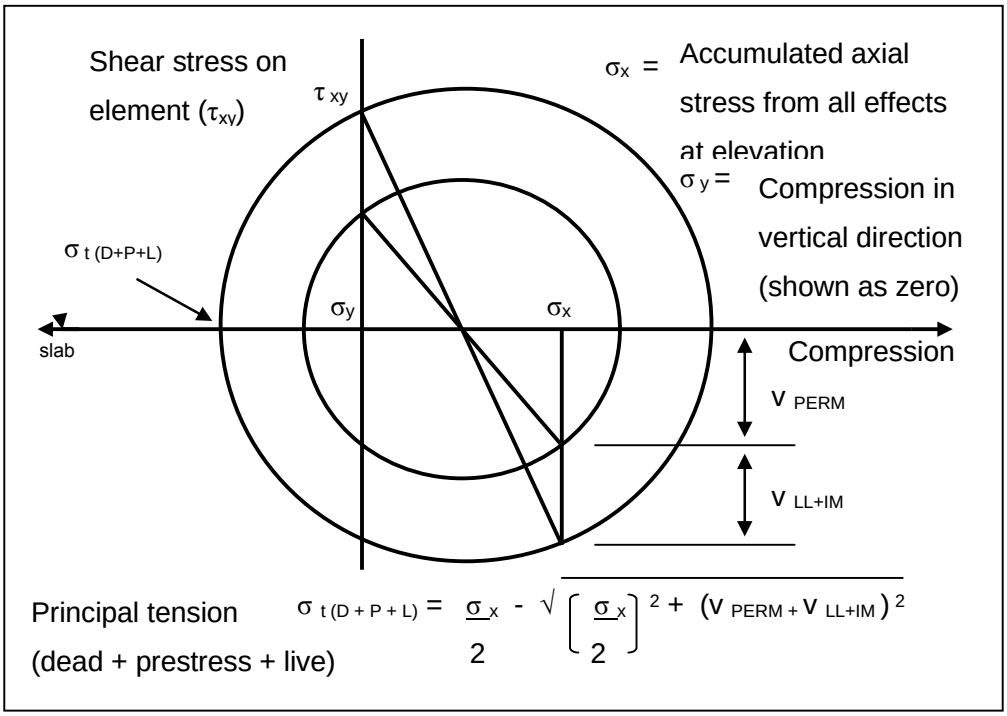

Figure 5.6.2-2 Mohr's Circle for Stress (Principal Tension)

In the end region of a typical prestressed I-girder the stress regime is complex as it is influenced by the prestress, the local bearing reaction, and the development length and de-bonding of the strands in addition to dead and live load moments and shear forces. All must be correctly accounted for in any attempt to determine either the flexural tensile stress in the bottom fiber or the principal tensile stress on an element within the depth of the girder. When the load on the girder is increased, near the support, cracks are generally initiated by the principal tension stress in the web as it reaches the cracking strength of the concrete. Further away from the bearing, cracks are generally initiated by flexural tension in the bottom fiber and propagate into the web, then curve over to follow the trajectory of the principal compression stress (being at right angles to the principal tensile stress).

This complexity in the end region of a pretensioned girder makes it difficult to define performance criteria for the service limit state. For concrete strengths above 10KSI a principal stress check should be considered. Limiting the magnitude of the shear stress itself cannot be used because shear resistance increases significantly with increasing axial prestress. The only possible means then is to limit the magnitude of the principal tensile stress. This would be in conjunction with existing limits for flexural tension stress per *AASHTO LRFD* Article 5.9.4.

Limits for principal tensile stress in a web at the elevation of the neutral axis of a segmental (box) girder in *AASHTO LRFD* Tables 5.9.5.4.1.2-1 and 5.9.5.4.2.2-1 were introduced in an endeavor to ensure a minimum web thickness for durability and to avoid or minimize web cracking; albeit that this check is applied under much simplified circumstances – namely, at the neutral axis where the longitudinal flexural stress is zero.

The designer of a pretensioned girder should exercise his judgment as to whether or not the service level stresses should be checked in the end regions of a girder to ensure satisfactory performance, durability and maintainability.

5.6.3 Torsion

Torsional behavior is very dependent on the section under torsion. Non-circular sections or open sections are weak in torsion. These open sections resist torsion by St. Venant Torsion (circular torsion) and warping torsion. Warping and St. Venant resistance have different displaced shapes and cannot be directly added (Figure 5.6.3-1).

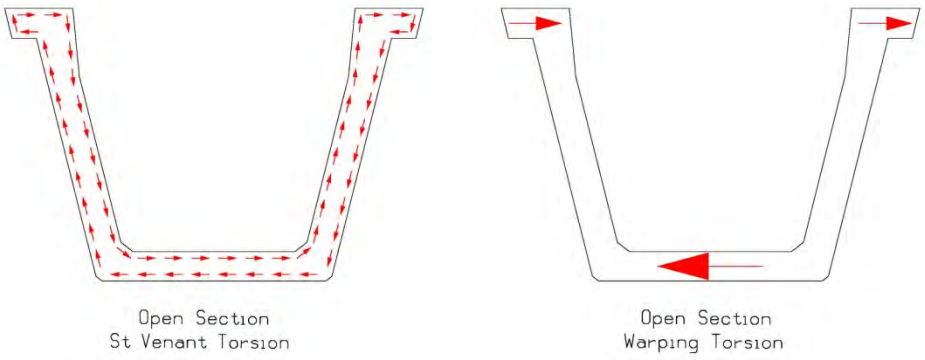

Figure 5.6.3-1 Comparison of St. Venant Torsion and Warping Torsion in an Open Cross Section

Cracking significantly reduces the torsional stiffness (on the order of 10% of the uncracked stiffness). The warping contribution becomes insignificant as the span length increases beyond a certain limit. Three-dimensional analysis can be used to determine the distorted shapes.

In a circular or closed section (Figure 5.6.3-2) the torsional stiffness will be 100 times greater than that of a similar section in an open shape.

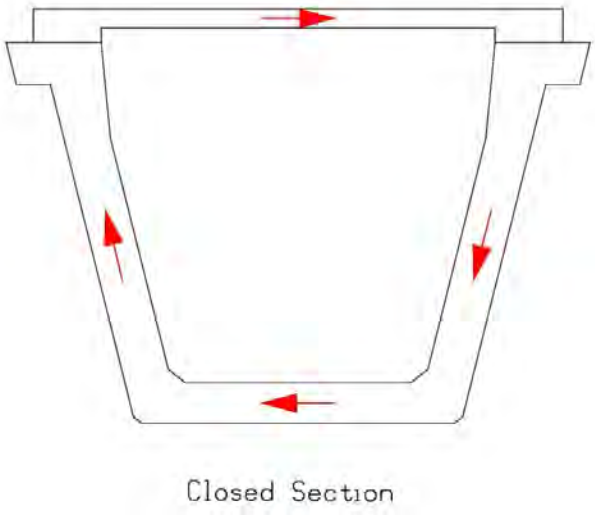

Figure 5.6.3-2 Closed Section Torsion Flow

AASHTO LRFD Section 5.8.2.1 requires torsion to be considered when:

$$T_u > 0.25\phi T_{cr} \qquad \textit{AASHTO LRFD} \text{ Equation 5.8.2.1-3}$$

Torsion in box sections is considered in shear design by increasing the shear demand from V_u to:

$$V_u + {T_u d_s}/{2A_0}$$ *AASHTO LRFD* Equation 5.8.2.1-7

The torsional reinforcement in precast segmental bridges is evaluated separate from the shear resistance. In structures where mild steel is provided through the closure pours between segments, the superstructure resistance is calculated as for ordinary bridges. The influence of geometry on closed cell girders is also discussed in *AASHTO LRFD* Article 4.6.1.2.4c, Closed Box and Tub Girders. This provision also applies to multiple lines of tub girders with significant warping. The effect of curvature may be ignored for main axis bending and shear if four provisions are met.

Figure 5.6.3-3 illustrates the components of shear stress flow in a closed section.

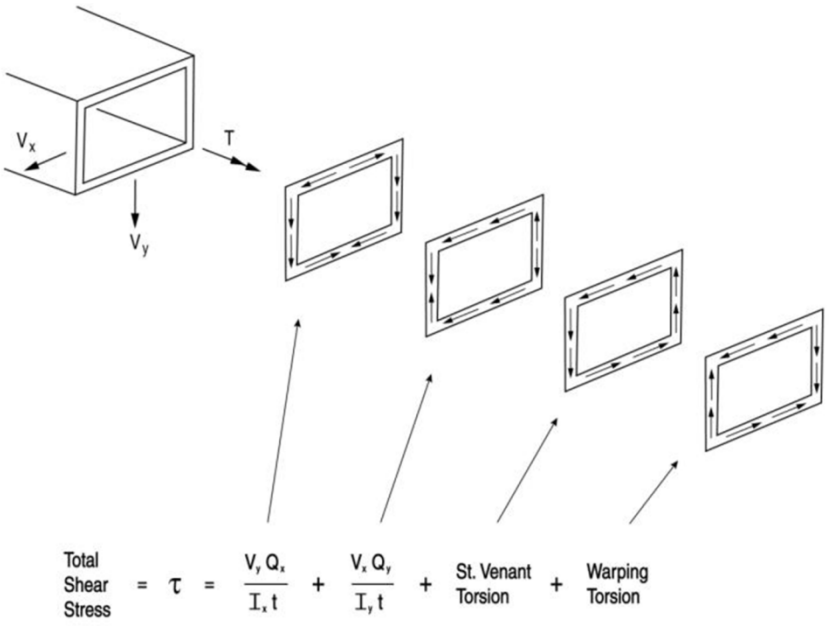

Figure 5.6.3-3 Components of Shear Flow in Closed Section with Bending about Both Axes

The total normal stress is illustrated in Figure 5.6.3-4.

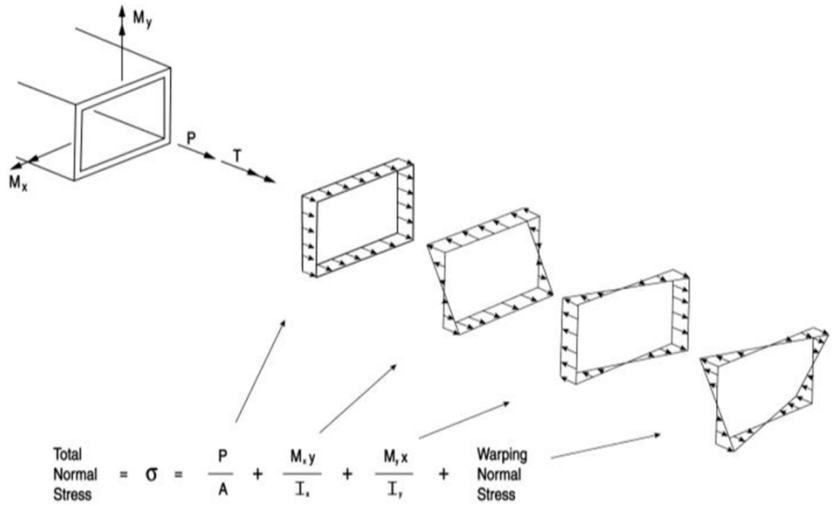

Figure 5.6.3-4 Components of Flexural Stress in Closed Section with Bending about Both Axes

Torsional resistance in *AASHTO LRFD* is based on a thin walled tube or space truss analogy. The cracking torque is calculated as:

$$T_{cr} = 0.125\sqrt{f_c'}\,\frac{A_{cp}^2}{p_c}\sqrt{1+\frac{f_{pc}}{0.125\sqrt{f_c'}}} \qquad \textit{AASHTO LRFD} \text{ Equation 5.8.2.1-4}$$

And the limit for principal tension is taken to be:

$$\text{Limit Principal Tension} = 0.125\sqrt{f_c'}\,(\text{ksi}) = 4\sqrt{f_c'}\,(\text{psi})$$

5.6.4 Interface Shear Transfer – Shear Friction

5.6.4.1 The Interface

Interface shear occurs where shear is transferred across a plane that is made up of two components of different materials or concrete cast at different times. *AASHTO LRFD* Article 5.8.4.1 states that interface shear transfer shall be considered at:

- An existing or potential crack
- An interface between dissimilar materials
- An interface between two concretes cast at different times
- The interface between different elements of the cross-section

In particular, for a composite girder, the girder and concrete slab are made up of two concretes that are cast at different times. Interface shear is, therefore, analyzed where the two components connect, i.e., at the interface of the top of the girder and the bottom of the slab.

5.6.4.2 Shear Mechanism

The best way to understand the origin of interface shear is to compare the behavior of a non-composite beam with a composite beam. Consider first a "non-composite" beam (i.e., prior to the slab being cast). The loads that the beam must resist are from the self-weight of the beam, the pretensioning effects, and the weight of the slab that will be placed on top of it (Figure 5.6.4.2-1).

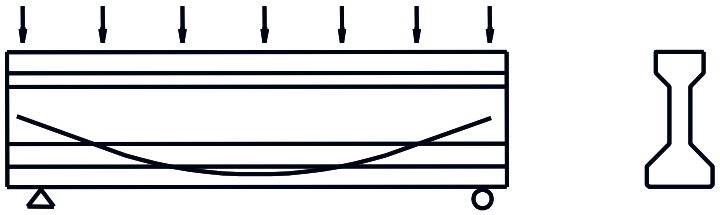

Figure 5.6.4.2-1 Noncomposite Beam Subjected to Beam Self-Weight, Pretensioning Effects and Slab Dead Weight

Once the slab has been placed and cured, the beam must now resist effects from utilities, barriers, wearing surface, and live loads (Figure 5.6.4.2-2).

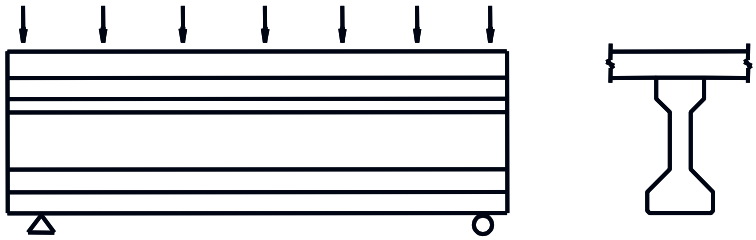

Figure 5.6.4.2-2 Deck Placed on Noncomposite Beam

If the slab simply rests on the beam, and the beam and slab are not connected, the non-composite beam behaves somewhat independently from the slab (assuming friction between the two contact surfaces is ignored.) Each component carries separately a part of the load. Under vertical load causing positive moment, the lower surface of the deck will theoretically be in tension and elongate while the top surface of the girder will be in compression and shorten. With friction neglected, only vertical internal forces will act between the deck and the girder, and slip will occur between the two components (Figure 5.6.4.2-3).

Figure 5.6.4.2-3 Independent (Noncomposite) Behavior between Precast Girder and Deck

Consider now the case where the beam has been made "composite", and the beam and slab are connected together structurally with some connectors (the design of which will be discussed later). In this case, the components will bend "together." The shear that must be designed for at the interface arises from the girder and slab being forced to act "together", as shown by the arrows in Figure 5.6.4.2-4, even though they are cast at different times and from different concretes.

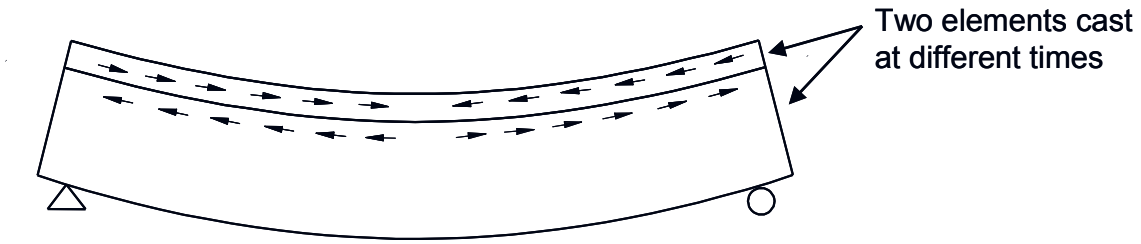

Figure 5.6.4.2-4 Interdependent (Composite) Behavior between Precast Girder and Deck

A beam that is composite with a slab has much greater resistance to bending than a plain beam (i.e., the moment of inertia is greatly increased). The result is weight and cost savings since shallower sections can be used.

The simplest way to calculate the magnitude of the horizontal shear is by using the *AASHTO LRFD* method, as found in *AASHTO LRFD* Article C5.8.4.1. The method gives an expression that relates the horizontal shear to the vertical shear, and it is based on equilibrium of a section of beam (Figure 5.6.4.2-5).

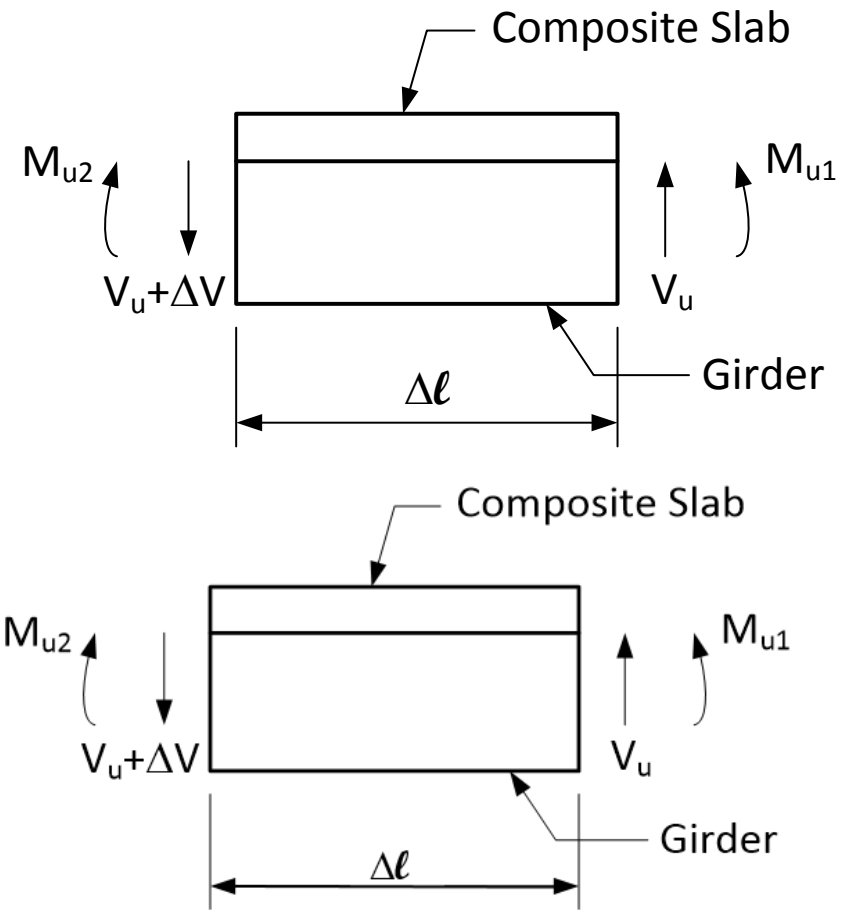

(a) Vertical Shear

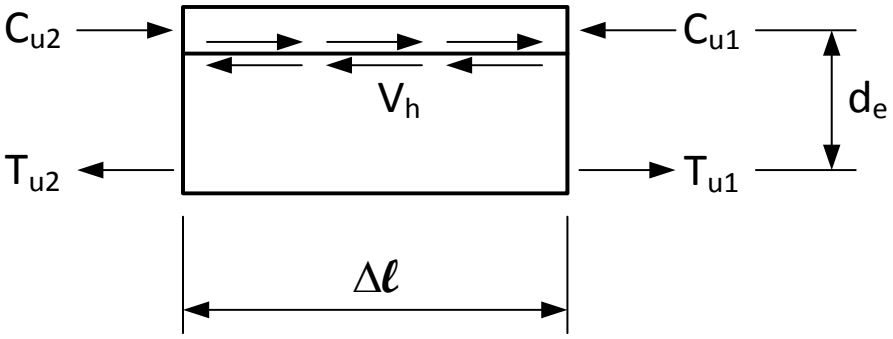

(b) Horizontal Shear

Figure 5.6.4.2-5 Relationship between Horizontal and Vertical Shear

First understand that diagram (a) in Figure 5.6.4.2-5 is roughly equivalent to diagram (b). The pertinent variables in the diagrams are V_h, the horizontal shear force within

length $\Delta\ell$, V_u, the factored vertical shear, and d_e, the distance between the centroid of the steel in the tension side of the beam to the center of the compression blocks in the deck. For simplicity, d_e can be taken as the distance between the centroid of the tension steel and the mid-thickness of the deck.

Taking moments about the left-hand side of (a),

$$M_{u2} = M_{u1} + V_u \Delta\ell \qquad \text{Equation 5.6.4.2-1}$$

Equating moments on the left-hand side of (a) with the left-hand side of (b),

$$C_{u2} \approx \frac{M_{u2}}{d_e} \qquad \text{Equation 5.6.4.2-2}$$

Substituting Equation 1 into Equation 2,

$$C_{u2} \approx \frac{M_{u1}}{d_e} + \frac{V_u \Delta\ell}{d_e} \qquad \text{Equation 5.6.4.2-3}$$

Equating moments on the right-hand side of (a) with the right-hand side of (b),

$$C_{u1} \approx \frac{M_{u1}}{d_e} \qquad \text{Equation 5.6.4.2-4}$$

Equating the horizontal forces at the interface in (b),

$$V_h = C_{u2} - C_{u1} \qquad \text{Equation 5.6.4.2-5}$$

Substituting Equation 3 and Equation 4 into Equation 5,

$$V_h = \frac{V_u \Delta\ell}{d_e} \qquad \text{Equation 5.6.4.2-6}$$

For a unit length segment ($\Delta\ell$ =1), Equation 6 reduces to:

$$V_h / \text{unit\_length} = V_{hi} = \frac{V_u}{d_e} \qquad \text{Equation 5.6.4.2-7}$$

The result is a simple way to calculate the magnitude of horizontal shear by using the vertical shear. V_{hi} is expressed as a force per length (i.e., kips/ft.) For V_u, use

only the loads that are applied to the composite section for Strength I Load Combination:

$$V_u = 1.25V_{DC} + 1.5V_{DW} + 1.75V_{LL+IM}$$ Equation 5.6.4.2-8

5.6.4.3 Resistance

When connectors are used, the resistance to interface shear is calculated in three parts. The first is the cohesion component, *c*, between the two surfaces, and the second is the connector strength component, $A_{vf}f_y$. A third contributor can be considered if the interface has a compressive force, P_c, normal to the shear plane. Recall from mechanics that the friction that is developed between two objects is proportional to the normal force.

Because the interface is rough, shear displacement will cause the discontinuity to widen. This opening will cause tension in the reinforcement crossing the discontinuity balanced by compressive stresses on the concrete discontinuity surfaces. The resistance of the face to shear is assumed to be a function of both cohesion and friction.

Reinforcement "ties" the beam and slab together, contributing to friction strength. Typically, mechanical shear connectors are used at the interface between the girder and slab. In a composite beam that is made up of a steel girder and a concrete slab, the most typical connectors that are used are shear studs that are welded onto the top flange that protrude into the slab. In a concrete girder, reinforcing bars (single or multiple leg stirrups) are typically cast into the top of the girder. The bars must be anchored in both the girder and the slab to develop the specified yield strength.

The interface shear resistance due to all of the above contributors is given in *AASHTO LRFD* Equation 5.8.4.1-3 as:

$$V_{ni} = cA_{cv} + \mu\left[A_{vf}f_y + P_c\right]$$

where:

V_{ni} = nominal shear resistance (kip)
c = cohesion factor (ksi)
A_{cv} = area of concrete engaged in shear transfer (in^2)
μ = friction factor
A_{vf} = area of shear reinforcement crossing the shear plane (in^2)
f_y = yield strength of reinforcement (ksi), not to exceed 60 ksi for design
P_c = permanent net compressive force normal to the shear plane; if force is tensile, P_c = 0.0 (kip)

Upper limits on the strength are given in *AASHTO LRFD* Equations 5.8.4.1-4 and 5.8.4.1-5 as:

$$V_{ni} \le K_1 f_c' A_{cv} \text{ , or}$$

$$V_{ni} \le K_2 A_{cv}$$

where:

f'_c = specified 28-day compressive strength of the weaker concrete (ksi)

The values given in *AASHTO LRFD* Article 5.8.4.3 for the cohesion and friction factors are dependent upon how the two different concretes are placed (see Table 5.6.4.3-1).

Table 5.6.4.3-1 Cohesion and Friction Factors

Description	*C (ksi)*	*μ*	K_1	K_2 *(ksi)*
For normal weight concrete placed monolithically	0.40	1.4	0.25	1.5
For cast-in-place concrete slab on clean concrete girder surfaces, free of laitance with surface roughened to an amplitude of 0.25 in.				
For normal weight concrete	0.28	1.0	0.3	1.8
For lightweight concrete	0.28	1.0	0.3	1.3
For concrete placed against a clean concrete surface, free of laitance, but not intentionally roughened	0.075	0.6	0.2	0.8

5.6.4.4 Reinforcement Required

For design, the required size and spacing of reinforcing steel must be determined. The horizontal shear (in units of force/length) is usually multiplied by the spacing of the reinforcement (in units of length) so that the resulting force can be equated to the expression for shear strength.

This amounts to "designing" a length of interface along the beam equal to the spacing of the reinforcement, such that $A_{cv} = b_v s$ (see Figure 5.6.4.4-1).

where:

b_v = width of the interface considered to be engaged (in)

s = spacing of interface shear reinforcement (in)

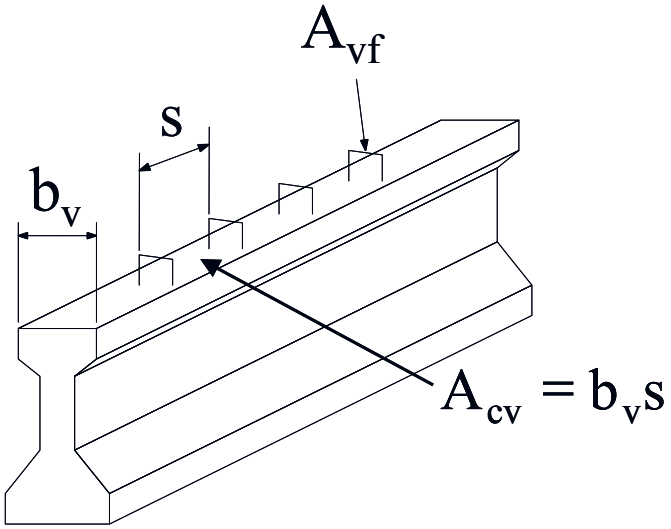

Figure 5.6.4.4-1 Reinforcement Required

The resulting equation is as follows:

$$\frac{V_{hi}s}{\phi} \le c(b_v s) + \mu\left(A_{vf} f_y + P_c\right) \qquad \textit{AASHTO LRFD} \text{ Equation 5.8.4.1-3}$$

where:

$V_{hi}s = V_{ui}$ (factored interface shear force) $\le \phi V_{ni}$

Solving for the required spacing of reinforcement:

$$s = \frac{\mu\left(A_{vf} f_y + P_c\right)}{V_{hi}/\phi - cb_v}$$

5.6.4.5 Minimum Requirements

The minimum cross-sectional area of reinforcement per unit length that must be provided, given in *AASHTO LRFD* Article 5.8.4.4, must satisfy:

$$A_{vf} \ge \frac{0.05 b_v}{f_y} \qquad \textit{AASHTO LRFD} \text{ Equation 5.8.4.4-1}$$

For the typical case of a cast-in-place concrete slab on a clean concrete girder surface free of laitance and with the surface intentionally roughened, the minimum value of A_{vf} need not be greater than that required to resist 1.33 times the value of

V_{ni} determined from *AASHTO LRFD* Equation 5.8.4.1-3 (see *AASHTO LRFD* Article 5.8.4.4 for details).

Alternatively, the minimum requirement may be waived if:

1. v_{ui}, as given by *AASHTO LRFD* Equation 5.8.4.2-1, is less than 0.210 ksi; and

2. All the minimum transverse steel required for vertical shear, A_v, given by *AASHTO LRFD* Equation 5.8.2.5-1, is extended across the interface and adequately anchored in the slab (see *AASHTO LRFD* Article 5.8.4.4 for details).

In accordance with *AASHTO LRFD* Article 5.8.4.2, for beams or girders the longitudinal center-to-center spacing of the interface shear reinforcement shall not exceed 48.0 inches or the depth of the member, h. Also, if the contact surface width (i.e., the top flange beam width) is greater than 48 inches, at least four bars in each row should be used.

Section 5.7 Prestressing

5.7.1 General Design Requirements

AASHTO LRFD Article 5.9.1 describes general design considerations for prestressed concrete structures and members. Prestressed concrete structural components must be designed for both initial and final prestressing forces. They are required to meet demands for service, fatigue, strength, and extreme event limit states, but for bridge superstructures the service and strength limits states will generally govern design.

Compressive stress limits for final prestressing forces are to be used with any applicable service load combination given in *AASHTO LRFD* Table 3.4.1-1 except Service Load Combination III, which applies only to tension. Service Load Combination III applies only when investigating tensile stresses under live load.

Service load stresses in the member must be checked against tensile and compressive stress limits given as a function of f'_{ci} and f'_c, respectively, for initial and final prestressing forces. f'_{ci} is normally taken as the concrete strength at the time of prestressing transfer (strand cutting) in the casting bed for pretensioned bridge girders. With a typical one-day turnaround of forms in the casting yard this value is likely to represent the concrete strength after just a day of curing. Post-tensioned structures are generally stressed at a later time so f'_{ci} may be significantly higher, even up to the 28-day strength. f'_c is usually taken as the 28-day strength for both

pretensioned and post-tensioned members. However, other concrete strengths, such as 56-day strength, may be specified for special applications.

AASHTO LRFD permits the use of either gross or transformed sections in calculating section properties for stress analysis. Nevertheless, individual state DOTs may have specific policies regarding the preferred or required use of one or the other method so it is best to verify this prior to commencing design. Different state DOTs also have different policies concerning crack control and limiting tensile stresses under service loads with the intent of limiting crack widths, preventing fatigue of reinforcement and eliminating or minimizing corrosion in the structure.

5.7.2 Stress Limitations

5.7.2.1 Stress Limits for Prestressing Tendons

Stress limits for prestressing tendons and bars are specified at the service and strength/extreme event limit states in *AASHTO LRFD* Tables 5.9.3-1 and 5.4.4.1-1, respectively.

Pretensioning. *AASHTO LRFD* Table 5.9.3-1 shows stress limits for Low Relaxation Strand and Deformed High-Strength Bars immediately prior to transfer (i.e., before cutting the strands in the precast bed) and at the service limit state after all losses have occurred. A couple of things to note about the information in this table are as follows:

- It is unlikely that you will have very many applications that use Deformed High-Strength Bars for pretensioning. These are more commonly post-tensioned.
- The table also shows stress limits for Stress-Relieved Strand and Plain High-Strength Bars. Stress-Relieved Strand is no longer manufactured in this country, and Plain-High Strength Bars are generally not used for bridge applications or for pretensioning.
- The tabulated values for Low Relaxation (Low-Lax) Strand are very important for all applications using pretensioned concrete bridge girders.
    - *Immediately prior to transfer* the stress in the steel is limited to $0.75f_{pu}$ with f_{pu} equal to 270 ksi for most bridge applications.
    - *At service limit state after all losses* (this can be any time from just after release to the end of the bridge service life, with the time just after release being the most critical) the stress in Low-Lax strand is limited to $0.80f_{py}$, where $f_{py} = 0.90f_{pu}$ (*AASHTO LRFD* Table 5.4.4.1-1), thus the maximum stress limit in the steel immediately after release = $0.80 \times 0.90 \times f_{pu} = 0.72\ f_{pu}$.

Post-tensioning. For post-tensioning applications *AASHTO LRFD* Table 5.9.3-1 provides maximum service load steel stress limits at three different stages for Low Relaxation and Deformed High-Strength Bars. (As noted above for pretensioned bars, the values given for Stress-Relieved Strand and Plain High-Strength Bars are no longer of value for bridge applications in the U.S.)

- *Temporary stresses prior to seating* the wedges (strand) or nut (bar) are limited to $0.90f_{py}$ = 0.90 x 0.90 x f_{pu} = $0.81f_{pu}$ (strand); = 0.90 x 0.80 x f_{pu} = $0.72f_{pu}$ (bars.) This is a short-term "over-stress" value that will be immediately reduced by seating and friction losses in the bar or strand after anchoring.
- *Immediately after seating* the tendons/bars (anchor set), maximum stresses are limited as follows:
  - At anchorages and couplers = 0.70 f_{pu}
  - Elsewhere along the length of a member (away from anchorages and couplers) = 0.74 f_{pu} (strand); = 0.70 f_{pu} (bars)
- *At service limit state after losses* = $0.80f_{py}$ = 0.80 x 0.90 x f_{pu} = $0.72f_{pu}$ (strand); = 0.80 x 0.80 x f_{pu} = $0.64f_{pu}$ (bars.) As with pretensioning, the time immediately after seating of the post-tensioning is when the stress in the tendon/bar will be at its maximum value so stresses should be checked against these values when the bridge first goes into service.

The distinction between stresses "at anchorages" and "away from anchorages" after seating will be explained in more detail in Section 5.7.3.3.1 with friction loss and anchor set.

5.7.2.2 Stress Limits for Concrete

Axial/flexural stress limits in concrete members are given for "Segmentally Constructed Bridges" and "Other Than Segmentally Constructed Bridges" in *AASHTO LRFD* Article 5.9.4 for "Temporary Stresses Before Losses" and at "Service Limit State After Losses." Limits are shown for tensile and compressive stresses at girder extreme fibers and principal tensile stresses in girder webs.

"Segmentally constructed" refers to bridges whose longitudinal members are made up of shorter box or girder segments that are assembled in stages and joined together using post-tensioning. Examples include segmental box girders and spliced precast prestressed girders, either of which may utilize cast-in-place closures or thin epoxy joints to connect longitudinal box or girder segments. Post-tensioning is used to compress the joints and hold the structure together without the need for mild steel reinforcement crossing the joint interface(s).

Segmentally constructed bridges are singled out in the concrete stress limit tables for three primary reasons:

- Because it is permissible to have closure joints without mild steel crossing them to resist tensile stresses, it is important to limit tensile stresses across the joints to a lower stress limit (zero tension or residual compression) than for monolithic concrete.
- Unlike composite beam girder bridges, which are essentially linear beam elements for prestressed concrete design purposes, segmental box girder bridges often utilize transverse post-tensioning to compress the deck. Therefore, it is necessary to define a stress limit criterion for transverse design of such structures.
- Segmental box girder and spliced I-girder bridges generally use very high levels of post-tensioning and relatively thin webs compared to conventional pretensioned composite girder bridges. Diagonal cracking of the webs may occur unless they are made sufficiently thick to resist the resulting diagonal tensile stresses. Thus, a principal tension check has been introduced into *AASHTO LRFD*. (Note: A near-term revision to *AASHTO LRFD* may limit principal tension stresses in the webs of all post-tensioned concrete bridge girders and in the webs of all pretensioned girders with a design concrete strength greater than 10 ksi.)

The compressive stress limits for concrete given in *AASHTO LRFD* Article 5.9.4 are fairly straightforward;

- Temporary stresses before losses: $0.60f'_{ci}$
- Service limit state after losses:
  - $0.45f'_c$ under sustained loads (i.e., effective prestress plus permanent loads)
  - $0.60f'_c$ due to the sum of sustained loads and transient (e.g. live, temperature) loads. (*Note: There is a modification factor for cross-sections with thin web or flange components*.)

Axial/flexural tensile stress limits given in *AASHTO LRFD* Table 5.9.4.1.2-1 (temporary, before losses) and *AASHTO LRFD* Table 5.9.4.2.2-1 (service limit state, after losses) are contingent on several factors, including:

- “Segmentally constructed” or “other than segmentally constructed”
- “Precompressed tensile zone” or “other than “precompressed tensile zone”
- “Less than or equal to moderate” or “severe” corrosion conditions
- “Bonded reinforcement” or “no bonded/insufficient reinforcement”

In addition to longitudinal stress limits in bridge girders, the tensile stress tables also provide limiting values for:

- Handling stresses in prestressed piles

- Transverse stresses in Segmentally Constructed Bridges
- Principal tensile stresses at the neutral axis in girder webs

AASHTO LRFD Article 5.9.4 provides a more complete treatment of concrete stress limits in prestressed concrete girders and members.

5.7.2.3 Tensile Stresses in Webs

As noted in the previous section, a principal tension stress limit is specified for the webs of "Segmentally Constructed Bridges." This limiting value currently appears in *AASHTO LRFD* Tables 5.9.4.1.2-1 and 5.9.4.2.2-1. However, the specifications are in the process of revision to expand the applicability of this requirement to more than just segmental box girder bridges. The limitations on principal tensile stresses in girder webs may be moved from the tables to a separate specification section and may apply to all girder webs with either internal or external post-tensioning and to pretensioned girders using concrete strengths higher than 10 ksi. Different stress limits may be defined for temporary conditions before losses and service limit states after losses.

5.7.3 Loss of Prestress

5.7.3.1 Total Loss Summation

Whether prestress is applied by pretensioning or post-tensioning, various losses of effective force occur as a natural response from the properties of the two materials; concrete and steel. The final effective prestress is influenced by:

- Elastic deformation of concrete
- Shrinkage of concrete
- Creep of concrete
- Relaxation (creep) of prestressing steel

Elastic deformation of concrete occurs initially at transfer of the prestress force and subsequently from the addition of structural loads and changes during construction. The modulus of elasticity of concrete depends primarily upon its strength – and this is influenced by many construction related factors, age, type of curing, type of cement, aggregate, environment and so on. Creep and shrinkage are affected by the same factors. Loss of prestress due to relaxation (creep) of prestressing steel depends upon the type of steel – whether normal or low-relaxation.

Additional loss of prestress arises in post-tensioning during the stressing process as a result of physical aspects of the post-tensioning system and ducts, such as the following:

- Wedge set (anchor set; pull-in)
- Friction in the jack
- Friction in the anchorage
- Duct friction due to curvature
- Duct friction due to unintentional variation from profile (wobble)

For design purposes, it is normal to make assumptions on the basis of past experience or specifications guidance in order to reasonably estimate the final effective prestress force as a consequence of these losses and effects. For simply-supported structures and relatively straightforward two- and three-span continuous structures, estimates can be made by hand. For more complex structures involving multiple stages of construction and time-dependent changes, special structural analysis computer programs are commercially available to facilitate the tedious analysis process.

For initial member selection, sizing of a cross section and preliminary design purposes, the final stress in the strands after all losses lies approximately in the range of 58% to 62% of F_{pu} for pretensioned girders (early concrete age at transfer; friction losses if tendon is harped.) For cast-in-place post-tensioned construction, the final stress in the strands after all losses lies approximately in the range of 55 to 60% of F_{pu} (early concrete age at transfer plus friction losses.) For precast segmental construction, where concrete is loaded at a later age, final forces after losses, including those due to friction and anchor set, tend to be approximately in the range of 60 to 64%F_{pu}. These are approximations. Final design should always properly account for loss of prestress according to recognized procedures.

5.7.3.2 Application to Composite Pretensioned Girder Structures

In pretensioned composite bridge construction, loss of prestress force is caused by elastic shortening, shrinkage of the girder and deck, creep of concrete and relaxation of prestressing steel. In a pretensioned girder these losses occur at transfer, during the time the girder is in storage or on site before the deck is cast, and then long-term after the deck has been cast. They are summarized in Table 5.7.3.2-1.
.

Table 5.7.3.2-1 Prestress Losses in Pre-Tensioned Girders

Prestress Loss (*AASHTO LRFD* Article 5.9.5)	At Transfer	Transfer to Deck Placement	Deck Placement to Final Time
Elastic Shortening	Δf_{pES}		
Shrinkage of Girder		Δf_{pSR}	Δf_{pSD}
Creep of Girder		Δf_{pCR}	Δf_{pCD}
Relaxation of Steel		Δf_{pR1}	Δf_{pR2}
Shrinkage of deck on Composite Section			Δf_{pSS}

Briefly summarizing, the terms for prestress loss (expressed in ksi) in the above table are:

Δf_{pES} = Elastic shortening under the initial prestress force at transfer
Δf_{pSR} = Shrinkage of girder concrete between transfer and deck placement
Δf_{pCR} = Creep of girder concrete between transfer and deck placement
Δf_{pR1} = Relaxation of prestressing strands between transfer and deck placement
Δf_{pR2} = Relaxation of prestressing strands in composite section after deck placement
Δf_{pSD} = Shrinkage of girder concrete after deck placement to final time
Δf_{pCD} = Creep of girder concrete after deck placement to final time
Δf_{pSS} = Shrinkage of deck composite section (prestress gain)

5.7.3.2.1 Instantaneous Losses

In pretensioned girders “Elastic Shortening” is the loss due to the initial elastic shortening (deformation) of the concrete as a result of the (instantaneous) release of pretensioned strands in the casting bed at the time of transfer. Usually, a component is relatively young (i.e., from a day to about a week old) and may have been steam cured or moist cured. Elastic shortening loss is given by *AASHTO LRFD* Article 5.9.5.2.3, as:

$$\Delta f_{pES} = \frac{E_p}{E_{ct}} f_{cgp}$$

where:

f_{cgp} = stress in the concrete at the centroid of the prestress at transfer
E_p = elastic modulus of strand
E_{ct} = elastic modulus of concrete

In the casting bed the strands are tensioned against bulkheads. After casting and after the concrete has attained the required transfer strength, the strands are cut – transferring their force to the concrete by bond. As a result, the concrete shortens. This shortening affects the strands too; the equation follows directly from consideration of elastic conditions. It can perhaps be better understood as follows:

- The total force in the strands, F_p, is applied to the concrete girder gross cross section, A_g, which has a moment of inertia I_g, at an average distance e_p below the neutral axis
- This creates a compressive stress in the concrete at the center of gravity of the strands of $f_{cgp} = F_p\ (1/A_g + e_p^2/I_g)$, which in turn causes a strain decrease in the concrete of $\varepsilon_{cgp} = f_{cgp}/E_{ct}$ at the level of the strands
- Because of strain compatibility, the strain decrease (shortening) in the steel strands equals the strain decrease in the concrete at the level of the strands, ε_{cgp}
- This shortening of the strands results in a stress loss in the strands of $\Delta f_{pES} = E_p\ \varepsilon_{cgp}$
- Substituting f_{cgp}/E_{ct} for ε_{cgp} in the above equation for the strain decrease in the concrete at the level of the strands gives *AASHTO LRFD* Equation 5.9.5.2.3 for elastic shortening loss

It should be noted that some jurisdictions permit the use of transformed sections (i.e., transforming steel area into concrete area) for the determination of stresses. If transformed section properties are used for stress analysis, then elastic shortening loss Δf_{pES} should not be applied at transfer since it is automatically accounted for by using the transformed steel area.

It is important for the bridge designer to understand what initial value to show in the plans for the initial strand stress – the jacking stress (before transfer) or the stress after girder release (after transfer.) Different DOTs and jurisdictions have different policies concerning this. If post-transfer stress is shown, the casting yard engineer must predict the elastic shortening loss of the girder and wedge set in his bed system in order to determine the initial strand jacking stress.

5.7.3.2.2 Approximate Estimate of Time-Dependent Losses

According to *AASHTO LRFD*, time-dependent prestress losses in pretensioned girders can be calculated using alternative procedures. The two main methods are:

- Approximate method (*AASHTO LRFD* Article 5.9.5.3)
- Refined method (*AASHTO LRFD* Article 5.9.5.4)

In order to enable a designer to determine a likely final prestressing force, the following summary of the approximate method is offered at this time. This basic process can then be adapted for other circumstances according to the type of construction.

The approximate method applies under the following circumstances:

- Precast components are of standard sections (AASHTO Type, PCI or DOT girders and similar) with composite cast-in-place deck
- Precast components are pre-tensioned (not post-tensioned)
- Concrete is normal weight (not light-weight or other special mix)
- The concrete is either steam- or moist-cured
- Components are pretensioned with bars or strands of either normal or low relaxation properties
- The project is in a location of average exposure conditions and temperatures

These circumstances apply to the vast majority of precast concrete girder bridges – which makes it ideal for illustration and initial design purposes.

Losses by the “Approximate Method” are calculated for:

- Shrinkage
- Creep
- Relaxation of prestressing steel

These three effects are time-dependent (long-term) losses influenced by the type of structure and environment. Long-term losses begin once the pretensioning force is transferred to the concrete. Elastic shortening is an instantaneous loss that occurs prior to any long-term losses and is calculated in accordance with the previous section.

For the approximate method, the total long term prestress loss (Δf_{pLT}) given by *AASHTO LRFD* Equation 5.9.5.3-1 contains three components for, respectively, creep of concrete, shrinkage of concrete and relaxation of steel – as compared to the seven terms for the refined estimate of *AASHTO LRFD* Article 5.9.5.4. The creep and shrinkage components depend upon the relative humidity (H) in both methods but not upon the volume to surface ratio (V/S) in the approximate method. The latter is accounted for by the limitations placed on the use of the approximate method (i.e., V/S relatively constant for most standard sections.) Also, the shrinkage of the deck

composite section (- Δf_{pSS}) is not accounted for in the approximate method – this is most probably because in the refined method, this term is taken with a negative sign indicating that for a simply supported beam, the effect actually increases the effective prestress force. Thus said, it depends upon the magnitude of the deck slab shrinkage relative to that of the girder and the strain induced at the elevation of the strands. The approximate method conservatively disregards this effect.

In the approximate method, relaxation of prestressing steel (Δf_{pR}) is taken as a lump sum amount of 2.5 ksi for low relaxation strands, 10.0 ksi for stress-relieved strands, or as given by the manufacturer for other types of strand – as compared to a formulation that also depends upon the stress in the strands at transfer (*AASHTO LRFD* Equation 5.9.5.4.2c-1) in the refined method.

The total long-term (time-dependent) loss can be estimated from *AASHTO LRFD* Article 5.9.5.3, as:

$$\Delta f_{pLT} = 10.0\frac{f_{pi}A_{ps}}{A_g}\gamma_h\gamma_{st} + 12.0\gamma_h\gamma_{st} + \Delta f_{pR}$$

where:

$$\gamma_h = 1.7 - 0.01H$$

$$\gamma_{st} = \frac{5}{\left(1 + f_{ci}^{`}\right)}$$

and:

Δf_{pR} = 2.5 ksi for low relaxation strand or 10.0 ksi for stress relieved strand
H = Relative humidity for bridge location (percent)

The first term in the equation corresponds to loss due to creep, the second to shrinkage loss and the third to relaxation loss. According to calibrations and tests, this equation gives a conservative approximation to results from the refined method. For most practical cases with ordinary precast girder bridges, the approximate method is sufficient.

5.7.3.2.3 Refined Estimate of Time-Dependent Losses

AASHTO LRFD Article 5.9.5.4 permits a refined estimate of time-dependent prestress loss where each of the above terms is evaluated more precisely for the effects of relevant material properties, structure proportions, age at loading and environmental conditions. The long-term prestress loss is given by *AASHTO LRFD* Equation 5.9.5.4.1-1 as:

$$\Delta f_{pLT} = (\Delta f_{pSR} + \Delta f_{pCR} + \Delta f_{pR1})_{initial \rightarrow deck} + (\Delta f_{pSD} + \Delta f_{pCD} + \Delta f_{pR2} - \Delta f_{pSS})_{deck \rightarrow final}$$

The various parameters that influence these terms include:

- Strength of the concrete (f'_{ci}) at time of initial loading (transfer)
- Age of the concrete (t_i) when load is initially applied (transfer)
- Maturity of the concrete (t, days) between the time of loading for creep calculations, or the end of curing for shrinkage calculations, and the time being considered for analysis of creep or shrinkage effects
- Volume to surface ratio of the component (V/S)
- Annual average ambient relative humidity (%)
- Modulus of elasticity of prestressing steel (E_p)
- Modulus of elasticity of concrete at transfer (E_{ci})
- Modulus of elasticity of concrete at transfer or load application (E_{ct})
- Modulus of elasticity of deck concrete (E_{cd})
- Type of prestressing strand, whether low relaxation or other

Along with composite and non-composite section properties, structural proportions, and area of prestressing steel, the above parameters are accounted for either directly in the various formulae in *AASHTO LRFD* Article 5.9.5.4 or indirectly via the creep coefficient $\Psi(t,t_i)$ defined in *AASHTO LRFD* Article 5.4.2.3.2 and the shrinkage strain ε_{sh} defined in *AASHTO LRFD* Article 5.4.2.3.3. Creep and shrinkage have similar time development patterns – especially for modern concrete mixes with high range water reducing admixtures and relatively low water/cement ratios (Commentary, *AASHTO LRFD* Article C.5.4.2.3.2).

The various refined formulaic relationships in *AASHTO LRFD* Article 5.9.5.4 for each of the prestressing losses in Table 5.7.3.2-1 of this Reference Manual chapter have been established algebraically or experimentally, and because of their complexity, will not be repeated here. Computation of losses using such complex formulae, applied at various elevations and sections along the girder, has really only been made feasible by the widespread use of computers and spreadsheets.

The approximate simplified relationships described in the previous section have been retained in *AASHTO LRFD* Article 5.9.5.3 for use in cases of standard precast, pretensioned girders, subject to the conditions specified therein.

AASHTO LRFD also permits the use of the CEB-FIP (European) model code or ACI 209 for estimates of creep and shrinkage in the absence of mix-specific data (*AASHTO LRFD* Article 5.4.2.3.1). A sample comparison of results for different codes based upon a limited number of structures is offered in Section 5.2.1.2.3 of this manual. The results show an apparent difference between CEB-FIP and ACI 209 for individual calculation of creep or shrinkage, but the overall sums of both

effects appear similar. Such differences, perhaps not so pronounced, can be expected when using different codes. For design and construction of a major project it is best to adopt a common formulation for long term creep and shrinkage that is acceptable to the different parties involved – for example, the Owner, the Designer and the Contractor's Engineer. This should help mitigate otherwise potential differences in the calculation of intermediate staged construction deformations, deflections and cambers.

5.7.3.2.4 Losses for Deflection Calculations

As discussed in Section 5.5.8.2 of this manual, deflection and camber change with time over a girder's service life. Creep causes displacement under constant (or near constant) loads to increase with time, whether it be downward (deflection) due to dead load or upward (camber) due to eccentric prestress. The resulting vertical displacement of the beam can be approximated at any time in the beam's life by superimposing the displacements from these two effects as adjusted for creep. The displacement with time due to prestress, however, is also affected by the level of stress in the tendon after losses. So while creep of the prestressing force on the girder tends to increase the camber of the girder with time, this increase is reduced somewhat by the loss of tension in the tendon itself due to creep, shrinkage and steel relaxation.

When estimating camber due to prestress in a pretensioned girder at a particular time during its service life, it is first necessary to estimate the stress level in the strands, or put another way, the initial strand stress at transfer less the change in stress (loss) that occurs from transfer until the time under consideration. *AASHTO LRFD* Article 5.9.5.5 recommends that stress values averaged along the length of the member be used, as follows:

- Concrete stress at center of gravity of pretensioning strands due to prestressing force at transfer and self-weight of member, f_{cgp}
- Change in concrete stress at level of pretensioning strands due to all dead loads except self-weight of the member (i.e., those added after transfer), Δf_{cdp}

Once the stress in the concrete at the level of the center of gravity of the prestressing strands has been determined, it is a simple exercise to multiply that value by the modular ratio of steel to concrete to obtain the stress in the steel.

5.7.3.3 Application to Post-Tensioned Structures

As with pretensioned girders, post-tensioned girders are affected by instantaneous losses that occur at the time of stressing and also by long-term losses that occur over time due to changes in concrete and prestressing steel properties. Long-term losses due to creep, shrinkage and relaxation for post-tensioned girders are similar

to those discussed in Section 5.7.3.2 for pretensioned girders. However, instantaneous losses due to elastic shortening that were discussed previously are different for post-tensioning than for pretensioning.

With pretensioning elastic shortening of the concrete and steel strand occur as the result of cutting the highly stressed strands in the casting bed, which causes the strands to retract into the concrete thereby transferring force into the concrete by bond between the steel and concrete. This shortening of the concrete member and strands reduces the tension in the strands, which is termed “elastic shortening loss.”

If prestress is applied by post-tensioning (i.e., installing tendons in ducts and tensioning after the concrete has hardened), the concrete member shortens as a result of the hydraulic ram acting against the embedded tendon anchor during stressing. Only after the beam has shortened due to stressing are the strands released to retract into the concrete member where force is transferred from the strands to the concrete through wedge anchors. Thus no elastic shortening loss occurs in the tendon itself while it is being post-tensioned.

Post-tensioning a group of multi-strand tendons in a concrete girder, however, does cause varying degrees of elastic shortening loss in the individual tendons. Although there is initially no elastic shortening loss in the first tendon stressed – because the girder shortens while the tendon is being jacked – when the second tendon passing through the same girder is stressed, the girder shortens elastically again. This shortening affects the first tendon, so it suffers an elastic shortening loss from the second tendon stressed. This process continues as subsequent tendons are stressed. The final tendon stressed suffers no elastic shortening loss itself but affects all tendons previously stressed.

Giving proper consideration to this phenomenon, loss from post-tensioning can be roughly estimated for preliminary design purposes in a manner similar to that for pretensioned girders. However, it is also necessary to consider instantaneous losses from duct friction and wobble, anchor friction and wedge pull-in effects prior to making estimates for subsequent long-term losses from shrinkage, creep, and relaxation. In addition, for staged construction and more complex structures, intermediate post-tensioning steps and changes in static schemes during construction require more detailed consideration and the summation of accumulated losses. These subjects are introduced in the following sections.

5.7.3.3.1 Instantaneous Losses

5.7.3.3.1.1 Elastic Shortening Losses

Elastic shortening is a loss that occurs upon the application of prestress. As the prestress is transferred to the concrete, the girder will shorten. This causes the

prestressed steel to also shorten, which causes the steel to lose stress. This loss may occur to a strand whose force is being transferred to the girder or to a strand that has been previously stressed, depending on the method of stressing the strands. This is important when considering the difference between elastic shortening in a pretensioned versus post-tensioned girder.

For a pretensioned girder typically all of the force from the strands is transferred to the girder at once when the strands are cut from the bulkheads. The concrete will shorten, and there will be a loss in all of the prestressing strands. However, for a post-tensioned girder, the tendons are stressed in stages, with each one being stressed directly against the concrete via their anchors. As a tendon is stressed, the force in it increases, which causes the girder to shorten; this will continue as the tendon is gradually stressed to its specified amount. The force in the tendon is measured up to the very end of the stressing operation, with the measurements already accounting for loss in the tendon stress due to shortening of the girder. During stressing of this tendon, however, the shortening of the girder will cause a loss in any strands that have already been stressed. For instance, when the first tendon is stressed, it will have no elastic shortening loss. When the second tendon is stressed, it will have none, either, but its stressing will cause loss in the first tendon that was stressed. Stressing of the third tendon will cause a loss in only the first and second tendons, and so on. The tendon that is tensioned last will not suffer any elastic shortening losses, while the tendon that was tensioned first will suffer the most. The overall elastic shortening loss in a post-tensioned system is less than that of a similar pretensioned system. *AASHTO LRFD* Article 5.9.5.2.3b gives the following equation for elastic shortening losses in post-tensioned members:

$$\Delta f_{pES} = \frac{(N-1)}{2N}\frac{E_p}{E_{ci}} f_{cgp}$$

where:

N	=	number of identical prestressing tendons
E_p	=	modulus of elasticity of prestressing tendons (ksi)
E_{ci}	=	modulus of elasticity of concrete at transfer (ksi)
f_{cgp}	=	sum of concrete stresses at the center of gravity of prestressing tendons due to the prestressing force after jacking and the self-weight of the member at the sections of maximum moment (ksi)

This equation accounts for sequential post-tensioning and its effect on the elastic shortening of previously stressed tendons. Altogether, the total elastic shortening loss is the average of all individual tendon loss except for the last tendon – i.e., the quotient “(N-1)/2N” in *AASHTO LRFD* Equation 5.9.5.2.3b-1.

5.7.3.3.1.2 Friction Losses

Post-tensioning tendons are often placed inside ducts that have been positioned to achieve a specified tendon profile. The profile may be curved along portions of its length. As the tendon is stressed, friction develops between the ducts and the strands, which produces a mechanical loss in the tendon stress, causing the stress to vary along its length. Friction losses are considered in two parts: "wobble" and "curvature", as shown in Figure 5.7.3.3.1.2-1. The wobble, or "length", effect arises when the duct is unintentionally misaligned, even though it is meant to be straight. This can occur when the ducts do not have adequate stiffness, when they are not properly supported and tied at sufficiently close intervals to prevent displacement or buoyancy during concrete placement, or at joints between precast box girder segments where it may be difficult to align the duct exactly at connections. The curvature effect results from the tendon making contact with the duct wall as it tries to straighten out in regions of intended curvature. The friction loss due to curvature is calculated for the accumulated angle change along the three-dimensional tendon path.

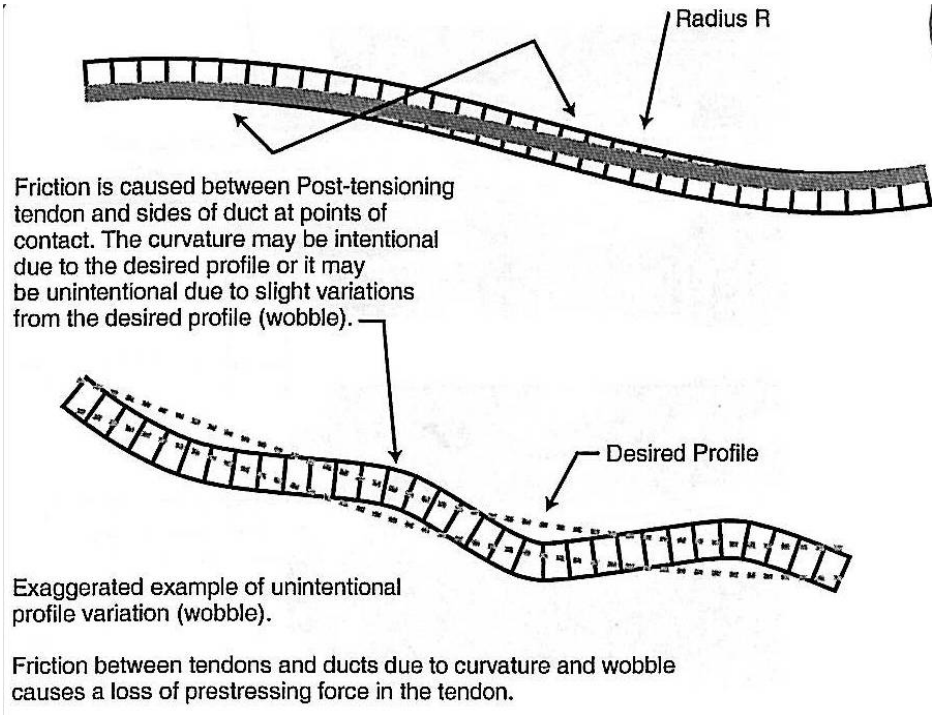

Figure 5.7.3.3.1.2-1 Friction Caused by Wobble and Duct Curvature

Loss due to friction may be calculated per *AASHTO LRFD* Article 5.9.5.2.2b, as follows:

$$\Delta f_{pF} = f_{pj}\left(1 - e^{-(Kx+\mu\alpha)}\right)$$

where:

f_{pj} = stress in the prestressing steel at jacking (ksi)
x = length of a prestressing tendon from the jacking end to any point under consideration (ft)
K = wobble friction coefficient (per ft of tendon)
μ = coefficient of friction
α = sum of the absolute values of angular change of prestressing steel path from jacking end, or from the nearest jacking end if tensioning is done equally at both ends, to the point under investigation (rad)

AASHTO LRFD Table 5.9.5.2.2b-1, repeated below in Table 5.7.3.3.1.2-1, provides suggested wobble and friction coefficients.

Table 5.7.3.3.1.2-1 Wobble and Friction Coefficients

Type of Duct	K	μ
Wire or strand: Rigid and semi-rigid galvanized metal sheathing	0.0002	0.15-0.25
Wire or strand: Polyethylene	0.0002	0.23
Wire or strand: Rigid steel pipe deviators for external tendons	0.0002	0.25
High-strength bars: Galvanized metal sheathing	0.0002	0.30

These equations are used to predict the elongation that a tendon will undergo during the stressing operation. Where large discrepancies occur between measured and calculated tendon elongations, in-place friction tests are required.

5.7.3.3.1.3 Anchor Set Losses

Anchor set, also known as wedge-set, is another instantaneous loss experienced by post-tensioning tendons. It occurs after the jack is released and when the prestressing is transferred to the anchorage. It is caused by the movement of the tendon prior to seating of the wedges or the anchorage gripping device. The friction wedges that ultimately hold the strands in place at the anchorage, shown in Figure 5.7.3.3.1.3-1 and Figure 5.7.3.3.1.3-2, slip slightly before the strands are firmly gripped. The magnitude of the minimum set depends on the prestressing system used. To ensure that the wedges will begin to grip immediately upon release of the jack, the wedges can be pre-seated by tapping with a steel pipe slid along the strand before installing the jack. Or, many commercial jacks have an internal power seating mechanism to ensure the wedges grip with minimal slip.

Anchorage set loss causes most of the difference between jacking stress and stress at transfer at any single location along the tendon. A common value for anchor set is 0.25 to 0.375 inches, although values as low as 0.0625 inches are more appropriate for some anchorage devices, such as those for bar tendons. For short tendons, the elongations are small, so a typical anchorage set would be large in comparison. So, it is particularly desirable to minimize the anchorage set for short tendons, such as by power wedge seating.

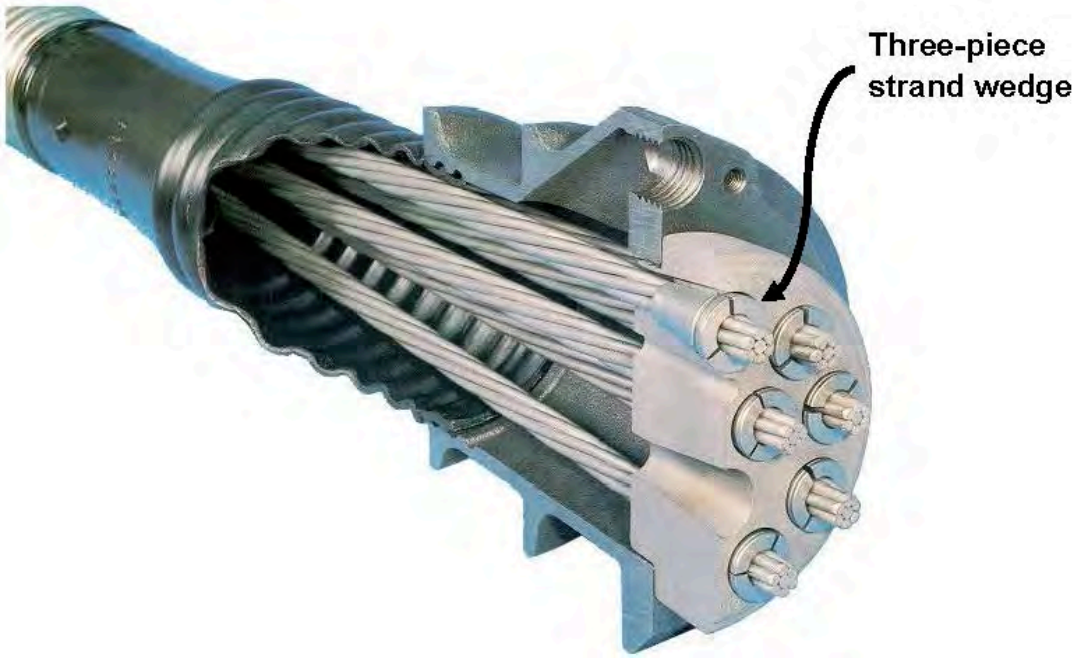

Figure 5.7.3.3.1.3-1 Cut-away of Post-tensioning Anchorage

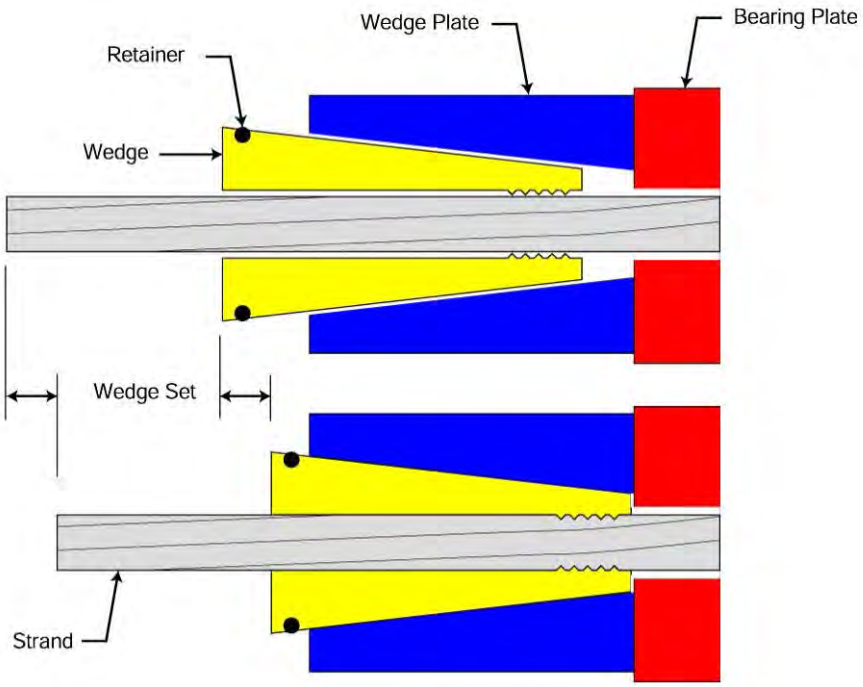

Figure 5.7.3.3.1.3-2 Gripping of Strands by Wedges

5.7.3.3.1.4 Tendon Elongations

Computation of prestressing tendon elongations in the field is necessary to ensure that the required forces are applied to the concrete. By measuring the elongation of the strands extending from the back of the ram after stressing, it is possible to correlate this value with the average force in the tendon along its length. Elongations are proportional to the modulus of elasticity of the strands as represented by Hooke's Law:

$$\text{Elongation} = \Delta = \frac{FL}{A_{ps}E_p}$$

where:

F	=	Average force along tendon length
L	=	Length of tendon
A_{ps}	=	Area of strands
E_p	=	Modulus of elasticity of strands

The length, strand area and elasticity are constant for any strand or tendon. The force is constant along the length of the strands if the strands are straight and not affected by friction curvature or wobble forces. A plot of the strand stress along the length of a straight tendon in an ideally straight duct shows that they have a very simple, constant stress diagram because of the lack of mechanical losses. The

stress diagram shown in Figure 5.7.3.3.1.4-1 is for a straight tendon that has been jacked to 202.5 ksi but not yet seated. Considering the basic relationship of Hooke's Law, we can arrange the terms to show that the modulus of elasticity times the elongation is equal to the stress in the strand times its length. This in turn is equal to the area below the stress diagram.

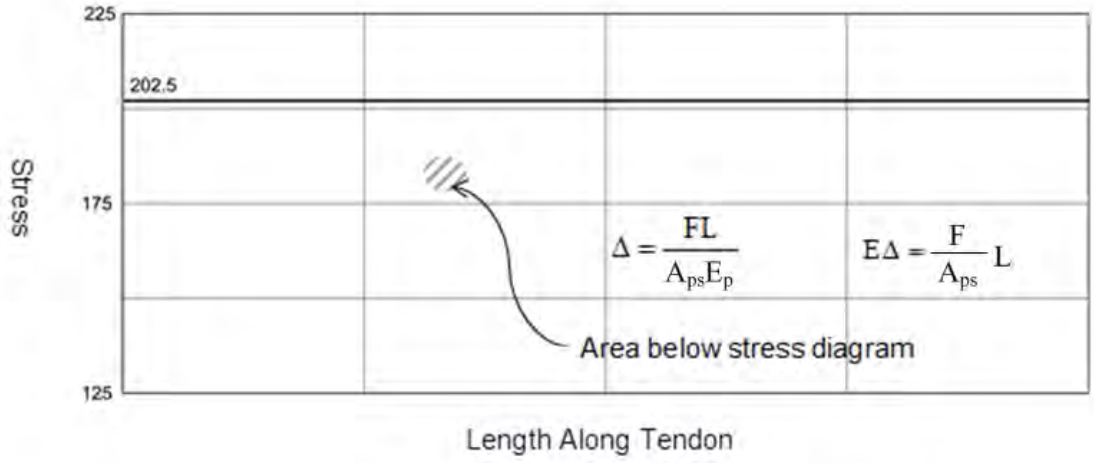

Figure 5.7.3.3.1.4-1 Stress Diagram of Straight Tendon

A post-tensioning tendon that deviates, or changes direction, along its length (Figure 5.7.3.3.1.4-2) experiences a loss in force at each of these deviations. Stress changes due to curvature friction are computed at major changes in tendon geometry. The diagram is developed with straight lines between these points (Figure 5.7.3.3.1.4-3). The theoretical elongation of the tendon can be evaluated as previously shown by calculating the area below the stress diagram and dividing it by the modulus.

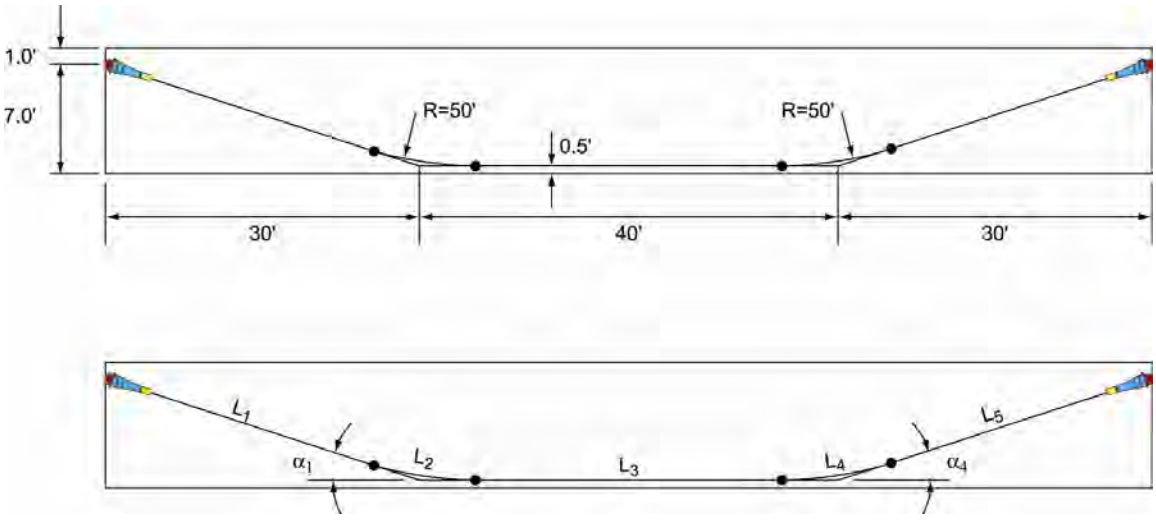

Figure 5.7.3.3.1.4-2 Example of Deviating Post-Tensioning Tendon

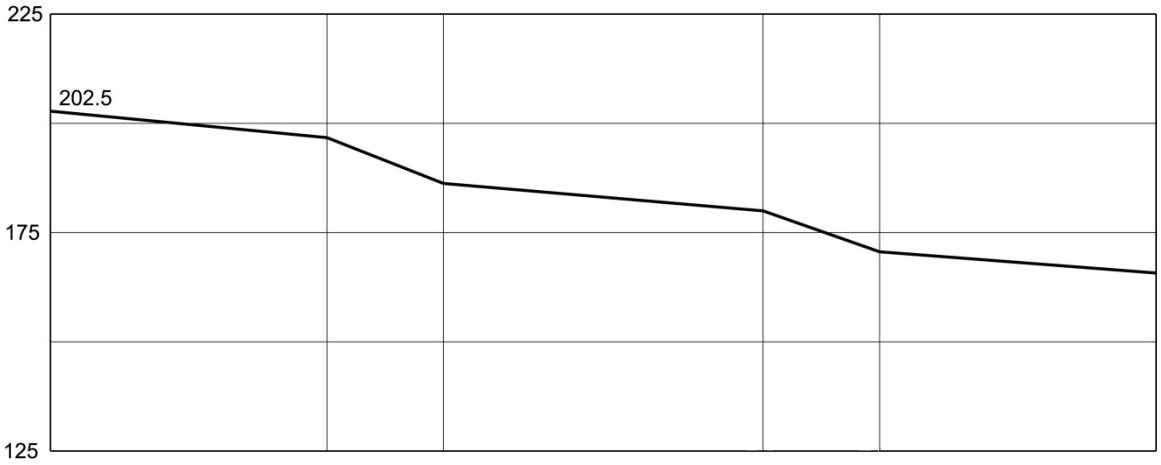

Figure 5.7.3.3.1.4-3 Stress Diagram of Deviating Tendon

5.7.3.3.2 Time-Dependent Losses

Time-dependent losses for post-tensioned structures are calculated similar to those for pretensioned structures, as detailed in Section 5.7.3.2.3. However, for more complex structures, staged construction, intermediate post-tensioning steps and changes in static schemes during construction, more detailed consideration and the summation of accumulated losses are required.

5.7.4 Pretensioning

5.7.4.1 Pretensioning Details

5.7.4.1.1 Strand Spacing

Minimum center-to-center and clear spacings between pretensioning strands is sufficiently addressed in *AASHTO LRFD* Article 5.10.3.3.1 that further discussion here is unwarranted. Clear spacing requirements are intended to ensure that strands are sufficiently separated to adequately transfer their force to the surrounding concrete while minimizing any potential for stress concentrations, bond deterioration or strand slipping. Most state transportation agencies, precasters and industry groups have standard girder shapes and products that inherently meet these requirements without additional consideration by the designer.

5.7.4.1.2 Debonding

Often the strand pattern necessary to meet the flexural requirements at mid-span can cause tension in the top of the beam near the beam ends where positive

bending moments from self-weight and gravity loads diminish to zero. There are two methods of reducing these prestressing moments at the beam ends (Figure 5.7.4.1.2-1): (1) “debonding” (i.e., preventing bond between the concrete and steel by the use of plastic sheathing around the strand) and (2) “deflecting” (or draping) the strands toward the member center of gravity to reduce the negative bending moment from strand eccentricity.

Since the concrete does not restrain debonded strands, the stress in the strands goes to zero at release and does not begin to develop until the end of the debonded length. By carefully choosing which strands to debond, the axial force from prestressing is lessened thereby reducing the prestressing moment causing tension in the top of the beam. Another way to reduce the prestressing moment is to reduce the eccentricity of the prestressing by deflecting. Deflecting prestressing steel also has the added beneficial effect of lifting up the beam where the strands are deviated and providing a vertical force component to resist gravity load shear. Unfortunately, deflecting strands has fallen out of favor with precasters because of the added cost and inconvenience associated with strand hold-down devices in the bed; debonding is the current standard of practice for much of the industry.

Development length is affected by debonding in two ways. The first and most obvious is that the transfer length and flexural bond length do not start until the end of the “debonded zone.” The second and more subtle change is that the κ factor in the development length calculation (*AASHTO LRFD* Equation 5.11.4.2-1) increases from 1.6 to 2.0 for debonded strands. There are also specifications requirements for the maximum numbers and locations of debonded strands in a girder. *AASHTO LRFD* Article 5.11.4.3 states the following:

- No more that 25% of the total number of strands at any section may be debonded
- No more than 40% of the total number of strands in any row may be debonded
- No more than 40% of the debonded strands or 4 strands, whichever is larger shall have the debonding terminated at any section
- Debonded strands shall be symmetrical about the centerline of the section
- Debonded lengths of pairs of strands that are symmetrical about the centerline shall be equal
- The exterior strands in each horizontal row shall be fully bonded

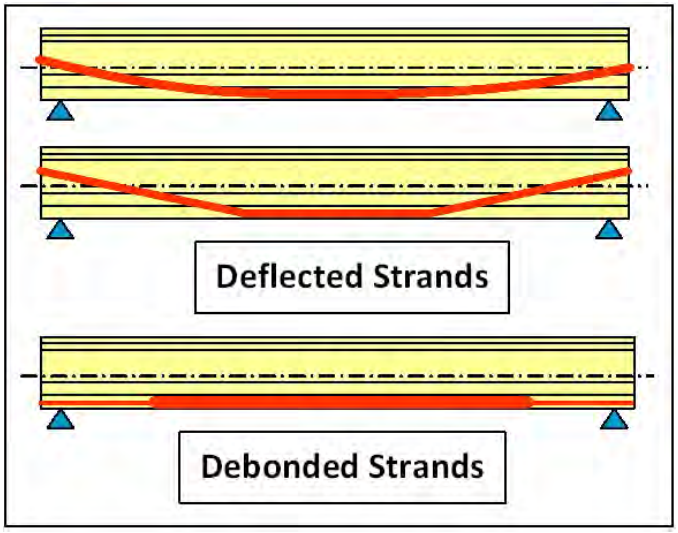

Figure 5.7.4.1.2-1 Typical Prestressing Steel Layouts

5.7.4.2 Transfer and Development

According to *AASHTO LRFD* Article 5.11.4.1, transfer length for bonded strand may be estimated at 60 strand diameters. This distance of thirty inches for ½" diameter strands is assumed to be the length where the stress in the prestressing steel varies from 0 to the effective stress in the prestressing steel after losses (f_{pe}). Beyond this zone there is another component that along with the transfer length makes up the development length (Figure 5.7.4.2-1). This zone is known as the flexural bond length. As its name suggests, the flexural bond length is the area where the additional bond is acquired to allow the strands to reach stresses required by flexural strength conditions (f_{ps}). Unlike the linear stress change in the transfer length, the flexural bond length uses a parabolic stress change. The total development length (ℓ_d) is defined in *AASHTO LRFD* Equation 5.11.4.2-1 as:

$$\ell_d \geq \kappa \, (f_{ps} - \tfrac{2}{3} f_{pe}) d_b$$

where:

κ	=	1.6 for precast, prestressed beams (fully bonded strands)
	=	2.0 for precast, prestressed beams (partially debonded strands)
f_{ps}	=	average stress in steel at nominal bending resistance (ksi)
f_{pe}	=	effective stress in steel after losses (ksi)
d_b	=	nominal strand diameter

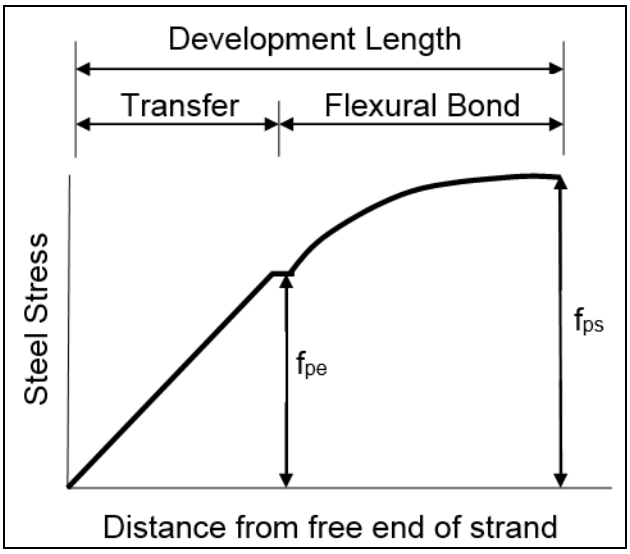

Figure 5.7.4.2-1 Transfer and Development Length

5.7.4.3 Pretensioned Anchorage Zones

Anchor zones in pretensioned girders represent the area where the prestressing force in the steel is transferred to the concrete section. In this area where large concentrated forces are being transferred and distributed, it is necessary to understand the fundamentals of the member behavior. The transfer and development lengths (zones) are where the concrete engages the prestressing force as the strands are cut in the bed. In some cases the bond is intentionally prevented, "debonding" as discussed previously, usually by means of an empty sheath surrounding the strand. In these cases "local" anchor zones may be staggered as each set of strands bonds with the concrete. Distribution of these forces from the concrete area in contact with the strands to the beam section in general, causes some areas of "splitting" tension within the anchorage zone, typically located above the strands in a prestressed I-beam. Using tools such as strut-and-tie or finite element analysis, these transverse (primarily vertical) tension stresses can be identified and properly reinforced ("tension ties".)

Another item of concern for anchor zones is that the concrete surrounding the prestressing steel must be able to resist the "bursting" tendency caused by the large concentrated axial strand forces before they can distribute uniformly to the entire member section. This can be aided by carefully placed "confining" reinforcement in the bottom flange.

5.7.4.3.1 Analysis (Strut-and-Tie)

Strut-and-tie models like the one in Figure 5.7.4.3.1-1 can help one visualize the end zone areas in tension and compression. The idea is to simplify a segment as though

it were a truss. For anchorage zones in a pretensioned girder, the application of the force is known and the distribution of that force some distance away (l) is known. "l" is typically taken as the depth of the girder, "h." Using some creativity and engineering judgment, a drawing of the force flow can be created which can then be turned into a strut-and-tie model. From the strut-and-tie model in the figure, it can be seen that there are two major sections of tension that must be reinforced: one perpendicular to the force of the prestressing modeled by T_1 and T_3 and one parallel to the force of prestressing modeled by T_2. In a beam the tension parallel to the prestressing force would be counter balanced by the dead load of the beam and checked at service level flexure. The tension perpendicular to the prestressing force ("splitting tension") is resisted by vertical reinforcement as prescribed in *AASHTO LRFD*. The area of high compression ("bulb" or bottom flange of girder) must also be reinforced with confining reinforcement.

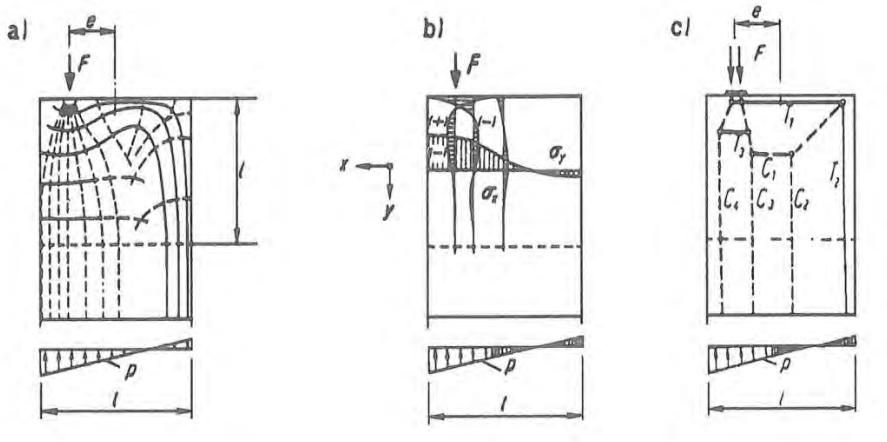

Figure 5.7.4.3.1-1 Development of Strut-and-Tie Model for Pretensioning

5.7.4.3.2 Splitting Reinforcement

AASHTO LRFD Article 5.10.10.1 addresses splitting resistance in the anchor regions of pretensioned girders. Splitting resistance is of primary importance in relatively thin and deep portions of pretensioned members, such as the webs of bulb-tee girders. However, it may also need to be considered in the lateral direction of thin bottom flanges (e.g. box beams or U-beams.) *AASHTO LRFD* specifies a 20 ksi service limit in the mild steel to control cracking. Smaller diameter bars that are well distributed within h/4 from the end of the beam are preferable to fewer large diameter bars.

The equation for required splitting reinforcement in the end of a pretensioned beam is given by:

$$P_r \geq f_s A_{s,}$$

where:

P_r = resisting force, not less than 4% of total prestressing force at transfer
f_s = stress in steel not to exceed 20 ksi
A_s = total area of reinforcement located within h/4 from end of beam (in^2)
h = overall dimension of precast member in the direction in which splitting resistance is being evaluated (e.g. beam depth for I-beam or bulb-tee girder)

AASHTO LRFD states that "reinforcement used to satisfy this requirement can also be used to satisfy other design requirements."

5.7.4.3.3 Confining Reinforcement

AASHTO LRFD Article 5.10.10.2 specifies requirements for confining the strands in the bottom flange. For other than box beams confinement steel must consist of bars not less than #3's at 6", shaped to enclose the strands and distributed along the beam for a distance of 1.5*d*. It is customary to assume the girder depth "*h*" for *d*.

5.7.4.3.4 Reinforcement Details

Most state departments of transportation have developed standard drawings of anchorage zones appropriate for use in their state. Using these standards will insure that local precasters are familiar with the reinforcing details.

5.7.5 Post-Tensioning

5.7.5.1 Post-Tensioning Details

5.7.5.1.1 Duct Spacing

AASHTO LRFD Articles 5.10.3.3.2 and 5.10.3.3.3 provide guidance for the minimum spacing of straight and curved post-tensioning ducts, respectively. For straight tendons the spacing requirements are primarily to ensure proper concrete consolidation and placement around the ducts. For curved tendons it is also necessary to consider the effects of radial tension from stressing on adjacent tendons and the requirements for providing transverse reinforcement to resist these forces.

AASHTO LRFD Article 5.10.4.3 specifies a maximum spacing of 4 times the slab thickness for post-tensioning tendons in slabs. This reflects current practice and the desirability of ensuring uniform compression across the width of the slab.

5.7.5.1.2 Tendon Confinement

AASHTO LRFD Article 5.10.4 gives requirements for confining post-tensioning tendons against radial pressures owing to intentional or unintentional curvature in the ducts.

5.7.5.2 Post-Tensioning Anchorage Zones

5.7.5.2.1 General

Anchor zones must be designed at the strength limit states for factored jacking forces as specified in *AASHTO LRFD* Article 3.4.3.

Post-tensioning anchorage end-zones for precast members and structures cast in place on falsework are designed and detailed in the same manner, using strut-and-tie methods or other appropriate techniques.

5.7.5.2.2 General Zone and Local Zone

Anchor zones for post-tensioning tendons are regions of complex stress as the localized, concentrated force from each anchorage, or group of anchorages, disperses over some distance to the full effective cross section, at which point stresses may be determined by ordinary beam theory. The length over which the dispersal takes place from the anchorage devices to the full effective section is referred to as the “general zone”. Immediately at the anchorages themselves (“local zone”), the post-tensioning force must be confined to prevent localized splitting of the concrete along the axis of the tendon. Figure 5.7.5.2.2-1 shows the general zone and local zones in a typical post-tensioned I-girder.

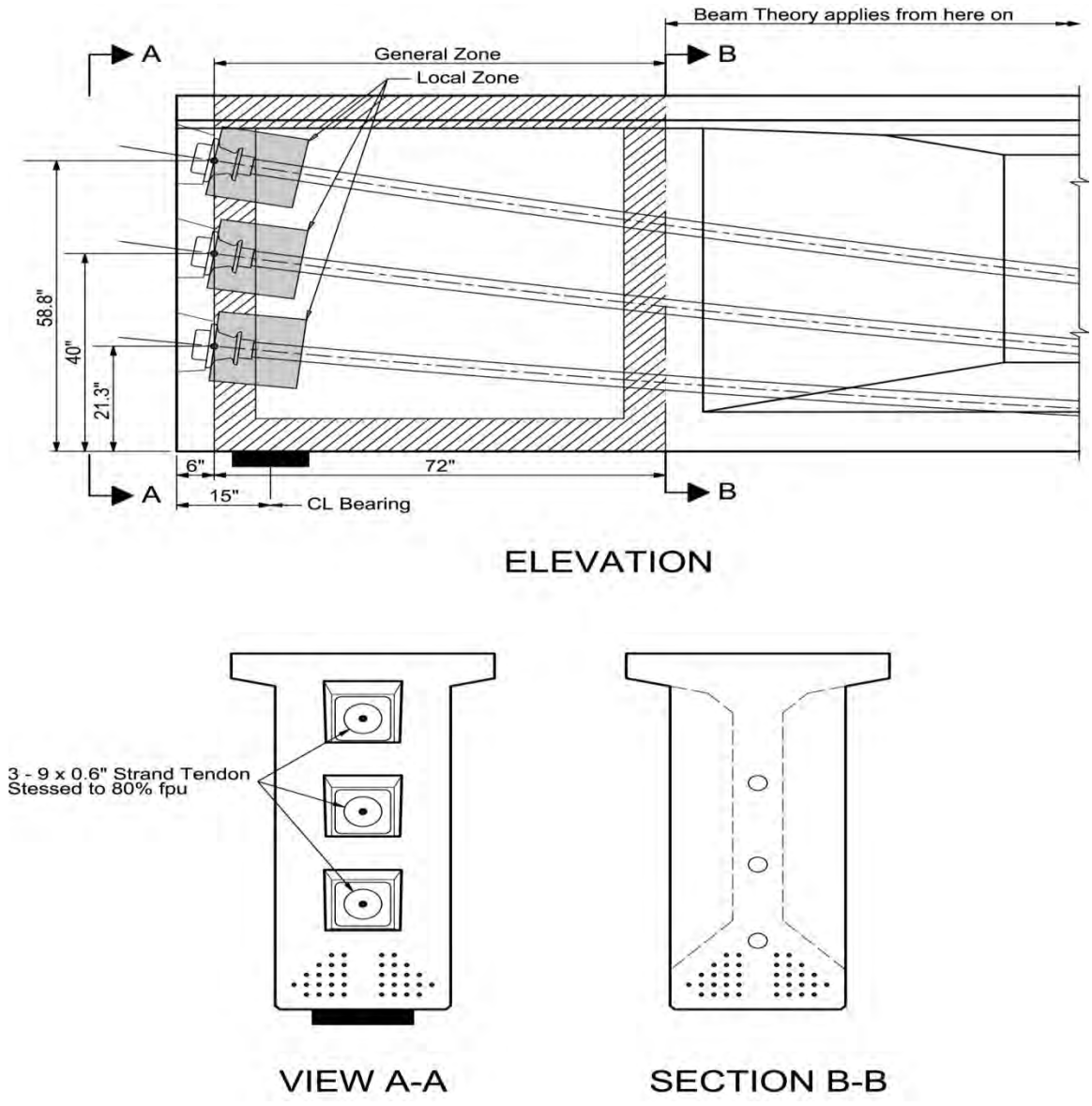

Figure 5.7.5.2.2-1 Anchor Zones for a Post-Tensioned Girder

5.7.5.2.3 Design of the General Zone

It is the responsibility of the Engineer (designer), to design reinforcement and details for the effect of the dispersal of forces through the general zone (*AASHTO LRFD* Article 5.10.9.2.4). For this purpose, in *AASHTO LRFD* Article 5.10.9.3.1, three techniques are recognized:

- Equilibrium-based inelastic models, generally known as “strut-and-tie” models
- Refined elastic stress analysis
- Other approximate methods, where applicable

In general, refined stress analysis and approximate methods have appropriate but limited application. By contrast, the “strut-and-tie” method is generally applicable to both routine and complex, three-dimensional shapes. The basic principles of this method are illustrated by considering the case at the end of a precast girder containing three anchorages stacked above each other and set at an angle following the draped profile of each tendon (as presented in Figure 5.7.5.2.2-1).

5.7.5.2.4 Application of Strut-and-Tie Model to Design of General Zone

When applying the strut-and-tie approach, various rudimentary questions arise:

1. What is the magnitude of the anchor force to be used for design?
2. Is there relief from the stressing sequence and forces after losses?
3. What role does the bearing reaction play?
4. Where is the location of the maximum bursting force, d_{burst}?
5. Where is the end of the general zone at which beam theory applies?
6. What is the size of the local zone?
7. What is the size of the anchor plate?
8. What is the effective cross-section at the end of the general zone?
9. Where are nodes located at the end of the general zone?
10. Where are nodes located relative to anchor plates?
11. How does one arrange struts and ties to simulate a credible, reliable, model?
12. What is the effective width and thickness of each compression strut?
13. What is the resistance of a strut (and limiting strain) in the concrete?
14. What limiting concrete stress can be sustained by a node?
15. What is the lateral bursting effect across the width of the end block?
16. What is the strength of a tension tie?
17. What other reinforcement might be needed, such as Corner Tension Ties?
18. What are the results of the strut-and-tie approach?
19. What should be the final disposition of reinforcement?
20. Are there any other observations?

With reference to *AASHTO LRFD* Articles 5.10.9.3 and 5.10.9.4, we can take each of these questions in turn and apply them to our example in Figure 5.7.5.2.2-1:

What is the magnitude of the anchor force to be used for design?

The load factor for the applied anchor force is given by *AASHTO LRFD* Article 3.4.3.2 as 1.2. The force for design is taken as 1.2 times the maximum jacking force. Before losses due to wedge seating, the maximum jacking stress in the strand may be as high as 80%fpu. The factored jacking force is then:

$$\text{Factored jacking force} = 1.2\,P_{jack} = 1.2*0.80*A_{ps}*f_{pu}$$

For example, using a tendon comprised of 9 * 0.6" dia. strands, with a specified tensile strength of 270 ksi, we find,

$$1.2\,P_{jack} = 1.2*0.80*9*0.217 * 270 = 506 \text{ kips per tendon}$$

Is there relief from the stressing sequence and forces after losses?

In an actual structure tendons would be stressed in sequence. Each one would experience wedge-seating loss at the anchor before the next tendon could be stressed. For 3/8" wedge set, a 9-strand tendon of this type might experience as much as 52 kips force loss. So that, after wedge seating the factored force of 506 kips could reduce to about 443 kips. This is a significant reduction. *AASHTO LRFD* Article 5.10.9.3 offers the possibility of relief of the required factored design forces by consideration of the stressing sequence – this would be appropriate.

It follows that the temporary condition between each stressing operation should be checked to ensure that the reinforcement and concrete strut capacities are satisfactory.

What role does the bearing reaction play?

At the end of the girder, the reaction of the bearing itself helps to locally confine bursting forces and reduce the reinforcement demand. If it is not known if the deck slab will have been cast to add to the magnitude of the reaction, then conservatively consider only a minimum reaction due to the self-weight of the girder. For strength limit state design of the general zone it is not appropriate to increase this reaction force above the anticipated minimum.

Under certain circumstances the presence of a support reaction might be used to beneficially modify the location of the maximum bursting force, as considered below.

Where is the location of the maximum bursting force, d_{burst}?

The location of the maximum bursting force determines where to locate reinforcement (according to *AASHTO LRFD* Article 5.10.9.3.2) in order to resist bursting forces and to facilitate development of a suitable strut-and-tie model. The location of the maximum bursting force is given by *AASHTO LRFD* Equation 5.10.9.6.3-2, as:

$$d_{burst} = 0.5(h - 2e) + 5e \sin \alpha$$

where:

h = lateral dimension of the cross section in the direction considered
e = eccentricity of tendon from the centroid (always taken positive)
α = inclination of tendon to axis; taken as negative if pointing away from the centroid

For each of the three tendons in our illustration, in the vertical plane:

Top tendon: h = 72 in, e = 22.8 in, α = 11.24°, d_{burst} = 35.4 in.
Middle tendon: h = 72 in, e = 4.0 in, α = 9.46°, d_{burst} = 35.3 in.
Bottom tendon*: h = 72 in, e = 14.7 in, α = -6.76°, d_{burst} = 12.6 in.

* Angle is negative since it is pointing away from the centroid.

This latter value (12.6 in) is very close to the anchorage. It is within the local zone (below) and might pose a difficulty in making a suitable strut-and-tie model. Can anything be done to improve the situation? Possibly – if the proximity of the support reaction, taken at its minimum value, (80 kips) is used to effectively modify the direction of the local tendon force, the angle changes to a positive value of α = 2.27°. Choosing to remain conservative, it would be reasonable to take α = 0°, giving a revised value for the bottom anchor d_{burst} = 21.3 in. Considering other needs (such as not to overlap anchor zones and struts except at nodes) we choose to locate the main vertical tension tie at 18 in from the anchor plate.

Now that the vertical plane has been assessed, the horizontal plane needs to be addressed. In plan view each tendon is at the center of the girder, so e = 0. Each is straight, so α = 0°. The width of the general zone is h = 28 in. Thus, d_{burst} = 14.0 in. In this case it turns out that the location of the maximum bursting effect is approximately at the end of the local zone found below. However, it is necessary to consider the dispersal of forces and the need to avoid overlapping anchor zones and struts before creating a strut-and-tie model. These items are addressed in the following.

Where is the end of the general zone at which beam theory applies?

According to *AASHTO LRFD* Article 5.10.9.1, the longitudinal extent of the anchor zone shall not be less than the greater of the transverse dimensions (i.e. the width or overall height of the concrete section at the anchors) nor more than 1.5 times that dimension. At the end the girder is widened to accommodate the anchorage zone. How much to widen a girder depends upon the particular type of girder, the size of the anchorages and available casting forms. For the purpose of this illustration, it is assumed that the end block would be as wide as the bottom flange. For a Type VI girder, this is 28 in. The girder height is 72 in. Consequently, we have:

Girder height, H = 72 in. (Type VI) ≤ GZ length ≤ 1.5H (= 108 in.)

The dispersal of anchorage forces to general beam behavior in the discontinuous region of the girder end will not occur in a length less than the depth of the girder. However, adopting this as the shortest length for the general zone usually leads to a conservative demand for reinforcement, particularly if the tendons are on a slope or deviate appreciably. Therefore, use 1.5H = 108 in.

What is the size of the local zone?

The width and height of the local zone is given by *AASHTO LRFD* Article 5.10.9.7.1. At the design stage the final supplier of the post-tensioning system is not known, so the transverse dimensions are taken as the greater of:

- The bearing plate size plus twice the minimum concrete cover
- The outer dimension of any confining reinforcement, plus the outer cover

If the size of the anchor plate is "*a*" and the cover "*c*", then the transverse dimension of the local zone is equal to (*a* + 2*c*); see *AASHTO LRFD* Figure C.5.10.9.7.1-1. In our illustration if the anchor plate size is 10in., cover 2in., the size of the local zone is 14 inches. The size of the bearing plate, "*a*", depends upon the limiting bearing resistance under the anchor plate given by *AASHTO LRFD* Equation 5.10.9.7.2 (below). Alternatively, if the manufacturer's recommended edge distance, "*e*", is known, then the size of the local zone is 2*e*. The length of the local zone is then taken as either (*a*+2*c*) or (2*e*) respectively. The size of the anchor plate also depends upon the bearing resistance of the concrete beneath the plate; determined as follows.

What is the size of the anchor plate?

The bearing resistance of an anchor plate is given by *AASHTO LRFD* Article 5.10.9.7.2 as:

$$P_r = \phi f_n A_b$$ *AASHTO LRFD* Equation 5.10.9.7.2-1

For which f_n is the lesser of:

$$f_n = 0.7f'_{ci} \sqrt{(A / A_g)}; \text{ and } f_n = 2.25f'_{ci}$$ *AASHTO LRFD* Equations 5.10.9.7.2-2 and 3

In this case, by *AASHTO LRFD* Article 5.5.4.2, for compression in anchorage zones, we find:

- ϕ = 0.80 for normal weight concrete (0.65 for lightweight aggregate concrete) (*AASHTO LRFD* Article 5.5.4.2)
- A = maximum area of the supporting surface that is similar to and concentric about the loaded area, but does not overlap adjacent areas for anchorage devices
- A_g = gross area of the anchor plate (including PT hole)
- A_b = effective net area of the anchor plate (A_g less PT hole)
- f'_{ci} = nominal concrete strength at time of application of tendon force (ksi)

For our illustration if it is assumed that the anchor plate is 10in. by 10in., then A_g = 100 in^2.

By scaling from a drawing or examination of the geometry, we find that if the anchor areas "*A*" are not to overlap, the maximum dimension is 18in., therefore A = 324 in^2.

For precast girders subsequently post-tensioned after erection, the concrete strength at the time of stressing is usually the 28-day strength. Taking f'_{ci} = 6.0 ksi, we find;

$$f_n = 0.7 * 6.0 * \sqrt{(324 / 100)} = 7.56 \text{ ksi.} \leq 2.25(6.0) = 13.5 \text{ ksi} \rightarrow \text{use } 7.56 \text{ ksi}$$

Allowing for, say, a 4.5 in. dia. hole in the plate, the effective area of the bearing plate, A_b, = 84.0 in^2. Assuming that all other aspects of *AASHTO LRFD* Article 5.10.9.7.2 can be properly satisfied, this gives a bearing resistance of:

$$P_r = \phi f_n A_b = 0.80 * 7.56 * 84.0 = 508.6 \text{ kips (> 506 k factored jacking force, OK)}$$

This means that the minimum dimension of the anchor plate, "*a*", may be taken as 10 in. This also verifies that, if the cover is 2 in., the size and length of the local zone = 14 in.

More importantly for our model, this enables us to determine where to locate nodes at the anchorages; namely at *a*/4 = 2.5 in. inwards from the bearing plate in each direction.

Also important for initiating the modeling process, it implies that if two struts frame into the anchor, then the maximum thickness for each would be roughly half the anchor plate size (i.e., 5 inch).

What is the effective cross-section at the end of the general zone?

If some or all of the tendons are to be tensioned only after the deck slab has been cast, there may be a case for considering the effectiveness of the deck slab itself at the end of the general zone. In which case, guidance may be sought from of *AASHTO LRFD* Figure 4.6.2.6.2-4. This shows normal forces dispersing at an angle of 30° to the longitudinal axis of the member into the slab. In which case, the width of slab to add to the width of the end block itself, at the end of the general zone, in our illustration would be:

$$2b_n = 2 * 72 * \tan 30° = 83 \text{ in.}$$

This would make the full effective top flange width:

$$2b_n + b_{n0} = 83 + 28 = 111 \text{ in.}$$

On the other hand, if the tendons are stressed before the deck slab is cast, then the effective section is that of the girder alone, with the widened end-block as shown in Figure 5.7.5.2.2-1 – Section BB. This is the section we will consider in this illustration. For simplicity, the small area of girder top flange is ignored in this case – making the section a rectangle. This simplifies the calculation of the effective longitudinal and shear stresses at various elevations in the section – the distribution of which is needed to locate nodes - as follows.

Where are nodes located at the end of the general zone?

To answer this, consider a free-body diagram of the end of the girder cut at the end of the general zone and determine the forces acting upon that small girder length. The factored jacking forces are resolved into horizontal and vertical components applied at the anchor locations. The bearing reaction is applied as an upward force on the free-body diagram. For these conditions, the bending moment, axial and shear force are determined at the location of the end of the general zone. Longitudinal fiber stresses and shear stresses are calculated by beam theory, using the appropriate section properties (in this case, the rectangular Section BB in Figure 5.7.5.2.2-1.)

Considering the vertical plane and using the magnitude of the longitudinal flexure and compression stresses and the effective width of the general zone (web), the height of the section is divided horizontally into portions so that the longitudinal force in each portion accumulates to half the magnitude of the longitudinal force from each anchorage. The reason for doing this is to facilitate the introduction of two local nodes at each anchor (Figure 5.7.5.2.4-1), each of which will carry half the factored anchor force. For three tendons, division leads six separate stress-blocks at the end

of the general zone (Figure 5.7.5.2.2-1, Section B-B). Nodes at Section B-B are then located at the center of force (i.e. P1 through P6) of each individual stress block.

The intensity of the shear stress is determined at this location. For the rectangular section this is a parabolic distribution from zero at the top to a maximum at mid-height to zero at the bottom. For analysis purposes, the vertical shear force is determined and proportionally allocated per node at this section (i.e. V1 through V6).

Where are nodes located relative to anchor plates?

In the vertical plane of the member, two local nodes are placed at each anchor - each to carry half of the anchor force. In actual fact, the three-dimensional (out of plane) nature of the general zone must also be taken into account. In which case, in a three-dimensional model, four nodes would be located at a distance of (a/4) from each edge of the anchor plate and along the path of the tendon from the back of the plate. In our illustration, (a/4) = 10/4 = 2.5in. One quarter of factored anchor force would be applied at each node.

However, for the time being we are considering only the vertical plane. For simplicity of analysis and because of the symmetrical nature of our illustration, in a side view of the vertical plane two nodes are located at each anchor; each to carry half the force. We will consider the three-dimensional nature of the lateral bursting effects later when we examine the dispersal of forces in the horizontal plane (plan view).

How does one arrange struts and ties to simulate a credible, reliable, model?

In this respect strut-and-tie analysis may be tedious and time consuming if the designer has to try several different models before arriving at a satisfactory solution. Guidance is offered in *AASHTO LRFD* Article 5.10.9.4 and associated figures in the Commentary.

An important consideration in finding a solution is to seek the simplest model that can be analyzed by statics alone. Models that contain redundant members and become statically indeterminate should not be used. On the contrary, it is preferable to seek models that could become mechanisms if the support from the mass of surrounding material was removed and they were truly pin-jointed. An example is that of *AASHTO LRFD* Figure C5.10.9.4.1-2(c) - the flow of force is evident and symmetry facilitates simplification, virtually to a mechanism. It should never be necessary, except perhaps as a check, to use a structural frame analysis program to analyze a strut-and-tie model.

Our illustration is chosen deliberately for a very common configuration of anchorages at the end of a precast post-tensioned girder. Three tendons in the web of a Type VI girder are draped to a longitudinal profile rising to the three anchor locations shown.

The drape is gradual such that, for practical purposes, they may be considered straight in the general anchorage zone. The end of the girder rests on a bearing so the bearing reaction should be considered when determining the strut-and-tie model. The arrangement constitutes a group of multiple anchors. Guidance for setting up the strut-and-tie model is sought from *AASHTO LRFD* Figures C5.10.9.4.2.1-2 and 3, as follows.

Choosing the length of the general zone as the depth of the girder, and considering all the forces acting at the end of that zone, it is found from beam theory that this section is in longitudinal compression with a lesser stress at the top fiber than the bottom. Being in compression, it means that the situation shown in *AASHTO LRFD* Figure C5.10.9.4.1-3 does not apply – because there is no longitudinal tensile force in the top of the girder. Also, because the tendons follow a gradually curved profile, there is a gradual distribution of the lateral tendon force (i.e., the force/radius of curvature, “P/R” effect.) There is no relatively sudden deviation of force in or near the general zone itself as shown in *AASHTO LRFD* Figure C5.10.9.4.1-2 (f) - so this does not apply.

Consequently, our problem involves satisfying: "Small Eccentricity", "Multiple Anchors", a "Support Reaction" and "Inclined and (Straight) Tendons". In other words, we can reference *AASHTO LRFD* Figures C5.10.9.4.1-2 (a), (c), (d) and (f) for our illustration.

In *AASHTO LRFD* Figures C5.10.9.4.1-2 (a) and (d) anchor forces are shown to disperse at a rate of 1:2 (1 laterally for 2 longitudinally). If we were to apply this dispersal rate to our model, we would find that the anchor zones (represented by the area "*A*" = maximum area of the supporting surface that is similar to, but does not overlap, adjacent areas for anchorage devices) would rapidly come to overlap each other - which is not feasible – anchor zones should not overlap. Moreover, this would occur within the length of the local zone. The location of nodes in our model must be modified such that this does not happen.

After some trial-and-error examination of the geometry and allowing for an estimated depth of compression strut (initially about 5 inches), it is found that if the dispersal rate for regions between the anchors is taken as about 1:4, instead of 1:2, then a series of nodes can be placed just beyond the end of the local zone, so that no overlap of anchor zones occurs. Nevertheless, force from the upper half of the top anchor is allowed to disperse at a rate of 1:2 - because it is unrestrained by any adjacent anchor (Figure 5.7.5.2.4-1). Force dispersal from the lower half of the bottom anchor is restrained by the local bearing reaction. The actual dispersal depends upon the results of the final statical analysis in which the locations of the bottom nodes (F and G of Figure 5.7.5.2.4-1) of the strut-and-tie model are adjusted so as to maintain equilibrium.

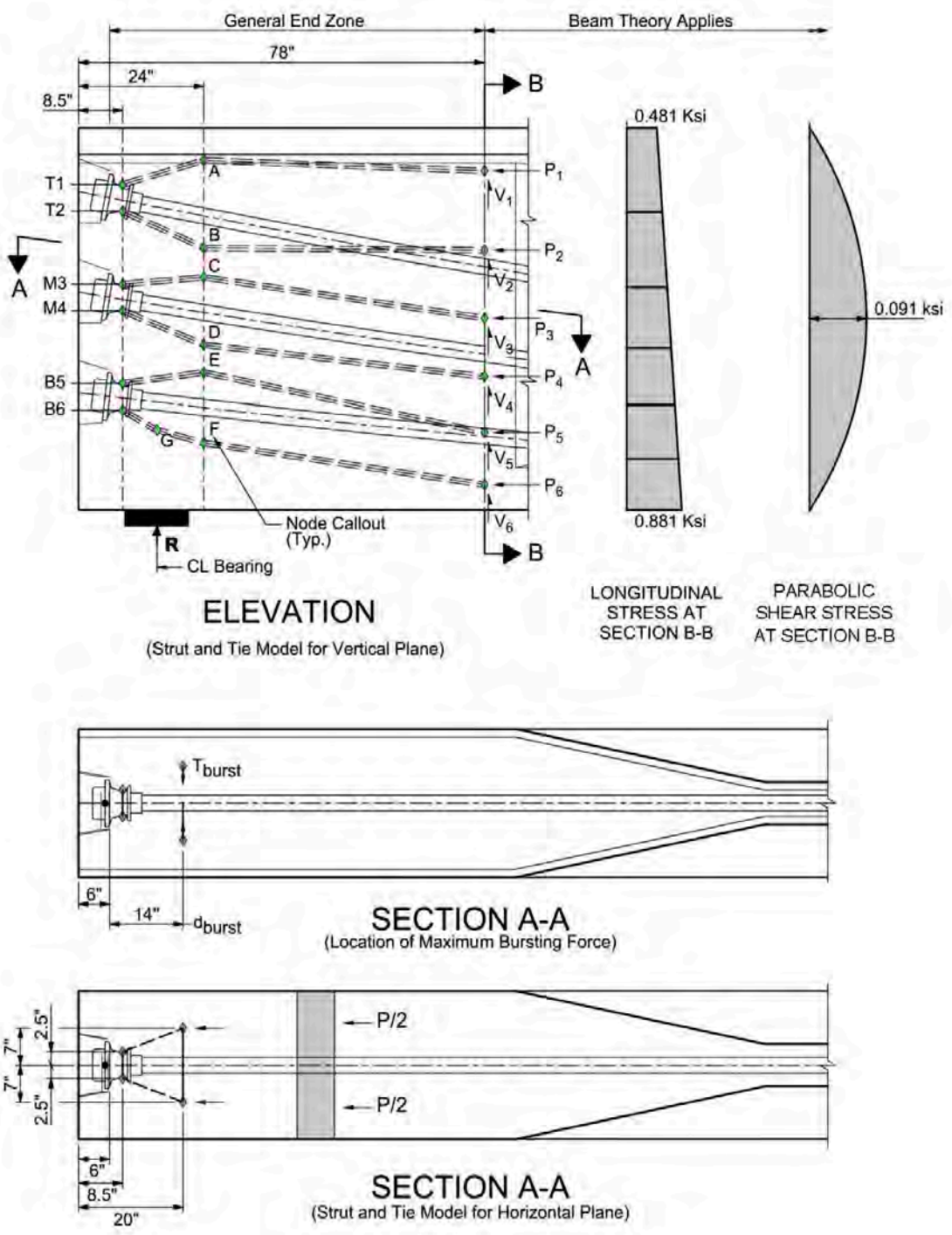

Figure 5.7.5.2.4-1 Strut-and-Tie Models for a Post-Tensioned Girder

A vertical tension tie is located at the point where the forces dispersed from the anchors must be restrained – just beyond the local zone (in this case, connecting nodes A through F at 18 in. from the anchor plates). Similarly, a vertical tie connects

all the nodes at the anchor face. For convenience and simplification of the analysis the nodes at the anchor face and at the location where the force dispersal is confined (nodes A through F) are aligned vertically. Analysis will reveal that these vertical “ties” actually behave as ties at some elevations (where dispersal of force from each anchor places them in tension) and as struts at others (i.e., between tendons, where they must resist the compression effect of the converging tendon paths).

Because the curvature of our tendons through the general zone is very slight (almost straight), longitudinal struts connect nodes A through F, directly with nodes at the end of the general zone located at the respective centers of force of the longitudinal stress distribution. These struts represent the effective inclined trajectory of the tendon forces and other loads, including the bearing reaction, self-weight and distributed lateral tendon force (“P/R”), as they transition from the anchorage to the section at the end of the general zone. At this section the vertical components of each strut force are balanced by shear forces determined by beam theory. From this section onward vertical web reinforcement as determined by normal beam theory can be used for the remainder of the girder.

Note that the model is statically determinate. In fact, if an attempt were made to analyze it using a frame analysis program with all pin-jointed nodes, it would be unstable and the program would not run. Nevertheless, it serves to envision the flow of forces and to determine the magnitude of force in each strut and tie from the anchors to the end of the general zone.

What is the effective width and thickness of each compression strut?

An answer to this question is essential to constructing a credible strut-and-tie model – one in which struts do not overlap except where they meet at properly sized nodes. This is dependent on the limiting concrete stress a strut or node can sustain, which is given in *AASHTO LRFD* Article 5.6.3.3, “Proportioning of Compressive Struts.”

Unfortunately, strut forces, and therefore required capacities and strut dimensions for the model, cannot be determined until after a model is analyzed. This presents a dilemma for the designer -- where to begin? We can make an initial estimate of the minimum strut thickness from the size of the nodes at the anchorages, as determined above. An initial strut thickness of 5 in (half the size of the minimum anchor plate size) may be used to establish initial node and tie locations. Applying the P.T. and bearing forces to this initial model and analyzing it provides further information concerning the corresponding maximum strut force and required resistance.

What is the resistance of a strut (and limiting strain) in the concrete?

The inclined struts in our model are not reinforced in the direction of compression, even though they are (will be) surrounded by orthogonally placed reinforcement. The nominal resistance of an unreinforced compressive strut is given by *AASHTO LRFD* Article 5.6.3.3.1 as:

$$P_n = f_{cu} A_{cs}$$

The limiting compressive stress, f_{cu}, is given by *AASHTO LRFD* Article 5.6.3.3.3 as:

$$f_{cu} = f'_c / (0.8 + 170\varepsilon_1) \; < 0.85f'_c$$

in which:

$$\varepsilon_1 = \varepsilon_s + (\varepsilon_s + 0.002) \cot^2\alpha_s$$

where:

α_s	=	smallest angle between a compressive strut and adjoining tension ties (degrees)
f'_c	=	specified compressive strength – in our example, f'_c = 6.0 ksi
ε_s	=	the tensile strain in the concrete in the direction of the tension tie

By examination of our initial model, α_s = 65.8° in our example. Initially, ε_s is not known. However, if we make a reasonable assumption that when reinforcement is provided, it acts at its yield strength (say f_y = 60 ksi) and that the strain in the concrete is the same as that in the reinforcement, then ε_s = 60/29,000 = 0.002. Inserting these values gives:

$$\varepsilon_1 = 0.002 + (0.002 + 0.002) \cot^2(65.8°) = 0.0028 \text{ in/in}$$

and

$$f_{cu} = 6.0 / (0.8 \; + \; 170*0.0028) \; = 4.70 \text{ ksi}$$

At this point we need to know the size of the strut, A_{cs}. Initially, when considering the local zones at the anchors and the location of the nodes (above), the anchor plate size was found to be 10 in. by 10 in. – implying that the minimum depth of a strut in the vertical plane terminating at an anchor zone would be about 5 in. Adjustment for strut inclination and the width of the strut perpendicular to the vertical plane have not yet been determined. For these we refer to the *AASHTO LRFD* Articles C5.10.9.4.2 and 3, and *AASHTO LRFD* Figure C5-10.9.4.2-1 in particular. The latter shows that the width of strut "w" is either constant or may widen, depending upon the details of

the model. Applying this guidance, in the vertical direction the width of the most critically loaded strut is 4.6 in (after also allowing for the inclination of the strut). The effective width in the horizontal direction *t'* (i.e., into the plane of the paper), at the distance "a" from the anchor is 16.4 in. so we have:

$$P_n = f_{cu} . A_{cs} = 4.70 * 4.6 * 16.4 = 354.0 \text{ kip}$$

Applying the strength reduction factor, $\phi = 0.80$ from *AASHTO LRFD* Article 5.5.4.2, for compression in anchorage zones, the reduced resistance is:

$$\phi P_n = 0.8 * 354 = 283 \text{ kip}$$

Examination of our initial model reveals that the maximum compressive force in the most heavily loaded strut is 270 kips (in the strut framing into the lower half of the middle anchor.) Now we must check the proportions of the nodal regions and their limiting stresses.

What limiting concrete stress can be sustained by a node?

For this, we refer to *AASHTO LRFD* Article 5.6.3.5, Proportioning of Node Regions.

For the support node (G) bounded by two compression struts and the bearing area, the compressive stress should not exceed $0.85\phi f'_c$ – where by *AASHTO LRFD* Article 5.5.4.2, $\phi = 0.70$. This gives a limiting compression stress of:

$$f_{limit} = 0.85*0.70* 6.0 = 3.57 \text{ ksi}$$

The smallest dimensional area at this node is estimated to have an area of at least 5.0 in by 16.43 in, subject to a maximum force of 225 kips, thereby imposing a stress of 2.74 ksi, which is less than 3.57 ksi and satisfactory.

Most other nodal regions in this model are bounded by a one directional tension tie and at least two compression struts, for which the limiting stress is $0.75 \phi f'_c$ – where again by *AASHTO LRFD* Article 5.5.4.2, $\phi = 0.70$. This gives a limiting compression stress of:

$$f_{limit} = 0.75*0.70* 6.0 = 3.15 \text{ ksi}$$

The smallest dimensional area for the most highly loaded node, in this case node D, is again estimated to be 5.0 in by 16.43 in, subject to a maximum force of 270 kips, thereby imposing a stress of:

$$f = 270 / (5.0 * 16.43) = 3.29 \text{ ksi} > 3.15 \text{ ksi}$$

Therefore, at first sight, this is not satisfactory. However, upon closer examination of the internal forces at this node, we find that the force between nodes D and E is in fact compressive – only the residual tension is taken by the tie C to D. Consequently, a case can be made for allowing the higher stress level (3.57 ksi) as if it were bounded by three compressive struts – in which case it is satisfactory. If this were not the case, a solution would be to revise the node locations and more closely examine the available strut depth and width, or adopt a slightly higher strength of concrete.

Before considering the sizing of tension ties we will consider the dispersal of forces across the width of the end block, perpendicular to the vertical plane (i.e., in plan view).

What is the lateral bursting effect across the width of the end block?

We have seen above that in plan view the location of the maximum bursting force is estimated to be at 14.0 in from the anchor plate, which incidentally coincides with the end of the local zone. This is not quite at the chosen location of the vertical ties (18 in from the anchor plate). Using 14 in. and following the principle that the force disperses at approximately 1:2, we find that the dispersal is sufficient to engage the full width of the member (i.e., 28 in.) Considering the tension tie at this location and resolving forces from the anchorage nodes, the tensile force generated by from one tendon is:

$$T = (P/2) \tan \alpha$$

In this case, $\alpha = \tan^{-1} \{(7.0 – 2.5) / (14.0 – 2.5)\} = 21.3°$

Thus, $T = 98.4$ kips (per tendon).

This is the total lateral tensile force to be resisted per tendon and can be satisfied by providing transverse reinforcement both above and below each tendon. The area of reinforcing steel required is determined as follows.

What is the strength of a tension tie?

The strength and proportioning of tension ties is addressed by *AASHTO LRFD* Article 5.6.3.4. For our example, for a lateral force of 98.4 kips the area of tensile steel required is:

$$A_{st} = T / (\phi * f_y) = 98.4 / (1.00 * 60.0) = 1.64 \text{ in}^2$$

The strength resistance factor is ϕ = 1.00, according to *AASHTO LRFD* Article 5.5.4.2. This area of reinforcement can be provided by 6 legs of #5 reinforcing bar, giving 1.86 in^2 - or 4 legs of #6 bar giving 1.76 in^2 (or similar, equivalent arrangement).

Before we consider rebar detailing we will determine the reinforcement required in the vertical direction. From the results of our strut-and-tie model we find that the maximum tensile force in this direction at the location of the end of the local zone is that between nodes A and B at the top anchor. Thus, the maximum force is 84.7 kips which, incidentally, only occurs if the top tendon is tensioned last in the sequence. This requires an area of reinforcement of:

$$A_{st} = 84.7 / (1.00 * 60.0) = 1.41 \text{ in}^2$$

The results also show that there is no tension, only compression, in the members in the vertical anchor face. The magnitude of the compression is well within the limits for the concrete between the anchors. However, none of this yet addresses or excludes corner tension.

What other reinforcement might be needed, such as corner tension ties?

It can be seen that our model does not yet contain any provision for tension ties around the top and bottom corners at the girder end. This stems from the fact that the anchorages are well centered and there is (theoretically) no net top or bottom tension. In practice, corner ties should always be provided. The minimum requirement would be to satisfy *AASHTO LRFD* Article 5.10.9.3.2 and to provide for 2 percent of the total factored tendon force.

The total factored tendon force in this case = 443 + 443 + 506 = 1392 kips – allowing for the reduction of force due to wedge set on two tendons, but not the third, as a result of sequential stressing. Providing for 2% of this results in a force of 28.0 kips, requiring 0.46 in^2 of reinforcement.

What are the results of the strut-and-tie approach?

Results of the strut and-tie model are summarized as follows.

Vertical effects:

	Force	Stressing Sequence
Member AB	84.7 kip tension	(Middle, Bottom, Top)
Member CD	53.9 kip tension	(Bottom, Top, Middle)
Member EF	10.5 kip compression	(Bottom, Middle, Top)
Between top and middle anchor	50.8 kip compression	
Between middle and bottom anchor	47.4 kip compression	

Corner ties at anchor face 28.0 kip tension

Reinforcement, maximum vertical tie:

$$A_{st} \text{ required} = 84.7 / 60.0 = 1.41 \text{ in}^2$$
$$= 0.71 \text{ in}^2 \text{ per face centered on tie (at 18 in. from anchor face)}$$

Corner ties:

$$A_{st} \text{ required} = 28.0 / 60.0 = 0.46 \text{ in}^2$$
$$= 0.23 \text{ in}^2 \text{ per face at top and bottom corners}$$

Transverse effects:

Transverse force per tendon = 98.4 kip tension
Transverse reinforcement, $A_{st} = 1.64 \text{ in}^2$ per tendon
(i.e., provide 0.76 in^2 both above and below each tendon.)

Location of bursting force:

Strut-and-tie model locates bursting force d_{burst} = 18 in. from anchor face for various reasons to do with dispersal of forces and non-overlap of anchor zones (above).

What should be the final disposition of reinforcement?

Choosing to use #4 as the minimum bar size and adopting a spacing of 6 in. for an anchor zone region, we find that the required area of rebar centered on the vertical tie 18 in. from the anchor face will require:

4 legs per face at 0.20 in^2 per leg $\rightarrow$ provides 0.80 in^2 per face > 0.71 in^2 O.K.

This is provided by closed links around the perimeter of the section (see Figure 5.7.5.2.4-2, Section B-B).

AASHTO LRFD Article 5.10.9.3.2 offers guidance for the distribution of bursting reinforcement – it should be located over a distance from the anchor face taken as the lesser of:

$$2.5d_{burst} = 2.5 * 18.0 = 45.0 \text{ in.}$$
$$1.5 * \text{width} = 1.5 * 28.0 = 42.0 \text{ in.}$$

However, being mindful of the range found for d_{burst} for the two top anchors (i.e., from 14.0 in. for the transverse direction to a maximum of 35.4 in. for the vertical direction), we choose to distribute the reinforcement required for bursting effects in the vertical direction over a distance of 48 in. from the anchor face – providing 9

closed links altogether. Since the primary purpose is to resist bursting forces in the vertical direction, including effects at corners of the cross section, these closed links should have corner hooks or continuous vertical legs with a splice in the top or bottom horizontal legs only. Also, in order to minimize congestion and allow for proper concrete placement and consolidation, these splices should be alternated from top to bottom.

By comparison and as a separate check, if the approximate method of *AASHTO LRFD* Article 5.10.9.6.3 is applied, taking the tendons as a group we find that d_{burst} = 35.7 in. and the required amount of reinforcement, A_{st} = 3.82 in^2. While the strut-and-tie model leads to a different location for the vertical tie resisting the bursting force, the total area of reinforcement provided over the 48 in from the anchor face is in fact, 2 * 9 * 0.20 = 3.60 in^2, which is a consistent result.

Lateral bursting effects, transverse to the girder, require 1.64 in^2 per tendon – half of which would be provided above and half below each tendon – centered on the lateral bursting location of d_{burst} = 14 in. from the anchor face. Since this will place some lateral reinforcement within the local zone, there is a possibility of conflict with any local spiral from the PT supplier. Thus, some thought should be given to minimizing congestion in this area.

Transverse bursting reinforcement might be provided by 4 closed links of #4 reinforcing bar around the anchor zone of each tendon (and by the residual transverse top and bottom legs of the links provided for vertical effects). This results in a minimum provision of:

$$A_{st} \text{ provided} = 4 * 2 * 0.20 = 1.60 \text{ per tendon (OK)}$$

Alternatively, we choose to use 3 #5 rebar links per anchor to reduce congestion. Since these bars are to resist lateral forces, a closing splice should be located on one of the vertical faces and not on the horizontal legs in order to properly develop the bars laterally.

Selection and disposition of reinforcement following the guidelines given in *AASHTO LRFD* leads to the final details shown in Figure 5.7.5.2.4-2. This figure shows reinforcement required for bursting effects determined and detailed as above. In this case the final details are somewhat conservative, especially for bursting in the vertical direction, and a refined distribution could probably be developed. However, any additional area of web reinforcement required for global beam shear force effect has not yet been included, nor has any minor (temperature and shrinkage) distribution reinforcement (e.g., across the anchor face).

Are There Any Other Observations?

In our example we chose to use an end block of constant width for a length equal to the depth of the girder (Section B-B in Figure 5.7.5.2.4-2). A valid alternative that would save a little weight would be to begin tapering the width of the end block before this location, perhaps at 3 or 4 feet from the anchors. Since the location at which beam behavior begins cannot change (i.e., it remains at 6 ft to 9 ft from the anchors (1.0 to 1.5 overall height), then new (smaller) section properties would have to be determined in order to facilitate recalculation of the longitudinal and shear stress dispersal. The centers of force and nodes would be relocated for a revised strut-and-tie model. Such a change would probably not significantly affect the total amount of reinforcement provided, but this has not been verified.

For lateral bursting if the approximate method of *AASHTO LRFD* Article 5.10.9.6.3 is applied (which has its origin in the work of Guyon, et al., circa 1960), we find that T = 73 kips per tendon, indicating an approximate level of correspondence between different approaches. For comparison if the factor were to be increased from 0.25 to 0.35, as had been suggested at times (e.g. FDOT Criteria of 1983), then T = 113 kips per tendon, which is a little too conservative. In our illustration “strut-and-tie” gives a more reasonable result of T = 98 kips.

In general, the amount of reinforcement incorporated into the final details for our example is in agreement with that required by the approximate method.

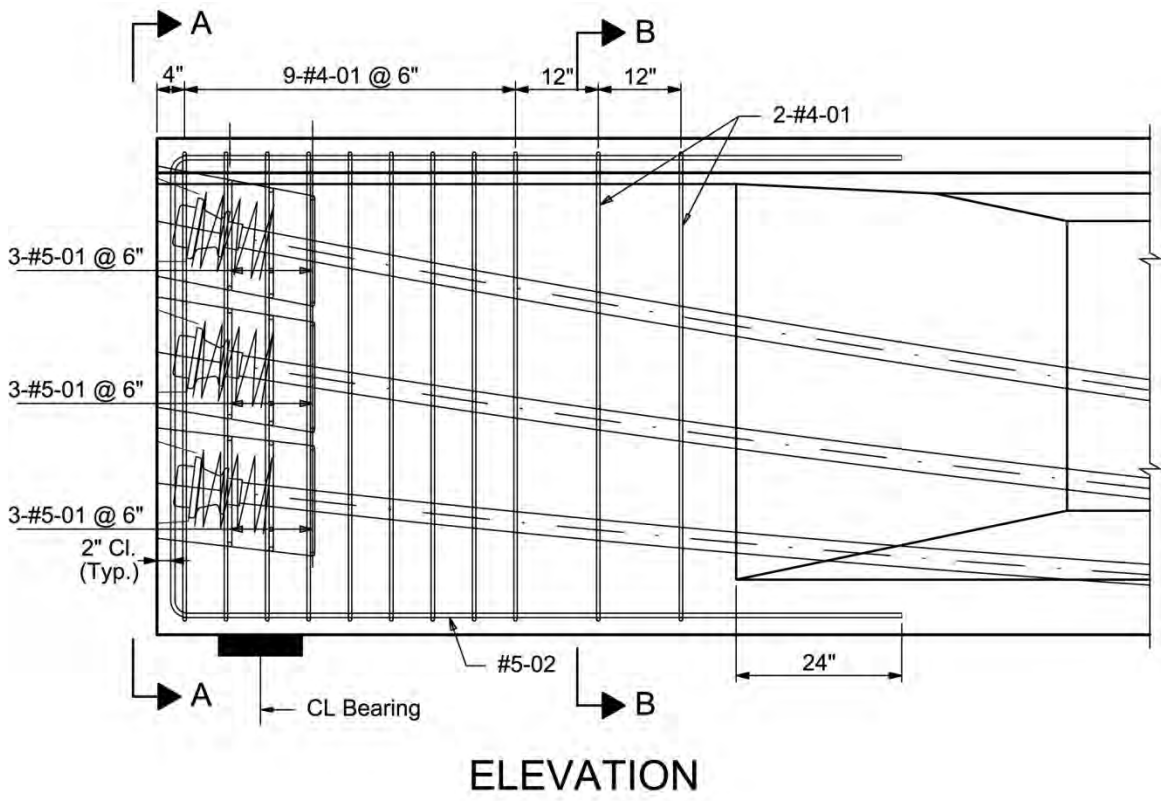

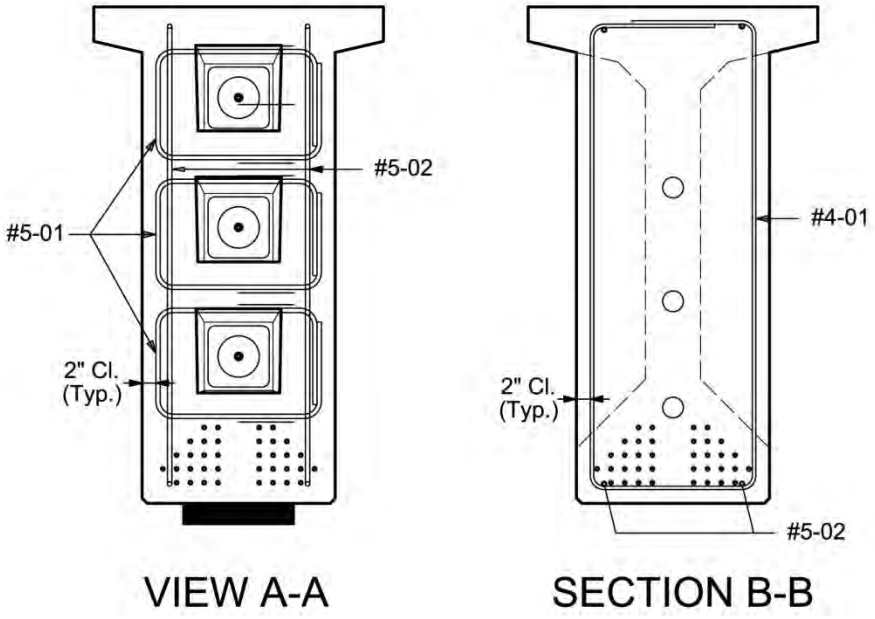

Figure 5.7.5.2.4-2 Strut-and-Tie Models for a Post-Tensioned Girder

5.7.5.2.5 Elastic Stress Analysis

Analyses based on elastic material properties, equilibrium and forces and loads, and compatibility of strains may be used for the analysis and design of anchorage zones (see *AASHTO LRFD* Article 5.10.9.5).

5.7.5.2.6 Approximate Stress Analyses and Design

For analysis of members with rectangular cross-sections, which does not include I-girders or bulb-tee girders with wide flanges, the approximate methods of *AASHTO LRFD* Article 5.10.9.6 may be used.

5.7.5.2.7 Design of Local Zones

Very high transverse tensile stresses develop in the concrete locally around an anchorage as the result of the "Poisson's ratio" effect. This effect is the same as that of driving a wedge into the end of a log to split it. The localized splitting effect, or bursting force, ("T burst"), must be confined by local reinforcement around the anchorage in the "local-zone". Most commercially available anchorage devices are supplied with a suitable spiral of reinforcement for this purpose. In the event that none is supplied, *AASHTO LRFD* Article 5.10.9.7 offers guidance for designing suitable local-zone reinforcement.

Section 5.8 Details of Reinforcement

During the design and detailing process for concrete girders, several details of reinforcement must be considered and incorporated into the design documents. The reinforcement details described in this section include concrete cover, hooks and bends, spacing of reinforcement, tendon confinement, transverse reinforcement, shrinkage and temperature reinforcement, and anchorage zones.

These details of reinforcement are clearly specified in *AASHTO LRFD* Article 5.10. Therefore, specific details are not repeated in this manual. However, this section serves as a general "road map" to describe where in the design and detailing process these various details must be considered.

5.8.1 Concrete Cover

Concrete cover is specified to ensure sufficient protection of the steel reinforcement embedded within the concrete. Failure to provide sufficient cover may result in spalling of the concrete and corrosion to the reinforcing steel.

Specific requirements for concrete cover are specified in *AASHTO LRFD* Articles 5.10.1 and 5.12.3.

Concrete cover directly affects the distance from the compression face to the centroid of the tension reinforcement, *d*, of a reinforced concrete member. This in turn directly affects the resistance of the member. Therefore, concrete cover must be considered during the design process.

5.8.2 Hooks and Bends

Hooks are specified to ensure sufficient development of reinforcement where flexural resistance from steel reinforcement is required to satisfy the flexural requirements of the member. Failure to provide hooks may result in "pop out" of the reinforcement under high loads or flexural failure of the member.

Bends are specified for feasibility of bending the reinforcement steel without breakage. Failure to satisfy the bend requirements may result in crushing of the concrete inside the bend.

Specific requirements for hooks and bends are specified in *AASHTO LRFD* Article 5.10.2. These requirements are consistent with the requirements of ACI 318 and Concrete Reinforcing Steel Institute's (CRSI) *Manual of Standard Practice*. Both hooks and bends are generally specified as a function of the bar diameter.

Hooks and bends generally do not affect the design process. However, they are very important for the successful construction of the bridge. Therefore, hooks and bends can be addressed during the detailing process and during development of design drawings. A possible exception is verification during design that a standard hook or minimum diameter of bend will fit within a specific member.

5.8.3 Spacing of Reinforcement

Spacing of reinforcement is specified to allow concrete to flow readily into spaces between bars and between bars and forms and to ensure against concentration of bars on a line that may cause shear or shrinkage cracking. Failure to satisfy the spacing requirements may result in honeycombing, cracking, or inconsistent and insufficient concrete within the member.

Specific requirements for spacing of reinforcement are specified in *AASHTO LRFD* Article 5.10.3. Both minimum and maximum spacing requirements are provided. Minimum spacing requirements are provided for cast-in-place concrete and precast concrete, for multiple layers of reinforcement, for splices, and for bundled bars. In addition, minimum and maximum spacing requirements for prestressing tendons and ducts are specified.

During design, the required area of reinforcement per foot is generally computed. The required bar size is then computed based on the selected spacing. Therefore, spacing of reinforcement must be considered during the design process.

5.8.4 Tendon Confinement

Tendon confinement is specified to ensure sufficient protection against wobble effects in slabs and out-of-plane forces for curved tendons. Failure to provide sufficient tendon confinement may result in slab delamination along the plane of the post-tensioning ducts, as well as cracking or side face rupture in the vicinity of sharp curvature of tendons.

Specific requirements for tendon confinement are specified in *AASHTO LRFD* Article 5.10.4. Requirements related to wobble effects in slabs and effects of curved tendons are provided.

Tendon confinement directly affects design decisions and therefore should be considered during the design process.

5.8.5 Transverse Reinforcement

Transverse reinforcement requirements apply primarily to compression members, such as piers and columns, but transverse reinforcement requirements are also provided for flexural members such as concrete girders. They are specified to ensure sufficient confinement of the primary reinforcing steel within the flexural member. Failure to provide sufficient transverse reinforcement may result in cracking, delamination, or spalls in the member.

Specific requirements for transverse reinforcement are specified in *AASHTO LRFD* Articles 5.10.7 and 5.10.6.

Transverse reinforcement for concrete girders must be designed during the design process.

5.8.6 Shrinkage and Temperature Reinforcement

Shrinkage and temperature reinforcement is specified to help prevent cracking in the concrete due to shrinkage as the concrete hardens and due to thermal expansion and contraction during the life of the bridge. Shrinkage and temperature reinforcement is placed normal to the primary reinforcement in the member. Failure to provide sufficient shrinkage and temperature reinforcement may result in cracks in the concrete and potential subsequent corrosion to the reinforcing steel.

Specific requirements for shrinkage and temperature reinforcement are specified in *AASHTO LRFD* Article 5.10.8.

Shrinkage and temperature reinforcement must be designed during the design process.

5.8.7 Anchorage Zones

Anchorage zones must be carefully designed for both post-tensioned and pretensioned concrete beams. Anchorage zones are located at the ends of the beam where the prestressing strands or bars are anchored. Failure to satisfy anchorage zone requirements may result in bursting, splitting, or spalling due to forced induced by tendon anchorages.

Specific requirements for post-tensioned anchorage zones and pretensioned anchorage zones are specified in *AASHTO LRFD* Articles 5.10.9 and 5.10.10, respectively. Requirements are provided for both general zones and local zones, in which the general zone is the region subjected to tensile stresses due to spreading of the tendon force into the beam and the local zone is the region of high compressive stresses immediately ahead of the anchorage device.

Post-tensioned anchorage zones are designed at the strength limit state for the factored jacking forces, and pretensioned anchorage zones have specific design requirements for splitting resistance and confinement reinforcement. Therefore, design of anchorage zones must be considered during the design process.

Section 5.9 Development and Splices of Reinforcement

In addition to details of reinforcement, development and splices of reinforcement must also be addressed and incorporated into the design documents. In the design of concrete beams, the calculated force effects in the reinforcement at each section must be developed on each side of that section by embedment length, hook, mechanical device, or a combination of these methods. However, hooks and mechanical devices may be used in developing bars in tension only. This section describes development of reinforcement, development of mechanical anchorages, development of prestressing strands, and splices of reinforcement.

Development and splices of reinforcement are clearly specified in *AASHTO LRFD* Article 5.11. Therefore, similar to the previous section, specific details are not repeated in this manual. However, this section serves as a general “road map” for addressing development and splices of reinforcement.

5.9.1 Development of Reinforcement

Development length is defined as the distance required to develop the specified strength of a reinforcing bar or prestressing strand. Critical sections for development of reinforcement in concrete beams must be taken at points of maximum stress and at points within the span where adjacent reinforcement ends or is bent. *AASHTO LRFD* Article 5.11.1.2.1 specifies that, except at simple span supports and at the free ends of cantilevers, reinforcement must be extended beyond the point at which it is no longer required to resist flexure for a distance not less than the following:

- Effective depth of the member
- 15 times the nominal diameter of the bar
- 1/20 of the clear span

AASHTO LRFD Article 5.11.1 provides additional requirements for development of reinforcement for positive moment regions, negative moment regions, and moment resisting joints. Specific requirements are provided for bars in tension and for bars in compression. In addition, various modification factors are provided which increase or decrease the development length. If the required development length cannot fit within the geometric constraints of the beam, then standard hooks can be used, for which specific requirements are also provided.

5.9.2 Development of Mechanical Anchorages

AASHTO LRFD Article 5.11.3 describes the requirements for development of mechanical anchorages. Mechanical anchorages must be able to develop the strength of the reinforcement without damaging the concrete. In addition, the performance of mechanical anchorages must be verified by laboratory tests.

Development of reinforcement may be achieved through a combination of mechanical anchorages and additional embedment length of the reinforcement between the point of maximum bar stress and the mechanical anchorage.

When mechanical anchorages are used, the contract documents must show complete details of the mechanical anchorage.

5.9.3 Development of Prestressing Strands

In addition to reinforcement bars, prestressing strands must also be developed sufficiently. *AASHTO LRFD* Article 5.11.4 specifies requirements for development of prestressing strands for both bonded strands and partially debonded strands.

For prestressing strands, both the transfer length and the development length must be considered. The transfer length is the length over which the pretensioning force is transferred to the concrete by bond and friction in a pretensioned member. The development length is the distance required to develop the specified strength of a prestressing strand. The relationship between the steel stress and the distance over which the strand is bonded to the concrete can be idealized by the relationship illustrated in Figure 5.9.3-1 (adapted from *AASHTO LRFD* Figure C5.11.4.2-1). This idealized variation of steel stress can be used to analyze sections within the transfer length and development length at the end of pretensioned members.

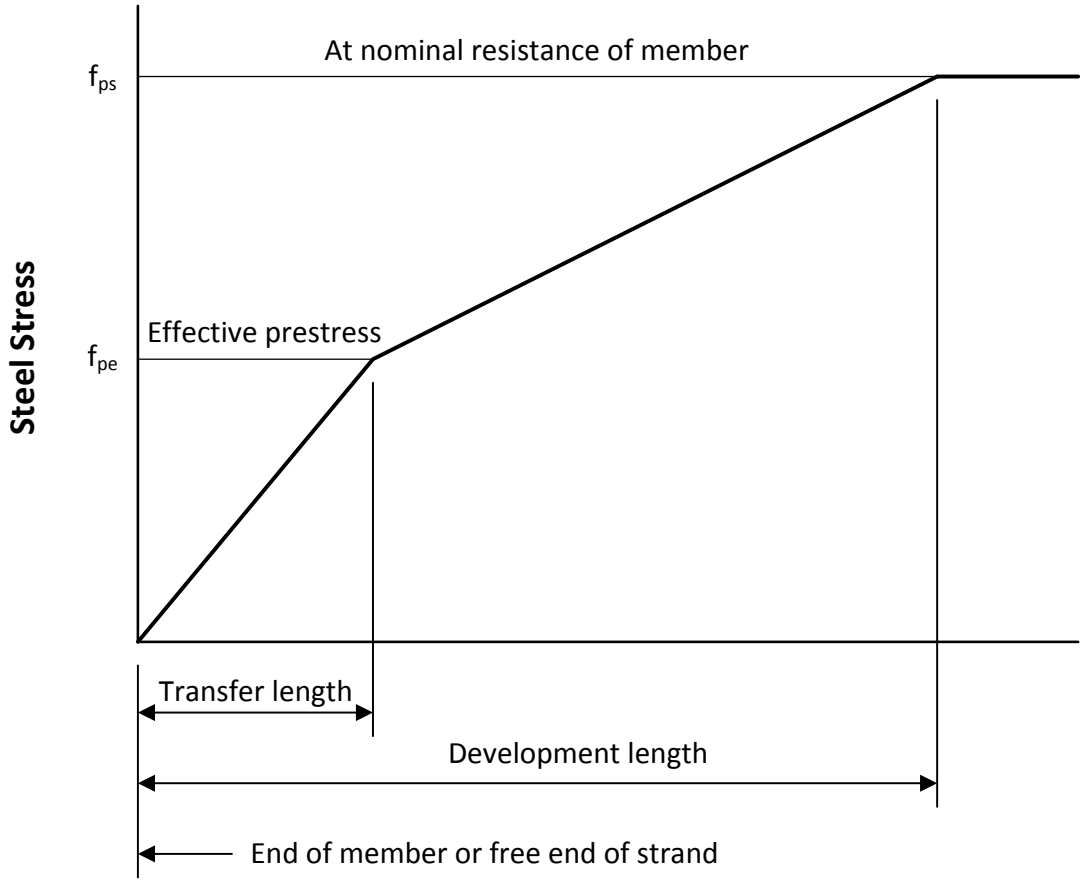

Figure 5.9.3-1 Idealized Relationship between Steel Stress and Distance from Free End of Strand

5.9.4 Splices of Reinforcement

If the required length of a reinforcing bar exceeds the maximum bar length provided by Fabricators, then a splice must be used. A splice is a specified length of overlap between two reinforcement bars that are approximately collinear that ensures full reinforcement bar strength over that length.

AASHTO LRFD Article 5.11.5 specifies requirements for splices of reinforcement. For lap splices in tension, three classes (Class A, B, and C) are provided, and the corresponding length of lap for each class is defined as a function of the development length. The selection of Class A, B, or C is based on the ratio of provided reinforcement to required reinforcement, as well as the percentage of reinforcement spliced with the required lap length.

In addition, provisions are provided for lap splices in compression, for mechanical connections or welded splices, for end-bearing splices, and for splices of welded wire fabric.

Section 5.10 Provisions for Structure Type

5.10.1 Slab Superstructures

Slab superstructures include cast-in-place flat slabs, cast-in-place voided slabs or precast deck bridges (i.e., slab beams or planks.) They may be mildly reinforced in either direction and/or post-tensioned.

AASHTO LRFD Article 5.14.4 governs the design of slab superstructures. *AASHTO LRFD* Sections 4 and 9 provide additional guidance concerning load analysis and design.

5.10.2 Precast Deck Bridges (Planks, Inverted-Ts and Double-T Girders)

For small span structures – generally in the range of 20 to 40 feet – precast prestressed concrete plank, inverted-T or double-T girders may prove useful (Figure 5.10.2-1).

Precast prestressed planks are placed side-by side, and the joints between them are filled with a cast-in-place concrete. Transverse post-tensioning is usually necessary, either of strand or bar tendons installed through ducts in each plank, to make them function structurally as a deep slab. Special care is essential with design details, fabrication, erection and installation in order to align ducts transversely and properly seal them to protect the tendons from corrosion.

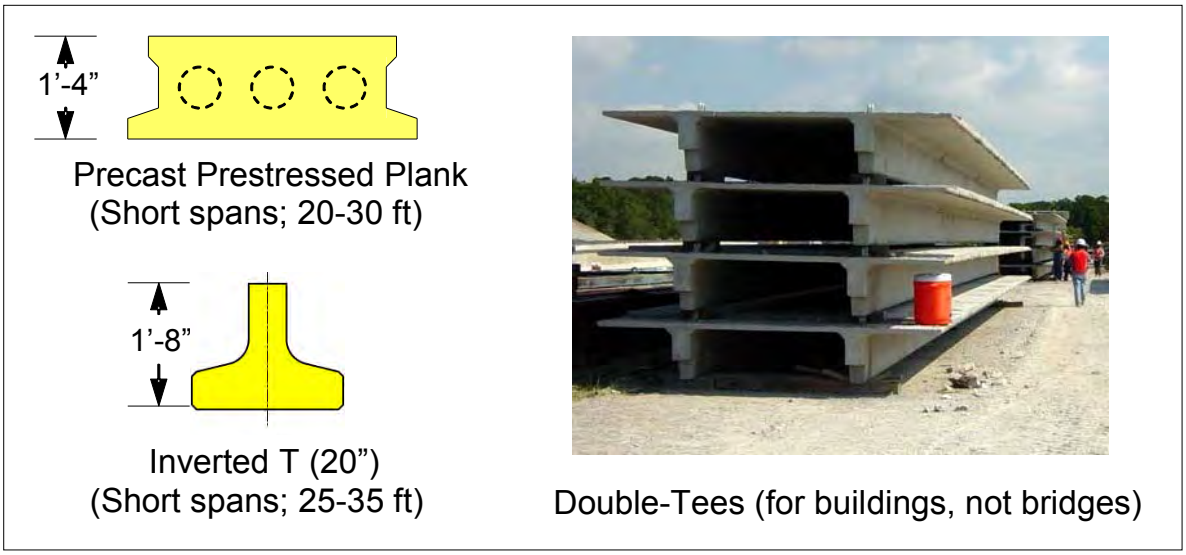

Figure 5.10.2-1 Other Miscellaneous Precast Concrete Sections

Inverted T-s beams are intended to be erected so that their bottom flanges are in contact. After placing transverse reinforcement, the spaces between them are completely filled with cast-in-place concrete. In this manner, inverted T girders are both the primary structural member and permanent formwork.

Double-T girders are widely used by the building industry. However, for bridges the top flange must be thickened to carry traffic loads or an additional reinforced concrete slab must be placed on site, using the thin top flange only as a form.

5.10.3 Beams and Girders

5.10.3.1 General

A typical concrete bridge deck may be comprised of several I-girders or bulb-tee girders with a reinforced concrete deck slab (Figure 5.10.3.1-1) Span length depends upon the type and size of the girder section, the spacing between girders, and the thickness of the deck slab. A deeper beam will span a greater length. Also, for the same size of girder and overall width of deck, if more girders are provided (say five instead of four) so that the girders are closer together, then a greater span is possible.

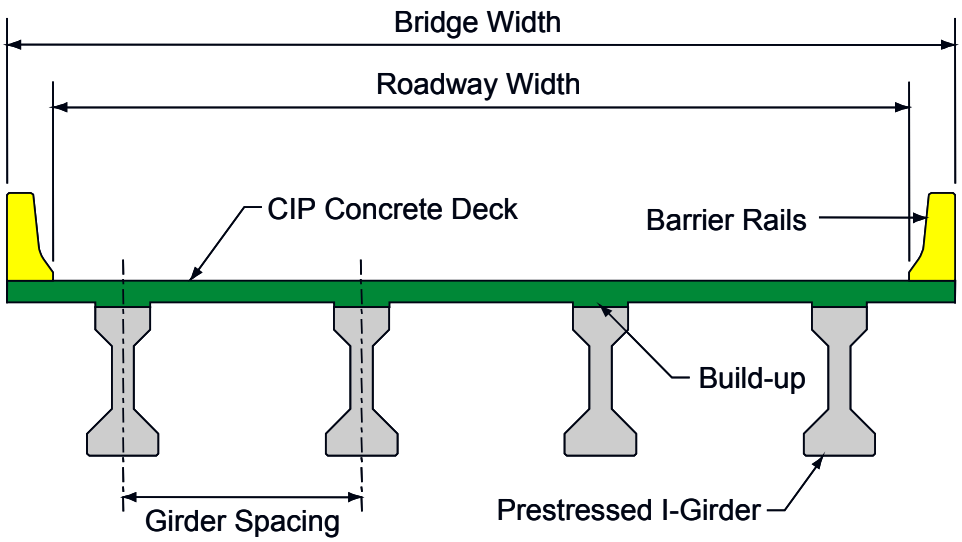

Figure 5.10.3.1-1 Typical Prestressed Concrete Girder Bridge Deck

Girders are usually spaced at 4 to 10 feet – possibly up to a maximum of 12 feet on center. The slab overhang is usually about 40% of the spacing but not more than 5 feet for most commercially available deck forming systems.

When girders are widely spaced, a deck slab must be thicker and heavier, than when girders are closely spaced. The minimum practical deck slab thickness (about 7") is governed by concrete cover, reinforcing bar diameters and construction tolerance. For this type of construction, deck slabs are rarely thicker than 8" or thereabouts. Usually, a slab is built-up over the girders to allow for camber. An economical bridge deck design strives for an overall balance between the thickness of the deck slab, girder spacing and span length.

5.10.3.1.1 AASHTO I-Girders

Standard AASHTO I-girder sections were developed in the 1950's. The most frequently used have been the Types II, III and IV for spans ranging from 40 to just over 100 feet (Figure 5.10.3.1.1-1). These particular sections have been widely adopted and the precast concrete industry is able to supply them in many areas.

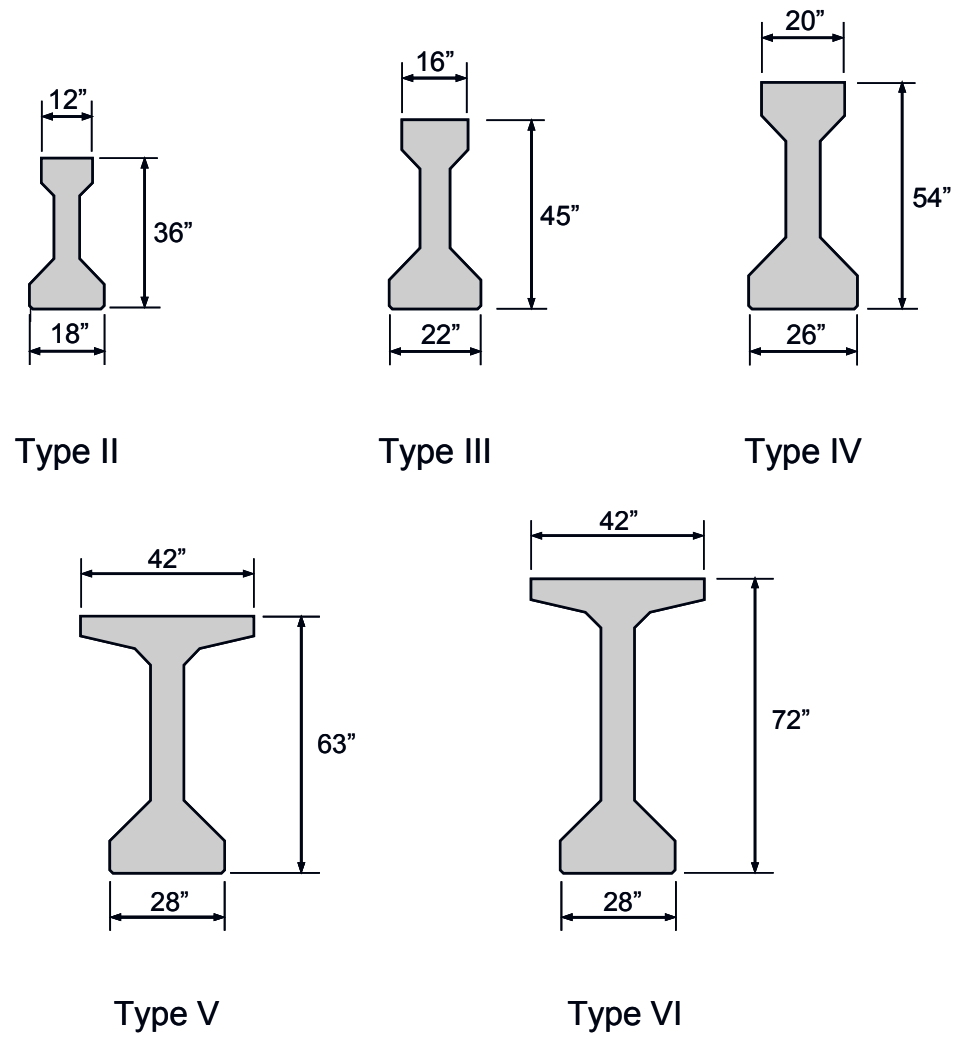

Figure 5.10.3.1.1-1 Standard AASHTO I-Girder Sections for Prestressed Bridges

At a shipping weight of 41 tons, a “Type IV” girder 100 feet long is about at the limit for convenient road transport and may require special routing or permits. Where transport by rail or water is feasible, or special road permits are possible, shipping lengths and weights can be greater and the use of a deeper, heavier, Type V or VI facilitate longer spans (Figure 5.10.3.1.1-1).

Several state departments of transportations have developed important variations on the basic AASHTO girder shapes. The designer should review state standards for the applicability of these shapes for a particular project.

5.10.3.1.2 Bulb-T Girders and U-Beams

In regions with a strong precast concrete industry, other types of sections have been developed to attain longer spans (such as bulb-T girders, as shown in Figure 5.10.3.1.2-1) or for enhanced aesthetics (such as U-beams, as shown in Figure 5.10.3.1.2-2).

Bulb-T girders facilitate simple spans up to about 135 feet, depending upon the depth of the girder section and spacing of the girders in the deck. U-beams are typically available in depths from 4 to 6 feet for simple spans up to about 125 feet. The wide top flanges of the bulb-T girders and the U-beam section provide increased lateral stability and can allow the development of very long girders. The Bow River Bridge near Calgary, Canada, for example, used 211' long, 9.2' deep precast, prestressed girders.

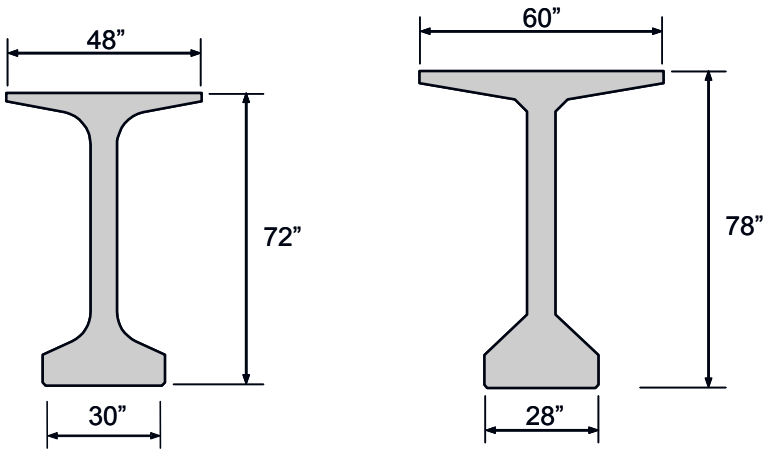

Figure 5.10.3.1.2-1 Bulb-T Girders

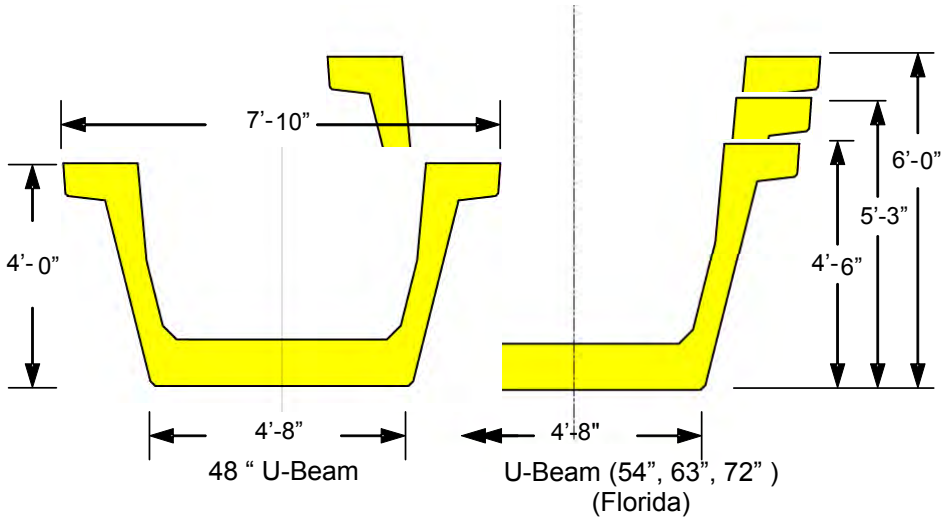

Figure 5.10.3.1.2-2 U-Beam Sections

5.10.3.1.3 Precast Beams

Standard precast concrete bridge components are produced in a factory using standardized fabrication processes. This offers efficiency, places fabrication off the critical path, provides economy and ensures good quality control.

Prestressed concrete girders are usually produced in a casting bed sufficiently long to make three or four girders in the same operation, using temporary intermediate bulkhead forms. Prestressing strands are laid in the bed from end to end at locations in the girder cross section according to design requirements (Figure 5.10.3.1.3-1).

Very often, portions of some strands near each end of each girder are de-bonded by shielding with plastic tubes to prevent contact with the concrete. The strands are tensioned to the required design force using a heavy duty stressing frame at each end of the bed (Figure 5.10.3.1.3-2).

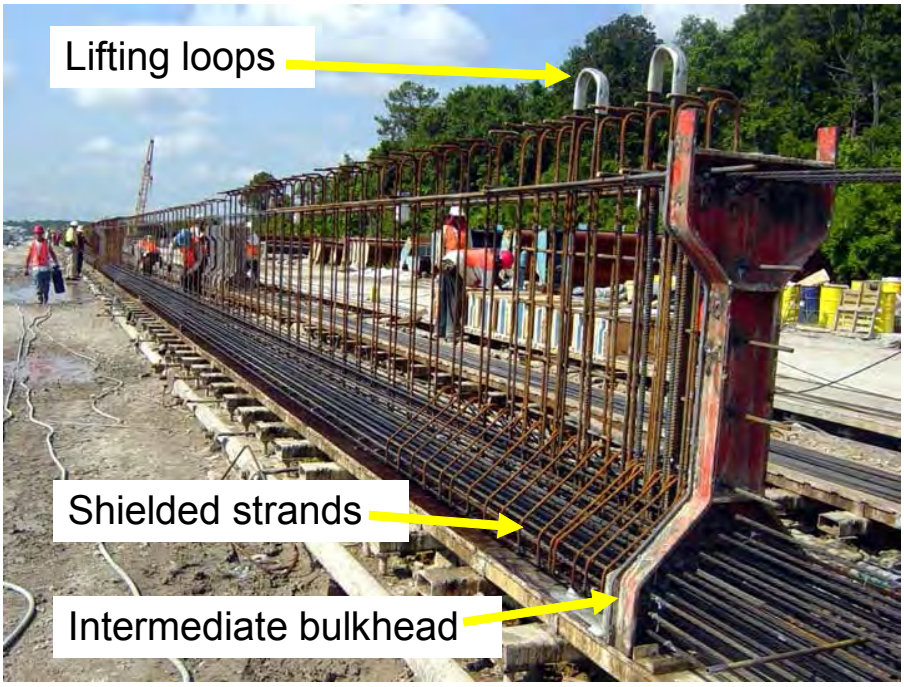

Figure 5.10.3.1.3-1 Precast I-Girder (Type IV) Fabrication

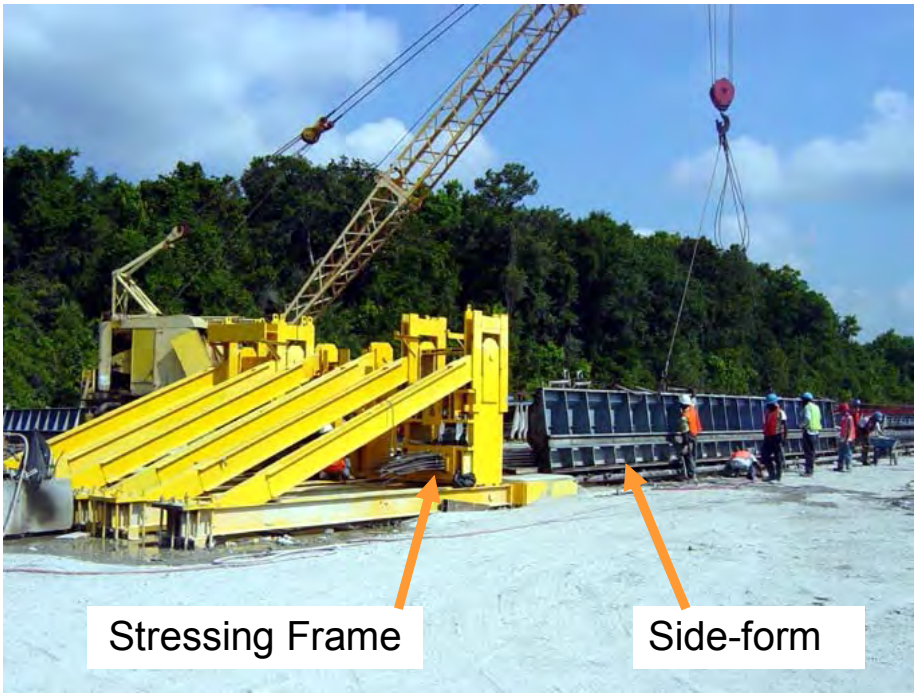

Figure 5.10.3.1.3-2 Stressing Frame and Side Forms

Mild steel web and flange reinforcement is placed at the necessary locations along each girder according to the design. Lifting devices, normally large loops of strand, are installed at each end. Web forms are installed on each side. Finally, when the

bed is ready and everything has been checked, concrete is placed and consolidated (Figure 5.10.3.1.3-3).

Figure 5.10.3.1.3-3 Placing and Consolidating Concrete

Short span components and girders may be sufficiently light to be picked by a single crane. Long girders usually require simultaneous lifting by a crane at each end. Lifting attachments, such as loops of strand or other devices are usually cast into the component at the precasting yard. Structurally, lateral stability of most precast concrete sections is assured by the width of the compression flange. However, during lifting and placing, care must be exercised to keep a girder web vertical – so as not to set it unevenly on bearings, uneven temporary supports or irregular dunnage.

Tilt of the girder, along with excessive sweep, can lead to instability, especially with some long “top-heavy” sections. Temporary lateral bracing may be necessary when erecting some sections, particularly long girders, until permanent diaphragms have been installed. Temporary steel or timber diaphragms have been used in some structures to provide construction stability until the deck slab has been cast (Figure 5.10.3.1.3-4). The cost of temporary intermediate steel diaphragm frames, their installation and removal should be considered in relation to the cost and benefits of alternative, permanent intermediate reinforced concrete diaphragms.

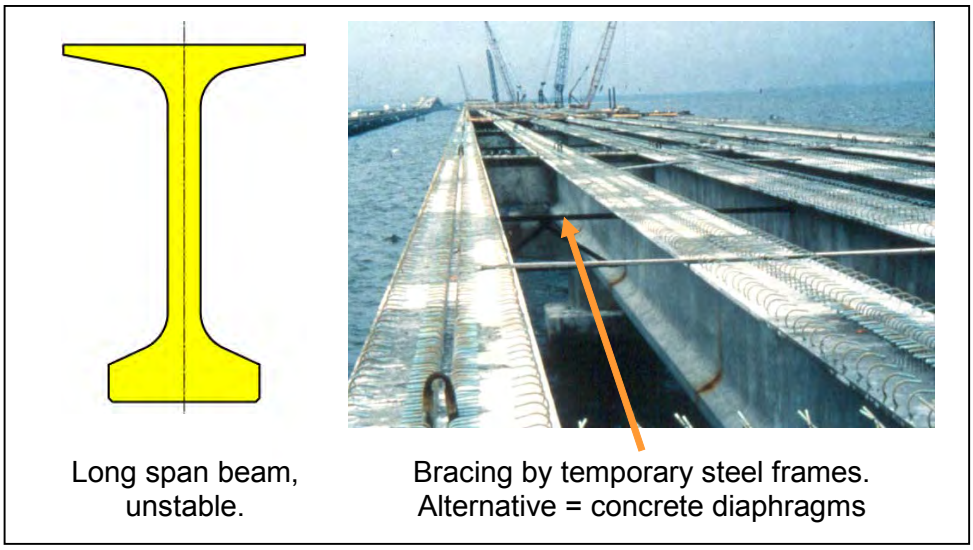

Figure 5.10.3.1.3-4 Temporary Bracing for Construction Stability

5.10.3.2 Precast Girders Made Continuous

This section addresses structures built as simply-supported spans but where continuity of the deck slab alone or the full depth of structure is made using cast-in-place reinforced joints over interior piers.

The advantages and disadvantages of making a structure partially or fully continuous are:

Advantages:

- Reduce positive bending
- Reduce prestress demand
- Reduce structural depth
- Enhance overall structural redundancy
- Eliminate expansion joints for improved ride
- Eliminate expansion joint leakage
- Reduce overall maintenance needs

Disadvantages:

- Introduces negative bending over interior piers
- Requires significant longitudinal reinforcing (or Post-Tensioning)
- Requires special reinforcement details in the ends of girders to develop continuity
- Requires additional design effort and construction control of deck slab casting sequence

- If casting sequence is not executed correctly, negative moment might induce additional cracking over piers

The primary advantages of continuity being the elimination of joints for improved traffic ride and reduced maintenance may often outweigh the disadvantages.

5.10.3.2.1 Partial Continuity of Deck Slabs Only

In order to eliminate expansion joints, improve rideability, control deck drainage and reduce maintenance costs, continuous deck slabs were introduced. In such bridges, girders are designed, erected and the deck slab cast, as simply supported spans. However, the slab itself is made continuous over the gap between the ends of the girders (Figure 5.10.3.2.1-1). Reinforcement is place in the slab over the gap to tie together the rebar mats in the slabs over each span. This detail is sometimes referred to as a “Poor-Boy” joint.

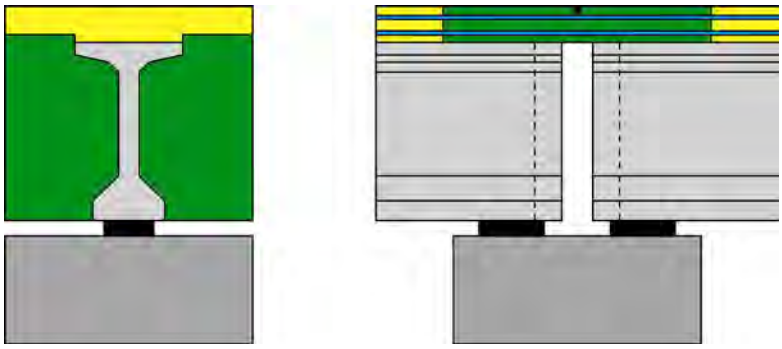

Figure 5.10.3.2.1-1 Deck Slab (“Poor-Boy”) Continuity Only

It is important that the ends of the girders themselves not come into direct contact (by inadvertent placement or deliberate blocking with hard material.) Such actions will establish a compression block at the bottom and attract negative dead load moments from live loads and/or creep redistribution. The magnitude of these moments could approach those in a fully continuous structure for which the deck and girders have not otherwise been designed.

Where only a deck slab is made continuous, continuity reinforcement is basically a nominal amount to control cracking. It is not structurally designed for a “particular load or effect” as such. Although theoretically, one could perform a rigorous analysis taking into account the distance between the adjacent bearings and their shear stiffness to develop or generate an opposing strut or tie force in the slab, the

engineering effort is hardly worthwhile. Nominal rebar is usually sufficient; with #4 or #5 rebar lap-spliced with the deck slab longitudinal steel. In practice, as the spans expand and contract and work under traffic loads, a crack will likely form over the gap. In order to control the crack, a crack-inducer, such as a small saw cut or formed strip is installed in the top of the slab over the gap.

This detail enables a few spans of continuous slab between true expansion joints in lengths up to about 400 feet. This facilitates, for example, a four-span bridge over an interstate highway with a continuous deck from end to end and expansion joints only at the abutments.

5.10.3.2.2 Full Continuity using Reinforced Concrete Joints

An alternative to the above deck-slab-only joint is to make the joint between the ends of the girders structurally continuous for all loads applied after construction of the deck. This is achieved by extending longitudinal reinforcement from the ends of the girders into a full-depth cast-in-place reinforced joint, as shown in Figure 5.10.3.2.2-1. Full depth joints may be built as diaphragms.

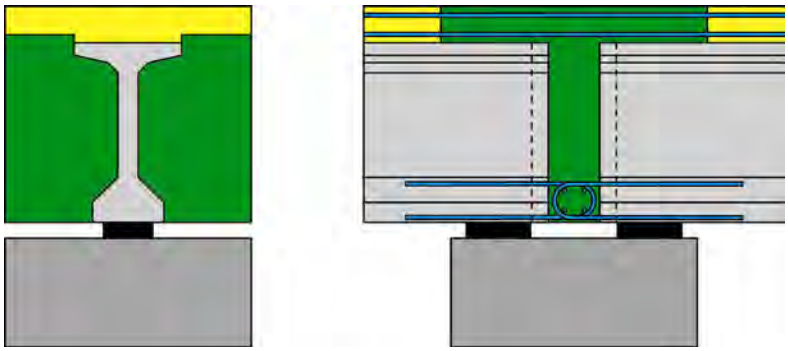

Figure 5.10.3.2.2-1 Full-Depth Reinforced Concrete Joint

This extends the concept of simply-supported prestressed concrete girders to applications where spans are made continuous by means of reinforced concrete joints connecting the superstructure of adjacent spans over interior piers. Consideration is given to accounting for the effect of the sequence of construction, statically indeterminate reactions and redistribution of moments due to creep.

Making a structure continuous by means of reinforced concrete joints requires that account be taken of the influence of the construction technique upon the design and the effects of redistribution of bending moments due to creep.

Summarizing, the impacts of the construction sequence on the design are:

- The self-weight of the girder, forms and deck slab, along with pretensioning effects are applied to the non-composite section on the simply-supported girder span.
- Subsequent loads are applied on a composite, continuous structure.
- It is necessary to evaluate the effects of redistribution due to creep and differential shrinkage of the deck slab.
- Reinforced splice joints should be designed and detailed for the positive and negative moments resulting from continuity.

An important aspect is to identify and evaluate the effects of creep redistribution (below).

5.10.3.2.3 Longitudinal Analysis (Bending Moments and Forces)

5.10.3.2.3.1 Analysis Methods

Making any superstructure continuous over one or more interior supports, introduces a number of redundant or indeterminate reactions equal to the number of interior supports. Support reactions can no longer be determined from statical analysis alone. If the interior supports are “simple bearings” (e.g. pins or rollers) that provide vertical support but little or no longitudinal restraint, then reactions can be determined using any classical formulae for continuous beams given in most structural engineering text books or manuals.

When girders are first erected as simply-supported beams with a bearing under the end of each girder and then made fully continuous, *AASHTO LRFD* allows the designer to utilize formulae for continuous beams as a close approximation to actual conditions. Where the assumption of a pin or roller between the superstructure and an interior pier is not valid, more rigorous analysis may be used at the discretion of the designer. Such rigor might be appropriate if, for example, (a) the distance between the bearings under the ends of the girders (b) the vertical stiffness of the bearings and (c) the rotational stiffness of the pier cap and columns are sufficient to generate a local couple. This couple would be taken by the substructure in flexure and would appear in the superstructure as a difference in negative moment from that at the bearing on one side of the pier to that on the other.

Classical analysis methods for determining bending moments at interior supports in (statically indeterminate) continuous beams may be summarized in the following steps:

- Consider the effect on the simply-supported span
- Calculate the end rotations
- Calculate the continuity moments from the end rotations
- Superimpose the simple-span and continuity moment diagrams to give final moments

Reference should be made to engineering text books for the analysis of continuous beams. Various methods are available such as slope-deflection, area-moment (flexibility) methods, moment distribution (Hardy-Cross), stiffness or matrix-methods. It is beyond the scope of this manual to address in detail methods of structural analysis for statically indeterminate structures. However, using the "Area-Moment Method", the above steps are expanded and summarized thus:

1. Reduce the structure to a statically determinate condition by removing redundant forces or constraints.
2. Develop the bending moment diagram, M, for this determinate condition.
3. Divide the ordinate of the bending moment, M, diagram by EI at each section to give the value of "M/EI". (This will facilitate analysis of both constant and variable depth structures.)
4. Divide the "M/EI" diagram into convenient geometrical areas and locate the centroid of each area.
5. Calculate the areas and moments of the areas of the "M/EI" diagram from each end of each simple span to determine rotations and displacements at each end respectively.
6. Apply unit redundant forces and moments to the structure and calculate the relevant bending moment diagrams.
7. Repeat steps 3, 4 and 5 for these diagrams to provide angular and linear displacements.
8. Equate the results of steps 5 and 7 to find values of actual redundant forces and moments.
9. Use these values to calculate the final bending moment diagram

The particular method of reducing a structure to a statically determinate condition is a matter of choice for the designer. The above is a general case. The designer may also utilize a suitable computer program. Most programs for the analysis of continuous beam or plane-frame structures are based on stiffness-matrix methods.

For the purpose of discussion, our illustration is simplified to superstructures of constant section – which is the case for the vast majority of precast girder bridges.

5.10.3.2.3.2 Continuity Effects

In continuous girders significant continuity effects arise from: (1) the construction process (i.e., the sequence of making continuity joints and casting the slab); (2)

secondary moments from prestress; (3) differential shrinkage of the deck slab relative to the girder; and (4) redistribution of moments due to creep. This final source (creep redistribution) may induce significant tensile stress in the bottom of the girders near the supports and reduce the effectiveness of prestress in the mid-span region. An adjustment of the pre-tensioning force by magnitude and/or eccentricity may be needed. These topics are addressed in greater detail in the following.

5.10.3.2.3.3 Construction Sequence Effects

When considering the effect of different construction sequences, the first possibility, "A", (Figure 5.10.3.2.3.3-1) is to erect the girders on individual bearings as simple spans then cast the majority of the deck slab except for a narrow closure gap over the piers (A.1.) The reinforced concrete splice joint connecting both the adjacent girders and deck slabs is then cast as a final closure operation (A.2.) Disregarding the effect of the short distance between the bearings (as discussed above) the bending moment in each girder from the weight of the slab plus formwork (say, w per unit length) is that for a simply supported span, namely:

Maximum positive moment, $M_{A\,pos} = + wL^2 / 8$

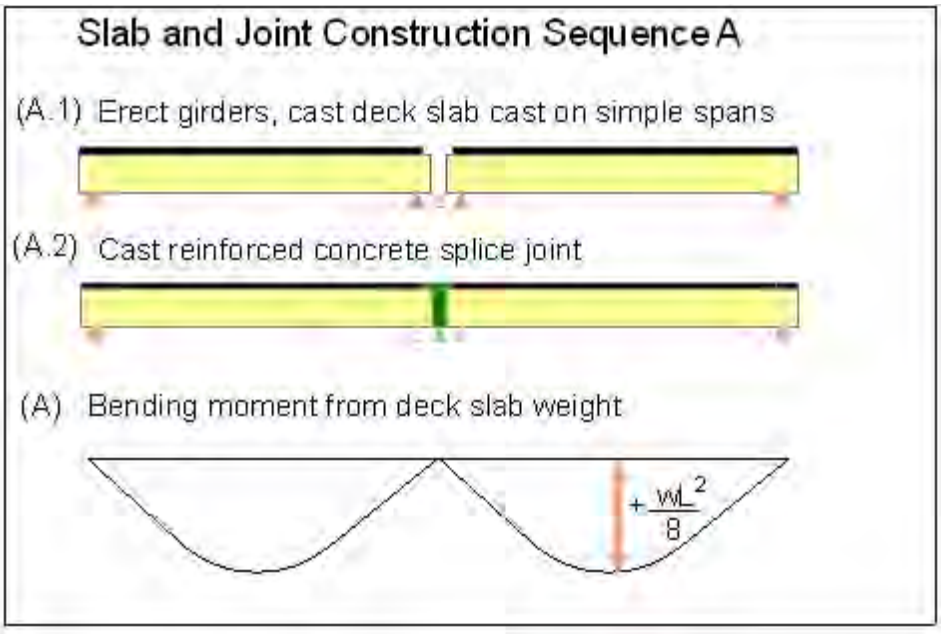

Figure 5.10.3.2.3.3-1 Construction Sequence Effects – Case (A)

An alternative possibility, "B", (Figure 5.10.3.2.3.3-2) is to erect the girders, cast the splice joint and allow it to harden, thus making the girders into continuous spans before casting the deck. In order to generate negative moment resistance, this would require significant longitudinal reinforcement to connect the tops of the girders. For the purpose of this illustration only, if it is assumed that such resistance is available,

then when the deck slab is cast on the now continuous girders the bending moments due to the weight of the slab are significantly different, namely:

$$\text{Maximum positive moment, } M_{B\ pos} = + 9wL^2 / 128$$

$$\text{Maximum negative moment, } M_{B\ neg} = - wL^2 / 8$$

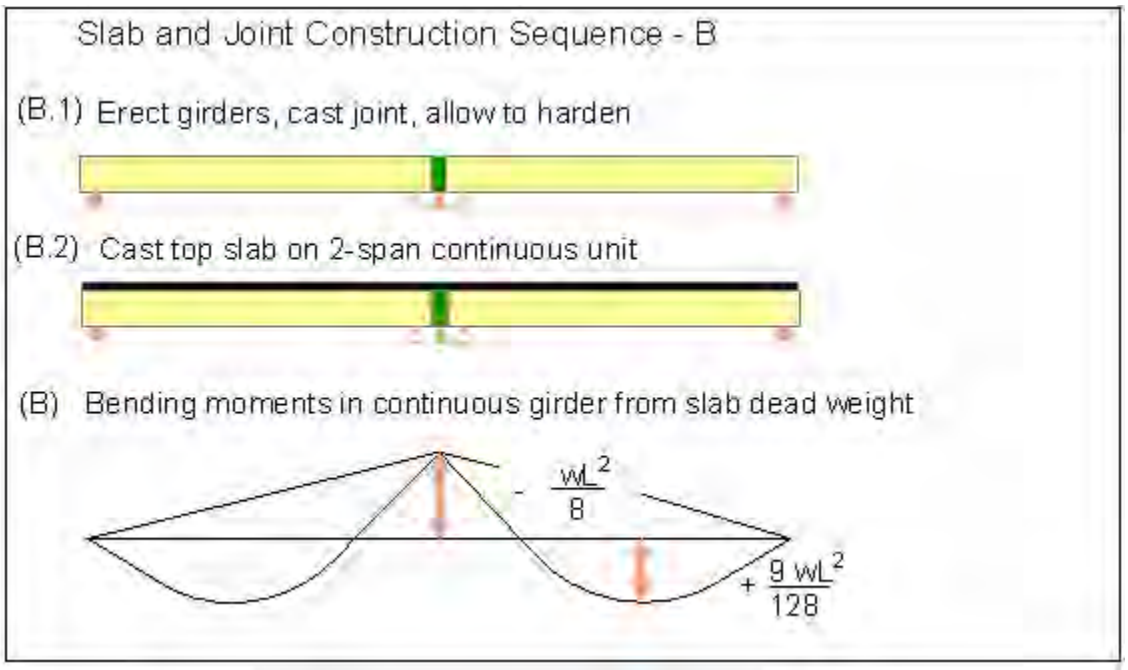

Figure 5.10.3.2.3.3-2 Construction Sequence Effects – Case (B)

These bending moments are those for a two-span girder as determined by any classical theory flexure under elastic conditions. It can be seen at a glance that the bending moments from the two construction sequences are significantly different. In reality it is possible to generate significant negative moment resistance over the center support using mild steel reinforcement in the deck connection between the ends of the girders. (Alternatively, significant negative moment resistance can be achieved using post-tensioning.)

The most practical sequence of construction for a real world two-span case would be Case “A”. This is justified below (see Figure 5.10.3.2.3.3-3).

In Phase 1 the pretensioned girders are erected. Since the flexural effect of the pretensioning is much greater than the moment of the girder self-weight, the net camber is upward. A wide joint is left over the pier to accommodate overlap of longitudinal reinforcement. Deck slab forms and reinforcement are installed. In Phase 2 negative moment reinforcing in the slab extends over the pier and the deck slab is cast over most of each span. The girders deflect under the weight of the wet

concrete, but the ends of the girders are free to rotate. In Phase 3 the closure joint reinforcement is completed and the joint is cast. Because this pour is small, there is negligible additional end rotation. The net camber is the sum of Phases 1 and 2 and is upward at this point. This is because the flexural effect of the pretensioning is greater than that of the girder and slab self-weight combined because there must be sufficient resistance to carry subsequently applied dead and live load. Permanent dead loads such as barriers, utilities, wearing surface and live load are applied to the two-span continuous unit.

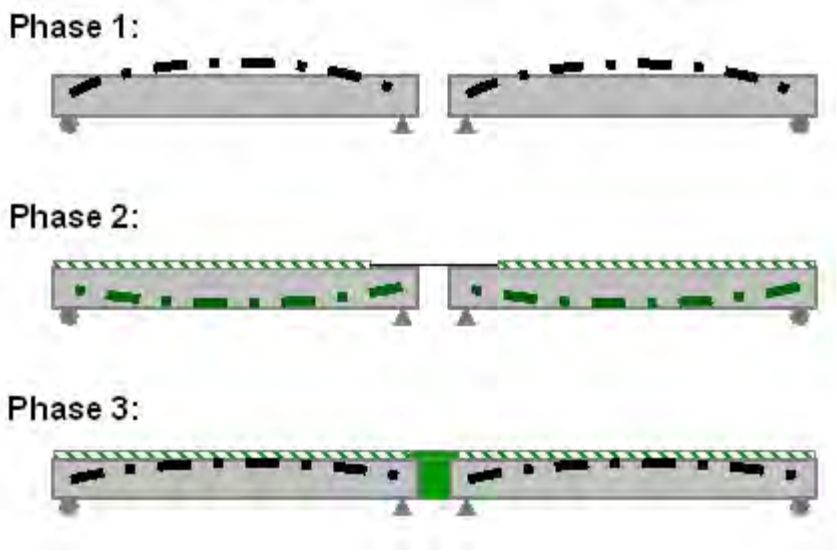

Figure 5.10.3.2.3.3-3 Practical Construction Sequence Considerations

The above two-span examples serve to illustrate the importance of considering the construction sequence, the method of making continuity and the application of loads to a structure in one (simple-span) configuration that becomes a different (continuous) structure at a later stage. The same principles extend to structures with a number of spans. In addition, effects from permanent dead load, prestress, creep and shrinkage occur at different times and stages of construction.

5.10.3.2.3.4 Secondary Prestress Reactions and Moments

Consider the case of a two-span girder continuous over a center support and prestressed with straight strands at a constant eccentricity from end to end of the continuous structure (Figure 5.10.3.2.3.4-1).

This is statically indeterminate structure. We are interested in finding the magnitude of the reaction at the center support from the prestress effect alone. In order to do this, imagine that the support is removed and that a constant prestress moment, $M_p = (F)(e)$, is applied to the simple span beam of length 2L.

The unrestrained upward deflection is determined by beam theory (e.g. area-moment or slope deflection). Then, applying the principle of compatibility, a downward load "P" is applied at the center to return the deflection to zero. By equating the deflections, the magnitude of the load P, in terms of the applied prestress, is found to be P = 3(F)(e)/L. This is the "Secondary Reaction" (acting downward) at the center support induced by straight prestress.

The accompanying bending moment is the "Secondary Moment" due to prestress, and is found to be:

$$M_{sec} = 3(F)(e) / 2$$

The net moment due to prestress at the center support is then

$$M_{net\ ps} = M_p - M_{sec} = (F)(e) - 3(F)(e)/2 = -(F)(e)/2$$

The net effect is to induce a negative bending moment (i.e., one that creates tension in the top fiber over the center support.) This net moment acts in the same sense as that due to a uniform load applied to the two spans. Consequently, the secondary moment from the above condition adversely affects the resistance of the girder at the center support.

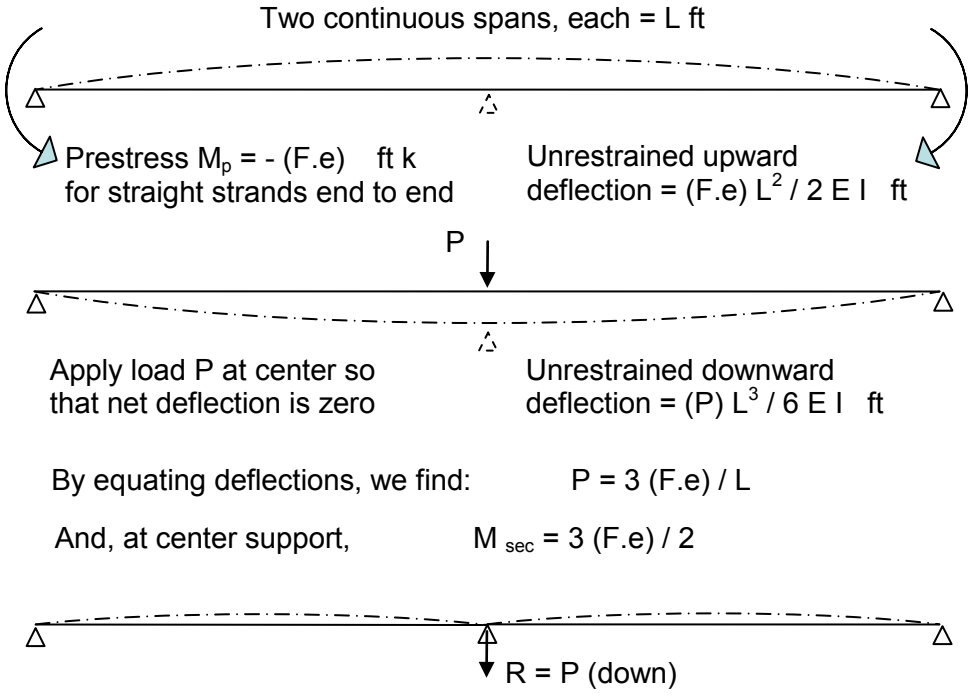

Figure 5.10.3.2.3.4-1 Secondary Reaction and Moment in Continuous Beam

This has profound implications for prestress applied to continuous structures and for the effects of creep redistribution in structures built in one statical condition that is later changed to another – as is encountered in cases where simply supported pre-tensioned girders are made continuous over interior piers by reinforced concrete joints.

A similar redistribution of moments occurs for structures made continuous with post-tensioning, except that the redistribution is driven by the difference between the combination of pre- (if any) and post-tensioning effects and dead load. However, in post-tensioned structures we shall see later that it is possible to reduce or eliminate secondary moments due to prestress by draping the tendon profile so that it is higher in the cross-section over the interior supports and lower within the span (Sections 5.10.5 and 5.10.6).

5.10.3.2.3.5 Differential Shrinkage

Since a deck slab is of younger and usually lower strength concrete than a girder, there is a certain amount of differential shrinkage between the deck slab and the girder – both shrink but at different rates. Because the deck is eccentric to the composite girder center of gravity, shrinkage of the deck relative to the girder results in a (uniform) positive moment that, if unrestrained, induces end rotations = $\theta_{sh.}$ However, since the structure has been made continuous over the pier, the adjacent spans restrain the rotations and induce a moment = M_{sh} over the interior pier. The result of this effect is illustrated in Figure 5.10.3.2.3.5-1.

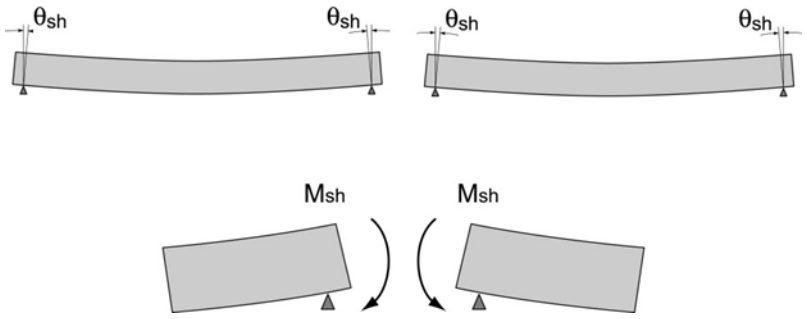

Figure 5.10.3.2.3.5-1 Differential Shrinkage

For the case of our two-span structure this differential shrinkage effect is analogous to the previous situation of secondary moments due to straight prestress at a constant eccentricity from end to end, but acting in the opposite sense (i.e., spans deflect instead of bowing up.) This can be envisioned by imagining the differential shrinkage effect as equivalent to a prestress force applied at the centerline of deck from end to end of the two spans. The net effect is to induce a tensile stress in the

bottom fiber of the girders at the interior pier. Calculation of the moment induced by this effect is addressed in detail below.

5.10.3.2.3.6 Redistribution of Moments Due to Creep

Since the girders are erected first in a statically determinate condition (simply-supported) that is later made continuous by means of a moment-resisting cast-in-place joint, a certain amount of redistribution of moments will occur due to creep. In this case what was originally erected as two simply-supported spans will tend to creep towards the condition that would have been the case had the entire superstructure (i.e., girders, prestress and deck slab) been placed "instantaneously" in its final (two-span) continuous configuration. This creep redistribution effect also applies to the differential shrinkage between the slab and girder.

It should be noted that for any superimposed dead load (barriers, utilities, surfacing etc.) applied to the completed, continuous structure in its final structural configuration there is no redistribution of the moments from these effects due to creep. Creep will cause increasing deflection (deformation) under their load, but there will be no redistribution of moments or forces from this effect.

Summarizing, redistribution of moment results from the restraint of creep deformations from loads that were applied to a structural configuration different than that which presently exists; support restraint of prestressing in statically indeterminate structures; or from differential shrinkage between cross-section elements cast at different times in a statically indeterminate structure. They include:

- Construction sequence effects – e.g. making simple-spans continuous, adding external supports or internal restraints
- Secondary reactions and moments due to prestress effects
- Differential shrinkage of the deck slab relative to the girder

Calculation of the effects is addressed in more detail in the following sections.

5.10.3.3 Creep Redistribution

5.10.3.3.1 Effect of Creep

Creep tends to make a structure, originally built in one condition (e.g. simply-supported) gradually act as if it had been built in its final condition (e.g. as a truly continuous structure from the outset.) In the previous two-span example bending moment over the interior pier due to the self-weight of the slab is initially zero in the "as-built" simply-supported condition, Case "A" in Figure 5.10.3.2.3.3-1. Gradually, creep redistributes the "as-built" moments.

In this illustration and considering only slab dead load, with time creep induces a negative moment over the interior pier accompanied by a corresponding reduction in positive moments within each span. However, since creep is a function of the maturity of the concrete when loaded, the stress level and duration of a particular load, 100% redistribution is never possible. That is to say, creep redistribution cannot attain the moments of Case "B" in Figure 5.10.3.2.3.3-2 which would be the condition if the slab load was applied "instantaneously" to a continuous two-span structure. The amount of redistribution is limited. For weight of the slab only, the final moments would be as illustrated in Figure 5.10.3.3.1-1.

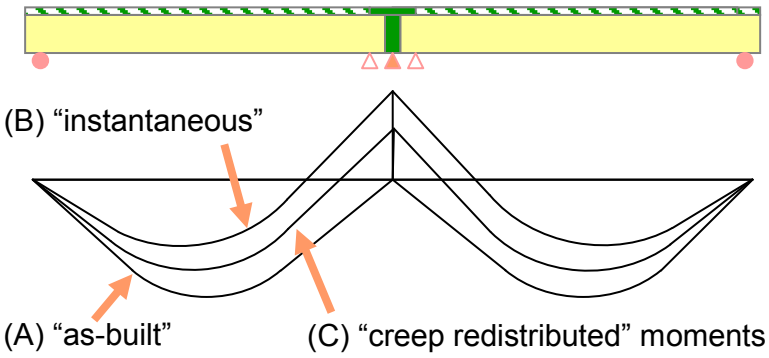

Figure 5.10.3.3.1-1 Creep Redistribution of Slab Weight in Continuous Spans

In this illustration the final bending moments (M_C) after redistribution due to creep are given by the expression:

$$M_C = (1 - e^{-\varphi})(M_B - M_A)$$

where φ = "creep coefficient," which represents the ratio of the creep strain to the instantaneous elastic strain (i.e., from the time that continuity is established in this illustration)

In this two-span illustration moments from creep redistribution gradually generate tension in the top longitudinal reinforcement in the slab over the piers and reduce the flexural tensile stress in the bottom fiber. This effect is a maximum at the interior pier and diminishes along the spans to zero at the exterior supports.

In an actual structure the situation is more complex since creep happens under all changes of internal stress from the combination of permanent load and prestress applied at different stages of construction. However, creep redistribution of moments only occurs after the stage and time of construction that continuity is established – i.e., the change from a statically determinate (simple span) to a statically indeterminate (continuous) superstructure.

A thorough, classic, theoretical and practical treatment of creep redistribution in a continuous structure was originally developed by Mattock (1961) and later extended by Freyermuth (1969) under research projects for PCA. The approach takes into account:

- Effect of stresses in the composite section, of creep of the precast girder due to prestress.
- Effect of stresses in the composite section, of creep of the precast girder due to dead load moments.
- Restraint moments in continuous girder due to creep.
- Stresses in the composite member due to differential shrinkage (between the slab and precast girder).
- Restraint moments in a continuous girder due to differential shrinkage (between the slab and precast girder).

This work led directly to the prior relatively simple equation for final moments (M_C) due to creep redistribution given the definition of the creep coefficient, φ, as the ratio of the final long-term creep strain to the initial elastic strain. Mattock and Freyermuth pointed out that φ typically varies from about 1.5 to 2.5. For most practical applications a value of 2.0 is reasonable. For our purposes a value of φ = 2.0 is used in the following example.

Consider the effects of creep in the spans shown in Figure 5.10.3.3.1-2. When erected, the simple spans deflect under loads and the ends rotate elastically by an amount equal to $\theta_{elastic}$. Unrestrained, these end rotations would grow because of creep by an amount equal to θ_{creep}. However, after the closure joint is cast the adjacent spans constrain the rotations, inducing a moment over the support equal to M_{cr}.

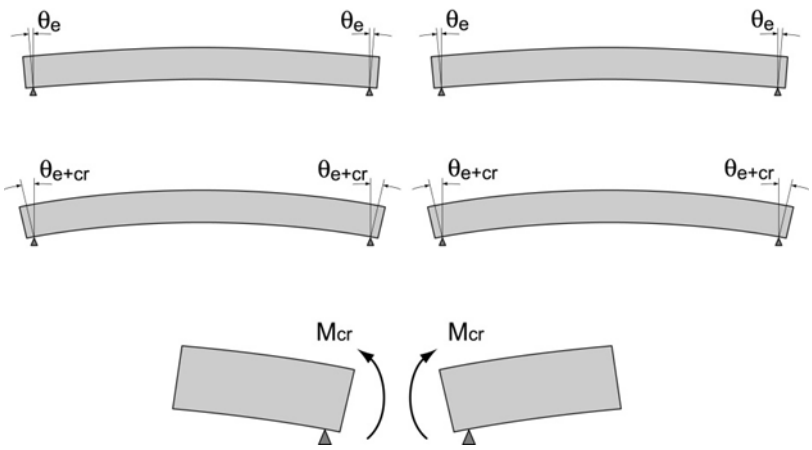

Figure 5.10.3.3.1-2 Creep Moments

5.10.3.3.2 Calculation of Creep Redistribution

For a continuous structure, redistribution of moments due to creep is determined using the "Ratio of Creep Method" established by Mattock, as follows:

- Evaluate simple span rotations due to non-composite dead loads.
- Evaluate simple span rotations due to prestressing
- Solve for moments on the continuous structure
- Factor moments by "ratio of creep" adjustment

The "ratio of creep" is given by the formula:

$$M_{cr} = M_{sw+ps} (1 - e^{-\Phi})$$

where:

Φ = $\varepsilon_{cr} / \varepsilon_e$ = creep ratio (typically in the range of 1.5 to 2.5)
ε_{cr} = creep strain after continuity is made (per unit stress)
ε_e = elastic strain per unit stress due to load

5.10.3.3.2.1 Illustration of Procedure

The process is illustrated by the following example. Consider a structure comprised of Type VI girders erected as two simple spans that are later made continuous, as illustrated in Figure 5.10.3.3.2.1-1. The simply supported, non-composite spans are 109'-0". After continuity has been made each span for composite conditions is assumed to be 110'-0".

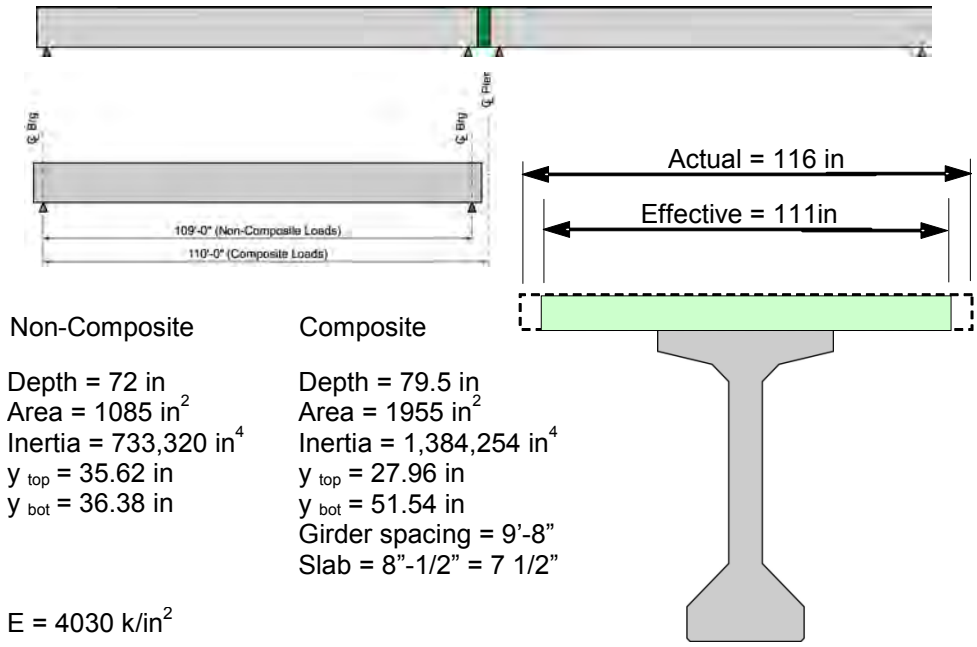

Figure 5.10.3.3.2.1-1 Two-Span Structure of Type VI Girders

The self-weight load on the simply-supported, non-composite section span is:

Uniform self-weight of girder	=	1.130 k/ft
Uniform load of slab	=	0.967 k/ft
Weight of haunch	=	0.175 k/ft
Total uniform load on non-composite section (w)	=	2.272 k/ft

Using any classical elastic beam formulae, such as the area-moment theorem, the end rotation of the girder for a uniform load of w per unit length (Figure 5.10.3.3.2.1-2), is given by:

$$\theta_{sw} = \frac{wL^3}{24EI} = \frac{2.272(110.0)^3}{24EI} x(12\ in/ft)^2 \rightarrow radians$$

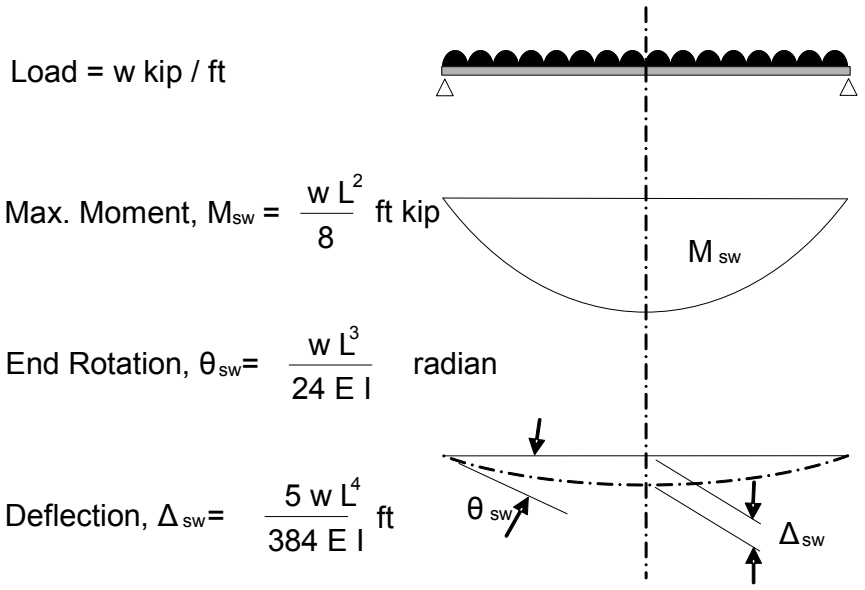

Figure 5.10.3.3.2.1-2 Simply-Supported Span under Uniform Load

Now apply a moment, M, at the closure of the 2-span girder to induce an equal and opposite end rotation to that of the simply supported girder under self-weight (Figure 5.10.3.3.2.1-3).

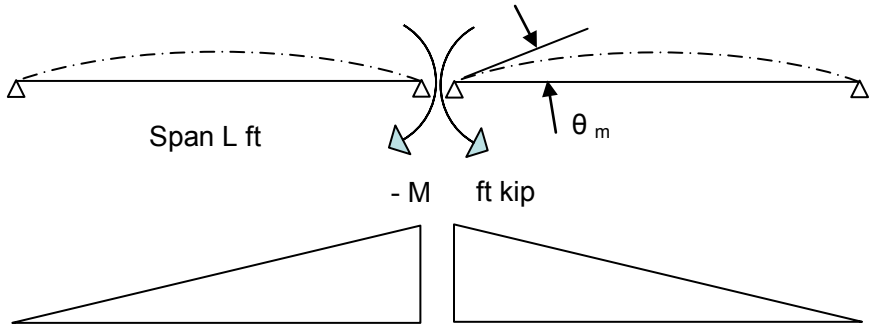

For Moment (- M) applied at closure, by area-moment =

$$\text{End Rotation, } \theta_m = \frac{(-M) L}{3 E I} \text{ radian}$$

Figure 5.10.3.3.2.1-3 Continuity Moment, M

The end rotation due to a moment (-M) applied at one (closure joint) end of a simply supported beam is given by:

$$\theta_m = \frac{(-M_{sw})L}{3EI}$$

Equating θ_m to θ_{sw} provides the magnitude of the continuity moment (-M), thus:

$$\text{End Rot } \theta_{sw} = \frac{wL^3}{24EI} = (-)\theta_m = \frac{(-M_{sw})L}{3EI}$$

$$\text{From which, } M = -\frac{wL^2}{8} \text{ ft} - \text{k}$$

This is the negative bending moment over the central pier for a uniform load (w) applied to a continuous girder of two spans, as given by any elastic beam theory formula for bending moments in continuous beams. Substituting values for w (= 2.272 k/ft) and L (= 110 ft) gives M = - 3,436 ft kip (Figure 5.10.3.3.2.1-1). In the two-span case (Figure 5.10.3.3.2.1-4) the negative moment at the interior pier happens to be of the same magnitude as the simply-supported self-weight moment at mid-span, but of opposite sign (assuming that the simple span and continuous span lengths are the same, which is approximately the case in our example.)

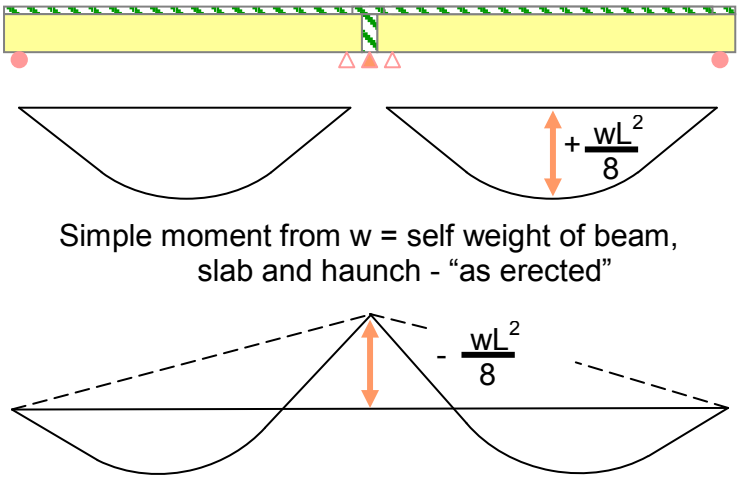

Figure 5.10.3.3.2.1-4 Two-Span, Self-Weight Continuity Moment

In a similar manner to the above we can calculate the simple-span end rotations due to prestressing and the moment necessary at the closure joint over the pier to provide an equal and opposite end rotation. In order to do this, we need to know the

layout of the prestress – this is illustrated in Figure 5.10.3.3.2.1-5. In this case the layout incorporates debonded (shielded) strands at the ends of the girder. The prestress force (F) and prestress moment (*F* x *e*) at each section of the girder is shown in Figure 5.10.3.3.2.1-6.

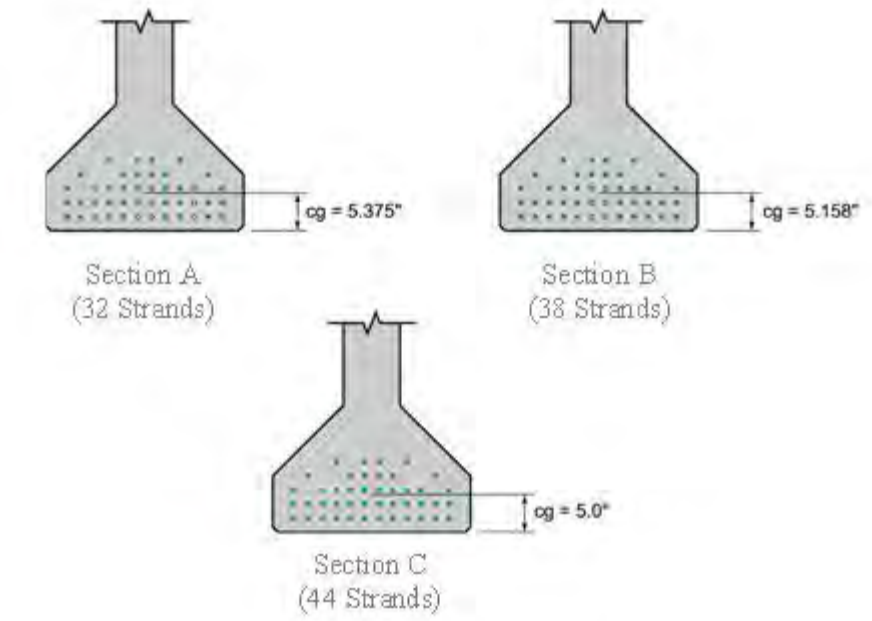

Figure 5.10.3.3.2.1-5 Prestressing Layout and Debonding

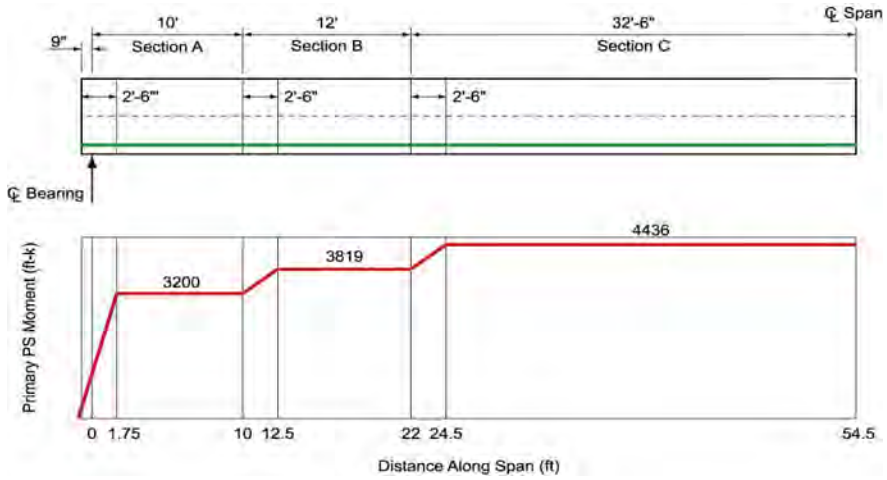

Figure 5.10.3.3.2.1-6 Prestress Moment for Simply-Supported Girder

The prestress moment varies along the girder due to deliberate debonding of strands to satisfy end conditions (i.e., to avoid excessive top tensile stress.) As the prestress is symmetrical about mid-span, only half of the diagram is shown in the figure. Since

it is symmetrical, the end rotation of the girder is calculated by applying the area-moment theorem in the manner described previously, giving an end rotation of:

$$\text{End Rotation, } \theta_{ps} = -\left(\frac{1}{2}\right)\frac{\sum(F * e)}{EI}$$

In this case the rotation, θ_{ps}, is negative (upwards) at the end of the girder. The continuity moment (M_{ps}) required at the closure joint is found by equating this end rotation to that for a moment of (M_{ps}) applied at the (closure joint) end of a simply supported beam (in the same manner but opposite in sign to that in Figure 5.10.3.3.2.1-3). This gives:

$$\text{End Rotation, } -\theta_{ps} = \left(\frac{1}{2}\right)\frac{\sum(F * e)}{EI} = \theta_m = \frac{M_{ps}L}{3EI}$$

$$\text{From which, } M_{ps} = \left(\frac{3}{2}\right)\frac{\sum(F * e)}{L}$$

Inserting the summation of prestress area-moment *Σ(F)(e)* = 441,919 ft k and the span length *L* of 110 ft. gives a (positive) continuity moment, M_{ps} = 6,026 ft k.

The net continuity moment at the center pier of a 2-span unit is the sum of the continuity (fixity) moments from self-weight and prestress, namely;

$$M_{sw+ps} = M_{sw} + M_{ps} = (-3{,}436 + 6{,}026) = 2{,}590 \text{ ft k}$$

This is the continuity moment that must be adjusted for creep. Applying the “Ratio of Creep Method”, the redistributed creep moment, M_{cr}, is given by:

$$M_{cr} = M_{sw+ps}\,(1 - e^{-\Phi})$$

If the creep ratio, Φ, is taken as 2.0, then the creep moment is :

$$M_{cr} = 2{,}590\ (0.8646) = 1{,}954 \text{ ft k}$$

5.10.3.3.3 Calculation of Moments Induced by Differential Shrinkage

Consider first a simply-supported span with a deck slab cast later and of different, less mature concrete than the precast girder. The slab tends to shrink relative to the girder but the girder also restrains that shrinkage. The net effect is to induce a bending moment, approximately constant, over the length of the span given by:

$$M_{sh} = \Delta\varepsilon_{sh} E_d A_d (e')$$

where:

$\Delta\varepsilon_{sh}$ = differential shrinkage strain of deck to girder
E_d = modulus of elasticity of deck slab
A_d = area of deck slab (full area plus haunch)
e' = distance from centroid of slab to centroid of composite section

Now:

$$\Delta\varepsilon_{sh} = \varepsilon_{sh,s,\infty} - (\varepsilon_{sh,b,\infty} - \varepsilon_{sh,b,t})$$

where:

$\varepsilon_{sh,s,\infty}$ = ultimate shrinkage of slab at time infinity
$\varepsilon_{sh,b,\infty}$ = ultimate shrinkage of precast beam at time infinity
$\varepsilon_{sh,b,t}$ = shrinkage of precast beam at time of casting deck slab

Shrinkage, according to *AASHTO LRFD* Article 5.4.2.3.3-1, is given by:

$$\varepsilon_{sh,s,\infty} = - k_s k_{hs} k_f k_{td} (0.48*10^{-3})$$

where for the girder;

$k_s = 1.45\text{-}0.13(V/S) = 0.877 < 1.0$; so for this case use 1.0

(Given V = 13,020 in^3/ft and S = 2,955 in^2/ft for the girder)

$k_{hs} = (2.00 – 0.14H) = 1.02$ taking H = 70% for relative humidity

$k_f = 5/(1+f'_{ci}) = 5/(1 + 4.8) = 0.862$

$k_{td} = t / [61\text{-}4(f'_{ci}) + t] = 1.0$ for $t = \infty$

or $k_{td} = 0.683$ for t = 90 days

Inserting these in *AASHTO LRFD* Article 5.4.2.3.3-1 for the girder, we find:

$\varepsilon_{sh,b,\infty}$ = 0.000422
$\varepsilon_{sh,b,t}$ = 0.000288
(assuming that the deck slab is cast when the girder is 90 days old)

Alternatively, for the slab:

$k_{vs} = 1.45\text{-}0.13(V/S) = 0.855 < 1.0$; so for this case use 1.00

(Given V = 10,440 in^3/ft and S = 2,280 in^2/ft for the slab)

k_{hs} = (2.00 – 0.14H) = 1.02 taking H = 70% for relative humidity

k_f = 5/(1+f'_{ci}) = 5/(1 + 3.20) = 1.19 (if f'_c = 4.0 ksi for slab)

k_{td} = t / (61-4(f'_{ci}) + t) = 1.0 for t = ∞

Applying *AASHTO LRFD* Article 5.4.2.3.3-1 to the slab, we find for our example that at time infinity;

$\varepsilon_{sh,s,\infty}$ = 0.000583

The modulus of elasticity for the slab is 3,834ksi.

Giving $\Delta\varepsilon_{sh}$ = 0.000583 – (0.000422 – 0.000288) = 0.000449

This induces a constant positive moment of:

M_{ss} = 0.000449(3,834)(116*7.5) (72 – 51.54 + (7.5/2))

= + 36,259 kip-in = + 3,021 ft-kip

The end rotations due to this constant moment, using area-moment theory, are:

$$\text{End Rotation, } -\theta_{ss} = -\left(\frac{1}{2}\right)\frac{\int M(x)dx}{EI} = -\left(\frac{1}{2}\right)\frac{M_{ss}L}{EI}$$

Applying a continuity moment, M_{cont}, at the end of a simply supported beam, the rotation at the point of application is given by:

$$\text{End Rotation, } \theta_{cont} = \frac{M_{cont}L}{3EI}$$

Applying compatibility and equating the rotations, we find that the continuity moment at the center support of a 2-span continuous girder induced as a result of shrinkage of the deck slab in the two spans after continuity has been established, is given by:

$$\text{Continuity Moment, } M_{cont} = \frac{-3M_{ss}}{2}$$

For the example, inserting the value of M_{ss} = 3021 ft kip, we find that the continuity moment M_{cont} = - 4,532 ft k. Note that this is a negative moment at the interior pier.

The final shrinkage moments are determined by applying the correction factor for shrinkage to the sum of the shrinkage driving moments (M_{ss}) and the shrinkage continuity moments (M_{cont}), namely:

$$M_{sh} = M_{ss} + cont\left(\frac{1-e^{-\varphi}}{\varphi}\right)$$

(The above correction factor is taken directly from the same work of Mattock (1961) and Freyermuth (1969) undertaken for PCA as for the formula for creep redistribution.)

In our example, if it is assumed that the creep ratio, φ = 2.0, then we find:

$$M_{sh} = (3{,}021 - 4{,}532)0.4323 = -653 \text{ ft - kip}$$

The summation of final bending moments due to creep redistribution from differential shrinkage effects on the two-span continuous girder is illustrated in Figure 5.10.3.3.3-1.

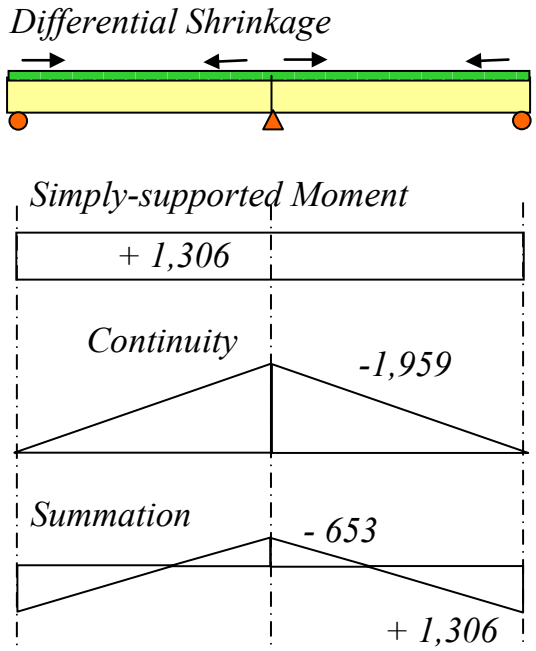

Figure 5.10.3.3.3-1 Redistributed Differential Shrinkage Moments

5.10.3.3.4 Effects of Permanent Loads Applied to Final Continuous Structure

For the two-span continuous I-girder example above, bending moments from permanent superimposed dead load (i.e. barriers, utilities, surfacing) applied to the structure after it has been made continuous, are determined from routine formulae for continuous beams. As mentioned above, since these effects are applied to the continuous structure in its final structural configuration there is no redistribution of their moments due to creep. Creep will cause increasing deflection (deformation) under their load, but no redistribution.

Similarly, the effects of permanent superimposed dead load applied to any continuous superstructure after all structural continuity has been made may be determined from classical beam theory for continuous beams, with no redistribution due to creep.

For the two-span example; the moment at the center pier due to a superimposed dead load of 0.217 kip per ft is:

$$M \text{ (sup. dead)} = - 0.217*110^2 / 8 = -328 \text{ ft-k}$$

5.10.3.3.5 Effectiveness of Closure Joints

According to *AASHTO LRFD* Article 5.14.1.4.5, the joint at the pier may be considered fully effective if compression is induced in the bottom under the combination of superimposed dead load, settlement, creep, shrinkage, 50% live load and thermal gradient, if applicable. Otherwise, the joint is considered only partially effective:

- For a fully effective joint, the structure is designed as continuous for all limit states for load applied after closure.
- For a partially effective joint, the structure is designed as continuous for strength limit states only.

If the resistance over the pier is less than the demand, then the positive resistance in the adjacent spans must be adjusted to accommodate redistribution.

For the two-span example, over the center pier:

Superimposed permanent load (DW)	=	-328 ft k
Settlement (n/a)	=	0 ft k
Creep moment	=	1,954 ft k
Differential shrinkage moment	=	-653 ft k
Live load moment (say)	=	0 ft k
Thermal gradient (n/a this example)	=	0 ft k
Sum	=	973 ft k

The presence of live load on this two-span structure would be to induce compression in the bottom fiber over the pier and therefore reduce the tensile demand. This is not a worst case rather zero live load is worse. So, absent live load, and assuming no settlement and no thermal gradient, the net moment at the center pier in this case is a positive moment inducing a tensile stress in the bottom fiber of the girders near the pier. Under this condition, the joint is partially effective; so the girder prestressing should be designed as for simply supported spans.

The magnitude of the positive moment at the pier is significant. The bottom of the closure joint should be appropriately reinforced. The amount of tensile reinforcement is determined as for a reinforced concrete (T) section under factored moments.

The factored demand moment, M_u, is:

$$M_u = 0.65(-328) + (1.0)(1{,}954) + (1.0)(-653) = 1{,}088 \text{ ft k}$$

The factored nominal resistance must be greater than the demand moment or 1.2 times the cracking moment (*AASHTO LRFD* Equation 5.7.3.3.2-1), which for this example is 1,560 ft-kips. The nominal moment resistance is given by:

$$M_n = A_s f_{y.} (d - a/2)$$

Using an average value of d of 79.5 inches, an effective top flange of 110 inches, a slab concrete strength of 4.0 ksi, and a reduction factor (φ) of 0.9, 8 number 7 bars provides the needed resistance. The arrangement of the reinforcement in the section over the pier is illustrated in Figure 5.10.3.3.5-1.

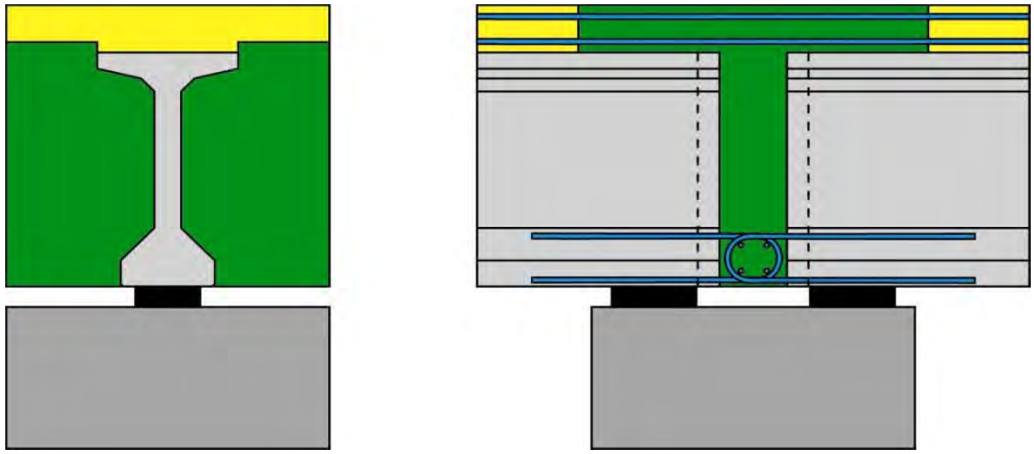

Figure 5.10.3.3.5-1 Bottom Reinforcement in Closure Joint at Pier

5.10.3.3.6 Creep Redistribution in Multiple Spans

Creep redistribution in superstructures of multiple spans is similar to that for the two-span example above. The final effects depend upon the sequence of casting deck slabs and making continuity. However, practical considerations may favor one sequence (Option B) over another (Option A) illustrated in Figure 5.10.3.3.6-1.

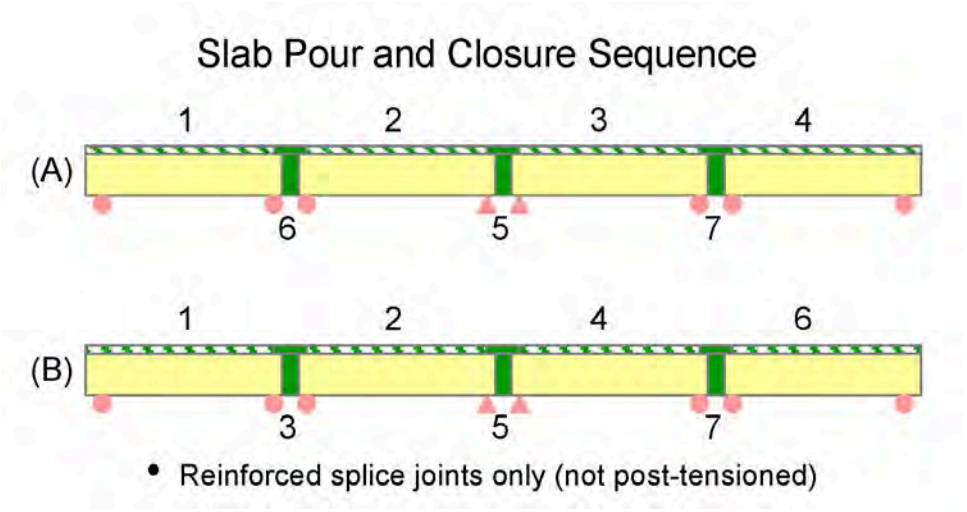

Figure 5.10.3.3.6-1 Multiple-Span Construction Continuity and Redistribution

For continuous structures, key points to remember are:

- The Designer should consider the sequence of casting the deck slab and closure joints and the effects it might have upon the girder and deck design.
- Required or preferred casting sequences should be shown on the plans or clearly addressed in construction specifications.
- Variations to facilitate alternative construction sequences may also be shown
- Requests from Contractors to vary the sequence from that shown on the plans should be reviewed by the Designer.

5.10.3.3.7 Creep Coefficient (φ)

The creep coefficient (φ) takes into account a variety of concrete properties and environmental conditions, in particular:

- Type of concrete, aggregate and cement
- Method of curing (steam, blankets, fog)
- Strength of concrete
- Maturity of the concrete from time of casting (i.e., strength gain)
- Notional thickness (ratio of volume to surface area, V/S)
- Humidity at the site

(Note: According to *AASHTO LRFD* Article 5.4.2.3.2, The Time Development Factor, k_{td}, for creep and shrinkage in *AASHTO LRFD* Equations 5.4.2.3.2-1 and 5.4.2.3.3-1, respectively, is valid for both accelerated (e.g. steam) curing and moist curing.)

The role of the creep coefficient (φ) may be understood in the context of the development of strain. For a concrete loaded at time t_0, with a constant stress of σ_0, the total strain $\varepsilon_{total}(t, t_0)$ at time t, may be expressed in a general form as:

$$\varepsilon_{total}(t,t_0) = \sigma_0\left(\frac{1}{E_c(t_0)} + \frac{\varphi(t,t_0)}{E_{c2}}\right)$$

where:

t_0	=	age of concrete at time of loading
t	=	age of concrete at time of evaluation
σ_0	=	applied stress
$E_c(t_0)$	=	modulus of elasticity of concrete at age of loading
E_{c2}	=	modulus of elasticity of concrete at 28 days
$\varphi(t,t_0)$	=	age of area of deck slab (full area plus haunch)

The creep coefficient, $\varphi(t, t_0)$ represents the increase in strain over the time period from t_0 to a future point in time, t. It is expressed with respect to the modulus of elasticity for the concrete according to its strength at 28 days. The modulus of elasticity at the time of loading, $E_c(t_0)$, is not necessarily the same as that at 28 days, depending upon the maturity of the concrete and time of loading. Within the brackets, the first term of the above expression represents the initial elastic strain under the stress at loading, σ_0.

Suppose it were possible to express the modulus of elasticity at the time of loading, $E_c(t_0)$, in terms of the 28-day modulus E_{c28}, then the above equation would lead to a slightly modified version, as follows:

$$\varepsilon_{total}(t,t_0) = \frac{\sigma_0}{E_{c28}}\left(\frac{1}{f_{28}} + \varphi(t,t_0)\right)$$

Where "f_{28}" is a function that relates $E_c(t_0)$ to E_{c28}. The term "$\varphi(t, t_0)$" would represent the development of the creep strain with time as ratio of that at time infinity (Figure 5.10.3.3.7-1). But, $\varphi(t,t_0)$ does not correspond to the term $\psi(t,ti)$ of *AASHTO LRFD* (ACI 209). There is an anomaly and no direct link between *AASHTO LRFD* (ACI 209) and FIB (CEB-FIP) – see also Figure 5.10.3.3.7-2.

The development of the creep strain as a ratio may be expressed algebraically as a function:

$$\text{Ratio of creep strain} = (1 - e^{-\varphi})$$

According to Mattock (1961) and Freyermuth (1969) any reasonable formulation for the creep coefficient, φ with time, may be adopted based on the results of tests or previous data and the final (infinite time) creep ratio typically lies between 1.5 and 2.5.

The development of shrinkage strain follows a similar pattern with time. As discussed previously, the effects of differential shrinkage are accounted for by applying a correction factor = $(1 - e^{-\varphi})/\varphi$ to the shrinkage drying and continuity moments.

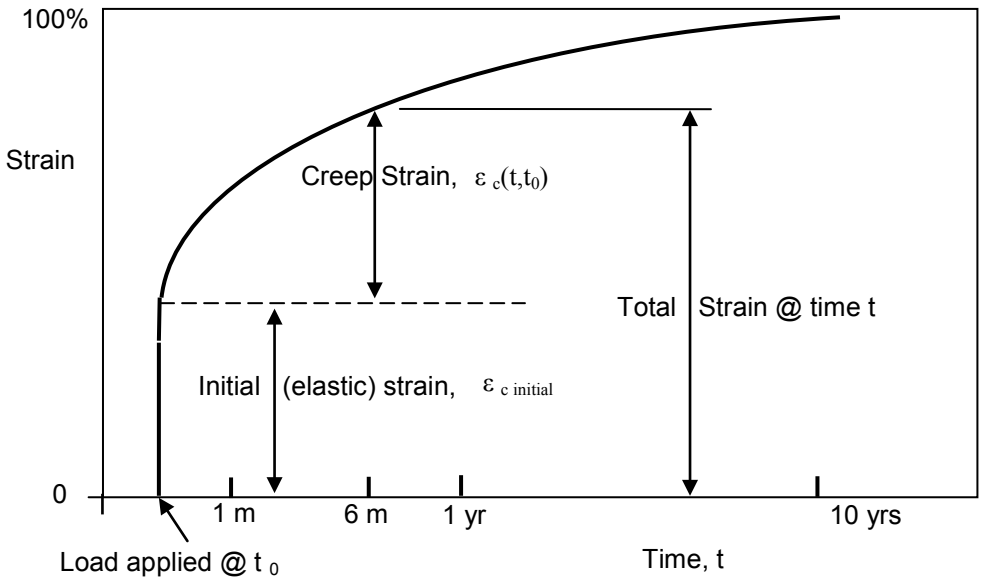

Figure 5.10.3.3.7-1 Development of Creep Strain with Time

In the absence of any information, *AASHTO LRFD* allows estimates for creep (and shrinkage) to be based on:

- *AASHTO LRFD* Articles 5.4.2.3.2 (creep) and 5.4.2.3.3 (shrinkage)
- The CEB-FIP (European) model code, or
- ACI 209

Terminology adopted by *AASHTO LRFD* and CEB-FIP for describing creep behavior is illustrated in greater detail in Figure 5.10.3.3.7-2. However, this does not mean that the codes are “equivalent”. Rather the contrary; experience indicates a noticeable difference between FIB (CEB-FIP) and ACI 209 upon which *AASHTO LRFD* is based.

For other structures, such as precast or cast-in-place segmental, structures cast in place on falsework, and particularly concrete cable-stayed structures, standard formulae may not accurately predict time-dependent behavior. Therefore, designers and field engineers need to be aware of their limitations and use appropriate material properties and formulations for creep and shrinkage in accordance with experience.

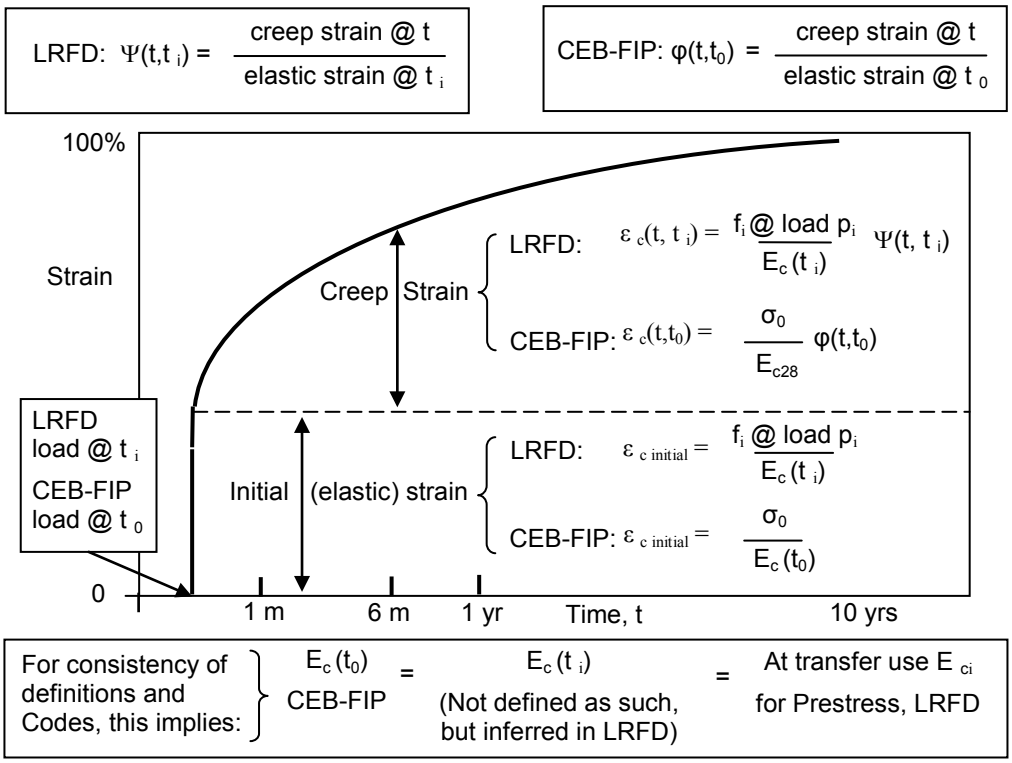

Figure 5.10.3.3.7-2 Terminology of CEB-FIP and *AASHTO LRFD*

With regard to the time, t_∞, at which the ultimate strain due to creep or shrinkage is attained, it is conventional to assume t = 4,000 days (or about 10 years).

In the absence of more accurate data shrinkage coefficients may be assumed to be 0.0002 after 28 days and 0.0005 after one year of drying. *AASHTO LRFD* provisions apply for concrete strengths up to 15 ksi (see *AASHTO LRFD* Appendix C5.)

5.10.3.4 Flexural Limit States

5.10.3.4.1 Differences Between Continuous and Simply-Supported Structures

Prestressed girder superstructures made continuous with reinforced concrete joints require additional considerations as compared to simply-supported superstructures. These include:

- Negative moments over interior supports from gravity loads such as self-weight, superimposed dead load and live load that create flexural tension in the top fiber and compression in the bottom fiber
- Secondary effects from prestress induce further negative moments over piers
- Differential shrinkage of the slab relative to the girder tends to induce a positive moment (bottom fiber tension) over interior piers.

As a result of the structure being built in a simply-supported condition and then changed to a continuous condition, there is a redistribution of structural moments due to long-term creep. Creep tends to reduce negative moments at piers due to structural dead load – but with a corresponding increase in positive moments within spans. Creep also redistributes secondary prestress and differential shrinkage effects.

Precast girders generally have straight strands in the bottom flange. Occasionally, some strands may be deflected to terminate high up in the webs at the ends. Deflected strands can minimize but may not eliminate adverse secondary prestress moment effects at interior piers.

5.10.3.4.2 Structural Analysis

Calculation of bending moments, shear forces and reactions for continuous structures may be accomplished by various methods based on classical beam theory, such as: flexibility analysis, displacement (stiffness) analysis, area-moment theorem, moment-distribution, matrix methods, etc. Computer models are generally based on matrix (stiffness) methods.

5.10.3.4.3 Application of Vehicular Live Load

For negative moment and support reactions at interior piers only, *AASHTO LRFD* Article 3.6.1.3.1, bullet point 3, requires loading for negative moment between points of contra-flexure consisting of 90% of two trucks spaced a minimum of 50 ft apart combined with 90% of the design lane load. For this purpose the location of the points of contra-flexure corresponds to that determined by applying a uniform load on all continuous spans.

5.10.3.4.4 Service Limit State

At the service limit state limiting flexural stresses for continuous structures are the same as for simply-supported structures (*AASHTO LRFD* Article 5.9.4), the difference being that these are now applied to the top or bottom fiber, as appropriate. Stresses due to secondary moments must be calculated and added to other effects when punitive. In continuous structures thermal gradient (TG), especially negative

thermal gradient, can induce additional top tension over interior supports, presenting difficulties for some structures and load combinations.

For a composite section, determination of the final state of stress can only be successfully accomplished by accumulating stresses from each individual effect (load or prestress) at each elevation of interest at each cross-section of interest. (It is incorrect to accumulate moments or shear forces and apply the total to the final section.) Stress accumulation is more tedious for continuous composite girders, but the principle is merely an extension of that for simply-supported pre-tensioned girders. In summary, stresses are first calculated and accumulated for the non-composite properties up to the time the slab has been cast and becomes effective. Thereafter, stresses are calculated and accumulated for the composite section properties, which are comprised of the non-composite section, the effective slab, and possibly, the transformed area of pre-tensioned strand.

Longitudinal stresses should be accumulated and checked at the top of deck slab, top of precast girder and bottom of precast girder as a minimum. If there is an interest in needing to know final principal tensile stress at various elevations, then it is necessary to accumulate longitudinal and shear stresses at those elevations, too. Such elevations would include the neutral axis of the non-composite and composite sections and perhaps top and bottom of web, as necessary. Given that the section properties (for flexure and shear) change with the construction process, meticulous accounting is necessary to track accumulated stress from initial to final long-term, in-service conditions. Nowadays, this process is greatly facilitated by spreadsheets.

5.10.3.4.5 Strength Limit State

In continuous prestressed structures, secondary moments due to prestress must be added to factored demand (with a load factor of 1.0) when checking the strength limit state. Also, for a continuous composite structure differential shrinkage of the deck slab tends to induce positive moment (bottom tension) at interior piers which undergoes redistribution due to creep. The magnitude of this effect depends upon the assumptions made for the creep coefficient and the sequence and timing of construction activities. Since the effect is beneficial in that it reduces other gravity loads, it is imperative not to overestimate the effects. With these exceptions calculation of the flexural resistance of a continuous structure cross-section is otherwise the same as for any prestressed girder and may be determined as outlined in *AASHTO LRFD* Article 5.7.3.

5.10.3.4.6 Contribution of Mild-Steel to Flexural Resistance

In superstructures made continuous by reinforced concrete joints, precast girders are usually provided with reinforcement in the form of L or U-bars that project into the splice region from the ends of the girders at the bottom. Continuous mild-steel

reinforcement is also required in the deck over the joint. Both sets of reinforcement may be counted toward flexural strength resistance, at positive and negative moment regions.

5.10.3.4.7 Redistribution of Negative Moment at the Strength Limit

AASHTO LRFD Article 5.7.3.5 addresses the ability of continuous concrete girders and frames to redistribute load after cracking. If tensile steel (in this case deck slab rebar) in the negative moment region provides sufficient ductility to enable a minimum net tensile strain (ε_t) of 0.0075, the moment determined by elastic theory at the strength limit state may be reduced by a percentage not greater than $1000\varepsilon_t$ or 20% at that section. In order to maintain equilibrium positive moments must be increased to account for the change in negative moments and positive moment resistance re-checked for the redistributed amounts.

5.10.3.5 Longitudinal Shear Design

5.10.3.5.1 Service Limit State

Design for shear at the service limit state is not required by *AASHTO LRFD* for pretensioned girders with 28-day strengths not exceeding 10 ksi. However, durability considerations may warrant a check to ensure that the structure will not experience shear cracking at the service level. High shear forces can cause diagonal cracking in webs as the result of large principal tensile stresses. The magnitude of the effect can be determined by applying classical theory using Mohr's circle for stress. Limiting the principal tensile stress between $0.110\sqrt{f'_c}$ and $0.125\sqrt{f'_c}$ (ksi) at the neutral axis location has traditionally and conveniently been used to establish an approximate web thickness for durability and detailing purposes.

5.10.3.5.2 Strength Limit State

AASHTO LRFD shear design using Modified Compression Field Theory was covered in Section 5.6 for precast, pretensioned girders. Shear design for pre-tensioned girders made continuous by reinforced concrete joints is similar with few refinements.

In a simply-supported girder, or any statically determinate structure, internal forces from prestressing do not cause reactions at the supports. However, when girders are continuous, the structure is statically indeterminate and prestressing causes secondary reactions. This is sometimes called the "continuity effect" or "secondary effect". Secondary reactions induce corresponding shear forces and secondary moments. This directly modifies the summation of shear forces from all loads.

Although common practice for simply-supported pretensioned girders is to use straight strands, they can be draped upwards at the ends, as discussed in Section 5.7.4.1.2. For pretensioned girders with deflected (draped) strands at the ends of the girders the force in the strands can be resolved to provide a vertical component - typically opposing the shear from dead and live loads. The effect is essentially a reduction in shear demand. However, *AASHTO LRFD* includes this effect as a component of strength rather than a reduction in demand. In this case, the vertical component of the effective prestressing force, V_p, is added to the strength of the concrete, V_c, and vertical reinforcement, V_s. The total shear strength is then:

$$V_n = V_c + V_s + V_p$$

If V_p is in the same direction as the dead and live load demand, then V_p should be taken as negative in this equation for total shear strength. Whether positive or negative, if V_p is considered to be a component of "strength", then shear effects from prestressing should *not* be included as a load "demand." Care should be exercised to make sure that the deflected (draped) strands can develop sufficiently to contribute to the vertical component, Vp, at the section required. Vertical prestressing by means of post-tensioned bars placed in webs is not a practical option for precast, pre- and post-tensioned I-girders.

5.10.4 Post-Tensioned Spliced Precast Girders

Previous sections addressed the construction of simply-supported precast concrete girder superstructures with cast-in-place deck slabs. This section deals with making such types of superstructures structurally continuous by the use of post-tensioning. The technique is often referred to as "spliced-girder construction" as it involves making small cast-in-place joints or "splices" to connect the ends of girders or portions of girders. Establishing structural continuity in this manner enables the length of otherwise simply-supported spans to be extended approximately 10 to 15% for the same girder size. In addition, if the section of girder over an interior pier is made deeper using a variable depth haunch, span lengths can be extended even further. Consequently, this type of construction facilitates spans ranging from 140 to a practical limit of about 350 feet.

5.10.4.1 Introduction

The objective of this topic is to present the basic concepts for the design and construction of precast concrete girder superstructures, made continuous by means of spliced joints and longitudinal post-tensioning. Typical girder sections, span lengths and post-tensioning layouts are described. Construction techniques using temporary supports, deck slab casting sequences and staged post-tensioning are discussed.

In addition to the advantages and disadvantages of continuity outlined previously, longitudinal post-tensioning offers the following additional advantages and disadvantages as compared to pretensioned girder construction:

Advantages:

- Shallower superstructure depth
- Significantly longer spans, with practical limits as follows:
    - Splices over piers – up to 140 feet (or longer, as limited by shipping considerations)
    - Simple spans with intermediate (quarter-point) splices – up to 225 feet
    - Variable depth with splices in spans – up to 350 feet

Disadvantages:

- More complex design and construction
- Requires thicker webs to accommodate post-tensioning ducts
- Requires inspection of ducts and anchors at precast yard
- Requires inspection of installation and grouting of tendons on site
- Friction loss in long, draped tendons may become significant

5.10.4.2 Design

Key aspects of post-tensioned, spliced girders that differ from considerations for pretensioned I-girders include: the influence of the construction technique upon the design; the effects of redistribution of bending moments due to creep; additional prestress loss due to friction and anchor set in post-tensioning tendons; and the treatment of anchor zones.

Girder splice joints themselves may be located over piers or at intermediate points within spans in such a manner that the length and weight of precast concrete girders or portions thereof are convenient for delivery and erection.

The method of construction is an integral feature of this type of bridge that must be properly considered in the design. Construction techniques for two of the most often used applications are presented as follows: (1) Four-Span Constant Depth I-Girder with spliced joints over interior piers (Figure 5.10.4.2-1). (2) Three-Span Haunched I-Girder utilizing variable pier segments with spliced joints near inflection points within the spans (Figure 5.10.4.2-2).

Example 1: Four-Span Spliced I-Girder (Figure 5.10.4.2-1)

For the purposes of design, “key activities” of the construction sequence that affect the design are summarized as:

1. Fabricate, cast and pretension precast girders (say, at time t0)
2. Erect all pretensioned girders (say, at time t1)
3. Cast in place spliced joints over piers between ends of girders (time t2)
4. Install first stage of post-tensioning (on non-composite section, time t3)
5. Form and cast deck slab (in a specific sequence, time t4)
6. Install second (final) stage of post-tensioning (on composite section, time t5)
7. Apply superimposed dead load (barriers, surfacing, etc., time t6)
8. End of Construction (EOC), open to traffic, (time t7)
9. Allow creep and shrinkage to take place to long term service, (time t∞)

Figure 5.10.4.2-1 Four-Span Constant Depth Spliced I-Girder

Example 2: Three-Span Variable-Depth Spliced I-Girder (Figure 5.10.4.2-2)

For the purposes of design, “key activities” of the construction sequence that affect the design are summarized as:

1. Fabricate, cast and pretension precast girders (could be at various times, say t0)
2. Erect pretensioned girders in side-spans (time, t1)
3. Erect pretensioned cantilever girders over main piers (time, t2)
4. Cast in place spliced joints in side spans girders (time t3)
5. Suspend main span girder on temporary hangers and cast splices (time t4)
6. Install and stress first stage longitudinal PT from end to end (time t5)

7. Form and cast deck slab (in a specific sequence, times could vary, say t6)
8. Install and stress second stage longitudinal PT from end to end (time t7)
9. Remove temporary support towers (time t8 - alternative might be after step 6)
10. Apply superimposed dead load (barriers, surfacing, etc., time t9)
11. End of Construction (EOC), open to traffic, (time t10)
12. Allow creep and shrinkage to take place to long term service, (time t∞)

Figure 5.10.4.2-2 Three-Span Haunched I-Girder

Each construction step should be considered in design calculations.

To a certain point, (Step 2 of Example 1; Step 3 of Example 2) the two structures are statically determinate. Once the splice joints are cast and gain strength, both structures become statically indeterminate. The joints begin to experience continuity effects by virtue of rebar projecting from the girders into the joints even before post-tensioning. But practically speaking, it is not until the tendons are stressed and the structure lifts off the supports that it begins its life as a continuous structure.

In the first example (four-span structure) initial conditions have already been addressed for pretensioned girders. For instance, initial transfer of pretensioning in the casting yard and subsequent loss of prestress from creep, shrinkage and relaxation from the time of casting to erection. This also applies to the pre-tensioned components of the second example (three-span structure).

In both examples changes due to creep and shrinkage occur in the intervals between each construction step. These cause loss of prestress (in both pretensioning and post-tensioning force), and redistribution of internal forces arises

from changes in the statical scheme due to creep and differential shrinkage of the deck slab (as addressed previously.)

More so than the first, the second example introduces design and construction considerations not previously encountered when discussing prestressed girders made continuous for live load – e.g. temporary support of partial length members; variable depth pier segments, etc. In the second example temporary support towers must be erected to support girder segments and then remain in place until the superstructure has been post-tensioned to be fully continuous for all subsequent loads (Figure 5.10.4.2-3). Depending upon the amount of post-tensioning and section capacities, the removal of temporary supports might conceivably occur after Step 6, but more safely after Step 8.

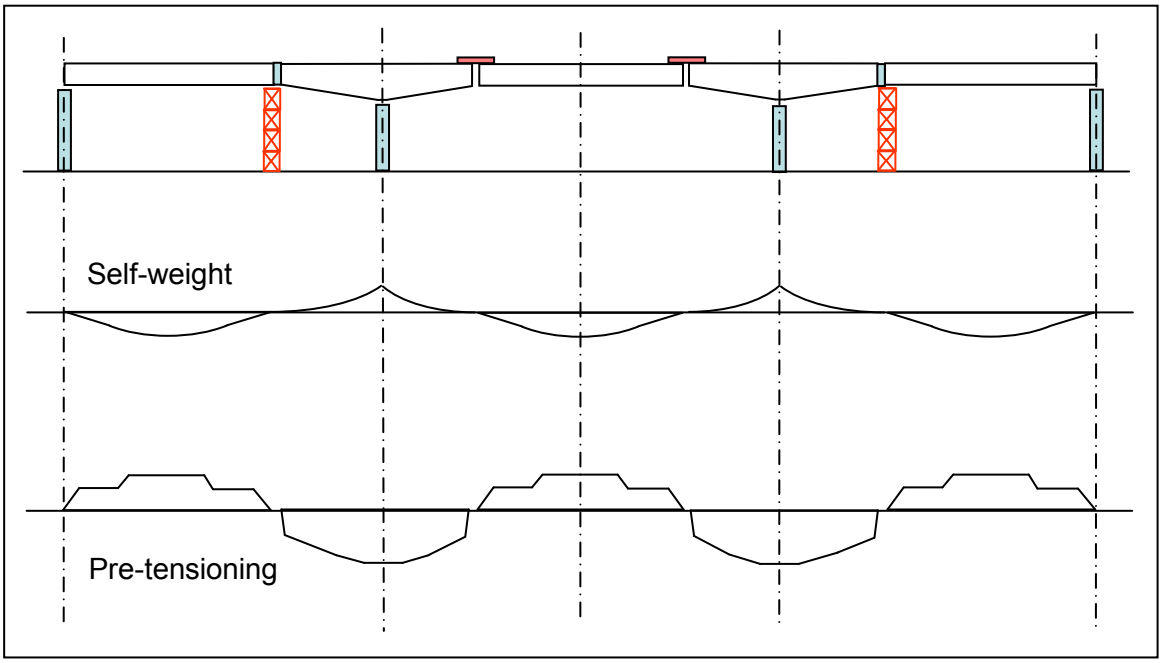

Figure 5.10.4.2-3 pliced Girder Construction - Self Weight and Pretensioning Moments

The reaction of the support tower needs to be determined. Initially, the reaction is statically determinate and equal to a portion of load from the self-weight of the end-span girder (Step 2). The reaction will change temporarily as the pier segment set in Step 3 is braced to the end of the end-span girder for stability (Figure 5.10.4.2-3). This reaction will change only slightly under Step 4. It will reduce under Step 5 (Figure 5.10.4.2-3) and will further reduce (perhaps lifting off) under Step 6 (Figure 5.10.4.2-4). The amount of reduction will depend upon the relative stiffness of the superstructure and support towers.

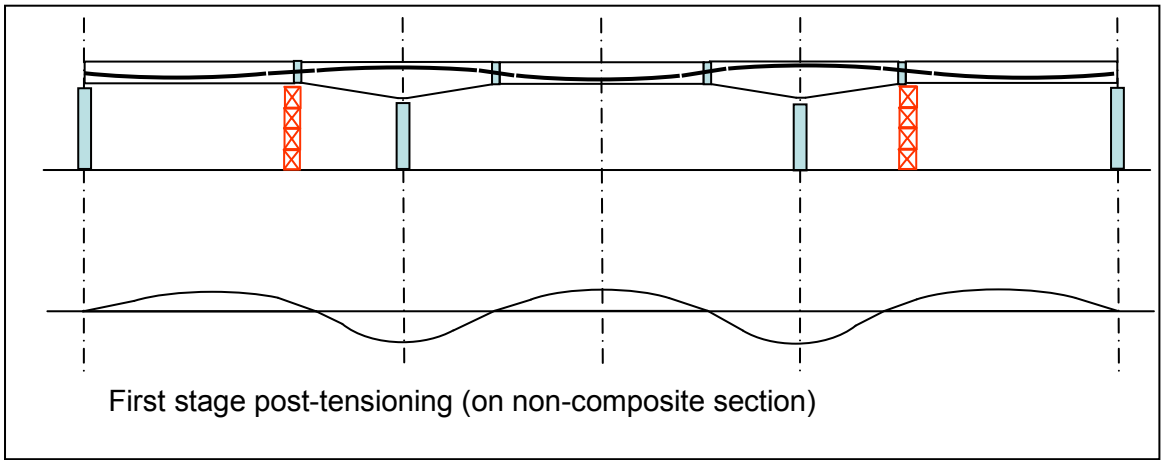

Figure 5.10.4.2-4 Spliced Girder Construction - Stage 1 PT Moments

The reaction will increase again under Step 7 (Figure 5.10.4.2-5) but will reduce (and might lift-off again) under Step 8. If it does not lift off at step 8, then removal of the residual (upward) reaction of the support tower imposes an equal and opposite (downward) load on the now completed continuous three-span structure. The important point here is that although use of the temporary tower began in a statically determinate condition, in this example, it is removed from a statically indeterminate structure. In such a circumstance, in order to determine the reaction, it is necessary to know or assume a vertical stiffness for the tower.

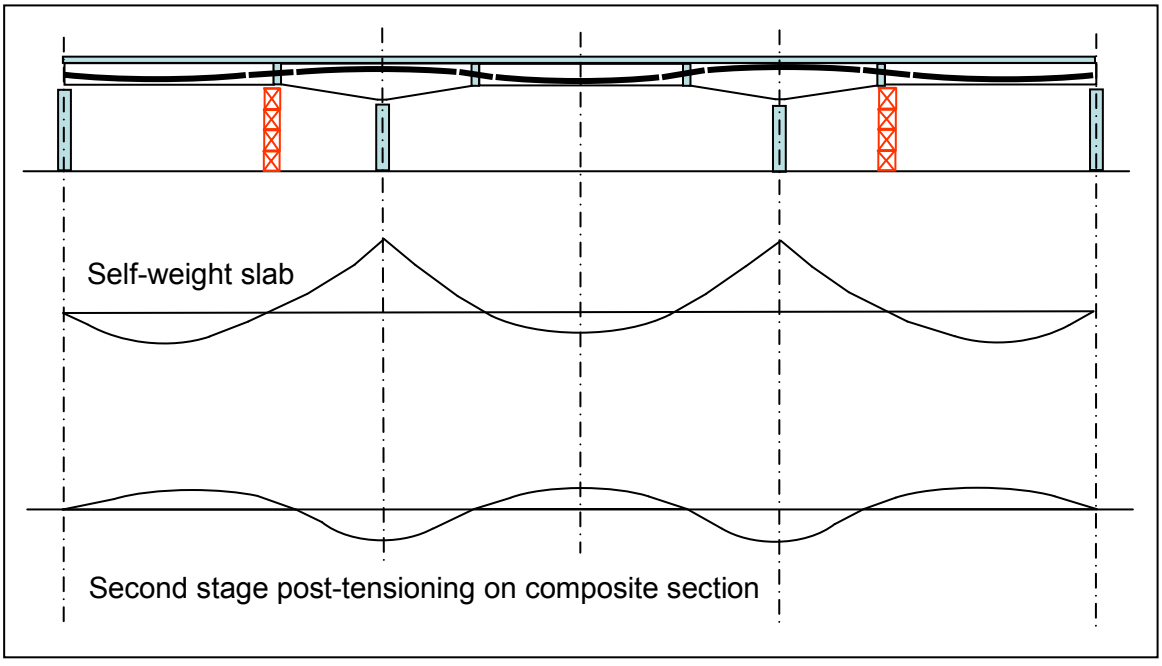

Figure 5.10.4.2-5 Spliced Girder Construction - Slab and Stage 2 PT Moments

On the other hand, if lift-off occurs at Step 6, and all subsequent loads can be carried safely by the superstructure and post-tensioning, then the maximum load on the tower occurs under Steps 2 through 5. The latter might be, approximately, statically determinate, if the precast lengths and support locations can be carefully proportioned by the designer.

Once the support towers are removed (either after Step 6 or Step 8), any residual reactions remaining in the towers must be applied as equal and opposite loads to the permanent continuous structure (Figure 5.10.4.2-6).

Obviously, safety is paramount for construction. Therefore, a Contractor should be given the opportunity to adjust proportions, support conditions and erection sequences for his elected means and methods of construction.

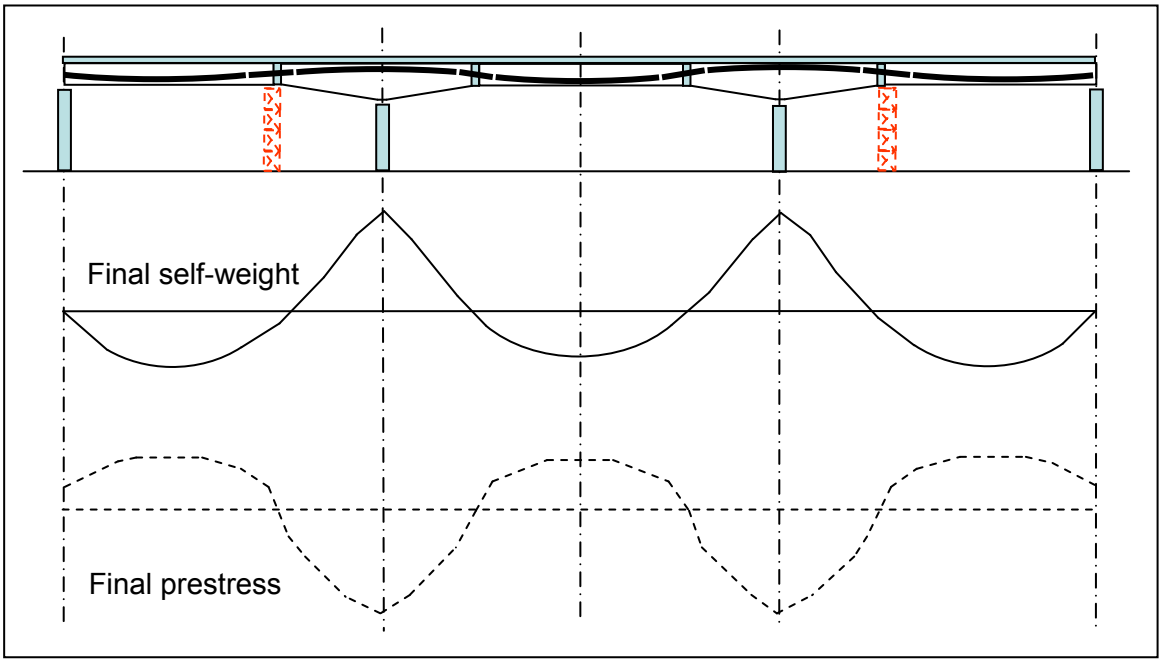

Figure 5.10.4.2-6 Spliced Girder Construction - Final Moments

Summarizing for design purposes:

- Each construction step should be identified and considered in calculations.
- Each time a load is added or the structure changed, forces, moments and stresses must be calculated and accumulated at each cross-section of interest.
- Creep recommences for each new loading, structural system and stress regime.
- Differential shrinkage of the deck slab and creep redistribution should be included.

- Use of temporary supports and their residual loads should be accounted for.

5.10.4.2.1 Longitudinal Analysis (Bending Moments and Shear Forces)

For any structure built in stages, longitudinal analysis must take into account the sequence of construction, the maturity of the concrete and the times at which key activities occur. This includes: making closures that change the statical structural configuration from simple to continuous spans; adding a span onto previously erected continuous spans; the introduction or removal of temporary supports and/or construction equipment loads; the sequence of pouring deck slab concrete; and the sequence of installing and stressing post-tensioning tendons.

Post-tensioning tendons extend from one end of a continuous superstructure to the other. However, because of loss of post-tensioning force due to friction between the tendon and internal ducts during stressing and other effects, the longer the structure, the less effective the prestress – particularly in the mid-region of a continuous-span unit where it is usually needed most. For this reason, the design layout should seek an effective balance between overall superstructure length and structural prestress requirements.

Precast girders are pretensioned sufficiently to carry their own self weight and some portion, but not all, of the subsequent structural dead load of the cast-in-place composite deck slab. Additional structural resistance and overall continuity for both flexure and shear is achieved by installing longitudinal post-tensioning tendons through the girders and splice joints from one end of the continuous superstructure to the other.

Bending moments from permanent superimposed dead load (i.e. barriers, utilities, surfacing) applied to the structure after it has been made continuous, may be determined from standard formulae or any appropriate analysis for continuous beams. It should be noted that since these loads are applied to the continuous structure, there is no subsequent redistribution of their effects by creep. Creep will cause increasing deflection (deformation) under their load, but because the load is constant, there will be no redistribution of bending moment.

In all other respects design utilizes the same concepts described previously for pre-tensioned girders, for example: effective cross-section; longitudinal pretensioning strands (for carrying all loads up to the time that additional resistance is provided by post-tensioning tendons); service and strength limit states for flexure and shear. Likewise, methods of longitudinal structural analysis for continuous girders are similar.

5.10.4.2.2 Continuity Effects

Continuity effects arise from the construction sequence (making continuity between spans), creep redistribution of permanent dead load and prestress secondary moments and differential shrinkage.

5.10.4.2.3 Application of Post-Tensioning Forces as Equivalent Loads

Loss of post-tensioning force from friction, wedge seating, elastic shortening, long-term creep and shrinkage are calculated for each section of interest along the superstructure using the same techniques as addressed in Section 5.7.3.

Force effects of draped post-tensioning may be applied to the continuous structure as a series of equivalent loads. In Figure 5.10.4.2.3-1 “P” is the effective force (usually taken after all losses) at any section of interest along the tendon. P varies along the tendon since it is reduced by friction loss. The vertical force that a tendon exerts on the concrete from the curve profile is p = P/R per unit length, where R is the radius of curvature. (The instantaneous radius at any location is the second derivative of the geometric profile.)

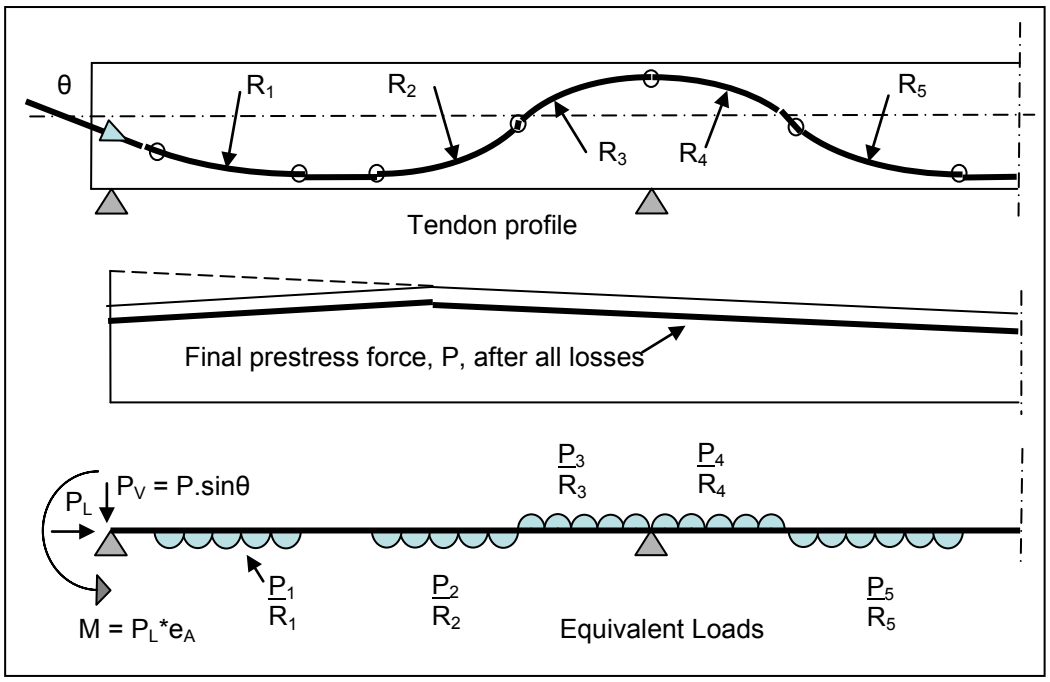

Figure 5.10.4.2.3-1 Equivalent Loads Represent Post-tensioning Effects

Numerically, for calculation purposes it is usually convenient to divide a profile into portions over which the force and radius may be assumed to be constant and into portions that exert upward or downward effects. This leads to a set of equivalent

loads of the type illustrated. This is repeated for each tendon, as necessary. A refinement would be to account for the actual eccentricity of a compacted bundle of strands within a duct and the true points of contact within of the tendon within the duct trajectory.

At an anchorage, there is both a longitudinal (horizontal or axial) component, P_L = Pcos θ where "P" is the (final) prestress force applied at eccentricity (e_A) at the anchor from the neutral axis. This gives a moment of P_L*e_A and vertical component of force P_V = Psin θ if a tendon terminates at a longitudinal slope of θ.

The illustration shows a structure of constant depth. For a structure of variable depth, equivalent loads (e.g. "P/R") should be determined according to the absolute (global) geometric tendon profile and then applied to a model of the bridge whose nodes preferably vary in elevation to follow the profile of the neutral axis. For hand calculations, the latter may not be feasible and an approximation is made where all the nodes are at the same elevation. Regardless, the eccentricity of a tendon (e) is taken relative to the actual neutral axis at each cross-section of interest.

At a deviation location, where a tendon may change direction rather sharply, the vertical force may be taken as the difference between the vertical components of force on one side of the deviator versus that on the other and approximated to an equivalent point load applied at the center of the deviator. (Deviators are used primarily for external tendons in box girder construction where tendons may have a 3D trajectory out of the plane of a web. In such a case there would be both a lateral and longitudinal force difference to take into account.)

After determining equivalent post-tensioning loads for each tendon the structure is analyzed as a continuous beam subject to the various combinations of equivalent load making up one or all tendons to provide the resulting bending moments, shear forces and reactions. From these, it is possible to determine "Secondary Moments" due to prestress as follows.

5.10.4.2.4 Secondary Moments from Prestressing

Secondary effects invariably reduce the effectiveness of the prestressing system. However, if the net prestressing profile (combination of pretensioning and post-tensioning) leads to a final condition where there are no secondary effects, the profile is said to be "concordant". In practice, it is easier to attain a concordant profile when all the prestress is provided by post-tensioning (as in the case of cast-in-place construction on falsework – Section 5.10.5) rather than by a combination of straight pretensioning and draped post-tensioning strands as discussed in this section.

In a continuous structure, post-tensioning induces secondary reactions. The magnitude of these reactions depends upon the trajectory of the tendons (and the

resulting equivalent loads derived to model their effects.) A means to determine the secondary reactions is to apply the equivalent loads for each tendon profile to the (weightless) continuous structure and calculate the resulting reactions using classical beam theory or a continuous beam program.

If we were to do this for the four-span structure in Figure 5.10.4.2.4-1, we would find non-zero reactions at each of the five supports. Some reactions would act upwards and some downwards – but the sum of all reactions would be zero. The bending moment diagram calculated from the resulting reactions alone (which is linear from pier to pier) gives the "Secondary Moment" (M_{sec}) due to prestress at any section of interest. The primary bending moment due to prestress at any location is the effective prestress force at that location multiplied by its eccentricity (e) from the neutral axis of the member (i.e., $M_{primary} = P_{eff} * e$). This is obtained directly from the position of the tendon profile relative to the neutral axis.

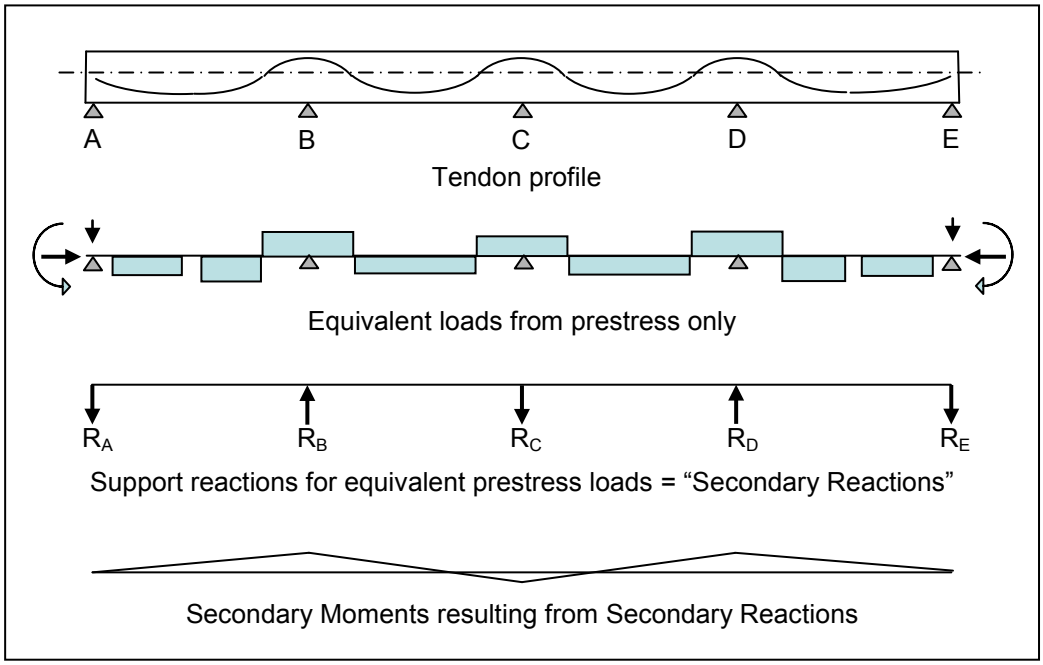

Figure 5.10.4.2.4-1 Secondary Moments from Prestress

If tendon profiles can be so arranged with a careful balance between upward and downward equivalent loads and eccentric moments at the anchors, so that each of the support reactions is zero, then there are no secondary reactions and no secondary moments. In such a case the profile is said to be "concordant". Although theoretically possible, this is very difficult to achieve in practice, so secondary reactions and moments are encountered in most post-tensioned structures. Even so, secondary effects can be minimized by using properly draped tendon profiles.

In strength resistance calculations, a load factor, γ_P = 1.0, is applied to the moments and shear forces from secondary effects and the results are added algebraically to the factored moments and shears due to dead and live loads. Secondary moments are considered under the term "EL" for accumulated locked-in construction effects per *AASHTO LRFD* Article 3.3.2 and Table 3.4.1-1.

5.10.4.2.5 Creep and Shrinkage - General

After stressing, shrinkage and creep will cause a loss of post-tensioning force. However, for a structure built entirely on falsework that is removed after construction, creep will cause an increase of the initial elastic deflection with time, but there will be no redistribution of bending moments or forces due to creep. The final long-term deflections (Δ_∞) are given by:

$$\Delta_\infty = \Delta_i * (1 + \varphi)$$

where:

Δ_i = Initial elastic deflection at transfer and removal of falsework
φ = creep coefficient (usually between 1.5 and 2.5; φ depends upon material properties and environmental characteristics, etc.)

For a structure built in stages a separate analysis or model is needed for each stage – i.e., first a single span, then two spans, then three spans and finally 4 spans, where the additional cast-in-place span (namely span 2, then 3, then 4) and associated post-tensioning is added at different intervals of time and maturity of previously cast concrete. The summation of the four stages represents the condition at the completion of construction. Not only will there be loss of prestress due to shrinkage and creep, but also, because of the staged construction, creep induced deflection will cause a redistribution of bending moments, shear forces and reactions. The final bending moments (M_∞) are given by:

$$M_\infty = M_{const} + (M_{inst} - M_{const})*(1 - e^{-\Phi})$$

where:

M_{const} = moments at end of construction (e.g. after release of span 4)
M_{inst} = moments as if the entire permanent structure had been cast on falsework, post-tensioned and released "instantaneously"

As can be seen, the form of the above equation for creep redistribution is the same as that discussed previously, because the driving effect (creep) is the same phenomena.

5.10.4.2.6 Creep and Shrinkage – Redistribution Effects

For structures made continuous with post-tensioning, redistribution of moments occurs similar to that for simple spans made continuous with (mild steel) reinforced joints – except that the redistribution is driven by the difference between the combination of pre- (if any) and post-tensioning effects and dead load.

In post-tensioned spliced I-girder structures, similar losses are experienced as in pretensioned structures, but of a different order of magnitude due to differences in the maturity of concrete and the sequence and timing of construction and application of post-tensioning.

For instance, if a girder is pre-tensioned for its own self-weight (and possibly for a portion of the deck slab dead load) it experiences the same initial loss in the casting bed. It then experiences the same losses due to shrinkage, creep and steel relaxation from the time of transfer as for any pre-tensioned girder. Under its own self weight and pretensioning, these losses continue to increase while the girder is erected and splice joints are made, up to the time that the first stage of any post-tensioning is installed. This changes the internal stress regime in the girder. Losses are calculated for this new stress regime up to the time that the deck slab is cast and the non-composite girder section alone carries the additional weight of the (wet) deck slab and any formwork or stay-in-place forms. This again changes the stress regime so new losses are experienced up to the time when the next (and usually final) post-tensioning is installed. The final stage of post-tensioning acts upon the now composite section. But this again changes the internal stress regime so creep, shrinkage and relaxation loss are recalculated from this point onward.

However, in a post-tensioned girder, additional losses are experienced at the time of installation and stressing of the tendons. These losses arise from the effect of friction between the tendon and the duct and from the effect of seating of anchor wedges, at the time of stressing. It is necessary to determine the magnitude of this loss and to properly account for it in the design.

5.10.4.2.7 Construction Sequence Effects

There is no unique or standard nomenclature for either major or intermediate construction activities or steps. Common terms include “construction step”, “construction phase” or “construction stage”. The techniques are often referred to as “phased construction”, “staged construction,” or similar. For illustration purposes herein the term “construction step” is used.

A Designer has to assume sequences and times for key activities according to a likely construction schedule. Engineering judgment is necessary; there is no absolute right or wrong answer. For instance, if it is expected that differential shrinkage effects between the slab and girder are likely to be significant, then it would be reasonable to assume a long time (say a year) between casting (t0) and

erecting (t1) girders. On the other hand, if a project is on a speedy schedule where girders are made and delivered just ahead of superstructure construction, then a shorter time interval (say 28 days) would be appropriate.

For design purposes it is usually sufficient to identify certain “key activities” as given in the two examples below. For an actual structure it may be necessary to examine some of these in greater detail. For instance, casting the deck slab (activity 5 in the first example and 7 in the second example) may need to be divided into several sub-activities for each of the anticipated deck slab pours, depending on the size of the structure and concrete delivery. Each activity then becomes a discrete “construction step”. Clearly, a large project may require many such discrete “construction steps”. The “key activities” in these examples are the significant points where a major event happens – new concrete is cast or loaded, or a change of structural continuity occurs - as such, they possibly indicate the fewest steps to consider.

Long term conditions after which all creep and shrinkage effects are assumed to have taken place (i.e., time t_∞) is conventionally taken as about 10 years or 4,000 days.

5.10.4.3 Construction

When precast girders are designed to span from pier to pier with splice joints at diaphragms over those piers (Figure 5.10.4.2-1), the erection of each individual girder is straightforward as for a simply-supported structure. However, when splice joints are located within spans, temporary supports are necessary. Often this requires one or more temporary falsework towers, depending upon the locations of splice joints. Alternatively, in some cases, special devices may be used to suspend partial length girders from an already erected (cantilever) portion of the structure (Figure 5.10.4.2-2).

Ducts for post-tensioning are usually set to a draped profile, being in the bottom flange of the girders at mid-span and in the top over interior piers. At cast-in-place joints, the ends of ducts are spliced together. It is preferable that this be done using special couplers or connectors that provide a continuously sealed duct for enhanced durability. After casting the splice joints, longitudinal post-tensioning tendons are installed in each duct from one end of the continuous-span superstructure to the other. It is usually necessary to stress the tendons in phases. For example, if there are four tendons per web, two of them may be tensioned before, and two after the deck slab has been cast and cured.

Since the final superstructure is structurally continuous over several spans, deck slab casting should proceed in a sequence that applies most of the load to positive (mid-span) moment regions first, then finishing with portions of the slab at negative

moment regions over the piers. This sequence, along with proper curing, is essential in order to eliminate or minimize potential transverse cracking of the deck slab.

Staged construction involving the sequential erection of precast girders, the use and removal of temporary supports, tendon installation and tensioning tendons in phases and the special casting sequence of the deck slab is essential in order to maintain stresses within acceptable limits and provide the required structural resistance. This “staged-construction” process is a very significant feature of this particular type of bridge. It must be properly taken into account during design and it must be faithfully executed during construction.

Attention to workable details is essential. The diameter of the tendon ducts must be limited to that which can be accommodated within the width of the web while leaving sufficient space for reinforcement, maximum aggregate size, fabrication tolerances and proper consolidation of concrete so as not to create local honeycomb voids or defects. This limitation on duct diameter automatically limits the size and number of strands that may be used to make up a tendon. In turn, this limits the maximum available tendon force, service stresses and strength resistance. Widening the web may relieve such limitations but only at the expense of additional weight. The use of vertically elongated (oval) ducts is not recommended because strands bear against the duct walls and exterior web cover when tensioned. This has caused longitudinal cracks and local web spalls in the past. Similar problems have also been encountered with circular ducts when crimped by rebar or badly aligned.

Splice-joints themselves need to be sufficiently long to facilitate alignment of tendon ducts from one precast girder to the next. A portion of duct will likely need to extend from the end of each girder in order to facilitate installation of a duct coupler to complete the splice. Cast-in-place splice joints over piers become an integral part of a transverse diaphragm. At intermediate splice locations within a span, a transverse diaphragm may or may not be necessary. Mild steel reinforcing usually extends from the ends of the precast girders into the splice and is supplemented by additional rebar as necessary.

At girder ends, webs typically flare to a width sufficient for anchor blocks to accommodate tendon anchorages and all necessary anchor-zone reinforcement. For all the above aspects, proper attention to design and detailing is essential for an efficient, practical and constructible solution.

The key aspects of spliced-girder construction are best illustrated by the two examples presented later in this section. In most other respects, such as formwork, placing and tying reinforcement, pouring, curing and finishing concrete, the construction of precast girder superstructures made continuous with post-tensioning employs techniques common to simply-supported girder construction.

5.10.4.3.1 Installation of Bearings, Lifting and Placing Girders (Lateral Stability)

In general, spliced-girder construction utilizes relatively long, slender I-girders. Most cross-sections for this type of application have wide top flanges that improve lateral stability. The installation of bearings and the lifting and placing of slender girders should always be done with care and attention to details and procedures. Temporary transverse bracing is usually necessary to prevent rolling of the girder.

5.10.4.3.2 Typical Layout and Construction of a Constant Depth, Four-Span Continuous Unit

Structures of this type are typically made from precast girders with individual lengths of 100 to 150 feet or so depending upon the particular girder section. A completed four-span unit may be 400 to 600 feet long or thereabouts.

A four-span continuous superstructure is made by first erecting girders spanning from pier to pier as with a simply-supported structure. Temporary lateral cross bracing or the construction of permanent transverse diaphragms between parallel girders is installed to prevent lateral instability or toppling – especially if the girders are slender or top heavy.

Longitudinally, girders are pretensioned for their own self weight and to help carry some, but not all, of the weight of the cast-in-place slab. Longitudinal post-tensioning is necessary to provide the capacity for additional slab, superimposed dead and live load. Tendons are installed to a profile that drapes from anchorages in the very ends of the continuous four-span unit, into the bottom flange in the positive moment (in-span) regions and up to the top over the interior piers (Figure 5.10.4.3.2-1).

When the spliced joints have been cast and cured, the first stage of post-tensioning – usually one half of the number of tendons – is stressed to impose a force solely upon the precast-girder section alone. This provides the section with the capacity to carry the load of the deck slab.

A feature of this particular erection technique is that each interior pier has a double row of bridge bearings – one under the end of each original precast girder. This creates a moment connection between the continuous superstructure and pier. The stiffness of the connection depends upon the vertical stiffness of the bearings and their lever arm (i.e., separation distance.) This moment connection and stiffness of the substructure should be appropriately taken into account for structural analysis of loads applied after continuity has first been made and the first stage post-tensioning installed.

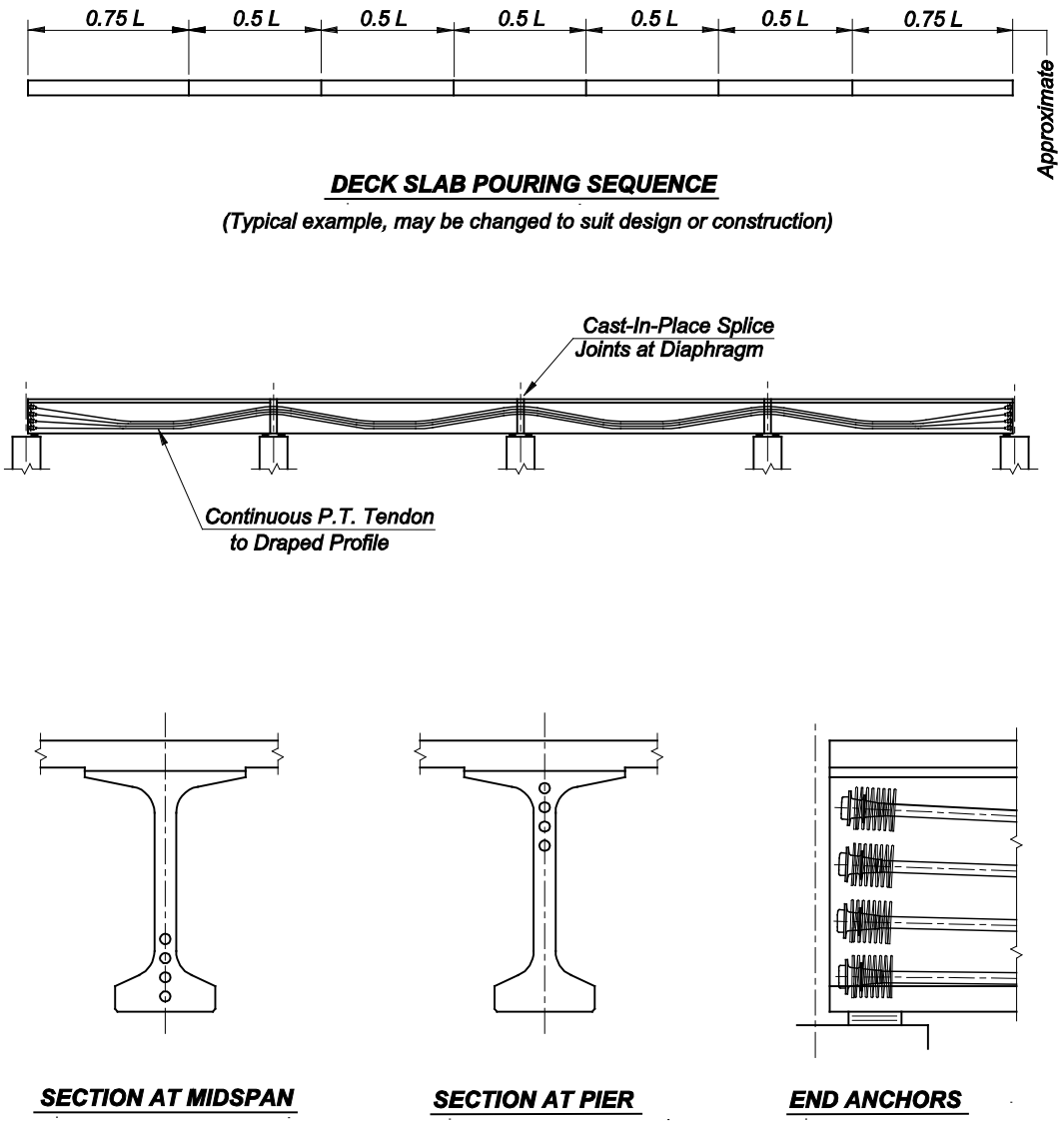

Figure 5.10.4.3.2-1 Post-Tensioning for Four-Span Continuous Girder Spliced at Piers

The next construction step is to form and install reinforcement for the deck slab. The slab is then cast in a pre-determined sequence – beginning with portions in positive moment regions and ending with those in negative moment regions over interior piers. The sequence in the figure is an example – a different sequence may be feasible and should be adapted according to the particular project.

When the deck slab has cured and gained sufficient strength, the remaining tendons are stressed. This second stage of post-tensioning applies prestress force to the composite section of the girder and the effective portion of the deck slab. The structure is now fully continuous for subsequent superimposed dead and live load.

Finally, the superstructure is completed with the installation of traffic barriers, wearing surface and utilities as necessary.

5.10.4.3.3 Typical Layout and Construction of a Three-Span Haunched Girder Unit

A girder deepened over the piers facilitates a longer main and side-spans in a typical three-span continuous unit (Figure 5.10.4.3.3-1).

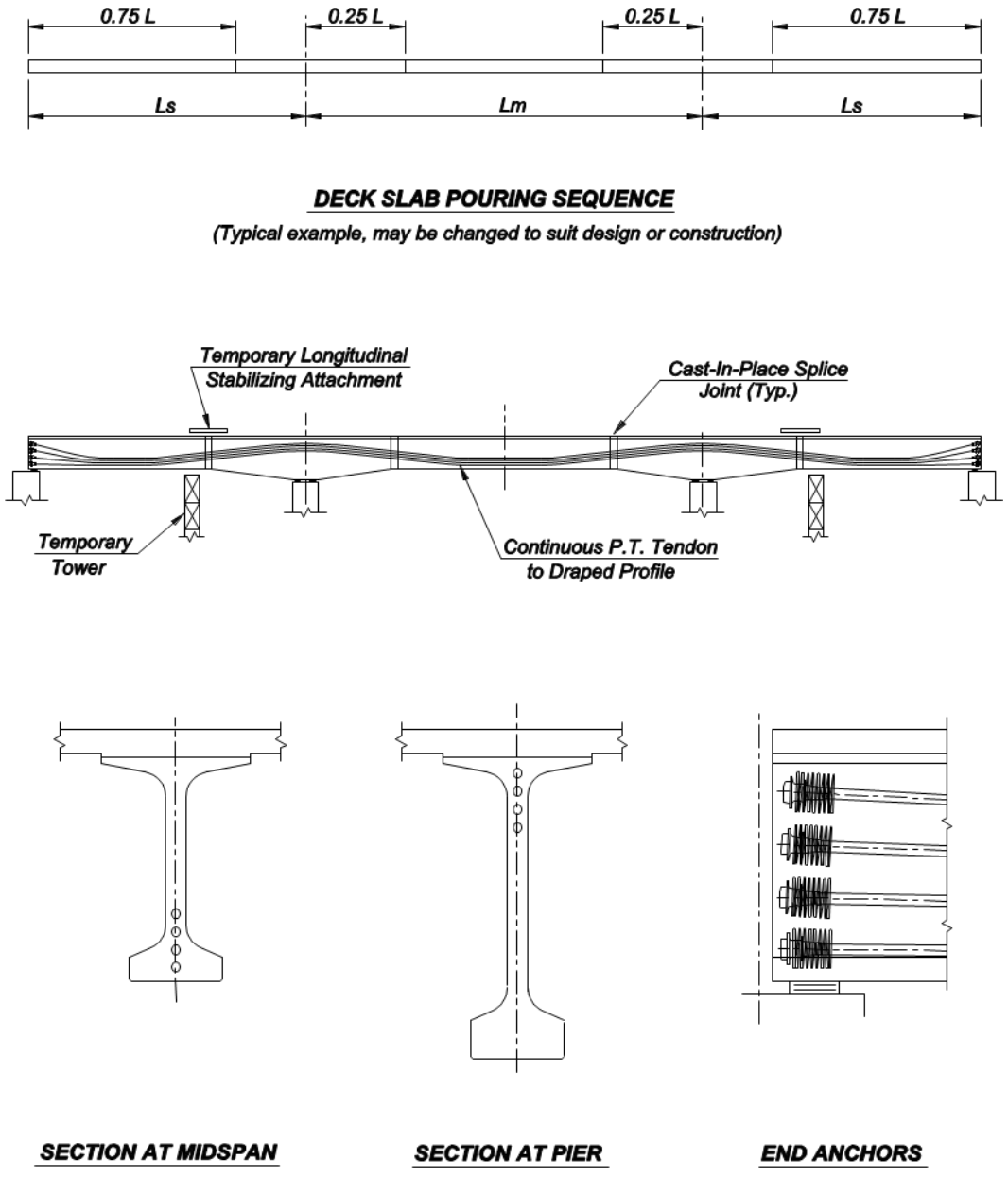

Figure 5.10.4.3.3-1 Post-Tensioning for Three-Span Haunched Girder Unit

This span configuration is often used for the main-span unit of a bridge over a navigation channel or similar situation. It is limited by the length and weight of splice girder portions to be precast, delivered and erected. It is relatively efficient for main spans of 200 to 250 feet, but longer spans (up to 350 feet) are possible, although they require heavier and far less efficient components. As side spans usually range from about 60 to 75% of the main span, the total length of a three-span unit might range from about 500 to 750 feet.

Longitudinal post-tensioning is essential because the precast girder portions themselves have insufficient pretensioning to carry little more than their own self weight. They cannot carry the weight of the deck slab or any live load without post-tensioning. Post-tensioning tendons follow a draped profile - being in the bottom flange of the girders in the positive moment (in-span) regions and in the top over the piers.

Longitudinally, erection proceeds in stages until all cast-in-place splices have been made connecting each precast girder continuously from one end of the three-span unit to the other. Post-tensioning is also installed in stages, before and after casting the deck slab. Typical construction stages are broadly illustrated in Figure 5.10.4.3.3-2.

Temporary supports and bracing are essential. Erection of the partial-length precast girders requires temporary towers or piers and devices to longitudinally stabilize the haunched cantilever portions over the main piers. Additional temporary lateral cross bracing or the construction of permanent transverse diaphragms between parallel girders is necessary to prevent lateral instability or toppling – especially for long slender girders.

Variations in the location of temporary towers, sequence of erecting girders, installing post-tensioning tendons and pouring the deck slab are possible. This type of construction requires an appropriate sequence be assumed for design. The assumed sequence should be shown on the plans.

After the precast girders have been erected and spliced to be continuous, the first stage (usually half) of the longitudinal post-tensioning is installed and stressed, acting on the precast section alone with no deck slab. This first-stage provides the precast section the capacity to carry the additional dead load of the deck slab itself.

Then, formwork and reinforcement for the deck slab is installed. The slab is cast in a specific sequence - beginning with the portions in positive moment regions and ending with those over the piers - as illustrated. Establishing and maintaining such a sequence is vital as variations significantly affect the resistance and performance of the final structure.

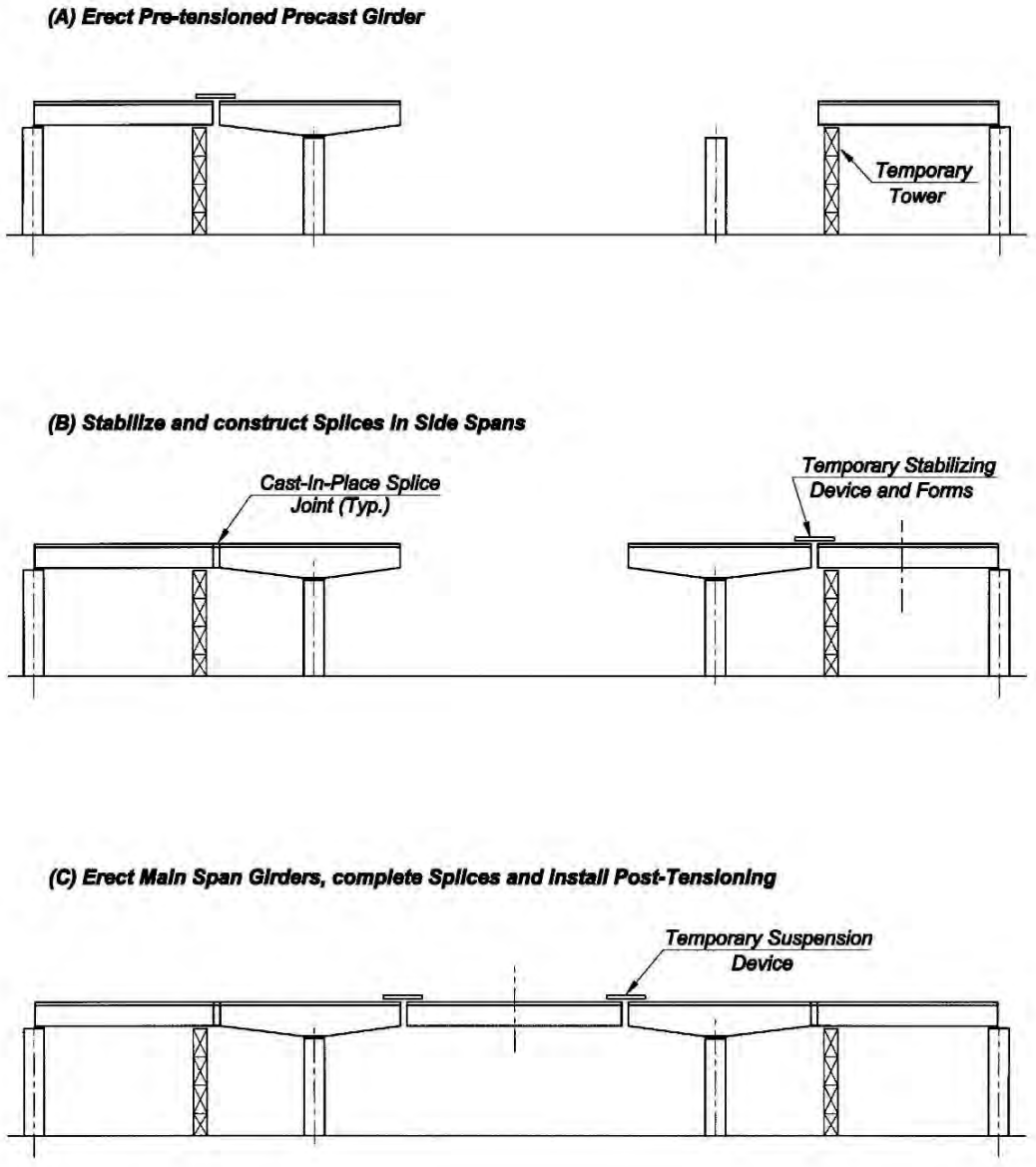

Figure 5.10.4.3.3-2 Erection of Precast Girders for Three-Span Unit

After the deck slab has cured and gained sufficient strength, the remaining tendons are stressed. This second stage post-tensioning applies prestress to the composite section of the girder and effective portions of the deck slab and makes the superstructure fully continuous for subsequent superimposed dead and live load. Traffic barriers, wearing surface and utilities are installed as necessary.

The following construction sequence is typical for the above example:

1. Construct pier and erect temporary tower in side-span
2. Place side span girder on pier and temporary tower (A)
3. Laterally install cross-braces or permanent diaphragms to stabilize girders
4. Erect haunched girder on main pier
5. Longitudinally stabilize haunched girder to side span girder (B)
6. Laterally install cross-braces or diaphragms to stabilize haunched girders
7. Make PT duct connections, install rebar, form and cast splice
8. Repeat above sequence for other side-span of unit
9. Erect main “drop-in” span girder with attachments to haunched girders (C)
10. Make PT duct connections, install rebar, form and cast splice
11. Install and tension first stage longitudinal PT tendons
12. Complete any remaining permanent diaphragms
13. Form deck slab, place reinforcement
14. Cast deck slab in sequence, finish and cure as necessary
15. Install and tension second (final) stage longitudinal PT tendons (see subsequent section titled, “Phased Post-Tensioning and Future Deck Replacement”)
16. Grout tendons, seal and protect anchorages

The above sequence is only an example. A different sequence may be necessary for a particular structure or to accommodate a Contractor’s elected means and methods of construction.

Administratively, for any type of continuous structure built in stages, changes from an assumed construction sequence shown on the plans to one that accommodates a Contractor’s elected means and methods, should be reviewed by the Engineer via a “Shop Drawing” process. Alternatively, if a change is sufficiently significant, a “Value Engineering Change Proposal” process may be more appropriate. For contract administration purposes, guidance should be offered on plans or in project specifications as to the structural nature of a change that would make it sufficiently significant to warrant the latter as opposed to the former. Final construction should be in accordance with agreed and approved procedures.

5.10.4.3.4 Phased Post-Tensioning and Future Deck Replacement

In regions of the country where the corrosion of deck reinforcement resulting from freeze-thaw cycles and the use of de-icing chemicals cause premature deck deterioration, some owners require that bridges be designed for full-depth deck replacement. However, for bridges where post-tensioning tendons have been stressed after the deck is cast, the complete removal of the deck in the future has significant consequences for the bridge. The removal of the prestressed area of the deck, and its associated dead load, may lead to significant overstress or even

possible failure of the girders. Furthermore, the precompression that existed in the original deck is lost, so the replacement deck is not expected to have the same life expectancy as the original precompressed deck.

In regions where deck replacement is typically considered in bridge design, there are three basic approaches to address this issue for spliced girders:

1. Require design for deck removal and prohibit stressing of post-tensioning tendons with the deck in place.
2. Require design for deck removal but allow stressing of post-tensioning tendons with the deck in place.
3. Allow stressing of post-tensioning tendons with the deck in place, but use alternate deck protection or rehabilitation measures to avoid complete removal of deck during the service life of the structure (e.g. high-performance concrete; integral overlay for partial depth replacement; sacrificial overlay; overlay with waterproof membrane.)

See NCHRP Report 517, “Extending Span Ranges of Precast Prestressed Concrete Girders,” Transportation Research Board, Washington, DC, 2004 for further discussion concerning this issue.

5.10.4.3.5 Tendon Grouting and Anchor Protection

After post-tensioning tendons have been installed and stressed, they must be properly grouted and the anchorages sealed and protected to ensure long-term durability.

With staged construction it may also be necessary to take temporary measures to protect tendons if a long period is anticipated between the first and second stage of post-tensioning. Measures might require, for example, opening duct drains, sealing grout vents and installing temporary caps on anchorage devices. The use of corrosion prevention chemicals should be in accordance with established practice and specifications. Such measures are an alternative to grouting the first stage immediately after stressing as there can be a potential risk of cross-grouting between internal ducts. Grout blockage might prevent further tendon installation or might trap tendons yet to be stressed.

Along with concrete cover and the deck’s role as a barrier to infiltration, completely filling a duct with grout is essential for ensuring protection of a post-tensioning tendon. Grout should be of an acceptable quality, mixed and injected carefully under controlled conditions to fill the duct. Grout material should have “no-bleed” properties to reduce or eliminate air and moisture voids. Injection should continue until all slugs of air and moisture have been expelled and the grout at the outlet is of a similar consistency to that at the inlet. Injection should proceed from low points, and

intermediate vents may be needed along the profile of a tendon. Outlets should be inspected for complete filling. During construction grouting should be done within a reasonable and short timeframe so as to minimize exposure risk of tendons after tensioning. At all times appropriate quality control and records should be kept.

Anchorages should also be completely filled with grout during the grouting process. In addition, components and details should enhance sealing and protection of the tendon. Anchor devices may need permanent concrete cover blocks (pour-backs) and additional sealing with suitable materials such as epoxy or elastomeric coatings.

All grouting and protection requirements should be addressed via appropriate details and notes on plans and in project specifications. For comprehensive information on the installation, stressing, grouting and protection of post-tensioning tendons and anchorages, including recommendations for the location of grout injection ports, vents, laboratory and field tests, quality control and records, etc., refer to "Post-Tensioning Tendon Installation and Grouting Manual," Second Edition, available from the Federal Highway Administration. Additional information is available from the Post-Tensioning Institute.

5.10.4.3.6 Deck Forming Systems

Deck forming systems for superstructures with girders made continuous with post-tensioning, are the same as for any other type of girder construction.

5.10.4.3.7 Rebar Placement

Rebar placement for superstructures of girders made continuous with post-tensioning are the same as for any other type of girder construction.

5.10.4.3.8 Deck Concreting and Curing

With the very important exception of the need to follow a predetermined sequence of placing deck concrete, superstructures of girders made continuous with post-tensioning are the same as for any other type of girder construction.

5.10.5 Cast-in-Place Box Girders and T-Beams

5.10.5.1 Introduction

This section is concerned primarily with post-tensioned superstructures built cast-in-place on falsework. This was the type of construction used when post-tensioning systems first became widely available in the 1950's. It is also a method of construction (cast-in-place boxes) that is widely used today in California, Nevada and other primarily western states. Many of the concepts involved in design and

construction have been described in other sections, however, there are some key aspects specific to this type of structure that deserve mention.

5.10.5.2 Longitudinal Analysis and Design

According to *AASHTO LRFD* Article 4.6.2, cast-in-place multi-cell concrete box girder bridge types may be designed as "whole-width" structures. In such closed sections, load sharing between "girders" is high and torsional loads are hard to estimate. Prestress should be evenly distributed between the girders and cell width-to-height ratios should be no more than about 2:1. The effects of the loss of area due to the presence of ducts prior to bonding (grouting) of tendons should be considered. After grouting, section properties may be taken on the gross or transformed section (*AASHTO LRFD* Article 5.9.1.4.) In this respect, the transformed section is that where the prestressing steel is taken as an equivalent area of concrete given by the area of steel multiplied by the modular ratio of steel (E_s) to concrete (E_c).

Superstructures of multi-cell boxes may be of constant or varying cross-section. Variation may result from variation in thickness of flanges, variation in overall depth or change of overall width as may occur, for example, at gore areas. Longitudinal moments, shear forces and reactions may be determined by any classical analysis technique for continuous beams or by using a continuous beam analysis computer program. Post-tensioning forces may be applied to each "girder line" as equivalent loads calculated following the outline above.

Other appropriate methods of analysis include a three-dimensional finite element models using, say, plate elements or a space-frame or grillage. Such methods would be particularly appropriate for structures of variable width or other changing geometry.

5.10.5.2.1 Differences between Continuous and Simply-Supported Structures

For continuous prestressed superstructures there are subtle differences in flexural limit states compared to simply-supported superstructures. The most obvious and significant difference is negative moment over interior supports. Negative moments from gravity loads, such as self-weight, superimposed dead load and live load, create flexural tension in the top fiber and compression in the bottom fiber at support regions.

The use of a draped post-tensioning layout where the tendons are low down in the section within a span and high up over the supports is purposefully intended to provide compressive stress where it is most needed - to offset permanent tensile stress from loads. It also minimizes the magnitude of adverse secondary moments from prestress.

5.10.5.2.2 Application of Vehicular Live Load

Live load effects may be determined using the approximate methods of analysis using the applicable cross section (d) of Table 4.6.2.2.1-1. By this method, a multi-cell box is treated as series of individual girders with section properties comprised of the web, the overhang of an exterior web and the associated top and bottom half-flanges between the web considered and the adjacent web. The procedure is closely analogous to that for beam and slab decks, but the distribution factors are formulated differently.

For negative moment and support reactions at interior piers, there is a particular nuance in the *AASHTO LRFD* Article 3.6.1.3.1, bullet point 3. Namely, that for negative moment between points of contra-flexure, 90% of two trucks spaced a minimum of 50 ft apart along with 90% of the effect of the design lane load shall be checked for negative moment. For this purpose, the points of contra-flexure correspond to that determined by applying a uniform load on all continuous spans.

Distribution factors for live load moment in an interior and exterior girder are taken according to Tables 4.6.2.2.2b-1 and 2d-1 respectively for the applicable section (d). If supports are skewed, distribution factors for moment may be reduced according to Table 4.6.2.2.2e-1.

Distribution factors for live load shear in interior and exterior girders are taken according to Tables 4.6.2.2.3a-1 and 3b-1 respectively for the applicable section (d). If the supports skewed, distribution factors for shear at the obtuse corner are reduced according to Table 4.6.2.2.3c-1.

5.10.5.2.3 Longitudinal Flexure Design

5.10.5.2.3.1 Service Limit State

At the service limit state, flexural stress limits for continuous structures are the same as for simply-supported structures (*AASHTO LRFD* Article 5.9.4), the only difference being that these are now applied to the top or bottom fiber as the case may be. Stresses due to secondary moments should be calculated and added to other effects as necessary. In continuous structures thermal gradient (TG) can induce additional tension over interior supports – presenting difficulties for some structures and load combinations.

5.10.5.2.3.2 Strength Limit State

Applying a load factor of 1.0, secondary moments due to prestress must be added to the factored load (or deducted from the factored resistance) when checking the strength limit state in continuous prestressed structures. With this particular exception the calculation of the flexural resistance of a cross section itself is otherwise the same as for any prestressed girder and may be determined as outlined in *AASHTO LRFD* Article 5.7.3.

In support (negative moment) regions of large single-cell and multi-cell box girders, it may be necessary to use formulae for flanged sections (*AASHTO LRFD* Article 5.7.3.2.2) as the compressive zone can extend higher than the thickness of the bottom slab. This depends upon the proportions of the section, lever-arm, and tensile elements. If negative moment resistance is not quite sufficient, local thickening of the bottom slab may offer a solution. In many structures, particularly single-cell boxes with large deck widths, the compressive zone may lie entirely within the depth of the top slab in positive moment (in-span) regions, thereby simplifying resistance calculation to that of a rectangular section (*AASHTO LRFD* Article 5.7.3.2.3).

5.10.5.2.4 Contribution of Mild-Steel to Flexural Resistance

In post-tensioned structures cast-in-place on falsework, continuous longitudinal mild-steel distribution reinforcement is usually provided for shrinkage, temperature and crack control. This reinforcement may be counted toward flexural strength resistance, if necessary, in both positive and negative moment regions.

5.10.5.2.5 Redistribution of Negative Moment at the Strength Limit

AASHTO LRFD Article 5.7.3.5 addresses this issue. If tensile steel (in this case prestress steel) in the negative moment region exceeds the net tensile strain (ε_t) of 0.0075, the moment determined by elastic theory at the strength limit state may be reduced by a percentage not greater than $1000\varepsilon_t$ or 20% at that section. In order to maintain equilibrium, positive moments must be adjusted to account for the change in negative moments. Positive moment resistance should be checked for the redistributed amounts.

5.10.5.2.6 Longitudinal Shear Design

5.10.5.2.6.1 Service Limit State

Design for shear at the service limit state is not currently a requirement of *AASHTO LRFD*. However, based upon ongoing discussions, the specifications may be revised to require a service limit state check of principal tension stresses in the webs of post-tensioned structures. High shear forces can cause diagonal cracking in webs as the result of these stresses. The magnitude of the effect can be determined by applying

classical theory using Mohr's circle for stress. Limiting the principal tensile stress to between 0.110 and $0.125\sqrt{f'_c}$ (ksi) at the elevation of the neutral axis has traditionally and conveniently been used to establish an approximate web thickness for durability and detailing purposes.

Where torsional shear stress effects are significant relative to vertical shear stress, a convenient approach is to consider the combined magnitude of the torsion and vertical shear stress at the elevation of the neutral axis in the worst loaded web.

5.10.5.2.6.2 Strength Limit State

AASHTO LRFD shear design using Modified Compression Field Theory has been covered in Section 5.6 for precast, pretensioned girders. Shear design for continuous, post-tensioned members is very similar with a few refinements.

In a simply-supported girder, or any statically determine structure, internal forces from the prestressing do not cause reactions at the supports. However, when girders are continuous, the structure becomes statically indeterminate so prestressing causes secondary reactions due to the tendon profile. This is sometimes called the "continuity effect". The secondary reactions induce corresponding shear forces and secondary moments (as discussed previously.) This directly modifies the summation of shear forces from all loads.

Although common practice for simply-supported pretensioned girders is to use straight strands, they can be draped upwards at the ends, as discussed in Section 5.7. Continuous or post-tensioned girders usually have draped prestressing at the ends of the girders and over the supports to counteract negative moments arising from dead and live loads. The force in the strands can be resolved to give a vertical component - typically being opposite the shear force from dead and live loads. Essentially, the effect is a reduction in shear demand. However, *AASHTO LRFD* includes this effect as a component of strength rather than a reduction in demand. In this case, the vertical component of the effective prestressing force, V_p, is added to the strength of the concrete, V_c, and vertical reinforcement, V_s. The total shear strength is then

$$V_n = V_c + V_s + V_p$$

If V_p is in the same direction as the dead and live load demand, then V_p should be taken as negative in this equation for total shear strength. Whether positive or negative, shear effects from prestressing should *not* be included as a load "demand" since they are considered to be a component of "resistance."

For special cases vertical prestressing can be placed in the webs for additional shear resistance. This is usually done using vertical post-tensioning bars. They

compress the webs under service level conditions, which is beneficial for principal tension checks. For the strength limit state, the bars supplement the vertical reinforcing steel (rebar). Vertical prestressing is more appropriate for segmental bridge structures, generally with superstructure depths of about 12-15 ft or greater.

5.10.5.3 Transverse Analysis and Design

In general, transverse design addresses the need for the deck slab to carry permanent structural dead and local wheel live loads and effectively transfer them to the webs in an appropriate manner - where they are then combined with global longitudinal conditions as necessary. Transverse analysis takes into account the transverse flexure of the multi-cell or single-cell box in acting like a frame to disperse local effects. Torsional effects from eccentric live loads are considered and appropriately distributed to be combined with shear forces in the webs.

It is a matter of design preference whether to commence with transverse or longitudinal design. In actuality, both need to proceed together as the results of one influence the other and vice-versa. Since it is in the interests of any project to minimize weight, performing a transverse analysis usually leads to the minimum required thickness for slabs and webs. These are refined when combined with longitudinal design conditions.

Appropriate methods of structural analysis for transverse conditions include:

- Classical elastic theory for the flexure of plates or shells
- Equivalent strip (*AASHTO LRFD*)
- Influence surfaces for flexure (derived from classical theory)
- Influence surface combined with a transverse frame
- Three-dimensional finite element modeling using plates or shell elements

Each technique may have an application appropriate for one project yet not for another. The following are general comments and should not be considered mandatory in any way. In all circumstances, engineering knowledge and good judgment is required.

5.10.5.3.1 Classical Theory

Classical linear-elastic analysis theory for out of plane bending of plates in two directions has been previously developed (Westergard, Timoshenko, et al.). The theory is applicable for any surface, such as the top slab of a bridge deck, in flexure and supported by one or more fixed edges, such as a cantilever wing or the top of webs and diaphragms. Classical theory is laborious and not easily suited to practical application; except that it has been used to develop influence surfaces.

5.10.5.3.2 Equivalent Strip

The approximate equivalent strip method of *AASHTO LRFD* Article 4.6.2.1 may be used to determine transverse effects in the deck slab of monolithic, multi-cell boxes (case (d) of Table 4.6.2.2.1-1) providing that the geometric proportions of the superstructure meet the requirements of this section.

Bending moments may be taken directly from *AASHTO LRFD* Table A4-1, basically if:

- There are at least 3 webs with not less than 14 ft between the centerlines of the outermost webs
- The overhang should be more than 21" but less than the smaller of 0.625 times the web spacing (S) or 6.0 ft
- The maximum web spacing (S) should not exceed 15 ft

Example: If it is assumed that the web spacing is 7ft 6in, and webs have a width of 10 in. then from Table A4-1, the maximum positive moment in the deck slab is M_{pos} = 5.44 kip-ft/ft. The corresponding maximum negative moment at the face of the web, by interpolation between the values given for the distance from the centerline of the web to the negative moment design section, is:

$$M_{neg} = 4.61 + (5.43 - 4.61)/3 = 4.88 \text{ kip-ft /ft.}$$

These are compared with those derived from influence surfaces (below), thus:

	Table A4-1	Influence Surface	Difference (%)
$M_{positive}$ =	5.44	5.24	3.8
$M_{negative}$ =	4.88	4.89	0.2

This close agreement lends credibility to both methods. The small variations may be accounted for by differences from reading influence charts, roundoff, the size of wheel prints applied to the influence surfaces, and by differences in assumed edge support conditions.

5.10.5.4 Construction

5.10.5.4.1 Construction Sequence

For a typical box-type superstructure, the cross-section is usually cast in phases beginning with the bottom slab, then the webs, then the top slab to facilitate convenient construction. The longitudinal length of a pour depends upon the rate of concrete delivery and placement within a given work period. This depends upon the

overall size of the superstructure and scale of the project. Temporary transverse bulkheads may be necessary to divide the superstructure into workable lengths. Transverse construction joints (i.e., over the entire cross-section) can usually be located to accommodate construction needs.

Locations of potential longitudinal construction joints (i.e., horizontal planes generally at top or bottom flange interfaces with webs or near mid-height of webs) must be carefully considered. For instance, web reinforcement must be adequate not only for global loads in the web, but also for local interface shear effects when longitudinal construction joints are made. Shear friction calculations should consider the coefficient of friction (μ) range between monolithic and jointed conditions. If necessary, restrictions on permissible joint locations should be clearly shown on the plans.

With cast-in-place construction on falsework, it is usually assumed that the entire superstructure is built and supported by falsework until longitudinal post-tensioning is installed and stressed to make it self-supporting – at which point the falsework is removed (Figure 5.10.5.4.1-1). This is equivalent to the case where the structure is "instantaneously" loaded with its own self weight and post-tensioning in its final configuration. The camber required for setting the formwork using this technique is the opposite of the anticipated final, long-term deflections under all dead and prestress loads.

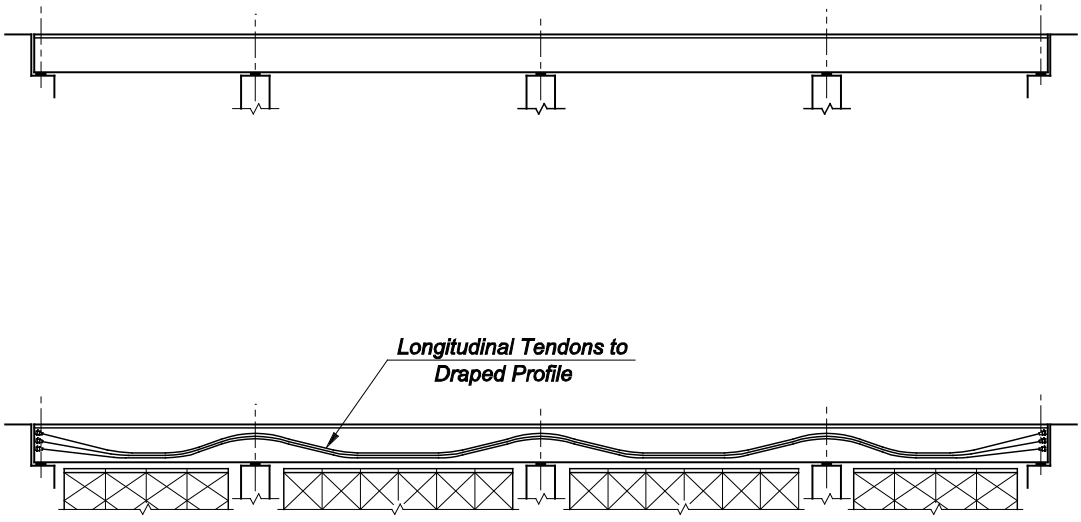

- ***Provide Falsework throughout***
- ***Construct Cast-In-Place Spans***
- ***Install and stress Longitudinal Tendons***
- ***Release Falsework***

Figure 5.10.5.4.1-1 Cast-in-Place on Falsework and Tendon Layout

With many continuous spans constituting a unit between expansion joints, construction might proceed in stages, with falsework supporting only one span - or a little more than one span – at a time. After the span has been post-tensioned, the falsework is released and re-cycled for a succeeding span. This requires detailed consideration of the layout of longitudinal tendons and their anchorages so as to properly overlap - with new ones picking up where previous ones terminate (Figure 5.10.5.4.1-2).

This technique also requires consideration of intermediate deflections and setting of formwork to an appropriate camber so that the final structure conforms as closely as possible to the desired profile after it has been constructed in stages (e.g. one span at a time). This camber is not the same as that where the entire structure is supported.

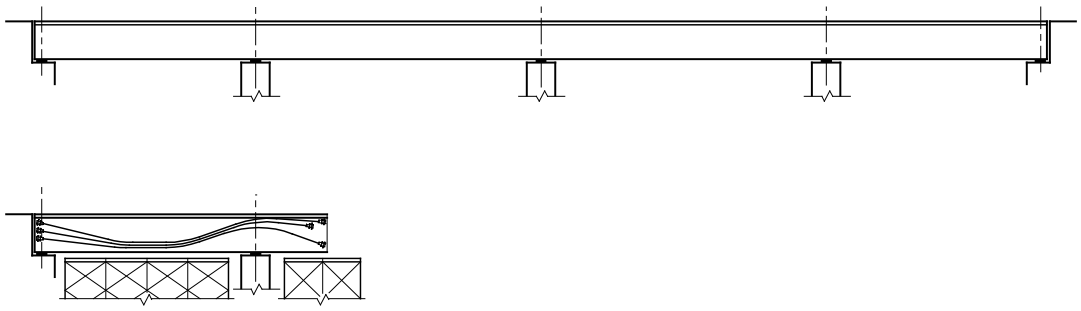

Stage 1 - Construct First Span, install and stress Tendons, release Falsework.

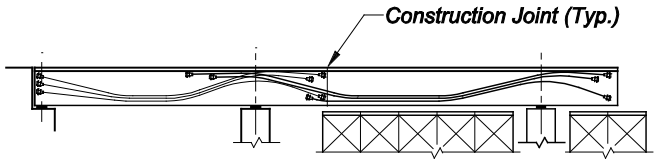

Stage 2 - Construct Second Span, install and stress Second Span Tendons, release Falsework.

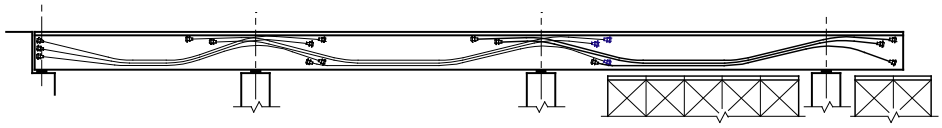

Stage 3 - Construct Third Span, install and stress Third Span Tendons, release Falsework.

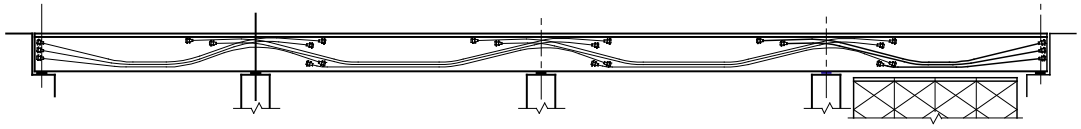

Stage 4 - Construct Fourth Span, install and stress Fourth Span Tendons, release Falsework.

Figure 5.10.5.4.1-2 Spans Cast Sequentially on Falsework and Tendon Layout

5.10.6 Cast-in-Place Segmental Box Girders

Although many of the concepts concerning cast-in-place (CIP) box girders and T-beams discussed in the previous section are applicable to CIP segmental girders, the longer spans and heavier cross-sections of the latter require additional considerations.

5.10.6.1 Design

5.10.6.1.1 Large Boxes - Section Properties for Analysis

For large single or double cell (two or three web) closed box sections of precast or cast-in-place construction, effective cross section properties may be determined by reference to *AASHTO LRFD* Article 4.6.2.6.2. This article of *AASHTO LRFD* is based upon investigations into the effects of shear lag in superstructures with relatively wide flange widths that were originally the basis of the German Code DIN 1075.

If reduced widths are used to determine effective section properties, the designer must remember to use the full (gross) section area for self-weight load calculations – along with an allowance for any intermediate diaphragms, anchorage blisters or tendon deviators, and so forth. Care should be exercised when using a computer program that automatically generates self-weight from (effective) section properties.

For determining stresses it is conservative to use the gross area for the prestress force effect, (i.e., P/A_g) but to use the effective (reduced) section properties for calculating flexural stress from applied loads and eccentric prestress (i.e., M/S_{eff} and Pe/S_{eff}). The procedures for calculating and applying appropriate section properties are neither exact nor prescriptive. A designer should always exercise a measure of engineering judgment for his particular project and span configuration.

An alternative way to analyze a box-type structure would be by three-dimensional finite element analysis using plates, space-frame members or similar with a sufficiently fine mesh to account for the global effects of shear lag. Providing that the model and applied loads are executed correctly, final stresses can be read directly from the element results.

Having determined the section properties, which may vary along a span, longitudinal moments, shear forces and reactions may be determined by classical analysis for continuous beams (area-moment theory, slope-deflection, moment distribution) or by using a continuous beam analysis computer program.

5.10.6.1.2 Torsional Effects of Eccentric Load

Under the action of eccentric (live) load, torsional effects are induced in single cell and multi-cell box superstructures. In a single cell (large) box section this sets up a torsional shear flow around the section in the direction of the applied torque. In a multi-cell box, the effect is to set up a torsional shear flow around each cell of the box section (Figure 5.10.6.1.2-1). At each of the inner webs the torsional shear flow from the cell on one side of the web acts in the opposite direction to the flow from the cell on the other side of the web. The sum of all the torsional shear flows equates to

the global torque at the cross section considered. If the webs are of approximately equal thickness, then the resulting torsional shear flow stress (v_f) around the perimeter of the section is given by:

$$v_f = T / 2A_o.t$$

where:

T	=	torque
t	=	member thickness (web or slab)
A_o	=	area contained by the centerline of the perimeter components

In practical terms, the torsional shear flow stress in the inner webs of a multi-cell box cancels out; leaving only a net effect in the outer webs and the top and bottom slabs. Torsional shear in the exterior web closest to the applied load adds to the shear force in that web, whereas it reduces the shear force in the opposite exterior web.

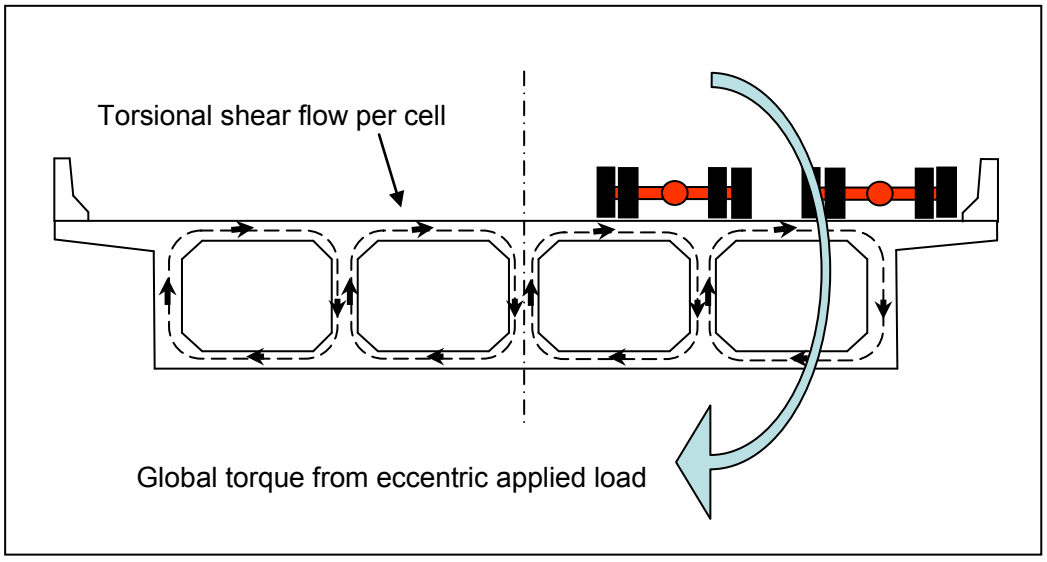

Figure 5.10.6.1.2-1 Shear Flow in Multi-cell Box

Torsion induces a slight deformation of the cross section, inducing transverse bending in the top and bottom flanges and webs – in the manner illustrated in Figure 5.10.6.1.2-2. Another way to envision this transverse action is to imagine the longitudinal girder lines attempting to deflect differently relative to each other as a result of carrying different proportions of the torsionally applied (eccentric) load – which can only be accommodated by a transverse flexure of the slabs and webs.

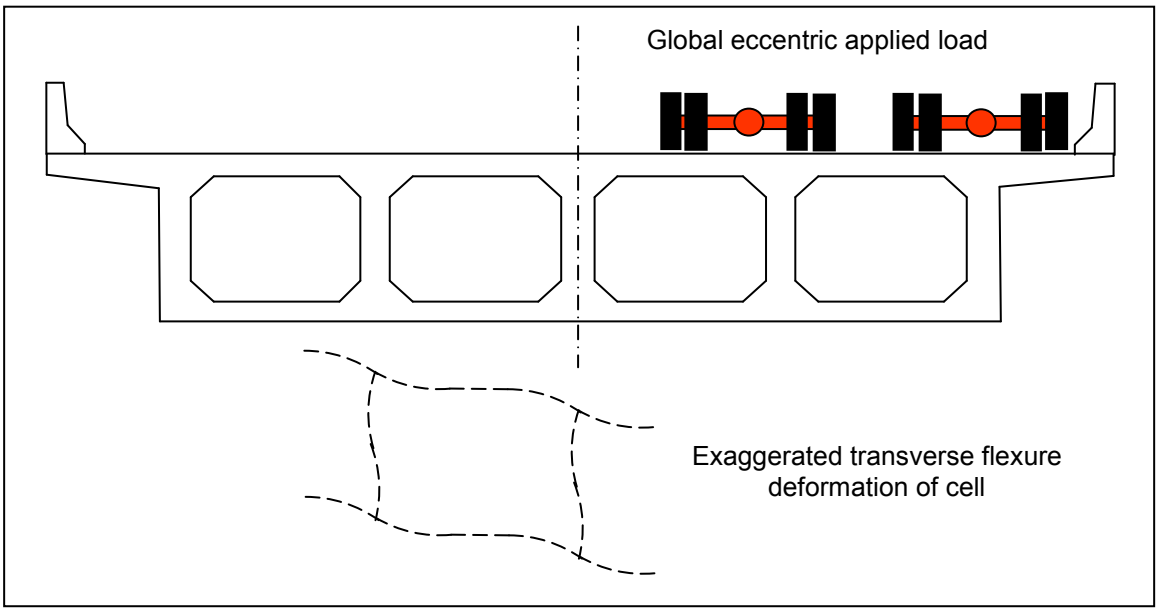

Figure 5.10.6.1.2-2 Transverse Deformation of Cells from Eccentric Load

This deformational effect is not as pronounced or significant for slab flexure as that of a deck slab supported by two, separate, stiff boxes of the type shown in *AASHTO LRFD* Commentary C9.7.2.4.

5.10.6.2 Construction

5.10.6.2.1 Falsework

Falsework is very often made from prefabricated modular shoring towers comprising well-braced interlocking frames in a square or rectangular arrangement of four legs. Each leg may have an individual resistance of up to about 100 kips. Multiple towers are located as necessary to support a temporary decking system for the superstructure formwork and work platform.

Alternatively, the main vertical falsework supports may be built from temporary steel towers, heavy section lumber, precast concrete piles or similar members as convenient and available (Figure 5.10.6.2.1-1). Temporary steel girders or trusses purposefully fabricated for the application or assembled from prefabricated modular systems may offer viable alternatives where temporary foundations can be placed only in certain locations due to poor conditions or as may be needed to span a traffic diversion.

Figure 5.10.6.2.1-1 Side-Span Falsework for Cast-in-Place Box (Acosta Bridge - Jacksonville, FL)

Guidance for design and construction of falsework is provided in two AASHTO publications:

- "Guide Design Specifications for Bridge Temporary Works"
- "Construction Handbook for Bridge Temporary Works"

Elevations of the falsework and formwork should be adjusted to compensate for any anticipated deflection of the falsework itself and for deflections of the superstructure itself arising from simply supported effects or construction in stages.

5.10.6.2.2 Superstructure Forming

Formwork for the superstructure may be made from lumber and plywood or prefabricated modular forming systems. Accuracy to line, level and thickness is essential to ensure the correct shape and size of concrete members. External surfaces are usually formed of a high quality, smooth and dense finished plywood, metal or any required aesthetic texture, as necessary. Internal surfaces should be within tolerance but are usually of a lesser quality finish and forming material.

Box girder sections are usually formed and cast in stages, commencing with the bottom slab, webs and finally the top slab; so formwork is arranged accordingly. Access to internal cells is usually necessary through diaphragms or manholes for future maintenance inspection and provides a convenient way through which internal formwork can be removed after casting. Purpose-built, permanent, internal top slab

soffit forms may remain in place provided that they have been accounted for in the design.

5.10.6.2.3 Rebar Placement

For a casting a typical box section, rebar is installed in stages as necessary – i.e., bottom slab, webs and top slab. It is helpful if reinforcement is detailed accordingly, giving attention to the location of bar splices to meet structural requirements and also facilitate forming and casting. Reinforcement should be installed within construction tolerances.

All necessary post-tensioning ducts, anchorage components and anchorage reinforcement should be installed in conjunction with the reinforcement. It is preferable that reinforcement and post-tensioning be designed and detailed to be free of conflicts. However, this is not always evident in advance. Whenever a conflict is encountered between reinforcement and post-tensioning, in general, the reinforcement should be adjusted locally as necessary to maintain the desired post-tensioning alignment. In cases of doubt, a decision should be sought from the Engineer.

5.10.6.2.4 Superstructure Concreting

Typically a box section superstructure of any number of webs or size is cast in stages – i.e., bottom slab, webs, top slab – allowing the concrete to harden each time. Longitudinal construction joints are normally created a few inches above the bottom slab and at the top of the webs. This is mainly for convenience of construction. In order to ensure proper structural integrity and function, joints should be prepared, cleaned and roughened prior to the next pour. This is usually sufficient; however, construction keyways, if necessary, should be shown on the plans.

Concrete placement, consolidation, finishing and curing should be addressed in project specifications. Care should be exercised when placing and consolidating concrete around post-tensioning ducts so that they are not displaced or damaged. The top of the bottom slab is usually float finished to line and level by hand as access between webs restricts mechanical devices. When the bottom slab concrete has set and sufficient hardened the webs are formed. Web concrete is then placed and consolidated. Web forms may have to remain in place for a minimum period for curing. This may restrict progress installing top slab soffit forms and reinforcement and should be coordinated accordingly.

With a wide, single-cell (two-web) box, concrete for the top slab should be placed at the outer wings and center first, finishing by placing portions over the webs last. This should minimize any tendency for deflection of formwork to cause longitudinal separation or cracking of partially set concrete if placed otherwise. With multi-cell

boxes and relatively closely spaced webs, this tendency is normally of little concern and concrete can be placed across the width from one side to the other as convenient. Finishing of a top slab may be done by hand or mechanical screed as used for slabs cast atop precast girders.

Longitudinally, vertical construction joints may be needed at various locations in a span or superstructure in order to keep the total volume of concrete placed within a work period to that which can be delivered, placed, consolidated and finished.

5.10.6.2.5 Superstructure Curing

Curing of concrete should be addressed in project specifications. With cast-in-place construction, it is necessary to attain a proper set and sufficient strength, prior to releasing forms before the next stage of casting and especially prior to imposing high local anchorage forces from post-tensioning or releasing falsework.

On site curing is usually done using blankets, wet-burlap, moisture, fogging and application of suitable curing compounds. Steam curing for large pours is less practical than at a precast production facility or when using enclosed form-travelers, and is not normally used on site. Protection of pours from adverse weather and heating may be necessary in some situations. Monitoring of internal concrete temperature using thermocouples or other devices at suitable locations over the curing period can be helpful in some cases, particularly for thick members and large pours. It provides a record of curing and can help avoid potential difficulties from a too rapid rise or fall from the heat of hydration. Curing and monitoring techniques should be addressed via appropriate specifications.

5.10.6.2.6 Post-Tensioning and Tendon Grouting Operations

Post-tensioning operations for cast-in-place construction involve the same procedures and techniques as discussed previously. After post-tensioning tendons have been installed and stressed, they must be properly grouted and anchorages sealed and protected to ensure long term durability.

For comprehensive information on the installation, stressing, grouting and protection of post-tensioning tendons and anchorages, including recommendations for the location of injection grout ports, vents, laboratory and field tests, quality control and records, refer to “Post-Tensioning Tendon Installation and Grouting Manual,” Version 2.0, FHWA-NHI-13-026, May 2013.

5.10.6.2.7 Staged Construction

Construction of a continuous cast-in-place superstructure in stages, for example, a span at a time, has been addressed in previous sections. Segmental construction

generally involves casting of full deck-width segments in 10 ft. to 20 ft. lengths. In such situations, it is necessary to calculate the amount of deflection of the structure as a consequence of the stages of construction and to make compensating adjustments (camber corrections) to the elevations of the forms. Such deflections depend upon the sequence in which permanent load (self-weight) and prestress is applied and the material properties (elasticity, creep and shrinkage) of the concrete. The latter are influenced by the type of concrete, maturity and age at loading. In addition, corrections to elevations for setting forms are necessary for anticipated deflection of falsework itself.

5.10.7 Curved Structures

For structures curved in plan, *AASHTO LRFD* Article 4.6.1.2 permits a rational analysis of the entire superstructure including appropriate supporting elements such as bearings or integral connections to piers. This approach can be applied to both large single girder (torsionally stiff) box section superstructures and multi-cell concrete box girders.

For continuous concrete superstructures of these types, (unlike steel girders) there is usually little distortion or deformation of the cross section – especially if diaphragms are provided at interior piers. Rational analyses methods include classical theory based upon small deflections or modeling using finite-elements, space-frame or grillage techniques.

5.10.7.1 Multi-Cell Concrete Box Girders

According to *AASHTO LRFD* Article 4.6.1.2.3, horizontally curved cast-in-place multi-cell box girders may be designed as single spine beams with straight segments for central angles up to 34° within one span using the distribution factors from *AASHTO LRFD* formulae. Ten straight segments per span were used in parametric analyses that underlie the conclusion in *AASHTO LRFD* Commentary C4.6.1.2.3. This is considered reasonable for most cases; but for sharp radii, more straight segments may be needed per span.

5.10.7.2 Post-Tensioning Effects in Curved Structures

5.10.7.2.1 Tendons within Curved Webs

When curved webs contain (draped) post-tensioning tendons, a lateral force develops given by:

$$F_{lateral} = P/R \text{ per unit length}$$

where:

$F_{lateral}$ = lateral force acting on the web per unit of length
P = force in the tendon
R = radius of curvature of the web in plan view

This lateral force effect will be at a maximum during stressing operations when the concrete itself might be young and not up to full strength. It can result in a tendon pulling through the side of the web – as happened on at least one occasion. This is easy to avoid by taking care to make sure that such ducts are regularly restrained by lateral ties. The effect is illustrated in *AASHTO LRFD* Figure C.5.10.4.3.1-2.

5.10.7.2.2 Internal Torsional Effects from Tendons

The above radial force effect in the horizontal direction also applies to tendons that lie mostly in the plane of the top or bottom slab. Because of their relatively large eccentricity from the shear center of the section, the horizontal effect induces torsion.

In the case of external tendons that pass over pier diaphragms and drape down to intermediate deviators at the bottom slab-web interface, there is a significant horizontal (lateral) as well as vertical force at each point of change in direction. In a straight bridge with a symmetrical section and symmetrical post-tensioning layout, these lateral effects cancel each other. However, this is not the case in a horizontally curved structure. The net lateral effects at their respective eccentricities from the shear center can induce significant (internal) torsional forces.

Consequently, care should be taken to minimize internal torsional effects as far as possible - first by attempting to modify or optimize the post-tensioning layout or system. But, no matter the modification, it is likely that residual torsional force effects of some magnitude will remain. Their effect should be appropriately added to other permanent torsional effects from gravity loads. Additional torsional reinforcement and possibly extra longitudinal post-tensioning may be needed to cater for these effects.

The magnitude of torsional force effects from post-tensioning may be calculated by determining the equivalent loads, applying them to a continuous girder and using classical theory (i.e. the “M/R Method” above) or by 3-dimension modeling.

Section 5.11 References

AASHTO, *Construction Handbook for Bridge Temporary Works*, 1995.

AASHTO, *Guide Design Specifications for Bridge Temporary Works*, 1st Edition, 2008 Interim Revisions.

"Design of Continuous Highway Bridges with Precast, Prestressed Concrete Girders," *Journal of the Prestressed Concrete Institute*, Vol. 14, No. 2, April 1969.

FHWA, *Post-Tensioning Tendon Installation and Grouting Manual*, Federal Highway Administration, FHWA-NHI-13-026, May 2013.

Hawkins, Neil M., Daniel A. Kuchma, Robert F. Mast, M. Lee Marsh, and Karl-Heinz Reineck, *Simplified Shear Design of Structural Concrete Members,* NCHRP Report 549, Transportation Research Board, Washington, DC, 2005.

HPC Bridge Views, Issue No. 22, FHWA-NCBC Publication, PCA, Skokie, IL.

NCHRP Report 517, "Extending Span Ranges of Precast Prestressed Concrete Girders," Transportation Research Board, Washington, DC, 2004.

PCI, *Bridge Design Manual*, MNL-133-14, 3rd Edition, Second Release, August 2014, Precast/Prestressed Concrete Institute, Chicago, IL.

PCI, *Manual for Quality Control for Plants and Production of Structural Precast Concrete Products*, MNL-116, Precast/Prestressed Concrete Institute, Chicago, IL.

PCI, *Manual for the Evaluation and Repair of Precast, Prestressed Concrete Bridge Products*, MNL-137-06, Precast/Prestressed Concrete Institute, Chicago, IL.

PCI, *PCI Design Handbook: Precast and Prestressed Concrete*, April 2014.

"Post-Tensioning Tendon Installation and Grouting Manual," Version 2.0, FHWA-NHI-13-026, May 2013.

Chapter 6
Steel Girder Superstructures

Section 6.1 Introduction

This chapter provides a comprehensive overview of the design process for steel-bridge superstructure components according to the *AASHTO LRFD Bridge Design Specifications* (*AASHTO LRFD*).

The chapter begins with a discussion of the structural steels, bolts and other miscellaneous materials used in steel bridges, and a brief review of some of the key mechanical properties of structural steels.

When designing steel bridges, several important decisions must be made prior to starting final design. These decisions involve layout considerations, as well as type and size considerations. This chapter presents guidelines for structural unit lengths, span arrangement, field-section sizes, girder spacing, deck overhangs, deck and haunch thicknesses, and cross-frames, diaphragms and lateral bracing. The chapter also provides guidance when making decisions about box girders vs. I-girders, span-to-depth ratio, optimum web depth, web proportioning, and flange proportioning.

Basic fundamental concepts related to the structural behavior of steel are reviewed to complement and expand on the specification commentary, and to aid in the understanding and implementation of the specification provisions in the design of various steel-bridge superstructure components at each limit state. Although the *AASHTO LRFD* design specifications are generally member and component based, the behavior of the entire steel-bridge system must also be considered in certain instances to ensure proper performance and overall stability, particularly during certain stages of construction, and in the case of skewed and horizontally curved girder bridges.

This chapter also discusses the basis of the LRFD flexural design resistance equations for steel I-girders and box girders. Specific LRFD design verifications for I-girders and box girders for constructibility, at the service limit state, at the fatigue limit state, and at the strength limit state are then presented. Strength limit state design verifications for flexure are discussed for sections subject to negative flexure, positive flexure, and stress reversal. Strength limit state design verifications for shear are also reviewed.

Finally, the chapter discusses the LRFD design requirements for detail items such as shear connectors, bracing members, bolted and welded connections, bolted girder splices, web stiffeners (i.e. transverse web stiffeners, bearing stiffeners and longitudinal web stiffeners), and truss gusset plates.

Section 6.2 Materials

6.2.1 Introduction

This section discusses structural steels, bolts and other miscellaneous materials used in steel bridges, along with the fundamental mechanical properties of structural steels. Included are discussions on available grades of steel for structural plate and rolled shapes used in bridges, and discussions on bolts, nuts and washers, stud shear connectors, weld metal and other miscellaneous materials. Fundamental properties of structural steels, including yield and tensile strength, ductility and toughness, and hardness, are also reviewed. Much of the discussion in this section is based on information presented in Wright (2012). The reader is referred to Wright (2012) for additional information on steel manufacturing practices, weldability and fabrication, corrosion resistance, and other mechanical properties not covered in detail herein.

6.2.2 Structural Steels

6.2.2.1 General

Structural steels for bridges generally have more stringent performance requirements compared to steels used in other structural applications. Bridge steels are subject to relatively large temperature changes, are subjected to millions of cycles of live loading, and are often exposed to corrosive environments containing chlorides. In addition to strength and ductility (i.e. toughness) requirements, bridge steels have to satisfy additional service requirements with respect to fatigue. Bridge steels also have to provide enhanced atmospheric corrosion resistance in many applications where they are used without expensive protective coatings. For these reasons, structural steels for bridges are required to satisfy fracture toughness requirements, and provide a level of corrosion resistance, that generally exceeds the requirements necessary for structural steels used in other applications.

6.2.2.2 Structural Plate and Rolled Shapes

6.2.2.2.1 General

The ASTM A709/A709M Standard Specification for Structural Steel for Bridges (ASTM, 2010) was established in 1974 as a separate specification covering all structural grades approved for use in main members of bridge structures. Many of

the ASTM A709/A709M provisions are identical to those in the individual structural steel specifications applicable for more general use; however, the ASTM A709/A709M specification includes the additional toughness requirements specified for bridge steels. The various steel grades covered by the specification include Grade 36, Grade 50, Grade 50S, Grade 50W, and the available grades of high-performance steel or HPS (including HPS 50W, HPS 70W and HPS 100W). The number in the grade designation indicates the nominal yield strength in ksi. The "W" indicates that the steel is a so-called "weathering steel". Minimum mechanical properties of the ASTM A709/A709M structural steels are specified in *AASHTO LRFD* Table 6.4.1-1. Thickness limitations relative to rolled shapes and groups are to satisfy the provisions of ASTM A6/A6M.

The American Society for Testing and Materials (ASTM) is a non-profit voluntary standards organization that develops consensus standards for steel products. Membership is comprised of experts from industry, government, academia, and end users to provide a balance of perspectives. The American Association of State Highway Transportation Officials (AASHTO) publishes a separate volume of standards that also include structural steel standards for bridge applications (AASHTO, 2011). These standards are developed by committees comprised solely of state government officials responsible for construction and maintenance of the highway system. The AASHTO standards are typically very similar or identical to the corresponding ASTM standards, particularly for bridge steel products. Some of the ASTM standards do not have an AASHTO counterpart. By maintaining independent standards, AASHTO maintains the right to modify the ASTM requirements if it is determined to be in the public's interest. The counterparts to the ASTM A709/A709M standards for structural steels for bridges are the AASHTO M270M/M270 standards.

Structural steel plates (and bars) that are to be cold or hot bent are to satisfy the requirements for bent plates specified in Article 11.4.3.3 of AASHTO (2010). This article limits the minimum bend radius for all grades and thicknesses of steels conforming to the ASTM A 709/A709M (AASHTO M 270/M270M) standards used in fracture-critical or nonfracture-critical applications, and where the bend lines are oriented perpendicular to the direction of final rolling of the plate. The specified minimum bend radius is increased where the bend lines are oriented parallel to the final rolling direction. These limits are provided to ensure that the bending of the plate has not significantly lowered the toughness and ductility of the plate. Smaller radius bends may be used with the approval of the Owner.

6.2.2.2.2 Grade 36

Grade 36 is the easiest and cheapest of all the steels in the ASTM A709/A709M specification to produce in steel mills that produce steel by melting iron ore in a blast furnace. Much of the steelmaking practice in the U.S. has now switched to electric

furnace production in which a large percentage of scrap is used to produce structural steel. Since scrap typically has more alloying elements than required by the Grade 36 specification, the resulting steel strength is typically much higher than that produced using the more traditional approach. The steels being delivered today as Grade 36 typically have strengths closer to 50 ksi than 36 ksi.

6.2.2.2.3 Grade 50

Grade 50 is a higher strength grade of weldable structural steel. The strength is obtained by adding small amounts of columbium, vanadium, and sometimes titanium to the basic carbon-manganese chemistry of Grade 36 steel. Grade 50 has become the material of choice for primary bridge members that are to be painted, galvanized, or metalized, and is the most common grade of structural steel available today.

6.2.2.2.4 Grade 50S

The ASTM A992 specification was introduced in 1998 to keep pace with changes in rolled shape production practices in the U.S. As was previously discussed for Grade 36 (Section 6.2.2.2.2), the shift to scrap-based production made Grade 36 materials somewhat obsolete. Steels under the ASTM A992 specification are dual certified to qualify for Grade 36 or Grade 50. It is more difficult to precisely control the chemical composition of scrap-based steel production since many alloys may be present in scrap steel. Therefore, the ASTM A992 specification allows a wide range of steel chemistry. However, too much alloying can adversely affect the performance of structural steel and maximum percentages are set for the various alloys. Grade 50S in the ASTM A709/A709M specification is equivalent to ASTM A992, but includes the additional toughness requirements specified for bridge steels. Non-weathering steel rolled I-shapes and structural tees should be specified as Grade 50S. Other non-weathering rolled shapes (e.g. angles and channels) are typically only available as either Grade 36 or Grade 50 and should be specified as such.

6.2.2.2.5 Grade 50W

Grade 50W is a special version of 50 ksi steel that was developed to have enhanced atmospheric corrosion resistance. Grade 50W, commonly referred to as "weathering steel", is capable of performing well without paint or other coatings in many bridge applications. Different steel companies initially developed competing proprietary grades that were included in the original ASTM A588 specification in 1968. The added corrosion resistance was achieved by adding different combinations of copper, chromium, and nickel to the Grade 50 chemistry to provide enhanced corrosion resistance. The added cost for Grade 50W compared to non-weathering Grade 50 is usually offset by the savings realized by eliminating the need to paint the steel.

6.2.2.2.6 HPS Grades

The high performance steel (HPS) grades were developed in the 1990s through a cooperative agreement between the Federal Highway Administration, the U.S. Navy, and the American Iron and Steel Institute. The goal was to enhance weldability and toughness compared to previous grades of Grade 70W and 100W steel (Wright, 1997). Prior to HPS, steels with yield strength greater than 50 ksi (e.g. ASTM A852 and ASTM A514) were very sensitive to welding conditions and fabricators often encountered welding problems. The HPS grades have essentially eliminated base metal weldability concerns. In addition, HPS grades provide significantly enhanced fracture toughness, and also enhanced corrosion resistance, compared to non-HPS grades (note that all HPS steels are "weathering steels"). Because of the greatly enhanced properties, the original Grade 70W steel (ASTM A852) has been replaced in the ASTM A709/A709M and AASHTO specifications, and HPS 70W is the only 70-ksi option for bridge use. For similar reasons, the HPS 100W grade has now replaced the previous Grade 100 (ASTM A514) for fabrication of structural bridge members where a 100-ksi minimum yield strength is desired. Rolled shapes are not available in HPS grades.

The properties of HPS are largely achieved by dramatically lowering the percentage of carbon in the steel chemistry. Since carbon is traditionally one of the primary strengthening elements in steel, the composition of other alloying elements must be more precisely controlled to meet the required strength and compensate for the reduced carbon content. There are also stricter controls on steelmaking practice and requirements for thermal and/or mechanical processing to meet the required strength. These refinements in steelmaking practice result in a very high quality product. However, this also limits the number of steel mills that have the capability of producing HPS steels in the US.

HPS steels typically come with a cost premium and additional lead-time is required in ordering versus non-HPS grades. However, experience is showing that HPS steels, due to their higher strength, can result in more efficient bridges with lower first cost. This benefit generally is greater as the size and span length of bridges increase. Hybrid girders utilizing Grade HPS 70W steel for the flanges and Grade 50W steel for the web have been shown to be a particularly economical option in regions of negative flexure in such cases (Section 6.4.4). The use of HPS should be carefully considered by the designer to ensure the benefits outweigh the additional cost of the product.

Grade HPS 50W is an as-rolled steel produced to the same chemical composition requirements as Grade HPS 70W. Similar to the higher-strength HPS grades, Grade HPS 50W has enhanced weldability and toughness compared to Grades 50 and 50W. However, the need for enhanced weldability is questionable at this strength level since few weldability problems are reported for the non-HPS grades.

The primary advantage of Grade HPS 50W is that it can be delivered with high toughness that exceeds the current AASHTO specification requirements for Grades 50 and 50W. Enhanced toughness may be beneficial for certain fracture critical members with low redundancy such as the tension ties in tied-arch bridges. Research is ongoing to integrate the benefits of the higher toughness into the AASHTO Fracture Control Plan contained in the *AASHTO/AWS D1.5M/D1.5 Bridge Welding Code* (AASHTO/AWS, 2010). Since Grade HPS 50W is a higher cost material compared to Grade 50W, engineers should carefully consider the need for higher toughness before specifying Grade HPS 50W.

6.2.2.3 Stainless Steels

Stainless steels are occasionally used to fabricate bearings and other parts for bridges where high corrosion resistance is required. Traditionally, the relative high cost of stainless steel has limited its use in primary bridge members. However, given the expanding trend toward life-cycle cost analysis, stainless steels merit consideration for some structural applications. According to *AASHTO LRFD* Article 6.4.7, stainless steels must conform to either ASTM A176, A240, A276 or A666, unless it can be shown that the steel conforms to one of the above-listed specifications or other published specifications that establish its properties and suitability based on analyses, tests and controls as prescribed by one of the above-listed specifications.

The most promising product for structural bridge use is ASTM A1010 Grade 50, a dual phase stainless steel with a 12% chromium content. This product meets the mechanical property requirements for ASTM A709/A709M Grade 50 and can meet the supplemental toughness requirements for Grade HPS 50W material. The product has been shown to have greatly enhanced corrosion resistance compared to weathering steel grades (Fletcher et al., 2003), and can provide adequate performance without paint in higher chloride bridge environments. The grade is currently available in thicknesses up to 2 in.

ASTM A1010 steel is weldable using all processes currently employed for bridge fabrication. However, this product is not currently included in the *AASHTO/AWS D1.5M/D1.5 Bridge Welding Code* (AASHTO/AWS, 2010); therefore supplemental provisions need to be invoked based on recommendations by the manufacturer. The grade can be processed using standard fabrication practices including cold bending, heat curving, and machining. One exception is that the material is not suitable for cutting using oxy-fuel processes. Plasma or laser cutting is required. Another exception is that blast cleaning needs to be performed with non-metallic media to avoid staining of the surface in service.

A limited number of bridges have been constructed using ASTM A1010 steel in Oregon (Seradj, 2010) and in California. Since there is currently limited experience

with the use of ASTM A1010 steel in bridges, and this grade has not yet been included in the AASHTO specifications, projects will require special provisions and may require supplemental testing at the discretion of the Owner. Also, since ASTM A1010 steel is currently a significantly higher cost material compared to conventional weathering steels, engineers should carefully consider the need for the higher corrosion resistance in a particular application before specifying ASTM A1010.

Stainless steels are subject to increased corrosion if a larger volume of stainless steel is placed in contact with regular carbon steel, galvanized steel or aluminum alloys in the presence of an electrolyte. This requires isolation of the two dissimilar metals in some manner in such cases to prevent galvanic corrosion from occurring.

6.2.2.4 Structural Tubing

Hollow structural sections (HSS) are commonly used in building construction and they can be considered as an option for some bridge members. The increased lateral bending and torsional resistance of HSS can make these members an attractive option for cross-frame members and other members subjected to compression. HSS have also been used to fabricate trusses used for pedestrian bridges that are subject to lower fatigue loading.

HSS has traditionally referred to cold-formed welded or seamless structural steel tubing produced under the ASTM A 500 specification. Grade C has minimum specified yield and tensile strengths of 50 ksi and 62 ksi, respectively. The shapes are usually formed by cold bending carbon steel plate into the required shape and making a longitudinal seam weld along the length using the electric resistance welding (ERW) process. Both round, square and rectangular shapes are available with various cross sections and wall thicknesses. Cold-formed welded or seamless steel tubing is also available under the ASTM A 847 specification (for weathering steel applications). Hot-formed steel tubing is to conform to ASTM A 501 or A 618 (*AASHTO LRFD* Article 6.4.1).

As indicated in *AASHTO LRFD* Article C6.4.1, the ASTM A500 specification cautions that structural tubing manufactured to that specification may not be suitable for applications involving “dynamically loaded elements in welded structures where low-temperature notch-toughness properties may be important.” Where this material is contemplated for use in applications where low-temperature notch-toughness properties are considered to be important, consideration should be given to requiring that the material satisfy the Charpy V-notch toughness requirements specified in *AASHTO LRFD* Article 6.6.2. The Owner should also be consulted regarding the use of this material.

The suitability of HSS produced under these specifications for bridge members subject to the fatigue and fracture limit states has not been well-established. Cold

bending of the corners of rectangular shapes can lead to reduced notch toughness in the corner regions. CVN or other toughness tests in the curved wall regions are not specified.

To try and alleviate some of these concerns, a new Standard Specification for Cold-Formed Welded Carbon Steel Hollow-Structural Sections (HSS) was published as an ASTM standard in May 2013, and is being proposed for potential inclusion in the *AASHTO LRFD* Specifications as of this writing (2015). The specification is identified as ASTM A1085/A1085M-13, "Standard Specification for Cold-Formed Welded Carbon Steel Hollow-Structural Sections (HSS)". The HSS covered in this specification is produced in welded sizes with a periphery of not more than 88 in., as well as a specified nominal wall thickness of at least 0.148 in. and not more than 0.875 in. Refinements in this specification include a minimum specified tensile strength of 65 ksi, a specified range of yield strengths from 50 to 70 ksi, an elongation in 2 inches of 23% minimum, and a CVN value of 20 ft-lbs at 20°F (with a supplementary requirement permitting a purchaser to determine absorbed energy and test temperature suitable for the application). The note relative to the suitability of the material for application in dynamically loaded welded structures (discussed above) was also removed. Corner radii are specified to be 1.6t to 3.0t for t less than or equal to 0.4 in., and 2.4t to 3.6t for t greater than 0.4 in. Currently a wall thickness of 0.93t must be used in the design of HSS produced according to the standards specified in *AASHTO LRFD* Article 6.4.1 to reflect a 10 percent wall thickness tolerance. Under this new specification, the use of the full nominal thickness is permitted in design calculations when HSS is produced to a standard permitting no more than 3-1/2% under the calculated mass and no less than 5% under the nominal thickness.

Another possible concern related to the use of HSS for bridges is the need to control internal corrosion within the tubes, since the interior of the tube cannot be accessed for visual inspection. Sealing of the tube ends or galvanizing are possible options to control internal corrosion. In addition, HSS requires different connection details for which limited fatigue data currently exists. Designers specifying HSS should consider the connection design procedures given in the AISC (2010a), Chapter K. Resistances for fatigue design of round, square, and rectangular HSS may be found in the *ANSI/AWS D1.1/D1.1M Structural Welding Code - Steel* (ANSI/AWS, 2010), Section 2.20.6, or in AASHTO (2013), Section 11. Where HSS is used in fracture-critical applications, the Engineer is referred to AASHTO (2009), Article 8.2.3.

6.2.3 Bolts, Nuts and Washers

6.2.3.1 Bolts

6.2.3.1.1 Unfinished Bolts

Unfinished bolts, also referred to as common, machine, ordinary, or rough bolts, are manufactured from low-carbon steel and are designated as ASTM A307 bolts. There is no corresponding AASHTO material standard to ASTM A307. Three grades – Grades A, B, and C – are covered in the ASTM standard.

Grade A is the quality that is typically used for general structural applications. Grade A bolt heads and nuts are manufactured with a regular square shape. Grade B bolts are typically used for flanged joints in piping-systems with cast iron flanges. As indicated in *AASHTO LRFD* Article 6.4.3.1, the specified minimum tensile strength of these bolts (specifically Grades A and B) is 60 ksi. These bolts are typically tightened using long-handled manual wrenches and hardened steel washers are not generally used. Since these bolts do not have a specified proof load, they should only be used for connecting relatively light auxiliary components or members subject to light static loads or for temporary fit-up. These bolts should not be used in connections subject to slip or vibration because of the tendency of the nuts to loosen.

ASTM A307 Grade C bolts are nonheaded anchor bolts, either bent or straight, intended for structural anchorage purposes. The properties of ASTM A307 Grade C bolts conform to the properties of ASTM A 36 material. The ASTM A307 Grade C specification, although still allowed in the AASHTO design code, has been replaced by the F1554 specification in ASTM. Anchor bolts used to connect steel components to concrete foundations with diameters up to 4 in. are required to comply with the ASTM F1554 specification. Three grades are available (36, 55, and 105) corresponding to the yield strength of the bolt in ksi. Similar to structural bolts, anchor bolts are required to be used with compatible nuts and washers. Both galvanized and non-galvanized options are available. The ASTM F1554 specification has supplemental provisions for notch toughness that can be invoked by the Owner for anchor bolts loaded in tension, if needed.

6.2.3.1.2 High-Strength Bolts

High-strength bolts are heavy hexagon-head bolts used with heavy semi-finished hexagon nuts. The threaded portion of high-strength bolts is shorter than for bolts used for nonstructural applications, which reduces the probability of having the threads present in the shear plane. High-strength bolts produce large and predictable tension when tightened. Initial tensioning of high-strength bolts results in

more rigid joints and greater assurance against nut loosening in connections subject to slip or vibration.

High-strength bolts have replaced rivets (Section 6.2.3.6) as the primary means of making non-welded structural connections. Initial experiments on high-strength bolted connections were first reported in Batho and Bateman (1934). Follow-up research (Wilson and Thomas, 1938) indicated that high-strength bolts had fatigue strengths equal to those of well-driven rivets as long as the bolts were sufficiently pretensioned. In 1947, the Research Council on Riveted and Bolted Structural Joints (currently known as the Research Council on Structural Connections or RCSC) was formed to carry out cooperative research into the behavior of various types of connections joined with rivets and bolts. The new Council began by using and extrapolating information from studies of riveted joints in order to evaluate the merits of high-strength bolts used in structural connections. This led to the publication by the Council in 1951 of the first edition of the "Specifications for Structural Joints Using A 325 Bolts", which permitted the replacement of rivets with bolts on a one-to-one basis. This specification assumed that friction transfer was necessary in all joints at service load conditions. The factor of safety against slip was set at a high enough level to ensure fatigue resistance that was similar to or better than the fatigue resistance of riveted joints.

Additional research (Munse, 1956) concluded that for high-strength bolts to be efficient and economical, the minimum initial bolt tension should be as high as practical. Therefore, by 1960, the minimum initial bolt tension was increased. Also, the bearing-type connection (i.e. a connection where the resistance of the connection is based on bearing of the bolt against the side of the hole and where high slip resistance at service loads is unnecessary – Section 6.6.4.2.1.2) was recognized as an acceptable substitute for a riveted connection. It was further recognized that the so-called friction-type connection (now referred to as a slip-critical connection – Section 6.6.4.2.1.1), in which the connection is designed on the basis of slip resistance at service loads, would only be necessary when stress reversals occur or when direct tension acts on the bolts.

In 1960, the turn-of-the-nut installation method was also introduced as an alternative to the torque wrench (or calibrated wrench) method. Furthermore, when the turn-of-the-nut method was used, only one washer located under the head of the element being turned was required, which further improved the economics of high-strength bolting. Previously, two washers were required in the connection. By 1962, the requirement for washers was eliminated, except for special circumstances (Section 6.2.3.3). In 1964, the higher strength ASTM A490 bolt was introduced. The philosophy of the design of bearing-type and friction-type connections was revised in later versions of the RCSC Specifications in the mid to late 1980s. The reader is referred to the RCSC Specifications (RCSC, 2014) and to Kulak et al. (1987) (both documents are available for download from http://www.boltcouncil.org/) for additional

more detailed information on the historical background, research and recommendations that form the basis of the current *AASHTO LRFD* Specification provisions for the design of high-strength bolted connections (Section 6.6.4.2).

As specified in *AASHTO LRFD* Article 6.4.3.1, ASTM A325 bolts in diameters of 0.5 inch through 1 inch have a required minimum tensile strength of 120 ksi. ASTM A325 bolts in diameters of 1.125 inch through 1.5 inch have a required minimum tensile strength of 105 ksi. ASTM A490 bolts in diameters of 0.5 inch to 1.5 inch have a required minimum tensile strength of 150 ksi. Both ASTM A325 and A490 bolts are available as Types 1 or 3 (Note: Type 2 bolts are no longer available). The ASTM A325 Type 1 bolt is a medium-carbon steel bolt. The ASTM A490 Type 1 bolt is an alloy steel bolt. Type 3 bolts have additional requirements for copper, nickel, and chromium to be compatible with the chemistry of weathering steel grades. ASTM A325 and A490 bolts (and the various bolt types) are distinguished by specific identifying marks described in RCSC (2014).

Type 1 bolts are to be used with steels other than weathering steels, and is the type of bolt furnished if not otherwise specified. Type 1 bolts are suitable for use with painted and galvanized coatings. Type 1 bolts may be either mechanically or hot-dip galvanized. However, galvanizing of ASTM A490 bolts (by either process) is not permitted due to the potential for hydrogen embrittlement (RCSC, 2014). When galvanized ASTM A325 bolts are used on weathering steel projects, only hot-dip galvanized bolts should be used as the relatively thin sacrificial coating on mechanically galvanized bolts will corrode too quickly in an uncoated weathering steel application. Galvanized bolts must be tension tested after galvanizing. The bolts, nuts and washers in any assembly must be galvanized using the same process. As discussed further in Section 6.2.3.2, galvanized nuts should be over-tapped to the minimum amount required for the assembly and lubricated with a lubricant containing a visible dye to allow for a visual check of the lubricant at the time of field installation.

Type 3 bolts have an atmospheric corrosion resistance and weathering characteristics comparable to weathering steels and are to be used only in weathering steel applications.

For high-strength bolts used in slip-critical connections, pretensioning of the bolt should be as high as possible without causing permanent deformation or failure of the bolt. As shown in Figure 6.2.3.1.2-1, the stress-strain or load-elongation behavior of bolt material in a direct-pull tension test has no well-defined yield point.

Instead, a so-called proof load is used in lieu of directly specifying a yield stress. The proof load is obtained by multiplying the tensile stress area by a yield stress obtained by using either a 0.2% offset strain or a 0.5% extension under load. The tensile stress area is equal to the following:

$$\text{Tensile stress area} = 0.785 + \left(d - \frac{0.9743}{n} \right)^2 \qquad \text{Equation 6.2.3.1.2-1}$$

where *d* is the bolt diameter and *n* is the number of threads per inch. For ASTM A325 and A490 bolts, the proof load stress is approximately a minimum of 70% and 80%, respectively, of the minimum tensile strength of the bolt, which is also established in a direct-pull tension test (Figure 6.2.3.1.2-1). In actual connections, the pretension in the bolt is established by turning the nut, which results in elongation of the bolt. Note that the use of ASTM A490 bolts greater than 1 in. in diameter is discouraged because they become too difficult to install.

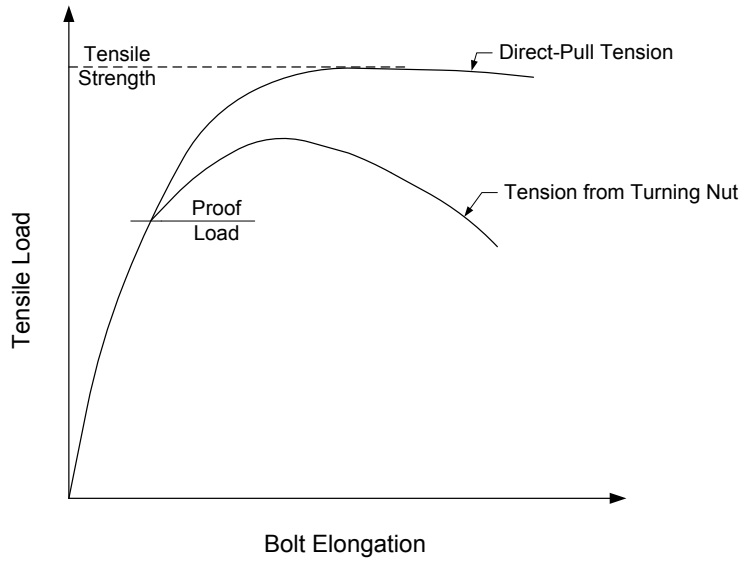

Figure 6.2.3.1.2-1 Typical Tensile Load-Elongation Curve for a High-Strength Bolt

Because of the torsional stresses in the bolt caused by tightening in this manner, the tensile strength and total elongation induced in the bolt by turning the nut are somewhat less than in a direct-pull tension test (Rumpf and Fisher, 1963; Sterling et al., 1965). *AASHTO LRFD* Table 6.13.2.8-1 (Table 6.2.3.1.2-1) specifies the minimum required bolt tension for ASTM A325 and A490 bolts used in slip-critical connections, which is taken equal to 70% of the minimum tensile strength of the respective bolts. The minimum required bolt tension is equal to the proof load for ASTM A325 bolts and about 85 to 90% of the proof load for ASTM A490 bolts.

In order to obtain the minimum required bolt tension, four general methods of installing the bolts can be used: 1) turn-of-the-nut tightening, 2) calibrated wrench tightening, 3) installation of twist-off fasteners, or 4) installation of direct tension indicators (DTIs).

Table 6.2.3.1.2-1 Minimum Required Bolt Tension

Bolt Diameter inches	Required Tension- P_t (kips)	
	A325	A490
5/8	19	24
3/4	28	35
7/8	39	49
1	51	64
1-1/8	56	80
1-1/4	71	102
1-3/8	85	121
1-1/2	103	148

The turn-of-the-nut method is the simplest and obtains the pretension by a specified rotation of the nut from the "snug tightened" condition, which is defined as the tightness that is attained with a few impacts of an impact wrench, or the full effort of an ironworker using an ordinary spud wrench to bring the plies into firm contact (RCSC, 2014). A sufficient number of bolts must initially be brought to the "snug tight" position to bring the connection components into full contact. All remaining bolts in the connection are then brought to the "snug tight" position. Once this phase is completed, all nuts in the joint are given an additional rotation depending on the bolt length and the type of connection. The additional rotation causes a specified strain in the bolt controlling the bolt elongation and obtaining bolt tension well beyond the specified proof load. In the plastic range, large changes in bolt strain cause small changes in bolt tension allowing high clamping forces to be consistently obtained under the additional specified rotation regardless of the variation of the initial "snug tightness".

Calibrated wrench tightening utilizes torque control to obtain the appropriate bolt tensions. Either manual torque wrenches or power wrenches adjusted to stall at a specified torque are used. To prevent large variations in bolt tensions, calibrated wrenches must be set to produce a bolt tension 5% in excess of the values prescribed in Table 6.2.3.1.2-1. Calibration must be repeated at least daily or whenever the wrench is used to tighten a different size bolt. A hardened washer must be used under the turned element (head or nut).

High-strength bolt installation utilizing twist-off fasteners and DTIs is discussed in more detail in Sections 6.2.3.4 and 6.2.3.5.

Regardless of the method used, the final tightening sequence should proceed in an orderly fashion from the most rigid part of the connection progressing systematically toward the less rigid areas or free edges. ASTM A490, F1852, F2280 fasteners, and galvanized ASTM A325 fasteners are not to be reused. Other ASTM A325 bolts

may be reused if approved by the Engineer. Additional more detailed information on high-strength bolt installation procedures and bolt inspection procedures (including required rotational-capacity testing) may be found in RCSC (2014) and AASHTO (2010).

It should be noted that a new combined structural bolt specification, ASTM F3125, has been approved and published by ASTM in January 2015. The specification replaces six separate bolt specifications: ASTM A325, 325M, A490, A490M, F1852, and F2280, that will eventually be removed. The intent of this specification is to streamline and unify language for structural bolts, and to simplify specification maintenance moving forward. The specification also adds some numerous needed changes and improvements. Grades within ASTM F3125 will still be referred to by familiar names; e.g., an A325 bolt will be designated as a "Grade A325" bolt and will simply reside within the combined specification. One important change in the new specification is an increase in the specified minimum tensile strength of 1-1/8 in. diameter and larger A325 bolts from 105 ksi to 120 ksi. Rotational-capacity testing requirements are also included as supplementary requirements, and are provided in an Annex. It is anticipated that references to the ASTM F3125 specification may eventually replace the existing references to the separate high-strength bolt specifications in the AASHTO Specifications.

6.2.3.2 Nuts

Different grades of high-strength bolts are combined with various heavy hexagon-shaped nuts, which guarantee failure by bolt yielding rather than by stripping of the nut threads.

As specified in *AASHTO LRFD* Article 6.4.3.2, nuts for use with ASTM A325 bolts must conform to the requirements of ASTM A563 Grades DH, DH3, C, C3 and D. Nuts to be used with ASTM A325 Type 3 bolts must be of Grade C3 or DH3. All plain nuts must have a minimum hardness of 89 HRB (Hardness Rockwell B).

Nuts to be galvanized must be heat-treated Grade DH nuts and must be lubricated with a lubricant containing a visible dye. The provisions of *AASHTO LRFD* Article 6.4.3.1 are also to apply. To accommodate the relatively thick non-uniform zinc coatings on bolt threads during hot-dip galvanizing, the blank nut is typically hot-dip galvanized and then tapped over-size. This results in a reduction in the thread engagement and the resulting stripping strength. Only the stronger hardened nuts (Grade DH) have adequate strength to meet ASTM thread-strength requirements after over-tapping. Less over-tapping is usually required for mechanically galvanized nuts. Galvanizing increases the friction between the bolt and nut threads, as well as the variability of the torque-induced pretension (Birkemoe and Herrschaft, 1970). If the nuts are lubricated, a lower required torque and more consistent results are obtained. Therefore, the supplier must test a galvanized bolt, lubricated galvanized

nut and a galvanized washer in an assembled steel joint prior to shipment to show that the galvanized nut with the lubricant provided can be rotated from the snug-tight condition well beyond the rotation required for pretensioned installation without stripping; i.e. rotational-capacity testing as described further in AASHTO (2010). Black bolts should be oily to the touch when delivered and installed.

Nuts for use with ASTM A490 bolts must conform to the requirements of ASTM A563 Grades DH and DH3. Nuts to be used with ASTM A490 Type 3 bolts must be of Grade DH3.

Nuts for use with anchor bolts (i.e. ASTM A307 Grade C or ASTM F1554 anchor bolts) are to conform to ASTM A563 for the appropriate grade and size of anchor bolt. Nuts to be galvanized are to be heat treated Grade DH or DH3 and the provisions of *AASHTO LRFD* Article 6.4.3.1 are to apply. All galvanized nuts should be lubricated with a lubricant containing a visible dye.

6.2.3.3 Washers

As specified in *AASHTO LRFD* Article 6.4.3.3, hardened steel washers must satisfy the requirements of ASTM F436. *AASHTO LRFD* Article 6.13.2.3.2 spells out the conditions under which hardened washers are required in high-strength bolted connections. These conditions are as follows:

- Hardened washers are to be be used when the outer face of the bolted parts has a slope greater than 1:20 with respect to a plane normal to the bolt axis.
- Hardened washers are to be be used under the turned element when tensioning is to be performed by the calibrated wrench or twist-off method (Section 6.2.3.4).
- Irrespective of the tensioning method, hardened washers are to be used under both the head and the nut when ASTM A490 or F2280 bolts (Section 6.2.3.4) are to be installed in material having a specified yield point less than 40 ksi, except that a washer is not required under the head of a round-head ASTM F2280 bolt.
- Where ASTM A325 or F1852 bolts (Section 6.2.3.4) of any diameter or ASTM A490 or F2280 bolts equal to or less than 1 in. in diameter are to be installed in oversize or short-slotted holes in an outer ply, a hardened washer conforming to ASTM F436 is to be used, except that a washer is not required under the head of a round-head ASTM F1852 or F2280 bolt.
- Where ASTM A490 or F2280 bolts over 1 in. in diameter are to be installed in an oversize or short-slotted hole in an outer ply, hardened washers conforming to ASTM F436, except with 5/16-in. minimum thickness, are to be used under both the head and the nut in lieu of standard thickness hardened washers, except that a washer is not required under the head of a round-head ASTM F2280 bolt. Multiple hardened washers with combined thickness

equal to or greater than 5/16 in. are not to be considered as satisfying this requirement. Alternatively, a minimum 3/8-in. thick plate washer of structural grade material and a standard thickness ASTM F436 washer may be used.

- Where ASTM A325 or F1852 bolts of any diameter or ASTM A490 or F2280 bolts equal to or less than 1 in. in diameter are to be installed in a long slotted hole in an outer ply, a plate washer or continuous bar of at least 5/16-in. thickness with standard holes is to be provided. These washers or bars are to have a size sufficient to completely cover the slot after installation and are to be of structural grade material, but need not be hardened.
- Where ASTM A490 or F2280 bolts over 1 in. in diameter are to be used in long slotted holes in an outer ply, a hardened washer conforming to ASTM F436 is to be used with a plate washer or continuous bar of at least 3/8-in. thickness and of structural grade material with standard holes. Multiple hardened washers with combined thickness equal to or greater than 3/8 in. are not to be considered as satisfying this requirement.

Note that ASTM F436 weathering steel washers should be used in conjunction with Type 3 high-strength bolts. The provisions of *AASHTO LRFD* Article 6.4.3.1 apply to galvanized washers. Installation procedures for washers are covered in AASHTO (2010).

6.2.3.4 Twist-Off Fasteners

Tension-control or so-called "twist-off fasteners" conforming to the requirements of ASTM F1852 or F2280, which offer the equivalent strength level of ASTM A325 and A490 bolts, respectively, are permitted if approved by the Owner and provided they satisfy the general provisions specified in *AASHTO LRFD* Article 6.4.3.4. Twist-off fasteners rely on a controlled torque-to-tension relationship to automatically provide the required tension or indirectly indicate the bolt tension.

6.2.3.5 Direct Tension Indicators (DTIs)

Direct tension indicators (DTIs) conforming to the requirements of ASTM F959, or other alternate direct tension indicating devices approved by the Owner, may be used according to *AASHTO LRFD* Article 6.4.3.5. DTIs conforming to ASTM F959 are hardened washers with several formed arches on one face that deform in a controlled manner when subjected to a compressive load. DTIs indicate that the maximum installation tension has been achieved without exceeding the ultimate strength of the bolt.

Type 325 is used with ASTM A325 high-strength bolts and Type 490 is used with ASTM A490 high-strength bolts. The DTIs must be incorporated into assemblies with hardened heavy hex ASTM A563 Grade DH nuts. As specified in *AASHTO*

LRFD Article 6.13.2.3.2, DTIs are not to be installed over oversize or slotted holes in an outer ply, unless a hardened washer or a structural plate washer is also provided.

The washers are not to be installed with the protrusions in contact with the structural steel. Installation of a DTI under the turned element is only permitted if a hardened washer is used to separate the turned element (head or nut) from the DTI, except in the case of captive DTI/nuts (see below) which are expressly designed for the DTI protrusions to bear against the turned nut.

DTIs measure load by compressing the protrusions on the washer with a proportional reduction in the gap in the spaces between the protrusions. Tightening of the bolt flattens the protrusions and reduces the gap. Attaining the required tension is verified by the number of gage refusals, or gaps which are too tight to permit the insertion of a feeler gage of the prescribed thickness.

The method of measurement is based upon the criterion that a DTI with more than half or more of its spaces less than 0.005 in. indicates a bolt tension above the required minimum tension. In order to verify that the DTI will provide this performance, the spaces are checked at 1.05 times the required installation tension. Half or fewer of the number of spaces must be greater than 0.005 in. at this load. Consequently, in the structure, if more than half or more of the spaces are less than 0.005 in. (number of refusals greater than half the number of spaces), the fastener is properly installed at a tension above the required minimum installation tension.

ASTM F959 indicates that for proper tension, the gap should be about 0.015 in. or less (Struik et al., 1973). The gap of 0.005 that is specified in AASHTO (rather than 0.015) is intended to address concerns about corrosion due to water intrusion into larger gaps. A visible gap must remain in at least one space after installation to help ensure that the bolts are not tensioned beyond their ultimate strength. Installation procedures for DTIs are covered in AASHTO (2010).

Alternate direct tension indicating devices may be used subject to the approval of the Owner. One such assembly is a so-called “captive DTI/nut” comprised of a DTI affixed to a hardened heavy hex structural nut by the fastener manufacturer. Another alternate assembly considered permissible for use is referred to as a “self-indicating DTI, or an assembly in which the DTI incorporates a self-indicating feature (i.e. silicone rubber) to signify significant bump compression.

6.2.3.6 Rivets

Rivets are rarely used today for new construction; however, a significant number of older bridges still exist with riveted construction. The ASTM A502-03 specification provides three rivet grades with different chemistry requirements. The Grade 1, 2, and 3 chemistries correspond to basic carbon steel, HSLA steel, and weathering

steel chemistries, respectively. Many bridge structures were built prior to this specification and the exact rivet grade and strength may be unknown. General information on rivets and riveted connections may be found in McGuire (1968). Further information on the strength of riveted connections is provided in Article 6A.6.12.5 of AASHTO (2011a).

6.2.4 Stud Shear Connectors

As specified in *AASHTO LRFD* Article 6.4.4, stud shear connectors are to be made from cold-drawn bars, either semi or fully killed, conforming to ASTM A108 Grade 1015, 1018 or 1020. The studs are to have a specified minimum yield strength, F_y, of 50 ksi, and a specified minimum tensile strength, F_u, of 60 ksi. If flux retaining caps are used on the studs, the caps are to be manufactured from a low carbon grade steel suitable for welding and are to conform to the requirements of ASTM A109. AASHTO (2010) covers physical properties, test methods and certification of stud shear connectors. The design of stud shear connectors is covered in Section 6.6.2.

6.2.5 Weld Metal

According to *AASHTO LRFD* Article 6.4.5, weld metal is to conform to the *AASHTO/AWS D1.5M/D1.5 Bridge Welding Code* (AASHTO/AWS, 2010). Filler metal electrodes and/or flux-electrode combinations are identified according to the appropriate AWS designation, which depends on the welding process. These designations are discussed further in Section 6.6.4.3.2. For weathering steel applications, electrodes with alloys added to give the filler metal atmospheric corrosion resistance are typically used.

Weld metal strength for design may be classified as “matching”, “undermatching” or “overmatching”. Matching weld (filler) metal has the same or slightly higher specified minimum yield and tensile strength as compared to the specified minimum properties of the base metal. Weld metal strength classifications for design are discussed further in Section 6.6.4.3.7.1.

6.2.6 Miscellaneous

6.2.6.1 Castings

Cast iron is primarily made from pig iron with carbon and silicon as the main alloying elements. Cast iron can provide strength similar to mild structural steel and can be poured into molds to produce parts with complex geometries. The disadvantage is that the material tends to be brittle with little ductility. As specified in *AASHTO LRFD* Article 6.4.6.3, cast iron castings are to conform to ASTM A48, Class 30. In bridges, the use of cast iron is generally limited to bearings, machine parts for movable

bridges, and other parts that are primarily loaded in compression. Historically in the 19th century, wrought iron, which has better ductility than cast iron, was used to fabricate bridges. However, its use was discontinued after the introduction of steel. Cast iron and wrought iron are generally considered to be non-weldable, although some materials can be welded using special techniques.

Ductile cast iron is a relatively new product that has more applicability for use in bridges. Unlike cast iron, ductile cast iron can be welded to structural steel members to form composite sections. Ductile cast iron has been used as a joint to connect structural steel tubes to form truss or frame systems. There has been some recent research to develop ductile iron end caps for HSS tubes that can simplify their connection details for use as bridge cross-frame elements. The cost of producing custom ductile iron parts may be prohibitive at the current time, but mass production may eventually make them cost-effective. According to *AASHTO LRFD* Article 6.4.6.1, ductile iron castings are to conform to ASTM A 536, Grade 60-40-18, unless otherwise specified.

Cast steel is to conform to either ASTM A27/A27, Grade 70-36 or ASTM A743/A743M, Grade CA15, unless otherwise specified (*AASHTO LRFD* Article 6.4.6.1). Malleable castings are to conform to ASTM A47, Grade 35018, with a specified minimum yield strength not to be less than 35 ksi (*AASHTO LRFD* Article 6.4.6.2).

6.2.6.2 Wires and Cables

Cables used in bridge construction are generally referred to as bridge strand (ASTM A586) or bridge rope (ASTM A603). Cables are constructed from individual cold-drawn wires that are spirally wound around a wire core. The nominal diameter can be specified between 1/2 in and 4 in. depending on the intended application. Strands and cables are almost always galvanized for use in bridges where internal corrosion between the wires is a possibility. Because cables are an assemblage of wires, it is difficult to define a yield strength for the assembly. Therefore, the capacity is defined as a minimum breaking strength that depends on the nominal diameter of the cables.

Since cables are axial tension members, the axial stiffness needs to be accurately known for most bridge applications. Because relative deformation between the individual wires will affect elongation, bridge strand and rope is pre-loaded to about 55% of the breaking strength after manufacturing to "seat" the wires and stabilize the deformation response. Following pre-loading, the axial deformation becomes linear and predictable based on an effective modulus for the wire bundles. Bridge rope has an elastic modulus of 20,000 ksi. The elastic modulus of bridge strand is 24,000 ksi (23,000 ksi for diameters greater than 2-9/16 in.).

Seven-wire steel strand is used in some structural steel applications although its primary use is for prestressed concrete. Possible uses include cable stays, hangers, and post-tensioning of steel components. Seven-wire strands consist of seven individual cold drawn round wires spirally wound to form a strand with nominal diameters between 0.25 and 0.60 in. Two grades are available (Grades 250 and 270) where the grade indicates the tensile strength of the wires (f_{pu}). Because of the voids between wires, the cross-sectional area of the strand will be less than that calculated based on the nominal diameter. The standard strand type is classified as low-relaxation. When a strand is stretched to a given length during tensioning, relaxation is an undesirable property that causes a drop in strand force over time. Strands are usually loaded by installing wedge-type chucks at the ends to grip the strand.

Mechanical properties for seven-wire strands are measured based on testing the strand, not the individual wires. The tensile strength is calculated by dividing the breaking load by the cross-sectional area of the strand wires. Compared to structural steels, strands do not exhibit a yield plateau and there is a gradual rounding of the stress-strain curve beyond the proportional limit. The yield strength (f_{py}) is determined by the 1% extension under load method where the strand elongates 1% during testing. Strands loaded to the yield stress will therefore experience increased permanent elongation compared to other structural steel products. AASHTO defines the yield strength as $f_{py} = 0.90f_{pu}$ for low relaxation strands. The elastic modulus of strands (E = 28,500 ksi) is lower than the modulus for the individual wires due to the bundling effect.

High strength steel bars are another product that has applications for steel construction, although their primary use is in prestressed concrete. Although they do not meet the definition of a wire or cable, high strength bars are included in this section since they are used for the same purposes as seven-wire strand. The bars are available in diameters ranging from 5/8 to 1-3/8 in. and can either be undeformed (Type 1), or have spiral deformations (Type 2) along their length that serve as a coarse thread for installing anchorage and coupling nuts. Unlike bolts, the bars cannot be tensioned by turning the nuts; the nuts act like the wedge anchors used for prestressing strand. Similar to seven-wire strands, high strength steel bars are specified based on their tensile strength (commonly f_{pu} = 150 ksi). AASHTO defines the yield strength as $f_{py} = 0.80f_{pu}$ for deformed bars and the modulus is E = 30,000 ksi.

6.2.6.3 Pins, Rollers, and Rockers

As specified in *AASHTO LRFD* Article 6.4.2, steel for pins, rollers, and rockers is to conform to the requirements specified in *AASHTO LRFD* Table 6.4.2-1 or 6.4.1-1, or in *AASHTO LRFD* Article 6.4.7 (stainless steel), as applicable.

6.2.7 Mechanical Properties of Structural Steels

6.2.7.1 Tensile Properties – Yield & Tensile Strengths

Figure 6.2.7.1-1 represents a schematic of an idealized tensile stress-strain curve for structural steels. The curve is obtained by tensile loading to failure specimens that have either rectangular or circular cross-sections. The ASTM A370 specification *Standard Test Methods and Definitions for Mechanical Testing of Steel Products* defines requirements for application of the procedures given in ASTM E8 *Standard Test Methods for Tension Testing of Metallic Materials* used for determining the strength of steel products. The test method requires determination of the yield strength, tensile strength, and percent elongation for each test. A complete stress-strain curve can be measured by graphically or digitally recording the load and elongation of an extensometer during the duration of the test.

The ASTM A6 *Standard Specification for General Requirements for Rolled Structural Steel Bars, Plates, Shapes, and Sheet Piling* defines the orientation, location, number, and type of test specimens, along with retest requirements and inspection and testing requirements for the determination of tensile properties. Flat rectangular specimens with an 8-in. gage length are typically used for testing plate products up to 1-1/2 in. thick, while 0.505-in.-diameter cylindrical specimens with a 2-in. gage length are used for testing plates thicker than ¾ in. Although both test-specimen geometries may be used for plate thicknesses between ¾ in. and 1-1/2 in., rectangular specimens are usually tested by the mills.

Steel plates and shapes used for bridges are required to have Mill Certificates documenting the test procedures performed according to the ASTM A6 specification. The default testing requirements are performed on the steel heat (H frequency), and one set of test results is used to qualify all plates produced from the heat. Some applications require additional testing to be performed on each plate (P frequency) invoking supplemental requirement S4. For H-frequency sampling, two tension tests are required to characterize all plates or shapes within the heat. Tensile specimens for all plates over 24-in. wide are made with the rolling direction transverse to the load axis of the specimen, unless otherwise specified. The sampling location is selected at one corner of the plate. One test is performed on the thickest plate, and one on the thinnest plate produced from the heat. For all plates under 24-inches wide, and for all structural shapes, tension specimens are made with the rolling direction parallel to the load axis. The sample location for W and HP shapes is in the flanges, 2/3 of the distance between the web and flange tip. The sample location for other shapes is taken from the web, or from one of the legs for angles, as applicable.

Heat treated steel grades in the ASTM A709/A709M specification are required to have an individual tension test performed on each plate (P-frequency). This

recognizes that the final properties are dependent on the specific heat treatments applied to each plate. Grades requiring P-frequency testing are HPS 70W and HPS 100W, and heat treated versions of HPS 50W.

If a tension test result falls below the nominal specification requirements, the ASTM A6 specification allows one re-test from a different location as long as the failed test is within 1 ksi of the nominal yield strength, 2 ksi of the nominal tensile strength, or 2% of the required percent elongation.

The curve given in Figure 6.2.7.1-1 is an engineering tensile stress-strain curve, as opposed to a true tensile stress-strain curve, because the stresses that are plotted are calculated by dividing the instantaneous load on the test specimen by its original unreduced cross-sectional area. The strains are also recorded by dividing the specimen's instantaneous elongation of its gage length by its original gage length. In actuality, the cross-sectional area is constantly being reduced by the Poisson contraction of the specimen as the specimen is loaded. The true stress at any given point at any given time can be calculated with respect to the contracted area at that point. The area reduction can be directly measured during testing, but it requires use of transverse extensometers, making it impractical except for research purposes. For some purposes, such as non-linear structural analysis, true stress-strain curves are required by the engineer. Lacking direct data, these can be calculated from the engineering stress-strain curves by equations that approximate the Poisson contraction effect.

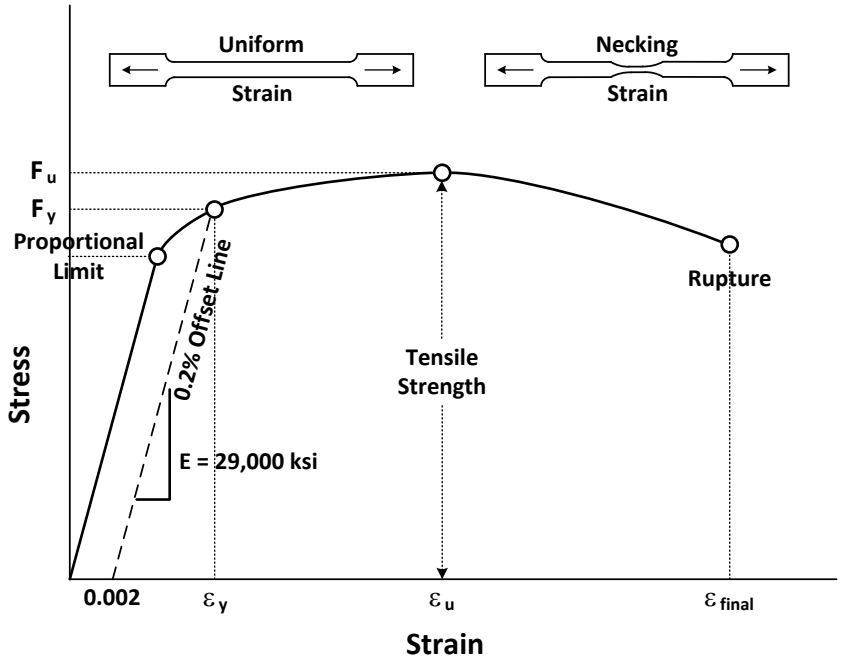

Figure 6.2.7.1-1 Engineering Tensile Stress vs. Strain Curve for Structural Steels Without a Defined Yield Plateau (Wright, 2012)

The initial straight line segment of the stress-strain curve in Figure 6.2.7.1-1 represents the elastic behavior of the specimen where stress is linearly related to strain. In this region, the strain is fully recoverable and the test specimen returns to its original length when the load is removed. The slope, or ratio of stress and strain, of the elastic portion of the stress-strain curve is referred to as the modulus of elasticity, E, or Young's modulus. Young's modulus is conservatively taken as E = 29,000 ksi for structural calculations for all structural steels used in bridge construction (at normal temperatures).

The ASTM E8 tension testing procedures are usually not capable of producing accurate measurements of Young's modulus. Modulus values are extremely sensitive to the accuracy of the extensometer used in testing. The ASTM E111 *Standard Test Method for Young's Modulus, Tangent Modulus, and Chord Modulus* provides special procedures for modulus measurement involving multiple, high accuracy extensometers to counteract bending effects, and multiple load cycles with a data averaging procedure. Modulus measurement by less rigorous procedures can result in considerable error. Experimental studies have reported modulus values between 29,000 and 30,000 ksi, however much of this variability can be attributed to variations in experimental techniques, and not material variability.

As the test load increases, the stresses and strains become non-linear, and the specimen exhibits plastic deformation. The stress corresponding to the initial deviation from linear behavior and the beginning of the plastic region is referred to as the yield strength of the material. Typically, the stress required to produce additional plastic strain increases with increasing strain; as a result, the steel strain hardens. The tangent slope of the curve at the onset of strain hardening represents the strain-hardening modulus, E_{st}, which is used for the analysis of the behavior steel at high strain levels.

Tensile stress-strain curves for structural steels can be divided into two types that exhibit different behavior in the plastic region. Figure 6.2.7.1-1 represents the first type in which the specimen exhibits a smooth deviation from linearity with the stress continuously increasing to a maximum value before decreasing until the specimen fractures; in this case, there is no defined yield plateau. Figure 6.2.7.1-2 shows the second type in which the stress in the specimen reaches a peak immediately after the stress-strain curve deviates from linearity, dips slightly, and then remains at a relatively constant value for a considerable amount of additional strain. The length of this plateau varies for different steels; $\varepsilon_{st} \approx 10\varepsilon_y$ is a typical value. There is typically some small load variation along the yield plateau, and it may exhibit a slight upward or downward slope, which is typically approximated by a horizontal line for structural analysis that defines perfect elastic-plastic behavior. Strain hardening begins at the end of the yield plateau. The stress increases with strain up to a maximum, and then decreases until the specimen fractures.

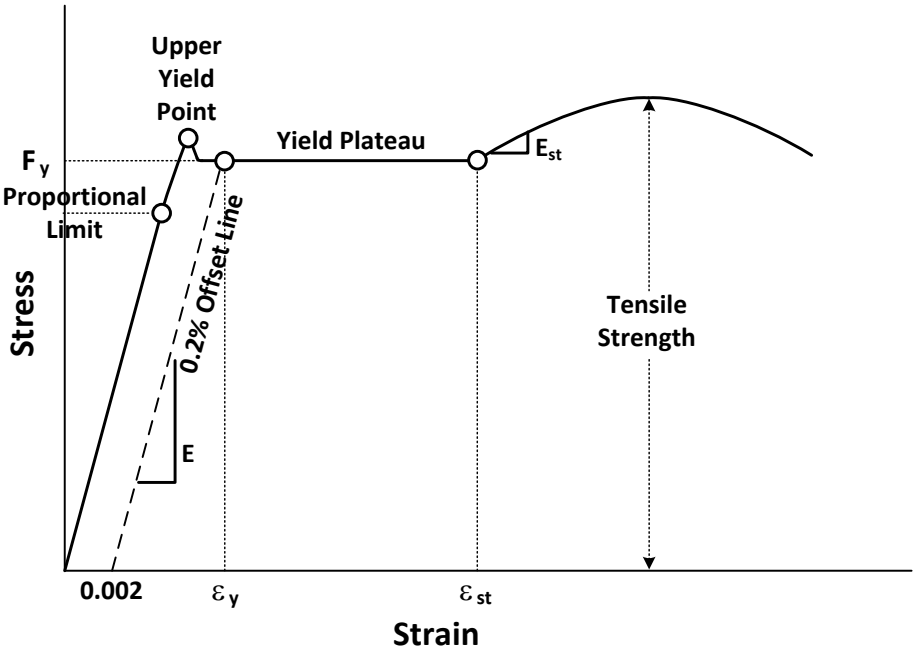

Figure 6.2.7.1-2 Engineering Tensile Stress vs. Strain Curve for Structural Steels With a Defined Yield Plateau (Wright, 2012)

The stress corresponding to the initial peak value is referred to as the upper yield point, as opposed to the yield strength, which is the stress at which the material exhibits a specific limiting deviation from linearity of stress and strain. The magnitude of the upper yield point is highly dependent on loading rate, therefore the upper yield point cannot be counted on for design purposes. The 0.2% offset method (see below) effectively excludes the upper yield point effect from yield strength determination. The maximum stress exhibited by the engineering stress-strain curve in both cases corresponds to the tensile strength of the given steel.

The yield strength is typically determined by the 0.2% offset method. A line is constructed parallel to the elastic portion of the stress-strain curve below the proportional limit with an x-axis offset of 0.2% (0.002) strain. The intersection of the offset line with the stress-strain curve defines the yield strength (Figure 6.2.7.1-2).

ASTM A709/A709M bridge steels with a minimum specified yield strength, F_y, less than or equal to 70 ksi show definite yield plateaus and exhibit similar ductility (Figure 6.2.7.1-2). Grade HPS 100W steel does not have a clearly defined yield plateau (Figure 6.2.7.1-1), and shows slightly lower ductility compared to the lower strength grades. The amount of strain hardening decreases with increasing yield strength.

Steel properties are not always uniform at all locations within a steel plate, nor are they always uniform between different plates. The *AASHTO LRFD* specifications are based on minimum specified nominal yield and tensile strength requirements. Most steel products are delivered with strength that exceeds the nominal minimums since steel makers target higher strengths in production to account for variability. Data from six different North American mills have been collected from over 3,000 tests on Grade 50 and Grade 50W plates with varying thickness (Suwan et al., 2003). Results show the measured yield strength averaged about 58 ksi. Plate variability is an inherent consequence of steel manufacturing, and it has been considered in the calibration of the *AASHTO LRFD* Specification.

The yield strength of steels is increased with an increased loading rate (i.e. decreased loading time). Yield strength increases by about 5 ksi for every order of magnitude increase in loading rate. As a result, the absolute increase in yield strength between slow loading and impact loading is about 25 to 30 ksi (Barsom and Rolfe, 1987). Since the absolute increases are essentially the same for all steels, the percentage increase is much larger for lower-strength steels. ASTM A370 specifies that the loading rate of tension test specimens must be between 10 and 100 ksi/min until the specimens have yielded. After yield, the strain rate must be maintained between 0.05 and 0.5 in/in/min. The yield strength obtained under these relatively slow loading rates is about 4 ksi higher than under static loading, or complete absence of loading rate (Nagaraja Rao et al., 1966). The load rate effect must be considered when comparing test results reported in mill reports, that are presumably performed close to the ASTM upper-bound loading rate, to supplemental product tests. The loading rate has little or no effect on the modulus of elasticity and Poisson's ratio.

The tensile properties of steel generally vary with temperature. The yield strength and tensile strength increase by approximately 60 ksi when the temperature decreases from 70°F to -320°F. Since absolute increases are about the same for all steels, the percentage increase is much larger for lower-strength steels. Structural steels exhibit lower strength and modulus of elasticity as their temperatures increase above room temperature. At temperatures between about 300°F and 700°F, slight increases in the yield and tensile strength, attributed to strain aging, have been observed. However, at high temperatures, such as during fires or other extreme heating events, structural steels can undergo a dramatic decrease in strength. In general, structural steels can be expected to have about a 50% reduction in yield strength at temperatures of 1,100°F. There is also a corresponding reduction in tensile strength and about a 30% reduction in Young's Modulus and the shear modulus. Additionally, creep can also occur at high temperatures leading to a time dependent increase in deflections. However, it is most important to keep in mind that the data show that in the temperature range of interest for most structures, i.e. -60°F < T < 120°F, the yield strength and tensile strength of structural steels remain essentially constant. Behavior of structural steels at elevated temperatures is

important for understanding and analysis of residual stresses, welding, and heat straightening.

6.2.7.2 Ductility and Toughness

The tensile stress-strain curve can be divided into a uniform and a non-uniform strain region, which combine to give the total strain to fracture (Figure 6.2.7.1-1). In the uniform strain region, the cross-sectional area along the entire gage length of the specimen decreases uniformly as loading elongates the specimen. The strain hardening initially compensates for the decrease in cross-sectional area, and the engineering stress continues to increase with increasing strain until the specimen reaches its tensile strength. Beyond that point, the plastic strain becomes localized in a small region of the gage length, and the specimen begins to neck locally with a corresponding decrease in the total stress until the specimen fractures.

Two measures of ductility obtained from the tension test are the total percentage of elongation, and the reduction of area at fracture. The percent elongation is calculated from the difference between the initial gage length and the gage length of the specimen after fracture. The percent reduction of area is calculated from the difference between the initial and final cross-sectional area of the specimen after fracture. The gage length and specimen geometry influence both the elongation and reduction of area. Tension specimens with a 2 in. gage length will exhibit a lower percent elongation compared to those with an 8 in gage length. The ASTM A370 specification provides a conversion between the elongation of an 8-in. gage length strap specimen and a 2-in. gage length round specimen.

Ductility is a required mechanical property that is not directly used in structural steel design. However, it is an important property, measured as the percent elongation prior to rupture, to assure that steel members and connections can perform as required in structural systems. Ductility allows for redistribution of high localized stresses that occur in welded connections and at regions of stress concentration, such as at holes and geometric changes. Any time a hole or other notch is placed in a structural member, it creates a reduced net section where localized yielding is expected to occur first under increasing loads. Without strain hardening, the localized material at the net section will yield and reach the rupture strain before the gross section of the member yields. To provide structural ductility, the steel must have sufficient strain hardening capability to increase the local net section strength sufficiently to allow the gross section to reach yield before rupture occurs at the net section. The ASTM A709/A709M specification assures that structural steel for bridges has an adequate level of material ductility to perform well in structural applications.

The most significant parameter to ensure structural ductility is the yield-tensile ratio (YT ratio), defined as F_y/F_u. In general, the rotational capacity of flexural members

decreases with increasing YT ratios. Similarly, higher YT ratios tend to increase the likelihood of the rupture limit state controlling bolted connection behavior. In general, the strength equations given in the *AASHTO LRFD* Specification are valid to predict behavior for steels with YT ≤ 0.93, and steels with YT ≈ 1.0 have been used successfully for some structural applications (Brockenbrough, 1995). A recent study shows that Grade 50 and 50W structural plates produced in North American mills have YT ratios varying between 0.63 and 0.81 (Suwan et al., 2003). At higher strengths, the YT ratio typically increases, approaching YT ≈ 0.93 for Grade HPS 100W. The *AASHTO LRFD* Specification does not allow the use of an inelastic strength basis for the design of steels with F_y > 70 ksi. For steels specified in the ASTM A709/A709M specification, there is no need for special consideration of the YT ratio for most bridge structural applications. Steels not covered by ASTM A709/A709M should be appropriately evaluated by the Engineer for their intended use.

Toughness is the ability of a material to absorb energy prior to fracture, and is related to the area under the tensile stress-strain curve. The larger the area under the curve, the tougher is the material. Fracture toughness is discussed in greater detail in Section 6.5.5.3.2.

6.2.7.3 Hardness

Hardness is the property of steel to resist indentation in the presence of a localized concentrated force. Hardness testing methods include the Brinell, Vickers, and Rockwell methods. The most accurate methods employ a laboratory testing apparatus. However, portable techniques have been developed for measuring hardness on large components. All of the methods in general involve pressing an indenter ball or pin into the material surface under a known force, and measuring the resulting indentation. Hardness is not a directly useful property for bridge engineers, but hardness can be used as an indirect measure to help approximate the tensile strength, ductility, and wear resistance of steels. Higher hardness generally indicates higher tensile strength and reduced ductility. Hardness is often used as a measure of the strength increase following heat treatments of high-strength steels when the heating history is not precisely known.

Hardness testing can be useful as a screening tool to estimate the properties of steels that have been exposed to different heating conditions in service or in fabrication. Examples in fabrication include evaluation of thermally cut edges, weld heat-affected zones, and plates that have been heat curved. Hardness testing is commonly used to assess the residual properties of structural steel that has been exposed to fire. Hardness measurement is also useful to assess the heat-treated condition of high-strength fasteners.

Section 6.3 Preliminary Design Decisions

6.3.1 Introduction

During the preliminary phase of a bridge design, several critical decisions must be made which set the course for the final design phase. These decisions directly influence whether the bridge design and construction will be successful or burdened with problems. Ill-conceived preliminary designs cannot be made efficient during final design, regardless of how well the individual bridge components are designed.

This section describes some of those preliminary design considerations and decisions that can lead to a more efficient design of a steel-girder bridge. These decisions involve layout considerations, as well as type and size considerations.

In this section, guidelines are presented for primary layout considerations, including structural unit lengths, span arrangement, field-section sizes, girder spacing, deck overhangs, deck and haunch thicknesses, and cross-frames, diaphragms and lateral bracing. Girder depth and substructure considerations are also discussed. This section also provides guidance when making type and size decisions, including the choice of box girders vs. I-girders, along with the consideration of the span-to-depth ratio, optimum web depth, web proportioning, and flange proportioning in the preliminary sizing of the girders.

6.3.2 Primary Layout Considerations for Preliminary Design

6.3.2.1 General

The first portion of this section focuses on the primary layout considerations during the preliminary design of steel-girder bridges. Careful attention to these issues during preliminary design will provide a cost-effective bridge and will reduce rework during final design. Additional important general layout considerations during preliminary design are covered in Chapter 2.

The typical bridge serves hundreds or even thousands of drivers daily and is often viewed by many more. In fact, bridges are one of the most ubiquitous symbols of the modern infrastructure. More stringent constraints have been placed on bridges as land values rise and other structures provide obstacles. Fortunately, the options available to the bridge engineer have kept pace. Structural steel is perhaps the most versatile bridge material today. It finds application in sites that have limited clearance due to its potential to be shaped into shallow structures. It can even have its depth smoothly changed with little influence on cost. Steel can be contorted into the tightest alignments. Steel can be combined with concrete in numerous ways resulting in a marvelous melding of the two materials. Steel bridges can be built with

minimal interruption to traffic. This is possible because it can be erected quickly and without shoring, although occasional temporary towers permit safe erection.

Because steel can be fabricated and erected in an almost endless number of shapes, it should be always in the mind of the bridge engineer that the structure should be pleasing to the user and to the viewer because it is likely to be viewed for many years.

Other critical factors are initial costs and maintenance costs. In part, because of steel's versatility there are many ways to cause unnecessary increases in cost as well as many more ways to design economy into the bridge. The bridge engineer owes the public no less than attractive low-cost structures. This section of the Manual provides recommended means to obtain these objectives within the framework of the *AASHTO LRFD* Specifications.

6.3.2.2 Structural Unit Lengths

One of the first decisions that must be made during preliminary design is the structural unit lengths for the bridge.

Where possible, a single multi-span unit should be employed in lieu of many simple spans or several continuous-span units. Modern design techniques and modern bearings permit the use of much longer multi-span structures than commonly used in the past. Elimination of as many end spans and associated joints as possible is desirable for both first-cost and maintenance considerations. Thermal considerations should lead to the use of separate units only after careful consideration of thermal requirements.

The length of bridge without expansion joints is not defined by specification. The elimination of deck joints – in addition to providing savings in the number of bearings, cross-frames and expansion devices – removes simple supports, which tend to require spans that are shorter than the adjacent spans in order to balance moments and provide economy. Shorter spans within a viaduct-type bridge detract from the aesthetics of equal spans.

Longitudinal forces can be distributed to several piers in proportion to their stiffnesses by the use of fixed pier bearings when designing long continuous units. Of course the piers must be sufficiently flexible. This option allows less expensive fixed elastomeric bearings to be used. Continuous steel bridges well over 2,000 feet in length have been successfully built in cold climates with expansion joints provided only at the ends.

6.3.2.3 Span Arrangement

6.3.2.3.1 Balanced Spans

Steel has the versatility to be built in most any span arrangement. However, steel is most efficient when it is used in properly proportioned span arrangements. Continuous-span steel bridges (Figure 6.3.2.3.1-1) are usually more efficient than simple-span steel bridges since there is less material required. In addition, fewer joints are required with continuous spans.

Figure 6.3.2.3.1-1 Continuous-Span Steel Bridge

Usually the optimum span arrangement for long steel-girder bridges is equal-length interior spans with the length of the end spans approximately 75 to 82 percent of the length of the interior spans. Often a span arrangement is provided with all equal spans, which is optimal for prestressed concrete. Such an arrangement, although buildable with steel, is far from optimal. It leads to larger positive moments in the end spans and at times a non-optimal depth of girder. A carefully arranged span arrangement has a positive impact on the economics of the bridge.

For continuous-span units with more than two spans, span lengths should be proportioned as recommended above to yield approximately equal maximum positive dead load moments in the end and interior spans for straight and horizontally curved continuous spans. Such arrangements are termed “balanced span arrangements”. A balanced span arrangement provides for a single optimum depth. If unbalanced spans are required, it may be desirable to taper the depth of the girder so that different depths are employed more efficiently in different spans.

Frequently, a girder depth between two optimal depths is neither optimum for the longer nor the shorter spans because an average girder depth can lead to flanges that are too large for the longer spans and too small for the shorter spans. Also, a shallow depth in the longer spans may cause problematic deflections.

In many cases, unbalanced spans and non-optimal girder depths cannot be avoided. The versatility of steel provides the best and often the only solution. There are choices that can make the situation less dire. Grade separation structures frequently have short end spans. An option in these situations is to examine the use of tall abutments eliminating the short "jump spans". Lengthening the bridge is an option, but is often found to be expensive. The traditional option is to use simple end spans, which adds two joints and is not desirable. When underclearance is critical, tie-down end supports with haunched interior span(s) have been employed. Of course, this option demands a foundation that can resist uplift. Adding concrete integral diaphragms adds significant weight to the end-span reactions and has been found to help resist uplift in many cases.

To illustrate the balanced span concept further, the unfactored moments in a three-span continuous girder caused by the dead load applied to the non-composite section (DC_1) are shown in Figure 6.3.2.3.1-2. The span arrangement for this girder (190′-0″ - 236′-0″ - 190′-0″) is reasonably balanced with an end-to-center span ratio of approximately 0.81. The moments assuming the same total length for the girder, but with a different span arrangement (200′-0″ - 216′-0″ - 200′-0″), are also shown. For this particular unbalanced span arrangement, the end-to-center span ratio is approximately 0.93. Note that the ratio of the maximum positive DC_1 moment in the end span to the maximum positive DC_1 moment in the center span increases from 1.2 to 2.5 when going from the balanced to the unbalanced span arrangement. For a steel-girder design, the larger uneven distribution of the moments from span to span in the unbalanced arrangement will have a significant overall effect on the girder efficiency and economy. Assuming the girder depth is optimized for either the interior or exterior spans, or else averaged, the chosen girder depth will be inefficient for the moments in either some or all spans.

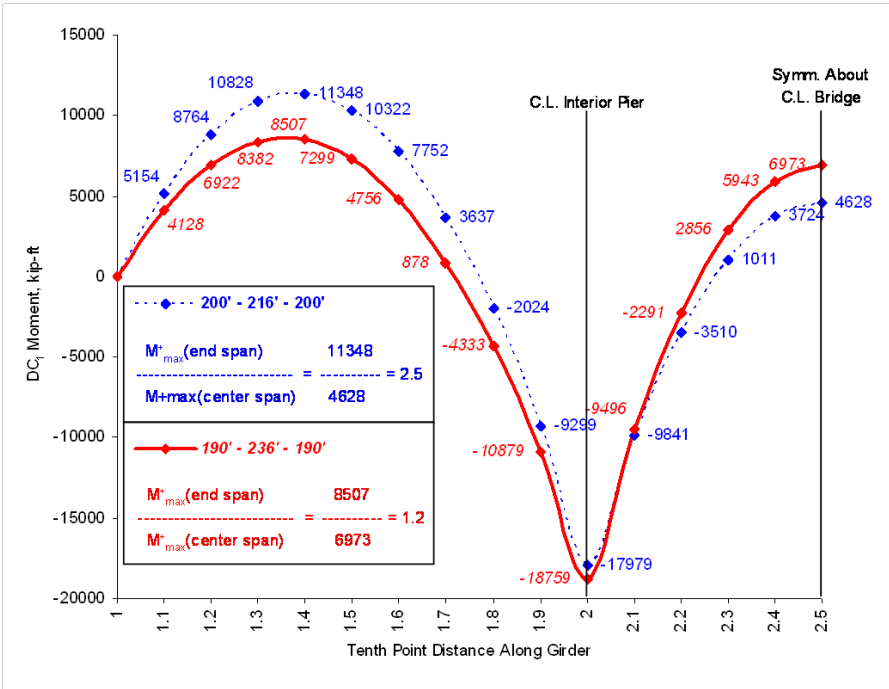

Figure 6.3.2.3.1-2 Component Dead Load (DC_1) Moments for Different Span Arrangements

6.3.2.3.2 Substructure Type and Costs

Obviously, if the substructure costs are relatively low, the optimum span is shorter than for a case with much larger substructure costs. When other things are not considered, the cost of the substructure should approximately equal the cost of the superstructure steel. An important corollary is that reduction of the pier cost has a double effect in that the savings in the piers justifies less costly (by an equal amount) shorter spans.

Clearly, the size, height, and shape of the piers and the foundation type and size affect the substructure cost, and thereby, the optimum span length. Estimates of pier cost must include the cost of formwork, reinforcement, concrete and concrete placement. Simplicity and repetition are keys to economy of the piers. Changes to the unit costs that may result from an improved knowledge of specific site conditions should be incorporated in the analysis and the above curves regenerated before selecting the final span arrangement.

Foundation costs are a function of geological conditions and loads. Steel superstructures often provide an advantage over concrete superstructures in that their weight is less. However, this is not always an advantage. In some cases, the lighter gravity load leads to more critical overturning loads. As discussed further in Section 6.3.3.3.1, an objective for an efficient foundation is one that requires minimal additional material beyond that required for vertical loads. Overturning forces should

be handled by a judicious positioning of piles or drilled shafts, or by the shape and size of a spread footing; preferably, they should not require additional piles, shafts or footing size.

To minimize the number of piles or drilled shafts, it is necessary to eliminate redundancy in the substructure. For example, a wall pier is typically more expensive than a single column, or hammerhead-type pier. The foundation for a hammerhead pier is usually also more economical .than that for a wall pier. Obviously, when piers are high and/or expensive, there is more incentive to reduce their costs and to introduce some simplicity into the design.

Hence, when alternate designs are investigated, the substructure for the steel design must be evaluated and designed concurrently with the superstructure if efficiency is to be obtained. Since substructure costs have such a substantial impact on the most economical span arrangement, the proper steps must be taken if the Engineer is to ensure that the substructure design is the most efficient possible when combined with the steel superstructure.

6.3.2.3.3 Span Optimization (Cost Curves)

For projects with a specified total bridge length in which spans may be varied, it is prudent to develop superstructure and substructure cost curves comparing cost to span length for a series of preliminary designs having different span lengths and arrangements. The cost of the deck is ignored in these investigations since its cost is constant with respect to span. The most economical span arrangement is at the minimum point of the total cost curve, or the curve representing the sum of the variable superstructure and fixed substructure cost per pier over the span range under investigation.

For the case illustrated in Figure 6.3.2.3.3-1, the optimum span length is 165 feet for straight girders. For multiple continuous-span units, this would be the span length chosen for the interior spans. The length of the end spans would then be chosen to provide a balanced span arrangement. The steel cost of curved-girder superstructures typically increases slightly over straight-girder superstructures. This increase generally results in a decreased optimum span length relative to straight girders for a given set of fixed substructure costs. If individual pier costs vary greatly due to height or subsurface conditions, this approach is of questionable value and a discrete pier investigation is warranted.

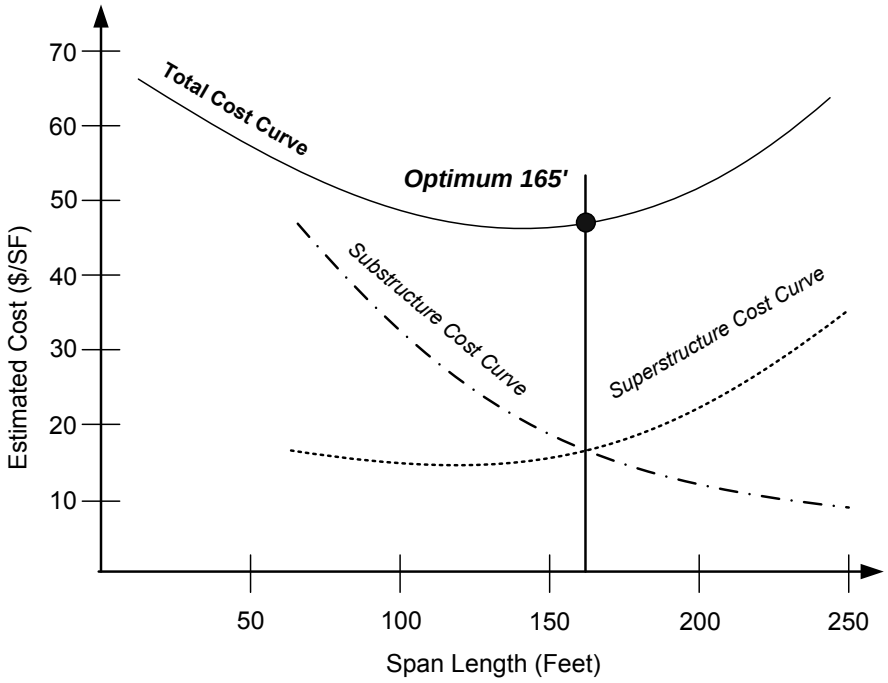

Figure 6.3.2.3.3-1 Sample Cost Curves for Span Optimization

6.3.2.4 Field-Section Size

6.3.2.4.1 General

Field sections or “shipping sections” (sometimes simply called “girders”) are pieces of the bridge girder that are fabricated as a unit and shipped to the bridge site in that manner. A field section is shown in Figure 6.3.2.4.1-1. The limiting length, depth and weight of a field section are a function of the fabricator’s ability to handle the piece in the shop and to ship it. Generally, fabricators are able to fabricate and ship field sections much larger than the optimal size. In rare cases where erection precludes the use of field splices, the larger sections can be made. However, for most structures, the design should be led by optimal-size field sections.

Figure 6.3.2.4.1-1 Girder Field Section in Route to the Construction Site

The Design Engineer usually does not know which fabricator will actually be doing the fabrication so he/she usually makes decisions on field-section size based on ensuring that at least one fabricator that is likely to bid on the work is capable of handling and shipping the field sections. Sometimes the Design Engineer may provide optional field splices that may be eliminated at the discretion of the fabricator. In design-build situations, the Design Engineer usually works closely with the team in making the decision regarding the size of field sections. This simplifies the decisions, but may limit the efficiency of the design compared to that of designs prepared by other teams. An example is girder depth. Another fabricator may be able to ship deeper more efficient girders by barge than the team fabricator may be able to ship.

The number of field sections and the location of splices can have a significant effect on the efficiency of the design. Fewer field splices reduces the cost for splices, other

things being equal. For example, a simple span that is too long to fabricate and ship as a single field section may be spliced at the center of the span at the point of maximum moment saving a second splice that would be required if spliced at points of lower moment. Not only is the number of splices reduced, but the splice is made at the point of minimum dead load shear reducing the demand on the web-splice bolts. Further, it may even save a shop splice if the flange plates are too large to come from the mill. In that case, a uniform-size flange plate would have to be shop-spliced with a hidden cost to the Design Engineer. Not only does the erector have less work, there is one less truck involved in shipping the two field sections than the three field sections to make up one girder line for the span. It should be kept in mind however that the flexural resistance of the tension flange at a bolted splice is limited to the flange yield stress according to the specifications (*AASHTO LRFD* Article 6.10.1.8), which also has to be given some consideration when locating a bolted splice at mid-span, particularly in a straight girder. The choice of field splice locations and the corresponding field section lengths is in many ways project specific.

The weight and length of sections should be determined after consultation with fabricators who are expected to be bidding the work. For example, the crane capacity in the shop legally limits the weight the fabricator can lift with each crane. Sometimes a section can be made slightly lighter to accommodate that capacity relieving the fabricator of calling for an additional crane every time the section is to be moved. Calling for additional cranes to move a section interrupts other production. Sections too long to fit in normal lay-down areas also interrupt normal operations. Flanges too wide to fit in blasting machines or girders too deep to clear overhead cranes are examples of the interrelated factors that affect the cost of fabricating girders.

Material availability from the mills and its cost is significant in some instances, but it is often difficult for the Design Engineer to ascertain availability and cost. For example, plates are typically considered standard between 0.375 and 2 inches thick. Above two inches in thickness, there is an extra charged. There may be only one producer that produces bridge quality plates above three inches thick, introducing a substantial extra even though plates up to 4 inches thick are permitted by specification. A deep web plate may be available from one mill, but its cost might lead the fabricator to choose to build the girder web up by splicing plates together. Another example is the issue of camber. Camber is typically cut into the web plate. If camber is large, the fabricator may choose to partially shape the web camber by sections of web plate rather than ordering a deep plate to burn out the camber with a large amount of waste. Camber issues are beyond the Engineer to consider at design.

6.3.2.4.2 Shipping

Shipping is very site sensitive and is perhaps the most nebulous of the issues involving steel-girder bridges. The shipping regulations of the various states differ greatly. It is impractical for the Design Engineer to know all the different aspects and issues related to the shipping of girder sections. That said, there are specific shipping limits that trip additional costs. For example, it may be that a field section length is slightly over the limit where an escort is not required. If the splice is moved a few feet, a significant savings in shipping cost might be gained. Similar trip points exist for girder weight, depth and width. This information should be ascertained from a fabricator. The width of curved field sections may be a factor. Obviously, the limiting width of a shipping piece might limit the length of a curved girder. Generally, curved girder bridges tend to require shorter field sections, but that is certainly not always true.

The fabricator's contract usually calls for delivery of the fabricated steel to the bridge site. This familiarity with shipping makes the fabricator the source for shipping information. Excessively long, wide or heavy field sections require determination of a specific route, shipping times and frequency of load transporting. Designs can sometimes provide for optional field splices to reduce handling and shipping costs. The Design Engineer is encouraged to discuss large bridge design projects in their early stages with the fabricators who are likely to bid on the project. These fabricators will provide parameter information particular to the project. An astutely designed steel girder bridge is one that more than one fabricator is able to bid competitively.

Steel I-girders are preferably shipped in the vertical position, although they can be shipped canted or horizontal (Figure 6.3.2.4.2-1).

The ability to ship a particular girder is dependent on the particular route. This requires that the fabricator study the route in order to give definitive information to the Design Engineer regarding practical girder-size limits.

Examples of special transportation provisions include additional blocking and tie-downs, special multi-axle trailers, escort vehicles, restricted hours for highway use, and special types of railroad cars, etc. Although such special provisions result in additional costs along with added shop handling costs, these costs may be offset by the need to erect fewer sections with fewer field splices, which can result in significant savings.

Figure 6.3.2.4.2-1 Steel I-Girder Transported in the Horizontal Position

6.3.2.4.2.1 Highway

The American highway system has matured to the point that it is the means of choice to ship the majority of steel-bridge components from the fabricator to the bridge site. Essentially all fabricators are capable of shipping by truck (Figure 6.3.2.4.2.1-1).

Figure 6.3.2.4.2.1-1 Transporting Steel Bridge Girders by Truck

Some fabricators have their own fleet of trucks so they keep trucking costs in-house. Having a dedicated fleet also permits control over delivery dates, even time of delivery.

Since highways are generally publicly owned and used by the public, they are subject to strict regulation to ensure safety and equal use. Load weight, length, and width are controlled, usually by the state, and regulations differ between the states. There are discrete limits on size. Certain sizes may be shipped without an escort; others may require more escorts, and so forth. There may also be limits on the time of day certain loads may be shipped and the number of shipments in a day. For example, it would be nonsensical to design a field section that requires extra shop-crane capacity and an extra escort to ship 250 miles to the bridge site when shortening it by three feet and lightening it by five tons would eliminate both of these extra costs. Therefore, for the Design Engineer to know these limits and take them into account at design is important. Generally, curvature limits the length of a shipping field section to a length less than what would be practical for a similar size straight field section. Of course, this may entail the need for additional field splices in order to reduce the length. For longer field sections, consider showing optional field splice locations on the plans.

The following recommendations related to shipping pieces (for shipment by truck) were provided by a large steel fabricator:

- Whenever the radius of the field section is less than 900 feet, and/or the mid-ordinate is greater than or equal to 18 inches, and/or if the flanges over the majority of the section are light (i.e., less than or equal to 1-inch thick), the Design Engineer should get in touch with a potential fabricator to discuss shipping considerations;
- The total height of the load should be kept below 13′-6″. The height includes the height of the trailer plus the girder depth, including camber and potentially the thickness of the tie-down chains. If the total height limit is exceeded, the use of “drop” trailers (typically 3′-10″ high) can be considered;
- If the planned length of the field section is to exceed 120 feet, the Design Engineer should again communicate with a potential fabricator;
- Field sections weighing more than 35 tons typically require more truck axles than the standard seven axles. A girder weight of 300 to 400 pounds per foot is optimal for shipping. Extreme weight sections are problematic. For long loads that are light (approximately 200 pounds per foot), stability and stresses need to be evaluated. For shorter and heavier loads, it becomes difficult to get the axles under the load. Extra rigging for stability is the fabricator’s responsibility, but is reflected in the project cost.

In at least one state, a load for truck shipment is classified as a “super load” if any of the following conditions are met:

- The load length (measured from the front of the tractor to the end of the girder) exceeds 160 feet;
- The total weight of the load, including all equipment, exceeds 100 tons;

- The load width exceeds 16 feet.

In this state, each company is allowed to ship two "super loads" per day. The shipper must pay for any bridge analysis that may be required along the route. State police inspection by each state traversed is usually required. Different travel times may be specified in different areas. Driver regulations may also impact travel times. Different states will likely have different regulations regarding "super loads." Fabricators should always be consulted with regard to trucking of a "super load."

6.3.2.4.2.2 Rail

A fabricator might choose rail transportation for particularly deep girders, or girders that are to be shipped a great distance (Figure 6.3.2.4.2.2-1). Since rail access at the bridge site is often not available, such pieces are usually off-loaded and trucked to the site. An interesting aspect of rail transportation is that it can change the competitive situation for a bridge. If the bridge cannot be shipped by truck and must be shipped by rail for whatever reason, the interest is opened for fabricators from greater distances since loading and unloading of the railcars, and demurrage are the largest factors in the cost of rail shipping; rail mileage is a less significant cost than highway mileage.

Figure 6.3.2.4.2.2-1 Rail Shipment of a Steel Girder

Longer loads may be shipped in standard gondola cars, or supported on bolsters on two flat cars at opposite ends of the load and connected by an idler car. Since the bolsters can be up to 1′-6″ above the floor of the car, the net height available for the load is reduced by up to that amount. The bolsters must be able to accommodate relative movement. Truck/train "piggyback" cars, which vary in length up to 85 feet and can handle loads over 100 feet in length when idler cars are used to

accommodate the overhang beyond the end of the car, have also been used. For restricted rail movements, load heights up to 16 feet and weights up to 100 tons may be possible depending on the available routing. Widths up to approximately 12 or 13 feet may also be possible depending on the route and the configuration of the load.

Again, it should be emphasized that the requirements for a particular project related to rail movement should be investigated with the likely fabricators on an individual project basis.

6.3.2.4.2.3 Waterway

Presently, there are few steel bridge fabricators located on navigable water in the United States. For certain appropriate structures, such as crossings over navigable water, water transportation may be practical. Such projects may involve enough sections to fill a barge and be on the water (Figure 6.3.2.4.2.3-1). Otherwise, hybrid shipping may need to be employed entailing trucks as well as a barge. Water shipment may be beneficial when site conditions permit erection directly from the barge. The potential for transporting sub-assemblies or assembling entire bridge spans, floating them into position and erecting them onto their bearings directly from the barge may offer significant economies in certain cases.

Figure 6.3.2.4.2.3-1 Steel-Girder Sections Loaded on a Barge

6.3.2.4.3 Handling and Erection

6.3.2.4.3.1 General

Each field section as defined between field splices must be able to be handled without buckling and without yielding. Field splices should be located close enough to each other that the individual pieces will be stable for handling both in the shop

and in the field and for erection without requiring any special stiffening trusses or falsework. The guideline contained in Article C6.10.3.4.1 of the *AASHTO LRFD* Specifications (Equation 6.3.4.4.2-2) may be used to help indicate relatively stable straight I-girder field sections.

For tub sections, *AASHTO LRFD* Article C6.7.5.3 discusses cases where a full-length top lateral bracing system may not necessarily be employed. As discussed in *AASHTO LRFD* Article C6.11.3.2, in cases where a full-length top lateral bracing system is not employed within a tub section, *L* in Equation 6.3.4.4.2-2 should be taken as the larger of the distances along the field piece between panels of lateral bracing or between a panel of lateral bracing and the end of the piece. For cases where a full-length top lateral bracing system is employed, Equation 6.3.4.4.2-2 need not be considered for top flanges of tub sections.

Special site conditions may affect the options available for handling, erection and transportation of large field sections. Examples include sites located in difficult terrain, ecologically sensitive areas or areas where there might be industrial facilities or active rail lines or highways underneath the bridge. The Engineer should become familiar with the site and any special conditions that might affect the size of the field sections.

6.3.2.4.3.2 Lifting of Curved Girders

The pick points on curved girders are selected so that the girder section is stable and relatively plumb. They are often found by trial-and-error. Location of the lifting points is complicated by the fact that the center-of-gravity is not located in the plane of the girder web. By treating a curved I-girder as a circular arc, two pick points can be roughly located at the intersections of the arc with a line through the center of gravity of the field section as shown in Figure 6.3.2.4.3.2-1. However, this computation based simply on geometry is not always valid because of the fact that the actual dimensions of the section often vary from the nominal dimensions and sections are also often non-prismatic, which can shift the center of gravity. Thus, trial lifts are often made, in which a piece is lifted a few inches to test for the most stable lifting locations and adjustments are made as necessary. Lifting points are typically located in the vicinity of the quarter points of the girder.

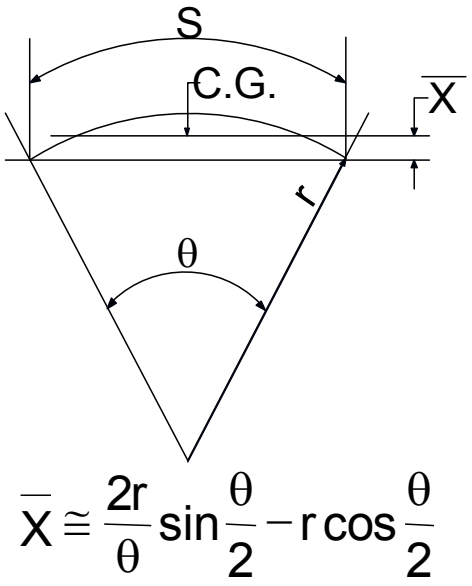

Figure 6.3.2.4.3.2-1 Locating Pick Points on a Curved I-Girder

Analytical and experimental field studies on lifting of curved I-girders have been conducted (Stith et al., 2010). The studies examined prismatic and non-prismatic field sections and lifting with single and multiple cranes with two or more pick points. The studies indicated that *a*/*L* (Figure 6.3.2.4.3.2-2) is the critical parameter to control the twist and deformations and to ensure stability; the radius was not a significant parameter.

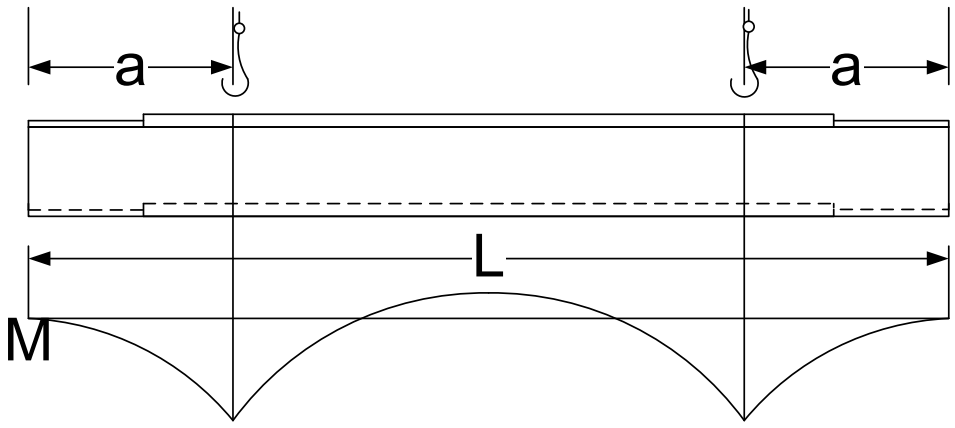

Figure 6.3.2.4.3.2-2 Moment Diagram Due to Lifting

It was further noted that the critical buckling load rarely controls the design for lifting of curved girders, but is a reasonable estimate for the lifting of straight girders.

A spreadsheet that provides for the analysis of the lifting of a horizontally curved I-girder with one crane and two lift clamps has been developed and is available for free download (Stith et al., 2010), and is just one tool that is freely available. The spreadsheet analyzes a girder segment lifted at specified locations with up to 8 different cross-sections and 18 cross-frames attached. Output from the spreadsheet includes the total girder length and weight and the location of the center of gravity of the girder segment, the predicted total rotations and stresses for the lifted segment, the reactions of the lift clamps, and an estimate of the critical buckling load.

The rotations include both the rigid body rotation, which is a function of the girder geometry and lifting locations, and an approximation of the cross-sectional twist determined from strength-of-materials. Maximum rotations are reported at both the segment ends and at the midpoint between the lift clamps. In order to determine the rigid body rotation, the user must input the location of the axis of rotation above the top of the girder, or the location where rotation is free to occur (Figure 6.3.2.4.3.2-3). This location is typically near the top of the lifting clamps. As illustrated in Figure 6.3.2.4.3.2-3, the direction of the rigid body rotation depends on the location of the center of gravity of the girder with respect to the line of support drawn through the pick points. The spreadsheet also provides the lift clamp locations that result in zero rigid body rotation and equal lift clamp forces. The cross-sectional twist is calculated using a linear finite element analysis and does not account for second-order effects.

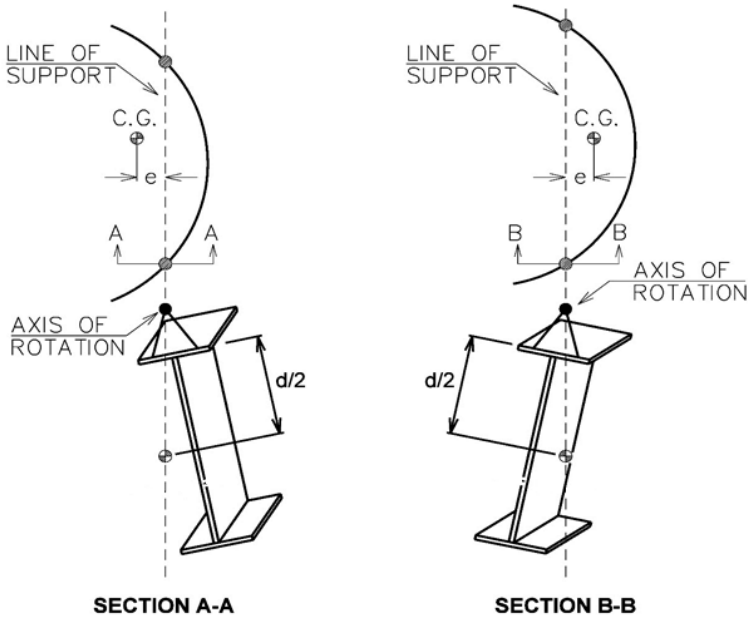

Figure 6.3.2.4.3.2-3 Rigid Body Rotation of a Horizontally Curved Girder During Lifting

Maximum stresses are reported at both lift locations and at the midpoint between the lift clamps. The stresses included strong-axis bending stresses, weak-axis bending stresses, and warping normal stresses. Additional information on lifting of curved girders may be found in NHI (2015).

6.3.2.5 Girder Spacing

6.3.2.5.1 General

Girder spacing (i.e. the number of girders) is a very important parameter in designing an economical steel-girder bridge. Generally, the fewest girders results in the most economical bridge.

Fewer girders generally provide the following economic benefits:

- Reduced fabrication, inspection, painting, shipping and erection;
- Fewer bearings to purchase, install and maintain;
- Fewer bolts and welded flange splices;
- Reduced fabrication and erection time;
- Reduced structural steel weight;
- Lower total bridge cost.

Another intrinsic benefit of utilizing wider girder spacings is that because each individual girder must carry more load, deeper girders are often economical. The greater depth leads to an increased moment of inertia of each girder, which in turn typically makes for a stiffer structure with smaller deflections.

Like any good idea, there are limits. The associated trade-offs need to be examined in each case. For example, wider girder spacing leads to thicker, heavier concrete decks. Frequently, the girder depth cannot be increased due to the clearance envelope. Flange sizes are limited to practical plate sizes. Live load deflection limits must be met.

In prior editions of the *AASHTO* bridge specifications, the exterior girder was less critical than the interior girders. The more recent *AASHTO* Specifications, including the *AASHTO LRFD* Specification, correctly assign more dead and live load to the exterior girders making them, typically, the critical girders in the cross-section. This is particularly true when the overhang is large. As a practical matter, the girders in the cross-section are best made the same size. This means that if the exterior girders control the design, the interior girders are overdesigned if they are made the same size as the exterior girders. If they are sized smaller than the exterior girders, the greater stiffness of the exterior girders will draw load away from the interior ones, leading to the exterior girders being technically under-designed. Thus, the optimal cross-section is one having a girder spacing and overhang such that the exterior and

interior girders have nearly the same total demand moments. Of course, increasing the girder spacing reduces the overhangs.

Because of steel's greater stiffness than concrete, it is often chosen where depth is limited. Live load deflection often becomes an issue in these circumstances. The tendency often is to add girder lines to reduce deflection, as discussed further in Section 6.3.2.5.5.2. The most efficient way to increase stiffness of the bridge without increasing girder depth is to increase the size of the bottom flanges.

The maximum flange size is controlled first by the availability of plate and secondly by a number of other matters. As discussed further in Section 6.3.4.4.3, the maximum practical flange thickness is 3 inches. It is suggested not to exceed this limit unless absolutely necessary. When strength and/or stiffness requirements cannot be met with practical size flanges and girder depth cannot be increased, the only alternative is to increase the number of girders.

6.3.2.5.2 Effect on Deck Design

Most states provide standard deck designs. Several owner-agencies have standard deck thicknesses which are tabulated in standard design tables, often as a function of girder spacing or similar parameters. Usually the decks of stringer bridges are designed as transversely reinforced only. Hence, deck thickness increases with increased girder spacing. However, the thickness increases in increments so the spacing can be widened to some degree without attendant increased thickness, which leads to increased concrete and deck reinforcing costs. However, these costs are usually less than the cost of an additional girder line.

When the girder spacing becomes very wide, the cost of forming may increase. When cast-in-place decks are used, the weight of concrete in the flutes of metal galvanized stay-in-place deck forms must be considered. Much of this weight can be eliminated by placing Styrofoam in the form flutes. Deeper permanent metal deck forms are available that can clear span up to about 13.5 feet between girder top flanges. Precast concrete deck panels are sometimes used as alternative stay-in-place forms, but there forms can only be used for girder spacings up to approximately 10 feet.

Plywood forms are required by some states. Extra wide spacing has been accomplished with wood forms by employing overhang brackets between the girders to reduce the effective span of the wood. Traditionally, the weight of wood forming has not been considered in the design because it is temporary. However, its weight acting on the non-composite section might be considered in longer spans. The weight is removed from the composite section. The form weight is applied to the non-composite section, but removed from the composite section so it can have an effect on the determination of vertical cambers.

To reduce the weight associated with a thicker deck and wide girder spacing, transversely post tensioned decks have been employed. Post-tensioning in place on steel creates certain issues that need to be addressed. The steel connecting the girders is much stiffer than the deck so it resists shortening, creating hogging in the deck. This is not an insurmountable problem, but it does require a rather refined analysis.

One way that post-tensioned decks have been made more practical is to introduce a vaulted deck. This shape allows the strands to be straight while they produce compression in the top of the deck in the thicker portions in negative moment regions and compression in the bottom of the deck in positive moment regions where the deck is thinner. This approach increases forming costs so it is economical only when spacing is around 30 feet or more. Of course such girder spacing is associated with very large overhangs—perhaps 15 feet. This type of deck has only been designed in conjunction with tub girders. Vaulted deck forming systems are rarely permanent.

Transverse posttensioning of lesser spans also has been used without vaulting. Other precast decks using mild steel transversely with nominal longitudinal posttensioning have been used successfully. Precast decks augment the speed of steel erection by removing the set trades from much of the contract, thereby speeding completion of the bridge.

Further information on the design of decks and deck systems may be found in Chapter 7.

6.3.2.5.3 Redecking under Traffic

High usage of the nation's roads has led many states to require that roads remain open to traffic while the deck is being replaced (Figure 6.3.2.5.3-1). This is usually accomplished by placing a temporary barrier on the deck, saw cutting the deck over a girder line and removing and replacing that portion of the deck. This process is repeated until the entire deck has been replaced. Various patterns have been employed, but most require that cutting be performed over a girder line and that traffic be maintained without damage to the bridge.

When considering redecking, the Engineer should investigate the Owner Agency's policy. Issues to consider when redecking under traffic include girder capacity, stability, uplift and cross-frame forces. A number of Owners are requiring an analysis to check for the temporary conditions that may exist during redecking as part of the design to ensure that the bridge has adequate capacity for a redecking plan. Skewed and/or horizontally curved girder bridges can be particularly problematic structures during redecking.

Figure 6.3.2.5.3-1 Staged Redecking Under Traffic

The most critical issue with redecking is the exterior girder on the side with deck and traffic. The removal of weight from the opposite side of the bridge allows the bridge to twist causing an increase in moment in that exterior girder. A second potential issue is uplift at bearings where some of their load has been removed. The uplift issue is more prevalent with skewed supports. Skewed supports can experience uplift that is not found when the total cross-section is effective. Another factor that may exacerbate the uplift issue is the crowding of lanes together during redecking. Design lanes are usually 12 feet, while during redecking, lane widths of 10 or 11 feet are common.

When a portion of the deck is removed, the load in the girders under the removed portion is relieved. The unloaded girders tend to rise while the cross-frames tend to restrain them. Not infrequently, the cross-frames may experience their greatest design load during this condition. The wet concrete is then placed on the bare girders as a non-composite load. The adjacent composite girders are much stiffer and tend to draw some additional load in excess of the unloading experienced by the earlier deck removal. This additional load must be added to the live load and the load from any temporary barriers. The empirical wheel-load distribution factors that may have been used for the design are no longer appropriate since the girders have varying stiffness at the time. When the entire deck is eventually replaced, it simply returns the bridge to its original stress state and deflected shape. Rarely are cross-frames overloaded as the deck is replaced.

Lane-width requirements and the requirement that cuts must be done over a girder line may control the number of girders in the cross-section. Redecking is more practical if the deck can be split at a girder line. An odd number of girders in the

cross-section permits such a split at the bridge centerline. For example, a narrow bridge may require only four girder lines, but the girders may not be located such that a lane can remain open when the deck is being replaced. The result is that a fifth girder in the center of the deck is required. Alternatively, if the bridge is wide enough, four girders may be used with wide spacing that permit a single traffic lane with an additional barrier to be supported on two girders. This might cause the exterior girders to be under-designed due to a small overhang, but it almost always more economical than adding an additional girder. Where alternate routes are available and the bridge does not need to be redecked under traffic, an even number of girder lines is more viable.

If a four-girder cross section is not wide enough to redeck using two girders, it can be modified by increasing the girder spacing in one bay to accommodate a lane of traffic. The remaining two-bay spacing is reduced. This technique requires a refined analysis because wheel load distribution factors provided in the *AASHTO LRFD* Specification are based on the assumption that the girder spacing is constant in all bays. This technique is particularly useful on curved bridges where the spacing in the bay closest to the center of curvature (i.e. on the concave side of the bridge) is increased while the spacing in the outside bays is decreased. This tends to reduce the moment in the convex critical girder, while perhaps permitting an entire girder line to be eliminated.

6.3.2.5.4 Phased Construction

6.3.2.5.4.1 General

Phased construction deals with construction of bridges in phases with a longitudinal joint. This method of construction has become increasingly common when replacing existing bridges without detouring traffic. In phased construction, traffic is typically maintained on the existing structure while part of the replacement structure is constructed. Frequently, a portion of the existing bridge is removed so that the existing substructure can be used. Traffic is then shifted to the new phase of the replacement structure, with appropriate temporary barriers added. This phase is followed by demolition of the existing structure. Girders, deck and parapets for the remaining phase of the replacement structure are then constructed and built next to the first phase. Unlike the situation in deck replacement, the first phase has not the benefit of removal of some load. If the second adjacent phase is connected to the first phase with cross-frames prior to casting the deck, significant load is shifted to the already composite bridge. This increases moments and deflections in the first phase. It is difficult to predict the final position of the bridge due to creep of the deck in the first phase. Extreme forces are often created in the cross-frames connecting the two phases.

The preferred method of construction is to build the second phase independent of the earlier phase. As the final step, the two phases are connected with cross-frames and a closure pour is cast (Section 6.3.2.5.4.2). In some cases, the deck will simply be cast onto the last phase without providing a closure pour (Section 6.3.2.5.4.3). The phased construction is then completed by the removal of any temporary barriers that were placed on the structure during construction. These final steps to join the completed phases and remove any temporary barriers occur on the composite replacement structure.

In both cases for the example bridge shown below in Sections 6.3.2.5.4.2 and 6.3.2.5.4.3, the new completed phase of the replacement structure represented by Girders G1 through G3 and the cross-frames in-between those girders must be investigated separately for the dead load acting on that phase only plus the live load placed in the temporary portion of the bridge. The completed bridge must also be evaluated for the combined effects resulting from the addition and removal of the various dead loads during the completion of the phased construction. Usually, the analyses of the phased construction will provide the critical case and is designed first. A check of the completed bridge will usually (but not always) show the girders to be less critically stressed.

Cambering girders for phased construction can be complex. Typically, the closure pour option is employed on longer spans where the dead load is most significant. Deflections are larger and the potential of problematic cross-frame forces in the bay between phases is great. When spans are small to moderate, a closure pour may not be necessary.

The girders may twist under heavy deck loading during phased construction. This is partly due to the uneven deck load on the bridge. The overhang is on one side and the deck is terminated at a girder. This can twist the girders significantly. If the twist occurs only on the second phase, chords as shown in Figure 6.3.2.5.4.3-2 may restrain the second phase sufficiently. Otherwise, top and bottom lateral bracing in the bays on each side of the closure bay may be required. If the girders are curved, of course the issue is exacerbated.

Phased construction of horizontally curved bridges presents serious issues that must be addressed. If the bridge is built from the concave side, i.e. the side toward the center of curvature, the first phase will cause severe overloading and over-deflection of the convex girder in that phase because it will temporarily be an exterior girder, whereas if the bridge were built in one step, that girder would shift a portion of its load to the adjacent convex girder. The result is that the first phase must be cambered and designed for the controlling first phase. It is important that the Contractor construct the bridge in the manner assumed in the design to calculate the dead load deflections (cambers). Specific considerations related to the phased construction of skewed and curved bridges are discussed further in NHI (2011).

6.3.2.5.4.2 With a Closure Pour

In cases where a closure pour is provided between the two phases (Figure 6.3.2.5.4.2-1), the weight of the closure pour, any associated deck forms, and the added cross-frames between the existing and replacement structure should be applied as a composite load to all six girders in the cross-section in the analysis, Removal of any temporary barriers and the addition of any future wearing surface load should also be applied to the completed composite structure.

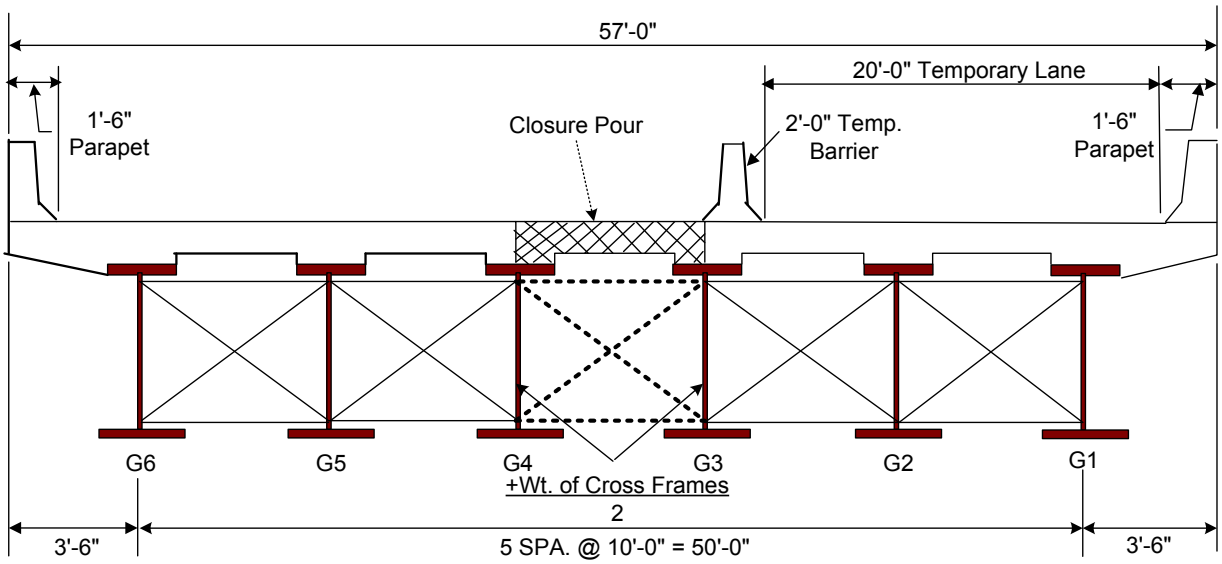

Figure 6.3.2.5.4.2-1 Phased Construction with a Closure Pour

6.3.2.5.4.3 Without a Closure Pour

When the deck is to be cast in phases without providing a closure pour, cross-frame forces in the bay between phases can be mitigated by attaching only the top and bottom chords, as shown in Figure 6.3.2.5.4.3-1. The diagonals in those cross-frames should not be effective until the deck of both phases has been cast. This procedure still requires that the erector return to the site. To ensure fit-up of the cross-frame diagonals, it may be desirable to use the diagonal holes as a template to field drill the connection-plate bolt holes.

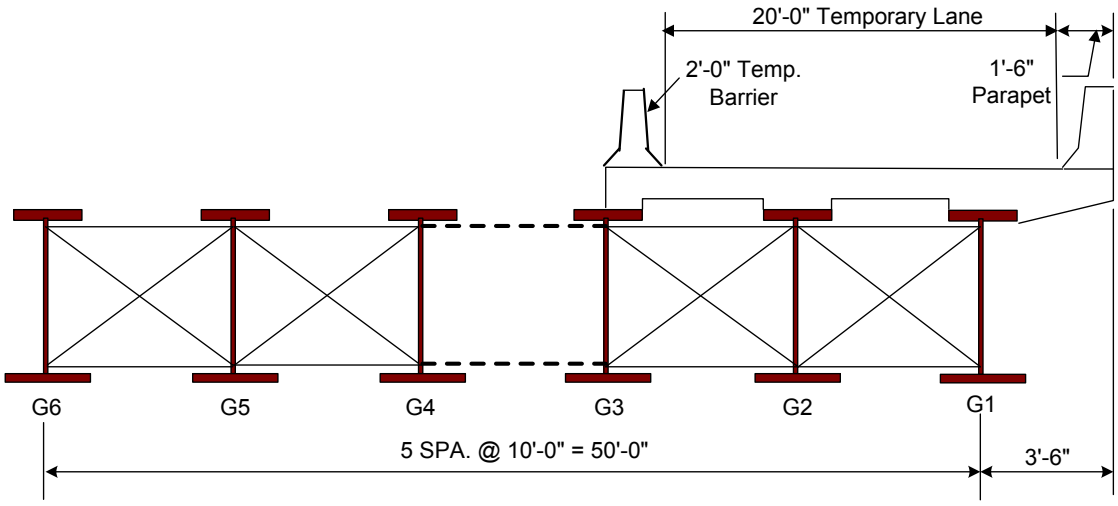

Figure 6.3.2.5.4.3-1 Phased Construction Without a Closure Pour

Unlike the scenario with a closure pour, in this case, the adjacent girders in the two phases each have a different stiffness prior to the final deck pour; one girder (Girder G3) is composite and the adjacent girder (Girder G4) is non-composite. Therefore, the stiffer composite girder will tend to draw more load when the final portion of the deck is cast (Figure 6.3.2.5.4.3-2). Eliminating the cross-frame diagonals for this phase helps reduce some of this load transfer so that the deflections of the adjacent girders will be closer to the case where both girders are assumed to have approximately the same stiffness. The two chords help maintain the alignment and spacing between the girders during the final deck cast.

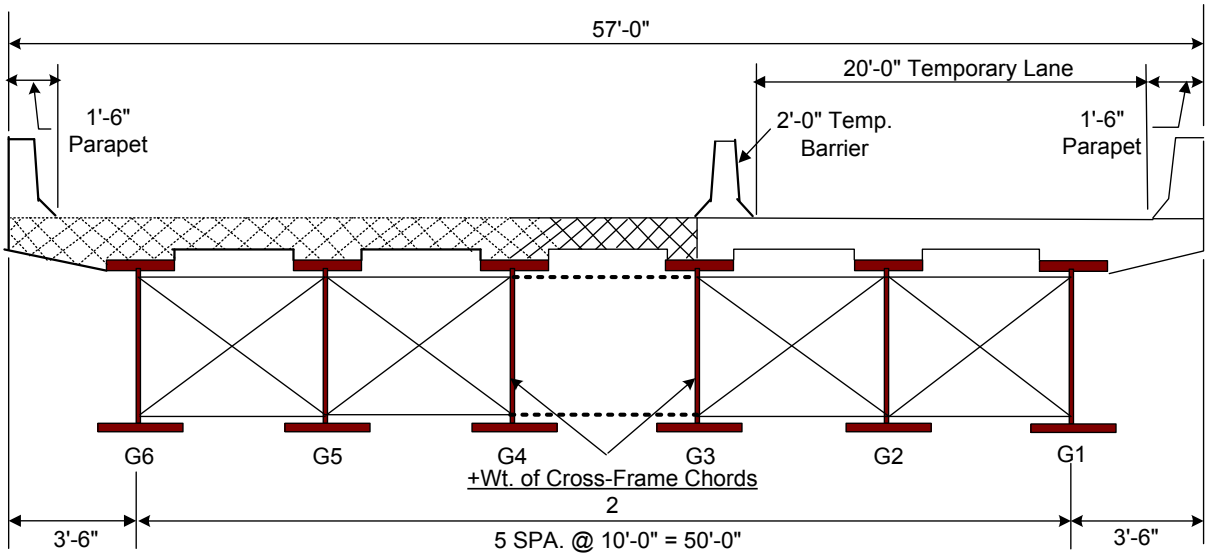

Figure 6.3.2.5.4.3-2 Phased Construction Without a Closure Pour – Deck Cast onto Last Phase

The deck and deck haunch weight (and any associated form weight) from the final portion of the deck cast should be applied as a non-composite load to Girders G4 through G6 and as a composite load to Girders G1 through G3. The weight of the cross-frame chords should also be added as a non-composite load to Girder G4 and as a composite load to Girder G3 in the analysis. Removal of any temporary barriers, addition of any permanent barriers and the addition of any future wearing surface load should be applied to the completed composite structure.

6.3.2.5.5 Deflection Issues

6.3.2.5.5.1 Dead Load Distribution

Unlike curved girders, straight girders support their own weight without any torsional rotations. When the girders are loaded unevenly, the cross-frames provide restoring forces to the girders. For example, if the exterior girder receives less deck weight than its neighbor, it is likely that the two girders will deflect nearly the same amount due to the restoring forces in the cross-frames. Thus, in straight bridges with no skew, the adjacent non-composite girders deflect relatively equally along their length in the vertical direction under dead load (outside of some twisting of the fascia girders that may occur due to eccentric vertical loads applied to deck overhangs), and the cross-frames simply deflect along with the girders. That is, the intermediate cross-frames or diaphragms act to equalize the girder deflections within the cross-section, and thus, nearly equalize the load in equal-stiffness non-composite girders regardless of the amount of load applied to the individual girders. This equalization of deflections creates restoring forces in the cross-frames or diaphragms.

AASHTO LRFD Article 4.6.2.2.1 recognizes this fact by stating that for multi-girder bridges satisfying certain conditions (e.g. width of the deck is constant, girders are parallel and have approximately the same stiffness, number of girders is not less than four, etc.), the permanent load of the wet concrete deck may be distributed equally to each of the girders in the cross-section (Sections 4.3.2 and 4.4.2.1). Although not currently stated, an additional condition of some importance in ensuring a reasonably equal distribution of these loads is that the bearing lines should not be significantly skewed (approximately 10 degrees from normal is a suggested limit) when the intermediate cross-frame/diaphragm lines are normal to the girders. (Note: where intermediate cross-frames/diaphragms are placed in collinear skewed lines parallel to the skewed supports, the assumption of equal distribution of dead loads may be extended to bridges having bearing lines skewed up to 20 degrees.). This assumption is particularly important when determining the non-composite deflections used in determining girder cambers.

AASHTO LRFD Article 4.6.2.2.1 also indicates that for bridges satisfying the stated conditions, permanent loads applied to the deck after the deck is made composite may also be distributed equally to each girder. For the wearing surface load, DW,

this is a reasonable assumption and has been the customary practice. However, Engineers have often applied this assumption to the concrete barrier load as well.

This provision dates back to the 1940s when concrete deck overhangs were much smaller and the provision was applied to much lighter curbs and railings, not barriers. When refined methods of analysis are employed, these loads may be applied at their true location, which usually results in the computed portion of the load resisted by the exterior girders to be significantly larger than an equal distribution assumption would indicate.

To better simulate the actual distribution of these loads when line-girder analyses are employed, consideration should be given to performing a reasonable approximation of this effect. Assigning a percentage of the barrier loads to the exterior girders and to the adjacent interior girder is a better assumption based on refined analyses of several cases. At least one State DOT requires that the barrier load be equally distributed to an exterior girder and the adjacent interior girder. Other State DOTs assign 60 percent of the barrier weight to the exterior girder and 40 percent to the adjacent interior girder. The Engineer may choose to use the live load distribution lever rule to determine the effect of the dead load on the exterior of the deck if the overhang is particularly large. In these cases, the portion of dead load applied to the exterior girder may be larger than the load itself. The interior girders would then sense an uplift condition in those cases. Regardless of the analysis assumption, recognizing the concentrated effect of heavy edge loads is suggested.

6.3.2.5.5.2 Live Load Deflection

The live load deflection criteria in the *AASHTO LRFD* Specification are optional (Section 6.5.4.2.2). No rational theoretical argument for a particular live load deflection limit has been presented and some believe that such a limit is unnecessary. It is probably best viewed as a serviceability limit.

As mentioned previously in Section 6.3.2.5.1, the tendency often is to add girder lines to reduce deflection. Traditionally, the averaging approach has been used most frequently to determine the appropriate live load assigned to a girder in a straight bridge to compute live load deflection (Section 6.5.4.2.2). Unlike previous specifications, which were ambiguous in this regard, the *AASHTO LRFD* Specification specifies that a multiple presence factor is to be applied. Thus, the more traffic lanes on a bridge, the smaller the live load assigned to a girder. The fewer the girders in the cross-section, the more live load assigned when computing deflection.

However, if the wheel load distribution factor for moment or a refined analysis is used to compute live load deflections, the number of girders in the cross-section has

a much less significant effect on live load deflection and fewer girders may in fact be needed than when the averaging approach is used.

The *AASHTO LRFD* live load deflection provisions also differ from previous specifications in other ways. The *AASHTO LRFD* Specification suggests that live load deflection be computed with a lighter live load than that specified for the strength limit states (*AASHTO LRFD* Article 3.6.1.3.2). The *AASHTO LRFD* Specifications permit the concrete to be considered fully effective in regions of negative flexure when computing live load deflections. The specification also permits continuous cast-in-place parapets to be considered in the computation of the stiffness resisting the deflection (*AASHTO LRFD* Article 2.5.2.6.2).

6.3.2.5.6 Varying Roadway Width

Variable deck width introduces challenges to the bridge designer. The versatility of steel is particularly beneficial in these cases. At times the roadway alignment may differ over the supporting girders. For example, a curved deck alignment may be used on straight girders when the curvature is within tolerable limits. In other cases, it may be necessary to splay the girders in plan in order to accommodate the roadway. In extreme cases, the alignment might separate within the same structure. This situation is a so-called bifurcated alignment (Figure 6.3.2.5.6-1).

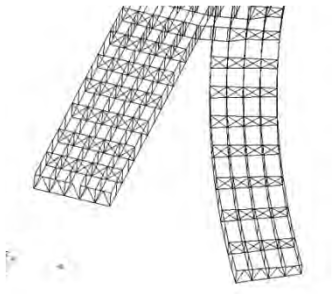

Figure 6.3.2.5.6-1 Splayed-Girder (Bifurcated) Framing Plan

In this case the roadway, before the bifurcation, is narrower than the sum of the two separate roadways. This necessitates the termination of some girders, as shown in Figure 6.3.2.5.6-2. In such cases, the discontinuous girder(s) are usually framed into a bulkhead between girders (Figure 6.3.2.5.6-2). The exterior girders are best not discontinued. First, there is no clean way of attaching the discontinued girder. Second, the exterior girders are frequently the critical girder in the cross-section and adding more load is certainly not desirable. Discontinuing a girder adjacent to an exterior girder is best avoided since it will likely place additional load on the already critical exterior girder.

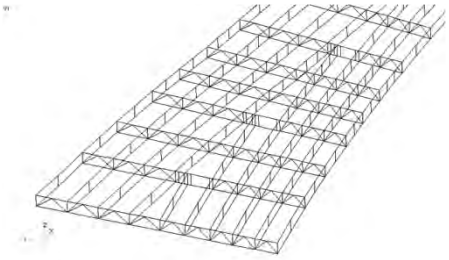

Figure 6.3.2.5.6-2 Discontinuous Girders

To minimize the moment and shear introduced into the bulkhead, it is usually best to discontinue the girders at a point of dead-load contraflexure. This location also reduces the impact on the deck, which is composite with the discontinued girder.

Design of these bulkheads is not treated directly by *AASHTO*. There have been issues raised as to whether or not the bulkheads are fracture critical members. By attaching the bulkhead(s) to the deck with shear connectors, this question is silenced. However, design of the member and its connections deserves careful consideration to avoid fatigue issues. Any moment in the girder at its terminus is transferred into the bulkhead and resisted by twist in the member, which is removed by its end connections and shear connectors. Discontinuous girders are best handled utilizing refined analysis methods.

In situations where the girder spacing varies, it is best to keep the variation within one bay, minimizing the number of different size cross-frames and minimizing changes in formwork and rebar changes.

In cases where distribution factors are employed, Article 4.6.2.2.1 of the *AASHTO LRFD* Specifications permits the distribution factor to either be varied at selected locations along the span, or else a single value of the distribution factor to be used in conjunction with a suitable value for the girder spacing (e.g. when the girder spacing varies, the average value of the girder spacing within the splay might be used).

Wheel load distribution factors for steel box girders are given in *AASHTO LRFD* Article 4.6.2.2.2b, which states that N_L be used in lieu of the girder spacing when determining a single value of the distribution factor for the case of varying roadway width, where N_L is the number of design lanes at the section under consideration determined as specified in *AASHTO LRFD* Article 3.6.1.1.1.

Furthermore, it should be noted that for box girders, special geometric restrictions on the use of live-load distribution factors are specified in *AASHTO LRFD* Article 6.11.2.3 and are summarized in Figure 6.3.2.5.6-3. Included are some basic cross-sectional limitations and a requirement that the bearing lines not be skewed. Also included is a requirement that where nonparallel box sections are used, the distance

center-to-center of adjacent flanges at supports is not to exceed 135 percent nor be less than 65 percent of the distance center-to-center of the flanges of each adjacent box (Figure 6.3.2.5.6-3). The reason for these limitations is the applicability of the wheel load distribution factors. For cases not satisfying these limitations, refined analysis methods are to be employed. As for I-girders, it has been found that widely spaced box girders are the most economical, and these configurations are often beyond the limitations of the empirical wheel load distribution factors.

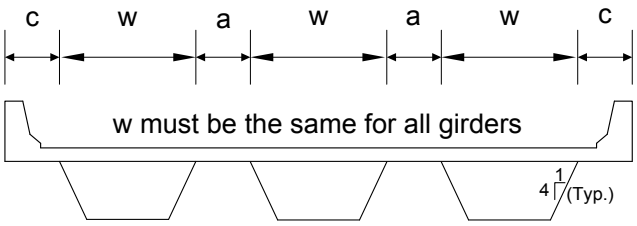

c/a ≤ min. (0.6, 6ft)

(a) Typical Bridge Cross Section

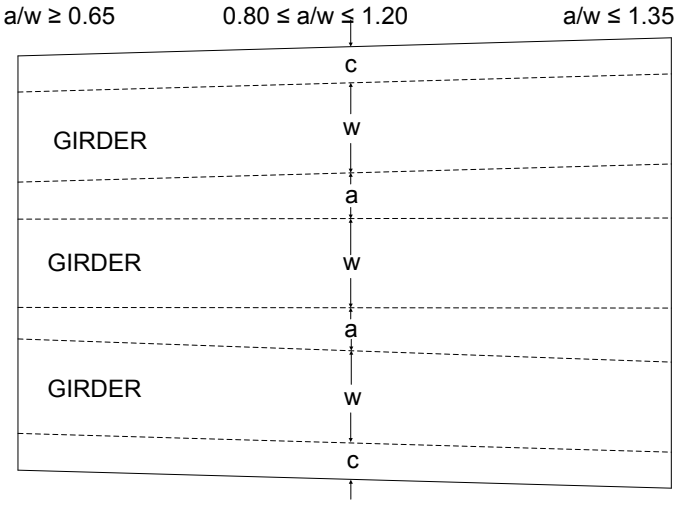

(b) Example of Possible Variation in Box Girder Bridge Width

Figure 6.3.2.5.6-3 Box Girder Geometric Restrictions on Use of Live Load Distribution Factor

6.3.2.5.7 Girder-Substringer Bridge Cross-Sections

A girder-substringer framing system, as illustrated in Figure 6.3.2.5.7-1, has been found to be a cost-effective alternative in some cases for continuous-span bridges with spans above 200 to 300 feet. This system consists of widely spaced composite main girders braced laterally by heavy K-shaped cross-frames. Main girder spacings

from 16 feet to 28 feet have been used. Halfway in-between the main girders, rolled-beam composite substringers are used to span continuously between the cross-frames and provide support for the deck and live load. The cross-frames are considered primary load-carrying members in this system.

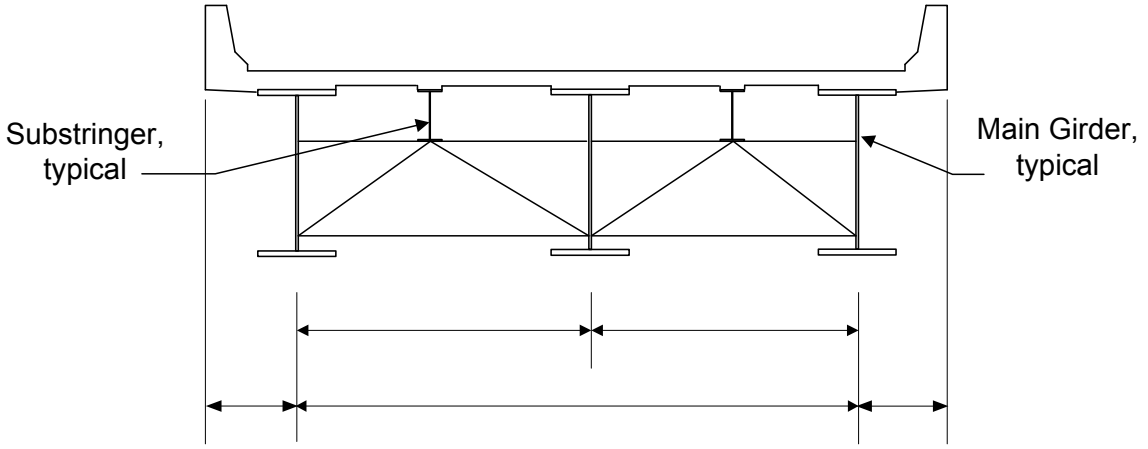

Figure 6.3.2.5.7-1 Girder-Substringer Cross-Section

6.3.2.5.8 Two-Girder Systems

Two-girder systems have fallen into disuse in the United States due to their perceived lack of redundancy. Historically, two-girder systems were very common and many are still in use. Two-girder systems may be divided into two categories; deck-type (Figure 6.3.2.5.8-1) and through-type (Figure 6.3.2.5.8-2) systems.

Figure 6.3.2.5.8-1 Deck-Type Two-Girder System

Figure 6.3.2.5.8-2 Through-Type Two-Girder System

One significant advantage of the through-type system is the increased clearance that this system provides. Railroads found this particularly advantageous since elevating the rail grade is even more expensive than doing the same for a highway. The compression flange of the girders in a through-girder system must receive its bracing from stiffening brackets. One disadvantage of the through-type system is that the girders must be spaced wider apart than the roadway width, forcing a relatively heavy floor system. The deck-type system has less clearance than the through-type system. However, the deck overhangs permit a girder spacing less than the deck width. Hence, a relatively lighter floor system can be used. The deck-type system also provides a more traditional appearance.

Many of the older bridges were built of riveted girders with rolled shapes for the floor system. The multiple elements in the riveted flanges provided redundancy. One reason that these bridges were so common was their economy. The cost of labor for riveting and the cost of material for the two-girder cross-section were reduced with this system compared to those costs for a comparable multi-girder cross-section.

Most existing two-girder bridges in the United States are non-composite since they were built prior to composite design being widely employed in bridge construction. Most are simple-span construction for the same reason; continuous-span construction was uncommon in the days of riveted construction.

Another issue related to the early two-girder bridges is the tendency of the floor-beam ends to create end moments at the girders. These moments were rarely accounted for in the design and have led to fatigue cracking of the girder webs in some cases. The fatigue cracks usually occur at the flange-web juncture. Often the floor beams are attached to wide plates or brackets that extend into the floor-beam span. These types of attachments tend to increase the end moments in the floor beams and these moments must be removed by couples in the girder through the

development of lateral moments in the girder flanges. Often the connection plates are not attached to the flanges, forcing the load through the flange-to-web welds.

Two-girder bridges often are found to have bottom flange lateral bracing. These members resist lateral wind force since the bottom portion of the girders may be unsupported by the floor beams. The lateral bracing members also may act with the sway bracing in the vicinity of the supports. In addition, these members act in resisting torsional loads by converting the cross-section of the structure into a pseudo-box section. Dead loads that are not applied symmetrically to the deck cause torsion, and subsequently, forces in the lateral bracing system. Live loads are usually unsymmetrical with respect to the cross-section and cause torsion in a similar fashion. Live load forces in the lateral bracing system need to be investigated for fatigue. Removal of the lateral bracing usually leads to an increase in the live load girder moments and wind forces in the girder flanges.

Decks of two-girder bridges behave somewhat differently than decks on typical multi-girder bridges. The full width of the deck is often not fully effective near bearings due to shear-lag effects. The result is slightly higher horizontal shear stresses in the deck. If the floor beam deflects significantly, stresses transverse to the girders are generated in the deck since the deflection of the deck varies across its width. If the floor beams and the stringers (if necessary) are at the level of the bottom of the deck and the stringers are bolted to the floor beams, the stringers are likely not acting as continuous beams and there may be excessive longitudinal stresses in the top of the deck.

There are a few bridges of this type recently built in the United States. Most are composite with the main girders and often are composite with the floor beams (and stringers where provided). More bridges of this type have been built in Switzerland, where the deck is often precast and attached to the girders with shear studs welded through pockets in the deck. The deck sections are then posttensioned and the stud pockets grouted.

The advantages of two-girder cross sections are the same as in earlier days. They provide a minimum number of webs, which introduces significant economy. The amount of welding is substantially reduced with only two main girders in the cross-section and by utilizing rolled shapes for the floor beams/stringers. Fatigue is less critical in the main girders since they are usually proportioned to carry a number of traffic lanes, hence they are heavier than girders in multi-girder bridges and the effect of a single truck is much less. Two-girder bridges also require fewer bearings and can be erected in less time.

The main girders may be built-up using angles and plates bolted together (much as a riveted girder) in order to provide an additional level of redundancy via the multiple-element technique. The only two-girder bridges that are known to have experienced

fractures continued to carry live loads after fracture occurred. A refined analysis with assumed hypothetical cracked components can demonstrate that many of these bridges are redundant in their own right. Research is currently ongoing to determine whether the improved toughness offered by newer high-performance steels (HPS) can be effectively and safely utilized to take advantage of some of the inherent economies offered by two-girder systems (and other systems that have traditionally been considered non-redundant).

6.3.2.6 Deck Overhangs

Deck overhangs in steel multi-girder bridges are often overlooked as insignificant. In fact, deck overhangs are an important factor in the overall economy of the bridge. Overhangs should be established to provide a reasonable balance of the total factored dead and live load major-axis bending moments in the exterior and interior girders. Otherwise, the exterior and interior girders are designed for different loads leading to inefficient designs for the more lightly loaded girders if all girders are kept the same size, or to different size girders with differing stiffnesses. The wheel-load distribution factors in the *AASHTO LRFD* Specifications are sometimes not applicable for bridges with cross-sections having girders with differing stiffnesses. If the stiffnesses are comparable, the wheel-load distribution factors in the specifications are adequate.

There are a number of factors that affect the design of exterior girders. The *AASHTO LRFD* wheel-load distribution factors for the exterior girder in steel bridges tend to more correctly apply a greater live load to those girders than did the wheel-load distribution factors in previous specifications, which were developed for smaller overhangs on much shallower girders than used on modern steel bridges (see Section 4.4.2.2.2). As discussed in Section 6.3.2.5.5.1, deck weight can be assigned equally between all stringers in the cross section if the girders are of approximately equal stiffness at cross-frame/diaphragm connection points. Additionally, a larger portion of the barrier weight should also be assigned to the exterior girders. As a result, the exterior girders are often designed for significantly more load than the interior girders if the overhang is as large as 35 percent of the girder spacing (or larger).

Article 2.5.2.7.1 of the *AASHTO LRFD* Specifications states that unless future widening of the bridge is not plausible, the load carrying capacity of the exterior girders is not to be less than the load carrying capacity of the interior girders. This requirement can be used to establish the lower limit on the length of the deck overhangs. However, as mentioned above, if the overhang is of a typical size, the total factored major-axis bending moments will tend to be larger in the exterior girders than the interior girders. Hence, it is necessary to limit the length of the deck overhangs to ensure a reasonable balance between interior and exterior girder moments.

In general, if the overhang is too large, the exterior girders will be critical and will be required to be larger than the interior girders. As discussed elsewhere, this leads to uneconomical designs. Therefore, keeping a reasonably small overhang with a minimal number of girders yields the most economical steel I-girder cross-section in most cases. Experience shows that deck overhangs for cast-in-place concrete decks limited to between approximately 28 and 35 percent of the girder spacing tend to yield reasonable balance between the total interior and exterior girder moments.

The transverse bending moment in the deck over the exterior girders is a function of the vertical loads on the overhang and impact on the barrier. The list below summarizes the typical non-composite and composite loads that may be applied to deck overhangs.

Non-composite loads that are supported by the overhang brackets attached to the exterior girders include:

- Deck forms
- Wet concrete
- Finishing machine
- Screed rail
- Walkway
- Overhang brackets

Composite loads applied to the overhang concrete include:

- Barriers
- Self-weight of concrete
- Barrier impact
- Sidewalk
- Sound walls
- Sign posts
- Live loads (vehicular and potentially pedestrian)

As overhangs become larger, it becomes more difficult to control the twist and web deflection of the exterior non-composite girder induced by loads on the cantilevered forming brackets. As illustrated in Figure 6.3.2.6-1, these brackets are typically spaced at three or four foot increments along the exterior girders (or exterior webs in the case of a box girder). The non-composite overhang loads are resisted by vertical shear and a couple created by horizontal forces applied to the top flange and to the bottom flange or web causing torsion on the exterior girders. The torsion is resisted by lateral bending in the flanges and by the cross-frames. Bearing on the web can lead to web distortion and lowering of the screed rail. This problem has been addressed in some cases by adding intermediate web stiffeners or struts between the girder webs. Most contractors either have full-depth brackets or can

rent them. The deeper the couple, the less the horizontal force. Hence it is advisable to use girder-depth brackets. The effect of these overhang loads on the girder design is addressed in Section 6.5.3.4.

Figure 6.3.2.6-1 Cantilevered Deck Overhang Brackets

6.3.2.7 Deck Thickness

The deck thickness is a function of the girder spacing and the design assumptions. Typically, owner-agencies have tables of deck thickness versus girder spacing. The "empirical deck design method" provided in *AASHTO LRFD* Article 9.7.2 is recommended to be used with caution. The method is based on the assumption that there is a fixed rotation restraint at the edges of the deck span. This is not always true. When the girders twist, the deck moments increase, hence requiring more reinforcement than provided by the method. Differential deflection of the girders creates similar increased moments. In bridges with skewed supports, the horizontal shear force can be significant in the vicinity of the simple supports. The tendency for relative longitudinal movement of the girders is resisted by horizontal shear. Also, relative vertical deflection of the adjacent girders in skewed bridges increases the vertical shear in the deck. Typically this shear is resisted by the cross-frames, which are significantly stiffer than the deck. Similar issues occur in curved-girder bridges, but typically they are not as severe. A more traditional design approach without such a tacit assumption is presented in the *AASHTO LRFD* Article 9.7.3.

When the deck is properly modeled, shear and flexural stresses can be computed in the deck for superimposed dead load and live load. These analyses must consider the compatible deformation of the steel concurrently with the deck. Usually, a simple rational analysis is sufficient to provide adequate reinforcement. However, in cases where the girders are particularly flexible and/or the skew is particularly sharp, a

refined deck analysis may be justified. The deck thickness is typically not changed during the course of the design once it has been set initially, but the amount of reinforcement may change.

6.3.2.8 Haunch Dimensions

Haunch width is usually set to match the top flange width. In some cases, the anticipated deck forming method may affect the choice of the haunch width (e.g., stay-in-place metal deck forms usually include clip angles which are attached to the top flange, dictating that the haunch width match the flange width). Sometimes aesthetic requirements (tapered overhang soffits, desire for constant haunch width even if top flange width varies, etc.) may affect the configuration of the haunch.

Haunch depth is usually set to accommodate all variations in the top flange thickness and any minor deviations from the theoretical dead load deflections, along with consideration of the deck cross slope and the anticipated deck forming method (which may involve a minimum haunch thickness requirement). Splice plates and bolt height must be considered, in addition to the requirements for minimum and maximum stud penetration into the deck (Section 6.6.2.2.4). The haunch height is usually increased slightly to ensure clearance for the deck reinforcing. The haunch height (only) is typically included in computing the composite section properties.

6.3.2.9 Cross-Frames and Diaphragms

6.3.2.9.1 General

In the following, the functions of cross-frames/diaphragms, selection of the longitudinal cross-frame/diaphragm spacing, layout or arrangement of the cross-frames/diaphragms, basic configurations of cross-frames/diaphragms and design considerations for cross-frames/diaphragms will be reviewed.

Although cross-frames and diaphragms account for only a small percentage of the total structure weight, they account for a significant portion of the total erected steel cost of the steel-girder superstructure. Therefore, careful attention should be paid to their design and detailing. The number, arrangement, member size and spacing of cross-frames/diaphragms are important design considerations. These decisions influence not only the design of these members, but the design of the entire superstructure.

Figure 6.3.2.9.1-1 illustrates a cross-frame, a diaphragm and lateral bracing. These are defined in *AASHTO LRFD* Article 6.2 as follows:

- Cross-frame – a transverse truss framework connecting adjacent longitudinal flexural components (or inside a closed box or tub section) used to transfer vertical and lateral loads and to provide stability to the compression flanges;
- Diaphragm – a vertically oriented solid transverse member connecting adjacent longitudinal flexural components (or inside a closed box or tub section) used to transfer vertical and lateral loads and to provide stability to the compression flanges.
- Lateral bracing – a truss placed in horizontal plane between two I-girders (or two flanges of a tub girder) to maintain cross-sectional geometry, and provide additional stiffness and stability to the bridge system;

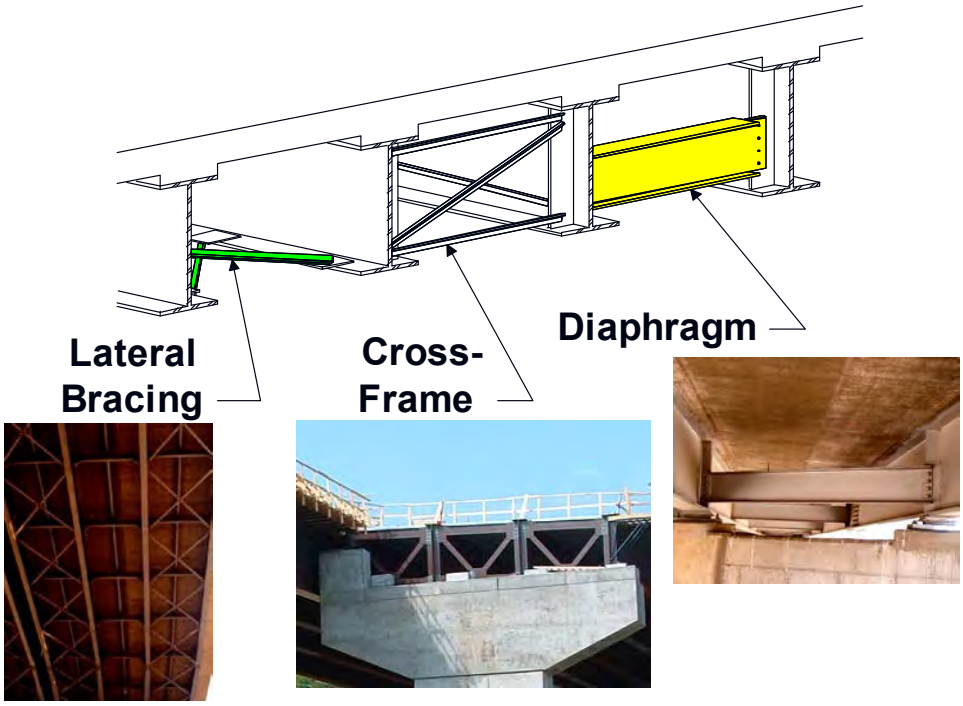

Figure 6.3.2.9.1-1 Definitions of Cross-Frame, Diaphragm and Lateral Bracing

6.3.2.9.2 Functions

6.3.2.9.2.1 Right, Straight I-Girder Bridges

Traditionally, cross frames/diaphragms in right, straight bridges provide support to the girders against lateral torsional buckling. They also provide geometric stability to the girders prior to the hardening of the deck. Without them, the girders would deflect independently of each other, making it very difficult to properly cast the deck. Properly erected cross-frames/diaphragms ensure that the girders in these bridges deflect nearly equally as the deck is cast. This ensures that the girders each resist about the same steel and deck non-composite load. The cross-frames/diaphragms transfer load between the girders to ensure that this occurs. As discussed

previously in Section 6.3.2.5.5.1, *AASHTO LRFD* Article 4.6.2.2.1 indicates that the total deck weight may be distributed equally to the girders when certain specified conditions are satisfied. Cross-frames/diaphragms, along with the deck, also distribute barrier weight, etc. within the superstructure. They also distribute live load within the superstructure.

Cross-frames/diaphragms stabilize the exterior girder when overhang bracket loads are applied. The top flange acts essentially as a continuous beam supported by the cross-frames/diaphragms. The top flange on the exterior girder must resist lateral bending induced by the overhang brackets between each cross-frame/diaphragm. This load may induce significant lateral bending in the top flange. A wider flange is useful to a degree. Intermediate support points have been introduced by various means. However, the spacing of cross-frames/diaphragms may control the girder design if the top flange is slender and/or if the overhangs are large (heavy).

The cross-frames/diaphragms transfer wind load from the superstructure through the bearings to the substructure. They also are effective in earthquakes in that they are the elements attaching the massive deck to the massive substructure.

Although the cross-frames/diaphragms provide lateral stability to the girders, they alone cannot with certainty, provide global stability to the steel girders before the deck is placed. If the girders are permitted to move longitudinally with respect to each other, the angle between the cross-frames/diaphragms and the girders is no longer a right angle and the girders may become unstable. Some additional stability is required. Bearings may be locked against longitudinal movement and/or lateral bracing may be added over a portion of the length of a span or spans.

At ends of the bridge, the edges of the deck and the live load must be supported by the top chord of the end cross-frames/diaphragms (refer to *AASHTO LRFD* Article 9.4.4). This member acts in flexure and is often a rolled I-shape or a rolled or bent-plate channel.

Although these are important functions, the cross-frame/diaphragm has not traditionally been treated as a primary member deserving special design attention in straight bridges with no skew; that is, structural actions are rarely calculated and standardized designs are generally used. That does not mean that these members have not been problematic. The most common problem has been fatigue cracks initiating in the area where the web and flange meet. The connection plates were not attached to the flanges for many years. Moment in the connection plates caused high transverse stresses in the web within small web gaps. Cyclic loading led to fatigue cracks in a number of cases. It should be noted also that cross-frames in the exterior bays transfer parapet (or other) loads on the deck overhangs to the girders. If these loads are large or if the overhang is large, the cross-frame forces in the

exterior bay may be significant. Frequently, signs are placed in these locations creating excessive forces in specific cross-frames.

6.3.2.9.2.2 Horizontally Curved I-Girder Bridges

In curved I-girder bridges, the cross-frames/diaphragms serve all of the above functions, as well as several additional critical functions. In horizontally curved I-girder bridges, the cross-frames/diaphragms provide the primary resistance to torsion. Unlike their typical characterization as secondary members in straight bridges, cross-frames in a horizontally curved bridge with or without skewed supports, must be designed as primary load-carrying members as specified in *AASHTO LRFD* Article 6.7.4.1.

The cross-frames/diaphragms connect adjacent girders so that the concave girder shifts some of its load to its neighboring girder, which must resist that load in order to stabilize the concave girder. The amount of load that is shifted is essentially a function of curvature and length of the span; as the curvature becomes tighter, the cross-frame/diaphragm spacing must be reduced. Regardless of the number of cross-frames/diaphragms in a span, the total load shifted is nearly constant. For example, if there are five cross-frames in a one bay of one span and the total load shift from the inside girder to the outside girder in that bay is 30 kips, the sum of the vertical components in the cross-frame diagonals will equal 30 kips, or 6 kips per cross-frame if they are equally spaced. If there are four equally spaced cross-frames in the same bay of that span, the sum of the vertical components will remain 30 kips, but the vertical force per cross-frame will be 7.5 kips.

If the span is 100 feet and five cross-frames are equally spaced at about 16.7 feet, the lateral flange bending moment is a function of the spacing squared (FHWA/NHI, 2010). If the number of cross-frames is reduced to four so that the cross-frame spacing is increased to 20 feet, the lateral flange bending will be increased by the ratio of $(20/16)^2 - 1 = 0.56$ or 56 percent.

6.3.2.9.2.3 Skewed I-Girder Bridges

In I-girder bridges with skewed supports, the restoring forces in the cross-frames/diaphragms tend to equalize the girder deflections as in right bridges. However, the cross-frames/diaphragms in skewed bridges frequently experience significant forces as they attempt to equalize deflections at the points at which the cross-frames/diaphragms are attached (FHWA/NHI, 2010). If the cross-frames/diaphragms are contiguous across the bridge, they act as a transverse truss transferring load across the bridge.

As mentioned previously, although cross-frames/diaphragms in straight I-girder bridges transfer load between the girders, particularly in bridges with sharply skewed

supports, their design has traditionally been given insufficient consideration. The specification does not require that the cross-frames/diaphragms in straight bridges with skewed supports be designed as primary members in spite of the fact that the cross-frame/diaphragm forces may be much higher than found in many curved-girder bridges. Cross-frames/diaphragms in these bridges restore the structure by transferring load between girders, brace the girder flanges, resist lateral bending and help resist deck overhang bracket forces.

6.3.2.9.2.4 Box-Girder Bridges

Cross-frames/diaphragms are employed inside and between boxes. They serve two different sets of functions.

Internal cross-frames maintain the shape of the box. A box section tends to distort when subjected to torsion. This distortion must be limited or the box will lose its capacity in either torsion or in bending and the distortion stresses will become excessive. Distortion occurs as the shear flow changes direction at the corners of the box (Section 6.5.5.2.2.3). The box distorts between the cross-frames and is returned to its proper shape at the cross-frame minus the elastic shortening of the cross-frame. Unlike bending moment that usually varies along the girder, torque can remain constant over the girder length between the points of application of the torque and points of torsional restraint. The magnitude of distortional warping is related to the magnitude of the torque and the amount of distortion permitted in the box cross-section.

Intermediate internal cross-frames are required in box-section members by specification (*AASHTO LRFD* Article 6.7.4.3). Spacing of the cross-frames may be increased as torsion decreases. Spacing may be more critical in larger and/or torsionally flexible boxes.

Wright et al (1968) used the analogy of the equations for box distortion and cross-frame forces to those for a beam on an elastic foundation (BEF) to develop charts for the solution of the box distortion problem. Transverse bending in the webs and flanges is analogous to the flex in the BEF beam, while the cross-frame members are analogous to BEF supports. The BEF analogy is discussed further in Section 6.5.5.2.2.3.

Internal cross-frames are attached to transverse stiffeners serving as connection plates. The connection plates are, in turn, welded to the web and to the top and bottom flanges. Hence, the stiffened web is stiffer in transverse bending than the web alone. The bottom flange is not typically stiffened transversely unless a bottom transverse member is provided within the internal cross-frames. When used, these transverse elements typically would be welded to the bottom flange or bolted to the longitudinal flange stiffeners if present. Without transverse stiffening, the bottom

flange plate may be susceptible to distortion, which can cause significant through-thickness transverse bending. The transverse bending stresses can be critical at points where the web stiffener is welded to the bottom flange. The fatigue resistance of the base metal at the termination of these welds with regard to the transverse through-thickness bending stresses in the flange is not currently quantified in the specifications, but is anticipated to be as low as Detail Category E. Through-thickness transverse bending stresses are most severe when the torque in the box is significant; e.g. boxes resting on skewed supports. Steps that can be taken to ameliorate this situation, and the specific cases for which this situation must be considered, are discussed in more detail in Section 6.5.5.2.2.3.

Overhang loads before the deck hardens may cause significant lateral bending in the outer top flange of tub girders, as is the case with I-girders. Overhang brackets are attached to the exterior top flange, applying an outward lateral pull to the flange. The brackets apply a countervailing force on the lower portion of the tub. The same issues apply that were discussed in Section 6.3.2.6 with regard to I-girders. Internal cross-frames or top struts act as reaction points for the top flange.

Wind loads during construction may also cause significant lateral moments in the top flanges.

As specified in *AASHTO LRFD* Article 6.7.4.3, internal diaphragms are to be provided at each support to resist cross-section distortion; they are to be designed to resist torsion in the box and to transmit vertical and lateral forces from the box to the bearings.

External cross-frames/diaphragms attempt to retain the relative position of adjacent box girders. In addition to vertical load, these members resist and/or introduce torsion in the boxes. To resist the distorting action they tend to cause on the box cross-section, *AASHTO LRFD* Article 6.7.4.3 requires that an interior cross-frame/diaphragm be used in-line with each exterior cross-frame/diaphragm.

According to *AASHTO LRFD* Article 6.7.4.3, for cross sections consisting of two or more boxes, external cross-frames/diaphragms are required at end supports (along with internal diaphragms) to support the deck and the live loads. External cross-frames/diaphragms also act to restrain the rotation of the boxes. External cross-frames/diaphragms must also be provided between girder lines at interior supports, particularly during erection, unless analysis indicates that the boxes are torsionally stable without these members. This is especially true if a box or tub girder has only one bearing per support.

When single bearings are used, the effective distance that the deck spans may be close to the distance between the bearings, which can be twice the distance between adjacent top flanges (assuming equal spacing between box webs). The

effective distance depends on the rotation permitted by the external cross-frames/diaphragms and the torsional stiffness of the boxes. Deck stresses and the demand on the external cross-frame/diaphragm increase with increased rotation of the box girders.

Temporary intermediate external cross-frames are sometimes used to control the relative deflection and rotation of adjacent boxes before the deck hardens. These members are removed to maintain the uncluttered appearance of the boxes that is diminished by the presence of too many external cross-frames. Removal of temporary bracing after the deck hardens is usually awkward. If the members are effective (i.e. contain large forces), they can present a danger to workers attempting to remove them when bolts in a partially connected member might fail. Removal of temporary members having large forces introduces restoring forces into the bridge. For example, a member having a force of 100 kips tension introduces a reversed force of 100 kips when it is removed. Removal of temporary cross-frames having large forces may increase deck stresses.

Analysis of the twist in the box due to erection and deck placement can be used to determine if temporary external cross-frames are required. Some suggest that external diaphragms are more attractive on box girder bridges than are cross-frames, which are seen as incongruent with the smooth surfaces of the box girders.

6.3.2.9.3 Spacing Requirements

6.3.2.9.3.1 I-Girder Bridges

The long-standing requirement limiting the maximum cross-frame/diaphragm spacing in I-girder bridges to 25 feet has been removed. The present provisions (*AASHTO LRFD* Article 6.7.4.1) do not limit cross-frame/diaphragm spacing for straight I-girder bridges. Spacing of cross-frames/diaphragms is to be established by rational investigation of critical construction stages and the final condition to meet the demands of design at each location. The factors determining cross-frame/diaphragm spacing in I-girder bridges are: lateral torsional buckling of the girder compression flange; skew; wind load; lateral loads due to deck overhang brackets; and in the case of curved girders, flange lateral bending due to curvature.

AASHTO LRFD Article C6.7.4.2 recommends that intermediate cross-frames/diaphragms be provided at nearly uniform spacing in I-girder bridges for constructibility, for efficiency of the design, and to allow the more accurate use of approximate methods of analysis for estimating lateral flange bending moments in curved bridges. The approximate V-load equation for estimating the lateral flange bending moments due to curvature (FHWA/NHI, 2010) assumes a uniform spacing of cross-frames/diaphragms. A tighter spacing may be desirable adjacent to interior

piers to reduce the unbraced length of the compression (bottom) flange. There are other reasons to vary the spacing of cross-frames/diaphragms.

Table 6.3.2.9.3.1-1 summarizes some of the trade-offs regarding cross-frame/diaphragm spacing. The importance of cross-frame/diaphragm spacing with regard to economy cannot be overemphasized. Although flange overstress can be addressed by the use of a larger flange in many cases, it can also be rectified by judicial arrangement of the cross-frames/diaphragms. Additional cross-frames/diaphragms often are less economical than heaver flanges. However, increasing spacing in some region(s) while reducing the spacing in other region(s) is often economical. For example, assume a uniform spacing of 25 feet on a straight bridge. For this spacing, analysis shows that the compression flange at the pier is overstressed with regard to lateral torsional buckling, but the top flange in the positive moment region has excess capacity. Thus, it may be possible to decrease the spacing adjacent to the pier and increase the spacing slightly beyond 25 feet in the positive moment region and still achieve a satisfactory design.

Table 6.3.2.9.3.1-1 Cross-Frame/Diaphragm Spacing Trade-Offs

Closer Spacing	Larger Spacing
Lower cross-frame forces	Lower cross-frame cost
Lower lateral flange moments	Larger cross-frame forces
Higher compression-flange moments	Larger lateral flange moments
Higher cross-frame cost	Lower compression-flange capacity

Relatively, the narrower the flanges, the closer the cross-frame/diaphragm spacing must be. However, cross-frames/diaphragms are more costly than flange steel, so wider flanges are usually desirable over additional cross-frames/diaphragms. But, by varying the spacing of a given number of cross-frames/diaphragms, economy in flange material can usually be gained.

The lateral force due to curvature is a function of the force in the flange and the curvature. The force in the flange is directly proportional to the vertical moment and inversely proportional to the girder depth. The lateral flange moment is proportional to the lateral force and the square of the distance between lateral supports; i.e., the cross-frame/diaphragm spacing. The forces in the cross-frames/diaphragms and the magnitude of the lateral flange moment can be modified by changing the cross-frame/diaphragm spacing and/or the girder depth, with no other changes made to the framing.

The total vertical shear within a span is nearly constant within a given span, regardless of the number of cross-frames/diaphragms. Hence, the shear per cross-frame/diaphragm is proportional to the number of cross-frames/diaphragms within a bay within a span. Where the vertical bending moments in a girder are large, a

smaller cross-frame/diaphragm spacing reduces the lateral flange bending moment, and also improves the lateral torsional buckling resistance of the compression flange. Simply increasing the spacing in regions where the vertical bending moment is smaller and the lateral flange moment is less critical may be satisfactory in lieu of adding a row of cross-frames/diaphragms.

Equation 3.1.1 is given in *AASHTO LRFD* Article C6.7.4.2 and may be used as a guide to determine preliminary cross-frame spacings in horizontally curved I-girder bridges.

$$L_b = \sqrt{\frac{5}{3} r_\sigma R b_f} \qquad \text{Equation 6.3.2.9.3.1-1}$$

AASHTO LRFD Equation C6.7.4.2-1

where:

r_σ = desired bending stress ratio $f_\ell / f_{bu} \le 0.3$
R = girder radius (ft)
b_f = flange width (ft)

The equation is derived from V-load theory (NHI, 2011) and has been shown to yield good correlation with refined 3D finite element analysis results when the cross-frame spacing is relatively uniform and there is no skew.

In the computation of r_σ, f_ℓ is flange lateral bending stress, and f_{bu} is the largest value of the compressive stress due to vertical bending within the unbraced length under consideration.

As an example, Table 6.3.2.9.3.1-2 gives results from Equation 6.3.2.9.3.1-1 for r_σ = 0.15 and b_f = 18 in.

Table 6.3.2.9.3.1-2 L_b Values from Equation 6.3.2.9.3.1-1 (for r_σ = 0.15; b_f = 18 in.)

	R = 500 ft	R = 1000 ft	R = 1500 ft
L_b (ft)	14	19	24

However as the user of this equation, one observes that the flange width is considered a given. It might be worthwhile investigating a change in the flange width to make a given cross-frame/diaphragm spacing work before additional cross-frames/diaphragms are added by rearranging Equation 6.3.2.9.3.1-1 as follows:

$$b_f = \frac{\left[3/5L_b^2\right]}{r_\sigma R} \qquad \text{Equation 6.3.2.9.3.1-2}$$

A subsequent check of the flange resistance requirements based on the initial cross-frame/diaphragm spacing determined from Equation 6.3.2.9.3.1-1 will likely necessitate adjustments to either the flange size or to the cross-frame/diaphragm spacing. Spacing may be varied with flange size and moment. It is desirable to examine the flange width, as well as its area. A wider flange reduces the lateral bending stress.

Although the *AASHTO LRFD Specification* does not prescribe a maximum cross-frame/diaphragm spacing for straight I-girder bridges, a maximum spacing requirement is specified for horizontally curved I-girder bridges in the erected condition in *AASHTO LRFD* Article 6.7.4.2. The requirement is given below:

$(L_b)_{max}$ = a minimum of:

- $L_r = \pi r_t \sqrt{(E/F_{yr})}$
- 30.0 feet
- R/10 feet, where *R* is the minimum girder radius within the panel

The limit of *R*/10 is consistent with past practice. L_r is the limiting unbraced length from *AASHTO LRFD* Eq. 6.10.8.2.3-5 to achieve the onset of nominal yielding in either flange under uniform bending with consideration of compression-flange residual stress effects prior to lateral torsional buckling of the compression flange. The terms r_t and F_{yr} are defined in *AASHTO LRFD* Article 6.10.8.2.3. Limiting the cross-frame/diaphragm spacing to L_r theoretically precludes elastic lateral torsional buckling of the compression flange. At unbraced lengths beyond L_r, significant lateral flange bending is likely to occur, and the amplification factor for flange lateral bending will tend to become large. The absolute upper limit on the cross-frame/diaphragm spacing in curved I-girder bridges has been established at 30.0 feet.

6.3.2.9.3.2 Box-Girder Bridges

For bridges other than those listed in *AASHTO LRFD* Article 6.11.2.3 (for which the wheel-load distribution factors are applicable), the spacing of internal cross-frames is limited to 40 feet according to *AASHTO LRFD* Article 6.7.4.3. Spacing of the internal cross-frames in box girders is primarily designed to control of distortion of the box. Each internal cross-frame restores the box shape to near its original unstressed shape. The further apart the cross-frames, the greater the distortion that must be corrected. This induces greater forces in the cross-frame. Of course, the stiffer the

box, the greater are the restoring cross-frame forces. Larger restoring forces induce greater box distortion in the vicinity of the cross-frame. Such distortion is associated with potential fatigue and should not be ignored in certain cases, particularly when the torques are large. If the computed cross-frame forces cause problems designing the member connections, the designer might consider reducing the cross-frame spacing. Live load causes much of the cross-frame force (distortion) in straight bridges without skew. Uneven loading of the deck weight on the two webs and parapet weight also may cause large torque. Skew and/or curvature will present significant torque for both dead and live load. The best internal cross-frame spacing is roughly inversely proportional to the torque in the box.

AASHTO LRFD Article 6.11.1.1 limits the through-thickness transverse bending stresses to 20 ksi at the strength limit state and requires that these stresses be considered for fatigue at the appropriate detail for bridges other than those listed in *AASHTO LRFD* Article 6.11.2.3 for which the wheel-load distribution factors are applicable.

AASHTO LRFD Article C6.7.4.3 recommends limiting the internal cross-frame spacing to control longitudinal warping stresses to approximately 10 percent of the stresses due to major-axis bending. *AASHTO LRFD* Article 6.11.5 requires that longitudinal warping stresses be considered for fatigue, again for bridges other than those listed in *AASHTO LRFD* Article 6.11.2.3 for which the wheel-load distribution factors are applicable. The calculation of transverse bending stresses and longitudinal warping stresses is examined in Section 6.5.5.2.2.3.

For straight boxes without skew satisfying the requirements of *AASHTO LRFD* Article 6.11.2.3 and with fully effective box flanges, and with relatively symmetrical deck weight acting on each box, cross-section distortion stresses have been found to be negligible. A reduction in the number of permanent internal cross-frames and/or top lateral bracing members is therefore permitted in such boxes when checked by proper analysis (see *AASHTO LRFD* Article C6.7.4.3); i.e. the spacing of the internal cross-frames may be permitted to exceed 40.0 feet if confirmed by analysis. However, the cost benefits probably rarely outweigh the risks. Erection conditions are an unknown to the Design Engineer.

Additional struts between the top flanges of tub sections may be necessary to satisfy constructibility provisions (*AASHTO LRFD* Article 6.11.3.2) when internal cross-frames are widely spaced. *AASHTO LRFD* Article C6.11.3.2 suggests that struts that are part of the top lateral bracing may be considered to act as top flange brace points at the discretion of the Design Engineer. The commentary suggests that this assumption may even be appropriate when significant flange lateral bending exists (due to deck overhang loads, curvature, etc.).

Internal cross-frames should be placed at points of maximum moment in each span. They are usually placed near both sides of field splices to aid in fit up in the shop and in the field. Additional internal cross-frames may be used to facilitate transportation and construction.

Additional internal cross-frames, or struts, may be required to reduce the lateral bending in the top flanges of tub sections resulting from transverse loads on these flanges (*AASHTO LRFD* Article C6.11.3.2). According to the commentary, this situation occurs when webs are inclined more than 1-to-4, or where the unbraced length of the top flanges exceeds 30 feet. The lateral load occurs with the inclined web due to web shear creating lateral force on the flanges. In lieu of a refined analysis, the maximum lateral flange bending moments, M_ℓ, due to the transverse load can be estimated as follows:

$$M_\ell = \frac{F_\ell L_b^2}{12}$$ Equation 6.3.2.9.3.2-1

AASHTO LRFD Equation C6.10.3.4.1-2

where:

F_ℓ = magnitude of the factored uniformly distributed transverse load (kip/in.)
L_b = unbraced length (in.)

This equation assumes that the flange is continuous at both brace points; the equation is unconservative at simple supports. The entire transverse load at the top is assumed applied to the top flanges (Fan and Helwig, 1999) so the transverse member is assumed to resist the entire transverse load.

Internal cross-frame spacing is influenced by the top lateral bracing arrangement. As the angle between the lateral bracing diagonals and the girder tangents is reduced, the bracing forces due to both torsion and flexure are increased. The brace length is decreased as the angle between the lateral bracing diagonals and the girder flanges increases, increasing the compressive capacity of a given diagonal member. The trade-off is that a flatter angle reduces the number of elements. The configuration of top flange lateral bracing is discussed further in Section 6.3.2.10.3.

6.3.2.9.4 Layout

6.3.2.9.4.1 General

Judicious layout of the cross-frames/diaphragms can have a significant effect on the economy of I-girder bridges. Although the spacing of the cross-frames/diaphragms

is important in controlling the number of cross-frames/diaphragms, their layout can influence the forces in the members and in the girders. The impact of layout is particularly important in I-girder bridges with skewed supports. Large cross-frame/diaphragm forces not only cause large members, they cause extremely expensive, even impractical connections in some cases.

Clearly, cross-frame/diaphragm forces can only be created when there is resistance at the end of the member. In I-girder bridges, this resistance has a few sources. The most critical one is the lateral restraint of a bearing on a rigid abutment. Next, is the resistance of such a bearing on a pier that has lateral flexibility to partially relieve the forces. Third, are opposing cross-frame members in adjacent bays or in the same cross-frame connected at a common node. Finally, the weakest form of resistance is the lateral restraint offered by the flanges.

Changing the number, size and arrangement of the cross-frames/diaphragms often has a significant effect on their forces. Hence, it is advisable to check the forces in these members early in the design, particularly for I-girder bridges with sharply skewed supports; that is, prior to resizing girders. If the forces are too large to design practical members or connections, their arrangement should be further investigated before proceeding with the resizing of the girders.

6.3.2.9.4.2 I-Girder Bridges without Skew

AASHTO LRFD Article 6.7.4.2 states that where supports are not skewed, intermediate cross-frames/diaphragms in I-girder bridges should be placed in contiguous lines normal to the girder tangents (Figure 6.3.2.9.4.2-1).

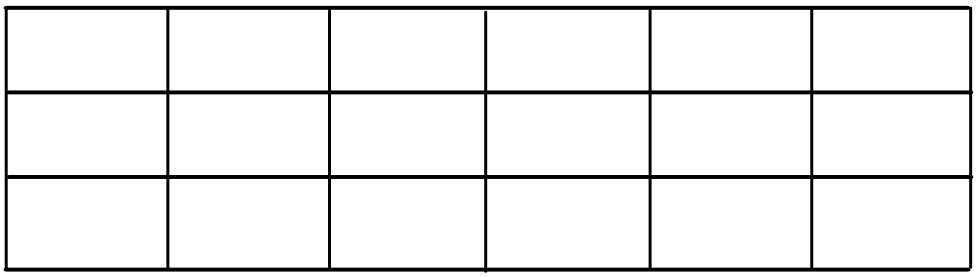

Figure 6.3.2.9.4.2-1 Contiguous Cross-Frame/Diaphragm Lines Normal to the Girder Tangents (Skew = 0°)

As discussed in Section 6.3.2.9.3.1, the cross-frame spacing along the girders may be varied in these cases. Reducing the spacing in the center of this simple span while increasing spacing near the supports may improve the capacity of the flanges

in the center of the span while not adding to the number of cross-frames, remembering that cross-frames are expensive compared to flange steel.

6.3.2.9.4.3 I-Girder Bridges with Skew

6.3.2.9.4.3.1 Supports Skewed Not More Than 20°

AASHTO defines skew as the angle made by the support relative to a line normal to a local tangent to the longitudinal axis of the bridge; thus, a skew angle of 0° denotes a right (or radial) support.

AASHTO LRFD Article 6.7.4.2 permits cross-frames/diaphragms to be arranged in contiguous skewed lines parallel to the skewed supports, as shown in Figure 6.3.2.9.4.3.1-1, where both supports within a span are skewed not more than 20 degrees.

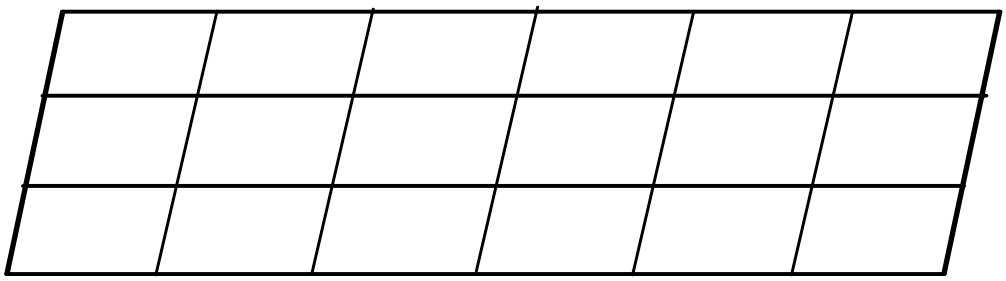

Figure 6.3.2.9.4.3.1-1 Contiguous Cross-Frame/Diaphragm Lines Parallel to Skew (for Skew ≤ 20°)

This requirement is consistent with past practice and is likely based on welding access to the acute corner between the cross-frame/diaphragm connection plates and web. Intermediate cross-frames skewed at greater angles also begin to reduce the torsional bracing stiffness of the cross-frames/diaphragms, reducing their effectiveness to prevent lateral-torsional buckling of the girders. The forces in the cross-frames/diaphragms also affect the girder forces when the cross-frames/diaphragms are highly skewed because their actions have longitudinal components acting along the girders.

This arrangement permits the cross-frames/diaphragms to be attached to the girders at points of similar length along the girders, i.e., equal stiffness, thus reducing the relative deflections between cross-frame/diaphragm ends and the restoring forces in these members. Cross-frame/diaphragms with greater parallel skew angles (up to 30°) have been used with no deleterious effect, but are currently forbidden by the Specifications.

6.3.2.9.4.3.2 Supports Skewed More than 20°

Cross-frames/diaphragms must be placed normal to the girder tangents where one or both supports within a span are skewed more than 20 degrees. Cross-frames/diaphragms may be placed in a contiguous pattern within the span, as shown in Figure 6.3.2.9.4.3.2-1, with the cross-frames/diaphragms opposing each other on both sides of the interior girders. At the bearings a different arrangement is recommended, as discussed further below. This cross-frame/diaphragm arrangement provides the greatest transverse stiffness; hence, the largest cross-frame/diaphragm forces.

In addition, with this cross-frame arrangement, the girders have differing deflections at points along a line perpendicular to the girders. This is due to the longitudinal shift of the girders resulting from the skewed supports, which results in the girders having different vertical stiffnesses along the line perpendicular to the girders. As such, two adjacent girders that have the same cross-section size and load deflect different amounts along any perpendicular line between them.

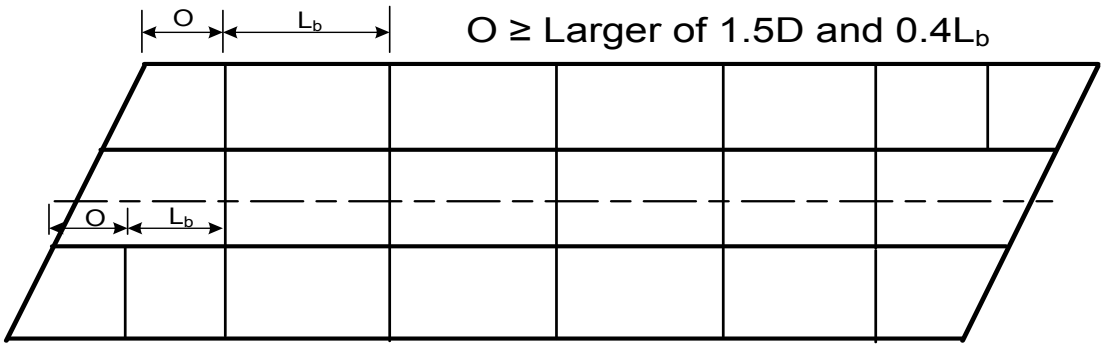

Figure 6.3.2.9.4.3.2-1 Contiguous Cross-Frame/Diaphragm Lines (Within the Span) Normal to the Girder Tangents (for Skew > 20°)

The cross-frames/diaphragms along the perpendicular lines going to the bearings at skewed supports act to transfer load across the bridge in proportion to the relative longitudinal and transverse stiffnesses of the bridge. Thus, the stiffer the transverse load path, the larger the load transferred to the bearings. This unwanted stiffness near skewed supports, producing undesirable load paths in the structural system, has often been referred to as “nuisance stiffness” (Krupicka and Poellot, 1993). Nuisance stiffness can produce dramatically increased cross-frame forces and can result in potential fit-up difficulties during the steel erection. Other attributes of the bridge geometry such as high span length to girder depth ratios, simply-supported spans, or poor span balance in continuous-spans, can lead to difficulties in

assembling the bridge. Basically, substantial differences in stiffness of different portions of a large bridge structure can be problematic.

AASHTO LRFD Article C6.7.4.2 recommends that when cross-frames/diaphragms are provided along a skewed support, the first intermediate cross-frame/diaphragm placed perpendicular to the girders adjacent to a that support ideally be offset at least the distance, O, taken equal to the larger of $1.5D$ or $0.4L_b$ from the support (Figure 6.3.2.9.4.3.2-1), where practicable, where D is the web depth of the girder under consideration and L_b is the unbraced length between the first and the second intermediate cross-frame/diaphragm connected to the girder under consideration. Providing this minimum offset will reduce the potential for excessively large cross-frame forces adjacent to severely skewed supports in I-girder bridges resulting from the "nuisance stiffness" effects (NCHRP, 2012). Elimination of such "nuisance stiffness" effects also tends to result in somewhat easier cross-frame installation along (and adjacent to) the skewed support line.

Another reason for higher cross-frame forces near bearings in skewed bridges is the restraint that they may provide. This restraint tends to forbid transverse movement; hence, causing higher cross-frame forces. Bearing restraint should be considered when computing cross-frame forces in severely skewed bridges. Changing bearing orientation and restraints often has a significant impact on cross-frame forces near supports. Thus, any investigation of cross-frame arrangement should include simultaneous consideration of bearing restraints. Implicit in this discussion is the use of an analysis that properly recognizes the effect of bearing restraints located off the neutral axis of the girders.

It may be advantageous in some cases to consider the use of non-contiguous (or discontinuous) cross-frame/diaphragm lines along the entire span as shown in Figure 6.3.2.9.4.3.2-2, which is also permitted in *AASHTO LRFD* Article 6.7.4.2. This pattern, which is often referred to as a staggered pattern, effectively reduces the transverse stiffness of the bridge. Alternatively, cross frames may be staggered only near the skewed supports while remaining contiguous in the middle of the span (a pattern not shown).

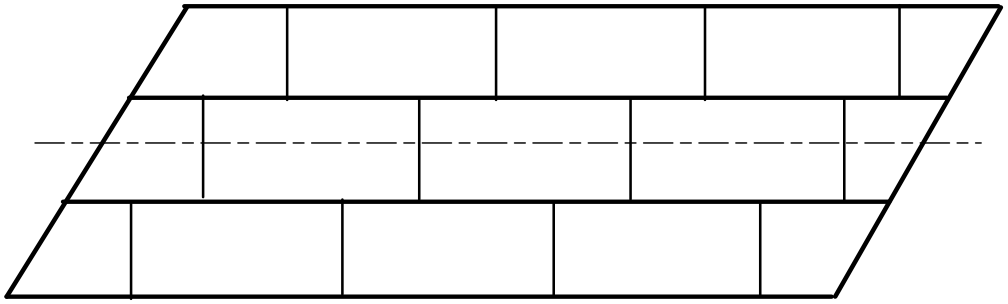

Figure 6.3.2.9.4.3.2-2 Discontinuous (Staggered) Cross-Frame/Diaphragm Lines Along the Entire Span Normal to Girder Tangents (for Skew > 20°)

The reduction of transverse stiffness that results whenever a discontinuous cross-frame/diaphragm arrangement is employed is accomplished by the transverse flex that occurs in the flanges. This reduction of stiffness is accompanied by a reduction in the cross-frame/diaphragm forces and associated connection complexity (cost). However, the flex of the flanges must also be accompanied by lateral flange bending, particularly near the locations where the lines are discontinued. However, often the lateral bending is not critical, and the net result is a desirable reduction in the cross-frame/diaphragm forces and resulting costs. The vertical bending capacity of the flanges is reduced by the lateral bending as evidenced by the one-third rule resistance equation discussed in Section 6.5.2.1. As indicated in *AASHTO LRFD* Article C6.10.1, flange lateral bending effects due to skew should be considered in all regions of the girders where cross-frames/diaphragms are discontinuous. Lateral bending effects due to skew are typically less critical in regions where cross-frames/diaphragms are contiguous.

Exterior girders (i.e., fascia girders) always have cross-frames/diaphragms on one side, but since there are no opposing cross-frames/diaphragms on the other side, flange lateral bending due to skew effects is usually smaller in these girders, which is fortuitous since the outside girder often has critical major-axis bending moments compared to the other girders. Interior girders are generally subject to significantly larger lateral flange moments due to skew effects relative to exterior girders, in particular whenever a discontinuous cross-frame/diaphragm arrangement is employed along the entire length of the bridge (i.e., a staggered arrangement).

Simple methods to determine flange lateral bending moments and restoring forces in the cross-frames/diaphragms in skewed bridges do not currently exist. These actions are best determined by refined analysis. In the absence of calculated values, estimates for lateral bending stresses are provided in *AASHTO LRFD* Article C6.10.1. These estimates are based on a limited examination of refined analysis results for bridges with skews approaching 60 degrees from normal and an average D/b_f ratio of approximately 4.0. As such, the flange lateral bending stress

recommendations provided in *AASHTO LRFD* Article C6.10.1 represent, at best, a rough approximation of the actual flange lateral bending stresses, and as a result they should be used in a conservative, simplified manner.

The use of a “lean-on bracing system” is another option to consider for reducing the cross-frame forces in straight skewed I-girder bridges (Herman et al., 2005). In the “lean-on bracing system”, cross-frames perpendicular to the girders in selected bays are provided with only a top and bottom chord, but no diagonals. The selected cross-frames continue to function as bracing members for the girder compression flanges, but without the shear stiffness of typical cross-frames. When this system is used, a refined analysis should be considered to determine the influence of the “lean-on” cross-frames on the girder deflections (cambers), cross-frame forces and transverse deck stresses at various stages, and to check for any excessive differential deflections between girders that are braced in a "lean-on” fashion.

Additional options to reduce cross-frame/diaphragm forces in highly skewed bridges, such as leaving some cross-frames/diaphragms unconnected until after the deck has been cast, and/or providing vertical slotted holes in the cross-frame/diaphragm connections, are not recommended herein. Leaving some cross-frames/diaphragms unconnected has the disadvantage of the possibility of poorly braced girders until the deck hardens, and potential loss of geometry control during the deck casting. The Erector will also have to return to the site after the deck is cast and work from underneath the deck to tighten the bolts. Holes usually need to be drilled or at least reamed. If vertical slotted holes are provided and the bolts are tightened prior to the deck casting, the slots must be of the proper size and location to allow the computed deflections to occur freely without binding, which is unlikely to be the case. The resistance of the bolts will also be less in the slotted holes for all loads that are applied after the bolts are tightened.

6.3.2.9.4.3.3 Skewed Interior Support Lines

AASHTO LRFD Article 6.7.4.2 states that at the discretion of the Owner, cross-frames/diaphragms need not be provided along skewed interior support lines of I-girder bridges if cross-frames/diaphragms normal to the girders are provided at bearings that resist lateral forces, as shown for a skewed and curved I-girder bridge in Figure 6.3.2.9.4.3.3-1. At severely skewed interior supports, e.g., with skews greater than 20°, the detailing of the intersections with the cross-frames/diaphragms oriented normal to the girders is complex. Welding of skewed connection plates to the girder may be problematic where the plate forms an acute angle with the girder. The cross-frames/diaphragms normal to the girders in such cases must be proportioned to transmit all the lateral components of force from the superstructure to the bearings that provide lateral restraint. Otherwise, the lateral bending in the bottom flange near the restrained bearings may be excessive.

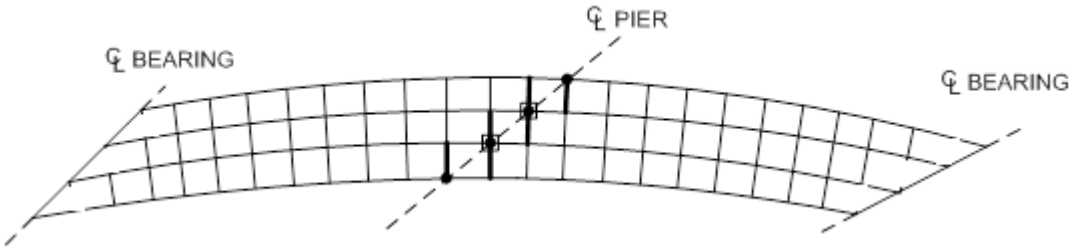

Figure 6.3.2.9.4.3.3-1 Skewed and Curved I-Girder Bridge: No Cross-Frame Along the Skewed Interior Support Line

Where discontinuous cross-frames/diaphragms are employed normal to the girders in the vicinity of skewed interior supports to reduce "nuisance stiffness" effects, care should be taken to match at least one cross-frame/diaphragm with each bearing that resists lateral force. Otherwise, the effect of the lateral moment induced in the bottom flange due to the eccentricity between the intermediate cross-frame/diaphragm and the bearing should be considered. Also, whenever any bearing along the support line is not matched with a cross-frame/diaphragm, care must be taken to ensure that the bottom flange of the girder is adequately braced. For such cases, the provision of cross-frames/diaphragms along the skewed support line may be necessary, as shown in Figure 6.3.2.9.4.3.3-2. There are no rules for how to arrange bearing restraints and cross-frames/diaphragms at these locations. Ingenuity and trial-and-error are the only tools. In critical cases, often only a least bad arrangement is available.

As illustrated in Figure 6.3.2.9.4.3.3-2, the skewed cross-frame/diaphragm in this case braces the bottom flange of the inside and outside girders, and also matches up with the bearings on the two interior girders that resist lateral force. Refined analysis is recommended to allow for a more detailed examination of cross-frame/diaphragm forces, lateral bearing reactions and lateral flange bending whenever removal of cross-frames/diaphragms along, and/or in the vicinity of, severely skewed interior support lines is considered.

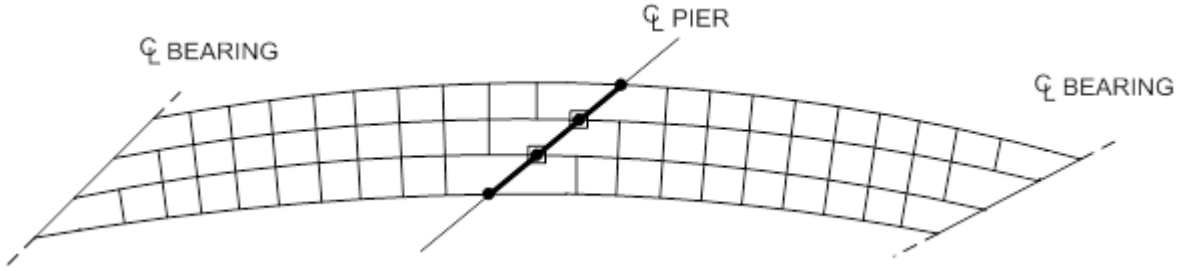

Figure 6.3.2.9.4.3.3-2 Skewed and Curved I-Girder Bridge with Discontinuous Cross-Frames: Cross-Frame Along the Skewed Interior Support Line

For skews not exceeding 20°, cross-frames/diaphragms along the skewed support line alone may be sufficient. If cross-frames/diaphragms are also provided normal to the girder tangents, they may be spaced too close together along the girders, introducing significant lateral flange bending stresses into the girders. As discussed in Section 6.3.2.9.6.3.1, for skewed cross-frames/diaphragms, connection plates should be oriented in the plane of the transverse bracing. The connection plates must be able to transfer the force between the girder and the bracing without undue distortion.

Whatever the case, consideration should always be given to providing a means to allow jacking of the girders at the supports to replace or repair the bearings.

6.3.2.9.4.3.4 Skewed Support Lines at Abutments

At skewed abutments (simple supports), a row of cross-frames/diaphragms is always required along the support line to support the free edge of the deck. Thus, a missing intermediate normal (radial) cross-frame/diaphragm is not a concern.

End rotations of the girders create forces in these cross-frames/diaphragms. At cross-frames/diaphragms along skewed end support lines, tangential components of the skewed end support cross-frame/diaphragm forces act along each girder. In order to maintain static equilibrium, vertical bending moments and shears must develop in the girders at the end supports. Note that the larger the rotation and concomitant deflection of the girders, the larger the end moments. In certain cases, these end moments may be important. Since these end moments are usually negative, they can potentially introduce tensile stresses in the deck or subject the bottom flange to compression adjacent to the supports. Generally, these moments cannot be avoided altogether. However, by placing the deck at the ends of the bridge last, the tensile stresses in the deck can be minimized. *AASHTO LRFD* Article 6.7.4.2 requires that the effect of the tangential components of force transmitted by the skewed end support members be considered.

The net components of the skewed end support cross-frame/diaphragm forces transverse to the girders introduce a torque at the girder ends. The effect of these transverse forces may need to be considered in the design of the transverse deck reinforcement, particularly when the end cross-frame/diaphragm forces are large.

6.3.2.9.5 Configuration

6.3.2.9.5.1 I-Girder Bridges

Article 6.7.4.2 in *AASHTO LRFD* requires that cross-frames/diaphragms for rolled beams and plate girders should be as deep as practicable, but preferably not less

than 0.5 of the beam depth for rolled beams and 0.75 of the girder depth for plate girders (Figure 6.3.2.9.5.1-1). This requirement is called out to ensure that the cross-frames/diaphragms provide adequate torsional resistance to the beam or girder. The deeper these members are, the lower the forces in them because the moments transferred through them are transferred more efficiently in a deeper section. However, as their sizes are increased, the forces in these members increase. The connection plates also need to be robust enough to transfer the loads to the girders.

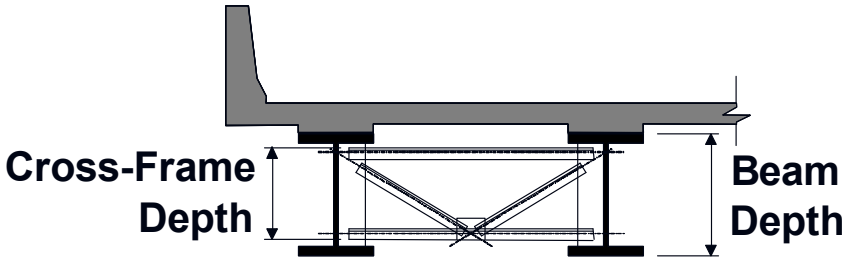

Figure 6.3.2.9.5.1-1 Cross-Frame and Beam Depth

The X-type configuration, as shown in Figure 6.3.2.9.5.1-2, is the least expensive configuration of intermediate cross-frames (i.e. cross-frames located at other than end supports). However, if the girder spacing-to-depth is too great, K-type cross frames are preferred in order to steepen the diagonal members. When the angle of the diagonals with respect to the horizontal becomes too shallow for an X-type configuration to be effective (less than about 30 degrees), the unsupported length of the diagonals can become large and the transfer of vertical force between girders imposes a large axial stress in the diagonals. Long members may also be subject to vibration. In such cases, the K-type cross frame is often preferred (AASHTO/NSBA, 2003). Specific rules in reference to this often are provided by the states.

Figure 6.3.2.9.5.1-2 X-Type Cross-Frames in an I-Girder Bridge

A typical K-type cross-frame in an I-girder bridge is shown in Figure 6.3.2.9.5.1-3.

Figure 6.3.2.9.5.1-3 K-Type Cross-Frames in an I-Girder Bridge

The K-node can either be located in the top or bottom chord. The latter configuration is preferred so the diagonals can brace the bottom chord in the vertical direction. However, it is observed that the diagonals have equal and opposite forces hence their horizontal components of force accumulate in one-half of the bottom chord. For this reason, it is often desirable to place the K-node in the top chord to allow these horizontal diagonal forces to accumulate in the lower-stressed top chord. The top chord is more lowly stressed because the deck assists the top chord for superimposed dead load and live load.

At the ends of bridges, the edges of the concrete deck must be supported in order to support the wheel loads coming onto the deck (refer to *AASHTO LRFD* Article 9.4.4). In an I-girder bridge, a rolled I-shape or a rolled or bent plate channel is typically used as the top chord of the end cross-frames in order to provide the necessary support. At end supports, locating the K-node in the center of the upper chord is preferred because it halves the span of the top chord, which must support the deck and the expansion device. The diagonals can also more efficiently carry the wind loads down to the bearings in this configuration; a similar configuration might be considered for the cross-frames at interior-pier supports for this reason.

The cross-frames provide lateral support to the girder compression flanges to resist lateral torsional buckling. They also provide geometric stability to the girders prior to the hardening of the deck. No top chord is used on cross-frames in some cases. If a top chord is not used with K-type cross-frames, the stability of the cross-frame prior to the deck hardening is dependent entirely on the bending stiffness of the bottom chord; this is an unstable condition. Thus, a top chord should always be provided with K-type cross-frames. X-type cross-frames without a top chord may be beneficial in some cases in straight bridges to soften “nuisance stiffness” effects. However, when the upper triangle of the cross-frame truss is eliminated, the stability

of the cross-frame may be compromised and so a top chord should always be provided whenever X-type cross-frames are used on horizontally curved bridges.

Diaphragms, such as the one shown in Figure 6.3.2.9.5.1-4, are used most often in rolled-beam bridges or in plate-girder bridges when the girders are less than about 48 inches deep. Hot-rolled channel sections or rolled I-shapes are most commonly used for diaphragms. Solid-plate diaphragms are rarely used, unless needed as special jacking diaphragms to accommodate bearing replacement.

Figure 6.3.2.9.5.1-4 Diaphragms in an I-Girder Bridge

Channel sections can either be rolled channels (C & MC sections), or bent-plate channels (i.e. a plate bent into the shape of a channel by the fabricator) attached directly to the connection plates or attached directly to the stringers using end angles. Bent-plate channels have been used on girders greater than 48 inches deep. The Engineer is encouraged to consult with local fabricators regarding their preference.

Rolled I-shapes can either be attached to connection plates using gusset plates, attached directly to the stringers using end angles, or attached directly to the connection plates. Attaching directly to the connection plates requires coping at the top and bottom. Diaphragms are typically designed for moment and shear. The moments introduce bending into the connection plates.

An advantage of diaphragms for I-girder bridges is that there is typically minimal fabrication involved. Disadvantages are that they often are not full depth, it is difficult to develop the moment in the connections, and they typically require location-specific connection plates with holes located to accommodate any cross-slope or superelevation.

6.3.2.9.5.2 Box-Girder Bridges

The use of internal K-type cross-frames with the K-node at the top chord usually provides the best access for internal inspection, while providing the required stiffness.

Should it become necessary to reduce the transverse bending stress range in the box flange adjacent to the cross-frame connection plate welds to the flange, the use of transverse cross-frame members attached to the bottom flange as part of the internal cross-frames can reduce the range of transverse bending stress. When bottom transverse cross-frame members are provided, they are to be attached to the bottom flange, unless a longitudinal flange stiffener(s) is used, in which case the transverse members are bolted to the longitudinal stiffener(s) (*AASHTO LRFD* Article 6.11.5). For closed-box sections, should the top transverse cross-frame members also be called upon to reduce the range of transverse bending stress, they should be similarly attached. In addition, the moment of inertia of the transverse cross-frame member must not be less than the moment of inertia of the largest connection plate for the internal cross-frame under consideration taken about the edge in contact with the web. The moment of inertia of the transverse cross-frame member should be taken about the edge in contact with the flange when it is attached to the flange, or about its neutral axis when bolted to the longitudinal stiffener(s). When transverse bracing members are welded directly to the bottom flange, the transverse bending stress range at the termination of these welds should be checked. When transverse bracing members are connected to longitudinal flange stiffeners, the box flange may be considered stiffened when computing the transverse bending stresses (*AASHTO LRFD* Article C6.11.5).

Internal diaphragms are used at supports. Access holes are provided in the diaphragms at interior supports. *AASHTO LRFD* Article 6.7.4.3 specifies that access holes in internal intermediate diaphragms be at least 18.0 in. wide and 24.0 in. deep; however, a larger hole at least 36.0 in. deep is preferable. In addition to restraining distortion of the box section, the diaphragms at supports also transfer load from the girder webs to the bearing(s). If a single centered bearing is used, the diaphragm must be stout enough to resist the reaction and transfer the load around any access hole. Bearing stiffeners are usually attached to the diaphragms. If a single centered bearing is employed, two stiffeners are generally used. A bearing stiffener on each side of the access hole generally removes the shear from the diaphragm before it is engaged by the hole. Torsion generally causes a different magnitude of shear in the webs of the box on the two sides of the diaphragm. In cases where there is a large torque, the shear may be equal on both sides of the hole. In these cases, some shear must pass over the section containing the hole. If the shear in the diaphragm is high, it may be advisable to investigate the edge stresses around the hole. Reinforcement around the hole may be required, particularly if the access hole requires a large portion of the diaphragm or if a single bearing is located under the

diaphragm. Auxiliary stiffeners on the diaphragm or webs may be employed if necessary to spread out the reaction. Refined analysis of internal diaphragms at supports is desirable because they are primary members necessary for the integrity of the bridge.

AASHTO LRFD Article 6.7.4.3 requires that an internal plate diaphragm provided for continuity or to resist torsional forces be connected to the flanges and webs of the box section. It is important to remember that the diaphragm-to-web welds are to be designed for the sum of the web shears on the left and right of the support.

External plate diaphragms with aspect ratios, or ratios of length to depth, less than 4.0 and internal plate diaphragms act as deep beams (*AASHTO LRFD* Article C6.7.4.3) and should be evaluated by considering principal stresses rather than by simple beam theory. Fatigue-sensitive details on these diaphragms and at the connection of the diaphragms to the flanges should be investigated by considering the principal tensile stresses.

6.3.2.9.6 Special Design Considerations

6.3.2.9.6.1 Preliminary Sizing

As a minimum, cross-frames/ diaphragms are to be designed to resist wind loads, to transfer lateral loads between the bearings and the superstructure, and to meet slenderness requirements (*AASHTO LRFD* Articles 6.8.4 or 6.9.3, as applicable) and minimum thickness requirements (*AASHTO LRFD* Article 6.7.3). *AASHTO LRFD* Article 6.7.4.1 also requires that cross-frames/diaphragms that are included in the structural analysis model be designed for the computed force effects. They are to be designed for all applicable limit states.

In a curved-girder bridge, a refined analysis should be used to obtain the actions required to design the bridge (*AASHTO LRFD* Article 4.6.3.3.2). Such analyses typically yield forces in the cross-frame/diaphragm members, which are primary members. The stiffness and size of these members influences the magnitude of the computed actions in them. Disproportionately large cross-frame/diaphragm members will result in large forces that can be reduced by reducing the member sizes. It is best to initially investigate smaller member sizes and increase the sizes as necessary. Significant changes in cross-frame or diaphragm sizes are best investigated with another analysis to assure that the forces have not changed excessively.

Preliminary sizes can be obtained from the permitted slenderness specified in *AASHTO LRFD* Articles 6.8.4 and 6.9.3. Single angles, double angles and tees are typically considered for use as cross-frame members. Double angles and tees provide larger compressive and tensile resistances than single angles. Double

angles also permit the bolts in their connections to work in double shear reducing the number. However, fabricators generally prefer single-element members (i.e. single angles or tees) for cross-frame members. Double angles are more expensive to fabricate since they typically require more handling and some reverse-side welding. Fabricators generally prefer to perform one-side welding of individual single-element members to gusset plates in a jig. The assembled cross-frame can then be shipped for erection rather than shipping individual cross-frame members for assembly in the field. When double-angle members are used, a special coating application is also typically required for the backs of the two angles in order to provide corrosion resistance, which adds time and cost. Although double-angle members, where necessary, certainly can and have been painted, their use preferably should be limited to uncoated weathering steel applications. Therefore, unless the additional compressive or tensile resistance provided by double-angle members is absolutely required, fabricators generally prefer the use of single angles or tees for cross-frame members.

The reader is referred to Section 6.6.3 for further information on the design of single-angle, tee and double-angle members, and to Section 6.6.3.6 for further information on the design of diaphragms.

6.3.2.9.6.2 Detailing

Fitting up and welding cross-frames as a unit in the shop is preferred over “knock-down” cross-frames that are shipped in pieces. Cross-frames that are assembled in a jig and brought to the site assembled minimize the chances of errors and field misfits. “Knock-down” cross-frames require more shop and field handling and are more difficult to erect due to the large number of different pieces that need to be tracked, handled and hoisted. Cross-frames that can be welded from one side are also preferred to prevent having to turn the cross-frame assembly over in the shop; that is, single-angle or tee-section members are again preferred rather than double-angle members.

Many fabricators prefer that cross-frames be detailed as parallelograms, rather than as rectangles. Part A of Figure 6.3.2.9.6.2-1 shows the preferred shape that follows the cross-slope of the bridge. This shape has the advantage of being deeper than possible with the rectangular shape. Note that the cross-frame chords are closer to the flanges. The parallelogram allows holes in the connection plates to be in a single location, increasing fabrication efficiency. A jig can be used to adjust for the cross-slope and accommodate the different required member lengths found with the parallelogram shape. In cases where there are significant drops between adjacent girders (e.g., a bridge with skewed haunched girders), the cross-frame jig is a necessity.

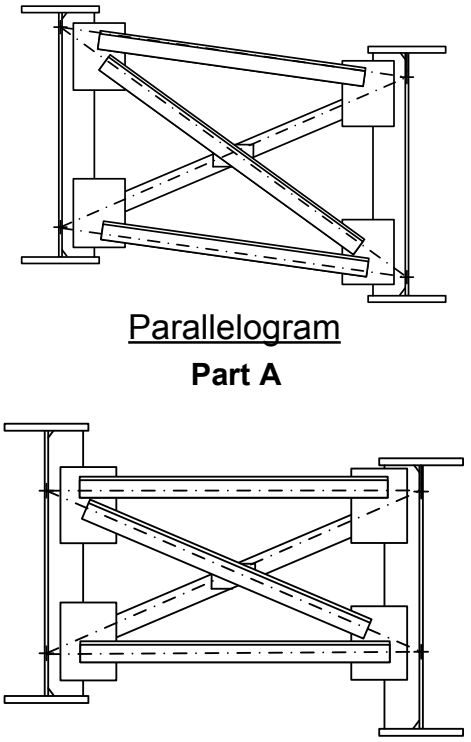

Figure 6.3.2.9.6.2-1 Cross-Frame Detailing

Part B of Figure 6.3.2.9.6.2-1 shows how the diagonal members in a rectangular cross frame are the same length, but the depth is shallow. As a result, different hole locations are required in most of the connection plates. Locating these holes is obviously expensive.

Rectangular cross-frames with a cross-slope cause opposing horizontal cross-frames that are not in alignment, as shown in Part A of Figure 6.3.2.9.6.2-2. This subjects the connection plate and web to bending (Part B of Figure 6.3.2.9.6.2-2) because the chords are not aligned on the two sides of the girders. The lateral forces on exterior girders are less than on interior girders.

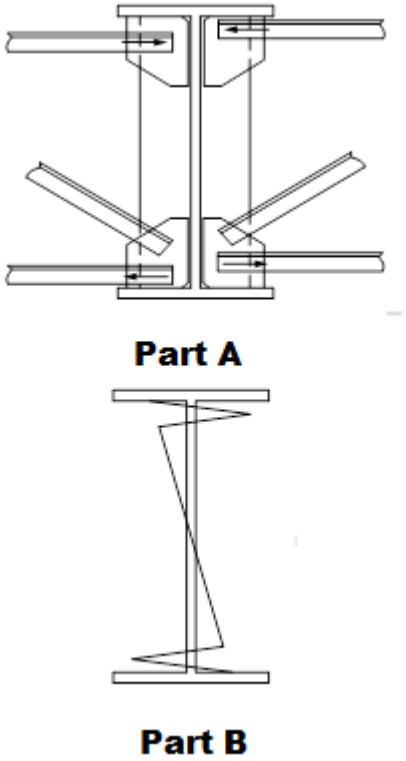

Figure 6.3.2.9.6.2-2 Connection-Plate Bending Resulting from Cross-Frame Alignment

6.3.2.9.6.3 Connection Plate Design

6.3.2.9.6.3.1 I-Girder Bridges

The complete load path for the cross-frame forces includes a transfer of the net cross-frame force from the connection plates to the girders. Even if the cross-frames are aligned, the net force must be transferred to the flanges. Part B of Figure 6.3.2.9.6.2-2 shows that when cross-frame members are misaligned on opposite sides of interior girders in I-girder bridges, the moment in the connection plate/web element may be computed by treating the element as a fixed-end beam. The web of the connection plate/web element for an interior girder may be ignored.

Where end moments are significant, the connection plate fillet welds to the flanges should be checked for combined shear and tension at the strength limit state. Connection plate welds to the web also might also be checked for the net resultant vertical cross-frame force.

All of these forces discussed above must be based on a proper resolution of the dead and live load (plus impact) cross-frame forces. The horizontal forces should be resolved to ensure equilibrium; that is, the proper combination of live loads must be used to obtain equilibrium. Since both maximum and minimum values of the live

load forces are obtained, consideration of the proper combinations of these forces is necessary. Although separate influence surfaces are loaded for each member in a refined analysis, equilibrium can still be obtained by combination of the proper live load forces. This issue is examined in more detail in Section 6.6.4.4.

Local buckling of connection plates for I-girder bridges should be checked when the cross-slope is large and rectangular cross-frames or diaphragms are used. There is usually a significant distance between the cross frame/diaphragm and the flange. The maximum moment in the connection plate may be checked against the resistance factor for flexure, ϕ_f, from *AASHTO LRFD* Article 6.5.4.2 times the nominal local buckling resistance of the connection plate about an axis parallel with the web.

The equations from *AASHTO LRFD* Article 6.12.2.2.1 giving the nominal local buckling resistance of I- and H-shaped members about an axis parallel with the web are appropriate to be applied to rectangular connection plates as follows:

- If $\lambda_f \le \lambda_{pf}$, then:

$$M_n = M_p \qquad \text{Equation 6.3.2.9.6.3.1-1}$$

AASHTO LRFD Equation 6.12.2.2.1-1

- If $\lambda_{pf} < \lambda_f \le \lambda_{rf}$, then:

$$M_n = \left[1 - \left(1 - \frac{S_y}{Z_y}\right)\left(\frac{\lambda_f - \lambda_{pf}}{0.45\sqrt{\frac{E}{F_{ys}}}}\right)\right] F_{ys} Z_y \qquad \text{Equation 6.3.2.9.6.3.1-2}$$

AASHTO LRFD Equation 6.12.2.2.1-2

where:

λ_f = slenderness ratio of the connection plate = b_t/t_t

$\lambda_{pf} = 0.38\sqrt{\frac{E}{F_{ys}}}$

$\lambda_{rf} = 0.83\sqrt{\frac{E}{F_{ys}}}$

F_{ys} = specified minimum yield strength of the connection plate (ksi)

M_p = plastic moment of the effective section (defined below) about the axis parallel with the web (kip-in.)

S_y = elastic section modulus of the effective section (defined below) about the axis parallel with the web (in.^{3})

Z_y = plastic section modulus of the effective section (defined below) about the axis parallel with the web (in.^{3})

For interior girders, S_y, M_p and Z_y may be calculated based on an effective rectangular section consisting of the connection plates on both side of the web. In this case, $M_p = 1.5F_{ys}S_y$ and $Z_y = 1.5S_y$. For exterior girders, S_y, M_p and Z_y may be calculated based on an effective section consisting of the connection plate plus a portion of the web. A portion of the web equal to $18t_w$ is suggested for inclusion with the connection plate in this case. In this case, all properties should be computed about the appropriate neutral axis of the effective tee section. Note that if F_{yw} is smaller than F_{ys}, where F_{yw} is the specified minimum yield strength of the web, the strip of web included in the effective section should be reduced by the ratio of F_{yw}/F_{ys}.

Figure 6.3.2.9.6.3.1-1 is a plot of a "Factor" versus b/t assuming that F_{ys} is 50 ksi and that b is the total width (inches) of double-sided connection plates (including the thickness of the web). Multiplying the "Factor" from the plot by the quantity "b^2t" gives the nominal local buckling resistance, M_n (in kip-ft), of the connection plates according to the above equations. The local buckling resistance of single-sided connection plates cannot be found using this plot.

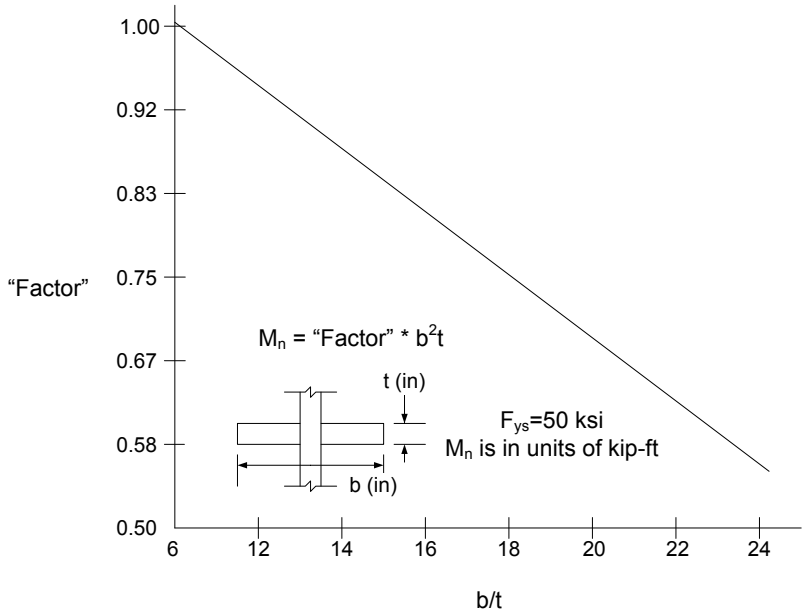

Figure 6.3.2.9.6.3.1-1 "Factor" for Computing Nominal Local Buckling Resistance of Double-Sided Connection Plates from Equation 6.3.2.9.6.3.1-1 and Equation 6.3.2.9.6.3.1-2

Note that connection plates serving as bearing or intermediate transverse shear stiffeners must also satisfy the applicable stiffener design requirements discussed further in Section 6.6.6.

A row of cross-frames/diaphragms is always needed along a skewed abutment in order to support the free edge of the deck. In order for the connection plates for a skewed cross-frame/diaphragm to transfer the forces between the cross-frame/diaphragm members without undue distortion, the connection plates should be oriented in the plane of the cross-frames/diaphragms. Two options for this detail are: a skewed connection plate (Figure 6.3.2.9.6.3.1-2); or a bent gusset plate (Figure 6.3.2.9.6.3.1-3). The skewed connection plate should be limited to maximum skew angle of 20°. For skew angles not exceeding 20°, it is desirable to give the fabricator the option to use either detail. These details are taken from AASHTO/NSBA (2003).

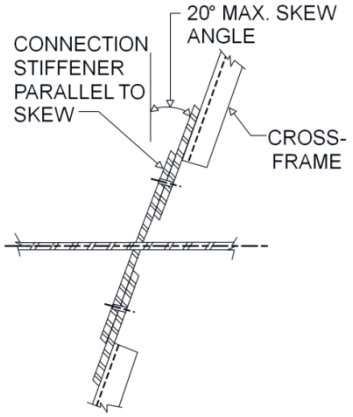

Figure 6.3.2.9.6.3.1-2 Skewed Connection Plate

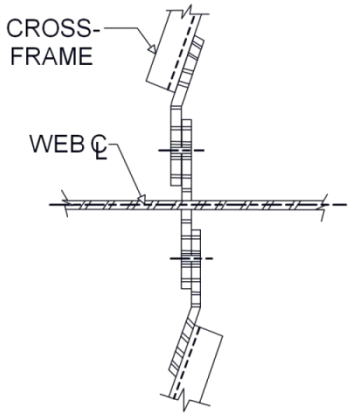

Figure 6.3.2.9.6.3.1-3 Bent Gusset Plate

The use of half-rounds (i.e. split pipes) as stiffeners has been investigated for this application (Battistini, 2009). Such stiffeners also provide improved torsional resistance to the girders.

6.3.2.9.6.3.2 Box-Girder Bridges

The attachment of internal cross-frame connection plates to box flanges is discussed in *AASHTO LRFD* Article C6.6.1.3.1. Fabrication of tub sections is often done by first welding the webs and top flanges. Web stiffeners and connection plates are then welded. The tub shape is then created by bolting in the internal cross frames. The superelevation and twist that might be required in the tub can be introduced in this manner. Finally, the common box flange of the box can be welded to the webs.

AASHTO LRFD Article 6.6.1.3.1 requires that the connection plates be attached to the flanges. Obviously, if the web stiffening extends to the bottom of the webs, automatic continuous welding of the bottom flange would be impossible. If the Design Engineer has permitted, the stiffening and/or connection plates are made short of the bottom of the webs, permitting the web-to-flange welds to be made uninterrupted. Subsequently, the connection plates are extended with lapped tabs that are welded to the bottom flange and the plates. Figures 3.5.A and 3.5.B in AASHTO/NSBA (2003) show suggested connection details for this particular situation. Figure 3.5.D in AASHTO/NSBA (2003) shows a suggested connection detail for cases where the box flange is welded to the webs prior to attaching the connection plates and stiffeners.

Details on tub girders have a significant effect on cost. The Design Engineer is encouraged to consult with fabricators likely to build the project regarding the preferred details for fabricating the tub sections. It may be desirable to show alternate details for the connection plates on the design plans.

6.3.2.10 Lateral Bracing

6.3.2.10.1 General

According to *AASHTO LRFD* Article 6.7.5.1, the need for lateral bracing is to be investigated for all stages of construction and the final condition.

6.3.2.10.2 Functions

6.3.2.10.2.1 I-Girder Bridges

In I-girder bridges, lateral bracing is generally used at the discretion of the Engineer. Lateral bracing forces the girders it connects to act as a truss. Lateral bracing also acts to resist relative movement of the girders.

When deemed necessary, lateral bracing has traditionally been used on the bottom flanges in I-girder bridges (Figure 6.3.2.10.2.1-1). However, as discussed further below, there are compelling reasons in many cases that lateral bracing might (and should) be used on the top flanges instead. Lateral bracing tends to force the connected girders to act as a pseudo-box if it is used on both top and bottom flanges, or if used only on the bottom flanges after the deck has hardened. Lateral bracing members experience significant load as a result of this box-type action. Lateral bracing is rarely used in all bays of the bridge. Typically, it is used in one or both exterior bays. The bracing need not necessarily extend over the full length of a span or the bridge in most cases.

Figure 6.3.2.10.2.1-1 Bottom Lateral Bracing on an I-Girder Bridge

Lateral bracing prevents the flanges of the girders to which it is attached from moving longitudinally with respect to each other. Hence, the two flanges have roughly the same stress. Frequently, the cross-frame forces are slightly elevated in the bay with lateral bracing because their diagonals provide the means to transfer the balancing load between the girders.

The outside girder of an I-girder bridge is usually the most highly loaded. This is particularly true with the convex girder of a curved bridge (i.e. the girder furthest from the center of curvature). The outside (convex) girder of these bridges often requires heavier flange plates which, in turn, causes increased stiffness drawing even more load, leading to more deflection and increased cross-frame forces. Lateral flange bracing in the outside bay of curved bridges can reduce the load in the convex girder and its deflection as well, if necessary, because it forces the adjacent girder to share the superimposed dead load and live load. If steel weight and deck weight are

causing the convex girder to be highly loaded, top and bottom lateral bracing may be required to create the pseudo box for the non-composite loads.

Lateral bracing can also help control deflections, provide stability and minimize girder out-of-plumbness during construction. Should the bridge be constructed by incremental launching, lateral bracing will likely be required in one or more bays along significant portions of each span in order to provide the necessary geometry control of the bridge cross-section during the launch.

The bare steel girders are subject to lateral wind forces before the deck hardens. *AASHTO LRFD* Article 4.6.2.7.3 requires the Engineer to consider the need for temporary wind bracing during construction. The stiffness of an I-girder bridge is equal to the sum of the stiffnesses of the girders. This is often inadequate to prevent damage to the girders and the bearings under the wind forces. Lateral bracing can provide additional stiffness to markedly reduces the lateral deflections and flange lateral bending stresses due to wind load acting on the non-composite bridge system; in particular, for longer spans. Lateral bracing together with the cross-frames provides a rigid truss action to resist the lateral wind force. It is often economical to use lateral bracing over only portions of the spans. One or two panels of lateral bracing adjacent to a support (preferably in the plane of the top flanges) can provide an effective line of support at the cross-frame or diaphragm line within the span where the lateral bracing terminates, thereby reducing the effective span length resisting the lateral wind loads. Large lateral deflections due to wind are undesirable during construction and could potentially result in damage to the bearings. At least one state DOT limits the maximum lateral wind load deflections in the final erected non-composite structure during construction under an assumed design wind pressure. An approximate approach to determine how many panels of lateral bracing, if any, might be necessary to reduce lateral wind load deflections in a straight I-girder bridge during construction to an acceptable level is presented in Section 6.5.3.6

The concept of lateral bracing for wind loads probably arose with truss design where the lateral bracing system is necessary to resist wind. Lateral bracing is not as effective in resisting wind load on a completed multi-girder composite bridge. The lateral wind force on completed girder bridges is resisted primarily by the deck as the cross-frames/diaphragms transfer the force to the deck, which is must stiffer than any lateral bracing system. The deck resists the wind force as a large diaphragm in shear and bending. The wind force is transferred from the deck to the laterally-restrained bearings through the end cross-frames/diaphragms.

Radial forces in cross-frames of curved-girder bridges cause longitudinal forces in the bridge that may not be balanced out by other cross-frames. Hence, the longitudinal forces may not be in equilibrium, causing potential loss of equilibrium during erection and in any condition before the deck hardens. For smaller-span

straight bridges, cross-frames or diaphragms acting alone in plan with the girders through Vierendeel truss action may be sufficient to prevent longitudinal translation of the girders. However, in larger spans, both straight and curved, the bending strength of the cross-fames may be insufficient. Frequently, the erector will lock down bearings so as to prevent longitudinal movement of the girders, providing another means of obtaining stability. Nevertheless, in larger straight bridges and in sharply curved bridges, locking down bearings may not be adequate. A small amount of lateral bracing in several or all bays is effective in these cases. Lateral bracing might only be necessary adjacent to interior supports for continuous-span girders.

AASHTO LRFD Article C6.7.5.2 suggests that lateral bracing be considered to prevent significant relative horizontal movement of I-girders in spans greater than 200 feet (i.e., to provide global stability). Individual circumstances, such as significant horizontal curvature or skew, or high wind loads acting on the non-composite structure, may warrant inclusion of lateral bracing for smaller spans. Each situation is unique that requires the sound judgment of the Design Engineer. Temporary lateral bracing may be used at the Owner's discretion.

The analysis must be able to recognize the influence of even temporary lateral bracing. If lateral bracing is left on the structure, it will continue to work. This is particularly true for live loads, which usually produce relatively large forces in lateral bracing for reasons discussed above. These forces make the members and their connections to the girders susceptible to fatigue if they have not been designed for fatigue. Lateral bracing might be placed in the plane of the top flange in cases when it is to be employed only for construction. In this location, it senses little effect from live loads so fatigue is unlikely, and it most likely need not be considered in the analysis of the final bridge.

Erection of lateral bracing may be problematic because the girders are usually erected and stressed due to self-weight, which may change the bolt-hole positions enough that fit-up is difficult. Some erectors have found that field drilling holes in the gusset plates to match the holes in the flanges works out well. Of course, the holes must be considered in determining the net section of the flanges where flanges are subject to tension (refer to *AASHTO LRFD* Article 6.10.1.8 and Section 6.4.7). Welding the gusset plates to the flanges presents fatigue issues that are expensive to address. This is another reason that top flange lateral bracing is appealing. Fatigue stresses are far less critical on the top of the girder than at the bottom. Usually, gusset plates can be welded to the top flange with minor changes to handle fatigue. Further, top flange lateral bracing will have smaller stresses so fewer bolts will be required. Often a single row of bolts is found adequate. Removal of top lateral bracing members may be expensive and problematic if bolted to the top flange.

6.3.2.10.2.2 Box-Girder Bridges

Lateral bracing of the top flanges of tub girders changes them from an “open section” to a torsionally closed section. They become a closed section for the non-composite loads. Otherwise, tub girders would not become a closed section until the deck hardens. The shear center of an open tub section is located below the bottom flange (Heins, 1975). The addition of top lateral bracing shifts the shear center to the inside of the tub resulting in a pseudo-box closed section. When the section becomes closed, the torsional stiffness is significantly increased. Without lateral bracing, a tub section acts as an open section and is torsionally weak. Top-flange bracing retains the shape of the tub.

AASHTO LRFD Article 6.7.5.3 requires lateral bracing over the entire length of the tubs in horizontally curved girders. A full-length lateral bracing system limits distortions that may result from temperature changes occurring prior to deck placement. *AASHTO LRFD* Article C6.7.5.3 recommends full-length lateral bracing be provided with straight tub sections on spans greater than 150 feet.

AASHTO LRFD Article 6.7.5.3 permits the use of partial-length lateral bracing in straight tub girders if torsion is known to be small and it can be shown that the section can resist excessive distortion with the partial lateral bracing. Attention should be given to possible loads that might be induced during shipping, erection and placement of the concrete deck. *AASHTO LRFD* Article 6.7.5.3 requires that the local stability of the top flanges and the global stability of the individual tub sections be investigated in tubs with partial length lateral bracing. This requirement applies to the Design Engineer’s assumed construction sequence. At least one panel of lateral bracing should be provided on each side of anticipated lifting points. The need for additional lateral bracing to resist the shear flow resulting from any net torque on the steel section due to unequal factored deck weight loads acting on each side of the top flanges, or any other known eccentric loads acting on the steel section during construction, should be considered. A full-length lateral bracing system should be considered for cases where the torques acting on the steel section are deemed particularly significant, e.g. tub-section members resting on skewed supports and/or tub-section members on which the deck is unsymmetrically placed.

Top flange lateral bracing is designed to resist the shear flow in the pseudo-box section resulting from any torsion acting on the steel section due to the design load effects. The bracing also act with the tub in resisting vertical bending. Hence, forces in the bracing due to flexure of the tub during construction must also be considered (based on the assumed construction sequence). Top flange lateral bracing also resists wind loads acting on the non-composite tub section.

When the bridge is analyzed by 3D finite element analysis in which the individual lateral bracing members are included in the model, their forces can be taken from

the analysis. When the forces in the bracing members are not computed directly, the shear flow, *f* (kips/in.), in the top of the pseudo-box section can be computed as follows:

$$f = \frac{T}{2A_o}$$ Equation 6.3.2.10.2.2-1

AASHTO LRFD Equation C6.11.1.1-1

where:

A_o = enclosed area within the box section (in.^{2})
T = internal torque due to the factored loads (kip-in.)

A_o is to be computed for the non-composite box section. If the top lateral bracing is attached to the webs of the tub, A_o is to be computed using its actual location according to *AASHTO LRFD* Article 6.7.5.3. The development of this equation is discussed further in Section 6.4.8.3.2.

The torsional shear (kips) across the top of the tub equals the shear flow times the distance between the tops of the webs. That shear may then be resolved into the vector along the diagonal bracing member. There is also a vector due to flexure that must be included. Bracing member forces due to flexure of the non-composite tub can be estimated by an approach presented in Fan and Helwig (1999). Note that since top lateral bracing contributes to the flexural stiffness of the tub section, the bracing member should be resolved into the section properties when determining stiffness for analysis and for section properties when computing stresses. The lateral system is also subjected to forces after the section becomes composite with the hardened deck. These forces can be significant when the lateral bracing members are large. The distribution of shear flow resisted by the deck and lateral system can be estimated by the ratio of the shear stiffnesses of the two elements.

The equivalent area, A_o, of a plate that will represent the shear stiffness of the top lateral bracing may be computed using an equivalent energy method (Kolbrunner and Basler, 1966; Dabrowski, 1968). The method provides formulas to calculate the equivalent plate thickness for several common configurations of top lateral bracing.

6.3.2.10.3 Configuration

AASHTO LRFD Article 6.7.5.1 states that if permanent lateral bracing members are included in the structural model used to determine live load force effects, they must be designed for all applicable limit states and be considered primary load-carrying members. Since bottom lateral bracing carries significant live load, it must also be detailed very carefully with respect to fatigue if it is left in place.

The configuration of lateral bracing may be important economically. This is particularly true in bridges that are subjected to large torsional loads. Lateral bracing configurations with a single diagonal per bay are usually adequate. Other X-type configurations have twice as many members and connections and are usually avoided.

The first decision the Design Engineer needs to make is the bay size for the lateral bracing. The longer the bay, the fewer members required; the longer the members, the greater the unbraced length. However, as mentioned previously in Section 6.3.2.9.3.2, the bracing forces due to both shear flow and flexure are increased with a "flatter" diagonal angle. Generally, the lateral bracing bay length is set equal to half of the cross-frame spacing, so that alternate bays of lateral bracing connect at an internal cross-frame. There is no formula to determine an optimal bay size. However, when members become large and connections become unwieldy, the need for a shorter bay is indicated. Or, if the lateral bracing member can be oriented so that it is in tension for the shear flow in regions where the same member is in compression due to flexure, there is less need to control its length and spanning from cross-frame to cross-frame may be a more economical arrangement. Rarely, is it good design practice to make the angle between the diagonal and the girder tangent greater than 45 degrees.

One commonly asked question is whether lateral bracing members attached to the top flange midway between cross-frames/diaphragms act as a brace point for the top flange in compression when checking for lateral torsional buckling in the presence of flange lateral bending (due to deck overhang loads, curvature, lateral bracing forces, etc.). Usually they are not considered as brace points for the top flanges of the tub. However, there is obviously some argument that the truss action of the lateral system will provide some lateral restraint. *AASHTO LRFD* Article 6.11.3.2 takes the conservative position when it states that the unbraced length of the top flanges of tub sections should be taken as the distance between interior cross-frames/diaphragms. As discussed previously, at locations where only struts exist between the top flanges, top lateral bracing attached to the flanges at these points may be considered to act as brace points at the discretion of the Design Engineer according to *AASHTO LRFD* Article C6.11.3.2.

The Design Engineer has two options regarding the configuration of a full-length single-diagonal lateral bracing system: a Pratt truss pattern, Figure 6.3.2.10.3-1 Part A; or a Warren truss pattern, Figure 6.3.2.10.3-1 Part B. In the Pratt truss configuration, only one member applies force against a flange at a cross-frame/diaphragm. The force is resisted mainly by the strut or top chord of the cross-frame, and to some degree, by lateral bending of the top flange.

The Warren truss pattern applies the force from two lateral bracing members at the intersection, increasing lateral flange moments and strut or cross-frame top chord

forces. An approach for estimating the flange lateral bending stresses due to these forces (in lieu of a refined 3D analysis) when a Warren truss pattern is utilized is presented in Fan and Helwig (1999).

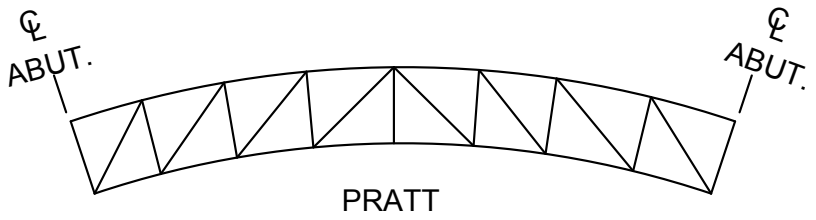

Part A

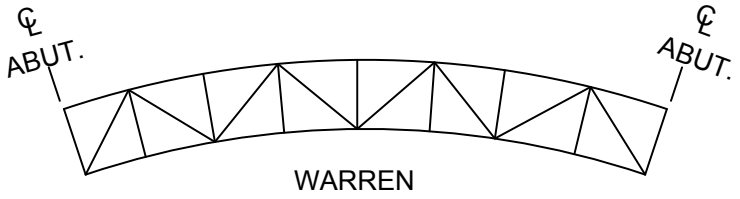

Part B

Figure 6.3.2.10.3-1 Full-Length Single-Diagonal Lateral Bracing Patterns

When torques are large and a dominate torque direction occurs, it is possible to orient the lateral bracing members such that they are in tension for shear flow, although they may be in compression due to flexure, and vice versa. By configuring the lateral bracing in the Pratt truss pattern with the directions of the diagonals determined from the sign of the torque, significant economy can often be realized with the Pratt truss pattern over the more typical Warren truss pattern that leads to half of the diagonal members in compression. As discussed previously, as the diagonal angle is increased, the bracing force due to both torsion and flexure is reduced, as well as the length of the brace. This becomes important for bracing that must resist compression. A flatter angle, however, reduces the number of elements required in the bracing system. It is for this reason that a Pratt truss pattern that allows tension bracing is economical. It should be noted that usually the direction of the Pratt truss pattern changes over a span. At the central location, it may be desirable to introduce one bay of X-bracing.

AASHTO LRFD Article C6.7.5.3 recommends that the following requirement be satisfied to ensure that a reasonable minimum area is provided for the diagonal members of the top lateral bracing for tub sections:

$$A_d \geq 0.03w \qquad \text{Equation 6.3.2.10.3-1}$$

AASHTO LRFD Equation C6.7.5.3-1

where:

A_d = minimum required cross-sectional area of one diagonal (in.^{2})
w = center-to-center distance between the top flanges (in.)

This requirement was included in the original *AASHTO* Guide Specifications for horizontally curved girders and was intended to ensure that top lateral bracing would be sized so that the tub would act as a pseudo-box section with normal stresses due to warping torsion less than or equal to 10 percent of the major-axis bending stresses and with minimal warping torsional displacements. The criterion was originally developed based on tub sections with vertical webs, with ratios of section width-to-depth between 0.5 and 2.0, and with X-type lateral bracing configurations with the diagonal members at an angle of 45 degrees to the longitudinal centerline of the girder flanges (Heins, 1978). Although most tub-girder configurations will likely differ from the configurations for which the above criterion was developed, the criterion at least ensures that some reasonable minimum area will be provided for these members regardless of the configuration. In most cases, larger members will likely be required to resist the applied member forces.

Finally, top lateral bracing should always be continuous across field splice locations. Otherwise, large lateral flange bending stresses might occur in the top flanges of the tub where the bracing is discontinued.

6.3.2.10.4 Detailing

AASHTO LRFD Article 6.6.1.3.2 deals with the detailing of lateral connection plates. Although not required by code, the most desirable connection of lateral bracing members (diagonals and struts) to the girders is to bolt the lateral connection plates (or members) to the flanges rather than to the webs. Welding of the connection plates to the flanges or web typically results in a fatigue Category E detail with a very low fatigue resistance. Bolting improves the fatigue resistance of the connection plate or member (Detail Category B or D) and eliminates the need to provide an expensive radiused transition at the ends of a welded connection plate to improve the fatigue resistance above Detail Category E. Note however that when the bracing members are bolted to a flange subject to tension, *AASHTO LRFD* Equation 6.10.1.8-1 must be satisfied at the strength limit state to ensure that fracture on the net section of the flange is prevented – refer to Section 6.4.7.

When the connection plate is bolted to the flange, a minimum gap of 4.0 in. should exist between the edge of the flange and first bolt line in the bracing member (Figure 6.3.2.10.4-1) to reduce stresses produced by vibration movement of the lateral bracing (NHI, 1990).

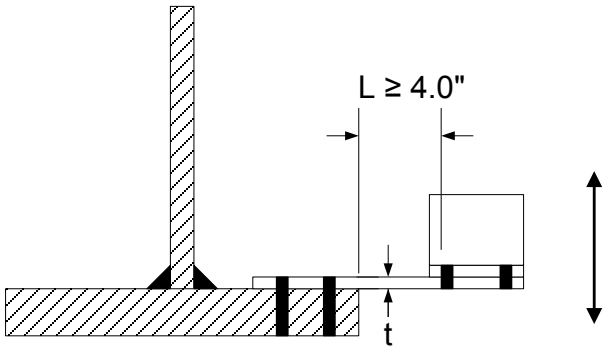

Figure 6.3.2.10.4-1 Lateral Connection Plate Bolted to Flange – Minimum Recommended Gap to Reduce Vibration Stresses

Some Owners specify removable deck forms, even within tub sections. These forms are very difficult to remove when lateral bracing is attached to the flanges, particularly from inside a tub section. To avoid connections of the bracing to the web, it is recommended that the requirement for removable forms be rescinded whenever possible in favor of using permanent metal deck forms, especially within tub sections. One-inch (±) thick fill plates between the lateral connection plate and the underside of the top flange can be used to stay clear of the stay-in-place form installation.

When lateral connection plates are attached to the webs, forces in the lateral bracing members are transferred to the web or connection plates before the forces can be resisted by the flanges. This creates a circuitous load path and potential fatigue prone details; both which must be considered in the design. Also, as specified in *AASHTO LRFD* Article 6.7.5.3, if the bracing is attached to the webs of tub sections, the cross-sectional area of the tub for shear flow A_o must be reduced to reflect the actual location of the bracing, and a means of transferring the forces from the bracing to the top flange must be provided; that is, an adequate load path, with fatigue considered, must be provided between the bracing-to-web connections and the top flanges of the tub.

Where it is not practical to attach lateral connection plates to the flanges, *AASHTO LRFD* Article 6.6.1.3.2 recommends that the connection plates be located a minimum specified distance from the flanges to minimize the effect of out-of-plane distortion stresses on the fatigue resistance of the base metal adjacent to the welds (refer to Section 6.5.5.2.3 for further discussion on distortion-induced fatigue). It is recommended that the connection plate be located a vertical distance not less than one-half the flange width above or below the flange, as applicable, to ensure adequate electrode access and to move the connection plate closer to the neutral axis of the girder to reduce the impact of the weld termination on the fatigue resistance (Figure 6.3.2.10.4-2). The recommended gap also facilitates painting and field inspection. However, even if this is done, a welded Category E detail will not

likely suffice at most locations requiring the connection plate to either be cut with a radius or bolted to the web. Should the connection plate be located on the opposite side of the web from a transverse stiffener, the connection plate must be centered on the stiffener and the stiffener must be rigidly attached to both the compression and tension flanges (Figure 6.3.2.10.4-2).

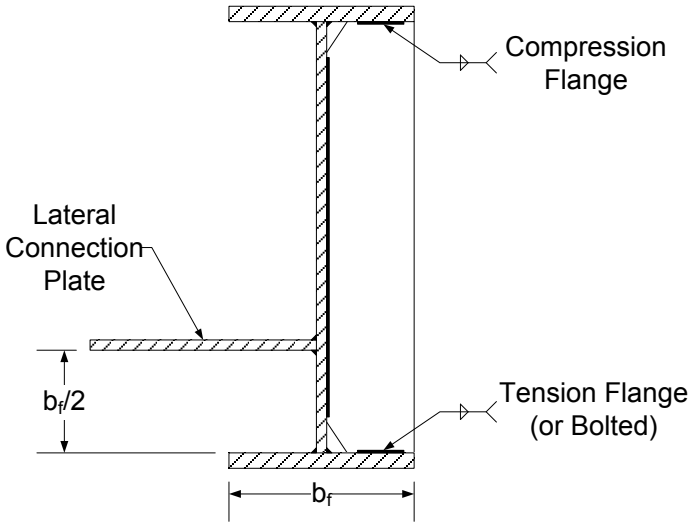

Figure 6.3.2.10.4-2 Recommended Lateral Connection Plate Detail for Plate Attached to the Girder Web – Plate Opposite Transverse Stiffener

The same recommendations apply when the connection plate is located on the same side of the web as a transverse stiffener. The line of action of the laterals should intersect at the transverse stiffener. The stiffener must be made discontinuous with the connection plate welded to the discontinuous stiffener, with sufficient copes and a minimum gap of 1 in. provided between the stiffener-to-web and lateral connection plate-to-web weld toes (Figure 6.3.2.10.4-3 – see also *AASHTO LRFD* Figure C6.6.1.3.2-1). As an alternative, the bracing member can be extended and bolted to the stiffener with the connection plate coped around the stiffener (Figure 6.3.2.10.4-4). The ends of the bracing members must be kept a minimum of 4.0 in. from the web and any transverse stiffener to reduce distortion-induced gap stresses resulting from vibrations of the bracing members (Figure 6.3.2.10.4-3 and Figure 6.3.2.10.4-4).

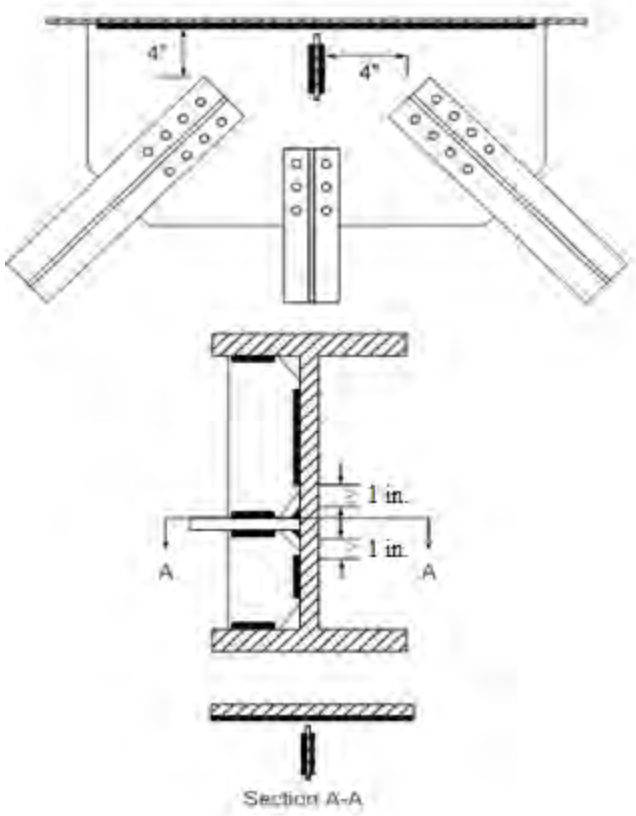

Figure 6.3.2.10.4-3 Recommended Lateral Connection Plate Detail for Plate Attached to the Girder Web – Plate on Same Side of Web as Transverse Stiffener

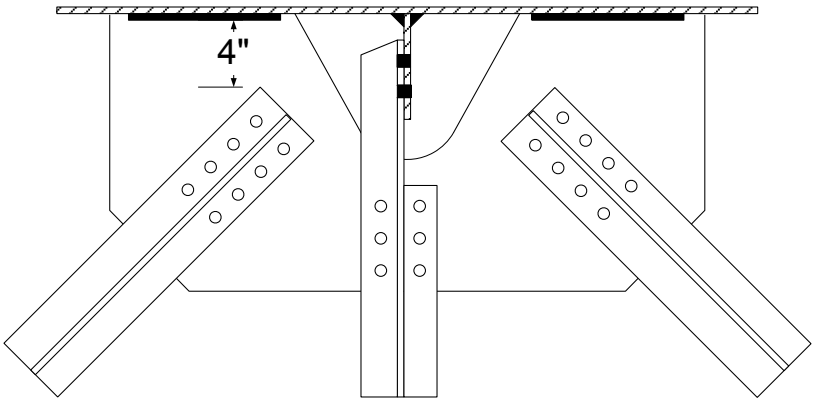

Figure 6.3.2.10.4-4 Alternative Recommended Lateral Connection Plate Detail for Plate Attached to the Girder Web – Plate on Same Side of Web as Transverse Stiffener

Should the web be unstiffened opposite the connection plate, the connection plate should be located a minimum of 6.0 inches above or below the flange, as applicable, but not less than one-half the flange width (Figure 6.3.2.10.4-5) in order to prevent large distortion-induced stresses from forming in the web between the connection plate and the flange.

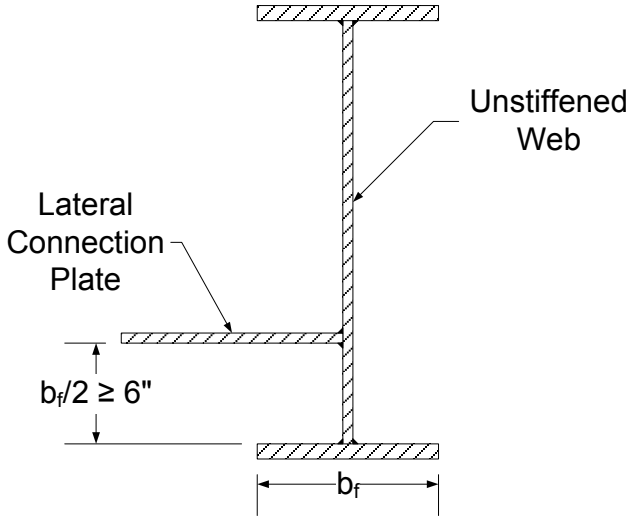

Figure 6.3.2.10.4-5 Recommended Lateral Connection Plate Detail for Plate Attached to Unstiffened Girder Web

The above detailing recommendations for welded lateral connection plates also satisfy the provisions of *AASHTO LRFD* Article 6.6.1.2.4 to avoid so-called "constraint-induced fracture" (Section 6.5.5.2.2.1.3). To avoid details subject to this form of brittle fracture, welds should not be allowed to intersect. Also, attachments that are parallel to the direction of primary stress should be made continuous with any intersecting transverse attachments made discontinuous. The intersecting joint in this case must be detailed to allow a minimum gap of 1 in. between weld toes to reduce constraint (see *AASHTO LRFD* Figure C6.6.1.3.2-1).

6.3.2.11 Box Girders vs. I-Girders

6.3.2.11.1 General

Steel box bridge members have been used in large trusses and straddle beams since at least the 1930s. Early box members were built up of four plates riveted to four hot-rolled angles. Access holes were provided for riveting. More recently, however, welded steel box girders, which were not practical until welding became acceptable for connecting major bridge elements, replaced riveted members. The first welded box girder bridges in America were probably constructed in Massachusetts in the 1950s. They were made up of four plates welded into a rectangular box. The two bridges that were constructed had rather severe horizontal

curves, which was most likely the reason that the torsionally stiff box sections were used. At that time, behavior of open curved sections was not well understood. Analysis of curved closed-box sections could be done more confidently, although warping behavior was often not explicitly considered; instead, closely spaced internal cross frames were used in the early box girders to control and minimize warping. Inspection of the Massachusetts box-girder structures in the late 1980s showed the interiors of the boxes to be in pristine condition after more than 30 years of service in the relatively harsh New England environment.

It was likely observed that the amount of steel required for these bridges was excessive. A slightly different box design was introduced by New York State who designed two box-girder bridges in the western tier of the state in the early 1960s. The designs employed lateral bracing between the top flanges of the individual boxes in the positive-moment regions. Hence, the boxes were actually tubs with top flanges. The torsional shear was resisted by a pseudo-box section created by the addition of top-flange lateral bracing members. The lateral bracing was simply designed by resolving the force due to the torsional shear flow into the individual lateral bracing members. Interestingly, the portions of the girders in the dead load negative-moment regions of these continuous-span bridges over the interior supports were closed-box sections built up from four plates. Perhaps the large torsion at the supports was believed better handled with a solid top plate, or perhaps the non-composite behavior in those regions was of concern. One of the bridges was field tested at the time of construction to confirm its behavior. In the 1990s, the bridge was field tested again and a refined analysis was performed; both confirmed that the original design was appropriate.

The early bridges were designed having radial supports. They used either two bearings or a wide rubber bearing at each support so that it could be assumed that most of the torsion would be resisted at supports by the bearings rather than by the diaphragms between the girders. Adequate internal bracing was used to ensure that the boxes did not distort to such a degree that the adequacy of the closed-section analysis could be disputed.

The smooth appearance of tub girders fabricated from welded plates soon became popular with both the public and Design Engineers. As with I-girders and other bridge types, tub girders were found susceptible to fatigue cracking when not properly detailed. For example, some longitudinal tub girders were welded to transverse box members without fully appreciating the implications of fatigue. As with many technological advances, the application preceded full investigation and improper detailing led to premature fatigue cracking in some of these bridges.

6.3.2.11.2 Advantages of Box Girders

Box girders offer some distinct structural advantages over I-girders, particularly when the girders are horizontally curved (Figure 6.3.2.11.2-1).

Figure 6.3.2.11.2-1 Curved Steel Box-Girder Bridge

The high torsional resistance of individual box sections permits the box to carry more of the load applied to it rather than shifting much of it to the adjacent girders having greater radius, as is the case with torsionally weaker I-girders. The tendency of box girders to more uniformly share gravity loads reduces the relatively large, and often troubling deflection, of the girder on the outside of the curve. Also, fewer cross-frames/diaphragms are required between the girders; i.e., less material needs to be added to box girders to resist torsional effects. When a single box girder is used, there is of course no visible bracing.

There are two main advantages of box girders: They can accommodate extremely tight radii of curvature; and they can potentially be more economical than I-girders on longer spans due to their increased torsional stability during erection.

Box girders also offer benefits in durability and maintainability. Fewer elements are available for debris build-up on the outside of the box. Box girders are also easier to

inspect since much of the inspection is performed from inside the box and does not impact traffic.

Because of their smooth uninterrupted profile and the fact that the number of exposed components is minimized, box girders are often chosen based on aesthetic preferences. Their smooth exteriors provide fewer moisture/debris traps and fewer locations for birds to perch.

Box girders are inherently more stable during erection and may often be erected with fewer but larger cranes than required for I-girders. I-girders must be stabilized until they are braced by their neighbors. Overall erection costs for box girders may also be less because there are generally fewer girders and fewer cross-frames/diaphragms than there are for a similar bridge constructed with I-girders. There are also fewer cross-frames/diaphragms to erect than in I-girder alternates. Box girders may also be quicker to construct as there are fewer external bracing members to erect. Box girders are also tend to be more stable under wind loads before the deck has hardened. The most frequent criticism concerning erection of box girders is that their weight usually requires larger crane capacities.

6.3.2.11.3 Disadvantages of Box Girders

Some disadvantages of box girders include ineffective bottom-flange material in the contraflexure regions where bending moments are relatively low. Box girders that are too small to navigate through are difficult to inspect. In addition, internal inspection of box girders requires consideration of access, lighting, and air quality.

Boxes can be problematic when resting on skewed supports. Skew introduces torques which can create problems in the field during construction making fit-ups difficult as well as introducing large torsional forces in the lateral bracing. The large torques due to skew also increase the shear stresses in the deck for load applied after the deck has hardened.

Fabrication of box girders is specialized and generally more costly per pound of steel than fabrication of I-girders. The complexity of fabricating trapezoidal box shapes (the most commonly used shape) to accommodate vertical and horizontal curvature, superelevation transitions, and/or skews can contribute to a cost premium versus I-girders. Webs should always be mathematically developable surfaces. This means that a flat plate can be cut to the shape of a web and bent to the proper shape. This is usually accomplished by maintaining a constant slope on the web.

Bridge cross-sections with one or two box girders are frequently defined as fracture critical. Although the jury is out regarding this issue, many Owners have rules defining non-redundant steel structures. Such bridges may therefore contain fracture-critical components, which add additional fabrication and inspection costs.

The detailing of tub or box girders is expensive and has found less standardization of details than for more common I-girder bridges. Hence, it is important that designers spend significant effort detailing tub girders. Usually conversations during design with fabricators who are likely bidders will lead to more fabrication-friendly details.

6.3.2.12 Rolled Beams vs. Welded I-Girders

Rolled wide-flange structural steel shapes, typically W-shapes, are widely used in bridge construction as various components, including primary bridge beams (stringers), substringers, transverse deck beams on long-span bridges, orthotropic bridge deck members, secondary members, and truss chord/diagonal members. For spans less than or equal to about 100 feet in steel I-girder bridge superstructures, the Engineer has the option to choose rolled shapes (Figure 6.3.2.12-1) over welded girders (Figure 6.3.2.12-2) for the primary bridge beams.

Wide-flange shapes are hot rolled from billets by repeatedly passing the blooms through rolls to form the final shape. Wide-flange shapes differ from standard sections in that they are made on a mill with extra rolls having a vertical axis in addition to the rolls with horizontal axes. Such rolls permit rolling sections with wider flanges; hence the name. Wide-flange shapes are designated by the nominal depth and weight per foot; e.g. a W36 X 182 is nominally 36 inches deep (with an actual depth of 36.33 inches) and weighs 182 pounds per foot. The available domestic shapes are listed in the AISC *Manual of Steel Construction* (2010) and also in the literature available from the domestic shape producers. The wide-flange sections used for bridge stringers typically range between 24-inch (W24) and the deepest shapes available domestically, which have a 44-inch (W44) nominal depth. (Note: the Engineer is alerted to the special requirements contained in Article A3.1c of AISC (2010a) related to welded joints in rolled heavy wide-flange shapes subjected to tensile forces and having a flange thicker than 2 inches).

Figure 6.3.2.12-1 Rolled-Beam Superstructure

Figure 6.3.2.12-2 Fabricated (Welded) Girder Superstructure

Wide-flange sections are doubly symmetric and have relatively thick webs compared to most welded I-shape sections. The rolling process imposes a maximum web depth-to-thickness ratio of approximately 60. In the past, partial length cover plates were often welded to the flanges of rolled wide-flange shapes used in bridges in order to increase their bending capacity. However, research has shown that cover-plate weld termination must be assigned a very low permissible stress range (Detail Category E or E′), which has essentially limited the current use of welded partial length cover plates on highway bridges to in-kind replacements.

A common application of rolled beams is as substringers between welded girders in larger bridges (e.g. Figure 6.3.2.5.7-1). In these structures, the rolled beams usually span between 20 and 30 feet and are supported on cross-frames that are bolted to the welded girders. Rolled shapes for this application are often between 18 and 24 inches deep.

Table 2.5.2.6.3-1 of the *AASHTO LRFD* Specifications provides suggested minimum depths for constant depth superstructures. A 40-inch deep rolled beam will meet the suggested minimum depth for a 120-foot composite continuous span. For a composite simple span, the same table suggests the maximum span for a 40-inch deep beam to be approximately 100 feet. The size of the rolled beam must also meet critical stress or live load deflection criteria. Before designing a rolled-beam bridge, the Engineer should consider consulting with shape producers to ascertain the availability of a specific section size and length. The maximum available length of rolled wide-flange shapes is approximately 120 feet and varies by section size (again, consult with the shape producers for maximum length availability for a specific section). Stock lengths are typically available from steel service centers in 5-foot increments between 30 and 60 feet, but they may not meet toughness requirements and may not be domestically produced.

Rolled shapes for use in bridges should typically be ordered as ASTM A709/A709M Grade 50S, which is the equivalent grade to ASTM A992 for structural shapes. Note that uncoated weathering steel Grade 50W wide-flange shapes are available under the ASTM A709/A709M specification. However, rolled wide-flange shapes are not available in any of the high-performance steel grades (i.e. Grades HPS 50W, HPS 70W or HPS 100W).

A shape equivalent to a rolled wide-flange shape can be fabricated from plate stock to form an I-shape. It can be shown for a given web depth-to-thickness ratio that the minimum cross-sectional area of a doubly symmetric non-composite I-shape that is required to support a given moment can be computed as follows (Haaijer, 1961):

$$A_{min} = \left(\frac{18S^2}{\alpha} \right)^{1/3} \qquad \text{Equation 6.3.2.12-1}$$

where:

α = web depth-to-thickness ratio (D/t_w)
S = section modulus (in^3)

This relationship shows, for example, that using an optimized welded girder having a web with a slenderness D/t_w of 150 saves almost 30 percent of the steel required in an optimal shape having a D/t_w of 55 that is typical of a wide-flange shape. Therefore, significant material savings can obviously be obtained by fabricating I-shaped girders with larger web depth-to-thickness ratios. Whereas rolled beams are practically limited to a maximum web depth-to-thickness ratio of approximately 60, welded I-shapes of much more slender web proportions can be fabricated. However, if the web depth-to-thickness is too thin, vertical stiffeners are required to prevent shear buckling and longitudinal stiffeners may be required to prevent web bend buckling. Rolled shapes typically do not require stiffeners.

The use of a singly symmetric girder section with a smaller flange in a composite section provides additional economy over the doubly symmetric rolled shape without a cover plate. The potential to use deeper welded sections also reduces live-load deflections, which can lead to the use of uneconomical rolled beam sections or to required depths that may not be available.

However, for all the apparent economic advantages of the welded I-shape in terms of savings in material, rolled shapes generally require less fabrication. For situations where rolled beams are adequate and available, fabricators often prefer them. However, fabricators like to have the option to substitute an equivalent welded girder in case availability, delivery or other specific requirements (e.g. radius, maximum available length, or camber) become problematic. Some Owners consider rolled beams to be more economical than welded girders in situations where a choice can

be made. Therefore, for bridges with spans where a choice between a rolled beam or a welded shape is possible, and where the structure has a radius greater than 1200 feet and the required camber is not excessive, consider specifying rolled beams, ensure that the selected sections are available, and allow the fabricator to substitute an equivalent welded girder should the situation warrant (AASHTO/NSBA, 2003). However, since differences in the preferences of some fabricators and Owners do occur and market conditions are forever changing, it is considered prudent to check with the Owner and/or the fabricators who may be potential bidders on the job prior to making a final decision.

The industry has formed a Short Span Steel Bridge Alliance (SSSBA), which is a group of bridge and culvert industry leaders - including steel manufacturers, fabricators, service centers, coaters, researchers, and representatives of related associations and government organizations - who have joined together to provide educational information on the design and construction of short span steel bridges in installations up to 140-feet in length. A free web-based design tool, eSPAN140, has been developed by the SSSBA that houses standard designs of rolled-beam and welded-girder superstructures and details for steel bridges up to 140 feet long, as well as buried soil structures and manufactured bridge solutions.

6.3.3 Girder Depth and Substructure Considerations

6.3.3.1 Span-to-Depth Ratio

To help control elastic deformations at the service limit state, the optional span-to-depth ratios suggested in *AASHTO LRFD* Article 2.5.2.6.3 should be met to establish a reasonable minimum web depth for the design in the absence of specific depth restrictions. However, the Engineer is permitted to use shallower girders where clearance limits girder depth.

The recommended minimum depths in *AASHTO LRFD* Article 2.5.2.6.3 (refer to Section 2.3.2.6.3) are based on traditional maximum span-to-depth ratios. Span-to-depth ratios for highway bridges date back at least to 1908 when Milo S. Ketchum published "*The Design of Highway Bridges*"; the first such book of its kind (Ketchum, 1908). In this book, Ketchum presented "General Specifications for Steel Highway Bridges". Article 54, Depth Limits, from those Specifications indicated that the depth of steel beams preferably should not be less than one-twentieth of the span. This article went on to require that when that limit was not met, the beam must be designed to limit the deflections as if the limiting depth had been met. This stringent depth limit was most likely derived from earlier railroad bridge design provisions. Railroad loads tended to be heavier than highway loads. Further, most railroad bridges had no concrete deck and were not ballasted. The precise reasoning for the requirement is probably lost in antiquity. However, it is believed related to a desire to provide adequate stiffness.

Design stresses for the steel in 1908 were less than 20 ksi. Live loads were roughly equivalent to HS20 (AASHTO, 2002). The deepest available rolled section at that time was the 21-inch standard beam (wide-flange shapes had not yet been invented). Ketchum (1908) gives examples of multi-girder bridges using rolled shapes with spans up to 45 feet. Longer span girder bridges in that era were typically two-girder deck-type or through-type bridges with a floor system spanning between girders. The girders were built-up riveted I-sections. Frequently the girders were not composite with the deck and the two-girder bridges assigned more load to the girders than would occur in a multi-girder bridge.

In 1908, the specified minimum ultimate tensile strength of the steel was about 60 ksi and the minimum specified yield stress was about 30 ksi. Modern bridge steels are designed at twice the design stresses used in 1908. Hence, an efficiently proportioned girder today tends to provide less stiffness and be relatively shallower than would have been the case a century ago. Although design engineers were aware of composite action, they rarely took advantage of it in computation of strength or deflections.

In the First Edition of the AASHO *Specifications for Bridges and Structures* (AASHO, 1931), the preferred maximum span-to-depth ratio of steel beams was set at 20. The provisions permitted shallower sections if deflections were limited to those that would have been computed if the girder were designed with a depth of Span/20. This limit was probably taken from Ketchum (1908), although it was the same as the limit given in the AREA Specifications (for railroads) at that time. After about 1910, Universal Mill rolled shapes were available with depths of three feet. The maximum span-to-depth ratio of 20 limited the use of these shapes to spans of about 60 feet in simple-span bridges (most early steel bridges were simple-span bridges).

In the Second Edition AASHO *Specifications for Bridges and Structures* (AASHO, 1935), the span-to-depth ratio was relaxed from 20 to 25, presumably in recognition of the much deeper wide-flange shapes with much larger and more efficient flanges that had become available after about 1910. The AASHO Specifications (AASHO, 1935) required that If the steel beams were shallower than Span/25, they had to be designed such that the deflection would be the same as if they were designed for Span/25. Increasing the ratio to 25 increased the effective span of the available rolled shapes to about 75 feet. The change was not as dramatic as it appeared since the limit was generally applied to many beams rather than only two, and it was also generally applied to bridges with de facto composite decks.

In the Third Edition AASHO Specification (AASHO, 1941), a live load deflection limit of Span/800 was also introduced. The span-to-depth and live load deflection limits were relatively consistent with each other for the typical girder bridges constructed of the traditional steel grades. ASTM A7 steel, having a specified minimum yield

strength of 33.0 ksi, was the most commonly used steel for bridge design at that time, although the use of other grades was not forbidden. The Span/800 deflection limit obviously would have had a greater effect on the designs of that era had the design stresses been higher.

The advent of composite design eventually led to shallower girders being accepted and economical. Recognition of composite action in design implied a stiffer bridge. In earlier times, many bridges were built with decks not integral with the top flange so the depth limits were based on the assumption that no structural interaction existed between the deck and girders; composite design recognized this interaction when it existed. In the early 1950s, it became evident that composite wide flange beams with span-to-depth ratios greater than 25 could be economical. As a result, the preferred maximum span-to-depth ratio was relaxed to Span/30 for the steel beam, and left at Span/25 for the composite beam. As shown in Section 2.3.2.6.3, these preferred ratios remain to the present day.

The enabling use of computers for the analysis and design of bridges in the 1960s led to wider use of more economical continuous span steel-girder bridges. Continuous spans complicated the application of the relatively straightforward span-to-depth ratios. Questions arose with regard to the span length to be used in determining the limiting span-to-depth ratio and live load deflection. Since these were recommended (as opposed to specified) limits, the determination of the appropriate span length in each case was left up to the Owner and the Design Engineer. This resulted in a variety of approaches. A common approach was to liberally define the span length as the distance between points of permanent load contraflexure for determining the maximum span-to-depth ratio, and as the span between supports in determining the Span/800 live load deflection limit.

In the determination of the suggested minimum depths given in *AASHTO LRFD* Table 2.5.2.6.3-1, *L* is taken as the span length between bearings. The suggested minimum depths in *AASHTO LRFD* Table 2.5.2.6.3-1 are based on the historical values discussed previously. For simple spans, the requirement in the *AASHTO* Standard Specifications (AASHTO, 2002) is that the span divided by the steel girder depth should not exceed 30. The reciprocal of this value is the constant of 0.033 applied to the span length in *AASHTO LRFD* Table 2.5.2.6.3-1. For continuous spans, the constant of 0.027 applied to the span length is obtained by reducing the constant 0.033 by 80 percent to account for the effect of end restraint. The suggested minimum overall depth of the composite I-girder for simple spans, i.e. including the deck, is based on applying a constant of 0.040 to the span length. The constant 0.040 is the reciprocal of the traditional maximum span-to-depth ratio of 25 suggested for the overall depth of simple-span composite girders in the Standard Specifications (AASHTO, 2002). Similarly, the constant of 0.032 for continuous spans in this case is 80 percent of the simple-span value. Note that an end depth-to-span ratio of 90 percent of the simple-span ratio might be considered in either

case to better account for only one end of the span being restrained by continuity. Although the limits are taken to apply to the overall depth of the girder, it is suggested herein that they be applied to the web depth for simplicity.

In the absence of depth restrictions, the above suggested minimum depths for steel I-girders may be used to establish a reasonable minimum vertical web depth for the design of box girders – keeping in mind that the optimum web depth for a box section will typically be slightly less than the optimum web depth of an I-section for the same span because of the inherent torsional stiffness of a box section.

In *AASHTO LRFD* Article 2.5.2.6.3, there are specific suggested minimum depths, *D*, recommended for curved steel girder systems (refer to Section 2.3.2.6.3.2). These suggested minimum depths are larger than the traditional values contained in *AASHTO LRFD* Table 2.5.2.6.3-1. This reflects the fact that the outermost steel girder receives a disproportionate share of the load in a curved steel girder system and should be stiffer. In the equations for these suggested minimum depths, *D* is defined as the overall depth of the steel girder, but it is again recommended herein that *D* instead be taken as the web depth for simplicity.

In curved skewed bridges in particular, cross-frame forces are directly related to the relative girder deflections. Therefore, increasing the depth and stiffness of all the girders in a curved skewed bridge leads to smaller relative differences in the deflections and smaller cross-frame forces. Deeper girders also result in reduced out-of plane rotations, which tend to make the bridge easier to erect. Sections deeper than the suggested minimum depth may be desired to provide greater stiffness during erection.

Whenever steels having yield stresses greater than 50 ksi are used for curved girders in regions of positive flexure, an increased suggested minimum girder depth is recommended (Section 2.3.2.6.3.2). The use of higher strength steels in these regions tends to lead toward the use of shallower girders with larger flanges than those required with a deeper web. The recommended relationship for this case is intended to ensure approximately the same dead and live load deflection as would be obtained at an *L*/*D* ratio of 25 when 50 ksi steel is used. In some cases, a hybrid girder using a 50 ksi top flange and web with a 70 ksi bottom flange is more efficient in positive-flexure. For this reason, the specified minimum yield strength of the bottom (tension) flange, F_{yt}, is used in the equation for the suggested minimum depth.

The greatest depth determined from the applicable equation for each span in a continuous girder should be used for the bridge. If the span lengths vary greatly, a tapered girder can be considered. The span-to-depth ratios discussed above are not directly applicable to variable depth girders. Obviously, a conservative approach is to use the recommended minimum depths based on those ratios, as specified, to set

the minimum depth. But the depth of the deeper portion of the variable depth girder should be greater than the depth determined from those values for the span between bearings. A suggested more reasonable approach for tapered-depth girders is to apply the recommended values to the depth at a point on the girder approximately 10 percent of the span away from the bearing. In the limit, the deflections of a tapered girder should not be less than the deflections of a constant-depth girder would be if the constant-depth girder met the recommended depth. Such a limit (i.e. based on deflections) is also suggested for application to girders with parabolic haunches.

Girder depths at or most often exceeding these suggested minimum depths typically provide the most economical girders. The efficiency of the design decreases rapidly as the depth decreases (Fountain and Thunman, 1987). When shallower girders are used, the Design Engineer needs to carefully evaluate cross-frame forces and girder rotations to ascertain that these matters are within acceptable ranges. Conversely, if a depth far greater than the suggested minimum depth is employed, the flanges designed for flexure are likely to be too small to meet the recommended minimum sizes discussed in later sections of this chapter.

After considering all of the above, many bridges have been successfully built that did not meet these suggested girder depths.

6.3.3.2 Girder Depth

The proper web depth is an important consideration affecting not only the economy, but also the constructibility and performance of steel-girder bridges. This is especially true for skewed and curved steel bridges. The web depth dictates the flange sizes. Since there are minimum flange width-to-web depth and flange width-to-thickness ratios, web depth cannot be selected indiscriminately. As higher strength steels (e.g. ASTM A709/A709M Grade HPS 70W) are employed, the design flange sizes are smaller than those for a similar web depth with Grade 50 steel. Hence, there is a tendency to reduce the web depth. Such reductions tend to infringe on the recommended span-to-depth ratio.

In the absence of site restrictions on depth, the suggested minimum depths discussed above in Section 6.3.3.1 (based on traditional values of span-to-depth ratios) should be met or preferably exceeded where practical. Deeper girders not only lead to a stiffer bridge, but result in flanges that meet specified depth-to-width limits and girders that are easier to handle. When Grade 70 steels are used, the flange sizes tend to be smaller, potentially infringing on the specified limits. Girder depths greater than the suggested minimum provide benefits during construction. This is particularly true for curved girders. Shallow skewed bridges may have large cross-frame forces. Increasing the girder depth and reducing the deflections tends to reduce cross-frame forces.

Highway bridge vertical clearance requirements are defined in *AASHTO*, *A Policy on Geometric Design of Highways and Streets* (AASHTO, 2011c). Typically, the required vertical clearance is 14'-6". The specified minimum clearance should include 6 inches for future overlays. Clearance requirements for railway bridges are set forth in American Railway Engineering and Maintenance-of-Way Association (AREMA), *Manual for Railway Engineering* (AREMA, 2014). Vertical and lateral clearances for navigable waterways are established with the U.S. Coast Guard. Permits for construction including temporary supports or causeways for bridges in navigable waterways must be cleared with the Coast Guard. Roadway specifications control roadway profiles to ensure adequate visibility and for other reasons. Hence, it is impractical in many cases to gain vertical clearance by changing profile significantly. It is this exact situation that creates a demand for steel.

The larger Young's Modulus of steel compared to that of concrete allows steel to be the material of choice where structure depth is limited. Frequently, the addition of girders in these situations is considered a necessity. This flawed logic is probably due to the provision in *AASHTO LRFD* Article 2.5.2.6.2 that allows the live load deflection to be computed by using a wheel load factor equal to the number of wheel lines that can be placed on the bridge divided by the number of girders in the cross-section (live load deflection is discussed further in Section 6.5.4.2.2). This method is not applicable to curved-girder bridges and is of questionable use for bridges with skewed supports. The most economical girder bridge, regardless of depth, is one with the fewest girders in the cross-section. There are of course practical limits to the prior statement; for example, if the flanges become too large to be practical, if there are too few girders, and/or if the deck cannot span between the girders.

6.3.3.2.1 Optimum Depth

6.3.3.2.1.1 General

At times, obstacles prevent proper span ratios in continuous-span structures. The temptation is to use an average depth based on the best depth for several spans. This choice rarely gives the best result. Shallow girders, particularly in curved bridges or in bridges with skewed supports, lead to issues during construction and at times in the completed bridge. It is usually desirable to use the near optimal depth for the largest span in the unit if feasible.

The optimum depth is the depth that provides a minimum cost girder for a particular structural unit and is quite elusive. Fortunately, the efficiency of girders does not vary greatly when near the optimum. Composite steel girders are actually designed for two conditions:

- Non-composite condition before the deck hardens
- Composite condition after the deck hardens.

There probably is no algorithm that gives the optimum girder depth. The optimum depth can be estimated by preparing a series of designs with different web depths to arrive at an optimum cost-effective depth based on weight and/or cost.

The optimum depth depends on the span lengths of the unit, target web slenderness, girder spacing, shipping constraints, site constraints, live load deflections, ratio of composite to non-composite load, and many other issues. For example, the optimum depth for the negative moment regions is often not the same as that for the positive moment regions. This is probably where the idea of haunched girders arose. Usually the optimum depth for the positive moment region is a better choice when combined with heavier flanges in the shorter negative moment regions. Where a deeper web in the positive moment region requires smaller flanges, this may lead to stability issues during shipping and erection. A compromise depth is usually necessary.

In many cases, the optimum web depth will be greater than the minimum depth based on the traditional span-to-depth ratios.

6.3.3.2.1.2 Box Girders

Box webs may either be inclined or vertical. *AASHTO LRFD* Article 6.11.2.1.1 indicates that the inclination of the web plates to a plane normal to the bottom flange should not exceed 1-to-4. Webs attached to top flanges of tub sections must be attached at mid-width of the flanges. Should the flanges be attached to the webs at locations other than mid-width of the flanges, additional lateral bending effects are introduced in the flanges that would require special investigation.

The optimum depth for a box section will typically be slightly less than the optimum depth of an I-section for the same span because of the inherent torsional stiffness of a box section. The web depth obviously dictates the flange sizes for a given design. Therefore, establishing a sound optimum depth for box sections is particularly important because the size of box flanges can typically be varied less over the bridge length. Shallow boxes may be subject to larger torsional shear. Box web depths should not be less than about 5 feet to facilitate fabrication and inspection.

It is interesting to note that the two webs of a box are stressed roughly equally. This means that there will be only one critical location of the live load to produce the maximum moment in the box, whereas there are two critical positions of the live load for two I-girders. The result is that the total live load moment that must be resisted by two I- girders is greater than the live load moment that must be must be resisted by a box girder supporting the same width of deck. This occurrence is of particular interest when comparing an exterior box girder to an exterior I-girder and the adjacent interior girder. Typically, the exterior I-girder is critical and all girders are

often made the same size. The result of comparing a box girder design to an I-girder design is often that the total required moment capacity of the box girder design is less than that required for the I-girder design. This is particularly true when four I-girders are compared to two boxes.

6.3.3.2.2 Constant Web Depth vs. Variable Web Depth Members

The decision to use a variable depth girder in a steel multi-girder bridge is usually driven by consideration of clearance requirements, economics, poor span arrangement, and/or aesthetics. Girder depth is typically varied utilizing either a straight-line taper or a parabolic haunch along the bottom flange. Both I-girder and box-girder members can be designed with a variable depth. Usually box girders are given parabolic haunches rather than tapers. If the webs of a box girder are inclined, the inclination is usually held constant with the bottom flange width varied with the change in depth. Flexural stresses and lateral bending stresses need to be checked at both brace points of I-girder flanges in regions where the girder depth varies.

Variable depth girders may be desirable where clearance issues or awkward span arrangements exist. The most economical means to vary the girder depth is with a straight-line taper (Part A of Figure 6.3.3.2.2-1). The taper can extend over an entire field section or a portion of a field section. The best detail is to splice the flange over a short distance so that the splice plates are not kinked to the change in slope. The change in depth requires that the cross-frame depth varies. The shorter the length of the taper, the fewer cross-frames will be affected. However, if the change in depth is slight, a long taper can make the change in depth almost invisible to the eye.

Haunched girders have a greater depth at interior supports. Haunching most often is done for aesthetic considerations. A parabolic haunch (Part B of Figure 6.3.3.2.2-1) is considered the most aesthetic, although other haunch types are often used. Figure 6.3.3.2.2-2 shows haunched I-girders with a parabolic haunch and with longitudinal web stiffeners.

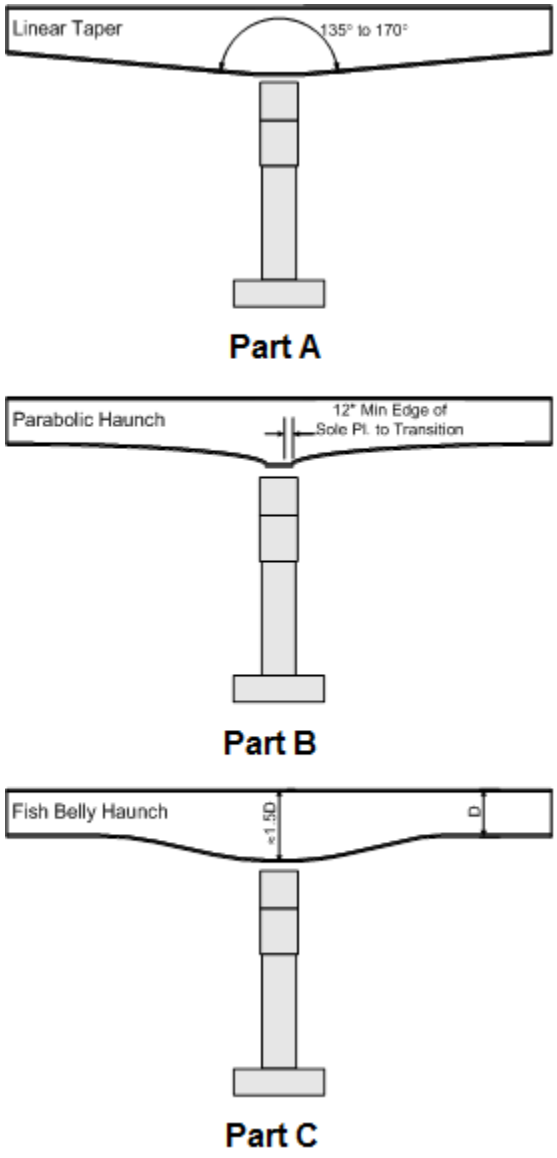

Figure 6.3.3.2.2-1 Variable Web-Depth Member Configurations

Figure 6.3.3.2.2-2 Haunched I-Girders with a Parabolic Haunch and Longitudinal Web Stiffeners

Haunched girders contribute little to the efficiency of steel girders because the haunch is cut from a wider plate, creating scrap. The distance over which the haunch is effective is relatively short so it does not draw much load away from the adjacent positive moment regions; hence, the positive moment regions receive little reduction in moment.

The inclined bottom flange with its vertical component of force, P_v, carries some of the shear that normally is resisted by the web (Figure 6.3.3.2.2-3). This increased flange force is not evident from a typical beam analysis since the shear component of stress is not a flexural stress. This phenomenon is called the Resal effect after the man who studied variable depth girders. The effect can be beneficial for concrete girders because it reduces the shear in the web, which is important to the shear-weak concrete. However in steel haunched girder design, the effect may be problematic. In concrete, the haunch usually rests on the foundation so the force can be easily transferred into the foundation without any bearing. In a haunched steel girder, the situation is different. Approaching the bearing, the flange is returned to a horizontal attitude and the Resal force is transferred from the flange into the web. This perturbation in the force field leads to large compression forces in the web in the vicinity of the change in flange attitude. This is addressed either by stiffening the web (as discussed further below), or by using a smoother transition or “fish belly” to change the slope so that the force can be introduced into the web over a greater distance (Part C of Figure 6.3.3.2.2-1).

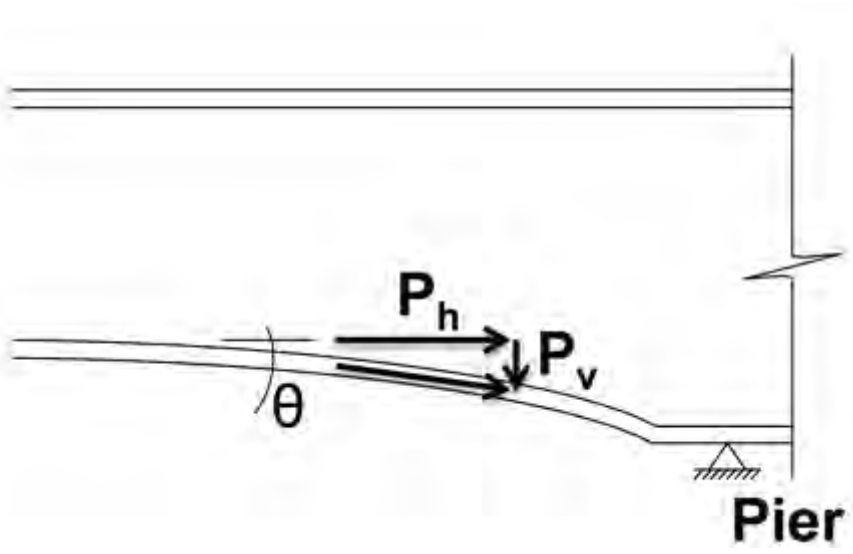

Figure 6.3.3.2.2-3 Vertical and Horizontal Components of Force in the Inclined Bottom Flange of a Parabolic Haunch at an Interior Pier

As discussed in Section 6.3.3.2, application of higher strength (high-performance) steel permits smaller flanges for a given depth girder in a given application. However, the smaller flanges reduce the girder stiffness leading to larger dead and live load deflections for a given depth. Thus, if a 50-ksi design is controlled by deflection, the girder must be deeper if 70-ksi steel is employed. Constant web depth members utilizing Grade HPS 70W steel flanges (with Grade 50W steel typically utilized in the web) are sometimes economical for spans up to and even exceeding 500 feet in length when applied in the proper depth. Thus, a parametric study of these applications investigating constant versus variable depth girders is usually justified. Application of the *AASHTO LRFD* suggested minimum depths (AASHTO LRFD Article 2.5.2.6.3) to variable depth girders is discussed near the end of Section 6.3.3.1.

In fabricating a variable web depth member, the desired girder depth is cut into the web plate and then the bottom flange plate is pulled into place and welded to the web plate. In a tapered or haunched girder, a transition is typically made from the sloping part of the taper or haunch to a horizontal bottom flange near the bearing to accommodate the bearing sole plate. The transition is made by using either a welded joint or by bending the flange plate. Bending of the plate depends on the required radius and the length of plate available from the mill. Proportioning of the flange plate at the transition location should allow for the possibility that the fabricator may bend the plate. As mentioned above, bending of the flange plate into a ″fish belly″ type of transition can help to smooth out the transition, in lieu of a more abrupt transition which can result in an extremely sharp increase in the web stress as the vertical component of the flange force is transferred back into the web. The

distance from the edge of the sole plate to the transition should be at least 12 inches in order to clear any distortion that may result from bending or welding of the flange plate, and to accommodate any possible future jacking needs for bearing maintenance (Part B of Figure 6.3.3.2.2-1).

Fabrication costs for variable web depth members are higher than for constant web depth members due to the additional cutting and fitting operations discussed above. Straight tapers are less costly than parabolic haunches because it is easier to cut the webs, locate and fit web stiffeners, weld flange transitions and fit-up the member at the web-to-flange joint.

For bridges with spans exceeding approximately 400 feet, the haunched section may be so deep as to require a longitudinal field splice in the section, which increases fabrication costs significantly. A horizontal field splice may be required because of the maximum plate width availability from the mill and/or because the depth of the haunched section may preclude shipping of the section without a longitudinal field splice (typically when the depth exceeds about 14 feet). Plates are generally available from many plate mills in maximum widths up to 150 inches. Generally, the maximum usable plate width from such a plate is about 144 inches. Larger plate widths may be available from select mills. The Design Engineer is encouraged to contact the fabricator regarding maximum practical plate widths. Longitudinal web splices may either be welded or field bolted. A field bolted splice can either be fabricated using a sub-flange on the bottom of the top section and the top of the bottom section of the web plates (which are then field bolted together), or using side plates similar to a conventional bolted web splice. Note that it may be easier to ship two I-sections than deep tee sections, which may need to be temporarily braced during shipment. Thus, when designing exceptionally deep variable web depth girders, consult with fabricators in the area regarding feasibility of shipping, field-section size/depth and jobsite access.

Variable web depth members are important aesthetically because they visually demonstrate the flow of the forces in the bridge and make the bridge appear thinner. To ensure that the tapers or haunches are long enough in proportion to the span, they preferably should be brought out to the point of dead-load inflection in the span (i.e. where a field splice would typically be located in a continuous span). Parabolic haunches at interior piers typically offer a smoother transition to the rest of the girder and are generally more visually pleasing. Haunches should typically not be deeper than 1.5 times the midspan depth of the girder to prevent the haunch from appearing too heavy in proportion to the midspan section (Part C of Figure 6.3.3.2.2-1). Conversely, a haunch that is too shallow does not save enough material to justify the added fabrication cost and is not aesthetically pleasing. The total angle at the point of haunch (i.e. between the haunches on either side of the interior pier) preferably should be between approximately 135 and 160 degrees to prevent the appearance of too sharp a haunch at the bearing point (Part A of Figure 6.3.3.2.2-1).

When haunched I-girders are employed in conjunction with skewed supports, significant drops are likely to occur between adjacent girders. Thus, the cross-frames would typically be detailed as parallelograms to follow the drops. The effect of these sloping cross-frame members should be considered in the analysis.

In variable web depth tub girders with inclined webs, the inclination of the webs preferably should remain constant to simplify the analysis and fabrication. Assuming a constant distance between the webs at the top of the tub, which is also preferred, along with a varying web depth, the width of the bottom flange must also vary along the length and the web heights at a given cross-section must be kept equal in order to maintain constant web slopes. As described previously, when a vertical curve must also be built into the web because of camber or roadway profile and camber, the establishment of the developed shape of the plate becomes more difficult; that is, the shape of the flat plate pattern from which the web must be cut. Experienced steel detailers and fabricators generally have software available to establish the necessary pattern. It should be noted that a curved inclined web for a tub section can be cut from a flat plate as part of a cone shape. If, however, the slope varies, the webs are no longer developable and must be heated to conform to the desired shape.

Erection of variable web depth members is affected to some degree by their more complex geometry. However, these complications are generally considered minimal by most erectors. Therefore, erection considerations typically need not enter into the decision process as to whether or not variable web or constant web depth members should be used. An exception might be when the bridge is to be erected by incremental launching, in which case the use of constant web depth members is recommended.

As discussed above, the bottom flange of variable web depth members carries a portion of the vertical shear in the region of the sloping web (Figure 6.3.3.2.2-3). Thus, the force in the bottom flange in this region is increased due to the vertical shear component. The major-axis bending moment in this region is developed from the smaller horizontal component of the resultant bottom-flange force, P_h (Figure 6.3.3.2.2-3). Therefore, if the normal stress in an inclined bottom flange (without considering flange lateral bending) is determined by simply dividing the major-axis bending moment by the elastic section modulus, the bending stress in the flange will generally be underestimated. According to *AASHTO LRFD* Article C6.10.1.4, the horizontal component of the flange force, P_h, can be determined as:

$$P_h = MA_f / S_x \qquad \text{Equation 6.3.3.2.2-1}$$

AASHTO LRFD Equation C6.10.1.4-1

where:

A_f = area of the inclined bottom flange (in.^{2})
M = major-axis bending moment at the section under consideration (kip-in.)
S_x = elastic section modulus to the inclined bottom flange (in.^{3})

According to Blodgett (1982), the normal stress in the inclined flange, f_n, may then be determined as:

$$f_n = P_h / A_f \cos\theta \qquad \text{Equation 6.3.3.2.2-2}$$

AASHTO LRFD Equation C6.10.1.4-2

where θ is the angle of inclination of the bottom flange with respect to the horizontal (Figure 6.3.3.2.2-3).

The vertical component of the flange force affects the vertical web shear. According to *AASHTO LRFD* Article C6.10.1.4, the vertical component of the flange force, P_v, may be determined as:

$$P_v = P_h \tan\theta \qquad \text{Equation 6.3.3.2.2-3}$$

AASHTO LRFD Equation C6.10.1.4-3

As pointed out in Blodgett (1982), for fish-belly haunches, P_v is equal to zero near the supports. In regions of positive flexure with tapered or parabolic haunches sloping downward toward the supports, the vertical web shear is increased by P_v. For all other cases, the vertical web shear is reduced by P_v. The specification allows the Design Engineer to reduce the web dead-load shear by the vertical component of the flange force where desired and permitted by static equilibrium. Reduction of the live-load shear is not recommended in these cases because many combinations of concurrent shear and moment must be evaluated in order to determine the critical (or smallest) shear reduction.

In parabolic haunches, the downward slope of the bottom flange is larger at positions closer to supports. At interior supports, this change in the inclination of the bottom flange along with the compressive stress in the flange introduces a compressive distributed transverse force on the web (Blodgett, 1982). Therefore, *AASHTO LRFD* Article C6.10.1.4 recommends that transverse stiffeners be provided within these types of haunches with a spacing d_o not to exceed approximately 1.5D. Otherwise, the Engineer should check the stability of the web under this force.

The bottom flange of a variable web depth member is usually made horizontal in the vicinity of the bearings. Where this transition occurs, the vertical component of the inclined flange force is transferred back into the web as a concentrated load, which

causes additional stress in the web and the web-to-bottom flange welds. Thus, additional local stiffening may be required in this area. According to *AASHTO LRFD* Article C6.10.1.4, additional stiffening is not required if the web local yielding provisions of *AASHTO LRFD* Article D6.5.2 (Appendix D6) are satisfied using a length of bearing *N* equal to zero. For compressive concentrated loads, the provisions of *AASHTO LRFD* Article D6.5.2 generally govern relative to the web crippling provisions of *AASHTO LRFD* Article D6.5.3 when *N* is taken equal to zero. Again, smoothing out the transition with a "fish-belly" flange rather than providing a sharp transition can help to reduce the increase in web stress at these locations.

6.3.3.3 Substructure Considerations

6.3.3.3.1 Substructure Form

The importance of the foundation and the pier regarding cost and aesthetics cannot be overstated. The first consideration is the geology. If a pile foundation is anticipated, a small footprint pier is often economical to reduce the number of piles. This can be accomplished by drawing the superstructure loads to a single column (i.e. a hammerhead pier). If a spread footing is anticipated, a larger footprint pier is usually more economical.

A narrow pier tends to drive the superstructure design to also be narrow. A superstructure consisting of a single box girder requiring no pier cap leads to not only an economical pier design, but also to a very economical superstructure. There has been reluctance to use single steel box-girder cross-sections even though there has been a paucity of fractures in the U.S. of newer bridges constructed with modern bridge steels. There are many examples of single-girder bridges built in the U.S. The Storrow Drive Bridge in Boston over the Charles River is perhaps the largest such American structure. There are a number of similar, less noticeable bridges in the Boston Central Artery project, in Ft. Lauderdale, FL and in Seattle, WA.

Each situation presents unique challenges to the Design Engineer. To achieve a truly efficient steel design, the superstructure and substructure type must be viewed in unison with respect to economic, structural and aesthetic demands.

The type of substructure is defined by considering its many functions and the existing soil conditions. The substructure is designed for various specified combinations of the resulting vertical and lateral load effects. Different load factors are applied to each force effect to account for the probability of the combination of individual design loads occurring simultaneously. Further, maximum live loads are reduced from the maximum vertical live load in order to cause the maximum overturning moment; e.g. live load is applied in only one span or on only one half of the cross-section to obtain maximum overturning with concomitant reductions in the maximum vertical load. Vertical loads are primarily dead and live loads plus impact.

Lateral loads include wind on the structure and on the live loads; braking; bearing friction; thermal forces; ice; stream flow; earth pressure; ship impact; debris; and seismic forces. Lateral loads are resisted by overturning moments and shear in the piers and abutments.

Overturning moments can cause an increase in the size of the foundation beyond that required for only vertical loads. An objective for an efficient foundation is one that requires minimal additional piles or drilled shafts beyond that required for vertical loads alone. Transferring the vertical loads to the ground through a minimum number of pier columns is usually desirable, if not necessary, to accomplish this objective. For example, single-shaft piers carry the entire vertical load as well as resist lateral loads. The critical moment in the shaft is partially due to transversely and longitudinally eccentric vertical loads. Usually the maximum moment and maximum axial load are not coincident. In multiple-column piers, there are multiple or redundant paths for live loads, which in essence provide an uneconomical vertical load capacity in excess of the design vertical load.

Where appropriate, the uneconomical redundant load path dilemma can be avoided by considering the use of single shaft piers that support multiple girders with a pier cap, or optimally a single box girder without a pier cap.

6.3.3.3.2 Clearance Envelopes

Since the purpose of a bridge is to span an obstacle, there is usually some clearance requirement involved. For example, river crossings must account for flood volumes of water; intersections must account for traffic height and safety limits on columns; and navigation channels have specified clearances.

Highway grade separations require that the Engineer thread the structure through a space that provides vertical and lateral clearances without demanding too much grade on the overpassing roadway. These restraints limit the girder depth, which in turn limits span lengths. The lower roads limit placement of piers. The Design Engineer is compelled toward the use of poor span ratios, skewed supports, and often times, to some kind of support structure that straddles the roadway. These straddle-beam structures have been used in some congested metropolitan areas for decades. However, they are becoming more common throughout the nation as right-of-way becomes harder to obtain and the road system becomes more complex.

6.3.3.3.3 Straddle Beams

Straddle beams usually straddle a roadway that passes under the planned bridge (Figure 6.3.3.3.3-1). They rest on two or more columns. There are several varieties of straddle beams; they may be made of concrete or steel; they may be integral with the columns supporting them; they may support the girders on their top or integrally.

Like single box-girder cross-sections, some are concerned about the use of non-redundant steel straddle beams, although the *AASHTO* fracture control plan with its demanding Charpy values for steel used in fracture-critical components and more stringent fabrication and inspection requirements has precluded any recent failures.

Figure 6.3.3.3.3-1 Straddle Beam Supporting a Curved Steel I-Girder Bridge

The simplest straddle beam is probably the single box beam supporting girders on bearings resting on the top of the box. Stability of the box is one problem. Typically four bearings, two at each support, are used. The stability of the straddle beam depends on its bearings not experiencing uplift. Tie-down bearings are usually not practical, but some have opted to build a bent with steel columns integral with the straddle beam. The options with girders on top of the straddle beam usually provide transversely free bearings to minimize lateral forces on the bent. However, some friction should be considered in designing the bent. One interesting aspect of design is the forces in the cross-frames at the straddle beam. Since the straddle beam deflects unequally under the girders as the bridge is built, significant load is transferred to the girders over the stiffest portions of the straddle beam. This affects the forces in the cross-frames as well as the moments in the girders, and to some degree, the straddle beam.

The advantage of these bents is their simplicity and speed of erection. This is particularly important where traffic is extreme.

A more common straddle bent is one with integral girders. This arrangement eliminates the concerns of stability once the bridge is constructed. Again, the straddle beam may be either steel or concrete. Again, the perceived advantage of

concrete is that it is not fracture critical. The disadvantage is that the girder sections must be held in place while the concrete is formed, cast and until it has hardened. This time removes much of the advantage of steel construction. Casting off-site has been examined, but the weight of the beam is challenging. More typically, the steel straddle beam is used with the girders either penetrating it or abutted against it. Generally, bolting the intersections is preferred. Earlier, welding was employed, but it was learned that the steel working orthogonally created stress states leading to metal fatigue. Most commonly, the top flange is spliced over the straddle beam with heavy splice plates. Depending on whether the straddle beam bottom flange is below the bottom flange of the girders or intersecting it, the details vary. If a common flange plate is used, the biaxial stress state in the plate should be checked; *AASHTO LRFD* Equation C6.11.8.1.1-1 (Section 6.5.6.2.4.2) is suggested for possible use in making this check. Web connections to the straddle beam are usually bolted with the bolts designed for shear and flexure.

AASHTO LRFD Article 6.6.2 requires that non-redundant fracture-critical members be identified on the plans and that they are fabricated according to the fracture control plan given in Section 12 of the *AASHTO/AWS D1.5M/D1.5 Bridge Welding Code*. Not infrequently, designers opt to use multiple plates bolted together to circumvent the redundancy issue. For example, two I-girders might be used as the box webs; the two independent girders would then be bolted together with common flange plates to form a box.

Cambering straddle beams and girders requires special attention. The straddle beam is usually erected without the girders and undergoes deflection prior to erection of the girders due to its own self-weight. The weight of the girders increases the straddle beam deflection further. When the straddle beam is long and flexible, addition of the girders may cause enough deflection that fit-up of the girders becomes a challenge. At any rate, camber of the girders must allow for the deflection of the straddle beam as loads are applied. This means that at the connection point, the girders should be cambered for the total deflection that they undergo due to the loads applied after connection of the girders to the straddle beam, minus the deflection of the straddle beam due to its own self-weight (i.e. prior to the erection of the girders) at that point. Within the girder span(s), the girder cambers should be similarly adjusted using a straight-line proration of the straddle-beam deflection (due to its own weight) at the connection point back to the adjacent support(s). If the adjacent support(s) is rigid, the deflection is zero at that point; if the adjacent support(s) is another straddle beam, the self-weight deflection of that straddle beam is used at that point for determining the straight-line proration. Fit-up of the girders to the straddle beam must account for the camber in the straddle beam at the time of fit-up.

Possible alternative fabrication procedures for closed-box straddle beams are discussed in AASHTO/NSBA (2003). The design of such straddle beams is assumed covered by the *AASHTO LRFD* Specifications.

6.3.3.3.4 Steel or Concrete Integral Cap Beams

Integral cap beams are pier caps that are integral with the girders. Usually they rest on a single pier column. They may be either concrete or steel. If they are concrete, they are generally integral with the pier column (Figure 6.3.3.3.4-1). If they are of steel, they are generally not integral with the pier column. As illustrated below in Figure 6.3.3.3.4-2 Part C, skewed piers often can be avoided with integral pier caps that are radial (or normal) with the girders. This keeps the dropped cap out of the clearance envelope. The pier may have a variety of configurations. Typically, a steel cap is used to support the exterior girders, while the center girders are erected first and supported directly on the pier column. Unlike the straddle beam, the cap is often composed of separated sections bolted between the girders.

Alternatively, the cap is made of post-tensioned concrete. This requires that the steel be erected before the concrete cap is formed and cast. Usually, the post-tensioning is performed in two stages; first for dead load and second for live load. The two stages permit a higher post-tensioning force without crushing the concrete. An often overlooked issue with these caps is the Poisson effect due to the post-tensioning. The concrete is often highly stressed orthogonally to the stressing due to this effect, which can result in a longitudinal stress in the steel girders (*AASHTO LRFD* Article 3.4.1). Transverse reinforcing should be introduced to prevent cracking.

Figure 6.3.3.3.4-1 Single-Column Integral Pier Cap

Figure 6.3.3.3.4-2 highlights three possible pier configurations for a skewed underpassing roadway or stream. Figure 6.3.3.3.4-2 Part A shows a skewed multi-column pier aligned with the roadway below. This configuration results in increased pier length and cost. Figure 6.3.3.3.4-2 Part B shows a multi-column pier aligned radial (or normal) to the girders. This configuration may result in vertical clearance violations. Figure 6.3.3.3.4-2 Part C shows a single-column integral pier cap aligned radial (or normal) to the girders. This final configuration eliminates the vertical clearance problems and allows for the elimination of the skewed support.

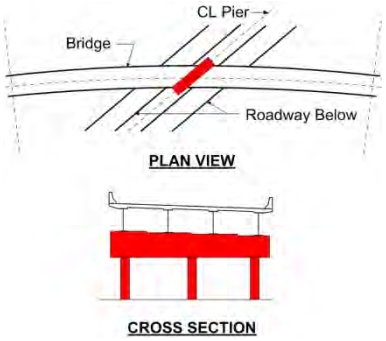

Part A

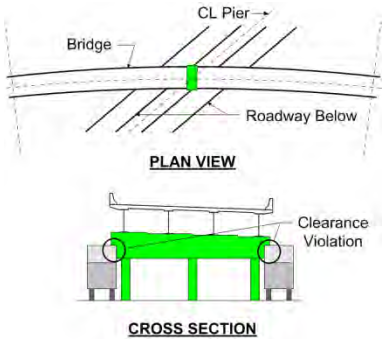

Part B

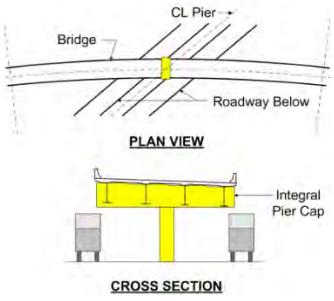

Part C

Figure 6.3.3.3.4-2 Possible Pier Configurations for Skewed Alignments

Figure 6.3.3.3.4-1 presents a photograph of the pier configuration depicted in Figure 6.3.3.3.4-2 Part C. This single-column integral pier cap is aligned radial (or normal) to the girders. It eliminates the vertical clearance problems, and it also allows for the elimination of the skewed support.

6.3.3.3.5 Integral Abutments

Most agree that bridge joints are a major factor affecting bridge maintenance. For this reason, many agencies have established policy stating that it is best practice to minimize the number of bridge joints. This policy has been carried to the point of elimination of joints at abutments by attaching the bridge to the approach slab in combination with an integral abutment.

Continuous structural units have become longer over the past two decades. Steel bridge structures up to nearly 2,000 feet long have been built in the U.S. without an intervening joint. Other structures of several hundred feet in length have been built without joints at their ends. Of course the critical issue is thermal movements. All bridges built with few or no joints are not without problems. Long curved structures with relatively low transverse stiffness have been shown to have advantages in allowing greater expansion lengths (FHWA/NHI, 2010). Design of the substructure becomes even more important in these cases where substructure movement is important.

Bridges designed as jointless are popular in some agencies. They have the advantage of preventing water from corroding the ends of the bridge. There are several ways to detail such bridges. Typically, the bridge abutments are made integral with the superstructure. Thermal forces are transferred between the sub and superstructures via connection of the concrete diaphragms at the abutments. There is often reinforcing passing through the girder webs. Sometimes shear studs are added to the girder webs to assist in transferring the load. Design of the studs can be performed by treating the studs as a fastener group designed to develop the end moment in the girders. In the case of a fully integral abutment, piles are generally used. The piles are attached to concrete that acts as the endwall as well as the end diaphragm for the bridge girders. Hence, the ends of the girders act as nearly fixed-end beams resisting the rotation and translation of the girders. Piles are usually oriented in the weak direction parallel to the girders to minimize resistance to expansion and contraction. The piles bear laterally against the soil. The deck is often attached to the approach slabs to further hinder movement, or placed on some interface intended to permit movement when the bridge girders change length due to thermal movements. To properly model this arrangement in an analysis, the friction of the approach slab and the active resistance of the soil acting on the piles should be considered, as well as the flexural stiffness of the piles. The approach slab and the active soil resistance are usually modeled with foundation elements of the proper

stiffness to represent the soil behavior. The piles are usually modeled with beam elements.

The effect of fully integral abutments on the girders is often substantial. Negative end moments and thrusts are created in the girders. These end moments and thrusts must be transferred from the girders into the concrete over a relatively short distance. This is done with shear studs. The number of studs can be determined from the force in the girders going into the concrete since it is known that the force at the end of the girder must be zero. Further, the negative moments create tension in the deck, which may cause significant cracking if the deck is not properly detailed. The effect of thermal forces on a jointless bridge having integral abutments may be significant when the deck is removed on a warm day.

Skewed abutments provide additional challenges to the Design Engineer when designing integral abutments. Severe bending may be created in the abutment itself due to its longitudinal component of force. This flexure also causes significant additional shear in the abutment that must be reinforced. The piles at the acute angle tend to lift up which increases the force on the piles at the obtuse angle. Hence, an increased number of piles are required. The shear connection also must be beefed up.

Semi-integral abutments are primarily composed of integral concrete end diaphragms, compressible backfill and moveable bearings in a horizontal joint at the superstructure and a pile-supported abutment interface. A steel cross-frame or diaphragm is often provided to stabilize the girders prior to casting the concrete end diaphragm. Semi-integral abutments are less problematic on skews than are fully integral abutments. Semi-integral abutments do not require modeling of the supporting piles in the analysis. Instead, the superstructure/abutment interfaces are typically modeled with foundation elements. However, end moments are still developed in the girders that need to be removed by shear connectors. Shear forces in the concrete develop when moments in adjacent girders are different. As with fully integral abutments, the concrete forming the abutment must be inserted in the analysis model only for the proper analyses. Often the concrete is placed in the abutments after the steel and deck weights have been recognized by the girders.

6.3.3.3.6 Simple Spans Made Continuous for Live Load

The use of span-by-span construction can provide economies for shorter span steel bridges; i.e. utilizing simple spans versus continuous spans. Continuity has most often been favored for steel bridges because it uses less structural steel, eliminates deck joints and the associated deterioration and results in the use of fewer bearings. The majority of the bridges in the U.S. have spans under 140 feet. For prestressed concrete girders, designers almost always use span-by-span construction due to the difficulties with the splicing of concrete girders. The use of modular elements and

span-by-span construction for shorter-span steel bridges can offer significant advantages in terms of accelerated bridge construction (ABC). ABC methods, including modular deck/beam elements, SPMT installations and lateral sliding installations all make use of span-by-span construction (Section 2.4). Span-by-span construction should be considered for certain shorter-span steel-bridge applications where there are shipping limitations and/or where traffic impacts during construction must be minimized.

The simple span for dead load and continuous for live load concept has been used successfully in span-by-span construction to eliminate deck joints (Javidi et al., 2014; Yakel and Azizinamini, 2014). In this concept, the individual steel girders are analyzed as simple spans for the self-weight of the steel and the concrete deck. Continuity for live load and superimposed dead load is then typically accomplished by placing reinforcing bars over the pier and then casting concrete diaphragms over the pier. Special details are typically required at the pier to transfer the compressive forces generated by the live load and superimposed dead load negative pier moments without crushing the concrete in the diaphragm in the vicinity of the steel-girder bottom flanges, as recommended in Azizinamini, 2014 and studied further in Lampe et al., 2014; and Farimani et al., 2014. Variations on these recommended special details have been used by different State DOTs on bridges that are in service with varying degrees of success (Azizinamini, 2014).

An alternative concept utilizes prefabricated girder units (typically box girders) pre-topped with a portion of the deck slab (Azizinamini, 2014). The portion of the deck can be cast onto the girders at the fabrication shop or at a temporary staging location. After setting the individual units on the supports adjacent to one another, a longitudinal deck closure pour is cast between the units joining them together. The concrete diaphragm over the interior pier is cast at the same time to provide continuity.

Advantages of the simple span for dead load and continuous for live load concept include the elimination of bolted field splices, the potential to use the same cross-section throughout the entire girder length, reduced negative moments over the interior piers, provision of a stable configuration during construction, protection of the girder ends against possible corrosion, and allowing for the sequence of deck casting for multi-span bridges to be ignored. Disadvantages include the need for some type of bottom-flange connection details as described above, additional field work, and the potential for concrete deck cracking over the pier under live load.

Another option to consider is a so-called “link-slab design” which provides jointless, but not continuous, construction. This concept is generally less complicated, less expensive and is designed to accommodate the end rotations of the beams (Caner and Zia, 1998; Culmo, 2014).

6.3.3.3.7 Thermal Forces/Bearing Restraints

Narrow straight bridges with perpendicular supports undergo minimal lateral movement under a uniform temperature change. Hence, lateral thermal movements can be ignored with respect to design of the bearings. However, if the bridge is wide, has skewed supports, or is curved, lateral expansion and contraction should not be ignored.

Bearing orientation is important to direct and accomodate thermal movements and to mitigate thermal forces. Excessive reactions and distortions can be created when the bearings are not able to accommodate the deflections and rotations induced in the bridge. Bearings also resist horizontal forces due to dead and live loads, thermal effects, wind, centrifugal force, braking force, extreme events, etc. Restraints and orientation must be chosen with consideration to all of these forces. Generally, the more constraint provided in the bearings, the larger the forces involved.

A point of fixity (i.e. zero translation) with respect to thermal movement can be arbitrarily chosen. A uniform temperature increase will cause expansion of the structure radially from that point if there are no horizontal restraints. Obviously, if guided bearings are assumed aligned along these rays, there will be no thermal restraint in the bearings. This simple principle applies to wide, skewed and curved bridges. Thermal effects can be minimized in continuous units by making a bearing on an interior pier, rather than a bearing at an abutment, serve as a single point of zero translation.

In many cases, it may be necessary to fix additional bearings transversely on a pier to provide sufficient resistance for other horizontal force effects (e.g., seismic). In such cases, it may be necessary to locate the assumed point of zero translation off a bearing, e.g., at mid-span, and again, guide all the expansion bearings toward that point. Several analytical investigations may be necessary to determine the optimum orientation of the bearings to successfully mitigate the resulting horizontal thermal reactions.

Longitudinal restraint at the reactions may introduce moments at the girder ends. This situation is particularly critical with skewed supports. The bearing restraint acts eccentric with respect to the neutral axis of the girders. Typically, this causes negative moments because the bottom flange is mostly in tension and is attempting to lengthen. The longitudinal reactions can be due to thermal and/or vertical loads. Even dead load effects may not be permanent as bearings or anchorages fail or if the bearings are replaced after the bridge is built. So it is not advisable to take advantage of the negative moments in design. However, it is desirable to check the girder design for the case where the bearings are constrained. The negative moments near piers may be larger and cross-frame/diaphragm actions may be critical for the constrained bearing case. The girders may be analyzed assuming

minimal bearing restraint to obtain the maximum positive moments for the design of the girders.

A fixed bearing located on a pier actually moves as a function of the pier stiffness when subjected to load. The displacement of such bearings equals the horizontal bearing force multiplied by the corresponding pier stiffness. The flexibility of the piers must be recognized in the analyses of bridges for horizontal loads. Recognition of the inherent flexibility of the piers in the analysis provides relief of the horizontal reactions at constrained bearings and also the cross-frame/diaphragm forces adjacent to laterally constrained bearings. The pier stiffnesses must be calculated in the direction of the constraint(s). Thus, both longitudinal and transverse pier stiffnesses may be required. Depending on the configuration of the pier, the response of the pier in the longitudinal and transverse directions may be quite different.

The longitudinal pier stiffness (i.e., assuming a right bridge, the stiffness of the pier in the direction parallel to the longitudinal centerline of the bridge) for a typical pier configuration can be represented schematically as a “flagpole” of length, *L* (Figure 6.3.3.3.7-1 Part A). The “flagpole” is fixed at the bottom at an assumed point of fixity, which is dependent on the pier configuration and soil conditions, and free at the top with a longitudinal load, *P*, assumed applied at the top. The deflection, Δ, is in the longitudinal direction, as defined above.

The transverse pier stiffness (i.e., assuming a right bridge, the stiffness in the direction perpendicular to the longitudinal centerline of the bridge) can be represented schematically as a “portal frame”, as shown for a two-column bent in Figure 6.3.3.3.7-1 Part B. The “portal frame” is also fixed at an assumed point of fixity, which is again dependent on the pier configuration and soil conditions. The deflection, Δ, is in the transverse direction in this case. Points of contraflexure are assumed to exist in the pier columns and in the cap beam as the “portal frame” deflects in the transverse direction under the load, *P*.

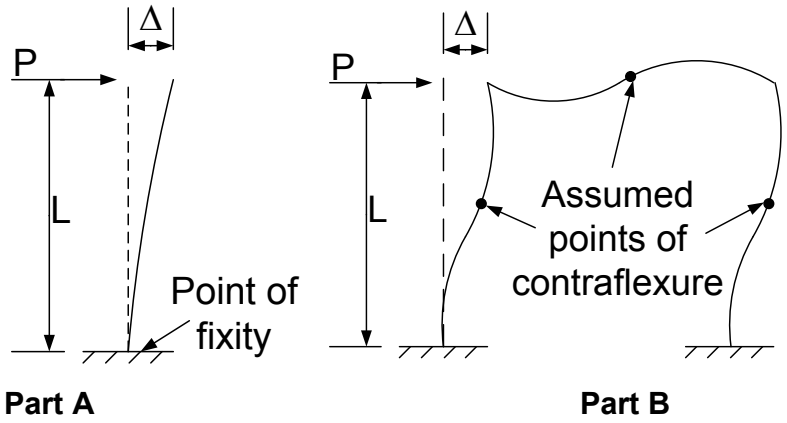

Figure 6.3.3.3.7-1 Schematic Representations of a Typical Pier in the Longitudinal and Transverse Directions
A) "Flagpole" - Longitudinal Pier Stiffness; B) "Portal Frame" - Transverse Pier Stiffness

Of course, refined finite element models of each pier could be built and analyzed in order to determine more accurate values of the pier stiffnesses, or the substructure could be explicitly modeled and combined with the refined model of the superstructure. However, for most typical pier configurations, the horizontal pier stiffnesses may be reasonably estimated in a quicker fashion using the classical conjugate-beam method. An approximate approach for calculating longitudinal and transverse pier stiffnesses based on the conjugate-beam method is illustrated in NHI (2011).

It is significant to note that a free bearing (i.e., with no horizontal restraint) can create significant force on a pier. If the dead load vertical reaction is 400 kips for example, the lateral force on the substructure is 40 kips for a sliding bearing if the coefficient of friction is 10 percent. This is usually not significant on the superstructure, but it may be significant on the overturning of the pier if the force was assumed to be zero.

The bearings of sharply skewed bridges, curved or straight, are often more problematic than those of straight or curved bridges without skew. Large horizontal reactions can be created in the bearings due to vertical and horizontal loads in skewed bridges in addition to thermal effects. These reactions increase with increased skew angle and vertical deflection of the girders. The greater the girder rotations at bearings, the greater the lateral reactions tend to be. This situation is particularly critical at end supports.

These large horizontal forces are evidenced by the failure of anchor bolts, concrete, bearings and end cross-frames on skewed bridges when these forces are not adequately taken into account at design (Figure 6.3.3.3.7-2).

It is not uncommon for the lateral forces on pot bearings resting on skewed supports to distort the pot, leading to leakage and bearing failure.

Fundamentally, the difference between the thermal behavior of a skewed bridge and one with right supports is that the longest expansion length of a skewed bridge is diagonally from acute bearing to acute bearing, while the shortest expansion length is either transversely or diagonally from obtuse angle to obtuse angle. This leads to a twist of the bridge which is usually resisted by laterally restrained bearings. One can imagine a simple-span skewed bridge with two fixed bearings on the extreme girders at one end and a single guided bearing on the center girder at the other support (Figure 6.3.3.3.7-3 -- perhaps not realistic but demonstrative). As the bridge expands, assuming a uniform temperature increase, the bridge will tend to twist as it expands from the two fixed bearings. The twist is resisted by the lateral restraint at the opposite end of the span as seen in Figure 6.3.3.3.7-3. The lateral reaction creates a couple at the opposite end with very large longitudinal forces. If the bearings at the extreme girders are released and the interior girders are fixed, the distance, ΔL, is smaller, but so too is the moment arm. The resulting longitudinal forces are reduced somewhat. Again, judicious arrangement of bearings can and does reduce these forces. These forces can be, and often are, large enough to break out anchor bolts and fail the bearings.

Figure 6.3.3.3.7-2 Distressed Bearing on a Skewed Support

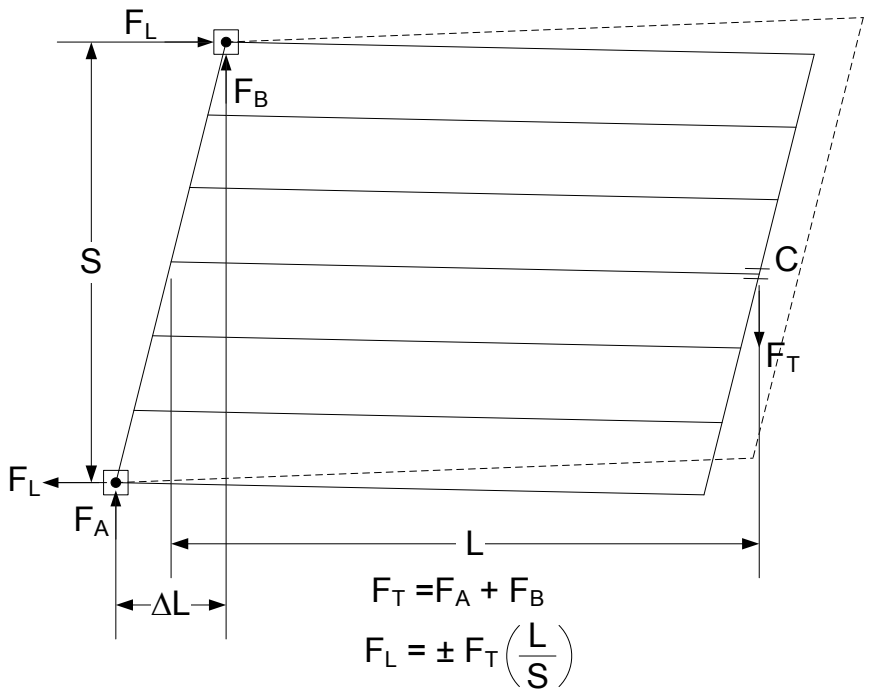

Figure 6.3.3.3.7-3 Twist of a Simple-Span Skewed Bridge Under Uniform Thermal Expansion & Resulting Lateral Reactions

It is important to investigate the bearing arrangement on skewed and/or curved bridges to minimize thermal forces on the piers while controlling the reacting forces on the superstructure. These issues are examined in greater detail in NHI (2011).

EXAMPLE

Consider the plan view of a straight simple-span skewed bridge with eight girders in the cross-section and staggered cross-frames shown in Figure 6.3.3.3.7-4. The model used in the analysis is a 3D finite element type. This model recognizes the eccentricity of the bearings with respect to the neutral axis of the composite girders.

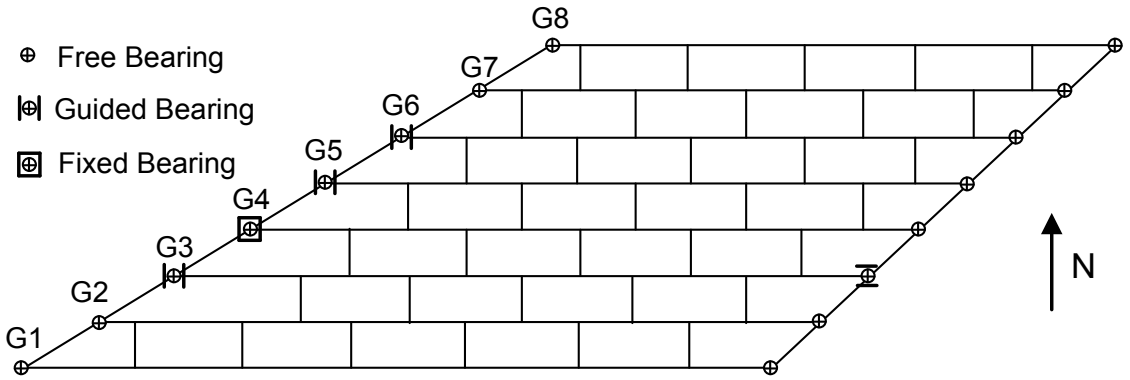

Figure 6.3.3.3.7-4 Plan View of Straight Simple-Span Skewed Bridge w/ Bearing Constraints Shown

The modulus of elasticity of the concrete deck (not shown in Figure 6.3.3.3.7-4) is based on the short-term modular ratio, *n* (no creep effects are assumed for thermal effects, which are assumed to be relatively ephemeral). The other parameters given for the exercise are as follows:

α	=	0.0000065 in/in/degree F (steel)
α	=	0.0000060 in/in/degree F (concrete)
ΔT	=	+70° F
Length of G1	=	136 ft
Length of G8	=	102 ft
Depth of steel girders	=	66.25 inches
Deck thickness	=	7.5 inches
Neutral axis	=	47.6 inches from the bottom of steel

For ease of discussion, the girders are assumed to lie west-east. The southernmost girder, G1, is the longest girder at approximately 136 feet, while the northernmost girder, G8, is the shortest girder at approximately 102 feet.

Referring to Figure 6.3.3.3.7-4, the orthogonal constraints of the bearings are oriented along and perpendicular to the girder lines. The middle four bearings constrain their respective girders longitudinally at the west end, while only one girder (G4) is constrained transversely. All girders are free longitudinally, and only one girder (G3) is constrained transversely at the east end. All other bearings are free.

In an actual bridge design, more than one bearing would typically be employed at each end to resist transverse movement and forces. However, only one such constraint is used in this analysis to separate the effect of the overall lateral bridge movement from the lateral constraint forces that would be generated due to expansion of the bridge between adjacent bearings, as discussed further below.

The superstructure, including the concrete deck, is subjected to a uniform 70 degree F temperature increase in the 3D analysis of the bridge.

The difference in the longitudinal expansion of G1 and G8 is significant, as would be expected, due to their different girder lengths. As shown in Figure 6.3.3.3.7-5, G1 expanded the most in the longitudinal direction: [0.57 – (-0.16)] = 0.73 inches. The theoretical expansion of G1 assuming it is isolated from the system is: 0.0000065 x 136 x 12 x 70 = 0.74 inches. G8 expanded the least: [0.78 – 0.19] = 0.59 inches (not shown in Figure 6.3.3.3.7-5). The theoretical expansion of G8 assuming it is isolated from the system is: 0.0000065 x 102 x 12 x 70 = 0.56 inches. The expansions from

the analysis are reported at the bottom of the steel. They are slightly less than computed because of the smaller coefficient expansion of the concrete, which was ignored in the hand calculations.

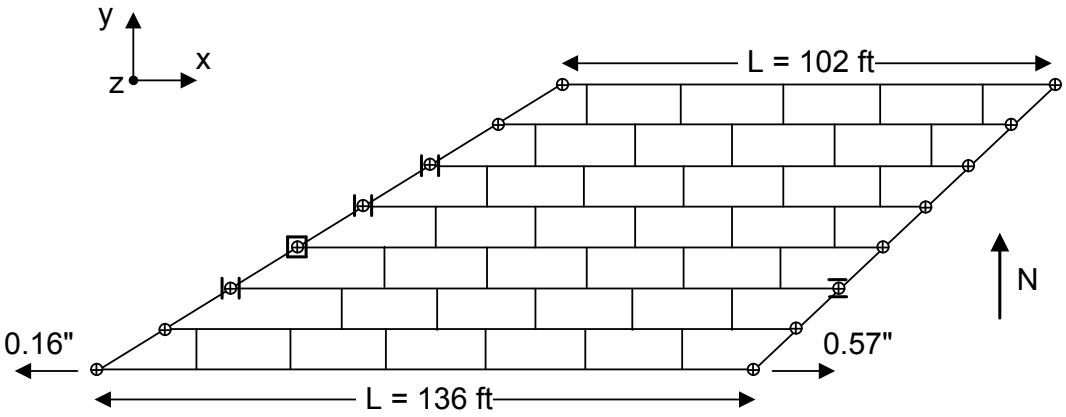

G1: Theoretical = αx136x12x70=0.74"
Net Computed = [0.57-(-0.16)]=0.73"

Figure 6.3.3.3.7-5 Longitudinal Thermal Expansion of G1 – Theoretical vs. Net Computed Expansion from the 3D Analysis

Particularly interesting, however, is that the difference in longitudinal expansion between G1 and G8 was arrived at by the expansion of each girder in a completely different fashion. The west end of G1 expanded negatively or to the west, while the west end of G8 expanded positively or to the east. The reason for these movements is the skew and the bearing constraints at the west end. The largest positive expansion was observed at the east end of G8, which represents the most distant corner from the longitudinal constraints at the west end.

The effect of lateral expansion should not be ignored in wide bridges. Assuming more than one bearing must eventually be constrained in the transverse direction, if the lateral thermal movement between adjacent bearings is larger than the freedom provided in the lateral constraints, local lateral forces resulting from the bearings pushing against their neighbors will develop. These forces are separate from the lateral forces that develop due to global rotation of bridges with skewed supports.

In this example, the east bearing of G3 is fixed transversely, while its neighbors are permitted to move transversely. As seen in Figure 6.3.3.3.7-6, the transverse (lateral) movement (y-direction) of the east bearing of G2 was -0.021 inches, and the similar movement at G4 was 0.087 inches. The relative movement of G2 can be ignored. The relative movement of G4 is more than one-sixteenth-inch and, depending on the type of bearing, may be enough to bind the bearing and cause

significant lateral forces if the bearing under that girder was transversely constrained. A second analysis with a gap element or a weak lateral constraint introduced may be made to recognize the freedom or play in the bearing in order to determine a more realistic lateral force should it be desired to constrain the bearing at G4 in the transverse direction.

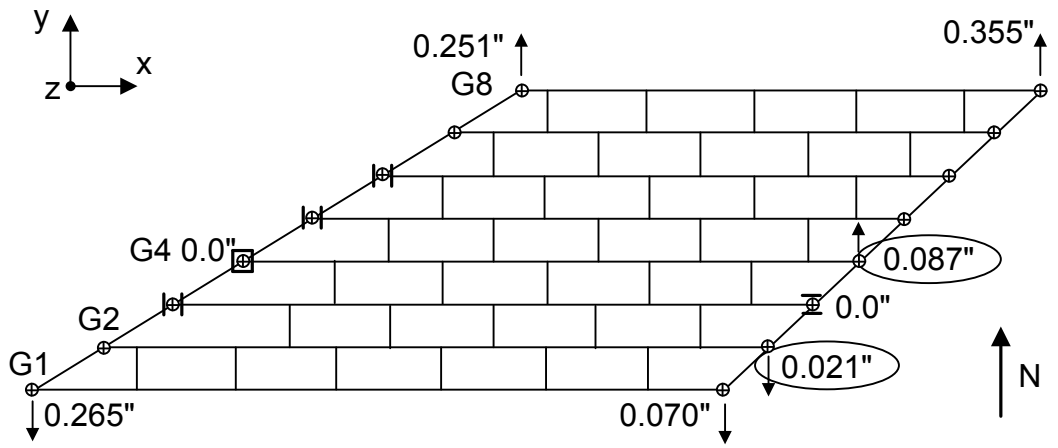

Figure 6.3.3.3.7-6 Transverse (Lateral) Thermal Expansion with a Single Bearing Constrained Transversely at Each End

The magnitudes of the resulting horizontal reactions (i.e., in the x-y plane) are presented in Figure 6.3.3.3.7-7. Recall that the bearing constraints are oriented orthogonal to the girders. The bridge expands in both the longitudinal and transverse directions because of the skew and the configuration of the bearing constraints and the longer Girder 1. The superstructure twists slightly in the counterclockwise direction in the horizontal plane. Further twist is resisted by the transverse constraints at each end. Note that only the center four girders are constrained in the longitudinal direction at the west end. Constraint of the bearings under the extreme outward girders would result in even larger horizontal forces.

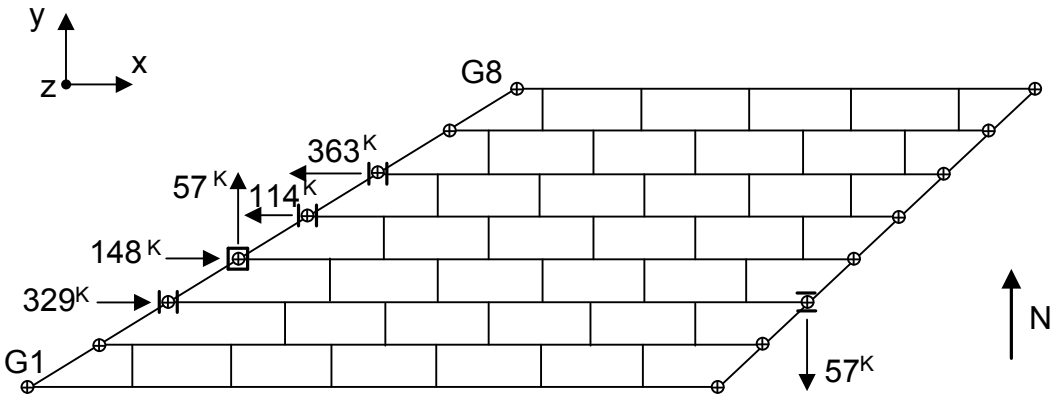

Figure 6.3.3.3.7-7 Horizontal Bearing Reactions (X-Y Plane) due to Thermal Expansion – Bearing Constraints Orthogonal to Girders

The 57-kip force at the east bearing of G3 generates a torque of:

57 kips x 47.6 in./12 = 226 k-ft

It is of interest to note that this torque would not be computed with a grid analysis that applied the bearing restraints at the neutral axes. This torque is resisted by vertical reactions at all bearings and lateral reactions at the west end which generate similar torques. The sums of the forces in the x and y directions are zero. The sum of moments is difficult to compute because of the three-dimensional character of the problem that combines internal torsional moments with external moments.

Consider a different case with the orientation of the bearings revised such that all the guided bearings are guided toward the fixed bearing at the west end of G4, which is the recommended solution in this case. That is, the three guided bearings at the west end under G3, G5 and G6 are all guided along the support line toward the fixed bearing under G4, and the guided bearing at the east end under G3 is guided along the ray emanating from the fixed bearing under the west end of G4 toward the bearing at the east end of G3 (Figure 6.3.3.3.7-8). This means that the west bearing of G4 is the point of thermal fixity (zero translation) discussed above.

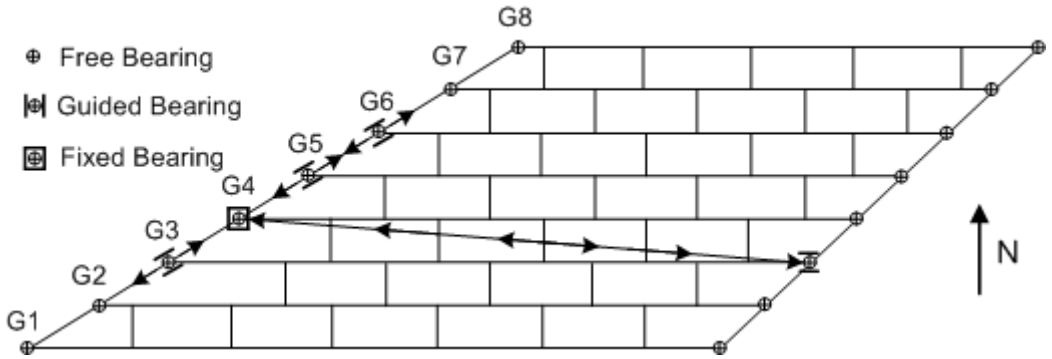

Figure 6.3.3.3.7-8 Guided Bearings All Guided Toward Fixed Bearing at West End of G4

Note the significant reduction in the horizontal reactions (i.e. in the x-y plane) that results (Figure 6.3.3.3.7-9) compared to the case shown previously (Figure 6.3.3.3.7-7). The longitudinal and transverse components of the reactions at all the guided bearings at both the west and east ends are shown in Figure 6.3.3.3.7-9. The reactions are not zero because of the slightly different coefficients of thermal expansion assigned to the steel girders and concrete deck. In a separate analysis,

the coefficients of thermal expansion were made the same and all horizontal reactions went to zero. A significant reduction in the vertical reactions (not shown in Figures 6.3.3.3.7-7 or 6.3.3.3.7-9) was also noted in this case. It is important to note that this bearing configuration would also need to be checked to ensure that it is satisfactory for dead and live loads and other potential horizontal loads.

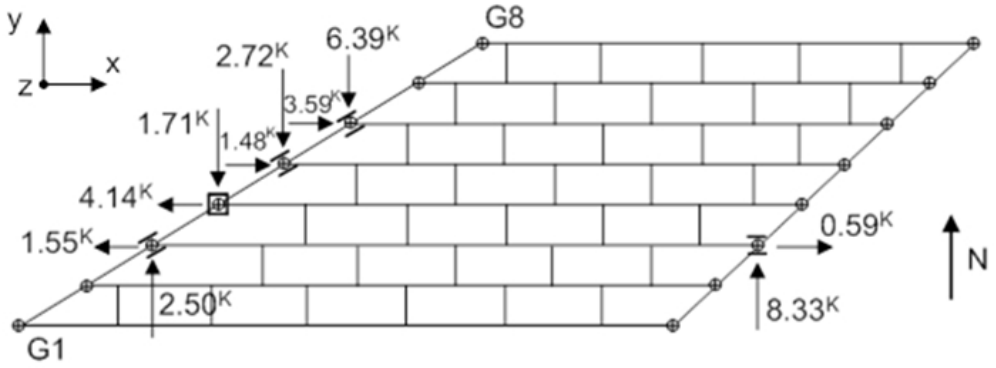

Figure 6.3.3.3.7-9 Horizontal Bearing Reactions (X-Y Plane) due to Thermal Expansion – Guided Bearings All Guided Toward Fixed Bearing at West End of G4

For the guided case, the net longitudinal expansion of G1 was [0.55 – (-0.21)] = 0.76” and the net longitudinal expansion of G8 was [0.84 – 0.27] = 0.57”. The lateral expansion of G1 at the west and east corners was -0.145” and -0.148”, respectively. The lateral expansion of G8 at the west and east corners was +0.193” and +0.185”, respectively.

6.3.4 I-Girder Design and Sizing

6.3.4.1 General

This section will discuss sizing of I-girders, including discussions related to the selection of the steel grade(s), web proportioning and flange proportioning.

6.3.4.2 Steel Grades

The steel industry has developed some new structural steels available to the bridge market. The processes of producing the steels have changed in some instances, resulting in slight differences in availability. The newer higher strength steel, called high-performance steel (or HPS), comes in three strengths -- 50, 70 and 100 ksi yield steels -- with improved toughness and good weathering characteristics (Section 6.2.2.2.6). Grade HPS50W should only be considered as an option where tough weather-resistant steel is required (e.g. in a fracture-critical application). The most

common structural bridge steels in use in the U.S. are the traditional 50 ksi steel and the 50 ksi weathering steel (Sections 6.2.2.2.3 and 6.2.2.2.5).

All structural steels have the same Young's Modulus. This means that bridges built from higher strength steel designed to its strength level deflect more unless the structure is made stiffer. In the case of girder bridges, the girders must be made deeper. As discussed above in Section 6.3.3.2, deeper girders of greater strength tend to have relatively slender flanges.

One way to take advantage of the greater strength is to use hybrid sections with Grade HPS70W flanges and traditional Grade 50W steel webs. *AASHTO LRFD* Article 6.10.1.3 covers the design of hybrid sections (see also Section 6.4.4). Designs utilizing Grade HPS70W compression flanges require closer bracing spacing than those utilizing Grade 50 or Grade 50W flanges, potentially requiring more cross-frames/diaphragms. It was suggested earlier in Section 6.3.2.9.3.1 that a variable spacing can be applied to the bracing where it is needed without adding cross-frames/diaphragms. A Grade HPS70W compression flange over an interior pier might demand a closer spacing to take advantage of the strength of the steel. A bracing spacing that allows only a 50 to 55 ksi factored stress in a Grade HPS70W flange is an inefficient design.

It has been found in many instances that the use of Grade HPS 70W for the tension flange in the negative moment region in conjunction with traditional Grade 50W steel in the web and compression flange is the most economical option. Potentially large tensile stresses in the deck caused by the use of Grade HPS70W in a top tension flange create another issue that is not addressed in the specifications. Experience has shown that the use of one percent longitudinal deck reinforcing has helped to control much of the cracking in the deck when steel strengths of 50 ksi or less are used. If Grade HPS70W is used and a significant portion of the design stress is applied to the composite section, the computed longitudinal tensile deck stress can exceed 1 or even 1.2 ksi. Thermal stresses could raise this level even higher. There are no known investigations of this issue available to the authors at this time.

The use of Grade HPS70W flanges has particular benefits in curved and skewed bridges. The lateral bending stresses can be resisted by a Grade HPS70W flange while allowing approximately 50 ksi for the vertical bending stress. Hence, the stiffness of the bridge is not compromised by the use of higher strength steel.

Fabrication of Grade HPS70W is slightly more expensive than the traditional bridge steels because different consumables are used in welding and the harder steel dulls drills faster. The base price of the steel is also somewhat greater than traditional steel. Hence, it should be used judiciously and where the higher strength can be used to advantage.

Availability of HPS is slightly different from the normal bridge steels (Section 6.3.4.4.5). HPS over about two inches thick (check with the producers for the latest information) generally must be quenched and tempered and is available in lengths not greater than 50 feet (note that Grade HPS 100W is only available in lengths not greater than 45 feet). This means that Grade HPS 50W or Grade HPS 70W plates over two inches in thickness should be limited to 50 feet in length without a section change. Typically such plates are employed at piers. Thus, shop splices should be introduced in the flanges within 25 feet of the interior-pier bearing line when HPS greater than two inches in thickness is used. Otherwise, the fabricator will be required to make full-thickness butt welds with no benefit in weight savings.

6.3.4.3 Web Proportioning

6.3.4.3.1 Web Thickness

As shown in Figure 6.3.4.3.1-1, a limiting D/t_w ratio of 150 is specified for webs without longitudinal stiffeners in *AASHTO LRFD* Article 6.10.2.1. For webs with longitudinal stiffeners, the limiting D/t_w ratio is 300, where D is the web depth and t_w is the web thickness.

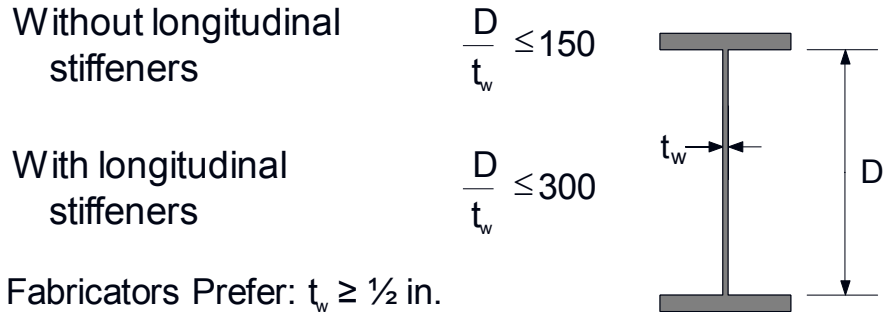

Figure 6.3.4.3.1-1 I-Girder Web Proportioning

These limits are practical upper limits on the web slenderness expressed as a function of D, which served as an upper limit on the slenderness of unstiffened webs in previous versions of the *AASHTO LRFD Specifications* and in the *Standard Specifications* (AASHTO, 2002). In these Specifications, the slenderness limit for webs without longitudinal stiffeners was generally expressed as a function of the specified minimum yield strength of the steel and the elastic depth of the web in compression D_c (to accommodate singly symmetric sections). The limit exceeded 150 for girders with a specified minimum yield strength of 50 ksi or below. This limit was established as an upper bound below which fatigue due to excessive transverse web deflections was deemed not to be a consideration (Yen and Mueller, 1966;

Mueller and Yen, 1968). However, expressing the limit in this fashion makes the initial proportioning of the web more difficult as D_c is not known until the entire cross-section has been defined. Also, the true D_c is a combination of the depth of the web in compression for the non-composite and composite sections prorated based on the portion of load applied in the two conditions. Expressing the limit as a function of D allows for straightforward determination of web thickness in preliminary design. To control transverse web displacements in slender-web girders (i.e. girders with larger values of $2D_c/t_w$) at critical limit states, including the fatigue limit state, separate web bend-buckling and shear buckling checks are now specified in the Specifications, as discussed in Section 6.5.

By limiting the slenderness of transversely stiffened webs to 150, transverse stiffeners need only be provided where the web shear requires stiffeners; maximum transverse stiffener spacings up to 3D are permitted. By limiting the web slenderness to 150, the need for additional transverse stiffeners for handling (Basler, 1961) has been eliminated; stiffeners need only be provided for shear and can potentially be spaced up to the maximum limit of 3D for straight and horizontally curved girders. Second, by satisfying the slenderness limit of 150, the web bend-buckling check can be disregarded in the design of composite sections without longitudinal stiffeners in positive flexure after the section is composite. The web bend-buckling resistance F_{crw}, discussed further in Section 6.4.5.5, for such sections is generally close to or larger than F_{yc} at the strength limit state.

The slenderness limit of 150 is considered valid for sections with specified minimum yield strengths up to and including 100 ksi. Vertical flange buckling limits (AISC, 2010a) are not considered in the *AASHTO LRFD Specifications*. For girders that satisfy the web slenderness limit of 150, the vertical flange buckling limits do not control unless F_y is greater than 85.0 ksi. Also, tests (Cooper, 1967; Lew and Toprac, 1968) have indicated that the influence of the vertical flange buckling mode, or folding of the compression flange vertically into the web, on the nominal flexural resistance of the girder is small even when the web slenderness significantly violates the vertical flange buckling limits.

For deep girders, longitudinal stiffeners are sometimes employed. Generally they would be much more slender than the 150 limit for transverse stiffened webs. *AASHTO LRFD* Article 6.10.2.1.2 limits these webs such that their slenderness does not exceed 300. Again, the limit is independent of the yield strength and D_c, which allows for simpler determination of appropriate web thickness. Even for longitudinally stiffened girders with webs that significantly exceed the limit of 300, tests (Cooper, 1967; Owen et al., 1970) have demonstrated that the nominal flexural resistance is not significantly affected by the vertical flange buckling failure mode. Extensive yielding of the compression flange in flexure preceded the vertical flange buckling failure. However, it should be noted that webs that have values of D/t_w larger than 300 are relatively inefficient, are likely to be more susceptible to distortion

induced fatigue and are more susceptible to the limit states of web crippling and web local yielding discussed in *AASHTO LRFD* Article D6.5 (Appendix D6).

Fabricators prefer a minimum web thickness of ½" to reduce the deformation of the web and potential weld defects according to the *AASHTO/NSBA Guidelines for Design for Constructibility* (AASHTO/NSBA, 2003). However, a minimum web thickness of 9/16" has been found to prevent shadowing of the transverse stiffeners on the girder web.

The web thickness over piers may have to be increased over the thickness provided in adjacent regions of positive flexure. This is particularly true if the concrete deck is considered effective in negative flexure at the service limit state, as permitted in *AASHTO LRFD* Article 6.10.4.2.1 when certain specified conditions are satisfied. The web bend-buckling check at the service limit state, specified in *AASHTO LRFD* Article 6.10.4.2.2 (and discussed in Section 6.5.4.3.2.2) will likely control the thickness of the web in these regions. Web thickness should only be changed at field splices.

Depending on the thickness selected, webs may require so-called “partial stiffening” with transverse stiffeners provided in the panels near the abutments and interior piers. Transverse stiffeners are no longer required where the web shear is reduced below the shear-yield or shear-buckling resistance. The Design Engineer should remember that cross-frame/diaphragm connection plates may be considered to act as transverse stiffeners for shear design. Web shear design is discussed further in Section 6.5.7.

A useful guideline for determining the trade-off between adding more transverse stiffeners versus increasing the thickness of the web material is that approximately 10 pounds of web material should be saved for every 1 pound of stiffener material added. Generally, an unstiffened web with no transverse stiffeners (other than the connection plates) is not the most economical alternative. The optimal solution usually includes some stiffeners over the piers and perhaps near the abutments.

6.3.4.4 Flange Proportioning

6.3.4.4.1 General

Sizing of flanges is one of the most important issues in obtaining economical curved girder bridges. Basic cross-section proportion limits for flanges of steel I-girders are specified in *AASHTO LRFD* Article 6.10.2.2 and discussed further below. The limits apply to both tension and compression flanges.

6.3.4.4.2 Flange Width

The minimum width of flanges is specified as:

$$b_f \geq D/6 \qquad \text{Equation 6.3.4.4.2-1}$$

AASHTO LRFD Equation 6.10.2.2-2

where:

b_f = width of the flange (in.)
D = web depth (in.)

The cross-section aspect ratio, D/b_f, has a significant effect on the strength and moment-rotation characteristics of I-girders (White and Barth, 1998). Tests on I-sections with very narrow flanges have indicated nominal flexural and shear resistances below those given by the current and previous specifications. Limiting the aspect ratio, D/b_f, to 6 helps to ensure that post-buckling shear resistance due to tension-field action can be developed. In many cases, a wider flange will be required based on other criteria.

A minimum width of 12 inches is suggested to prevent flange distortion and cupping due to welding. Typically, somewhat larger minimum flange widths will often be desired for curved girders.

The controlling condition for the top compression flange in regions of positive flexure is usually the non-composite condition. Under this condition, the flange is designed to support its self-weight, the deck and lateral wind on the steel frame. The top flanges of the exterior girders are also designed to resist the lateral force caused by the overhang brackets supporting the wet overhang portion of the deck. The critical non-composite design moment is a function of the deck-casting sequence.

Loads applied to the overhang brackets attached to the flanges cause lateral flange moments. The overhang lateral moment in the convex girder of a curved bridge in regions of positive flexure is of the same sense as the lateral flange moments due to curvature. The top flange must have the capacity to resist the vertical and lateral moments.

Equation 6.3.4.4.2-2 is a suggested guideline regarding the minimum width of flanges in compression (Figure 6.3.4.4.2-1). This suggested guideline is based on the experience of erectors (*AASHTO LRFD* Article C6.10.3.4.1)

$$b_{fc} \geq \frac{L}{85} \qquad \text{Equation 6.3.4.4.2-2}$$

AASHTO LRFD Equation C6.10.3.4.1-1

where:

b_{fc} = width of compression flange (in.)
L = length of girder shipping piece (in.)

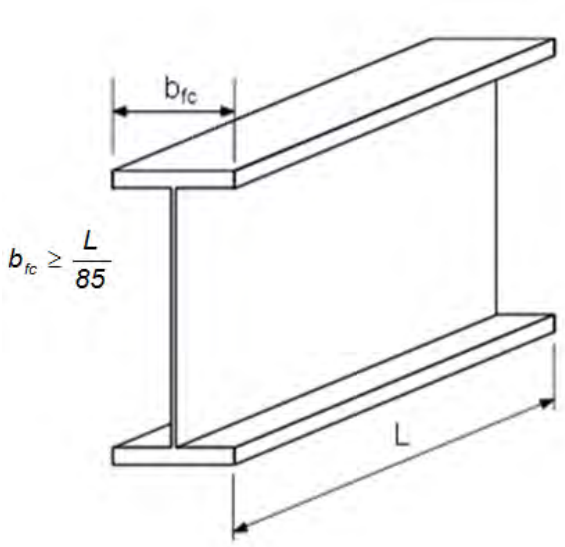

Figure 6.3.4.4.2-1 Field Section L/b Ratio

Satisfaction of this empirical guideline helps ensure that individual field sections are stable during handling in the fabrication shop and for the erector.

Equation 6.3.4.4.2-2 should be used in conjunction with Equation 6.3.4.4.2-1 to establish a minimum top-flange width.

Equation 6.3.4.4.2-3 from *AASHTO LRFD* Article 6.10.2.2 limits the width-to-thickness ratio of compression and tension flanges as follows:

$$\frac{b_f}{2t_f} \le 12.0 \qquad \text{Equation 6.3.4.4.2-3}$$

AASHTO LRFD Equation 6.10.2.2-1

This requirement is taken from *AASHTO* Allowable Stress Design provisions (AASHTO, 2002). It provides a practical upper limit to control flange distortion due to welding.

Equation 6.3.4.4.2-4 from *AASHTO LRFD* Article 6.10.2.2 limits the ratio of the moment of inertia of the compression flange about its strong axis to the moment of inertia of the tension flange about its strong axis as follows:

$$0.1 \le \frac{I_{yc}}{I_{yt}} \le 10 \qquad \text{Equation 6.3.4.4.2-4}$$

AASHTO LRFD Equation 6.10.2.2-4

where:

I_{yc} = moment of inertia of the compression flange of the steel section about the vertical axis in the plane of the web (in.^{4})

I_{yt} = moment of inertia of the tension flange of the steel section about the vertical axis in the plane of the web (in.^{4})

This provision prevents the design of unusually unsymmetrical girders where the yield moment, M_y, may in fact be larger than the plastic moment, M_p. Sections with an I_{yc}/I_{yt} ratio beyond the specified limits behave more like tee sections with the shear center located at the intersection of the larger flange and the web. Such sections may be particularly difficult to handle. Satisfaction of Equation 6.3.4.4.2-4 also ensures the validity of the lateral-torsional buckling equations (discussed in Section 6.5.6.2) for cases involving moment gradients.

Additional discussion related to efficient sizing of curved I-girder flange widths for fabrication is provided in Section 6.3.4.4.5.

6.3.4.4.3 Flange Thickness

The minimum thickness of girder flanges is specified in *AASHTO LRFD* Article 6.10.2.2 as follows:

$$t_f \ge 1.1 t_w \qquad \text{Equation 6.3.4.4.3-1}$$

AASHTO LRFD Equation 6.10.2.2-3

Equation 6.3.4.4.3-1 ensures that the boundary conditions assumed at the web-flange juncture in the compression-flange local buckling and web bend buckling formulations within the *AASHTO LRFD* Specifications are reasonably accurate. This relationship also ensures that the flanges will provide some level of restraint against web shear buckling. This is only a lower limit, but is often exceeded. The flange thickness should never be less than ¾ inches (AASHTO/NSBA, 2003).

Since the minimum width of plate available from the steel mill is 48 inches, the design is most economical when the entire plate width is utilized. To accomplish this, the Design Engineer should use a minimum number of plate thicknesses and steel grades on a project (Section 6.3.4.4.5). Curved girder bridges often lead to different demands on the girders in a cross-section and hence different flange sizes.

Where practical, it is best to vary flange sizes in a cross-section by varying the width, keeping the thickness constant.

Flange plate thicknesses are to a large degree dictated by the demanded flange. Although plate pricing from the mills is very complex and should not be a consideration of the Design Engineer, there are several useful limits that the Design Engineer should be aware of in order to keep the mill costs low. Plate thicknesses between 0.375 and 2 inches are considered standard. Thus, although not absolutely necessary, it may be good practice, for example, to change a flange size from 2.25″ x 20″ to 2″ x 22.5″. The practical thickness limit is 3 inches, although the specification provides for thickness up to 4 inches. The 3-inch limit is based on continuous cast steel. Casters produce slabs that are 9-inches thick. Bridge steel toughness requirements necessitate that the plate thickness be reduced by a factor of three, or from 9 inches down to not more than 3 inches. Plate over 3-inches thick must be made by other more expensive processes.

The area of the smaller flange plate should not be less than one-half the area of the larger flange plate at welded flange shop splices. A number of states have this as a requirement. It is a reasonable way to control stress concentrations at the splices.

Further discussion related to efficient sizing of curved I-girder flange thicknesses for fabrication is provided in Section 6.3.4.4.5, including discussion related to the efficient location of flange-thickness transitions at shop-welded splices.

6.3.4.4.4 Additional Flange Proportioning Considerations

6.3.4.4.4.1 Negative Moment Regions

A shop splice is almost always used off the pier to reduce the amount of steel. The thickness of the smaller plate is best defined at about one-half the thickness of the pier plate. The width of each plate (top and bottom) is best held constant within the pier field sections assuming that the fabricator will slab weld the flanges (Section 6.3.4.4.5). The smaller plates usually extend to the field splices. The flange plates in the pier field sections are usually controlled by the strength limit state; the service and fatigue limit state checks and constructibility checks usually are not critical.

There are at least three issues involved in determining the sizes of these plates. The first issue is cross-frame spacing. Spacing off the pier must be set to brace the bottom (compression) plate such that it can be designed to nearly its yield stress. The cross-frame spacing and the plate width define the lateral torsional buckling capacity. Wider plates and smaller cross-frame spacings (for a given size flange) provide larger capacity.

The second issue is to find a pier plate that can be spliced down to half of its thickness while maintaining the nominal flexural resistance of the pier plate in the thinner plate. If the thinner bottom plate is too slender, local buckling controls and the nominal flexural resistance will be reduced, making the plate inefficient. The remedy is to use a narrower, thicker pier plate. This may mean that the cross-frame spacing must be reduced to accommodate the narrower plate. It is simplest to locate the cross-frames near splice locations. Of course the smaller plate must have the capacity to handle the moment at the splice. Unfortunately, higher strength steels need stockier plates and hence more bracing to reach the potential capacity of the material. This significantly complicates the design when Grade HPS 70W and higher yield-strength steels are used. The preceding approach is even more important when these more expensive steels are used.

The third issue is to select a plate thickness that will give efficient flanges in at least several of the girders in the cross-section. In straight girders with no skew, the problem is negligible since the girders in a span are most often the same. In curved girder bridges and in some bridges with skewed supports, this issue is more complex. The Design Engineer will find that changing the width of a flange rather than the thickness (while keeping the selected width of the flange constant within the girder pier field sections) is likely to provide the most efficient design if it is desirable to change the capacity of the girders within a span (Section 6.3.4.4.5).

Lateral flange bending occurs when either curvature or skewed supports are encountered. Lateral flange bending due to curvature is a function of the square of the cross-frame spacing (FHWA/NHI, 2010). Lateral bending increases with the square of the increase in spacing. The one-third rule equations given in the *AASHTO LRFD* Specifications (Section 6.5.2.1) reduce the flange capacity for vertical bending in proportion to one-third of the squared spacing. Cross-frames are often discontinued near skewed supports to avoid complex detailing at the bearings (Section 6.3.2.9.4.3). This discontinuity may cause significant lateral flange bending. There are no known algorithms to solve this issue. Trial and error is needed. Lateral bending moments should be re-estimated when the cross-frame spacing is changed. This can be accomplished in curved girders by multiplying the original lateral moment by the square of the ratio of the new spacing by the old spacing. A re-analysis is required to obtain lateral flange moments if a discontinuous cross-frame arrangement is used and the cross-frame spacing is changed.

Top-flange sizes in regions of negative flexure are typically controlled by tension-flange yielding at the strength limit state. For girders that are composite throughout their length, the longitudinal deck reinforcement (which must satisfy the minimum one-percent longitudinal reinforcement requirement specified in *AASHTO LRFD* Article 6.10.1.7) within the effective deck width can be included when calculating the composite section properties in these regions. As a result, a top flange with an area slightly smaller than the area of the bottom flange can be assumed. Also live load

stresses and stress ranges for fatigue design can be computed assuming the concrete deck is effective for both positive and negative flexure. This results in a significant reduction in the computed stress range at and near the top flange.

The bottom-flange sizes in these regions are typically controlled by either the flange local buckling or lateral-torsional buckling resistance at the strength limit state. Initial trial flange sizes in these regions are primarily educated guesses based on experience. Often, depending on the span arrangement and other factors, the flanges may be somewhat wider than the corresponding flanges in regions of positive flexure.

Flange width transitions should be made at the field splices (Section 6.3.4.4.4.3). Changes in the top-flange width at the field splices can lead to some inconveniences with respect to the deck forming, but these problems are not insurmountable and are relatively minor when compared to the overall economy of the girder design.

6.3.4.4.4.2 Positive Moment Regions

The flange plates in the positive moment region are easier to design. Design of the top flange (compression) is usually controlled by constructibility; design of the bottom flange (tension) is usually controlled by the strength limit state checks for noncompact sections, or by either the fatigue or service limit state checks for compact sections. The critical parameters in the design of the top flange are flange width and cross-frame spacing. The design stress in the top flange is the sum of the stresses due to the loads applied to the non-composite and composite sections. Lateral flange moments are only considered for the non-composite case since the flange is encased in concrete when the section becomes composite and lateral flange bending cannot be mobilized.

Preliminary analysis gives the moments at the point of maximum positive moment. It is sufficient to design the flanges for maximum moment and check any splice points. Consideration of the moments due to the deck staging is necessary, particularly in the end spans of continuous units, as discussed in Section 6.5.3.3. Lateral flange moments from the overhang brackets acting on the exterior girders also need to be considered, as discussed in Section 6.5.3.4.

Preliminary sizing of top flanges in the positive moment regions of short spans may give small flanges that require close cross-frame spacing to reach an efficient critical stress. Rearranging or addition of a row of cross-frames may be of some benefit, but a larger flange is often most efficient. The flange plates in longer spans are larger so cross-frame spacing is less critical and the present provisions allow the spacing to increase without a numerical limit in straight bridges.

Overhang bracket moments may be problematic leading to reduced cross-frame spacing. Large overhang loads may indicate that the overhangs are too large and increasing the girder spacing may be the best solution. This is particularly true if the exterior girder moments are significantly larger than the moments in the interior girders (Section 6.3.2.6). Properly recognizing the effect of barrier loads leads to larger moments in the exterior girders. Live load action in the exterior girders is often greater than in the interior girders. Efficient girder spacing was discussed earlier in Section 6.3.2.5.

Modern software makes it easy to modify plate sizes based on an analysis. However, the important part of preliminary sizing is the proportioning of flange sizes along the span to ensure that the moments are approximately correct for resizing. Final size of the top flange and/or the spacing of the cross-frames/diaphragms in these regions will be controlled by either local buckling or lateral torsional buckling.

For exterior girders, which usually control, the critical construction condition will most often be the combined vertical and lateral bending stress in the top flange due to the effect of the deck-casting sequence plus the deck overhang loads. Therefore, it is recommended that the final top-flange size and cross-frame/diaphragm spacing in these regions be determined based on this condition, and then subsequent design verifications be made at the strength, fatigue and service limit states, as applicable. All these design verifications at the various limit states are discussed in greater detail in Section 6.5.

Typically, for composite construction, the bottom flange will be somewhat wider than the top flange. The controlling limit state for the design of bottom (tension) flanges in these regions depends on whether the section qualifies as a compact or noncompact section (Section 6.5.6.3). For a compact section (straight bridges only), the design of the flange will typically be controlled by either the fatigue limit state or service limit state verifications. For horizontally curved bridges, sections in positive flexure must be treated as noncompact sections at the strength limit state. Sections in severely skewed bridges should also be treated as noncompact sections. For a noncompact section, the design of the flange will typically be controlled by tension-flange yielding at the strength limit state. In certain cases, the size of the bottom flange may have to be increased from this level in some areas due to stress-range limitations at the fatigue limit state at certain critical welded details (e.g. cross-frame/diaphragm connection plate welds to the bottom flange near points of permanent load contraflexure). Service limit state verifications will not control for noncompact sections in positive flexure under the load combinations specified in *AASHTO LRFD* Table 3.4.1-1. Constructibility verifications on the bottom flanges will typically not control in these regions regardless of whether the section is compact or noncompact.

There are usually a number of additional splice locations in large spans. For example, frequently it is found to be efficient to splice the bottom flange near abutments. The same objectives as described above are used to keep flange width constant within all field sections where slab welding is anticipated.

AASHTO LRFD Article 6.6.2 specifies that all primary longitudinal superstructure components sustaining tensile stress under the Strength I load combination be designated on the plans (to indicate where Charpy V-notch testing of the material is required). The top flange tension region often extends into the positive dead load region some distance where the factored live load tensile stress overcomes the factored dead load compressive stress.

6.3.4.4.4.3 At Field Splices

Field splices are usually bolted although some states permit field welding. The design of bolted field splices for flexural members is discussed in Section 6.6.5. *AASHTO LRFD* Article 6.10.1.8 requires that the ultimate strength of the net section of the bolted joint be checked at the last row of bolts in the splice in order to prevent the possibility of net section fracture (Section 6.4.7). This provision should never be allowed to control the plate thickness at a splice. When this requirement appears to control, the number of bolt lines can be reduced (note however that *AASHTO LRFD* Article 6.13.6.1.4a requires that there be at least two row of bolts on each side of the web), or the bolts lines may be staggered. This provision seems to be more critical at bottom flange splices of box girders.

There is no structural reason to maintain a constant flange width over an entire span. In areas where there is anticipated significant pedestrian traffic under the bridge, it may be desirable to employ a constant width bottom flange to improve the looks of the bridge. This choice is a relatively expensive choice in some instances because the *b*/*t* requirements may force the designer to use thicker plates than required. The sudden change in flange width can be softened by using a radiused wider plate or by tapering the wider plate to the narrower width. The top and bottom flange widths at a section are often different.

It may be best to change the width of the flanges and keep the thickness constant at the field splice to avoid the need for a filler plate. Filler plates add some to the cost of the splice and additional bolts are usually required to develop these plates (Section 6.6.5.5). The savings may not justify the effort, except if the splice is repeated a number of times.

6.3.4.4.5 Sizing Flanges for Efficient Fabrication

As a practical matter, fabricators order plate for flange material from the mills in widths 48 inches and above, with maximum widths ranging from 150 to 190 inches;

typically, the most economical plate size to buy from a mill is between 72 and 96 inches. The availability of plate material varies from mill to mill. A fabricator and/or producer should be consulted regarding the most up-to-date plate availability information. The maximum available plate length is generally a function of the plate width and thickness, steel grade and production process. For example, high performance steel (HPS) is currently produced by quenching and tempering (Q&T) or by thermo-mechanical-controlled-processing (TMCP) (Wilson, 2002). TMCP HPS is currently available in plate thicknesses up to 2 inches and in maximum plate lengths from approximately 600 to 1500 inches depending on weights. Q&T HPS is available in plate thicknesses from 2 to 4 inches (or less for larger plate widths), but because of the furnaces that are used in the tempering process, is subject to a maximum plate-length limitation of 600 inches (50 feet) or less depending on weights (note that Grade HPS 100W is only available in lengths not greater than 540 inches or 45 feet). Therefore, whenever Q&T HPS is used (i.e. generally when HPS plates over 2 inches in thickness are specified), the maximum plate-length limitation should be considered when laying out flange (and web) transitions in a girder.

Plate with additional width and length is ordered to account for cutting (about 1/8 inch per cut between plates and along sides), plate sweep tolerance, and waste (about ½ inch on each outside edge). For example, a plate 74 inches wide might be ordered to cut five 14-inch-wide flange plates.

It is not economical to design flanges such that something less than 48 inches in width of a given grade and thickness of plate material will be required. Flanges should be designed so that the material can be cut from plate of a single plate of given grade and thickness, preferably between 72 and 96 inches wide, even where girder flanges vary from girder to girder. In other words, size flanges so that as many pieces as possible can be obtained from a wide plate with minimal waste. For curved flanges, consider the flange offset due to curvature.

To minimize waste, it is also important to limit the number of different flange plate thicknesses specified for a given project. Larger order quantities of plate cost less, and minimizing the number of different thicknesses simplifies fabrication and inspection and reduces mill quantity extras. For curved-girder flanges it is especially important to minimize the number of thicknesses of plate that must be ordered to minimize waste. Thus, re-use flange thicknesses where possible in the design and adjust the flange width accordingly, while preferably maintaining constant top and bottom flange widths within a given field section.

Fabricators will either weld the shop splices in the individual flanges after cutting them to width, or utilize slab welding, which is the process of butt-welding wide plates of different thicknesses together from which individual flanges may be stripped. Stripping the individual plates from a single wide plate allows for fewer weld starts and stops and results in only one set of run-on and run-off tabs. It is estimated

that up to 35% of the labor required to join the flanges can be saved by specifying changes in thickness rather than width within a field section (AASHTO/NSBA, 2003).

Figure 6.3.4.4.5-1 demonstrates the amount of scrap generated when a 1″ x 16″ curved flange 113-ft long with a 700-ft radius is cut from a single plate. The offset, *H*, is equal to 27 inches. The amount of scrap generated is 12,458 lbs of steel, or twice the weight of the flange. If flanges from all four girders in the bridge are cut from individual plates, the amount of scrap generated is 49,832 lbs of steel.

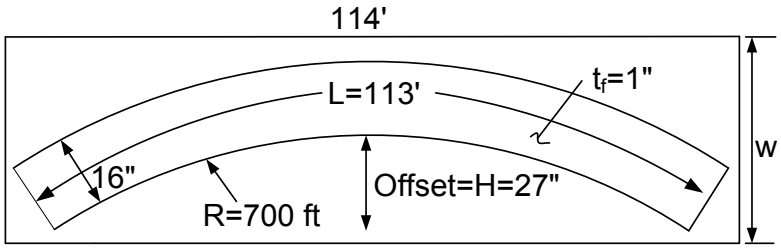

Allow 3 in. for cutting and plate camber

w = 27″+16″+3″ = 46″ (min. plate = 48″)

Plate wt. = (48″)(1″)(114′)(3.4 lbs/in^2/ft) = 18,605 lbs
Flange wt. = (16″)(1″)(113′)(3.4 lbs/in^2/ft) = 6,147 lbs
Scrap = 12,458 lbs

Scrap from 4 flanges = 4 x 12,458 = 49,832 lbs

Figure 6.3.4.4.5-1 Scrap Calculations – Curved Flange Cut from a Single Plate

Figure 6.3.4.4.5-2 reviews the calculation of the amount of scrap generated if four such flanges are nested and cut from a single plate. Nesting is the technique of laying out cutting patterns on a plate to minimize scrap. The individual flanges will be heat curved slightly to different radii.

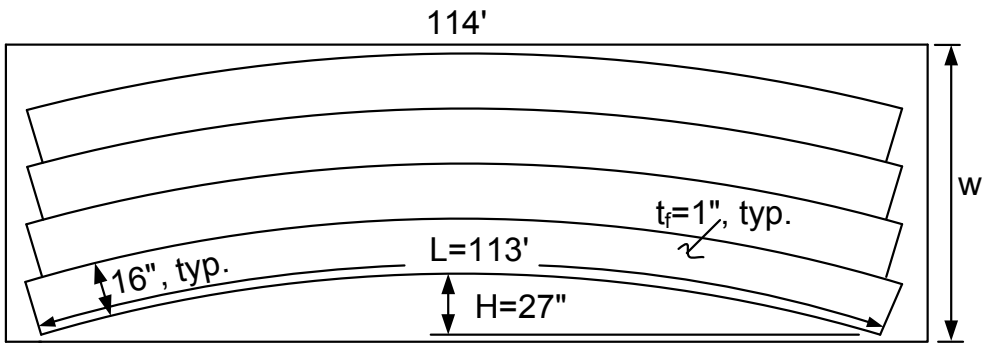

w = 27″+(16″x4)+3″ = 94″

Plate wt. = (94″)(1″)(114′)(3.4 lbs/in^2/ft) = 36,434 lbs
Flange wt. = 6,147 lbs x 4 = 24,588 lbs
Scrap = 11,846 lbs

Figure 6.3.4.4.5-2 Scrap Calculations – Nested Curved Flanges Cut from a Single Wide Plate

The amount of scrap generated is reduced from 49,832 lbs when the flanges are cut from individual plates to 11,846 lbs.

All flanges in the section must have the same thickness.

Figure 6.3.4.4.5-3 shows a pattern that provides eight half-length flanges of the same size. This pattern requires four welded flange splices. Note that the offset is only 6.8 inches. The amount of scrap from this pattern is reduced to only 4,094 lbs, or a savings of 7,752 lbs over the scrap from four full-length flanges nested on a single plate. The savings at 40 cents per pound is $3,100. The Fabricator may only choose this option if the design uses equal-thickness flanges.

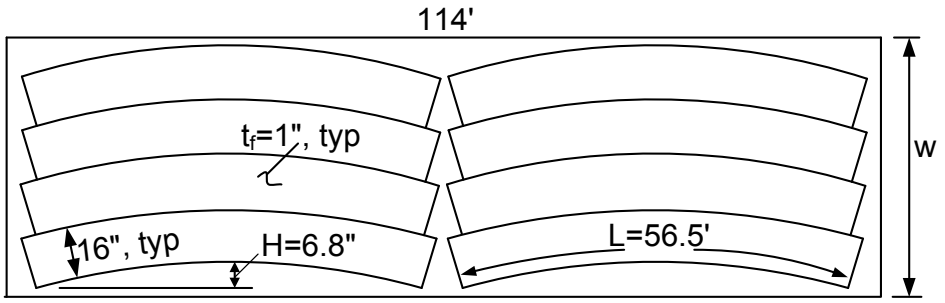

Assume 8 half-length flanges are taken from a single plate – flanges to be spliced

$$w = 6.8″+(16″x4)+3″ \approx 74″$$

Plate wt. = $(74″)(1″)(114′)(3.4\ lbs/in^2/ft)$ = 28,682 lbs
Flange wt. = 24,588 lbs
Scrap = 4,094 lbs

Figure 6.3.4.4.5-3 Scrap Calculations – Nested Half-Length Curved Flanges Cut from a Single Wide Plate

Table 6.3.4.4.5-1 provides a summary of the scrap generated by each of the three cut-curving options presented on the preceding three figures.

Table 6.3.4.4.5-1 Summary of Cut-Curving Options

Option	Description	Scrap (lbs)
1 (Figure 6.3.4.4.5-1)	4 individual plates	49,832
2 (Figure 6.3.4.4.5-2)	4 flanges from single plate	11,846
3 (Figure 6.3.4.4.5-3)	8 half-length flanges from single plate (with splice)	4,094

Dividing the scrap savings of 7,752 pounds between Options 2 and 3 by the four welded shop splices that must be introduced in the flange plates in Option 3 yields a scrap savings per splice of 1,938 lbs. This savings may be enough to justify the introduction of the welded splices.

This example demonstrates that cutting four flanges from a single plate significantly reduces scrap. Long constant-size plates, as often found in the positive moment regions, may be spliced by the Fabricator to further reduce scrap. The Design

Engineer may change plate size in cases where shop splices are anticipated for economy to take advantage of the splices.

The Design Engineer should be aware if the Fabricator plans to use slab welding and if so, where, as it can affect the sizing of the flanges. The process is most often employed for the pier sections. When utilized, the flange widths for an individual girder must be kept constant within the field section. Necessary changes in flange widths can be made at field splices, as discussed in Section 6.3.4.4.4.1.

Figure 6.3.4.4.5-4 shows how nested curved flange plates can be laid out for slab welding. This layout can only be employed by the Fabricator if the Design Engineer has planned ahead. Note that the butt splices are nearly equidistant from the pier, but the length of the pier plates need not be equal on both sides of the bearing.

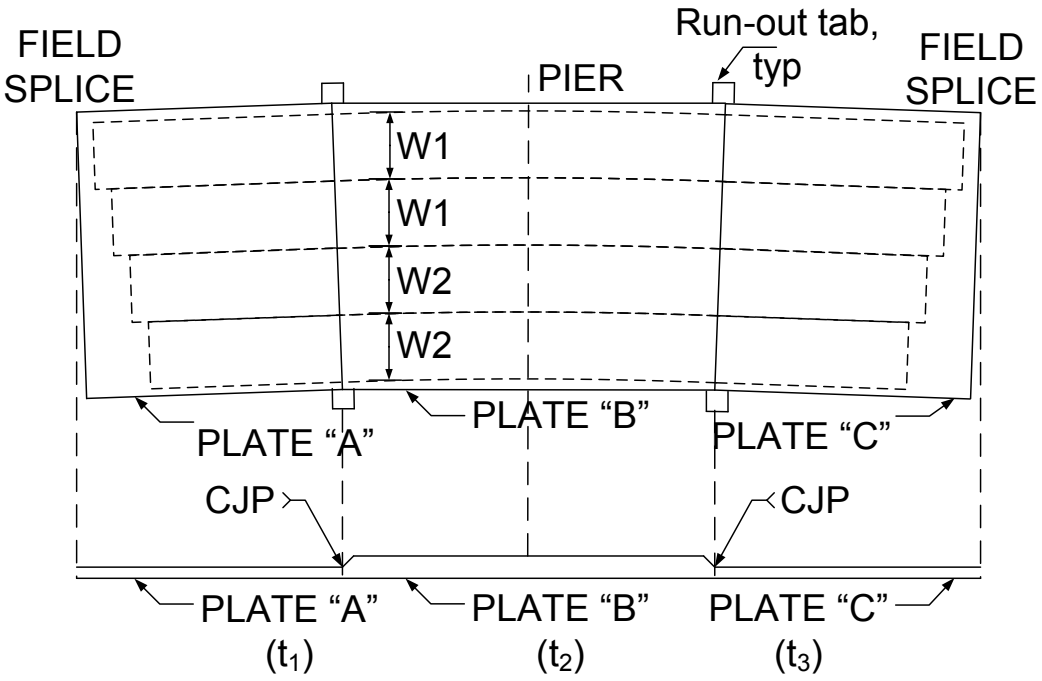

Figure 6.3.4.4.5-4 Slab Welding – Nesting of Curved Flange Plates for a Pier Section

Slab welding can only be used when flange plates have the same thickness, but they may have different widths as long as the spliced plates in each girder have the same width as the pier plate.

Four flanges from either Plate "A" or "C" are best kept to about the same length to minimize scrap. Of course, Plates A and C need not be the same length.

If heat curving is employed to fabricate the curved girders, the pier-section flanges are likely to be slab welded in the straight condition as shown in Figure 6.3.4.4.5-5. The girders will be heat curved after fabrication. The same recommendations regarding flange-plate length, width and thickness discussed in the preceding paragraphs apply. A similar nesting of the flange plates might be done to fabricate the pier-section flanges for straight girders with the flange widths likely kept constant.

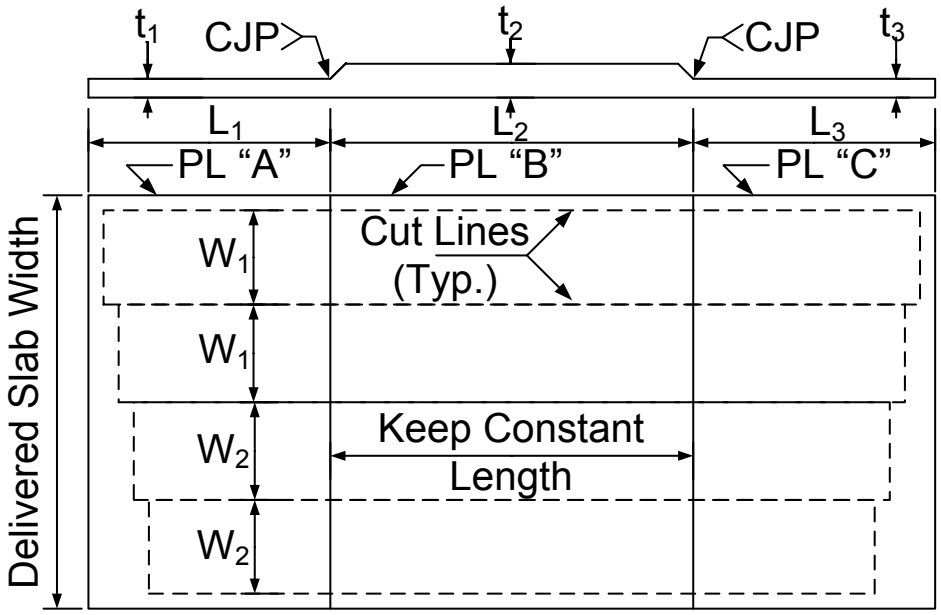

Figure 6.3.4.4.5-5 Slab Welding – Nesting of Straight Flange Plates for a Pier Section

The Design Engineer might well consult with fabricators that may bid the work regarding their preferences that might affect cost. Most fabricators are helpful in this regard. The information may be contradictory at times and the Design Engineer must be aware of suggestions that make the project unique to one fabricator.

Welded transitions in flange thickness are preferred over transitions in width. The design plans should consider allowing the option to move a shop splice, subject to the approval of the Design Engineer. When evaluating such a request, the Design Engineer must consider the effect of the longer thick plate on deflections. Usually a change in the location of a splice does not change deflections significantly. However, removal of a welded splice may have a pronounced effect on deflections.

Parameters affecting the cost of shop-welded splices vary from shop to shop and for a number of subtle reasons. AASHTO/NSBA, 2003 provides a table (Table 1.5.2.A) of estimated equivalency of weight savings per inch of butt weld to flange material to aid in the evaluation of flange shop splices. Roughly, a butt weld costs 1,000

pounds of material. The Design Engineer is always advised to consult a fabricator whenever practical. The maximum length of flange plate is optimally about 80 feet or less.

Typically, no more than three different flange sizes are necessary in a field section.

6.3.5 Box-Girder Design and Sizing

6.3.5.1 General

This section will discuss sizing of box girders, including discussions related to the box and bridge cross-section configuration, the selection of the steel grade(s), web proportioning, flange proportioning, bearing arrangements, and concrete deck options.

6.3.5.2 Box and Bridge Cross-Section Configuration

Box and bridge cross-section configuration is the most critical issue in the design of steel box-girder bridges. The shape and number of boxes in the cross-section is central to an efficient and aesthetic bridge. Traditionally, *AASHTO* provisions have limited the box and bridge cross-section configuration because the live load distribution factors for boxes were developed based on a limited range of parameters. The efficient cross-section usually lies outside of these limitations. Fortunately, when a refined analysis is used, the live load distribution is not dependent on wheel load distribution factors; hence the Design Engineer is freed up to select a more economical cross- section. This usually entails fewer box girders. The girders may be wider or narrower than the spacing between them.

Steel box girders are used as stringers, as straddle beams and in various other applications. Boxes may either be closed (steel on four sides), as shown in Figure 6.3.5.2-1 Part A, or open top tub sections, as shown in Figure 6.3.5.2-1 Part B. Closed boxes are generally employed as straddle beams in the U.S. Tub girders are used as stringers with a composite deck attached to the top flanges. The tubs generally have lateral lacing connecting the top flanges to form a pseudo box that is able to resist torsion before the deck hardens.

In many other countries, closed box girders are more common, but OSHA regulations tend to make them expensive in the U.S. Some of the earliest box girders in the U.S. were the closed type. Others had closed sections in the negative moment regions and tub sections in the positive moment regions. Over time, the tub section has become the dominant steel box configuration in the U.S.

Typically, box-stringer webs are inclined so that the bottom flange is as narrow as practical. *AASHTO LRFD* Article 6.11.2.1.1 suggests that the taper on the webs should not exceed 1-to-4.

The composite deck acts as the box top, closing the tub and forming a box. There are certain cases denoted in the specifications that permit lateral bracing to be eliminated. In these cases, the tub acts as an open section until the deck hardens. Other sections, such as boxes formed with truss-type webs with pipe flanges, or multi-cell boxes are not addressed in the *AASHTO LRFD* Specifications. I-girders connected with top and bottom lateral bracing act as a closed-box section and may be treated as such. This situation was discussed in Section 6.3.2.10.2.1. Hence, a composite I-girder cross-section with one or more bay(s) of bottom lateral bracing may be more accurately analyzed by treating each pair of I-girders as a box section.

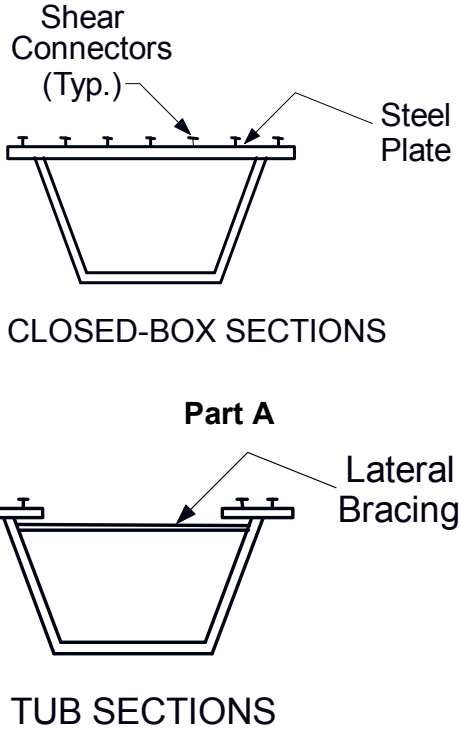

Figure 6.3.5.2-1 Box Girder Types

Closed-box sections are defined in the *AASHTO LRFD* Specifications as flexural members having a cross-section composed of two vertical or inclined webs enclosed at the top with a steel plate. The top plate typically acts as deck forms between the webs. A closed steel box may have a cost advantage over a laterally braced tub when torsion is very large.

A closed box girder has the advantage of being hermetically sealed. Experience has demonstrated that corrosion inside of closed steel box sections is insignificant when the box is hermetically sealed. The sections need not be hermetically sealed to prevent corrosion of the interior if provision is made for drainage and air circulation. Tub girders cannot be hermetrically sealed because moisture may enter through the concrete deck. However, corrosion of the interior of tub girders has been shown to be minimal when the tubs are adequately drained and ventilated.

Trapezoidal tub girders, as depicted in Figure 6.3.5.2-2, are the most popular steel box girder configuration in the U.S. A full-length top lateral bracing system must be provided for curved tub girders to form a pseudo-box to ensure that the member acts as a torsionally closed member for non-composite and composite loads. Painting the interior of tub sections a light color facilitates inspection to allow for easier detection of any fatigue cracks. Light colored paint also reduces solar-caused temperature gain of the tub before the deck forms are installed. The paint quality need not match that normally used for exterior surfaces, particularly when provisions are made to drain and ventilate the interior of the box.

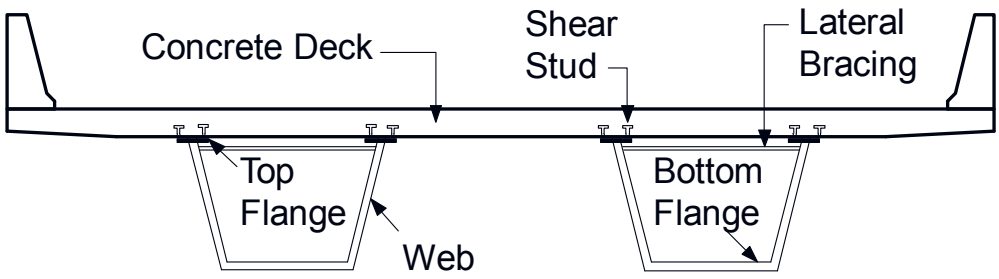

Figure 6.3.5.2-2 Trapezoidal Tub Girders

One reason that tub girders are popular is that they permit a wide spacing between webs on top, and a relatively narrow steel flange at the bottom.

Box-girder bridges typically employ multiple single-cell steel boxes as shown in Part A of Figure 6.3.5.2-3. However, single-box bridges as shown in Part B of Figure 6.3.5.2-3 are frequently economical and have found application in numerous ramp bridges. There are very few multi-cell steel box bridges in the U.S. The specifications do not address this configuration. One of the few such structures in the U.S. is the ramp structure on the western side of the Fort Duquesne Bridge in Pittsburgh, Pennsylvania, which was constructed in the late 1960s. Analysis of a multi-cell single box requires consideration of the torques in adjacent cells and the complex addition of torsional and flexural shears. Fabrication, shipping and erection of these structures are also difficult. The use of a nearly full-width bottom flange required by these structures is rarely economical.

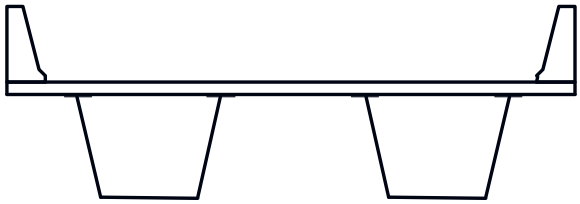

MULTIPLE
SINGLE-CELL

Part A

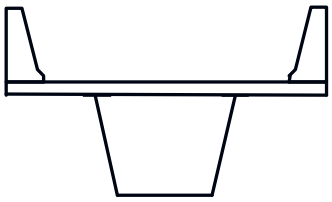

SINGLE-CELL
(Larger Overhangs)

Part B

Figure 6.3.5.2-3 Box Girder Cross-Sections

Single (one-cell) box girders are often found economical when they can be used in place of two boxes. The single box has been found to be very competitive with multi-stringer I-girder bridges. The economy of single-box cross-sections results from reduced fabrication, reduced steel and simpler erection. Further, a single box carries all of the live load regardless of the transverse position of the load. The torsional stiffness of the box transfers the load to the box. The torsion is carried predominately by shear, which is capable of transferring the loads from the outside of the bridge to the central box girder. In a multi-girder section, the girders carry different portions of the live load depending on where the live load is placed. Since the single box carries all of the dead load and live load, the ratio of dead to live is usually greater than if multiple girders are used. This results in a design that is less susceptible to fatigue. Further, the substructure supporting a single box is more economical than a wider redundant substructure likely required when more than one box is used in the cross-section.

The issue of redundancy is always raised with a single box girder cross-section. Depending on circumstances, a single box may be non-redundant. Most of the discussion revolves around the potential of a brittle fracture of the steel. If a fracture should occur in a continuous-span single box bridge, failure could occur if the box is overstressed at the piers. However, modern bridge steels have proven to be quite

ductile and no brittle fractures have been reported in steels that are twenty years or less in age. Furthermore, continuously braced top flanges of single boxes in regions of negative flexure need not be considered fracture critical where there is adequate reinforcing to act as a top flange; in such cases, adequate shear connection must also be provided. Single box sections are permitted in the *AASHTO LRFD* Specifications without limitation; shear due to St. Venant torsion and cross-section distortion stresses must be considered. The steel box must be positioned in a central location with respect to the cross-section, and the center of gravity of the dead load should be as close to the shear center of the box as possible. The use of single box cross-section needs two bearings at some supports for stability and equilibrium.

As with prestressed concrete box-girder bridges, a transversely post-tensioned concrete deck may be used when large deck overhangs or girder spacings are employed. This type of construction is used in Europe; it has not been employed in the U.S. at this time.

A bridge width that is too great for a single box may be designed with a minimum number of boxes. The Macmillan Yard Bridge, Toronto, Canada has a cross-section with a 100-foot vaulted deck resting on two steel box girders. The span between the boxes is approximately 30 feet. Overhangs are approximately 15 feet. This vaulted deck was transversely post-tensioned as a prestressed concrete box girder bridge might have been built. Vaulting permits straight (undeviated) transverse strands to be effective in positive and negative bending. This particular bridge was bid successfully against a similar post-tensioned segmental concrete design. The Storrow Drive Bridge across the Charles River in Boston is another example of a single-box steel bridge carrying a wide deck (approximately 80 feet in width). The deck on this bridge is supported on transverse floor beams and is not post-tensioned.

A box cross section is more economical with fewer narrower boxes. A steel box-girder bridge with a cross-section configuration similar to that of a segmental concrete box bridge is often competitive. A steel bridge with two boxes usually cannot be competitive with a single box segmental box girder bridge. The reason is the configuration.

The design of box sections for flexure and torsion (both straight and horizontally curved) is covered in *AASHTO LRFD* Article 6.11. The flexural resistance of non-composite closed-box sections used as compression or tension members is specified in *AASHTO LRFD* Article 6.12.2.2.2. *AASHTO LRFD* Article C6.11.1 indicates that the provisions are applicable when applied to box sections in continuous, simple or tied-down curved or straight spans up to approximately 350 feet long. Furthermore, the provisions may be applied to longer spans if a thorough evaluation, consistent with basic structural engineering fundamentals, is conducted.

The article also refers to an alternative straight box-girder specification for further information on the design of long-span straight steel box-girder bridges (FHWA, 1980). Differences between this specification and the *AASHTO LRFD* Specification primarily relate to the calculation of the effective width for box flanges, the nominal flexural resistance of unstiffened and stiffened box flanges and the web shear capacity.

The *AASHTO LRFD* provisions in Article 6.11 require that composite box sections used as primary longitudinal flexural members have a composite concrete deck throughout their length in the final condition. *AASHTO LRFD* Article 6.10.1.5 specifies the concrete deck be assumed effective in compression and tension over the entire bridge for analysis of the composite case. Torsion exists along the entire bridge in composite box girders. Therefore, shear connectors are required over the entire bridge. As indicated in *AASHTO LRFD* Article C6.11.1, as of this writing (2015), the specifications do not address the use of composite concrete on the bottom flanges of box girders.

In the 10th Edition of the AASHO Bridge Specifications (1969), provisions for computing the wheel load distribution factor for straight box girders were introduced. A similar equation (in units of lanes) was carried forward to *AASHTO LRFD* Article 4.6.2.2.2b (Table 4.6.2.2.2b-1). The equation was derived based on folded-plate theory, which was shown at the time to be valid to analyze the behavior of multiple box-section bridges based on analytical and experimental model studies of simple-span bridges (Johnston and Mattock, 1967). To ensure that the equation was applied within the limitations and bridge characteristics of the research study upon which it was based, limits were placed on the cross-section as part of the specifications. Since refined analysis methods were not readily available or widely used at that time, designs outside the specified limits were rarely done. It was further determined from the research that when the cross-section restrictions are satisfied, secondary bending stresses due to cross-section distortion and shear due to St. Venant torsion may be neglected if the box flange is fully effective.

Bridge cross-section limitations were not included in the initial version of the AASHTO *Guide Specifications for Horizontally Curved Bridges* (1980). In lieu of distribution factors, rational analysis was required to distribute the loads in horizontally curved bridges. The *AASHTO LRFD* Specifications unified the provisions for the design of straight and horizontally curved bridges into a single specification in 2005. In addition, with the more common availability and use of refined methods of analysis, the overall scope of the provisions was broadened to allow the consideration of a wider variety of box-girder bridge types and cross-sections that were outside of the initial specified limitations. However, since the distribution factor equation was also implemented in the *AASHTO LRFD* Specifications as an acceptable approximate analysis method for determining live load moments in straight bridges, it was necessary to continue the restrictions on the

cross-section in order to permit its use. These restrictions are specified in *AASHTO LRFD* Article 6.11.2.3, and are summarized in Figure 6.3.2.5.6-3.

Bridges not satisfying one or more of the special restrictions specified in *AASHTO LRFD* Article 6.11.2.3 (and/or that do not have fully effective box flanges) must be investigated using one of the available methods of refined structural analysis, or other acceptable methods of approximate structural analysis specified in *AASHTO LRFD* Articles 4.4 or 4.6.2.2.4. This includes single box cross-sections and multiple box cross-sections in horizontally curved bridges. The additional torsional effects resulting from support skew are not comprehended by the specified live load distribution factor. Hence, a more refined analysis is required whenever one or more supports are skewed, even if the bridge satisfies the specified cross-sectional limitations. Skewed supports are particularly problematic for box-girder bridges and special care should be taken in analyzing and detailing box girders with skewed supports in order to provide a successful bridge. A refined analysis is also recommended in *AASHTO LRFD* Article C6.11.2.3 if the straight portion of a bridge satisfies the preceding requirements, but also contains horizontally curved segments, as the effects of horizontal curvature generally extend beyond the curved segments. Torsion, unlike bending moment, is not mitigated by length Refined analysis methods may be employed, even if the bridge satisfies all the specified restrictions. For bridges not satisfying the specified restrictions and/or without fully effective box flanges, secondary bending stresses due to cross-section distortion and shear due to St. Venant torsion must be considered. The consideration of these actions in the design of the various components of the box section is discussed further in Sections Section 6.5 and Section 6.6.

Transverse through-thickness bending stresses are of particular concern for boxes subject to large torques; e.g. single box sections, sharply curved boxes and boxes resting on skewed supports. Longitudinal warping stresses must be considered for fatigue, particularly at the corners of the box section where critical details are often located (Wright and Abdel-Samad, 1968). Tests have indicated that longitudinal warping stresses do not adversely affect the strength of boxes of proportions defined in the provisions. The application of the beam-on-elastic-foundation (BEF) analogy to compute cross-section distortional stresses (Wright and Abdel-Samad, 1968) is discussed further in Section 6.5.5.2.2.3.

6.3.5.3 Steel Grades

The advantages of using higher-strength high performance steel (HPS) for box flanges in compression are less evident as the local buckling resistance of box flanges (unstiffened or stiffened) is a function of Young's modulus rather than the yield strength of the steel. Since the modulus is not increased with yield strength, the compressive resistance of a plate of increased yield strength may not significantly improve with an increase in yield strength.

Longitudinal flange stiffeners are primary load carrying members. Therefore their specified minimum yield strength must not be less than the specified minimum yield strength of the box flange to which they are attached as specified in *AASHTO LRFD* Article 6.11.11.2. Rolled structural tees are not available in HPS; therefore, when HPS is used for box flanges, tees must be fabricated from plates or from cut plate.

6.3.5.4 Web Proportioning

6.3.5.4.1 Web Thickness

Cross-section proportion limits for webs of box sections are specified in *AASHTO LRFD* Article 6.11.2.1. As specified in *AASHTO LRFD* Article 6.11.2.1.2, for webs without longitudinal stiffeners, the webs must be proportioned such that:

$$\frac{D}{t_w} \le 150 \qquad \text{Equation 6.3.5.4.1-1}$$

AASHTO LRFD Equation 6.11.2.1.2-1

where D is the web depth and t_w is the web thickness.

Longitudinal web stiffeners are required on webs that do not satisfy Equation 6.3.5.4.1-1. Webs with longitudinal stiffeners must be proportioned to satisfy Equation 6.3.5.4.1-2, as specified in *AASHTO LRFD* Article 6.11.2.1.3.

$$\frac{D}{t_w} \le 300 \qquad \text{Equation 6.3.5.4.1-2}$$

AASHTO LRFD Equation 6.11.2.1.3-1

Additional discussion regarding web slenderness limits is given in Section 6.3.4.3.1.

Note that for sections with inclined webs, *AASHTO LRFD* Article 6.11.2.1.1 requires that the distance along the web be used for checking all design requirements. Therefore, in checking Equation 6.3.5.4.1-1 and Equation 6.3.5.4.1-2 for the case of an inclined web, the web height, D, must be taken as $D/\cos\theta$, where θ is the angle of inclination of the web plate with respect to the vertical.

As discussed later on in Section 6.5.7.1.2, computation of the shear must also take into account the slope of the web; that is, the vertical shear determined from the analysis must be divided by $\cos\theta$. Torsional shear is to be added if it is computed separately from the vertical bending shear. Vertical bending shear in the box is divided evenly between the two webs. St. Venant torsion causes web shears to

have opposite signs in opposing webs. Hence, torsional shear is additive to flexural shear in one web and subtractive in the other. A 3D finite element refined analysis provides both shears since both webs are modeled. Usually, the design is for the critical web and the other web is stiffened the same. Of course, live load causes opposite torques that must be checked. These different shears are also reflected in the reactions when two bearings are used at a support. One bearing will have a larger reaction than its neighbor.

Additional guidelines for I-sections provided in Section 6.3.4.3.1 regarding minimum web thickness, change in web thickness along the girder, and determining the trade-off between adding more stiffeners versus increasing the thickness of web material should be considered applicable to webs of box sections as well.

6.3.5.5 Flange Proportioning

6.3.5.5.1 Top Flanges of Tub Sections

AASHTO LRFD Article 6.11.2.2 specifies that top flanges of tub sections subject to tension or compression satisfy the following requirements:

$$\frac{b_f}{2t_f} \le 12.0 \qquad \text{Equation 6.3.5.5.1-1}$$

AASHTO LRFD Equation 6.11.2.2-1

$$b_f \ge D/6 \qquad \text{Equation 6.3.5.5.1-2}$$

AASHTO LRFD Equation 6.11.2.2-2

and:

$$t_f \ge 1.1t_w \qquad \text{Equation 6.3.5.5.1-3}$$

AASHTO LRFD Equation 6.11.2.2-3

These requirements are the same as those specified for flanges of I-sections in *AASHTO LRFD* Article 6.10.2.2. They are discussed further in Section 6.3.4.4. For sections with inclined webs, *AASHTO LRFD* Article 6.11.2.1.1 requires that the distance along the inclined web be used for checking all design requirements. Therefore, in checking Equation 6.3.5.5.1-2 for an inclined web, *D* is taken as $D/\cos\theta$, where θ is the angle of inclination of the web plate with respect to vertical.

Recommendations regarding minimum flange width and thickness and flange transitions given in Section 6.3.4.4 are applicable to top flanges of tub sections. The two top flanges of a tub section should be the same size. The top flange width

should not be less than 16 inches to accommodate the connection of lateral bracing members. In cases where lateral bracing members are not bolted to the flanges, which is not recommended, the flanges may be smaller. For cases where a full-length top lateral bracing system is provided (required for horizontally curved tub sections and strongly recommended for straight tub sections resting on skewed supports), Equation 6.3.4.4.2-2 need not be considered for the top flanges.

The sizes of top flanges of tub sections in regions of positive flexure are generally governed by constructibility. The establishment of a reasonable preliminary design width and thickness for the flanges in these regions is based on experience, keeping the minimum width and thickness discussed in Section 6.3.4.4. The final size of the top flanges and/or the spacing of the cross-frames/diaphragms in these regions will generally be controlled by either local buckling or lateral-torsional buckling under construction conditions. A critical construction condition is often the combined vertical and lateral bending. The outermost flange of the exterior tub often has the largest vertical bending stress due to deck-casting plus the lateral bending stress due to curvature and deck overhang loads. It is suggested that the top-flange size in positive moment regions be investigated early in the design based on the critical construction condition. Subsequent design verifications can be made for strength, fatigue and service limit states. The specific design verifications at the various limit states are discussed in greater detail in Section 6.5.

The sizes of top flanges of tub sections in negative flexure are typically controlled by tension-flange yielding at the strength limit state. The specification requires that box girders be composite throughout, including in the negative moment regions. Again, preliminary sizes in these regions are based on experience. The top flanges in the negative moment regions near the piers of continuous spans may be wider and thicker than those in regions of positive flexure. Widths should be constant within a field section to permit slab welding of the flanges. Transitions in width should be made at the field splices. Changes in the top-flange width cause some inconvenience in that the length of the forming must be changed. This issue is minor when compared to the improved economy of the structural steel. Other limit states, including the fatigue limit state (discussed in Section 6.5.5), may be critical in the design of the top flanges in regions of negative flexure in some cases. Web bend-buckling at the service limit state may be critical in the negative moment region if the deck is considered to be effective in tension (refer to Section 6.5.4.3.3.2). This is caused by the higher neutral axis, which causes more than half of the web to be in compression.

The top flange lateral bracing resists the torsional shear before the top flanges become continuously braced by the hardened concrete deck. Once the concrete hardens, it assists the top lateral bracing in resisting the torsional shear. The torsional shear produces horizontal shear in the deck that should be considered when designing the deck reinforcing steel. Lateral bending stresses occur in the top

flanges prior to hardening of the concrete deck and must be considered. Once the deck has hardened, flanges are continuously braced so lateral flange bending, local buckling and lateral-torsional buckling usually need not be considered. If a precast deck is used, the engineer may choose to investigate local buckling if the deck does not adequately brace the flange.

AASHTO LRFD Article 6.10.1.7 requires that the longitudinal deck reinforcement be equal to or greater than one-percent of the total cross-sectional area of the deck. This requirement is provided to control deck cracking. This reinforcement should be included in the composite section properties and often permits a reduction in the size of the top flanges. When the top flange has a yield strength greater than 50 ksi, slightly more longitudinal reinforcing may be desirable to account for the larger strains in the deck, which are compatible with the strains associated with the higher strength steel.

Top flanges should be evaluated for lateral loads from the webs in cases where the webs are sloped more than 1-to-4 for loads applied prior to hardening of the deck (see *AASHTO LRFD* Article C6.11.3.2).

6.3.5.5.2 Bottom/Top Box Flanges

A box flange is defined in the *AASHTO LRFD* Specifications as a flange that is connected to two webs. The flange may be a flat unstiffened plate, a stiffened plate or a flat plate with reinforced concrete attached to the plate with shear connectors. Thus, unstiffened or stiffened bottom flanges of tub and closed-box sections and top flanges of closed-box sections are classified as box flanges under this definition.

For box sections with inclined webs, the width of bottom box flanges is a function of the web spacing and depth as well as the slope of the webs. Inclined webs are advantageous in reducing the bottom flange width while maintaining the spacing at the top of the box to economically support the deck. *AASHTO LRFD* Article 6.11.2.1.1 specifies that the inclination of the web plates to a plane normal to the bottom flange should not exceed 1-to-4. Where the live load distribution factor equation is used to determine the live load flexural moments, the inclination of the web plates may not exceed 1-to-4. However, this limitation does not apply to curved tub girders and should not be applied to boxes resting on skewed supports. A narrower bottom box flange is desirable. However, caution should be exercised when deviating too much from the constraint applied to the web slope. Lateral bending stresses in the top tub flanges increase as the slope of the web exceeds 1-to-4. This is due to the transverse component of shear force in the web.

Recommendations regarding flange thickness transitions given in Section 6.3.4.4 should also be considered for box flanges. A savings of 800 to 1,200 pounds of flange steel justifies a flange butt splice in top flanges of tub girders

(AASHTO/NSBA, 2003). For wider box flanges, there are additional issues involved. One fabricator has suggested that to warrant the introduction of a shop splice between 48-inch-wide straight box flanges 1½ and 2 inches in thickness composed of ASTM A572 Grade 50 material, at least 2,250 pounds of material must be saved. This number will vary depending on the width, thickness and grade of the plates being joined, and whether the plates are straight or curved. Box flanges must be cut curved from large plates. Thus, depending on the radius, it may be desirable to introduce additional shop splices in the flange to reduce waste. Therefore, it is recommended that fabricators who are likely bidders on the job be consulted with regard to the issue of shop splices in box flanges.

Box flanges should extend at least one inch beyond the outside of each web to facilitate welding (*AASHTO LRFD* Article C6.11.2.2) Wider flange lips provide a place for birds to perch, which might otherwise be prevented with a steel tub.

The closed box presents special design considerations. Closed-box sections are often used as straddle beams rather than as girders in the U.S. Top flanges of straddle-beam box sections are designed similarly to bottom flanges of tub girders. However, composite closed-box girders present some different issues. They must be stiff enough to support the weight of the wet concrete. They also must act compositely with the deck. This means that the flange must be thick enough to receive shear studs; a minimum ¾-inch-thick flange is acceptable. In positive flexure, the top flange is generally controlled by constructibility verifications (as discussed in Section 6.5) if it is to be composite in the final condition. For closed-box sections in positive flexure (or tub sections in negative flexure), the thickness of the non-composite box flange is usually controlled by its local buckling resistance (see Sections 6.5.2.2 and 6.5.6.2.4.2). It is recommended that the initial flange thickness in these cases be determined based on the local buckling resistance. Subsequent design verifications will then need to be made at the other limit states, as described in more detail in Section 6.5 Deflection of the flange should be checked to ensure that the integrity of the box shape is maintained when concrete is placed on the flange. The shear connection pattern needs to be determined to ensure proper attachment of the deck to the flange (see Section 6.6.2.2.3). If the flange is wide enough to experience shear lag, the shear connectors should be distributed across the flange width according to the shear distribution in the flange plate. Shear is highest near the webs at supports. The horizontal shear through the top flange should be checked.

Non-composite box flanges in compression may require longitudinal stiffening to prevent buckling under combined uniform axial compression and St. Venant torsional shear. Unstiffened box flanges are preferred**.** However, an unstiffened box flange should not be so slender that its buckling resistance becomes impractical. Longitudinal flange stiffeners may be added to increase the compressive resistance of thin flanges. As discussed further in the next paragraph, the cost of these

stiffeners is significant and they should be employed only after a thickness increase is evaluated. A minimum thickness of ¾" is recommended for unstiffened box flanges for ease of handling and to minimize distortion and possible cupping of the flange during welding, with the maximum ratio of width to thickness of the flange recommended not to exceed around 120 (Coletti et al., 2005). A lesser thickness might be considered for a stiffened box flange; however, it is recommended that fabricators first be consulted before utilizing box flange thicknesses below ¾".

Provisions for longitudinally stiffened box flanges have been part of the *AASHTO* design specifications since box girders were first included. However, they are best avoided where possible. They are costly and can be a time-consuming design matter. Narrower flanges can often be designed efficiently without stiffening in either tension or compression. Usually box flanges narrower than 60 inches can be designed to be efficient without stiffening and often flanges up to 70 inches do not require stiffening. Box sections do not need to be as deep as do I-sections because the two webs act as an integral unit, sharing the load. This is particularly true for curved alignments. The shallower the box, the stockier the box flange can be (i.e. greater b/t) and the more efficient the flange can be without stiffening. There probably is not a good rule regarding longitudinal flange stiffeners, but a weight savings of flange equal to at least 10 times the stiffener weight would be required to approach parity. High strength steel (above 50 ksi) is usually not economical in box flanges. Flanges that can be designed for 86 to 90 percent of the yield stress at the strength limit state without a longitudinal stiffener usually should not be stiffened. In short, shallower, narrower boxes provide for better economy. If the inside of the box is to be painted, the cost of cleaning and painting the tee section(s) (i.e. stiffeners) offsets some of the advantage of adding the stiffeners (AASHTO/NSBA, 2003). Another economic advantage of smaller box girders occurs in the contraflexure regions where flange demand is a minimum. A wider box flange requires more steel to simply close the box in these areas than does a narrower one.

Structural tees are recommended for longitudinal flange stiffeners. They provide better lateral torsional buckling resistance than do bars or angles. Tees also provide a high ratio of out-of-plane stiffness to stiffener cross-sectional area. These issues are discussed in *AASHTO LRFD* Article C6.11.11.2. Further discussion of the design of longitudinal flange stiffeners is provided in Section 6.5.6.2.4.2. The tee(s) must be spliced to ensure that the stiffeners are continuous at field section splices, which can complicate both the fabrication and field assembly. The stiffeners should be continuous through internal diaphragms; consideration should be given to attaching the stiffeners to the internal diaphragms as recommended in *AASHTO LRFD* Article C6.11.11.2.

If more than one longitudinal stiffener in a flange section is used, their required moment of inertia is increased substantially. The reason for this is that the webs are assumed to be perfectly rigid and the flange panels with one stiffener are assumed

rigidly connected at the webs. When two or longitudinal stiffeners are used to achieve the desired buckling coefficient, their size increases dramatically becoming impractical (as discussed further in Section 6.5.6.2.4.2). Rare is the instance where more than one longitudinal stiffener is economical.

The provisions allow different assumptions regarding the plate-buckling coefficient for uniform normal stress for a longitudinally stiffened flange. A value from 2 to 4 is typically selected by the Design Engineer. The value of 4 assumes that the stiffener is rigid enough that the flange will buckle with no deformation of the stiffener. Lower values assumed the stiffener is permitted to flex before the plate reaches its capacity. This option improves potential economy because a smaller stiffener may be adequate. The Design Engineer is advised to develop or obtain an interactive spreadsheet or program to investigate the design with different coefficients. The optimum choice provides the flange/stiffener combination that is both adequate and economical for the location.

Termination of the longitudinal flange stiffener is another consideration. The stiffener is not required after the compression stress in the flange drops to a level that the flange is adequate without stiffening. The Design Engineer must check deck staging to be sure that the flange is not subjected to excess compression caused by significant ephemeral negative moments at the terminus during deck placement. Lifting field sections with slender box flanges during shipping or erection can be problematic. The thickness of a stiffened flange may have to be increased at the termination of a longitudinal flange stiffener.

The terminus of a welded longitudinal stiffener with no special transition radius provided creates a fatigue Category E or E′ detail (depending on the detail thickness), which essentially forbids the practice. The fatigue category can be improved by introducing a radius at the terminus and grinding the weld to a smooth radius (see Condition 4.3 in *AASHTO LRFD* Table 6.6.1.2.3-1). It is obviously expensive to terminate the stiffener in regions of net tensile stress. As discussed in Section 6.5.6.2.4.2.1, it is optimal to terminate a longitudinal stiffener at a bolted splice, which frequently occurs at or near points of dead load contraflexure. The flexural stresses at the joint are zero since the ends of the plates are stress free. However, there are live load stresses in these regions so it cannot be said that the adjacent flange plates are free of flexural stress. It may be that the live load negative moment is large enough to cause the unstiffened flange to be thickened in order to terminate the stiffener. Other potential alternatives for termination of the longitudinal flange stiffener are discussed in Section 6.5.6.2.4.2.1.

Box flanges in tension are designed against yielding. The flexural stress is combined with the St. Venant torsional shear stress so that a check can be made. Longitudinal stiffeners are not required when the flange is in tension. However, they may assist in maintaining the flatness of a slender flange.

The controlling limit state for the design of bottom box flanges in tension depends on whether the section qualifies as a compact or noncompact section. Box girders in horizontally curved bridges in positive flexure regions must be treated as noncompact sections at the strength limit state. This means that tension flanges will be controlled by yielding. Fatigue may be critical in some cases. Constructibility verifications will not typically control the design of box flanges in these regions.

For closed-box sections in regions of negative flexure, the controlling limit state for the design of the top flange in tension will typically be yielding at the strength limit state once the top flange is continuously braced by the hardened deck.

AASHTO LRFD Article 6.11.1.4 specifies that inspection access holes in box sections should be located in areas of low stress in the bottom flange. The access holes should be large enough to provide easy access (at least 18 inches by 36 inches). Access holes should be provided at each end of the bridge. The effect of access holes on stresses in the flange should be investigated to determine if reinforcement around the hole is required. Rarely should access holes be located in compression flanges. When they must be so located, the flexural resistance of the remaining flange on each side of the hole is to be determined. *AASHTO LRFD* Article 6.10.8.2.2 (discussed further in Section 6.5.6.2.2.2) can be used to determine the local buckling resistance, with the flange slenderness based on the projecting width of flange on either side of the hole.

6.3.5.5.3 Effective Width of Box Flanges

Shear lag may be significant in wider box flanges, especially near interior supports. This phenomenon occurs most severely when a concentrated load or reaction is experienced by the girder. Simply, the full flange width does not experience flexural stress suddenly. Instead the portion of the box flange nearest the web sees more stress while the central portion of the flange experiences less of the load. Over some distance, more of the load is distributed to the central portion of the flange, which tends to equalize the stress across the flange. This condition is treated in most specifications by indicating that only a portion of the flange may be used in determining section properties.

If a 3D finite element model is used to model the box, several elements can be used to model the box flange. Edge stresses in the elements provides a pattern of the shear lag at particular points.

In cases where a refined analysis is not available, *AASHTO LRFD* Article 6.11.1.1 specifies that the entire box flange may be considered effective in flexure with a uniform flexural stress when the width of the box flange does not exceed one-fifth of the effective span, which is defined as the span length for simple spans. The

effective span in continuous spans is defined as the distance between points of dead load contraflexure or between a simple support and a point of dead load contraflexure.

A flange width of one-fifth of the effective span is to be considered effective in cases where the flange width exceeds one-fifth of the effective span. The effective flange width is used for section properties to calculate factored flexural stresses as suggested in *AASHTO LRFD* Article C6.11.1.1. The entire flange width is used to calculate the flexural stiffness of the box for analysis and for calculating the nominal flexural resistance of the box flange.

The effective width requirement is based on analyses of simple-span box-girder bridges using a series of folded-plate equations (Goldberg and Leve, 1957). Span-to-flange width ratios between 5.65 and 35.3 were included in the study. The effective flange width (as compared to the full flange width) ranged from 0.89 for the bridge with the smallest span-to-width ratio to 0.99 for the bridge with the largest span-to-width ratio. It should be noted that continuous spans were not investigated. As discussed above, interior reactions present the most significant situation for shear lag. Based on the parametric results described, the researchers deemed it reasonable to assume that a flange is fully effective as long as the width of the flange does not exceed one-fifth of the span. The rule was extended to continuous spans by assuming that the effective span be defined as described above. *AASHTO LRFD* Article C6.11.1.1 states that for extremely wide box flanges, a special investigation of shear lag is warranted regardless of the effective span-to-flange width ratio.

6.3.5.6 Bearing Arrangements

The arrangement of bearings can have a significant influence on the design of box girders and their cross frames/diaphragms. A single bearing might be centered over the shear center to minimize the torque resisted by the support. However, the torsion in the box must be removed. At such a support, torque is resisted via the cross-frame(s) or diaphragm(s) connecting the box to its neighboring box(es). Of course, a single box is unstable with a single bearing.

AASHTO LRFD Article 6.11.1.2 specifies that if single bearings narrower than the bottom flange are used, they are to be aligned with the center of the box and all other supports must have adequate resistance against overturning under any design load combination. *AASHTO LRFD* Article 6.11.1.2 allows double bearings to be placed between or outboard of the webs. Placing the bearings outboard of the box reduces overturning loads on the bearings and reduces uplift reactions. Wide box spacing, large overhangs, and curvature all can create large uplift forces in addition to the severe uplift issue related to skewed supports. Potential uplift should be investigated with and without a future wearing surface.

A skewed support with two bearings under a box along the skew line will generate a torque because the advance bearing will be more heavily loaded than the rear bearing. The net force in the two bearings will be eccentric with the shear center; hence the torque. If a single bearing is used in these cases, the diaphragm between boxes will resist the torque. The moment and shear in the connecting diaphragm will be large.

Single-box cross sections are often economical structures, but their design introduces some unique concerns. All torsional loads are resisted by bearing pairs. Skewed single boxes are so problematic that they are best not used. Significant torsional loads may occur during construction as well as in the completed bridge under thermal and live loads. Positions of live load must be investigated for both flexure and torsion.

Orientation of guided bearings can usually be addressed in a manner similar to the orientation of bearings on I-girder bridges.

6.3.5.7 Concrete Deck Options

The cross-section of the deck may be a traditional flat soffit deck or vaulted. If moderate spacing of the boxes is employed, a deck with a flat soffit (inside and between the girders) and mild reinforcing is best. However, if a bolder spacing and/or overhang is used, a vaulted deck with transverse post-tensioning may be the most economical choice.

If a single-bearing design is used, the transverse bending moment in the deck is usually much larger than that determined by the free span between webs due to the rotation of the boxes when vertical load is placed on the deck between the webs of adjacent boxes. Cross-frames/diaphragms between the boxes can reduce the rotation and associated deck stresses. Large skews and other extreme torques can cause large shear flow in the deck. Even with top lateral bracing, the stiffer deck resists most of the shear flow once it hardens. *AASHTO LRFD* Article C6.11.1.1 states that for tub sections, the deck should be assumed to resist all the torsional shear acting on top of the composite box section. The deck reinforcement should be designed for this horizontal shear.

In a limited number of cases, a precast concrete deck has been employed with steel tub girders. Typically such decks are not economical. However, when speed of construction is important, precast decks have been found to be practical. Deck panels may be placed on one or two tubs and spliced together using a longitudinal joint. This splice can be accomplished with mild reinforcing and a field-cast joint. Deck units may be joined together with epoxy as the units are installed and post-tensioned. The post-tensioning force should be adequate to prevent transverse cracking due to thermal changes in the steel. The first precast deck application was

the steel alternate design of the Wallace Viaduct in Idaho (not built). This bridge had precast vaulted deck units ten feet long. The deck was post-tensioned in both the longitudinal and transverse directions. In this design, prestressing to overcome thermal stresses was required. This requirement was found to be too severe in that the ducts could not be practically located and the cost was excessive. The ramps on this project employed single box cross-sections. The mainline unit required more boxes. However, they were widely spaced with deck spans up to 30 feet. Separate deck sections were designed for placement on each tub and subsequent post-tensioning both transversely and longitudinally. Some deck sections were over 40 feet wide.

Another vaulted deck design was utilized on the MacMillan Yard Bridge near Toronto, Ontario (mentioned previously in Section 6.3.5.2). The advantage of a vaulted deck is that undeviated post-tensioning can act at the top of the deck in negative bending and at the bottom of the deck in positive bending. The MacMillan Yard Bridge had two boxes in the cross-section with deck overhangs of 15 feet and a free deck span between box webs of approximately 30 feet for a total deck width approaching 100 feet. This deck was cast-in-place, but post-tensioned transversely, with only mild reinforcement provided longitudinally. This design was bid successfully against a segmental concrete design.

A precast deck design was also utilized on the box girder bridges on the Westchester Parkway in New York State. These box-girder bridges were designed originally with a cast-in-place deck, but the contractor opted for a precast deck that was post-tensioned longitudinally in order to speed construction and take advantage of a per diem payment for early completion. Transverse joints were grouted and tensioned. Shear connectors were welded through pockets in the deck and grouted. The bridges were built in phases with longitudinal joints. Adjacent phases were connected with small closure pours containing mild reinforcing only. The transverse length of the deck sections traversed two tub girders, or a width of about 40 feet. Again, this project was satisfactorily completed and is functioning well.

Section 6.4 General Design Considerations/Fundamentals

6.4.1 Introduction

This section will discuss general design considerations and basic fundamental concepts related to the structural behavior of steel. Included in this section are discussions on composite construction, non-composite sections and hybrid sections. Miscellaneous fundamental calculations are also reviewed including the computation of the plastic moment, yield moment, the depth of the web in compression in the elastic range (D_c) and at the plastic moment (D_{cp}), the web bend-buckling resistance (F_{crw}), the web load-shedding factor (R_b) and the hybrid factor (R_h).

Lastly, other topics that are discussed in this section include girder stiffness assumptions for analysis, net section fracture, torsion, general information on skewed and curved girder bridges, cover plates and the minimum thickness of steel.

6.4.2 Composite Construction

6.4.2.1 General

In general, the term composite construction refers to structural systems in which there is a structural interaction between materials having diverse engineering properties, such as steel and concrete or steel and timber. Technically, reinforced concrete, prestressed concrete and fiber-reinforced polymers are composites, but are not included under the rubric of composite construction.

In this discussion, the term composite construction refers a structural system consisting of two components, steel and concrete, which are structurally connected. The earliest patents related to composite construction date to the 1880s and relate generally to what are called “concrete encased beams”. The bond between the concrete and steel was realized to create the composite action. Engineers were aware of the composite behavior, particularly its increased stiffness, but generally did not take full advantage of its additional strength. Steel beams fully encased in concrete were widely used in building design from the early 1900s until the development of lightweight materials for fire protection after World War II.

Viest et al. (1958) site the first patent relating to composite highway bridges to J. Kahn in 1926. In Australia, a paper by Knight (1934) on composite slab and steel-girder bridges discusses the design of shear connectors, the effect of varying the modular ratio on the composite section properties, the propping of main girders and the prestressing of steel girders by upward cambering. The Germans expressed an interest in composite construction and even published a code of standard practice due to the pressures of a steel shortage immediately following World War II, which forced engineers to use the most economical design methods available to cope with the large number of structures that had to be reconstructed following the war. Interestingly, the German bridges built by propping were not found to be successful. The concrete crept to such an extent that after a few months, the negative moment applied to the composite section by releasing the props was resisted almost entirely by the steel section.

In the U.S., the first AASHO bridge-design code in 1944 contained an approved method for the design of composite girders. With its publication, official recognition was given to this method of construction for highway bridges and an increasing number of composite highway bridges were built in the U.S. However, only simple spans were addressed in the AASHO code for a number of years and concurrent research indicated that there were a number of issues that needed to be addressed.

Modern procedures for the design of composite steel bridges can be traced back to the 1957 edition of the AASHO Bridge Specifications. Viest (1960) in a review of research on composite girders noted that that a critical factor in ensuring composite action is that the bond between the concrete and steel remain unbroken. As investigators began to perform additional research on the behavior of mechanical shear connectors during the decade of the 1960s and the specifications continued to evolve, the use of composite construction for steel bridges began to accelerate until it is now the dominant form of construction used for steel-girder bridges in the U.S.

The composite action between the deck and steel girders is ensured by the use of welded mechanical shear connectors between the girder and the deck (Figure 6.4.2.1-1). The function of the shear connectors is to transfer the horizontal shear between the deck and the girder forcing the steel girder and the concrete deck to act together as a structural unit by preventing slip along the concrete-steel interface. By ensuring a linear strain from the top of the concrete deck to the bottom of the girder, the planes of the composite girder remain essentially plane under load in the elastic realm, at least through the depth of the steel girder.

Although composite action was understood and composite action was recognized as present in girder bridges, composite design was not permitted by AASHO until the mid-1940s. At that time, most girder bridges were simple-span construction. Some cantilever girder bridges were built with hinges, but early composite behavior was generally limited to simple spans. Mechanical shear connection of various shapes was employed to augment the present, but undependable, bond between the deck and the top flange. It was observed that flexible shear connectors were best to accommodate the strain that occurred in the concrete between the shear connector rows. By making the deck composite, the neutral axis is shifted upward making the doubly symmetric steel section uneconomical. To better balance the section, partial length cover plates were often welded to the bottom flange. These cover plates increased the economy of composite rolled beams. However, because the cover plates were terminated, this required the force in the cover plates to be transferred to the base flange. This, in turn, created stress risers in the fillet welds connecting the plates to the flanges and subsequent fatigue cracks in the heat-affected regions of the base flange.

Figure 6.4.2.1-1 Steel Girder with Stud Shear Connectors

In the 1960s, continuous girder spans became commonplace. The AASHO Specifications provided for the optional elimination of shear connectors in the region between dead-load contraflexure points. Sometimes the longitudinal reinforcement in that region was made composite in the same regions with minimal shear connection. This thinking had been adopted from the building industry where specifications regarding composite construction were adopted earlier. In building design, the live load is applied much as the dead load and there are actual regions where continuous spans see no negative moment for the design loading. Discontinuing the shear connectors near the dead load point of contraflexure in a bridge, however, effectively causes the deck slab to act as a partial length cover plate. Where this is done, enough additional shear connectors should be provided to transfer the force in the slab back into the steel girder. However, this has two negative effects. First, in regions of negative flexure, the tensile stress in the deck may become large enough to cause unwanted cracking just past the location where the shear connectors end. Second, the shear connectors at the discontinuity may be overloaded similar to the welds at the termination of a partial length cover plate, particularly if the appropriate slab forces are not considered in the design.

Thus, *AASHTO LRFD* Article 6.10.10.1 strongly recommends that shear connectors be employed throughout the span of composite girders. The commentary states that shear connectors help control deck cracking in regions of negative flexure where the deck is subject to tensile stress and has longitudinal reinforcement. It further states that this practice is conservative, which is certainly the case. A cursory review of moment influence lines will show that when the live load is placed for critical shear range, it will produce positive moment in the girder (Figure 6.4.2.1-2). Thus, there are actually no critical negative moments for shear connector design in continuous spans with regard to a moving fatigue truck load. Hence, there is no reason to treat

the location between points of dead-load contraflexure solely as a negative moment region in a highway bridge.

At other points along the girder, shear connectors are spaced according to the absolute value of the composite shear and stud spacing typically becomes tighter near abutment bearings. Research has demonstrated that shear connectors can be placed more uniformly according to the fatigue requirements related to the shear range acting on the stud. Ultimate shear capacity is then checked by assuming that the studs between the point of maximum moment and the end of a defined region will deform until they are all engaged up to their full static capacity.

AASHTO LRFD Article 6.6.1.2 permits the recognition of continuous shear connectors by allowing the use of the uncracked section to compute fatigue stresses and stress ranges in the girder, and of course, in the shear connectors. This not only simplifies design calculations, it properly recognizes behavior of the composite girder. An additional requirement extending the one percent longitudinal reinforcement to the regions where the deck is in tension under factored construction loads and overloads (i.e. Service II loads) is certainly logical (*AASHTO LRFD* Article 6.10.1.7).

Composite design offers a number of inherent advantages. Significant weight savings along with shallower sections can be achieved utilizing composite sections. When plate girders are used, composite design typically allows for the use of a smaller top flange. Stiffer composite sections allow for the use of longer spans and reduced live load and composite dead load deflections. The nominal flexural resistance of a composite section, particularly in regions of positive flexure, greatly exceeds the resistance of the steel girder and concrete deck considered separately, which provides a significant overload capacity. A composite concrete deck also provides positive lateral support to top flanges.

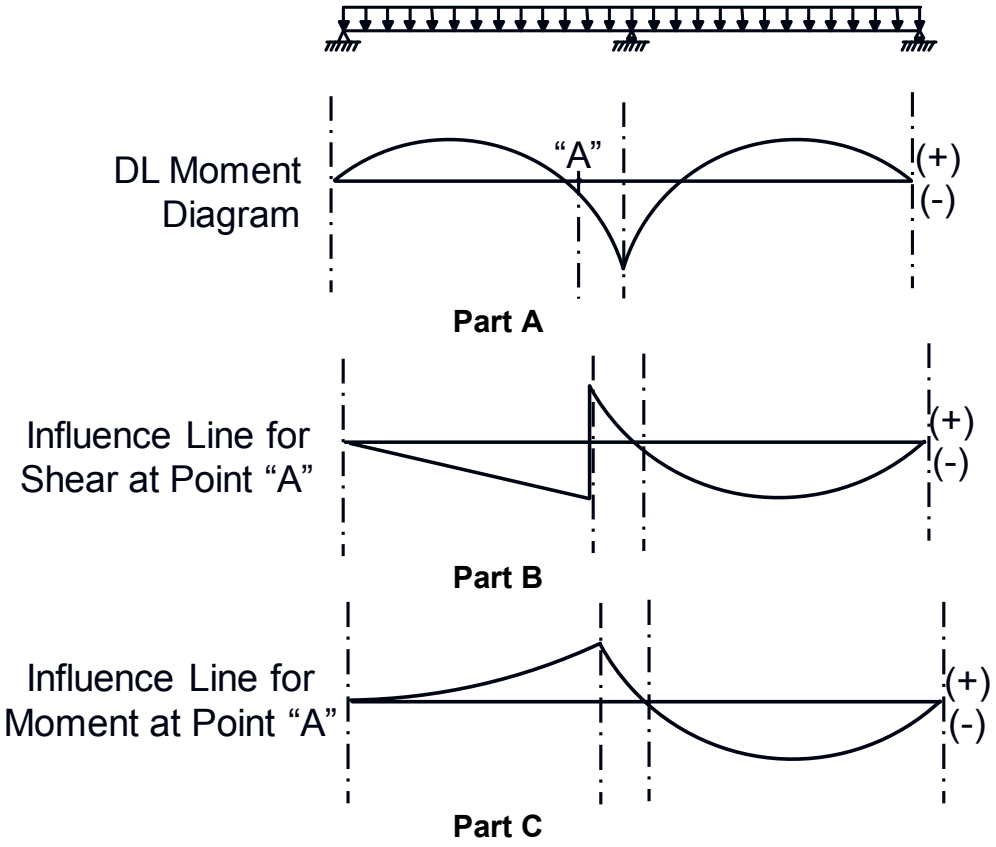

Figure 6.4.2.1-2 Positive Live Load Moment Resulting from the Loading Causing the Maximum Shear Range in a Dead Load Negative Moment Region

A) Dead Load Moment Diagram; B) Influence Line for Shear at Point A;

C) Influence Line for Moment at Point A

While there are many advantages of composite construction, there are also some construction concerns that the Engineer needs to be aware of during the design of a composite bridge superstructure. Although shallower sections are achieved from composite design, they yield larger deflections due to the steel self-weight and the weight of the wet concrete. The deck placement sequence is also of concern (Section 6.5.3.3). Certain deck placement sequences may induce temporary moments in the girders that are considerably higher than the final non-composite dead load moments after the entire deck is placed. The smaller top flanges resulting from composite design typically place more than half the web depth in compression during the deck placement in regions of positive flexure. This can lead to out-of-plane distortions of the small girder compression flange and web if not accounted for in the design. Redecking is also more difficult since the concrete around the shear connectors must be removed along the entire length of each girder.

6.4.2.2 Unshored vs. Shored Construction

Composite bridges can either be designed assuming unshored or shored construction. Construction where the bare steel girders are shored along their length until the concrete deck is acting compositely with the steel girders is called shored composite construction and is permitted according to *AASHTO LRFD* Article 6.10.1.1.1a. Construction where the bare steel girder resists load applied before the concrete deck hardens or is made composite is called unshored composite construction and is the recommended approach. In unshored composite construction, permanent loads and transient loads applied after the concrete deck hardens or is made composite are assumed resisted by the composite girder.

In either case, the deck may either be cast onto the girders, or alternatively, the concrete deck may be precast and attached to the steel girders. Other materials such as fiber-reinforced plastics and aluminum have also been employed as bridge decks. According to previous specifications, a concrete deck that is cast onto the girders may be considered sufficiently hardened after attaining 75 percent of its specified 28-day compressive strength f'_c. *AASHTO LRFD* Article C6.10.1.1.1a states that other indicators may now be used in the judgment of the Engineer.

In unshored composite construction, the dead load of the steel and the concrete (and other loads such as stay-in-place forms) are placed on the steel section in its final erected condition, and it is assumed that there are no temporary supports used during construction. For example, if a composite steel six-girder multi-girder bridge is erected using a temporary tower under three of the girders while the remaining three girders are erected, and then the shoring tower is removed, the stresses in the steel may be different from the case of all girders erected without shoring. The difference depends on the detailing. If the girders are cambered and the cross-frames are detailed assuming that all girders are erected under zero gravity and connections are made without reaming of the bolt holes, there is little difference in girder stresses. If, however, the girders are cambered and the cross-frames are detailed to be erected with the first three girders shored, and the others erected without shoring and then connected, the stress state may be different than in the first instance.

Shoring of girders until the deck is cast and has hardened creates similar situations. In this case, the girders are composite for the deck weight and for the steel weight if the shoring is in place to keep the steel in the no-load condition. If the shoring is added after the steel is erected, only the deck weight is applied to the shored condition. A similar situation exists when a bridge is redecked under traffic as described in Section 6.3.2.5.3. Some of the girders are composite when deck load is added to the adjacent girders. When cross-frames are connecting the composite and non-composite girders, the bridge acts in some ways as shored. Much of the non-composite load is transferred to the composite girders because of their greater

stiffness. This transfer increases the forces in the connecting cross-frames and changes the dead load deflections of the girders.

The major disadvantage of shored composite construction is that most of the dead load is carried by the composite section, which puts large forces in the shear connectors and the concrete deck increasing deflections due to creep of the concrete. This affects the rideability of the bridge over time and tends to put much of the stress saved in the original design back into the steel girders. It is difficult to predict the amount of creep. For this reason, shored composite construction is not popular in bridges. However, it is important to recognize when the design becomes effectively a shored bridge and take appropriate action to ensure proper consideration of loads and deflections.

When shored construction is used, it must be indicated as such in the contract documents. If the girders are cambered for final elevation, they are often very high at the time of construction. If they are not cambered properly for creep, the roadway may deflect too much as the structure ages. Although shored construction is permitted according to the *AASHTO LRFD* Specifications, its use is not recommended.

There have been only a very limited number of demonstration bridges built with shored construction in the U.S. There has been limited research on the effects of concrete creep on composite steel girders under significant dead loads. Shored composite bridges constructed in Germany are known not to have retained composite action. In addition, when shored construction is used, there is an increased likelihood of large localized tensile stresses occurring in the concrete deck at permanent support points. Also, close tolerances on girder cambers may be difficult to achieve. Therefore, all subsequent discussion in this section will refer to unshored composite construction.

Unshored construction is the common practice for composite bridge construction because it better utilizes the advantages of steel in that shoring is not required and dead load deflections are much better predicted.

6.4.2.3 Elastic Section Properties

6.4.2.3.1 General

The following discussion relates to the calculation of the basic elastic section properties for composite sections in regions of positive and negative flexure for use in the design calculations. The calculation of the yield moment and plastic moment for a composite section is covered in Section 6.4.5.

Composite girders must be treated specially with regard to the computation of section properties. This discussion will be limited to unshored composite construction. As discussed in Section 6.4.2.2, unshored composite construction essentially is the design of two girders—the non-composite girder and the composite girder. Separate analyses are required for each case. The steel girders do not need to have capacity to carry both dead and live load, particularly in positive bending with respect to the compression flange and web. Hence, stability of these girders during erection is more critical than erection of steel that is capable of carrying all of the load. Since most steel-girder bridges today have continuous spans, the issue of how to deal with negative bending must also be addressed since the concrete deck is placed in tension. There has not been a great deal of research on this basic issue because composite construction was originally developed for simple spans and the specifications were developed for buildings. Where continuous spans existed, the design provisions simply assumed they were non-composite.

The situation with bridges with moving live loads is quite different. Instead of a moment or shear diagram, the designer must deal with moment and shear envelopes. Thus, the term negative moment region has little meaning in bridge design. Chapter 6 of the *AASHTO LRFD* Specifications provides an improved treatment of this issue compared to past specifications. Live load can often produce approximately equal positive and negative moments in the regions near points of dead load contraflexure. Thus, much of a girder may be either in positive or negative bending. The live load is applied to the composite section, while much of the dead load is applied to the non-composite section. Superimposed dead load, however, is applied to the composite section.

To determine which section properties to use depends on the condition. For analysis, it has been shown that the stiffness properties of the full composite section in positive and negative moment gives the best results when compared to field measurements for composite dead and live loads. As discussed in Section 6.4.6, *AASHTO LRFD* Article 6.10.1.5 requires this assumption. Field measurements indicate that the full composite section assumption gives the best correlation with service stresses. Thus, *AASHTO LRFD* Articles 6.6.1.2.1 and 6.10.4.2.1 permit the use of the full composite section to determine flexural stresses for both positive and negative moment at the fatigue and service limit states, respectively, when certain conditions are met.

For strength, the section assuming the concrete is cracked and ineffective is best used for negative moment acting on the composite section in order to be conservative. The issue with regard to section properties is when to use the cracked section. In regions where the moments due to the transient and permanent loads applied to the composite section are of opposite sign at the strength limit state (i.e. in potential regions of stress reversal), the appropriate composite section to apply to each moment depends on the net unfactored stress in the concrete deck due to

these loads. According to *AASHTO LRFD* Article 6.10.1.1.1b, if the net stress in the concrete deck due to the sum of the unfactored moments caused by these loads is compressive, the associated composite section may be used with each of the moments. That is, positive moments should be applied to the appropriate composite section including the transformed area of the concrete deck, and negative moments should be applied to the composite section consisting of the steel girder plus the longitudinal reinforcement only. If the net unfactored stress in the concrete deck is tensile, then the concrete deck is assumed cracked and ineffective. In this case, the moments due to these loads (both positive and negative moments) must be applied to the composite section consisting of the steel girder plus the longitudinal reinforcement only. The computation of concrete deck stresses is discussed further in Section 6.4.2.4.2. Since bolted field splices are often made in regions of low moment where the transient and permanent load moments are often opposite in sign, the use of proper section properties near points of zero dead load moment is important.

Computation of deflections of composite girders is also dependent on section properties. Best correlation between measured and computed deflections has been obtained when the full composite section is assumed. Deflections at the time of construction are closest to those computed with a modular ratio of n and deflections are closest to those computed with a modular ratio of $3n$ about three years after the deck is cast due to the effects of concrete creep (the modular ratio is discussed in Section 6.4.2.3.2).

6.4.2.3.2 Sections in Positive Flexure

6.4.2.3.2.1 General

The elastic behavior of a composite steel/concrete girder subject to positive flexure is similar to the behavior of an equivalent homogenous steel girder composed of the actual steel girder and a transformed area of the concrete deck. As opposed to reinforced concrete design, in which the reinforcing steel is transformed to an equivalent concrete area, the concrete deck in a composite steel section is transformed into equivalent steel. The deck area is typically transformed by using a deck width equal to b_{eff}/n, where b_{eff} is the effective flange of the deck (Section 4.2.2) and n is the modular ratio. The deck width is reduced rather than the deck thickness so as to have a less significant effect on the computed moment of inertia. In relatively rare cases where the steel girder is relatively small in relation to the concrete deck, the elastic neutral axis of the transformed composite section may fall within the deck. As specified in *AASHTO LRFD* Article 6.10.1.1.1b, concrete on the tension side of the neutral axis is not to be considered effective at the strength limit state; the concrete below the neutral axis is assumed cracked in tension and therefore ineffective. In such cases, the effective transformed area of the concrete becomes a function of the neutral-axis position (see example below). Since the

transformed area approach assumes a linear variation of stress with strain, it is not applicable to the computation of the ultimate strength of a composite section.

As specified in *AASHTO LRFD* Article 6.10.1.1.1b, the modular ratio should be taken as:

$$n = \frac{E}{E_c}$$ Equation 6.4.2.3.2.1-1

AASHTO LRFD Equation 6.10.1.1.1b-1

where:

E = modulus of elasticity of the steel = 29,000 ksi
E_c = modulus of elasticity of the concrete determined as specified in *AASHTO LRFD* Article 5.4.2.4 (ksi)

According to *AASHTO LRFD* Article 5.4.2.4, the modulus of elasticity, E_c, for concrete with a unit weight between 0.090 and 0.155 kcf may be taken as:

$$E_c = 33{,}000 w_c^{1.5} \sqrt{f'_c}$$ Equation 6.4.2.3.2.1-2

AASHTO LRFD Equation 5.4.2.4-1

where:

w_c = unit weight of the concrete (kcf)
f'_c = minimum specified 28-day compressive strength of the concrete (ksi)

For normal weight concrete, w_c should usually be assumed to be 0.145 kcf for the calculation of E_c. An additional 0.005 kcf is often included in w_c to account for the weight of the rebars, but this weight should not be included when calculating E_c.

EXAMPLE

Calculate the modular ratio, n, assuming normal weight concrete and a specified minimum 28-day compressive strength for the concrete, f'_c, equal to 4.0 ksi.

$$E_C = 33{,}000 w_C^{1.5} \sqrt{f'_C}$$

$$E_C = 33{,}000(0.145)^{1.5} \sqrt{4.0} = 3{,}644 \text{ ksi}$$

$$n = \frac{E}{E_C}$$

$$n = \frac{29{,}000}{3{,}644} = 7.96$$

Note that *AASHTO LRFD* Article C6.10.1.1.1b permits rounding of the modular ratio values for normal weight concrete as follows in lieu of using the exact calculated value:

$$2.4 \le f_c' < 2.9 \quad n = 10$$
$$2.9 \le f_c' < 3.6 \quad n = 9$$
$$3.6 \le f_c' < 4.6 \quad n = 8$$
$$4.6 \le f_c' < 6.0 \quad n = 7$$
$$6.0 \le f_c' \quad n = 6$$

EXAMPLE

Locate the elastic neutral axis of the transformed composite section for the composite rolled beam substringer shown in Figure 6.4.2.3.2.1-1 (W24 x 68), which is assumed to be located in a region of positive flexure. In this case, the elastic neutral axis is located in the deck so the portion of the concrete below the neutral axis is assumed cracked in tension and ineffective. Assume a 10-inch-thick structural concrete deck and that the effective flange width of the deck is equal to 124.5 inches. The deck haunch from the top of the web to the bottom of the deck is 4.0 inches. The modular ratio, *n*, is equal to 8.

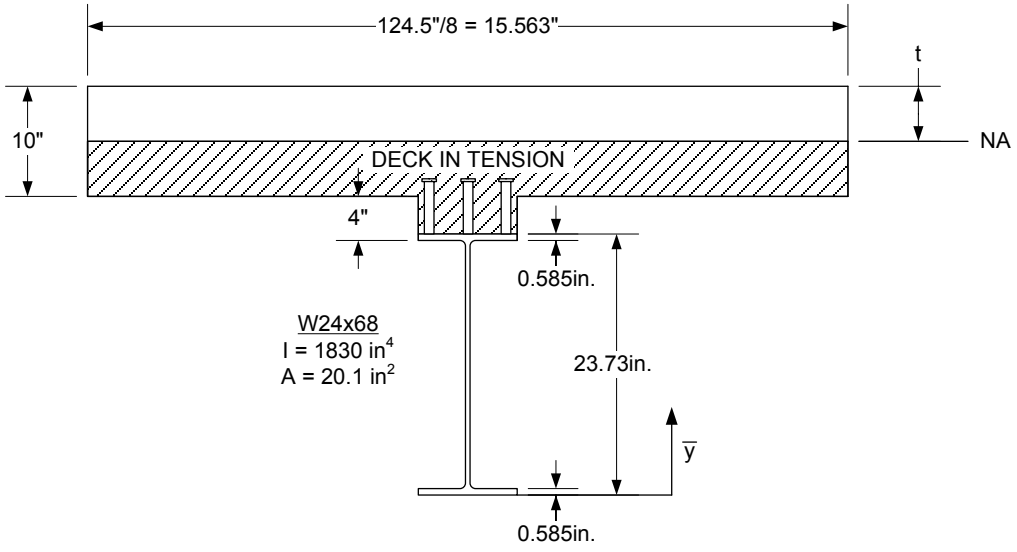

Figure 6.4.2.3.2.1-1 Composite Rolled-Beam Substringer Subject to Positive Flexure

$$\frac{\sum \bar{yA}}{A} = \frac{20.1(11.865) + (15.563t)(23.145 + 4.0 + 10.0 - \frac{t}{2})}{20.1 + 15.563t}$$

$$= \frac{238.5 + 578.14t - 7.78t^2}{20.1 + 15.563t}$$

The neutral axis is located at the following location measured from the bottom of the beam:

$$\begin{aligned} N.A. &= 23.145 + 4.0 + 10.0 - t \\ &= 37.145 - t \end{aligned}$$

Therefore: $37.145 - t = \frac{238.5 + 578.14t - 7.78t^2}{20.1 + 15.563t}$

Rearranging: $0 = 7.783t^2 + 20.15t - 508.1$

$$t = \frac{-20.15 + \sqrt{406.02 + 15818.2}}{15.566} = 6.89"$$

Calculate the moment of inertia of the transformed composite section about the neutral axis:

$$I = 1830 + \frac{1}{3}(15.563)(6.89)^3 + 20.1(10.0 - 6.89 + 4.0 + 11.28)^2 = 10{,}324 \text{ in.}^4$$

6.4.2.3.2.2 Effects of Creep and Shrinkage

When concrete is placed under a sustained long-term stress, there is an instantaneous elastic strain, followed by a time-dependent increase in strain known as creep. Theoretical and experimental studies of concrete creep have been widely reported in the literature and the reader is referred elsewhere, including to Chapter 5 of this Manual on concrete bridge superstructure design, for more detailed discussions on the phenomenon of concrete creep. Suffice it to say, when a composite steel girder is subject to a constant sustained loading, such as permanent loads applied to the composite section (e.g. barriers, railings, wearing surface, etc.), the concrete deck stress is not constant. As time passes, the concrete creeps. The strain in the steel girder increases and the steel stresses become larger, while the strains and concomitant stresses in the concrete deck are reduced. The reduction of

stress in the concrete is a function of the relative stiffness of the girder and the concrete deck.

The actual calculation of creep stresses in composite girders is theoretically complex and not necessary for the design of composite girders. Instead, a simple approach has been adopted for design in which a modular ratio appropriate to the duration of the load is used to compute the corresponding elastic section properties. As specified in *AASHTO LRFD* Article 6.10.1.1.1b, for transient loads applied to the composite section, the so-called ″short-term″ modular ratio n is used. For permanent loads applied to the composite section, the so-called ″long-term″ modular ratio of $3n$ is used. The short-term modular ratio is based on the initial tangent modulus, E_c, of the concrete, while the long-term modular ratio is based on an effective apparent modulus, E_c/k, to account for the effects of creep. In U.S. practice, a value of k equal to 3 has been accepted as a reasonable value.

As concrete cures, it will contract or shrink with time. Although shrinkage is included in most of the basic load combinations given in *AASHTO LRFD* Table 3.4.1-1, the effects of shrinkage on the behavior of composite steel girders are less well understood than creep and are often ignored in U.S. design practice as of this writing. However, some state DOTs require that shrinkage be included as part of the camber considerations. As the concrete deck shrinks, it introduces compression in the flange attached to it while corresponding tensile stresses are introduced in the concrete deck as long as there is no loss of bond between the two materials. The effect of the shortening of both the concrete deck and top flange is to generate a positive moment in the composite girder with its concomitant increase in deflection. The amount of deflection is a function of a number of parameters including the distance of the deck-flange interface from the neutral axis and the stiffness of both the deck and the girder. Shrinkage stresses cannot exceed the modulus of rupture of the deck concrete.

Although shrinkage increases the stresses in the girder, it does not appreciably diminish its capacity in the positive moment region because added load will reverse the shrinkage stresses in the deck, which will release its pull on the girder. In the negative moment regions of a girder, the deck is considered ineffective by the fact that it is assumed cracked.

6.4.2.3.2.3 Section Property Calculations

As specified in *AASHTO LRFD* Articles 6.10.1.1.1a and 6.10.1.1.1b, for the calculation of the stresses in the composite girder in regions of positive flexure, the properties of the bare steel section would be used for permanent loads applied before the concrete deck has hardened or is made composite. The properties of the long-term $3n$ composite section would be used for permanent loads applied after the concrete deck has hardened or is made composite. The properties of the short-term

n composite section would be used for transient loads applied after the concrete deck is made composite. *AASHTO LRFD* Article 6.10.1.1.1d requires that *n* be used to compute concrete deck stresses for permanent loads, whereas 3*n* is to be used for calculating the stresses in the steel girder due to permanent loads. The reason for this is to check concrete stresses at the time of construction prior to creep when such stresses are highest, and to check steel stresses after creep has occurred when such stresses are the highest. For the calculation of the longitudinal stresses in the concrete deck due to transient loads in regions of positive flexure, again the properties of the short-term *n* composite section are to be used (refer to *AASHTO LRFD* Article 6.10.1.1.1d).

In the calculation of the long-term and short-term composite properties, the appropriate transformed area of the concrete deck is used. Note that it is permitted to include the longitudinal reinforcement lying within the effective flange width in the computation of the long-term and short-term composite section properties. However, this reinforcement usually is not considered effective in compression at the strength limit state because it is not tied; therefore, its contribution is typically neglected in positive bending regions for strength limit state checks. Typically, the area of the concrete deck haunch is not considered in the computation of the composite section properties; the haunch depth is considered, however. Consideration may be given to including the longitudinal reinforcement in positive bending regions when computing stresses at the service and fatigue limit states.

EXAMPLE

Calculate the elastic section properties for the composite section shown in Figure 6.4.2.3.2.3-1, which represents a section from an exterior girder in a region of positive flexure. These properties would be used for design calculations in regions designed for positive flexure. Calculate the properties of the bare steel section, the long-term composite section and the short-term composite section. The effective width of the 9-inch-thick structural deck over the exterior girder is 114.0 inches. The modular ratio, *n*, is equal to 8.0.

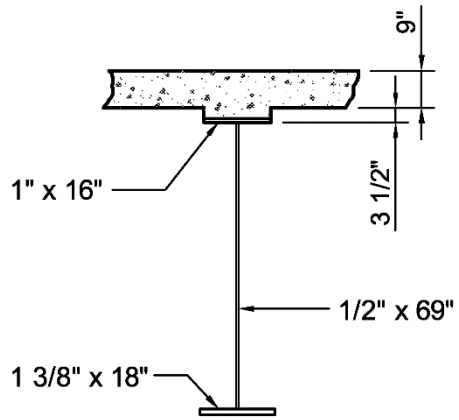

Figure 6.4.2.3.2.3-1 Example Composite Cross-Section – Exterior Girder – Positive Flexure Region

Steel Section

Component	A	d	Ad	Ad^2	I_o	I
Top Flange 1" x 16"	16.00	35.00	560.0	19,600	1.33	19,601
Web ½" x 69"	34.50				13,688	13,688
Bottom Flange 1-3/8" x 18"	24.75	-35.19	-871.0	30,649	3.90	30,653
Σ	75.25		-311.0			63,942

-4.13(311.0) = -1,284

I_{NA} = 62,658 in.^{4}

$$d_s = \frac{-311.0}{75.25} = -4.13 \text{ in.}$$

$d_{\text{Top of Steel}} = 35.50 + 4.13 = 39.63$ in. $\qquad d_{\text{Bot of Steel}} = 35.88 - 4.13 = 31.75$ in.

$$S_{\text{Top of Steel}} = \frac{62{,}658}{39.63} = 1{,}581 \text{ in.}^3 \qquad S_{\text{Bot of Steel}} = \frac{62{,}658}{31.75} = 1{,}973 \text{ in.}^3$$

Long-Term Composite Section; 3*n* = 24

Component	A	d	Ad	Ad^2	I_o	I
Steel Section	75.25		-311.0			63,942
Concrete Slab 9" x (114"/24)	42.75	42.50	1,817	77,217	288.6	77,506
Σ	118.0		1,506			141,448

-12.76(1,506) = -19,216

I_{NA} = 122,232 in.^{4}

$$d_{3n} = \frac{1{,}506}{118.0} = 12.76 \text{ in.}$$

$$d_{\text{Top of Steel}} = 35.50 - 12.76 = 22.74 \text{ in.} \qquad d_{\text{Bot of Steel}} = 35.88 + 12.76 = 48.64 \text{ in.}$$

$$S_{\text{Top of Steel}} = \frac{122{,}232}{22.74} = 5{,}375 \text{ in.}^3 \qquad S_{\text{Bot of Steel}} = \frac{122{,}232}{48.64} = 2{,}513 \text{ in.}^3$$

Short-Term Composite Section; *n* = 8

Component	A	d	Ad	Ad^2	I_o	I
Steel Section	75.25		-311.0			63,942
Concrete Slab 9" x (114"/8)	128.3	42.50	5,453	231,742	865.7	232,608
Σ	203.5		5,142			296,550

-25.27(5,142) = -129,938

I_{NA} = 166,612 in.^{4}

$$d_n = \frac{5{,}142}{203.5} = 25.27 \text{ in.}$$

$$d_{\text{Top of Steel}} = 35.50 - 25.27 = 10.23 \text{ in.} \qquad d_{\text{Bot of Steel}} = 35.88 + 25.27 = 61.15 \text{ in.}$$

$$S_{\text{Top of Steel}} = \frac{166{,}612}{10.23} = 16{,}287 \text{ in.}^3 \qquad S_{\text{Bot of Steel}} = \frac{166{,}612}{61.15} = 2{,}725 \text{ in.}^3$$

As an aside, for tub and closed-box sections with inclined webs, the area of the inclined webs should be used in computing all section properties. The moment of inertia of *each* inclined web, I_{ow}, with respect to a horizontal axis at mid-depth of the web may be taken as follows:

$$I_{ow} = I_w\left(\frac{S^2}{S^2+1}\right) \qquad \text{Equation 6.4.2.3.2.3-1}$$

where:

I_w = moment of inertia of each inclined web with respect to an axis normal to the web (in.^{4})

S = web slope with respect to the horizontal (typically equal to 4.0)

Also, inspection manholes are often inserted in the bottom flanges of tub and closed-box sections near supports (Figure 6.4.2.3.2.3-2). These manholes should be subtracted from the bottom-flange area when computing the elastic section properties for use in the region of the access hole. Finally, as discussed in *AASHTO LRFD* Article C6.11.1.1, consideration should be given to including the longitudinal component of the top lateral bracing area when computing the section properties of tub sections (for determining the stiffness for the analysis and for determining flexural stresses) since the top lateral bracing contributes to the flexural stiffness of these sections. The longitudinal component of the top-flange bracing area, A_d, may be computed as follows:

For single-diagonal lateral bracing systems:

$$A_d = A\cos\theta \qquad \text{Equation 6.4.2.3.2.3-2}$$

For X-type lateral bracing systems:

$$A_d = 2A\cos\theta \qquad \text{Equation 6.4.2.3.2.3-3}$$

where:

A = area of a single top-flange bracing diagonal member (in.^{2})

θ = angle of the top-flange bracing member(s) with respect to a tangent to the girder (degrees)

When the lateral bracing members are attached directly to the top flanges (which is preferred), A_d can simply be included with the top-flange areas in computing the section properties.

Figure 6.4.2.3.2.3-2 Inspection Manhole in Box Girder Bottom Flange

6.4.2.3.3 Sections in Negative Flexure

6.4.2.3.3.1 General

For a composite steel/concrete girder subject to negative flexure in continuous spans, *AASHTO LRFD* Article 6.10.1.1.1c states that the short-term and long-term sections are to generally consist of the steel section and the longitudinal reinforcement within the effective width of the concrete deck. That is, the concrete deck in tension is typically assumed cracked and not participating in the resistance of moment at the strength limit state. An exception is permitted for design calculations at the service and fatigue limit states and for the computation of tensile stresses in the concrete deck, as discussed further in Section 6.4.2.3.3.2.

6.4.2.3.3.2 Minimum Negative Concrete Deck Reinforcement

To control concrete deck cracking in regions of negative flexure, *AASHTO LRFD* Article 6.10.1.7 specifies that the total cross-sectional area of the longitudinal reinforcement that is provided in these regions shall be not less than 1 percent of the total cross-sectional area of the (structural) deck. The reinforcement is to have a specified minimum yield strength not less than 60 ksi and the size of the reinforcement should not exceed No. 6 bars. It is further stated that the required reinforcement should be placed in two layers uniformly distributed across the deck width, with two-thirds of the reinforcement placed in the top layer. The effective width of concrete deck is actually close to the entire deck width in most girder bridges; that is the reason the reinforcement is distributed across the entire concrete section. As mentioned in *AASHTO LRFD* Article C6.10.1.7, when precast deck panels are used as deck forms, it may not be possible to place the required

reinforcement in two layers, in which case this placement requirement may be waived at the discretion of the Engineer. The individual bars should be spaced at intervals not exceeding 12.0 in. The use of small bars at relatively close spacing is intended to ensure closely spaced cracks of small width.

It is of interest to examine the effect of the deck reinforcing. One No. 6 bar has an area of 0.44 square inches. Thus, assuming an area of reinforcement exactly equal to 1 percent of the total cross-sectional area of the deck has been provided, it is effective for 44 square inches of deck cross section. If the deck is 8 inches thick, the bars are spaced at approximately 5 inches. If the concrete is stressed to its modulus of rupture of 0.5 ksi at the time it cracks, it will introduce 22 kips or 50 ksi into the reinforcing bar. Since the bar has a yield stress of 60 ksi, it will not yield and a full-depth crack should be arrested when it is about 0.001 inches wide. If the deck tensile stress is larger, more reinforcing bars will be required to resist the crack progression and possible yield or debonding of the reinforcing. The use of steels with higher yield stress in negative moment regions tends to cause higher deck stresses.

Precast deck panels may be advantageous over a cast-in-place concrete deck due to the speed of construction and better quality control. Design of a precast concrete deck with respect to longitudinal stresses in the deck is similar to design of the longitudinal reinforcement. Tensile stresses in the deck need to be overcome by pretensioning. This is done before the deck is attached to the steel girders with grouted shear connectors.

As illustrated in the example below, the total cross-sectional area of the (structural) deck is to be used to satisfy the minimum 1 percent area requirement. Note in the example that the deck overhang tapers are included in calculating the total cross-sectional area of the deck. As specified in *AASHTO LRFD* Article 6.10.1.1.1c, only the reinforcement within the appropriate effective flange width is to be considered acting with each girder. In the example, the effective flange width for the exterior girder is computed to be the tributary width of the deck over the girder, or 114.0 inches (Section 4.2.2).

EXAMPLE

Assume the cross-section shown in Figure 6.4.2.3.3.2-1 for a steel I-girder bridge. Calculate the minimum required negative moment longitudinal reinforcement over the exterior girder. The width of the exterior girder top flange is assumed to be 18.0 inches.

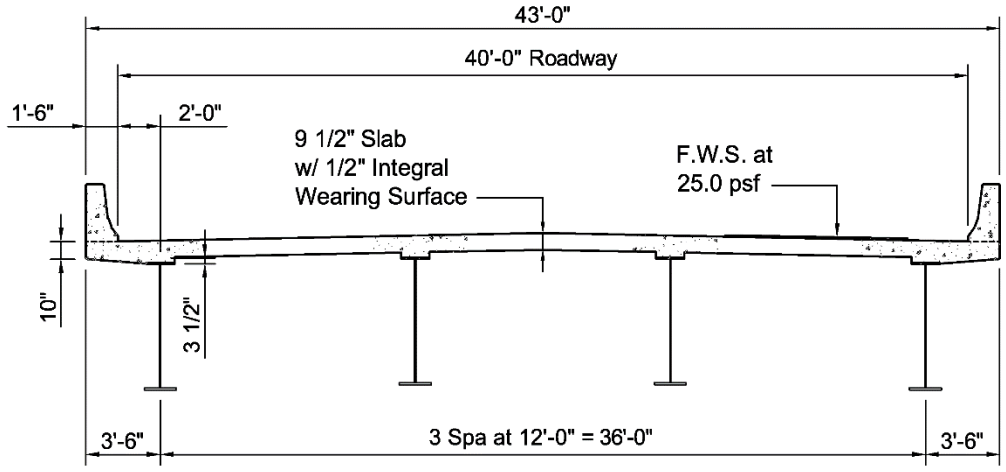

Figure 6.4.2.3.3.2-1 Steel I-Girder Bridge Example Cross-Section

$$A_{deck} = \frac{9.0}{12}(43.0) + 2\left[\frac{1}{12}\left(\frac{3.0}{2} + 0.5\right)\left(3.5 - \frac{18/2}{12}\right)\right] = 33.17 \text{ ft}^2 = 4{,}776 \text{ in.}^2$$

$$0.01(4{,}776) = 47.76 \text{ in.}^2$$

$$\frac{47.76}{43.0} = 1.11 \text{ in.}^2/\text{ft} = 0.0926 \text{ in.}^2/\text{in.}$$

$$0.0926(114.0) = 10.56 \text{ in.}^2$$

The location of the point of termination of the longitudinal reinforcement is specified in *AASHTO LRFD* Article 6.10.1.7, which requires that this reinforcement be provided wherever the longitudinal tensile stress in the concrete deck due to either the factored construction loads or Load Combination Service II given in *AASHTO LRFD* Table 3.4.1-1 exceeds ϕf_r. f_r is the modulus of rupture of the concrete taken as $0.24\sqrt{f'_c}$ (*AASHTO LRFD* Article 6.10.1.7), and ϕ is the resistance factor for concrete in tension specified in *AASHTO LRFD* Article 5.5.4.2.1 equal to 0.9. Previous specifications limited the placement of longitudinal deck reinforcement to regions of negative flexure only, which were taken as between points of permanent load contraflexure. However, the deck on steel girder bridges can often experience significant tensile stresses outside the points of permanent load contraflexure. This can occur under moving live loads and during the placement of the concrete deck in stages, in which case regions of the deck that have already been placed may be subject to negative flexure during subsequent casts, even though these regions may be subjected primarily to positive flexure in the final condition. Tensile stresses in the deck due to thermal and shrinkage strains can also occur in regions where these

stresses otherwise might not be anticipated. The conditions cited above are particularly prevalent in highly skewed continuous girder bridges.

Terminating the longitudinal deck reinforcement based on the requirement to prevent the calculated tensile stresses in the deck from exceeding the modulus of rupture during construction and under design overload (i.e. Service II) conditions is a rational approach. The prior assumption in this regard often permitted large tensile deck stresses in under-reinforced regions that led to premature deck cracking.

Examples illustrating how to locate the minimum longitudinal reinforcement based on the calculated level of deck stress are given in Sections 6.5.3.3.4 and 6.5.4.4.

Calculations of composite sections properties are based on the first-order assumption that plane sections remain plane. Stresses in the longitudinal reinforcement and the deck, be they in tension or compression, are based on this assumption. For this assumption to be valid, the deck-steel interface must not slip. Slip is prevented by the introduction of adequate shear connectors.

Prior *AASHTO LRFD* provisions in this regard required that shear connectors in the negative moment regions be provided based on the first moment of only the longitudinal reinforcement used in the design of the composite section. Of course, the first moment of the entire effective deck is much larger and would require closer spacing of shear studs. The deck in these negative moment regions generally remains effective as a result of the significant bond that normally exists between the concrete and steel. If shear connectors are present when the bond is broken, they are heavily loaded and may cause fatigue cracks in the top flange. If they are not present and the bond should fail, the shear connectors at the contraflexure points must carry all of the shear and are generally overloaded.

AASHTO LRFD Article 6.10.10.1 recommends that shear connectors be provided along the entire length of straight continuous composite bridges, including the negative moment regions. Shear connectors must be provided along the entire length of curved continuous composite bridges. When shear connectors are provided along the entire length, satisfaction of the requirements of *AASHTO LRFD* Article 6.10.1.7 regarding the provision and placement of minimum negative flexure longitudinal reinforcement can then be used to an advantage in the design calculations at the fatigue and service limit states. As permitted in *AASHTO LRFD* Article 6.6.1.2.1, when the preceding requirements are satisfied, fatigue live load stresses and stress ranges may be computed assuming the concrete deck to be fully effective for both positive and negative flexure. Also, as permitted in *AASHTO LRFD* Article 6.10.4.2.1, flexural stresses on the composite section due to Load Combination Service II may potentially be determined assuming the concrete deck to be fully effective for both positive and negative flexure.

Concrete provides significant resistance to tensile stress at service load levels. By providing the minimum negative flexure longitudinal reinforcement according to the provisions of *AASHTO LRFD* Article 6.10.1.7, in conjunction with shear connectors along the entire length of the member, crack length and width can be controlled so that full-depth cracks should not occur. These practices are common in reinforced concrete design. Where cracks occur, the stress in the longitudinal reinforcement increases until the cracked concrete and reinforcement ultimately reach equilibrium. As a result, the deck may experience staggered transverse cracking that is prevented from coalescence to damaging size by the proper design of the longitudinal reinforcement. Recognizing that the concrete is effective in tension has a significant beneficial effect on the computation of fatigue stress ranges *in top flanges* subject to tensile stresses. It can also significantly reduce the Service II flexural stresses in these regions. However, when the concrete deck is assumed effective in negative flexure, more than half of the web may be in compression increasing the susceptibility of the web to bend buckling under the Service II Load Combination. This issue is explored in greater depth in Sections 6.4.5.4 and 6.4.5.5.

When shear connectors are omitted in so-called negative moment regions, additional shear connectors are required at points of permanent load contraflexure according to the provisions of *AASHTO LRFD* Article 6.10.10.3. The commentary explains that the extra shear connectors are determined for the maximum force in the longitudinal reinforcement. The force in the concrete deck on the positive moment region is also removed at this point if the deck is uncracked. However, the additional shear connectors are not investigated for this force. The design of these additional connectors, and the design of shear connectors in general, is discussed in more detail in Section 6.6.2. According to *AASHTO LRFD* Article 6.10.1.7, under this condition, the negative flexure longitudinal reinforcement is to be extended into the positive flexure regions beyond these additional connectors by a distance not less than the reinforcement development length specified in Section 5 of the *AASHTO LRFD* Specifications.

To further control concrete deck cracking, *AASHTO LRFD* Article C6.10.1.7 discusses the importance of preventing nominal yielding of the 1 percent longitudinal reinforcement, and suggests that nominal yielding of this reinforcement be prevented under Load Combination Service II. Since the minimum longitudinal reinforcement must have a specified minimum yield strength not less than 60 ksi according to *AASHTO LRFD* Article 6.10.1.7, any nominal yielding of this reinforcement is judged to be insignificant under the Service II Load Combination for the following conditions: 1) unshored construction where the steel section utilizes steel with a specified minimum yield stress less than or equal to 70 ksi in either flange, and 2) shored construction where the steel section utilizes steel with a specified minimum yield strength less than or equal to 50 ksi in either flange. For all other cases, it is recommended that the Engineer perform an explicit check for nominal yielding of the longitudinal reinforcement under the Service II Load Combination. This check would

be made only for the permanent loads and transient loads applied after the concrete deck has been made composite.

6.4.2.3.3.3 Section Property Calculations

As specified in *AASHTO LRFD* Articles 6.10.1.1.1a and 6.10.1.1.1c, the properties of the bare steel section would be used for permanent loads applied before the concrete deck has hardened or is made composite. In regions of negative flexure, the properties of the steel section plus the longitudinal reinforcement would always be used at the strength limit state for permanent loads and transient loads applied after the concrete deck has hardened or is made composite. The properties of the steel section plus the longitudinal reinforcement would also be used for these loads at the fatigue and service limit states in regions of negative flexure, unless the Engineer invokes the provisions of *AASHTO LRFD* Articles 6.6.1.2.1 and/or 6.10.4.2.1 permitting the concrete to be considered effective in tension for negative flexure at the fatigue and/or service limit states, respectively (as discussed in Section 6.4.2.3.3.2). In that case, the properties of the long-term 3*n* composite section (including the transformed area of the concrete deck) would be used for permanent loads applied after the concrete deck has hardened or is made composite. The properties of the short-term *n* composite section (including the transformed area of the concrete deck) would be used for transient (live) loads applied after the concrete deck has hardened or is made composite. These properties would be computed exactly as illustrated above for sections in positive flexure; again, the longitudinal reinforcement may be conservatively neglected in these computations.

Although not shown here or required by the *AASHTO LRFD* Specifications, for stress calculations involving the application of permanent loads to the long-term composite section in regions of negative flexure, consideration might be given to conservatively adjusting the area of the longitudinal reinforcement for the effects of concrete creep by dividing the rebar area by 3. The concrete is assumed to transfer the force from the longitudinal deck steel to the rest of the cross-section and concrete creep acts to reduce that force over time effectively increasing the stress in the steel section.

For the calculation of the longitudinal stresses in the concrete deck due to both permanent and transient loads in regions of negative flexure, the properties of the short-term *n* composite section are to be used, as discussed in Section 6.4.2.4.2 (refer also to *AASHTO LRFD* Article 6.10.1.1.1d).

EXAMPLE

Calculate the elastic section properties for the composite section shown in Figure 6.4.2.3.3.3-1, which represents a section from an exterior girder in a region of negative flexure. These properties would be used for design calculations in regions

of negative flexure. Calculate the properties of the bare steel section and the steel section plus the longitudinal reinforcement (Note: the longitudinal reinforcement is not shown in Figure 6.4.2.3.3.3-1).

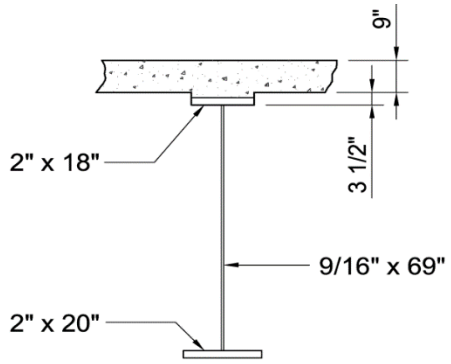

Figure 6.4.2.3.3.3-1 Example Composite Cross-Section – Exterior Girder – Negative Flexure Region

For the purpose of the example calculations given below, the previously calculated minimum 1 percent longitudinal reinforcement, which would typically be placed in two layers, is assumed combined into a single layer placed at the centroid of the two layers (with each layer also including the assumed transverse deck reinforcement). From separate calculations, the centroid of the two layers is computed to be 4.63 in. from the bottom of the deck. Also, although a larger reinforcement area may be provided in the actual deck design, the calculated minimum required area is used in the subsequent calculations.

Steel Section

Component	A	d	Ad	Ad^2	I_o	I
Top Flange 2" x 18"	36.00	35.50	1,278	45,369	12.00	45,381
Web 9/16" x 69"	38.81				15,399	15,399
Bottom Flange 2" x 20"	40.00	-35.50	-1,420	50,410	13.33	50,423
Σ	114.8		-142.0			111,203

-1.24(142.0) = -176.1

I_{NA} = 111,027 $in.^4$

$$d_s = \frac{-142.0}{114.8} = -1.24 \text{ in.}$$

$$d_{\text{Top of Steel}} = 36.50 + 1.24 = 37.74 \text{ in.} \qquad d_{\text{Bot of Steel}} = 36.50 - 1.24 = 35.26 \text{ in.}$$

$$S_{\text{Top of Steel}} = \frac{111{,}027}{37.74} = 2{,}942 \text{ in.}^3 \qquad S_{\text{Bot of Steel}} = \frac{111{,}027}{35.26} = 3{,}149 \text{ in.}^3$$

Steel Section + Longitudinal Reinforcement

Component	A	d	Ad	Ad^2	I_o	I
Steel Section	114.8		-142.0			111,203
Longitudinal Reinforcement	10.56	42.63	450.2	19,191		19,191
Σ	125.4		308.2			130,394

-2.46(308.2) = -758.2

I_{NA} = 129,636 in.^{4}

$$d_{reinf} = \frac{308.2}{125.4} = 2.46 \text{ in.}$$

$$d_{Top\ of\ Steel} = 36.50 - 2.46 = 34.04 \text{ in.} \qquad d_{Bot\ of\ Steel} = 36.50 + 2.46 = 38.96 \text{ in.}$$

$$S_{Top\ of\ Steel} = \frac{129,636}{34.04} = 3,808 \text{ in.}^3 \qquad S_{Bot\ of\ Steel} = \frac{129,636}{38.96} = 3,327 \text{ in.}^3$$

Note that for tub or closed-box sections, longitudinal flange stiffeners, if present, are often included when computing the elastic section properties. The longitudinal component of the top lateral bracing area may also be included in the top flange area when computing the section properties for tub sections and the properties of the inclined webs should also be considered, as discussed previously in Section 6.4.2.3.2.3.

6.4.2.4 Elastic Stress Calculations

6.4.2.4.1 Steel Girder

The elastic bending stresses in the steel girder of a composite section are dependent on the manner of construction. For unshored construction, the steel girders are erected first and must support their own weight, the weight of the deck forms and wet concrete, or the weight of precast deck panels. Once the concrete deck has hardened or is made composite, bending stresses in the steel girder due to all permanent and transient loads are computed based on the appropriate transformed composite section properties; that is, the long-term composite section properties are applied to permanent loads and the short-term composite section properties are applied to transient loads. For shored construction, in which the steel girders are supported on temporary shoring along their length, all bending stresses in the steel girder due to all permanent and transient loads are computed based on the appropriate transformed composite section properties.

Regardless of the method of construction, since plane sections are assumed to remain plane, the calculated elastic stresses due to the various loadings acting on the composite section may be summed. However, at elastic stress levels, the

principle of superposition does not apply to the bending moments due to the various loadings, as these moments are each applied to different sections; that is, the girder stiffness is changing as each of the moments are applied. Therefore, at elastic stress levels, the individual bending moments may not be summed.

EXAMPLE

Calculate the bending stress in the bottom flange of the girder shown in Figure 6.4.2.3.2.3-1 under the Strength I Load Combination (Section 3.9.1.2.2). The load modifier η is assumed to be 1.0 (Section 1.3.6). Assume unshored construction. The section is located in a region of positive flexure. Use the section properties computed earlier for this section. Assume the following unfactored bending moments:

M_{DC1} = +2,202 kip-ft
M_{DC2} = +335 kip-ft
M_{DW} = +322 kip-ft
M_{LL+IM} = +3,510 kip-ft

DC_1 represents the permanent loads applied before the concrete deck has hardened or is made composite, *DC_2* represents the permanent loads (other than wearing surface and utility loads) applied after the concrete deck has hardened or is made composite, *DW* represents the wearing surface and utility loads, and *LL+IM* represents the live load plus impact loads. Both the *DW* and *LL+IM* loads are assumed applied after the concrete deck has hardened or is made composite.

Bottom Flange:

$$f = 1.0\left[\frac{1.25(+2{,}202)}{1{,}973} + \frac{1.25(+335)}{2{,}513} + \frac{1.5(+322)}{2{,}513} + \frac{1.75(+3{,}510)}{2{,}725}\right]12 = +48.10 \text{ ksi}$$

Calculate the bending stress in the bottom flange of the girder shown in Figure 6.4.2.3.3.3-1 under the Strength I Load Combination. The load modifier η is assumed to be 1.0. Assume unshored construction. The section is located in a region of negative flexure. Use the section properties computed earlier for this section. Note that the section is a hybrid section utilizing Grade HPS 70W steel flanges and a Grade 50W web. Assume the following unfactored bending moments:

M_{DC1} = -4,840 kip-ft
M_{DC2} = -690 kip-ft
M_{DW} = -664 kip-ft
M_{LL+IM} = -4,040 kip-ft

Bottom Flange:

$$f = 1.0\left[\frac{1.25(-4{,}840)}{3{,}149} + \frac{1.25(-690)}{3{,}327} + \frac{1.5(-664)}{3{,}327} + \frac{1.75(-4{,}040)}{3{,}327}\right]12 = -55.26 \text{ ksi}$$

6.4.2.4.2 Concrete Deck

For calculating longitudinal flexural stresses in the concrete deck of a composite section, the calculated stress in the transformed (structural) concrete deck must be divided by the modular ratio. In a composite girder, longitudinal flexural stresses in the deck are assumed to result only from the permanent loads and transient loads applied after the concrete deck has hardened or is made composite.

According to *AASHTO LRFD* Article 6.10.1.1.1d, the short-term modular ratio *n* is to always be used to calculate the deck stresses. Previous specifications required that the longitudinal flexural stresses in the concrete deck due to permanent loads be calculated using either the *n* or 3*n* section, whichever gave the more critical stress in the deck. The *n* composite section generally governs the deck stress calculation when the deck stresses due to the permanent and transient loads are of the same sign. However, in situations where smaller compressive permanent load stresses can result in larger net tensile stresses in the deck in the vicinity of points of contraflexure (i.e. in potential regions of stress reversal), the use of the 3*n* composite section when calculating the permanent load stresses will produce a more critical tension stress in the deck. It was felt, however, that such a level of refinement in the calculation of longitudinal deck stresses was no longer warranted.

EXAMPLE

Calculate the maximum bending stress in the (structural) concrete deck for the composite girder shown in Figure 6.4.2.3.2.3-1 under the Service II Load Combination (Section 3.10.1.3.3). The load modifier η is assumed to be 1.0. Assume unshored construction. The section is assumed to be located in a region of positive flexure. Use the section properties computed earlier for this section, and the unfactored bending moments given in the preceding example at this section. Assume *n* = 8.

Concrete Deck:

$$f = \frac{1}{8}(1.0)\left[\frac{1.0(+335)}{166{,}612} + \frac{1.0(+322)}{166{,}612} + \frac{1.3(+3{,}510)}{166{,}612}\right](-21.73)(12) = -1.021 \text{ ksi}$$

6.4.3 Non-Composite Sections

As defined in *AASHTO LRFD* Article 6.10.1.2, a non-composite section is a section where the concrete deck is not connected to the steel section by shear connectors. Although permitted by the *AASHTO LRFD* Specifications, non-composite sections are not recommended because they are uneconomical and there is no positive attachment of the deck to the girder.

Continuous members in which non-composite sections are utilized in negative flexure regions only are referred to as composite girders. In a non-composite girder, or a girder in which there are no shear connectors along the entire length of the member, if friction between the deck and girder is neglected, the girder and deck are each assumed to separately carry a part of the load. In this case, there are two neutral axes; one at the centroid of the deck and one at the centroid of the girder. Under vertical load causing positive moment, the lower surface of the deck will theoretically be in tension and elongate while the top surface of the girder will be in compression and shorten. With friction neglected, only vertical internal forces will act between the deck and the girder and slip will occur between the two components. In other words, a plane section does not remain plane under load.

Although numerous field tests have shown that considerable bond develops on the concrete-steel faying surface such that unintended composite action occurs in a non-composite section, this bond is conservatively ignored and the stiffness of the deck is not included when calculating the section properties for design.

6.4.4 Hybrid Sections

A hybrid girder is defined as a fabricated steel girder with a web that has a specified minimum yield strength less than one or both flanges. As a result, yielding of the lower strength web will occur before the maximum flange strength has been reached. Therefore, the web will participate to a lesser extent than in a homogeneous girder when the moment capacity of the hybrid girder is attained. The hybrid factor, R_h, is used to account for the effect of earlier yielding of the lower strength steel in the web (Section 6.4.5.7). Hybrid girders may be used in straight or horizontally curved bridges.

Hybrid girders are covered in general in *AASHTO LRFD* Article 6.10.1.3. Although the specifications can be applied safely to all types of hybrid girders (ASCE, 1968), for greater design efficiency, it is recommended in *AASHTO LRFD* Article 6.10.1.3 that the difference in the specified minimum yield strengths of the web and the higher strength flange be limited to one steel grade. That is, the specified minimum yield strength of the web should not be less than the larger of 70 percent of the specified minimum yield strength of the higher strength flange and 36.0 ksi. This minimum limit on the web yield strength helps guard against early inelastic web bend-buckling of slender hybrid webs.

As for a homogeneous girder, a hybrid girder unloads elastically. If the yield stress in the web was exceeded during the initial loading, a small residual curvature will remain in the girder after unloading. However, under all subsequent loading and unloading cycles, the girder will behave elastically if the moment upon reloading does not exceed the previously applied maximum moment. Also, as in a homogeneous girder, residual stresses will cause inelastic behavior in a hybrid girder during the initial application of the load, but the ultimate resistance of the girder will generally not be affected by the presence of residual stresses. Additional more detailed information on the overall behavior of hybrid girders, along with initial design recommendations, may be found in Frost and Schilling (1964); Schilling (1967); ASCE (1968); Carskaddan (1968); Schilling (1968); Toprac and Engler (1961); and Toprac and Natarajan (1971).

Hybrid girders utilizing Grade HPS 70W steel for the flanges and Grade 50W steel for the web have recently proven to be a popular and economical option, primarily in regions of negative flexure (Horton et al., 2000; Lwin, 2002). Hybrid girders utilizing a tension flange with a higher yield stress than the web and a compression flange with the same yield stress as the web may also prove economical, particularly for composite sections in positive flexure. Because of stability issues before the concrete deck cures, it is often necessary to use a top flange that is not fully stressed at the strength limit state in regions of positive flexure. Some specific design issues to consider when hybrid sections are utilized are discussed further in Sections 6.3.4.2 and 6.3.5.3.

Test data for hybrid sections with nominally larger yield strengths in the web than in one or both flanges are limited. Therefore, in such cases, *AASHTO LRFD* Article 6.10.1.3 limits the nominal yield strength that may be used for the web in determining the flexural and shear resistance of the section to 120 percent or less of the specified minimum yield strength of the lower strength flange. This is felt to be a range that is supported by the limited available test data. An exception is permitted for composite sections in positive flexure with a higher strength steel in the web than in the compression flange, in which case the full web strength may be used in determining the flexural and shear resistance.

6.4.5 Miscellaneous Fundamental Calculations

6.4.5.1 General

This section will cover the calculation of some other important miscellaneous parameters that are often utilized in steel-bridge-girder design. These parameters include the plastic moment, M_p, the yield moment, M_y, the depth of the web in compression in the elastic range D_c and at the plastic moment D_{cp}, the web bend-buckling resistance, F_{crw}, and the flange-stress reduction factors – namely the web load-shedding factor, R_b, and the hybrid factor, R_h.

6.4.5.2 Plastic Moment

6.4.5.2.1 General

The plastic moment, M_p, is defined in the *AASHTO LRFD* Specifications as the resisting moment of a fully yielded cross-section (about the major axis). M_p is calculated as the moment of the plastic forces acting on the cross-section about the plastic neutral axis (Note: for sections subject to flexure only, M_p may be calculated as the moment of the plastic forces about any axis parallel to the plastic neutral axis). Plastic forces in steel portions of the cross-section are calculated using the yield strengths of the flanges, web and longitudinal reinforcing steel, as appropriate. Plastic forces in concrete portions of the cross-section (in compression only) are based on a rectangular stress block, with the magnitude of the compressive stress taken equal to $0.85f'_c$. Concrete in tension is neglected. The position of the plastic neutral axis is calculated based on the equilibrium condition that there is no net axial force acting on the cross-section.

The plastic moment is used as a theoretical measure of the maximum potential resistance of non-composite or composite sections satisfying specific steel grade, flange and web slenderness, compression-flange bracing and ductility requirements, as applicable. In the *AASHTO LRFD* Specifications, such sections in straight bridges that are composite in regions of positive flexure are termed compact sections. Non-composite sections or composite sections in regions of negative flexure in straight bridges satisfying these requirements are termed compact web sections, which are less commonly used. For sections that can achieve the full plastic-moment resistance, it is assumed that the section is completely elastic up to M_p and then rotates inelastically at M_p with no increase in the moment resistance. The effects of strain hardening are conservatively ignored. This idealized moment-rotation behavior is termed elastic-perfectly plastic behavior.

6.4.5.2.2 Non-Composite Sections

For homogenous non-composite sections, M_p may simply be calculated as follows:

$$M_p = F_y Z \qquad \text{Equation 6.4.5.2.2-1}$$

where:

Z = plastic section modulus (in.^{3})

Z is calculated as the sum of the first moments of the flange and web areas about the plastic neutral axis. For rolled wide-flange sections, values of *Z* are tabulated in the AISC *(*2010*).* For hybrid non-composite sections, the products of the yield strength and *Z* value for each individual component would be summed to calculate M_p.

The plastic moment of a non-composite section may also be calculated by simply eliminating the terms pertaining to the concrete deck and longitudinal reinforcement from the equations in Table 6.4.5.2.3.2-1 and Table 6.4.5.2.3.3-1 for composite sections.

6.4.5.2.3 Composite Sections

6.4.5.2.3.1 General

For composite sections, the stress distribution in the cross-section at M_p is assumed independent of the manner in which the stresses are induced into the beam. Thus, M_p is computed in the same manner for both unshored and shored construction even though the elastic stress distribution differs for each method of construction. Also, creep and shrinkage are assumed to have no effect on the internal stress distribution at M_p. Thus, when checking the flexural resistance of a composite section against M_p, the moments acting on the non-composite, long-term composite and short-term composite sections may be directly summed for comparison to M_p. The effect of the sequence of application of the different types of loads on the stress states and partial yielding within the cross-section on the resistance is not considered.

6.4.5.2.3.2 Sections in Positive Flexure

For composite sections in positive flexure, the attainment of M_p is possible only if the steel girder is provided with an adequate number of shear connectors so that the horizontal shear force from the concrete deck is effectively transmitted to the steel girder. The natural bond between the steel and concrete is not sufficient by itself. The design of shear connectors for ultimate strength is covered in Section 6.6.2.4. M_p for a composite section in positive flexure can be determined as follows:

- Calculate the plastic forces of each individual component in the cross-section and use them to determine whether the plastic neutral axis is in the web, top flange or concrete deck;
- Calculate the location of the plastic neutral axis within the element determined in Step 1; and
- Calculate M_p. *AASHTO LRFD* Article D6.1 in Appendix D6 provides equations for seven possible cases in *AASHTO LRFD* Table D6.1-1 (Table 6.4.5.2.3.2-1).

In Table 6.4.5.2.3.2-1, *d* is the distance from the element plastic force to the plastic neutral axis. The element forces are assumed to act at the mid-thickness of the flanges and concrete deck, at the mid-depth of the web and at the center of the longitudinal reinforcement.

The element forces in the table are to be computed as follows:

$$P_{rt} = F_{yrt}A_{rt}$$

$$P_s = 0.85f'_c b_s t_s$$

$$P_{rb} = F_{yrb}A_{rb}$$

$$P_c = F_{yc}b_c t_c$$

$$P_w = F_{yw}Dt_w$$

$$P_t = F_{yt}b_t t_t$$

Table 6.4.5.2.3.2-1 Calculation of $\overline{Y}$ and M_p for Sections in Positive Flexure

CASE	PNA	CONDITION	$\overline{Y}$ AND M_p
I	In Web	$P_t + P_w \geq P_c + P_s + P_{rb} + P_{rt}$	$\overline{Y} = \left(\frac{D}{2}\right)\left[\frac{P_t - P_c - P_s - P_{rt} - P_{rb}}{P_w} + 1\right]$ $M_p = \frac{P_w}{2D}\left[\overline{Y}^2 + (D - \overline{Y})^2\right] + \left[P_s d_s + P_{rt} d_{rt} + P_{rb} d_{rb} + P_c d_c + P_t d_t\right]$
II	In Top Flange	$P_t + P_w + P_c \geq P_s + P_{rb} + P_{rt}$	$\overline{Y} = \left(\frac{t_c}{2}\right)\left[\frac{P_w + P_t - P_s - P_{rt} - P_{rb}}{P_c} + 1\right]$ $M_p = \frac{P_c}{2t_c}\left[\overline{Y}^2 + (t_c - \overline{Y})^2\right] + \left[P_s d_s + P_{rt} d_{rt} + P_{rb} d_{rb} + P_w d_w + P_t d_t\right]$
III	Concrete Deck, Below P_{rb}	$P_t + P_w + P_c \geq \left(\frac{c_{rb}}{t_s}\right)P_s + P_{rb} + P_{rt}$	$\overline{Y} = (t_s)\left[\frac{P_c + P_w + P_t - P_{rt} - P_{rb}}{P_s}\right]$ $M_p = \left(\frac{\overline{Y}^2 P_s}{2t_s}\right) + \left[P_{rt} d_{rt} + P_{rb} d_{rb} + P_c d_c + P_w d_w + P_t d_t\right]$
IV	Concrete Deck, at P_{rb}	$P_t + P_w + P_c + P_{rb} \geq \left(\frac{c_{rb}}{t_s}\right)P_s + P_{rt}$	$\overline{Y} = c_{rb}$ $M_p = \left(\frac{\overline{Y}^2 P_s}{2t_s}\right) + \left[P_{rt} d_{rt} + P_c d_c + P_w d_w + P_t d_t\right]$
V	Concrete Deck, Above P_{rb} Below P_{rt}	$P_t + P_w + P_c + P_{rb} \geq \left(\frac{c_{rt}}{t_s}\right)P_s + P_{rt}$	$\overline{Y} = (t_s)\left[\frac{P_{rb} + P_c + P_w + P_t - P_{rt}}{P_s}\right]$ $M_p = \left(\frac{\overline{Y}^2 P_s}{2t_s}\right) + \left[P_{rt} d_{rt} + P_{rb} d_{rb} + P_c d_c + P_w d_w + P_t d_t\right]$
VI	Concrete Deck, at P_{rt}	$P_t + P_w + P_c + P_{rb} + P_{rt} \geq \left(\frac{c_{rt}}{t_s}\right)P_s$	$\overline{Y} = c_{rt}$ $M_p = \left(\frac{\overline{Y}^2 P_s}{2t_s}\right) + \left[P_{rb} d_{rb} + P_c d_c + P_w d_w + P_t d_t\right]$
VII	Concrete Deck, Above P_{rt}	$P_t + P_w + P_c + P_{rb} + P_{rt} < \left(\frac{c_{rt}}{t_s}\right)P_s$	$\overline{Y} = (t_s)\left[\frac{P_{rb} + P_c + P_w + P_t + P_{rt}}{P_s}\right]$ $M_p = \left(\frac{\overline{Y}^2 P_s}{2t_s}\right) + \left[P_{rt} d_{rt} + P_{rb} d_{rb} + P_c d_c + P_w d_w + P_t d_t\right]$

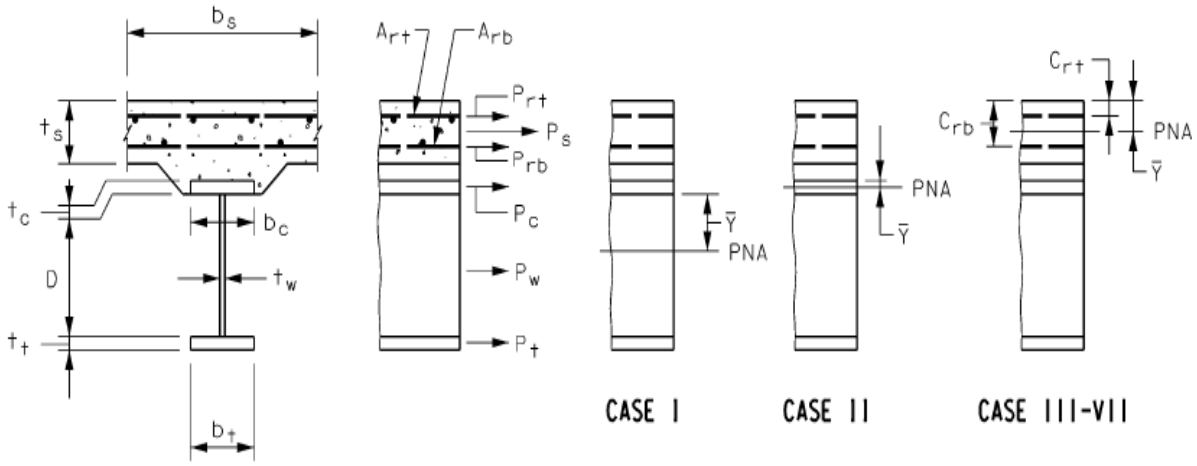

All element forces, dimensions, and distances are to be taken as positive. The conditions should be checked in the order listed in the table. The forces in the longitudinal reinforcement may be conservatively neglected by setting the terms, P_{rb} and P_{rt}, equal to zero in the equations given in the table. Application of the table to the composite cross-section given in Figure 6.4.2.3.2.3-1 is illustrated below.

EXAMPLE

Calculate the plastic moment M_p for the composite section shown in Figure 6.4.2.3.2.3-1, which is in a region of positive flexure, using the equations given in *AASHTO LRFD* Table D6.1-1 (Table 6.4.5.2.3.2-1). The longitudinal reinforcement will be conservatively neglected. Assume the web and flange steel is Grade 50W steel and that f'_c for the concrete deck is 4.0 ksi. The effective flange width of the concrete deck, b_{eff}, is 114.0 inches.

$$P_t + P_w + P_c = A_{steel}F_y = 75.25(50) = 3{,}763 \text{ kips}$$

$$P_s = 0.85f'_c\, b_{eff}\, t_s = 0.85(4.0)(114.0)(9.0) = 3{,}488 \text{ kips}$$

$$3{,}488 \text{ kips} < 3{,}763 \text{ kips}$$

Therefore, the plastic neutral axis (PNA) is in the top flange, use Case II in *AASHTO LRFD* Table D6.1-1 (Table 6.4.5.2.3.2-1)

$$\bar{y} = \frac{t_c}{2}\left[\frac{P_w + P_t - P_s}{P_c} + 1\right]$$

$$\bar{y} = \frac{1.0}{2}\left[\frac{50(69.0)(0.5) + 50(1.375)(18.0) - 3{,}488}{50(1.0)(16.0)} + 1\right]$$

$$= 0.17 \text{ in. from the top of the top flange}$$

Check equilibrium by calculating and comparing the total plastic forces acting on the compression and tension sides of the plastic neutral axis:

Compression side:

$$3{,}488 + (0.17)(16.0)(50) = 3{,}624 \text{ kips}$$

Tension side:

$$(1.0 - 0.17)(16.0)(50) + (69.0)(0.5)(50) + (18.0)(1.375)(50) = 3{,}626 \text{ kips} \quad \text{ok}$$

$$M_p = \frac{P_c}{2t_c}\left[\bar{y}^2 + (t_c - \bar{y})^2\right] + \left[P_s d_s + P_w d_w + P_t d_t\right]$$

Calculate the distances from the PNA to the centroid of each element:

$$d_s = \frac{9.0}{2} + 3.5 + 0.17 - 1.0 = 7.17 \text{ in.}$$

$$d_w = 1.0 + \frac{69.0}{2} - 0.17 = 35.33 \text{ in.}$$

$$d_t = 1.0 + 69.0 + \frac{1.375}{2} - 0.17 = 70.52 \text{ in.}$$

$$M_p = \left[\frac{50(1.0)(16.0)}{2(1.0)}\right]\left[(0.17)^2 + (1.0 - 0.17)^2\right] +$$
$$\left[(3{,}488)(7.17) + 69.0(0.5)(50)(35.33) + 1.375(18.0)(50)(70.52)\right]$$

$$M_p = 173{,}509 \text{ kip} - \text{in.} = 14{,}459 \text{ kip} - \text{ft}$$

6.4.5.2.3.3 Sections in Negative Flexure

For composite sections in negative flexure, a similar procedure can be used. In this case, however, the tensile strength of the concrete is ignored and the contribution of the longitudinal reinforcement should be included. *AASHTO LRFD* Table D6.1-2

(Table 6.4.5.2.3.3-1) contains the equations for the two cases most likely to occur in practice. Again, the conditions should be checked in the order listed in the table.

Table 6.4.5.2.3.3-1 Calculation of $\overline{Y}$ and M_p for Sections in Negative Flexure

CASE	PNA	CONDITION	$\overline{Y}$ AND M_p
I	In Web	$P_c + P_w \geq P_t + P_{rb} + P_{rt}$	$\overline{Y} = \left(\frac{D}{2}\right)\left[\frac{P_c - P_t - P_{rt} - P_{rb}}{P_w} + 1\right]$ $M_p = \frac{P_w}{2D}\left[\overline{Y}^2 + (D-\overline{Y})^2\right] + \left[P_{rt}d_{rt} + P_{rb}d_{rb} + P_t d_t + P_c d_c\right]$
II	In Top Flange	$P_c + P_w + P_t \geq P_{rb} + P_{rt}$	$\overline{Y} = \left(\frac{t_t}{2}\right)\left[\frac{P_w + P_c - P_{rt} - P_{rb}}{P_t} + 1\right]$ $M_p = \frac{P_t}{2t_t}\left[\overline{Y}^2 + (t_t-\overline{Y})^2\right] + \left[P_{rt}d_{rt} + P_{rb}d_{rb} + P_w d_w + P_c d_c\right]$

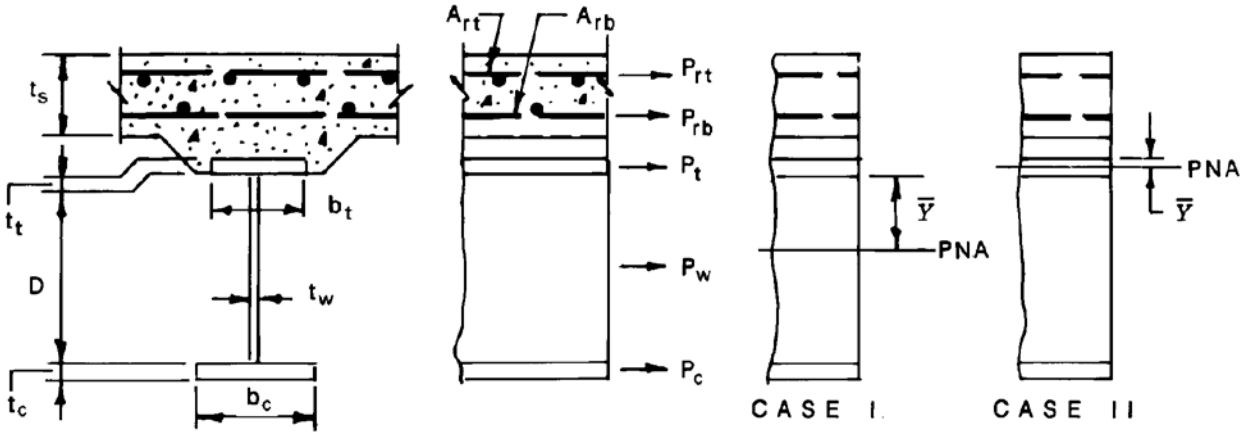

6.4.5.2.4 Closed Box and Tub Sections

Table 6.4.5.2.3.2-1 and Table 6.4.5.2.3.3-1 can also be applied to compute M_p for a closed-box or tub section by applying the equations to calculate M_p for one-half of the box section. For sections with inclined webs, the web depth D should be measured along the web slope.

6.4.5.3 Yield Moment

6.4.5.3.1 General

The yield moment, M_y, is defined in the *AASHTO LRFD* Specifications as the moment at which an outer fiber, in a member subjected to flexure about the major-axis, attains the nominal yield stress neglecting the effect of any residual stresses. In the *AASHTO LRFD* Specifications, M_y is used in the resistance calculations for

certain types of sections – primarily compact composite sections in regions of positive flexure in straight continuous-span bridges.

AASHTO LRFD Article D6.2 in Appendix D6 discusses the computation of the yield moment. In all cases, the calculations are to disregard the effects of any flange lateral bending or local web yielding in hybrid sections.

6.4.5.3.2 Non-Composite Sections

For a non-composite section, *AASHTO LRFD* Article D6.2.1 states that M_y is to be taken as the smaller of the moment required to cause nominal first yielding in the compression flange (M_{yc}), or the moment required to cause nominal first yielding in the tension flange (M_{yt}) at the strength limit state.

6.4.5.3.3 Composite Sections

6.4.5.3.3.1 Sections in Positive Flexure

AASHTO LRFD Article D6.2.2 states that for composite sections in positive flexure, M_y is to be taken as the sum of the moments applied separately to the steel, short-term and long-term composite sections to cause nominal first yielding in either flange at the strength limit state. M_y is taken as the lesser of either M_{yc} or M_{yt}. As discussed in the previous section, in a composite girder, moments are applied to different sections and this fact must be appropriately accounted for in the computation of M_y. M_y for a composite section in positive flexure can therefore be determined as follows: 1) calculate the moment, M_{D1}, caused by the factored permanent load applied before the concrete deck has hardened or is made composite and apply this moment to the steel section; 2) calculate the moment, M_{D2}, caused by the remainder of the factored permanent load and apply this moment to the long-term composite section; 3) calculate the additional moment, M_{AD}, that must be applied to the short-term composite section to cause nominal yielding in either steel flange; and 4) calculate M_y as the sum of the total permanent load moment and M_{AD}. This procedure can be represented in equation form as follows:

- Solve for M_{AD} from the following equation:

$$F_{yf} = \frac{M_{D1}}{S_{NC}} + \frac{M_{D2}}{S_{LT}} + \frac{M_{AD}}{S_{ST}} \qquad \text{Equation 6.4.5.3.3.1-1}$$

AASHTO LRFD Equation D6.2.2-1

- Calculate:

$$M_y = M_{D1} + M_{D2} + M_{AD} \qquad \text{Equation 6.4.5.3.3.1-2}$$

AASHTO LRFD Equation D6.2.2-2

where:

S_{NC} = section modulus for the steel section (in.^{3})
S_{ST} = section modulus for the long-term composite section (in.^{3})
S_{LT} = section modulus for the short-term composite section (in.^{3})

In regions of positive flexure, the longitudinal reinforcement may be neglected in the calculation of S_{ST} and S_{LT}.

EXAMPLE

Calculate the yield moment, M_y, for the composite section shown in Figure 6.4.2.3.2.3-1, which is in a region of positive flexure, using the equations given in *AASHTO LRFD* Article D6.2.2. For a composite section in positive flexure, M_{yt}, or the yield moment calculated for the tension flange, typically controls. From earlier calculations, the section moduli to the bottom flange were calculated as follows: S_{NC} = 1,973 in.^{3}; S_{LT} = 2,513 in.^{3}; S_{ST} = 2,725 in.^{3}. Use the unfactored dead load bending moments at this section given in a previous example (Section 6.4.2.4.1). Assume the calculation is to be done for Load Combination Strength I (Section 3.9.1.2.2), and that the load modifier η is to be taken equal to 1.0 (Section 1.3.6).

$$F_{yf} = \frac{M_{D1}}{S_{NC}} + \frac{M_{D2}}{S_{LT}} + \frac{M_{AD}}{S_{ST}}$$

$$50 = 1.0\left[\frac{1.25(2{,}202)(12)}{1{,}973} + \frac{1.25(335)(12) + 1.50(322)(12)}{2{,}513} + \frac{M_{AD}}{2{,}725}\right]$$

$$M_{AD} = 78{,}897 \text{ kip-in.} = 6{,}575 \text{ kip-ft}$$

$$M_y = M_{D1} + M_{D2} + M_{AD}$$

$$M_y = 1.0[1.25(2{,}202) + 1.25(335) + 1.50(322) + 6{,}575]$$

$$M_y = 10{,}229 \text{ kip-ft}$$

The ratio of M_p/M_y is a property of the cross-sectional shape known as the shape factor. For doubly symmetric non-composite I-shapes bent about their major axis, the shape factor is approximately 1.12. For singly symmetric composite girders in

regions of positive flexure, the shape factor is much larger. Values on the order of 1.4 to 1.6 are quite common.

6.4.5.3.3.2 Sections in Negative Flexure

For a composite section in negative flexure, *AASHTO LRFD* Article D6.2.3 states that a procedure similar to the above is to be used to compute M_y, only in this case, both S_{ST} and S_{LT} are to be taken for the section consisting of the steel girder plus the longitudinal reinforcement within the effective flange width of the concrete deck. Also, M_{yt} is to be taken with respect to either the tension flange or the longitudinal reinforcement, whichever is the smallest value. *AASHTO LRFD* Article D6.2.4 addresses the procedure to be used for sections with cover plates.

6.4.5.4 Depth of the Web in Compression

6.4.5.4.1 In the Elastic Range, D_c

6.4.5.4.1.1 General

The depth of the web in compression in the elastic range, D_c, is used primarily in computing the web bend-buckling resistance, F_{crw}, and the web load-shedding factor, R_b (Sections 6.4.5.5 and 6.4.5.6). For composite sections in negative flexure and non-composite sections, D_c is also used to determine whether the section qualifies as a slender or a non-slender web section for determining the nominal flexural resistance. Slender and non-slender web sections are discussed further in Section 6.5.6.

D_c for composite sections is a function of the dead-to-live load stress ratio in the elastic range of stress at the service, fatigue and strength limit states. This is because in a composite girder, the dead and live loads are applied to different sections. This is an especially important consideration for composite sections since the dead-load stress has a significant effect on the location of the elastic neutral axis. Note that when checking the section for web bend-buckling during construction, however, while the girder is still in the non-composite condition before the concrete deck hardens or is made composite, D_c of the steel section alone (which is a section property independent of the stress) is used in the calculations.

6.4.5.4.1.2 Sections in Positive Flexure

D_c of the composite section (refer to Figure 6.4.5.4.1.2-1 – the terms shown in the figure are described below) at sections in positive flexure increases with increasing span length because of the increasing dead-to-live load ratio. With increasing spans, the larger non-composite dead load stresses acting on the steel section alone effectively cause the neutral axis to be much lower than it would if all loads were

applied to the composite section, which obviously increases the depth of the web in compression. Therefore, in general, it is important in certain cases to recognize the effect of the dead load stress on the location of the neutral axis at these sections.

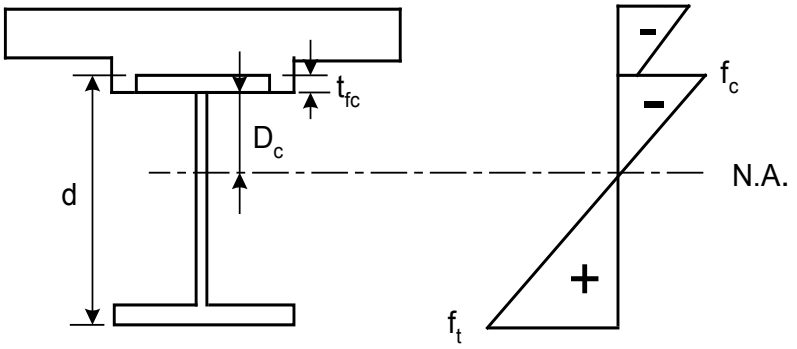

Figure 6.4.5.4.1.2-1 D_c for a Composite Section in Positive Flexure

AASHTO LRFD Article D6.3.1 in Appendix D6 states that D_c for composite sections in positive flexure is to be taken as the depth over which the algebraic sum of the stresses acting on the steel, long-term composite and short-term composite sections due to the dead and live loads, plus impact, is compressive. The following equation, which can simply be derived from an examination of the stress diagram and cross-section given in Figure 6.4.5.4.1.2-1, is provided in this article to compute D_c in lieu of calculating D_c utilizing the individual stress diagrams:

$$D_c = \left(\frac{-f_c}{|f_c| + f_t} \right) d - t_{fc} \geq 0 \qquad \text{Equation 6.4.5.4.1.2-1}$$

AASHTO LRFD Equation D6.3.1-1

where:

d = total depth of the steel section (in.)

f_c = sum of the compression-flange vertical bending stresses caused by the different loads, i.e. DC_1, the permanent load acting on the non-composite section; DC_2, the permanent load acting on the long-term composite section; DW, the wearing surface load acting on the long-term composite section; and LL+IM, live load plus impact acting on the short-term composite section (ksi). For stresses in compression, f_c is to be taken as negative.

f_t = sum of the tension-flange vertical bending stresses caused by the different loads (ksi) – see the preceding definition.

t_{fc} = thickness of the compression flange (in.)

Flange lateral bending stresses are to be ignored in the computation of f_c and f_t.

According to the *AASHTO LRFD* Specifications, for composite sections in positive flexure at the fatigue, service and strength limit states, D_c only needs to be employed in the computation of the nominal flexural resistance for sections in which longitudinal web stiffeners are required based on *AASHTO LRFD* Article 6.10.2.1.1.

For composite sections in positive flexure without longitudinal web stiffeners that meet the section proportioning limits of *AASHTO LRFD* Article 6.10.2, and also the ductility requirement of *AASHTO LRFD* Article 6.10.7.3 to prevent premature crushing of the concrete deck, the web bend-buckling resistance, F_{crw} (Section 6.4.5.5), is generally close to or larger than the yield stress of the compression flange, F_{yc}, at the strength limit state. Also, for loads applied at the service and fatigue limit states after the deck has hardened or is made composite, the increased compressive stresses in the web tend to be compensated for by the increase in F_{crw} resulting from the corresponding decrease in D_c after the section becomes composite. These compensating effects simply continue at the strength limit state. As a result, since theoretical web bend-buckling of these sections is essentially prevented at all elastic stress levels, the web load-shedding factor, R_b (Section 6.4.5.6), is specified to be 1.0 for composite sections in positive flexure without longitudinal web stiffeners. Since computations of F_{crw} and R_b are not required for these sections, it follows that a computation of D_c is also not required.

The section proportioning requirements of *AASHTO LRFD* Article 6.10.2.1.2 for sections with longitudinal web stiffeners are not generally sufficient to ensure that web bend buckling will not occur. As a result, the specifications require the calculation of F_{crw} and R_b, and consequently D_c, for these sections. The calculation of D_c for composite sections in positive flexure can potentially complicate bridge load rating calculations because of the dependency of the flexural resistance on the applied load. Therefore, avoiding the computation of D_c is desirable where practical.

EXAMPLE

Calculate the depth of the web in compression, D_c, for the composite section shown in Figure 6.4.2.3.2.3-1, which is in a region of positive flexure, using Equation 6.4.5.4.1.2-1. Assume the calculation is to be done for Load Combination Strength I (Section 3.9.1.2.2) and that the load modifier η is to be taken equal to 1.0 (Section 1.3.6).

From earlier calculations (Section 6.4.2.4.1), the sum of the factored stresses in the tension flange, f_t, was computed to be +48.10 ksi. From separate calculations similar to those illustrated in Section 6.4.2.4.1, the sum of the factored stresses in the compression flange, f_c, is computed to be –27.43 ksi.

$$D_C = \left(\frac{-f_c}{|f_c| + f_t} \right) d - t_{fc} \geq 0 \quad \text{(Equation 6.4.5.4.1.2-1)}$$

$$d = 1.375 + 69.0 + 1.0 = 71.375 \text{ in.}$$

$$t_{fc} = 1.0 \text{ in.}$$

$$D_C = \left(\frac{-(-27.43)}{|-27.43| + 48.10} \right) 71.375 - 1.0 = 24.92 \text{ in.}$$

Note from the previous elastic section property calculations (Section 6.4.2.3.2.3) that D_c for the short-term (n = 8) composite section is (10.23 in. – 1.0 in.) = 9.23 in. Therefore, the non-composite dead load stress has a significant effect on the actual value of D_c for this composite section.

6.4.5.4.1.3 Sections in Negative Flexure

The concrete deck is typically not considered to be effective in tension for composite sections in negative flexure, except perhaps at the fatigue and service limit states as permitted by the Specifications when certain conditions are satisfied. The distance between the neutral-axis locations for the steel and composite sections is small when the concrete deck is not considered effective, as the composite section only consists of the steel section plus the longitudinal reinforcement. As a result, the location of the neutral axis for the composite section is essentially unaffected by the dead load stress. In fact, accounting for the effect of the dead load stress actually results in a smaller value of D_c in regions of negative flexure.

Therefore, for the majority of situations involving composite sections in negative flexure, *AASHTO LRFD* Article D6.3.1 (Appendix D6) of the Specifications conservatively specifies the use of D_c computed for the section consisting of the steel girder plus the longitudinal reinforcement, without considering the algebraic sum of the stresses acting on the non-composite and composite sections. Again, this avoids potential difficulties in bridge load rating calculations since the resulting value of D_c is independent of the applied loading.

A single exception to the preceding requirement is specified in *AASHTO LRFD* Article D6.3.1; that is, if the concrete deck is assumed effective in tension in regions of negative flexure at the service limit state, as permitted for composite girders satisfying the conditions specified in *AASHTO LRFD* Article 6.10.4.2.1 (Section 6.5.4.3), Equation 6.4.5.4.1.2-1 must be used to compute D_c. The terms to be used in Equation 6.4.5.4.1.2-1 in this case are shown in Figure 6.4.5.4.1.3-1. When calculating the web bend-buckling resistance, F_{crw} (Section 6.4.5.5), at the service

limit state, a more precise calculation of D_c, accounting for the beneficial effect of the dead load stress in this case, is required when the concrete deck is considered effective in tension. Otherwise, the reduction in F_{crw} will be too large and not reflective of the actual potential web bend-buckling resistance at this limit state.

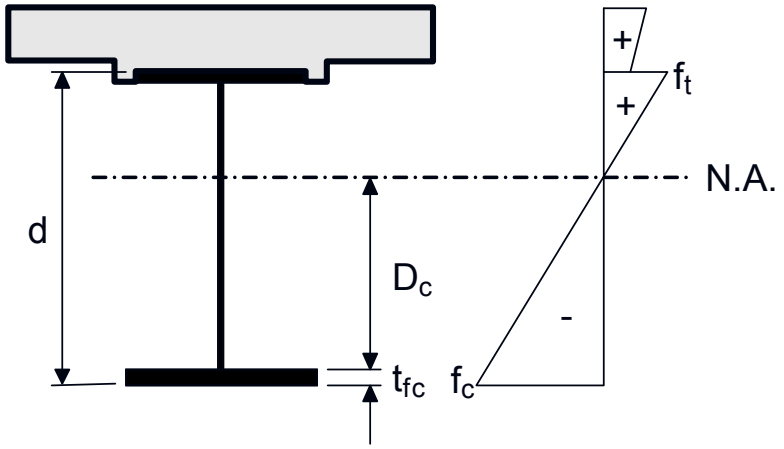

Figure 6.4.5.4.1.3-1 D_c for a Composite Section in Negative Flexure

D_c of the steel section alone should always be used for non-composite sections.

EXAMPLE

Calculate the depth of the web in compression, D_c, for the composite section shown in Figure 6.4.2.3.3.3-1, which is in a region of negative flexure, using Equation 6.4.5.4.1.2-1. Assume the calculation is to be done for Load Combination Service II (Section 3.10.1.3.3), and that the appropriate conditions specified in *AASHTO LRFD* Article 6.10.4.2.1 are met to allow the concrete deck to be considered effective in tension for this load combination (Section 6.5.4.3).

From separate calculations similar to those illustrated in Sections 6.4.2.3.2.3 and 6.4.2.3.3.3, the composite elastic section moduli for the long-term (3*n*) and short-term (*n*) composite sections for the section shown in Figure 6.4.2.3.3.3-1, including the concrete deck and longitudinal reinforcement, are as follows:

Composite Section; 3*n* = 24: $S_{TOP\ OF\ STEEL}$ = 7,587 in.^{3} $S_{BOT\ OF\ STEEL}$ = 3,684 in.^{3}
Composite Section; *n* = 8: $S_{TOP\ OF\ STEEL}$ = 16,836 in.^{3} $S_{BOT\ OF\ STEEL}$ = 3,921 in.^{3}

Using section properties for the steel section only (computed previously in Section 6.4.2.3.3.3), along with the section properties given above and the unfactored moments given earlier in Section 6.4.2.4.1, calculate the factored Service II stresses f_t in the top flange and f_c in the bottom flange as follows:

Top flange:

$$f_t = \left[\frac{1.0(-4{,}840)}{-2{,}942} + \frac{1.0(-690 + -664)}{-7{,}587} + \frac{1.3(-4{,}040)}{-16{,}836}\right]12 = 25.63 \text{ ksi}$$

Bottom flange:

$$f_c = \left[\frac{1.0(-4{,}840)}{3{,}149} + \frac{1.0(-690 + -664)}{3{,}684} + \frac{1.3(-4{,}040)}{3{,}921}\right]12 = -38.93 \text{ ksi}$$

Calculate D_c using Equation 6.4.5.4.1.2-1:

$$D_c = \left(\frac{-f_c}{|f_c| + f_t}\right)d - t_{fc} \geq 0$$

$$d = 2.0 + 69.0 + 2.0 = 73.0 \text{ in.}$$

$$t_{fc} = 2.0 \text{ in.}$$

$$D_c = \left(\frac{-(-38.93)}{|-38.93| + 25.63}\right)73.0 - 2.0 = 42.02 \text{ in.}$$

Note from separate calculations that D_c for the short-term (n = 8) composite section is equal to 57.21 in. Therefore, this example clearly illustrates the substantial benefit of calculating D_c taking into account the effect of the dead load stress when the concrete is considered effective in tension in regions of negative flexure at the service limit state.

6.4.5.4.2 At the Plastic Moment, D_{cp}

6.4.5.4.2.1 General

In the *AASHTO LRFD* Specifications, the depth of the web in compression at the plastic moment, D_{cp}. is used primarily in one of the criteria to determine if a composite section in positive flexure qualifies as a compact section at the strength limit state, and to determine if a non-slender composite section in negative flexure or a non-slender non-composite section qualifies as either a compact web or a noncompact web section at the strength limit state. All the preceding section classifications for determining the nominal flexural resistance are discussed in more detail in Section 6.5.6.

6.4.5.4.2.2 Sections in Positive Flexure

At sections in positive flexure, the depth of the web in compression typically reduces (i.e., from D_c) as plastic strains associated with moments larger than R_hM_y are incurred. R_h is the hybrid factor discussed in Section 6.4.5.7. In fact, for composite sections in positive flexure, the neutral axis at the plastic moment, M_p, will often be located either in the concrete deck or in the top flange of the steel girder, as illustrated in the example M_p calculation given in Section 6.4.5.2.3.2. In such cases, the entire web of the girder is in tension and D_{cp} is to be taken as zero according to *AASHTO LRFD* Article D6.3.2. When D_{cp} is equal to zero, all web-slenderness requirements in the Specifications based on D_{cp} are assumed automatically satisfied.

The location of the plastic neutral axis for composite sections in positive flexure can be determined from the conditions listed in *AASHTO LRFD* Table D6.1-1 (Table 6.4.5.2.3.2-1). Again, the position of the plastic neutral axis is calculated based on the equilibrium condition that there be no net axial force acting on the assumed fully yielded cross-section. For deeper girders (e.g. with longitudinal web stiffeners), it is possible that the conditions in *AASHTO LRFD* Table D6.1-1 (Table 6.4.5.2.3.2-1) may indicate that the plastic neutral axis is located in the web. In this case, D_{cp} may be calculated from the following equation given in *AASHTO LRFD* Article D6.3.2:

$$D_{cp} = \frac{D}{2}\left(\frac{F_{yt}A_t - F_{yc}A_c - 0.85f'_cA_s - F_{yrs}A_{rs}}{F_{yw}A_w} + 1\right) \quad \text{Equation 6.4.5.4.2.2-1}$$

AASHTO LRFD Equation D6.3.2-1

where:

A_c = area of the compression flange (in.^{2})
A_{rs} = total area of the longitudinal reinforcement within the effective concrete deck width (in.^{2})
A_s = area of the concrete deck (in.^{2})
A_t = area of the tension flange (in.^{2})
A_w = area of the web (in.^{2})
F_{yc}, F_{yt}, F_{yw}, F_{yrs} = specified minimum yield strength of the compression flange, tension flange, web and longitudinal reinforcement, respectively (ksi)

6.4.5.4.2.3 Sections in Negative Flexure

At sections in negative flexure, the depth of the web in compression typically increases (i.e., from D_c) as plastic strains associated with moments larger than R_hM_y are incurred. The location of the plastic neutral axis for composite sections in negative flexure and for non-composite sections can be determined from the

conditions listed in *AASHTO LRFD* Table D6.1-2 (Table 6.4.5.2.3.3-1 – note that for non-composite sections, all terms related to the longitudinal reinforcement in Table 6.4.5.2.3.3-1 should be set equal to zero).

In calculating D_{cp} in regions of negative flexure, the concrete deck is assumed not to be effective in tension. Therefore, in most all cases, the plastic neutral axis will be located in the web. For rare cases in which the plastic neutral axis is located in the top flange and the entire web is in compression, D_{cp} is to be taken equal to the web depth D according to *AASHTO LRFD* Article D6.3.2. For composite sections in negative flexure where the plastic neutral axis is located in the web, D_{cp} may be computed as follows (all terms are defined in Section 6.4.5.4.2.2):

$$D_{cp} = \frac{D}{2A_w F_{yw}}\left[F_{yt}A_t + F_{yw}A_w + F_{yrs}A_{rs} - F_{yc}A_c\right] \qquad \text{Equation 6.4.5.4.2.3-1}$$

AASHTO LRFD Equation D6.3.2-2

EXAMPLE

Calculate the depth of the web in compression at the plastic moment, D_{cp}, for the composite section shown in Figure 6.4.2.3.3.3-1, which is in a region of negative flexure, using Equation 6.4.5.4.2.3-1. Recall that this section is assumed to be a hybrid section utilizing Grade HPS 70W steel flanges and a Grade 50W web. The area of longitudinal reinforcement, A_{rs}, was determined previously (Section 6.4.2.3.3.2) to be 10.56 in.^{2} with a specified minimum yield strength, F_{yrs} = 60 ksi.

$$A_t = (2.0)(18.0) = 36.0 \text{ in.}^2$$

$$A_w = (0.5625)(69.0) = 38.8 \text{ in.}^2$$

$$A_c = (2.0)(20.0) = 40.0 \text{ in.}^2$$

$$D_{cp} = \frac{D}{2A_w F_{yw}}\left[F_{yt}A_t + F_{yw}A_w + F_{yrs}A_{rs} - F_{yc}A_c\right]$$

$$D_{cp} = \frac{69.0}{2(38.8)(50)}\left[(70)(36.0) + (50)(38.8) + (60)(10.56) - (70)(40.0)\right] = 40.79 \text{ in.}$$

Check equilibrium by calculating and comparing the total plastic forces acting on the tension and compression sides of the plastic neutral axis:

Tension side:

$$(69.0 - 40.79)(0.5625)(50) + (36.0)(70) + (10.56)(60) = 3{,}947 \text{ kips}$$

Compression side:

$$(40.79)(0.5625)(50) + (40.0)(70) = 3{,}947 \text{ kips} \quad \text{ok}$$

Note that for the section consisting of the steel girder plus the longitudinal reinforcement, the elastic depth of the web in compression D_c is (38.96 in. – 2.0 in.) = 36.96 in., which is smaller than D_{cp} as expected.

6.4.5.5 Web Bend-Buckling Resistance, F_{crw}

6.4.5.5.1 General

The buckling behavior of a slender web plate subject to pure bending is similar to the buckling behavior of a flat plate. A perfectly flat plate with no initial imperfections would not deflect laterally from its initial flat position until its theoretical buckling load is reached. However, in many experimental tests, bending deformations and associated transverse displacements of web plates occur from the onset of load application due to initial web out-of-flatness, and increase progressively throughout the entire range of applied bending moment. As expected, these deformations are largest in the compression zone of the web. Because of the stable post-buckling behavior of the web, however, a significant change in the rate of increase of the transverse displacements of the web as a function of the applied loads is not observed as the theoretical web bend-buckling stress is exceeded (Basler et al., 1960). Therefore, web bend-buckling behavior is essentially a load-deflection rather than a bifurcation phenomenon; that is, a distinct buckling load is not observed.

Since web plates in bending do not collapse when the theoretical buckling load is reached, the available post-buckling strength can be considered in determining the nominal flexural resistance of sections with slender webs at the strength limit state, as discussed further in Section 6.4.5.6. However, in certain situations, it is desirable to limit the bending deformations and transverse displacements of the web. This is particularly true during the construction condition and at the service limit state.

The advent of composite design has led to a significant reduction in the size of compression flanges in regions of positive flexure. As a result, more than half of the web of the non-composite section will be in compression in these regions during the construction condition before the concrete deck has hardened or is made composite. As a result, the web is more susceptible to bend buckling in this condition and is to be explicitly checked in all regions of the non-composite girder during the construction condition (Section 6.5.3.5).

At the service limit state, a significant structural performance requirement is to prevent objectionable permanent deflections of the girders due to expected severe traffic loadings that could impair the riding quality of the bridge. Therefore, a control on the amount of transverse web displacement is again desirable. In a composite girder at the service limit state, regions in negative flexure are most susceptible to web bend-buckling, especially when the concrete deck is assumed effective in tension, as permitted for composite sections satisfying the provisions of *AASHTO LRFD* Article 6.10.4.2.1 (Section 6.5.4.3). In this case, more than half the web is likely to be in compression, again increasing the susceptibility of the web to bend-buckling.

Control of transverse web displacements at the fatigue limit state is also desirable to prevent significant elastic out-of-plane flexing of the web under repeated live loading, which could potentially lead to fatigue cracks at the web-to-flange junctions. *AASHTO LRFD* Article 6.10.5.3 does provide a check for shear buckling of the web under the shear due to unfactored permanent load plus the factored fatigue load. The factored fatigue load for this particular check is specified to be the Fatigue I Load Combination (Section 3.9.1.5.2), which is based on the fatigue live load given in *AASHTO LRFD* Article 3.6.1.4 (Section 3.4.4.1). The Fatigue Load Combination is intended to represent the live loading causing the maximum stress range for fatigue over the assumed 75-year design life of the bridge. This check is discussed in more detail in Section 6.5.5.2.2.2. A check is not specified for bend-buckling under this load condition because the bend-buckling check at the service limit state discussed in the preceding paragraph will always control. This includes composite sections in positive flexure with longitudinal web stiffeners that do not satisfy *AASHTO LRFD* Article 6.10.2.1.1. In this case, the smaller value of F_{crw} resulting from the larger value of D_c at the fatigue limit state (i.e. larger than the value at the service limit state) tends to be compensated for by the lower web compressive stress due to the load condition specified for the fatigue limit state check given in *AASHTO LRFD* Article 6.10.5.3.

The *AASHTO LRFD* Specifications use the theoretical web bend-buckling load as a simple index to control the web plate bending strains and transverse displacements during construction and at the service limit state. The web bend-buckling resistance is specified in *AASHTO LRFD* Article 6.10.1.9. The equation for the web bend-buckling resistance, F_{crw}, is provided in *AASHTO LRFD* Article 6.10.1.9.1. This equation is derived from the following equation for the elastic buckling stress of a flat plate subject to pure bending (Timoshenko and Gere, 1961):

$$F_{cr} = \frac{k\pi^2 E}{12\left(1-\mu^2\right)(b/h)^2} \qquad \text{Equation 6.4.5.5.1-1}$$

AASHTO LRFD Article C6.9.4.2

where:

b = width of the plate along the edge subject to bending (in.)
E = Young's modulus (29,000 ksi for steel)
h = thickness of the plate (in.)
k = bend-buckling coefficient (Section 6.4.5.5.2)
μ = Poisson's ratio (0.3 for steel)

Substituting the slenderness ratio D/t_w of the web for b/h, and the values of E, π and μ in Equation 6.4.5.5.1-1 yields the following:

$$F_{crw} = \frac{0.9Ek}{\left(\frac{D}{t_w}\right)^2} \qquad \text{Equation 6.4.5.5.1-2}$$

AASHTO LRFD Equation 6.10.1.9.1-1

F_{crw} is not to exceed the smaller of R_hF_{yc} and $F_{yw}/0.7$, where F_{yc} and F_{yw} are the specified minimum yield strengths of the compression flange and web, respectively, and R_h is the hybrid factor (Section 6.4.5.7). Since the web carries only a relatively small portion of the total bending moment, the transition zone resulting from inelastic buckling is not considered significant and only an elastic buckling equation is provided.

F_{crw} is to be checked against the maximum compression-flange vertical bending stress due to the factored loads. Utilizing the maximum compressive stress in the web rather than the stress in the compression flange in order to obtain greater precision is not warranted for this check. In hybrid sections with a lower yield-strength web, the longitudinal and plate bending strains in the inelastic web at the web-flange juncture are constrained by a stable nominally elastic compression flange (ASCE, 1968). Since the flange will tend to restrain the longitudinal strains resulting from web bend-buckling at compression-flange stress levels up to R_hF_{yc}, the use of an F_{crw} value that is potentially greater than F_{yw} in hybrid sections is felt to be justified. The upper limit of $F_{yw}/0.7$ is a conservative limit to cover hybrid sections with F_{yw}/F_{yc} less than 0.7, which are permitted according to *AASHTO LRFD* Article 6.10.1.3, but are not recommended.

6.4.5.5.2 Bend-Buckling Coefficient

6.4.5.5.2.1 Webs without Longitudinal Stiffeners

The bend-buckling coefficient, *k*, to be substituted in Equation 6.4.5.5.1-2 for webs without longitudinal stiffeners is given by *AASHTO LRFD* Equation 6.10.1.9.1-2 as follows:

$$k = \frac{9}{(D_c/D)^2} \qquad \text{Equation 6.4.5.5.2.1-1}$$

AASHTO LRFD Equation 6.10.1.9.1-2

where:

D_c = depth of the web in compression in the elastic range (Section 6.4.5.4.1) (in.)

Equation 6.4.5.5.2.1-1 yields a *k* value of 36.0 for a doubly symmetric I-girder (i.e. $D_c = 0.5D$). This value is approximately equal to $k_{ss} + 0.8(k_{sf} - k_{ss})$, where $k_{ss} = 23.9$ and $k_{sf} = 39.6$ are the bend-buckling coefficients for simply supported and fully restrained longitudinal edge conditions, respectively, along the flanges (Timoshenko and Gere, 1961). The use of the *k* value from Equation 6.4.5.5.2.1-1 has been found to provide a reasonable approximation of the theoretical bend-buckling resistance for singly symmetric I-girders.

To ensure that the above boundary conditions at the web-flange juncture are satisfied, *AASHTO LRFD* Article 6.10.2.2 provides minimum flange proportioning requirements that were presented in Section 6.3.4.4. Specifically, the requirement given by Equation 6.3.4.4.3-1 that the thickness of the flanges be greater than or equal to 1.1 times the thickness of the web, and the requirement given by Equation 6.3.4.4.2-1 that the flange widths equal or exceed 1/6 of the web depth help ensure that the boundary conditions assumed in the web bend-buckling formulation are sufficiently accurate.

Substituting $k = 36.0$ and the effective web slenderness for a singly symmetric section $2D_c/t_w$ for D/t_w in Equation 6.4.5.5.1-2 and rearranging yields the web-slenderness limit, λ_{rw}, for a noncompact-web section given in *AASHTO LRFD* Article 6.10.6.2.3 as follows:

$$\frac{2D_c}{t_w} \le \lambda_{rw} = 5.7\sqrt{\frac{E}{F_{yc}}} \qquad \text{Equation 6.4.5.5.2.1-2}$$

AASHTO LRFD Equation 6.10.6.2.3-1

This limit applies to composite sections in negative flexure and non-composite sections and distinguishes a non-slender versus a slender-web section. For sections with webs satisfying this limit (i.e. non-slender web sections), theoretical web bend buckling will not occur for elastic stress levels, computed according to beam theory, at or below F_{yc}. Therefore, for these sections, the web load-shedding

factor R_b (Section 6.4.5.6) will always equal 1.0 and the web bend-buckling checks described above need not be made. Both compact-web and noncompact-web sections fall into this category. Sections not satisfying this limit are termed slender-web sections, which rely on significant post bend-buckling resistance at the strength limit state. The slenderness limit, λ_{rw}, from Equation 6.4.5.5.2.1-2 is given in for different grades of steel as follows:

Table 6.4.5.5.2.1-1 Slenderness Limit, λ_{rw}, from Equation 6.4.5.5.2.1-2 for Different Grades of Steel

F_{yc} (ksi)	λ_{rw}
36.0	162
50.0	137
70.0	116
90.0	102
100.0	97

Although relatively rare, in certain cases, near points of permanent-load contraflexure, both edges of the web (top and bottom) may be in compression when the stresses in the steel and composite sections due to the moments of opposite sign are accumulated. This is particularly true when the concrete is considered to be effective in tension at the service limit state, as permitted in *AASHTO LRFD* Article 6.10.4.2.1 when certain specified conditions are satisfied. In such cases, the neutral axis lies above the web and Equation 6.4.5.5.2.1-1 cannot be used to compute *k*. Therefore, *AASHTO LRFD* Article 6.10.1.9.1 states that when both edges of the web are in compression, *k* for use in Equation 6.4.5.5.1-2 is to be taken equal to 7.2. This value is approximately equal to the theoretical bend-buckling coefficient for a web plate under uniform compression assuming fully restrained longitudinal edge conditions along the flanges (Timoshenko and Gere, 1961). Although such cases are infrequent and the accumulated web compressive stresses are usually small and unlikely to be critical when this occurs, a *k* value is still provided in the specification to allow these cases to be considered in computer software.

EXAMPLE

Calculate the web bend-buckling resistance, F_{crw}, for the composite section shown in Figure 6.4.2.3.2.3-1, which is in a region of positive flexure, using Equation 6.4.5.5.1-2 and Equation 6.4.5.5.2.1-1. Grade 50W steel is assumed for the flanges and web (i.e., the hybrid factor R_h = 1.0). Perform the calculation for the non-composite section for the constructibility check; i.e. check *AASHTO LRFD* Equation 6.10.3.2.1-3 (Section 6.5.3.5).

The maximum accumulated unfactored positive moment at this section due to the deck-casting sequence plus the steel weight, which is assumed to be +2,889 kip-ft,

is used in this check. The load combination to investigate for maximum force effects acting on the fully erected steel frame during construction, specified in AASHTO LRFD Article 3.4.2.1 (Section 3.9.2.2), will be applied. From separate calculations, the stress in the top (compression) flange due to the factored loads for this load combination is computed to be f_{bu} = 1.4(-21.93) = -30.70 ksi. From earlier section property calculations (Section 6.4.2.3.2.3), D_c for the steel section is computed to be (39.63 in. – 1.0 in.) = 38.63 in. Since the web slenderness $2D_c/t_w$ of 154.5 exceeds λ_{rw} = 137 for 50-ksi steel from Equation 6.4.5.5.2.1-2 (Table 6.4.5.5.2.1-1), the steel section is a slender-web section and web bend-buckling must be checked. The resistance factor for flexure ϕ_f is equal to 1.0 (*AASHTO LRFD* Article 6.5.4.2).

$$k = \frac{9}{(D_c/D)^2}$$

$$k = \frac{9}{(38.63/69.0)^2} = 28.7$$

$$F_{crw} = \frac{0.9Ek}{\left(\frac{D}{t_w}\right)^2}$$

$$F_{crw} = \frac{0.9(29{,}000)(28.7)}{\left(\frac{69.0}{0.5}\right)^2} = 39.33 \text{ ksi}$$

$$F_{yw}/0.7 = 50/0.7 = 71.43 \text{ ksi}$$

$$R_h F_{yc} = (1.0)(50) = 50.00 \text{ ksi (controls)} > 39.33 \text{ ksi} \quad \text{ok}$$

According to *AASHTO LRFD* Equation 6.10.3.2-1-3:

$$f_{bu} \le \phi_f F_{crw}$$

$$f_{bu} = |-30.70 \text{ ksi}| < \phi_f F_{crw} = (1.0)(39.33) = 39.33 \text{ ksi} \quad \text{ok}$$

As specified in *AASHTO LRFD* Article 6.10.4.2.2, for composite sections in positive flexure without longitudinal stiffeners (i.e. satisfying the web slenderness requirement of *AASHTO LRFD* Article 6.10.2.1.1), a web bend-buckling check is not required at the service limit state.

EXAMPLE

Calculate the web bend-buckling resistance, F_{crw}, for the hybrid composite section shown in Figure 6.4.2.3.3.3-1, which is in a region of negative flexure, using Equation 6.4.5.5.1-2 and Equation 6.4.5.5.2.1-1.

First, perform the calculation for the non-composite section for the constructibility check; i.e. check *AASHTO LRFD* Equation 6.10.3.2.1-3. The maximum accumulated unfactored negative moment at this section due to the deck-casting sequence plus the steel weight, which is assumed to be -4,918 kip-ft, is used in this check. The load combination to investigate for maximum force effects acting on the fully erected steel frame during construction, specified in AASHTO LRFD Article 3.4.2.1 (Section 3.9.2.2), will be applied. From separate calculations, the stress in the bottom (compression) flange due to the factored loads is computed to be f_{bu} = 1.4(-18.74) = -26.24 ksi. From earlier section property calculations (Section 6.4.2.3.3.3), D_c for the steel section is computed to be (35.26 in. – 2.0 in.) = 33.26 in. Since the web slenderness $2D_c/t_w$ of 118.3 exceeds λ_{rw} = 116 for 70-ksi steel from Equation 6.4.5.5.2.1-2 (Table 6.4.5.5.2.1-1), the steel section is a slender-web section and web bend-buckling must be checked. The resistance factor for flexure ϕ_f is equal to 1.0 (AASHTO LRFD Article 6.5.4.2). The hybrid factor, R_h (Section 6.4.5.7), for the steel section alone is computed to be 0.983 from separate calculations.

$$k = \frac{9}{(D_c/D)^2}$$

$$k = \frac{9}{(33.26/69.0)^2} = 38.7$$

$$F_{crw} = \frac{0.9Ek}{\left(\frac{D}{t_w}\right)^2}$$

$$F_{crw} = \frac{0.9(29{,}000)(38.7)}{\left(\frac{69.0}{0.5625}\right)^2} = 67.13 \text{ ksi}$$

$$F_{yw}/0.7 = 50/0.7 = 71.43 \text{ ksi}$$

$$R_h F_{yc} = (0.983)(70) = 68.81 \text{ ksi (controls)} > 67.13 \text{ ksi} \quad \text{ok}$$

According to *AASHTO LRFD* Equation 6.10.3.2-1-3:

$$f_{bu} \le \phi_f F_{crw}$$

$$f_{bu} = \left|-26.24 \text{ ksi}\right| < \phi_f F_{crw} = (1.0)(67.13) = 67.13 \text{ ksi} \quad \text{ok}$$

For sections in negative flexure, a web bend-buckling check is also required at the service limit state according to *AASHTO LRFD* Article 6.10.4.2.2. Therefore, perform the calculation for Load Combination Service II (Section 3.10.1.3.3) and assume that the appropriate conditions specified in *AASHTO LRFD* Article 6.10.4.2.1 are met to allow the concrete deck to be considered effective in tension for this load combination. Check *AASHTO LRFD* Equation 6.10.4.2.2-4 for this condition (Section 6.5.4.3.2.2). From earlier computations (Section 6.4.5.4.1.3), D_c for this case, which is a function of the accumulated stresses, was calculated to be 42.02 in., and the Service II stress in the compression flange due to the factored loads, f_c, was calculated to be -38.93 ksi. From separate calculations, the hybrid factor, R_h (Section 6.4.5.7), for the composite section is computed to be 0.977.

$$k = \frac{9}{\left(42.02/69.0\right)^2} = 24.3$$

$$F_{crw} = \frac{0.9(29{,}000)(24.3)}{\left(\dfrac{69.0}{0.5625}\right)^2} = 42.15 \text{ ksi}$$

$$F_{yw}/0.7 = 50/0.7 = 71.43 \text{ ksi}$$

$$R_h F_{yc} = (0.977)(70) = 68.39 \text{ ksi (controls)} > 42.15 \text{ ksi} \quad \text{ok}$$

According to *AASHTO LRFD* Equation 6.10.4.2.2-4:

$$f_c \le F_{crw}$$

$$f_c = \left|-38.93 \text{ ksi}\right| < F_{crw} = 42.15 \text{ ksi} \quad \text{ok}$$

6.4.5.5.2.2 Webs with Longitudinal Stiffeners

The bend-buckling coefficient, *k*, for webs with longitudinal stiffeners (Figure 6.4.5.5.2.2-1) depends on the distance from the centerline of the closest longitudinal stiffener to the inner surface of compression flange, d_s, with respect to the optimum location of the stiffener, which is at d_s/D_c = 0.4. The value of *k* to be substituted in

Equation 6.4.5.5.1-2 is therefore given by *AASHTO LRFD* Equation 6.10.1.9.2-1 or *AASHTO LRFD* Equation 6.10.1.9.2-2 as follows:

- If $\frac{d_s}{D_c} \geq 0.4, \text{then:}$

$$k = \frac{5.17}{(d_s/D)^2} \geq \frac{9}{(D_c/D)^2} \qquad \text{Equation 6.4.5.5.2.2-1}$$

AASHTO LRFD Equation 6.10.1.9.2-1

- If $\frac{d_s}{D_c} < 0.4, \text{then:}$

$$k = \frac{11.64}{\left(\frac{D_c - d_s}{D}\right)^2} \qquad \text{Equation 6.4.5.5.2.2-2}$$

AASHTO LRFD Equation 6.10.1.9.2-2

For existing riveted girders, d_s should be taken between the gage line of the closest angle longitudinal stiffener to the inner leg of the compression-flange element. The development of these equations is discussed in Frank and Helwig (1995). In cases where Equation 6.4.5.5.2.2-1 controls, the longitudinal stiffener is below its optimum location and web bend-buckling occurs in the panel between the stiffener and the compression flange. In cases where Equation 6.4.5.5.2.2-2 controls, the stiffener is above its optimum location and web bend-buckling occurs in the panel between the stiffener and the tension flange. In cases where d_s is equal to $0.4D_c$ (i.e. the stiffener is located at its optimum position), web bend-buckling theoretically occurs simultaneously in both panels, in which case, both equations yield a k value of 129.3 for the case of a doubly symmetric girder. Note that both equations for k assume simply supported longitudinal edge conditions along the flanges.

Figure 6.4.5.5.2.2-1 I-Girder with Longitudinal Web Stiffeners

Studies on non-composite girders have indicated that the optimum location of one longitudinal stiffener is $0.4D_c$ for bending and $0.5D$ for shear. The distance $0.4D_c$ is recommended as the optimum location because shear is almost always accompanied by moment and because a properly proportioned longitudinal stiffener can effectively control lateral web deflections under both bending (Cooper, 1967) and shear.

Changes in flange size can cause D_c to vary along the girder length. Also, as discussed below, D_c in a composite girder is a function of the applied load. Because D_c may vary along the span, it is suggested that the longitudinal stiffener be located based on D_c computed at the section with the largest compressive flexural stress. Since the longitudinal stiffener is normally located a fixed distance from the compression flange, the stiffener cannot be at its optimum location at other sections along the girder length with a lower stress and a different D_c. These sections must also be examined to ensure that they satisfy the specified limit states. *AASHTO LRFD* Article 6.10.11.3.1 requires that longitudinal stiffeners be located at a vertical position on the web such that Equation 6.4.5.5.1-2 is satisfied to prevent web bend-buckling when checking constructibility, and at the service limit state. In addition, the stiffener must be located to satisfy all other appropriate design requirements at the strength limit state. Several trial locations of the stiffener may need to be investigated to determine an appropriate location, particularly for composite sections in regions of positive flexure.

The calculated web bend-buckling resistance for composite sections in positive flexure is different before and after placement of the deck and is a function of the applied loading. D_c of the steel section is typically large for non-composite loadings during construction and web bend-buckling must be checked. In a longitudinally stiffened girder, D_c for the composite girder can also be large enough at the service

limit state in regions of positive flexure that web bend-buckling may still be of concern. D_c in this case must be calculated based on the accumulated flexural stresses due to the factored loads using Equation 6.4.5.4.1.2-1.

It is suggested that for composite sections in negative flexure, the longitudinal stiffener initially be located at $0.4D_c$ from the inner surface of the compression flange at the section with the maximum factored compressive vertical bending stress at the strength limit state, with D_c calculated for the section consisting of the steel girder plus the longitudinal reinforcement. For non-composite sections, D_c would be based on the section consisting of the steel girder alone. Based on the required bend-buckling checks and other strength limit state checks, the stiffener may have to be moved up or down from this initial trial position, especially in cases where the concrete deck is assumed effective in tension in regions of negative flexure at the service limit state. D_c in this case must also be calculated based on the accumulated stresses using Equation 6.4.5.4.1.2-1.

Because simply supported boundary conditions were assumed in the development of Equation 6.4.5.5.2.2-1 and Equation 6.4.5.5.2.2-2, it is possible at locations where the longitudinal stiffener is located at an inefficient position for a particular condition, that the web bend-buckling resistance of the longitudinally stiffened web is less than that computed for a web of the same dimensions without longitudinal stiffeners. This anomaly is due to the fact that Equation 6.4.5.5.2.1-1 for determining k for webs without longitudinal stiffeners was derived assuming partial rotational restraint of the web panel by the flanges. Therefore, the k value from Equation 6.4.5.5.2.1-1 serves as a lower limit on the k value for a longitudinally stiffened web panel computed from Equation 6.4.5.5.2.2-1. This lower limit is not applied to Equation 6.4.5.5.2.2-2 because it would never control in this case. Also, as discussed previously for webs without longitudinal stiffeners, k is to be taken equal to 7.2 for the rare case in which both edges of the longitudinally stiffened web are in compression.

It may be necessary, or desirable, in regions where the web undergoes stress reversal to use two longitudinal stiffeners on the web. Equation 6.4.5.5.2.2-1 and Equation 6.4.5.5.2.2-2 conservatively neglect any benefit of placing more than one longitudinal stiffener on the web. However, *AASHTO LRFD* Article 6.10.1.9.2 does permit the Engineer to perform a direct buckling analysis of a web panel with multiple longitudinal stiffeners, if desired, to determine F_{crw} or k for this case. Simply supported boundary conditions should be assumed at the flanges and at the longitudinal stiffener locations in such an analysis. If F_{crw} determined from the bucking analysis is greater than or equal to F_{yc}, then the girder may be proportioned using a web load-shedding factor, R_b (Section 6.4.5.6), equal to 1.0. The termination of longitudinal stiffeners in these regions is problematic in that a punitive Category E or E' detail exists at the end of the stiffener-to-web welds **unless an appropriate transition radius is provided at the termination** (refer to *AASHTO LRFD* Table 6.6.1.2.3-1 – Condition 4.3). One way to address this issue is to continue a single

longitudinal stiffener from the positive moment region to the negative moment region. A single longitudinal stiffener can be extended over both regions by bending the stiffener from the top portion of the web in the positive moment region to the bottom portion in the negative moment region. Hence, in the contraflexure region, the stiffener will pass through the mid-height of the web. As noted above, the current specification provisions permit the computation of the web bend-buckling resistance with the longitudinal stiffener located at any position on the web.

Rearranging Equation 6.4.5.5.1-2 yields the web slenderness, D/t_w, at or below which theoretical web bend buckling will not occur for elastic stress levels, computed according to beam theory, at or below F_{yc}:

$$\frac{D}{t_w} \le 0.95\sqrt{\frac{Ek}{F_{yc}}} \qquad \text{Equation 6.4.5.5.2.2-3}$$

AASHTO LRFD Equation 6.10.1.10.2-1

The web load-shedding factor, R_b (Section 6.4.5.6), will always equal 1.0 for sections satisfying this limit. Based on the k value of 129.3 for the case of a doubly symmetric girder, i.e. $D_c = 0.5D$, with a single longitudinal stiffener located at the optimum position on the web, i.e. $d_s = 0.4D_c$, the slenderness limit from Equation 6.4.5.5.2.2-3 is given as follows for different grades of steel:

Table 6.4.5.5.2.2-1 Slenderness Limit from Equation 6.4.5.5.2.2-3 for Different Grades of Steel

F_{yc} (ksi)	$0.95\sqrt{Ek/F_{yc}}$
36.0	300
50.0	260
70.0	220
90.0	194
100.0	184

The limiting D/t_w will generally be less than the value shown in the preceding table for singly symmetric girders with $D_c/D > 0.5$, and/or where a single longitudinal stiffener is not located at its optimum position.

The design of longitudinal web stiffeners for both I- and box sections is covered in *AASHTO LRFD* Article 6.10.11.3 and discussed in Section 6.6.6.4.

EXAMPLE

Calculate the web bend-buckling resistance, F_{crw}, for the longitudinally stiffened section shown in Figure 6.4.5.5.2.2-2, which is in a region of positive flexure, using Equation 6.4.5.5.1-2 and Equation 6.4.5.5.2.2-1 or Equation 6.4.5.5.2.2-2, as applicable. Grade 50W steel is assumed for the flanges and web (i.e. the hybrid factor R_h = 1.0).

First, calculate F_{crw} for the non-composite section for the constructibility check; i.e. check *AASHTO LRFD* Equation 6.10.3.2.1-3. The maximum accumulated unfactored positive moment at this section due to the deck-casting sequence, which is assumed to be +11,750 kip-ft, is used in this check. The unfactored moment due to the steel weight at this section is assumed to be +6,480 kip-ft. The load combination to investigate for maximum force effects acting on the fully erected steel frame during construction, specified in AASHTO LRFD Article 3.4.2.1 (Section 3.9.2.2), will be applied. From separate calculations, the stress in the top (compression) flange due to the factored loads is computed to be f_{bu} = 1.4(-24.24) = -33.94 ksi. D_c for the steel section is computed to be 85.29 in. The resistance factor for flexure ϕ_f is equal to 1.0 (*AASHTO LRFD* Article 6.5.4.2).

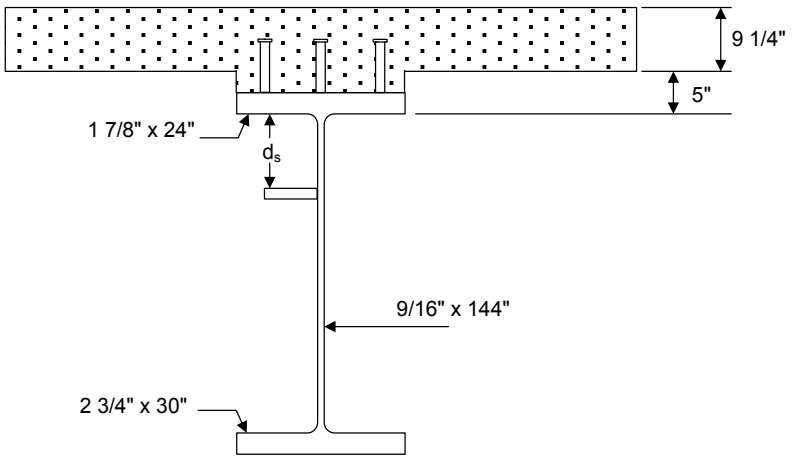

Figure 6.4.5.5.2.2-2 Longitudinally Stiffened Girder Section – Positive Flexure Region

Try locating the stiffener initially at the theoretical optimum location:

$$d_s = 0.4D_c = 0.4(85.29) = 34.12 \text{ in.}$$

Therefore, use Equation 6.4.5.5.2.2-1 to calculate the bend-buckling coefficient, *k*.

$$k = \frac{5.17}{(d_s/D)^2} \geq \frac{9}{(D_c/D)^2}$$

$$k = \frac{5.17}{(34.12/144.0)^2} = 92.09$$

$$\frac{9}{(85.29/144.0)^2} = 25.65 < 92.09 \quad \text{ok}$$

$$F_{crw} = \frac{0.9Ek}{\left(\frac{D}{t_w}\right)^2}$$

$$F_{crw} = \frac{0.9(29{,}000)(92.09)}{\left(\frac{144.0}{0.5625}\right)^2} = 36.68 \text{ ksi}$$

$$F_{yw}/0.7 = 50/0.7 = 71.43 \text{ ksi}$$

$$R_h F_{yc} = (1.0)(50) = 50.00 \text{ ksi (controls)} > 36.68 \text{ ksi} \quad \text{ok}$$

According to *AASHTO LRFD* Equation 6.10.3.2.1-3:

$$f_{bu} \leq \phi_f F_{crw}$$

$$f_{bu} = |-33.94 \text{ ksi}| < \phi_f F_{crw} = (1.0)(36.68) = 36.68 \text{ ksi} \quad \text{ok}$$

For sections with longitudinal stiffeners, a web bend-buckling check is also required at the service limit state for composite sections in positive flexure; i.e. check *AASHTO LRFD* Equation 6.10.4.2.2-4. From separate computations, under Load Combination Service II (Section 3.10.1.3.3), the stress in the compression flange, f_c, is –32.36 ksi, and the stress in the tension flange, f_t, is +37.66 ksi. Since D_c for the composite section in this case is a function of the accumulated factored stresses, use Equation 6.4.5.4.1.2-1 as follows:

$$D_c = \left(\frac{-f_c}{|f_c| + f_t}\right) d - t_{fc} \geq 0$$

$$d = 2.75 + 144.0 + 1.875 = 148.63 \text{ in.}$$

$$t_{fc} = 1.875 \text{ in.}$$

$$D_c = \left(\frac{-(-32.36)}{|-32.36| + 37.66} \right) 148.63 - 1.875 = 66.81 \text{ in.}$$

Since d_s = 34.12 in. is also greater than $0.4D_c$ = 0.4(66.81) = 26.72 in. in this case, again use Equation 6.4.5.5.2.2-1 to compute k:

$$k = \frac{5.17}{(34.12/144.0)^2} = 92.09$$

$$\frac{9}{(66.81/144.0)^2} = 41.81 < 92.09 \quad \text{ok}$$

$$F_{crw} = 36.68 \text{ ksi}$$

According to *AASHTO LRFD* Equation 6.10.4.2.2-4:

$$f_c \le F_{crw}$$

$$f_c = |-32.36 \text{ ksi}| < F_{crw} = 36.68 \text{ ksi} \quad \text{ok}$$

Separate checks are also necessary to ensure that the section has adequate nominal flexural resistance at the strength limit state with the longitudinal stiffener in this position. In this particular instance, using the theoretical optimum location of the stiffener as the initial trail location worked well. However, this may not always be the case. Checks at other sections in the positive flexure region (where the stiffener may not be located at the optimum position) could also potentially require the stiffener to be moved to a different position.

Checks for sections in negative flexure are similar to those illustrated above for webs without longitudinal stiffeners, except that the appropriate *k* value from Equation 6.4.5.5.2.2-1 or Equation 6.4.5.5.2.2-2 is used to compute F_{crw}. As recommended above, it is suggested that the longitudinal stiffener initially be located at $0.4D_c$ from the inner surface of the compression flange at the section with the maximum flexural compressive stress due to the factored loads at the strength limit state, with D_c calculated for the section consisting of the steel girder plus the longitudinal reinforcement for composite sections and the steel girder alone for non-composite sections.

6.4.5.6 Web Load-Shedding Factor, R_b

As discussed in Section 6.4.5.5, once the theoretical web bend-buckling load is reached, a slender-web section does not fail but has significant post-buckling resistance that can be utilized at the strength limit state. As buckling of the compression zone of the web increases, the ability of the web to carry its portion of the load, as computed by ordinary beam theory, decreases. However, this does not mean failure. Instead, a redistribution of stress to the stiffer longitudinal elements (i.e. the compression flange and the immediately adjacent portion of the web) occurs. The tension flange stress is not increased significantly by the shedding of the web compressive stresses. As a result, for a given moment, the stress in the compression portion of the web that is deflecting laterally is less than that calculated for a linear distribution and the stress in the compression flange is greater, as illustrated in Figure 6.4.5.6-1. Therefore, yielding may occur in the compression flange before the yield moment calculated from ordinary beam theory is attained.

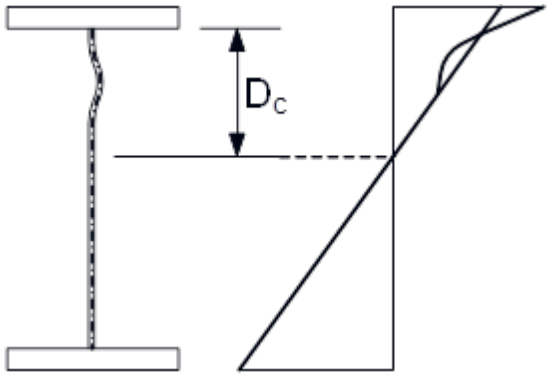

Figure 6.4.5.6-1 Load Shedding from the Web to the Compression Flange

To account for this postbuckling resistance in the design of a slender-web section at the strength limit state, or a section with a web slenderness exceeding λ_{rw} as given by Equation 6.4.5.5.2.1-2, an approximate method was needed to account for the extra load the compression flange must carry after the web becomes partially ineffective. Basler and Thurlimann (1961) developed such an approach by assuming a linear distribution of stress acting on an effective cross-section, with the nominal flexural resistance, M_n, reached when the extreme fiber of this effective section in compression reached either the yield stress or a critical buckling stress, as applicable. The effective section assumed that a portion of the web in which the buckling (or out-of-plane deformation) occurs becomes ineffective (Figure 6.4.5.6-2).

An effective width, b_e, equal to $30t_w$ for a web with a slenderness D/t_w of about 345 was assumed. This value was the limiting slenderness to preclude the failure mode of vertical flange buckling, or buckling of the compression flange into the web, for 33,000-psi yield strength steel at an assumed web-to-flange area ratio A_w/A_f of 2

(where A_f is the area of each flange), and at an assumed residual tension stress level of 16.5 ksi. The nominal flexural resistance was then assumed to increase linearly from the resistance of this effective section up to a value of M_y at a web slenderness of λ_{rw}. A more general linear equation containing A_w/A_f as a parameter was then developed as follows:

$$\frac{M_n}{M_y} = 1 - 0.0005\frac{A_w}{A_f}\left(\frac{D}{t_w} - \lambda_{rw}\right) \qquad \text{Equation 6.4.5.6-1}$$

The expression on the right-hand side of Equation 6.4.5.6-1 has come to be known as the web load-shedding factor, R_b. The load-shedding factor, which is less than or equal to 1.0, can be used to either reduce the section modulus to the compression flange effectively increasing the compression-flange stress, or to reduce the nominal flexural resistance of the compression flange. Design specifications, including the *AASHTO LRFD* Specifications, have traditionally followed the latter course. In the *AASHTO LRFD* Specifications, the web load-shedding factor to be applied to the nominal flexural resistance of the compression flange at the strength limit state is specified in *AASHTO LRFD* Article 6.10.1.10.2. Note that the effect of load shedding to the compression flange is not considered significant and is ignored whenever the nominal flexural resistance exceeds the yield moment M_y.

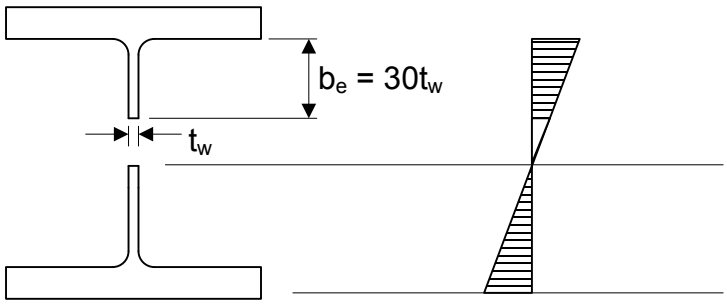

Figure 6.4.5.6-2 Effective Cross-Section Assumed in the Derivation of R_b

The preceding equation assumes that the ratio of A_w/A_f does not exceed approximately 3. To accommodate larger ratios up to 10, the *AASHTO LRFD* Specifications utilize a form of the more general equation developed by Basler (Cooper, 1967), in which the coefficient of 0.0005 in Equation 6.4.5.6-1 is replaced by the following coefficient:

$$\frac{a_r}{1200 + 300a_r} \qquad \text{Equation 6.4.5.6-2}$$

where:

a_r = A_w/A_{fc}
A_{fc} = area of the compression flange (in.^{2})

The ratio of the web area to the compression-flange area will always be less than or equal to 5.45 for sections with flanges satisfying the minimum flange proportioning requirements given by *AASHTO LRFD* Equations 6.10.2.2-2 and 6.10.2.2-3 in the *AASHTO LRFD* Specifications (i.e. $b_f \geq D/6$ and $t_f \geq 1.1t_w$, respectively). Hence, even though the modified coefficient given by Equation 6.4.5.6-2 is used, it is not necessary to specify the limiting ratio of 10.

Furthermore, to better accommodate singly symmetric sections, the *AASHTO LRFD* Specifications have replaced a_r in Equation 6.4.5.6-2 with a_{wc}, where a_{wc} is typically equal to the ratio of two times the web area in compression to the area of the compression flange. In addition, D/t_w in Equation 6.4.5.6-1 is replaced by the effective web slenderness ratio, $2D_c/t_w$, resulting in the following equation for R_b given as Equation 6.10.1.10.2-3 in the *AASHTO LRFD* Specifications:

$$R_b = 1 - \left(\frac{a_{wc}}{1200 + 300a_{wc}}\right)\left(\frac{2D_c}{t_w} - \lambda_{rw}\right) \leq 1.0 \qquad \text{Equation 6.4.5.6-3}$$

AASHTO LRFD Equation 6.10.1.10.2-3

where:

a_{wc} = $2D_c t_w / b_{fc} t_{fc}$
b_{fc} = width of the compression flange (in.)
t_{fc} = thickness of the compression flange (in.)

For compression flanges that have cover plates, the cover-plate area may be added to the compression-flange area in the denominator of the equation for a_{wc}.

The denominator (under the radical) of λ_{rw} in Equation 6.4.5.6-3 in previous specifications was the actual compression-flange bending stress due to the factored loads rather than F_{yc}. While this refinement can lead to an increase in the value of R_b in some cases, the increase is not likely to be overly significant. Also, using the actual flange stress to compute the nominal flexural resistance can lead to difficulties in load rating since the flexural resistance is a function of the applied load. Therefore, F_{yc} is now conservatively utilized in the equation for λ_{rw}.

The concrete deck acting as a compression-flange element typically contributes a large fraction of the flexural resistance at composite sections subject to positive flexure. To account for this in an approximate fashion in a longitudinally stiffened composite section in these regions, which may be subject to web bend-buckling at the strength limit state, a fraction of the transformed concrete deck area based conservatively on the long-term 3*n* composite section may be included with the steel compression-flange area in computing the a_{wc} term in Equation 6.4.5.6-3 as follows:

$$a_{wc} = \frac{2D_c t_w}{b_{fc} t_{fc} + b_s t_s \left(1 - f_{DC1}/F_{yc}\right)/3n}$$ Equation 6.4.5.6-4

AASHTO LRFD Equation 6.10.1.10.2-6

where:

b_s = effective flange width of the concrete deck (in.)
f_{DC1} = compression flange vertical bending stress caused by the factored permanent load applied before the concrete deck has hardened or is made composite (ksi)
t_s = thickness of the concrete deck (in.)

For these sections, D_c in Equation 6.4.5.6-4 is a function of the accumulated stresses and must therefore be calculated using Equation 6.4.5.4.1.2-1.

As discussed previously in Section 6.4.5.5, for composite sections in positive flexure *without* longitudinal stiffeners, web bend-buckling is not considered a concern, and therefore, the R_b factor is always taken equal to 1.0 for these sections according to *AASHTO LRFD* Article 6.10.1.10.2. Even if this were not specified to be the case, including the transformed concrete area in the a_{wc} term for these sections as shown in Equation 6.4.5.6-4, would likely ensure a value of R_b equal to 1.0 in most every case.

For composite sections in negative flexure, D_c in Equation 6.4.5.6-3 should conservatively be computed using the section consisting of the steel girder plus the longitudinal deck reinforcement.

One-half of the effective box flange width should be used in conjunction with one top flange and a single web in calculating R_b for a tub section, as indicated in *AASHTO LRFD* Article C6.11.8.2.2. The effective box flange width is defined in *AASHTO LRFD* Article 6.11.1.1. One-half of the effective top and bottom box flange width should be used in conjunction with a single web for a closed-box section.

AASHTO LRFD Article 6.10.1.10.2 lists the four specific conditions for which the R_b factor may be explicitly taken equal to 1.0 as follows:

- When the section is composite and in a region of positive flexure and the web slenderness D/t_w does not exceed 150 (i.e. longitudinal web stiffeners are not required);
- When checking constructibility according to the provisions of *AASHTO LRFD* Article 6.10.3.2 (since the web bend-buckling resistance F_{crw} must not be exceeded during construction as discussed in Section 6.4.5.5);
- When one or more longitudinal web stiffeners are provided and Equation 6.4.5.5.2.2-3 is satisfied (i.e. whenever the web slenderness D/t_w does not

exceed the slenderness at or below which theoretical web bend buckling will not occur for elastic stress levels at or below F_{yc} at the strength limit state);

- When Equation 6.4.5.5.2.1-2 is satisfied for webs without longitudinal web stiffeners (i.e. whenever the web slenderness $2D_c/t_w$ does not exceed the noncompact-web slenderness limit λ_{rw} at or below which theoretical web bend buckling will not occur for elastic stress levels at or below F_{yc} at the strength limit state).

Otherwise, R_b must be calculated from Equation 6.4.5.6-3.

Bend buckling of longitudinally stiffened webs is prevented during construction and at the service limit state in the *AASHTO LRFD* Specifications, but is permitted at the strength limit state as discussed above. It should be noted, however, that the current longitudinal stiffener proportioning requirements given in *AASHTO LRFD* Article 6.10.11.3 do not ensure that a horizontal line of near zero lateral deflection will be maintained throughout the post-buckling response of the web. As a result, when computing R_b from Equation 6.4.5.6-3 at the strength limit state for longitudinally stiffened webs in regions of positive or negative flexure, the presence of the longitudinal stiffeners is conservatively ignored (i.e. the noncompact-web slenderness limit λ_{rw} is used in Equation 6.4.5.6-3 rather than the limiting slenderness to prevent theoretical web bend buckling in longitudinally stiffened webs given by Equation 6.4.5.5.2.2-3). Further research is ongoing at Georgia Tech as of this writing (2015) on the post-buckling response of longitudinally stiffened webs.

In the specifications, bend buckling of the web is not considered to have any effect on the shear buckling resistance of the web (and vice versa). The shear resistance of slender-web sections is not reduced as a result of bend buckling (and vice versa) because in such webs, most of the shear resistance results from tension-field action (refer to Section 6.5.7) with only a small contribution from the portion of the web adjacent to the flange.

EXAMPLE

Calculate the web load-shedding factor, R_b, at the strength limit state for the hybrid composite section (without longitudinal web stiffeners) shown in Figure 6.4.2.3.3.3-1, which is in a region of negative flexure.

First, determine if R_b is indeed less than 1.0 by checking Equation 6.4.5.5.2.1-2. For sections in negative flexure at the strength limit state, use D_c for the section consisting of the steel girder plus the longitudinal reinforcement (*AASHTO LRFD* Article D6.3.1).

$$\frac{2D_c}{t_w} = \frac{2(36.96)}{0.5625} = 131.4$$

$$\frac{2D_c}{t_w} > \lambda_{rw} = 5.7\sqrt{\frac{E}{F_{yc}}} = 5.7\sqrt{\frac{29{,}000}{70}} = 116.0$$

Therefore, the section is a slender-web section subject to web bend-buckling at elastic stress levels at the strength limit state and R_b is less than 1.0. Calculate R_b from Equation 6.4.5.6-3:

$$R_b = 1 - \left(\frac{a_{wc}}{1200 + 300a_{wc}}\right)\left(\frac{2D_c}{t_w} - \lambda_{rw}\right) \le 1.0$$

where:

$$a_{wc} = \frac{2D_c t_w}{b_{fc} t_{fc}}$$

$$a_{wc} = \frac{2(36.96)(0.5625)}{20(2)} = 1.04$$

$$R_b = 1 - \left(\frac{1.04}{1200 + 300(1.04)}\right)(131.4 - 116.0) = 0.989$$

EXAMPLE

Calculate the web load-shedding factor, R_b, for the longitudinally stiffened section shown in Figure 6.4.5.5.2.2-2, which is in a region of positive flexure. Grade 50W steel is assumed for the flanges and web. The web bend-buckling coefficient was calculated in an earlier example (Section 6.4.5.5.2.2) to be k = 92.09 for this section.

First, determine if R_b is potentially less than 1.0 by checking Equation 6.4.5.5.2.2-3:

$$\frac{D}{t_w} = \frac{144}{0.5625} = 256.0$$

$$\frac{D}{t_w} > 0.95\sqrt{\frac{Ek}{F_{yc}}} = 0.95\sqrt{\frac{29{,}000(92.09)}{50}} = 219.6$$

Therefore, the section is subject to web bend-buckling at elastic stress levels at the strength limit state. Calculate R_b from Equation 6.4.5.6-3:

$$R_b = 1 - \left(\frac{a_{wc}}{1200 + 300 a_{wc}} \right) \left(\frac{2D_c}{t_w} - \lambda_{rw} \right) \leq 1.0$$

For composite longitudinally stiffened sections in positive flexure, the term, a_{wc}, is calculated from Equation 6.4.5.6-4 as follows, which includes a fraction of the transformed concrete deck along with the steel compression-flange area:

$$a_{wc} = \frac{2D_c t_w}{b_{fc} t_{fc} + b_s t_s \left(1 - f_{DC1} / F_{yc}\right) / 3n}$$

From separate computations, under Load Combination Strength I (Section 3.9.1.2.2), the stress in the compression flange, f_c, is –41.63 ksi, and the stress in the tension flange, f_t, is +49.34 ksi. Since D_c for the composite section in this case is a function of the accumulated factored stresses, use Equation 6.4.5.4.1.2-1 as follows:

$$D_c = \left(\frac{-f_c}{|f_c| + f_t} \right) d - t_{fc} \geq 0$$

$$d = 2.75 + 144.0 + 1.875 = 148.63 \text{ in.}$$

$$t_{fc} = 1.875 \text{ in.}$$

$$D_c = \left(\frac{-(-41.63)}{|-41.63| + 49.34} \right) 148.63 - 1.875 = 66.14 \text{ in.}$$

$$\frac{2D_c}{t_w} = \frac{2(66.14)}{0.5625} = 235.2$$

$$\lambda_{rw} = 5.7 \sqrt{\frac{E}{F_{yc}}} = 5.7 \sqrt{\frac{29{,}000}{50}} = 137.3$$

From separate calculations, the compression-flange stress at the strength limit state (Strength I) caused by the factored permanent load applied before the concrete deck has hardened is f_{DC1} = -25.52 ksi. The modular ratio n is equal to 8. The effective flange width of the concrete deck is b_s = 123.0 in. Therefore:

$$a_{wc} = \frac{2(66.14)(0.5625)}{(24.0)(1.875)+(123.0)(9.25)\left(1-\left|-25.52\right|/50\right)/24} = 1.091$$

$$R_b = 1-\left(\frac{1.091}{1200+300(1.091)}\right)(235.2-137.3) = 0.930$$

6.4.5.7 Hybrid Factor, R_h

Hybrid girders were defined and discussed previously in Section 6.4.4. Section 6.4.5.6 discussed the redistribution of stress that occurs in slender-web sections from the compression zone of the web to the compression flange as a result of localized bend buckling of the web. A similar redistribution of stress from the web to the flanges occurs in hybrid sections as a result of the early localized yielding of the lower strength web; the primary difference being that in the case of the hybrid section, the redistribution occurs to both the compression and tension flanges (Figure 6.4.5.7-1). In the first case, the web load-shedding factor, R_b, is used to account for the reduced contribution of the web to the nominal flexural resistance resulting from web bend buckling. In the case of the hybrid section, the hybrid factor, R_h, is used to account for the effect of earlier yielding of the lower strength steel in the web.

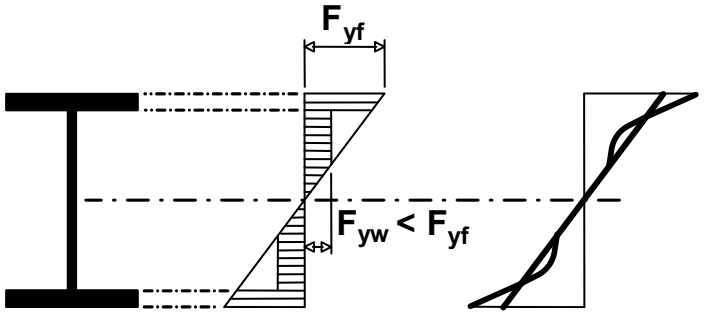

Figure 6.4.5.7-1 Load Shedding from the Web to the Flanges Due to Early Web Yielding in a Hybrid Section

As is the case with the load-shedding factor, the hybrid factor, which is less than or equal to 1.0, can be used to either reduce the section modulus to each flange effectively increasing the flange stresses, or to reduce the nominal flexural resistance of each flange. Again, design specifications, including the *AASHTO LRFD* Specifications, have traditionally followed the latter course. In the *AASHTO LRFD* Specifications, the hybrid factor to be applied to the nominal flexural resistance of each flange of a hybrid section is specified in *AASHTO LRFD* Article 6.10.1.10.1. For rolled shapes, which are obviously homogeneous sections based on the nominal yield strength, homogeneous built-up sections and built-up sections

with a higher-strength steel in the web than in both flanges, R_h is to be explicitly taken equal to 1.0 according to *AASHTO LRFD* Article 6.10.1.10.1.

The specification allows the Design Engineer to compute R_h for all other cases based on a direct iterative strain compatibility analysis. In lieu of such an analysis, the R_h factor is to be determined as follows:

$$R_h = \frac{12 + \beta\left(3\rho - \rho^3\right)}{12 + 2\beta} \qquad \text{Equation 6.4.5.7-1}$$

AASHTO LRFD Equation 6.10.1.10.1-1

where:

$\beta = \dfrac{2D_n t_w}{A_{fn}}$

ρ = the smaller of F_{yw}/f_n and 1.0

A_{fn} = sum of the flange area and the area of any cover plates on the side of the neutral axis corresponding to D_n (in.^{2}). For composite sections in negative flexure, the area of the longitudinal reinforcement may be included in calculating A_{fn} for the top flange.

D_n = larger of the distances from the elastic neutral axis of the cross-section to the inside face of either flange (in.). For sections where the neutral axis is at the mid-depth of the web, D_n is to be taken as the distance from the neutral axis to the inside face of the flange on the side of the neutral axis where yielding occurs first.

f_n = for sections where yielding occurs first in the flange, a cover plate or the longitudinal reinforcement on the side of the neutral axis corresponding to D_n, the largest of the specified minimum yield strengths of each component in the calculation of A_{fn} (ksi). Otherwise, the largest of the elastic stresses in the flange, cover plate or longitudinal reinforcement on the side of the neutral axis corresponding to D_n at first yield on the opposite side of the neutral axis.

Equation 6.4.5.7-1 is the basic fundamental equation for R_h originally derived for doubly symmetric I-sections (Frost and Schilling, 1964; Schilling, 1968) (or for sections where the elastic neutral axis is reasonably close to the mid-depth of the web), and included for such sections in previous *AASHTO LRFD Specifications*. Previous specifications also included a separate more complex R_h equation for singly symmetric composite sections subject to positive flexure (Schilling, 1968). The more complex equation for composite sections has been eliminated in the *AASHTO LRFD* Specifications in lieu of the basic Equation 6.4.5.7-1, which has been generalized to consider all possible combinations associated with different positions of the elastic neutral axis and different yield strengths of the top and bottom flange elements in a non-iterative fashion.

A “flange element” is considered to be a flange, a cover plate or plates attached to that flange or the longitudinal reinforcement (associated with the top flange only). Singly symmetric sections (both non-composite and composite) are handled using the base equation by focusing on the side of the neutral axis where nominal yielding occurs first, or the side of the neutral axis subject to the most extensive web yielding prior to first yielding of any flange element. All flange elements on the side of the neutral axis where nominal yielding occurs first are conservatively assumed to be located at the edge of the web in the calculation of R_h. In addition, any shift in the neutral axis caused by the effect of web yielding is considered negligible. These assumptions are similar to the assumptions made originally in the development of the R_h equation for singly symmetric composite sections (Schilling, 1968), and are not considered overly punitive since computed R_h values are typically close to 1.0.

The first step in computing R_h using Equation 6.4.5.7-1 is to determine D_n. According to the definition, D_n is to be taken as the larger of the distances from the elastic neutral axis of the cross-section to the inside face of either flange. The following suggestions are made regarding the calculation of D_n for composite sections:

- For composite sections in positive flexure, D_n may conservatively be taken as the distance from the neutral axis of the short-term *n*-composite section to the inside face of the bottom flange.
- Except as noted in the next bullet item, for composite sections in negative flexure, it is recommended that the elastic neutral axis based on the section consisting of the steel girder plus the longitudinal reinforcement be used in determining D_n.
- For composite sections in negative flexure at the service limit state in which the concrete deck is considered to be effective as permitted in *AASHTO LRFD* Article 6.10.4.2.1, D_n may conservatively be taken as the distance from the neutral axis of the short-term *n*-composite section to the inside face of the bottom flange. Note that when the concrete deck is *not* considered to be effective in negative flexure, the same value of R_h is used at the strength and service limit states.

In all of the above cases, a more accurate solution can be obtained by calculating the neutral axis location based on the sum of the accumulated factored stresses at the appropriate limit state. However, using the above suggested neutral axes locations for the computation in each case will prevent the flexural resistance from being a function of D_n, with D_n being a function of the applied load, which can result in potential complications in load rating. Also, significant differences in the calculated values of R_h, which are generally close to 1.0 in most cases as mentioned above, as a function of the neutral-axis location are not anticipated nor deemed worthy of introducing any additional complexity into the calculation.

In cases where the neutral axis is located at the mid-depth of the web, D_n is to be taken as the distance from the neutral axis to the inside face of the flange on the side of the neutral axis where yielding occurs first. Should yielding occur simultaneously on both sides of the neutral axis, D_n should be taken as the distance to the flange element with the smaller value of A_{fn}.

Once the value of D_n has been established, the next step is to calculate A_{fn}. A_{fn} is defined as the sum of the areas of the flange elements on the side of the neutral axis corresponding to D_n. This would include the flange area, the area of any cover plates, and for composite sections in negative flexure, the area of the longitudinal reinforcement if D_n happens to be measured to the top flange. With D_n and A_{fn} established, the constant β used in Equation 6.4.5.7-1 can then be calculated.

In order to calculate the constant ρ used in Equation 6.4.5.7-1, the stress f_n must first be calculated. According to the stated definition of f_n, for sections where nominal yielding occurs first in a flange element on the side of the neutral axis corresponding to D_n, which is the case in most instances, f_n is to be taken as the largest of the specified minimum yield strengths of each flange element included in the calculation of A_{fn}. Should yielding occur first on the other side of the neutral axis, f_n is to be taken as the largest of the calculated elastic stresses in the various flange elements on the side of the neutral axis corresponding to D_n when nominal first yielding occurs on the opposite side. f_n is then divided into the specified minimum yield strength of the web F_{yw} in order to determine ρ, which cannot exceed 1.0.

One-half of the effective box flange width should be used in conjunction with one top flange and a single web in calculating R_h for a tub section, as indicated in *AASHTO LRFD* Article C6.11.8.2.2. The effective box flange width is defined in *AASHTO LRFD* Article 6.11.1.1. One-half of the effective top and bottom box flange width should be used in conjunction with a single web for a closed-box section.

Finally, as discussed in *AASHTO LRFD* Article C6.10.3.2.1, for hybrid sections that are composite in the final condition, but that are non-composite during construction (i.e. sections in bridges built using unshored composite construction), R_h must be calculated separately for the non-composite and composite sections. For the constructibility design checks, R_h for the non-composite section would be applied, and for all subsequent checks in which the member is composite, R_h for the composite section would be applied. For constructibility checks of a hybrid girder where the factored flange flexural stress, f_{bu}, does not exceed the specified minimum yield strength of the web, R_h is to be taken equal to 1.0 (*AASHTO LRFD* Article 6.10.3.2).

EXAMPLE

Calculate the hybrid factor for the composite section shown in Figure 6.4.2.3.3.3-1, which is in a region of negative flexure. The flanges are Grade HPS 70W steel and the web is Grade 50W steel.

First, calculate D_n or the larger of the distances from the elastic neutral axis of the cross-section to the inside face of either flange. As recommended above, in most cases for composite sections in negative flexure, use the section consisting of the steel girder plus the longitudinal reinforcement to calculate D_n. From earlier calculations for this section, the distance from the neutral axis to the inside face of the top flange is 32.04 in. and to the inside face of the bottom flange is 36.96 in. Therefore, D_n is 36.96 in.

Next, calculate A_{fn} or the sum of the area of the flange elements on the side of the neutral axis corresponding to D_n. Since there are no cover plates and D_n is measured to the bottom flange, the only flange element contributing to A_{fn} is the bottom flange. Therefore, A_{fn} = 20(2) = 40.0 in^2.

$$\beta = \frac{2D_n t_w}{A_{fn}}$$

$$\beta = \frac{2(36.96)(0.5625)}{40.0} = 1.04$$

Since the flanges are the same yield strength, nominal yielding will occur first on the side of the neutral axis corresponding to D_n (separate calculations show that the 60-ksi longitudinal reinforcement does not yield first). For sections where nominal yielding occurs first in a flange element on the side of the neutral axis corresponding to D_n, f_n is taken as the largest of the specified minimum yield strengths of each flange element included in the calculation of A_{fn}. Therefore, f_n = 70.0 ksi.

$$\rho = \frac{F_{yw}}{f_n} = \frac{50.0}{70.0} = 0.714 \le 1.0$$

$$R_h = \frac{12 + \beta\left(3\rho - \rho^3\right)}{12 + 2\beta}$$

$$R_h = \frac{12 + 1.04\left[3(0.714) - (0.714)^3\right]}{12 + 2(1.04)} = 0.984$$

Assuming the concrete deck is *not* considered to be effective in negative flexure at the service limit state, this same value of R_h would be used for this section at the strength and service limit states.

If the concrete deck is considered to be effective in negative flexure at the service limit state, as permitted in *AASHTO LRFD* Article 6.10.4.2.1, a different value of R_h should be calculated for use in the service limit state design checks. As recommended above, in this case, D_n may conservatively be taken as the distance from the neutral axis of the short-term *n*-composite section to the inside face of the bottom flange. From separate calculations, this value is computed to be D_n = 57.21 in. Since D_n is measured to the bottom flange, A_{fn} = 20(2.0) = 40.0 in^2 and f_n = 70.0 ksi. Therefore:

$$\beta = \frac{2(57.21)(0.5625)}{40.0} = 1.61$$

$$\rho = 50.0/70.0 = 0.714$$

$$R_h = \frac{12 + 1.61\left[3(0.714) - (0.714)^3\right]}{12 + 2(1.61)} = 0.977$$

From earlier calculations (Section 6.4.5.4.1.3), the neutral axis location for this section (assuming the concrete is effective in negative flexure) was determined based on the sum of the accumulated factored stresses at the service limit state. Based on these calculations, D_n would be taken equal to 42.02 in. (versus 57.21 in. when based on the short-term composite section). Performing calculations similar to the above based on this smaller value of D_n would result in a value of R_h equal to 0.982. Although a slightly larger value of R_h is obtained in this case using the more accurate neutral axis location, the R_h factor is now a function of the applied load, which can potentially complicate rating calculations.

EXAMPLE

Calculate the hybrid factor for the section shown in Figure 6.4.2.3.2.3-1, which is in a region of positive flexure. Assume the top flange and web are Grade 50W steel and the bottom flange is Grade HPS 70W steel.

First, calculate R_h for the non-composite girder, which would be used in all the constructibility design checks for this section. From earlier calculations for the steel girder at this section, the distance from the neutral axis to the inside face of the top flange is 38.63 in. and to the inside face of the bottom flange is 30.38 in. Therefore, D_n is 38.63 in.

Next, calculate A_{fn} or the sum of the area of the flange elements on the side of the neutral axis corresponding to D_n. Since there are no cover plates and D_n is measured to the top flange, the only flange element contributing to A_{fn} is the top flange. Therefore, A_{fn} = 16(1) = 16.0 in.^{2}

$$\beta = \frac{2D_n t_w}{A_{fn}}$$

$$\beta = \frac{2(38.63)(0.5)}{16.0} = 2.414$$

Separate calculations indicate that nominal first yielding will occur in the Grade 50W top flange. For sections where nominal yielding occurs first in a flange element on the side of the neutral axis corresponding to D_n, f_n is taken as the largest of the specified minimum yield strengths of each flange element included in the calculation of A_{fn}. Therefore, f_n = 50.0 ksi.

$$\rho = \frac{F_{yw}}{f_n} = \frac{50.0}{50.0} = 1.0$$

$$R_h = \frac{12 + \beta\left(3\rho - \rho^3\right)}{12 + 2\beta}$$

$$R_h = \frac{12 + 2.414\left[3(1.0) - (1.0)^3\right]}{12 + 2(2.414)} = 1.0$$

Note that if the factored flange flexural stress for constructibility, f_{bu}, does not exceed the specified minimum yield strength of the web (i.e. F_{yw} = 50 ksi in this case), R_h is to simply be taken equal to 1.0 (in lieu of performing the preceding calculation), as specified in *AASHTO LRFD* Article 6.10.3.2.

Next, calculate R_h for the composite girder, which would be used in all the service and strength limit state design checks. As recommended above, in this case, D_n may conservatively be taken as the distance from the neutral axis of the short-term *n*-composite section to the inside face of the bottom flange. From earlier calculations (Section 6.4.2.3.2.3), this value is computed to be D_n = 59.78 in. Since D_n is measured to the bottom flange, A_{fn} = 18(1.375) = 24.75 in.^{2}

$$\beta = \frac{2(59.78)(0.5)}{24.75} = 2.415$$

Separate calculations indicate that nominal first yielding will occur in the Grade HPS 70W bottom flange. Therefore, f_n = 70.0 ksi.

$$\rho = \frac{F_{yw}}{f_n} = \frac{50.0}{70.0} = 0.714$$

$$R_h = \frac{12 + 2.415\left[3(0.714) - (0.714)^3\right]}{12 + 2(2.415)} = 0.968$$

6.4.6 Girder Stiffness Assumptions for Analysis

AASHTO LRFD Article 6.10.1.5 states that for loads applied to non-composite sections, the stiffness properties of the steel beam alone are to be used in the analysis of flexural members even though considerable unintended composite action occurs in such sections. This requirement applies to all loads applied to a non-composite girder, and to all loads applied to the bare steel section of a composite girder before the deck has hardened or is made composite.

In continuous spans, the composite section in negative moment regions will typically have a different stiffness for design calculations at the strength limit state because the concrete deck in tension is assumed cracked and not participating. Until recently, it was sometimes also assumed that the concrete in the negative moment regions between points of dead load contraflexure was not effective in analyses for loads applied to the composite section. *AASHTO LRFD* Article 6.10.1.5 now requires that the stiffness properties of the full composite section be used over the entire span length in the analysis for permanent loads and transient loads applied to composite members, even when shear connectors are omitted from the negative flexure regions of continuous composite girders. The effect of concrete creep is accounted for by adjusting Young's Modulus.

Field tests of live loads on continuous composite bridges have shown that the portions of the girders in the so-called negative moment regions act compositely under service loads (Baldwin et al., 1978; Roeder and Eltvik, 1985; Yen et al., 1985). Moments and deflections computed assuming full composite action agree much better with field measurements than those computed with a assuming no composite action in these regions. The composite action in these regions gives greater girder moments at the pier and slightly smaller mid-span moments compared to analyses based on assuming composite action in the so-called positive moment regions only. The increase in negative girder moments occurs over a relatively short length of what is typically a larger cross-section, while the reduction in moment occurs over a much longer positive moment region.

Steel properties should match the actual girders as closely as possible for the analysis; a uniform beam property over the span length will give erroneous results. It is also important to recognize the effects of any changes to the relative girder stiffness on the analysis results. Re-analysis should be made whenever revisions are considered to girder and/or cross-frame/diaphragm sizes (i.e. whenever refined analysis models are employed that include the cross-frames/diaphragms in the model). It should always be remembered that any increase in stiffness attracts load to the point of increased stiffness and vice versa. For example, should the depth of one girder be larger than the adjacent girders in the cross-section, that girder will tend to attract more load than it would if all the girders were of the same depth. Curved-girder bridges, in particular, are sensitive to changes in relative girder stiffness because the outside girder typically carries a larger than average share of the load. If the outside girder is sized up, its stiffness will increase and it will draw additional load. This situation will also cause an increase in cross-frame forces in the exterior bay as more load is shifted through the cross-frames to the outside girder.

6.4.7 Net Section Fracture

6.4.7.1 General

Components subject to tension with holes must be checked for fracture on the net section at the strength limit state. The component can fracture by failure of the net area at a load smaller than that required to yield the gross area depending on the ratio of net to gross area, the properties of the steel (i.e. the ratio of F_u/F_y), and the bolted connection geometry. Holes in a component cause stress concentrations at service loads, with the tensile stress adjacent to a round unreinforced hole (e.g. a bolt hole) typically about three times the average stress on the net area. As the load increases and the deformation continues, all fibers across the section will achieve or eventually exceed the yield strain. Failure occurs when the localized yielding results in a fracture through the net area. Since the width of the component occupied by the net area at bolt holes is generally negligible relative to the overall width of the component, strain hardening is easily achieved in the vicinity of the holes and yielding on the net area at bolt holes is not considered to be significant, except perhaps for built-up members of unusual proportions. Typically, a higher margin of safety is used when considering the net section fracture resistance versus the yield resistance.

6.4.7.2 Tension Flange of Flexural Members

AASHTO LRFD Article 6.10.6.2.1 specifies that if there are holes in the tension flange of a flexural member at the section under consideration, the tension flange must satisfy the following requirement at the strength limit state (*AASHTO LRFD* Article 6.10.1.8):

$$f_t \le 0.84\left(\frac{A_n}{A_g}\right)F_u \le F_{yt} \qquad \text{Equation 6.4.7.2-1}$$

AASHTO LRFD Equation 6.10.1.8-1

where:

- A_n = net area of the tension flange determined as specified in *AASHTO LRFD* Article 6.8.3 (in.^{2})
- A_g = gross area of the tension flange (in.^{2})
- f_t = vertical bending stress on the gross area of the tension flange due to the factored loads (ksi)
- F_u = specified minimum tensile strength of the tension flange determined as specified in *AASHTO LRFD* Table 6.4.1-1 (ksi)

It is assumed that the holes are the size of those typically used for connectors, such as bolts. For larger holes, the provisions of *AASHTO LRFD* Article 6.8.1 should be applied instead. Equation 6.4.7.2-1 provides a limit on the maximum bending stress permitted on the gross section of the girder, neglecting the loss of area due to the holes. This equation replaces the 15 percent rule in previous specifications, which allowed holes with an area less than or equal to 15 percent of the gross area of the flange to be neglected. For higher strength steels, with a higher yield to ultimate strength ratio than Grade 36 steel, the 15 percent rule is not valid; such steels are better handled using Equation 6.4.7.2-1. The factor of 0.84 in Equation 6.4.7.2-1 is approximately equivalent to the ratio of the resistance factor for fracture of tension members, ϕ_u = 0.80, to the resistance factor for yielding of tension members, ϕ_y = 0.95 (*AASHTO LRFD* Article 6.5.4.2).

As will be discussed further in Sections 6.5.6.2 and 6.5.6.3, at compact composite sections in positive flexure and at composite I-sections in negative flexure designed according to the optional provisions of *AASHTO LRFD* Appendix A6, with no holes in the tension flange, the nominal flexural resistance is permitted to exceed the moment at first yield at the strength limit state. However, pending further research, the specification currently requires that Equation 6.4.7.2-1 still be checked at such sections where there are holes in the tension flange, which will likely prevent holes from being located in these sections at or near points of maximum applied moment where significant yielding of the web (i.e. beyond the localized yielding of the web permitted in hybrid sections) may occur.

Where lateral bracing members are bolted to a flange subject to tension, Equation 6.4.7.2-1 must be satisfied at the strength limit state.

Where an access hole is provided in a box flange in tension, the hole should be deducted in determining the gross area of the flange for checking this requirement, as specified in *AASHTO LRFD* Article 6.8.1. Thus, yielding is effectively being checked on the net area of the flange at the hole through the use of Equation 6.4.7.2-1. However, Equation 6.4.7.2-1 was not specifically developed for the case at hand; i.e. large access holes in the flange. At the edges of a round unreinforced hole, the theoretical stress concentration factor is approximately 3.0. Therefore, the material adjacent to either side of the hole will yield first. As discussed in Section 6.4.7.1, at bolt holes, which are relatively small in width in relation to the width of the flange, the section will continue to resist load as the yielding spreads across the plate due to strain hardening at those sections. If Equation 6.4.7.2-1 is satisfied, yielding across the gross section will theoretically be achieved prior to fracture on the net section and each fiber of the cross-section can be assumed to be at the yield stress. Access holes, on the other hand, are much larger relative to the width of the flange and there has been no research to determine whether sufficient strain hardening exists to permit development of the yield stress across the entire net section. Therefore, it is recommended herein that until further research is conducted, the tensile stress, f_t, on the adjusted gross area of the box flange due to the factored loads at the strength limit state at access holes conservatively be limited to $0.33F_{yt}$, where F_{yt} is the minimum specified yield stress of the box flange in tension, in lieu of using Equation 6.4.7.2-1.

6.4.7.3 Tension Members and Connected Elements

Net section fracture is also a concern for members with holes subject to axial tension and connected elements with holes subject to tension (e.g. splice plates and gusset plates). The net section fracture resistance of members subject to axial tension is discussed further in Section 6.6.3.3.2. The net section fracture resistance of connected elements subject to tension is discussed further in Sections 6.6.4.2.5.6.1, 6.6.5, and 6.6.7.4.

6.4.8 Torsion

6.4.8.1 General

Strength-of-materials teaches that application of a load in a plane other than one through the shear center of the cross-section will cause torsion in the cross-section. The member will twist to the extent that torsional restraints prevent such twisting. The torsional stresses consist of shear and flexural stresses. These stresses must be combined with the stresses due to flexure.

The shear center is defined as the unique point for a cross-section through which any load will create no torsion. The shear center is the point about which a section rotates when subjected to torque. Flexural bending does not create torsion when the

applied loads pass through the shear center. This can be tacitly assumed in the analysis with little error in many cases. However, there are many cases where loads do not pass through the shear center, in which case they may create significant torsional stresses.

The shear center of a section must be located in order to evaluate the torsional stress. The shear center does not necessarily coincide with the centroid of the cross-section. For doubly-symmetric sections, such as the I-sections shown in the left and center sketches of Figure 6.4.8.1-1, the shear center coincides with the centroid. For singly-symmetric and unsymmetrical sections, such as channels, tees and single angles, the shear center does not coincide with the centroid. For the channel shown in the right sketch of Figure 6.4.8.1-1, the shear center is actually located outside of the section. All of the sections shown in this figure are categorized as open sections. This simply means that the elements of the section do not form a closed or box-type shape. Open sections warp out-of-plane when subjected to torsion.

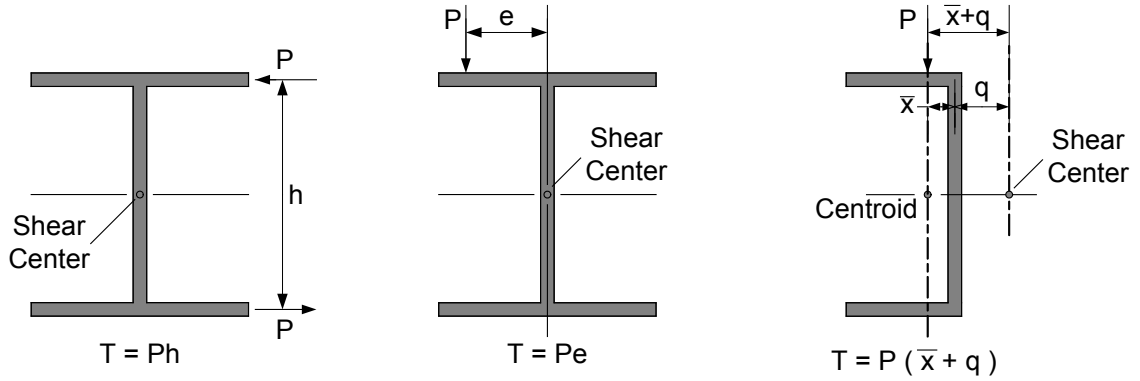

Figure 6.4.8.1-1 Torsional Loadings on an I-Section and a Channel

Potential sources of torsion in steel bridges include curvature, support skew, lateral loads (such as wind) and eccentric loads (such as loads induced by deck overhang brackets acting on exterior girders during construction). Due to the torsional effects resulting from curvature, a single curved girder by itself is not stable without some form of torsional restraint. This restraint is typically provided by the cross-frames between the individual girders.

6.4.8.2 I-Sections

6.4.8.2.1 St. Venant Torsion

The simplest form of torsion is referred to as pure torsion or St. Venant torsion. Pure torsion can best be visualized by a solid prismatic round member free to twist at one end and restrained against twisting at the other end (Figure 6.4.8.2.1-1). If a torque, or torsional moment, is applied to the free end, the torque will travel unreduced to the opposite (torsionally restrained) end where it will be resisted by a torque equal

but opposite to the applied torque. The only stresses generated are torsional shear stresses, τ. Hence, the energy induced can be described by a single term. The magnitude of the resulting total angle of twist, ϕ, is computed as:

$$\phi = \frac{TL}{GJ} \qquad \text{Equation 6.4.8.2.1-1}$$

where:

G = shear modulus (ksi)

J = torsion constant or polar moment of inertia; for a solid round = $\pi r^4/2$, where *r* is the radius (in.^{4})

L = member length (in.)

T = applied torque (kip-in.)

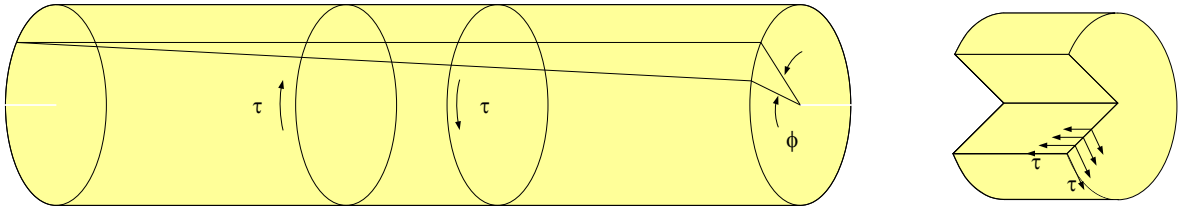

Figure 6.4.8.2.1-1 Solid Round Member Subjected to Torsion

The rate of twist per unit length, $d\phi/dz$, may be assumed constant for an open cross-section, such as the I-girder section shown in Figure 6.4.8.2.1-2, when the cross-section is assumed not to distort and the torsion is pure and not interrupted by other loads or torsional restraints. The assumption of no distortion allows a torsional constant to be computed. The section may be thought of as three interconnected rectangular elements (i.e., two flanges and a web) with respect to twist. This assumption is not true for many steel bridge girders where the web is deep and will distort. When the assumption of no distortion is appropriate, the St. Venant torsion shear distribution in an I-section will be almost identical to that which exists in three separate narrow rectangles.

For a narrow rectangle subject to pure torsion, the relationship between the resisting torque T_s and the twist per unit length can be expressed as follows (McGuire, 1968):

$$T_s = G\left(bt^3/3\right)\frac{d\phi}{dz} \qquad \text{Equation 6.4.8.2.1-2}$$

where:

b = width of the rectangle (in.)

t = thickness of the rectangle (in.)

For an I-section, the total St. Venant resisting torque consists of the individual contributions from three narrow rectangles is given as follows:

$$T_s = G\Sigma\frac{bt^3}{3}\frac{d\phi}{dz} = GJ\frac{d\phi}{dz} \qquad \text{Equation 6.4.8.2.1-3}$$

where:

J = St. Venant torsional constant = $\sum bt^3/3\,(\text{in.}^4)$

and b and t are the individual width and thickness of each flange and web element. In *AASHTO LRFD* Appendix A6, a more accurate approximation of J for an I-section, neglecting the effect of web-to-flange fillets, is given as:

$$J = \frac{Dt_w^3}{3} + \frac{b_{fc}t_{fc}^3}{3}\left(1 - 0.63\frac{t_{fc}}{b_{fc}}\right) + \frac{b_{ft}t_{ft}^3}{3}\left(1 - 0.63\frac{t_{ft}}{b_{ft}}\right) \qquad \text{Equation 6.4.8.2.1-4}$$

AASHTO LRFD Equation A6.3.3-9

where:

b_{fc} = width of the compression flange (in.)
b_{ft} = width of the tension flange (in.)
D = depth of the web (in.)
t_{fc} = thickness of the compression flange (in.)
t_{ft} = thickness of the tension flange (in.)
t_w = thickness of the web (in.)

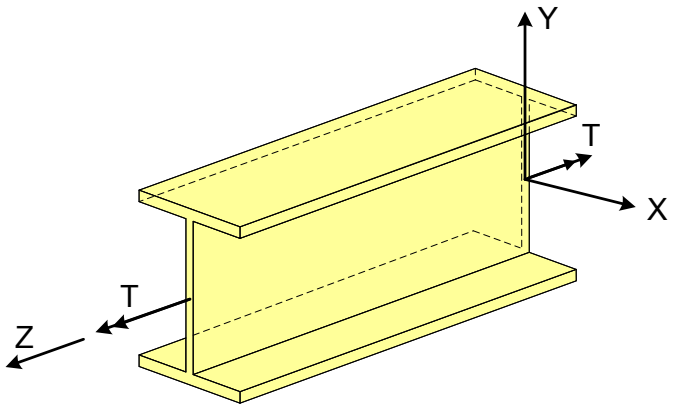

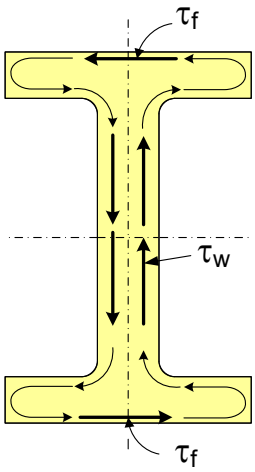

Figure 6.4.8.2.1-2 Torsion and Torsional Shear Stress on an I-Girder

For flanges with $b_f/2t_f$ greater than 7.5, the term in parentheses for that flange in the preceding equation may be taken equal to one. More accurate values of J for rolled I-shapes, including the effect of the web-to-flange fillets, are tabulated in the AISC *Steel Construction Manual* (AISC, 2010).

St. Venant torsional shear stresses in the flanges (τ_f) and web (τ_w) can be approximated from the following formulas:

$$\tau_f = \frac{T_s t_f}{J} \qquad \tau_w = \frac{T_s t_w}{J} \qquad \text{Equation 6.4.8.2.1-5}$$

which are for a narrow rectangle, again summing the contributions from the separate rectangular components. As shown in Figure 6.4.8.2.1-2, peaks of shear stress occur on the outer fibers at the center of the flange and on the outer fibers at the mid-height of the web.

6.4.8.2.2 Warping Torsion

If a non-circular cross-section is subjected to a torsional moment, the cross-section will twist. However, it will also deform longitudinally so that plane sections do not remain plane, as shown in Part A of Figure 6.4.8.2.2-1. This cross-sectional deformation is referred to as warping, as shown in Part B of Figure 6.4.8.2.2-1. If warping is restrained (which is typically the case), additional torsional resistance results from transverse shears that develop in the girder flanges. These shears develop due to the flexural resistance of the flanges. This additional component of the torsion resistance resulting from restraint of warping is known as warping torsion.

Part A of Figure 6.4.8.2.2-2 shows a doubly symmetric I-section free at one end and prevented from twisting, but not warping, at the base subjected to a torque, *T*. In Part B of Figure 6.4.8.2.2-2, the same I-section is restrained from warping as well as twisting at its base. As a result, the forces, *F*, are developed and exerted by the support due to restraint of warping. The forces, *F*, acting in the directions shown represent the lateral flange bending moments. These forces cause flange shear stresses, which result in transverse shear forces, *H*, in each flange, as shown in Part B of Figure 6.4.8.2.2-2. These transverse shears bend each flange much like a rectangular beam about its own major axis. Bending in the web is neglected due to its lack of rigidity in the weak direction. In this case, the transverse shear times the distance, *h*, between flange centers results in a couple having the same direction as the resisting torque. Thus, the restraint at the end provides the warping torsion resistance.

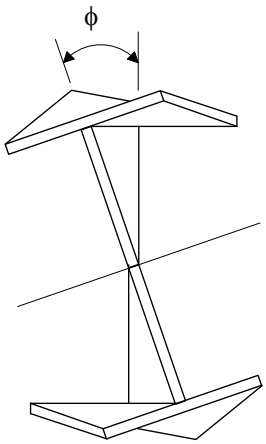

Twisting

Part A

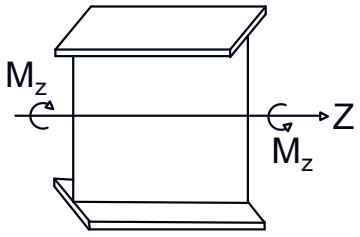

Warping

Part B

Figure 6.4.8.2.2-1 Twisting and Warping of an I-Section

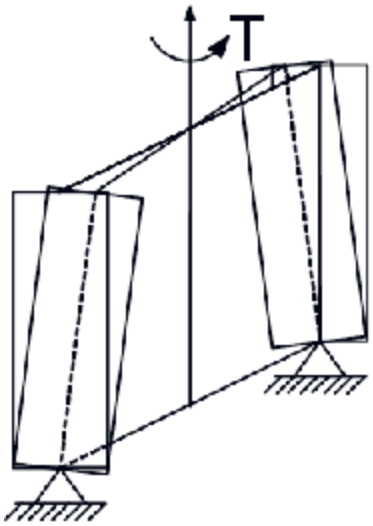

Warping

PART A

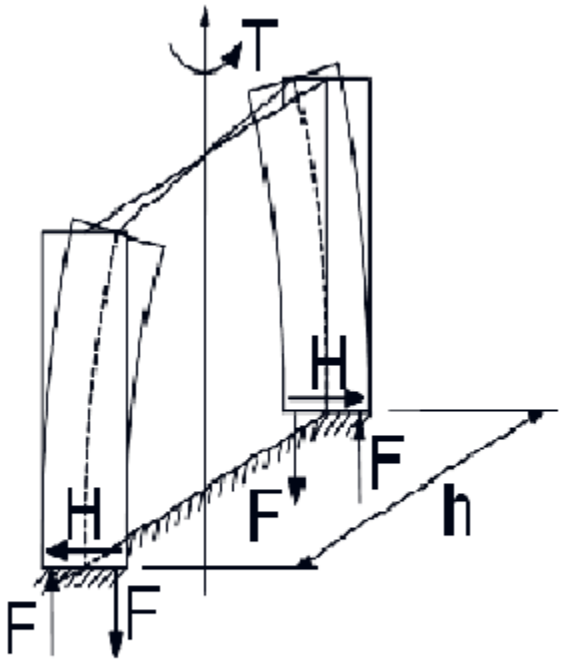

No Warping

PART B

Figure 6.4.8.2.2-2 Warping Torsion Resistance

Thus, whenever warping restraint is present in an I-section, only part of the applied torque need be resisted in St. Venant torsion. The remainder is carried by so-called warping torsion that is developed due to the transverse shears that result from the flexural resistance of the flanges. The equation for the warping component of the total torque for an I-section is given as follows (McGuire, 1968):

$$T_w = -EC_w \frac{d^3\phi}{dz^3} \qquad \text{Equation 6.4.8.2.2-1}$$

where:

C_w = warping torsional constant = $I_y h^2/4$ (in.^{6}). Warping torsional constants are available in the literature for other shapes.
h = distance between the centerlines of the flanges (in.)
I_y = moment of inertia of the I-section about a vertical axis in the plane of the web (in.^{4})

Warping torsion is also commonly referred to as “non-uniform torsion” since the shear stress patterns under St. Venant torsion are disturbed because of warping restraint. Thus, non-uniform torsion results from a variation of torque along the span and/or where there are discontinuities in the torque introduced along the span (such as at cross-frames in horizontally curved bridges).

6.4.8.2.3 Torsion Resistance for Design

The total torsion resistance for I-sections is the sum of the St. Venant torsion resistance and the warping torsion resistance, or the resistance that results from the restraint of warping. The differential equation defining the total torsional moment resistance, T, whenever warping restraint is present is given by the following equation (McGuire, 1968):

$$T = T_s + T_w = GJ\frac{d\phi}{dz} - EC_w \frac{d^3\phi}{dz^3} \qquad \text{Equation 6.4.8.2.3-1}$$

Knowing the boundary conditions, the differential equation can be solved for the twist angle, ϕ, and its various derivatives leading to exact theoretical solutions for the various torsional stresses and lateral flange bending moments.

In design, it is often convenient and always conservative to base the design on the dominant type of torsion resistance for the section under consideration and neglect the effects of the other type of torsion resistance. For closed cross-sections, such as box girders, and for certain smaller singly-symmetric and unsymmetrical open cross-sections, such as rolled channels, tees or angles, St. Venant torsion generally

predominates. For larger open cross-sections, such as I-sections, warping torsion is generally predominant.

For I-girder design, the St. Venant torsion component is typically ignored for sections with slender webs and all torsion is assumed resisted by warping torsion. Without a significant force couple distance between the shear flows across the thickness of any given element of the I-section, the ability of I-sections to develop St. Venant torsion shear resistance is low. The reason for this is that web distortion causes the section to no longer obey strength-of-materials theory (Figure 6.4.8.2.3-1).

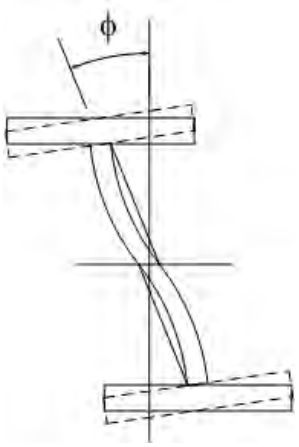

Figure 6.4.8.2.3-1 Web Distortion in an I-Section

The more slender the web, the less significant the St. Venant torsion stiffness becomes. For this reason, St. Venant torsion stiffness is conservatively neglecting in determining the elastic lateral-torsional buckling resistance of slender-web I-sections in the *AASHTO LRFD* Specifications.

For compact web and noncompact web sections, an additional safeguard is specified as follows to allow the use of the full St. Venant torsional stiffness in determining the elastic lateral-torsional buckling resistance in *AASHTO LRFD* Appendix A6:

$$\frac{I_{yc}}{I_{yt}} \geq 0.3 \qquad \text{Equation 6.4.8.2.3-2}$$

AASHTO LRFD Equation 6.10.6.2.3-2 & Equation A6.1-2

where:

I_{yc} = moment of inertia of the compression flange of the steel section about the vertical axis in the plane of the web (in.^{4})

I_{yt} = moment of inertia of the tension flange of the steel section about the vertical axis in the plane of the web (in.^{4})

This limit guards against the use of extremely monosymmetric non-composite I-sections. Cross-section distortion can significantly reduce the influence of the St. Venant torsional stiffness on the lateral-torsional buckling resistance of these sections.

As shown in Figure 6.4.8.2.3-2, warping torsion results in the development of transverse shears in the flanges, along with lateral flange bending moments. The warping torque is typically not used in the design of open sections.

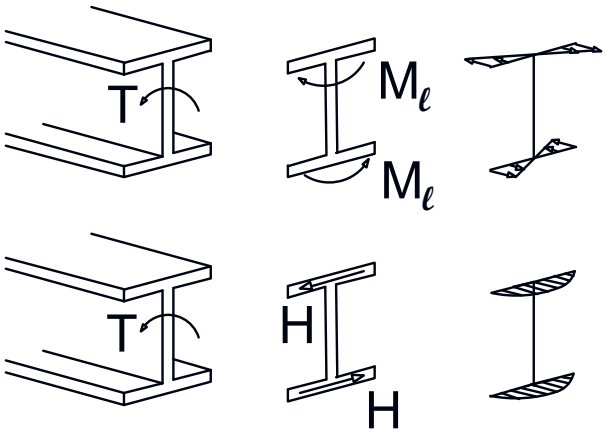

Figure 6.4.8.2.3-2 I-Sections with Effects of Warping Torsion

The lateral flange bending moment times the distance between the flange centers is often referred to as the "bimoment" (in units of kip-in^2), which is most commonly used in the computation of certain fundamental torsional section properties. These properties are not employed in conventional designs.

Individual I-girders with slender webs subject to torsion are typically designed for the force effects shown in Figure 6.4.8.2.3-3. The girders are designed for the normal stresses, as shown in Part A of Figure 6.4.8.2.3-3, and for shears, as shown in Part B of Figure 6.4.8.2.3-3, resulting from the vertical (major-axis) bending moment.

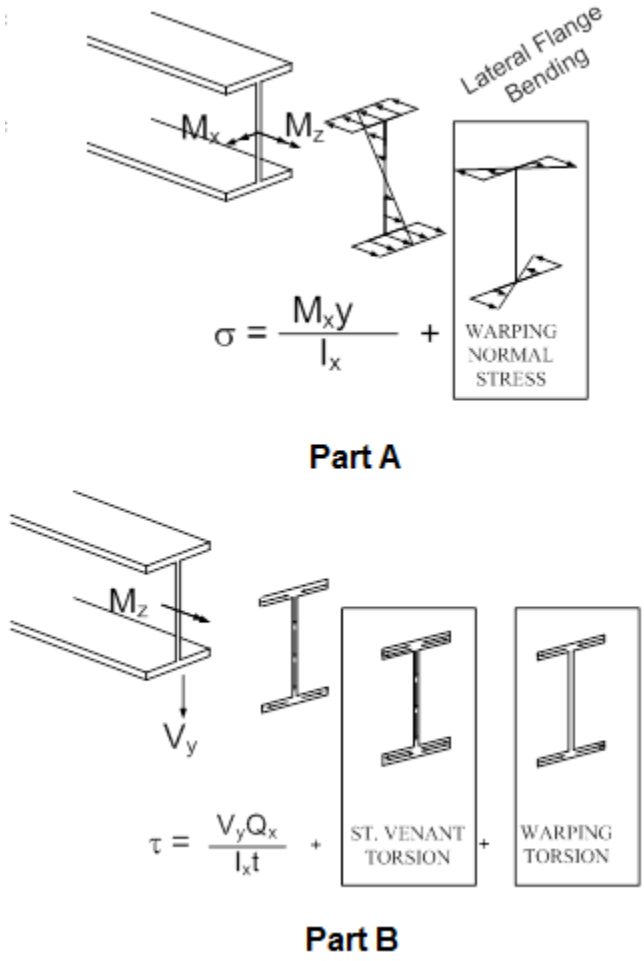

Figure 6.4.8.2.3-3 I-Section Bending Stresses and Shears for Design

The girder flanges are also designed for the lateral flange moments resulting from warping torsion. Shears due to St. Venant torsion and warping torsion in I-sections are generally small and may usually be neglected. Lateral flange bending stresses are the primary action consideration in the design of I-sections for torsion.

Lateral flange bending can be determined by solving a complex differential equation, by reasonable approximations, or by direct computation in a 3D finite element model of the section that properly recognizes the lateral bending stiffness. The latter two methods are commonly employed in practical design.

6.4.8.3 Box Sections

6.4.8.3.1 General

Closed, or box, sections are many times stiffer in torsion that are open sections. St. Venant torsion is dominant over warping torsion. Additionally, box sections are subject to cross-section distortion that should be considered in design in certain cases.

Figure 6.4.8.3.1-1 shows qualitatively the deformations of a box section due to vertical bending and torsion. Flexure causes vertical deflection; torsion causes twist and cross-section distortion. The final deflected condition is a combination of the three effects.

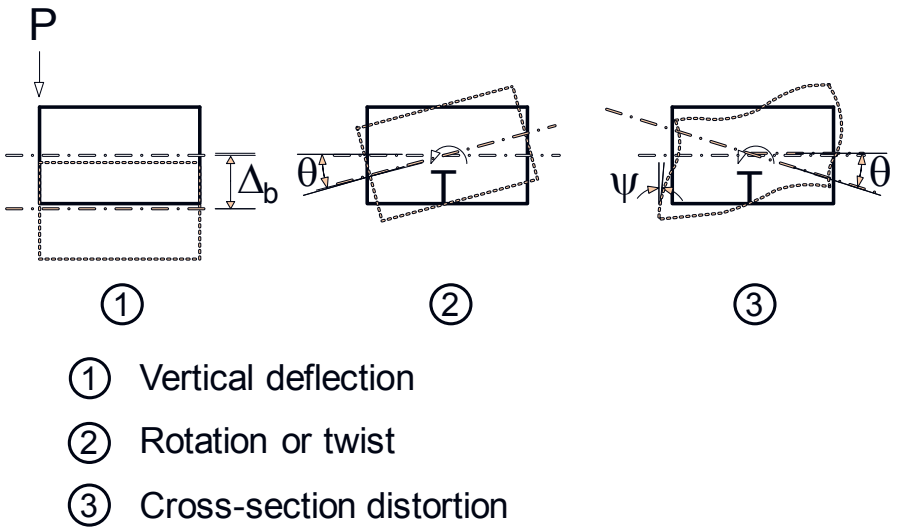

Figure 6.4.8.3.1-1 Deformation of Box Sections

The series of drawings in Figure 6.4.8.3.1-2 illustrates simplistically how a vertical load applied off the shear center can be separated into vertical bending and torsion components using superposition. The load, *P*, is divided equally to the two webs for bending. The torque is represented with a couple of magnitude *Pb*/2.

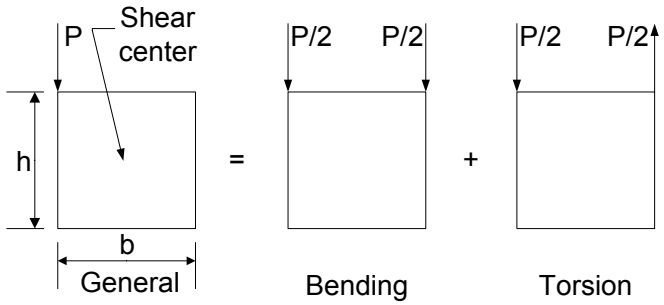

Figure 6.4.8.3.1-2 Vertical Bending and Torsion Components – Box Section

The resulting bending and torsion components to be considered are two normal stresses, three shear stresses, and a set of through-thickness bending stresses.

Figure 6.4.8.3.1-3 shows qualitatively the normal and shear stress distributions in the box section due to vertical bending near mid-span (Parts A and B) and at a support (Parts C and D).

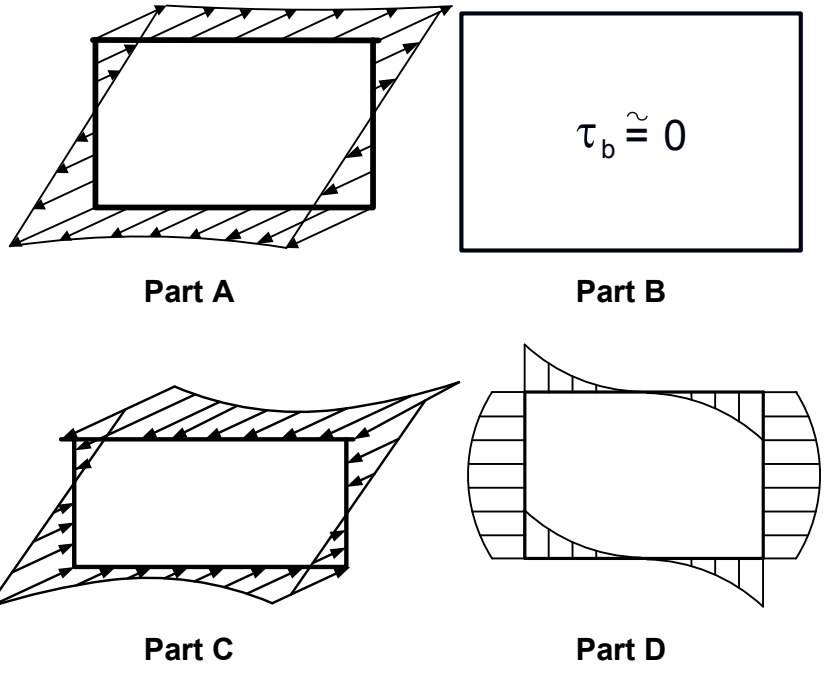

Figure 6.4.8.3.1-3 Normal and Shear Stress Distributions – Box Section

The curvature in the normal and shear stress distributions is due to the effects of shear lag caused by a perturbation in the shear, such as that due to the effect of any concentrated load (such as reactions). The average normal stress across the flange is nearly the same as the integrated normal stress times the area since statics must be satisfied.

This shear lag effect is also present in the deck, but recent research has shown that in most cases its effect may be ignored (Section 4.2.2).

The series of drawings in Figure 6.4.8.3.1-4 illustrates how the torsion load can be further separated into St. Venant torsion and distortion components. The vertical and horizontal forces shown in the figure are applied directly to the webs and flanges, respectively. The magnitude, *H*, of the horizontal forces applied to the flanges is found from the condition that the total applied torsional moment must be the same as for the box to the left. That is,

$$(P/2)b = (P/4)b + Hh \qquad \text{Equation 6.4.8.3.1-1}$$

$$\therefore\ H = (P/4)b/h \qquad \text{Equation 6.4.8.3.1-2}$$

In the distortion case of Figure 6.4.8.3.1-4, the applied forces are self-equilibrating and only cause distortion of the cross-section.

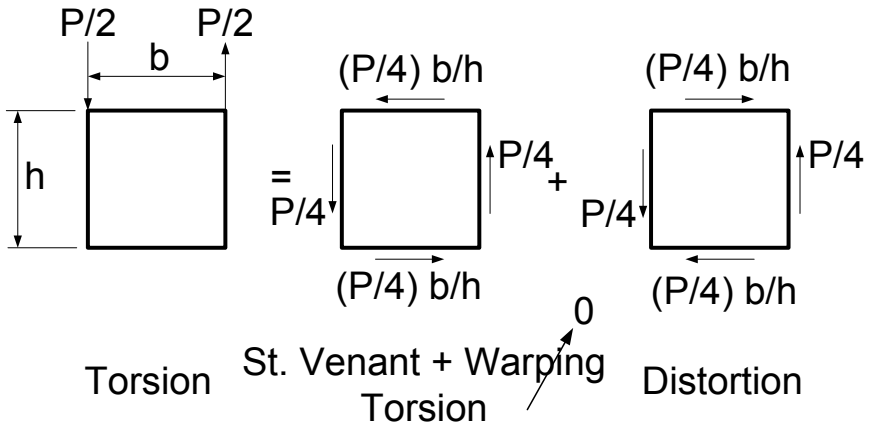

Figure 6.4.8.3.1-4 Torsion Components – Box Section

6.4.8.3.2 St. Venant Torsion

Figure 6.4.8.3.2-1 illustrates the St. Venant torsion stress for a box section. As discussed above in Section 6.4.8.2.1, in open sections, torsional shear flows around the individual elements. In closed sections, torsional shear flows around the whole section. In a single-cell section, the torsional shear flows around the circumference of the section. For a single cell box section, the uniform St. Venant torsional shear flow, $f = t\tau$ in units of force/length, that develops around the circumference of the box can be determined from the equation shown inside the box in Figure 6.4.8.3.2-1 where *T* is the torque, *A* is the enclosed area of the box, and *t* is the thickness of the element under consideration.

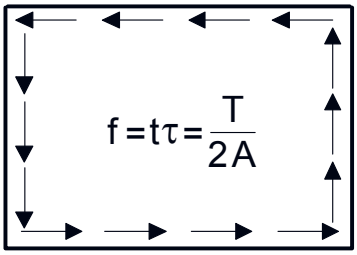

Figure 6.4.8.3.2-1 St. Venant Torsion Shear Flow – Box Section

To develop this equation, first consider the hollow cylindrical tube shown in Part A of Figure 6.4.8.3.2-2 subject to a torque, *T*.

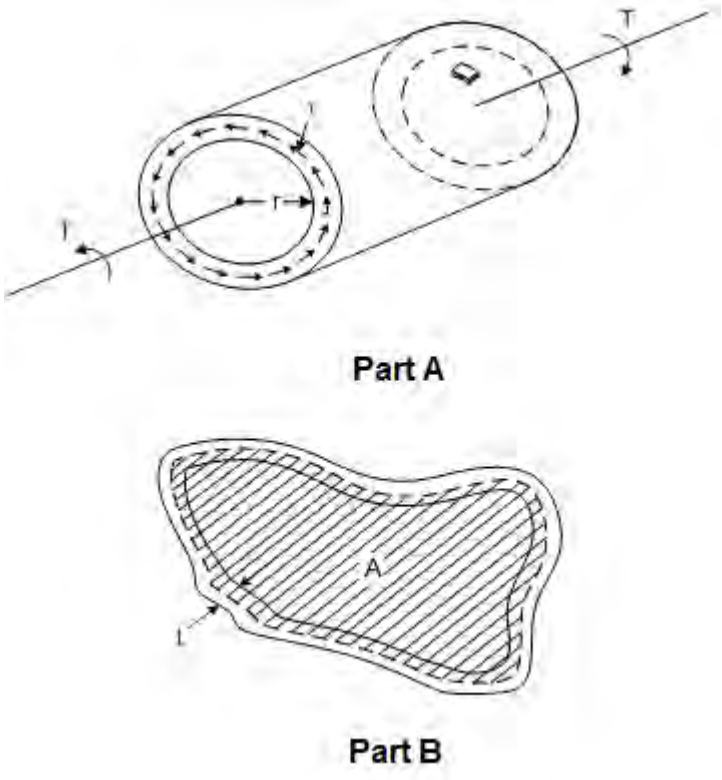

Figure 6.4.8.3.2-2 Cylindrical Tube and Enclosed Area of a Hollow Shaft

The torque is resisted by shear stresses, τ, concentrated within the tubular wall. Assuming the wall is thin with respect to the radius, but thick enough to prevent local buckling, the radial variation of the shear stresses through the thickness may be neglected, and the shear flow in the wall may be assumed acting at a distance *r* from the longitudinal axis. *r* is the radius to the middle of the wall from the shear center. For equilibrium in the general case, the shear flow must be taken as the integration

of the torsion over the circumference of the section within the enclosed area. For the cylindrical tube shown in Part A of Figure 6.4.8.3.2-2:

$$T = (\tau t 2\pi r)r \qquad \text{Equation 6.4.8.3.2-1}$$

or

$$f = \tau t = \frac{T}{2A} \qquad \text{Equation 6.4.8.3.2-2}$$

AASHTO LRFD Equation C6.11.1.1-1

where $A = \pi r^2$ or the enclosed area within the effective radius (Part B of Figure 6.4.8.3.2-2 as opposed to the actual cross-sectional area of the material in the tube wall).

Similarly, for the thin-walled rectangular box section shown in Figure 6.4.8.3.2-3 subjected to a torque, *T*:

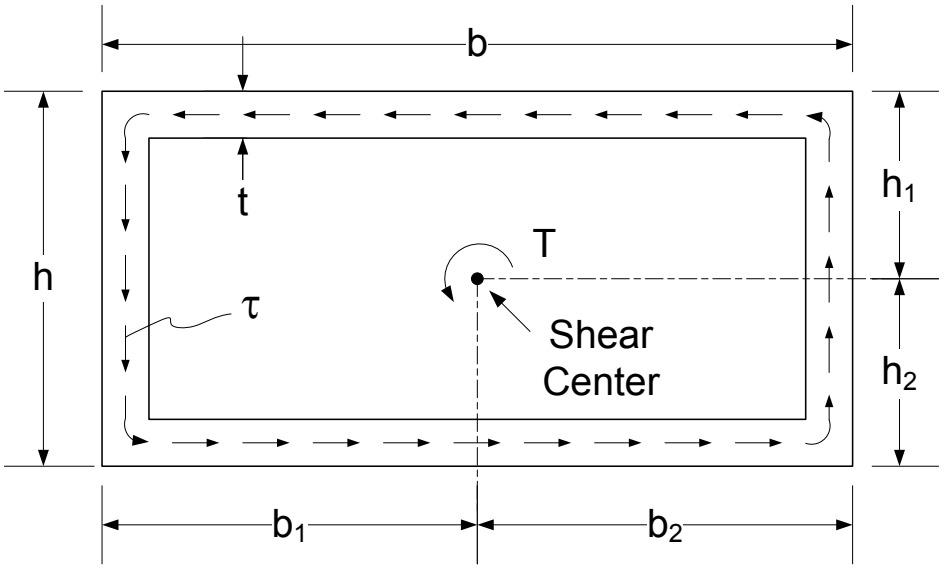

Figure 6.4.8.3.2-3 Shear Flow for a Thin-Walled Rectangular Box Section

$$T = \tau t * [h * (b_1 + b_2) + b * (h_1 + h_2)] \qquad \text{Equation 6.4.8.3.2-3}$$

Since:

$$A = bh = (b_1 + b_2)(h_1 + h_2) \qquad \text{Equation 6.4.8.3.2-4}$$

$$T = \tau t * [(b * h) + (b * h)] \qquad \text{Equation 6.4.8.3.2-5}$$

Therefore:

$$f = \tau t = \frac{T}{2(b * h)} = \frac{T}{2A} \qquad \text{Equation 6.4.8.3.2-6}$$

Thus, for any thin-walled single-cell closed shape, the torsional shear stress at any point is equal to the torque divided by the product of the wall thickness at that point and twice the enclosed area. The preceding is true even when the wall thickness varies as long as the change is not abrupt enough to cause a concentration of stress; the shear flow follows the peripheral line and is constant.

The St. Venant torsional constant, *J*, for a rectangular box section with adequate torsional stiffness is determined from Bredt's formula and is given as follows:

$$J = 4\frac{A_o^2}{\sum \frac{b}{t}} \qquad \text{Equation 6.4.8.3.2-7}$$

AASHTO LRFD Equation C6.7.4.3-1

where *b* is the width of the plate element under consideration. *AASHTO LRFD* Article C6.7.4.3 permits this equation to be used to compute *J* for tub-girder sections if the distortion of the section is adequately controlled. Cross-section distortion of boxes is usually constrained by internal cross-bracing members. The necessary spacing of internal bracing is difficult to determine, but is a function of the box stiffness and the applied torsion. This issue is examined in more detail in Sections 6.3.2.9 and Section 6.5.

In the U.S., most box girders used in bridge superstructures are tub girders having open tops. The open top is braced with a top lateral bracing system that forms a pseudo-box section. The top lateral bracing is designed to resist the shear flow combined with the flexural bending moment in the box. Formulas are available in Kolbrunner and Basler (1966) and Dabrowski (1968) to calculate the thickness of an equivalent plate for different possible configurations of top lateral bracing for use in determining *J*. True (rectangular) box beams in the U.S. are usually limited in application to straddle beams or integral pier caps.

The torsional stiffness of a box section is between 100 and 1,000 times the torsional stiffness of a comparable I-section. This great stiffness is a double-edged sword. When used on horizontally curved alignments, a single box has the ability to resist torsion alone, unlike open sections that depend on adjacent open sections for stability. Box girders are often used with little or no external cross-frames/diaphragms, except at supports, even on a significantly curved alignment.

This frequently simplifies erection compared to curved I-girders, which may require more lateral bracing and sometimes additional temporary supports. The other edge of the sword limits the twist the box will permit during fit-up. The torsional stiffness in this regard is particularly evident with boxes resting on skewed supports.

Shear flow increases shear in one box web and reduces shear in the other web. In the composite section, the shear flow is resisted, in part, by the deck. The amount of horizontal shear in the concrete deck is determined by the relative shear stiffness of the top flange lateral bracing or top box flange and the deck. In bridges with skewed supports, the horizontal shear in the deck can sometimes be substantial and should be considered in the design of the reinforcing steel. The horizontal shear in the bottom box flange is considered by specification in the design of the bottom flange plate. The horizontal shear in the top flanges of tub girders is typically neglected; the top lateral bracing is designed to resist the shear flow induced before the concrete deck hardens.

According to *AASHTO LRFD* Article 6.11.1.1, shear due to St. Venant torsion must be considered at all limit states for all single box or multiple box sections in skewed and/or curved bridges, and/or for sections that do not have fully effective box flanges (discussed further in Section 6.3.5.5.3). As specified in *AASHTO LRFD* Articles 6.13.6.1.4b and 6.13.6.1.4c, shear due to St. Venant torsion is also to be considered at all limit states in the design of bolted web splices and bolted box-flange splices for the preceding cases.

6.4.8.3.3 Warping Torsion

The warping torsion constant for box sections is usually assumed equal to zero (Figure 6.4.8.3.1-4). This means that shear and normal stresses due to warping torsion are typically quite small and are usually neglected for box sections. However, as discussed further below in Section 6.4.8.3.4, in certain cases including for box sections in skewed and/or curved bridges, normal warping stresses due to cross-section distortion must be considered for fatigue and for checking slip in bolted flange splices. These stresses may be ignored at the strength limit state.

6.4.8.3.4 Cross-Section Distortion

Figure 6.4.8.3.4-1 shows the three stress components associated with distortion of a box cross-section; normal warping stress, warping shear and through-thickness bending stress. The through-thickness bending stress distribution shown on the right-hand side of Figure 6.4.8.3.4-1 represents the transverse bending stresses in the outside fiber of the flanges and webs.

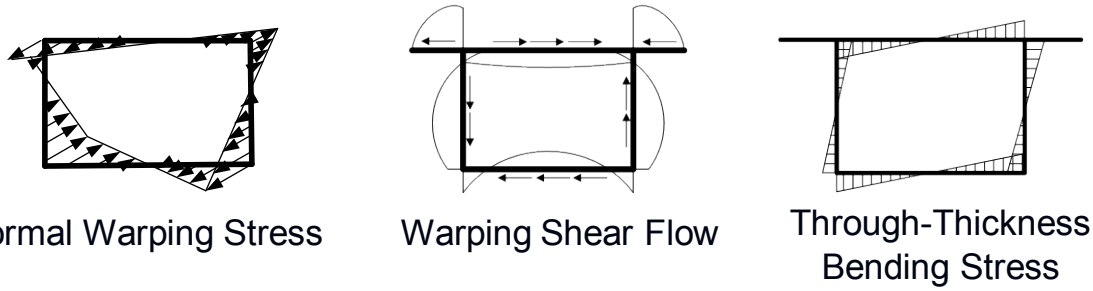

Figure 6.4.8.3.4-1 Distortion Stresses – Box Section

Distortion stresses occur when the section is not round and shear flow changes direction at the box corners, which warps the section. The amount of warping is related primarily to the amount of distortion in the cross-section of the box.

The transverse bending stresses are associated with the shear flow vector changing direction. Since torsion is not mitigated along the section, the section tends to continue to distort and warp until interrupted. In box sections, since the transverse bending stiffness of the flanges and webs alone is not sufficient to retain the box shape, this interruption is accomplished with intermediate internal cross-frames or diaphragms. These members provide quite rigid restraint against movement of the four corners of the box, hence restoring the box to its original shape. Astute location of these braces controls the distortion and associated warping actions.

According to *AASHTO LRFD* Articles 6.11.1.1 and 6.13.6.1.4c, the normal warping stresses due to cross-section distortion must be considered for fatigue and for checking slip in bolted flange splices for all single box or multiple box sections in skewed and/or curved bridges, and/or for sections that do not have fully effective box flanges (6.3.5.5.3). Normal warping stresses are largest at the corners of the box section where critical welded details are often located. The range of live load longitudinal warping stresses should therefore be added to the range of live load major-axis bending stresses in the bottom flange when checking fatigue. Normal warping stresses due to cross-section distortion may be ignored at the strength limit state. It is apparent that the warping stresses in a flange average out and have been shown to be not deleterious with respect to achieving the capacity of the flange plate. Warping shear stresses due to cross-section distortion are ignored in the specifications.

As discussed previously, when box sections are subject to torsion, the cross-section becomes distorted and is restored at cross-frames/diaphragms, giving rise to secondary transverse bending stresses. Loading the opposite side of the bridge produces reversal of these bending stresses. Thus, according to *AASHTO LRFD* Articles 6.11.1.1 and 6.11.5, transverse bending stresses due to cross-section distortion are to be considered for fatigue for all single box or multiple box sections in skewed and/or curved bridges, and/or for sections that do not have fully effective box

flanges. In addition, for these cases, the transverse bending stresses due to the factored loads are to be limited to 20 ksi at the strength limit state. Adequate internal cross bracing usually controls the magnitude of these stresses in boxes of typical proportion such that they are not critical to the ultimate resistance of the box section at the strength limit state.

Transverse bending stresses have caused fatigue cracking in the webs of tub girders where transverse web stiffeners were not attached to the flange. Transverse web stiffeners add significantly to the stiffness of the web so the box distortion is concentrated at their terminus. Attachment of the stiffeners to the flanges, including stiffeners not serving as cross-frame connection plates, prevents this distortion at the stiffener locations. Hence, the welded attachment resists the distortion force. The fatigue resistance of the base metal at the termination of the fillet welds connecting transverse stiffeners to webs and flanges when subject to transverse bending is not currently quantified in the specifications, but is anticipated to be as low as Category E. Transverse bending stresses are particularly large in boxes subject to large torque, including single box bridges, sharply curved boxes and boxes resting on skewed supports.

The Beam-on-Elastic Foundation (BEF) analogy (Wright and Abdel-Samad, 1968) is typically used to calculate the distortion stresses and stress ranges, as illustrated in Section 6.5.5.2.2.3. Refined analysis methods are generally not used to calculate these stresses due to the refinement of the mesh necessary for their accurate calculation.

6.4.9 Skewed and Curved Girder Bridges

6.4.9.1 General

Tighter constraints on right-of-way, particularly in urban environments, have led to a significantly increased utilization of skewed and/or curved alignments in highway bridge construction. Due to the relative ease of configuring the structure to the roadway geometry, steel I-girder bridges are often a preferred option for these cases.

This section discusses in a general sense the applications, advantages, and challenges of skewed and curved steel bridges, issues that are unique to these bridges, and the basic effects of curvature and skew on these bridges, with an emphasis on the importance of considering system behavior in the analysis of these bridges.

The reader is referred to NHI (2011) for further more detailed information on these bridges and the topics that are discussed in general below.

6.4.9.2 Curved Bridges

A horizontally curved girder is defined in *AASHTO LRFD* as an I-, closed-box, or tub girder that is curved in a horizontal plane. A horizontally curved bridge can consist of simple-span straight girders kinked at the supports to follow the curve, continuous kinked (chorded) girders or curved girders. In each case, the concrete deck is ordinarily horizontally curved, with the deck overhang being variable in the first two cases and constant in the third.

According to *AASHTO LRFD* Article C6.10.1, bridges containing both straight (tangent) and curved segments are to be treated as horizontally curved bridges since the effects of curvature on the support reactions and girder deflections, as well as the effects of flange lateral bending, usually extend beyond the curved segments. Continuous kinked (chorded) girders are also to be treated as horizontally curved girders.

Curved girders generally are not stable by themselves and need the support of adjacent members to establish equilibrium, particularly during the erection.

The earliest curved girders were probably made from rolled shapes that were cold bent about their weak axis. As girder welding became more acceptable, curved girders grew in popularity. Horizontally curved girders are used in buildings, such as for balconies. However, the most widespread use of curved girders is in the highway bridge market. They are commonly used in interchanges requiring complex geometries to minimize right-of-way acquisition and where smooth transitions in direction must be accomplished at high speeds.

Curved steel girder bridges have been built in the United States since the 1950s. Some of the earliest horizontally curved girder bridges in the U.S. were box sections made by welding together four plates. Today, curved-girder bridges represent a significant percentage of the total steel-bridge market. Figure 6.4.9.2-1 shows a curved I-girder bridge prior to the deck being placed.

Figure 6.4.9.2-1 Integral Steel Cap on a Curved I-Girder Bridge Without the Deck

Horizontally curved girders offer certain advantages over kinked or chorded girders including:

- Overall simplification of the structure by allowing curved girders to follow the roadway alignment;
- Use of longer spans;
- Continuity over several spans permitting simplified framing, efficient use of material, increased vertical clearance and fewer joints;
- Reduced number of piers;
- Simplified forming of the deck with a constant deck overhang; and
- Simpler reinforcing bar schedule.

Aesthetics of highway bridges are being assigned an ever-higher priority. In addition to their structural and economic advantages, curved steel girder bridges provide improved aesthetics at constricted sites. Their graceful appearance is typically well received by the public.

Curved girder bridges, such as the one shown in Figure 6.4.9.2-2, demonstrate the aesthetic benefits of matching the structural lines with the traffic flow. The increasing need for horizontally curved bridges is driven by the demand for efficient high-speed highway interchanges and magnificent approaches to major stream crossings. This figure visually shows the versatility welded structural steel can provide when an aesthetic curved bridge is desired.

Figure 6.4.9.2-2 Curved I-Girder Bridge

While there is no aesthetic comparison of a curved girder bridge to a segmented curved structure (as shown in Figure 6.4.9.2-3) with its seemingly myriad piers and its interrupted girder lines, the fact is that this inherent aesthetic beauty of curved girders can be obtained for usually less cost than the perfunctory alternative.

However, there are challenges in designing and building horizontally curved girder bridges:

Fabrication requires either additional labor or additional material depending on how the girders are fabricated. Additional labor is used if the girders are fabricated straight and heat curved. Additional material is required of the flanges are cut curved and then the girders are fabricated into a curved shape. Additional labor is also required in the latter case due to handling. Shipping may add some cost to horizontally curved girders.

Figure 6.4.9.2-3 Segmented Curved I-Girder Bridge

Torsion introduces issues when lifting the girders and during erection. Often additional lifting points and temporary supports are needed, increasing costs. Much of these costs would also be encountered if segmented girders were used.

The design of curved girders is slightly more complex than straight girders, but the simpler reinforcing schedule and overhang design of horizontally curved decks on curved girders often balances the increased effort to design the curved girders and cross-frames. Curved girder bridges are competitive with straight girder bridges on a horizontal curve, but each structure may need to be evaluated as an individual case.

During inspections of curved bridges, greater attention must be paid to cross-frames, diaphragms, cross-girders and lateral bracing since these members are considered to be primary load-carrying members in these bridges. They are also primary members in kinked-girder bridges. Bottom lateral bracing members must also be considered to be primary load-carrying members since they resist significant loads throughout the life of the bridge.

6.4.9.3 Skewed Supports

Skewed supports are employed to match the supports to the underlying alignment of roads, railroads or streams. Skewed supports are often used with either straight or curved alignments.

Skewed supports allow for reduced span lengths and bridge deck area. Reduced spans, in turn, permit reduced girder depths. Skewed supports introduce increased

cost with longer abutments and piers compared to right supports. A schematic of a curved bridge with skewed supports is illustrated in Figure 6.4.9.3-1.

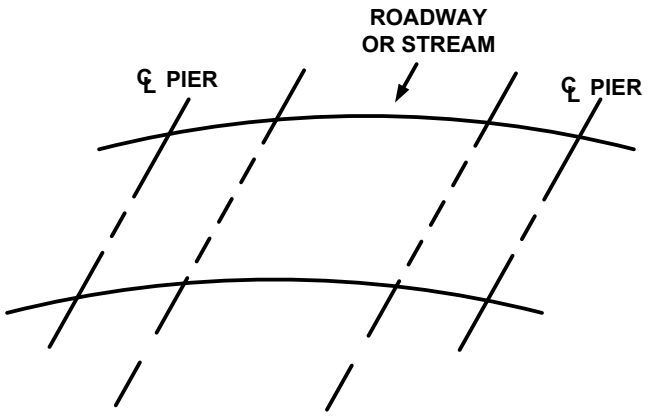

Figure 6.4.9.3-1 Curved Bridge with Skewed Supports to Match Roadway/Stream

Skewed supports present additional challenges in the design and construction of straight or curved girders due to the differential deflections of adjacent girders. Interconnection of the girders creates restoring forces in the cross-frames and deck when the structure is loaded. These restoring forces cause torsion in the girders. These load effects lead to girder rotations, larger cross-frame forces and unique thermal movements.

6.4.9.4 Unique Issues

The objectives of good bridge design include economy, elegance, constructibility and durability. Economy relates to efficient use of the materials and labor while minimizing delays through the reduction of Requests for Information (RFIs). An ill-conceived bridge is never economical or elegant. A well-conceived bridge has an efficient span arrangement with a minimal number of open joints. Unless site constraints make it extremely impractical, spans should be set that permit reasonable and economical girder depths. This is particularly important for bridges having either curved girders and/or skewed supports since shallower girders tend to accentuate issues associated with these bridges. Selection of an efficient number of girders in the cross-section is particularly important and often overlooked in the early stages of design when this important decision is made. Identification of field-splice and shop-splice locations was examined in Section 6.3. Utilizing proper types of bearings and joints to permit the bridge to function properly is important. Investigation of construction issues at design is very important for both skewed and curved bridges. Such investigations usually will reduce bid costs by providing additional information on design plans and specifications that will lead the contractors to prepare bids based on knowledge rather than uncertainty.

Clearly, to accomplish all these objectives in practical levels of time and cost demands a true professional who is steeped in the technology, construction and enabling technologies that permit him/her to succeed. Success is not measured in the plan set, but only after bidding, construction, acceptance by the public and years of service. Fortunately, the tools and enabling technologies are available to the enterprising engineer.

First, unique fundamental behavioral issues related to skewed and curved steel bridges must be considered. In addition to vertical bending and shear, torsion in skewed and curved bridge girders results in shear and warping stresses not significant in typical girder bridges, but that must be considered during the design of curved and/or skewed bridges (Section 6.4.8). As discussed in Section 6.4.8.2.2, warping of I-sections results in transverse shears in the flange and concomitant lateral bending stresses (Figure 6.4.9.4-1). In box sections, the torsion results in torsional shear stresses and cross-section distortion stresses (Section 6.4.8.3). Warping is less severe in closed sections such as box girders.

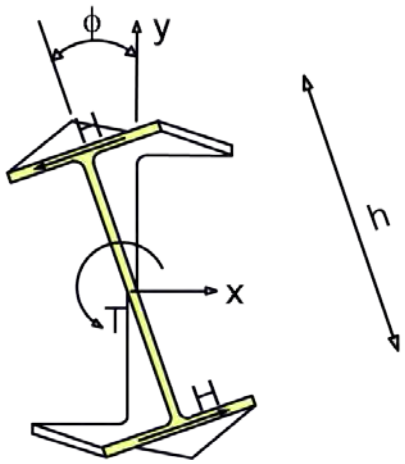

Figure 6.4.9.4-1 I-Girder Subjected to Torsion

In skewed and curved bridges, significant load is often transferred between the girders. Curved girders depend on their neighbor girders for stability, which is accomplished by shifting load to the next girder away from the center of curvature. This action prevents the girders from twisting further. However, they do twist due to the curvature. Connection to the adjacent girders, usually at cross-frames, interrupts the torsion creating what is referred to as “non-uniform torsion”. Of course, this causes increased cross-frame forces and deck stresses. Vertical deflections of adjacent girders differ, resulting in lateral deflection and twist of the girders. Hence, deflection control becomes more critical. Torsion changes the vertical and horizontal

reactions, as do thermal loads, wind loads and centrifugal force; all of which have a significant impact on bearing design.

The integrated behavior of the entire system must be recognized in the analysis of curved-girder bridges due to the significant interaction between components. Bracing members between girders must be included in the analysis and designed as primary load-carrying members. Greater durability and integrity of the bridge can be attained by including all of the structure in the analysis. By computing the force effects on the bearings, bracing and the deck, these components may be designed from rationally computed forces. For example, lateral forces due to vertical as well as lateral loads on laterally restrained bearings can be computed. This information permits rational design of the bearings for lateral forces, particularly those due to vertical loads. This design information leads to much better bearing performance; this is particularly true for bearings in bridges with skewed supports. Rational design of cross-frame members and their connections can be made. The deck reinforcing can be rationally designed for both shear and transverse bending.

A refined analysis model is shown below in Figure 6.4.9.4-2. Refined analysis employing such models ensures much more accurate recognition of system behavior.

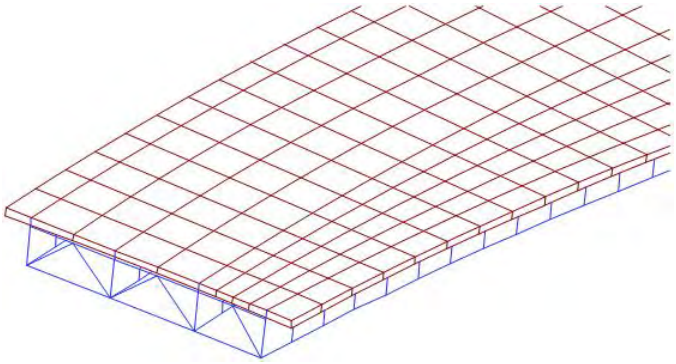

Figure 6.4.9.4-2 3D Analysis Model of Curved I-Girder Bridge with Deck

Rational (sanity) checks of statics, strength of materials and deflections are particularly important when refined analyses are employed since the analysis involves calculations performed by a computer and depends on input assumptions made within the computer, and the correctness of the algorithms within the software. There are two methods most commonly employed for checking. First is simply to check global statics; e.g. ensuring that the sum of the vertical reactions equals the vertical applied loads. The second methodology is to use the program to solve classical problems that have been solved by classical methods.

In skewed and curved girder bridges, the effects of torsion and amplification of deflections must be considered in the girder design. As mentioned previously, for I-girders, lateral flange bending stresses due to torsion are the primary concern. For box girders, shear stresses and cross-section distortion stresses due to torsion are the primary concern.

For certain bridges with skewed supports and/or curved girders, it may be desirable to provide a Construction Plan in the bid documents indicating what constructibility considerations were made during design. This Construction Plan would be based on the assumptions made at design. For example, it might include components such as an erection plan assumed in developing cambers and stresses, the assumption in design for temporary supports and the deck casting sequence assumed in design. It typically would not include means and methods that are customarily determined by the contractor and should remain as such.

Bracing members provide system stability for curved girders and are critical to controlling deflections; thus, they are designed as primary members. This is not directly true for bridges with skewed supports. However, skews may introduce unusually large cross-frame forces, deck stresses and lateral bearing forces compared to “right” bridges. The composite interaction of the cross-frames with the deck through the shear studs is considered in the design of shear connectors in both skewed and curved girder bridges. Transverse deck moments can be significant enough that additional reinforcing beyond the nominal amount required for the deck may be required.

There are several factors that the fabricator, erector and general contractor should be aware of in order to build bridges with horizontally curved girders and/or skewed supports.

The first decision the fabricator must address when confronted with a curved-girder project is the method of fabrication of the girders. Welded girders may be built by either cut curving the flanges or heat curving flanges of girders built straight. Cut curving is shown in Figure 6.4.9.4-3. This method requires additional plate beyond that required for the final girder flanges, which must be ascertained at the time of ordering of the plate from the steel mill. If the decision is made to heat curve the flanges, the plate order will be different. These issues are examined in more detail in Section 6.3.4.4.5.

Whichever method the fabricator selects to curve the flanges, handing and shipping of curved girders presents an additional set of challenges.

Figure 6.4.9.4-3 Cut Curved I-Girder Flanges in the Fabrication Shop

Erection of horizontally curved steel girders is more complex than the erection of straight steel girders due to the inherent instability of the girders. Frequently the erector is called on to retain an engineer to analyze the system during different stages of the erection to ensure that effects such as girder twist and stability are properly considered during the erection process. Temporary supports are often found to be necessary that might not have been required if the girders were straight (Figure 6.4.9.4-4).

Girders in skewed and curved bridges erected with their webs plumb in the so-called “no-load condition” will be out-of-plumb when the dead load is applied, except at radial supports. Special detailing of the cross-frames in skewed and curved bridges may be required to achieve girder webs in the plumb position after the dead load has been applied.

Skewed supports can complicate the deck-casting. In structures with severe skews, the contractor may choose to skew the screed parallel to the supports in an attempt to equalize the load on the girders. This leads to a longer screed. If the bridge is wide, transverse casts may be required introducing longitudinal construction joints. This also complicates the calculation of deflections, girder moments and cross-frame forces.

Deck overhang brackets create lateral flange bending moments in the top and bottom flanges of the exterior girders. It is desirable to place the bottom of the bracket at the bottom flange in order to maximize the moment arm and reduce the

lateral force on the flanges, which in turn reduces the lateral flange moments. The lateral flange moments may be significant on the top flange of the outside convex curved girder where the brackets caused lateral flange moments that are additive to those due to curvature in the positive moment regions of the girder.

Figure 6.4.9.4-4 Temporary Supports on Curved I-Girder Bridge

All of these unique issues relative to skewed and curved steel bridges are discussed in greater detail in NHI (2011).

6.4.9.5 Effects of Curvature and Skew

6.4.9.5.1 I-Girder Bridges

6.4.9.5.1.1 Straight Skewed Bridges

In straight-skewed I-girder bridges, the girders deflect only vertically under their self-weight as long as the cross-frames are not connected to the girders in a manner such that they are engaged and can transfer internal shears and moments (Figure 6.4.9.5.1.1-1).

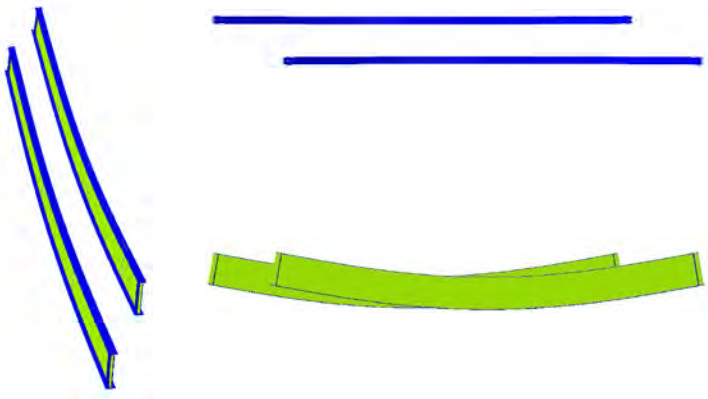

Figure 6.4.9.5.1.1-1 Magnified Girder Vertical Deflections for Two Simple-Span I-Girders on Parallel Skewed Supports Subjected to Steel Dead Load Prior to Interconnecting the Cross-Frames

When the cross-frames are connected to the girders, the interconnected girders deflect as a three-dimensional system under all subsequent loads. The cross-frames brace the girders, but they also serve as an additional transverse load path in the system. As a result, the girders deflect vertically and simultaneously twist under the dead loads (Figure 6.4.9.5.1.1-2).

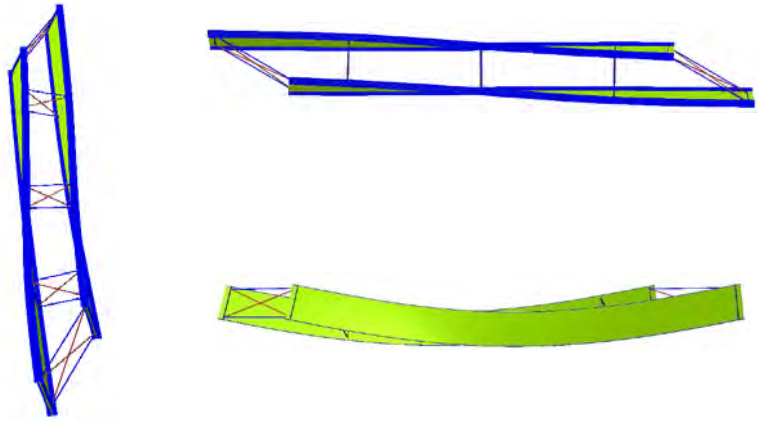

Figure 6.4.9.5.1.1-2 Magnified Girder Vertical Deflections and Twist for Two Simple-Span I-Girders on Parallel Skewed Supports Subjected to Steel Dead Load when Cross-Frames are Connected to the Girders

Where the cross-frames are perpendicular to the girders, the twisting occurs primarily because of the differential vertical deflections between the girders at each of the intermediate cross-frames, since these cross-frames connect to different positions within the span of each of the girders. In straight skewed bridges with parallel skews and contiguous cross-frames aligned with the skewed bearing lines, which is permitted by AASHTO for skew angles less than or equal to 20 degrees

from normal (Section 6.3.2.9.4.3.1), the differential vertical deflections at the ends of the cross-frames are essentially zero. However, in this case, girder twisting is induced by the rotational continuity between the skewed cross-frames and the girders. Similarly, along skewed bearing lines where the vertical deflections of the girders are zero, the girders must also twist to maintain rotational continuity between the support cross-frames and the girders. At any position along the bridge where the cross-frames are skewed relative to the girders, if the girders have non-zero major-axis rotations, the girders must twist to maintain rotational continuity with the cross-frames.

6.4.9.5.1.2 Horizontally Curved Bridges

The bridge cross-section in horizontally-curved I-girder bridges is subjected to significant internal torsional moments due to the fact that the resultant of the bridge vertical loads within the spans has an eccentricity relative to a straight chord between the supports. In a straight skewed bridge, the total internal torsion tends to be relatively small and it is induced entirely by the compatibility of deformations between the girders and the cross-frames; that is, if the girders are not interconnected by the cross-frames, there is no tendency for them to twist under the primary vertical loads. However, the internal torsion in curved bridges exists independently of the interconnection of the girders by the cross-frames.

The predominant resistance to the above internal torsion in horizontally-curved I-girder bridges is developed by interconnecting the girders by the cross-frames across the entire bridge width. Vertical forces are applied to the girders at the cross-frames by the diagonal cross-frame members. This produces a shift in the internal vertical forces toward the girders on the outside of the horizontal curve. Associated radial forces are applied from the cross-frames to the girders that prevent excessive individual girder torsional rotations by attaching the girders to the overall bridge cross-section. Because the overall bridge cross-section wants to rotate torsionally (Figure 6.4.9.5.1.2-1), curved I-girders and curved I-girder bridge units generally cannot be erected without providing some type of intermediate vertical support within the spans, typically via holding cranes or temporary shoring at critical stages of the erection.

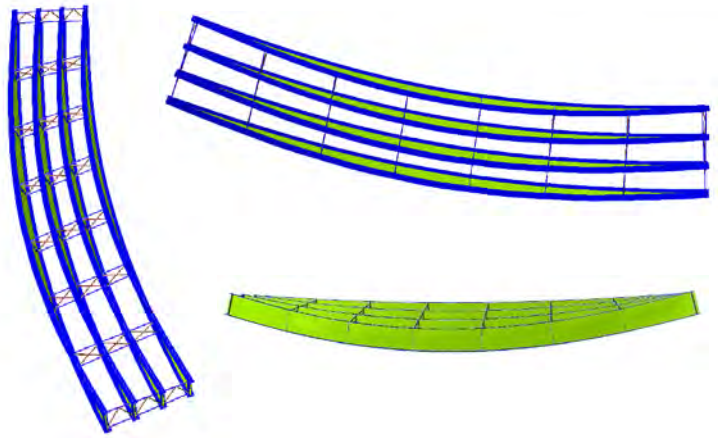

Figure 6.4.9.5.1.2-1 Magnified Girder Vertical Deflections and Twist for Four Horizontally Curved Simple Span I-Girders on Non-Skewed Supports Subjected to Steel Dead Load

The torsion on the girders is resisted internally by the development of non-uniform (warping) torsion in the girders (Section 6.4.8.2.2), which results in the development of flange lateral bending moments (and stresses) along the girder lengths. In this case, the flange lateral bending moments are approximately proportional to the major-axis bending moment and the square of the cross-frame spacing, and are inversely proportional to the radius and the girder depth (*AASHTO LRFD* Eq. C4.6.1.2.4b-1). These lateral bending moments must always be considered in the design. The flange lateral bending moments resulting from torsion due to curvature are distinctly different from flange lateral bending moments resulting from torsion due to skew effects. In curved bridges, a direct coupling exists between major-axis bending and flange lateral bending due to the horizontal curvature. Major-axis bending of curved girders generally cannot occur without also inducing twisting of the girders, and twisting of curved girders generally cannot occur without also inducing major-axis bending.

Figure 6.4.9.5.1.2-2 (FHWA/NHI, 2010) shows the free-body diagram of a curved I-girder compression flange between two cross-frames. The flange is subject to a constant axial compressive force, P, induced by an assumed uniform major-axis bending moment acting in-between the cross-frames. The radial forces, H, shown on the free body are the restoring forces at the cross-frames. Vertical forces (not shown) are also applied at the cross-frame locations by the diagonal cross-frame members. Load is transferred between the curved girders through the cross-frames. The non-collinearity of the flange forces, P, at the cross-frames due to the curvature is accentuated in Figure 6.4.9.5.1.2-2 Part A. The distributed radial components of these flange forces, which are directly proportional to the major-axis bending moment, bow the flange outward. The flange lateral moments due to the non-uniform torsion, M_L, shown at the cross-frames in Figure 6.4.9.5.1.2-2 Part A,

restrain the outward bowing of the flange in this case. The sense of the lateral moments at the cross-frames in compression flanges in usually taken as negative.

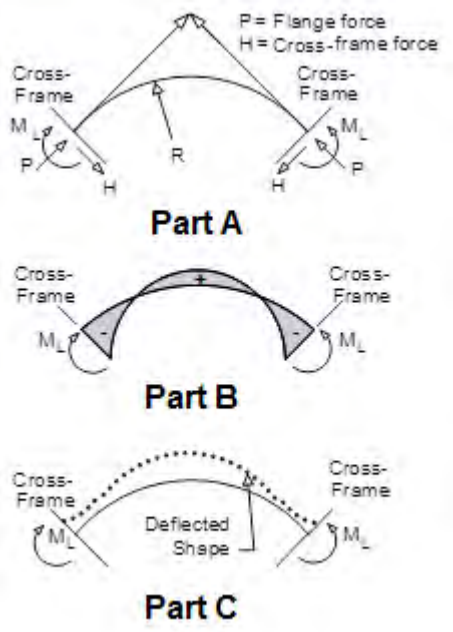

Figure 6.4.9.5.1.2-2 Curved I-Girder Compression Flange In-Between Two Cross-Frames
(A) Free Body Diagram; (B) Flange Lateral Bending Moment Diagram; (C) Deflected Shape in the Lateral Direction

As illustrated in Figure 6.4.9.5.1.2-2 Part B, the sign of the flange lateral bending moments reverses over the central region between cross-frames, much as the sign of the major-axis bending moments reverses in a continuous-span beam. An elementary analysis of the flange lateral bending due to curvature can in fact be made by assuming a beam (i.e. the flange) that is continuous across rigid supports (i.e. the cross-frames).

The net effect of the non-uniform torsion due to the horizontal curvature in compression flanges is to increase the curvature of the flange, as illustrated in Figure 6.4.9.5.1.2-2 Part C. The net lateral movement of the entire flange in-between the cross-frames is outward away from the center of curvature, with a reversal of curvature occurring in the flange near the cross-frames due to the lateral restraint offered by the cross-frames.

For a curved I-girder tension flange, diagrams similar to those shown in Figure 6.4.9.5.1.2-2 can be drawn with all of the actions reversed. The bending sense of the lateral bending moments at the cross-frames in tension flanges is usually taken as positive, with the sign of the moment again reversing in-between the cross-

frames. In this case, the distributed radial components of the flange force tend to reduce the curvature, i.e. they straighten the flange or bend the flange toward the center of curvature, while the flange lateral bending moments at the brace points tend to restore the curvature. The net effect on the flange can be to either increase or decrease the curvature of the flange depending on the flange stiffness and curvature. The net lateral movement of the tension flange is typically not large. Regardless, the net lateral movements of the top and bottom flanges lead to an overall canting of the girder web from its initial plumb orientation.

Thus, in straight skewed bridges, the cross-frames tend to force twist rotations into the girders in order to satisfy displacement compatibility requirements resulting from the skewed-bridge geometry. The resulting non-uniform torsion and flange lateral bending moments are indirectly related to the girder major-axis bending. In curved radially supported bridges, the cross-frames restrain the tendency of the individual girders to twist as a result of the curvature and act to reduce the twist rotations of the girders; approximately equal twist rotations are enforced across the bridge cross-section at the locations where the cross-frames are attached to the individual girders. The resulting non-uniform torsion and flange lateral bending moments are directly coupled to the girder major-axis bending. Although the cross-frame forces may be significant in both cases, only the cross-frames in horizontally curved bridges are currently required by AASHTO to be treated as primary members for design, since these components are more critical to the overall stability of the bridge system.

6.4.9.5.1.3 Horizontally Curved Bridges with Skewed Supports

Horizontally curved bridges with skewed supports are probably the most complex category of I-girder bridges. In curved I-girder bridges with skewed supports, non-uniform torsion is introduced into the girders by both the curvature and the skew, as described previously. The curvature and skew can exhibit either additive and/or subtractive skew and curvature effects depending on the overall bridge geometry. A skewed abutment, in combination with the framing of the cross-frames, can cause girder twist rotations that act in the same direction as the twist due to horizontal curvature. However, a similar skewed abutment with a skew angle that is the negative of the above, in combination with the framing of the cross-frames, can induce girder twist rotations that act in the opposite direction from those due to the horizontal curvature. Refined analysis is strongly recommended to more accurately capture the combined system effects in these bridges.

Discontinuous cross-frames adjacent to the skewed supports can be a useful tool in these bridges to provide a desirable reduction in the cross-frame forces in the vicinity of the skewed supports, and to reduce “nuisance stiffness” effects, as discussed previously (Section 6.3.2.9.4.3.2). Elimination of skewed interior supports in continuous-span horizontally-curved bridges is always desirable, if practical. An integral pier cap in conjunction with a single-shaft pier is one possible option that

may be considered to eliminate a skewed interior support and also eliminate potential vertical clearance problems in some cases (Figure 6.3.3.3.4-2 Part C). Of course, extending the end spans and eliminating skewed end supports is also a desirable option where possible and practical.

6.4.9.5.1.4 Skewed and/or Curved Steel Bridge Fit

Skewed and curved I-girder bridges have been built successfully for many years and have performed well in service. However, challenging attributes of the framing arrangements combined with long-used detailing practices and common erection procedures can result in issues during construction at certain extremes. Some of the issues encountered have included:

- Girders and cross-frames that are difficult to assemble during the erection, requiring unplanned operations such as substantial force fitting of connections, field drilling and field welding;
- Erected girders with webs that are significantly out-of-plumb (although out-of-plumbness of girder webs is not necessarily problematic);
- Additive locked-in stresses in the cross-frames and girders, which may be significant in some cases;
- Bearing rotations that are larger than allowable design limits; and
- Deck joints and barrier rails that are out-of-alignment between the approach and the end of the bridge.

In certain instances, these issues have resulted in construction delays, rework, cost overruns, and disputes and litigation.

Skewed and/or curved I-girder bridges generally exhibit torsional displacements, or twisting, of the individual girders and of the overall bridge cross-section under load, including the loads during construction. The above issues can be avoided by developing a better understanding of the effects of this twisting, and the ways in which framing arrangements, cross-frame detailing practices, and erection procedures influence the behavior of the bridge.

The “fit” or “fit condition” is of particular importance as part of the above considerations. These terms are used commonly to refer to the deflected or undeflected geometry under which the cross-frames are detailed to attach to theoretically plumb girders with theoretically no load in the cross-frame members. The most commonly referenced fit conditions are No-Load Fit (NLF) or Fully-Cambered Fit, where the cross-frames are detailed to attach to the girders without any force-fitting in their initially fabricated, plumb, undeflected geometry under zero load, Steel Dead Load Fit (SDLF) or Erected Fit, where the cross-frames are detailed to attach to the girders in a plumb position in which the girders are deflected only vertically under the bridge steel dead loads, and Total Dead Load Fit (TDLF) or

Final Fit, where the cross-frames are detailed to fit to the girders in a plumb position in which the girders are deflected only vertically under the bridge total dead loads.

The “fit” or “fit condition” is selected to offset, or compensate for, the tendency of the I-girders to twist in skewed and/or curved I-girder bridges, with due consideration of potential impacts on constructibility, the constructed geometry, and the internal forces induced in the structure.

Different skewed and/or curved I-girder bridges experience the above issues to different degrees. Bridges with smaller skew and/or with larger radii and/or with shorter spans are not as severely affected. For a given skew and/or horizontal curvature, bridges with longer spans potentially can experience more difficulties with respect to key responses during and at the completion of the construction, such as: fit-up (i.e., assembly) of the steel during the erection, achievement of the targeted constructed geometry under dead load, and development of significant changes in the internal force states in the structure under dead load due to detailing and erection procedures.

It is important to recognize that twisting of the girders in a sharply skewed and/or tightly curved I-girder bridge is not necessarily indicative of a structural problem or deficiency. If this were the case, essentially all of these bridges with extreme geometries would be deficient under the design live loads. However, it is important to recognize and understand the effects of the girder twisting that occurs in these bridges. This is necessary so that an informed decision on an appropriate fit condition can be made as a function of the bridge geometry to avoid construction problems, thus ensuring a successful project.

The Design Engineer typically analyzes and designs a bridge as if the bridge is fully constructed in the unstressed (No-Load) position, without any force-fitting, and then the gravity load is simply “turned on.” This is a simplifying assumption which does not account for the influence of fabricated geometry and the cross-frame detailing method on the bridge response. *AASHTO LRFD* Article 6.7.2 specifies that for straight skewed I-girder bridges and horizontally curved I-girder bridges with or without skewed supports, the contract documents should state an intended erected position of the girders and the load condition under which that position is to be achieved. The intent of this provision is to ensure that the preferences of the Owner and Engineer of Record regarding the anticipated erected position of the girders are clearly conveyed to those involved in the fabrication and construction of the bridge.

Since the fit decision directly influences the cross-frame fabricated geometry, as well as the bridge constructibility and subsequent internal forces, the fit condition should ideally be selected by the designer, who best knows the loads and capacities of the structural members, with proper consideration of the bridge erection. To facilitate an informed decision, the designer can (and should) discuss their bridge with

experienced fabricators, detailers, erectors, and contractors. The desired outcome, safe, easy and economical construction of skewed and/or curved steel I-girder bridges, is more likely to be achieved if all parties involved in the design and construction of the bridge communicate early to ensure that an appropriate fit decision is made for a particular bridge project.

A fit decision always must be made so that the Fabricator/Detailer can complete the shop drawings and fabricate the bridge components in a way that allows the Erector/Contractor to assemble the steel and achieve a desired geometry in the field. The fit decision also affects design decisions that must be made regarding the rotation demands on the bearings as well as the internal forces for which the cross-frames and girders must be designed. The Design Engineer needs to understand how the bridge will respond to a specific fit condition, particularly how the fit decision may influence the erectability of the steel, how it influences the deflected geometry of the structure under its dead load, and how it affects the internal stresses in the various bridge components.

The key question, then, is under what (load) condition should an I-girder bridge be detailed to fit? Certainly, the Total Dead Load condition is of great interest: to perform effectively in service, girders and cross-frames need to be in place, properly connected and properly functioning, with internal loads which do not exceed the capacity of the structure. Therefore, one might infer that bridges should be detailed simply to fit in their final constructed condition. For some bridges fitting the cross-frames to the final condition is fine and indeed may be the best choice; however, for others, fitting to the final condition significantly increases the internal cross-frame forces and can potentially make the bridge unconstructable. For every bridge, the fit condition must be selected to effectively manage the structure's constructed geometry and internal forces, and to facilitate the construction of the bridge.

NSBA (2014) has been prepared to assist the Owner and the Engineer of Record, in consultation with fabrication and construction professionals, to make a more informed consensus decision in specifying the fit condition for a particular skewed and/or curved steel I-girder bridge. The document is also useful for a Field Engineer to better understand the observed behavior of these bridges during construction. The document provides tables of recommended and acceptable fit conditions for straight skewed and curved steel I-girder bridges (with or without skew) as a function of broad generalized characteristics of the bridge geometry. The tables also indicate which fit condition(s) should be avoided for a particular bridge type. The reader is referred to NCHRP (2012), NSBA (2014), and to NHI (2011) for additional more detailed information regarding fit and the various fit conditions for which the cross-frames may be detailed to attach to the girders to offset, or compensate for (to different extents), the tendency of the I-girders to twist in these bridge types.

6.4.9.5.2 Box-Girder Bridges

The major difference between box girders and I-girders subjected to torsion is that the individual box is capable of resisting much larger torques than a typical I-girder of similar vertical bending capacity. The system behavior of curved-box girder bridges must still be recognized in their analysis, but the treatment of the individual girder element changes and is somewhat more complex in the case of box girders. Since the live load distribution factor for multiple box-girder bridges (*AASHTO LRFD* Article 6.11.2.3) does not address skewed and curved bridges, a refined analysis is inferred at least to determine the live-load effects. Internal and external cross-frames/diaphragms and lateral bracing members are subject to design forces and are to be treated as primary members. A typical two-tub curved box-girder bridge is shown in Figure 6.4.9.5.2-1.

Box-girders on skewed supports are subject to large torques and tend to be particularly problematic to design and to build. Special care should be taken in analyzing and detailing box girders, particularly intermediate cross frames and lateral bracing in order to design a successful bridge.

Figure 6.4.9.5.2-1 Underside of a Two-Tub Curved Box-Girder Bridge

There are three means whereby torsion is generally introduced into box-girder bridges. First is the application of vertical or lateral loads that do not pass through the shear center of the box cross-section. This includes essentially all dead, live, and wind loads. The second means is through horizontal curvature. The third means is through the bearings or supports. A single bearing resists no torsion; stability must be obtained via a set of bearings on a support. A pair of bearings

supporting a box girder on a skewed support introduces significant torsion into a box. The reason for this is that the bearing nearest the span receives greater load than does the rear bearing; hence, a torque is introduced by the presence of unbalanced reactions in the two bearings. Since neither of these reactions pass through the shear center of the box, torsion is created. Connections between the boxes tend to restore the girder to its original position. As a result, the forces in cross frames/diaphragms are often referred to as restoring forces.

The concrete deck of composite box girders is subjected to horizontal shear due to the shear flow in the box in addition to horizontal shears similar to those in an I-girder deck. Hence, it is particularly important to check the deck reinforcement for these additional shear forces.

6.4.10 Cover Plates

In lieu of increasing the width and/or thickness of flange plates in order to increase the flexural resistance of welded beams, or in order to increase the flexural resistance of rolled beams, cover plates can be attached to one or both flanges. The design of cover plates is covered in *AASHTO LRFD* Article 6.10.12. Because of concerns about the fatigue resistance of cover-plated details, the use of cover plates has generally fallen into disfavor, except perhaps for rehabilitation purposes. Utilizing the moment redistribution provisions described in Section 6.5.6.6 can help to eliminate the need for cover plates in straight continuous rolled-beam bridges.

As specified in *AASHTO LRFD* Article 6.10.12.1, the length of any cover plate, L_{cp}, in feet that is added to a member must satisfy the following:

$$L_{cp} \geq \frac{d}{6.0} + 3.0 \qquad \text{Equation 6.4.10-1}$$

AASHTO LRFD Equation 6.10.12.1-1

where *d* is the total depth of the steel section in inches. The maximum thickness of a single cover plate is not to be greater than two times the thickness of the flange to which it is attached. Multiple welded cover plates on a single flange are not permitted.

Cover plates can either be wider or narrower than the flange to which they are attached, but where they are wider, welds are not to be wrapped around the ends of the cover plate. Transverse end welds may or may not be provided in this particular case, but if they are provided, they should be stopped short of the flange edges. Where transverse end welds are not provided in this case, the fatigue resistance at the cover-plate end is reduced from Detail Category E to Category E′ (*AASHTO LRFD* Table 6.6.1.2.3-1). Cover plates may be tapered at their ends, but the width

at the ends of the tapered plates must not be less than 3.0 inches. Tapering the cover plate ends does not significantly increase the fatigue resistance at welded ends. The stress concentration at the weld end that is transverse to the applied stress is not significantly altered by varying the shape of the cover-plate end (Fisher, 1977).

As specified in *AASHTO LRFD* Article 6.10.12.2.1, the theoretical end or cutoff point of the cover plate is to be taken as the section where the major-axis bending stress, f_{bu}, or the moment, M_u, due to the factored loads is equal to the factored flexural resistance of the flange. The cover plate must then be extended a terminal distance beyond the theoretical end such that:

- The stress range at the actual end of the cover plate (i.e. at the point located at the terminal distance beyond the theoretical end) satisfies the load-induced fatigue requirements specified in *AASHTO LRFD* Article 6.6.1.2 (Section 6.5.5); and
- The longitudinal force in the cover plate due to the factored loads at the theoretical end can be developed by sufficient welds and/or bolts placed between the theoretical and actual ends.

As mentioned earlier, the fatigue resistance of cover-plated details is a significant consideration in locating the termination (i.e. the actual ends) of partial-length cover plates. Cover plates are typically attached to flanges using welds. The continuous longitudinal welds connecting the cover plate to the flange away from the cover-plate ends are fatigue Detail Category B. Between the theoretical and actual ends of the cover plate, these welds must be adequate to develop the computed force in the cover plate at the theoretical end (*AASHTO LRFD* Article 6.10.12.2.2).

The ends of the longitudinal welds and the toe of the transverse end weld (if provided) connecting partial-length welded cover plates to the flange provide comparable fatigue conditions. These conditions result in a very low fatigue resistance. According to *AASHTO LRFD* Table 6.6.1.2.3-1, for base metal at the actual ends of partial-length welded cover plates narrower than the flange, with or without transverse end welds, or wider than the flange with transverse end welds, the nominal fatigue resistance is based on fatigue Detail Category E (for flange thicknesses less than or equal to 0.8 inches) or Detail Category E′ (for flange thicknesses greater than 0.8 inches). As mentioned previously, where the cover plates are wider than the flange and transverse end welds are not provided, the nominal fatigue resistance is computed based on Detail Category E′. For flanges more than 0.8 inches thick used in nonredundant load path structures subject to repetitive loadings that produce tension or stress reversal in the flange, partial-length welded cover plates are not to be used (*AASHTO LRFD* Article 6.10.12.1).

According to *AASHTO LRFD* Table 6.6.1.2.3-1, the nominal fatigue resistance at the ends of partial-length cover plates may be based on fatigue Detail Category B if bolted slip-critical end connections are provided. The bolts provided between the theoretical and actual ends of the cover plate must be sufficient to develop the force due to the factored loads in the cover plate at the theoretical end (*AASHTO LRFD* Article 6.10.12.2.3), and the continuous longitudinal welds connecting the cover plate to the flange must stop a distance of one bolt spacing before the first row of bolts in the end-bolted portion (Wattar et al., 1985). The slip resistance of the bolts in the end-bolted portion is to be determined according to the provisions of *AASHTO LRFD* Article 6.13.2.8 (Section 6.6.4.2.4.2). As specified in *AASHTO LRFD* Article 6.10.12.2.3, the contract documents must indicate that end-bolted cover plates be installed in the following sequence:

- Drill holes;
- Clean faying surfaces;
- Install bolts; and
- Weld the cover plates.

If the cover plate is welded first to simplify fabrication, cutting oils used during the hole drilling process will reduce the slip coefficient and Detail Category B stress levels will not be developed regardless of the surface preparation used (Wattar et al., 1985).

6.4.11 Minimum Thickness of Steel

AASHTO LRFD Article 6.7.3 specifies requirements related to the minimum thickness of steel.

The minimum thickness of structural steel is specified to be 5/16 inches. This includes bracing, cross-frames and all types of gusset plates, except for gusset plates used in trusses for which the thickness is not to be less than 3/8 inches. Webs of rolled shapes, closed ribs in orthotropic decks, fillers and structural steel used in railings are also exempt from the minimum 5/16-inch requirement. The web thickness of rolled beams or channels is not to be less than ¼ inches. The reader is referred to *AASHTO LRFD* Article 6.7.3 for the minimum thickness requirements for orthotropic decks.

Where the steel is expected to be exposed to severe corrosive influences, it is to be specially protected against corrosion, or else a sacrificial metal thickness is to be specified.

Section 6.5 Girder Design Verifications

6.5.1 Introduction

This section discusses the basis of the LRFD flexural design resistance equations for steel I-girders and box girders. The specific LRFD design verifications for I-girders and box girders for constructibility, at the service limit state, at the fatigue limit state and at the strength limit state are then presented. Strength limit state design verifications for flexure are discussed for sections subject to negative flexure, positive flexure and stress reversal. Strength limit state design verifications for shear are also reviewed.

6.5.2 LRFD Flexural Design Resistance Equations

6.5.2.1 I-Girders

6.5.2.1.1 General

The *AASHTO LRFD* flexural resistance equations for the design of steel I-girders are discussed in this section. The same equations are used to check both straight and horizontally curved I-girders with or without skew.

In I-girder bridges, significant flange lateral bending may be caused by wind, by the use of discontinuous cross-frame/diaphragm lines in conjunction with skews exceeding 20° from normal (radial), by torsion due to curvature and by torsion due to eccentric concrete deck overhang loads acting on cantilever forming brackets placed along fascia girders. After the flange lateral bending stresses due to one or more of these effects have been determined, the issue then becomes how to effectively and rationally combine these stresses with the flange major-axis (vertical) bending stresses to check the capacity of the flange (or section). For I-girders, the so-called "one-third rule equations" are used in the *AASHTO LRFD* Specifications to combine the lateral flange bending stresses, f_ℓ, with the vertical bending stresses, f_{bu}, to check the flexural resistance. These equations were introduced in the 2005 Interim Specifications.

The form of the one-third rule equation shown in Equation 6.5.2.1.1-1 is used at sections for which the vertical flexural resistance is expressed in terms of flange stress:

$$f_{bu} + \frac{1}{3} f_\ell \le F_r \qquad \text{Equation 6.5.2.1.1-1}$$

where:

f_{bu} = flange vertical bending stress determined as specified in *AASHTO LRFD* Article 6.10.1.6 (ksi)

f_ℓ = flange lateral bending stress (ksi)

F_r = factored flexural resistance in terms of flange vertical bending stress = $\phi_f F_n$ (ksi)

F_n = nominal flexural resistance in terms of flange vertical bending stress (ksi)

ϕ_f = resistance factor for flexure = 1.0 (*AASHTO LRFD* Article 6.5.4.2)

The second form of the one-third rule equation shown in Equation 6.5.2.1.1-2 is used at sections for which in the vertical flexural resistance is expressed in terms of moment:

$$M_u + \frac{1}{3} f_\ell S_x \le M_r \qquad \text{Equation 6.5.2.1.1-2}$$

Where:

M_r = factored flexural resistance in terms of vertical bending moment = $\phi_f M_n$ (kip-in.)

M_n = nominal flexural resistance in terms of vertical bending moment (kip-in.)

M_u = member vertical bending moment determined as specified in *AASHTO LRFD* Article 6.10.1.6 (kip-in.)

S_x = elastic section modulus about the major-axis of the section to the flange under consideration ($in.^3$)

The proper application of each form of the one-third rule equation is discussed below in Section 6.5.2.1.4. When the effects of flange lateral bending are judged to be insignificant or incidental, the flange lateral bending term, f_ℓ, is simply set to zero in the applicable equation.

The one-third rule equations address the combined effects of vertical bending and lateral bending by handling discretely braced compression flanges as equivalent beam-columns. A discretely braced flange is defined as a flange supported at discrete intervals by bracing sufficient to restrain lateral deflection of the flange and twisting of the entire cross section. A flange encased in concrete or attached by shear connectors is considered to be a continuously braced flange. The stress, f_{bu}, and moment, M_u, are analogous to the axial loading in the beam-column and the stress, f_ℓ, is analogous to the beam-column bending moment. M_u is considered analogous to axial loading since it produces axial stresses in the flanges.

For discretely braced tension flanges, the one-third rule equations approximate the full plastic strength of a rectangular cross section subjected to combined vertical and lateral bending.

The resistance equations are written in an interaction format in which the left-hand side of the equations pertains to the applied load effects, and the right-hand side of the equations is the appropriate member resistance in vertical bending. The conceptual basis of these equations and development of the 1/3 factor applied to f_ℓ will be explained in further detail in Section 6.5.2.1.2.

In both forms of the equations, all terms are to be taken positive in sign. However, when summing dead and live load stresses to obtain the total vertical and lateral bending stresses, f_{bu} and f_ℓ, to apply in the equations, the signs of the individual dead and live load stresses must be considered.

6.5.2.1.2 Conceptual Basis

To explain the conceptual basis of the one-third rule equations, consider an isolated flange of an I-girder subjected to combined vertical and lateral bending. If the flange behaves compactly (e.g. a tension flange), it can be assumed to eventually develop the resistances associated with the idealized fully-plastic stress distribution shown on the right-hand side of Figure 6.5.2.1.2-1.

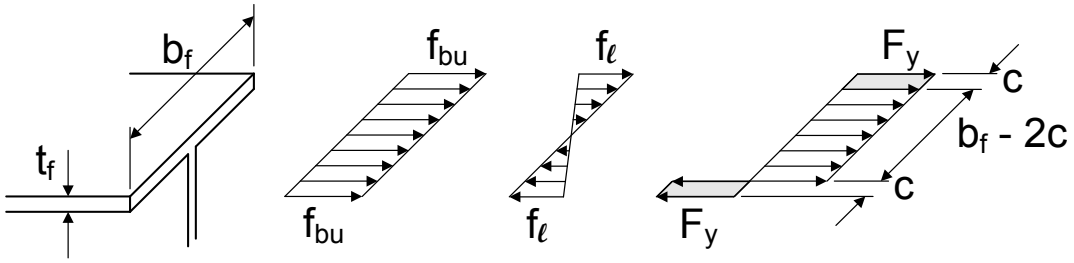

Figure 6.5.2.1.2-1 Fully-Plastic Stress Distribution under Combined Vertical and Lateral Bending (Compact Flange)

Referring to Figure 6.5.2.1.2-1, within this idealized stress distribution, the lateral moment resistance is generated by the strips of width c at the tips of the flange, and the remaining width, ($b_f - 2c$), develops the resistance to the flange force associated with vertical bending. By equating the flange lateral bending moment related to the elastically computed lateral bending stress, $f_\ell S_\ell$, where S_ℓ is the lateral section modulus of the flange, to this lateral moment resistance, one obtains:

$$M_\ell = \frac{f_\ell b_f^2 t_f}{6} = F_y c t_f (b_f - c) \qquad \text{Equation 6.5.2.1.2-1}$$

where b_f is the flange width and t_f is the flange thickness. This quadratic equation can then be solved for the width *c* to obtain:

$$c = \frac{b_f}{2}\left(1 - \sqrt{1 - \frac{2}{3}\frac{f_\ell}{F_y}}\right) \qquad \text{Equation 6.5.2.1.2-2}$$

Similarly, by equating the elastic flange force, *P*, due to vertical bending to the fully-plastic flange force based on the remaining flange width as follows:

$$P = f_{bu} b_f t_f = F_y (b_f - 2c) t_f \qquad \text{Equation 6.5.2.1.2-3}$$

and substituting the value of *c* from Equation 6.5.2.1.2-2, the elastically-computed vertical bending stress associated with the flange fully-plastic resistance may be expressed as:

$$f_{bu} = F_y \frac{b_f - 2c}{b_f} = F_y \sqrt{1 - \frac{2}{3}\frac{f_\ell}{F_y}} \qquad \text{Equation 6.5.2.1.2-4}$$

If one considers practical bridge I-girders, where f_ℓ is typically much smaller than F_y (e.g., $f_\ell \le 0.6F_y$), the preceding equation is approximated accurately by the simple linear equation:

$$f_{bu} = F_y - \frac{1}{3} f_\ell \qquad \text{Equation 6.5.2.1.2-5}$$

The top curve in Figure 6.5.2.1.2-1 shows a plot of the theoretical fully-plastic strength of a discretely braced tension flange for various combinations of the major-axis bending stress, f_{bu}, and flange lateral bending stress, f_ℓ, as given by the exact Equation 6.5.2.1.2-4. The values of f_{bu} and f_ℓ have both been normalized by the flange yield strength, F_{yf}. Also plotted is the simpler linear Equation 6.5.2.1.2-5 based on the use of $1/3f_\ell$, which is shown to give a reasonable approximation of the more exact solution up to the specified limit on f_ℓ of $0.6F_{yf}$ given in *AASHTO LRFD* Article 6.10.1.6. The total of the lateral bending stresses from all sources, including curvature, wind, skew and/or deck overhang forces, is limited to $0.6F_{yf}$ because beyond that limit, the reduction in vertical bending resistance due to the flange lateral bending tends to be greater than that comprehended by the one-third rule equation.

Research has shown that the 1/3 coefficient on f_ℓ also accurately captures the strength interaction between f_{bu} and f_ℓ for discretely braced compression flanges, including the various yielding and stability effects, again up to the limit of $0.6F_{yf}$ on f_ℓ. In this case, the resistance of the compression flange may be governed by either flange local buckling or flange lateral-torsional bucking and the flange may not be able to reach F_{yf} under the combined effects. In the case shown in Figure 6.5.2.1.2-2, the compression flange is only assumed able to reach $0.7F_{yf}$, for

example, due to the effects of local or lateral-torsional buckling. In such cases, the slope of the line relating f_{bu} and f_ℓ, again based on the 1/3 coefficient, was found to be an excellent lower-bound fit to a large series of analytical, numerical and experimental results (represented by the series of dots in the figure). As such, the one-third rule equations may be considered both semi-analytical and semi-empirical.

The final stress form of the one-third rule equation (Equation 6.5.2.1.1-1) was obtained by changing F_{yf} (or $0.7F_{yf}$ for the compression flange in this case) to the factored flexural resistance of the flange, $F_r = \phi_f F_n$, and by bringing the flange lateral bending stress term, $1/3f_\ell$, over to the left-hand side of the equation since it represents a load effect (refer to the box in the upper right-hand corner of Figure 6.5.2.1.2-2). The moment form of the equation (Equation 6.5.2.1.1-2) was obtained by multiplying Equation 6.5.2.1.1-1 through by the elastic section modulus about the major-axis of the section. A more detailed discussion of the derivation and validation of the one-third rule equations is provided in White and Grubb (2005).

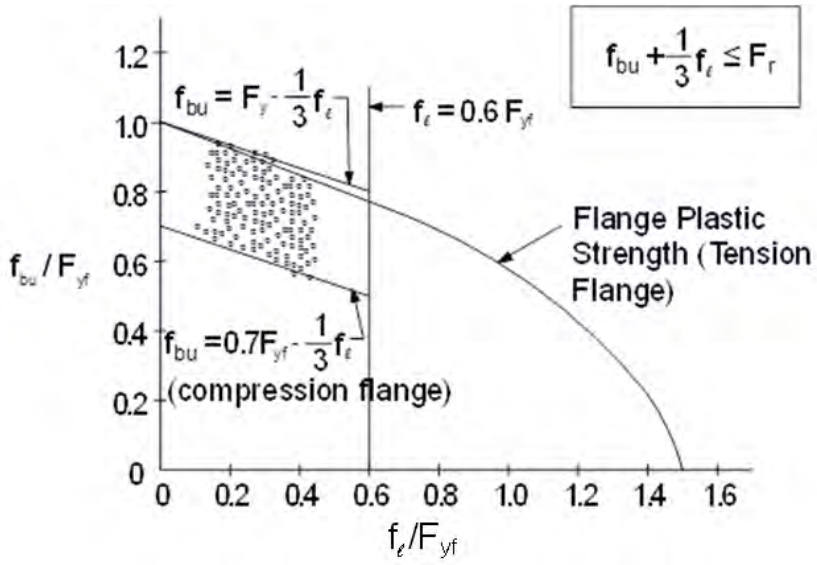

Figure 6.5.2.1.2-2 Normalized Plot of f_{bu} vs. f_ℓ

6.5.2.1.3 Secondary Flange Lateral Bending Stresses

6.5.2.1.3.1 General

In addition to flange lateral bending resulting from non-uniform torsion due to curvature and other effects, other secondary effects generate additional flange lateral bending. These effects include the amplification effect and the radial effect.

6.5.2.1.3.2 Amplification Effect

The secondary effect causing the most significant lateral flange bending is the amplification effect as illustrated schematically in Figure 6.5.2.1.3.2-1, which results due to the lateral deflection of a discretely braced compression flange. As the compression flange curvature increases under load, additional lateral moment occurs due to the axial force in the compression flange acting through the lateral deflection of the flange (similar to the P-delta effect or amplification effect in beam-columns). This effect occurs in both straight and horizontally curved discretely braced compression flanges. The amplification effect is considered negligible in the tension flange as the lateral deflections of that flange tend to be much smaller. Taking the equivalent beam-column analogy one step further, as applied to girder flanges in the one-third rule equation development, consideration must therefore be given to amplifying the compression-flange lateral bending stresses in certain situations.

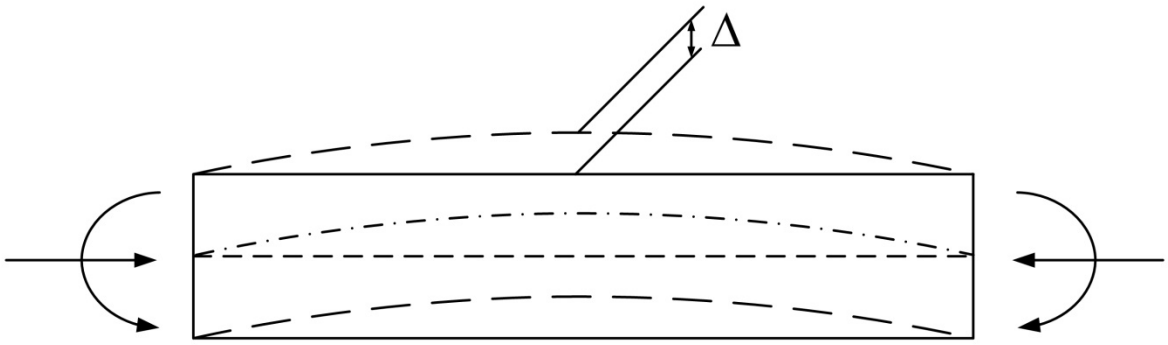

Figure 6.5.2.1.3.2-1 Amplification Effect in a Discretely Braced Compression Flange

The additional lateral bending in the compression flange due to the amplification effect may be estimated directly from a geometric nonlinear (i.e., elastic large deflection or second-order) analysis of the superstructure, or more simply and conveniently, by amplifying first-order compression-flange lateral bending stresses by the approximate amplification factor shown below in Equation 6.5.2.1.3.2-2. In bridge members, it is generally impractical to calculate second-order flange lateral bending stresses directly for the case of moving live loads.

In beam-column members subject to axial compression, secondary bending moments arise equal to the compression force times the lateral deflection of the member. Therefore, internal bending moments are amplified. In an analogous fashion, first-order flange lateral bending stresses in discretely braced compression

flanges may need to be amplified to guard against large unbraced lengths in which second-order lateral bending effects may be significant.

AASHTO LRFD Article 6.10.1.6 specifies that for discretely braced compression flanges, if the following equation is not satisfied, then second-order elastic compression-flange lateral bending stresses must be determined:

$$L_b \le 1.2L_p\sqrt{\frac{C_bR_b}{f_{bu}/F_{yc}}} \qquad \text{Equation 6.5.2.1.3.2-1}$$

AASHTO LRFD Equation 6.10.1.6-2

where:

C_b = moment-gradient modifier specified in *AASHTO LRFD* Article 6.10.8.2.3
F_{yc} = specified minimum yield stress of the compression flange (ksi)
L_b = unbraced length (in.)
L_p = limiting unbraced length to reach a lateral-torsional buckling resistance equal to F_{max} specified in *AASHTO LRFD* Article 6.10.8.2.3 (in.)
R_b = web load-shedding factor specified in *AASHTO LRFD* Article 6.10.1.10.2

The second-order elastic lateral bending stresses may be determined by conservatively amplifying the first-order values based on the following equation in lieu of a direct geometric non-linear analysis:

$$f_\ell = \left(\frac{0.85}{1-\frac{f_{bu}}{F_{cr}}}\right) f_{\ell 1} \ge f_{\ell 1} \qquad \text{Equation 6.5.2.1.3.2-2}$$

AASHTO LRFD Equation 6.10.1.6-4

where:

f_{bu} = largest value of the factored compressive vertical bending stress throughout the unbraced length in the flange under consideration (ksi)
$f_{\ell 1}$ = factored first-order compression flange lateral bending stress (ksi)
F_{cr} = elastic lateral-torsional buckling stress determined from *AASHTO LRFD* Eq. 6.10.8.2.3-8 (ksi)

Note that the right-hand side of Equation 6.5.2.1.3.2-1 is the limiting value of the unbraced length, L_b, for which f_ℓ equals $f_{\ell 1}$ in Equation 6.5.2.1.3.2-2. It also should be noted that F_{cr} for use in Equation 6.5.2.1.3.2-2 is not limited to $R_bR_hF_{yc}$ as it would be when calculating the elastic lateral-torsional buckling resistance for the design of the compression flange (refer to *AASHTO LRFD* Article C6.10.1.6 and Section 6.5.6.2.2.2).

Similar equivalent expressions are specified for use in *AASHTO LRFD* Article 6.10.1.6 (i.e. *AASHTO LRFD* Equations 6.10.1.6-3 and 6.10.1.6-5) whenever the vertical flexural resistance is expressed in terms of moment rather than flange stress (e.g. when the provisions of *AASHTO LRFD* Appendix A6 are employed – Section 6.5.6.2.3).

Equation 6.5.2.1.3.2-2 represents an established form of the amplification equation used to estimate maximum second-order elastic moments in braced beam-column members whose ends are restrained by other framing (White and Grubb, 2005). The purpose of this equation is to guard conservatively against large unbraced lengths in which second-order flange lateral bending effects are significant; for example, in certain construction situations such as when determining the effect of eccentric concrete deck overhang loads acting on exterior-girder flanges. For cases where the amplification of construction dead-load stresses is large, an additional alternative would be to consider conducting a direct geometric nonlinear analysis to more accurately determine the second-order effects. In the final constructed condition, the amplification factor need only be considered for the bottom flange in negative-flexure regions in continuous spans. In these cases, however, F_{cr} is increased significantly due to the moment gradient that exists in these regions, through the moment-gradient modifier C_b.

As shown in White et al. (2001), these equations give accurate to conservative estimates of flange second-order lateral bending stresses. The equations tend to be significantly conservative for larger unbraced lengths in which f_{bu} also approaches F_{cr}. In cases where the amplification resulting from this equation is large, consideration may be given to using an effective length factor k less than 1.0 in the calculation of the elastic lateral-torsional buckling resistance to appropriately increase F_{cr}. The base lateral-torsional buckling equations in the *AASHTO LRFD* Specifications conservatively assume k = 1.0. *AASHTO LRFD* Article C6.10.8.2.3 makes reference to a procedure (SSRC, 1998; Nethercot and Trahair, 1976) that can be used to calculate a reduced effective length factor for lateral-torsional buckling that accounts for the restraint from adjacent unbraced lengths that are less critically loaded than the unbraced length under consideration. The resulting lower value of k can be used to appropriately increase F_{cr} and to modify the unbraced length L_b in special situations. The use of this procedure is demonstrated in Grubb and Schmidt (2012).

When determining the amplification of $f_{\ell 1}$ in horizontally-curved I-girders with $L_b/R \geq 0.05$, F_{cr} in Equation 6.5.2.1.3.2-1 and *AASHTO LRFD* Equation 6.10.1.6-5 may be determined from Equation 6.5.6.2.2.2.2-7 or Equation 6.5.6.2.3.3.2-6 by replacing L_b with $KL_b = 0.5L_b$. For girders with $L_b/R < 0.05$, L_b may be used. The use of $KL_b = 0.5L_b$ for $L_b/R \geq 0.05$ gives a better estimate of the amplification of the bending deformations associated with the boundary conditions for the flange lateral bending at intermediate cross-frame locations, which are approximately symmetrical, and assumes that an unwinding stability failure of the compression flange is unlikely for

this magnitude of the girder horizontal curvature. Figure 6.5.2.1.3.2-2 illustrates qualitatively, using a straight elastic member for simplicity, the amplified second-order elastic flange lateral deflections associated with horizontal curvature effects, as well as the unwinding stability failure mode.

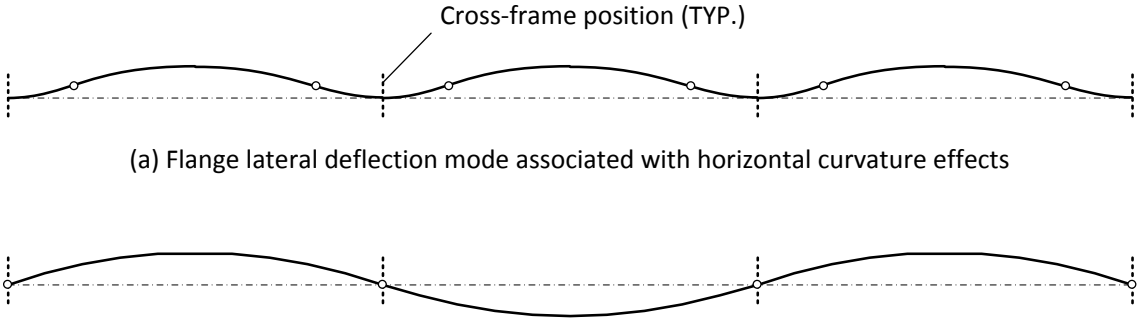

(a) Flange lateral deflection mode associated with horizontal curvature effects

Figure 6.5.2.1.3.2-2 Second-order Elastic Lateral Deflections due to Horizontal Curvature Effects Versus the Unwinding Stability Failure Mode of the Compression Flange

6.5.2.1.3.3 Radial Effect

A secondary effect causing additional flange lateral bending in horizontally curved girders is the so-called radial effect. A curved girder subjected to bending tends to deform radially as soon as loading commences, causing both flanges to undergo increased bowing. This effect can be thought of as resulting from a uniform load applied to both flanges in the radial direction.

The flange lateral moments due to the radial effect vary between brace points as shown in Part B of Figure 6.4.9.5.1.2-2 for the compression flange. The signs of the flange lateral moments are reversed in the tension flange. However, unlike the non-uniform torsion effect, the lateral moments in both flanges due to the radial effect have the same sign. Therefore, as a result of the radial effect, the lateral moments in the compression flange are amplified and the lateral moments in the tension flange are decreased. For a doubly-symmetric girder, the radial effect also causes the cross-frame forces acting on the compression and tension flanges to be different.

Flange lateral bending due to the combination of non-uniform torsion and the radial effect can be estimated reasonably accurately using a 3D refined analysis if the flanges and web are modeled discretely in-between brace points. Approximate analysis approaches to estimate flange lateral bending due to the radial effect are not currently available; however, this is generally compensated for by the conservative approximations often used to estimate lateral bending due to non-uniform torsion and the amplification effect.

6.5.2.1.4 Application of One-Third Rule Equations

This section discusses the application of the one-third flexural resistance equations for I-girder design at each limit state in the *AASHTO LRFD* Specification. Depending on the limit state and the specific application, one or more different forms of the one-third rule equations may be applied. The different forms of the equations that appear in the specifications are summarized in Table 6.5.2.1.4-1 and discussed in more detail below. The one-third rule equations are intended for application only to I-girders with a concrete deck; through-girders are not comprehended.

Table 6.5.2.1.4-1 Summary of Limit State Application of One-Third Rule Equations

Discretely braced flanges:	Equation
Strength limit state (main provisions) and constructibility (strength)	$f_{bu} + \frac{1}{3} f_\ell \le F_r$
Strength limit state (Appendix A6)	$M_u + \frac{1}{3} f_\ell S_x \le M_r$
Constructibility (yielding)	$f_{bu} + f_\ell \le \phi_f R_h F_{yf}$
Service limit state	$f_{bu} + \frac{1}{2} f_\ell \le F_r$
Continuously braced flanges:	Equation
All limit states	$f_{bu} \le F_r$

The first equation in Table 6.5.2.1.4-1 is the stress-based form of the one-third rule equation (Equation 6.5.2.1.1-1). This form of the equation must be used at all sections in kinked (chorded) continuous or horizontally curved-girder bridges, and at all composite sections subject to negative flexure and at all non-composite sections in straight-girder bridges whose supports are skewed more than 20° from normal. This form of the equation must also be used at sections in straight-girder bridges whose supports are normal or skewed not more than 20° from normal, and with intermediate cross-frames/diaphragms placed in contiguous lines placed parallel to the supports, that do not satisfy certain conditions that are spelled out in the specifications (refer to *AASHTO LRFD* Articles 6.10.6.2.2 and 6.10.6.2.3). Note that Equation 6.5.2.1.1-1 may optionally and conservatively be used at sections in such bridges that do satisfy those conditions. Equation 6.5.2.1.1-1 appears only in the Main Provisions of Section 6 of the *AASHTO LRFD* Specification, and is applied at the strength limit state to check the resistance of discretely braced flanges (*AASHTO LRFD* Articles 6.10.7.2 and 6.10.8.1 – Sections 6.5.6.3.3 and 6.5.6.2.2). This

equation is also applied when checking the strength of discretely braced compression flanges for constructibility (*AASHTO LRFD* Article 6.10.3.2.1 – Section 6.5.3.5).

The second equation in Table 6.5.2.1.4-1 is the moment-based form of the one-third rule equation (Equation 6.5.2.1.1-2). This form of the equation may not be used at any section in a kinked (chorded) continuous or horizontally curved-girder bridge. This form of the equation may be used at composite sections subject to negative flexure or at non-composite sections in straight-girder bridges whose supports are normal or skewed not more than 20° from normal, and with intermediate cross-frames/diaphragms placed in contiguous lines placed parallel to the supports. Other conditions, spelled out in *AASHTO LRFD* Articles 6.10.6.2.3 and *AASHTO LRFD* Appendix A6, must also be satisfied in order to utilize Equation 6.5.2.1.1-2 to check discretely braced flanges of such sections at the strength limit state. Equation 6.5.2.1.1-2 appears throughout *AASHTO LRFD* Appendix A6, which accounts for the ability of stockier web I-sections in straight bridges with limited skews to develop flexural resistances significantly greater than M_y (Section 6.5.6.2.3). Equation 6.5.2.1.1-2 may also be used at composite sections in positive flexure in straight-girder bridges at the strength limit state when the conditions spelled out in *AASHTO LRFD* Article 6.10.6.2.2 are satisfied (Section 6.5.6.3).

The third equation in Table 6.5.2.1.4-1 is used to check for nominal yielding of discretely braced flanges (in compression or tension) of I-sections in flexure during construction. The 1/3 factor applied to the lateral bending stress is changed to 1.0 in this equation to prevent nominal yielding at the flange tips. The hybrid factor, R_h, is also introduced to account for the effect of the limited localized yielding that occurs in webs of hybrid sections on the flange stress. Note that the first and third equations in Table 6.5.2.1.4-1 are also to be used to check the top flanges of tub sections for flexure during construction.

The fourth equation in Table 6.5.2.1.4-1 is used to check the resistance of discretely braced flanges of I-girder sections at the service limit state (Section 6.5.4.3.2). This equation is intended to limit the combined stresses in discretely braced flanges at the service limit state (under the Service II load combination) to prevent objectionable permanent deflections due to expected severe traffic loadings that might impair rideability. The factored resistance of the flange, F_r, on the right side of the equation in this case is taken as $0.95R_hF_{yf}$ for composite sections and $0.80R_hF_{yf}$ for non-composite sections. The 1/3 factor applied to the lateral bending stress is conservatively changed to ½ in this equation. Changing the factor to ½ allows the equation to approximate more rigorous yield-interaction equations corresponding to a load at the onset of yielding at the web-flange juncture under combined major-axis and lateral bending (Schilling, 1996; Yoo and Davidson, 1997). The effect of any minor yielding that occurs at the flange tips prior to this stage is comprehended. By

controlling the yielding at the web-flange juncture in this fashion, the resulting permanent deflections under the combined stresses will be small.

Amplification of the first-order lateral bending stresses may be required in discretely braced compression flanges, as discussed in Section 6.5.2.1.3.2, prior to the application of each of the preceding equations. First-order lateral bending stresses in discretely braced tension flanges are not to be amplified (i.e. the amplification factor is to be taken as 1.0).

Finally, the resistance equation for checking continuously braced flanges for flexure at all limit states is presented as the last equation in Table 6.5.2.1.4-1. When compared with the resistance equations for discretely braced flanges, the f_ℓ term is eliminated altogether for continuously braced flanges. For continuously braced flanges, in which the flange is encased in concrete or attached to the deck by shear connectors, lateral flange bending need not be considered.

Discretely braced compression flanges are subject to flange local buckling and lateral torsional buckling. Discretely braced tension flanges and continuously braced flanges (in tension or compression) are subject only to yielding. The determination of the factored flexural resistance, F_r, of discretely and continuously braced flanges at the strength limit state and for checking strength for constructibility will be discussed later in Sections Section 6.5 and 6.5.6.

6.5.2.2 Box Girders

Design provisions for straight composite steel tub girders were first introduced in the 10th Edition of the *AASHO* Bridge Specifications dated 1969. These provisions, developed as part of a joint effort between the American Iron and Steel Institute (AISI) and the University of Washington, were based on analytical work as well as some model tests. The provisions applied solely to tangent multi-box cross-sections. By implication, skewed supports were not considered. Torsion was implicitly considered and recognized in the distribution of live loads, but was thought to be insignificant in the design of tub girders based on the parameters covered by the research and limited in the specifications. The capacity of the bottom plate in compression was based on classical plate buckling equations (Timoshenko and Gere, 1961). Special wheel-load distribution factors were developed to assign live load to the tub girders (Johnston and Mattock, 1967). To ensure that the wheel-load distribution factors were applied within the limits of the research study from which they were developed, limits were placed on the cross-section within the provisions.

Design provisions for horizontally curved box girders were included in the First Edition of the *AASHTO Guide Specifications for Horizontally Curved Bridges* dated 1980. These provisions considered more general design parameters. Torsion was explicitly considered. However, skewed supports were not specifically addressed,

although clearly skewed supports create more torsion than does curvature in many typical bridges. This does not imply that skewed supports could not be considered within these provisions, but they clearly did not recognize the criticalness of skews. The original allowable stress design provisions were developed under the Consortium of University Research Team (CURT) Project, which was under the direction of the FHWA, a group of state DOTs, and industry representatives (CURT, 1975). The Guide Specifications also included Load Factor Design provisions, which were developed separately under AISI Project 190 (Galambos, 1978). The bridge cross-section was not limited in the curved-girder provisions; instead, a rational analysis was required to distribute the loads. Box flange plate capacity was again based on classical plate buckling equations, only including the effect of shear stress (Culver and Mozer, 1971). (A box flange is explicitly defined in AASHTO LRFD Article 6.2 and herein as a flange that is connected to two webs). The consideration of torsion implied consideration of forces developed in internal cross-frames and lateral bracing, as well as bracing between adjacent girders. Since consideration of distortional stresses was also required by these provisions, the computation of the distorsional warping stiffness of the box sections became necessary. This could be determined by using the BEF analogy (Wright and Abdel-Samad, 1968). Torsional moments resulting from the superstructure analysis could be used in conjunction with the BEF analogy to compute cross-frame forces as well as through-thickness bending stresses due to cross-section distortion.

There were several failures of major steel box bridges around the world, generally during construction, which demonstrated that these bridges were not without their concerns. The British formed a special commission called the Merrison Commission to investigate these failures. From the work of that commission came the Rules by the same name. These new rules were extremely conservative in their attempt to ensure that no additional failures of box- girder bridges would occur. When applied literally, the rules ensured that no such bridges would fail because they would be too expensive to build. This conundrum prompted a major research project in Britain, which included both analytical studies and supportive testing. The research, completed in about 1980, resulted in the development of the modern BS54 box-girder design provisions.

In the late 1970s, the FHWA formed a task force to develop a new American design specification, specifically for steel box-girder bridges. The firm of Wolchuk and Mayrbaurl developed the *Proposed Design Specifications for Steel Box Girder Bridges* in 1980 (FHWA, 1980). The vast majority of this work was derived from the British research. Although the proposed specifications were mainly directed toward larger box girder bridges than were typically built in the United States, it has been employed in the design of several bridges in the U.S.

The 2003 *AASHTO Guide Specifications for Horizontally Curved Steel Girder Highway Bridges* employed much of the earlier work from the 1980 AASHTO Guide

Specifications. These specifications were developed by BSDI, Ltd. and Auburn University under the direction and sponsorship of the National Cooperative Highway Research Program (NCHRP), and included Load Factor Design provisions only (Hall et al., 1999). Several refinements were introduced in these provisions related specifically to tub girders. Shear connectors were required to be designed for torsional shear as well as vertical bending. These provisions also included special considerations for box girders during construction. Single-box and composite closed-box cross-sections were also covered more extensively than in any previous *AASHTO* provisions.

The design provisions from the 2003 *AASHTO* Guide Specifications were later incorporated, with some slight modification, into the *AASHTO LRFD* Specifications as part of the 2005 Interims to the Third Edition of the specifications. This was done as part of a larger overall effort to unify the design provisions for straight and horizontally curved girder bridges. With the completion of this effort, the *AASHTO LRFD* flexural resistance equations for box girders now provide a unified approach for consideration of the combined effects of normal stress and St. Venant torsional shear stress in box flanges during construction, and in the final constructed condition at the strength limit state. This was done by utilizing the classical plate buckling equations from the earlier Guide Specifications, again with some slight modification. Combined major-axis and flange lateral bending from any source can also now be considered in the top flanges of tub sections during construction by applying the one-third rule equations that were developed for I-sections. Hence, the same equations can now be used to check the flexural resistance of box sections in both straight and horizontally curved girders at the appropriate limit states. These flexural resistance equations will be presented and discussed in greater detail in Sections Section 6.5 and 6.5.6.

6.5.3 LRFD Constructibility Design

6.5.3.1 General

Although not identified as a formal limit state, the *AASHTO LRFD* Specifications provide significant emphasis on constructibility, and specify it as a primary objective of bridge design in *AASHTO LRFD* Article 1.3.1.

AASHTO LRFD Article 2.5.3 states that bridges should be designed such that fabrication and erection can be performed without undue difficulty or distress, and so that locked-in construction force effects are within tolerable limits. If a particular sequence of construction has been assumed by the Design Engineer in order to induce a particular set of dead load stresses (e.g. a particular deck-placement sequence), that sequence must be identified in the contract documents. For design, Engineers typically assume the most conservative deck placement sequence possible.

Also, for bridges considered to be of unusual complexity, at least one means of constructing the bridge must be provided by the Design Engineer in the contract documents to assist the Contractor in preparing a reasonable bid. Responsibility for the actual construction of the bridge (i.e. the "means and methods") is left to the Contractor, who may still use a more innovative or custom construction sequence in order to gain an advantage over the competitors, if desired. The actual responsibilities of the Design Engineer in this regard are not well defined and are generally left up to the Owner to specify. In addition, according to *AASHTO LRFD* Article 2.5.3, if the design requires temporary bracing, strengthening or support (e.g. falsework) during the erection by the specified sequence, this must also be identified in the contract documents.

AASHTO LRFD Article 6.5.1 requires that steel bridges be investigated for each stage that may be critical during construction, handling, transportation and erection. This is particularly important with respect to modern steel-girder designs, which are typically more slender in their non-composite condition than in the past due to the advent of composite construction, the introduction of higher-strength steels, and the increased use of limit-states design approaches leading to a lower load factor applied to dead-load effects than traditional working stress design approaches. In composite construction, the steel girders alone must be strong enough to carry the full non-composite dead loads. Since the composite section assists in resisting the live loads, smaller top flanges can be used in regions of positive flexure. Thus, more than half the depth of the web is in compression in these regions during construction. For tub sections in particular, with a wide bottom flange relative to the top flanges, typically more than half of the depth of the web is in compression in regions of positive flexure during construction. Therefore, investigation of critical construction stages when the girders are non-composite, such as during the sequential deck placement (Section 6.5.3.3), is particularly important.

Wind-load effects on the non-composite structure prior to casting of the deck are an important consideration (Section 6.5.3.6). As specified in *AASHTO LRFD* Article 4.6.2.7.3, the need for temporary wind bracing to control lateral bending and lateral deflections during construction must be investigated. In some cases, such bracing may be left in-place as permanent bracing. Since box girders are torsionally stiff and tub girders must always be provided with at least some degree of top lateral bracing, wind load generally has less effect on box girders than on I-girders during construction. An investigation of the effects of deck overhang loads on the exterior (fascia) girders in their non-composite condition is also an important design consideration (Section 6.5.3.4).

Potential uplift at bearings is also an important consideration and must be investigated at each critical construction stage according to *AASHTO LRFD* Article 6.10.3.1 (Section 6.5.3.3.3).

Should concentrated loads not be applied to the web through a deck or deck system, and bearing stiffeners also not be provided at such locations, the web must satisfy the provisions of *AASHTO LRFD* Article D6.5 (Appendix D6) to prevent web crippling and web local yielding (Section 6.6.6.3.5).

AASHTO LRFD Article 6.10.3.5 refers to the provisions of *AASHTO LRFD* Article 6.7.2, which state that vertical camber must be specified to account for the dead-load deflections. The deflections due to the steel weight, concrete weight, future wearing surface or other loads not applied at the time of construction are reported separately. When phased construction is specified, i.e. when the superstructure is built in separate longitudinal units with a longitudinal joint, the sequence of the load application must be recognized in determining the stresses and the required cambers. This requires analysis of the planned construction stages. Phased construction issues are discussed in greater detail in Section 6.3.2.5.4.

6.5.3.2 Applicable Load Combinations

All design checks for strength during construction are to be made using the appropriate factored loads specified in *AASHTO LRFD* Articles 3.4.1 and 3.4.2.

The applicable strength load combinations for these design checks specified in *AASHTO LRFD* Table 3.4.1-1 include Strength I and Strength III, modified as specified in *AASHTO LRFD* Article 3.4.2.1 (see below). Strength I is the base strength load combination (Section 3.9.1.2.2). Strength III is for the investigation of dead load in combination with wind load (Section 3.9.1.2.4).

As specified in *AASHTO LRFD* Article 3.4.2.1, when investigating the Strength I and Strength III load combinations for maximum force effects during construction, load factors for the weight of the structure and appurtenances, *DC* and *DW*, are not to be less than 1.25. The load factor for wind during construction in the Strength III load combination is not to be less than 1.25 when investigating maximum force effects, unless specified otherwise by the Owner. Any applicable construction loads should be included with a load factor not less than 1.25.

When considering construction loads, or dead loads and temporary loads that act on the structure only during construction, the construction loads (including any dynamic effects if applicable) are to be added in the Strength I load combination with a load factor not less than 1.5 when investigating for maximum force effects, unless specified otherwise by the Owner (*AASHTO LRFD* Article 3.4.2.1). Construction loads include, but are not limited to, the weight of materials, removable forms, personnel, and equipment such as deck finishing machines or loads applied to the structure through falsework or other temporary supports. The weight of the wet concrete deck and any stay-in-place forms should be considered as *DC* loads.

Often the construction loads are not known accurately at the time of design. The Owner may consider noting the construction loads assumed in the design on the contract documents.

AASHTO LRFD Article 3.4.2.1 further states that primary steel superstructure components are to be investigated for maximum force effects during construction for an additional special load combination consisting of the applicable *DC* loads and any construction loads that are applied to the fully erected steelwork. The load factor for force effects caused by *DC* loads and construction loads, including dynamic effects (if applicable), is not to be less than 1.4 for this additional special load combination.

Previous service-load design approaches have effectively applied a load factor ranging from about 1.67 (1/0.60) to 1.82 (1/0.55) to the dead load force effects, with the *AASHTO* service-load design method effectively applying the latter (often discounted as much as 25 percent for temporary construction conditions). The base strength load combinations in more recent limit-state design approaches have applied a load factor ranging from about 1.25 to 1.3 to these force effects. With the advent of higher-strength steels and composite construction also generally contributing to the use of lighter members, the application of this special load combination when checking the constructibility of primary steel superstructure components for loads applied to the fully erected steelwork helps to ensure a level of strength and stability during critical construction stages (where unintended events could potentially lead to significantly larger force effects than those predicted during the design) that at least approaches that attained in the past using previous design approaches.

For the calculation of deflections during construction, all load factors are to be taken as 1.0 (i.e. the Service I load combination applies), including load factors applied to any construction loads, according to *AASHTO LRFD* Article 3.4.2.2. Slip of bolted connections during the deck placement is to be checked using the appropriate factored loads, with the slip resistance of the connection to be determined as specified in *AASHTO LRFD* Article 6.13.2.8.

6.5.3.3 Deck Placement Analysis

6.5.3.3.1 General

Steel girders in unshored composite construction must support their own weight plus the weight of the wet concrete deck slab, cross-frames, deck forms and construction equipment. The girders become composite once the concrete deck hardens and their behavior changes. The complicating factor is that, depending on the length of the bridge, the construction of the deck may likely require placement in sequential stages, as seen in Figure 6.5.3.3.1-1. Site conditions and access and other factors typically limit how much concrete can be cast in a single day.

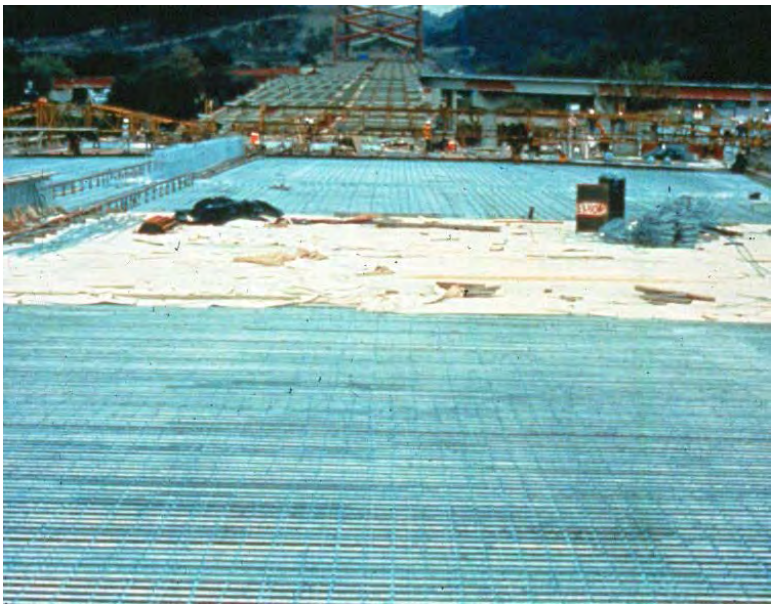

Figure 6.5.3.3.1-1 Bridge Deck Under Construction in Sequential Stages

If the deck is placed in sequential stages, then certain sections of the girder will become composite before other sections, which must be considered in the load analysis. Temporary construction moments must be computed for each stage. These temporary construction moments, along with the torsional effects induced in the girders and bracing members during the deck casting, can be significantly greater than if the deck were placed in adjacent spans concurrently and must be considered during design. In addition, construction reactions and deflections must also be considered.

Therefore, as specified in *AASHTO LRFD* Article 6.10.3.4.1, sections in positive flexure that are composite in the final condition, but non-composite during construction (i.e. unshored construction), must be investigated during the various stages of the deck placement. Changes in load, stiffness and bracing during the various stages of the deck placement are to be considered. Potential uplift at the bearings is also to be investigated according to *AASHTO LRFD* Article 6.10.3.1. Once the critical deck-casting moments are determined from the analysis, the maximum flexural stresses, f_{bu}, in the flanges of the bare steel girders due to the factored moments are to be determined in order to perform the necessary constructibility verifications to ensure adequate strength for flexure, as specified in *AASHTO LRFD* Article 6.10.3.2 for I-sections and *AASHTO LRFD* Article 6.11.3.2 for box sections. Design verifications for shear are also required for shear according to *AASHTO LRFD* Articles 6.10.3.3 and 6.11.3.3 for I-sections and box sections, respectively. The deck placement is usually evaluated on the fully erected steelwork since the erection sequence is typically not defined at the design state, except for complex bridges.

Common practice when casting includes both positive and negative moment regions is to cast the slab in the positive moment regions first, and then cast the slab in the negative moment region over the support in order to minimize cracking at the top of the slab. This is illustrated for a two-span continuous horizontally curved bridge at the top of Figure 6.5.3.3.1-2. However, when concrete is cast in a span adjacent to a span that already has a hardened deck, induced negative moments in the adjacent spans will cause tensile stresses (and torsional shear stresses in the case of a curved bridge) in the cured concrete that may result in transverse deck cracking. Thus, checks on the concrete deck stresses during the deck placement must also be made as specified in *AASHTO LRFD* Article 6.10.3.2.4. As discussed below in Section 6.5.3.3.4, provision of the minimum required one percent longitudinal reinforcement in the deck at these sections can help control the cracking.

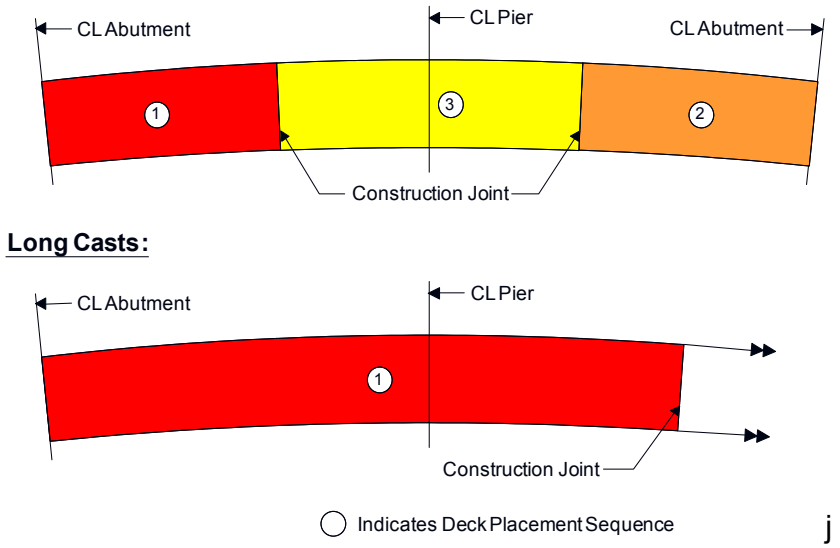

Figure 6.5.3.3.1-2 Casts with Both Positive and Negative Moment Regions

In a long cast, e.g. extending from one end of the bridge over an interior support into an adjacent span (refer to the bottom of Figure 6.5.3.3.1-2), it is possible that the concrete in the negative moment region over the support will harden and be subject to tensile stresses during the remainder of the cast, which may result in early age cracking of the deck. A retarder admixture may be required in the casts over the piers to reduce the potential for early cracking. Also, for such casts, or for casts on bridges that are short and narrow enough that the deck may be cast from one end of the bridge to the other (instead of in stages), the end span must still be checked for the critical instantaneous unbalanced case where wet concrete exists over the entire end span, with no concrete yet on the remaining spans.

Skewed supports and/or curvature can complicate the deck-casting sequence. Keeping the deck placement reasonably symmetrical laterally minimizes eccentric or

unbalanced loading and helps reduce differential deflections between adjacent girders. It is preferable on skewed bridges where the differential deflections between girders are reasonably small to keep the finishing machine normal to the girders as it reduces the length of the machine. However, in cases with severe skews leading to large differential deflections, it may be necessary to consider skewing the finishing machine to avoid casting significantly more concrete than needed to meet the specified minimum deck thickness or roadway elevations and achieve the proper bridge geometry. Thus, for these structures, using refined analysis methods to perform the deck-staging analysis is obviously desirable.

Multiple casts may have to be made in the lateral direction also in wide structures that have multiple girders and/or with severe skews. Such casts result in the introduction of longitudinal construction joints.

6.5.3.3.2 Composite Stiffness

During deck placement, the actual composite stiffness depends on the amount of time that the concrete has had to cure before the next portion is cast, but such refinements are usually not considered in the analysis. If a retarder is not used, placed concrete usually obtains composite action in a matter of hours. Thus, the full composite stiffness is often used.

The stiffness of previously cast portions of the concrete deck when computing deflections considering deck staging should be based on a modular ratio closer to the short-term modular ratio since the concrete does not have enough time to creep significantly between casts. At least one State DOT has found the use of a concrete modulus of elasticity equal to 70 percent of the modulus of elasticity at 28 days (which results in a modular ratio of approximately 1.4n) to be appropriate in computing the stiffness.

6.5.3.3.3 Uplift

Uplift can occur at end supports during deck casting if the end spans are lightly loaded and may be particularly critical for curved structures and/or structures with skewed end supports. Thus, the potential for uplift during the deck casting must be investigated.

Options to consider when uplift occurs include:

- Rearranging the concrete placements
- Modifying the framing
- Specifying a temporary load over that support
- Specifying a tie-down bearing
- Removing the bearing

- If the uplift can be tolerated, performing another deck-staging analysis recognizing the absence of vertical restraint at the support experiencing lift-off in order to determine the correct moments and deflections

It is suggested that a load factor of 1.0 be applied to all downward support reactions due to component dead loads causing uplift, and a load factor of 0.9 be applied to all upward support reactions due to component dead loads resisting uplift for the investigation of uplift at critical construction stages.

6.5.3.3.4 Control of Deck Cracking

When the concrete deck is placed in a span adjacent to a span where the concrete has already been placed, as illustrated schematically in Figure 6.5.3.3.4-1, negative moment in the adjacent span causes tensile stresses in the previously placed concrete.

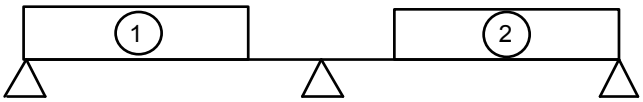

Figure 6.5.3.3.4-1 Sequential Deck Casting

Or in situations where long placements are made such that a negative-flexure region is included in the initial placement, it is possible for the concrete in that region to be subject to tensile stresses during the remainder of the deck placement, which could potentially lead to early cracking of the deck.

AASHTO LRFD Article 6.10.3.2.4 requires that the longitudinal tensile stress in a composite concrete deck due to the factored construction loads satisfy the following equation to control the cracking in the previously placed concrete, unless the total cross-sectional area of the longitudinal reinforcement is at least equal to 1 percent of the total cross-sectional area of the concrete deck (refer also to *AASHTO LRFD* Article 6.10.1.7):

$$f_{deck} \le \phi f_r = 0.9 f_r \qquad \text{Equation 6.5.3.3.4-1}$$

where:

ϕ = resistance factor for concrete in tension = 0.9 for reinforced concrete (*AASHTO LRFD* Article 5.5.4.2.1)

f_r = deck concrete modulus of rupture specified in *AASHTO LRFD* Article 5.4.2.6 (ksi)

For normal-weight concrete:

$$f_r = 0.24\sqrt{f'_c}$$ Equation 6.5.3.3.4-2

The short-term modular ratio should be used when computing the concrete deck tensile stress; that is, *n* should be used to compute the composite section properties as opposed to 3*n* (refer to *AASHTO LRFD* Article 6.10.1.1.1d). The calculated stress on the transformed section must be divided by *n* to obtain the stress in the concrete. f_r is the modulus of rupture, computed using the lower-bound equation for normal-weight concrete shown in Equation 6.5.3.3.4-2. For lightweight concrete, refer to *AASHTO LRFD* Article 5.4.2.6. A more accurate estimate of the concrete strength at the time the deck casts are made can be used to compute f_r and the modular ratio for this check, if desired.

Sufficient shear connectors should also be present at the end of each cast to transfer the tensile force from the deck to the top flange and prevent potential crushing of the concrete around the studs or fracturing of the studs. To estimate the length over which the tensile force must be transmitted via the factored shear resistance of the connectors, a 45-degree angle might be assumed from the end of the cast to where the concrete deck is assumed effective. If necessary, the tensile force in the deck can be lowered by modifying the placement sequence.

EXAMPLE

Consider the sample deck placement sequence shown in Figure 6.5.3.3.4-2 for a three-span continuous bridge. For this bridge, it is assumed that the positive moment regions are placed first with each of the casts in the end spans (from the abutment to the field splice) placed simultaneously. Then, the positive moment region of the interior span is assumed placed. After the positive moment regions have been placed, the negative moment regions over the piers are assumed placed simultaneously.

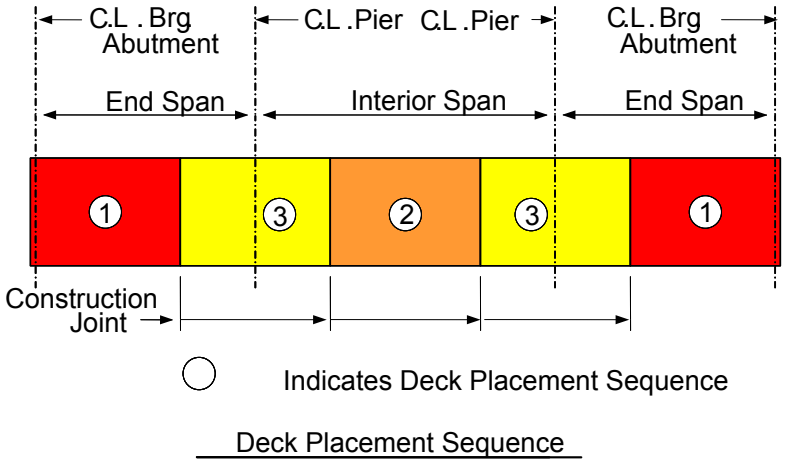

Figure 6.5.3.3.4-2 Sample Deck Placement Sequence

Although simultaneous placement in the end spans followed later by simultaneous placement over the piers is shown in this example for simplicity, it is sometimes more desirable to cast the deck from one end of the bridge. Simultaneous placement in the end spans, as assumed here, would require two finishing machines. Also, for this case, a more critical situation in actuality would be where the concrete would be assumed cast in only one end span since it would be practically impossible to ensure simultaneous placement of the two end casts. If the deck were cast from one end for the case shown in Figure 6.5.3.3.4-2, the second cast would likely extend from the end of the first cast in one end span over the adjacent pier to either the first or second construction joint shown in the center span (depending on how much concrete could be cast in a single day). Casting would then continue on from there accordingly in appropriate stages. In this case, a retarder admixture may be required in the concrete mix for the casts over the piers to reduce the potential for early cracking caused by tensile stresses induced by subsequent casts. Should the bridge be short and narrow enough that the deck could be cast from one end of the bridge to the other in a single day (instead of in stages), the end span would still have to be checked for the critical instantaneous unbalanced case where wet concrete exists over the entire end span, with no concrete yet on the remaining spans.

Figure 6.5.3.3.4-3 (and all subsequent figures for this example) shows an elevation view of an exterior girder, which will be used to show the results for each stage of the deck placement sequence assumed for this example in Figure 6.5.3.3.4-1. In Figure 6.5.3.3.4-3, the girders are in place but no deck concrete has yet been placed. The entire girder length is non-composite at this stage. Before the deck is placed, the non-composite girder must resist the moments due to the girder self-weight and the weight of any stay-in-place (SIP) forms (if present). The moments due to these effects are shown at Location A, which is the location of maximum positive moment in the first end span.

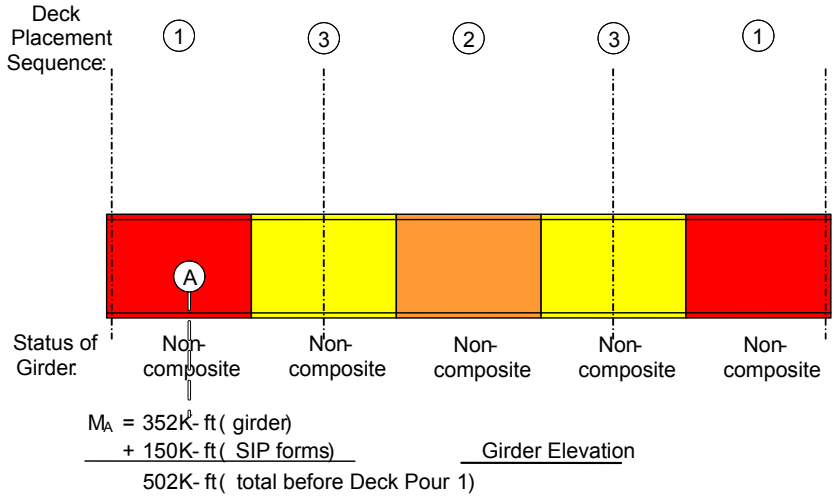

Figure 6.5.3.3.4-3 Example Girder Elevation View

Figure 6.5.3.3.4-4 shows the first deck placement (Cast 1), which is located in the positive moment regions of the end spans. The moment due to the wet concrete load, which consists of the weight of the deck and deck haunches, is added to the moments due to the girder self-weight and SIP forms. Since the concrete in this first placement has not yet hardened, the moment due to the first deck placement is resisted by the non-composite girder. The cumulative positive moment in the exterior girder at Location A after the first deck placement is +2,889 kip-ft, which is the maximum positive moment this section will experience during the assumed placement sequence. This moment is significantly larger than the moment of +2,202 kip-ft that would be computed at this location assuming a simultaneous placement of the entire deck (i.e. ignoring the sequential stages).

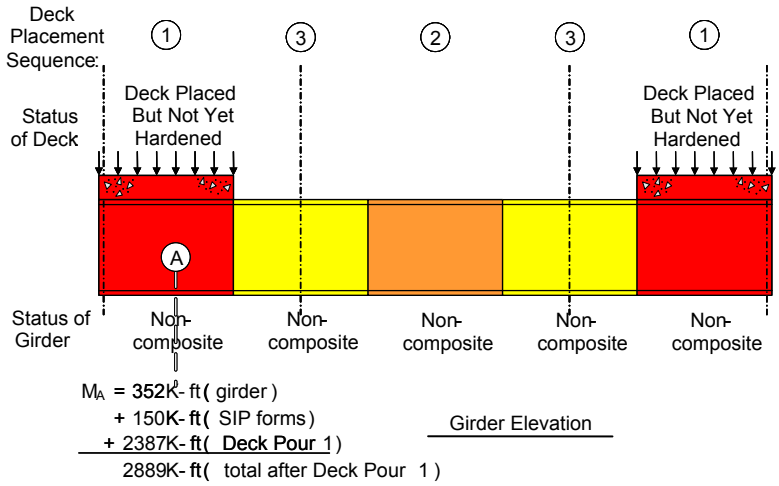

Figure 6.5.3.3.4-4 Sample Deck Placement Analysis (Cast 1)

The next deck placement (Cast 2) is located in the positive moment region of the interior span, as shown in Figure 6.5.3.3.4-5. The concrete in the first placement is now assumed hardened so that those portions of the girder are now composite. Therefore, as required in *AASHTO LRFD* Article 6.10.3.4.1, those portions of the girder are assumed composite in the analysis for this particular deck placement. The remainder of the girder is non-composite. Since the deck casts are relatively short-term loadings, the short-term modular ratio, n, is used to compute the composite stiffness. The previous casts are assumed fully hardened in this case, but adjustments to the composite stiffness to reflect the actual strength of the concrete in the previous casts at the time of this particular placement could be made, if desired. The cumulative moment at Location A has decreased from +2,889 kip-ft after Cast 1 to +2,103 kip-ft after Cast 2 because the placement in the middle span causes a negative moment in the end spans.

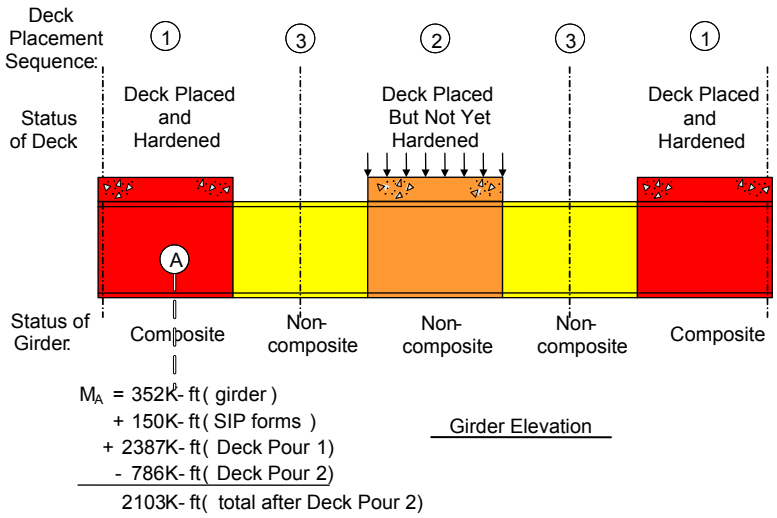

Figure 6.5.3.3.4-5 Sample Deck Placement Analysis (Cast 2)

The last deck placement (Cast 3) is located in the negative moment regions over the piers (Figure 6.5.3.3.4-6). Again, the concrete in Casts 1 and 2 is assumed fully hardened in the analysis for Cast 3. The cumulative moment at Location A has increased slightly from +2,103 kip-ft to +2,170 kip-ft, which is less than the moment of +2,889 kip-ft experienced at Location A after Cast 1.

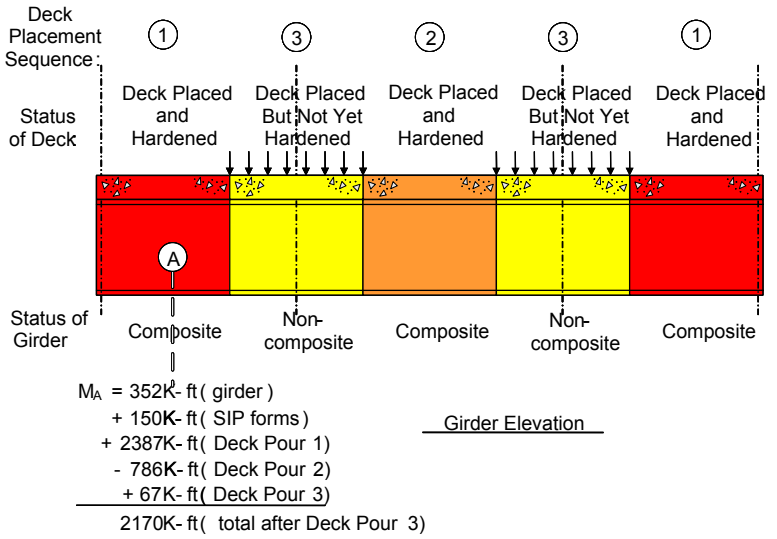

Figure 6.5.3.3.4-6 Sample Deck Placement Analysis (Cast 3)

Table 6.5.3.3.4-1 shows a more complete set of the unfactored dead-load moments in the end span (Span 1) from the abutment to the end of Cast 1 computed from the example deck placement analysis. Data are given at 12.0-ft increments along the span measured from the abutment. The end of Cast 1 is at the field splice, which is located 100.0 feet from the abutment. Location A is 56.0 feet from the abutment.

Cross-frames are spaced at 24.0 feet along the girder and the length to each cross-frame from the abutment is indicated in bold in the table.

In addition to the moments due to each of the individual casts, Table 6.5.3.3.4-1 gives the moments due to the steel weight, the moments due to the weight of the SIP forms, the sum of the moments due to the three casts plus the weight of the SIP forms, the maximum accumulated positive moments during the sequential deck casts (not including the steel weight) when they are added in sequence, the sum of the moments due to the dead loads, DC_2 and DW, applied to the final composite structure, and the moments due to the weight of the concrete deck, haunches and SIP forms assuming that the concrete is placed simultaneously on the non-composite girders instead of in sequential steps. The assumed weight of the SIP forms includes the weight of the concrete in the form flutes. Although the forms are initially empty, the weight of the deck reinforcement is essentially equivalent to the weight of the concrete in the form flutes.

The slight differences in the moments on the last line of Table 6.5.3.3.4-1 and the sum of the moments due to the three casts plus the weight of the SIP forms are due to the changes in the girder stiffness with each sequential cast. The principle of superposition does not apply directly in the deck-placement analyses since the girder stiffness changes at each step of the analysis. However, note the significant differences between the moments on the last line of Table 6.5.3.3.4-1 (which assumes a simultaneous placement of these loads along the entire girder), and the maximum accumulated positive moments resulting from the sequential deck casts when added in sequence (′Max. +M′ in Table 6.5.3.3.4-1). In regions of positive flexure, the non-composite girder should be checked for the effect of the largest accumulated positive moment acting on the non-composite girder before the deck cures, which happens to be equal to ′Max. +M′ in this case at all points shown in Table 6.5.3.3.4-1. However, this is not always the case, and the Engineer must be careful that the appropriate moment is used when investigating the non-composite girder for the placement sequence. In cases where ′Max. +M′ is not the most critical moment, the critical moment will always be less than ′Max. +M′. As mentioned previously, previous deck casts are typically assumed to be composite for subsequent casts. Thus, even if subsequent casts cause additional positive moments at a particular point, the moments due to these cases should not be added to the critical moment acting on the non-composite girder if the girder is assumed to be composite at the point during that particular cast.

This critical moment acting on the non-composite girder at Location A ('Max. +M' in this case) is shown in bold in Table 6.5.3.3.4-1, along with the moment due to the steel weight. The sum of these moments is computed as:

$$M = 352 + 2{,}537 = 2{,}889 \text{ kip-ft}$$

which agrees with the moment at this location shown in Figure 6.5.3.3.4-4.

Table 6.5.3.3.4-1 Moments from Sample Deck-Placement Analysis

Span -> 1	Unfactored Dead-Load Moments (kip-ft)									
Length (ft)	**0.00**	12.00	**24.00**	42.00	**48.00**	56.00	**72.00**	84.00	**96.00**	100.0
Steel Weight	0	143	250	341	353	**352**	296	206	74	21
SIP Forms (SIP)	0	63	110	147	151	150	124	84	27	4
Cast										
1	0	870	1544	2189	2306	2387	2286	1983	1484	1275
2	0	-168	-336	-589	-673	-786	-1010	-1179	-1347	-1403
3	0	14	28	50	57	67	86	101	115	120
Sum of Casts + SIP	0	779	1346	1797	1841	1818	1486	989	279	-4
Max +M	0	933	1654	2336	2457	**2537**	2410	2067	1511	1279
DC_2 + DW	0	275	477	643	661	657	551	386	148	52
Deck, haunches + SIP	0	786	1360	1822	1870	1850	1528	1038	335	53

The unfactored vertical dead-load deflections in Span 1 from the abutment to the end of Cast 1 for the example problem, including the deflections resulting from the assumed deck-placement sequence, are summarized in Table 6.5.3.3.4-2. The format of the data in Table 6.5.3.3.4-2 is similar to the format used in Table 6.5.3.3.4-1. Negative values are downward deflections and positive values are upward deflections. Again, since the deck casts are relatively short-term loadings, the *n*-composite stiffness is used for all preceding casts in computing the moments and deflections shown for Casts 2 and 3 in Table 6.5.3.3.4-1 and Table 6.5.3.3.4-2. Note that the moments and deflections on the final composite structure due to the sum of the DC_2 and *DW* loads shown in Table 6.5.3.3.4-1 and Table 6.5.3.3.4-2 are computed using the 3*n*-composite stiffness to account for the long-term effects of concrete creep. Also, the entire cross-sectional area of the deck associated with the exterior girder was assumed effective in the analysis in determining the stiffness of the composite sections.

Table 6.5.3.3.4-2 Vertical Deflections from Sample Deck-Placement Analysis

Span -> 1	Unfactored Vertical Dead-Load Deflections (in.)									
Length (ft)	**0.00**	12.00	**24.00**	42.00	**48.00**	56.00	**72.00**	84.00	**96.00**	100.0
Steel Weight	0	-.17	-.32	-.47	-.50	-.51	-.47	-.39	-.29	-.25
SIP Forms (SIP)	0	-.07	-.14	-.20	-.21	-.21	-.20	-.16	-.12	-.10
Cast										
1	0	-1.32	-2.50	-3.78	-4.04	-4.27	-4.30	-3.95	-3.33	-3.08
2	0	.27	.52	.86	.96	1.08	1.25	1.32	1.32	1.31
3	0	-.01	-.03	-.04	-.04	-.05	-.05	-.05	-.04	-.03
Sum of Casts + SIP	0	-1.14	-2.14	-3.16	-3.34	-3.46	-3.30	-2.84	-2.17	-1.91
DC_2 + DW	0	-.17	-.32	-.46	-.48	-.49	-.45	-.38	-.28	-.24
Total	0	-1.48	-2.78	-4.09	-4.32	-4.46	-4.22	-3.61	-2.74	-2.40
Deck, haunches + SIP	0	-.92	-1.71	-2.47	-2.59	-2.64	-2.43	-2.02	-1.47	-1.27

Note the differences in the calculated deflections on the last line of Table 6.5.3.3.4-2 (assuming the deck is cast simultaneously on the non-composite structure), and the sum of the accumulated deflections during the sequential deck casts. In many cases, the deflections shown on the last line can be used to estimate the girder cambers, as required in *AASHTO LRFD* Article 6.10.3.5, to account for the dead-load deflections. When the differences in these deflections are not significant, the deflections due to the accumulated deck casts will likely converge toward the deflections shown on the last line as concrete creep occurs. However, if the differences in the deflections are deemed significant, the Engineer may need to evaluate which set of deflections should be used, or else estimate deflections somewhere in-between when establishing camber and screed requirements to avoid potential errors in the final girder elevations.

It is interesting to note that a refined 3D analysis of the example bridge yielded a maximum vertical deflection in Span 1 (at Location A) due to the weight of the concrete deck, haunches and SIP forms (assuming that the concrete is placed simultaneously on the non-composite girders) of 2.61 inches in the exterior girders and 2.65 inches in the interior girders. From Table 6.5.3.3.4-2, the comparable maximum vertical deflection from a line-girder analysis is 2.64 inches, which indicates the assumption of equal distribution of the DC_1 loads to all the girders (which was assumed for this analysis) is the proper assumption in this case (see Section 6.3.2.5.5.1 for further discussion on this issue).

AASHTO LRFD Article 6.10.3.1 requires that potential uplift at bearings be investigated at each critical construction stage. The unfactored vertical dead-load reactions resulting from the deck-placement analysis for the example problem are given in Table 6.5.3.3.4-3. Negative reactions represent upward reactions that resist

the maximum downward force at the support under consideration. Conversely, positive reactions represent downward reactions that resist the maximum uplift force at the support.

Table 6.5.3.3.4-3 Unfactored Vertical Dead-Load Reactions from Sample Deck-Placement Analysis (kips)

	Abut 1		Pier 1		Pier 2		Abut 2	
Steel Weight	-13		-53		-53		-13	
Sum		-13		-53		-53		-13
SIP Forms (SIP)	-6		-21		-21		-6	
Sum		-19		-74		-74		-19
Cast 1	-80		-55		-55		-80	
Sum		-99		-129		-129		-99
Cast 2	13		-75		-75		14	
Sum		-85		-204		-204		-85
Cast 3	-1		-110		-110		-1	
Sum		-86		-314		-314		-86
Sum of Casts + SIP		-73		-261		-261		-73
DC_2+DW		-26		-90		-90		-26
Total		-112		-404		-404		-112
Deck, haunches + SIP		-74		-261		-261		-74

Shown in Table 6.5.3.3.4-3 (under ‘sum’) are the accumulated reactions for the steel weight plus the individual deck casts, which should be used to check for uplift under the deck placement. A net positive reaction indicates that the girder may lift-off at the support. Lift-off does not occur in this particular example; lift-off is most common when end spans of continuous units are skewed or relatively short. If the girder is permitted to lift-off its bearing seat, the staging analysis is incorrect unless a hold-down of the girder is provided at the location of a positive reaction. Although not illustrated here, it is recommended that for investigation of uplift in this case, a load factor of 1.0 be applied to all downward (i.e. positive) support reactions, and a load factor of 0.9 be applied to all upward (i.e. negative) support reactions.

Options to consider when uplift occurs are discussed in Section 6.5.3.3.3. Note that the sum of the reactions from the analysis of the staged deck casts may differ somewhat from the reactions assuming the deck is cast simultaneously on the non-composite structure (as given on the last line of Table 6.5.3.3.4-3); however, in most cases, the reactions should not differ greatly.

The maximum factored flexural stresses in the flanges of the non-composite steel section resulting from the deck-placement sequence will next be calculated. Strength I, along with the special load combination specified in AASHTO LRFD

Article 3.4.2.1 for the investigation of maximum force effects during construction due to loads applied to the fully erected steelwork, will be considered (Section 6.5.3.2). The cross-section of the girder at Location A is shown in Figure 6.4.2.3.2.3-1. The elastic section properties for this section were computed earlier (Section 6.4.2.3.2.3).

As specified in *AASHTO LRFD* Article 6.10.1.6 (and discussed further below in Section 6.5.6), for design checks where the flexural resistance is based on lateral torsional buckling, the major-axis stress, f_{bu}, is to be determined as the largest value of the compressive stress throughout the unbraced length in the flange under consideration, calculated without consideration of flange lateral bending. For design checks where the flexural resistance is based on yielding, flange local buckling or web bend buckling, f_{bu} may be determined as the stress at the section under consideration.

Cross-frames adjacent to Location A are located 48 ft and 72 ft from the abutment. From inspection of Table 6.5.3.3.4-1, since the girder is prismatic between the two cross-frames, the largest stress within the unbraced length occurs right at Location A. The load modifier, η, is assumed equal to 1.0 in this example. Therefore:

For Strength I (Section 6.5.3.2):

$$\text{Top flange:} \quad f_{bu} = \frac{1.0(1.25)(2{,}889)(12)}{1{,}581} = -27.41\,\text{ksi}$$

$$\text{Bot. flange:} \quad f_{bu} = \frac{1.0(1.25)(2{,}889)(12)}{1{,}973} = 21.96\,\text{ksi}$$

For the Special Load Combination in *AASHTO LRFD* Article 3.4.2.1 (Section 6.5.3.2):

$$\text{Top flange:} \quad f_{bu} = \frac{1.0(1.4)(2{,}889)(12)}{1{,}581} = -30.70\,\text{ksi}$$

$$\text{Bot. flange:} \quad f_{bu} = \frac{1.0(1.4)(2{,}889)(12)}{1{,}973} = 24.60\,\text{ksi}$$

AASHTO LRFD Article 6.10.3.2.4 requires that the factored longitudinal tensile stress in a composite concrete deck not exceed ϕf_r during critical stages of construction, unless longitudinal reinforcement is provided according to the provisions of *AASHTO LRFD* Article 6.10.1.7. Assume normal weight concrete is used with a 28-day compressive strength, f'_c, equal to 4.0 ksi. f_r is the modulus of rupture of the concrete determined as follows for normal weight concrete (*AASHTO LRFD* Article 5.4.2.6):

$$f_r = 0.24\sqrt{f'_c} = 0.24\sqrt{4.0} = 0.480 \text{ ksi}$$

ϕ is the appropriate resistance factor for concrete in tension specified in *AASHTO LRFD* Article 5.5.4.2.1. For reinforced concrete in tension, ϕ is equal to 0.90. Therefore:

$$\phi f_r = 0.90(0.480) = 0.432 \text{ ksi}$$

Check the tensile stress in the concrete deck at the end of Cast 1 in Span 1 (100.0 feet from the abutment) caused by the critical negative moment due to Cast 2 acting on the composite section. Only moments acting on the composite section (positive or negative moments) from the staging analysis at the point under investigation should be accumulated in order to determine the critical negative moment.

From Table 6.5.3.3.4-1, the critical negative moment at the end of Cast 1 due to Cast 2 acting on the composite section is –1,403 kip-feet. The longitudinal concrete deck stress is to be determined as specified in *AASHTO LRFD* Article 6.10.1.1.1d; that is, using the short-term modular ratio n = 8. The special load combination specified in *AASHTO LRFD* Article 3.4.2.1 controls by inspection.

$$f_{deck} = \frac{1.0(1.4)(-1{,}403)(21.73)(12)}{166{,}612(8)} = 0.384 \text{ ksi} < 0.432 \text{ ksi}$$

Therefore, the minimum one percent longitudinal reinforcement (refer to *AASHTO LRFD* Article 6.10.1.7) is not required at this section in order to satisfy this check. Although not done in this example, a more accurate estimate of the concrete strength at the time Cast 2 is made, and the resulting modular ratio, can be used in this check.

The effective width of the deck is 114.0 in. and the structural deck thickness is 9.0 in. Therefore, the total tensile force in the concrete deck at the end of Cast 1 is (0.384)(114.0)(9.0) = 394 kips. This force will be transferred from the deck through the shear connectors to the top flange. Sufficient shear connectors should be present at this location to resist this force and prevent potential crushing of the concrete around the studs or fracturing of the studs. To estimate the length over which this force must be transmitted, assume a 45-degree angle from the end of the cast to where the concrete deck is assumed effective. Therefore, the length in this particular case is estimated to be 57.0 inches. The pitch of the studs is 12.0 inches in this region and that there are three studs per row. The factored shear resistance of an individual 7/8-inch stud is computed to be 30.6 kips for f'_c equal to 4.0 ksi (Section 6.6.2.4.3). Thus, the force resisted by the 15 studs within the 57-inch

length is 15(30.6) = 459 kips > 394 kips. If necessary, the tensile force in the deck can be lowered by modifying the placement sequence.

6.5.3.3.5 Global Displacement Amplification in Slender I-Girder Bridge Units

Specific guidelines for checking the global stability of spans of certain slender unsupported straight or horizontally curved multiple I-girder bridge units interconnected by cross-frames or diaphragms, when in their non-composite condition during the deck placement operation, are provided in *AASHTO LRFD* Article 6.10.3.4.2.

In certain situations, spans of slender unsupported straight or horizontally curved steel I-girder bridge units can be vulnerable to overall (i.e. global) elastic stability related failures during their construction (Figure 6.5.3.3.5-1). The non-composite dead loads must be resisted predominantly by the steel structure during deck placement prior to hardening of the concrete deck. Relatively slender I-girder bridge units (i.e. units with large span-to-width ratios, and with three or fewer girders) may be susceptible to global stability problems rather than cross-section or individual unbraced length strength limit states during the deck placement (Yura et al., 2008). Due to second-order lateral-torsional amplification of the displacements and stresses, the limit of the structural resistance may be reached well before the theoretical elastic buckling resistance. Large displacement amplifications can make it difficult to predict and control the structure geometry.

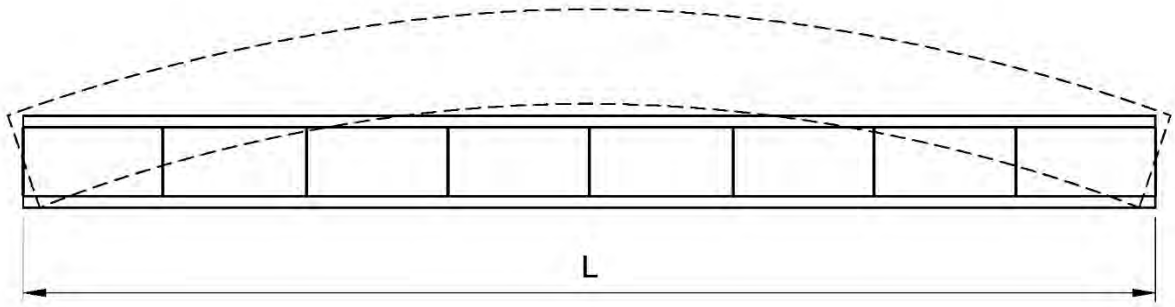

Figure 6.5.3.3.5-1 Global Displacement Ampilification in a Slender I-Girder Bridge Unit

The provisions of *AASHTO LRFD* Article 6.10.3.4.2 provide one means of estimating the global lateral-torsional buckling resistance of slender unsupported multiple I-girder units with three or fewer girders interconnected by cross-frames or diaphragms when in their non-composite condition during the deck placement operation. The primary intent of these provisions is to avoid excessive amplification of the lateral and vertical displacements of slender I-girder bridge units during the

deck placement operation before the concrete deck has hardened. Two-girder units are particularly susceptible to excessive global lateral-torsional amplification during the deck placement; however, units with large span/width ratios having up to three girders also may be susceptible to significant global amplification in some cases. Situations involving phased construction utilizing narrow unsupported units with only two or three girders, and possibly unevenly applied deck weight, are situations where this may be of particular concern. Large global torsional rotations signified by large differential vertical deflections between the girders, and also large lateral deflections as determined from a first-order analysis, are indicative of the potential for significant second-order global amplification.

The elastic global buckling resistance may be used as an indicator of the susceptibility of general straight, curved and/or skewed I-girder systems to second-order amplification under noncomposite loading conditions (NCHRP, 2012). The global buckling mode in this case refers to buckling of the bridge unit as a structural unit, and not buckling of the girders between intermediate braces. Global lateral-torsional buckling is defined as a buckling mode in which a system of girders buckle as a unit with an unbraced length equal to the clear span of the girders.

The provisions of *AASHTO LRFD* Article 6.10.3.4.2 apply to spans of I-girder bridge units with three or fewer girders, interconnected by cross-frames or diaphragms, that also meet both of the following conditions in their noncomposite condition during the deck placement operation:

- The unit is not braced by other structural units and/or by external bracing within the span; and
- The unit does not contain any flange level lateral bracing or lateral bracing from a hardened composite deck within the span.

Considering all of the girders across the width of the unit within the span under consideration, the sum of the largest total factored positive girder moments during the deck placement should not exceed 50 percent of the elastic global lateral-torsional buckling resistance of the span acting as a system. Limiting the sum of the total factored positive girder moments across the width of the unit within the span under consideration to 50 percent of the elastic global buckling resistance of the span acting as a system theoretically limits the amplification under the corresponding nominal loads to a maximum value of approximately 1.5.

The elastic global lateral-torsional buckling resistance of the span acting as a system, M_{gs}, may be calculated as follows (Yura et al., 2008):

$$M_{gs} = \frac{\pi^2 w_g E}{L^2}\sqrt{I_{eff}\, I_x} \qquad \text{Equation 6.5.3.3.5-1}$$

AASHTO LRFD Equation 6.10.3.4.2-1

where:

- For doubly symmetric girders:

$$I_{eff} = I_y \qquad \text{Equation 6.5.3.3.5-2}$$

AASHTO LRFD Equation 6.10.3.4.2-2

- For singly symmetric girders:

$$I_{eff} = I_{yc} + \left(\frac{t}{c}\right) I_{yt} \qquad \text{Equation 6.5.3.3.5-3}$$

AASHTO LRFD Equation 6.10.3.4.2-3

c = distance from the centroid of the non-composite steel section under consideration to the centroid of the compression flange (in.). The distance is to be taken as positive.

I_x = non-composite moment of inertia about the horizontal centroidal axis of a single girder within the span under consideration (in.^{4})

I_{yc}, I_{yt}= moments of inertia of the compression and tension flange, respectively, about the vertical centroidal axis of a single girder within the span under consideration (in.^{4})

I_y = non-composite moment of inertia about the vertical centroidal axis of a single girder within the span under consideration (in.^{4})

L = length of the span under consideration (in.)

t = distance from the centroid of the non-composite steel section under consideration to the centroid of the tension flange (in.). The distance is to be taken as positive.

w_g = girder spacing for a two-girder system, or the distance between the two exterior girders of the unit for a three-girder system (in.)

Should the sum of the largest total factored positive girder moments across the width of the unit within the span under consideration exceed 50 percent of M_{gs}, the following alternatives may be considered:

- The addition of flange level lateral bracing adjacent to the supports of the span may be considered as discussed in *AASHTO LRFD* Article 6.7.5.2 (Section 6.3.2.10);
- The unit may be revised to increase the system stiffness; or

- The amplified girder second-order displacements of the span during the deck placement may be evaluated to verify that they are within tolerances permitted by the Owner.

Yura et al. (2008) suggest adjustments to be made to Equation 6.5.3.3.5-1 when estimating the elastic global lateral-torsional buckling resistance of the system where a partial top-flange lateral bracing system is present at the ends of the span, along with some associated bracing design recommendations.

Once a concrete deck is acting compositely with the steel girders, a given span of a bridge unit is practically always stable as an overall system; Equation 6.5.3.3.5-1 is not intended for application to I-girder bridge spans in their composite condition. Equation 6.5.3.3.5-1 is also not applicable to I-girder bridge units with more than three girders, which are typically not susceptible to excessive global lateral-torsional amplification during the deck placement.

Equation 6.5.3.3.5-1 was derived assuming prismatic girders and that all girder cross-sections in the unit are the same. For cases where the girders are nonprismatic and/or the girder cross-sections vary across the unit, it is recommended in *AASHTO LRFD* Article C6.10.3.4.2 that length-weighted average moments of inertia within the positive-moment sections of all the girders in the span under consideration be used for I_x, I_y, I_{yc} and I_{yt}, as applicable, in calculating the elastic global lateral-torsional buckling resistance from Equation 6.5.3.3.5-1. Also, in cases where the girder spacing is less than the girder depth, it is recommended that the more general elastic global lateral-torsional buckling equation provided in Yura et. al. (2008) be used, as Equation 6.5.3.3.5-1 becomes more conservative in this case. Yura et al. (2008) further indicate the adjustments that need to be made to the more general buckling equation for singly symmetric girders and/or for three-girder systems.

AASHTO LRFD Article C6.10.3.4.2 further indicates that other methods, such as an eigenvalue buckling analysis or a global second-order load-deflection analysis, may be used in lieu of Equation 6.5.3.3.5-1 to determine the response of the system.

It should be noted that as of this writing (2015), the current provisions for checking for global displacement amplification may be on the conservative side in some cases. It is anticipated that future revisions to there provisions, such as the inclusion of a special moment-gradient modifier, C_b, in Equation 6.5.3.3.5-1 may alleviate some of this inherent conservatism.

6.5.3.4 Deck Overhang Loads

6.5.3.4.1 General

AASHTO LRFD Article 6.10.3.4.1 also requires that the effect of forces from deck overhang brackets acting on the fascia girders be considered (Figure 6.5.3.4.1-1).

The overhang brackets, which are usually spaced at 3 to 4 feet along the exterior girders, are typically attached to the top flanges of the girders. The brackets may either bear directly on the web or be carried to the intersection of the bottom flange and the web, which is preferred. The horizontal components of the bracket reactions transmitted directly onto the exterior girder web may cause the web to exhibit significant plate deformations. Excessive deformations of the web or top flange resulting from the bracket support forces may cause the deck finish to be problematic. Therefore, if the brackets bear on the girder web, particularly in the compression zone of the web, a means should be provided to ensure that the web is not damaged and that the associated deformations permit proper placement of the concrete deck. Also, when the brackets bear on the web, the lateral flange force and the force on the web increase significantly.

The eccentricity of the deck weight and other loads acting on the overhang brackets creates applied torsional moments on the fascia girders. The torsional moments bend the top flanges of exterior I-girders, or the outermost top flanges of tub girders, outward resulting in lateral bending stresses that must be considered in the design of the flanges. The top flange must have sufficient capacity to resist these lateral loads acting in combination with the vertical loads resulting from the deck casting. The effect of the reactions from the brackets on the cross-frame forces should also be considered.

Overhang bracket loads on curved bridges are particularly critical for the girder on the outside of the curve. The top flange is bent outward as the loads are applied to the brackets causing lateral flange moments of the same sense as the lateral flange moments due to curvature in regions of positive flexure. The opposite is true for the girder on the inside of the curve.

Figure 6.5.3.4.1-1 Overhang Brackets on a Curved I-Girder Bridge

6.5.3.4.2 Lateral Flange Forces

The sketch shown in Figure 6.5.3.4.2-1 shows a deck overhang bracket bearing directly on the bottom flange, which again is the preferred configuration.

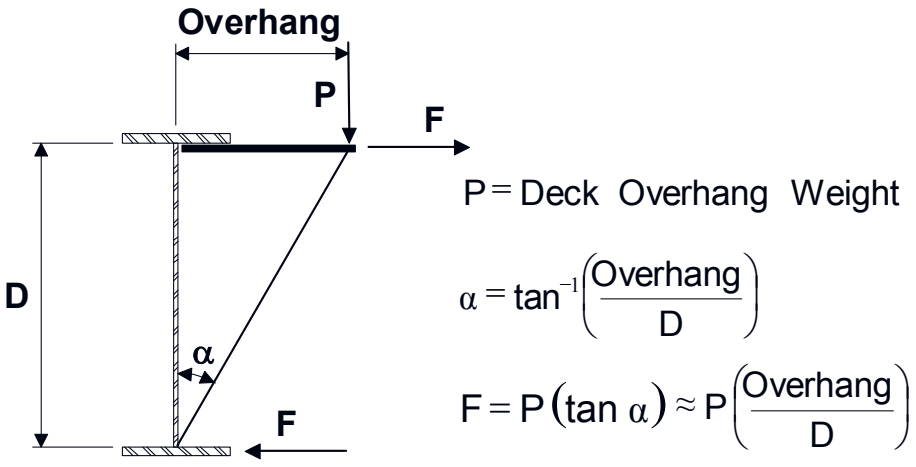

Figure 6.5.3.4.2-1 Lateral Flange Forces from Deck Overhang

The deck overhang weight is resisted by the brackets. If the bracket is assumed to extend near the edge of the deck overhang, it can be assumed that half of the deck overhang weight is placed on the fascia girder and half is placed on the overhang brackets. One-half of the deck haunch weights can also conservatively be included in the total overhang weight.

Besides the weight of the deck, typical loads that act on the overhang only during construction include the overhang deck forms, the screed rail, the railing, the walkway, the overhang brackets and the finishing machine. The finishing machine and railing loads may be ignored when the finishing machine is applied directly over the fascia girder. The Design Engineer should consider talking with local contractors to obtain accurate load values. Refer to *AASHTO LRFD* Article 3.4.2 for the appropriate load factors to be applied to these construction loads (Section 6.5.3.2).

The lateral force, *F*, on the flanges due to the vertical load, *P*, on the overhang brackets may be computed as shown in Figure 6.5.3.4.2-1. From the equation for *F* shown in the figure, it is evident how *F* increases and the force on the web increases when the bracket bears directly on the web. Since the lateral force is dependent on the assumed angle that the brackets make with the web, the assumed magnitude and application of the overhang loads should be indicated on the contract documents. Should the Contractor deviate significantly from the assumed angle and/or loads, an additional investigation by the Contractor may be necessary.

The deck overhang construction loads are often applied to the non-composite section and removed when the bridge has become composite. Typically, the major-axis bending moments due to these loads are small relative to other design loads. However, the Design Engineer may find it desirable in some cases to consider the effect of these moments, particularly in computing deflections for cambers in special situations involving large overhangs. The lateral bending moments due to these loads are often more critical. Where design checks for exterior girder including the overhang force effects are made under the Strength I load combination, where a smaller load factor is applied to the component dead load effects than under the special load combination specified in *AASHTO LRFD* Article 3.4.2.1, consideration might be given to conservatively considering the effect of the additional vertical bending moments resulting from the deck overhang loads.

6.5.3.4.3 Lateral Flange Bending Moments

The approximate equations shown below may be used to estimate the maximum lateral bending moments, M_ℓ, in the flanges (acting at the cross-frames/diaphragms) due to the lateral bracket forces in the absence of a more refined analysis. These equations are presented in *AASHTO LRFD* Article C6.10.3.4.1. The equation to use depends on how the lateral bracket forces are assumed applied to the top flange.

The first equation applies if a statically equivalent uniformly distributed bracket force, F_ℓ (kips/in.), is assumed.

$$M_\ell = \frac{F_\ell L_b^2}{12} \qquad \text{Equation 6.5.3.4.3-1}$$

AASHTO LRFD Equation C6.10.3.4.1-2

where:

L_b = unbraced length (in.)

The second equation applies if a statically equivalent concentrated lateral bracket force, P_ℓ (kips), is assumed to act at the middle of the unbraced length:

$$M_\ell = \frac{P_\ell L_b}{8} \qquad \text{Equation 6.5.3.4.3-2}$$

AASHTO LRFD Equation C6.10.3.4.1-3

Bracket dead loads are typically assumed applied uniformly. The finishing machine truss load may be assumed to be applied as a single concentrated load.

The two equations are based on the assumption of interior unbraced lengths in which the flange is continuous with adjacent unbraced lengths. In addition, approximately equal adjacent unbraced lengths are also assumed, such that the ends of the unbraced length under consideration are effectively torsionally fixed. When these assumptions do not approximate actual conditions for the unbraced length under consideration, the Design Engineer should consider other more appropriate idealizations.

In special cases involving larger deck overhangs, refined 3D analyses of the non-composite bridge for these overhang loads provides more accurate flange lateral bending moments and may identify any rotation of the overhang that could potentially affect the elevation of the screed when finishing the deck.

6.5.3.4.4 Lateral Flange Bending Stresses

Once the lateral bending moments are obtained, the lateral bending stress in the flange under consideration can be computed based on the lateral section modulus of the rectangular flange:

$$f_\ell = \frac{M_\ell}{S_\ell} \le 0.6F_y \qquad \text{Equation 6.5.3.4.4-1}$$

where:

f_ℓ = flange lateral bending stress (ksi)
M_ℓ = flange lateral bending moment (kip-in.)
S_ℓ = lateral section modulus of flange = $t_f b_f^2/6$ (in.^{3})

Total lateral bending stresses from all sources (e.g. deck overhang bracket effects, curvature and/or skew as applicable in this case) are limited to a maximum value of $0.6F_{yf}$ according to *AASHTO LRFD* Article 6.10.1.6. Beyond that limit, the reduction in the major-axis bending resistance of the flange due to flange lateral bending tends to be greater than that comprehended by the one-third rule equations used to check the resistance of the flange for the combined vertical and lateral bending effects.

6.5.3.4.4.1 Amplification of Lateral Bending Stresses

As discussed previously in Section 6.5.2.1.3.2, according to *AASHTO LRFD* Article 6.10.1.6, lateral bending stresses determined from a first-order analysis may be used in discretely braced compression flanges for which Equation 6.5.2.1.3.2-1 is satisfied. In applying this equation for the case of lateral bending stresses due to deck overhang effects (acting in combination with lateral bending stresses due to curvature and/or skew as applicable), f_{bu} is to be taken as the critical factored major-axis compressive bending stress determined from the deck-casting analysis.

If the equation is not satisfied (which will often be the case for typical cross-frame/diaphragm spacings used in bridges), then *AASHTO LRFD* Article 6.10.1.6 requires that second-order elastic compression-flange lateral bending stresses be determined. These stresses may be determined by conservatively amplifying the first-order values based on Equation 6.5.2.1.3.2-2 in lieu of a direct geometric nonlinear analysis.

The amplified or second-order lateral bending stress in the compression flange, including the effects of the deck overhangs, curvature and/or skew as applicable, is then appropriately combined with the flexural stress, f_{bu}, in that flange determined from the deck-casting analysis to perform the necessary constructibility verifications specified in *AASHTO LRFD* Article 6.10.3.2 (for I-girders) or *AASHTO LRFD* Article 6.11.3.2 (for top flanges of tub girders). These verifications are described in more detail below in Section 6.5.3.5.

Tension flange lateral bending stresses are not to be amplified. Therefore, bottom flanges in regions of positive flexure, which are often also wider than top flanges, are typically not critical for the constructibility verifications.

EXAMPLE

Calculate the lateral flange bending stresses due to the deck overhang loads within the 24-foot unbraced length of an exterior girder in the end span of a three-span continuous I-girder bridge encompassing Location A from the preceding example. The cross-section of the girder within this unbraced length is shown in Figure 6.5.3.4.4.1-1. The elastic section properties for this section were computed earlier (Section 6.4.2.3.2.3). The girder is homogeneous with the yield strength of the flanges and web equal to 50 ksi. Assume the deck overhang bracket configuration shown in with the brackets (Figure 6.5.3.4.4.1-1) extending to the bottom flange, which is preferred.

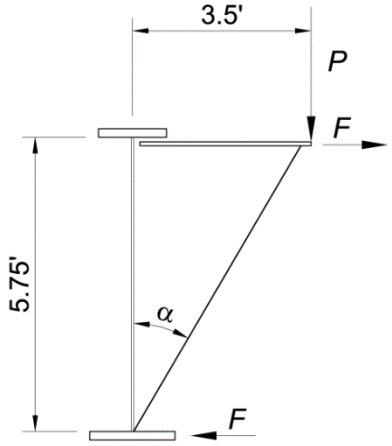

Figure 6.5.3.4.4.1-1 Example Deck Overhang Bracket

Although the brackets are typically spaced at 3 to 4 feet along the exterior girder, all bracket loads except for the finishing machine load are assumed applied uniformly. Calculate the vertical loads acting on the overhang brackets. Because in this case the bracket is assumed to extend near the edge of the deck overhang, assume that half the deck overhang weight is placed on the exterior girder and half the weight is placed on the overhang brackets. Conservatively include one-half the deck haunch weight in the total overhang weight. Assume the bridge cross-section shown in Figure 6.5.3.4.4.1-2.

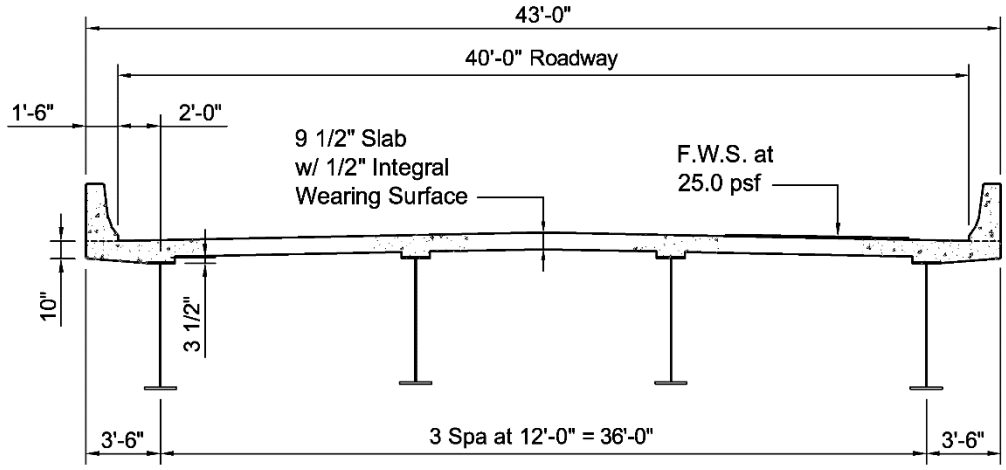

Figure 6.5.3.4.4.1-2 Example Bridge Cross-Section

The top flange of the girder within the unbraced length under consideration is ¾" x 16" (Figure 6.4.2.3.2.3-1). The ½" integral wearing surface is not included in the indicated 10" dimension at the edge of the overhang. Therefore, the deck overhang weight assumed to be acting on the bracket is computed as:

$$P = 0.5 * 150\left[\frac{9.5}{12}(3.5)+\left[\frac{1}{12}\left(\frac{3.0}{2}+0.5\right)\left(3.5-\frac{16/2}{12}\right)\right]+\frac{2.75}{12}\left(\frac{16/2}{12}\right)\right] = 255 \text{ lbs / ft}$$

The other half of the overhang weight can be assumed to act at the edge of the top flange (at a distance of 8.0 inches from the shear center of the girder in this case). The effective deck weight acting on the other side of the girder can be assumed applied at the other edge of the top flange. The net torque can be resolved into flange lateral moments that generally act in the opposite direction to the lateral moments caused by the overhang loads. This effect is conservatively neglected in this example.

Construction loads, or dead loads and temporary loads that act on the overhang only during construction, are assumed as follows:

Overhang deck forms:	*P*	=	40 lbs/ft
Screed rail:	*P*	=	85 lbs/ft
Railing:	*P*	=	25 lbs/ft
Walkway:	*P*	=	125 lbs/ft
Finishing machine:	*P*	=	3000 lbs

The finishing machine load is estimated as one-half of the total finishing machine truss weight, plus some additional load to account for the weight of the engine, drum

and operator assumed to be located on one side of the truss. Note that the above loads are estimated loads used here for illustration purposes only. Again, it is recommended that the Engineer consider talking to local Contractors to obtain more accurate values for these construction loads.

The lateral force on the top flange due to the vertical load on the overhang brackets is estimated as (Figure 6.5.3.4.2-1):

$$F = P\left(\frac{\text{Overhang}}{D}\right) = P\left(\frac{3.5}{5.75}\right) = 0.609P$$

Assuming the flanges are continuous with the adjacent unbraced lengths and that the adjacent unbraced lengths are approximately equal, the lateral bending moment due to a statically equivalent uniformly distributed lateral bracket force may be estimated as (Equation 6.5.3.4.3-1):

$$M_\ell = \frac{F_\ell L_b^2}{12}$$

The lateral bending moment due to a statically equivalent concentrated lateral bracket force assumed placed at the middle of the unbraced length may be estimated as (Equation 6.5.3.4.3-2):

$$M_\ell = \frac{P_\ell L_b}{8}$$

According to *AASHTO LRFD* Article 6.10.1.6, lateral bending stresses determined from a first-order analysis may be used in discretely braced compression flanges for which (Equation 6.5.2.1.3.2-1):

$$L_b \le 1.2L_p\sqrt{\frac{C_b R_b}{f_{bu}/F_{yc}}}$$

L_p is the limiting unbraced length specified in *AASHTO LRFD* Article 6.10.8.2.3 determined as (Equation 6.5.6.2.2.2.2-5):

$$L_p = 1.0r_t\sqrt{\frac{E}{F_{yc}}}$$

where r_t is the effective radius of gyration for lateral torsional buckling specified in *AASHTO LRFD* Article 6.10.8.2.3 determined as (Equation 6.5.6.2.2.2.2-8):

$$r_t = \frac{b_{fc}}{\sqrt{12\left(1+\frac{1}{3}\frac{D_c t_w}{b_{fc} t_{fc}}\right)}}$$

For the steel section within the unbraced length under consideration, the depth of the web in compression in the elastic range D_c is 38.63 inches. Therefore,

$$r_t = \frac{16}{\sqrt{12\left(1+\frac{1}{3}\frac{38.63(0.5)}{16(1)}\right)}} = 3.90 \text{ in.}$$

$$L_p = \frac{1.0(3.90)}{12}\sqrt{\frac{29{,}000}{50}} = 7.83 \text{ ft}$$

C_b is the moment gradient modifier specified in *AASHTO LRFD* Article 6.10.8.2.3. Separate calculations show that $f_{mid}/f_2 > 1$ in the unbraced length under consideration. Therefore, C_b must be taken equal to 1.0 (Section 6.5.6.2.2.2.2).

According to *AASHTO LRFD* Article 6.10.1.10.2, the web load-shedding factor, R_b, is to be taken equal to 1.0 when checking constructibility since web bend buckling is prevented during construction by a separate limit state check (Section 6.5.3.5.1.2).

Finally, f_{bu} is the largest value of the factored compressive stress throughout the unbraced length in the flange under consideration, calculated without consideration of flange lateral bending. In this case, use f_{bu} = -30.70 ksi due to the deck-placement sequence, as computed earlier for the special load combination specified in *AASHTO LRFD* Article 3.4.2 (which controls in this particular computation). Therefore:

$$1.2(7.83)\sqrt{\frac{1.0(1.0)}{|-30.70|/50}} = 11.99 \text{ ft} < L_b = 24.0 \text{ ft}$$

Because the preceding equation is not satisfied, *AASHTO LRFD* Article 6.10.1.6 requires that second-order elastic compression-flange lateral bending stresses be determined. The second-order compression-flange lateral bending stresses may be determined by amplifying first-order values (i.e. f_{f1}) as follows (Equation 6.5.2.1.3.2-2):

$$f_\ell = \left(\frac{0.85}{1 - \frac{f_{bu}}{F_{cr}}} \right) f_{\ell 1} \geq f_{\ell 1}$$

or: $$f_\ell = (AF) f_{\ell 1} \geq f_{\ell 1}$$

where *AF* is the amplification factor and F_{cr} is the elastic lateral torsional buckling stress for the flange under consideration specified in *AASHTO LRFD* Article 6.10.8.2.3 determined as (Equation 6.5.6.2.2.2.2-7):

$$F_{cr} = \frac{C_b R_b \pi^2 E}{\left(\frac{L_b}{r_t} \right)^2}$$

$$F_{cr} = \frac{1.0(1.0)\pi^2(29{,}000)}{\left(\frac{24(12)}{3.90} \right)^2} = 52.49 \text{ ksi}$$

As indicated in *AASHTO LRFD* Article C6.10.1.6, note that the calculated value of F_{cr} for use in *AASHTO LRFD* Equation 6.10.1.6-4 is not limited to $R_b R_h F_{yc}$ as specified in *AASHTO LRFD* Article 6.10.8.2.3.

The amplification factor is then determined as follows:

For Strength I:

$$AF = \frac{0.85}{\left(1 - \frac{|-27.41|}{52.49} \right)} = 1.78 > 1.0 \quad \text{ok}$$

For the Special Load Combination in *AASHTO LRFD* Article 3.4.2.1:

$$AF = \frac{0.85}{\left(1 - \frac{|-30.70|}{52.49} \right)} = 2.05 > 1.0 \quad \text{ok}$$

AF is taken equal to 1.0 for tension flanges. The above equation for the amplification factor conservatively assumes an elastic effective length factor for lateral-torsional buckling equal to 1.0.

Note that first- or second-order flange lateral bending stresses, as applicable, are limited to a maximum value of $0.6F_{yf}$ according to *AASHTO LRFD* Equation 6.10.1.6-1.

In the Strength I load combination, a load factor of 1.5 is applied to all construction loads (refer to *AASHTO LRFD* Article 3.4.2 – Section 6.5.3.2).

For Strength I:

Dead loads: $P = 1.0\left[1.25(255) + 1.5(40 + 85 + 25 + 125)\right] = 731.3 \text{ lbs / ft}$

$$F = F_\ell = 0.609P = 0.609(731.3) = 445.4 \text{ lbs / ft}$$

$$M_\ell = \frac{F_\ell L_b^2}{12} = \frac{0.445(24)^2}{12} = 21.4 \text{ kip} - \text{ft}$$

$$\text{Top flange: } f_\ell = \frac{M_\ell}{S_\ell} = \frac{21.4(12)}{1(16)^2/6} = 6.02 \text{ ksi}$$

$$\text{Bot. flange: } f_\ell = \frac{M_\ell}{S_\ell} = \frac{21.4(12)}{1.375(18)^2/6} = 3.46 \text{ ksi}$$

Finishing machine: $P = 1.0\left[1.5(3000)\right] = 4{,}500 \text{ lbs}$

$$F = P_\ell = 0.609P = 0.609(4{,}500) = 2{,}740 \text{ lbs}$$

$$M_\ell = \frac{P_\ell L_b}{8} = \frac{(2{,}740 / 1000)(24)}{8} = 8.22 \text{ kip} - \text{ft}$$

$$\text{Top flange: } f_\ell = \frac{M_\ell}{S_\ell} = \frac{8.22(12)}{1(16)^2/6} = 2.31 \text{ ksi}$$

$$\text{Bot. flange: } f_\ell = \frac{M_\ell}{S_\ell} = \frac{8.22(12)}{1.375(18)^2/6} = 1.33 \text{ ksi}$$

Top flange:

f_ℓ total $= 6.02 + 2.31 = 8.33$ ksi * AF = (8.33)(1.78) = 14.83 ksi < $0.6F_{yf}$ = 30 ksi ok

Bot. flange:

f_ℓ total $= 3.46 + 1.33 = 4.79$ ksi * AF = (4.79)(1.0) = 4.79 ksi < $0.6F_{yf}$ = 30 ksi ok

For the Special Load Combination in *AASHTO LRFD* Article 3.4.2.1 (Section 6.5.3.2):

Dead loads: $P = 1.0[1.4(255 + 40 + 85 + 25 + 125)] = 742$ lbs / ft

$$F = F_\ell = 0.609P = 0.609(742) = 451.9 \text{ lbs / ft}$$

$$M_\ell = \frac{F_\ell L_b^2}{12} = \frac{0.452(24)^2}{12} = 21.7 \text{ kip} - \text{ft}$$

$$\text{Top flange: } f_\ell = \frac{M_\ell}{S_\ell} = \frac{21.7(12)}{1(16)^2/6} = 6.10 \text{ ksi}$$

$$\text{Bot. flange: } f_\ell = \frac{M_\ell}{S_\ell} = \frac{21.7(12)}{1.375(18)^2/6} = 3.51 \text{ ksi}$$

Finishing machine: Not considered to be a *DC* load

Top flange: f_ℓ total $= 6.10$ ksi * AF = 6.10(2.05) = 12.51 ksi < $0.6F_{yf}$ = 30 ksi ok
Bot. flange: f_ℓ total $= 3.51$ ksi * AF = 3.51(1.0) = 3.51 ksi < $0.6F_{yf}$ = 30 ksi ok

6.5.3.5 Design Verifications

6.5.3.5.1 I-Sections

6.5.3.5.1.1 General

The provisions for design for constructibility for I-section flexural members are given in *AASHTO LRFD* Article 6.10.3. The provisions are intended to provide adequate strength and stability of the main load-carrying members during construction, to properly account for dead load deflections, and to control the slip in load-resisting

bolted connections at each critical construction stage to ensure that the proper geometry of the structure is maintained. *AASHTO LRFD* Article 6.10.3.1 states that nominal yielding or reliance on post-buckling resistance is not to be permitted for main load-carrying members during the critical stages of construction. An exception is permitted for the localized yielding of the web that may occur in hybrid members. To achieve these objectives, the requirements of *AASHTO LRFD* Articles 6.10.3.2 (Flexure) and 6.10.3.3 (Shear) must be satisfied at each critical construction stage, as detailed below. The required check on the concrete deck tensile stress during construction specified in AASHTO LRFD Article 6.10.3.2.4 was discussed previously in Section 6.5.3.3.4. A helpful flowchart detailing the required LRFD constructibility design verifications for I-sections, discussed below, is provided in AASHTO LRFD Figure C6.4.1-1 (Appendix C6).

6.5.3.5.1.2 Flexure

An important distinction is made between discretely braced and continuously braced flanges in the constructibility design provisions for flexure given in *AASHTO LRFD* Article 6.10.3.2. As discussed previously in Section 6.5.2.1.1, a discretely braced flange is braced at discrete intervals by bracing sufficient to restrain lateral deflection of the flange and twisting of the entire cross-section at the brace points. Both flanges along the entire length of the girder are considered to be discretely braced flanges for the non-composite steel I-girder during construction. A continuously braced flange is encased in hardened concrete or anchored by shear connectors. Lateral flange bending need not be considered for a continuously braced flange. A continuously braced compression flange is also assumed not to be subject to local or lateral-torsional buckling (local buckling and lateral-torsional buckling are discussed further in Section 6.5.6.2.2.2).

There are three equations that must be satisfied for discretely braced flanges in compression, as shown below and as presented in *AASHTO LRFD* Article 6.10.3.2.1. Each of these requirements must be satisfied for critical stages of construction.

The first equation for discretely braced flanges in compression is as follows:

$$f_{bu} + f_{\ell} \le \phi_f R_h F_{yc} \qquad \text{Equation 6.5.3.5.1.2-1}$$

AASHTO LRFD Equation 6.10.3.2.1-1

where:

ϕ_f = resistance factor for flexure specified in *AASHTO LRFD* Article 6.5.4.2 = 1.0

f_{bu} = factored compression-flange vertical stress determined as specified in *AASHTO LRFD* Article 6.10.1.6 (ksi). f_{bu} is always taken as positive.

f_ℓ = factored flange lateral bending stress determined as specified in *AASHTO LRFD* Article 6.10.1.6 (ksi). f_ℓ is always taken as positive.

R_h = hybrid factor specified in *AASHTO LRFD* Article 6.10.1.10.1 (Section 6.4.5.7). For hybrid sections in which f_{bu} does not exceed the specified minimum yield strength of the web, R_h is to be taken equal to 1.0.

Equation 6.5.3.5.1.2-1 ensures that the maximum combined factored vertical and lateral bending stress in the compression flange during construction will not exceed the specified minimum yield strength of the flange times the hybrid factor, R_h. As such, this equation is a yielding limit state check. For girders subject to significant lateral bending stresses and for members with compact or noncompact webs, Equation 6.5.3.5.1.2-1 will often control. However, the equation does not need to be checked for slender-web sections when f_ℓ is equal to zero. The definitions of compact, noncompact and slender-web sections are discussed further in Section 6.5.6.2.2.1.1. In categorizing the web as compact, noncompact or slender for these checks, the properties of the non-composite steel section are used. Non-composite sections in all kinked (chorded) continuous and horizontally curved-girder bridges and in straight-girder bridges whose supports are skewed more than 20° from normal must always be treated as slender web sections, regardless of their web slenderness, in applying the specifications.

The hybrid factor, R_h, is discussed further in Section 6.4.5.7. Note that for sections that are composite in the final condition, but non-composite during construction, different values of R_h must be computed for the checks in which the member is non-composite and for the checks in which the member is composite.

The second equation for discretely braced flanges in compression is as follows:

$$f_{bu} + \frac{1}{3} f_\ell \le \phi_f F_{nc} \qquad \text{Equation 6.5.3.5.1.2-2}$$

AASHTO LRFD Equation 6.10.3.2.1-2

where:

F_{nc} = nominal flexural resistance of the compression flange determined as specified in *AASHTO LRFD* Article 6.10.8.2 (ksi)

Equation 6.5.3.5.1.2-2 ensures that the member has sufficient strength with respect to flange local buckling and lateral-torsional buckling under the maximum combined factored vertical and lateral bending stress in the compression flange during construction. Equation 6.5.3.5.1.2-2 is based on the stress-based form of the one-third rule equation (Section 6.5.2.1.4) since the nominal flexural resistance for constructibility is always expressed in terms of the flange stress. The calculation of the flange local buckling (FLB) resistance and lateral-torsional buckling (LTB)

resistance, F_{nc}, according to the *AASHTO LRFD* Specification provisions is discussed in detail in Section 6.5.6.2.2.2. Equation 6.5.3.5.1.2-2 will generally control for members with noncompact flanges having large unsupported lengths during construction in combination with zero or small values of f_ℓ. A noncompact flange is a compression flange with a slenderness ratio between the limiting values of λ_{pf} and λ_{rf} specified in *AASHTO LRFD* Article 6.10.8.2.2 (and discussed further in Section 6.5.6.2.2.2.1).

Note that for sections in straight I-girder bridges with compact or noncompact webs, *AASHTO LRFD* Article 6.10.3.2.1 permits the LTB resistance to be determined from the provisions of *AASHTO LRFD* Article A6.3.3 (Appendix A6), which include the beneficial effect of the St. Venant torsional constant, *J* (Section 6.5.6.2.3.3.2). For straight members having larger unbraced lengths that utilize such sections, the additional LTB resistance obtained by including the contribution of *J* may be beneficial. The LTB resistance, M_{nc}, computed from the provisions of Appendix A6 is expressed in terms of moment because, in general, Appendix A6 permits flexural resistances to exceed the yield moment resistance, M_{yt} or M_{yc}, as applicable. Therefore, if the LTB resistance is computed from Appendix A6 in such cases, the resulting LTB resistance, M_{nc}, must be divided by S_{xc} (taken equal to M_{yc}/F_{yc}) to express the resistance in terms of stress for application in Equation 6.5.3.5.1.2-2. The calculated resistance F_{nc} may exceed F_{yc} in some cases, however Equation 6.5.3.5.1.2-1 will control ensuring that the combined factored stress in the flange will not exceed F_{yc} during construction.

AASHTO LRFD Article 6.10.1.6 specifies that for design checks involving lateral-torsional buckling, the vertical bending compressive stress, f_{bu}, and flange lateral bending stress, f_ℓ, are to be taken as the largest values throughout the unbraced length in the flange under consideration, which is consistent with established practice in applying beam-column interaction equations involving member stability checks. For design checks involving flange local buckling, f_{bu} and f_ℓ may be taken as the corresponding values at the section under consideration. However, when maximum values of these stresses occur at different locations within the unbraced length, which is often the case, it is conservative to use the maximum values in the local buckling check.

As discussed previously in Section 6.5.3.4.4.1, amplification of the flange lateral bending stresses in discretely braced compression flanges may be required in some cases. The sign of f_{bu} and f_ℓ is always taken as positive in these equations. However, when summing the lateral flange bending stresses due to curvature, skew and/or deck overhang effects to determine f_ℓ to apply in the equations, the signs of the individual stresses must be considered. *AASHTO LRFD* Article 6.10.1.6 further specifies that the sum of the factored flange lateral bending stresses due to all sources (after amplification) cannot exceed $0.6F_{yf}$.

The third equation for discretely braced flanges in compression is as follows:

$$f_{bu} \le \phi_f F_{crw}$$ Equation 6.5.3.5.1.2-3

AASHTO LRFD Equation 6.10.3.2.1-3

where:

F_{crw} = nominal bend-buckling resistance for webs determined as specified in *AASHTO LRFD* Article 6.10.1.9 (ksi)

Equation 6.5.3.5.1.2-3 ensures that theoretical web bend-buckling will not occur during construction. The calculation of the web bend-buckling resistance, F_{crw}, is discussed in Section 6.4.5.5. F_{crw} is to be checked against the maximum compression-flange vertical bending stress due to the factored loads, f_{bu}. Utilizing the maximum compression stress in the web rather than the stress in the compression flange in order to obtain greater precision is not warranted for this check.

Because the compression-flange stress is limited to F_{crw} during construction according to Equation 6.5.3.5.1.2-3, the web load-shedding factor, R_b, is always taken equal to 1.0 when computing the nominal flexural resistance of the compression flange for the constructibility checks (the web load-shedding factor, R_b, is discussed further in Section 6.4.5.6). As a result, the R_b factor is not included in Equation 6.5.3.5.1.2-1 or Equation 6.5.3.5.1.2-2. Note also that the web slenderness of compact and noncompact web sections is limited such that theoretical web bend-buckling will not occur at elastic stress levels, computed according to beam theory, at or below F_{yc}. Therefore, the specification indicates that Equation 6.5.3.5.1.2-3 need not be checked for these sections.

Options to consider should Equation 6.5.3.5.1.2-3 be violated under the construction condition are given at the end of *AASHTO LRFD* Article C6.10.3.2.1 and include the following:

- Providing a larger compression flange or a smaller tension flange to reduce the elastic depth of the web in compression, D_c;
- Adjusting the deck-placement sequence to reduce the compressive stress in the web;
- Providing a thicker web; or
- As a last resort, should the previous options not prove practical or cost-effective, providing a longitudinal web stiffener.

According to *AASHTO LRFD* Article 6.10.1.6, for design checks involving web bend-buckling or yielding, f_{bu} and f_ℓ may be taken as the corresponding values at the

section under consideration. As discussed above, it is conservative to use the maximum values of these stresses within the unbraced length in this check.

AASHTO LRFD Article 6.10.3.2.2 requires that a discretely braced tension flange satisfy the following relationship during critical stages of construction to prevent nominal yielding under the combined factored vertical bending and lateral bending stresses:

$$f_{bu} + f_{\ell} \le \phi_f R_h F_{yt} \qquad \text{Equation 6.5.3.5.1.2-4}$$

AASHTO LRFD Equation 6.10.3.2.2-1

AASHTO LRFD Article 6.10.3.2.3 requires that the following relationship be satisfied for continuously braced flanges in compression or tension during critical stages of construction to prevent nominal yielding of the flange:

$$f_{bu} \le \phi_f R_h F_{yf} \qquad \text{Equation 6.5.3.5.1.2-5}$$

AASHTO LRFD Equation 6.10.3.2.3-1

As mentioned previously, flange lateral bending need not be considered for a continuously braced flange. The lateral resistance of the concrete deck is generally adequate to compensate for the neglect of any initial lateral bending stresses in the steel prior to placement of the deck and any additional lateral bending stresses induced after the deck has been placed.

The design of discretely braced flanges in tension, continuously braced flanges, and discretely braced flanges in compression in regions of negative flexure is usually not controlled by constructibility verifications.

EXAMPLE

Given the deck placement analysis results and the flange lateral bending stresses due to the deck overhang loads calculated in the preceding two examples (Sections 6.5.3.3.4 and 6.5.3.4.4.1), check the exterior-girder section at Location A within the end span of a three-span continuous bridge for flexure according to the *AASHTO LRFD* Specification provisions (refer to the example in Section 6.5.3.3.4 to determine Location A).

The cross-section of the girder at this location (and within the entire 24-foot unbraced length encompassing this location) is shown in Figure 6.4.2.3.2.3-1. The elastic section properties for this section were computed earlier (Section 6.4.2.3.2.3). The girder is homogeneous with the yield strength of the flanges and web equal to

50 ksi. As determined earlier, the largest stress within this unbraced length occurs right at Location A.

First, determine if the non-composite section at Location A is a compact or noncompact web section according to *AASHTO LRFD* Equation 6.10.6.2.3-1 (or alternatively, see *AASHTO LRFD* Table C6.10.1.10.2-2 (Table 6.5.6.2.2.1.3-1) or Equation 6.5.6.2.2.1.3-1):

$$\frac{2D_c}{t_w} \le 5.7\sqrt{\frac{E}{F_{yc}}}$$

$$\frac{2D_c}{t_w} = \frac{2(38.63)}{0.5} = 154.5$$

$$5.7\sqrt{\frac{E}{F_{yc}}} = 5.7\sqrt{\frac{29{,}000}{50}} = 137.3 < 154.5$$

Therefore, the section at Location A is a slender-web section. As a result, for the top flange, Equation 6.5.3.5.1.2-1 must be checked since f_ℓ is not zero. Equation 6.5.3.5.1.2-3 must also be checked, and the optional provisions of *AASHTO LRFD* Appendix A6 (Section 6.5.6.2.3.3.2) cannot be used to determine the LTB resistance of the top (compression) flange.

The factored stresses, f_{bu} and f_ℓ, used in the following checks were computed in the preceding examples in Sections 6.5.3.3.4 and 6.5.3.4.4.1, respectively.

Top Flange

Flange Tip Yielding (*Equation* 6.5.3.5.1.2-1)

Check for nominal yielding at the top flange tips according to Equation 6.5.3.5.1.2-1:

For Strength I:

$$f_{bu} + f_\ell \le \phi_f R_h F_{yc}$$

$$f_{bu} + f_\ell = |-27.41| \text{ ksi} + 14.83 \text{ ksi} = 42.24 \text{ ksi}$$
$$\phi_f R_h F_{yc} = 1.0(1.0)(50) = 50.0 \text{ ksi}$$
$$42.24 \text{ ksi} < 50.0 \text{ ksi} \quad \text{ok}$$

For the Special Load Combination in *AASHTO LRFD* Article 3.4.2.1:

$$f_{bu} + f_{\ell} \le \phi_f R_h F_{yc}$$

$$f_{bu} + f_{\ell} = |-30.70| \text{ ksi} + 12.51 \text{ ksi} = 43.21 \text{ ksi}$$
$$\phi_f R_h F_{yc} = 1.0(1.0)(50) = 50.0 \text{ ksi}$$
$$43.21 \text{ ksi} < 50.0 \text{ ksi} \quad \text{ok}$$

The top flange at this location is a discretely braced compression flange. Therefore, calculate the FLB and LTB resistances (Section 6.5.6.2.2.2), and check the strength of the flange for FLB and LTB according to Equation 6.5.3.5.1.2-2 as follows:

Flange Local Buckling (FLB) Resistance (*AASHTO LRFD Article 6.10.8.2.2*)

Determine the slenderness ratio of the top flange:

$$\lambda_f = \frac{b_{fc}}{2t_{fc}}$$

$$\lambda_f = \frac{16}{2(1)} = 8.0$$

Determine the limiting slenderness ratio for a compact flange (Equation 6.5.6.2.2.2.1-6 - alternatively, see Table 6.5.6.2.2.2.1-1):

$$\lambda_{pf} = 0.38\sqrt{\frac{E}{F_{yc}}}$$

$$\lambda_{pf} = 0.38\sqrt{\frac{29{,}000}{50}} = 9.2$$

Since $\lambda_f < \lambda_{pf}$, use Equation 6.5.6.2.2.2.1-7:

$$(F_{nc})_{FLB} = R_b R_h F_{yc}$$

As specified in *AASHTO LRFD* Article 6.10.3.2.1, in computing F_{nc} for constructibility, the web load-shedding factor, R_b, is to be taken equal to 1.0 because the flange stress is always limited to the web bend-buckling stress according to Equation 6.5.3.5.1.2-3 (see below). Therefore,

$$(F_{nc})_{FLB} = 1.0(1.0)(50) = 50.0 \text{ ksi}$$

For Strength I:

$$f_{bu} + \frac{1}{3} f_\ell \le \phi_f (F_{nc})_{FLB}$$

$$f_{bu} + \frac{1}{3} f_\ell = |-27.41| \text{ ksi} + \frac{14.83}{3} \text{ ksi} = 32.35 \text{ ksi}$$
$$\phi_f F_{nc} = 1.0(50.0) = 50.0 \text{ ksi}$$
$$32.35 \text{ ksi} < 50.0 \text{ ksi} \quad \text{ok}$$

For the Special Load Combination in *AASHTO LRFD* Article 3.4.2.1 (Section 6.5.3.2):

$$f_{bu} + \frac{1}{3} f_\ell \le \phi_f (F_{nc})_{FLB}$$

$$f_{bu} + \frac{1}{3} f_\ell = |-30.70| \text{ ksi} + \frac{12.51}{3} \text{ ksi} = 34.87 \text{ ksi}$$
$$\phi_f F_{nc} = 1.0(50.0) = 50.0 \text{ ksi}$$
$$34.87 \text{ ksi} < 50.0 \text{ ksi} \quad \text{ok}$$

Lateral Torsional Buckling (LTB) Resistance (AASHTO LRFD Article 6.10.8.2.3)

The limiting unbraced length, L_p, was computed in the preceding example to be 7.83 feet (Section 6.5.3.4.4.1). The effective radius of gyration for lateral torsional buckling, r_t, for the non-composite section at Location A was also computed earlier to be 3.90 in.

Determine the limiting unbraced length, L_r (Equation 6.5.6.2.2.2.2-6):

$$L_r = \pi r_t \sqrt{\frac{E}{F_{yr}}}$$

where:
$$F_{yr} = 0.7F_{yc} \le F_{yw}$$

$$F_{yr} = 0.7(50) = 35.0 \text{ ksi} < 50 \text{ ksi} \quad \text{ok}$$

F_{yr} must also not be less than $0.5F_{yc}$ = 0.5(50) = 25.0 ksi ok.

Therefore:

$$L_r = \frac{\pi(3.90)}{12}\sqrt{\frac{29{,}000}{35.0}} = 29.39 \text{ ft}$$

Since L_p = 7.83 feet < L_b = 24.0 feet < L_r = 29.39 feet, use Equation 6.5.6.2.2.2.2-3:

$$(F_{nc})_{LTB} = C_b\left[1-\left(1-\frac{F_{yr}}{R_h F_{yc}}\right)\left(\frac{L_b - L_p}{L_r - L_p}\right)\right]R_b R_h F_{yc} \le R_b R_h F_{yc}$$

As discussed in the preceding example (Section 6.5.3.4.4.1), since $f_{mid}/f_2 > 1$ in the unbraced length under consideration, the moment-gradient modifier, C_b, must be taken equal to 1.0. Therefore,

$$(F_{nc})_{LTB} = 1.0\left[1-\left(1-\frac{35.0}{1.0(50)}\right)\left(\frac{24.0-7.83}{29.39-7.83}\right)\right](1.0)(1.0)(50) = 38.75 \text{ ksi} < 1.0(1.0)(50) = 50 \text{ ksi}$$

For Strength I:

$$f_{bu} + \frac{1}{3}f_\ell \le \phi_f (F_{nc})_{LTB}$$

$$f_{bu} + \frac{1}{3}f_\ell = \left|-27.41\right| \text{ ksi} + \frac{14.83}{3} \text{ ksi} = 32.35 \text{ ksi}$$
$$\phi_f F_{nc} = 1.0(38.75) = 38.75 \text{ ksi}$$
$$32.35 \text{ ksi} < 38.75 \text{ ksi} \quad \text{ok}$$

For the Special Load Combination in *AASHTO LRFD* Article 3.4.2.1 (Section 6.5.3.2):

$$f_{bu} + \frac{1}{3}f_\ell \le \phi_f (F_{nc})_{LTB}$$

$$f_{bu} + \frac{1}{3}f_\ell = \left|-30.70\right| \text{ ksi} + \frac{12.51}{3} \text{ ksi} = 34.87 \text{ ksi}$$
$$\phi_f F_{nc} = 1.0(38.75) = 38.75 \text{ ksi}$$
$$34.87 \text{ ksi} < 38.75 \text{ ksi} \quad \text{ok}$$

Web Bend-Buckling Resistance (AASHTO LRFD Article 6.10.1.9)

Determine the nominal elastic web bend-buckling resistance at Location A according to the provisions of *AASHTO LRFD* Article 6.10.1.9.1 as follows (Equation 6.4.5.5.1-2):

$$F_{crw} = \frac{0.9Ek}{\left(\frac{D}{t_w}\right)^2}$$

but not to exceed the smaller of R_hF_{yc} and $F_{yw}/0.7$, where:

$$k = \frac{9}{(D_c/D)^2} \quad \text{(Equation 6.4.5.5.2.1-1)}$$

$$k = \frac{9}{(38.63/69.0)^2} = 28.7$$

Therefore,

$$F_{crw} = \frac{0.9(29{,}000)(28.7)}{\left(\frac{69.0}{0.5}\right)^2} = 39.33 \text{ ksi} < \min\left(R_hF_{yc}, F_{yw}/0.7\right) = R_hF_{yc} = 1.0(50) = 50 \text{ ksi}$$

Check for web bend buckling at Location A using Equation 6.5.3.5.1.2-3 as follows:

For Strength I:

$$f_{bu} \le \phi_f F_{crw}$$

$$\phi_f F_{crw} = 1.0(39.33) = 39.33 \text{ ksi}$$
$$|-27.41| \text{ ksi} < 39.33 \text{ ksi} \quad \text{ok}$$

For the Special Load Combination in *AASHTO LRFD* Article 3.4.2.1 (Section 6.5.3.2):

$$f_{bu} \le \phi_f F_{crw}$$

$$\phi_f F_{crw} = 1.0(39.33) = 39.33 \text{ ksi}$$
$$|-30.70| \text{ ksi} < 39.33 \text{ ksi} \quad \text{ok}$$

Bottom Flange

The bottom flange at this location is a discretely braced tension flange. Check for yielding at the bottom flange tips according to Equation 6.5.3.5.1.2-4 as follows:

For Strength I:

$$f_{bu} + f_\ell \le \phi_f R_h F_{yt}$$

$$f_{bu} + f_\ell = 21.96 \text{ ksi} + 4.79 \text{ ksi} = 26.75 \text{ ksi}$$
$$\phi_f R_h F_{yt} = 1.0(1.0)(50) = 50.0 \text{ ksi}$$
$$26.75 \text{ ksi} < 50.0 \text{ ksi} \quad \text{ok}$$

For the Special Load Combination in *AASHTO LRFD* Article 3.4.2.1 (Section 6.5.3.2):

$$f_{bu} + f_\ell \le \phi_f R_h F_{yt}$$

$$f_{bu} + f_\ell = 24.60 \text{ ksi} + 3.51 \text{ ksi} = 28.11 \text{ ksi}$$
$$\phi_f R_h F_{yt} = 1.0(1.0)(50) = 50.0 \text{ ksi}$$
$$28.11 \text{ ksi} < 50.0 \text{ ksi} \quad \text{ok}$$

Although the checks are illustrated here for completeness, the bottom flange will typically not control in this region.

Although not illustrated here, consideration might be given to increasing f_{bu} for the Strength I load combination checks to conservatively account for the additional major-axis bending moments resulting from the deck overhang loads.

6.5.3.5.1.3 Shear

AASHTO LRFD Article 6.10.3.3 requires that webs satisfy the following equation during critical stages of construction:

$$V_u \le \phi_v V_{cr} \qquad \text{Equation 6.5.3.5.1.3-1}$$

AASHTO LRFD Equation 6.10.3.3-1

where:

ϕ_v = resistance factor for shear specified in *AASHTO LRFD* Article 6.5.4.2 (= 1.0)

V_u = factored shear in the web at the section under consideration due to the permanent loads and construction loads applied to the non-composite section (kips)

V_{cr} = shear-yielding or shear-buckling resistance determined from *AASHTO LRFD* Equation 6.10.9.3.3-1 (Equation 6.5.7.2-8) (kips)

The nominal shear resistance for this check is limited to the shear-yielding or shear-buckling resistance. The use of tension-field action is not permitted to resist construction loads. Use of tension-field action is permitted at the strength limit state after the deck has hardened or is made composite (if the section along the entire panel is proportioned according to the requirements for tension-field action). The calculation of V_{cr}, and the post-buckling shear resistance due to tension-field action is discussed further in Section 6.5.7.

EXAMPLE

Check the shear during construction in the critical interior panel of the first 100-foot-long field section in the 140-foot end span of a three-span continuous I-girder bridge. The web plate in this field section is ½" x 69". The yield strength of the web, F_{yw}, is 50 ksi.

The critical panel for this check is assumed to be the panel immediately to the left of the fourth intermediate cross-frame from the abutment, which is located 96.0 feet from the abutment (assuming cross-frames spaced longitudinally along the girder at 24.0 feet). The transverse stiffener in this panel is assumed to be located at the maximum permitted spacing of $d_o = 3D = 3(69.0) = 207.0$ inches to the left of this cross-frame (Section 6.5.7.1). Since shear is rarely increased significantly due to deck staging, the factored DC_1 shear at the cross-frame will be used in this check (the special load combination specified in *AASHTO LRFD* Article 3.4.2.1 governs by inspection – refer to Section 6.5.3.2). The load modifier, η, is assumed equal to 1.0:

$$(V_u)_{DC_1} = 1.0(1.4)(-79) = -111 \text{ kips at } 96'\text{-}0'' \text{ from the abutment}$$

The shear buckling resistance of the 207-inch-long panel is determined as (Equation 6.5.7.2-8):

$$V_n = V_{cr} = CV_p$$

C is the ratio of the shear buckling resistance to the shear yield strength determined from *AASHTO LRFD* Equation 6.10.9.3.2-4, 6.10.9.3.2-5 or 6.10.9.3.2-6, as applicable. First, compute the shear buckling coefficient, k (Equation 6.5.7.2-4):

$$k = 5 + \frac{5}{\left(\frac{d_o}{D}\right)^2}$$

$$k = 5 + \frac{5}{\left(\frac{207.0}{69.0}\right)^2} = 5.56$$

Since,

$$1.40\sqrt{\frac{Ek}{F_{yw}}} = 1.40\sqrt{\frac{29{,}000(5.56)}{50}} = 79.5 < \frac{D}{t_w} = \frac{69.0}{0.5} = 138.0$$

$$C = \frac{1.57}{\left(\frac{D}{t_w}\right)^2}\left(\frac{Ek}{F_{yw}}\right) \text{ (Equation 6.5.7.2-5)}$$

$$C = \frac{1.57}{(138.0)^2}\left(\frac{29{,}000(5.56)}{50}\right) = 0.266$$

V_p is the plastic shear force determined as follows (Equation 6.5.7.1-2):

$$V_p = 0.58F_{yw}Dt_w$$

$$V_p = 0.58(50)(69.0)(0.5) = 1{,}001 \text{ kips}$$

Therefore,

$$V_{cr} = 0.266(1{,}001) = 266 \text{ kips}$$

$$\phi_v V_{cr} = 1.0(266) = 266 \text{ kips}$$

$$|-111| \text{ kips} < 266 \text{ kips} \quad \text{ok}$$

6.5.3.5.2 Box Sections

6.5.3.5.2.1 General

The provisions for design for constructibility for box-section flexural members are given in *AASHTO LRFD* Article 6.11.3. These provisions essentially refer back to the design provisions for constructibility given in *AASHTO LRFD* Article 6.10.3 for I-section flexural members, with a few exceptions as discussed below. The design provisions for constructibility are intended to provide adequate strength and stability of the main load-carrying members during construction, to properly account for dead-load deflections, and to control the slip in load-resisting bolted connections at each critical construction stage to ensure that the proper geometry of the structure is maintained. *AASHTO LRFD* Article 6.10.3.1 states that nominal yielding or reliance on post-buckling resistance is not permitted for main load-carrying members during critical stages of construction. An exception is permitted for the localized yielding of the web that may occur in hybrid members.

The geometry of individual box sections must be maintained throughout all stages of construction as specified in *AASHTO LRFD* Article 6.11.3.1. Eccentric loads that may occur during construction should be considered. The need for temporary or permanent intermediate internal and/or external cross-frames/diaphragms, top lateral bracing, or other means must be investigated to ensure that deformations of the box are controlled. Important considerations in investigating the need for these members are discussed in Sections 6.3.2.9 and 6.3.2.10. As indicated in *AASHTO LRFD* Article C6.11.3.1, temporary cross-frames/diaphragms that are not part of the original design should be removed because the structural behavior of the box section, including the load distribution, may be affected if these members are left in place. As discussed further in Section 6.3.2.9.2.4, released temporary members may have large built-up forces in them after the deck has hardened, which may introduce restoring forces into the bridge upon removal.

AASHTO LRFD Article C6.11.3.1 suggests that for painted box sections, an allowance be made in the dead load for the weight of the paint. An allowance of three percent of the steel weight has been found to be a reasonable allowance.

To ensure the goal of providing adequate strength and stability of box-section flexural members during construction, without permitting nominal yielding (except for localized web yielding in hybrid sections) or relying on post-buckling resistance, the requirements of *AASHTO LRFD* Articles 6.11.3.2 (Flexure) and 6.10.3.3 (Shear) must be satisfied at each critical construction stage. The required check on the concrete deck tensile stress during construction specified in *AASHTO LRFD* Article 6.10.3.2.4, which is also applicable to box girders, was discussed previously in Section 6.5.3.3.4 and will not be repeated here. Further information regarding the

construction of composite steel box-girder bridges may be found in United States Steel (1978).

6.5.3.5.2.2 Flexure

6.5.3.5.2.2.1 Top Flanges of Tub Sections

AASHTO LRFD Article 6.11.3.2 specifies that for critical stages of construction, the constructibility design provisions of *AASHTO LRFD* Articles 6.10.3.2.1 through 6.10.3.2.3 for flexure of I-sections are to be applied to the top flanges of tub sections. A single exception is that the provisions of *AASHTO LRFD* Article A6.3.3 (Appendix A6 – Section 6.5.6.2.3.3.2) are not to be applied in determining the lateral torsional buckling resistance of top flanges of straight tub sections in compression with compact or noncompact webs.

The equations of *AASHTO LRFD* Articles 6.10.3.2.1 through 6.10.3.2.3 are discussed in detail above in Section 6.5.3.5.1.2 and are not repeated here. Essentially, a single top flange of a tub section is considered equivalent to the top flange of an I-section in applying the equations; therefore, it is recommended that the checks using these equations be made for half of the tub section. *AASHTO LRFD* Article 6.11.3.2 conservatively suggests that the unbraced length be taken as the distance between interior cross-frames/diaphragms in calculating the lateral torsional buckling resistance of the flanges. Further discussion on brace points for top flanges of tub sections subject to compression is provided in Sections 6.3.2.9.3.2 and 6.3.2.10.3. The web depth, D, and the depth of the web in compression, D_c, should each be measured along the web slope in computing the web bend-buckling resistance, F_{crw}, for use in Equation 6.5.3.5.1.2-3 for sections with inclined webs; that is, D_c should be divided by cos θ, where θ is the angle of inclination of the web plate with respect to the vertical. The calculation of the web bend-buckling resistance, F_{crw}, is discussed further in Section 6.4.5.5. The effects of St. Venant torsional shear stress in the top flanges are neglected in checking all these equations.

The equations of *AASHTO LRFD* Articles 6.10.3.2.1 and 6.10.3.2.2 (i.e. Equation 6.5.3.5.1.2-1, Equation 6.5.3.5.1.2-2 and Equation 6.5.3.5.1.2-4) allow for the direct consideration of flange lateral bending in discretely braced top flanges of tub sections due to various sources, if deemed significant. Potential sources of lateral flange bending include curvature, wind loads and eccentric concrete deck overhang loads acting on the outermost flanges of fascia girders. Additional potential sources of significant lateral bending in discretely braced top flanges occur in tub girders with inclined webs and with web slopes exceeding 1 to 4, in tub girders where the unbraced length of the top flange exceeds 30 feet, and in tub girders with Warren Truss top lateral bracing configurations, as discussed further in Sections 6.3.2.9.3.2 and 6.3.2.10.3.

6.5.3.5.2.2.2 Box Flanges

AASHTO LRFD Article 6.11.3.2 specifies that non-composite box flanges in compression satisfy the following requirements for critical stages of construction:

$$f_{bu} \le \phi_f F_{nc} \qquad \text{Equation 6.5.3.5.2.2.2-1}$$

AASHTO LRFD Equation 6.11.3.2-1

and:

$$f_{bu} \le \phi_f F_{crw} \qquad \text{Equation 6.5.3.5.2.2.2-2}$$

AASHTO LRFD Equation 6.11.3.2-2

where:

ϕ_f = resistance factor for flexure specified in *AASHTO LRFD* Article 6.5.4.2 = 1.0

f_{bu} = factored longitudinal flange stress at the section under consideration calculated without consideration of longitudinal warping (ksi)

F_{crw} = nominal web bend-buckling resistance determined as specified in *AASHTO LRFD* Article 6.10.1.9 (Section 6.4.5.5) (ksi)

F_{nc} = nominal flexural resistance of box flanges in compression determined as specified in *AASHTO LRFD* Article 6.11.8.2 (Section 6.5.6.2.4.2**)** (ksi). In computing F_{nc} for constructibility, the web load-shedding factor, R_b (Section 6.4.5.6), is to be taken equal to 1.0.

Equation 6.5.3.5.2.2.2-1 is a check for local buckling of the flange during critical stages of construction. Note that lateral flange bending and lateral-torsional buckling are not a consideration for box flanges. Equation 6.5.3.5.2.2.2-2 ensures that theoretical web bend-buckling will not occur during construction at sections where non-composite box flanges are subject to compression. This check only need be made for sections with slender webs. The calculation of the web bend-buckling resistance, F_{crw}, is discussed further in Section 6.4.5.5.

Non-composite box flanges in tension and continuously braced box flanges in tension or compression must satisfy the following requirement for each critical stage of construction:

$$f_{bu} \le \phi_f R_h F_{yf} \Delta \qquad \text{Equation 6.5.3.5.2.2.2-3}$$

AASHTO LRFD Equation 6.11.3.2-3

where:

$$\Delta = \sqrt{1 - 3\left(\frac{f_v}{F_{yf}}\right)^2} \qquad \text{Equation 6.5.3.5.2.2.2-4}$$

AASHTO LRFD Equation 6.11.3.2-4

f_v = factored St. Venant torsional shear stress in the flange at the section under consideration not to exceed the factored torsional shear resistance of the flange, F_{vr}, given by *AASHTO LRFD* Equation 6.11.1.1-1 (Equation 6.5.6.1.2-1) (ksi)

$$= \frac{T}{2A_o t_f} \qquad \text{Equation 6.5.3.5.2.2.2-5}$$

AASHTO LRFD Equation 6.11.3.2-5

A_o = enclosed area within the box section (in.^{2})

R_h = hybrid factor determined as specified in *AASHTO LRFD* Article 6.10.1.10.1 (Section 6.4.5.7). For hybrid sections in which f_{bu} does not exceed the specified minimum yield strength of the web, R_h is to be taken equal to 1.0.

t_f = thickness of the flange under consideration (in.)

T = internal torque due to the factored loads (kip-in.)

Equation 6.5.3.5.2.2.2-3 is a yielding check based on the von Mises yield criterion (Boresi et al., 1978), which is used to consider the effect of the St. Venant torsional shear in combination with flexure. The enclosed area, A_o, in Equation 6.5.3.5.2.2.2-5 is to be computed for the non-composite box section. If top lateral bracing in a tub section is attached to the webs, A_o is to be reduced to reflect the actual location of the bracing (*AASHTO LRFD* Article 6.7.5.3).

The effects of longitudinal warping stresses in the flanges due to cross-section distortion are not considered in checking Equation 6.5.3.5.2.2.2-1 and Equation 6.5.3.5.2.2.2-3. However, the effects of these distortion-related stresses must be considered in certain cases when checking bolt slip in flange splices for the construction condition, as discussed further in Section 6.6.5.2.2.5. Also, in checking these equations, the torque, T, should comprehend the critical torque induced in the girder during the deck-placement sequence.

Non-composite box flanges on top of closed-box sections receive the weight of the wet concrete and other loads during construction before the deck hardens. Therefore, the flange must be designed as a non-composite box flange for those loads. *AASHTO LRFD* Article 6.11.3.2 specifies that the maximum vertical deflection of the non-composite box flange due to the unfactored permanent loads, including the self-weight of the flange, and any unfactored construction loads must

not exceed 1/360 times the transverse span between webs. Through-thickness bending stresses in the flange due to the factored permanent loads and factored construction loads must not exceed 20.0 ksi. The flange may be considered to act as a simple span between webs in making these checks. Transverse and/or longitudinal stiffening of the box flange may be necessary to control the flange stresses and deflections under these loads.

6.5.3.5.2.3 Shear

AASHTO LRFD Article 6.11.3.3 refers back to the shear requirement specified in *AASHTO LRFD* Article 6.10.3.3 (Section 6.5.3.5.1.3).

The provisions of *AASHTO LRFD* Article 6.11.9, as applicable, are to be applied in checking Equation 6.5.3.5.1.3-1. That is, for box sections with inclined webs, the web must be designed for the total vertical shear in the plane of the web, V_{ui}, taken equal to V_u divided by $\cos\theta$, where θ is the angle of inclination of the web plate with respect to the vertical (Equation 6.5.7.1.2-1). Also, in computing the shear-yielding or shear-buckling resistance, V_{cr}, for the case of inclined webs from *AASHTO LRFD* Equation 6.10.9.3.3-1, the web depth, D, must be taken as the depth of the web measured along the slope, or $D/\cos\theta$. The calculation of V_{cr} is discussed further in Section 3.2.7.

V_u is to be taken as the sum of the flexural and St. Venant torsional shears in checking this requirement for all box sections for which the effects of St. Venant torsion must be considered (including all box sections in curved and/or skewed bridges). In cases where there is significant St. Venant torsional shear, the dead load shear in one web is greater than the flexural dead load shear by the amount of the torsional shear and less than the flexural shear by the same amount in the other web at the same cross-section. For practicality, both webs are generally detailed as if they had the same critical shear. Shears in the web due to warping torsion and due to cross-section distortion may be ignored in making this check for typical box sections, as indicated in *AASHTO LRFD* Article C6.11.9.

6.5.3.6 Wind Loads

AASHTO LRFD Article 4.6.2.7.3 requires that the need for wind bracing to resist wind loads acting on the non-composite structure prior to placing the concrete deck be investigated.

Although the AASHTO design specifications are generally member or component based, in some cases it becomes necessary to consider the overall behavior of the entire bridge system. As demonstrated in the following example, the entire non-composite bridge structure acts as a system for resisting wind loads during construction. In certain cases, the addition of lateral bracing can help provide a

stiffer load path for wind loads acting on the non-composite structure to help reduce lateral deflections and lateral flange bending stresses.

For checking stresses due to wind load during construction, the Strength III load combination is used (Section 3.9.1.2.4). According to *AASHTO LRFD* Article 3.4.2, the load factor applied to wind acting on the structure, *WS*, during construction is not to be taken less than 1.25, which is reduced from the load factor of 1.4 applied to *WS* in the base Strength III load combination (Section 6.5.3.2). For checking deflections due to wind load during construction, all load factors are taken equal to 1.0 according to *AASHTO LRFD* Article 6.10.3.1.

EXAMPLE

Wind load acting on Span 1 of the following three-span continuous non-composite I-girder structure prior to casting of the concrete deck will be investigated (see the framing plan of one-half of the symmetrical erected structure shown in Figure 6.5.3.6-1). A rational approximate approach will be illustrated to help the Engineer evaluate how many panels of lateral wind bracing (if any) might be necessary to reduce the lateral deflections and lateral flange bending stresses due to the wind loads to a level deemed acceptable for the construction situation under consideration (in lieu of a refined analysis).

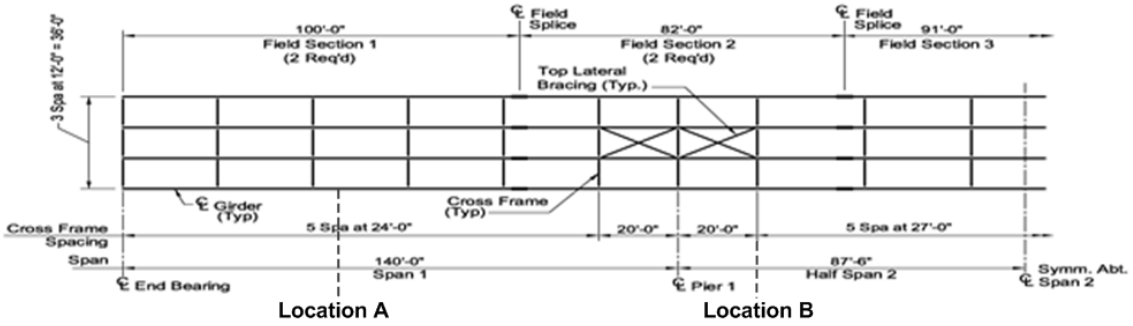

Figure 6.5.3.6-1 Fully Erected Non-Composite Framing Plan for Wind Load Example

For this example, the design horizontal wind pressure, P_D, used to compute the wind load acting on the structure, *WS*, is determined as specified in *AASHTO LRFD* Article 3.8.1. It will be assumed that the example bridge superstructure is 35 feet above the low ground and that it is located in open country.

In the absence of more precise data, the design horizontal wind pressure is to be determined as follows:

$$P_D = P_B\left(\frac{V_{DZ}}{V_B}\right)^2 = P_B\frac{V_{DZ}^2}{10{,}000} \qquad \text{Equation 6.5.3.6-1}$$

AASHTO LRFD Equation 3.8.1.2.1-1

where:

P_B = base wind pressure = 0.050 ksf for beams (*AASHTO LRFD* Table 3.8.1.2.1-1)
V_{DZ} = design wind velocity at design elevation, Z (mph)
V_B = base wind velocity at 30 ft height = 100 mph

For bridges or parts of bridges more than 30 feet above low ground, V_{DZ} is to be adjusted as follows:

$$V_{DZ} = 2.5V_o\left(\frac{V_{30}}{V_B}\right)\ln\left(\frac{Z}{Z_o}\right) \qquad \text{Equation 6.5.3.6-2}$$

AASHTO LRFD Equation 3.8.1.1-1

where:

V_o = friction velocity = 8.20 mph for open country (*AASHTO LRFD* Table 3.8.1.1-1)
V_{30} = wind velocity at 30 feet above low ground = V_B = 100 mph in the absence of better information
Z = height of the structure measured from low ground (> 30 feet)
Z_o = friction length of upstream fetch = 0.23 feet for open country (*AASHTO LRFD* Table 3.8.1.1-1)

Therefore,

$$V_{DZ} = 2.5(8.20)\left(\frac{100}{100}\right)\ln\left(\frac{35}{0.23}\right) = 103.0 \text{ mph}$$

$$P_D = 0.050\left[\frac{(103.0)^2}{10{,}000}\right] = 0.053 \text{ ksf}$$

The full design base wind velocity, V_B = 100 mph, is used in the above calculation for illustration purposes only. For an actual temporary construction condition, however, strong consideration might be given to using a smaller design wind pressure depending on the specific situation and the anticipated maximum wind velocity at the site. The reader is referred to NHI (2015) for further guidance on the calculation of more realistic wind pressures and velocities for temporary construction conditions.

P_D is to be assumed uniformly distributed on the area exposed to the wind. The exposed area is to be the sum of the area of all components as seen in elevation taken perpendicular to the assumed wind direction. The direction of the wind is to be varied to determine the extreme force effect in the structure or its components. As specified in *AASHTO LRFD* Article 3.8.1.2.1, the total wind load, *WS*, acting on girder spans is not to be taken less than 0.3 klf. Again, consideration might be given to waiving this requirement for the temporary construction condition. Conservatively using the smallest steel section in Span 1 (7/8" x 18" bottom flange; ½" x 69" web; 1" x 16" top flange), the total wind load per unit length, *w*, for the case of wind applied normal to the structure assuming no superelevation is computed as:

$$w = P_D h_{exp.} = 0.053\left[(0.875 + 69.0 + 1.0)/12\right] = 0.313 \text{ kips/ft} > 0.3 \text{ kips/ft} \qquad \text{ok}$$

Determine the maximum major-axis bending stress, f_{bu}, in the top and bottom flanges due to the factored steel weight within the unbraced length encompassing Location A in Span 1 (refer to the preceding example in Section 6.5.3.3.4 to determine Location A).

The cross-section of the girder at this location (and within the entire 24-foot unbraced length encompassing this location) is shown in Figure 6.4.2.3.2.3-1. The elastic section properties for this section were computed earlier (Section 6.4.2.3.2.3). The girder is homogeneous with the yield strength of the flanges and web equal to 50 ksi. The largest moment due to the steel weight within the unbraced length is equal to 352 kip-feet right at Location A (Table 6.5.3.3.4-1). Therefore, since the member is assumed prismatic in-between these two cross-frames, the largest stress in both flanges also occurs at Location A. The Strength III load combination applies to the case of dead plus wind load with no live load on the structure. The load modifier, η, is taken equal to 1.0 in this example. Therefore,

For Strength III:

Top flange:

$$f_{bu} = \frac{1.0(1.25)(352)(12)}{1{,}581} = -3.34 \text{ ksi}$$

Bot. flange:

$$f_{bu} = \frac{1.0(1.25)(352)(12)}{1{,}973} = 2.68 \text{ ksi}$$

Since there is no deck at this stage to provide horizontal diaphragm action, assume the cross-frames act as struts in distributing the total wind force on the structure to the flanges on all girders in the cross-section. The force is then assumed

transmitted through lateral bending of the flanges to the ends of the span or to the closest point(s) of lateral wind bracing.

Determine the total factored wind force on the structure assuming the wind is applied to the deepest steel section within Span 1 (i.e. the section over the interior pier -- 2" x 20" bottom flange; 9/16" x 69" web; 2" x 18" top flange -- Figure 6.4.2.3.3.3-1) and normal to the structure (with no superelevation). For the Strength III load combination, the load factor for wind during construction is not to be taken less than 1.25 (*AASHTO LRFD* Article 3.4.2).

$$W = \frac{1.0(1.25)(0.053)(2.0 + 69.0 + 2.0)}{12} = 0.403 \text{ kips / ft}$$

To illustrate the effect that a couple of panels of top lateral bracing can have in providing a stiffer load path for wind loads acting on the non-composite structure during construction, assume the system of top lateral bracing shown in Figure 6.5.3.6-1; that is, top lateral bracing in the interior bays on each side of each interior-pier section. Bottom lateral bracing would serve a similar function, but unlike top bracing, would be subject to significant live-load forces in the finished structure that would have to be considered should the bracing be left in place. Again, it should be emphasized that this example is used only to demonstrate the suggested approximate procedure. It is unlikely that a 140-foot span would require lateral wind bracing under a reduced (and more reasonable) assumed design wind pressure during construction.

Assume that Span 1 of the structure (acting as a system) resists the lateral wind force as a propped cantilever, with an effective span length L_e of 120.0 feet. That is, the top lateral bracing is assumed to provide an effective line of fixity at the cross-frame 20.0 feet from the pier for resisting the lateral force. Calculate the moment on the propped cantilever at Location A (Note: the following formula actually gives the moment at $0.375L_e$ = 45 feet from the abutment, but is used here to give a conservative approximation of the moment at Location A):

$$M_A = \frac{9}{128} W L_e^2 = \frac{9}{128}(0.403)(120.0)^2 = 408.0 \text{ kip} - \text{ft}$$

Calculate the moment on the propped cantilever at the assumed line of fixity (call it Location B -- 20.0 feet from the pier into Span 1):

$$M_B = \frac{1}{8} W L_e^2 = \frac{1}{8}(0.403)(120.0)^2 = 725.4 \text{ kip} - \text{ft}$$

The lateral wind moments are proportional to the square of the effective length, L_e. Note that a refined 3D analysis of the example non-composite structure subjected to the factored wind load yielded a total lateral moment in the top and bottom flanges of all four girders of 405 kip-ft at Location A and 659 kip-ft at Location B.

Proportion the total lateral moment to the top and bottom flanges at Location A according to the relative lateral stiffness of each flange (refer to Figure 6.4.2.3.2.3-1). Assume that the total flange lateral moment is then divided equally to each girder. The single bay of top bracing along with the line of cross frames adjacent to that bay (acting as an effective line of fixity) permits all the girders to work together as a system to resist the lateral wind force along the entire span.

Location A:

Top flange

$$I_\ell = \frac{1(16)^3}{12} = 341.3 \text{ in.}^4$$

$$M_\ell = \frac{408.0(341.3)}{(341.3+668.3)4} = 34.48 \text{ kip} - \text{ft}$$

Bottom flange

$$I_\ell = \frac{1.375(18)^3}{12} = 668.3 \text{ in.}^4$$

$$M_\ell = \frac{408.0(668.3)}{(341.3+668.3)4} = 67.52 \text{ kip} - \text{ft}$$

A similar computation can be made at Location B (however, this section is not checked for this condition in this example).

According to *AASHTO LRFD* Article 6.10.1.6, lateral bending stresses determined from a first-order analysis may be used in discretely braced compression flanges for which (Equation 6.5.2.1.3.2-1):

$$L_b \le 1.2 L_p \sqrt{\frac{C_b R_b}{f_{bu}/F_{yc}}}$$

Again, f_{bu} is the largest value of the compressive stress due to the factored loads throughout the unbraced length in the flange under consideration, calculated without

consideration of flange lateral bending. In this case, f_{bu} = -3.34 ksi. In a preceding example (Section 6.5.3.5.1.2), it was determined that the moment gradient modifier, C_b, and the web load-shedding factor, R_b, within the unbraced length encompassing Location A are both equal to 1.0. The limiting unbraced length, L_p, was also determined in that same example to be 7.83 feet. Therefore,

$$1.2(7.83)\sqrt{\frac{1.0(1.0)}{|-3.34|/50}} = 36.35 \text{ ft} > L_b = 24.0 \text{ ft}$$

Therefore, lateral bending stresses determined from a first-order analysis may be used. First- or second-order flange lateral bending stresses, as applicable, are limited to a maximum value of $0.6F_{yf}$ according to *AASHTO LRFD* Equation 6.10.1.6-1.

Location A:

Top flange:

$$f_\ell = \frac{34.48(12)}{1(16)^2/6} = 9.70 \text{ ksi} < 0.6F_{yf} = 30.0 \text{ ksi} \quad \text{ok}$$

Bottom flange:

$$f_\ell = \frac{67.52(12)}{1.375(18)^2/6} = 10.91 \text{ ksi} < 0.6F_{yf} = 30.0 \text{ ksi} \quad \text{ok}$$

Calculate the shear in the propped cantilever at Location B:

$$V_B = \frac{5}{8}WL_e = \frac{5}{8}(0.403)(120.0) = 30.23 \text{ kips}$$

Resolve the shear into a compressive force in the diagonal of the top bracing:

$$P = 30.23\left(\frac{\sqrt{(20.0)^2 + (12.0)^2}}{12.0}\right) = -58.76 \text{ kips}$$

In addition, the member carries a force due to the steel weight. Calculate the average stress in the top flange adjacent to the braced bay using the average

moment due to the factored steel weight along the 20-foot unbraced length adjacent to the pier section assumed applied to the larger section within this unbraced length (i.e. the interior-pier section; S_{tf} = 2,942 in^3). The unfactored major-axis bending moment due to the steel weight at the section 20 feet from the interior pier into Span 1 (i.e. at Location B) is –312 kip-ft. The unfactored major-axis bending moment due to the steel weight at the interior pier is –777 kip-ft. Therefore,

$$f_{tf_{avg.}} = \frac{1.0(1.25)(12)(-312 + -777)/2}{2{,}942} = 2.78 \text{ ksi}$$

Resolve this stress into the diagonal:

$$f_{diag.} = 2.78\left(\frac{20.0}{\sqrt{(20.0)^2 + (12.0)^2}}\right) = 2.38 \text{ ksi}$$

Assuming an area of 8.0 in.^{2} for the diagonal yields a compressive force due to the steel weight of –19.04 kips resulting in a total estimated compressive force of (-58.76) + (-19.04) = -77.80 kips. The diagonal must be designed to carry this force. Note that the refined 3D analysis, mentioned previously, yielded a total compressive force in the diagonal bracing member of approximately -67.0 kips.

Finally, estimate the maximum lateral deflection of Span 1 of the structure (i.e. the propped cantilever) due to the unfactored wind load using the total of the lateral moments of inertia of the top and bottom flanges of all four girders at Location A. For simplicity, this section is assumed to be an average section for the span (a weighted average section would likely yield greater accuracy):

$$\Delta_{\ell max.} = \frac{WL_e^4}{185EI} = \frac{(0.403/1.25)(120.0)^4(1{,}728)}{185(29{,}000)(341.3 + 668.3)4} = 5.3 \text{ in.}$$

Note that the refined 3D analysis yielded a maximum lateral deflection of approximately 5.6 inches in Span 1. If the top bracing were not present, L_e would increase to 140.0 feet and the estimated maximum lateral deflection calculated from the above equation would increase to 9.9 inches. Large lateral deflections may potentially result in damage to the bearings. Therefore, such an approach may be helpful to determine how many panels of top lateral bracing, if any, might be necessary to reduce the lateral deflection to a level deemed acceptable for the particular situation under consideration.

To analyze the center span for this condition, a similar approach can be taken using the actions of an assumed fixed-fixed beam rather than a propped cantilever.

6.5.4 LRFD Service Limit State Design

6.5.4.1 General

AASHTO LRFD Article 1.3.2.2 specifies that the service limit state be taken as restrictions on stress, deformations and crack width under regular service conditions. As mentioned in the Commentary to this article, service limit state criteria are more experience-based and somewhat less scientifically oriented.

AASHTO LRFD Article 6.5.2 specifies that for steel structures, the provisions of *AASHTO LRFD* Article 2.5.2.6, dealing primarily with the control of elastic live-load deformations and the consideration of span-to-depth ratios, are to apply as applicable. Permanent deformations must also be controlled for I- and box-section flexural members to prevent objectionable permanent deformations caused by localized yielding and potential web bend-buckling under expected severe traffic loadings, which might impair rideability (*AASHTO LRFD* Articles 6.10.4.2 and 6.11.4). These checks are made under the Service II load combination (Section 3.10.1.3.3). A check on the tensile concrete deck stresses under the Service II load combination must also be made as specified in *AASHTO LRFD* Article 6.10.1.7 to ensure that the minimum required one percent longitudinal reinforcement is provided in the deck at the appropriate sections to help control the cracking of the deck. Slip in slip-critical bolted connections is also checked at the service limit state (Section 6.6.4.2.1.1).

A helpful flowchart detailing the required LRFD service limit state design verifications discussed below is provided in *AASHTO LRFD* Figure C6.4.2-1 (Appendix C6).

6.5.4.2 Elastic Deformations

6.5.4.2.1 General

AASHTO LRFD Article 6.10.4.1 deals with checks related to the control of elastic deformations in steel I-girder bridges under normal service conditions. For box-girder bridges, *AASHTO LRFD* Article 6.11.4 refers back to *AASHTO LRFD* Article 6.10.4.1. Specifically, this article then refers back to the applicable provisions of *AASHTO LRFD* Article 2.5.2.6 dealing with optional live-load deflection criteria and the criteria for span-to-depth ratios. Span-to-depth ratios were discussed previously in Section 6.3.3.1. Live load deflection is discussed below.

6.5.4.2.2 Live Load Deflection

Limitation of live load deflection is a service limit state; such criteria are specified in *AASHTO LRFD* Article 2.5.2.6.2 and limit the computed elastic live-load vertical deflections. Although the criteria are optional, most states require their application.

The obvious reason for these provisions is to provide a level of stiffness. However, the reason(s) for a required stiffness is less clear.

Until the 1960s, bridges were designed to a working level; i.e., they were designed for a desired service level. Live load deflection has been a service design consideration from early times in the design of steel highway bridges in the U.S. Limits on live load deflection can be traced back to the railway specifications of the late 1800s, which gave limitations similar to those now given in the *AASHTO LRFD* Specifications (Fountain and Thunman, 1987). The requirement to limit the deflection of a railroad bridge seems rather self-evident when one considers the rocking forces that could have led to catastrophe on a bridge that was too flexible. Large deflections could also have led to secondary stresses that might have caused fatigue cracking that was not well understood in the early days of iron and steel bridges. The first specified live load deflection limit for steel highway bridges in the U.S. was in the Third Edition *AASHO Specification,* 1941. The suggested limit of Span/800 under vehicular load, which remains in the specification today (*AASHTO LRFD* Article 2.5.2.6.2 – Section 2.3.2.6.2), is thought to have been recommended by the Bureau of Public Roads after studying several steel-beam bridges that were reportedly subjected to objectionable vibrations (Fountain and Thunman, 1987). This limit, along with the maximum span-to-depth ratio of 25 that was recommended at that time, were the first attempts to control service load deformations. This was only reasonable since the entire philosophy of working stress design was based on serviceability and not strength.

The advent of higher strength steels and concomitant increases in design stresses led to concern about the effect of live load deflection on economics. As early as the 1950s, *ASCE* began an investigation of the basis for these deflection limits and found numerous shortcomings, including no clear basis for their use, and no evidence of structural damage that could be attributed to excessive deflections (ASCE, 1958). Competition with prestressed concrete bridges in the 1960s led to further investigations as to the need for this serviceability limit. Field investigations at that time, again, showed no direct correlation.

Not only did the limitation remain, but in the early 1960s, an additional limit was introduced; the live load deflection limit on steel bridges with both pedestrian and vehicular loads was set at Span/1000 as a result of isolated concerns related to human response. The criteria remained optional. One legend has it that this limit arose when a mother and wife of a political figure who was pushing her baby in a carriage across a bridge attributed the awakening of her baby to vibration of the bridge (Fountain and Thunman, 1987). This complaint prompted the state's governor to chastise the State Bridge Engineer. The issue of human comfort becomes a serviceability issue when people who might use a bridge find its motion objectionable. This is a departure from the other structural criteria provided in the Specification.

The complex issue of the human response of occupants of moving vehicles and of pedestrians to motion has been extensively studied. However, there still are no definitive guidelines on the tolerable limits of dynamic motion or static deflection to ensure creature comfort. Guidelines for limiting the natural frequency of bridges to provide tolerable motion are contained in the *Ontario Highway Bridge Design Code* (Ontario Ministry, 1991), in which the deflection limits are tied to the first fundamental frequency of the superstructure. These limits are provided in the form of graphs and are separated in conjunction with the anticipated pedestrian use. These provisions require that the designer compute the natural frequency of the composite bridge.

Wright and Walker (1971) found a tenuous theoretical relationship between deflection and natural frequency. They observed that user comfort was an important factor. They reported that psychologists had found that humans think that vertical deflection they sense is about ten times the actual deflection. Wright and Walker postulated that human discomfort is due to acceleration, not deflection alone. They proposed a parameter, defined as the dynamic component of acceleration in the fundamental mode of vibration, be limited to 100 in^2/sec. The authors suggested that such acceleration is within the tolerable range experienced in building elevators contemporary with the writing of the paper (1960s). They further suggested that only bridges designed for pedestrian traffic or stationary vehicles be limited in motion by such a serviceability criterion. The issue of bridge vibrations and their relation to human response, along with the development of a reasonable means of controlling bridge vibrations to ensure adequate creature comfort, remains a complex and subjective issue in need of further study.

Other suggested live load deflection limits contained in *AASHTO LRFD* Article 2.5.2.6.2 include a limit of Span/300 for vehicular loads on cantilever arms, and a limit of Span/375 for combined vehicular and pedestrian loads on cantilever arms.

The ‘Span’ is typically taken as the full span length of the girder (arc span length for curved girders) when checking all the deflection limits. The limit on span-to-depth ratio for continuous spans is usually determined by defining the span as the length between points of permanent load contraflexure. This leads to shallower bridges with an increased flexibility when the limiting live load deflection is defined based on the actual span. Some states conservatively limit deflection by using the distance between points of permanent load contraflexure in computing the permissible deflection. Field tests have confirmed that decks of continuous composite girders in negative moment regions actually behave compositely. Tradition has assumed those regions to be non-composite. Use of the entire deck obviously reduces the computed deflections and brings them closer to actual with regard to the behavior of the deck.

The combination of moving from 33- to 70-ksi yield-stress steel, along with the introduction of composite design, the introduction of Load Factor Design (LFD) and then LRFD, and the increase of the span-to-depth ratio for steel girders from 25 to 30 had a net effect of roughly increasing the permitted live load deflection by about threefold. Field experience of bridges built has provided scant evidence that the increased flexibility of steel bridges had led to any reduced functionality. It seems that some logical limit exists, but such a limit has proved elusive. It has also been shown that computation of live load deflection as specified in *AASHO* and *AASHTO* is not likely to predict the actual deflection. And so, as the live load deflection limit has become an increasingly critical factor in the design of steel bridges utilizing the higher-strength high performance steels (HPS), an additional investigation has recently been launched into the potential need for improved live load deflection criteria for steel bridges (Roeder et al., 2002).

The live load used to compute live load deflection has traditionally been the same as the design live load. This made sense for design based on service loads only. However, for strength-based design, a different and lighter load for service limit state checks is logical since the criteria are based on a different philosophy. In strength design, the capacity of the structure is challenged. Serviceability relates to the structure response to likely loads; these likely loads are reasonably less than the load used to check structural strength. As specified in *AASHTO LRFD* Article 3.6.1.3.2 and discussed further in Section 3.4.3.3, the live load deflection check consists of evaluating two separate live load conditions:

- Design truck alone; and
- Design lane plus 25% of design truck

The dynamic load allowance of 33 percent is applied to the design truck only in each case. A load factor of 1.0 is applied to the live load according to the Service I load combination (Section 3.9.1.3.2). As discussed further in Section 3.4.3.3, the specified load is intended to produce live load deflections similar to those produced by the HS20 loading in the *Standard Specifications* (AASHTO, 2002).

However, even in service load design, live load application for the computation of deflections has often been different from application for design of the elements. For example, the 1941 *AASHO* Bridge Specifications permitted the Engineer to compute the moment in a stringer for deflection purposes by assuming that all of the lanes are loaded with the design load and that the resulting load is uniformly distributed equally to all stringers where adequate depth diaphragms or cross-frames exist. This provision has since been interpreted to allow a reduction in load based on the multiple presence factor provision. The practice of loading all lanes appears to be at odds, at least in some cases, with the provision in the 1935 Edition (Art. 3.2.11), which states: “In calculating stresses in structures which support cantilevered sidewalks, the sidewalk shall be considered as fully loaded on only one side of the

structure if this condition produces maximum stress." This provision reveals an understanding that loading on the far side of a multi-stringer bridge unloads the near side; this understanding has been borne out in refined analyses. If one visualizes the entire cross-section rotating as a rigid body under each of the above load cases, it is apparent that the opposite side of the bridge rises when one side is loaded. Hence, from the time it was introduced, the assumption of uniform loading of girders for computation of deflection was known to be simply a means to require less stiffness.

The provisions of *AASHTO LRFD* Article 2.5.2.6.2 allow all integer 12-foot wide design lanes to be loaded with all girders assumed to deflect equally. This clause should only be applied for straight-girder bridges when the longitudinal stiffness of the individual girders at all cross-sections is the same. Cases where the clause should not be applied include cases with skewed supports and skew angles exceeding 20 degrees from normal, different girder depths, or girders with different flange sizes. The assumption of equal live load deflection should not be applied to horizontally curved bridges. The *AASHTO LRFD* specifications are currently silent with regard to the application of this assumption to bridges with skewed supports. The live load deflection of individual girders should be computed for curved girders based on analysis of the superstructure as a structural system with live loads applied according the loading provisions of the Specifications (*AASHTO LRFD* Article 2.5.2.6.2). There are other bridges where the equal deflection assumption is not rational. As mentioned above, loading of all lanes simultaneously of relatively wide bridges may not give a rational deflection. The second example below demonstrates the fallacy of assuming equal deflection of girders in a wide bridge.

It is probably well accepted that live load deflection cannot be accurately predicted using the assumption of uniform deflection of all girders due to all girders loaded. The argument might be made that the actual live load deflection is not important; it is the relative deflection that is important. The assumption of uniform deflection yields widely varying accuracies depending on the particular bridge cross-section, and can potentially lead to significant design errors in certain situations. It is incorrect to add girders to reduce the live load deflection of a multi-girder steel bridge. When this is done, the actually live load deflection may not be affected much, but the bridge cost is substantially increased. The most efficient way to increase stiffness of the bridge without increasing girder depth is to increase the size of the bottom flange. The number of girders for an economical cross section is best determined without consideration of live load deflection. Note that when a refined analysis is used to compute live load deflections, the number of girders in the cross-section has a much less significant effect on deflection and fewer girders may in fact be needed than when the averaging approach is used. This issue is examined in more detail for a straight simple-span steel I-girder bridge with right supports in the third example given below.

Some states specify that the distribution factor used for moment is to be used to calculate live load deflections. When the distribution factor for moment is used, the lanes are implicitly located in the critical position. The width of the bridge and the number of girders are less significant since the wheel load distribution factors are based on two lanes of traffic regardless of the bridge width. When a refined analysis is used or when the exterior girder is investigated, it is also possible to place the live load in the striped lane(s) rather than in the critical transverse position. Such analyses would represent a more realistic service condition than the hypothetical situation that would be employed for a strength check.

Concrete barriers and sidewalks, and even railings, often contribute to the stiffness of composite superstructures at service load levels. Therefore, *AASHTO LRFD* Article 2.5.2.6.2 permits the entire width of the roadway and the structurally continuous portions of railings, sidewalks and barriers (i.e. continuous cast-in-place barriers) to be included in determining the composite stiffness for deflection calculations. The assumption of the full deck width for determining the composite cross-section stiffness for the analysis, gives more functionally correct results. Because the inclusion of the concrete items other than the deck can cause complications in the calculation of the composite stiffness (and in modeling with regard to their inclusion in refined analyses), it is suggested that these items be ignored. If the parapets are on the exterior of the deck, they tend to stiffen the exterior girders drawing load to those girders. Hence, computation of the deflections of the critical exterior based on refined analysis methods show that the computed deflections are not materially reduced by the consideration of the parapets.

EXAMPLE

Determine the distribution factor for live load deflection for the cross-section of a straight steel I-girder bridge (Figure 6.5.4.2.2-1) with equal stiffness girders based on the permitted assumption that all design lanes are loaded and that all girders are assumed to deflect equally:

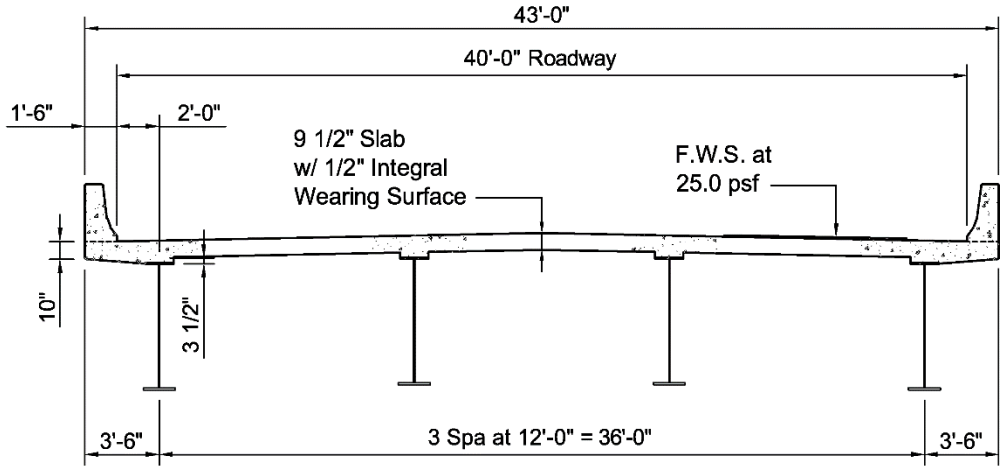

Figure 6.5.4.2.2-1 Straight Steel I-Girder Bridge Example Cross-Section

The 40-ft wide roadway can support up to three 12-foot-wide design traffic lanes. *AASHTO LRFD* Article 2.5.2.6.3 specifies that the multiple presence factors, *m*, given in *AASHTO LRFD* Article 3.6.1.1.2 should be applied in calculating live load deflections. These factors are given in *AASHTO LRFD* Table 3.6.1.1.2-1 as follows: for one lane loaded, *m* = 1.2; for two lanes loaded, *m* = 1.0; for three lanes loaded, *m* = 0.85; for more than three lanes loaded, *m* = 0.65 (Section 3.4.1.2). Therefore:

$$(DF)_{LLdef} = m\left(\frac{N_L}{N_b}\right) \qquad \text{Equation 6.5.4.2.2-1}$$

where:

DF = distribution factor (lanes)
m = multiple presence factor specified in *AASHTO LRFD* Article 3.6.1.1.2
N_L = number of design lanes (roadway width/12 with fractions dismissed)
N_b = number of girders in the cross-section

For three traffic lanes, the multiple presence factor, *m*, is equal to 0.85. Therefore, from Equation 6.5.4.2.2-1:

$$(DF)_{LLdef} = m\left(\frac{N_L}{N_b}\right) = 0.85\left(\frac{3}{4}\right) = 0.638 \text{ lanes}$$

The bridge is a three-span continuous composite bridge with spans of 140 ft – 175 ft – 140 ft. The web depth of the girders is 69 in. Using this distribution factor, a separate line-girder analysis is performed for the two separate live load conditions to be used to calculate live load deflections according to *AASHTO LRFD* Article 3.6.1.3.2. The maximum live-load deflections in the end span and center span of the

exterior girder due to the design truck plus the dynamic load allowance are computed to be:

$$(\Delta_{LL+IM}) \text{ end span} = 0.91 \text{ in. (governs)}$$
$$(\Delta_{LL+IM}) \text{ center span} = 1.23 \text{ in. (governs)}$$

The maximum live-load deflections in the end span and center span of the exterior girder due to the design lane load plus 25 percent of the design truck plus the dynamic load allowance are computed to be:

$$(\Delta_{LL+IM}) \text{ end span} = 0.60 + 0.25(0.91) = 0.83 \text{ in.}$$
$$(\Delta_{LL+IM}) \text{ center span} = 0.85 + 0.25(1.23) = 1.16 \text{ in.}$$

The dynamic load allowance of 33 percent was applied to the design truck in each case. A load factor of 1.0 was applied to the live load. The actual *n*-composite moments of inertia along the entire length of the girder were used in the analysis. The stiffness of the barriers was not included in the composite stiffness. However, the full width of the concrete deck associated with the exterior girder was used in determining the composite stiffness, as recommended in *AASHTO LRFD* Article 2.5.2.6.2 for the calculation of live-load deflections. Check the suggested limit of Span/800 given in *AASHTO LRFD* Article 2.5.2.6.2:

End Spans: $\Delta_{ALLOW} = \dfrac{140.0(12)}{800} = 2.10 \text{ in.} > 0.91 \text{ in.}$

Center Span: $\Delta_{ALLOW} = \dfrac{175.0(12)}{800} = 2.63 \text{ in.} > 1.23 \text{ in.}$

Application of the live load deflection provisions shown above results in deflection not being critical; that is, other limit states controlled the design. Infringement on the recommended girder depth might be possible in this case, while still meeting the live load deflection provisions. Of course, larger flanges would likely be required to meet the strength or perhaps the fatigue limit states.

Separate calculations indicate that the live load distribution factor for bending moment in the exterior girder of this example bridge (to be used for live load stress calculations) is 0.950 lanes, or approximately 1.5 times larger than the factor computed above. If this factor were used instead, the computed live load deflection in the center span would be 1.83 in. versus 1.23 in. The deflection limit would still be satisfied for this particular bridge.

EXAMPLE

Consider a 518-foot span made continuous by adjoining spans of slightly less length. The straight bridge has seven design lanes and seven girders in the cross-section. All girders have the same longitudinal stiffness and are connected with cross-frames and a composite concrete deck. The live load deflection limit is Span/800, where 'Span' is the distance between bearings. In this case, the limit is 7.77 inches.

For this case, the live load distribution factor for deflection may again be computed as follows by assuming all lanes are loaded and all girders are deflecting equally. For more than three lanes loaded, the multiple presence factor, *m*, is equal to 0.65. Therefore, from Equation 6.5.4.2.2-1:

$$(DF)_{LLdef} = 0.65\left(\frac{7}{7}\right) = 0.65 \text{ lanes}$$

Analysis of a single girder from the bridge with the preceding distribution factor gives a live load deflection of 6.8 inches, which is well below the deflection limit.

As shown in Table 6.5.4.2.2-1, a refined 3D analysis of this bridge gives a live load deflection of 8.30 inches in one exterior girder (Girder 1) for four lanes loaded using an impact factor of 10 percent and a multiple presence factor of 0.65.

Table 6.5.4.2.2-1 Refined 3D Analysis Results for Live Load Deflection of a Wide Bridge

No. of Lanes Loaded	m	Live Load Deflection (in.)
1	1.2	-5.70
2	1.0	-8.18
3	0.85	-7.26
4	0.65	-8.30
Opposite Side: 2	1.0	1.30

Evidently, for this particular bridge, four lanes loaded results in the largest deflection (it should be noted that the center lanes were loaded two spans away from the span investigated to compute this deflection). When the multiple presence factors are considered, two lanes loaded gives almost the same live load deflection as does four lanes loaded in this case. Clearly, it does not appear reasonable to assume seven lanes loaded to calculate a live load deflection that meets the deflection limit, while the loading of only two lanes fails the same criteria. An argument can be made that deflection is only a relative issue and no hard rules are available as to the true deflection that should be permitted. However, it appears to be unreasonable to

compute a smaller deflection on a bridge because it is wider than another bridge with the same span and girder spacing.

Also, as noted in the last row of Table 6.5.4.2.2-1, when the live load is restrained to the two lanes on the far (opposite) side of the deck in the area of the other exterior girder (i.e. Girder 7), the computed live load deflection in Girder 1 in an upward deflection of 1.3 inches (downward deflections are negative and upward deflections are positive in the table). This deflection was the result of loading in the same span; loading in adjacent spans on the opposite side of the bridge was inconsequential. Thus, the addition of live load on the opposite side of the span of interest would actually unload Girder 1. This phenomenon is the reason that the 1935 AASHO Specification disallowed loading sidewalks on both sides in order to reduce the effect of a single sidewalk, as discussed previously.

EXAMPLE

Consider a straight simple-span I-girder bridge with right supports having a span of 161 feet. Live load deflections computed from a refined analysis, such as would be used to calculate the deflections in a curved-girder bridge, are compared to the deflections computed for the same bridge from a line girder analysis utilizing the distribution factor given by Equation 6.5.4.2.2-1. The width of the bridge deck is 60.5 feet out-to-out; the roadway is 57.5 feet; the overhangs are 4.25 feet. Four 12-foot design traffic lanes can be placed on this roadway. Five-girder and seven-girder cross sections are examined. The overhang is held constant for both cross sections. The girder spacing for the 5-girder case is 13’-0”. The girder spacing for the 7-girder case is 8’-8”.

The girders are sized for the strength limit state based on *AASHTO LRFD* design criteria and the results of 3D refined finite element analyses. The design live load is HL-93. These analyses show the exterior girder is critical with respect to both strength and live load deflection. Therefore, only an exterior girder is sized; interior girders are assumed to be the same size.

The 5-girder homogeneous 50-ksi case consists of five 69-inch deep I-girders. The 7-girder homogeneous 50-ksi case consists of seven 69-inch deep I-girders. This depth gives a span-to-depth ratio of 28; thus, the girders are slightly deeper than the suggested span-to-depth ratio of 30, or depth-to-span ratio of 0.033 as given in *AASHTO LRFD* Article 2.5.2.6.3. A further comparison was made with similar deck cross-sections and hybrid girders having 70 ksi bottom flanges and 50 ksi webs and top flanges; the girder depths were decreased to 64 inches, which is the minimum depth that meets the optional span-to-depth ratio of 30.

As indicated previously, in the *AASHTO LRFD* Specifications, a special loading is used for the calculation of live load deflections, which is a lighter load than the HL-93

design live load. Either the design lane load in combination with one-fourth of the design truck or the design truck alone – whichever gives the greater deflection – is used. Impact of 33% is applied only to the truck. Since live load deflection is a service criterion, the load factor applied to the live load is 1.0. The suggested live load deflection limit of Span/800 is 2.4 inches.

As discussed previously, the *AASHTO LRFD* specifications permit the application of the multiple presence factors prescribed in *AASHTO LRFD* Article 3.6.1.1.2 in computing live load deflections. Therefore, according to the *AASHTO LRFD* Specification, for the 5-girder case, the distribution factor (DF) for live load deflection is computed from Equation 6.5.4.2.2-1 as follows:

DF = 0.65 x (4 lanes/5 girders) = 0.52 lanes per girder

The similar computation for the 7-girder case is as follows:

DF = 0.65 x (4 lanes/7 girders) = 0.37 lanes per girder

The assumption of uniform participation indicates that an increase in the number of girders reduces significantly the live load deflection. If the computed deflection exceeds the suggested allowable deflection, additional girders are often added. In this example, the increase from 5 to 7 girders reduces the DF by:

[(0.52 – 0.37)/0.52] x 100% = 29 %

Although live load deflection limits are subjective, addition of girders lines is not; it adds significantly to the cost of the bridge. The addition of two girder lines reduces the girder spacing and hence reduces the required size of each girder based on the strength limit state.

The computed maximum live load deflections from the analyses described above are summarized below in Table 6.5.4.2.2-2.

Table 6.5.4.2.2-2 Maximum Live Load Deflections (in.)

No. of girders	All 50 ksi		Hybrid	
	3D Refined	Line Girder	3D Refined	Line Girder
5	1.46	0.815	2.01	1.16
7	1.47	0.758	1.97	1.04

The reported live load deflections for the 3D refined analysis are the maximum of the computed deflections for one, two, three and four lanes loaded including impact and multiplied by the appropriate multiple-presence factor. The line girder analysis columns give the live load deflections computed by assuming all lanes (4 lanes) are loaded and uniform participation of all girders. The appropriate multiple-presence

factors are again applied for each case. Note that the addition of two girder lines had no benefit whatsoever on the accurately computed live load deflections from the refined 3D analysis.

A comparison of the girder weights for the four cases given in Table 6.5.4.2.2-3 is instructive.

Table 6.5.4.2.2-3 Comparison of Girder Weights

Design	Girder Weight (lbs)	Total Weight (lbs)	Weight (psf)	Weight Efficiency Ratio
5-girder Hybrid	58,150	290,750	29.8	1.00
5-girder All 50 ksi	66,402	332,010	34.1	1.14
7-girder Hybrid	46,939	328,573	33.7	1.13
7-girder All 50 ksi	54,467	381,269	39.1	1.31

The girder weight does not reflect the additional two bays of cross frames, four additional bearings, additional erection and deck forming costs associated with the 7-girder options. Note that these additional costs did not provide any measurable reduction in actual live load deflections.

It is also instructive to examine the composite moments of inertia of the individual girders and of the total cross-sections. Table 6.5.4.2.2-4 gives the moment of inertia for a single girder and for the sum of the girders in each cross-section.

Table 6.5.4.2.2-4 Moments of Inertia Per Girder and Total Moments of Inertia

No. Girders MOI (in^4)	All 50 ksi	Hybrid
	69" Web	64" Web
5 Total MOI	303,303 in^4/gir 1,516,515 in^4	217,104 in^4/gir 1,085,520 in^4
7 Total MOI	219,532 in^4/gir 1,536,724 in^4	176,824 in^4/gir 1,237,768 in^4
% Increase in total stiffness	1.3	3.9

The 5-girder all 50-ksi cross-section girder has 38% greater stiffness than the comparable girder in the 7-girder cross-section. A similar comparison for the hybrid designs shows a 23% greater stiffness. The larger girder spacing for the 5-girder cross section results in more load to the exterior girder. However, the larger load is

resisted by the greater stiffness resulting in nearly identical live load deflections for the 5- and 7-girder cross-sections under the same live loads.

The concept of uniform deflection may be examined by comparing the total stiffness of the composite cross-sections. The 5-girder cross-section in the all 50-ksi case is 99% as stiff as the comparable 7-girder cross-section. The 5-girder cross-section in the hybrid case is 88% as stiff as the comparable 7-girder cross-section.

As anticipated, the live load deflections computed from the 3D refined analysis are directly related to the inverse of the moment of inertia for all cases. For example, the ratio of the girder moments of inertia for the 5-girder all 50-ksi design to the 5-girder hybrid design (303,303/217,104 = 1.40) is inversely proportional to the ratio of the corresponding maximum live load deflections (2.01/1.46 = 1.38).

Although each case is different, the essence of this study probably remains true for all cases. It is incorrect to add girders to reduce the live load deflection of a multi-girder steel bridge. One might argue that the girder spacing could have been increased beneficially in the 7-girder case. That is true, but so could it have been increased in the 5-girder case.

The preceding discussion is not intended to insinuate that flexibility should not be controlled. Wherever possible, it is best to meet or preferably exceed the minimum girder depths recommended in the specifications (Section 6.3.3.1). Of course, there are situations such as curved girder bridges and bridges with differing girder stiffnesses where the uniform deflection assumption is not permitted or recommended. In these cases, specific loading is required for computation of live load deflections. It would likely be more consistent to consider the same assumption for all bridges.

6.5.4.2.3 Dead Load Deflection

All versions of the AASHTO Specifications, including the *AASHTO LRFD* Specification, are essentially silent regarding dead load deflections (*AASHTO LRFD* Article 6.7.2 does state that vertical camber be provided to account for the dead load deflections). Prior to the advent of composite design, the steel bridge girder was designed to support both dead and live load. With the advent of composite design, much of the dead load is applied on the non-composite structure while the live load is applied to the composite one. This has led to the reduction of the recommended depth of the steel section from $1/25^{th}$ of the span to $1/30^{th}$ of the span. This combined with higher strength steels and a smaller factor applied to dead load for design has, in many cases, results in very slender steel sections. Although there are no provisions for limiting of dead load deflection, the Engineer is wise to consider vertical deflection of the steel and its potential effects during the various stages of construction of the bridge.

6.5.4.3 Permanent Deformations

6.5.4.3.1 General

Checks are to be made on the flange stresses and for potential web bend-buckling in steel-girder superstructures under the Service II load combination to control permanent deformations under repeated severe traffic loadings, which is important to ensure good riding quality.

The standard design Service II loading is defined as 1.0*DC* + 1.0*DW* + 1.3(*LL+IM*), where *DC* represents the component dead loads, *DW* represents the wearing surface and utility loads and (*LL+IM*) represents the design live load plus the dynamic load allowance placed in multiple lanes (Section 3.10.1.3.3). Checks must also be made to prevent slip in slip-critical bolted connections under the Service II loading. The Service II load combination is intended to represent live loads that may be allowed on the structure on infrequent occasions without causing permanent damage.

Under certain conditions, *AASHTO LRFD* Article 6.10.4.2.1 permits flexural stresses in the girders caused by Service II loads applied to the composite section to be computed assuming the concrete deck is effective for both positive and negative flexure for the permanent deflection design checks. *AASHTO LRFD* Article 6.10.4.2.1 lists these conditions as follows:

- Shear connectors must be provided along the entire girder length;
- One-percent longitudinal reinforcement must be provided wherever the tensile stress in the concrete deck due to the Service II loads or due to the factored construction loads exceeds ϕf_r (*AASHTO LRFD* Article 6.10.1.7). ϕ is the resistance factor for concrete in tension (= 0.9), and f_r is the modulus of rupture of the concrete taken equal to $0.24\sqrt{f'_c}$ for normal-weight concrete (*AASHTO LRFD* Article 5.4.2.6); and
- The maximum longitudinal tensile stress in the concrete deck at the section under consideration, caused by the Service II loads, must not exceed $2f_r$.

Under these conditions, the crack size is felt to be controlled to a degree such that the concrete deck may be considered effective in tension for computing the flexural stresses acting on the composite section at the service limit state. The limit of $2f_r$ between the use of an uncracked or cracked section for calculation of flexural stresses in the structural steel is similar to the limit suggested in CEN (2004) beyond which the effects of concrete cracking should be considered. When the above conditions are satisfied, the Engineer is strongly encouraged to consider the

concrete deck to be fully effective in calculating all Service II flexural stresses, as this assumption better reflects the actual conditions in the bridge.

When one of more of the preceding conditions are not satisfied, the flexural stresses in the structural steel caused by Service II loads applied to the composite section in regions of negative flexure must be computed using the section consisting of only the steel section and the longitudinal reinforcement within the effective width of the concrete deck. The properties of the steel section alone are to be used to calculate the flexural stresses in the structural steel for sections that are non-composite for negative flexure. Longitudinal stresses in the concrete deck are to be determined as specified in *AASHTO LRFD* Article 6.10.1.1.1d (Section 6.4.2.4.2).

6.5.4.3.2 I-Sections

6.5.4.3.2.1 Flange Stresses

AASHTO LRFD Article 6.10.4.2.2 specifies that flange stresses due to the Service II loads in I-sections be limited as shown in Table 6.5.4.3.2.1-1 to control permanent deformations in the steel girder at the service limit state.

Table 6.5.4.3.2.1-1 Flange Stress Checks at the Service Limit State (I-Sections)

Sketch	Description	Equation
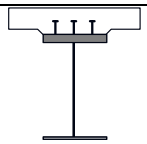	For top steel flange of composite sections	$f_f \le 0.95 R_h F_{yf}$ Equation 6.5.4.3.2.1-1
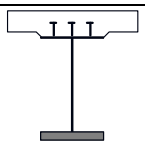	For bottom steel flange of composite sections	$f_f + \frac{f_\ell}{2} \le 0.95 R_h F_{yf}$ Equation 6.5.4.3.2.1-2
	For both steel flanges of non-composite sections	$f_f + \frac{f_\ell}{2} \le 0.80 R_h F_{yf}$ Equation 6.5.4.3.2.1-3

f_f is the flange stress due to vertical bending caused by the Service II loads at the section under consideration. f_ℓ is the flange lateral bending stress due to the Service II loads. The other terms are as defined previously. A resistance factor, ϕ, is not

shown in these equations because *AASHTO LRFD* Article 1.3.2.1 specifies that the resistance factor be taken equal to 1.0 at the service limit state. The sign of f_f and f_ℓ is always taken as positive in these equations. However, when summing dead and live load stresses to obtain the total vertical and lateral bending stresses, f_f and f_ℓ, to apply in the equations, the signs of the individual dead and live load stresses must be considered.

f_ℓ is not included in Equation 6.5.4.3.2.1-1 because the top flange of composite sections is continuously braced by the concrete deck at the service limit state. Therefore, flange lateral bending stresses are small and may be neglected. Lateral bending in the bottom flange is only a consideration at the service limit state for all horizontally curved I-girder bridges (with or without skew) and for straight I-girder bridges with discontinuous cross-frame/diaphragm lines in conjunction with skews exceeding 20° from normal. Other significant sources of flange lateral bending, such as concrete deck overhang loads and wind loads, are not a consideration at the service limit state.

A factor of ½ is conservatively included in front of the f_ℓ term in Equation 6.5.4.3.2.1-2 and Equation 6.5.4.3.2.1-3. As discussed previously in Section 6.5.2.1.4, when this factor is included, the equations approximate more rigorous yield interaction equations corresponding to a load at the onset of yielding at the web-flange juncture under combined major-axis and lateral bending (Schilling, 1996; Yoo and Davidson, 1997). The effect of any minor yielding that occurs at the flange tips prior to this stage is comprehended. By controlling the yielding in this fashion under the combined effects of vertical and lateral bending, with the factored lateral flange bending stresses not exceeding the permissible upper limit of $0.6F_{yf}$ (after any amplification) given in *AASHTO LRFD* Article 6.10.1.6, the resulting permanent deflections will be small. According to *AASHTO LRFD* Article 6.10.1.6, amplification of the first-order flange lateral bending stresses may be required in discretely braced compression flanges. Amplification of tension-flange lateral bending stresses is not required. Amplification of these stresses was discussed previously in Section 6.5.2.1.3.2.

For continuous-span members in which non-composite sections are utilized in negative flexure regions only, *AASHTO LRFD* Article C6.10.4.2.2 recommends that Equation 6.5.4.3.2.1-1 and Equation 6.5.4.3.2.1-2, as applicable, be applied in those regions.

As discussed in Vincent (1969) and Hansell and Viest (1971), the base stress limits of $0.95F_{yf}$ for composite sections and $0.80F_{yf}$ for non-composite sections arose from bridge experiments conducted as part of the AASHO Road Test at Ottawa, Illinois in the early 1960s (AASHO, 1962). The six steel bridges in the Road Test were subjected to more than 390,000 vehicle passages, which is roughly equivalent to 20

overload crossings every day for more than 50 years. Two of the bridges were composite and four were non-composite. Each bridge had a span of 50 feet. The total accumulated permanent sets measured at the end of the test traffic are plotted in Figure 6.5.4.3.2.1-1**.** The differences in the magnitudes of the measured permanent sets in the composite and non-composite bridges are evident in the figure. At stresses approaching 90 percent of F_{yf}, the permanent set was relatively low in composite bridge 2B compared to the permanent set in non-composite bridge 3A. On the basis of this data, the limits were set as shown in Table 6.5.4.3.2.1-1. Note that at these two limiting conditions, the measured permanent sets were of comparable magnitude.

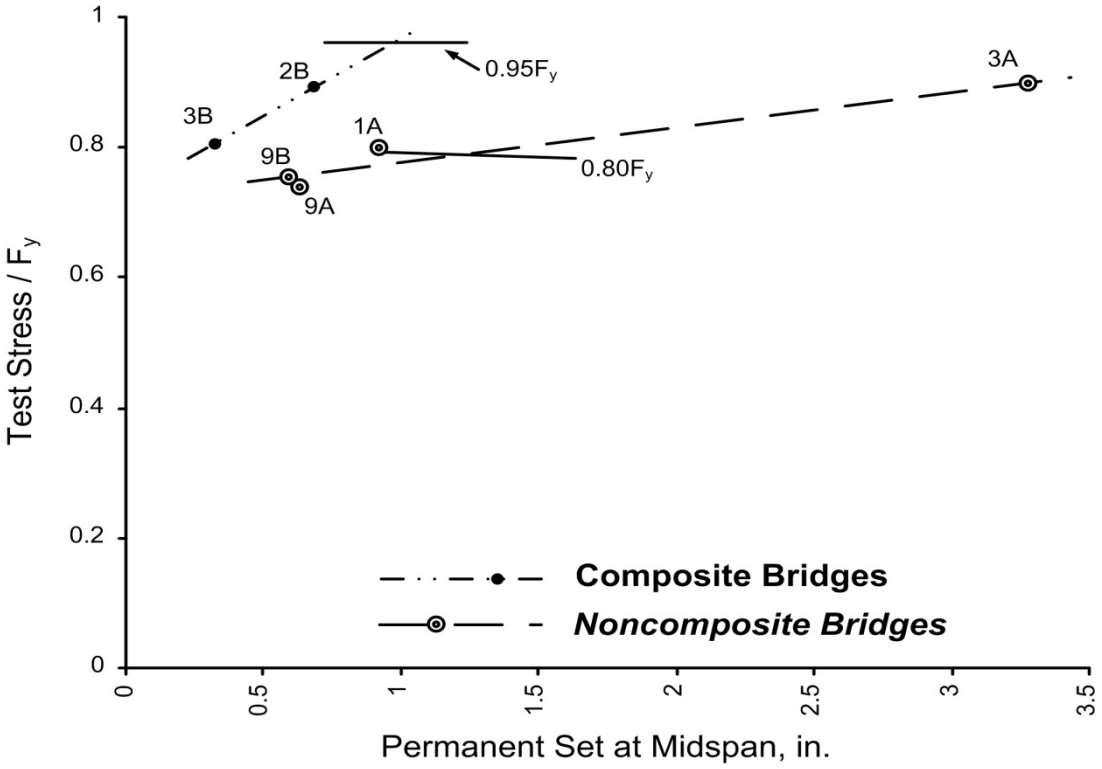

Figure 6.5.4.3.2.1-1 Measured Permanent Set of AASHO Road Test Bridges

The hybrid factor, R_h, has been conservatively added to the stress limits in the *AASHTO LRFD* Specifications to account for the increase in flange stress caused by early web yielding in hybrid sections. ***R*h is discussed further in Section 6.4.5.7.**

AASHTO LRFD Article C6.10.4.2.2 lists sections for which Equation 6.5.4.3.2.1-1 through Equation 6.5.4.3.2.1-3 do not control the design under the load combinations specified in *AASHTO LRFD* Table 3.4.1-1 and need not be checked. These sections include:

- Composite sections in negative flexure for which the main provisions of *AASHTO LRFD* Article 6.10.8 (assuming slender-web behavior) are applied to determine the nominal flexural resistance at the strength limit state;
- Non-composite sections with f_ℓ equal to zero for which the main provisions of *AASHTO LRFD* Article 6.10.8 (assuming slender-web behavior) are applied to determine the nominal flexural resistance at the strength limit state; and
- Noncompact composite sections in positive flexure.

As discussed later (Section 6.5.6.2), sections in negative flexure in all kinked (chorded) continuous and horizontally curved-girder bridges **and in straight-girder bridges whose supports are skewed more than 20° from normal** must always be treated as slender-web sections, regardless of their web slenderness. Thus, such sections must always be designed according to the provisions of *AASHTO LRFD* Article 6.10.8 at the strength limit state (i.e. *AASHTO LRFD* Appendix A6 may not be used). Composite sections in positive flexure in all kinked (chorded) continuous and horizontally curved-girder systems must be treated as noncompact sections at the strength limit state according to *AASHTO LRFD* Article 6.10.6.2.2 (Section 6.5.6.3). Although not currently stated in the specifications, consideration should also be given to treating all composite sections in positive flexure in straight-girder bridges whose supports are skewed more than 20° from normal as noncompact sections. Thus, in all these cases, the preceding conditions are met and the nominal flexural resistance of the section at the strength limit state is not permitted to exceed the moment at first yield. As a result, for these cases under the load combinations specified in *AASHTO LRFD* Table 3.4.1-1, the flange-stress checks at the service limit state described above do not control and need not be checked. Web bend buckling, described in Section 6.5.4.3.2.2, must always be checked however, where applicable.

AASHTO LRFD Article 6.10.4.2.2 optionally permits moment redistribution according to the provisions of *AASHTO LRFD* Appendix B6 prior to making the service limit state design verifications. However, this is only permitted for continuous-span members in straight I-girder bridges with skews not exceeding 10° from normal. Other limitations spelled out in *AASHTO LRFD* Article B6.2 must also be satisfied. Further information on the provisions of *AASHTO LRFD* Appendix B6 may be found in Section 6.5.6.6.

One final requirement in *AASHTO LRFD* Article 6.10.4.2.2 relates to the rare case of compact composite sections in positive flexure utilized in shored construction. In this case, longitudinal compressive stresses in the concrete deck due to the Service II loads are limited to $0.6f'_c$ to ensure linear behavior of the concrete. As discussed in *AASHTO LRFD* Article C6.10.1.1.1a, the use of shored construction is not recommended. Also, as discussed previously, composite sections in positive flexure in all kinked (chorded) continuous and horizontally curved-girder systems must be

treated as noncompact sections. As mentioned above, composite sections in positive flexure in straight I-girder bridges whose supports are skewed more than 20° should also be treated as noncompact sections.

EXAMPLE

Check the flange stresses due to the Service II loads in the composite section shown in Figure 6.4.2.3.2.3-1. The load modifier η is specified to always equal 1.0 at the service limit state (*AASHTO LRFD* Article 1.3.2). Assume unshored construction. The section is an exterior girder located in a region of positive flexure. Use the section properties computed earlier for this section. Since the girder is homogeneous, R_h is equal to 1.0. The girder is straight and the supports are not skewed; therefore, f_ℓ in the bottom flange is equal to zero. Assume the following unfactored bending moments:

M_{DC1} = +2,202 kip-ft
M_{DC2} = +335 kip-ft
M_{DW} = +322 kip-ft
M_{LL+IM} = +3,510 kip-ft

$$0.95R_hF_{yf} = 0.95(1.0)(50) = 47.50 \text{ ksi}$$

Top flange:

$$f_f \le 0.95R_hF_{yf}$$

$$f_f = 1.0\left[\frac{1.0(2{,}202)}{1{,}581} + \frac{1.0(335+322)}{5{,}375} + \frac{1.3(3{,}510)}{16{,}287}\right]12 = -21.54 \text{ ksi}$$

$$\left|-21.54\right| \text{ ksi} < 47.50 \text{ ksi} \qquad \text{ok}$$

Bottom flange:

$$f_f + \frac{f_\ell}{2} \le 0.95R_hF_{yf}$$

$$f_f = 1.0\left[\frac{1.0(2{,}202)}{1{,}973} + \frac{1.0(335+322)}{2{,}513} + \frac{1.3(3{,}510)}{2{,}725}\right]12 = 36.62 \text{ ksi}$$

$$36.62 \text{ ksi} + 0 < 47.50 \text{ ksi} \qquad \text{ok}$$

EXAMPLE

Check the flange stresses due to the Service II loads in the composite section shown in Figure 6.4.2.3.3.3-1, which is for an exterior girder in a region of negative flexure. The flanges are Grade HPS 70W steel and the web is Grade 50W steel. Assume unshored construction and that the appropriate conditions specified in *AASHTO LRFD* Article 6.10.4.2.1 are met such that the concrete deck can be considered effective in negative flexure at the service limit state. The minimum 1 percent longitudinal deck reinforcement is also included in the computation of the composite section properties. The hybrid factor, R_h, for this section at the service limit state was computed previously to be 0.977 (Section 6.4.5.7). Use the section properties computed earlier for this section. Again, the girder is straight and the supports are not skewed; therefore, f_ℓ in the bottom flange is equal to zero. Assume the following unfactored bending moments:

M_{DC1} = -4,840 kip-ft
M_{DC2} = -690 kip-ft
M_{DW} = -664 kip-ft
M_{LL+IM} = -4,040 kip-ft

$$0.95R_hF_{yf} = 0.95(0.977)(70) = 64.97 \text{ ksi}$$

Top flange:

$$f_f \le 0.95R_hF_{yf}$$

$$f_f = 1.0\left[\frac{1.0(-4{,}840)}{2{,}942} + \frac{1.0(-690 + -664)}{7{,}587} + \frac{1.3(-4{,}040)}{16{,}836}\right]12 = 25.63 \text{ ksi}$$

$$25.63 \text{ ksi} < 64.97 \text{ ksi} \quad \text{ok}$$

Bottom Flange:

$$f_f + \frac{f_\ell}{2} \le 0.95R_hF_{yf}$$

$$f_f = 1.0\left[\frac{1.0(-4{,}840)}{3{,}149} + \frac{1.0(-690 + -664)}{3{,}684} + \frac{1.3(-4{,}040)}{3{,}921}\right]12 = -38.93 \text{ ksi}$$

$$\left|-38.93\right| \text{ ksi} + 0 < 64.97 \text{ ksi} \quad \text{ok}$$

6.5.4.3.2.2 Web Bend Buckling

AASHTO LRFD Article 6.10.4.2.2 specifies that except for composite sections in positive flexure in which the web satisfies the requirement of *AASHTO LRFD* Article

6.10.2.1.1 (i.e. $D/t_w \leq 150$ – no longitudinal web stiffeners), all sections must also satisfy the following check at the service limit state:

$$f_c \leq F_{crw} \qquad \text{Equation 6.5.4.3.2.2-1}$$

AASHTO LRFD Equation 6.10.4.2.2-4

where:

f_c = compression-flange vertical bending stress due to Service II loads (ksi)
F_{crw} = nominal bend-buckling resistance of the web determined as specified in *AASHTO LRFD* Article 6.10.1.9 (ksi)

Again, a resistance factor is not specified (i.e. it is implicitly assumed equal to 1.0) because this is a serviceability check.

A web bend buckling check is specified at the service limit state to control bending deformations and transverse displacements of the web. Regions in negative flexure are particularly susceptible to web bend buckling in composite girders at the service limit state, especially when the concrete deck is considered to be effective in tension as permitted for composite sections in *AASHTO LRFD* Article 6.10.4.2.1 (i.e. when the conditions discussed in Section 6.5.4.3.1 are satisfied). When the concrete deck is considered effective in tension, more than half of the web is likely to be in compression increasing the susceptibility of the web to bend buckling. As a result, the check in this case may often end up governing the web thickness of the girder in these regions when the concrete is assumed effective (as recommended when the appropriate conditions are satisfied). Because an explicit web bend buckling check is specified, the web load-shedding factor, R_b, is not included in Equation 6.5.4.3.2.1-1 through Equation 6.5.4.3.2.1-3. R_b is discussed further in Section 6.4.5.6.

Options to consider should F_{crw} be exceeded are similar to those discussed previously in Section 6.5.3.5.1.2 related to the construction condition, except obviously for the adjustment of the deck-placement sequence.

The reader is referred to Section 6.4.5.5 for further discussion on the particulars of this check. Example calculations illustrating this check at the service limit state are also given for a web of a composite section without longitudinal stiffeners subject to negative flexure (in which the concrete deck is assumed to be effective in tension), and for a web of a composite section with longitudinal stiffeners subject to positive flexure.

6.5.4.3.3 Box Sections

6.5.4.3.3.1 Flange Stresses

According to *AASHTO LRFD* Article 6.11.4, flange stresses due to the Service II loads are limited as specified in *AASHTO LRFD* Article 6.10.4.2.2 to control permanent deformations in box sections at the service limit state, with the following exceptions: 1) the f_ℓ term in *AASHTO LRFD* Equation 6.10.4.2.2-2 (Equation 6.5.4.3.2.1-2) is to be taken as zero, and 2) *AASHTO LRFD* Equation 6.10.4.2.2-3 (Equation 6.5.4.3.2.1-3) does not apply. Therefore, the specified stress checks reduce to the following:

For the top and bottom steel flange:

$$f_f \le 0.95 R_h F_{yf} \qquad \text{Equation 6.5.4.3.3.1-1}$$

where:

f_f = flange vertical bending stress at the section under consideration due to the Service II Loads (ksi). f_f is always taken as positive in this equation. However, when summing dead and live load stresses to obtain the total vertical bending stress, f_f, to apply in the equation, the signs of the individual dead and live load stresses must be considered.

R_h = hybrid factor determined as specified in *AASHTO LRFD* Article 6.10.1.10.1

The genesis of the base stress limit given by Equation 6.5.4.3.3.1-1 is discussed further in Section 6.5.4.3.2.1. The hybrid factor, R_h, has been conservatively added to the stress limit in Equation 6.5.4.3.3.1-1 in the *AASHTO LRFD* Specifications to account for the increase in flange stress caused by early web yielding in hybrid sections. A resistance factor, ϕ, is not shown in this equation because *AASHTO LRFD* Article 1.3.2.1 specifies that the resistance factor be taken equal to 1.0 at the service limit state. Note that at sections where access holes are present in the box flange, f_f should be computed using section properties calculated assuming the area of the access hole is subtracted from the box-flange area.

The f_ℓ term is not considered in the stress check for both flanges because flange lateral bending is not a consideration for box flanges and because top flanges are continuously braced at the service limit state. Equation 6.5.4.3.2.1-3, which applies to both steel flanges of non-composite sections, does not apply because box-section members must be composite along their entire length according to *AASHTO LRFD* Article 6.11.10.

Longitudinal warping stresses due to cross-section distortion and St. Venant torsional shear stresses need not be considered in checking Equation 6.5.4.3.3.1-1. As indicated in *AASHTO LRFD* Article C6.11.4, the effect of these stresses on the overall permanent deflections at the service limit state is considered to be insignificant. The effect of longitudinal warping stresses must be considered, however, in certain cases when checking slip of the connections in bolted non-composite box flange splices at the service limit state, as discussed further in Section 6.6.5.2.2.5.4.

Under the load combinations specified in *AASHTO LRFD* Table 3.4.1-1, Equation 6.5.4.3.3.1-1 need only be checked for compact sections in positive flexure as indicated in *AASHTO LRFD* Article C6.11.4. Composite sections in positive flexure in all horizontally curved-girder systems must be treated as noncompact sections at the strength limit state according to *AASHTO LRFD* Article 6.11.6.2.2. Although not currently stated in the specifications, consideration should also be given to treating all composite sections in positive flexure in straight-girder bridges whose supports are skewed more than 20° from normal as noncompact sections. Thus, for all sections in negative flexure and for noncompact sections in positive flexure, Equation 6.5.4.3.3.1-1 does not control and need not be checked under the load combinations specified in *AASHTO LRFD* Table 3.4.1-1. However, web bend buckling must always be considered as discussed in Section 6.5.4.3.3.2.

AASHTO LRFD Article 6.10.4.2.2 optionally permits moment redistribution for continuous-span members in straight I-girder bridges that satisfy specific limitations spelled out in *AASHTO LRFD* Appendix B6 (Article B6.2) prior to making the service limit state design verifications. However, according to *AASHTO LRFD* Article 6.11.4, the applicability of these moment redistribution procedures to box sections has not yet been demonstrated; therefore, the optional Appendix B6 provisions are not to be applied to box sections at the service limit state.

One final requirement in *AASHTO LRFD* Article 6.10.4.2.2 relates to the rare case of compact composite sections in positive flexure utilized in shored construction. In this case, longitudinal compressive stresses in the concrete deck due to the Service II loads are limited to $0.6f'_c$ to ensure linear behavior of the concrete. As discussed in *AASHTO LRFD* Article C6.10.1.1.1a, the use of shored construction is not recommended. Also, as discussed previously, composite sections in positive flexure in all kinked (chorded) continuous and horizontally curved-girder systems must be treated as noncompact sections. Composite sections in positive flexure in straight I-girder bridges whose supports are skewed more than 20° should also be treated as noncompact sections.

6.5.4.3.3.2 Web Bend Buckling

AASHTO LRFD Article 6.11.4 specifies that except for composite sections in positive flexure in which the web satisfies the requirement of *AASHTO LRFD* Article 6.11.2.1.2 (i.e. $D/t_w \leq 150$ – no longitudinal web stiffeners), all sections must also satisfy Equation 6.5.4.3.2.2-1 at the service limit state. At sections where access holes are present in the box flange, f_c should be computed using section properties calculated assuming the area of the access hole is subtracted from the box-flange area.

The web depth, D, and the depth of the web in compression, D_c, should each be measured along the web slope in computing the web bend-buckling resistance, F_{crw}, from Equation 6.4.5.5.1-2 for sections with inclined webs; that is, the vertical web depth in each case must be divided by $\cos\theta$, where θ is the angle of inclination of the web plate with respect to the vertical. The reader is referred to Sections 6.4.5.5 and 6.4.5.4.1 for further information on this particular check, the web bend-buckling resistance, F_{crw}, and the depth of the web in compression in the elastic range, D_c.

6.5.4.4 Control of Deck Cracking

AASHTO LRFD Article 6.10.1.7 requires that the longitudinal tensile stress in a composite concrete deck due to the Service II load combination satisfy the following equation to control the cracking in the concrete deck:

$$f_{deck} \leq \phi f_r = 0.9 f_r \qquad \text{Equation 6.5.4.4-1}$$

where:

ϕ = resistance factor for concrete in tension = 0.9 for reinforced concrete (*AASHTO LRFD* Article 5.5.4.2.1)

f_r = deck concrete modulus of rupture specified in *AASHTO LRFD* Article 5.4.2.6 (ksi)

For normal-weight concrete:

$$f_r = 0.24\sqrt{f'_c} \qquad \text{Equation 6.5.4.4-2}$$

The short-term modular ratio should be used when computing the concrete deck tensile stress; that is, n should be used to compute the composite section properties as opposed to $3n$ (refer to *AASHTO LRFD* Article 6.10.1.1.1d). The calculated stress on the transformed section must be divided by n to obtain the stress in the concrete. f_r is the modulus of rupture, computed using the lower-bound equation for normal-weight concrete shown in Equation 6.5.4.4-2. For lightweight concrete, refer to *AASHTO LRFD* Article 5.4.2.6.

A similar requirement is enforced under the factored construction loads (i.e. the deck-placement sequence), as discussed previously in Section 6.5.3.3.4. Basically, the requirement under the service limit state will determine if the cut-off point for the minimum 1 percent longitudinal deck reinforcing steel determined for the factored construction loads will need to be extended further into the span.

As discussed in *AASHTO LRFD* Article C6.10.1.7, in addition to providing one percent longitudinal deck reinforcement, nominal yielding of the reinforcement should be prevented under Service II loadings to control concrete deck cracking (Grubb, 1993). The use of longitudinal deck reinforcement with a specified minimum yield strength not less than 60 ksi may be taken to preclude nominal yielding of the longitudinal reinforcement under Service II loading for cases of: 1) unshored construction where the steel section utilizes steel with a specified minimum yield strength less than or equal to 70 ksi in either flange; or 2) shored construction where the steel section utilizes steel with a specified minimum yield strength less than or equal to 50 ksi in either flange. The effects of any nominal yielding within the longitudinal reinforcing steel are judged to be insignificant in these cases. Otherwise, the Engineer should check to ensure that nominal yielding of the longitudinal reinforcement does not occur under Service II loading.

EXAMPLE

An earlier example (Section 6.5.3.3.4) showed that the longitudinal reinforcement in the 140-ft end span must extend from the interior-pier section to a section approximately 95.0 feet from the abutment in order to satisfy this requirement under the factored construction loads. The factored modulus of rupture was computed to be ϕf_r = 0.432 ksi in that particular example. Check the tensile stress in the deck to the Service II load combination at the section 95.0 feet from the abutment in the end span. The Service II moments are this section are as follows:

M_{DC2} = +87.0 kip-ft
M_{DW} = +83.0 kip-ft
M_{LL+IM} = -1,701 kip-ft

Note that only the DC_2, *DW* and *LL+IM* loads are assumed to cause stress in the concrete deck. Stresses in the concrete deck are determined as specified in *AASHTO LRFD* Article 6.10.1.1.1d (Section 6.4.2.4.2). The short-term modular ratio n = 8. The short-term composite moment of inertia at this section is I = 166,612 in.^{4} The distance from the short-term composite elastic neutral axis to the top of the structural concrete deck is 21.73 in.

$$f_{deck} = \frac{1.0[1.0(87) + 1.0(83) + 1.3(-1{,}701)](21.73)(12)}{166{,}612(8)} = 0.399 \text{ ksi} < 0.90f_r = 0.432 \text{ ksi}$$

Therefore, the longitudinal reinforcement does not need to be extended any further toward the abutment. The Engineer should ensure that the longitudinal reinforcement is adequately developed at this point.

6.5.5 LRFD Fatigue and Fracture Limit State Design

6.5.5.1 General

AASHTO LRFD Article 1.3.2.3 specifies that the fatigue limit state is to be taken as restrictions on the stress range resulting from a single design truck occurring at an expected number of stress range cycles, which are intended to limit crack growth under repetitive loads to prevent fracture during the design life of the bridge. The fracture limit state is taken as a set of material toughness requirements intended to ensure that the steel has the ability to absorb energy without fracture at minimum specified service temperatures.

AASHTO LRFD Article 6.5.3 states that components and details are to be investigated for fatigue as specified in *AASHTO LRFD* Article 6.6. The investigations are to be made for the applicable Fatigue load combination specified in *AASHTO LRFD* Table 3.4.1-1 using the fatigue live load given in *AASHTO LRFD* Article 3.6.1.4. The fatigue live load is discussed in Section 3.4.4. The two Fatigue load combinations are discussed in Section 3.9.1.5. Fracture toughness requirements are to be in conformance with *AASHTO LRFD* Article 6.6.2.

The preceding requirements are reiterated for I-sections, in *AASHTO LRFD* Articles 6.10.5.1 and 6.10.5.2. The design of box sections for the fatigue limit state is covered in *AASHTO LRFD* Article 6.11.5. In addition, a special fatigue requirement for webs is specified in *AASHTO LRFD* Article 6.10.5.3 that is applicable to both I- and box sections. Requirements for fatigue design of shear connectors are covered in Section 6.6.2.3.

A helpful flowchart detailing the required LRFD fatigue and fracture limit state design verifications discussed below is provided in *AASHTO LRFD* Figure C6.4.3-1 (Appendix C6).

6.5.5.2 Fatigue Limit State

6.5.5.2.1 General

Fatigue is defined in the *AASHTO LRFD* Specifications as the initiation and/or propagation of cracks due to repeated variation of normal stress with a tensile

component. The fatigue life of a detail is defined as the number of repeated stress cycles that result in fatigue failure of a detail, and the fatigue design life is defined as the number of years that a detail is expected to resist the assumed traffic loads without fatigue cracking. In the *AASHTO LRFD* Specifications, the base fatigue design life is taken to be 75 years.

AASHTO LRFD Article 6.6.1.1 specifies that fatigue be categorized as either "load-induced fatigue" (*AASHTO LRFD* Article 6.6.1.2) or "distortion-induced fatigue" (*AASHTO LRFD* Article 6.6.1.3). Load-induced fatigue is defined as fatigue effects due to in-plane stresses for which components and details are explicitly designed. For load-induced fatigue, specific design verifications are required for both flexure and shear to ensure adequate fatigue resistance for the expected number of stress range cycles, and to control web buckling and the resulting elastic flexing of the web under repeated loading. Distortion-induced fatigue is defined as fatigue effects due to secondary stresses not normally quantified in the typical analysis and design of a bridge. Distortion-induced fatigue is typically controlled by providing rigid load paths to preclude the development of significant secondary stresses that could induce fatigue crack growth.

6.5.5.2.2 Load-Induced Fatigue

6.5.5.2.2.1 Flexure

6.5.5.2.2.1.1 Stress Range and S-N Curves

Early attempts to quantify the fatigue resistance of a particular structural joint were based on tests on relatively small-scale specimens that simulated a prototype connection (Munse and Grover, 1964; Gurney, 1968). The experiments contained a limited number of specimens and many variables were introduced that made it difficult to establish the significance of details, type of steels, stress conditions and the quality of fabrication. Because of the limitations of the test data, only approximate design relationships could be developed. Prior to the Ninth Edition of the *AASHO* Specifications (1965), welded bridges were checked for fatigue by limiting alternating stresses using American Welding Society (AWS) specifications. The Ninth Edition specifications introduced the concept of cycles of maximum stress combined with the modified Goodman diagram to limit maximum fatigue stresses for nine different conditions. These provisions were based primarily on the tests mentioned above. However, fatigue cracks were still being found in some beams with partial length cover plates after as little as 13 years of service. Fatigue cracks were also found at the ends of web-to-stiffener welds in stiffeners cut short of the beam flange.

Additional experimental data were therefore developed starting in 1968 under National Cooperative Highway Research Program (NCHRP) Project 12-7, which

involved the fatigue testing of approximately 500 test beams and girders under constant amplitude loading (Fisher et al., 1970; Fisher et al., 1974). Large-scale rolled and welded beam specimens were tested both with and without attachments, such as cover plates and transverse stiffeners. The use of large-scale specimens overcame some of the difficulties associated with the previous data, including the effects of residual stresses, defect size and distribution and shear lag. The test data demonstrated that all fatigue cracks commence at an initial discontinuity in the weldment, or at the periphery of the weld, and grow perpendicular to the applied stresses. Such discontinuities are always present regardless of the welding process or techniques used during the fabrication. The data also showed that the termination of groove and fillet welds provides an even more critical crack growth condition than initial discontinuities in the weld due to high stress concentrations resulting from the geometrical conditions.

Analysis of the data from the NCHRP Project showed that the most important factors governing the fatigue resistance are the stress range and type of detail. Other parameters such as the minimum stress, maximum stress, type of steel and stress ratio (i.e. the ratio of minimum stress to maximum stress) do not play an important role. The stress range is the algebraic difference between the maximum stress and minimum stress at a detail. Stress range means that only the live load plus impact stresses need to be considered; dead load does not contribute to the stress range (Figure 6.5.5.2.2.1.1-1). The fact that stress range is the only significant design parameter is due to the existence of residual stresses in welded steel structures. The welding process results in high tensile residual stresses due to shrinkage of the weld upon cooling, which are at or near the yield point of the weldment and the adjacent base metal. Tensile residual stresses of this magnitude occur regardless of the steel type, which is why the fatigue resistance is independent of the type of steel. Most of the fatigue life occurs in these regions of high tensile residual stress and is exhausted by the time the fatigue crack propagates out of this zone.

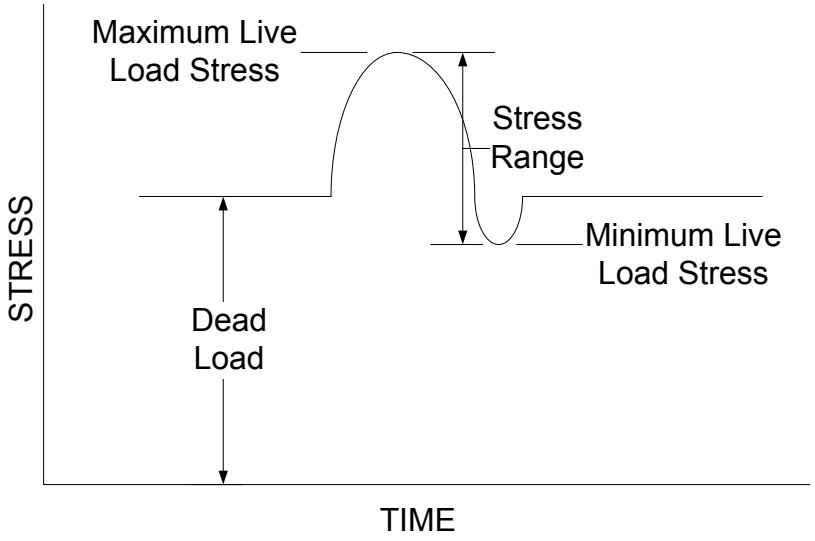

Figure 6.5.5.2.2.1.1-1 Components of a Stress Cycle

The tensile portion of a stress cycle propagates a fatigue crack. Therefore, material subjected to a cyclic loading at or near an initial discontinuity will be subject to a fully effective stress cycle in tension, even in cases of stress reversal, because the superposition of the tensile residual stress will elevate the entire cycle into the tensile stress region (Figure 6.5.5.2.2.1.1-2). The test data even showed an effective stress cycle in tension in cover-plated beams subjected to cyclic compression alone. Fatigue cracks occurred in the tensile residual stress zone at the cover plate weld terminations, but were arrested as they propagated into the adjacent compressive residual stress regions. No loss in load-carrying capacity was observed. This concept of considering only stress range has also been extended to bolted and riveted details where much different residual stress fields exist; the application of this concept to non-welded details is conservative.

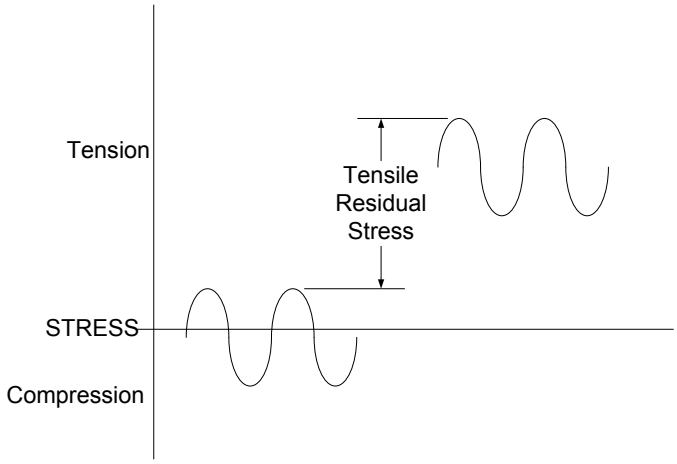

Figure 6.5.5.2.2.1.1-2 Effect of Tensile Residual Stress on a Stress Cycle

As a result of the observed behavior, fatigue design criteria need only be considered for details subject to effective stress cycles in tension and/or stress reversal. If a detail is subject to stress reversal, fatigue must be considered no matter how small the tension component of the stress cycle since a crack generated in the tensile residual stress zone could still be propagated to failure by the small tensile component of stress. Of course, the detail also must be subject to a net applied tensile stress to begin with when considering the maximum anticipated fatigue live load stress occurring over the fatigue design life acting in conjunction with the stress due to the unfactored permanent loads.

Once it was established that the stress range was the critical parameter defining the fatigue life, a relationship between the nominal fatigue resistance expressed in terms of stress range, $(\Delta F)_n$, and the number of stress cycles to failure, N, or S-N curve, could be established. Regression analyses showed that such a relationship could be developed with a constant slope in log-log space as follows:

$$\log N = \log A - B \log(\Delta F)_n \qquad \text{or} \qquad N = A(\Delta F)_n^{-B} \quad \text{Equation 6.5.5.2.2.1.1-1}$$

where *log A* is the *log N*-axis intercept of the *S*-*N* curve, and *B* is the slope constant of the curve. Failure in this case is defined as the growth of a crack large enough in size to result in the inability of a member to carry the load, but does not include brittle fracture where there is limited crack growth.

A least squares linear regression analysis was performed for each type of detail to obtain a curve defining the estimated mean life for that particular detail group; i.e., where half the test data failed prior to reaching the estimated fatigue life and half the data failed after reaching this estimated life. A parallel curve was then drawn two standard deviations below this mean curve, which represented the 95 percent lower confidence limit. This lower bound curve defined a 97.5 percent probability of survival, or conversely, a 2.5 percent probability of failure. A set of such curves was developed for five different detail categories ranging from A to E, with Detail Category A representing details with the highest fatigue resistance and Detail Category E representing details with the lowest fatigue resistance for the details tested as part of the NCHRP research program. Each curve had a slope constant *B* of approximately 3. These curves first appeared in the 1973 *AASHTO* Interim Specifications. Additional fatigue research conducted in the U.S. and abroad between 1973 and 1986 led to minor adjustments to the fatigue design curves and the inclusion of two additional curves for Detail Categories B′ and E′. The slope constant of each curve was also set equal to 3. The complete set of current AASHTO *S*-*N* curves given in the *AASHTO LRFD* Specification is shown in Figure 6.5.5.2.2.1.1-3.

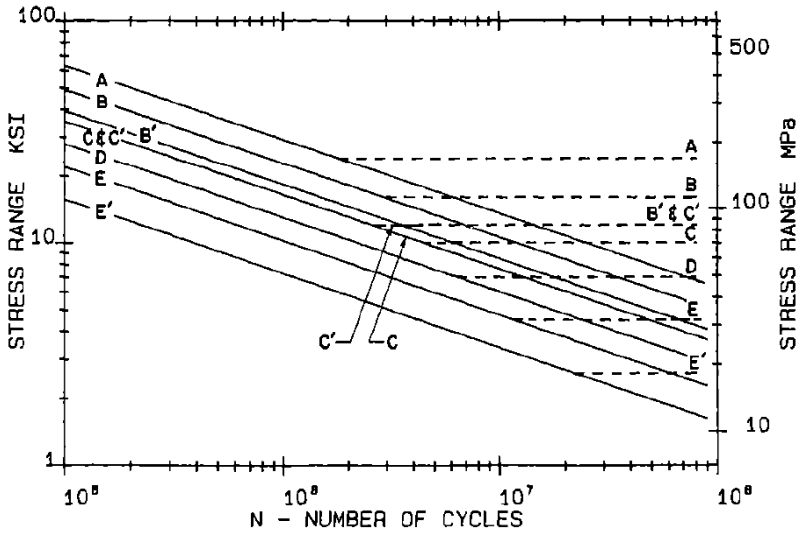

Figure 6.5.5.2.2.1.1-3 *AASHTO LRFD* S-N Curves

It was also observed from the test data that as the stress range decreased in magnitude, there was a level at which no fatigue cracking was observed in the test specimens. The maximum stress range at which no fatigue crack growth will occur under constant amplitude loading is termed the constant-amplitude fatigue threshold, $(\Delta F)_{TH}$, and is indicated by the dashed horizontal line in Figure 6.5.5.2.2.1.1-3 for each detail category. Note that $(\Delta F)_{TH}$ decreases as the severity of the detail category increases. For higher traffic-volume bridges, if the maximum stress range experienced by a detail due to the heaviest truck expected to cross the bridge over the fatigue design life is less than $(\Delta F)_{TH}$, then that detail has a theoretically infinite fatigue life. Therefore, the dashed-line portion of the *S-N* curves will be referred to here as the "infinite-life region". Values for $(\Delta F)_{TH}$ for each detail category are given in *AASHTO LRFD* Table 6.6.1.2.5-3 as follows:

Table 6.5.5.2.2.1.1-1 Values for $(\Delta F)_{TH}$ for Each Detail Category

Detail Category	$(\Delta F)_{TH}$ (ksi)
A	24.0
B	16.0
B′	12.0
C	10.0
C′	12.0
D	7.0
E	4.5
E′	2.6

With an identical slope constant of 3 for each curve in Figure 6.5.5.2.2.1.1-3, the equation for the sloping portion of the *S-N* curves can be written as follows:

$$(\Delta F)_n = \left(\frac{A}{N}\right)^{\frac{1}{3}} \qquad \text{Equation 6.5.5.2.2.1.1-2}$$

Values of the *Log N*-axis intercept coefficient, *A,* or as referred to in the *AASHTO LRFD* Specification, Detail Category Constant, are given in *AASHTO LRFD* Table 6.6.1.2.5-1 as follows:

Table 6.5.5.2.2.1.1-2 Detail Category Constant, A

Detail Category	Constant A times 10^8 (ksi^3)
A	250.0
B	120.0
B′	61.0
C	44.0
C′	44.0
D	22.0
E	11.0
E′	3.9

Equation 6.5.5.2.2.1.1-2 controls for lower traffic-volume bridges. The sloping portion of the *S-N* curves will be referred to here as the “finite-life region”.

The above tables reveal that both A and $(\Delta F)_{TH}$ are greatest for Detail Category A and are least for Detail Category E′. Therefore, nominal fatigue resistance is also greatest for Detail Category A and is least for Detail Category E′. The fatigue detail categories are discussed in the next section.

6.5.5.2.2.1.2 Fatigue Detail Categories

Detail Category A defines the fatigue resistance of the base metal in rolled plates and shapes without welded or bolted details or attachments and provides the maximum possible fatigue resistance of any detail.

Detail Category B applies to the base metal at the majority of welded details, including longitudinal fillet (Figure 6.5.5.2.2.1.2-1) and full penetration groove welds, transverse groove welds ground flush and transitioned flange splices. Pre-tensioned high-strength bolted connections designed as slip-critical connections installed in holes drilled full size or subpunched and reamed to size are classified as Detail Category B (e.g. bolted flange and web splices, bolted stiffeners and end-bolted cover plates). The fatigue resistance applies to the base metal at the gross section of the connection near the hole(s). Detail Category B also applies to the base metal at the net section of high-strength bolted connections designed as bearing-type connections, but fabricated and installed to the requirements for slip-critical connections, with pre-tensioned bolts installed in holes drilled full size or subpunched and reamed to size. The nominal fatigue resistance of uncoated weathering steel base metal designed and detailed in accordance with FHWA (1989) is also classified as Detail Category B.

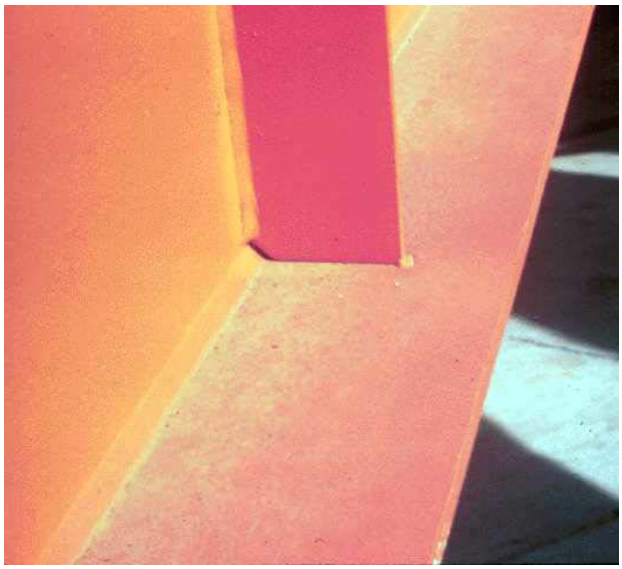

Figure 6.5.5.2.2.1.2-1 Longitudinal Flange-to-Web Fillet Weld (Fatigue Detail Category B)

Detail Category B′, introduced in 1988, applies to longitudinal partial penetration groove welds, full penetration groove welds with backing bars left in place, and straight flange transition splices made with steels with a specified minimum yield strength greater than or equal to 100 ksi. Detail Categories A through B′ rarely control the design.

Detail Category C applies to the base metal at short attachments, unimproved transverse groove welds, welded shear studs and certain attachments with specified radius transitions. Detail Category C marks the transition where geometrical stress concentrations begin to influence the fatigue resistance more than initial discontinuities in the weldment (NHI, 1990).

Detail Category C′ applies specifically to the base metal at the toe of transverse stiffener-to-flange and transverse stiffener-to-web welds.

Detail Category D represents a transition between high and low fatigue strength details. The fatigue resistance of Category D details is influenced by any improvements to reduce the geometrical stress concentration and the attachment length. Detail Category D also applies to the base metal at the gross or net section (as applicable) of pre-tensioned high-strength bolted connections installed in holes punched full size (Brown et al., 2007); the base metal at the net section of joints using ASTM A307 bolts or non-pretensioned high-strength bolts; and the base metal at the net section of open holes in members (Brown et al., 2007).

Detail Category E applies to base metal at the ends of partial length welded cover plates; base metal at the ends of welded longitudinal web or flange stiffeners without specified radius transitions, lateral connection-plate welds, long attachments and small radius transitions; and the base metal at the net section of eyebar heads or pin plates. Base metal in angle or tee section members connected to a gusset or connection plate by longitudinal fillet welds along both sides of the connected element of the member cross-section is also classified as Detail Category E. The fatigue stress range is calculated in this case based on an effective net area of the member as defined in *AASHTO LRFD* Table 6.6.1.2.3-1 and discussed further in Section 6.6.3.3.5. (Note that as of this writing (2015), AASHTO is considering a potential reduction in the nominal fatigue resistance of the base metal in single-angle members connected by longitudinal fillet welds from Detail Category E to Detail Category E′ - see Section 6.6.3.3.5.1).

Detail Category F given in previous specifications for checking shear on the throat of a fillet weld has been eliminated. When fillet welded are properly sized for strength considerations, Detail Category F should not govern. Fatigue will be governed by cracking in the base metal at the weld toe and not by shear on the throat of the weld.

Category E′ details are the lowest fatigue-strength details and are similar to Category E details, but exhibit a reduced fatigue resistance due to a plate-thickness effect, which results in a higher geometrical stress concentration. Category E′ details include the base metal at longitudinal welded attachments with a thickness greater than 1.0 in., at welded cover plate ends on flanges with a thickness greater than 0.8 in. and at the welded ends of cover plates wider than the flange with no transverse end welds.

AASHTO LRFD Table 6.6.1.2.3-1 lists the detail categories for different details. Included in the table is a description of the specific situation, the corresponding detail category and a brief description of potential crack initiation points. For easy reference, the constant-amplitude fatigue threshold, $(\Delta F)_{TH}$, along with the detail category constant, A, have been provided in the table for each detail. Many of the details are shown in 3D, along with the orientation of the applied stress range. In addition, the potential location of crack initiation is shown in the illustrations.

For example, Figure 6.5.5.2.2.1.2-2 shows the illustrative examples given in the table for: 1) base metal at the termination of partial length welded cover plates having square or tapered ends that are narrower than the flange, with or without welds across the ends, or cover plates that are wider than the flange with welds across the ends (Condition 3.5 in the table); and 2) base metal and weld metal in longitudinal web or longitudinal box-flange stiffeners connected by continuous fillet welds parallel to the direction of applied stress (Condition 4.2 in the table). As shown in Figure 6.5.5.2.2.1.2-3, the examples confirm for the cases shown in the photograph that the detail category for the ends of a welded partial-length cover plate is Detail Category E′ (since the cover plate is narrower than the flange and the flange thickness is greater than 0.8 inches), and that the detail category for the base metal and weld metal for the continuous fillet weld connecting the longitudinal stiffener to the web is Category B. The illustrative examples are not intended to serve as standard details or necessarily as examples of good detailing practice.

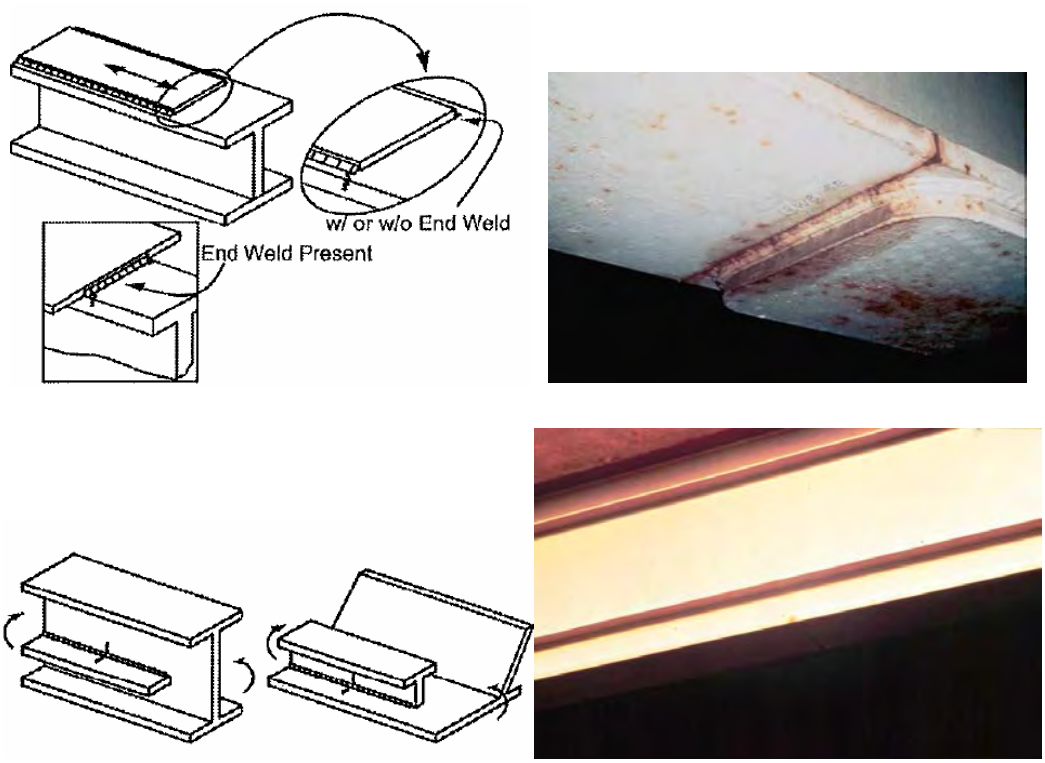

Figure 6.5.5.2.2.1.2-2 Sample Illustrative Examples of Fatigue Details

Description	Category	Constant A (ksi3)	Threshold $(\Delta F)_{TH}$ ksi	Potential Crack Initiation Point
3.5 Base metal at the termination of partial length welded cover plates having square or tapered ends that are narrower than the flange, with or without welds across the ends, or cover plates that are wider than the flange with welds across the ends:				In the flange at the toe of the end weld or in the flange at the termination of the longitudinal weld or in the edge of the flange with wide cover plates
Flange thickness ≤ 0.8 in	E	11×10^8	4.5	
Flange thickness > 0.8 in.	(E')	3.9×10^8	2.6	

Description	Category	Constant A (ksi3)	Threshold $(\Delta F)_{TH}$ ksi	Potential Crack Initiation Point
4.2 Base metal and weld metal in longitudinal web or longitudinal box-flange stiffeners connected by continuous fillet welds parallel to the direction of applied stress.	(B)	120×10^8	16	From the surface or internal discontinuities in the weld away from the end of the weld

Figure 6.5.5.2.2.1.2-3 Category E' and B Details

6.5.5.2.2.1.3 Good Detailing Practices

Examples of design details to optimize the fatigue resistance can be found in NHI (1990); Fisher (1977); and Schilling (1986a). The following basic general principles of good fatigue design taken from NHI (1990) are restated as follows:

- Avoid the introduction of details less than fatigue Detail Category C where possible.
- Design the bridge and its assemblage of members as a whole so as to provide easy paths for stress flow. Avoid gross discontinuities by providing gradual changes in cross-section. Put material at the points at which loads are to be resisted and avoid sudden changes in stiffness.
- Although all connections produce stress concentrations, their number and severity should be minimized.
- Avoid the introduction of unnecessary stresses, such as those associated with unnecessary eccentricities.
- Position connections and weld terminations jnear points of low fatigue stress if possible. For example, field splices in continuous girders should preferably be positioned near points of permanent-load contraflexure.

Although details with a fatigue resistance greater than or equal to that for Detail Category C are preferred, details with a fatigue resistance less than Detail Category C should not necessarily be precluded from use if they can be used in regions of low stress range. A Category C detail that is overstressed provides less safety than an understressed Category E detail.

Intersecting welds at details should always be avoided. Such details are possible, for example, at the intersection of transverse and longitudinal web stiffeners, and at the intersection of lateral connection plates and transverse stiffeners. The restraining effect of the intersecting welds on the plate elements can result in the development of large restraint stresses during cooling, which can potentially result in cracking and low fatigue resistance. In most cases, it is desirable for the longitudinal weld, or the weld parallel to the applied stress, to be continuous to avoid a Category E detail at the weld termination if it is interrupted. End terminations of transverse welds are typically classified as Category C′ details.

AASHTO LRFD Article 6.6.1.2.4 discusses detailing to reduce these constraint-like conditions. This article specified that to the extent practical, welded structures are to be detailed to avoid conditions that create highly constrained joints and crack-like geometric discontinuities susceptible to so-called "constraint-induced fracture" (i.e. brittle fracture that can occur without any perceptible fatigue crack growth and without any warning). This type of failure was documented during the Hoan Bridge failure investigation (Wright et al., 2003; Kaufmann et al., 2004). Criteria to identify

bridges and details susceptible to this failure mode are discussed in Mahmoud et al. (2005). Again, intersecting welds are to be avoided. Welds that are parallel to the primary stress, but interrupted by intersecting members, are to be detailed to allow a minimum gap of 1 in. between the weld toes to reduce constraint. Attached welded elements are less susceptible to fatigue and fracture if the attachment parallel to the primary stress is continuous and the transverse attachment is discontinuous (Figure 6.5.5.2.2.1.3-1). Refer to *AASHTO LRFD* Figure C6.6.1.3.2-1 and Section 6.3.2.10.4 for the preferred details at the intersection of transverse stiffener/connection plates with lateral connection plates.

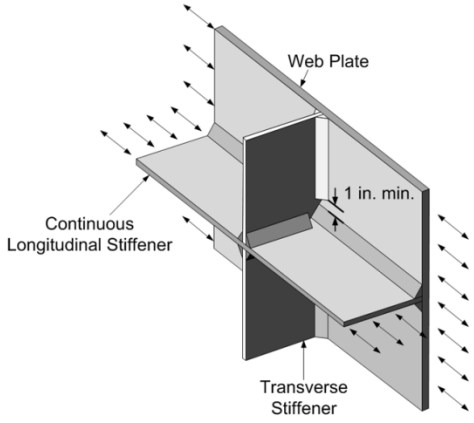

Figure 6.5.5.2.2.1.3-1 Weld Detail at a Continuous Attachment Parallel to the Applied Stress with a Discontinuous Transverse Attachment

Fillet welds or partial penetration welds providing continuity between intersecting plate members (e.g. at transverse and longitudinal stiffener intersections and at transversely loaded web attachments) are often referred to as cruciform joints (Figure 6.5.5.2.2.1.3-2).

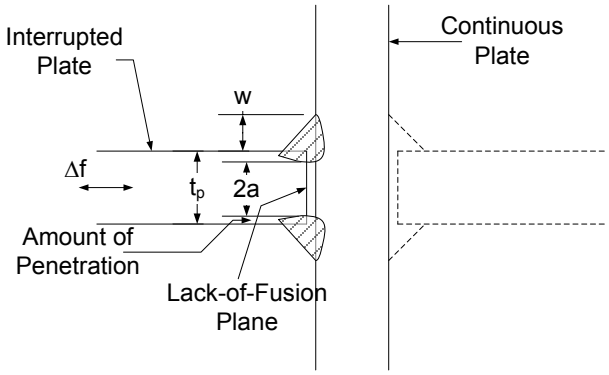

Figure 6.5.5.2.2.1.3-2 Cruciform Joint Detail

Such joints are typically fabricated with one plate continuous while the other plate is interrupted, with fillet welds or partial penetration welds provided at the corners. As

shown in Figure 6.5.5.2.2.1.3-2, a lack-of-fusion plane (or penetration at the weld root) may result depending on the thickness of the interrupted plate, weld size and depth of penetration. When only the continuous plate is loaded, the lack of fusion plane is parallel with the stress field and the fatigue resistance of the base metal at the weld is Detail Category C. If the interrupted plate is loaded, the lack-of-fusion plane is perpendicular to the stress field (i.e. the fillet welds or partial penetration welds are transversely loaded). and the fatigue resistance of the base metal at the weld must be taken from the following equation given in *AASHTO LRFD* Article 6.6.1.2.5:

$$(\Delta F)_n = (\Delta F)_n^C \left(\frac{0.65 - 0.59\left(\frac{2a}{t_p}\right) + 0.72\left(\frac{w}{t_p}\right)}{t_p^{0.167}} \right) \le (\Delta F)_n^C \quad \text{Equation 6.5.5.2.2.1.3-1}$$

AASHTO LRFD Equation 6.6.1.2.5-4

where:

$(\Delta F)_n^C$ = nominal fatigue resistance for Detail Category C determined from *AASHTO LRFD* Eq. 6.6.1.2.5-1 or 6.6.1.2.5-2, as applicable (ksi)

$2a$ = length of the non-welded root face in the direction of the thickness of the loaded plate (in.). For fillet-welded connections, the quantity ($2a/t_p$) is to be taken equal to 1.0.

t_p = thickness of the loaded plate (in.)

w = leg size of the reinforcement or contour fillet, if any, in the direction of the thickness of the loaded plate (in.)

Equation 6.5.5.2.2.1.3-1 accounts for the potential of a crack initiating from the weld root and includes the effects of weld penetration. As a result, the equation is also applicable to partial joint penetration groove welds. The effect of any weld penetration is conservatively ignored by taking the quantity ($2a/t_p$) equal to 1.0. Equation 6.5.5.2.2.1.3-1 limits the nominal fatigue resistance based on the crack initiating from the weld root to the nominal fatigue resistance for Detail Category C, which assumes crack initiation from the weld toe. The development of Equation 6.5.5.2.2.1.3-1 is discussed in Frank and Fisher (1979).

The severity of the cruciform joint can be reduced by the proper selection of the continuous plate element. For example, as discussed above, at intersections of longitudinal and transverse stiffeners, the longitudinal stiffener (i.e. the loaded element) should be continuous while the transverse stiffener (i.e. the unloaded element) is interrupted. At intersections of transverse stiffeners with lateral connection plates, it is required that the transverse stiffener be interrupted and

attached to the lateral connection plate (*AASHTO LRFD* Article 6.6.1.3.2). It should be emphasized that Equation 6.5.5.2.2.1.3-1 does *not* apply to the base metal at the toe of transversely loaded transverse stiffener-to-flange or transverse stiffener-to-web fillet welds, which are classified as Detail Category C′.

NHI (1990) discusses the need to provide a sufficient minimum length for the web gap between the end termination of the transverse weld and the weld toe of the longitudinal weld. For example, where transverse stiffeners are welded to the flange, the end of the transverse weld should be terminated at least one inch from the web-to-flange weld toe to prevent intersecting welds and the formation of significant restraint stresses, and also approximately ¼ inch from the plate edge (Figure 6.5.5.2.2.1.3-3). The stiffener plate should be coped to avoid interference with the web-to-flange weld. At the other end of the stiffener, the weld can either be terminated approximately ¼ inch from the plate edge, or else wrapped around the stiffener plate if it is desired to provide sealing against the penetration of moisture.

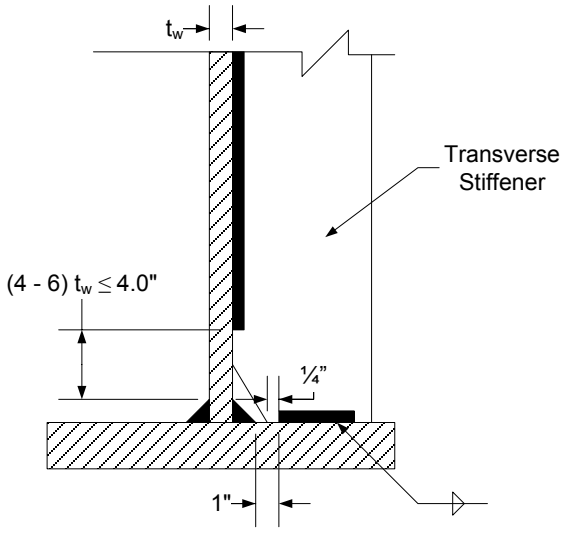

Figure 6.5.5.2.2.1.3-3 Transverse Stiffener Detail

As shown in Figure 6.5.5.2.2.1.3-3, the minimum distance between the end of the web-to-stiffener weld and the near edge of the web-to-flange fillet weld is limited to four times the web thickness, as specified in *AASHTO LRFD* Article 6.10.11.1.1. This limit is specified to eliminate the possibility of a weld intersection and the concomitant high restraint stresses resulting from weld shrinkage. In addition, this limit helps to relieve flexing of the unsupported portion of the web in the gap to avoid fatigue-induced cracking of the stiffener-to-web welds, particularly during handling and shipping of the girders when the stiffeners are cut short from the tension flange (the web gaps should be blocked during shipment in this case). An upper limit on this distance equal to the lesser of six times the web thickness and 4.0 inches is also specified. The $6t_w$ limit is specified to avoid vertical buckling of the unsupported

portion of the web. The 4.0-inch limit was arbitrarily selected to avoid large unsupported web segments in cases where the web thickness has been selected for reasons other than stability; an example being the webs of bascule girders at trunnions. Additional information regarding the detailing of stiffeners (transverse, longitudinal and bearing) is provided in Section 6.6.6. Further information regarding the detailing of lateral connection plates for lateral bracing members is provided in Section 6.3.2.10.4.

6.5.5.2.2.1.4 Nominal Fatigue Resistance

Most of the early laboratory fatigue tests were based on constant-amplitude loading, which consisted of a series of identical load cycles or a constant applied stress range. However, bridges are actually subject to variable-amplitude loading because of the variation of vehicle weights and different possible loading combinations. Variable-amplitude loading consists of a series of cycles of different magnitudes, usually applied in a random sequence. The effects of variable-amplitude loading are typically accounted for using a cumulative damage rule. The most widely used method to account for the effects of cumulative damage is the linear rule proposed by Miner (1945). According to Miner's rule, fatigue damage occurs when the sum of the cumulative stress cycle ratios for the various stress cycles equals unity, or $\sum n_i / N_i = 1.0$, where n_i is the number of cycles applied at a stress range, S_{ri}, and N_i is the number of constant amplitude cycles to failure at S_{ri}.

Variable-amplitude fatigue tests were carried out on large-scale beams under NCHRP Project 12-12 (Schilling et al., 1975) to evaluate the effectiveness of Miner's linear damage hypothesis in relating variable stress cycles to constant cycle data. The beams were identical to those tested under the original NCHRP Project 12-7. It was determined from the results of this study that an equivalent constant-amplitude stress range, or an effective stress range, S_{re}, which causes the same fatigue damage as an equal number of variable-amplitude cycles could be developed by combining Miner's linear damage rule with Equation 6.5.5.2.2.1.1-2 as follows:

$$S_{re} = \left(\sum \gamma_i S_{ri}^3\right)^{1/3} \qquad \text{Equation 6.5.5.2.2.1.4-1}$$

where γ_i is equal to the frequency of occurrence of the stress range, S_{ri}. Using an effective stress range allows constant-amplitude fatigue data and resistance curves to be used to define variable-amplitude conditions and also allows the fatigue damage resulting from an arbitrary load spectrum to be related to a single stress range.

Similarly, the gross weight of a fatigue design truck selected so that the fatigue damage caused by a given number of passages of this truck is the same as the

damage caused by an equal number of passages of different-sized trucks in actual traffic can be computed as follows:

$$W_F = \left(\sum \alpha_i W_i^3\right)^{1/3} \qquad \text{Equation 6.5.5.2.2.1.4-2}$$

where α_i is the fraction of trucks with a gross weight of W_i. The stress range caused by the passage of such a truck would be representative of the effective stress range given by Equation 6.5.5.2.2.1.4-1. To use Equation 6.5.5.2.2.1.4-2, a histogram of truck-weight data for a particular site would be required to arrive at the weight of the fatigue design truck. Since such data are generally not available, a gross weight of 54 kips was originally proposed for the fatigue design truck in AASHTO (89), which was calculated from Equation 6.5.5.2.2.1.4-2 based on weigh-in-motion data and the results of several nationwide traffic surveys (Schilling, 1986a). A constant rear-axle spacing of 30 feet was also proposed for the fatigue design truck in AASHTO (1989) since that spacing was assumed to approximate the spacing for the 4- and 5-axle semitrailers that do most of the fatigue damage to bridges. Further, an impact factor of 1.15 was proposed for fatigue design since the impact factor in this case is for stress range rather than peak stress. Also, it was felt by the Guide Specification writers that an average impact factor rather than a maximum factor would be more appropriate for fatigue design.

These concepts were carried forward to the *AASHTO LRFD* Specifications, with some slight modification. As discussed in Section 3.4.4, the fatigue design truck is specified to be a single HL-93 design truck, weighing 72 kips, with a constant rear-axle spacing of 30 feet (*AASHTO LRFD* Article 3.6.1.4.1). A dynamic load allowance (impact factor) of 1.15 is to be applied to the truck (*AASHTO LRFD* Article 3.6.2). *AASHTO LRFD* Article 3.6.1.4.3a specifies that when the bridge is analyzed by a refined analysis method, the truck is to be positioned transversely and longitudinally to maximize the stress range at the detail under consideration regardless of the position of the actual traffic lanes on the deck. *AASHTO LRFD* Article 3.6.1.4.3b specifies that when wheel-load distribution factors are used for the analysis, the appropriate factor specified for one-lane loaded in *AASHTO LRFD* Article 4.6.2.2 is to be used. Further, *AASHTO LRFD* Article 3.6.1.1.2 specifies that the multiple presence factor of 1.2 for one-lane loaded (*AASHTO LRFD* Table 3.6.1.1.2-1) is not to be applied for the fatigue limit state check. Therefore, when using the tabularized equation for the distribution factor for one-lane loaded for the interior girders, the 1.2 multiple presence factor must be divided out of the calculated factor. Or, when using the lever rule or the special analysis equation to compute the factor for one-lane loaded for the exterior girders, or when applying the fatigue design truck to an influence surface in a refined analysis, the 1.2 factor must not be applied.

The preceding discussion on the effective stress range leads to the first principle of fatigue resistance, which applies in the finite-life region, and states that for lower traffic volumes, the nominal fatigue resistance, $(\Delta F)_n$, is inversely proportional to the cube of the effective stress range. This principle is reflected by Equation 6.5.5.2.2.1.1-2, which represents the equation for the sloping portion of the *S-N* curve. In the *AASHTO LRFD* Specifications, the effective stress range is represented by a factored fatigue design truck weighing 54 kips (plus impact), which is specified as the Fatigue II load combination in *AASHTO LRFD* Table 3.4.1-1. The specified load factor for the Fatigue II load combination is 0.75; 0.75 * 72 kips = 54 kips.

In the extreme life (or infinite life) region, for which many details on bridges located on high-volume routes are designed, most of the stress cycles in a spectrum will be below the constant-amplitude fatigue threshold, $(\Delta F)_{TH}$. These cycles do not cause fatigue damage under constant-amplitude loading. However, under variable-amplitude loading, larger stress cycles that exceed $(\Delta F)_{TH}$ will contribute to fatigue crack growth, which will cause the threshold to decrease in magnitude until all stress cycles will eventually contribute to crack growth. Therefore, in the infinite-life region, fatigue design of welded details subject to variable-amplitude loading requires that the maximum stress range be considered in addition to the effective stress range.

As a result, three different cases related to fatigue life are possible depending on the relative values of the effective stress range, maximum stress range and $(\Delta F)_{TH}$: Case 1 -- effective stress range and maximum stress range greater than $(\Delta F)_{TH}$; Case 2 -- effective stress range less than $(\Delta F)_{TH}$ and maximum stress range greater than $(\Delta F)_{TH}$; or Case 3 -- effective and maximum stress ranges both less than $(\Delta F)_{TH}$. These three cases are illustrated in Figure 6.5.5.2.2.1.4-1. For the first two cases, the fatigue life is defined by sloping portion of the *S-N* curve and its straight-line extension below $(\Delta F)_{TH}$. Only for the third case will no fatigue crack growth be assured; that is, the detail will have a theoretically infinite fatigue life.

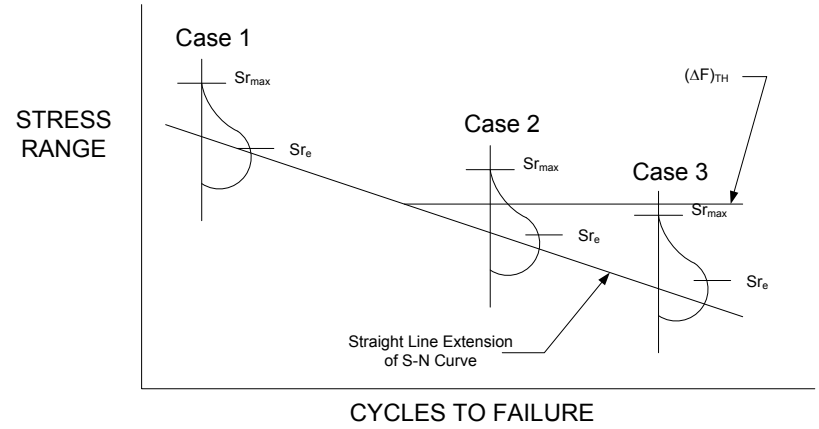

Figure 6.5.5.2.2.1.4-1 Three Possible Cases of Variable-Amplitude Loading

The discussion in the preceding paragraph leads to the second principle of fatigue resistance, which applies in the infinite-life region, and states that for higher traffic volumes, the fatigue resistance $(\Delta F)_n$ is infinite if the maximum stress range is less than $(\Delta F)_{TH}$. In the *AASHTO LRFD* Specifications, the maximum stress range is assumed to be twice the effective stress range, or twice the live load stress range due to the passage of the effective design truck (plus impact), which is specified as the Fatigue I load combination in *AASHTO LRFD* Table 3.4.1-1. The specified load factor for the Fatigue I load combination is 1.5; 2 * 0.75 * 72 kips = 1.5 * 72 kips = 108 kips. That is, the maximum stress range for fatigue design is assumed to be the stress range due to a 108-kip truck (plus impact) with a constant rear-axle spacing of 30 feet. This represents the heaviest truck expected to cross the bridge over its base 75-year fatigue design life.

Therefore, in the *AASHTO LRFD* Specifications, the nominal fatigue resistance, $(\Delta F)_n$, based on the two principles of fatigue resistance is given in *AASHTO LRFD* Article 6.6.1.2.5 as follows:

For the Fatigue I load combination and infinite life:

$$(\Delta F)_n = (\Delta F)_{TH} \qquad \text{Equation 6.5.5.2.2.1.4-3}$$

AASHTO LRFD Equation 6.6.1.2.5-1

For the Fatigue II load combination and finite life:

$$(\Delta F)_n = \left(\frac{A}{N}\right)^{\frac{1}{3}} \qquad \text{Equation 6.5.5.2.2.1.4-4}$$

AASHTO LRFD Equation 6.6.1.2.5-2

The number of stress cycles, *N*, in Equation 6.5.5.2.2.1.4-4 for the required fatigue life as defined in the *AASHTO LRFD* Specifications is to be computed from the following equation:

$$N = (365)(75)n(ADTT)_{SL} \qquad \text{Equation 6.5.5.2.2.1.4-5}$$

AASHTO LRFD Equation 6.6.1.2.5-3

The number *365* represents the number of days in a year, the number *75* represents the fatigue design life of 75 years (a number other than 75 should be substituted if a fatigue design life other than 75 years is sought), *n* is the number of stress cycles per truck passage taken from *AASHTO LRFD* Table 6.6.1.2.5-2, and $(ADTT)_{SL}$ is the

single-lane *ADTT* (Average Daily Truck Traffic) averaged over the design life specified in *AASHTO LRFD* Article 3.6.1.4.2.

The number of stress range cycles per truck passage, *n*, is again specified in *AASHTO LRFD* Table 6.6.1.2.5-2. In many cases, *n* will be taken equal to 1.0. Short-span longitudinal members (with spans less than or equal to 40 feet in length according to *AASHTO LRFD* Table 6.6.1.2.5-2), transverse members loaded directly by a wheel (with a longitudinal spacing less than or equal to 20 feet according to *AASHTO LRFD* Table 6.6.1.2.5-2), and areas near interior supports of continuous spans (with 'near' defined in *AASHTO LRFD* Article C6.6.1.2.5 as a distance equal to one-tenth of the span on each side of an interior support) will be subject to more than one stress cycle, *n*, per truck passage. As span length increases, the effect of the axle loads is attenuated. For cantilever girders, *n* is to be taken equal to 5.0 because these members are susceptible to large vibrations, which cause additional cycles after the truck leaves the bridge.

As specified in *AASHTO LRFD* Article 3.6.1.4.2 and also discussed in Section 1.3.2.3.3, in the absence of better information, $(ADTT)_{SL}$ may be taken as follows:

$$(ADTT)_{SL} = p * ADTT \qquad \text{Equation 6.5.5.2.2.1.4-6}$$

AASHTO LRFD Equation 3.6.1.4.2-1

where:

$(ADTT)_{SL}$ = the number of trucks per day in a single-lane averaged over the design life

p = fraction of truck traffic in a single lane specified in *AASHTO LRFD* Table 3.6.1.4.2-1 (Table 6.5.5.2.2.1.4-1)

$ADTT$ = the number of trucks per day in one direction averaged over the design life in the traffic lane carrying the majority of the truck traffic

AASHTO LRFD Article C3.6.1.4.2 contains recommendations on how to compute the *ADTT* based on the average daily traffic (*ADT*) in the absence of site-specific data, and discusses extension of the traffic growth data to the fatigue design life of 75 years (Section 3.4.4.2). The single-lane *ADTT* is to be taken for the traffic lane in which the majority of the truck traffic crosses the bridge, which is typically the shoulder lane. As discussed in *AASHTO LRFD* Article C3.6.1.4.2, in the absence of truck traffic data in one direction from traffic engineers, designing for 55 percent of the bi-directional *ADTT* is suggested

The fraction of truck traffic in a single lane, *p*, is given in Table 6.5.5.2.2.1.4-1, and is a function of the number of lanes available to trucks on the bridge travelling in one direction. The frequency of the fatigue load for a single lane is assumed to apply to

all lanes since future traffic patterns on the bridge are uncertain; therefore, the number of design lanes that can be accommodated on the bridge is typically used to establish the value of *p*.

Table 6.5.5.2.2.1.4-1 Coefficient, *p*, for Average Daily Truck Traffic

No. of Lanes	p
1	1.00
2	0.85
3 or more	0.80

The probability that all lanes will contain only truck traffic decreases as the number of lanes available to trucks increases. Therefore, it is reasonable that the values for *p* should decrease as the number of lanes available to trucks increases.

The fatigue design for most details (except potentially for Detail Categories E and E′) for higher traffic volumes will be governed by the infinite life check; that is, the nominal fatigue resistance determined from Equation 6.5.5.2.2.1.4-3 utilized in conjunction with the Fatigue I load combination. Table 6.5.5.2.2.1.4-2 (*AASHTO LRFD* Table 6.6.1.2.3-2) shows the values of $(ADTT)_{SL}$ for each detail category *above* which the nominal fatigue resistance is governed by $(\Delta F)_{TH}$ (or the infinite-life check):

Table 6.5.5.2.2.1.4-2 75-Year $(ADTT)_{SL}$ Equivalent to Infinite Life

Detail Category	75-Year $(ADTT)_{SL}$ Equivalent to Infinite Life (Trucks per Day)
A	530
B	860
B’	1035
C	1290
C’	745
D	1875
E	3530
E’	6485

The values in Table 6.5.5.2.2.1.4-2 were computed assuming a 75-year fatigue design life and a number of stress cycles per truck passage, *n*, equal to one, and are rounded up to the nearest five trucks per day. For other values of *n*, the values in the table should be modified by dividing them by *n*. If a fatigue life other than 75

years is sought, the table values must be multiplied by the ratio of 75 divided by the fatigue life sought (in years). The indicated values were determined by equating the infinite life and fatigue life resistances (from Equation 6.5.5.2.2.1.4-3 and Equation 6.5.5.2.2.1.4-4) taking into account the difference in load factors used with the Fatigue I and Fatigue II load combinations as follows:

$$75\_\text{Year}(\text{ADTT})_{SL} = \frac{A}{\left[\frac{(\Delta F)_{TH}}{2}\right]^3 (365)(75)(n)} \qquad \text{Equation 6.5.5.2.2.1.4-7}$$

AASHTO LRFD Equation C6.6.1.2.3-1

using the values for A and $(\Delta F)_{TH}$ specified in Table 6.5.5.2.2.1.1-2 and Table 6.5.5.2.2.1.1-1, respectively.

AASHTO LRFD Article 6.6.1.2.3 specifies that components and details on fracture-critical members (defined later in Section 6.5.5.3.3) should be designed for infinite life using the Fatigue I load combination regardless of the $(ADTT)_{SL}$.

It should be noted that as of this writing (2015), a future increase in the load factors for the Fatigue I and Fatigue II load combinations is anticipated, which may also affect Equation 6.5.5.2.2.1.4-7 and the corresponding values given in Table 6.5.5.2.2.1.4-2.

6.5.5.2.2.1.5 Design Verification for Flexure

For load-induced fatigue considerations, each detail must satisfy the following equation specified in *AASHTO LRFD* Article 6.6.1.2.2:

$$\gamma(\Delta f) \le (\Delta F)_n \qquad \text{Equation 6.5.5.2.2.1.5-1}$$

AASHTO LRFD Equation 6.6.1.2.2-1

where:

γ = load factor for the applicable fatigue load combination (1.5 for Fatigue I or 0.75 for Fatigue II)

(Δf) = live load stress range due to the passage of the fatigue design live load plus impact (ksi)

$(\Delta F)_n$ = nominal fatigue resistance determined as specified in *AASHTO LRFD* Article 6.6.1.2.5 (ksi)

The load modifier, η, and the resistance factor, ϕ, are always taken equal to 1.0 at the fatigue limit state.

The lateral bending stress range in the bottom flange due to the factored fatigue live load plus impact must be included in *(Δf)* for curved bridges, where applicable (*AASHTO LRFD* Article 6.10.5.1). Bottom flange-to-web welds, obviously, need only be checked for the average stress range (due to vertical bending) since the welds are near the mid-width of the flange. However, at points where attachments are welded to the girder bottom flanges, such as at cross-frame connection plates, the flange should be checked for the average stress range plus the lateral flange bending stress range at the critical transverse location on the flange. Bottom flange butt welds should also be checked for the lateral bending stress range in addition to the average stress range. Consideration should also be given to including the bottom-flange lateral bending stress range in straight skewed bridges in regions where cross-frames are discontinuous. The stress range due to flange lateral bending is generally not a consideration for details on the top flange because the flange is continuously braced.

For example, the flange lateral bending stress range, $(\Delta M)_{Lat}$, increases the stress range in the base metal adjacent to the outer termination of the connection plate-to-bottom flange weld, as shown in Figure 6.5.5.2.2.1.5-1. I_{Lat} is the lateral moment of inertia of the bottom flange = $t_f b_f^3 / 12$.

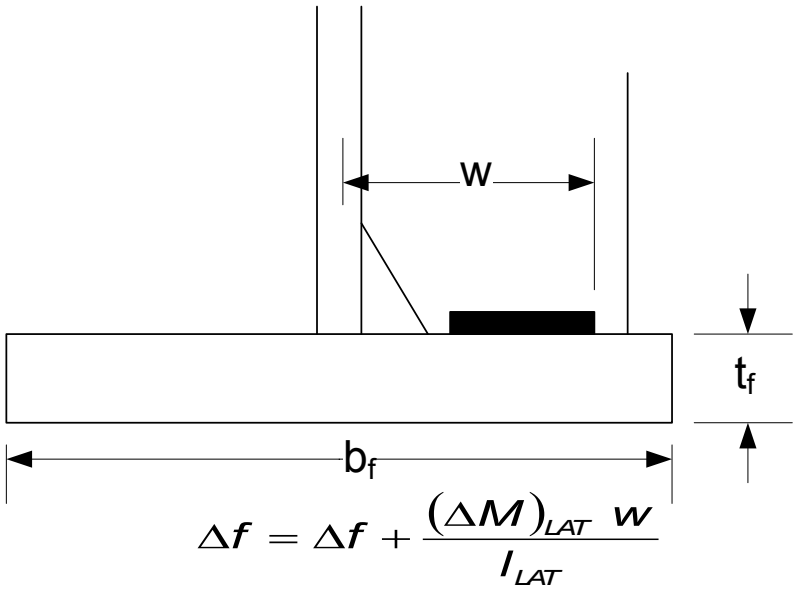

Figure 6.5.5.2.2.1.5-1 Effect of Bottom Flange Lateral Bending on the Stress Range

Under certain conditions, *AASHTO LRFD* Article 6.6.1.2.1 permits dead load stresses, live load stresses, and live load stress ranges for the fatigue limit state

checks to be computed using the appropriate corresponding composite section assuming the concrete deck is effective (i.e., uncracked) for both positive and negative flexure, as discussed previously for the service limit state (Section 6.5.4.3.1). The long-term (3*n*) composite section is to be used for the dead loads, and the short-term (*n*) composite section is to be used for the live loads. *AASHTO LRFD* Article 6.10.1.7 specifies those conditions as the following: 1) shear connectors must be provided along the entire length of the girder; and 2) the minimum 1 percent longitudinal deck reinforcement must be placed wherever the tensile stress in the concrete deck due to either the factored construction loads or load combination Service II exceeds the factored lower-bound modulus of rupture of the concrete. The crack size is felt to be controlled to such a degree under these conditions that full-depth cracks will not occur. Where cracks do occur, the stress in the longitudinal reinforcement will increase until the crack is arrested and the cracked concrete and reinforcement reach equilibrium. With a small number of staggered cracks that do not coalesce at any given section, the concrete can provide significant resistance to tensile stress at service load levels. If one or both of the above conditions is not satisfied, then the concrete deck is not to be considered effective for computing stresses on the composite section for negative flexure.

Using the short-term *n*-composite section to compute the factored fatigue load stresses due to both positive and negative flexure results in a significant reduction in the computed stress range at and near the top flange. The stress range at or near the bottom flange is largely unaffected because the increase in stiffness for negative flexure is essentially offset by the increase in the distance from the *n*-composite neutral axis to the bottom flange.

The computation of the nominal fatigue resistance, $(\Delta F)_n$, is summarized schematically in Figure 6.5.5.2.2.1.5-2. Except as specified for fracture-critical members (Section 6.5.5.2.2.1.4), where the projected 75-year single lane Average Daily Truck Traffic $(ADTT)_{SL}$ is less than or equal to the applicable value specified in Table 6.5.5.2.2.1.4-2 for the Detail Category under consideration, the Fatigue II load combination specified in *AASHTO LRFD* Table 3.4.1-1 (Section 3.9.1.5.3) should be used in combination with the nominal fatigue resistance for finite life given by Equation 6.5.5.2.2.1.4-4. The load factor of 0.75 for the Fatigue II load combination, applied to the single design truck, reflects a load level found to be representative of the effective stress range of the truck population with respect to a small number of stress range cycles and to their cumulative effects in steel elements, components and connections for finite fatigue life design. Otherwise, the Fatigue I load combination is to be used in combination with the nominal fatigue resistance for infinite life given by Equation 6.5.5.2.2.1.4-3. The load factor of 1.5 for the Fatigue I load combination, applied to the single design truck, reflects load levels found to be representative of the maximum stress range of the truck population for infinite fatigue life design. The factor was chosen on the assumption that the maximum stress

range in the random variable spectrum is twice the effective stress range caused by Fatigue II load combination.

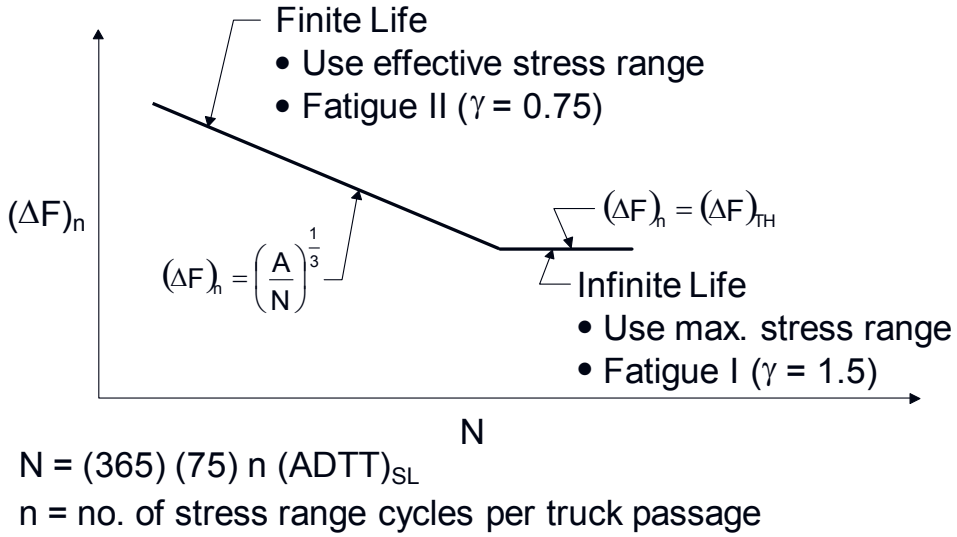

Figure 6.5.5.2.2.1.5-2 Nominal Fatigue Resistance, $(\Delta F)_n$

6.5.5.2.2.1.6 Check for Net Applied Tensile Stress

AASHTO LRFD Article 6.6.1.2.1 specifies that Equation 6.5.5.2.2.1.5-1 need only be checked for details subject to a net applied tensile stress. That is, in regions where the unfactored permanent loads produce compression, fatigue need only be considered at a particular detail if the compressive stress at that detail is less than the maximum tensile live load stress caused by the Fatigue I load combination. The Fatigue I load combination again represents the heaviest truck expected to cross the bridge over its 75-year fatigue design life. The effect of any future wearing surface may be conservatively ignored when making this check. If the tensile component of the Fatigue I stress range does not exceed the compressive stress due to the unfactored permanent loads, there is no net tensile stress. As a result, the stress cycle is compression/compression and a fatigue crack will not propagate beyond a heat-affected zone.

Live load almost always produces negative moments in girders in adjacent spans and often in the same span when supports are sharply skewed. Live load also produces positive moment in girders in regions defined as negative moment regions between points of dead load contraflexure and supports. Thus, it is necessary to test each point in a span to determine if net tension might exist for the fatigue loading.

EXAMPLE

Check fatigue of the base metal at the cross-frame connection-plate welds to the flanges at the connection plate located 72.0 feet from the abutment in the 140-ft end span of a straight three-span continuous (140 ft – 175 ft – 140 ft) I-girder bridge with no skew. The cross-section of the composite girder at this section is shown in Figure 6.4.2.3.2.3-1. The elastic section properties for this section were calculated Section 6.4.2.3.2.3.

The bridge has a 40-ft roadway width capable of handling three (3) design lanes. The average daily truck traffic *ADTT* in one direction averaged over the 75-year fatigue design life is assumed to be 2,000 trucks per day. Assume that the appropriate conditions specified in *AASHTO LRFD* Article 6.10.1.2.1 are met such that the concrete deck can be considered effective in positive and negative flexure for computing the live load stresses and stress ranges at the fatigue limit state. The unfactored permanent load moments at this section are as follows:

M_{DC1} = +1,824 kip-ft
M_{DC2} = +281 kip-ft
M_{DW} = +270 kip-ft

The unfactored moments at this section due to the fatigue load specified in *AASHTO LRFD* Article 3.6.1.4 (i.e. a 72-kip truck with a constant rear-axle spacing of 30 ft) placed in a single lane, including the 15 percent dynamic load allowance, are as follows:

$+M_{LL+IM}$ = +1,337 kip-ft
$-M_{LL+IM}$ = -496 kip-ft

First, check the top-flange connection-plate weld. Since the unfactored permanent loads produce compression at the top flange, determine if the top flange is subject to a net applied tensile stress according to the provisions of *AASHTO LRFD* Article 6.6.1.2.1. The total unfactored permanent-load compressive stress at the top-flange weld at this location (conservatively neglecting the future wearing surface) is computed as:

$$f_{DC1} = \frac{1{,}824(12)(38.63)}{62{,}658} = -13.49 \text{ ksi}$$

$$f_{DC2} = \frac{281(12)(21.74)}{122{,}232} = \underline{-0.600 \text{ ksi}}$$

$$-14.09 \text{ ksi}$$

The maximum tensile stress at the top-flange weld at this location due to the negative moment Fatigue I load combination is:

$$f_{LL+IM} = \frac{1.5|-496|(12)(9.23)}{166{,}612} = 0.495 \text{ ksi}$$

$$|-14.09| \text{ ksi} > 0.495 \text{ ksi}$$

Therefore, fatigue of the base metal at the connection-plate weld to the top flange at this location need not be checked.

Next, check the bottom-flange connection-plate weld. By inspection, it is determined that the base metal at the connection-plate weld to the bottom flange at this location is subject to a net applied tensile stress.

Determine the fatigue detail category from *AASHTO LRFD* Table 6.6.1.2.3-1. Under Section 4 of the table on Welded Stiffener Connections, the fatigue detail category for base metal at transverse stiffener-to-flange welds is Detail Category C′.

For a Category C′ detail, *AASHTO LRFD* Table 6.6.1.2.5-1 (Table 6.5.5.2.2.1.1-1) gives a Detail Category Constant *A* equal to 44.0 * 10^8 ksi^3, and *AASHTO LRFD* Table 6.6.1.2.5-3 (Table 6.5.5.2.2.1.1-1) gives a constant-amplitude fatigue threshold $(\Delta F)_{TH}$ equal to 12.0 ksi. From *AASHTO LRFD* Article 3.6.1.4.2, the single-lane average daily truck traffic $(ADTT)_{SL}$ is computed as (Equation 6.5.5.2.2.1.4-6):

$$(\text{ADTT})_{\text{SL}} = p * \text{ADTT}$$

where *p* is the fraction of truck traffic in a single lane taken from *AASHTO LRFD* Table 3.6.1.4.2-1. For a 3-lane bridge, *p* is equal to 0.80 (Table 6.5.5.2.2.1.4-1). Therefore:

$$(\text{ADTT})_{\text{SL}} = 0.80(2{,}000) = 1{,}600 \text{ trucks per day}$$

The number of stress cycles, *N*, is computed as follows (Equation 6.5.5.2.2.1.4-5):

$$N = (365)(75)n(\text{ADTT})_{\text{SL}}$$

For continuous spans with span lengths greater than 40.0 feet, the number of stress cycles per truck passage, *n*, is equal to 1.0 at sections away from the pier (*AASHTO LRFD* Table 6.6.1.2.5-2). Sections ′away from the pier′ are defined as sections

greater than a distance of one-tenth the span on each side of the interior support. Therefore:

$$N = (365)(75)(1.0)(1{,}600) = 43.8 * 10^6 \text{ cycles}$$

AASHTO LRFD Table 6.6.1.2.3-2 (Table 6.5.5.2.2.1.4-2) shows the values of $(ADTT)_{SL}$ for each fatigue detail category above which the fatigue resistance is governed by $(\Delta F)_{TH}$ (such that the detail will theoretically provide infinite fatigue life) under the Fatigue I load combination. By using this table, it will usually not be necessary to determine the values of *A* and *N*. The values in the table assume a 75-year design life and one stress cycle, *n*, per truck passage. Therefore, from *AASHTO LRFD* Table 6.6.1.2.3-2, the 75-year $(ADTT)_{SL}$ equivalent to infinite fatigue life for a Category C′ detail is 745 trucks per day < 1,600 trucks per day. Therefore:

$$(\Delta F)_n = (\Delta F)_{TH} = 12.00 \text{ ksi}$$

$$\gamma(\Delta f) \le (\Delta F)_n$$

The stress range, $\gamma(\Delta f)$, at the connection-plate weld due to the Fatigue I load combination is computed using the properties of the short-term composite section as follows:

$$\gamma(\Delta f) = \frac{1.5(1{,}337)(12)(59.78)}{166{,}612} + \frac{1.5|-496|(12)(59.78)}{166{,}612}$$
$$= 11.84 \text{ ksi}$$

$$11.84 \text{ ksi} < 12.00 \text{ ksi} \qquad \text{ok}$$

An alternative is to bolt the connection plates to the bottom flange, only in this region of high stress range, to raise the nominal fatigue resistance to that for a Category B detail. Bolting these particular connection plates to the tension flange will raise the nominal fatigue resistance to 16.00 ksi in this case, and may allow the designer to use a smaller bottom-flange plate in this region. However, the designer is cautioned that a Category C' detail still exists at the termination of the connection-plate weld to the web just above the bottom flange. Also, the bolted connections must be detailed properly to ensure a positive attachment to the flange that offers rotational fixity to prevent distortion-induced fatigue caused by out-of-plane deformations (*AASHTO LRFD* Article 6.6.1.3). NHI (1990) contains further discussion on these connections and provides examples of bolted connection details that provide the desired positive attachment. In most instances, bolting the connection plates to the flange is more expensive than welding the connection plates to the flange; thus, it is prudent for the Engineer to consult a fabricator to determine the most overall cost-effective solution.

Had the stress range exceeded the nominal fatigue resistance in this case, an efficient alternative to investigate might be to move the cross-frame connection plate a few feet toward the abutment in order to reduce the range of stress.

EXAMPLE

Check fatigue of the base metal at the stud shear-connector weld to the top flange at the section located 100.0 feet from the abutment in the 140-ft end span of the three-span continuous I-girder bridge from the preceding example. The cross-section of the composite girder at this section is again shown in Figure 6.4.2.3.2.3-1. Other design conditions are the same as in the preceding example.

The unfactored permanent load moments at this section are as follows:

M_{DC1} = +74 kip-ft
M_{DC2} = +27 kip-ft
M_{DW} = +28 kip-ft

The unfactored moments at this section due to the fatigue load specified in *AASHTO LRFD* Article 3.6.1.4 (i.e. a 72-kip truck with a constant rear-axle spacing of 30 ft) placed in a single lane, including the 15 percent dynamic load allowance, are as follows:

$+M_{LL+IM}$ = +912 kip-ft
$-M_{LL+IM}$ = -688 kip-ft

Since the unfactored permanent loads produce compression at the top flange, determine if the top flange is subject to a net applied tensile stress according to the provisions of *AASHTO LRFD* Article 6.6.1.2.1. The total unfactored permanent-load compressive stress in the top flange at this location (neglecting the future wearing surface) is computed as:

$$f_{DC_1} = \frac{74(12)}{1{,}581} = -0.56 \text{ ksi}$$

$$f_{DC_2} = \frac{27(12)}{5{,}375} = \underline{-0.06 \text{ ksi}}$$

$$-0.62 \text{ ksi}$$

The maximum tensile stress at the top-flange weld at this location due to the negative moment caused by the Fatigue I load combination is:

$$f_{LL+IM} = \frac{1.5|-688|(12)}{16{,}287} = 0.76 \text{ ksi}$$

$$|-0.62| \text{ ksi} < 0.76 \text{ ksi}$$

Therefore, fatigue of the base metal at the stud shear-connector weld to the top flange at this location must be checked.

Determine the fatigue detail category from *AASHTO LRFD* Table 6.6.1.2.3-1. Under Section 8, Miscellaneous, of the table, the fatigue detail category for base metal adjacent to welded stud-type shear connectors is Detail Category C.

From *AASHTO LRFD* Table 6.6.1.2.3-2 (Table 6.5.5.2.2.1.4-2), the 75-year $(ADTT)_{SL}$ equivalent to infinite fatigue life for a Category C detail for *n* equal to 1.0 is 1,290 trucks per day < 1,600 trucks per day. Therefore:

$$(\Delta F)_n = (\Delta F)_{TH}$$

For a Category C detail, $(\Delta F)_{TH}$ = 10.0 ksi (*AASHTO LRFD* Table 6.6.1.2.5-3 – Table 6.5.5.2.2.1.1-1). Therefore:

$$(\Delta F)_n = 10.00 \text{ ksi}$$

$$\gamma(\Delta f) \le (\Delta F)_n$$

The stress range $\gamma(\Delta f)$ at the stud shear connector weld to the top flange at this location due to the Fatigue I load combination is computed using the properties of the short-term composite section as:

$$\gamma(\Delta f) = \frac{1.5(912)(12)}{16{,}287} + \frac{1.5|-688|(12)}{16{,}287} = 1.77 \text{ ksi}$$

$$1.77 \text{ ksi} < 10.00 \text{ ksi} \qquad \text{ok}$$

6.5.5.2.2.2 Shear

AASHTO LRFD Article 6.10.5.3 contains a special fatigue requirement for webs of flexural members. The check is intended to prevent shear buckling of the web under the heaviest truck expected to cross the bridge over its 75-year fatigue design life. In doing so, significant elastic flexing of the web under repeated live loading is not

expected to occur. **Curved webs are assumed to be initially true.** If post-buckling tension-field action were permitted under this load condition, the principal tensile stress range acting along the buckle would result in significant out-of-plane flexing of the web under repeated live loads. By limiting the factored shear under this load condition to the shear buckling resistance, the member is assumed to be able to sustain an infinite number of smaller loadings without fatigue cracking due to this effect.

Interior panels of webs with transverse stiffeners, with or without longitudinal stiffeners, must satisfy the following requirement:

$$V_u \le V_{cr} \qquad \text{Equation 6.5.5.2.2.2-1}$$

AASHTO LRFD Equation 6.10.5.3-1

where:

V_u = shear in the web at the section under consideration due to the unfactored permanent load plus the Fatigue I load combination – i.e. $V_{DC} + V_{DW} + 1.5V_{FAT}$ (kips)

V_{cr} = shear-yield or shear-buckling resistance determined from *AASHTO LRFD* Equation 6.10.9.3.3-1 (kips)

The nominal shear resistance for this check is limited to the shear-yielding or shear-buckling resistance. The use of tension-field action is not permitted. The calculation of V_{cr} is discussed further in Section 6.5.7.2. The live load shear due to the Fatigue I load combination for this check is intended to be that of the heaviest truck expected to cross the bridge in 75 years.

This requirement need not be checked for unstiffened webs or end panels of stiffened webs because the shear in these cases is already limited to V_{cr} at the strength limit state. Thus, Equation 6.5.5.2.2.2-1 would not control.

The provisions of *AASHTO LRFD* Article 6.11.9, as applicable, are to be applied in checking Equation 6.5.5.2.2.2-1 for box sections. Inclined webs must be designed for the component of the vertical shear in the plane of the web, V_{ui}, taken equal to V_u divided by $\cos\theta$, where θ is the angle of inclination of the web plate with respect to the vertical (Equation 6.5.7.1.2-1). Also, in computing the shear-yielding or shear-buckling resistance, V_{cr}, for the case of inclined webs, the web depth, D, must be taken as the depth of the web measured along the slope or $D/\cos\theta$. V_u is to be taken as the sum of the flexural and St. Venant torsional shears due to the unfactored permanent load plus the Fatigue I load combination in checking this requirement for all box sections for which the effects of St. Venant torsion must be considered (including all box sections in curved and/or skewed bridges). Proper determination of this value considers coincident flexure and torsion. Conservatively, critical torsion and critical flexural shears can be added. In these cases, the dead and live load

shears in one web are greater than in the other web at the same cross-section since the torsional shear is of opposite sign in the two webs. For practical reasons, however, both webs are usually detailed for the critical shear. Shears in the web due to warping torsion and cross-section distortion may be ignored in all cases in making this check.

An explicit check on web bend buckling is not specified at the fatigue limit state under this load condition, as the web bend-buckling check at the service limit state (Sections 6.5.4.3.2.2 and 6.5.4.3.3.2) will always control. This includes composite sections in positive flexure with longitudinal web stiffeners. The smaller value of F_{crw} resulting from the larger value of D_c at the fatigue limit state (i.e. larger than the value at the service limit state) in this case tends to be compensated for by the lower web compressive stress due to the load condition specified for the fatigue limit state shear check.

EXAMPLE

Check the special fatigue requirement for webs specified in *AASHTO LRFD* Article 6.10.5.3 at the first interior-pier section of the three-span continuous I-girder bridge from the preceding two examples. The cross-section of the composite girder at this section is shown in Figure 6.4.2.3.3.3-1. The girder is hybrid at this section with the flanges having a yield strength of 70 ksi and the web having a yield strength of 50 ksi.

The transverse-stiffener spacing adjacent in the panel adjacent to the interior-pier section is d_o = 10.0 feet. The unfactored permanent load shears at the interior-pier section are as follows:

V_{DC1} = -159 kips
V_{DC2} = -23 kips
V_{DW} = -22 kips

The unfactored shear at this section due to the fatigue load specified in *AASHTO LRFD* Article 3.6.1.4 (i.e. a 72-kip truck with a constant rear-axle spacing of 30 ft) placed in a single lane, including the 15 percent dynamic load allowance, is as follows:

V_{LL+IM} = -56 kips

In this check, interior panels of webs with transverse stiffeners must satisfy the following requirement to control elastic flexing of the web under repeated live loading (Equation 6.5.5.2.2.2-1):

$$V_u \le V_{cr}$$

V_u is to be taken as the shear due to the unfactored permanent load plus the shear due to the Fatigue I load combination, which is assumed to represent the heaviest truck expected to the cross the bridge over its 75-year fatigue design life. Therefore:

$$V_u = -159 + -23 + -22 + 1.5(-56) = -288 \text{ kips}$$

The shear buckling resistance, V_{cr}, of the 10-foot web panel is determined as follows (Equation 6.5.7.2-8):

$$V_n = V_{cr} = CV_p$$

C is the ratio of the shear buckling resistance to the shear yield strength determined from *AASHTO LRFD* Equation 6.10.9.3.2-4, 6.10.9.3.2-5 or 6.10.9.3.2-6, as applicable. First, compute the shear buckling coefficient, *k* (Equation 6.5.7.2-4):

$$k = 5 + \frac{5}{\left(\frac{d_o}{D}\right)^2}$$

$$k = 5 + \frac{5}{\left(\frac{10(12)}{69.0}\right)^2} = 6.65$$

Since, $\quad 1.40\sqrt{\frac{Ek}{F_{yw}}} = 1.40\sqrt{\frac{29{,}000(6.65)}{50}} = 86.9 < \frac{D}{t_w} = \frac{69.0}{0.5625} = 122.7$

$$C = \frac{1.57}{\left(\frac{D}{t_w}\right)^2}\left(\frac{Ek}{F_{yw}}\right) \text{ (Equation 6.5.7.2-5)}$$

$$C = \frac{1.57}{(122.7)^2}\left(\frac{29{,}000(6.65)}{50}\right) = 0.402$$

V_p is the plastic shear force determined as follows (Equation 6.5.7.1-2):

$$V_p = 0.58F_{yw}Dt_w$$

$$V_p = 0.58(50)(69.0)(0.5625) = 1{,}126 \text{ kips}$$

Therefore, $V_{cr} = 0.402(1{,}126) = 453 \text{ kips} > V_u = |-288| \text{ kips}$ ok

6.5.5.2.2.3 Cross-Section Distortion Stresses (Box Sections)

6.5.5.2.2.3.1 General

As specified in *AASHTO LRFD* Article 6.11.5 and discussed previously in Section 6.4.8.3.4, both longitudinal warping stresses and transverse bending stresses due to cross-section distortion must be considered at the fatigue limit state for all box sections that do not have fully effective box flanges, and/or for all the following sections:

- Single box sections in straight or horizontally curved bridges;
- Multiple box sections in straight bridges not satisfying the restrictions specified in *AASHTO LRFD* Article 6.11.2.3; or
- Multiple box section in horizontally curved bridges.

Skewed box-girder bridges are comprehended in the above list. As discussed in Section 6.4.9.5.2, skewed supports create significant torque in box sections regardless of whether the bridge is straight or curved.

The cross-section becomes distorted giving rise to secondary bending stresses when box sections are subject to torsion. Horizontal curvature produces torque when the curvature causes load to be applied eccentric to the shear center at the supports. The torque decreases at increasing distances from the supports into simple spans. The phenomenon is less evident in continuous spans where the interaction between spans is complex. Torque in straight girders is produced by applying load eccentric to the shear center. If loads are applied through the shear center; for example, applied equally to the top and bottom flanges along the entire length of a symmetric straight box, there is no torque created. Skewed supports create such an unsymmetrical loading condition however. If there are two bearings, the reactions in the two bearings are significantly different, creating torque in the box. If there is one bearing, torque is created by diaphragms connecting adjacent boxes. It is easily seen that loading the opposite side of a box produces reversal of these secondary distortional bending stresses. Therefore, in the cases listed above, distortional stresses must be considered when checking fatigue. Although the stresses might be thought of as “distortion-induced”, they are calculable and are treated herein as load-induced. Transverse bending stresses are typically most

critical for cases where the St. Venant torques are significant, e.g. boxes resting on skewed supports, single box sections and sharply curved boxes.

AASHTO LRFD Article 6.11.5 requires that the stress range due to longitudinal warping be considered in checking the fatigue resistance of the base metal at all details on the box section according to Equation 6.5.5.2.2.1.5-1 for the above cases; the longitudinal warping stresses are generally assumed to be additive to the longitudinal vertical bending stresses. This assumption is conservative since the critical longitudinal warping stresses are usually produced by eccentric live loads, whereas the critical vertical bending stresses are produced by more centrally located (i.e. different) live load positions

AASHTO LRFD Article 6.11.5 also requires that the transverse bending stress range be investigated in the base metal adjacent to flange-to-web fillet welds and adjacent to the termination of fillet welds connecting transverse elements to webs and box flanges for the above cases. This investigation is separate from the fatigue check for longitudinal stress ranges in the box.

The condition at welded transverse elements is usually the critical case for transverse bending. A stress concentration occurs at the termination of these welds as a result of the transverse bending. The *AASHTO LRFD* Specification does not specifically address the fatigue resistance of this detail when subject to transverse bending. *AASHTO LRFD* Article C6.11.5 indicates that the fatigue resistance of the base metal adjacent to the welds for this case may be perhaps as low as fatigue Detail Category E. A means of reducing the criticalness of these details is to attach all transverse web stiffeners to the top and bottom flanges. Attachment of the transverse stiffeners to the flanges reduces the sharp through-thickness bending within the unstiffened portions of the web adjacent to the termination of the stiffener-to-web welds, which is typically the most critical region. *AASHTO LRFD* Article 6.6.1.3.1 already requires attachment of cross-frame connection plates to the top and bottom flanges. This provision was found necessary in order to transfer load from the cross-frames directly to the flanges rather than through the web via transverse bending. The same logic applies to all transverse stiffener termini when transverse bending exists in the web. The same check must then be made in the box flange at the terminus of the stiffener-to-flange fillet weld.

AASHTO LRFD Article 6.11.5 further specifies that at the termination of fillet welds connecting cross-frame connection plates to box flanges subjected to calculated torque (i.e. in the above cases only), the need for a transverse member across the bottom of the tub (and/or across the top of a closed box) as part of the internal cross-frames to resist the transverse bending stress range in the box flange must be considered. These members would typically be provided adjacent to the box flanges. When necessary, these members, which are part of the internal cross-bracing, can significantly reduce the transverse bending stress range and help

ensure integrity of the cross-section. Closer spacing of the cross-frames also leads to lower transverse bending stresses. To better control the distortion of box flanges in such cases, transverse cross-frame members next to box flanges, that are required to control cross-section distortion stresses, must be attached to the flange. If a longitudinal flange stiffener(s) is present, the transverse members must be bolted to the longitudinal stiffener(s) and not welded to the box flange. This detail avoids the use of more discontinuous fillet welds. Where the transverse bracing members are welded directly to the box flange, the stress range due to transverse bending should also be considered in checking the fatigue resistance of the base metal adjacent to the termination of these welds. Where the transverse bracing members are connected to longitudinal flange stiffeners, the box flange may be considered stiffened (Section 6.5.5.2.2.3.2) when computing the transverse bending stresses (*AASHTO LRFD* Article C6.11.5). The moment of inertia of these transverse bracing members is not to be less than the moment of inertia of the largest transverse connection plate for the internal cross-frame under consideration taken about the edge in contact with the web. The moment of inertia of the transverse cross-frame member should be taken about the edge in contact with the flange when it is attached to the flange, or about its neutral axis when bolted to the longitudinal stiffener(s). The transverse connection plates must still be attached to both flanges as required in *AASHTO LRFD* Article 6.6.1.3.1.

AASHTO LRFD Article 6.11.1.3 requires that the total throat thickness of the flange-to-web welds be not less than the smaller of the web or flange thickness when fewer than two intermediate internal cross-frames are provided in a span. The reason for this is to ensure that the smaller section is fully developed for transverse bending. This article permits flange-to-web fillet welds on both sides of the web when two or more intermediate internal cross-frames are provided in each span. The welds must meet the minimum and maximum size requirements specified in *AASHTO LRFD* Article 6.13.3.4.

Consideration might be given to ignoring the distortional stresses in certain cases if it can be demonstrated that the torques are of comparable magnitude to the torques for cases where research has shown that these stresses are small enough to be neglected (Johnston and Mattock, 1967); e.g. a straight bridge of similar proportion satisfying the restrictions specified in *AASTHO LRFD* Article 6.11.2.3; or if the torques are deemed small enough in the judgment of the Owner and the Design Engineer. In such cases, however, it is strongly recommended that all web stiffeners be attached to both flanges in order to enhance fatigue performance.

6.5.5.2.2.3.2 BEF Analogy

The beam on elastic foundation (BEF) analogy for determining distortional stresses in box girders is based on the work reported in Wright and Abdel-Samad (1968) that

was sponsored by the American Iron and Steel Institute. The approach is described in detail in Heins and Hall (1981), which forms the basis for the following discussion.

Consider the deflection δ_1 due to the uniform torsional load with no cross-frames/diaphragms present, as shown in Figure 6.5.5.2.2.3.2-1.

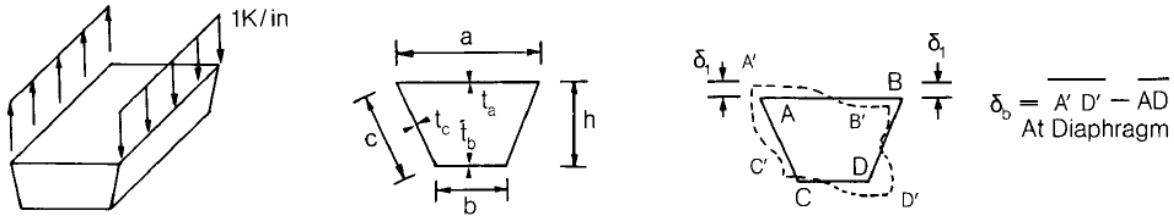

Figure 6.5.5.2.2.3.2-1 Box Under Uniform Torsional Loading

δ_1 is the reciprocal of the torsional stiffness of the box and is analogous to the reciprocal of the foundation modulus in the BEF problem. δ_1 (in units of in^2/kip) is computed as follows:

$$\delta_1 = \frac{ab}{24(a+b)}\left\{\frac{c}{D_c}\left[\frac{2ab}{a+b} - v(2a+b)\right] + \frac{a^2}{D_a}\left[\frac{b}{a+b} - v\right]\right\} \qquad \text{Equation 6.5.5.2.2.3.2-1}$$

where:

a, *b*, *c* = dimensions of box section as shown in Figure 6.5.5.2.2.3.2-1 (in.)

v = compatibility shear at the center of the bottom flange for unit loads applied at the top corners of a box section of unit length (Figure 6.5.5.2.2.3.2-1)

$$= \frac{\frac{1}{D_c}\left[(2a+b)abc\right] + \frac{1}{D_a}\left[ba^3\right]}{(a+b)\left\{\frac{a^3}{D_a} + \frac{2c\left(a^2+ab+b^2\right)}{D_c} + \frac{b^3}{D_b}\right\}} \qquad \text{Equation 6.5.5.2.2.3.2-2}$$

D_a, D_b, D_c = transverse flexural rigidities of an unstiffened plate (kip-$in.^2$/in.)

$$D_a = \frac{Et_a^3}{12(1-\mu^2)} \qquad \text{Equation 6.5.5.2.2.3.2-3}$$

$$D_b = \frac{Et_b^3}{12(1-\mu^2)} \qquad \text{Equation 6.5.5.2.2.3.2-4}$$

$$D_c = \frac{Et_c^3}{12(1-\mu^2)} \qquad \text{Equation 6.5.5.2.2.3.2-5}$$

t_a, t_b, t_c = thickness of top flange, bottom flange and web, respectively

(Figure 6.5.5.2.2.3.2-1) (in.)

μ = Poisson's ratio (= 0.2 for concrete – see *AASHTO LRFD* Article 5.4.2.5; 0.3 for steel)

The center of the bottom flange was chosen as the location for computing the compatibility shear because the transverse bending moment and thrust are zero at this point (Wright and Abdel-Samad, 1968).

When transverse stiffeners are present on either the flanges or the webs, they should be considered in calculating the transverse flexural rigidities for resisting transverse bending. The rigidity, *D*, of the stiffened plate is computed as:

$$D = \frac{EI_s}{d} \qquad \text{Equation 6.5.5.2.2.3.2-6}$$

where:

d = stiffener spacing (in.)

I_s = moment of inertia of the stiffened plate for transverse bending (based on the effective width of the plate defined by Equation 6.5.5.2.2.3.2-7 below) including the transverse stiffener (in.^{4})

The stiffness of the transverse stiffener is assumed distributed evenly along the stiffened plate.

The effective width of plate, d_o, acting with the stiffener can be determined from the following semi-empirical relationship (Wright and Abdel-Samad, 1968) as:

$$d_o = \frac{d \tanh\left(5.6\frac{d}{h}\right)}{\frac{5.6d}{h}\left(1-\mu^2\right)} \qquad \text{Equation 6.5.5.2.2.3.2-7}$$

where:

h = length of web or box-flange element, as applicable (i.e. dimension "b" or "c" as shown in Figure 6.5.5.2.2.3.2-1 (in.)

The BEF stiffness parameter β (in units of in.$^{-1}$) is a measure of the torsional stiffness of the beam and is analogous to the beam-foundation parameter in the BEF problem. β is calculated as follows:

$$\beta \approx \left(\frac{1}{EI\delta_1}\right)^{\frac{1}{4}} \qquad \text{Equation 6.5.5.2.2.3.2-8}$$

where:

I = moment of inertia of the box section (in.^{4})

The cross-frames/diaphragms in the box girder restrict the box distortion and are analogous to the supports in the BEF. The cross-frames/diaphragms are incorporated in the solution by the dimensionless ratio, q, of the cross-frame/diaphragm stiffness to the box stiffness per unit length, which is defined as follows:

$$q = \left[\frac{E_b A_b}{L_b \ell \delta_1}\right]\delta_b^2 \qquad \text{Equation 6.5.5.2.2.3.2-9}$$

where:

A_b = cross-sectional area of one cross-frame/diaphragm bracing member (in.^{2})

E_b = Young's modulus of the cross-frame/diaphragm material (ksi)

ℓ = cross-frame/diaphragm spacing (in.)

L_b = length of the cross-frame/diaphragm bracing member (in.)

δ_b = deformation of the bracing member due to the applied torque (Figure 6.5.5.2.2.3.2-1) (in.2/kip)

$$= \frac{2(1+a/b)}{\sqrt{1+\left[\frac{a+b}{2h}\right]^2}}\delta_1 \qquad \text{Equation 6.5.5.2.2.3.2-10}$$

h = vertical web depth of the box section (in.)

Equation 6.5.5.2.2.3.2-9 assumes that the cross-bracing member is effective in both compression and tension. If the bracing slenderness is large and the member is only considered effective in tension, then A_b in Equation 6.5.5.2.2.3.2-9 should be taken as one-half the area of one brace.

The distortional stresses in the box section can be determined analogously by solving the BEF problem. The moment in the BEF is analogous to the distortional longitudinal warping stress, σ_{dw}. The deflection of the BEF is analogous to the distortional transverse bending stress, σ_t. The reactions in the BEF are analogous to the forces in the cross-bracing, F_b. Solutions to the BEF problem for these three components are presented in graphical form in Figure 6.5.5.2.2.3.2-2 through Figure 6.5.5.2.2.3.2-10 below. These figures each give a BEF factor (or "C" value), which is then used in the appropriate corresponding equation given below (i.e. Equation 6.5.5.2.2.3.2-11, Equation 6.5.5.2.2.3.2-12, or Equation 6.5.5.2.2.3.2-15) to calculate the distortion-related stresses (and stress ranges) or forces (and force ranges). The graphs give relationships for the distortional stresses at either the cross-bracing or at midpanel between the cross-braces, and also for the cross-bracing force, under

either a uniform torque per unit length *m*, or a concentrated torque *T* (or a range of *m* or *T*). Relationships are given for the concentrated torque *T* (or range of torque *T*) applied at either midpanel or at the cross-bracing. Given the box geometry, the value of β from Equation 6.5.5.2.2.3.2-8, the loading, the cross-bracing stiffness ratio, *q*, from Equation 6.5.5.2.2.3.2-9 and the spacing of the cross-bracing, ℓ, the appropriate value of "C" can be obtained from the graphs for use in the following equations. Since only two loading positions are considered in the graphs for *T*, it may be necessary in some cases to interpolate between the appropriate graphs for each position. The principle of superposition applies for more than one torque.

The distortional longitudinal warping stress, σ_{dw}, at any point on the cross-section is obtained as follows:

$$\sigma_{dw} = \frac{C_w y}{I\beta a}(m\ell \text{ or } T) \qquad \text{Equation 6.5.5.2.2.3.2-11}$$

where:

C_w = BEF factor for distortional longitudinal warping stress obtained from Figure 6.5.5.2.2.3.2-2, Figure 6.5.5.2.2.3.2-3, or Figure 6.5.5.2.2.3.2-4, as applicable

y = distance along the transverse vertical axis of the box from the neutral axis to the point under consideration (in.)

All other terms are as defined previously. The range of longitudinal warping stress is obtained by substituting the range of *m* or *T*, as applicable, in Equation 6.5.5.2.2.3.2-11.

The distortional transverse bending stresses, σ_t, in the web or box flange at the top or bottom corners of the box section are obtained as follows:

$$\sigma_t = C_t F_d \beta \frac{1}{2a}(m\ell \text{ or } T) \qquad \text{Equation 6.5.5.2.2.3.2-12}$$

where:

C_t = BEF factor for distortional transverse bending stress obtained from Figure 6.5.5.2.2.3.2-5, Figure 6.5.5.2.2.3.2-6, Figure 6.5.5.2.2.3.2-7, or Figure 6.5.5.2.2.3.2-8, as applicable

F_d = transverse bending stress in the web or box flange, as applicable, due to the applied torque (in.$^{-1}$)

= $\frac{bv}{2S}$ for the bottom corner of the box Equation 6.5.5.2.2.3.2-13

= $\frac{a}{2S}\left(\frac{b}{a+b} - v\right)$ for the top corner of the box Equation 6.5.5.2.2.3.2-14

S = section modulus per unit length of the web or box flange, as applicable, for transverse bending (in.^{3}/in.). For a stiffened plate, the section modulus per unit length should be based on the effective width of the plate defined by Equation 6.5.5.2.2.3.2-7 and include the transverse stiffener.

All other terms are as defined previously. The critical transverse bending stress may be in either the web or the adjacent box flange(s). The range of transverse bending stress is obtained by substituting the range of m or T, as applicable, in Equation 6.5.5.2.2.3.2-12.

The axial force in the cross-bracing due to distortional forces applied to the box, F_b, is obtained as follows:

$$F_b = C_b \left[\frac{\sqrt{1+\left(\frac{a+b}{2h}\right)^2}}{2\left(1+\frac{a}{b}\right)} \right] \frac{(m\ell \text{ or } T)}{a} \qquad \text{Equation 6.5.5.2.2.3.2-15}$$

where:

C_b = BEF factor distortional cross-bracing force determined from Figure 6.5.5.2.2.3.2-9, or Figure 6.5.5.2.2.3.2-10, as applicable

h = vertical web depth of the box section (in.)

Again, all other terms are as defined previously. The range of axial force is obtained by substituting the range of m or T, as applicable, in Equation 6.5.5.2.2.3.2-15. Note that Figure 6.5.5.2.2.3.2-11 shows the effect of β on the influence line for cross-bracing forces when the cross-bracing is rigid.

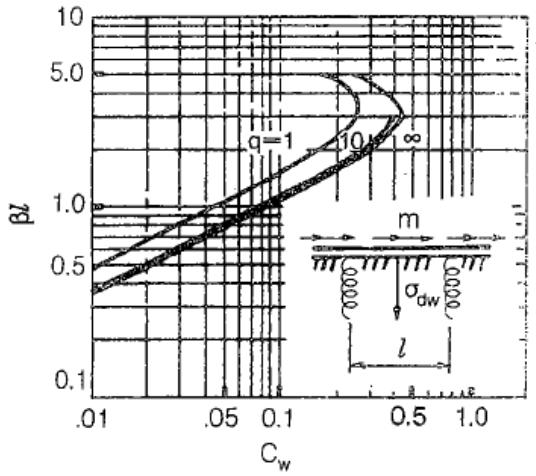

Figure 6.5.5.2.2.3.2-2 BEF Factor, C_w, for Distortional Longitudinal Warping Stress at Midpanel due to a Uniform Torque, *m*

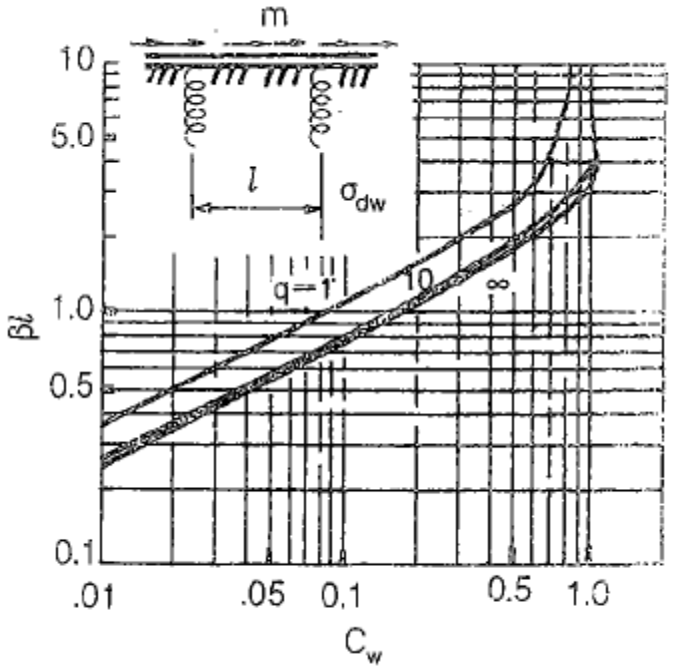

Figure 6.5.5.2.2.3.2-3 BEF Factor, C_w, for Distortional Longitudinal Warping Stress at Cross-Bracing due to a Uniform Torque, *m*

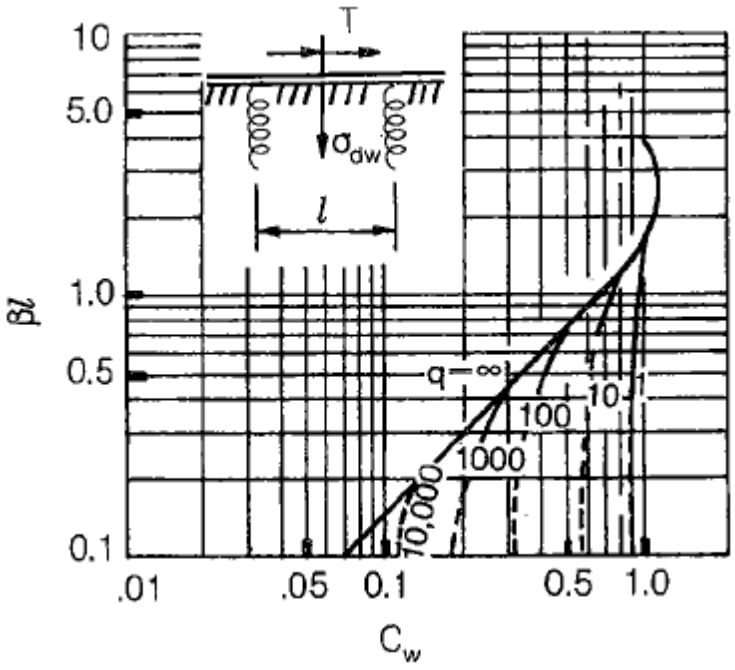

Figure 6.5.5.2.2.3.2-4 BEF Factor, C_w, for Distortional Longitudinal Warping Stress at Midpanel due to a Concentrated Torque, *T*, at Midpanel

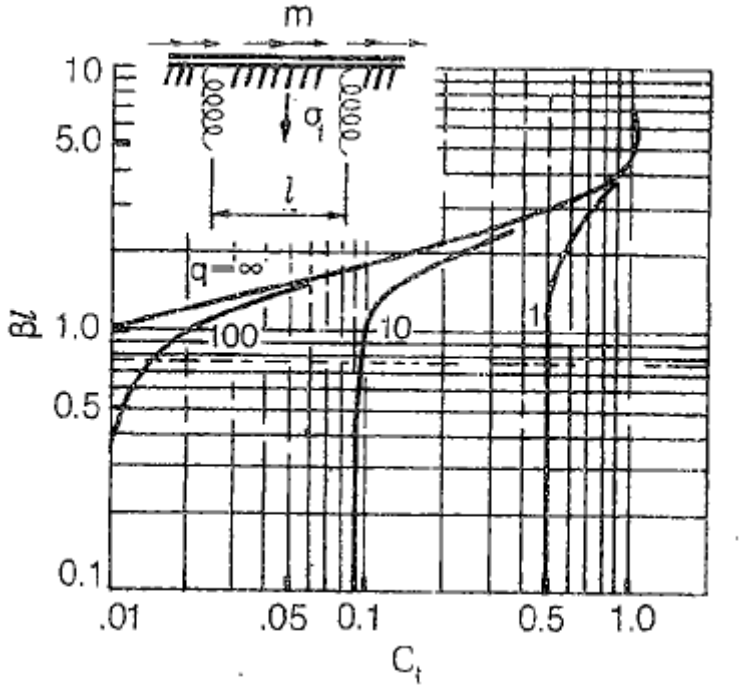

Figure 6.5.5.2.2.3.2-5 BEF Factor, C_t, for Distortional Transverse Bending Stress at Midpanel due to a Uniform Torque, *m*

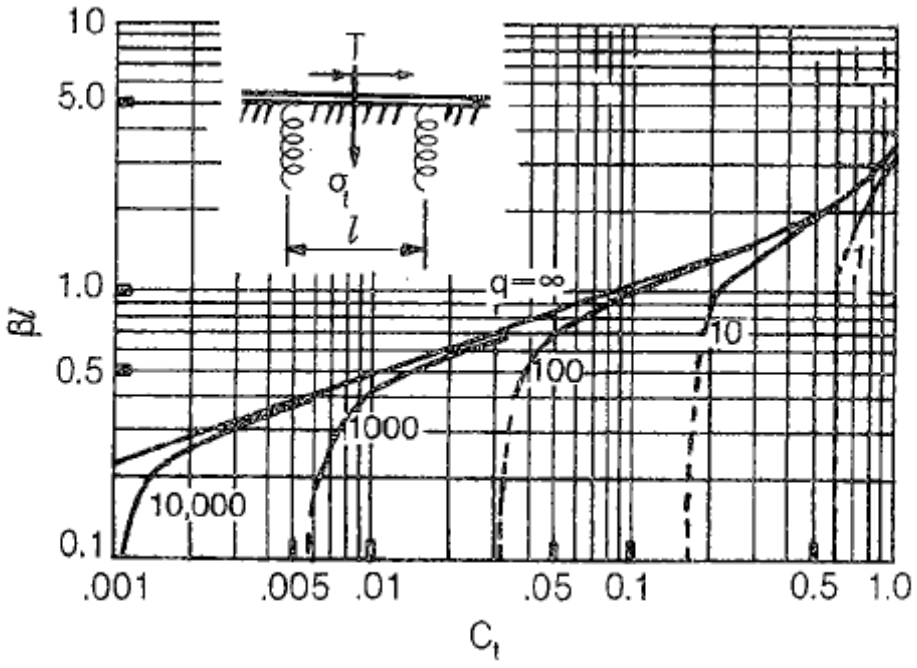

Figure 6.5.5.2.2.3.2-6 BEF Factor, C_t, for Distortional Transverse Bending Stress at Midpanel due to a Concentrated Torque, T, at Midpanel

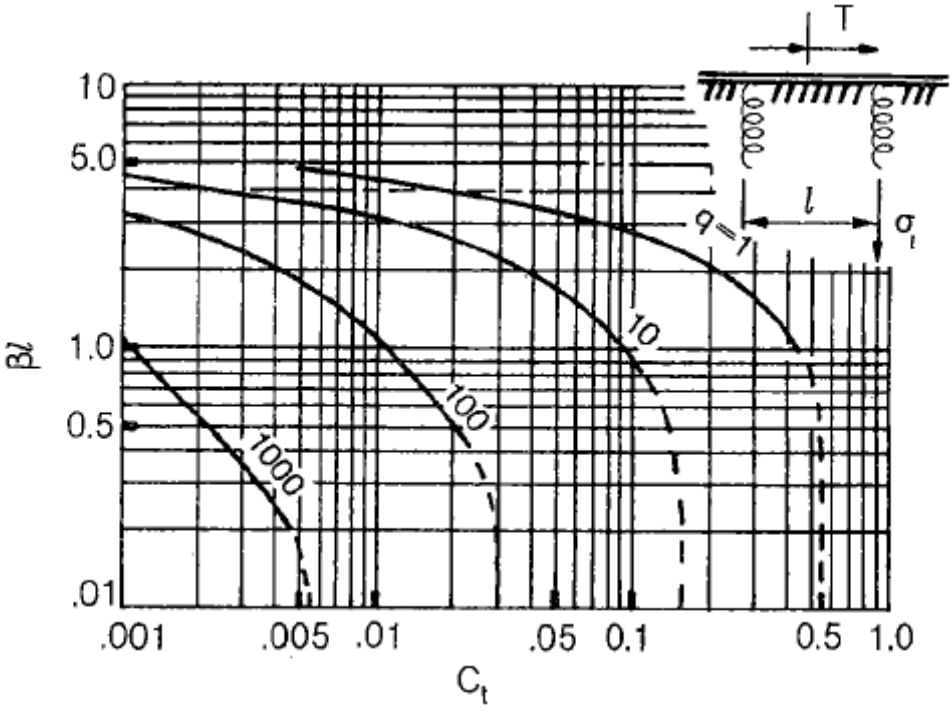

Figure 6.5.5.2.2.3.2-7 BEF Factor, C_t, for Distortional Transverse Bending Stress at Cross-Bracing due to a Concentrated Torque, T, at Midpanel

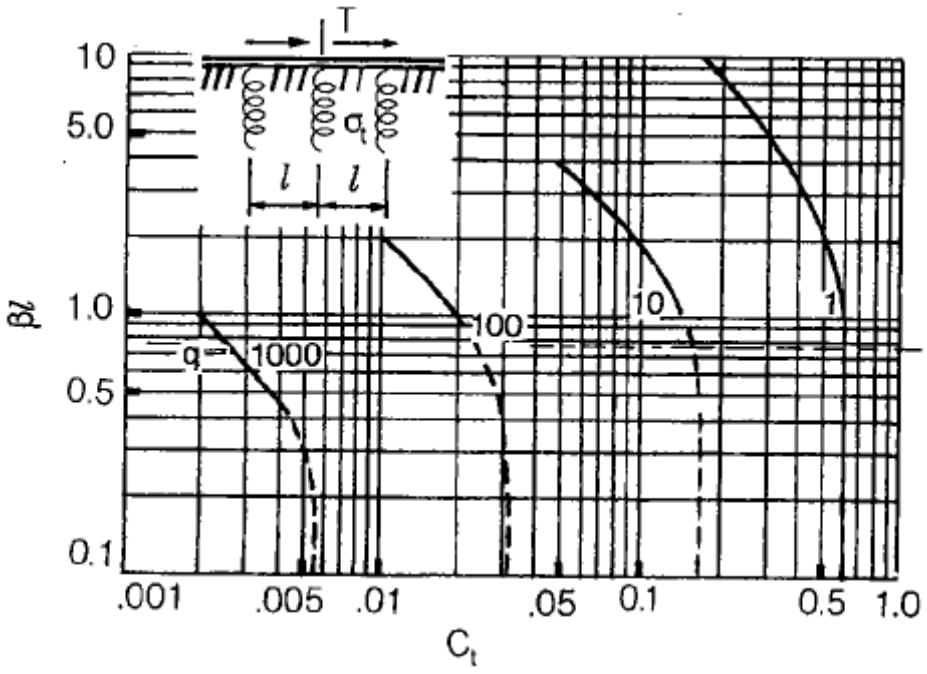

Figure 6.5.5.2.2.3.2-8 BEF Factor, C_t, for Distortional Transverse Bending Stress at Cross-Bracing due to a Concentrated Torque, *T*, at Cross-Bracing

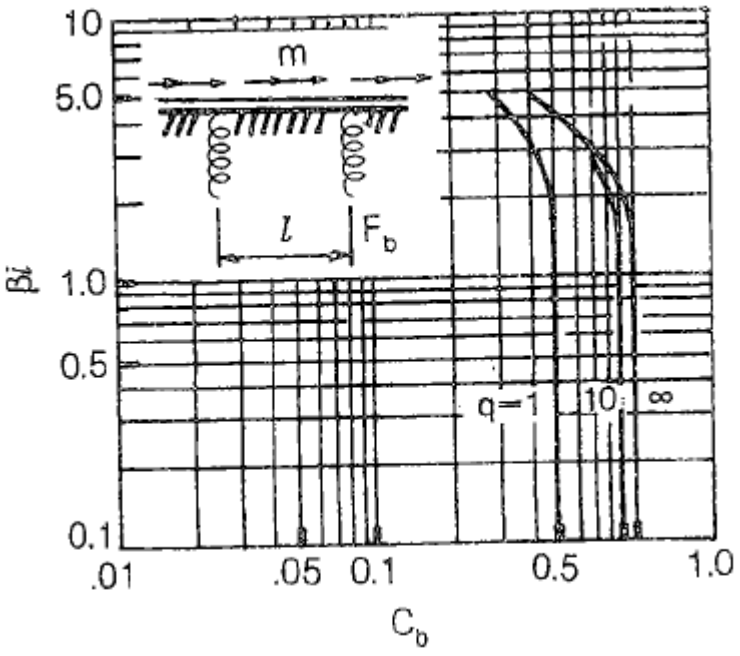

Figure 6.5.5.2.2.3.2-9 BEF Factor, C_b, for Distortional Axial Cross-Bracing Force due to a Uniform Torque, *m*

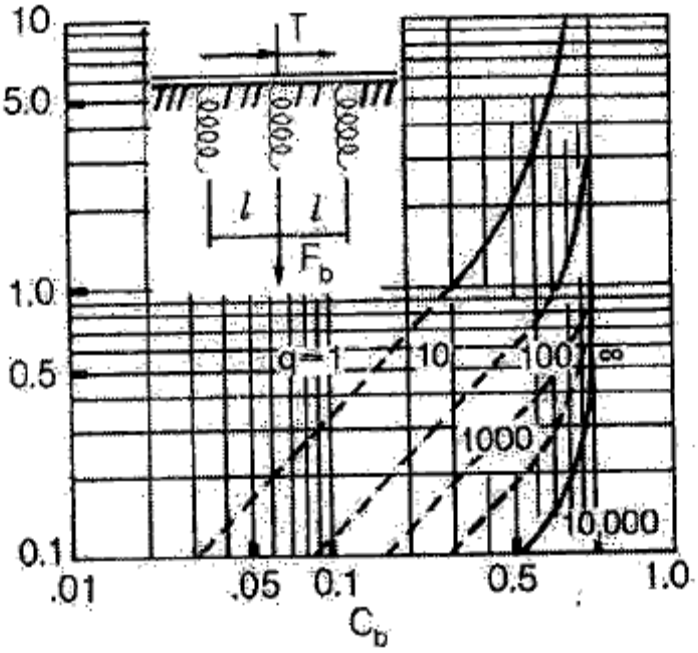

Figure 6.5.5.2.2.3.2-10 BEF Factor, C_b, for Distortional Axial Cross-Bracing Force due to a Concentrated Torque, T, at Cross-Bracing

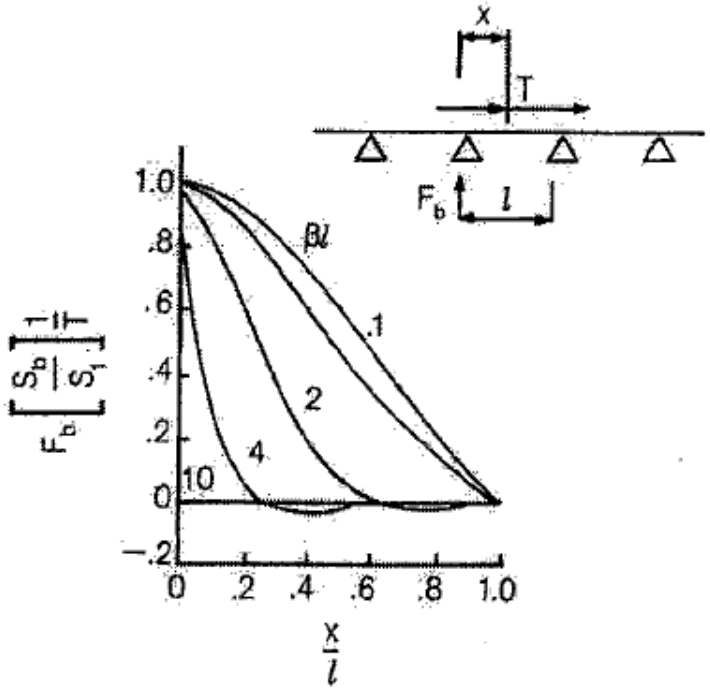

Figure 6.5.5.2.2.3.2-11 Influence Line for Distortional Axial Cross-Bracing Force for a Rigid Cross-Brace due to a Concentrated Torque, T

EXAMPLE

Check the distortional transverse bending stress range for fatigue at the termination of the fillet welds connecting the transverse stiffeners to the web of the composite tub girder cross-section shown in Figure 6.5.5.2.2.3.2-12, which is part of a straight multiple tub-girder bridge resting on skewed supports.

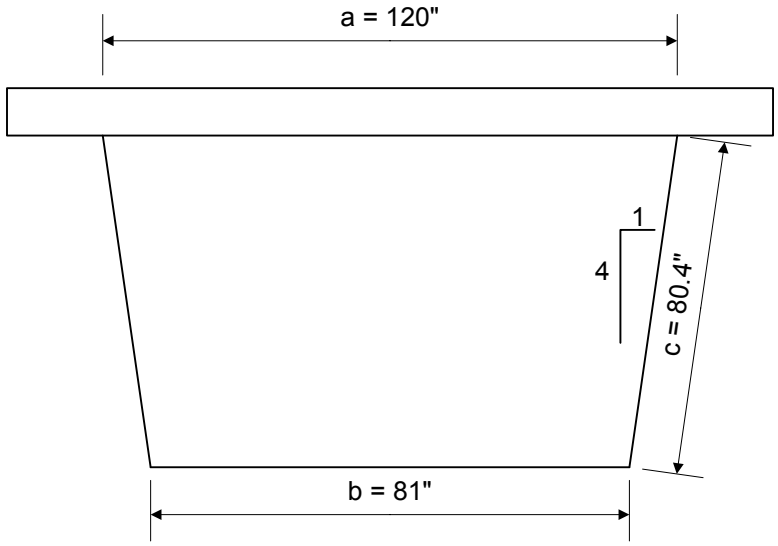

Figure 6.5.5.2.2.3.2-12 Example Box-Girder Cross-Section

Since the bridge is resting on skewed supports, the restrictions specified in *AASHTO LRFD* Article 6.11.2.3 are not satisfied and distortional stresses must be considered for fatigue. It is assumed that the distortional longitudinal warping stress range has been considered separately and is negligible for this example.

The thicknesses of the cross-section components are as follows:

Slab (structural):	t_a	=	9.5 in.
Web	t_c	=	0.5625 in.
Bottom flange	t_b	=	1.5 in.

The vertical web depth is 78.0 inches. The moment of inertia of the composite tub cross-section is I = 836,080 in.^{4} The transverse stiffener plates are ½" x 5.5" bars on one side of the web. The transverse stiffener spacing, d, adjacent to the section is 62.0 in. The cross-frame spacing, ℓ, adjacent to the section is 18.0 feet = 216.0 in. The bottom box flange is unstiffened both longitudinally and transversely.

From the results of a refined analysis of the superstructure (which is recommended for tub girders resting on skewed supports), the unfactored torques at this section

due to the fatigue load specified in *AASHTO LRFD* Article 3.6.1.4 (i.e. a 72-kip truck with a constant rear-axle spacing of 30 feet) placed in a single lane, including the 15 percent dynamic load allowance, are as follows:

$+T_{LL+IM}$ = +278 kip-ft
$-T_{LL+IM}$ = -236 kip-ft

Therefore, the total range of torque is $278 + |-236| = 514 \text{ kip} - \text{ft}$. *AASHTO LRFD* Article C6.6.1.2.1 recommends that the critical range of torque be determined in this case with the fatigue truck positioned as specified in *AASHTO LRFD* Article 3.6.1.4.3a, and with the truck confined to one critical transverse position per each longitudinal position throughout the length of the bridge in the analysis.

A stress concentration occurs at the termination of the transverse stiffener welds to the top flange as a result of the transverse bending. The fatigue resistance of this detail when subject to transverse bending is not currently quantified. As recommended in *AASHTO LRFD* Article C6.11.5, assume fatigue Detail Category E for computing the nominal fatigue resistance. Assume the number of stress cycles per truck passage in this region *n* is equal to 1.0. From separate calculations, the single-lane average daily truck traffic $(ADTT)_{SL}$ is computed to be 1,600 trucks/day (Section 6.5.5.2.2.1.4). According to *AASHTO LRFD* Table 6.6.1.2.3-2 (Table 6.5.5.2.2.1.4-2), since the $(ADTT)_{SL}$ does not exceed the 75-year $(ADTT)_{SL}$ equivalent to infinite life of 3,530 trucks/day for a Category E detail with *n* equal to 1.0, the nominal fatigue resistance, $(\Delta F)_n$, is computed from Equation 6.5.5.2.2.1.4-4 based on finite life as follows:

$$(\Delta F)_n = \left(\frac{A}{N}\right)^{\frac{1}{3}}$$

The detail category constant, *A*, for a Category E detail is taken as 11.0 x 10^8 ksi^3 from *AASHTO LRFD* Table 6.6.1.2.5-1 (Table 6.5.5.2.2.1.1-2). The number of stress cycles, *N*, is computed from Equation 6.5.5.2.2.1.4-5 as follows:

$$N = (365)(75)n(ADTT)_{SL}$$

$$N = (365)(75)(1.0)(1{,}600) = 43.8 \text{ x } 10^6 \text{ cycles}$$

Therefore:

$$(\Delta F)_n = \left(\frac{11.0 \text{ x } 10^8}{43.8 \text{ x } 10^6}\right)^{\frac{1}{3}} = 2.93 \text{ ksi}$$

In the finite life region of the S-N curve, the Fatigue II load combination specified in *AASHTO LRFD* Table 3.4.1-1 is to be applied (Section 3.9.1.5.3). The load factor for the Fatigue II load combination is 0.75. Therefore:

$$T_{range} = 514 \text{ kip} - \text{ft} * 0.75 = 385.5 \text{ kip} - \text{ft} = 4{,}626 \text{ kip} - \text{in.}$$

Calculate the transverse flexural rigidities, D_a and D_b, of the concrete deck and unstiffened bottom box flange, respectively. The modulus of elasticity, E_c, of the concrete is 3,834 ksi. The Poisson's ratio, μ, for the concrete is taken as 0.2 for the concrete and 0.3 for the steel. Therefore, from Equation 6.5.5.2.2.3.2-3 and Equation 6.5.5.2.2.3.2-4:

$$D_a = \frac{Et_a^3}{12(1-\mu^2)} = \frac{3{,}834(9.5)^3}{12\left(1-0.2^2\right)} = 285{,}345 \text{ k} - \text{in.}^2 / \text{in.}$$

$$D_b = \frac{Et_b^3}{12(1-\mu^2)} = \frac{29{,}000(1.5)^3}{12\left(1-0.3^2\right)} = 8{,}963 \text{ k} - \text{in.}^2 / \text{in.}$$

Calculate the transverse flexural rigidity, D_c, of the stiffened webs. Since the webs are stiffened, D_c will be computed from Equation 6.5.5.2.2.3.2-6; that is, the transverse stiffeners will be considered effective in resisting the transverse bending. First, calculate the effective width of the web plate, d_o, acting with the transverse stiffener from Equation 6.5.5.2.2.3.2-7 (refer also to Figure 6.5.5.2.2.3.2-13). For the web plate, $h = c = 78/\cos 14° = 80.4$ in.

$$d_o = \frac{d \tanh\left(5.6\frac{d}{h}\right)}{\frac{5.6d}{h}\left(1-\mu^2\right)} = \frac{62.0 \tanh\left[5.6\left(\frac{62.0}{80.4}\right)\right]}{\frac{5.6(62.0)}{80.4}\left(1-0.3^2\right)} = 15.8 \text{ in.}$$

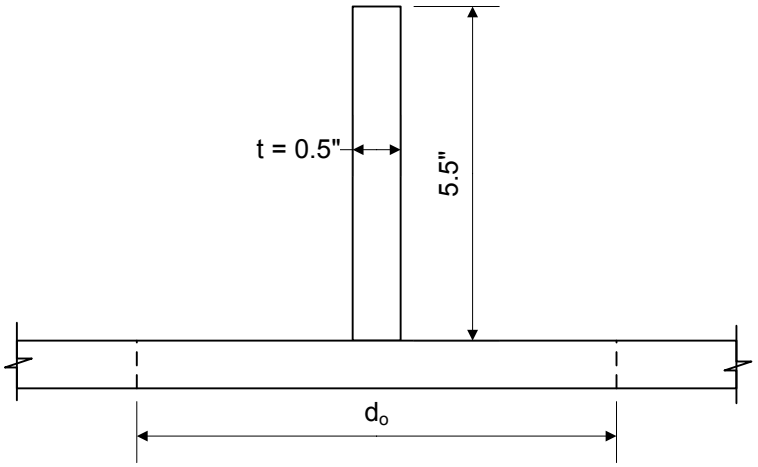

Figure 6.5.5.2.2.3.2-13 Calculation of Effective Width, d_o, of the Web Plate

Compute the location of the neutral axis of the effective section from the outer web face.

Area of the stiffener	=	5.5 * 0.5	= 2.75 in.^{2}
Area of effective web	=	15.8 * 0.5625	= 8.89 in.^{2}
			11.64 in.^{2}

$$\text{N.A.} = \frac{2.75(0.5625 + 5.5/2) + 8.89(0.5625/2)}{11.64} = 1.0 \text{ in.}$$

Calculate the moment of inertia, I_s, of the effective stiffened web plate for transverse bending, including the transverse stiffener:

$$I_s = \frac{1}{12}(5.5)^3 + 2.75(5.5/2 + 0.5625 - 1.0)^2 + 8.89(0.5625/2 - 1.0)^2 + \frac{1}{12}(15.8)(0.5625)^3 = 33.40 \text{ in.}^4$$

From Equation 6.5.5.2.2.3.2-6:

$$D_c = \frac{EI_s}{d} = \frac{29{,}000(33.40)}{62.0} = 15{,}623 \text{ kip} - \text{in.}^2/\text{in.}$$

Compute the compatibility shear, v, at the center of the bottom box flange according to Equation 6.5.5.2.2.3.2-2:

$$v = \frac{\frac{1}{D_c}\left[(2a+b)abc\right] + \frac{1}{D_a}\left[ba^3\right]}{(a+b)\left\{\frac{a^3}{D_a} + \frac{2c\left(a^2+ab+b^2\right)}{D_c} + \frac{b^3}{D_b}\right\}}$$

$$v = \frac{\frac{1}{15{,}623}\left[(2*120+81)(120*81*80.4)\right] + \frac{1}{285{,}345}\left(81*120^3\right)}{(120+81)\left\{\frac{120^3}{285{,}345} + \frac{2*80.4\left(120^2+120*81+81^2\right)}{15{,}623} + \frac{81^3}{8.963}\right\}} = 0.22$$

Calculate the box distortion per kip per inch of load, δ_1, assuming no cross-bracing is present from Equation 6.5.5.2.2.3.2-1:

$$\delta_1 = \frac{ab}{24(a+b)}\left\{\frac{c}{D_c}\left[\frac{2ab}{a+b} - v(2a+b)\right] + \frac{a^2}{D_a}\left[\frac{b}{a+b} - v\right]\right\}$$

$$\delta_1 = \frac{120*81}{24(120+81)}\left\{\frac{80.4}{12{,}381}\left[\frac{2*120*81}{120+81} - 0.223(2*120+81)\right] + \frac{120^2}{285{,}345}\left(\frac{81}{120+81} - 0.223\right)\right\} = 0.347 \text{ in.}^2/\text{kip}$$

Compute the BEF stiffness parameter, β, from Equation 6.5.5.2.2.3.2-8:

$$\beta = \left(\frac{1}{EI\delta_1}\right)^{\frac{1}{4}} = \left(\frac{1}{29{,}000*836{,}050*0.347}\right)^{\frac{1}{4}} = 0.00330 \text{ in.}^{-1}$$

$$\beta\ell = 0.00330(216.0) = 0.713$$

The transverse bending stress range at the top and bottom corners of the tub section may be computed from Equation 6.5.5.2.2.3.2-12 as follows:

$$\sigma_t = C_t F_d \beta \frac{1}{2a} T_{range}$$

It will be assumed for this example that the transverse stiffeners are attached to the top and bottom flanges of the tub, which is recommended for these cases. Transverse stiffeners attached to the top and bottom flanges reduce the sharp through-thickness bending that would otherwise occur due to cross-section distortion in the unstiffened portions of the web at the termination of the stiffener-to-web welds. Connection plates are required to be attached to the flanges for this reason.

First compute the section modulus, *S*, per unit length of the stiffened web (including the transverse stiffener). In the following equation, *y* is the distance from the neutral axis to the extreme fiber of the section consisting of the transverse stiffener and the effective portion of the web plate and *d* is the transverse stiffener spacing.

$$S = \frac{I_s}{yd} = \frac{26.47}{(5.5 + 0.5625 - 1.0)(62.0)} = 0.084 \text{ in.}^3 / \text{in.}$$

The calculated section modulus must at least equal or exceed the calculated section modulus per unit length of the unstiffened web, which is the lower bound. Compute the section modulus, *S*, per unit length of the unstiffened portions of the web, which by inspection is more critical than the unstiffened bottom box flange:

$$S = \frac{1}{6}(1)(0.5625)^2 = 0.053 \text{ in.}^3 / \text{in.}$$

For the bottom corner of the box, the transverse bending stress in the web due to the applied torque, F_d, is computed from Equation 6.5.5.2.2.3.2-13 as follows:

$$F_d = \frac{bv}{2S}$$

For the stiffened portions of the web:

$$F_d = \frac{81(0.223)}{2(0.084)} = 108 \text{ in.}^{-1}$$

For the top corner of the box, the transverse bending stress in the web due to the applied torque, F_d, is computed from Equation 6.5.5.2.2.3.2-14 as follows:

$$F_d = \frac{a}{2S}\left(\frac{b}{a+b} - v\right)$$

For the stiffened portions of the web:

$$F_d = \frac{120}{2(0.084)}\left(\frac{81}{120+81} - 0.223\right) = 129 \text{ in.}^{-1} \quad \text{(controls)}$$

Obtain the BEF factor, C_t, for distortional transverse bending stress. The transverse stiffener will be assumed at mid-panel with the torques conservatively assumed applied at mid-panel. This is the most critical case if one visualizes the analogous

deflection of a beam on an elastic foundation. Therefore, Ct will be obtained from the graph given in Figure 6.5.5.2.2.3.2-6. If desired, greater precision could be obtained for an actual condition different than that assumed by interpolating between the appropriate graphs. First, calculate the deformation of the internal bracing member, δ_b, due to the applied torque from Equation 6.5.5.2.2.3.2-10:

$$\delta_b = \frac{2(1 + a/b)}{\sqrt{1 + \left[\frac{a+b}{2h}\right]^2}} \delta_1$$

$$\delta_b = \frac{2(1 + 120/81)}{\sqrt{1 + \left[\frac{120+81}{2(78.0)}\right]^2}} (0.347) = 1.056 \text{ in.}^2/\text{kip}$$

Calculate the cross-bracing stiffness ratio, *q*, from Equation 6.5.5.2.2.3.2-9. Assume an internal K-brace with the area of one diagonal, A_b, equal to 6.94 in.^{2}, and the length of the diagonal, L_b, equal to 87.9 in. Assume the bracing member has been designed to be effective in compression; therefore, the full area may be used for A_b.

$$q = \left[\frac{E_b A_b}{L_b \ell \delta_1}\right] \delta_b^2$$

$$q = \left[\frac{29{,}000(6.94)}{87.9(216.0)(0.347)}\right] (1.056)^2 = 34.1$$

From the graph in Figure 6.5.5.2.2.3.2-6, for q = 34.1 and $\beta\ell$ = 0.713 (as computed previously), C_t is approximately equal to 0.15. Therefore, from Equation 6.5.5.2.2.3.2-12:

$$\sigma_t = 0.15(129)(0.00330)\left(\frac{1}{2(120)}\right) 4{,}626 = 1.23 \text{ ksi}$$

$$\sigma_t = 1.23 \text{ ksi} < (\Delta F)_n = 2.93 \text{ ksi} \qquad \text{ok}$$

If necessary, the transverse bending stress could be reduced by decreasing the cross-frame spacing and/or increasing the thickness of the web plate.

6.5.5.2.3 Distortion-Induced Fatigue

Distortion-induced fatigue is defined in the *AASHTO LRFD* Specifications as fatigue effects due to secondary stresses not normally quantified in the typical analysis and

design of a bridge. These secondary stresses are typically caused by out-of-plane distortions generated by forces resulting from the three-dimensional interaction of bridge members. The resulting localized stresses can be significant in magnitude and generally are not explicitly considered in the design process.

There must be an unstiffened gap, constraints at boundaries of the unstiffened gap, and out-of-plane distortion for a bridge detail and/or weldment to be susceptible to distortion-induced fatigue. In the past, short unstiffened gaps were often intentionally designed into bridge structures to avoid a fatigue-sensitive weldment on the tension flange. In fact, transverse welds on tension flanges were prohibited by *AASHTO* up until 1974. As a result, welded cross-frame/diaphragm and floorbeam connection plates often had web gaps introduced adjacent to the tension flange. Web gaps were also introduced when lateral connection plates for lateral bracing were coped and not connected to transverse stiffeners. Bolted connections resulted in the introduction of additional web gaps. Intersecting components of a bridge at such details will result in small displacements perpendicular to the web plate that cause bending stresses within the gaps (Figure 6.5.5.2.3-1), which can result in fatigue crack propagation in the web plate, and in some cases when left unarrested, further propagation into the flange. For the bending stresses to develop, sufficient constraint must exist at the ends of the web gap.

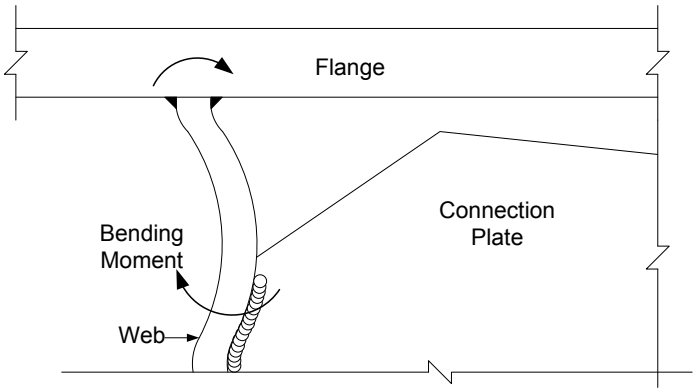

Figure 6.5.5.2.3-1 Web Gap Distortion

Some cases of web gap cracking have been attributed to high frequency vibration of plate elements. For example, vertical vibrations of relatively flexible lateral bracing members have resulted in out-of-plane movements of lateral connection plates attached to either the web or the flange (NHI, 1990). Even with small amounts of vibration, a very small gap between the lateral bracing member and the flange connection can lead to large out-of-plane bending stresses. Suggested lateral bracing details to limit the effects of out-of-plane distortion are discussed in Section 6.3.2.10.4, which is an especially important consideration for tub girders. Load-induced fatigue is usually not critical for top lateral bracing in tub girders since the concrete deck is much stiffer than the bracing; thus, the live load forces in the

bracing members are usually relatively small. However, since the concrete deck resists the majority of the torsional shear in such cases, it is recommended that the transverse reinforcement in the deck be checked for the torsional shear.

In multiple-girder bridges, out-of-plane distortions of web gaps result from differential displacements between adjacent longitudinal members under eccentric loading causing forces to develop at the intersections between transverse and longitudinal members. NHI (1990) details conditions resulting in out-of-plane distortions in other types of bridge structures. The magnitude of the resulting secondary stresses that develop in the web gap is difficult to estimate and the fatigue resistance of the details under these conditions is also difficult to quantify. As a result, the design approach taken is to avoid such details and to provide rigid load paths to preclude the development of significant secondary stresses. *AASHTO LRFD* Article 6.6.1.3 requires that sufficient load paths be provided by connecting all transverse members to the appropriate components comprising the cross-section of the longitudinal member, with the load paths provided by attaching the components through either welding or bolting.

AASHTO LRFD Article 6.6.1.3.1 deals with the detailing of transverse connection plates to prevent distortion-induced fatigue. Transverse connection plates (or transverse stiffeners serving as connection plates) attached to cross-frames, diaphragms, or floorbeams are to be bolted or welded to both the compression and tension flanges of the cross-section in order to eliminate any web gaps. To ensure that the connection is not undersized, particularly at locations where larger out-of-plane forces may develop, it is recommended in *AASHTO LRFD* Article 6.6.1.3.1 that in the absence of better information, the welded or bolted connection in straight, non-skewed bridges be designed for a minimum of a 20.0 kip lateral force (NHI, 1990). For straight, skewed bridges and horizontally curved bridges with or without skew, it is recommended in *AASHTO LRFD* Article C6.6.1.3.1 that the force be determined by analysis. The attachment of internal cross-frame connection plates to box flanges is discussed in *AASHTO LRFD* Article C6.6.1.3.1 and Section 6.3.2.9.6.3.2.

An exception is permitted where intermediate connecting diaphragms are used on rolled beams in straight bridges with composite reinforced decks whose supports are normal or skewed not more than 10° from normal, and with the intermediate diaphragms placed in contiguous lines parallel to the supports. In such cases, *AASHTO LRFD* Article 6.6.1.3.1 permits less than full-depth end angles or connection plates to be bolted or welded to the beam web to connect the diaphragms. This provision reflects the fact that less than full-depth end angles or connection plates have been bolted or welded to the webs of rolled beams to connect intermediate diaphragms for a number of years. Rolled beams typically have thicker webs resulting in larger resistance to out-of-plane distortion and larger lateral-torsional buckling resistance. The end angles or plates must be at least 2/3

the depth of the web to provide some additional torsional resistance to the beam. For bolted angles, a minimum gap of 3.0 in. must be provided between the top and bottom bolt holes and each flange to preclude potential problems with distortion-induced fatigue. All bolt spacing requirements specified in *AASHTO LRFD* Article 6.13.2.6 are to be satisfied. For welded angles or plates, a minimum gap of 3.0 in. is to be provided between the top and bottom of the end-angle or plate welds and each flange, and the heel and toe of the end angles or both sides of the connection plate, as applicable, is to be welded to the beam web. Welds are not to be placed along the top and bottom of the end angles or connection plates. The detail is limited to intermediate diaphragm connections in straight rolled-beam bridges with composite reinforced concrete decks where the skews do not exceed 10° from normal, and where the intermediate diaphragm lines are contiguous. Under such conditions, live load forces in the intermediate diaphragms are typically relatively small.

6.5.5.3 Fracture Limit State

6.5.5.3.1 General

Fracture is defined as a tensile mode in which the metal of an element breaks into two parts. By definition, any force in the fractured element is redistributed into the remaining structure. The ability of the structure to absorb this energy without further damage and carry some additional load is called structural redundancy. In a steel bridge member, fracture can either be a ductile fracture, brittle fracture or a combination of the two modes.

Ductile fracture is characterized by plastic deformation prior to separation of the member or component. Ductile fracture is preferable over brittle fracture because there is generally a warning in the form of excessive deformations or deflection prior to failure. The existence of large plastic deformations is indicative that the material has basically followed its stress-strain curve through yielding until the ultimate strength is reached, as shown qualitatively in Figure 6.5.5.3.1-1 for a typical mild steel. Ductile failures generally occur at connections where there is cross-section loss due to plastic deformation in the vicinity of holes and/or concentrations of stress. The design of members or components for ductile fracture is based on the net section.

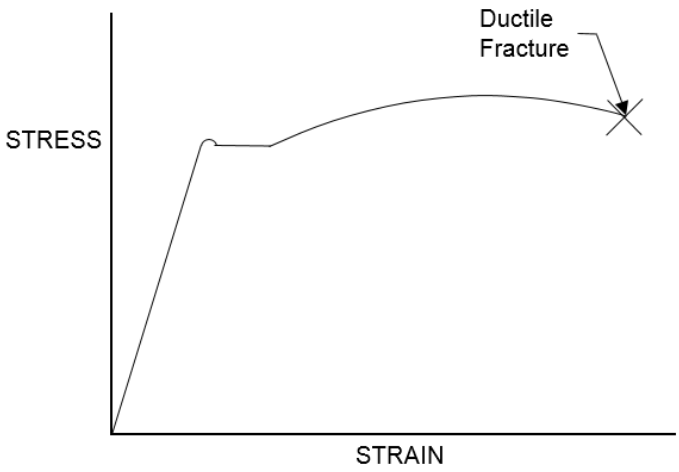

Figure 6.5.5.3.1-1 Typical Stress-Strain Curve for Mild Steel

Brittle fracture is sudden and without warning. With brittle fracture, there is little or no plastic deformation or yielding prior to separation of the member or component. Thus, the ultimate strength of the member is typically not reached (Figure 6.5.5.3.1-2). Since the average stress level at the time of brittle fracture is usually below the yield stress, there is less internal energy and the strength of the member or component is reduced. Brittle fracture typically initiates at an initial flaw or discontinuity in the steel. When a critical stress level is reached at a flaw, crack growth will continue in an unstable fashion at a nearly instantaneous rate until complete separation occurs. Thus, there is an interaction between the crack size and the tensile stress level. As crack size increases, the tensile stress level at which brittle fracture occurs decreases, while smaller cracks can tolerate higher tensile stress levels prior to failure. Hence, it is obviously important to control the size of any discontinuities during the fabrication process.

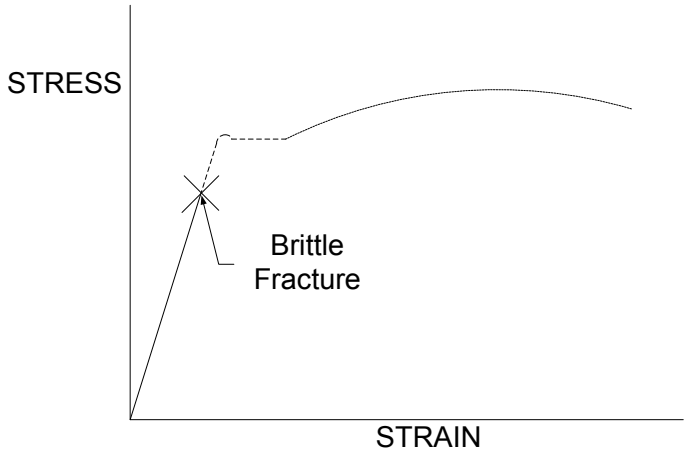

Figure 6.5.5.3.1-2 Stress-Strain Curve Indicative of a Brittle Fracture

6.5.5.3.2 Fracture Toughness

Fracture toughness is a material property, much like the properties of yield or tensile strength, which is defined in the *AASHTO LRFD* Specifications as a measure of the ability of a structural material or element to absorb energy without fracture. As the fracture toughness of steel increases, its ability to tolerate/accommodate combinations of higher tensile stress and larger cracks prior to unstable crack growth also increases. The fracture toughness of the steel is ideally defined as the area under the stress-strain curve. Thus, a material experiencing a ductile fracture has a much larger area under the stress-strain curve (Figure 6.5.5.3.1-1), and thus, a larger fracture toughness (versus a material experiencing a brittle fracture). Materials such as steel, aluminum and copper have relatively high fracture toughness versus materials such as concrete, cast iron and stone.

Linear-elastic fracture mechanics analysis is the basis for predicting brittle fracture in structural steels. Conventional stress analysis cannot be applied to crack-like defects since the theoretical stress concentration factor is infinite. This led to development of the stress intensity factor, K_I, as a means to characterize the crack tip singularity (Barsom and Rolfe, 1987). For a given plate geometry, the stress intensity present at a crack tip is a function of the crack size and the applied stress. The material fracture resistance is characterized by the critical stress intensity factor, K_{Ic}, that can be sustained without fracture. When the applied stress intensity, K_I, equals or exceeds the material fracture resistance, K_{Ic}, fracture is predicted.

The fracture toughness of steel is a function of the material properties, temperature, load rate and degree of constraint. As the yield strength of the steel increases, the ductility of the steel and its ability to plastically deform generally decreases. Alloying and heat treatment of these steels during manufacture is used to increase the fracture toughness.

Fracture toughness decreases with temperature. At high and low temperatures, the fracture toughness can be characterized by the relatively constant "upper shelf" and "lower shelf" toughness levels (Figure 6.5.5.3.2-1). The metallurgical fracture mode transitions from brittle cleavage on the lower shelf to ductile tearing on the upper shelf at a certain temperature, called the transition temperature. Mixed mode fracture is expected in the transition zone region.

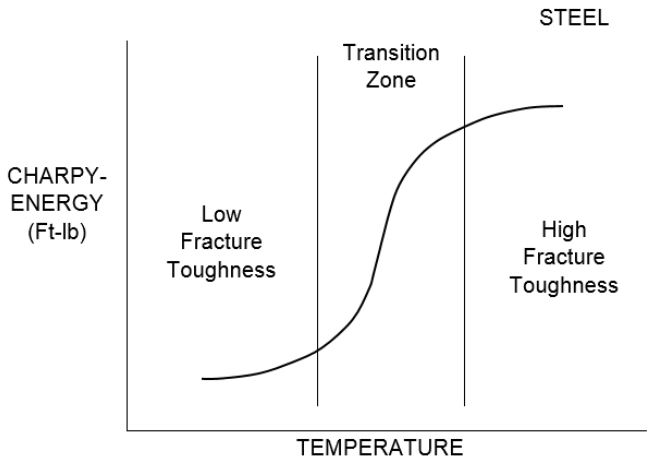

Figure 6.5.5.3.2-1 Typical Plot of Charpy Energy Versus Temperature for a Steel

Slow static load rates result in a higher fracture toughness than rapid dynamic load rates. Truck loading on bridges generally results in an intermediate load rate.

Highly constrained details, such as those utilizing thick plates, large welds and/or complex geometries, will also exhibit a lower fracture toughness because of the reduced ability of the steel to deform around a crack. As plate thickness increases, the ability of the plate to plastically deform also decreases.

Pre-existing cracks are introduced during the welding process and cannot be avoided. Quality control procedures during fabrication are intended to minimize the size of the initial flaws to increase both the fatigue and fracture resistance of welded details. The intent of the fatigue-design provisions in *AASHTO* is to prevent or limit stable crack growth, or small incremental crack growth (i.e. fatigue crack propagation) under cyclic loading over the service life of the structure, as continued fatigue crack growth will eventually result in brittle fracture if it not detected and arrested. Using a detail with a higher fatigue resistance or lowering the stress range at the detail can increase the fatigue design life or number of cycles required for failure. The inherent fracture toughness of the steel will limit the fatigue design life due to the maximum crack size that can be tolerated prior to brittle fracture (i.e. unstable crack growth).

Steels for use in primary bridge members are required to have sufficient fracture toughness to reduce the probability of brittle failure in the presence of a fatigue crack or other notch-like defect. *AASHTO* adopted a fracture control plan in the aftermath of the Silver Bridge collapse in 1967 due to brittle fracture. The fracture control plan was originally issued as an *AASHTO* Guide Specification in 1978 and is now instead given in Section 12 of the *AASHTO/AWS D1.5M/D1.5 Bridge Welding Code* (AASHTO/AWS, 2010).

The plan places controls on material properties and initial flaw sizes to provide adequate performance. The fracture control plan specifies: design and review responsibilities; welding inspector, fabricator and NDT personnel qualification and certification; welding requirements; welding procedures; welding repair procedures and required fracture toughness of the steel and weld metal. Stringent preheat and interpass temperature requirements are included to minimize the potential for hydrogen-induced cracking, which results from the presence of hydrogen (moisture) in the molten weld metal. As the weld cools and solidifies, the hydrogen migrates to the grain boundaries of the metal resulting in a weakened plane in the weld, which eventually cracks due to the presence of restraint and tensile residual stresses. The crack reduces the strength of the weld and may potentially lead to fatigue crack growth.

Since the plan has been applied to U.S. bridge construction, there have been no such failures. Recent failures of steel bridges associated with tensile stress, such as the Hoan Bridge in Milwaukee, have been traced to inadequate detailing that did not provide an adequate load path. There have been far more sudden collapses of bridges associated with stability failures, particularly during construction, than due to fracture. Nonetheless, redundant bridges are desirable. However, when a less redundant design is found desirable, it can be built under the current provisions.

6.5.5.3.2.1 Charpy V-Notch Testing

The fracture control plan utilizes the Charpy V-Notch impact test to determine the fracture toughness requirements for various bridge steels. A small 10 x 10 mm bending specimen with a machined notch is impacted by a hammer at very high strain rates, and the energy required to initiate fracture is measured (Figure 6.5.5.3.2.1-1). The maximum height the pendulum rises after impact indicates the amount of energy absorbed in foot-pounds. When sets of specimens are tested at different temperatures, there is a shift or transition in energy absorption with temperature, as shown in Figure 6.5.5.3.2-1. It is obviously desirable for bridge steels to be operating in the area to the right of the transition zone.

Figure 6.5.5.3.2.1-1 Charpy V-Notch Testing Machine

The Charpy V-Notch (CVN) impact test is a relatively severe test of fracture toughness and does not define the conditions under which bridge steels actually operate. The load rate that a CVN specimen is subject to in the transition zone is approximately five times that expected during bridge loading. The fracture toughness decreases as the load rate increases at a given temperature. The constraint around the fracture zone of the CVN specimen is typically more severe than found in bridges. Although plates thicker than the thickness of a CVN specimen are used in bridges, a minimum level of fracture toughness is reached in the CVN test, as the test represents a plane-strain condition. No further reduction in fracture toughness than the level attained in the CVN test is realized with increasing plate thickness.

The CVN test cannot directly predict the K_{Ic} fracture toughness of steel. More elaborate fracture mechanics tests are required using fatigue-cracked specimens with measurement of the load and displacement during testing. These tests are too

expensive to use for quality control in steel production. However, correlations have been developed to predict the K_{Ic} fracture toughness from CVN test data (Barsom and Rolfe, 1987).

The *AASHTO* fracture control plan uses three different temperature zones (designated Zones 1, 2 and 3) to qualify the fracture toughness of bridge steels. The three zones are differentiated by their minimum operating (or service) temperatures, which are given in *AASHTO LRFD* Table 6.6.2-1. The required fracture toughness increases as the minimum expected service temperature for the bridge decreases. The fracture toughness requirements (*AASHTO LRFD* Table C6.6.2-1) for various bridge steels are given in terms of the energy (in foot-pounds) absorbed by the CVN specimens at specified test temperatures for the three different temperature zones.

The CVN test temperatures are on average 70 degrees higher than the minimum service temperature for each zone to compensate for the higher load rates experienced by the test specimens (AISI, 1975). The requirements for non-fracture critical members were set to keep the K_{Ic} fracture toughness above the lower shelf at bridge service temperatures. The requirements for fracture critical members were set higher in the transition region to provide added resistance to brittle fracture. The use of the temperature shift concept, mentioned above, results in CVN test temperatures that are higher than the actual service temperatures in bridges. Experience has shown that thick plates are more vulnerable to brittle fracture; thus, for higher strength steels, the requirements are generally more stringent for thicker plates. For the newer high performance steels (HPS), which provide significant improvements in fracture toughness, it was decided that these steels would be required to meet more stringent Zone 3 requirements in all three temperature zones (Wilson, 2002).

Once members are designated as either non-fracture critical (T), or fracture critical (F) (Section 6.5.5.3.3), the member classification (T or F) followed by the temperature zone (1, 2, or 3) must be designated to invoke the proper CVN requirements. For example, a Grade 50 non-fracture critical plate for use in temperature zone 2 is designated as ASTM A709/A709M Grade 50-T2. A Grade HPS 70W fracture critical plate for use in temperature zone 3 is designated as ASTM A709/A709M Grade HPS 70W-F3. The ASTM A673 *Standard Specification for Sampling Procedure for Impact Testing of Structural Steel* governs the CVN sampling and testing requirements. Similar to the tension test sampling requirements (Section 6.2.7.1), CVN testing is required to be performed at either H or P frequency depending on the grade and application. In addition, P frequency sampling is required at two locations (each end) in some plates depending on grade and heat treatment (*AASHTO LRFD* Article C6.6.2).

6.5.5.3.3 Fracture-Critical Members

Separate fracture toughness requirements are given in *AASHTO LRFD* Table C6.6.2-1 for nonfracture-critical and fracture-critical members (or components). A fracture-critical member (FCM) is an element that should it fracture, would release energy into the structure that the structure could not safely absorb without further damage. The *AASHTO LRFD* Specification defines a FCM as a component in tension whose failure is expected to result in the collapse of the bridge, or the inability of the bridge to perform its function. FCMs are an essential part of a non-redundant bridge system. The FHWA interprets the term "component in tension" to be a steel member in tension, or a sub-element within a built-up member that is in tension (Lwin, 2012). Further, the phrase "inability of the bridge to perform its function" is interpreted by the FHWA to mean the inability of the bridge to safely carry some level of live load in its damaged condition; usually less than the full design load for the strength limit state load combination (load factors and combinations used to evaluate the damaged condition must be agreed upon by the Owner and Engineer and reviewed by the FHWA). For these reasons, further precautions are taken in the fabrication of fracture-critical members (FCMs).

FCMs are subject to more stringent Charpy V-Notch fracture toughness requirements than nonfracture-critical members. FCMs must also be fabricated in accordance with the fracture control plan given in AASHTO/AWS (2010). According to *AASHTO LRFD* Article 6.6.2, the Engineer has the responsibility to identify all bridge members or components that are fracture critical and clearly delineate their location on the contract plans. Examples of FCMs in bridges include certain truss members in tension, suspension cables, tension components of girders in two-girder systems, pin and link systems in suspended spans, cross-girders and welded tie girders in tied-arches. In addition, any attachment, except for bearing sole plates, having a length in the direction of the tension stress greater than 4 inches and welded to the tension area of a component of a FCM is also to be considered fracture critical. Bearing sole plates welded to tension flanges are typically located in regions of low (to zero) tensile stress. Furthermore, these components are likely to be field welded, and an unnecessary fracture-critical designation of those welds can result in complications in the field welding. For example, in the cases of an elastomeric bearing pad vulcanized to a plate, or a field repair to the area near an already installed bearing, the required minimum fracture-critical preheat for the weld may exceed the maximum allowable temperature for the bearing material.

AASHTO LRFD Article 6.6.2 requires that all primary longitudinal superstructure components and connections, except as noted, sustaining tensile force effects due to the Strength I load combination, along with transverse floorbeams subject to such effects, be subject to mandatory Charpy V-Notch fracture toughness testing. The components and connections requiring such testing (e.g. flange and web material subject to tension) must be so designated on the contract plans. The exceptions are

noted as follows (unless designated otherwise on the contract plans): splice plates and filler plates connected in double shear in bolted splices; intermediate transverse web stiffeners not serving as connection plates; bearings, sole plates and masonry plates; expansion dams; and drainage material. The specification of mandatory fracture toughness testing for other primary components and connections sustaining tensile force effects under the specified load combination, e.g. primary connections and components other than floorbeams that are transverse to the primary longitudinal components (e.g. cross-frames/diaphragms and lateral bracing in skewed and/or curved bridges) is left to the discretion of the Owner.

6.5.5.3.4 Redundancy Considerations

The term redundancy implies the exceeding of what is considered necessary or normal. Hence, the implication in the term redundancy as applied to a particular structure is the inclusion of something that is not necessary for the normal functioning of the structure. In order to design structures with the least cost, that style of redundancy is a type the Engineer tries best to avoid.

Redundancy became a matter of some discussion when several structures suffered major fractures. It was observed that a fracture failure in bridges such as the Silver Bridge, which had no redundancy, led to the loss of life. On the other hand, fracture failures experienced by other bridges, such as the I-79 Bridge over Neville Island, which was structurally redundant, only led to minimal inconvenience. Since those days, much effort has been spent defining redundancy, when it exists, and how it can best be obtained. This approach falls under the rubric of designing for failure, since if the bridge does not fail, redundancy is not called upon. But the importance of bridges and the human lives they carry seems to call out for at least some level of redundancy in every structure.

Wherever possible, bridge details and concepts should be developed to provide some level of redundancy. In the *AASHTO LRFD* Specifications, redundancy is defined as the quality of a bridge that enables it to perform its design function in a damaged state. A redundant member is defined as a member whose failure does not cause failure of the bridge. The implication is that the failure of a single member will be identified before a second member fails.

Generally, the *AASHTO LRFD* Specification specifies capacity of individual elements or members. However, *AASHTO LRFD* Article 1.3.4 addresses the entire structure. This article recommends either multi-load-path structures or continuous ones in order to provide redundancy. One term that could potentially be used to identify bridges that are thought to collapse if one main element should fail is “failure-critical”. The member(s) that causes the structure to be failure-critical is identified as “fracture-critical” (Section 6.5.5.3.3). Another term that has often been used to define such a structure is one susceptible to “progressive collapse”. A load modifier,

η_R, is provided that suggests a factor of 1.05 be applied for members in non-redundant structures (Section 1.3.6.2). However, there are no instructions as to how to make the proper analysis, or the level of live load that the bridge should be able to carry in its damaged condition. Load factors to be applied to the analysis of the damaged structure are also currently lacking.

At least three types of redundancy can be defined:

- Load path redundancy – a bridge has load path redundancy if it has multiple main load-carrying member (or load paths), usually parallel, between points of support ;
- Structural redundancy – a bridge has structural redundancy if its main members provide continuity of the load path from span to span (i.e. statical indeterminacy), or other three-dimensional mechanisms; and
- Internal member redundancy – a bridge member has internal redundancy if it contains multiple elements, which are mechanically fastened together to act as crack arrestors and limit fracture propagation across the member cross-section.

The most conservative, and often uneconomical choice, is multiple load path redundant structures.

According to the FHWA (Lwin, 2012), for design and fabrication, only load path redundancy may currently be considered in the classification of FCMs. It is further emphasized that it is not the failure of only the element in tension that needs to be considered with regard to the performance of the damaged bridge, but the failure of the entire member containing that tension element at the cross-section under consideration. The NBIS defines load path redundancy as three or more load paths; however, some states use four or more. Structural redundancy demonstrated by refined analysis may be considered for in-service inspection protocol, although criteria for such analyses have not yet been codified in the *AASHTO LRFD* Specification. Internal redundancy is not currently recognized by the FHWA in the classification of FCMs for design, fabrication, or in-service inspection protocol. Further research on intenral redundancy is ongoing at Purdue University as of this writing (2015).

Redundancy exists in most highway bridges. However, it is not always simple to determine the presence or absence of adequate redundancy as defined herein. For example, it may not exist in a single box girder cross-section of either steel or post-tensioned concrete; it may or may not exist in a horizontally curved multi-girder bridge. Therefore, it becomes necessary to consider a methodology for the determination of whether redundancy exists.

AASHTO LRFD Article 6.6.2 does permit the use of refined analyses with assumed hypothetical cracked components to demonstrate redundancy, or to confirm that part of a hypothetically damaged structure is not fracture critical. Owners are becoming more receptive to such analyses. However, as discussed in *AASHTO LRFD* Article C6.6.2, and mentioned above, the criteria for these analyses have not yet been codified so that items such as the loading cases to be considered, the location of the potential cracks, the degree of the dynamic effects to be included, the software to be used along with the degree of refinement of the model should all be agreed upon by the Owner and the Design Engineer. Relief from the full factored loads in the applicable strength limit state load combinations should be considered. The number of loaded design lanes versus the number of striped traffic lanes should also be given some consideration in the analysis.

A bridge would be expected to support its design load after a fracture occurs. Assume that it will not be expected to support more than the design live load. The bridge must also support its dead load. A load factor of 1.3 is one possible suggestion for both of these loads based approximately on the dead-load factor applied in the LFD (Load Factor Design) and LRFD methodologies. The lower factor applied to the live load is based on expected overloading. The method of loading must be considered in a fracture investigation. Much of the load (i.e. the dead load) is applied to a non-composite structure, but the fracture effect acts entirely on the composite structure. The live load is applied to the composite structure in both cases.

The dead load is applied as in design. However, the fracture introduces a redistribution of internal actions and external reactions as a result of the fracture. In a steel structure, introduction of the fracture is rather straightforward. The stress at the fracture face must be zero. Thus, forces are applied to the fractured structure at the location of the assumed fracture in a reverse sense to those applied under dead load, forcing the net resultant stresses at the fracture face to be zero. The resulting load case is additive to the dead load cases originally employed during the design.

Ensuring that adequate reinforcing within the deck and adequate shear connection of the deck to the girders are provided to resist the effects of the fracture are important factors in determining the redundancy of composite steel bridges.

The process is similar, but more complex, in a post-tensioned concrete structure. The typical case would be a segmental box girder with a portion of the bottom flange destroyed. The force in the broken strands would be reversed and applied to the remaining structure. Grouting of the strands must be considered. The multiple strands provide some redundancy against failure of a strand. The same concept can be employed in steel structures by using multiple elements to form a member and provide internal member redundancy. Typically, this type of redundancy occurs with riveted members. Modern truss members and arch ties have been made of built-up

bolted members to provide internal member redundancy, as have girder bridges that were considered non-redundant. In these structures, the remaining elements in the member need to be examined to ensure that they are adequate. Additional bolt shear forces are encountered should an element fail when the force in the failed element is redistributed through the bolts in the vicinity of the failure to the functioning elements. As mentioned above, the FHWA does not recognize internal member redundancy as of this writing (2015) in the classification of FCMs. Research is ongoing to better understand the level of redundancy provided by this approach.

Perhaps the best approach is to design and build the structure such that it does not fail; hence avoiding the need for providing redundancy as defined herein. This approach also has been investigated intensely since the 1960s—and with great success. It was observed that most all of the steel bridges that failed were either welded using the older technologies that existed at the time, as in the case of Neville Island girder-bridge, or of old material and/or out-of-date design practice, as in the case of the Silver Bridge. Investigations showed that tougher steel, better design of details, and more intense inspection makes steel bridges much tougher and extremely resistant to fracture. This research is borne out as is evidenced in the paucity of fractures of newer bridges in the United States. Generally, the additional costs associated with the work and material specification necessary to satisfy the fracture control plan is not great, and can usually be more than offset by the increased efficiency of the structural form. Cross-sections having a single tub or widely-spaced tubs are a good example of such economy. Single tubs save not only on steel and fabrication costs; they permit significantly reduced-cost substructures. These savings usually more than offset the costs associated with FCM fabrication and stringent material requirements related to fracture-critical components in these structures. A number of these bridges have been built across the nation and are functioning safely.

AASHTO LRFD Article 6.11.5 specifies that box flanges in tension in single-box cross sections are to be considered FCMs, unless by analysis the bridge can be shown to support the dead load and the live load after sustaining a fracture at any point along the girder. If the bridge cannot be shown to be redundant, it does not mean that it cannot be built within the specification. It simply means that the elements leading to the non-redundant condition must be designated FCMs. The continuously braced tension (top) flanges in the negative-moment regions of a single-box bridge may be shown to be nonfracture-critical due to the presence of the longitudinal reinforcement provided in the composite deck acting as the top flanges in the event of a fracture. There must be adequate shear connection of the deck to permit the section to remain structurally intact. In cross-sections comprised of two box girders, the bottom flanges in positive moment regions are to be considered fracture-critical components according to *AASHTO LRFD* Article 6.11.5, unless adequate strength and stability of the hypothetically damaged structure can be

verified by refined analysis. Where cross-sections contain more than two box sections, none of the components of the box sections are to be considered fracture critical according to this article.

6.5.6 LRFD Strength Limit State Design for Flexure

6.5.6.1 General

AASHTO LRFD Article 1.3.2.4 specifies that the strength limit state is intended to ensure that strength, as well as both global and local stability, are provided to resist the statistically significant load combinations that a bridge is expected to experience over its design life. As mentioned in the Commentary to this article, structural damage and distress may be expected to occur at the strength limit state, but overall structural integrity should be maintained.

AASHTO LRFD Article 6.5.4 states that the strength load combinations specified in *AASHTO LRFD* Table 3.4.1-1 (discussed in Section 3.9.1.2) in combination with the resistance factors specified in *AASHTO LRFD* Article 6.5.4.2 are to be used to check the strength limit state. In all the subsequent discussions below, the resistance factor for flexure, ϕ_f, is to be taken as 1.0, as specified in *AASHTO LRFD* Article 6.5.4.2.

As discussed in *AASHTO LRFD* Articles C6.10.6.2.1 and C6.11.6.2.1, the flexural design provisions in the *AASHTO LRFD Specifications* assume low or zero levels of axial force in the member. Should a concentrically applied axial force due to the factored loads, P_u, in excess of ten percent of the factored axial resistance of the member, P_r, be applied at the strength limit state, the section should instead be checked according to the beam-column interaction equations given in *AASHTO LRFD* Article 6.8.2.3 or 6.9.2.2, as applicable. According to the beam-column interaction equations in these articles, when P_u is ten percent of P_r, the flexural resistance of the member is reduced by five percent. The specification writers felt that it would be reasonable to ignore the effect of the axial force in the design below this level.

For cases where the axial force is deemed significant, the reader is referred to White (2012) for a more in-depth discussion regarding the design of composite steel bridge girders subjected to combined axial compression and flexure, such as might occur in a cable-stayed system with a composite I- or box-girder deck system. A combination of flexural and thermal loads can also produce this situation; this is particularly true when there are stiff restraints against thermal movement.

6.5.6.1.1 I-Sections

AASHTO LRFD Article 6.10.6 provides a "roadmap" to direct the Design Engineer to the appropriate articles giving the specific strength limit state checks that are to be made for composite or non-composite I-section flexural members in regions of negative or positive flexure, as discussed in more detail below in Sections 6.5.6.2 and 6.5.6.3.

Helpful flowcharts detailing the design checks for flexure to be made at the strength limit state for I-sections are provided in Appendix C6 of the *AASHTO LRFD Specifications*. A flowchart summarizing the basic "roadmap" presented in *AASHTO LRFD* Article 6.10.6 is given in *AASHTO LRFD* Figure C6.4.4-1. The design checks for non-composite sections and composite sections in negative flexure (according to the slender-web provisions given in *AASHTO LRFD* Article 6.10.8) are summarized in the flowchart given in *AASHTO LRFD* Figure C6.4.6-1. A related flowchart for determining unbraced length requirements to develop the maximum potential lateral-torsional buckling resistance in the presence of a moment gradient (according to the provisions of *AASHTO LRFD* Article D6.4.1 in Appendix D6) is given in *AASHTO LRFD* Figure C6.4.8-1. The design checks for composite sections in positive flexure are summarized in the flowchart given in *AASHTO LRFD* Figure C6.4.5-1.

6.5.6.1.2 Box Sections

AASHTO LRFD Article 6.11.6 provides a "roadmap" to direct the Design Engineer to the appropriate articles giving the specific strength limit state checks that are to be made for box-section flexural members in regions of positive or negative flexure, as discussed in more detail below in Sections 6.5.6.2.4 and 6.5.6.3.

The effect of the St. Venant torsional shear stress, f_v, in box flanges must be considered for sections in bridges outside the special restrictions discussed in *AASHTO LRFD* Article 6.11.2.3 (which includes all box sections in skewed and/or curved bridges). f_v may be taken equal to zero for sections in bridges meeting the special restrictions. In cases where f_v is judged to be insignificant or incidental, or is not to be considered, all terms related to f_v are simply set equal to zero in the appropriate equations given in Sections 6.5.6.2.4 and 6.5.6.3. The equations then reduce to the equations for determining the nominal flexural resistance of straight box sections in the absence of St. Venant torsion. Again, the Design Engineer should consider torque whenever the supports are skewed.

f_v is determined by dividing the St. Venant torsional shear flow given by *AASHTO LRFD* Equation C6.11.1.1-1 (Equation 6.4.8.3.2-2) by the thickness of the box flange. The nominal flexural resistance of the box flange for such cases is based on the von Mises yield criterion, which is used to consider the effect of the St. Venant torsional shear in combination with flexure. Maximum bending moments and

torques are typically not produced by concurrent loads. However, the coincident flexure and torsion due to moving loads to produce the critical von Mises stress is too complex to treat in a practical manner; therefore, maximum envelope values may be used to make all design checks. The Specification is currently silent regarding the inclusion of the elastic shear flow in the box flange due to flexure (i.e. $f = VQ/I$). As pointed out in White (2012), consideration of the flexural shear stress in the flange may be prudent in cases there the thickness of the box flange is equal to or only slightly larger than the thickness of the web. In such cases, the shear flow in the box flange will be essentially the same as the shear flow in the web at the web-flange junctures.

AASHTO LRFD Article C6.11.1.1 states that for torques applied to the non-composite section, the enclosed area, A_o, used in computing the shear flow is to be computed for the non-composite box section. If top lateral bracing in a tub section is attached to the webs, A_o is to be reduced to reflect the actual location of the bracing (*AASHTO LRFD* Article 6.7.5.3). Because shear connectors are required along the entire length of box sections as specified in *AASHTO LRFD* Article 6.11.10, the concrete deck is considered effective in resisting torsion along the entire span. Thus, for torques applied to the composite section in regions of positive or negative flexure, A_o is to be computed for the composite section using the depth from the bottom flange to the mid-thickness of the concrete deck. The depth may be conservatively determined by neglecting the thickness of the concrete deck haunch or by using a lower bound estimate of the actual thickness of the haunch, if desired.

The torsion acting on the composite section introduces horizontal shear in the concrete deck that should be considered in the design of the deck transverse reinforcement, particularly for boxes resting on skewed supports. For tub sections, the deck should be assumed to resist all the torsional shear acting on top of the composite box section. If top flange lateral bracing is present, it may be modified to an equivalent plate for the analysis (Kolbrunner and Basler, 1966). For closed-box sections, the torsional shear in the concrete deck can be determined by multiplying the torsional shear acting on top of the composite box section by the ratio of the thickness of the transformed concrete deck to the total thickness of the top flange plus the transformed deck, as suggested in *AASHTO LRFD* Article C6.11.10. Consideration may be given to adjusting the thickness of the deck for the difference in the Poisson's ratio of the concrete ($\mu = 0.2$) and the steel ($\mu = 0.3$). Adequate shear connection must be provided to ensure that the two materials act in concert.

AASHTO LRFD Article 6.11.1.1 specifies that in cases where the St. Venant torsional shears must be considered, the St. Venant torsional shear stress, f_v, in box flanges due to the factored loads at the strength limit state must not exceed the factored torsional shear resistance of the flange, F_{vr}, given as follows:

$$F_{vr} = 0.75\phi_v \frac{F_{yf}}{\sqrt{3}}$$ Equation 6.5.6.1.2-1

AASHTO LRFD Equation 6.11.1.1-1

where:

ϕ_v = resistance factor for shear specified in *AASHTO LRFD* Article 6.5.4.2 (= 1.0)

It is unlikely that such a level of torsional shear stress will actually be experienced in practical box-girder designs.

6.5.6.2 Composite Sections in Negative Flexure and Non-Composite Sections

6.5.6.2.1 General

This section describes the AASHTO LRFD strength limit design verifications for composite I- and box-girder sections subject to negative flexure and for non-composite I-girder sections. The base design provisions for I-sections are given in *AASHTO LRFD* Article 6.10.1.8 within the main body of Section 6 (referred to hereafter as the 'Main Provisions'), and are described further in Section 6.5.6.2.2. Optional design provisions for I-sections that meet certain specified qualifications described in Section 6.5.6.2.3 are given in *AASHTO LRFD* Appendix A6. The design provisions for composite box sections subject to negative flexure are described further in Section 6.5.6.2.4.

6.5.6.2.2 I-Sections: Main Provisions (AASHTO Article 6.10.1.8)

6.5.6.2.2.1 General

6.5.6.2.2.1.1 Section Classifications

Composite I-sections subject to negative flexure at the strength limit state, and also non-composite I-sections, are classified in the Specification as follows:

- *Compact Web Sections*: a non-composite section or a composite section in negative flexure that has a web with a slenderness at or below which the section can achieve a maximum flexural resistance, M_{max}, equal to the plastic moment, M_p, prior to web bend buckling having a statistically significant influence on the response;
- *Noncompact Web Sections*: a non-composite section or a composite section in negative flexure that has a web satisfying specific steel grade requirements and with a slenderness at or below which theoretical web bend-buckling does

not occur at elastic stress levels, computed according to beam theory, smaller than the maximum flexural resistance;

- *Slender Web Sections*: a non-composite section or a composite section in negative flexure that has a web with a slenderness at or above which the theoretical bend-buckling stress is reached in the web prior to reaching the yield moment, M_y.

Figure 6.5.6.2.2.1.1-1 illustrates the basic relationship between the maximum potential flexural resistance, M_{max} (or equivalently F_{max}), and the web slenderness, $2D_c/t_w$, for all three types of sections; compact web, noncompact web and slender web (assuming yielding with respect to the compression flange controls and that lateral-torsional buckling and local buckling are prevented). The plot shown in Figure 6.5.6.2.2.1.1-1 assumes that compression-flange yielding controls.

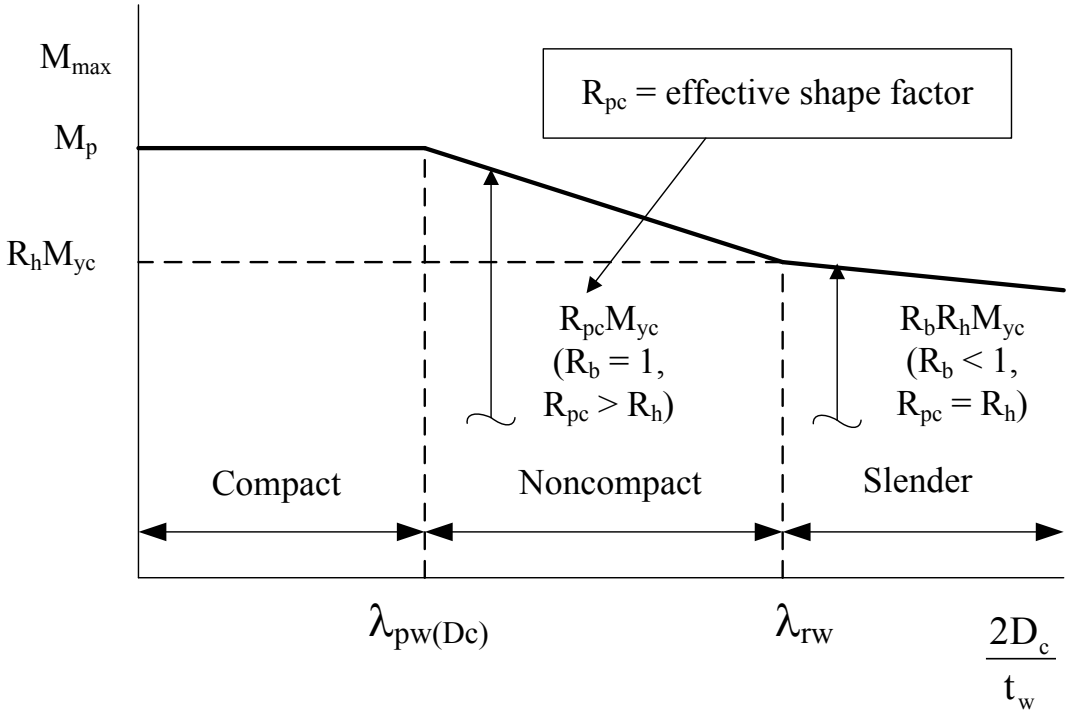

Figure 6.5.6.2.2.1.1-1 M_{max} versus Web Slenderness for Composite I-Sections Subject to Negative Flexure and Non-Composite I-Sections

6.5.6.2.2.1.2 Compact Web Sections

'Compact web sections' are typically shallower sections with thicker webs; that is, rolled beams and welded girder sections with proportions similar to rolled beams that are typically used on bridges with shorter spans. Sections with compact webs are able to develop a maximum potential flexural resistance equal to their full plastic moment capacity, M_p (Section 6.4.5.2), provided that specific steel grade, ductility,

flange and web slenderness and lateral bracing requirements are satisfied. The web slenderness requirement for a compact web section is stated in *AASHTO LRFD* Article A6.2.1 (*AASHTO LRFD* Appendix A6) as follows:

$$\frac{2D_{cp}}{t_w} \le \lambda_{pw(D_{cp})} \qquad \text{Equation 6.5.6.2.2.1.2-1}$$

AASHTO LRFD Equation A6.2.1-1

where D_{cp} is the depth of the web in compression at the plastic moment determined as specified in *AASHTO LRFD* Article D6.3.2 (*AASHTO LRFD* Appendix D6), and $\lambda_{pw(D_{cp})}$ is the limiting slenderness ratio for a compact web section given as follows:

$$\lambda_{pw(D_{cp})} = \frac{\sqrt{\frac{E}{F_{yc}}}}{\left(0.54\frac{M_p}{R_h M_y} - 0.09\right)^2} \le \lambda_{rw}\left(\frac{D_{cp}}{D_c}\right) \qquad \text{Equation 6.5.6.2.2.1.2-2}$$

AASHTO LRFD Equation A6.2.1-2

Equation 6.5.6.2.2.1.2-2 is modified relative to the slenderness limit given in previous specifications for these sections. The modified limit accounts for the higher demands on the web placed on singly symmetric I-sections with larger shape factors M_p/M_y (White and Barth, 1998; Barth et al., 2005).

For a shape factor equal to 1.12, which is the typical shape factor for a doubly symmetric non-composite I-section, and a shape factor equal to 1.30, which is representative of the shape factor for a composite I-section subject to negative flexure, the limit from Equation 6.5.6.2.2.1.2-2 is as follows (Table 6.5.6.2.2.1.2-1):

Table 6.5.6.2.2.1.2-1 Web Slenderness Limit for Compact Web Sections, $\lambda_{pw(Dc)}$, from Equation 6.5.6.2.2.1.2-2 for Shape Factors M_p/M_y of 1.12 and 1.30

F_{yc} (ksi)	M_p/M_y = 1.12	M_p/M_y = 1.30
36	107	76
50	91	64
70	77	54
90	68	48
100	54	45

The upper limit of $\lambda_{rw}(D_{cp}/D_c)$ in Equation 6.5.6.2.2.1.2-2 (see Section 6.5.6.2.2.1.3 for a discussion of the slenderness limit, λ_{rw}) is to protect against extreme cases

where D_c/D is significantly less than 0.5. In such cases, D_{cp}/D is typically smaller than D_c/D. As such, in certain situations, the web slenderness associated with the elastic cross-section, $2D_c/t_w$, may be larger than λ_{rw} while the slenderness associated with the plastic cross-section, $2D_{cp}/t_w$, may be smaller than $\lambda_{pw(D_{cp})}$. In other words, the elastic web would be classified as slender at the same time the plastic web would be classified as compact. To guard against such situations and the possibility of theoretical bend buckling of the web prior to reaching M_p, the upper limit of $\lambda_{rw}(D_{cp}/D_c)$ is placed on $\lambda_{pw(D_{cp})}$.

A qualitative bending moment versus rotation relationship for a homogeneous compact web section taken from a member satisfying the following conditions is shown in Figure 6.5.6.2.2.1.2-1: 1) the member is subject only to transverse loads perpendicular to one principal axis; 2) the loads all pass through the shear center of the cross-section, and thus, the member is not subject to torsion; 3) the member has sufficient lateral support along its length to prevent lateral-torsional buckling; and 4) the section has been proportioned to prevent local buckling of the compression flange prior to reaching its maximum potential flexural resistance, M_{max}. A homogeneous section is a considered to be a section in which the flanges and web have the same nominal yield strength.

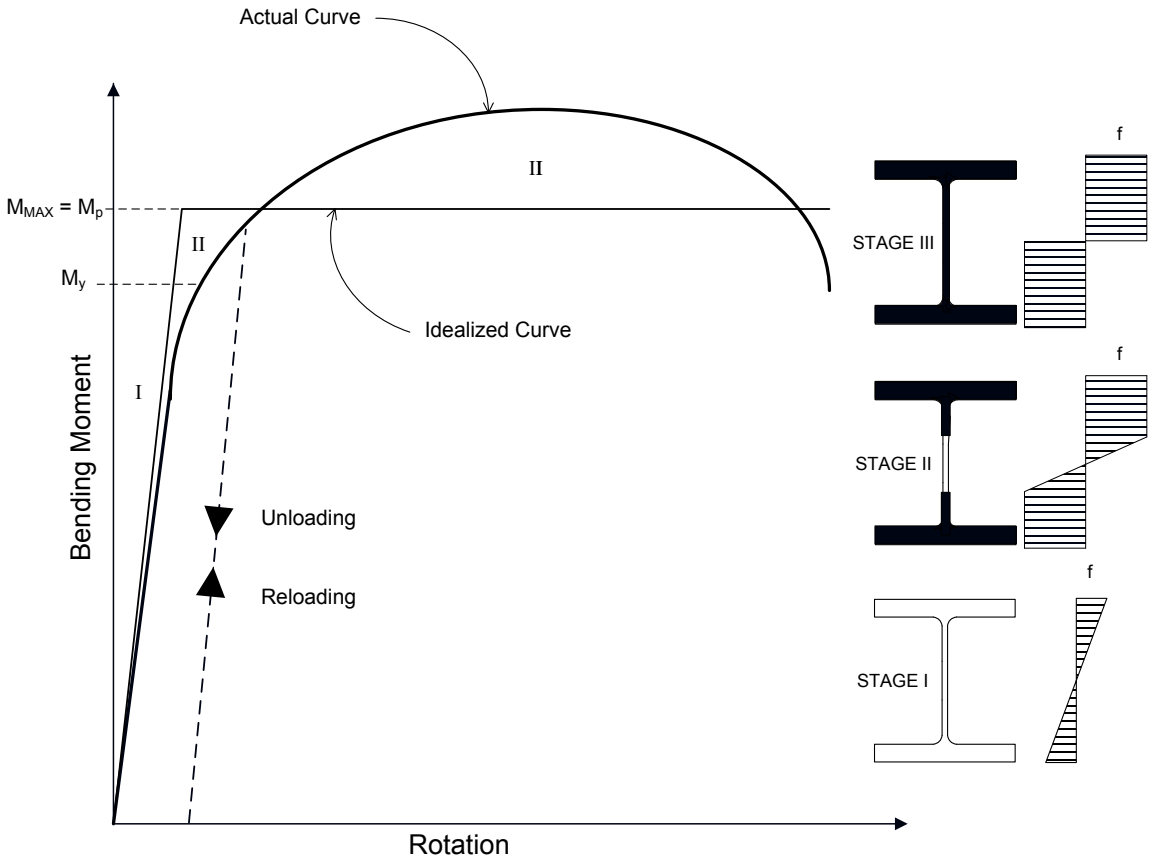

Figure 6.5.6.2.2.1.2-1 Bending Moment versus Rotation for a Homogenous Compact Web Section

Proceeding along the actual curve shown in Figure 6.5.6.2.2.1.2-1, the initial Stage I behavior represents completely elastic behavior. As the section approaches the theoretical yield moment M_y (Section 6.4.5.3), the presence of residual stresses will result in some inelastic behavior in the outer fibers of the cross-section before the calculated M_y is reached (in the girder cross-sections shown in Figure 6.5.6.2.2.1.2-1, black indicates yielding). At Stage II, yielding continues and begins to progress throughout the section as the section approaches M_p. The actual curve shown in Figure 6.5.6.2.2.1.2-1 assumes the presence of a moment gradient along the length of the member with peak moments occurring at individual cross-sections. Under moment gradient conditions, the formation of a local buckle causing a decline in the flexural resistance requires yielding of the flange over a portion of the length of the member. Before such a local buckle can form, there may be significant strain hardening in the region of maximum moment. In such cases, as illustrated in the figure, compact web sections are typically able to exceed M_p due to the strain hardening before eventually unloading due to local buckling of the compression flange. However, because this excess flexural resistance is difficult to accurately predict, it is ignored in design. Also, under uniform moment conditions, local

buckling will invariably occur before there is any significant increase in the flexural resistance attributable to strain hardening. Under these conditions, the resistance essentially plateaus at M_p before unloading eventually occurs.

As a result, the idealized curve shown in Figure 6.5.6.2.2.1.2-1 is assumed for design. Because the residual stresses do not reduce the plastic moment, the section is assumed elastic up to M_p, and is then assumed to rotate inelastically at a constant moment equal to M_p. At this stage (Stage III in Figure 6.5.6.2.2.1.2-1), the entire cross-section has yielded; that is, each component of the cross-section is assumed to be at F_y. In some cases, if certain requirements are met, the available inelastic rotation capacity in these sections (i.e. the difference between the elastic rotation at M_p and the rotation where the moment drops below M_p) can be utilized to allow a redistribution of the bending moments from interior piers to more lightly loaded sections in positive flexure prior to making the design verifications at the service and strength limit states (Section 6.5.6.6). In addition, composite sections in positive flexure may be able to achieve a nominal flexural resistance at or just below M_p in certain cases when compact web sections are used at interior piers (Section 6.5.6.3.2).

In a hybrid section (Section 6.4.4), an additional stage between Stage I and Stage II occurs in which yielding develops in the lower-strength web while the flanges remain elastic (assuming both flanges have a yield strength higher than the web). Then at Stage II (in Figure 6.5.6.2.2.1.2-1), yielding will progress through the flanges while the web remains partially elastic. Otherwise, the behavior is similar. Again, the presence of residual stresses does not reduce $M_{max} = M_p$. Also, the redistribution of the stress to the flanges resulting from the local yielding of the web is ignored whenever the nominal flexural resistance exceeds the yield moment M_y. Therefore, the hybrid factor R_h is not applied to M_p for compact web sections.

The dotted line shown in Figure 6.5.6.2.2.1.2-1 illustrates the behavior of a member that is loaded with a moment greater than M_y and then unloaded. Note that elastic behavior is observed both during the unloading and subsequent reloading and a small residual curvature will remain in the member. Also, because the member behaves elastically during unloading and subsequent reloading, the effect of residual stresses is only observed during the initial application of the load as long as the moment due to any subsequent loads does not exceed the previously applied moment.

6.5.6.2.2.1.3 Noncompact Web Sections

′Noncompact web sections′ are sections of intermediate depth with a web slenderness satisfying the following requirement:

$$\frac{2D_c}{t_w} \le \lambda_{rw} = 5.7\sqrt{\frac{E}{F_{yc}}} \qquad \text{Equation 6.5.6.2.2.1.3-1}$$

AASHTO LRFD Equation A6.2.2-1

The limiting value of λ_{rw} from Equation 6.5.6.2.2.1.3-1, which defines the limit below which theoretical web bend buckling does not occur for elastic stress values smaller than F_{yc}, is given as follows for different grades of steel (Table 6.5.6.2.2.1.3-1):

Table 6.5.6.2.2.1.3-1 Web Slenderness Limit for Noncompact Web Sections, λ_{rw}, from Equation 6.5.6.2.2.1.3-1

F_{yc} (ksi)	λ_{rw}
36	162
50	137
70	116
90	102
100	97

Because web bend buckling is not assumed to occur, R_b is taken equal to 1.0 for these sections (Section 6.4.5.6).

The maximum potential flexural resistance of a noncompact web section is taken as the smaller of $R_{pc}M_{yc}$ and $R_{pt}M_{yt}$ (assuming specific steel grade, compression-flange slenderness and compression-flange bracing requirements are satisfied), and falls between M_{max} for a compact web and a slender web section as a linear function of the web slenderness ratio, $2D_c/t_w$. M_{yc} and M_{yt} are the yield moments with respect to the compression and tension flanges, respectively. R_{pc} and R_{pt} are termed web plastification factors for the compression and tension flange, respectively. The web plastification factors are essentially effective shape factors that define a smooth linear transition in the maximum flexural resistance between M_y and M_p (Section 6.5.6.2.3.2). Referring to Figure 6.5.6.2.2.1.1-1, which assumes that compression-flange yielding controls, at the slenderness limit, $\lambda_{pw(Dc)}$, delineating a compact web and a noncompact web section, R_{pc} is taken equal to the cross-section shape factor, M_p/M_{yc}, corresponding to the compression flange. At the slenderness limit, λ_{rw}, delineating a noncompact web and a slender web section, R_{pc} is equal to the hybrid factor, R_h (Section 6.4.5.7).

6.5.6.2.2.1.4 Slender Web Sections

Sections having a web with a slenderness exceeding λ_{rw} from Equation 6.5.6.2.2.1.3-1 are termed ″slender web sections″. Sections with slender webs rely

upon significant web post bend-buckling resistance at the strength limit state. Because web bend buckling (Section 6.4.5.5) is assumed to occur in such sections prior to reaching M_{max}, the web load-shedding factor, R_b (Section 6.4.5.6), must be introduced to account for the effect of the post bend-buckling resistance or redistribution of the web compressive stresses to the compression flange resulting from the bend buckling of the web. The hybrid factor, R_h (Section 6.4.5.7), must also be introduced to account for the redistribution of stress to both flanges resulting from local yielding of the web in a hybrid section. Therefore, the maximum potential flexural resistance, M_{max}, is taken as the smaller of $R_bR_hM_{yc}$ and R_hM_{yt}.

Figure 6.5.6.2.2.1.4-1 shows a qualitative moment versus rotation relationship for a homogeneous slender web section taken from a member satisfying the previously stated conditions.

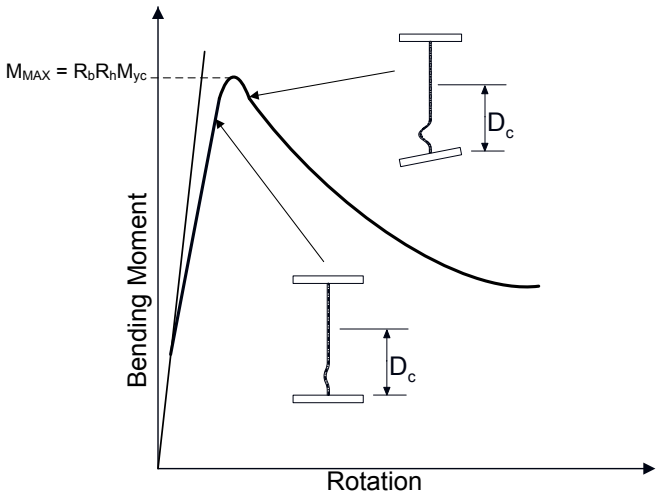

Figure 6.5.6.2.2.1.4-1 Moment versus Curvature for a Homogenous Slender Web Section

Unlike a compact web section, a slender web section has little or no available inelastic rotation capacity after reaching M_{max} as the web deformations begin to dramatically increase. Therefore, the flexural resistance drops off quite rapidly after reaching M_{max}, and redistribution of moments is obviously not permitted when these sections are used at interior piers.

6.5.6.2.2.1.5 Application – Main Provisions vs. Appendix A6

The design of composite I-sections subject to negative flexure at the strength limit state and non-composite I-sections is covered in either *AASHTO LRFD* Article 6.10.8 or *AASHTO LRFD* Appendix A6. The majority of steel bridge I-sections utilize either slender webs or noncompact webs that approach the slenderness limit, λ_{rw}. Therefore, for the design of these sections, the simpler and more streamlined provisions of *AASHTO LRFD* Article 6.10.8 are the most appropriate for determining the nominal flexural resistance at the strength limit state. The provisions of *AASHTO*

LRFD Article 6.10.8 presume slender-web behavior, and therefore, limit the nominal flexural resistance to be less than or equal to the nominal moment at first yield, M_y. However, it is considered more appropriate to express the maximum resistance in terms of stress for sections in which the maximum resistance is always less than or equal to M_y. In composite construction, the combined effects of the loadings acting on different states of the member cross-section (i.e. non-composite, long-term composite and short-term composite) are better handled by working with flange stresses rather than moments. Bridge engineers are also generally more accustomed to working with stresses. Therefore, in the AASHTO LRFD Specifications, the flexural resistance for slender web sections is expressed in terms of stress (with the maximum potential flexural resistance given the moniker, F_{max}).

For compact web and noncompact web sections in which the maximum potential flexural resistance equals or exceeds M_y, expressing the flexural resistance in terms of stress would generally result in stress limits greater than the yield stress for cases where the resistance exceeds M_y. Therefore, the resistance equations are more conveniently written in terms of bending moment for these sections. For sections in which the flexural resistance is expressed in terms of moment, moments acting on the non-composite, long-term composite and short-term composite sections may be directly summed for comparison to the nominal resistance. Effects of partial yielding within the cross-section and the sequence of application of loads acting on the different sections need not be considered. Therefore, in *AASHTO LRFD* Appendix A6, which may optionally be applied to compact web and noncompact web sections satisfying specific steel grade and web and flange proportioning requirements in straight I-girder bridges with limited skews (Section 6.5.6.2.3), the nominal flexural resistance equations are expressed in terms of bending moment and the nominal flexural resistance is permitted to exceed M_y (with the maximum potential flexural resistance given the moniker, M_{max}).

Since the types of sections that would qualify for the use of *AASHTO LRFD* Appendix A6 are less commonly used, the somewhat more complex provisions for their design have been placed in an appendix in the specification in order to streamline and simplify the Main Provisions. The slender web provisions of *AASHTO LRFD* Article 6.10.8 may be applied to sections in bridges utilizing compact webs or noncompact webs that are nearly compact, but at the expense of some economy with the potential loss in economy increasing with decreasing web slenderness. It is strongly recommended though that compact web sections and noncompact web sections that are nearly compact be designed according to the provisions of *AASHTO LRFD* Appendix A6 in order to minimize the potential loss in economy when these sections are used.

As discussed previously in Section 6.5.2.1.4, composite I-sections in negative flexure and non-composite I-sections in all kinked (chorded) continuous and horizontally curved I-girder bridges, and in straight I-girder bridges whose supports

are skewed more than 20° from normal, must always be treated as slender web sections, regardless of their web slenderness, in applying the specifications. Thus, the nominal flexural resistance of these sections in these bridges is not permitted to exceed M_y. As a result, the optional provisions of *AASHTO LRFD* Appendix A6 may not be applied to compact web or noncompact web sections in these bridges.

AASHTO LRFD Appendix A6 may optionally be applied to composite I-sections subject to negative flexure and non-composite I-sections with compact or noncompact webs in straight-girder bridges whose supports are normal or skewed not more than 20° from normal, and with intermediate cross-frames/diaphragms placed in contiguous lines placed parallel to the supports. Other conditions, spelled out in *AASHTO LRFD* Articles 6.10.2.2.3 and *AASHTO LRFD* Appendix A6, must also be satisfied in order to utilize these provisions to check discretely braced flanges of such sections. The following discussion will focus only on the slender web provisions of *AASHTO LRFD* Article 6.10.8. Further information on the provisions of *AASHTO LRFD* Appendix A6 - and the specific conditions under which Appendix A6 may be used - may be found in Section 6.5.6.2.3.

Note that *AASHTO LRFD* Articles 6.10.6.2.3 also optionally permits moment redistribution according to the provisions of *AASHTO LRFD* Appendix B6 prior to making the strength limit state design verifications. However, this is only permitted for continuous-span members in straight I-girder bridges with skews not exceeding 10° from normal. Other limitations spelled out in *AASHTO LRFD* Article B6.2 must also be satisfied. Further information on the provisions of optional *AASHTO LRFD* Appendix B6 may be found in Section 6.5.6.6.

6.5.6.2.2.2 Discretely Braced Compression Flanges

AASHTO LRFD Article 6.10.8.1.1 in the Main Provisions specifies that at the strength limit state, discretely braced compression flanges must satisfy the one-third rule equation expressed in terms of stress (Section 6.5.2.1.1) as follows:

$$f_{bu} + \frac{1}{3} f_{\ell} \le \phi_f F_{nc} \qquad \text{Equation 6.5.6.2.2.2-1}$$

AASHTO LRFD Equation 6.10.8.1.1-1

where:

f_{bu} = factored compression-flange vertical bending stress determined as specified in *AASHTO LRFD* Article 6.10.1.6 (ksi). f_{bu} is always taken as positive.

f_{ℓ} = factored flange lateral bending stress determined as specified in *AASHTO LRFD* Article 6.10.1.6 (ksi). f_{ℓ} is always taken as positive.

F_{nc} = nominal flexural resistance of the compression flange determined as specified in *AASHTO LRFD* Article 6.10.8.2 (ksi)

A discretely braced flange is a flange braced at discrete intervals by bracing sufficient to restrain lateral deflection of the flange and twisting of the entire cross-section at the brace points. At the strength limit state, discretely braced compression flanges would typically be the bottom flanges in regions of negative flexure in continuous-span members. During construction, top flanges of the non-composite section in regions of positive flexure would also be classified as discretely braced compression flanges.

Equation 6.5.6.2.2.2-1 must be satisfied for both local buckling and lateral-torsional buckling using the appropriate value of F_{nc} determined for each case, as specified in *AASHTO LRFD* Articles 6.10.8.2.2 and 6.10.8.2.3, respectively. The computation of F_{nc} for local buckling and lateral-torsional buckling is discussed further in Sections 6.5.6.2.2.2.1 and 6.5.6.2.2.2.2, respectively.

AASHTO LRFD Article 6.10.1.6 specifies that for design checks involving lateral-torsional buckling, the compressive vertical bending stress, f_{bu}, and flange lateral bending stress, f_{ℓ}, are to be taken as the largest values throughout the unbraced length in the flange under consideration. This is consistent with established practice in applying beam-column interaction equations involving member stability checks. For design checks involving flange local buckling, f_{bu} and f_{ℓ} may be taken as the corresponding values at the section under consideration. However, when maximum values of these stresses occur at different locations within the unbraced length,

which is often the case, it is conservative to use the maximum values in the local buckling check.

The sign of f_{bu} and f_ℓ is always taken as positive in Equation 6.5.6.2.2.2-1. However, when summing dead and live load stresses to obtain the total factored vertical and lateral bending stresses, f_{bu} and f_ℓ, to apply in the equation, the signs of the individual dead and live load stresses must be considered.

Potential sources of flange lateral bending in discretely braced compression flanges at the strength limit state include curvature, wind loading and the effect of discontinuous cross-frames/diaphragms used in conjunction with support skew. During construction, overhang bracket loads on exterior girders acting on the non-composite section also cause flange lateral bending. According to *AASHTO LRFD* Article 6.10.1.6, amplification of the first-order flange lateral bending stresses may be required in discretely braced compression flanges. Amplification of these stresses was discussed previously in Section 6.5.2.1.3.2. *AASHTO LRFD* Article 6.10.1.6 further specifies that the sum of the factored flange lateral bending stresses due to all sources (after amplification) cannot exceed $0.6F_{yf}$.

6.5.6.2.2.2.1 Local Buckling Resistance

Both rolled and built-up steel I-sections are composed of flat plate elements. When these elements are compressed, for example a discretely braced flange, they may buckle locally out of their original planes, as illustrated in Figure 6.5.6.2.2.2.1-1.

Figure 6.5.6.2.2.2.1-1 Local Buckling of Compression Flange of a Laboratory Specimen

The width-to-thickness ratio of the compression flange in a flexural member is the controlling parameter for local buckling. The critical elastic buckling stress for a

perfectly flat plate with no residual stress subjected to a uniform uniaxial compressive stress is given as follows (Timoshenko and Gere, 1961):

$$F_{cr} = \frac{k_c \pi^2 E}{12\left(1-\mu^2\right)\left(b_{fc}/t_{fc}\right)^2} \qquad \text{Equation 6.5.6.2.2.2.1-1}$$

where:

b_{fc} = width of the plate along the edge subject to compression (in.)
E = Young's modulus (29,000 ksi for steel)
t_{fc} = thickness of the plate (in.)
k_c = plate buckling coefficient (discussed below)
μ = Poisson's ratio (0.3 for steel)

The plate buckling coefficient, k_c, depends on the boundary conditions of the plate element. For one-half of a girder compression flange, the longitudinal edge representing the flange-web juncture may be assumed pinned or restrained against rotation. The other longitudinal edge of the flange is free. For idealized pinned conditions at one edge and the other edge free, k_c is equal to 0.425 for a long plate typical of practical structural members; for fully-restrained conditions along one edge, k_c increases to 1.277 (Timoshenko and Gere, 1961). If an objective is to reach F_{yc} prior to elastic local buckling of the flange, substituting F_{yc} for F_{cr} and $b_{fc}/2$ for b_{fc} in Equation 6.5.6.2.2.2.1-1 and rearranging yields:

$$\frac{b_{fc}}{2t_{fc}} \le 0.95\sqrt{\frac{Ek_c}{F_{yc}}} \qquad \text{Equation 6.5.6.2.2.2.1-2}$$

Research by Johnson (1985) has resulted in the following general expression for k_c for built-up I-sections:

$$k_c = \frac{4}{\sqrt{\frac{D}{t_w}}} \qquad \text{Equation 6.5.6.2.2.2.1-3}$$

AASHTO LRFD Equation A6.3.2-6

This expression accounts for the fact that thinner webs in built-up sections tend to offer less rotational restraint to prevent flange local buckling. The calculated value of k_c from Equation 6.5.6.2.2.2.1-3 must fall between the range of 0.35 and 0.76.

The lower-bound value of 0.35 (which controls at D/t_w values greater than approximately 130) is back-calculated by equating the local buckling resistances

given in the *AASHTO LRFD* Specifications to measured resistances from tests conducted by Johnson (1985) and others with D/t_w values ranging from 72 to 245. The fact that the lower-bound value is less than 0.425 (which assumes idealized simply-supported boundary conditions along the web-flange juncture) is indicative of the fact that web local buckling in more slender webs tends to destabilize the compression flange. The upper-bound value of 0.76 corresponds to the traditional value that has been assumed for rolled shapes (AISC, 2010a).

A k_c value of 0.35 is conservatively assumed for all sections in *AASHTO LRFD* Article 6.10.8.2.2, which is assumed to apply only to slender web sections. This results in the following limiting slenderness ratio, λ_{rf}, for a so-called ′noncompact flange′ (when k_c is taken equal to 0.35 and F_{yr} is substituted for F_{yc} in Equation 6.5.6.2.2.2.1-2):

$$\lambda_{rf} = 0.56\sqrt{\frac{E}{F_{yr}}} \qquad \text{Equation 6.5.6.2.2.2.1-4}$$

AASHTO LRFD Equation 6.10.8.2.2-5

where:

F_{yr} = compression-flange vertical bending stress at the onset of nominal yielding within the cross-section, including residual stress effects, taken as the smaller of $0.7F_{yc}$ and F_{yw}, but not less than $0.5F_{yc}$ (ksi)

F_{yr} is discussed further in Section 6.5.6.2.2.2.2. In the *AASHTO LRFD* Specifications (Article 6.2), a ′noncompact flange′ is defined as a discretely braced compression flange with a slenderness at or below which localized yielding within the cross-section associated with a hybrid web, residual stresses and/or cross-section monosymmetry has a statistically significant effect on the nominal flexural resistance.

The local buckling resistance is governed by elastic buckling for a compression-flange slenderness, $b_{fc}/2t_{fc}$, greater than λ_{rf} from Equation 6.5.6.2.2.2.1-4, resulting in a so-called ′slender flange′. However, elastic local buckling typically does not control for practical bridge-girder sections. The flange-proportioning limit specified in *AASHTO LRFD* Article 6.10.2.2 (Section 6.3.4.4.2), which limits $b_{fc}/2t_{fc}$ to a practical maximum value of 12.0, precludes elastic flange local buckling for specified minimum yield strengths of the compression flange, F_{yc}, up to and including 90 ksi. In fact, because of this, elastic flange local buckling resistance equations are not provided in the *AASHTO LRFD* Specification. The use of the inelastic flange local buckling resistance equation (discussed below) is permitted for the rare case in which $b_{fc}/2t_{fc}$ may be in the elastic buckling range for F_{yc} greater than 90 ksi.

Flanges may be required to undergo significant plastic compressive strain without having local buckling occur in order to achieve the maximum potential local buckling resistance, F_{max}. For plastic design, a girder will have adequate rotation capacity at a plastic hinge if its flanges are capable of straining to the point of incipient strain hardening prior to buckling, which is typically at a point approximately 15 to 20 times the yield strain. To achieve this condition, the compression-flange slenderness should not exceed the following limit:

$$\frac{b_{fc}}{2t_{fc}} \le 0.30\sqrt{\frac{E}{F_{yc}}} \qquad \text{Equation 6.5.6.2.2.2.1-5}$$

The development of this limit is beyond the scope of this document, but is described in detail elsewhere (Hall, 2000; Salmon and Johnson, 1996). Because residual stress effects and material imperfections have less effect in the plastic range, and because compressive plastic strains only about one-half the strain necessary to reach strain hardening are required to simply reach maximum flexural resistance equal to the plastic moment, this limit was felt to be too severe to reach F_{max} (Salmon and Johnson, 1996). Therefore, the limit was increased to the following slenderness limit, λ_{pf}, for a so-called ′compact flange′:

$$\lambda_{pf} = 0.38\sqrt{\frac{E}{F_{yc}}} \qquad \text{Equation 6.5.6.2.2.2.1-6}$$

AASHTO LRFD Equation 6.10.8.2.2-4

The limiting ratio, λ_{pf}, is given in Table 6.5.6.2.2.2.1-1 for different grades of steel:

Table 6.5.6.2.2.2.1-1 Compression-Flange Slenderness Limit for a Compact Flange, λ_{pf}, from Equation 6.5.6.2.2.2.1-6

F_{yc} (ksi)	λ_{pf}
36	10.8
50	9.2
70	7.7
90	6.8
100	6.5

A ′compact flange′ is defined in the *AASHTO LRFD* Specifications (Article 6.2) as a discretely braced compression flange with a slenderness at or below which the flange can sustain sufficient strains such that the maximum potential flexural

resistance is achieved prior to flange local buckling having a statistically significant influence on the response (assuming bracing requirements are also satisfied to develop the maximum potential resistance).

Limits on the width-to-thickness ratio of compression flanges were typically specified in previous specifications as a function of the yield strength of the flange and were taken to be an indirect check on the local buckling resistance of the flange. In the *AASHTO LRFD* Specifications, the compression-flange local buckling resistance is now explicitly calculated as a function of $b_{fc}/2t_{fc}$ and the yield strength of the flange, with $b_{fc}/2t_{fc}$ capped at the specified upper limit of 12.0. For local buckling, the equations defining the nominal flexural resistance of the compression flange, Fnc, in AASHTO LRFD Article 6.10.8.2.2 (Main Provisions) are expressed in terms of stress as follows (the equations are shown graphically in Figure 6.5.6.2.2.2.1-2**):**

- If $\lambda_f \leq \lambda_{pf}$, then:

$$F_{nc} = F_{max} = R_b R_h F_{yc} \qquad \text{Equation 6.5.6.2.2.2.1-7}$$

AASHTO LRFD Equation 6.10.8.2.2-1

- Otherwise:

$$F_{nc} = \left[1 - \left(1 - \frac{F_{yr}}{R_h F_{yc}}\right)\left(\frac{\lambda_f - \lambda_{pf}}{\lambda_{rf} - \lambda_{pf}}\right)\right] R_b R_h F_{yc} \qquad \text{Equation 6.5.6.2.2.2.1-8}$$

AASHTO LRFD Equation 6.10.8.2.2-2

where:

λ_f = slenderness ratio for the compression flange = $b_{fc}/2t_{fc}$
λ_{pf} = limiting slenderness ratio for a compact flange (Equation 6.5.6.2.2.2.1-6)
λ_{rf} = limiting slenderness ratio for a noncompact flange (Equation 6.5.6.2.2.2.1-4)
R_b = web load-shedding factor determined as specified in *AASHTO LRFD* Article 6.10.1.10.2 (Section 6.4.5.6)
R_h = hybrid factor determined as specified in *AASHTO LRFD* Article 6.10.1.10.1 (Section 6.4.5.7)

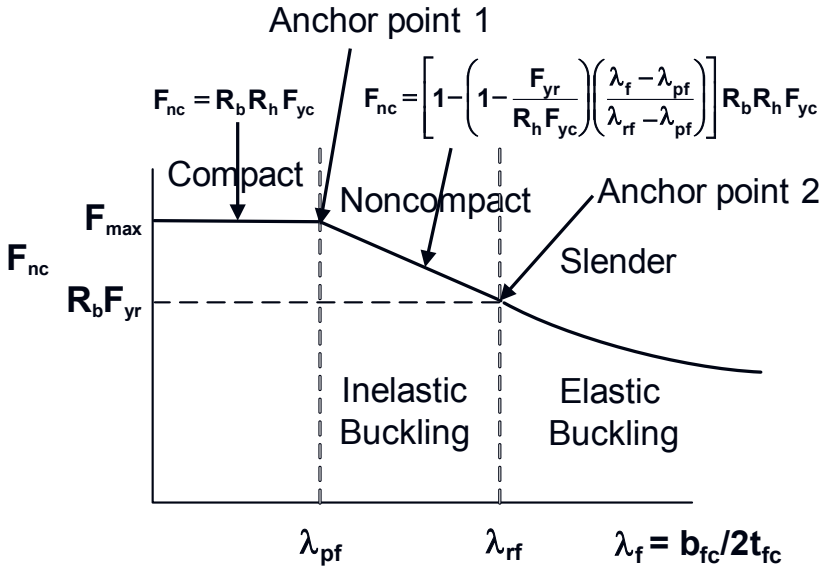

Figure 6.5.6.2.2.2.1-2 Local Buckling Resistance, F_{nc}

λ_{pf} and λ_{rf} are Anchor Points 1 and 2, respectively, as shown on Figure 6.5.6.2.2.2.1-2. For intermediate values of $b_{fc}/2t_{fc}$ between λ_{pf} and λ_{rf}, residual stresses and initial imperfections give rise to inelastic local buckling, represented in the *AASHTO LRFD* Specifications by a linear transition curve given by Equation 6.5.6.2.2.2.1-8. As mentioned previously, an elastic local buckling equation is not provided. The relatively minor influence of moment gradient effects is also neglected for flange local buckling.

6.5.6.2.2.2.2 Lateral Torsional Bucking Resistance

An I-section member may deflect laterally in a torsional mode before the compressive bending stress reaches the yield stress if the compression flange does not have adequate lateral support. The bracing must be sufficient to restrain lateral deflection of the flange and twisting of the entire cross-section at the brace points for a compression flange to be considered adequately braced.

Figure 6.5.6.2.2.2.2-1 shows a doubly symmetric I-section member in pure bending, simply supported and held against twisting at both ends. It is assumed that the compression flange is sturdy enough that it will not buckle locally and that the cross-section will not distort prior to buckling of the entire member between points of lateral support of the compression flange. Under uniform compression, the top flange would buckle downward in its weak direction if this motion were not prevented by the web. Instead, if the force in the compression flange is large enough, the flange will tend to buckle horizontally, or in the only direction that it is free to move. The bottom flange, which is in tension, tends to remain straight. Therefore, the top flange

tending to buckle, bends further than the bottom flange, which tends to remain straight. As a result, the entire cross-section rotates as one rigid unit, as shown in Figure 6.5.6.2.2.2.2-1.

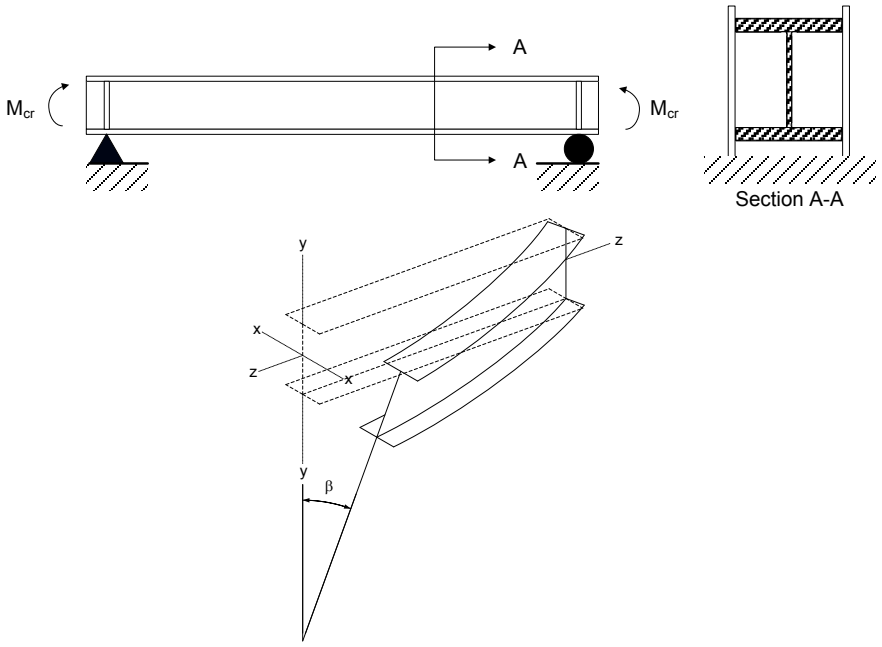

Figure 6.5.6.2.2.2.2-1 Lateral-Torsional Buckling of a Doubly Symmetric I-Section Member

The principal variable affecting the lateral-torsional buckling resistance is the distance between the points of lateral support. However, other variables affect the resistance as well including, but not limited to, the end restraints, type and position of the loads, material properties, residual stresses, initial imperfections and cross-section distortion.

For an ideal straight and centered member, there is no tendency for this lateral-torsional motion until the moment reaches a critical magnitude, M_{cr}, at which the member becomes unstable and can undergo lateral deflections and rotations leading to collapse. The tendency for an I-section member to twist is resisted by a combination of St. Venant torsion and warping torsion. The general equation for the elastic lateral-torsional buckling resistance, M_{cr}, for a doubly symmetric I-section bent about the strong axis is given as (Brockenbrough and Johnston, 1981):

$$M_{cr} = \frac{C_b\pi}{kL_b}\sqrt{EI_yGJ}\sqrt{1+\frac{\pi^2 C_w E}{GJ(kL_b)^2}(C^2+1)} \pm \left(\frac{C\pi}{kL_b}\right)\sqrt{\frac{C_w E}{GJ}} \qquad \text{Equation 6.5.6.2.2.2.2-1}$$

where:

C = coefficient to account for load height effect
C_b = moment-gradient modifier
C_w = warping constant = $I_y h^2/4$ (in.^{6})
E = Young's modulus
G = shear modulus
H = vertical distance between flanges
I_y = moment of inertia about the vertical axis in the plane of the web (in.^{4})
J = St. Venant torsion constant (in.^{4})
K = effective length factor
L_b = unbraced length

Other more complex formulations have been developed for singly symmetric sections (SSRC, 1998; Kitipornchai and Trahair, 1980; Kitipornchai and Trahair, 1986). The resistance to the differential bending of the flanges in their own plane increases with the bending rigidity of each flange in its own plane and with the distance between the flanges, as reflected in the warping constant, C_w.

It is assumed in the development of Equation 6.5.6.2.2.2.2-1 that the end supports for the member are torsionally simple, which means the end sections are prevented from twisting about the z-axis (Figure 6.5.6.2.2.2.2-1), but are free to warp out of plane. The effect of any warping restraint can be accounted for with the effective length factor, k. For the case of no warping restraint, k = 1.0, and for full warping restraint, k = 0.5 (Kitipornchai and Trahair, 1986). The base lateral-torsional buckling equations in the *AASHTO LRFD* Specifications conservatively assume k = 1.0. Warping restraint exists from adjacent unbraced lengths that are less critically loaded than the unbraced length under consideration, which can result in a reduced effective length factor for lateral-torsional buckling. A reduced effective length factor can be used to modify the unbraced length, L_b (i.e. kL_b), and to increase the elastic lateral-torsional buckling stress, F_{cr}, by a factor of ($1/k^2$) (Grubb and Schmidt, 2012). As mentioned previously in Section 6.5.2.1.3.2, *AASHTO LRFD* Article C6.10.8.2.3 makes reference to a procedure (SSRC, 1998; Nethercot and Trahair, 1976; Grubb and Schmidt, 2012) that can be used to calculate a reduced effective length factor for lateral-torsional buckling in special circumstances (e.g. when it becomes necessary to reduce the amplification of first-order flange lateral bending stresses).

The beneficial effect of a variation in the moment gradient along the length between brace points is accounted for by using the moment gradient modifier, C_b, which can take a value between 1.0 and 2.3 depending on the ratio and relative sign of the end moments. The C_b factor is discussed in greater detail below.

The coefficient, C, in Equation 6.5.6.2.2.2.2-1 accounts for the tipping or stabilizing effect that occurs if transverse loads are applied at the top or bottom flange of the member. Top flange loading aggravates the tendency toward lateral bucking and

therefore the last term in the brackets of Equation 6.5.6.2.2.2.2-1 should be subtracted if the load is applied through the top flange. Bottom flange loading has a stabilizing effect and therefore the last term should be added if load is applied through the bottom flange. For a simple span, C = 0.45 for a uniformly distributed load and 0.55 for a concentrated load. If the load is applied through the centroid or if the beam is loaded by end moments, C is taken equal to zero.

Most specifications, including the *AASHTO LRFD* Specifications, neglect the effect of load height. The neglect of this effect is believed justified because of the conservative approximations made in simplifying the theoretical formulas for use in design and also by the relative severity of the loading condition on which the provisions are based. Also, when loads are applied to the top flange, the members transmitting the load typically provide restraint to the twisting (e.g. the concrete deck). More recent formulations have accounted for the effect of the load height instead through the C_b factor (SSRC, 1998). *AASHTO LRFD* Article C6.10.8.2.3, points out that for unusual situations with no intermediate cross-bracing and for unbraced cantilevers with significant loading applied to the top flange, load-height effects should be considered in the calculation of C_b. In such cases, C_b can actually be less than 1.0. Solutions for unbraced cantilevers are given in Doswell (2002).

Equation 6.5.6.2.2.2.2-1 (minus the load height effect) is simplified in the *AASHTO LRFD* Specifications and extended to cover singly symmetric sections by introducing an effective radius of gyration for lateral-torsional buckling, r_t, which is essentially the radius of gyration of the compression flange plus 1/3 of the depth of the web in compression.

Also, within the provisions of *AASHTO LRFD* Article 6.10.8, the St. Venant torsional constant, J, in Equation 6.5.6.2.2.2.2-1 is assumed equal to zero. As discussed previously, the provisions of *AASHTO LRFD* Article 6.10.1.8 are assumed to apply to slender web sections. For very slender web sections, such as deep longitudinally stiffened girders, the contribution of J to the elastic lateral-torsional buckling resistance is generally small. Distortion of the web into an S shape and the corresponding raking of the flanges relative to each other is likely to reduce the buckling resistance further (Figure 6.4.8.2.3-1). For composite I-sections subject to negative flexure, the specification equation is generally conservative since it neglects the restraint provided to the bottom (compression) flange by the lateral and torsional stiffness of the concrete deck. However, for very slender web sections, the effect of this restraint is reduced by cross-section distortion and the fact that the deck may not provide an effectively fixed torsional restraint to such relatively large girders. For less slender sections approaching the noncompact web section slenderness limit, λ_{rw} (Equation 6.5.6.2.2.1.3-1), ignoring J is convenient, but tends to be conservative. For sections below the noncompact slenderness limit, the use of the equations given in *AASHTO LRFD* Article A6.3.3 (Section 6.5.6.2.3.3.2) should be considered instead. For such sections (i.e. compact web and noncompact web sections)

designed according to the optional provisions of *AASHTO LRFD* Appendix A6, *J* is included in the elastic buckling equation since these stockier sections are not subject to significant web distortion.

Lateral-torsional buckling in the elastic range is of primary importance for relatively slender girders braced at longer than normal intervals. Therefore, the elastic lateral-torsional buckling resistance is most useful when considering the resistance of such girders during the construction phase. In most cases, girders will be braced at intervals such that the girder will buckle laterally and torsionally only after some portions of the girder have exceeded the yield strain. This phenomenon is referred to as inelastic lateral-torsional buckling.

Inelastic lateral-torsional buckling is complex, as it is influenced by the magnitude and distribution of residual stresses, initial geometric imperfections, and the reduction in various stiffness properties (i.e. Young's modulus, shear modulus, minor-axis bending stiffness, St. Venant torsional stiffness and warping torsional stiffness) as a result of yielding due to in-plane flexure prior to buckling. Many researchers have employed a tangent-modulus approach to investigate the effect of inelastic lateral-torsional buckling. The AASHTO LRFD Specifications have adopted a simple linear expression to approximate the lateral-torsional buckling resistance of discretely braced compression flanges in the inelastic range.

The equations defining the nominal flexural resistance of the compression flange, F_{nc}, for lateral-torsional buckling in *AASHTO LRFD* Article 6.10.8.2.3 (Main Provisions) are expressed in terms of stress as follows (the equations are shown graphically in Figure 6.5.6.2.2.2.2-2**):**

- If $L_b \le L_p$, then:

$$F_{nc} = R_b R_h F_{yc} \qquad \text{Equation 6.5.6.2.2.2.2-2}$$

AASHTO LRFD Equation 6.10.8.2.3-1

- If $L_p < L_b \le L_r$, then:

$$F_{nc} = C_b\left[1 - \left(1 - \frac{F_{yr}}{R_h F_{yc}}\right)\left(\frac{L_b - L_p}{L_r - L_p}\right)\right] R_b R_h F_{yc} \le R_b R_h F_{yc} \qquad \text{Equation 6.5.6.2.2.2.2-3}$$

AASHTO LRFD Equation 6.10.8.2.3-2

- If $L_b > L_r$, then:

$$F_{nc} = F_{cr} \le R_b R_h F_{yc}$$ Equation 6.5.6.2.2.2.2-4

AASHTO LRFD Equation 6.10.8.2.3-3

where:

L_b = unbraced length (in.)

L_p = limiting unbraced length to achieve the nominal flexural resistance F_{max} equal to $R_b R_h F_{yc}$ under uniform bending (in.)

$$= 1.0 r_t \sqrt{\frac{E}{F_{yc}}}$$ Equation 6.5.6.2.2.2.2-5

AASHTO LRFD Equation 6.10.8.2.3-4

L_r = limiting unbraced length to achieve the onset of nominal yielding in either flange under uniform bending with consideration of compression-flange residual stress effects (in.)

$$= \pi r_t \sqrt{\frac{E}{F_{yr}}}$$ Equation 6.5.6.2.2.2.2-6

AASHTO LRFD Equation 6.10.8.2.3-5

C_b = moment gradient modifier (discussed below)

F_{cr} = elastic lateral-torsional buckling stress (ksi)

$$= \frac{C_b R_b \pi^2 E}{\left(\frac{L_b}{r_t}\right)^2}$$ Equation 6.5.6.2.2.2.2-7

AASHTO LRFD Equation 6.10.8.2.3-8

F_{yr} = compression-flange stress at the onset of nominal yielding within the cross-section, including residual stress effects, but not including compression-flange lateral bending, taken as the smaller of $0.7F_{yc}$ and F_{yw}, but not less than $0.5F_{yc}$ (ksi)

R_b = web load-shedding factor determined as specified in *AASHTO LRFD* Article 6.10.1.10.2 (Section 6.4.5.6)

R_h = hybrid factor determined as specified in *AASHTO LRFD* Article 6.10.1.10.1 (Section 6.4.5.7)

r_t = effective radius of gyration for lateral torsional buckling (in.)

$$= \frac{b_{fc}}{\sqrt{12\left(1 + \frac{1}{3}\frac{D_c t_w}{b_{fc} t_{fc}}\right)}}$$ Equation 6.5.6.2.2.2.2-8

AASHTO LRFD Equation 6.10.8.2.3-9

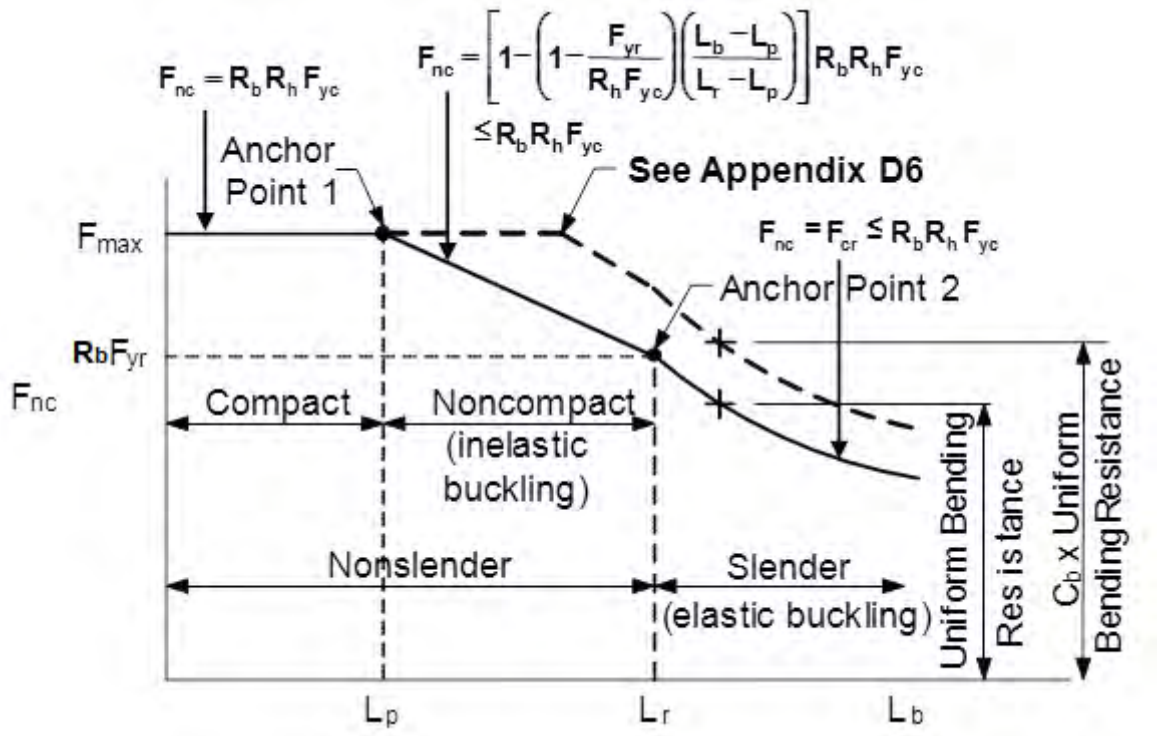

Figure 6.5.6.2.2.2.2-2 Lateral Torsional Buckling Resistance, F_{nc}

Brace points defining the unbraced length, L_b, of the compression flange are considered to be points where lateral deflection of the girder flange and twisting of the entire cross-section are restrained. In the past, points of contraflexure have sometimes been considered to act as brace points. Since this practice can lead to significantly unconservative estimates of the lateral-torsional buckling resistance, the *AASHTO LRFD Specifications* do not imply that points of contraflexure should be considered as brace points. Instead, the effects of moment gradient are to be handled directly through the use of the moment gradient modifier C_b (discussed below). Suggested values of C_b for rolled I-sections or for compact web sections subject to reverse curvature bending with no intermediate bracing or bracing on only one flange are provided in Yura and Helwig (2010), and in the Commentary to Article F1 of AISC (2010a).

The solid curve in Figure 6.5.6.2.2.2.2-2 represents the lateral-torsional buckling resistance for the case of uniform vertical bending. The dashed curve represents the lateral-torsional buckling resistance under moment gradient conditions (Figure 6.5.6.2.2.2.2-3). L_p and L_r are Anchor Points 1 and 2, respectively, as shown on Figure 6.5.6.2.2.2.2-2. L_p and L_r are given by Equation 6.5.6.2.2.2.2-5 and Equation 6.5.6.2.2.2.2-6, respectively.

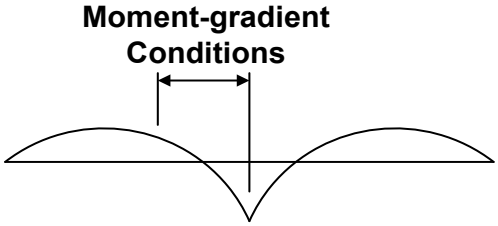

Figure 6.5.6.2.2.2.2-3 Moment Gradient Conditions

L_p defines the ′compact unbraced length′ limit. A member braced at or below the compact unbraced length limit is able to achieve the maximum potential lateral-torsional buckling resistance (F_{max} in Figure 6.5.6.2.2.2.2-2) of $R_bR_hF_{yc}$ under uniform vertical bending, which is independent of the unbraced length. The limit is more restrictive than the limit given in previous Specifications. It was developed based on a linear regression analysis for a wide range of data from experimental tests under uniform major-axis bending (with an effective length factor k for lateral-torsional buckling effectively equal to 1.0) that fell within the inelastic lateral-torsional buckling region (White, 2004). Note that in many cases, particularly under uniform vertical bending, it will not be economical to brace the girder at a distance equal to L_p or below in order to reach F_{max}.

L_r defines the ′noncompact unbraced length′ limit. The lateral-torsional buckling resistance of a member braced at or below the noncompact unbraced length limit is expressed in Equation 6.5.6.2.2.2.2-3 as a linear function of the unbraced length, as illustrated in Figure 6.5.6.2.2.2.2-2, which represents the inelastic lateral-torsional buckling resistance. L_r is the unbraced length at which the inelastic and elastic lateral-torsional buckling resistances are the same. The resistance at this point is assumed to be R_bF_{yr}. F_{yr} is taken as the smaller of $0.7F_{yc}$ and F_{yw}, but not less than $0.5F_{yc}$. With the exception of hybrid sections with F_{yw} significantly smaller than F_{yc}, $F_{yr} = 0.7F_{yc}$. This limit corresponds to an assumed nominal compression flange residual stress effect of $0.3F_{yc}$. As pointed out in *AASHTO LRFD* Article C6.10.8.2.3, the $0.5F_{yc}$ limit on F_{yr} avoids anomalous situations for some types of cross-sections in which the inelastic buckling equation gives a larger resistance than the corresponding elastic buckling curve.

Unbraced lengths greater than L_r are termed ′slender unbraced lengths′ and their resistance is controlled by elastic lateral-torsional buckling. As mentioned previously, lateral-torsional buckling in the elastic range is of primary importance for relatively slender girders braced at longer than normal intervals, which most typically occurs during a temporary construction condition. Equation 6.5.6.2.2.2.2-7 for the elastic lateral-torsional buckling stress, F_{cr}, is a conservative approximation of Equation 6.5.6.2.2.2.2-1 (assuming load-height effects are not considered). To

handle singly symmetric I-sections, an effective radius of gyration, r_t, is introduced as follows:

$$r_t = \frac{b_{fc}}{\sqrt{12\left(\frac{h}{d} + \frac{1}{3}\frac{D_c t_w}{b_{fc} t_{fc}}\frac{D^2}{hd}\right)}}$$ Equation 6.5.6.2.2.2.2-9

AASHTO LRFD Equation C6.10.8.2.3-1

where d is the overall depth of the steel section, and h is the depth between the flange centerlines. The expression for r_t given in Equation 6.5.6.2.2.2.2-8 is a simplification of Equation 6.5.6.2.2.2.2-9 obtained by assuming that $D = h = d$. However, Equation 6.5.6.2.2.2.2-9 is still provided in the Commentary to the specification (*AASHTO LRFD* Article C6.10.8.2.3) should the Design Engineer require a more precise calculation of the elastic lateral-torsional buckling stress. The web term, $D_c t_w$, in both expressions for r_t accounts for the destabilizing effects of the flexural compression in the web on the lateral-torsional buckling resistance.

Moment Gradient Modifier, C_b

The effect of a variation in the vertical bending moment along the length between brace points, or a moment gradient (Figure 6.5.6.2.2.2.2-3), is accounted for by applying the moment gradient modifier, C_b, to the base inelastic and elastic lateral-torsional buckling equations. When the moment and corresponding flange compressive vertical bending stress are constant along the unbraced length, C_b has a base value of 1.0. Under moment gradient conditions, C_b may be taken greater than 1.0, which effectively increases the lateral-torsional buckling resistance with the increase capped at $F_{max} = R_b R_h F_{yc}$ (refer to the dashed curves in Figure 6.5.6.2.2.2.2-2). C_b may conservatively be taken equal to 1.0 in all cases, except for some rare cases involving no cross-bracing within the span, as discussed below.

C_b is specified as follows in *AASHTO LRFD* Article 6.10.8.2.3:

- For unbraced cantilevers and for members when $f_{mid}/f_2 > 1$ or $f_2 = 0$:

$$C_b = 1.0$$ Equation 6.5.6.2.2.2.2-10

AASHTO LRFD Equation 6.10.8.2.3-6

- For all other cases:

$$C_b = 1.75 - 1.05\left(\frac{f_1}{f_2}\right) + 0.3\left(\frac{f_1}{f_2}\right)^2 \le 2.3$$ Equation 6.5.6.2.2.2.2-11

AASHTO LRFD Equation 6.10.8.2.3-7

where:

f_2 = except as noted in the following, largest factored compressive vertical bending stress at either end of the unbraced length of the flange under consideration, calculated from the critical moment envelope value (ksi). f_2 shall be taken as positive. If the stress is zero or tensile in the flange under consideration at both ends of the unbraced length, f_2 shall be taken as zero.

f_0 = factored vertical bending stress at the brace point opposite to the one corresponding to f_2, calculated from the moment envelope value that produces the largest compression at this point in the flange under consideration, or the smallest tension if this point is never in compression (ksi). f_0 shall be taken as positive in compression and negative in tension.

f_1 = factored vertical bending stress at the brace point opposite to the one corresponding to f_2, calculated as the intercept of the most critical assumed linear stress variation passing through f_2 and either f_{mid} or f_0, whichever produces the smaller value of C_b (ksi). f_1 may be determined as follows:

- When the variation in the moment along the entire length between brace points is concave in shape:

$$f_1 = f_0$$ Equation 6.5.6.2.2.2.2-12

AASHTO LRFD Equation 6.10.8.2.3-10

- Otherwise:

$$f_1 = 2f_{mid} - f_2 \ge f_0$$ Equation 6.5.6.2.2.2.2-13

AASHTO LRFD Equation 6.10.8.2.3-11

where:

f_{mid} = factored vertical bending stress at the middle of the unbraced length under consideration, calculated from the moment envelope value that produces the largest compression at this point, or the smallest tension if the point is never in compression (ksi). f_{mid} shall be taken as positive in compression and negative in tension.

Vertical bending stresses are used in Equation 6.5.6.2.2.2.2-11 since dead and live load bending moments are applied to different sections in composite girders, which is significant when the nominal flexural resistance is not permitted to exceed the moment at first yield. However, as pointed out in *AASHTO LRFD* Article C6.10.8.2.3, the ratio of the major-axis bending moments at the brace points may be used in lieu of the bending stresses for convenience, if the Design Engineer feels that the use of the moment ratios does not have a significant effect on the calculated value of C_b.

It is convenient and always conservative to use the critical moment envelope values to compute the above stresses, particularly since concurrent moment values at the brace points are not normally tracked in the analysis. It can be shown that the use of the critical moment envelope values to compute f_2, f_{mid} and f_o is always conservative since a more critical stress distribution along the unbraced length, in terms of computing C_b, cannot exist for all possible concurrent loadings.

The application of the C_b equation to different cases will be illustrated through the examples given in Figure 6.5.6.2.2.2.2-4. In examining these cases, recall that according to the definitions given above, in the calculation of C_b, compressive stresses are to be taken as positive and tensile stresses are to be taken as negative.

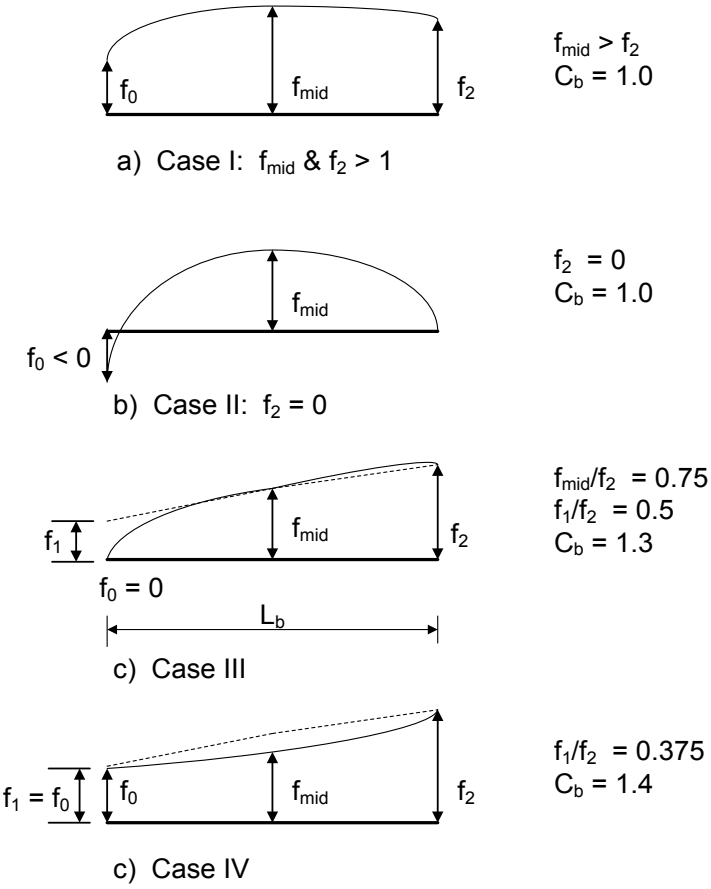

Figure 6.5.6.2.2.2.2-4 Moment Gradient Modifier, C_b – Example Cases

The first two cases illustrate when C_b must be taken equal to 1.0. In Case I shown in Figure 6.5.6.2.2.2.2-4 Part A, the compressive stress at the middle of the unbraced length, f_{mid}, is greater than the largest compressive stress at either end of the unbraced length, f_2. Therefore, C_b must be taken equal to 1.0. This is a common situation in regions of positive flexure when investigating the lateral-torsional buckling resistance of the top flange of the non-composite girder in critical unbraced lengths during construction.

In Case II shown in Figure 6.5.6.2.2.2.2-4 Part B, the stress in the top flange at one end of the unbraced length is zero and the stress in the top flange at the other end of the unbraced length is tensile. As stated in the above definition of the stress f_2, when this situation occurs, f_2 is to be taken as zero. And further, when f_2 is equal to zero, C_b must be taken equal to 1.0. The situation shown in Figure 6.5.6.2.2.2.2-4 Part B represents the rare case of a continuous span with no cross-bracing within the span. A case (not shown) where the stress would be zero at both ends of the unbraced length (and f_2 must then also be taken equal to zero according to the definition) would be a simply supported span with no cross-bracing within the span.

The last case (also not shown) for which C_b must be taken equal to 1.0 is for an unbraced cantilever, which is carried over from previous specifications. As discussed previously, for situations involving no cross-bracing within the span or unbraced cantilevers with significant loading applied to the top flange, consideration should be given to including load-height effects in the calculation of C_b (SSRC, 1998; Doswell, 2002). In such situations, the calculated C_b values may actually be less than 1.0. As pointed out in *AASHTO LRFD* Article C6.10.8.2.3, when C_b is less than 1.0, F_{nc} may be smaller than F_{max} even when L_b is less than L_p. Therefore, in these cases, it is recommended that F_{nc} be calculated from Equation 6.5.6.2.2.2.2-3 whenever L_b is less than or equal to L_r.

Equation 6.5.6.2.2.2.2-11 requires in certain situations the approximation of the stress variation along the unbraced length as the most critical of: 1) a line that passes through f_2 and f_{mid}, or 2) a line that passes between f_2 and f_0, whichever produces the smaller value of C_b. The intercept of the most critical line at the opposite end from f_2 is denoted as f_1. The preceding approximation is represented by Equation 6.5.6.2.2.2.2-13. For example, Case III shown in Figure 6.5.6.2.2.2.2-4 Part C represents a simply-supported member braced only at its ends and at midspan (only one-half of the member is assumed shown in the figure). In previous specifications, using the compressive stresses at each end of the unbraced length would have given a C_b value of 1.75 according to Equation 6.5.6.2.2.2.2-11. However, more accurate equations yield a C_b value of 1.3 for this case (AISC, 2010a) since the flange compression is significantly larger within the unbraced length than the linear variation implicitly assumed by Equation 6.5.6.2.2.2.2-11 due to the parabolic shape of the moment diagram. As shown in Figure 6.5.6.2.2.2.2-4 Part C, a line passing through f_2 and f_{mid} will produce a smaller value of C_b for this case than a line passing between f_2 and f_0 since the slope of a line through f_2 and f_{mid} is flatter and closer to that produced by a uniform moment. This fact is reflected when using Equation 6.5.6.2.2.2.2-13, which yields $f_1 = 2(0.75f_2) - f_2 = 0.5f_2 > f_0$. Substituting $f_1/f_2 = 0.5$ into Equation 6.5.6.2.2.2.2-11 yields $C_b = 1.3$.

It should be noted, however, that in most cases, Equation 6.5.6.2.2.2.2-13 will not need to be employed. The most common application of Equation 6.5.6.2.2.2.2-11 in design is for unbraced lengths in continuous spans in regions of negative flexure adjacent to interior piers, which are typically subject to significant moment gradients (Figure 6.5.6.2.2.2.2-3). The Design Engineer is strongly encouraged to calculate C_b for unbraced lengths adjacent to interior piers. The unbraced lengths on either side of the pier should be checked to determine which side will yield the lower value of C_b. As shown in Case IV in Figure 6.5.6.2.2.2.2-4 Part D, in these cases, where f_{mid} is smaller in magnitude than the average of f_0 and f_2 (or where the moment diagram is concave in shape along the entire length between brace points, which is the case in these regions), f_1 will always equal f_0. Therefore, the specification indicates that for cases where the moment diagram is concave in shape along the entire length between brace points, f_1 in Equation 6.5.6.2.2.2.2-11 may simply be taken equal to

f_0, or the stress at the brace point opposite to the one corresponding to f_2, and Equation 6.5.6.2.2.2.2-13 need not be employed. This of course assumes that the section within the unbraced length is prismatic, or if a flange transition is present that it is located a relatively short distance (i.e. $0.2L_b$) from the brace point with the smaller moment. As discussed further below, when this is not the case, C_b must be taken equal to 1.0. Sample illustrations of the calculation of the C_b factor for other cases, including cases of reverse curvature bending, are provided at the end of *AASHTO LRFD* Appendix C6. Further more detailed discussion on the derivation and calculation of the C_b factor may also be found in White (2012).

As represented by the dashed curves shown in Figure 6.5.6.2.2.2.2-2, under moment gradient conditions (i.e., $C_b > 1.0$), in addition to an increase in the base lateral-torsional buckling resistance, the maximum potential lateral-torsional buckling resistance, $F_{max} = R_b R_h F_{yc}$, can be reached at larger unbraced lengths. The provisions of *AASHTO LRFD* Article D6.4.1 (Appendix D6) can be used to calculate the maximum unbraced lengths to achieve F_{max} under moment gradient conditions, and are strongly recommended for use whenever C_b is greater than 1.0. The modifications to Anchor Points 1 and 2 to account for the effect of the moment gradient are given as follows in *AASHTO LRFD* Article D6.4.1:

- If $L_b \le L_p$, then:

$$F_{nc} = R_b R_h F_{yc} \qquad \text{Equation 6.5.6.2.2.2.2-14}$$

AASHTO LRFD Equation D6.4.1-1

- If $L_p < L_b \le L_r$, then:

  - If $L_b \le L_p + \dfrac{\left(1 - \dfrac{1}{C_b}\right)}{\left(1 - \dfrac{F_{yr}}{R_h F_{yc}}\right)}\left(L_r - L_p\right)$, then:

$$F_{nc} = R_b R_h F_{yc} \qquad \text{Equation 6.5.6.2.2.2.2-15}$$

AASHTO LRFD Equation D6.4.1-2

  - Otherwise:

$$F_{nc} = C_b\left[1-\left(1-\frac{F_{yr}}{R_hF_{yc}}\right)\left(\frac{L_b-L_p}{L_r-L_p}\right)\right]R_bR_hF_{yc} \le R_bR_hF_{yc}$$ Equation 6.5.6.2.2.2.2-16

AASHTO LRFD Equation D6.4.1-3

- If $L_b > L_r$, then:

  - If $L_b \le \pi r_t\sqrt{\frac{C_bE}{R_hF_{yc}}}$, then:

$$F_{nc} = R_bR_hF_{yc}$$ Equation 6.5.6.2.2.2.2-17

AASHTO LRFD Equation D6.4.1-4

  - Otherwise:

$$F_{nc} = F_{cr} \le R_bR_hF_{yc}$$ Equation 6.5.6.2.2.2.2-18

AASHTO LRFD Equation D6.4.1-5

Effect of Section Transitions within the Unbraced Length

The base lateral-torsional buckling equations in the specifications assume that the member is prismatic within the unbraced length. According to Carskaddan and Schilling (1974), under uniform vertical bending, the reduction in the elastic lateral-torsional buckling resistance due to a transition to a smaller section is approximately 5 percent when the transition is placed at 20 percent of the unbraced length from one of the brace points, and when the lateral moment of inertia of the flange in the smaller section is equal to one-half the corresponding value in the larger section. The reduction is less under moment gradient conditions as long as the larger bending moment occurs within the larger section, the lateral moment of inertia of the flange in the smaller section is greater than one-half the corresponding value in the larger section, and/or the section transition is placed closer to the brace point.

Therefore, *AASHTO LRFD* Article 6.10.8.2.3 permits the effect of the section transition on the lateral-torsional buckling resistance to be ignored when the stated conditions above are satisfied. If there is more than one section transition within the unbraced length, any transition within 20 percent of the unbraced length from the brace point with the smaller moment may be ignored, and the lateral-torsional buckling resistance based on the remaining sections may then be computed as described in the next paragraph.

For unbraced lengths containing a transition to a smaller section at a distance greater than 20 percent of the unbraced length from the brace point with the smaller moment, the lateral-torsional buckling resistance, F_{nc}, at each section within the unbraced length may be taken as the smallest resistance within the unbraced length according to *AASHTO LRFD* Article 6.10.8.2.3 (note that the transition can either be in the compression or tension flange). The resulting lateral-torsional buckling resistance must then not be exceeded at any section within the unbraced length. In addition, the C_b factor must be taken equal to 1.0 and the unbraced length must not be modified by an effective length factor.

Essentially, the nonprismatic member is being replaced with an equivalent prismatic member. The cross-section of the equivalent member that gives the correct lateral-torsional buckling resistance is generally some weighted average of all the cross-sections along the unbraced length. If the cross-section that gives the smallest uniform vertical bending resistance is used (i.e., calculated assuming C_b is equal to 1.0) and the calculated resistance based on that cross-section is not exceeded anywhere along the unbraced length, a conservative solution is obtained. A suggested procedure to obtain a more refined estimate of the lateral-torsional buckling resistance for this case is given in Grubb and Schmidt (2012).

The preceding requirements are summarized in Figure 6.5.6.2.2.2.2-5 for an unbraced length with a single section change. To avoid a significant reduction in the lateral-torsional buckling resistance in such cases according to the above criteria, consider locating flange transitions within 20 percent of the unbraced length from the brace point with the smaller moment and ensure that the lateral moment of inertia of the flange (or flanges) of the smaller section is equal to or larger than one-half the corresponding value(s) for the flange(s) of the larger section at the transition.

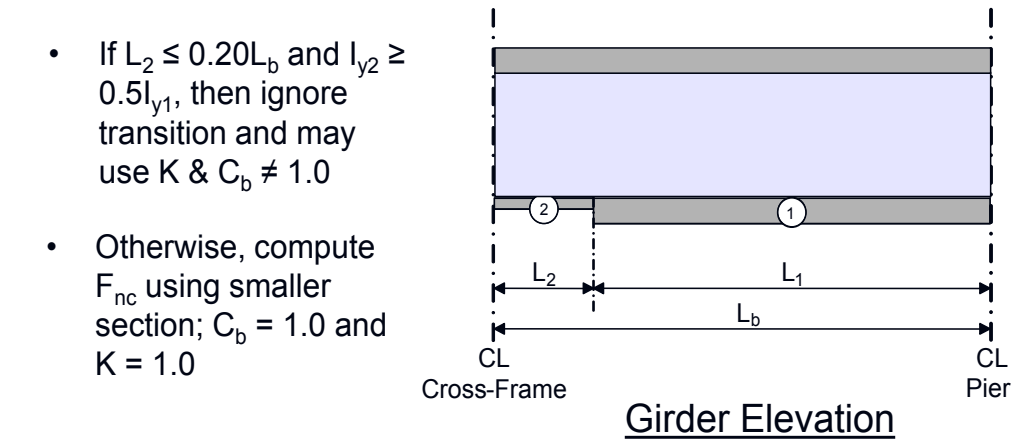

Figure 6.5.6.2.2.2.2-5 Unbraced Length with a Single Section Transition

Finally, for unbraced lengths consisting of singly symmetric non-composite I-sections subject to reverse curvature bending, the LTB resistance must be checked for both flanges, unless the top flange is considered to be continuously braced. Because the flanges of these sections are different sizes, the LTB resistance may be governed by compression in the smaller flange, even though the compressive stress may be smaller than the maximum compressive stress in the larger flange.

6.5.6.2.2.3 Tension Flanges

6.5.6.2.2.3.1 Continuously Braced Tension Flanges

Tension (top) flanges in regions of negative flexure in continuous-span composite members are typically classified as continuously braced flanges. A continuously braced flange is defined as a flange encased in concrete or anchored by shear connectors. Since in negative flexure regions, the top flange is in tension and the flange is usually continuously braced, only yielding of the flange is a concern and any flange lateral bending stresses need not be considered.

Continuously braced flanges in tension or compression must satisfy the following relationship at the strength limit state (*AASHTO LRFD* Article 6.10.8.1.3 in the Main Provisions):

$$f_{bu} \le \phi_f R_h F_{yf} \qquad \text{Equation 6.5.6.2.2.3.1-1}$$

AASHTO LRFD Equation 6.10.8.1.3-1

where:

F_{yf} = specified minimum yield strength of the flange under consideration (ksi)
R_h = hybrid factor determined as specified in *AASHTO LRFD* Article 6.10.1.10.1 (Section 6.4.5.7)

The specification considers the effects of any potential web bend buckling to be negligible for such cases, and therefore, the web load-shedding factor, R_b, is not included in Equation 6.5.6.2.2.3.1-1. Again, lateral bending does not need to be considered in Equation 6.5.6.2.2.3.1-1 because the flanges in these cases are continuously supported by the concrete deck.

6.5.6.2.2.3.2 Discretely Braced Tension Flanges

Discretely braced tension flanges of non-composite sections in positive or negative flexure must satisfy the following relationship at the strength limit state (*AASHTO LRFD* Article 6.10.8.1.2 in the Main Provisions):

$$f_{bu} + \frac{1}{3} f_{\ell} \le \phi_f F_{nt} \qquad \text{Equation 6.5.6.2.2.3.2-1}$$

AASHTO LRFD Equation 6.10.8.1.2-1

where:

f_{bu} = tension-flange stress calculated without consideration of flange lateral bending determined as specified in *AASHTO LRFD* Article 6.10.1.6 (ksi). f_{bu} is always taken as positive.

f_{ℓ} = factored flange lateral bending stress determined as specified in *AASHTO LRFD* Article 6.10.1.6 (ksi). f_{ℓ} is always taken as positive.

F_{nt} = nominal flexural resistance of the tension flange determined as specified in *AASHTO LRFD* Article 6.10.8.3 = $R_h F_{yt}$ (ksi)

F_{yt} = specified minimum yield strength of the tension flange (ksi)

R_h = hybrid factor determined as specified in *AASHTO LRFD* Article 6.10.1.10.1 (Section 6.4.5.7)

The nominal flexural resistance of the flange, F_{nt}, is based on yielding. According to *AASHTO LRFD* Article 6.10.1.6, for design checks involving yielding, f_{bu} and f_{ℓ} may be taken as the corresponding values at the section under consideration.

The sign of f_{bu} and f_{ℓ} is always taken as positive in Equation 6.5.6.2.2.3.2-1. However, when summing dead and live load stresses to obtain the total factored vertical and lateral bending stresses, f_{bu} and f_{ℓ}, to apply in the equation, the signs of the individual dead and live load stresses must be considered.

Potential sources of flange lateral bending in discretely braced tension flanges of non-composite sections at the strength limit state include curvature, wind loading and the effect of discontinuous cross-frames/diaphragms used in conjunction with support skew. During construction, overhang bracket loads on exterior girders acting on the non-composite section also cause flange lateral bending. According to *AASHTO LRFD* Article 6.10.1.6, amplification of the first-order flange lateral bending stresses is not required in discretely braced tension flanges. *AASHTO LRFD* Article 6.10.1.6 further specifies that the sum of the factored flange lateral bending stresses due to all sources cannot exceed $0.6F_{yf}$.

EXAMPLE

Check the composite section shown in Figure 6.4.2.3.3.3-1, which is the interior-pier section for an exterior girder in a straight continuous-span bridge (without skew), for the Strength I load combination (Section 3.9.1.2.2). The girder is hybrid with the flanges having a yield strength of 70 ksi and the web having a yield strength of 50 ksi. The load modifier, η, is assumed to be 1.0. Assume unshored construction. Use the section properties computed earlier for this section (Section 6.4.2.3.3.3). The web load-shedding factor, R_b, for this section was computed earlier to be 0.990

(Section 6.4.5.6). The hybrid factor, R_h, for this section was computed earlier to be 0.984 (Section 6.4.5.7). Assume the following unfactored bending moments:

M_{DC1} = -4,840 kip-ft
M_{DC2} = -690 kip-ft
M_{DW} = -664 kip-ft
M_{LL+IM} = -4,040 kip-ft

First, determine if the section satisfies the noncompact web section slenderness limit given as follows (Equation 6.5.6.2.2.1.3-1):

$$\frac{2D_c}{t_w} < 5.7\sqrt{\frac{E}{F_{yc}}}$$

where D_c is the depth of the web in compression in the elastic range. For composite sections, D_c is to be determined as specified in *AASHTO LRFD* Article D6.3.1. According to *AASHTO LRFD* Article D6.3.1 (Appendix D6), for composite sections in negative flexure at the strength limit state, D_c is to be computed for the section consisting of the steel girder plus the longitudinal reinforcement. For this section, D_c is equal to 36.96 inches. Therefore,

$$5.7\sqrt{\frac{29{,}000}{70}} = 116.0$$

$$\frac{2(36.96)}{0.5625} = 131.4 > 116.0$$

Since the section does not satisfy the noncompact web section slenderness limit, the section is classified as a slender-web section and the provisions of *AASHTO LRFD* Article 6.10.8 must be used to compute the nominal flexural resistance (i.e., the optional provisions of *AASHTO LRFD* Appendix A6, which permit the nominal flexural resistance to exceed the moment at first yield, cannot be used).

Calculate the local buckling resistance (FLB) of the bottom (compression) flange. Determine the slenderness ratio of the flange:

$$\lambda_f = \frac{b_{fc}}{2t_{fc}}$$

$$\lambda_f = \frac{20}{2(2)} = 5.0$$

Determine the limiting slenderness ratio for a compact flange (alternatively, see *AASHTO LRFD* Table C6.10.8.2.2-1 or Table 6.5.6.2.2.2.1-1):

$$\lambda_{pf} = 0.38\sqrt{\frac{E}{F_{yc}}}$$

$$\lambda_{pf} = 0.38\sqrt{\frac{29{,}000}{70}} = 7.73$$

Since $\lambda_f < \lambda_{pf}$ the flange is compact. Therefore (Equation 6.5.6.2.2.2.1-7),

$$F_{nc} = R_b R_h F_{yc}$$

$$(F_{nc})_{FLB} = (0.990)(0.984)(70.0) = 68.19 \text{ ksi}$$

Calculate the lateral-torsional buckling (LTB) resistance of the bottom flange. The unbraced length, L_b, on either side of the interior-pier is 20.0 feet. A flange transition is located 15.0 feet from each side of the interior pier. At the transition, the top flange steps down to a 1" x 18" plate and the bottom flange steps down to a 1" x 20" plate. The web remains at 9/16" x 69". Since the flange transition is located at a distance greater than 20 percent of the unbraced length from the brace point with the smaller moment, the LTB resistance is to be taken as the smallest resistance within the unbraced length under consideration according to *AASHTO LRFD* Article 6.10.8.2.3. The moment gradient modifier C_b is also to be taken equal to 1.0 and L_b is not to be modified by an effective length factor. Calculate F_{nc} based on the smaller section at the flange transition. From separate calculations, D_c for the section consisting of the steel girder plus the longitudinal reinforcement is computed to be 38.29 inches for the smaller section at the transition. Therefore (Equation 6.5.6.2.2.2.2-8):

$$r_t = \frac{b_{fc}}{\sqrt{12\left(1+\frac{1}{3}\frac{D_c t_w}{b_{fc} t_{fc}}\right)}}$$

$$r_t = \frac{20}{\sqrt{12\left(1+\frac{1}{3}\frac{38.29(0.5625)}{20(1)}\right)}} = 4.95 \text{ in.}$$

$$L_p = 1.0 r_t \sqrt{\frac{E}{F_{yc}}} \quad \text{(Equation 6.5.6.2.2.2-5)}$$

$$L_p = \frac{1.0(4.95)}{12}\sqrt{\frac{29{,}000}{70}} = 8.40 \text{ ft}$$

$$L_r = \pi r_t \sqrt{\frac{E}{F_{yr}}} \quad \text{(Equation 6.5.6.2.2.2-6)}$$

$$F_{yr} = 0.7F_{yc} \le F_{yw}$$

$$F_{yr} = 0.7(70) = 49.0 \text{ ksi} < 50 \text{ ksi} \qquad \text{ok}$$

F_{yr} must also not be less than $0.5F_{yc}$ = 0.5(70) = 35.0 ksi ok.

$$L_r = \frac{\pi(4.95)}{12}\sqrt{\frac{29{,}000}{49.0}} = 31.53 \text{ ft}$$

Since L_p = 8.40 feet < L_b = 20.0 feet < L_r = 31.53 feet (Equation 6.5.6.2.2.2-3),

$$F_{nc} = C_b\left[1-\left(1-\frac{F_{yr}}{R_h F_{yc}}\right)\left(\frac{L_b - L_p}{L_r - L_p}\right)\right]R_b R_h F_{yc} \le R_b R_h F_{yc}$$

From separate calculations similar to those illustrated previously, R_b and R_h for the smaller section at the flange transition are computed to be 0.977 and 0.971, respectively. Therefore,

$$(F_{nc})_{LTB} = 1.0\left[1-\left(1-\frac{49.0}{0.971(70.0)}\right)\left(\frac{20.0-8.40}{31.53-8.40}\right)\right](0.977)(0.971)(70)$$

$$= 57.11 \text{ ksi} < 0.977(0.971)(70) = 66.41 \text{ ksi}$$

$$(F_{nc})_{LTB} = 57.11 \text{ ksi}$$

The calculated lateral torsional buckling resistance must not be exceeded anywhere along the unbraced length. The major-axis bending stress in the bottom flange due to the factored loads at the interior-pier section for the Strength I load combination is computed to be:

Bottom flange at interior pier:

$$f = 1.0\left[\frac{1.25(-4{,}840)}{3{,}149} + \frac{1.25(-690)}{3{,}327} + \frac{1.5(-664)}{3{,}327} + \frac{1.75(-4{,}040)}{3{,}327}\right]12 = -55.26 \text{ ksi}$$

Assume the following unfactored bending moments at the flange transition:

M_{DC1} = -2,656 kip-ft
M_{DC2} = -373 kip-ft
M_{DW} = -358 kip-ft
M_{LL+IM} = -2,709 kip-ft

Using the elastic section properties for the smaller section at the flange transition (from separate calculations), the major-axis bending stress in the bottom flange due to the factored loads at this section for the Strength I load combination is computed to be:

Bottom flange at flange transition:

$$f = 1.0\left[\frac{1.25(-2{,}656)}{1{,}789} + \frac{1.25(-373)}{1{,}995} + \frac{1.5(-358)}{1{,}995} + \frac{1.75(-2{,}709)}{1{,}995}\right]12 = -56.82 \text{ ksi}$$

As specified in *AASHTO LRFD* Article 6.10.1.6, for design checks where the flexural resistance is based on lateral torsional buckling, f_{bu} is to be determined as the largest value of the compressive stress throughout the unbraced length in the flange under consideration, calculated without consideration of flange lateral bending. Therefore, f_{bu} = -56.82 ksi. As specified for discretely braced compression flanges at the strength limit state in *AASHTO LRFD* Article 6.10.8.1.1 (Equation 6.5.6.2.2-1):

$$f_{bu} + \frac{1}{3}f_{\ell} \le \phi_f F_{nc}$$

Since the bridge is straight and not skewed and wind load is not considered for the Strength I load combination, there are no sources of flange lateral bending. Therefore, f_{ℓ} is equal to zero. Since f_{ℓ} is equal to zero, amplification is also not a concern. Therefore,

$$f_{bu} + \frac{1}{3} f_\ell = \left|-56.82\right| \text{ ksi} + \frac{1}{3}(0) = 56.82 \text{ ksi}$$
$$\phi_f (F_{nc})_{LTB} = 1.0(57.11) = 57.11 \text{ ksi}$$
$$56.82 \text{ ksi} < 57.11 \text{ ksi} \qquad \text{ok}$$

For design checks where the flexural resistance is based on flange local buckling, f_{bu} may be determined as the corresponding value at the section under consideration according to *AASHTO LRFD* Article 6.10.1.6. Therefore, at the interior-pier section:

$$f_{bu} + \frac{1}{3} f_\ell = \left|-55.26\right| \text{ ksi} + \frac{1}{3}(0) = 55.26 \text{ ksi}$$
$$\phi_f (F_{nc})_{FLB} = 1.0(68.19) = 68.19 \text{ ksi}$$
$$55.26 \text{ ksi} < 68.19 \text{ ksi} \qquad \text{ok}$$

At the bottom flange transition:

$$f_{bu} + \frac{1}{3} f_\ell = \left|-56.82\right| \text{ ksi} + \frac{1}{3}(0) = 56.82 \text{ ksi}$$
$$\phi_f (F_{nc})_{FLB} = 1.0(68.19) = 68.19 \text{ ksi}$$
$$56.82 \text{ ksi} < 68.19 \text{ ksi} \qquad \text{ok}$$

For illustration, assume that the flange transition in this case is instead located 17.0 feet from each side of the interior pier. Since the flange transition is now located at a distance less than or equal to 20 percent of the unbraced length from the brace point with the smaller moment, *AASHTO LRFD* Article 6.10.8.2.3 permits the effect of the section transition on the LTB resistance to be ignored. Therefore, the LTB resistance may be computed based on the larger section at the interior pier.

$$r_t = \frac{20}{\sqrt{12\left(1 + \frac{1}{3}\frac{36.55(0.5625)}{20(2)}\right)}} = 5.33 \text{ in.}$$

$$L_p = \frac{1.0(5.33)}{12}\sqrt{\frac{29{,}000}{70}} = 9.04 \text{ ft}$$

$$L_r = \frac{\pi(5.33)}{12}\sqrt{\frac{29{,}000}{49.0}} = 33.95 \text{ ft}$$

Since the effect of the transition is ignored, the moment gradient modifier, C_b, may also now be applied (Equation 6.5.6.2.2.2.2-11).

$$C_b = 1.75 - 1.05\left(\frac{f_1}{f_2}\right) + 0.3\left(\frac{f_1}{f_2}\right)^2 \le 2.3$$

f_2 is generally taken as the largest compressive stress without consideration of lateral bending due to the factored loads at either end of the unbraced length of the flange under consideration, calculated from the critical moment envelope value. Since the stress at both ends of the unbraced length is not zero or tensile, f_2 in this case is equal to the compressive stress in the bottom flange at the interior-pier section due to the factored loads, which was computed earlier to be 55.26 ksi (f_2 is always taken as positive in this calculation).

As stated in *AASHTO LRFD* Article 6.10.8.2.3, when the variation in the moment along the entire length between brace points is concave in shape (which is the case here), f_1 may simply be taken equal to f_0, where f_0 is the stress without consideration of lateral bending due to the factored loads at the brace point opposite to the one corresponding to f_2. f_0 is to be calculated from the moment envelope value that produces the largest compression, or the smallest tension if the point is never in compression. Assume the following unfactored bending moments at the first brace point located 20.0 feet from the interior pier:

M_{DC1} = -2,390 kip-ft
M_{DC2} = -334 kip-ft
M_{DW} = -321 kip-ft
M_{LL+IM} = -2,615 kip-ft

Since it is assumed that the flange transition does not exist in this case, calculate the major-axis bending stress in the bottom flange due to the factored loads at this brace point for the Strength I load combination using the section properties of the (larger) interior-pier section:

Bottom flange at brace point:

$$f_1 = f_o = 1.0\left[\frac{1.25(-2{,}390)}{3{,}149} + \frac{1.25(-334)}{3{,}327} + \frac{1.5(-321)}{3{,}327} + \frac{1.75(-2{,}615)}{3{,}327}\right]12 = -31.13 \text{ ksi}$$

f_0 is to be taken as positive in compression in the calculation of C_b. Therefore, $f_1 = f_0$ = 31.13 ksi.

$$C_b = 1.75 - 1.05\left(\frac{31.13}{55.26}\right) + 0.3\left(\frac{31.13}{55.26}\right)^2 = 1.25 < 2.3$$

Since C_b is greater than 1.0, the provisions of *AASHTO LRFD* Article D6.4.1 (Appendix D6) will be used to calculate the maximum unbraced lengths to achieve F_{max} under moment gradient conditions.

Since L_p = 9.04 feet < L_b = 20.0 feet < L_r = 33.95 feet, check the following:

$$L_b \le L_p + \frac{\left(1 - \frac{1}{C_b}\right)}{\left(1 - \frac{F_{yr}}{R_h F_{yc}}\right)}\left(L_r - L_p\right)$$

$$L_b = 20.0 < 9.04 + \frac{\left(1 - \frac{1}{1.25}\right)}{\left(1 - \frac{49.0}{0.984(70.0)}\right)}\left(33.95 - 9.04\right) = 26.30 \text{ ft} \quad \text{ok}$$

Therefore (Equation 6.5.6.2.2.2.2-15),

$$F_{nc} = R_b R_h F_{yc}$$

$$\left(F_{nc}\right)_{LTB} = (0.990)(0.984)(70.0) = 68.19 \text{ ksi}$$

$$(F_{nc})_{LTB} = 68.19 \text{ ksi}$$

By locating the flange transition within 20 percent of the unbraced length from the brace point with the smaller moment, the LTB resistance increased by 19.4 percent in this case.

Check the top (tension) flange. The nominal flexural resistance of the tension flange is based on yielding. As specified in *AASHTO LRFD* Article 6.10.1.6, for design checks where the flexural resistance is based on yielding, the major-axis bending stress f_{bu} may be determined as the corresponding stress at the section under consideration. The major-axis bending stress in the top flange due to the factored loads at the interior-pier section for the Strength I load combination is computed to be:

Top flange at interior pier:

$$f_{bu} = 1.0\left[\frac{1.25(-4{,}840)}{2{,}942} + \frac{1.25(-690)}{3{,}808} + \frac{1.5(-664)}{3{,}808} + \frac{1.75(-4{,}040)}{3{,}808}\right]12 = 52.81 \text{ ksi}$$

As specified for continuously braced tension flanges at the strength limit state in *AASHTO LRFD* Article 6.10.8.1.3 (Equation 6.5.6.2.2.3.1-1):

$$f_{bu} \le \phi_f R_h F_{yf}$$

$$\phi_f R_h F_{yf} = 1.0(0.984)(70) = 68.88 \text{ ksi}$$

$$52.81 \text{ ksi} < 68.88 \text{ ksi} \quad \text{ok}$$

6.5.6.2.3 I-Sections: AASHTO Appendix A6

6.5.6.2.3.1 General

As specified in *AASHTO LRFD* Article 6.10.6.2.3 (and repeated in *AASHTO LRFD* Article A6.1), sections in straight bridges whose supports are normal or skewed not more than 20° from normal and with intermediate cross-frame/diaphragms placed in contiguous lines parallel to the supports, for which:

- The specified minimum yield strengths of the flanges do not exceed 70 ksi;
- The web satisfies the noncompact slenderness limit, λ_{rw}, given by Equation 6.5.6.2.2.1.3-1, and for which;
- The flanges satisfy the following ratio:

$$\frac{I_{yc}}{I_{yt}} \ge 0.3 \qquad \text{Equation 6.5.6.2.3.1-1}$$

AASHTO LRFD Equation 6.10.6.2.3-2 and Equation A6.1-2

where:

I_{yc} = moment of inertia of the compression flange of the steel section about the vertical axis in the plane of the web (in.^{4})

I_{yt} = moment of inertia of the tension flange of the steel section about the vertical axis in the plane of the web (in.^{4})

can optionally be proportioned according to the provisions for compact web and noncompact web sections given in *AASHTO LRFD* Appendix A6.

Sections designed according to the provisions of *AASHTO LRFD* Appendix A6 must qualify as either compact web or noncompact web I-sections (Section 6.5.6.2.2.1). Basically, the provisions of *AASHTO LRFD* Appendix A6 account for the ability of certain compact and noncompact web I-sections to develop flexural resistances

significantly greater than M_y. As a result, the equations giving the nominal flexural resistance in *AASHTO LRFD* Appendix A6 are all more appropriately expressed in terms of bending moment. The provisions also account for the contribution of the St. Venant torsional resistance to the lateral-torsional buckling resistance of these sections, which may be useful for compact and noncompact web sections with larger unbraced lengths, particularly under certain construction conditions.

The potential benefits of the *AASHTO LRFD* Appendix A6 provisions tend to be small for I-sections with webs that approach the noncompact web slenderness limit, λ_{rw}, given by Equation 6.5.6.2.2.1.3-1. In such cases, the simpler and more streamlined provisions of *AASHTO LRFD* Article 6.10.8 are recommended (Section 6.5.6.2.2). The potential gains in economy in using *AASHTO LRFD* Appendix A6 increase with decreasing web slenderness. The Engineer is strongly encouraged to utilize *AASHTO LRFD* Appendix A6 for sections in which the web is compact or nearly compact.

The provisions of *AASHTO LRFD* Appendix A6 are fully consistent with and are a direct extension of the procedures specified in *AASHTO LRFD* Article 6.10.8 in concept and in implementation. Calculation of potential flexural resistances greater than the yield moment, M_y (Section 6.4.5.3) is accomplished through the use of the web plastification factors, R_{pc} and R_{pt}, described further in Section 6.5.6.2.3.2.

I-section members with a specified minimum yield strength of the flanges greater than 70 ksi are more likely to be limited by Equation 6.5.6.2.2.1.3-1, and are likely to be controlled by design conditions other than the strength limit state conditions. In cases where Equation 6.5.6.2.2.1.3-1 is satisfied with F_{yc} greater than 70 ksi, the implications of designing such members at the strength limit state using a nominal flexural resistance greater than M_y have not been sufficiently studied to allow the use of *AASHTO LRFD* Appendix A6.

Research has also not yet been conducted to extend the provisions of *AASHTO LRFD* Appendix A6 to sections in kinked (chorded) continuous or horizontally curved-girder bridges, or to composite sections subject to negative flexure or non-composite sections in straight-girder bridges with skew angles exceeding 20 degrees from normal. The effects of the transverse redistribution of loads that occurs as interior-pier sections begin to yield in these bridges have not been examined. Severely skewed bridges with contiguous cross-frames have greater transverse stiffness relative to those with discontinuous cross-frames and thus already have relatively large cross-frame forces in the elastic range. As pier sections yield and begin to lose stiffness and shed their load, the forces in the adjacent cross-frames will increase. There is currently no established procedure to predict the resulting increase in the forces short of doing a refined non-linear 3D analysis. Such analyses cannot be performed with moving live loads since the influence surface method requires an elastic structure.

With discontinuous cross-frames, significant lateral flange bending effects usually occur. The resulting lateral bending moments (and stresses) are amplified in the bottom (compression) flange adjacent to the pier as the flange deflects laterally. There is currently no means to accurately predict these amplification effects as the flange is also yielding. Accurate prediction of even the first-order lateral bending effects requires a refined analysis model that should include the modeling of any actual lateral bearing restraints. Skewed supports also result in twisting of the girders, which is not recognized in plastic-design theory. The relative vertical deflections of the girders create eccentricities that are also not recognized in the theory. Thus, until further research work is done to examine these effects in greater detail, the conservative approach has been taken in the specification.

The reason for the limiting ratio given by Equation 6.5.6.2.3.1-1 was discussed previously in Section 6.4.8.2.3.

Example applications of the *AASHTO LRFD* Appendix A6 provisions are demonstrated in Barth (2012) and Barth (2012a).

6.5.6.2.3.2 Web Plastification Factors

AASHTO LRFD Article A6.2 defines the web plastification factors, R_{pc} and R_{pt}, for the compression and tension flange, respectively. The web plastification factors are essentially effective shape factors that define a smooth linear transition in the maximum flexural resistance between M_y and M_p.

For a compact web section, or a section with a web satisfying Equation 6.5.6.2.2.1.2-1, the web plastification factors are equivalent to the cross-section shape factors as follows (*AASHTO LRFD* Article A6.2.1):

$$R_{pc} = \frac{M_p}{M_{yc}} \qquad \text{Equation 6.5.6.2.3.2-1}$$

AASHTO LRFD Equation A6.2.1-4

$$R_{pt} = \frac{M_p}{M_{yt}} \qquad \text{Equation 6.5.6.2.3.2-2}$$

AASHTO LRFD Equation A6.2.1-5

Thus, whenever R_{pc} and R_{pt} given by the preceding equations are used in the appropriate flexural resistance equations, the maximum flexural resistance of a compact web section, M_{max}, will equal the plastic moment, M_p (Section 6.4.5.2). By

using R_{pc} and R_{pt} in the flexural resistance equations, separate flexural resistance equations are not required for compact and noncompact web sections.

For a noncompact web section, or a section with a web not satisfying Equation 6.5.6.2.2.1.2-1, but satisfying Equation 6.5.6.2.2.1.3-1, the web plastification factors are given as follows (*AASHTO LRFD* Article A6.2.2):

$$R_{pc} = \left[1 - \left(1 - \frac{R_h M_{yc}}{M_p}\right)\left(\frac{\lambda_w - \lambda_{pw(D_c)}}{\lambda_{rw} - \lambda_{pw(D_c)}}\right)\right]\frac{M_p}{M_{yc}} \le \frac{M_p}{M_{yc}} \qquad \text{Equation 6.5.6.2.3.2-3}$$

AASHTO LRFD Equation A6.2.2-4

$$R_{pt} = \left[1 - \left(1 - \frac{R_h M_{yt}}{M_p}\right)\left(\frac{\lambda_w - \lambda_{pw(D_c)}}{\lambda_{rw} - \lambda_{pw(D_c)}}\right)\right]\frac{M_p}{M_{yt}} \le \frac{M_p}{M_{yt}} \qquad \text{Equation 6.5.6.2.3.2-4}$$

AASHTO LRFD Equation A6.2.2-5

where λ_w is equal to the web slenderness, $2D_c/t_w$, based on the elastic moment, λ_{rw} is equal to the web slenderness limit for a noncompact web section given in Equation 6.5.6.2.2.1.3-1, and $\lambda_{pw(Dc)}$ is the limit slenderness ratio for a compact web corresponding to $2D_c/t_w$ given as follows:

$$\lambda_{pw(D_c)} = \lambda_{pw(D_{cp})}\left(\frac{D_c}{D_{cp}}\right) \le \lambda_{rw} \qquad \text{Equation 6.5.6.2.3.2-5}$$

AASHTO LRFD Equation A6.2.2-6

D_{cp} is the depth of the web in compression at the plastic moment, and $\lambda_{pw(Dcp)}$ is the limiting slenderness ratio for a compact web corresponding to $2D_{cp}/t_w$ given by Equation 2.104.

Equation 6.5.6.2.3.2-3 and Equation 6.5.6.2.3.2-4 define a linear transition in the maximum potential flexural resistance, M_{max}, of a noncompact web section between M_y and M_p as a function of the web slenderness. As $2D_c/t_w$ approaches the noncompact web section limit, λ_{rw}, the web plastification factors approach values equal to the hybrid factor, R_h, and therefore, M_{max} within the appropriate flexural resistance equations approaches a limiting value of R_hM_{yc} or R_hM_{yt}, as applicable. As $2D_{cp}/t_w$ approaches the compact web section limit, $\lambda_{pw(Dcp)}$, the web plastification factors approach the cross-section shape factors (Equation 6.5.6.2.3.2-1 and Equation 6.5.6.2.3.2-2), and therefore, M_{max} within the appropriate flexural resistance equations approaches a limiting value of M_p. Equation 6.5.6.2.3.2-5 converts the

web compactness limit defined in terms of D_{cp}, as given by Equation 6.5.6.2.2.1.2-2, to a value that can be used consistently in Equation 6.5.6.2.3.2-3 and Equation 6.5.6.2.3.2-4 with the web slenderness, λ_w, which is expressed in terms of D_c. The reason for the upper limit of λ_{rw} in Equation 6.5.6.2.3.2-5 was discussed previously in Section 6.5.6.2.2.1.2.

Upper limits of M_p/M_{yc} and M_p/M_{yt} are placed on R_{pc} and R_{pt}, respectively, in Equation 6.5.6.2.3.2-3 and Equation 6.5.6.2.3.2-4. These upper limits will limit the larger of the base resistances, $R_{pc}M_{yc}$ or $R_{pc}M_{yt}$, to M_p for the rare case of an extremely monosymmetric section in which M_{yc} or M_{yt} is greater than M_p. However, the flange-proportioning limit given by Equation 6.3.4.4.2-4 will generally tend to prevent the use of such sections

6.5.6.2.3.3 Sections with Discretely Braced Compression Flanges

As specified in *AASHTO LRFD* Article A6.1.1, at the strength limit state, discretely braced compression flanges must satisfy the one-third rule equation (Section 6.5.2.1.4) expressed in terms of bending moment as follows:

$$M_u + \frac{1}{3} f_\ell S_{xc} \le \phi_f M_{nc} \qquad \text{Equation 6.5.6.2.3.3-1}$$

AASHTO LRFD Equation A6.1.1-1

where:

M_u = bending moment about the major axis of the cross-section determined as specified in *AASHTO LRFD* Article 6.10.1.6 (kip-in.). M_u is always taken as positive.

f_ℓ = flange lateral bending stress determined as specified in *AASHTO LRFD* Article 6.10.1.6 (ksi). f_ℓ is always taken as positive.

M_{nc} = nominal flexural resistance based on the compression flange determined as specified in *AASHTO LRFD* Article A6.3 (kip-in.)

S_{xc} = elastic section modulus about the major axis of the section to the compression flange taken as M_{yc}/F_{yc} (in.^{3})

A discretely braced flange is a flange braced at discrete intervals by bracing sufficient to restrain lateral deflection of the flange and twisting of the entire cross-section at the brace points. At the strength limit state, discretely braced compression flanges would typically be the bottom flanges in regions of negative flexure in continuous-span members. During construction, top flanges of the non-composite section in regions of positive flexure would also be classified as discretely braced compression flanges.

Equation 6.5.6.2.3.3-1 must be satisfied for both local buckling and lateral-torsional buckling using the appropriate value of M_{nc} determined for each case, as specified in *AASHTO LRFD* Articles A6.3.2 and A6.3.3, respectively. The computation of M_{nc} for local buckling and lateral-torsional buckling is discussed further in Sections 6.5.6.2.3.3.1 and 6.5.6.2.3.3.2, respectively.

AASHTO LRFD Article 6.10.1.6 specifies that for design checks involving lateral-torsional buckling, the major-axis bending moment, M_u, and flange lateral bending stress, f_ℓ, are to be taken as the largest values throughout the unbraced length in the flange under consideration. This is consistent with established practice in applying beam-column interaction equations involving member stability checks. For design checks involving flange local buckling, M_u and f_ℓ may be taken as the corresponding values at the section under consideration. However, when maximum values of these stresses occur at different locations within the unbraced length, which is often the case, it is conservative to use the maximum values in the local buckling check.

The sign of M_u and f_ℓ is always taken as positive in Equation 6.5.6.2.3.3-1. However, when summing dead and live load moment/stresses to obtain the total factored major-axis bending moments and lateral bending stresses, M_u and f_ℓ, to apply in the equation, the signs of the individual dead and live load moments/stresses must be considered**.**

Potential sources of flange lateral bending in discretely braced compression flanges at the strength limit state include curvature, wind loading and the effect of discontinuous cross-frames/diaphragms used in conjunction with support skew. During construction, overhang bracket loads on exterior girders acting on the non-composite section also cause flange lateral bending. According to *AASHTO LRFD* Article 6.10.1.6, amplification of the first-order flange lateral bending stresses may be required in discretely braced compression flanges. Amplification of these stresses was discussed previously in Section 6.5.2.1.3.2. *AASHTO LRFD* Article 6.10.1.6 further specifies that the sum of the factored flange lateral bending stresses due to all sources (after amplification) cannot exceed $0.6F_{yf}$.

The elastic section modulus, S_{xc}, in Equation 6.5.6.2.3.3-1 is defined as M_{yc}/F_{yc} so that for a composite section with a web proportioned exactly at the noncompact web slenderness limit given in Equation 6.5.6.2.2.1.3-1, the flexural resistance given by *AASHTO LRFD* Appendix A6 will be approximately the same as the flexural resistance given by the Main Provisions (*AASHTO LRFD* Article 6.10.8). Slight differences between the resistance predictions may occur for reasons pointed out in *AASHTO LRFD* Article CA6.1.1.

6.5.6.2.3.3.1 Local Buckling Resistance

The basic form of the flange local buckling equations as a function of the compression-flange slenderness is discussed further in Section 6.5.6.2.2.2.1. According to *AASHTO LRFD* Article A6.3.2, the flexural resistance based on compression flange local buckling, M_{nc}, for use in *AASHTO LRFD* Appendix A6 is to be taken as follows:

- If $\lambda_f \le \lambda_{pf}$, then

$$M_{nc} = R_{pc} M_{yc} \qquad \text{Equation 6.5.6.2.3.3.1-1}$$

AASHTO LRFD Equation A6.3.2-1

- Otherwise:

$$M_{nc} = \left[1 - \left(1 - \frac{F_{yr} S_{xc}}{R_{pc} M_{yc}}\right)\left(\frac{\lambda_f - \lambda_{pf}}{\lambda_{rf} - \lambda_{pf}}\right)\right] R_{pc} M_{yc} \qquad \text{Equation 6.5.6.2.3.3.1-2}$$

AASHTO LRFD Equation A6.3.2-2

where:

λ_f = slenderness ratio for the compression flange = $b_{fc}/2t_{fc}$

λ_{pf} = limiting slenderness ratio for a compact flange

$$= 0.38\sqrt{\frac{E}{F_{yc}}} \qquad \text{Equation 6.5.6.2.3.3.1-3}$$

AASHTO LRFD Equation A6.3.2-4

λ_{rf} = limiting slenderness ratio for a noncompact flange

$$= 0.95\sqrt{\frac{Ek_c}{F_{yr}}} \qquad \text{Equation 6.5.6.2.3.3.1-4}$$

AASHTO LRFD Equation A6.3.2-5

F_{yr} = compression-flange stress at the onset of nominal yielding within the cross-section, including residual stress effects, but not including compression-flange lateral bending, taken as the smaller of $0.7F_{yc}$, $R_h F_{yt} S_{xt}/S_{xc}$ and F_{yw}, but not less than $0.5F_{yc}$ (ksi)

k_c = flange local buckling coefficient taken as follows:

- For built-up sections:

$= 4/\sqrt{D/t_w}$ with $0.35 \leq k_c \leq 0.76$

- For rolled sections:
  = 0.76

R_h = hybrid factor determined as specified in *AASHTO LRFD* Article6.10.1.10.1 (Section 6.4.5.7)
R_{pc} = web plastification factor for the compression flange determined as specified in *AASHTO LRFD* Article A6.2.1 or A6.2.2, as applicable (Section 6.5.6.2.3.2)
S_{xc} = elastic section modulus about the major axis of the section to the compression flange taken as M_{yc}/F_{yc} (in.^{3})
S_{xt} = elastic section modulus about the major axis of the section to the tension flange taken as M_{yt}/F_{yt} (in.^{3})

λ_{pf} and λ_{rf} are Anchor Points 1 and 2, respectively, as shown on Figure 6.5.6.2.2.2.1-1. The derivation of these Anchor Points was discussed previously in Section 6.5.6.2.2.2.1. λ_{pf} defines the limiting slenderness ratio for a compact flange. A compact flange is able to achieve the maximum potential local buckling resistance (M_{max} in Figure 6.5.6.2.2.2.1-1) of $R_{pc}M_{yc}$, which is independent of the flange slenderness. Values of λ_{pf} for different grades of steel were given previously in Table 6.5.6.2.2.2.1-1.

λ_{rf} defines the limiting slenderness ratio for a noncompact flange. The local buckling resistance of a noncompact flange is expressed in Equation 6.5.6.2.3.3.1-2 as a linear function of the flange slenderness, as illustrated in Figure 6.5.6.2.2.2.1-1, which represents the inelastic local buckling resistance. λ_{rf} is the compression-flange slenderness at which the inelastic and elastic local buckling resistances are the same. The resistance at this point is assumed to be $R_bF_{yr}S_{xc}$. F_{yr} (and its associated limits), along with the derivation of the flange local buckling coefficient k_c, are discussed in more detail in Sections 6.5.6.2.2.2.2 and 6.5.6.2.2.2.1, respectively).

Compression flanges with a slenderness greater than λ_{rf} are termed slender flanges and their resistance is controlled by elastic local buckling. However, as pointed out previously, because $b_{fc}/2t_{fc}$ is limited to a practical maximum value of 12.0 in *AASHTO LRFD* Article 6.10.2.2, elastic flange local buckling typically does not control for specified minimum yield strengths of the compression flange F_{yc} up to and including 70 ksi, which is the limiting yield strength for the application of the provisions of *AASHTO LRFD* Appendix A6.

6.5.6.2.3.3.2 Lateral Torsional Buckling Resistance

The basic form of the lateral torsional buckling (LTB) equations as a function of the unbraced length is discussed further in Section 6.5.6.2.2.2.2. According to *AASHTO LRFD* Article A6.3.3, the flexural resistance based on lateral-torsional buckling, M_{nc}, for use in *AASHTO LRFD* Appendix A6 is to be taken as follows:

- If $L_b \le L_p$, then

$$M_{nc} = R_{pc}M_{yc} \qquad \text{Equation 6.5.6.2.3.3.2-1}$$

AASHTO LRFD Equation A6.3.3-1

- If $L_p < L_b \le L_r$, then

$$M_{nc} = C_b\left[1-\left(1-\frac{F_{yr}S_{xc}}{R_{pc}M_{yc}}\right)\left(\frac{L_b-L_p}{L_r-L_p}\right)\right]R_{pc}M_{yc} \le R_{pc}M_{yc} \qquad \text{Equation 6.5.6.2.3.3.2-2}$$

AASHTO LRFD Equation 6.3.3-2

- If $L_b > L_r$, then

$$M_{nc} = F_{cr}S_{xc} \le R_{pc}M_{yc} \qquad \text{Equation 6.5.6.2.3.3.2-3}$$

AASHTO LRFD Equation A6.3.3-3

where:

L_b = unbraced length (in.)

L_p = limiting unbraced length to achieve the nominal flexural resistance

M_{max} = $R_{pc}M_{yc}$ under uniform bending (in.)

$$= 1.0r_t\sqrt{\frac{E}{F_{yc}}} \qquad \text{Equation 6.5.6.2.3.3.2-4}$$

AASHTO LRFD Equation A6.3.3-4

L_r = limiting unbraced length to achieve the onset of nominal yielding in either flange under uniform bending with consideration of compression-flange residual stress effects (in.)

$$= 1.95r_t\frac{E}{F_{yr}}\sqrt{\frac{J}{S_{xc}h}}\sqrt{1+\sqrt{1+6.76\left(\frac{F_{yr}}{E}\frac{S_{xc}h}{J}\right)^2}} \qquad \text{Equation 6.5.6.2.3.3.2-5}$$

AASHTO LRFD Equation A6.3.3-5

C_b = moment gradient modifier (discussed below)

F_{cr} = elastic lateral-torsional buckling stress (ksi)

$$= \frac{C_b \pi^2 E}{(L_b/r_t)^2}\sqrt{1+0.078\frac{J}{S_{xc}h}(L_b/r_t)^2} \quad \text{Equation 6.5.6.2.3.3.2-6}$$

AASHTO LRFD Equation A6.3.3-8

F_{yr} = compression-flange stress at the onset of nominal yielding within the cross-section, including residual stress effects, but not including compression-flange lateral bending, taken as the smaller of $0.7F_{yc}$, $R_hF_{yt}S_{xt}/S_{xc}$ and F_{yw}, but not less than $0.5F_{yc}$ (ksi)

J = St. Venant torsional constant (in.^{4})

$$= \frac{Dt_w^3}{3}+\frac{b_{fc}t_{fc}^3}{3}\left(1-0.63\frac{t_{fc}}{b_{fc}}\right)+\frac{b_{ft}t_{ft}^3}{3}\left(1-0.63\frac{t_{ft}}{b_{ft}}\right) \quad \text{Equation 6.5.6.2.3.3.2-7}$$

AASHTO LRFD Equation A6.3.3-9

R_h = hybrid factor determined as specified in *AASHTO LRFD* Article 6.10.1.10.1 (Section 6.4.5.7)

R_{pc} = web plastification factor for the compression flange determined as specified in *AASHTO LRFD* Article A6.2.1 or A6.2.2, as applicable (Section 6.5.6.2.3.2)

S_{xc} = elastic section modulus about the major axis of the section to the compression flange taken as M_{yc}/F_{yc} (in.^{3})

S_{xt} = elastic section modulus about the major axis of the section to the tension flange taken as M_{yt}/F_{yt} (in.^{3})

h = depth between the centerline of the flanges (in.)

r_t = effective radius of gyration for lateral torsional buckling (in.)

$$= \frac{b_{fc}}{\sqrt{12\left(1+\frac{1}{3}\frac{D_c t_w}{b_{fc}t_{fc}}\right)}} \quad \text{Equation 6.5.6.2.3.3.2-8}$$

AASHTO LRFD Equation A6.3.3-10

Brace points defining the unbraced length, L_b, of the compression flange are considered to be points where lateral deflection of the girder flange and twisting of the entire cross-section are restrained. In the past, points of contraflexure have sometimes been considered to act as brace points. Since this practice can lead to significantly unconservative estimates of the lateral-torsional buckling resistance, the *AASHTO LRFD* Specifications do not imply that points of contraflexure should be considered as brace points. Instead, the effects of moment gradient are to be handled directly through the use of the moment gradient modifier, C_b (discussed below). Suggested values of C_b for rolled I-sections or for compact web sections subject to reverse curvature bending with no intermediate bracing or bracing on only one flange are provided in Yura and Helwig (2010), and in the Commentary to Article F1 of AISC (2010a).

L_p and L_r are Anchor Points 1 and 2, respectively, as shown on Figure 6.5.6.2.2.2.2-2. L_p defines the compact unbraced length limit. A member braced at or below the compact unbraced length limit is able to achieve the maximum potential lateral-torsional buckling resistance (M_{max} in Figure 6.5.6.2.2.2.2-2) of $R_{pc}M_{yc}$ under uniform bending, which is independent of the unbraced length. Note that in many cases, it will not be economical to brace the girder at a distance equal to L_p or below in order to reach M_{max}, particularly under uniform bending conditions for which C_b is equal to 1.0.

L_r defines the noncompact unbraced length limit. The lateral-torsional buckling resistance of a member braced at or below the noncompact unbraced length limit is expressed in Equation 6.5.6.2.3.3.2-2 as a linear function of the unbraced length, as illustrated in Figure 6.5.6.2.2.2.2-2, which represents the inelastic lateral-torsional buckling resistance. L_r is the unbraced length at which the inelastic and elastic lateral-torsional buckling resistances are the same. The resistance at this point is assumed to be $R_bF_{yr}S_{xc}$. F_{yr} (and its associated limits) is discussed in more detail in Section 6.5.6.2.2.2.2.

Unbraced lengths greater than L_r are termed slender unbraced lengths and their resistance is controlled by elastic lateral-torsional buckling. As mentioned previously, lateral-torsional buckling in the elastic range is of primary importance for relatively slender girders braced at longer than normal intervals, which most typically occurs during a temporary construction condition. The equation for the elastic lateral-torsional buckling stress, F_{cr} (Equation 6.5.6.2.3.3.2-6), is the exact beam-theory solution for the elastic lateral-torsional buckling resistance of a doubly symmetric I-section under uniform bending (when load-height effects are not considered), when an effective radius of gyration, r_t, given by Equation 6.5.6.2.2.2.2-9 is introduced into Equation 6.5.6.2.2.2.2-1. The expression for r_t given in the specifications (Equation 6.5.6.2.3.3.2-8), is a simplification of Equation 6.5.6.2.2.2.2-9 obtained by assuming that $D = h = d$. However, Equation 6.5.6.2.2.2.2-9 is still provided in the *AASHTO LRFD* Article C6.10.8.2.3 should the Engineer require a more precise calculation of the elastic lateral-torsional buckling stress. The web term, D_ct_w, in both expressions for r_t accounts for the destabilizing effects of the flexural compression in the web on the lateral-torsional buckling resistance, and also extends the equation to cover singly symmetric I-section members. For composite I-sections in negative flexure, the equations for F_{cr} and L_r are somewhat conservative compared to rigorous beam-theory solutions since they neglect the restraint provided to the bottom (compression) flange by the lateral and torsional stiffness of the concrete deck.

Unlike the Main Provisions, which assume slender-web behavior, the equations for F_{cr} and L_r in *AASHTO LRFD* Appendix A6 include the St. Venant torsional constant J, which is appropriate for stockier compact web and noncompact web sections that

are generally not subject to significant web distortion. Setting J equal to zero in the above expression for F_{cr} results in the equation for F_{cr} given in the Main Provisions (Equation 6.5.6.2.2.2.2-7). The above expression for J (Equation 6.5.6.2.3.3.2-7) provides an accurate approximation of the St. Venant torsional stiffness neglecting the effect of the web-to-flange fillets (El Darwish and Johnston, 1965). Note that for flanges with $b_f/2t_f$ greater than 7.5, the term in parentheses for that particular flange in Equation 6.5.6.2.3.3.2-7 may be taken equal to one. More accurate values for J for rolled W-sections, including the effect of the web-to-flange fillets, are tabulated in AISC (2010a). As pointed out in *AASHTO LRFD* Article CA6.3.3, for the unusual case of a non-composite compact or noncompact web section with $I_{yc}/I_{yt} > 1.5$ and $D/b_{fc} < 2$, $D/b_{ft} < 2$, or $b_{ft}/t_{ft} < 10$, consideration should be given to using more exact beam-theory solutions for the elastic LTB resistance, or else J may be factored by 0.8 to account for the tendency of the above equation for F_{cr} to overestimate the LTB resistance in this case (White and Jung, 2003).

The above LTB equations assume an effective length factor, k, for lateral-torsional buckling equal to 1.0. As discussed Section 6.5.6.2.2.2.2, warping restraint exists from adjacent unbraced lengths that are less critically loaded than the unbraced length under consideration, which can result in a reduced effective length factor for lateral-torsional buckling. A reduced effective length factor can be used to modify the unbraced length, L_b (i.e. kL_b), and to increase the elastic lateral-torsional buckling stress, F_{cr}, by a factor of $(1/k^2)$ (Grubb and Schmidt, 2012). As mentioned previously in Section 6.5.2.1.3.2, *AASHTO LRFD* Article C6.10.8.2.3 makes reference to a procedure (SSRC, 1998; Nethercot and Trahair, 1976; Grubb and Schmidt, 2012) that can be used to calculate a reduced effective length factor for lateral-torsional buckling in special circumstances (e.g. when it becomes necessary to reduce the amplification of first-order flange lateral bending stresses).

Moment Gradient Modifier

The effect of a variation in the major-axis bending moment along the length between brace points, or a moment gradient (Figure 6.5.6.2.2.2.2-3), is accounted for by applying the moment gradient modifier, C_b, to the base inelastic and elastic LTB equations. When the moment and corresponding flange compressive major-axis bending stress are constant along the unbraced length, C_b has a base value of 1.0. Under moment gradient conditions, C_b may be taken greater than 1.0, which effectively increases the LTB resistance with the increase capped at $M_{max} = R_{pc}M_{yc}$ (refer to the dashed curves in Figure 6.5.6.2.2.2.2-2). C_b may conservatively be taken equal to 1.0 in all cases, except for some rare cases involving no cross-bracing within the span. In *AASHTO LRFD* Appendix A6, C_b is specified as follows:

- For unbraced cantilevers and for members when $M_{mid}/M_2 > 1$ or $M_2 = 0$:

$$C_b = 1.0$$ Equation 6.5.6.2.3.3.2-9

AASHTO LRFD Equation A6.3.3-6

- For all other cases:

$$C_b = 1.75 - 1.05\left(\frac{M_1}{M_2}\right) + 0.3\left(\frac{M_1}{M_2}\right)^2 \le 2.3$$ Equation 6.5.6.2.3.3.2-10

AASHTO LRFD Equation A6.3.3-7

where:

M_2 = except as noted below, largest major-axis bending moment at either end of the unbraced length causing compression in the flange under consideration, calculated from the critical moment envelope value (kip-in.). M_2 shall be due to the factored loads and shall be taken as positive. If the moment is zero or causes tension in the flange under consideration at both ends of the unbraced length, M_2 shall be taken as zero.

M_0 = moment at the brace point opposite to the one corresponding to M_2, calculated from the moment envelope value that produces the largest compression at this point in the flange under consideration, or the smallest tension if this point is never in compression (kip-in.). M_0 shall be due to the factored loads and shall be taken as positive when it causes compression and negative when it causes tension in the flange under consideration.

M_1 = moment at the brace point opposite to the one corresponding to M_2, calculated as the intercept of the most critical assumed linear moment variation passing through M_2 and either M_{mid} or M_0, whichever produces the smaller value of C_b (ksi). M_1 may be determined as follows:

- When the variation in the moment along the entire length between brace points is concave in shape:

$$M_1 = M_0$$ Equation 6.5.6.2.3.3.2-11

AASHTO LRFD Equation A6.3.3-11

- Otherwise:

$$M_1 = 2M_{mid} - M_2 \ge M_0$$ Equation 6.5.6.2.3.3.2-12

AASHTO LRFD Equation A6.3.3-12

where:

M_{mid} = major-axis bending moment at the middle of the unbraced length, calculated from the moment envelope value that produces the largest compression at this point in the flange under consideration, or the smallest tension if the point is never in compression (kip-in.). M_{mid} shall be due to the factored loads and shall be taken as positive when it causes compression and negative when it causes tension in the flange under consideration.

The basic form of the equation for C_b given by Equation 6.5.6.2.3.3.2-10 has been retained from previous Specifications. However, the definition of the cases where C_b must be taken equal to 1.0, and the calculation of the moments M_1 and M_2 in Equation 6.5.6.2.3.3.2-10, have each been modified to remove ambiguities and to address specific cases where Equation 6.5.6.2.3.3.2-10 was previously unconservative. The reader is referred to Section 6.5.6.2.2.2.2 for further information on these issues. Section 6.5.6.2.2.2.2 also contains further information on the application of the C_b equation to various cases (refer also to the examples given in Figure 6.5.6.2.2.2.2-4).

In the Main Provisions (Article 6.10.8), major-axis bending stresses are used to calculate C_b since dead and live load bending moments are applied to different sections in composite girders, which is significant when the nominal flexural resistance is not permitted to exceed the moment at first yield. In *AASHTO LRFD* Appendix A6, where the nominal flexural resistance is permitted to exceed the moment at first yield for certain compact and noncompact web sections, the major-axis bending moments are used to calculate C_b since the effect of applying the bending moments to different sections is less critical in these cases.

It is convenient and always conservative to use the critical moment envelope values to calculate C_b, particularly since concurrent moment values at the brace points are not normally tracked in the analysis. It can be shown that the use of the critical moment envelope values for M_2, M_{mid}, and M_o is always conservative since a more critical moment distribution along the unbraced length, in terms of computing C_b, cannot exist for all possible concurrent loadings.

As shown in Figure 6.5.6.2.2.2.2-2, under moment gradient conditions (i.e., C_b > 1.0), in addition to an increase in the base LTB resistance, the maximum potential LTB resistance, $M_{max} = R_{pc}M_{yc}$, can be reached at larger unbraced lengths. The provisions of *AASHTO LRFD* Article D6.4.2 (Appendix D6) can be used to calculate the maximum unbraced lengths to achieve M_{max} under moment gradient conditions, and are recommended for use whenever C_b is greater than 1.0. The modifications to Anchor Points 1 and 2 to account for the effect of the moment gradient are given as follows in *AASHTO LRFD* Article D6.4.2:

- If $L_b \le L_p$, then:

$$M_{nc} = R_{pc}M_{yc}$$ Equation 6.5.6.2.3.3.2-13

AASHTO LRFD Equation D6.4.2-1

- If $L_p < L_b \le L_r$, then:

  - If $L_b \le L_p + \frac{\left(1-\frac{1}{C_b}\right)}{\left(1-\frac{F_{yr}S_{xc}}{R_{pc}M_{yc}}\right)}\left(L_r - L_p\right)$, then:

$$M_{nc} = R_{pc}M_{yc}$$ Equation 6.5.6.2.3.3.2-14

AASHTO LRFD Equation D6.4.2-2

  - Otherwise:

$$M_{nc} = C_b\left[1-\left(1-\frac{F_{yr}S_{xc}}{R_{pc}M_{yc}}\right)\left(\frac{L_b - L_p}{L_r - L_p}\right)\right]R_{pc}M_{yc} \le R_{pc}M_{yc}$$ Equation 6.5.6.2.3.3.2-15

AASHTO LRFD Equation D6.4.2-3

- If $L_b > L_r$, then:

  - If $L_b \le 1.95r_t\frac{C_bS_{xc}E}{R_{pc}M_{yc}}\sqrt{\frac{J}{S_{xc}h}}\sqrt{1+\sqrt{1+6.76\left(\frac{R_{pc}M_{yc}}{C_bS_{xc}E}\frac{S_{xc}h}{J}\right)^2}}$, then:

$$M_{nc} = R_{pc}M_{yc}$$ Equation 6.5.6.2.3.3.2-16

AASHTO LRFD Equation D6.4.2-4

  - Otherwise:

$$M_{nc} = F_{cr}S_{xc} \le R_{pc}M_{yc}$$ Equation 6.5.6.2.3.3.2-17

AASHTO LRFD Equation D6.4.2-5

Effect of Section Transitions within the Unbraced Length

The base LTB equations in the Specifications assume that the member is prismatic within the unbraced length. For reasons discussed previously in Section 6.5.6.2.2.2.2, *AASHTO LRFD* Article A6.3.3 permits the effect of a section transition on the LTB resistance to be ignored when the transition is located at a distance less than or equal to 20 percent of the unbraced length from the brace point with the smaller moment, and the lateral moment of inertia of the flange or flanges of the smaller section is equal to or larger than one-half the corresponding value in the larger section. If there is more than one transition within the unbraced length, any transition within 20 percent of the unbraced length from the brace point with the smaller moment may be ignored and the LTB resistance based on the remaining sections may then be computed as described in the next paragraph.

For unbraced lengths containing a transition to a smaller section at a distance greater than 20 percent of the unbraced length from the brace point with the smaller moment, the flexural resistance based on lateral-torsional buckling may be taken as the smallest resistance within the unbraced length according to *AASHTO LRFD* Article A6.3.3 (note that the transition can either be in the compression or tension flange). The flexural resistance, M_{nc}, at each section within the unbraced length is then to be taken as this resistance multiplied by the ratio of S_{xc} at the section under consideration to S_{xc} at the section governing the lateral-torsional buckling resistance. In addition, the C_b factor must be taken equal to 1.0 and the unbraced length must not be modified by an effective length factor.

Essentially, the nonprismatic member is being replaced with an equivalent prismatic member. The cross-section of the equivalent member that gives the correct LTB resistance is generally some weighted average of all the cross-sections along the unbraced length. If the cross-section that gives the smallest uniform bending resistance is used (i.e., calculated assuming C_b is equal to 1.0) and the calculated resistance based on that cross-section is not exceeded anywhere along the unbraced length, a conservative solution is obtained. A suggested procedure to obtain a more refined estimate of the LTB resistance for this case is given in Grubb and Schmidt (2012).

The preceding requirements are summarized in Figure 6.5.6.2.2.2.2-5 for a section change due to a single flange transition. To avoid a significant reduction in the LTB resistance in such cases according to the above criteria, consider locating flange transitions within 20 percent of the unbraced length from the brace point with the smaller moment, and ensure that the lateral moment of inertia of the flange (or flanges) of the smaller section is equal to or larger than one-half the corresponding value(s) for the flange(s) of the larger section at the transition.

Finally, for unbraced lengths consisting of singly symmetric non-composite I-sections subject to reverse curvature bending, the LTB resistance must be checked for both flanges, unless the top flange is considered to be continuously braced. Because the flanges of these sections are different sizes, the LTB resistance may be governed by compression in the smaller flange, even though the compressive stress may be smaller than the maximum compressive stress in the larger flange.

6.5.6.2.3.4 Sections with Continuously Braced Tension Flanges

Tension (top) flanges in regions of negative flexure in continuous-span composite members are typically classified as continuously braced flanges. A continuously braced flange is defined as a flange encased in concrete or anchored by shear connectors. Since in negative flexure regions, the top flange is in tension and the flange is usually continuously braced, only yielding of the flange is a concern and any flange lateral bending stresses need not be considered.

Continuously braced flanges in tension must satisfy the following relationship at the strength limit state (*AASHTO LRFD* Article A6.1.4 in Appendix A6):

$$M_u \leq \phi_f R_{pt} M_{yt} \qquad \text{Equation 6.5.6.2.3.4-1}$$

AASHTO LRFD Equation A6.1.4-1

where:

M_{yt} = yield moment with respect to the tension flange determined as specified in *AASHTO LRFD* Article D6.2 (kip-in.) (Section 6.4.5.3)

R_{pt} = web plastification factor for the tension flange determined as specified in *AASHTO LRFD* Article A6.2.1 or A6.2.2, as applicable (Section 6.5.6.2.3.2)

Lateral bending does not need to be considered in Equation 6.5.6.2.3.4-1 because the flanges are continuously supported by the concrete deck.

6.5.6.2.3.5 Sections with Continuously Braced Compression Flanges

Continuously braced compression flanges would typically be top flanges in regions of positive flexure in continuous-span non-composite members, or the top flanges of simple-span non-composite members, in which the flanges are considered continuously braced. According to *AASHTO LRFD* Article A6.1.3, continuously braced flanges in compression must satisfy the following relationship at the strength limit state (*AASHTO LRFD* Article A6.1.3 in Appendix A6):

$$M_u \le \phi_f R_{pc} M_{yc} \qquad \text{Equation 6.5.6.2.3.5-1}$$

AASHTO LRFD Equation A6.1.3-1

where:

M_{yc} = yield moment with respect to the compression flange determined as specified in *AASHTO LRFD* Article D6.2 (kip-in.) (Section 6.4.5.3)

R_{pc} = web plastification factor for the compression flange determined as specified in *AASHTO LRFD* Article A6.2.1 or A6.2.2, as applicable (Section 6.5.6.2.3.2)

Lateral bending does not need to be considered in Equation 6.5.6.2.3.5-1 because the flanges in these cases are considered continuously supported by the concrete deck.

6.5.6.2.3.6 Sections with Discretely Braced Tension Flanges

Discretely braced tension flanges of non-composite sections in positive or negative flexure must satisfy the following relationship at the strength limit state (*AASHTO LRFD* Article A6.1.2 in Appendix A6):

$$M_u + \frac{1}{3} f_\ell S_{xt} \le \phi_f M_{nt} \qquad \text{Equation 6.5.6.2.3.6-1}$$

AASHTO LRFD Equation A6.1.2-1

where:

M_u = bending moment about the major axis of the cross-section determined as specified in *AASHTO LRFD* Article 6.10.1.6 (kip-in.). M_u is always taken as positive.

f_ℓ = flange lateral bending stress determined as specified in *AASHTO LRFD* Article 6.10.1.6 (ksi). f_ℓ is always taken as positive.

M_{nt} = nominal flexural resistance based on tension yielding determined as specified in *AASHTO LRFD* Article A6.4 (kip-in.) (see below)

S_{xt} = elastic section modulus about the major axis of the section to the tension flange taken as M_{yt}/F_{yt} (in.^{3})

The nominal flexural resistance, M_{nt}, is based on yielding and is to be taken as (*AASHTO LRFD* Article A6.4):

$$M_{nt} = R_{pt} M_{yt} \qquad \text{Equation 6.5.6.2.3.6-2}$$

AASHTO LRFD Equation A6.4-1

where:

M_{yt} = yield moment with respect to the tension flange determined as specified in *AASHTO LRFD* Article D6.2 (kip-in.) (Section 6.4.5.3)

R_{pt} = web plastification factor for the tension flange determined as specified in *AASHTO LRFD* Article A6.2.1 or A6.2.2, as applicable (Section 6.5.6.2.3.2)

Equation 6.5.6.2.3.6-2 represents a linear transition in the flexural resistance between M_{yt} and M_p as a function of the web slenderness. As the web slenderness approaches the noncompact web section limit, λ_{rw}, given in Equation 6.5.6.2.2.1.3-1, Equation 6.5.6.2.3.6-2 approaches the nominal flexural resistance based on tension flange yielding equal to R_hF_{yt}.

According to *AASHTO LRFD* Article 6.10.1.6, for design checks involving yielding, M_u and f_ℓ may be taken as the corresponding values at the section under consideration. Note that when M_{yc} is less than or equal to M_{yt} and f_ℓ is equal to zero, the flexural resistance based on the tension flange does not control and Equation 6.5.6.2.3.6-1 need not be checked.

The sign of M_u and f_ℓ is always taken as positive in Equation 6.5.6.2.3.6-1**.** However, when summing dead and live load stresses to obtain the total factored major-axis bending moments and lateral bending stresses, M_u and f_ℓ, to apply in the equation, the signs of the individual dead and live load moments/stresses must be considered.

Potential sources of flange lateral bending in discretely braced tension flanges of non-composite sections at the strength limit state include curvature, wind loading and the effect of discontinuous cross-frames/diaphragms used in conjunction with support skew. During construction, overhang bracket loads on exterior girders acting on the non-composite section also cause flange lateral bending. According to *AASHTO LRFD* Article 6.10.1.6, amplification of the first-order flange lateral bending stresses is not required in discretely braced tension flanges. *AASHTO LRFD* Article 6.10.1.6 further specifies that the sum of the factored flange lateral bending stresses due to all sources cannot exceed $0.6F_{yf}$.

The elastic section modulus, S_{xt}, in Equation 6.5.6.2.3.6-1 is defined as M_{yt}/F_{yt} so that for a composite section with a web proportioned exactly at the noncompact web slenderness limit given in Equation 6.5.6.2.2.1.3-1, the flexural resistance given by *AASHTO LRFD* Appendix A6 will be approximately the same as the flexural resistance given by the Main Provisions (*AASHTO LRFD* Article 6.10.8). Slight differences between the resistance predictions may occur for reasons pointed out in *AASHTO LRFD* Article CA6.1.1.

6.5.6.2.4 Box Sections

6.5.6.2.4.1 General

AASHTO LRFD Article 6.11.6.2.3 specifies that for closed-box and tub sections subject to negative flexure at the strength limit state, the provisions of *AASHTO LRFD* Article 6.11.8 are to be applied. The provisions of *AASHTO LRFD* Article 6.11.8 limit the nominal flexural resistance to always be less than or equal to the moment at first yield for all types of box girder bridges. Therefore, the nominal flexural resistance for these sections is always expressed in terms of the elastically computed flange stress.

Further, according to *AASHTO LRFD* Article 6.11.6.2.3, the optional provisions of *AASHTO LRFD* Appendices A6 and B6 (Sections 6.5.6.2.3 and 6.5.6.6) are not to be applied to box sections. These optional appendices apply only to the design of I-section flexural members. Their applicability to the design of box-section flexural members has not yet been demonstrated.

6.5.6.2.4.2 Box Flanges in Compression

AASHTO LRFD Article 6.11.8.1.1 specifies that for box sections subject to negative flexure, box flanges in compression (i.e. bottom flanges) must satisfy the following requirement at the strength limit state:

$$f_{bu} \le \phi_f F_{nc} \qquad \text{Equation 6.5.6.2.4.2-1}$$

AASHTO LRFD Equation 6.11.8.1.1-1

where:

ϕ_v = resistance factor for flexure specified in AASHTO LRFD Article 6.5.4.2 (=1.0)

f_{bu} = factored longitudinal flange stress at the section under consideration calculated without consideration of longitudinal warping (ksi)

F_{nc} = nominal flexural resistance of the box flange in compression determined as specified in *AASHTO LRFD* Article 6.11.8.2 (Section 6.5.6.2.4.2.1) (ksi)

Equation 6.5.6.2.4.2-1 is intended to ensure that box flanges in compression have sufficient local buckling resistance. Flange lateral bending and lateral-torsional buckling are not a consideration for box flanges. Longitudinal warping stresses are typically ignored at the strength limit state, as permitted in *AASHTO LRFD* Article 6.11.1.1.

In general, bottom box flanges at interior-pier sections are subject to a complex stress state. The flanges are subject to biaxial bending due to vertical bending of the box section and due to vertical bending of the internal diaphragm over the bearing sole plate. Bending of the internal diaphragm over the bearing sole plate may be particularly significant for boxes supported on single bearings. The flange is also subject to shear stresses due to the vertical shear in the internal diaphragm, and in cases where it must be considered, the St. Venant torsional shear. Thus, for cases where the bending of the internal diaphragm and/or the flange shear stresses are deemed significant, *AASHTO LRFD* Article C6.11.8.1.1 suggests that the following equation be used to check the combined stress state in the box flange at interior-pier sections at the strength limit state. The equation represents the general form of the Huber-von Mises-Hencky yield criterion for combined stress (Ugural and Fenster, 1978):

$$\sqrt{f_{bu}^2 - f_{bu}f_{by} + f_{by}^2 + 3(f_d + f_v)^2} \le \phi_f R_b R_h F_{yc} \qquad \text{Equation 6.5.6.2.4.2-2}$$

AASHTO LRFD Equation C6.11.8.1.1-1

where:

f_{by} = factored stress in the box flange caused by the vertical bending of the internal diaphragm over the bearing sole plate (ksi)

f_d = factored shear stress in the box flange caused by the internal diaphragm vertical shear (ksi)

$$= \frac{VQ}{It_{fc}} \qquad \text{Equation 6.5.6.2.4.2-3}$$

AASHTO LRFD Equation C6.11.8.1.1-2

f_v = factored St. Venant torsional shear stress in the box flange (ksi)

I = moment of inertia of the effective internal diaphragm section (discussed below) (in.^{4})

F_{yc} = minimum specified yield strength of the compression flange (ksi)

Q = first moment of one-half the effective box-flange area about the neutral axis of the effective internal diaphragm section (discussed below) (in.^{3})

R_b = web load-shedding factor determined as specified in *AASHTO LRFD* Article 6.10.1.10.2 (Section 6.4.5.6)

R_h = hybrid factor determined as specified in *AASHTO LRFD* Article 6.10.1.10.1 (Section 6.4.5.7)

V = factored vertical shear in the internal diaphragm due to flexure plus St. Venant torsion (kips)

f_{bu} and f_{by} are to be taken as signed quantities in Equation 6.5.6.2.4.2-2. As indicated in *AASHTO LRFD* Article C6.11.8.1.1, for a box supported on two bearings, f_{by} in Equation 6.5.6.2.4.2-2 is typically relatively small and may be

neglected in making this check. f_{by} should be considered for boxes resting on single bearings and may be computed using the effective section discussed in the next paragraph.

In calculating f_d from Equation 6.5.6.2.4.2-3, and also f_{by}, a portion of the box flange may be considered effective with the internal diaphragm. *AASHTO LRFD* Article C6.11.8.1.1 currently suggests that a flange width equal to six times its thickness may be considered effective with the internal diaphragm. Further, whenever an access hole is provided within the internal diaphragm for inspection purposes, the effect of the hole should be considered in computing the section properties of the effective diaphragm section.

Recall as discussed previously in Sections 6.4.5.6 and 6.4.5.7 that to calculate the web load-shedding factor, R_b, and the hybrid factor, R_h, for a tub section, where applicable, one-half of the effective box flange width should be used in conjunction with one top flange and a single web (refer to *AASHTO LRFD* Article C6.11.8.2.2). One-half of the effective top and bottom box flange width should be used in conjunction with a single web for a closed-box section. The effective box flange width is defined in *AASHTO* LRFD Article 6.11.1.1 and discussed further in Section 6.3.5.5.3.

6.5.6.2.4.2.1 Nominal Flexural Resistance, F_{nc}

The nominal flexural resistance of box flanges in compression, F_{nc}, in the *AASHTO LRFD* Specifications is based on local buckling of the flange under combined uniform axial compression and torsional shear stress (lateral-torsional buckling is not a consideration for box flanges). In general, the resistance is defined for three distinct regions based on the flange slenderness. For unstiffened flanges, the slenderness is based on the full flange width between webs, b_{fc}. For longitudinally stiffened flanges, the slenderness is based on the larger of the width of the flange between longitudinal flange stiffeners or the distance from a web to the nearest longitudinal flange stiffener, w. The local buckling resistance of longitudinally stiffened flanges is dependent on the rigidity of the longitudinal stiffener(s).

As for the compression-flange local buckling and lateral-torsional buckling resistance curves for I-section members, the local buckling resistance curves for box flanges are fitted to two anchor points (Figure 6.5.6.2.4.2.1-1).

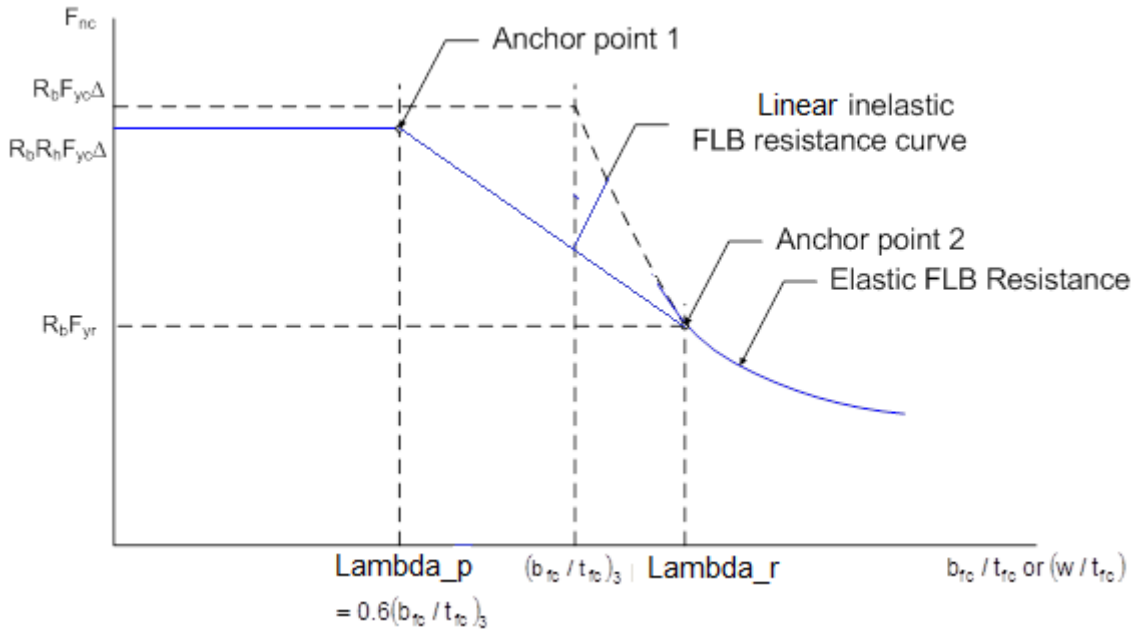

Figure 6.5.6.2.4.2.1-1 Local Buckling Resistance Curves for Box Flanges in Compression

These anchor points are discussed in more detail below. Note that the inelastic local buckling resistance of the box flange is represented by a linear interpolation between the two anchor points, as is the case for I-section members. The equations are based on the tacit assumptions that the flange panel is of infinite length and that the panel is subjected to a uniform stress field over its full width and length. Since the moment gradient in negative moment regions increases rather sharply near interior supports, the true stress usually decreases over the panel length from a maximum at one end of the panel. Further the panel is not of infinite length. So the true strength of actual box flanges in negative flexure is greater than implied. Still, it is advisable to use the critical stress in the panel to make the following checks.

At access holes in box flanges subject to compression, it is recommended that the nominal flexural resistance of the remaining flange on each side of the hole be determined according to the provisions of *AASHTO LRFD* Article 6.10.8.2.2, with λ_f taken as the projecting width of the flange on that side of the hole divided by the flange thickness. The equations in *AASHTO LRFD* Article 6.10.8.2.2 are the local buckling resistance equations for I-girder compression flanges (Section 6.5.6.2.2.2.1), with the flange width based on the projecting width of the flange on the side of the hole under consideration.

Unstiffened Box Flanges

According to *AASHTO LRFD* Article 6.11.8.2.1, the nominal flexural resistance of box flanges in compression without flange longitudinal stiffeners (i.e. unstiffened flanges), F_{nc}, is to be determined as specified in *AASHTO LRFD* Article 6.11.8.2.2, and is to be taken as:

$$F_{nc} = F_{cb}\sqrt{1-\left(\frac{f_v}{\phi_v F_{cv}}\right)^2} \qquad \text{Equation 6.5.6.2.4.2.1-1}$$

AASHTO LRFD Equation 6.11.8.2.2-1

where:

ϕ_v = resistance factor for shear specified in AASHTO LRFD Article 6.5.4.2 (=1.0)

f_v = factored St. Venant torsional shear stress in the flange at the section under consideration not to exceed the factored torsional shear resistance of the flange, F_{vr}, given by Equation 6.5.6.1.2-1 (ksi)

$$= \frac{T}{2A_o t_{fc}} \qquad \text{Equation 6.5.6.2.4.2.1-2}$$

AASHTO LRFD Equation 6.11.8.2.2-12

A_o = enclosed area within the box section (in.)

F_{cb} = nominal axial compression buckling resistance of the flange under compression alone (discussed below) (ksi)

F_{cv} = nominal shear buckling resistance of the flange under shear alone (discussed below) (ksi)

t_{fc} = thickness of the compression flange (in.)

T = internal torque due to the factored loads (kip-in.)

Equation 6.5.6.2.4.2.1-1 is derived from the following nonlinear interaction curve relating the normal axial compressive stress, f_c, and the St. Venant torsional shear stress, f_v (NHI, 2011a):

$$\left(\frac{f_v}{\phi_v F_{cv}}\right)^2 + \left(\frac{f_c}{\phi_f F_{cb}}\right)^2 \le 1.0 \qquad \text{Equation 6.5.6.2.4.2.1-3}$$

AASHTO LRFD Equation C6.11.8.2.2-1

Rearranging Equation 6.5.6.2.4.2.1-3 in terms of f_c, and substituting F_{nc} for f_c, results in Equation 6.5.6.2.4.2.1-1. SSRC (1998) contains a general discussion on the reduction of the critical local buckling stress due to the presence of torsional shear.

AASHTO LRFD Article 6.11.8.2.2 defines the nominal axial compression buckling resistance of the flange under compression alone, F_{cb}, (i.e. local buckling resistance) as follows:

- If $\lambda_f \le \lambda_p$, then:

$$F_{cb} = R_b R_h F_{yc} \Delta \qquad \text{Equation 6.5.6.2.4.2.1-4}$$

AASHTO LRFD Equation 6.11.8.2.2-2

- If $\lambda_p < \lambda_f \le \lambda_r$, then:

$$F_{cb} = R_b R_h F_{yc}\left[\Delta - \left(\Delta - \frac{\Delta - 0.3}{R_h}\right)\left(\frac{\lambda_f - \lambda_p}{\lambda_r - \lambda_p}\right)\right] \qquad \text{Equation 6.5.6.2.4.2.1-5}$$

AASHTO LRFD Equation 6.11.8.2.2-3

- If $\lambda_f > \lambda_r$, then:

$$F_{cb} = \frac{0.9 E R_b k}{\lambda_f^2} \qquad \text{Equation 6.5.6.2.4.2.1-6}$$

AASHTO LRFD Equation 6.11.8.2.2-4

where:

λ_f = slenderness ratio for the compression flange

$$= \frac{b_{fc}}{t_{fc}} \qquad \text{Equation 6.5.6.2.4.2.1-7}$$

AASHTO LRFD Equation 6.11.8.2.2-8

$$\lambda_p = 0.57\sqrt{\frac{Ek}{F_{yc}\Delta}} \qquad \text{Equation 6.5.6.2.4.2.1-8}$$

AASHTO LRFD Equation 6.11.8.2.2-9

$$\lambda_r = 0.95\sqrt{\frac{Ek}{F_{yr}}} \qquad \text{Equation 6.5.6.2.4.2.1-9}$$

AASHTO LRFD Equation 6.11.8.2.2-10

$$\Delta = \sqrt{1-3\left(\frac{f_v}{F_{yc}}\right)^2} \qquad \text{Equation 6.5.6.2.4.2.1-10}$$

AASHTO LRFD Equation 6.11.8.2.2-11

b_{fc} = compression-flange width between webs (in.)
F_{yc} = minimum specified yield strength of the compression flange (ksi)
F_{yr} = smaller of the compression-flange yield stress at the onset of nominal yielding, with consideration of residual stress effects, or the specified minimum yield strength of the web (ksi)

$$= (\Delta - 0.3)F_{yc} \qquad \text{Equation 6.5.6.2.4.2.1-11}$$

AASHTO LRFD Equation 6.11.8.2.2-13

k = plate-buckling coefficient for uniform normal stress
= 4.0
R_b = web load-shedding factor determined as specified in *AASHTO LRFD* Article 6.10.1.10.2 (Section 6.4.5.6)
R_h = hybrid factor determined as specified in *AASHTO LRFD* Article 6.10.1.10.1 (Section 6.4.5.7)

F_{cb} is defined for three distinct regions based on the slenderness of the flange (Figure 6.5.6.2.4.2.1-1). Equation 6.5.6.2.4.2.1-6 defines the elastic local buckling resistance of the flange under compression alone and is based on the theoretical elastic Euler buckling equation for an infinitely long plate under a uniform normal stress (Timoshenko and Gere, 1961). For stocky plates, full yielding of the plate as defined by the von Mises yield criterion for combined normal and shear stress (Boresi et al., 1978) can be achieved (Equation 6.5.6.2.4.2.1-4). In between these two regions is a transition region that reflects the fact that partial yielding due to residual stresses and initial imperfections does not permit the attainment of the elastic buckling stress. F_{cb} in this region is expressed as a linear function of the flange slenderness (Equation 6.5.6.2.4.2.1-5). A residual stress level of $0.3F_{yc}$ is assumed in the presence of no shear (Equation 6.5.6.2.4.2.1-11).

λ_p (Anchor Point 1 in Figure 6.5.6.2.4.2.1-1) is defined as 0.6 times the flange slenderness at which the elastic flange local buckling stress given by Equation 6.5.6.2.4.2.1-6 is equal to $R_bF_{yc}\Delta$. For the case of f_v equal to zero and thus Δ equal to 1.0, the limiting Anchor Point 1 value of b_{fc}/t_{fc} for F_{yc} = 50 ksi and k = 4.0 is 27.5.

λ_r (Anchor Point 2 in Figure 6.5.6.2.4.2.1-1) is defined as the flange slenderness at which the elastic flange local buckling stress given by Equation 6.5.6.2.4.2.1-6 is equal to R_bF_{yr}, where F_{yr} is given by Equation 6.5.6.2.4.2.1-11. For the case of f_v equal to zero and thus Δ equal to 1.0, the limiting Anchor Point 2 value of b_{fc}/t_{fc} for F_{yc} = 50 ksi and k =4.0 is 54.7.

The computation of the flange torsional shear stress, f_v, from Equation 6.5.6.2.4.2.1-2 due to torques applied separately to the non-composite and composite sections is discussed in *AASHTO LRFD* Article C6.11.1.1. In cases where f_v is relatively small, consideration may be given to assuming Δ equal to 1.0 and F_{nc} equal to F_{cb} for preliminary design.

AASHTO LRFD Article 6.11.8.2.2 defines the nominal shear buckling resistance of the flange under shear alone, F_{cv}, as follows:

- If $\lambda_f \le 1.12\sqrt{\frac{Ek_s}{F_{yc}}}$, then:

$$F_{cv} = 0.58F_{yc} \qquad \text{Equation 6.5.6.2.4.2.1-12}$$

AASHTO LRFD Equation 6.11.8.2.2-5

- If $1.12\sqrt{\frac{Ek_s}{F_{yc}}} < \lambda_f \le 1.40\sqrt{\frac{Ek_s}{F_{yc}}}$, then:

$$F_{cv} = \frac{0.65\sqrt{F_{yc}Ek_s}}{\lambda_f} \qquad \text{Equation 6.5.6.2.4.2.1-13}$$

AASHTO LRFD Equation 6.11.8.2.2-6

- If $\lambda_f > 1.40\sqrt{\frac{Ek_s}{F_{yc}}}$, then:

$$F_{cv} = \frac{0.9Ek_s}{\lambda_f^2} \qquad \text{Equation 6.5.6.2.4.2.1-14}$$

AASHTO LRFD Equation 6.11.8.2.2-7

where:

k_s = plate-buckling coefficient for shear stress
= 5.34

The preceding equations for F_{cv} are determined from the equations for the constant, *C*, given in AASHTO LRFD Article 6.10.9.3.2 (Section 6.5.7.2). *C* is defined as the ratio of the shear buckling resistance to the shear yield strength of the flange, which is taken as $F_{yc}/\sqrt{3}$.

The specified plate-buckling coefficient for uniform normal stress, k = 4.0, and the specified shear-buckling coefficient, k_s = 5.34, both assume simply supported boundary conditions at the edges of the flanges (Timoshenko and Gere, 1961).

Longitudinally Stiffened Box Flanges

The nominal flexural resistance of the flange in compression may decrease to an impractical level when an unstiffened box flange becomes too slender. Longitudinal stiffeners can then be added to the flange to increase the nominal flexural resistance.

The design of longitudinal compression-flange stiffeners for box sections is covered in *AASHTO LRFD* Article 6.11.11.2. Longitudinal compression-flange stiffeners on box sections are to be equally spaced across the flange width. Since the stiffeners are primary load carrying members, the specified minimum yield strength of the stiffeners must not be less than the specified minimum yield strength of the box flange to which they are attached. Also, the stiffeners should be included in the section properties of the closed-box or tub section where they are used since they contribute to the flexural stiffness and strength of the section.

Structural tees are preferred for use as longitudinal flange stiffeners because tees increase the lateral torsional buckling resistance of the stiffeners, and also provide a high ratio of out-of-plane stiffness to stiffener cross-sectional area. Using flat bars as stiffeners is an undesirable alternative. Structural tees are not available in grades of steel exceeding 50 ksi. In cases where higher strength tee sections are required (e.g. tees on Grade HPS 70W steel flanges), the tees must be fabricated from plates or bars cut from plate.

As indicated in *AASHTO LRFD* Article C6.11.11.2, longitudinal flange stiffeners should be continuous through internal diaphragms (cut-outs can be provided in the diaphragm to accommodate the stiffeners). Consideration should be given to attaching the longitudinal flange stiffeners to the internal diaphragms; tees can conveniently attached to the diaphragms with a pair of clip angles, as illustrated in Figure 6.5.6.2.4.2.1-2.

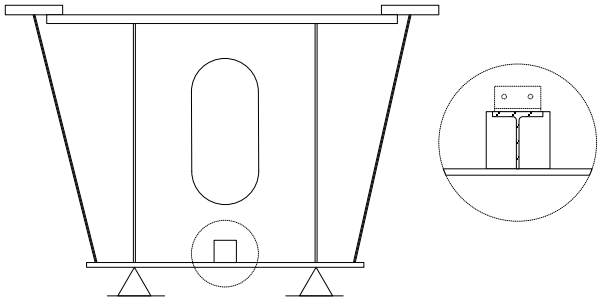

Figure 6.5.6.2.4.2.1-2 Suggested Longitudinal Flange Stiffener Detail at an Internal Diaphragm

Longitudinal flange stiffeners are best discontinued at field splice locations at the free edge of the flange where the flange stress is zero, particularly when the span balance is such that the box flange on the other side of the field splice does not require stiffening. In such cases, the compressive resistance of the unstiffened box flange on the other side of the splice must always be checked (see above) to determine if the flange is satisfactory without a stiffener, or if a slight increase in the flange thickness will suffice without providing a stiffener. Figure 6.5.6.2.4.2.1-3 illustrates a suggested box-flange bolted splice detail to accommodate a termination of the stiffener at the free edge of the flange. When the stiffener is terminated as such, fatigue of the base metal at the stiffener-to-flange weld termination need not be checked in regions subject to a net applied tensile stress (as defined in *AASHTO LRFD* Article 6.6.1.2.1) because the flange stress is zero at the termination.

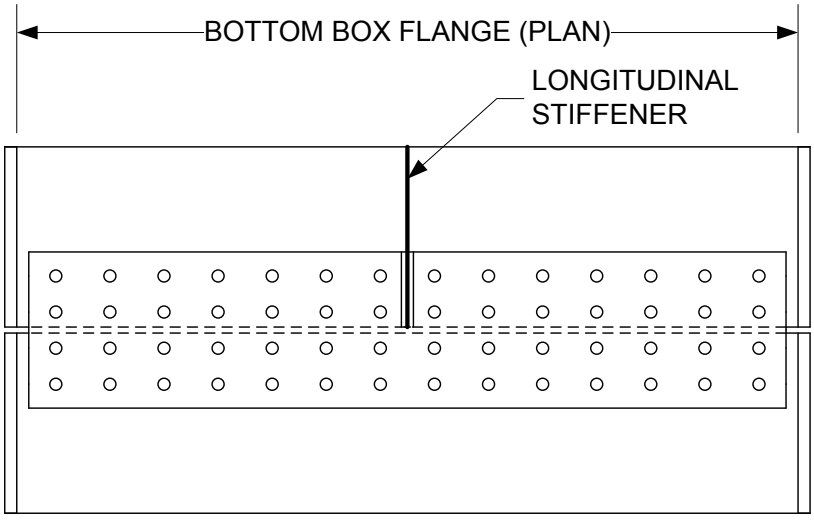

Figure 6.5.6.2.4.2.1-3 Suggested Box-Flange Bolted Splice Detail at Flange Stiffener Termination

Should it become necessary to terminate the stiffener beyond the field splice in a region subject to a net applied tensile stress (or should the stiffener be terminated before the field splice in such a region), the termination becomes more difficult. The base metal at the termination of the stiffener-to-flange weld must be checked for fatigue according to the stiffener terminus detail (usually a low Category E or E′ detail unless an appropriate transition radius is provided at the termination – refer to *AASHTO LRFD* Table 6.6.1.2.3-1 – Condition 4.3).

Possible options to consider in this case include thickening the flange in the region of the termination to eliminate the need for the stiffener, running the stiffener the full length of the span if the remaining length of unstiffened flange is reasonable (note that this option may help to stiffen a relatively thin tension flange. If a smaller tee section will suffice over the remaining length, it can be spliced onto the existing stiffener), and lastly, including an appropriate transition radius at the end of the stiffener to raise the fatigue detail category accordingly, which is the most costly and least desirable option. The Design Engineer is advised to consult with a fabricator regarding the relative cost of each of these options. Splicing the flange stiffener across the field splice is recommended whenever it becomes necessary to run the stiffener beyond the splice.

AASHTO LRFD Article 6.11.8.2.3 specifies that the nominal flexural resistance of a longitudinally stiffened box flange in compression, F_{nc}, be determined using the same basic equations specified for unstiffened box flanges in compression given in *AASHTO LRFD* Article 6.11.8.2.2 (see above), with the following substitutions:

- The width, w, is to be substituted for b_{fc};
- The plate-buckling coefficient for uniform normal stress, k, is to be taken as:
  - If n = 1, then:

$$k = \left(\frac{8 I_s}{w t_{fc}^3} \right)^{\frac{1}{3}} \qquad \text{Equation 6.5.6.2.4.2.1-15}$$

AASHTO LRFD Equation 6.11.8.2.3-1

  - If n = 2, then:

$$k = \left(\frac{0.894 I_s}{w t_{fc}^3} \right)^{\frac{1}{3}} \qquad \text{Equation 6.5.6.2.4.2.1-16}$$

AASHTO LRFD Equation 6.11.8.2.3-2

with $1.0 \leq k \leq 4.0$

The plate-buckling coefficient for shear stress, k_s, is to be taken as:

$$k_S = \frac{5.34 + 2.84\left(\frac{I_s}{wt_{fc}^3}\right)^{\frac{1}{3}}}{(n+1)^2} \leq 5.34 \qquad \text{Equation 6.5.6.2.4.2.1-17}$$

AASHTO LRFD Equation 6.11.8.2.3-3

where:

I_s = moment of inertia of a single longitudinal flange stiffener about an axis parallel to the flange and taken at the base of the stiffener (in.^{4})
n = number of equally spaced longitudinal flange stiffeners
w = larger of the width of the flange between the longitudinal flange stiffeners, or the distance from a web to the nearest longitudinal flange stiffener (in.)

The prescribed values of k and k_s for a longitudinally stiffened flange are typically smaller than the prescribed values for an unstiffened flange due to the finite flexibility of the longitudinal stiffeners. The shear-buckling coefficient for the stiffened plate, k_s, given by Equation 6.5.6.2.4.2.1-17 is taken from Culver (1972). The plate-buckling coefficient for uniform stress, k, is related to the stiffness of the longitudinal flange stiffeners, I_s, and the number of stiffeners, n, according to Equation 6.5.6.2.4.2.1-15 and Equation 6.5.6.2.4.2.1-16. Equation 6.5.6.2.4.2.1-15 and Equation 6.5.6.2.4.2.1-16 are derived directly by algebraic manipulation of the following equation for the requirement moment of inertia, I_ℓ, of each longitudinal flange stiffener about an axis parallel to the flange and taken at the base of the stiffener (*AASHTO LRFD* Article 6.11.11.2):

$$I_\ell \geq \psi w t_{fc}^3 \qquad \text{Equation 6.5.6.2.4.2.1-18}$$

AASHTO LRFD Equation 6.11.11.2-2

where:

ψ = $0.125k^3$ for $n = 1$
= $1.120k^3$ for $n = 2$

Equation 6.5.6.2.4.2.1-18 is a simplified approximate expression that yields values of the elastic critical stress for a longitudinally stiffened box flange close to those obtained using the exact but more complex equations of elastic stability

(Timoshenko and Gere, 1961). The simplified expression assumes that the box flange and the stiffeners are infinitely long and ignores the effect of any transverse bracing or stiffening. As a result, when n exceeds one, the required moment of inertia from Equation 6.5.6.2.4.2.1-18 begins to increase dramatically. When n exceeds 2, for which the value of ψ for application in Equation 6.5.6.2.4.2.1-18 is equal to $0.07k^3n^4$, the required moment of inertia becomes nearly impractical. For the rare situation where an exceptionally wide box flange is required and n may need to exceed 2, *AASHTO LRFD* Article C6.11.11.2 suggests that transverse flange stiffeners be considered to reduce to size of the longitudinal stiffeners to a more practical value. The design of a box flange with longitudinal and transverse flange stiffeners is discussed in more detail below.

Equation 6.5.6.2.4.2.1-18 provides the minimum required moment of inertia, I_ℓ. As discussed previously, when an actual assumed longitudinal flange stiffener moment of inertia, I_s, is used in determining the plate-buckling coefficient, k, from Equation 6.5.6.2.4.2.1-15 or Equation 6.5.6.2.4.2.1-16, as applicable, Equation 6.5.6.2.4.2.1-18 is automatically satisfied for that value of k since Equation 6.5.6.2.4.2.1-15 and Equation 6.5.6.2.4.2.1-16 are simply algebraic manipulations of Equation 6.5.6.2.4.2.1-18. As an alternative to using Equation 6.5.6.2.4.2.1-15 and Equation 6.5.6.2.4.2.1-16, however, the Design Engineer can assume a value of k ranging from 1.0 to 4.0 (although a k value ranging from 2.0 to 4.0 typically should be assumed), and then determine the minimum required moment of inertia for each longitudinal stiffener to provide that assumed value of k (as a minimum) from Equation 6.5.6.2.4.2.1-18.

AASHTO LRFD Article C6.11.8.2.3 states that k will be at or near a value of 4.0 if the longitudinal flange stiffeners are very rigid and plate buckling will therefore be forced to occur between the stiffeners. For lower values of k, the stiffeners are less rigid and the nominal flexural resistance of the flange will be reduced. Therefore, using Equation 6.5.6.2.4.2.1-15 and Equation 6.5.6.2.4.2.1-16, or alternatively Equation 6.5.6.2.4.2.1-18, the Engineer should attempt to efficiently balance the required stiffener size against the required flange resistance in order to provide an economical design. Selecting a k value of 4.0 to provide the largest longitudinal stiffener(s), or selecting a longitudinal stiffener(s) to provide the largest permitted k value of 4.0, may not always provide the most economical solution.

Also, as discussed above, as the number of longitudinal stiffeners, n, increases beyond one, the required moment of inertia to achieve a desired k value begins to increase dramatically and eventually becomes impractical. Therefore, equations for k are only provided for values of n up to and including two. For boxes of typical proportions, where longitudinal flange stiffeners are required, it is strongly recommended that the number of longitudinal flange stiffeners not exceed one. In rare cases where an exceptionally wide box flange is required and the number of longitudinal flange stiffeners may need to exceed two, the addition of transverse

flange stiffeners should be considered as discussed below. Further discussion on longitudinally stiffened box flanges may be found in Section 6.3.5.5.2.

AASHTO LRFD Article 6.11.11.2 specifies that the projecting width, b_ℓ, of a longitudinal flange stiffener element satisfy the following requirement:

$$b_\ell \le 0.48 t_s \sqrt{\frac{E}{F_{yc}}} \qquad \text{Equation 6.5.6.2.4.2.1-19}$$

AASHTO LRFD Equation 6.11.11.2-1

where:

t_s = thickness of the projecting longitudinal stiffener element (in.)

For structural tees, b_ℓ is to be taken as one-half the width of the flange. Equation 6.5.6.2.4.2.1-19 is intended to prevent local buckling of the projecting elements of the longitudinal stiffener.

Transversely and Longitudinally Stiffened Box Flanges

In rare cases where an exceptionally wide box flange is needed and the number of longitudinal flange stiffeners, *n*, may need to exceed 2, the use of transverse flange stiffeners should be considered to reduce the required size of the longitudinal flange stiffeners to a more practical value. The required size of the longitudinal stiffeners is based on an infinite length of panel. This assumption becomes significantly conservative when more than two longitudinal stiffeners are used. Also, for cases where *n* is equal to 2 and a plate-buckling coefficient *k* greater than about 2.5 is required, the use of transverse flange stiffeners can help to reduce the size of the longitudinal flange stiffeners over that required by Equation 6.5.6.2.4.2.1-18.

The use of transverse stiffeners reduces the length of the panel from infinity to the spacing of the transverse stiffeners. Equations for the design of transversely and longitudinally stiffened box flanges at the strength limit state are provided in *AASHTO LRFD* Article C6.11.11.2 and are reviewed below. These equations are based on classical plate-buckling equations (Timoshenko and Gere, 1961).

As indicated in *AASHTO LRFD* Article C6.11.11.2, for the exceptional case where transverse flange stiffeners are deemed necessary, the plate-buckling coefficient, *k*, for uniform normal stress to be used in determining the nominal axial compressive buckling resistance of the flange (from Equation 6.5.6.2.4.2.1-4, Equation 6.5.6.2.4.2.1-5, or Equation 6.5.6.2.4.2.1-6 as applicable) at the strength limit state may be taken as follows:

$$k = \frac{\left[1 + (a/b_{fc})^2\right]^2 + 87.3}{(n+1)^2 (a/b_{fc})^2 [1 + 0.1(n+1)]} \le 4.0 \quad \text{Equation 6.5.6.2.4.2.1-20}$$

AASHTO LRFD Equation C6.11.11.2-3

where:

a = longitudinal spacing of the transverse flange stiffeners (in.) $\le 3b_{fc}$

Further, in determining the required moment of inertia of the longitudinal flange stiffeners, I_ℓ, from Equation 6.5.6.2.4.2.1-18 when transverse stiffeners are present, the constant, ψ, is to be taken as 8.0. The number of longitudinal flange stiffeners, n, preferably should not exceed 5 when transverse flange stiffeners are provided. When n does not exceed 5, transverse flange stiffeners spaced at a distance not exceeding $4w$ (see the beginning of this section for the definition of w) will provide a k of approximately 4.0 according to Equation 6.5.6.2.4.2.1-20.

When the k value from Equation 6.5.6.2.4.2.1-20 is used to determine the nominal flexural resistance of the flange, the moment of inertia, I_t, of each transverse flange stiffener about an axis through its centroid and parallel to its bottom edge must satisfy the following:

$$I_t \ge 0.05(n+1)^3 w^3 \frac{f_s}{E} \frac{A_f}{a} \quad \text{Equation 6.5.6.2.4.2.1-21}$$

AASHTO LRFD Equation C6.11.11.2-4

where:

A_f = area of the box flange including the longitudinal flange stiffeners (in.^{2})

f_s = largest of the longitudinal flange stresses due to the factored loads in the panels on either side of the transverse flange stiffener under consideration (ksi)

In addition, the specified minimum yield strength of the transverse flange stiffeners should not be less than the specified minimum yield strength of the box flange according to *AASHTO LRFD* Article C6.11.11.2.

Transverse flange stiffeners can take one of two forms; either individual tees can serve as transverse flange stiffeners, or a bottom strut provided within the internal cross-bracing of the box satisfying the requirements of *AASHTO LRFD* Article 6.7.4.3 can serve as a transverse flange stiffener if the strut also satisfies the stiffness requirement given by Equation 6.5.6.2.4.2.1-21. Regardless of which form is used, the transverse flange stiffeners should be attached to the longitudinal flange stiffeners by bolting, with the connection to each longitudinal flange stiffener designed to resist the following vertical force, F_s, at the strength limit state:

$$F_s = \frac{\phi_f F_{ys} S_s}{n b_{fc}}$$ Equation 6.5.6.2.4.2.1-22

AASHTO LRFD Equation C6.11.11.2-1

where:

F_{ys} = specified minimum yield strength of the transverse flange stiffener (ksi)
S_s = section modulus of the transverse flange stiffener (ksi)

Individual tees serving as transverse flange stiffeners should also be attached to the webs of the box section. As indicated in *AASHTO LRFD* Article C6.11.11.2, the connection of the transverse flange stiffeners to each web should be designed to resist the following vertical force, F_w, at the strength limit state:

$$F_w = \frac{\phi_f F_{ys} S_s}{2 b_{fc}}$$ Equation 6.5.6.2.4.2.1-23

AASHTO LRFD Equation C6.11.11.2-2

Should a bottom strut be provided within the internal cross-bracing of the box to control distortion of the box flange and reduce the transverse bending stress ranges in the flange for fatigue, as discussed previously in Section 6.5.5.2.2.3, the bottom strut and its connections need not satisfy the requirements of Equation 6.5.6.2.4.2.1-21, Equation 6.5.6.2.4.2.1-22, and Equation 6.5.6.2.4.2.1-23 unless the strut is also intended to serve as a transverse flange stiffener at the strength limit state and the *k* value from Equation 6.5.6.2.4.2.1-20 is utilized in the design of the box flange.

6.5.6.2.4.3 Continuously Braced Tension Flanges

AASHTO LRFD Article 6.11.8.1.2 specifies that for box sections subject to negative flexure, continuously braced flanges in tension (i.e. top flanges) must satisfy the following requirement at the strength limit state:

$$f_{bu} \le \phi_f F_{nt}$$ Equation 6.5.6.2.4.3-1

AASHTO LRFD Equation 6.11.8.1.2-1

where:

F_{nt} = nominal flexural resistance of the flange in tension determined as specified in *AASHTO LRFD* Article 6.11.8.3 (discussed below) (ksi)

A continuously braced flange is defined as a flange encased in concrete or anchored by shear connectors. Lateral flange bending stresses and St. Venant torsional shears need not be considered for continuously braced top flanges of tub sections.

The torsional shear must be considered in the continuously braced top flange of a closed-box section however.

For sections in negative flexure, the nominal flexural resistance of the (top) tension flange(s) is controlled by yielding. According to *AASHTO LRFD* Article 6.11.8.3, the nominal flexural resistance of the tension flanges of tub sections, F_{nt}, is to be taken as:

$$F_{nt} = R_h F_{yt} \qquad \text{Equation 6.5.6.2.4.3-2}$$

AASHTO LRFD Equation 6.11.8.3-1

where:

R_h = hybrid factor determined as specified in *AASHTO LRFD* Article 6.10.1.10.1 (Section 6.4.5.7)

The nominal flexural resistance of the (top) tension flange of closed-box sections, F_{nt}, is to be taken as:

$$F_{nt} = R_h F_{yt} \Delta \qquad \text{Equation 6.5.6.2.4.3-3}$$

AASHTO LRFD Equation 6.11.7.2.2-5

where:

$$\Delta = \sqrt{1 - 3\left(\frac{f_v}{F_{yt}}\right)^2} \qquad \text{Equation 6.5.6.2.4.3-4}$$

AASHTO LRFD Equation 6.11.7.2.2-6

f_v = factored St. Venant torsional shear stress in the flange at the section under consideration not to exceed the factored torsional shear resistance of the flange, F_{vr}, given by Equation 6.5.6.1.2-1 (ksi)

$$= \frac{T}{2A_o t_{ft}} \qquad \text{Equation 6.5.6.2.4.3-5}$$

AASHTO LRFD Equation 6.11.7.2.2-7

A_o = enclosed area within the box section (in.^{2})
t_{ft} = thickness of the tension flange (in.)
T = internal torque due to the factored loads (kip-in.)

EXAMPLE

Check the composite tub section shown in Figure 6.5.6.2.4.3-1 (note: longitudinal reinforcement and top lateral bracing not shown), which is at the interior pier of an exterior girder in a straight continuous-span bridge, for the Strength I load combination. The girder is homogeneous with the flanges and web having a yield strength of 50 ksi. The load modifier, η, is assumed to be 1.0. Assume unshored construction and that the tub girder is supported on two bearings at the pier.

It is also assumed that the section is from a multiple box-section bridge that does not satisfy one or more of the special restrictions specified in *AASHTO LRFD* Article 6.11.2.3 (Section 6.3.5.2). Therefore, the effects of St. Venant torsional shear and cross-sectional distortion stresses must be considered at the strength limit state. Had the bridge met the special restrictions, all terms related to the St. Venant torsional shear stress, f_v, would simply be set equal to zero in the following resistance equations (assuming the box flange is also fully effective as confirmed below). Cross-sectional distortion stresses would also not need to be considered.

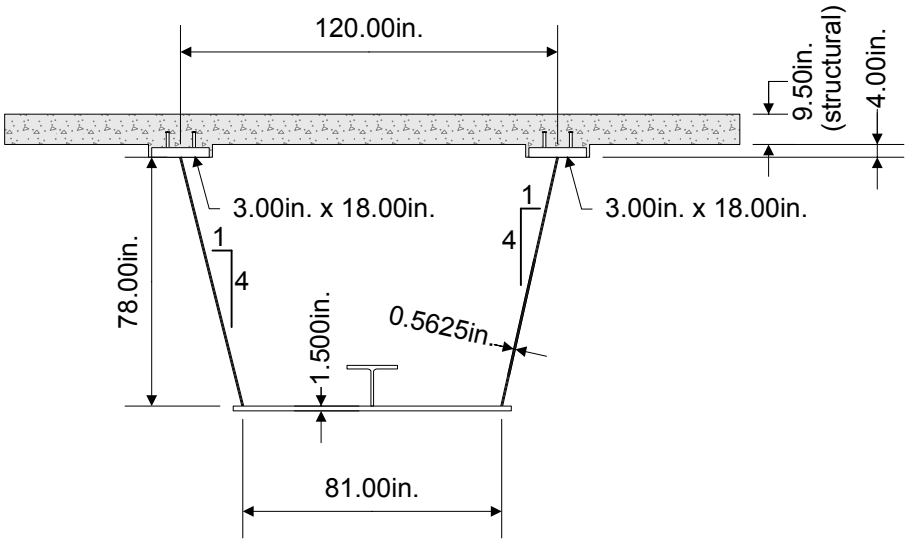

Figure 6.5.6.2.4.3-1 Example Composite Tub Section at an Interior Pier

The area of the longitudinal deck reinforcement is 20.0 in.^{2} assumed placed at the neutral axis of the deck. The applicable elastic section properties for the strength limit state check are as follows:

Steel girder:

I = 438,966 in.^{4}
S_{top} = 10,047 in.^{3}
S_{bot} = 11,311 in.^{3}
N.A. is 38.81 in. from the bottom of the bottom flange

Steel girder plus longitudinal reinforcement:

I = 484,714 in.^{4}
S_{top} = 11,837 in.^{3}
S_{bot} = 11,666 in.^{3}
N.A. is 41.55 in. from the bottom of the bottom flange

The section properties include the longitudinal component of the top-flange lateral bracing area (as recommended in *AASHTO LRFD* Article C6.11.1.1); a single top-flange bracing member with a cross-sectional area A of 8.0 in.^{2} placed at an angle of 30 degrees from tangent to the girder is assumed. The bracing members are assumed bolted to the top flanges. Therefore, the additional cross-sectional area included with the top-flange areas in calculating the section properties is computed from Equation 6.4.2.3.2.3-2 as A_d = 8.0cos30° = 6.93 in.^{2} The section properties also include the single longitudinal flange stiffener (size is determined in the next Example), and the 1-inch-wide bottom-flange lips (measured from the centerline of the webs) that are provided for web-to-flange welding access.

The area of the inclined webs is used in computing all section properties. The moment of inertia of each inclined web, I_{ow}, with respect to a horizontal axis at mid-depth of the web is taken from Equation 6.4.2.3.2.3-1 as:

$$I_{ow} = I_w\left(\frac{S^2}{S^2+1}\right)$$

where:

I_w = moment of inertia of each inclined web with respect to an axis normal to the web (in.^{4})
S = web slope with respect to the horizontal (= 4.0 in this case)

Since the bottom box-flange width does not exceed one-fifth of the distance between the points of permanent load contraflexure on either side of the pier section, the flange is considered fully effective and shear lag effects need not be considered in calculating the section properties for the determination of the flexural stresses (*AASHTO LRFD* Article 6.11.1.1 – Section 6.3.5.5.3). Therefore, the longitudinal bending stress may be assumed uniform across the full flange width.

Assume the following unfactored bending moments:

M_{DC1} = -17,007 kip-ft
M_{DC2} = -2,712 kip-ft
M_{DW} = -2,220 kip-ft
M_{LL+IM} = -9,444 kip-ft

Assume the following unfactored torques. Since the section is at an interior support, positive and negative torques exist at the section for each load case. Only the maximum and minimum values of the HL-93 live load plus impact torques are given:

T_{DC1} = +26/-3 kip-ft
T_{DC2} = +246/-190 kip-ft
T_{DW} = +201/-156 kip-ft
T_{LL+IM} = +854/-966 kip-ft

It is assumed that all the deck weight is applied to the girder top flanges in the analysis for this example. Thus, the DC_1 torque does not include the torque due to the weight of deck overhang acting on the boxes. The torque results primarily from the application of unequal deck weight loads to the girder top flanges.

Check the flexural resistance of the bottom box flange in compression. First, compute the flexural stress in the bottom flange due to the factored loads (ignoring the effect of longitudinal warping). For the Strength I load combination:

$$f_{bu} = 1.0\left[\frac{1.25(-17{,}007)}{11{,}311} + \frac{1.25(-2{,}712)}{11{,}666} + \frac{1.5(-2{,}220)}{11{,}666} + \frac{1.75(-9{,}444)}{11{,}666}\right]12 = -46.47 \text{ ksi}$$

Calculate the St. Venant torsional shear stress due to the factored loads, f_v, in the bottom flange. For the DC_1 torque, which is applied to the non-composite section, the enclosed area, A_o, is computed for the non-composite box section. The vertical depth between the mid-thickness of the flanges is used. It is also assumed that the top lateral bracing is connected to the top flanges so that a reduction in A_o is not required. Therefore:

$$A_o = \frac{(120+81)}{2} * (78.0 + 1.5 + 0.75) * \frac{1 \text{ ft}^2}{144 \text{ in.}^2} = 56.0 \text{ ft}^2$$

$$f_v = \frac{T}{2A_o t_{fc}} \quad \text{(Equation 6.5.6.2.4.2.1-2)}$$

$$f_v = \frac{1.0(1.25)(26)}{2(56.0)(1.5)} * \frac{1}{12 \text{ in./ft}} = 0.016 \text{ ksi}$$

For the torques applied to the composite section, calculate A_o for the composite section from the mid-thickness of the bottom flange to the mid-thickness of the concrete deck (considering the deck haunch):

$$A_o = \frac{(120+81)}{2} * (78.0 + 0.75 + 4.0 + \frac{9.5}{2}) * \frac{1 \text{ ft}^2}{144 \text{ in.}^2} = 61.1 \text{ ft}^2$$

The negative torque case controls. Therefore:

$$f_v = \frac{1.0\left|1.25(-190) + 1.5(-156) + 1.75(-966)\right|}{2(61.1)(1.5)} * \frac{1}{12 \text{ in./ ft}} = 0.983 \text{ ksi}$$

$$f_{v \text{ total}} = 0.016 + 0.983 = 0.999 \text{ ksi}$$

Note that although the critical torques acting on the non-composite and composite box sections act in opposite directions in this case, the shear flows are conservatively added together since a future wearing surface is included in the negative torque applied to the composite section. Check that $f_{v\ total}$ does not exceed the factored torsional shear resistance of the flange, F_{vr} (Equation 6.5.6.1.2-1):

$$F_{vr} = 0.75\phi_v \frac{F_{yf}}{\sqrt{3}}$$

$$F_{vr} = 0.75(1.0)\frac{50}{\sqrt{3}} = 21.65 \text{ ksi} > f_{v \text{ total}} = 0.999 \text{ ksi} \quad \text{ok}$$

Calculate the nominal flexural compressive resistance, F_{nc}, of the longitudinally stiffened bottom flange according to the provisions of *AASHTO LRFD* Article 6.11.8.2.3. For a longitudinally stiffened flange, the resistance is to be determined with the spacing, w, taken as the larger of the width of the flange between the longitudinal flange stiffeners, or the distance from a web to the nearest longitudinal flange stiffener, substituted for the flange width, b_{fc}. Therefore, in this case:

$$w = \frac{(81.0 - 0.5625)}{2} = 40.2 \text{ in.}$$

$$\lambda_f = \frac{w}{t_{fc}} = \frac{40.2}{1.5} = 26.8$$

$$\Delta = \sqrt{1 - 3\left(\frac{f_v}{F_{yc}}\right)^2} \quad \text{(Equation 6.5.6.2.4.2.1-10)}$$

$$\Delta = \sqrt{1 - 3\left(\frac{0.999}{50}\right)^2} \cong 1.0$$

Calculate the nominal axial compression buckling resistance of the flange under compression alone, F_{cb}, and the nominal shear resistance of the flange under shear alone, F_{cv}. To determine which equation to use, calculate the corresponding Anchor Points, which requires the values of the corresponding buckling coefficients, k and k_s.

For longitudinally stiffened flanges, k from Equation 6.5.6.2.4.2.1-15 or Equation 6.5.6.2.4.2.1-16, as applicable, and k_s from Equation 6.5.6.2.4.2.1-17 are be used in place of k = 4.0 and k_s = 5.34 (for unstiffened flanges), respectively. Since the longitudinal stiffener size is unknown at this point, instead of assuming a stiffener size, reasonable values of k and k_s will instead be assumed. The size of the longitudinal stiffener required to provide the assumed value of k (as a minimum) will be computed in the following Example. The resulting stiffener size will then be used to compute the actual values of k and k_s in the same example using Equation 6.5.6.2.4.2.1-15 and Equation 6.5.6.2.4.2.1-17, respectively. The factored flexural resistance will then be checked using the actual values of k and k_s to determine if there is a significant change in the resistance from what is computed below.

A value of k below the maximum permitted value of 4.0 will result in a smaller nominal flexural resistance, but will also result in a significantly smaller longitudinal flange stiffener than might otherwise be required. Assume k = 3.0. Assume k_s = 2.5. Using the assumed value of k, and the previously computed value of Δ, Anchor Point 1 for the calculation of F_{cb} is computed as follows (Equation 6.5.6.2.4.2.1-8):

$$\lambda_p = 0.57\sqrt{\frac{Ek}{F_{yc}\Delta}} = 0.57\sqrt{\frac{29{,}000(3.0)}{50(1.0)}} = 23.8$$

$$F_{yr} = (\Delta - 0.3)F_{yc} \quad \text{(Equation 6.5.6.2.4.2.1-11)}$$

$$F_{yr} = (1.0 - 0.3)50 = 35.0 \text{ ksi}$$

Using F_{yr} and the previously assumed value of k, Anchor Point 2 for the calculation of F_{cb} is computed as follows (Equation 6.5.6.2.4.2.1-9).

$$\lambda_r = 0.95\sqrt{\frac{Ek}{F_{yr}}} = 0.95\sqrt{\frac{29{,}000(3.0)}{35.0}} = 47.4$$

Since $23.8 < \lambda_f = 26.8 < 47.4$, then (Equation 6.5.6.2.4.2.1-5):

$$F_{cb} = R_b R_h F_{yc}\left[\Delta - \left(\Delta - \frac{\Delta - 0.3}{R_h}\right)\left(\frac{\lambda_f - \lambda_p}{\lambda_r - \lambda_p}\right)\right]$$

For a homogeneous girder, the hybrid factor R_h is equal to 1.0. Calculate the web load-shedding factor, R_b. First, determine if R_b is indeed less than 1.0 by checking Equation 6.4.5.5.2.1-2. For composite sections in negative flexure, the elastic depth of the web in compression, D_c, at the strength limit state is to conservatively be computed for the section consisting of the steel girder plus the longitudinal reinforcement (*AASHTO LRFD* Article D6.3.1). Also, for box sections with inclined webs, D_c must be measured along the web slope. Therefore:

$$\frac{2D_c}{t_w} = \frac{2(41.55 - 1.5)/\cos 14^\circ}{0.5625} = \frac{2(41.28)}{0.5625} = 146.8$$

$$\frac{2D_c}{t_w} > \lambda_{rw} = 5.7\sqrt{\frac{E}{F_{yc}}} = 5.7\sqrt{\frac{29{,}000}{50}} = 137.3$$

Therefore, the section is a slender-web section subject to web bend-buckling at elastic stress levels at the strength limit state and R_b is less than 1.0. Calculate R_b from Equation 6.4.5.6-3:

$$R_b = 1 - \left(\frac{a_{wc}}{1200 + 300a_{wc}}\right)\left(\frac{2D_c}{t_w} - \lambda_{rw}\right) \le 1.0$$

where:

$$a_{wc} = \frac{2D_c t_w}{b_{fc} t_{fc}}$$

As indicated in *AASHTO LRFD* Article C6.11.8.2.2, in calculating R_b for a tub section, one-half of the effective box flange width is to be used in conjunction with one top flange and a single web. Thus:

$$a_{wc} = \frac{2(41.28)(0.5625)}{((81.0 - 0.5625)/2)(1.5)} = 0.770$$

$$R_b = 1 - \left(\frac{0.770}{1200 + 300(0.770)}\right)(146.8 - 137.3) = 0.995$$

Therefore:

$$F_{cb} = (0.995)(1.0)(50)\left[1.0 - \left(1.0 - \frac{(1.0 - 0.3)}{1.0}\right)\left(\frac{26.8 - 23.8}{47.4 - 23.8}\right)\right] = 47.85 \text{ ksi}$$

Using the assumed value of k_s, Anchor Point 1 for the calculation of F_{cv} is computed as follows:

$$1.12\sqrt{\frac{Ek_s}{F_{yc}}} = 1.12\sqrt{\frac{29{,}000(2.5)}{50}} = 42.6$$

Since $\lambda_f = 26.8 < 42.6$, then (Equation 6.5.6.2.4.2.1-12):

$$F_{cv} = 0.58F_{yc} = 0.58(50) = 29.0 \text{ ksi}$$

The nominal flexural resistance of the flange, F_{nc}, is computed as (Equation 6.5.6.2.4.2.1-1):

$$F_{nc} = F_{cb}\sqrt{1 - \left(\frac{f_v}{\phi_v F_{cv}}\right)^2} = 47.85\sqrt{1 - \left(\frac{0.999}{1.0(29.0)}\right)^2} = 47.82 \text{ ksi}$$

The factored flexural resistance of the flange, F_r, is computed as:

$$F_r = \phi_f F_{nc} = 1.0(47.82) = 47.82 \text{ ksi} > |f_{bu}| = 46.47 \text{ ksi} \quad \text{ok}$$

The bottom flange at the interior pier acting in combination with the internal diaphragm is subject to bending in two directions plus the torsional and diaphragm shear (ignoring any through-thickness bending of the flange plate under its own self weight). *AASHTO LRFD* Article C6.11.8.1.1 suggests the use of Equation

6.5.6.2.4.2-2 for checking this combined stress state in the box flange at the strength limit state as follows (with f_{bu} and f_{by} taken as signed quantities):

$$\sqrt{f_{bu}^2 - f_{bu}f_{by} + f_{by}^2 + 3(f_d + f_v)^2} \le \phi_f R_b R_h F_{yc}$$

For a box supported on two bearings, as is the case in this example, the bottom-flange stress, f_{by}, due to major-axis bending of the diaphragm over the bearing sole plate is typically relatively small and will be neglected. Therefore, f_{by} will be taken equal to zero in the preceding equation for this example. From previous calculations, the St. Venant torsional shear stress, f_v, due to the factored loads at the strength limit state was computed to be 0.999 ksi.

The shear stress in the bottom flange due to the internal diaphragm vertical shear, f_d, may be computed from Equation 6.5.6.2.4.2-3 as follows:

$$f_d = \frac{VQ}{It_{fc}}$$

As suggested in *AASHTO LRFD* Article C6.11.8.1.1, a bottom flange width equal to 6 times its thickness will be assumed effective with the internal diaphragm; i.e. 6 * 1.5 in. = 9.0 in. The internal diaphragm is 78 inches deep and 1.0 in. thick with a 36-inch deep access hole centered in the middle of the diaphragm. The diaphragm has a 1" x 12" top flange. Calculate the section properties of the effective section at the bearing stiffener adjacent to the critical web.

Component	A	d	Ad	Ad^2	I_o	I
Top Flange 1" x 12"	12.00	39.50	474.0	18,723	1.00	18,724
Web 1" x 78"	78.00				39.546	39,546
Bot. Flange 1-1/2" x 9"	13.50	39.75	-536.6	21,331	2.53	21,334
	103.50		-62.6			79,604
						-0.605(62.6) = -37.87
						I_{NA} = 79,566 in.^{4}

$$d_s = \frac{-62.6}{103.50} = -0.605 \text{ in.}$$

$$d_{TOP\ OF\ STEEL} = 40.00 + 0.605 = 40.61 \text{in.} \qquad d_{BOT\ OF\ STEEL} = 40.50 - 0.605 = 39.90 \text{ in.}$$

$$S_{TOP\ OF\ STEEL} = \frac{79{,}566}{40.61} = 1{,}959 \text{ in.}^3 \qquad S_{BOT\ OF\ FLANGE} = \frac{79{,}566}{39.90} = 1{,}994 \text{ in.}^3$$

The first moment, *Q*, of one-half the effective box-flange area about the neutral axis of the effective internal diaphragm section is computed as:

$$Q = \frac{1}{2}(9.0)(1.5)(39.90 - 0.75) = 264.3 \text{ in.}^3$$

The factored vertical shear, *V*, in the internal diaphragm due to flexure plus St. Venant torsion on the critical side is given as 1,411 kips (the calculation of the internal diaphragm shear is discussed further in the Example given in Section 6.6.3.6.2). Thus:

$$f_d = \frac{1{,}411(264.3)}{79{,}566(1.5)} = 3.12 \text{ ksi}$$

Calculate the section properties of the effective section through the center of the access hole. There is significant shear lag around the access hole and plane sections through the hole do not remain plane. Although the material above the hole is effective in bending (and shear), it will be conservatively ignored in the calculation of the section properties of the section composed of the bottom flange and the diaphragm below the hole:

Component	A	d	Ad	Ad^2	I_o	I
Web – below hole	21.00	28.50	-598.5	17,057	771.8	17,829
Bot. Flange 1-1/2" x 9"	13.50	39.75	-536.6	21,331	2.53	21,334
	34.50		-1,135			39,163
					-32.90(1,135) =	-37,342
					I_{NA} =	1,821 in.^{4}

$$d_s = \frac{-1{,}135}{34.50} = -32.90 \text{ in.}$$

$$d_{BOT\ OF\ HOLE} = 22.50 - 7.60 = 14.90 \text{ in.} \qquad d_{BOT\ OF\ FLANGE} = 40.50 - 32.90 = 7.60 \text{ in.}$$

$$S_{BOT\ OF\ HOLE} = \frac{1{,}821}{14.90} = 122 \text{ in.}^3 \qquad S_{BOT\ OF\ FLANGE} = \frac{1{,}821}{7.60} = 108 \text{ in.}^3$$

The first moment, *Q*, of one-half the effective box-flange area about the neutral axis of the effective internal diaphragm section is computed as:

$$Q = \frac{1}{2}(9.0)(1.5)(7.60 - 0.75) = 46.2 \text{ in.}^3$$

The total factored bearing reaction on the critical side under the Strength I load combination is computed as R_u = 1,255 kips (refer to the example given in Section 6.6.3.6.2). Therefore, the total factored vertical diaphragm shear at the section through the access hole is:

$$V = 1{,}411 \text{ kips} - 1{,}255 \text{ kips} = 156 \text{ kips}$$

$$f_d = \frac{156(46.2)}{1{,}821(1.5)} = 2.64 \text{ ksi}$$

The shear stress in the flange at the bearing stiffener is critical.

$$\sqrt{(-46.47)^2 - (-46.47)(0) + (0)^2 + 3(3.12 + 0.999)^2} = 46.78 \text{ ksi}$$

$$\phi_f R_b R_h F_{yc} = 1.0(0.995)(1.0)(50) = 49.75 \text{ ksi} > 46.78 \text{ ksi} \quad \text{ok}$$

Confirm the preceding calculation using the following alternative form of the Huber-von Mises-Hencky yield criterion (Ugural and Fenster, 1978):

$$\sqrt{\sigma_1^2 - \sigma_1\sigma_2 + \sigma_2^2} \le \phi_f R_b R_h F_{yc}$$

where:

σ_1, σ_2 = maximum and minimum principal stresses in the bottom flange (ksi)

$$= \left(\frac{f_{bu} + f_{by}}{2}\right) \pm \sqrt{\left(\frac{f_{bu} - f_{by}}{2}\right)^2 + (f_d + f_v)^2}$$

$$\sigma_{1,2} = \left(\frac{-46.47 + 0}{2}\right) \pm \sqrt{\left(\frac{-46.47 - 0}{2}\right)^2 + (3.12 + 0.999)^2} = -46.68, 0.21 \text{ ksi}$$

$$\sqrt{(-46.68)^2 - [(-46.68)(0.21)] + (0.21)^2} = 46.78 \text{ ksi} < \phi_f R_b R_h F_{yc} = 49.75 \text{ ksi} \quad \text{ok}$$

Check the flexural resistance of the top flanges of the tub section in tension. First, compute the flexural stress in the top flanges due to the factored loads (ignoring the effect of longitudinal warping). For the Strength I load combination:

$$f_{bu} = 1.0\left[\frac{1.25(-17{,}007)}{10{,}047} + \frac{1.25(-2{,}712)}{11{,}837} + \frac{1.5(-2{,}220)}{11{,}837} + \frac{1.75(-9{,}444)}{11{,}837}\right]12 = 48.96 \text{ ksi}$$

According to *AASHTO LRFD* Article 6.11.8.3, the nominal flexural resistance, F_{nt}, of the tension flanges of tub sections in regions of negative flexure is to be taken as (Equation 6.5.6.2.4.3-2):

$$F_{nt} = R_h F_{yt}$$

$$F_{nt} = 1.0(50) = 50 \text{ ksi}$$

The factored flexural resistance, F_r, of the tension flanges is computed as:

$$F_r = \phi_f F_{nt} = 1.0(50) = 50.00 \text{ ksi} > f_{bu} = 48.96 \text{ ksi} \quad \text{ok}$$

Regarding the cross-sectional distortion stresses, refer to the Example given in Section 6.5.5.2.2.3.2.

EXAMPLE

Select a longitudinal flange stiffener for the box section shown in the preceding Example, which is at the interior pier of an exterior girder in a straight continuous-span bridge.

In the preceding example, a value of the plate-buckling coefficient for uniform normal stress, *k*, was assumed in order to design the box flange (i.e. *k* = 3.0 was assumed). Determine the minimum required moment of inertia, I_ℓ, of the longitudinal flange stiffener from Equation 6.5.6.2.4.2.1-18 necessary to provide this assumed value of *k* as follows:

$$I_\ell = \psi w t_{fc}^3$$

For a single longitudinal flange stiffener (i.e. *n* = 1):

$$\psi = 0.125k^3 = 0.125(3.0)^3 = 3.375$$

Therefore:

$$I_\ell = 3.375(40.2)(1.5)^3 = 457.9 \text{ in.}^4$$

Try a WT8 x 33.5 rolled structural tee for the longitudinal stiffener. From the AISC Manual shape property tables:

b_f = 10.235 in.
t_s = 0.665 in.
I_x = 48.6 in.^{4}
A = 9.84 in.^{2}
N.A. is 6.605 in. from the tip of the tee stem

Check the projecting width of the tee flange according to Equation 6.5.6.2.4.2.1-19:

$$b_\ell \le 0.48 t_s \sqrt{\frac{E}{F_{yc}}}$$

$$0.48(0.665)\sqrt{\frac{29{,}000}{50}} = 7.69 \text{ in.} > b_\ell = \frac{b_f}{2} = \frac{10.235}{2} = 5.12 \text{ in.} \quad \text{ok}$$

Calculate the actual moment of inertia, I_s, of the longitudinal flange stiffener about the base of the stiffener:

$$I_s = 48.6 + 9.84(6.605)^2 = 477.9 \text{ in.}^4 > I_\ell = 457.9 \text{ in.}^4 \quad \text{ok}$$

Note that substituting the calculated value of I_s into Equation 6.5.6.2.4.2.1-15 as follows gives:

$$k = \left(\frac{8 I_s}{w t_{fc}^3} \right)^{\frac{1}{3}}$$

$$k = \left(\frac{8(477.9)}{40.2(1.5)^3} \right)^{\frac{1}{3}} = 3.04 \quad (1.0 \le k \le 4.0 \quad \text{ok})$$

versus the assumed value of k = 3.0.

In the preceding example, a value of the plate shear-buckling coefficient for shear stress, k_s, was also assumed in order to design the box flange (i.e. k_s = 2.5 was assumed). Using Equation 6.5.6.2.4.2.1-17 and the calculated value of I_s, determine the actual value of k_s as follows:

$$k_s = \frac{5.34 + 2.84\left(\frac{I_s}{w t_{fc}^3} \right)^{\frac{1}{3}}}{(n+1)^2} \le 5.34$$

$$k_s = \frac{5.34 + 2.84\left(\frac{477.9}{40.2(1.5)^3} \right)^{\frac{1}{3}}}{(1+1)^2} = 2.42 < 5.34 \quad \text{ok}$$

versus the assumed value of k_s = 2.5.

Repeating the calculations from the preceding example for k = 3.04 and k_s = 2.42 (calculations not shown) results in a final factored flexural resistance, F_r, for the box flange of 47.91 ksi (versus F_r = 47.82 ksi calculated previously for k = 3.0 and k_s = 2.5), which is still satisfactory. Use a single WT8 x 33.5 longitudinal flange stiffener.

6.5.6.3 Composite Sections in Positive Flexure

6.5.6.3.1 General

In the *AASHTO LRFD* Specifications, the nominal flexural resistance of composite sections in straight girders subject to positive flexure that satisfy specific steel grade, web slenderness and ductility requirements is permitted to exceed the moment at first yield at the strength limit state. Sections meeting these requirements are termed ′compact sections′ (Section 6.5.6.3.2). The nominal flexural resistance of sections not meeting one or more of these requirements, termed ′noncompact sections′ (Section 6.5.6.3.3), is not permitted to exceed the moment at first yield. For compact sections, the nominal flexural resistance is most appropriately expressed in terms of moment and for noncompact sections, the nominal flexural resistance is most appropriately expressed in terms of the elastically computed flange stress (for reasons discussed previously in Section 6.5.6.2.2.1.5).

According to AASHTO LRFD Articles 6.10.6.2.2 and 6.11.6.2.2, composite I- and box sections in positive flexure in kinked (chorded) continuous or horizontally curved steel girder bridges are always to be considered as noncompact sections at the strength limit state. Research has not yet been conducted to support the design of these sections as compact sections with flexural resistances exceeding the moment at first yield. Although the specification is currently silent on the issue, consideration should be given to conservatively treating composite sections in positive flexure in straight-girder bridges whose supports are skewed more than 20° from normal as noncompact sections for similar reasons. For sections that do qualify and/or are considered to be compact sections, consideration may always be given to conservatively treating the section as a noncompact section, which simplifies the calculations somewhat and should not result in a significant loss of economy as other limit-state criteria (e.g. service limit state or fatigue limit state criteria) are likely to control the design of the section.

In addition to the basic design requirements, both compact and noncompact sections must satisfy a ductility requirement to prevent premature crushing of the concrete deck prior to reaching the specified nominal flexural resistance (Section 6.5.6.3.4). For noncompact sections, the maximum longitudinal compressive stress in the concrete deck at the strength limit state is also limited to $0.6f'_c$ to ensure linear behavior of the concrete, which is assumed in the calculation of the steel flange stresses (Section 6.5.6.3.3.4).

Top (compression) flanges of composite sections in positive flexure are continuously braced flanges. For a continuously braced compression flange, one side of the flange is effectively prevented from local buckling, or else both sides of the flange must buckle in the direction away from the concrete deck, resulting in highly restrained boundary conditions at the web-flange juncture. The concrete deck also helps restrain lateral deflections of the flange associated with local and lateral-torsional buckling. As a result, continuously braced compression flanges need not be checked for local or lateral-torsional buckling according to the AASHTO LRFD Specifications. Lateral flange bending stresses also need not be considered for continuously braced flanges, including any lateral flange bending stresses induced in the non-composite flange before it becomes continuously braced. The lateral resistance of the composite concrete deck is generally sufficient to compensate for the neglect of any initial lateral bending stresses in the flange, as well as any additional lateral bending stresses that may be induced after the deck has been placed.

6.5.6.3.2 Compact Sections

6.5.6.3.2.1 General

Compact sections were defined in the preceding section as composite sections in straight girders subject to positive flexure that satisfy specific steel grade, web slenderness and ductility requirements such that the nominal flexural resistance is permitted to exceed the moment at first yield at the strength limit state. Composite sections in positive flexure in kinked (chorded) continuous or horizontally curved bridges, or sections not meeting one or more of these requirements, must be treated as noncompact sections. The design requirements for compact sections are discussed below for I-sections (Section 6.5.6.3.2.2) and for box sections (Section 6.5.6.3.2.3). The design requirements for noncompact sections are discussed in Section 6.5.6.3.3.

6.5.6.3.2.2 I-Sections

AASHTO LRFD Article 6.10.6.2.2 defines the specific requirements that must be met in order for a composite section in positive flexure in a straight I-girder bridge to qualify as compact. These requirements are restated as follows:

- The specified minimum yield strengths of the flanges must not exceed 70.0 ksi;
- The web must satisfy the requirement of *AASHTO LRFD* Article 6.10.2.1.1 (i.e. $D/t_w \leq 150$ or no longitudinal web stiffeners); and
- The web must satisfy the following web slenderness limit:

$$\frac{2D_{cp}}{t_w} \le 3.76\sqrt{\frac{E}{F_{yc}}} \qquad \text{Equation 6.5.6.3.2.2-1}$$

AASHTO LRFD Equation 6.10.6.2.2-1

where:

D_{cp} = depth of the web in compression at the plastic moment determined as specified in *AASHTO LRFD* Article D6.3.2 (Section 6.4.5.4.2.2) (in.)

Compact composite sections in positive flexure must also satisfy a ductility requirement (Section 6.5.6.3.4) to prevent premature crushing of the concrete deck prior to achieving the calculated nominal flexural resistance, which will ensure a ductile mode of failure.

The use of yield strengths larger than 70 ksi may result in significant nonlinearity and potential crushing of the concrete deck prior to reaching nominal flexural resistance values above the moment at first yield. The section must not have any longitudinal web stiffeners (i.e. the web slenderness, D/t_w, must not exceed 150) because there are insufficient test data to support designing sections with longitudinal stiffeners for moments above R_hM_y. Composite sections with longitudinal stiffeners are deeper sections that tend to be used on longer spans and thus, are subject to larger non-composite dead load stresses. Therefore, the depth of the web in compression, D_c, is likely to be such that substantial inelastic strains would not be able to develop in the web prior to bend buckling of the web occurring at moment levels close to R_hM_y.

Equation 6.5.6.3.2.2-1 is a web slenderness limit for compact sections retained from previous Specifications. In a composite girder subject to positive flexure, the concrete deck causes an upward shift in the neutral axis, which reduces the depth of the web in compression. This reduction continues as plastic strains associated with moments larger than R_hM_y are incurred. As a result, most composite sections in positive flexure without longitudinal stiffeners in straight bridges will qualify as compact according to Equation 6.5.6.3.2.2-1. Since the majority of the web is in tension in these sections, there is typically significant available reserve capacity.

As specified in *AASHTO LRFD* Article 6.10.7.1.1, at the strength limit state, compact sections in positive flexure must satisfy the one-third rule equation expressed in terms of bending moment (Section 6.5.2.1.4) as follows:

$$M_u + \frac{1}{3}f_\ell S_{xt} \le \phi_f M_n \qquad \text{Equation 6.5.6.3.2.2-2}$$

AASHTO LRFD Equation 6.10.7.1.1-1

where:

f_ℓ = lateral bending stress in the tension flange (ksi). f_ℓ is always taken as positive.

M_n = nominal flexural resistance of the section determined as specified in *AASHTO LRFD* Article 6.10.7.1.2 (see below) (kip-in.)

M_u = member major-axis bending moment due to the factored loads at the section under consideration (kip-in.). M_u is always taken as positive.

S_x = elastic section modulus about the major-axis of the section to the tension flange taken as M_{yt}/F_{yt}

The sign of M_u and f_ℓ is always taken as positive in Equation 6.5.6.3.2.2-2. However, when summing dead and live load moment/stresses to obtain the total factored major-axis bending moments and lateral bending stresses, M_u and f_ℓ, to apply in the equation, the signs of the individual dead and live load moments/stresses must be considered.

The moment format is used because for these types of sections, the major-axis bending moment is physically a more meaningful quantity than the elastically computed flange bending stress. Also, the nominal flexural resistance of these sections is generally greater than the yield moment with respect to the tension flange M_{yt}. If desired, the equation could be considered in a stress format by dividing both sides of the equation by S_{xt}. Equation 6.5.6.3.2.2-2 is a conservative but accurate representation of a section analysis in which a pair of fully-yielded widths are discounted from the tension flange to accommodate flange lateral bending, with the remainder of the flange assumed to resist the vertical loads.

Note that only lateral bending in the bottom (tension) flange is considered in Equation 6.5.6.3.2.2-2. Lateral bending does not need to be considered in the top (compression) flange of these sections at the strength limit state because that flange is continuously supported by the concrete deck. Sources of lateral bending in the bottom flange of these sections at the strength limit state include curvature, wind loading and the effect of staggered cross-frames/diaphragms and/or support skew. The determination of flange lateral bending moments due to curvature is addressed in *AASHTO LRFD* Article 4.6.1.2.4b. Determination of flange lateral bending moments due to wind is discussed in *AASHTO LRFD* Article C4.6.2.7.1 (Section 6.5.6.5). Lateral flange bending due to staggered cross-frames/diaphragms and/or support skew is discussed in *AASHTO LRFD* Article C6.10.1 and is preferably handled by a direct structural analysis of the bridge superstructure. *AASHTO LRFD* Article C6.10.1 does contain a suggested value of f_ℓ to use for the preceding case in lieu of a direct structural analysis, if desired. Additional discussion on lateral flange bending in skewed bridges may be found in Section 6.3.2.9.4.3.2. As specified in *AASHTO LRFD* Article 6.10.1.6, the sum of the flange lateral bending stresses due

to all sources cannot exceed $0.6F_{yf}$. Amplification of the flange lateral bending stresses is not required in this case since the bottom flange is in tension.

Note that in all the one-third rule equations within the specification, when the effects of flange lateral bending are judged to be insignificant or incidental, the flange lateral bending term, f_ℓ, is simply set equal to zero in the appropriate equations. The format of the equations then reduces to the more conventional and familiar format for checking the nominal flexural resistance of I-sections in the absence of flange lateral bending.

As specified in *AASHTO LRFD* Article 6.10.7.1.2, the nominal flexural resistance, M_n, of compact composite sections in positive flexure is given as follows:

- If $D_p \leq 0.1D_t$, then:

$$M_n = M_p \qquad \text{Equation 6.5.6.3.2.2-3}$$

AASHTO LRFD Equation 6.10.7.1.2-1

- Otherwise:

$$M_n = M_p\left(1.07 - 0.7\frac{D_p}{D_t}\right) \qquad \text{Equation 6.5.6.3.2.2-4}$$

AASHTO LRFD Equation 6.10.7.1.2-2

where:

D_p = distance from the top of the concrete deck to the neutral axis of the composite section at the plastic moment (in.)
D_t = total depth of the composite section (in.)
M_p = plastic moment of the composite section determined as specified in *AASHTO LRFD* Article D6.2 (Section 6.4.5.2.3.2) (kip-in.)

The nominal flexural resistance, M_n, of compact composite sections in positive flexure depends on the ratio of the depth of the plastic neutral axis below the top of the deck, D_p, to the total depth of the composite section, D_t. Sections with a ratio of D_p/D_t less than or equal to 0.1 can reach the plastic moment, M_p, of the composite section as a minimum without any ductility concerns (Equation 6.5.6.3.2.2-3). When the ratio of D_p/D_t exceeds 0.1, the nominal flexural resistance is reduced from M_p as a linear function of D_p/D_t to provide an additional margin of safety against premature crushing of the concrete deck (Equation 6.5.6.3.2.2-4), which follows a general philosophy espoused by Wittry (1993). The linear equation, which is simpler in form

than the equation given in previous Specifications, depends only on M_p and the ratio of D_p/D_t, as also suggested by Yakel and Azizinamini (2005).

For sections in continuous spans, the nominal flexural resistance is also given by Equation 6.5.6.3.2.2-3 or Equation 6.5.6.3.2.2-4, as applicable, but the section must also satisfy the following:

$$M_n \leq 1.3R_hM_y \qquad \text{Equation 6.5.6.3.2.2-5}$$

AASHTO LRFD Equation 6.10.7.1.2-3

where:

- M_n = nominal flexural resistance given by Equation 6.5.6.3.2.2-3 or Equation 6.5.6.3.2.2-4, as applicable (kip-in.)
- M_y = yield moment determined as specified in *AASHTO LRFD* Article D6.2 (Section 6.4.5.3.3.1) (kip-in.)
- R_h = hybrid factor determined as specified in *AASHTO LRFD* Article 6.10.1.10.1 (Section 6.4.5.7)

The nominal flexural resistance of these sections in straight continuous spans is subject to the limitation given by Equation 6.5.6.3.2.2-5, unless the span and all adjacent interior-pier sections have sufficient ductility and robustness to ensure that the redistribution of moments caused by partial yielding within the positive flexure regions is insignificant (see below). Composite I-sections in positive flexure can have a shape factor, or ratio of M_p/M_y, exceeding 1.5 in certain cases (as a point of comparison, the shape factor of a doubly symmetric non-composite I-section is typically around 1.12). As a result, a considerable amount of yielding and inelastic curvature is required to reach M_p, which reduces the stiffness of the composite section.

The resulting reduction in stiffness can shift moment from the positive to the negative flexure regions in continuous spans. The shedding of moment to adjacent interior-pier sections could potentially result in incremental collapse under repeated live loads if the interior-pier sections do not have the additional capacity needed to sustain these larger moments; for example, interior-pier sections with slender webs and moment-rotation curves that unload rapidly once the peak moment resistance is exceeded (Figure 6.5.6.2.2.1.4-1). Therefore, in such situations, the amount of additional moment allowed above R_hM_y at compact composite sections in positive flexure in continuous spans is limited to 30 percent of R_hM_y. To ensure adequate strength and ductility of the composite section, the resulting nominal flexural resistance of $1.3R_hM_y$ must not exceed the nominal flexural resistance determined from Equation 6.5.6.3.2.2-3 or Equation 6.5.6.3.2.2-4, as applicable. In most cases, unless D_p/D_t is relatively large or M_p/M_y is relatively small, the limiting value of

$1.3R_hM_y$ will control. The factor of 1.3 was established based on engineering judgment.

Additional flexural resistance beyond that determined above is usually not needed at the strength limit state as the size of the bottom flange of these sections will most often be controlled by fatigue or service limit state design criteria. In fact, because other limit state criteria will likely control in this instance, treating these sections conservatively as noncompact sections (Section 6.5.6.3.3.2) simplifies the calculations somewhat and should not result in a significant loss of economy in most cases.

As alluded to previously, the limiting value of $1.3R_hM_y$ may be waived if special steps outlined in *AASHTO LRFD* Article 6.10.7.1.2 are taken to ensure that the span and all adjacent interior-pier sections have adequate ductility to absorb the effects of potential moment shifting. The specific steps involve restrictions on the skew and cross-frame alignment, and on the steel grade, compression-flange slenderness and bracing, web slenderness, shear and minimum available plastic rotation capacity of the adjacent pier sections. As an example, most rolled shapes or welded shapes of comparable proportions will satisfy the restrictions related specifically to the cross-section. The specific steps are as follows:

- The span under consideration and all adjacent interior-pier sections satisfy the requirements of *AASHTO LRFD* Article B6.2 (Section 6.5.6.6.2), and;
- The appropriate value of θ_{RL} from *AASHTO LRFD* Article B6.6.2 (Section 6.5.6.6.4) exceeds 0.009 radians at all adjacent interior-pier sections.

Sections meeting the above requirements are assumed to have sufficient ductility and robustness such that the redistribution of moments to adjacent pier sections caused by partial yielding within the positive flexure regions is inconsequential. θ_{RL} is defined in *AASHTO LRFD* Article B6.6.2 as the plastic rotation at which the interior-pier section moment begins to decrease with increasing plastic rotation. The specified value of 0.009 radians for θ_{RL} is assumed to be an upper bound value of the potential increase in the plastic rotations at adjacent interior-pier sections caused by any positive-moment yielding. *AASHTO LRFD* Article C6.10.7.1.2 indicates the types of interior-pier sections that meet these restrictions. Included in this list are most rolled shapes or welded shapes of comparable proportions.

An example illustrating the application of the above procedures for the design of compact composite I-sections in positive flexure is given in Section 6.5.6.5.1.

6.5.6.3.2.3 Box Sections

AASHTO LRFD Article 6.11.6.2.2 defines the specific requirements that must be met in order for a composite section in positive flexure in a straight box-girder bridge to qualify as compact. These requirements are restated as follows:

- The specified minimum yield strength of the flanges and web do not exceed 70.0 ksi;
- The web must satisfy the requirement of *AASHTO LRFD* Article 6.11.2.1.2 (i.e. $D/t_w \leq 150$ or no longitudinal web stiffeners, with D measured along the web slope for box sections with inclined webs);
- The section must be part of a bridge that satisfies the requirements of *AASHTO LRFD* Article 6.11.2.3 such that the effects of shear due to St. Venant torsion and cross-sectional distortion stresses need not be considered (Section 6.3.5.2);
- Box flanges must be fully effective as specified in *AASHTO LRFD* Article 6.11.1.1 (Section 6.3.5.5.3); and
- The section must satisfy the following web slenderness limit:

$$\frac{2D_{cp}}{t_w} \leq 3.76\sqrt{\frac{E}{F_{yc}}} \qquad \text{Equation 6.5.6.3.2.3-1}$$

AASHTO LRFD Equation 6.11.6.2.2-1

where:

D_{cp} = depth of the web in compression at the plastic moment determined as specified in *AASHTO LRFD* Article D6.3.2 (Section 6.4.5.4.2.2) (in.). D_{cp} should be measured along the web slope for box sections with inclined webs.

Compact composite sections in positive flexure must also satisfy a ductility requirement (Section 6.5.6.3.4) to prevent premature crushing of the concrete deck prior to achieving the calculated nominal flexural resistance, which will ensure a ductile mode of failure.

The reasoning behind the first, second and fifth requirements listed above was discussed previously (Section 6.5.6.3.2.2). As indicated by the third and fourth requirements above, if the section is not part of a bridge that satisfies the restrictions specified in *AASHTO LRFD* Article 6.11.2.3, or if any box flanges in the section are not fully effective as defined in *AASHTO LRFD* Article 6.11.1.1, the section must be designed as a noncompact section (Section 6.5.6.3.3.3). The ability of such sections to develop a nominal flexural resistance greater than the moment at first yield in the presence of potentially significant St. Venant torsional shear and cross-sectional

distortion stresses has not been demonstrated. The same concern and conclusion holds true for sections that are part of a horizontally curved bridge and/or a bridge with skewed supports.

As specified in *AASHTO LRFD* Article 6.11.7.1.1, at the strength limit state, compact sections in positive flexure must satisfy the following requirement:

$$M_u \le \phi_f M_n \qquad \text{Equation 6.5.6.3.2.3-2}$$

AASHTO LRFD Equation 6.11.7.1.1-1

where:

M_n = nominal flexural resistance of the section determined as specified in *AASHTO LRFD* Article 6.11.7.1.2 (see below) (kip-in.)

M_u = bending moment about the major-axis of the cross-section due to the factored loads at the section under consideration (kip-in.)

Equation 6.5.6.3.2.3-2 is expressed in terms of moment because for these types of sections, the major-axis bending moment is physically a more meaningful quantity than the elastically computed flange bending stress. Also, the nominal flexural resistance of these sections is generally greater than the yield moment with respect to the tension flange, M_{yt}. If desired, the equation could be considered in a stress format by dividing both sides of the equation by S_{xt}.

Lateral bending does not need to be considered in the top (compression) flanges of tub sections at the strength limit state because the flanges are continuously supported by the concrete deck. Flange lateral bending is not a consideration for box flanges.

With one exception, *AASHTO LRFD* Article 6.11.7.1.2 refers back to the provisions of *AASHTO LRFD* Article 6.10.7.1.2 for the calculation of the nominal flexural resistance, M_n, of compact composite sections in positive flexure as follows:

- If $D_p \le 0.1D_t$, then:

$$M_n = M_p \qquad \text{Equation 6.5.6.3.2.3-3}$$

AASHTO LRFD Equation 6.10.7.1.2-1

- Otherwise:

$$M_n = M_p\left(1.07 - 0.7\frac{D_p}{D_t}\right) \qquad \text{Equation 6.5.6.3.2.3-4}$$

AASHTO LRFD Equation 6.10.7.1.2-2

where:

D_p = vertical distance from the top of the concrete deck to the neutral axis of the composite section at the plastic moment (in.)

D_t = total vertical depth of the composite section (in.)

M_p = plastic moment of the composite section determined as specified in *AASHTO LRFD* Article D6.2 (Section 6.4.5.2.4) (kip-in.)

For sections in continuous spans, the nominal flexural resistance is also given by Equation 6.5.6.3.2.3-3 or Equation 6.5.6.3.2.3-4, as applicable, but the section must also satisfy the following:

$$M_n \leq 1.3R_hM_y \qquad \text{Equation 6.5.6.3.2.3-5}$$

AASHTO LRFD Equation 6.10.7.1.2-3

where:

M_n = nominal flexural resistance given by Equation 6.5.6.3.2.3-3 or Equation 6.5.6.3.2.3-4, as applicable (kip-in.)

M_y = yield moment determined as specified in *AASHTO LRFD* Article D6.2 (Section 6.4.5.3.3.1) (kip-in.)

R_h = hybrid factor determined as specified in *AASHTO LRFD* Article 6.10.1.10.1 (Section 6.4.5.7)

The reason for the limitation given by Equation 6.5.6.3.2.2-5 is discussed at some length in Section 6.5.6.3.2.2.

The preceding equations do not account for any transverse redistribution of load through the bracing members as yielding occurs at positive moment sections. St. Venant torsion and cross-sectional distortion stresses need not be considered for compact sections.

The single exception alluded to above is that Equation 6.5.6.3.2.2-5 must always be enforced for compact box sections in positive flexure in continuous spans. For compact I-sections in continuous spans, the nominal flexural resistance need not be subject to the limitation given by Equation 6.5.6.3.2.2-5 when certain specific conditions in the span under consideration and at all adjacent interior-pier sections are met (as spelled out in *AASHTO LRFD* Article 6.10.7.1.2 – Section 6.5.6.3.2.2). These conditions are not presently applicable to box sections.

EXAMPLE

Check the composite tub section shown in Figure 6.5.6.3.2.3-1 (note: top lateral bracing not shown), which is in a region of positive flexure in the end span of a straight continuous-span bridge, for the Strength I load combination. The girder is homogeneous with the flanges and web having a yield strength of 50 ksi. The 28-day compressive strength f'_c of the concrete deck is 4.5 ksi. The modular ratio n = 8. The load modifier, η, is assumed to be 1.0. Assume unshored construction.

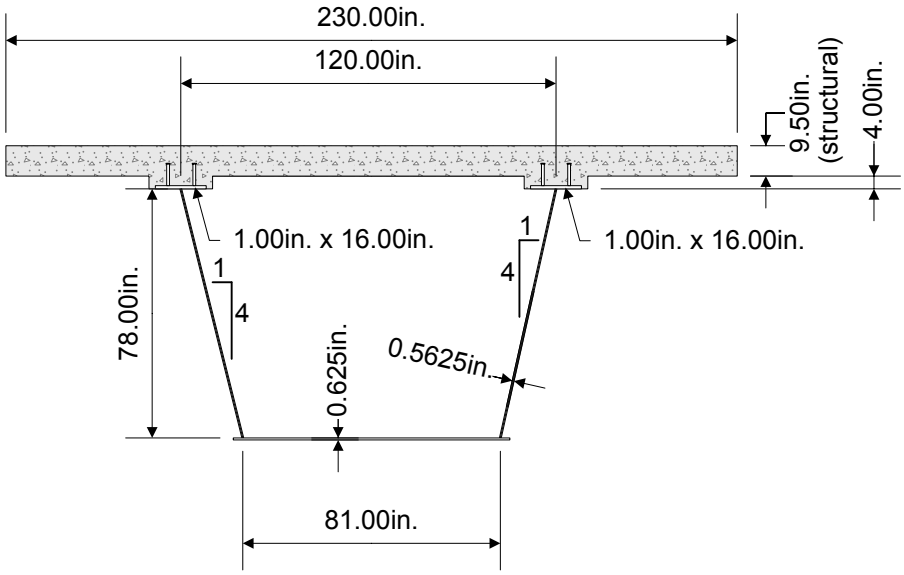

Figure 6.5.6.3.2.3-1 Example Composite Tub Section in a Region of Positive Flexure

Assume the following unfactored bending moments:

M_{DC1} = +7,365 kip-ft
M_{DC2} = +1,219 kip-ft
M_{DW} = +995 kip-ft
M_{LL+IM} = +6,748 kip-ft

The applicable elastic section properties for the strength limit state check (neglecting the longitudinal reinforcement) are as follows:

Steel girder:

I = 185,356 in.^{4}
S_{top} = 4,333 in.^{3}

S_{bot} = 5,030 in.^{3}
N.A. is 36.85 in. from the bottom of the bottom flange

3*n*-composite section:

I = 339,167 in.^{4}
S_{top} = 13,126 in.^{3}
S_{bot} = 6,306 in.^{3}
N.A. is 53.79 in. from the bottom of the bottom flange

n-composite section:

I = 463,544 in.^{4}
S_{top} = 37,504 in.^{3}
S_{bot} = 6,891 in.^{3}
N.A. is 67.27 in. from the bottom of the bottom flange

The section properties include the longitudinal component of the top-flange lateral bracing area (as recommended in *AASHTO LRFD* Article C6.11.1.1); a single top-flange bracing member with a cross-sectional area A of 8.0 in.^{2} placed at an angle of 30 degrees from tangent to the girder is assumed. The bracing members are assumed bolted to the top flanges. Therefore, the additional cross-sectional area included with the top-flange areas in calculating the section properties is computed from Equation 6.4.2.3.2.3-2 as $A_d = 8.0\cos 30^\circ = 6.93$ in.^{2} The section properties also include the 1-inch-wide bottom-flange lips (measured from the centerline of the webs) that are provided for web-to-flange welding access. The area of the inclined webs is used in computing all section properties. The moment of inertia of each inclined web, I_{ow}, with respect to a horizontal axis at mid-depth of the web is taken from Equation 6.4.2.3.2.3-1 as:

$$I_{ow} = I_w\left(\frac{S^2}{S^2+1}\right)$$

where:

I_w = moment of inertia of each inclined web with respect to an axis normal to the web (in.^{4})
S = web slope with respect to the horizontal (= 4.0 in this case)

Since the bottom box-flange width does not exceed one-fifth of the distance from the abutment to the point of permanent load contraflexure, the flange is considered fully effective and shear lag effects need not be considered in calculating the section properties for the determination of the flexural stresses (*AASHTO LRFD* Article

6.11.1.1 – Section 6.3.5.5.3). Therefore, the longitudinal bending stress may be assumed uniform across the full flange width.

Calculate the plastic moment, M_p, for the composite section. The equations given in *AASHTO LRFD* Table D6.1-1 (Table 6.4.5.2.3.2-1) for I-sections will be utilized to calculate M_p for one-half of the composite box section. The longitudinal reinforcement will be conservatively neglected. The longitudinal component of the top-flange lateral bracing area will be included. The web depth, D, will be taken as the depth measured along the web slope.

$$P_t = F_{yt} b_t t_t = 50(83.0/2)(0.625) = 1{,}297 \text{ kips}$$

$$P_w = F_{yw} D t_w = 50(78.0/\cos 14^\circ)(0.5625) = 2{,}261 \text{ kips}$$

$$P_c = F_{yc} b_c t_c + F_y A_d = 50(16.0)(1.0) + 50(6.93) = 1{,}147 \text{ kips}$$

$$P_s = 0.85 f'_c b_s t_s = 0.85(4.5)(230.0/2)(9.5) = 4{,}179 \text{ kips}$$

Since $P_t + P_w + P_c = 4{,}705$ kips > $P_s = 4{,}179$ kips, the plastic neutral axis (PNA) is in the top flange. Therefore, use Case II in *AASHTO LRFD* Table D6.1-1 (Table 6.4.5.2.3.2-1):

$$\bar{y} = \frac{t_c}{2}\left[\frac{P_w + P_t - P_s}{P_c} + 1\right]$$

$$\bar{y} = \frac{1.0}{2}\left[\frac{2{,}261 + 1{,}297 - 4{,}179}{1{,}147} + 1\right] = 0.229 \text{ in. from the top of the top flange}$$

Check equilibrium by calculating and comparing the total plastic forces acting on the compression and tension sides of the plastic neutral axis:

Compression side:

$$4{,}179 + 50(16.0)(0.229) + 50(6.93)(0.229/1.0) = 4{,}442 \text{ kips}$$

Tension side:

$$50(16.0)(1.0 - 0.229) + 50(6.93)[(1.0 - 0.229)/1.0] + 2{,}261 + 1{,}297 = 4{,}442 \text{ kips} \quad \text{ok}$$

Calculate the distances from the PNA for the centroid of each element:

$$d_s = \frac{9.5}{2} + 4.0 + 0.229 - 1.0 = 7.98 \text{ in.}$$

$$d_w = 1.0 + \frac{78.0}{2} - 0.229 = 39.77 \text{ in.}$$

$$d_t = 1.0 + 78.0 + \frac{0.625}{2} - 0.229 = 79.08 \text{ in.}$$

$$M_p = \frac{P_c}{2t_c}\left[\bar{y}^2 + (t_c - \bar{y})^2\right] + \left[P_s d_s + P_w d_w + P_t d_t\right]$$

$$M_p = \frac{1{,}147}{2(1.0)}\left[(0.229)^2 + (1.0 - 0.229)^2\right] +$$
$$\left[4{,}179(7.98) + 2{,}261(39.77) + 1{,}297(79.08)\right] = 226{,}206 \text{ kip} - \text{in.}$$

M_p = 18,851 kip-ft for ½ the box = 37,702 kip-ft for the whole box

Calculate the yield moment, M_y, for the composite section using the equations given in *AASHTO LRFD* Article D6.2.2 (Section 6.4.5.3.3.1). For a composite section in positive flexure, M_{yt}, or the yield moment calculated for the tension flange, typically controls. From Equation 6.4.5.3.3.1-1:

$$F_{yf} = \frac{M_{D1}}{S_{nc}} + \frac{M_{D2}}{S_{LT}} + \frac{M_{AD}}{S_{ST}}$$

$$50 = 1.0\left[\frac{1.25(7{,}365)(12)}{5{,}030} + \frac{1.25(1{,}219)(12) + 1.50(995)(12)}{6{,}306} + \frac{M_{AD}}{6{,}891}\right]$$

M_{AD} = 153,649 kip-in. = 12,804 kip-ft

From Equation 6.4.5.3.3.1-2:

$$M_y = M_{D1} + M_{D2} + M_{AD}$$

$$M_y = 1.0\left[1.25(7{,}365) + 1.25(1{,}219) + 1.50(995) + 12{,}804\right] = 25{,}027 \text{ kip} - \text{ft}$$

Since the section is in a straight bridge, determine if the section qualifies as a compact section. According to *AASHTO LRFD* Article 6.11.6.2.2, composite sections in positive flexure in straight bridges qualify as compact when: 1) the specified minimum yield strengths of the flanges do not exceed 70 ksi (ok); 2) the web satisfies the requirement of *AASHTO LRFD* Article 6.11.2.1.2 such that longitudinal stiffeners are not required; i.e. $D/t_w \leq 150$ (D/t_w = (78.0/cos14°)/0.5625 = 142.9 < 150 ok); 3) the section is part of a bridge that satisfies the requirements of *AASHTO LRFD* Article 6.11.2.3 (Section 6.3.5.2 – it will be assumed for this portion of the example that all these requirements are satisfied); 4) the box flange is fully

effective as specified in *AASHTO LRFD* Article 6.11.1.1 (Section 6.3.5.5.3 – ok); and 5) the section satisfies the web-slenderness limit given by Equation 6.5.6.3.2.3-1 (earlier computations indicated that the plastic neutral axis of the composite section is located in the top flange. Therefore, according to *AASHTO LRFD* Article D6.3.2, D_{cp} is taken equal to zero for this case, and thus, Equation 6.5.6.3.2.3-1 is considered to be automatically satisfied). Therefore, the section qualifies as a compact section.

Compact composite sections in positive flexure must also satisfy the ductility requirement (Section 6.5.6.3.4) to protect the concrete deck from premature crushing. At this section:

$$D_p = 9.5 + 4.0 - 1.0 + 0.229 = 12.73 \text{ in.}$$

$$D_t = 0.625 + 78.0 + 4.0 + 9.5 = 92.13 \text{ in.}$$

$$0.42D_t = 0.42(92.13) = 38.69 \text{ in.} > 12.73 \text{ in.} \quad \text{ok}$$

For Strength I:

$$M_u = 1.0\left[1.25(7{,}365 + 1{,}219) + 1.50(995) + 1.75(6{,}748)\right] = 24{,}032 \text{ kip} - \text{ft}$$

As specified in *AASHTO LRFD* Article 6.11.7.1.2, the nominal flexural resistance of compact composite box sections in positive flexure is to be determined according to the provisions of *AASHTO LRFD* Article 6.10.7.1.2. St. Venant torsion and cross-sectional distortion stresses need not be considered for compact sections.

$$0.1D_t = 0.1(92.13) = 9.21 \text{ in.} < D_p = 12.73 \text{ in.}$$

Therefore, from Equation 6.5.6.3.2.3-4:

$$M_n = M_p\left(1.07 - 0.7\frac{D_p}{D_t}\right)$$

$$M_n = 37{,}702\left[1.07 - 0.7\left(\frac{12.73}{92.13}\right)\right] = 36{,}695 \text{ kip} - \text{ft}$$

However, in a continuous span, the nominal flexural resistance of the section must be limited to the following according to *AASHTO LRFD* Article 6.11.7.1.2 (Equation 6.5.6.3.2.3-5):

$$M_n = 1.3R_hM_y$$

For a homogeneous girder, the hybrid factor, R_h, is equal to 1.0. Therefore:

$$M_n = 1.3(1.0)(25{,}027) = 32{,}535 \text{ kip} - \text{ft} \quad \text{(governs)}$$

$$M_n = 32{,}535 \text{ kip} - \text{ft}$$

The factored flexural resistance is computed as:

$$M_r = \phi_f M_n$$

AASHTO LRFD Equation 6.11.7.1.1-1

$$M_r = 1.0(32{,}535) = 32{,}535 \text{ kip} - \text{ft} > M_u = 24{,}032 \text{ kip} - \text{ft} \quad \text{ok}$$

The section has significant excess flexural resistance at the strength limit state. Other limit-state criteria (e.g. service limit state or fatigue limit state criteria) must of course be checked and constructibility verifications must also be made, as discussed previously. Service or fatigue limit state criteria are likely to control the design of the section in this case. Because other limit-state criteria will likely control in this instance, treating these sections conservatively as noncompact sections at the strength limit state simplifies the calculations, in general, and should not result in a significant loss of economy in many cases.

6.5.6.3.3 Noncompact Sections

6.5.6.3.3.1 General

Composite sections in positive flexure not meeting one or more of the requirements listed in Section 6.5.6.3.2.2 or Section 6.5.6.3.2.3 for I- or box sections, respectively, must be treated as noncompact sections at the strength limit state. Composite sections in positive flexure in kinked (chorded) continuous or horizontally curved bridges must also be treated as noncompact sections. The design requirements for noncompact sections are discussed below for I-sections (Section 6.5.6.3.3.2) and for box sections (Section 6.5.6.3.3.3).

In addition to the basic design requirements, noncompact sections must satisfy a ductility requirement to prevent premature crushing of the concrete deck prior to reaching the specified nominal flexural resistance (Section 6.5.6.3.4). The maximum longitudinal compressive stress in the concrete deck at the strength limit state is also limited to $0.6f'_c$ to ensure linear behavior of the concrete, which is assumed in the calculation of the steel flange stresses (Section 6.5.6.3.3.4).

6.5.6.3.3.2 I-Sections

6.5.6.3.3.2.1 Continuously Braced Compression Flanges

AASHTO LRFD Article 6.10.7.2.1 specifies that at the strength limit state, the (top) compression flange of noncompact composite I-sections in positive flexure must satisfy the following:

$$f_{bu} \le \phi_f F_{nc} \qquad \text{Equation 6.5.6.3.3.2.1-1}$$

AASHTO LRFD Equation 6.10.7.2.1-1

where:

f_{bu} = factored flange vertical bending stress at the section under consideration (ksi).

F_{nc} = nominal flexural resistance of the compression flange determined as specified in *AASHTO LRFD* Article 6.10.7.2.2 (discussed below) (ksi)

Again, flange lateral bending is not considered for the compression flange in Equation 6.5.6.3.3.2.1-1 because at the strength limit state, the flange is continuously supported by the concrete deck.

AASHTO LRFD Article 6.10.7.2.2 specifies that the nominal flexural resistance of the compression flange, F_{nc}, of a noncompact composite I-section in positive flexure is to be taken as:

$$F_{nc} = R_b R_h F_{yc} \qquad \text{Equation 6.5.6.3.3.2.1-2}$$

AASHTO LRFD Equation 6.10.7.2.2-1

where:

R_b = web load-shedding factor determined as specified in *AASHTO LRFD* Article 6.10.1.10.2 (Section 6.4.5.6)

R_h = hybrid factor determined as specified in *AASHTO LRFD* Article6.10.1.10.1 (Section 6.4.5.7)

Local and lateral buckling of the top flanges is not a concern because the flanges are continuously braced; therefore, the nominal flexural resistance is based on nominal yielding.

Note that for composite sections in positive flexure with $D/t_w \le 150$ (i.e. no longitudinal web stiffeners), R_b is to be taken equal to 1.0 because web bend buckling and subsequent load shedding are unlikely for these sections at the strength limit state.

6.5.6.3.3.2.2 Discretely Braced Tension Flanges

The (bottom) tension flange of noncompact composite I-sections in positive flexure must satisfy the one-third rule equation expressed in terms of stress (Section 6.5.2.1.4) as follows:

$$f_{bu} + \frac{1}{3} f_{\ell} \le \phi_f F_{nt}$$ Equation 6.5.6.3.3.2.2-1

AASHTO LRFD Equation 6.10.7.2.1-2

where:

f_{ℓ} = factored flange lateral bending stress at the section under consideration (ksi)

F_{nt} = nominal flexural resistance of the tension flange determined as specified in *AASHTO LRFD* Article 6.10.7.2.2 (discussed below) (ksi)

The stress format is more appropriate in members for which the maximum resistance is always less than or equal to the yield moment in vertical bending.

The sign of f_{bu} and f_{ℓ} is always taken as positive in Equation 6.5.6.3.3.2.2-1**.** However, when summing dead and live load stresses to obtain the total factored vertical and lateral bending stresses, f_{bu} and f_{ℓ}, to apply in the equation, the signs of the individual dead and live load stresses must be considered.

Since the bottom (tension) flange is not continuously supported, lateral bending must be considered in flexural resistance computations for the tension flange. Possible sources of lateral bending in the bottom flange of these sections at the strength limit state include curvature, wind loading and the effect of staggered cross-frames/diaphragms and/or support skew. *AASHTO LRFD* Article 6.10.1.6 specifies that the sum of the flange lateral bending stresses due to all sources cannot exceed $0.6F_{yf}$. Amplification of the flange lateral bending stresses is not required in this case since the bottom flange is in tension.

AASHTO LRFD Article 6.10.7.2.2 specifies that the nominal flexural resistance of the tension flange, F_{nt}, is to be taken as:

$$F_{nt} = R_h F_{yt}$$ Equation 6.5.6.3.3.2.2-2

AASHTO LRFD Equation 6.10.7.2.2-2

Load shedding of the web compressive stresses to the tension flange as a result of bend buckling of the web is considered insignificant; therefore, the R_b factor is not included in Equation 6.5.6.3.3.2.2-2.

6.5.6.3.3.3 Box Sections

6.5.6.3.3.3.1 General

The nominal flexural resistance of noncompact composite box sections in positive flexure is specified in *AASHTO LRFD* Article 6.11.7.2. Longitudinal warping stresses are typically ignored at the strength limit state, as permitted in *AASHTO LRFD* Article 6.11.1.1. St. Venant torsion and cross-section distortion stresses must be considered, however, for noncompact sections.

6.5.6.3.3.3.2 Continuously Braced Compression Flange(s)

AASHTO LRFD Article 6.11.7.2.1 specifies that at the strength limit state, the (top) compression flange(s) of noncompact composite box sections in positive flexure must satisfy the following:

$$f_{bu} \le \phi_f F_{nc} \qquad \text{Equation 6.5.6.3.3.3.2-1}$$

AASHTO LRFD Equation 6.10.7.2.1-1

where:

f_{bu} = factored longitudinal flange vertical bending stress at the section under consideration calculated without consideration of longitudinal warping (ksi).

F_{nc} = nominal flexural resistance of the compression flange determined as specified in *AASHTO LRFD* Article 6.11.7.2.2 (discussed below) (ksi)

Again, flange lateral bending is not considered for the compression flange(s) in Equation 6.5.6.3.3.3.2-1 because at the strength limit state, the flange is continuously supported by the concrete deck.

AASHTO LRFD Article 6.11.7.2.2 specifies that the nominal flexural resistance of the compression flanges, F_{nc}, of a noncompact composite tub section in positive flexure is to be taken as:

$$F_{nc} = R_b R_h F_{yc} \qquad \text{Equation 6.5.6.3.3.3.2-2}$$

AASHTO LRFD Equation 6.10.7.2.2-1

where:

R_b = web load-shedding factor determined as specified in *AASHTO LRFD* Article 6.10.1.10.2 (Section 6.4.5.6)

R_h = hybrid factor determined as specified in *AASHTO LRFD* Article6.10.1.10.1 (Section 6.4.5.7)

Local and lateral buckling of the top flanges is not a concern because the flanges are continuously braced; therefore, the nominal flexural resistance is based on nominal yielding. St. Venant torsional shears are also typically neglected in tub girder top flanges.

The nominal flexural resistance of the compression flange of noncompact composite closed-box sections in positive flexure, F_{nc}, is to be taken as:

$$F_{nc} = R_b R_h F_{yc} \Delta \qquad \text{Equation 6.5.6.3.3.3.2-3}$$

AASHTO LRFD Equation 6.11.7.2.2-2

where:

$$\Delta = \sqrt{1 - 3\left(\frac{f_v}{F_{yc}}\right)^2} \qquad \text{Equation 6.5.6.3.3.3.2-4}$$

AASHTO LRFD Equation 6.11.7.2.2-3

f_v = factored St. Venant torsional shear stress in the flange at the section under consideration not to exceed the factored torsional shear resistance of the flange, F_{vr}, given by Equation 6.5.6.1.2-1 (ksi)

$$= \frac{T}{2A_o t_{fc}} \qquad \text{Equation 6.5.6.3.3.3.2-5}$$

AASHTO LRFD Equation 6.11.7.2.2-4

A_o = enclosed area within the box section (in.^{2})

t_{fc} = thickness of the compression flange (in.)

T = internal torque due to the factored loads (kip-in.)

Local buckling of the top box flange is not a concern because the flange is continuously braced at the strength limit state; therefore, the nominal flexural resistance is based on nominal yielding.

Note that in both of the above cases, for composite sections in positive flexure with $D/t_w \le 150$ (i.e. no longitudinal web stiffeners), R_b is to be taken equal to 1.0 because web bend buckling and subsequent load shedding are unlikely for these sections at the strength limit state.

6.5.6.3.3.3.3 Box Flanges in Tension

AASHTO LRFD Article 6.11.7.2.1 specifies that at the strength limit state, the (bottom) tension flange of noncompact composite box sections in positive flexure must satisfy the following:

$$f_{bu} \le \phi_f F_{nt} \qquad \text{Equation 6.5.6.3.3.3.3-1}$$

AASHTO LRFD Equation 6.11.7.2.1-2

where:

F_{nt} = nominal flexural resistance of the tension flange determined as specified in *AASHTO LRFD* Article 6.11.7.2.2 (discussed below) (ksi)

The stress format is more appropriate in members for which the maximum resistance is always less than or equal to the yield moment in vertical bending. Lateral bending is not a consideration for the tension flange in Equation 6.5.6.3.3.3.3-1 because the tension flange is always a box flange in this case (and lateral bending is not a consideration for box flanges).

AASHTO LRFD Article 6.11.7.2.2 specifies that the nominal flexural resistance of the tension flange of noncompact composite closed-box and tub sections in positive flexure, F_{nt}, based on nominal yielding is to be taken as:

$$F_{nt} = R_h F_{yt} \Delta \qquad \text{Equation 6.5.6.3.3.3.3-2}$$

AASHTO LRFD Equation 6.11.7.2.2-5

where:

$$\Delta = \sqrt{1 - 3\left(\frac{f_v}{F_{yt}}\right)^2} \qquad \text{Equation 6.5.6.3.3.3.3-3}$$

AASHTO LRFD Equation 6.11.7.2.2-6

f_v = factored St. Venant torsional shear stress in the flange at the section under consideration not to exceed the factored torsional shear resistance of the flange, F_{vr}, given by Equation 6.5.6.1.2-1 (ksi)

$$= \frac{T}{2A_o t_{ft}} \qquad \text{Equation 6.5.6.3.3.3.3-4}$$

AASHTO LRFD Equation 6.11.7.2.2-7

t_{ft} = thickness of the tension flange (in.)

Load shedding of the web compressive stresses to the tension flange as a result of bend buckling of the web is considered insignificant; therefore, the R_b factor is not included in Equation 6.5.6.3.3.3.3-2.

EXAMPLE

Assume that the composite tub girder section shown in Figure 6.5.6.3.2.3-1 is subject to positive flexure and the section is from a multiple box-section bridge that does satisfy one or more of the special restrictions specified in *AASHTO LRFD* Article 6.11.2.3 (Section 6.3.5.2). Therefore, the section must be treated as a noncompact section, and the effects of St. Venant torsional shear and cross-sectional distortion stresses must be considered at the strength limit state.

Assume the following unfactored torques:

T_{DC1} = +330 kip-ft
T_{DC2} = +65 kip-ft
T_{DW} = +54 kip-ft
T_{LL+IM} = +546 kip-ft

It is assumed that all the deck weight is applied to the girder top flanges in the analysis for this example. Thus, the DC_1 torque does not include the torque due to the weight of deck overhang acting on the boxes. The torque results primarily from the application of unequal deck weight loads to the girder top flanges.

Check the flexural resistance of the bottom box flange in tension. First, compute the flexural stress in the bottom flange due to the factored loads (ignoring the effect of longitudinal warping). For the Strength I load combination:

$$f_{bu} = 1.0\left[\frac{1.25(7{,}365)}{5{,}030} + \frac{1.25(1{,}219)}{6{,}306} + \frac{1.5(995)}{6{,}306} + \frac{1.75(6{,}748)}{6{,}891}\right]12 = 48.27 \text{ ksi}$$

Calculate the St. Venant torsional shear stress due to the factored loads, f_v, in the bottom flange. For the DC_1 torque, which is applied to the non-composite section, the enclosed area, A_o, is computed for the non-composite box section. The vertical depth between the mid-thickness of the flanges is used. It is also assumed that the top lateral bracing is connected to the top flanges so that a reduction in A_o is not required. Therefore:

$$A_o = \frac{(120 + 81)}{2} * (78.0 + 0.3125 + 0.5) * \frac{1 \text{ ft}^2}{144 \text{ in.}^2} = 55.0 \text{ ft}^2$$

$$f_v = \frac{T}{2A_o t_{fc}} \text{ (Equation 6.5.6.3.3.3.2-5)}$$

$$f_v = \frac{1.0(1.25)(330)}{2(55.0)(0.625)} * \frac{1}{12 \text{ in.} / \text{ft}} = 0.500 \text{ ksi}$$

For the torques applied to the composite section, calculate A_o for the composite section from the mid-thickness of the bottom flange to the mid-thickness of the concrete deck (considering the deck haunch):

$$A_o = \frac{(120+81)}{2} * (78.0 + 0.3125 + 4.0 + \frac{9.5}{2}) * \frac{1 \text{ ft}^2}{144 \text{ in.}^2} = 60.8 \text{ ft}^2$$

$$f_v = \frac{1.0\left|1.25(65) + 1.5(54) + 1.75(546)\right|}{2(60.8)(0.625)} * \frac{1}{12 \text{ in.} / \text{ft}} = 1.23 \text{ ksi}$$

$$f_{v \text{ total}} = 0.500 + 1.23 = 1.73 \text{ ksi}$$

Check that $f_{v\ total}$ does not exceed the factored torsional shear resistance of the flange, F_{vr} (Equation 6.5.6.1.2-1):

$$F_{vr} = 0.75\phi_v \frac{F_{yf}}{\sqrt{3}}$$

$$F_{vr} = 0.75(1.0)\frac{50}{\sqrt{3}} = 21.65 \text{ ksi} > f_{v \text{ total}} = 1.73 \text{ ksi} \quad \text{ok}$$

Calculate the nominal flexural tensile resistance of the bottom flange according to the provisions of *AASHTO LRFD* Article 6.11.7.2.2. The nominal flexural resistance F_{nt} of the tension flange of noncompact tub sections in positive flexure is to be taken as (Equation 6.5.6.3.3.3.3-2):

$$F_{nt} = R_h F_{yt} \Delta$$

$$\Delta = \sqrt{1 - 3\left(\frac{f_v}{F_{yt}}\right)^2} \text{ (Equation 6.5.6.3.3.3.3-3)}$$

$$\Delta = \sqrt{1-3\left(\frac{1.73}{50}\right)^2} = 0.998$$

$$F_{nt} = 1.0(50)(0.998) = 49.90 \text{ ksi}$$

The factored flexural resistance, F_r, is computed as:

$$F_r = \phi_f F_{nt} = 1.0(49.90) = 49.90 \text{ ksi} > f_{bu} = 48.27 \text{ ksi} \quad \text{ok}$$

Check the flexural resistance of the top flanges in compression. First, compute the flexural stress in the top flanges due to the factored loads (ignoring the effect of longitudinal warping). For the Strength I load combination:

$$f_{bu} = 1.0\left[\frac{1.25(7{,}365)}{4{,}333} + \frac{1.25(1{,}219)}{13{,}126} + \frac{1.5(995)}{13{,}126} + \frac{1.75(6{,}748)}{37{,}504}\right]12 = -32.03 \text{ ksi}$$

St. Venant torsional shears are typically neglected in continuously braced top flanges of tub sections.

Calculate the nominal flexural compressive resistance of the top flanges according to the provisions of *AASHTO LRFD* Article 6.11.7.2.2. The nominal flexural resistance, F_{nc}, of the compression flanges of noncompact tub sections in positive flexure is to be taken as (Equation 6.5.6.3.3.2.1-2):

$$F_{nc} = R_b R_h F_{yc}$$

As specified in *AASHTO LRFD* Article 6.10.1.10.2, R_b is to be taken as 1.0 at the strength limit state when the section is composite and is in positive flexure and the web slenderness D/t_w does not exceed 150 (i.e. when there are no longitudinal web stiffeners present). Therefore:

$$F_{nc} = 1.0(1.0)(50) = 50.00 \text{ ksi}$$

The factored flexural resistance, F_r, is computed as:

$$F_r = \phi_f F_{nc} = 1.0(50.00) = 50.00 \text{ ksi} > |f_{bu}| = 32.03 \text{ ksi} \quad \text{ok}$$

As specified in *AASHTO LRFD* Article 6.11.6.2.2, noncompact sections in positive flexure must also satisfy the ductility requirement (Section 6.5.6.3.4) to ensure a ductile failure of the section. This requirement was checked in the preceding example and found to be satisfactory.

Regarding the cross-sectional distortion stresses, the longitudinal warping stresses due to cross-section distortion will be ignored at the strength limit state, as permitted in *AASHTO LRFD* Article 6.11.1.1. It is assumed that the internal cross-frames are spaced so that the longitudinal warping stresses do not exceed 10 percent of the major-axis bending stresses at the strength limit state, as recommended in *AASHTO LRFD* Article C6.7.4.3 (with the spacing not to exceed 30.0 feet). The transverse bending stresses due to cross-section distortion are limited to 20.0 ksi at the strength limit state according to *AASHTO LRFD* Article 6.11.1.1. Although not explicitly checked in this example, both the longitudinal warping and transverse bending stresses at the strength limit state can be computed using the BEF analogy, as discussed previously in Section 6.5.5.2.2.3.2. Specifically, Equation 6.5.5.2.2.3.2-11 and Equation 6.5.5.2.2.3.2-12 may be applied at the strength limit state to compute these stresses. The distortional stresses must be considered at the fatigue limit state in this case (Section 6.5.5.2.2.3).

6.5.6.3.3.4 Longitudinal Compressive Deck Stress

According to *AASHTO LRFD* Articles 6.10.7.2.1 (for I-sections) and 6.11.7.2.1 (for box sections), the maximum factored longitudinal compressive stress in the deck at noncompact composite sections in positive flexure at the strength limit state, f_c, is limited as follows:

$$f_c \le 0.6f'_c \qquad \text{Equation 6.5.6.3.3.4-1}$$

This limit is intended to ensure linear behavior of the concrete, which is assumed in the calculation of the steel flange stresses.

As pointed out in *AASHTO LRFD* Articles C6.10.7.2.1 and C6.11.7.2.1, this check is unlikely to control except in cases involving: 1) shored construction, or unshored construction where the non-composite steel dead load stresses are low, combined with 2) geometries causing the neutral axis of the short-term and long-term composite section to be significantly below the bottom of the concrete deck. Equation 6.5.6.3.3.4-1 ensures that noncompact composite I-sections in positive bending with a relatively large F_{yt}/f'_c or F_{yc}/f'_c and a relatively small concrete deck, resulting in a location of the neutral axis well below the concrete deck, will not be permitted. In such rare cases, Equation 6.5.6.3.3.4-1 may be satisfied by increasing the concrete f'_c, the slab thickness, the size of the steel top flange, and/or the girder spacing.

6.5.6.3.4 Ductility Requirement

According to *AASHTO LRFD* Articles 6.10.6.2.2 (for I-sections) and 6.11.7.2.2 (for box sections), both compact and noncompact composite sections in positive flexure must also satisfy the following ductility requirement specified in *AASHTO LRFD* Article 6.10.7.3:

$$D_p \leq 0.42D_t \qquad \text{Equation 6.5.6.3.4-1}$$

AASHTO LRFD Equation 6.10.7.3-1

where:

D_p = distance from the top of the concrete deck to the neutral axis of the composite section at the plastic moment (in.)
D_t = total depth of the composite section (in.)

This requirement is intended to prevent premature crushing of the concrete deck prior to reaching the specified nominal flexural resistance. Satisfying this requirement also helps permit the web bend buckling check to be neglected for composite sections in positive flexure without longitudinal stiffeners after the deck hardens.

Although noncompact sections in positive flexure are not permitted to exceed the moment at first yield, the ductility requirement shown in Equation 6.5.6.3.4-1 must still be satisfied to ensure a ductile failure, and to prevent premature crushing of the deck for sections that may utilize up to 100-ksi steel and/or that are utilized in shored construction. The D_p/D_t ratio is limited to 0.42 to ensure significant yielding of the bottom flange when the crushing strain is reached at the top of the concrete deck. D_t should be computed using a lower-bound estimate of the deck and haunch thickness, or be determined conservatively by neglecting the thickness of the haunch.

6.5.6.4 Regions of Stress Reversal

Girder regions of stress reversal are typically located near points of permanent load contraflexure in continuous spans. These regions can extend over much of the span in some cases depending on the span ratio.

Careful attention must be paid to the design of welded details for load-induced fatigue in these regions since fatigue stress ranges are often significant in these regions. In particular, as discussed previously in Sections 6.4.5.5.2.2 and 6.5.6.2.4.2.1, special attention must be paid to the termination of welded longitudinal web and flange stiffeners in these regions. Welded cross-frame/diaphragm connection plates (Category C′) located in these regions may also be critical for

fatigue. In such cases, the location of the connection plate along the girder may need to be adjusted slightly to satisfy the fatigue limit state requirements.

Shear connectors should not be discontinued in these regions for reasons discussed further in Section 6.6.2.2.5.

The girder should be checked in these regions at the strength limit state for the dead load plus positive live load condition and the dead load plus negative live load condition. The signs of the individual dead and live load stresses must be considered when summing to obtain the total factored vertical and lateral bending stresses for each condition. When the sign of a particular dead load stress is opposite in sign to the live load stress when factoring and combining the stresses, the dead load stress should be unloaded by applying the appropriate minimum load factor, γ_p, specified in *AASHTO LRFD* Table 3.4.1-2 (Section 3.9.1.6), in combination with a load modifier equal to $1/\eta \leq 1.0$ (*AASHTO LRFD* Equation 1.3.2.1-3 – Section 1.3.6) applied to that stress.

Different section properties are used for computing composite section stresses at the strength limit state in these regions due to positive and negative moments. *AASHTO LRFD* Article 6.10.1.1.1b specifies that the associated composite section properties may be used to compute the factored vertical bending stresses at the strength limit state due to live and permanent loads if the resulting net unfactored stress in the concrete deck is compressive. When the net unfactored stress in the concrete deck is tensile, the factored vertical bending stresses must be computed ignoring the concrete deck according to *AASHTO LRFD* Article 6.10.1.1.1c. For example, if the unfactored live load compressive stress in the deck overcomes the unfactored tensile stress in the deck due to the DC_2 and *DW* loads, the factored DC_2 and *DW* stresses in the girder at that location may be computed using the long-term composite (3*n*) section. Conversely, if the unfactored live load tensile stress in the deck overcomes the unfactored compressive stress in the deck due to the DC_2 and *DW* loads, the factored DC_2 and *DW* stresses in the girder at that location are to be computed using only the steel section plus the longitudinal reinforcement within the effective width of the deck.

Bottom flanges slightly beyond the point of dead load contraflexure are subjected to a net factored compressive stress. Flanges in these regions must be checked to ensure they have adequate local and/or lateral torsional buckling resistance; unstiffened box flanges are often found problematic.

Bolted girder splices are often located around points of dead load contraflexure. Flanges subject to a net tensile stress at bolted splices must be checked for net section fracture (refer to Section 6.4.7). The number of bolt holes in a row can be decreased along with a concomitant lengthening of the splice to gain relief.

6.5.6.5 Wind Loads

6.5.6.5.1 I-Sections

In I-girder bridges with composite concrete decks, non-composite decks with concrete haunches, and other decks that can provide horizontal diaphragm action, wind load on the upper half of the exterior girder, the deck, the barriers, and the vehicles may be assumed transmitted directly to the deck, which acts as a lateral diaphragm to carry the load to the supports. Wind load on the lower half of the exterior girder may be assumed applied laterally to the bottom flange, which transmits the load to the adjacent brace points by flexural action. Brace points occur at cross-frame/diaphragm locations or at wind (lateral) bracing nodes. The lateral forces applied at the brace points by the flanges are then assumed transmitted to the supports by truss action of any wind bracing in the plane of the bottom flange, and/or the frame action of the cross-frames or diaphragms. The frame action of the cross-frames or diaphragms transmits the forces into the deck, and/or into any wind bracing in the plane of the top flange, which in turn transmits the forces to the supports through diaphragm action of the deck and/or truss action of the wind bracing.

In lieu of a refined analysis, *AASHTO LRFD* Article C4.6.2.7.1 provides the following approximate formula for estimating the factored wind force per unit length, *W*, applied to the loaded flange:

$$W = \frac{\eta\gamma P_D d}{2} \qquad \text{Equation 6.5.6.5.1-1}$$

AASHTO LRFD Equation C4.6.2.7.1-1

where:

η = load modifier relating to ductility, redundancy, and operational importance specified in *AASHTO LRFD* Article 1.3.2.1 (Section 1.3.6)

γ = load factor specified in *AASHTO LRFD* Table 3.4.1-1 for the group loading combination under consideration

P_D = design horizontal wind pressure specified in *AASHTO LRFD* Article 3.8.1 (Section 3.5.1.2) (ksf)

d = depth of the girder (ft)

For composite or non-composite exterior members with cast-in-place concrete or orthotropic steel decks, *W* need not be applied to the top flange.

P_D is to be assumed uniformly distributed on the area exposed to the wind. The exposed area is to be the sum of the area of all components as seen in elevation taken perpendicular to the assumed wind direction (including the effects of any superelevation). The direction of the wind is to be varied to determine the extreme

force effect in the structure or its components. For cases where the wind is not taken as normal to the structure, lateral and longitudinal components of the base wind pressure, P_B, for various angles of wind direction (assuming a base wind velocity V_B = 100 mph) are given in *AASHTO LRFD* Table 3.8.1.2.2-1. The angles are assumed measured from a perpendicular to the longitudinal axis. As specified in *AASHTO LRFD* Article 3.8.1.2.1, the total wind load per unit length acting on girder spans, *WS*, is not to be taken less than 0.3 klf.

AASHTO LRFD Article C4.6.2.7.1 also provides the following approximate formula for estimating the maximum factored wind moment on the loaded flange, M_w, for the above cases in lieu of a refined analysis:

$$M_w = \frac{WL_b^2}{10} \qquad \text{Equation 6.5.6.5.1-2}$$

AASHTO LRFD Equation C4.6.2.7.1-2

where:

L_b = spacing of the brace points (ft)
W = factored wind force per unit length applied to the flange (Equation 6.5.6.5.1-1) (kip/ft)

For bridges with decks that cannot provide horizontal diaphragm action (e.g. precast concrete plank decks and timber decks), the lever rule is to be applied to distribute the wind load to the top and bottom flanges according to *AASHTO LRFD* Article 4.6.2.7.1. Where there is no wind bracing in the plane of either flange, the lateral forces applied at the brace points by the flanges are assumed transmitted to the supports by lateral bending of all the flanges in the same plane; i.e. the cross-frames/diaphragms are assumed to act as struts in distributing the wind force on the exterior girder flanges to the adjacent flanges. *AASHTO LRFD* Article C4.6.2.7.1 provides the following approximate formula for estimating the maximum factored wind moment on the loaded flange, M_w, for such a case in lieu of a refined analysis:

$$M_w = \frac{WL_b^2}{10} + \frac{WL^2}{8N_b} \qquad \text{Equation 6.5.6.5.1-3}$$

AASHTO LRFD Equation C4.6.2.7.1-3

where:

L = span length (ft)
L_b = spacing of cross-frames/diaphragms (ft)
N_b = number of longitudinal members

W = factored wind force per unit length applied to the flange (Equation 6.5.6.5.1-1) (kip/ft)

If there are no cross-frames/diaphragms, the first term in Equation 6.5.6.5.1-3 is to be taken as 0.0, and N_b should be taken as 1.0.

AASHTO LRFD Article C4.6.2.7.1 also provides the following approximate formula for estimating the factored lateral wind force applied to each brace point in lieu of a refined analysis:

$$P_w = WL_b \qquad \text{Equation 6.5.6.5.1-4}$$

AASHTO LRFD Equation C4.6.2.7.1-4

where:

L_b = spacing of cross-frames/diaphragms (ft)
W = factored wind force per unit length applied to the flange (Equation 6.5.6.5.1-1) (kip/ft)

Lateral wind bracing systems required to support both flanges due to the transfer of wind loading through cross-frames/diaphragms should be designed for a horizontal force of $2P_w$ at each brace point.

EXAMPLE

Check the composite section shown in Figure 6.4.2.3.2.3-1, which is from an exterior girder in a continuous-span bridge in a region of positive flexure, for the Strength V load combination (Section 3.9.1.2.6). The girder is homogeneous with the flanges and web having a yield strength of 50 ksi. The load modifier, η (Section 1.3.6), is assumed to be 1.0. Assume unshored construction. Use the section properties computed earlier for this section. Assume the following unfactored bending moments:

M_{DC1} = +2,202 kip-ft
M_{DC2} = +335 kip-ft
M_{DW} = +322 kip-ft
M_{LL+IM} = +3,510 kip-ft

Determine first if the section qualifies as a compact section (Section 6.5.6.3.2.2). According to *AASHTO LRFD* Article 6.10.6.2.2, composite sections in positive flexure in straight bridges qualify as compact when: 1) the specified minimum yield strengths of the flanges do not exceed 70 ksi (ok), 2) the web satisfies the requirement of *AASHTO LRFD* Article 6.10.2.1.1 such that longitudinal stiffeners are not required; i.e. $D/t_w \leq 150$ (D/t_w = 69.0/0.5 = 138.0 < 150 ok), and 3) the section

satisfies the web-slenderness limit given by Equation 6.5.6.3.2.2-1 (earlier computations indicated that the plastic neutral axis of the composite section is located in the top flange. Therefore, according to *AASHTO LRFD* Article D6.3.2, D_{cp} is taken equal to zero for this case, and thus, Equation 6.5.6.3.2.2-1 is considered to be automatically satisfied). Therefore, the section qualifies as a compact section.

Compact composite sections in positive flexure must satisfy the ductility requirement given by Equation 6.5.6.3.4-1 to protect the concrete deck from premature crushing. At this section:

$$D_p = 9.0 + 3.5 - 1.0 + 0.44 = 11.94 \text{ in.}$$

$$D_t = 1.375 + 69.0 + 3.5 + 9.0 = 82.88 \text{ in.}$$

$$0.42D_t = 0.42(82.88) = 34.81 \text{ in.} > 11.94 \text{ in.} \quad \text{ok}$$

AASHTO LRFD Article C4.6.2.7.1 provides the following approximate formula for estimating the factored wind force per unit length applied to the bottom flange of composite exterior members with cast-in-place concrete decks (Equation 6.5.6.5.1-1):

$$W = \frac{\eta\gamma P_D d}{2}$$

where P_D is the design horizontal wind pressure specified in *AASHTO LRFD* Article 3.8.1, and d is the depth of the girder. Assume for this example that P_D is calculated to be 0.053 ksf. (see the wind-load example in Section 6.5.3.6 for the procedures used to calculate P_D).

Assuming no superelevation for the example bridge and a barrier height of 42 inches above the concrete deck, the minimum exposed height of the composite superstructure is computed as:

$$h_{exp.} = (0.875 + 69.0 + 3.5 + 9.5 + 42.0)/12 = 10.41 \text{ ft}$$

The total wind load per unit length, *WS*, for the case of wind applied normal to the structure is computed as (as specified in *AASHTO LRFD* Article 3.8.1.2.1, the total wind load per unit length acting on girder spans, *WS*, is not to be taken less than 0.3 klf):

$$WS = P_D h_{exp.} = 0.053(10.41) = 0.55 \text{ kips/ft} > 0.3 \text{ kips/ft} \quad \text{ok}$$

For the wind-load path identified above, *AASHTO LRFD* Article C4.6.2.7.1 also provides the following approximate equation for estimating the maximum flange lateral bending moment due to the factored wind load, M_w, within the unbraced length under consideration:

$$M_w = \frac{WL_b^2}{10}$$

The unbraced length, L_b, at this section is 24.0 feet. Assemble the factored actions needed to check Equation 6.5.6.3.2.2-2 at this section.

Wind pressure on live load (*WL*) is specified in *AASHTO LRFD* Article 3.8.1.3 (Section 3.5.1.3). Wind pressure on live load is to be represented by a moving force of 0.1 klf acting normal to and 6 feet above the roadway, which results in an overturning force on the vehicle similar to the effect of centrifugal force on vehicles traversing horizontally curved bridges. The horizontal line load is to be applied to the same tributary area as the design lane load for the force effect under consideration. When wind on live load is not taken normal to the structure, the normal and parallel components of the force applied to the live load may be taken from *AASHTO LRFD* Table 3.8.1.3-1.

In this example, *WL* is assumed transmitted directly to the deck and is therefore not considered in the Strength V load combination. For simplicity, the effect of the overturning force due to *WL* on the vehicle wheel loads is also not considered in this example. It should be mentioned that for load cases where the direction of the wind is taken perpendicular to the bridge and there is no wind on live load considered, a vertical wind pressure of 0.020 ksf applied to the entire width of the deck is to be applied in combination with the horizontal wind loads to investigate potential overturning of the bridge (*AASHTO LRFD* Article 3.8.3 – Section 3.5.2). This load case is not investigated in this example.

The amplification factor, *AF*, for f_ℓ (*AASHTO LRFD* Article 6.10.1.6) is taken equal to 1.0 for flanges in tension (Section 6.5.2.1.3.2). Note again that first- or second-order flange lateral bending stresses, as applicable, are limited to a maximum value of $0.6F_{yf}$ according to *AASHTO LRFD* Equation 6.10.1.6-1. Therefore,

For Strength V:

Dead and live loads:

$$M_u = 1.0\left[1.25(2{,}202 + 335) + 1.5(322) + 1.35(3{,}510)\right] = 8{,}393 \text{ kip} - \text{ft}$$

Wind loads:

$$W = \frac{1.0(0.4)(0.053)(1.375+69.0+1.0)/12}{2} = 0.063 \text{ kips / ft}$$

$$M_w = \frac{0.063(24.0)^2}{10} = 3.63 \text{ kip} - \text{ft}$$

$$f_\ell = \frac{M_w}{S_\ell} = \frac{3.63(12)}{1.375(18)^2/6} = 0.587 \text{ ksi} * AF = 0.587(1.0) = 0.587 \text{ ksi} < 0.6F_{yf} = 30.0 \text{ ksi} \quad \text{ok}$$

From an examination of the above flange lateral bending stress, it is apparent that for typical cross-frame spacings, the majority of the wind force on the lower half of a composite structure is transmitted directly to the deck through the cross-frames, and only a small portion of the force is resisted through lateral bending of the bottom flange.

Determine the nominal flexural resistance of the section according to the provisions of *AASHTO LRFD* Article 6.10.7.1.2. For this example section, M_p and M_y were computed earlier to be 14,199 kip-ft and 10,171 kip-ft, respectively (see Sections 6.4.5.2 and 6.4.5.3).

$$0.1D_t = 0.1(82.88) = 8.29 \text{ in.} < D_p = 11.94 \text{ in.}$$

Therefore, Equation 6.5.6.3.2.3-4 controls:

$$M_n = M_p\left(1.07 - 0.7\frac{D_p}{D_t}\right)$$

$$M_n = 14{,}199\left[1.07 - 0.7\left(\frac{11.94}{82.88}\right)\right] = 13{,}761 \text{ kip} - \text{ft}$$

However, in a continuous span, the nominal flexural resistance of the section is limited to the following (Equation 6.5.6.3.2.3-5):

$$M_n = 1.3R_hM_y$$

or,

$$M_n = 1.3(1.0)(10{,}171) = 13{,}222 \text{ kip} - \text{ft} \qquad \text{(governs)}$$

$$M_n = 13{,}222 \text{ kip} - \text{ft}$$

Calculate S_{xt}. The yield moment, M_y, was calculated with respect to the tension flange; therefore, $M_{yt} = M_y$:

$$S_{xt} = \frac{M_{yt}}{F_{yt}} = \frac{10{,}171(12)}{50} = 2{,}441 \text{ in}^3$$

Check Equation 6.5.6.3.2.2-2 now that all the required information has been assembled:

$$M_u + \frac{1}{3} f_\ell S_{xt} \le \phi_f M_n$$

For Strength V:s

$$M_u + \frac{1}{3} f_\ell S_{xt} = 8{,}393 \text{ kip} - \text{ft} + \frac{1}{3}\frac{(0.587)(2{,}441)}{12} = 8{,}433 \text{ kip} - \text{ft}$$
$$\phi_f M_n = 1.0(13{,}222) = 13{,}222 \text{ kip} - \text{ft}$$
$$8{,}433 \text{ kip} - \text{ft} < 13{,}222 \text{ kip} - \text{ft} \quad \text{ok}$$

The section has significant excess flexural resistance under this load combination at the strength limit state. Other limit-state criteria (e.g. service limit state or fatigue limit state criteria) are likely to control the design of the section in this case. As a result, consideration might be given to treating this section conservatively as a noncompact section, which simplifies the calculations somewhat and should not result in a significant loss of economy.

6.5.6.5.2 Box Sections

In lieu of a refined analysis, *AASHTO LRFD* Article 4.6.2.7.2 states that one quarter of the wind force on a box section is to be applied to the bottom flange of the exterior box beam. *AASHTO LRFD* Article 6.11.1.1 states that the section of the exterior box beam assumed to resist the factored horizontal wind force is to be taken as the bottom box flange, assumed to act as a web, and 12 times the thickness of the web, assumed to act as flanges. The other three quarters of the wind force on a box section, plus the wind force acting on vehicles, barrier and appurtenances, is to be assumed transmitted to the supports by diaphragm action of the deck. Interbox lateral bracing is to be provided if the section assumed to resist the wind force is not adequate.

6.5.6.6 Moment Redistribution: AASHTO Appendix B6

6.5.6.6.1 General

AASHTO LRFD Appendix B6 of the *AASHTO LRFD* Specifications provides optional provisions for the calculation of redistribution moments from the interior-pier sections of straight continuous-span I-girder bridges (meeting certain specified restrictions) at the service and/or strength limit states. These provisions replace the traditional flat ten-percent redistribution allowance given in previous *AASHTO* Standard Specifications and, in general, provide simpler and more rational approaches for calculating the percentage of moment redistribution from interior-pier sections than the inelastic analysis procedures given in previous *AASHTO LRFD* Specifications. In the more simplified approach that is presented in *AASHTO LRFD* Appendix B6 (the Effective Plastic Moment Method), elastic moment envelopes are utilized and the direct use of any iterative inelastic analysis methods is not required. A more rigorous approach (the Refined Method) is also permitted to allow the Engineer to conduct a direct shakedown analysis, if desired, again utilizing the elastic moment envelope values.

Several restrictions are specified on the use of these approaches in order to ensure adequate ductility and robustness at interior-pier sections (Section 6.5.6.6.2). Where these requirements are met, the provisions may be applied to sections with compact, noncompact or slender webs. Previous provisions were limited only to sections with compact webs, as defined in those earlier provisions. The provisions may also be applied to sections that are either composite or non-composite in positive or negative flexure. As mentioned above, according to the provisions, the redistribution moments may be calculated using either a simplified effective plastic moment method that intrinsically accounts for the interior-pier section moment-rotation characteristics, or a more refined method in which a direct shakedown analysis is conducted to ensure the simultaneous satisfaction of continuity and moment-rotation relationships at all interior-pier sections from which moments are redistributed. Additional more detailed information on the development of these provisions may be found in Barker et al. (1997), Schilling et al. (1997), White et al. (1997), and Barth et al. (2004), which contain extensive references to other supporting research. Example applications of these provisions are demonstrated in Barth (2012) and Barth (2012a).

Moment redistribution in straight continuous I-girder spans results from minor localized yielding at interior piers. However, in conventional elastic analysis and design, moment and shear envelopes are typically determined by elastic analysis with no redistribution due to the effects of local yielding considered. As a result, cross-sections in regions adjacent to interior-pier sections are proportioned for a resistance equal or greater than that required by the elastic moment envelopes. Therefore, cover plates may be added to rolled beams in these regions to increase

the flexural resistance, which introduces details that often have low fatigue resistance. In welded beams, multiple flange transitions are typically added in these regions according to the elastic moment demand, which can result in increased fabrication costs. Accounting for the redistribution of moments according to these optional provisions, where appropriate, can make it possible to eliminate such details by using prismatic sections along the entire length of the bridge or between field splices, which can provide fabrication economies and improve the overall fatigue resistance. This is made possible by removing restrictions on the flexural resistance in the regions adjacent to interior piers from which moments are redistributed by accounting for the strength and ductility of the pier sections directly within the procedures used to calculate the redistribution moments.

6.5.6.6.2 Restrictions

6.5.6.6.2.1 General

The following restrictions specified in *AASHTO LRFD* Article B6.2 must be satisfied in order to apply the optional provisions of *AASHTO LRFD* Appendix B6 to calculate the redistribution moments. Also, as discussed previously in Section 6.5.6.3.2, when these restrictions are satisfied and when the appropriate value of θ_{RL} from *AASHTO LRFD* Article B6.6.2 (discussed below under the Refined Method) exceeds 0.009 radians at all adjacent interior-pier sections, the nominal flexural resistance M_n of composite sections in positive flexure in continuous spans need not be limited to $1.3R_hM_y$. Pier sections meeting the above requirements are assumed to have sufficient ductility and robustness such that the redistribution of moments to adjacent pier sections caused by partial yielding within the positive flexure regions is considered inconsequential.

The provisions of *AASHTO LRFD* Appendix B6 may be applied only to straight continuous-span I-section members whose support lines are not skewed more than 10 degrees from radial and along which there are no staggered cross-frames. Research to date has primarily focused only on straight non-skewed I-girder bridge superstructures without staggered cross-frames.

The cross-sections throughout the unbraced lengths immediately adjacent to interior-pier sections from which moments are redistributed must have a specified minimum yield strength not exceeding 70 ksi. The original development of these provisions considered only nonhybrid and hybrid girders with specified minimum yield strengths up to and including 70 ksi.

Because the effect of holes in the tension flange on potential net section fracture at cross-sections experiencing significant inelastic strains is not well understood, holes in the tension flange are not permitted over a distance of $2D$ on either side of the interior-pier sections from which moments are redistributed, where D is the web

depth. The distance of 2*D* approximately encompasses the zone of primary inelastic behavior at pier sections.

In addition, all of the following requirements must be met throughout the unbraced lengths immediately adjacent to interior-pier sections from which moments are redistributed. If the effective plastic moment approach (Section 6.5.6.6.3) is utilized to calculate the redistribution moments, the unbraced lengths immediately adjacent to *all* interior-pier sections of the continuous-span member must satisfy the following requirements. This restriction is due to the approximations involved in the development of the simplified effective plastic moment approach, and the fact that inelastic redistribution moments from one interior pier generally produce nonzero redistribution moments at all interior piers. If the refined method (Section 6.5.6.6.4) is used to calculate the redistribution moments, the unbraced lengths immediately adjacent to all interior-pier sections are not required to satisfy the following requirements. However, moments may only be redistributed from interior-pier sections with adjacent unbraced lengths that do satisfy them.

In addition to the requirements given below, as specified in *AASHTO LRFD* Article B6.2.3, the steel I-section member must be prismatic within the unbraced length under consideration, as only prismatic members within unbraced lengths adjacent to interior piers were considered in the supporting research. Also, as specified in *AASHTO LRFD* Article B6.2.6, bearing stiffeners designed according to the provisions of *AASHTO LRFD* Article 6.10.11.2 (Section 6.6.6.3) must be provided at the interior-pier section under consideration (even on rolled beams). The bearing stiffeners help to ensure adequate robustness of the pier section as inelastic rotations occur.

6.5.6.6.2.2 Web Proportions

As specified in *AASHTO LRFD* Article B6.2.1, the web within the unbraced length under consideration must satisfy all the following requirements:

$$\frac{D}{t_w} \le 150$$ Equation 6.5.6.6.2.2-1

AASHTO LRFD Equation B6.2.1-1

$$\frac{2D_c}{t_w} \le 6.8\sqrt{\frac{E}{F_{yc}}}$$ Equation 6.5.6.6.2.2-2

AASHTO LRFD Equation B6.2.1-2

$$D_{cp} \le 0.75D \qquad \text{Equation 6.5.6.6.2.2-3}$$

AASHTO LRFD Equation B6.2.1-3

where:

D_c = depth of the web in compression in the elastic range (in.). For composite sections, D_c is to be determined according to the provisions of *AASHTO LRFD* Article D6.3.1.

D_{cp} = depth of the web in compression at the plastic moment determined as specified in *AASHTO LRFD* Article D6.3.2 (in.)

Equation 6.5.6.6.2.2-1 parallels the web-slenderness requirement given in *AASHTO LRFD* Article 6.10.2.1.1 and prevents the application of the provisions of *AASHTO LRFD* Appendix B6 to interior-pier sections with longitudinal web stiffeners. The moment-rotation characteristics of sections with longitudinal web stiffeners have not been studied in sufficient detail at this writing. Equation 6.5.6.6.2.2-2, Equation 6.5.6.6.2.2-2, and Equation 6.5.6.6.2.2-3 are limits on the web slenderness, $2D_c/t_w$, and depth of the web in compression at the plastic moment, D_{cp}, that were considered in the research conducted to date.

6.5.6.6.2.3 Compression-Flange Proportions

As specified in *AASHTO LRFD* Article B6.2.2, compression flanges within the unbraced length under consideration must satisfy the following requirements:

$$\frac{b_{fc}}{2t_{fc}} \le 0.38\sqrt{\frac{E}{F_{yc}}} \qquad \text{Equation 6.5.6.6.2.3-1}$$

AASHTO LRFD Equation B6.2.2-1

$$b_{fc} \ge \frac{D}{4.25} \qquad \text{Equation 6.5.6.6.2.3-2}$$

AASHTO LRFD Equation B6.2.2-2

Equation 6.5.6.6.2.3-1 conservatively ensures that all compression flanges within the unbraced length will be compact flanges (Section 6.5.6.2.2.2). Equation 6.5.6.6.2.3-2 corresponds to the largest aspect ratio, D/b_{fc}, considered in the supporting research. Larger values of this ratio reduce the strength and moment-rotation characteristics of I-sections.

6.5.6.6.2.4 Compression-Flange Bracing

As specified in *AASHTO LRFD* Article B6.2.4, the unbraced length L_b under consideration must satisfy:

$$L_b \le \left[0.1 - 0.06\left(\frac{M_1}{M_2}\right)\right]\frac{r_t E}{F_{yc}} \qquad \text{Equation 6.5.6.6.2.4-1}$$

AASHTO LRFD Equation B6.2.4-1

where:

M_1 = bending moment about the major-axis of the cross-section at the brace point with the lower moment due to the factored loads, taken as either the maximum or minimum moment envelope value, whichever produces the smallest permissible unbraced length (kip-in.)

M_2 = bending moment about the major-axis of the cross-section at the brace point with the higher moment due to the factored loads, taken as the critical moment envelope value (kip-in.)

r_t = effective radius of gyration for lateral torsional buckling within the unbraced length under consideration determined from *AASHTO LRFD* Equation A6.3.3-10 (in.)

The ratio of (M_1/M_2) is to be taken as negative when the moments cause reverse curvature bending. Equation 6.5.6.6.2.4-1 is similar to the compression-flange bracing requirement given for compact sections in previous *AASHTO LRFD* Specifications, but is written in terms of r_t rather than the radius of gyration of the entire steel section about the vertical axis, r_y, which is felt by the specification writers to be more correct for handling composite sections in negative flexure. Since the negative-moment envelope is typically concave in shape near interior-pier sections, consideration of the moment at the mid-point of the unbraced length is not required for consideration of moment-gradient effects, as is required in general for the calculation of the moment-gradient modifier C_b in *AASHTO LRFD* Article A6.3.3. Using the ratio of the end moments (M_1/M_2) in Equation 6.5.6.6.2.4-1 is considered to be sufficient and conservative for considering the moment-gradient effects.

6.5.6.6.2.5 Shear

As specified in *AASHTO LRFD* Article B6.2.5, webs with or without transverse stiffeners within the unbraced length under consideration must satisfy the following requirement at the strength limit state:

$$V_u \le \phi_v V_{cr} \qquad \text{Equation 6.5.6.6.2.5-1}$$

AASHTO LRFD Equation B6.2.5-1

where:

ϕ_v = resistance factor for shear specified in *AASHTO LRFD* Article 6.5.4.2 (= 1.0)

V_{cr} = shear-buckling resistance determined from *AASHTO LRFD* Equation 6.10.9.2-1 for unstiffened webs and from *AASHTO LRFD* Equation 6.10.9.3.3-1 for stiffened webs (kips)

V_u = shear due to the factored loads (kips)

Equation 6.5.6.6.2.5-1 limits the shear due to the factored loads within the unbraced length to the shear-buckling resistance to improve the moment-rotation characteristics of pier sections from which moments are redistributed. Therefore, the use of post-buckling shear resistance, or tension-field action, is not permitted within the vicinity of these pier sections.

6.5.6.6.3 Effective Plastic Moment Method

6.5.6.6.3.1 General

The redistribution moments at the service and/or strength limit states may be computed using a simplified effective plastic moment approach using an effective plastic moment that is based on a lower-bound estimate of the moment-rotation characteristics of interior-pier sections satisfying the restrictions of *AASHTO LRFD* Article B6.2. At each limit state, the redistribution moments are computed according to the corresponding procedures given below, and are then added to the elastic moments due to the appropriate factored loads.

6.5.6.6.3.2 Service Limit State

Calculation of the redistribution moments at the service limit state using the effective plastic moment method is covered in *AASHTO LRFD* Article B6.3. As specified in *AASHTO LRFD* Article B6.3.1, load combination Service II (*AASHTO LRFD* Table 3.4.1-1) is to be applied in the calculations. In checking permanent deflections under the Service II load combination (Section 6.5.4.3), localized yielding is permitted at interior-pier sections satisfying the restrictions of *AASHTO LRFD* Article B6.2, which results in a redistribution of the elastic moments. As discussed in Section 6.5.6.6.2.1, when the effective plastic moment method is employed, these restrictions must be met at all interior-pier sections in the member. According to *AASHTO LRFD* Article B6.3.3.1, the redistribution moment M_{rd} at the interior-pier sections at the service limit state is to be taken as:

$$M_{rd} = |M_e| - M_{pe} \qquad \text{Equation 6.5.6.6.3.2-1}$$

AASHTO LRFD Equation B6.3.3.1-1

where:

M_e = critical elastic moment envelope value at the interior-pier section due to the Service II loads (kip-in.)

M_{pe} = negative-flexure effective plastic moment for the service limit state determined as specified in *AASHTO LRFD* Article B6.5 (see below) (kip-in.)

Equation 6.5.6.6.3.2-1 is based on the concepts related to shakedown analysis of continuous-span girders under repeated applications of moving live loads (Schilling et al., 1997; ASCE, 1971) utilizing an effective plastic moment, M_{pe}. Shakedown has been determined to be the most appropriate limit state related to moment redistribution in continuous-span bridges (Galambos et al., 1993). Flange lateral bending effects at interior piers under the Service II load combination were considered negligible by the specification writers due to the restrictions of *AASHTO LRFD* Article B6.2, and are therefore not included in Equation 6.5.6.6.3.2-1.

At the service limit state, unless the requirements of *AASHTO LRFD* Article B6.5.1 are satisfied to provide enhanced moment-rotation characteristics, the effective plastic moment M_{pe} at interior-pier sections satisfying the restrictions of *AASHTO LRFD* Article B6.2 is to be taken as (*AASHTO LRFD* Article B6.5.2):

$$M_{pe} = \left(2.90 - 2.3\frac{b_{fc}}{t_{fc}}\sqrt{\frac{F_{yc}}{E}} - 0.35\frac{D}{b_{fc}} + 0.39\frac{b_{fc}}{t_{fc}}\sqrt{\frac{F_{yc}}{E}}\frac{D}{b_{fc}} \right) M_n \le M_n$$

Equation 6.5.6.6.3.2-2

AASHTO LRFD Equation B6.5.2-1

where:

M_n = nominal flexural resistance of the interior-pier section taken as the smaller of $F_{nc}S_{xc}$ and $F_{nt}S_{xt}$, with F_{nc} and F_{nt} determined as specified in *AASHTO LRFD* Article 6.10.8. For sections with compact or noncompact webs, M_n may be taken as the smaller of M_{nc} and M_{nt} determined as specified in *AASHTO LRFD* Appendix A6 (kip-in.)

For interior-pier sections satisfying the special requirements of *AASHTO LRFD* Article B6.5.1 to provide enhanced moment-rotation characteristics, namely:

- where transverse web stiffeners spaced at $D/2$ or less are provided over a minimum distance of $D/2$ on each side of the interior-pier section, and
- an ultracompact web satisfying the following requirement is provided:

$$\frac{2D_{cp}}{t_w} \le 2.3\sqrt{\frac{E}{F_{yc}}} \qquad \text{Equation 6.5.6.6.3.2-3}$$

AASHTO LRFD Equation B6.5.1-1

M_{pe} at the service limit state may instead be taken as follows:

$$M_{pe} = M_n \qquad \text{Equation 6.5.6.6.3.2-4}$$

AASHTO LRFD Equation B6.5.1-2

Closely spaced transverse stiffeners adjacent to the interior-pier section help to restrain the local buckling distortions of the compression flange and web. A stocky ultracompact web also helps reduce web distortions and restrains flange local buckling distortions such that the moment-rotation characteristics of the pier section are enhanced relative to sections that only satisfy the restrictions of *AASHTO LRFD* Article B6.2 (Barth et al., 2004; White et al., 1997).

In both Equation 6.5.6.6.3.2-2 and Equation 6.5.6.6.3.2-4, the influence of the web slenderness on M_{pe} for both noncompact web and slender web sections is captured through the inclusion of the term M_n. Equation 6.5.6.6.3.2-2 and Equation 6.5.6.6.3.2-4 are based on an estimated upper-bound required plastic rotation of 0.009 radians at the pier sections at the service limit state that was determined by a direct inelastic analysis of various trial designs (Schilling, 1986). The development of these equations is discussed in further detail in Barth et al., 2004.

According to *AASHTO LRFD* Article B6.3.3.1, the calculated pier-section redistribution moment M_{rd} must be greater than or equal to zero and less than or equal to $0.2|M_e|$. This requirement is intended to prevent the use of an interior-pier section in the design that is so small that it might violate the assumed upper-bound plastic rotation of 0.009 radians assumed in the development of the equations for M_{pe} at the service limit state. If the upper limit of $0.2|M_e|$ is violated, a larger section must be selected at the interior pier until this limit is satisfied.

The redistribution moments remain in the member after the live loads are removed and cause the member to shakedown or behave elastically under subsequent passages of heavy overload vehicles. The moments are held in equilibrium by the support reactions; hence, they must vary linearly between the supports. Therefore, as specified in *AASHTO LRFD* Article B6.3.3.2, the redistribution moments at all locations other than at interior piers are to be determined by connecting with straight lines the redistribution moments at adjacent interior-pier sections. The lines are to be extended to any points of zero redistribution moment at adjacent supports, including the abutments. A typical redistribution moment diagram for a three-span

continuous member is illustrated in Figure 6.5.6.6.3.2-1. Note that the redistribution moments are positive at both interior-pier sections in this case.

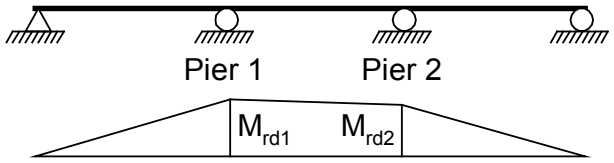

Figure 6.5.6.6.3.2-1 Typical Redistribution Moment Diagram for a Three-Span Continuous Bridge

At the service limit state, permanent deflections are controlled by limiting the flange stresses due to the Service II load combination according to the provisions of *AASHTO LRFD* Article 6.10.4.2 (Section 6.5.4.3.2.1). Also, except for composite sections in positive flexure in which the web satisfies the requirement of *AASHTO LRFD* Article 6.10.2.1.1 (i.e. $D/t_w \leq 150$), a web bend-buckling check is required (Section 6.5.4.3.2.2). As specified in *AASHTO LRFD* Article B6.3.2.1, after the redistribution moments are calculated, the flange-stress limitations of *AASHTO LRFD* Article 6.10.4.2 are not to be checked within the regions extending in each adjacent span from interior-pier sections satisfying the restrictions of *AASHTO LRFD* Article B6.2 to the nearest flange transition or point of permanent-load contraflexure, whichever is closest. These checks are not considered necessary in these regions because the redistribution moments cause the member to shakedown under repeated live loads and because the ductility and strength of the interior-pier sections has been considered within the calculation of those moments. The web bend-buckling check is still required in these regions however and should be based on the elastic moments prior to redistribution.

At all other locations outside these regions, the provisions of *AASHTO LRFD* Article 6.10.4.2 must be checked after the redistribution moments are calculated (*AASHTO LRFD* Article B6.3.2.2). As discussed previously, the redistribution moments are added to the elastic moments due to the Service II loads before the checks are made. At composite sections, the stresses due to the locked-in redistribution moments tend to decrease with time due to creep in the concrete. These stresses are likely to be continually renewed however with the subsequent passages of similar heavy live loads. Therefore, at composite sections in positive flexure, the redistribution moments are to be added to the DC_2 and DW (if present) moments and the corresponding flexural stresses in the steel section calculated using the long-term composite section (i.e. using a modular ratio of $3n$), as specified in *AASHTO LRFD* Article B6.3.2.2.

As mentioned in *AASHTO LRFD* Article CB6.3.2.1, additional cambering of the girder steel to account for the small permanent deformations associated with

localized yielding at the piers under the Service II loads and the corresponding redistribution of the pier-section moments is not recommended. Very small permanent deflections under an overload condition were observed during the testing of an actual full-scale bridge on a logging road that was designed to permit redistribution of negative moments (Roeder and Eltvik, 1985).

6.5.6.6.3.3 Strength Limit State

Calculation of the redistribution moments at the strength limit state using the effective plastic moment method is covered in *AASHTO LRFD* Article B6.4. In checking the strength limit state, localized yielding is permitted at interior-pier sections satisfying the restrictions of *AASHTO LRFD* Article B6.2, which results in a redistribution of the elastic moments. As discussed in Section 6.5.6.6.2.1, when the effective plastic moment method is employed, these restrictions must be met at all interior-pier sections in the member. According to *AASHTO LRFD* Article B6.4.2.1, the redistribution moment, M_{rd}, at the interior-pier sections at the strength limit state is to be taken as the *larger* of the following:

$$M_{rd} = |M_e| + \frac{1}{3} f_\ell S_{xc} - \phi_f M_{pe} \qquad \text{Equation 6.5.6.6.3.3-1}$$

AASHTO LRFD Equation B6.4.2.1-1

or

$$M_{rd} = |M_e| + \frac{1}{3} f_\ell S_{xt} - \phi_f M_{pe} \qquad \text{Equation 6.5.6.6.3.3-2}$$

AASHTO LRFD Equation B6.4.2.1-2

where:

ϕ_f = resistance factor for flexure specified in *AASHTO LRFD* Article 6.5.4.2 (= 1.0)

f_ℓ = lateral bending stress in the flange under consideration at the interior-pier section (ksi). For continuously braced flanges, f_ℓ is to be taken as zero.

M_e = critical elastic moment envelope value at the interior-pier section due to the factored loads (kip-in.)

M_{pe} = negative-flexure effective plastic moment for the strength limit state determined as specified in *AASHTO LRFD* Article B6.5 (see below) (kip-in.)

S_{xc} = elastic section modulus about the major-axis of the cross-section to the compression flange taken as M_{yc}/F_{yc} (in.^{3})

S_{xt} = elastic section modulus about the major-axis of the cross-section to the tension flange taken as M_{yt}/F_{yt} (in.^{3})

Flange lateral bending effects at interior piers are conservatively included in Equation 6.5.6.6.3.3-1 and Equation 6.5.6.6.3.3-2 (according to the one-third rule – Section 6.5.2.1) to account for the reduction in the flexural resistance at the interior-pier section due to these effects. In this case, at the strength limit state, flange lateral bending effects are primarily due to wind loads, which must be considered in certain strength load combinations.

At the strength limit state, unless the requirements of *AASHTO LRFD* Article B6.5.1 are satisfied to provide enhanced moment-rotation characteristics, the effective plastic moment, M_{pe}, at interior-pier sections that satisfy the restrictions of *AASHTO LRFD* Article B6.2 is to be taken as (*AASHTO LRFD* Article B6.5.2):

$$M_{pe} = \left(2.63 - 2.3\frac{b_{fc}}{t_{fc}}\sqrt{\frac{F_{yc}}{E}} - 0.35\frac{D}{b_{fc}} + 0.39\frac{b_{fc}}{t_{fc}}\sqrt{\frac{F_{yc}}{E}}\frac{D}{b_{fc}} \right) M_n \le M_n$$

Equation 6.5.6.6.3.3-3

AASHTO LRFD Equation B6.5.2-2

For interior-pier sections that satisfy the special requirements of *AASHTO LRFD* Article B6.5.1 to provide enhanced moment-rotation characteristics, namely:

- where transverse web stiffeners spaced at D/2 or less are provided over a minimum distance of D/2 on each side of the interior-pier section, and
- an ultracompact web satisfying Equation 6.5.6.6.3.2-3 is provided, M_{pe} at the strength limit state may instead be taken as follows:

$$M_{pe} = \left(2.78 - 2.3\frac{b_{fc}}{t_{fc}}\sqrt{\frac{F_{yc}}{E}} - 0.35\frac{D}{b_{fc}} + 0.39\frac{b_{fc}}{t_{fc}}\sqrt{\frac{F_{yc}}{E}}\frac{D}{b_{fc}} \right) M_n \le M_n$$

Equation 6.5.6.6.3.3-4

AASHTO LRFD Equation B6.5.1-3

In both Equation 6.5.6.6.3.3-3 and Equation 6.5.6.6.3.3-4, the influence of the web slenderness on M_{pe} for both noncompact web and slender web sections is captured through the inclusion of the term, M_n. Equation 6.5.6.6.3.3-3 and Equation 6.5.6.6.3.3-4 are based on an estimated upper-bound required plastic rotation of 0.03 radians at the pier sections at the strength limit state that was determined by a direct inelastic analysis of various trial designs (Schilling, 1986). The development of these equations is discussed in further detail in Barth et al. (2004).

According to *AASHTO LRFD* Article B6.4.2.1, the calculated pier-section redistribution moment, M_{rd}, must be greater than or equal to zero and less than or equal to $0.2|M_e|$. This requirement is intended to prevent the use of an interior-pier section in the design that is so small that it might violate the assumed upper-bound plastic rotation of 0.03 radians assumed in the development of the equations for M_{pe} at the strength limit state. If the upper limit of $0.2|M_e|$ is violated, a larger section must be selected at the interior pier until this limit is satisfied.

The redistribution moments at all locations other than at interior piers are to be determined in the same manner as discussed previously for the service limit state (*AASHTO LRFD* Article B6.4.2.2 – refer to Figure 6.5.6.6.3.2-1**)**.

As specified in *AASHTO LRFD* Article B6.4.1.1, after the redistribution moments are calculated, the strength limit state flexural resistance requirements (Section 6.5.6.2) are not to be checked within the unbraced lengths immediately adjacent to interior-pier sections satisfying the restrictions of *AASHTO LRFD* Article B6.2. Again, these checks are not considered necessary in these regions because the redistribution moments cause the member to shakedown under repeated live loads and because the ductility and strength of the interior-pier sections has been considered within the calculation of the those moments.

At all other locations outside these regions, the strength limit state provisions of *AASHTO LRFD* Articles 6.10.7.1, 6.10.8.1 or A6.1, as applicable (Section 6.5.6), *must* be checked after the redistribution moments are calculated (*AASHTO LRFD* Article B6.4.1.2). The redistribution moments are added to the elastic moments due to the factored loads at the strength limit state before the checks are made. As discussed previously for the service limit state, at composite sections in positive flexure where stress calculations are required at the strength limit state (e.g. at noncompact sections*)*, the redistribution moments are to be added to the DC_2 and DW (if present) moments and the corresponding flexural stresses in the steel section calculated using the long-term composite section (i.e. using a modular ratio of 3*n*), as specified in *AASHTO LRFD* Article B6.4.1.2.

6.5.6.6.4 Refined Method

AASHTO LRFD Article B6.6 alternatively allows the use of a refined method to calculate the redistribution moments, in which a direct shakedown analysis is conducted to ensure the simultaneous satisfaction of rotational continuity and inelastic moment-rotation relationships at all interior-pier sections from which moments are redistributed. The refined method may be applied at the service and/or strength limit states, and utilizes the critical elastic moment envelope values due to the appropriate factored loads in the analysis. As specified in *AASHTO LRFD* Article B6.2, when the refined method is employed, all interior-pier sections are *not* required

to satisfy the restrictions of *AASHTO LRFD* Article B6.2, but moments may not be redistributed from those particular sections and those sections must be assumed to remain elastic in the analysis. Also, those sections (and the corresponding portions of each span adjacent to those sections) must satisfy all applicable design requirements at the service and/or strength limit states after a final solution is obtained. As pointed out in *AASHTO LRFD* Article CB6.6.1, when the refined method is used, the calculated plastic rotations at the pier sections will typically be smaller than the upper-bound rotations assumed in the development of the effective plastic moment method (Section 6.5.6.6.3).

The refined method is similar in concept to the unified autostress method permitted in previous *AASHTO LRFD* Specifications and described in detail in Schilling (1991). In this method, at each pier from which moments are to be redistributed, continuity relationships are written relating the plastic rotations, θ_p, at all pier sections assumed to be undergoing yielding to the moment at the pier section under consideration. In this relationship, the pier-section moment is taken equal to the critical elastic moment envelope value at the pier section under consideration plus the sum of the redistribution moments at that pier due to any plastic rotations (and corresponding redistribution moments) occurring at all pier sections assumed to be undergoing yielding. Redistribution moments resulting from plastic rotations at one interior support generally produce nonzero redistribution moments at all interior supports. For example, assume for a three-span continuous bridge that moments are to be redistributed from both interior piers. The continuity relationship for Pier 1 can then be written as follows:

$$M_1 = |M_{e1}| - k_{\theta 11}\theta_{p1} - k_{\theta 12}\theta_{p2} \qquad \text{Equation 6.5.6.6.4-1}$$

where:

M_1 = total continuity moment at Pier 1 (kip-in.)

M_{e1} = critical elastic moment envelope value at the Pier 1 due to the Service II loads or due to the factored loads at the strength limit state, as applicable (kip-in.)

$k_{\theta 11}$, $k_{\theta 12}$ = unit rotational stiffness constants at Pier 1 due to plastic rotations at Pier 1 and Pier 2, respectively (kip-in./radian)

θ_{p1}, θ_{p2} = plastic rotations at Pier 1 and Pier 2, respectively (radians)

A similar relationship would be written for Pier 2. The unit rotational stiffness constants are a function of the stiffness properties of the girder and are calculated in this particular case, for example, by applying a unit relative rotation at each pier in turn and calculating the resulting moment at Pier 1 using any appropriate indeterminate analysis approach. According to *AASHTO LRFD* Article B6.6.1, these coefficients are to be determined using the elastic stiffness properties of the short-term composite section assuming the concrete deck is effective over the entire span

length, as the redistribution moments are assumed formed by short-term loads. For reasons discussed at some length in *AASHTO LRFD* Article CB6.6.1, the influence of any partial yielding in regions of positive flexure is neglected in developing the continuity relationships in the refined method.

The total continuity moment and corresponding plastic rotation must fall on the moment-rotation curve for the cross-section at each location where yielding is assumed to occur. The nominal moment-rotation curve taken from *AASHTO LRFD* Article B6.6.2 and shown below in Figure 6.5.6.6.4-1 may be used in the analysis when the restrictions of *AASHTO LRFD* Article B6.2 are satisfied. The development of this curve is discussed in Barth et al. (2004) and White et al. (1987).

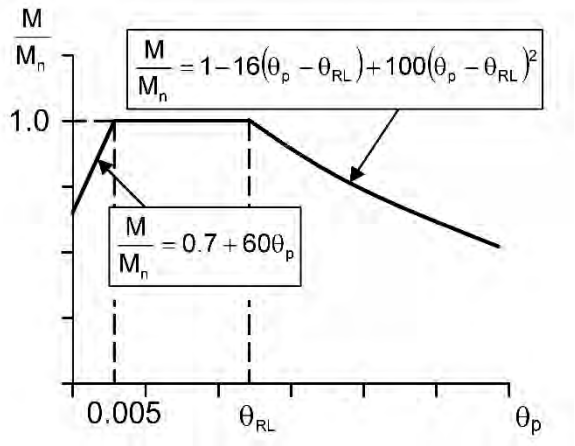

Figure 6.5.6.6.4-1 Nominal Moment-Rotation Curve for Interior-Pier Sections Satisfying *AASHTO LRFD* Article B6.2

where:

θ_p = plastic rotation at the interior-pier section (radians)

θ_{RL} = plastic rotation at which the interior-pier section moment nominally begins to decrease with increasing θ_p determined as shown below (radians)

M = bending moment about the major-axis of the cross-section due to the appropriate factored loads (kip-in.)

M_n = nominal flexural resistance of the interior-pier section taken as the smaller of $F_{nc}S_{xc}$ and $F_{nt}S_{xt}$, with F_{nc} and F_{nt} determined as specified in *AASHTO LRFD* Article 6.10.8. For sections with compact or noncompact webs, M_n may be taken as the smaller of M_{nc} and M_{nt} determined as specified in *AASHTO LRFD* Appendix A6 (kip-in.). For load combinations that induce significant flange lateral bending, deduct the larger of $\frac{1}{3}f_\ell S_{xc}$ or $\frac{1}{3}f_\ell S_{xt}$ from the above values for M_n.

f_ℓ = lateral bending stress in the flange under consideration at the interior-pier section (ksi). For continuously braced flanges, f_ℓ is to be taken as zero.

For interior-pier sections satisfying the requirements of *AASHTO LRFD* Article B6.5.1 in order to provide enhanced moment-rotation characteristics, θ_{RL} is to be taken as follows:

$$\theta_{RL} = 0.137 - 0.143\frac{b_{fc}}{t_{fc}}\sqrt{\frac{F_{yc}}{E}} - 0.0216\frac{D}{b_{fc}} + 0.0241\frac{D}{b_{fc}}\frac{b_{fc}}{t_{fc}}\sqrt{\frac{F_{yc}}{E}}$$

Equation 6.5.6.6.4-2

AASHTO LRFD Equation B6.6.2-1

Otherwise, θ_{RL} is to be taken as:

$$\theta_{RL} = 0.128 - 0.143\frac{b_{fc}}{t_{fc}}\sqrt{\frac{F_{yc}}{E}} - 0.0216\frac{D}{b_{fc}} + 0.0241\frac{D}{b_{fc}}\frac{b_{fc}}{t_{fc}}\sqrt{\frac{F_{yc}}{E}}$$

Equation 6.5.6.6.4-3

AASHTO LRFD Equation B6.6.2-2

As specified in *AASHTO LRFD* Article B6.6.1, the nominal moment-rotation curve in Figure 6.5.6.6.4-1 is to be multiplied by the resistance factor for flexure ϕ_f specified in *AASHTO LRFD* Article 6.5.4.2 in applying the refined method at the strength limit state. At the service limit state, the nominal moment-rotation curve is to be used. *AASHTO LRFD* Article B6.6.2 permits the use of other moment-rotation curves in lieu of the curve given in Figure 6.5.6.6.4-1, as long as all potential factors influencing the moment-rotation characteristics within the restrictions given by *AASHTO LRFD* Article B6.2 are considered.

By setting the appropriate continuity relationship equal to the selected moment-rotation relationship at each pier assumed to be undergoing plastic rotation, a set of simultaneous equations results. These equations can be solved to yield the continuity moments and plastic rotations at those piers. In some cases, iteration may be required in order to arrive at a solution. Once the plastic rotations have been determined, the redistribution moments at the piers can be determined from the corresponding continuity relationship. For example, in the preceding three-span example, the redistribution moment at Pier 1 would be taken equal to the sum of the last two terms in Equation 6.5.6.6.4-1. The redistribution moments at all locations other than at interior piers can then be determined in the same manner as discussed

previously for the service limit state (*AASHTO LRFD* Article B6.4.2.2 – refer to Figure 6.5.6.6.3.2-1).

AASHTO LRFD Article B6.6.1 states that sections adjacent to interior piers satisfy the requirements of *AASHTO LRFD* Article B6.3.2.1 at the service limit state and *AASHTO LRFD* Article B6.4.1.1 at the strength limit state after the redistribution moments are calculated. As specified in *AASHTO LRFD* Article B6.3.2.1, after the redistribution moments are calculated, the service limit state flange-stress limitations of *AASHTO LRFD* Article 6.10.4.2 (Section 6.5.4.3.2.1) are not to be checked within the regions extending in each adjacent span from interior-pier sections satisfying the restrictions of *AASHTO LRFD* Article B6.2 to the nearest flange transition or point of permanent-load contraflexure, whichever is closest. This is because the limit-state response is properly accounted for in Equation 6.5.6.6.4-1. The web bend-buckling check (Section 6.5.4.3.2.2) is still required in these regions however and should be based on the elastic moments prior to redistribution. As specified in *AASHTO LRFD* Article B6.4.1.1, after the redistribution moments are calculated, the strength limit state flexural resistance requirements (Section 6.5.6.2) are not to be checked within the unbraced lengths immediately adjacent to interior-pier sections satisfying the restrictions of *AASHTO LRFD* Article B6.2.

At all other locations outside these regions, the applicable provisions of *AASHTO LRFD* Articles 6.10.4.2, 6.10.7.1, 6.10.8.1 or A6.1 (Section 6.5.6) must be checked after the redistribution moments are calculated (*AASHTO LRFD* Article B6.6.1). The redistribution moments are added to the elastic moments due to the appropriate factored loads before the checks are made. As discussed previously, at composite sections in positive flexure where stress calculations are required at the service and/or strength limit states, the redistribution moments are to be added to the DC_2 and DW (if present) moments and the corresponding flexural stresses in the steel section calculated using the long-term composite section (i.e. using a modular ratio of 3*n*), as specified in *AASHTO LRFD* Article B6.6.1.

6.5.7 LRFD Strength Limit State Design for Shear

6.5.7.1 General

The algebraic sum of the applied loads and reactions on either side of the transverse cross-section of a girder is the shear force, *V*, at that section. Shear can only occur in the presence of bending, but is usually considered independent of bending in design practice (note that this discussion only deals with shear due to bending and not shear caused by torsion, which is discussed in Section 6.4.8). *V* is resisted by internal shear stresses that are maximum on horizontal and vertical planes passing through the neutral axis of the section. The elastic flexural shear stress, f_v, is given by the following fundamental equation:

$$f_v = \frac{VQ}{It}$$ Equation 6.5.7.1-1

where:

I = moment of inertia of the section about the strong axis (in.^{4})
Q = first statical moment of the cross-sectional area above the point where the shear stress is calculated taken about the neutral axis of the cross-section (in.^{3})
t = thickness of the girder where the shear stress is calculated (in.)

The distribution of elastic flexural shear stresses through the depth of an I-section is shown in Figure 6.5.7.1-1. The distribution of these stresses in a closed box section was shown previously in Figure 6.4.8.3.1-3 Part D. Note that in both cases the shear stress in the flanges is generally small and is typically ignored (unless perhaps if the thickness of a box flange is equal to or only larger than the thickness of the web, it may be prudent to consider the flexural shear flow in the design of the box flange). The variation in the shear stress in the web is also small so the shear stress in the web may be approximated as an average shear stress equal to the shear force divided by the web area, or V/Dt_w. Shear forces resisted in this manner are typically referred to as shears carried by beam action.

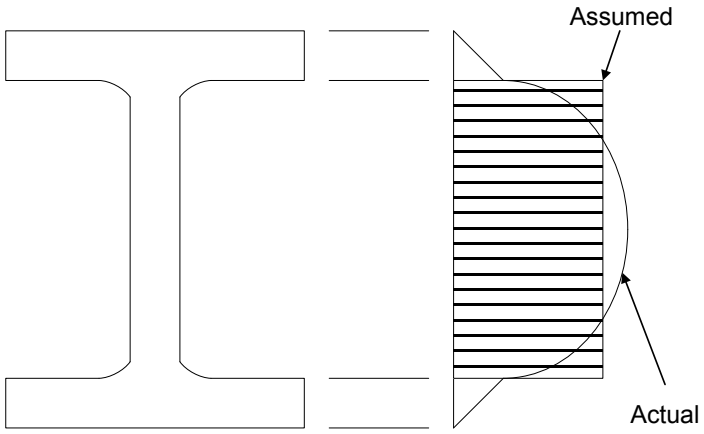

Figure 6.5.7.1-1 Distribution of Elastic Flexural Shear Stresses (I-Section)

The shear force causing yielding in shear is known as the plastic shear force, V_p. The shear yield stress, τ_y, is taken equal to $F_{yw}/\sqrt{3}$. Therefore, V_p is calculated as follows:

$$V_p = \frac{F_{yw}}{\sqrt{3}} Dt_w = 0.58 F_{yw} Dt_w$$ Equation 6.5.7.1-2

AASHTO LRFD Equation 6.10.9.2-2

Deflections due to shear are typically much smaller than bending deflections and usually do not need to be considered, except for beams with large depth-to-length ratios.

The vertical shear force in composite girders is assumed resisted by the web of the steel girder. The horizontal shear force per unit length, *VQ*/*I*, where *I* is the moment of inertia of the transformed composite section, that develops during bending of the girder (sometimes referred to as shear flow) must be transferred between the deck and girder by shear connectors to prevent slip along the concrete/steel interface. This facilitates composite action between the girder and the deck. The design of shear connectors for this horizontal shear flow is discussed in Section 6.6.2. Flange-to-web welds are also typically designed for the horizontal shear flow.

Webs must satisfy the following relationship at the strength limit state:

$$V_u \le \phi_v V_n \qquad \text{Equation 6.5.7.1-3}$$

AASHTO LRFD Equation 6.10.9.1-1

where:

V_n = nominal shear resistance (kips)
V_u = factored shear in the web at the section under consideration (kips)

The resistance factor for shear, ϕ_v, is to be taken as 1.0, as specified in *AASHTO LRFD* Article 6.5.4.2.

The nominal shear resistance, V_n, depends on if the web is considered stiffened or unstiffened. The maximum transverse stiffener spacing requirements that determine whether or not a web is considered stiffened or unstiffened are a function of the web depth, *D*. *AASHTO LRFD* Article 6.10.9.1 specifies that interior web panels of non-hybrid (homogeneous) and hybrid members: 1) without a longitudinal stiffener and with a transverse stiffener spacing not exceeding 3*D*; or 2) with one or more longitudinal stiffeners and with a transverse stiffener spacing not exceeding 1.5*D* are considered stiffened (Figure 6.5.7.1-2 Part A). Otherwise, the panel is considered unstiffened. An interior web panel is defined as a panel not adjacent to the discontinuous end of a girder.

Stiffened web panels are able to develop post-buckling shear resistance (Section 6.5.7.3). The shear resistance of unstiffened webs is limited to the shear-yield or shear-buckling resistance, V_{cr} (Section 6.5.7.2). The spacing of transverse stiffeners for end panels of stiffened webs, with or without a longitudinal stiffener must not exceed 1.5*D* (Figure 6.5.7.1-2 Part B). The shear resistance of end panels is limited

to V_{cr}. An end panel is defined as a panel adjacent to the discontinuous end of a girder.

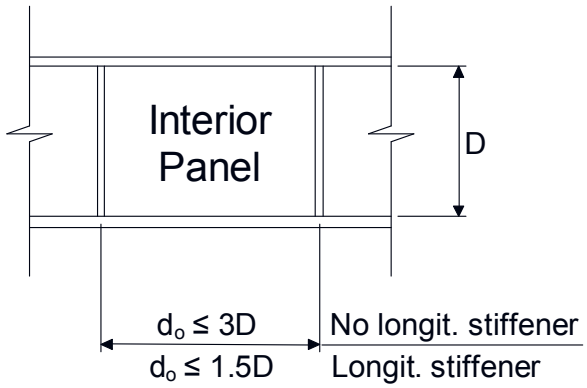

Part A

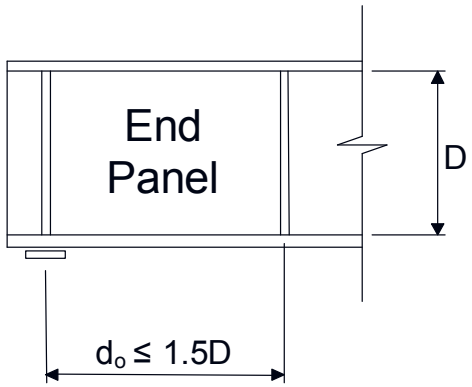

Part B

Figure 6.5.7.1-2 Maximum Transverse Stiffener Spacing Requirements A) Interior Panel with or without Longitudinal Web Stiffeners; B) End Panel

Since longitudinal stiffeners divide a web panel into subpanels, the shear resistance of the entire panel could potentially be taken as the sum of the shear resistances of the subpanels. Although a longitudinal stiffener located at its optimum position on the web for flexure also increases the buckling resistance of the web in shear, the increase is relatively small compared to the increase in the bend-buckling resistance resulting from the longitudinal stiffener(s). Therefore, the specifications conservatively neglect the influence of the longitudinal stiffener in computing the nominal shear resistance of the web; that is, the total web depth, *D*, is used in computing the shear resistance.

A flowchart for shear design is given in *AASHTO LRFD* Figure C6.10.9.1-1. This flowchart applies for both hybrid and non-hybrid I- and box girders, and to both

straight and horizontally curved girders. In the *AASHTO LRFD* Specifications, shear design is identical for both straight and horizontally curved girders.

6.5.7.1.1 I-Sections

Shear design provisions for I-section flexural members at the strength limit state are covered in *AASHTO LRFD* Article 6.10.9. The design of transverse web stiffeners for I-sections is covered in *AASHTO LRFD* Article 6.10.11.1 and discussed in Section 6.6.6.2.

6.5.7.1.2 Box Sections

Shear design provisions for box-section flexural members at the strength limit state are covered in *AASHTO LRFD* Article 6.11.9. For determining the factored shear resistance of a single web of a box section, *AASHTO LRFD* Article 6.11.9 essentially refers back to the provisions of *AASHTO LRFD* Article 6.10.9 for I-sections (with a few exceptions as discussed further in the following).

For box sections with inclined webs, the web must be designed for the component of the vertical shear in the plane of the web according to *AASHTO LRFD* Article 6.11.9. That is, each web must be designed for a factored shear, V_{ui}, taken as follows:

$$V_{ui} = \frac{V_u}{\cos\theta} \qquad \text{Equation 6.5.7.1.2-1}$$

AASHTO LRFD Equation 6.11.9-1

where:

V_u = vertical shear due to the factored loads on one inclined web (kips)
θ = angle of inclination of the web plate to the vertical (degrees)

Box-section webs are usually detailed to be of equal height. However, if the deck is superelevated, the box is typically rotated to match the deck slope, which simplifies fabrication by maintaining symmetry of the box sections. However, rotating the box increases the inclination angle of the web over what it would have been if the box were not rotated. In such cases, consideration should be given to adjusting the vertical shear in that web accordingly.

Also, according to *AASHTO LRFD* Article 6.11.9, for all box sections in bridges outside the special restrictions discussed in *AASHTO LRFD* Article 6.11.2.3 (which includes all box sections in skewed and/or curved bridges), V_u is to be taken as the sum of the flexural and St. Venant torsional shears. Proper determination of this value considers coincident flexure and torsion. Conservatively, critical torsion and critical flexural shears can be added. In these cases, the dead and live load shears in one web are greater than in the other web at the same cross-section since the

torsional shear is of opposite sign in the two webs. For practical reasons, however, both webs are usually detailed for the critical shear. Shears in the web due to warping torsion and due to cross-section distortion may be ignored in all cases, as indicated in *AASHTO LRFD* Article C6.11.9.

In computing the nominal shear resistance, V_n, and the maximum transverse stiffener spacing requirements for the case of inclined webs, the web depth, *D,* must be taken as the depth of the web measured along the slope, or $D/\cos\theta$.

AASHTO LRFD Article 6.11.9 specifies that for box flanges, b_{fc} or b_{ft} in Equation 6.5.7.3-3 (Section 6.5.7.3), as applicable, is to be taken as one-half the effective flange width between webs, but not to exceed $18t_f$, where t_f is the thickness of the box flange. The effective flange width is determined as specified in *AASHTO LRFD* Article 6.11.1.1 (Section 6.3.5.5.3).

The design of transverse web stiffeners for box sections is covered in *AASHTO LRFD* Article 6.10.11.1 and discussed in Section 6.6.6.2.

6.5.7.2 Shear-Buckling (or Shear-Yield) Resistance, V_{cr}

Consider a theoretically flat web panel hypothetically subjected to pure shear, as shown in Figure 6.5.7.2-1 Part A. The length of the panel between transverse stiffeners is d_o, and the clear height of the panel between flanges is *D*. As shown in Figure 6.5.7.2-1 Part B and Figure 6.5.7.2-1 Part C, an element in pure shear is equivalent to an element rotated 45 degrees and acted upon by a principal tensile stress and an equal principal compressive stress acting in the perpendicular direction.

Assume then that the web will buckle in shear perpendicular to the direction of the principal compressive stress. The panel, if properly supported around the edges, does not fail at this point unless the stress is well above the proportional limit. The buckled plate is able to support the diagonal compression through beam action since unrestrained out-of-plane deflection of the panel is prevented by the diagonal tension. For web panels with significant post-buckling resistance (Section 6.5.7.3), it is assumed that the diagonal compression retains the value of beam action shear resistance it had when the plate buckled all the way up to complete failure.

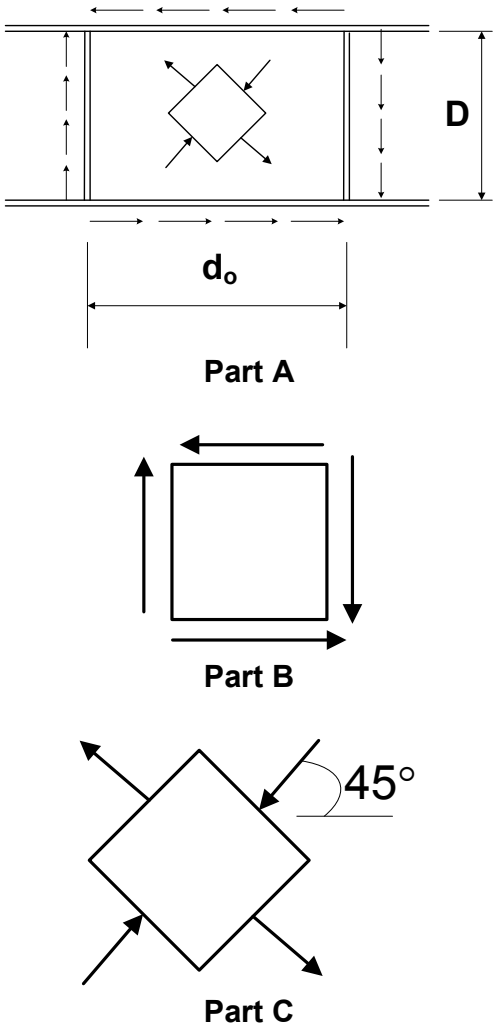

Figure 6.5.7.2-1 A) Web Panel Subjected to Pure Shear; B) Web Element Subject to Pure Shear; C) Equivalent Principal Stresses

The elastic buckling stress of a flat plate subject to pure shear is given as follows (Timoshenko and Gere, 1961):

$$\tau_{cr} = \frac{k\pi^2 E}{12\left(1-\mu^2\right)\left(D/t_w\right)^2} \qquad \text{Equation 6.5.7.2-1}$$

The shear-buckling coefficient, *k*, is dependent on the web plate boundary conditions, such as fixed, simply supported, or free edge. Assuming simply supported boundary conditions along the edges, which is the typical assumption

used in design practice (including in the *AASHTO LRFD* Specifications), *k* is given as (Timoshenko and Gere, 1961):

$$\text{For } \frac{d_o}{D} \le 1: \quad k = 4.0 + \frac{5.34}{\left(\frac{d_o}{D}\right)^2} \qquad \text{Equation 6.5.7.2-2}$$

$$\text{For } \frac{d_o}{D} > 1: \quad k = \frac{4.0}{\left(\frac{d_o}{D}\right)^2} + 5.34 \qquad \text{Equation 6.5.7.2-3}$$

Equation 6.5.7.2-2 and Equation 6.5.7.2-3 have been consolidated into a single simplified expression for *k* in the *AASHTO LRFD* Specifications, which is independent of the panel aspect ratio, as follows:

$$k = 5 + \frac{5}{\left(\frac{d_o}{D}\right)^2} \qquad \text{Equation 6.5.7.2-4}$$

AASHTO LRFD Equation 6.10.9.3.2-7

It can be seen from the preceding equation that decreasing the transverse stiffener spacing increases the value of *k*. This, in turn, also increases V_{cr}. For an unstiffened web, *k* is taken equal to 5.0, which is a conservative approximation of the exact value of *k* = 5.34 for an infinitely long strip with simply supported edges (Timoshenko and Gere, 1961).

For design, Equation 6.5.7.2-1 is expressed in non-dimensional form by introducing the constant, *C*, which is defined as the ratio of the shear buckling stress, τ_{cr}, to the shear yield stress, τ_y. Therefore, substituting ν = 0.3 in Equation 6.5.7.2-1 gives:

$$C = \frac{\tau_{cr}}{\tau_y} = \frac{k\pi^2 E\sqrt{3}}{F_{yw}(12)(1-0.91)(D/t_w)^2} = \frac{1.57}{\left(\frac{D}{t_w}\right)^2}\left(\frac{Ek}{F_{yw}}\right) \qquad \text{Equation 6.5.7.2-5}$$

AASHTO LRFD Equation 6.10.9.3.2-6

which is given as *AASHTO LRFD* Equation 6.10.9.3.2-6.

As is the case for lateral-torsional buckling and flange local buckling, residual stresses and geometric imperfections can cause inelastic buckling in shear as the critical stress approaches the yield stress. A transition curve for inelastic buckling was developed by Basler (1961) based on the assumption that $\tau_{cr} = \sqrt{0.8\tau_y \tau_{cr}}$. That is, it was assumed that the proportional limit for shear is $0.8\tau_y$, which is higher than for flanges in compression because the effect of residual stresses is less for shear. Therefore, dividing τ_{cr} under the preceding radical by τ_y to obtain *C*, and substituting the value of *C* from Equation 6.5.7.2-5 gives:

$$C = \sqrt{0.8C} = \sqrt{0.8\frac{1.57}{\left(\frac{D}{t_w}\right)^2}\left(\frac{Ek}{F_{yw}}\right)} = \frac{1.12}{\frac{D}{t_w}}\sqrt{\frac{Ek}{F_{yw}}} \qquad \text{Equation 6.5.7.2-6}$$

AASHTO LRFD Equation 6.10.9.3.2-5

which is given as *AASHTO LRFD* Equation 6.10.9.3.2-5. When *C* exceeds 0.8, *C* is taken from Equation 6.5.7.2-6. Therefore, substituting a *C* value of 0.8 in Equation Equation 6.5.7.2-5 and solving for D/t_w gives $D/t_w = 1.40\sqrt{Ek/F_{yw}}$ above which *C* is calculated from Equation 6.5.7.2-6, and at or below which *C* is calculated from Equation 6.5.7.2-5.

When *C* is equal to 1.0, the shear resistance is equal to the shear yield stress. Therefore, substituting a *C* value of 1.0 into Equation 6.5.7.2-6 and solving for D/t_w gives $D/t_w = 1.12\sqrt{Ek/F_{yw}}$ below which *C* is taken equal to 1.0 and shear yielding controls; that is, V_{cr} is taken equal to the shear-yield resistance or the plastic shear force, V_p.

The relationship between the buckling strength in shear and the web slenderness ratio, D/t_w, based on the preceding equations for the constant *C*, is shown graphically in Figure 6.5.7.2-2. Note that as the web slenderness increases, the shear resistance decreases.

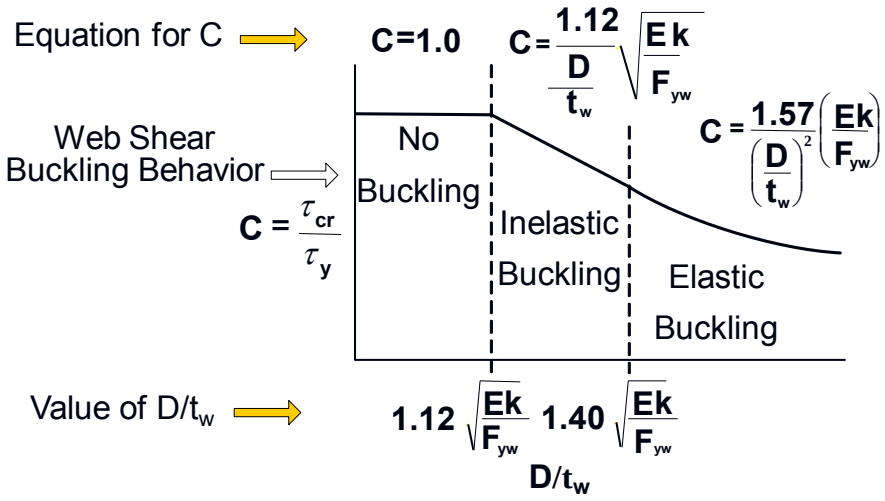

Figure 6.5.7.2-2 Web Shear Buckling Resistance – the Constant C

The nominal shear resistance of the girder based on shear buckling (elastic or inelastic) or shear yielding can be computed as:

$$V_n = V_{cr} = \tau_{cr} D t_w \qquad \text{Equation 6.5.7.2-7}$$

Substituting $C = \tau_{cr}/\tau_y$ gives:

$$V_n = V_{cr} = C\tau_y D t_w = CV_p \qquad \text{Equation 6.5.7.2-8}$$

AASHTO LRFD Equation 6.10.9.2-1

6.5.7.3 Post-Buckling Shear Resistance (Tension-Field Action)

A web plate stiffened adequately by flanges and transverse stiffeners can carry shear forces considerably greater than its shear buckling resistance; that is, the panel has considerable post-buckling shear resistance. After the web buckles, the girder acts in a manner similar to a Pratt truss with part of each web panel acting as a diagonal tension member carrying the tension forces by membrane action of the web (so-called tension-field action), with the compression forces carried by the transverse stiffeners in conjunction with the adjacent portions of the web (Figure 6.5.7.3-1). The ability of a plate girder to carry shear in the post-buckling range by truss action was recognized as early as 1898 (Basler, 1961). Early applications of the diagonal tension-field theory were primarily in the aircraft industry where strength-to-weight ratios are critical factors and thin metal construction is employed.

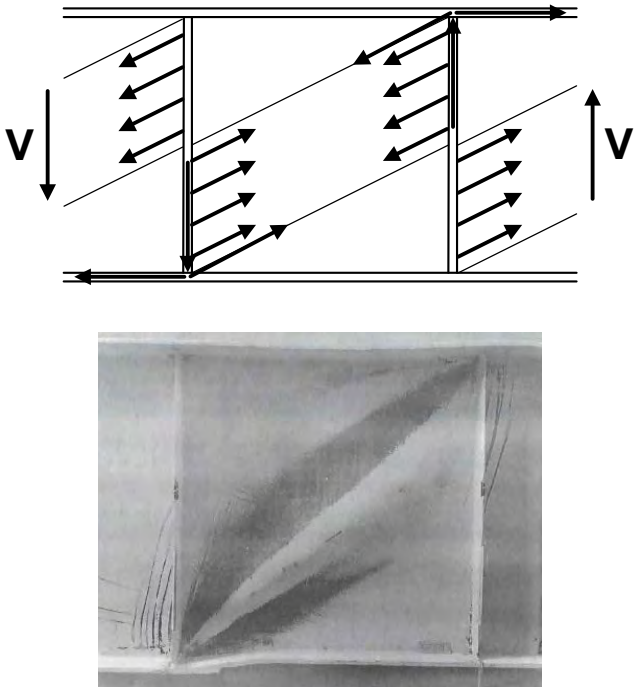

Figure 6.5.7.3-1 Web Post-Buckling Shear Resistance – Tension-Field Action

As mentioned in Section 6.5.7.2, it is assumed that the diagonal compression retains the value of beam action shear resistance it had when the plate first buckles all the way up to complete failure. Therefore, the nominal shear resistance for post buckling can be computed by summing the contributions of beam action, V_{cr}, and tension-field action, V_{tf}.

The development of V_{tf} has been the subject of numerous research studies worldwide and many different theories have been espoused. An in-depth discussion of all these theories or even the development of the classical value of V_{tf} as developed by Basler (Salmon and Johnson, 1996; McGuire, 1968; Basler, 1961), which is still used in many design specifications including the *AASHTO LRFD* Specifications, is beyond the scope of this document. The Basler formulation, which neglects any contribution of the flanges in resisting the diagonal tensile stresses, and conservatively assumes that the angle of the diagonal tension field is at 45 degrees from the horizontal, results in the following expression for V_{tf}:

$$V_{tf} = \frac{0.87V_p(1-C)}{\sqrt{1+\left(\frac{d_o}{D}\right)^2}} \qquad \text{Equation 6.5.7.3-1}$$

Therefore, the total nominal shear resistance can be written as:

$$V_n = V_p\left[C + \frac{0.87(1-C)}{\sqrt{1+\left(\frac{d_o}{D}\right)^2}}\right] \qquad \text{Equation 6.5.7.3-2}$$

AASHTO LRFD Equation 6.10.9.3.2-2

Previous specifications included a moment-shear interaction relationship for web panels subject to tension-field action. According to this relationship, the bending and shear resistance of web panels subject simultaneously to both high shear and bending stresses was reduced due to the yielding that could potentially occur under the action of the combined stresses. Relatively recent research (White et al., 2004) has led to the removal of this relationship in the *AASHTO LRFD* Specifications. Instead, web panels with the entire section along the panel proportioned to satisfy the following criterion:

$$\frac{2Dt_w}{(b_{fc}t_{fc} + b_{ft}t_{ft})} \le 2.5 \qquad \text{Equation 6.5.7.3-3}$$

AASHTO LRFD Equation 6.10.9.3.2-1

are assumed able to develop the full post-buckling shear resistance due to tension-field action given by Equation 6.5.7.3-2. If Equation 6.5.7.3-3 is satisfied, along with the requirement on the cross-section aspect ratio given by Equation 6.3.4.4.2-1, and if the maximum moment within the web panel is used to check the flexural resistance, then it is felt that the shear resistance equations given in the specification adequately reflect the majority of the available experimental test results without the need to consider moment-shear interaction effects. The moment-shear interaction relationship was not originally developed to handle the effect of moving loads. Although maximum moment and shear envelope values were typically used to check this relationship, these values generally were not caused by concurrent loadings, which added a level of conservatism. Determining the most critical combination of concurrent moment and shear to check this relationship was not practical. In addition, the anchorage of the tension field and additional shear resistance provided by the composite concrete deck is conservatively neglected in all the shear resistance equations.

If Equation 6.5.7.3-3 is not satisfied, the total area of the flanges within the panel is small relative to the area of the web and the full post-buckling resistance generally

cannot be developed. Rather than reducing the shear resistance to V_{cr}, it was felt to be conservative to use a reduced level of the post-buckling shear resistance as shown in the following equation (Salmon and Johnson, 1996):

$$V_n = V_p\left[C + \frac{0.87(1-C)}{\sqrt{1+\left(\frac{d_o}{D}\right)^2}+\frac{d_o}{D}}\right] \qquad \text{Equation 6.5.7.3-4}$$

AASHTO LRFD Equation 6.10.9.3.2-8

which is given as *AASHTO LRFD* Equation 6.10.9.3.2-8. The extra d_o/D term in the denominator reflects the solution that neglects the shear contribution within the wedges outside of the tension band that was implicitly included by Basler in the development of Equation 6.5.7.3-2.

Another development also incorporated in the *AASHTO LRFD* Specifications is the extension of the post-buckling shear resistance due to tension-field action to webs of hybrid girders (White et al., 2004; White and Barker, 2004; Jung and White, 2006). In previous specifications, the shear resistance of hybrid girder webs was conservatively limited to V_{cr} given by Equation 6.5.7.2-8.

Equation 6.5.7.3-2 and Equation 6.5.7.3-4 are applied to stiffened interior web panels. End panels, adjacent to a discontinuous end of a girder, are not permitted to develop any post-buckling resistance. Instead, the shear resistance of these panels is limited to V_{cr} (Equation 6.5.7.2-8) in order to provide a sufficient anchor for the development of the tension field in the immediately adjacent interior panels; that is, to absorb any imbalance of the computed horizontal component of the diagonal tension stress in the adjacent panels. In determining V_{cr} for the end panel, the shear buckling coefficient, k, is to be calculated from Equation 6.5.7.2-4 based on the spacing from the discontinuous end of the girder to the first transverse stiffener adjacent to that end, which cannot exceed $1.5D$.

6.5.7.4 Shear Design Requirements

6.5.7.4.1 Unstiffened Webs

The nominal shear resistance, V_n, of nonhybrid and hybrid unstiffened webs is specified in *AASHTO LRFD* Article 6.10.9.2. The nominal shear resistance is limited to the shear-buckling (or shear-yield) resistance, V_{cr}, which was derived in Section 6.5.7.2 and is given by Equation 6.5.7.2-8. Consideration of post-buckling shear resistance due to tension-field action is not permitted for unstiffened webs.

The shear buckling coefficient, k, is to be taken as 5.0 in calculating the appropriate value of the constant C for an unstiffened web (from Equation 6.5.7.2-5 or Equation 6.5.7.2-6, as applicable). When C is equal to 1.0, the nominal shear resistance is controlled by shear yielding. The plastic shear force, V_p, for use in Equation 6.5.7.2-8 is calculated from Equation 6.5.7.1-2. For special considerations related to the determination of the shear resistance of box-section webs, refer to Section 6.5.7.1.2.

In determining whether or not transverse stiffeners are required at a particular section, the Design Engineer will first have to determine the nominal shear resistance of the web, assuming it is unstiffened, to determine if it is less than the factored shear in the web at that section. If so, transverse stiffeners are required. Note that cross-frame/diaphragm connection plates can be considered to act as transverse stiffeners as long as they satisfy the proportioning requirements for transverse stiffeners discussed in Section 6.6.6.2.

6.5.7.4.2 Stiffened Webs

The nominal shear resistance, V_n, of non-hybrid and hybrid stiffened webs is specified in *AASHTO LRFD* Article 6.10.9.3. Requirements for interior web panels are given in *AASHTO LRFD* Article 6.10.9.3.2 and requirements for end panels are given in *AASHTO LRFD* Article 6.10.9.3.3. The maximum factored shear in the panel is to be used to determine the required stiffener spacing, which cannot exceed the maximum values stated in Section 6.5.7.1. The total web depth, D, is to be used in determining the nominal shear resistance of web panels with longitudinal stiffeners (i.e. the influence of the longitudinal stiffener is conservatively neglected). For special considerations related to the determination of the shear resistance of box-section webs, refer to Section 6.5.7.1.2.

6.5.7.4.2.1 Interior Panels

Stiffened interior web panels of both non-hybrid and hybrid sections are capable of developing post-buckling shear resistance due to tension-field action. As discussed previously in Section 6.5.7.3, in order to develop the full post-buckling resistance, the section along the entire panel must be proportioned to satisfy the relationship given by Equation 6.5.7.3-3.

The nominal shear resistance may be taken as the shear yielding resistance or the sum of the shear bucking resistance and the full post-buckling shear resistance (Equation 6.5.7.3-2) if the web-to-flange area ratio given by Equation 6.5.7.3-3 is satisfied everywhere within the panel. If Equation 6.5.7.3-3 is not satisfied, the total area of the flanges is small relative to the area of the web within the panel such that it is assumed that the full post-buckling resistance cannot be developed. In such cases, V_n is to be based on the available (or reduced) post-buckling resistance

(Equation 6.5.7.3-4) in lieu of limiting V_n to V_{cr}. The calculation of the constant C for use in Equation 6.5.7.3-2 or Equation 6.5.7.3-4, as applicable, is to be based on the shear buckling coefficient, k, given by Equation 6.5.7.2-4, which is a function of the transverse stiffener spacing, d_o.

6.5.7.4.2.2 End Panels

End panels of stiffened webs, or the panels immediately adjacent to wherever the girder is discontinuous, are not permitted to develop any post-buckling shear resistance. The shear resistance of these panels is instead limited to V_{cr} (Equation 6.5.7.2-8) in order to provide a sufficient anchor for the development of the tension field in the immediately adjacent interior panels. The shear buckling coefficient, k, used to compute the constant C in this case is to be calculated based on the spacing from the discontinuous end of the girder to the first transverse stiffener adjacent to that end.

EXAMPLE

Given the shears due to the factored dead plus live loads, V_u, for the Strength I load combination shown in Figure 6.5.7.4.2.2-1, which are for an interior girder, determine the required transverse stiffener spacing in Field Section 1. The web in Field Section 1 is ½" x 69". The example bridge is a three-span continuous bridge (the shears for half the bridge are shown in Figure 6.5.7.4.2.2-1). The bridge is symmetrical about the longitudinal centerline.

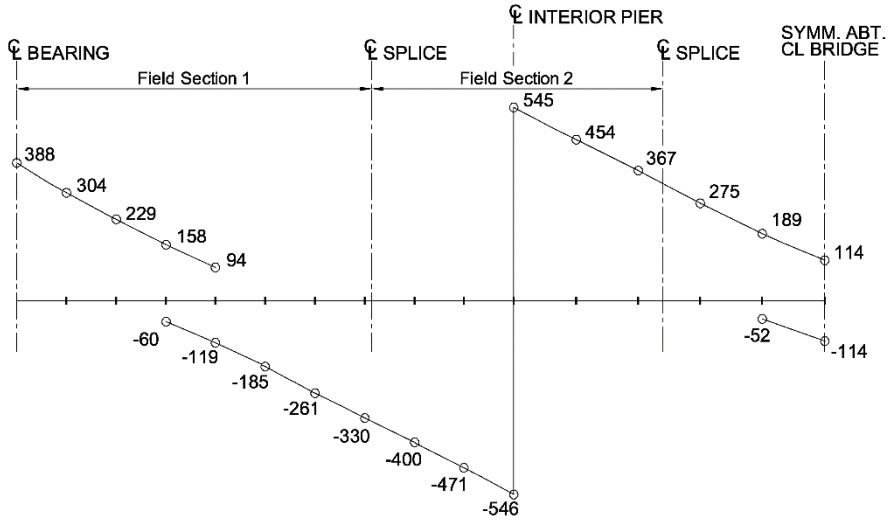

Figure 6.5.7.4.2.2-1 Example Problem Shears due to the Factored Loads – Strength I

First, to determine the regions where transverse stiffeners are required, calculate the nominal shear resistance of an unstiffened web. According to *AASHTO LRFD* Article 6.10.9.2, the nominal shear resistance of an unstiffened web is limited to the shear yielding or shear buckling resistance, V_{cr}, determined as (Equation 6.5.7.2-8):

$$V_n = V_{cr} = CV_p$$

C is the ratio of the shear buckling resistance to the shear yield strength determined from *AASHTO LRFD* Equation 6.10.9.3.2-4, 6.10.9.3.2-5 or 6.10.9.3.2-6, as applicable, with the shear buckling coefficient, *k*, taken equal to 5.0 for unstiffened webs.

Since,

$$1.40\sqrt{\frac{Ek}{F_{yw}}} = 1.40\sqrt{\frac{29{,}000(5.00)}{50}} = 75.4 < \frac{D}{t_w} = \frac{69.0}{0.5} = 138.0$$

$$C = \frac{1.57}{\left(\frac{D}{t_w}\right)^2}\left(\frac{Ek}{F_{yw}}\right) \text{ (Equation 6.5.7.2-5)}$$

$$C = \frac{1.57}{(138.0)^2}\left(\frac{29{,}000(5.0)}{50}\right) = 0.239$$

V_p is the plastic shear force determined as follows (Equation 6.5.7.1-2):

$$V_p = 0.58F_{yw}Dt_w$$

$$V_p = 0.58(50)(69.0)(0.5) = 1{,}001 \text{ kips}$$

Therefore,

$$V_n = V_{cr} = 0.239(1{,}001) = 239 \text{ kips}$$

$$\phi_v V_n = 1.0(239) = 239 \text{ kips}$$

Thus, transverse stiffeners are required in Field Section 1 wherever V_u exceeds $\phi_v V_n$ = 239 kips.

At the abutment, V_u is equal to 388 kips (Figure 6.5.7.4.2.2-1). Therefore, a transverse stiffener is required. According to *AASHTO LRFD* Article 6.10.9.3.3, the nominal shear resistance of a web end panel is limited to the shear yielding or shear buckling resistance, V_{cr}. First, compute the shear buckling coefficient, k. The transverse stiffener spacing for end panels is not to exceed $1.5D = 1.5(69.0) = 103.5$ inches. Assume the spacing from the abutment to the first transverse stiffener is d_o = 7.25 feet = 87.0 inches. Therefore:

$$k = 5 + \frac{5}{\left(\frac{87.0}{69.0}\right)^2} = 8.15$$

Since, $$1.40\sqrt{\frac{Ek}{F_{yw}}} = 1.40\sqrt{\frac{29{,}000(8.15)}{50}} = 96.3 < \frac{D}{t_w} = \frac{69.0}{0.5} = 138.0$$

$$C = \frac{1.57}{(138.0)^2}\left(\frac{29{,}000(8.15)}{50}\right) = 0.390$$

$$V_p = 0.58(50)(69.0)(0.5) = 1{,}001 \text{ kips}$$

Therefore, $$V_n = V_{cr} = 0.390(1{,}001) = 390 \text{ kips}$$

$$\phi_v V_n = 1.0(390) = 390 \text{ kips} > V_u = 388 \text{ kips} \quad \text{ok}$$

According to *AASHTO LRFD* Article 6.10.9.1, the transverse stiffener spacing for interior panels without a longitudinal stiffener is not to exceed $3D = 3(69.0) = 207.0$ inches. For the first interior panel to the right of the end panel, assume a transverse stiffener spacing of d_o = 16.75 feet = 201.0 inches, which is the distance from the first transverse stiffener to the first intermediate cross-frame in Field Section 1 (assume that the cross-frame connection plate serves as a transverse stiffener). At the first transverse stiffener located d_o = 7.25 feet from the abutment, V_u is equal to 345 kips, which exceeds $\phi_v V_n$ = 239 kips for an unstiffened web. Therefore, an additional transverse stiffener is required.

For interior panels of both nonhybrid and hybrid members with the section along the entire panel proportioned such that (Equation 6.5.7.3-3):

$$\frac{2Dt_w}{(b_{fc}t_{fc} + b_{ft}t_{ft})} \le 2.5$$

the nominal shear resistance is to be taken as the shear yielding resistance or the sum of the shear-buckling resistance and the full post-buckling shear resistance due to tension-field action (Equation 6.5.7.3-2):

$$V_n = V_p\left[C + \frac{0.87(1-C)}{\sqrt{1+\left(\frac{d_o}{D}\right)^2}}\right]$$

Otherwise, the nominal shear resistance is to be based on the reduced post-buckling shear resistance as determined from *AASHTO LRFD* Equation 6.10.9.3.2-8 (Equation 6.5.7.3-4).

For the interior web panel under consideration, the top-flange plate size is 1" x 16" and the bottom-flange plate size is 7/8" x 18". Therefore:

$$\frac{2(69.0)(0.5)}{[16(1.0)+18(0.875)]} = 2.17 < 2.5$$

$$k = 5 + \frac{5}{\left(\frac{201.0}{69.0}\right)^2} = 5.59$$

Since, $$1.40\sqrt{\frac{Ek}{F_{yw}}} = 1.40\sqrt{\frac{29{,}000(5.59)}{50}} = 79.7 < \frac{D}{t_w} = \frac{69.0}{0.5} = 138.0$$

$$C = \frac{1.57}{(138.0)^2}\left(\frac{29{,}000(5.59)}{50}\right) = 0.267$$

$$V_p = 0.58(50)(69.0)(0.5) = 1{,}001 \text{ kips}$$

Therefore, $$V_n = 1{,}001\left[0.267 + \frac{0.87(1-0.267)}{\sqrt{1+\left(\frac{201.0}{69.0}\right)^2}}\right] = 475 \text{ kips}$$

$$\phi_v V_n = 1.0(475) = 475 \text{ kips} > V_u = 345 \text{ kips} \quad \text{ok}$$

V_u at the first intermediate cross-frame in Field Section 1 located 24.0 feet from the abutment is equal to 250 kips, which is greater than $\phi_v V_n$ = 239 kips for an unstiffened web. Therefore, assume a transverse stiffener spacing of d_o = 3D = 17.25 feet = 207.0 inches from the cross frame to the next stiffener.

$$k = 5 + \frac{5}{\left(\frac{207.0}{69.0}\right)^2} = 5.56$$

Since, $$1.40\sqrt{\frac{Ek}{F_{yw}}} = 1.40\sqrt{\frac{29{,}000(5.56)}{50}} = 79.5 < \frac{D}{t_w} = \frac{69.0}{0.5} = 138.0$$

$$C = \frac{1.57}{(138.0)^2}\left(\frac{29{,}000(5.56)}{50}\right) = 0.266$$

$$V_p = 1{,}001 \text{ kips}$$

Therefore, $$V_n = 1{,}001\left[0.266 + \frac{0.87(1-0.266)}{\sqrt{1+\left(\frac{207.0}{69.0}\right)^2}}\right] = 468 \text{ kips}$$

$$\phi_v V_n = 1.0(468) = 468 \text{ kips} > V_u = 250 \text{ kips} \quad \text{ok}$$

V_u at this stiffener is equal to 162 kips, which is less than $\phi_v V_n$ = 239 kips for an unstiffened web. Therefore, no additional transverse stiffeners are required at the left end of Field Section 1.

At the right end of Field Section 1, V_u at the fourth intermediate cross-frame located 96.0 feet from the abutment is equal to 320 kips, which exceeds $\phi_v V_n$ = 239 kips for an unstiffened web. Assume a transverse stiffener spacing of d_o = 3D = 17.25 feet = 207.0 inches to the left of this cross frame. For this panel, the top-flange plate size is 1” x 16” and the bottom-flange plate size is 1-3/8” x 18”. Therefore:

$$\frac{2(69.0)(0.5)}{[16(1.0)+18(1.375)]} = 1.69 < 2.5$$

The nominal shear resistance may be taken as the shear yielding resistance or the sum of the shear bucking resistance and the full post-buckling shear resistance due to tension-field action. As determined above for this stiffener spacing,

$$\phi_v V_n = 1.0(468) = 468 \text{ kips} > V_u = 320 \text{ kips} \quad \text{ok}$$

V_u at this stiffener is equal to 233 kips, which is less than $\phi_v V_n$ = 239 kips for an unstiffened web. Therefore, no additional transverse stiffeners are required at the right end of Field Section 1.

Section 6.6 Design of Detail Items

6.6.1 Introduction

This section of the Manual discusses LRFD design requirements for detail items such as shear connectors, bracing member design (i.e. tension members, compression members, and diaphragms), connections (i.e. bolted connections and welded connections), bolted girder splices, stiffeners (i.e., transverse web stiffeners, bearing stiffeners and longitudinal web stiffeners), and truss gusset plates.

The design of many of these items is particularly important for skewed and/or curved bridges. The load shifting between girders in such bridges due to the torsional effects resulting from curvature and support skew directly affects the design of many of these items and increases their relative importance. These effects must be considered in the design of these items as discussed herein.

6.6.2 Shear Connectors

6.6.2.1 General

The composite action between the deck and steel girders in composite construction is ensured by the use of welded mechanical shear connectors between the girder and the deck (Figure 6.6.2.1-1). The primary function of the shear connectors is to transfer the horizontal shear between the deck and the girder forcing the steel girder and concrete deck to act together as a structural unit by preventing slip along the concrete-steel interface. Shear connectors also help control deck cracking in regions of negative flexure in regions where the deck is subject to tensile stress and also has longitudinal reinforcement present.

The design of shear connectors for I-sections is covered in *AASHTO LRFD* Article 6.10.10. The design of shear connectors for box sections is covered in *AASHTO LRFD* Article 6.11.10.

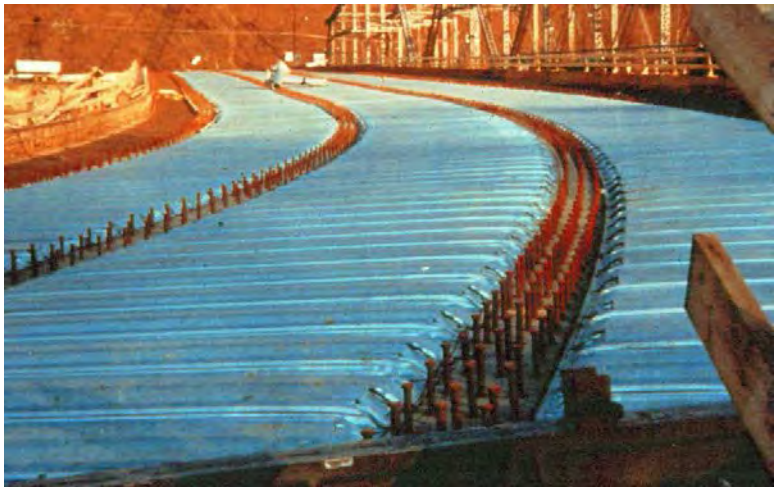

Figure 6.6.2.1-1 Stud Shear Connectors on Steel Girders

The shear connectors must be capable of resisting both horizontal and vertical movement between the concrete deck and the steel, and allow compaction of the concrete around them so that their entire surfaces are in contact with the concrete. Typically, stud shear connectors are used, but channel shear connectors are also permitted and may be designed according to the provisions of *AASHTO LRFD* Article 6.10.10. However, channel shear connectors are not commonly used on modern bridges. Common sizes of studs may be found in manufacturer's catalogs.

6.6.2.2 Layout Requirements

6.6.2.2.1 General

Requirements for the layout of stud shear connectors are discussed in the following. These requirements include such items as the minimum height-to-diameter ratio, transverse spacing and clear distance, cover and penetration and the maximum and minimum pitch. If any of these requirements are not satisfied, then composite action may not be assumed.

6.6.2.2.2 Minimum Height-to-Diameter Ratio

AASHTO LRFD Article 6.10.10.1.1 specifies that the ratio of the height to the diameter of a stud shear connector must be greater than or equal to 4.0 (Figure 6.6.2.2.2-1). The stud height includes the head, but the stud diameter is measured at the shaft rather than the head.

$$\frac{\text{Height}}{\text{Diameter}} \geq 4.0$$

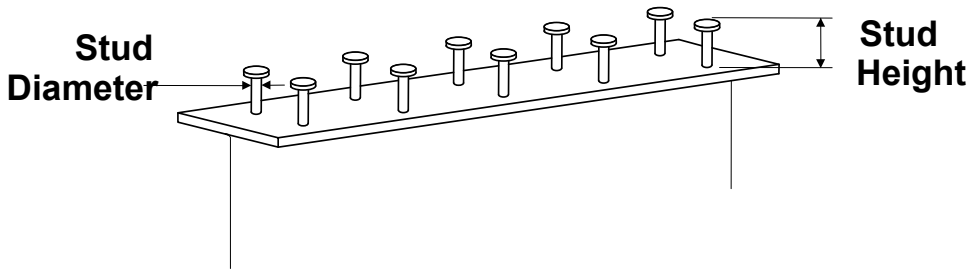

Figure 6.6.2.2.2-1 Minimum Height-to-Diameter Ratio

6.6.2.2.3 Transverse Spacing and Clear Distance

6.6.2.2.3.1 General

AASHTO LRFD Article 6.10.10.1.3 specifies that stud shear connectors are to be spaced no closer than 4.0 stud diameters center-to-center transversely across the top flange(s) of I-sections and tub-girder sections (Figure 6.6.2.2.3.1-1). As also illustrated in Figure 6.6.2.2.3.1-1, the clear distance between the edge of the top flange and the edge of the nearest shear connector is not to be less than 1.0 in.

Transverse Spacing ≥ 4.0 x (Stud Diameter)

Clear Distance ≥ 1.0 Inch

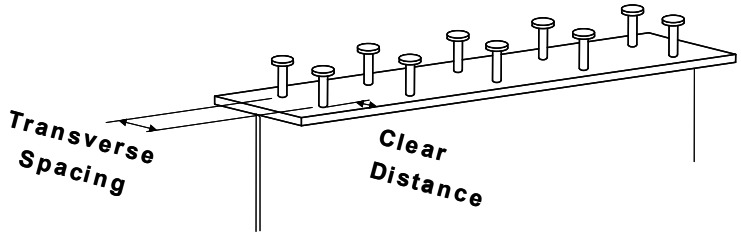

Figure 6.6.2.2.3.1-1 Transverse Spacing and Clear Distance

6.6.2.2.3.2 Closed-Box Sections

Shear connectors for closed-box sections should be uniformly distributed across the width of the top (box) flange to ensure composite action of the entire flange with the concrete. *AASHTO LRFD* Article 6.11.10 specifies that the maximum transverse

spacing, s_t, between shear connectors on composite box flanges of closed-box sections must satisfy the following requirement to help prevent local buckling of the flange plate between connectors when subject to compression:

$$\frac{s_t}{t_f}\sqrt{\frac{F_{yf}}{kE}} \le \lambda_p \qquad \text{Equation 6.6.2.2.3.2-1}$$

AASHTO LRFD Equation 6.11.10-1

where:

k = plate-buckling coefficient for uniform normal stress on box flanges determined as specified in *AASHTO LRFD* Article 6.11.8.2 (Section 6.5.6.3.3.3.2)

λ_p = limiting slenderness ratio for the box flange determined from *AASHTO LRFD* Equation 6.11.8.2.2-9 (Equation 6.5.6.2.4.2.1-8)

6.6.2.2.4 Cover and Penetration

AASHTO LRFD Article 6.10.10.1.4 specifies that the clear depth of concrete cover over the tops of shear connectors must not be less than 2.0 in., and the shear connectors should penetrate at least 2.0 in. into the concrete deck (Figure 6.6.2.2.4-1). Otherwise, the deck haunch should be appropriately reinforced to contain the studs and develop their load in the deck.

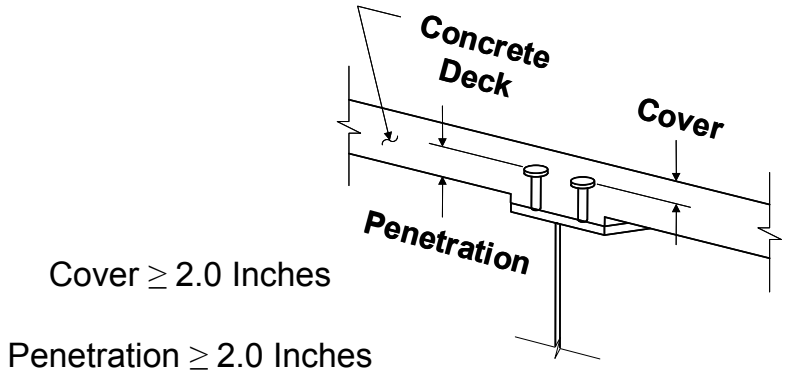

Figure 6.6.2.2.4-1 Cover and Penetration

The Design Engineer should be aware that steep cross-slopes and wide flanges on curved girder bridges may result in little or no haunch above the flange on the low side of the slope if not properly accounted for when setting the initial haunch dimensions.

6.6.2.2.5 Minimum and Maximum Pitch

Shear connectors may be spaced at regular or variable intervals longitudinally along the girder. The longitudinal center-to-center spacing of shear connectors is referred to as the pitch. *AASHTO LRFD* Article 6.10.10.1.2 specifies that the pitch must not exceed 24.0 in., and must not be less than six stud diameters (Figure 6.6.2.2.5-1). As described in more detail below (Section 6.6.2.3), the pitch of the shear connectors is typically determined first to satisfy the fatigue limit state, as specified in *AASHTO LRFD* Article 6.10.10.2 and 6.10.10.3 (as applicable). The resulting number of shear connectors is then checked to ensure that it is not less than the number required to satisfy the strength limit state, as specified in *AASHTO LRFD* Article 6.10.10.4 (Section 6.6.2.4).

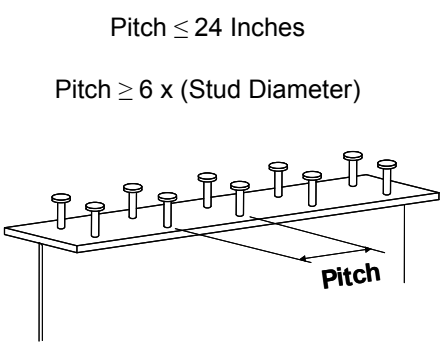

Figure 6.6.2.2.5-1 Minimum and Maximum Pitch

AASHTO LRFD Article 6.10.10.1 specifies that simple-span composite bridges are to have shear connectors provided throughout the length of the span. Straight continuous composite I-girder bridges are to normally be provided with shear connectors throughout the length of the bridge, again to help control cracking in regions of negative flexure, but it is not required. However, if the longitudinal reinforcement in the deck in regions of negative flexure is considered in determining the composite I-section properties in these regions, then shear connectors must also be provided in these regions.

Should shear connectors not be provided in these regions, the longitudinal reinforcement cannot be considered in the computation of the composite section properties. In addition, if shear connectors are omitted in regions of negative flexure in straight I-girder bridges, additional connectors must be placed in the region of the points of permanent load contraflexure according to the provisions of *AASHTO LRFD* Article 6.10.10.3 (Section 6.6.2.3.3), and the longitudinal deck reinforcement must be extended into the positive flexure region beyond the additional connectors a distance not less than the development length specified in Section 5 of the *AASHTO LRFD* Specifications (*AASHTO LRFD* Article 6.10.1.7).

AASHTO LRFD Article 6.10.10.1 further specifies that curved continuous composite bridges must be provided with shear connectors throughout the length of the bridge because torsional shear exists and is developed in the full composite section along the entire bridge (note that the same requirement applies to all types of composite box-girder bridges). For bridges containing one or more curved segments, the effects of curvature usually extend beyond the curved segment. Therefore, it is conservatively specified that shear connectors be provided along the entire length of the bridge in this case as well. As torsional shear also exists along the entire span of straight continuous skewed I-girder bridges and must be developed in the full composite section, consideration should also be given to providing shear connectors along the entire length of these structures.

6.6.2.3 Fatigue Limit State Design

6.6.2.3.1 General

According to the provisions of *AASHTO LRFD* Article 6.10.10.1.2, the pitch of the shear connectors along the longitudinal axis of the girder is to be initially determined to satisfy the fatigue limit state. The resulting number of shear connectors is then to be checked against the number required to satisfy the strength limit state.

The required pitch of the shear connectors at the fatigue limit state is based on the horizontal fatigue live load shear range between the deck and top flange of the girder. In straight girders, if torsion is ignored, the shear range is due only to vertical bending. However, in certain cases, skew can introduce significant torsion. Curvature and other conditions can also introduce torsion. St. Venant torsional shears are significant in certain types of box sections and must be considered in the design of the shear connectors. The shear connector design provisions in the *AASHTO LRFD* Specifications allow for flexural and torsional components of the shear to be considered in these cases and to be added vectorially, as discussed in more detail below.

In addition to determining the required pitch, the base metal at stud welds to flanges subject to net tension must be checked for load-induced fatigue for Detail Category C (*AASHTO LRFD* Table 6.6.1.2.3-1 – Condition 8.1). Refer to *AASHTO LRFD* Article 6.6.1.2 and to Section 6.5.5.2.2.

6.6.2.3.2 Pitch

6.6.2.3.2.1 General

According to *AASHTO LRFD* Article 6.10.10.1.2, the pitch, *p*, of the shear connectors at the fatigue limit state must satisfy the following:

$$p \le \frac{nZ_r}{V_{sr}}$$ Equation 6.6.2.3.2.1-1

AASHTO LRFD Equation 6.10.10.1.2-1

where:

n = number of shear connectors in a cross-section (Figure 6.6.2.3.2.1-1)
V_{sr} = horizontal fatigue shear range per unit length (Equation 6.6.2.3.2.1-2) (kips/in.)
Z_r = fatigue shear resistance of an individual shear connector determined as specified in *AASHTO LRFD* Article 6.10.10.2 (Section 6.6.2.3.2.4) (kips)

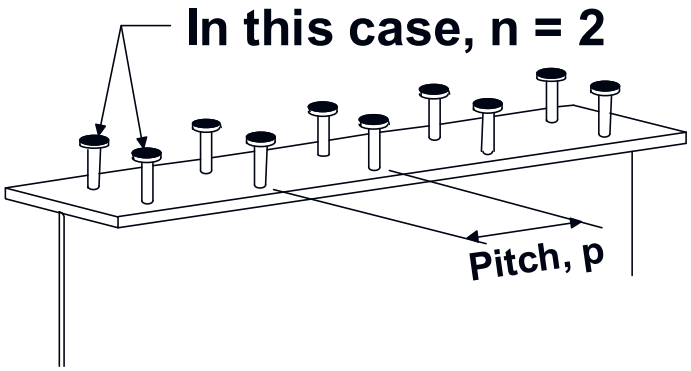

Figure 6.6.2.3.2.1-1 Number of Shear Connectors in a Cross-Section, *n*

The horizontal fatigue shear range per unit length, V_{sr}, is determined as follows:

$$V_{sr} = \sqrt{(V_{fat})^2 + (F_{fat})^2}$$ Equation 6.6.2.3.2.1-2

AASHTO LRFD Equation 6.10.10.1.2-2

where:

V_{fat} = longitudinal fatigue shear range per unit length (Section 6.6.2.3.2.2) (kips/in.)
F_{fat} = radial fatigue shear range per unit length (Section 6.6.2.3.2.3) (kips/in.)

That is, the horizontal shear range is taken as the vectorial sum of the longitudinal and radial fatigue shear ranges.

For curved and/or skewed bridges, it is recommended that V_{sr}, and the resulting pitch, p, for the fatigue limit state, be determined at each cross-frame.

For composite box flanges in closed-box sections, V_{sr} is to be determined as the vector sum of the longitudinal fatigue shear range given by Equation 6.6.2.3.2.2.1-1

(see below) and the torsional fatigue shear range in the concrete deck, in lieu of using Equation 6.6.2.3.2.1-2 (*AASHTO LRFD* Article 6.11.10). According to *AASHTO LRFD* Article C6.11.10, the torsional shear range resisted by the concrete deck can be determined by multiplying the torsional shear range acting on the top of the box section by the ratio of the thickness of the transformed concrete deck to the total thickness of the top flange plus the transformed concrete deck.

6.6.2.3.2.2 Longitudinal Fatigue Shear Range, V_{fat}

6.6.2.3.2.2.1 General

The longitudinal fatigue shear range per unit length, V_{fat} (kips/in.), is determined as follows:

$$V_{fat} = \frac{V_f Q}{I} \qquad \text{Equation 6.6.2.3.2.2.1-1}$$

AASHTO LRFD Equation 6.10.10.1.2-3

where:

I = moment of inertia of the short-term composite section (in.^{4})
Q = first moment of the transformed short-term area of the concrete deck about the neutral axis of the short-term composite section (in.^{3})
V_f = vertical shear force under the applicable Fatigue load combination specified in *AASHTO LRFD* Table 3.4.1-1 (Fatigue I or Fatigue II), with the fatigue live load taken as specified in *AASHTO LRFD* Article 3.6.1.4 (kips)

As discussed in Section 3.4.4, the fatigue live load is specified to be a single HL-93 design truck, weighing 72 kips, with a constant rear-axle spacing of 30 feet (*AASHTO LRFD* Article 3.6.1.4.1). For the Fatigue I load combination, which is used for infinite life design, a load factor of 1.5 is applied to the vertical shears resulting from the single design truck. For the Fatigue II load combination, which is used for finite life design, a load factor of 0.75 is applied to the vertical shears resulting from the single design truck. A dynamic load allowance (impact factor) of 1.15 is also to be applied (*AASHTO LRFD* Article 3.6.2). The appropriate Fatigue load combination to use in determining V_f is discussed below in Section 6.6.2.3.2.4.

As mentioned in *AASHTO LRFD* Article C6.10.10.1.2, in negative flexure regions of straight girders only (preferably without skew), Q and I are permitted to be determined using only the longitudinal reinforcement within the effective flange width in line with previous specifications, unless the concrete is considered effective in tension in determining stress ranges for checking fatigue as permitted in *AASHTO LRFD* Article 6.6.1.2.1 (refer to Section 6.5.5.2.2). When only the longitudinal reinforcement is considered, it must be ensured that the pitch of the shear

connectors in these regions does not exceed the permitted maximum pitch of 24.0 in.

For girders in curved bridges, the parameters Q and I in Equation 6.6.2.3.2.2.1-1 are always to be determined including the effective width of the concrete deck in all regions of the girder, including in regions of negative flexure (similar values of Q and I should also be considered for use for girders in straight skewed bridges). Vfat is produced by placing the factored fatigue live load immediately to the left and right of the point under consideration. With the load in these positions, positive moments are produced over significant portions of the girder length (Figure 6.4.2.1-2). As a result, it is reasonable to assume that the concrete deck within the effective width is fully effective along the entire span in determining the stiffness used in the analysis to determine the shear range. In addition, the horizontal shear force in the deck is typically assumed to be effective along the entire span in the analysis. In order to satisfy this assumption, the shear force in the deck should be developed along the entire span.

The effective width of the concrete deck is likely to be different for the interior and exterior girders in the cross-section, which in conjunction with different fatigue shear ranges in the girders, may result in slightly different pitches for each girder. However, for practical purposes, unless the differences are deemed significant, it is recommended that the same pitches be used on all the girders.

6.6.2.3.2.2.2 Box Sections

AASHTO LRFD Article 6.11.10 specifies that for all single box sections, horizontally curved box sections, and multiple box sections in bridges not satisfying the limitations of *AASHTO LRFD* Article 6.11.2.3, or with box flanges that are not fully effective according to the provisions of *AASHTO LRFD* Article 6.11.1.1, shear connectors are to be designed for the sum of the flexural and St. Venant torsional shears. In such cases, for which the St. Venant torsional shears are considered to be more significant, V_f in Equation 6.6.2.3.2.2.1-1 is to be computed by summing the maximum flexural and torsional shears in the web subject to additive shears. The maximum flexural and torsional shears are used, although they are typically not produced by concurrent loads, because the interaction between flexure and torsion due to moving live loads is too complex to treat in a practical manner. The shear range and resulting pitch should be computed using one-half the moment of inertia *I* of the box. The top flange over the web opposite to the web subject to additive flexural and torsional shears, or the other half of the flange for a closed-box section, should contain an equal number of shear connectors.

6.6.2.3.2.3 Radial Fatigue Shear Range, F_{fat}

Curvature, skew and other conditions may cause torsion, which introduces a radial component of the horizontal shear. The radial shear range, F_{fat}, so determined is typically computed with the fatigue live load positioned to produce the largest positive and negative major-axis bending moments in the span. The longitudinal shear range, V_{fat}, is produced by placing the fatigue live load immediately to the left and to the right of the point under consideration. Therefore, vectorial addition of the longitudinal and radial components of the shear range is conservative because the longitudinal and radial shears are not produced by concurrent loads.

The radial fatigue shear range per unit length, F_{fat} (kips/in.), is to be taken as the larger of the following:

$$F_{fat1} = \frac{A_{bot}\sigma_{flg}\ell}{wR} \qquad \text{Equation 6.6.2.3.2.3-1}$$

AASHTO LRFD Equation 6.10.10.1.2-4

$$F_{fat2} = \frac{F_{rc}}{w} \qquad \text{Equation 6.6.2.3.2.3-2}$$

AASHTO LRFD Equation 6.10.10.1.2-5

where:

σ_{flg} = range of longitudinal fatigue stress in the bottom flange under the applicable Fatigue load combination without consideration of flange lateral bending (ksi)
A_{bot} = area of the bottom flange (in.^{2})
F_{rc} = net-range of cross-frame/diaphragm force at the top flange (kips)
ℓ = distance between brace points (ft)
R = minimum girder radius within the panel (ft)
w = effective length of concrete deck (in.) taken as 48.0 in., except at end supports where w may be taken as 24.0 in.

F_{fat1} is used to determine the radial fatigue shear range due to curvature between brace points, and is taken as zero for straight spans or segments. F_{fat2} is the radial fatigue shear range where significant torsion is caused by effects other than curvature, such as skew. F_{fat2} is likely to control when discontinuous cross-frames are used in conjunction with skew angles exceeding 20 degrees in either a straight or a horizontally curved bridge. For all other cases, F_{fat2} may be taken equal to zero.

These two equations are provided to ensure that a load path is provided through the shear connectors to satisfy equilibrium at a section through the girders, deck and cross-frame. The equations yield approximately the same value if the span or segment is curved and there are no other sources of torsion. An example illustrating the calculation and application of F_{fat} is provided in Section 5.1 of NHI (2011).

6.6.2.3.2.3.1 Radial Fatigue Shear Range due to Curvature, F_{fat1}

F_{fat1} is the radial fatigue shear range resulting from the effect of any curvature between brace points. The shear range is taken as the radial component of the longitudinal range of force, $A_{bot}\sigma_{flg}$, in the bottom flange under the applicable Fatigue load combination calculated without consideration of flange lateral bending. The range in the bottom flange is used as a measure of the vertical bending moment due to the fatigue load. σ_{flg} is preferably computed at a cross-frame and also at the mid-thickness of the bottom flange since it is being used to compute a flange force *F*.

Referring to the top of Figure 6.6.2.3.2.3.1-1, which represents a segment of a curved bottom flange between two cross-frames, the radial component of flange force due to curvature can be assumed to act as a radial distributed force, *q*, over the length of the flange segment. Although the radial force, *q*, actually varies along the flange as a function of the axial flange force, *F*, due to vertical bending, for a small segment of the flange, both *q* and *F* may be considered constant. Based on this assumption, the magnitude of *q* is derived in as follows (NHI, 2011):

$$q = \frac{F}{R} \qquad \text{Equation 6.6.2.3.2.3.1-1}$$

or:

$$q = \frac{A_{bot}\,\sigma_{flg}}{R} \qquad \text{Equation 6.6.2.3.2.3.1-2}$$

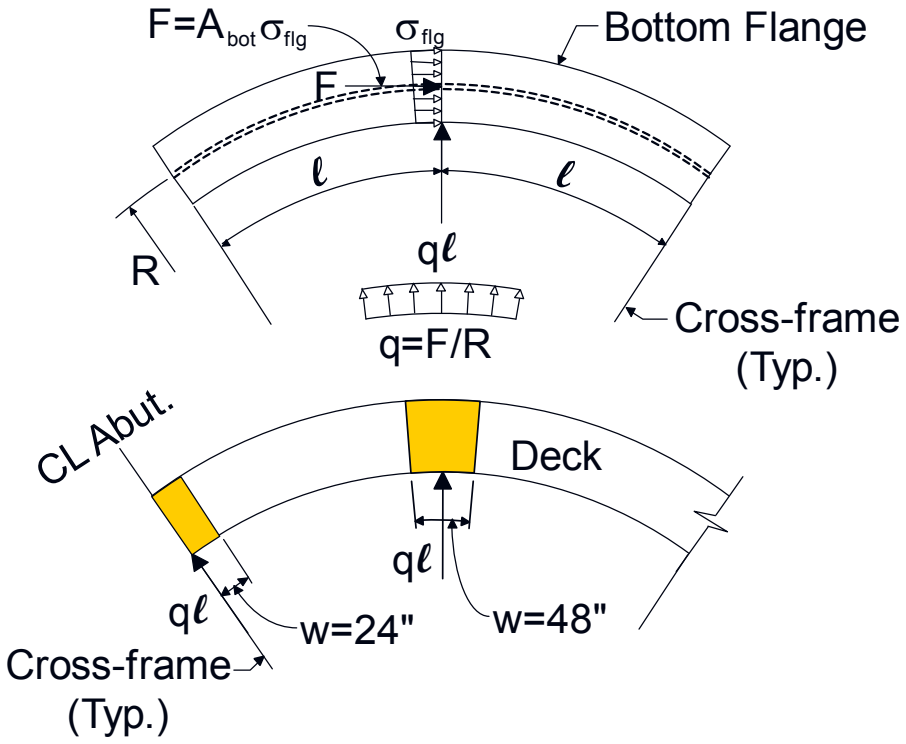

Figure 6.6.2.3.2.3.1-1 Derivation of F_{fat1} (Equation 6.6.2.3.2.3-1)

As shown at the bottom of Figure 6.6.2.3.2.3.1-1, multiplying q from Equation 6.6.2.3.2.3.1-1 by the cross-frame spacing, ℓ, and distributing the resulting radial shear range over an effective length of deck, w, gives F_{fat1} in kips/inch as given by Equation 6.6.2.3.2.3-1. w is taken as 48.0 inches, except at end supports where w is halved to 24.0 inches. This length is considered representative of the effective length of the deck assumed acting with the flange in the transverse direction.

F_{fat1} may be taken equal to zero for straight spans or segments. F_{fat1} may be ignored for box sections used in horizontally curved spans or segments, as permitted in AASHTO LRFD Article 6.11.10, because of the inherent conservatism in the shear connector design requirements for box sections.

6.6.2.3.2.3.2 Radial Fatigue Shear Range due to Effects Other than Curvature, F_{fat2}

F_{fat2} is the radial fatigue shear range where significant torsion is caused by effects other than curvature, such as skew. F_{fat2} is computed from the net range of cross-frame/diaphragm force at the top flange under the applicable Fatigue load combination, F_{rc}.

As illustrated in Figure 6.6.2.3.2.3.2-1, F_{rc} is to be taken as the resultant range of horizontal force at the level of the top chord from all members and/or cross-frames at the point under consideration that is resisted by the shear connectors. F_{rc} is then distributed over the effective length of deck, *w*, shown in Figure 6.6.2.3.2.3.1-1 to give F_{fat2} in kips/inch as given by Equation 6.6.2.3.2.3-2.

As shown at the bottom of Figure 6.6.2.3.2.3.2-1, at skewed cross-frames, the normal (radial) component of the resultant range of force in that cross-frame at the level of the top chord must be computed. Should a normal (radial) cross-frame intersect the skewed cross-frame at the point under consideration, the normal (radial) component of the skewed cross-frame resultant force range should then be appropriately combined with the resultant range of horizontal force at the level of the top chord in the normal (radial) cross-frame to determine F_{rc}.

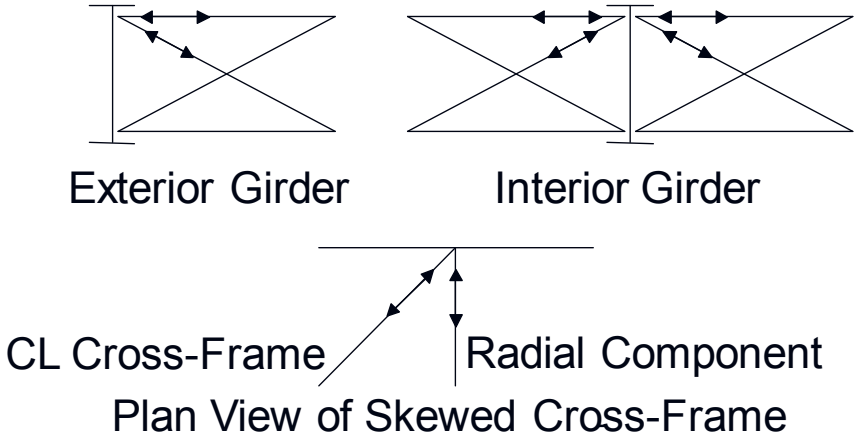

Figure 6.6.2.3.2.3.2-1 Resolution of the Horizontal Cross-Frame Force Ranges due to the Factored Fatigue Load at the Level of the Top Chord to Determine F_{rc}

According to *AASHTO LRFD* Article C6.10.10.1.2, in lieu of a refined analysis, F_{rc} may be taken equal to 25.0 kips for an exterior girder, which is typically the critical girder (Figure 6.6.2.3.2.3.2-1). This is typically a conservative value so more accurate determination of this value via refined analysis is suggested. F_{rc} should not be multiplied by the factor of 0.75 that is recommended for application when determining ranges of force in cross-frames in *AASHTO LRFD* Article C6.6.1.2.1.

F_{fat2} is most likely to control when discontinuous cross-frame lines are used in conjunction with skew angles exceeding 20 degrees. For all other cases, F_{fat2} may be taken equal to zero according to *AASHTO LRFD* Article 6.10.10.1.2.

6.6.2.3.2.4 Stud Fatigue Shear Resistance, Z_r

The fatigue shear resistance of an individual stud shear connector, Z_r, to be used in Equation 6.6.2.3.2.1-1 for determining the shear connector pitch is to be taken as follows (Slutter and Fisher, 1966):

- Where the projected 75-year single-lane Average Daily Truck Traffic $(ADTT)_{SL}$ is greater than or equal to 960 trucks per day, the Fatigue I load combination is to be used and the fatigue shear resistance for infinite life is to be taken as:

$$Z_r = 5.5d^2 \qquad \text{Equation 6.6.2.3.2.4-1}$$

AASHTO LRFD Equation 6.10.10.2-1

- Otherwise, the Fatigue II load combination is to be used and the fatigue shear resistance for finite life is to be taken as:

$$Z_r = \alpha d^2 \qquad \text{Equation 6.6.2.3.2.4-2}$$

AASHTO LRFD Equation 6.10.10.2-2

where:

α = constant = $34.5 - 4.28 \log N$

d = diameter of the stud (in.)

N = number of stress cycles specified in *AASHTO LRFD* Article 6.6.1.2.5

= $(365)(75)n(ADTT)_{SL}$ Equation 6.6.2.3.2.4-3

AASHTO LRFD Equation 6.6.1.2.5-3

n = number of stress range cycles per truck passage taken from *AASHTO LRFD* Table 6.6.1.2.5-2

If a fatigue design life other than 75 years is sought, a number other than 75 may be inserted in Equation 6.6.2.3.2.4-3.

The specified value of the 75-year $(ADTT)_{SL}$ above which the infinite life check governs (i.e. 960 trucks per day) is calculated assuming a 75-year life and one stress range cycle per truck passage (i.e. n = 1.0 in Equation 6.6.2.3.2.4-3). For other values of the fatigue design life, the specified value of $(ADTT)_{SL}$ = 960 trucks/day should instead be taken as the ratio of 71,768 divided by the fatigue life sought in years. For other values of n, the specified of $(ADTT)_{SL}$ should be divided by the appropriate value of n taken from *AASHTO LRFD* Table 6.6.1.2.5-2.

The reader is referred to *AASHTO LRFD* Article 6.10.10.2 for the appropriate values of Z_r for channel shear connectors.

6.6.2.3.3 Special Requirements at Points of Contraflexure

In straight continuous composite I-girder bridges, *AASHTO LRFD* Article 6.10.10.1 permits the elimination of shear connectors in the negative moment regions between permanent-load contraflexure points in cases where the longitudinal reinforcement is not included in the computation of the section properties for negative flexure. Thus, since there are no shear connectors within the regions between points of permanent-load contraflexure in this case, the member must be considered non-composite when subjected to positive or negative flexure within these regions. *AASHTO LRFD* Article 6.10.10.3 requires that for this case, additional shear connectors be provided in the region of points of permanent load contraflexure. According to *AASHTO LRFD* Article 6.10.10.3, the number of additional connectors, n_{ac}, that must be provided is to be taken as:

$$n_{ac} = \frac{A_s f_{sr}}{Z_r} \qquad \text{Equation 6.6.2.3.3-1}$$

AASHTO LRFD Equation 6.10.10.3-1

where:

A_s = total area of longitudinal reinforcement over the interior support within the effective concrete deck width (in.^{2})

f_{sr} = stress range in the longitudinal reinforcement over the interior support under the applicable Fatigue load combination specified in *AASHTO LRFD* Table 3.4.1-1 with the fatigue live load taken as specified in *AASHTO LRFD* Article 3.6.1.4 (ksi)

Z_r = fatigue shear resistance of an individual shear connector determined as specified in *AASHTO LRFD* Article 6.10.10.2 (kips)

This requirement is apparently intended to use the clump of shear connectors to develop the fatigue force in the longitudinal reinforcement due to the negative factored fatigue live load moment over the interior support, and is not related to girder shear in the normal sense. The additional connectors are to be placed within a distance equal to one-third of the effective concrete deck width on each side of the point of permanent load contraflexure (i.e. preferably centered about the point within the specified distance), with field splices placed so as not to interfere with the connectors.

Strength-of-materials principles demand that the shear force between the reinforcing steel and the steel girder be sufficient to develop the force in the reinforcing bars. The reinforcing bars must extend far enough past the clump of shear connectors that

the force in the bars may be developed. Strength-of-materials also demands sufficient additional connectors be provided to transfer the force in the concrete deck, at both the fatigue and strength limit states, back into the steel girder in the regions of points of permanent load contraflexure since there are no shear connectors beyond those points. The current provision appears to violate those principles.

Discontinuing the shear connectors in these regions effectively causes the deck slab to act as a partial-length cover plate, which has two potential problematic effects. First, the slab is likely to crack near the point at which it is no longer acting compositely with the steel girder. Second, the shear connectors and their welds at the discontinuity may be overloaded much as the welds at the termination of a partial length cover plate, particularly if sufficient shear connectors are not provided to transfer the appropriate deck forces back into the girder. In fact, field tests have confirmed that the deck continues to act compositely without shear connection in these regions. When it ceases to act compositely, a tell-tail rust line often develops between the deck and the girder flange that is evident in inspections. This situation may be followed with the deterioration of the deck. Points of permanent load contraflexure should not be related to shear connector design. As demonstrated previously in Figure 6.4.2.1-2, over most of the region of negative moment due to permanent load, the live load to obtain the maximum shear range produces positive moment, and not negative moment.

EXAMPLE

Determine the required pitch of the stud shear connectors to satisfy the fatigue limit state for the exterior girder of a straight three-span continuous I-girder bridge (140 ft – 175 ft – 140 ft) with no skew. Shear connectors will be provided throughout the entire length of the bridge. Therefore, the longitudinal deck reinforcement may be considered as part of the composite section in regions of negative flexure. The average daily truck traffic in a single lane $(ADTT)_{SL}$ will be assumed equal to 1,600 trucks/day.

First, determine the required stud proportions. The structural thickness of the concrete deck is 9.0 in. The deck haunch thickness from the top of the web to the bottom of the deck is 3.5 in. The minimum top-flange thickness along the girder is 7/8”. Terminating the studs at approximately the mid-thickness of the concrete deck will place them well within the limits for cover and penetration specified in *AASHTO LRFD* Article 6.10.10.1.4 and will also clear the reinforcing steel. Therefore,

$$\frac{9.0}{2} + (3.5 - 0.875) = 7.125 \text{ in.}$$

Use 7/8″ x 7″ studs. Check that the ratio of the height to the diameter is not less than 4.0, as required in *AASHTO LRFD* Article 6.10.10.1.1.

$$\frac{h}{d} = \frac{7.0}{0.875} = 8.0 > 4.0 \quad \text{ok}$$

As specified in *AASHTO LRFD* Article 6.10.10.1.2, the pitch, *p*, of the shear connectors must satisfy the following (Equation 6.6.2.3.2.1-1):

$$p \le \frac{nZ_r}{V_{sr}}$$

V_{sr} is to be computed as follows (Equation 6.6.2.3.2.1-2):

$$V_{sr} = \sqrt{(V_{fat})^2 + (F_{fat})^2}$$

Since the bridge in this example is straight and does not have skewed supports, the radial fatigue shear range per unit length, F_{fat}, will be taken equal to zero, as permitted in *AASHTO LRFD* Article 6.10.10.1.2. Therefore, in this case, V_{sr} is equal to V_{fat}. V_{fat} is computed as (Equation 6.6.2.3.2.2.1-1):

$$V_{fat} = \frac{V_f Q}{I}$$

Since the minimum required one-percent longitudinal reinforcement is assumed provided in the deck according to the provisions of *AASHTO LRD* Article 6.10.1.7, and shear connectors will be provided along the entire length of the bridge, the concrete deck will be assumed effective in tension for negative flexure when computing longitudinal stress ranges for separate load-induced fatigue computations. Therefore, the cross-section parameters *I* and *Q* must be determined using the short-term area of the concrete deck (within the effective flange width) along the entire girder.

A sample calculation of *Q* for the transformed short-term area of the concrete deck about the neutral axis of the short-term composite section at the interior-pier section is given below. The effective width of the deck over the interior pier is 114.0 in. The modular ratio *n* is equal to 8. The distance from the neutral axis of the short-term composite section to the mid-thickness of the deck is 20.65 in.

Therefore:

$$Q = (9.0 \text{ x } 114.0 / 8.0)(20.65) = 2{,}648 \text{ in.}^3$$

Calculated values of *Q* and *I* at tenth points along the entire girder are given below in Table 6.6.2.3.3-1 (only one-half of the girder is shown since the girder is symmetrical about the longitudinal centerline of the center span).

Since the (ADTT)SL of 1,600 trucks/day exceeds 960 trucks/day, the Fatigue I load combination is to be used, and the fatigue resistance of an individual stud shear connector, Z_r, for infinite life is to be taken as (Equation 6.6.2.3.2.4-1):

$$Z_r = 5.5d^2$$

$$\therefore \text{ use } Z_r = 5.5(0.875)^2 = 4.21 \text{ kips} \quad \text{(at all locations)}$$

The number of shear connectors in a cross-section, *n*, will be assumed equal to three (3). Requirements for the transverse spacing of shear connectors across the top flange are given in *AASHTO LRFD* Article 6.10.10.1.3 (Section 6.6.2.2.3.1).

The vertical shear force range, V_f, is determined for the factored fatigue load (factored by the 1.5 load factor specified for the Fatigue I load combination), including the specified dynamic load allowance of 15 percent. Calculated values of V_f from the analysis at tenth-point locations along the girder are shown in the table below (again, the girder is symmetrical about the longitudinal centerline of the center span).

Based on Equation 6.6.2.3.2.1-1, Equation 6.6.2.3.2.1-2, and Equation 6.6.2.3.2.2.1-1 (recall that F_{fat} in Equation 6.6.2.3.2.1-2 is taken equal to zero), Table 6.6.2.3.3-1 summarizes the required stud pitch along the girder to satisfy the fatigue limit state. As specified in *AASHTO LRFD* Article 6.10.10.1.2, the pitch must not be less than six stud diameters = 6(0.875) = 5.25 inches or more than 24.0 inches.

Table 6.6.2.3.3-1 Required Shear Connector Pitch – Fatigue Limit State - Example

Length (ft)	V_f (kips)	Q (in^3)	I (in^4)	V_{sr} (kips/in)	p (in/row)
0.0	85.6	1,849	131,725	1.20	10.5
14.0	75.0	1,849	131,725	1.05	12.0
28.0	64.6	1,849	131,725	0.91	13.9
42.0	63.0	1,849	131,725	0.88	14.4
56.0	64.6	2,210	166,612	0.86	14.7
70.0	64.6	2,210	166,612	0.86	14.7
84.0	67.6	2,210	166,612	0.90	14.0
98.0	72.0	2,210	166,612	0.96	13.2
112.0	75.0	2,085	153,311	1.02	12.4
126.0	79.6	2,648	227,766	0.93	13.6
140.0	90.0	2,648	227,766	1.05	12.0
157.5	84.0	2,085	153,311	1.14	11.1
175.0	76.6	2,085	153,311	1.04	12.1
192.5	70.6	2,116	156,266	0.96	13.2
210.0	69.0	2,116	156,266	0.93	13.6
227.5	69.0	2,116	156,266	0.93	13.6

6.6.2.4 Strength Limit State Design

6.6.2.4.1 General

The resulting number of shear connectors determined to satisfy the fatigue limit state must be checked against the number required to satisfy the strength limit state.

The design requirement at the strength limit state computes the minimum number of shear connectors, *n*, necessary to develop a specified nominal longitudinal force, *P*, within regions on either side of the point of maximum positive design live load plus impact moment **(**Figures 6.6.2.4.2.1-1 and Figure 6.6.2.4.2.1-2**).** The regions are defined off the point of maximum live load plus impact moment because it applies to the composite section and is easier to locate than a maximum of the sum of all the moments acting on the composite section. The equation for determining *n* in each region is given in *AASHTO LRFD* Article 6.10.10.4.1 as follows:

$$n = \frac{P}{Q_r}$$ Equation 6.6.2.4.1-1

AASHTO LRFD Equation 6.10.10.4.1-2

where:

P = total nominal shear force within the region under consideration determined as specified in *AASHTO LRFD* Article 6.10.10.4.2 (Section 6.6.2.4.2) (kips)

Q_r = factored shear resistance of one shear connector (Section 6.6.2.4.3) (kips)

Similar to V_{sr} for the fatigue limit state, P has both a longitudinal and a radial component, as discussed below in Section 6.6.2.4.2.1.

Since P is in terms of total nominal shear force over a specified region, and Q_r is in terms of shear resistance per shear connector, it is clear that n will result in the required number of shear connectors over the specified region.

6.6.2.4.2 Nominal Shear Force, P

6.6.2.4.2.1 General

According to *AASHTO LRFD* Article 6.10.10.4.2, for simple spans and for continuous **spans** between points of maximum positive design live load plus impact moment and an adjacent end of the member, the total nominal shear force, P, is to be taken as:

$$P = \sqrt{P_p^2 + F_p^2}$$ Equation 6.6.2.4.2.1-1

AASHTO LRFD Equation 6.10.10.4.2-1

where:

P_p = total longitudinal force in the concrete deck at the point of maximum positive live load plus impact moment (discussed below) (kips)

F_p = total radial force in the concrete deck at the point of maximum positive live load plus impact moment (discussed below) (kips)

P_p is taken as the lesser of the following forces based on either the ultimate-strength properties of the concrete deck (P_{1p}), or the ultimate-strength properties of the steel girder (P_{2p}):

$$P_{1p} = 0.85 f'_c b_s t_s$$ Equation 6.6.2.4.2.1-2

AASHTO LRFD Equation 6.10.10.4.2-2

or:

$$P_{2p} = F_{yw} D t_w + F_{yt} b_{ft} t_{ft} + F_{yc} b_{fc} t_{fc}$$ Equation 6.6.2.4.2.1-3

AASHTO LRFD Equation 6.10.10.4.2-3

where:

b_s = effective width of the concrete deck (in.)
t_s = thickness of the concrete deck (in.)

F_p is taken as follows:

$$F_p = P_p \frac{L_p}{R}$$ Equation 6.6.2.4.2.1-4

AASHTO LRFD Equation 6.10.10.4.2-4

where:

L_p = arc length between an end of the girder and an adjacent point of maximum positive live load plus impact moment (Figure 6.6.2.4.2.1-1) (ft)
R = minimum girder radius over the length, L_p (ft)

F_p is provided in Equation 6.6.2.4.2.1-1 to account for the radial effect of curvature, and is required for curved spans or segments to bring the smallest of the longitudinal forces in either the deck or the girder (from Equation 6.6.2.4.2.1-2 or Equation 6.6.2.4.2.1-3) into equilibrium. The resulting longitudinal force, P_p, is assumed to be constant over the length, L_p, when computing the radial component, F_p, using Equation 6.6.2.4.2.1-4. Note that for straight spans or segments, F_p may be taken equal to zero.

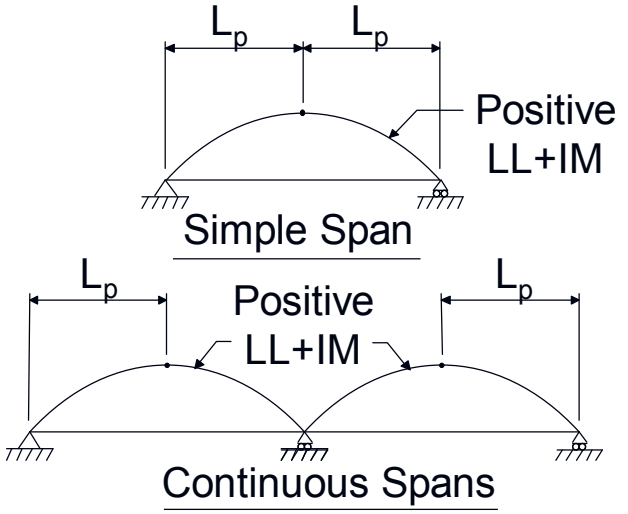

Figure 6.6.2.4.2.1-1 Definition of Arc Length, L_p

For continuous spans between the point of maximum positive design live load plus impact moment and the centerline of an adjacent interior support, the total nominal shear force, *P*, is to be taken as:

$$P = \sqrt{P_T^2 + F_T^2}$$ Equation 6.6.2.4.2.1-5

AASHTO LRFD Equation 6.10.10.4.2-5

where:

P_T = total longitudinal force in the concrete deck between the point of maximum positive live load plus impact moment and the centerline of an adjacent interior support (discussed below) (kips)

F_T = total radial force in the concrete deck between the point of maximum positive live load plus impact moment and the centerline of an adjacent interior support (discussed below) (kips)

P_T is taken as follows:

$$P_T = P_p + P_n$$ Equation 6.6.2.4.2.1-6

AASHTO LRFD Equation 6.10.10.4.2-6

where:

P_n = total longitudinal force in the concrete deck over an interior support (discussed below) (kips)

The number of shear connectors required between points of maximum positive design live load plus impact moment and the centerline of an adjacent interior support is computed from the sum of the critical forces at the maximum positive and negative moment locations according to Equation 6.6.2.4.2.1-6. The sum of the critical forces at the maximum moment locations is conservatively used in order to provide adequate shear resistance for any live load position. Many shear connectors in this region resist reversing forces in the concrete deck depending on the live load position since there is no one point where the moment always changes sign.

P_n is taken as the lesser of the following forces based on either the ultimate-strength properties of the steel girder (P_{1n}), or a conservative approximation of the combined contribution of both the longitudinal reinforcement and the concrete that remains effective in tension based on its modulus or rupture (P_{2n}):

$$P_{1n} = F_{yw} D t_w + F_{yt} b_{ft} t_{ft} + F_{yc} b_{fc} t_{fc}$$ Equation 6.6.2.4.2.1-7

AASHTO LRFD Equation 6.10.10.4.2-7

or:

$$P_{2n} = 0.45 f'_c b_s t_s \qquad \text{Equation 6.6.2.4.2.1-8}$$

AASHTO LRFD Equation 6.10.10.4.2-8

In this region, sufficient shear connectors are necessary to transfer the ultimate tensile force in the longitudinal reinforcement from the concrete deck to the steel section. The tension force given by Equation 6.6.2.4.2.1-8 is a conservative approximation to account for the combined contribution of the longitudinal reinforcement and the concrete deck that remains effective in tension based on its modulus of rupture. *AASHTO LRFD* Article C6.10.10.4.2 permits a more precise value to be substituted for P_{2n}.

The radial force, F_T, is taken as follows:

$$F_T = P_T \frac{L_n}{R} \qquad \text{Equation 6.6.2.4.2.1-9}$$

AASHTO LRFD Equation 6.10.10.4.2-9

where:

L_n = arc length between the point of maximum positive live load plus impact moment and the centerline of an adjacent interior support (Figure 6.6.2.4.2.1-2) (ft)

R = minimum girder radius over the length, L_n (ft)

F_T may be taken equal to zero for straight spans or segments.

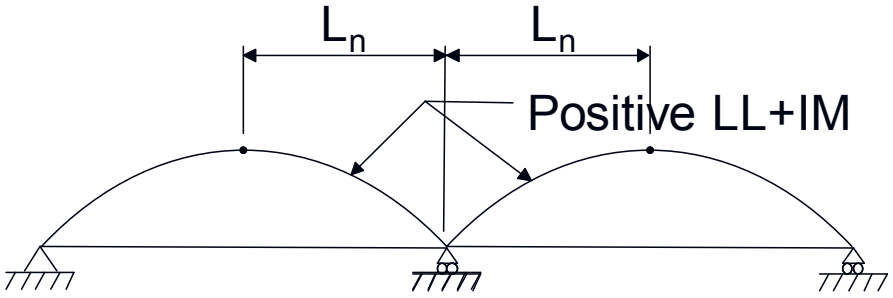

Figure 6.6.2.4.2.1-2 Definition of Arc Length, L_n

6.6.2.4.2.2 Box Sections

According to *AASHTO LRFD* Article 6.11.10, for box sections, the cross-sectional area of the steel box under consideration and the effective area of the concrete deck associated with that box are to be used to calculate the longitudinal force in Equation

6.6.2.4.2.1-2, Equation 6.6.2.4.2.1-3, Equation 6.6.2.4.2.1-7, and Equation 6.6.2.4.2.1-8.

Also, for composite box flanges in closed-box sections at the strength limit state, in addition to satisfying the provisions of *AASHTO LRFD* Article 6.10.10.4, the vector sum of the longitudinal and torsional shears due to the factored loads in the concrete deck per connector are not to exceed Q_r from Equation 6.6.2.4.3-1 (see below). The torsional shear in the concrete deck can be determined by multiplying the torsional shear acting on the top of the composite box section by the ratio of the thickness of the transformed concrete deck to the total thickness of the top flange plus the transformed deck. The deck should include adequate transverse reinforcement to resist this torsional shear.

6.6.2.4.3 Factored Shear Resistance of a Stud, Q_r

According to *AASHTO LRFD* Article 6.10.10.4.1, the factored shear resistance, Q_r, of a single shear connector at the strength limit state is to be taken as:

$$Q_r = \phi_{sc} Q_n \qquad \text{Equation 6.6.2.4.3-1}$$

AASHTO LRFD Equation 6.10.10.4.1-1

where:

ϕ_{sc} = resistance factor for shear connectors determined as specified in *AASHTO LRFD* Article 6.5.4.2 (= 0.85)

Q_n = nominal shear resistance of a single shear connector determined as specified in *AASHTO LRFD* Article 6.10.10.4.3 (discussed below) (kips)

AASHTO LRFD Article 6.10.10.4.3 specifies that the nominal shear resistance, Q_n, of one stud shear connector embedded in a concrete deck is to be taken as (Ollgaard et al., 1971):

$$Q_n = 0.5 A_{sc} \sqrt{f'_c E_c} \le A_{sc} F_u \qquad \text{Equation 6.6.2.4.3-2}$$

AASHTO LRFD Equation 6.10.10.4.3-1

where:

A_{sc} = cross-sectional area of a stud shear connector (in.^{2})

E_c = modulus of elasticity of the deck concrete determined as specified in *AASHTO LRFD* Article 5.4.2.4 (ksi)

F_u = specified minimum tensile strength of a stud shear connector determined as specified in *AASHTO LRFD* Article 6.4.4 (ksi)

The specified minimum tensile strength of the connector, F_u, is equal to 60 ksi for a typical stud shear connector (*AASHTO LRFD* Article 6.4.4).

The reader is referred to *AASHTO LRFD* Article 6.10.10.4.3 for the appropriate value of Q_n for channel shear connectors.

EXAMPLE

Check the number of stud shear connectors that were determined to satisfy the fatigue limit state in the preceding example (Section 6.6.2.3.3) against the number required to satisfy the strength limit state. The preceding example determined the required pitch of the shear connectors to satisfy the fatigue limit state for the exterior girder of a straight three-span continuous I-girder bridge (140 ft – 175 ft – 140 ft) with no skew. Shear connectors are provided throughout the entire length of the bridge so the girder is assumed composite in regions of negative flexure in the final condition. As determined in the preceding example, 7/8" x 7" studs are to be used (3 studs per row). The specified minimum 28-day compressive strength, f'_c, of the concrete deck is 4.0 ksi.

According to *AASHTO LRFD* Article 6.10.10.4.1, the factored shear resistance of a single shear connector, Q_r , at the strength limit state is to be taken as (Equation 6.6.2.4.3-1):

$$Q_r = \phi_{sc} Q_n$$

As specified in *AASHTO LRFD* Article 6.10.10.4.3, the nominal shear resistance of one stud shear connector embedded in a concrete deck is to be taken as (Equation 6.6.2.4.3-2):

$$Q_n = 0.5 A_{sc} \sqrt{f'_c E_c} \le A_{sc} F_u$$

The modulus of elasticity of the deck concrete, E_c, is determined as follows (Equation 6.4.2.3.2.1-2):

$$E_c = 33{,}000 w_c^{1.5} \sqrt{f'_c}$$

A unit weight, w_c, of 0.145 kcf will be assumed for the normal weight concrete. Therefore:

$$E_c = 33{,}000(0.145)^{1.5} \sqrt{4.0} = 3{,}644 \text{ ksi}$$

The specified minimum tensile strength of a stud shear connector, F_u, is taken as 60.0 ksi, as specified in *AASHTO LRFD* Article 6.4.4. Thus:

$$A_{sc} = \frac{\pi}{4}(0.875)^2 = 0.60 \text{ in.}^2$$

$$A_{sc}F_u = (0.60)(60.0) = 36.00 \text{ kips}$$

$$Q_n = 0.5(0.60)\sqrt{4.0(3{,}644)} = 36.22 \text{ kips} > 36.00 \text{ kips}$$

$$\therefore Q_n = 36.00 \text{ kips}$$

$$Q_r = 0.85(36.00) = 30.60 \text{ kips}$$

At the strength limit state, the minimum number of shear connectors, *n*, over the region under consideration is to be taken as:

$$n = \frac{P}{Q_r} \qquad \text{Equation 6.6.2.4.3-3}$$

AASHTO LRFD Equation 6.10.10.4.1-2

where *P* is the total nominal shear force determined as specified in *AASHTO LRFD* Article 6.10.10.4.2. According to *AASHTO LRFD* Article 6.10.10.4.2, for continuous spans that are composite for negative flexure in the final condition, the total nominal shear force, *P*, between the point of maximum positive design live load plus impact moment and an adjacent end of the member is to be determined as (Equation 6.6.2.4.2.1-1):

$$P = \sqrt{P_p^2 + F_p^2}$$

where P_p is the total shear force in the concrete deck at the point of maximum positive live load plus impact moment taken as the lesser of (Equation 6.6.2.4.2.1-2):

$$P_{1p} = 0.85f_c^{'}b_s t_s$$

where b_s and t_s are the effective width and thickness of the concrete deck, respectively, (assumed to be equal to 114.0 inches and 9.0 inches in this region for this example), or (Equation 6.6.2.4.2.1-3):

$$P_{2p} = F_{yw}Dt_w + F_{yt}b_{ft}t_{ft} + F_{yc}b_{fc}t_{fc}$$

$$P_{1p} = 0.85(4.0)(114.0)(9.0) = 3{,}488 \text{ kips}$$

For the steel section yielding the smallest force in this region (top flange = 1" x 16"; web = ½" x 69"; bottom flange = 7/8" x 18"):

$$P_{2p} = (50.0)(69.0)(0.5) + (50.0)(18.0)(0.875) + (50.0)(16.0)(1.0) = 3{,}313 \text{ kips}$$

Since the girder is straight, the radial force, F_p, is taken equal to zero.

$$\therefore P = P_p = P_{2p} = 3{,}313 \text{ kips}$$

$$n = \frac{P}{Q_r} = \frac{3{,}313}{30.60} = 108 \text{ studs}$$

Compute the required pitch, *p*, in this region at the strength limit state with 3 studs per row. The point of maximum positive live load plus impact moment in Span 1 is located 60.2 feet from the abutment. Therefore:

$$\text{No. of rows} = \frac{108}{3} = 36 \text{ rows}$$

$$p = \frac{60.2(12)}{(36-1)} = 20.6 \text{ in.}$$

The total nominal shear force, *P*, between the point of maximum positive design live load plus impact moment and the centerline of an adjacent interior support is to be determined as (Equation 6.6.2.4.2.1-5):

$$P = \sqrt{P_T^2 + F_T^2}$$

where P_T is the total longitudinal force in the concrete deck between the point of maximum positive live load plus impact moment and the centerline of the adjacent interior support taken as (Equation 6.6.2.4.2.1-6):

$$P_T = P_p + P_n$$

P_n is the total longitudinal shear force in the concrete deck over an interior support taken as the lesser of (Equation 6.6.2.4.2.1-7):

$$P_{1n} = F_{yw} D t_w + F_{yt} b_{ft} t_{ft} + F_{yc} b_{fc} t_{fc}$$

or (Equation 6.6.2.4.2.1-8):

$$P_{2n} = 0.45 f'_c b_s t_s$$

For the steel section (top flange = 1" x 16"; web = ½" x 69"; bottom flange = 1-3/8"" x 18") and effective concrete deck yielding the smallest forces in this region:

$$P_{1n} = (50.0)(69.0)(0.5) + (50.0)(18.0)(1.375) + (50.0)(16.0)(1.0) = 3{,}763 \text{ kips}$$

$$P_{2n} = 0.45(4.0)(114.0)(9.0) = 1{,}847 \text{ kips}$$

$$\therefore P_n = 1{,}847 \text{ kips}$$

Since the girder is straight, the radial force, F_T, is taken equal to zero.

$$\therefore P = P_T = P_p + P_n = 3{,}313 + 1{,}847 = 5{,}160 \text{ kips}$$

$$n = \frac{P}{Q_r} = \frac{5{,}160}{30.60} = 169 \text{ studs}$$

Compute the required pitch, *p*, in this region at the strength limit state with 3 studs per row. The distance between the point of maximum positive live load plus impact moment in Span 1 and the adjacent interior support is (140.0 - 60.2) = 79.8 feet. Therefore:

$$\text{No. of rows} = \frac{169}{3} = 56 \text{ rows}$$

$$p = \frac{79.8(12)}{(56-1)} = 17.4 \text{ in.}$$

The distance between the point of maximum positive live load plus impact moment in Span 2 and each of the adjacent interior supports is 87.5 feet. Using calculations similar to the above:

P_p = 3,488 kips
P_n = 1,847 kips
P = 5,335 kips
n = 174 studs
No. of rows = 58 rows
p = 18.4 in.

The final recommended pitches are governed by the fatigue limit state and are shown in Figure 6.6.2.4.3-1. The effective width of the concrete deck is larger for the interior girders, which in conjunction with different fatigue shear ranges, may result in slightly different recommended pitches. However, for practical purposes, unless the differences are deemed significant, it is recommended that the same pitches be used on all the girders.

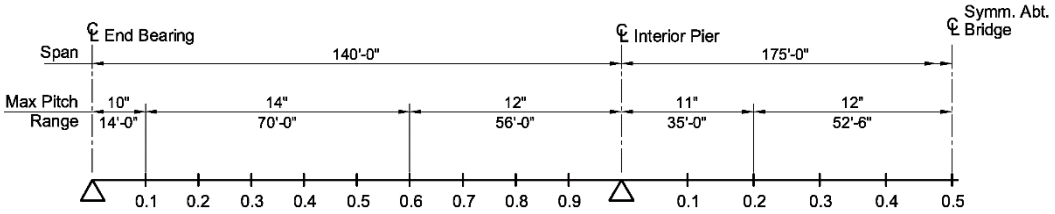

Figure 6.6.2.4.3-1 Final Recommended Pitches - Example

6.6.3 Bracing Member Design

6.6.3.1 General

Bracing members (i.e. cross-frames/diaphragm and lateral bracing members) perform many important functions in steel I- and box-girder bridges. In addition to reviewing those functions, Sections 6.3.2.9 and 6.3.2.10 discuss the process of selecting the type of bracing member (cross-frame or diaphragm), laying out the spacing of cross-frame/diaphragm members, the different possible configurations of cross-frame and lateral bracing members, and some suggestions on the detailing and preliminary sizing of these members.

Section 6.6.3 reviews in more detail the *AASHTO LRFD* Specification provisions for the detailed design of the bracing members themselves. The discussion covers the design of tension members, compression members and solid-plate diaphragms. Design of the connections and connection elements for bracing members (bolted or welded) is discussed in Section 6.6.4.

The minimum permitted thickness of steel must sometimes be considered in the design of bracing members and their connections. The reader is referred to Section 6.4.11 for further information.

As discussed in Section 6.3.2.9.6.1, single angles, or when necessary, structural tees, are preferred for cross-frame and lateral bracing members. Double angles are more expensive to fabricate and painting the backs of the angles can cause difficulties.

6.6.3.2 Stability Bracing Requirements

Appendix 6.3 of AISC (2010a) provides design recommendations for torsional and lateral bracing related to the required strength and stiffness of the various bracing components. The provided equations are intended to ensure that the strength and stiffness provided by these members is sufficient to ensure their ability to adequately function as brace points for the compression elements to which they are attached. Equations are given for computing stability bracing forces which are additive to the conventional bracing design forces determined from a first-order analysis. These design recommendations are described in greater detail in Yura and Helwig (2012). As of this writing (2015), these design recommendations have not been incorporated into the *AASHTO LRFD* Specifications. However, in the interim, the Engineer may wish to consider checking these recommendations for bracing members in straight bridges with or without skewed supports; in particular, whenever a line-girder analysis is employed.

Nodal braces, such as cross-frames or diaphragms, control the deformation of a single point along the member. Cross-frames or diaphragms also restrain the twist of the girders; therefore, they are classified in the recommendations as nodal torsional braces. Effective stability bracing must possess sufficient stiffness and strength.

The required stiffness, $(\beta_T)_{req}$, for nodal torsional stability bracing as presented in the recommendations is:

$$(\beta_T)_{req} = \frac{\beta_T}{\left(1 - \frac{\beta_T}{\beta_{sec}}\right)} \qquad \text{Equation 6.6.3.2-1}$$

The required strength, $(M_{br})_{req}$, for nodal torsional stability bracing as presented in the recommendations is:

$$(M_{br})_{req} = \frac{(0.005) L_b L M_f^2}{n E I_{eff} C_b^2 h_o} \qquad \text{Equation 6.6.3.2-2}$$

where:

β_T = overall required brace system stiffness (kip-in./rad)

$$= \frac{2.4 L M_f^2}{\phi n E I_{eff} C_b^2} \qquad \text{Equation 6.6.3.2-3}$$

β_{sec} = web distortional stiffness (kip-in./rad). For full-depth web stiffeners, β_{sec} is equal to infinity. For partial-depth web stiffeners, calculate β_i for various portions of the web as follows:

$$\beta_i = \frac{3.3E}{h_i}\left(\frac{h_o}{h_i}\right)^2\left(\frac{1.5h_i t_w^3}{12}+\frac{t_s b_s^3}{12}\right) \qquad \text{Equation 6.6.3.2-4}$$

Refer to Figure 11 in Yura and Helwig (2012) for definitions of the height, h_i, of the various portions of the web; and then $1/\beta_{sec} = \sum(1/\beta_i)$

L = span length (in.)

M_f = maximum factored major-axis bending moment in the region (i.e. positive or negative moment region) and span under consideration for the limit-state load combination under consideration (kip-in.)

ϕ = resistance factor for bracing = 0.80

n = number of torsional braces within the span

I_{eff} = effective moment of inertia calculated from Equation 6.5.3.3.5-2 or 6.5.3.3.5-3, as applicable (in.^{4})

C_b = moment gradient modifier (Section 6.5.6.2.2.2.2)

L_b = unbraced length (in.)

h_o = distance between the flange centroids (in.)

b_s = width of transverse stiffener (in.)

t_s = thickness of transverse stiffener (in.)

t_w = web thickness (in.)

The required stiffness, $(\beta_T)_{req}$, from Equation 6.6.3.2-1 is checked against the actual overall brace system stiffness, $(\beta_T)_{act}$, given as:

$$(\beta_T)_{act} = \frac{1}{\left(\frac{1}{\beta_b}+\frac{1}{\beta_{sec}}+\frac{1}{\beta_g}\right)} \qquad \text{Equation 6.6.3.2-5}$$

where:

β_b = cross-frame or diaphragm stiffness (kip-in./rad).

$$= \frac{A_d E s^2 h_b^2}{L_d^3} \text{ (X-type cross-frame: tension-compression)} \qquad \text{Equation 6.6.3.2-6}$$

$$= \frac{E s^2 h_b^2}{\frac{2L_d^3}{A_d}+\frac{s^3}{A_c}} \text{ (X-type cross-frame: tension only)} \qquad \text{Equation 6.6.3.2-7}$$

$$= \frac{2Es^2h_b^2}{\frac{8L_d^3}{A_d}+\frac{s^3}{A_c}} \text{ (K-type cross-frame)} \qquad \text{Equation 6.6.3.2-8}$$

Refer to Yura (2001), or to Yura and Helwig (2012), for the appropriate formula to use to calculate β_b for diaphragms. Adjustments to be made for skewed cross-frames are discussed in Section 2.4 of Yura and Helwig (2012).

β_g = in-plane girder stiffness (kip-in./rad).

$$= \frac{24(n_g-1)^2}{n_g}\frac{s^2EI_x}{L^3} \qquad \text{Equation 6.6.3.2-9}$$

Refer to Section 2.3.4 of Yura and Helwig (2004) for more information on β_g. This term is likely negligible for most multi-girder systems. If β_g dominates the actual overall brace system stiffness, then a system mode of buckling is possible (Section 6.5.3.3.5)

A_c = area of cross-frame bottom chord member (in.^{2})
A_d = area of cross-frame diagonal member (in.^{2})
h_b = height of cross-frame (in.)
I_x = strong-axis moment of inertia of one girder (in.^{4})
L_d = length of cross-frame diagonal (in.)
n_g = number of girders in the cross-section
s = girder spacing (in.)

For cross-frames, the required strength, $(M_{br})_{req}$, from Equation 6.6.3.2-2 is converted to chord forces in the cross-frame members by dividing $(M_{br})_{req}$ by the distance between the centroids of the top and bottom chords to obtain the required stability chord forces, $(F_{br})_{req}$. The required stability forces in the diagonals may be obtained by multiplying $(F_{br})_{req}$ by L_d/s for an X-type cross-frame configuration (tension-compression), and by $2L_d/s$ for a K-type cross-frame configuration and for an X-type cross-frame configuration (tension only).

Appendix 6.3 of AISC (2010a) specifies a resistance factor, ϕ, of 0.75 in Equation 6.6.2.3-3. However, resistance factors in the *AASHTO LRFD* Specification are typically set at a level that is 0.05 higher than those in the *AISC LRFD* Specification; therefore, the use of a resistance factor of 0.80 is recommended.

It is further recommended that a load factor of 1.0 be applied to the stability bracing forces when combined with the other factored forces for the limit state under consideration when checking the total factored forces in the bracing member against the factored resistance of the bracing member. This is because the stability bracing forces were calculated using a factored major-axis bending moment, M_f. It is also

recommended that the calculated values of the stability bracing forces for each investigated limit state be combined only with the other factored forces calculated for that same limit state to avoid excessive conservatism.

When the values of the variables in the two unbraced segments adjacent to a nodal brace are different, the brace may be designed for the average of values determined for both segments. In positive moment regions, it is recommended that the stability bracing forces only be considered in load combinations acting on the non-composite section (the top flange in compression is continuously braced in these regions by the hardened concrete deck for load combinations acting on the composite section). Also, it is recommended that the non-composite girder section properties at the point of maximum positive moment be used. In negative-moment regions, it is recommended that the stability bracing forces be considered in load combinations acting on both the non-composite and composite sections, and that the appropriate corresponding girder section properties at the point of largest negative moment be used (i.e. at the pier). Also, in negative-moment regions, consider avoiding excessive conservatism by checking the stability bracing requirements at the first cross-frame adjacent to the pier, and not at the pier. Anchor bolts and pier cross-frames should provide sufficient bracing stability by inspection.

The reader is referred to Appendix 6.3 of AISC (2010a) and to Yura and Helwig (2012) for similar recommendations pertaining to lateral bracing systems (or so-called relative bracing systems).

6.6.3.3 Tension Members

6.6.3.3.1 General

The design of tension members is covered in *AASHTO LRFD* Article 6.10.8. Tension members may consist of a single structural shape or they may be built-up from several structural shapes. Built-up tension members generally consist of rolled or welded shapes connected by continuous plates with or without perforations or by tie plates with or without lacing bars on the open sides. Perforated plates are now more commonly used. The design of built-up tension members is covered in *AASHTO LRFD* Article 6.8.5 (Section 6.6.3.3.4).

Although not classified as bracing members, tension members in bridges also include eyebars and pin-connected members. The design of eyebars is covered in *AASHTO LRFD* Article 6.8.6 and the design of pin-connected plates is covered in *AASHTO LRFD* Article 6.8.7. Additional information on the design of these members may be found in McGuire (1968), AISC (2010a), and White (2012). The design of eyebars and pin-connected plates is not covered in this Manual. As pointed out in McGuire (1968), eyebars and pin-connected plates were commonly used in the nineteenth century when Engineers were often concerned with

minimizing secondary stresses. They were also often more economical and faster to erect than hand-riveted construction. Since there is greater knowledge and less concern in modern design about the minimization of secondary stresses, the use of these members in new construction has largely disappeared.

Although steel cables, strands and rods also qualify as tension members, they are not typically used as permanent bracing members and so they are not covered in this particular section of the Manual.

6.6.3.3.2 Axial Tension

6.6.3.3.2.1 General

AASHTO LRFD Article 6.8.2.1 specifies that the factored tensile resistance, P_r, at the strength limit state for members subject to axial tension is to be taken as the lesser of the following:

- The factored tensile resistance for yielding on the gross section taken as:

$$P_r = \phi_y F_y A_g \qquad \text{Equation 6.6.3.3.2.1-1}$$

AASHTO LRFD Equation 6.8.2.1-1

or:

- The factored tensile resistance for fracture on the net section taken as:

$$P_r = \phi_u F_u A_n R_p U \qquad \text{Equation 6.6.3.3.2.1-2}$$

AASHTO LRFD Equation 6.8.2.1-2

where:

ϕ_y = resistance factor for yielding of tension members as specified in *AASHTO LRFD* Article 6.5.4.2 (=0.95)

ϕ_u = resistance factor for fracture of tension members as specified in *AASHTO LRFD* Article 6.5.4.2 (=0.80)

A_g = gross cross-sectional area of the member (in.^{2})

A_n = net area of the member determined as specified in *AASHTO LRFD* Article 6.8.3 (Section 6.6.3.3.2.3) (in.^{2})

F_y = specified minimum yield strength of the member (ksi)

F_u = tensile strength of the member specified in *AASHTO LRFD* Table 6.4.1-1 (ksi)

R_p = reduction factor for holes taken equal to 0.90 for bolt holes punched full size, and 1.0 for bolt holes drilled full size or subpunched and reamed to size

U = reduction factor to account for shear lag; 1.0 for components in which force effects are transmitted to all elements, and as specified in *AASHTO LRFD* Article 6.8.2.2 for other cases (Section 6.6.3.3.2.4)

The governing value of P_r must not exceed the factored block shear rupture resistance, R_r, of the member determined as specified in *AASHTO LRFD* Article 6.13.4 (Section 6.6.3.3.2.5).

A ductile steel loaded in axial tension can resist a force greater than the product of its gross area and yield strength prior to fracture due to strain hardening as long as excessive elongation due to uncontrolled yielding does not occur. However, depending on the ratio of net area to gross area, the geometry of the end connection and the mechanical properties of the steel, the component can fail by fracture of the net area at a load smaller than that required to yield the gross area. Thus, both yielding and fracture must be checked.

Holes in a member cause stress concentrations at service loads, with the tensile stress adjacent to the hole typically about three times the average stress on the net area. As load increases and the deformation continues, all fibers across the section will achieve or eventually exceed the yield strain. Failure occurs when the localized yielding results in a fracture through the net area. Since the width of the member occupied by the net area at bolt holes is generally negligible relative to the overall width of the member, strain hardening is easily achieved in the vicinity of the holes and yielding on the net area at bolt holes is not considered to be significant, except perhaps for built-up members of unusual proportions. A higher margin of safety is typically used when considering the net section fracture resistance versus the yield resistance, as reflected in the specified resistance factors.

The gross area, A_g, in Equation 6.6.3.3.2.1-1 is to be determined considering all holes larger than those typically used for connectors, such as bolts. Holes that must typically be deducted when computing the gross area include access holes, pin holes and perforations. The calculation of the net area, A_n, in Equation 6.6.3.3.2.1-2 is discussed in Section 6.6.3.3.2.3.

The reduction factor, R_p, in Equation 6.6.3.3.2.1-2 conservatively accounts for the reduced fracture resistance in the vicinity of bolt holes punched full size (Brown et al., 2007). No reduction in the net section fracture resistance is required for holes that are drilled full size or subpunched and reamed to size. In previous specifications, the reduction in the factored resistance for punched holes was accounted for by increasing the hole size for design by 1/16 inches, which penalized drilled and subpunched and reamed holes and did not provide a uniform reduction for punched holes since the reduction varied with the hole size. This reduction has since been removed in favor of the factor, R_p. *AASHTO LRFD* Article 6.6.1.2.3 specifies that unless information is available to the contrary, bolt holes in cross-

frame and lateral bracing members and their connection plates are to be assumed for design to be punched full size.

The shear lag reduction factor, *U*, in Equation 6.6.3.3.2.1-2 is discussed in Section 6.6.3.3.2.4.

6.6.3.3.2.2 Limiting Slenderness Ratios

AASHTO LRFD Article 6.8.4 specifies limiting slenderness ratios, ℓ/r, for tension members other than rods, eyebars, cables and plates, where ℓ is the unbraced length and *r* is the minimum radius of gyration for the cross-section. The slenderness limits are not intended to ensure the structural integrity of tension members, but to ensure a minimum degree of stiffness to reduce the potential for undesirable lateral movements or vibrations of the members. The resistance of tension members is not affected by out-of-straightness within reasonable tolerances as the applied tension tends to reduce the out-of-straightness, whereas out-of-straightness tends to be amplified by applied compression.

For primary tension members subject to stress reversals, the maximum ℓ/r is limited to 140. For primary tension members not subject to stress reversals, the maximum ℓ/r is limited to 200. In the *AASHTO LRFD* Specifications, a primary member is defined as a member designed to carry the internal forces determined from an analysis. For secondary members (i.e. members in which stress is not normally evaluated in the analysis), the maximum ℓ/r is limited to 240. Note that for single angles, the radius of gyration about the z-axis typically produces the maximum ℓ/r.

6.6.3.3.2.3 Net Area, A_n

AASHTO LRFD Article 6.8.3 specifies that the net area, A_n, be taken as the product of the thickness of the member/element and its smallest net width. The width of each standard bolt hole is to be taken as the nominal diameter of the hole. Maximum holes sizes for different bolt diameters are specified in *AASHTO LRFD* Table 6.13.2.4.2-1 (Section 6.6.4.2.3.1). For example, for a 7/8-inch diameter bolt, the maximum hole size of a standard hole is 15/16 inches.

The net width is to be determined for each chain of holes extending across the connected angle leg along any transverse, diagonal or zigzag line. For each chain, the net width is to be determined by subtracting from the total width, the sum of all holes in the chain, and adding the quantity $s^2/4g$ for each space between consecutive holes in the chain (i.e. when holes are staggered), where *s* is equal to the pitch of ay two consecutive holes and *g* is the gage of the same two holes (Figure 6.6.3.3.2.3-1). The development of the $s^2/4g$ rule is described in McGuire (1968). When holes are staggered in both legs of an angle, the gage for holes in

opposite adjacent legs is to be taken as the sum of the gages from the back of the angles less the thickness of the angle. For welded connections, A_n is to be taken as the gross area less any access holes within the connection region.

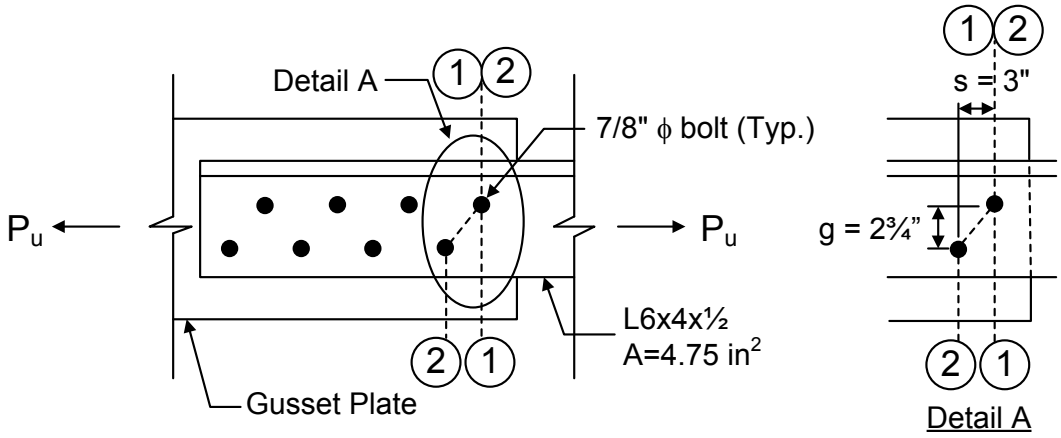

$$\text{Chain } 1-1: \quad A_n = 4.75 - [1(0.9375)(0.5)] = 4.28 \text{ in.}^2$$

$$\text{Chain } 2-2: \quad A_n = 4.75 - [2(0.9375)(0.5)] + \left[\frac{(3.0)^2}{4(2.75)}(0.5)\right] = 4.22 \text{ in.}^2 \quad \text{(Governs)}$$

Figure 6.6.3.3.2.3-1 Net Area Computation – Single Angle with Staggered Bolt Holes

It is conservative to use the least net width in conjunction with the full tensile force to check the connected element. Assuming each bolt transfers an equal share of the load whenever the bolts are arranged symmetrically with respect to the centroidal axis of the connected element, a less conservative alternative is to check each possible chain with a tensile force obtained by subtracting the force removed by each bolt ahead of that chain from the full tensile force (refer to the example in Section 6.6.4.2.5.6.1).

6.6.3.3.2.4 Shear Lag Reduction Factor, *U*

The shear lag reduction factor, *U,* accounts for shear lag effects associated with end connection geometry. Shear lag is a consideration where the tensile force in the member is applied eccentrically or transmitted by connection to some, but not all of the connection elements; e.g. an angle having a connection to only one leg, or when the connection elements do not lie in a common plane. In such cases, the tensile force is not uniformly distributed over the net area and the critical net section may not be fully effective. The shear lag factor is to be applied when computing the net section fracture resistance given by Equation 6.6.3.3.2.1-2 at the strength limit state. Shear lag does not need to be considered when checking yielding on the gross section because the non-uniform tensile stresses over the cross-section tend to be

equalized by the yielding. Research on the effects of shear lag in end connections of tension members is described in Munse and Chesson (1963) and Easterling and Giroux (1993).

As specified in *AASHTO LRFD* Table 6.8.2.2-1 (Case 1), if the tensile force is transmitted directly to every component plate of a member cross-section by bolts or welds, *U* is to be taken equal to 1.0. For tension members, except for plates and HSS, where the tensile load is transmitted to some but not all of the component plates of a member cross-section by bolts or longitudinal welds, *AASHTO LRFD* Table 6.8.2.2-1 (Case 2) permits U to be calculated by the following formula (Munse and Chesson, 1963):

$$U = 1 - \frac{\bar{x}}{L} \qquad \text{Equation 6.6.3.3.2.4-1}$$

where:

$\bar{x}$ = perpendicular distance from the connection plane or face of the member to the centroid of the member section resisting the connection force (in.). Illustrative examples for different cases are given in *AASHTO LRFD* Figure C6.8.2.2-1.

L = out-to-out distance between the bolts in the connection parallel to the line of force, or maximum length of the longitudinal welds (in.)

Illustrative examples of $\bar{x}$ and *L* for single angles connected with bolts and welds are shown in Figure 6.6.3.3.2.4-1. Note that for members connected with combinations of longitudinal and transverse welds, *L* is taken as the maximum length of the longitudinal welds. The transverse weld does little to influence the transfer of the load into the unattached elements of the member cross-section, and thus, does not significantly affect the fracture resistance based on shear lag.

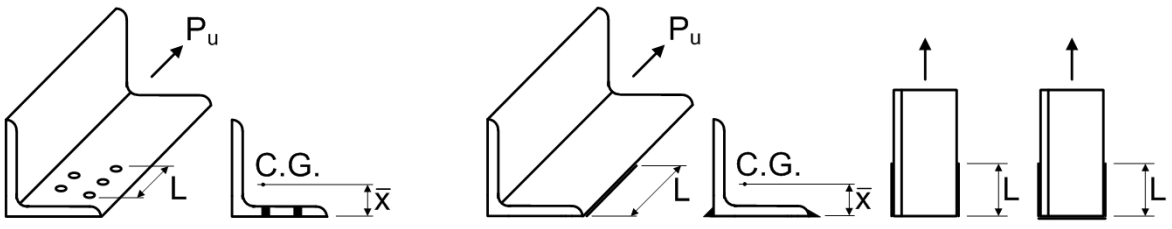

Figure 6.6.3.3.2.4-1 Determination of $\bar{x}$ and *L* in the Calculation of the Shear Lag Reduction Factor, *U*, from Equation 6.6.3.3.2.4-1

In lieu of using Equation 6.6.3.3.2.4-1, *AASHTO LRFD* Table 6.8.2.2-1 (Case 7) instead specifies the following alternative values of *U* for bolted connections in W, M, S, and HP shapes, or tees cut from these shapes:

- For shapes with flange widths, b_f, greater than or equal to 2/3 of the section depth, *d*, connected to the flanges with three or more bolts in the direction of the line of force:

$$U = 0.90$$

- For shapes with b_f < 2/3 of *d* connected to the flanges with three or more bolts in the direction of the line of force:

$$U = 0.85$$

- For shapes with the web connected and with four or more bolts in the direction of the line of force:

$$U = 0.70$$

AASHTO LRFD Table 6.8.2.2-1 (Case 8) specifies alternative values of *U* for single angles connected with bolts. That is, for single angles with four or more bolts in the direction of the line of force, *U* may be taken as 0.80. For single angles with two or three bolts in the direction of the line of force, *U* may be taken as 0.60.

Note that If *U* is calculated from Equation 6.6.3.3.2.4-1, and any of the above alternative values are also considered, the larger value is permitted to be used.

AASHTO LRFD Table 6.8.2.2-1 (Case 3) specifies that when the load is transmitted only by transverse welds to some but not all of the component plates (which is relatively rare in bridges), *U* is to be taken as 1.0 and A_n is to be taken as only the area of the directly connected component plates (which indirectly accounts for the shear lag effect by using the reduced area). Furthermore, for the case of lapped-plate tension members, where the load is transmitted by longitudinal welds only, *AASHTO LRFD* Table 6.8.2.2-1 (Case 4) specifies reduced values of *U* (i.e. less than 1.0) when *L* is less than twice the distance, *w*, between the longitudinal welds (i.e. the plate width). Values of *U* for round and rectangular HSS are also specified in *AASHTO LRFD* Table 6.8.2.2-1 (Cases 5 and 6, respectively).

AASHTO LRFD Article 6.8.2.2 further specifies that for members composed or more than one element, the calculated value of *U* should not be taken to be less than the ratio of the gross area of the connected element (or elements) to the member gross area. In addition, *U* is permitted to be alternatively determined by refined analysis or tests.

6.6.3.3.2.5 Block Shear Rupture Resistance, R_r

A connected element subject to tension must be checked for a tearing limit state known as block shear rupture. A block shear rupture failure for an angle in tension bolted to a gusset plate is shown in Figure 6.6.3.3.2.5-1. In Figure 6.6.3.3.2.5-1, the tearing failure along the bolt holes occurs along section a-b-c. The tearing or shear rupture resistance on section a-b, plus the tensile yield resistance on section b-c, will result in the total block shear rupture resistance. Note that the failure path is defined by the centerlines of the bolt holes. Tests have shown that it is reasonable to add the resistance in tension yielding on one plane to the shear rupture resistance of the perpendicular plane (Ricles and Yura, 1983; Hardash and Bjorhovde, 1985).

AASHTO LRFD Article 6.13.4 specifies that block shear rupture is to be checked for the web connection of coped beams and for all tension connections, including connection plates, splice plates and gusset plates. Tests on coped beams have indicated that a block shear failure can occur around the perimeter of the bolt holes (Birkemoe and Gilmour, 1978). The block shear rupture mode is not limited to the coped ends of beams, however. Tension member connections are also susceptible, and the block shear rupture mode should also be checked around the periphery of welded connections.

The connection is to be investigated by considering all possible failure planes in the connected elements, including those parallel and perpendicular to the applied forces, and determining the most critical set of planes. Planes parallel to the applied force are to be considered to resist only shear stresses and planes perpendicular to the applied force are to be considered to resist only tensile stresses. Block shear rupture is most likely to control in the design of bolted end connections to thin webs of girders (e.g. coped beams) and in the design of short compact bolted connections. It is unlikely to control in the design of bolted flange and web splices of typical proportions.

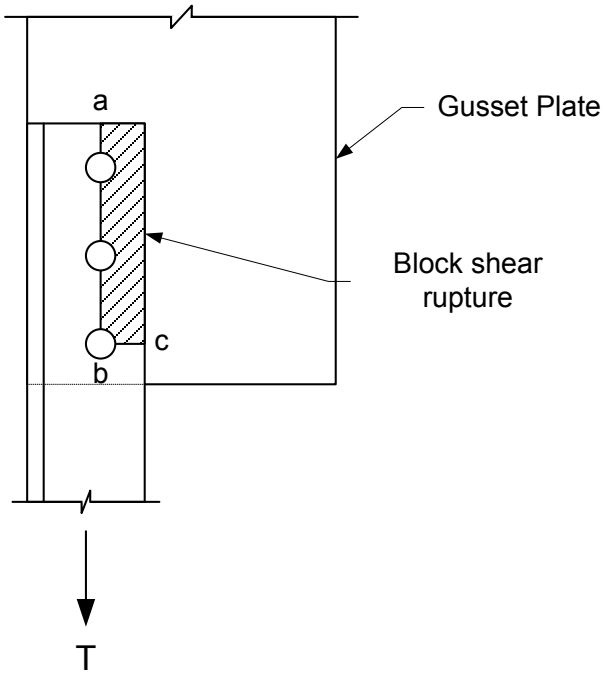

Figure 6.6.3.3.2.5-1 Tension Failure of a Bolted Single Angle Member by Block Shear Rupture

The factored tensile resistance, P_r, computed from Equation 6.6.3.3.2.1-1 or Equation 6.6.3.3.2.1-2, whichever controls, must not exceed the factored block shear rupture resistance, R_r, of the member, which must be investigated at the end connections. The factored block shear rupture resistance is determined according to the provisions of *AASHTO LRFD* Article 6.13.4 as follows:

$$R_r = \phi_{bs} R_p \left(0.58 F_u A_{vn} + U_{bs} F_u A_{tn}\right)$$

$$\leq \phi_{bs} R_p \left(0.58 F_y A_{vg} + U_{bs} F_u A_{tn}\right) \qquad \text{Equation 6.6.3.3.2.5-1}$$

AASHTO LRFD Equation 6.13.4-1

where:

ϕ_{bs} = resistance factor for block shear rupture specified in *AASHTO LRFD* Article 6.5.4.2 (=0.80)

A_{vg} = gross area along the plane resisting shear stress (in.^{2})

A_{vn} = net area along the plane resisting shear stress (in.^{2})

A_{tn} = net area along the plane resisting tension stress (in.^{2})

U_{bs} = reduction factor for block shear rupture resistance taken equal to 0.50 when the tension stress is non-uniform and 1.0 when the tension stress is uniform

The terms F_y, F_u and R_p are as defined previously.

In determining R_r, the resistance to rupture along the shear plane is added to the resistance to rupture on the tensile plane (Figure 6.6.3.3.2.5-2). Block shear rupture is a rupture or tearing phenomenon and not a yielding phenomenon. However, gross yielding along the shear place can occur when tearing on the tensile plane commences if $0.58F_uA_{vn}$ exceeds $0.58F_yA_{vg}$. Therefore, the preceding equation limits $0.58F_uA_{vn}$ to not exceed $0.58F_yA_{vg}$.

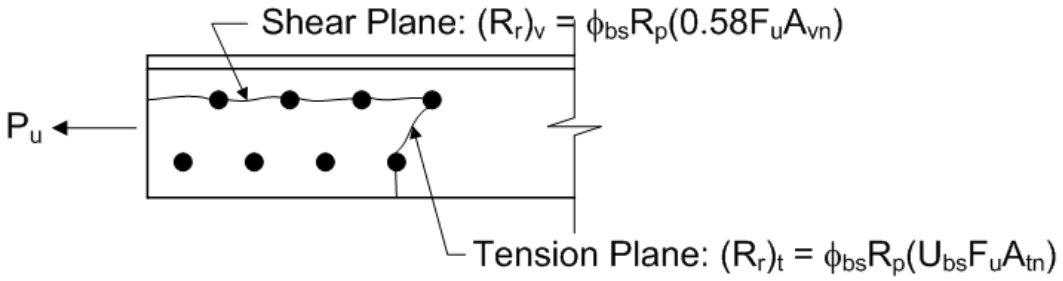

Figure 6.6.3.3.2.5-2 Factored Resistance of Shear and Tension Planes

The reduction factor, U_{bs}, has been included in Equation 6.6.3.3.2.5-1 to approximate the effect of a non-uniform stress distribution on the tensile plane in certain cases; e.g., coped beam connections with multiple rows of bolts. In such cases, the tensile stress on the end plane is non-uniform because the rows of bolts nearest the beam end pick up most of the shear (Ricles and Yura, 1983; Kulak and Grondin, 2001). For the majority of connections encountered in steel bridges, U_{bs} will equal 1.0.

In determining the net area of cuts carrying shear stress, the full effective diameter of staggered holes centered within two hole diameters of the cut is to be deducted; holes further removed are to be disregarded. In determining the net area of cuts carrying tension stress, the effect of staggered holes adjacent to the cuts is to be determined using the $s^2/4g$ correction.

EXAMPLE

Determine the factored tensile resistance, P_r, of the single-angle bracing member shown in Figure 6.6.3.3.2.5-3 at the strength limit state. The steel is ASTM A709/A709M Grade 50 steel. All bolts are 7/8-inch diameter ASTM A325 high-strength bolts placed in standard holes assumed for design to be punched full size (refer to *AASHTO LRFD* Article 6.6.1.2.3). From *AASHTO LRFD* Table 6.4.1-1, F_u for Grade 50 steel is 65 ksi.

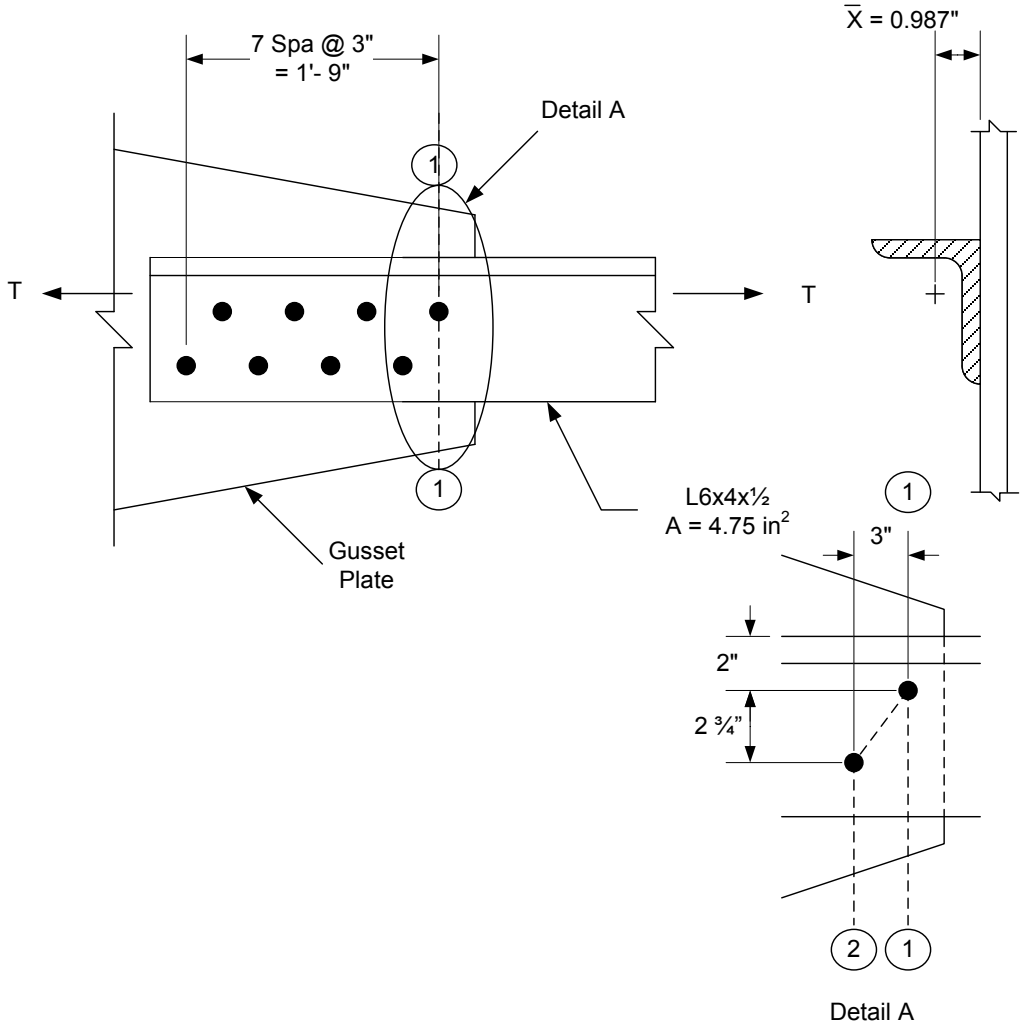

Figure 6.6.3.3.2.5-3 Example – Factored Tensile Resistance of Single Angle Bracing Member

The factored tensile resistance for yielding on the gross section is calculated as (Equation 6.6.3.3.2.1-1):

$$P_r = \phi_y P_{ny} = \phi_y F_y A_g$$

$$P_r = 0.95(50)(4.75) = 225.6 \text{ kips}$$

The factored tensile resistance for fracture on the net section is computed as (Equation 6.6.3.3.2.1-2):

$$P_r = \phi_u P_{nu} = \phi_u F_u A_n R_p U$$

The calculation of the net area, A_n, for this case is illustrated in Figure 6.6.3.3.2.3-1. Both cases in Figure 6.6.3.3.2.3-1 are assumed to act in conjunction with the full tensile force, *T*. The governing value of A_n is computed to be 4.22 in.^{2}

As specified in *AASHTO LRFD* Article 6.8.2.2, the shear-lag factor, *U*, for this case would be taken as 0.80 (for single angles with four or more bolts per line in the direction of the load – Case 8 in *AASHTO LRFD* Table 6.8.2.2-1), or else a larger value could be used if the *U* factor were calculated from Equation 6.6.3.3.2.4-1 as follows (Case 2 in *AASHTO LRFD* Table 6.8.2.2-1):

$$U = 1 - \frac{\bar{x}}{L} = 1 - \frac{0.987}{21} = 0.95$$

Since the holes are assumed punched full size, the reduction factor, R_p, is taken equal to 0.90. Therefore, from Equation 6.6.3.3.2.1-2:

$$P_r = 0.80(65)(4.22)(0.90)(0.95) = 187.6 \text{ kips}$$

Calculate the factored block shear rupture resistance of the connection. Assume the block shear failure planes shown in Figure 6.6.3.3.2.5-4. For the calculation of the net areas, the width of each standard bolt hole is taken as the nominal diameter of the hole. For a 7/8-inch diameter bolt, the maximum hole size of a standard hole is 15/16 inches (Section 6.6.4.2.3.1).

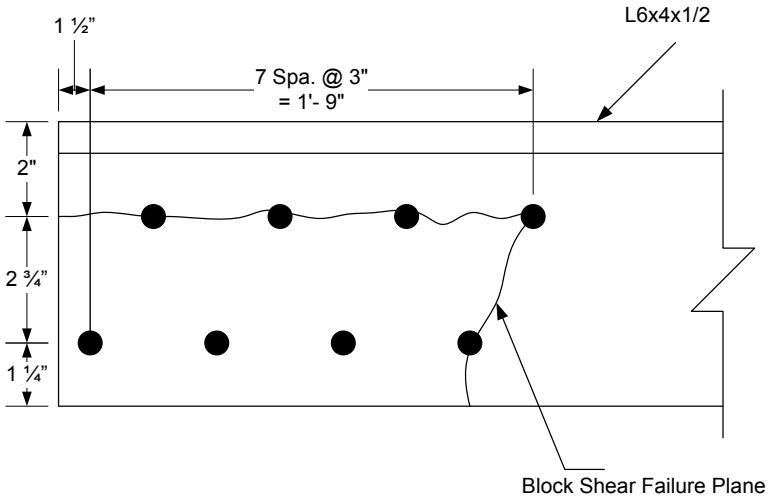

Figure 6.6.3.3.2.5-4 Example – Assumed Block Shear Failure Planes in Single-Angle Bracing Member

$$A_{tn} = \left[2.75 + 1.25 - 1.5(0.9375) + \frac{(3.0)^2}{4(2.75)}\right](0.5) = 1.71\,\text{in.}^2$$

A_{vn} is the net area along the place resisting the shear stress. As specified in *AASHTO LRFD* Article 6.13.4, the full effective diameter of the staggered holes adjacent to the cut need not be deducted in determining A_{vn} in this case since these holes are centered more than two hole diameters from the cut. Therefore:

$$A_{vn} = [3(6.0) + 4.5 - 3.5(0.9375)](0.5) = 9.61\,\text{in.}^2$$

A_{vg} is the gross area along the plane resisting the shear stress.

$$A_{vg} = [3(6.0) + 4.5](0.5) = 11.25\,\text{in.}^2$$

The factored block shear rupture resistance, R_r, is determined as (Equation 6.6.3.3.2.5-1):

$$R_r = \phi_{bs} R_p (0.58 F_u A_{vn} + U_{bs} F_u A_{tn}) \le \phi_{bs} (0.58 F_y A_{vg} + U_{bs} F_u A_{tn})$$

ϕ_{bs} is the resistance factor for block shear rupture taken equal to 0.80 (*AASHTO LRFD* Article 6.5.4.2). The reduction factor, U_{bs}, is taken equal to 1.0 since the tension stress is uniform. Therefore:

$$\begin{aligned} R_r &= 0.80(0.90)[0.58(65)(9.61) + 1.0(65)(1.71)] = 341\,\text{kips} \\ &> 0.80(0.90)[0.58(50)(11.25) + 1.0(65)(1.71)] = 315\ \text{kips} \\ &\therefore R_r = 315\ \text{kips} \end{aligned}$$

Therefore, the factored tensile resistance of the member is governed by fracture on the net section; that is P_r = 187.6 kips.

As discussed further in Section 6.6.3.3.3, the effects of the combined flexure and axial force due to the eccentricity of the loading acting on a single-angle bracing member subject to tension are accounted for in determining the factored tensile resistance of the member at the strength limit state through the use of the shear lag factor, *U*.

6.6.3.3.3 Combined Axial Tension and Flexure

As specified in *AASHTO LRFD* Article 6.8.2.3, a member or component subject to combined tension and flexure must satisfy the following two interaction relationships:

- If $\frac{P_u}{P_r} < 0.2$, then:

$$\frac{P_u}{2.0P_r} + \left(\frac{M_{ux}}{M_{rx}} + \frac{M_{uy}}{M_{ry}}\right) \le 1.0 \qquad \text{Equation 6.6.3.3.3-1}$$

AASHTO LRFD Equation 6.8.2.3-1

- If $\frac{P_u}{P_r} \ge 0.2$, then:

$$\frac{P_u}{P_r} + \frac{8.0}{9.0}\left(\frac{M_{ux}}{M_{rx}} + \frac{M_{uy}}{M_{ry}}\right) \le 1.0 \qquad \text{Equation 6.6.3.3.3-2}$$

AASHTO LRFD Equation 6.8.2.3-2

where:

ϕ_f = resistance factor for flexure determined as specified in *AASHTO LRFD* Article 6.5.4.2 (= 1.0)

M_{rx} = factored flexural resistance about the x-axis taken as ϕ_f times the nominal flexural resistance about the x-axis determined as specified in *AASHTO LRFD* Article 6.10, 6.11 or 6.12, as applicable (kip-in.)

M_{ry} = factored flexural resistance about the y-axis taken as ϕ_f times the nominal flexural resistance about the y-axis determined as specified in *AASHTO LRFD* Article 6.12, as applicable (kip-in.)

M_{ux} = factored moment about the x-axis (kip-in.)

M_{uy} = factored moment about the y-axis (kip-in.)

P_r = factored tensile resistance determined as specified in *AASHTO LRFD* Article 6.8.2.1 (see Equations 6.6.3.3.2.1-1 and Equation 6.6.3.3.2.1-2 above) (kips)

P_u = factored axial force (kips)

AASHTO LRFD Article 6.8.2.3 further specifies that a flange subject to a compressive stress under combined tension and flexure must be investigated for local buckling.

For prismatic members along the unbraced length, the largest value of P_u/P_r based on the axial tensile resistance limit states of yielding or net section fracture is to be used in Equation 6.6.3.3.3-1 or Equation 6.6.3.3.3-2, as applicable. Also, the largest values of M_{ux}/M_{rx} and M_{uy}/M_{ry} based on the flexural resistance limit states of yielding, local buckling or lateral-torsional buckling are to be used. Strictly speaking, for a particular load combination, concurrent values of P_u, M_{ux}, and M_{uy} should be used in

computing and determining the critical ratios to use. However, since concurrent actions are not typically tracked in the analysis, it is conservative and convenient to use the maximum envelope values for these actions in combining the ratios in these equations. For nonprismatic members, the reader is referred to White (2012) for additional information regarding the proper application of the preceding equations to such members.

As indicated in *AASHTO LRFD* Article C6.8.2.3, for sections where the nominal flexural resistance about the x-axis is expressed in terms of stress, the factored flexural resistance about the x-axis, M_{rx}, in Equation 6.6.3.3.3-1 or Equation 6.6.3.3.3-2, as applicable, is to be taken as:

$$M_{rx} = \text{the smaller of } \phi_f F_{nc} S_{xc} \text{ and } \phi_f F_{nt} S_{xt} \qquad \text{Equation 6.6.3.3.3-3}$$

AASHTO LRFD Equation C6.8.2.3-1

where:

F_{nc} = nominal flexural resistance of the compression flange (ksi)
F_{nt} = nominal flexural resistance of the tension flange (ksi)
S_{xc} = elastic section modulus about the major axis of the section to the compression flange taken as M_{yc}/F_{yc} (in.^{3})
S_{xt} = elastic section modulus about the major axis of the section to the tension flange taken as M_{yt}/F_{yt} (in.^{3})
M_{yc} = yield moment with respect to the compression flange determined as specified in *AASHTO LRFD* Article D6.2 (Section 6.4.5.3) (kip-in.)
M_{yt} = yield moment with respect to the tension flange determined as specified in *AASHTO LRFD* Article D6.2 (Section 6.4.5.3) (kip-in.)

S_{xc} and S_{xt}, as defined above, are equivalent values that account for the combined effects of the loads acting on different sections in composite members.

For sections where the nominal flexural resistance about the x-axis is determined according to the provisions of *AASHTO LRFD* Appendix A6 (Section 6.5.6.2.3), the factored flexural resistance about the x-axis, M_{rx}, in Equation 6.6.3.3.3-1 or Equation 6.6.3.3.3-2, as applicable, is to be taken as:

$$M_{rx} = \text{the smaller of } \phi_f M_{nc} \text{ and } \phi_f M_{nt} \qquad \text{Equation 6.6.3.3.3-4}$$

AASHTO LRFD Equation C6.8.2.3-2

where:

M_{nc} = nominal flexural resistance based on the compression flange (kip-in.)
M_{nt} = nominal flexural resistance based on the tension flange (kip-in.)

In cases where the member is subject to flexure about the y-axis, the nominal flexural resistance about the y-axis for I-shaped members is determined according to the provisions of *AASHTO LRFD* Article 6.12.2.2.1 (Section 6.6.3.5 - this section also contains further information on determining the nominal flexural resistance of miscellaneous members such as tees, double angles, and channels.). Otherwise, the y-axis terms are set to zero in Equation 6.6.3.3.3-1 or Equation 6.6.3.3.3-2, as applicable.

The effect of connection eccentricity is a function of connection and member stiffness, and may sometimes need to be considered in the design of the tension connection or member. Historically, engineers have neglected the effect of eccentricity in both the member and the connection when designing tension-only bracing. The flexibility of the member and the connections will often allow the member to deform such that the resulting eccentricity is relieved to a considerable extent. Symmetry of the applied tensile load at each end connection of the member can also help to restrain the end rotations of the member through application of the shear lag reduction factor, *U* (Section 6.6.3.3.2.4), when determining the factored tensile resistance of the member at the strength limit state can indirectly account for the effects of the eccentricity of the loading in angle and tee bracing members, in lieu of applying Equations 6.6.3.3.3-1 and 6.6.3.3.3-2. This factor is used to account for the effects of the eccentric net tensile force acting on these members at the fatigue limit state, as discussed further in Section 6.6.3.3.5. If in the judgment of the Engineer, it is felt that the relative connection and member stiffness is such that the effect of the eccentricity should be considered at the strength limit state (particularly for tee and double-angle bracing members which typically have larger eccentricities), Equations 6.6.3.3.3-1 and 6.6.3.3.3-2 may be conservatively applied.

6.6.3.3.4 Built-Up Members

Built-up tension members are covered in *AASHTO LRFD* Article 6.8.5. Built-up tension members typically consist of rolled or welded shapes connected on the open sides by continuous plates with or without perforations. Tie plates (sometimes referred to as batten or stay plates), or end tie plates and lacing bars, are also permitted on the open sides where special circumstances warrant, but are now less commonly used. Only the design requirements for perforated plates are covered in this Manual. Specific design requirements for tie plates and lacing bars may be found in AASHTO (2002) and AISC (2010a). Additional information on the design of laced and battered members may also be found in McGuire (1968), Salmon and Johnson (1996), and SSRC (1998).

As specified in *AASHTO LRFD* Article 6.8.5.1, welded connections between the plates and shapes of built-up tension members must be continuous and bolted connections between the shapes and plates must satisfy the provisions of *AASHTO*

LRFD Article 6.13.2, including the appropriate bolt spacing requirements (Section 6.6.4.2.2.2.4).
Specific design requirements for perforated plates in built-up members (subject to tension or compression) are given in *AASHTO LRFD* Article 6.8.5.2 (SSRC, 1998). These requirements are summarized as follows:

- The ratio of the length of the holes in the direction of stress to the width of the holes is not to exceed 2.0;
- The clear distance between the holes in the direction of stress is not to be less than the transverse distance between the nearest line of connection bolts or welds;
- The clear distance between the end of the plate and the first hole is not to be less than 1.25 times the transverse distance between the bolts or welds;
- The periphery of the holes is to have a minimum radius of 1.5 in.;
- The unsupported widths at the edges of the holes may be assumed to contribute to the net area of the member, and;
- Where the holes are staggered in opposite perforated plates, the net area of the member is to be considered the same as for a section having holes in the same transverse plane.

6.6.3.3.5 Fatigue of Single-Angle and Tee Member Connections

6.6.3.3.5.1 General

AASHTO LRFD Table 6.6.1.2.3-1 now provides a simplified procedure for checking fatigue of welded (Condition 7.2) or bolted (Condition 2.5) connections of single-angle or tee members to gusset or connection plates that are subject to a net applied tensile stress (as defined in *AASHTO LRFD* Article 6.6.1.2.1).

Where force effects in cross-frames or diaphragms are computed from a refined analysis, it is desirable to check any fatigue-sensitive details on these members that are subjected to a net applied tensile stress. In such cases, the effect of positioning the fatigue truck in two different transverse positions located directly over the adjacent connected girders, or directly over the adjacent connected girder webs in the case of a box section, usually creates the largest range of stress or torque in these bracing members. There is an extremely low probability of the truck being located in these two critical relative transverse positions over millions of cycles. Also field observation has not indicated a significant problem with the details on these members caused by load-induced fatigue or fatigue due to cross-section distortion.

Therefore, *AASHTO LRFD* Article C6.6.1.2.1 recommends that the fatigue truck be positioned to determine the maximum range of stress or torque, as applicable, in these members as specified in *AASHTO LRFD* Article 3.6.1.4.3a, with the truck

confined to one critical transverse position per each longitudinal position throughout the length of the bridge in the analysis.

6.6.3.3.5.2 Welded Connections

For single-angle or tee members connected to a gusset or connection plate by longitudinal fillet welds along both sides of the connected element of the member cross-section (Figure 6.6.3.3.5.2-1), the fatigue stress range, Δf, is to be calculated as follows:

$$\Delta f = \frac{\Delta P}{A_e} = \frac{\Delta P}{UA_g} \qquad \text{Equation 6.6.3.3.5.2-1}$$

where:

A_e = effective net area of the member = UA_g (in.^{2})
A_g = gross cross-sectional area of the member (in.^{2})
ΔP = range of axial force in the member under the applicable Fatigue load combination (kips)
U = shear-lag reduction factor determined from Equation 6.6.3.3.2.4-1

$\bar{x}$ is to be taken as the distance from the centroid of the member to the surface of the gusset or connection plate, and L is to be taken as the maximum length of the longitudinal welds (Figure 6.6.3.3.5.2-1) in the calculation of the shear-lag reduction factor, U.

The effect of the moment due to the eccentricities in the connection may be ignored in computing the stress range when Equation 6.6.3.3.5.2-1 is used (McDonald and Frank, 2009).

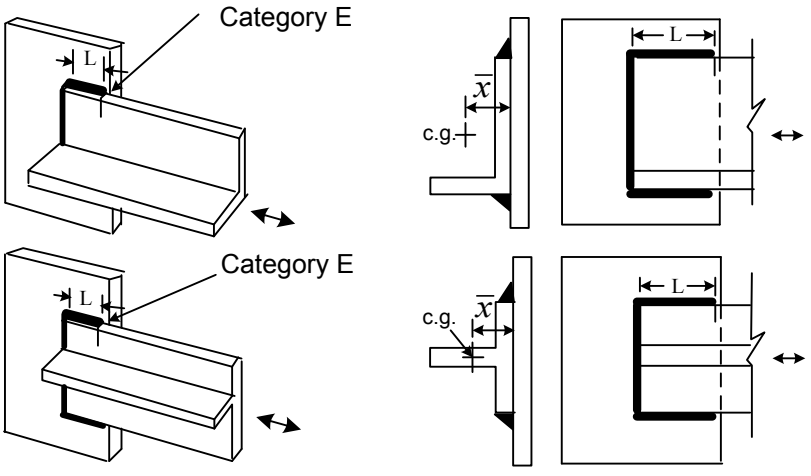

Figure 6.6.3.3.5.2-1 Welded Connection of a Single-Angle and a Tee Member to a Gusset Plate

The nominal fatigue resistance of the base metal in single-angle members connected by longitudinal fillet welds along both sides of the connected element of the member cross-section, and with or without backside welds, is to be based on Detail Category E (Condition 7.2 in *AASHTO LRFD* Table 6.6.1.2.3-1). While the research showed that balancing of the welds offers some increase in the fatigue life (McDonald and Frank, 2009), it is probably not worth the increase in the gusset or connection plate length required to accommodate the longer weld along one leg.

As of this writing (2015), AASHTO is considering a potential reduction in the nominal fatigue resistance of the base metal in single-angle members connected by longitudinal fillet welds from Detail Category E to Detail Category E′. Full-scale fatigue tests on 25 different welded cross-frame configurations, including configurations utilizing single-angle and double-angle members, have indicated that the current classification of these welded cross-frame details as Detail Category E may be unconservative (Battastini et al., 2014). The eccentricity of these members when fatigue tested in an actual full-scale cross-frame arrangement (rather than testing the members as individual components) seems to indicate a lower bound to fatigue Category E′. Double-angle members behave similarly to tee-section members, and thus although not physically tested as part of this research, tee-section members are implicitly included in this category.

6.6.3.3.5.3 Bolted Connections

For single-angle members connected to a gusset or connection plate with high-strength bolted slip-critical connections (Figure 6.6.3.3.5.3-1), the fatigue stress range, Δf, is to be calculated from Equation 6.6.3.3.5.2-1. Slip-critical connections are discussed further in Section 6.6.4.2.1.1. A_g is to be replaced with the net area of the member, A_n, in Equation 6.6.3.3.5.2-1 for all other types of bolted connections.

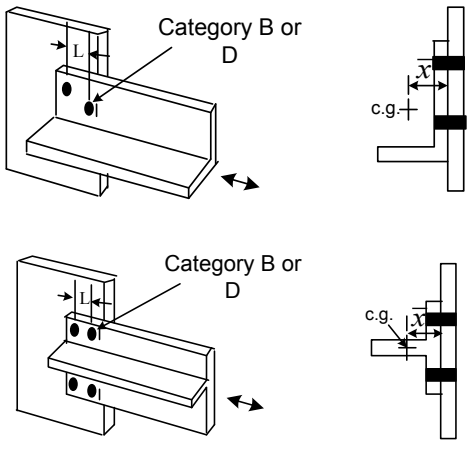

Figure 6.6.3.3.5.3-1 Bolted Connection of a Single-Angle and a Tee Member to a Gusset Plate

$\bar{x}$ is to be taken as the distance from the centroid of the member to the surface of the gusset or connection plate, and *L* is to be taken as out-to-out distance between the bolts in the connection parallel to the line of force (Figure 6.6.3.3.5.3-1) in the calculation of the shear-lag reduction factor, *U*.

The effect of the moment due to the eccentricities in the connection may be ignored in computing the stress range when Equation 6.6.3.3.5.2-1 is used.

The nominal fatigue resistance of the base metal in members connected by pre-tensioned high-strength bolts in slip-critical connections is to be determined based on whether the bolt holes are drilled full size or subpunched and reamed to size (Detail Category B), or punched full size (Detail Category D) (Condition 2.1 in *AASHTO LRFD* Table 6.6.1.2.3-1). *AASHTO LRFD* Article 6.6.1.2.3 specifies that unless information is available to the contrary, bolt holes in cross-frame and lateral bracing members and their connection plates are to be assumed for design to be punched full size.

Refer to Condition 2.2 or 2.3 in *AASHTO LRFD* Table 6.6.1.2.3-1, as applicable, for all other types of bolted connections. The fatigue resistance of bolted connections is discussed further in Section 6.6.4.2.1.3.

6.6.3.4 Compression Members

6.6.3.4.1 General

This section addresses the design of steel compression members, which are covered primarily in *AASHTO LRFD* Article 6.9. Compression members may consist of a single structural shape or may be built-up from plates or shapes. Common built-up compression members include back-to-back angles, “boxed” channels, and members connected by lacing (flat bars, angles, channels or other shapes), tie plates (also referred to as batten or stay plates) or perforated cover plates. The design of built-up compression members is covered in *AASHTO LRFD* Article 6.9.4.3 (Section 6.6.3.4.4).

Compression members include solid-web arch ribs (refer to *AASHTO LRFD* Article 6.14.4 and White, 2012), and compression chords of half-through trusses (refer to *AASHTO LRFD* Article 6.14.2.9). However, these members are not addressed herein as this document is primarily concerned with the design of bracing members.

The design of composite columns (i.e. concrete-filled steel tubes and concrete encased steel shapes) is covered in *AASHTO LRFD* Articles 6.9.5 and 6.9.6. The *AASHTO LRFD* Specification provisions for composite columns in *AASHTO LRFD* Article 6.9.5 are based on the work of SSRC Task Group 20 and others (SSRC,

1979; Galambos and Chapuis, 1980). As discussed further in White (2012), the *AISC LRFD* Specification (AISC, 2010a) provides significantly revised provisions for the design of composite columns that provide improved accuracy in the prediction of the nominal compressive resistance of these members. This improved accuracy is reflected by a reduced value of the resistance factor. The design procedures for composite columns are not covered in this Manual. The reader is referred instead to White (2012) for additional more detailed discussion related to the design of composite columns.

The provisions of *AASHTO LRFD* Articles 6.9.6 and 6.12.2.3.3 provide an alternative for the design of composite concrete-filled steel tubes (CFSTs), with or without internal reinforcement, subject to axial compression or combined axial compression and flexure. The use of composite CFSTs for piers permits rapid construction of the pier, since no formwork or internal reinforcement is required. Further, composite CFST piers result in the less weight and material since the diameter of the pier will be 25% to 35% smaller than a comparable reinforced concrete pier of the same strength and stiffness. CFSTs expected to develop full plastic hinging of the composite section as a result of a seismic event are to instead satisfy the provisions of AASHTO (2011b). The development of these alternative provisions, which are not discussed further herein, is described in Roeder et al. (2009), Roeder et al. (2010), and Roeder and Lehman (2012).

White (2012) also discusses the issue of composite steel bridge girders subjected to combined axial compression and flexure, such as might occur in a cable-stayed system with a composite I- or box-girder deck system.

The design of tapered compression members is not covered herein. The reader is referred to White (2012) for assistance regarding the design of nonprismatic and/or tapered compression members.

The subsequent discussion focuses on the design of non-composite elements subject to axial compression or combined axial compression and flexure. *AASHTO LRFD* Article 6.9 applies to prismatic members with at least one plane of symmetry and subject to either axial compression or combined axial compression and flexure about an axis of symmetry.

6.6.3.4.2 Axial Compression

6.6.3.4.2.1 General

As specified in *AASHTO LRFD* Article 6.9.2.1, the factored resistance of components subject to axial compression at the strength limit state, P_r, is to be taken as:

$$P_r = \phi_c P_n \qquad \text{Equation 6.6.3.4.2.1-1}$$

AASHTO LRFD Equation 6.9.2.1-1

where:

ϕ_c = resistance factor for axial compression specified in *AASHTO LRFD* Article 6.5.4.2 (=0.95)

P_n = nominal compressive resistance based on the limit state of flexural buckling, torsional buckling or flexural-torsional buckling, whichever controls (kips). Refer to *AASHTO LRFD* Article 6.9.4.1.1 and *AASHTO LRFD* Table 6.9.4.1.1-1 for the selection of the appropriate buckling mode, and for the appropriate equations to use for the calculation of P_e and Q, as applicable (Section 6.6.3.4.2.3.1).

The calculation of the nominal compressive resistance, P_n, for the limit states of flexural buckling, torsional buckling and flexural-torsional buckling is discussed in Section 6.6.3.4.2.3.

6.6.3.4.2.2 Limiting Slenderness Ratios

AASHTO LRFD Article 6.9.3 specifies limiting slenderness ratios, $K\ell/r$, for compression members, where K is the effective length factor determined as specified in *AASHTO LRFD* Article 4.6.2.5 (Section 6.6.3.4.2.3.3), ℓ is the unbraced length, and r is the minimum radius of gyration for the cross-section. In computing the maximum slenderness for checking the appropriate limiting ratio only as given below, *AASHTO LRFD* Article 6.9.3 permits the radius of gyration to be computed on a notional section that neglects part of the area of a component provided that the resistance of the component based on the actual area and radius of gyration exceeds the factored loads, and the resistance of the notional component based on the reduced area and corresponding radius of gyration also exceeds the factored loads.

For primary compression members, the maximum $K\ell/r$ is limited to 120. In the *AASHTO LRFD* Specification, a primary member is defined as a member designed to carry the internal forces determined from an analysis. For compression members used as secondary members (i.e. members in which stress is not normally evaluated in the analysis), the maximum $K\ell/r$ is limited to 140.

Note that for single angles where the effective slenderness ratio approach is used to design the angle (Section 6.6.3.4.5.2), the actual maximum slenderness ratio, $K\ell/r$, should be checked against the appropriate limiting value, rather than the effective slenderness ratio, $(K\ell/r)_{eff}$. Thus, if $(K\ell/r)_{eff}$ exceeds the limiting ratio, but the actual maximum slenderness ratio of the angle, $K\ell/r$, does not, the design is satisfactory.

6.6.3.4.2.3 Nominal Compressive Resistance

6.6.3.4.2.3.1 General

For non-composite members composed of nonslender elements that satisfy the width-to-thickness requirements for axial compression specified in *AASHTO LRFD* Article 6.9.4.2.1 (Section 6.6.3.4.2.4), the nominal compressive resistance, P_n, is to be taken as follows according to the provisions of *AASHTO LRFD* Article 6.9.4.1.1:

- If $\frac{P_e}{P_o} \geq 0.44$, then:

$$P_n = \left[0.658^{\left(\frac{P_o}{P_e}\right)}\right] P_o \qquad \text{Equation 6.6.3.4.2.3.1-1}$$

AASHTO LRFD Equation 6.9.4.1.1-1

- If $\frac{P_e}{P_o} < 0.44$, then:

$$P_n = 0.877\ P_e \qquad \text{Equation 6.6.3.4.2.3.1-2}$$

AASHTO LRFD Equation 6.9.4.1.1-2

where:

P_e = elastic critical buckling resistance determined as specified in *AASHTO LRFD* Article 6.9.4.1.2 for flexural buckling (Section 6.6.3.4.2.3.3), and as specified in *AASHTO LRFD* Article 6.9.4.1.3 for torsional buckling or flexural-torsional buckling, as applicable (Section 6.6.3.4.2.3.4) (kips)
P_o = equivalent nominal yield resistance = QF_yA_g (kips)
A_g = gross cross-sectional area of the member (in.^{2})
F_y = specified minimum yield strength (ksi)
Q = slender element reduction factor ≤ 1.0 specified in *AASHTO LRFD* Article 6.9.4.2 (Section 6.6.3.4.2.4). Q is to be taken equal to 1.0 for bearing stiffeners

Equation 6.6.3.4.2.3.1-1 for P_n provides a transition between elastic buckling and yielding, reflecting essentially the effects of residual stress and initial out-of-straightness. Equation 6.6.3.4.2.3.1-2 represents an elastic bucking equation for longer columns. The two equations represent a single curve that closely fits SSRC (Structural Stability Research Council) Column Curve 2P (SSRC, 1998) modified to reflect an initial out-of-straightness criterion of L/1500. The development of the mathematical form of the equations representing this curve is discussed in Tide

(1985) and Tide (2001). Salmon and Johnson (1996) shows a reasonable comparison of the results from Equations 6.6.3.4.2.3.1-1 and 6.6.3.4.2.3.1-2 with physical column test data compiled by Hall (1981). More detailed discussion on column buckling theory and the genesis of Equations 6.6.3.4.2.3.1-1 and 6.6.3.4.2.3.1-2 is provided below in Section 6.6.3.4.2.3.2.

Equations 6.6.3.4.2.3.1-1 and 6.6.3.4.2.3.1-2 are equivalent to the equations given in AISC (2010a) for computing the nominal compressive resistance. In the *AASHTO LRFD* Specification, the equations are written in a different format in terms of the critical elastic buckling resistance, P_e, and the equivalent nominal yield resistance, P_o, (discussed below) to allow for more convenient calculation of the nominal resistance for members subject to buckling modes in addition to, or other than, flexural buckling, and to allow for the consideration of compression members with slender elements (Section 6.6.3.4.2.4.3).

6.6.3.4.2.3.2 Column Buckling Theory

Column buckling theory originated from the work of Leonhard Euler (Euler, 1744). Euler investigated the buckling strength of an initially straight, concentrically loaded, pinned-end member, in which all fibers are assumed to remain elastic until buckling instability occurs. Instability occurs at the load at which the lateral bending moment in the column (due to an infinitesimal lateral deflection) is large enough to cause infinite lateral deflection. The derivation of the critical Euler buckling stress is discussed elsewhere (Bleich, 1952; McGuire, 1968; Johnston, 1983; and Salmon and Johnson, 1996), and will not be repeated here.

Euler's theory pertains to columns with uniform stress over the cross-section and stresses below the elastic limit. These conditions never occur in bridges, but are approached in compression members with large slenderness ratios. Test results prove that typical columns are not as strong as predicted by Euler's theory.

Considere (1891) and Engesser (1889) independently found that portions of steel columns were strained beyond the proportional limit prior to buckling. They postulated that a variable modulus of elasticity should be used to account for the fact that columns fail by inelastic rather than elastic buckling. Engesser proposed the Euler equation with the substitution of the tangent modulus for the elastic modulus. The tangent modulus is defined as the tangent to the stress-strain curve of a stub-column test at F_{cr}. Thus, Engesser modified the Euler buckling equation by inserting the tangent modulus of elasticity, E_t, at the stress, F_{cr}, as follows:

$$F_{cr} = \frac{\pi^2 E_t}{\left(\frac{K\ell}{r_s}\right)^2}$$ Equation 6.6.3.4.2.3.2-1

The basic assumptions with regard to material, shape and end conditions that were made in the determination of the basic column buckling strength of an ideal column given by Equation 6.6.3.4.2.3.2-1 were that the same compressive stress-strain properties exist throughout the section, all fibers remain elastic until buckling occurs, no twisting or distortion of the cross-section occurs during bending, small-deflection theory applies with shear neglected, determinate end conditions exist so that an equivalent pinned-end length can be established, no residual stresses are present in the member due to welding or cooling after rolling, and loading of the member occurs through the centroidal axis until the member begins to bend. The theory ignores the effect of residual stresses on the stiffness of the column. The portion of the section containing compressive residual stresses will yield first. This yielding will be evidenced by a non-linear appearance to the stress-strain curve. However, it will not have any influence on the moment of inertia of the section. Typically, compressive residual stresses exist at the critical exterior fibers of column sections. Hence, the tangent modulus does not accurately reflect the column strength of those sections with high residual stresses. It is noted that the above method is empirical in that it can only be found by test.

Engesser's tangent modulus theory still gave computed buckling loads lower than measured ultimate resistances. Therefore, in 1895, he revised his tangent modulus theory to incorporate the phenomenon of strain reversal; that is, to account for the fact that at the onset of bending, some fibers undergo increased strain at the lower tangent modulus while other fibers are unloaded at a higher modulus under the reduced strain. This led to the development of his double modulus theory, in which a combined reduced modulus was used to calculate the critical buckling load. The double modulus theory was generally accepted, but gave computed resistances somewhat higher than the test values. The double modulus theory only considered equilibrium positions near the ideal straight position, and still did not address the effect of residual stresses on the column moment of inertia. Some attempts to address the column problem analytically were made in the 1960s by computing the tangent modulus of a shape with the effect of residual stresses on the moment of inertia considered; however, strain reversal was not addressed.

An explanation of the true behavior of concentrically loaded columns was presented in 1946, when Shanley reasoned that as the column bends beyond infinitesimal values of curvature upon reaching the buckling load, which includes the inelastic effects on the cross-section, it is still possible for the column to resist increasing axial compression if its initial bending is due to non-linear behavior (Shanley, 1946). As

bending occurs and the curvature increases to a finite value, strain reversal must again occur to develop a resisting moment to maintain equilibrium with the moment due to the external load times the lateral deflection. However, the load on the column will continue to increase above the buckling load in a non-linear fashion for small but finite values of curvature as long as the increment of load represented by the stress acting on the area of increasing strain exceeds the increment of load represented by the stress acting on the area of decreasing strain. For practical design, this increase in the load carrying capacity above the buckling load is neglected, but the true flexural buckling behavior of an ideal concentrically loaded column was now well understood.

Practically speaking, however, actual conditions do not generally correspond to the ideal conditions represented by the preceding assumptions. Test results typically include the effects of residual stresses, initial imperfections (i.e. out-of-straightness), unintended eccentricity of the load, end restraint and local buckling. As a result of these effects, the term ″buckling″ represents more of a transition between stable and unstable deflections of a compression member rather than an instantaneous (or bifurcation) type behavior.

Residual stresses are stresses that remain in an unloaded member after that member has been formed into a finished product by cold bending and/or cooling after rolling or welding. Residual stresses are also introduced by cutting operations and by the punching of holes during fabrication. However, residual stresses introduced by uneven cooling are the most significant stresses.

As shown in Figure 6.6.3.4.2.3.2-1, after hot rolling, the thicker flanges of rolled wide-flange or H-shaped sections cool more slowly than the web region. Also, the flange tips cool more rapidly than the region at the flange-to-web juncture. As a result, compressive residual stresses exist at the flange tips and at mid-depth of the web, or the regions that cool the fastest, while tensile residual stresses exist where the flanges and web are joined.

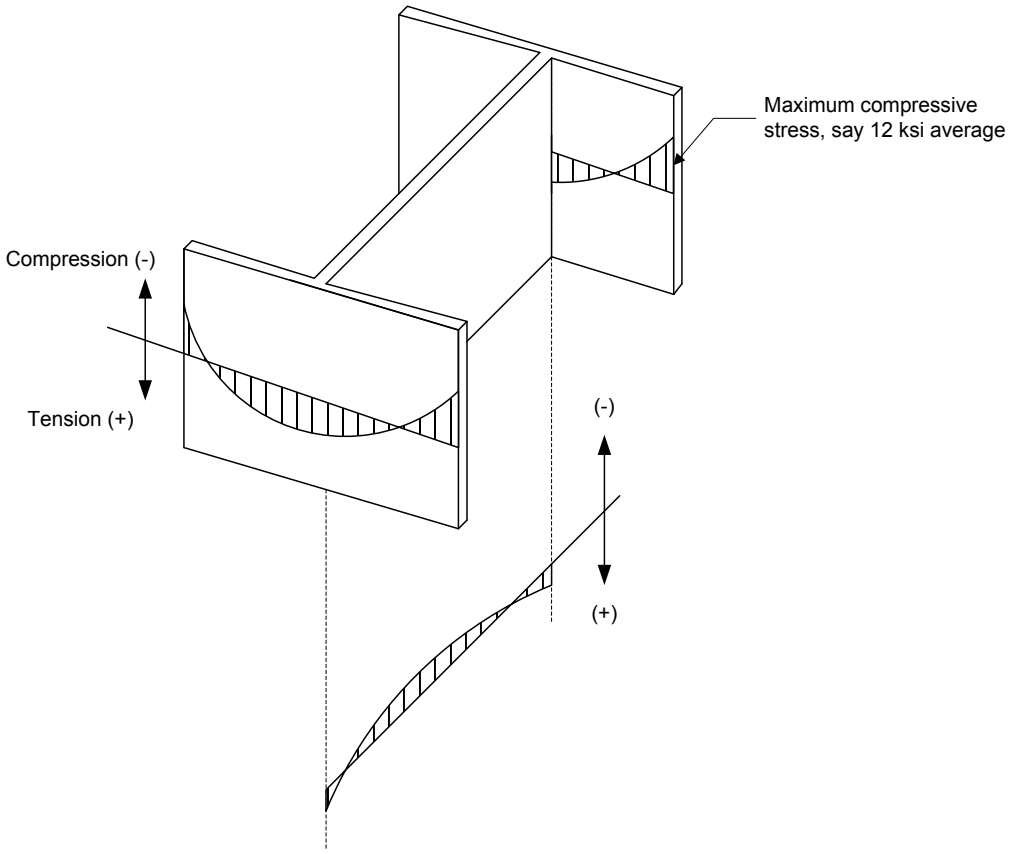

Figure 6.6.3.4.2.3.2-1 Typical Residual Stress Distribution for Rolled Shapes

Figure 6.6.3.4.2.3.2-1 shows a typical residual stress pattern for an unstraightened hot-rolled shape. The magnitude of these stresses varies based on the dimensions of the section. Residual stresses are essentially independent of yield strength (Yang et al., 1952), and have been measured as high as 20 ksi at the tips of rolled shapes (SSRC, 1998). Residual stresses shown in this figure are due to differential cooling of the steel subsequent to rolling. This variable cooling causes the shapes to go out-of-straight and they must be straightened. Smaller shapes, such as angles and tees commonly used in bracing, are passed through a rotary straightener. This machine flexes the shape back and forth removing the residual stresses due to cooling. Generally, the final residual stresses are much less than those due to cooling. For example, when a smaller wide flange shape is flexed in the strong direction, as is done in a rotary straightener, the maximum residual stress is due to springback from the plastic moment, M_p. The shape factor M_p/M_y is 1.12 so the residual stresses are not greater than 12 percent of the yield stress.

Figure 6.6.3.4.2.3.2-2 shows qualitatively the effect of residual stresses on the stress-strain curve for a rolled shape, plotted using the average stress versus the average compressive strain.

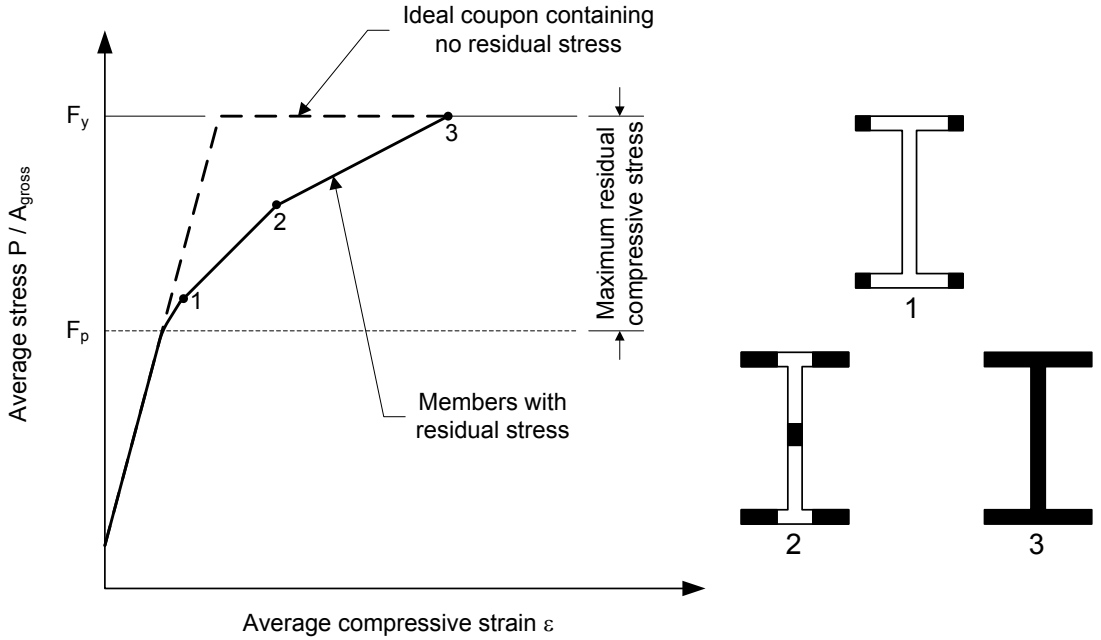

Figure 6.6.3.4.2.3.2-2 Residual Stress Effects on the Average Stress-Strain Curve for a Rolled Shape

The so-called secant formula was an early attempt to account for the effects of residual stresses, accidental eccentricities, and initial out-of-straightness. However, cooling residual stresses, more than initial imperfections or unintended eccentricity of load, have been shown to be the primary contributor to the non-linear portion of the average stress-strain curve for axially loaded compression members in tests (Huber and Beedle, 1954). The tangent modulus theory based on inelastic buckling applies because the average stress-strain curve is non-linear when F_{cr} is reached, however, the tangent modulus on one fiber is not the same as on the adjacent fiber and all fibers cannot be assumed stressed to the same level due to the effect of the residual stresses.

In welded built-up shapes, the plates themselves have little or no initial residual stress due to cooling. Modern steel is rolled in wide plates and sheared to approximate widths for sale to fabricators. The fabrication process involves cutting the sheared plates into individual flange widths. This may be performed with a torch or with other means such as a laser. The local heat input of the cutting creates rather high local tensile stresses at the cut lines (Figure 6.6.3.4.2.3.2-3 Part A). Welding causes high tensile residual stresses with a magnitude at or near the yield stress in the vicinity of the welds. The remainder of the section must balance the tensile force with compressive stresses. The resulting nonuniform cooling results in a residual stress pattern such as that shown in Figure 6.6.3.4.2.3.2-3 Part B for the flange of a welded I-section. When the heat due to welding is large in comparison to the heat sink formed by the attached material, distortions in the plate may occur.

Residual stresses balance in tension and compression within a section. Hence, as a section is loaded in flexure, residual stresses have no effect on the ultimate strength of the section, but may cause it to deflect more than would be predicted ignoring residual stresses. Euler showed that a column fails in bending. Hence, the flexural strength of a column is not affected by residual stresses. The deleterious effect of residual stresses on columns is in their reduction in the bending stiffness *I* of the column. The location of residual stresses in a cross-section, as well as their magnitude, affects the column strength of a section. Shanley showed that the flexural strength of a column shape is greater than the tangent modulus strength because of strain reversal. When a part of the section yields prematurely due to residual stresses and the column commences to bend, the fibers on the outside of the bend go into tension increasing the strength. Shanley's discovery explains why the column strength of shapes with large residual stresses are not affected as much as tangent modulus theory would indicate.

Recognizing the overall importance of residual stresses and in an attempt to better fit the test results, various column strength design curves were developed for strong- and weak-axis buckling based on various assumed distributions of residual stress. In 1960, the AISC Allowable Stress Design (ASD) specification implemented the following SSRC parabolic equation initially proposed by Bleich (1952) to define the transition region in column strength between elastic buckling and yielding:

$$F_{cr} = F_y\left[1 - \frac{F_y}{4\pi^2 E}\left(\frac{K\ell}{r_s}\right)^2\right] \qquad \text{Equation 6.6.3.4.2.3.2-2}$$

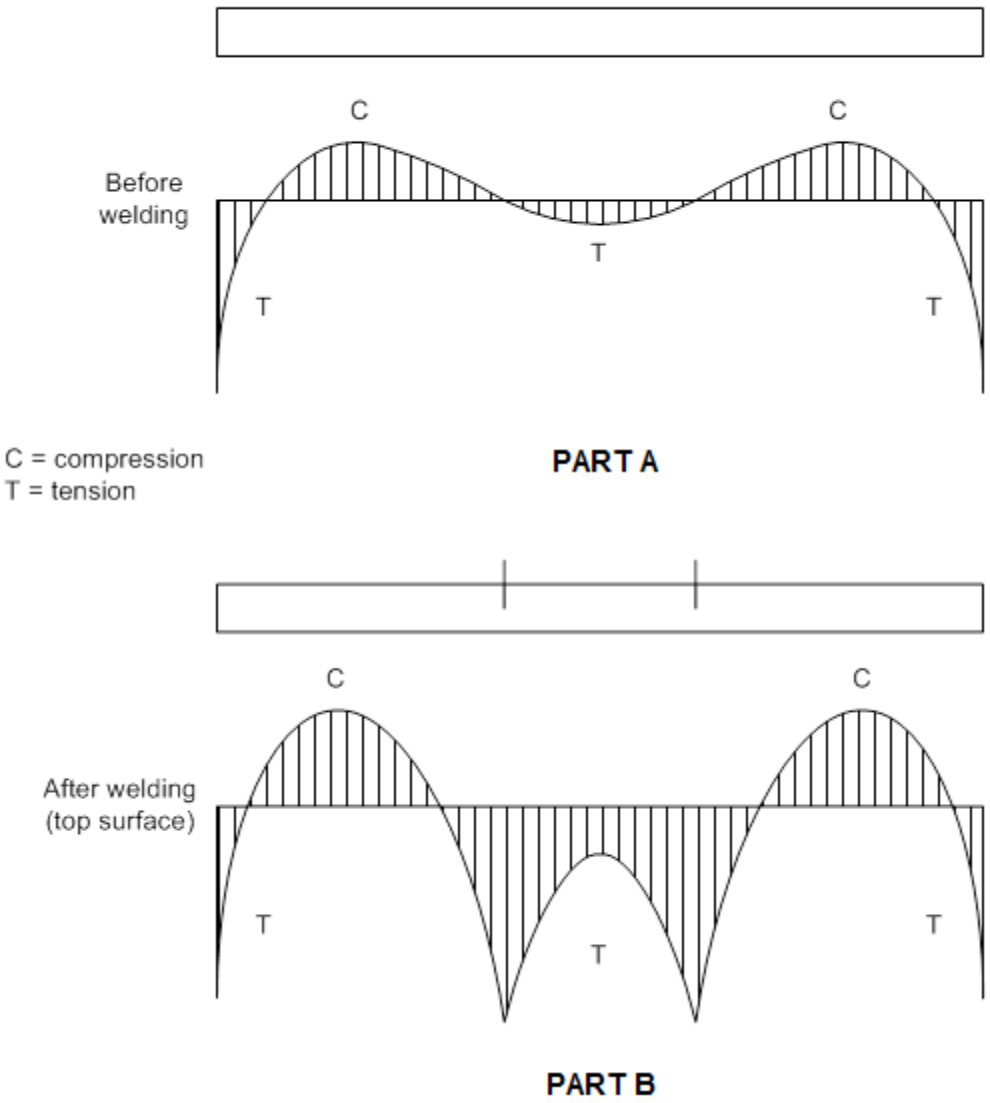

Figure 6.6.3.4.2.3.2-3 Typical Residual Stress Distribution in Welded Flange Plates

This equation was also implemented in earlier versions of the AASHTO Standard Specifications, including the Guide Specifications for horizontally curved girders. The effects of initial imperfections and unintended eccentricity of the load increase with increasing slenderness. In the AISC ASD Specification, these effects were accounted for via a variable factor of safety that increased with slenderness from 1.67 to 1.92. AASHTO ASD conservatively applied a constant factor of safety of 2.12. Note that Equation 6.6.3.4.2.3.2-2 is a parabolic equation, whereas the Euler equation is a hyperbola. In the AISC Specification, where Equation 6.6.3.4.2.3.2-2 was tangent to the Euler hyperbola, it was terminated. However, AASHTO extended

the parabolic equation beyond where AISC switched to the hyperbola. At these large slenderness values, the parabolic equation is very conservative.

In the transition to the AISC LRFD Specification, it was decided to provide a constant margin of safety for all columns and to instead account for the variation of resistance with slenderness through the calculation of the nominal axial resistance, P_n. Bjorhovde's probability-based work examining the resistance of steel columns (Bjorhovde, 1972; Bjorhovde, 1978; Bjorhovde, 1988) resulted in his recommendation of three column strength curves. The three curves represented a central strength for theoretical column strength based on measured residual stresses. The work assumed a mean out-of-straightness of 1/1470 based on measured out-of-straightness of unstraightened columns (SSRC, 1998). The permitted out-of-straightness is L/1000 so the expected effect of out-of-straightness is much less than assumed in that study.

The three column curves were the approximate means of bands of strength curves for columns of similar manufacture based on extensive analyses and confirmed by full-scale tests, not including straightening. SSRC presented these curves. SSRC Column Category 1P represented the data band of highest resistance, included hot- and cold-formed heat-treated HSS columns. SSRC Column Category 2P represented the data band of lowest resistance, included welded built-up H-sections made from universal mill plates with a yield strength less than 50 ksi for major-axis buckling and a yield strength less than 60 ksi for minor-axis buckling, and heavy W-shapes with a yield strength less than 50 ksi. SSRC Column Category 2P included the largest group of columns. Additional information on the recommended use of SSRC Column Categories 1P and 2P for a range of I-shaped steel-column sections subject to major- or minor-axis bending, and the reliability provided by each curve, may be found in SSRC (1998). Since welded built-up shapes are no longer manufactured from universal mill plates and the minimum yield strength of constructional steels used in new construction is typically 50 ksi or larger, SSRC Column Catgeory 3P is no longer shown in SSRC (2010).

Probabilistic analysis would have resulted in a resistance factor ϕ_c = 0.90, or even slightly higher, had the original *AISC LRFD* Specification opted for using all three column curves for the respective column categories (Galambos, 1983; Bjorhovde, 1988; SSRC, 2010). However, it was decided to use only one column curve, SSRC Column Category 2P, for all column types. The *AASHTO LRFD* Specification followed suit. Equations 6.6.3.4.2.3.1-1 and 6.6.3.4.2.3.1-2 represent the mathematical form of this curve. The use of only one column curve results in a larger data spread and thus a larger coefficient of variation, and so a resistance factor ϕ_c = 0.85 was adopted in the original 1986 *AISC LRFD* Specification for the column equations to achieve a level of reliability comparable to that of beams. Resistance factors in the *AASHTO LRFD* Specification are typically set at a level

that is 0.05 higher than those in the *AISC LRFD* Specification; thus, ϕ_c was set to 0.90 in the original *AASHTO LRFD* Specification.

The resistance factor, ϕ_c, was increased from 0.85 to 0.90 in the AISC (2005). This increase gave recognition to the changes in industry practice combined with the substantial numbers of additional column strength analyses and tests that had taken place since the original calibrations were performed in the 1970s and 1980s (Bjorhovde, 1988). The changes in industry practice that made this increase warranted, indeed even somewhat conservative, included the following: (1) built-up shapes are no longer manufactured from universal mill plates; (2) the most commonly used structural steel is now ASTM A 709 Grade 50 or 50W, with a specified minimum yield stress of 50 ksi; and (3) changes in steelmaking practice have resulted in materials of higher quality and much better defined properties. The level and variability of the yield stress thus have led to a reduced coefficient of variation for the relevant material properties (Bartlett et al., 2003). As a result, for consistency, ϕ_c for steel members (or components) subject to axial compression was raised from 0.90 to 0.95 in the *AASHTO LRFD* Specification in 2014.

6.6.3.4.2.3.3 Elastic Flexural Buckling Resistance

Flexural buckling of concentrically loaded compression members refers to a buckling mode in which the member deflects laterally without twist or a change in the cross-sectional shape. In general, flexural buckling involves lateral displacements of the member cross-section in the direction of the geometric x- and y-axes that are resisted by the respective flexural rigidities, EI_x or EI_y, of the member.

The equation used to calculate the elastic critical flexural buckling resistance, P_e, is specified in *AASHTO LRFD* Article 6.9.4.1.2 as follows:

$$P_e = \frac{\pi^2 E}{\left(\frac{K\ell}{r_s}\right)^2} A_g \qquad \text{Equation 6.6.3.4.2.3.3-1}$$

AASHTO LRFD Equation 6.9.4.1.2-1

where:

A_g = gross cross-sectional area of the member (in.^{2})
K = effective length factor in the plane of buckling determined as specified in *AASHTO LRFD* Article 4.6.2.5 (see below)
ℓ = unbraced length in the plane of buckling (in.)
r_s = radius of gyration about the axis normal to the plane of buckling (in.)

Equation 6.6.3.4.2.3.3-1 is to be used to calculate the elastic critical flexural buckling resistances about the x- and y-axes, with the smaller value taken as P_e for use in Equation 6.6.3.4.2.3.1-1 or 6.6.3.4.2.3.1-2, as applicable.

Effective Length Factor, K

The effective length factor, *K*, which is applied to the actual member unbraced length, ℓ, accounts for the influence of end conditions. *K* is used to compensate for translational and rotational boundary conditions. It represents the ratio of the idealized pinned-end compression member length to the actual length of a member with other than pinned ends.

In many cases, some degree of end restraint exists causing an effective length factor other than 1.0. *AASHTO LRFD* Table C4.6.2.5-1 provides a table of theoretical *K* values taken from SSRC (1998) for idealized end conditions in which translational and/or rotational end conditions are either fully restrained or free. Because actual member end conditions are seldom perfectly fixed or perfectly unrestrained as represented by the ideal conditions, *AASHTO LRFD* Table C4.6.2.5-1 also provides recommended design values as suggested by the Structural Stability Research Council. These simple modifications of the ideal values lead to either equal or somewhat higher *K* values.

In the absence of refined inelastic analysis, *AASHTO LRFD* Article 4.6.2.5 provides recommended *K* values in the braced plane of triangulated trusses, trusses and frames where lateral stability is provided. The recommended values are as follows:

- For bolted or welded end connections at both ends: $K = 0.750$
- For pinned connections at both ends: $K = 0.875$
- For single angles, regardless of end connection: $K = 1.0$

The recommended values for *K* do not account for any relative translation or rotation of the ends of the member. These relative motions are not usually present in building columns. They more closely resemble the actions found in transmission towers. Caution should be exercised in applying these recommended values to cases with larger unbraced lengths where elastic buckling may control.

A conservative *K* value of 1.0 is suggested for single angles since these members are often loaded through only one leg and are subject to eccentric loading as well as twist. These effects may not be properly recognized in design. The recommended value of $K = 1.0$ for single angles also closely matches that provided in ASCE (2000) (the design of single-angle compression members is discussed in more detail in Section 6.6.3.4.5).

SSRC (1998) gives more specific recommendations of *K* values to use for in-plane buckling of various truss members. In some cases, the *K* values are higher than the recommended values given above. This reference also gives recommendations for buckling of truss members in the out-of-plane direction. Suggested *K* values for in-plane buckling of arch members are provided in *AASHTO LRFD* Article 4.5.3.2.2c. The reader is referred to White (2012) for additional discussion of *K* values.

Where non-rigid rotational restraint exists, *K* may be determined from traditional alignment charts for sidesway-inhibited or sidesway-uninhibited cases that are provided in *AASHTO LRFD* Article C4.6.2.5. Closed-form equations are also provided. The assumptions made in the alignment charts and equations are discussed in detail in the commentary to Chapter C of AISC (2005). Modifications are also presented there that extend the range of applicability of the alignment charts. The reader is urged to review these assumptions and modifications prior to using the alignment charts and/or equations.

6.6.3.4.2.3.4 Elastic Torsional Buckling & Flexural-Torsional Buckling Resistance

Torsional or flexural-torsional buckling may be critical in certain open-section members. Torsional buckling is usually found in doubly symmetric open-section members in which the effective torsional unbraced length is larger than the effective lateral unbraced length. Singly symmetric compression members such as double angles, channels and tees may be governed by flexural-torsional buckling rather than flexural buckling. The equations for torsional buckling and for flexural-torsional buckling, as written below, apply only to members composed of nonslender elements (for members composed of one or more slender elements, refer also to Section 6.6.3.4.2.4.3). Note that according to *AASHTO LRFD* Article 6.9.4.4, flexural-torsional buckling does not need to be checked for single angles subject to compression (Section 6.6.3.4.5). Because of the relatively large torsional stiffness, *GJ*, in closed sections, torsional buckling and flexural-torsional buckling need not be considered for closed sections, including built-up members connected by lacing bars, batten plates, perforated plates, or any combination thereof. Torsional buckling and flexural-torsional buckling are also not applicable to bearing stiffeners.

The torsional and flexural-torsional buckling resistance equations given in *AASHTO LRFD* Article 6.9.4.1.3 (and summarized in the following) provide the elastic critical buckling resistance, P_e, to be substituted into the applicable Equation 6.6.3.4.2.3.1-1 or 6.6.3.4.2.3.1-2 in order to determine the nominal compressive resistance, P_n.

Elastic Torsional Buckling Resistance

The limit state of torsional buckling, or twisting about the shear center, applies only to concentrically loaded open-section doubly symmetric compression members for

which the locations of the centroid and shear center coincide. For such members, the elastic critical torsional buckling resistance, P_e, is computed as:

$$P_e = \left[\frac{\pi^2 E C_w}{(K_z \ell_z)^2} + GJ\right]\frac{A_g}{I_x + I_y} \qquad \text{Equation 6.6.3.4.2.3.4-1}$$

AASHTO LRFD Equation 6.9.4.1.3-1

where:

A_g = gross cross-sectional area of the member, in.^{2}
C_w = warping torsional constant for the cross-section (equal to zero for a cruciform section), in.^{6} For a doubly symmetric I-section, C_w may be taken as $I_y h^2/4$, where h is the distance between flange centroids in lieu of a more precise analysis.
$K_z\ell_z$ = effective length for torsional buckling, in.
G = shear modulus of elasticity for steel = 0.385E (ksi)
J = St. Venant torsional constant for the cross-section, in.^{4} (Section 6.4.8.2.1)
I_x, I_y = moments of inertia about the major and minor principal axes of bending, respectively, in.^{4}

The effective length for torsional buckling $K_z\ell_z$ is the length between locations where the member is prevented from twisting. Typically, $K_z\ell_z$ can conservatively be taken as $1.0\ell_z$. White (2012) indicates that for a cantilever member fully restrained against twisting and warping at one end with the other end free, $K_z\ell_z$ is equal to 2ℓ, where ℓ is the length of the member. For a member with twisting and warping restrained at both ends, $K_z\ell_z$ is equal to 0.5ℓ.

Torsional buckling will rarely control (as opposed to flexural buckling), and need not be considered for doubly-symmetric I-section members that satisfy the proportioning limits specified in *AASHTO LRFD* Article 6.10.2, unless the effective length for torsional buckling is significantly larger than the effective length for weak-axis flexural buckling (White, 2012).

Elastic Flexural-Torsional Buckling Resistance

Flexural-torsional buckling of concentrically loaded compression members refers to a buckling mode in which the member twists and bends simultaneously without a change in the shape of the cross-section. Concentrically loaded compression members composed of singly symmetric open cross-sections, where the y-axis is defined as the axis of symmetry of the cross-section (e.g. tees, double angles, and channels), can either fail by flexural buckling about the x-axis, or by torsion combined with flexure about the y-axis. Unsymmetric open-section compression

members, or members with no cross-section axis of symmetry, that are concentrically loaded can fail by torsion combined with flexure about both the x- and y-axes. In all of these cases, the shear center and centroid of the cross-section do not coincide, and the torsional rigidity of the section is relatively low.

As buckling occurs, the axial load has a lateral component resulting from the deflection of the member. The torsional moment caused by this lateral component of axial force acting about the shear center of the section causes twisting of the member. The degree of interaction between the torsional and flexural deformations determines the amount of reduction of the buckling load in comparison to the flexural buckling load (SSRC, 1998). As the distance between the centroid and shear center increases, the twisting tendency increases and the flexural-torsional buckling load decreases. Because of their relatively low torsional rigidity, flexural-torsional buckling may be a critical mode of failure for thin-walled singly-symmetric open sections.

The critical elastic flexural-torsional buckling resistance for open-section singly symmetric members, is always smaller than the critical elastic flexural buckling resistance about the y-axis, P_{ey}. Therefore, for these members, only the elastic flexural buckling resistance about the x-axis, P_{ex} (Section 6.6.3.4.2.3.3), need be considered along with the elastic flexural-torsional buckling resistance in determining the governing nominal compressive resistance, P_n. For open-section unsymmetric members, except for single-angle members design according to the provisions of *AASHTO LRFD* Article 6.9.4.4 (Section 6.6.3.4.5), only flexural-torsional buckling is considered in computing P_e and P_n; flexural buckling about the x- and y-axes need not be checked

For open-section members composed of singly symmetric cross-sections where the y-axis is defined as the axis of symmetry of the cross-section, the elastic critical flexural-torsional buckling resistance, P_e, may be computed as:

$$P_e = \left(\frac{P_{ey} + P_{ez}}{2H}\right)\left[1 - \sqrt{1 - \frac{4P_{ey}P_{ez}H}{(P_{ey} + P_{ez})^2}}\right] \qquad \text{Equation 6.6.3.4.2.3.4-2}$$

AASHTO LRFD Equation 6.9.4.1.3-2

where:

$$P_{ey} = \frac{\pi^2 E}{\left(\frac{K_y \ell_y}{r_y}\right)^2} A_g \quad \text{(kips)} \qquad \text{Equation 6.6.3.4.2.3.4-3}$$

AASHTO LRFD Equation 6.9.4.1.3-4

$$P_{ez} = \left(\frac{\pi^2 E C_w}{(K_z \ell_z)^2} + GJ\right)\frac{1}{\bar{r}_o^2} \text{ (kips)} \qquad \text{Equation 6.6.3.4.2.3.4-4}$$

AASHTO LRFD Equation 6.9.4.1.3-5

$$H = 1 - \frac{y_o^2}{\bar{r}_o^2} \qquad \text{Equation 6.6.3.4.2.3.4-5}$$

AASHTO LRFD Equation 6.9.4.1.3-3

$$\bar{r}_o^2 = y_o^2 + \frac{I_x + I_y}{A_g} \qquad \text{Equation 6.6.3.4.2.3.4-6}$$

AASHTO LRFD Equation 6.9.4.1.3-6

A_g = gross cross-sectional area of the member (in.^{2})
C_w = warping torsional constant (see below) (in.^{6})
G = shear modulus of elasticity for the steel = 0.385E (ksi)
I_x = moment of inertia about the x-axis (in.^{4})
I_y = moment of inertia about the y-axis (in.^{4})
J = St. Venant torsional constant (in.^{4})
$K_y\ell_y$ = effective length for flexural buckling about the y-axis, in.
$K_z\ell_z$ = effective length for torsional buckling, in.
r_y = radius of gyration about the y-axis (in.)
y_o = distance along the y-axis between the shear center and centroid of the cross-section (for a tee section, see Figure 6.6.3.4.2.3.4-1) (in.)

Values of J, H and $\bar{r}_o^2$ for rolled tee sections are tabulated in the AISC (2010). The warping torsional constant, C_w, is to conservatively be taken as zero for tees and double angles.

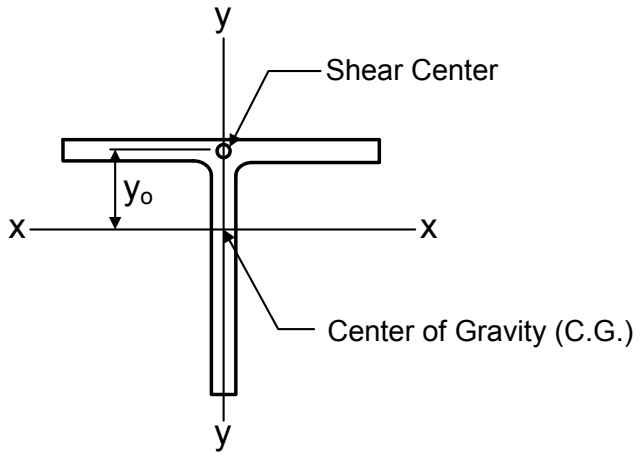

Figure 6.6.3.4.2.3.4-1 Calculation of y_o for a Tee Section

The y-axis is again defined as the axis of symmetry of the cross-section in the preceding equations. Therefore, for a single channel section, the y-axis would actually be taken as the x-axis of the cross-section (or the axis of symmetry of the channel section, as shown in the AISC Manual shape property tables) in calculating the preceding values. For a single channel section, refer to Section 6.6.3.5.6 regarding the computation of C_w.

Should double-angle bracing members subject to compression be interconnected at intervals along their length (i.e. between their ends) in the plane defined by the y-axis of the cross-section, the modified slenderness ratio, $(K\ell/r)_m$, specified for built-up members in *AASHTO LRFD* Article 6.9.4.3.1 (Section 6.6.3.4.4) should be used in place of $(K_y\ell_y/r_y)$ in Equation 6.6.3.4.2.3.4-3 to account for the effect of shear displacements between the two angles. Flexural buckling about the x-axis would be checked in conventional fashion, as shear effects would have no effect on buckling about the x-axis. In addition, *AASHTO LRFD* Article 6.9.4.3.1 specifies that the slenderness ratio of each component shape between connecting bolts or welds not exceed 75 percent of the governing slenderness ratio of the built-up member (Section 6.6.3.4.4). When bolts are used, the maximum longitudinal spacing or pitch of the bolts must satisfy the requirements for stitch bolts specified in *AASHTO LRFD* Article 6.13.2.6.3 (Section 6.6.4.2.2.2.4). The reader is referred to White (2012) for further information.

For unsymmetric members, or members with no cross-section axis of symmetry (except for single angles designed according to the provisions of *AASHTO LRFD* Article 6.9.4.4 – Section 6.6.3.4.5), the failure mode always involves torsion combined with flexure about both the x- and y-axes (i.e. flexural buckling need not be considered). In this case, the elastic critical flexural-torsional buckling resistance, P_e, may be computed as the lowest root of the following cubic equation:

$$(P_e - P_{ex})(P_e - P_{ey})(P_e - P_{ez}) - P_e^2(P_e - P_{ey})\left(\frac{x_o}{\bar{r}_o}\right)^2 - P_e^2(P_e - P_{ex})\left(\frac{y_o}{\bar{r}_o}\right)^2 = 0$$

Equation 6.6.3.4.2.3.4-7

AASHTO LRFD Equation 6.9.4.1.3-7

where:

$$P_{ex} = \frac{\pi^2 E}{\left(\frac{K_x \ell_x}{r_x}\right)^2} A_g$$

Equation 6.6.3.4.2.3.4-8

AASHTO LRFD Equation 6.9.4.1.3-8

$\bar{r}_o$ = polar radius of gyration about the shear center, in.

$$\bar{r}_o^2 = x_o^2 + y_o^2 + \frac{I_x + I_y}{A_g} \qquad \text{Equation 6.6.3.4.2.3.4-9}$$

AASHTO LRFD Equation 6.9.4.1.3-9

$K_x\ell_x$ = effective length for flexural buckling about the x-axis, in.
r_x = radius of gyration about the x-axis, in.
x_o = distance along the x-axis between the shear center and the centroid of the cross-section, in.

All other terms are as defined previously.

As discussed further in White (2012), for singly-symmetric I-sections with equal flange widths (i.e. differing flange thicknesses), flexural-torsional buckling does not need to be considered as long as $0.67 \le t_{f1}/t_{f2} \le 1.5$, where t_{f1} and t_{f2} are the flange thicknesses, and $K_z\ell_z \le K_y\ell_y$. However, it is recommended that flexural-torsional buckling always be checked for singly symmetric I-sections with differing flange widths that are loaded in axial compression. The warping torsional constant, C_w, for such sections (with equal flange thicknesses) may be computed as follows (Salmon and Johnson, 1996):

$$C_w = \frac{t_f h^2}{12}\left(\frac{b_1^3 b_2^3}{b_1^3 + b_2^3}\right) \qquad \text{Equation 6.6.3.4.2.3.4-10}$$

AASHTO LRFD Equation C6.9.4.1.3-1

where:

b_1, b_2= individual flange widths (in.)
h = distance between flange centroids (in.)
t_f = flange thickness (in.) Use an average thickness if the flange thicknesses differ.

6.6.3.4.2.4 Nonslender and Slender Member Elements

6.6.3.4.2.4.1 General

AASHTO LRFD Article 6.9.4.2.1 specifies width-to-thickness ratio limits that enable cross-section elements (or components) subject to uniform axial compression to develop their full nominal yield strength before the onset of local buckling. Elements satisfying these particular limits are classified as nonslender elements. All the buckling resistance equations presented above apply as shown to compression members composed entirely of nonslender elements. Elements not satisfying these

particular limits are classified as slender elements. The procedures to calculate the nominal compressive resistance of compression members consisting of one or more slender elements are reviewed below.

It is important to note that under uniform compression, cross-section elements are classified as either slender or nonslender in the AASHTO and AISC Specifications. Compactness requirements apply only when determining the nominal resistance of flexural members for which compression flange and web elements may need to withstand larger inelastic strains in order to ensure that local buckling does not adversely affect the nominal flexural resistance.

6.6.3.4.2.4.2 Nonslender Member Elements

In general, as specified in *AASHTO LRFD* Article 6.9.4.2.1, to qualify as a nonslender element, plates in members subject to uniform compression must satisfy the following requirement:

$$\frac{b}{t} \le k\sqrt{\frac{E}{F_y}} \qquad \text{Equation 6.6.3.4.2.4.2-1}$$

AASHTO LRFD Equation 6.9.4.2.1-1

where:

k = plate buckling coefficient specified in *AASHTO LRFD* Table 6.9.4.2.1-1 (Table 6.6.3.4.2.4.2-1)
b = width of plate as specified in *AASHTO LRFD* Table 6.9.4.2.1-1 (Table 6.6.3.4.2.4.2-1)
t = plate thickness (in.)

More specifically, the half-width of flanges of built-up I-sections, and plate or angle legs projecting from built-up I-sections, must satisfy the following:

$$\frac{b}{t} \le 0.64\sqrt{\frac{k_c E}{F_y}} \qquad \text{Equation 6.6.3.4.2.4.2-2}$$

AASHTO LRFD Equation 6.9.4.2.1-2

and:

$$0.35 \le k_c \le 0.76 \qquad \text{Equation 6.6.3.4.2.4.2-3}$$

AASHTO LRFD Equation 6.9.4.2.1-3

where:

$$k_c = \frac{4}{\sqrt{\frac{D}{t_w}}} \qquad \text{Equation 6.6.3.4.2.4.2-4}$$

AASHTO LRFD Equation 6.9.4.2.1-4

b = half-width of flange (in.)
D = web depth (in.)

Equation 6.6.3.4.2.4.2-4 accounts for the effects of web-flange interaction on local buckling in built-up I-sections subject to axial compression, and its development is discussed further in Section 6.5.6.2.2.2.1. Since web-flange interaction effects are considered negligible in rolled sections, these sections are not required to satisfy Equations 6.6.3.4.2.4.2-2 and 6.6.3.4.2.4.2-3. Note however that the upper limit on k_c of 0.76 given in Equation 6.6.3.4.2.4.2-3 (which would apply to built-up I-sections with web slenderness ratios less than or equal to about 28) yields a k value of 0.56 (i.e. $0.64\sqrt{k_c} = 0.56$), which is equivalent to the value of k given for the half-flange width of rolled I-sections in Table 6.6.3.4.2.4.2-1 for use in Equation 6.6.3.4.2.4.2-1. Note that none of the rolled tee sections in the AISC Manual shape property tables have slender flanges. The values of the plate buckling coefficient, k_c, assumed for all other cases listed in Table 6.6.3.4.2.4.2-1 can be calculated as $(k/0.64)^2$, where k is the tabulated plate buckling coefficient given in Table 6.6.3.4.2.4.2-1.

The wall thickness of circular tubes, including round HSS, is to satisfy:

$$\frac{D}{t} \le 0.11\frac{E}{F_y} \qquad \text{Equation 6.6.3.4.2.4.2-5}$$

AASHTO LRFD Equation 6.9.4.2.1-5

where:

D = outside diameter of the tube (in.)
t = thickness of the tube (in.)

The limit given by Equation 6.6.3.4.2.4.2-5 to prevent local buckling of circular tubes is based on test results (Sherman, 1976) rather than theoretical calculations. When D/t exceeds the value given by Equation 6.6.3.4.2.4.2-5, Equation 6.6.3.4.2.4.3-11 should be used to compute the slender element reduction factor, Q_a. This equation for Q_a is valid up to a D/t limit of $0.45E/F_y$. Circular tubes with D/t values greater than this limit should not be used as compression members. Circular tubes may be designed using the specified provisions for HSS in the AASHTO LRFD Specifications provided that they conform to ASTM A 53 Class B, and the

appropriate parameters are used in design. Information on connection design for round, square, and rectangular HSS may be found in Chapter K of AISC (2010a).

The last paragraph of *AASHTO LRFD* Article 6.9.4.2.1 states that for members designed for combined axial compression and flexure according to the equations of *AASHTO LRFD* Article 6.9.2.2 (Section 6.6.3.4.3), F_y in Equations 6.6.3.4.2.4.2-1 and 6.6.3.4.2.4.2-2 may be replaced with the calculated compressive stress due to the factored axial load and concurrent bending moment. As discussed further in White (2012), if this done, the linear axial force versus bending moment interaction curve given by *AASHTO LRFD* Equation 6.9.4.2.1-6 must be used rather than the bilinear interaction curves given in *AASHTO LRFD* Article 6.9.2.2 (Section 6.6.3.4.3). This is because the application of the bilinear interaction curves to members containing slender cross-section elements is not valid if the nonslender member element limits given by Equations 6.6.3.4.2.4.2-1 and 6.6.3.4.2.4.2-2 are modified in this fashion.

Table 6.6.3.4.2.4.2-1 Plate Buckling Coefficients and Width of Plates for Axial Compression

Plates Supported Along One Edge (Unstiffened Elements)	*k*	*b*
Flanges of Rolled I-, Tee, and Channel Sections; Plates Projecting from Rolled I-Sections; and Outstanding Legs of Double Angles in Continuous Contact	0.56	• Half-flange width of rolled I- and tee sections • Full-flange width of channel sections • Distance between free edge and first line of bolts or welds in plates • Full width of an outstanding leg for double angles in continuous contact
Stems of Rolled Tees	0.75	Full depth of tee
Outstanding Legs of Single Angles; Outstanding Legs of Double Angles with Separators; and All Other Unstiffened Elements	0.45	• Full width of outstanding leg for single angle or double angles with separators • Full projecting width for all others

Plates Supported Along Two Edges (Stiffened Elements)	*k*	*b*
Flanges and Webs of Square and Rectangular Built-Up Box Sections and HSS; and Nonperforated Flange Cover Plates	1.40	• Distance between adjacent lines of bolts or welds in flanges of built-up box sections • Distance between adjacent lines of bolts or clear distance between flanges when welds are used in webs of built-up box sections • Clear distance between webs or flanges minus inside corner radius on each side for HSS. Use the outside dimension minus three times the appropriate design wall thickness specified in *AASHTO LRFD* Article 6.12.2.2.2 if the corner radius is not known • Distance between lines of welds or bolts for flange cover plates
Webs of I- and Channel Sections; and All Other Stiffened Elements	1.49	• Clear distance between flanges minus the fillet or corner radius at each flange for webs of rolled I- and channel sections • Distance between adjacent lines of bolts or clear distance between flanges when welds are used for webs of built-up I- and channel sections • Clear distance between edge supports for all others
Perforated Cover Plates	1.86	Clear distance between edge supports; see also the paragraph at the end of *AASHTO LRFD* Article 6.9.4.3.2

6.6.3.4.2.4.3 Slender Member Elements

For compression members with one or more elements not satisfying the width-to-thickness limitations specified in *AASHTO LRFD* Article 6.9.4.2.1 (i.e. slender elements), potential local buckling of those elements may adversely affect the overall

buckling resistance of the member. Therefore, the nominal compressive resistance P_n (based on flexural, torsional or flexural-torsional buckling, as applicable) must be reduced. Many of the rolled wide-flange sections given in the AISC Manual shape property tables (i.e. rolled W-sections with $d/b_f \geq 1.7$) have slender webs under uniform axial compression. The webs of welded I- and box girders are almost always classified as slender for uniform axial compression. The stems of a large number of rolled tee sections and one or both legs of many rolled angle sections also classify as slender elements according to the preceding criteria.

In such cases, P_n is to be determined according to Equation 6.6.3.4.2.3.1-1 or 6.6.3.4.2.3.1-2, as applicable, with the equivalent nominal yield resistance, P_o, taken as follows:

$$P_o = QF_yA_g \qquad \text{Equation 6.6.3.4.2.4.3-1}$$

where:

A_g = gross cross-sectional area of the members, in.^{2}
Q = slender element reduction factor determined as specified in *AASHTO LRFD* Article 6.9.4.2.2
= 1.0 for members with all nonslender elements and for bearing stiffeners
= Q_sQ_a for members with one or more slender elements (where Q_s and Q_a are defined below)

For compression members containing slender elements, the nominal compressive resistance is calculated by using a reduced equivalent yield capacity, $P_o = QP_y$, where the slender element reduction factor, Q, is less than or equal to 1.0. The AISC Specification has used this approach, as adopted from AISI (1969). Prior to 1969, a more conservative approach was used in which any portion of the plate width that exceeded the appropriate slenderness limit was disregarded.

In calculating Q, *AASHTO LRFD* Article 6.9.4.2.2 distinguishes between unstiffened elements, which refer to elements supported along only one longitudinal edge parallel to the direction of the compression force, and stiffened elements, which refer to elements supported along two longitudinal edges parallel to the direction of the force. Unstiffened elements are assumed to reach their limit of resistance when they attain their theoretical local buckling resistance. Stiffened elements take advantage of the post-buckling resistance that is available to a plate supported along two longitudinal edges. The post-buckling resistance is determined using an effective width approach. An effective width approach was adopted for both unstiffened and stiffened elements in AISI (2001); however, subsequent editions of the AISC Specification did not adopt this approach primarily because the advantages of post-buckling resistance for unstiffened elements do not become significant unless the plate elements are very slender. Such dimensions are not commonly encountered in structures fabricated from hot-rolled plates. Other reasons for not adopting this approach are summarized in White (2012).

For cross-sections composed of only unstiffened slender elements, Q is to be taken equal to Q_s (i.e. Q_a = 1.0). For cross-sections composed only of stiffened slender elements, Q is to be taken equal to Q_a (i.e. Q_s = 1.0). For cross-sections composed of both unstiffened and stiffened slender elements, Q is to be taken equal to Q_sQ_a.

Equations for Q_s and Q_a from *AASHTO LRFD* Article 6.9.4.2.2 are reproduced below. Further information regarding the development and application of these equations may be found in the Commentary to Section E7 of AISC (2010a), and in Salmon and Johnson (1996) and White (2012). White (2012) also provides recommendations for the application of these equations to hybrid I-sections with slender web elements subject to axial compression.

Slender Unstiffened Elements, Q_s

For slender unstiffened elements, the slender element reduction factor, Q_s, is equal to the ratio of the smallest local buckling resistance of all the unstiffened elements in the cross-section divided by F_y. In other words, for a compression member consisting entirely of unstiffened elements, the reduced equivalent yield strength of the member is taken as the average axial stress at which the most critical unstiffened element reaches its local buckling resistance (i.e. the elastic or inelastic local buckling resistance depending on the values of b/t, k_c and F_y).
In the following, unless otherwise specified, b is the width of the unstiffened compression element as defined in Table 6.6.3.4.2.4.2-1, and t is the thickness of the element. Only the equations for single angles, outstanding legs of double angles with separators, and stems of tees are given below, as these are likely to be the most common equations utilized in steel-bridge design. Equations for flanges of rolled I-, tee and channel sections, flanges of built-up I-sections, and plates projecting from rolled or built-up I-sections may be found in *AASHTO LRFD* Article 6.9.4.2.2, along with equations for outstanding legs of double angles in continuous contact.

For outstanding legs of single angles, or outstanding legs of double angles with separators:

- For $\frac{b}{t} \le 0.45\sqrt{\frac{E}{F_y}}$:

$$Q_s = 1.0 \qquad \text{Equation 6.6.3.4.2.4.3-2}$$

- For $0.45\sqrt{\frac{E}{F_y}} < \frac{b}{t} \le 0.91\sqrt{\frac{E}{F_y}}$:

$$Q_s = 1.34 - 0.76\left(\frac{b}{t}\right)\sqrt{\frac{F_y}{E}}$$ Equation 6.6.3.4.2.4.3-3

AASHTO LRFD Equation 6.9.4.2.2-5

- For $\frac{b}{t} > 0.91\sqrt{\frac{E}{F_y}}$:

$$Q_s = \frac{0.53E}{F_y\left(\frac{b}{t}\right)^2}$$ Equation 6.6.3.4.2.4.3-4

AASHTO LRFD Equation 6.9.4.2.2-6

where *b* is the full width of the longest angle leg (in. - Figure 6.6.3.4.2.4.3-1).

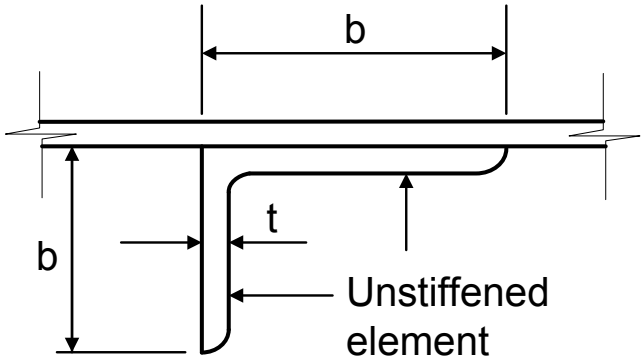

Figure 6.6.3.4.2.4.3-1 Unstiffened Elements for a Single-Angle Member

For stems of rolled tees:

- For $\frac{d}{t} \le 0.75\sqrt{\frac{E}{F_y}}$:

$$Q_s = 1.0$$ Equation 6.6.3.4.2.4.3-5

- For $0.75\sqrt{\frac{E}{F_y}} < \frac{d}{t} \le 1.03\sqrt{\frac{E}{F_y}}$:

$$Q_s = 1.908 - 1.22\left(\frac{d}{t}\right)\sqrt{\frac{F_y}{E}}$$ Equation 6.6.3.4.2.4.3-6

AASHTO LRFD Equation 6.9.4.2.2-3

- For $\frac{d}{t} > 1.03\sqrt{\frac{E}{F_y}}$:

$$Q_s = \frac{0.69E}{F_y\left(\frac{d}{t}\right)^2}$$ Equation 6.6.3.4.2.4.3-7

AASHTO LRFD Equation 6.9.4.2.2-4

where *d* is the full nominal depth of the tee (in. - Figure 6.6.3.4.2.4.3-2)

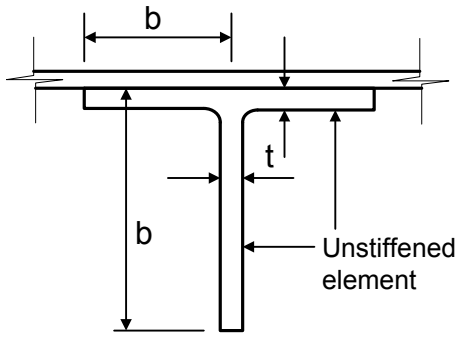

Figure 6.6.3.4.2.4.3-2 Unstiffened Elements for a Tee Member

Slender Stiffened Elements, Q_a

The reduction factor, Q_a, for slender stiffened elements except for circular tubes and round HSS, is taken as:

$$Q_a = \frac{A_{eff}}{A}$$ Equation 6.6.3.4.2.4.3-8

AASHTO LRFD Equation 6.9.4.2.2-9

where:

A = total gross cross-sectional area of the member (in.^{2})

A_{eff} = summation of the effective areas of the cross-section based on a reduced effective width, b_e, for each slender stiffened element in the cross-section = $A - \sum(b\text{-}b_e)t$ (in.^{2})

The reduced effective width, b_e, is the width of the rectangular stress blocks over which the maximum stress, f, at the longitudinal edges can be assumed to act uniformly to produce the same force at the actual stresses acting over the full width of the plate. The actual average stresses in the middle of the plate, averaged through the thickness, are smaller due to the post-buckling deformations (Figure 6.6.3.4.2.4.3-3).

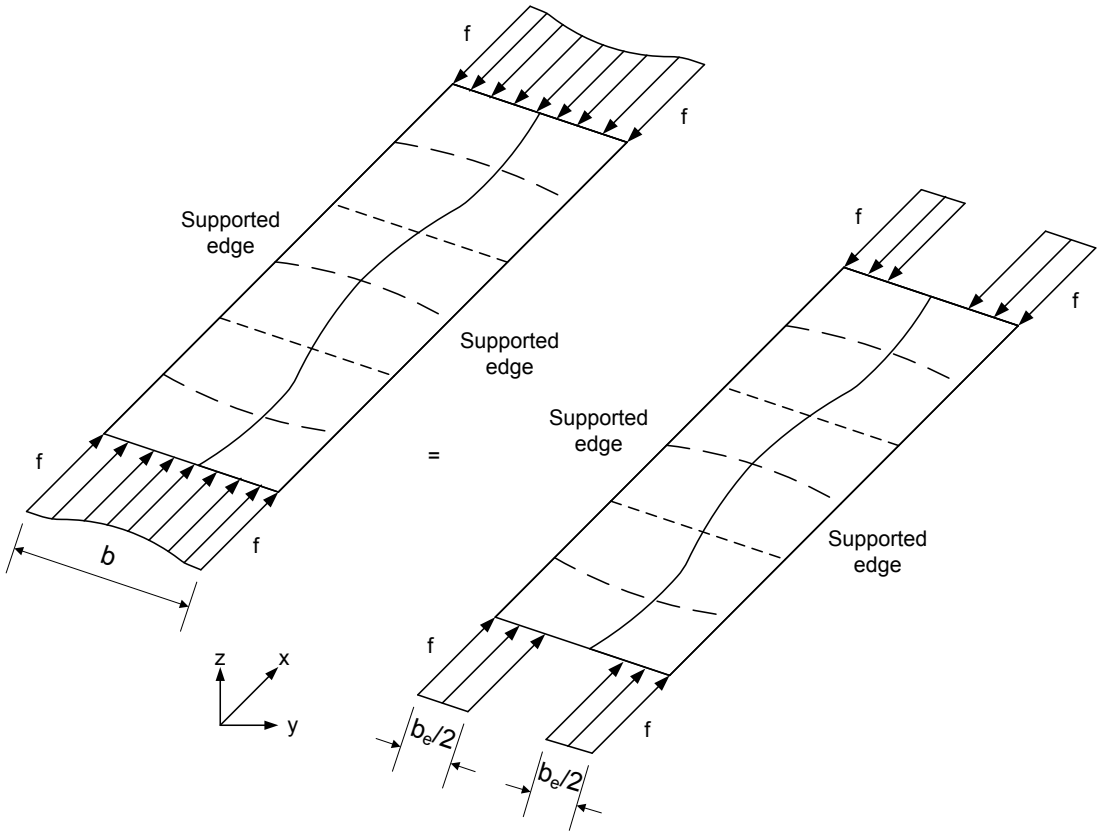

Figure 6.6.3.4.2.4.3-3 Average vs. Idealized Stress Distribution Across the Width of a Post-Buckled Stiffened Plate Element

b_e is determined as follows:

- For flanges of square and rectangular box sections and HSS of uniform thickness with $\frac{b}{t} \geq 1.40\sqrt{\frac{E}{f}}$; and nonperforated cover plates:

$$b_e = 1.92t\sqrt{\frac{E}{f}}\left[1 - \frac{0.38}{(b/t)}\sqrt{\frac{E}{f}}\right] \leq b \qquad \text{Equation 6.6.3.4.2.4.3-9}$$

AASHTO LRFD Equation 6.9.4.2.2-10

- For webs with $\frac{b}{t} \geq 1.49\sqrt{\frac{E}{f}}$; perforated cover plates, and all other stiffened elements:

$$b_e = 1.92t\sqrt{\frac{E}{f}}\left[1 - \frac{0.34}{(b/t)}\sqrt{\frac{E}{f}}\right] \leq b \qquad \text{Equation 6.6.3.4.2.4.3-10}$$

AASHTO LRFD Equation 6.9.4.2.2-11

In both of the above equations, f is taken equal to $Q_s F_y$. Where all unstiffened elements, if any, in the cross-section are classified as nonslender, Q_s is equal to 1.0.

For axially loaded circular tubes, including round HSS:

- For $0.11\frac{E}{F_y} < \frac{D}{t} < 0.45\frac{E}{F_y}$:

$$Q = Q_a = \frac{0.038E}{F_y(D/t)} + \frac{2}{3} \qquad \text{Equation 6.6.3.4.2.4.3-11}$$

AASHTO LRFD Equation 6.9.4.2.2-12

where D is the outside diameter of the tube, and t is the thickness of the tube (in.)

6.6.3.4.3 Combined Axial Compression and Flexure

6.6.3.4.3.1 General

For members subject to combined axial compression and flexure, often referred to as beam-columns, the resistance is typically defined by interaction equations that reduce to the compressive resistance in the limit of pure axial compression (with no flexure), or to the flexural resistance about the corresponding principal axis of the section in the limit of pure flexure about that axis (with no axial compression).

AASHTO LRFD Article 6.9.2.2 specifies the following bilinear relationship to define the resistance of members subject to combined axial compression and flexure:

- If $\frac{P_u}{P_r} < 0.2$, then:

$$\frac{P_u}{2.0P_r} + \left(\frac{M_{ux}}{M_{rx}} + \frac{M_{uy}}{M_{ry}}\right) \le 1.0 \qquad \text{Equation 6.6.3.4.3.1-1}$$

AASHTO LRFD Equation 6.9.2.2-1

- If $\frac{P_u}{P_r} \ge 0.2$, then:

$$\frac{P_u}{P_r} + \frac{8.0}{9.0}\left(\frac{M_{ux}}{M_{rx}} + \frac{M_{uy}}{M_{ry}}\right) \le 1.0 \qquad \text{Equation 6.6.3.4.3.1-2}$$

AASHTO LRFD Equation 6.9.2.2-2

where:

ϕ_f = resistance factor for flexure determined as specified in *AASHTO LRFD* Article 6.5.4.2 (= 1.0)

M_{rx} = factored flexural resistance about the x-axis taken as ϕ_f times the nominal flexural resistance about the x-axis determined as specified in *AASHTO LRFD* Article 6.10, 6.11 or 6.12, as applicable (kip-in.)

M_{ry} = factored flexural resistance about the y-axis taken as ϕ_f times the nominal flexural resistance about the y-axis determined as specified in *AASHTO LRFD* Article 6.12, as applicable (kip-in.)

M_{ux} = maximum factored second-order elastic moment along the member unbraced length taken about the x-axis of the cross-section (Section 6.6.3.4.3.2) (kip-in.)

M_{uy} = maximum factored second-order elastic moment along the member unbraced length taken about the y-axis of the cross-section (Section 6.6.3.4.3.2) (kip-in.)

P_r = factored compressive resistance determined as specified in *AASHTO LRFD* Article 6.9.2.1 (Section 6.6.3.4.2.1) (kips)
P_u = factored axial compressive force (kips)

The calculation of M_{rx} for use in Equations 6.6.3.4.3.1-1 and 6.6.3.4.3.1-2 was discussed previously in Section 6.6.3.3.3 of this chapter (refer to Equations 6.6.3.3.3-3 and 6.6.3.3.3-4). For cases where the member is subject to flexure about the y-axis, the nominal flexural resistance about the y-axis for I-shaped members is determined according to the provisions of *AASHTO LRFD* 6.12.2.2.1 (Section 6.6.3.5 - this section also contains further information on determining the nominal flexural resistance of miscellaneous bracing members such as tees, double angles and channels).

For prismatic members along the unbraced length, the largest value of P_u/P_r based on the axial compressive resistance limit states of flexural buckling, torsional bucking or flexural-torsional buckling is to be used in Equations 6.6.3.4.3.1-1 or 6.6.3.4.3.1-2, as applicable. Also, the largest values of M_{ux}/M_{rx} and M_{uy}/M_{ry} based on the flexural resistance limit states of yielding, local buckling or lateral-torsional buckling are to be used. Strictly speaking, for a particular load combination, concurrent values of P_u, M_{ux} and M_{uy} should be used in computing and determining the critical ratios to use. However, since concurrent actions are not typically tracked in the analysis, it is conservative and convenient to use the maximum envelope values for these actions in combining the ratios in these equations. For nonprismatic members, the reader is referred to White (2012) for additional information regarding the proper application of the preceding equations to such members.

The bilinear form of the interaction curve given by Equations 6.6.3.4.3.1-1 and 6.6.3.4.3.1-2 combines member strength and stability considerations into one single curve. Previous specifications utilized two curves; one that addressed stability or strength considerations, and one that addressed yielding as a member cross-section check. The bilinear form is simpler to use and better represents the fact that beam-columns actually fail through a combination of inelastic bending and stability effects (White, 2012).

As discussed further in White (2012), Equations 6.6.3.4.3.1-1 and 6.6.3.4.3.1-2 were established based on curve fitting to results from a large number of rigorous beam-column solutions; primarily for non-composite doubly symmetric I-section members composed of compact elements. The equations provide an excellent fit to solutions using a second-order moment magnification factor applied to first-order analysis results for doubly-symmetric I-sections subject to strong-axis bending with an ℓ/r ranging from 0 to 100. The equations are accurate to conservative for such shapes subject to weak-axis bending, and become increasingly conservative in these cases when ℓ/r is less than about 40 due to the large shape factor (or ratio of M_p/M_y), and increasing convexity of the curve representing the fully plastic weak-axis bending

resistance of these sections. The equations are moderately conservative for both axes when ℓ/r is greater than 120. For the no sidesway case, the equations also tend to be more conservative for beam-columns subject to reverse-curvature bending since they do not account for the influence of moment gradient on the shape of the strength or resistance curve (Clarke and Bridge, 1992). Additional information on the interaction behavior of doubly symmetric I-sections may be found in Liew et al. (1992), ASCE (1997), Maleck and White (2003), and White (2012).

6.6.3.4.3.2 Moment Magnification

AASHTO LRFD Article 6.9.2.2 specifies that the moments about the x- and y-axes, M_{ux} and M_{uy}, due to the eccentricity of the applied factored axial compressive force, P_u, is to be calculated considering second-order effects arising from the additional secondary moment cause by the axial force acting through the member deflection. The subsequent discussion will focus on the moment about the major x-axis, M_{ux} (Figure 6.6.3.4.3.2-1).

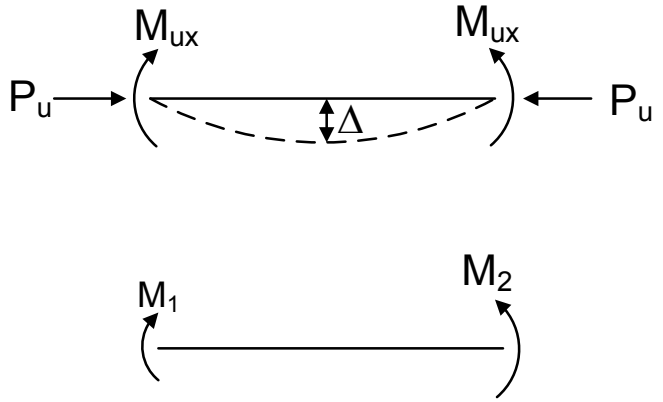

Figure 6.6.3.4.3.2-1 Magnification of M_{ux}, and End Moments M_1 and M_2

The magnification of the first-order moment, $(M_{ux})_1$, can be determined from a second-order elastic analysis, or more simply, from the approximate single-step adjustment specified in *AASHTO LRFD* Article 4.5.3.2.2b as follows (the sidesway term in the equation is generally not applicable for bracing members):

$$(M_{ux})_2 = \delta_b (M_{ux})_1 \qquad \text{Equation 6.6.3.4.3.2-1}$$

AASHTO LRFD Equation 4.5.3.2.2b-1

where:

$$\delta_b = \frac{C_m}{1-\frac{P_u}{\phi_K P_e}} \geq 1.0 \qquad \text{Equation 6.6.3.4.3.2-2}$$

AASHTO LRFD Equation 4.5.3.2.2b-3

C_m = equivalent uniform moment factor. For members braced against sidesway and without transverse loading between supports in the plane of bending:

$$= 0.6 + 0.4(M_1/M_2) \qquad \text{Equation 6.6.3.4.3.2-3}$$

AASHTO LRFD Equation 4.5.3.2.2b-6

P_e = Euler buckling load for buckling about the x-axis (i.e. the axis of bending)

$$= \frac{\pi^2 E I_x}{(K_x \ell_x)^2} \text{ (kips)} \qquad \text{Equation 6.6.3.4.3.2-4}$$

AASHTO LRFD Equation 4.5.3.2.2b-5

ϕ_K = stiffness reduction factor taken equal to 1.0 for steel members
I_x = moment of inertia of the member about the x-axis (in.^{4})
K_x = effective length factor about the x-axis determined as specified in AA*SHTO LRFD* Article 4.6.2.5 (Section 6.6.3.4.2.3.3)
ℓ_x = unbraced length for buckling about the x-axis (in.)
M_1 = smaller end moment (kip-in.)
M_2 = larger end moment (kip-in.)
P_u = applied factored axial compressive force (kips)

The equivalent uniform moment factor, C_m, given by Equation 6.6.3.4.3.2-3 depends on the ratio of the moments at the end of the member, with M_1 taken as the smaller end moment and M_2 taken as the larger end moment (Figure 6.6.3.4.3.2-1). The ratio, (M_1/M_2), is taken as positive when the member is bent in single curvature and negative when the member is bent in reverse curvature. Therefore, for a uniform moment, which is typically the case for an eccentrically loaded bracing member, C_m is equal to 1.0.

6.6.3.4.3.3 Interaction Curves for Tees and Double Angles

For tees and double angles subject to combined axial tension and flexure or combined axial compression and flexure, in which the axial and flexural stresses in the flange of the tee are additive in tension or compression (as applicable), a bulge

in the interaction curve occurs as noted qualitatively in Figure 6.6.3.4.3.3-1 (see upper right and lower left quadrants).

Such a condition occurs when a tee is used as a bracing member and the connection of the member is made to the flange. The resulting moment due to the eccentricity of the connection typically places the member design in the upper right or lower left quadrant, and often in the vicinity of the largest bulge in the resistance envelope. As a result, the *AASHTO LRFD* interaction curves may significantly underestimate the resistance in these cases.

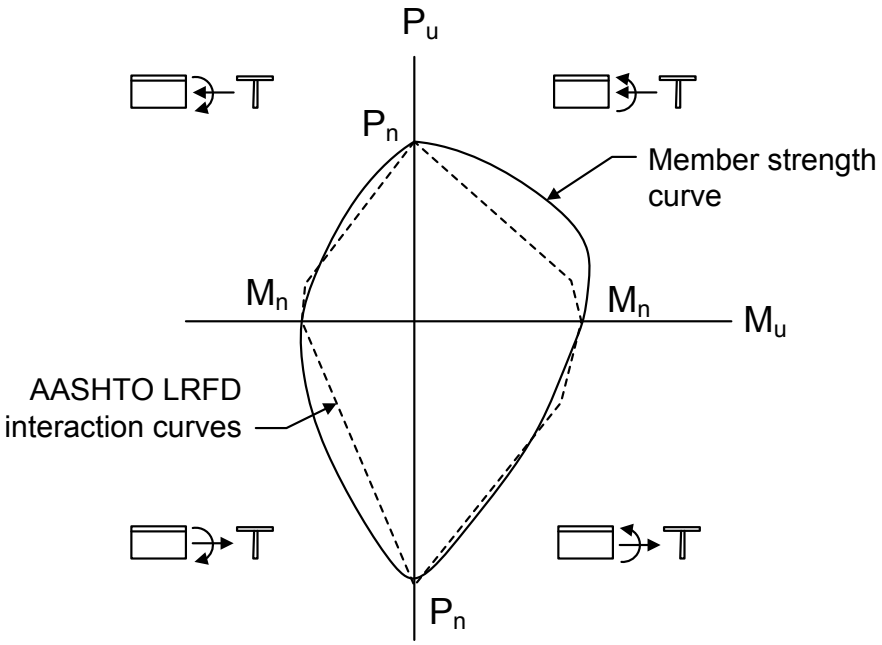

Figure 6.6.3.4.3.3-1 Interaction Curves for Tees Subjected to Combined Axial Forces and Flexure

The *AASHTO LRFD* interaction curves provide a reasonably accurate estimate of the actual resistance in cases where the stem of the tee is subject to additive axial and flexural tension or compression (see upper left and lower right quadrants of Figure 6.6.3.4.3.3-1).

As discussed in *AASHTO LRFD* Articles C6.8.2.3 and C6.9.2.2, alternative approaches attempting to capture the bulge in the interaction curve have proven thus far to be generally inconclusive or incomplete. Thus, in the interim, it is recommended that the *AASHTO LRFD* interaction curves be conservatively applied to cases where the axial and flexural stresses in the flange of the tee are additive in tension or compression. Should significant additional resistance be required, the use of one or more of these alternative approaches, as described in greater detail in White (2012), might be considered.

6.6.3.4.4 Built-Up Members

Built-up compression members are covered in *AASHTO LRFD* Article 6.9.4.3. As mentioned previously, built-up compression members typically consist of two or more shapes. Included in this category are back-to-back angles connected by intermittent bolted or welded filler plates, boxed channels, and flange components (i.e. two rolled shapes or plates) spaced widely apart and connected by lacing (flat bars, angles, channels or other shapes), tie plates (also referred to as batten or stay plates), or perforated cover plates.
To utilize the full calculated factored compressive resistance of a built-up member (determined as discussed below), each component of the member must satisfy the corresponding width-to-thickness requirement for axial compression specified in *AASHTO LRFD* Equation 6.9.4.2.1 (Section 6.6.3.4.2.4.2). Should the member consist of one or more elements not satisfying the width-to-thickness requirements of *AASHTO LRFD* Article 6.9.4.2.1 (i.e. slender elements), the nominal compressive resistance of the member must be reduced according to the procedures given in AASHTO LRFD Article 6.9.4.2.2 (Section 6.6.3.4.2.4.3) to account for the fact that the slender elements might potentially undergo local buckling, which may adversely affect the overall buckling resistance of the member.

In many instances, the axial resistance of built-up columns used as compression members is also affected by any relative deformation between the shapes that produces shear forces in the connectors between the individual shapes. Shear in a compression member can result due to lateral loads, end eccentricity of the axial load, and/or by the slope of the member with respect to the line of thrust of the axial load caused by bending during buckling or any unintended initial curvature. Shear has an insignificant effect on reducing the compressive resistance of sections with solid webs (Salmon and Johnson, 1996), and on box-section members built-up using perforated cover plates. However, the effect of shear on the compressive resistance for all other types of built-up compression members should not be neglected.

As discussed further in McGuire (1968), Salmon and Johnson (1996), and SSRC (1998), the shear effect can be accounted for by an adjustment to the effective length of the member. *AASHTO LRFD* Article 6.9.4.3 specifies the following modified slenderness ratio, $(K\ell/r)_m$, for built-up members composed of two or more shapes where the buckling mode involves relative deformation that produces shear forces in connectors between the individual shapes. This modified ratio applies when the intermediate connectors between the shapes are welded or fully-tensioned bolted (Aslani and Goel, 1991):

$$\left(\frac{K\ell}{r}\right)_m = \sqrt{\left(\frac{K\ell}{r}\right)_o^2 + 0.82\left(\frac{\alpha^2}{1+\alpha^2}\right)\left(\frac{a}{r_{ib}}\right)^2} \qquad \text{Equation 6.6.3.4.4-1}$$

AASHTO LRFD Equation 6.9.4.3.1-1

where:

$(K\ell/r)_o$= slenderness ratio of the built-up member (with shear deformation neglected) acting as a unit in the buckling direction being considered

α = separation ratio = $h/2r_{ib}$

a = distance (center-to-center) between connectors (in.)

r_{ib} = radius of gyration of an individual component shape relative to its centroidal axis parallel to the member axis of buckling (in.)

h = distance between centroids of individual component shapes perpendicular to the member axis of buckling (in.)

For example, for a built-up double-angle or double-channel compression member interconnected at intervals along its length in the plane defined by the y-axis of the cross-section, $(K\ell/r)_m$ would be used in place of $(K\ell/r)_y$ for flexural buckling about the y-axis to account for the effect of the shear displacements between the shapes. Flexural buckling about the x-axis would be checked in conventional fashion, as shear effects would have no effect on buckling about the x-axis. For the case of the singly-symmetric back-to-back double-angle member, P_{ey} calculated from Equation 6.6.3.4.2.3.4-3 -- using the modified $(K\ell/r)_m$ in place of $(K\ell/r)_y$ -- would be used in the flexural-torsional buckling Equation 6.6.3.4.2.3.4-2. The nominal compressive resistance in this case would then be computed as the smaller value based on either flexural buckling about the x-axis or flexural-torsional buckling, which involves torsion of the member in combination with flexure about the y-axis.

As discussed in White (2012), Equation 6.6.3.4.4-1 is a refinement of an equation originally derived in Bleich (1952) for battened columns neglecting the influence of the strain energy developed due to localized bending of the batten plates and assuming zero shearing deformation of the end tie plates. Aslani and Goel (1991) summarize the theoretical derivation of Equation 6.6.3.4.4-1 and illustrate that the equation gives accurate to slightly conservative predictions compared to experimental test data for built-up double-angle compression members. However, since the derivation of the equation is general in nature, Aslani and Goel (1991) suggest that the equation is also applicable to built-up compression members utilizing widely spaced components.

AASHTO LRFD Article C6.9.4.3.1 gives the following alternate equation for $(K\ell/r)_m$ assumed applicable to compression members, for which shear-force effects are a concern, that are built-up using other types of intermediate connectors, including those members on existing structures that are interconnected with rivets:

$$\left(\frac{K\ell}{r}\right)_m = \sqrt{\left(\frac{K\ell}{r}\right)_o^2 + \left(\frac{a}{r_i}\right)^2} \qquad \text{Equation 6.6.3.4.4-2}$$

AASHTO LRFD Article C6.9.4.3.1-1

where:

r_i = minimum radius of gyration of an individual component shape (in.)

Equation 6.6.3.4.4-2 is based on the equation given in Section E6 of ASIC (2010a) for application to built-up compression members in which the intermediate connectors are snug-tight bolted. The equation is empirically based on test results, as discussed further in Zandonini (1985).

In addition, *AASHTO LRFD* Article 6.9.4.3.1 specifies that for built-up compression members composed of two or more shapes interconnected at intervals, the slenderness ratio of each component shape between connecting fasteners or welds (i.e. the maximum value of a/r_{ib} for each shape) must not exceed 75 percent of the governing slenderness ratio of the built-up member. Also, lacing members and/or tie plates are to be spaced such that the slenderness ratio of each component shape between the lacing and/or tie-plate connection points does not exceed 75 percent of the governing slenderness ratio of the built-up member. In each case, the least radius of gyration is to be used in computing the slenderness ratio of each component shape between the connectors or connection points. Formulas giving approximate radii of gyration for various potential configurations of built-up members are provided in Table A1 of Salmon and Johnson (1996). This requirement is intended to mitigate the possibility of so-called compound buckling, or the interaction between global buckling of the built-up member and local buckling of the individual components between intermediate connectors or lacing and/or tie-plate connection points (Duan et al., 2002).

As mentioned in *AASHTO LRFD* Article C6.9.4.3.1, the connectors in built-up compression members must be designed to resist the shear forces that develop in the buckled member, but no additional guidance is offered. White (2012) suggests that the additional transverse shear force due to stability effects (given by Equation 6.6.3.4.4-3 below) might be used to design the connectors.

Along the length of the member between the end connections, the maximum longitudinal spacing or pitch of bolts must satisfy the spacing requirements for stitch bolts specified in *AASHTO LRFD* Article 6.13.2.6.3 (Section 6.6.4.2.2.2.4). These maximum pitch requirements are intended to ensure that the individual components of the member act as a unit to transfer the required forces without buckling of the member. Note that the maximum pitch must also not exceed the maximum pitch for sealing specified in *AASHTO LRFD* Article 6.13.2.6.2 (Section 6.6.4.2.2.2.2).

Reference 26 suggests that the specified maximum pitch requirements might also be applied to the spacing of intermittent welds used to connect built-up compression members.

As indicated in the Commentary to Section E6 of AISC (2010a), in the case of both of the preceding equations, the ends of the member must be connected rigidly by welding or full-tension bolting, or by the use of end tie plates. Section E6 of AISC (2010a) suggests designing bolted end connections of built-up compression members for the full compressive load as a bearing-type connection, with the bolts fully pretensioned and a Class A or B faying surface provided. The Class A or B surface is not recommended to develop slip resistance in the bolts, but to help prevent relative moment between the components at the end as the member takes a curved shape [the shear is highest at the ends of the member where the slope of the buckled member is the greatest (Bleich, 1952)]. At the ends of built-up compression members, bolts must also satisfy the maximum pitch requirements specified for the ends of these members in *AASHTO LRFD* Article 6.13.2.6.4 (Section 6.6.4.2.2.2.4).

Perforated cover plates are more likely to be used for built-up members in new bridge construction than laced or battened compression members. Specific design requirements for perforated cover plates used in built-up compression or tension members are given in *AASHTO LRFD* Article 6.8.5.2 (see Section 6.6.3.3.4 for a summary of these requirements).

In addition, for built-up compression members utilizing perforated cover plates, *AASHTO LRFD* Article 6.9.4.3.2 specifies that the perforated plates must be designed for the sum of the shear force due to the factored loads (i.e. shear due to self-weight of the member plus any additional applied force), and an additional transverse shear force, *V* (kips), due to stability effects, assumed divided equally to each plane containing a perforated plate, taken as:

$$V = \frac{P_r}{100}\left(\frac{100}{(\ell/r)+10} + \frac{8.8(\ell/r)F_y}{E}\right) \qquad \text{Equation 6.6.3.4.4-3}$$

AASHTO LRFD Equation 6.9.4.3.2-1

where:

P_r = factored compressive resistance determined as specified in *AASHTO LRFD* Article 6.9.2.1 or 6.9.2.2 (Section 6.6.3.4.2.1 or 6.6.3.4.3.1) (kips)
ℓ = member length (in.)
r = radius of gyration about an axis perpendicular to the plane of the perforated plate (in.)

The requirements of *AASHTO LRFD* Article 6.9.4.2.1 (Section 6.6.3.4.2.4.2) are also to be checked for the clear distance between the two edge supports of the

perforated cover plate utilizing a plate-buckling coefficient, *k*, of 1.86. These requirements should also be separately checked for the projecting width from the edge of the perforation to a single edge support utilizing a plate-buckling coefficient, *k*, of 0.45.

Equation 6.6.3.4.4-3 is carried over from AASHTO (2002), and should also be applied to any built-up compression member design in which lacing might be used. Specific design requirements for lacing bars and tie or batten plates, which are not covered in this Manual, may be found in AISC (2010a) and AASHTO (2002). Additional information on the design of laced and battened compression members may also be found in McGuire (1968), Salmon and Johnson (1996), and SSRC (1998). Duan et al. (2000) provide an approach for determining the section properties of latticed built-up members, including the moment of inertia and torsional constant.

6.6.3.4.5 Single-Angle Compression Members

6.6.3.4.5.1 General

Single angles, as shown in Figure 6.6.3.4.5.1-1, are commonly used as cross-frame and lateral bracing members for steel bridges. Since in most practical applications the angle is connected through one leg only, single-angle bracing members are typically subject to combined axial compression/tension and flexure, or moments about both principal axes due to the eccentricities of the applied axial load. The angle is also usually restrained by differing amounts about its geometric x- and y-axes. As a result, the prediction of the nominal resistance of these members under these conditions is difficult, particularly when the member is subject to compression.

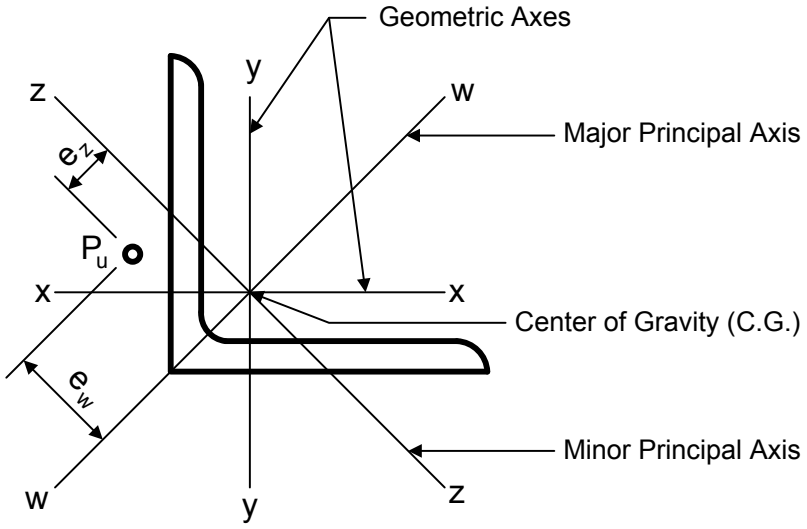

Figure 6.6.3.4.5.1-1 Single-Angle Member Geometry

As discussed in Section 6.6.3.3.3, the condition of flexure due to eccentric axial tension for single angles at the strength limit state may be (and is typically) addressed through the use of the shear lag coefficient, *U*, specified in *AASHTO LRFD* Article 6.8.2.2 (Section 6.6.3.3.2.4).

The condition of flexure due to eccentric axial compression is now efficiently handled through the use of an effective slenderness ratio, $(K\ell/r)_{eff}$, as specified in *AASHTO LRFD* Article 6.9.4.4 (Section 6.6.3.4.5.2). The use of the specified effective slenderness ratio allows single angles satisfying certain conditions that are subject to combined axial compression and flexure to be designed as pin-ended concentrically loaded compression members for flexural buckling only. Furthermore, when the effective slenderness ratio is used, single angles need not be checked for flexural-torsional buckling, and the calculation of the nominal flexural resistance, M_n, of a single-angle member is typically not required. These provisions are based on the provisions for the design of single-angle members used in latticed transmission towers (ASCE, 2000). Similar provisions are also employed in Section E5 of AISC (2010a), the Eurocode 3 standard (CEN, 1993), and in British Standard BS5950 (BSI, 1990).

6.6.3.4.5.2 Effective Slenderness Ratio

According to *AASHTO LRFD* Table 6.9.4.1.1-1, single angles in compression need only be checked for flexural buckling (Section 6.6.3.4.2.3.3) if the provisions of *AASHTO LRFD* Article 6.9.4.4 are employed. These provisions permit the effects of all eccentricities in the member to be neglected when these members are evaluated as axially loaded compression members for flexural buckling only using an appropriate effective slenderness ratio, $(K\ell/r)_{eff}$. The effective slenderness ratio indirectly accounts for the bending in the angles due to the eccentricity of the loading allowing the member to be proportioned as if it were a pinned-end concentrically loaded compression member. Furthermore, when the effective slenderness ratio is used, single angles need not be checked for flexural-torsional buckling.

The member must satisfy all of the following conditions specified in *AASHTO LRFD* Article 6.9.4.4, which are typically satisfied by members used in cross-frames and lateral bracing in steel-bridge applications, in order to use the effective slenderness ratio:

- The end connections are to a single leg,
- The member is loaded at the ends in compression through the same leg,
- The end connections are welded or use a minimum of two bolts,
- The member is not subjected to any intermediate transverse loads, and
- When used as web members in trusses, all adjacent web members are attached to the same side of the gusset plate or chord.

The equations for the effective slenderness ratio presume significant end rotational restraint about the y-axis, or the axis perpendicular to the connected leg and gusset plate (Figure 6.6.3.4.5.2-1). As a result, as shown in various tests (Usami and Galambos, 1971; Woolcock and Kitipornchi, 1986; and Mengelkoch and Yura, 2002), the angle tends to buckle primarily about the x-axis due to the eccentricity of the load about the x-axis coupled with the high degree of restraint about the y-axis (Usami and Galambos, 1971; and Mengelkoch and Yura, 2002 included tests of unequal-leg angles).

Thus, the radius of gyration in the effective slenderness ratio equations is taken as r_x, or the radius of gyration about the geometric axis parallel to the connected leg, as opposed to the minimum radius of gyration about the minor principal axis of the angle, r_z (Figure 6.6.3.4.5.2-2). When an angle has significant rotational restraint about the y-axis, the stress along the connected leg will be approximately uniform (Lutz, 1996).

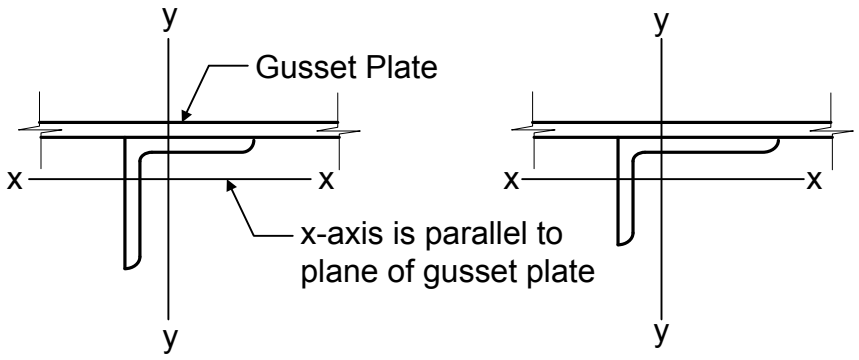

Figure 6.6.3.4.5.2-1 Single-Angle Geometric Axes Utilized in the Effective Slenderness Ratio Expressions - for Equal-Leg Angle and Unequal-Leg Angle Connected Through the Longer Leg

Lutz (2006) compared the results from the effective slenderness ratio equations to test results for single-angle members in compression with essentially pinned-end connections reported in Foehl (1948) and Trahair et al. (1969), and found an average value of P_r/P_{test} of 0.998 with a coefficient of variation of 0.109. A separate set of equations presented in AISC (2010a), which assume a higher degree of x-axis rotational restraint and thus are intended for application only to single angles used as web members in box or space trusses, are not provided in the *AASHTO LRFD* Specifications.

The equations for the effective slenderness ratio, $(K\ell/r)_{eff}$, for the case of equal-leg angles and unequal-leg angles connected through the longer leg (Figure 6.6.3.4.5.2-1) are as follows.

- If $\ell/r_x \le 80$, then:

$$\left(\frac{K\ell}{r}\right)_{eff} = 72 + 0.75\left(\frac{\ell}{r_x}\right)$$ Equation 6.6.3.4.5.2-1

AASHTO LRFD Equation 6.9.4.4-1

- If $\ell/r_x > 80$, then:

$$\left(\frac{K\ell}{r}\right)_{eff} = 32 + 1.25\left(\frac{\ell}{r_x}\right)$$ Equation 6.6.3.4.5.2-2

AASHTO LRFD Equation 6.9.4.4-2

where:

ℓ = distance between the work points of the joints measured along the length of the angle (in.)

r_x = radius of gyration about the geometric axis of the angle parallel to the connected leg (in.)

r_x in the equations should be taken as the smaller value about the angle geometric axes, which is typically listed as r_y for rolled angle shapes, in applying the equations for an unequal-leg angle connected through the longer leg.

The equations for the effective slenderness ratio, $(K\ell/r)_{eff}$, for the case of unequal-leg angles connected through the shorter leg and with ratios of leg lengths, (b_ℓ/b_s), less than 1.7 (Figure 6.6.3.4.5.2-2) are as follows:

- If $\ell/r_x \le 80$, then:

$$\left(\frac{k\ell}{r}\right)_{eff} = 72 + 0.75\left(\frac{\ell}{r_x}\right) + 4\left[\left(\frac{b_\ell}{b_s}\right)^2 - 1\right] \ge 0.95\left(\frac{\ell}{r_z}\right)$$ Equation 6.6.3.4.5.2-3

AASHTO LRFD Equation 6.9.4.4-3

- If $\ell/r_x > 80$, then:

$$\left(\frac{k\ell}{r}\right)_{eff} = 32 + 1.25\left(\frac{\ell}{r_x}\right) + 4\left[\left(\frac{b_\ell}{b_s}\right)^2 - 1\right] \geq 0.95\left(\frac{\ell}{r_z}\right) \quad \text{Equation 6.6.3.4.5.2-4}$$

AASHTO LRFD Equation 6.9.4.4-4

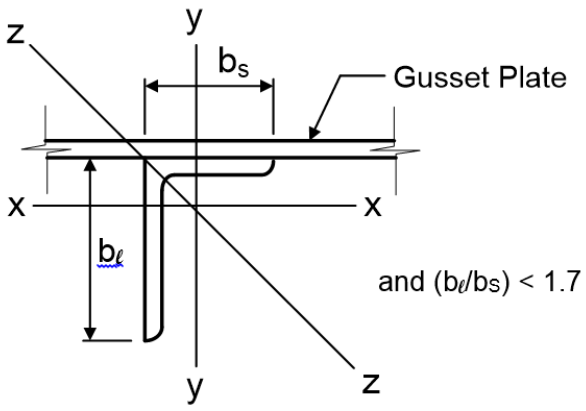

Figure 6.6.3.4.5.2-2 Unequal-Leg Angles Connected Through the Shorter Leg with Ratio of Leg Lengths < 1.7

The limited available test data for this case (Usami and Galambos, 1971; Mengelkoch and Yura, 2002) give lower capacities for comparable ℓ/r_x values than equal-leg angles (Lutz, 2006). Stiffening the shorter leg rotationally tends to force the buckling axis of the angle away from the x-axis and closer to the z-axis, or minor principal axis of the angle (Lutz, 2006) (Figure 6.6.3.4.5.2-2). Thus, the effective slenderness ratio equations for this case (Equations 6.6.3.4.5.2-3 and 6.6.3.4.5.2-4) are modified by adding an additional term based on the ratio of the leg lengths, along with a governing slenderness limit based on ℓ/r_z for slender unequal-leg angles. The upper limit on (b_ℓ/b_s) of 1.7 is based on the limits of the available physical tests.

Single-angle compression members not meeting one or more of the specified conditions, or with (b_ℓ/b_s) greater than or equal to 1.7, should instead be explicitly evaluated for combined axial load and flexure as beam-columns according to Section H2 of AISC (2010a). The reader is referred to *AASHTO LRFD* Article C6.9.4.4 for further information on the suggested procedure to follow in the unlikely event that this would be required.

Single-angle members are often employed in X-type configurations in cross-frames. Since the necessary rotational restraint about the y-axis assumed in the effective slenderness ratio equations may not be present at the crossover point of the diagonals (e.g. if the members are only connected with a single bolt at that point), it is currently recommended in *AASHTO LRFD* Article C6.9.4.4 that the full length of the diagonal between the connection work points be used for ℓ in applying the

effective slenderness ratio equations. Section 2.7 of Yura and Helwig (2012) presents a different viewpoint on this issue for consideration.

Finally, it is important to note that *AASHTO LRFD* Article 6.9.4.4 specifies that the actual maximum slenderness ratio of the angle, as opposed to $(K\ell/r)_{eff}$, is not to exceed the applicable limiting slenderness ratio specified in *AASHTO LRFD* Article 6.9.3 (Section 6.6.3.4.2.2). Thus, if the actual maximum slenderness ratio of the angle exceeds the limiting ratio, a larger angle must be selected until the ratio is satisfied. If $(K\ell/r)_{eff}$ exceeds the limiting ratio, but the actual maximum slenderness ratio of the angle does not, the design is satisfactory.

EXAMPLE

Determine the factored compressive resistance, P_r, at the strength limit state of a 5 x 5 x 7/16 single angle used as a bottom strut in an I-girder cross frame. The angle is 8.0 feet long, and the steel for the angle is ASTM A709/A709M Grade 50W steel. The distance, ℓ, between the work points of the joints measured along the length of the angle is 10.0 feet.

The angle is subject to a compressive force due to the factored loads, P_u, under the Strength I load combination of 58.0 kips. From the AISC Manual shape property tables, the gross cross-sectional area of the angle, A_g, is equal to 4.18 in.^{2}, the radius of gyration about the x-axis, r_x, is equal to 1.55 in., and the radius of gyration about the z-axis, r_z, is equal to 0.986 in. Therefore:

$$\frac{\ell}{r_x} = \frac{10.0(12)}{1.55} = 77.4$$

For an equal-leg angle with $\ell/r_x < 80$, use the effective slenderness ratio calculated from Equation 6.6.3.4.5.2-1 as follows:

$$\frac{K\ell}{r} = 72 + 0.75\frac{\ell}{r_x}$$

$$\frac{K\ell}{r} = 72 + 0.75(77.4) = 130.0$$

Assume an X-type configuration for the cross-frame, and that the angle is welded to gusset plates, which are assumed bolted to the cross-frame connection plates in the field. Using the physical length of the angle to represent the unbraced length of the bottom strut in this case, the actual maximum slenderness ratio is computed as follows. The effective length factor, K, is taken as 1.0, as specified for single angles in *AASHTO LRFD* Article 4.6.2.5 (Section 6.6.3.4.2.3.3):

$$\frac{K\ell}{r_z} = \frac{1.0(8.0)12}{0.986} = 97.4$$

Since the force in the angle is assumed to be determined from an analysis, the member is considered to be a primary member. The maximum permitted slenderness ratio for primary compression members specified in AASHTO LRFD Article 6.9.3 is 120 (Section 6.6.3.4.2.2), which is greater than 97.4 (ok).

Check if the angle has any slender elements. As specified in *AASHTO LRFD* Article 6.9.4.2.1, to qualify as a nonslender element, plates in members subject to uniform compression must satisfy the following requirement (Equation 6.6.3.4.2.4.2-1):

$$\frac{b}{t} \le k\sqrt{\frac{E}{F_y}}$$

From Table 6.6.3.4.2.4.2-1, for the outstanding legs of single angles, *k* in the preceding equation is taken equal to 0.45. Therefore:

$$0.45\sqrt{\frac{29{,}000}{50}} = 10.8 < \frac{b}{t} = \frac{5}{0.4375} = 11.4$$

Therefore, the nominal compressive resistance of the angle must be reduced due to potential local buckling of the slender outstanding legs. Since *b*/*t* is less than $0.91\sqrt{E/F_y} = 21.9$, calculate the form factor, Q_s, for the slender unstiffened element from Equation 6.6.3.4.2.4.3-3 as follows:

$$Q_s = 1.34 - 0.76\left(\frac{b}{t}\right)\sqrt{\frac{F_y}{E}}$$

$$Q_s = 1.34 - 0.76(11.4)\sqrt{\frac{50}{29{,}000}} = 0.98$$

Since there are no stiffened elements, *Q* is taken equal to Q_s; therefore, *Q* = 0.98.

Since the effective slenderness ratio approach is used, the effect of all load eccentricities can be neglected and flexural-torsional buckling does not need to be considered. Therefore, calculate the nominal flexural resistance, P_n, based on flexural buckling (Section 6.6.3.4.2.3.3).

The elastic critical flexural buckling resistance, P_e, is computed from Equation 6.6.3.4.2.3.3-1 as follows, with the effective slenderness ratio, $(K\ell/r)_{eff}$, substituted for $K\ell/r_s$:

$$P_e = \frac{\pi^2 E}{\left(\frac{K\ell}{r_s}\right)^2} A_g$$

$$P_e = \frac{\pi^2(29{,}000)}{(130.0)^2}(4.18) = 70.8 \text{ kips}$$

Since $Q < 1.0$, the equivalent nominal yield resistance, P_o, is computed from Equation 6.6.3.4.2.4.3-1 as follows:

$$P_o = QF_yA_g$$

$$P_o = 0.98(50)(4.18) = 204.8 \text{ kips}$$

$$\frac{P_e}{P_o} = \frac{70.8}{204.8} = 0.34 < 0.44$$

Therefore, P_n is computed from Equation 6.6.3.4.2.3.1-2 as follows:

$$P_n = 0.877P_e$$

$$P_n = 0.877(70.8) = 62.1 \text{ kips}$$

The factored compressive resistance, P_r, is computed from Equation 6.3.4.2.1-1 as:

$$P_r = \phi_c P_n$$

where ϕ_c is the resistance factor for axial compression specified in *AASHTO LRFD* Article 6.5.4.2 = 0.95. Therefore:

$$P_r = 0.95(62.1) = 59.0 \text{ kips} > P_u = 58.0 \text{ kips} \quad \text{ok}$$

6.6.3.5 Flexural Resistance of Miscellaneous Bracing Members

6.6.3.5.1 General

AASHTO LRFD Article 6.12 provides provisions for determining the nominal flexural resistance of miscellaneous rolled or built-up non-composite or composite members subject to flexure, most often in combination with axial loads (Sections 6.6.3.3.3 and 6.6.3.4.3). Included are doubly symmetric non-composite box-shaped members utilized in trusses, frames, and arches, and angles, tees, and channels utilized as bracing members. This section reviews these provisions for select non-composite members only – namely the provisions for determining the nominal flexural resistance of miscellaneous sections utilized as bracing members. Tees and double angles are covered in Section 6.6.3.5.3, channels in Section 6.6.3.5.4, and single angles in Section 6.6.3.5.5. Also covered herein are the provisions for determining the nominal flexural resistance of I- and H-shaped members subject to weak-axis flexure (Section 6.6.3.5.2).

Discussions on the determination of the nominal flexural resistance of non-composite box-shaped members, including square and rectangular HSS (*AASHTO LRFD* Articles 6.12.2.2.2 and 6.12.1.2.3b), non-composite circular tubes (*AASHTO LRFD* Articles 6.12.2.2.3 and 6.12.1.2.3c), and non-composite rectangular bars and solid rounds (*AASHTO LRFD* Article 6.12.2.2.7) are generally considered to be outside the scope of this Manual. The reader is referred to White (2012) for additional information regarding the flexural resistance of these members.

The reader is also referred to *AASHTO LRFD* Article 6.12.2.3 and to AISC (2010a) and White (2012) for additional information on determining the nominal flexural resistance of miscellaneous composite flexural members (e.g. concrete encased shapes and concrete filled steel tubes or CFSTs). *AASHTO LRFD* Article 6.12.3 covers the determination of the shear resistance of these miscellaneous composite flexural members.

6.6.3.5.2 I- and H-Shaped Members Subject to Weak-Axis Flexure

As specified in *AASHTO LRFD* Article 6.12.2.2.1, the nominal flexural resistance of non-composite I- and H-shaped members subject to flexure about an axis parallel with the web (i.e. weak-axis flexure) is to be determined as follows:

- If $\lambda_f \le \lambda_{pf}$, then:

$$M_n = M_p \qquad \text{Equation 6.6.3.5.2-1}$$

AASHTO LRFD Equation 6.12.2.2.1-1

- If $\lambda_{pf} < \lambda_f \le \lambda_{rf}$, then:

$$M_n = \left[1 - \left(1 - \frac{S_y}{Z_y}\right)\left(\frac{\lambda_f - \lambda_{pf}}{0.45\sqrt{\frac{E}{F_{yf}}}}\right)\right] \qquad \text{Equation 6.6.3.5.2-2}$$

AASHTO LRFD Equation 6.12.2.2.1-2

where:

λ_f = largest flange slenderness ratio

= $b_f/2t_f$ *AASHTO LRFD* Equation 6.12.2.2.1-3

λ_{pf} = limiting slenderness ratio for a compact flange

$$= 0.38\sqrt{\frac{E}{F_{yf}}} \qquad \text{Equation 6.6.3.5.2-3}$$

AASHTO LRFD Equation 6.12.2.2.1-4

λ_{rf} = limiting slenderness ratio for a noncompact flange

$$= 0.83\sqrt{\frac{E}{F_{yf}}} \qquad \text{Equation 6.6.3.5.2-4}$$

AASHTO LRFD Equation 6.12.2.2.1-5

F_{yf} = specified minimum yield strength of the lower-strength flange (ksi)

M_p = plastic moment about the axis parallel with the web (weak axis) = $F_{yf}Z_y$ (kip-in.)

S_y = elastic section modulus about the axis parallel with the web (weak axis) (in.^{3})

Z_y = plastic section modulus about the axis parallel with the web (weak axis) (in.^{3})

For sections where the largest slenderness ratio, λ_f, of the two flanges is less than or equal to the compact flange slenderness limit, λ_{pf}, given by Equation 6.6.3.5.2-3, the nominal flexural resistance is to be taken as the full plastic moment resistance, M_p, which is equal to $1.5F_{yf}S_y$ for a doubly-symmetric I- or H-shaped member bent about its weak axis (i.e. $Z_y = 1.5S_y$). For a hybrid section, the lower-strength flange is used in determining λ_{pf}, and in calculating M_p (the web contribution to M_p about the weak axis is small).

For sections where the largest slenderness ratio, λ_f, of the two flanges is greater than the compact flange slenderness limit, λ_{pf}, but less than or equal to the noncompact flange slenderness limit, λ_{rf}, given by Equation 6.6.3.5.2-4, the nominal

flexural resistance is controlled by inelastic flange local buckling. Hence, the linear Equation 6.6.3.5.2-2 is used to determine the nominal flexural resistance.

λ_{rf} is derived from the right-hand side of Equation 6.5.6.2.2.2.1-2 with the plate buckling coefficient, k_c, taken equal to 0.76. For a linear stress distribution across the flange width with the maximum compressive stress at the flange tip and zero stress at the web/flange juncture, the theoretical elastic flange local buckling coefficient, k_c, is 0.57 assuming simply-supported edge conditions and 1.61 assuming fixed edge conditions at the web/flange juncture (SSRC, 1998). A k_c of 0.76 is felt to be a reasonable value due to the restraint offered to the flanges by the web and due to the fact that a portion of the flanges is in tension (White, 2012). The effect of residual stresses is neglected since k_c is relatively small compared to the potential theoretical value and because of the strain gradient across the flange width (White, 2012). The web load-shedding factor, R_b (Section 6.4.5.6), is not included in Equation 6.6.3.5.2-2 since the web flexural stress is zero.

An elastic flange local buckling equation (for $\lambda_f > \lambda_{rf}$) is not included since Equation 6.6.3.5.2-4 gives a λ_{rf} value equal to 14.1 for F_{yf} = 100 ksi, and λ_f is limited to 12.0 for I-sections according to the flange proportioning limits specified in *AASHTO LRFD* Article 6.10.2.2 (Equation 6.3.4.4.2-3).

Note that for I-sections subject to strong-axis flexure in combination with flange lateral bending due to torsion or weak-axis flexure, the one-third rule equations provided in the specifications (Section 6.5.2.1) should be utilized in lieu of the preceding equations.

6.6.3.5.3 Tees and Double Angles

Structural tees, as shown in Figure 6.6.3.5.3-1, are sometimes used as cross-frame and lateral bracing members for steel bridges, particularly as the loads in these members become larger. Since in most practical applications, the tee is connected through the flange, tees used as bracing members are also typically subject to combined axial compression/tension and flexure, or a moment about the major-axis of the tee due to the eccentricity of the applied axial load (Figure 6.6.3.5.3-2). Double angles can be treated similarly to structural tees. Double angles permit bolts to work in double shear reducing the number. However, as mentioned in Section 6.3.2.9.6.1, they are typically more expensive to fabricate and painting between the angles is difficult.

Figure 6.6.3.5.3-1 Cross-Frame Composed of Structural Tees

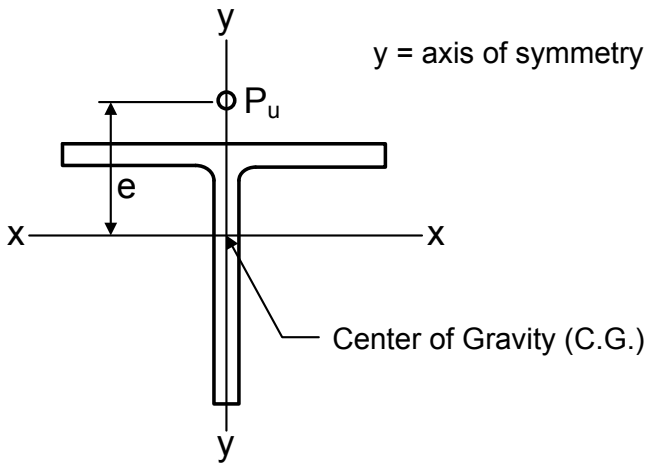

Figure 6.6.3.5.3-2 Tee Member Geometry and Eccentricity of Applied Load, P_u

As discussed in the Section 6.6.3.3.3, at the judgment of the Engineer, the condition of flexure due to eccentric axial tension for tees and double angles at the strength limit state may be addressed through the use of the shear lag reduction factor, *U*, or the beam-column interaction curves specified in *AASHTO LRFD* Article 6.8.2.3 (Section 6.6.3.3.3; see also Section 6.6.3.4.3).

Flexure due to eccentric axial compression for tees and double angles at the strength limit state is always addressed through the use of the beam-column interaction curves specified in *AASHTO LRFD* Article 6.9.2.2 (Section 6.6.3.4.3; see also Section 6.6.3.4.3.3). Thus, the calculation of the nominal flexural resistance, M_n, of these members is typically required. Also, tees and double angles subject to axial compression can fail either by flexural buckling about their x-axis, or by torsion combined with flexure about their y-axis (or the axis of symmetry of the section); a

condition known as flexural-torsional buckling (Section 6.6.3.4.2.3.4). An effective slenderness ratio approach, such as the approach discussed in Section 6.6.3.4.5 for the design of single angles subject to eccentric axial compression, is not available for the design of tees and double angles.

Tees and double angles are singly symmetric members, with the plane of symmetry assumed to be that formed by their weak axis (or y-axis), as shown in Figure 6.6.3.5.3-2. Legs of double angles in continuous contact or with separators may together be assumed treated as the stem of a tee in applying the specification provisions discussed below. In computing the flange slenderness, $b_f/2t_f$, for double angles, b_f is to be taken as the sum of the widths of the outstanding legs in checking these provisions.

AASHTO LRFD Article 6.12.2.2.4 covers the nominal flexural resistance of tees and double angles loaded in the plane of symmetry. For flexure of these members about their weak-axis or y-axis, which is considered to be a rare case in bridge applications, the reader is referred to the Commentary to Section F9 of AISC (2010a).

The nominal flexural resistance is to be taken as the smallest value based on yielding, lateral torsional buckling or flange local buckling, as applicable.

For yielding, the nominal flexural resistance is given as:

$$M_n = M_p = F_y Z_x \qquad \text{Equation 6.6.3.5.3-1}$$

AASHTO LRFD Equation 6.12.2.2.4-1

where:

M_p = plastic moment (kip-in.)
Z_x = plastic section modulus about the x-axis (in.^{3})

For yielding, M_n is limited to $1.6M_y$ for stems in tension, and to M_y for stems in compression, where M_y is equal to the yield moment of the cross-section based on the distance to the tip of the tee stem. The limit on M_n of $1.6M_y$ for cases where the stem is in tension is intended to indirectly control situations where significant yielding of the stem might occur at service load levels.

For lateral-torsional buckling, a simplified version of the elastic lateral-torsional buckling equation developed in Kitipornchai and Trahair (1980), and discussed further in Ellifritt et al. (1992), is given as:

$$M_n = \frac{\pi\sqrt{EI_yGJ}}{L_b}\left[B + \sqrt{1+B^2}\right] \qquad \text{Equation 6.6.3.5.3-2}$$

AASHTO LRFD Equation 6.12.2.2.4-2

where:

$$B = \pm 2.3\frac{d}{L_b}\sqrt{\frac{I_y}{J}} \qquad \text{Equation 6.6.3.5.3-3}$$

AASHTO LRFD Equation 6.12.2.2.4-3

d = total depth of the section (in.)
G = shear modulus of elasticity for steel = 0.385E (ksi)
I_y = moment of inertia of the cross-section about the y-axis (in.^{4})
J = St. Venant torsional constant (in.^{4}) (Equation 6.5.6.2.3.3.2-7 - more accurate values for rolled tee sections including the effect of the web-to-flange fillets are given in AISC, 2010)
L_b = unbraced length (in.)

The plus sign on the value of B in Equation 6.6.3.5.3-3 applies when the stem is in tension, and the minus sign applies when the stem is in compression. If the tip of the stem is in compression anywhere along the unbraced length, a negative value of B must be used.

Note that Equation 6.6.3.5.3-2 does not contain the moment gradient modifier, C_b (Section 6.5.6.2.2.2.2). As discussed in *AASHTO LRFD* Article C6.12.2.2.4, the C_b factor specified for I-sections is unconservative for tees with the stem in compression. Also, for reverse curvature bending, the portion with the stem in compression may govern the lateral-torsional buckling resistance even though the corresponding moments may be small in relation to the moments in the other portions of the unbraced length. The lateral-torsional buckling resistance for the case where the stem is in compression is substantially smaller than for the stem in tension. As a result, C_b is conservatively taken equal to 1.0 for all cases. *AASHTO LRFD* Article C6.12.2.2.4 also cautions that for cases where the stem is in tension, connection details should be designed to minimize end restraint moments that may cause the stem to be in flexural compression at the ends of the member.

For sections where the flange is in compression, and the flange slenderness, λ_f, exceeds λ_{pf}, flange local buckling must also be checked. For flange local buckling of tees, the nominal flexural resistance is taken as:

$$M_n = M_p - \left(M_p - 0.7F_yS_{xc}\right)\left(\frac{\lambda_f - \lambda_{pf}}{\lambda_{rf} - \lambda_{pf}}\right) \le 1.6M_y \qquad \text{Equation 6.6.3.5.3-4}$$

AASHTO LRFD Equation 6.12.2.2.4-4

For flange local buckling of double angles, the nominal flexural resistance is taken as:

$$M_n = F_yS_{xc}\left(2.43 - 1.72\left(\frac{b_f}{2t_f}\right)\sqrt{\frac{F_y}{E}}\right) \le 1.5F_yS_{xc} \qquad \text{Equation 6.6.3.5.3-5}$$

AASHTO LRFD Equation 6.12.2.2.4-5

where:

M_p = plastic moment (kip-in.)

$= F_yZ_x \le 1.6M_y$ Equation 6.6.3.5.3-6

AASHTO LRFD Equation 6.12.2.2.4-6

λ_f = flange slenderness ratio = $b_f/2t_f$

λ_{pf} = limiting slenderness for a compact flange

$$= 0.38\sqrt{\frac{E}{F_y}} \qquad \text{Equation 6.6.3.5.3-7}$$

AASHTO LRFD Equation 6.12.2.2.4-7

λ_{rf} = limiting slenderness for a noncompact flange

$$= 1.0\sqrt{\frac{E}{F_y}} \qquad \text{Equation 6.6.3.5.3-8}$$

AASHTO LRFD Equation 6.12.2.2.4-8

b_f = flange width (in.)

S_{xc} = elastic section modulus with respect to the compression flange (in.^{3})

t_f = flange thickness (in.)

For cases where the flange is in compression and λ_f does not exceed λ_{pf}, flange local buckling does not control and need not be checked.

Equation 6.6.3.5.3-4 represents an inelastic flange local buckling resistance equation provided for tees in AISC (2010a). Equation 6.6.3.5.3-5 represents a local buckling resistance equation provided for determining the inelastic local buckling resistance of

single-angle legs in Section F10 of AISC (2010a), which is conservatively applied to determine the inelastic local buckling resistance of the compression flange of double angles loaded in the plane of symmetry, as recommended in AISC (2010a).

Elastic flange local buckling resistance equations for cases with λ_f exceeding λ_{rf}, i.e. for slender flanges, are not provided because the limiting slenderness value, λ_{rf}, beyond which elastic flange local buckling controls is larger than the limiting slenderness value of 12.0 given by Equation 6.3.4.4.2-3. The flanges of all rolled tee sections given in AISC (2010) satisfy Equation 6.3.4.4.2-3; therefore, this equation need only be checked for fabricated sections. An elastic flange local buckling resistance equation is provided in AISC (2010a).

Separate equations for checking local buckling of stems in compression are not provided herein. Lateral torsional buckling and local buckling of the stem are essentially the same phenomenon for these sections. Hence, satisfaction of Equation 6.6.3.5.3-2 will ensure that local buckling of the stem in compression will not occur.

EXAMPLE

The design of a tee serving as a top lateral bracing member in a steel tub girder for eccentric axial compression is illustrated in this example. Top flange lateral bracing is designed to resist the shear flow in the pseudo-box section resulting from any torsion acting on the steel section due to the design load effects, including during the deck-casting sequence (Section 6.3.2.10.2.2). The bracing also acts with the tub in resisting vertical bending. Hence, forces in the bracing due to flexure of the tub must also be considered. Since the bracing is permanent, composite dead load force effects (i.e. due to DC_2 and DW), and live load force effects are considered at the strength limit state, although these effects are relatively small in this case since the bracing is located at the top of the tub section.

Since the bridge is analyzed by 3D finite element analysis in which the individual lateral bracing members are included in the model, the unfactored compressive forces in this example diagonal member taken directly from the analysis are as follows (note: the force effects in the member resulting from top-flange lateral bending due to the deck overhang bracket forces are not considered in this particular analysis):

P_{steel} = -10 kips
$P_{deck\ casting(max)}$ = -71 kips
P_{DC1} = -52 kips
P_{DC2} = -1 kip
P_{DW} = -2 kips
P_{LL+IM} = -4 kips

The factored compressive force, P_u, due to the Strength I load combination is computed as (the load modifier, η, is taken equal to 1.0):

$$P_u = 1.0[1.25(-52 + -1) + 1.5(-2) + 1.75(-4)] = -76 \text{ kips}$$

The factored compressive force, P_u, due to the steel weight plus the deck-casting sequence is computed according to the special load combination for constructibility of steel bridges specified in *AASHTO LRFD* Article 3.4.2.1 as:

$$P_u = 1.0[1.4(-10 + -71)] = -113 \text{ kips (governs)}$$

Determine the suitability of a WT7 x 37 rolled structural tee for use as the top-flange diagonal lateral bracing member. Assume the steel for the tee is ASTM A709/A709M Grade 50W. The width, *w*, of the tub section at the top between the centerlines of the flanges is 111 inches, and the top flange width is 18 inches.

From the AISC Manual shape property tables, the following section properties are obtained for a WT7 x 37:

A_g = 10.90 in.^{2} (> 0.03*w* = 0.03(111) = 3.3 in.^{2} -> Equation 6.3.2.10.3-1)
d = 7.085 in.
t_w = 0.450 in.
b_f = 10.070 in.
t_f = 0.785 in.
I_x = 36.0 in.^{4}
S_x = 6.25 in.^{3}
r_x = 1.82 in.
y = 1.32 in.
I_y = 66.9 in.^{4}
r_y = 2.48 in.
J = 1.94 in.^{4}
$\bar{r}_o$ = 3.21 in.
H = 0.917

The thickness of the tee stem exceeds the minimum permissible thickness of 5/16″ specified for structural steel in *AASHTO LRFD* Article 6.7.3 (Section 6.4.11).

First, check the maximum slenderness ratio of the tee to ensure it does not exceed the permissible value of 120 for primary members in compression (*AASHTO LRFD* Article 6.9.3 – Section 6.6.3.4.2.2). Since the member is assumed to be in a horizontally curved bridge, and the forces in the tee were determined from an analysis, the member is considered to be a primary member.

Assume the stem of the tee section is pointed down with the flange of the tee bolted to the bottom of the tub top flanges, which is the preferred method of connection. The clear distance between the top flanges is 111 in. – 18 in. = 93 inches. The spacing along the top flange between the strut of the Pratt truss lateral bracing system at this location and the adjacent cross-frame is 111.5 inches. Thus, the length, ℓ, of the bracing member is computed as:

$$\ell = \sqrt{93^2 + 111.5^2} = 145.2 \text{ in.}$$

AASHTO LRFD Article 4.6.2.5 allows the effective length factor, *K*, to be taken as 0.750 for members with bolted or welded connections at both ends (Section 6.6.3.4.2.3.3). Assume K_y = 0.750. However, since only the tub flanges are providing restraint for buckling about the x-axis, K_x will conservatively be taken equal to 1.0. The slenderness ratios about each axis in this case are therefore:

$$\frac{K_y \ell_y}{r_y} = \frac{0.750(145.2)}{2.48} = 43.9$$

$$\frac{K_x \ell_x}{r_x} = \frac{1.0(145.2)}{1.82} = 79.8 < 120 \quad \text{ok}$$

AASHTO LRFD Article 6.9.2.1 specifies that the factored compressive resistance, P_r, at the strength limit state be taken as (Equation 6.6.3.4.2.1-1):

$$P_r = \phi_c P_n$$

ϕ_c is the resistance factor for axial compression specified in *AASHTO LRFD* Article 6.5.4.2 = 0.95.

The nominal compressive resistance, P_n, is to be determined as (Equations 6.6.3.4.2.3.1-1 and 6.6.3.4.2.3.1-2):

- If $\frac{P_e}{P_o} \geq 0.44$, then:

$$P_n = \left[0.658^{\left(\frac{P_o}{P_e}\right)} \right] P_o$$

- If $\frac{P_e}{P_o} < 0.44$, then:

$$P_n = 0.877P_e$$

For the design of tees, P_e is taken as the smaller of the elastic critical buckling resistance for flexural buckling about the x-axis determined as specified in *AASHTO LRFD* Article 6.9.4.1.2 (Equation 6.6.3.4.2.3.3-1):

$$P_{ex} = \frac{\pi^2 E}{\left(\frac{K_x \ell_x}{r_x}\right)^2} A_g$$

and the elastic critical buckling resistance for flexural-torsional buckling determined as specified in *AASHTO LRFD* Article 6.9.4.1.3 (Equation 6.6.3.4.2.3.4-2):

$$P_e = \left(\frac{P_{ey} + P_{ez}}{2H}\right)\left[1 - \sqrt{1 - \frac{4P_{ey}P_{ez}H}{(P_{ey} + P_{ez})^2}}\right]$$

P_o is the equivalent nominal yield resistance determined as specified in *AASHTO LRFD* Article 6.9.4.1.1 (Equation 6.6.3.4.2.4.3-1). Q is the slender element reduction factor specified in *AASHTO LRFD* Article 6.9.4.2.2 (Section 6.6.3.4.2.4.3):

$$P_o = QF_y A_g$$

Calculate the equivalent nominal yield resistance, P_o. For compression members composed of one or more slender elements; that is, elements not meeting the corresponding width-to-thickness ratio limits specified in *AASHTO LRFD* Table 6.9.4.2.1-1 (Table 6.6.3.4.2.4.2-1), the slender element reduction factor, Q, accounts for the effect of potential local buckling of those elements on the overall buckling resistance of the member and has a value less than 1.0. The value of Q in this instance is determined according to the provisions of *AASHTO LRFD* Article 6.9.4.2.2 (Section 6.6.3.4.2.4.3).

Q is taken equal to 1.0 as specified in *AASHTO LRFD* Article 6.9.4.2.1 for compression member cross-sections without any slender elements; that is, composed entirely of nonslender elements. In such cases, local buckling does not adversely affect the nominal compressive resistance.

For compression member cross-sections composed entirely of unstiffened elements, or plates supported along only one edge parallel to the direction of the compression force, Q is taken equal to the factor for unstiffened elements, Q_s. Tees are composed entirely of unstiffened elements (Figure 6.6.3.4.2.4.3-2).

None of the rolled tee sections in the AISC Manual shape property tables have slender flanges. When the b/t ratio of the stem of the tee is less than or equal to the following limit (from Equation 6.6.3.4.2.4.2-1 with k taken equal to 0.75), the element is nonslender, and $Q = Q_s = 1.0$. b is taken as the full depth of the tee (including the flange) and t is taken as the stem thickness (Figure 6.6.3.4.2.4.3-2) in checking this limit. Check if the stem of the tee under investigation is a slender element:

$$\frac{b}{t} \le 0.75\sqrt{\frac{E}{F_y}}$$

$$0.75\sqrt{\frac{29{,}000}{50}} = 18.1 > \frac{b}{t} = \frac{7.085}{0.450} = 15.7$$

Therefore, the nominal compressive resistance of the tee does not have to be reduced due to potential local buckling of the stem. Since the stem is a nonslender element, the slender element reduction factor, $Q = Q_s$, is equal to 1.0.

From Equation 6.6.3.4.2.4.3-1:

$$P_o = QF_yA_g = 1.0(50)(10.90) = 545 \text{ kips}$$

Tee sections loaded in axial compression can either fail by flexural buckling about the x-axis or by torsion combined with flexure about the y-axis or flexural-torsional bucking (where the y-axis is defined as the axis of symmetry of the tee section).

The elastic critical buckling resistance for flexural buckling about the x-axis, P_{ex}, is determined as (Equation 6.6.3.4.2.3.3-1):

$$P_{ex} = \frac{\pi^2(29{,}000)}{(79.8)^2}(10.90) = 490 \text{ kips}$$

Calculate the elastic critical buckling resistance, P_e, for flexural-torsional buckling. First, calculate P_{ey} as follows (Equation 6.6.3.4.2.3.4-3):

$$P_{ey} = \frac{\pi^2 E}{\left(\frac{K_y \ell_y}{r_y}\right)^2} A_g$$

$$P_{ey} = \frac{\pi^2 (29{,}000)}{(43.9)^2}(10.90) = 1{,}619 \text{ kips}$$

The warping torsional constant, C_w, is taken as zero for tees. Therefore, calculate P_{ez} as follows (Equation 6.6.3.4.2.3.4-4 with C_w taken equal to zero). The shear modulus, G, is equal to $0.385E$ = 0.385(29,000) = 11,165 ksi for steel:

$$P_{ez} = \frac{GJ}{\bar{r}_o^2}$$

$$P_{ez} = \frac{11{,}165(1.94)}{(3.21)^2} = 2{,}102 \text{ kips}$$

Therefore from Equation 6.6.3.4.2.3.4-2:

$$P_e = \left(\frac{1{,}619 + 2{,}102}{2(0.917)}\right)\left[1 - \sqrt{1 - \frac{4(1{,}619)(2{,}102)(0.917)}{(1{,}619 + 2{,}102)^2}}\right] = 1{,}392 \text{ kips}$$

Since P_{ex} is less than P_e for flexural-torsional buckling, flexural buckling about the x-axis controls. Therefore, P_e is equal to P_{ex} = 490 kips.

Since:

$$\frac{P_e}{P_o} = \frac{490}{545} = 0.90 > 0.44$$

the nominal compressive resistance, P_n, is computed as follows (Equation 6.6.3.4.2.3.1-1):

$$P_n = \left[0.658^{\left(\frac{545}{490}\right)}\right](545) = 342 \text{ kips}$$

The factored compressive resistance, P_r, is taken as:

$$P_r = \phi_c P_n = 0.95(342) = 325 \text{ kips}$$

Since the tee flange is bolted to the top flanges of the tub, the tee is also subject to a uniform bending moment about the major principal axis (x-axis) due to the eccentricity of the connection at each end of the member (Figure 6.6.3.5.3-2). The thickness of the top flanges is 1.0 inch; therefore, the first-order moment, $(M_{ux})_1$, due to the eccentricity is computed as:

$$(M_{ux})_1 = |P_u|(y + \frac{1.0}{2}) = |-113|(1.32 + 0.5) = 206.0 \text{ kip} - \text{in.}$$

Second-order effects arise from the additional secondary moment caused by the axial force acting through the member deflection (Figure 6.6.3.4.3.2-1). *AASHTO LRFD* Article 4.5.3.2.2b specifies that the single-step adjustment or moment magnification method may be used to determine the second-order elastic moment as follows (Equation 6.6.3.4.3.2-1):

$$(M_{ux})_2 = \delta_b (M_{ux})_1$$

The magnification factor, δ_b, is computed as follows (Equation 6.6.3.4.3.2-2):

$$\delta_b = \frac{C_m}{1 - \frac{P_u}{\phi_K P_e}} \geq 1.0$$

ϕ_K is a stiffness reduction factor taken equal to 1.0 for steel members. C_m is the equivalent uniform moment factor, which for members braced against sidesway and without transverse loading (other than the self-weight of the member) between supports in the plane of bending, is to be taken as (Equation 6.6.3.4.3.2-3):

$$C_m = 0.6 + 0.4 \frac{M_1}{M_2}$$

The tee section is bent in single curvature by equal moments at the end of the member due to the eccentricity. For single curvature, the ratio of the end moments M_1/M_2 = 1.0 is to be taken as positive. Therefore, from the preceding equation, C_m = 1.0.

P_e is the Euler buckling load for buckling about the x-axis (i.e. the plane of bending), which is to be taken as follows (Equation 6.6.3.4.3.2-4):

$$P_e = \frac{\pi^2 EI}{(K_x \ell_x)^2}$$

K_x is the effective length factor for buckling about the x-axis, and ℓ_x is the unbraced length for buckling about the x-axis. For this case, K_x is equal to 1.0 and I is equal to I_x = 24.9 in.^{4}. Therefore:

$$P_e = \frac{\pi^2(29{,}000)(36.0)}{(1.0 * 145.2)^2} = 489 \text{ kips}$$

$$\delta_b = \frac{1.0}{1 - \frac{|-113|}{1.0(489)}} = 1.30$$

Thus:

$$(M_{ux})_2 = 1.30(206.0) = 268 \text{ kip} - \text{in.}$$

Calculate the factored flexural resistance, M_{rx}, of the tee-section member about the strong axis (Section 6.6.3.5.3). The factored flexural resistance, M_{rx}, of tees about the x-axis at the strength limit state is to be taken as follows:

$$M_{rx} = \phi_f M_{nx}$$

The nominal flexural resistance about the x-axis, M_{nx}, is to be taken as the lowest value based on yielding, lateral torsional buckling or flange local buckling.

For yielding, the nominal flexural resistance is given as (Equation 6.6.3.5.3-1):

$$M_{nx} = M_p$$

where $M_p = F_y Z_x$. The plastic section modulus, Z_x, for the tee section neglecting the effect of the web-to-flange fillets is computed by first locating the plastic neutral axis (assumed to be a distance $\bar{y}$ from the top of the flange) as follows:

Depth of stem = (7.085 – 0.785) = 6.30 in.

$$\bar{y}(10.070) = 10.070(0.785 - \bar{y}) + (6.30)(0.450)$$

$$\bar{y} = 0.533 \text{ in.}$$

Taking moments of the cross-sectional areas about the plastic neutral axis yields:

$$Z_x = \frac{10.070(0.533)^2}{2} + \frac{10.070(0.785-0.533)^2}{2} + 0.450(6.30)\left[(0.785-0.533)+\frac{(6.30)}{2}\right] = 11.39 \text{ in.}^3$$

$$M_p = (50)(11.39) = 569.5 \text{ kip} - \text{in.}$$

M_n for yielding is limited to $1.6M_y$ for stems in tension, and to M_y for stems in compression. Determine if the tip of the stem is in compression or tension:

$$f_{tip} = \frac{-113}{10.90} + \frac{268.0}{6.25} = 32.5 \text{ ksi} \quad \text{(tension)}$$

Therefore:

$$1.6M_y = 1.6F_yS_x = 1.6(50)(6.25) = 500.0 \text{ kip} - \text{in.} < M_p$$

$$\therefore M_{nx} = 500.0 \text{ kip} - \text{in.} \quad \text{(for yielding)}$$

For lateral-torsional buckling (Equation 6.6.3.5.3-2):

$$M_{nx} = \frac{\pi\sqrt{EI_yGJ}}{L_b}\left[B + \sqrt{1+B^2}\right]$$

From Equation 6.6.3.5.3-3:

$$B = \pm 2.3\frac{d}{L_b}\sqrt{\frac{I_y}{J}}$$

The plus sign on the value of B applies when the stem is in tension. Therefore:

$$B = +2.3\frac{7.085}{145.2}\sqrt{\frac{66.9}{1.94}} = +0.659$$

$$M_{nx} = \frac{\pi\sqrt{29{,}000(66.9)(11{,}165)(1.94)}}{145.2}\left[0.659 + \sqrt{1+0.659^2}\right] = 8{,}235 \text{ kip} - \text{in.}$$

(lateral torsional buckling)

Since the flange is in compression, the limit state of flange local buckling must also be considered. The flange slenderness, $\lambda_f = b_f/2t_f = 10.070/2(0.785) = 6.4$, does not

exceed the slenderness limit for a compact flange, $\lambda_{pf} = 0.38\sqrt{E / F_y}$ = 9.2. Therefore, flange local buckling does not control and need not be checked.

Thus, the nominal flexural resistance, M_{nx}, of the tee section is controlled by yielding and is equal to 500.0 kip-in. The factored flexural resistance, M_{rx}, is equal to:

$$M_{rx} = \phi_f M_{nx} = 1.0(500.0) = 500.0 \text{ kip} - \text{in.}$$

Interaction curves for tee members subject to eccentric axial compression are discussed in Sections 6.6.3.4.3.1 and 6.6.3.4.3.3. The beam-column resistance for the singly symmetric tee-section member will conservatively be checked in this case using Equations 6.6.3.4.3.1-1 and 6.6.3.4.3.1-2.

Since $P_u/P_r = |-113| / 325 = 0.35 > 0.2$, Equation 6.6.3.4.3.1-2 controls:

$$\frac{P_u}{P_r} + \frac{8.0}{9.0}\frac{M_{ux}}{M_{rx}} \le 1.0$$

$$\frac{|-113|}{325} + \frac{8.0}{9.0}\left(\frac{268}{500}\right) = 0.82 < 1.0 \qquad \text{ok}$$

Further investigation would likely lead to the use of a slightly smaller tee section. If a timber were used to brace the member at mid-length in the vertical plane during construction, and upward movement of the tee section was prevented at the brace point, the unbraced length with respect to flexural buckling about the x-axis would be reduced and an even smaller tee section could potentially be used.

The above calculations illustrate the design of a lateral bracing member for the largest observed compressive force. Smaller members should be used where feasible at other locations where lower forces are present. Consideration might be given to the development of a practical grouping of different member sizes for the lateral bracing according to the largest demand within various regions of the bridge.

6.6.3.5.4 Channels

AASHTO LRFD Article 6.12.2.2.5 covers the nominal flexural resistance of channels. For channels in flexure about their strong or x-axis, the nominal flexural resistance is to be taken as the smaller value based on yielding or lateral torsional buckling, as applicable.

For yielding, the nominal flexural resistance is given as:

$$M_n = M_p = F_y Z_x \qquad \text{Equation 6.6.3.5.4-1}$$

AASHTO LRFD Equation 6.12.2.2.5-1

where:

M_p = plastic moment (kip-in.)
Z_x = plastic section modulus about the x-axis (in.^{3})

For lateral-torsional buckling, when the unbraced length, L_b, exceeds L_p, lateral-torsional buckling must be checked. The nominal flexural resistance based on lateral-torsional buckling is taken as:

- If $L_b \le L_r$, then:

$$M_n = C_b\left[M_p - \left(M_p - 0.7F_yS_x\right)\left(\frac{L_b - L_p}{L_r - L_p}\right)\right] \le M_p \qquad \text{Equation 6.6.3.5.4-2}$$

AASHTO LRFD Equation 6.12.2.2.5-2

- If $L_b > L_r$, then:

$$M_n = F_{cr}S_x \le M_p \qquad \text{Equation 6.6.3.5.4-3}$$

AASHTO LRFD Equation 6.12.2.2.5-3

where:

F_{cr} = elastic lateral torsional buckling stress (ksi)

$$= \frac{C_b\pi^2 E}{\left(\frac{L_b}{r_{ts}}\right)^2}\sqrt{1 + 0.078\frac{Jc}{S_x h_o}\left(\frac{L_b}{r_{ts}}\right)^2} \qquad \text{Equation 6.6.3.5.4-4}$$

AASHTO LRFD Equation 6.12.2.2.5-4

$$c = \frac{h_o}{2}\sqrt{\frac{I_y}{C_w}} \qquad \text{Equation 6.6.3.5.4-5}$$

AASHTO LRFD Equation 6.12.2.2.5-5

C_w = warping torsional constant (in.^{6})

$$= \frac{t_f b^3 h_o^2}{12}\left(\frac{3bt_f + 2h_o t_w}{6bt_f + h_o t_w}\right) \qquad \text{Equation 6.6.3.5.4-6}$$

AASHTO LRFD Equation 6.12.2.2.5-6

(More accurate values for rolled channel sections based on the sloping flanges and web-to-flange fillets are tabulated in AISC, 2010)

L_p = limiting unbraced length to achieve the nominal flexural resistance, M_p, under uniform bending (in.)

$$= 1.76 r_r \sqrt{\frac{E}{F_y}} \qquad \text{Equation 6.6.3.5.4-7}$$

AASHTO LRFD Equation 6.12.2.2.5-7

L_r = limiting unbraced length to achieve the nominal onset of yielding under uniform bending with consideration of compression-flange residual stress effects (in.)

$$= 1.95 r_{ts} \frac{E}{0.7F_y} \sqrt{\frac{Jc}{S_x h_o}} \sqrt{1+\sqrt{1+6.76\left(\frac{0.7F_y}{E}\frac{S_x h_o}{Jc}\right)^2}} \qquad \text{Equation 6.6.3.5.4-8}$$

AASHTO LRFD Equation 6.12.2.2.5-8

$$r_{ts}^2 = \frac{\sqrt{I_y C_w}}{S_x} \qquad \text{Equation 6.6.3.5.4-9}$$

AASHTO LRFD Equation 6.12.2.2.5-9

C_b = moment gradient modifier (Section 6.5.6.2.2.2.2)
L_b = unbraced length (in.)
b = distance between the toe of the flange and the centerline of the web (in.)
h_o = distance between flange centroids (in.)
I_y = moment of inertia of the cross-section about the y-axis (in.^{4})
J = St. Venant torsional constant (in.^{4}) (Equation 6.5.6.2.3.3.2-7 - more accurate values for rolled channel sections including the effect of the sloping flanges and web-to-flange fillets are given in AISC, 2010)
r_{ts} = radius of gyration used in the determination of L_r (in.)
r_y = radius of gyration of the cross-section about the y-axis (in.)
S_x = elastic section modulus about the x-axis (in.^{3})
t_f = thickness of the flange (in.); for rolled channels, use the average thickness
t_w = thickness of the web (in.)

For cases where L_b is less than or equal to L_p, lateral-torsional buckling does not control and need not be checked.

The lateral-torsional buckling equations given above assume that the channels have compact flanges and webs; hence, flange and web local buckling need not be checked. All the rolled channels given in the AISC Manual shape property tables

have compact flanges and webs for $F_y \leq 65$ ksi. To qualify as compact, the flange slenderness, $\lambda_f = b_f/t_f$, of fabricated or bent-plate channels must not exceed the limiting slenderness for a compact flange, $\lambda_{pf} = 0.38\sqrt{E/F_y}$, and the web slenderness, D/t_w, of fabricated or bent-plate channels must not exceed the limiting slenderness for a compact web, $\lambda_{pw} = 3.76\sqrt{E/F_y}$. The above equations also assume that the channel is restrained at the brace points such that twisting of the member does not occur at those points.

For flexure of channels about their weak-axis or y-axis, *AASHTO LRFD* Article 6.12.2.2.5 specifies that the nominal flexural resistance be determined according to the provisions of *AASHTO LRFD* Article 6.12.2.2.1 (Section 6.6.3.5.2). An additional limit of $1.6F_yS_y$, where S_y is the elastic section modulus about the y-axis, is placed on the computed nominal flexural resistance of channels bent about their weak-axis to indirectly prevent substantial yielding of the member at service load levels. For I-sections, the shape factor Z_y/S_y is nearly always less than 1.6 (only four rolled W-shapes have $Z_y/S_y > 1.6$), whereas for channel sections, Z_y/S_y is commonly greater than 1.6 (White, 2012).

6.6.3.5.5 Single Angles

AASHTO LRFD Article 6.12.2.2.6 states that single angles should not be used as pure flexural members. Single angles are not typically intended to serve as flexural members in bridge construction. However, in practical bracing member applications, they are typically subject to flexure about both principal axes due to the eccentricity of applied axial loads.

The condition of flexure plus eccentric axial tension is primarily addressed through the use of the shear lag coefficient, U (Section 6.6.3.3.2.4), as discussed further in Section 6.6.3.3.3.

The condition of flexure plus eccentric axial compression is handled primarily through the use of an effective slenderness ratio, $(K\ell/r)_{eff}$, as discussed further in Section 6.6.3.4.5. In certain unusual cases spelled out in Section 6.6.3.4.5.2, single angles subject to combined flexure and axial compression must instead be evaluated as beam-columns according to Section H2 of AISC (2010a), in lieu of using $(K\ell/r)_{eff}$. In such cases, the nominal flexural resistance of the angle, M_n, should be determined according to the procedures given in Section F10 of AISC (2010a), which are not discussed in detail herein. For these unusual cases, the reader is referred instead to Section F10 of AISC (2010a), and the corresponding commentary, for additional information on the determination of M_n for single-angle members.

6.6.3.6 Diaphragms

6.6.3.6.1 I-Girder Bridges

Functions and configurations of diaphragms in I-girder bridges were discussed previously in Sections 6.3.2.9.2 and 6.3.2.9.5.1, respectively. Some general design considerations were discussed in Section 6.3.2.9.6.1.

AASHTO LRFD Article 6.7.4.2 specifies that diaphragms for I-girder bridges with span-to-depth ratios greater than or equal to 4.0 may be designed as beams. Diaphragms with span-to-depth ratios less than 4.0 act as deep beams and should be evaluated by considering principal stresses rather than by beam theory (refer to Section 6.6.3.6.2). The end moments in the diaphragm are also to be considered in the design of the connection between the girders and the diaphragm (*AASHTO LRFD* Article 6.7.4.2).

End diaphragms must be designed for forces and distortion transmitted by the deck and deck joint. They also must be designed to support the deck and the wheel loads coming onto the ends of the deck.

6.6.3.6.2 Box-Girder Bridges

Functions and configurations of diaphragms in box-girder bridges were discussed previously in Sections 6.3.2.9.2.4 and 6.3.2.9.5.2, respectively. Some general design considerations were discussed in Section 6.3.2.9.6.1.

Solid-plate diaphragms are most commonly used as internal and external diaphragms in box-girder bridges at supports, or as internal diaphragms in steel box-section integral bent caps. External diaphragms at end supports act with the internal diaphragm to support the deck and the wheel loads coming onto the ends of the deck. End moments should be considered in the design of the external diaphragms and their end connections to the girders.

Beams deeper than about one-fourth of their span are classified as deep beams in reinforced concrete design. Ordinary beam theory does not apply for deep beams, meaning that shear deformations should be considered and principal stresses should be evaluated. Thus, *AASHTO LRFD* Article C6.7.4.3 indicates that consideration should be given to evaluating the principal stresses in all internal support diaphragms, and in external support diaphragms with aspect ratios (ratios of length to depth) less than 4.0 (external support diaphragms with aspect ratios greater than or equal to 4.0 may be designed as ordinary I-section flexural members). The combined principal stresses in the diaphragm in these cases can be

evaluated at the strength limit state using the following general form of the Huber-von Mises-Hencky yield criterion (Ugural and Fenster, 1978):

$$\sqrt{\sigma_1^2 - \sigma_1\sigma_2 + \sigma_2^2} \le \phi_f F_y \qquad \text{Equation 6.6.3.6.2-1}$$

where:

ϕ_f = resistance factor for flexure specified in *AASHTO LRFD* Article 6.5.4.2 (= 1.0)

σ_1, σ_2 = critical maximum and minimum principal stresses in the diaphragm (ksi)

$$= \left(\frac{f_{by} + f_{bz}}{2}\right) \pm \sqrt{\left(\frac{f_{by} - f_{bz}}{2}\right)^2 + f_d^2} \qquad \text{Equation 6.6.3.6.2-2}$$

f_{by} = for internal diaphragms, factored stress in the diaphragm caused by major-axis bending of the diaphragm over the bearing sole plate (ksi). For external diaphragms, factored stress in the diaphragm caused by major-axis bending of the diaphragm (ksi)

f_{bz} = factored stress in the diaphragm caused by bending of the diaphragm about its longitudinal axis (ksi)

f_d = factored shear stress in the diaphragm caused by the total vertical shear in the diaphragm (ksi)

F_y = specified minimum yield strength of the diaphragm (ksi)

f_{by} and f_{bz} are to be taken as signed quantities in Equation 6.6.3.6.2-2. The term f_{bz} is neglected in most all cases. f_{by} may be particularly significant for a box section supported on a single bearing. In calculating f_{by} for internal diaphragms, a width of the bottom box flange equal to six times its thickness may be considered effective with the diaphragm in resisting bending (*AASHTO LRFD* Article C6.7.4.3). More than one loading condition may need to be investigated in order to determine the critical principal stresses in the diaphragm. Should the diaphragm web have a different yield strength than the box flange (for the case of internal diaphragms) or the diaphragm flanges (for the case of external diaphragms), consideration should be given to including the hybrid factor, R_h, (Section 6.4.5.7) on the right-hand side of Equation 6.6.3.6.2-1.

Post bend-buckling resistance should not be considered in the design of these critical diaphragm members. Therefore, when considering bending of the diaphragm, *AASTHO LRFD* Article 6.7.4.3 specifies that the diaphragm web satisfy the following requirement:

$$\frac{2D_c}{t_w} \le \lambda_{rw} = 5.7\sqrt{\frac{E}{F_y}} \qquad \text{Equation 6.6.3.6.2-3}$$

AASHTO LRFD Equation 6.10.1.10.2-2

where:

D_c = elastic depth of the diaphragm web in compression (in.)

Satisfaction of Equation 6.6.3.6.2-3 ensures that theoretical bend buckling of the diaphragm web will not occur. Thus, the web load-shedding factor, R_b (Section 6.4.5.6), is implicitly taken equal to 1.0 in Equation 6.6.3.6.2-1.

The factored shear resistance of the diaphragm must be checked at the strength limit state as follows:

$$V \le \phi_v V_n \qquad \text{Equation 6.6.3.6.2-4}$$

where:

ϕ_v = resistance factor for shear specified in *AASHTO LRFD* Article 6.5.4.2 (= 1.0)
V = total factored vertical shear in the diaphragm (kips)
V_n = nominal shear resistance of the diaphragm (kips)

Post-buckling shear resistance due to tension-field action also should not be considered in the design of these critical diaphragm members. Therefore, *AASTHO LRFD* Article 6.7.4.3 specifies that the nominal shear resistance, V_n, be limited to the shear buckling (or shear yielding) resistance, V_{cr}, given as follows (Section 6.5.7.2):

$$V_n = V_{cr} = CV_p \qquad \text{Equation 6.6.3.6.2-5}$$

AASHTO LRFD Equation 6.10.9.3.3-1

where:

V_p = plastic shear force (kips) = $0.58F_yDt_w$
C = ratio of the shear buckling resistance to the shear yield strength determined from *AASHTO LRFD* Equation 6.10.9.3.2-4, 6.10.9.3.2-5 or 6.10.9.3.2-6, as applicable
D = vertical depth of the diaphragm (in.)
t_w = thickness of the diaphragm (in.)

In calculating the constant C, the shear buckling coefficient k should be taken as 5.0 for unstiffened webs, and determined using Equation 6.5.7.2-4 for stiffened webs. Bearing stiffeners on internal plate diaphragms may be considered to act as transverse stiffeners.

The section through an access hole in an internal diaphragm at an interior support is especially critical for a section supported on a single bearing, and additional stiffening and/or reinforcement around the hole may be necessary. In such cases, the bearing is typically wider than the access hole so bearing stiffeners provided on each side of the hole can be considered to act as transverse stiffeners to increase

the shear resistance of the diaphragm at the hole. If necessary, horizontal stiffeners above and below the hole might be used to increase the flexural resistance of the diaphragm at the hole in lieu of thickening the diaphragm plate.

Because of the presence of access holes and complex details such as stiffening around the holes, and because of the number of load points and more complicated mechanism of load transfer, a more refined analysis of internal plate diaphragms at supports may be desirable to obtain more accurate estimates of the diaphragm flexural and shear stresses. This is particularly true for box sections supported on single bearings. Procedures are available for estimating the moment and shear resistance of steel beams with unreinforced and reinforced web openings (Darwin, 1990). However, these procedures were primarily developed for rolled I-section flexural members used in multistory buildings with smaller web openings used to pass utilities through the beams, and not for deeper and shorter solid-plate diaphragms used in bridges, with relatively large access holes that exhibit deep-beam behavior.

.

AASHTO LRFD Article 6.11.11.1 specifies that bearing stiffeners for box sections with inclined webs should be attached to either an internal or external diaphragm rather than to the webs so that the bearing stiffeners will be perpendicular to the sole plate. Where a single centered bearing is used and a centered access hole is also provided in an internal diaphragm, the diaphragm must be stout enough to transfer the load around any access hole and to resist the reaction. As mentioned previously, a refined analysis of the diaphragm is desirable is such situations. Stiffening around the hole may be required. Auxiliary bearing stiffeners might be provided to spread out the reaction. Thermal movements of the bridge at expansion bearings may cause the diaphragm to be eccentric with respect to the bearings. *AASHTO LRFD* Article 6.11.11.1 states that the bearing stiffeners and diaphragms should be designed for the resulting eccentricity. The effect of the eccentricity can be recognized by treating the effective bearing stiffener/diaphragm assembly as a beam-column according to the provisions of *AASHTO LRFD* Article 6.9.2.2 (Section 6.6.3.4.3). The effective bearing assembly consists of the stiffeners plus the portion of the diaphragm web specified in *AASHTO LRFD* Article 6.10.11.2.4b assumed to act with the stiffeners as an effective column section (Section 6.6.6.3.4.2).

Details on diaphragms should be appropriately investigated for the fatigue limit state. On diaphragms for which principal stresses are considered, fatigue-sensitive details should be investigated by considering the principal tensile stress range due to the applicable factored fatigue live load that results from the diaphragm acting as a deep beam, which may preclude the use of certain fatigue-sensitive details on the diaphragm. Note that the direction of the principal tensile stress may change for different positions of the live load. Details need only be checked for fatigue if they are subject to a net tensile stress according to the criterion specified in *AASHTO LRFD* Article 6.6.1.2.1.

EXAMPLE

Design the solid-plate internal diaphragm at the interior pier of an exterior tub girder in a straight continuous-span bridge for the strength limit state (Figure 6.6.3.6.2-1). The tub girder is supported on two bearings at the pier, and a single pair of bearing stiffeners is to be provided on the diaphragm over each bearing. The bearing stiffeners are assumed spaced 60 inches apart. An 18-inch wide by 36-inch deep access hole is provided in the center of the diaphragm. The girder is homogeneous with the flanges and web having a yield strength of 50 ksi.

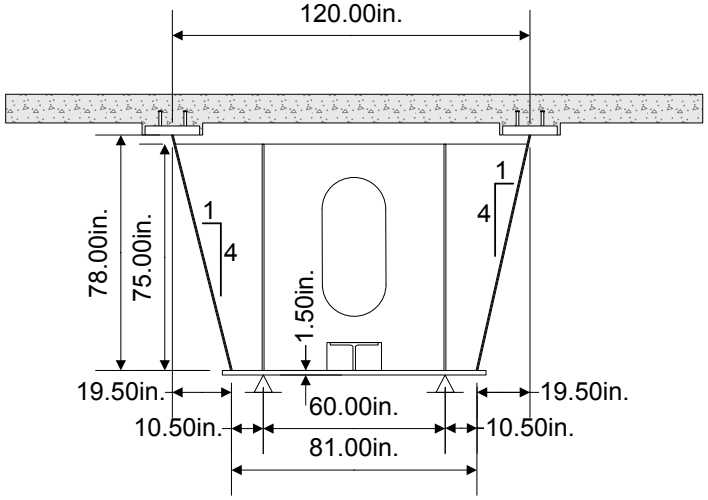

Figure 6.6.3.6.2-1 Example Tub Girder Section at an Interior Pier

The load modifier η is assumed to be 1.0 and the Strength I load combination will be assumed to control.

It is assumed that the section is from a multiple box-section bridge that does *not* satisfy one or more of the special restrictions specified in *AASHTO LRFD* Article 6.11.2.3. Therefore, the effects of St. Venant torsional shear must be considered in the design of the girder and the diaphragm.

Assume the following total unfactored vertical shears in the critical web of the tub section. The critical web is considered to be the web subject to additive flexural and St. Venant torsional shears for each load case. Since the section is at an interior support, positive and negative shears exist at the section for each load case. Only the maximum and minimum values of the HL-93 live load plus impact shears are given:

V_{DC1} = +255/-254 kips
V_{DC2} = +62/-58 kips

V_{DW} = +50/-48 kips
V_{LL+IM} = +183/-175 kips

Compute the total maximum factored vertical shear in the diaphragm. The total unfactored vertical dead load shear in the diaphragm will be computed by summing the vertical dead load shears in the critical web of the tub section acting on each side of the interior-pier section

DC_1: $V = 255 + |-254| = 509$ kips

DC_2: $V = 62 + |-58| = 120$ kips

DW: $V = 50 + |-48| = 98$ kips

Total unfactored dead load shear: = 727 kips

In this case, the HL-93 live load plus impact shear in the critical web at the interior pier is governed by two lanes loaded. Thus, the total unfactored vertical live load plus impact shear in the diaphragm will be computed by summing the vertical live load plus impact shears in the critical web of the tub section acting on each side of the interior-pier section, and then subtracting two times the rear-axle load of the HL-93 design truck plus impact (assumed positioned directly over the interior pier to maximize the live load shear at the pier section). The rear axle of the HL-93 design truck weighs 32.0 kips and the dynamic load allowance applied to the design truck at the strength limit state is 33 percent. Therefore:

LL+IM: $V = 183 + |-175| - 2(32.0)(1.33) = 273$ kips

The total factored vertical shear in the diaphragm under the Strength I load combination is computed as:

$$V = 1.0[1.25(509 + 120) + 1.50(98) + 1.75(273)] = 1{,}411 \text{ kips}$$

Assume a 7/8-inch-thick ASTM A709/A709M Grade 50 diaphragm plate (i.e. F_y = 50 ksi). The vertical depth of the plate is 75 inches. Check the factored shear resistance of the diaphragm. The nominal shear resistance, V_n, is computed from Equation 6.6.3.6.2-5 as follows:

$$V_n = V_{cr} = CV_p$$

The plastic shear force, V_p, is computed as:

$$V_p = 0.58F_yDt_w = 0.58(50)(75.0)(0.875) = 1{,}903 \text{ kips}$$

Calculate the constant, *C*. The bearing stiffeners will be assumed to act as transverse stiffeners. The critical region for shear in this case is the region outside the bearing stiffeners adjacent to the critical web. Therefore, use the spacing from the mid-depth of the girder web to the first pair of bearing stiffeners; that is, d_o = 19.5/2 + 10.5 = 20.25 in. Therefore, the shear buckling coefficient, *k*, is computed from Equation 6.5.7.2-4 as:

$$k = 5 + \frac{5}{\left(\frac{d_o}{D}\right)^2}$$

$$k = 5 + \frac{5}{\left(\frac{20.25}{75}\right)^2} = 73.59$$

Since:

$$1.12\sqrt{\frac{Ek}{F_y}} = 1.12\sqrt{\frac{29{,}000(73.59)}{50}} = 231.4 > \frac{D}{t_w} = \frac{75.0}{0.875} = 85.7$$

$$C = 1.0$$

AASHTO LRFD Equation 6.10.9.3.2-4

$$V_n = V_{cr} = (1.0)(1{,}903) = 1{,}903 \text{ kips}$$

$$V_r = \phi_v V_n = 1.0(1{,}903) = 1{,}903 \text{ kips} > V = 1{,}411 \text{ kips} \quad \text{ok}$$

An interior support diaphragm is subject to major-axis bending over the bearing sole plates in addition to shear. Therefore, evaluate the principal stresses. Compute the maximum total vertical shear stress, f_d, in the diaphragm at critical sections. First, separate out the flexural shear, V_b, due to major-axis bending of the tub section, and the St. Venant torsional shear, V_T, from the total vertical diaphragm shear, *V*. Referring to the example given at the end of Section 6.5.6.2.4.3, the factored torsional shear flow in the non-composite tub section was computed as:

$$f = \frac{T}{2A_o} = \frac{1.0(1.25)(26)}{2(56.0)(12)} = 0.024 \text{ kips / in.}$$

Therefore:

$$V_T = 0.024(78.0/\cos 14^\circ) = 0.024(80.4) = 1.93 \text{ kips}$$

The vertical component of V_T is computed as:

$$(V_T)_v = 1.93\left(\frac{78.0}{80.4}\right) = 1.87 \text{ kips}$$

The horizontal component of V_T is computed as:

$$(V_T)_h = 1.93\left(\frac{19.5}{80.4}\right) = 0.47 \text{ kips}$$

The total factored DC_1 vertical diaphragm shear acting on the non-composite section on the critical side is V_{DC1} = 1.0[1.25(509)] = 636.3 kips. Therefore, the flexural shear is:

$$V_b = 636.3 - 1.87 = 634.4 \text{ kips}$$

The total factored DC_1 vertical diaphragm shear acting on the non-composite section on the non-critical side is:

$$V_{DC_1} = 634.4 - 1.87 = 632.5 \text{ kips}$$

From the previous example (Section 6.5.6.2.4.3), the factored torsional shear flow in the composite tub section was computed as:

$$f = \frac{T}{2A_o} = \frac{1.0\left|1.25(-190) + 1.5(-156) + 1.75(-966)\right|}{2(61.1)(12)} = 1.474 \text{ kips/in.}$$

Therefore:

$$V_T = 1.474(80.4) = 118.5 \text{ kips}$$

The vertical component of V_T is computed as:

$$(V_T)_v = 118.5\left(\frac{78.0}{80.4}\right) = 115.0 \text{ kips}$$

The horizontal component of V_T is computed as:

$$(V_T)_h = 118.5\left(\frac{19.5}{80.4}\right) = 28.74 \text{ kips}$$

The total factored vertical diaphragm shear acting on the composite section on the critical side is V_c = 1.0[1.25(120)+1.50(98)+1.75(273)] = 774.8 kips. Therefore, the flexural shear is:

$$V_b = 774.8 - 115.0 = 659.8 \text{ kips}$$

The total factored vertical diaphragm shear acting on the composite section on the non-critical side is:

$$V_c = 659.8 - 115.0 = 544.8 \text{ kips}$$

Therefore, on each side of the diaphragm, the total factored vertical shear due to flexure is:

$$(V_b)_{tot} = 634.4 + 659.8 = 1{,}294 \text{ kips}$$

The total factored vertical shear in the diaphragm on the critical side (including the vertical component of the torsional shear) is:

$$V_{tot} = 636.3 + 774.8 = 1{,}411 \text{ kips} \qquad \text{(as computed previously)}$$

The total factored vertical shear in the diaphragm on the non-critical side is:

$$V_{tot} = 632.5 + 544.8 = 1{,}177 \text{ kips}$$

The factored shear stress in the diaphragm due to St. Venant torsion $(f_d)_T$ is equal to:

$$(f_d)_T = (0.024 / 0.875 + 1.474 / 0.875) = 1.71 \text{ ksi}$$

Note that although the torques on the non-composite and composite box sections act in different directions in this case, the DC_1 shear flow is small and the shear flow acting on the composite section includes the effect of an assumed future wearing surface. Therefore, for simplicity, the shear flows are conservatively assumed to act in the same direction and are added together in this example.

The average factored flexural shear stress in the diaphragm web (on the critical side) at the bearing stiffener due to major-axis bending, $(f_d)_b$, is taken as:

$$(f_d)_b = \frac{1{,}294}{75.0(0.875)} = 19.72 \text{ ksi}$$

Therefore, the total factored shear stress f_d in the diaphragm web (on the critical side) at the bearing stiffener is equal to:

$$f_d = (f_d)_T + (f_d)_b = 1.71 + 19.72 = 21.43 \text{ ksi}$$

Calculate the shear stress at the section through the access hole. Assume the following unfactored bearing reactions:

Critical side:	R_{DC1}	=	509 kips
	R_{DC2}	=	25 kips
	R_{DW}	=	18 kips
	R_{LL+IM}	=	320 kips

The total factored reaction on the critical side under the Strength I load combination is computed as:

$$R_u = 1.0\left[1.25(509 + 25) + 1.50(18) + 1.75(320)\right] = 1{,}255 \text{ kips}$$

Non-critical side:	R_{DC1}	=	349 kips
	R_{DC2}	=	120 kips
	R_{DW}	=	98 kips
	R_{LL+IM}	=	277 kips

The total factored reaction on the non-critical side under the Strength I load combination is computed as:

$$R_u = 1.0\left[1.25(349 + 120) + 1.50(98) + 1.75(277)\right] = 1{,}218 \text{ kips}$$

Therefore, the total factored vertical diaphragm shear due to flexure at the section through the access hole is:

$$V = 1{,}294 \text{ kips} - 1{,}255 \text{ kips} = 39.0 \text{ kips}$$

The average factored flexural shear stress in the diaphragm web at the section through the access hole due to major-axis bending, $(f_d)_b$, is taken as:

$$(f_d)_b = \frac{39.0}{(75.0 - 36.0)(0.875)} = 1.14 \text{ ksi}$$

Therefore, the total factored shear stress, f_d, in the diaphragm web at the section through the access hole is equal to:

$$f_d = (f_d)_T + (f_d)_b = 1.71 + 1.14 = 2.85 \text{ ksi}$$

Calculate the stress due to major-axis bending of the diaphragm over the bearing sole plate, f_{by}. The stress f_{bz} is typically neglected. Assume a strip of the bottom box flange equal to six times its thickness (i.e. 6 * 1.5 in. = 9.0 in.) acts with the diaphragm in resisting major-axis bending of the diaphragm (*AASHTO LRFD* Article C6.7.4.3). Calculate the section properties of the effective section at the bearing stiffener adjacent to the critical web:

Component	A	d	Ad	Ad^2	I_o	I
Web 7/8" x 75"	65.62				30,762	30,762
Bot. Flange 1-1/2" x 9"	13.50	38.25	-516.4	19,751	2.53	19,753
	79.12		-516.4			50,515
					-6.53(516.4) =	-3,372
					I_{NA} =	47,143 in.^{4}

$$d_S = \frac{-516.4}{79.12} = -6.53 \text{ in.}$$

$$d_{\text{Top of Steel}} = 37.50 + 6.53 = 44.03 \text{ in.} \qquad d_{\text{Bot of Steel}} = 39.00 - 6.53 = 32.47 \text{ in.}$$

$$S_{\text{Top of Steel}} = \frac{47{,}143}{44.03} = 1{,}071 \text{ in.}^3 \qquad S_{\text{Bot of Steel}} = \frac{47{,}143}{32.47} = 1{,}452 \text{ in.}^3$$

Calculate the section properties of the effective section through the center of the access hole:

Component	A	d	Ad	Ad^2	I_o	I
Web – above hole	17.06	27.75	473.4	13,137	540.7	13,678
Web – below hole	17.06	27.75	-473.4	13,137	540.7	13,678
Bot. Flange 1-1/2" x 9"	13.50	38.25	-516.4	19,751	2.53	19,753
	47.62		-516.4			47,109
					-10.84(516.4) =	-5,598
					I_{NA} =	41,511 in.^{4}

$$d_S = \frac{-516.4}{47.62} = -10.84 \text{ in.}$$

$$d_{\text{Top of Steel}} = 37.50 + 10.84 = 48.34 \text{ in.} \qquad d_{\text{Bot of Steel}} = 39.00 - 10.84 = 28.16 \text{ in.}$$

$$S_{\text{Top of Steel}} = \frac{41{,}511}{48.34} = 859 \text{ in.}^3 \qquad S_{\text{Bot of Steel}} = \frac{41{,}511}{28.16} = 1{,}474 \text{ in.}^3$$

Check Equation 6.6.3.6.2-3 to ensure that bend buckling of the diaphragm web does not occur (the section at the bearing stiffener is critical for this check):

$$\frac{2D_C}{t_w} = \frac{2(32.47 - 1.5)}{0.875} = 70.8 < \lambda_{rw} = 5.7\sqrt{\frac{29{,}000}{50}} = 137.3 \quad \text{ok}$$

Check the section at the bearing stiffener. Moments of the factored St. Venant torsional shears and flexural shears will be taken about a point lying on the neutral axis of the diaphragm at this section directly above the bearing. First, compute the moment in the diaphragm due to the factored St. Venant torsional shears. For simplicity, the torsional shear flows due to the dead and live loads (computed previously) will be assumed to act around the same perimeter (i.e. the perimeter of the diaphragm). The horizontal and vertical components of the torsional web shears (computed previously) acting at the mid-depth of the web will be considered.

Top:

$$M = (0.024 \text{ kips/in.} + 1.474 \text{ kips/in.})(10.5 \text{ in.} + 19.5 \text{ in.})(44.03 \text{ in.}) = -1{,}979 \text{ kip} - \text{in.}$$

Web:

$$M = (1.87 \text{ kips} + 115.0 \text{ kips})(10.5 \text{ in.} + 19.5 \text{ in.}/2) - (0.47 \text{ kips} + 28.74 \text{ kips})(6.53 \text{ in.}) = -2{,}176 \text{ kip} - \text{in.}$$

Bot.:

$$M = (0.024 \text{ kips/in.} + 1.474 \text{ kips/in.})(10.5 \text{ in.})(30.97 \text{ in.}) = -487 \text{ kip} - \text{in}$$

Total:

$$M = (-1{,}979) + (-2{,}176) + (-487) = -4{,}642 \text{ kip} - \text{in.}$$

The moment in the diaphragm due to the factored flexural shears is computed as:

$$M = 1{,}294 \text{ kips}\left[10.5 \text{ in.} + 19.5 \text{ in.}/2. - \frac{19.5}{78.0}(6.53) \text{ in.}\right] = -24{,}091 \text{ kip} - \text{in}$$

The total factored moment in the diaphragm at the bearing stiffener is:

$$M = (-4{,}642) + (-24{,}091) = -28{,}733 \text{ kip} - \text{in.}$$

The maximum bending stress at the top of the diaphragm is:

$$f_{by} = \frac{|-28{,}733 \text{ kip} - \text{in.}|}{1{,}071 \text{ in.}^3} = +26.83 \text{ ksi}$$

From Equation 6.6.3.6.2-2:

$$\sigma_{1,2} = \left(\frac{f_{by} + f_{bz}}{2}\right) \pm \sqrt{\left(\frac{f_{by} - f_{bz}}{2}\right)^2 + f_d^2}$$

$$\sigma_{1,2} = \left(\frac{26.83 + 0}{2}\right) \pm \sqrt{\left(\frac{26.83 - 0}{2}\right)^2 + (21.43)^2} = 38.70, -11.87 \text{ ksi}$$

Checking the combined principal stresses according to Equation 6.6.3.6.2-1 gives:

$$\sqrt{\sigma_1^2 - \sigma_1\sigma_2 + \sigma_2^2} \le \phi_f F_y$$

$$\sqrt{(38.70)^2 - (38.70)(-11.87) + (-11.87)^2} = 45.80 \text{ ksi} < 1.0(50) = 50.00 \text{ ksi} \quad \text{ok}$$

Check the section through the center of the access hole. Moments of the factored St. Venant torsional shears and flexural shears will be taken about a point lying on the neutral axis of the diaphragm at this section. First, compute the moment in the diaphragm due to the factored St. Venant torsional shears.

Top:

$$M = (0.024 \text{ kips/in.} + 1.474 \text{ kips/in.})(120 \text{ in.}/2)(48.34 \text{ in.}) = -4{,}345 \text{ kip} - \text{in.}$$

Web:

$$M = (1.87 \text{ kips} + 115.0 \text{ kips})(120 \text{ in.}/2 - 19.5 \text{ in.}/2) - (0.47 \text{ kips} + 28.74 \text{ kips})(10.84 \text{ in.}) = -5{,}556 \text{ kip} - \text{in.}$$

Bot.:

$$M = (0.024 \text{ kips/in.} + 1.474 \text{ kips/in.})(81 \text{ in.}/2)(26.66 \text{ in.}) = -1{,}617 \text{ kip} - \text{in}$$

Total:

$$M = (-4{,}345) + (-5{,}556) + (-1{,}617) = -11{,}518 \text{ kip} - \text{in.}$$

The moment in the diaphragm due to the factored flexural shears is computed as:

$$M = 1{,}294 \text{ kips}\left[81 \text{ in.}/2 + 19.5\Big/2 \text{ in.} - \frac{19.5}{78.0}(10.84) \text{ in.}\right] = -61{,}517 \text{ kip} - \text{in}$$

The total moment factored in the diaphragm at the center of the access hole (considering also the moment due to the critical bearing reaction) is:

$$M = (-11{,}518) + (-61{,}517) + (1{,}255 \text{ kips})(60 \text{ in.}/2) = -35{,}385 \text{ kip} - \text{in.}$$

The maximum bending stress at the top of the diaphragm is:

$$f_{by} = \frac{|-35{,}385 \text{ kip} - \text{in.}|}{859 \text{ in.}^3} = +41.19 \text{ ksi}$$

From Equation 6.6.3.6.2-2:

$$\sigma_{1,2} = \left(\frac{f_{by} + f_{bz}}{2}\right) \pm \sqrt{\left(\frac{f_{by} - f_{bz}}{2}\right)^2 + f_d^2}$$

$$\sigma_{1,2} = \left(\frac{41.19 + 0}{2}\right) \pm \sqrt{\left(\frac{41.19 - 0}{2}\right)^2 + 2.85^2} = 41.39, -0.20 \text{ ksi}$$

Checking the combined principal stresses according to Equation 6.6.3.6.2-1 gives:

$$\sqrt{\sigma_1^2 - \sigma_1\sigma_2 + \sigma_2^2} \le \phi_f F_y$$

$$\sqrt{(41.39)^2 - (41.39)(-0.20) + (-0.20)^2} = 41.49 \text{ ksi} < 1.0(50) = 50.00 \text{ ksi} \quad \text{ok}$$

The section at the bearing stiffener controls. Use a 7/8" x 75" diaphragm plate. Similar computations should be done at the fatigue limit state to obtain the principal tensile stress range due to the factored fatigue live load to check potential fatigue-sensitive diaphragm details subject to a net tensile stress.

Design the bearing stiffeners (Section 6.6.6.3). ASTM A 709 Grade 50 steel will be assumed for the stiffeners (i.e. F_{ys} = 50 ksi). Assume that the bearings are fixed at

the piers. Thus, there will be no thermal expansion causing eccentric loading on the bearing stiffeners. The width, b_t, of each projecting stiffener element must satisfy Equation 6.6.6.3.2-1 as follows:

$$b_t \le 0.48 t_p \sqrt{\frac{E}{F_{ys}}}$$

Welded bearing stiffeners are also commonly made up of less expensive flat bar stock, which is generally produced in whole-inch width increments and 1/8-in. thickness increments. Try two 10.5-inch-wide bars welded to each side of the diaphragm web. Rearranging Equation 6.6.6.3.2-1 gives:

$$(t_p)_{min.} = \frac{b_t}{0.48\sqrt{\frac{E}{F_{ys}}}}$$

$$(t_p)_{min.} = \frac{10.5}{0.48\sqrt{\frac{29{,}000}{50}}} = 0.908 \text{ in.}$$

Try a stiffener thickness t_p of 1.0 inches, which satisfies the preferred minimum thickness of ½ inch for stiffeners given in AASHTO/NSBA (2003).

According to *AASHTO LRFD* Article 6.10.11.2.3, the factored bearing resistance for the fitted ends of bearing stiffeners is to be taken as (Equation 6.6.6.3.3-1):

$$(R_{sb})_r = \phi_b (R_{sb})_n$$

where $(R_{sb})_n$ is equal to the nominal bearing resistance for the fitted end of bearing stiffeners taken as (Equation 6.6.6.3.3-2):

$$(R_{sb})_n = 1.4 A_{pn} F_{ys}$$

A_{pn} is the area of the projecting elements of the stiffener outside of the web-to-flange fillet welds. Assume for this example that the clip provided at the base of the stiffeners to clear the web-to-flange fillet welds is 1.5 inches in length. The resistance factor for bearing on milled surfaces, ϕ_b = 1.0. Therefore:

$$A_{pn} = 2(10.5 - 1.5)(1.0) = 18.00 \text{ in.}^2$$

$$(R_{sb})_n = 1.4(18.00)(50.0) = 1{,}260 \text{ kips}$$

$$(R_{sb})_r = \phi_b (R_{sb})_n = 1.0(1{,}260) = 1{,}260 \text{ kips} > R_u = 1{,}255 \text{ kips} \quad \text{ok}$$

For computing the axial resistance of bearing stiffeners that are welded to the diaphragm web, *AASHTO LRFD* Article 6.10.11.2.4b states that a portion of the web is to be included as part of the effective column section. For stiffeners consisting of two plates welded to the web, the effective column section is to consist of the two stiffener elements, plus a centrally located strip of web extending not more than $9t_w$ on each side of the stiffeners (Figure 6.6.6.3.4.2-1).

As specified in *AASHTO LRFD* Article 6.10.11.2.4a, the radius of gyration of the effective column section is to be computed about the mid-thickness of the web and the effective length is to be taken as 0.75*D*, where *D* is the web depth. The area of the effective column section is computed as:

$$A_g = 2\left[(10.5)(1.0) + 9(0.875)(0.875)\right] = 34.78 \text{ in.}^2$$

The moment of inertia of the effective column section (conservatively neglecting the web strip) is computed as:

$$I_s = \frac{1.0(10.5 + 0.875 + 10.5)^3}{12} = 872.3 \text{ in.}^4$$

The radius of gyration of the effective column section is therefore computed as:

$$r_s = \sqrt{\frac{I_s}{A_g}} = \sqrt{\frac{872.3}{34.78}} = 5.01 \text{ in.}$$

The effective length of the effective column section is computed as:

$$K\ell = 0.75D = 0.75(75.0) = 56.25 \text{ in.}$$

Check the limiting slenderness ratio of 120 specified for main members in compression in *AASHTO LRFD* Article 6.9.3:

$$\frac{K\ell}{r_s} = \frac{56.25}{5.01} = 11.2 < 120 \text{ ok}$$

As specified in *AASHTO LRFD* Article 6.10.11.2.4a, calculate the factored axial resistance P_r of the effective column section according to the provisions of *AASHTO LRFD* Article 6.9.2.1 as follows (Equation 6.6.6.3.4.1-1):

$$P_r = \phi_c P_n$$

where P_n is equal to the nominal compressive resistance determined as specified in *AASHTO LRFD* Article 6.9.4.1, and ϕ_c is equal to the resistance factor for axial compression = 0.95.

Calculate the elastic critical flexural buckling resistance, P_e (Equation 6.6.6.3.4.1-4):

$$P_e = \frac{\pi^2 E}{\left(\frac{K\ell}{r_s}\right)^2} A_g$$

$$P_e = \frac{\pi^2 (29{,}000)}{(11.2)^2} (34.78) = 79{,}358 \text{ kips}$$

Calculate the equivalent nominal yield resistance, P_o (the slender element reduction factor, Q, is taken equal to 1.0 for bearing stiffeners).

$$P_o = QF_{ys}A_g$$

$$P_o = (1.0)(50.0)(34.78) = 1{,}739 \text{ kips}$$

$$\frac{P_e}{P_o} = \frac{79{,}358}{1{,}739} = 45.6 > 0.44$$

Therefore, use Equation 6.6.6.3.4.1-2 to compute P_n as follows:

$$P_n = \left[0.658^{\left(\frac{P_o}{P_e}\right)} \right] P_o$$

$$P_n = \left[0.658^{\left(\frac{1{,}739}{79{,}358}\right)} \right] 1{,}739 = 1{,}723 \text{ kips}$$

$$P_r = \phi_c P_n$$

$$P_r = 0.95(1{,}723) = 1{,}637 \text{ kips} > R_u = 1{,}255 \text{ kips} \quad \text{ok}$$

Use 1" x 10-1/2" bearing stiffeners (one pair) over each bearing.

6.6.4 Connections

6.6.4.1 General

Connection design is covered in *AASHTO LRFD* Article 6.13. The design of bolted connections is covered in *AASHTO LRFD* Article 6.13.2. The design of welded connections is covered in *AASHTO LRFD* Article 6.13.3. *AASHTO LRFD* Articles 6.13.4 and 6.13.5 deal with the topics of block shear rupture resistance and the design of connection elements (e.g. splice plates, gusset plates and lateral connection plates) for tension and shear, respectively.

AASHTO LRFD Article 6.13.1 covers several general considerations related to connection design. Where practical, connections should be made symmetrical about the axis of the members. Members, including bracing, should be connected so that their gravity axes will intersect at a point. Eccentric connections should be avoided, however, where this is not possible, the members and connections must be designed for the combined effects of the shear and moment due to the eccentricity. Bolted connections, except for connections on lacing and handrails, are to contain not less than two bolts.

End connections of stringers, floorbeams and girders should be connected with high-strength bolts. Where bolting is not practical, welded connections may be used, but they must be designed for the vertical loads and any bending moment resulting from restraint against end rotation.

AASHTO LRFD Article 6.13.1 specifies that where cross-frames/diaphragms, lateral bracing, stringers or floorbeams for straight or horizontally curved members are included in a structural model used to determine force effects, or are designed for explicitly calculated force effects from the results of a separate investigation (e.g. an approximate wind load analysis), the end connections for those members are to be designed for the calculated factored member force effects. Otherwise, the end connections for these members are to be designed for 75 percent of the factored resistance corresponding to the force effect under consideration. The preceding exception results from experience indicating that application of 75 percent and average load provisions to the end connections of these members in which force effects have been determined by analysis, as required in previous specifications,

tended to result in large connections with large eccentricities and force concentrations. Therefore, it was felt by the specification writers that the above exception was justified to prevent the complications resulting from such large connections.

6.6.4.2 Bolted Connections

6.6.4.2.1 General

The design of bolted connections is covered in *AASHTO LRFD* Article 6.13.2. *AASHTO LRFD* Article 6.13.2.1 specifies that bolted steel parts must fit solidly together after the bolts are tightened. The bolted parts may be coated or uncoated. It must be specified in the contract documents that all joint surfaces, including surfaces adjacent to the bolt head and nut, be free of scale (except for tight mill scale), dirt or other foreign material. All material within the grip of the bolt must be steel.

High-strength bolts are to be installed to have a specified initial tension, which results in an initial precompression between the joined parts. At service load levels, the transfer of the loads between the joined parts may then occur entirely via friction with no bearing of the bolt shank against the side of the hole. Until the friction force is overcome, the shear resistance of the bolt and the bearing resistance of the bolt hole will not affect the ability to transfer the load across the shear plane between the joined parts.

In general, high-strength bolted connections designed according to the *AASHTO LRFD* Specification provisions will have a higher reliability than the connected parts because the resistance factors for the design of bolted connections were selected to provide a higher level of reliability than those chosen for member design. Also, the controlling strength limit state in the connected part, e.g. yielding or deflection, is typically reached well before the controlling strength limit state in the connection, e.g. the bolt shear resistance or the bearing resistance of the connected material.

The *AASHTO LRFD* Specifications recognize two types of high-strength bolted connections; slip-critical connections (Section 6.6.4.2.1.1), and bearing-type connections (Section 6.6.4.2.1.2). The resistance of all high-strength bolted connections in transmitting shear across a shear plane between bolted steel parts is the same whether the connection is a slip-critical or bearing-type connection. The slip-critical connection has an additional requirement that slip must not occur between the joined parts at service load levels.

6.6.4.2.1.1 Slip-Critical Connections

In high-strength bolted slip-critical connections subject to shear, the load is transferred between the joined parts by friction up to a level of force that is dependent upon the clamping force and the coefficient of friction of the faying surfaces. The coefficient of friction depends on the faying surface condition, with mill scale, paint or other surface treatments determining the value of the friction coefficient.
Prior to joint slip, the bolts are not subject to shear nor are the joined parts subject to bearing stress. Once the load exceeds the frictional resistance between the faying surfaces, slip occurs; that is, the friction bond is broken and the two surfaces slip with respect to one another by a relatively large amount. A rupture failure does not occur. Therefore, the connection is able to continue resisting an even greater load through the shear resistance of the bolts and the bearing resistance against the connected material. Final failure of the connection will be by shear failure of the bolts, yielding or tear-out of the connected material or by an unacceptable deformation around the holes; the ultimate resistance of the connection is not related to the slip load.

The slip and bearing resistances are computed separately for application at different load combinations (the calculation of the slip, shear and bearing resistances of bolted connections and the resistance of the connected material is discussed in more detail in Sections 6.6.4.2.4 and 6.6.4.2.5). Because a high tensile force on the bolt is required to develop a significant resisting friction force, only bolts with a high tensile yield strength (i.e. ASTM A325 and A490 high-strength bolts) can be used in slip-critical connections.

AASHTO LRFD Article 6.13.2.1.1 specifies that slip-critical connections are to be proportioned to prevent slip under Load Combination Service II (Section 3.10.1.3.3), and to provide bearing, shear and tensile resistance under the applicable strength load combinations. Slip is to be prevented under Load Combination Service II to control permanent deformations caused by slip in bolted joints that could adversely affect the serviceability of the structure. It is further assumed that under the strength load combinations, slip between the bolted parts occurs at the higher loads and that the bolts have gone into bearing against the connected material. Thus, the shear resistance of the bolts and bearing resistance of the bolt holes must be checked under the appropriate strength load combination. In addition, the resistance of the connected material must be checked at the strength limit state.

According to *AASHTO LRFD* Article 6.13.2.1.1, bolted joints subject to stress reversal, heavy impact loads, severe vibration or located where stress or strain due to joint slippage would be detrimental to the serviceability of the structure are to be designated as slip-critical (the reader is referred to this article for the specific list of joints that should be designated as slip-critical). Repeated loading may introduce

fatigue concerns if slip occurs in these cases, particularly when oversize or slotted holes are used. Bracing member connections should always be designed as slip-critical connections.

6.6.4.2.1.2 Bearing-Type Connections

In high-strength bolted bearing-type connections, the load is resisted by a combination of the shear resistance of the bolt, the bearing resistance of the connected material and an unknown amount of friction between the faying surfaces. The failure of a bearing-type connection will be by shear failure of the bolts, yielding or tear-out of the connected material or by an unacceptable deformation around the holes, with the final failure load independent of the clamping force provided by the bolts (Kulak et al., 1987).

AASHTO LRFD Article 6.13.2.1.2 specifies that bearing-type connections are only to be permitted on bridges for joints subject to axial compression or joints on secondary members. Such connections are to be designed to provide the required factored resistance in shear and bearing at the strength limit state. Connections utilizing A 307 bolts are to be designed as bearing-type connections.

6.6.4.2.1.3 Fatigue Resistance of Bolted Connections

The behavior of a bolted connection under fatigue loading is influenced by the type of load transfer in the connection. In tests of slip-critical lap joints subject to in-plane cyclic loading, crack initiation and growth typically occurred in the gross section in front of the first bolt hole of the connection (Kulak et al., 1987). The cracks initiated on the faying surfaces. Failures that occur at the interface of metallic surfaces that are in contact and that slip a small amount relative to each other under an oscillating load are referred to as fretting failures. The point where fretting is initiated depends on the discontinuities of the mill scale, the clamping zone of the bolt and the frictional resistance of the faying surface.

In bearing-type connections where the load is transmitted primarily by shear and bearing, the crack typically initiates instead at the edge of the bolt hole and grows in the region of the net section, with failure eventually occurring due to fracture of the net section. However, it was observed that slip-critical connections designed based on the gross section (i.e. stress ranges computed on the gross section) and bearing-type connections designed based on the net section (i.e. stress ranges computed on the net section) provide approximately the same nominal fatigue resistance. It was determined that fatigue detail Category B provides a reasonable and conservative lower bound to the test data in both cases (Kulak et al., 1987).

Therefore, *AASHTO LRFD* Table 6.6.1.2.3-1 indicates that base metal at the gross section of high-strength bolted slip-critical connections (Condition 2.1), and at the net

section of high-strength bolted bearing-type connections (Condition 2.2), subject to a net applied tensile stress (as defined in *AASHTO LRFD* Article 6.6.1.2.1) be designed for fatigue based on Detail Category B. Both of the above conditions assume the connections are made with pre-tensioned high-strength bolts and that the bolts are installed in holes drilled full size or subpunched and reamed to size. Should the bolts be installed in holes punched full size, the connection for each of the above cases is instead to be designed for fatigue based on Detail Category D according to Condition 2.3 in *AASHTO LRFD* Table 6.6.1.2.3-1 (Brown et al., 2007).

Condition 2.3 in *AASHTO LRFD* Table 6.6.1.2.3-1 also covers the fatigue resistance of the base metal at the net section of other mechanically fastened joints, except for eyebars and pin plates; e.g. joints using ASTM A307 bolts or non pre-tensioned high-strength bolts. For these cases, the connection is also to be designed for fatigue based on Detail Category D.

The checking of fatigue of bolted bracing member connections for single- and double-angle members, and for tee members, is discussed above in Section 6.6.3.3.5.

Axially loaded joints subject to fatigue loading in direct tension (versus shear), in addition to prying action, are treated differently according to the provisions of *AASHTO LRFD* Article 6.13.2.10.3 (Section 6.6.4.2.5.4).

6.6.4.2.2 Bolt Requirements

6.6.4.2.2.1 Size of Bolts

AASHTO LRFD Article 6.13.2.5 gives some specific requirements regarding the size of bolts. Bolts are not to be less than 0.625 in. in diameter. Bolts 0.625 in. in diameter are not to be used in primary members, except for 2.5-in. legs of angles and in flanges of sections whose dimensions require 0.625-in. bolts to satisfy other detailing provisions given in the specifications. Structural shapes that do not permit the use of 0.625-in. bolts are to be limited to use in handrails.

The diameter of bolts in angles that serve as primary members is not to exceed one-fourth of the width of the leg in which the bolts are placed. Finally, angles whose size is not determined by a calculated demand may use the following bolt sizes: 1) 0.625-in. diameter bolts in 2.0-in. legs; 2) 0.75-in. diameter bolts in 2.5-in. legs; 3) 0.875-in. diameter bolts in 3.0-in. legs; and 4) 1.0-in. diameter bolts in 3.5-in. legs.

6.6.4.2.2.2 Spacing of Bolts

6.6.4.2.2.2.1 Minimum Spacing and Clear Distance

AASHTO LRFD Article 6.13.2.6.1 specifies that the minimum spacing between centers of bolts in standard holes is not to be less than 3.0*d*, where *d* is the diameter of the bolt (Figure 6.6.4.2.2.2.1-1).

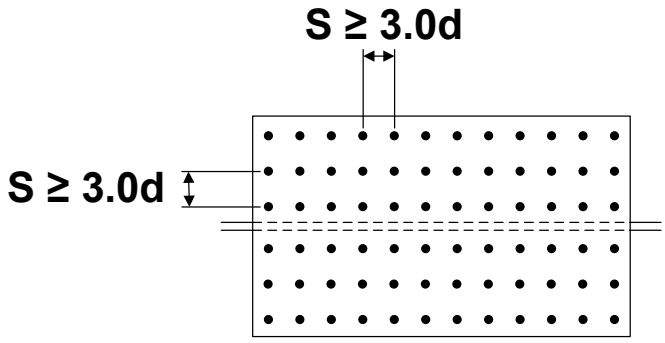

Figure 6.6.4.2.2.2.1-1 Minimum Spacing Requirement Between Centers of Bolts

The minimum clear distance, L_c, between the edges of adjacent bolt holes in the direction of the force and transverse to the direction of the force is not to be less than 2.0*d* when oversize or slotted holes are used.

6.6.4.2.2.2.2 Maximum Spacing for Sealing Bolts

AASHTO LRFD Article 6.13.2.6.2 specifies that to seal against the penetration of moisture in joints, the spacing, *s*, of a single line of bolts adjacent to a free edge of an outside plate or shape must satisfy the following requirement (Figure 6.6.4.2.2.2.2-1 Part A):

$$s \le (4.0 + 4.0t) \le 7.0 \text{ in.} \qquad \text{Equation 6.6.4.2.2.2.2-1}$$

AASHTO LRFD Equation 6.13.2.6.2-1

where:

t = thickness of the thinner outside plate or shape (in.)

Where there is a second line of bolts uniformly staggered with the line adjacent to the free edge, at a gage less than 1.5 + 4.0*t*, the staggered spacing, *s*, in the two lines considered together must satisfy the following requirement (Figure 6.6.4.2.2.2.2-1 Part B):

$$s \le 4.0 + 4.0t - \left(\frac{3.0g}{4.0}\right) \le 7.0 \text{ in.}$$ Equation 6.6.4.2.2.2.2-2

AASHTO LRFD Equation 6.13.2.6.2-2

where:

g = gage between bolts (in.)

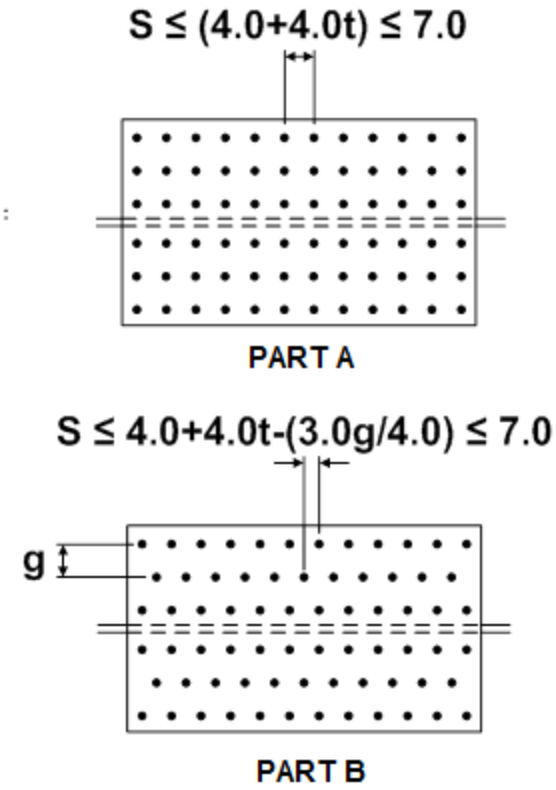

Figure 6.6.4.2.2.2.2-1 Maximum Spacing Requirements for Sealing Bolts

In uncoated weathering steel structures, it is critical that the bolt spacing be such that the connection joint is tight and excess moisture cannot enter between the plies of material. If sufficient moisture enters the joint, the resulting corrosion may cause prying, or pack-out, of the joint or bolt failure. Bolt spacing guidelines to insure proper tightness and stiffness of uncoated weathering steel bolted joints to avoid joint prying and corrosion pack-out are provided in Brockenbrough (1983). The maximum spacing requirements for sealing bolts, given above, automatically satisfy these guidelines.

Maximum pitch requirements for stitch bolts, which fasten together built-up compression or tension members at intervals along their length to ensure that the separate components act as a unit and to prevent buckling of compression

members, are specified in *AASHTO LRFD* Article 6.13.2.6.3. The pitch is not to exceed the maximum pitch specified for sealing bolts.

6.6.4.2.2.2.3 Edge and End Distance Requirements

The edge distance of bolts is defined as the distance perpendicular to the line of force between the center of a hole and the edge of the component (Figure 6.6.4.2.2.2.3-1). The minimum edge distance is a function of the diameter of the bolt and the condition of the plate edge (i.e. sheared or rolled or gas cut). *AASHTO LRFD* Article 6.13.2.6.6 specifies that the minimum edge distance is to be taken specified in *AASHTO LRFD* Table 6.13.2.6.6-1 (Table 6.6.4.2.2.2.3-1):

Table 6.6.4.2.2.2.3-1 Minimum Edge Distances

Bolt Diameter	Sheared Edges	Rolled Edges of Plates or Shapes, or Gas Cut Edges
in.	in.	in.
5/8	1-1/8	7/8
3/4	1-1/4	1
7/8	1-1/2	1-1/8
1	1-3/4	1-1/4
1-1/8	2	1-1/2
1-1/4	2-1/4	1-5/8
1-3/8	2-3/8	1-3/4

The maximum edge distance is not to be more than the lesser of eight times the thickness of the thinnest outside plate and 5.0 in.

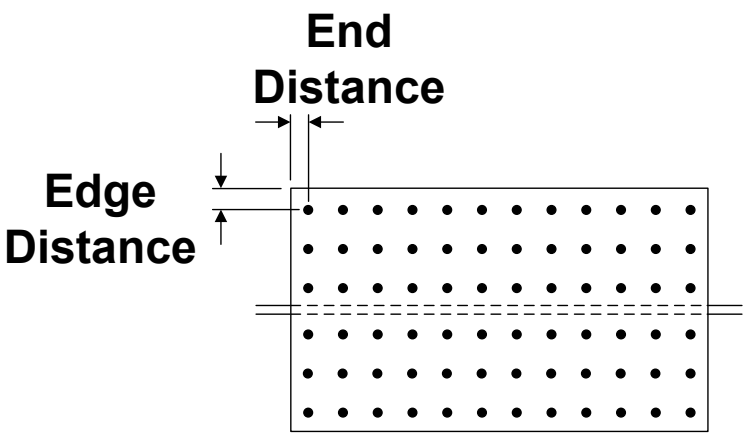

Figure 6.6.4.2.2.2.3-1 Edge and End Distance

The end distance of bolts is defined as the distance along the line of force between the center of a hole and the end of the component (Figure 6.6.4.2.2.2.3-1). *AASHTO LRFD* Article 6.13.2.6.5 specifies that the end distance for all types of holes is not to less than the appropriate minimum edge distance specified in Table 6.6.4.2.2.2.3-1. When oversize or slotted holes are used, the minimum clear end distance, which is defined as the distance between the edge of the bolt hole and the end of the member, must not be less than the bolt diameter.

The maximum end distance is to be taken the same as the maximum edge distance, or the lesser of eight times the thickness of the thinnest outside plate and 5.0 in.

At this writing (2015), AASHTO is considering the potential removal of the separate minimum edge (and end) distance requirements for bolt holes adjacent to sheared edges, as was done in AISC (2010a). The minimum edge (and end) distance requirements for bolt holes adjacent to rolled or gas cut edges would be retained and applied to all types of edges. Also, for bolts over 1-1/4 in. in diameter, the minimum edge (and end) distance would be taken as 1-1/4 times the diameter of the bolt, and the last line of the preceding table would be removed. The minimum edge distances are based on standard fabrication practices and workmanship tolerances. Edge (and end) distances larger than the specified minimum edge distances, but not larger than the specified maximum edge distances, should be permitted to help ensure that the specified minimum distances are not violated during fabrication after allowing for unavoidable workmanship tolerances. Also, satisfaction of the provisions of *AASHTO LRFD* Article 6.13.2.9 related to the bearing resistance of bolt holes (Section 6.6.4.2.5.3) ensures that sufficient end distances are provided such that bearing and tear-out limits are not exceeded for bolts adjacent to all types of edges.

6.6.4.2.2.2.4 Maximum Pitch for Stitch Bolts

Stitch bolts are used to fasten together built-up compression or tension members where two or more plates or shapes are in contact (Sections 6.6.3.3.4 and 6.6.3.4.4). A maximum pitch of the bolts is specified to ensure that the parts act as a unit and to prevent buckling of compression members. The pitch is not to exceed the maximum pitch specified for sealing bolts (Section 6.6.4.2.2.2.2).

As specified in *AASHTO LRFD* Article 6.13.2.6.3, the pitch, *p*, of stitch bolts in compression members is not to exceed 12.0*t*, and the gage, *g*, between adjacent lines of bolts is not to exceed 24.0*t*. For two adjacent lines of staggered holes, the staggered pitch, *p*, of the stitch bolts must satisfy the following requirement:

$$p \le 15.0t - \left(\frac{3.0g}{8.0}\right) \le 12.0t \qquad \text{Equation 6.6.4.2.2.2.4-1}$$

AASHTO LRFD Equation 6.13.2.6.3-1

According to *AASHTO LRFD* Article 6.13.2.6.4, at the ends of compression members, the pitch, *p*, of the stitch bolts must not exceed 4.0*d* for a length equal to 1.5 times the maximum width of the member, where *d* is the diameter of the bolt. Beyond this length, *p* may be increased gradually over a length equal to 1.5 times the maximum width of the member until the maximum pitch given by either 12.0*t* or Equation 6.6.4.2.2.2.4-1, as applicable, is reached.

For tension members, the pitch, *p*, must not exceed twice the maximum pitch specified above for compression members, and the gage, *g*, between adjacent lines of bolts must not exceed 24.0*t*.

6.6.4.2.3 Holes

6.6.4.2.3.1 Size

The maximum permitted size of standard, oversize, short-slotted and long-slotted holes is given in *AASHTO LRFD* Table 6.13.2.4.2-1 (Table 6.6.4.2.3.1-1). In the table, *d* is the diameter of the bolt.

Table 6.6.4.2.3.1-1 Maximum Hole Sizes

Bolt Dia.	Standard	Oversize	Short Slot	Long Slot
d	Dia.	Dia.	Width × Length	Width × Length
in.	in.	in.	in.	in.
5/8	11/16	13/16	11/16 × 7/8	11/16 × 1-9/16
3/4	13/16	15/16	13/16 × 1	13/16 × 1-7/8
7/8	15/16	1-1/16	15/16 × 1-1/8	15/16 × 2-3/16
1	1-1/16	1-1/4	1-1/16 × 1-5/16	1-1/16 × 2-1/2
≥ 1-1/8	*d*+1/16	*d*+5/16	*d*+1/16 × *d*+3/8	*d*+1/16 × 2.5*d*

AASHTO LRFD Article 6.8.3 specifies that for design calculations, the width of standard bolt holes is to be taken as the nominal diameter of the hole. The width of oversize and slotted holes is to be taken as the nominal diameter or width of the hole, as applicable, given in Table 6.6.4.2.3.1-1.

At this writing (2015), AASHTO may be considering a potential future increase in hole size for bolts greater than or equal to 1 in. in diameter to the nominal diameter of the bolt plus 1/8 in., which eliminates the need to field ream holes to fit large-diameter hot-forged bolts, which often have a longitudinal forging seam that interferes with holes 1/16 in. larger than the bolt diameter.

6.6.4.2.3.2 Standard Holes

According to *AASHTO LRFD* Article 6.13.2.4.1a, standard holes (Table 6.6.4.2.3.1-1) are to be used for high-strength bolted connections, unless specified otherwise.

AASHTO LRFD Article 6.13.1 specifies that unless expressly permitted otherwise by the contract documents, standard holes are to be used in connections in horizontally curved bridges to ensure that the steel fits together in the field during erection. Curved girders depend on their connections to adjacent girders through bracing members for their stability. Therefore, cross-frames/diaphragms on curved girders should be firmly connected to the girders in order for the girders to remain stable during erection. Loosely connected cross-frames/diaphragms and oversize or slotted holes are not recommended for use in horizontally curved bridges as they may compromise the girder alignment and plumbness, making cross-frame/diaphragm fit-up difficult (NHI, 2011).

6.6.4.2.3.3 Slotted Holes

6.6.4.2.3.3.1 General

NHI (2011) discusses the potential use of vertical slotted holes for cross-frame connections in straight skewed I-girder bridges in an attempt to minimize the twist of the girders and reduce the cross-frame forces. Such an approach is not recommended as it becomes difficult to control the vertical deflections during the deck placement and care must be taken to ensure the construction plan reflects the analysis assumptions made as to when the bolts are to be tightened.

6.6.4.2.3.3.2 Short-Slotted Holes

AASHTO LRFD Article 6.13.2.4.1c specifies that short-slotted holes (Table 6.6.4.2.3.1-1) may be used in any or all plies of either slip-critical or bearing-type connections. In slip-critical connections, the slots may be used without regard to the direction of loading. However, in bearing-type connections, the length of the slot must be normal to the direction of the load.

6.6.4.2.3.3.3 Long-Slotted Holes

AASHTO LRFD Article 6.13.2.4.1d specifies that long-slotted holes (Table 6.6.4.2.3.1-1) may be used only one ply of either slip-critical or bearing-type connections. As for short-slotted holes, in slip-critical connections, the slots may be used without regard to the direction of loading. However, in bearing-type connections, the length of the slot must be normal to the direction of the load.

6.6.4.2.4 Service Limit State

6.6.4.2.4.1 General

AASHTO LRFD Article 6.13.2.2 specifies that for slip-critical connections at the service limit state, the factored resistance, R_r, of a bolt at the Service II load combination is to be taken as:

$$R_r = R_n \qquad \text{Equation 6.6.4.2.4.1-1}$$

AASHTO LRFD Equation 6.13.2.2-1

where:

R_n = nominal slip resistance of the bolt specified in *AASHTO LRFD* Article 6.13.2.8 (Section 6.6.4.2.4.2) (kips)

6.6.4.2.4.2 Slip Resistance of Bolts

The slip resistance of bolts is covered in *AASHTO LRFD* Article 6.13.2.8. The bolt pretension and surface condition of the faying surface (i.e. coefficient of friction) have the greatest effect on the slip-resistance of high-strength bolted connections.

AASHTO LRFD Article 6.13.2.8 specifies that the nominal slip resistance, R_n, of a bolt in a slip-critical connection (subject to shear) is to be taken as:

$$R_n = K_h K_s N_s P_t \qquad \text{Equation 6.6.4.2.4.2-1}$$

AASHTO LRFD Equation 6.13.2.8-1

where:

N_s = number of slip planes per bolt
P_t = minimum required bolt tension specified in *AASHTO LRFD* Table 6.13.2.8-1 (Table 6.2.3.1.2-1) (kips)
K_h = hole size factor specified in *AASHTO LRFD* Table 6.13.2.8-2 (Table 6.6.4.2.4.2-1)
K_s = surface condition factor specified in *AASHTO LRFD* 6.13.2.8-3 (Table 6.6.4.2.4.2-2)

In a slip-critical connection subject to combined axial tension and shear, the tensile force reduces the contact pressure between the connected plates thereby reducing the slip resistance to the shear forces. The reduction in slip resistance is approximately proportional to the ratio of the applied tensile force to the bolt installation tension (RCSC, 2014). Therefore, according to *AASHTO LRFD* Article 6.13.2.11, the nominal slip resistance of a bolt in a slip-critical connection subjected to combined axial tension and shear under service loads (i.e. under Load Combination Service II) must not exceed the nominal slip resistance given by Equation 6.6.4.2.4.2-1 times the following factor:

$$1 - \frac{T_u}{P_t} \qquad \text{Equation 6.6.4.2.4.2-2}$$

AASHTO LRFD Equation 6.13.2.11-3

where:

T_u = tensile force due to the factored loads under Load Combination Service II (kips)
P_t = minimum required bolt tension specified in *AASHTO LRFD* Table 6.13.2.8-1 (Table 6.2.3.1.2-1) (kips)

The resistance to combined tension and shear once the connection slips and goes into bearing at the strength limit state is discussed in Section 6.6.4.2.5.5.

Since all locations must develop the slip resistance before a total joint slip can occur at that plane, the assumption is made that the slip resistance at each bolt is equal and additive with the slip resistance at the other bolts in the connection. It is also assumed that the full slip resistances must be mobilized at each slip plane before full joint slip can occur, although the forces at each slip plane do not necessarily develop simultaneously. Equation 6.6.4.2.4.2-1 is formulated for the case of a single slip plane. Therefore, the total slip resistance of a joint with multiple slip planes can be taken equal to the resistance of a single slip plane multiplied by the number of slip planes N_s.

Hole size factors, K_h, less than 1.0 are provided for bolts in oversize or slotted holes in *AASHTO LRFD* Table 6.13.2.8-2 (Table 6.6.4.2.4.2-1) because of the greater possibility of significant deformation occurring in joints with oversize or slotted holes. For long-slotted holes, even though the slip load is the same for bolts loaded transverse or parallel to the axis of the slot, the hole size factor for loading parallel to the axis has been reduced, based upon judgment, because of the greater consequences of slip in this case.

Table 6.6.4.2.4.2-1 Hole Size Factor, K_h

Description of Hole	K_h
for standard holes	1.00
for oversize and short-slotted holes	0.85
for long-slotted holes with the slot perpendicular to the direction of the force	0.70
for long-slotted holes with the slot parallel to the direction of the force	0.60

The surface condition factor, K_s, is provided in *AASHTO LRFD* Table 6.13.2.8-3 (Table 6.6.4.2.4.2-2), and is a function of the class of the surface. Three different classes of surfaces are defined based on the mean value of slip coefficients from many tests of clean mill scale, blast-cleaned steel surfaces and galvanized and roughened surfaces. The classes of surfaces are described as follows:

- Class A Surface: unpainted clean mill scale and blast-cleaned surfaces with Class A coatings;

- Class B Surface: unpainted blast-cleaned surfaces and blast-cleaned surfaces with Class B coatings;
- Class C Surface: hot-dip galvanized surfaces roughened by wire brushing after galvanizing.

Table 6.6.4.2.4.2-2 Surface Condition Factor, K_s

Surface Condition	K_s
for Class A surface conditions	0.33
for Class B surface conditions	0.50
for Class C surface conditions	0.33

It has been found that if tightly adherent mill scale is on the faying surface of a bolted connection on uncoated weathering steel, the connection slips into bearing at a lower shear stress than on a carbon steel with mill scale (Yura et al., 1981). However, if the faying surface is blast-cleaned, slip-critical connections on uncoated weathering steel can be designed using a Class B surface condition (Mathay, 1993). Otherwise, a Class A surface condition, which is appropriate for clean mill-scale surfaces, must be used. The slip resistance of bolted joints is not affected by the weathering of uncoated steel surfaces prior to erection, but any loose rust on the connection or faying surfaces must be removed. Pre-construction primers may be used for the cleaned bolted surfaces. Yura et al. (1981) indicate that the Class B surface condition can be maintained in such cases for up to one year prior to joint assembly.

Unpainted clean mill-scale faying surfaces and unpainted blast-cleaned faying surfaces must be protected from inadvertent paint overspray. *AASHTO LRFD* Article 6.13.2.8 requires that in uncoated joints, paint (including any inadvertent overspray) be excluded from areas closer than one bolt diameter but not less than 1.0 in. from the edge of any hole and all areas within the bolt pattern. Tests have demonstrated that for material with thickness in the range of 3/8 in. to ¾ in., the transfer of shear by friction between contact surfaces is concentrated in an annular ring around and close to the bolts (Polyzois and Frank, 1986). Paint on the contact surfaces away from the edge of the bolt hole by not less than 1.0 in. nor the bolt diameter did not reduce the slip resistance. For joints in thicker material, the minimum bolt pretension may not be adequate to completely flatten and pull the thick material into tight contact around every bolt in the pattern. Therefore, it is specified that all bolt areas within the pattern be kept free of paint, including any overspray.

Joints with painted faying surfaces must be blast-cleaned and coated with a paint that has been qualified by test as a Class A or Class B coating. A Class A coating

will not reduce the slip coefficient below that provided by clean mill scale, and a Class B coating will not reduce the slip coefficient below that provided by blast-cleaned steel surfaces. A test method to determine the mean slip coefficient in order to qualify a particular coating for use according to the *AASHTO LRFD* Specifications is provided in Appendix A of RCSC (2014). The method includes long-term creep test requirements to ensure that the creep deformations caused by the bolt clamping force and joint shear are such that the coating will provide satisfactory long-term performance under sustained loading (Yura and Frank, 1985). Re-qualification of the coating is required if any essential variable is changed. According to *AASHTO LRFD* Article 6.13.2.8, the contract documents must state that coated joints not be assembled before the coatings have cured the minimum time used in the qualifying test. Research has indicated that all curing of faying surface coatings ceases at the time the joints are assembled and tightened and that coatings that are not fully cured act as lubricants severely reducing the slip resistance of the joint (Frank and Yura, 1981). The specification permits the use of faying-surface coatings with a slip resistance less than Class A, (i.e. K_s = 0.33) subject to the approval of the Engineer, provided that the mean slip coefficient is determined by the specified test procedure.

Galvanized faying surfaces must be hot-dip galvanized according to the procedures given in the ASTM A123 Specification and then must be subsequently roughened by means of hand wire brushing. The mean slip coefficient for clean hot-dip galvanized surfaces is on the order of 0.19 compared to 0.33 for clean mill scale (RCSC, 2014). Research has indicated that the slip coefficient for galvanized surfaces can be significantly improved by hand wire brushing or light “brush-off” grit blasting (Birkemoe and Herrschaft, 1970). The treatment must be controlled in order to achieve visible scoring or roughening. Power wire brushing is not satisfactory because it may polish rather than roughen the surface or remove the coating. Tests on surfaces that have been hand wire brushed after coating have indicated a mean slip coefficient of 0.35 (Kulak et al., 1987). The surface condition factor, K_s, for treated galvanized surfaces has been conservatively set at 0.33, which is the same as for Class A surfaces. A separate class (Class C) has been provided for galvanized surfaces to avoid potential confusion. Previous Specifications indicated a slip coefficient of 0.40 for galvanized surfaces, which assumed blast-cleaning of the surface after galvanizing; however, this is not the typical practice. Note that field experience and test results have indicated that galvanized surfaces may have a tendency to continue to slip under sustained loading illustrating a creep-type behavior (Kulak et al., 1987). Relaxation of bolt tension may also occur where hot-dip galvanized coatings are used, particularly if there are many plies of thickly coated material in the joint. In such cases, this can either be allowed for in the design or else the bolts can be re-tightened after a period of settling-in subsequent to the initial tightening.

Since faying surfaces (that are not galvanized) are typically blast-cleaned as a minimum, a Class A surface condition should only be used to compute the slip

resistance when Class A coatings are applied or when unpainted mill scale is left on the faying surface. Most commercially available primers will qualify as Class B coatings.

EXAMPLE

Calculate the factored slip resistance for a 7/8-in. diameter ASTM A325 high-strength bolt assuming a Class B surface condition for the faying surface, standard holes and two slip planes per bolt.

The nominal slip resistance per bolt, R_n, is computed as (Equation 6.6.4.2.4.2-1):

$$R_n = K_h K_s N_s P_t$$

For standard holes: K_h = 1.0 (Table 6.6.4.2.4.2-1)
For a Class B surface: K_s = 0.50 (Table 6.6.4.2.4.2-2)
For two slip planes: N_s = 2
For a 7/8" A325 bolt: P_t = 39 kips (Table 6.2.3.1.2-1)

Therefore: $R_n = 1.0(0.50)(2)(39) = 39.0 \text{ kips/bolt}$

Since from Equation 6.6.4.2.4.1-1:

$$R_r = R_n$$

$$R_r = 39.0 \text{ kips/bolt}$$

6.6.4.2.5 Strength Limit State

6.6.4.2.5.1 General

AASHTO LRFD Article 6.13.2.2 specifies that the factored resistance, R_r, of a bolt at the strength limit state (in a slip-critical or bearing-type connection) is to be taken as either:

$$R_r = \phi R_n \qquad \text{Equation 6.6.4.2.5.1-1}$$

AASHTO LRFD Equation 6.13.2.2-2

or:

$$T_r = \phi T_n \qquad \text{Equation 6.6.4.2.5.1-2}$$

AASHTO LRFD Equation 6.13.2.2-3

where:

ϕ = resistance factor for bolts specified in *AASHTO LRFD* Article 6.5.4.2
- = ϕ_s for bolts in shear = 0.80 (for ASTM A325 and A490 bolts); 0.65 (for ASTM A307 bolts)
- = ϕ_t for bolts in tension = 0.80 (for ASTM A325, A490 and A307 bolts)
- = ϕ_{bb} for bolts bearing on connected material = 0.80
- = ϕ_y for yielding in gross section for connected elements in tension = 0.95
- = ϕ_u for fracture in net section for connected elements in tension =0.80
- = ϕ_{vu} for connected elements in shear, rupture in connection element = 0.80

R_n = nominal resistance of the bolt, connected element or connected material (kips)
- = for bolts in shear as specified in *AASHTO LRFD* Article 6.13.2.7 (Section 6.6.4.2.5.2)
- = for connected material in bearing joints as specified in *AASHTO LRFD* Article 6.13.2.9 (6.6.4.2.5.3)
- = for connected elements in tension or shear as specified in *AASHTO LRFD* Article 6.13.5.2 (Sections 6.6.4.2.5.6.1 and 6.6.4.2.5.6.2)

T_n = nominal resistance of the bolt (kips)
- = for bolts in axial tension as specified in *AASHTO LRFD* Article 6.13.2.10 (Section 6.6.4.2.5.4)
- = for bolts in combined axial tension and shear as specified in *AASHTO LRFD* Article 6.13.2.11 (Section 6.6.4.2.5.5)

6.6.4.2.5.2 Shear Resistance of Bolts

The shear resistance of bolts is covered in *AASHTO LRFD* Article 6.13.2.7 (note that the shear resistance of anchor bolts, which are not covered herein, is specified in *AASHTO LRFD* Article 6.13.2.12). The shear failure of a bolt is illustrated in Figure 6.6.4.2.5.2-1.

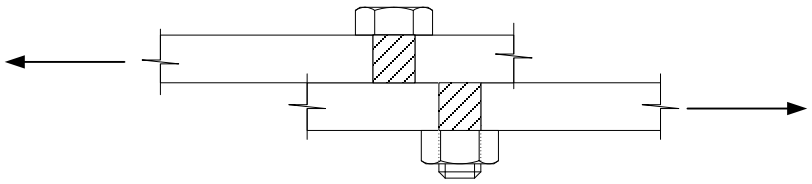

Figure 6.6.4.2.5.2-1 Shear Failure of a Bolt

AASHTO LRFD Article 6.13.2.7 specifies that the nominal shear resistance of a high-strength bolt (A 325 or A 490 bolt) or an A 307 bolt at the strength limit state in joints whose length between extreme fasteners measured parallel to the line of action of the force is less than 50.0 in. is to be taken as:

Where threads are excluded from the shear plane:

$$R_n = 0.48 A_b F_{ub} N_s \qquad \text{Equation 6.6.4.2.5.2-1}$$

AASHTO LRFD Equation 6.13.2.7-1

Where threads are included in the shear plane:

$$R_n = 0.38 A_b F_{ub} N_s \qquad \text{Equation 6.6.4.2.5.2-2}$$

AASHTO LRFD Equation 6.13.2.7-2

where:

A_b = area of the bolt corresponding to the nominal diameter (in.^{2})
F_{ub} = specified minimum tensile strength of the bolt specified in *AASHTO LRFD* Article 6.4.3 (ksi)
N_s = number of shear planes per bolt

For a bolt in a connection greater than 50.0 in. in length, the nominal shear resistance is to be taken as 0.80 times the value given by Equation 6.6.4.2.5.2-1 or Equation 6.6.4.2.5.2-2, as applicable. The nominal shear resistance is based on the observation that the shear strength of a single high-strength bolt is about 0.60 times the tensile strength F_{ub} of the bolt (Kulak at al., 1987).

The shear resistance is not affected by the pretension in the bolts provided the connected material is in contact at the faying surfaces. In shear connections with more than two bolts in the line of force, the average bolt strength decreases as the joint length increases due to the nonuniform bolt shear force distribution caused by deformation of the connected material. For joints up to 50.0 in. in length, a single reduction factor of 0.80 is implicitly applied to the 0.60 multiplier rather than providing a function that reflects the decrease in average bolt strength with joint length (0.80 * 0.60 equals the 0.48 multiplier given in Equation 6.6.4.2.5.2-1). This was felt not to adversely affect the economy of very short joints. For bolts in joints longer than 50.0 in., the nominal shear resistance must be reduced by an additional 20 percent. For bolted flange splices, note that the 50.0 in. length is to be measured between the extreme bolts on only one side of the connection (*AASHTO LRFD* Article C6.13.2.7). The greater than 50.0 in. length reduction does not apply when the distribution of shear force is essentially uniform along the joint, such as in a bolted web splice (RCSC, 2014).

When bolts are positioned so that they cross two planes of contact (i.e. N_s = 2), this is referred to as ′double shear′. Double shear is a symmetrical loading situation with regard to the shear planes and direction of shear transfer. When there is a single

plane of contact involved in the load transfer (i.e. N_s = 1), this is referred to as ′single shear′, which is an unsymmetrical loading situation.

The average ratio of the nominal shear resistance for bolts with threads included in the shear plane to the nominal shear resistance for bolts with threads excluded from the shear plane is 0.83 with a standard deviation of 0.03 (Frank and Yura, 1981). Therefore, a reduction factor of 0.80 is conservatively used to account for the nominal shear resistance when threads are included in the shear plane but calculated with the area corresponding to the nominal bolt diameter (0.48 * 0.80 equals the 0.38 multiplier given in Equation 6.6.4.2.5.2-2).

In determining whether the threads are excluded from the shear planes, the thread length of the bolt is to be determined as two thread pitches greater than the specified thread length. If the threads of a bolt are included in a shear plane of a joint, the nominal shear resistance of the bolts in all shear planes of the joint is to conservatively be taken from Equation 6.6.4.2.5.2-2. That is, for bolts in double shear with a non-threaded shank in one shear plane and a threaded section in the other shear plane, the sharing of the load between the two dissimilar shear areas is uncertain. Also, knowledge about the specific bolt placement, which might result in both shear planes being in the threaded section, is not ordinarily available to the Design Engineer.

Since the threaded length of an A 307 bolt is not as predictable as that of a high-strength bolt, the nominal shear resistance of an A 307 bolt must always be based on Equation 6.6.4.2.5.2-2. Also, A 307 bolts with a long grip (i.e. the total thickness of the plies of a joint through which the bolt passes exclusive of any washers or load-indicating devices) tend to bend reducing their shear resistance. Therefore, *AASHTO LRFD* Article 6.13.2.7 requires that when the grip length of an A 307 bolt exceeds 5.0 bolt diameters, the nominal shear resistance must be lowered 1.0 percent for each 1/16 in. of grip in excess of 5.0 bolt diameters.

EXAMPLE

Calculate the factored shear resistance for a 7/8-in. diameter A325 high-strength bolt in double shear assuming the threads are excluded from the shear planes. Assume the length between extreme fasteners measured parallel to the line of action of the force is less than 50 in. Therefore, the nominal shear resistance is taken as (Equation 6.6.4.2.5.2-1):

$$R_n = 0.48 A_b F_{ub} N_s$$

For a 7/8” A325 bolt: $A_b = \frac{\pi(0.875)^2}{4} = 0.601\,\text{in}^2$

F_{ub} = 120 ksi (*AASHTO LRFD* Article 6.4.3.1)
For double shear: N_s = 2

Therefore:

$$R_n = 0.48(0.601)(120)(2) = 69.2 \text{ kips / bolt}$$

Since from Equation 6.6.4.2.5.1-1:

$$R_r = \phi_s R_n$$

$$R_r = 0.80(69.2) = 55.4 \text{ kips/bolt}$$

6.6.4.2.5.3 Bearing Resistance of Connected Material

The bearing resistance of the connected material in a bolted connection is covered in *AASHTO LRFD* Article 6.13.2.9. A bearing failure relates generally to either deformation of the bolt or deformation around a bolt hole, as illustrated in Figure 6.6.4.2.5.3-1 Parts A and B, respectively.

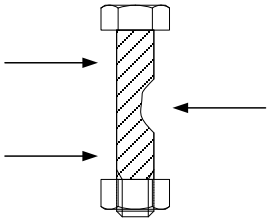

PART A

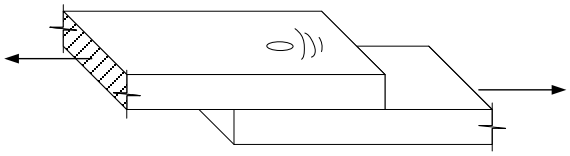

PART B

Figure 6.6.4.2.5.3-1 Bearing Failure of Bolt (Part A) and Connected Material (Part B)

After a major slip has occurred in a slip-critical connection, one or more bolts are in bearing against the side of the hole. The contact pressure between the bolt and connected material can be expressed as the bearing stress on the bolt or connected material. Tests have always shown that the bearing stress on the bolt is not critical

(Kulak et al., 1987). For simplicity, the bearing stress is assumed to be a uniform stress distribution equal to the load transmitted by the bolt divided by the bearing area taken as the bolt diameter times the thickness of the connected material. *AASHTO LRFD* Article 6.13.2.9 specifies that the effective thickness of connected material with countersunk holes is to be taken as the thickness of the connected material minus one-half the depth of the countersink.

The actual failure mode depends on the end distance or clear distance between bolts, the bolt diameter and the thickness of the connected material. Either the bolt will split out through the end of the plate because of insufficient end distance, or else excessive deformations are developed in the connected material adjacent to the bolt hole (Figure 6.6.4.2.5.3-1 Part B) because of insufficient clear distance between the bolts.

The end distance required to prevent the plate from splitting out can be approximated by equating the maximum load, R_n, transmitted by the end bolt to the force corresponding to shear failure of the plate material of thickness, t, along the dotted Lines 1-1 and 2-2 shown in Figure 6.6.4.2.5.3-2. Although actual splitting would occur along the Lines 1-1 and 2-2 in Figure 6.6.4.2.5.3-2, the angle, α, will be assumed equal to zero in order to compute a lower-bound resistance and failure will be assumed to occur along the two solid lines instead.

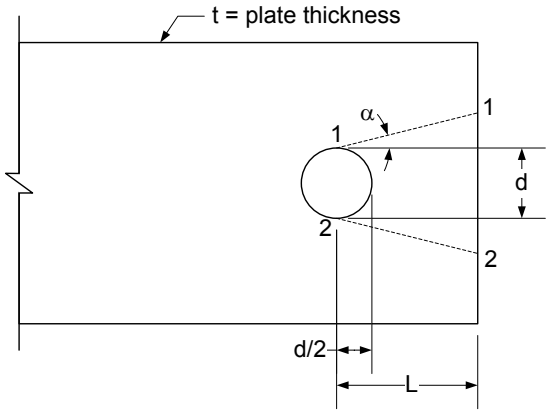

Figure 6.6.4.2.5.3-2 Bearing Resistance Related to End Distance

Therefore:

$$R_n = 2t(L - \frac{d}{2})\tau_u \qquad \text{Equation 6.6.4.2.5.3-1}$$

where τ_u is the ultimate shear resistance of the plate material. For commonly used steels, τ_u can be assumed approximately equal to $0.75F_u$, where F_u is the ultimate tensile strength of the plate material. Therefore, substituting $0.75F_u$ for τ_u and the clear distance, L_c, from the edge of the hole to the end of the plate in the direction of

the force for (L – d/2) in Equation 6.6.4.2.5.3-1 (to simplify the calculations for oversize and slotted holes) gives:

$$R_n = 1.5 L_c t F_u \qquad \text{Equation 6.6.4.2.5.3-2}$$

Equation 6.6.4.2.5.3-2 can be used to determine the bearing resistance between bolt holes by substituting the clear distance between adjacent holes for the clear end distance. The same bearing resistance applies regardless of the bolt shear resistance or the presence or absence of bolt threads in the bearing area. An alternative equivalent relationship relating the bearing stress r_n to F_u as a function of the L/d ratio based conservatively on test results of finger-tight bolts (Kulak et al., 1987) is given in *AASHTO LRFD* Article C6.13.2.9 as follows:

$$\frac{L}{d} \geq \frac{r_n}{F_u} \qquad \text{Equation 6.6.4.2.5.3-3}$$

AASHTO LRFD Equation C6.13.2.9-1

Kulak et al. (1987) further recommends that the ratio of r_n/F_u be limited to 3.0 in order to limit deformations under the factored loads. Substituting $r_n = R_n/dt$ in this ratio and rearranging gives an upper-bound bearing resistance of:

$$R_n = 3.0 F_u d t \qquad \text{Equation 6.6.4.2.5.3-4}$$

Equations 6.6.4.2.5.3-2 and 6.6.4.2.5.3-4 are given as the bearing resistance equations in RCSC (2014) for cases where deformation at the bolt holes at service load is not a design consideration for standard holes, oversize holes, or short-slotted holes loaded in any direction and long-slotted holes loaded parallel to the applied bearing force.

The more conservative equations from RCSC (2014) for the preceding cases when deformation at the bolt holes at service load *is* a design consideration are instead specified as follows in *AASHTO LRFD* Article 6.13.2.9 (and are to be applied under the factored loads at the strength limit state):

$$R_n = 1.2 L_c t F_u \leq 2.4 d t F_u \qquad \text{Equation 6.6.4.2.5.3-5}$$

AASHTO LRFD Equations 6.13.2.9-1 & 6.13.2.9-2

Equation 6.6.4.2.5.3-5 is derived based on tests that showed that the total elongation of a standard hole that is loaded to obtain the maximum recommended bearing resistance given by Equation 6.6.4.2.5.3-4 is on the order of the diameter of the bolt

(Kulak et al., 1987). Based on these tests, to prevent elongations exceeding 0.25 inches, a reduced limit on the bearing resistance of $2.4dtF_u$ is specified according to Equation 6.6.4.2.5.3-5.

For long-slotted holes perpendicular to the applied bearing force, the bending component of the deformation in the connected material becomes more critical (RCSC, 2014). Therefore, for this case, the bearing resistance is further limited as follows:

$$R_n = L_c t F_u \le 2.0 dt F_u \qquad \text{Equation 6.6.4.2.5.3-6}$$

AASHTO LRFD Equations 6.13.2.9-3 & 6.13.2.9-4

The design bearing resistance is expressed in terms of a single bolt, although it is truly for the connected material adjacent to the bolt. Therefore, in calculating the nominal bearing resistance for the connected part, the total bearing resistance may be taken as the sum of the bearing resistances of the individual bolts (holes) parallel to the line of the applied force.

EXAMPLE

Calculate the total factored bearing resistance of the flange splice plate shown in Figure 6.6.4.2.5.3-3 subject to a tensile force, *P*. The plate material is ASTM ASTM A709/A709M Grade 50W steel. From *AASHTO LRFD* Table 6.4.1-1, F_u for Grade 50W steel is 70 ksi. The bolts are 7/8-inch diameter ASTM A325 bolts placed in standard holes.

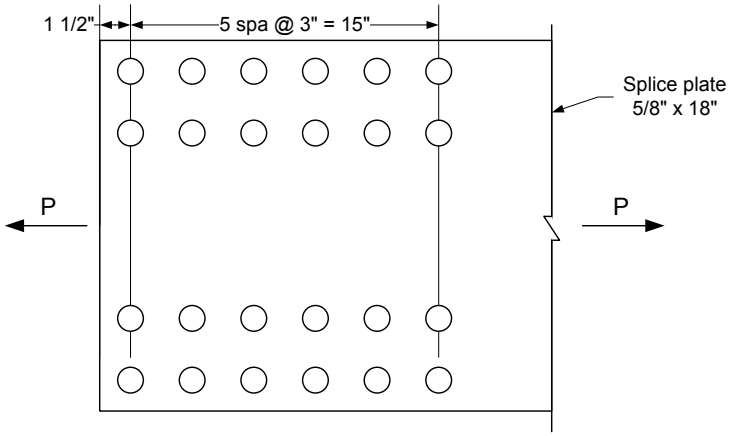

Figure 6.6.4.2.5.3-3 Bearing Resistance Example – Flange Splice Plate

The bearing resistance of the connected part is calculated as the sum of the bearing resistances of the individual bolt holes parallel to the line of the applied force. As specified in *AASHTO LRFD* Article 6.8.3, for design calculations, the width of standard bolt holes is to be taken as the nominal diameter of the hole. Therefore, the width of the holes is to be taken as 0.9375 in. (Table 6.6.4.2.3.1-1)

For standard holes, the nominal bearing resistance, R_n, parallel to the applied bearing force is to be taken as follows (Equation 6.6.4.2.5.3-5):

$$R_n = 1.2L_c tF_u \le 2.4dtF_u$$

For the four bolts adjacent to the end of the splice plate, the end distance is 1.5 in. Therefore, the clear end distance, L_c, between the edge of the hole and the end of the splice plate is:

$$L_c = 1.5 - \frac{0.9375}{2} = 1.03 \text{ in.}$$

Therefore:

$$R_n = 4(1.2L_c tF_u) = 4\left[1.2(1.03)(0.625)(70)\right] = 216.3 \text{ kips (governs)}$$

or: $$R_n = 4(2.4dtF_u) = 4\left[2.4(0.875)(0.625)(70)\right] = 367.5 \text{ kips}$$

For the other twenty bolts, the center-to-center distance between the bolts in the direction of the applied force is 3.0 in. Therefore, the clear distance L_c between the edges of the adjacent holes is:

$$L_c = 3.0 - 0.9375 = 2.0625 \text{ in.}$$

Therefore:

$$R_n = 20(1.2L_c tF_u) = 20\left[1.2(2.0625)(0.625)(70)\right] = 2{,}165 \text{ kips}$$

or:

$$R_n = 20(2.4dtF_u) = 20\left[2.4(0.875)(0.625)(70)\right] = 1{,}837 \text{ kips (governs)}$$

The total nominal bearing resistance of the splice plate is therefore:

$$R_n = 216.3 \text{ kips} + 1{,}837 \text{ kips} = 2{,}053 \text{ kips}$$

Since from Equation 6.6.4.2.5.1-1:

$$R_r = \phi_{bb} R_n$$

$$R_r = 0.80(2{,}053) = 1{,}642 \text{ kips}$$

6.6.4.2.5.4 Tensile Resistance of Bolts

6.6.4.2.5.4.1 General

The tensile resistance of bolts is covered in *AASHTO LRFD* Article 6.13.2.10. The tensile failure of a bolt is illustrated in Figure 6.6.4.2.5.4.1-1.

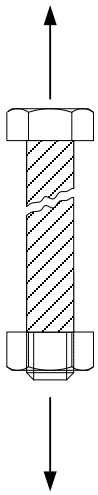

Figure 6.6.4.2.5.4.1-1 Tensile Failure of a Bolt

Axial tension occurring without simultaneous shear occurs in bolts for tension members such as hangers or other members whose line of action is perpendicular to the member to which it is fastened. The applied tensile force must be taken as the force due to externally applied loads plus any tension resulting from prying action produced by deformation of the connected parts. Prying action is not discussed herein; further information on prying action may be found in AISC (2010) and Kulak et al. (1987). The tensile resistance of bolts (as discussed herein) must typically be considered in combination with simultaneous shear for bolted bracing member connections (Section 6.6.4.2.5.5).

AASHTO LRFD Article 6.13.2.10.1 specifies that high-strength bolts subject to axial tension must be pretensioned to the level given in Table 6.2.3.1.2-1 regardless of whether the design is for a slip-critical or a bearing-type connection. According to *AASHTO LRFD* Article 6.13.2.10.2, the nominal tensile resistance of a bolt, T_n, independent of any initial tightening force is to be taken as:

$$T_n = 0.76 A_b F_{ub}$$ Equation 6.6.4.2.5.4.1-1

AASHTO LRFD Equation 6.13.2.10.2-1

where:

A_b = area of the bolt corresponding to the nominal diameter (in.^{2})
F_{ub} = tensile strength of the bolt specified in *AASHTO LRFD* Article 6.4.3 (ksi)

The tensile resistance of a bolt is the product of the tensile strength of the bolt and the tensile stress area through the threaded portion of the bolt given by Equation 6.2.3.1.2-1. The tensile stress area is approximately 76 percent of the nominal cross-sectional area of the bolt for the usual sizes of structural bolt (RCSC, 2014). Hence, the nominal tensile resistance per unit area (based on the nominal area of the bolt) is taken as 76 percent of the tensile strength of the bolt.

The specified nominal tensile resistance is approximately equal to the initial tightening force specified in Table 6.2.3.1.2-1. Thus, when a tensile force is applied to a high-strength bolt that has been properly pretensioned, the increase in the bolt tension is generally much smaller than the applied load.

Consider a single high-strength bolt and a portion of two connected parts of thickness *t* subject to an externally applied tensile force, *P*, as shown in Figure 6.6.4.2.5.4.1-2 Part A. Prior to application of the external force, the bolt is installed with a pretension force, T_b. As shown in Figure 6.6.4.2.5.4.1-2 Part B, this causes the two parts to be initially compressed by an amount C_i. C_i must equal T_b for equilibrium. The external force *P* is then applied as shown in Figure 6.6.4.2.5.4.1-2 Part C, and for equilibrium, *P* plus C_f must equal T_f, where the subscript *f* refers to the final condition after the application of the force.

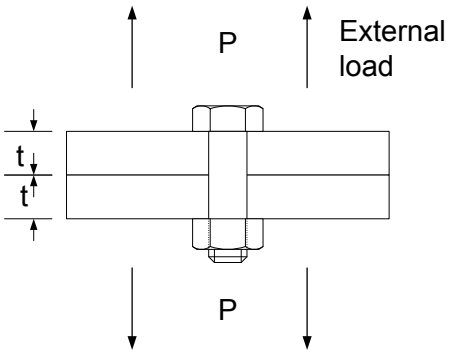

PART A

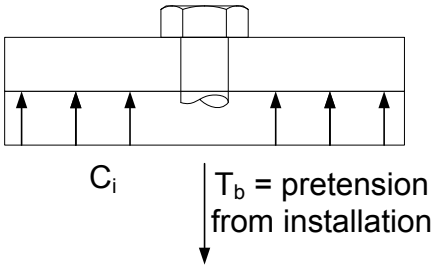

PART B

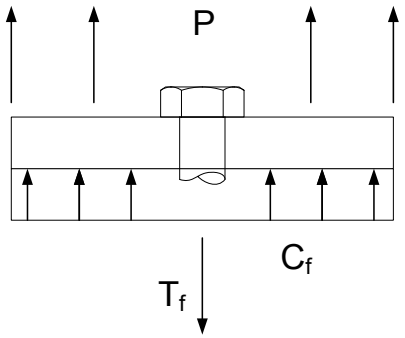

PART C

Figure 6.6.4.2.5.4.1-2 Pretensioning Effect on a Bolted Joint

The bolt elongates as the tensile force is applied to the joint and the compressed plates simultaneously expand as the initial contact pressure is reduced. The applied force is offset by the increase in the bolt tension and the decrease in contact pressure. As illustrated in Salmon and Johnson (1996), the increase in the bolt tension is a function of the relative stiffness of the bolt and connected plates, but it is typically minimal until the parts separate (Kulak et al., 1987). There will be little increase in bolt force above the pretension load at service load levels. After the

parts separate, the bolt will act as a tension member with the applied force equaling the bolt tension. As a result, bolts in connections subject to axial tension are required to be fully pretensioned.

As mentioned above, pretensioning imposes a small axial elongation of the bolt. A joint subsequently loaded in tension, shear or combined tension and shear imposes significant deformations in the bolt prior to failure that override the small initial elongation and remove the pretensioning. Tests confirm that the initial pretension that would be sustained after the applied load is removed is essentially zero before the bolts fail in shear (Kulak et al., 1987). Therefore, the tensile and shear resistances of the bolt are unaffected by the initial pretensioning of the bolt. Any residual torsion induced in the bolt during installation is also small and will be removed when the bolt is loaded to the point of plate separation. Hence, any effect of torsion on the tensile resistance of the bolt need not be considered (Kulak et al., 1987).

6.6.4.2.5.4.2 Bolt Tensile Fatigue

As specified in *AASHTO LRFD* Article 6.13.2.10.3, properly pretensioned high-strength bolts subject to fatigue in axial tension must satisfy *AASHTO LRFD* Equation 6.6.1.2.2-1 (Equation 6.5.5.2.2.1.5-1). The stress range (Δf) in the equation is to be taken as the stress range in the bolt due to the passage of the 72-kip fatigue design load (plus the 15 percent dynamic load allowance) specified in *AASHTO LRFD* Article 3.6.1.4, plus any prying force resulting from the cyclic application of the fatigue load (the initial tension in the bolts is not to be included). The stress range is to be computed using the nominal diameter of the bolt. In calculating the nominal fatigue resistance $(\Delta F)_n$ from *AASHTO LRFD* Equation 6.6.1.2.5-1 (Equation 6.5.5.2.2.1.4-3) or 6.6.1.2.5-2 (Equation 6.5.5.2.2.1.4-4), as applicable, the detail category constant A and the constant-amplitude fatigue threshold $(\Delta F)_{TH}$ for ASTM A325 and A490 bolts in axial tension are to be taken directly from *AASHTO LRFD* Tables 6.6.1.2.5-1 and 6.6.1.2.5-3, respectively, when the bolts are fully pretensioned and all threads are located within the grip. Otherwise, Condition 9.2 in *AASHTO LRFD* Table 6.6.1.2.3-1 applies.

Tests of various single-bolt assemblies and joints with bolts in tension subjected to repeated external loads that resulted in eventual failure of the pretensioned high-strength bolts indicated that properly tightened high-strength bolts are not adversely affected by repeated application of service-load tensile stress (Kulak et al., 1987); that is, the nominal fatigue resistance of the bolts in such applications is relatively high. However, since a limited range of prying effects was investigated in these studies, the assumption is made that the connected material is sufficiently stiff that any prying force is a relatively small part of the applied tension. *AASHTO LRFD* Article 6.13.2.10.3 limits the calculated prying force to 30 percent of the externally applied load when bolts are subject to tensile fatigue loading. As indicated in RCSC

(2014), this limit is based on limited investigations of prying effects under fatigue loading.

Since low carbon ASTM A307 bolts are of lower strength and are not pretensioned, *AASHTO LRFD* Article 6.13.2.10.3 prohibits their use in connections subjected to fatigue loading.

6.6.4.2.5.5 Combined Tensile and Shear Resistance of Bolts

The resistance of bolts under combined axial tension and shear is covered in *AASHTO LRFD* Article 6.13.2.11. Examples of connections in which the bolts would be subject to combined tension and shear are shown in Figure 6.6.4.2.5.5-1.

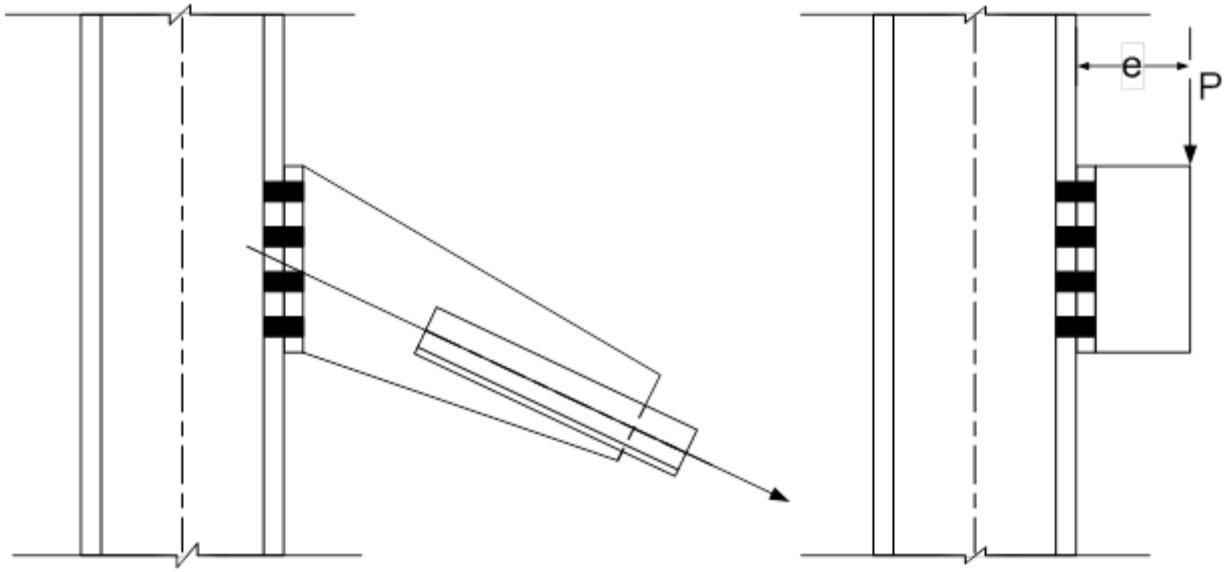

Figure 6.6.4.2.5.5-1 Bolted Connections Subject to Combined Tension and Shear

Once a bolt slips and goes into bearing, the bolt yields under the effects of combined tension and shear at a lower load than if only shear or tension were present. Tests on single high-strength bolts subject to various combinations of tension and shear in this condition were conducted at the University of Illinois (Chesson et al., 1965). From these tests, it was determined that when both shear and tensile forces act on a high-strength bolt at the strength limit state, the interaction can be conveniently expressed by an elliptical interaction relationship as follows (RCSC, 2014):

$$\left[\frac{T_u}{(R_r)_t}\right]^2 + \left[\frac{P_u}{(R_r)_s}\right]^2 \qquad \text{Equation 6.6.4.2.5.5-1}$$

where:

P_u = shear force on the bolt due to the factored loads (kips)
T_u = tensile force on the bolt due to the factored loads (kips)
$(R_r)_s$ = factored resistance of the bolt in shear (kips)
$(R_r)_t$ = factored resistance of the bolt in tension (kips)

Equation 6.6.4.2.5.5-1 accounts for the connection length effect on bolts loaded in shear, the ratio of the shear resistance to tensile resistance of threaded bolts, the ratio of root area to nominal body area of the bolt and the ratio of the tensile stress area to the nominal body area of the bolt. Equations for various cases based on Equation 6.6.4.2.5.5-1 can be found in RCSC (1988).

A conservative simplification of the interaction relationship given by Equation 6.6.4.2.5.5-1 is used in *AASHTO LRFD* Article 6.13.2.11. The nominal tensile resistance, T_n, of a bolt subjected to combined shear and axial tension is taken as follows:

- If $\frac{P_u}{R_n} \le 0.33$, then:

$$T_n = 0.76 A_b F_{ub}$$ Equation 6.6.4.2.5.5-2

AASHTO LRFD Equation 6.13.2.11-1

- If $\frac{P_u}{R_n} > 0.33$, then:

$$T_n = 0.76 A_b F_{ub} \sqrt{1 - \left(\frac{P_u}{\phi_s R_n} \right)^2}$$ Equation 6.6.4.2.5.5-3

AASHTO LRFD Equation 6.13.2.11-2

where:

ϕ_s = resistance factor for bolts in shear specified in *AASHTO LRFD* Article 6.5.4.2 (= 0.80)
A_b = area of the bolt corresponding to the nominal diameter (in.^{2})
F_{ub} = tensile strength of the bolt specified in *AASHTO LRFD* Article 6.4.3 (ksi)
P_u = factored shear force on the bolt (kips)
R_n = nominal shear resistance of the bolt determined as specified in Article 6.13.2.7 (Section 6.6.4.2.5.2) (kips)

In other words, no reduction in the nominal tensile resistance of the bolt is required when the factored shear force does not exceed 33 percent of the nominal shear resistance of the bolt.

The nominal resistance of a bolt in a slip-critical connection subject to combined tension and shear under service loads (i.e. under Load Combination Service II) was discussed previously in Section 6.6.4.2.4.2.

In the bracket connection shown in Figure 6.6.4.2.5.5-2 Part A, the eccentric load, *P*, results in a moment on the connection that produces both shear and tension in the upper bolts. The tension is largest on the top row of bolts. As shown in Figure 6.6.4.2.5.5-2 Part B, the neutral axis under the bending moment, *M*, due to the factored loads occurs at the centroid of the rectangular contact area (i.e. at *d*/2). The initial pretension in the high-strength bolts introduces a precompression stress, f_{bi}, in the contact area of the joined plates (Figure 6.6.4.2.5.5-2 Part C). Assuming this initial compression stress is uniform over the contact area, *bd*, this stress can be computed as:

$$f_{bi} = \frac{\sum T_i}{bd} \qquad \text{Equation 6.6.4.2.5.5-4}$$

where ΣT_i is the minimum required pretension from Table 6.2.3.1.2-1 times the number of bolts in the connection. The tensile stress at the top of the contact area, f_{tb}, due to the applied moment (Figure 6.6.4.2.5.5-2 Part D) is computed as:

$$f_{tb} = \frac{M\,d/2}{I} = \frac{6M}{bd^2} \qquad \text{Equation 6.6.4.2.5.5-5}$$

As shown in Figure 6.6.4.2.5.5-2 Part E, it should be checked that f_{tb} does not exceed f_{bi} in order to ensure that compression remains between the joined parts at the top of the connection. The tensile load, T_u, on the top bolt due to the factored loads is equal to f_{tb} times the bolt tributary area, or the width, *b*, times the bolt spacing, *p*, divided by the number of vertical rows of bolts, *n*; i.e. $T_u = f_{tb}bp/n$. Substituting f_{tb} from Equation 6.6.4.2.5.5-5 gives:

$$T_u = \frac{6Mp}{nd^2} \qquad \text{Equation 6.6.4.2.5.5-6}$$

Assuming the top bolt is approximately *p*/2 from the top, T_u can be modified as follows (Salmon and Johnson, 1996):

$$T_u = \frac{6Mp}{nd^2}\left(\frac{d-p}{d}\right) \qquad \text{Equation 6.6.4.2.5.5-7}$$

For the typical case where all bolts in the connection are the same size, and where f_{bi} is not overcome by f_{tb}, it is shown in Salmon and Johnson (1996) that T_u can also be computed from the following simplified formula:

$$T_u = \frac{My_b}{\sum y^2} \qquad \text{Equation 6.6.4.2.5.5-8}$$

where y_b is the vertical distance from the centroid of the connection to the extreme row of bolts, and y is the vertical distance from the centroid of the connection to each bolt.

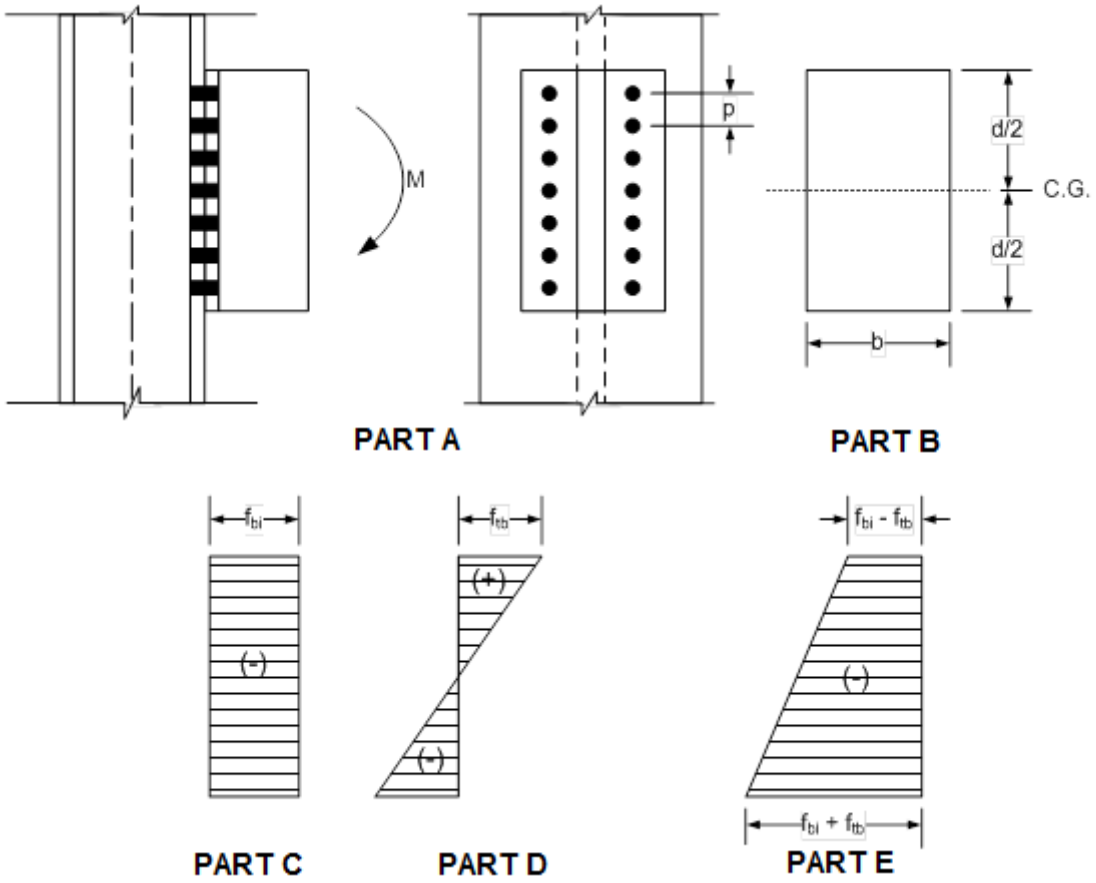

Figure 6.6.4.2.5.5-2 Tension and Shear from Eccentric Loading – Stresses on Contact Area

The same equations can be used to calculate T_u for use in Equation 6.6.4.2.4.2-2 at the service limit state (i.e. under the Service II Load Combination). The shear force, P_u, in each bolt due to the factored loads can be taken simply as the total load, P, divided by the number of bolts in the connection.

EXAMPLE

Check the bolts in the slip-critical bracket connection shown in Figure 6.6.4.2.5.5-1 at the strength limit state (i.e. assuming the bolts have slipped and gone into bearing). The number of vertical rows of bolt in the connection *n* is equal to two. The total force *P* due to the factored loads is 150 kips applied at an eccentricity *e* of 3 in. Assume 7/8-inch diameter ASTM A325 bolts in standard holes with the threads not excluded from the shear plane. The vertical pitch between bolts *p* is 3 in. The end distance for the top and bottom bolts is 1.5 in. The bracket dimensions are *b* = 5.5 in. and *d* = 12 in. Assume that the connected parts are adequate and stiff enough to preclude any additional tensile force due to prying action.
From Table 6.2.3.1.2-1, the minimum required initial pretension for 7/8-inch diameter ASTM A325 bolts is 39.0 kips. Therefore, from Equation 6.6.4.2.5.5-4, the initial precompression stress f_{bi} on the contact area is equal to (8)(39.0)/(5.5)(12) = 4.73 ksi. From Equation 6.6.4.2.5.5-5, the tensile stress at the top of the bracket f_{tb} is equal to $6(150)(3)/(5.5)(12)^2$ = 3.41 ksi, which is less than f_{bi}. The pieces remain in compression (contact) at the top of the bracket.

For threads included in the shear plane, the nominal shear resistance of a bolt is computed from Equation 6.6.4.2.5.2-2 as follows:

$$R_n = 0.38 A_b F_{ub} N_s$$

For a 7/8" A325 bolt: $A_b = \dfrac{\pi(0.875)^2}{4} = 0.60 \text{ in.}^2$

F_{ub} = 120 ksi (*AASHTO LRFD* Article 6.4.3.1)

For single shear: N_s = 1

Therefore:

$$R_n = 0.38(0.60)(120)(1) = 27.4 \text{ kips/bolt}$$

The shear due to the factored loads, P_u, in each bolt is taken as *P* divided by the number of bolts. Therefore, P_u = 150 /8 = 18.75 kips. Since P_u/R_n = 18.75/27.4 = 0.68 > 0.33, the nominal tensile resistance of each bolt, T_n, under combined tension and shear is taken from Equation 6.6.4.2.5.5-3 as follows:

$$T_n = 0.76 A_b F_{ub} \sqrt{1 - \left(\frac{P_u}{\phi_s R_n} \right)^2}$$

$$T_n = 0.76(0.60)(120)\sqrt{1-\left(\frac{18.75}{(0.80)(27.4)}\right)^2} = 28.3 \text{ kips}$$

Since from Equation 6.6.4.2.5.1-2:

$$T_r = \phi_t T_n$$

$$T_r = 0.80(28.3) = 22.6 \text{ kips/bolt}$$

The tensile force in each bolt to the factored loads, T_u, may be computed from Equation 6.6.4.2.5.5-7 as follows:

$$T_u = \frac{6Mp}{nd^2}\left(\frac{d-p}{d}\right)$$

$$T_u = \frac{6(150)(3)(3)}{2(12)^2}\left(\frac{12-3}{12}\right) = 21.1 \text{ kips} < T_r = 22.6 \text{ kips} \quad \text{ok}$$

Alternatively, T_u may be computed from Equation 6.6.4.2.5.5-8 as follows:

$$T_u = \frac{My_b}{\sum y^2}$$

where y_b = 4.5 in., and $\Sigma y^2 = 4[(1.5)^2 + (4.5)^2] = 90$ in.^{2} Therefore:

$$T_u = \frac{150(3)(4.5)}{90} = 22.5 \text{ kips} < T_r = 22.6 \text{ kips} \quad \text{ok}$$

6.6.4.2.5.6 Resistance of a Connected Element

6.6.4.2.5.6.1 Tensile Resistance of a Connected Element

AASHTO LRFD Article 6.13.5.2 specifies that the factored tensile resistance, R_r, of a connected element (i.e. a splice plate, gusset plate or lateral connection plate) is to be taken as the smallest of the resistances based on yielding, net section fracture or block shear rupture.

Yield Resistance

A connected element subject to tension must be checked for yielding on the gross section. Excessive elongation due to uncontrolled yielding of the gross area can

limit the structural usefulness of the connected element so that it no longer serves its intended purpose.

According to *AASHTO LRFD* Article 6.13.5.2, the factored yield resistance of a connected element in tension is to be computed from *AASHTO LRFD* Equation 6.8.2.1-1 as follows:

$$R_r = \phi_y F_y A_g \qquad \text{Equation 6.6.4.2.5.6.1-1}$$

AASHTO LRFD Equation 6.8.2.1-1

where:

ϕ_y = resistance factor for yielding of tension members specified in *AASHTO LRFD* Article 6.5.4.2 (= 0.95)
F_y = specified minimum yield strength of the connected element (ksi)
A_g = gross cross-sectional area of the connected element (in.^{2})

Net Section Fracture Resistance

A connected element subject to tension must be checked for fracture on the net section. The connected element can fracture by failure of the net area (Figure 6.6.4.2.5.6.1-1) at a load smaller than that required to yield the gross area depending on the ratio of net to gross area, the properties of the steel (i.e. the ratio of F_u/F_y), and the end connection geometry. Holes in a member cause stress concentrations at service loads, with the tensile stress adjacent to the hole typically about three times the average stress on the net area. As the load increases and the deformation continues, all fibers across the section will achieve or eventually exceed the yield strain. Failure occurs when the localized yielding results in a fracture through the net area.

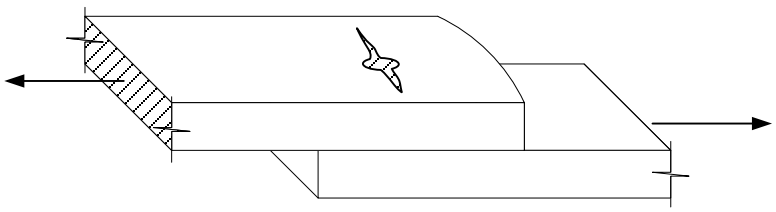

Figure 6.6.4.2.5.6.1-1 Tensile Failure of a Connected Element by Net Section Fracture

Typically, a higher margin of safety is used when considering the net section fracture resistance versus the yield resistance. According to *AASHTO LRFD* Article 6.13.5.2, the factored net section fracture resistance of a connected element in tension is to be computed from *AASHTO LRFD* Equation 6.8.2.1-2 as follows:

$$R_r = \phi_u F_u A_n R_p U$$ Equation 6.6.4.2.5.6.1-2

AASHTO LRFD Equation 6.8.2.1-2

where:

- ϕ_u = resistance factor for fracture of tension members specified in *AASHTO LRFD* Article 6.5.4.2 (= 0.80)
- F_u = tensile strength of the connected element specified in *AASHTO LRFD* Table 6.4.1-1 (ksi)
- A_n = net cross-sectional area of the connected element determined as specified in *AASHTO LRFD* Article 6.8.3 (Section 6.6.3.3.2.3) (in.^{2})
- R_p = reduction factor for holes taken equal to 0.90 for bolt holes punched full size and 1.0 for bolt holes drilled full size or subpunched and reamed to size (Section 6.6.3.3.2.1)
- U = reduction factor to account for shear lag (Section 6.6.3.3.2.4)

The calculation of the net area, A_n, is discussed in Section 6.6.3.3.2.3. According to AASHTO LRFD Article 6.13.5.2, for lateral connection plates, splice plates and gusset plates, A_n is not to be taken greater than 85 percent of the gross area, A_g, of the plate in checking Equation 6.6.4.2.5.6.1-2. Because the length of these particular elements is small compared to the overall member length, inelastic deformation of the gross area is limited. Tests have shown that when holes are present in such short elements where general yielding on the gross section cannot occur, there will be at least a 15 percent reduction in tensile capacity from that obtained based on yielding of the gross section (Kulak et al., 1987).

The reduction factor, U, in Equation 6.6.4.2.5.6.1-2 accounts for the effect of shear lag in connections, and is discussed further in Section 6.6.3.3.2.4. Shear lag is a consideration when the connection elements do not lie in a common plane and where the tensile force in the member is applied eccentrically or transmitted by connection to some but not all of the connection elements; e.g. an angle having a connection to only one leg. As specified in AASHTO LRFD Article 6.13.5.2, for short connection elements such as lateral connection plates, splice plates and gusset plates, where the elements of the cross-section essentially lie in a common plate, U is to be taken equal to 1.0.

The reduction factor, R_p, in Equation 6.6.4.2.5.6.1-2 is a reduction factor for holes, and is discussed further in Section 6.6.3.3.2.1. *AASHTO LRFD* Article 6.6.1.2.3 specifies that unless information is available to the contrary, bolt holes in cross-frame and lateral bracing members and their connection plates are to be assumed for design to be punched full size.

EXAMPLE

Calculate the net section fracture resistance of the bolted flange splice plate shown in Figure 6.6.4.2.5.6.1-2 subject to a factored tensile force, *T*. Assume that the flange has adequate net area and does not control the net section fracture resistance. Assume 7/8-inch diameter ASTM A325 bolts placed in standard holes that are drilled full size. Assume ASTM A709/A709M Grade 50W steel for the flange and splice plate. From *AASHTO LRFD* Table 6.4.1-1, F_u for Grade 50W steel is 70 ksi.

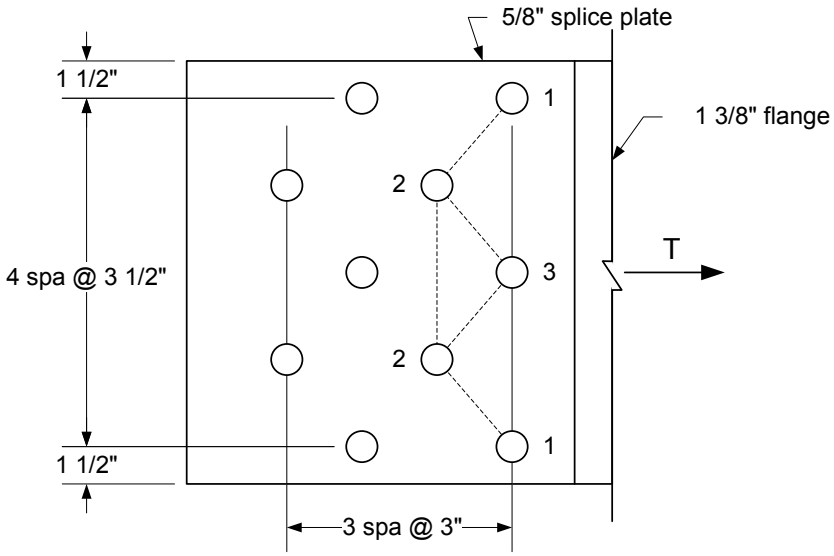

Figure 6.6.4.2.5.6.1-2 Net Section Fracture Resistance Example – Bolted Flange Splice Plate

Calculate the deduction in width for one hole. For 7/8 in. high-strength bolts in standard holes,

$$\text{Deduction} = \frac{15}{16}\text{ in.} = 0.9375\text{ in.}$$

For chain 1-1: $$A_n = [17.0 - 3(0.9375)](0.625) = 8.87\text{ in.}^2$$

For chain 1-2-3-2-1: $$A_n = \left[17.0 - 5(0.9375) + 4\frac{(3.0)^2}{4(3.5)}\right](0.625) = 9.30\text{ in.}^2$$

For chain 1-2-2-1: $$A_n = \left[17.0 - 4(0.9375) + 2\frac{(3.0)^2}{4(3.5)}\right](0.625) = 9.08 \text{ in.}^2$$

The first two cases act in conjunction with the full tensile force, *T*. The last case can be considered to act in conjunction with a reduced force of 0.9*T* since one bolt (at location 3) has transferred its share of the load prior to reaching chain 1-2-2-1. Therefore, A_n of 9.08 in^2 acting in conjunction with 0.9*T* is equivalent to A_n of 9.08/0.9 = 10.09 in^2 acting in conjunction with *T*. As a result, chain 1-1 controls and the minimum A_n is equal to 8.87 in^2.

For splice plates, *U* is to be taken equal to 1.0 (*AASHTO LRFD* Article 6.13.5.2) Since the holes are drilled full size, the reduction factor, R_p, is equal to 1.0. Therefore, from Equation 6.6.4.2.5.6.1-2:

$$R_r = \phi_u F_u A_n R_p U$$

$$R_r = 0.80(70)(8.87)(1.0)(1.0) = 497 \text{ kips}$$

According to *AASHTO LRFD* Article 6.13.5.2, for splice plates subject to tension, A_n must not exceed $0.85A_g$.

$$0.85(17.0)(0.625) = 9.03 \text{ in}^2 > A_n = 8.87 \text{ in}^2 \quad \text{ok}$$

Block Shear Rupture Resistance

The factored block shear rupture resistance, R_r, of the connected element is calculated according to Equation 6.6.3.3.2.5-1. The reader is referred to Section 6.6.3.3.2.5 for further discussion regarding block shear rupture.

EXAMPLE

Calculate the block shear rupture resistance for the outside and inside bolted flange splice plates (Figure 6.6.4.2.5.6.1-3), and the smaller girder flange at the splice (Figure 6.6.4.2.5.6.1-4) subjected to a factored tensile force, *T*. Assume 7/8-inch diameter ASTM A325 bolts placed in standard holes that are drilled full size. Assume ASTM A709/A709M Grade 50W steel for the splice plates and flange. From *AASHTO LRFD* Table 6.4.1-1, F_u for Grade 50W steel is 70 ksi.

Calculate the deduction in width for one hole. For 7/8-in. high-strength bolts in standard holes,

$$\text{Deduction} = \frac{15}{16} \text{ in.} = 0.9375 \text{ in.}$$

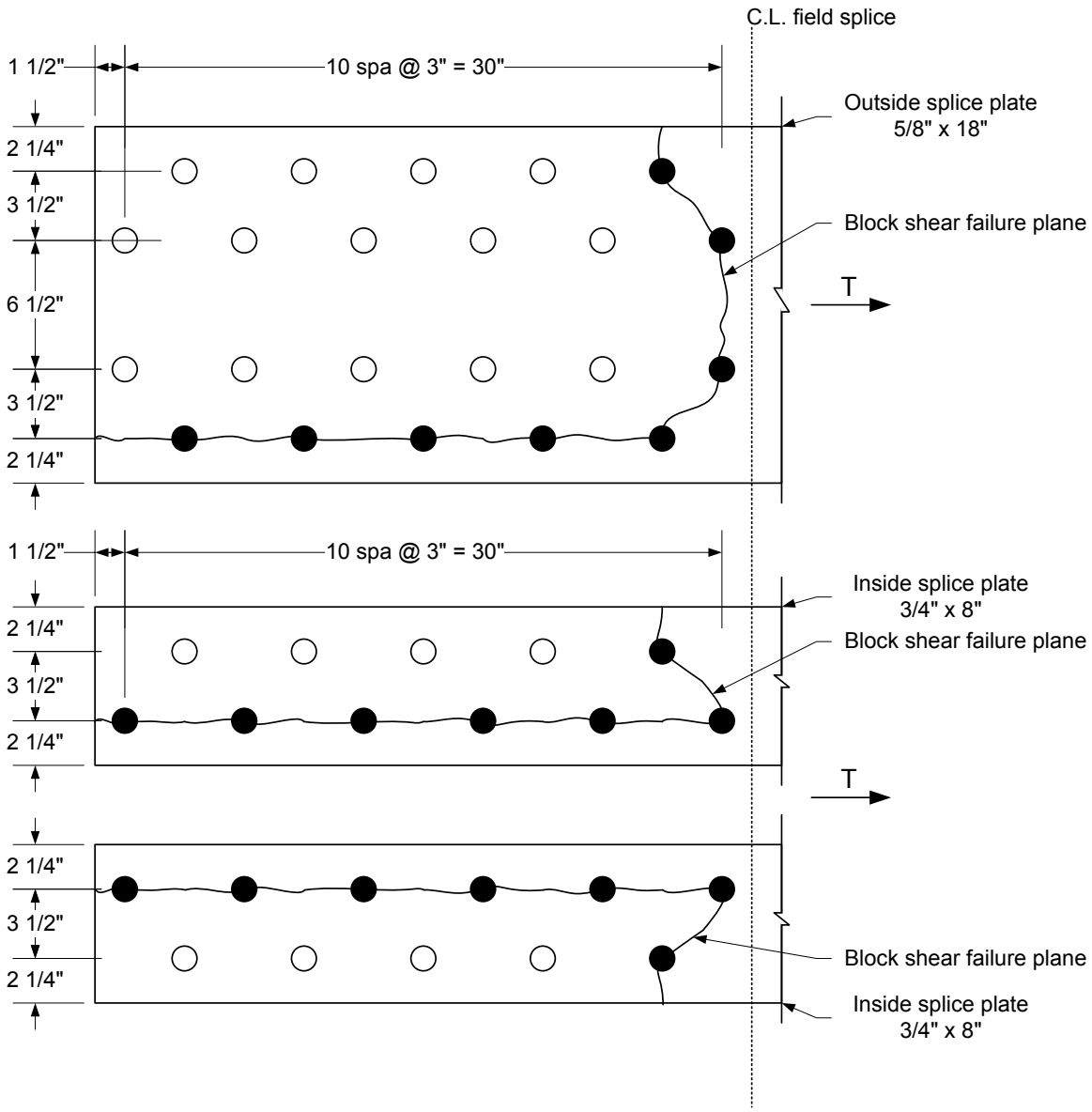

Figure 6.6.4.2.5.6.1-3 Block Shear Rupture Resistance Example – Bolted Flange Splice Plates

Calculate the factored block shear rupture resistance for the outside splice plate assuming the failure planes shown in Figure 6.6.4.2.5.6.1-3. A_{tn} is the net area along the place resisting the tensile stress. The effect of the staggered holes must be considered in determining A_{tn}.

$$A_{tn} = \left[18.0 - 2.25 - 3.5(0.9375) + 2\frac{(3.0)^2}{4(3.5)}\right](0.625) = 8.60 \text{ in.}^2$$

A_{vn} is the net area along the place resisting the shear stress. As specified in *AASHTO LRFD* Article 6.13.4, the full effective diameter of the staggered holes adjacent to the cut need not be deducted in determining A_{vn} in this case since these holes are centered more than two hole diameters from the cut. Therefore:

$$A_{vn} = [4(6.0) + 4.5 - 4.5(0.9375)](0.625) = 15.18 \text{ in.}^2$$

A_{vg} is the gross area along the plane resisting the shear stress.

$$A_{vg} = [4(6.0) + 4.5](0.625) = 17.81 \text{ in.}^2$$

The factored block shear rupture resistance, R_r, is determined as (Equation 6.6.3.3.2.5-1):

$$R_r = \phi_{bs} R_p (0.58 F_u A_{vn} + U_{bs} F_u A_{tn}) \le \phi_{bs} (0.58 F_y A_{vg} + U_{bs} F_u A_{tn})$$

ϕ_{bs} is the resistance factor for block shear rupture taken equal to 0.80 (*AASHTO LRFD* Article 6.5.4.2). The reduction factor, R_p, is taken equal to 1.0 for holes drilled full-size. The reduction factor, U_{bs}, is taken equal to 1.0 since the tension stress is uniform. Therefore:

$$\begin{aligned} R_r &= 0.80(1.0)[0.58(70)(15.81) + 1.0(70)8.60)] = 975 \text{ kips} \\ &> 0.80(1.0)[0.58(50)(17.81) + 1.0(70)(8.60)] = 895 \text{ kips} \\ &\therefore R_r = 895 \text{ kips} \end{aligned}$$

Calculate the factored block shear rupture resistance of the inside splice plates assuming the failure planes shown in Figure 6.6.4.2.5.6.1-3.

$$A_{tn} = 2\left[3.5 + 2.25 - 1.5(0.9375) + \frac{(3.0)^2}{4(3.5)}\right](0.75) = 7.48 \text{ in.}^2$$

$$A_{vn} = 2[5(6.0) + 1.5 - 5.5(0.9375)](0.75) = 39.52 \text{ in.}^2$$

A_{vg} is the gross area along the plane resisting the shear stress.

$$A_{vg} = 2[5(6.0) + 1.5](0.75) = 47.25 \text{ in.}^2$$

$$R_r = 0.80(1.0)\left[0.58(70)(39.52) + 1.0(70)7.48)\right] = 1{,}702 \text{ kips}$$
$$> 0.80(1.0)\left[0.58(50)(47.25) + 1.0(70)(7.48)\right] = 1{,}515 \text{ kips}$$
$$\therefore R_r = 1{,}515 \text{ kips}$$

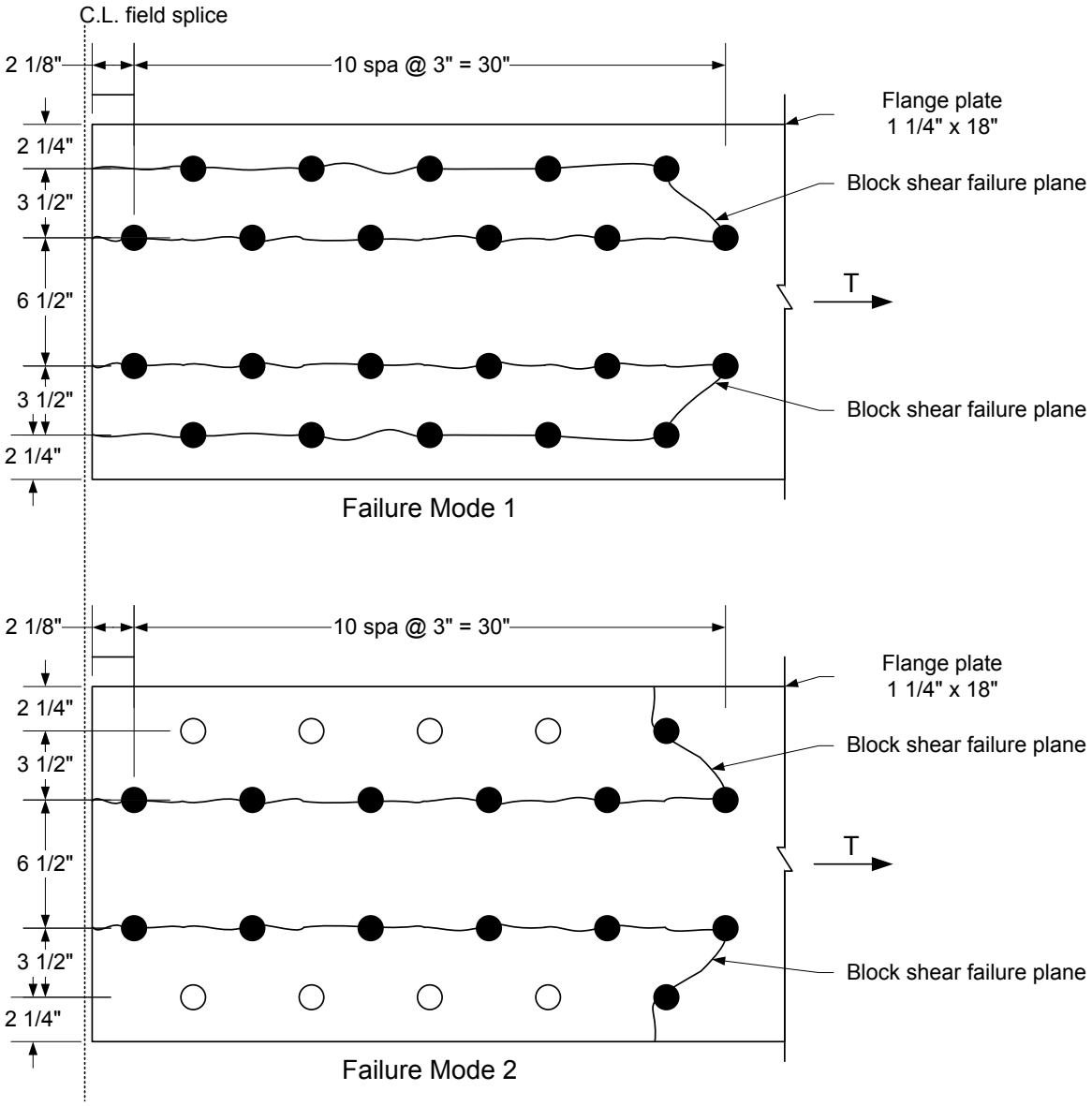

Figure 6.6.4.2.5.6.1-4 Block Shear Rupture Resistance Example – Smaller Flange at a Bolted Splice

Calculate the factored block shear rupture resistance of the smaller girder flange at the splice assuming the failure planes shown in Figure 6.6.4.2.5.6.1-4. Two potential failure modes are investigated for the flange as shown in Figure 6.6.4.2.5.6.1-4. For Failure Mode 1:

$$A_{tn} = 2\left[3.5 - 0.9375 + \frac{(3.0)^2}{4(3.5)}\right](1.25) = 8.01\,\text{in.}^2$$

$$A_{vn} = 2[4(6.0) + 5.125 - 4.5(0.9375)](1.25) + 2[5(6.0) + 2.125 - 5.5(0.9375)](1.25) = 129.7\ \text{in.}^2$$

A_{vg} is the gross area along the plane resisting the shear stress.

$$A_{vg} = 2[4(6.0) + 5.125](1.25) + 2[5(6.0) + 2.125](1.25) = 153.1\,\text{in.}^2$$

$$\begin{aligned} R_r &= 0.80(1.0)[0.58(70)(129.7) + 1.0(70)(8.01)] = 4{,}661\ \text{kips} \\ &> 0.80(1.0)[0.58(50)(153.1) + 1.0(70)(8.01)] = 4{,}000\ \text{kips} \\ &\therefore R_r = 4{,}000\ \text{kips} \end{aligned}$$

For Failure Mode 2:

$$A_{tn} = 2\left[3.5 + 2.25 - 1.5(0.9375) + \frac{(3.0)^2}{4(3.5)}\right](1.25) = 12.47\ \text{in.}^2$$

$$A_{vn} = 2[5(6.0) + 2.125 - 5.5(0.9375)](1.25) = 67.42\ \text{in.}^2$$

A_{vg} is the gross area along the plane resisting the shear stress.

$$A_{vg} = 2[5(6.0) + 2.125](1.25) = 80.31\,\text{in.}^2$$

$$\begin{aligned} R_r &= 0.80(1.0)[0.58(70)(67.42) + 1.0(70)(12.47)] = 2{,}888\ \text{kips} \\ &> 0.80(1.0)[0.58(50)(80.31) + 1.0(70)(12.47)] = 2{,}562\ \text{kips} \\ &\therefore R_r = 2{,}562\ \text{kips} \end{aligned}$$

The block shear rupture resistance will typically not control for bolted flange splices of typical proportion. Block shear rupture typically controls for short compact bolted connections and bolted end connections to thin webs of girders.

6.6.4.2.5.6.2 Shear Resistance of a Connected Element

AASHTO LRFD Article 6.13.5.3 specifies that the factored shear resistance, R_r, of a connected element (i.e. a splice plate, gusset plate or lateral connection plate) is to be taken as the smaller value based on shear yielding or shear rupture.

Shear Yielding

For shear yielding, the factored shear resistance of the connected element, R_r, is conservatively based on the shear yield stress (i.e. $F_y/\sqrt{3} = 0.58F_y$) as follows:

$$R_r = \phi_v 0.58 F_y A_{vg}$$ Equation 6.6.4.2.5.6.2-1

AASHTO LRFD Equation 6.13.5.3-1

where:

ϕ_v = resistance factor for shear specified in *AASHTO LRFD* Article 6.5.4.2 (= 1.0)
A_{vg} = gross area of the connected element subject to shear (in.^{2})
F_y = specified minimum yield strength of the connected element (ksi)

Shear Rupture

A shear rupture failure of a connected element is illustrated in Figure 6.6.4.2.5.6.2-1.

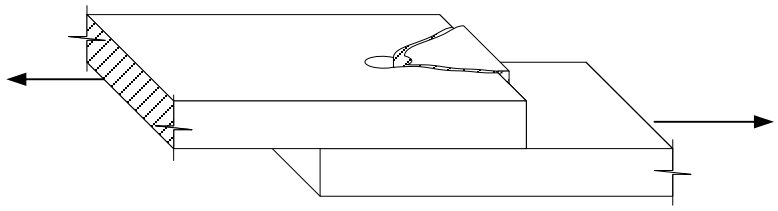

Figure 6.6.4.2.5.6.2-1 Shear Rupture Failure of a Connected Element

For shear rupture, the factored shear resistance of the connected element, R_r, is to be taken as follows:

$$R_r = \phi_{vu} 0.58 R_p F_u A_{vn}$$ Equation 6.6.4.2.5.6.2-2

AASHTO LRFD Equation 6.13.5.3-2

where:

ϕ_{vu} = resistance factor for shear rupture of connected elements specified in *AASHTO LRFD* Article 6.5.4.2 (= 0.80)
A_{vn} = net area of the connected element subject to shear (in.^{2})
F_u = tensile strength of the connected element specified in *AASHTO LRFD* Table 6.4.1-1 (ksi)
R_p = reduction factor for holes taken equal to 0.90 for bolt holes punched full size and 1.0 for bolt holes drilled full size or subpunched and reamed to size (Section 6.6.3.3.2.1)

6.6.4.2.5.6.3 Compressive Resistance of a Connected Element

The compressive resistance of cross-frame gusset plates and lateral connection plates for lateral bracing members is not currently covered in the *AASHTO LRFD* Specifications. One possible suggestion is to adapt the procedures given in AISC (2010) for determining and checking the compressive resistance of these items to fit with the *AASHTO LRFD* Specifications. Another possible option is to adapt the procedure for checking the compressive resistance of truss gusset plates discussed in Section 6.6.7.3.

Local buckling of cross-frame connection plates serving as transverse stiffeners adjacent to web panels subject to postbuckling tension-field action is considered in *AASHTO LRFD* Article 6.10.11.1 (Section 6.6.6.2.3). A suggested check for local buckling of cross-frame connection plates in I-girder bridges when the cross-slope is large and rectangular cross-frames or diaphragms are used is discussed in Section 6.3.2.9.6.3.1.

6.6.4.2.6 Eccentric Shear

In Figure 6.6.4.2.6-1 Part A, the force, *P*, is applied on a line of action that does not pass through the center of gravity of the bolt group. The resultant action may be represented as a moment (torque) equal to *P* times the eccentricity, *e*, and a concentric force, *P*, acting on the connection, as shown in Figure 6.6.4.2.6-1 Part B, and Figure 6.6.4.2.6-1 Part C.

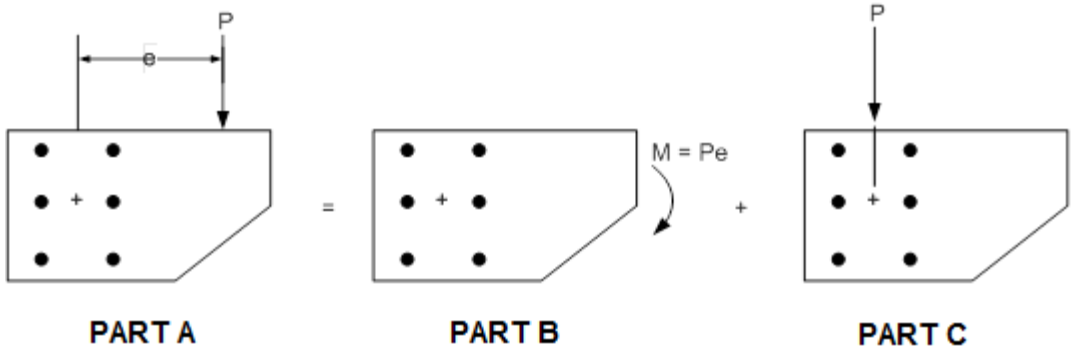

Figure 6.6.4.2.6-1 Bolted Connection Subject to Eccentric Shear

Since both the moment and concentric force cause shears on the bolt group, this particular situation is referred to as eccentric shear. As will be discussed in Section 6.6.5.2.3, a common example of a connection in a steel bridge subject to eccentric shear is a bolted web splice. Bolted cross-frame member connections are also often subject to eccentric shear.

Bolt groups subject to eccentric shear have typically been analyzed using a traditional elastic vector analysis assuming no friction, that the bolts are elastic and that the plates are rigid ensuring a linear strain variation on the bolts (Kulak et al., 1987). The concentric force, *P*, is assumed to stress the bolts uniformly and the stress due to the torsion is then superimposed vectorially. The torque has traditionally been treated using an adaptation of the theory of twisting of circular steel shafts, as discussed below.

Kulak et al. (1987) discuss an alternative ultimate strength approach in which the translation and rotation of the bolt group is reduced to a pure rotation about a point referred to as the instantaneous center of rotation. An empirical load-deformation relationship is used to relate the shear resistance of each bolt to its deformation (Fisher, 1965; Crawford and Kulak, 1971). However, it was felt by the *AASHTO LRFD* specification writers that the traditional elastic approach provides a more consistent factor of safety and is therefore recommended for use (*AASHTO LRFD* Article C6.13.6.1.4b).

Consider the bolt group acted on by a torque, *M*, as shown in Figure 6.6.4.2.6-2 Part A. Assume the plate, which transmits the torque to the bolts, rotates about an axis through the centroid of the bolt group, and that the bolts all have different areas. It is assumed in this development that constraints on the members or connection do not force rotation about some point other than the centroid of the bolt group, which is typically the case in most practical connections.

Neglecting friction between the plates, the torque on the bolt group is equal to (Figure 6.6.4.2.6-2 Part B):

$$M = R_1 d_1 + R_2 d_2 + R_3 d_3 + ... + R_6 d_6 \qquad \text{Equation 6.6.4.2.6-1}$$

Assume that the shear stress in each bolt due to the torque acts normal to the radius drawn from the centroid and that the stresses vary linearly with the distance from the centroid. Thus, the bolt furthest removed from the centroid (say Bolt 6 in Figure 6.6.4.2.6-2 Part B for the purposes of this discussion) is the one most heavily stressed. The shear force in Bolt 6 is equal to $R_6 = \tau_6 A_6$. The stresses in the other bolts are then proportional to the stress in Bolt 6. Therefore, the forces acting on the other bolts can be computed as:

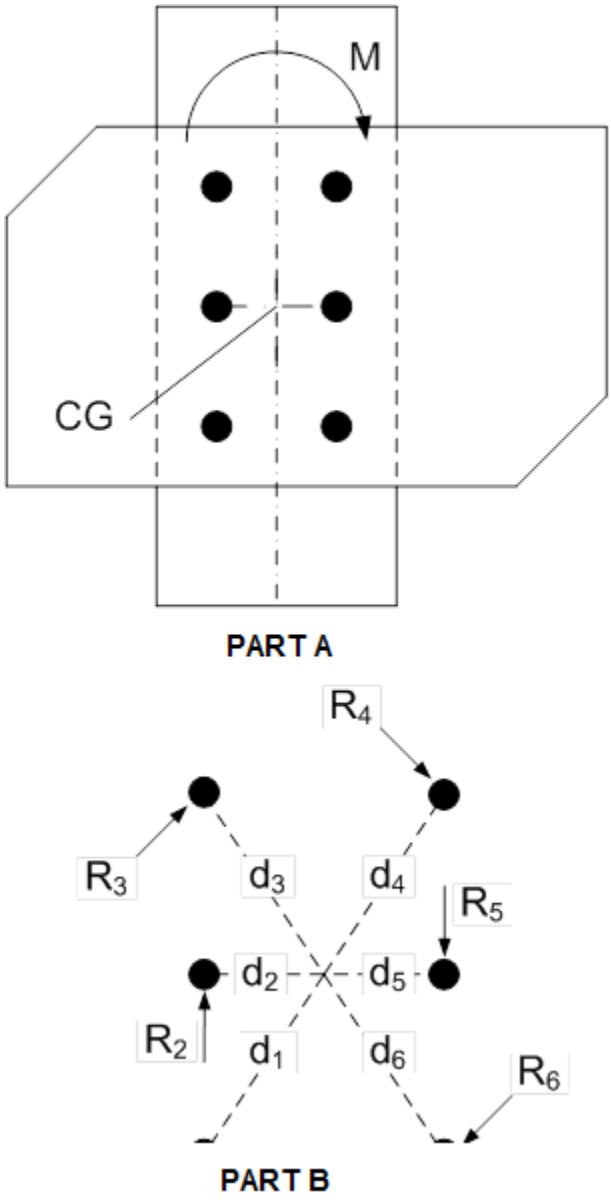

Figure 6.6.4.2.6-2 Analytical Model for Torque on a Bolt Group

$$R_1 = \frac{d_1 \tau_6}{d_6} A_1; R_2 = \frac{d_2 \tau_6}{d_6} A_2; R_3 = \frac{d_3 \tau_6}{d_6} A_3; R_4 = \frac{d_4 \tau_6}{d_6} A_4; R_5 = \frac{d_5 \tau_6}{d_6} A_5$$

Equation 6.6.4.2.6-2

Substituting the forces into Equation 6.6.4.2.6-1 gives:

$$M = \frac{\tau_6}{d_6} \sum_{i=1}^{n} d_i^2 A_i$$

Equation 6.6.4.2.6-3

where *n* is the total number of bolts in the connection (*n* = 6 in this case).

Rearranging and substituting the polar moment of inertia, I'_p, for the term, $\sum_{i=1}^{n} d_i^2 A_i$, gives the following equation for the stress in the most heavily stressed bolt in the group:

$$\tau_6 = \frac{Md_6}{I_p'} \qquad \text{Equation 6.6.4.2.6-4}$$

which is analogous to the equation for the shear stress in a circular shaft subject to pure torsion (McGuire, 1968).

In most cases, the bolts in the connection will be the same size. Therefore, it becomes convenient to factor the bolt cross-sectional area, *A*, out of I'_p. Therefore, letting $I'_p = A\sum_{i=1}^{n} d_i^2 = AI_p$ results in the following expression for the shear force in the most heavily stressed bolt:

$$R_6 = \frac{Md_6}{I_p} \qquad \text{Equation 6.6.4.2.6-5}$$

Referring to Figure 6.6.4.2.6-3, since $d^2 = x^2 + y^2$:

$$I_p = \sum_{i=1}^{n} x_i^2 + \sum_{i=1}^{n} y_i^2 \qquad \text{Equation 6.6.4.2.6-6}$$

Note that *AASHTO LRFD* Article C6.13.6.1.4b provides the following alternative formula for computing the polar moment of inertia, I_p, about the centroid of the connection assuming a uniform vertical pitch of the bolts (AISC, 1963):

$$I_p = \frac{nm}{12}\left[s^2\left(n^2 - 1\right) + g^2(m^2 - 1)\right] \qquad \text{Equation 6.6.4.2.6-7}$$

AASHTO LRFD Equation C6.13.6.1.4b-3

where:

m = number of vertical rows of bolts
n = number of bolts in one vertical row
s = vertical pitch of bolts (in.)
g = horizontal pitch of bolts (in.)

To facilitate combination with the direct shear in each bolt due to the concentric force *P*, it becomes convenient to use the *x* and *y* components of the bolt shears due to torsion. Referring again to Figure 6.6.4.2.6-3, $R_6 = R_y\, d_6/x_6$ and $R_6 = R_x\, d_6/y_6$ Substituting into Equation 6.6.4.2.6-5 gives:

$$R_x = \frac{My_6}{I_p} \qquad \text{Equation 6.6.4.2.6-8}$$

$$R_y = \frac{Mx_6}{I_p} \qquad \text{Equation 6.6.4.2.6-9}$$

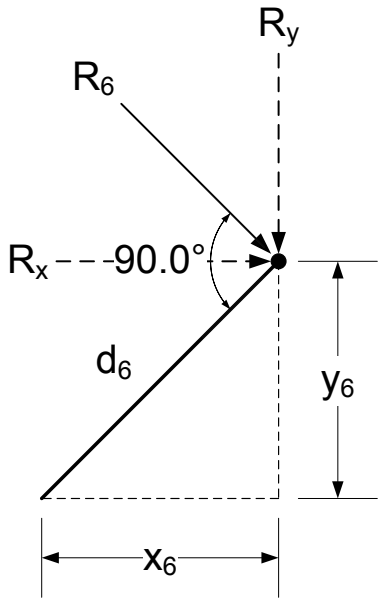

Figure 6.6.4.2.6-3 Horizontal and Vertical Components of Shear Force, *R*

The direct shear force on a bolt in an eccentric shear connection due to the concentric force, *P*, can be computed as:

$$R_v = \frac{P}{n} \qquad \text{Equation 6.6.4.2.6-10}$$

where *n* is again the total number of bolts in the connection.

The total resultant force on the bolt is then computed from the vector sum of the direct shear force and the *x* and *y* components of the shear force due to torsion as follows:

$$R = \sqrt{(R_V + R_y)^2 + R_x^2} \qquad \text{Equation 6.6.4.2.6-11}$$

In certain cases, additional horizontal components of shear force may act on a bolt group subject to eccentric shear (e.g. in bolted web splices for sections where the neutral axis is not as the mid-depth of the web, or in cross-frame connections where the line of action of force in a diagonal member does not pass through the center of gravity of the corresponding bolt group). In such cases, the additional horizontal component would be appropriately combined with R_x in Equation 6.6.4.2.6-11 to determine the resultant bolt force.

As illustrated in the example below, for bolted bracing member connections subjected to eccentric shear, the location of the working point is a critical factor in determining the overall economy of the connection.

EXAMPLE

Assume the gusset-plate connection configuration and bolt pattern shown in Figure 6.6.4.2.6-4. All bolts are 7/8-inch diameter ASTM A325 high-strength bolts placed in standard holes. Assume that all bolt spacing and edge and end distance requirements are satisfied, and that the bearing resistance of the bolt holes at the strength limit state has been checked and is satisfactory.

The working point (W.P. in the figure) of the connection has been initially selected as shown. The selection of efficient working points for cross-frame connections can be determined in consultation with a fabricator/detailer. As illustrated later, if there is enough space to place the working point closer to the center of the bolt group, it obviously is desirable. Depending on how the cross-frame is detailed, i.e. if the cross-frame is detailed as a rectangle rather than a parallelogram (which is not preferred), the space available for bolts beyond the working point may vary with the particular bridge cross slope.

From separate calculations (Section 6.6.4.4), the critical resultant strength limit state force combination for the selected gusset-plate connection configuration is a horizontal force of –126.3 kips acting in combination with a vertical force of –46.4 kips.

Check the bolts for shear at the strength limit state assuming the bolts in the connection have slipped and gone into bearing. The bolts are subject to eccentric shear to the in-plane eccentricity and to combined shear and tension due to the out-of-plane eccentricity.

For the eccentric shear (in-plane eccentricity), the traditional elastic vector method is used for calculating the maximum resultant bolt force. The polar moment of inertia, I_p, of the bolts with respect to the centroid of the connection is computed using Equation 6.6.4.2.6-7. For the example connection (referring to Figure 6.6.4.2.6-4), n = 4; m = 4; s = 3.0 in.; and g = 3.0 in. Therefore:

$$I_p = \frac{4(4)}{12}\left[(3.0)^2\left(4^2-1\right)+(3.0)^2(4^2-1)\right] = 360.0 \text{ in.}^2$$

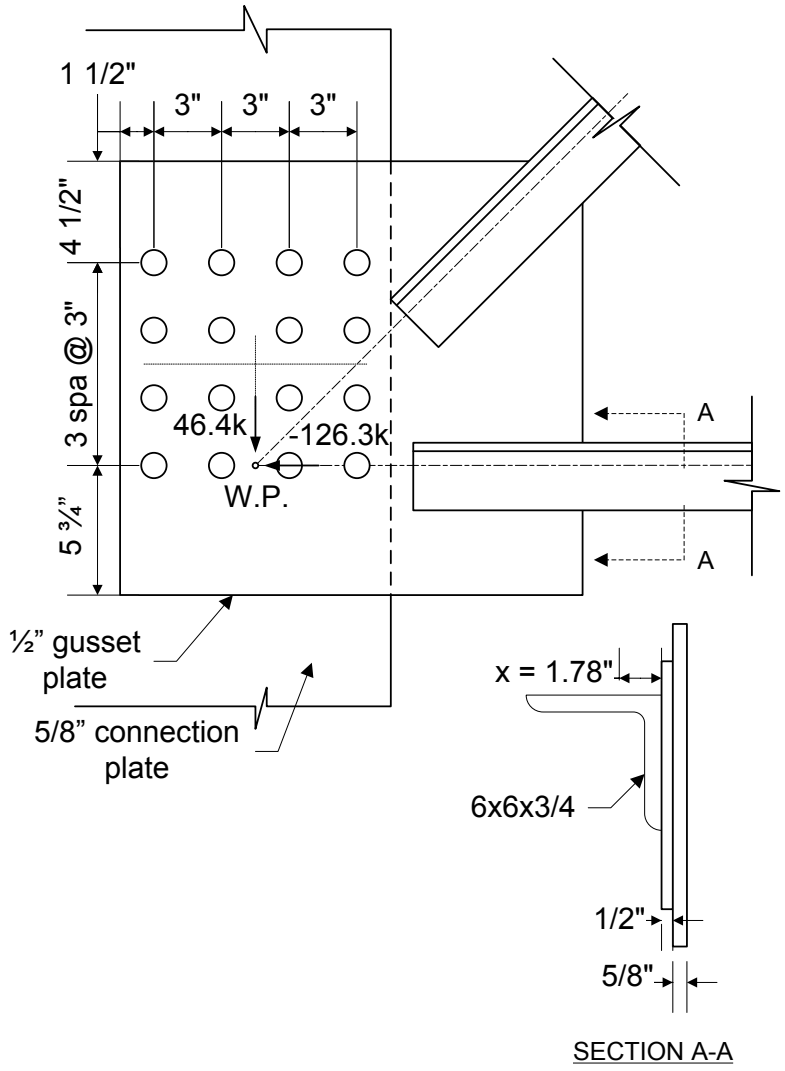

Figure 6.6.4.2.6-4 Example Gusset-Plate Configuration for Bolted Bracing Member Connection – Option 1

Determine vertical bolt force, R_v:

$$R_v = \frac{46.4}{16} = 2.90 \text{ kips / bolt}$$

Determine the horizontal bolt force, R_h:

$$R_h = \frac{126.3}{16} = 7.89 \text{ kips / bolt}$$

Determine the vertical and horizontal components of the force on the extreme bolt due to the total moment on the connection, M_{tot}:

$$M_{tot} = 126.3(4.5) - 46.4(0.0) = 568.4 \text{ kip} - \text{in.}$$

$$R_{M_v} = \frac{M_{tot} x}{I_p} = \frac{568.4(4.5)}{360.0} = 7.11 \text{ kips}$$

$$R_{M_h} = \frac{M_{tot} y}{I_p} = \frac{568.4(4.5)}{360.0} = 7.11 \text{ kips}$$

The resultant bolt force on the extreme bolt is:

$$R = \sqrt{(R_v + R_{M_v})^2 + (R_h + R_{M_h})^2} = \sqrt{(2.90 + 7.11)^2 + (7.89 + 7.11)^2} = 18.03 \text{ kips}$$

The factored shear resistance, R_r, for a 7/8-in. diameter ASTM A325 high-strength bolt in single shear assuming the threads are excluded from the shear plane is computed by applying the resistance factor, ϕ_s=0.80, to the nominal shear resistance, R_n, computed from Equation 6.6.4.2.5.2-1. The result is 27.70 kips/bolt. Therefore:

$$R = 18.03 \text{ kips} < R_r = 27.70 \text{ kips} \qquad \text{ok}$$

In addition to shear, the bolts are also subject to tension as a result of the out-of-plane eccentricity. By inspection, the 126.3 kip force controls this computation.

From Table 6.2.3.1.2-1, the minimum required initial pretension, P_t, for 7/8-inch diameter ASTM A325 bolts is 39.0 kips. Therefore, from Equation 6.6.4.2.5.5-4 and referring to Figure 6.6.4.2.6-4, the initial precompression stress, f_{bi}, on the contact area is equal to (16)(39.0)/(19.25)(12) = 2.70 ksi. Referring to Section A-A in Figure 6.6.4.2.6-4, the eccentricity to the center of the 5/8-inch-thick connection plate is

conservatively computed as e = 1.78 + 0.5 + 0.625/2 = 2.59 in. (the eccentricity of the larger bottom chord member is used). From Equation 6.6.4.2.5.5-5, the tensile stress on the contact area, f_{tb}, is equal to $6(126.3)(2.59)/(19.25)(12)^2$ = 0.71 ksi, which is less than f_{bi}. Therefore, the pieces remain in compression (contact).

The nominal shear resistance of each bolt, R_n, is taken as the factored shear resistance, R_r = 27.70 kips/bolt, divided by ϕ_s. Therefore, R_n = 27.70/0.8 = 34.62 kips/bolt. The shear due to the factored loads, P_u, in each bolt is taken as the maximum resultant force, R, computed above. Therefore, P_u = 18.03 kips. Since P_u/R_n = 18.03/34.62 = 0.52 > 0.33, the nominal tensile resistance of each bolt, T_n, under combined tension and shear is taken from Equation 6.6.4.2.5.5-3.

For a 7/8" A325 bolt: $A_b = \dfrac{\pi(0.875)^2}{4} = 0.601 \text{ in.}^2$

F_{ub} = 120 ksi (*AASHTO LRFD* Article 6.4.3.1)

$$T_n = 0.76(0.601)(120)\sqrt{1-\left(\frac{18.03}{(0.80)(34.62)}\right)^2} = 41.6 \text{ kips}$$

Since:

$$T_r = \phi_t T_n$$

$$T_r = 0.80(41.6) = 33.3 \text{ kips/bolt}$$

The tensile force in each bolt to the factored loads, T_u, may be computed from Equation 6.6.4.2.5.5-7 as follows:

$$T_u = \frac{6(126.3)(2.59)(3)}{4(12)^2}\left(\frac{12-3}{12}\right) = 7.7 \text{ kips} < T_r = 33.3 \text{ kips} \quad \text{ok}$$

Alternatively, T_u may be computed from Equation 6.6.4.2.5.5-8, where y_b = 4.5 in. and $\Sigma y^2 = 8[(1.5)^2 + (4.5)^2] = 180.0 \text{ in.}^2$ Therefore:

$$T_u = \frac{126.3(2.59)(4.5)}{180.0} = 8.2 \text{ kips} < T_r = 33.3 \text{ kips} \quad \text{ok}$$

Since the bolted connection is a slip-critical connection, *AASHTO LRFD* Article 6.13.2.1.1 also requires that the connection be proportioned to prevent slip under Load Combination Service II specified in *AASHTO LRFD* Table 3.4.1-1 (Section 3.10.1.3.3).

From separate calculations, the critical resultant Service II force combination for the selected gusset-plate connection configuration is a horizontal force of –97.8 kips acting in combination with a vertical force of –35.9 kips.

Determine the vertical bolt force, R_v:

$$R_v = \frac{35.9}{16} = 2.24 \text{ kips / bolt}$$

Determine the horizontal bolt force, R_h:

$$R_h = \frac{97.8}{16} = 6.11 \text{ kips / bolt}$$

Determine the vertical and horizontal components of the force on the extreme bolt due to the total moment on the connection, M_{tot}:

$$M_{tot} = 97.8(4.5) - 35.9(0.0) = 440.1 \text{ kip} - \text{in.}$$

$$R_{M_v} = \frac{M_{tot} x}{I_p} = \frac{440.1(4.5)}{360.0} = 5.50 \text{ kips}$$

$$R_{M_h} = \frac{M_{tot} y}{I_p} = \frac{440.1(4.5)}{360.0} = 5.50 \text{ kips}$$

The resultant bolt force on the extreme bolt is:

$$R = \sqrt{(R_v + R_{M_v})^2 + (R_h + R_{M_h})^2} = \sqrt{(2.24 + 5.50)^2 + (6.11 + 5.50)^2} = 13.95 \text{ kips}$$

The factored slip resistance, R_r, for a 7/8-in. diameter ASTM A325 high-strength bolt assuming a Class B surface condition for the faying surface, standard holes and a single slip plane per bolt is equal to the nominal slip resistance, R_n, computed from Equation 6.6.4.2.4.2-1. The result is 19.50 kips/bolt. However, in the presence of tension (due to the out-of-plane eccentricity), the slip resistance must be reduced according to Equation 6.6.4.2.4.2-2.

P_t in Equation 6.6.4.2.4.2-2 is equal to the minimum required bolt tension specified in *AASHTO LRFD* Table 6.13.2.8-1 (specified as 39.0 kips for a 7/8-inch diameter ASTM A325 bolt – Table 6.2.3.1.2-1). Under the Service II load combination, the tensile force due to the factored loads, T_u, may be computed from Equation 6.6.4.2.5.5-8 as follows:

$$T_u = \frac{97.8(2.59)(4.5)}{180} = 6.3 \text{ kips}$$

Therefore, the factored slip resistance, R_r, modified for the effect of the tension is computed from Equation 6.6.4.2.4.2-2 as:

$$R_r = 19.50\left(1 - \frac{6.3}{39.0}\right) = 16.35 \text{ kips}$$

$$R = 13.95 \text{ kips} < R_r = 16.35 \text{ kips} \qquad \text{ok}$$

The slip resistance under the Service II load combination controls the design of the bolted connection in this case. Note that similar computations would need to be done if the cross-frame members had been bolted directly to the connection plate.

If it were possible, the moment on the connection could be reduced significantly in this particular case by moving the working point to the left. For example, if the working point could be moved 3 inches to the left along the bottom row of bolts, the total moment on the connection under the Service II load combination would be reduced from 440 kip-in. to:

$$M_{tot} = 97.8(4.5) - 35.9(3.0) = 332.4 \text{ kip} - \text{in.}$$

which may allow for an overall reduction in the number of bolts.

Assume that enough space is available to move the bottom row of bolts down (or move the bottom cross-frame member up) such that the working point can be located at the center of the bolt group (Figure 6.6.4.2.6-5).

As slip controls, check the slip resistance of the bolts in the resulting reduced bolt pattern shown in Figure 6.6.4.2.6-5 (the critical Service II resultant cross-frame forces are shown in the figure). Note that by going to this pattern, the size of the gusset plate is obviously reduced and the size of the connection plate is also reduced.

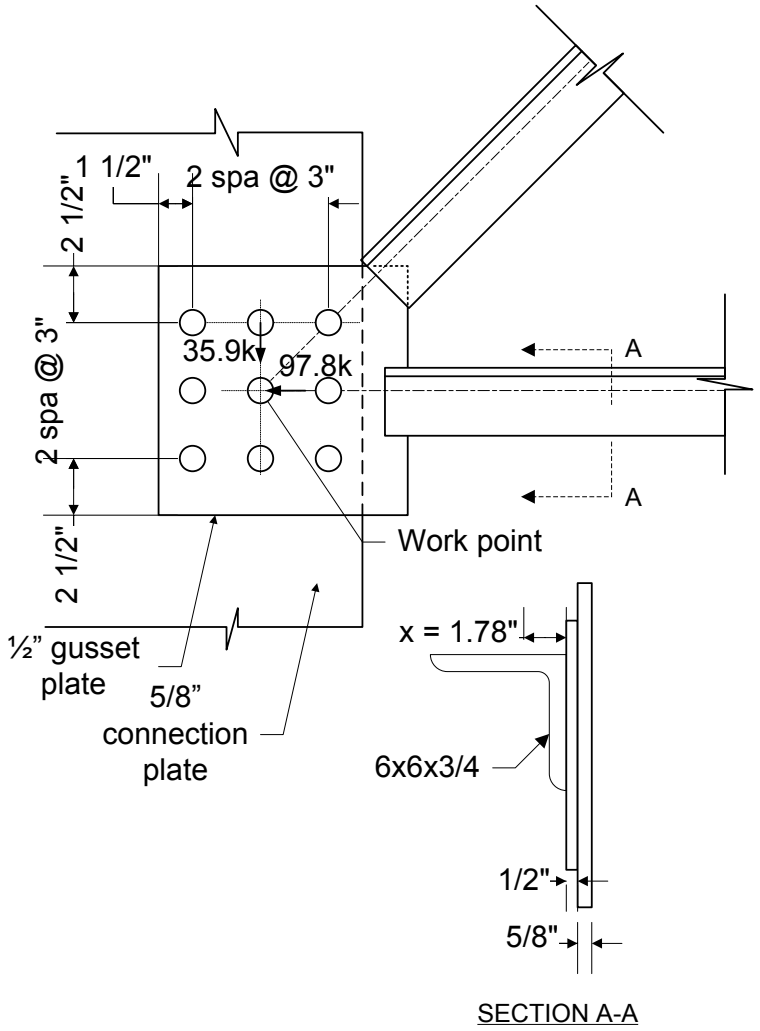

Figure 6.6.4.2.6-5 Example Gusset-Plate Configuration for Bolted Bracing Member Connection – Option 2

Determine the vertical bolt force, R_v:

$$R_v = \frac{35.9}{9} = 3.99 \text{ kips / bolt}$$

Determine the horizontal bolt force, R_h:

$$R_h = \frac{97.8}{9} = 10.87 \text{ kips / bolt}$$

The total moment on the connection, M_{tot}, is:

$$M_{tot} = 97.8(0.0) - 35.9(0.0) = 0.0 \text{ kip} - \text{in.}$$

The resultant bolt force on the extreme bolt is:

$$R = \sqrt{R_v^2 + R_h^2} = \sqrt{(3.99)^2 + (10.87)^2} = 11.58 \text{ kips}$$

To account for the tension on the bolts, y_b = 3.0 in. and $\Sigma y^2 = 3[(3.0)^2 + (3.0)^2] = 54.0$ in.^{2} T_u is therefore computed from Equation 6.6.4.2.5.5-8 as follows:

$$T_u = \frac{97.8(2.59)(3.0)}{54.0} = 14.07 \text{ kips}$$

Therefore, the factored slip resistance, R_r, modified for the effect of the tension is computed from Equation 6.6.4.2.4.2-2 as:

$$R_r = 19.50\left(1 - \frac{14.07}{39.0}\right) = 12.47 \text{ kips}$$

$$R = 11.58 \text{ kips} < R_r = 12.47 \text{ kips} \qquad \text{ok}$$

6.6.4.3 Welded Connections

6.6.4.3.1 General

Welding is the process of joining two pieces of material, usually metals, by heating the pieces to a suitable temperature such that the materials are soft enough to coalesce or fuse into one material. The pieces are held in position for welding and may or may not be pressed together depending on the process that is used. Also, the pieces may be joined directly to each other or they may be joined using filler material.

Although there are some forty different welding processes, arc welding, in which electrical energy in the form of an electric arc is introduced to generate the heat necessary for welding, is the most commonly used process in the steel-bridge construction industry. The heat of the electric arc as the current passes through the system simultaneously melts a consumable electrode (deposited as filler material) and the parts of the material being joined, with the joint resulting from the cooling and solidification of the fused material. To protect the molten region from impurities, the zone to be welded is typically blanketed in an atmosphere supplied by a flux, which may be a fusible coating on the welding rod, a fusible powder spread over the line of the weld or a gas sprayed over the weld. To produce a weld of the desired quality, the properties of the electrode must be carefully controlled. Proper control of the current and voltage along with a skilled welder are also required in order to produce a quality weld.

Welding in its simplest form has been around for several thousand years, primarily in the form of forge welding in which pieces of metal were heated and hammered into the desired shapes. Brazing of metals was also done for many years. Significant advancements in welding technology did not occur, however, until the late 1800s. Resistance welding, which combines electrical energy with mechanical pressure, originated around 1877 (Iron Age, 1955). Examples of resistance welding include spot and seam welding, which are primarily used for welding of light-gage steel plates and open-web steel joists.

In the late 1880s and early 1890s, the metal arc process made its initial appearance in Russia and in the U.S. at about the same time using uncoated bare electrodes (Miskoe, 1986). Around the same time period, coated metal electrodes were introduced to eliminate many of the problems associated with the use of bare electrodes (Iron Age, 1955). During World War I (1914-1918), welding techniques were primarily applied to repairing damaged ships. Right after the war, experimentation with electrodes and gases to shield the arc and weld area led to the development of gas metal arc welding and gas tungsten arc welding. In 1932, the use of granular flux to protect the weld was introduced, which along with the use of a continuously fed electrode led to the development of the commonly used submerged arc welding process in which the arc is buried under the granular flux (Miskoe, 1986). Research and advancements continue today with the increased usage of automated welding techniques and welding robotics.

The introduction of welding has led to significant advancements in steel-bridge design and fabrication. Welding is now used for the vast majority of shop connections. Welded connections are usually neater in appearance than bolted connections. Welded connections also allow the Design Engineer more freedom to be innovative and build-up cross-sections to transmit the loads in the most efficient manner.

Several factors influence the cost of welding, including but not limited to, the amount of weld material required, the costs of preparing the edges to be welded, the ratio of actual arc time to overall welding time, and the amount of handling required. Shop welding is almost always less expensive than field welding. Reasons for this include the more ready availability of automatic welding machines and special jigs for holding the pieces in more favorable positions, a less hostile environment, the ability to more easily perform proper preheating of the joint, and the ability to schedule a smooth continuous operation versus having to wait for cranes or special erection equipment to become available. More extensive information and discussion related to the variables influencing welding costs may be found in AWS (2001); and Miller and Ogborn (1994).

The weldability of a steel is a measure of the ease of producing a crack-free and sound structural joint. The weldability of structural steel is primarily controlled by its

carbon content. While carbon (C) is beneficial to the strength of the steel, it is detrimental to ductility. A high carbon content combined with the heat generated during welding may cause a brittle zone in which weld cracks may develop. A carbon content of about 0.20 percent results in a very weldable steel. Good weldability can be obtained with an upper limit on carbon content of about 0.25 percent. In certain steels, the addition of alloys to enhance the strength and/or corrosion resistance can increase the hardness of the steel. Increased hardness results in an increased likelihood of brittle zones forming. Higher concentrations of carbon and other alloying elements such as manganese (Mn), chromium (Cr), silicon (Si), molybdenum (Mo), vanadium (V), copper (Cu) and nickel (Ni) tend to increase the hardness and decrease the weldability of the steel. Each of these alloying elements tends to influence the hardness and weldability of the steel to different magnitudes. Therefore, an approximate guide to the weldability of alloy steels against that of plain carbon steels is necessary. The most common standard used is the carbon equivalent (%CE) given as follows (Lincoln Electric Company, 1994):

$$\%CE = \%C + \left(\frac{\%Mn + \%Si}{6}\right) + \left(\frac{\%Cr + \%Mo + \%V}{5}\right) + \left(\frac{\%Cu + \%Ni}{15}\right)$$

Equation 6.6.4.3.1-1

For %CE less than 14 percent, the steel is considered to have excellent weldability. For %CE between 14 and 45 percent, modest preheat and low hydrogen electrodes become necessary. For %CE greater than 45 percent, weld cracking is likely; therefore, larger preheats and low hydrogen electrodes are required.

Weldability should be determined on the basis of actual rather than specified chemical compositions as compositions listed on actual mill certification reports are typically below the maximum alloy contents set by the specifications. Most of the bridge steels specified in the ASTM A709/A709M Specification can be welded without special precautions or procedures. However, special procedures should be followed to improve weldability and ensure high-quality welds when high-performance steels (HPS) are used (AASHTO/AWS, 2010).

The design of welded connections is covered in *AASHTO LRFD* Article 6.13.3. *AASHTO LRFD* Article 6.13.3.1 requires that all base metal, weld metal and weld design details conform to the requirements of AASHTO/AWS (2010) (i.e. the *AASHTO/AWS D1.5M/D1.5 Bridge Welding Code*).

6.6.4.3.2 Welding Processes

Welding processes that are used for arc welding carbon and low-alloy steels typically used in bridge construction include: shielded metal arc welding (SMAW), submerged

arc welding (SAW), flux cored arc welding (FCAW), gas metal arc welding (GMAW), narrow-gap improved electroslag welding (NGI-ESW), and stud welding (SW). Note that the Design Engineer does not typically specify the welding process to be used or the exact filler metal (electrode/flux material) to be employed. These decisions are usually left with the fabricator. However, a basic understanding of the commonly used welding processes and corresponding AWS filler-metal designations is helpful. More extensive discussion of these processes and the decisions that go into selecting a particular process may be found in AWS (2004); AWS (2007); and Miller and Ogborn (1994). More detailed information on filler-metal designations used with each process may be found in Miller and Ogborn (1994); and AASHTO/AWS (2010).

6.6.4.3.3 Types of Welds

6.6.4.3.3.1 General

As shown in Figure 6.6.4.3.3.1-1, there are four basic types of welds – groove, fillet, slot and plug. Fillet welds represent the largest percentage of welds used in welded construction, and are the most commonly used welds for bracing member connections. Slot and plug welds are primarily used in lap joints in combination with fillet welds to assist in transmitting the shear when the size of the connection limits the length available for fillet or other edge welds. Slot and plug welds can also help prevent the overlapping parts from buckling. However, because of fatigue concerns, slot and plug welds are rarely used in bridge construction, and then, only to resist compression or shear stress; therefore, they are not covered any further herein.

Weld symbols are used to allow the Design Engineer to instruct the fabricator and detailer as to the type and size of weld required for a particular connection (and vice versa). A standard system of designating welds by symbols that communicate the desired weld size, location and type has been developed by the AWS (2012). *AASHTO LRFD* Article 6.13.3.1 specifies that all welding symbols must conform to this system.

If a particular welded connection is used in many different parts of the structure, it may only be necessary to show a typical detail utilizing the welding symbols. For special complex or confusing connections, additional sketches may be necessary to indicate what is required. Welding symbols should be used to communicate and not to confuse. The Design Engineer will typically use welding symbols to convey a minimum amount of information to the fabricator/detailer regarding the welded connection on the design drawings (e.g. type and size of weld, etc.). The fabricator/detailer will then provide welding symbols for the same connection, often conveying more detailed information about the connection, on the shop drawings for review and approval by the Design Engineer. Therefore, the Design Engineer should have a complete understanding of weld symbols. More detailed information

on welding symbols may be found in AASHTO/AWS (2010); AWS (2012); and in most any structural steel textbook.

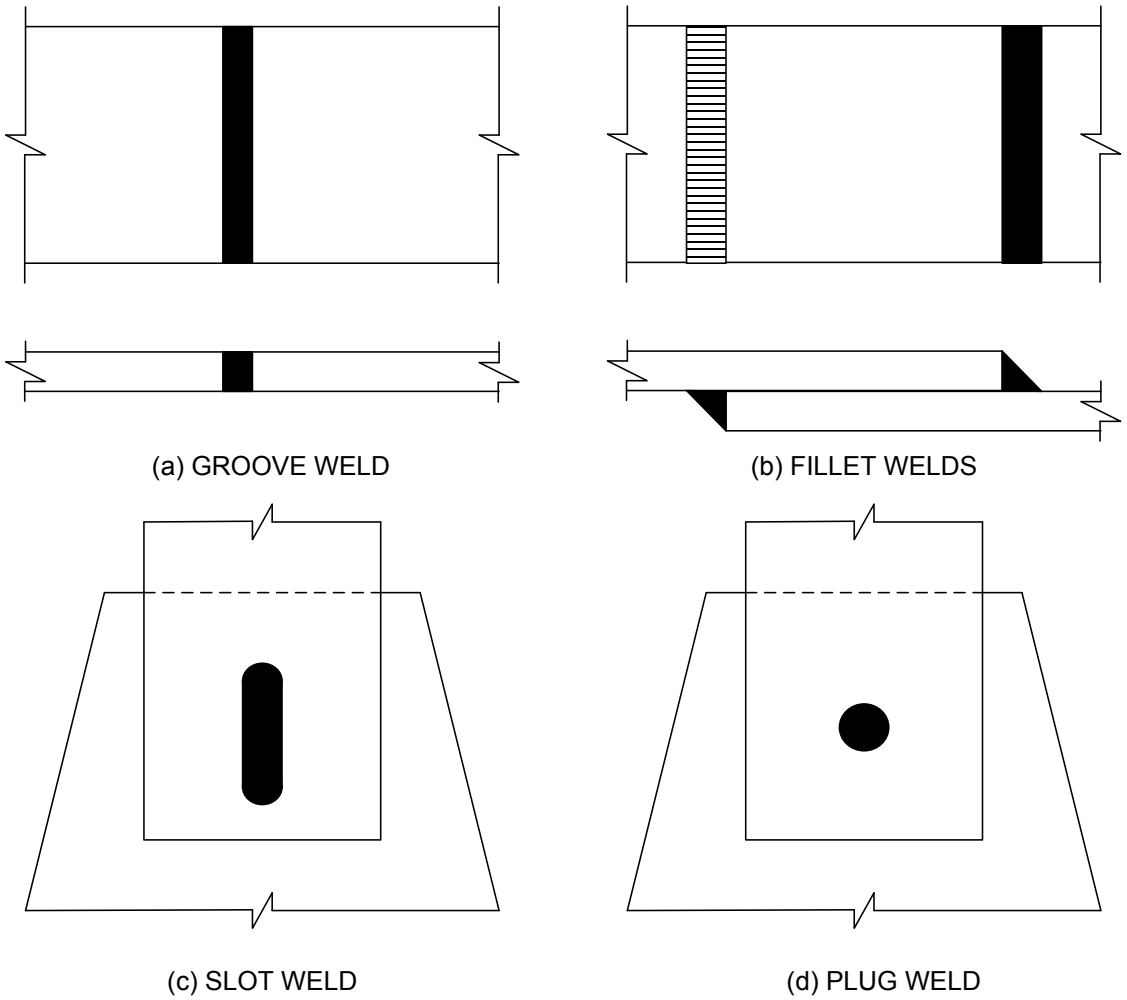

Figure 6.6.4.3.3.1-1 Types of Welds

6.6.4.3.3.2 Groove Welds

6.6.4.3.3.2.1 General

Groove welds are most often used to connect structural members that are aligned in the same plane (i.e. butt joints). They can also be used in tee and corner joints. As shown in Figure 6.6.4.3.3.2.1-1, there are two basic subcategories of groove welds: complete penetration groove welds (CJP) and partial penetration groove welds (PJP).

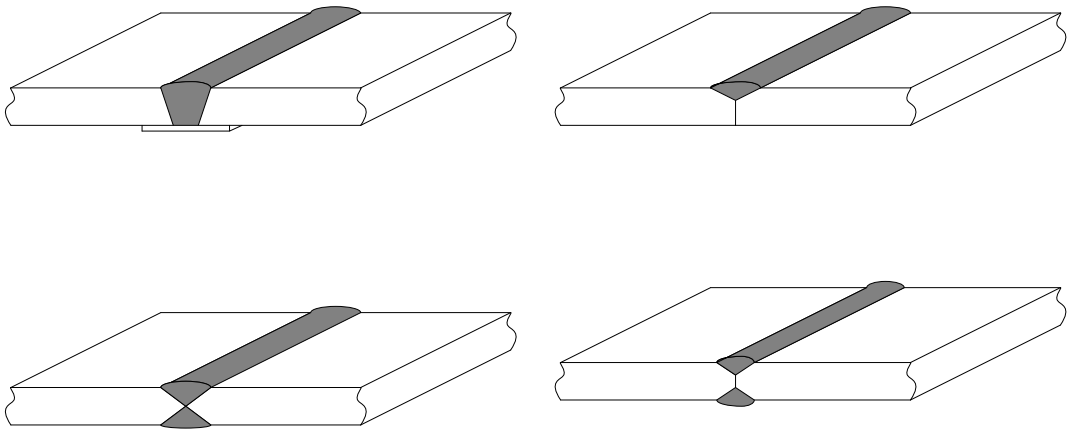

Complete Joint Penetration Groove Welds (CJP)

Partial Joint Penetration Groove Welds (PJP)

Figure 6.6.4.3.3.2.1-1 Subcategories of Groove Welds

CJP groove welds have the same resistance as the pieces joined and are intended to transmit the full load of the members that are joined. PJP groove welds do not extend completely through the thickness of the pieces being joined and are subject to special design requirements. PJP welds are sometimes used when stresses are low and there is no need to develop the complete strength of the base material. Note that both types of welds may be single- or double-sided welds. Double-sided welds, which require access to both sides of the joint, may require less weld metal and result in less distortion and are of particular importance when joining thick members. Basic groove weld nomenclature is shown in Figure 6.6.4.3.3.2.1-2.

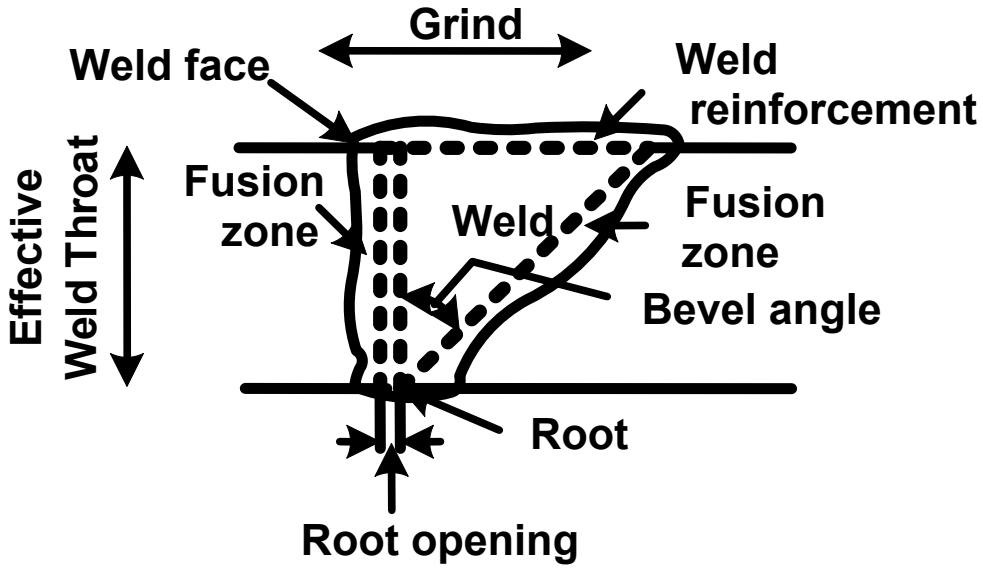

Figure 6.6.4.3.3.2.1-2 Groove Weld Nomenclature

6.6.4.3.3.2.2 Types

Groove welds are classified according to their particular shape. Most groove welds require a specific edge preparation and are named accordingly (Figure 6.6.4.3.3.2.2-1).

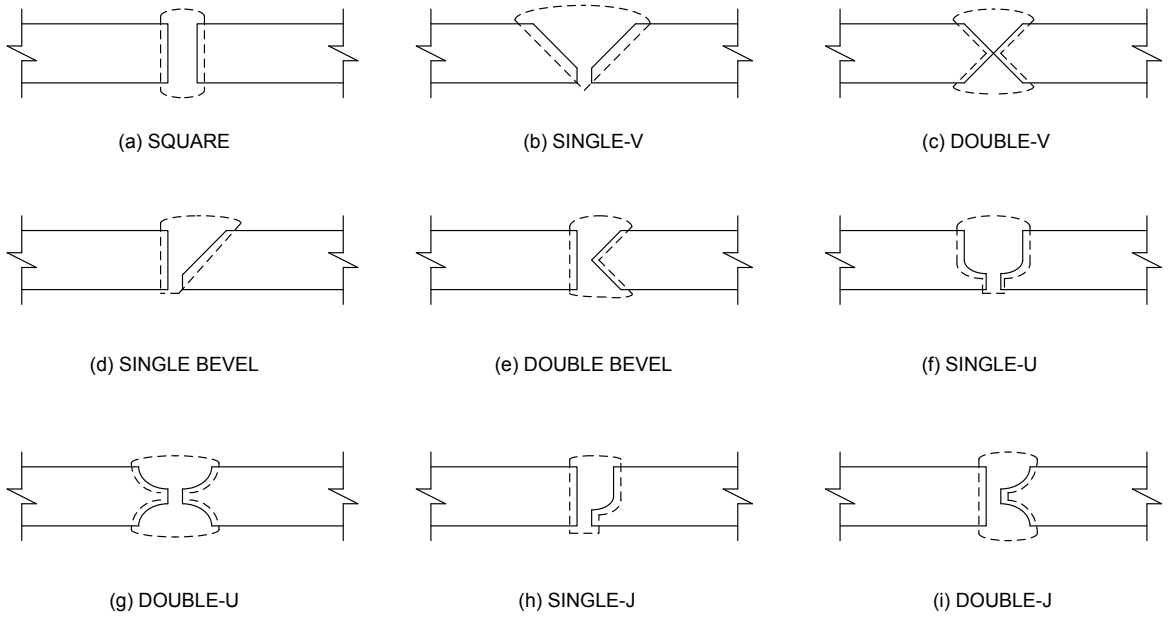

Figure 6.6.4.3.3.2.2-1 Types of Groove Welds

The square groove (Figure 6.6.4.3.3.2.2-1a) requires no edge preparation and is rarely used in bridge construction, except for thin sections. For the bevel groove (Figures 6.6.4.3.3.2.2-1d and 6.6.4.3.3.2.2-1e), one plate is cut at a 90-degree angle and the second plate is provided with a bevel cut. The V groove (Figures 6.6.4.3.3.2.2-1b and 6.6.4.3.3.2.2-1c) is similar to the bevel groove, except that both plates are bevel cut. The J groove (Figures 6.6.4.3.3.2.2-1h and 6.6.4.3.3.2.2-1i) resembles a bevel groove, except that the root has a radius instead of a straight cut. The U groove (Figures 6.6.4.3.3.2.2-1f and 6.6.4.3.3.2.2-1g) is similar to two J grooves put together. In all grooves but the square groove, the small opening or separation of the pieces being joined is called the root opening, which is provided for electrode access to the base of the joint. Note that the smaller the root opening, the larger the angle of the bevel that must be provided.

The selection of the proper groove weld is dependent on the cost of the edge preparations, the welding process used and the cost of making the weld. The decision as to which groove type to use is usually left to the fabricator/detailer, who will select the type of groove that will generate the required quality at a reasonable cost.

6.6.4.3.3.2.3 Effective Area

The resistance of welds is based on the effective area of the weld, which is taken as the effective length of the weld times the effective throat according to *AASHTO LRFD* Article 6.13.3.3. The effective throat is defined nominally as the shortest distance from the joint root to the face of the weld (neglecting any weld reinforcement), or the minimum width of the expected failure plane.

The effective length of a groove weld is the width of the part joined perpendicular to the direction of stress. By definition, the effective throat of a CJP groove weld is equal to the thickness of the thinner part joined (Figures 6.6.4.3.3.2.3-1a and 6.6.4.3.3.2.3-1b), with no increase allowed for any weld reinforcement. To ensure fusion throughout the thickness of the part being joined, backing is usually required if the CJP weld is made from one side, and back gouging is usually required from the second side if the CJP weld is made from both sides. Otherwise, qualification testing is required to show that the full throat can be developed.

The effective throat of PJP groove welds is defined in AASHTO/AWS (2010). The effective throat of PJP groove welds depends on the probable depth of fusion that will be achieved; that is, the depth of groove preparation and depth of penetration that can be achieved by the selected welding process and welding position. In certain cases, the effective throat may be specified to be 1/8 in. less than the depth of joint preparation; that is, it is assumed that the last 1/8 in. of the joint will not be fused (Figure 6.6.4.3.3.2.3-1c). Therefore, in such cases, the depth of joint preparation will have to be increased by 1/8 in. to offset the loss of penetration.

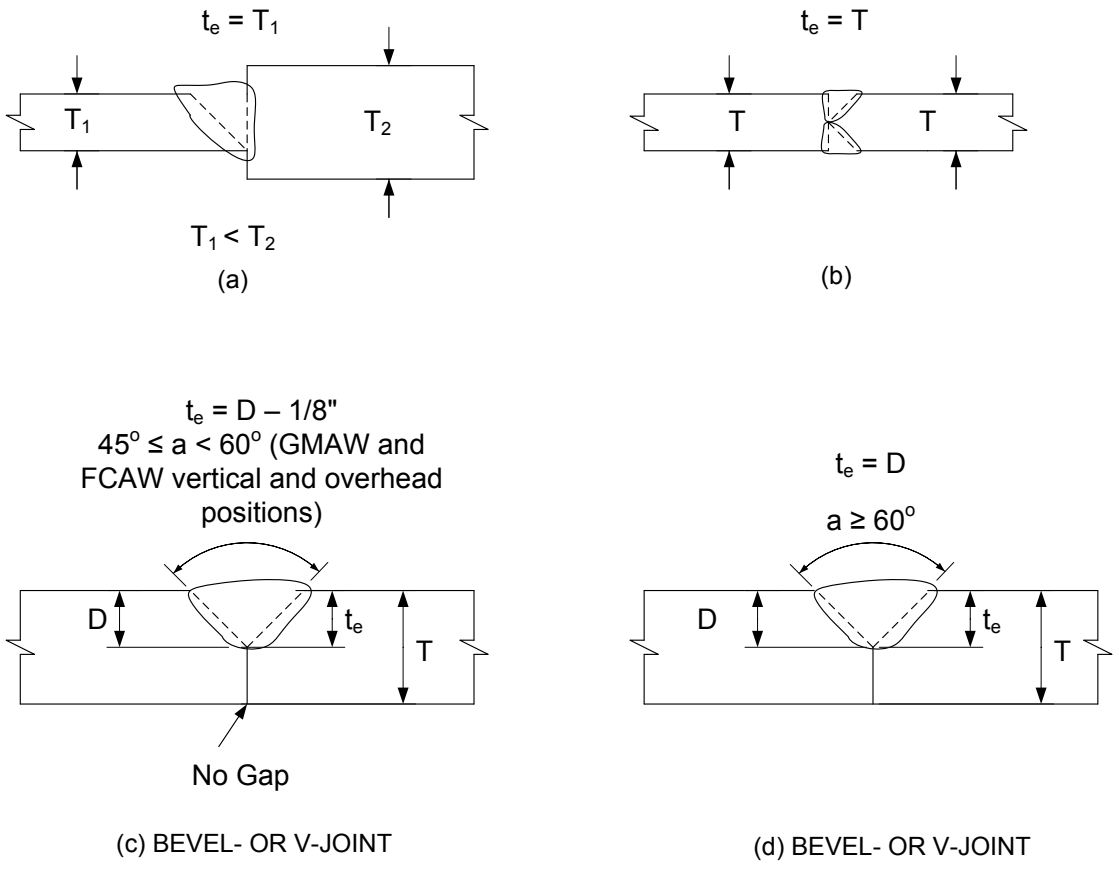

Figure 6.6.4.3.3.2.3-1 Effective Throat Dimensions for Groove Welds (SMAW, SAW, GMAW & FCAW)

The effective throat of a PJP weld is designated utilizing a capital 'E' and the required depth of penetration is designated by a capital 'S'. The Engineer will typically only specify the dimension for 'E'. The Fabricator will then specify the appropriate 'S' dimension on the shop drawings based on the welding process and position that is selected. Both the 'E' and 'S' dimension are typically shown on the welding symbols on the shop drawings, with the effective throat shown in parentheses. Minimum effective throat thickness requirements for PJP welds are also given in AASHTO/AWS (2010).

6.6.4.3.3.3 Fillet Welds

6.6.4.3.3.3.1 General

Fillet welds are the most widely used welds due to their ease of fabrication and overall economy, and are certainly the most widely used welds for bracing member connections. Fillet welds generally require less precision during fit-up and the edges of the joined pieces seldom need special preparation such as beveling or squaring. Fillet welds have a triangular cross-section and do not fully fuse the cross-sectional

area of the parts they join, although full-strength connections can be developed with fillet welds.

AASHTO LRFD Article 6.13.3.6 specifies that fillet welds deposited on the opposite sides of a common plane of contact between two parts are to be interrupted at a corner common to both welds (e.g. double-sided fillet welds connecting transverse stiffeners, connection plates or bearing stiffeners to a flange).

Basic fillet weld nomenclature is shown in Figure 6.6.4.3.3.3.1-1. The size of a fillet weld is given as the leg size of the fillet. If the two legs are unequal, the nominal size of the weld is given by the shorter of the legs.

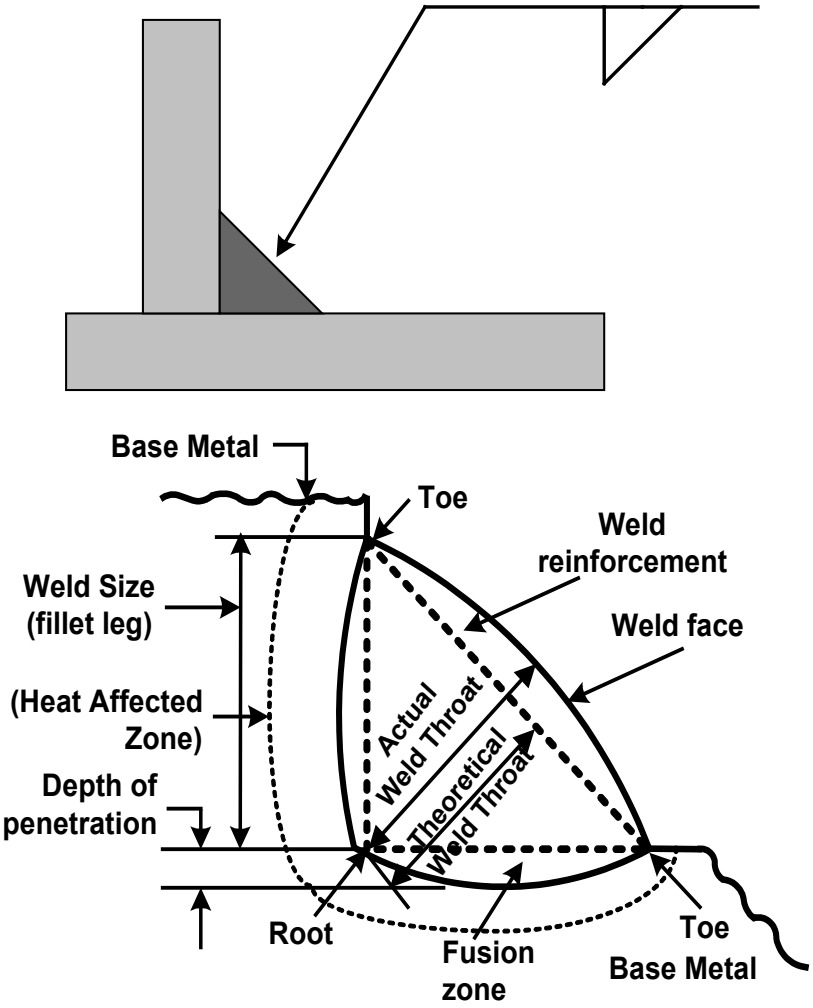

Figure 6.6.4.3.3.3.1-1 Fillet Weld Nomenclature

6.6.4.3.3.3.2 Effective Area

As for groove welds, the effective area of a fillet weld is taken equal to the effective length of the weld times the effective throat (*AASHTO LRFD* Article 6.13.3.3). The effective length is to be taken as the overall length of the full-size fillet. The effective throat is taken as defined below.

Effective Throat

The effective throat dimension of a fillet weld for a typical fillet weld with equal legs of nominal size, *a*, is taken equal to 0.707*a* (Figure 6.6.4.3.3.3.2-1 Part A), or nominally the shortest distance from the joint root to the weld face (neglecting any reinforcement). For the rare case of a fillet weld with unequal leg sizes, the effective throat would be computed as shown in Figure 6.6.4.3.3.3.2-1, Part B.

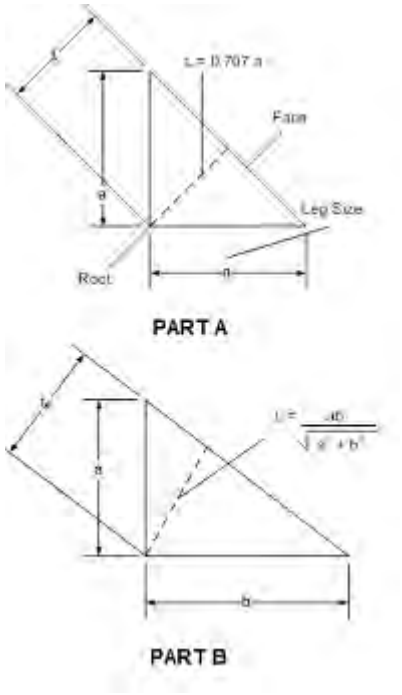

Figure 6.6.4.3.3.3.2-1 Effective Throat Dimensions for Fillet Welds

A) Equal Legs; B) Unequal Legs

Minimum Effective Length

When placing a fillet weld, the welder builds up the weld to the full dimension as near to the beginning of the weld as possible. However, there is always a slight tapering off of the weld where the weld starts and ends. Therefore, a minimum effective

length of the weld is required. As specified in *AASHTO LRFD* Article 6.13.3.5, the minimum effective length of a fillet weld is to be taken as four times its leg size, but not less than 1.5 inches (Figure 6.6.4.3.3.3.2-2).

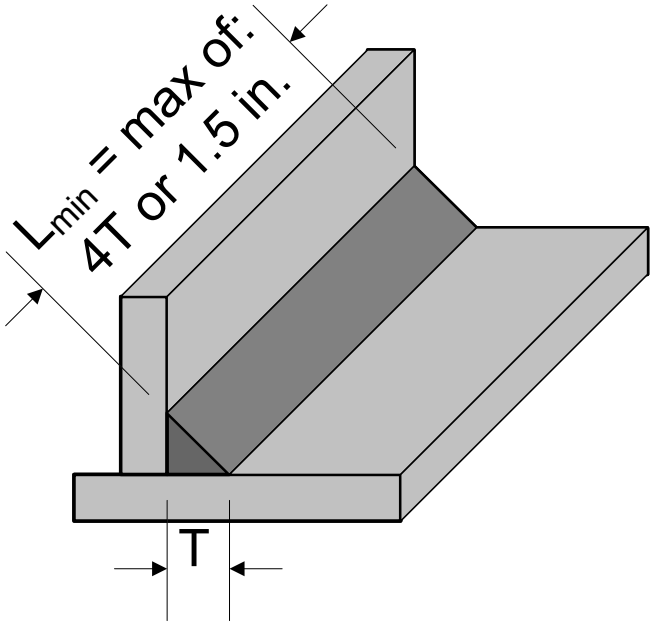

Figure 6.6.4.3.3.3.2-2 Minimum Effective Length of Fillet Welds

6.6.4.3.3.3.3 Maximum Thickness Requirements

As specified in *AASHTO LRFD* Article 6.13.3.4 and shown in Figure 6.6.4.3.3.3.3-1, Part A and Part B, maximum thickness (size) requirements for fillet welds along edges of connected parts depend on the thickness of the parts being connected (unless the weld is specifically designated on the contract documents to be built out to obtain full throat thickness). The requirements prevent melting of the base metal where the fillet would meet the corner of the plate if the fillet were made the full plate thickness (Salmon and Johnson, 1996).

Note that for the case shown in Figure 6.6.4.3.3.3.3-1, Part C, no specific limit applies, except as limited by the resistance requirements for the base metal in some instances.

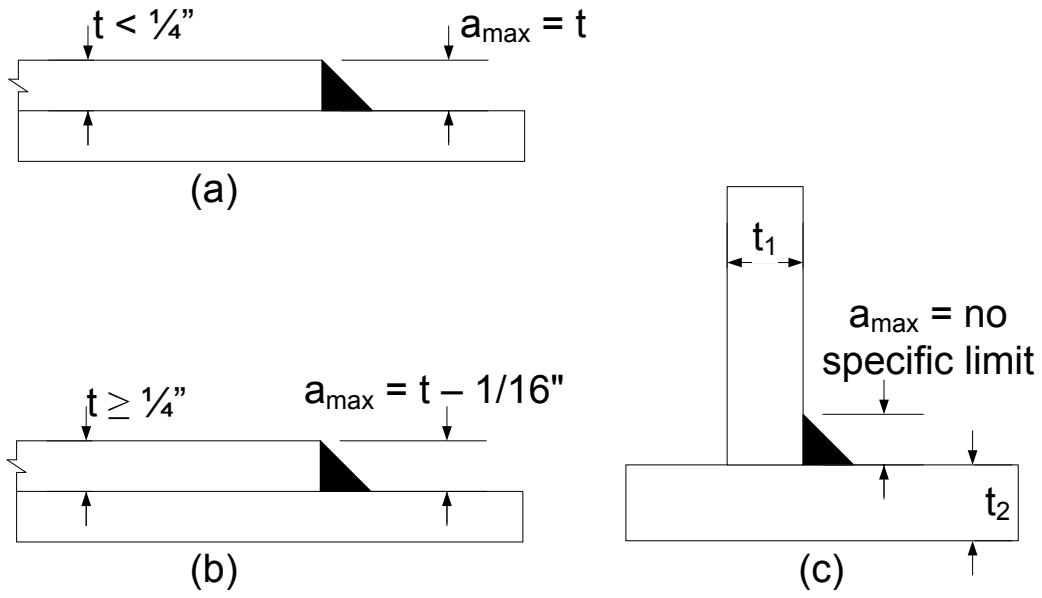

Figure 6.6.4.3.3.3.3-1 Maximum Size Requirements for Fillet Welds

A) For *t* < ¼″; B) For *t* ≥ ¼″; C) No specific limit

6.6.4.3.3.3.4 Minimum Thickness Requirements

The minimum thickness (size) of a fillet weld is not to be less than that required to transmit the required forces, nor the minimum thickness specified in *AASHTO LRFD* Table 6.13.3.4-1 (Table 6.6.4.3.3.3.4-1).

Table 6.6.4.3.3.3.4-1 Minimum Thickness Requirements for Fillet Welds

Base Metal Thickness of Thicker Part Joined (*T*)	Minimum Size of Fillet Weld
in.	in.
T ≤ 3/4	1/4
3/4 < *T*	5/16

The minimum weld size need not exceed the thickness of the thinner part joined. Note that the specified minimum weld sizes assume that the required preheats and interpass temperatures are provided (Section 6.6.4.3.5) (Miller and Ogborn, 1994). According to *AASHTO LRFD* Article 6.13.3.4, smaller welds than the minimum size welds may be approved by the Design Engineer if they are shown to be adequate for the applied stress and if the appropriate additional preheat is applied.

Minimum thickness requirements for fillet welds are based on preventing too rapid a rate of cooling in order to prevent a loss of ductility (i.e. the formation of a brittle microstructure) or a lack of fusion. The thicker the plate joined, the faster the heat is removed from the welding area. As a minimum, a weld of sufficient size is needed to prevent the thicker plate from removing heat at a faster rate than it is being supplied to cause the base metal to become molten. Thus, the minimum weld sizes implicitly imply a specified minimum heat input. In addition, restraint to weld metal shrinkage may result in weld cracking if the welds are too small. Minimum weld sizes are frequently used for the case of longitudinal fillet welds that resist shear (e.g. girder flange-to-web welds). Reducing the amount of weld metal will decrease the amount of distortion in welded assemblies; thus, the smallest acceptable weld size that will provide the required factored resistance should be used.

Since the minimum size requirements for fillet welds imply a minimum level of heat input, the minimum size welds must be made in a single pass, as multiple passes to make the minimum size weld would not provide the assumed minimum level of heat input, essentially defeating the purpose of the requirement. The largest single-pass fillet weld that can be made with the manual SMAW process is typically 5/16 in. (single-pass welds up to about ½ in. can be made with the SAW process).

6.6.4.3.3.4 Seal Welds

As specified in *AASHTO LRFD* Article 6.13.3.7, fillet welds to be used as seal welds are to be continuous and are to combine the functions of sealing and strength. Seal welds are to change section only as required by strength or by the minimum size requirements discussed above.

6.6.4.3.4 Types of Welded Joints

As shown in Figure 6.6.4.3.4-1, there are five basic types of welded joints – butt, lap, tee, corner and edge joints. In practice, different variations and combinations of these joints may be used. Edge joints are more commonly used in sheet metal applications and are not discussed herein.

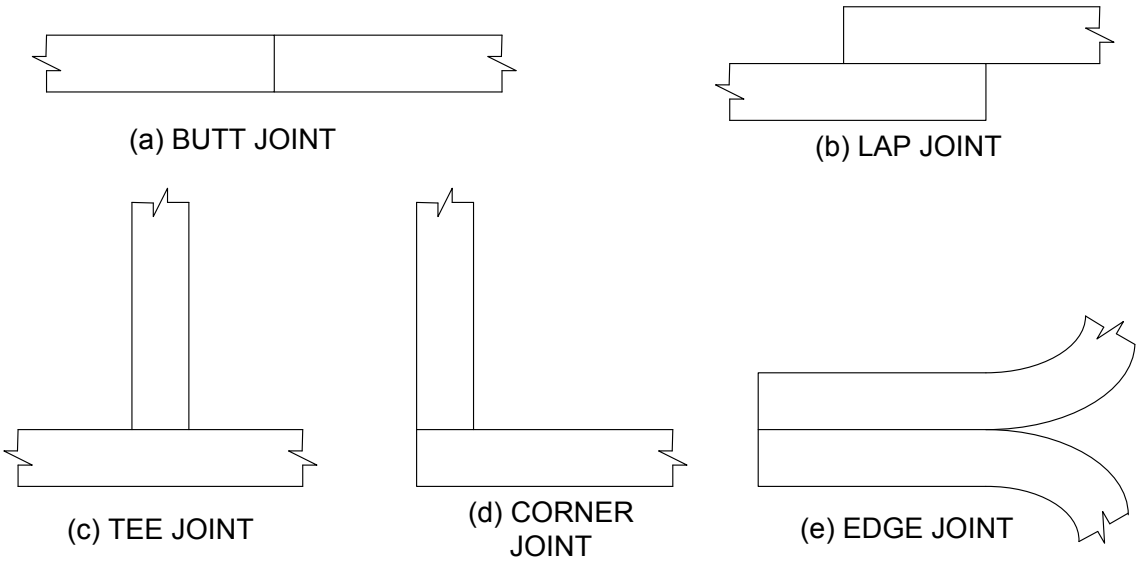

Figure 6.6.4.3.4-1 Types of Welded Joints

The joint type does not necessarily imply a specific type of weld. The selection of the weld type for certain types of joints (e.g. tee and corner joints) is usually dictated by the loading type and magnitude.

Butt joints are used to join the ends of flat plates together (e.g. girder flange and web shop splices). Butt joints in tension subject to fatigue loading are best made with complete penetration groove welds with the weld reinforcement removed. When subject to compression or shear only, partial penetration groove welds may be used providing adequate throats can be developed. The principal disadvantage of butt joints is that the connected edges typically require special preparation (i.e. beveling or grinding), and must be carefully aligned prior to welding.

Lap joints (e.g. cover plates and bracing member-to-gusset plate joints) do not require quite the preciseness in fabrication as other types of joints. The edges of the joined pieces are usually sheared or flame cut and do not require any special edge preparation. Lap joints utilize fillet welds and are the primary joint type for bracing member connections.

Tee joints are used to fabricate built-up sections, or in general, any pieces framing in at right angles (e.g. plate girder web-to-flange connections, stiffener-to-web connections, hangers, brackets). For tee joints subject to longitudinal shear, continuous fillet welds or groove welds can be used to join the pieces; however, fillet welds are usually the most economical option when the fillet weld leg size is less than ¾ in. (Miller and Ogborn, 1994). As larger throats are required, partial penetration groove welds (perhaps with external fillet welds) are the most cost-effective option (Miller and Ogborn, 1994). Complete penetration groove welds are

not recommended for use in tee joints because of the relatively high cost and resulting welding deformations. It should be noted that partial penetration groove welds are assigned a slightly lower fatigue category in this configuration (Detail Category B′ vs. Detail Category B), but this rarely controls.

Corner joints are typically used to form built-up non-composite rectangular closed box sections. For corner joints, internal access to the box section has a major influence on the weld selection. AASHTO/NSBA (2003) discusses suggested details for welding of corner joints in closed box configurations, including large boxes in which a person can safely work and boxes that are too small for a person to work safely inside. The suggested details primarily involve the use of fillet welds alone in all four corners of the box, or a combination of fillet welds for one flange and partial penetration groove welds for the second flange. Combinations involving the use of fillet welds and complete penetration groove welds are included, but are generally not recommended due to the expense, and the fact that backing bars must generally be left in place. For details where single fillet welds in all four corners, or double fillet welds for one flange in combination with partial penetration groove welds for the second flange, are recommended, the Design Engineer should evaluate the loading conditions (e.g. torsion) and ensure that sufficient internal diaphragms are provided to limit rotations at the corner joints. Corner joints should also be carefully detailed to prevent the possibility of lamellar tearing (Kaufmann et al., 1981; AISC, 1973; Thornton, 1973; ASCE, 1982).

6.6.4.3.5 Control of Distortion

Weld metal shrinkage can also result in distortion due to the non-uniform expansion and contraction of the weld metal and the adjacent base metal during the heating and cooling cycles of the welding process. As the weld metal cools and contracts, the resulting strains can cause distortion if the surrounding base material is free to move (Figure 6.6.4.3.5-1a). In heavily restrained materials, the strains induce stresses that can potentially lead to cracking. Stresses that result from material shrinkage are inevitable in welding. Distortions can be minimized, however, through efficient design and fabrication practices (Blodgett, 1960).

The Engineer can design welded assemblies to help minimize the amount of distortion. Reducing the amount of weld metal will decrease the amount of distortion. Therefore, the smallest acceptable weld size should be used. Groove weld details with no greater root opening that necessary that require the minimum volume of weld metal per unit length are also beneficial.

Symmetry in welding is also important in minimizing distortion. Consider using double-sided joints versus single-sided joints where practical. Balancing welds about the planes of symmetry of the cross-section can help the shrinkage forces from one set of welds counteract the shrinkage forces from the other set (Figure

6.6.4.3.5-1b and Figure 6.6.4.3.5-1c). Unbalanced welds removed from the neutral axis can cause longitudinal camber or sweep of the member.

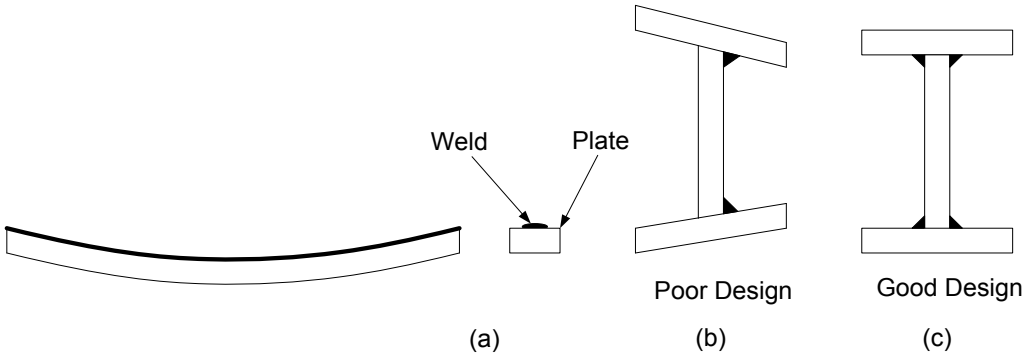

Figure 6.6.4.3.5-1 Welding Distortion

The Fabricator can also use techniques to help minimize distortion. Using as few weld passes as possible can help limit the number of heating and cooling cycles and the concomitant accumulation of shrinkage stresses. Overwelding should be avoided as it can result in more distortion than necessary. A well-planned welding sequence can help to balance the shrinkage forces. Parts to be welded may be pre-cambered prior to welding so that the parts will be drawn back into the proper alignment as weld shrinkage occurs. Clamps and jigs can be used to avoid rotation of the part and force the weld metal to stretch as it cools. Use of low heat input welding procedures that utilize high currents and high travel speeds can reduce the size of the heat affected zone and the amount of distortion.

To help minimize shrinkage and ensure adequate ductility, the AWS has established minimum preheat and minimum and maximum interpass temperatures (AASHTO/AWS, 2010). Preheat refers to the temperature of the steel immediately before the arc is struck on the steel. Preheat slows the cooling rates in the heat affected zone to prevent hardening and potential heat affected zone cracking (Section 6.6.4.3.6.1). Conditions of higher restraint, enriched base metal chemistries and adverse fabrication conditions may require additional preheat beyond the minimum requirements.

Interpass temperatures are measured after the welding (or the welding for each pass) has begun. The required minimum interpass temperature should be the same as the minimum specified preheat. The minimum interpass temperature is the temperature below which welding should not be done unless additional heat is added to raise the temperature of the steel. Large weldments and long joints can fall below the minimum interpass temperature before starting the next pass necessitating the addition of more heat before welding can resume. The maximum interpass temperature is the temperature beyond which welding should not be performed. Small weldments and short joints can exceed the maximum interpass

temperature, in which case welding must stop until the joint is cooled down to an acceptable level.

6.6.4.3.6 Weld Quality

6.6.4.3.6.1 Potential Defects in Welds

Discontinuities within a weld may result from a number of potential defects unless good welding techniques and practices are followed. Among the more common defects are incomplete fusion, inadequate joint preparation, porosity, undercutting, slag inclusions, and cracks.

As illustrated in Figure 6.6.4.3.6.1-1a, incomplete fusion results due to failure of the base metal and weld metal to fuse together properly. Potential causes of incomplete fusion include the use of welding equipment with insufficient current so that the base metal does not reach its melting point, too rapid a rate of welding and surfaces to be joined that are contaminated or coated with mill scale, slag, oxides or other foreign material.

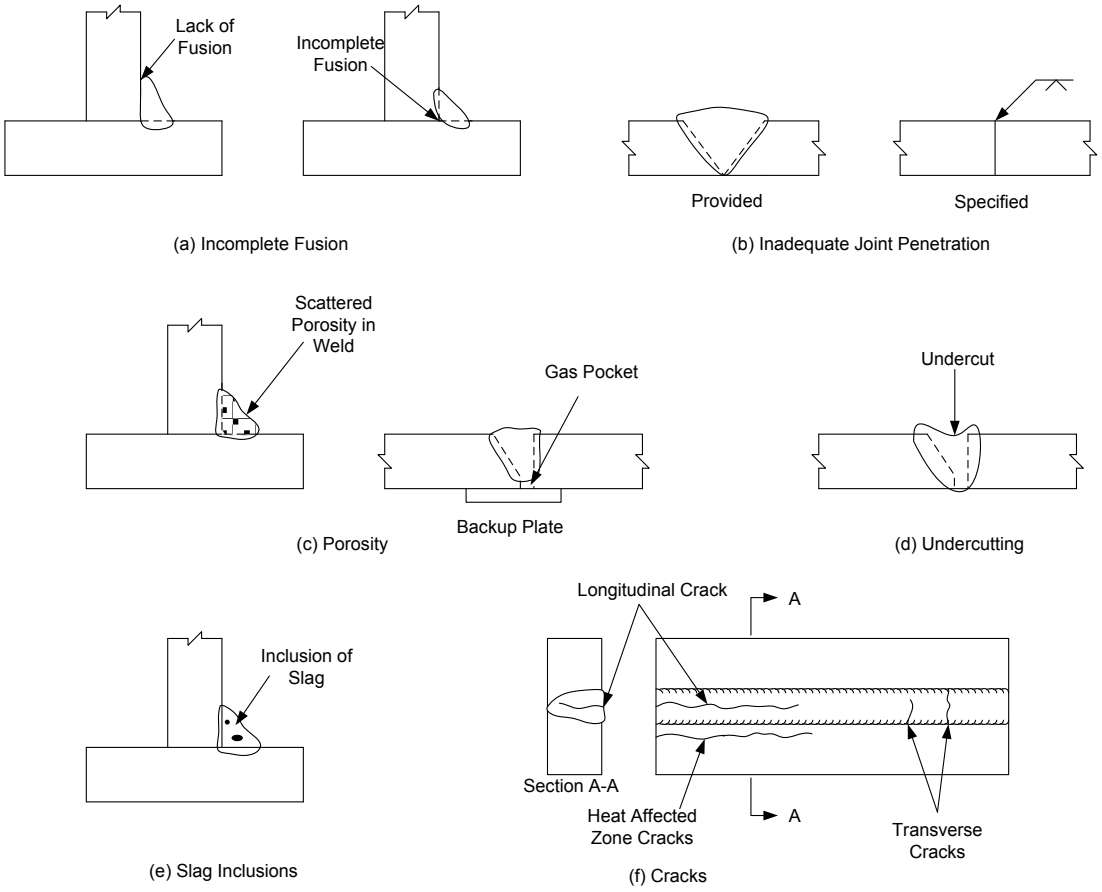

Figure 6.6.4.3.6.1-1 Potential Weld Defects

Incomplete joint penetration (Figure 6.6.4.3.6.1-1b) is associated primarily with groove welds, and occurs when CJP groove welds are specified and the weld extends a shallower distance through the depth of the groove than specified. This defect can result from the use of insufficient welding current, too rapid a rate of welding, excessively large electrodes or the use of an improper groove design for the selected welding process. The use of the pre-qualified joints given by AWS in AASHTO/AWS (2010), or joints that have a proven history of acceptable performance that can be used without again proving their adequacy by test, can help to minimize such defects. The specified combination of root opening, included angle, applicable thickness, etc. in a pre-qualified joint helps to ensure adequate fusion, welder access and joint penetration. Specified tolerances may be applied to pre-qualified joints. When the actual joint detail fits within those tolerances, the joint is considered to be pre-qualified. Otherwise, the joint requires qualification by test. The fabricator/detailer will typically select the proper pre-qualified joint for a particular application and show it on the shop drawings.

Porosity in a weld occurs when voids or a number of small gas pockets are trapped in the weld during cooling (Figure 6.6.4.3.6.1-1c). The porosity may be scattered through the weld, or concentrated as a large pocket at the root of a fillet weld, or at the root of a groove weld adjacent to a backup plate. Porosity typically results from using too long of an arc or an excessively high current.

Undercutting results when a groove is melted into the base material adjacent to a fillet weld toe or into the weld itself (Figure 6.6.4.3.6.1-1d), and is left unfilled by weld metal. This defect usually results from the use of excessive current, or too long of an arc, and can usually be corrected by depositing additional weld metal.

Slag inclusions result when the slag that forms during the welding process, which has a lower density than the molten weld metal and normally floats to the surface, is trapped within the weld due to too rapid a cooling of the joint (Figure 6.6.4.3.6.1-1e). In multiple pass welds, the slag must be removed by the welder in-between each pass. Otherwise, slag inclusions may result. Overhead welds are particularly susceptible to slag inclusions.

Weld cracks, which are the most significant of the weld defects, result from internal shrinkage strains that occur as the weld metal cools. Weld cracks, as distinguished from weld failures that may occur due to underdesign, overload or fatigue, typically occur close to the time of fabrication. Hot cracks are cracks that occur at elevated temperatures and are usually related to solidification as cooling begins to occur. Hot cracks are usually caused by brittle states of various constituents (e.g. alloying elements) forming along grain boundaries and can usually be prevented by more uniform heating and slower cooling. Cold cracks are cracks that occur after the weld metal has cooled to ambient temperature and may be related to the effects of hydrogen, restraint to shrinkage and distortion, and the formation of a brittle

martensite microstructure. Cold cracking typically occurs in low-alloy steels and can be minimized through the use of low-hydrogen electrodes, use of the proper preheating and interpass temperatures, careful attention to welding sequences and procedures, use of the proper filler material, and in some cases, post weld heat treatment.

Weld cracks may be characterized as centerline (or longitudinal) cracks, heat affected zone cracks, and transverse cracks (Figure 6.6.4.3.6.1-1f).

Centerline cracking is a separation occurring in the center of a given weld bead.

Heat affected zone cracking (also known as delayed or underbead cracking) is a separation occurring immediately adjacent to the weld bead in the base material. This region, termed the heat affected zone (HAZ), results from the thermal cycle experienced by this region during welding. This region is typically raised to a temperature above the transformation temperature of the steel, but below its melting point. The final properties of this region depend on the cooling rate that it experiences. In base material with higher carbon and carbon equivalency levels, the HAZ is susceptible to increased hardness and reduced ductility upon cooling, which can increase the probability of HAZ cracking. Hydrogen on the steel, electrode, shielding material or in the atmosphere that is dissolved in the molten weld metal can also contribute to HAZ cracking in low-alloy steels that are subject to such cracking. Diffusion of the hydrogen through the weld metal toward any discontinuities in the HAZ occurs as the weld metal solidifies. As free hydrogen combines to form molecular hydrogen, a significant increase in internal pressure occurs within the HAZ. In susceptible steels, cracking can occur in the presence of this hydrogen in combination with the residual stresses due to welding. Since the diffusion of the hydrogen through the weld metal takes time, such cracking may occur hours or even days after fabrication is completed; hence the term “delayed hydrogen cracking”.

Transverse cracking is a separation occurring within the weld metal perpendicular to the direction of travel. It is generally associated with weld metal that is high in strength that significantly overmatches the base metal, and is the least frequently encountered type of cracking.

More detailed information on the causes of different types of weld cracks and potential corrective solutions may be found in Miller and Ogborn (1994).

6.6.4.3.6.2 Inspection and Control

The success of welding in steel-bridge construction can be attributed to the inspection and control procedures that have been implemented to ensure the production of a sound quality weld.

Welding Procedure Specifications (WPS) are developed by welding engineers or technicians to communicate to the welders and inspectors the various parameters under which the welding is to be performed. The WPS is essentially the recipe for making a particular weld and should be made available to the welder and inspector near the point of welding for easy referral. The procedures are then tested to ensure their validity.

The supporting test data for a particular welding procedure is contained in a so-called Procedure Qualification Record (PQR). The tests typically include bend tests, transverse tension tests, all-weld-metal tension tests, Charpy impact tests, and a marcoetch specimen. PQRs are typically filed in the fabrication office and are not made available to the welders. All welders should be pre-qualified; that is, they must pass an AWS Qualification Test prior to making a structural connection.

Welds must be inspected to ensure that they comply with the requirements of a given specification. Discontinuities are irregularities in the weld that may or may not be acceptable according to a given specification, whereas defects are discontinuities that are rejectable according to a given specification. A qualified welding inspector can utilize five primary non-destructive testing methods to locate and evaluate weld discontinuities. Each method has unique advantages and disadvantages. The methods are visual inspection (VT), penetrant testing (PT), magnetic particle inspection (MT), radiographic inspection (RT), and ultrasonic inspection (UT). Phased array ultrasonic testing (PAUT) is a newer inspection method that has recently been gaining some traction (not discussed herein).

Visual inspection (VT) is the most powerful and simplest inspection method. Visual inspection commences well before welding begins by examining the materials to be welded, the alignment and fit-up of the parts, joint preparation and procedural data. During welding, visual inspection can ensure compliance with procedural requirements. Upon completion of welding, the size, appearance, bead profile and surface quality of the weld can be visually inspected.

Penetrant testing (PT) involves the application of a liquid dye penetrant to the weld, which is drawn to a surface discontinuity (i.e. porosity or a crack) by capillary action. A developer is then applied which absorbs the penetrant within the discontinuity and results in a stain indicating the presence of the discontinuity. This means of inspection is generally not specified for bridge fabrication since it is limited to the recognition of surface discontinuities, which can also be recognized by magnetic particle inspection.

Magnetic particle inspection (MT) involves the application of magnetic iron powders to the surface of the part. When a magnetic field is then applied, the change in magnetic flux that occurs in the presence of a discontinuity shows up as a different

pattern within the powders. MT is most effective in locating surface discontinuities, and those that are slightly subsurface. It is typically used to enhance visual inspection. Fillet welds and intermediate passes on large groove welds are often inspected using MT.

Radiographic inspection (RT) utilizes X-rays or gamma rays that are passed through a groove weld to expose a photographic film on the opposite side of the joint producing a permanent record for future reference. Thin parts (e.g. porosity, slag and cracks) absorb less radiation than thick parts and therefore will appear darker on the radiograph, which is in effect a negative. RT is generally most effective in detecting porosity and slag inclusions, and requires significant skill in order to properly interpret the radiograph.

Ultrasonic inspection (UT) utilizes high frequency sound waves that are transmitted through the materials. Discontinuity-free material will transmit the sound through the part in an uninterrupted fashion. A receiver hears the sound reflected off the back surface of the part being examined. A discontinuity between the transmitter and the back surface of the part will result in an intermediate signal being sent to the receiver. The magnitude of the signal indicates the size of the discontinuity and the location of the discontinuity is indicated by the relationship of the signal with respect to the back surface. UT can be used to spot even small discontinuities and is generally most sensitive to cracks. UT is often used to inspect (and re-inspect) groove welds prior to code-mandated RT inspection.

More detailed information on each of these inspection methods, including the relative advantages and disadvantages of each, may be found in AWS (2001) and Miller and Ogborn (1994).

6.6.4.3.7 Factored Resistance

6.6.4.3.7.1 General

The factored resistance of a welded connection, R_r, at the strength limit state in the *AASHTO LRFD* Specifications is based on either the factored resistance of the base metal, or the product of the weld metal strength and the effective area of the weld that resists the load. The weld metal strength is the capacity of the weld metal itself, typically given in units of ksi. As discussed in Section 6.6.4.3.3.2.3, the effective area of the weld that resists the load is the product of the effective length and the effective throat of the weld.

Weld metal strength may be classified as “matching”, “undermatching”, or “overmatching”. Matching weld (filler) metal has the same or slightly higher specified minimum yield and tensile strength, as compared to the specified minimum properties of the base metal. For example, matching weld metal for ASTM

A709/A709M Grade 50 steel would be E70 filler material, where the specified minimum weld/base metal properties for yield strength are 60/50 ksi and for tensile strength are 70/65 ksi. Although the weld metal has slightly higher properties than the base metal in this case, this is considered to be a matching combination. Note that according to AASHTO/AWS (2010), matching consumables for ASTM A709/A709M Grade 50W base metal (as specified in AASHTO/AWS, 2010) are considered to be matching strength for hybrid designs, where ASTM A709/A709M Grade HPS 70W base metal is joined to ASTM A709/A709M Grade 50W base metal.

AASHTO LRFD Article 6.13.3.1 specifies that matching weld metal must be used in groove and fillet welds, except that undermatching weld metal is permitted for fillet welds if the welding procedure and weld metal are selected to ensure the production of sound welds. According to *AASHTO LRFD* Article C6.13.3.1, the use of undermatched weld metal is strongly encouraged for fillet welds connecting steels with specified minimum yield strength greater than 50 ksi. Lower strength weld metal will generally be more ductile than higher strength weld metal. Since the residual stresses in a welded connection are assumed to be on the order of the yield point of the weaker material in the connection (Miller and Ogborn, 1994), using lower strength weld metal will lower the level of residual stresses in the base metal at the connection reducing the cracking tendencies. Therefore, undermatched welds will be much less sensitive to delayed hydrogen cracking, and are more likely to consistently produce sound welds. In such cases, the Design Engineer should indicate where undermatched welds are acceptable on the contract drawings.

Overmatching weld metal offers no significant advantages, and increases the level of residual stresses and distortion at the connection. As mentioned above, higher yield strength weld metal is typically less ductile and more crack sensitive. Overmatching weld metal may also force the failure plane into the heat affected zone, or fusion boundary, which is an undesirable condition (Miller and Ogborn, 1994). Slight overmatching is acceptable in some cases. For example, in the process of adding alloys for improved atmospheric corrosion resistance, most filler metals for welding ASTM A709/A709M Grade 50W weathering steel will deposit weld metal with a specified minimum tensile strength of 80 ksi, versus the specified minimum tensile strength of 70 ksi for the base metal. Since this combination performs well, and there are limited alternatives, this slight overmatch is acceptable. Since some acceptable weld metals for weathering steel applications are classified as E70, basing the weld design calculations on E70 will give the fabricator the flexibility of using either E70 or E80 weld metal.

Section 6.6.4.3.7.2 discusses the factored resistance of welded connections made with fillet welds, which are the most widely used welds. For determining the factored resistance of welded connections made with CJP or PJP groove welds, the reader is referred to *AASHTO LRFD* Articles 6.13.3.2.2 and 6.13.3.2.3, respectively.

6.6.4.3.7.2 Fillet Welded Connections

6.6.4.3.7.2.1 General

For design purposes, fillet welds are assumed to transfer loads through shear on the effective area of the weld regardless of whether the shear transfer is parallel or perpendicular to the axis of the weld. The factored resistance is actually greater for shear transfer perpendicular to the weld, but there is less deformation capability. In both cases, although the weld fails in shear, the plane of rupture is not the same. However, in the *AASHTO LRFD* Specifications, the additional factored resistance of fillet welds loaded perpendicular to the axis of the weld is ignored and both loading situations are treated the same.

Figure 6.6.4.3.7.2.1-1 Part A shows qualitatively a typical elastic shear stress distribution in the longitudinal fillet welds in a lap joint (i.e. for shear transfer parallel to the weld axis). The actual variation of shear stress from Point A to Point B depends on the ratio of the widths of the plates being joined and the length of the weld. Figure 6.6.4.3.7.2.1-1 Part B shows a typical elastic shear distribution for fillet welds loaded perpendicular to the weld axis.

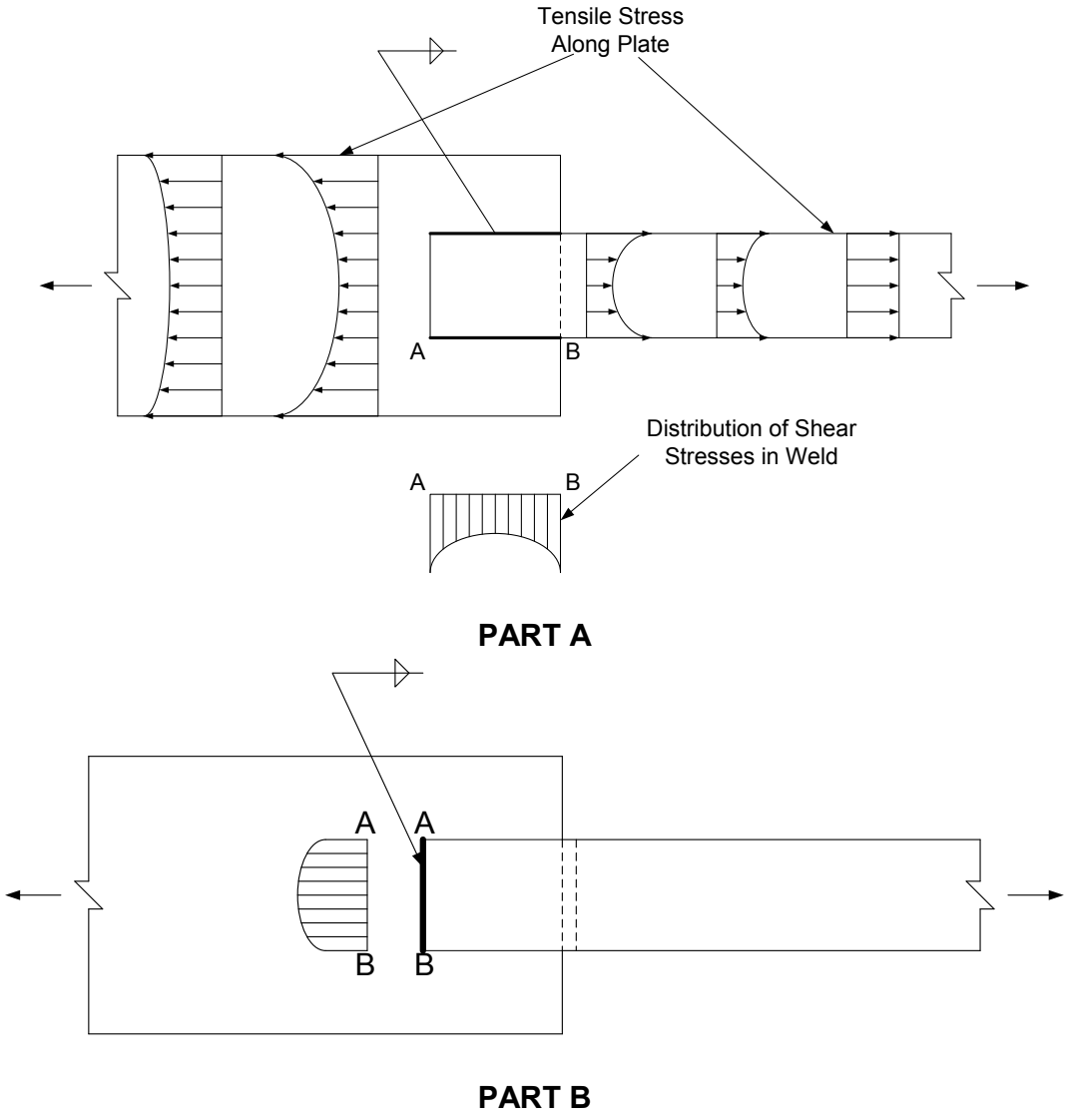

Figure 6.6.4.3.7.2.1-1 Typical Fillet Weld Shear Stress Distributions in a Lap Joint

A) Shear Stress Distribution for Load Parallel to Weld Axis; B) Shear Stress Distribution of Load Perpendicular to Weld Axis

Shear yielding is not critical in the welds because strain hardening occurs without significant overall deformation occurring in either case. Although the elastic shear stress distributions along the length of the weld are not uniform, the available ductility or plastic deformation capability permits lines of fillet weld loaded parallel or perpendicular to the weld to be assumed to resist the load equally along their lengths.

According to *AASHTO LRFD* Article 6.13.3.2.4a, the factored resistance, R_r, of fillet-welded connections at the strength limit state subject to tension or compression parallel to the axis of the weld is to be taken as the corresponding factored resistance of the base metal. Note that fillet welds joining component elements of built-up members (e.g. girder flange-to-web welds) need not be designed for the tensile or compressive stress in those elements parallel to the axis of the welds.

According to *AASHTO LRFD* Article 6.13.3.2.4b, the factored resistance, R_r, of fillet-welded connections at the strength limit state subject to shear on the effective area is to be taken as follows:

$$R_r = 0.6\phi_{e2}F_{exx} \qquad \text{Equation 6.6.4.3.7.2.1-1}$$

AASHTO LRFD Equation 6.13.3.2.4b-1

where:

ϕ_{e2} = resistance factor for shear on the throat of the weld metal in fillet welds specified in *AASHTO LRFD* Article 6.5.4.2 (= 0.80)

F_{exx} = classification strength of the weld metal (ksi) (e.g. for E70 weld metal, F_{exx} = 70 ksi)

The welds must have typical weld profiles and may be matched or undermatched. The factored shear rupture resistance of the base metal (i.e. $R_r = \phi_u 0.6F_u$) adjacent to the weld leg will seldom control since the effective area of the base metal at the weld leg is typically about 30 percent greater than the weld throat. Therefore, the specification does not require this resistance to be checked. In cases where overmatching weld metal is used, or where the weld throat has excessive convexity such that the resistance is governed by the weld leg, the shear rupture resistance should be checked to avoid overstressing of the base metal.

If a certain size fillet weld must be used in adjacent areas of a particular joint, it is desirable to use the same size weld to allow the same electrodes and welding equipment to be used for that joint and to simplify the inspection.

EXAMPLE

Design the bearing stiffener-to-web fillet welds for the bearing stiffeners that are designed in the example given in Section 6.6.6.3.4.2. The maximum factored Strength I end reaction, R_u, is 388 kips. The girder web at the abutment is ½" x 69". The bearing stiffeners are 5/8" thick. The girder flanges and web and the stiffeners are ASTM A709/A709M Grade 50W steel with a specified minimum tensile strength, F_u = 70 ksi (*AASHTO LRFD* Table 6.4.1-1). Assume E70 electrodes (i.e. matching weld metal) with a classification strength, F_{exx}, equal to 70 ksi.

According to *AASHTO LRFD* Table 6.13.3.4-1 (Table 6.6.4.3.3.3.4-1), the minimum size fillet weld is ¼ in. when the base metal thickness, *T*, of the thicker part joined is less than or equal to ¾ in. Therefore, try the minimum size fillet weld equal to ¼ in. The effective throat of a ¼ in. equal-leg fillet weld is equal to:

$$t_e = 0.707(0.25) = 0.177 \text{ in.}$$

According to *AASHTO LRFD* Article 6.13.3.2.4b, the factored resistance, R_r, of fillet-welded connections at the strength limit state subject to shear on the effective area is to be taken as (Equation 6.6.4.3.7.2.1-1):

$$R_r = 0.6\phi_{e2}F_{exx}$$

where ϕ_{e2} is equal to the resistance factor for shear on the throat of the weld metal in fillet welds specified in *AASHTO LRFD* Article 6.5.4.2 = 0.80. Therefore:

$$R_r = 0.6(0.80)(70) = 33.6 \text{ ksi}$$

The factored resistance of a ¼-in. fillet weld in shear in units of kips/inch at the strength limit state is computed as:

$$V_r = R_r t_e = 33.6(0.177) = 5.95 \text{ kips / in.}$$

Note that the governing factored shear rupture resistance of the base metal adjacent to the weld leg at the strength limit state is computed as (Equation 6.6.4.2.5.6.2-2):

$$V_r = \phi_{vu}0.58F_u t = 0.80(0.58)(70)(0.5) = 16.2 \text{ kips / in.}$$

and does not control. As mentioned previously, this will be the case in most situations unless overmatching weld metal is used, or where the weld throat has excessive convexity such that the resistance is controlled by the weld leg instead of the effective throat.

The total length of a single bearing stiffener-to-web weld, allowing 2.5 inches for clips at the top and bottom of the stiffeners to clear the flange-to-web welds, is:

$$L_w = 69.0 - 2(2.5) = 64.0 \text{ in.}$$

The total factored resistance of the four ¼-in. fillet welds connecting the stiffeners to the web (in kips) is therefore:

$$4(5.95)(64.0) = 1523 \text{ kips} > R_u = 388 \text{ kips} \quad \text{ok}$$

Since the stiffeners are located at an abutment, fatigue of the base metal adjacent to these welds need not be checked. From *AASHTO LRFD* Table 6.6.1.2.3-1 (Condition 4.1), the nominal fatigue resistance for base metal at the toe of stiffener-to-web welds is based on fatigue Detail Category C′. Thus, when these welds are subject to a net applied tensile stress (as defined in *AASHTO LRFD* Article 6.6.1.2.1), the longitudinal stress range due to the factored fatigue load plus impact at the toe of the welds should be checked against the nominal fatigue resistance based on fatigue Detail Category C′ (Section 6.5.5.2.2).

EXAMPLE

Design the flange-to-web fillet welds for the composite girder cross-section shown in Figure 6.4.2.3.2.3-1, which is in a region of positive flexure. The elastic section properties for this section are given in Section 6.4.2.3.2.3. The steel for the flanges and web is ASTM A709/A709M Grade 50W steel with a specified minimum tensile strength F_u = 70 ksi (*AASHTO LRFD* Table 6.4.1-1). Assume E70 electrodes (i.e. matching weld metal) with a classification strength, F_{exx}, equal to 70 ksi.
Flange-to-web welds are designed for the horizontal shear flow (i.e. $s = VQ/I$). The maximum unfactored vertical design shears acting on this section are as follows:

V_{DC1} = 87 kips
V_{DC2} = 13 kips
V_{DW} = 13 kips
V_{LL+IM} = 139 kips

For the steel section only:

I = 62,658 in.^{4}
Top flange: Q = 1(16)(39.13) = 626 in.^{3}
Bot. flange: Q = 1.375(18)(31.06) = 769 in.^{3}

For the composite section ($3n$ = 24):

I = 122,232 in.^{4}
Top flange: Q = 1(16)(22.24) = 356 in.^{3}
Conc. deck: Q = 9(114/24)(29.74) = + 1,271 in.^{3}
1,627 in.^{3}
Bot. flange: Q = 1.375(18)(47.95) = 1,187 in.^{3}

For the composite section (n = 8):

I = 166,612 in.^{4}
Top flange: Q = 1(16)(9.73) = 156 in.^{3}
Conc. deck: Q = 9(114/8)(17.23) = + 2,210 in.^{3}
2,366 in.^{3}

Bot. flange: $Q = 1.375(18)(60.46) = 1{,}496 \text{ in.}^3$

Calculate the total factored Strength I shear flow at the top and bottom welds.

At the top welds:

$$s_u = \left[\frac{1.25(87)(626)}{62{,}658} + \frac{1.25(13)(1{,}627)}{122{,}232} + \frac{1.5(13)(1{,}627)}{122{,}232} + \frac{1.75(139)(2{,}366)}{166{,}612}\right] = 5.02 \text{ kips / in.}$$

At the bottom welds:

$$s_u = \left[\frac{1.25(87)(769)}{62{,}658} + \frac{1.25(13)(1{,}187)}{122{,}232} + \frac{1.5(13)(1{,}187)}{122{,}232} + \frac{1.75(139)(1{,}496)}{166{,}612}\right] = 3.86 \text{ kips / in.}$$

The shear flow at the top welds governs. For two welds, the shear flow at each weld is 5.02/2 = 2.51 kips/in.

According to *AASHTO LRFD* Article 6.13.3.2.4b, the factored resistance, R_r, of fillet-welded connections at the strength limit state subject to shear on the effective area is to be taken as (Equation 6.6.4.3.7.2.1-1):

$$R_r = 0.6\phi_{e2}F_{exx}$$

where ϕ_{e2} is equal to the resistance factor for shear on the throat of the weld metal in fillet welds specified in *AASHTO LRFD* Article 6.5.4.2 = 0.80. Therefore:

$$R_r = 0.6(0.80)(70) = 33.6 \text{ ksi}$$

Equating the factored resistance of a fillet weld in shear in units of kips/inch at the strength limit state to the shear flow due to the factored loads gives:

$$V_r = R_r t_e = 33.6(0.707a) = 2.51 \text{ kips / in.}$$

where t_e is the thickness of the effective throat, and *a* is the required leg size of the weld. Solving for *a* gives:

$$a = 0.11 \text{ in.}$$

However, according to *AASHTO LRFD* Table 6.13.3.4-1 (Table 6.6.4.3.3.3.4-1), the minimum size fillet weld is 5/16 in. (0.3125 in.) when the base metal thickness, *T*, of the thicker part joined is greater than ¾ in. The top flange is 1" thick and the bottom flange is 1-3/8" thick (the web is ½" thick). Therefore, use the minimum size fillet

weld equal to 5/16 in. for both the top and bottom flange welds. The minimum size weld will often control the size of flange-to-web welds.

From *AASHTO LRFD* Table 6.6.1.2.3-1 (Condition 3.1), the nominal fatigue resistance for base metal connected by continuous fillet-welded connections parallel to the direction of applied stress is based on fatigue Detail Category B. Although not illustrated here, for flange-to-web welds subject to a net applied tensile stress, the longitudinal stress range due to the factored fatigue load plus impact should be checked against the nominal fatigue resistance based on fatigue Detail Category B (Section 6.5.5.2.2).

6.6.4.3.7.2.2 Fatigue Resistance

According to *AASHTO LRFD* Table 6.6.1.2.3-1 (Condition 7.2), the nominal fatigue resistance of the base metal in single- or double-angle members or tee members connected by longitudinal fillet welds along both sides of the connected element of the member cross-section (e.g. a typical lap joint used in a bracing member connection) is to be based on Detail Category E. The checking of fatigue of fillet-welded bracing member connections for single- and double-angle members, and for tee members, is discussed above in Section 6.6.3.3.5. As discussed in that section, while research showed that balancing of the welds offers some increase in the fatigue life of these connections (McDonald and Frank, 2009), it is probably not worth the increase in the gusset or connection plate length required to accommodate the longer weld along one leg. (Note that as of this writing (2015), AASHTO is considering a potential reduction in the nominal fatigue resistance of the base metal in single-angle members connected by longitudinal fillet welds from Detail Category E to Detail Category E′ - refer to Section 6.6.3.3.5.1).

The reader is referred to *AASHTO LRFD* Table 6.6.1.2.3-1 to determine the fatigue detail category for other types of fillet-welded connections, and for various groove-welded connections (e.g. welded lateral connection plates for lateral bracing members).

6.6.4.3.7.2.3 Eccentric Shear

As indicated in *AASHTO LRFD* Article 6.13.1, eccentric connections should be avoided, but where they cannot be avoided, members and connections are to be designed for the combined effects of shear and moment due to the eccentricity.

AASHTO LRFD Article C6.13.3.2.4b indicates that if fillet welds are subject to eccentric loads that produce a combination of shear and bending stresses, they are to be proportioned based on a direct vector addition of the shear forces on the weld. Eccentric shear can result, for example, when the loading of fillet welds is neither parallel to nor transverse to the axis of the welds. Basically, eccentric shear

conditions occur when the welds are subject to pure torsion, a combination of shear and torsion, or a combination of shear and bending.

As discussed in Section 6.6.4.2.6 for eccentric shear on bolted connections, the resistance of an eccentrically-loaded fillet-weld connection subject to a combination of shear and torsion can be conservatively determined using a traditional elastic vector analysis approach. The following assumptions are made in this approach: 1) assuming each segment of weld is of the same size, it is assumed that concentrically applied load (i.e. direct shear) is resisted equally by each weld segment; 2) any rotation caused by a torsional moment is assumed to occur about the centroid of the weld configuration; 3) load on a weld segment caused by a torsional moment is assumed proportional to the distance of that segment from the centroid of the weld configuration; 4) the direction of the force on a weld segment caused by a torsional moment is assumed perpendicular to the radial distance of the segment from the centroid of the weld configuration; and 5) the resultant force is obtained by combining vectorially the components of the forces caused by direct shear and torsion. Also, for computing forces or stresses on the weld segments, the segment lines are assumed defined by the edges along which the fillets are placed, rather than to the center of the effective throats.

Consider the general case of an eccentrically loaded welded connection subject to combined shear and torsion shown in Figure 6.6.4.3.7.2.3-1.

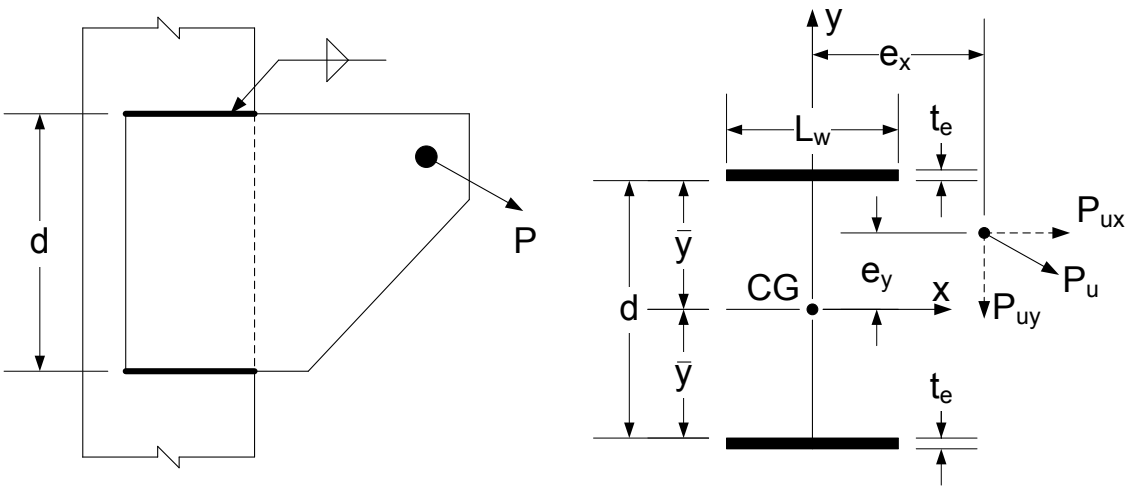

Figure 6.6.4.3.7.2.3-1 Eccentrically Loaded Fillet Welded Connection Subject to Combined Shear & Torsion

For this case, the components of stress in the weld segments caused by direct shear are determined as:

$$f_{vx} = \frac{P_{ux}}{A}$$ Equation 6.6.4.3.7.2.3-1

$$f_{vy} = \frac{P_{uy}}{A}$$ Equation 6.6.4.3.7.2.3-2

where *A* is the effective weld area taken as the thickness of the effective throat, t_e, times the total length, L_w, of the weld configuration.

The x- and y-components of stress due to the torsional moment can be computed as follows:

$$f_{Tx} = \frac{Ty}{I_p} = \frac{\left(P_{ux}e_y + P_{uy}e_x\right)y}{I_p}$$ Equation 6.6.4.3.7.2.3-3

$$f_{Ty} = \frac{Tx}{I_p} = \frac{\left(P_{ux}e_y + P_{uy}e_x\right)x}{I_p}$$ Equation 6.6.4.3.7.2.3-4

where I_p is the polar moment of inertia of the weld configuration about the centroid of the weld configuration calculated as follows:

$$I_p = \sum\left(I_x + I_y\right) + \sum A\left(\bar{x}^2 + \bar{y}^2\right)$$ Equation 6.6.4.3.7.2.3-5

I_x and I_y are the moments of inertia of each weld segment about their own centroidal axes, *A* is the area of each weld segment, and $\bar{x}$ and $\bar{y}$ are the distances from the centroid of the weld configuration to each individual weld segment. For the case shown in Figure 6.6.4.3.7.2.3-1:

$$I_p \cong \frac{t_e}{6}\left[12L_w\bar{y}^2 + L_w^3\right]$$ Equation 6.6.4.3.7.2.3-6

When the above stresses are multiplied by effective throat thickness, t_e, the result is a component of force, *R*, in units of kips/inch.

It becomes convenient in these calculations to treat the welds as lines having length, but with an effective throat thickness (width), t_e, equal to unity (Figure 6.6.4.3.7.2.3-2).

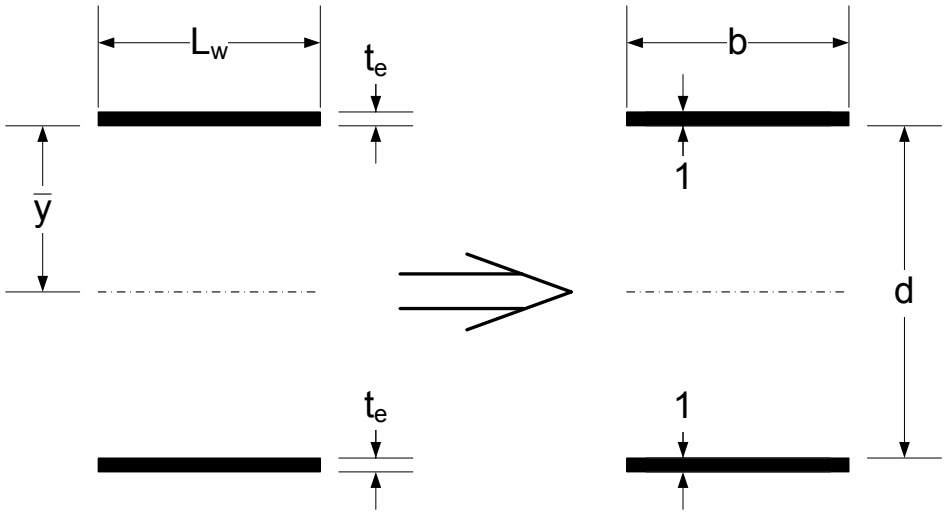

Figure 6.6.4.3.7.2.3-2 Weld Configuration Considered as Lines of Unit Thickness

For the above case, setting t_e equal to 1.0 and using the more general terms, *b* and *d*, as shown in Figure 6.6.4.3.7.2.3-3, Equation 6.6.4.3.7.2.3-6 can be written as follows:

$$I_p \cong \frac{1}{6}\left[12b\left(\frac{d}{2}\right)^2 + b^3\right] = \frac{b}{6}\left[3d^2 + b^2\right] \qquad \text{Equation 6.6.4.3.7.2.3-7}$$

Properties for other common weld line configurations are tabulated in Salmon and Johnson (1996), or can be derived in a similar fashion by the Design Engineer.

A less conservative alternative approach to determine the resistance of a weld configuration subject to eccentric shear is provided in AISC (2010a). In this approach, an instantaneous center of rotation is located and the load-deformation relationship of a fillet weld is used.

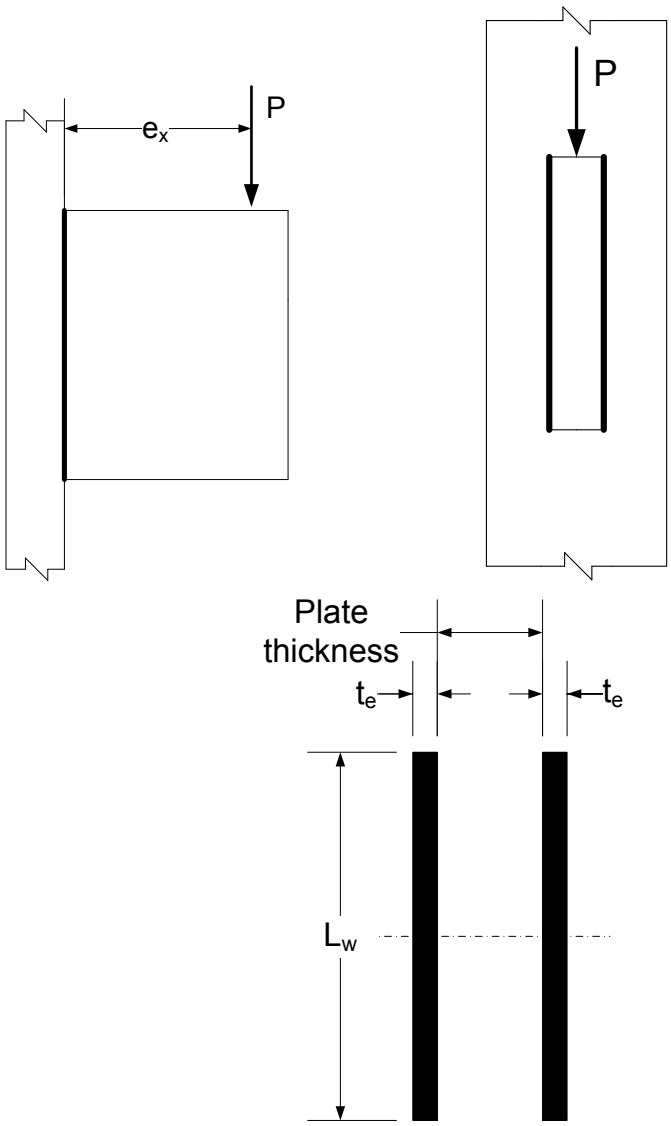

Figure 6.6.4.3.7.2.3-3 Eccentrically Loaded Fillet Welded Connection Subject to Combined Shear & Bending

The traditional elastic vector analysis method can also be used for the case where the applied load is eccentric to the plane of the weld configuration subjecting the configuration to combined shear and bending moment (Figure 6.6.4.3.7.2.3-3). In essence, the weld configuration is loaded in shear and tension. The compression force from the bending is typically assumed carried by direct compression of the pieces being welded rather than through the welds. The weld segments are again treated as lines with a thickness of unity.

EXAMPLE

Using the elastic vector analysis method, design the fillet welds for the eccentrically loaded bracket shown in Figure 6.6.4.3.7.2.3-4, which is subject to combined shear and torsion, for the strength limit state. The fatigue limit state is not checked in this example. Assume E70 electrodes.

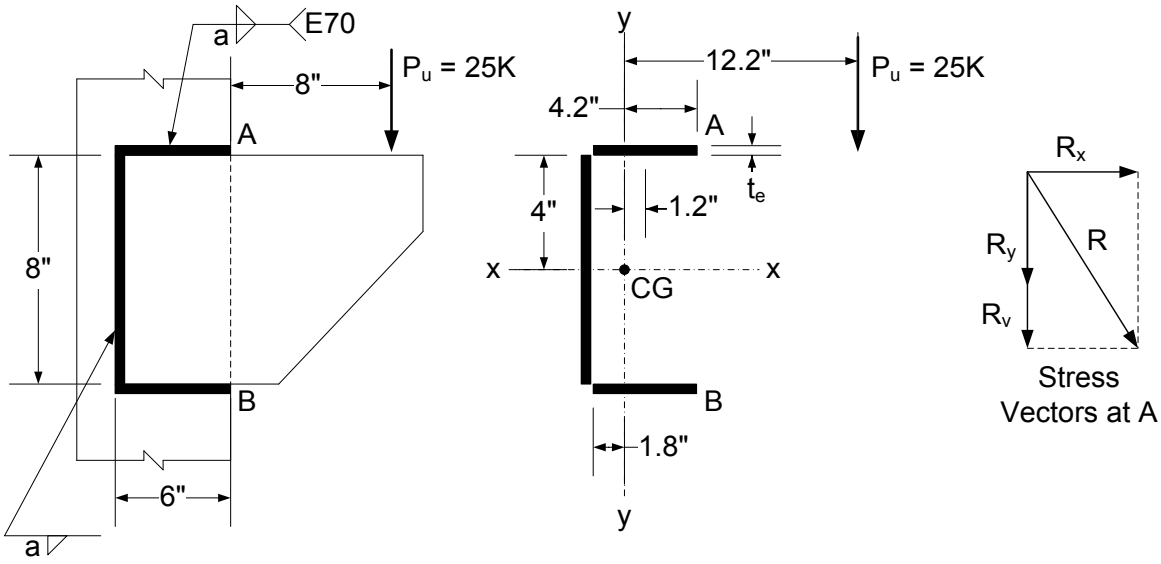

Figure 6.6.4.3.7.2.3-4 Eccentrically Loaded Fillet-Welded Bracket Example 1

Salmon and Johnson (1996) provide the following formulas for computing the location of the centroid (from the vertical weld) and polar moment of inertia of the above weld configuration treating the welds as lines:

$$\bar{x} = \frac{b^2}{2b + d}$$

Therefore:

$$\bar{x} = \frac{6^2}{2(6) + 8} = 1.8 \text{ in.}$$

$$I_p = \frac{8b^3 + 6bd^2 + d^3}{12} - \frac{b^4}{2b + d}$$

Therefore:

$$I_p = \frac{8(6)^3 + 6(6)(8)^2 + 8^3}{12} - \frac{6^4}{2(6)+8} = 314 \text{ in}^3$$

The maximum resultant force, *R*, on the weld configuration is at Points A and B. Compute the vertical force on the weld line configuration, R_v, due to the direct shear:

$$R_v = \frac{P_u}{L_w} = \frac{25}{2(6)+8} = 1.25 \text{ kips / in.}$$

Referring to Figure 6.6.4.3.7.2.3-4, compute the x- and y-components of force R_{Tx} and R_{Ty} due to the torsion acting on the weld line configuration:

$$R_{Tx} = \frac{Ty}{I_p} = \frac{25(12.2)4}{314} = 3.89 \text{ kips / in.}$$

$$R_{Ty} = \frac{Tx}{I_p} = \frac{25(12.2)4.2}{314} = 4.08 \text{ kips / in.}$$

Compute the resultant force, *R*, by taking the vector sum of the horizontal and vertical components of force:

$$R = \sqrt{(3.89)^2 + (1.25 + 4.08)^2} = 6.60 \text{ kips / in.}$$

According to *AASHTO LRFD* Article 6.13.3.2.4b, the factored resistance, R_r, of fillet-welded connections at the strength limit state subject to shear on the effective area is to be taken as (Equation 6.6.4.3.7.2.1-1):

$$R_r = 0.6\phi_{e2}F_{exx}$$

where ϕ_{e2} is equal to the resistance factor for shear on the throat of the weld metal in fillet welds specified in *AASHTO LRFD* Article 6.5.4.2 = 0.80. Therefore:

$$R_r = 0.6(0.80)(70) = 33.6 \text{ ksi}$$

Equating the factored resistance of a fillet weld in shear in units of kips/inch at the strength limit state to the resultant force, *R*, on the weld line configuration due to the factored loads gives:

$$V_r = R_r t_e = 33.6(0.707a) = 6.60 \text{ kips / in.}$$

where t_e is the thickness of the effective throat and *a* is the required leg size of the weld. Solving for *a* gives:

a = 0.28 in. Use 5/16 in. fillet welds

EXAMPLE

Using the elastic vector analysis method, design the fillet welds for the eccentrically loaded bracket shown in Figure 6.6.4.3.7.2.3-5, which is subject to combined shear and bending (i.e. shear and tension), for the strength limit state. The fatigue limit state is not checked in this example. Assume E70 electrodes.

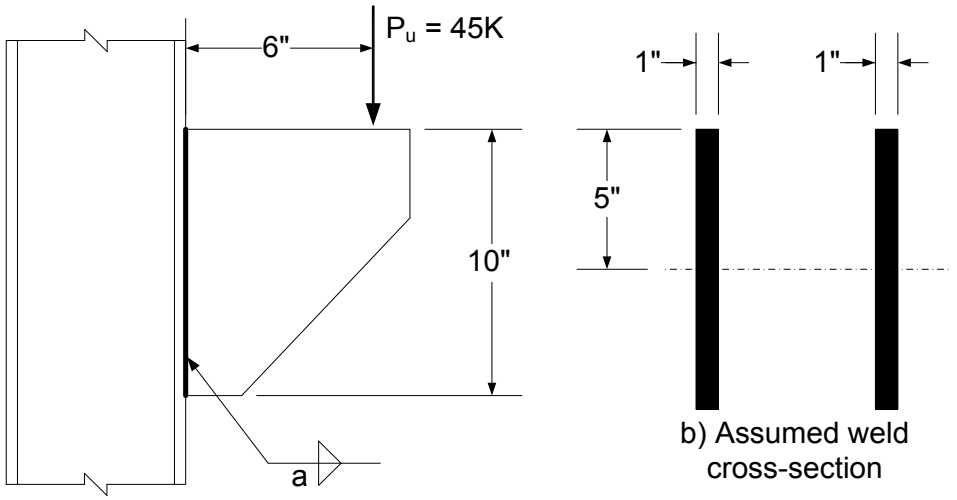

a) Bracket

Figure 6.6.4.3.7.2.3-5 Eccentrically Loaded Fillet-Welded Bracket Example 2

The welds are treated as lines with a thickness of one inch. The direct shear (vertical) component R_v is assumed carried equally by each weld segment. Therefore:

$$R_v = \frac{P_u}{L_w} = \frac{45}{2(10)} = 2.25 \text{ kips / in.}$$

The moment of inertia of the weld line segments is calculated as:

$$I = 2\left[\frac{(10)^3}{12}\right] = 166.7 \text{ in.}^3$$

Therefore, the tension (horizontal) component, R_{mt}, due to the moment (i.e. out of the paper referring to Figure 6.6.4.3.7.2.3-5b) is calculated as:

$$R_{mt} = \frac{45(6)(5)}{166.7} = 8.10 \text{ kips / in.}$$

Compute the resultant force, *R*, by taking the vector sum of the horizontal and vertical components of force:

$$R = \sqrt{(8.10)^2 + (2.25)^2} = 8.41 \text{ kips / in.}$$

According to *AASHTO LRFD* Article 6.13.3.2.4b, the factored resistance, R_r, of fillet-welded connections at the strength limit state subject to shear on the effective area is to be taken as (Equation 6.6.4.3.7.2.1-1):

$$R_r = 0.6\phi_{e2}F_{exx}$$

where ϕ_{e2} is equal to the resistance factor for shear on the throat of the weld metal in fillet welds specified in *AASHTO LRFD* Article 6.5.4.2 = 0.80. Therefore:

$$R_r = 0.6(0.80)(70) = 33.6 \text{ ksi}$$

Equating the factored resistance of a fillet weld in shear in units of kips/inch at the strength limit state to the resultant force, *R*, on the weld line configuration due to the factored loads gives:

$$V_r = R_r t_e = 33.6(0.707a) = 8.41 \text{ kips / in.}$$

where t_e is the thickness of the effective throat and *a* is the required leg size of the weld. Solving for *a* gives:

$$a = 0.35 \text{ in.} \qquad \text{Use 3/8 in. fillet welds}$$

6.6.4.4 Cross-Frame Equilibrium

Individual cross frames are often created in 3D finite element models, permitting them to be individually analyzed. This level of investigation is particularly important in skewed and curved bridges in which these members are often heavily loaded. In

addition to dead load analysis, individual influence surfaces may be built for these members to obtain live load forces. Like other member actions, each maximum and minimum live load response for individual members is for different live load positions. Hence, live load responses, unlike dead load responses, are not in equilibrium for the cross- frame.

Consideration of the proper combination of live load forces is necessary to establish equilibrium. Exact equilibrium cannot be assured in some cases if the loader moves the live loads slightly on the influence surfaces for each individual member. With proper equilibrium established, the appropriate resultant dead and live load factored forces can be combined for the design of the cross-frame connections to the connection plates.

The issue can best be visualized by considering an X-type cross-frame between two I-girders as shown in Figure 6.6.4.4-1. Load applied to the left girder causes compression in the diagonal attached to the top flange of the left girder and tension in the other diagonal. A load applied to the right girder causes forces of the opposite sign (Figure 6.6.4.4-1). These forces can be thought of as “restoring forces” if the system was in equilibrium before the loads are applied. Restoring forces are forces that attempt to return the system to its original equilibrium condition from its new equilibrium condition. Interestingly, the chord members reach their maximum response when the live load is placed in a different position.

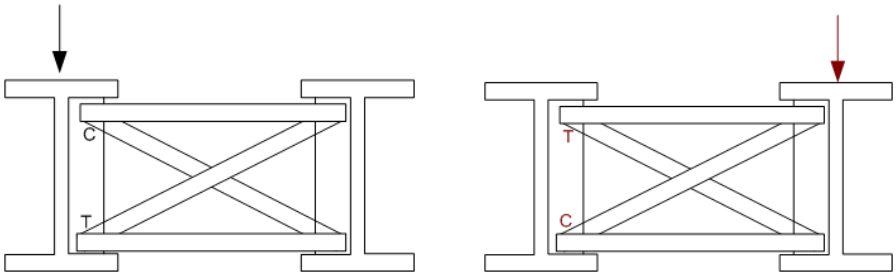

Figure 6.6.4.4-1 Cross-Frame Diagonal Forces in an X-Type Cross-Frame due to a Concentrated Load Over Each Girder

Clearly, the maximum force in the diagonals cannot exist at the same time since the live load must be in a different position to attain each maximum. However, the maximum force in one diagonal may well co-exist with the minimum force in the other.

Cross-frame forces alone cannot be in equilibrium for loads applied after the deck hardens because the deck then forms part of the restoring section. Hence, the deck has a horizontal force component in either tension or compression as well as a vertical component in the form of vertical shear. A check of equilibrium is easiest done for the non-composite loads. An equilibrium check for the composite dead

loads is usually not possible. The best check for this case is to check for equilibrium in the bottom-flange connections. Cross-frame forces at the bottom of an exterior girder can be checked by combining the horizontal chord force (usually the axial force if the member is horizontal), and the horizontal component of any diagonal member force. The net force must oppose any lateral reaction resulting from lateral bending of the bottom flange at the cross-frame.

Significant lateral bending occurs in interior girder flanges of skewed, straight girders when the cross-frames are staggered. In this case, much of the cross-frame force is due to the effect of the skew. If the girders are horizontally curved, much of the lateral flange bending is due to curvature. If the bridge is both curved and skewed, lateral moments may be large and occur for all of the above reasons.

Figure 6.6.4.4-2 shows a sample cross-frame equilibrium calculation for the component cross-frame forces for dead load (DC_1 + DC_2) at the bottom of an exterior girder from a 3D analysis of a straight skewed bridge. The arrows in Figure 6.6.4.4-2 indicate the calculated resultant horizontal and vertical forces in the cross-frame diagonal where the diagonal intersects the bottom of the girder. In this case, the net horizontal force is approximately zero, since there is no offsetting horizontal force on the other side of the girder, and the lateral flange bending moment (not given) is nearly zero. In this particular case, the bridge is straight and the cross-frames are placed in contiguous lines normal to the girders so that the lateral moments are negligible.

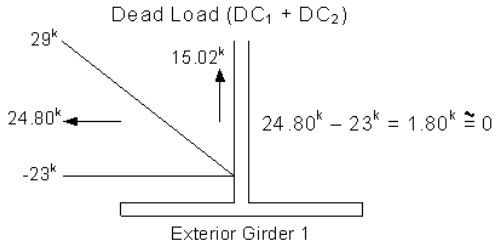

Figure 6.6.4.4-2 Equilibrium Check for DC_1 + DC_2 Cross-Frame Horizontal Forces at the Bottom of an Exterior Girder

The connection of the diagonal member to the gusset plate at this point would have to resist a 24.8 kip lateral dead load force, and a 15 kip vertical dead load force (the appropriate load factors would of course have to be applied). The connection of the gusset plate to the girder would only need to be designed for the 15 kip vertical force in this case.

The vertical component of force is not in equilibrium since gravity loads are being transferred between the girders. The difference in the vertical loads from zero at a

cross-frame is the net vertical load applied to or removed from the girder at that point.

Figure 6.6.4.4-3 shows cross-frame forces due to maximum and minimum live load plus impact *(+LL+IM* and *–LL+IM*) for a cross-frame at the bottom of an exterior girder from the same straight skewed bridge. Since the lateral moment is nearly zero, the sum of horizontal forces must be nearly zero. Maximum (positive) force in the diagonal must be combined with the minimum (negative) force in the bottom chord to establish horizontal equilibrium (and vice versa). The values show that this is indeed the case. This means that the same load position produced the minimum force in one member while it produced the maximum force in the other member. This must be the case.

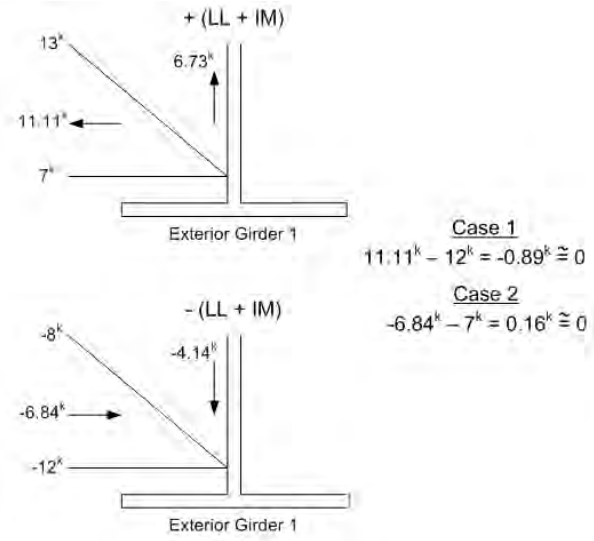

Figure 6.6.4.4-3 Equilibrium Check for (+*LL*+*IM*) and (-*LL*+*IM*) Cross-Frame Horizontal Forces at the Bottom of an Exterior Girder

Once equilibrium is confirmed at the bottom flange, the top-flange connection can be designed using the resultant forces at the top flange without further checking equilibrium. In the case of skewed and/or curved girders, where there is a net lateral force on the top flange, this force may be used to determine the transverse (radial) force to be resisted by the shear connectors (Sections 6.6.2.3.2.3 and 6.6.2.4.2).

Figure 6.6.4.4-4 shows cross frames at the bottom flange of the adjacent interior girder. The figure shows the horizontal and vertical forces due to (DC_1 + DC_2), *(+LL+IM*) and *(-LL+IM*) in that order going from top to bottom of the figure. The cross-frame forces at interior girders with contiguous opposing cross frames experience opposing forces, so equilibrium is obtained by considering the forces on both sides of the girder.

Unlike the situation at the exterior girder, the forces for the maximum (positive) live load condition in the diagonal and bottom chord on both sides of the interior girder provide a net horizontal force of approximately zero at the bottom of the girder, and the net minimum (negative) live load condition in the diagonal and bottom chord on both sides of the girder do likewise. Referring to Figure 6.6.4.4-1, the reason for this occurrence is that when the adjacent girders each receive live load, they each transfer load to the interior girder through compression. The reverse situation happens when the live load is in place over the interior girder; load is transferred away from the interior girder through tension. Note that the cross-frame force is larger for the case where load is transferred to the girder than when it is transferred away from it. The reason is that two lanes of live load are transferring load to the girder, but only one lane of live load can be placed on the interior girder to transfer load away from it.

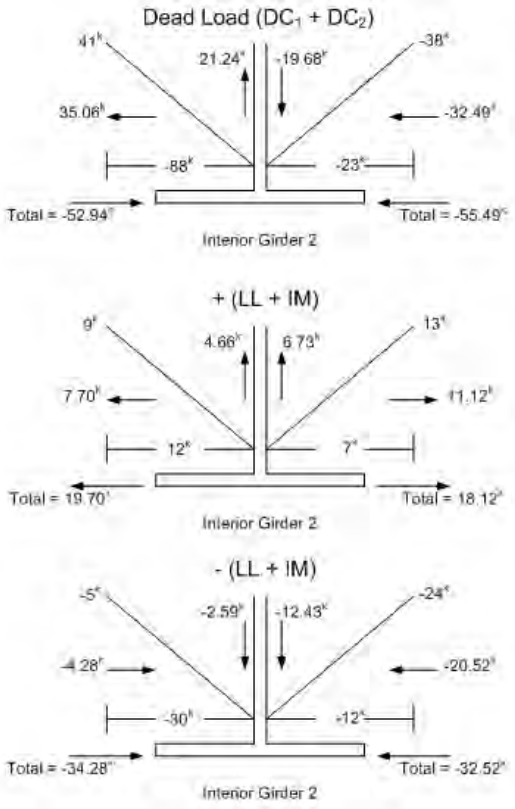

Figure 6.6.4.4-4 Equilibrium Check for $DC_1 + DC_2$, (*+LL+IM*) and *(-LL+IM)* Cross-Frame Horizontal Forces at the Bottom of an Interior Girder

With equilibrium confirmed, the Design Engineer can then proceed to confidently design the cross-frame connections. The resultant horizontal force acting in combination with the corresponding resultant vertical force is to be used in the design of the connection on each side of the girder. The difference in horizontal

force on the two opposing sides of the web in this case must be resisted by attachment of the connection plates to the flanges.

Influence surfaces can be designed for special requirements instead of summing forces as described. For example, an influence surface consisting of the chord force plus the horizontal component of the diagonal force coming into the same joint can be defined. The resulting loading would then be the maximum and minimum horizontal force at the joint. The vertical force is simply the vertical component of the diagonal force. These results can be used to design the bolt group attaching that gusset plate to the connection plate. There still is a need for an influence surface for each individual member however to design the member attachment to the gusset plate. Usually, fatigue is the controlling condition.

As mentioned above, the difference in the horizontal force on the two opposing sides of the web equals the force resisted by the web-flange of the girder. Usually, this force is transferred through a load path connecting the connection plate(s) to the flange. These connections are usually welds, although bolts in clip angles are not unheard of. The situation where this force might be significant is with staggered cross-frames on interior girders often found on sharply skewed bridges. The cross-frames on the opposite side of the girder restrain the girder from moving laterally to relieve the cross-frame force, as would be the case for an exterior girder. The net force is resisted by the lateral bending of the flange. The magnitude of the force is dependent on the stiffness of the flange and the spacing of the cross-frames. Staggered cross-frames are a common means of reducing cross-frame forces, as discussed in Section 6.3.2.9.4.3.

The resultant dead and live load forces on the right-hand side of the interior girder (Figure 6.6.4.4-4) will now be combined according to the Strength I load combination. The load modifier, η, is taken equal to 1.0. The minimum load factor for component dead load, γ_p = 0.90, from *AASHTO LRFD* Table 3.4.1-2, in combination with $1/\eta$, is considered for application to the (DC_1 + DC_2) resultant force whenever the sign of the force is opposite to the sign of the live load plus impact force to determine if a more critical load combination is produced.

Horizontal resultant force:

(DC_1 + DC_2):	(1/1.0)[0.9(-55.49)]	=	-49.9 kips
(+LL+IM):	1.0[1.75(18.12)]	=	31.7 kips
			∑=-18.2 kips

or:

(DC_1 + DC_2):	1.0[1.25(-55.49)]	=	-69.4 kips
(+LL+IM):	1.0[1.75(18.12)]	=	31.7 kips
			∑=-37.7 kips (controls)

(DC_1 + DC_2):	1.0[1.25(-55.49)]	=	-69.4 kips
(-LL+IM):	1.0[1.75(-32.52)]	=	-56.9 kips
			∑=**-126.3 kips**

Vertical resultant force:

(DC_1 + DC_2):	(1/1.0)[0.9(-19.68)]	=	-17.7 kips
(+LL+IM):	1.0[1.75(6.73)]	=	11.8 kips
			∑=-5.9 kips

or:

(DC_1 + DC_2):	1.0[1.25(-19.68)]	=	-24.6 kips
(+LL+IM):	1.0[1.75(6.73)]	=	11.8 kips
			∑=-12.8 kips (controls)

(DC_1 + DC_2):	1.0[1.25(-19.68)]	=	-24.6 kips
(-LL+IM):	1.0[1.75(-12.43)]	=	-21.8 kips
			∑=**-46.4 kips**

There are three reasons for the lack of perfect equilibrium in the preceding sample cases: 1) all forces are rounded off to integers; 2) the live load positions may be slightly different for the critical forces in the diagonal and bottom strut; and 3) the effect of small lateral bending moment (in this case) in the bottom flange at the cross-frame is ignored. Again, the bridge was straight and the cross-frames were placed in contiguous lines normal to the girders so that the lateral moments were negligible. Larger lateral moments and resulting deviations from equilibrium of the cross-frame members alone would be expected with cross-frames placed in discontinuous lines (i.e. staggered) and/or with curvature. Although the lateral flange moments would be increased with the cross-frames placed in discontinuous lines, the cross-frame forces would be lessened with the magnitude of the differences being a function of the flange stiffness and relative cross-frame spacings.

In such cases, computation of the net lateral force resisted by the flanges can be estimated by resolving the lateral moment. For the case of staggered cross-frames, the lateral reaction at the cross-frames for establishing equilibrium can be estimated from the equations for the interior reaction and moment in a three-span continuous beam loaded by equal concentrated loads, *P*, at the center of each span as follows:

$$R = 1.14P \qquad \text{Equation 6.6.4.4-1}$$

where:

$$P = \frac{3.33M_{lat}}{\ell} \text{ (kips)} \qquad \text{Equation 6.6.4.4-2}$$

ℓ = cross-frame spacing (in.)
M_{lat} = lateral flange moment at the cross-frame (kip-in.)

The lateral reaction would act in the opposite direction at the top-flange connection.

In horizontally curved bridges, there is also a lateral reaction at the cross-frames resulting from the lateral flange moments due to curvature. This lateral reaction can be estimated from the equations for the interior reaction and moment in a three-span continuous beam loaded by a uniform load, *w*, in each span as follows:

$$R = 1.1w\ell \qquad \text{Equation 6.6.4.4-3}$$

where:

$$w = \frac{M}{RD} \text{ (kips/in.)} \qquad \text{Equation 6.6.4.4-4}$$

D = web depth (in.)
M = vertical bending moment in the girder at the cross-frame (kip-in.)
R = girder radius (in.)

Statics requires that the lateral reaction at the top-flange connection act in the opposite direction.

The above lateral reactions would only be used as necessary to establish equilibrium (in an approximate fashion) for determining the proper combination of the forces at a particular joint. The lateral reactions do not influence the design of the cross-frame member end connections. However, the reactions so computed should be considered when checking the cross-frame connection plate welds to the flanges, as discussed above. Attachment of connection plates to the flanges avoids transfer of the lateral loads through the web. In older bridges, these connections were not made by code and frequently caused cracks in the web-flange juncture. In recent years, the code has been changed to require these connections.

6.6.5 Splices

6.6.5.1 General

A splice is defined in *AASHTO LRFD* Article 6.2 as a group of bolted connections, or a welded connection, sufficient to transfer the moment, shear, axial force or torque

between two structural elements joined at their ends to form a single, longer element. In steel-bridge design, splices are typically used to connect girder sections together in the field; hence, the term field splices is often used.

The design of splices is covered in *AASHTO LRFD* Article 6.13.6. The design of bolted splices is covered in *AASHTO LRFD* Article 6.13.6.1. Section 6.6.5.2 discusses the design of bolted field splices for girders (i.e. flexural members – Figure 6.6.5.1-1), as outlined in *AASHTO LRFD* Article 6.13.6.1.4. Sections 6.6.5.3 and 6.6.5.4 discuss the design of bolted splices for tension members and compression members, as outlined in *AASHTO LRFD* Articles 6.13.6.1.2 and 6.13.6.1.3, respectively. Principles of bolted connection design, discussed above in Section 6.6.4.2, are applied in the design of these splices. Section 6.6.5.5 discusses the design of filler plates for bolted splices, as outlined in *AASHTO LRFD* Article 6.13.6.1.5. Section 6.6.5.6 discusses the design of welded splices, as outlined in *AASHTO LRFD* Article 6.13.6.2. Section 6.3.2.4 discusses issues related to the selection of field-section size and field-splice locations.

Figure 6.6.5.1-1 Bolted Splice on a Curved Steel I-Girder

6.6.5.2 Flexural Members

6.6.5.2.1 General

A schematic of a typical bolted girder splice for a girder (flexural member) is shown in Figure 6.6.5.2.1-1 (shown for an I-section). Bolted girder splices generally include top flange splice plates, web splice plates and bottom flange splice plates. In addition, if the plate thicknesses on one side of the joint are different than those on the other side, then filler plates are usually needed. Filler plates are discussed in

Section 6.6.5.5. For the flange splice plates, there is typically one plate on the outside of the flange and two smaller plates on the inside, one on each side of the web. For the web splice plates, there are two plates, one on each side of the web. High-strength bolts are used to connect the splice plates to the member in the final condition.

AASHTO LRFD Article 6.13.6.1.1 specifies that at the strength limit state, bolted splices are to be designed to satisfy the general requirements of *AASHTO LRFD* Article 6.13.1; that is, unless specified otherwise, the splices are to be designed for not less than the larger of: 1) the average of the flexural moment-induced stress, shear or axial force due to the factored loads at the point of splice and the factored flexural, shear or axial resistance of the member or element at the same point, or 2) 75 percent of the factored flexural, shear or axial resistance of the member or element. In addition, where a section changes at the splice, the smaller of the two connected sections is to be used in the design. *AASHTO LRFD* Article C6.13.6.1.4a provides guidance for determining the smaller section to be used in the splice design. The moment of inertia of the steel section alone should be computed on both sides of the splice. In addition, the minimum flange yield strength should be determined on both sides of the splice. That is, if different yield strengths are used for the top and bottom flange, then the minimum of those two values should be used. Finally, on both sides of the splice, the product of the moment of inertia of the steel section alone and the minimum flange yield strength should be computed. The side of the splice for which this product is minimum is defined as the smaller section and is used in the splice design.

Bolted splices in continuous spans should be made at or near points of permanent load contraflexure if possible, which helps to minimize the flange design forces. Splices located in areas of stress reversal near points of permanent load contraflexure are to be investigated for both positive and negative flexure in order to determine the governing condition; that is, for the dead load plus positive (maximum) live load condition and the dead load plus negative (minimum) live load condition.

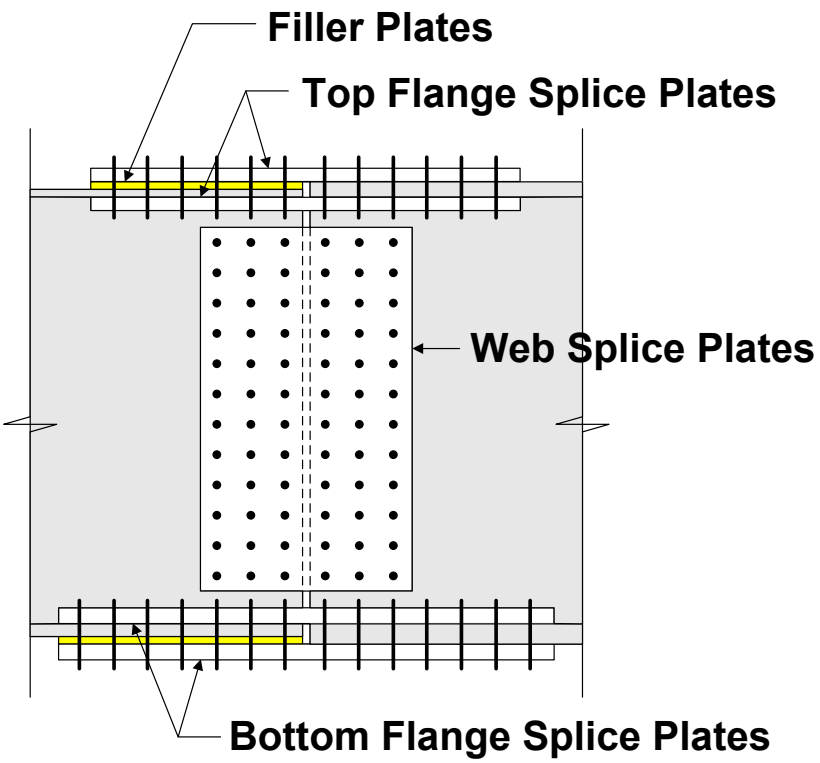

Figure 6.6.5.2.1-1 Typical Bolted Girder Splice

Web and flange splices are not to have less than two rows of bolts on each side of the joint to ensure proper alignment and stability of the girder during construction. Also, oversize or slotted holes are not to be used in either the member or the splice plates at bolted splices. This is also for improved geometry control during erection, and because a strength reduction (not recognized by the specifications) may occur when oversize or slotted holes are used in eccentrically loaded bolted web connections.

Bolted splice connections for flexural members are to be designed as slip-critical connections. Slip-critical bolted connections were previously discussed in Section 6.6.4.2.1.1. Slip-critical connections are to be proportioned to prevent slip under Load Combination Service II (Section 3.10.1.3.3), and to provide bearing, shear and tensile resistance at the strength limit state. In addition, bolted connections for flange and web splices in flexural members are to be proportioned to prevent slip during the erection of the steel and during the casting of the concrete deck; once again for improved geometry control.

Although there are holes in the tension flange at the point of splice, for simplicity, *AASHTO LRFD* Article 6.13.6.1.4a states that flexural stresses due to the factored loads at the strength limit state and for checking slip of the bolted connections under the Service II load combination at the point of splice are to be determined using the

properties of the gross section. However, the factored flexural resistance of the tension flange at the last row of bolt holes for the splice is limited to be less than or equal to the specified minimum yield stress of the tension flange at the strength limit state and when checking constructibility according to the provisions of *AASHTO LRFD* Article 6.10.1.8 (Section 6.4.7.2 – Equation 6.4.7.2-1) in order to prevent the possibility of net section fracture. As discussed in Section 6.3.4.4.4.3, this provision should never be allowed to control the plate thickness at a splice. When this requirement appears to control, the number of bolt lines can be reduced (note however that *AASHTO LRFD* Article 6.13.6.1.4a requires that there be at least two row of bolts on each side of the web), or the bolts lines may be staggered. This provision appears to be more critical at bottom flange splices of box girders.

As discussed in Section 6.6.4.2.1.3, the nominal fatigue resistance of base metal at the gross section adjacent to slip-critical bolted connections is based on fatigue detail Category B (*AASHTO LRFD* Table 6.6.1.2.3-1 – Condition 2.1) assuming the bolts are installed in holes drilled full size or subpunched and reamed to size (which is typically the case for bolted girder splices). However, as mentioned in *AASHTO LRFD* Article C6.13.6.1.4a, fatigue will generally not control the design of the bolted splice plates for flexural members. The areas of the flange and web splice plates typically equal or exceed the areas of the flanges and web to which they are attached, and the flanges and web are usually checked separately for either equivalent or more critical fatigue category details. Therefore, fatigue of the splice plates will generally not need to be checked unless either of the preceding conditions is not satisfied.

6.6.5.2.2 Flange Splices

6.6.5.2.2.1 General

The design of bolted flange splices is covered in *AASHTO LRFD* Article 6.13.6.1.4c. Filler plates for flange splices are discussed in Section 6.6.5.5.2. Lateral bending effects on bolted flange splices are discussed in Section 6.6.5.2.2.4. Special considerations related to the design of bolted flange splices for box girders are discussed in Section 6.6.5.2.2.5.

6.6.5.2.2.2 Strength Limit State

6.6.5.2.2.2.1 Controlling Flange

For the strength limit design of flange splices, the controlling flange is defined as the flange in the smaller section at the point of splice that has the maximum ratio of the factored flexural stress at its midthickness to its factored flexural resistance. The flange in the smaller section at the point of splice opposite the controlling flange is termed the noncontrolling flange.

As discussed in Section 6.6.5.2.1, the splice must be checked independently for both positive and negative flexure at splices located in regions of stress reversal. For each condition, a different flange may qualify as the controlling flange. For composite sections in positive flexure, the controlling flange is typically the bottom flange. For sections in negative flexure, either flange may qualify as the controlling flange.

Bolted splice plates and their connections on the controlling flange are to be proportioned at the strength limit state to provide a minimum design resistance (force) taken equal to the design stress, F_{cf}, times the effective area, A_e, of the controlling flange. The design stress for the controlling flange, F_{cf}, is to be computed as follows:

$$F_{cf} = \frac{\left(\left|\frac{f_{cf}}{R_h}\right| + \alpha\phi_f F_{yf} R_g\right)}{2} \geq 0.75\alpha\phi_f F_{yf} R_g \qquad \text{Equation 6.6.5.2.2.2.1-1}$$

AASHTO LRFD Equation 6.13.6.1.4c-1

where:

α = 1.0, except that a lower value equal to F_n/F_{yf} may be used for flanges where F_n is less than F_{yf} (discussed below)

ϕ_f = resistance factor for flexure specified in *AASHTO LRFD* Article 6.5.4.2 (= 1.0)

f_{cf} = maximum factored vertical bending stress at the midthickness of the controlling flange at the point of splice (ksi)

F_n = nominal flexural resistance of the flange (ksi)

F_{yf} = specified minimum yield strength of the flange (ksi)

R_g = flange resistance modification factor (discussed below) taken as:

$$= \frac{\left\lfloor \alpha A_e F_{yf} \right\rfloor_{LS}}{\left\lfloor \alpha A_e F_{yf} \right\rfloor_{SS}} \leq 1.0 \qquad \text{Equation 6.6.5.2.2.2.1-2}$$

AASHTO LRFD Equation 6.13.6.1.4c-3

$\left\lfloor \alpha A_e F_{yf} \right\rfloor_{LS}$ = product of the effective area times αF_{yf} for the flange under consideration in the larger section at the point of splice

$\left\lfloor \alpha A_e F_{yf} \right\rfloor_{SS}$ = product of the effective area times αF_{yf} for the flange under consideration in the smaller section at the point of splice

A_e = effective area of the controlling flange (discussed below) (in.^{2})

R_h = hybrid factor determined as specified in *AASHTO LRFD* Article 6.10.1.10.1 (Section 6.4.5.7). For hybrid sections in which F_{cf} does not exceed the specified minimum yield strength of the web, R_h is to be taken as 1.0.

Equation 6.6.5.2.2.2.1-1 is based on the general design requirements specified in *AASHTO LRFD* Article 6.13.1 and discussed above in Section 6.6.5.2.1. The 75 percent rule (i.e. the right-hand side of Equation 6.6.5.2.2.2.1-1), which normally governs in regions of lower moment or stress, is interpreted as providing a longitudinal stiffness at the splice that is consistent with the stiffness assumed at that point in the structural analysis. The average rule (i.e. the left-hand side of Equation 6.6.5.2.2.2.1-1), which normally governs in regions of higher moment or stress, is interpreted as providing adequate flexural resistance at the splice. The application of Equation 6.6.3.2.2.2.1-1 to provide a minimum design resistance for the controlling flange allows for possible unintended shifts in girder moment at the splice and for differences between the actual and predicted moment at the splice, which are certain to be more significant near points of permanent-load contraflexure.

The factor, α, is included in Equation 6.6.5.2.2.2.1-1 to allow for a reduction in the minimum design stress for cases where the nominal flexural resistance of the flange, F_n, is significantly below F_{yf}. An example is a bottom box flange in compression at the point of splice for which the nominal local buckling resistance, F_n, is usually well below F_{yf}. As a result, it would be overly conservative to use F_{yf} in Equation 6.6.5.2.2.2.1-1 to determine the minimum design force for designing the splice as the box flange is not permitted to approach a stress level anywhere near F_{yf}. In such cases, α may be taken equal to F_n/F_{yf} (i.e. less than 1.0). For I-section flanges in compression, the reduction in F_n below F_{yf} based on local or lateral torsional buckling is typically not as large as for box flanges. Thus, for simplicity, a conservative value of 1.0 may be used for α in this case even though the specification would permit the use of a lower value. For tension flanges, α should always be taken equal to 1.0.

The factor, R_g, is Equation 6.6.5.2.2.2.1-1, as given by Equation 6.6.5.2.2.2.1-2, is a flange resistance modification factor, which ensures that the flange splice is not designed for a force larger than the minimum design force for the weaker flange on either side of the splice. The factor, R_g, also takes into account the fact that the specified minimum yield strengths of the adjacent flange plates, or the factor, α, or a combination thereof, may potentially differ on either side of the splice.

In Equation 6.6.5.2.2.2.1-1, the factored vertical bending stress at the midthickness of the controlling flange, f_{cf}, is divided by the hybrid factor, R_h, instead of reducing F_{yf} by R_h. In actuality, yielding in the web of a hybrid section results in an increase in the flange stress and the flange is permitted to reach F_{yf} (Section 6.4.5.7). When the design stress, F_{cf}, is less than or equal to the specified minimum yield strength of the web, F_{yw}, there is theoretically no yielding in the web, and R_h is taken equal to 1.0. The web load-shedding factor, R_b (Section 6.4.5.6), is not included in Equation 6.6.5.2.2.2.1-1 since the possibility of web bend buckling, and the concomitant shedding of the web compressive stresses to the compression flange, is precluded by the presence of the web splice plates.

To calculate the minimum design force, P_{cf}, for the controlling flange, F_{cf} is multiplied by an effective flange area, A_e, of the controlling flange. For compression flanges, A_e is to be taken as the gross area of the flange. For tension flanges, A_e is to be calculated as follows:

$$A_e = \left(\frac{\phi_u F_u}{\phi_y F_{yt}}\right) A_n \le A_g \qquad \text{Equation 6.6.5.2.2.2.1-3}$$

AASHTO LRFD Equation 6.13.6.1.4c-2

where:

ϕ_u = resistance factor for fracture of tension members specified in *AASHTO LRFD* Article 6.5.4.2 (= 0.80)

ϕ_y = resistance factor for yielding of tension members specified in *AASHTO LRFD* Article 6.5.4.2 (= 0.95)

A_n = net area of the tension flange determined as specified in *AASHTO LRFD* Article 6.8.3 (in.^{2})

A_g = gross area of the tension flange (in.^{2})

F_u = tensile strength of the flange determined as specified in *AASHTO LRFD* Table 6.4.1-1 (ksi)

F_{yt} = specified minimum yield strength of the tension flange (ksi)

The calculation of the net area, A_n, of bolted connection elements was discussed previously in Section 6.6.4.2.5.6.1. For tension flanges, the use of A_e given by Equation 6.6.5.2.2.2.1-3 ensures that fracture on the net section of the flange will theoretically be prevented at the splice.

6.6.5.2.2.2.2 Noncontrolling Flange

Bolted splice plates and their connections on the noncontrolling flange at the strength limit state are to be proportioned to provide a minimum design resistance (force), P_{ncf}, taken equal to the design stress, F_{ncf}, times the effective area, A_e, of the noncontrolling flange. The design stress for the noncontrolling flange, F_{ncf}, is to be computed as follows:

$$F_{ncf} = R_{cf}\left|\frac{f_{ncf}}{R_h}\right| \ge 0.75\alpha\phi_f F_{yf} R_g \qquad \text{Equation 6.6.5.2.2.2.2-1}$$

AASHTO LRFD Equation 6.13.6.1.4c-4

where:

f_{ncf} = factored vertical bending stress at the midthickness of the noncontrolling flange at the point of splice concurrent with f_{cf} (ksi)

R_{cf} = the absolute value of the ratio of F_{cf} to f_{cf} for the controlling flange

R_g = flange resistance modification factor determined from Equation 6.6.5.2.2.2.1-2 (discussed above in Section 6.6.5.2.2.2.1)

R_h = hybrid factor determined as specified in *AASHTO LRFD* Article 6.10.1.10.1 (Section 6.4.5.7). For hybrid sections in which F_{cf} does not exceed the specified minimum yield strength of the web, R_h is to be taken as 1.0.

According to Equation 6.6.5.2.2.2.2-1, the factored vertical bending stress at the midthickness of the noncontrolling flange, f_{ncf}, concurrent with the stress in the controlling flange is being factored up in the same proportion as the flexural stress in the controlling flange, f_{cf}, (i.e. according to Equation 6.6.5.2.2.2.1-1) in order to satisfy the general design requirements of *AASHTO LRFD* Article 6.13.1. To satisfy the requirements of *AASHTO LRFD* Article 6.13.1, the factored-up stress in the noncontrolling flange must be equal to or greater than $0.75\alpha\phi_f F_{yf} R_g$ as a minimum. As was the case for the controlling flange, the factored vertical bending stress, f_{ncf}, is divided by the hybrid factor, R_h.

6.6.5.2.2.2.3 Flange Splice Plates and Bolts

The calculated minimum design forces in the controlling and noncontrolling flanges, P_{cf} and P_{ncf}, are to be used to check: 1) the resistance of the flange splice plates; 2) the shear resistance of the high-strength bolts (Section 6.6.4.2.5.2); and 3) the bearing resistance of the connected material at the bolt holes (Section 6.6.4.2.5.3) assuming the bolts have slipped and gone into bearing at the strength limit state.

For a typical flange splice with inner and outer splice plates, an approach is needed to proportion the minimum design force to the inner and outer plates. According to *AASHTO LRFD* Article C6.13.6.1.4c, at the strength limit state, the minimum flange design force may be assumed equally divided to the inner and outer flange splice plates when the areas of the inner and outer plates do not differ by more than 10 percent. In this case, the shear resistance of the bolted connection should be checked for the total minimum flange design force assumed acting in double shear.

Should the areas of the inner and outer plates differ by more than 10 percent, the minimum design force in each plate at the strength limit state should be determined by multiplying the total minimum flange design force by the ratio of the area of the splice plate under consideration to the total area of the inner and outer plates. In this case, the shear resistance of the bolted connection should be checked for the larger of the calculated splice-plate minimum design forces assumed acting on a single shear plane.

Flange Splice Plates

Splice Plates in Tension

The minimum design force at the strength limit state in flange splice plates subject to tension is not to exceed the factored resistance of the splice plates in tension specified in *AASHTO LRFD* Article 6.13.5.2; that is, the splice plates are to be checked for yielding on the gross section, fracture on the net section, and for block shear rupture (refer to Section 6.6.4.2.5.6.1). Block shear rupture will not typically control the design of flange splice plates of typical proportion.

Note also that according to *AASHTO LRFD* Article 6.13.5.2, for splice plates subject to tension, A_n must not exceed $0.85A_g$. For narrow splice plates on relatively narrow flanges requiring a relatively large number of bolts, it may be desirable to taper the splice plates at their ends in order to reduce the number of holes until the plates can be sufficiently unloaded to accommodate more holes across the width. The smallest value of A_e at the end of the taper should probably be used to conservatively compute the flange design forces in this case.

Splice Plates in Compression

AASHTO LRFD Article 6.13.6.1.4c specifies that for flange splice plates subject to compression at the strength limit state, the minimum design force must not exceed the factored resistance in compression given as:

$$R_r = \phi_c F_y A_s \qquad \text{Equation 6.6.5.2.2.2.3-1}$$

AASHTO LRFD Equation 6.13.6.1.4c-5

where:

ϕ_c = resistance factor for compression specified in *AASHTO LRFD* Article 6.5.4.2 (= 0.95)
A_s = gross area of the splice plate (in.^{2})
F_y = specified minimum yield strength of the splice plate (ksi)

Equation 6.6.5.2.2.2.3-1 is a check for yielding on the gross section of the splice plates assuming an unbraced length of zero for the relatively short plates.

Flange Splice Bolts

The shear resistance of the flange splice bolts and the bearing resistance of the flange splice bolt holes is to be calculated according to the procedures discussed in

Sections 6.6.4.2.5.2 and 6.6.4.2.5.3, respectively. Note that slip of the flange splice bolts is to be checked at the service limit state using a lower minimum design force as discussed below in Section 6.6.5.2.2.3.

If the ply thickness (i.e. splice plate thickness) closest to the nut is greater than or equal to ½-in. thick, the nominal shear resistance of the bolts should be determined assuming the threads are excluded from the shear planes for bolts less than 1 in. in diameter. For bolts greater than or equal to 1 in. in diameter, the nominal shear resistance of the bolts should be determined assuming the threads are excluded from the shear planes if the ply thickness closest to the nut is greater than ¾-in. in thickness. Otherwise, the threads should be assumed included in the shear planes. The preceding assumes there is one washer under the turned element (i.e. the nut), and that there is no stick-out beyond the nut (which represents the worst case for this determination).

Recall that for a bolt in a connection greater than 50.0 in. in length, the nominal shear resistance is to be taken as 0.80 times the value given by Equation 6.6.4.2.5.2-1 or Equation 6.6.4.2.5.2-2, as applicable. For bolted flange splices, the 50.0 in. length is to be measured between the extreme bolts on only one side of the connection (*AASHTO LRFD* Article C6.13.2.7).

The bearing resistance is calculated as the sum of the bearing resistances of the individual bolt holes parallel to the line of the flange design force. When splicing two homogeneous sections of the same specified minimum yield strength, the bearing resistance of the thinner flange splice plate controls if the sum of the inner and outer splice-plate thicknesses is less than the thickness of the thinner flange at the point of splice; otherwise, the thinner flange plate controls. For all other cases, the comparison must be made between the sum of the inner and outer splice-plate thicknesses times the tensile strength, F_u, of the splice plates to the thickness of each flange times the corresponding F_u of each flange at the point of splice in order to determine which plate controls. The largest corresponding force in the plate under consideration, be it tension or compression, is then checked against the total factored bearing resistance.

6.6.5.2.2.3 Service Limit State

The slip resistance of the flange splice bolts (Section 6.6.4.2.4.2) at the service limit state is to be checked under the Service II load combination. The slip resistance of the bolts should also be checked during the deck casting.

For this check, the minimum design force for the flange under consideration is to be taken as the design stress, F_s, times the gross area, A_g, of that flange in the smaller section at the point of splice. The design stress, F_s, is to be taken as:

$$F_s = \frac{f_s}{R_h} \qquad \text{Equation 6.6.5.2.2.3-1}$$

AASHTO LRFD Equation 6.13.6.1.4c-6

where:

f_s = maximum vertical bending stress due to Load Combination Service II or the factored vertical bending stress due to the deck-casting sequence (whichever controls) at the midthickness of the flange under consideration in the smaller section at the point of splice (ksi)

R_h = hybrid factor determined as specified in *AASHTO LRFD* Article 6.10.1.10.1 (Section 6.4.5.7). For hybrid sections in which f_s in the flange with the larger stress does not exceed the specified minimum yield strength of the web, R_h is to be taken equal to 1.0.

Since net section fracture is not a concern when checking for slip under this service limit state load combination, the gross area of the flange under consideration in the smaller section at the point of splice is to be used to compute the minimum design force for that flange.

As discussed in *AASHTO LRFD* Article C6.13.6.1.4c, when checking the slip resistance of the bolts for a typical flange splice with inner and outer splice plates, the minimum design force at the service limit state should always be assumed divided equally to the two slip planes regardless of the ratio of the splice plate areas. Unless slip occurs on both planes, slip of the connection cannot occur. Therefore, in this case, the slip resistance of the bolted connection should always be checked for the total minimum flange design force assuming two slip planes (i.e. N_s = 2 in Equation 6.6.4.2.4.2-1).

A check of the flexural stresses in the flange splice plates under the Service II load combination to control permanent deformations in the plates is not currently required. However, such a check is recommended whenever the combined area of the inner and outer splice plates is less than the area of the smaller flange at the splice. It is recommended that the check be made in this instance by dividing the total minimum design force, P_s (calculated from the design stress, F_s, obtained from Equation 6.6.5.2.2.3-1), equally to the inner and outer plates, dividing the resulting splice-plate minimum design forces by the gross area of the corresponding plate(s), and then checking that the resulting stresses do not exceed $0.95F_y$, where F_y is the specified minimum yield strength of the splice plate(s).

6.6.5.2.2.4 Flange Lateral Bending

According to *AASHTO LRFD* Article 6.13.6.1.4c, in cases for straight girders where flange lateral bending is deemed significant (e.g. in straight bridges with significant skew), and for horizontally curved girders (with or without skew), the effects of flange

lateral bending must be considered in the design of the bolted splices for discretely braced flanges of I-sections and for discretely braced top flanges of tub sections (a discretely braced flange is defined in *AASHTO LRFD* Section 6.2). Top flanges of I-sections and tub sections are typically discretely braced during the construction condition. Flange lateral bending may be ignored in the design of top-flange splices once the flange is continuously braced. Bottom flanges of I-girders are always discretely braced.

The traditional elastic vector method for eccentric shear (refer to Section 6.6.4.2.6) may be used to account for the effects of flange lateral bending in the design of the flange splice bolts. The direct shear on the flange bolts is caused by either the actual factored flange force, or by the appropriate minimum flange design force, depending on the limit state under investigation (*P* in Figure 6.6.5.2.2.4-1). The flange force is calculated without consideration of the flange lateral bending. The moment, M_ℓ (Figure 6.6.5.2.2.4-1), on the bolt group is taken as the calculated factored flange lateral bending moment.

Note in Figure 6.6.5.2.2.4-1 that the lateral moments in the top and bottom flanges are opposing. The use of the flange lateral moments at the cross-frame closest to the splice is obviously conservative based on the general shape of the lateral moment diagram in-between cross-frames in which the lateral moment actually reverses sign, and the fact that the splice cannot be located right at a cross-frame. If the flange lateral moment is available mid-way between the cross-frames adjacent to the desired splice location (e.g. if a flange node is located halfway between the cross-frames in a refined 3D model), a line plotted between the lateral moment at that point and the lateral moment at the cross-frame closest to the splice (with the proper sense of the moments considered) can be used to determine an optimal splice location to minimize the effect of the lateral moment on the design of the splice.

For curved bridges with radial supports where the effects of lateral flange bending are due primarily to curvature, the splice is likely to often be at a location where the effects of the flange lateral bending on the splice are minimal and can be ignored. To confirm this, the splice location can be checked using the procedure just described, or it can be checked in a more approximate fashion against the location of the point of contraflexure in a fixed-end beam loaded with a uniform load, which is at approximately $0.21L_b$ from the fixed end (i.e., from the cross-frame), where L_b is the cross-frame spacing

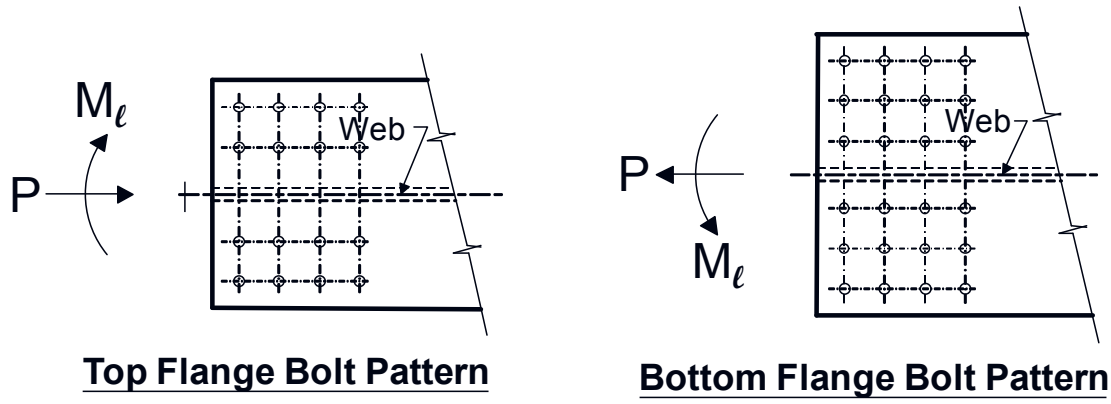

Figure 6.6.5.2.2.4-1 Top and Bottom Flange Splices Subject to Flange Lateral Bending

Under the combined actions of the flange force, *P*, and the flange lateral bending moment, M_ℓ, top flange splice bolts in I- and tub sections are to be checked for slip for constructibility under the combined actions when the top flange is discretely braced prior to hardening of the deck. Lateral flange bending effects can be ignored in the design of top flange splices once the deck hardens and the flange is continuously braced.

Since the bottom flanges of I-girders are always discretely braced, lateral flange bending effects must be considered in the design of bottom flange splices at all limit states. Thus, bottom flange splice bolts are to be checked for slip under the combined actions for the Service II load combination or for constructibility, whichever governs. At the strength limit state, the bolts are to be checked for shear and the bolt holes are to be checked for bearing under the combined actions.

The top and bottom flange splice plates are to be checked at the strength limit state. Since the bottom flange is discretely braced, the splice plates on the bottom flange should be checked for the combined stress due to *P* and M_ℓ. Lateral flange bending can be ignored in the design of the top flange splice plates since the flange is continuously braced at the strength limit state.

The calculation of *P* and M_ℓ for each case is discussed in the following.

For constructibility, *P* may to be taken equal to:

$$P = \frac{f}{R_h} A_g \qquad \text{Equation 6.6.5.2.2.4-1}$$

where:

f = factored vertical bending stress at the splice at the mid-thickness of the flange under consideration determined from the deck-casting analysis (ksi)

R_h = hybrid factor for the non-composite section determined as specified in *AASHTO LRFD* Article 6.10.1.10.1 (Section 6.4.5.7)

A_g = smaller gross flange area on either side of the splice (in.^{2})

and M_ℓ may be taken equal to the factored flange lateral bending moment at the splice determined from the deck-casting analysis for the same loads. For splices in exterior girders, the factored lateral flange moment due to the deck overhang loads should also be considered.

The stress, f, should include the stress due to the steel weight plus stay-in-place form weight plus the weight of the wet concrete.

For Service II, P may be taken equal to:

$$P = \frac{f_s}{R_h} A_g \qquad \text{Equation 6.6.5.2.2.4-2}$$

where:

A_g = smaller gross flange area on either side of the splice (in.^{2})

f_s = maximum flexural stress due to load combination Service II at the midthickness of the flange under consideration for the smaller section at the point of splice (ksi)

R_h = hybrid factor specified in *AASHTO LRFD* Article 6.10.1.10.1 (Section 6.4.5.7)

and M_ℓ may be taken equal to the factored flange lateral bending moment at the splice for the Service II load combination.

For the strength limit state and depending on which flange is under consideration, P may be taken equal to:

$$P = F_{cf} A_e \text{ or } F_{ncf} A_e \qquad \text{Equation 6.6.5.2.2.4-3}$$

where:

F_{cf} = design stress for the controlling flange given by *AASHTO LRFD* Eq. 6.13.6.1.4c-1 (Equation 6.6.5.2.2.2.1-1) (ksi)

F_{ncf} = design stress for the noncontrolling flange given by *AASHTO LRFD* Eq. 6.13.6.1.4c-3 (Equation 6.6.5.2.2.2.2-1) (ksi)

A_e = effective area of the flange under consideration (in.^{2})

and M_ℓ may be taken as the factored flange lateral bending moment at the splice for the Strength I load combination. Note that according to *AASHTO LRFD* Article C6.13.6.1.4c, the flange lateral bending moment at the strength limit state need not be multiplied by the factor, R_{cf}, given in Equation 6.6.5.2.2.2.2-1 when computing the moment for the design of the splice.

Flange Splice Plates

The equations given below for splice plates subject to tension and for splice plates subject to compression considering the effect of flange lateral bending assume that the areas of the inner and outer flange splice plates do not differ by more than 10 percent. Otherwise, P and M_ℓ should be proportioned to the inner and outer splice plates by the ratio of the area(s) of the inner and outer plate(s) to the total area of the splice plates, with the splice plates than checked individually using their respective actions.

Splice Plates in Tension

Splice plates subject to tension at the strength limit state are to be checked for yielding on the gross section (*AASHTO LRFD* Eq. 6.8.2.1-1), fracture on the net section (*AASHTO LRFD* Eq. 6.8.2.1-2) and block shear rupture (refer to *AASHTO LRFD* Article 6.13.4) (Section 6.6.4.2.5.6.1).

Lateral flange bending is ignored for the top flange splice plates at the strength limit state because the flange is continuously braced. Thus, the following checks may to be made for the top flange splice plates subject to tension:

For yielding:

$$\frac{P}{(A_g)_{PL}} \le \phi_y F_y \qquad \text{Equation 6.6.5.2.2.4-4}$$

For net section fracture:

$$\frac{P}{(A_n)_{PL}} \le \phi_u F_u R_p U \qquad \text{Equation 6.6.5.2.2.4-5}$$

For block shear rupture:

$$P \le R_r \qquad \text{Equation 6.6.5.2.2.4-6}$$

where:

ϕ_y = resistance factor for yielding on the gross section in tension specified in *AASHTO LRFD* Article 6.5.4.2 (= 0.95)

ϕ_u = resistance factor for fracture on the net section in tension specified in *AASHTO LRFD* Article 6.5.4.2 (= 0.80)
$(A_g)_{PL}$= total gross area of the inner and outer flange splice plates (in.^{2})
$(A_n)_{PL}$= total net area of the inner and outer flange splice plates (in.^{2})
F_y = specified minimum yield strength of the flange splice plates (ksi)
F_u = tensile strength of the flange splice plates specified in *AASHTO LRFD* Table 6.4.1-1 (ksi)
R_p = reduction factor for holes = 1.0 for splice plates (since holes are drilled full-size – Section 6.6.4.2.5.6.1)
U = reduction factor to account for shear lag = 1.0 for splice plates (see *AASHTO LRFD* Article 6.13.5.2 – Section 6.6.3.3.2.4)
R_r = factored block shear rupture resistance determined as specified in *AASHTO LRFD* Article 6.13.4 (Section 6.6.4.2.5.6.1) (kips)

The total net area of the splice plates, $(A_n)_{PL}$, must not be taken as greater than 85 percent of the total gross area of the plates, $(A_g)_{PL}$ when checking net section fracture (*AASHTO LRFD* Article 6.13.5.2).

Since the bottom flange is discretely braced, splice plates in tension on the bottom flange are checked for the combined stress (i.e. including the flange lateral bending stress). Thus, the following checks may be made for bottom flange splice plates subject to tension (with flange lateral bending considered):

For yielding:

$$\frac{P}{(A_g)_{PL}} + \frac{M_\ell}{S_{PL}} \le \phi_y F_y \qquad \text{Equation 6.6.5.2.2.4-7}$$

For net section fracture:

$$\frac{P}{(A_n)_{PL}} + \frac{M_\ell}{(S_n)_{PL}} \le \phi_u F_u R_p U \qquad \text{Equation 6.6.5.2.2.4-8}$$

For block shear rupture:

$$\frac{P}{(A_g)_{PL}} + \frac{M_\ell}{S_{PL}} \le \frac{R_r}{(A_g)_{PL}} \qquad \text{Equation 6.6.5.2.2.4-9}$$

where:

S_{PL} = total gross lateral section modulus of the inner and outer splice plates (in^3)
$(S_n)_{PL}$= total net lateral section modulus of the inner and outer flange splice plates (in.^{3})

$$= \frac{\left[\left(I_g\right)_{Outer\ PL} - \sum_{i=1}^{N_b} A_{hole} Y_i^2\right]}{c} + 2\left(\frac{\left[\left(I_g\right)_{Inner\ PL} - \sum_{i=1}^{N_b} A_{hole} Y_i^2\right]}{c}\right)$$

Equation 6.6.5.2.2.4-10

$(I_g)_{Outer\ PL}$ = gross lateral moment of inertia of the outer flange splice plate (in.^{4})
$(I_g)_{InnerPL}$ = gross lateral moment of inertia of an inner flange splice plate (in.^{4})
A_{hole} = area of an individual bolt hole (in.^{2})
c = half the width of the splice plate under consideration (in.)

The distances, Y_i, for each hole in Equation 6.6.5.2.2.4-10 are shown on the schematic in Figure 6.6.5.2.2.4-2.

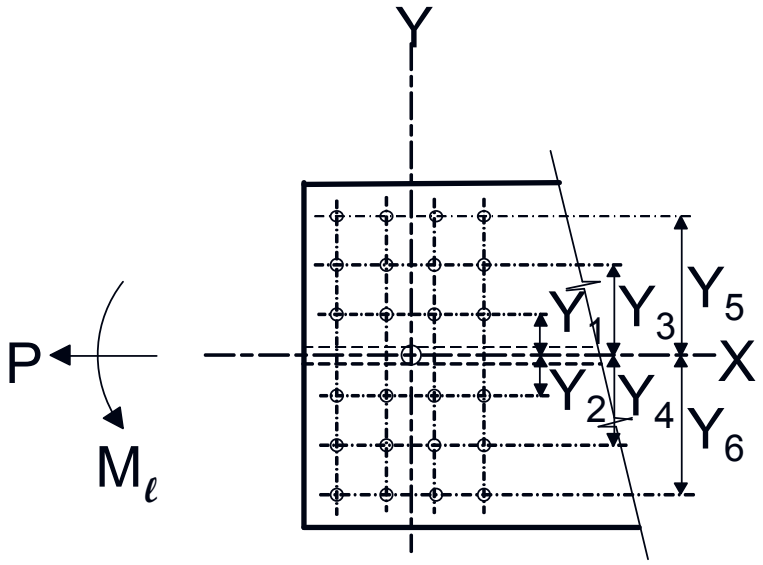

Figure 6.6.5.2.2.4-2 Distances, Y_i, in Equation 6.6.5.2.2.4-10

Splice Plates in Compression

Yielding on the gross section of flange splice plates subject to compression may be checked at the strength limit state using the following equations. Again, lateral flange bending is ignored for the top flange splice plates at the strength limit state because the flange is continuously braced. Since the bottom flange is discretely braced, the bottom flange splice plates must be checked for the combined stress. The equations assume an unbraced length of zero for the splice plates.

For top flange splice plates:

$$\frac{P}{(A_g)_{PL}} \le \phi_c F_y \qquad \text{Equation 6.6.5.2.2.4-11}$$

For bottom flange splice plates:

$$\frac{P}{(A_g)_{PL}} + \frac{M_\ell}{S_{PL}} \le \phi_c F_y \qquad \text{Equation 6.6.5.2.2.4-12}$$

where:

ϕ_c = resistance factor for compression specified in *AASHTO LRFD* Article 6.5.4.2 (= 0.95)

$(A_g)_{PL}$ = total gross area of the inner and outer flange splice plates (in.^{2})

S_{PL} = total gross lateral section modulus of the inner and outer flange splice plates (in.^{3})

F_y = specified minimum yield strength of the flange splice plates (ksi)

Flange Splice Bolts

To utilize the elastic vector method to determine the maximum resultant force in the extreme bolt under the combined actions, the polar moment of inertia, I_p, of the entire bolt group must first be computed.

For example, for the sample bottom-flange bolt pattern shown in Figure 6.6.5.2.2.4-3, I_p for the bolt group can be computed using Equation 6.6.4.2.6-6 as follows:

$$I_p = \left[2 * 6 * \left(1.5^2 + 4.5^2\right)\right] + \left[2 * 4 * \left(2.5^2 + 5.5^2 + 8.5^2\right)\right]$$
$$= 1140 \text{ in}^2$$

After I_p has been computed, the bolt force in the critical extreme bolt in the group due to the flange lateral moment can then be computed.

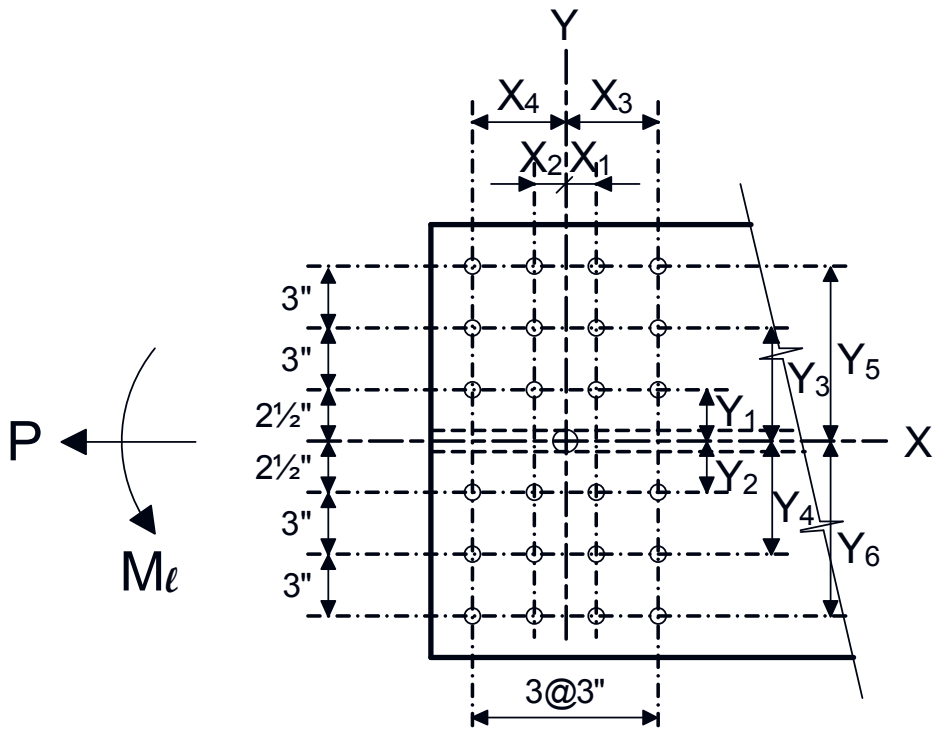

Figure 6.6.5.2.2.4-3 Sample Bottom Flange Bolt Pattern for Computation of I_p

The bolt force due to the moment is computed in two components, as shown below. The longitudinal component, P_{Mx}, is computed as:

$$P_{Mx} = \frac{M_\ell Y}{I_p} \qquad \text{Equation 6.6.5.2.2.4-13}$$

Similarly, the transverse component, P_{My}, is computed as:

$$P_{My} = \frac{M_\ell X}{I_p} \qquad \text{Equation 6.6.5.2.2.4-14}$$

X and Y in Equations 6.6.5.2.2.4-13 and 6.6.5.2.2.4-14 are defined below in Figure 6.6.5.2.2.4-4.

The bolt force due to shear, P_v, is taken equal to:

$$P_V = \frac{P}{N_b} \qquad \text{Equation 6.6.5.2.2.4-15}$$

where

P = applicable flange force (kips)
N_b = number of bolts in the bolt group

After the bolt forces due to the lateral moment and the shear have been computed, the maximum resultant bolt force in the critical extreme bolt, P_r (Figure 6.6.5.2.2.4-4), is then computed as:

$$P_r = \sqrt{(P_v + P_{Mx})^2 + P_{My}^2} \qquad \text{Equation 6.6.5.2.2.4-16}$$

P_r may then be used to check for slip of the bolts, or to check shear in the bolts and bearing at the bolt holes, as applicable.

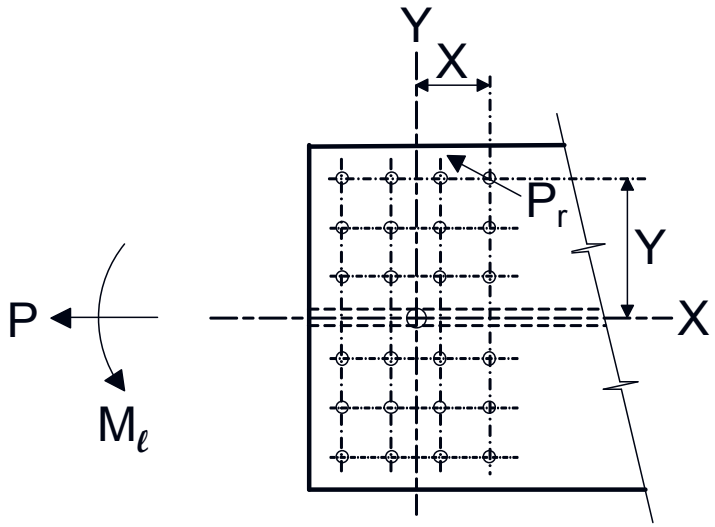

Figure 6.6.5.2.2.4-4 Resultant Bolt Force, P_r, and Distances X and Y

When checking the shear resistance of the bolts at the strength limit state, the bolts may be checked using P_r assuming double shear if the areas of the inner and outer flange splice plates do not differ by more than 10 percent. Otherwise, P_r should be proportioned to the inner and outer splice plates by the ratio of the area(s) of the inner and outer plate(s) to the total area of the splice plates. The shear resistance of the bolts would then be checked for the maximum splice plate force assuming single shear.

When checking the slip resistance of the bolts at the service limit state, the resultant force, P_r, at the service limit state should always be assumed divided equally to the two slip planes regardless of the ratio of the splice plate areas.

When checking the bearing resistance of the flange at bolt holes, the resistance of the outermost hole, calculated using the clear edge or end distance as applicable,

can conservatively be checked against the maximum resultant force, P_r, acting on the extreme bolt at the strength limit state. This assumes the bearing resistance of the flange controls; otherwise, P_r must be appropriately proportioned to the splice plates before making the check as discussed in Section 6.6.5.2.2.2.3. This check is conservative since the resultant force acts in the direction of an inclined distance that is larger than the clear edge or end distance. If the bearing resistance is exceeded, options include increasing the edge or end distance, calculating the bearing resistance based on the inclined distance, or resolving P_r in the direction parallel to the edge or end distance for making the check.

An example illustrating the application of the above procedures is given in NHI (2011).

6.6.5.2.2.5 Special Considerations for Box-Girder Flange Splices

6.6.5.2.2.5.1 General

Special considerations related to flange lateral bending, St. Venant torsional shear and longitudinal warping stress due to cross-section distortion may apply to the design of bolted flange splices for box girders in certain cases as discussed below. Fatigue considerations related to the termination of longitudinal flange stiffeners at bolted flange splices are discussed in Section 6.5.6.2.4.2.

6.6.5.2.2.5.2 Flange Lateral Bending

AASHTO LRFD Article 6.13.6.1.4c specifies that where applicable, lateral flange bending must be considered in the design of bolted flange splices for discretely braced top flanges of tub sections. Top flanges of tub sections are discretely braced during construction prior to the hardening of the deck. The procedures illustrated in Section 6.6.5.2.2.4 may be applied in this case.

6.6.5.2.2.5.3 St. Venant Torsional Shear

AASHTO LRFD Article 6.13.6.1.4c specifies that for all single box sections, and for multiple box sections in bridges not satisfying the requirements of *AASHTO LRFD* Article 6.11.2.3 (including box sections in horizontally curved bridges or on skewed supports), or with box flanges that are not fully effective according to the provisions of *AASHTO LRFD* Article 6.11.1.1, St. Venant torsional shear must also be considered in the design of the bolted splices for box flanges at all limit states.

The factored St. Venant torsional shear in the flange can be determined by multiplying the shear flow given by *AASHTO LRFD* Equation C6.11.1.1-1 (Equation 6.4.8.3.2-2) by the width of the box flange. The enclosed area of the box section, A_o,

should be computed as discussed in Section 6.5.6.1.2 for torques applied separately to the non-composite and composite sections.

The bolts for box-flange splices can be designed for the effects of the torsional shear using the traditional elastic vector method for eccentric shear (refer to Section 6.6.4.2.6). The direct shear on the flange bolts is caused by either the factored flange force due to the factored loads, or by the appropriate minimum flange design force, depending on the limit state under investigation. The moment on the bolt group is taken as the moment resulting from the eccentricity of the factored St. Venant torsional shear, assumed applied at the centerline of the splice. Note that according to *AASHTO LRFD* Article C6.13.6.1.4c, the flange St. Venant torsional shear at the strength limit state need not be multiplied by the factor, R_{cf}, given in Equation 6.6.5.2.2.2.2-1 when computing the moment for the design of the splice.

The box flange splice plates in these cases should also be designed at the strength limit state for the combined effects of the appropriate flange force and the moment resulting from the eccentricity of the factored St. Venant torsional shear. An example illustrating the application of this procedure is given in NHI (2011).

St. Venant torsional shears are typically ignored in the design of the top flanges of tub sections once the flange is continuously braced and the section is closed, and therefore, need not be considered in the design of the splices for these flanges. The composite deck is assumed to resist the majority of the torsional shear acting on the top of tub sections once the section is closed.

6.6.5.2.2.5.4 Longitudinal Warping Stress

For the same box sections cited in Section 6.6.5.2.2.5.3, longitudinal warping stresses due to cross-section distortion (see Section 6.5.5.2.2.3) are to be considered when checking the slip resistance of the bolts for constructibility and at the service limit state, and when checking fatigue of the splices. These stresses can potentially be significant under construction and service conditions in these box sections, and therefore, should be considered in these cases when checking fatigue and when checking for slip of the bolts.

The warping stresses under these conditions can be ignored when checking the top-flange splices after the flange is continuously braced. At the strength limit state, longitudinal warping stresses due to cross-section distortion may be ignored when checking both the top and bottom flange splices, as these stresses are typically limited at the strength limit state through the provision of sufficient internal cross bracing (*AASHTO LRFD* Article C6.7.4.3).

6.6.5.2.3 Web Splices

6.6.5.2.3.1 General

The design of bolted web splices for flexural members is covered in *AASHTO LRFD* Article 6.13.6.1.4b. Filler plates for web splices are discussed in Section 6.6.5.5.3. Special considerations related to the design of bolted web splices for box girders are discussed in Section 6.6.5.2.3.4.

As illustrated in Figure 6.6.5.2.3.1-1, web splice plates and their connections for flexural members are to be designed in general for a design shear, the moment due to the eccentricity of the design shear at the point of splice, and the portion of the flexural moment assumed resisted by the web at the point of splice.

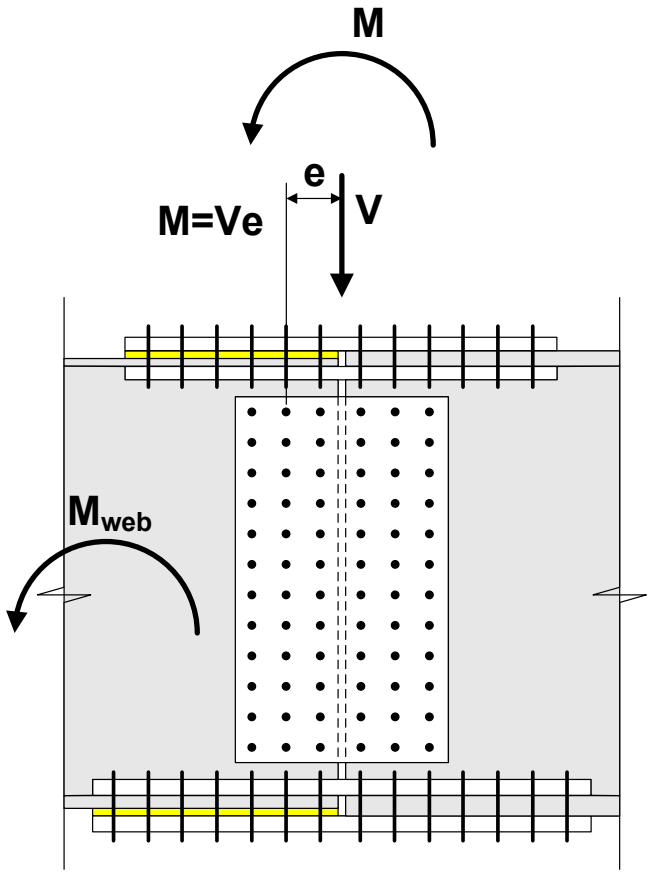

Figure 6.6.5.2.3.1-1 Design Actions for Bolted Web Splices for Flexural Members

The web moment is assumed applied at mid-depth of the web. Therefore, as discussed further in Section 6.6.5.2.3.2.3, at sections where the neutral axis is not at

the mid-depth of the web, a horizontal force resultant (not shown in Figure 6.6.5.2.3.1-1) must also be applied at the mid-depth of the web in order to establish equilibrium.

Webs must be spliced symmetrically by plates on each side of the web. The splice plates must extend as near as practical for the full depth between flanges. Since the web splice is assumed to resist a portion of the flexural moment, maximizing the depth of the web splice plates also maximizes the flexural resistance of the web splice. However, it is important that the splice not impinge on bolt assembly clearances between the top/bottom row of web bolts and the adjacent flange splice bolts. Bolt assembly clearances are given in Tables 7-16 and 7-17 of AISC (2010).

Fatigue considerations related to the termination of longitudinal web stiffeners are discussed in Section 6.4.5.5.2.2. If possible, longitudinal web stiffeners are best discontinued at field splice locations at the free edge of the web where the flexural stress in the web is zero, which will require splitting of the web splice plates. The issues related to this are similar to the issues related to the termination of longitudinal stiffeners on box flanges at bolted field splices discussed in Section 6.5.6.2.4.2. As for the box-flange stiffener, splicing the longitudinal web stiffener across the field splice is recommended whenever it becomes necessary to run the stiffener beyond the splice.

6.6.5.2.3.2 Strength Limit State

6.6.5.2.3.2.1 Design Shear

Bolted web splice plates and their connections for flexural members are to be proportioned at the strength limit state for a minimum design shear, V_{uw}, taken equal to the following:

- If $V_u < 0.5\phi_v V_n$, then:

$$V_{uw} = 1.5V_u \qquad \text{Equation 6.6.5.2.3.2.1-1}$$

AASHTO LRFD Equation 6.13.6.1.4b-1

- Otherwise:

$$V_{uw} = \frac{\left(V_u + \phi_v V_n\right)}{2} \qquad \text{Equation 6.6.5.2.3.2.1-2}$$

AASHTO LRFD Equation 6.13.6.1.4b-2

where:

ϕ_v = resistance factor for shear specified in *AASHTO LRFD* Article 6.5.4.2 (= 1.0)

V_u = factored shear at the point of splice (kips)
V_n = nominal shear resistance determined as specified in *AASHTO LRFD* Articles 6.10.9.2 and 6.10.9.3 for unstiffened and stiffened webs, respectively (Section 6.5.7.4) (kips)

Equation 6.6.5.2.3.2.1-1 represents an exception to the general design requirements specified in *AASHTO LRFD* Article 6.13.1 and discussed above in Section 6.6.5.2.1. For cases where the factored shear, V_u, is less than 50 percent of the factored shear resistance, $V_r = \phi_v V_n$, the 75 percent rule is not applied. Instead, the increase in the shear is limited to 50 percent of V_u. This is done for several reasons. First, the opportunities for the shear V_u to change from its calculated value are less than for moment; that is, large unintended shifts in the shear at the splice are unlikely. Second, the maximum shear is usually not concurrent with the maximum moment at the splice, and therefore, the use of lower value of the design shear in these regions was felt by the specification writers to be reasonable. Lastly, a lower value of the design shear is more reasonable for rolled beams. Designing web splices for rolled beams for 75 percent of their factored shear resistance is unreasonable because the factored shear resistance of a rolled beam can be up to 4 to 5 times greater than V_u.

For cases where V_u is greater than or equal to 50 percent of V_r, the average rule is retained for determining the design shear; that is, the minimum design shear is taken as the average of V_u and V_r (Equation 6.6.5.2.3.2.1-2).

The web with the smallest nominal shear resistance on either side of the splice should be used to compute the minimum design shear to ensure that the shear resistance of that web is not exceeded.

6.6.5.2.3.2.2 Moment due to Eccentricity of the Shear

Bolted web splices for flexural members are also to be designed at the strength limit state for a design moment, M_{uv}, due to the eccentricity of the design shear at the point of splice as follows:

$$M_{uv} = V_{uw} e \qquad \text{Equation 6.6.5.2.3.2.2-1}$$

where:

e = eccentricity of the design shear at the point of splice (in.) (refer to Figure 6.6.5.2.3.2.2-1)
V_{uw} = design shear for the web splice determined from Equation 6.6.5.2.3.2.1-1 or 6.6.5.2.3.2.1-2, as applicable (kips)

As specified in *AASHTO LRFD* Article 6.13.6.1.4b and illustrated in Figure 6.6.5.2.3.2.2-1, when computing the moment due to the eccentricity of the design shear at the point of splice, the correct eccentricity to use is the horizontal distance

from the centerline of the splice to the centroid of the web bolt group on the side of the joint under consideration (Sheikh-Ibrahim and Frank, 1998).

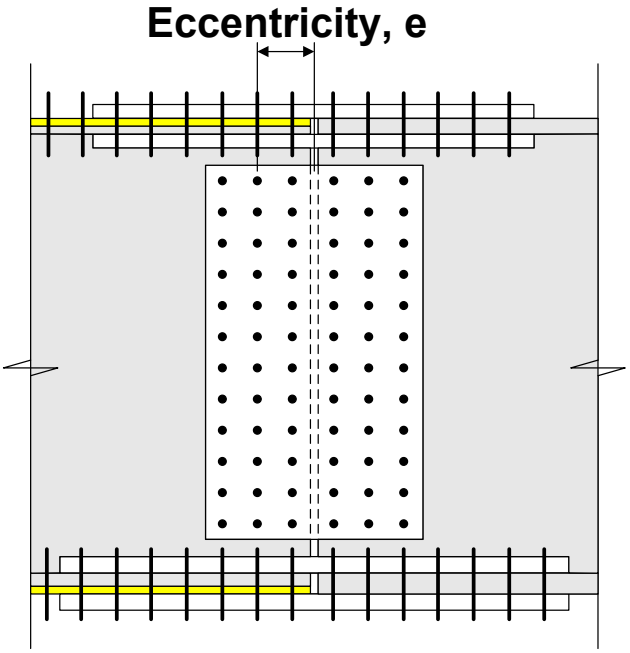

Figure 6.6.5.2.3.2.2-1 Eccentricity of the Design Shear for a Web Splice

6.6.5.2.3.2.3 Design Moment and Horizontal Force Resultant

The determination of the proportion of the flexural moment resisted by the web at the point of splice is not necessarily straightforward, particularly for a singly symmetric composite girder. Many different approaches have been used, which have sometimes led to significant variations in the number of web bolts provided in different designs for similar splice geometries.

To simplify the overall computations and eliminate any potential ambiguities, it is suggested in *AASHTO LRFD* Article C6.13.6.1.4b that the calculated portion of the flexural moment resisted by the web be applied at mid-depth of the web. Thus, to establish equilibrium at sections where the neutral axis is not at mid-depth of the web (e.g. in singly symmetric composite sections), a horizontal force resultant must also be applied. In such cases, the horizontal force resultant is also applied at mid-depth of the web and may be assumed applied equally to all the web bolts.

The following equations are provided in *AASHTO LRFD* Article C6.13.6.1.4b to determine a design moment, M_{uw}, and a design horizontal force resultant, H_{uw}, to be applied at mid-depth of the web:

$$M_{uw} = \frac{t_w D^2}{12}\left|R_h F_{cf} - R_{cf} f_{ncf}\right| \qquad \text{Equation 6.6.5.2.3.2.3-1}$$

AASHTO LRFD Equation C6.13.6.1.4b-1

$$H_{uw} = \frac{t_w D}{2}\left(R_h F_{cf} + R_{cf} f_{ncf}\right) \qquad \text{Equation 6.6.5.2.3.2.3-2}$$

AASHTO LRFD Equation C6.13.6.1.4b-2

where:

D = web depth of the smaller section at the point of splice (in.)

f_{ncf} = factored vertical bending stress at the midthickness of the noncontrolling flange at the point of splice concurrent with f_{cf} (see below); positive for tension, negative for compression (ksi)

F_{cf} = design stress for the controlling flange at the point of splice determined as specified in *AASHTO LRFD* Article 6.13.6.1.4c (Equation 6.6.5.2.2.2.1-1); positive for tension, negative for compression (ksi)

R_{cf} = the absolute value of the ratio of F_{cf} to the maximum factored vertical bending stress, f_{cf}, at the midthickness of the controlling flange at the point of splice

R_h = hybrid factor determined as specified in *AASHTO LRFD* Article 6.10.1.10.1 (Section 6.4.5.7). For hybrid sections in which F_{cf} does not exceed the specified minimum yield strength of the web, R_h is taken equal to 1.0.

t_w = web thickness of the smaller section at the point of splice (in.)

M_{uw} and H_{uw} from the preceding equations, applied together, yield a combined stress distribution equivalent to the unsymmetrical stress distribution in the web. For symmetrical sections with equal compressive and tensile stresses at the top and bottom of the web, H_{uw} will equal zero.

Note that M_{uw} and H_{uw} are conservatively computed using the flexural stresses at the midthickness of the flanges. By utilizing the stresses at the midthickness of the flanges, the same computed stresses are used for the design of the flange and web splices, which simplifies the calculations. The stresses at the inner fibers of the flanges may be used instead, if desired.

In either case, for composite sections, the factored vertical bending stresses are to be computed considering the application of the moments to the respective cross-sections supporting those loads. Note that all stresses in Equations 6.6.5.2.3.2.3-1 and 6.6.5.2.3.2.3-2 are to be taken as signed quantities**.** Since the sign of M_{uw} corresponds to the sign of the flexural moment for the loading condition under consideration, absolute value signs are applied to the resulting difference of the stresses in Equation 6.6.5.2.3.2.3-1 for convenience. H_{uw} from Equation

6.6.5.2.3.2.3-2 is taken as a signed quantity; positive for tension, negative for compression.

M_{uw} and H_{uw} are to be computed independently for both positive and negative flexure in areas of stress reversal in order to determine the governing condition. For a composite section subject to positive flexure at the strength limit state, the controlling flange is typically the bottom flange; thus, the top of the web is usually in compression and the neutral axis is usually near the top flange (Figure 6.6.5.2.3.2.3-1). To compute minimum design values of M_{uw} and H_{uw} for this case, the stress at the midthickness of the controlling (bottom) flange is assumed equal to its minimum flange design stress, F_{cf} (from Equation 6.6.5.2.2.2.1-1), times the hybrid factor, R_h (Figure 6.6.5.2.3.2.3-1). The stress, f_{ncf}, at the midthickness of the noncontrolling flange (the top flange in this case), which is taken as the factored vertical bending stress concurrent with the maximum applied flexural stress, f_{cf}, at the midthickness of the controlling (bottom) flange, is assumed factored up by the ratio, R_{cf}, which is taken as the absolute value of the ratio of F_{cf} to f_{cf}.

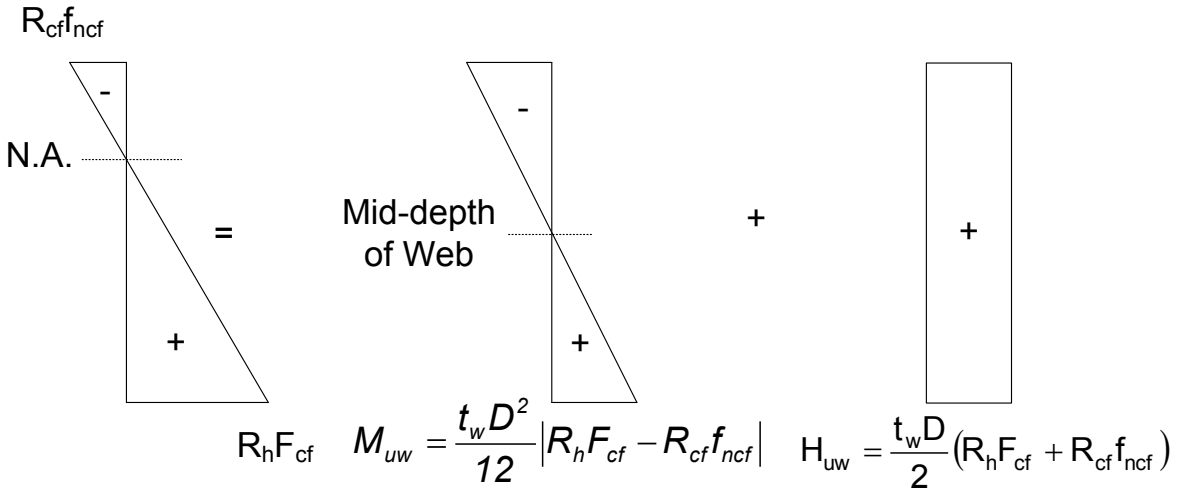

Figure 6.6.5.2.3.2.3-1 Assumed Flexural Stress Distribution in the Web for the Design of a Bolted Web Splice in a Composite Section Subject to Positive Flexure

Essentially, by factoring up the stress f_{ncf} by R_{cf}, the stresses in the web are being factored up in the same proportion as the flexural stress in the controlling flange so that the web splice is designed in a consistent fashion; that is, designed to also satisfy the general strength limit state design requirements specified in *AASHTO LRFD* Article 6.13.1. By integrating the resulting stress distribution over the depth of the web, Equation 6.6.5.2.3.2.3-1 is derived to determine the value of M_{uw} to be applied at the mid-depth of the web. H_{uw} in Equation 6.6.5.2.3.2.3-2 is then simply taken as the average of the factored-up stresses at the midthickness of the top and bottom flange.

For the case of negative flexure at the strength limit state, the controlling flange can either be the top or bottom flange. The top of the web is usually in tension and the neutral axis is usually at or near the mid-depth of the web (Figure 6.6.5.2.3.2.3-2). To compute minimum design values of M_{uw} and H_{uw} for this case, the stress at the midthickness of the controlling flange is again assumed equal to its minimum flange design stress, F_{cf} (from Equation 6.6.5.2.2.2.1-1), times the hybrid factor, R_h. If the top flange is assumed to be the controlling flange (Figure 6.6.5.2.3.2.3-2), the stress, f_{ncf}, at the midthickness of the noncontrolling flange (the bottom flange in this case) is assumed factored up by the ratio, R_{cf}, which would be taken as the absolute value of the ratio of F_{cf} to f_{cf} for the top flange. M_{uw} and H_{uw} would again then be computed from Equations 6.6.5.2.3.2.3-1 and 6.6.5.2.3.2.3-2, respectively.

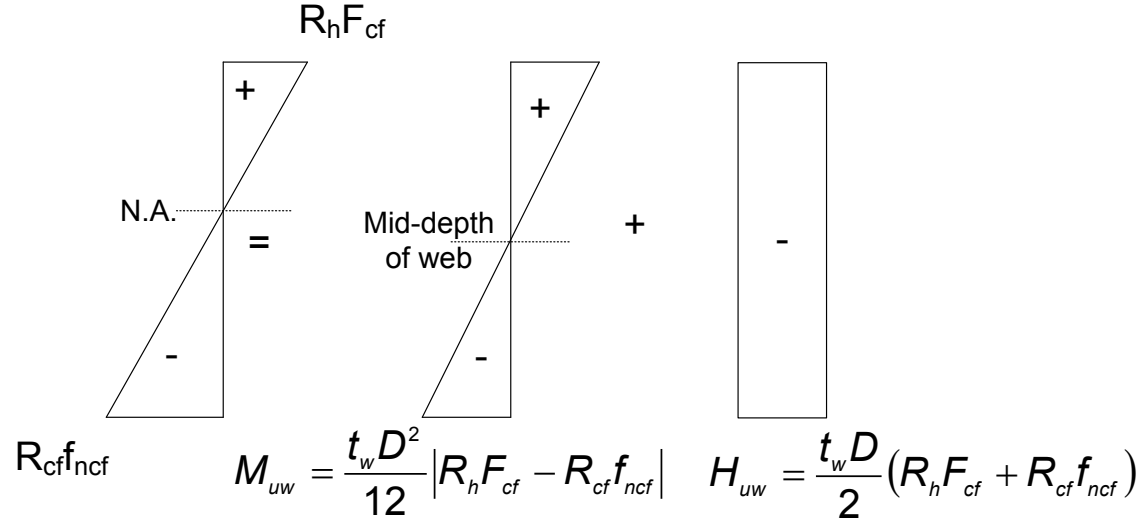

Figure 6.6.5.2.3.2.3-2 Assumed Flexural Stress Distribution in the Web for the Design of a Bolted Web Splice in a Section Subject to Negative Flexure

For splices not in areas of stress reversal, M_{uw} and H_{uw} need only be computed for the loading condition causing the maximum flexural stress in the controlling flange at the strength limit state; that is, only a single load condition need be checked.

AASHTO LRFD Article 6.13.6.1.4b permits an alternative approach for the design of web splices for compact web sections at the strength limit state only (refer to Section 6.5.6.2.2.1.1 for the definition of a compact web section). In this approach, all the flexural moment is assumed resisted by the flange splices, provided the flanges are capable of resisting the design moment (Sheikh-Ibrahim and Frank, 1998; Sheikh-Ibrahim and Frank, 2001). Should the flanges not be capable of resisting the entire design moment, the web splice is assumed to resist any remaining flexural moment in addition to the design shear and the moment due to the eccentricity of the design shear. Note that when this alternate approach is used, the slip resistance of the

bolts is still to be checked using conventional assumptions (i.e. that the web resists all its portion of the flexural design moment at the service limit state – Section 6.6.5.2.3.3).

6.6.5.2.3.2.4 Web Splice Plates and Bolts

The calculated minimum design actions in the web, V_{uw}, M_{uv}, M_{uw} and H_{uw}, are to be used to check: 1) the resistance of the web splice plates; 2) the shear resistance of the high-strength bolts (Section 6.6.4.2.5.2); and 3) the bearing resistance of the connected material at the bolt holes (Section 6.6.4.2.5.3) assuming the bolts have slipped and gone into bearing at the strength limit state.

Web Splice Plates

AASHTO LRFD Article 6.13.6.1.4b specifies that at the strength limit state, the combined stress in the web splice plates due to M_{uv}, M_{uw} and H_{uw} must not exceed the specified minimum yield strength of the splice plates times the resistance factor, ϕ_f (=1.0), as follows:

$$f = \frac{M_{uv} + M_{uw}}{S_{PL}} + \frac{H_{uw}}{A_g} \le \phi_f F_y \qquad \text{Equation 6.6.5.2.3.2.4-1}$$

where:

A_g = gross area of the web splice plates (in.^{2})
F_y = specified minimum yield strength of the web splice plates (ksi)
H_{uw} = design horizontal force resultant (Equation 6.6.5.2.3.2.3-2) (kips)
M_{uv} = design moment due to the eccentricity of the design shear at the point of splice (Equation 6.6.5.2.3.2.2-1) (kip-in.)
M_{uw} = design moment (Equation 6.6.5.2.3.2.3-1) (kip-in.)
S_{PL} = section modulus of the web splice plates based on the gross section (in.^{3})

In addition, the design shear, V_{uw}, must not exceed the lesser of the block shear rupture resistance specified in *AASHTO LRFD* Article 6.13.4 (Section 6.6.4.2.5.6.1) or the factored shear resistance of the splice plates specified in *AASHTO LRFD* Article 6.13.5.3 (Section 6.6.4.2.5.6.2). Note that because of the overall length of the connection, the block shear rupture resistance normally does not control for web splice plates of typical proportion.

Web Splice Bolts

The shear resistance of the web splice bolts and the bearing resistance of the web splice bolt holes is to be calculated according to the procedures discussed in

Sections 6.6.4.2.5.2 and 6.6.4.2.5.3, respectively. Note that slip of the flange splice bolts is to be checked at the service limit state using lower minimum design actions as discussed below in Section 6.6.5.2.3.3.

Web splice bolts should be assumed to be included in the shear plane when calculating the factored shear resistance of the bolts, unless the splice plates are greater than or equal to ½ in. thick for bolts less than 1-in. in diameter, or greater than ¾ in. thick for bolts greater than or equal to 1 in. in diameter. The preceding assumes that there is one washer under the turned element (i.e. the nut), and that there is no stick-out beyond the nut (which represents the worst case for this determination).

In calculating the shear resistance of the web splice bolts, the greater than 50.0 in. length reduction does not apply when the distribution of shear force is essentially uniform along the joint, such as in a bolted web splice (RCSC, 2014).

The traditional elastic vector method is recommended for calculating the maximum resultant bolt force since the web splice bolts are subject to eccentric shear (Section 6.6.4.2.6). In applying this method to the web bolts, all actions are to be applied at the mid-depth of the web and the polar moment of inertia of the bolt group, I_p, should be computed about the centroid of the connection (Equation 6.6.4.2.6-7 may be used when the vertical pitch of the bolts is uniform). Shifting I_p to the neutral axis of the composite section (which is typically not at the mid-depth of the web) may cause the bolt forces to be underestimated unless the location of the neutral axis is determined from the summation of the stresses due to the appropriate loadings acting on the respective cross-sections supporting those loadings.

The design horizontal force resultant, H_{uw} (when applicable), may be assumed applied equally as a horizontal shear force to all the web bolts. In determining the maximum resultant bolt force, R, in the outermost bolt, the horizontal shear force in bolt due to H_{uw} would be appropriately combined with the horizontal component of the bolt shear due to torsion, R_x, in Equation 6.6.4.2.6-11.

The number of bolts in the web splice can potentially be decreased significantly by spacing a group of bolts closer to the mid-depth of the web (where the flexural stress is relatively low) at the maximum spacing specified for sealing (*AASHTO LRFD* Article 6.13.2.6.2 – Section 6.6.4.2.2.2), and by spacing the remaining two groups of bolts near the top and bottom of the web at a closer spacing.

There are several options for checking the bearing resistance of the web at bolt holes. The resistance of an outermost hole, calculated using the clear edge distance, can conservatively be checked against the maximum resultant bolt force acting on the extreme bolt in the connection (Figure 6.6.5.2.3.2.4-1 Part A). Since

the resultant force acts in the direction of an inclined distance that is larger than the clear edge distance, the check is conservative.

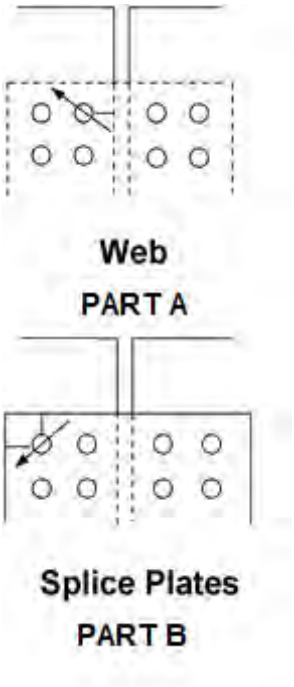

Figure 6.6.5.2.3.2.4-1 Critical Locations for Checking Bearing Resistance of Outermost Web Splice Bolt Holes

Alternatively, the bearing resistance can be calculated based on the inclined distance, or else the resultant bolt force can be resolved in the direction parallel to the edge distance. Regardless of which approach is used, should the bearing resistance be exceeded, it is strongly recommended that the edge distance be increased slightly in lieu of increasing the number of bolts or thickening the web, as this is clearly the simplest and most economical solution.

In unusual cases where the bearing resistance of the web splice plate controls (i.e. where the sum of the web splice-plate thicknesses is less than the thickness of the thinner web at the splice), the smaller of the clear edge or end distance on the splice plates should be used to compute the bearing resistance of the outermost hole Figure 6.6.5.2.3.2.4-1 Part B).

6.6.5.2.3.3 Service Limit State

The slip resistance of the web splice bolts (Section 6.6.4.2.4.2) at the service limit state is to be checked under the Service II load combination. The slip resistance of the bolts should also be checked during the deck casting.

The design shear for the service limit state, V_s, is to be taken as the shear at the point of splice under Load Combination Service II (Section 3.10.1.3.3), or the factored shear due to the deck-casting sequence (whichever controls).
The design moment, M_{sv}, at the service limit state due to the eccentricity of the design shear at the point of splice is to be taken as follows:

$$M_{sv} = V_s e \qquad \text{Equation 6.6.5.2.3.3-1}$$

where:

e = eccentricity of the design shear at the point of splice (in.) (Figure 6.6.5.2.3.2.2-1)
V_s = design shear for the web splice taken as the shear due to Load Combination Service II or the factored shear due to the deck-casting sequence (whichever controls) at the point of splice (kips)

According to *AASHTO LRFD* Article C6.13.6.1.4b, for checking slip of the web-splice bolts at the service limit state, the portion of the flexural moment resisted by the web (i.e. the design moment M_{sw}) and the design horizontal force resultant, H_{sw}, may be computed as follows:

$$M_{sw} = \frac{t_w D^2}{12}\left|f_s - f_{os}\right| \qquad \text{Equation 6.6.5.2.3.3-2}$$

$$H_{sw} = \frac{t_w D}{12}\left(f_s + f_{os}\right) \qquad \text{Equation 6.6.5.2.3.3-3}$$

where:

D = web depth (in.)
f_s = maximum vertical bending stress due to Load Combination Service II or maximum factored vertical bending stress due to the deck-casting sequence (whichever controls) at the midthickness of the flange under consideration for the smaller section at the point of splice; positive for tension, negative for compression (ksi)
f_{os} = vertical bending stress due to Load Combination Service II or factored vertical bending stress due to the deck-casting sequence (whichever controls) at the midthickness of the other flange at the point of splice concurrent with f_s in the flange under consideration; positive for tension, negative for compression (ksi)
t_w = web thickness (in.)

M_{sw} and H_{sw} are signed quantities in a similar fashion to M_{uw} and H_{uw} at the strength limit state. It is not necessary to determine the controlling and noncontrolling flange when checking for slip; hence the terms F_{cf} and R_{cf} do not appear in Equations 6.6.5.2.3.3-2 and 6.6.5.2.3.3-3.

As for the strength limit state, in areas of stress reversal, M_{sw} and H_{sw} must be computed independently for both positive and negative flexure to determine the governing condition. If the splice is not located in an area of stress reversal, M_{sw} and H_{sw} need only be computed for the loading condition causing the maximum vertical bending stress in the flange under consideration.

The maximum resultant bolt force for checking the slip resistance of the web splice bolts should be determined using the traditional elastic vector method for eccentric shear, in a fashion similar to that described above for the strength limit state in Section 6.6.5.2.3.2.4.

A check of the combined stress due to M_{sv}, M_{sw} and H_{sw} in the web splice plates under the Service II load combination to control permanent deformations in the plates is not currently required. However, such a check is recommended for the unusual case where the combined area of the web splice plates is less than the area of the smaller web at the splice. In this check, the maximum combined stress on the gross section of the web splice plates should not exceed $0.95F_y$, where F_y is the specified minimum yield strength of the splice plates.

6.6.5.2.3.4 Special Considerations for Box-Girder Web Splices

Special considerations related to St. Venant torsional shear may apply to the design of bolted web splices for box girders in certain cases as discussed below.

AASHTO LRFD Article 6.13.6.1.4b specifies that for all single box sections, and for multiple box sections in bridges not satisfying the requirements of *AASHTO LRFD* Article 6.11.2.3 (including box sections in horizontally curved bridges or on skewed supports), or with box flanges that are not fully effective according to the provisions of *AASHTO LRFD* Article 6.11.1.1, the shear due to the factored loads is to be taken as the sum of the flexural and St. Venant torsional shears in the web subjected to additive shears in the design of bolted web splices at all limit states.

Also, for boxes with inclined webs, the web splice is to be designed at all limit states for the component of the vertical shear in the plane of the web by dividing the design shear by the cosine of the angle of inclination of the web plate to the vertical.

EXAMPLE

The following is a complete example design of a bolted field splice for the interior girder of an I-section flexural member. The splice is located 100 feet from the abutment (near the point of permanent load contraflexure) in the 140-foot end span of a three-span continuous bridge. The unbraced length adjacent to either side of the splice is 24’-0”. The girder plate sizes on the left- and right-hand side of the point of splice are as follows:

Left Side:	Top Flange	1” x 16”	Right Side:	Top Flange	1” x 18”
	Web	½” x 69”		Web	9/16” x 69”
	Bot. Flange	1-3/8” x 18”		Bot. Flange	1” x 20”

The section on the left-hand side of the splice is homogeneous utilizing ASTM ASTM A709/A709M Grade 50W steel for the flanges and web. The section on the right-hand side of the splice is a hybrid section utilizing ASTM A709/A709M Grade HPS 70W steel for the flanges and ASTM A709/A709M Grade 50W steel for the web.

The smaller section will be taken as the side of the splice that has the smaller product of the calculated moment of inertia for the non-composite steel section and the smallest specified minimum flange yield strength on the side of the splice under consideration. Separate computations indicate that the left-hand side of the splice qualifies as the smaller section according to this criterion. Thus, only the calculations for the left-hand side of the splice (i.e. the non-hybrid side) are shown below.

At the section on the left-hand side of the splice, the effective flange width of the concrete deck is 114.0 in. The structural slab thickness is 9.0 in. The modular ratio n is equal to 8. The deck haunch is 3.5 in. from the top of the web to the bottom of the deck. The area of the longitudinal deck reinforcement is 10.56 in.^{2} and is assumed to be located at the centroid of the two layers of longitudinal reinforcement, or at 4.63 in. from the bottom of the deck. From separate calculations similar to those illustrated previously in this chapter, the elastic section properties of the gross section on the left-hand side of the splice are as follows:

	I (in.^{4})	S_{top} (in.^{3})	S_{bot} (in.^{3})	Neutral Axis* (in.)
Steel	62,658	1,581	1,973	31.75
Steel + Long. Reinforcement	82,907	2,447	2,211	37.50
3n Composite	122,232	5,375	2,513	48.64
n Composite	166,612	16,287	2,725	61.15

* Neutral axis is measured from the bottom of the steel

The unfactored moments and shears at the point of splice are as follows:

M_{DC1}	=	+248 kip-ft	V_{DC1}	=	-82 kips
$M_{deck\ casting}$	=	+1,300 kip-ft	$V_{deck\ casting}$	=	-82 kips
M_{DC2}	=	+50 kip-ft	V_{DC2}	=	-12 kips
M_{DW}	=	+52 kip-ft	V_{DW}	=	-11 kips
M_{+LL+IM}	=	+2,469 kip-ft	V_{+LL+IM}	=	+19 kips
M_{-LL+IM}	=	-1,754 kip-ft	V_{-LL+IM}	=	-112 kips

The DC_2 and DW moments are positive at the point of splice. However, these moments are relatively small since the splice is located near a point of permanent load contraflexure. By inspection, it is apparent that the unfactored flexural compressive stress is the concrete deck due to the sum of these moments is overcome by the tensile stress in the deck due to the negative live load moment plus impact. Therefore, as specified in *AASHTO LRFD* Article 6.10.1.1.1b, the flexural stresses due to the DC_2 and DW moments will be computed using the 3n composite section properties for combination with the positive live load plus impact flexural stress. For combination with the negative live load plus impact flexural stress, the stresses due to these moments will be computed using the section properties for the steel girder plus the longitudinal reinforcement.

Calculate the unfactored flexural stresses at the mid-thickness of the bottom flange:

$$f_{DC1} = \frac{248(12)(31.063)}{62{,}658} = +1.48 \text{ ksi}$$

$$f_{DC2} = \frac{50(12)(47.953)}{122{,}232} = +0.24 \text{ ksi} \quad (3n)$$

$$f_{DC2} = \frac{50(12)(36.813)}{82{,}907} = +0.27 \text{ ksi} \quad (\text{steel} + \text{reinf.})$$

$$f_{DW} = \frac{52(12)(47.953)}{122{,}232} = +0.24 \text{ ksi} \quad (3n)$$

$$f_{DW} = \frac{52(12)(36.813)}{82{,}907} = +0.28 \text{ ksi} \quad (\text{steel} + \text{reinf.})$$

$$f_{+LL+IM} = \frac{2{,}469(12)(60.463)}{166{,}612} = +10.75 \text{ ksi}$$

$$f_{-LL+IM} = \frac{-1{,}754(12)(36.813)}{82{,}907} = -9.34 \text{ ksi}$$

Calculate the unfactored flexural stresses at the mid-thickness of the top flange:

$$f_{DC1} = \frac{248(12)(39.13)}{62{,}658} = -1.86 \text{ ksi}$$

$$f_{DC2} = \frac{50(12)(22.24)}{122{,}232} = -0.11\,\text{ksi}\ (3n)$$

$$f_{DC2} = \frac{50(12)(33.38)}{82{,}907} = -0.24\ \text{ksi}\ \ (\text{steel} + \text{reinf.})$$

$$f_{DW} = \frac{52(12)(22.24)}{122{,}232} = -0.11\,\text{ksi}\ \ (3n)$$

$$f_{DW} = \frac{52(12)(33.38)}{82{,}907} = -0.25\ \text{ksi}\ \ (\text{steel} + \text{reinf.})$$

$$f_{+LL+IM} = \frac{2{,}469(12)(9.73)}{166{,}612} = -1.73\ \text{ksi}$$

$$f_{-LL+IM} = \frac{-1{,}754(12)(33.38)}{82{,}907} = +8.47\ \text{ksi}$$

Since the splice is located in an area of stress reversal, checks must be made for both the positive and negative flexure conditions. Compute the combined factored flexural stresses at the midthickness of the bottom and top flanges at the strength limit state for each of these conditions using the appropriate load factors given in *AASHTO LRFD* Tables 3.4.1-1 and 3.4.1-2. The Strength I load combination is used. Note that the minimum load factors, γ_p, from *AASHTO LRFD* Table 3.4.1-2 in conjunction with a load modifier of 1/η are applied to the permanent loads when the corresponding stresses are of opposite sign to the live load plus impact stress.

Bottom Flange

A. Dead Load + Positive Live Load:

$$f = 1.0\left[1.25(1.48 + 0.24) + 1.5(0.24) + 1.75(10.75)\right] = +21.32\ \text{ksi}$$

B. Dead Load + Negative Live Load:

$$f = \frac{1}{1.0}\left[0.90(1.48 + 0.27) + 0.65(0.28)\right] + 1.0\left[1.75(-9.34)\right] = -14.59\ \text{ksi}$$

Top Flange

A. Dead Load + Positive Live Load:

$$f = 1.0\left[1.25(-1.86 + -0.11) + 1.5(-0.11) + 1.75(-1.73)\right] = -5.65 \text{ ksi}$$

B. Dead Load + Negative Live Load:

$$f = \frac{1}{1.0}\left[0.90(-1.86 + -0.24) + 0.65(-0.25)\right] + 1.0[1.75(+8.47)] = +12.77 \text{ ksi}$$

The controlling flange is defined as the top or bottom flange in the smaller section at the point of splice, whichever flange has the maximum ratio of the elastic flexural stress at its midthickness due to the factored loads to its factored flexural resistance. From separate calculations, the factored flexural resistance, F_r, of each flange on the left-hand side of the splice, and the ratio of f/F_r for each condition (positive and negative flexure) are as follows:

Bottom Flange

A. Dead Load + Positive Live Load:

F_r = 50 ksi; $|f/F_r|$ = 0.43

B. Dead Load + Negative Live Load:

F_r = 49.8 ksi; $|f/F_r|$ = 0.29

Top Flange

A. Dead Load + Positive Live Load:

F_r = 50 ksi; $|f/F_r|$ = 0.11

B. Dead Load + Negative Live Load:

F_r = 50 ksi; $|f/F_r|$ = 0.25

Therefore, the bottom flange is the controlling flange for both the positive and negative flexure conditions.

Positive Flexure

Controlling Flange

For the case of positive flexure, the minimum design stress for the controlling (bottom) flange is computed as (Equation 6.6.5.2.2.2.1-1):

$$F_{cf} = \frac{\left(\left|\frac{f_{cf}}{R_h}\right| + \alpha\phi_f F_{yf} R_g\right)}{2} \geq 0.75\alpha\phi_f F_{yf} R_g$$

The hybrid factor, R_h, is taken as 1.0 for homogeneous sections and α is taken equal to 1.0 for flanges in tension. f_{cf} is the maximum flexural stress due to the factored loads at the midthickness of the controlling flange at the point of splice = +21.32 ksi.

The flange modification factor, R_g, is taken as (Equation 6.6.5.2.2.2.1-2):

$$R_g = \frac{\lfloor \alpha A_e F_{yf} \rfloor_{LS}}{\lfloor \alpha A_e F_{yf} \rfloor_{SS}} \leq 1.0$$

$\lfloor \alpha A_e F_{yf} \rfloor_{LS}$ is the product of the effective area, A_e, times αF_{yf} for the flange under consideration in the larger section at the point of splice. For flanges subject to tension, A_e is computed as (Equation 6.6.5.2.2.2.1-3):

$$A_e = \left(\frac{\phi_u F_u}{\phi_y F_{yt}}\right) A_n \leq A_g$$

From *AASHTO LRFD* Table 6.4.1-1, F_u for ASTM A709/A709M Grade HPS 70W steel is 85 ksi. Assume the bottom flange splice will consist of 4 rows of 7/8-in. diameter ASTM A325 high-strength bolts across the width of the flange. As specified in *AASHTO LRFD* Article 6.8.3, the width of standard bolt holes (which must be used for bolted splices in flexural members) for design is to be taken as the nominal diameter of the hole, which is equal to 15/16 in. for a 7/8-in. diameter bolt. Therefore:

$$A_n = [20.0 - 4(0.9375)](1.0) = 16.25 \text{ in.}^2$$

$$A_g = 20.0(1.0) = 20.00 \text{ in.}^2$$

$$A_e = \left(\frac{0.80(85)}{0.95(70)}\right)16.25 = 16.62 \text{ in.}^2 < 20.00 \text{ in.}^2$$

$$\lfloor \alpha A_e F_{yf} \rfloor_{LS} = 1.0(16.62)(70) = 1163.4$$

$\lfloor \alpha A_e F_{yf} \rfloor_{SS}$ is the product of the effective area, A_e, times αF_{yf} for the flange under consideration in the smaller section at the point of splice. From *AASHTO LRFD* Table 6.4.1-1, F_u for ASTM A709/A709M Grade 50W steel is 70 ksi. Therefore:

$$A_n = [18.0 - 4(0.9375)](1.375) = 19.59 \text{ in.}^2$$

$$A_g = 18.0(1.375) = 24.75 \text{ in.}^2$$

$$A_e = \left(\frac{0.80(70)}{0.95(50)}\right)19.59 = 23.09 \text{ in.}^2 < 24.75 \text{ in.}^2$$

$$\lfloor \alpha A_e F_{yf} \rfloor_{SS} = 1.0(23.09)(50) = 1154.5$$

$$R_g = \frac{1163.4}{1154.5} = 1.008 > 1.0 \quad \therefore \; R_g = 1.0$$

$$\frac{\left|\frac{f_{cf}}{R_h}\right| + \alpha F_{yf} R_g}{2} = \frac{\left|\frac{+21.32}{1.0}\right| + 1.0(50)(1.0)}{2} = 35.66 \text{ ksi}$$

$$0.75\alpha F_{yf} R_g = 0.75(1.0)(50)(1.0) = 37.50 \text{ ksi} \quad \text{(governs)}$$

The minimum design force for the controlling flange, P_{cf}, is taken equal to the design stress, F_{cf}, times the effective area of the controlling flange:

$$P_{cf} = F_{cf} A_e = 37.50(23.09) = 866 \text{ kips}$$

Noncontrolling Flange

For the case of positive flexure, the minimum design stress for the noncontrolling (top) flange is computed as:

$$F_{ncf} = R_{cf}\left|\frac{f_{ncf}}{R_h}\right| \geq 0.75\alpha\phi_f F_{yf} R_g$$

f_{ncf} is the flexural stress due to the factored loads at the midthickness of the noncontrolling flange at the point of splice concurrent with f_{cf} and is equal to -5.65 ksi. The top flange is in compression and is continuously braced for this condition. Therefore, since $F_{nc} = F_{yf}$, α must be taken equal to 1.0.

For flanges subject to compression, A_e is taken equal to A_g. For the larger section at the splice:

$$A_e = A_g = 18(1.0) = 18.00 \text{ in.}^2$$

$$\lfloor \alpha A_e F_{yf} \rfloor_{LS} = 1.0(18.00)(70) = 1260.0$$

For the smaller section at the splice:

$$A_e = A_g = 16(1.0) = 16.00 \text{ in.}^2$$

$$\lfloor \alpha A_e F_{yf} \rfloor_{SS} = 1.0(16.00)(50) = 800.0$$

$$R_g = \frac{1260.0}{800.0} = 1.575 > 1.0 \quad \therefore \; R_g = 1.0$$

$$R_{cf} = \left| \frac{F_{cf}}{f_{cf}} \right| = \left| \frac{37.50}{+21.32} \right| = 1.76$$

$$R_{cf} \left| \frac{f_{ncf}}{R_h} \right| = 1.75 \left| \frac{-5.65}{1.0} \right| = 9.89 \text{ ksi}$$

$$0.75 \alpha F_{yf} R_g = 0.75(1.0)(50)(1.0) = 37.50 \text{ ksi} \;\; \text{(governs)}$$

The minimum design force for the noncontrolling flange, P_{ncf}, is taken equal to the design stress, F_{ncf}, times the effective of the noncontrolling flange.

$$P_{ncf} = F_{ncf} A_e = 37.50(16.00) = 600 \text{ kips}$$

Negative Flexure

Controlling Flange

For the case of negative flexure, the controlling (bottom) flange is subject to compression. Although F_{nc} is slightly less than F_{yf} for this case, α will be conservatively taken equal to 1.0. f_{cf} = -14.59 ksi.

For flanges subject to compression, A_e is taken equal to A_g. For the larger section at the splice:

$$A_e = A_g = 20(1.0) = 20.00 \text{ in.}^2$$

$$\lfloor \alpha A_e F_{yf} \rfloor_{LS} = 1.0(20.00)(70) = 1400.0$$

For the smaller section at the splice:

$$A_e = A_g = 18(1.375) = 24.75 \text{ in.}^2$$

$$\lfloor \alpha A_e F_{yf} \rfloor_{SS} = 1.0(24.75)(50) = 1237.5$$

$$R_g = \frac{1400.0}{1237.5} = 1.13 > 1.0 \quad \therefore \; R_g = 1.0$$

Therefore:

$$\frac{\left|\frac{f_{cf}}{R_h}\right| + \alpha F_{yf} R_g}{2} = \frac{\left|\frac{-14.59}{1.0}\right| + 1.0(50)(1.0)}{2} = 32.29 \text{ ksi}$$

$$0.75\alpha F_{yf} R_g = 0.75(1.0)(50)(1.0) = 37.50 \text{ ksi} \quad \text{(governs)}$$

$$P_{cf} = F_{cf} A_e = 37.50(24.75) = 928 \text{ kips}$$

Noncontrolling Flange

For the case of negative flexure, the noncontrolling (top) flange is subject to tension; therefore, α is equal to 1.0. f_{ncf} = +12.77 ksi.

Assume the top flange splice will consist of 4 rows of 7/8-in. diameter ASTM A325 high-strength bolts across the width of the flange. For the larger section at the splice:

$$A_n = [18.0 - 4(0.9375)](1.0) = 14.25 \text{ in.}^2$$

$$A_g = 18.0(1.0) = 18.00 \text{ in.}^2$$

$$A_e = \left(\frac{0.80(85)}{0.95(70)}\right)14.25 = 14.57 \text{ in.}^2 < 18.00 \text{ in.}^2$$

$$\left[\alpha A_e F_{yf}\right]_{LS} = 1.0(14.57)(70) = 1019.9$$

For the smaller section at the splice:

$$A_n = [16.0 - 4(0.9375)](1.0) = 12.25 \text{ in.}^2$$

$$A_g = 16.0(1.0) = 16.00 \text{ in.}^2$$

$$A_e = \left(\frac{0.80(70)}{0.95(50)}\right)12.25 = 14.44 \text{ in.}^2 < 16.00 \text{in.}^2$$

$$\left[\alpha A_e F_{yf}\right]_{SS} = 1.0(14.44)(50) = 722.0$$

$$R_g = \frac{1019.9}{722.0} = 1.41 > 1.0 \quad \therefore \; R_g = 1.0$$

$$R_{cf} = \left|\frac{F_{cf}}{f_{cf}}\right| = \left|\frac{37.50}{-14.59}\right| = 2.57$$

$$R_{cf}\left|\frac{f_{ncf}}{R_h}\right| = 2.57\left|\frac{12.77}{1.0}\right| = 32.82 \text{ ksi}$$

$$0.75\alpha F_{yf} R_g = 0.75(1.0)(50)(1.0) = 37.50 \text{ ksi} \;\; (\text{governs})$$

$$P_{ncf} = F_{ncf} A_e = 37.50(14.44) = 542 \text{ kips}$$

A summary of the design forces for the bottom and top flange splices is as follows:

Bottom Flange: P_{cf} = 866 kips (tension)
P_{cf} = 928 kips (compression)

Top Flange: P_{ncf} = 600 kips (compression)
P_{ncf} = 542 kips (tension)

Flange Splice Design

Bottom Flange Splice

The width of the outside splice plate should be at least as wide as the width of the narrowest flange at the splice. Therefore, try a 9/16” x 18” outside splice plate with two 11/16” x 8” inside splice plates. Include a 3/8” x 18” filler plate on the outside (Figure 6.6.5.2.3.4-1). All plates are ASTM A709/A709M Grade 50W steel.

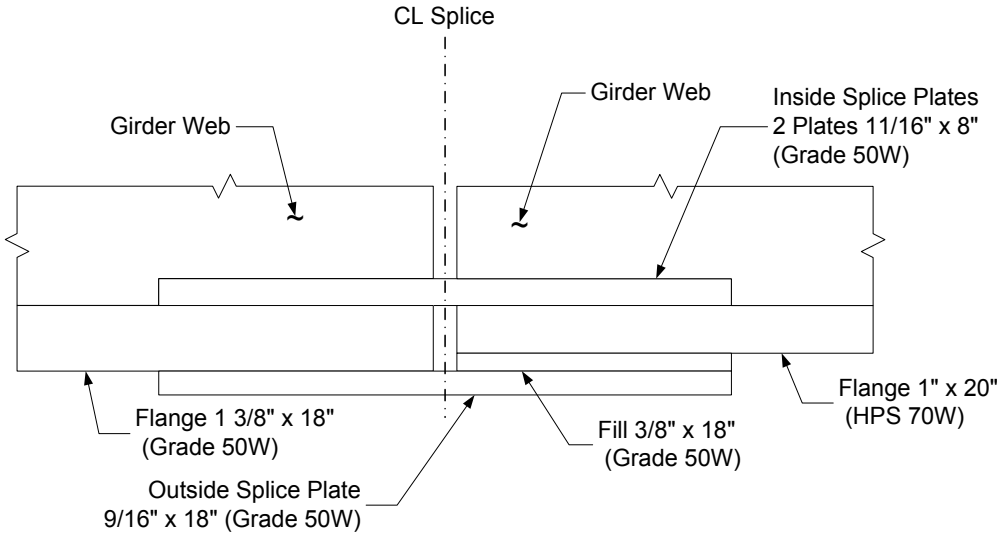

Figure 6.6.5.2.3.4-1 Example Bottom Flange Splice

As specified in *AASHTO LRFD* Article C6.13.6.1.4c, at the strength limit state, the minimum flange design force may be assumed equally divided to the inner and outer flange splice plates when the areas of the inner and outer plates do not differ by more than 10 percent. In this case, the areas of the inner and outer plates are equal. Therefore, the design force will be equally divided to the inner and outer plates and the shear resistance of the bolted connection will be checked for the total minimum flange design force assumed acting in double shear. For checking the slip resistance of the bolts at the service limit state, the total Service II design force will be distributed equally to the two slip places, as slip of the connection cannot occur unless slip occurs on both planes.

As specified in *AASHTO LRFD* Article 6.13.5.2, the factored tensile resistance of splice plates, R_r, at the strength limit state is to be taken as the smallest of the resistance based on yielding, net section fracture or block shear rupture (Section 6.6.4.2.5.6.1). The factored yield resistance of splice plates in tension is to be computed from Equation 6.6.4.2.5.6.1-1 as follows:

$$R_r = \phi_y F_y A_g$$

Outside plate:

$$R_r = 0.95(50)(18.0)(0.5625) = 481\,\text{kips} > 866/2 = 433\,\text{kips} \quad \text{ok}$$

Inside plates:

$$R_r = 0.95(50)(2)(8.0)(0.6875) = 522\,\text{kips} > 866/2 = 433\,\text{kips} \quad \text{ok}$$

The factored net section fracture resistance of splice plates in tension is to be computed from Equation 6.6.4.2.5.6.1-2 as follows:

$$R_r = \phi_u F_u A_n R_p U$$

where the reduction factor, *U*, to account for shear lag is to be taken as 1.0 for splice plates (*AASHTO LRFD* Article 6.13.5.2). R_p is a hole reduction factor taken equal to 1.0 for bolt holes drilled full-size (Section 6.6.4.2.5.6.1).

Outside plate:

$$R_r = 0.80(70)[18.0 - 4(0.9375)](0.5625)(1.0)(1.0) = 449\,\text{kips} > 866/2 = 433\,\text{kips} \quad \text{ok}$$

Inside plates:

$$R_r = 0.80(70)[2(8.0) - 4(0.9375)](0.6875)(1.0)(1.0) = 472\,\text{kips} > 866/2 = 433\,\text{kips} \quad \text{ok}$$

Also, according to *AASHTO LRFD* Article 6.13.5.2, for splice plates subject to tension, A_n must not exceed $0.85A_g$.

Outside plate:

$$0.85(18.0)(0.5625) = 8.61\,\text{in}^2 > A_n = [18.0 - 4(0.9375)](0.5625) = 8.02\,\text{in.}^2 \quad \text{ok}$$

Inside plates:

$$0.85(2)(8.0)(0.6875) = 9.35\,\text{in}^2 > A_n = [2(8.0) - 4(0.9375)](0.6875) = 8.42\,\text{in.}^2 \quad \text{ok}$$

The block shear rupture resistance of the splice plates will be checked later.

As specified in *AASHTO LRFD* Article 6.13.6.1.4c, for flange splice plates subject to compression at the strength limit state, the minimum design force must not exceed the factored resistance in compression given as (Equation 6.6.5.2.2.2.3-1):

$$R_r = \phi_c F_y A_s$$

Outside plate:

$$R_r = 0.95(50)(18)(0.5625) = 481 \text{ kips} > 928/2 = 464 \text{ kips} \quad \text{ok}$$

Inside plates:

$$R_r = 0.95(50)(2)(8)(0.6875) = 523 \text{ kips} > 928/2 = 464 \text{ kips} \quad \text{ok}$$

Determine the number of bolts for the bottom flange splice plates that are required to develop the governing minimum design force in the flange in shear at the strength limit state assuming the bolts in the connection have slipped and gone into bearing. A minimum of two rows of bolts must be provided to ensure proper alignment and stability of the girder during construction.

Since 7/8-inch diameter bolts are used with one washer assumed under the turned element, and the ply thickness closest to the nut (i.e. the inner flange splice plates) are greater than 1/2-in. thick, the threads are excluded from the shear planes (Section 6.6.5.2.2.2.3). The factored shear resistance, R_r, for a 7/8-in. diameter ASTM A325 high-strength bolt in double shear assuming the threads are excluded from the shear planes was computed in an earlier example to be 55.4 kips/bolt (Section 6.6.4.2.5.2).

It is assumed that the length between the extreme bolts (on one side of the connection) measured parallel to the line of action of the force will be less than 50.0 in. so that no reduction in the factored shear resistance is required (this will be checked later). Therefore, the minimum number of bolts required to develop the governing minimum design force in the flange in shear on the side of the splice without the filler plate is:

$$N = \frac{P}{R_r} = \frac{928}{55.4} = 16.8 \text{ bolts}$$

As discussed below in Section 6.6.5.5.2, filler plates 0.25 in. or greater in thickness in girder flange splices must be secured by additional bolts to ensure that shear planes are well defined and that no reduction in the factored shear resistance of the bolts results. As specified in *AASHTO LRFD* Article 6.13.6.1.5, this can be accomplished by either: 1) extending the fillers beyond the splice plate with the filler

extension secured by enough additional bolts to distribute the total stress uniformly over the combined section of the member or filler, or 2) in lieu of extending and developing the fillers, reducing the factored shear resistance of the bolts by the following factor:

$$R = \left[\frac{(1+\gamma)}{(1+2\gamma)}\right]$$

where the terms in the above equation are defined in Section 6.6.5.5.2. In this example, the factored shear resistance of the bolts on the side of the splice with the filler plate will be reduced by the factor, *R*.

$$A_f = 0.375(18.0) = 6.75 \text{ in.}^2$$

A_p = flange area $= 1.0(20.0) = 20.0 \text{ in.}^2$ (governs) or

A_p = splice plate area $= 2(0.6875)(8.0) + 0.5625(18.0) = 21.12 \text{ in.}^2$

$$\gamma = \frac{6.75}{20.0} = 0.338$$

$$R = \frac{1+0.338}{1+2(0.338)} = 0.80$$

Therefore, the number of bolts required to develop the governing minimum design force in the flange in shear on the side of the splice with the filler plate is:

$$N = \frac{P}{R * R_r} = \frac{928}{0.80(55.4)} = 20.9 \text{ bolts}$$

For practical reasons, use the same number of bolts on either side of the splice. Therefore, a minimum of 21 bolts is required to provide the necessary factored shear resistance for the bottom flange splice under the controlling minimum design force.

AASHTO LRFD Article 6.13.6.1.4c requires that high-strength bolted connections for flange splices be designed to prevent slip at the service limit state under a Service II design force. In addition, *AASHTO LRFD* Article 6.13.6.1.4a requires that high-strength bolted splices for flexural members be proportioned to prevent slip during the erection of the steel (assuming an erection analysis is conducted) and during the casting of the concrete deck. For the service limit state check, the Service II design stress F_s is to be taken as (Equation 6.6.5.2.2.3-1):

$$F_s = \frac{f_s}{R_h}$$

where f_s is the maximum flexural stress due to Load Combination Service II at the midthickness of the flange under consideration for the smaller section at the point of splice. For the left-hand side of the splice, which is deemed the smaller section, the Service II stress in the bottom flange is computed as follows. It will be assumed that the conditions specified in *AASHTO LRFD* Article 6.10.4.2.1 are met such that flexural stresses caused by Service II loads applied to the composite section can be computed using the short-term or long-term composite section, as appropriate, assuming the concrete deck is effective for both positive and negative flexure (Section 6.5.4.3.1).

A. Dead Load + Positive Live Load:

$$f = \left[1.0(1.48 + 0.24 + 0.24) + 1.3(10.75)\right] = +15.94 \text{ ksi} \quad (\text{governs})$$

B. Dead Load + Negative Live Load:

$$f = \left[1.0(1.48 + 0.24 + 0.24) + 1.3(-7.64)\right] = -7.97 \text{ ksi}$$

Therefore, f_s is equal to +15.94 ksi and F_s is equal to f_s/R_h = +15.94/1.0 = +15.94 ksi.

The stress at the mid-thickness of the bottom flange due to the deck-casting sequence (the special load combination for checking constructibility of steel bridges specified in *AASHTO LRFD* Article 3.4.2.1 controls) is:

$$f = \frac{1.4(1{,}300)(12)(31.063)}{62{,}658} = +10.83 \text{ ksi} \qquad \frac{f}{R_h} = \frac{+10.83}{1.0} = +10.83 \text{ ksi}$$

which is less than F_s; therefore, the Service II design stress controls the slip resistance check.

The design force, P_s, for the flange splice is taken as F_s times the gross area of the flange under consideration in the smaller section at the point of splice, or

$$P_s = F_s A_g = 15.94(1.375)(18.0) = 395 \text{ kips}$$

Determine the number of bolts for the bottom flange splice plates that are required to prevent slip under the design force, P_s. The factored slip resistance, R_r, for a 7/8-in. diameter ASTM A325 high-strength bolt assuming a Class B surface condition for the faying surface, standard holes and two slip planes per bolt was computed in an earlier example to be 39.0 kips/bolt (Section 6.6.4.2.4.2). As specified in *AASHTO*

LRFD Article 6.13.6.1.5 (and discussed in Section 6.6.5.5.2), the factored slip resistance need not be adjusted for the effect of filler plates. Therefore, the minimum number of bolts required is:

$$N = \frac{P}{R_r} = \frac{395}{39.0} = 10.1 \text{ bolts}$$

which is less than the minimum number of bolts required to provide adequate factored shear resistance at the strength limit state (i.e. *N* = 21 bolts). Thus, use twenty-four (24) 7/8-in. diameter high-strength bolts on each side of the bottom flange splice (6 rows of bolts with 4 bolts per row -- no stagger).

In order to check the factored bearing resistance of the bolt holes and the block shear rupture resistance of the splice plates and the flange, the bolt spacings and bolt edge and end distances must first be established and checked (Figure 6.6.5.2.3.4-2).

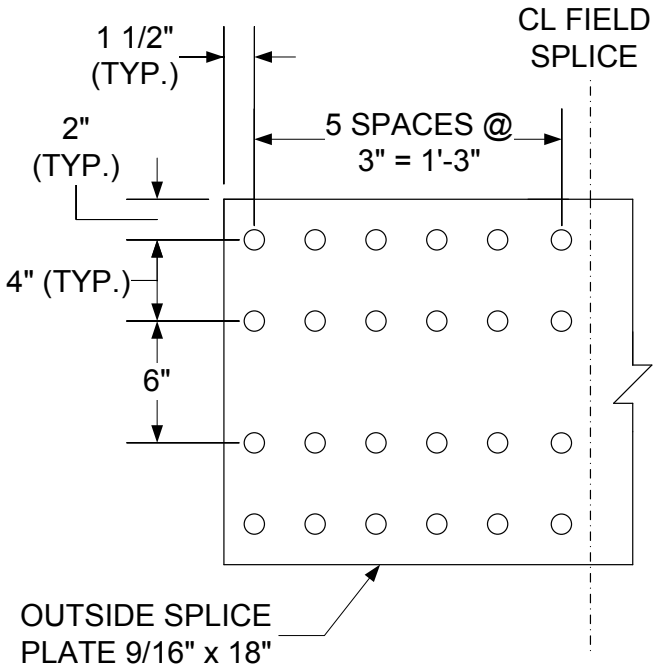

Figure 6.6.5.2.3.4-2 Outside Bottom Flange Splice Plate – Plan View

As specified in *AASHTO LRFD* Article 6.13.2.6.1 (Section 6.6.4.2.2.2.1), the minimum spacing between centers of bolts in standard holes is not to be less than 3.0*d*, where *d* is the diameter of the bolt. For 7/8-in. diameter bolts:

$$s_{min} = 3d = 3(0.875) = 2.63 \text{ in.} \quad \text{use } 3.0 \text{ in.}$$

Since the length between the extreme bolts (on one side of the connection) measured parallel to the line of action of the force is less than 50.0 in., no reduction in the factored shear resistance of the bolts is required, as originally assumed.

As specified in *AASHTO LRFD* Article 6.13.2.6.2 (Section 6.6.4.2.2.2.2), to seal against the penetration of moisture in joints, the spacing *s* of a single line of bolts adjacent to a free edge of an outside plate or shape (when the bolts are not staggered) must satisfy the following requirement (Equation 6.6.4.2.2.2.2-1):

$$s \le (4.0 + 4.0t) \le 7.0 \text{ in.}$$

where *t* is the thickness of the thinner outside plate or shape. First check for sealing along the edges of the outer splice plate (which is the thinner plate) parallel to the direction of the applied force. A ¾" gap is assumed between the flange splice plates to allow the splice to be more easily flushed out for maintenance:

$$s_{max} = 4.0 + 4.0(0.5625) = 6.25 \text{ in.} > 4.75 \text{ in.} \quad \text{ok}$$

Check for sealing along the free edge at the end of the splice plate:

$$s_{max} = 4.0 + 4.0(0.5625) = 6.25 \text{ in.} > 6.0 \text{ in.} \quad \text{ok}$$

Note that the maximum pitch requirements for stitch bolts specified in *AASHTO LRFD* Article 6.13.2.6.3 (Section 6.6.4.2.2.2.4) apply only to the connection of plates in mechanically fastened built-up members and would not be applied here.

The edge distance of bolts is defined as the distance perpendicular to the line of force between the center of a hole and the edge of the component. In this example, the edge distance of 2.0 inches satisfies the minimum edge distance requirement of 1-1/8 inches specified for 7/8-in. diameter bolts and gas cut edges in *AASHTO LRFD* Table 6.13.2.6.6-1 (Section 6.6.4.2.2.2.3). This distance also satisfies the maximum edge distance requirement of 8.0*t* (not to exceed 5.0 in.) = 8.0(0.5625) = 4.5 in. specified in *AASHTO LRFD* Article 6.13.2.6.6.

The end distance of bolts is defined as the distance along the line of force between the center of a hole and the end of the component. In this example, the end distance of 1½ inches satisfies the minimum end distance requirement of 1-1/8 inches specified for 7/8-in. diameter bolts and gas cut edges in *AASHTO LRFD* Table 6.13.2.6.6-1 (Section 6.6.4.2.2.2.3). The maximum end distance requirement of 8.0*t* (not to exceed 5.0 in.) = 8.0(0.5625) = 4.5 in. specified in *AASHTO LRFD* Article 6.13.2.6.5 is also obviously satisfied. Although not specifically required, note that the distance from the corner bolts to the corner of the splice plate, equal to

$\sqrt{(1.5)^2 + (2.0)^2} = 2.5$ in., also satisfies the maximum end distance requirement. If desired, the corners of the plate can be clipped to meet this requirement.

The bearing resistance of the connected material at the strength limit state is calculated as the sum of the bearing resistances of the individual bolts (holes) parallel to the line of the applied force (Section 6.6.4.2.5.3). As specified in *AASHTO LRFD* Article 6.8.3, for design calculations, the width of standard bolt holes is to be taken as the nominal diameter of the holes, or 15/16 in. for a 7/8-in. diameter bolt. Check the sum of the inner and outer splice plate thicknesses times the specified minimum tensile strength, F_u, of the splice plates versus the thickness of each flange times its corresponding F_u, to determine which plate controls the bearing resistance of the connection.

Splice Plates: $(0.6875 + 0.5625)(70) = 87.5$ kips / in.

Bottom Flange Left: $(1.375)(70) = 96.3$ kips / in.

Bottom Flange Right: $(1.0)(85) = 85.0$ kips / in. (governs)

For standard holes, the nominal bearing resistance, R_n, parallel to the applied bearing force is taken as follows (Equation 6.6.4.2.5.3-5):

$$R_n = 1.2L_c tF_u \le 2.4dtF_u$$

For the four bolts adjacent to the end of the flange, the end distance is 1.5 in. Therefore, the clear distance, L_c, between the edge of the hole and the end of the splice plate is:

$$L_c = 1.5 - \frac{0.9375}{2} = 1.03 \text{ in.}$$

Therefore:

$$R_n = 4(1.2L_c tF_u) = 4\left[1.2(1.03)(1.0)(85)\right] = 420 \text{ kips (governs)}$$

or:

$$R_n = 4(2.4dtF_u) = 4\left[2.4(0.875)(1.0)(85)\right] = 714 \text{ kips}$$

For the other twenty bolts, the center-to-center distance between the bolts in the direction of the applied force is 3.0 in. Therefore, the clear distance, L_c, between the edges of the adjacent holes is:

$$L_c = 3.0 - 0.9375 = 2.0625 \text{ in.}$$

Therefore:

$$R_n = 20(1.2L_c tF_u) = 20\left[1.2(2.0625)(1.0)(85)\right] = 4208 \text{ kips}$$

or:

$$R_n = 20(2.4dtF_u) = 20\left[2.4(0.875)(1.0)(85)\right] = 3570 \text{ kips (governs)}$$

The total nominal bearing resistance of the flange plate, R_n, is therefore:

$$R_n = 420 \text{ kips} + 3570 \text{ kips} = 3990 \text{ kips}$$

Since:

$$R_r = \phi_{bb} R_n$$

$$R_r = 0.80(3990) = 3192 \text{ kips} > 928 \text{ kips} \quad \text{ok}$$

Check the block shear rupture resistance of the bottom flange splice plates and the bottom flange when subject to the minimum design force in tension at the strength limit state (Section 6.6.4.2.5.6.1). Assume the potential block shear failure planes on the outside and inside splice plates shown in Figure 6.6.5.2.3.4-3.

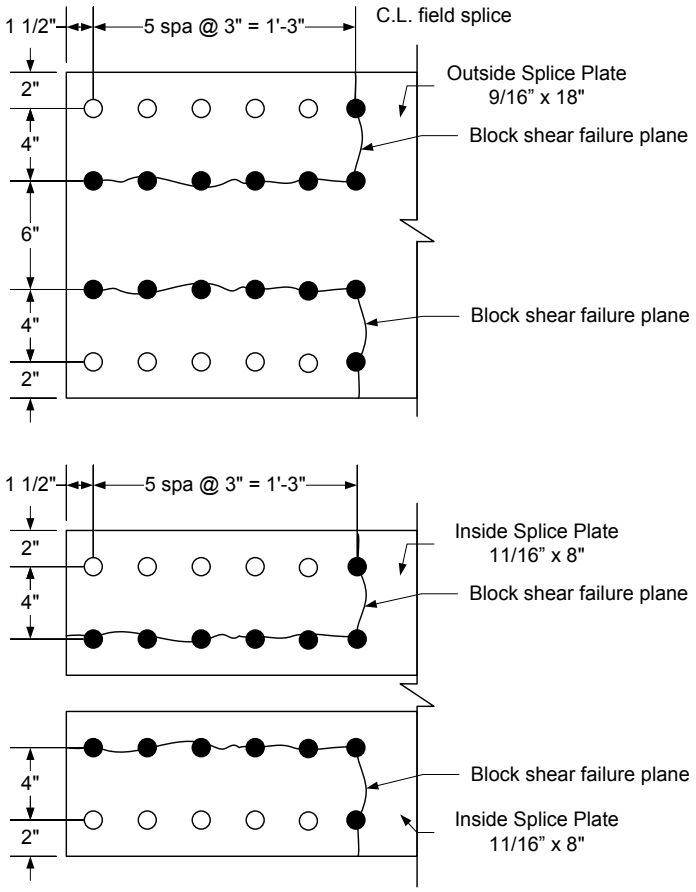

Figure 6.6.5.2.3.4-3 Bottom Flange Splice – Assumed Block Shear Failure Planes in the Splice Plates

Check the outside splice plate. A_{tn} is the net area along the place resisting the tensile stress.

$$A_{tn} = 2[4.0 + 2.0 - 1.5(0.9375)](0.5625) = 5.17 \text{ in}^2$$

A_{vn} is the net area along the place resisting the shear stress.

$$A_{vn} = 2[5(3.0) + 1.5 - 5.5(0.9375)](0.5625) = 12.76 \text{ in}^2$$

A_{vg} is the gross area along the plane resisting the shear stress.

$$A_{vg} = 2[5(3.0) + 1.5](0.5625) = 18.56 \text{ in}^2$$

The factored block shear rupture resistance, R_r, is determined as (Equation 6.6.3.3.2.5-1):

$$R_r = \phi_{bs} R_p \left(0.58 F_u A_{vn} + U_{bs} F_u A_{tn}\right) \le \phi_{bs} \left(0.58 F_y A_{vg} + U_{bs} F_u A_{tn}\right)$$

ϕ_{bs} is the resistance factor for block shear rupture taken equal to 0.80 (*AASHTO LRFD* Article 6.5.4.2). The reduction factor, R_p, is taken equal to 1.0 for holes drilled full-size. The reduction factor, U_{bs}, is taken equal to 1.0 since the tension stress is uniform. Therefore:

$$\begin{aligned} R_r &= 0.80(1.0)\left[0.58(70)(12.76) + 1.0(70)(5.17)\right] = 704 \text{ kips} \\ &< 0.80(1.0)\left[0.58(50)(18.56) + 1.0(70)(5.17)\right] = 720 \text{ kips} \\ \therefore R_r &= 704 \text{ kips} > \frac{866}{2} = 433 \text{ kips} \quad \text{ok} \end{aligned}$$

Check the inside splice plates.

$$A_{tn} = 2\left[4.0 + 2.0 - 1.5(0.9375)\right](0.6875) = 6.32 \text{ in}^2$$

$$A_{vn} = 2\left[5(3.0) + 1.5 - 5.5(0.9375)\right](0.6875) = 15.60 \text{ in}^2$$

$$A_{vg} = 2\left[5(3.0) + 1.5\right](0.6875) = 22.68 \text{ in}^2$$

$$\begin{aligned} R_r &= 0.80(1.0)\left[0.58(70)(15.60) + 1.0(70)(6.32)\right] = 861 \text{ kips} \\ &< 0.80(1.0)\left[0.58(50)(22.68) + 1.0(70)(6.32)\right] = 880 \text{ kips} \\ \therefore R_r &= 861 \text{ kips} > \frac{866}{2} = 433 \text{ kips} \quad \text{ok} \end{aligned}$$

Check the critical girder flange at the splice. Since the areas and yield strengths of the flanges on each side of the splice differ, both sides would need to be checked. Only the calculations for the flange on the right-hand side of the splice, which is determined to be the critical flange, are shown below. Two potential failure modes are investigated for the flange as shown in Figure 6.6.5.2.3.4-4.

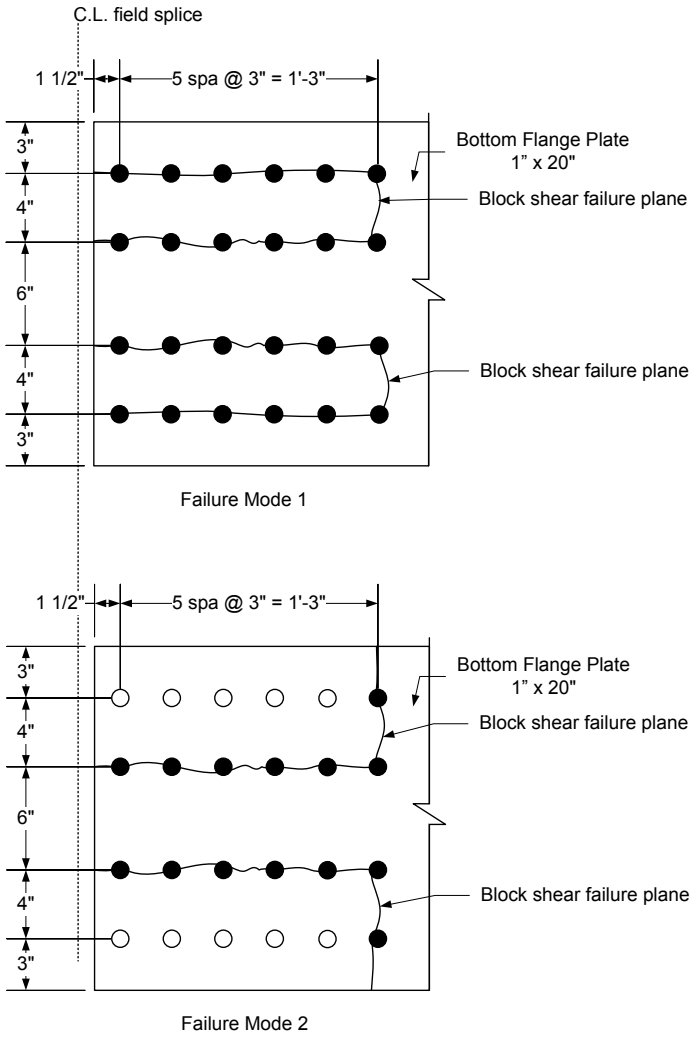

Figure 6.6.5.2.3.4-4 Bottom Flange Splice – Assumed Block Shear Failure Planes in the Flange on the Right-Hand Side of the Splice

For Failure Mode 1:

$$A_{tn} = 2[4.0 - 0.9375](1.0) = 6.13 \text{ in}^2$$

$$A_{vn} = 4[5(3.0) + 1.5 - 5.5(0.9375)](1.0) = 45.37 \text{ in}^2$$

$$A_{vg} = 4[5(3.0) + 1.5](1.0) = 66.00 \text{ in}^2$$

$$R_r = 0.80(1.0)\left[0.58(85)(45.37) + 1.0(85)(6.13)\right] = 2{,}206 \text{ kips}$$
$$< 0.80(1.0)\left[0.58(70)(66.00) + 1.0(85)(6.13)\right] = 2{,}560 \text{ kips}$$
$$\therefore R_r = 2{,}206 \text{ kips} > 866 \text{ kips} \quad \text{ok}$$

For Failure Mode 2:

$$A_{tn} = 2\left[4.0 + 3.0 - 1.5(0.9375)\right](1.0) = 11.19 \text{ in}^2$$

$$A_{vn} = 2\left[5(3.0) + 1.5 - 5.5(0.9375)\right](1.0) = 22.69 \text{ in}^2$$

$$A_{vg} = 2\left[5(3.0) + 1.5\right](1.0) = 33.00 \text{ in}^2$$

$$R_r = 0.80(1.0)\left[0.58(85)(22.69) + 1.0(85)(11.19)\right] = 1{,}656 \text{ kips}$$
$$< 0.80(1.0)\left[0.58(70)(33.00) + 1.0(85)(11.19)\right] = 1{,}833 \text{ kips}$$
$$\therefore R_r = 1{,}656 \text{ kips} > 866 \text{ kips} \quad \text{ok}$$

Check for net section fracture of the bottom flange of the smaller section at the point of splice when subject to tension at the strength limit state according to the following requirement (Equation 6.4.7.2-1):

$$f_t \le 0.84\left(\frac{A_n}{A_g}\right)F_u \le F_{yt}$$

$$0.84\left(\frac{A_n}{A_g}\right)F_u = 0.84\left(\frac{19.59}{24.75}\right)70 = 46.5 \text{ ksi} < F_{yt} = 50 \text{ ksi}$$

From separate calculations, f_t in the bottom flange of the smaller section at the strength limit state (Strength I) is equal to +21.58 ksi, which is less than 46.5 ksi.

Since the combined area of the inside and outside flange splice plates is less than the area of the bottom flange of the smaller section at the splice, check the fatigue stresses in the base metal of the bottom flange splice plates adjacent to the slip-critical bolted connections. Also, check the flexural stresses in the splice plates at the service limit state under the Service II load combination. Although the area of the splice plates is less than the area of the bottom flange in this case, design of the splice for the specified minimum design force is assumed to provide adequate stiffness and strength.

By inspection, the bottom flange is subject to a net tensile stress. According to *AASHTO LRFD* Table 6.6.1.2.3-2, the 75-year $(ADTT)_{SL}$ equivalent to infinite life for a Category B detail is 860 trucks/day. The actual $(ADTT)_{SL}$ for this example is assumed to be 1,600 trucks/day, which is greater than this value such that the detail is to be designed for the Fatigue I load combination and infinite life. The load factor for the Fatigue I load combination is 1.5. The moments at the point of splice due to the factored fatigue load (factored by the 1.5 load factor specified for the Fatigue I load combination) plus the 15 percent dynamic load allowance are:

M_{+LL+IM} = +1,442 kip-ft
M_{-LL+IM} = -1,010 kip-ft

The maximum flange stresses rather than the stresses at the midthickness of the flange (acting on the gross section) will be conservatively used in the fatigue check. It will be assumed that the conditions spelled out in *AASHTO LRFD* Article 6.6.1.2.1 are met such that the fatigue live load stresses can be computed using the short-term composite section assuming the concrete deck is effective for both positive and negative flexure. Therefore, using the section properties of the smaller section at the point of splice:

$$f_{+LL+IM} = \frac{1{,}442(12)}{2{,}725} = 6.35 \text{ ksi} \qquad \text{(tension)}$$

$$f_{-LL+IM} = \frac{-1{,}010(12)}{2{,}725} = -4.45 \text{ ksi} \quad \text{(compression)}$$

$$\gamma(\Delta f) = f_{+LL+IM} + \left|f_{-LL+IM}\right| = 6.35 + \left|-4.45\right| = 10.80 \text{ ksi}$$

According to *AASHTO LRFD* Article 6.6.1.2.5, the nominal fatigue resistance for the Fatigue I load combination and infinite life is to be taken as:

$$(\Delta F)_n = (\Delta F)_{TH}$$

where $(\Delta F)_{TH}$ is the constant-amplitude fatigue threshold taken from AASHTO LRFD Table 6.6.1.2.5-3. For a Category B detail, $(\Delta F)_{TH}$ is equal to 16.0 ksi.

The range of flange force in the bottom flange of the smaller section at the point of splice is computed from the stress range as follows:

$$\Delta P = 10.80(1.375)(18.0) = 267.3 \text{ kips}$$

The range of fatigue force and stress in the outside splice plate is computed as:

$$\Delta P = \frac{267.3}{2} = 133.6 \text{ kips}$$

$$\Delta f = \frac{133.6}{(0.5625)(18.0)} = 13.19 \text{ ksi} < (\Delta F)_n = 16.00 \text{ ksi} \quad \text{ok}$$

The range of fatigue force and stress in the inside splice plates is computed as:

$$\Delta P = \frac{267.3}{2} = 133.6 \text{ kips}$$

$$\Delta f = \frac{133.6}{2(0.6875)(8.0)} = 12.14 \text{ ksi} < (\Delta F)_n = 16.00 \text{ ksi} \quad \text{ok}$$

At the service limit state, the stress in the splice plates under the Service II load combination will be checked against a limiting stress of $0.95F_y$, where F_y is the specified minimum yield strength of the splice plates (Section 6.5.4.3.2.1). The minimum service limit state design force, P_s, for the splice was computed earlier to be 395 kips. As discussed previously in Section 6.6.5.2.2.3, the minimum design force at the service limit state should always be assumed divided equally to the two slip planes regardless of the ratio of the splice plate areas. Therefore, the force on the outside and inside splice plates will be taken as 395/2 = 197.5 kips. The resulting stress on the gross area of the outside splice plate is:

$$f = \frac{197.5}{(0.5625)(18.0)} = 19.5 \text{ ksi} < 0.95(50) = 47.5 \text{ ksi} \quad \text{ok}$$

The stress on the gross area of the inside splice plates is:

$$f = \frac{197.5}{2(0.6875)(8.0)} = 18.0 \text{ ksi} < 0.95(50) = 47.5 \text{ ksi} \quad \text{ok}$$

Top Flange Splice

The width of the outside splice plate should be at least as wide as the width of the narrowest flange at the splice. Therefore, try a 7/16” x 16” outside splice plate with two 1/2” x 7” inside splice plates (Figure 6.6.5.2.3.4-5). A filler plate is not required. All plates are ASTM A709/A709M Grade 50W steel.

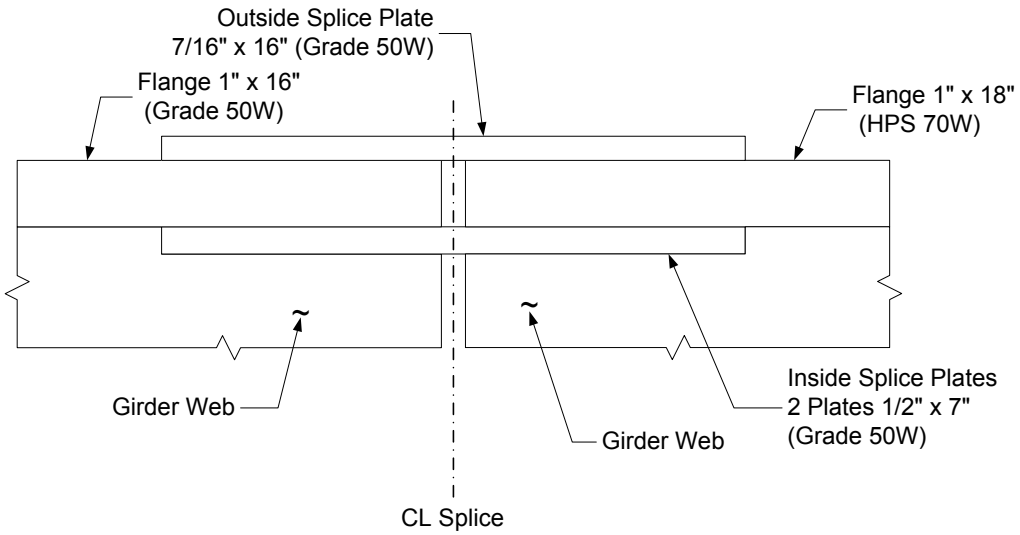

Figure 6.6.5.2.3.4-5 Example Top Flange Splice

As the areas of the inner and outer plates are equal, the design force will be equally divided to the inner and outer plates, and the shear resistance of the bolted connection at the strength limit state will be checked for the total minimum flange design force assumed acting in double shear.

The factored yield resistance of the splice plates in tension at the strength limit state is checked as follows (Equation 6.6.4.2.5.6.1-1):

Outside plate:

$$R_r = 0.95(50)(16.0)(0.4375) = 332.5 \text{ kips} > 542/2 = 271 \text{ kips} \quad \text{ok}$$

Inside plates:

$$R_r = 0.95(50)(2)(7.0)(0.5) = 332.5 \text{ kips} > 542/2 = 271 \text{ kips} \quad \text{ok}$$

The factored net section fracture resistance of the splice plates in tension at the strength limit state is checked as follows (Equation 6.6.4.2.5.6.1-2):

Outside plate:

$$R_r = 0.80(70)[16.0 - 4(0.9375)](0.4375)(1.0)(1.0) = 300.1 \text{ kips} > 542/2 = 271 \text{ kips} \quad \text{ok}$$

Inside plates:

$$R_r = 0.80(70)[2(7.0) - 4(0.9375)](0.5)(1.0)(1.0) = 287.0 \text{ kips} > 542/2 = 271 \text{ kips} \quad \text{ok}$$

Also, according to *AASHTO LRFD* Article 6.13.5.2, for splice plates subject to tension, A_n must not exceed $0.85A_g$.

Outside plate:

$$0.85(16.0)(0.4375) = 5.95 \text{ in}^2 > A_n = [16.0 - 4(0.9375)](0.4375) = 5.36 \text{ in.}^2 \quad \text{ok}$$

Inside plates:

$$0.85(2)(7.0)(0.5) = 5.95 \text{ in}^2 > A_n = [2(7.0) - 4(0.9375)](0.5) = 5.13 \text{ in.}^2 \quad \text{ok}$$

The block shear rupture resistance of the splice plates will be checked later.

The factored resistance of the splice plates in compression at the strength limit state is checked as follows (Equation 6.6.5.2.2.2.3-1):

Outside plate:

$$R_r = 0.95(50)(16)(0.4375) = 332.5 \text{ kips} > 600/2 = 300 \text{ kips} \quad \text{ok}$$

Inside plates:

$$R_r = 0.95(50)(2)(7.0)(0.5) = 332.5 \text{ kips} > 600/2 = 300 \text{ kips} \quad \text{ok}$$

Since 7/8-inch diameter bolts are used with one washer assumed under the turned element, and the ply closest to the nut (i.e. the inner flange splice plates) are 1/2-in. thick, the threads are excluded from the shear planes (Section 6.6.5.2.2.2.3). The factored shear resistance, R_r, for a 7/8-in. diameter ASTM A325 high-strength bolt in double shear assuming the threads are excluded from the shear planes was computed in an earlier example to be 55.4 kips/bolt (Section 6.6.4.2.5.2).

The minimum number of bolts required to develop the governing minimum design force in the flange in shear at the strength limit state (in the absence of a filler plate) is:

$$N = \frac{P}{R_r} = \frac{600.0}{55.4} = 10.8 \text{ bolts} \qquad \text{Use N = 12 bolts}$$

The Service II stress in the top flange of the smaller section at the point of splice is computed as follows:

A. Dead Load + Positive Live Load:

$$f = [1.0(-1.86 + -0.11 + -0.11) + 1.3(-1.73)] = -4.33 \text{ ksi} \quad \text{(controls)}$$

B. Dead Load + Negative Live Load:

$$f = [1.0(-1.86 + -0.11 + -0.11) + 1.3(+1.23)] = -0.48 \text{ ksi}$$

Therefore, f_s is equal to –4.33 ksi and F_s is equal to f_s/R_h = -4.33/1.0 = -4.33 ksi.

The stress at the mid-thickness of the top flange due to the deck-casting sequence (the special load combination for checking constructibility of steel bridges specified in *AASHTO LRFD* Article 3.4.2.1 controls) is:

$$f = \frac{1.4(1{,}300)(12)(39.13)}{62{,}658} = -13.64 \text{ ksi} \qquad \frac{f}{R_h} = \frac{-13.64}{1.0} = -13.64 \text{ ksi}$$

which is greater than F_s; therefore, the stress due to the deck-casting sequence controls the slip resistance check.

The design force, P_s, for the flange splice is taken as this stress times the gross area of the flange in the smaller section at the point of splice, or

$$P_s = |-13.64|(1.0)(16.0) = 218.2 \text{ kips}$$

The minimum number of bolts required to provide adequate slip resistance under this design force is:

$$N = \frac{P}{R_r} = \frac{218.2}{39.0} = 5.6 \text{ bolts}$$

which is less than the minimum number of bolts required to provide adequate factored shear resistance at the strength limit state (i.e. N = 12 bolts). Thus, use twelve (12) 7/8-in. diameter high-strength bolts on each side of the top flange splice (3 rows of bolts with 4 bolts per row -- no stagger).

The bolt spacing and bolt edge and end distances shown in Figure 6.6.5.2.3.4-6 satisfy the appropriate requirements as illustrated earlier for the bottom flange splice.

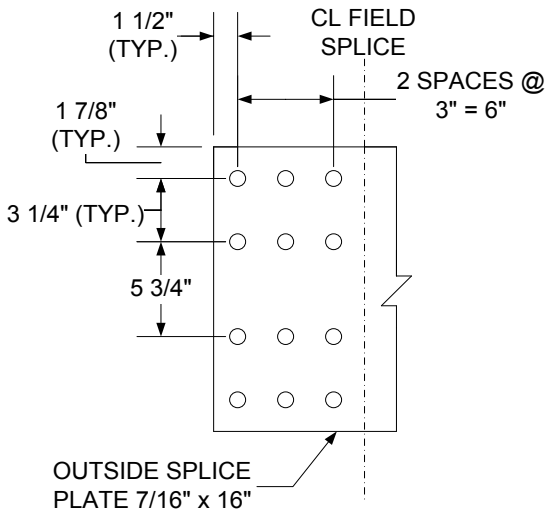

Figure 6.6.5.2.3.4-6 Outside Top Flange Splice Plate – Plan View

Check the bearing resistance at the bolt holes at the strength limit state. Check the sum of the inner and outer splice plate thicknesses times the specified minimum tensile strength, F_u, of the splice plates versus the thickness of each flange times its corresponding F_u, to determine which plate controls the bearing resistance of the connection.

$$\text{Splice Plates: } (0.5+0.4375)(70)=65.6 \text{ kips/in. (governs)}$$
$$\text{Bottom Flange Left: } (1.0)(70)=70.0 \text{ kips/in.}$$
$$\text{Bottom Flange Right: } (1.0)(85)=85.0 \text{ kips/in.}$$

The thinner outside splice plate controls the bearing resistance of the connection.

For the four bolts adjacent to the end of the splice plate, the end distance is 1.5 in. Therefore, the clear distance, L_c, between the edge of the hole and the end of the splice plate is:

$$L_c = 1.5 - \frac{0.9375}{2} = 1.03 \text{ in.}$$

Therefore, from Equation 6.6.4.2.5.3-5:

$$R_n = 4(1.2L_c tF_u) = 4\left[1.2(1.03)(0.4375)(70)\right] = 151.4 \text{ kips (governs)}$$

or:

$$R_n = 4(2.4dtF_u) = 4\left[2.4(0.875)(0.4375)(70)\right] = 257.3 \text{ kips}$$

For the other eight bolts, the center-to-center distance between the bolts in the direction of the applied force is 3.0 in. Therefore, the clear distance, L_c, between the edges of the adjacent holes is:

$$L_c = 3.0 - 0.9375 = 2.0625 \text{ in.}$$

Therefore:

$$R_n = 8(1.2L_c tF_u) = 8\left[1.2(2.0625)(0.4375)(70)\right] = 606.4 \text{ kips}$$

or:

$$R_n = 8(2.4dtF_u) = 8\left[2.4(0.875)(0.4375)(70)\right] = 514.5 \text{ kips (governs)}$$

The total nominal bearing resistance of the splice plate, R_n, is therefore:

$$R_n = 151.4 \text{ kips} + 514.5 \text{ kips} = 665.9 \text{ kips}$$

$$R_r = 0.80(665.9) = 532.7 \text{ kips} > \frac{600}{2} = 300 \text{ kips} \quad \text{ok}$$

Check the block shear rupture resistance of the top flange splice plates and the top flange when subject to the minimum design force in tension at the strength limit state. Assume the same potential block shear failure planes on the outside and inside splice plates as shown previously for the bottom flange splice plates (refer to Figure 6.6.5.2.3.4-3).

Check the outside splice plate. A_{tn} is the net area along the place resisting the tensile stress.

$$A_{tn} = 2\left[3.25 + 1.875 - 1.5(0.9375)\right](0.4375) = 3.25 \text{ in}^2$$

A_{vn} is the net area along the place resisting the shear stress.

$$A_{vn} = 2\left[2(3.0) + 1.5 - 2.5(0.9375)\right](0.4375) = 4.51 \text{ in}^2$$

A_{vg} is the gross area along the planes resisting the shear stress.

$$A_{vg} = 2\left[2(3.0) + 1.5\right](0.4375) = 6.56 \text{ in}^2$$

The factored block shear rupture resistance, R_r, is determined as (Equation 6.6.3.3.2.5-1):

$$R_r = \phi_{bs} R_p \left(0.58 F_u A_{vn} + U_{bs} F_u A_{tn}\right) \le \phi_{bs} \left(0.58 F_y A_{vg} + U_{bs} F_u A_{tn}\right)$$

ϕ_{bs} is the resistance factor for block shear rupture taken equal to 0.80 (*AASHTO LRFD* Article 6.5.4.2). The reduction factor, R_p, is taken equal to 1.0 for holes drilled full-size. The reduction factor, U_{bs}, is taken equal to 1.0 since the distribution of the shear force on the splice plates is essentially uniform. Therefore:

$$\begin{aligned} R_r &= 0.80(1.0)\left[0.58(70)(4.51) + 1.0(70)(3.25)\right] = 328.5 \text{ kips} \\ &< 0.80(1.0)\left[0.58(50)(6.56) + 1.0(70)(3.25)\right] = 334.2 \text{ kips} \\ \therefore R_r &= 328.5 \text{ kips} > \frac{542}{2} = 271 \text{ kips} \quad \text{ok} \end{aligned}$$

Check the inside splice plates.

$$A_{tn} = 2\left[3.25 + 1.875 - 1.5(0.9375)\right](0.5) = 3.72 \text{ in}^2$$

$$A_{vn} = 2\left[2(3.0) + 1.5 - 2.5(0.9375)\right](0.5) = 5.16 \text{ in}^2$$

$$A_{vg} = 2\left[2(3.0) + 1.5\right](0.5) = 7.50 \text{ in}^2$$

$$\begin{aligned} R_r &= 0.80(1.0)\left[0.58(70)(5.16) + 1.0(70)(3.72)\right] = 375.9 \text{ kips} \\ &< 0.80(1.0)\left[0.58(50)(7.50) + 1.0(70)(3.72)\right] = 382.3 \text{ kips} \\ \therefore R_r &= 375.9 \text{ kips} > \frac{542}{2} = 271 \text{ kips} \quad \text{ok} \end{aligned}$$

Check the critical girder flange at the splice. Since the areas and yield strengths of the flanges on each side of the splice differ, both sides would need to be checked. Only the calculations for the flange on the left-hand side of the splice, which is determined to be the critical flange, are shown below. The same two potential failure modes are investigated as for the bottom flange (refer to Figure 6.6.5.2.3.4-4).

For Failure Mode 1:

$$A_{tn} = 2\left[3.25 - 0.9375\right](1.0) = 4.63 \text{ in}^2$$

$$A_{vn} = 4\left[2(3.0) + 1.5 - 2.5(0.9375)\right](1.0) = 20.63 \text{ in}^2$$

$$A_{vg} = 4[2(3.0) + 1.5](1.0) = 30.00 \text{ in}^2$$

$$\begin{aligned} R_r &= 0.80(1.0)[0.58(70)(20.63) + 1.0(70)(4.63)] = 929.3 \text{ kips} \\ &< 0.80(1.0)[0.58(50)(30.00) + 1.0(70)(4.63)] = 955.3 \text{ kips} \\ \therefore R_r &= 929.3 \text{ kips} > 542 \text{ kips} \quad \text{ok} \end{aligned}$$

For Failure Mode 2:

$$A_{tn} = 2[3.25 + 1.875 - 1.5(0.9375)](1.0) = 7.44 \text{ in}^2$$

$$A_{vn} = 2[2(3.0) + 1.5 - 2.5(0.9375)](1.0) = 10.31 \text{ in}^2$$

$$A_{vg} = 2[2(3.0) + 1.5](1.0) = 15.00 \text{ in}^2$$

$$\begin{aligned} R_r &= 0.80(1.0)[0.58(70)(10.31) + 1.0(70)(7.44)] = 751.5 \text{ kips} \\ &< 0.80(1.0)[0.58(50)(15.00) + 1.0(70)(7.44)] = 764.6 \text{ kips} \\ \therefore R_r &= 751.5 \text{ kips} > 542 \text{ kips} \quad \text{ok} \end{aligned}$$

Check for net section fracture of the top flange of the smaller section at the point of splice when subject to tension at the strength limit state according to Equation 6.4.7.2-1.

$$0.84\left(\frac{A_n}{A_g}\right)F_u = 0.84\left(\frac{12.25}{16.0}\right)70 = 45.0 \text{ ksi} < F_{yt} = 50 \text{ ksi}$$

From separate calculations, f_t in the top flange at the strength limit state (Strength I) is equal to +12.98 ksi in the top flange of the smaller section at the splice, which is less than 45.0 ksi.

Since the combined area of the inside and outside flange splice plates is less than the area of the top flange of the smaller section at the splice, check the fatigue stresses in the base metal of the top flange splice plates adjacent to the slip-critical bolted connections. Also, check the flexural stresses in the splice plates at the service limit state under the Service II load combination.

The factored fatigue live load plus impact moments were given earlier. The maximum flange stresses rather than the stresses at the midthickness of the flange (acting on the gross section) will be conservatively used in the fatigue check. It will again be assumed that the conditions spelled out in *AASHTO LRFD* Article 6.6.1.2.1 are met such that the fatigue live load stresses can be computed using the short-

term composite section assuming the concrete deck is effective for both positive and negative flexure.

First, determine if the top flange splice plate is subject to a net tensile stress under the unfactored permanent loads plus the Fatigue I load combination, as specified in *AASHTO LRFD* Article 6.6.1.2.1. The future wearing surface will be conservatively neglected in this calculation.

$$f_{DC1} = \frac{248(12)}{1{,}581} = -1.88 \text{ ksi}$$

$$f_{DC2} = \frac{50(12)}{5{,}375} = -0.11 \text{ ksi}$$

$$f_{-LL+IM} = \frac{-1{,}010(12)}{16{,}287} = +0.74 \text{ ksi}$$

Since |-1.88 + -0.11| = 1.99 ksi > 0.74 ksi, the top flange splice plates are not subject to a net tensile stress under the specified load combination and fatigue need not be checked.

At the service limit state, the stress in the splice plates under the Service II load combination will be checked against a limiting stress of $0.95F_y$, where F_y is the specified minimum yield strength of the splice plates. The minimum service limit state design force, P_s, for the splice is equal to F_s (computed earlier) times the gross area of the top flange in the smaller section at the point of splice =|-4.33|(1.0)(16.0) = 69.3 kips. As discussed previously in Section 6.6.5.2.2.3, the minimum design force at the service limit state should always be assumed divided equally to the two slip planes regardless of the ratio of the splice plate areas. Therefore, the force on the outside and inside splice plates will be taken as 69.3/2 = 34.6 kips. The resulting stress on the gross area of the outside splice plate is:

$$f = \frac{34.6}{(0.4375)(16.0)} = 4.9 \text{ ksi} < 0.95(50) = 47.5 \text{ ksi} \quad \text{ok}$$

The stress on the gross area of the inside splice plates is:

$$f = \frac{34.6}{2(0.5)(7.0)} = 4.9 \text{ ksi} < 0.95(50) = 47.5 \text{ ksi} \quad \text{ok}$$

Web Splice Design

The web splice will be designed based on the conservative assumption that the maximum moment and shear at the splice will occur under the same loading condition.

Determine the design shear in the web, V_{uw}, at the point of splice at the strength limit state. Compute the maximum factored shear at the splice, V_u, at the strength limit state using the appropriate load factors given in *AASHTO LRFD* Tables 3.4.1-1 and 3.4.1-2. The Strength I load combination is used. Note that the minimum load factors, γ_p, from *AASHTO LRFD* Table 3.4.1-2 in conjunction with a load modifier of $1/\eta$ are applied to the permanent load shears when the corresponding shears are of opposite sign to the live load plus impact shear.

A. Dead Load + Negative Live Load Shear:

$$V_u = 1.0\left[1.25(-82 + -12) + 1.5(-11) + 1.75(-112)\right] = -330 \text{ kips (governs)}$$

B. Dead Load + Positive Live Load Shear:

$$V_u = \frac{1}{1.0}\left[0.90(-82 + -12) + 0.65(-0.11)\right] + 1.0\left[1.75(+19)\right] = -58.5 \text{ kips}$$

Calculate the factored shear resistance of the web, $V_r = \phi_v V_n$, adjacent to the splice. From separate calculations, the smallest nominal shear resistance is for the web on the left-hand side of the splice. The transverse stiffener spacing adjacent to the splice on the left-hand side is d_o = 17'-3" = 207 in., which is equal to the maximum permitted spacing of 3*D* = 3(69.0) = 207 in. As discussed previously in Section 6.5.7.3, in order for a stiffened panel to develop the full post-buckling shear resistance, the section along the panel must satisfy the following relationship (Equation 6.5.7.3-3):

$$\frac{2Dt_w}{(b_{fc}t_{fc} + b_{ft}t_{ft})} \le 2.5$$

$$\frac{2(69.0)(0.5)}{\left[16(1.0) + 18(1.375)\right]} = 1.69 < 2.5$$

Therefore:

$$V_n = V_p\left[C + \frac{0.87(1-C)}{\sqrt{1+\left(\frac{d_o}{D}\right)^2}}\right] \quad \text{(Equation 6.5.7.3-2)}$$

$$k = 5 + \frac{5}{\left(\frac{d_o}{D}\right)^2} \quad \text{(Equation 6.5.7.2-4)}$$

$$k = 5 + \frac{5}{\left(\frac{207.0}{69.0}\right)^2} = 5.56$$

Since,

$$1.40\sqrt{\frac{Ek}{F_{yw}}} = 1.40\sqrt{\frac{29{,}000(5.56)}{50}} = 79.5 < \frac{D}{t_w} = \frac{69.0}{0.5} = 138.0$$

$$C = \frac{1.57}{\left(\frac{D}{t_w}\right)^2}\left(\frac{Ek}{F_{yw}}\right) \quad \text{(Equation 6.5.7.2-5)}$$

$$C = \frac{1.57}{(138.0)^2}\left(\frac{29{,}000(5.56)}{50}\right) = 0.266$$

$$V_p = 0.58F_{yw}Dt_w \quad \text{(Equation 6.5.7.1-2)}$$

$$V_p = 0.58(50)(69.0)(0.5) = 1{,}001\,\text{kips}$$

$$\text{Therefore, } V_n = 1{,}001\left[0.266 + \frac{0.87(1-0.266)}{\sqrt{1+\left(\frac{207.0}{69.0}\right)^2}}\right] = 468 \text{ kips}$$

$$V_r = \phi_v V_n = 1.0(468) = 468 \text{ kips} > |V_u| = 330 \text{ kips}$$

As specified in *AASHTO LRFD* Article 6.13.6.1.4b, the equation to use to compute the design shear, V_{uw}, depends on the value of V_u with respect to $V_r = \phi_v V_n$ as follows:

$$0.5\phi_v V_n = 0.5(468) = 234 \text{ kips}$$
$$|V_u| = 330 \text{ kips} > 234 \text{ kips}$$

Therefore:

$$V_{uw} = \frac{(V_u + \phi_v V_n)}{2} \quad \text{(Equation 6.6.5.2.3.2.1-2)}$$

$$V_{uw} = \frac{(|-330| + 468)}{2} = 399 \text{ kips}$$

Two vertical rows of bolts with 18 bolts per row will be investigated. According to *AASHTO LRFD* Article 6.13.6.1.4a, a minimum of two rows of bolts is required on each side of the joint to ensure proper alignment and stability of the girder during construction. The bolts are spaced horizontally and vertically as shown below in Figure 6.6.5.2.3.4-7.

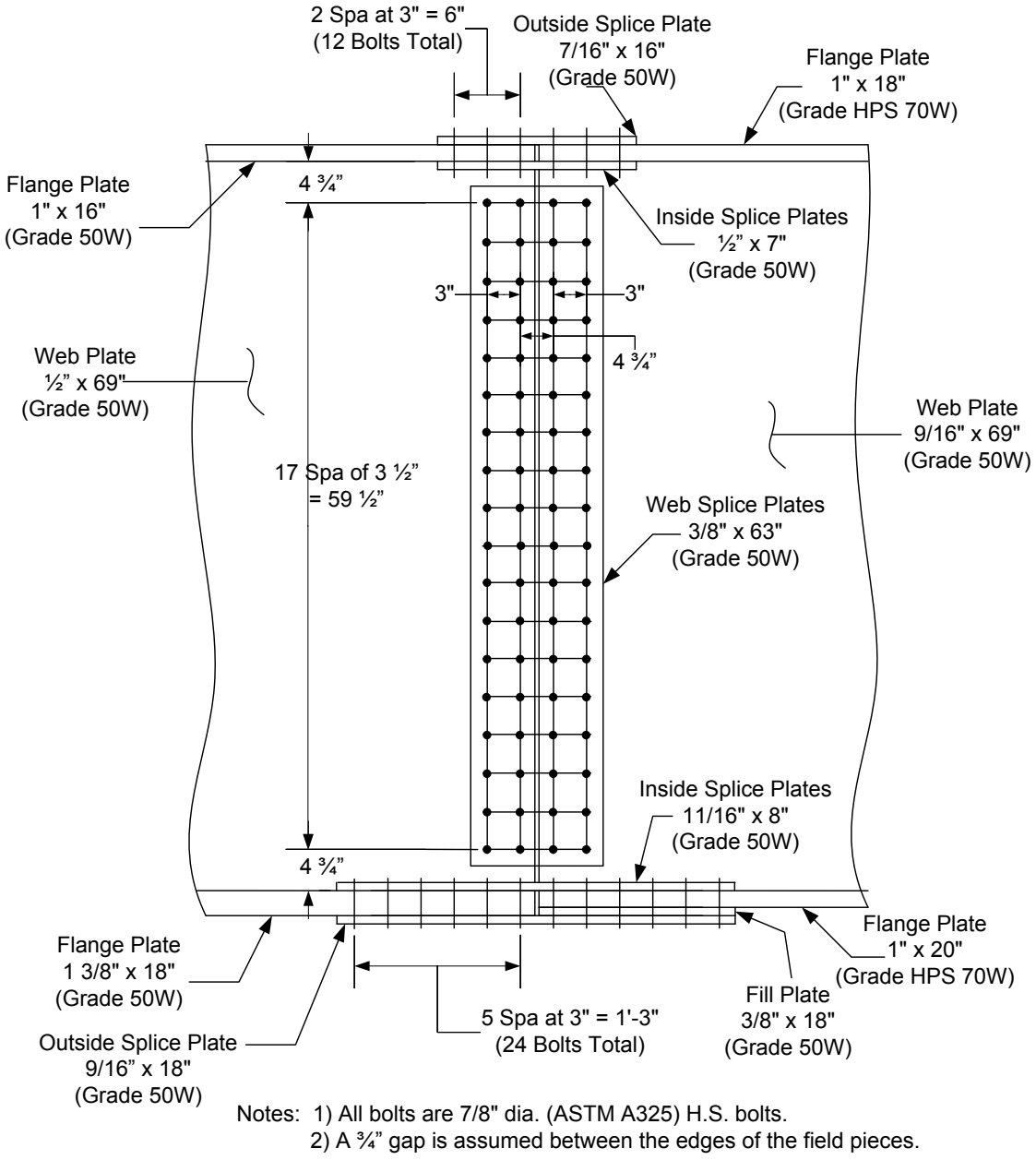

Notes: 1) All bolts are 7/8" dia. (ASTM A325) H.S. bolts.
2) A ¾" gap is assumed between the edges of the field pieces.

Figure 6.6.5.2.3.4-7 Example Web Splice

The outermost bolts are located 4-3/4" inches from the flanges to provide clearance for assembly [see AISC (2010) for bolt assembly clearances]. The web is spliced symmetrically by plates with a thickness not less than one-half the web thickness. Assume 3/8" x 63" splice plates on each side of the web. The splice plates are ASTM A709/A709M Grade 50W steel. As permitted in *AASHTO LRFD* Article 6.13.6.1.5 (and discussed below), a fill plate is not included since the difference in thickness of the web plates on either side of the splice does not exceed 0.0625 in. (i.e. 1/16 in.).

Although not illustrated here, the number of bolts in the web splice could be decreased by spacing a group of bolts closer to the mid-depth of the web (where the flexural stress is relatively low) at the maximum spacing specified for sealing (*AASHTO LRFD* Article 6.13.2.6.2 – Section 6.6.4.2.2.2.2), and by spacing the remaining two groups of bolts near the top and bottom of the web at a closer spacing.

Calculate the design moment, M_{uv}, due to the eccentricity of the design shear at the point of splice at the strength limit state as follows (Equation 6.6.5.2.3.2.2-1):

$$M_{uv} = V_{uw}e$$

Referring to Figure 6.6.5.2.3.4-7, the correct eccentricity to use is the horizontal distance from the centerline of the splice to the centroid of the web bolt group on the side of the joint under consideration as follows. A gap of ¾ in. is assumed between the webs at the splice, which allows the splice to be more easily flushed out for maintenance:

$$e = \left(2.375 + \frac{3.0}{2}\right)\frac{1}{12} = 0.323 \text{ ft}$$

$$M_{uv} = 399.0(0.323) = 128.9 \text{ kip} - \text{ft}$$

Determine the portion of the flexural moment to be resisted by the web, M_{uw}, and the horizontal design force resultant, H_{uw}, in the web at the strength limit state. Use the equations provided in *AASHTO LRFD* Article C6.13.6.1.4b (Equations 6.6.5.2.3.2.3-1 and 6.6.5.2.3.2.3-2). Again, since the splice is located in an area of stress reversal, checks must be made for both the positive and negative flexure conditions.

Positive Flexure

For the case of positive flexure, the controlling flange was previously determined to be the bottom flange. The maximum flexural stress due to the factored loads at the midthickness of the controlling flange, f_{cf}, and the minimum design stress for the controlling flange, F_{cf}, were previously computed for this loading condition to be:

$$f_{cf} = +21.32 \text{ ksi}$$
$$F_{cf} = +37.50 \text{ ksi}$$

For the same loading condition, the concurrent flexural stress at the mid-thickness of the noncontrolling (top) flange, fncf, was previously computed to be:

$$f_{ncf} = -5.65 \text{ ksi}$$

The portion of the flexural moment assumed to be resisted by the web is computed as (Equation 6.6.5.2.3.2.3-1):

$$M_{uw} = \frac{t_w D^2}{12}\left|R_h F_{cf} - R_{cf} f_{ncf}\right|$$

where the hybrid factor, R_h, is taken as 1.0 for a homogeneous section and ratio, R_{cf}, is computed as follows:

$$R_{cf} = \left|\frac{F_{cf}}{f_{cf}}\right| = \left|\frac{+37.50}{+21.32}\right| = 1.76$$

Therefore:

$$M_{uw} = \frac{0.5(69.0)^2}{12}\left|1.0(+37.50) - 1.76(-5.65)\right| = 9{,}412 \text{ kip} - \text{in.} = 784.3 \text{ kip} - \text{ft}$$

The design horizontal force resultant for this loading condition, H_{uw}, is computed as (Equation 6.6.5.2.3.2.3-2):

$$H_{uw} = \frac{t_w D}{2}\left(R_h F_{cf} + R_{cf} f_{ncf}\right)$$

$$H_{uw} = \frac{0.5(69.0)}{2}\left[1.0(+37.50) + 1.76(-5.65)\right] = +475.3 \text{ kips}$$

Note that all stresses in the above equations are to be taken as signed quantities. Since the sign of M_{uw} corresponds to the sign of the flexural moment for the loading condition under consideration, absolute value signs are applied to the resulting difference of the stresses for convenience. H_{uw} is always taken as a signed quantity; positive for tension, negative for compression. Check the above computed values of M_{uw} and H_{uw}. For the web, the section modulus $S = (0.5)(69.0)^2/6 = 396.8$ in.^{3} and the area $A = 0.5(69.0) = 34.5$ in.^{2}. Therefore:

$$f_{bot} = \frac{784.3(12)}{396.8} + \frac{475.3}{34.5} = 37.50 \text{ ksi} = R_h F_{cf} \quad \text{ok}$$

$$f_{top} = -\frac{784.3(12)}{396.8} + \frac{475.3}{34.5} = -9.94 \text{ ksi} = R_{cf} f_{ncf} = 1.76(-5.65) \quad \text{ok}$$

The use of $R_h F_{cf}$ and the application of the factor R_{cf} to f_{ncf} in essence is factoring up the stresses in the web by the same amount as the stresses in the controlling flange so that the web splice is designed in a consistent fashion at the strength limit state.

The total moment on the web splice for this condition is equal to the sum of M_{uv} and M_{uw}:

$$M_{tot} = M_{uv} + M_{uw} = 128.9 + 784.3 = 913.2 \text{ kip} - \text{ft}$$

Negative Flexure

For the case of negative flexure, the controlling flange was also previously determined to be the bottom flange. The maximum flexural stress due to the factored loads at the midthickness of the controlling flange, f_{cf}, and the minimum design stress for the controlling flange, F_{cf}, were previously computed for this loading condition to be:

$$f_{cf} = -14.59 \text{ ksi}$$
$$F_{cf} = -37.50 \text{ ksi}$$

For the same loading condition, the concurrent flexural stress at the mid-thickness of the noncontrolling (top) flange was previously computed to be:

$$f_{ncf} = +12.77 \text{ ksi}$$

The ratio, R_{cf}, is computed as follows:

$$R_{cf} = \left|\frac{F_{cf}}{f_{cf}}\right| = \left|\frac{-37.50}{-14.59}\right| = 2.57$$

Therefore:

$$M_{uw} = \frac{0.5(69.0)^2}{12}\left|1.0(-37.50) - 2.57(+12.77)\right| = 13{,}949 \text{ kip} - \text{in.} = 1{,}162 \text{ kip} - \text{ft}$$

The design horizontal force resultant for this loading condition, H_{uw}, is computed as:

$$H_{uw} = \frac{0.5(69.0)}{2}\left[1.0(-37.50) + 2.57(+12.77)\right] = -80.7 \text{ kips}$$

Check the above computed values of M_{uw} and H_{uw}:

$$f_{bot} = -\frac{1{,}162(12)}{396.8} - \frac{80.7}{34.5} = -37.50 \text{ ksi} = R_h F_{cf} \quad \text{ok}$$

$$f_{top} = \frac{1{,}162(12)}{396.8} - \frac{80.7}{34.5} = +32.80 \text{ ksi} = R_{cf} f_{ncf} = 2.57(+12.77) \quad \text{ok}$$

The total moment on the web splice for this condition is equal to the sum of M_{uv} and M_{uw}:

$$M_{tot} = M_{uv} + M_{uw} = 128.9 + 1{,}162 = 1{,}291 \text{ kip} - \text{ft}$$

Check the web-splice bolts for shear at the strength limit state assuming the bolts in the connection have slipped and gone into bearing. The web-splice bolts are to be designed for the effects of the design shear, the moment due to the eccentric design shear, and the flexural moment and horizontal design force resultant in the web, which are all assumed applied at the mid-depth of the web. The traditional elastic vector method is used for calculating the maximum resultant bolt force (Section 6.6.4.2.6). The polar moment of inertia, I_p, of the bolts with respect to the centroid of the connection is computed as follows (Equation 6.6.4.2.6-7):

$$I_p = \frac{nm}{12}\left[s^2\left(n^2 - 1\right) + g^2(m^2 - 1)\right]$$

For the example web splice (Figure 6.6.5.2.3.4-7), n = 18; m = 2, s = 3.5 in.; and g = 3.0 in. Therefore:

$$I_p = \frac{18(2)}{12}\left[(3.5)^2\left(18^2 - 1\right) + (3.0)^2(2^2 - 1)\right] = 11{,}951 \text{ in.}^2$$

Determine the vertical bolt force, R_v, due to the design shear, V_{uw}, assuming two vertical rows with 18 bolts per row for a total number of bolts, N_b, equal to 36:

$$R_v = \frac{V_{uw}}{N_b} = \frac{399}{36} = 11.08 \text{ kips / bolt}$$

Positive Flexure

Determine the bolt force due to the horizontal design force resultant, H_{uw}:

$$R_h = \frac{H_{uw}}{N_b} = \frac{475.3}{36} = 13.20 \text{ kips / bolt}$$

Determine the vertical and horizontal components of the force on the extreme bolt due to the total moment on the web splice, M_{tot}:

$$R_{M_v} = \frac{M_{tot}x}{I_p} = \frac{913.2(12)(3.0/2)}{11{,}951} = 1.38 \text{ kips}$$

$$R_{M_h} = \frac{M_{tot}y}{I_p} = \frac{913.2(12)(29.75)}{11{,}951} = 27.28 \text{ kips}$$

The resultant bolt force on the extreme bolt is:

$$R = \sqrt{(R_v + R_{M_v})^2 + (R_h + R_{M_h})^2} = \sqrt{(11.08 + 1.38)^2 + (13.20 + 27.28)^2} = 42.35 \text{ kips}$$

Negative Flexure

Determine the bolt force due to the horizontal design force resultant, H_{uw}:

$$R_h = \frac{H_{uw}}{N_b} = \frac{|-80.7|}{36} = 2.24 \text{ kips / bolt}$$

Determine the vertical and horizontal components of the force on the extreme bolt due to the total moment on the web splice, M_{tot}:

$$R_{M_v} = \frac{M_{tot}x}{I_p} = \frac{1{,}291(12)(3.0/2)}{11{,}951} = 1.94 \text{ kips}$$

$$R_{M_h} = \frac{M_{tot}y}{I_p} = \frac{1{,}291(12)(29.75)}{11{,}951} = 38.56 \text{ kips}$$

The resultant bolt force on the extreme bolt is:

$$R = \sqrt{(R_v + R_{M_v})^2 + (R_h + R_{M_h})^2} = \sqrt{(11.08 + 1.94)^2 + (2.24 + 38.56)^2} = 42.83 \text{ kips (governs)}$$

Since 7/8-in. diameter bolts are used and the web splice plates are less than ½-in. thick, the bolts are included in the shear plane (Section 6.6.5.2.3.2.4). The factored shear resistance, R_r, for a 7/8-in. diameter ASTM A325 high-strength bolt in double shear with the threads included in the shear planes is 55.4(0.38/0.48) = 43.9 kips/bolt (Section 6.6.4.2.5.2). Note that the greater than 50.0 in. length reduction does not apply when computing the factored shear resistance of the bolts in a web splice since the distribution of shear force is essentially uniform along the joint. Therefore:

$$R = 42.83 \text{ kips} < R_r = 43.9 \text{ kips} \quad \text{ok}$$

AASHTO LRFD Article 6.13.6.1.4b requires that high-strength bolted connections for web splices be designed to prevent slip at the service limit state under the maximum resultant bolt force due to Load Combination Service II. In addition, *AASHTO LRFD* Article 6.13.6.1.4a requires that high-strength bolted splices for flexural members be proportioned to prevent slip during the erection of the steel (assuming an erection analysis is conducted) and during the casting of the concrete deck. As a minimum, for checking slip of the bolts, the design shear, V_s, is to be taken as the shear at the point of splice due to Load Combination Service II. The Service II shears at the point of splice for the positive and negative flexure conditions are computed as follows:

A. Dead Load + Negative Live Load Shear:

$$V_S = [1.0(-82 + -12 + -11) + 1.3(-112)] = -251 \text{ kips (governs)}$$

B. Dead Load + Positive Live Load Shear:

$$V_S = [1.0(-82 + -12 + -0.11) + 1.3(+19)] = -80.3 \text{ kips}$$

The factored shear due to the deck-casting sequence (the special load combination for checking constructibility of steel bridges specified in *AASHTO LRFD* Article 3.4.2.1 controls) is computed as:

$$V = 1.4(-82) = -115 \text{ kips}$$

which is less than the governing value of V_s. Therefore, the design shear for checking slip of the web bolts will be taken as V_s.

Calculate the design moment, M_{sv}, due to the eccentricity of the design shear at the point of splice at the service limit state as follows (Equation 6.6.5.2.3.3-1):

$$M_{SV} = V_S e$$

$$M_{SV} = |-251.0|(0.323) = 81.1 \text{ kip} - \text{ft}$$

Determine the portion of the flexural moment to be resisted by the web, M_{sw}, and the horizontal design force resultant, H_{sw}, in the web at the service limit state (Equations 6.6.5.2.3.3-1 and 6.6.5.2.3.3-2). The maximum Service II flexural stress at the midthickness of the bottom flange, f_s, was computed previously to be +15.94 ksi due to the positive flexure load condition. The flexural stress in the other (top) flange at the point of splice, f_{os}, concurrent with f_s in the bottom flange for this load condition is –4.33 ksi. The portion of the flexural moment assumed to be resisted by the web is computed as (Equation 6.6.5.2.3.3-2):

$$M_{sw} = \frac{t_w D^2}{12}\left|f_s - f_{os}\right|$$

$$M_{sw} = \frac{0.5(69.0)^2}{12}\left|+15.94 - (-4.33)\right| = 4{,}021\,\text{kip} - \text{in.} = 335.1\,\text{kip} - \text{ft}$$

The design horizontal force resultant for this loading condition is computed as (Equation 6.6.5.2.3.3-3):

$$H_{sw} = \frac{t_w D}{12}\left(f_s + f_{os}\right)$$

$$H_{uw} = \frac{0.5(69.0)}{2}\left[+15.94 + (-4.33)\right] = +200.3\ \text{kips}$$

Check the above computed values of M_{sw} and H_{sw}:

$$f_{bot} = \frac{335.1(12)}{396.8} + \frac{200.3}{34.5} = 15.94\ \text{ksi} = f_s \quad \text{ok}$$

$$f_{top} = -\frac{335.1(12)}{396.8} + \frac{200.3}{34.5} = -4.33\ \text{ksi} = f_{os} \quad \text{ok}$$

The total moment on the web splice for this condition is equal to the sum of M_{sv} and M_{sw}:

$$M_{tot} = M_{sv} + M_{sw} = 81.1 + 335.1 = 416.2\,\text{kip} - \text{ft}$$

In this case, the loading condition causing the maximum Service II flexural stress in the top flange is the same loading condition (i.e. the positive flexure condition). Therefore, slip of the web bolts only needs to be checked for the one load condition.

The traditional elastic vector method is again used for calculating the maximum resultant bolt force. Determine the vertical bolt force, R_v, due to the design shear, V_s, assuming two vertical rows with 18 bolts per row for a total number of bolts, N_b, equal to 36:

$$R_v = \frac{V_s}{N_b} = \frac{\left|-251\right|}{36} = 6.97\ \text{kips / bolt}$$

Determine the bolt force due to the horizontal design force resultant, H_{sw}:

$$R_h = \frac{H_{sw}}{N_b} = \frac{200.3}{36} = 5.56 \text{ kips / bolt}$$

Determine the vertical and horizontal components of the force on the extreme bolt due to the total moment on the web splice, M_{tot}:

$$R_{M_v} = \frac{M_{tot}x}{I_p} = \frac{416.2(12)(3.0/2)}{11{,}951} = 0.63 \text{ kips}$$

$$R_{M_h} = \frac{M_{tot}y}{I_p} = \frac{416.2(12)(29.75)}{11{,}951} = 12.43 \text{ kips}$$

The resultant bolt force on the extreme bolt is:

$$R = \sqrt{\left(R_v + R_{M_v}\right)^2 + \left(R_h + R_{M_h}\right)^2} = \sqrt{(6.97 + 0.63)^2 + (5.56 + 12.43)^2} = 19.53 \text{ kips}$$

The factored slip resistance, R_r, for a 7/8-in. diameter ASTM A325 high-strength bolt assuming a Class B surface condition for the faying surface, standard holes and two slip planes per bolt was computed in an earlier example to be 39.0 kips/bolt (Section 6.6.4.2.4.2). Therefore:

$$R = 19.53 \text{ kips} < R_r = 39.0 \text{ kips} \quad \text{ok}$$

Check the bolt spacings and bolt edge and end distances for the web splice (refer to Figure 6.6.5.2.3.4-7).

As specified in *AASHTO LRFD* Article 6.13.2.6.1 (Section 6.6.4.2.2.2.1), the minimum spacing between centers of bolts in standard holes is not to be less than 3.0*d*, where *d* is the diameter of the bolt. For 7/8-in. diameter bolts:

$$s_{min} = 3d = 3(0.875) = 2.63 \text{ in.} < 3.0 \text{ in.} \quad \text{ok}$$

As specified in *AASHTO LRFD* Article 6.13.2.6.2 (Section 6.6.4.2.2.2.2), to seal against the penetration of moisture in joints, the spacing, *s*, of a single line of bolts adjacent to a free edge of an outside plate or shape (when the bolts are not staggered) must satisfy the following requirement (Equation 6.6.4.2.2.2.2-1):

$$s \le \left(4.0 + 4.0t\right) \le 7.0 \text{ in.}$$

where *t* is the thickness of the thinner outside plate or shape. Check for sealing along the vertical edges of the web splice plates:

$$s_{max} = 4.0 + 4.0(0.375) = 5.5 \text{ in.} > 4.75 \text{ in.} \quad \text{ok}$$

The edge distance of bolts is defined as the distance perpendicular to the line of force between the center of a hole and the edge of the component. In this example, the edge distance from the center of the vertical line of holes in the web plate to the edge of the field piece of 2.0 inches satisfies the minimum edge distance requirement of 1-1/8 inches specified for 7/8-in. diameter bolts and gas cut edges in *AASHTO LRFD* Table 6.13.2.6.6-1 (Section 6.6.4.2.2.2.3). This distance also satisfies the maximum edge distance requirement of 8.0*t* (not to exceed 5.0 in.) = 8.0(0.375) = 3.0 in. specified in *AASHTO LRFD* Article 6.13.2.6.6. The edge distance for the outermost vertical row of holes on the web splice plates is set at 2.0 inches.

The end distance of bolts is defined as the distance along the line of force between the center of a hole and the end of the component. In this example, the end distance of 1-3/4 inches at the top and bottom of the web splice plates satisfies the minimum end distance requirement of 1-1/8 inches specified for 7/8-in. diameter bolts and gas cut edges in *AASHTO LRFD* Table 6.13.2.6.6-1 (Section 6.6.4.2.2.2.3). The maximum end distance requirement of 8.0*t* (not to exceed 5.0 in.) = 8.0(0.375) = 3.0 in. specified in *AASHTO LRFD* Article 6.13.2.6.5 is also satisfied. Although not specifically required, note that the distance from the corner bolts to the corner of the web splice plate, equal to $\sqrt{(2.0)^2 + (1.75)^2} = 2.65$ in., also satisfies the maximum end distance requirement.

Check the bearing resistance at the web-splice bolt holes at the strength limit state. Since in this case the thickness of the thinner web at the point of splice times its specified minimum tensile strength, F_u, is less than the sum of the web splice-plate thicknesses times the corresponding F_u of the splice plates, and the thickness of the thicker web at the point of splice times its corresponding F_u, the thinner web (on the left-hand side) controls the bearing resistance of the connection.

The resistance of an outermost hole, calculated using the clear edge distance (which is smaller than the clear vertical distance between the bolt holes), can conservatively be checked against the maximum resultant bolt force acting on the extreme bolt in the connection (**Error! Reference source not found.** Part A). Since the resultant force acts in the direction of an inclined distance that is larger than the clear edge distance, the check is conservative. Other options for checking the bearing resistance were discussed previously (Section 6.6.5.2.3.2.4). Based on the edge distance from the center of the hole to the edge of the field piece of 2.0 inches, the clear edge distance, L_c, is computed as:

$$L_c = 2.0 - \frac{0.9375}{2} = 1.53 \text{ in.}$$

For standard holes, the nominal bearing resistance, R_n, parallel to the applied bearing force is taken as follows (Equation 6.6.4.2.5.3-5):

$$R_n = 1.2L_c tF_u \leq 2.4dtF_u$$

$$R_n = 1.2L_c tF_u = 1.2(1.53)(0.5)(70) = 64.26 \text{ kips (governs)}$$

or:

$$R_n = 2.4dtF_u = 2.4(0.875)(0.5)(70) = 73.50 \text{ kips}$$

$$R_r = \phi_{bb} R_n$$

$$R_r = 0.80(64.26) = 51.41 \text{ kips} > R = 42.83 \text{ kips} \quad \text{ok}$$

Had the bearing resistance been exceeded, the preferred option would be to increase the edge distance slightly in lieu of increasing the number of bolts or thickening the web.

Check the block shear rupture resistance of the web splice plates at the strength limit state. Because of the overall length of the connection, the block shear rupture resistance normally does not control for web splice plates of typical proportion, but the check is illustrated here for completeness. Assume the block shear failure plane on the web splice plates shown in Figure 6.6.5.2.3.4-8:

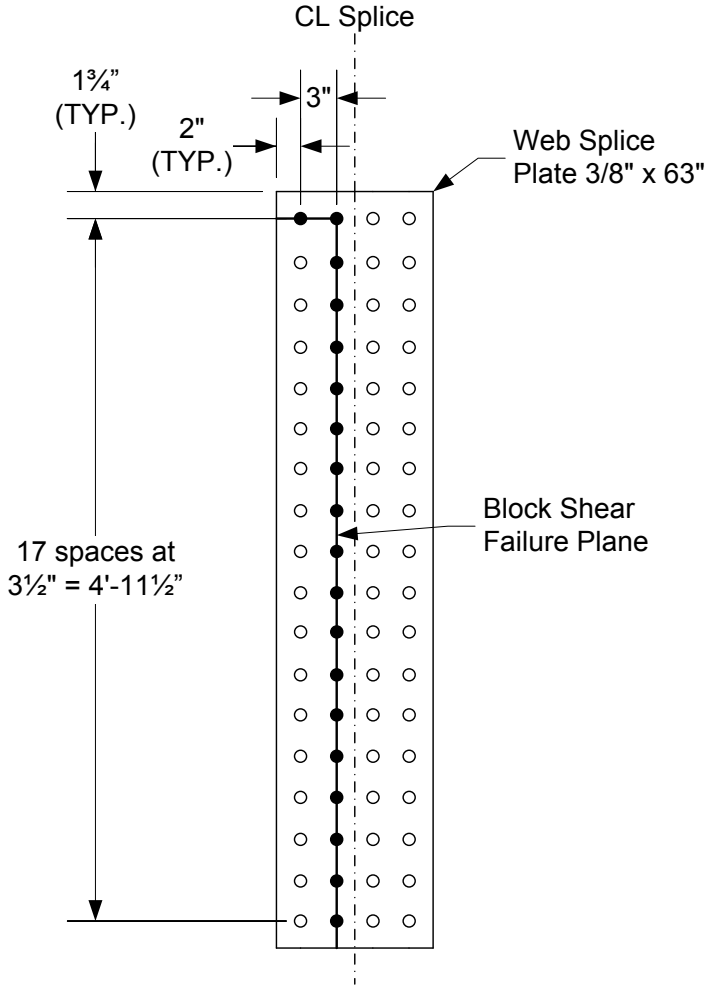

Figure 6.6.5.2.3.4-8 Web Splice Plate – Assumed Block Shear Failure Plane in the Web Splice Plates

A_{tn} is the net area along the place resisting the tensile stress.

$$A_{tn} = 2[3.0 + 2.0 - 1.5(0.9375)](0.375) = 2.69 \text{ in}^2$$

A_{vn} is the net area along the place resisting the shear stress.

$$A_{vn} = 2[63.0 - 1.75 - 17.5(0.9375)](0.375) = 33.63 \text{ in}^2$$

A_{vg} is the gross area along the plane resisting the shear stress.

$$A_{vg} = 2[63.0 - 1.75](0.375) = 45.94 \text{ in}^2$$

The factored block shear rupture resistance, R_r, is determined as (Equation 6.6.3.3.2.5-1):

$$R_r = \phi_{bs} R_p \left(0.58 F_u A_{vn} + U_{bs} F_u A_{tn}\right) \le \phi_{bs} \left(0.58 F_y A_{vg} + U_{bs} F_u A_{tn}\right)$$

ϕ_{bs} is the resistance factor for block shear rupture taken equal to 0.80 (*AASHTO LRFD* Article 6.5.4.2). The reduction factor, R_p, is taken equal to 1.0 for holes drilled full-size. The reduction factor, U_{bs}, is taken equal to 1.0 since the distribution of the shear force on the splice plates is essentially uniform. Therefore:

$$\begin{aligned} R_r &= 0.80(1.0)\left[0.58(70)(33.63) + 1.0(70)(2.69)\right] = 1{,}243 \text{ kips} \\ &> 0.80(1.0)\left[0.58(50)(45.94) + 1.0(70)(2.69)\right] = 1{,}216 \text{ kips} \\ &\therefore R_r = 1{,}216 \text{ kips} > V_{uw} = 399 \text{ kips} \quad \text{ok} \end{aligned}$$

Check for flexural yielding on the gross section of the web splice plates at the strength limit state (Equation 6.6.5.2.3.2.4-1).

$$A_{PL} = 2(0.375)(63.0) = 47.25 \text{ in.}^2$$

$$S_{PL} = \frac{2(0.375)(63.0)^2}{6} = 496.1 \text{ in.}^3$$

$$f_{PL} = \frac{M_{tot}}{S_{PL}} + \frac{H_{uw}}{A_{PL}}$$

For positive flexure:

$$f_{PL} = \frac{913.2(12)}{496.1} + \frac{475.3}{47.25} = 32.15 \text{ ksi} < \phi_f F_y = 1.0(50) = 50 \text{ ksi} \quad \text{ok}$$

For negative flexure:

$$f_{PL} = \frac{1{,}291(12)}{496.1} + \frac{|-80.7|}{47.25} = 32.94 \text{ ksi} < \phi_f F_y = 1.0(50) = 50 \text{ ksi} \quad \text{ok}$$

Check for shear yielding on the gross section of the web splice plates under the design shear, V_{uw}, at the strength limit state. As specified in *AASHTO LRFD* Article 6.13.5.3, the factored shear resistance of a connected element, R_r, is conservatively based on the shear yield stress (i.e. $F_y/\sqrt{3} = 0.58F_y$) as follows (Section 6.6.4.2.5.6.2):

$$R_r = \phi_v 0.58 F_y A_{vg}$$

$$R_r = 1.0(0.58)(50)(2)(0.375)(63.0) = 1{,}370 \text{ kips}$$

$$R_r = 1{,}370 \text{ kips} > V_{uw} = 399 \text{ kips} \quad \text{ok}$$

Check for shear rupture on the web splice plates under the design shear, V_{uw}, at the strength limit state. As specified in *AASHTO LRFD* Article 6.13.5.3, the factored shear resistance of a connected element, R_r, for shear rupture is taken as follows (Section 6.6.4.2.5.6.2):

$$R_r = \phi_{vu} 0.58 R_p F_u A_{vn}$$

$$R_r = 0.80(0.58)(1.0)(70)(2)[63.0 - 36(0.9375)](0.375) = 712.5 \text{ kips}$$

$$R_r = 712.5 \text{ kips} > V_{uw} = 399 \text{ kips} \quad \text{ok}$$

Since the combined area of the web splice plates is greater than the area of the web on both sides of the splice, the fatigue stresses in the base metal of the web splice plates adjacent to the slip-critical bolted connections need not be checked. Also, the flexural stresses in the splice plates at the service limit state under the Service II load combination need not be checked.

6.6.5.3 Tension Members

The design of bolted splices for tension members is covered in *AASHTO LRFD* Article 6.13.6.1.2. All bolted splices for tension members are to be designed using slip-critical connections (Section 6.6.4.2.1.1), and are to satisfy the tensile resistance requirements for connected elements specified in *AASHTO LRFD* Article 6.13.5.2 (Section 6.6.4.2.5.6.1). The splices are to be designed for the load as determined by the general requirements of *AASHTO LRFD* Article 6.13.1 for the smaller section at the point of splice.

6.6.5.4 Compression Members

The design of bolted splices for compression members is covered in *AASHTO LRFD* Article 6.13.6.1.2. Splices for compression members (e.g. arch members, truss chords and columns) may either be designed at the strength limit state as: 1) open joints (i.e. no contact between adjoining parts) with enough bolts provided in the splice to carry 100 percent of the load as determined by the general requirements of *AASHTO LRFD* Article 6.13.1 for the smaller section at the point of splice, or 2) milled joints in full contact bearing with the bolts designed to carry no less than 50

percent of the lower factored resistance of the sections spliced. If the latter option is chosen, *AASHTO LRFD* Article 6.13.6.1.2 requires that the contract documents call for inspection of the joint during fabrication and erection. According to AASHTO/NSBA (2003), fabricators generally prefer the first option because it is less expensive and has the potential for fewer problems in the field.

The splices in these members are to be located as near as practicable to the panel points and usually on the side of the panel point where the smaller force effect occurs. The arrangement of all splice elements must make proper provision for all force effects in the component parts of the spliced members.

6.6.5.5 Filler Plates

6.6.5.5.1 General

The design of filler plates is covered in *AASHTO LRFD* Article 6.13.6.1.5. Filler plates are typically used on bolted flange splices of flexural members (and sometimes on web splices) when the thicknesses of the adjoining plates at the point of splice are different (Figure 6.6.5.5.1-1). At bolted flange splices, it is often advantageous to transition one or more of the flange thicknesses down adjacent to the point of splice, if possible, so as to reduce the required size of the filler plate, or possibly change the width of the flanges and keep the thickness constant in order to eliminate the need for a filler plate altogether.

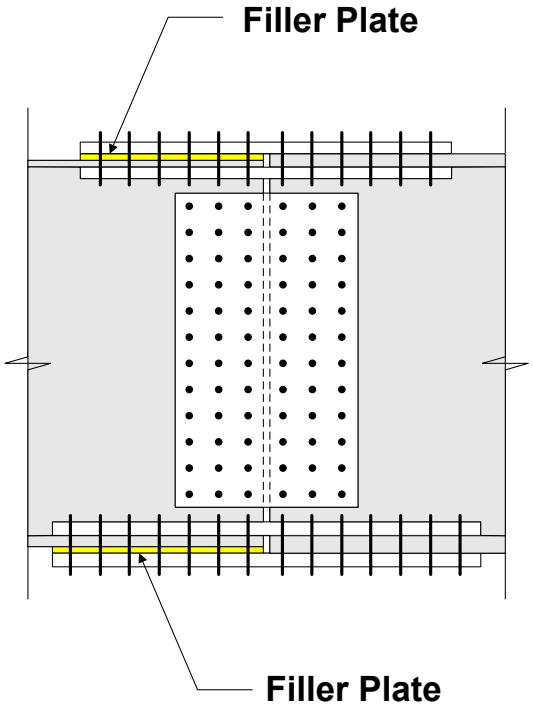

Figure 6.6.5.5.1-1 Filler Plates in Bolted Flange Splices

6.6.5.5.2 Filler Plates for Flange Splices

Fillers in axially loaded connections at the strength limit state must be secured by additional bolts to ensure that the fillers are an integral part of the connection; that is, to ensure that the shear planes are well-defined and that no reduction in the factored shear resistance of the bolts results.

AASHTO LRFD Article 6.13.6.1.5 provides two choices for developing fillers 0.25 in. or more in thickness in axially loaded bolted connections, which include girder flange splices. The choices are to either: 1) extend the fillers beyond the gusset or splice plate with the filler extension secured by enough additional bolts to distribute the total stress uniformly over the combined section of the member or filler; or 2) in lieu of extending and developing the fillers, reduce the factored shear resistance of the bolts (Section 6.6.4.2.5.2) by the following factor:

$$R = \left[\frac{(1+\gamma)}{(1+2\gamma)}\right] \qquad \text{Equation 6.6.5.5.2-1}$$

AASHTO LRFD Equation 6.13.6.1.5-1

where:

γ = A_f/A_p

A_f = sum of the area of the fillers on both sides of the connected plate (in.^{2})

A_p = smaller of either the connected plate area or the sum of the splice plate areas on both sides of the connected plate (in.^{2}). For truss gusset plate chord splices, when considering the gusset plate(s), only the portion of the gusset plate(s) that overlaps the connected plate is to be considered in the calculation of the splice plate areas.

Equation 6.6.5.5.2-1 was developed mathematically (Sheikh-Ibrahim, 2002) and compared to the results from an experimental program on axially loaded bolted splice connections with undeveloped fillers (Yura et al., 1982). The reduction factor, *R*, accounts for the reduction in the nominal shear resistance of the bolts due to bending in the bolts and will likely result in having to provide additional bolts in the connection to develop the filler(s). Note that the reduction factor is only to be applied on the side of the connections with the filler(s). For practical reasons, consideration should be given to using the same number of bolts on either side of the splice. Unlike the empirical reduction factor given in AISC (2010a), Equation 6.6.5.5.2-1 will typically be less than 1.0 for connections utilizing 0.25-in.-thick fillers in order to limit the deformation of the connection. Note that fillers 0.25-in. or more in thickness are not to consist of more than two plates, unless approved by the Design Engineer.

AASHTO LRFD Article 6.13.6.1.5 also requires that the specified minimum yield strength of fillers 0.25 in. or more in thickness not be less than the larger of 70

percent of the specified minimum yield strength of the connected plate and 36.0 ksi. To provide fully developed fillers that act integrally with the connected plate, the specified minimum yield strength of the fillers should theoretically be greater than or equal to the specified minimum yield strength of the connected plates times the factor [1/(1+γ)], where γ is taken as defined above. However, this may not be practical or convenient in some cases due to thinner filler-plate material availability issues. Therefore, in some cases at the strength limit state, premature yielding of the fillers, bolt bending and increased deformation of the connection may occur. To control the potential for excessive deformation of the connection, the lower limit on the specified minimum yield strength of the fillers (given above) is specified. Although in some cases there may be an increased probability of larger deformations in the connection at the strength limit state, the connection bolts will still have adequate reserve shear resistance as long as the fillers are appropriately extended and developed, or in lieu of extending the fillers, additional bolts are added according to Equation 6.6.5.5.2-1. According to *AASHTO LRFD* Article C6.13.6.1.5, the effects of yielding of the fillers and connection deformation are not considered to be significant for connections with fillers less than 0.25 in. in thickness. Note that for connections involving the use of weathering steels, a weathering grade product should be specified for the filler-plate material.

The resistance to slip between the filler and either connected part at the service limit state is comparable to the slip resistance that would exist between the connected parts if the filler were not present. Therefore, as specified in *AASHTO LRFD* Article 6.13.6.1.5, for slip-critical connections, the factored slip resistance of the bolts (Section 6.6.4.2.4.2) is not to be adjusted for the effect of the fillers.

6.6.5.5.3 Filler Plates for Web Splices

AASHTO LRFD Article 6.13.6.1.5 permits the omission of filler plates in bolted web splices where the thicknesses of the adjoining web plates differ by 0.0625 in. (1/16 in.) or less.

6.6.5.6 Welded Splices

The design of welded splices is covered in *AASHTO LRFD* Article 6.13.6.2. Welded splices must also conform to the requirements given in the latest edition of AASHTO/AWS (2010).

As a minimum, welded splices are to be designed according to the general design requirements given in *AASHTO LRFD* Article 6.13.1 for the smaller section at the point of splice. Groove welds are typically used for the butt joints at welded splices (Section 6.6.4.3.3.1). According to *AASHTO* LRFD Article 6.13.6.2, complete penetration groove welds may be used to splice tension and compression members; the use of splice plates should be avoided. Fatigue should be checked at all welded

splices subject to an applied net tensile stress (determined as specified in *AASHTO LRFD* Article 6.6.1.2.1) based on the appropriate fatigue detail category for the splice configuration given in *AASHTO LRFD* Table 6.6.1.2.3-1 (Section 6.5.5.2.2.1).

As discussed previously in Section 6.3.4.4.4, changing flange widths at welded shop splices should be avoided if at all possible. Should it become necessary to splice material of different widths using welded butt joints, symmetric transitions must be used that conform to one of the details shown in *AASHTO LRFD* Figure 6.13.2.6.2-1. The transition often starts at the butt splice. However, note that *AASHTO LRFD* Figure 6.13.2.6.2-1 shows a preferred detail in which the butt splice is located a minimum of 3.0 in. from the transition for greater ease in fitting the run-off tabs. At welded butt splices joining material of different thicknesses, the transition (including the weld) must be ground to a uniform slope between the offset surfaces of not more than 1 in 2.5 (and must be indicated as such in the contract documents).

Welded field splices are less commonly used. If used, they should be arranged to minimize overhead welding.

6.6.6 Web Stiffeners

6.6.6.1 General

The design of transverse stiffeners, bearing stiffeners, and longitudinal stiffeners is discussed in each of the following sections.

6.6.6.2 Transverse Web Stiffeners

6.6.6.2.1 General

The design of transverse web stiffeners for I-girders is covered in *AASHTO LRFD* Article 6.10.11.1. For box girders, *AASHTO LRFD* Article 6.11.11.1 refers to the I-girder provisions of *AASHTO LRFD* Article 6.10.11.1 for the design of transverse web stiffeners.

Transverse stiffeners are used to increase the shear resistance of a girder and are aligned vertically on vertical webs, or along the slope of inclined webs. Transverse stiffeners consist of plates or angles welded or bolted to either one or both sides of the web (Figure 6.6.6.2.1-1). The term connection plate is given to a transverse stiffener to which a cross-frame or diaphragm is connected. A connection plate can serve as a transverse stiffener for shear design calculations.

AASHTO LRFD Article 6.10.11.1.1 specifies that transverse web stiffeners used as connection plates must be attached to both flanges. According to *AASHTO LRFD* Article 6.6.1.3.1, attachment of the connection plate to the flanges must be made by

welding or bolting. The connection to the compression flange is typically welded. The connection to the tension flange is either welded or bolted through a tab plate that has been welded to the connection plate. Design engineers have specified the use of bolted tab plates to raise the nominal fatigue resistance of the flange base metal at the attachment detail from Detail Category C′ to Detail Category B. This should only be considered at connection plates where fatigue is a significant issue. The bolted tab plate is significantly more expensive to furnish and install than a welded connection. Also, the fatigue category of the base metal at the termination of the weld attaching the connection plate to the web is of the same fatigue category as the base metal at the weld to the tension flange (i.e. Detail Category C′). In most cases, the live load stress range at these two adjacent locations is not significantly different. Therefore, an adjustment of the location of a problem connection plate to eliminate the need for a bolted tab connection should be considered.

Figure 6.6.6.2.1-1 Transverse Web Stiffeners on an I-Girder

Stiffeners in straight girders not used as connection plates are to be tight fit or attached at the compression flange, but need not be in bearing with the tension flange. Generally, attachment of such stiffeners to the compression flange is accomplished by welding. Also, these stiffeners are generally either tight fit or cut short of the tension flange. A tight fit can help straighten the flange tilt without the application of heat (AASHTO/NSBA, 2003).

According to *AASHTO LRFD* Article 6.10.11.1.1, single-sided stiffeners on horizontally curved girders should be attached to both flanges to help retain the cross-sectional shape of the girder when subjected to torsion and to avoid high localized bending within the web, particularly near the top flange due to the torsional restraint of the concrete deck. For the same reason, it is required that pairs of transverse stiffeners on horizontally curved girders be tight fit or attached to both flanges. Similar consideration should be given to stiffeners on straight girders

resting on severely skewed supports since they are also subjected to significant torsion.

Special considerations related to the attachment of transverse stiffeners and connection plates to tub-girder flanges are discussed in Section 6.3.2.9.6.3.2.

As discussed in Section 6.5.5.2.2.1.3 (Figure 6.5.5.2.2.1.3-2), the distance between the end of the web-to-stiffener weld and the near edge of the adjacent web-to-flange weld is not to be less than $4t_w$ or more than the lesser of $6t_w$ and 4.0 in.

AASHTO/NSBA (2003) recommends that stiffeners and connection plates be detailed to be normal to the girder flanges unless unusual conditions require them to be detailed otherwise. Also, a minimum spacing of 8 inches or 1-1/2 times the stiffener plate width should be provided between stiffeners or connection plates for welding access.

Web panels with longitudinal stiffeners must include transverse stiffeners at a spacing of 1.5*D* or less (where *D* is the web depth), whether or not they are required for shear, in order to provide support to the longitudinal stiffeners along their length. Also, all available supporting experimental data for the design of longitudinally stiffened girders were generated from specimens that included transverse stiffeners, with panel aspect ratios generally less than or equal to 1.5.

6.6.6.2.2 Proportioning Requirements

AASHTO LRFD Article 6.10.11.1.2 specifies that the width, b_t, of each projecting transverse stiffener element (Figure 6.6.6.2.2-1) satisfy the following requirements:

$$b_t \geq 2.0 + \frac{D}{30} \qquad \text{Equation 6.6.6.2.2-1}$$

AASHTO LRFD Equation 6.10.11.1.2-1

and:

$$16t_p \geq b_t \geq b_f/4 \qquad \text{Equation 6.6.6.2.2-2}$$

AASHTO LRFD Equation 6.10.11.1.2-2

where:

b_f = for I-sections, full width of the widest compression flange within the field section under consideration; for tub sections, full width of the widest top flange within the field section under consideration; for closed box sections, the limit of $b_f/4$ does not apply (in.)

t_p = thickness of the projecting stiffener element (in.)

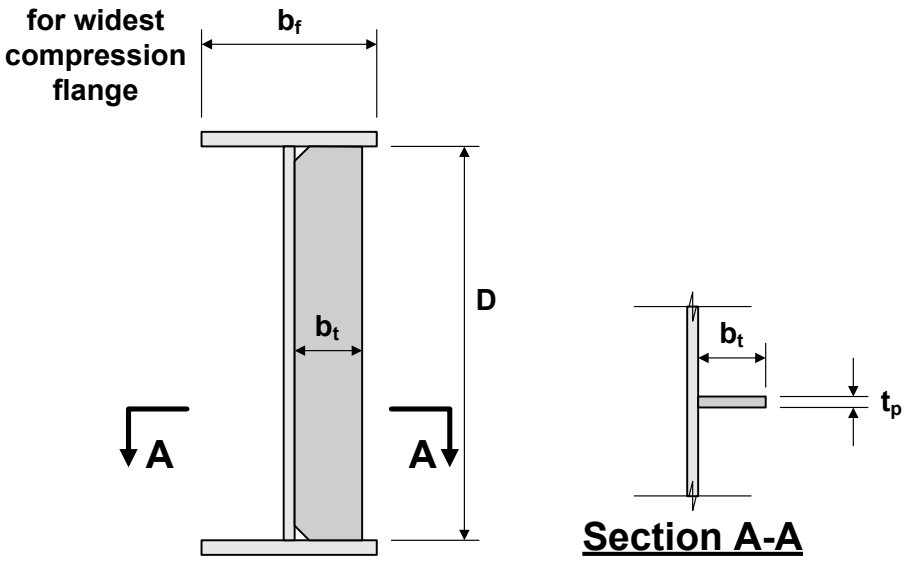

Figure 6.6.6.2.2-1 Projecting Width of Transverse Stiffeners

Equation 6.6.6.2.2-1 (Ketchum, 1908) tends to control relative to Equation 6.6.6.2.2-2 for I-girders with large ratios of D/b_f.

In Equation 6.6.6.2.2-2, the full width of the widest compression flange within the field section under consideration is used for b_f to allow for the use of the same minimum stiffener width throughout the entire field section, if desired, and to help restrain the widest compression flange. Since the bottom flange of tub sections is restrained by a web along both edges, the widest top flange is used for b_f in Equation 6.6.6.2.2-2. Since the web restrains the edges of both flanges of a closed box section, the limit of $b_f/4$ does not apply.

Welded stiffeners and connection plates are commonly made up of less expensive flat bar stock. Flat bars are generally produced in whole-inch width increments and 1/8-in. thickness increments. A ½-inch minimum thickness for stiffeners and connection plates is preferred (AASHTO/NSBA, 2003).

6.6.6.2.3 Moment of Inertia Requirements

The transverse stiffener must have sufficient rigidity to maintain a vertical line of near zero lateral deflection of the web along the line of the stiffener in order for the web to adequately develop the shear-buckling resistance, or the combined shear-buckling and postbuckling tension-field resistance as determined in *AASHTO LRFD* Article 6.10.9. Therefore, the bending rigidity (or moment of inertia) is the dominant parameter governing the performance of transverse stiffeners.

AASHTO LRFD Article 6.10.11.1.3 specifies that for transverse stiffeners adjacent to web panels not subject to postbuckling tension-field action, the moment of inertia of the transverse stiffener, I_t, must satisfy the smaller of the following limits:

$$I_t \geq I_{t1}$$ Equation 6.6.6.2.3-1

AASHTO LRFD Equation 6.10.11.1.3-1

and:

$$I_t \geq I_{t2}$$ Equation 6.6.6.2.3-2

AASHTO LRFD Equation 6.10.11.1.3-2

where:

$$I_{t1} = bt_w^3 J$$ Equation 6.6.6.2.3-3

AASHTO LRFD Equation 6.10.11.1.3-3

$$I_{t2} = \frac{D^4 \rho_t^{1.3}}{40}\left(\frac{F_{yw}}{E}\right)^{1.5}$$ Equation 6.6.6.2.3-4

AASHTO LRFD Equation 6.10.11.1.3-4

J = stiffener bending rigidity parameter taken as:

$$= \frac{2.5}{(d_o/D)^2} - 2.0 \geq 0.5$$ Equation 6.6.6.2.3-5

AASHTO LRFD Equation 6.10.11.1.3-5

F_{crs} = local buckling stress for the stiffener (ksi) taken as:

$$= \frac{0.31E}{\left(\frac{b_t}{t_p}\right)^2} \leq F_{ys}$$ Equation 6.6.6.2.3-6

AASHTO LRFD Equation 6.10.11.1.3-6

b = the smaller of d_o and D (in.)
b_t = width of the projecting stiffener element (in.)
d_o = the smaller of the adjacent panel widths (in.)
F_{ys} = specified minimum yield strength of the stiffener (ksi)
F_{yw} = specified minimum yield strength of the web (ksi)

I_t = moment of inertia of the transverse stiffener taken about the edge in contact with the web for single stiffeners and about the mid-thickness of the web for stiffener pairs (in.^{4})

I_{t1} = minimum moment of inertia of the transverse stiffener required for the development of the web shear-buckling resistance (in.^{4})

I_{t2} = minimum moment of inertia of the transverse stiffener required for the development of the full web postbuckling tension-field action resistance (in.^{4})

ρ_t = the larger of F_{yw}/F_{crs} and 1.0

t_p = thickness of the projecting stiffener element (in.)

For transverse stiffeners adjacent to web panels subject to postbuckling tension-field action, the moment of inertia, I_t, of the transverse stiffeners must satisfy the following:

- If $I_{t2} > I_{t1}$, then:

$$I_t \geq I_{t1} + (I_{t2} - I_{t1})\rho_w \qquad \text{Equation 6.6.6.2.3-7}$$

AASHTO LRFD Equation 6.10.11.1.3-7

- Otherwise:

$$I_t \geq I_{t2} \qquad \text{Equation 6.6.6.2.3-8}$$

AASHTO LRFD Equation 6.10.11.1.3-8

where:

- If both web panels adjacent to the stiffener are subject to postbuckling tension-field action, then:

ρ_W = maximum ratio of $\left(\dfrac{V_u - \phi_v V_{cr}}{\phi_v V_n - \phi_v V_{cr}}\right)$ within the two web panels

- Otherwise:

ρ_W = ratio of $\left(\dfrac{V_u - \phi_v V_{cr}}{\phi_v V_n - \phi_v V_{cr}}\right)$ within the one panel subject to postbuckling tension-field action

V_{cr} = shear-yielding or shear-buckling resistance of the web panel under consideration (Section 6.5.7.2) (kips)

$= CV_p$ Equation 6.6.6.2.3-9

AASHTO LRFD Equation 6.10.11.1.3-9

V_p = plastic shear force (kips)

$= 0.58F_{yw}Dt_w$ Equation 6.6.6.2.3-10

AASHTO LRFD Equation 6.10.11.1.3-10

ϕ_v = resistance factor for shear specified in *AASHTO LRFD* Article 6.5.4.2 (= 1.0)

C = ratio of the shear-buckling resistance to the shear yield strength determined from *AASHTO LRFD* Equation 6.10.9.3.2-4, 6.10.9.3.2-5, or 6.10.9.3.2-6 as applicable.

V_n = nominal shear-yielding or shear buckling plus postbuckling tension-field action resistance of the web panel under consideration determined as specified in *AASHTO LRFD* Article 6.10.9.3.2 (Section 6.5.7.3) (kips)

V_u = maximum shear due to the factored loads in the web panel under consideration (kips)

For single-sided stiffeners, a significant portion of the web is implicitly assumed to contribute to the bending rigidity so that the neutral axis of the stiffener is assumed located close to the edge in contact with the web. Therefore, for this case, the moment of inertia is taken about this edge and the contribution of the web to the moment of inertia about the neutral axis is neglected for simplicity.

The smaller moment of inertia from Equation 6.6.6.2.3-1 or Equation 6.6.6.2.3-2 is considered sufficient to develop the shear-buckling resistance of the web, $V_{cr} = CV_p$, when a larger shear resistance is not required in either panel adjacent to the stiffener (Kim and White, 2014). For members with $D/t_w = 1.12\sqrt{Ek/F_{yw}}$, which is the D/t_w value at which C is equal to 1.0 and V_{cr} is equal to the plastic shear force, V_p (Equation 6.6.6.2.3-10), Equation 6.6.6.2.3-1 and Equation 6.6.6.2.3-2 give approximately the same value of the I_t required to develop V_{cr}. For members with $D/t_w > 1.12\sqrt{Ek/F_{yw}}$, Equation 6.6.6.2.3-1 gives the smaller value of the I_t to develop the elastic or inelastic value of the shear-buckling resistance V_{cr}, and for members with $D/t_w < 1.12\sqrt{Ek/F_{yw}}$, Equation 6.6.6.2.3-2 gives the smaller value of the I_t required to develop $V_{cr} = V_p$. For the latter case, Equation 6.6.6.2.3-1 requires excessively large stiffener sizes since this equation is based on developing the elastic shear-buckling resistance of the web. Bleich (1952) gives inelastic buckling solutions, which show that such large stiffeners are not required as D/t_w is reduced below the limit of $1.12\sqrt{Ek/F_{yw}}$. Research based on refined finite-element studies has also confirmed this fact (Kim and White, 2014).

Much larger values of I_t are required to develop the shear-buckling resistance for ratios of (d_o/D) less than or equal to 1.0 (Bleich, 1952), which is represented by Equation 6.6.6.2.3-1. For ratios of (d_o/D) greater than 1.0, the term, b, in Equation 6.6.6.2.3-1, along with Equation 6.6.6.2.3-5, provide a reasonably constant value of the required I_t to develop the shear-buckling resistance.

The stiffener must generally have a larger I_t than defined by Equation 6.6.6.2.3-1 to develop the web postbuckling or tension-field resistance in one or both panels adjacent to the stiffener (Kim and White, 2014). Equation 6.6.6.2.3-2 provides the larger required I_t necessary in such cases to maintain a line of near zero lateral deflection within the postbuckled web at the stiffener location. Equation 6.6.6.2.3-2 provides an accurate to slightly conservative required stiffener size relative to refined finite-element solutions for straight and horizontally curved I-girders at all values of D/t_w permitted by the *AASHTO LRFD* Specifications (Kim and White, 2014). Although the required stiffener rigidity is insensitive to the parameter, (d_o/D), according to Equation 6.6.6.2.3-2, the equation provides an approximate upper bound to the results from a comparable equation proposed in Kim and White (2014) for all values of (d_o/D). The term, ρ_t, in Equation 6.6.6.2.3-2 accounts for the effect of potential local buckling of stiffeners having a relatively large width-to-thickness ratio, b_t/t_p, and also for the effect of potential early yielding in stiffeners with F_{ys} less than or equal to F_{yw}.

Equation 6.6.6.2.3-2 is intended to provide a required I_t that will allow the development of a factored shear resistance at or near the postbuckling tension-field shear resistance, $\phi_v V_n$, in the adjacent web panel(s). However, in cases where V_u is smaller than $\phi_v V_n$, this value of I_t is not required. Equation 6.6.6.2.3-7 accounts for the fact that the I_t necessary to develop a factored shear resistance greater than or equal to V_u is smaller when V_u is smaller than the full factored combined web shear buckling and postbuckling resistance, $\phi_v V_n$ (Kim and White, 2014). Equation 6.6.6.2.3-7 allows for the calculation of a conservative but more economical stiffener size for large girder depths that is sufficient to develop a girder shear resistance greater than or equal to V_u. Equation 6.6.6.2.3-8 addresses a small number of cases with stocky webs where V_n is approximately equal to the plastic shear force, V_p.

Previous Specifications included an area requirement for transverse stiffeners adjacent to panels subject to postbuckling tension-field action, which has since been removed. Multiple experimental and refined finite-element based research studies have shown that transverse stiffeners are loaded primarily in lateral bending by the postbuckled web panels, and not by axial forces associated with postbuckling tension-field action, even for web panels with D/t_w up to 300. Therefore, the stiffener moment of inertia has a much stronger correlation with the stiffener performance than the stiffener area. In addition, the research described in Kim and White (2014) indicated that panels designed for shear postbuckling resistance using one-sided stiffeners and two-sided stiffeners based on the traditional area requirement had significantly different values of shear resistance. In fact, in some cases (primarily cases with two-sided stiffeners as D/t_w increased beyond $1.12\sqrt{Ek/F_{yw}}$), the area requirement provided a stiffener size that was insufficient to hold the postbuckled web in position at the stiffener location. Equation 6.6.6.2.3-2 recognizes the fact that one- and two-sided stiffeners, sized such that they have the same value of I_t, provide

essentially the same shear resistance for a given stiffener spacing (Kim and White, 2014; Horne and Grayson, 1983; Rahal and Harding, 1990; Stanway et al., 1996; and Lee at al., 2003).

The size of intermediate stiffeners should be kept the same along the length of the girders to eliminate multiple plate sizes and eliminate the possibility of placement errors.

Transverse stiffeners used in panels with longitudinal web stiffeners must also satisfy the following relationship:

$$I_t \geq \left(\frac{b_t}{b_\ell}\right)\left(\frac{D}{3d_o}\right)I_\ell \qquad \text{Equation 6.6.6.2.3-11}$$

AASHTO LRFD Equation 6.10.11.1.3-11

where:

b_ℓ = projecting width of the longitudinal stiffener (in.)
b_t = projecting width of the transverse stiffener (in.)
I_ℓ = moment of inertia of the longitudinal stiffener determined as specified in *AASHTO LRFD* Article 6.10.11.3.3 (Section 6.6.6.4) (in.^{4})

Lateral loads along the length of a longitudinal stiffener are transferred to the adjacent transverse stiffeners as concentrated reactions at the stiffener intersections (Cooper, 1967). Equation 6.6.6.2.3-11 provides a relationship between the moments of inertia of the transverse and longitudinal stiffeners to ensure that the transverse stiffeners do not fail under these concentrated reactions. The relationship applies whether the stiffeners are on the same or opposite side of the web.

EXAMPLE

Size the transverse stiffeners for Field Section 1 of the exterior girder of a three-span continuous I-girder bridge (refer to Figure 6.5.7.4.2.2-1). The web in Field Section 1 is ½" x 69". The top flange in Field Section 1 is 16 inches wide. The same size stiffeners will be used within the field section for practical purposes. Grade 50W steel will be used for the stiffeners (i.e. F_{ys} = 50.0 ksi), and for the flanges and web of the girder. All stiffeners are on one side of the web.

Determine the initial trail stiffener proportions. Size the stiffener width, b_t, to be greater than or equal to $b_f/4$ as required in Equation 6.6.6.2.2-2. For I-sections, b_f is to be taken as the full width of the widest compression flange within the field section under consideration.

$$b_t \geq \frac{16.0}{4} = 4.0 \text{ in.}$$

Again, stiffeners and connection plates are commonly made up of less expensive flat bar stock, which is generally produced in whole-inch width increments and 1/8-in. thickness increments. Therefore:

$$\text{Use } b_t = 6.0 \text{ in.} > 4.0 \text{ in.} \quad \text{ok}$$

Check Equation 6.6.6.2.2-1:

$$b_t \geq 2.0 + \frac{D}{30}$$

$$2.0 + \frac{69.0}{30} = 4.3 \text{ in.} < 6.0 \text{ in.} \qquad \text{ok}$$

Try a stiffener thickness t_p of 0.5 inches, which satisfies the preferred minimum thickness of ½ inch for stiffeners given in AASHTO/NSBA (2003).

Check that:

$$16t_p \geq b_t \quad \text{(Equation 6.6.6.2.2-2)}$$

$$16(0.5) = 8.0 \text{ in.} > 6.0 \text{ in.} \quad \text{ok}$$

According to the shear calculations in the previous example in Section 6.5.7.4.2.2 containing Figure 6.5.7.4.2.2-1, most of the web panels in this field section are subject to postbuckling tension-field action. To adequately develop the postbuckling tension-field shear resistance within these web panels, the transverse stiffeners (and any connection plates serving as transverse stiffeners) adjacent to these panels must satisfy the following:

- If $I_{t2} > I_{t1}$, then:

$$I_t \geq I_{t1} + (I_{t2} - I_{t1})\rho_w \quad \text{(Equation 6.6.6.2.3-12)}$$

- Otherwise:

$$I_t \geq I_{t2} \quad \text{(Equation 6.6.6.2.3-13)}$$

For the critical panel in Field Section 1:

V_u = 345 kips
$\phi_v V_{cr}$ = 239 kips
$\phi_v V_n$ = 475 kips
d_o = 16′-9″ = 201.0 in.

$$I_{t1} = bt_w^3 J \quad \text{(Equation 6.6.6.2.3-3)}$$

$$J = \frac{2.5}{(d_o/D)^2} - 2.0 \geq 0.5 \quad \text{(Equation 6.6.6.2.3-5)}$$

$$J = \frac{2.5}{(201.0/69.0)^2} - 2.0 = -1.71 < 0.5$$

$$\therefore J = 0.5$$

b is taken equal to the smaller of D and d_o. In this case, b is equal to D = 69.0 in. Therefore:

$$I_{t1} = 69.0(0.5)^3(0.5) = 4.31 \text{ in.}^4$$

$$I_{t2} = \frac{D^4 \rho_t^{1.3}}{40}\left(\frac{F_{yw}}{E}\right)^{1.5} \quad \text{(Equation 6.6.6.2.3-4)}$$

The local buckling stress, F_{crs}, for the stiffener is calculated as follows:

$$F_{crs} = \frac{0.31E}{\left(\frac{b_t}{t_p}\right)^2} \leq F_{ys} \quad \text{(Equation 6.6.6.2.3-6)}$$

$$F_{crs} = \frac{0.31(29{,}000)}{\left(\frac{6.0}{0.5}\right)^2} = 62.4 \text{ ksi} > F_{ys} = 50 \text{ ksi}$$

$$\therefore F_{crs} = 50 \text{ ksi}$$

The term, ρ_t, is equal to the larger of F_{yw}/F_{crs} (i.e. 50 ksi/50 ksi = 1.0) and 1.0. Therefore, in this case, ρ_t is equal to 1.0.

$$I_{t2} = \frac{(69.0)^4(1.0)^{1.3}}{40}\left(\frac{50}{29{,}000}\right)^{1.5} = 40.57 \text{ in}^4$$

Since $I_{t2} > I_{t1}$, then:

$$I_t \geq I_{t1} + (I_{t2} - I_{t1})\rho_w \quad \text{(Equation 6.6.6.2.3-14)}$$

Since only one panel adjacent to this stiffener (i.e. the right panel) is subject to postbuckling tension-field action (the left panel is an end panel), then ρ_W is equal to the ratio of $\left(\frac{V_u - \phi_v V_{cr}}{\phi_v V_n - \phi_v V_{cr}}\right)$ within the one panel subject to postbuckling tension-field action. Therefore:

$$I_t \geq 4.31 + (40.57 - 4.31)\left(\frac{345 - 239}{475 - 239}\right) = 20.60 \text{ in.}^4$$

For single-sided stiffeners, the moment of inertia of the stiffener is to be taken about the edge in contact with the web. Therefore:

$$I_t = \frac{1}{3}(0.5)(6.0)^3 = 36.00 \text{ in.}^4 > 20.60 \text{ in.}^4 \qquad \text{ok}$$

Use 1/2" x 6" stiffeners.

6.6.6.3 Bearing Stiffeners

6.6.6.3.1 General

The design of bearing stiffeners for I- and box girders is covered in *AASHTO LRFD* Article 6.10.11.2. *AASHTO LRFD* Article 6.11.1.1 contains a special provision related to bearing stiffeners for box girders (discussed below).

Bearing stiffeners, which are aligned vertically on the web (or preferably on diaphragms in the case of box girders with inclined webs), are designed as columns to resist the reactions at bearing locations and at other locations subjected to concentrated loads where the loads are not transmitted through a deck or deck system (Figure 6.6.6.3.1-1).

Figure 6.6.6.3.1-1 Bearing Stiffener on I-Girder Web

AASHTO LRFD Article 6.10.11.2.1 specifies that bearing stiffeners be placed on the webs of built-up sections at all bearing locations. At bearing locations on rolled shapes and at other locations on built-up sections or rolled shapes subjected to concentrated loads, where the loads are not transmitted through a deck or deck system, either bearing stiffeners must be provided or else the web must satisfy the provisions of *AASHTO LRFD* Article D6.5 (Appendix D6). Webs without bearing stiffeners at those locations are to be investigated for the limit states of web local yielding and web crippling according to the provisions of *AASHTO LRFD* Article D6.5 (Section 6.6.6.3.5). The section must either be modified to comply with these requirements, or else bearing stiffeners must be placed on the web at the locations under consideration. The Design Engineer should be especially aware of these provisions when concentrated loads (not transmitted through a deck or deck system) are applied during a temporary construction situation; e.g., when girders are incrementally launched over supports.

Bearing stiffeners must consist of one or more plates or angles welded or bolted to both sides of the web, with the connections to the web designed to transmit the full factored bearing force. The stiffeners must extend the full depth of the web and as closely as practical to the outer edges of the flanges.

AASHTO LRFD Article 6.11.11.1 specifies that when inclined webs are used on box sections, the bearing stiffeners should be attached to either an internal or external diaphragm rather than to the webs so that the bearing stiffeners are perpendicular to the sole plate. In such cases, at expansion bearings, thermal movements of the

bridge may cause the diaphragm to be eccentric with respect to the bearings. The effect of this eccentricity on the design of the bearing stiffeners and diaphragms should be recognized. Eccentricity effects can be recognized by designing the bearing stiffener assembly as a beam-column according to the provisions of *AASHTO LRFD* Articles 6.10.11.2 and 6.9.2.2. For bearing stiffeners attached to diaphragms, the requirements regarding the effective column section of the bearing stiffeners discussed in Section 6.6.6.3.4.2 are to be applied to the diaphragm rather than to the web (*AASHTO LRFD* Article 6.11.1.1).

Connection of the bearing stiffener to the flange through which it receives its load can either be made by finish-to-bear plus a fillet weld on each side of the stiffener plate (note that fillet welds are not necessary if a cross-frame/diaphragm is not connected to the stiffener plate), or by a full penetration groove weld. Finish-to-bear means allowing the fabricator the option of grinding or milling. It is recommended that the finish-to-bear option (with or without fillet welds as applicable) always be specified as this approach dramatically reduces the deformations of the flange induced by a full penetration groove weld, and also costs significantly less than a full penetration groove weld.

AASHTO/NSBA (2003) recommends that permission be granted for the bearing stiffeners (and bearing diaphragms in box sections) to be detailed either vertical or normal to the girder top flange at the fabricator's option. AASHTO/NSBA (2003) further indicates that most fabricators prefer the bearing stiffeners to be detailed normal. Also, in cases where multiple bearing stiffeners are used at a given location, a minimum spacing of 8 inches or 1-1/2 times the stiffener plate width should be provided between the stiffener plates for welding access.

6.6.6.3.2 Projecting Width Requirement

AASHTO LRFD Article 6.10.11.2.2 specifies that the projecting width, b_t, of each bearing stiffener element (Figure 6.6.6.3.2-1) satisfy the following requirement in order to prevent local buckling of the bearing stiffener plates:

$$b_t \le 0.48 t_p \sqrt{\frac{E}{F_{ys}}} \qquad \text{Equation 6.6.6.3.2-1}$$

AASHTO LRFD Equation 6.10.11.2.2-1

where:

F_{ys} = specified minimum yield strength of the stiffener (ksi)
t_p = thickness of the projecting stiffener element (in.)

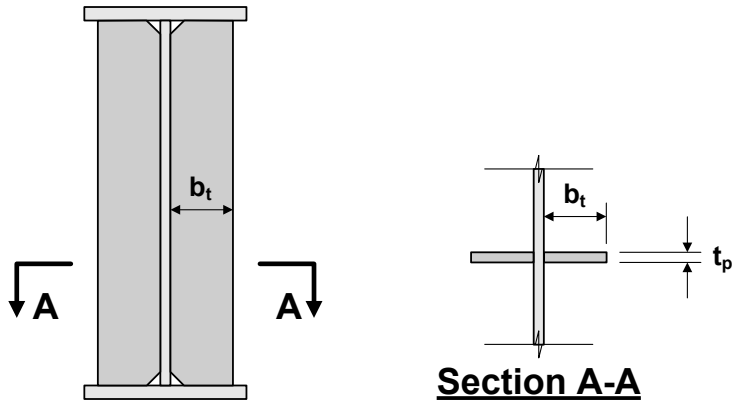

Figure 6.6.6.3.2-1 Projecting Width of Bearing Stiffener

6.6.6.3.3 Bearing Resistance

Bearing stiffeners must be clipped to clear the web-to-flange fillet welds and to bring the stiffener plates tight against the flange through which they receive their load. As a result, the area of the plates in direct bearing on the flange is less than the gross area of the plates. *AASHTO LRFD* Article 6.10.11.2.3 specifies that the factored bearing resistance of the fitted ends of bearing stiffeners be taken as:

$$\left(R_{sb}\right)_r = \phi_b\left(R_{sb}\right)_n \qquad \text{Equation 6.6.6.3.3-1}$$

AASHTO LRFD Equation 6.10.11.2.3-1

where:

ϕ_b = resistance factor for bearing on milled surfaces specified in *AASHTO LRFD* Article 6.5.4.2 (= 1.0)

$(R_{sb})_n$ = nominal bearing resistance for the fitted ends of bearing stiffeners (kips) taken as:

$$= 1.4A_{pn}F_{ys} \qquad \text{Equation 6.6.6.3.3-2}$$

AASHTO LRFD Equation 6.10.11.2.3-2

A_{pn} = area of the projecting elements of the stiffener outside of the web-to-flange fillet welds but not beyond the edge of the flange (in.^{2}). A_{pn} is computed by subtracting the clips from the nominal cross-sectional area of the stiffeners

F_{ys} = specified minimum yield strength of the stiffener (ksi)

The nominal bearing resistance for the fitted ends of bearing stiffeners is given in AISC (2010a) as $R_n = 1.8F_yA_{pb}$, where A_{pb} is equal to the projected bearing area. The specified nominal bearing resistance is twice the *AISC ASD* (Allowable Stress Design) value of $R_n = 0.9F_yA_{pb}$. Applying the specified *AISC* resistance factor of 0.75 to the nominal *AISC LRFD* nominal bearing resistance gives a factored bearing resistance of $1.35F_yA_{pb}$. Since the *AASHTO LRFD* resistance factors for connection

elements are generally 0.05 higher than the *AISC LRFD* resistance factors, the nominal bearing resistance for the fitted ends of bearing stiffeners in the *AASHTO LRFD* Specification was raised to 0.8 *1.8F_yA_{pb} = 1.4F_yA_{pb}, which is then used in conjunction with a specified *AASHTO LRFD* resistance factor for bearing on milled surfaces of ϕ_b = 1.0.

6.6.6.3.4 Axial Resistance

6.6.6.3.4.1 General

Bearing stiffeners are designed as columns. *AASHTO LRFD* Article 6.10.11.2.4a specifies that the factored axial resistance of the stiffeners, P_r, is to be determined as specified in *AASHTO LRFD* Article 6.9.2.1 using the specified minimum yield strength of the stiffener plates, F_{ys}, in order to account for the effect of any early yielding of lower strength stiffener plates. The factored resistance of components in axial compression is given in *AASHTO LRFD* Article 6.9.2.1 as:

$$P_r = \phi_c P_n \qquad \text{Equation 6.6.6.3.4.1-1}$$

AASHTO LRFD Equation 6.9.2.1-1

where:

ϕ_c = resistance factor for axial compression specified in *AASHTO LRFD* Article 6.5.4.2 (= 0.95)

P_n = nominal compressive resistance specified in *AASHTO LRFD* Article 6.9.4.1 (kips)

The nominal compressive resistance, P_n, of bearing stiffeners is to be computed as follows (*AASHTO LRFD* Article 6.9.4.1.1):

- If $\frac{P_e}{P_o} \geq 0.44$, then:

$$P_n = \left[0.658^{\left(\frac{P_o}{P_e}\right)}\right] P_o \qquad \text{Equation 6.6.6.3.4.1-2}$$

AASHTO LRFD Equation 6.9.4.1.1-1

- If $\frac{P_e}{P_o} < 0.44$, then:

$$P_n = 0.877P_e$$ Equation 6.6.6.3.4.1-3

AASHTO LRFD Equation 6.9.4.1.1-2

where:

P_e = elastic critical buckling resistance for flexural buckling (kips) specified in *AASHTO LRFD* Article 6.9.4.1.2 as:

$$= \frac{\pi^2 E}{\left(\frac{K\ell}{r_s}\right)^2} A_g$$ Equation 6.6.6.3.4.1-4

AASHTO LRFD Equation 6.9.4.1.2-1

(The flexural buckling resistance is used to compute P_e for bearing stiffeners - see the last entry in *AASHTO LRFD* Table 6.9.4.1.1-1.)

P_o = equivalent nominal yield resistance = $QF_{ys}A_g$ (kips). (The slender element reduction factor, Q, is taken equal to 1.0 for bearing stiffeners).

A_g = cross-sectional area of the effective column section of the bearing stiffeners (Section 6.6.6.3.4.2) (in.^{2})

F_{ys} = specified minimum yield strength of the stiffener (ksi)

$K\ell$ = effective length of the effective column section of the bearing stiffeners taken as 0.75D, where D is the web depth (*AASHTO LRFD* Article 6.10.11.2.4a) (in.)

r_s = radius gyration of the effective column section of the bearing stiffeners about the plane of buckling computed about the mid-thickness of the web (*AASHTO LRFD* Article 6.10.11.2.4a) (in.)

The reduced effective length $K\ell$ = 0.75D of the effective column is a result of the end restraint against column buckling provided by the flanges.

Note that the width-to-thickness requirements of *AASHTO LRFD* Article 6.9.4.2.1 are not enforced in bearing stiffener design because the stiffener projecting width requirement specified in *AASHTO LRFD* Article 6.10.11.2.2 (i.e. Equation 6.6.6.3.2-1) is typically more severe. As a result, the slender element reduction factor, Q, is taken equal to 1.0 in computing the equivalent nominal yield resistance, P_o, for bearing stiffeners.

6.6.6.3.4.2 Effective Column Section

The effective column section of the bearing stiffeners is defined in *AASHTO LRFD* Article 6.10.11.2.4b. For stiffeners bolted to the web (or diaphragm), the effective column section is to consist of only the stiffener elements. For stiffeners welded to the web (or diaphragm), a portion of the web (or diaphragm) is to be included as part of the effective column section, with some exceptions noted below. For stiffeners consisting of two plates welded to the web (or diaphragm), the effective column

section is to consist of the two stiffener plates, plus a centrally located strip of web (or diaphragm) extending not more than $9t_w$ on each side of the stiffeners (Figure 6.6.6.3.4.2-1).

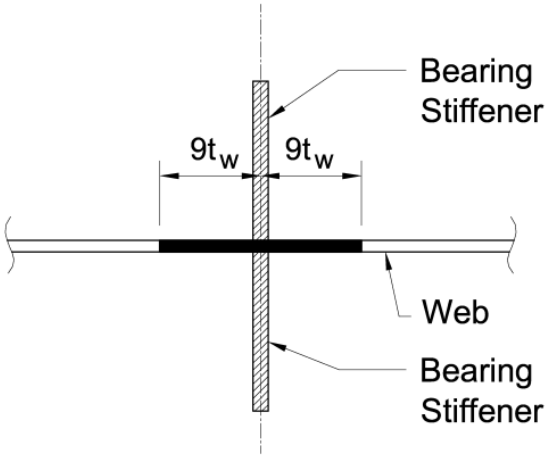

Figure 6.6.6.3.4.2-1 Effective Column Section for Welded Bearing Stiffener Design (One Pair of Stiffeners Welded to a Web)

If more than one pair of stiffeners is used, the effective column section is to consist of all the stiffener plates, plus a centrally located strip of web (or diaphragm) extending not more than $9t_w$ on each side of the outer projecting elements of the group.

The strip of web is not to be included in the effective section at interior supports of continuous-span hybrid members for which the specified minimum yield strength of the web is less than 70 percent of the specified minimum yield strength of the higher strength flange due to the amount of web yielding that may be expected due to the longitudinal flexural stress. The preceding exception does not apply at the end supports of hybrid members. For unusual cases in which F_{ys} is larger than F_{yw}, the yielding of the lower strength web is to be accounted for by reducing the width of the web strip included in the effective section by the ratio of F_{yw}/F_{ys}.

EXAMPLE

Design a pair of welded bearing stiffeners at the end support of a three-span continuous I-girder bridge. The girder flanges and web are Grade 50W steel, and Grade 50W steel will also be used for the stiffeners (i.e. F_{ys} = 50.0 ksi).

The unfactored bearing reactions at the end support are as follows:

R_{DC1} = 87 kips
R_{DC2} = 13 kips

R_{DW} = 13 kips
R_{LL+IM} = 139 kips

Assemble the bearing reactions due to the factored loads at the end support. The Strength I load combination controls. Therefore:

$$R_u = 1.0\left[1.25(87+13)+1.5(13)+1.75(139)\right] = 388 \text{ kips}$$

The width, b_t, of each projecting stiffener element must satisfy Equation 6.6.6.3.2-1 as follows:

$$b_t \le 0.48 t_p \sqrt{\frac{E}{F_{ys}}}$$

Welded bearing stiffeners are also commonly made up of less expensive flat bar stock, which is generally produced in whole-inch width increments and 1/8-in. thickness increments. Try two 7.0-inch-wide bars welded to each side of the web. The selected plates should be wide enough to accommodate the connection of any cross-frame/diaphragm members attached to the stiffeners.

Rearranging Equation 6.6.6.3.2-1 gives:

$$\left(t_p\right)_{min.} = \frac{b_t}{0.48\sqrt{\frac{E}{F_{ys}}}}$$

$$\left(t_p\right)_{min.} = \frac{7.0}{0.48\sqrt{\frac{29{,}000}{50.0}}} = 0.61 \text{ in.}$$

Try a stiffener thickness, t_p of 0.625 inches, which satisfies the preferred minimum thickness of ½ inch for stiffeners given in AASHTO/NSBA (2003).

According to *AASHTO LRFD* Article 6.10.11.2.3, the factored bearing resistance for the fitted ends of bearing stiffeners is to be taken as (Equation 6.6.6.3.3-1):

$$\left(R_{sb}\right)_r = \phi_b \left(R_{sb}\right)_n$$

where $(R_{sb})_n$ is equal to the nominal bearing resistance for the fitted end of bearing stiffeners taken as (Equation 6.6.6.3.3-2):

$$\left(R_{sb}\right)_n = 1.4 A_{pn} F_{ys}$$

A_{pn} is the area of the projecting elements of the stiffener outside of the web-to-flange fillet welds but not beyond the edge of the flange. Assume for this example that the clip provided at the base of the stiffeners to clear the web-to-flange fillet welds is 1.5 inches in length. The resistance factor for bearing on milled surfaces ϕ_b = 1.0. Therefore:

$$A_{pn} = 2(7.0 - 1.5)(0.625) = 6.88 \text{ in.}^2$$

$$(R_{sb})_n = 1.4(6.88)(50.0) = 482 \text{ kips}$$

$$(R_{sb})_r = (1.0)(482) = 482 \text{ kips} > R_u = 388 \text{ kips} \qquad \text{ok}$$

For computing the axial resistance of bearing stiffeners that are welded to the web, *AASHTO LRFD* Article 6.10.11.2.4b states that a portion of the web is to be included as part of the effective column section. For stiffeners consisting of two plates welded to the web, the effective column section is to consist of the two stiffener elements, plus a centrally located strip of web extending not more than $9t_w$ on each side of the stiffeners, as shown in Figure 6.6.6.3.4.2-1.

As specified in *AASHTO LRFD* Article 6.10.11.2.4a, the radius of gyration of the effective column section is to be computed about the mid-thickness of the web and the effective length is to be taken as 0.75*D*, where *D* is the web depth. The gross area of the effective column section is computed as:

$$A_g = 2[(7.0)(0.625) + 9(0.5)(0.5)] = 13.25 \text{ in.}^2$$

The moment of inertia of the effective column section (conservatively neglecting the web strip) is computed as:

$$I_s = \frac{0.625(7.0 + 0.5 + 7.0)^3}{12} = 158.8 \text{ in.}^4$$

The radius of gyration of the effective column section is therefore computed as:

$$r_s = \sqrt{\frac{I_s}{A_g}} = \sqrt{\frac{158.8}{13.25}} = 3.46 \text{ in.}$$

The effective length of the effective column section is computed as:

$$K\ell = 0.75D = 0.75(69.0) = 51.75 \text{ in.}$$

Check the limiting slenderness ratio of 120 specified for main members in compression in *AASHTO LRFD* Article 6.9.3:

$$\frac{K\ell}{r_s} = \frac{51.75}{3.46} = 15.0 < 120 \text{ ok}$$

As specified in *AASHTO LRFD* Article 6.10.11.2.4a, calculate the factored axial resistance P_r of the effective column section according to the provisions of *AASHTO LRFD* Article 6.9.2.1 as follows (Equation 6.6.6.3.4.1-1):

$$P_r = \phi_c P_n$$

where P_n is equal to the nominal compressive resistance determined as specified in *AASHTO LRFD* Article 6.9.4.1, and ϕ_c is equal to the resistance factor for axial compression = 0.95.

Calculate the elastic critical flexural buckling resistance, P_e (Equation 6.6.6.3.4.1-4):

$$P_e = \frac{\pi^2 E}{\left(\frac{K\ell}{r_s}\right)^2} A_g$$

$$P_e = \frac{\pi^2 (29{,}000)}{(15.0)^2} (13.25) = 16{,}855 \text{ kips}$$

Calculate the equivalent nominal yield resistance, P_o (the slender element reduction factor, Q, is taken equal to 1.0 for bearing stiffeners).

$$P_o = QF_{ys}A_g$$

$$P_o = (1.0)(50.0)(13.25) = 662.5 \text{ kips}$$

$$\frac{P_e}{P_o} = \frac{16{,}855}{662.5} = 25.4 > 0.44$$

Therefore, use Equation 6.6.6.3.4.1-2 to compute P_n as follows:

$$P_n = \left[0.658^{\left(\frac{P_o}{P_e}\right)}\right] P_o$$

$$P_n = \left[0.658^{\left(\frac{662.5}{16{,}855}\right)}\right] 662.5 = 652 \text{ kips}$$

$$P_r = \phi_c P_n$$

$$P_r = 0.95(652) = 619 \text{ kips} > R_u = 388 \text{ kips} \qquad \text{ok}$$

Use 5/8" x 7" bearing stiffeners (one pair).

6.6.6.3.5 Concentrated Loads Applied to Webs without Bearing Stiffeners

6.6.6.3.5.1 General

At bearing locations on rolled shapes, and at other locations on built-up sections or rolled shapes subjected to concentrated loads, where the loads are not transmitted through a deck or deck system, either bearing stiffeners must be provided or else the web must be investigated for the limit states of web local yielding and web crippling as discussed below in Sections 6.6.6.3.5.2 and 6.6.6.3.5.3, respectively (refer to *AASHTO LRFD* Article D6.5 – Appendix D6).

The equations given in *AASHTO LRFD* Article D6.5 are essentially identical to the equations given in AISC (2010a). *AASHTO LRFD* Article CD6.5.1 notes that the limit state of sidesway web buckling given in AISC (2010a) is not included because it governs only for: 1) members subjected to concentrated loads applied directly to the steel section; 2) members for which the compression flange is braced at the load point; 3) members for which the tension flange is unbraced at the load point; and 4) members for which the ratio of D/t_w to L_b/b_{ft} is less than or equal to 1.7. The preceding conditions do not commonly occur in bridge construction.

6.6.6.3.5.2 Web Local Yielding

The limit state of web local yielding is covered in *AASHTO LRFD* Article D6.5.2, and is intended to prevent localized yielding of the web due to a high compressive or tensile stress caused by a concentrated load or bearing reaction. In order to satisfy

this limit state without providing bearing stiffeners, webs subject to compressive or tensile concentrated loads must satisfy the following:

$$R_u \le \phi_b R_n \qquad \text{Equation 6.6.6.3.5.2-1}$$

AASHTO LRFD Equation D6.5.2-1

where:

ϕ_b = resistance factor for bearing specified in *AASHTO LRFD* Article 6.5.4.2 (= 1.0)
R_u = factored concentrated load or bearing reaction (kips)
R_n = nominal resistance to the concentrated loading (kips) taken as follows:

- For interior-pier reactions and for concentrated loads applied at a distance from the end of the member that is greater than *d*:

$$R_n = (5k + N)F_{yw}t_w \qquad \text{Equation 6.6.6.3.5.2-2}$$

AASHTO LRFD Equation D6.5.2-2

- Otherwise:

$$R_n = (2.5k + N)F_{yw}t_w \qquad \text{Equation 6.6.6.3.5.2-3}$$

AASHTO LRFD Equation D6.5.2-3

d = depth of the steel section (in.)
k = distance from the outer face of the flange resisting the concentrated load or bearing reaction to the toe of the fillet (in.). For a rolled shape, *k* is published in the available tables giving dimensions for the shapes. For a built-up section, *k* may be taken as the distance from the outer face of the flange to the web toe of the web-to-flange fillet weld.
N = length of bearing (in.). *N* must be greater than or equal to *k* at end bearing locations.

The preceding equations are largely based on the work described in References 84 and 85. The concentrated load acting on a rolled shape or a built-up section is assumed critical at the toe of the fillet, located a distance *k* from the outer face of the flange resisting the concentrated load or bearing reaction (Figure 6.6.6.3.5.2-1). For interior concentrated loads or interior-pier reactions, the load is assumed to distribute along the web at a slope of 2.5 to 1 and over a distance of (5*k* + *N*) according to Equation 6.6.6.3.5.2-2 (see also Figure 6.6.6.3.5.2-1). An interior concentrated load is assumed to be a load applied at a distance from the end of the member greater than the depth of the steel section *d*. For end concentrated loads or end reactions, the load is assumed to distribute along the web at the same slope over a distance of (2.5*k* + *N*) according to Equation 6.6.6.3.5.2-3 (Figure 6.6.6.3.5.2-1).

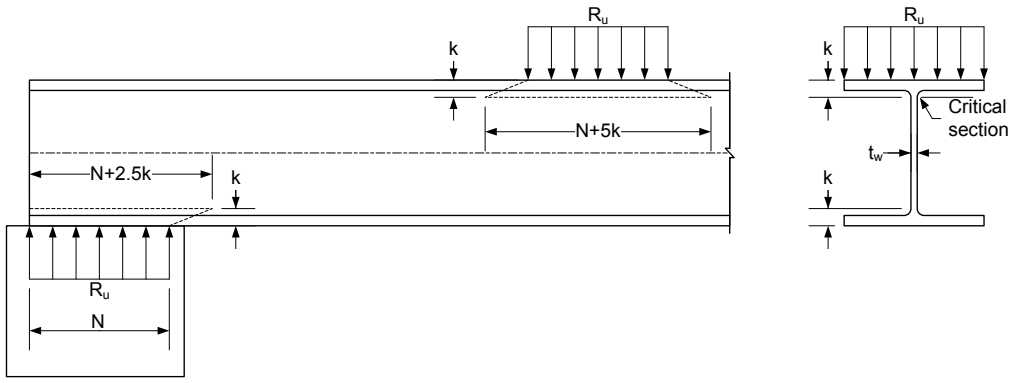

Figure 6.6.6.3.5.2-1 Local Web Yielding – Bearing Length and *k*

6.6.6.3.5.3 Web Crippling

The limit state of web crippling is covered in *AASHTO LRFD* Article D6.5.3, and is intended to prevent local instability or crippling of the web due to a high compressive stress caused by a concentrated load or bearing reaction. In order to satisfy this limit state without providing bearing stiffeners, webs subject to compressive concentrated loads must satisfy the following:

$$R_u \le \phi_w R_n \qquad \text{Equation 6.6.6.3.5.3-1}$$

AASHTO LRFD Equation D6.5.3-1

where:

ϕ_w = resistance factor for web crippling specified in *AASHTO LRFD* Article 6.5.4.2 (= 0.80)
R_u = factored concentrated load or bearing reaction (kips)
R_n = nominal resistance to the concentrated loading (kips) taken as follows:

- For interior-pier reactions and for concentrated loads applied at a distance from the end of the member that is greater than or equal to $d/2$:

$$R_n = 0.8 t_w^2 \left[1 + 3\left(\frac{N}{d}\right)\left(\frac{t_w}{t_f}\right)^{1.5}\right]\sqrt{\frac{EF_{yw}t_f}{t_w}} \qquad \text{Equation 6.6.6.3.5.3-2}$$

AASHTO LRFD Equation D6.5.3-2

- Otherwise:
  - If $N/d \le 0.2$, then:

$$R_n = 0.4t_w^2\left[1+3\left(\frac{N}{d}\right)\left(\frac{t_w}{t_f}\right)^{1.5}\right]\sqrt{\frac{EF_{yw}t_f}{t_w}} \qquad \text{Equation 6.6.6.3.5.3-3}$$

AASHTO LRFD Equation D6.5.3-3

- If N/d > 0.2, then:

$$R_n = 0.4t_w^2\left[1+\left(\frac{4N}{d}-0.2\right)\left(\frac{t_w}{t_f}\right)^{1.5}\right]\sqrt{\frac{EF_{yw}t_f}{t_w}} \qquad \text{Equation 6.6.6.3.5.3-4}$$

AASHTO LRFD Equation D6.5.3-4

where:

d = depth of the steel section (in.)
N = length of bearing (in.). *N* must be greater than or equal to *k* at end bearing locations.
t_f = thickness of the flange resisting the concentrated load or bearing reaction (in.)

Equation 6.6.6.3.5.3-2 and Equation 6.6.6.3.5.3-3 are based on research described in Roberts (1981). Equation 6.6.6.3.5.3-4 was developed after additional testing to better represent the effect of longer bearing lengths at the ends of members (Elgaaly and Salkar, 1981).

6.6.6.4 Longitudinal Web Stiffeners

6.6.6.4.1 General

The design of longitudinal web stiffeners is covered in *AASHTO LRFD* Article 6.10.11.3. For box girders, *AASHTO LRFD* Article 6.11.11.1 refers to the I-girder provisions of *AASHTO LRFD* Article 6.10.11.3 for the design of longitudinal web stiffeners.

Longitudinal stiffeners are aligned horizontally on the web along the length of the girder and divide the web panel into smaller sub-panels (Figure 6.6.6.4.1-1). In the *AASHTO LRFD* Specifications, longitudinal stiffeners are required whenever the web slenderness, D/t_w, exceeds 150, and are used to provide additional bend-buckling resistance to the webs of deeper girders.

Figure 6.6.6.4.1-1 Longitudinal Web Stiffeners on an I-Girder

Longitudinal stiffeners, where required, are to consist of a plate welded to one side of the web or a bolted angle. Welded longitudinal stiffeners are commonly made up of less expensive flat bar stock, which is generally produced in whole-inch width increments and 1/8-in. thickness increments. Longitudinal stiffeners should always be used in conjunction with transverse stiffeners to support the longitudinal stiffeners along their length.

AASHTO LRFD Article 6.10.11.3.1 specifies that longitudinal stiffeners are to be located vertically on the web such that adequate web bend-buckling resistance is provided for constructibility and at the service limit state; i.e., the stiffeners must be located such that Equation 6.5.3.5.1.2-3 (for I-sections) or Equation 6.5.3.5.2.2.2-2 (for box sections) is satisfied when checking constructibility, and Equation 6.5.4.3.2.2-1 is satisfied at the service limit state (see Section 6.4.5.5.2.2 regarding the calculation of the web bend-buckling resistance, F_{crw}, for a web with longitudinal stiffeners). It also must be verified that the section has adequate nominal flexural resistance at the strength limit state with the longitudinal stiffener in the selected position (Section 6.5.6).

The depth of the web in compression, D_c, in the elastic range for composite sections in positive flexure changes relative to the vertical position of the longitudinal stiffener after the concrete deck has been placed. D_c for composite sections is a function of the dead-to-live load stress ratio because the dead and live loads are applied to different sections in a composite girder (Section 6.4.5.4.1.1). The dead load stress has a significant effect on the location of the elastic neutral axis for composite sections in positive flexure in particular. The non-composite dead load stresses acting on the steel section alone cause the neutral axis to be lower than it would if all loads were applied to the composite section. This effect increases with increasing span length.

The neutral axis moves higher on the web after the deck has hardened and dead and live loads are applied to the composite section. Thus, D_c changes relative to the vertical position of the longitudinal stiffener, which is usually located a fixed distance from the compression flange in these regions. As a result, the computed web bend-buckling resistance is different before and after placement of the deck and is dependent on the loading. Therefore, several trial locations of the stiffener on the web may be necessary in these regions in order to determine a location of the stiffener to satisfy Equation 6.5.3.5.1.2-3 (for I-sections) or Equation 6.5.3.5.2.2.2-2 (for box sections) when checking constructibility, Equation 6.5.4.3.2.2-1 at the service limit state, and all applicable strength limit state criteria. *AASHTO LRFD* Article C6.10.11.3.1 provides the following equation for determining an initial trial location of a longitudinal stiffener in regions of positive flexure:

$$\frac{d_s}{D_c} = \frac{1}{1 + 1.5\sqrt{\frac{f_{DC1} + f_{DC2} + f_{DW} + f_{LL+IM}}{f_{DC1}}}} \qquad \text{Equation 6.6.6.4.1-1}$$

AASHTO LRFD Equation C6.10.11.3.1-1

where:

d_s = distance from the centerline of a plate longitudinal stiffener, or the gage line of an angle longitudinal stiffener, to the inner surface or leg of a compression-flange element (in.)

D_c = depth of the web of the non-composite steel section in compression in the elastic range (in.)

f_{xx} = factored compression-flange vertical bending stresses at the strength limit state caused by the different loads acting on their respective sections at the section with the maximum compressive vertical bending stress (ksi).

The stiffener will likely need to be moved vertically up or down from this initial trial location in order to satisfy all the specified limit-state criteria.

It is recommended that the longitudinal stiffener initially be located at $0.4D_c$ from the inner surface of the compression flange at composite sections in negative flexure and at non-composite sections. D_c would be conservatively calculated for the section consisting of the steel girder plus the longitudinal reinforcement for composite sections in negative flexure. D_c would be based on the section consisting of the steel girder alone for non-composite sections.

Based on theoretical and experimental studies on non-composite girders, the optimum location of a single longitudinal stiffener is $0.4D_c$ for bending and $0.5D$ for shear. Tests have also shown that longitudinal stiffeners located at $0.4D_c$ on these sections can effectively control lateral web deflections due to bending (Cooper,

1967). Because shear is always accompanied by moment and because a properly proportioned longitudinal stiffener will also reduce lateral web deflections due to shear, the distance of $0.4D_c$ is recommended. The stiffener may need to be moved vertically up or down from this initial trial location, especially for cases where the concrete deck may be assumed effective in tension in regions of negative flexure at the service limit state as permitted in *AASHTO LRFD* Article 6.10.4.2.1. *AASHTO LRFD* Article D6.3.1 specifies that in this case, D_c at the service limit state must be calculated based on the accumulated stresses using Equation 6.4.5.4.1.2-1.

Because D_c may vary along the span, it is suggested that the longitudinal stiffener be located based on D_c computed at the section with the largest compressive vertical bending stress. Other sections must also be examined to ensure they satisfy the specified limit states since the stiffener cannot be at its optimum location at other sections along the girder length with a lower stress and a different value of D_c.

In some cases, particularly in regions of stress reversal, it may be necessary or desirable to use two longitudinal stiffeners on the web. The use of two longitudinal stiffeners on the web is discussed in greater detail in Section 6.4.5.5.2.2.

It is preferred that longitudinal stiffeners be placed on the opposite side of the web from transverse stiffeners. At bearing stiffeners and connection plates where the longitudinal stiffener and transverse web element must intersect, a decision must be made as to which element to interrupt. According to *AASHTO LRFD* Article 6.10.11.3.1, wherever practical, longitudinal stiffeners are to extend uninterrupted over their specified length, unless otherwise permitted in the contract documents, since longitudinal stiffeners are designed as continuous members to improve the web bend buckling resistance. In such cases, the interrupted transverse elements must be fitted and attached to both sides of the longitudinal stiffener with fillet welds on both sides of the longitudinal stiffener and the transverse element.

If the longitudinal stiffener is interrupted instead, it should be similarly attached to all transverse elements. All interruptions must be carefully designed with respect to fatigue, especially if the longitudinal stiffener is not attached to the transverse web elements, as a punitive Category E or E′ detail may exist at the termination points of each longitudinal stiffener-to-web weld (refer to *AASHTO LRFD* Table 6.6.1.2.3-1 – Condition 4.3). Copes should always be provided to avoid intersecting welds. If an interrupted longitudinal stiffener is attached to a transverse web element, Equation 6.5.5.2.2.1.3-1 may apply in checking fatigue (refer to Figure 6.5.5.2.2.1.3-1). Should longitudinal stiffeners be discontinued at bolted field splices, consideration should be given to taking the stiffener to the free edge of the web where the normal stress is zero to avoid the fatigue-sensitive details at the termination of the stiffener-to-web welds. This would require splitting of the web splice plates.

Longitudinal stiffeners are subject to the same flexural strain as the web at their vertical position on the web. As a result, the stiffeners must have sufficient strength and rigidity to resist bend buckling of the web (at the appropriate limit state) and to transmit the stresses in the stiffener and an effective portion of the web as an equivalent column (Cooper, 1967). Therefore, *AASHTO LRFD* Article 6.10.11.3.1 specifies that the factored vertical bending stress in the longitudinal stiffener, f_s, must satisfy the following requirement at the strength limit state and when checking constructibility:

$$f_s \le \phi_f R_h F_{ys} \qquad \text{Equation 6.6.6.4.1-2}$$

AASHTO LRFD Equation 6.10.11.3.1-1

where:

ϕ_f = resistance factor for flexure specified in *AASHTO LRFD* Article 6.5.4.2 (= 1.0)
F_{ys} = specified minimum yield strength of the longitudinal stiffener (ksi)
R_h = hybrid factor determined as specified in *AASHTO LRFD* Article 6.10.1.10.1 (Section 6.4.5.7)

The hybrid factor, R_h, is included in Equation 6.6.6.4.1-2 to account for the influence of local web yielding on the longitudinal stiffener stress in hybrid sections. The appropriate corresponding value of R_h should be applied for the strength limit state and constructibility verifications.

6.6.6.4.2 Projecting Width Requirement

AASHTO LRFD Article 6.10.11.3.2 specifies that the projecting width, b_ℓ, of the longitudinal stiffener satisfy the following requirement in order to prevent local buckling of the stiffener plate:

$$b_\ell \le 0.48 t_s \sqrt{\frac{E}{F_{ys}}} \qquad \text{Equation 6.6.6.4.2-1}$$

AASHTO LRFD Equation 6.10.11.3.2-1

where:

F_{ys} = specified minimum yield strength of the stiffener (ksi)
t_s = thickness of the longitudinal stiffener (in.)

6.6.6.4.3 Moment of Inertia Requirement

AASHTO LRFD Article 6.10.11.3.3 specifies that to ensure that a longitudinal stiffener will have adequate rigidity to maintain a horizontal line of near zero lateral deflection in the web to resist bend buckling of the web (at the appropriate limit

state), the moment of inertia of the stiffener acting in combination with an adjacent strip of web must satisfy the following requirement (SSRC, 1998):

$$I_\ell \geq Dt_w^3\left[2.4\left(\frac{d_o}{D}\right)^2 - 0.13\right]\beta \qquad \text{Equation 6.6.6.4.3-1}$$

AASHTO LRFD Equation 6.10.11.3.3-1

where:

d_o = transverse stiffener spacing (in.)

I_ℓ = moment of inertia of the longitudinal stiffener including an effective width of the web equal to $18t_w$ taken about the neutral axis of the combined section (in.^{4}). If F_{yw} is smaller than F_{ys}, the strip of web included in the effective section must be reduced by the ratio of F_{yw}/F_{ys}.

β = curvature correction factor for longitudinal stiffener rigidity calculated as follows (equal to 1.0 for longitudinal stiffeners on straight webs):

- For cases where the longitudinal stiffener is on the side of the web away from the center of curvature:

$$\beta = \frac{Z}{6} + 1 \qquad \text{Equation 6.6.6.4.3-2}$$

AASHTO LRFD Equation 6.10.11.3.3-3

- For cases where the longitudinal stiffener is on the side of the web toward the center of curvature:

$$\beta = \frac{Z}{12} + 1 \qquad \text{Equation 6.6.6.4.3-3}$$

AASHTO LRFD Equation 6.10.11.3.3-4

Z = curvature parameter taken as:

$$= \frac{0.95d_o^2}{Rt_w} \leq 10 \qquad \text{Equation 6.6.6.4.3-4}$$

AASHTO LRFD Equation 6.10.11.3.3-5

R = minimum girder radius in the panel (in.)

Cooper (1967) suggests that the moment of inertia (and radius of gyration – Section 6.6.6.4.4) of the longitudinal stiffener be taken about the neutral axis of an equivalent

column cross-section consisting of the stiffener and an adjacent strip of web with a width of $18t_w$. For a web having a lower yield strength than the yield strength of the longitudinal stiffener, the web strip that contributes to the effective column section is reduced by F_{yw}/F_{ys} in computing the moment of inertia of the longitudinal stiffener. Previous specifications required that the moment of inertia (and radius of gyration) of the stiffener be taken about the edge in contact with the web plate.

Longitudinal stiffeners on horizontally curved webs require greater rigidity than on straight webs because of the tendency of curved webs to bow. This is reflected by including the factor, β, in Equation 6.6.6.4.3-1, which is a simplification of a requirement for longitudinal stiffeners on curved webs given in Hanshin (1988). For longitudinal stiffeners on straight webs, β is taken equal to 1.0.

6.6.6.4.4 Radius of Gyration Requirement

AASHTO LRFD Article 6.10.11.3.3 specifies that to ensure the longitudinal stiffener acting in combination with an adjacent strip of web as an effective column section can withstand the axial compressive stress without lateral buckling, the radius of gyration of the effective column section must satisfy the following requirement:

$$r \geq \frac{0.16 d_o \sqrt{\frac{F_{ys}}{E}}}{\sqrt{1 - 0.6\frac{F_{yc}}{R_h F_{ys}}}} \qquad \text{Equation 6.6.6.4.4-1}$$

AASHTO LRFD Equation 6.10.11.3.3-2

where:

d_o = transverse stiffener spacing (in.)
r = radius of gyration of the longitudinal stiffener including an effective width of the web equal to $18t_w$ taken about the neutral axis of the combined section (in.)
F_{ys} = specified minimum yield strength of the longitudinal stiffener (ksi)
R_h = hybrid factor determined as specified in *AASHTO LRFD* Article 6.10.1.10.1 (Section 6.4.5.7)

Equation 6.6.6.4.4-1 is a modification of the original requirement given in Cooper (1967) that accounts for the possibility of different specified minimum yield strengths for the longitudinal stiffener and compression flange. The hybrid factor, R_h, is also included in the equation to approximate the influence of a lower yield strength web in a hybrid section. For a section with F_{yc}/F_{ys} greater than one, a significantly larger radius of gyration is required than in previous specifications because in this case, the longitudinal stiffener is subjected to larger stresses compared to its resistance than

in an equivalent homogeneous column. Equation 6.6.6.4.4-1 is valid as long as Equation 6.6.6.4.1-2 is satisfied to prevent full nominal yielding of the longitudinal stiffener at the strength limit state.

6.6.7 Truss Gusset Plates

6.6.7.1 General

Gusset plates are used to interconnect vertical, diagonal, and horizontal truss members at a panel point. Provisions are provided in *AASHTO LRFD* Article 6.14.2.8 for the design of double gusset-plate connections used in trusses. The validity of the requirements for application to single gusset-plate connections has not been verified. The provisions are based on the findings from NCHRP Project 12-84 (Ocel, 2013). Example calculations illustrating the application of the resistance equations for gusset-plate connections described in the following are provided in Ocel (2013), and in Appendix A of AASHTO (2011a).

The gusset-plate fasteners connecting each member are to be symmetrical with the axis of the member, so far as practicable, and the connection of all the elements of the member should be given consideration to facilitate the load transfer. Bolted gusset plate connections are to satisfy the applicable requirements of *AASHTO LRFD* Articles 6.13.1 and 6.13.2 (Section 6.6.4.2.1). Where filler plates are required, the provisions of *AASHTO LRFD* Article 6.13.6.1.5 are to apply (Section 6.6.5.5).

Gusset plates are to satisfy the minimum plate thickness requirement for gusset plates used in trusses specified in Article 6.7.3 (Section 6.4.11). Gusset plates are to be designed for shear, compression, and/or tension occurring in the vicinity of each connected member, as applicable, according to the requirements specified in *AASHTO LRFD* Articles 6.14.2.8.3 through 6.14.2.8.5 (Sections 6.6.7.2 through 6.6.7.4). Gusset plates serving as a chord splice are to also be independently designed as a splice according to the provisions of *AASHTO LRFD* Article 6.14.2.8.6 (Section 6.6.7.5). The edge slenderness requirement specified in *AASHTO LRFD* Article 6.14.2.8.7 is to be considered (Section 6.6.7.6).

Where multi-layered gusset and splice plates are used, the resistances of the individual plates may be added together when determining the factored resistances provided that enough fasteners are present to develop the force in the layered gusset and splice plates. Kulak et al. (1987) contains additional guidance on determining the number of fasteners required to develop the force in layered gusset and splice plates.

Resistance factors for truss gusset plates specified in *AASHTO LRFD* Article 6.5.4.2 were developed and calibrated to a target reliability index of 4.5 for the Strength I

load combination at a dead-to-live ratio, *DL*/*LL*, of 6.0. More liberal ϕ factors could be justified at a *DL*/*LL* less than 6.0.

6.6.7.2 Shear Resistance

As specified in AASHTO LRFD Article 6.14.2.8.3, the factored shear resistance, Vr, of truss gusset plates is to be taken as the smaller value based on shear yielding or shear rupture. For shear yielding, the factored shear resistance is to be taken as*:*

$$V_r = \phi_{vy} 0.58 F_y A_{vg} \Omega \qquad \text{Equation 6.6.7.2-1}$$

AASHTO LRFD Equation 6.14.2.8.3-1

where:

- ϕ_{vy} = resistance factor for truss gusset plate shear yielding specified in Article 6.5.4.2 (=0.80)
- Ω = shear reduction factor for gusset plates taken as 0.88
- A_{vg} = gross area of the shear plane (in.^{2})
- F_y = specified minimum yield strength of the gusset plate (ksi)

For shear rupture, the factored shear resistance is to be determined from Equation 6.6.4.2.5.6.2-2*.*

The Ω shear reduction factor in Equation 6.6.7.2-1 is only used in the evaluation of truss gusset plates for shear yielding. This factor accounts for the nonlinear distribution of shear stresses that form along a failure plane, as compared to an idealized plastic shear stress distribution. The nonlinearity primarily develops due to shear loads not being uniformly distributed on the plane, and also due to strain hardening and stability effects. The Ω factor was developed using shear yield data generated in Ocel (2013). The Ω factor was 1.02 on average for a variety of gusset-plate geometries; however, there was significant scatter in the data due to proportioning of load between members, and variations in plate thickness and joint configuration. The specified Ω factor of 0.88 was calibrated to account for shear plane length-to-thickness ratios varying from 85 to 325.

Shear is to be checked on relevant partial and full failure plane widths. Partial shear planes are to be checked around compression members, and only Equation 6.6.7.2-1 is to apply to partial shear planes. Research has shown that the buckling of connections with tightly spaced members is correlated with shear yielding around the compression members (Ocel, 2013), which is important because the buckling criteria specified in AASHTO LRFD Article 6.14.2.8.4 (Section 6.6.7.3) would overestimate the compressive buckling resistance of these types of connections.

Once a plane yields in shear, the reduction in the plate modulus reduces the out-of-plane stiffness such that the stability of the plate is affected.

The partial shear plane length is to be taken along adjoining member fastener lines between plate edges and other fastener lines. Failure of a full width shear plane requires relative mobilization between two zones of the plate, typically along chords. Mobilization cannot occur when a shear plane passes through a continuous member; for instance, a plane passing through a continuous chord member that would require shearing of the member itself.

The following partial shear planes, as applicable, are to be evaluated to determine which shear plane controls:

- The plane that parallels the chamfered end of the compression member, as shown in Figure 6.6.7.2-1*;*
- The plane on the side of the compression member that has the smaller framing angle between the member and the other adjoining members, as shown in Figure 6.6.7.2-2*;* and
- The plane with the least cross-sectional shear area if the member end is not chamfered and the framing angle is equal on both sides of the compression member.

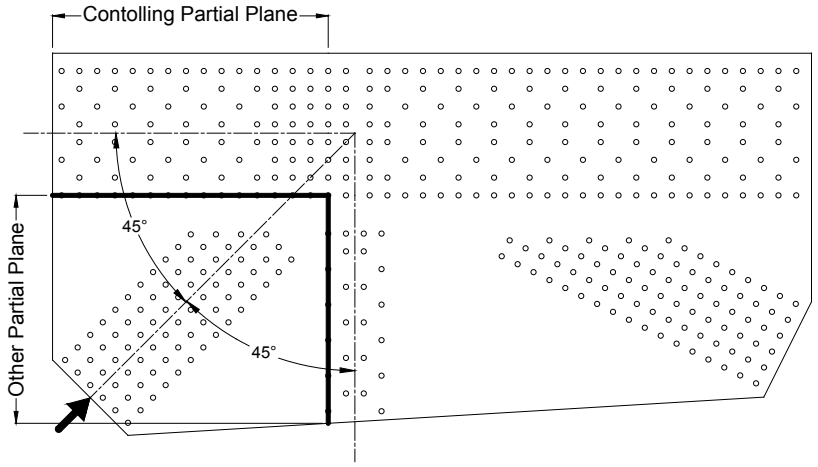

Figure 6.6.7.2-1 Example of a Controlling Partial Shear Plane that Parallels the Chamfered End of the Compression Member Since that Member Frames in at an Angle of 45 Degrees to Both the Chord and the Vertical

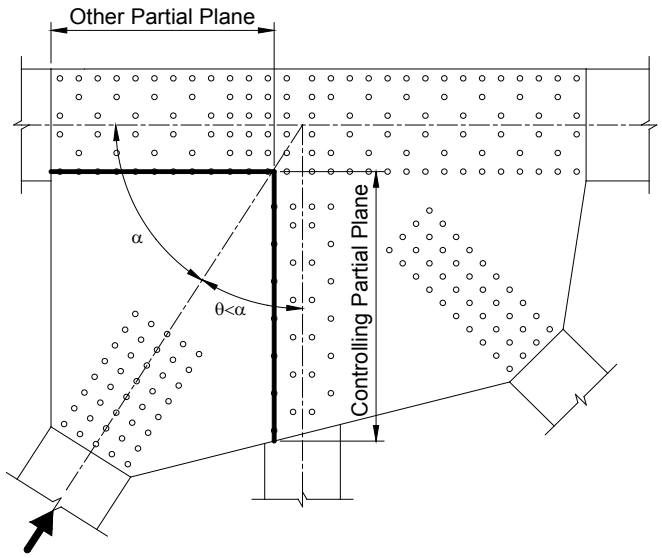

Figure 6.6.7.2-2 Example of a Controlling Partial Shear Plane on the Side of a Compression Member Without a Chamfered End that has the Smaller Framing Angle between that Member and the Other Adjoining Members (i.e. $\theta < \alpha$)

Generally, truss verticals and chord members are not subject to the partial plane shear yielding check because there is no adjoining member fastener line that can yield in shear and cause the compression member to become unstable. For example, the two compression members shown in Figure 6.6.7.2-3 would not be subject to a partial plane shear check.

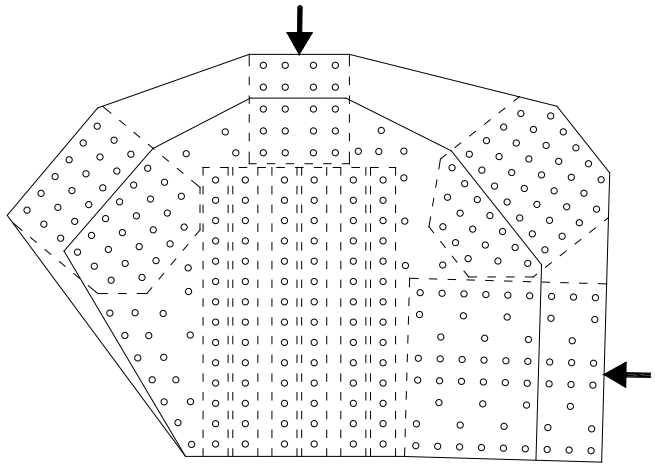

Figure 6.6.7.2-3 Example Showing Truss Vertical and Chord Members in Compression that Do Not Require a Partial Shear Plane Check

6.6.7.3 Compressive Resistance

Gusset plate zones in the vicinity of compression members must be designed for plate stability. Experimental testing and finite element simulations performed by Ocel (2013); Yamamoto et al. (1988); and Higgins et al. (2013) have found that truss gusset plates subject to compression always buckle in a sidesway mode in which the end of the compression member framing into the gusset plate moves out-of-plane. The buckling resistance is dependent upon the chamfering of the member, the framing angles of the members entering the gusset, and the standoff distance of the compression member relative to the surrounding members; i.e. the distance, L_{mid} (refer to Figure 6.6.7.3-2). An example connection showing a typical chamfered member end and member framing angle is provided in Figure 6.6.7.3-1.

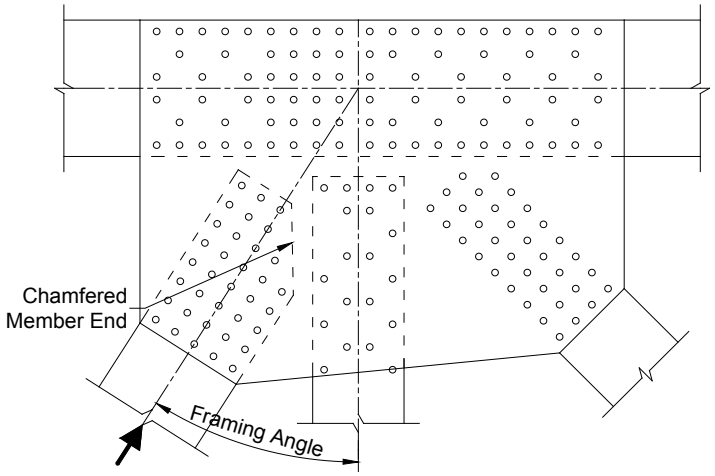

Figure 6.6.7.3-1 Example Connection Showing a Typical Chamfered Member End and Member Framing Angle

The research found that the compressive resistance of gusset plates with large L_{mid} distances was reasonably predicted using modified column buckling equations and Whitmore section analysis. When the members were heavily chamfered reducing the L_{mid} distance, the buckling of the plate was initiated by shear yielding on the partial shear plane adjoining the compression member causing a destabilizing effect (Section 6.6.7.2).

As specified in AASHTO LRFD Article 6.14.2.8.4, the factored compressive resistance, P_r, of truss gusset plates is to be taken as:

$$P_r = \phi_{cg} P_n \qquad \text{Equation 6.6.7.3-1}$$

AASHTO LRFD Equation 6.14.2.8.4-1

where:

ϕ_{cg} = resistance factor for truss gusset plate compression specified in Article 6.5.4.2 (=0.75)

P_n = nominal compressive resistance of a Whitmore section determined from Equation 6.6.3.4.2.3.1-1 or 6.6.3.4.2.3.1-2, as applicable (kip).

In the calculation of P_n, the slender element reduction factor, Q (Section 6.6.3.4.2.4.3), is to be taken as 1.0, and the elastic critical buckling resistance, P_e, is to be taken as:

$$P_e = \frac{3.29E}{\left(\frac{L_{mid}}{t_g}\right)^2} A_g \qquad \text{Equation 6.6.7.3-2}$$

AASHTO LRFD Equation 6.14.2.8.4-2

where:

A_g = gross cross-sectional area of the Whitmore section determined based on 30 degree dispersion angles, as shown in Figure 6.6.7.3-2 (in.^{2}). The Whitmore section shall not be reduced if the section intersects adjoining member bolt lines.

L_{mid} = distance from the middle of the Whitmore section to the nearest member fastener line in the direction of the member, as shown in Figure 6.6.7.3-2 (in.)

t_g = gusset-plate thickness (in.)

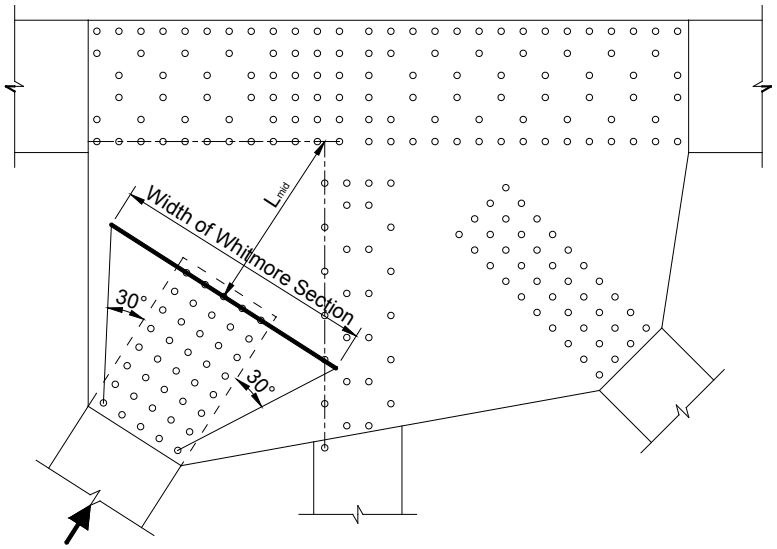

Figure 6.6.7.3-2 Example Connection Showing the Whitmore Section for a Compression Member Derived from 30 Degree Dispersion Angles, and the Distance L_{mid}

For truss gusset plate design, the Whitmore section (Whitmore, 1952) is defined as the portion of a truss gusset plate at the end of a member fastener pattern, based on 30 degree dispersion patterns from the lead fastener, through which it may be assumed for the purposes of design that all force from the member is evenly distributed into the gusset plate.

Equation 6.6.7.3-2 was derived by substituting plate properties into Equation 6.6.3.4.2.3.3-1, along with an effective length factor, *K*, of 0.5 that was found to be relevant for a wide variety of gusset-plate geometries (Ocel, 2013).

In situations where the gusset plate resistance is controlled by buckling (i.e. the partial shear check described in Section 6.6.7.2, or the Whitmore check described herein), a more refined analysis may be warranted. The gusset plate compression checks can be quite conservative in certain situations, frequently underestimating plate capacity by more than 25 percent, and in one case, underestimating plate capacity by more than 40 percent (Ocel, 2013). Therefore, in situations where the governing checks are known to have substantial conservatism, consideration should be given to using any of the more rigorous analysis approaches described in AASHTO (2011a) (e.g. the Basic Corner Check, or the Truncated Whitmore Section Method), or any other comparable analysis approved by the Owner that is consistent with a rational application of established engineering principles.

For the design of chord splices subject to compression, refer instead to Section 6.6.7.5.

6.6.7.4 Tensile Resistance

As specified in AASHTO LRFD Article 6.14.2.8.5, the factored tensile resistance, R_r, of truss gusset plates is to be taken as the smallest factored resistance in tension based on yielding, fracture or block shear rupture determined according to the provisions of AASHTO LRFD Article 6.13.5.2 (Section 6.6.4.2.5.6.1).

When checking Equations 6.6.3.3.2.1-1 and 6.6.3.3.2.1-2, the Whitmore section defined in Figure 6.6.7.4-1 is to be used to define the effective area. The Whitmore section is not to be reduced if the width intersects adjoining member bolt lines.

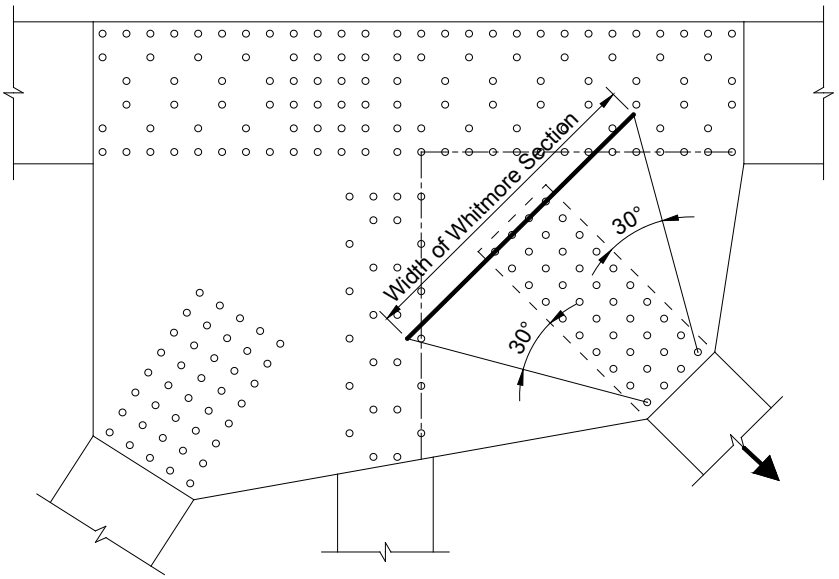

Figure 6.6.7.4-1 Example Connection Showing the Whitmore Section for a Tension Member Derived from 30 Degree Dispersion Angles

For the design of chord splices subject to tension, refer instead to Section 6.6.7.5.

6.6.7.5 Chord Splices

A chord splice is defined as a connection between two discontinuous chord members in a truss structure, which may occur within or outside of a gusset plate. For chord splices that occur outside of the gusset plate, the provisions of *AASHTO LRFD* Article 6.13.6.1.2 (Section 6.6.5.3) or 6.13.6.1.3 (Section 6.6.5.4) apply in lieu of those discussed herein.

For gusset plates also serving the role of a chord splice, the forces from all members framing into the connection must be considered. The chord splice forces are the resolved axial forces acting on each side of the spliced section, as illustrated in Figure C6.14.2.8.6-1. The chord splice should be investigated for the larger of the two resolved forces on either side of the splice.

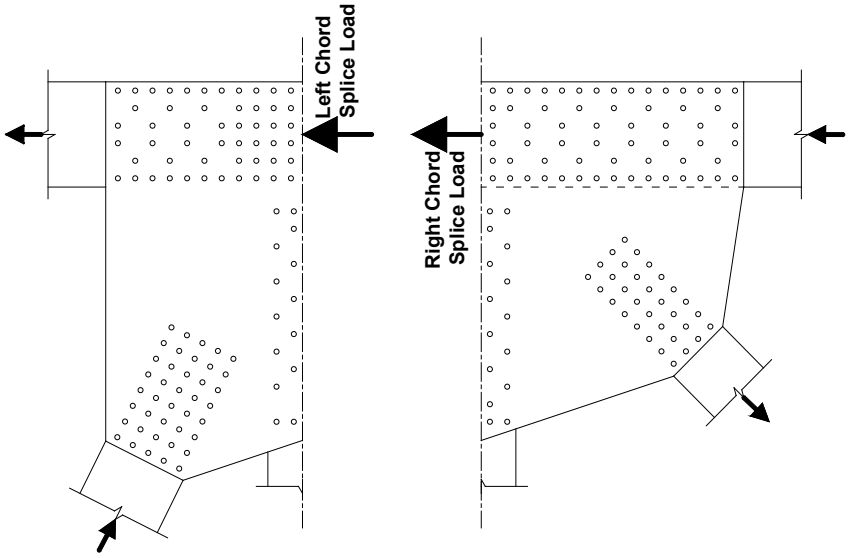

Figure 6.6.7.5-1 Example Connection Showing the Resolution of the Member Forces into Forces Acting on Each Side of a Chord Splice

Gusset plates that splice two chord sections together are to be checked using a section analysis considering the relative eccentricities between all plates crossing the splice and the loads on the spliced plane.

As specified in *AASHTO LRFD* Article 6.14.2.8.6, for compression chord splices, the factored compressive resistance, P_r, of the spliced section is to be taken as:

$$P_r = \phi_{cs} F_{cr} \left(\frac{S_g A_g}{S_g + e_p A_g} \right) \qquad \text{Equation 6.6.7.5-1}$$

AASHTO LRFD Equation 6.14.2.8.6-1

where:

F_{cr} = stress in the spliced section at the limit of usable resistance (ksi). F_{cr} is to be taken as the specified minimum yield strength of the gusset plate when the following equation is satisfied:

$$\frac{KL_{splice}\sqrt{12}}{t_g} < 12$$ Equation 6.6.7.5-2

AASHTO LRFD Equation 6.14.2.8.6-2

ϕ_{cs} = resistance factor for truss gusset plate chord splices specified in Article 6.5.4.2 (=0.65)
A_g = gross area of all plates in the cross-section intersecting the spliced plane (in.^{2})
e_p = distance between the centroid of the cross-section and the resultant force perpendicular to the spliced plane (in.)
K = effective column length factor taken as 0.50 for chord splices
L_{splice} = center-to-center distance between the first lines of fasteners in the adjoining chords as shown in Figure 6.6.7.5-2 (in.)
S_g = gross section modulus of all plates in the cross-section intersecting the spliced plane (in.^{3})
t_g = gusset plate thickness (in.)

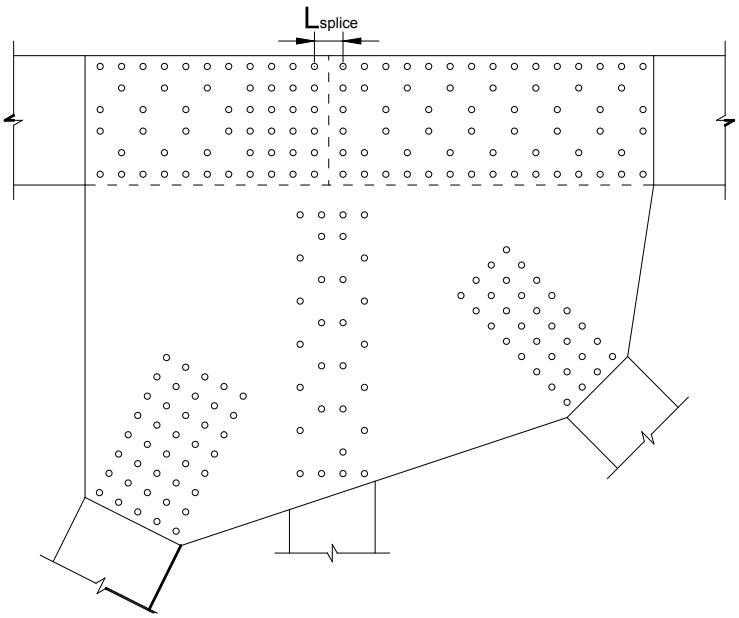

Figure 6.6.7.5-2 Example Connection Showing Chord Splice Parameter, L_{splice}

The Whitmore section check specified in *AASHTO LRFD* Article 6.14.2.8.4 (Section 6.6.7.3) is not considered applicable for the design of a compression chord splice.

For tension chord splices, the factored tensile resistance, P_r, is to be taken as the lesser of the values given by the following equations:

$$P_r = \phi_{cs} F_y \left(\frac{S_g A_g}{S_g + e_p A_g} \right)$$ Equation 6.6.7.5-3

AASHTO LRFD Equation 6.14.2.8.6-3

$$P_r = \phi_{cs} F_u \left(\frac{S_n A_n}{S_n + e_p A_n} \right)$$ Equation 6.6.7.5-4

AASHTO LRFD Equation 6.14.2.8.6-4

where:

ϕ_{cs} = resistance factor for truss gusset plate chord splices specified in Article 6.5.4.2 (=0.65)
A_g = gross area of all plates in the cross-section intersecting the spliced plane (in.^{2})
A_n = net area of all plates in the cross-section intersecting the spliced plane (in.^{2})
e_p = distance between the centroid of the cross-section and the resultant force perpendicular to the spliced plane (in.)
F_y = specified minimum yield strength of the gusset plate (ksi)
F_u = specified minimum tensile strength of the gusset plate (ksi)
S_g = gross section modulus of all plates in the cross-section intersecting the spliced plane (in.^{3})
S_n = net section modulus of all plates in the cross-section intersecting the spliced plane (in.^{3})

Tension chord splice members are also to be checked for block shear rupture as specified in AASHTO LRFD Article 6.13.4 (Section 6.6.3.3.2.5). The yielding and net section fracture checks on the Whitmore section specified in *AASHTO LRFD* Article 6.14.2.8.5 (Section 6.6.7.4) are not considered applicable for the design of a tension chord splice.

The preceding equations assume the gusset and splice plates behave as one combined spliced section to resist the applied axial load and eccentric bending that occurs due to the fact that the resultant forces on the section are offset from the centroid of the combined section, as illustrated in Figure 6.6.7.5-3. The combined spliced section is treated as a beam, and for compression chord splices, the factored resistance at the strength limit state is determined assuming the stress in the combined section at the limit of usable resistance is equal to the specified minimum yield strength of the gusset plate if the slenderness limit for the spliced section given by Equation 6.6.7.5-2 is met, which will typically be the case. If not, the Engineer will need to derive a reduced value of F_{cr} to account for possible elastic buckling of the gusset plate within the splice.

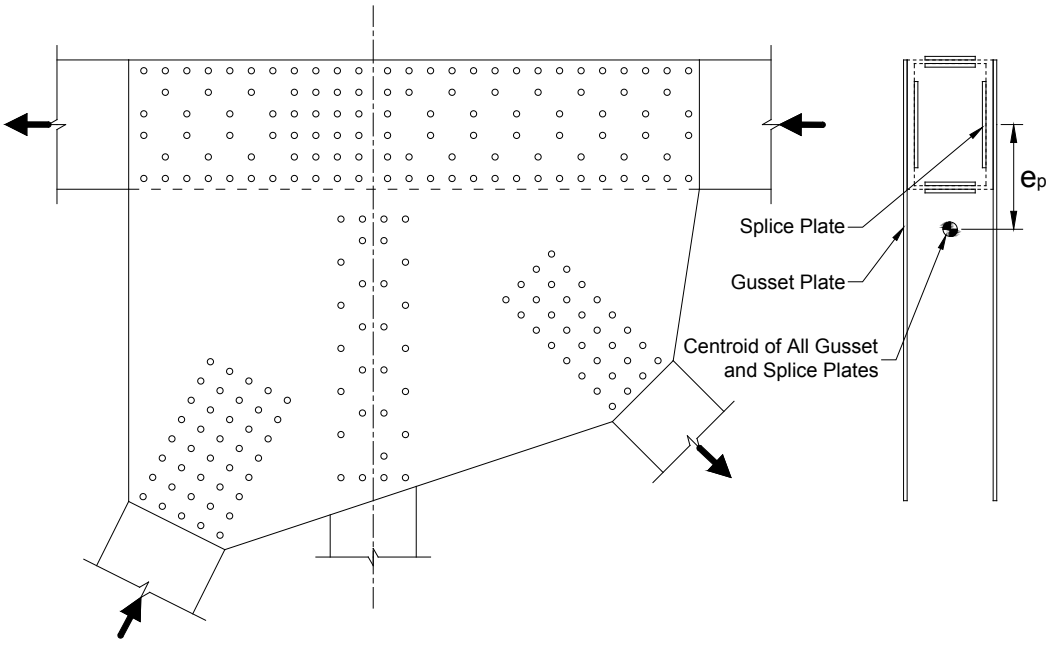

Figure 6.6.7.5-3 ***Illustration of the Combined Spliced Section at a Chord Splice***

6.6.7.6 Edge Slenderness

As specified in AASHTO LRFD Article 6.14.2.8.7, if the length of the unsupported edge of a gusset plate exceeds $2.06t_g(E/F_y)^{1/2}$, where t_g is the gusset plate thickness and F_y is the specified minimum yield strength of the gusset plate, the edge should be stiffened.

The preceding provision is intended to provide good detailing practice to reduce deformations of free edges during fabrication, erection, and service as opposed to providing an increase in the member compressive buckling resistance at the strength limit state. No direct correlation has been found between the buckling resistance of the gusset plate and the free edge slenderness (Ocel, 2013). There are no criteria specified for sizing of the edge stiffeners, but the traditional practice of using angles with leg thicknesses of 0.50 in. has generally provided adequate performance.

Section 6.7 Acknowledgments

The past contributions of Mr. Dann H. Hall and Mr. A. Richard Lawin of Bridge Software Development International, Ltd. to significant portions of the material provided within this chapter are acknowledged.

Section 6.8 References

AASHO. 1931. *Specifications for Bridges and Structures*, First Edition, American Association of State Highway Officials, Washington, D.C.

AASHO. 1935. *Specifications for Bridges and Structures*, Second Edition, American Association of State Highway Officials, Washington, D.C.

AASHO. 1941. *Specifications for Bridges and Structures*, Third Edition, American Association of State Highway Officials, Washington, D.C.

AASHO Road Test. 1962. "Report No. 4, Bridge Research, Highway Research Board Special Report 61D." Publication No. 953, National Academy of Sciences, National Research Council, Washington, D.C.

AASHTO. 1989. *Guide Specifications for Fatigue Design of Steel Bridges*. American Association of State Highway and Transportation Officials, Washington, D.C.

AASHTO. 2002. *Standard Specifications for Highway Bridges*. 17th Edition, American Association of State Highway and Transportation Officials, Washington, D.C.

AASHTO. 2009. *LRFD Guide Specifications for Design of Pedestrian Bridges*. 2nd Edition, American Association of State Highway and Transportation Officials, Washington, DC.

AASHTO. 2010. *LRFD Bridge Construction Specifications and Interim Specifications*. 3rd Edition. American Association of State Highway and Transportation Officials, Washington, D.C.

AASHTO. 2011. *Standard Specifications for Transportation Materials and Methods of Sampling.* American Association of State Highway and Transportation Officials, Washington, DC, 31st Ed.

AASHTO. 2011a. *The Manual for Bridge Evaluation*. Second Edition, MBE-2-M, American Association of State Highway and Transportation Officials, Washington, DC.

AASHTO. 2011b. *Guide Specifications for LRFD Seismic Bridge Design*, Second Edition, LRFDSEIS-2, American Association of Highway and Transportation Officials, Washington, DC.

AASHTO. 2011c. *A Policy on Geometric Design of Highways and Streets*, Sixth Edition, GDHS-6-UL, American Association of Highway and Transportation Officials, Washington, DC.

AASHTO. 2013. *Standard Specifications for Structural Supports for Highway Signs, Luminaires, and Traffic Signals*. Sixth Edition, American Association of State Highway and Transportation Officials, Washington, DC.

AASHTO/AWS. 2010. *Bridge Welding Code*, BWC-6 (AASHTO/AWS D1.5M/D1.5:2010). American Association of State Highway and Transportation Officials and American Welding Society, Washington, DC.

AASHTO/NSBA Steel Bridge Collaboration. 2003. "Guidelines for Design for Constructibility, G12.1." American Highway of State Highway and Transportation Officials, Washington, D.C., Publication No. GDC-1.

AISC. 1963. *Manual of Steel Construction*. 6th ed. American Institute of Steel Construction, Chicago, IL.

AISC. 1973. "Commentary on Highly Restrained Welded Connections." *AISC Engineering Journal*, American Institute of Steel Construction, Chicago, IL, Vol. 10, No. 3, 3rd Qtr.

AISC. 2005. *Specification for Structural Steel Buildings*. ANSI/ASCE 360-05, American Institute of Steel Construction, Chicago, IL, March 9.

AISC. 2010. *Manual of Steel Construction – Load and Resistance Factor Design*. 3rd Ed. American Institute of Steel Construction, Chicago, IL.

AISC. 2010a. *Specification for Structural Steel Buildings*. ANSI/ASCE 360-10, American Institute of Steel Construction, Chicago, IL, June 22.

AISI. 1969. *Specification for the Design of Cold-Formed Steel Structural Members*. American Iron and Steel Institute, Washington, DC.

AISI. 1975. *The Development of AASHTO Fracture-Toughness Requirements for Bridge Steels*. American Iron and Steel Institute, Washington, D.C., February.

AISI. 2001. North American Specification for the Design of Cold-Formed Steel Structural Members. American Iron and Steel Institute, Washington, DC.

ANSI/AWS. 2010. *Structural Welding Code – Steel*. American Welding Society, Miami, FL.

AREMA. 2014. *Manual for Railway Engineering*. American Railway and Maintenance-of-Way Association, Lanham, MD.

ASCE. 1958. "Deflection Limits of Bridges. Progress Report of the Committee on Deflection Limitations of Bridge of the Structural Division." *Journal of the Structural Division*, ASCE, New York, NY, Vol. 84, No. ST3, May.

ASCE. 1968. "Design of Hybrid Steel Beams." Joint ASCE-AASHO Subcommittee on Hybrid Beams and Girders, *Journal of the Structural Division*, American Society of Civil Engineers, Vol. 94, No. ST6, New York, NY.

ASCE. 1971. *Plastic Design in Steel – A Guide and Commentary*. 2nd Edition. ASCE Manual No. 41, American Society of Civil Engineers, New York, NY.

ASCE. 1982. "Causes and Prevention of Lamellar Tearing." *Civil Engineering*, American Society of Civil Engineers, New York, NY, April.

ASCE. 1997. *Effective Length and Notional Load Approaches for Assessing Frame Stability: Implications for American Steel Design*. American Society of Civil Engineers Structural Engineering Institute's Task Committee on Effective Length under the Technical Committee on Load and Resistance Factor Design.

ASCE. 2000. *Design of Latticed Steel Transmission Structures*, ASCE 10-97, American Society of Civil Engineers, Reston, VA.

Aslani, F., and S.C. Goel. 1991. "An Analytical Criteria for Buckling Strength of Built-Up Compression Members." *Engineering Journal*, American Institute of Steel Construction, Chicago, IL, Vol. 28, No. 4, 4th Qtr.

ASTM. 2010. *Standard Specification for Structural Steel for Bridges.* West Conshohocken : American Society for testing and Materials, A 709/A709M.

AWS. 2001. "Welding Handbook, 9th ed., Vol. 1, Welding Science & Technology", American Welding Society, Miami, FL.

AWS. 2004. "Welding Handbook, 9th ed., Vol. 2, Welding Processes, Part 1", American Welding Society, Miami, FL.

AWS. 2007. "Welding Handbook, 9th ed., Vol. 2, Welding Processes, Part 2", American Welding Society, Miami, FL.

AWS. 2012. "Standard Symbols for Welding, Brazing and Nondestructive Examination: ANSI/AWS A2.4". American Welding Society, Miami, FL.

Azizinamini, A. 2014. "Simple for Dead Load and Continuous for Live Load Steel Bridge Systems." *AISC Engineering Journal*. 2nd and 3rd Quarters.

Baldwin, J.W., H.J. Salame, and R.C. Duffield. 1987. "Fatigue Test of a Three-Span Composite Highway Bridge." Report 73-1, Department of Civil Engineering, University of Missouri, Columbia, MO, June.

Barker, M.G., B.A. Hartnagel, C.G. Schilling, and B.E. Dishongh. 1997. "Inelastic Design and Experimental Testing of Compact and Noncompact Steel Girder Bridges." *Report 93-1*, Missouri Cooperative Highway Research Program.

Barsom, J.M., and S.T. Rolfe. 1987. *Fracture and Fatigue Control in Structures – Applications of Fracture Mechanics*. 2nd Edition, Prentice-Hall, Inc., Englewood, Cliffs, NJ.

Barth, K.E., B.A. Hartnagel, D.W. White, and M.G. Barker. 2004. "Improved Simplified Inelastic Design of Steel I-Girder Bridges." *Journal of Bridge Engineering*, American Society of Civil Engineers, Reston, VA, Vol. 9, No. 3.

Barth, K.E., D.W. White, J.E. Righman, and L. Yang. 2005. "Evaluation of Web Compactness Limits for Singly and Doubly Symmetric Steel I-Girders." *Journal of Constructional Steel Research*, Elsevier, Orlando, FL, Vol. 61, No. 10.

Barth, K.E. 2012. "Steel Bridge Design Handbook Design Example 2A: - Two-Span Continuous Straight Composite Steel I-Girder Bridge." Publication No. FHWA-IF-12-052 – Vol. 21, U.S. Department of Transportation, Federal Highway Administration, Washington, DC, November.

Barth, K.E. 2012a. "Steel Bridge Design Handbook Design Example 2B: - Two-Span Continuous Straight Composite Steel Wide-Flange Beam Bridge." Publication No. FHWA-IF-12-052 – Vol. 22, U.S. Department of Transportation, Federal Highway Administration, Washington, DC, November.

Bartlett, R.M., R.J. Dexter, M.D. Graeser, J.J. Jelinek, B.J. Schmidt, and T.V. Galambos. 2003. "Updating Standard Shape Material Properties Database for Design and Reliability," *Engineering Journal,* AISC, Vol. 40, No. 1, pp. 2–14.

Basler, K., B.T. Yen, J.A. Mueller, and B. Thurlimann. 1960. "Web Buckling Tests on Welded Plate Girders." *WRC Bulletin No. 64*, Welding Research Council, New York, NY.

Basler, K. 1961. "Strength of Plate Girders in Shear." *Journal of the Structural Division*, ASCE, Vol. 87. No. ST7, October.

Basler, K., and B. Thurlimann. 1961. "Strength of Plate Girders in Bending." *Journal of the Structural Division*, American Society of Civil Engineers, New York, NY, Vol. 87, No. ST6, August.

Batho, C., and E.H. Bateman. 1934. *Investigations on Bolts and Bolted Joints*. Second Report of the Steel Structures Research Committee, London; His Majesty's Stationary Office.

Battistini, A.D. 2009. "Skewed Cross Frame Connection Stiffness." Ph.D. Dissertation, Phil M. Ferguson Structural Engineering Laboratory, University of Texas at Austin, Austin, TX (http://fsel.engr.utexas.edu/publications).

Battistini, A., W. Wang, S. Donahue, T. Helwig, M. Engelhardt, and K. Frank. 2014. "Improved Cross Frame Details for Steel Bridges." Report No. FHWA/TX-13/0-6564-1, Center for Transportation Research, University of Texas at Austin, Austin, TX, May, pp. 306-307.

Birkemoe, P.C., and D.C. Herrschaft. 1970. "Bolted Galvanized Bridges: Engineering Acceptance Near." *Civil Engineering*, American Society of Civil Engineers, New York, NY, Vol. 40, No. 4, April.

Birkemoe, P.C., and M.I. Gilmour. 1978. "Behavior of Bearing Critical Double-Angle Beam Connections." *AISC Engineering Journal*, American Institute of Steel Construction, Chicago, IL, Vol. 15, No. 4, 4th Qtr.

Bjorhovde, R. 1972. "Deterministic and Probabilistic Approaches to the Strength of Steel Columns." Ph.D. Dissertation, Lehigh University, Bethlehem, PA, May.

Bjorhovde, R. 1978. "The Safety of Steel Columns." *Journal of the Structural Division*, American Society of Civil Engineers, New York, NY, Vol. 104, No. ST9, September.

Bjorhovde, R. 1988. "Columns: From Theory to Practice," *Engineering Journal*, AISC, Vol. 25, No. 1, 1st Quarter, pp. 21–34.

Bleich, F. 1952. *Buckling Strength of Metal Structures*. McGraw-Hill, New York, NY.

Blodgett, O.W. 1960. "Shrinkage Control in Welding." *Civil Engineering*, American Society of Civil Engineers, New York, NY, November.

Blodgett, O.W. 1982. *Design of Welded Structures*. The James F. Lincoln Arc Welding Foundation, Cleveland, OH.

Boresi, A.P., O.M. Sidebottom, F.B. Seely, and J.O. Smith. 1978. *Advanced Mechanics of Materials*, Third Edition, John Wiley and Sons, New York, NY.

Brockenbrough, R.L., and B.G. Johnston. 1981. *USS Steel Design Manual*. United States Steel Corporation, ADUSS 27-3400-04, Pittsburgh, PA, January.

Brockenbrough, R.L. 1983. "Considerations in the Design of Bolted Joints for Weathering Steel." *AISC Engineering Journal*, American Institute of Steel Construction, Chicago, IL, Vol. 20, 1st Qtr.

Brockenbrough, R.L. 1995. "Effect of Yield-tensile Ratio on Structural Behavior." American Iron and Steel Institute, Washington, D.C., 1995.

Brown, J.D., D.J. Lubitz, Y.C. Cekov, and K.H. Frank. 2007. "Evaluation of Influence of Hole Making Upon the Performance of Structural Steel Plates and Connections." Report No. FHWA/TX-07/0-4624-1, University of Texas at Austin, Austin, TX.

BSI. 1990. "BS5950: Part 1: 1990, Structural Use of Steelwork in Buildings, Part 1, Code of Practice for Design in Simple and Continuous Construction: Hot Rolled Sections." British Standards Institution, London.

Caner, A., and P. Zia. 1998. "Behavior and Design of Link Slabs for Jointless Bridge Decks." *PCI Journal,* pp. 68-80, May-June.

Carskaddan, P.S. 1968. "Shear Buckling of Unstiffened Hybrid Beams." *Journal of the Structural Division*, American Society of Civil Engineers, New York, NY, Vol. 94, ST8, August.

Carskaddan, P.S., and C.G. Schilling. 1974. "Lateral Buckling of Highway Bridge Girders." Research Laboratory Report 22-G-001 (019-3), United States Steel Corporation, Monroeville, PA.

CEN. 1993. *Eurocode 3: Design of Steel Structures, Part 1.1 – General Rules and Rules for Buildings*, ENV 1992-1-1, European Committee for Standardization, Brussels, Belgium.

CEN. 2004. Eurocode 4, EN: 1994-1-1:2004, European Committee for Standardization, Brussels, Belgium.

Chesson, E., N.L. Faustino, and W.H. Munse. 1965. "High-Strength Bolts Subject to Tension and Shear." *Journal of the Structural Division*, American Society of Civil Engineers, New York, NY, Vol. 91, No. ST5, October.

Clarke, M.J., and R.Q. Bridge. 1992. "The Inclusion of Imperfections in the Design of Beam-Columns." *Proceedings of the Annual Technical Session and Meeting*, Pittsburgh, PA, Structural Stability Research Council, University of Missouri, Rolla, MO.

Coletti, D., Z. Fan, W. Gatti, J. Holt, and J. Vogel. 2005. "Practical Steel Tub Girder Design." available from the National Steel Bridge Alliance (NSBA), Chicago, IL, April.

Considere, A. 1891. "Resistance des pieces comprimees." *Congres International des Procedes de Construction*, Paris.

Consortium of University Research Teams (CURT). 1975. "Tentative Design Specifications for Horizontally Curved Highway Bridges." CURT Project, Part of Final Report, Research Project HPR2-(111), March.

Cooper, P.B. 1967. "Strength of Longitudinally Stiffened Plate Girders." *Journal of the Structural Division*, ASCE, Vol. 93, No. ST2, April.

Crawford, S.F., and G.L. Kulak, 1971. "Eccentrically Loaded Bolted Connections." *Journal of the Structural Division*, American Society of Civil Engineers, New York, NY, Vol. 97, No. ST3, March.

Culmo, M.P. 2014. "Piece BY Piece." *Modern Steel Construction*, American Institute of Steel Construction, Chicago, IL, September.

Culver, C.G., and J. Mozer. 1971. "Horizontally Curved Highway Bridges, Stability of Box Girders." Department of Civil Engineering, Carnegie Mellon University, Pittsburgh, PA, Report No. B2 submitted to the FHWA, Contract No. FH-11-7389, July.

Culver, C.G. 1972. "Design Recommendations for Curved Highway Bridges." *Final Report for PennDOT Research Project 68-32*, Civil Engineering Department, Carnegie-Mellon University, Pittsburgh, PA, June.

Dabrowski, R. 1968. *Curved Thin-Walled Girders*. Translation No. 144, Cement and Concrete Association, London, England.

Darwin, D. 1990. *Steel and Composite Beams with Web Openings*. AISC Steel Design Guide Series No. 2, American Institute of Steel Construction, Chicago, IL.

Doswell, B. 2002. "Lateral-Torsional Buckling of Wide Flange Cantilever Beams." *Proceedings of the 2002 Annual Stability Conference*, Structural Stability Research Council, University of Missouri, Rolla, MO.

Duan, L., M. Reno, and L. Lynch. 2000. "Section Properties for Latticed Members of San-Francisco-Oakland Bay Bridges." *Journal of Bridge Engineering*, American Society of Civil Engineers, Reston, VA, Vol. 4, No. 2, May.

Duan, L., M. Reno, and C.M. Uang. 2002. "Effect of Compound Buckling on Compression Strength of Built-Up Members." *Engineering Journal*, American Institute of Steel Construction, Chicago, IL, Vol. 39, No. 1, 1st Qtr.

Easterling, W.S., and L.G. Giroux. 1993. "Shear Lag Effects in Steel Tension Members." *AISC Engineering Journal*, American Institute of Steel Construction, Chicago, IL, Vol. 30, No. 3, 3rd Qtr.

El Darwish, I.A., and B.G. Johnston. 1965. "Torsion of Structural Shapes." *Journal of the Structural Division*, American Society of Civil Engineers, New York, NY, Vol. 91, No. ST1, February.

Elgaaly, M., and R. Salkar. 1991. "Web Crippling Under Edge Loading." *Proceedings of the AISC National Steel Construction Conference*, Washington, D.C.

Ellifritt, D.S., G. Wine, T. Sputo, and S. Samuel. 1992. "Flexural Strength of WT Sections." *Engineering Journal*, American Institute of Steel Construction, Chicago, IL, Vol. 29, No. 2, 2nd Qtr.

Engesser, F. 1889. "Ueber die Knickfestigkeit gerader Stabe." *Zeitschrift des Architekten-und Ingenieur- Vereins zu Hannover*, Volume 35; and "Die Knickfestigkeit gerader Stabe." *Zentralblatt der Bauverwaltung*, Berlin, December 5, 1891.

Euler, L. 1744. De Curvis Elasiticis, Additamentum I, Methodus Inveniendi Lineas Curvas Maximi Minimive Proprietate Gaudentes. Lausanne and Geneva; and "Sur le Forces des Colonnes," Memories de l'Academie Royale des Sciences et Belles Lettres, Vol. 13, Berlin, 1759; English translation of the letter by J.A. Van den Broek, "Euler's Classic Paper 'On the Strength of Columns'," American Journal of Physics, Volume 15, January/February, 1947.

Fan, Z., and T.A. Helwig. 1999. "Behavior of Steel Box Girders with Top Flange Bracing." *Journal of Structural Engineering*, ASCE, Vol. 125, No. ST8, August, pp. 829-837.

Farimani, F., S. Javidi, D. Kowalski, and A. Azizinamini. 2014. "Numerical Analysis and Design Provision Development of Simple for Dead – Continuous for Live Bridge System." *AISC Engineering Journal*, to be published in second quarter.

FHWA. 1980. “Proposed Design Specifications for Steel Box Girder Bridges.” FHWA-TS-80-205, Federal Highway Administration, Washington, D.C.

FHWA. 1989. *Technical Advisory on Uncoated Weathering Steel in Structures*. Federal Highway Administration, U.S. Department of Transportation, Washington, D.C., October.

Fisher, J.W. 1965. “Behavior of Fasteners and Plates with Holes.” *Journal of the Structural Division*, American Society of Civil Engineers, New York, NY, Vol. 91, No. ST6, December.

Fisher, J.W., K.H. Frank, M.A. Hirt, and B.M. McNamee. 1970. “Effect of Weldments on Fatigue Strength of Steel Beams.” NCHRP Report 102, Highway Research Board, Washington, D.C.

Fisher, J.W., P.A. Albrecht, B.T. Yen, D.J. Klingerman, and B.M. McNamee. 1974. “Fatigue Strength of Steel Beams with Transverse Stiffeners and Attachments.” NCHRP Report 147, Highway Research Board, Washington, D.C.

Fisher, J.W. 1977. “Bridge Fatigue Guide – Design and Details.” American Institute of Steel Construction, Chicago, IL.

Fletcher, F.B., H.E. Townsend, and A.D. Wilson. 2003. “Corrosion Performance of Improved Weathering Steels for Bridges.” World Steel Bridge Symposium, Nov. 19-20, Orlando, National Steel Bridge Alliance, Chicago, IL.

Foehl, P.J. 1948. “Direct Method of Designing Single Angle Struts in Welded Trusses.” *Design Book for Welding*, Lincoln Electric Company, Cleveland, OH, November.

Fountain, R.S., and C.E. Thunman, Jr. 1987. “Deflection Criteria for Steel Highway Bridges.” Proceedings of the AISC National Engineering Conference, New Orleans, LA, April 29-May 7.

Frank, K.H., and J.W. Fisher. 1979. “Fatigue Strength of Fillet Welded Cruciform Joints.” Journal of the Structural Division, American Society of Civil Engineers, New York, NY, Vol. 105, No. ST9, September.

Frank, K.H., and J.A. Yura. 1981. “An Experimental Study of Bolted Shear Connections.” FHWA/RD-81/148, Federal Highway Administration, Washington, D.C., December.

Frank, K.H., and T.A. Helwig. 1995. "Buckling of Webs in Unsymmetric Plate Girders." *AISC Engineering Journal*, American Institute of Steel Construction, Chicago, IL, Vol. 32, 2nd Qtr.

Frost, R.W., and C.G. Schilling. 1964. "Behavior of Hybrid Beams Subjected to Static Loads." *Journal of the Structural Division*, American Society of Civil Engineers, New York, NY, Vol. 90, ST3, June.

Galambos, T.V. 1978. "Tentative Load Factor Design Criteria for Curved Steel Bridges." Research Report No. 50, Department of Civil Engineering, St. Louis, MO, May.

Galambos, T.V., and J. Chapuis. 1980. *LRFD Criteria for Composite Columns and Beam Columns*. Revised draft. Washington University Department of Civil Engineering, St. Louis, MO, December.

Galambos, T.V. 1983. "Reliability of Axially Loaded Columns," *Engineering Structures*, Vol. 5, No. 1, pp. 73–78.

Galambos, T.V., R.T. Leon, C.E. French, M.G. Barker, and B.E. Dishongh. 1993. "Inelastic Rating Procedures for Steel Beam and Girder Bridges." *NCHRP Report 352*, Transportation Research Board, National Research Council, Washington, D.C.

Goldberg, J.E., and H.L. Leve. 1957. "Theory of Prismatic Folded Plate Structures." *IABSE*, Vol. 16, International Association for Bridge and Structural Engineers, Zurich, Switzerland.

Grubb, M.A. 1993. "Review of Alternate Load Factor (Autostress) Design," *Transportation Research Record 1380*, Transportation Research Board, National Research Council, Washington, DC, pp. 45-48.

Grubb, M.A., and R.E. Schmidt. 2012. "Steel Bridge Design Handbook Design Example 1: Three-Span Continuous Straight Composite Steel I-Girder Bridge". Publication No. FHWA-IF-12-052 – Vol. 20, U.S. Department of Transportation, Federal Highway Administration, Washington, DC, November.

Gurney, T.R. 1968. "Fatigue of Welded Structures." Cambridge University Press.

Haaijer, G. 1961. "Economy of High Strength Steel Structural Members." *Journal of the Structural Division*, American Society of Civil Engineers, New York, NY, Vol. 87, No. ST 8.

Higgins, C., A. Hafner, O. T. Turan, and T. Schumacher. 2013. "Experimental Tests of Truss Bridge Gusset Plate Connections with Sway-Buckling Response," *Journal*

of Bridge Engineering, American Society of Civil Engineers, Reston, VA, 18(10), pp. 980-991.

Hall, D.H. 1981. "Proposed Steel Column Strength Criteria." *Journal of the Structural Division*, American Society of Civil Engineers, New York, NY, Vol. 107, No. ST4, April.

Hall, D.H., M.A. Grubb, M.A., and C.H. Yoo. 1999. "Improved Design Specifications for Horizontally Curved Steel Girder Highway Bridges." *NCHRP Report 424*, Transportation Research Board, Washington, D.C.

Hall, D.H. 2000. "The Effect of Material Properties on the Stability of Steel Girder Bridges." *Proceedings of the SSRC Annual Technical Session*, Memphis, TN, Structural Stability Research Council, University of Missouri, Rolla, MO.

Hansell, W.C., and I.M. Viest. 1971. "Load Factor Design for Steel Highway Bridges." *AISC Engineering Journal*, American Institute of Steel Construction, Chicago, IL, October.

Hanshin Expressway Public Corporation and Steel Structure Study Subcommittee. 1988. "Guidelines for the Design of Horizontally Curved Girder Bridges (Draft)." Hanshin Expressway Public Corporation, October.

Hardash, S., and R. Bjorhovde. 1985. "New Design Criteria for Gusset Plates in Tension." *AISC Engineering Journal*, American Institute of Steel Construction, Chicago, IL, Vol. 22, 2nd Qtr.

Heins, C.P. 1975. *Bending and Torsional Design in Structural Members*. Lexington Books, D.C. Heath and Company, Lexington, MA.

Heins, C.P. 1978. "Box Girder Bridge Design – State of the Art." AISC Engineering Journal, American Institute of Steel Construction, Chicago, IL, 4th Qtr.

Heins, C.P., and D.H. Hall. 1981. "Designers Guide to Steel Box Girder Bridges." Booklet No. 3500, Bethlehem Steel Corporation, Bethlehem, PA, February.

Herman, R., T. Helwig, J. Holt, R. Medlock, M. Romage, and C. Zhou. 2005. "Lean-On Cross-Frame Bracing for Steel Girders with Skewed Supports." *Proceedings of the 2005 World Steel Bridge Symposium*, Orlando, FL, available from the National Steel Bridge Alliance, Chicago, IL.

Horne, M.R., and W.R. Grayson. 1983. "Parametric Finite Element Study of Transverse Stiffeners for Webs in Shear." *Instability and Plastic Collapse of Steel*

Structures, Proceedings of the Michael R. Horne Conference, L.J. Morris (ed.), Granada Publishing, London, England.

Horton, R., E. Power, K. V. Ooyen, and A. Azizinamini. 2000. "High Performance Steel Cost Comparison Study." Conference Proceedings, Steel Bridge Design and Construction for the New Millennium with Emphasis on High Performance Steel, November 30 - December 1, Federal Highway Administration, Washington, D. C.

Huber, A.W., and L.S. Beedle. 1954. "Residual Stress and the Compressive Strength of Steel." *Welding Journal*, December.

Iron Age. 1955. "100 Years of Metalworking – Welding, Brazing and Joining." June.

Javidi, S., A. Yakel, and A. Azizinamini. 2014. "Experimental Investigation, Application and Monitoring of Simple-made-continuous Bridge Connection for Modular Bridge Construction Method." *AISC Engineering Journal*, to be published in third quarter.

Johnson, D.L. 1985. "An Investigation into the Interaction of Flanges and Webs in Wide Flange Shapes." *Proceedings of the SSRC Annual Technical Session*, Cleveland, OH, Structural Stability Research Council, University of Missouri, Rolla, MO.

Johnston, S.B., and A.H. Mattock. 1967. "Lateral Distribution of Load in Composite Box Girder Bridges." *Highway Research Record, No. 167*, Bridges and Structures, Transportation Research Board, Washington, D.C.

Johnston, B.G. 1983. "Column Buckling Theory: Historic Highlights." *Journal of Structural Engineering*, American Society of Civil Engineers, New York, NY, Vol. 109, No. 9, September.

Jung, S.-K., and D.W. White. 2006. "Shear Strength of Horizontally Curved Steel I-Girders – Finite Element Studies." *Journal of Constructional Steel Research*, 62(4).

Kaufman, E.J., A.W. Pense, and R.D. Stout. 1981. "An Evaluation of Factors Significant to Lamellar Tearing." *Welding Journal*, Research Supplement, Vol. 60, March.

Kaufmann, E.J., R.J. Connor, and J.W. Fisher. 2004. *Failure Investigation of the SR 422 over the Schuylkill River Girder Fracture – Draft Final Report.* ATLSS Engineering Research Center, Lehigh University, Bethlehem, PA.

Ketchum, M.S. 1908. *The Design of Highway Bridges*. First Edition, McGraw-Hill, New York, NY.

Kim, Y.D., and D.W. White. 2014. “Transverse Stiffener Requirements to Develop the Shear Buckling and Post-Buckling Resistance of Steel I-Girders.” *Journal of Structural Engineering*, American Society of Civil Engineers, Reston, VA, Vol. 140, No. 4, pp. 04013098.

Kitipornchai, S., and N.S. Trahair. 1980. “Buckling Properties of Monosymmetric I-Beams.” *Journal of the Structural Division*, American Society of Civil Engineers, New York, NY, Vol. 106, No. ST5, May.

Kitipornchai, S., and N.S. Trahair. 1986. “Buckling Properties of Monosymmetric I-Beams Under Moment Gradient.” *Journal of the Structural Division*, American Society of Civil Engineers, New York, NY, Vol. 112, No. ST4.

Knight, A.W. 1934. “The Design and Construction of Composite Slab and Girder Bridges.” *J. Instn Engrs Aust.*, Vol. 6, No. 1.

Kolbrunner, C., and K. Basler. 1966. *Torsion in Structures*. Springer-Verlag, New York, NY.

Krupicka, G., and B. Poellot. 1993. “Nuisance Stiffness.” *Bridgeline*, 4(1), HDR Engineering, Inc., Omaha, NE.

Kulak, G.L., J.W. Fisher, and J.H.A. Struik. 1987. *Guide to Design Criteria for Bolted and Riveted Joints*. 2nd Edition, John Wiley & Sons, New York, NY.

Kulak, G.L., and G.Y. Grondin. 2001. “AISC LRFD Rules for Block Shear – A Review.” *AISC Engineering Journal*, American Institute of Steel Construction, Chicago, IL, Vol. 38, No. 4, 4th Qtr.

Lampe, N., N. Mossahebi, A. Yakel, R. Farimani, and A. Azizinamini. 2014. "Development and Experimental Testing of Connections for Simple for Dead Load – Continuous for Live Load Steel Bridge System." *AISC Engineering Journal*, 2nd and 3rd Quarters.

Lee, S.C., C.H. Yoo, and D.Y. Yoon. 2003. “New Design Rule for Intermediate Transverse Stiffeners Attached on Web Panels.” *Journal of Structural Engineering*, American Society of Civil Engineers, Reston, VA, 129(12).

Lew, H.S., and A.A. Toprac. 1968. “Static Strength of Hybrid Plate Girders.” *SFRL Technical Report*, University of Texas, Austin, TX.

Liew, J.Y.R., D.W. White, and W.F. Chen. 1992. "Beam-Columns." *Constructional Steel Design, An International Guide*, Chapter 2.5, P.J. Dowling, J.E. Harding and R. Bjorhovde (ed.), Elsevier, Essex, England.

Lincoln Electric Company. 1994. *The Procedure Handbook of Arc Welding*. Lincoln Electric Company, Cleveland, OH.

Lutz, L.A. 1996. "A Closer Examination of the Axial Capacity of Eccentrically Loaded Single Angle Struts." *AISC Engineering Journal*, American Institute of Steel Construction, Chicago, IL, Vol. 33, No. 2, 2nd Qtr.

Lutz, L.A. 2006. "Evaluating Single Angle Compression Struts Using an Effective Slenderness Approach." *AISC Engineering Journal*, American Institute of Steel Construction, Chicago, IL, Vol. 43, No. 4, 4th Qtr.

Lwin, M. M. 2002. *High Performance Steel Designer's Guide.* Federal Highway Administration, Western Resource Center, San Francisco, CA, April.

Lwin, M. M. 2012. "Clarification of Requirements for Fracture Critical Members." FHWA Memorandum, June 20.

Mahmoud, H.N., R.J. Connor, and J.W. Fisher. 2005. "Finite Element Investigation of the Fracture Potential of Highly Constrained Details." *Journal of Computer-Aided Civil and Infrastructure Engineering*, Blackwell Publishing, Inc., Malden, MA, Vol. 20.

Maleck, A.E., and D.W. White. 2003. "Alternative Approaches for Elastic Analysis and Design of Steel Frames, I: Overview." *Journal of Structural Engineering*, American Society of Civil Engineers, Reston, VA, Vol. 130, No. 8.

Mathay, W.L. 1993. *Uncoated Weathering Steel Bridges*. Highway Structures Design Handbook, Volume 1, Chapter 9, available from the National Steel Bridge Alliance, Chicago, IL.

McDonald, G.S., and K.H. Frank. 2009. "The Fatigue Performance of Angle Cross-Frame Members in Bridges." Ferguson Structural Engineering Laboratory Report FSEL No: 09-1, University of Texas at Austin, Austin, TX, December 2009.

McGuire, W. 1968. *Steel Structures*. Prentice-Hall, Inc., Englewood Cliffs, NJ.

Mengelkoch, N.S., and J.A. Yura. 2002. "Single-Angle Compression Members Loaded Through One Leg." *Proceedings of the Annual Technical Session and Meeting*, Seattle, WA Structural Stability Research Council, University of Missouri, Rolla, MO, April 24-27.

Miller, D.K., and J. Ogborn. 1994. "Welding of Steel Bridges." Highway Structures Design Handbook, available from the National Steel Bridge Alliance, Chicago, IL, Volume 1, Chapter 15.

Miner, M.A. 1945. "Cumulative Damage in Fatigue." *Journal of Applied Mechanics*. Volume 12, September.

Miskoe, W.L. 1986. "The Centenary of Modern Welding, 1885-1985 – A Commemoration." *Welding Journal*, Volume 65, April.

Mueller, J.A., and B.T. Yen. 1968. "Girder Web Boundary Stresses and Fatigue." *WRC Bulletin No. 127*. January.

Munse, W. H. 1956. "Research on Bolted Connections." *Transactions*, American Society of Civil Engineers, New York, NY, No.121.

Munse, W.H., and E. Chesson, Jr. 1963. "Riveted and Bolted Joints: Net Section Design." *Journal of the Structural Division*, American Society of Civil Engineers, New York, NY, Vol. 83, No. ST2, February.

Munse, W.H., and L.H. Grover. 1964. "Fatigue of Welded Steel Structures." Welding Research Council, New York, NY.

Nagaraja Rao, N.R., M. Lohrmann, and L. Tall. 1966. "Effect of Strain Rate on the Yield Stress of Structural Steels," *Journal of Materials*, March.

NCHRP. 2012. "Guidelines for Analytical Methods and Construction Engineering of Curved and Skewed Steel Girder Bridges," NCHRP Report 725, Transportation Research Board, National Research Council, Washington, DC.

NHI. 1990. "Economic and Fatigue Resistant Steel Bridge Details – Participant Notebook." National Highway Institute Course No. 13049, Federal Highway Administration, Publication No. FHWA-1-11-90-043, June.

NHI. 2011. "Analysis and Design of Skewed and Curved Steel Bridges with LRFD – Reference Manual." National Highway Institute Course No. 130095, Federal Highway Administration, Publication No. FHWA-NHI-10-087, February.

NHI. 2011a. "Design Criteria for Arch and Cable Stayed Signature Bridges – Reference Manual." National Highway Institute Course No. 130096, Federal Highway Administration, Publication No. FHWA-NHI-11-023.

NHI. 2015. "Engineering for Structural Safety in Construction of Bridge Superstructures – Reference Manual." National Highway Institute Course No. 130102, Federal Highway Administration.

Nethercot, D.A., and N.S. Trahair. 1976. "Lateral Buckling Approximations for Elastic Beams." *The Structural Engineer*. Vol. 54, No. 6.

NSBA. 2014. "Skewed and Curved Steel I-Girder Bridge Fit." produced by a Fit Task Force, NSBA Technical Subcommittee (Chavel, B., D. Coletti, K. Frank. M. Grubb, W. McEleney, R. Medlock, and D. White), August 20.

Ocel, J. M. 2013. Guidelines for the Load and Resistance Factor Design and Rating of Welded, Riveted and Bolted Gusset-Plate Connections for Steel Bridges, NCHRP Web-Only Document 197, Transportation Research Board, National Research Council, Washington D.C.

Ollgaard, J.G., R.G. Slutter, and J.W. Fisher. 1971. "Shear Strength of Stud Connectors in Lightweight and Normal Weight Concrete." *AISC Engineering Journal*, American Institute of Steel Construction, Chicago, IL, Vol. 8, No. 2, April.

Ontario Ministry of Transportation. 1991. *Ontario Highway Bridge Design Code*. Quality and Standards Division, Structural Office, Toronto, Canada.

Owen, D.R.J., K.C. Rockey, and M. Skaloud. 1970. "Ultimate Load Behavior of Longitudinally Reinforced Webplates Subjected to Pure Bending." IABSE Publications, Vol. 30-1.

Polyzois, D., and K.H. Frank. 1986. "Effect of Overspray and Incomplete Masking of Faying Surfaces on the Slip Resistance of Bolted Connections." *AISC Engineering Journal*, American Institute of Steel Construction, Chicago, IL, Vol. 23, 2nd Qtr.

Rahal, K.N., and J.E. Harding. 1990. "Transversely Stiffened Girder Webs Subjected to Shear Loading – Part 1: Behaviour." *Proceedings of the Institution of Civil Engineers*, Part 2, 89, March.

RCSC (Research Council on Structural Connections). 1988. *Load and Resistance Factor Design Specification for Structural Joints Using ASTM A325 or A490 Bolts*. c/o American Institute of Steel Construction, Chicago, IL, June.

RCSC (Research Council on Structural Connections). 2014. *Specification for Structural Joints Using High-Strength Bolts*. c/o American Institute of Steel Construction, Chicago, IL, August 1.

Ricles, J.M., and J.A. Yura. 1983. “Strength of Double-Row Bolted Web Connections.” *Journal of the Structural Division*, American Society of Civil Engineers, New York, NY, Vol. 109, No. ST1, January.

Roberts, T.M. 1981. “Slender Plate Girders Subjected to Edge Loading.” *Proceedings, Institution of Civil Engineers*, Part 2, 71, London.

Roeder, C.W., and L. Eltvik. 1985. “An Experimental Evaluation of Autostress Design.” *Transportation Research Record 1044*, Transportation Research Board, National Research Council, Washington, D.C.

Roeder, C.W., K. Barth, and A. Bergman. 2002. “Improved Live Load Deflection Criteria for Steel Bridges.” Final Report for NCHRP Project 20-7[133], National Cooperative Highway Research Program, Transportation Research Board, Washington, D.C., November.

Roeder, C.W, D.E. Lehman, and R. Thody. 2009. "Composite Action in CFT Components and Connections," AISC, *Engineering Journal*, Vol. 46, No. 4, Chicago, IL, pgs 229-42.

Roeder, C.W., D.E. Lehman and E. Bishop. 2010. “Strength and Stiffness of Circular Concrete Filled Tubes," ASCE, *Journal of Structural Engineering*, Vol. 135, No. 12, pgs 1545-53, Reston, VA.

Roeder, C.W., and D.E. Lehman. 2012. "Initial Investigation of Reinforced Concrete Filled Tubes for use in Bridge Foundations," *Research Report WA-RD 776.1*, Washington Department of Transportation, Olympia, WA.

Rumpf, J.L., and J.W. Fisher. 1963. “Calibration of A 325 Bolts.” *Journal of the Structural Division*, American Society of Civil Engineers, Vol. 89, No. ST6, December.

Salmon, C.G., and J.E. Johnson. 1996. *Steel Structures – Design and Behavior*, Fourth Edition, HarperCollins College Publishers, New York, NY.

Schilling, C.G. 1967. “Web Crippling Tests on Hybrid Girders.” *Journal of the Structural Division*, American Society of Civil Engineers, New York, NY, Vol. 93, ST1, February.

Schilling, C.G. 1968. “Bending Behavior of Composite Hybrid Beams.” *Journal of the Structural Division*, American Society of Civil Engineers, New York, NY, Vol. 94, ST8, August.

Schilling, C.G., K.H. Klippstein, J.M. Barsom, and G.T. Blake. 1975. "Fatigue of Welded Steel Bridge Members Under Variable-Amplitude Loadings." Final Report – NCHRP Project 12-12, Transportation Research Board, Washington, D.C., August.

Schilling, C.G. 1986. "Exploratory Autostress Girder Designs." Project 188 Report, American Iron and Steel Institute, Washington, D.C.

Schilling, C.G. 1986a. "Fatigue." Chapter I/6. *Highway Structures Design Handbook*. Available from the National Steel Bridge Alliance, Chicago, IL, February.

Schilling, C.G. 1991. "Unified Autostress Method." *AISC Engineering Journal*, American Institute of Steel Construction, Chicago, IL, Vol. 28, No. 4.

Schilling, C.G. 1996. "Yield-Interaction Relationships for Curved I-Girders." *Journal of Bridge Engineering*, American Society of Civil Engineers, New York, NY, Vol. 1, No. 1, pp. 26-33.

Schilling, C.G., M.G. Barker, B.E. Dishongh, and B.A. Hartnagel. 1997. "Inelastic Design Procedures and Specifications." Final Report submitted to the American Iron and Steel Institute, Washington, D.C.

Seradj, H. 2010. "Weldability of ASTM A 1010 Steel." 8th International Conference on Short & Medium Span Bridges, Niagara Falls, NY, Canadian Society of Civil Engineering.

Shanley, F.R. 1946. "The Column Paradox." *Journal of the Aeronautical Sciences*, Volume 13, No. 12, December.

Sheikh-Ibrahim, F.I., and K.H. Frank. 1998. "The Ultimate Strength of Symmetric Beam Bolted Splices." *AISC Engineering Journal*, American Institute of Steel Construction, Chicago, IL, Vol. 35, No. 3, 3rd Qtr.

Sheikh-Ibrahim, F.I., and K.H. Frank. 2001. "The Ultimate Strength of Unsymmetric Beam Bolted Splices." *AISC Engineering Journal*, American Institute of Steel Construction, Vol. 38, No. 2, 2nd Qtr.

Sheikh-Ibrahim, F.I. 2002. "Design Method for Bolts in Bearing-Type Connections with Fillers." *AISC Engineering Journal*, American Institute of Steel Construction, Chicago, IL, Vol. 39, No. 4, 4th Qtr.

Sherman, D.R. 1976. "Tentative Criteria for Structural Applications of Steel Tubing and Pipe." American Iron and Steel Institute, Washington, D.C.

Slutter, R.G., and J.W. Fisher. 1966. "Fatigue Strength of Shear Connectors." *Highway Research Record No. 147*, Highway Research Board, Washington, D.C.

SSRC. 1979. "A Specification for the Design of Steel Concrete Composite Columns." Task Group 20, *AISC Engineering Journal*, American Institute of Steel Construction, Chicago, IL., Vol. 16, 4th Qtr.

SSRC (Structural Stability Research Council). 1998. *Guide to Stability Design for Metal Structures*. Fifth Edition, Galambos, T.V., ed., John Wiley and Sons, Inc., New York, NY.

SSRC (Structural Stability Research Council). 2010. *Guide to Stability Design Criteria for Metal Structures*, Sixth Edition, Ziemian, R.D. (ed.), John Wiley & Sons, Inc., Hoboken, NJ.

Stanway, G.S., J.C. Chapman, and P.J. Dowling. 1996. "A Design Method for Intermediate Web Stiffeners." *Proceedings of the Institution of Civil Engineers, Structures and Buildings*, 116, February.

Sterling, G.H. et al. 1965. "Calibration Tests of A 490 High Strength Bolts." *Journal of the Structural Division*, American Society of Civil Engineers, Vol. 91, No. ST5, October.

Stith, J., A. Schuh, J. Farris, B. Petruzzi, T. Helwig, E. Williamson, K. Frank, M. Englehardt, and H.J. Kim. 2010. "Guidance for Erection and Construction of Curved I-Girder Bridges." Report No. FHWA/TX-10/0-5574-1, Center for Transportation Research, University of Texas at Austin, Austin, TX, May. (software link: http://fsel.engr.utexas.edu/software/index.cfm)

Struik, J.H.A., A.O. Oyeledun, and J.W. Fisher. 1973. "Bolt Tension Control with a Direct Tension Indicator." *Engineering Journal,* American Institute of Steel Construction, Chicago, IL, Vol. 10, First Quarter.

Suwan, S., L. Manual, and K. Frank. 2003. "Statistical Analysis of Structural Plate Mechanical Properties". Ferguson Structural Engineering Laboratory Report No. 03-1, University of Texas at Austin, Austin, TX.

Thornton, C.H. 1973. "Quality Control in Design and Supervision Can Eliminate Lamellar Tearing." *AISC Engineering Journal*, American Institute of Steel Construction, Chicago, IL, Vol. 10, No. 4, 4th Qtr.

Tide, R.H.R. 1985. "Reasonable Column Design Equations." Proceedings of the Annual Technical Session and Meeting. Cleveland, OH, April 16-17, Structural Stability Research Council, University of Missouri, Rolla, MO.

Tide, R.H.R. 2001. “A Technical Note: Derivation of the LRFD Column Design Equations.” *AISC Engineering Journal*, American Institute of Steel Construction, Chicago, IL, Vol. 38, No. 3, 3rd Qtr.

Timoshenko, S.P., and J.M. Gere. 1961. *Theory of Elastic Stability*. McGraw-Hill, New York, NY.

Toprac, A.A., and R.A. Engler. 1961. “Plate Girders With High-Strength Steel Flanges and Carbon Steel Webs.” *Proceedings*, American Institute of Steel Construction, pp. 83-94.

Toprac, A.A., and M. Natarajan. 1971. “Fatigue Strength of Hybrid Plate Girders.” *Journal of the Structural Division*, American Society of Civil Engineers, New York, NY, Vol. 97, ST4, April.

Trahair, N.S., T. Usami, T., and T.V. Galambos. 1969. “Eccentrically Loaded Single-Angle Columns.” *Research Report No. 11*, Civil and Environmental Engineering Department, Washington University, St. Louis, MO.

Ugural, A.C., and S.K. Fenster. 1978. *Advanced Strength and Applied Elasticity*. Elsevier-North Holland Publishing Co., Inc., New York, NY.

United States Steel. 1978. *Steel/Concrete Composite Box-Girder Bridge: A Construction Manual*. available from the National Steel Bridge Alliance, Chicago, IL, December.

Usami, T., and T.V. Galambos. 1971. “Eccentrically Loaded Single-Angle Columns.” International Association for Bridge and Structural Engineering, Zurich, Switzerland.

Viest, I. M., R.S. Fountain, and R.C. Singleton. 1958. *Composite Construction in Steel and Concrete for Bridges and Buildings*. McGraw-Hill, New York.

Viest, I.M. 1960. “Review of Research on Composite Steel-Concrete Construction.” *Journal of the Structural Division*, American Society of Civil Engineers, Vol. 86, No. ST6, June 1960.

Vincent, G.S. 1969. “Tentative Criteria for Load Factor Design of Steel Highway Bridges.” *AISI Bulletin No. 15,* American Iron and Steel Institute, Washington, D.C., March.

Wattar, F., P. Albrecht, and A.H. Sahli. 1985. “End-Bolted Cover Plates.” *Journal of the Structural Division*, American Society of Civil Engineers, New York, NY, Vol. 3, No. 6, June.

White, D.W., J.A. Ramirez, and K.E. Barth. 1997. "Moment Rotation Relationships for Unified Autostress Design Procedures and Specifications." Final Report, Joint Transportation Research Program, Purdue University, West Lafayette, IN.

White, D.W., and K.E. Barth. 1998. "Strength and Ductility of Compact-Flange I Girders in Negative Bending." *Journal of Constructional Steel Research*, Vol. 45, No. 3.

White, D.W., A.H. Zureick, N. Phoawanich, and S.K. Jung. 2001. "Development of Unified Equations for Design of Curved and Straight Steel Bridge I-Girders." Final Report to the American Iron and Steel Institute Transportation and Infrastructure Committee, Professional Service Industries, Inc. and the Federal Highway Administration. School of Civil and Environmental Engineering, Georgia Institute of Technology, Atlanta, GA.

White, D.W., and S.-K Jung. 2003. "Simplified Lateral-Torsional Buckling Equations for Singly-Symmetric I-Section Members." Structural Engineering, Mechanics and Materials Report No. 24b, School of Civil and Environmental Engineering, Georgia Institute of Technology, Atlanta, GA.

White, D.W. 2004. "Unified Flexural Resistance Equations for Stability Design of I-Section Members – Overview." Structural Engineering, Mechanics and Materials Report No. 24a, School of Civil and Environmental Engineering, Georgia Institute of Technology, Atlanta, GA.

White, D.W., M. Barker, and A. Azizinamini. 2004. "Shear Strength and Moment Shear Interaction in Transversely-Stiffened Steel I-Girders." Structural Engineering, Mechanics and Materials Report No. 27, School of Civil and Environmental Engineering, Georgia Institute of Technology, Atlanta, GA.

White, D.W., and M. Barker. 2004. "Shear Resistance of Transversely Stiffened Steel I-Girders." Structural Engineering, Mechanics and Materials Report No. 26, School of Civil and Environmental Engineering, Georgia Institute of Technology, Atlanta, GA.

White, D.W., and M.A. Grubb. 2005. "Unified Resistance Equations for Design of Curved and Tangent Steel Bridge I-Girders." *Proceedings of the Transportation Research Board Sixth International Bridge Engineering Conference*, Boston, MA, July.

White, D.W. 2012. "Steel Bridge Design Handbook: Structural Behavior of Steel." Publication No. FHWA-IF-12-052 – Vol. 4, U.S. Department of Transportation, Federal Highway Administration, Washington, DC, November.

Whitmore, R. E. 1952. "Experimental Investigation of Stresses in Gusset Plates," *Bulletin 16*, University of Tennessee, Knoxville, TN.

Wilson, W.M., and F.P. Thomas. 1938. “Fatigue Tests on Riveted Joints.” *Bulletin 302*, University of Illinois, Engineering Experiment Station, Urbana, IL.

Wilson, A.D. 2002. “Availability and Future Development of High Performance Steel.” Proceedings of the 2002 NABRO/FHWA HPS Conference, Salt Lake City, UT.

Wittry, D.M. 1993. “An Analytical Study of the Ductility of Steel Concrete Composite Sections.” Masters thesis. University of Texas, Austin, TX. December.

Woolcock, S.T., and S. Kitipornchai. 1986. “Design of Single-Angle Web Struts in Trusses.” *Journal of Structural Engineering*, American Society of Civil Engineers, New York, NY, Vol. 112, No. ST6, June.

Wright, R.N., and S.R. Abdel-Samad. 1968. “BEF Analogy for Analysis of Box Girders.” *Journal of the Structural Division*, ASCE, Vol. 94, No. ST7, pp. 1719-1743.

Wright, R.N., and W.H. Walker. 1971. “Criteria for Deflection of Steel Bridges.” *AISI Bulletin No. 19*, American Iron and Steel Institute, Washington, D.C., November.

Wright, W.J. 1997. “High Performance Steel: Research to Practice.” *Public Roads,* Spring, Vol. 60, No. 4.

Wright, W.J., J.W. Fisher, and E.J. Kaufmann. 2003. “Failure Analysis of the Hoan Bridge Fractures.” *Recent Developments in Bridge Engineering*, Mahmoud ed. Swets & Zeitlinger, Lisse.

Wright, W.J. 2012. “Steel Bridge Design Handbook: Bridge Steels and Their Mechanical Properties.” Publication No. FHWA-IF-12-052 – Vol. 1, U.S. Department of Transportation, Federal Highway Administration, Washington, DC, November.

Yakel, A., and A. Azizinamini. 2005. “Improved Moment Strength Prediction of Composite Steel Plate Girders in Positive Bending.” *Journal of Bridge Engineering*, American Society of Civil Engineers, Reston, VA, January/February.

Yakel, A., and A. Azizinamini. 2014. "Field Application Case Studies and Long Term Monitoring of Bridges Utilizing the Simple for Dead – Continuous for Live Bridge System." *AISC Engineering Journal*, 3rd Quarter.

Yamamoto, et al. 1998. “Buckling Strengths of Gusseted Truss Joints,” *Journal of Structural Engineering*, American Society of Civil Engineers, Reston, VA, Vol. 114.

Yang, C.H., L.S. Beedle, and B.G. Johnston. 1952. “Residual Stress and the Yield Strength of Steel Beams.” *Welding Journal*, April.

Yen, B.T., and J.A. Mueller. 1966. “Fatigue Tests of Large Size Welded Plate Girders.” *WRC Bulletin No. 118*, November.

Yen, B.T., T. Huang, and D.V. VanHorn. 1995. “Field Testing of a Steel Bridge and a Prestressed Concrete Bridge.” Research Report No. 86-05, Final Report, Vol. II, Pennsylvania Department of Transportation Office of Research and Special Studies, Fritz Engineering Laboratory Report No. 519.2, Lehigh University, Bethlehem, PA, May.

Yoo, C.H., and J.S. Davidson. 1997. “Yield Interaction Equations for Nominal Bending Strength of Curved I-Girders.” *Journal of Bridge Engineering*, American Society of Civil Engineers, New York, NY, Vol. 2, No. 2, pp. 37-44.

Yura, J.A., K.H. Frank, and L. Cayes. 1981. “Bolted Friction Connections with Weathering Steel.” *Journal of the Structural Division*, American Society of Civil Engineers, Vol. 107, No. ST11, November.

Yura, J.A., M.A. Hansen, and K.H. Frank. 1982. “Bolted Splice Connections with Undeveloped Fillers.” *Journal of the Structural Division*, American Society of Civil Engineers, New York, NY, Vol. 108, No. ST12, December.

Yura, J.A., and K.H. Frank. 1985. “Testing Method to Determine Slip Coefficient for Coatings Used in Bolted Joints.” *AISC Engineering Journal*, American Institute of Steel Construction, Chicago, IL, Vol. 22, No. 3, 3rd Qtr.

Yura, J. A. 2001. “Fundamentals of Beam Bracing”, *AISC Engineering Journal*, American Institute of Steel Construction, Chicago, IL, Vol. 38, No.1, pp.11-26.

Yura, J.A., T. Helwig, R. Herman, and C. Zhou. 2008. “Global Lateral Buckling of I-Shaped Girder Systems,” *Journal of Structural Engineering*, ASCE, 134(9), 1487-1494.

Yura, J.A., and T.A. Helwig, 2010. “Buckling of Beams with Inflection Points”, *Proceedings*, 2010 Annual Stability Conference, Structural Stability Research Council, pp 245--261, AISC North American Steel Construction Conference. Orlando FL, May 12-15, 2010.

Yura, J.A., and T.A. Helwig. 2012. “Steel Bridge Design Handbook: Bracing System Design.” Publication No. FHWA-IF-12-052 – Vol. 13, U.S. Department of Transportation, Federal Highway Administration, Washington, DC, November.

Zandonini, R. 1985. “Stability of Compact Built-Up Struts: Experimental Investigation and Numerical Simulation.” *Construczione Metalliche*, Milan, Italy, No. 4.

Chapter 7
Decks and Deck Systems

Section 7.1 Introduction

A bridge deck provides a smooth and safe riding surface for the traffic utilizing the bridge, and it transfers the live load and dead load of the deck to the underlying bridge components. During deck design, the engineer must consider the most suitable deck material, overhang design and construction, formwork, and deck staging.

Section 7.2 General Design Requirements

The most common materials used for decks are concrete, metal, and wood. However, several general design considerations are common to all deck materials.

7.2.1 Composite Action

AASHTO LRFD Bridge Design Specifications (*AASHTO LRFD*) Article 9.4.1 specifies that all decks, with the exception of wood and open grid decks, must be made composite with the supporting components, unless there are compelling reasons not to do so. Composite action is beneficial for several reasons. It enhances the stiffness of the superstructure, it improves the economy of the bridge, and it prevents vertical separation between the deck and its supporting components.

Composite action is made possible by providing shear connectors at the interface between the deck and its supporting components. Shear connectors can be in the form of studs or angles, and they must be designed for both strength and fatigue limit states. Shear connectors must be designed for force effects computed on the basis of full composite action, regardless of whether composite action was considered in the design and proportioning of the primary members. This requirement ensures the integrity of the connection under all possible load cases.

7.2.2 Deck Drainage

Since a primary function of the deck is to provide a safe riding surface, deck drainage must be considered during the deck design. Computations can be performed to determine the allowable length of the bridge without scuppers. This

length is a function of the roughness coefficient of the deck surface, the deck cross slope, the grade as a function of the location on the bridge, the design speed, the rate of rainfall, and the width of deck to be drained. If this computation shows that deck drainage is required, then scuppers or other forms of drainage are designed and detailed to meet the drainage requirements of the bridge.

Based on past experience, the deck joint regions are particularly affected by poor deck drainage and are commonly susceptible to deterioration from excessive water. Therefore, special care should be given to the design and detailing of deck drainage

7.2.3 Deck Appurtenances

To safely direct traffic on the bridge, appurtenances are provided along the edges of the bridge. They are also sometimes provided between directions of traffic. Deck appurtenances are usually concrete, and they can be provided in the form of curbs, parapets, barriers, and dividers. Deck appurtenances should generally be made structurally continuous. Since the deck appurtenances may be damaged due to vehicular collision, their structural contribution should not be considered for strength or extreme event limit states. However, their structural contribution may be considered for service and fatigue limit states.

7.2.4 Limit State Requirements

For decks designed using the traditional design method, the deck must be designed to satisfy requirements for service, strength, fatigue, and extreme event limit states. For the service limit state, deflections caused by live load plus dynamic load allowance must be limited as specified in *AASHTO LRFD* Article 9.5.2. For the strength limit state, the deck must be designed to meet the structural requirements of *AASHTO LRFD* Sections 5, 6, 7, and 8 pertaining to the deck type and material selected. For the fatigue limit state, design requirements are provided for metal grid, filled grid, partially filled grid, steel grid, and steel orthotropic decks, but there are no fatigue requirements for concrete decks and wood decks. For the extreme event limit state, force effects transmitted by traffic and by combination railings must be considered during deck design.

Section 7.3 Concrete Deck Slabs

7.3.1 General

Reinforced concrete is the most common material used for deck design. The primary advantages of concrete decks are their strength and their ability to provide a smooth riding surface. In recent years, automation of deck concrete placement and finishing has improved the cost-effectiveness of this deck type. However, cast-in-

place concrete decks can experience excessive differential shrinkage with the supporting beams, and they can lead to slow construction.

Recent research into concrete mixes and curing methods has enhanced performance characteristics such as freeze-thaw resistance, high abrasion resistance, and low shrinkage. To improve the durability of concrete decks against environmental factors, additives and wearing surfaces are frequently used. Additives can potentially increase the life and lower the long-term costs of concrete bridge decks by enhancing resistance to water, corrosion, and deicing salt.

Concrete decks can be designed using several methods, including the traditional design method and the empirical design method. The following sections provide background information, equations, and design examples for each of these two methods.

7.3.1.1 Concrete Deck Reinforcement

Concrete deck slabs and appurtenances are required to be reinforced. Typically, concrete is reinforced with mild steel reinforcement bars. These bars should conform to the requirements of ASTM A615 or ASTM A706 which specify a yield strength of 60 ksi and a modulus of elasticity of 29,000 ksi.

Mild steel bars are susceptible to extremely corrosive environments due to the presence of deicing salts or marine environments. Since steel reinforcement degradation is the main cause of poor deck performance, states have taken steps to mitigate this deterioration. Many states require the application of an epoxy coating to the reinforcement bars, while other states have begun to adopt galvanizing the bars as a corrosion inhibitor. Stainless steel reinforcement manufactured to ASTM A995 has been used in several reinforced concrete decks because of their enhanced corrosion resistance. Some agencies may use non-metallic reinforcement. Other coating systems may also be used by some agencies for corrosion protection. Furthermore, some agencies allow the use of uncoated bars but require an increased concrete cover. The designer should consult the agency's standards and specifications to determine the preferred method of corrosion resistance.

7.3.1.2 Minimum Depth and Cover

The minimum concrete deck slab thickness is generally 7 inches, unless otherwise specified by the Owner. Minimum concrete cover is specified in *AASHTO LRFD* Article 5.12.3. Minimum cover requirements were determined from traditional concrete mixes and the absence of a protective reinforcement coating. A combination of special mix design, protective coatings, and environment can be considered to reduce the cover requirements per the Owner's specifications.

7.3.1.3 Skewed Decks

Highly skewed decks are subject to extensive cracking if inadequately reinforced. *AASHTO LRFD* Article 9.7.1.3 states that if the angle of skew does not exceed 25°, the primary reinforcement can be placed parallel to the skew angle; otherwise, the primary reinforcement needs to be placed perpendicular to the main supporting components. Heavily skewed reinforcement may result in the absence of substantial reinforcement acting in the direction of principal flexural stresses, as shown in Figure 7.3.1.3-1. The acute corners are often unreinforced because of the orthogonal bars lacking sufficient length to fully develop. The designer should consult the Owner or agency for various detailing techniques for highly skewed bridges.

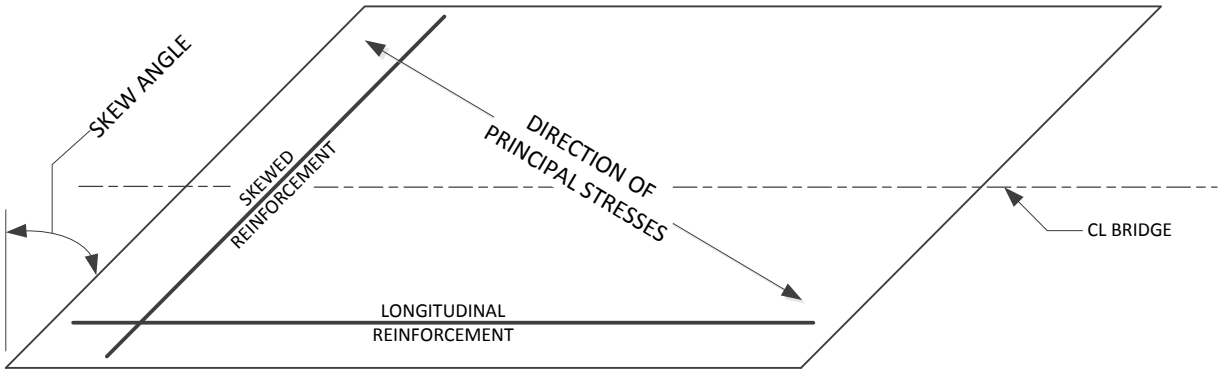

Figure 7.3.1.3-1 Reinforcement Layout for a Highly Skewed Deck

7.3.1.4 Edge Support

Edge supports must be provided along the edges of the deck, unless the deck is designed to support wheel loads in extreme positions with respect to its edges. The edge support may be either an edge beam or an integral part of the deck, such as a structurally continuous barrier. Expansion joint hardware may be considered to be a structural element of the edge support if it is integrated with the deck.

7.3.1.5 Deck Haunches

The deck haunch is typically the area between the girder and the bottom of the concrete deck and is formed and placed with the concrete deck. In the case of steel girder bridges, the haunch is usually defined as the distance from the top of the girder web to the bottom of the concrete deck. For concrete girder bridges, the haunch is the distance between the top of the girder and the bottom of the deck. When setting the haunch depth, it is important to consider all variations in the flange thicknesses, deck cross slope, and forming method. The haunch depth may need to

be adjusted in the field due to girder fabrication and erection tolerances. The haunch width is typically set as the same width as the top flange of the girder but can vary depending on the deck forming system.

Typically, haunches do not need shear reinforcement unless they are over a certain depth. The maximum depth that does not require shear reinforcement varies from state to state but is typically in the range of 3 to 6 inches. If the shear studs do not penetrate more than 2 inches into the deck, the haunch needs shear reinforcement to adequately allow the load to develop in the deck.

7.3.2 Traditional Design Method

7.3.2.1 General

The traditional design method of deck design is based on flexure and has been included in many previous editions of AASHTO's bridge specifications. The reinforcing steel normal to the supporting girders is considered the primary reinforcement and is computed based on the design moments. The reinforcing steel in the other direction is distribution reinforcement and is computed based on a specified percentage of the primary reinforcement area.

7.3.2.2 Equivalent Strip Method of Analysis

The Equivalent Strip Method is based on the flexure of the deck in the transverse direction. This method applies to decks at least 7 inches thick, meet minimum concrete cover requirements and have four layers of reinforcement; 2 in each direction on the top and bottom. Truck axle loads are assumed to be supported by a transverse strip of deck which is treated as a continuous beam with the girders acting as pinned supports at their centerlines.

7.3.2.3 Other Methods of Analysis

Refined methods of analysis are permitted according to *AASHTO LRFD* Article 9.6.1. For various limit states specified in *AASHTO LRFD* Article 9.5, approximate elastic methods of analysis specified in *AASHTO LRFD* Article 4.6.2.1 or refined methods specified in *AASHTO LRFD* Article 4.6.3.2 may be used to analyze a reinforced concrete deck slab. Refined methods include finite element analysis, grid analysis, or orthotropic plate theory. Also, local moments in the deck slab due to wheel loads can be calculated through the use of Homberg (1968) or Pucher (1964) influence surfaces, a series of contour plots of influence surfaces for various plates and loading geometries. Homberg or Pucher surfaces are typically used for segmentally constructed concrete bridges.

7.3.2.4 Primary Reinforcement Requirements

The design of the primary deck reinforcement by the traditional design method involves the following steps:

1. Obtain design criteria.
2. Determine minimum slab thickness.
3. Determine minimum overhang thickness.
4. Select slab and overhang thickness.
5. Compute dead load effects.
6. Compute live load effects.
7. Compute factored positive and negative design moments.
8. Design for positive flexure in deck.
9. Check for positive flexure cracking under service limit state.
10. Design for negative flexure in deck.
11. Check for negative flexure cracking under service limit state.

These design steps are presented and illustrated through the following design example.

1. Obtain design criteria

The design requirements for this deck design example are as follows:

Girder spacing = 9.75 feet
Number of girders = 5
Deck top cover = 2.5 inches (*AASHTO LRFD* Table 5.12.3-1)
Deck bottom cover = 1 inch (*AASHTO LRFD* Table 5.12.3-1)
Deck reinforced concrete unit weight = 150 pcf (*AASHTO LRFD* Article 3.5.1)
Deck concrete strength, f'_c = 4.0 ksi (*AASHTO LRFD* Article 5.4.2.1)
Reinforcement strength, f_y = 60 ksi (*AASHTO LRFD* Article 5.4.3)
Future wearing surface unit weight = 140 pcf (*AASHTO LRFD* Table 3.5.1-1)

The superstructure cross section is presented in Figure 7.3.2.4-1.

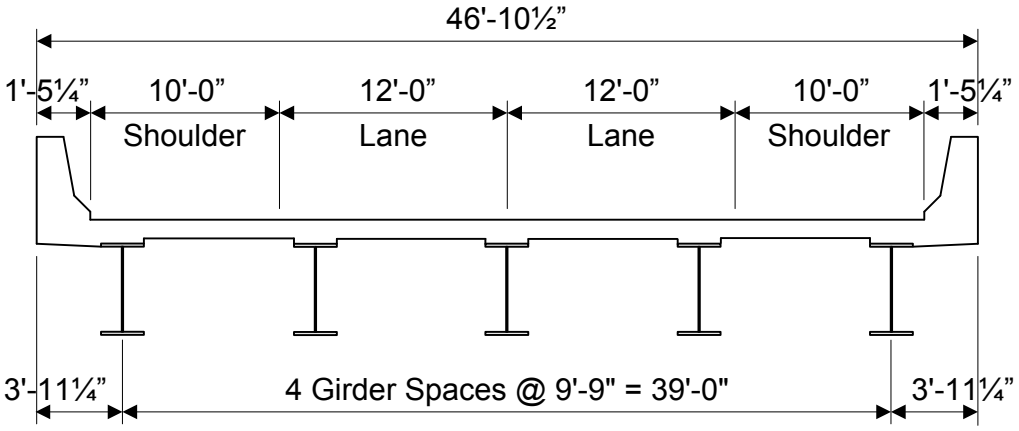

Figure 7.3.2.4-1 Superstructure Cross Section for Design Example

It should be noted that the ratio between the overhang and the girder spacing in this design example is as follows:

$$\frac{\text{Overhang}}{\text{Girder Spacing}} = \frac{3' - 11\ \ 1/4''}{9' - 9''} = 0.40$$

The overhang width is generally determined such that the moments and shears in the exterior girder are similar to those in the interior girder. In addition, the overhang is set such that the positive and negative moments in the deck slab are balanced. A common rule of thumb is to make the overhang approximately 30% to 50% of the girder spacing.

2. Determine minimum slab thickness

Based on *AASHTO LRFD* Article 9.7.1.1, the concrete deck thickness cannot be less than 7.0 inches, excluding any provision for grinding, grooving, and sacrificial surface.

3. Determine minimum overhang thickness

Similarly, based on *AASHTO LRFD* Article 13.7.3.1.2, the deck overhang thickness for concrete deck overhangs supporting concrete parapets or barriers cannot be less than 8.0 inches.

4. Select slab and overhang thickness

After the minimum slab and overhang thicknesses are determined, they can be increased as needed based on client standards and design computations. For this design example, an 8.5 inch deck thickness and a 9.0 inch overhang thickness will be used.

5. Compute dead load effects

The dead load moments in the deck must be computed, generally using structural analysis software. For this design example, an analysis produces the dead load moments presented in Table 7.3.2.4-1. These design moments are based on a 1-foot strip running across the width of the deck.

Table 7.3.2.4-1 Unfactored Dead Load Moments (K-ft/ft)

Dead Load	Bay	Location in Bay										
		0.0	0.1	0.2	0.3	0.4	0.5	0.6	0.7	0.8	0.9	1.0
Slab	Bay 1	-0.74	-0.33	-0.01	0.22	0.36	0.41	0.37	0.24	0.01	-0.30	-0.71
	Bay 2	-0.71	-0.30	0.02	0.24	0.38	0.42	0.38	0.24	0.01	-0.31	-0.72
	Bay 3	-0.72	-0.31	0.01	0.24	0.38	0.42	0.38	0.24	0.02	-0.30	-0.71
	Bay 4	-0.71	-0.30	0.01	0.24	0.37	0.41	0.36	0.22	-0.01	-0.33	-0.74
Barrier	Bay 1	-1.66	-1.45	-1.24	-1.03	-0.82	-0.61	-0.40	-0.19	0.02	0.22	0.43
	Bay 2	0.47	0.40	0.33	0.26	0.19	0.12	0.05	-0.02	-0.09	-0.16	-0.23
	Bay 3	-0.23	-0.16	-0.09	-0.02	0.05	0.12	0.19	0.26	0.33	0.40	0.47
	Bay 4	0.43	0.22	0.02	-0.19	-0.40	-0.61	-0.82	-1.03	-1.24	-1.45	-1.66
FWS	Bay 1	-0.06	0.04	0.11	0.15	0.17	0.17	0.14	0.08	0.00	-0.11	-0.24
	Bay 2	-0.24	-0.12	-0.02	0.05	0.09	0.11	0.10	0.07	0.01	-0.07	-0.18
	Bay 3	-0.18	-0.07	0.01	0.07	0.10	0.11	0.09	0.05	-0.02	-0.12	-0.24
	Bay 4	-0.24	-0.11	0.00	0.08	0.14	0.17	0.17	0.15	0.11	0.04	-0.06

The controlling dead load moments from Table 7.3.2.4-1 are presented in Table 7.3.2.4-2.

Table 7.3.2.4-2 Controlling Dead Load Moments

Dead Load	Controlling Positive Moment	Controlling Negative Moment
DC_1 (slab)	0.42 K-ft/ft	-0.74 K-ft/ft
DC_2 (barrier)	0.47 K-ft/ft	-1.66 K-ft/ft
DW (future wearing surface)	0.17 K-ft/ft	-0.24 K-ft/ft

It is assumed for the sake of simplicity that all controlling positive moments are coincident and all controlling negative moments are also coincident.

6. Compute live load effects

Similarly, the live load moments in the deck must also be computed. Again, an analysis program is frequently used to compute the live load moments. These design moments are based on the following live load design requirements:

- Minimum distance from the center of the design vehicle wheel to the inside face of the barrier = 1 foot (*AASHTO LRFD* Article 3.6.1.3.1)
- Dynamic load allowance, IM = 0.33 (*AASHTO LRFD* Table 3.6.2.1-1)
- Multiple presence factor, m, with one lane loaded = 1.20 (*AASHTO LRFD* Table 3.6.1.1.2-1)
- Multiple presence factor, m, with two lanes loaded = 1.00 (*AASHTO LRFD* Table 3.6.1.1.2-1)
- Multiple presence factor, m, with three lanes loaded = 0.85 (*AASHTO LRFD* Table 3.6.1.1.2-1)

The controlling live load moments for this design example are presented in Table 7.3.2.4-3. Multiple presence factors are included in the values in Table 7.3.2.4-3, but dynamic load allowance is excluded.

Table 7.3.2.4-3 Controlling Live Load Moments

Live Load	Controlling Positive Moment	Controlling Negative Moment
One truck (with m = 1.20)	36.76 K-ft	-28.51 K-ft
Two trucks (with m = 1.00)	26.46 K-ft	-29.40 K-ft

Using the values presented in Table 7.3.2.4-3, the maximum controlling positive moment is 36.76 K-ft, which is based on one truck and an m value of 1.20. The maximum controlling negative moment is -29.40 K-ft, which is based on two trucks and an m value of 1.00.

The dead load moments in Table 7.3.2.4-1 and Table 7.3.2.4-2 are in units of K-ft/ft, while the live load moments in Table 7.3.2.4-3 are in units of K-ft. To compute the live load moments in units of K-ft/ft, the values in Table 7.3.2.4-3 must be divided by an equivalent strip width. Based on *AASHTO LRFD* Table 4.6.2.1.3-1, the equivalent strip widths are presented in Figure 7.3.2.4-2.

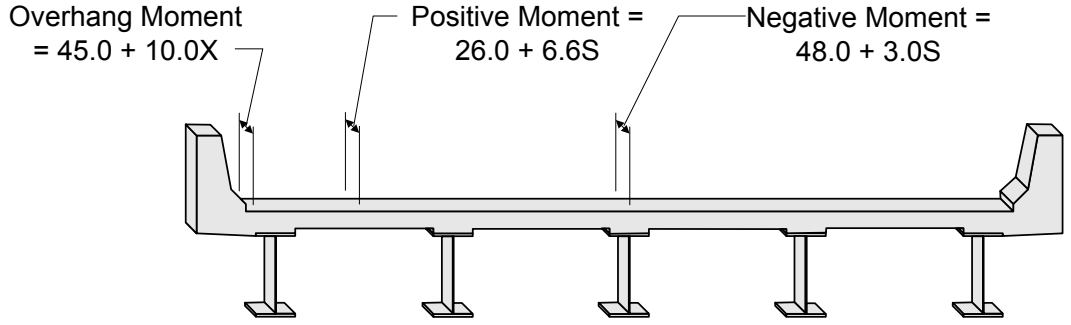

Figure 7.3.2.4-2 Equivalent Strip Widths

In Figure 7.3.2.4-2, X represents the distance from the load to the point of support and S represents the spacing of the supporting components, each measured in units of feet. The equivalent strip width is then computed in units of inches.

For negative moment, the live load moment is based on the distance from the centerline of the girder to the design section for negative moment. The design section for negative moment is as shown in Figure 7.3.2.4-3.

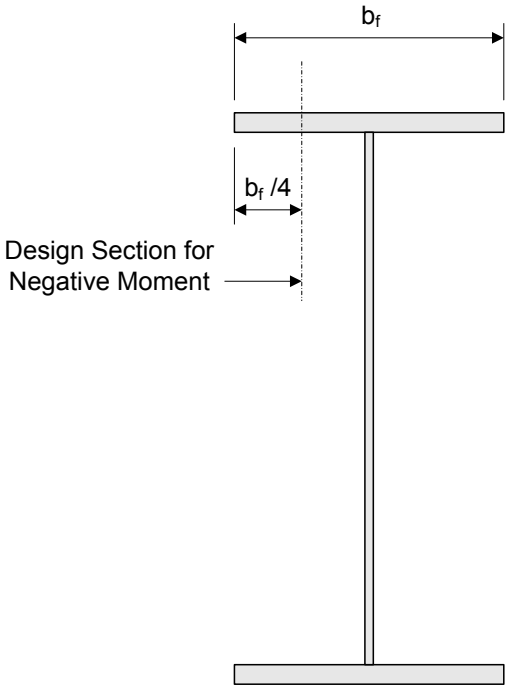

Figure 7.3.2.4-3 Design Section for Negative Moment

Assuming a top flange width of 12 inches, the design section for negative moment is 3 inches from the centerline of the girder. Therefore, for this design example, X and S can be computed as follows:

$$X = 2.25 \text{ ft} - 1.0 \text{ ft} = 1.25 \text{ ft} \qquad \text{and} \qquad S = 9.75 \text{ ft}$$

For positive moment, the equivalent strip width and the resulting live load plus dynamic load allowance moment are computed as follows:

$$\text{Equivalent Strip Width} = 26.0 + 6.6S = 26.0 + 6.6(9.75) = 90.35 \text{ inches} = 7.53 \text{ ft}$$

$$M_{LL+I} = \frac{1.33(36.76 \text{ K} - \text{ft})}{7.53 \text{ ft}} = 6.49 \frac{\text{K} - \text{ft}}{\text{ft}}$$

For negative moment, the equivalent strip width and the resulting live load plus dynamic load allowance moment are computed as follows:

$$\text{Equivalent Strip Width} = 48.0 + 3.0\text{S} = 48.0 + 3.0(9.75) = 77.25 \text{ inches} = 6.44 \text{ ft}$$

$$M_{LL+I} = \frac{1.33(-29.40 \text{ K} - \text{ft})}{6.44 \text{ ft}} = -6.07 \frac{\text{K} - \text{ft}}{\text{ft}}$$

Similarly, for the overhang moment, the equivalent strip width is computed as follows:

$$\text{Equivalent Strip Width} = 45.0 + 10.0\text{X} = 45.0 + 10.0(1.25) = 57.5 \text{ inches} = 4.79 \text{ ft}$$

The overhang moment will be computed in a subsequent section of this chapter.

*AASHTO Deck Slab Design Table (*AASHTO LRFD *Appendix A4):*

The above live load moment computations are based on a finite element analysis program. As an alternative or as an independent check, AASHTO provides a deck slab design table in *AASHTO LRFD* Appendix A4. This table may be used to determine the live load design moments for different girder arrangements. The table is based on a set of assumptions and limitations which were used to develop the table and which are presented in *AASHTO LRFD* Appendix A4. These assumptions include the following:

- The moments are computed using the equivalent strip method.
- The moments apply to concrete slabs supported on parallel girders.
- Multiple presence factors are included in the tabulated live load values.
- Dynamic load allowance is included in the tabulated live load values.
- The moments are applicable for decks supported by at least three girders and not having a width of less than 14 feet between exterior girder centerlines.
- The moments do not apply to overhangs.

For positive moment, the tabulated live load plus dynamic load allowance moment for a girder spacing, S, of 9'-9" is 6.74 K-ft/ft. This value is approximately 4% greater than the value of 6.49 K-ft/ft computed above using an analysis program.

For negative moment, the tabulated live load plus dynamic load allowance moment for a girder spacing, S, of 9'-9" and for a distance of 3 inches from the centerline of girder to the design section for negative moment is -6.65 K-ft/ft. This value is approximately 10% greater than the value of -6.07 K-ft/ft computed above using an analysis program.

It can be seen that the values from *AASHTO LRFD* Table A4-1 are slightly greater than the live load values computed using a finite element analysis program. Generally, using the values presented in *AASHTO LRFD* Table A4-1 may be beneficial due to time savings by not having to develop a finite element model. However, since the time was spent to develop the finite element model for this deck design, the values obtained from the analysis program will be used for this design example.

Based on *AASHTO LRFD* Articles 5.5.3.1 and 9.5.3, fatigue does not need to be investigated for concrete deck design in multi-girder applications.

7. Compute factored positive and negative design moments

After the dead load and live load moments have been computed, they must be factored and combined. The load factors for the Strength I load combination, as presented in *AASHTO LRFD* Tables 3.4.1-1 and 3.4.1-2, are as shown in Table 7.3.2.4-4.

Table 7.3.2.4-4 Load Factors for Strength I Load Combination

Load	Maximum Load Factor	Minimum Load Factor
DC_1 (slab)	1.25	0.90
DC_2 (barrier)	1.25	0.90
DW (future wearing surface)	1.50	0.65
LL (live load)	1.75	1.75
IM (dynamic load allowance)	1.75	1.75

Therefore, the maximum factored positive moment can be computed as follows:

$$M_{pos} = 1.25\left(0.42\,\frac{K-ft}{ft}\right) + 1.25\left(0.47\,\frac{K-ft}{ft}\right) + 1.50\left(0.17\,\frac{K-ft}{ft}\right) + 1.75\left(6.49\,\frac{K\text{-}ft}{ft}\right) = 12.73\,\frac{K-ft}{ft}$$

Similarly, the maximum factored negative moment can be computed as follows:

$$M_{neg} = 1.25\left(-0.74\,\frac{K-ft}{ft}\right) + 1.25\left(-1.66\,\frac{K-ft}{ft}\right) + 1.50\left(-0.24\,\frac{K-ft}{ft}\right) + 1.75\left(-6.07\,\frac{k\text{-}ft}{ft}\right) = -13.98\,\frac{K-ft}{ft}$$

8. Design for positive flexure in deck

Since positive flexure produces compression in the top fiber and tension in the bottom fiber, sufficient reinforcement must be provided in the bottom layer of the deck to resist the factored positive moment. The first step in designing the positive flexure reinforcement is to assume a bar size. From the bar size, the effective depth can be computed, then the required reinforcement area, and then the required reinforcement spacing.

For this design example, assume the use of #5 bars to resist positive flexure in the deck. Therefore, the effective depth is computed as follows:

$$d_s = \text{Slab Thickness} - \text{Bottom Cover} - \frac{\text{Bar Diameter}}{2} - \text{Top Integral Wearing Surface}$$

$$= 8.5 \text{ inches} - 1.0 \text{ inches} - \frac{0.625 \text{ inches}}{2} - 0.5 \text{ inches} = 6.69 \text{ inches}$$

Then the required reinforcement area is computed using the basic reinforcing steel equations that can be found and derived in most reinforced concrete textbooks.

$$M_r = \phi M_n = \phi A_s F_y \left(d_s - \frac{a}{2} \right) \qquad \text{Equation 7.3.2.4-1}$$

where:

$$a = \frac{A_s F_y}{0.85 f'_c \, b} \qquad \text{Equation 7.3.2.4-2}$$

For this design example:

$$a = \frac{A_s F_y}{0.85 f'_c \, b} = \frac{A_s (60 \text{ ksi})}{0.85(4.0 \text{ ksi}) \left(\frac{12 \text{ inches}}{1 \text{ ft}} \right)} = \left(1.47 \frac{\text{ft}}{\text{inch}} \right) A_s$$

$$M_r = \phi M_n = \phi A_s F_y \left(d_s - \frac{a}{2} \right) = 0.90 A_s (60 \text{ ksi}) \left[6.69 \text{ inches} - \frac{\left(1.47 \frac{\text{ft}}{\text{inch}} \right) A_s}{2} \right]$$

Setting M_r equal to the factored design moment of 12.73 K-ft/ft produces the following required reinforcement area:

$$A_s = 0.43\,\frac{\text{inches}^2}{\text{ft}}$$

The required reinforcement spacing can then be computed as follows:

$$\text{Required Spacing} = \frac{0.31\,\frac{\text{inches}^2}{\text{bar}}}{0.43\,\frac{\text{inches}^2}{\text{ft}}} = 0.72\text{ ft} = 8.7\text{ inches}$$

Therefore, use #5 at 8 inches for the positive flexural reinforcement. Computing the provided flexural resistance serves as an independent check:

$$A_s = \frac{0.31\,\text{inches}^2}{(8\text{ inches})\left(\frac{1\,\text{ft}}{12\text{ inches}}\right)} = 0.465\,\frac{\text{inches}^2}{\text{ft}}$$

$$a = \frac{\left(0.465\,\frac{\text{inches}^2}{\text{ft}}\right)(60\text{ ksi})}{0.85(4.0\text{ ksi})\left(\frac{12\text{ inches}}{1\,\text{ft}}\right)} = 0.684\text{ inches}$$

$$M_r = 0.90\left(0.465\,\frac{\text{inches}^2}{\text{ft}}\right)(60\text{ ksi})\left[6.69\text{ inches} - \frac{0.684\text{ inches}}{2}\right]$$

$$= 13.28\,\frac{\text{K}-\text{ft}}{\text{ft}} > 12.21\,\frac{\text{K}-\text{ft}}{\text{ft}} \qquad \therefore \text{OK}$$

9. <u>Check for positive flexure cracking under service limit state</u>

After the required reinforcing steel has been computed, the control of cracking by distribution of the reinforcement must be checked in accordance with *AASHTO LRFD* Article 5.7.3.4. The basic equations for this design check are as follows:

$$s \le \frac{700\gamma_e}{\beta_s f_{ss}} - 2d_c \qquad \text{Equation 7.3.2.4-3}$$

AASHTO LRFD Equation 5.7.3.4-1

$$\beta_s = 1 + \frac{d_c}{0.7(h - d_c)}$$ Equation 7.3.2.4-4

where:

γ_e = exposure factor
d_c = thickness of the concrete cover measured from the extreme tension fiber to the center of the closest flexural reinforcement, in inches
f_{ss} = tensile stress in steel reinforcement at the service limit state, in ksi
h = overall thickness of the component, in inches

These equations are based on a physical crack model rather than the statistically-based model used in previous editions of the AASHTO specifications.

Since the Class 2 exposure condition applies to concrete decks, the exposure factor equals 0.75. The values of d_c and h are illustrated in Figure 7.3.2.4-4.

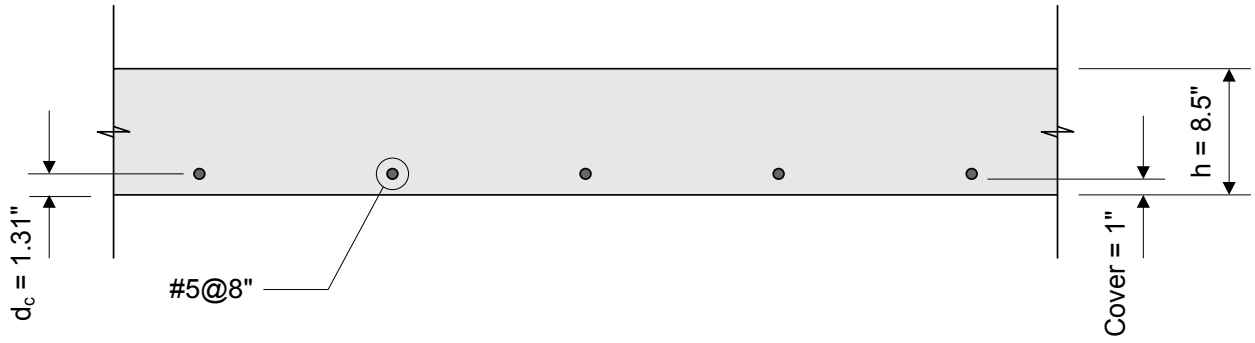

Figure 7.3.2.4-4 Crack Control by Distribution of Reinforcement

For this design example:

$$d_c = 1\,\text{inch} + \frac{0.625\ \text{inches}}{2} = 1.31\,\text{inches}$$

$$\beta_s = 1 + \frac{1.31\,\text{inches}}{0.7(8.5\ \text{inches} - 1.31\,\text{inches})} = 1.26$$

The tensile stress in the steel reinforcement at the service limit state, f_{ss}, is computed using load factors of 1.00, as follows:

$$M_{service} = 1.00\left(0.42\ \frac{K-ft}{ft}\right) + 1.00\left(0.47\ \frac{K-ft}{ft}\right) + 1.00\left(0.17\frac{K-ft}{ft}\right) + 1.00\left(6.49\frac{K\text{-}ft}{ft}\right) = 7.55\ \frac{K-ft}{ft}$$

The computation of the service limit state stress is then computed using the following equations. It should be noted that other methods are also available in reinforced concrete textbooks, all of which produce similar results.

$$n = 8$$

$$\rho = \frac{A_s}{bd_s} \qquad \text{Equation 7.3.2.4-5}$$

$$\rho = \frac{0.465 \text{ inches}^2}{(12 \text{ inches})(6.69 \text{ inches})} = 0.00579$$

$$k = \sqrt{(\rho n)^2 + (2\rho n)} - \rho n \qquad \text{Equation 7.3.2.4-6}$$

$$k = \sqrt{[(8)(0.00579)]^2 + [2(8)(0.00579)]} - [(8)(0.00579)] = 0.262$$

$$j = 1 - \frac{k}{3} \qquad \text{Equation 7.3.2.4-7}$$

$$j = 1 - \frac{0.262}{3} = 0.913$$

$$f_s = \frac{M}{A_s jd} \qquad \text{Equation 7.3.2.4-8}$$

$$f_s = \frac{\left(7.55 \frac{K - ft}{ft}\right)\left(\frac{12 \text{ inches}}{1 \text{ ft}}\right)}{\left(0.465 \frac{\text{inches}^2}{ft}\right)(0.913)(6.69 \text{ inches})} = 31.9 \text{ ksi}$$

The spacing of the steel reinforcement is then checked as follows:

$$\frac{700\gamma_e}{\beta_s f_s} - 2d_c = \frac{700(0.75)}{(1.26)(31.9)} - 2\,(1.31) = 10.4 \text{ inches} > 8 \text{ inches} \qquad \therefore OK$$

Equation 7.3.2.4-9

Therefore, the distribution of the positive flexure reinforcement meets the crack control requirements of *AASHTO LRFD* Article 5.7.3.4. The primary reinforcement in the bottom layer of the deck is as shown in Figure 7.3.2.4-5.

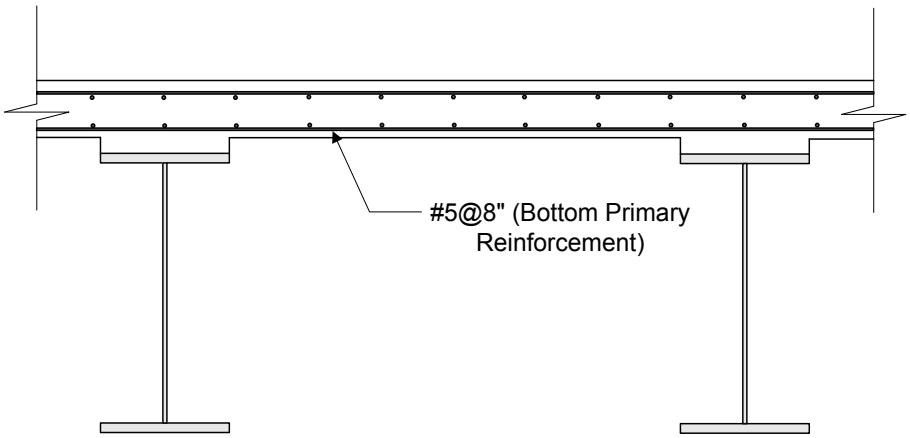

Figure 7.3.2.4-5 Primary Reinforcement in Bottom of Deck

10. Design for negative flexure in deck

After the positive flexure reinforcement has been designed, the negative flexure reinforcement must also be designed. Negative flexure produces compression in the bottom fiber and tension in the top fiber of the deck. Therefore, sufficient reinforcement must be provided in the top layer of the deck to resist the factored negative moment. Similar to the positive flexure reinforcement, the first step in designing the negative flexure reinforcement is to assume a bar size. For this design example, assume the use of #5 bars to resist negative flexure in the deck. Therefore, the effective depth is computed as follows:

$$d_s = \text{Slab Thickness} - \text{Top Cover} - \frac{\text{Bar Diameter}}{2}$$

$$= 8.5 \text{ inches} - 2.5 \text{ inches} - \frac{0.625 \text{ inches}}{2} = 5.69 \text{ inches}$$

Then the required reinforcement for negative flexure is computed similar to the procedure for the positive flexure reinforcement. For this design example:

$$a = \frac{A_s F_y}{0.85 f'_c b} = \frac{A_s(60\text{ ksi})}{0.85(4.0\text{ ksi})\left(\frac{12\text{ inches}}{1\text{ ft}}\right)} = \left(1.47\frac{\text{ft}}{\text{inch}}\right)A_s$$

$$M_r = \phi M_n = \phi A_s F_y\left(d_s - \frac{a}{2}\right) = 0.90A_s(60\text{ ksi})\left[5.69\text{ inches} - \frac{\left(1.47\frac{\text{ft}}{\text{inch}}\right)A_s}{2}\right]$$

For negative flexure, the absolute value of the negative moment is used as the design moment in the required reinforcement computations. Setting M_r equal to the factored design moment of 13.98 K-ft/ft produces the following required reinforcement area:

$$A_s = 0.59\frac{\text{inches}^2}{\text{ft}}$$

The required reinforcement spacing can then be computed as follows:

$$\text{Required Spacing} = \frac{0.31\frac{\text{inches}^2}{\text{bar}}}{0.59\frac{\text{inches}^2}{\text{ft}}} = 0.53\text{ ft} = 6.3\text{ inches}$$

Therefore, use #5 at 6 inches for the negative flexural reinforcement. Computing the provided flexural resistance serves as an independent check:

$$A_s = \frac{0.31\text{ inches}^2}{(6\text{ inches})\left(\frac{1\text{ ft}}{12\text{ inches}}\right)} = 0.62\frac{\text{inches}^2}{\text{ft}}$$

$$a = \frac{\left(0.62\frac{\text{inches}^2}{\text{ft}}\right)(60\text{ ksi})}{0.85(4.0\text{ ksi})\left(\frac{12\text{ inches}}{1\text{ ft}}\right)} = 0.91\text{ inches}$$

$$M_r = 0.90\left(0.62\frac{\text{inches}^2}{\text{ft}}\right)(60\text{ ksi})\left[5.69\text{ inches} - \frac{0.91\text{ inches}}{2}\right]$$

$$= 14.60\frac{\text{K}-\text{ft}}{\text{ft}} > 13.98\frac{\text{K}-\text{ft}}{\text{ft}} \qquad \therefore \text{ OK}$$

11. Check for negative flexure cracking under service limit state

Control of cracking by distribution of the reinforcement is then checked in accordance with *AASHTO LRFD* Article 5.7.3.4. (It should be noted that this step is not required for decks that are designed by the empirical design method and that meet the requirements of *AASHTO LRFD* Article 5.7.3.4.)

For this design example:

$$d_c = 2\text{ inches} + \frac{0.625\text{ inches}}{2} = 2.31\text{ inches}$$

$$\beta_s = 1 + \frac{2.31\text{ inches}}{0.7(8.5\text{ inches} - 2.31\text{ inches})} = 1.53$$

The tensile stress in the steel reinforcement at the service limit state, f_{ss}, is computed using load factors of 1.00, as follows:

$$M_{service} = 1.00\left(-0.74\frac{\text{K}-\text{ft}}{\text{ft}}\right) + 1.00\left(-1.66\frac{\text{K}-\text{ft}}{\text{ft}}\right) + 1.00\left(-0.24\frac{\text{K}-\text{ft}}{\text{ft}}\right)$$
$$+ 1.00\left(-6.07\frac{\text{K - ft}}{\text{ft}}\right) = -8.71\frac{\text{K}-\text{ft}}{\text{ft}}$$

The service limit state stress for negative flexure is computed similar to the procedure for computing the service limit state stress for positive flexure.

$$n = 8$$

$$\rho = \frac{A_s}{bd_s} = \frac{0.62\text{ inches}^2}{(12\text{ inches})(5.69\text{ inches})} = 0.00908$$

$$k = \sqrt{(\rho n)^2 + (2\rho n)} - \rho n = \sqrt{[(8)(0.00908)]^2 + [2(8)(0.00908)]} - [(8)(0.00908)] = 0.315$$

$$j = 1 - \frac{k}{3} = 1 - \frac{0.315}{3} = 0.895$$

$$f_{ss} = \frac{M}{A_s jd} = \frac{\left(8.71\frac{K-ft}{ft}\right)\left(\frac{12\ inches}{1\ ft}\right)}{\left(0.62\frac{inches^2}{ft}\right)(0.895)(5.69\ inches)} = 33.1\ ksi$$

The spacing of the steel reinforcement is then checked as follows:

$$\frac{700\gamma_e}{\beta_s f_{ss}} - 2d_c = \frac{700(0.75)}{(1.53)(33.1)} - 2\ (2.31) = 5.8\ \textit{inches} < 6\ \textit{inches} \qquad \therefore\ \textit{NG}$$

Therefore, the distribution of the negative flexure reinforcement needs reduced to meet the crack control requirements of *AASHTO LRFD* Article 5.7.3.4. The primary reinforcement in the top layer of the deck is as shown in Figure 7.3.2.4-6.

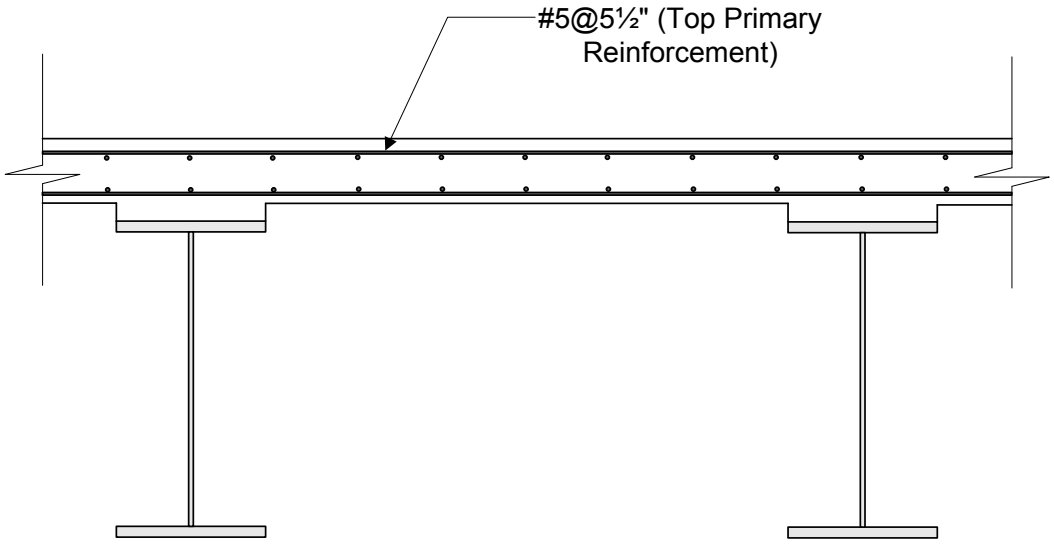

Figure 7.3.2.4-6 Primary Reinforcement in Top of Deck

7.3.2.5 Distribution Reinforcement Requirements

In addition to the primary reinforcement, which is placed normal to the supporting girders, distribution reinforcement must also be provided, which is placed in the opposite direction. According to *AASHTO LRFD* Article 9.7.3.2, the distribution reinforcement is placed in the bottom of the deck and is computed as a percentage of the primary reinforcement for positive moment. When the primary reinforcement is parallel to the traffic, the distribution reinforcement is computed as follows:

$$\frac{100}{\sqrt{S}} \le 50 \text{ percent} \qquad \text{Equation 7.3.2.5-1}$$

When the primary reinforcement is perpendicular to traffic, the distribution reinforcement is computed as follows:

$$\frac{200}{\sqrt{S}} \le 67 \text{ percent} \qquad \text{Equation 7.3.2.5-2}$$

As used in the above equations, S is defined as the effective span length, as described for the empirical design method (see Figure 7.3.3.3-1). For this design example, assume a top flange width of 12 inches and a web thickness of 7/16 inches. Therefore, the effective span length is computed as follows:

$$S = \text{Spacing}_{\text{girder}} - b_f + \left(\frac{b_f - t_w}{2}\right) \qquad \text{Equation 7.3.2.5-3}$$

$$S = 117 \text{ inches} - 12 \text{ inches} + \left(\frac{12 \text{ inches} - 0.4375 \text{ inches}}{2}\right) = 110.78 \text{ inches} = 9.23 \text{ ft}$$

Since the primary reinforcement is perpendicular to traffic for this design example, the distribution reinforcement is computed as follows:

$$\frac{200}{\sqrt{9.23}} = 72.4 > 67 \text{ percent} \qquad \therefore \text{ Use 67 percent}$$

$$67\% \text{ of } A_s = (0.67)\left(0.465 \frac{\text{inches}^2}{\text{ft}}\right) = 0.312 \frac{\text{inches}^2}{\text{ft}}$$

Therefore, use #5 at 10 inches. The provided distribution reinforcement is as follows:

$$A_s = \frac{0.31 \text{ inches}^2}{(10 \text{ inches})\left(\frac{1 \text{ ft}}{12 \text{ inches}}\right)} = 0.372 \frac{\text{inches}^2}{\text{ft}} > 0.312 \frac{\text{inches}^2}{\text{ft}} \qquad \therefore \text{ OK}$$

The distribution reinforcement in the bottom layer of the deck is as shown in Figure 7.3.2.5-1.

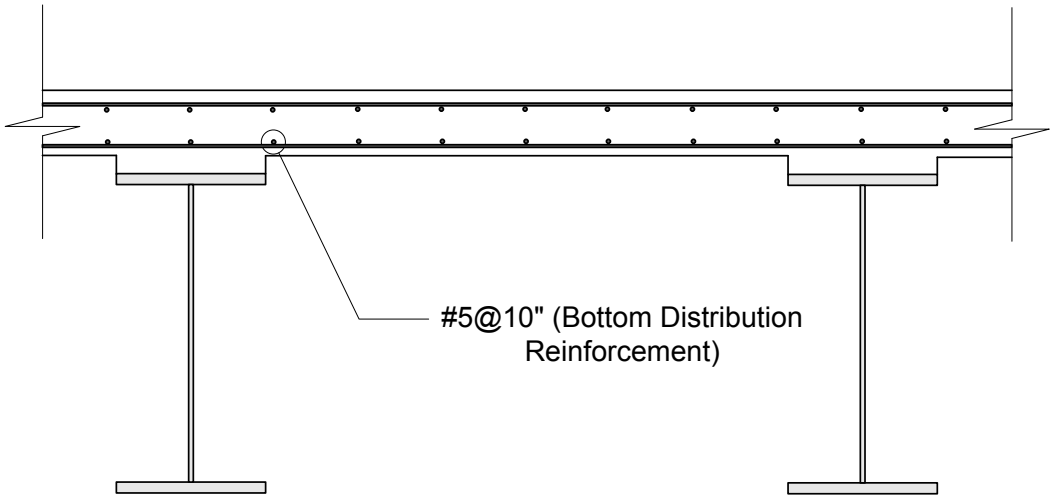

Figure 7.3.2.5-1 Distribution Reinforcement in Bottom of Deck

Since no specific requirements are provided in *AASHTO LRFD* for the distribution reinforcement in the top of the deck, the temperature and shrinkage requirement of *AASHTO LRFD* Article 5.10.8 must be satisfied, as follows:

$$A_s \geq \frac{1.30bh}{2(b+h)f_y} \qquad \text{Equation 7.3.2.5-4}$$

AASHTO LRFD Equation 5.10.8-1

and

$$0.11 \leq A_s \leq 0.60 \qquad \text{Equation 7.3.2.5-5}$$

AASHTO LRFD Equation 5.10.8-2

$$\frac{1.30(8.5 \text{ inches})\left(12\frac{\text{inches}}{\text{ft}}\right)}{2\left(8.5 \text{ inches} + 12\frac{\text{inches}}{\text{ft}}\right)60 \text{ ksi}} = 0.05\frac{\text{inches}^2}{\text{ft}} < 0.11$$

$$\therefore A_s = 0.11\frac{\text{inches}^2}{\text{ft}}$$

When using the above equation, the calculated area of reinforcing steel must be equally distributed on both concrete faces. In addition, the maximum spacing of the temperature and shrinkage reinforcement must be smaller than 3.0 times the deck thickness or 18.0 inches. Therefore, the amount of steel required for the top longitudinal reinforcement is:

$$A_s = \frac{0.11\frac{\text{inches}^2}{\text{ft}}}{2} = 0.055\frac{\text{inches}^2}{\text{ft}}$$

Use #4 at the maximum spacing of 18 inches. The provided temperature and shrinkage reinforcement is as follows:

$$A_s = \frac{0.20\ \text{inches}^2}{(18\ \text{inches})\left(\frac{1\,\text{ft}}{12\ \text{inches}}\right)} = 0.13\frac{\text{inches}^2}{\text{ft}} > 0.055\frac{\text{inches}^2}{\text{ft}} \quad \therefore \text{OK}$$

Therefore, #4 at 18 inches satisfies both the area and spacing requirements for the temperature and shrinkage reinforcement. The reinforcement in the top layer of the deck is as shown in Figure 7.3.2.5-2.

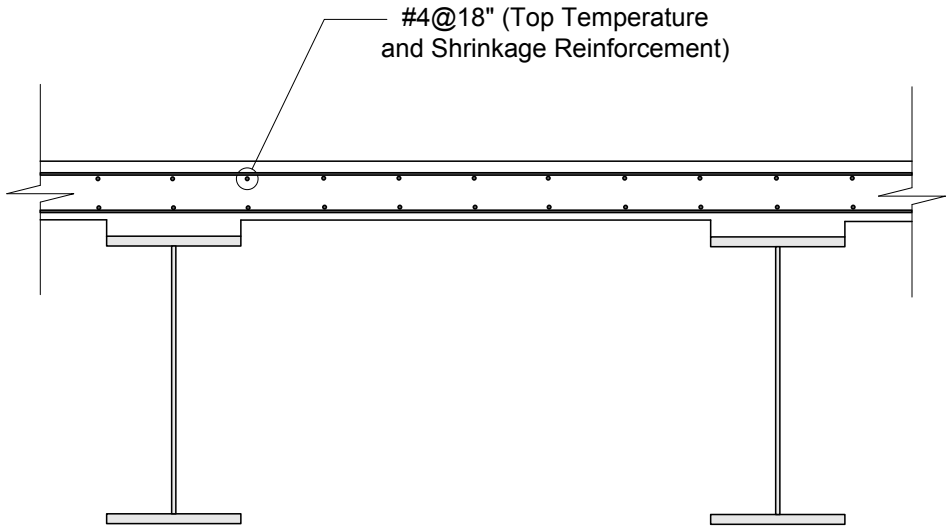

Figure 7.3.2.5-2 Temperature and Shrinkage Reinforcement in Top of Deck

7.3.2.6 Reinforcement Requirements over Piers

If the superstructure is comprised of simple span precast girders made continuous for live load, the top longitudinal reinforcement should be designed according to *AASHTO LRFD* Article 5.14.1.4. For continuous steel girder superstructures, the top longitudinal reinforcement should be designed according to *AASHTO LRFD* Article 6.10.1.7.

For this design example, continuous steel girders are used to span the piers of a multi-span bridge. Based on *AASHTO LRFD* Article 6.10.1.7, the total cross-sectional area of the longitudinal reinforcement over the piers should not be less than 1 percent of the total slab cross-sectional area. These bars must have a

specified minimum yield strength of at least 60 ksi, the bar size cannot exceed #6 bars, and the bar spacing cannot exceed 12 inches. For this design example:

$$1\%\text{ of } A_g = (0.01)(8.5\text{ inches})\left(12\frac{\text{inches}}{\text{ft}}\right) = 1.02\frac{\text{inches}^2}{\text{ft}}$$

AASHTO specifies that two-thirds of the required longitudinal reinforcement should be placed in the top layer of the deck. Therefore, for this design example, the following reinforcement is required for the top layer over the piers:

$$\left(\frac{2}{3}\right)\left(1.02\frac{\text{inches}^2}{\text{ft}}\right) = 0.68\frac{\text{inches}^2}{\text{ft}}$$

Use #5 at 5 inches in the top layer over the piers. The provided reinforcement is as follows:

$$A_s = \frac{0.31\,\text{inches}^2}{(5\text{ inches})\left(\frac{1\,\text{ft}}{12\text{ inches}}\right)} = 0.74\frac{\text{inches}^2}{\text{ft}} > 0.68\frac{\text{inches}^2}{\text{ft}} \quad \therefore \text{OK}$$

The remaining one-third of the required longitudinal reinforcement should be placed in the bottom layer of the deck. Therefore, for this design example, the following reinforcement is required for the bottom layer over the piers:

$$\left(\frac{1}{3}\right)\left(1.02\frac{\text{inches}^2}{\text{ft}}\right) = 0.34\frac{\text{inches}^2}{\text{ft}}$$

Use #5 at 10 inches in the bottom layer over the piers. The provided reinforcement is as follows:

$$A_s = \frac{0.31\,\text{inches}^2}{(10\text{ inches})\left(\frac{1\,\text{ft}}{12\text{ inches}}\right)} = 0.37\frac{\text{inches}^2}{\text{ft}} > 0.34\frac{\text{inches}^2}{\text{ft}} \quad \therefore \text{OK}$$

The required longitudinal reinforcement over the piers is as shown in Figure 7.3.2.6-1.

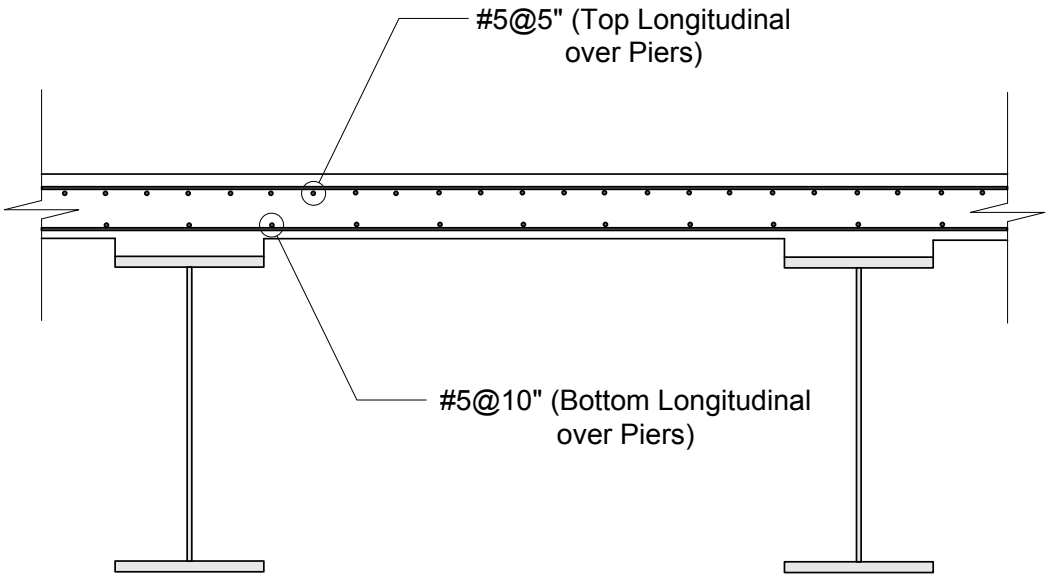

Figure 7.3.2.6-1 Longitudinal Reinforcement over Piers

After designing the primary reinforcement, the distribution reinforcement, and the longitudinal reinforcement over the piers, it is valuable to provide a schematic showing all of the reinforcement and identifying the bar size and spacing for each one. For this design example, a schematic of the final deck design based on the traditional design method is provided in Figure 7.3.2.6-2. A comparison with the deck design based on the empirical design method is provided in Table 7.3.3.4-1.

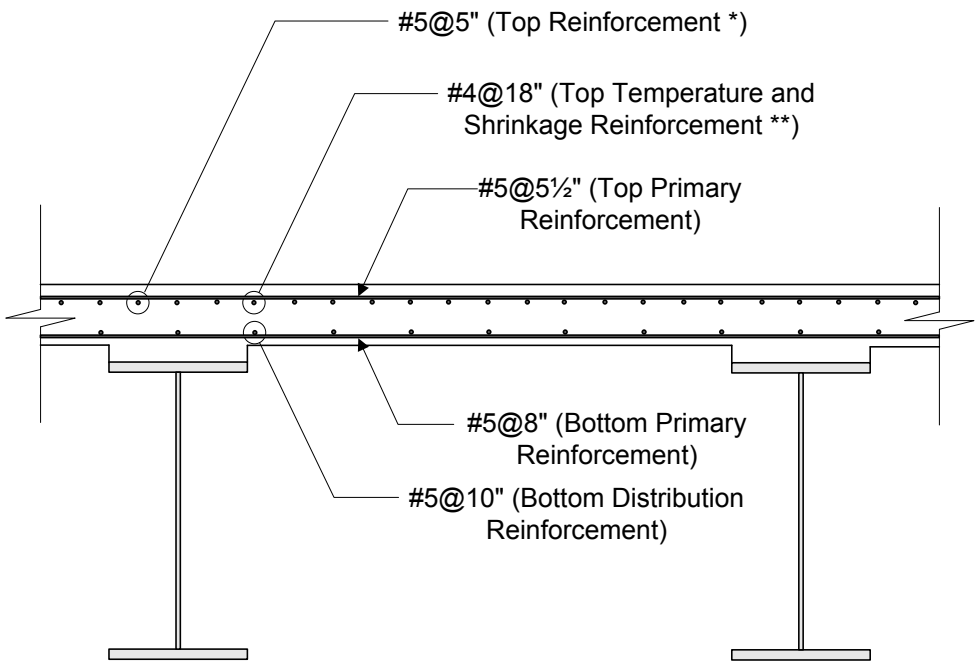

* Provide only in negative moment regions over piers

** Provide wherever negative moment reinforcement over piers is not present

Note: All other reinforcement is provided throughout the entire deck

Figure 7.3.2.6-2 Bridge Deck Based on Traditional Design Method

7.3.3 Empirical Design Method

7.3.3.1 General

In addition to the traditional design method, AASHTO also provides specifications for an empirical design method. This method does not require the computation of design moments and is simpler to apply than the traditional design method. However, it is applicable only under specified design conditions. The empirical design method is described in *AASHTO LRFD* Article 9.7.2.

7.3.3.2 Design Theory

While the traditional design method is based on flexural behavior with the girders acting as supports, the empirical design method is based on internal arching behavior with a complex internal membrane stress state.

Extensive research has shown that concrete bridge decks behave similar to an internal compressive dome. This behavior is made possible by the cracking of the concrete in the positive moment region of the deck, which causes the neutral axis to move upward in that portion of the deck. This results in structural behavior similar to

that of a compressive dome. The arching behavior is also made possible by the lateral confinement provided by the surrounding concrete deck, nearby rigid appurtenances, and supporting components acting compositely with the deck. While the failure mode for the traditional design method is flexural failure, the failure mode for the empirical design method is punching shear.

The reinforcing steel provided using the empirical design method serves two purposes:

- It provides for local flexural resistance.
- It provides global confinement required to develop arching effects.

The primary differences between the traditional design method and the empirical design method are summarized in Table 7.3.3.2-1.

Table 7.3.3.2-1 Traditional and Empirical Design Methods

Characteristic	Traditional Design Method	Empirical Design Method
Structural behavior	Flexural behavior with girders acting as supports	Internal membrane stress state, referred to as internal arching
AASHTO LRFD reference	*AASHTO LRFD* Article 9.7.3	*AASHTO LRFD* Article 9.7.2
Application	Slab must have four layers of reinforcing steel, two in each direction, and must satisfy minimum slab thickness requirements	Slab must satisfy a more extensive set of design conditions presented in *AASHTO LRFD* Article 9.7.2.4 and in the following section of this chapter
Deck overhang	May be used for the design of the deck overhang	May not be used for the design of the deck overhang
Purpose of reinforcing steel	Provide for flexural resistance	Provide for flexural resistance and provide global confinement required to develop arching effects
Mode of failure	Flexural failure	Punching shear failure
Basis of design	Computation of design moments using flexural design theory	Extensive research and experiments; no design moments are computed
Simplicity of design computations	More design computations are required than with the Empirical Design Method	Fewer design computations are required than with the Traditional Design Method

7.3.3.3 Design Conditions/Limitations

Although the empirical design method is simpler than the traditional design method, the empirical design method may be used only if a set of design conditions are satisfied, as specified in *AASHTO LRFD* Article 9.7.2.4. These design conditions include the following:

- Diaphragms must be used throughout the cross-section at lines of support.
- Supporting components must be made of steel and/or concrete.
- Deck must be fully cast-in-place and must be water cured.
- Deck must have a uniform depth except for girder haunches and areas of local thickening.
- 6.0 ≤ effective length to design depth ratio ≤ 18.0.
- Core depth of the deck ≥ 4.0 inches.
- Effective length ≤ 13.5 feet.
- Minimum depth of the deck ≥ 7.0 inches; excluding a sacrificial wearing surface.
- Overhang ≥ 5 x deck depth (without a continuous and composite barrier), or overhang ≥ 3 x deck depth (with a continuous and composite barrier).
- 28-day deck concrete strength, $f'_c \geq 4.0$ ksi.
- Deck is composite with the supporting structural components.
- Minimum of two shear connectors at 24-inch spacing in negative moment region.

As used with the empirical design method, the effective length for slabs supported on steel or concrete girders is defined as the distance between flange tips, plus the flange overhang, taken as the distance from the extreme flange tip to the face of the web, disregarding any fillets (see *AASHTO LRFD* Article 9.7.2.3). The effective slab length is illustrated in Figure 7.3.3.3-1.

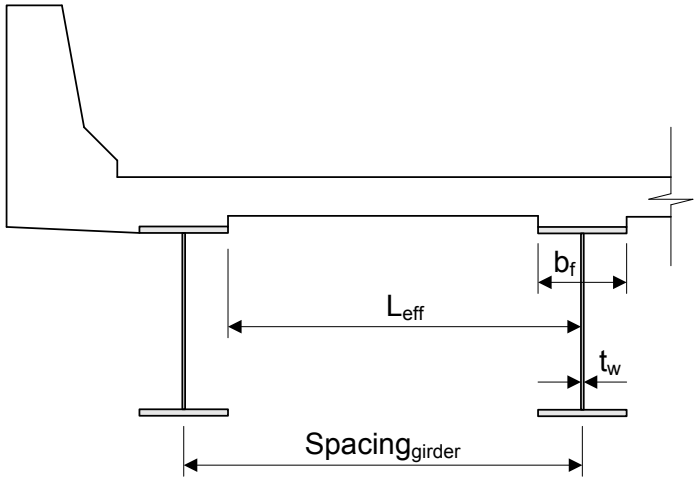

Figure 7.3.3.3-1 Effective Slab Length

$$\text{Effective Slab Length, } L_{eff} = Spacing_{girder} - b_f + \left(\frac{b_f - t_w}{2}\right) \qquad \text{Equation 7.3.3.3-1}$$

The empirical design method is based on extensive non-linear finite element analysis and extensive experimentation, and the above design conditions reflect the current scope of analysis and experimentation using this design method. Failure to meet the above design conditions does not necessarily mean that the empirical design method will result in deck failure. Rather, it simply means that sufficient testing has not yet been performed to verify a safe design, and it therefore should not be used for that application.

In addition to the design conditions previously presented, it should be noted that the empirical design method does not apply if the unit being designed is not "monolithic." The use of concrete stay-in-place forms is not consistent with the empirical design method.

In addition, if there is a second course wearing surface (that is, two-stage deck construction), the second stage should not be considered when evaluating the design conditions for the empirical design method. The first stage alone must satisfy the design conditions for empirical design.

7.3.3.4 Reinforcement Requirements

For bridges satisfying each of the above design conditions, the reinforcement requirements of the empirical design method are specified in *AASHTO LRFD* Article 9.7.2.5. These reinforcement requirements are as follows:

- Four layers of reinforcement (top in each direction and bottom in each direction).
- Area of each bottom layer of reinforcement ≥ 0.27 inches^2/foot.
- Area of each top layer of reinforcement ≥ 0.18 inches^2/foot.
- Spacing of reinforcement ≤ 18 inches.
- Grade 60 reinforcement or better.

The above reinforcement requirements demonstrate that neither dead load nor live load moments are required using the empirical design method. The minimum area of reinforcing steel is specified, regardless of the design moments or the girder spacing. This reflects the fact that the empirical design method is based on research showing that the above reinforcement requirements satisfy all AASHTO design requirements for any bridge which satisfies the specified design conditions.

An example of a bridge deck reinforcing pattern based on the empirical design method is presented in Figure 7.3.3.4-1.

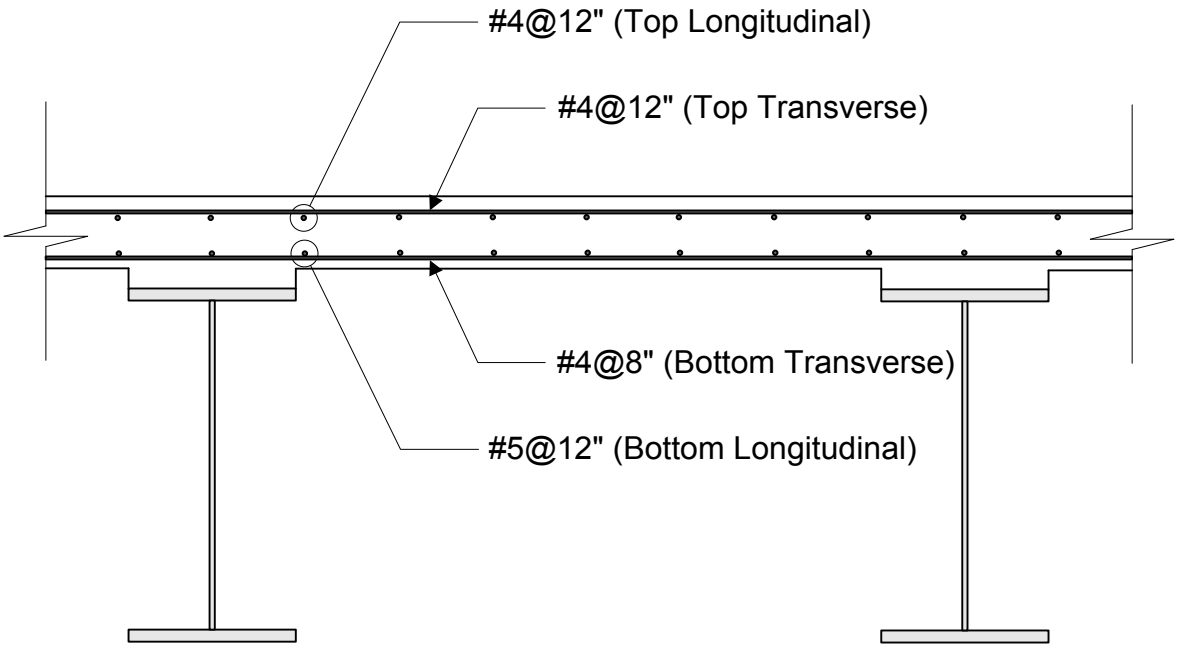

Figure 7.3.3.4-1 Bridge Deck Based on Empirical Design Method

The sufficiency of the reinforcing steel shown in Figure 7.3.3.4-1 can be checked as follows:

Top Transverse:

$$A_s = \frac{0.20 \text{ inches}^2}{(12 \text{ inches})\left(\frac{1 \text{ foot}}{12 \text{ inches}}\right)} = 0.20 \frac{\text{inches}^2}{\text{foot}} > 0.18 \frac{\text{inches}^2}{\text{foot}} \qquad \therefore \text{OK}$$

Top Longitudinal:

$$A_s = \frac{0.20 \text{ inches}^2}{(12 \text{ inches})\left(\frac{1 \text{ foot}}{12 \text{ inches}}\right)} = 0.20 \frac{\text{inches}^2}{\text{foot}} > 0.18 \frac{\text{inches}^2}{\text{foot}} \qquad \therefore \text{OK}$$

Bottom Longitudinal:

$$A_s = \frac{0.31 \text{ inches}^2}{(12 \text{ inches})\left(\frac{1 \text{ foot}}{12 \text{ inches}}\right)} = 0.31 \frac{\text{inches}^2}{\text{foot}} > 0.27 \frac{\text{inches}^2}{\text{foot}} \qquad \therefore \text{OK}$$

Bottom Transverse:

$$A_s = \frac{0.20 \text{ inches}^2}{(8 \text{ inches})\left(\frac{1 \text{ foot}}{12 \text{ inches}}\right)} = 0.30 \frac{\text{inches}^2}{\text{foot}} > 0.27 \frac{\text{inches}^2}{\text{foot}} \qquad \therefore \text{OK}$$

It should be noted that reinforcement must be provided in each face of the slab with the outermost layers placed in the direction of the effective slab length and placed as close to the concrete surfaces as permitted by the cover requirements.

The reinforcing steel in the deck overhang must be designed based on the traditional design method. Additional reinforcing steel required in the negative flexure region (over piers) is as presented with the traditional design method.

A comparison between the deck design example using the traditional design method and that using the empirical design method is presented in Table 7.3.3.4-1.

Table 7.3.3.4-1 Comparison of Design Methods for Deck Design Example

Reinforcement	Traditional Design Method	Empirical Design Method
Top Transverse	#5@5.5”	#4@12”
Bottom Transverse	#5@8”	#4@8”
Top Longitudinal	#4@18”	#4@12”
Bottom Longitudinal	#5@10”	#5@12”

It is clear from Table 7.3.3.4-1 that, for this particular design example, the transverse reinforcement requirements are greater using the traditional design method than using the empirical design method. For this design example, the longitudinal reinforcement requirements are similar using both methods.

7.3.4 Deck Overhang Design

7.3.4.1 General

Design of the deck overhang involves the following steps:

1. Design for flexure in deck overhang.
2. Check for cracking in overhang under service limit state.
3. Compute overhang cut-off length requirement.
4. Compute overhang development length.

These design steps are presented and illustrated through a continuation of the previous design example. The deck overhang dimensions from that design example, as well as the locations of the design sections and the live load on the overhang, are presented in Figure 7.3.4.1-1.

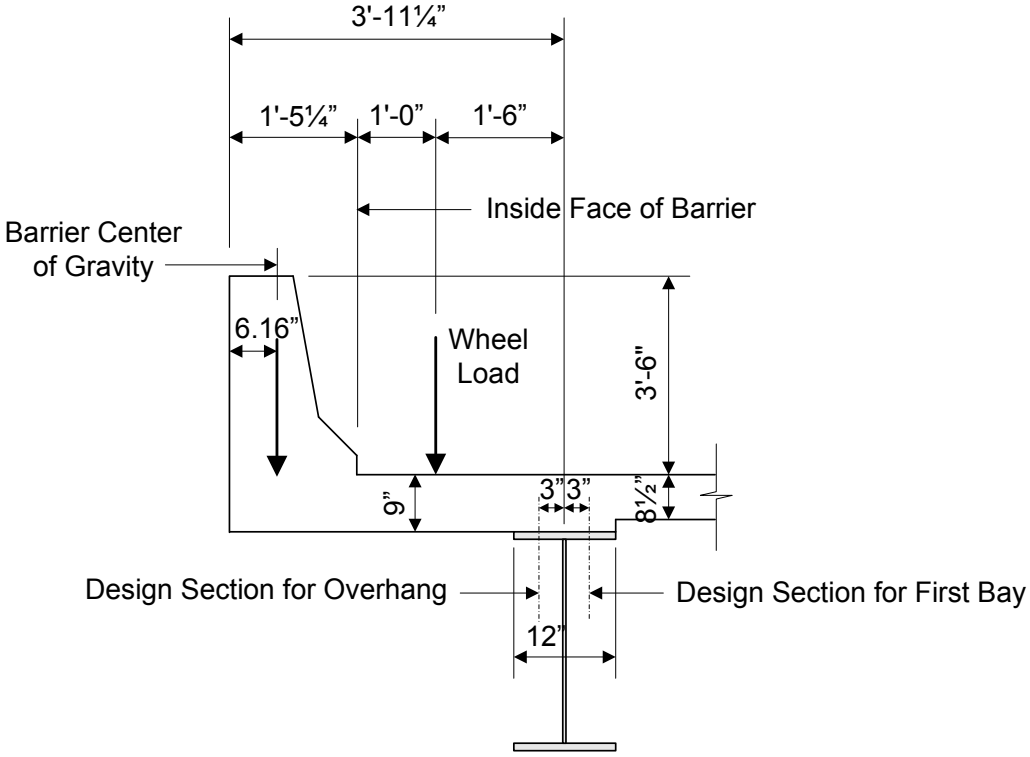

Figure 7.3.4.1-1 Deck Overang Dimensions and Live Load

7.3.4.2 Design for Flexure

1. Design for flexure in deck overhang

As described in Appendix A13 to *AASHTO LRFD* Article 13, deck overhangs must be designed to satisfy three different design cases. These three design cases are summarized in Table 7.3.4.2-1.

Table 7.3.4.2-1 Deck Overhang Design Cases

Design Case	Applied Loads	Limit State	Design Locations
Design Case 1	Horizontal (transverse and longitudinal) vehicular collision force	Extreme event limit state	• At inside face of barrier • At design section for overhang • At design section for first bay
Design Case 2	Vertical vehicular collision force	Extreme event limit state	Usually does not control
Design Case 3	Dead and live loads	Strength limit state	• At design section for overhang • At design section for first bay

In addition, the deck overhang must be designed to provide a resistance greater than the resistance of the concrete barrier.

7.3.4.2.1 Design for Vehicular Collision Forces

Design Case 1: Design overhang for horizontal vehicular collision force

The overhang must be designed for the vehicular collision moment plus the dead load moment, acting concurrently with the axial tension force from vehicular collision, in accordance with *AASHTO LRFD* Article A13.4.1. The barrier that has been selected for use with this design example is approved for Test Level TL-3 and is shown in Figure 7.3.4.2.1-1.

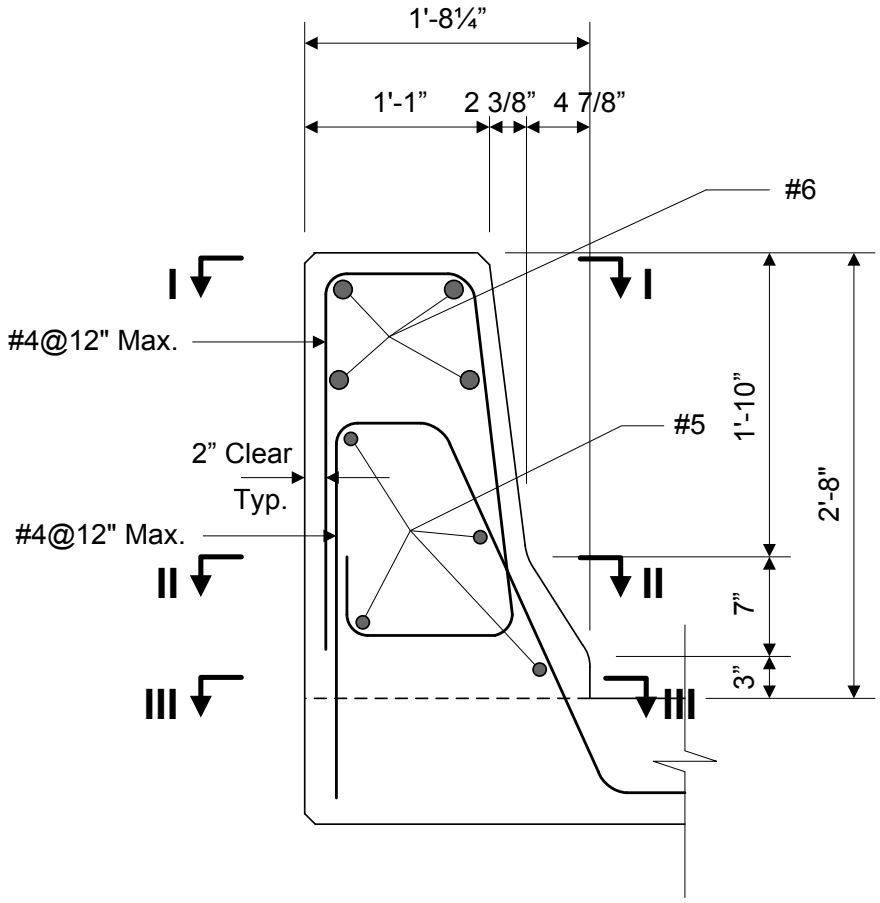

Figure 7.3.4.2.1-1 Barrier Configuration

Based on the dimensions shown in Figure 7.3.4.2.1-1, the cross-sectional area and weight of the barrier are:

$$\text{Area} = (13")(32") + \frac{1}{2}(2.375")(22") + \frac{1}{2}(4.875")(7") + (2.375")(7") + (7.25")(3") =$$
$$= 497.6 \text{ inches}^2 = 3.46 \text{ ft}^2$$

$$\text{Weight} = (3.46 \text{ ft}^2)(0.150 \text{ kcf}) = 0.52 \text{ kips/ft}$$

The moment resistance of the barrier is computed based on the formation of yield lines at the limit state. The fundamentals of yield line analysis can be found in many structural analysis textbooks. For an assumed yield line pattern that is consistent with the geometry of the barrier, a solution is obtained by equating the internal work along the yield lines with the external work due to the applied loads. While a full explanation of the barrier design equations and their derivation is beyond the scope of this manual, Figure 7.3.4.2.1-2 illustrates the assumed yield line pattern for a barrier wall.

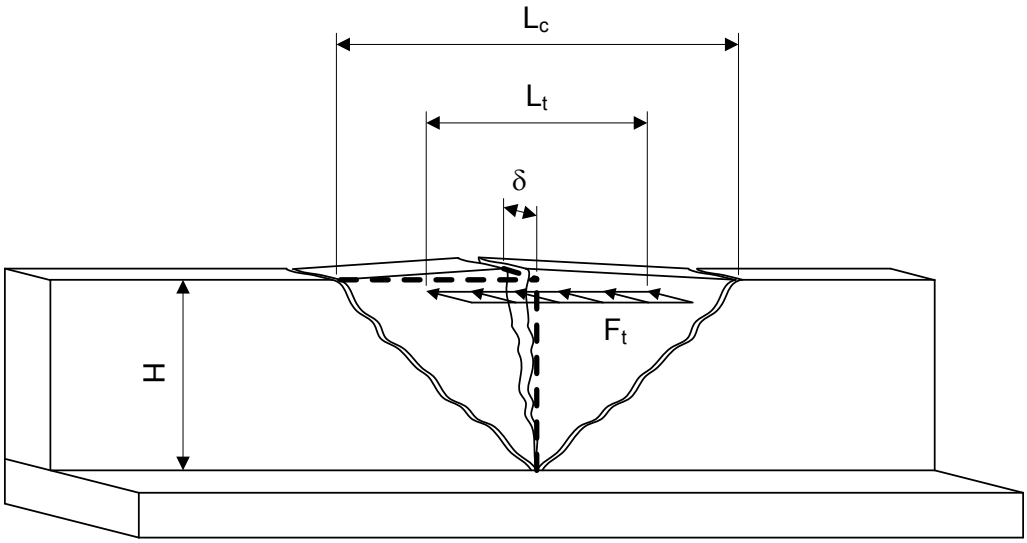

Figure 7.3.4.2.1-2 Assumed Yield Line Pattern for Barrier Wall

As used in Figure 7.3.4.2.1-2:

F_t = transverse vehicle impact force
L_t = longitudinal length of distribution of impact force, F_t
L_c = critical length of wall failure
H = height of wall

δ = lateral displacement of wall due to transverse force

If relatively thick parapets are used, then using a thicker deck can be beneficial to develop yield lines in the parapets. As an alternative, the deck can be designed for the forces, without the need to develop the parapet load since the parapet could be thicker than required.

The ultimate flexural resistance of the barrier about its horizontal axis, M_c, at Sections I, II, and III (see Figure 7.3.4.2.1-3) can be calculated as follows, assuming a constant thickness for each section:

At Section I:

$$a = \frac{A_s F_y}{0.85 f'_c b} = \frac{(0.20 \text{ inches}^2)(60 \text{ ksi})}{0.85(4.0 \text{ ksi})(12 \text{ inches})} = 0.29 \text{ inches}$$

$$d = 13 \text{ inches} - 2 \text{ inches} - \frac{1}{2}(0.50 \text{ inches}) = 10.75 \text{ inches}$$

$$M_c = \phi A_s F_y \left(d_s - \frac{a}{2} \right) \qquad \text{Equation 7.3.4.2.1-1}$$

$$M_c = \phi A_s F_y \left(d_s - \frac{a}{2} \right) = 1.0 \left(0.20 \frac{\text{in}^2}{\text{ft}} \right) (60 \text{ ksi}) \left[10.75 \text{ in} - \frac{0.29 \text{ in}}{2} \right] = 10.61 \frac{\text{K} - \text{ft}}{\text{ft}}$$

Similarly, at Section II, using an increased barrier thickness:

$$d = 15.375 \text{ inches} - 2 \text{ inches} - \frac{1}{2}(0.50 \text{ inches}) = 13.125 \text{ inches}$$

$$M_c = \phi A_s F_y \left(d_s - \frac{a}{2} \right) = 1.0 \left(0.20 \frac{\text{in}^2}{\text{ft}} \right) (60 \text{ ksi}) \left[13.125 \text{ in} - \frac{0.29 \text{ in}}{2} \right] = 12.98 \frac{\text{K} - \text{ft}}{\text{ft}}$$

Finally, at Section III:

$$d = 20.25 \text{ inches} - 2 \text{ inches} - \frac{1}{2}(0.50 \text{ inches}) = 18 \text{ inches}$$

$$M_c = \phi A_s F_y \left(d_s - \frac{a}{2} \right) = 1.0 \left(0.20 \frac{\text{in}^2}{\text{ft}} \right) (60 \text{ ksi}) \left[18 \text{ in} - \frac{0.29 \text{ in}}{2} \right] = 17.86 \frac{\text{K} - \text{ft}}{\text{ft}}$$

Assuming that the failure mechanism includes the entire height of the barrier, the moment resistance, M_c, is computed by averaging the above components over their respective heights:

$$M_c = \frac{\left[\left(\frac{10.61\frac{K-ft}{ft} + 12.98\frac{K-ft}{ft}}{2}\right)(22\text{ in}) + \left(\frac{12.98\frac{K-ft}{ft} + 17.86\frac{K-ft}{ft}}{2}\right)(10\text{ in})\right]}{32\text{ in}} =$$

$$12.93\frac{K-ft}{ft}$$

Similarly, assuming that the failure mechanism includes only between Section I and II (the top 22 inches of the barrier), the moment resistance, M_c, is computed as follows:

$$M_c = \frac{10.61\frac{K-ft}{ft} + 12.98\frac{K-ft}{ft}}{2} = 11.80\frac{K-ft}{ft}$$

For this design example, there is no top beam included on the barrier. Therefore, the ultimate moment resistance of the beam at the top of the wall, M_b, is zero.

To compute the ultimate flexural resistance of the barrier about its vertical axis, M_w, the barrier must be divided into three portions, as illustrated in Figure 7.3.4.2.1-3. The moment resistance is then computed for each portion about its vertical axis.

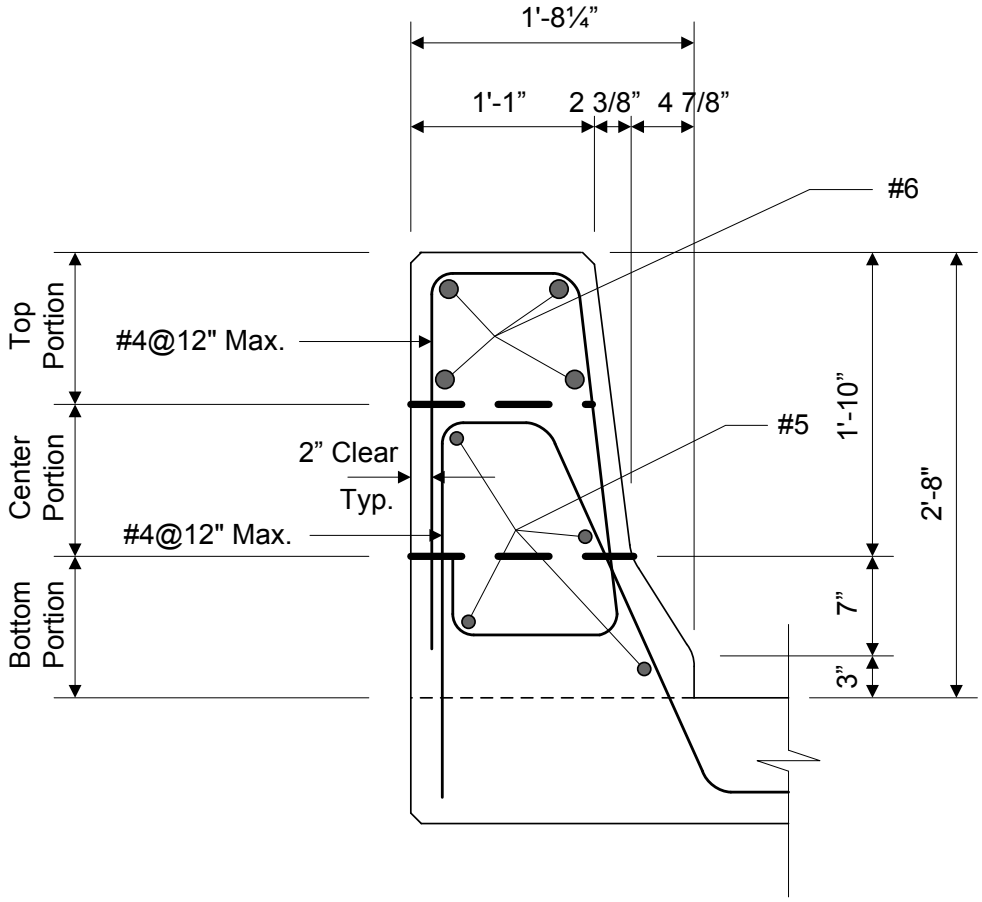

Figure 7.3.4.2.1-3 Three Portions of Barrier for Computation of M_w

For the top portion of the barrier, there are four #6 bars. To compute the ultimate flexural resistance of the barrier about its vertical axis, it can be assumed that two #6 bars are for positive flexure and two are for negative flexure. The effective depth can be computed based on an average of the structural depth of that portion.

$$a = \frac{A_s F_y}{0.85 f'_c b} = \frac{(0.88 \text{ inches}^2)(60 \text{ ksi})}{0.85(4.0 \text{ ksi})(11 \text{ inches})} = 1.41 \text{ inches}$$

$$d = 13.59 \text{ inches} - 2 \text{ inches} - \frac{1}{2}(0.75 \text{ inches}) = 11.22 \text{ inches}$$

$$M_w = \phi A_s F_y \left(d_s - \frac{a}{2} \right) \qquad \text{Equation 7.3.4.2.1-2}$$

$$M_w = 1.0(0.88 \text{ inches}^2)(60 \text{ ksi}) \left[11.22 \text{ in} - \frac{1.41 \text{ in}}{2} \right] = 46.27 \text{ K} - \text{ft}$$

For the center portion of the barrier, there are two #5 bars. Similar to the top portion, it can be assumed that one #5 bar is for positive flexure and one is for negative flexure.

$$a = \frac{A_s F_y}{0.85 f'_c b} = \frac{(0.31 \text{ inches}^2)(60 \text{ ksi})}{0.85(4.0 \text{ ksi})(11 \text{ inches})} = 0.50 \text{ inches}$$

$$d = 14.78 \text{ inches} - 2 \text{ inches} - \frac{1}{2}(0.625 \text{ inches}) = 12.47 \text{ inches}$$

$$M_w = \phi A_s F_y \left(d_s - \frac{a}{2} \right) = 1.0(0.31 \text{ inches}^2)(60 \text{ ksi}) \left[12.47 \text{ in} - \frac{0.50 \text{ in}}{2} \right] = 18.94 \text{ K} - \text{ft}$$

Similarly, for the bottom portion of the barrier, there are two #5 bars.

$$a = \frac{A_s F_y}{0.85 f'_c b} = \frac{(0.31 \text{ inches}^2)(60 \text{ ksi})}{0.85(4.0 \text{ ksi})(10 \text{ inches})} = 0.55 \text{ inches}$$

$$d = 17.81 \text{ inches} - 2 \text{ inches} - \frac{1}{2}(0.625 \text{ inches}) = 15.50 \text{ inches}$$

$$M_w = \phi A_s F_y \left(d_s - \frac{a}{2} \right) = 1.0(0.31 \text{ inches}^2)(60 \text{ ksi}) \left[15.50 \text{ in} - \frac{0.55 \text{ in}}{2} \right] = 23.59 \text{ K} - \text{ft}$$

For the case in which different reinforcement steel area is used for positive and negative flexure, the moments for both should be computed and then the average should be used. This is acceptable because the yield line mechanism for this case will have some positive moment hinges and some negative moment hinges.

However, for collision near the expansion joint, the flexural resistance for positive moment should be used. Positive moment will cause tension along the inside face of the barrier, and the only yield line to form is caused by a moment causing tension along the inside face.

Assuming that the failure mechanism includes the entire height of the barrier, the ultimate flexural resistance of the barrier about its vertical axis, M_w, is computed by adding each of the three components:

$$M_w = 46.27 \text{ K} - \text{ft} + 18.94 \text{ K} - \text{ft} + 23.59 \text{ K} - \text{ft} = 88.80 \text{ K} - \text{ft}$$

Similarly, assuming that the failure mechanism includes only the top two portions of the barrier (the top 22 inches of the barrier), the ultimate flexural resistance of the barrier about its vertical axis, M_w, is computed as follows:

$$M_w = 46.27\,K-ft + 18.94\,K-ft = 65.21\,K-ft$$

For impacts within a wall segment, the barrier resistance, R_w, and the critical length of yield line failure pattern, L_c, are computed based on *AASHTO LRFD* Article A13.3.1, as follows:

$$R_w = \left(\frac{2}{2L_c - L_t}\right)\left(8M_b + 8M_w + \frac{M_c L_c^{\,2}}{H}\right) \qquad \text{Equation 7.3.4.2.1-3}$$

AASHTO LRFD Equation A13.3.1-1

$$L_c = \frac{L_t}{2} + \sqrt{\left(\frac{L_t}{2}\right)^2 + \frac{8H(M_b + M_w)}{M_c}} \qquad \text{Equation 7.3.4.2.1-4}$$

AASHTO LRFD Equation A13.3.1-2

where:

L_t = longitudinal length of distribution of impact force (see *AASHTO LRFD* Table A13.2-1)

M_b = additional flexural resistance of beam in addition to M_w, if any, at top of wall

M_w = flexural resistance of the wall about its vertical axis

M_c = flexural resistance of cantilevered walls about an axis parallel to the longitudinal axis of the bridge

Assuming that the failure mechanism includes the entire height of the barrier and using the previously computed values for M_b, M_w, and M_c, the values for R_w and L_c are computed as follows:

$$L_c = \frac{4\text{ ft}}{2} + \sqrt{\left(\frac{4\text{ ft}}{2}\right)^2 + \frac{8(3.5\text{ ft})(0\,K\text{-ft} + 88.80\,K-ft)}{12.93\,\frac{k\text{-ft}}{ft}}} = 16.01\text{ ft}$$

$$R_w = \left(\frac{2}{2(16.01\text{ ft}) - 4\text{ ft}}\right)\left(8(0\,K\text{-ft}) + 8(88.80\,K-ft) + \frac{\left(12.93\,\frac{K\text{-ft}}{ft}\right)(16.01\text{ ft})^2}{3.5\text{ ft}}\right)$$

$$= 118.3 \text{ kips}$$

Similarly, assuming that the failure mechanism is only the top portion (the top 22 inches of the barrier) and using the previously computed values for M_b, M_w, and M_c, the values for R_w and L_c are computed as follows:

$$L_c = \frac{4\text{ ft}}{2} + \sqrt{\left(\frac{4\text{ ft}}{2}\right)^2 + \frac{8(1.83\text{ ft})(0\text{ K - ft} + 65.21\text{ K} - \text{ft})}{11.80\,\frac{\text{k - ft}}{\text{ft}}}} = 11.22\text{ ft}$$

$$R_w = \left(\frac{2}{2(11.22\text{ ft}) - 4\text{ ft}}\right)\left(8(0\text{ K - ft}) + 8(65.21\text{ K} - \text{ft}) + \frac{\left(11.80\,\frac{\text{K - ft}}{\text{ft}}\right)(11.22\text{ ft})^2}{1.83\text{ ft}}\right)$$

$$= 144.4\text{ kips}$$

The barrier load resistance is then taken as the minimum for the investigated failure mechanisms, or 118.3 kips. The barrier that has been selected for use with this design example is assumed to be approved for Test Level TL-3. Therefore, based on *AASHTO LRFD* Table A13.2-1, the transverse design force, F_t, is 54.0 kips.

$$R_w = 118.3\text{ kips} > 54.0\text{ kips} = F_t \qquad \therefore \text{OK}$$

For impacts at the end of a wall or at a joint, the barrier resistance, R_w, and the critical length of yield line failure pattern, L_c, are computed based on *AASHTO LRFD* Article A13.3.1, as follows:

$$R_w = \left(\frac{2}{2L_c - L_t}\right)\left(M_b + M_w + \frac{M_c L_c^{\,2}}{H}\right) \qquad \text{Equation 7.3.4.2.1-5}$$

AASHTO LRFD Equation A13.3.1-3

$$L_c = \frac{L_t}{2} + \sqrt{\left(\frac{L_t}{2}\right)^2 + H\left(\frac{M_b + M_w}{M_c}\right)} \qquad \text{Equation 7.3.4.2.1-6}$$

AASHTO LRFD Equation A13.3.1-4

Assuming that the failure mechanism includes the entire height of the barrier and using the previously computed values for M_b, M_w, and M_c, the values for R_w and L_c are computed as follows:

$$L_c = \frac{4\text{ ft}}{2} + \sqrt{\left(\frac{4\text{ ft}}{2}\right)^2 + (3.5\text{ ft})\left(\frac{0\text{ K-ft} + 88.80\text{ K} - \text{ft}}{12.93\,\frac{\text{k-ft}}{\text{ft}}}\right)} = 7.30\text{ ft}$$

$$R_w = \left(\frac{2}{2(7.30\text{ ft}) - 4\text{ ft}}\right)\left(0\text{ K-ft} + 88.80\text{ K} - \text{ft} + \frac{\left(12.93\,\frac{\text{K-ft}}{\text{ft}}\right)(7.30\text{ ft})^2}{3.5\text{ ft}}\right)$$

$$= 54.0\text{ kips}$$

Similarly, assuming that the failure mechanism is only the top portion (the top 22 inches of the barrier) and using the previously computed values for M_b, M_w, and M_c, the values for R_w and L_c are computed as follows:

$$L_c = \frac{4\text{ ft}}{2} + \sqrt{\left(\frac{4\text{ ft}}{2}\right)^2 + (1.83\text{ ft})\left(\frac{0\text{ K-ft} + 65.21\text{K} - \text{ft}}{11.80\,\frac{\text{k-ft}}{\text{ft}}}\right)} = 5.76\text{ ft}$$

$$R_w = \left(\frac{2}{2(5.76\text{ ft}) - 4\text{ ft}}\right)\left(0\text{ K-ft} + 65.21\text{K} - \text{ft} + \frac{\left(11.80\,\frac{\text{K-ft}}{\text{ft}}\right)(5.76\text{ ft})^2}{1.83\text{ ft}}\right)$$

$$= 74.2\text{ kips}$$

The barrier load resistance is then taken as the minimum for the investigated failure mechanisms, or 54.0 kips. The barrier that has been selected for use with this design example is assumed to be approved for Test Level TL-3. Therefore, based on *AASHTO LRFD* Table A13.2-1, the transverse design force, F_t, is 54.0 kips.

$$R_w = 54.0\text{ kips} \approx 54.0\text{ kips} = F_t \qquad \therefore \text{OK}$$

After computing the barrier load resistance, the horizontal vehicular collision force must be checked at the inside face of the barrier, at the design section for the overhang, and at the design section for the first girder bay. These design locations are presented in Figure 7.3.4.1-1. As shown in Table 7.3.4.2-1, these design checks are for the extreme event limit state.

Check at inside face of barrier:

The dead load moment at the inside face of the barrier is computed as follows:

$$M_{deck} = \frac{(0.150 \text{ kcf})(9 \text{ inches})\left(\frac{1 \text{ ft}}{12 \text{ inches}}\right)(1.4375 \text{ ft})^2}{2} = 0.116 \frac{K-ft}{ft}$$

$$M_{barrier} = \left(0.53 \frac{kips}{ft}\right)\left(1.4375 \text{ ft} - \frac{6.16 \text{ inches}}{\left(\frac{12 \text{ inches}}{1 \text{ ft}}\right)}\right) = 0.490 \frac{K-ft}{ft}$$

Therefore, the total factored design moment for the extreme event limit state is:

$$M_u = (1.25)\left[0.116 \frac{K-ft}{ft} + 0.490 \frac{k-ft}{ft}\right] + 17.86 \frac{K-ft}{ft} = 18.62 \frac{K-ft}{ft}$$

Based on *AASHTO LRFD* Article A13.4.2, the axial tensile force, T, is computed as follows:

$$T = \frac{R_w}{L_c + 2H}$$ Equation 7.3.4.2.1-7

AASHTO LRFD Equation A13.4.2-1

where:

R_w = total transverse resistance of the barrier
L_c = critical length of yield line failure pattern
H = height of wall

Using the previously computed values for R_w, L_c, and H for the controlling failure mechanism:

$$T = \frac{54.0 \text{ kips}}{7.30 \text{ ft} + 2(3.5 \text{ ft})} = 3.78 \frac{kips}{ft}$$

After these values have been computed, the required area of reinforcing steel is computed similar to the procedure for the deck. Based on the traditional design method, #5 at 6 inches was used for the top primary reinforcement. For the

overhang reinforcement, assume the use of #5 bars to resist the negative flexure in the deck. Therefore, the effective depth is computed as follows:

$$d_s = \text{Slab Thickness} - \text{Top Cover} - \frac{\text{Bar Diameter}}{2}$$

$$= 9.0 \text{ inches} - 2.5 \text{ inches} - \frac{0.625 \text{ inches}}{2} = 6.19 \text{ inches}$$

$$a = \frac{A_s F_y}{0.85 f'_c b} = \frac{A_s(60 \text{ ksi})}{0.85(4.0 \text{ ksi})\left(\frac{12 \text{ inches}}{1 \text{ ft}}\right)} = \left(1.47 \frac{\text{ft}}{\text{inch}}\right) A_s$$

$$M_r = \phi M_n = \phi A_s F_y \left(d_s - \frac{a}{2}\right) = 0.90 A_s (60 \text{ ksi}) \left[6.19 \text{ inches} - \frac{\left(1.47 \frac{\text{ft}}{\text{inch}}\right) A_s}{2}\right]$$

Setting M_r equal to the factored design moment of 28.97 K-ft/ft produces the following required reinforcement area:

$$A_s = 1.22 \frac{\text{inches}^2}{\text{ft}}$$

The required reinforcement spacing can then be computed as follows:

$$\text{Required Spacing} = \frac{0.31 \frac{\text{inches}^2}{\text{bar}}}{1.22 \frac{\text{inches}^2}{\text{ft}}} = 0.25 \text{ ft} = 3.0 \text{ inches}$$

Therefore, use two #5 bars bundled at 6 inches for the overhang reinforcement. Taking into account the axial tension force, the provided flexural resistance is computed as follows:

$$A_s = \frac{2(0.31 \text{ inches}^2)}{(6 \text{ inches})\left(\frac{1 \text{ ft}}{12 \text{ inches}}\right)} = 1.24 \frac{\text{inches}^2}{\text{ft}}$$

$$T_a = A_s F_y \qquad \text{Equation 7.3.4.2.1-8}$$

$$T_a = \left(1.24\,\frac{\text{inches}^2}{\text{ft}}\right)(60\text{ ksi}) = 74.40\,\frac{\text{kips}}{\text{ft}}$$

$$C = T_a - T \qquad \text{Equation 7.3.4.2.1-9}$$

$$C = 74.40\,\frac{\text{kips}}{\text{ft}} - 3.78\,\frac{\text{kips}}{\text{ft}} = 70.62\,\frac{\text{kips}}{\text{ft}}$$

$$a = \frac{C}{0.85f'_c\,b} \qquad \text{Equation 7.3.4.2.1-10}$$

$$a = \frac{70.62\,\frac{\text{kips}}{\text{ft}}}{0.85(4.0\text{ ksi})\left(\frac{12\text{ inches}}{1\,\text{ft}}\right)} = 1.73\text{ inches}$$

$$M_r = \phi\left[T_a\left(d_s - \frac{a}{2}\right) + T\left(\frac{d_s}{2} - \frac{a}{2}\right)\right] \qquad \text{Equation 7.3.4.2.1-11}$$

$$M_r = 0.90\left[\begin{array}{l}\left(74.40\,\frac{\text{kips}}{\text{ft}}\right)\left(6.19\text{ inches} - \frac{1.73\text{ inches}}{2}\right) \\ +\left(3.78\,\frac{\text{kips}}{\text{ft}}\right)\left(\frac{6.19\text{ inches}}{2} - \frac{1.73\text{ inches}}{2}\right)\end{array}\right]$$

$$= 30.35\,\frac{\text{K}-\text{ft}}{\text{ft}} > 28.97\,\frac{\text{K}-\text{ft}}{\text{ft}} \qquad \therefore \text{OK}$$

Check at design section for overhang:

The overhang must also be checked at the design section for the overhang, as illustrated in Figure 7.3.4.1-1. The collision forces are distributed over a distance L_c for moment and L_c+2H for axial force. Since the design section is moved away from the face of the barrier, the distribution length will increase. This design example assumes a distribution length increase based on a 30˚ angle from the face of the barrier, as illustrated in Figure 7.3.4.2.1-4.

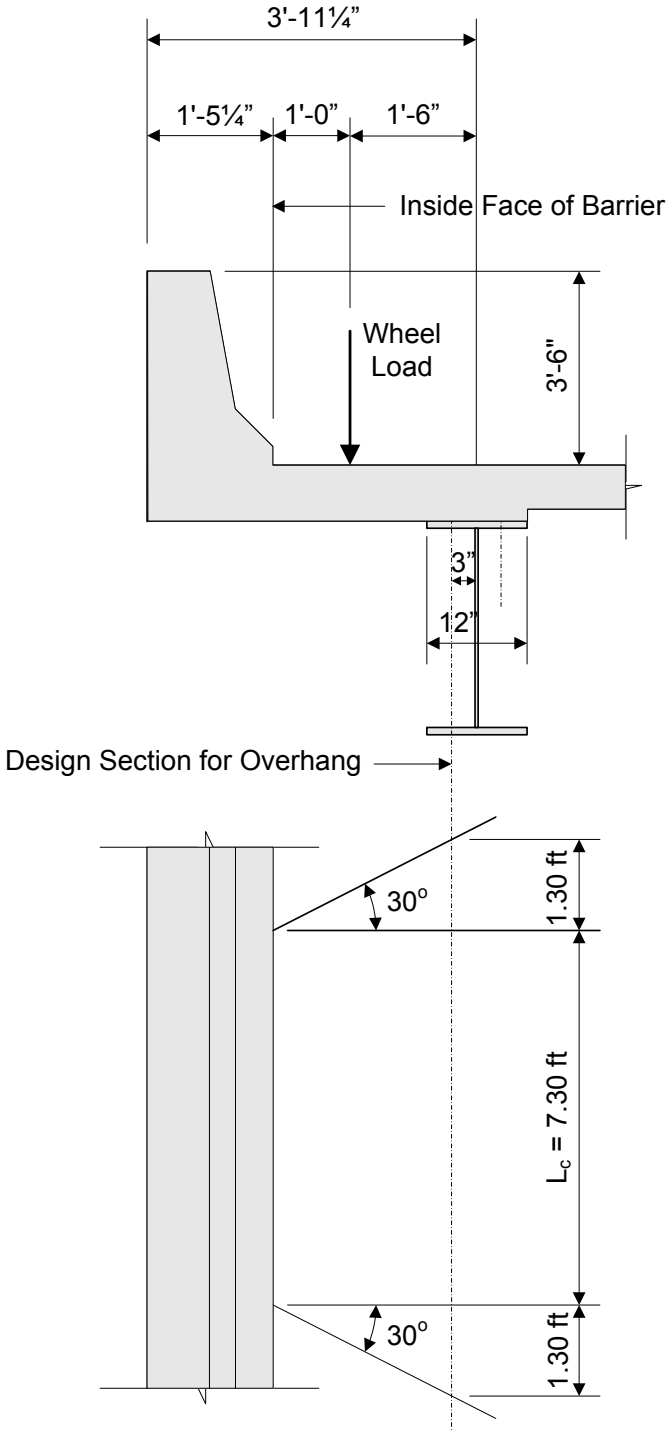

Figure 7.3.4.2.1-4 Assumed Distribution of Collision Moment Load in the Overhang

Using the same general procedures used for the check at the inside face of the barrier, the dead load moment at the design section in the overhang is computed as follows:

$$M_{deck} = \frac{(0.150 \text{ kcf})(9 \text{ inches})\left(\frac{1 \text{ ft}}{12 \text{ inches}}\right)(3.6875 \text{ ft})^2}{2} = 0.77 \frac{\text{K} - \text{ft}}{\text{ft}}$$

$$M_{barrier} = \left(0.53 \frac{\text{kips}}{\text{ft}}\right)\left(3.6875 \text{ ft} - \frac{6.16 \text{ inches}}{\left(\frac{12 \text{ inches}}{1 \text{ ft}}\right)}\right) = 1.68 \frac{\text{K} - \text{ft}}{\text{ft}}$$

$$M_{FWS} = \frac{(0.140 \text{ kcf})(2.5 \text{ inches})\left(\frac{1 \text{ ft}}{12 \text{ inches}}\right)(2.25 \text{ ft})^2}{2} = 0.07 \frac{\text{K} - \text{ft}}{\text{ft}}$$

The barrier moment resistance is adjusted as follows, based on the distribution shown in Figure 7.3.4.2.1-4:

$$M_{\text{barrier resistance}} = \frac{\left(17.86 \frac{\text{K} - \text{ft}}{\text{ft}}\right)(7.30 \text{ ft})}{7.30 \text{ ft} + 2(1.30 \text{ ft})} = 13.17 \frac{\text{K} - \text{ft}}{\text{ft}}$$

Therefore, the total factored design moment for the extreme event limit state is:

$$M_u = 1.25\left[0.77 \frac{\text{K} - \text{ft}}{\text{ft}} + 1.68 \frac{\text{k} - \text{ft}}{\text{ft}}\right] + 1.50\left(0.07 \frac{\text{K - ft}}{\text{ft}}\right) + 13.17 \frac{\text{K} - \text{ft}}{\text{ft}}$$
$$= 16.34 \frac{\text{K} - \text{ft}}{\text{ft}}$$

The axial tensile force, T, is computed as follows:

$$T = \frac{R_w}{L_c + 2(1.30 \text{ ft}) + 2H} = \frac{54.0 \text{ kips}}{7.30 \text{ ft} + 2(1.30 \text{ ft}) + 2(3.5 \text{ ft})} = 3.20 \frac{\text{kips}}{\text{ft}}$$

After these values have been computed, the required area of reinforcing steel is computed similar to the procedure for the deck. Similar to the face of the barrier, the effective depth and required reinforcement are computed as follows:

$$d_s = \text{Slab Thickness} - \text{Top Cover} - \frac{\text{Bar Diameter}}{2}$$

$$= 9.0 \text{ inches} - 2.5 \text{ inches} - \frac{0.625 \text{ inches}}{2} = 6.19 \text{ inches}$$

$$a = \frac{A_s F_y}{0.85 f'_c b} = \frac{A_s(60 \text{ ksi})}{0.85(4.0 \text{ ksi})\left(\frac{12 \text{ inches}}{1 \text{ ft}}\right)} = \left(1.47 \frac{\text{ft}}{\text{inches}}\right) A_s$$

$$M_r = \phi M_n = \phi A_s F_y \left(d_s - \frac{a}{2}\right) = 0.90 A_s (60 \text{ ksi}) \left[6.19 \text{ inches} - \frac{\left(1.47 \frac{\text{ft}}{\text{inches}}\right) A_s}{2}\right]$$

Setting M_r equal to the factored design moment of 24.48 K-ft/ft produces the following required reinforcement area:

$$A_s = 1.00 \frac{\text{inches}^2}{\text{ft}}$$

Therefore, the required reinforcing steel at the design section for the overhang is less than that at the inside face of the barrier.

Check at design section for first bay:

To design for flexure at the design section for the first bay, the distribution of the collision moment across the width of the deck is assumed to be similar to the distribution of the moment due to the barrier weight, as shown in Figure 7.3.4.2.1-5. The ratio, M_1/M_2, for the moment due to the barrier weight is assumed to equal the ratio, M_1/M_2, for the collision moment. The collision moment can then be computed by using the increased distribution length based on the 30˚ angle from the face of the barrier, as illustrated in Figure 7.3.4.2.1-4.

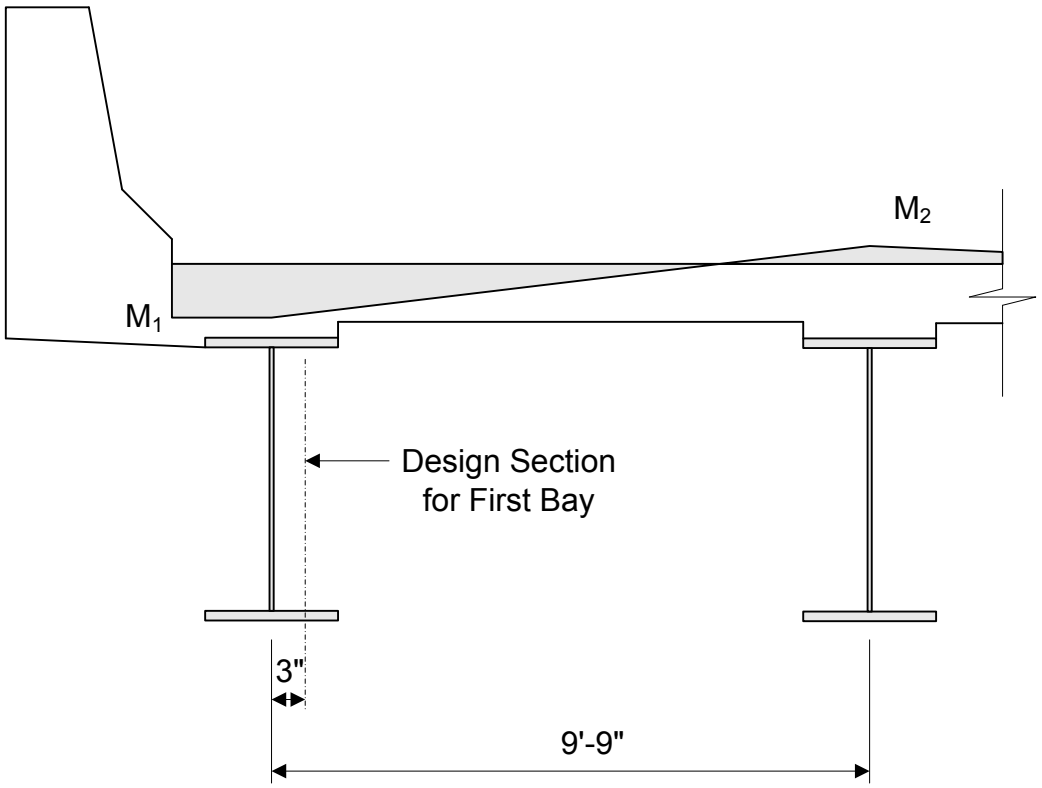

Figure 7.3.4.2.1-5 Assumed Distribution of Collision Moment

As described in previous sections of this chapter, the dead load moments in the deck can be computed using structural analysis software, based on a 1-foot strip running across the width of the deck. For this design example, the dead load moments are presented in Table 7.3.2.4-2, and the moments at the girders due to barrier weight are as follows:

$$M_{barrier\,1} = -1.66\,\frac{K-ft}{ft} \quad \text{and} \quad M_{barrier\,2} = 0.47\,\frac{K-ft}{ft}$$

Since the collision moment at the inside face of the barrier is -28.21 K-ft/ft, the collision moment at the design section for the first bay can be computed as follows:

$$M_{collision\,2} = M_{collision\,1}\frac{M_{barrier\,2}}{M_{barrier\,1}} = -17.86\,\frac{K-ft}{ft}\left(\frac{0.47\,\frac{K-ft}{ft}}{-1.66\,\frac{K-ft}{ft}}\right) = 5.06\,\frac{K-ft}{ft}$$

Based on interpolation, the collision moment at the design section for the first bay is:

$$M_{collision} = -17.86\frac{K-ft}{ft} + \left[\left(5.06\frac{K-ft}{ft} + 17.86\frac{K-ft}{ft}\right)\left(\frac{0.25\ ft}{9.75\ ft}\right)\right]$$
$$= -17.27\frac{K-ft}{ft}$$

Applying the 30° angle distribution, similar to the procedure used at the design section for the overhang, the barrier moment resistance is adjusted as follows:

$$M_{barrier\ resistance} = \frac{\left(-17.27\frac{K-ft}{ft}\right)(7.30\ ft)}{7.30\ ft + 2(1.59\ ft)} = -12.03\frac{K-ft}{ft}$$

Using the unfactored dead load moments presented in Table 7.3.2.4-2, the total factored design moment for the extreme event limit state is:

$$M_u = 1.25\left[-0.74\frac{K-ft}{ft} - 1.66\frac{k-ft}{ft}\right] + 1.50\left(-0.24\frac{K-ft}{ft}\right) - 12.03\frac{K-ft}{ft}$$
$$= -15.39\frac{K-ft}{ft}$$

The axial tensile force, T, is computed as follows:

$$T = \frac{R_w}{L_c + 2(1.59\ ft) + 2H} = \frac{54.0\ kips}{7.30\ ft + 2(1.59\ ft) + 2(3.5\ ft)} = 3.09\frac{kips}{ft}$$

After these values have been computed, the required area of reinforcing steel is computed:

$$d_s = \text{Slab Thickness} - \text{Top Cover} - \frac{\text{Bar Diameter}}{2}$$
$$= 8.5\ \text{inches} - 2.5\ \text{inches} - \frac{0.625\ \text{inches}}{2} = 5.69\ \text{inches}$$

$$a = \frac{A_s F_y}{0.85 f'_c b} = \frac{A_s(60\ ksi)}{0.85(4.0\ ksi)\left(\frac{12\ inches}{1\ ft}\right)} = \left(1.47\frac{ft}{inch}\right)A_s$$

$$M_r = \phi M_n = \phi A_s F_y \left(d_s - \frac{a}{2} \right)$$

$$= 0.90 A_s (60 \text{ ksi}) \left[5.69 \text{ inches} - \frac{\left(1.47 \frac{\text{ft}}{\text{inch}} \right) A_s}{2} \right]$$

Setting M_r equal to the factored design moment of 22.63 K-ft/ft produces the following required reinforcement area:

$$A_s = 1.02 \frac{\text{inches}^2}{\text{ft}}$$

Therefore, the required reinforcing steel at the design section for the first bay is also less than that at the inside face of the barrier.

Design Case 2: Design overhang for vertical collision force

The overhang is also designed for the vertical forces specified in *AASHTO LRFD* Article A13.4.1. As shown in Table 7.3.4.2-1, these design checks are also for the extreme event limit state. However, for concrete barriers, the case of vertical collision force never controls.

7.3.4.2.2 Design for Dead and Live Load

Design Case 3: Design overhang for dead load and live load

Finally, the overhang must be designed for dead load and live load. The dead load and live load must be checked at the design section for the overhang and at the design section for the first girder bay. These design locations are presented in Figure 7.3.4.1-1. As shown in Table 7.3.4.2-1, these design checks are for the strength limit state.

Check at design section for overhang:

As presented in Figure 7.3.2.4-2, the equivalent strip for live load on an overhang is:

$$\text{Equivalent Strip Width} = 45.0 + 10.0\text{SX}$$
$$= 45.0 + 10.0(1.25) = 57.5 \text{ inches} = 4.79 \text{ ft}$$

Applying a multiple presence factor of 1.20 for one lane loaded and a dynamic load allowance of 0.33, the moment due to live load and dynamic load allowance is computed as follows:

$$M_{LL+I} = \frac{(1.20)(1.33)(16 \text{ kips})(1.25 \text{ ft})}{4.79 \text{ ft}} = 6.66 \frac{K-ft}{ft}$$

Using the same dead load moments that were previously computed, the total factored design moment for the strength limit state is:

$$M_u = 1.25\left[0.77 \frac{K-ft}{ft} + 1.68 \frac{k-ft}{ft}\right] + 1.50\left(0.07 \frac{K\text{-}ft}{ft}\right)$$
$$+ 1.75\left(6.66 \frac{K\text{-}ft}{ft}\right) = 16.82 \frac{K-ft}{ft}$$

Since the total factored design moment for Design Case 3 is less than that computed for Design Case 1 at the design section for the overhang, Design Case 3 does not control at this design section.

Check at design section for first bay:

The dead load and live load moments are taken from Table 7.3.2.4-1, Table 7.3.2.4-2 and Table 7.3.2.4-3. The maximum negative live load moment occurs in Bay 4. Since the negative live load moment is produced by a load on the overhang, the equivalent strip is computed based on a moment arm to the centerline of the girder. As presented in Figure 7.3.2.4-2, the equivalent strip is:

$$\text{Equivalent Strip Width} = 45.0 + 10.0SX$$
$$= 45.0 + 10.0(1.50) = 60.0 \text{ inches} = 5.00 \text{ ft}$$

Therefore, the moment due to live load and dynamic load allowance is computed as follows:

$$M_{LL+I} = \frac{1.33\left(-29.40 \frac{K\text{-}ft}{ft}\right)}{5.00 \text{ ft}} = -7.82 \frac{K-ft}{ft}$$

Using the same dead load moments that were previously computed, the total factored design moment for the strength limit state is:

$$M_u = 1.25\left[-0.74\frac{K-ft}{ft} - 1.66\frac{k-ft}{ft}\right] + 1.50\left(-0.06\frac{K-ft}{ft}\right)$$
$$+1.75\left(-7.82\frac{K-ft}{ft}\right) = -16.78\frac{K-ft}{ft}$$

Since the total factored design moment for Design Case 3 is less than that computed for Design Case 1 at the design section for the first girder bay, Design Case 3 does not control at this design section.

Based on the computations for the three design cases, it is clear that the design of the deck overhang is controlled by Design Case 1 (horizontal vehicular collision force) at the inside face of the barrier for the extreme event limit state. As previously computed, the factored design moment is 28.97 K-ft/ft and the required reinforcing steel is 1.22 inches^2/foot. Also as previously computed, the required negative flexural reinforcement is #5 at 6 inches. Therefore the provided reinforcement due to negative flexure is:

$$A_s = \frac{0.31\,\text{inches}^2}{(6\text{ inches})\left(\frac{1\,\text{ft}}{12\text{ inches}}\right)} = 0.62\frac{\text{inches}^2}{\text{ft}} < 1.22\frac{\text{inches}^2}{\text{ft}}$$

Since the area of reinforcing steel required in the overhang is greater than the area of reinforcing steel provided for the negative moment regions, reinforcement must be added in the overhang area to satisfy the design requirements. The design requirements can be satisfied by bundling one #5 bar to each negative flexure reinforcing bar in the overhang area. Therefore, the provided reinforcement in the overhang is:

$$A_s = \frac{2(0.31\,\text{inches}^2)}{(6\text{ inches})\left(\frac{1\,\text{ft}}{12\text{ inches}}\right)} = 1.24\frac{\text{inches}^2}{\text{ft}} > 1.22\frac{\text{inches}^2}{\text{ft}} \qquad \therefore \text{OK}$$

7.3.4.3 Service Limit State Design

Check for cracking in overhang under service limit state

Cracking in the overhang must be checked for the service limit state in accordance with *AASHTO LRFD* Article 5.7.3.4. However, since this design check is presented in previous sections of this chapter and since it does not control most deck overhang designs, the cracking check computations are not shown in this deck overhang design example.

7.3.4.4 Reinforcement Cut-Off and Development

Compute overhang cut-off length requirement

The next step is to compute the cut-off location of the additional, bundled #5 bar in the first bay. This is done by determining the location where the total design moment (including dead load, live load, and collision load) is less than or equal to the resistance provided by #5 bars at 6 inches (negative design reinforcement).

The factored negative flexural resistance provided by #5 at 6 inch spacing is computed as follows:

$$A_s = \frac{0.31\,\text{inches}^2}{(6\text{ inches})\left(\frac{1\,\text{ft}}{12\text{ inches}}\right)} = 0.62\frac{\text{inches}^2}{\text{ft}}$$

$$a = \frac{\left(0.62\frac{\text{inches}^2}{\text{ft}}\right)(60\text{ ksi})}{0.85(4.0\text{ ksi})\left(\frac{12\text{ inches}}{1\,\text{ft}}\right)} = 0.91\,\text{inches}$$

$$M_r = 0.90\left(0.62\frac{\text{inches}^2}{\text{ft}}\right)(60\text{ ksi})\left[5.69\text{ inches} - \frac{0.91\,\text{inches}}{2}\right]$$
$$= 14.60\frac{\text{K}-\text{ft}}{\text{ft}}$$

Based on the factored flexural resistance and an interpolation of the factored design moments, the theoretical cut-off point for the additional #5 bar is approximately 3.75 feet from the centerline of the fascia girder.

Then, based on *AASHTO LRFD* Article 5.11.1.2, the additional cut-off length required beyond the theoretical cut-off point is the maximum of the following three values:

$$d_e = 5.69\text{ inches}$$

$$15(\text{nominal bar diameter}) = 15(0.625\text{ inches}) = 9.375\text{ inches}$$

$$\frac{1}{20}(\text{clear span}) = \frac{1}{20}(9.75\text{ ft})\left(12\frac{\text{inches}}{\text{ft}}\right) = 5.85\text{ inches}$$

Therefore, using 9.5 inches as the additional cut-off length, the total required length past the centerline of the fascia girder into the first bay is:

Total cut-off length = 45 inches + 9.5 inches = 54.5 inches

The location of the cut-off length is shown in Figure 7.3.4.4-1.

Compute overhang development length

In addition to the cutoff length, the overhang development length must also be computed. The basic development length is the larger of the following three values:

$$\frac{1.25A_b f_y}{\sqrt{f'_c}} = \frac{1.25(0.31)(60)}{\sqrt{4}} = 11.63 \text{ inches}$$

$$0.4d_b f_y = 0.4(0.625)(60) = 15 \text{ inches}$$

12 inches

Therefore, the basic development length for the overhang reinforcement is 15 inches. However, the following modification factors must also be applied:

Epoxy coated bars:	1.2
Bundled bars:	1.2
Spacing > 6 inches with more than 3 inches of clear cover in direction of spacing:	0.8

Applying these modification factors to the basic development length:

$$L_d = (15 \text{ inches})(1.2)(1.2)(0.8) = 17.3 \text{ inches} \qquad \text{Use 18 inches}$$

Since the 18-inch development length must extend beyond the design section, which is located 3 inches beyond the centerline of the girder, the required development distance beyond the centerline of the fascia girder is 21 inches.

Development distance = 21 inches < 54.5 inches = Cut-off distance ∴ OK

The development length is shown in Figure 7.3.4.4-1.

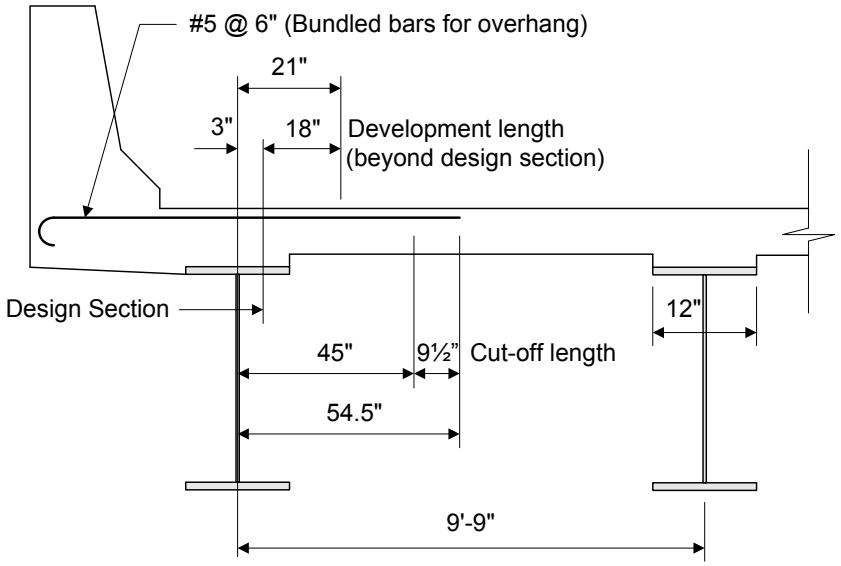

Figure 7.3.4.4-1 Length of Overhang Negative Moment Reinforcement

7.3.5 Formwork

7.3.5.1 General

The use of temporary or permanent formwork can be used for the construction of cast-in-place concrete bridge deck slabs. Permanent formwork, also known as stay-in-place formwork, can be either steel or concrete. Temporary formwork is typically constructed of wood components and the acceptability varies from state to state. Both formwork methods require the use of the deck overhang brackets to support the construction of the concrete cantilever portion of the deck.

7.3.5.2 Stay-in-Place Formwork

Stay-in-place forms can be used to span the distance between bridge girders providing formwork for cast-in-place concrete decks. Stay-in-place forms serve to support the uncured deck concrete during construction, and as the name suggests, they remain a part of the bridge after construction is completed.

Stay-in-place formwork is designed to behave elastically during construction. The forms are designed to support the self-weight of the form, the deck reinforcement, the deck concrete, including the concrete in the valleys of the form, as well as a construction load of 50 pounds per square foot. They are also designed to limit deflection to a specified maximum value, such as 1/180 of the form span or ½ inch. The flexural stress and elastic deformation requirements for stay-in-place forms are presented in *AASHTO LRFD* Article 9.7.4.1.

Some of the benefits of stay-in-place forms are:

- Ease of installation, since they are installed from the top rather than the bottom
- Reduced labor cost compared with traditional formwork which must be removed
- Reduced construction time compared with traditional formwork which must be removed
- Facilitates a uniform slab thickness

However, some disadvantages of stay-in-place forms include:

- Water than passes through the porous concrete deck is trapped in the forms and can cause corrosion of the reinforcement
- Underside inspection of the bridge deck is not possible, and therefore any cracks and corrosion in the underside of the deck are not visible

7.3.5.2.1 Steel Formwork

Stay-in-place formwork can be either steel or concrete. A typical steel stay-in-place form is illustrated in Figure 7.3.5.2.1-1. As shown in Figure 7.3.5.2.1-1, the stay-in-place forms often bear on angles welded to the girders. Due to their corrugated cross section, they can support dead load of the deck while the concrete cures. The corrugations of the form are oriented perpendicular to the girder length. Stay-in-place forms generally have closed tapered ends and are used for the interior girder bays only, where the forms can be supported on both sides by the girders. Welding is generally not permitted either to flanges in tension or to bridge elements fabricated with non-weldable grades of steel.

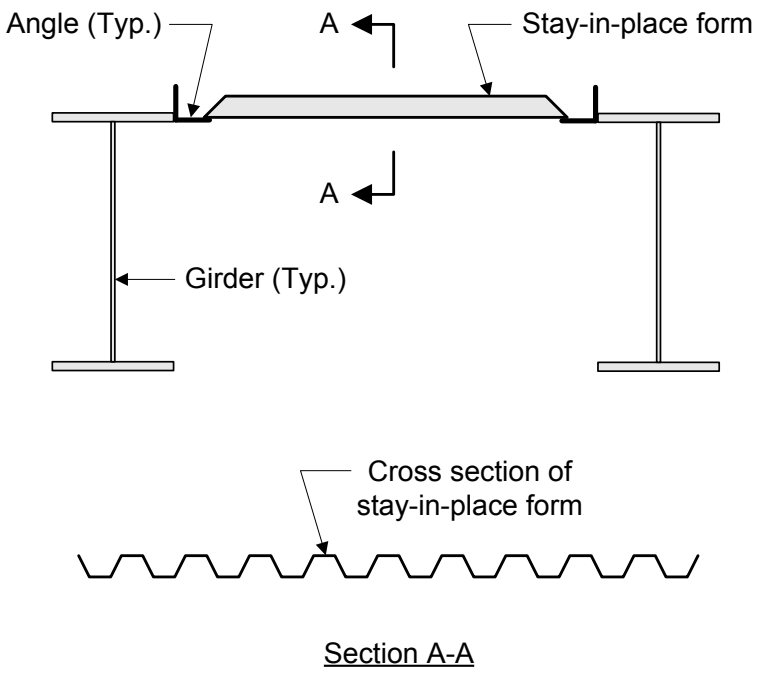

Figure 7.3.5.2.1-1 Steel Stay-in-place Formwork

7.3.5.2.2 Concrete Formwork

In addition to steel formwork, concrete formwork can also be used. Concrete formwork must satisfy the depth, reinforcement, creep and shrinkage control, and bedding requirements presented in *AASHTO LRFD* Article 9.7.4.3.

7.3.5.2.2.1 Depth

The depth of a precast concrete formwork should not be greater than 55% of the finished slab and should not exceed 3½ inches. The depth limitation is believed to be a practical limit that reduces the cracking of the cast-in-place concrete at the concrete interface.

7.3.5.2.2.2 Reinforcement

Precast concrete formwork reinforcement may be prestressed if oriented along the design span. Also, these strands can be considered as primary reinforcement in the deck slab. The concrete cover below the strands should be greater than ¾ of an inch and do not need to be extended into the cast-in-place concrete above the beams. If bottom distribution reinforcement is used, it can be placed directly onto of the panels. When placing top primary reinforcement, the splice locations are not to be located over the panel joints.

7.3.5.2.2.3 Creep and Shrinkage Control

To minimize interface shear stresses between the precast panels and the cast-in-place concrete the designer should consider the age of the panel concrete. This will minimize the difference between the shrinkage and creep of the cast-in-place concrete and the precast panel. The upper surface of the panels is to be roughened to create composite action between the stay-in-place formwork and the concrete deck. If prepared correctly, no bonding agents and/or mechanical couplers are needed.

7.3.5.2.2.4 Bedding of Panels

The precast formwork panels are to be rigidly supported. This can be accomplished by either setting the panels on a continuous mortar bed or support the panels during construction such that the cast-in-place concrete flows into the space between the panel and the supporting component to form a concrete bed. This objective is to alleviate excessive reflective cracking due to the panels transferring load to flexible supports. Creep due to prestress pulled the panel ends away from the cast-in-place concrete resulting in the direct transfer to the flexible supports.

7.3.5.3 Temporary Formwork

Temporary formwork is removed once the cast-in-place concrete deck has hardened. There are many materials that can be used as temporary formwork but the most common is wood. If temporary formwork is to be used, it should be specified in the contract documents. The designer may also choose to specify the load allowances he/she considered when investigating the girder constructibility provisions associated with the deck placement sequence. The contractor is typically responsible for the design of temporary formwork. An advantage that temporary formwork has over a stay-in-place system is the ability to see the underside of the deck allowing any distresses to be easily visible during routine bridge inspections. A disadvantage is the increased construction time due to the removal of the concrete forms.

7.3.5.4 Deck Overhang Brackets

Deck overhand brackets are used to construct the portion of the deck that extends beyond the exterior girders. The brackets must be designed to support the wet concrete overhang and the required formwork. Typically, they also support a construction walkway and the concrete paving machine. Usually the brackets are prefabricated parts and are selected from a manufacturer's catalogue. In many states, the contractor is responsible for selecting the proper overhang bracket but in some, a Professional Engineer is required to seal computations verifying the size

and spacing of the brackets. Typically, the overhang brackets are spaced at 3 of 4 feet along the exterior girder.

While the proper bracket design is the contractor's responsibility, the designer should consider the loads these brackets place on the girders supporting them when performing girder constructibility checks. The loads act eccentrically to the exterior girder resulting in torsional moments on the entire girder and local distortions of the web and flanges. If possible, the brackets should bear at the intersection of the web and bottom flange. If the bracket bears above the bottom flange, the overhang placement can cause web distortions due to out-of-plane bending. Refined analysis should be used to ensure damage to the web doesn't occur. Should a contractor select an overhang bracket that would load the web in such a way, the contract documents should include a provision requiring the contractor to submit computations seals by a Professional Engineer showing the brackets will not damage the web. Overhang brackets also induce lateral load acting on the girder top flange. Instead of using refined analysis techniques, *AASHTO LRFD* Article C6.10.3.4 provides equations that can be used to estimate the maximum lateral bending moments due to the eccentric loading.

7.3.6 Precast Deck Slabs

7.3.6.1 General

Precast concrete decks have been used on bridges since the 1950s. The primary benefit of precast decks is that they expedite bridge construction, thereby reducing construction-related traffic delays. Conventional cast-in-place deck construction with its associated curing requirements can consume more than one month on a typical bridge construction project. However, forming, casting, and curing operations of precast decks can be carried out at a remote location with reduced on-site impact to motorists. Precast decks are applicable to a wide variety of common bridge types and are applicable to deck replacement projects as well as new construction.

When constructing a precast concrete deck, the precast elements are brought to the construction site ready to be set in place and can be joined together quickly. A subsequent cast-in-place concrete pour can seal the joints and tie individual units together, forming a uniform homogenous bridge deck with improved ride quality. Deck joints can be oriented either transversely across the width of the bridge or longitudinally along the length of the bridge. The typical panel distance between joints is greater than 5 feet, sometimes exceeding 20 feet.

Several different systems of precast decks have been used. One system for full-depth concrete slab span bridges speeds construction by eliminating the need for deck forming. This system consists of precast inverted T-beam units with looped reinforcement extending from the sides of each unit. The inverted beams are

installed adjacent to each other in a manner that interlocks the looped reinforcement. The beams are made composite with cast-in-place concrete that seals the joints and fills the voids between the T's to form a solid full-depth concrete slab span structure.

Another system consists of precast deck sections that are installed on girders, with each panel extending the full width of the bridge. No on-site deck forming is needed, thereby reducing the required construction time. Similar to the previously described system, the units of this system are connected together with a series of looped reinforcement extending from the sides of the panels. They are then sealed with cast-in-place concrete.

A third system seals the joints between adjacent precast beams with a cast-in-place concrete pour. This system is applicable for box girders, as well as bulb-T girders and double-T beams.

Research on precast decks has resulted in the implementation of post-tensioning for connection durability and overlaid systems for ride quality. Other issues that have been addressed include panel casting and placement tolerances, shear connections, vertical alignment, final grade adjustment, drainage, and barrier connections.

7.3.6.2 Transversely Joined Precast Decks

AASHTO LRFD Article 9.7.5.2 allows the use of flexurally discontinuous decks made from precast panels joined together by shear keys. Shear key design and the grout used in the key must be approved by the bridge owner. Because of differential movement between panels due to wheel loads, warping, and environmental effects, shear keys tend to crack which leads to leaking and decreased shear transfer. It is recommended that this type of deck is not used in regions exposed to deicing salts.

7.3.6.3 Longitudinally Post-Tensioned Precast Decks

Precast decks made flexurally continuous by longitudinal post-tensioning are the more preferred over other precast systems because they behave monolithically and expected to require less maintenance over a long-term basis. *AASHTO LRFD* Article 9.7.5.3 specifies that the minimum average effective prestress should not be less than 0.25 ksi. The transverse joint between the components and the block-outs at the coupling of post-tensioning ducks are to be filled with a nonshrink grout having a minimum compressive strength of 5.0 ksi at 24 hours. Block-outs are also to be provided around shear connectors which will be filled with the same grout upon completion of post-tensioning. The panels should not be set in a mortar or grout to allow movement relative to the girders during prestressing.

7.3.7 Design Considerations

7.3.7.1 General

Unless there are compelling reasons otherwise, concrete decks are to be made composite with their supporting elements to enhance stiffness and economy of structures. Shear connectors used to create composite action are to be designed for force effects based on full composite action. Deck drainage is to be considered and any adverse structural effects due to the drain openings are to be considered. Fatigue in a concrete deck need not be considered if used in a multi-girder system.

7.3.7.2 Sequential Deck Placement

Deck staging must be considered to provide an acceptable deck placement sequence during construction. An analysis of the proposed deck sequence must address (but is not limited to) the following considerations:

- Stability and strength of the girder throughout deck construction.
- Change in the stiffness in the girder as different portions of the deck are placed.
- Temporary stresses and “locked-in” erection stresses in the girders.
- Bracing of the compression flange of the girders and its effect on the stability and strength of the girder.
- Bracing of the overhang deck forms
- Potential for uplift at bearings

The analysis of the deck staging is performed in an incremental manner using a concrete modulus of elasticity equal to 70% of the concrete modulus of elasticity at 28 days for concrete which is at least 24 days old. Therefore, the stiffnesses used in the model will change with each deck stage.

It is common practice to leave a block-out in the deck to facilitate proper placement and alignment of the deck joints after the dead load deflections have occurred.

The deck in the positive moment regions are generally placed before the deck in the negative moment regions. This sequence minimizes the potential for tensile stresses and cracking in the deck in the negative moment regions.

For prestressed concrete bridges made continuous for live load, the deck staging is frequently as follows:

1. Place intermediate diaphragms and shear blocks between beams, and place end diaphragms at abutments.

2. Place slab in positive moment regions.
3. Place continuity diaphragms at piers.
4. Place slab in negative moment regions.
5. Place barriers in the positive moment region and then in the negative moment region (unless continuous placement can be maintained).

A sample deck placement sequence plan is presented in Figure 7.3.7.2-1.

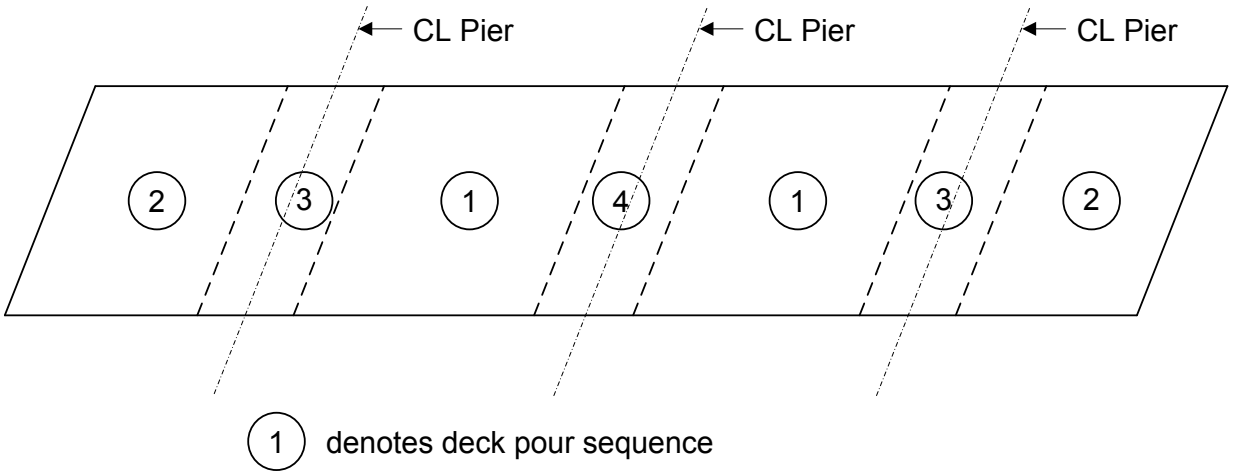

Figure 7.3.7.2-1 Sample Deck Placement Sequence Plan

7.3.7.3 Future Deck Replacement

During the service life of the bridge, a deck replacement may be required to continue to keep the bridge in service. Consideration of how the replacement might occur and incorporating those details into initial design and construction will prevent costly improvements and modifications when the replacement happens. Items such as deck removal and replacement can be considered and included in the contract plans.

Section 7.4 Metal Grid Decks

7.4.1 General

Metal grid decks are composed of main elements that span between beams, stringer, or cross-beams and secondary elements that interconnect and span between the main elements. The resulting grid can be a rectangular or diagonal pattern. The grid can be open, partially filled or filled, or unfilled with a composite slab.

7.4.2 Metal Grid Decks

Metal grid decks are made up of primary members that span between adjacent beams or transversely and secondary members that connect and span the primary members to form a grid pattern. The grid pattern is typically rectangular but diagonal patters can also be used. Metal grid decks are typically made of steel and can be open, filled or partially filled with reinforced concrete. Grid decks can also be unfilled and composite with a reinforced concrete slab.

7.4.2.1 General

Metal grid decks have been used in bridge construction since the 1930's and continue to be used in new construction or rehabilitation projects. They are especially useful where weight reduction and/or speed of construction are important considerations. Metal grid decks, filled or unfilled, are typically lighter than conventional reinforced concrete decks and offer a similar flexural resistance. Their strength-to-weight ratio is beneficial for moveable bridges and rehabilitated bridges where a lighter deck can reduce the need for structural repairs.

Metal grid decks typically consist of several panels that are fastened together as they're place on the bridge. Filled and partial filled decks may require a closer pour if precast. Filled and partial filled decks that use cast-in-place concrete offer reduced formwork to place the deck.

7.4.2.2 Open Grid Floors

Open grid floor systems consist of primary and secondary members only. The tops of the components are typically serrated to provide better vehicle traction. According to *AASHTO LRFD* Article 9.8.2.2, open metal grid decks must be connected to the supporting components by welds or mechanical fasteners at each main element. If welded, a single-sided 3 inch long or 1½ inch weld on each side is to be used. These welds should be considered a Category E detail, and the provisions of *AASHTO LRFD* Article 6.6 apply.

While their high strength-to-weight ratio is an obvious advantage, open grid decks have several disadvantages over filled metal grid decks or conventional reinforced deck slabs. The disadvantages include unpleasant ride quality, additional noise, possible safety issues when wet, and they allow debris, road salts and water through the deck and onto the superstructure and substructure normally protected by a closed deck. Fatigue is also an issue for open grid decks, both internally and in their connections to the main elements. Because of these disadvantages, open grid decks are rarely used in new construction except for in-kind replacements.

7.4.2.3 Filled and Partially Filled Grid Decks

Filled metal grid decks are when the entire depth of the grid system is filled with concrete. The system can either utilize precast panels or serve as formwork for cast-in-place concrete. To satisfy serviceability and durability requirements, reinforcing bars are added perpendicular to the main supporting bars and thin gage sheet metal is attached to the bottom to provide support for the full depth concrete. Filled metal grid decks were first introduced in the 1930's as a way to decrease construction time on large scale bridge projects.

Partially filled metal grid decks are when a portion of the depth of the grid system is filled with concrete. This system was introduced in the 1950's as a way to further reduce weight by eliminating concrete from the bottom of the deck which is in tension in simple span applications. The system can either utilize precast panels or serve as formwork for cast-in-place concrete. To satisfy serviceability and durability requirements, reinforcing bars are added parallel to the main supporting bars and thin gage sheet metal is attached at mid-depth to provide support for the concrete.

A 1¾ inch thick structural overfill should be provided on filled and partially filled metal grid decks per *AASHTO LRFD* 9.8.2.3.1, although 2 inches is more common. The concrete overfill provides protection against chlorides. It is also recommended to galvanize or paint the steel to add another layer of protection. Filled or partially filled grid decks can be attached to supporting elements by welding or shear studs, which is more prevalent. Should shear studs be used, a haunch should be provided to ensure that the studs are completely encased in concrete and extend into the steel grid similarly to a conventional reinforced deck, but not into the concrete overfill.

7.4.2.4 Unfilled Grid Decks Composite with Reinforced Concrete Slabs

An unfilled grid deck composite with a reinforced concrete slab has a reinforced concrete slab that is cast on top of an unfilled grid deck and made composite with the unfilled grid deck. In these types of decks, reinforced concrete is supported by thin gage sheet metal on top of secondary members. Reinforcing steel is provided for serviceability and durability, but also provides negative flexural resistance. Composite action is achieved through shear connectors or other means capable of resisting interface shear. Several shear connections are offered in *AASHTO LRFD* Article 9.8.2.4.2 which includes tertiary bars that studs are welded to or holes that are drilled in the main bars and allow concrete to flow between and lock the grid and deck together. The steel should also be galvanized or painted to protect the metal grid from corrosion. Shear studs are used to connect these types of decks to the main components. Similar to the partially filled and filled metal grid decks, a haunch should be provided so the studs are complete encased in concrete.

7.4.2.5 Design and Detailing Considerations

7.4.2.5.1 Determination of Force Effects

According to *AASHTO LRFD* Article 9.8.2.1, the force effects in open, filled, partially filled grid decks and grid decks composite with a reinforced concrete slab can be determined using one of the following methods:

- The approximate methods specified in *AASHTO LRFD* Article 4.6.2.1, as applicable;
- Orthotropic plate theory;
- Equivalent grillage;
- Design aids provided by the manufacturers, if the performance of the deck is documented and supported by sufficient technical evidence.

The equivalent strip method can be used for the determination of live load effects for open grid decks, similar to conventional reinforced concrete deck slabs. For fully and partially filled grids and for unfilled grid decks composite with reinforced concrete slabs, *AASHTO LRFD* Article 4.6.2.1.8 applies because of the orthotropic plate behavior of these types of decks.

7.4.2.5.2 Applications

Table 7.4.2.5.2-1 highlights typical applications for partially filled and filled grid decks, and grid decks composite with reinforced concrete slabs. The typical weight range and thickness considers 2 inches of overfill.

Table 7.4.2.5.2-1 Typical Components, Span Lengths, Weight Ranges, and Total Thickness for Various Metal Grid Decks

	Partial Depth	Full Depth	Unfilled and Composite Slab
Primary Member Component	Rolled I-shape	Rolled I-shape or WT	WT4, WT5, or WT 6 *
Maximum Span Length	Up to 10 feet	Up to 10 feet	Greater than 10 feet
Weight Range (psf)	65 to 75	70 to 110	60 to 70
Total Thickness (in.)	7.25	5.00 to 7.25	6.50 to 9.50

* These are the most common sizes; however larger WT shapes can be used for large spans.

7.4.2.5.3 Composite Action

Filled and partially filled grid decks, and grid decks composite with a reinforced concrete slab can be made composite with the supporting superstructure by

embedding shear studs in a haunch area with full depth concrete. Shear studs are to be designed and placed in accordance with *AASHTO LRFD* Articles 5.8.4 or 6.10.10 depending on the superstructure material. If made composite, the supporting elements can be designed assuming an effective slab width in accordance with *AASHTO LRFD* Article 4.6.2.6.1 and omitting any concrete slab area in tension.

7.4.2.5.4 Deck Overhang

Similar to conventional reinforced concrete decks, *AASHTO LRFD* Article A13.4.1 applies to metal grid decks with reinforced concrete. The design of the overhang must still consider the three design cases provided in the article. As a designer, special attention needs to be given for the connection of the barrier to the deck to ensure crashworthiness of the system is sufficient.

7.4.3 Orthotropic Steel Decks

While not common in the United States, orthotropic steel decks have been used throughout Europe, Asia, the Far East, and South America. An orthotropic steel deck consists of a thin, flat steel plate that is stiffened by longitudinal ribs that run parallel to traffic and orthogonal to floorbeams. The behavior of this type of deck is more anisotropic due to the significant difference in transverse and longitudinal elastic section properties. The name orthogonal came from the layout of the floorbeams and ribs supporting the deck system. Typically, an orthotropic steel deck is made integral with the supporting superstructure component.

7.4.3.1 General

In an orthotropic steel deck system, live loads are transferred through a wearing surface and top steel deck plate, to the longitudinal ribs, and then to the transverse floor beams and finally to the main load carrying system, typically a steel plate girder. According to *AASHTO LRFD* Article 9.8.3.1, the orthotropic deck is to act as a common flange for the ribs, floorbeams and main longitudinal components of the bridge. With proper maintenance, experience has shown that this system has a long service life.

Orthotropic deck construction requires less time than conventional reinforced concrete decks, mostly because they are prefabricated in a shop. Future deck replacement is typically not needed but the wearing surface requires replacement every 20 to 30 years. The success of this type of deck is contingent on construction and fabrication techniques.

7.4.3.2 Typical Deck Sections

Typical deck sections are either classified as open-rib or closed-rib systems. Open-rib systems are typically made from flat bars, bulb shapes, inverted T-sections, or angles. Closed-rib systems are typically made from trapezoidal, U-shaped, or V-shaped sections. Closed rib systems are preferred over open-rib systems because of their high torsional stiffness which effectively transfers loads to the adjacent ribs. While closed-rib systems distribute loads more efficiently, the partial penetration weld required to weld the shape to the plate is complicated and fatigue proned. Furthermore, because of the torsional rigidity, closed-rib systems are subject to secondary deformations and stresses that must be addressed during design. Both systems are made continuous and integral with the floorbeams by notching out the floorbeams to allow the ribs to pass through them.

Advantages of orthotropic steel decks are evident in long span bridges because of their high strength-to-weight ratio compared to conventional concrete decks. This reduction in dead weight makes orthotropic bridge cross sections good candidates for moveable bridges and suspended span bridges. Another popular use of orthotropic decks is in steel box girders because many of the slender plates require stiffening.

7.4.3.3 Design and Detailing Considerations

When analyzing orthotropic steel decks, *AASHTO LRFD* Article 9.8.3.4.1 requires the appropriate use of the three levels of analysis specified in *AASHTO LRFD* Articles 9.8.3.4.2 through 9.8.3.4.4. The fatigue limit state is to be designed for at least one of the three levels, while strength, service, and extreme event limit states and constructibility criteria are to be investigated using Level 2 (*AASHTO LRFD* Article 9.8.3.4.3). Level 1 design is empirical in nature and based on minimal structural analysis. The details selected for this type of design are based on previous experimental testing for specimens similar in design and detail. All details must maintain a consistent level of safety according to AASHTO specifications. Level 2 design is based on a simplified one-dimensional or two-dimensional analysis of certain panel details. Calculations for this level of analysis only consider nominal stresses and not local stress concentrations. Using the Pelikan-Esslinger method allows the designer to calculate conservative global force effects.

Level 3 design is the most intricate level of analysis. It employs the use of a refined three-dimensional model to quantify the local stresses. Level 3 design is required for panels that have not undergone previous experimental testing unless it can be proven that distortions will not lead to fatigue cracking. If a refined three-dimensional analysis is required, structural modeling techniques must include the following:

- Use of shell or solid elements with acceptable formulation to accommodate steep stress gradients
- Mesh density of t x t, where t is the thickness of the plate component
- Local structural stresses are to be determined as specified in *AASHTO LRFD* 9.8.3.4.4

7.4.3.4 Wearing Surfaces

The wearing surface on an orthotropic steel deck is imperative to improving the skid resistance, distributing wheel loads, and protecting the deck from corrosion. Also, the deck wearing surface must be sufficiently ductile and strong enough to expand, contract and deform without cracking or debonding. Sufficient wearing surface fatigue strength to withstand flexural stresses due to composite action between the deck plate and wearing surface is required. Also, the wearing surface must:

- Be durable enough to resist rutting and wearing from traffic
- Impervious to water and vehicular fuels and oils, and
- Resistant to deicing salts and deterioration due to solar radiation.

The two most common wearing surface systems are bituminous, which is generally 2.0 inches thick or greater, or a polymer system, usually ¾ inch thick. Typically, climate dictates the chosen wearing surface. When specified and installed correctly, and maintained properly, either wearing surface has shown to have a service life in excess of 30 years.

Section 7.5 Other Deck Systems

7.5.1 General

In addition to steel and concrete, there are other options available for providing a suitable bridge deck. Aluminum, wood and fiber reinforced polymers are examples of alternative materials that have been and shown acceptable for various applications.

7.5.2 Orthotropic Aluminum Decks

Orthotropic aluminum decks consist of a deck stiffened and supported by rib extrusions. The ribs may be parallel or perpendicular to the direction of traffic. According to *AASHTO LRFD* Article 9.8.4, the articles pertaining to orthotropic steel decks apply except that the wearing surface is not to be considered integral with the deck for analysis and design of the deck or rib. Additionally, when supported by components of another material, differences in thermal expansion of the two

materials and the potential for accelerated corrosion due to dissimilar materials are to be considered.

7.5.3 Corrugated Metal Decks

As stated in *AASHTO LRFD* Article 9.8.5.1, corrugated metal decks should only be used on secondary and rural roads. Corrugated metal decks are composed of corrugated metal pans filled with a bituminous asphalt or another approved surfacing material. The corrugated metal pans are to be fastened to the supporting components for stability of both under transient loads. Wheel loads are distributed through the surfacing material at a 45 degree angle from the contact area to the neutral axis of the corrugated metal pans. If contribution of the fill material through composite action is to be assumed, the provisions of *AASHTO LRFD* Article 9.8.3.3 must be satisfied.

7.5.4 Wood Decks

7.5.4.1 General

AASHTO LRFD Article 9.9 details the design of wood decks and deck systems. Materials used in wood decks, including their preservative treatment, must meet standards found in *AASHTO LRFD* Sections 2, 5, 6, and 8. Plank decks must have a minimum thickness of 4.0 inches for roadways and 2.0 inches for sidewalks. For any other wood deck, the minimum thickness is 6.0 inches.

According to *AASHTO LRFD* Article 9.9.3.1, load distribution through wood decks can be accomplished using one of the following methods:

- The approximate method specified in *AASHTO LRFD* Article 4.6.2.1,
- Orthotropic plate through, or
- Equivalent grillage model.

When selecting the appropriate load distribution method, the spacing of the supporting components should be considered. For spacing either 36.0 inches or 6.0 times the nominal depth of the deck, the entire system, including the supporting components, has to be modeled as an orthotropic plate or an equivalent grid.

7.5.4.2 Types of Wood Decks

7.5.4.2.1 Glued Laminated Decks

Glued laminated, or Glulam, timber panel decks consist of a series of panels, prefabricated with water-resistant adhesives, that are tightly abutted along their

edges. Glulam panels are continuous across the deck width and typically joined with a bituminous sealer providing a watertight deck surface.

7.5.4.2.2 Stress Laminated Decks

Stress laminated decks are a series of wood laminations that are placed edgewise and post-tensioned together, normal to the direction of the lamination. The majority of decks of this type include laminations that are 2.0 to 3.0 inches in thickness. Post-tensioning bars are placed through predrilled holes in the laminations. *AASHTO LRFD* Article 9.9.5 provides detailed specifications for nailing, staggering butt joints, prestressing hole locations, spacing, and stressing, and deck tie-downs. Stressed laminated decks are not permitted to be used where skew angles are in excess of 45 degrees.

Stress laminated decks have an increased load distribution and load sharing ability over other wood decks. The compression caused by the prestressing force develops friction allowing the laminations to act as an orthotropic plate. Considering this and their improved durability, stress laminated decks are preferred for high volume and heavy vehicular traffic.

7.5.4.2.3 Spike Laminated Decks

Spike laminated decks are a series of wood laminations that are placed edgewise and spiked together on their wide face with deformed spikes. According to *AASHTO LRFD* 9.9.6, the spikes must be long enough to fully penetrate at least four laminations and spaced no greater than 12.0 inches in an alternating pattern. Pilot holes are to be drilled through pairs of laminations prior to driving the spikes. This method of fastening laminations together does not lead to long-term durability on roads with high truck volumes. *AASHTO LRFD* Article C9.9.6.1 recommends this type of deck be used on secondary roads with an ADTT less than 100 trucks per day.

7.5.4.2.4 Plank Decks

Wood plank decks are a series of lumber planks placed flatwise on supports and fastened to the supporting member. *AASHTO LRFD* Article 9.9.7 provides tie-down spacing and size requirements. This type of deck can be economical for low volume roads with little or no heavy vehicles. Because they do not have a bituminous wearing surface, there is no protection against moisture resulting in continuous maintenance if used by heavy vehicles. *AASHTO LRFD* Article C9.9.7.1 states this deck should be limited to roads that carry little or no heavy vehicles or where the running surface is constantly monitored and maintained.

7.5.4.3 Wearing Surfaces

According to *AASHTO LRFD* Article 9.9.8, wood deck wearing surfaces are to be continuous in nature and no nails, except in wood planks, are to be used to fasten them to the deck. Bituminous wearing surfaces are recommended. To encourage adhesion and prevent bleeding of preservative treatment through the wearing surface, the wood deck should be free of surface oils. The plans and specifications should clearly state that the deck material should be treated using the empty cell process, followed by an expansion bath or steaming.

7.5.5 Fiber Reinforced Polymer (FRP) Decks

Fiber reinforced polymer (FRP) bridge decks are pre-engineered and prefabricated in a shop then then assembled and installed at the bridge site. After assembly, a wearing surface is typically applied in the field. FRP bridge decks are composed of various layers of E-glass fibers and a resin, typically either vinyl ester or polyester. FRP decks are dependent on multiple things such as fiber type, volume and orientation as well as resin type, manufacturing methods and bonding materials. Typically, FRP bridge decks are composed for two plates separated by a core material. The core material can be of a foam material or corrugated FRP sheets.

Because of FRP's high strength-to-weight ratio, FRP bridge decks can be as much as one quarter the weight of conventional concrete decks. This makes FRP decks an attractive option for rehabilitation projects. The decreased dead weight reserves a supporting girder system's capacity for heavier live loads and can raise a bridge posting weight restriction. Also, FRP bridge decks have a decreased construction time compared to conventional concrete decks; another advantage for rehabilitation projects where closure time is of concern.
A disadvantage to using FRP bridge decks is the higher initial cost compared to conventional concrete decks. Also, because this is a relatively new technology, designs have not been standardized and there is no long-term data supporting the design service life. FRP bridge decks degrade when overexposed to ultraviolet radiation. Finally, since they're preassembled, there is little tolerance when erecting in the field.

For more information regarding the advantages and disadvantages of FRP decks, construction methods, considerations for the use of FRP decks, and general design criteria, the reader should refer to the FHWA advisory titled "Current Practices in FRP Composite Technology FRP Bridge Decks and Superstructures".

Section 7.6 Bridge Railing Design

Many different railings are used on our nation's bridges today. The bridge engineer usually does not need to design the railings for a bridge. Instead the railings are

selected from a set of crashed-tested and approved railings. The crash-testing matrices and conditions are defined in either NCHRP Report 350, "Recommended Procedures for the Safety Performance Evaluation of Highway Features", or AASHTO's *Manual for Assessing Safety Hardware* (or MASH). All highway safety hardware accepted prior to the adoption of MASH and using criteria contained in NCHRP Report 350 criteria is not required to be retested using MASH criteria. New high safety hardware not previously evaluated must utilize MASH for testing and evaluation. For the purposes of this manual, MASH criteria will be presented but the major differences between MASH and NCHRP Report 350 will be discussed.

MASH was developed to revise criteria for impact performance of virtually all highway safety features, based primarily on changes in the vehicle fleet. Some of the major differences between MASH and NCHRP Report 350 pertaining to bridge railings include:

Changes in Test Matrices

- The small car impact angle is increased from 20 to 25 degrees
- The impact speed for the single-unit truck test is increased from 80 km/h to 90 km/h
- Length-of-need tests with the pickup truck are required to meet occupant risk criteria
- The barrier mounting height is recommended to be set at the maximum for small car tests and at the minimum for pickup truck tests

Changes in Test Installations

- Any rail element splices that are used in the field are required to be installed in the impact region during testing
- More detailed documentation of components used in the test installation is required
- Minimum installation length requirements are specified more clearly

Changes in Test Vehicles

- The size and weight of test vehicles is increased to reflect the increase in vehicle fleet size:
    - The 820C test vehicle is replaced by the 1100C
    - The 2000P test vehicle is replaced by the 2270P
    - The single unit truck mass is increased from 8000 kg to 10,000 kg
    - The light truck test vehicle must have a minimum center of gravity height of 28 inches
- The option for using passenger car test vehicles older than 6 years is removed
- Truck box attachments on test vehicles are required to meet published guidelines

- External vehicle crush must be documented using National Automotive Sampling System (NASS) procedures

Changes in Evaluation Criteria

- The occupant compartment damage evaluation uses quantitative, instead of qualitative, criteria
- All evaluation criteria will be pass/fail, eliminating the “marginal pass”
- All longitudinal barrier tests are required to meet flail space criteria
- Maximum roll and pitch angles are set at 75 degrees
- The subjective criteria for evaluating exit conditions are eliminated; reporting the exit box evaluation criterion is required

Changes in Test Documentation

- CAD drawings of the test device and test installation are required
- Additional documentation of the test and evaluation results is required

Changes in Performance Evaluation

- Language emphasizing the importance of in-service evaluation is added

With the guidelines provided in MASH, a given railing or barrier may be tested to one of six test levels. A test level is defined by the impact speed, the impact angle of approach, and the type of test vehicle. Bridge barriers designed and tested to satisfy Test Level 1 are generally used on low service level roadways, such as rural connectors, local roads, or restricted work zones. Barriers designed and tested to satisfy Test Level 6, however, are usually used on high service level roadways, such as freeways and major highways. To illustrate the six test levels, Table 7.6-1 contains testing information used for each level.

Table 7.6-1 Test Matrix for Barriers

Test Level	Test Vehicle Designation and Type	Test Conditions	
		Speed mph (km/h)	Angle (degrees)
TL-1	1100C (Passenger Car)	31 (50.0)	25
TL-1	2270P (Pickup Truck)	31 (50.0)	25
TL-2	1100C (Passenger Car)	44 (70.0)	25
TL-2	2270P (Pickup Truck)	44 (70.0)	25
TL-3	1100C (Passenger Car)	62 (100.0)	25
TL-3	2270P (Pickup Truck)	62 (100.0)	25
TL-4	1100C (Passenger Car)	62 (100.0)	25
TL-4	2270P (Pickup Truck)	62 (100.0)	25
TL-4	10000S (Single-Unit Truck)	56 (90.0)	15
TL-5	1100C (Passenger Car)	62 (100.0)	25
TL-5	2270P (Pickup Truck)	62 (100.0)	25
TL-5	36000V (Tractor-Van Trailer)	50 (80.0)	15
TL-6	1100C (Passenger Car)	62 (100.0)	25
TL-6	2270P (Pickup Truck)	62 (100.0)	25
TL-6	36000T (Tractor-Tank Trailer)	50 (80.0)	15

shows that, as the test level increases, either the heaviest test vehicle size increases or the nominal impact speed increases if the same vehicle is being used.

To be approved for use on a bridge, a barrier must satisfy three phases:

1. Research and development – the design evolves and is eventually subjected to a set of crash tests, which are assessed based on a set of evaluation criteria.
2. Experimental – the in-service performance of the experimental barrier is closely monitored.
3. Operational – the in-service performance of the approved barrier continues to be monitored.

When a barrier satisfies these three phases, it is approved to resist a set of design forces, as presented in Table 7.6-2. Just as Table 7.6-1 shows that a higher test level can resist a heavier test vehicle or a greater impact speed, Table 7.6-2 shows that a higher test level can resist greater design forces. The variables and designations used in Table 7.6-2 are defined in *AASHTO LRFD* Article 13.3 and are illustrated in *AASHTO LRFD* Figure A13.2-1.

Table 7.6-2 Design Forces for Traffic Railings
(Based on *AASHTO LRFD* Table A13.2-1)

Design Forces and Designations	Railing Test Level					
	TL-1	TL-2	TL-3	TL-4	TL-5	TL-6
F_t Transverse (kips)	13.5	27.0	54.0	54.0	124.0	175.0
F_L Longitudinal (kips)	4.5	9.0	18.0	18.0	41.0	58.0
F_v Vertical (kips) Down	4.5	4.5	4.5	18.0	80.0	80.0
L_t and L_L (feet)	4.0	4.0	4.0	3.5	8.0	8.0
L_v (feet)	18.0	18.0	18.0	18.0	40.0	40.0
H_e (min.) (inches)	18.0	20.0	24.0	32.0	42.0	56.0
Minimum H Height of Rail (inches)	27.0	27.0	27.0	32.0	42.0	90.0

Example:

The Typical Concrete Barrier, shown in Figure 7.6-1, has been tested and approved for Test Level 5.

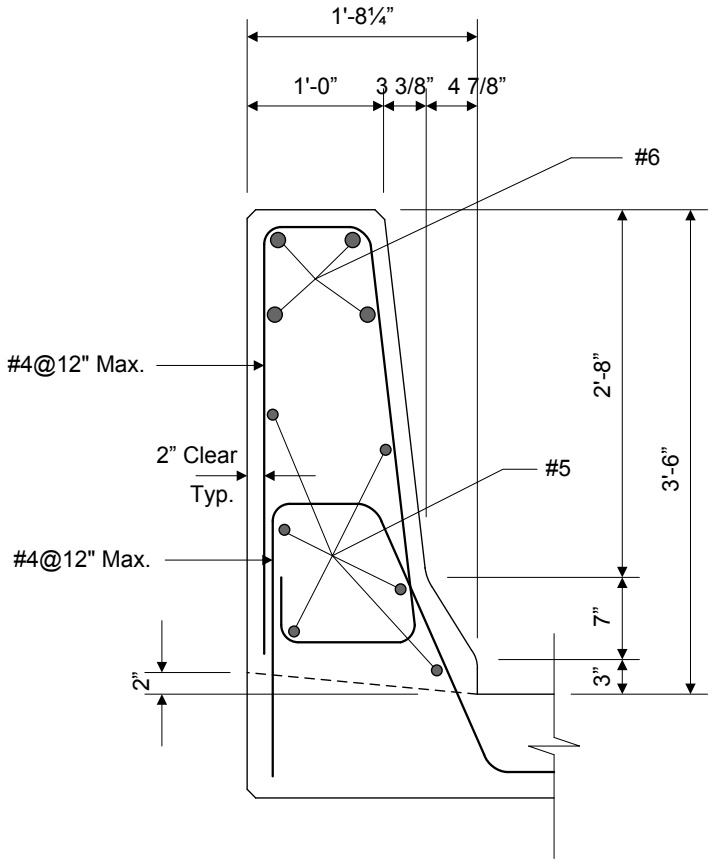

Concrete strength, f'_c = 4 ksi
Reinforcing steel strength, f_y = 60 ksi

Figure 7.6-1 Typical Concrete Barrier, Approved for Test Level 5

Similarly, the Alternate Concrete Barrier, shown in Figure 7.6-2, has been tested and approved for Test Level 4.

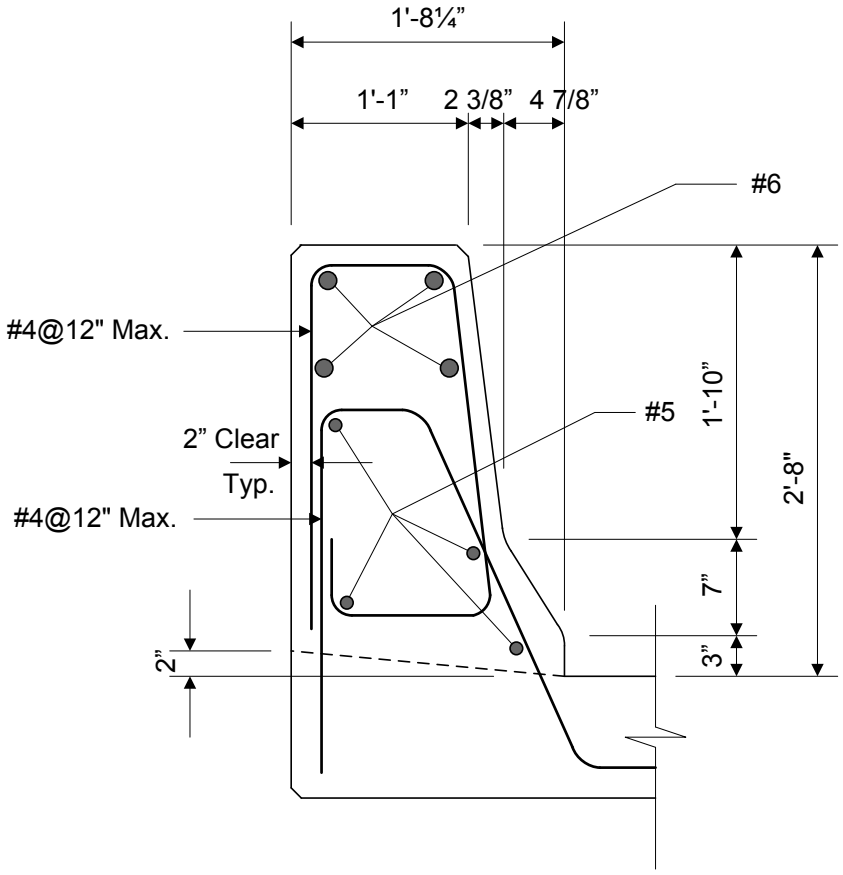

Concrete strength, f'_c = 4 ksi
Reinforcing steel strength, f_y = 60 ksi

Figure 7.6-2 Alternate Concrete Barrier, Approved for Test Level 4

Several observations can be made from these two barrier examples. First, the two barriers are similar, but the Typical Concrete Barrier, which is 3'-6" high, is approved for Test Level 5, while the Alternate Concrete Barrier, which is only 2'-8" high, is only approved for Test Level 4. It is intuitive that for similar barriers, the taller barrier can be utilized for higher service level roadways.

Second, the approved barrier details define more than just the barrier shape. They also define all dimensions of the barrier, all reinforcing steel required in the barrier, the required reinforcement clear distance, and the required concrete and reinforcing

steel strengths. If these barriers are utilized on a bridge, each of these requirements must be fully satisfied.

Third, the barrier has been approved for a specific test level and therefore satisfies specific performance characteristics. However, the test level does not necessarily define a specific barrier application. That determination rests with the appropriate transportation agency responsible for the bridge.

Finally, the engineer does not necessarily need to perform any barrier design. Instead, they select a barrier that has been tested and approved for the specific test level required by the governing agency for that particular bridge location.

However, it should be noted that some changes to tested barriers are permitted and can be submitted to FHWA for approval. Such changes generally relate to either the anchorage or the overhang, but they do not generally relate to the geometry of the front face of the barrier. These changes can often be demonstrated through analysis and need not receive a full crash test to be approved.

For a concrete barrier, sample design computations are presented in Section 7.3.4 of this chapter. The values computed in Section 7.3.4 are required for the design of the overhang portion of the deck.

Section 7.7 References

AASHTO. 2009. *Manual for Assessing Safety Hardware.* American Association of State Highway and Transportation Officials, Washington, DC.

Chavel, B. 2012. “Steel Bridge Design Handbook: Bridge Deck Design”. Federal Highway Administration, Office of Bridge Technology, Washington, DC.

Homberg, H. 1968. *Fahrbahnplatten mit Verandlicher Dicke*. Springer-Verlag, New York, NY.

Pucher, A. 1964. *Influence Surfaces of Elastic Plates*, 4th Edition. Springer-Verlag, New York, NY.

Chapter 8
Bearings and Joints

Section 8.1 Introduction

Bearings are located between the superstructure and the substructure of a bridge. They transmit loads from the superstructure to the substructure while also facilitating translations and/or rotations. This chapter describes some of the most common bearing types, it provides guidance for selecting the optimum bearing for a specific application, and it describes the design process for several common bearing types.

Joints are located within bridge decks to accommodate the translation and rotation of the structure at the joint. This chapter describes several common deck joints, and it provides guidance for selecting the number and location of joints.

Section 8.2 Bearings

8.2.1 General

Bearings come in a variety of types and sizes, but they all perform the same basic function. They all transmit loads from the superstructure to the substructure and facilitate translations and/or rotations. The bearing type and size is simply a function of the design requirements and the magnitudes of the loads and movements. A guided steel bearing is shown in Figure 8.2.1-1.

Figure 8.2.1-1 Guided Steel Pot Bearing

Bearing selection and design generally involves three basic steps:

1. Obtain the required design input.
2. Select the most feasible bearing type.
3. Design the selected bearing.

The bearing design input generally depends on whether the bearing is fixed or expansion. A common schematic used by bridge engineers to depict fixed and expansion bearings is presented in Figure 8.2.1-2.

Figure 8.2.1-2 Schematic of Fixed and Expansion Bearings

In addition, the capabilities of fixed and expansion bearings are summarized in Table 8.2.1-1.

Table 8.2.1-1 Capabilities of Fixed and Expansion Bearings

Capabilities	Fixed Bearings	Expansion Bearings
Resists vertical force	Yes	Yes
Resists horizontal force	Yes	No
Facilitates vertical movement	No	No
Facilitates horizontal movement	No	Yes
Facilitates rotation	Yes	Yes

Bearings can be fixed in both the longitudinal and transverse directions, fixed in one direction and expansion in the other, or expansion in both directions.

When deciding which bearings are fixed and which are expansion on a bridge, the following guidelines are commonly considered:

- The bearing layout for a bridge must be developed as a consistent system. Vertical movements are resisted by all bearings, horizontal movements are resisted by fixed bearings and facilitated in expansion bearings, and rotations are generally allowed to occur as freely as possible.
- For maintenance purposes, it is generally desirable to minimize the number of deck joints on a bridge, which can in turn affect the bearing layout.

- The bearing layout must facilitate the anticipated thermal movements, primarily in the longitudinal direction but also in the transverse direction for wide bridges.
- It is generally desirable for the superstructure to expand in the uphill direction wherever possible.
- If more than one substructure unit is fixed within a single superstructure unit, then forces will be induced into the fixed substructure units and must be considered during design.
- For curved and/or skewed bridges, the bearing layout can induce additional stresses into the superstructure which must be considered during design.
- Forces are distributed to the bearings based on the superstructure analysis.

8.2.2 Loads and Movements

Bearings must be designed for both the applied loads and the anticipated movements. Loads can be applied to bearings in several different directions, and translations and rotations can also occur in several directions. Bearing loads and movements result in bearing deformations, as illustrated in the elastomeric bearing in Figure 8.2.2-1.

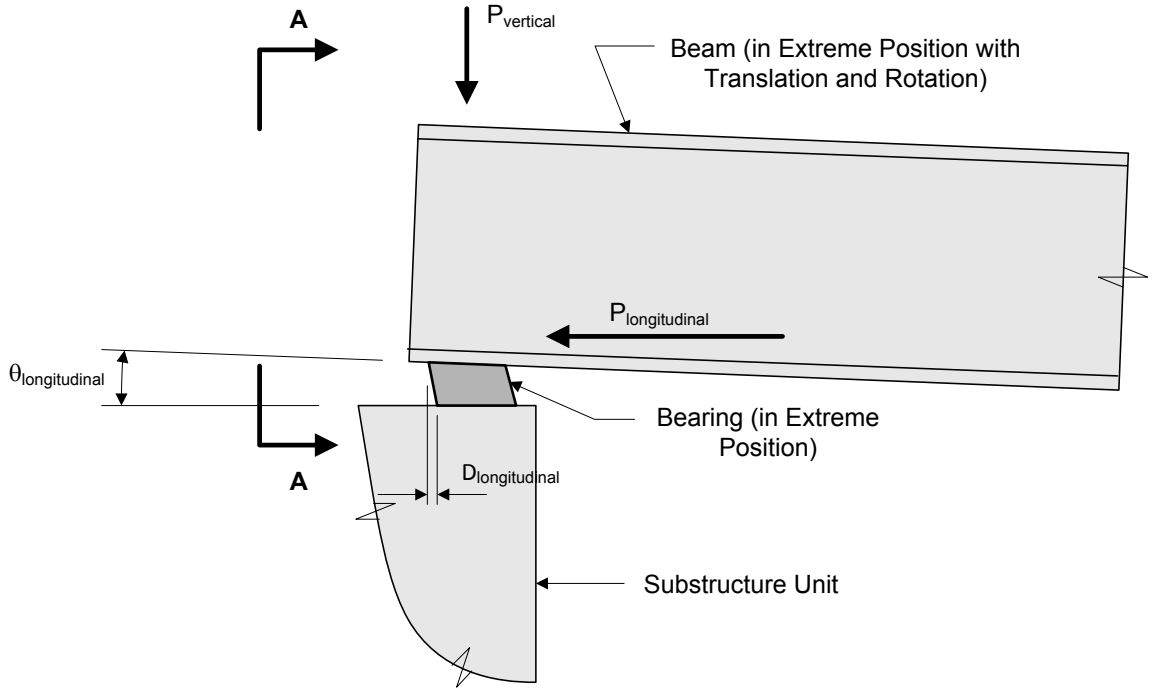

Elevation

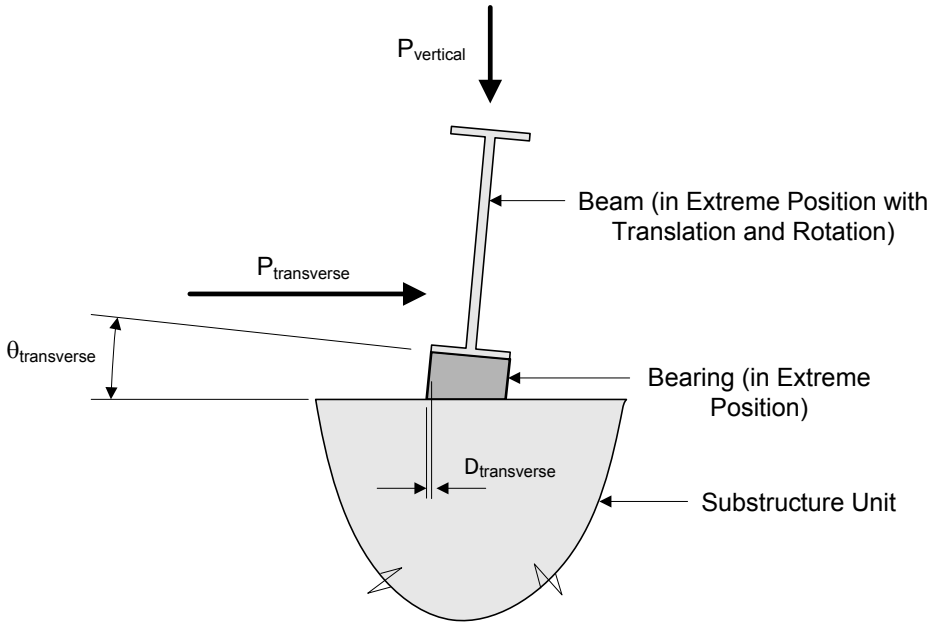

View A-A

Figure 8.2.2-1 Elastomeric Bearing Loads and Movements

8.2.2.1 Loads

Bearings must be designed to resist the loads transferred from the superstructure to the substructure. The primary load is generally the vertical load, which is caused by dead load, vehicular live load, dynamic load allowance, pedestrian live load, and any other vertical loads which may be present. For some bearings, a minimum vertical load is specified in addition to a maximum vertical load.

In addition, bearings must also resist horizontal loads in the direction of fixity. Horizontal loads can be caused by wind load on structure, wind on live load, uniform temperature, vehicular braking force, vehicular centrifugal force, earthquake, and any other horizontal loads which may be present.

It is important to note that expansion bearings do not resist horizontal loads in the direction of expansion (with the exception of frictional forces). For example, if a bearing facilitates expansion in the longitudinal direction, then that bearing will not resist longitudinal loads. Similarly, if a bearing facilitates expansion in the transverse direction, then it will not resist transverse loads. Horizontal loads are applied only to bearings that are fixed in the direction of the load.

A schematic showing the various loads acting on a bearing is presented in Figure 8.2.2-1.

8.2.2.2 Movements

In addition to resisting loads, bearings must also be designed to facilitate the anticipated movements that will occur at the bearing location. Bearing movements include both translation and rotation.

8.2.2.2.1 Translation

A bearing must facilitate translation in the girders or beams that are being supported. For example, if the superstructure lengthens due to temperature rise or shortens due to temperature fall, then the bearings must be designed to facilitate this longitudinal translation. Although translation is usually greatest in the longitudinal direction, translation in the transverse direction can also be significant, especially on wide, curved, or skewed bridges.

Fixed bearings are designed such that no translation is permitted in the direction of fixity. Expansion bearings are designed to facilitate the anticipated translation in the direction of expansion.

Bearing translation is illustrated in Figure 8.2.2-1.

8.2.2.2.2 Rotation

A bearing must also facilitate rotation in the girders or beams that are being supported. For example, if a girder deflects due to dead load or live load, then this deflection will cause the end of the girder to rotate in the longitudinal direction (about the transverse axis of the bridge). Similarly, for a curved or skewed bridge, the torsional effects in the girders may cause the end of the girder to rotate in the transverse direction (about the longitudinal axis of the bridge). The bearing must be designed to facilitate these anticipated rotations.

Bearing rotation is also illustrated in Figure 8.2.2-1.

8.2.3 Bearing Types

8.2.3.1 General

There are many different types of bearings, and each one has its own unique applications, based on the magnitude of the loads, translations, and rotations about the various axes of the bridge. Five common bearing types are illustrated in Figure 8.2.3.1-1.

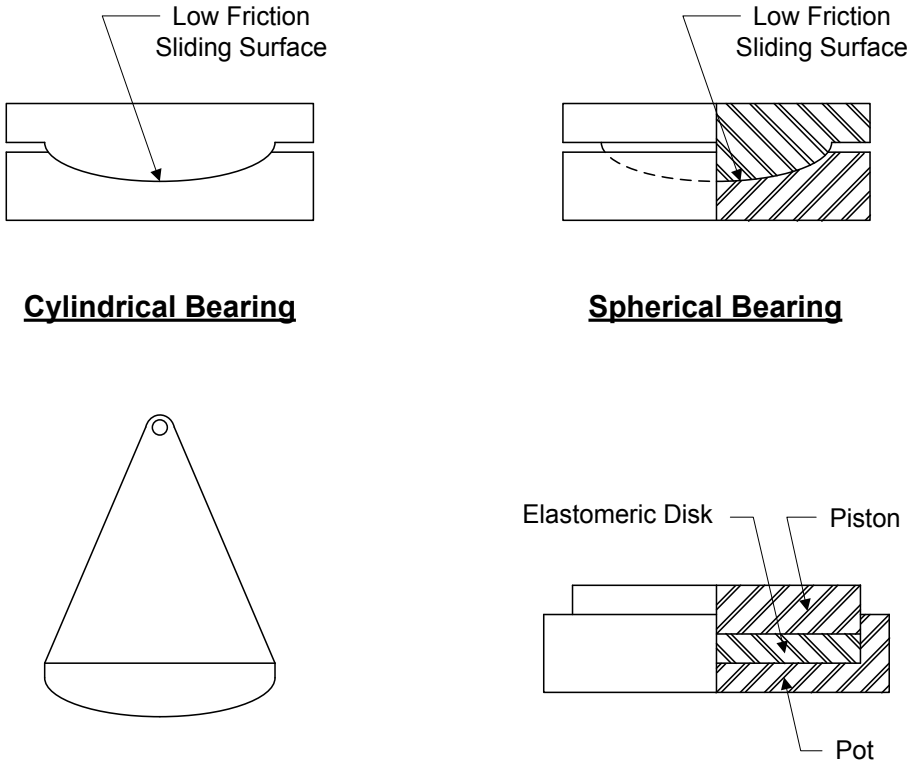

Figure 8.2.3.1-1 Common Bearing Types
(Based on *AASHTO LRFD* Figure 14.6.2-1)

Some of the most common bearing types are presented in Table 8.2.3.1-1, along with a general description of the bearing. Information about bearing selection, including maintenance requirements, is presented in Section 8.2.3.6.

Table 8.2.3.1-1 Bearing Type Descriptions

Bearing Type	General Description
Bronze bearing	A cylindrical or spherical bearing in which displacements or rotations take place by the sliding of a bronze surface against a mating surface.
Cotton-duck-reinforced pad (CDP)	An elastomeric pad made from closely spaced layers of elastomer and cotton-duck, bonded together during vulcanization.
Disc bearing	A bearing that accommodates rotation by deformation of a single elastomeric disc molded from a urethane compound. It may be guided, unguided, or fixed. Movement is accommodated by sliding of polished stainless steel on PTFE.
Double cylindrical bearing	A bearing made from two cylindrical bearings placed on top of each other with their axes at right angles to facilitate rotation about any two horizontal orthogonal axes.
Fiberglass-reinforced pad (FGP)	An elastomeric pad made from discrete layers of elastomer and woven fiberglass bonded together during vulcanization.
Knuckle bearing	A bearing in which a concave metal surface rocks on a convex metal surface to provide rotation capability about any horizontal axis.
Metal rocker or roller bearing	A bearing that carries vertical load by direct contact between two metal surfaces and that accommodates movement by rocking or rolling of one surface with respect to the other.
Plain elastomeric pad (PEP)	An elastomeric pad made exclusively of elastomer, which provides limited translation and rotation.
Pot bearing	A bearing that carries vertical load by compression of an elastomeric disc confined in a steel cylinder and that accommodates rotation by deformation of the disc.
PTFE sliding bearing	A bearing that carries vertical load through contact stresses between a PTFE sheet or woven fabric and its mating surface, and that permits movements by sliding of the PTFE over the mating surface.
Steel-reinforced elastomeric bearing	An elastomeric bearing made from alternate laminates of steel and elastomer bonded together during vulcanization. Vertical loads are carried by compression of the elastomer. Movements parallel to the reinforcing layers and rotations are accommodated by deformation of the elastomer.

8.2.3.2 Elastomeric Bearings

8.2.3.2.1 General

Elastomeric bearings are commonly used on small to moderate sized bridges. Design of elastomeric bearings is typically the responsibility of the design engineer, as opposed to the bearing manufacturer. There are several general types of elastomeric bearings, including the following:

- Plain pads
- Steel or fiberglass reinforced elastomeric bearings
- Cotton duck bearings

Each type is described in the following sections.

8.2.3.2.2 Plain Pads

As the name suggests, plain elastomeric pads consist entirely of elastomer, and they are usually rectangular in shape. Plain elastomeric pads can be used for small bridges, in which the vertical loads, translations, and rotations are relatively small.

Plain elastomeric pads rely upon friction at the contact surfaces to resist bulging of the pad. Loss of friction leads to slippage, which in turn results in increased strain and decreased load-carrying resistance of the bearing. Since the compressive resistance of the plain elastomeric pad is a function of the shape factor, plain pads must be relatively thin to carry the maximum compressive load. Therefore, plain pads can accommodate only limited translations and rotations.

8.2.3.2.3 Steel/Fiberglass Reinforced Elastomeric Bearings

Reinforced elastomeric pads are often used for larger bridges with more sizable vertical loads, translations, and rotations. Reinforced elastomeric pads consist of multiple layers of elastomer bonded to alternating layers of reinforcing material. Steel plate is most commonly used for the reinforcing material, although fiberglass can also be used. A sample reinforced elastomeric pad is illustrated in Figure 8.2.3.2.3-1.

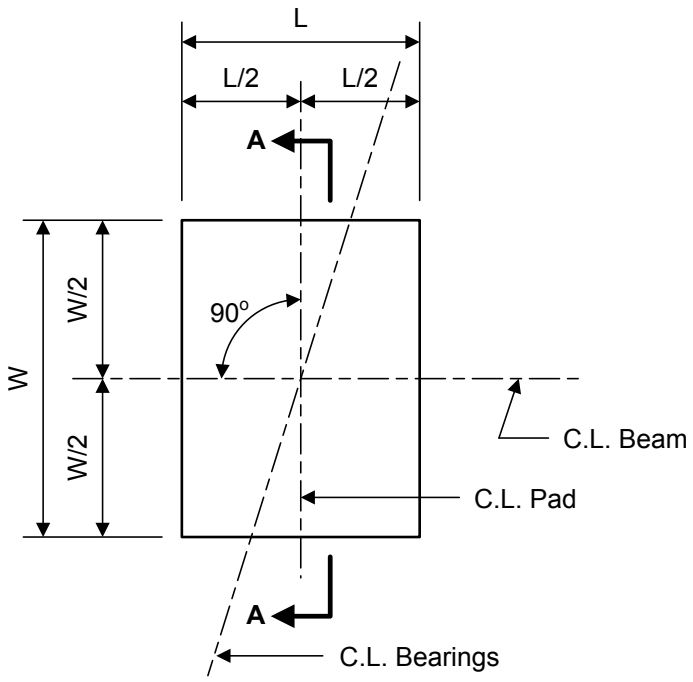

Plan

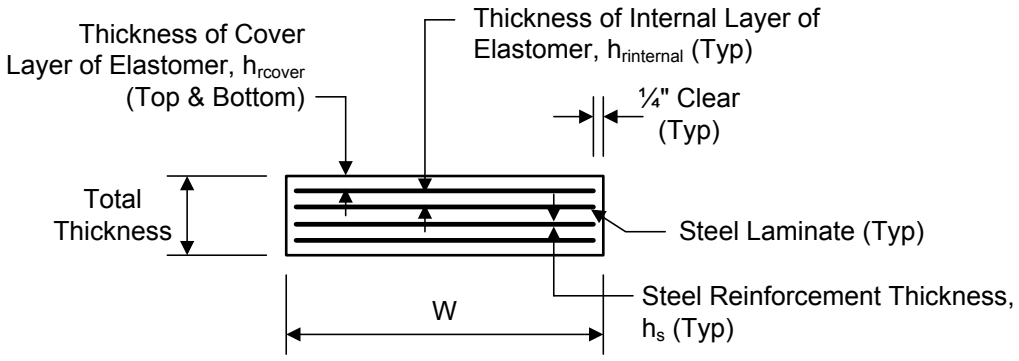

Section A-A

Figure 8.2.3.2.3-1 Reinforced Elastomeric Pad

Steel reinforced elastomeric bearings rely upon the restraint of the bonded steel plates, in addition to the contact surface friction, to resist bulging of the bearing. The presence of steel reinforcing results in thin, uniformly spaced elastomer layers, which facilitate greater compressive stresses and greater translation and rotational resistance than plain pads.

Based on the assumed coefficient of friction between the elastomer and the concrete or steel surface, the bearing is subject to slip if the horizontal shear force is greater

than approximately 20% of the minimum permanent dead load. In such cases, the bearing may need to be secured against horizontal movement.

8.2.3.2.4 Cotton Duck Bearings

Cotton duck bearings are fabricated by vulcanizing thin layers of elastomer with cotton fabric weave. Due to their high durometer hardness, they are generally stiff against shear and rotation and can resist high compressive loads. Because of their resistance to translation, cotton duck bearings are commonly used with a polytetrafluorethylene (PTFE) sliding surface, and they do not require a metallic substrate between the PTFE and the bearing.

8.2.3.3 High-Load Multi-Rotational Bearings

8.2.3.3.1 General

High-load multi-rotational (HLMR) bearings are commonly used on larger bridges for which elastomeric bearings are unable to satisfy the design requirements. Design of HLMR bearings is typically the responsibility of the bearing manufacturer. HLMR bearings can generally resist high loads and are able to rotate in any direction. They can be fixed or, when fabricated with sliding surfaces, they can accommodate translation for use as an expansion bearing. Guide bars can also be used with HLMR bearings to restrict movement in one direction.

There are several general types of HLMR bearings, including the following:

- Pot bearings
- Disc bearings
- Bearings with curved sliding surfaces

Each type is described in the following sections.

8.2.3.3.2 Pot Bearings

Pot bearings are commonly used for moderate to large bridges. They carry vertical load by compression of an elastomeric disc contained within a steel cylinder and accommodate rotation by deformation of the disc. Pot bearings are generally used for applications requiring a multi-directional rotational resistance and a medium to large range of load.

The primary components of a pot bearing are illustrated in Figure 8.2.3.3.2-1. The schematic in Figure 8.2.3.3.2-1 shows a sample pot bearing, but it does not necessarily represent the exact configuration of all pot bearings.

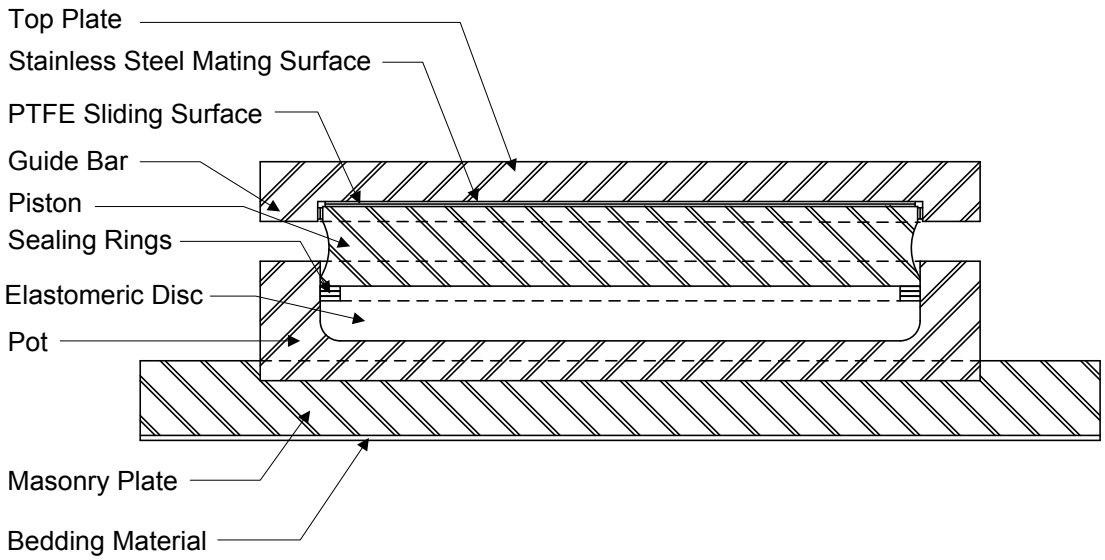

Figure 8.2.3.3.2-1 Components of a Pot Bearing

Pot bearings resist vertical load primarily through compressive stress in the elastomeric pad. The pad can deform and it has some shear stiffness, but it has very limited compressibility. Pot bearings generally have a large reserve of resistance to vertical load.

Pot bearings facilitate rotation through deformation of the elastomeric pad. During rotation, one side of the pad compresses and the other side expands. Pot bearings can sustain many cycles of small rotations with little or no damage. However, pot bearings can experience significant damage when subjected to relatively few cycles of large rotations.

Pot bearings can also resist horizontal loads. Pot bearings can either be fixed, guided, or non-guided. Fixed pot bearings cannot translate in any direction, and they resist horizontal load primarily through contact between the rim of the piston and the wall of the pot. Guided pot bearings can translate in only one direction, and they resist horizontal load in the other direction through the use of guide bars. Non-guided bearings can translate in any direction, and they do not resist horizontal loads in any direction.

8.2.3.3.3 Disc Bearings

Disc bearings consist of an unconfined elastomeric disc. Disc bearings are more economical than many other steel bearing types, and they are frequently used when smaller load resistance is required. Disc bearings may be guided, unguided, or fixed. Movement is accommodated by the sliding of polished stainless steel on PTFE. Horizontal forces are generally transmitted from an upper load plate to either

a shear pin in the center of the disc or to a restricting ring. The restricting ring is similar in detail to a pot bearing, except that the disc is unconfined with no requirement for sealing rings.

8.2.3.3.4 Bearings with Curved Sliding Surfaces

Bearings with curved sliding surfaces transmit vertical and horizontal loads through the spherical coupling of the convex and concave plates of the bearing. The interface of these two plates is typically a mating of PTFE and stainless steel, resulting in a low coefficient of friction. All vertical loads are assumed to be transmitted radially through the interface of these two surfaces, and all horizontal loads are resisted by the spherical geometry of the plates.

8.2.3.4 Metal Rocker and Roller Bearings

In addition to HLMR bearings, two other types of metal bearings are rocker bearings and roller bearings. In rocker bearings, a curved surface is generally placed on top of a flat surface. The two steel parts are constrained by a dowel pin to prevent horizontal movement of the bearing. Rocker bearings should be avoided or carefully designed for applications in which the anticipated horizontal translation is excessive and may result in tipping of the rocker bearing. For example, in seismic regions, the anticipated horizontal translation could result in tipping of rocker bearings.

In roller bearings, one or more steel cylinders is placed between two parallel steel plates. Since the rollers facilitate horizontal movement, roller bearings are generally used only at expansion supports. Roller bearings must be designed to ensure that the bearing alignment does not change during the design life of the bridge. Multiple roller bearings should be connected by gearing to ensure that individual rollers remain at their designed spacing and remain parallel to each other. Roller bearings can be damaged if the bridge rotates about the axis normal to the rotational axis of the bearing. Therefore, roller bearings are not suitable for curved or skewed bridges or for bridges in seismic regions.

Metal rocker bearings and roller bearings must be detailed such that they can be easily inspected and maintained.

8.2.3.5 Sliding Surfaces

Sliding bearings consist of two surfaces that slide against each other. PTFE and lubricated bronze or copper alloy are frequently used as sliding surfaces for sliding bearings. Sliding surfaces develop a frictional force that can be estimated as follows:

$$F = \mu N \qquad \text{Equation 8.2.3.5-1}$$

where:

F = friction force
μ = coefficient of friction
N = normal force on the sliding surface

As shown in the above equation, the greater the coefficient of friction between the two surfaces, the greater the friction force. Curved surfaces can also be used to facilitate sliding. Several types of sliding surfaces are described in the following sections.

8.2.3.5.1 PTFE

Polytetrafluorethylene (PTFE), also known as Teflon (Dupont's brand name), is often used for lubrication in sliding bearings, and it provides favorable chemical resistance and a low coefficient of friction. PTFE sliding surfaces are commonly used in the following bearing types:

- Elastomeric/PTFE bearings
- Sliding pot bearings
- Spherical PTFE bearings with slider

Because PTFE has a low coefficient of friction, it develops relatively small friction forces.

PTFE is used with a mating surface, generally consisting of stainless steel for flat sliding surfaces and for many curved surfaces. The mating surface can also be anodized aluminum for some spherical or cylindrical surfaces. The stainless steel surface must be larger than the PTFE surface to prevent exposure of the PTFE during movement. Wherever possible, the stainless steel should be placed on top of the PTFE to prevent contamination from dirt or dust.

The coefficient of friction varies from approximately 0.02 to 0.10 for dimpled lubricated PTFE, depending on the pressure and the temperature. Other types of PTFE have different coefficients of friction. PTFE generally has a lower coefficient of friction than bronze or copper alloy. Additional information about coefficient of friction values is presented in *AASHTO LRFD* Table 14.7.2.5-1.

PTFE sometimes creeps laterally when subjected to high compressive stresses. To control the potential for creep, the PTFE is sometimes recessed half of its thickness into the sliding plate. PTFE must be at least 1/16 inch thick after compression. However, recessed PTFE must be at least 3/16 inches thick when the maximum dimension does not exceed 24 inches, and it must be at least ¼ inch thick when the

maximum dimension exceeds 24 inches. It is recommended that the bridge engineer require certification tests for all types of PTFE to ensure that it satisfies the design requirements.

8.2.3.5.2 Bronze or Copper Alloy

Bronze or copper alloy can also be used for a sliding surface, and it can accommodate very large translations. Bronze or copper alloy sliding surfaces are commonly used for the following bearing types:

- Flat sliding surfaces to accommodate translational movements
- Curved sliding surfaces to accommodate translation and limited rotation
- Pins or cylinders for shaft bushings of rocker bearings or other bearings with large rotations

The mating surface can be structural steel. Lubricated bronze bearings use a pattern of recesses for lubricant. The recesses are usually approximately ½ inch deep, and they are formed by casting the bronze in a mold and then machining it to the proper geometry and surface finish. The lubricant is placed into the recesses under pressure, and it projects above the bronze approximately 1/16 inch. The mating surface grips the lubricant and spreads it over the sliding surface as movement occurs. However, the surface lubrication can dissipate with time and movement, sometimes resulting in direct contact between the bronze and the mating surface.

The coefficient of friction is initially approximately 0.07, but it generally increases to approximately 0.10 after the lubrication begins to erode. If the surface lubrication has completely dissipated, then the coefficient of friction can be on the order of 0.40.

Bronze bearings are economical compared with PTFE, and they do not require the high degree of quality control required for PTFE surfaces. They do not require a highly polished mating surface, nor do they require the tight geometric constraints of PTFE. However, the frictional resistance is often considerably larger than that provided by PTFE surfaces.

8.2.3.5.3 Curved Surfaces

Sliding bearings can be fabricated with flat surfaces to facilitate horizontal movement. They can also be fabricated with curved surfaces to facilitate rotation and a limited amount of horizontal movement. Curved surfaces must be manufactured such that the two surfaces have equal nominal radii, and they must have a low friction sliding interface. Therefore, the inside and outside radii must be accurately machined and controlled. Bearings with curved sliding surfaces include

both spherical and cylindrical bearings, and they are special cases of PTFE or lubricated bronze sliding surfaces.

8.2.3.6 Bearing Selection

After the bearing layout for the entire bridge has been established and the bearing design requirements have been defined, the next step is to select the most feasible bearing type. Several tools are available to the bridge engineer to assist in selecting feasible bearing types.

One such tool is presented in *AASHTO LRFD* Table 14.6.2-1, in which the suitability of various bearing types is presented in terms of movement, rotation, and resistance to loads. This information is presented in Table 8.2.3.6-1.

Table 8.2.3.6-1 Bearing Suitability
(Based on *AASHTO LRFD* Table 14.6.2-1)

Type of Bearing	Movement		Rotation about Bridge Axis Indicated			Resistance to Loads		
	Long.	Trans.	Long.	Trans.	Vert.	Long.	Trans.	Vert.
Plain elastomeric pad	S	S	S	S	L	L	L	L
Fiberglass-reinforced pad	S	S	S	S	L	L	L	L
Cotton-duck-reinforced pad	U	U	U	U	U	L	L	S
Steel-reinforced elastomeric bearing	S	S	S	S	L	L	L	S
Plane sliding bearing	S	S	U	U	S	R	R	S
Curved sliding spherical bearing	R	R	S	S	S	R	R	S
Curved sliding cylindrical bearing	R	R	U	S	U	R	R	S
Disc bearing	R	R	S	S	L	S	S	S
Double cylindrical bearing	R	R	S	S	U	R	R	S
Pot bearing	R	R	S	S	L	S	S	S
Rocker bearing	S	U	U	S	U	R	R	S
Knuckle pinned bearing	U	U	U	S	U	S	R	S
Single roller bearing	S	U	U	S	U	U	R	S
Multiple roller bearing	S	U	U	U	U	U	U	S

In the above table:

S represents suitable
U represents unsuitable
L represents suitable for limited applications
R represents may be suitable but requires special considerations or additional elements such as sliders or guideways

Another valuable tool is presented in the American Iron and Steel Institute's (AISI) *Steel Bridge Bearing Selection and Design Guide*, Table I-A. This table not only presents load, translation, and rotation capabilities of each bearing type, but it also presents information about initial costs and maintenance costs. This information is presented in Table 8.2.3.6-2.

Table 8.2.3.6-2 Summary of Bearing Capabilities
(Based on AISI's *Steel Bridge Bearing Selection and Design Guide*, Table I-A)

Bearing Type	Load (Kips)		Translation (Inches)		Rotation (Radians)	Costs	
	Min.	Max.	Min.	Max.	Limit	Initial	Maintenance
Plain elastomeric pads	0	100	0	0.6	0.01	Low	Low
Cotton duck elastomeric pads	0	315	0	0.2	0.003	Low	Low
Fiberglass elastomeric pads	0	135	0	1	0.015	Low	Low
Steel-reinforced elastomeric pads	50	780	0	4	0.04	Low	Low
Flat PTFE slider	0	>2250	1	>4	0	Low	Moderate
Curved lubricated bronze	0	1570	0	0	>0.04	Moderate	Moderate
Pot bearing	270	2250	0	0	0.02	Moderate	High
Pin bearing	270	1000	0	0	>0.04	Moderate	High
Rocker bearing	0	400	0	4	>0.04	Moderate	High
Single roller	0	100	1	>4	>0.04	Moderate	High
Curved PTFE	270	1570	0	0	>0.04	High	Moderate
Multiple rollers	110	2250	4	>4	>0.04	High	High

Another valuable tool from AISI's *Steel Bridge Bearing Selection and Design Guide* is a set of three preliminary bearing selection diagrams. Separate diagrams are presented for each of the following rotation requirements:

- Minimal design rotation (rotation ≤ 0.005 radians)
- Moderate design rotation (rotation ≤ 0.015 radians)
- Large design rotation (rotation > 0.015 radians)

These three diagrams are presented in Figure 8.2.3.6-1, Figure 8.2.3.6-2, and Figure 8.2.3.6-3. In each diagram, the limit lines which define the regions are approximate and could be moved approximately 5% in either direction. Therefore, if a specific bearing application falls near a limit line, the Engineer should investigate both bearing types.

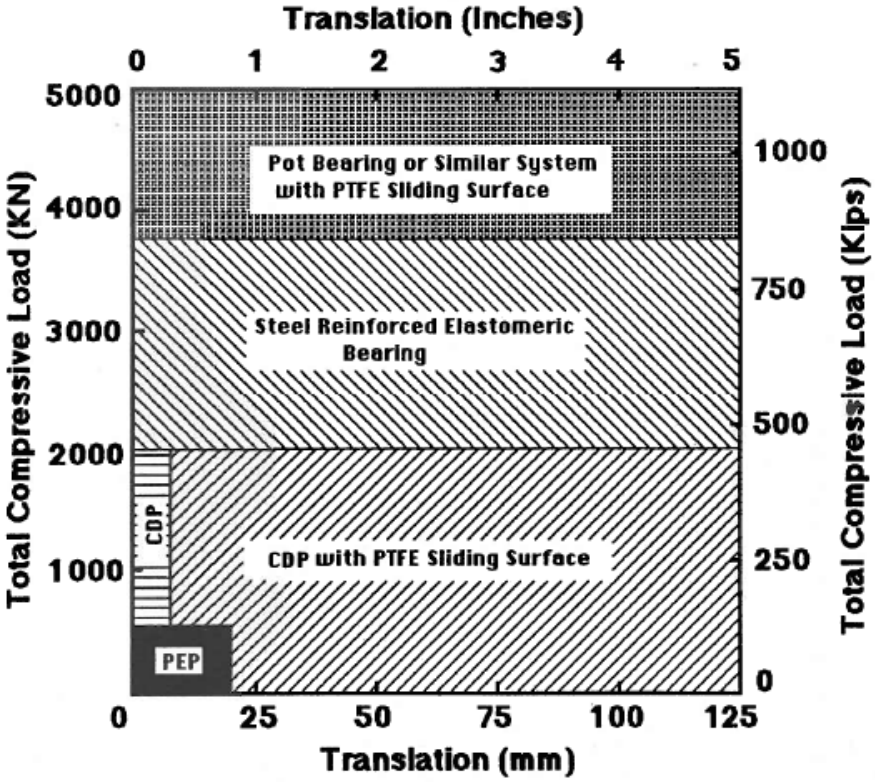

Figure 8.2.3.6-1 Preliminary Bearing Selection Diagram for Minimal Design Rotation (Rotation ≤ 0.005 Radians)
(From AISI's *Steel Bridge Bearing Selection and Design Guide*, Figure I-1)

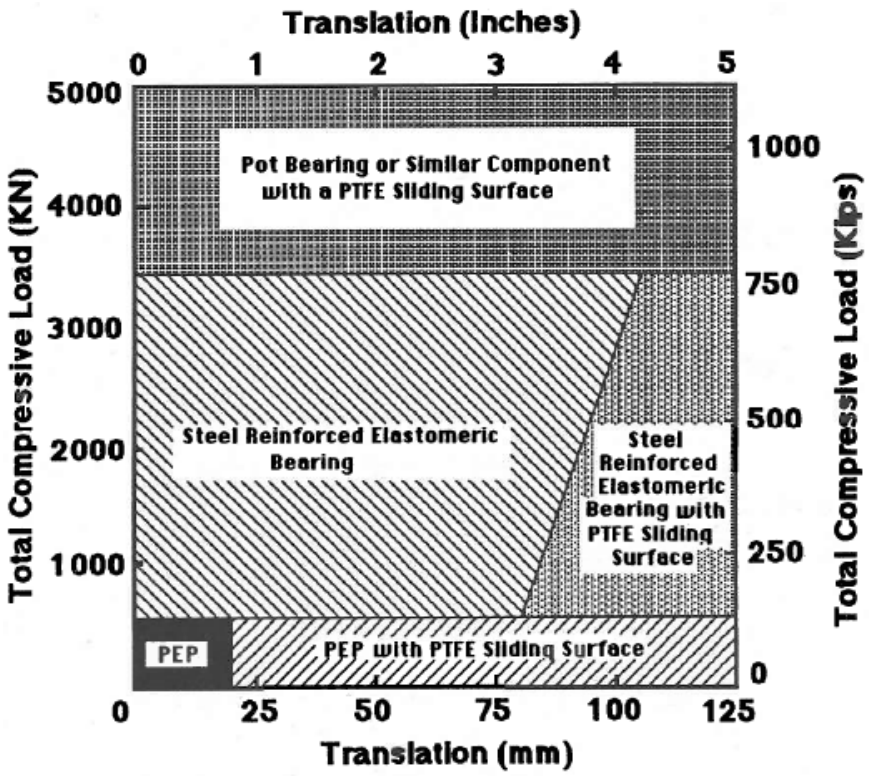

Figure 8.2.3.6-2 Preliminary Bearing Selection Diagram for Moderate Design Rotation (Rotation ≤ 0.015 Radians)
(From AISI's *Steel Bridge Bearing Selection and Design Guide*, Figure I-2)

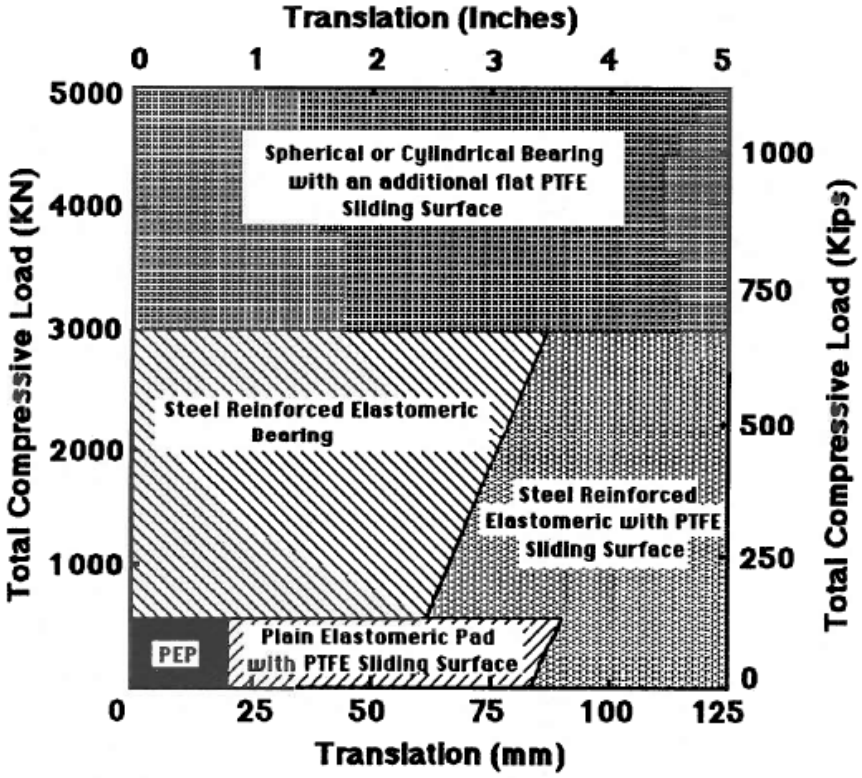

Figure 8.2.3.6-3 Preliminary Bearing Selection Diagram for Large Design Rotation (Rotation > 0.015 Radians)
(From AISI's *Steel Bridge Bearing Selection and Design Guide*, Figure I-3)

8.2.3.6.1 Bearing Selection Examples

For the first bearing selection example, consider a bearing in which large vertical loads (approximately 1750 kips) must be resisted and rotation must be facilitated about all three axes. According to Table 8.2.3.6-1, only four bearing types may be suitable – steel-reinforced elastomeric bearings, curved sliding spherical bearings, disc bearings, and pot bearings. For this same bearing selection example, Table 8.2.3.6-2 provides two bearings types which may be suitable – pot bearings and multiple rollers. However, according to Table 8.2.3.6-2, pot bearings have a moderate initial cost and a high maintenance cost, whereas multiple rollers have a high initial cost and a high maintenance cost. In addition, multiple rollers will not facilitate rotation about all three axes. It should also be noted that pot bearings are more commonly used than multiple rollers in current practice. Therefore, pot bearings might be the most feasible bearing type for this specific design application. However, all four of the bearing types listed above should be considered for further evaluation during preliminary design.

For the second bearing selection example, consider a bearing which must resist a vertical load of 740 kips, a translation of 1.25 inches, and a rotation of 0.010 radians.

Since the rotation is less than 0.015 radians but greater than 0.005 radians, the diagram in Figure 8.2.3.6-2 applies to this bearing application. According to Figure 8.2.3.6-2, for a total compressive load of 740 kips and a translation of 1.25 inches, the preliminary bearing selection is steel reinforced elastomeric bearings. However, since the application falls near the limit line, a plain elastomeric pad with a PTFE sliding surface should also be considered during preliminary design.

8.2.4 Design Requirements

After defining the bearing design requirements and evaluating the feasible bearing types, the next step is to design the most feasible bearing type. There are several general design requirements that apply to all bearing types. Bearing movements and loads from the following sources must be considered during the design of virtually all bearing types:

- **Bridge skew** – skewed bridges move both longitudinally and transversely, with the transverse movement becoming more significant as the skew angle increases.
- **Bridge curvature** – curved bridges move both tangentially and radially, with the radial movement becoming more significant as the radius of curvature decreases.
- **Beam camber or curvature** – initial camber may cause a large initial bearing rotation, but this rotation may decrease as the bridge construction progresses.
- **Construction** – construction movements must be considered, although they have a short duration.
- **Misalignment or construction procedures** – construction loads and movements due to tolerances must also be considered.
- **Traffic loading** – bearing movements caused by traffic loading can cause considerable wear to the bearing.
- **Thermal effects** – the magnitude of the thermal change in length, ΔL, is a function of the material properties, the temperature change, and the expansion length, as expressed in the following equation:

$$\Delta L = \alpha \, \Delta T \, L \qquad \text{Equation 8.2.4-1}$$

where:

ΔL = thermal change in length
α = coefficient of thermal expansion
ΔT = change in temperature
L = expansion length

Some general rules that should be followed during the design of virtually all bearing types are presented in Table 8.2.4-1.

Table 8.2.4-1 General Rules for Bearing Design

Observation	General Rule	Consequence of Ignoring Rule
LOAD COMBINATIONS – Some combinations of loads and movements are not possible.	Consider only feasible load and movement combinations, as specified in *AASHTO LRFD* Article 3.4.1.	Using unrealistic load combinations may result in a costly bearing which performs poorly.
LOAD DIRECTIONS – Loads do not necessarily all act in the same direction, and movements do not necessarily take place in the same direction.	Consider the directions of each loading component when computing load and movement combinations.	Adding the absolute values of all loads and movements may result in unrealistic conditions and uneconomical bearings.
INITIAL CONDITIONS – Temporary initial conditions can adversely affect the design of some bearings.	Consider adjusting the position of the bearing during the final stages of construction.	Designing the bearing to resist temporary initial conditions may result in an unnecessarily large and costly bearing.
PROTECTION – Bearings are typically located where dirt, debris, and moisture can collect.	Design and install the bearings to provide protection against the environment and to allow easy access for inspection.	Collection of dirt, debris, and moisture can lead to corrosion and deterioration of the bearing.
SERVICE LIFE – Due to severe demands on a bridge bearing, its service life is often less than that of other bridge components.	Provide allowances for bearing replacement (including space for lifting jacks and employment of appropriate details, such as jacking stiffeners), as specified in *AASHTO LRFD* Article 2.5.2.3.	Failure to provide jacking details may require expensive retrofits to provide sufficient jacking space and resistance.

The following descriptions and design requirements apply to specific bearing types. For additional details, refer to the appropriate sections of *AASHTO LRFD* Article 14.7.

8.2.4.1 Elastomeric Bearings

8.2.4.1.1 General

There are two common methods available for designing steel-reinforced elastomeric bearings – Design Method A and Design Method B. Design Method A usually results in a bearing with a lower resistance than a bearing designed with Method B. However, Method B requires additional testing and quality control.
The design of an elastomeric bearing generally involves the following basic steps:

1. Obtain required design input.
2. Select preliminary bearing properties.
3. Select design method (Design Method A or B).
4. Compute shape factor.
5. Check compressive stress.
6. Check compressive deflection.
7. Check shear deformation.
8. Check rotation or combined compression and rotation.
9. Check stability.
10. Check reinforcement.
11. Check anchorage or design for seismic provisions.

8.2.4.1.2 Method A

For Design Method A, the above basic steps are presented and illustrated through the following design example for a steel-reinforced elastomeric pad at an abutment. The bearings are expansion in the longitudinal direction only; they are fixed in the transverse direction. The following requirements for Design Method A are further described in *AASHTO LRFD* Article 14.7.6.

8.2.4.1.2.1 General

The required design input for this bearing for the service limit state is as follows:

DL = 78.4 kips
LL+I = 110.4 kips
LL = 83.0 kips (excluding dynamic load allowance)
Design longitudinal translation (at the service limit state) = 0.76 inches

Therefore, the total service limit state vertical load is as follows:

$$DL + LL+I = 78.4 \text{ kips} + 110.4 \text{ kips} = 188.8 \text{ kips}$$

8.2.4.1.2.2 Material Properties

The next step is to select the preliminary bearing properties. These are obtained from *AASHTO LRFD*, as well as from past experience. For this design, the following preliminary bearing pad configuration was selected (see Figure 8.2.3.2.3-1 for illustration of terminology):

Pad length, L = 14 inches
Pad width, W = 15 inches
Elastomer cover thickness, h_{rcover} = 0.25 inches
Elastomer internal layer thickness, $h_{rinternal}$ = 0.375 inches
Number of steel reinforcement layers = 9
Steel reinforcement thickness, h_s = 0.1196 inches

In addition, the following material properties were selected:

Elastomer hardness = 50 (*AASHTO LRFD* Article 14.7.6.2)
Elastomer shear modulus, G = 0.095 ksi (*AASHTO LRFD* Table 14.7.6.2-1)
Elastomer creep deflection at 25 years divided by initial deflection = 0.25 (*AASHTO LRFD* Table 14.7.6.2-1)
Steel reinforcement yield strength, F_y = 50 ksi
Steel reinforcement constant-amplitude fatigue threshold for Detail Category A, ΔF_{TH} = 24.0 ksi (*AASHTO LRFD* Table 6.6.1.2.5-3)

The next step is to compute the shape factor. The shape factor for individual elastomer layers is the plan area divided by the area of the perimeter free to bulge. For steel-reinforced elastomeric bearings, the following requirements must be satisfied:

- All internal layers of elastomer must be the same thickness.
- The thickness of the cover layers cannot exceed 70 percent of the thickness of the internal layers.

For this design example, all internal layers are 0.375 inches thick. The thickness of the cover layers (0.25 inches) is 66.7 percent of the thickness of the internal layers (0.375 inches). Therefore, both of these requirements are satisfied.

For rectangular bearings without holes, the shape factor for the i^{th} layer is:

$$S_i = \frac{L\,W}{2\,h_{ri}\,(L+W)} \qquad \text{Equation 8.2.4.1.2.2-1}$$

AASHTO LRFD Equation 14.7.5.1-1

For the internal layers of elastomer, the shape factor is computed as follows:

$$S_{internal} = \frac{(14\text{ inches})(15\text{ inches})}{2(0.375\text{ inches})(14\text{ inches} + 15\text{ inches})} = 9.66$$

For the cover layers of elastomer, the shape factor is computed as follows:

$$S_{cover} = \frac{(14\text{ inches})(15\text{ inches})}{2(0.25\text{ inches})(14\text{ inches} + 15\text{ inches})} = 14.48$$

Method A applies to the design of steel-reinforced elastomeric bearings if the primary rotation is about the axis parallel to the transverse axis of the bridge and if the following condition is satisfied:

$$\frac{S_i^2}{n} < 22 \qquad \text{Equation 8.2.4.1.2.2-2}$$

where:

n = number of interior layers of elastomer; when the thickness of the exterior layer of elastomer is equal to or greater than one-half the thickness of an interior layer, the parameter, *n*, may be increased by one-half for each such exterior layer

S_i = shape factor of the *i*th internal layer

For this design example,

$$n = 8 + \frac{1}{2} + \frac{1}{2} = 9$$

$$S_i^2 / n = (9.66)^2 / 9 = 10.4 < 22 \qquad \therefore \text{OK}$$

8.2.4.1.2.3 Compressive Stress

For steel-reinforced elastomeric bearings, the compressive stress in the elastomer at the service limit state is limited by each of the following two equations, in which S_i is based on an internal layer of the bearing:

$$\sigma_s \le 1.25\,G\,S_i \quad \text{and} \quad \sigma_s \le 1.25\,\text{ksi} \qquad \text{Equation 8.2.4.1.2.3-1}$$

AASHTO LRFD Equations 14.7.6.3.2-7 and 14.7.6.3.2-8

If shear deformation is prevented, these compressive stress limits may be increased by ten percent.

For this bearing design example,

$$\sigma_s = \frac{188.8\,\text{kips}}{(14\,\text{inches})(15\,\text{inches})} = 0.90\,\text{ksi} < 1.25\,\text{ksi} \qquad \therefore \text{OK}$$

$$\sigma_s = 0.90\,\text{ksi} < 1.15\,\text{ksi} = 1.25(0.095\,\text{ksi})(9.66) = 1.0\,\text{G S} \qquad \therefore \text{OK}$$

Therefore, the compressive stress requirements are satisfied for this bearing.

8.2.4.1.2.4 Compressive Deflection

The instantaneous live load deflection is computed using the following equation:

$$\delta_L = \sum \varepsilon_{Li}\, h_{ri} \qquad \text{Equation 8.2.4.1.2.4-1}$$

AASHTO LRFD Equation 14.7.5.3.6-1

where:

ε_{Li} = instantaneous live load compressive strain in the i^{th} elastomer layer
h_{ri} = thickness of the i^{th} elastomeric layer

Similarly, the initial dead load deflection is computed using the following equation:

$$\delta_d = \sum \varepsilon_{di}\, h_{ri} \qquad \text{Equation 8.2.4.1.2.4-2}$$

AASHTO LRFD Equation 14.7.5.3.6-2

where:

ε_{di} = initial dead load compressive strain in the i^{th} elastomer layer
h_{ri} = thickness of the i^{th} elastomeric layer

Since test results are not available for this design example, the compressive strains can be approximated using *AASHTO LRFD* Figure C14.7.6.3.3-1. First the live load compressive stress and dead load compressive stress are computed as follows:

$$\sigma_L = \frac{83.0\,\text{kips}}{(14\,\text{inches})(15\,\text{inches})} = 0.40\,\text{ksi}$$

$$\sigma_d = \frac{78.4\,\text{kips}}{(14\,\text{inches})(15\,\text{inches})} = 0.37\,\text{ksi}$$

Then based on the design aids presented in *AASHTO LRFD* Figure C14.7.6.3.3-1, the compressive strain is found to be approximately 2.0% for 50 durometer

reinforced bearings with a compressive stress of 0.40 ksi and shape factor of 9.66. Similarly, using the design aids presented in *AASHTO LRFD* Figure C14.7.6.3.3-1, the compressive strain is found to be approximately 1.8% for the cover layers, which have a shape factor of 14.48. Therefore, the instantaneous live load deflection is computed as follows:

$$\delta_L = [2(0.25\,\text{inches})(0.018)] + [8(0.375\,\text{inches})(0.020)] = 0.069\,\text{inches}$$

Similarly, the initial dead load deflection is computed as follows:

$$\delta_d = [2(0.25\,\text{inches})(0.016)] + [8(0.375\,\text{inches})(0.018)] = 0.062\,\text{inches}$$

In addition, the effects of creep should also be considered. For this design example, material-specific data is not available. As presented in Section 8.2.4.1.2.2, the elastomer creep deflection at 25 years divided by initial deflection equals 0.25 (*AASHTO LRFD* Table 14.7.6.2-1). Therefore, the long-term dead load deflection, which includes both the initial deflection and the effects of creep, can be computed as follows (based on *AASHTO LRFD* Equation 14.7.6.3.6-3):

$$\delta_{lt} = \delta_d + \alpha_{cr}\delta_d = (0.062\,\text{inches}) + (0.25)(0.062\,\text{inches}) = 0.078\,\text{inches}$$

The compressive deflection under instantaneous live load and initial dead load in an internal layer of a steel-reinforced elastomeric bearing at the service limit state without dynamic load allowance cannot exceed $0.09h_{ri}$. For this design example:

$$\delta_{internal} = \varepsilon_{internal}\, h_{ri} = (0.020 + 0.018)(0.375\,\text{inches}) = 0.014\,\text{inches}$$

$$0.09\, h_{ri} = (0.09)(0.375\,\text{inches}) = 0.034\,\text{inches} > 0.014\,\text{inches} \qquad \therefore \text{OK}$$

8.2.4.1.2.5 Shear

Shear deformation is checked to ensure that the bearing can facilitate the anticipated horizontal bridge movement. Also, the shear deformation is limited to avoid rollover at the edges and delamination due to fatigue. The maximum shear deformation of the pad at the service limit state, Δ_s, should be taken as the maximum horizontal superstructure displacement, reduced to account for pier flexibility and modified for construction procedures. In addition, if a low friction sliding surface is used, then Δ_s need not be taken greater than the deformation corresponding with first slip.

The total horizontal movement for this bridge design example is based on thermal effects only and is presented in Section 8.2.4.1.2.1 as 0.76 inches. For a steel-reinforced elastomeric bearing, the following equation must be satisfied:

$$h_{rt} \geq 2\,\Delta_s$$ Equation 8.2.4.1.2.5-1

AASHTO LRFD Equation 14.7.6.3.4-1

where:

h_{rt} = smaller of total elastomer or bearing thickness

Δ_s = maximum total shear deformation of the bearing from applicable service load combinations

In this example, this requirement is checked as follows:

$$h_{rt} = 2(0.25\text{ inches}) + 8(0.375\text{ inches}) = 3.50\text{ inches}$$

$$2\Delta_s = 2(0.76\text{ inches}) = 1.52\text{ inches} < 3.50\text{ inches} \qquad \therefore \text{OK}$$

8.2.4.1.2.6 Rotation

In previous editions of *AASHTO LRFD*, rotation was checked to ensure that no point in the bearing experienced net uplift. However, recent research (Stanton et al., 2008) has demonstrated that net uplift, or lift off, is not a concern for elastomeric bearings. Therefore, the rotation requirements ensuring no lift off have been removed from *AASHTO LRFD* for both Method A and Method B.

8.2.4.1.2.7 Stability

The total thickness of the rectangular pad must not exceed one-third of the pad length or one-third of the pad width, or expressed mathematically:

$$h_{total} \leq \frac{L}{3} \qquad \text{and} \qquad h_{total} \leq \frac{W}{3}$$ Equation 8.2.4.1.2.7-1

For this design example:

$$\begin{aligned} h_{total} &= 2(0.25\text{ inches}) + 8(0.375\text{ inches}) + 9(0.1196\text{ inches}) \\ &= 4.5764\text{ inches} \end{aligned}$$

$$\frac{L}{3} = \frac{14\text{ inches}}{3} = 4.67\text{ inches} > 4.5764\text{ inches} \qquad \therefore \text{OK}$$

$$\frac{W}{3} = \frac{15\text{ inches}}{3} = 5.0\text{ inches} > 4.5764\text{ inches} \qquad \therefore \text{OK}$$

Therefore, the bearing pad satisfies the stability requirements.

8.2.4.1.2.8 Reinforcement

The steel reinforcement thickness, h_s, cannot be less than 0.0625 inches, and the reinforcement must be able to sustain the tensile stresses induced by compression in the bearing.

For this design example, the thickness of the steel reinforcement, h_s, is 0.1196 inches. Therefore, the minimum thickness requirement is satisfied.

For the service limit state:

$$h_s \geq \frac{3\, h_{ri}\, \sigma_s}{F_y}$$ Equation 8.2.4.1.2.8-1

AASHTO LRFD Equation 14.7.5.3.5-1

$$h_s \geq \frac{3\, h_{ri}\, \sigma_s}{F_y} = \frac{3(0.375\,\text{inches})(0.90\,\text{ksi})}{50\,\text{ksi}} = 0.020\,\text{inches} \qquad \therefore \text{OK}$$

For the fatigue limit state:

$$h_s \geq \frac{2\, h_{ri}\, \sigma_L}{\Delta F_{TH}}$$ Equation 8.2.4.1.2.8-2

AASHTO LRFD Equation 14.7.5.3.5-2

$$\sigma_L = \frac{110.4\,\text{kips}}{(14\,\text{inches})(15\,\text{inches})} = 0.53\,\text{ksi}$$

As presented in Section 8.2.4.1.2.2, the steel reinforcement constant-amplitude fatigue threshold for Detail Category A, ΔF_{TH}, is 24.0 ksi.

$$h_s \geq \frac{2\, h_{ri}\, \sigma_L}{\Delta F_{TH}} = \frac{2(0.375\,\text{inches})(0.53\,\text{ksi})}{24.0\,\text{ksi}} = 0.017\,\text{inches} \qquad \therefore \text{OK}$$

Therefore, the steel reinforcement thickness satisfies the minimum thickness requirement, the service limit state requirement, and the fatigue limit state requirement.

8.2.4.1.2.9 Anchorage

Expansion bearings must provide adequate anchorage to resist horizontal forces (in excess of those accommodated by shear in the pad) for seismic loads and other extreme event loads. Anchor bolts must be designed for the combined effects of bending and shear for the seismic loads and other extreme event loads. An exception is if the bearing is intended to act as a fuse or if irreparable damage is permitted.

Fixed bearings must provide sufficient horizontal restraint to resist the full horizontal load.

The sole plate and base plate should be made wider than the pad to accommodate the anchor bolts. Inserts through the elastomer are not permitted.

For this design example, a schematic showing a plan view and sectional view of the final elastomeric bearing configuration is presented in Figure 8.2.4.1.2.9-1.

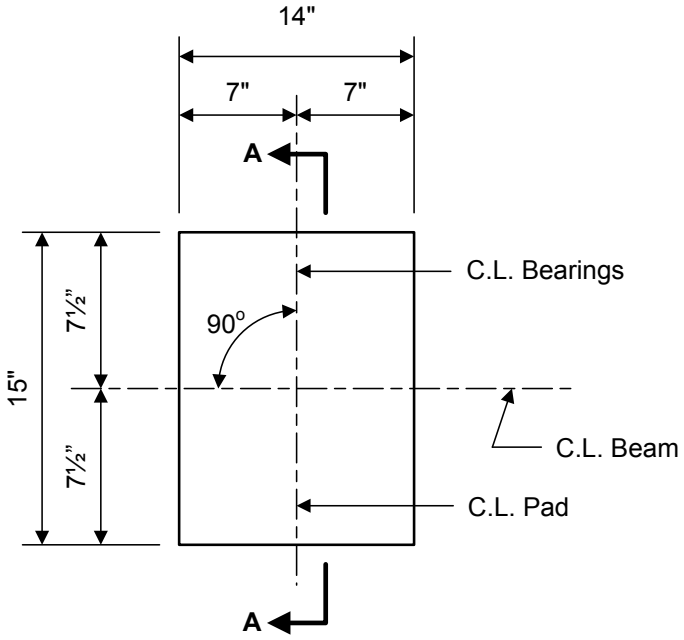

Plan

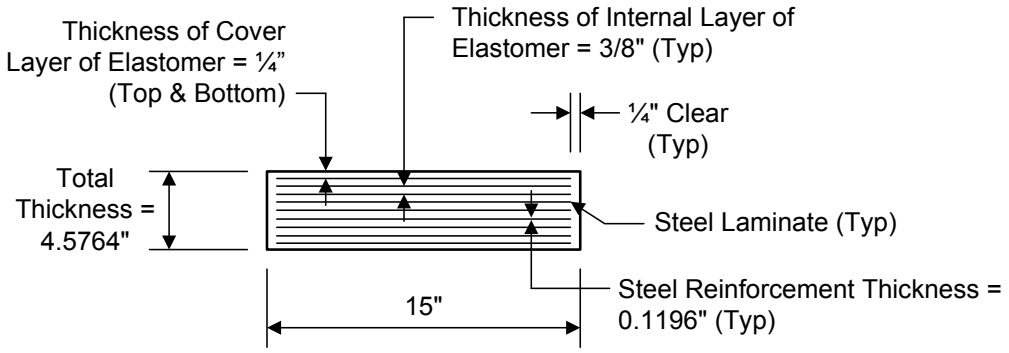

Section A-A

Figure 8.2.4.1.2.9-1 Final Configuration of Elastomeric Bearing Design Example

8.2.4.1.3 Method B

Many of the design procedures for Design Method B are similar to those of Design Method A. However, some primary differences between the two methods are summarized in Table 8.2.4.1.3-1.

Table 8.2.4.1.3-1 Elastomeric Bearing Design Methods A and B

Characteristic	Design Method A	Design Method B
Application	Applicable for: • Plain elastomeric pads • Pads reinforced with discrete layers of fiberglass • Most steel-reinforced elastomeric bearings (see Section 8.2.4.1.2.2) • Cotton-duck pads	Applicable only for: • Steel-reinforced elastomeric bearings
AASHTO LRFD reference	*AASHTO LRFD* Article 14.7.6	*AASHTO LRFD* Article 14.7.5
Bearing resistance	Stress limits for Design Method A usually result in a bearing with a lower resistance than with Method B	Stress limits for Design Method B usually result in a bearing with a higher resistance than with Method A
Additional testing and quality control	Does not require additional testing and quality control	Requires additional testing and quality control
Design steps unique to that method	• Unique stability requirements	• Check combined compression, rotation, and shear • Unique stability requirements • Restraint system requirements

Since the design procedures for Method A and Method B are similar, and since the design procedure for Method A is described in detail in Section 8.2.4.1.2, the design procedure for Method B is not detailed in this section. However, additional information about the design procedure for Method B is provided in *AASHTO LRFD* Article 14.7.5.

8.2.4.2 High-Load Multi-Rotational Bearings

In addition to elastomeric bearings, high-load multi-rotational bearings also have specific design requirements that are specified in *AASHTO LRFD*. The following sections describe design requirements for the following bearing types:

- Pot bearings
- Disc bearings
- Bearings with curved sliding surfaces

8.2.4.2.1 Pot Bearings

8.2.4.2.1.1 General

Although a pot bearing consists of many components (see Figure 8.2.3.3.2-1), only the elastomeric disc, sealing rings, pot, and piston have design requirements presented in the pot bearing design section of *AASHTO LRFD* (Article 14.7.4). It should be noted, however, that the masonry plate and top plate may also require some design.

For this design example, the requirements of *AASHTO LRFD* Article 14.7.4 are illustrated using the following design steps:

1. Obtain required design input.
2. Select preliminary bearing properties.
3. Design the elastomeric disc.
4. Design the sealing rings.
5. Design the pot.
6. Design the piston.
7. Check the concrete or grout support.

The required design input for this bearing design example is as follows:

Service limit state:
Total maximum vertical load = 830 kips
Minimum vertical load = 200 kips

Strength limit state:
Total maximum vertical load = 1250 kips
Maximum design rotation = 0.014 radians

Strength and extreme event limit states:
Total horizontal load = 70 kips

Based on *AASHTO LRFD* Article 14.7.4.1, the minimum vertical load on a pot bearing should not be less than 20 percent of the vertical design load. For this design example, this requirement is checked as follows:

$$\text{Minimum Vertical Load} = 200\,\text{kips} > 166\,\text{kips} = (0.20)(830\,\text{kips}) \qquad \therefore \text{OK}$$

8.2.4.2.1.2 Materials

The next step is to select the preliminary bearing properties. These are obtained from *AASHTO LRFD* Article 14.7.4.2, as well as from past experience. For this design example, the following material properties were selected:

Structural steel:
AASHTO M270 Grade 50
Pier cap:
Concrete strength, f'_c = 4.0 ksi

Elastomeric disc:
Nominal hardness = 50 on the Shore A scale

8.2.4.2.1.3 Geometric Requirements

Based on *AASHTO LRFD* Article 14.7.4.3, the depth of the elastomeric disc, h_r, must satisfy the following requirement:

$$h_r \geq 3.33\, D_p\, \theta_u \qquad \text{Equation 8.2.4.2.1.3-1}$$

AASHTO LRFD Equation 14.7.4.3-1

where:

D_p = internal diameter of pot in inches
θ_u = maximum strength limit state design rotation in radians

This equation limits the edge deflections due to rotation in the elastomeric pad to 15 percent of the nominal pad thickness.

For this design example, assume an internal diameter of the pot, D_p, of 18 inches. This assumption will be verified in the next section (Section 8.2.4.2.1.4).

The depth of the elastomeric disc requirement is checked as follows:

$$h_r \geq 3.33\,(18\ \text{inches})(0.014\ \text{radians}) = 0.84\ \text{inches}$$

Therefore, use a depth of elastomeric disc, h_r, of 0.875 inches and an internal diameter, D_p, of 18 inches.

8.2.4.2.1.4 Elastomeric Disc

Based on *AASHTO LRFD* Article 14.7.4.4, pot bearings are designed for an average compressive stress on the elastomer not exceeding 3.5 ksi at the service limit state. The area of the elastomeric disc, as well as the pot, is controlled by this compressive stress requirement.

$$A_{pad} = \frac{830\ \text{kips}}{3.5\ \text{ksi}} = 237\ \text{inches}^2$$

$$D_p = \sqrt{\frac{4\,A_{pad}}{\pi}} = \sqrt{\frac{4\left(237\ \text{inches}^2\right)}{\pi}} = 17.4\ \text{inches}$$

Therefore, the assumed 18-inch diameter elastomeric disc satisfies this compressive stress requirement. This is verified as follows:

$$\sigma_s = \frac{830\ \text{kips}}{\left[\frac{\pi(18\ \text{inches})^2}{4}\right]} = 3.26\ \text{ksi} < 3.5\ \text{ksi} \qquad \therefore \text{OK}$$

The top and bottom surfaces of the elastomeric disc should be treated with an appropriate lubricant to facilitate the required rotation in the pot bearing.

8.2.4.2.1.5 Sealing Rings

Sealing rings provide a seal between the pot and the piston and can be provided in one of two configurations:

- Three rings with rectangular cross sections
- One ring with circular cross section

For three rings with rectangular cross sections, the following geometric constraints are required:

$$\text{Width} \geq 0.02\,D_p \quad \text{and} \quad \text{Width} \geq 0.25\ \text{inches}$$

$$\text{Width} \le 0.75 \text{ inches}$$

$$\text{Depth} \ge 0.2 \text{ Width}$$

For one ring with a circular cross section, the cross-sectional diameter must satisfy the following equation:

$$\text{Diameter} \ge 0.0175\, D_p \quad \text{and} \quad \text{Diameter} \ge 0.15625 \text{ inches}$$

For this design example, three rings with rectangular cross sections are being used. The width and depth of each ring are computed as follows:

$$\text{Width} \ge 0.02\, D_p = 0.02(18 \text{ inches}) = 0.36 \text{ inches}$$

and $\text{Width} \ge 0.25$ inches

$$\text{Width} \le 0.75 \text{ inches}$$

Therefore, use a ring width of 0.4 inches.

$$\text{Depth} \ge 0.2 \text{ Width} = 0.2(0.4 \text{ inches}) = 0.08 \text{ inches}$$

Therefore, use a ring depth of 0.08 inches for each ring, resulting in a total depth for the three rings of 0.24 inches.

8.2.4.2.1.6 Pot

The pot walls must be thick enough to resist both the internal hydrostatic pressure of the elastomeric disc and the pressure from any lateral loads. These two requirements are satisfied using the following two equations:

$$t_w \ge \frac{D_p\, \sigma_s}{1.25\, F_y} \quad \text{and} \quad t_w \ge 0.75 \text{ inches} \qquad \text{Equation 8.2.4.2.1.6-1}$$

AASHTO LRFD Equations 14.7.4.6-5 and 14.7.4.6-6

$$t_w \ge \sqrt{\frac{25\, H_u\, \theta_u}{F_y}} \qquad \text{Equation 8.2.4.2.1.6-2}$$

AASHTO LRFD Equation 14.7.4.7-1

where:

σ_s = average compressive stress due to total load for service limit state

F_y = yield strength of the steel
H_u = lateral load from applicable strength and extreme event load combinations
θ_u = maximum strength limit state design rotation

For this design example,

$$t_w \geq \frac{D_p\ \sigma_s}{1.25\ F_y} = \frac{(18\text{ inches})(3.26\text{ ksi})}{1.25\ (50\text{ ksi})} = 0.94\text{ inches}$$

and $t_w \geq 0.75\text{ inches}$

$$t_w \geq \sqrt{\frac{25\ H_u\ \theta_u}{F_y}} = \sqrt{\frac{25\ (70\text{ kips})\ (0.014\text{ radians})}{50\text{ ksi}}} = 0.70\text{ inches}$$

Therefore, for this design example, use a pot wall thickness of 1 inch.

Since the pot base must be thick enough to resist the moments from the cantilever bending of the walls, the lateral load equation for the pot wall also applies to the pot base:

$$t_b \geq \sqrt{\frac{25\ H_u\ \theta_u}{F_y}}$$

In addition, for a pot base that bears directly against concrete or grout:

$$t_b \geq 0.06\ D_p \quad \text{and} \quad t_b \geq 0.75\text{ inches}$$

For a pot base that bears directly on steel girders or load distribution plates:

$$t_b \geq 0.04\ D_p \quad \text{and} \quad t_b \geq 0.50\text{ inches}$$

For this design example, assuming that the pot base bears directly on load distribution plates:

$$t_b \geq \sqrt{\frac{25\ H_u\ \theta_u}{F_y}} = \sqrt{\frac{25\ (70\text{ kips})\ (0.014\text{ radians})}{50\text{ ksi}}} = 0.70\text{ inches}$$

$$t_b \geq 0.04\ D_p = 0.04\ (18\text{ inches}) = 0.72\text{ inches}$$

and $t_b \geq 0.50\text{ inches}$

Therefore, for this design example, the pot wall thickness is 1 inch and the pot base thickness is 0.75 inches.

8.2.4.2.1.7 Piston

The piston has the same plan shape as the inside of the pot. Its thickness must be sufficient to provide the required rigidity and strength. Therefore, the piston thickness must satisfy the following minimum requirement:

$$t_{piston} \geq 0.06\, D_p$$

The height from the top of the rim to the underside of the piston, h_w, must satisfy all three of the following requirements:

$$h_w \geq \frac{1.5\, H_u}{D_p\, F_y} \quad \text{and} \quad h_w \geq 0.125 \text{ inches} \quad \text{and} \quad h_w \geq 0.03\, D_p \qquad \text{Equation 8.2.4.2.1.7-1}$$

AASHTO LRFD Equations 14.7.4.7-2, 14.7.4.7-3, and 14.7.4.7-4

Finally, the clearance, *c*, between the inside diameter of the pot and the diameter of the piston rim must satisfy the following requirements:

$$c \geq \theta_u \left(h_w - \frac{D_p\, \theta_u}{2} \right) \quad \text{and} \quad c \geq 0.02 \text{ inches} \qquad \text{Equation 8.2.4.2.1.7-2}$$

AASHTO LRFD Equation 14.7.4.7-5

For this design example:

$$t_{piston} \geq 0.06\, D_p = 0.06\,(18 \text{ inches}) = 1.08 \text{ inches}$$
$$\therefore \text{Use } t_{piston} = 1.25 \text{ inches}$$

$$\frac{1.5\, H_u}{D_p\, F_y} = \frac{1.5\,(70 \text{ kips})}{(18 \text{ inches})(50 \text{ ksi})} = 0.12 \text{ inches}$$
$$\text{and} \quad 0.03\, D_p = 0.03\,(18 \text{ inches}) = 0.54 \text{ inches}$$
$$\therefore \text{Use } h_w = 0.54 \text{ inches}$$

$$c \geq \theta_u \left(h_w - \frac{D_p \, \theta_u}{2} \right)$$

$$= (0.014 \text{ radians}) \left[0.54 \text{ inches} - \frac{(18 \text{ inches})(0.014 \text{ radians})}{2} \right]$$

$$= 0.0058 \text{ inches} \qquad \therefore \text{Use } c = 0.02 \text{ inches}$$

8.2.4.2.1.8 Concrete or Grout Support

The masonry plate of a pot bearing is designed similarly to masonry plates for other applications. Assuming that confinement reinforcement is absent in the concrete, the concrete bearing must satisfy the following requirement:

$$P_r = \phi P_n = \phi \left[0.85 f'_c \, A_1 \, m \right] \qquad \text{Equation 8.2.4.2.1.8-1}$$

AASHTO LRFD Equations 5.7.5-1 and 5.7.5-2

For this design example, assuming a masonry plate measuring 28 inches by 28 inches and assuming that the modification factor, *m*, equals 1:

$$P_r = \phi P_n = \phi \left[0.85 f'_c \, A_1 m \right] = 0.70 \left[0.85 (4.0 \text{ ksi}) (28 \text{ inches})^2 (1) \right]$$

$$= 1866 \text{ kips} > 1250 \text{ kips} \qquad \therefore \text{OK}$$

The final pot bearing configuration for this design example is presented in Figure 8.2.4.2.1.8-1.

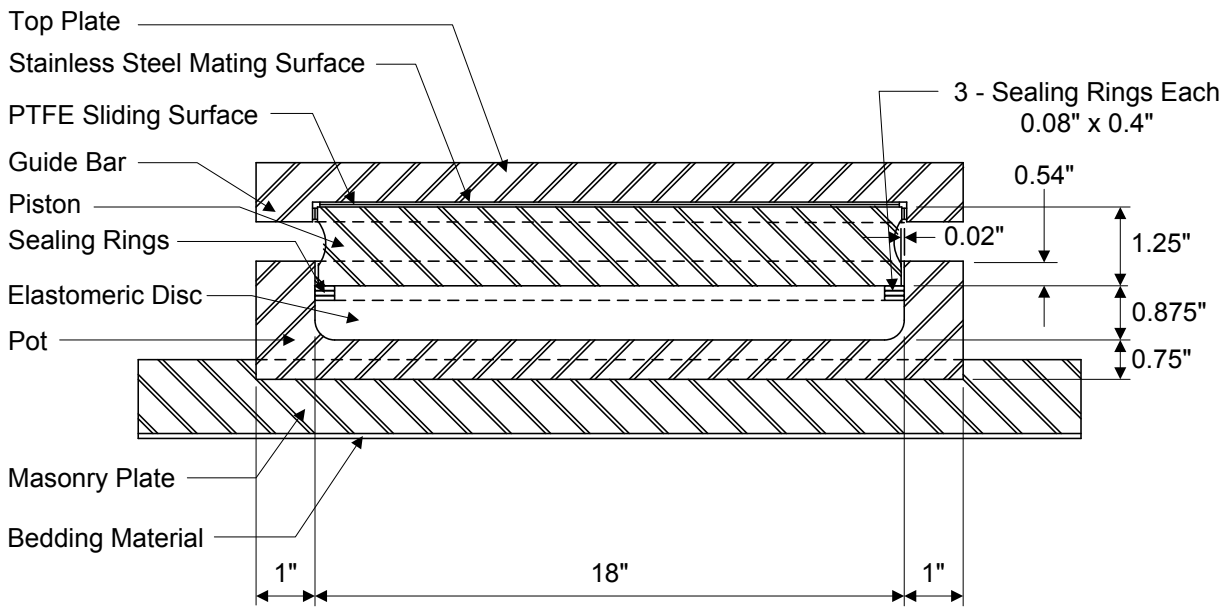

Figure 8.2.4.2.1.8-1 Final Configuration of Pot Bearing Design Example

8.2.4.2.2 Disc Bearings

For disc bearings, *AASHTO LRFD* Article 14.7.8 specifies design requirements for the elastomeric disc, the shear-resisting mechanism, the steel plates, and the limiting rings.

The elastomeric disc must have a hardness between 45 and 65 on the Shore D scale, it should be designed based on the service limit state, and its components must not lift off each other at any location. The average compressive stress in the elastomeric disc must be less than or equal to 5.0 ksi based on the smallest plan area of the disc. Instantaneous deflection under total load must be less than or equal to 10 percent of the thickness of the unstressed disc. Similarly, additional deflection due to creep must be less than or equal to 8 percent of the thickness of the unstressed disc. If a PTFE slider is used, it must be designed to satisfy the PTFE stress requirements presented in *AASHTO LRFD* Article 14.7.2.4. In addition, the effect of induced moments caused by the urethane disc must be included in the stress analysis.

A shear-resisting mechanism is required for fixed and guided bearings to transmit horizontal forces between the upper and lower steel plates. The shear-resisting mechanism must be able to resist a horizontal force in any direction equal to the larger of the following:

- Design shear force at strength limit state

- Design shear force at extreme event limit state
- 15 percent of the design vertical load at service limit state

The upper and lower steel plates must satisfy thickness requirements to ensure that they uniformly distribute the concentrated load in the bearing. If the steel plate is in direct contact with a steel girder or distribution plate, the thickness of each plate, t_{PL}, must satisfy the following:

$$t_{PL} \geq 0.045\, D_d \qquad \text{Equation 8.2.4.2.2-1}$$

where:

D_d = diameter of the disc element

However, if the steel plate bears directly against concrete or grout, the thickness of each plate must satisfy the following:

$$t_{PL} \geq 0.06\, D_d \qquad \text{Equation 8.2.4.2.2-2}$$

If limiting rings are used, they may consist of steel rings welded to the upper and lower plates, or a circular recess may be included in each of those plates. The limiting rings partially confine the elastomer against lateral expansion. The depth of the ring must satisfy the following requirement:

$$\text{Depth} \geq 0.03\, D_d \qquad \text{Equation 8.2.4.2.2-3}$$

This ring depth requirement prevents possible overriding by the urethane disc under extreme rotation conditions.

8.2.4.2.3 Bearings with Curved Sliding Surfaces

Bearing with curved sliding surfaces consist of two metal parts with matching curved surfaces and a low friction sliding interface. They may be either spherical or cylindrical, and the two metal parts must have the same nominal radius at the sliding interface. *AASHTO LRFD* Article 14.7.3 specifies design requirements for bearing resistance and resistance to lateral load.

For bearing resistance, the total compressive load at the service limit state on the horizontal projected area of the bearing, P_s, must satisfy the following requirements:

For spherical bearings: $$P_s \leq \phi \frac{\pi D^2 \sigma_{SS}}{4} \qquad \text{Equation 8.2.4.2.3-1}$$

AASHTO LRFD Equation 14.7.3.2-2

For cylindrical bearings: $P_s \le \phi DW\sigma_{SS}$ Equation 8.2.4.2.3-2

AASHTO LRFD Equation 14.7.3.2-1

where:

- D = diameter of the projection of the loaded surface of the bearing in the horizontal plane
- σ_{SS} = maximum average contact stress at the service limit state permitted on PTFE
- W = length of cylinder
- ϕ = resistance factor = 1.0

For bearings that must resist lateral load, either an external restraint system must be provided or the following requirements for horizontal load at the service limit state, H_s, must be satisfied:

For spherical bearings: $H_s \le \pi R^2 \sigma_{SS} \sin(\psi - \beta - \theta_u)\sin\beta$ Equation 8.2.4.2.3-3

AASHTO LRFD Equation 14.7.3.3-2

For cylindrical bearings: $H_s \le 2RW\sigma_{SS} \sin(\psi - \beta - \theta_u)\sin\beta$ Equation 8.2.4.2.3-4

AASHTO LRFD Equation 14.7.3.3-1

in which:

$$\beta = \tan^{-1}\left(\frac{H_s}{P_D}\right)$$ Equation 8.2.4.2.3-5

AASHTO LRFD Equation 14.7.3.3-3

$$\psi = \sin^{-1}\left(\frac{L}{2R}\right)$$ Equation 8.2.4.2.3-6

AASHTO LRFD Equation 14.7.3.3-4

where:

- L = projected length of the sliding surface perpendicular to the rotation axis
- P_D = compressive load at the service limit state due to permanent loads
- R = radius of curved sliding surface
- W = length of cylindrical surface
- β = angle between the vertical and resultant applied load
- θ_u = maximum strength limit state design rotation angle
- σ_{SS} = maximum average contact stress at the service limit state permitted on PTFE
- ψ = subtended semi-angle of the curved surface

The above design checks ensure that the curved bearing, combined with gravity loads, provides the required resistance to lateral load. However, for resisting large lateral loads at the bearing, an external restraint is a more reliable method.

8.2.4.3 Mechanical Bearings

Metal rocker and roller bearings, also known as mechanical bearings, must be carefully aligned with the axis about which the greatest rotation occurs. *AASHTO LRFD* Article 14.7.1 specifies the design requirements for mechanical bearings, including the following requirements for contact load, P_S, at the service limit state:

For spherical bearings:

$$P_s \le 40\left(\frac{D_1}{1-\frac{D_1}{D_2}}\right)^2 \frac{F_y^{\,3}}{E_s^{\,2}} \qquad \text{Equation 8.2.4.3-1}$$

AASHTO LRFD Equation 14.7.1.4-2

For cylindrical bearings:

$$P_s \le 8\frac{WD_1}{\left(1-\frac{D_1}{D_2}\right)}\left(\frac{F_y^{\,2}}{E_s}\right) \qquad \text{Equation 8.2.4.3-2}$$

AASHTO LRFD Equation 14.7.1.4-1

where:

D_1 = diameter of the rocker or roller surface
D_2 = diameter of the mating surface (positive if curvatures have the same sign and infinite if the mating surface is flat)
W = width of the bearing

8.2.5 Guides and Restraints

8.2.5.1 General

Bearings which are intended to be fixed in either the longitudinal or transverse direction must be designed for restraint in the direction of fixity. That is, if a bridge is designed such that the bearings at a specific substructure unit are fixed in one or both directions, then those bearings must be designed to provide restraint in those directions.

Guides are used to prevent movement in one direction, while restraints are used to permit only limited movement in one or more directions. Guides and restraints are designed for the following design loads:

- Maximum horizontal force at the strength limit state
- 15 percent of the total vertical force at the service limit state (distributed to each guided bearing at the substructure unit)
- Applicable seismic or other extreme event limit state forces

Low friction material must be used at the sliding contact surfaces, and it must be attached using at least any two of the following three methods:

- Mechanical fastening
- Bonding
- Mechanical interlocking with a metal substrate

8.2.5.2 Lateral Restraint

Several states have specific details for providing lateral restraint at bearings, and several different means of lateral restraint are possible.

Some states use external restraint systems with stainless steel on the guiding system and a corresponding low coefficient of friction for its mating material. For such a lateral restraint system, the stainless steel should cover the material in all movement extremes. In addition, vertical displacement due to construction loads and application of dead loads must be considered.

Other states use a steel pin built into the bearing to provide lateral restraint. The anchor pin is designed to resist the applied horizontal force, with a minimum diameter of 1½ inches often specified.

For bridges with horizontal curves or non-parallel girders, the bearings should be guided in the same direction with respect to the centerline of the corresponding substructure unit. Guiding at different directions results in binding of the bearings, and this effect is particularly problematic with large amounts of lateral movement. For a horizontally curved bridge, it is common practice to align the bearings along a chord from the fixed point to the expansion point. If any other alignment is used, the resulting additional forces must be accounted for in the design of the bearing, the lateral restraint system, and the substructure unit.

8.2.5.3 Uplift Restraint

Uplift at bearings due to service loads should be avoided as much as possible by strategic placement of additional dead loads.

Similarly, uplift at bearings due to construction loads should be avoided by either revising the deck pouring sequence or by using other uplift restraint methods that do not affect the bearings.

If required, uplift restraint for elastomeric bearings should be external to the bearing, such as the use of tie-down anchor rods from the superstructure directly to the substructure unit. For HLMR bearings, uplift restraint, if required, can be built into the bearing by designing restraint attachments.

8.2.6 Load Plates and Anchorage

8.2.6.1 General

Load plates are often used to distribute large concentrated forces from the girder to the substructure unit below through the bearing so as not to damage the supporting structure. Mechanical bearings generally cause the greatest concentrated loads, followed sequentially by pots, discs, spherical bearings, and elastomeric bearings. Anchorage is used to provide restraint against the horizontal design forces.

8.2.6.2 Sole Plates and Masonry Plates

To help prevent damage from large concentrated forces in the bearings, sole plates are often used to distribute the load from the girder to the bearing, and masonry plates are often used to distribute the load from the bearing to the concrete or grout surfaces below.

Sole plates are not always required with elastomeric bearings, but they are often used with other bearing types. The sole plate should be level under full permanent load at the mean annual temperature for the bridge site. Therefore, if the bearing surface is out of level by more than 0.01 radian, or 1 percent, a tapered plate should be used to provide a level surface. Sole plates are connected to the girder by welding or bolting, with welding being the most common and preferred method. Sole plates must be designed for bending if the width of the bearing extends beyond the edges of the girder flange.

Masonry plates are commonly used to prevent damage to the underlying concrete or grout due to high concentrated bearing forces or to facilitate replacement of the bearing during its service life. Masonry plates are generally connected to the concrete pier using embedded anchors or anchor bolts. The bearing is then attached to the masonry plate by placing it within a machined recess and bolting it down. To replace the bearings, the bridge needs to be lifted only by the depth of the recess. Bearing replacement should be considered during the design of bearings and girder stiffeners.

8.2.6.3 Anchor Bolts or Rods

Bearings are generally connected to the concrete pier using anchor bolts or rods. The design of the anchor bolts is illustrated below based on the previous elastomeric bearing design example presented in Section 8.2.4.1.2.

In addition to the requirements presented in Section 8.2.4.1.2, *AASHTO LRFD* Article 3.10.9 provides additional bearing anchorage requirements. For example, assuming that the bridge in the previous elastomeric bearing design example is located in Seismic Zone 1, *AASHTO LRFD* Article 3.10.9.2 specifies that the horizontal design connection force in the restrained directions must be at least equal to 0.15 times the vertical reaction due to the tributary permanent load and the tributary live loads assumed to exist during an earthquake. This minimum design value is intended to preclude the need for a more rigorous analysis for bridges in parts of the country with very low seismicity.

Since all abutment bearings are restrained in the transverse direction, the tributary permanent load can be taken as the reaction at the bearing. Assuming that γ_{EQ} equals zero (see *AASHTO LRFD* Article 3.4.1), no tributary live load will be considered.

$$H_{EQ} = 0.15\,DL \qquad \text{Equation 8.2.6.3-1}$$

$$H_{EQ} = 0.15\,(78.4\text{ kips}) = 11.8\text{ kips}$$

For two 7/8" diameter A 307 bolts with a minimum tensile strength of 60 ksi, the factored shear resistance for threads excluded from the shear plane is computed as follows in accordance with *AASHTO LRFD* Article 6.13.2.7:

$$R_n = 0.48A_bF_{ub}N_s \qquad \text{Equation 8.2.6.3-2}$$

AASHTO LRFD Equation 6.13.2.7-1

$$R_n = 0.48(2\text{ bolts})(0.60\text{ inches}^2/\text{bolt})(60\text{ ksi})(1\text{ shear plane/bolt}) = 34.6\text{ kips}$$

$$R_r = \phi_s R_n \qquad \text{Equation 8.2.6.3-3}$$

AASHTO LRFD Equation 6.13.2.2-2

$$R_r = (0.75)(34.6\text{ kips}) = 26.0\text{ kips} > 11.8\text{ kips} \qquad \therefore \text{OK}$$

After the anchor bolt size and quantity have been determined, the anchor bolt length must also be computed. As an approximation, the bearing stress may be assumed to vary linearly from zero at the end of the embedded length to its maximum value at the top surface of the concrete, in accordance with *AASHTO LRFD* Article C14.8.3.1. The bearing resistance of the concrete is based on *AASHTO LRFD* Article 5.7.5. Assuming that the modification factor, *m*, equals 1, the bearing stress is computed as follows:

$$P_r = \phi_b P_n = \phi_b 0.85 f'_c A_1 m$$ Equation 8.2.6.3-4

AASHTO LRFD Equations 5.7.5-1 and 5.7.5-2

$$f_{brg} = \frac{P_r}{A_1} = \frac{\phi_b 0.85 f'_c A_1 m}{A_1} = \phi_b 0.85 f'_c m$$ Equation 8.2.6.3-5

$$f_{brg} = (0.70)(0.85)(4.0\text{ ksi})(1) = 2.38\text{ ksi}$$

The total transverse horizontal force acting on each bolt is:

$$H_{EQ}\text{ /bolt} = \frac{11.8\text{ kips}}{2\text{ bolts}} = 5.9\text{ kips/bolt}$$

Using the linear bearing stress approximation from above, the required anchor bolt area resisting the transverse horizontal force can be calculated as follows:

$$A_1 = \frac{H_{EQ}/\text{bolt}}{\frac{0 + f_{brg}}{2}} = \frac{5.9\text{ kips/bolt}}{\frac{0 + 2.38\text{ ksi}}{2}} = 5.0\text{ inches}^2$$

A_1 is the product of the anchor bolt diameter and the anchor bolt length of embedment into the concrete pedestal or beam seat. Since the anchor bolt diameter is known, the minimum required anchor bolt embedment length can be computed as follows:

$$A_1 = (\text{Length}_{bolt})(\text{Diameter}_{bolt})$$ Equation 8.2.6.3-6

$$\text{Length}_{bolt} = \frac{A_1}{\text{Diameter}_{bolt}} = \frac{5.0\text{ inches}^2}{0.875\text{ inches}} = 5.7\text{ inches}$$

8.2.7 Corrosion Protection and Maintenance

Corrosion protection and future maintenance must be considered during design of the bearings.

The most reliable protection against corrosion in bearings is the use of stainless steel, because any coatings may be subject to damage from wear or impact. Bearings with metal-to-metal contact, such as mechanical bearings, are especially prone to wear and impact. If stainless steel is not used, then corrosion protection can be provided by zinc metallization, hot-dip galvanizing, an approved paint system, or a combination of zinc and paint system. Some bearings, such as pot bearings or spherical bearings, may not be suitable for hot-dip galvanizing. In addition, weathering steel should not be used for bearings, since the oxide coating that is formed may inhibit the proper function of the bearing.

Bearings should also be designed to facilitate ease of inspection, maintenance, and replacement. The Engineer should design the bridge such that access for inspection of the bearings is provided. In addition, there should be a means to relieve the bearings of load, and it must be feasible to remove the existing bearings and insert new replacement bearings. Jacking stiffeners are often provided on steel girders to facilitate bearing replacement.

Section 8.3 Joints

8.3.1 General

Deck joints are structural discontinuities between two elements in a bridge deck, with at least one of the elements being the deck itself. Deck joints are designed to permit relative translation and/or rotation of abutting structural elements.

Deck joints must be designed such that motorcycles, bicycles, and pedestrians can safely pass over them. They cannot significantly impair the riding characteristics of the roadway nor can they cause damage to vehicles crossing the bridge. Deck joints must also be carefully detailed to prevent damage to the structure from water, deicing chemicals, and roadway debris.

8.3.2 Types of Joints

There are many different types of joints, and each one has its own unique application, based on the type of deck being used and the magnitude of expansion and contraction of the deck. Some of the most common joint types are presented in Table 8.3.2-1, along with a general description of the joint.

Table 8.3.2-1 Joint Type Descriptions

Joint Type	General Description
Closed joint	A deck joint designed to prevent the passage of debris and water through the joint and to safeguard pedestrian and cycle traffic.
Compression seal	A preformed elastomeric device that is precompressed in the gap of a joint with expected total range of movement less than 2.0 inches.
Cycle-control joint	A transverse approach slab joint designed to permit longitudinal cycling of integral bridges and attached approach slabs.
Finger plate joint	An open joint consisting of two steel plates with interlocking fingers, facilitating relatively large movement ranges. Also known as a tooth plate joint or tooth dam.
Longitudinal joint	A joint parallel to the span direction of a structure provided to separate a deck or superstructure into two independent structural systems.
Modular bridge joint system (MBJS)	A sealed joint with two or more elastomeric seals held in place by edgebeams that are anchored to the structural elements (such as the deck or abutment) and one or more transverse centerbeams that are parallel to the edgebeams. MBJS are typically used for movement ranges greater than 4.0 inches.
Open joint	A joint designed to permit the passage of water and debris through the joint.
Joint Type	General Description
Poured seal	A seal made from a material that remains flexible (such as asphaltic or polymeric), which is poured into the gap of a joint and is expected to adhere to the sides of the gap. Poured seals are typically used only when the expected total range of movement is less than 1.5 inches.
Relief joint	A deck joint, usually transverse, that is designed to minimize either unintended composite action or the effect of differential horizontal movement between a deck and its supporting structural system.
Sealed joint	A joint provided with a joint seal.
Single-support-bar system (SSB)	An MBJS designed so that only one support bar is connected to all of the centerbeams. The centerbeam/support bar connection typically consists of a yoke through which the support bar slides.
Strip seal	A sealed joint with an extruded elastomeric seal retained by edgebeams that are anchored to the structural elements (such as the deck or abutment). Strip seals are typically used for expected total movement ranges from 1.5 to 4.0 inches, although single seals capable of spanning a 5.0 inch gap are also available.

Joint Type	General Description
Waterproofed joints	Open or closed joints that have been provided with some form of trough below the joint to contain and conduct deck discharge away from the structure.
Welded multiple-support-bar system (WMSB)	An MBJS designed so that each support bar is welded to only one centerbeam. Although some larger WMSB systems have been built and are performing well, WMSB systems are typically impractical for more than nine seals or for movement ranges larger than 27.0 inches.

Several commonly used deck joints are described in the following sections.

8.3.2.1 Open Joints

Open joints are not designed to be watertight, and they permit a free flow of water through the joint. They should not be used where deicing chemicals may be applied to the bridge. In addition, piers and abutments located beneath open joints must satisfy the following serviceability requirements to prevent the accumulation of water and debris:

- All surfaces of the piers and abutments, other than bearing seats, must have a minimum slope of 15 percent toward their edges.
- The bearings must be protected against contact with salt and debris.

While open joints are generally avoided due to the potential for maintenance problems for the underlying structure, they can provide an effective and economical solution under limited conditions, such as bridges on secondary highways where little sand and salt are used during the winter. However, open joints are not well suited for urban areas where deck joint drainage costs are high.

The use of open joints generally requires the following conditions:

- An effective deck drainage system
- Control of deck discharge through the joints
- Containment and disposal of runoff from the site
- Prevention of surface drainage and roadway debris from accumulating on any part of the structure below the open joint (using such means as deflectors, shields, covers, and coatings)

It should be noted, however, that drainage troughs designed to control deck discharge through the joints can fail and result in significant maintenance problems.

Two common types of open joints are butt joints and sliding plate joints. A butt joint is an exposed opening in the deck, sometimes with steel armoring to protect the exposed concrete surfaces. Butt joints can be used for movements of less than 1 inch. A butt joint is illustrated in Figure 8.3.2.1-1.

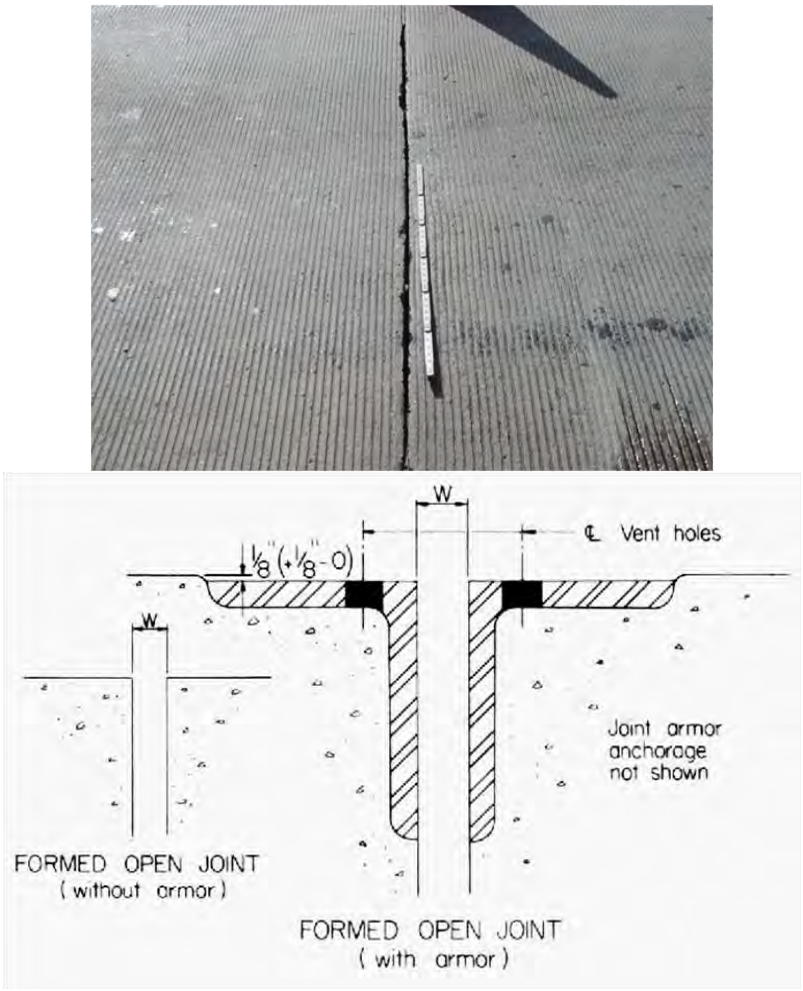

Figure 8.3.2.1-1 Butt Joint

A sliding plate joint is an opening in the deck, covered by a steel plate attached to one side and extending across the opening to the other side. Sliding plate joints can be used for movements of 1 to 3 inches. A sliding plate joint is illustrated in Figure 8.3.2.1-2.

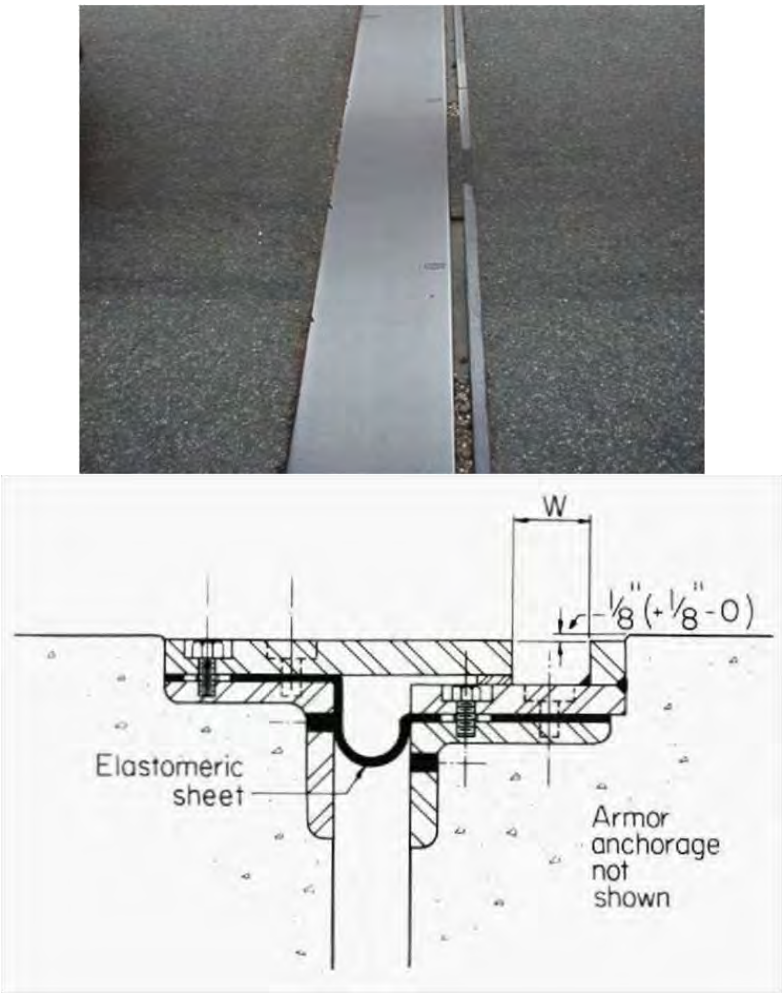

Figure 8.3.2.1-2 Sliding Plate Joint

8.3.2.2 Closed Joints

Unlike open joints, closed joints are designed to be watertight. They must not permit a free flow of water or debris through the joint. Over the past several decades, the increased use of deicing salt on bridges has led to a decrease in the use of open joints and an increase in the use of closed joints.

Three common types of closed joints include the following:

- Pourable joint sealer
- Compression seal
- Strip seal

A pourable joint sealer, or field-molded sealer, consists of a thick, sticky, and pourable waterproof material placed near the top of the joint as a sealant. Silicone is

a common material used for pourable joint sealers. Pourable joint sealers are generally limited in use to joint movements of 0.25 inches or less. A pourable joint sealer is illustrated in Figure 8.3.2.2-1.

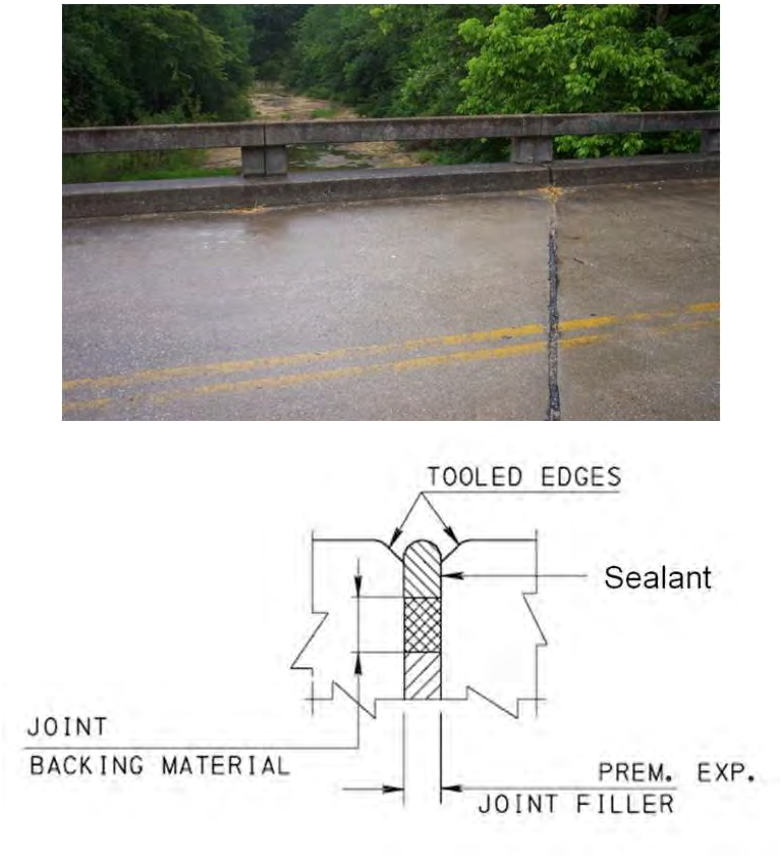

Figure 8.3.2.2-1 Pourable Joint Sealer

Compression seals generally consist of semi-hollow cross sections with internal diagonal and vertical neoprene webbing, resembling a truss, to allow the joint seal to compress freely. It also provides stability and pressure against the joint face during deck expansion and contraction. Compression seals are generally applicable for joint movements of 0.25 inches to 2.5 inches. A compression seal is illustrated in Figure 8.3.2.2-2.

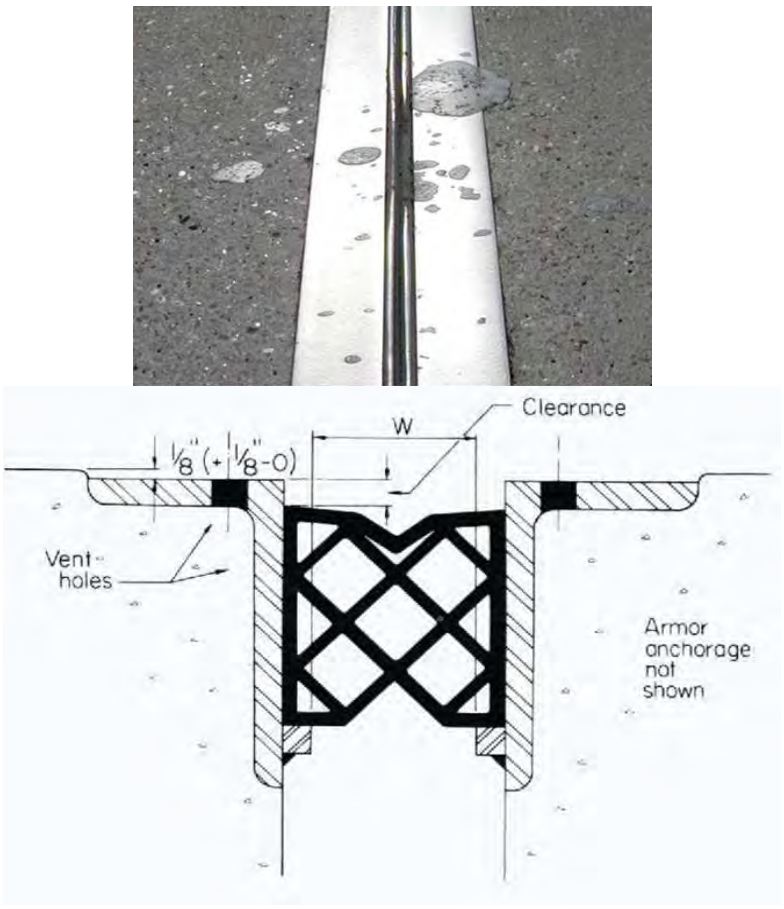

Figure 8.3.2.2-2 Compression Seal

A strip seal consists of a membrane or gland of neoprene rigidly attached to a steel armored facing on both sides of the opening. The strip seal is premolded into the shape of a "V". It opens as the joint width increases, and it closes as the joint width decreases. Strip seals can generally be used for movements of up to 4 inches. A strip seal is illustrated in Figure 8.3.2.2-3.

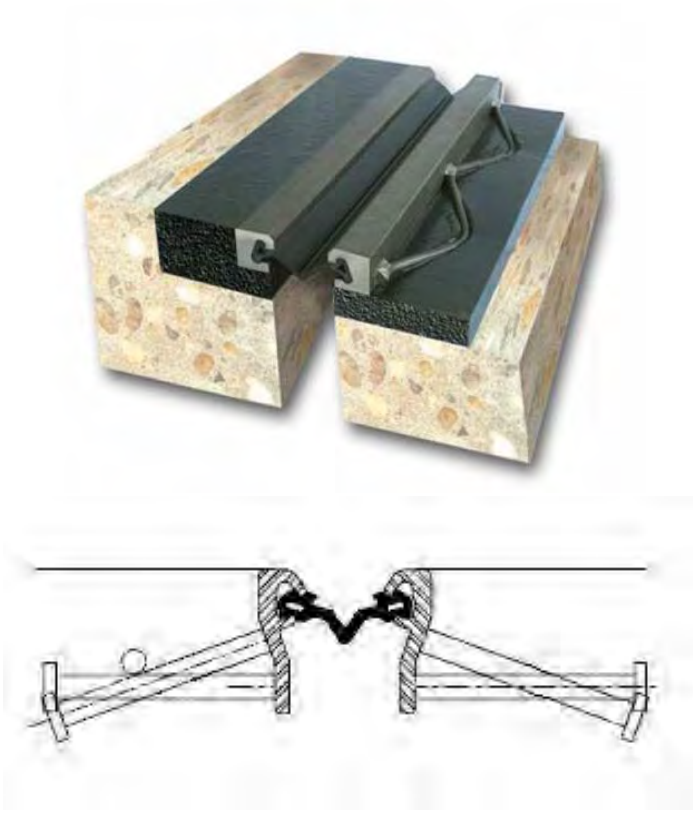

Figure 8.3.2.2-3 Strip Seal

In addition to sealing the surface of the deck, closed joints must also seal the surface of curbs, sidewalks, medians, parapets, and barrier wall, where present. The glands or membranes used for closed joints must not come in direct contact with the wheels of vehicles driving over them.

8.3.2.3 Modular Bridge Joint Systems

A modular bridge joint system (MBJS) is a unique type of closed joint that can accommodate movements between 4 and 24 inches. However, they have also been designed for use on very long span bridges with movements of more than 7 feet.

An MBJS consists of three primary components – sealers, separator beams, and support bars. Sealers are hollow, rectangular neoprene block seals. They are interconnected with steel separator beams, and the entire system is supported on support bars, which form its own stringer system. Two common types of MBJS are welded multiple-support-bar (WMSB) systems and single-support-bar (SSB) systems.

AASHTO LRFD Article 14.5.6.9 specifies performance requirements, strength limit state design requirements, and fatigue limit state requirements for MBJS.

An MBJS is illustrated in Figure 8.3.2.3-1.

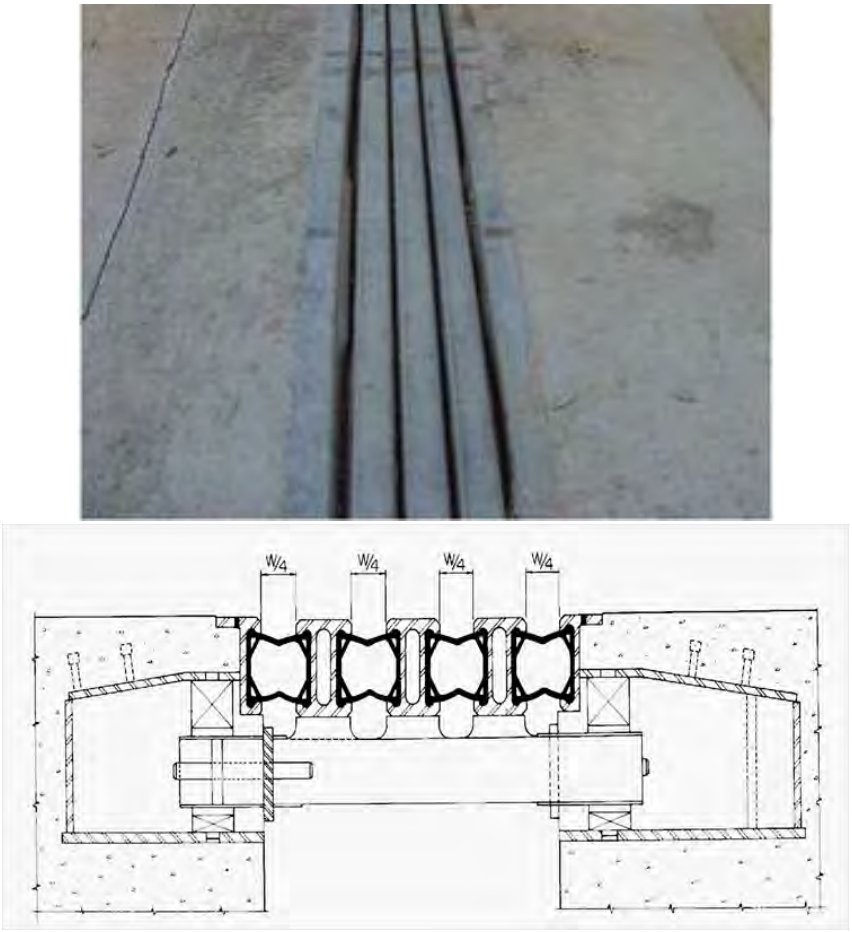

Figure 8.3.2.3-1 Modular Bridge Joint System

8.3.2.4 Finger Plate Joints

A finger plate joint, also known as a tooth plate joint or tooth dam, is a specific type of open joint. It consists of two steel plates with interlocking fingers. These joints are usually found on longer span bridges where greater movement is required. Two types of finger plate joints are cantilever finger plate joints and supported finger plate joints.

The cantilever finger plate joint is used when relatively little expansion is required. The fingers on this joint cantilever out from the deck side plate and the abutment side plate.

The supported finger plate joint is used on longer spans requiring greater movement. The fingers on this joint have their own support system in the form of transverse beams under the joint. Some types of finger plate joints are segmental, allowing for

maintenance and replacement if necessary. Finger plate joints are used to accommodate movement from 4 inches to over 24 inches.

Troughs are sometimes placed under open finger plate joints. Their purpose is to direct water that passes through the joint away from the superstructure, bearings, and substructure.

A finger plate joint is illustrated in Figure 8.3.2.4-1.

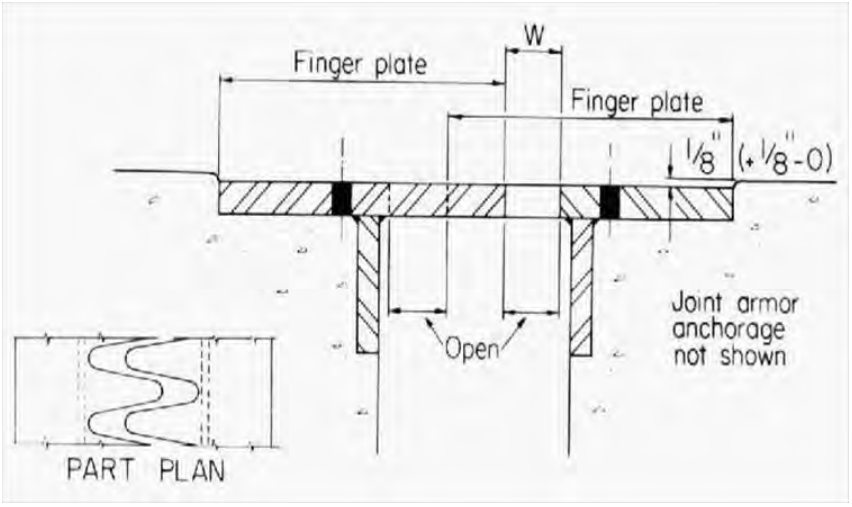

Figure 8.3.2.4-1 Finger Plate Joint

8.3.3 Selection

8.3.3.1 Number of Joints

Since deck joints frequently result in deterioration and maintenance problems for the underlying bridge elements, the number of deck joints on a bridge should be minimized.

In addition, the use of jointless bridges, which generally incorporate the use of integral abutments, should be considered. Tennessee DOT, a pioneer in the use of jointless bridges, routinely builds jointless bridges up to 400 feet long with steel girder superstructures and up to 800 feet long with concrete superstructures. They have built a jointless bridge with nine spans, totaling 1,200 feet in length. Some other states, however, have been more conservative in their implementation of integral abutments and jointless bridges, using a limit of approximately 300 feet.

8.3.3.2 Location of Joints

There are several guidelines that should be followed during the design process when locating deck joints on a bridge. As a general rule of thumb, deck joints should be avoided in the following locations:

- Over roadways, railroads, sidewalks, and other public areas
- At the low point of sag vertical curves

Other guidelines related to the location of deck joints are presented in Table 8.3.3.2-1:

Table 8.3.3.2-1 Location of Joints

Application	Guideline
Joints located over abutments	Prevent the discharge of deck drainage directly onto the bridge seats
Open joints	Locate only where deck drainage can be directed to bypass the bearings and discharged directly below the joint
Closed joints	Provide where joints are located directly over structural members and bearings that would be adversely affected by the accumulation of water and debris
Sealed or waterproof joints	Provide where deicing chemicals are used on the bridge deck
Straight bridges	Align longitudinal elements of deck joints, such as plate fingers, curb and barrier plates, and MBJS support bars, parallel to the longitudinal axis of the deck
Curved and skewed bridges	Allow for deck end movements anticipated with the selected bearings
Modular bridge joint systems (MBJS)	Do not locate in the middle of curved bridges (to avoid unforeseen movement demands) or near traffic signals or toll areas (to avoid extreme braking forces)

8.3.4 General Design Considerations

The primary design consideration for deck joints is the anticipated magnitude of movement, primarily due to thermal changes. The superstructure length affecting the movement at a joint is the distance from the joint being considered to the structure's neutral point.

For curved bridges that are laterally unrestrained by guided bearings, the direction of longitudinal movement should be assumed to be parallel to the chord of the deck centerline taken from the joint to the neutral point of the structure.

The design of deck joints is dependent on the type of deck joint selected, and deck joints are often designed by the manufacturer. However, several factors are generally considered when computing the movements and force effects for a deck joint, including the following:

- Material properties for the structure (such as coefficient of thermal expansion, modulus of elasticity, and Poisson's ratio)
- Effects of temperature, creep, and shrinkage
- Sizes of structural components
- Construction tolerances
- Method and sequence of construction
- Curvature
- Skew
- Resistance of joints to movements
- Approach pavement movement
- Substructure movements due to embankment construction
- Foundation movements due to consolidation and stabilization of subsoils
- Structural restraints
- Static and dynamic structural responses and their interaction
- Effects of end beam rotation on joint movement requirements for deep girders

Design movements are computed based on the strength limit state. The roadway surface gap, *W*, must be less than or equal to 4 inches for a single gap and less than or equal to 3 inches for multiple modular gaps.

The opening between adjacent fingers on a finger plate deck joint should not be greater than 2 inches for longitudinal openings greater than 8 inches, nor should it be greater than 3 inches for longitudinal openings of 8 inches or less. The finger overlap at the maximum movement based on the strength limit state should not be less than 1.5 inches.

Special covering floor plates should be considered in the shoulder areas if bicycle use is anticipated on the roadway.

When designing and specifying a deck joint, state agencies have reported that their primary factors of consideration, in order of importance, are the following (Purvis, 2003):

- Movement range
- Bridge span
- Type of bridge
- Joint performance and previous experience
- Durability
- Maintenance requirements
- Bridge alignment
- Joint details at curbs, concrete barriers, or deck edges
- Initial costs
- Climate conditions
- Expected joint life
- Installation time
- Life-cycle costs
- Type of bridge supports
- Service level

The design and specification of deck joints is commonly a team effort involving both the agency and the joint manufacturer.

8.3.5 Installation

AASHTO LRFD Article 14.5.5 provides guidance regarding the installation of deck joints. Information is provided about temperature adjustments, the use of temporary supports, and field splice restrictions.

Past experience with the installation of deck joints has revealed that several practical measures can improve deck joint performance and extend service life (Purvis, 2003). These measures include the following:

- Implement a proactive deck joint maintenance program
- Use deck joint blockouts adjacent to openings when placing a joint system
- Support each replacement joint system on sound existing concrete
- Install each seal to match ambient temperature
- Ensure that the joint opening size and shape is properly constructed
- Install the joint system after overlay is placed (if overlay is used)
- Protect against unusual joint movement that could damage the joint seal

- Follow the manufacturer's recommendations for selection and installation
- Avoid splices in premolded expansion material
- Protect against snowplow damage

Section 8.4 References

Purvis, R. 2003. *Bridge Deck Joint Performance, A Synthesis of Highway Practice*, NCHRP Synthesis 319, Transportation Research Board, National Research Council, Washington, DC.

Stanton, J. F., C. W. Roeder, P. Mackenzie-Helnwein, C. White, C. Kuester, and B. Craig. 2008. *Rotation Limits for Elastomeric Bearings*, NCHRP Report 596. Transportation Research Board, National Research Council, Washington, DC, February 2008.

This page intentionally left blank.

Glossary

A

Abutment—An end support for a bridge superstructure.

Active Earth Pressure—Lateral pressure resulting from the retention of the earth by a structure or component that is tending to move away from the soil mass.

Anchorage—In post-tensioning, a mechanical device used to anchor the tendon to the concrete; in pretensioning, a device used to anchor the tendon until the concrete has reached a predetermined strength, and the prestressing force has been transferred to the concrete; for reinforcing bars, a length of reinforcement, or a mechanical anchor or hook, or combination thereof at the end of a bar needed to transfer the force carried by the bar into the concrete.

Anchorage Zone—The portion of the structure in which the prestressing force is transferred from the anchorage device onto the local zone of the concrete, and then distributed more widely into the general zone of the structure.

B

Beam—A structural member whose primary function is to transmit loads to the support primarily through flexure and shear. Generally, this term is used when the component is made of rolled shapes.

Beam-Column—A structural member whose primary function is to resist both axial loads and bending moments.

Bearing—A structural device that transmits loads while facilitating translation and/or rotation.

Block Shear Rupture—Failure of a bolted web connection of coped beams or any tension connection by the tearing out of a portion of a plate along the perimeter of the connecting bolts.

Bracing Member—A member intended to brace a main member or part thereof against lateral movement.

Bridge—Any structure having an opening not less than 20.0 feet that forms part of a highway or that is located over or under a highway.

C

Cast-in-Place Concrete—Concrete placed in its final location in the structure while still in a plastic state.

Centrifugal Force—A lateral force resulting from a change in the direction of a vehicle's movement.

Charpy V-Notch Impact Requirement—The minimum energy required to be absorbed in a Charpy V-notch test conducted at a specified temperature.

Clear Distance of Bolts—The distance between edges of adjacent bolt holes.

Clear End Distance of Bolts—The distance between the edge of a bolt hole and the end of a member.

Clearance—An unobstructed horizontal or vertical space.

Collapse—A major change in the geometry of the bridge rendering it unfit for use.

Compact Section—A composite section in positive flexure satisfying specific steel grade, web slenderness and ductility requirements that is capable of developing a nominal resistance exceeding the moment at first yield, but not to exceed the plastic moment.

Compact Unbraced Length—For a composite section in negative flexure or a noncomposite section, the limiting unbraced length of a discretely braced compression flange at or below which the maximum potential flexural resistance can be achieved prior to lateral torsional buckling having a statistically significant influence on the response, provided that sufficient flange slenderness requirements are satisfied to develop the maximum potential flexural resistance.

Component—A structural unit requiring separate design consideration; synonymous with member.

Composite Construction—Concrete components or concrete and steel components interconnected to respond to force effects as a unit.

Composite Girder—A steel flexural member connected to a concrete slab so that the steel element and the concrete slab, or the longitudinal reinforcement within the slab, respond to force effects as a unit.

Compression Seal—A preformed elastomeric device that is precompressed in the gap of a joint with expected total range of movement less than 2.0 inches.

Concrete Cover—The specified minimum distance between the surface of the reinforcing bars, strands, posttensioning ducts, anchorages, or other embedded items, and the surface of the concrete.

Connection—A weld or arrangement of bolts that transfers normal and/or shear stresses from one element to another.

Construction Joint—A temporary joint used to permit sequential construction.

Continuously Braced Flange—A flange encased in concrete or anchored by shear connectors for which flange lateral bending effects need not be considered. A continuously braced flange in compression is also assumed not to be subject to local or lateral torsional buckling.

Cracked Section—A composite section in which the concrete is assumed to carry no tensile stress.

Creep—Time-dependent deformation of concrete under permanent load.

Cross-Frame—A transverse truss framework connecting adjacent longitudinal flexural components or inside a tub section or closed box used to transfer and distribute vertical and lateral loads and to provide stability to the compression flanges. Sometimes synonymous with the term diaphragm.

Curved Girder—An I-, closed-box, or tub girder that is curved in a horizontal plane.

D

Damper—A device that transfers and reduces forces between superstructure elements and/or superstructure and substructure elements, while permitting thermal movements. The device provides damping by dissipating energy under seismic, braking, or other dynamic loads.

Deck—A component, with or without wearing surface, directly supporting wheel loads.

Deck Joint—A structural discontinuity between two elements, at least one of which is a deck element. It is designed to permit relative translation and/or rotation of abutting structural elements.

Deck Slab—A solid concrete slab resisting and distributing wheel loads to the supporting components.

Deck Truss—A truss system in which the roadway is at or above the level of the top chord of the truss.

Deformation—A change in structural geometry due to force effects, including axial displacement, shear displacement, and rotations.

Degree-of-Freedom—One of a number of translations or rotations required to define the movement of a node. The displaced shape of components and/or the entire structure may be defined by a number of degrees-of-freedom.

Design—Proportioning and detailing the components and connections of a bridge to satisfy the requirements of the *AASHTO LRFD Bridge Design Specifications*.

Design Lane—A notional traffic lane positioned transversely on the roadway.

Design Life—Period of time on which the statistical derivation of transient loads is based: 75 year for the *AASHTO LRFD Bridge Design Specifications*.

Design Water Depth—Depth of water at mean high water.

Detail Category—A grouping of components and details having essentially the same fatigue resistance.

Development Length—The distance required to develop the specified strength of a reinforcing bar or prestressing strand.

Diaphragm—A vertically oriented solid transverse member connecting adjacent longitudinal flexural components or inside a closed-box or tub section to transfer and distribute vertical and lateral loads and to provide stability to the compression flanges.

Disc Bearing—A bearing that accommodates rotation by deformation of a single elastomeric disc molded from a urethane compound. It may be movable, guided, unguided, or fixed. Movement is accommodated by sliding of polished stainless steel on PFTE.

Dolphin—Protective object that may have its own fender system and that is usually circular in plan and structurally independent from the bridge.

Ductility—Property of a component or connection that allows inelastic response.

Dynamic Load Allowance—An increase in the applied static force effects to account for the dynamic interaction between the bridge and moving vehicles.

E

Edge Distance—The minimum distance between the centerline of reinforcement or other embedded elements and the edge of the concrete.

Effective Depth—The depth of a component effective in resisting flexural or shear forces.

Elastic—A structural response in which stress is directly proportional to strain and no deformation remains upon removal of loading.

Element—A part of a component or member consisting of one material.

Embedment Length—The length of reinforcement or anchor provided beyond a critical section over which transfer of force between concrete and reinforcement may occur.

Engineer—A licensed structural engineer responsible for the design of the bridge or review of the bridge construction.

Equivalent Fluid—A notional substance whose density is such that it would exert the same pressure as the soil it is seen to replace for computational purposes.

Evaluation—Determination of load-carrying capacity of an existing bridge.

Extreme Event Limit States—Limit states relating to events such as earthquakes, ice load, and vehicle and vessel collision, with return periods in excess of the design life of the bridge.

F

Factored Load—The nominal loads multiplied by the appropriate load factors specified for the load combination under consideration.

Factored Resistance—The nominal resistance multiplied by a resistance factor.

Fastener—Generic term for welds, bolts, rivets, or other connecting device.

Fatigue—The initiation and/or propagation of cracks due to a repeated variation of normal stress with a tensile component.

Fatigue Design Life—The number of years that a detail is expected to resist the assumed traffic loads without fatigue cracking. In the development of these Specifications it has been taken as 75 years.

Fatigue Life—The number of repeated stress cycles that results in fatigue failure of a detail.

Fender—Protection hardware attached to the structural component to be protected or used to delineate channels or to redirect aberrant vessels.

Finite Element Method—A method of analysis in which a structure is discretized into elements connected at nodes, the shape of the element displacement field is assumed, partial or complete compatibility is maintained among the element interfaces, and nodal displacements are determined by using energy variational principles or equilibrium methods.

Fixed Bearing—A bearing that prevents differential longitudinal translation of abutting structural elements. It may or may not provide for differential lateral translation or rotation.

Fixed Bridge—A bridge with a fixed vehicular or navigational clearance.

Flange Lateral Bending—Bending of a flange about an axis perpendicular to the flange plate due to lateral loads applied to the flange and/or nonuniform torsion in the member.

Flexural-Torsional Buckling—A buckling mode in which a compression member bends and twists simultaneously without a change in cross-sectional shape.

Force—Resultant of distribution of stress over a prescribed area. Generic term signifying axial loads, bending moment, torques, and shears.

Force Effect—A deformation, stress, or stress resultant (i.e., axial force, shear force, torsional, or flexural moment) caused by applied loads, imposed deformations, or volumetric changes.

Foundation—A supporting element that derives its resistance by transferring its load to the soil or rock supporting the bridge.

Fracture-Critical Member (FCM)—Component in tension whose failure is expected to result in the collapse of the bridge or the inability of the bridge to perform its function.

Fracture Toughness—A measure of the ability of a structural material or element to absorb energy without fracture. It is generally determined by the Charpy V-notch test.

G

Girder—A structural component whose primary function is to resist loads in flexure and shear. Generally, this term is used for fabricated sections.

Grid Method—A grid method of analysis of girder bridges in which the longitudinal girders are modeled individually using beam elements and the cross-frames are typically modeled as equivalent beam elements. For composite girders, a tributary deck width is considered in the calculation of individual girder cross-section properties.

Gusset Plate—Plate material used to interconnect vertical, diagonal, and horizontal truss members at a panel point, or to interconnect diagonal and horizontal cross-frame members for subsequent attachment of the cross-frame to transverse connection plates.

H

Hybrid Section—A fabricated steel section with a web that has a specified minimum yield strength lower than one or both flanges.

Hydraulics—The science concerned with the behavior and flow of liquids, especially in pipes and channels.

Hydrology—The science concerned with the occurrence, distribution, and circulation of water on the earth, including precipitation, runoff, and groundwater.

I

Inelastic—Any structural behavior in which the ratio of stress and strain is not constant, and part of the deformation remains after load removal.

Influence Surface—A continuous or discretized function over a bridge deck whose value at a point, multiplied by a load acting normal to the deck at that point, yields the force effect being sought.

Integral Bridge—A bridge without deck joints.

J

Jacking Force—The force exerted by the device that introduces tension into the tendons.

Joint—A structural discontinuity between two elements. The structural members used to frame or form the discontinuity.

K

L

Lane—The area of deck receiving one vehicle or one uniform load line.

Lane Live Load—The combination of tandem axle and uniformly distributed loads or the combination of the design truck and design uniformly distributed load.

Lateral Bending Stress—The normal stress caused by flange lateral bending.

Lateral Bracing—A truss placed in a horizontal plane between two I-girders or two flanges of a tub girder to maintain cross-sectional geometry, and provide additional stiffness and stability to the bridge system.

Lateral-Torsional Buckling—Buckling of a component involving lateral deflection and twist.

Lever Rule—The statical summation of moments about one point to calculate the reaction at a second point.

Limit State—A condition in which a component or structure becomes unfit for service and is judged either to be no longer useful for its intended function or to be unsafe. Limits of structural usefulness include brittle fracture, plastic collapse, excessive deformation, durability, fatigue, instability, and serviceability.

Linear Response—Structural behavior in which deflections are directly proportional to loads.

Load—The effect of acceleration, including that due to gravity, imposed deformation, or volumetric change.

Load and Resistance Factor Design (LRFD)—A reliability-based design methodology in which force effects caused by factored loads are not permitted to exceed the factored resistance of the components.

Load Effect—Moment, shear, axial force or torque induced in a member by loads applied to the structure.

Load Factor—A statistically-based multiplier applied to force effects accounting primarily for the variability of loads, the lack of accuracy in analysis, and the probability of simultaneous occurrence of different loads, but also related to the statistics of the resistance through the calibration process.

Load-Induced Fatigue—Fatigue effects due to the in-plane stresses for which components and details are explicitly designed.

Load Modifier—A factor accounting for ductility, redundancy, and the operational classification of the bridge.

Local Scour—Scour in a channel or on a floodplain that is localized at a pier, abutment, or other obstruction to flow.

Longitudinal—Parallel with the main span direction of a structure.

Longitudinal Joint—A joint parallel to the span direction of a structure provided to separate a deck or superstructure into two independent structural systems.

Low Relaxation Steel—Prestressing strand in which the steel relaxation losses have been substantially reduced by stretching at an elevated temperature.

M

Metal Rocker or Roller Bearing—A bearing that carries vertical load by direct contact between two metal surfaces and that accommodates movement by rocking or rolling of one surface with respect to the other.

Method of Analysis—A mathematical process by which structural deformations, forces, and stresses are determined.

Model—A mathematical or physical idealization of a structure or component used for the purpose of analysis.

Modular Bridge Joint System (MBJS)—A sealed joint with two or more elastomeric seals held in place by edgebeams that are anchored to the structural elements (deck, abutment, etc.) and one or more transverse centerbeams that are parallel to the edgebeams. Typically used for movement ranges greater than 4.0 inches.

Movable Bridge—A bridge with a variable vehicular or navigational clearance.

M/R Method—An approximate method for the analysis of curved box girders in which the curved girder is treated as an equivalent straight girder to calculate flexural effects and as a corresponding straight conjugate beam to calculate the concomitant St. Venant torsional moments due to curvature.

Multibeam Decks—Bridges with superstructure members consisting of adjacent precast sections with the top flange as a complete full-depth integral deck or a structural deck section placed as an overlay. Sections can be closed cell boxes or open stemmed.

Multiple-Load-Path Structure—A structure capable of supporting the specified loads following loss of a main load-carrying component or connection.

Negative Moment—Moment producing tension at the top of a flexural element.

N

Node—A point where finite elements or grid components meet; in conjunction with finite differences, a point where the governing differential equations are satisfied.

Nominal Load—An arbitrarily selected design load level.

Nominal Resistance—Resistance of a component or connection to force effects, as indicated by the dimensions specified in the contract documents and by permissible stresses, deformations, or specified strength of materials.

Noncompact Section—A composite section in positive flexure for which the nominal resistance is not permitted to exceed the moment at first yield.

Noncomposite Section—A steel beam where the deck is not connected to the steel section by shear connectors.

Nonlinear Response—Structural behavior in which the deflections are not directly proportional to the loads due to stresses in the inelastic range, or deflections causing significant changes in force effects, or by a combination thereof.

O

Orthotropic—Perpendicular to each other, having physical properties that differ in two or more orthogonal directions.

Orthotropic Deck—A deck made of a steel plate stiffened with open or closed steel ribs welded to the underside of a steel plate.

Owner—Person or agency having jurisdiction over the bridge.

P

Passive Earth Pressure—Lateral pressure resulting from the earth's resistance to the lateral movement of a structure or component into the soil mass.

Permanent Loads—Loads and forces that are, or are assumed to be, either constant upon completion of construction or varying only over a long time interval.

Permit Vehicle—Any vehicle whose right to travel is administratively restricted in any way due to its weight or size.

Pier—A column or connected group of columns or other configuration designed to be an interior support for a bridge superstructure.

Pin Connection—A connection among members by a notionally frictionless pin at a point.

Plastic Analysis—Determination of load effects on members and connections based on the assumption of rigid-plastic behavior; i.e., that equilibrium is satisfied throughout the structure and yield is not exceeded anywhere. Second-order effects may need to be considered.

Point of Contraflexure—The point where the sense of the flexural moment changes; synonymous with point of inflection.

Positive Moment—Moment producing tension at the bottom of a flexural element.

Post-Tensioning—A method of prestressing in which the tendons are tensioned after the concrete has reached a predetermined strength.

Pot Bearing—A bearing that carries vertical load by compression of an elastomeric disc confined in a steel cylinder and that accommodates rotation by deformation of the disc.

Precast Members—Concrete elements cast in a location other than their final position.

Prestressed Concrete—Concrete components in which stresses and deformations are introduced by application of prestressing forces.

Pretensioning—A method of prestressing in which the strands are tensioned before the concrete is placed.

Primary Member—A member designed to carry the loads applied to the structure as determined from an analysis.

Q

R

Rating Vehicle—A sequence of axles used as a common basis for expressing bridge resistance.

Redistribution of Moments—A process that results from formation of inelastic deformations in continuous structures.

Redundancy—The quality of a bridge that enables it to perform its design function in a damaged state.

Redundant Member—A member whose failure does not cause failure of the bridge.

Refined Methods of Analysis—Methods of structural analysis that consider the entire superstructure as an integral unit and provide the required deflections and actions.

Regular Service—Condition excluding the presence of special permit vehicles, wind exceeding 55 mph, and extreme events, including scour.

Rehabilitation—A process in which the resistance of the bridge is either restored or increased.

Reinforced Concrete—Structural concrete containing no less than the minimum amounts of prestressing tendons or nonprestressed reinforcement specified herein.

Reinforcement—Reinforcing bars and/or prestressing steel.

Relaxation—The time-dependent reduction of stress in prestressing tendons.

Reliability Index—A quantitative assessment of safety expressed as the ratio of the difference between the mean resistance and mean force effect to the combined standard deviation of resistance and force effect.

Residual Stress—The stresses that remain in an unloaded member or component after it has been formed into a finished product by cold bending, and/or cooling after rolling or welding.

Resistance Factor—A statistically-based multiplier applied to nominal resistance accounting primarily for variability of material properties, structural dimensions and workmanship, and uncertainty in the prediction of resistance, but also related to the statistics of the loads through the calibration process.

Roadway Width—Clear space between barriers and/or curbs.

S

Scupper—A device to drain water through the deck.

Sealed Joint—A joint provided with a joint seal.

Secondary Member—A member in which stress is not normally evaluated in the analysis.

Second-Order Analysis—Analysis in which equilibrium conditions are formulated on the deformed structure; that is, in which the deflected position of the structure is used in writing the equations of equilibrium.

Service Life—The period of time that the bridge is expected to be in operation.

Service Limit States—Limit states relating to stress, deformation, and cracking under regular operating conditions.

Service Loads—Loads expected to be supported by the structure under normal usage.

Shear Connector—A mechanical device that prevents relative movements both normal and parallel to an interface.

Sidewalk Width—Unobstructed space for exclusive pedestrian use between barriers or between a curb and a barrier.

Skew Angle—Angle between the centerline of a support and a line normal to the roadway centerline.

Slab—A deck composed of concrete and reinforcement.

Spacing of Beams—The center-to-center distance between lines of support.

Specified Strength of Concrete—The nominal compressive strength of concrete specified for the work and assumed for design and analysis of new structures.

Splice—A group of bolted connections, or a welded connection, sufficient to transfer the moment, shear, axial force, or torque between two structural elements joined at their ends to form a single, longer element.

Stay-in-Place Formwork—Permanent metal or precast concrete forms that remain in place after construction is finished.

Steel-Reinforced Elastomeric Bearing—A bearing made from alternate laminates of steel and elastomer bonded together during vulcanization. Vertical loads are carried by compression of the elastomer. Movements parallel to the reinforcing layers and rotations are accommodated by deformation of the elastomer.

Stiffener—A member, usually an angle or plate, attached to a plate or web of a beam or girder to distribute load, to transfer shear, or to prevent buckling of the member to which it is attached.

Strain—Elongation per unit length.

Strength Limit States—Limit states relating to strength and stability during the design life.

Stress Range—The algebraic difference between the maximum and minimum stresses due to transient loads.

Strip Seal—A sealed joint with an extruded elastomeric seal retained by edgebeams that are anchored to the structural elements (deck, abutment, etc.). Typically used for expected total movement ranges from 1.5 to 4.0 inches, although single seals capable of spanning a 5.0 inch gap are also available.

Strut-and-Tie Model—A model used principally in regions of concentrated forces and geometric discontinuities to determine concrete proportions and reinforcement quantities and patterns based on assumed compression struts in the concrete, tensile ties in the reinforcement, and the geometry of nodes at their points of intersection.

Substructure—Structural parts of the bridge that support the horizontal span.

Superelevation—A tilting of the roadway surface to partially counterbalance the centrifugal forces on vehicles on horizontal curves.

Superflood—Any flood or tidal flow with a flow rate greater than that of the 100-yr flood but not greater than a 500-year flood.

Superposition—The situation where the force effect due to one loading can be added to the force effect due to another loading. Use of superposition is only valid when the stress-strain relationship is linearly elastic and the small deflection theory is used.

Superstructure—Structural parts of the bridge that provide the horizontal span.

Surcharge—A load used to model the weight of earth fill or other loads applied to the top of the retained material.

T

Tandem—Two closely spaced and mechanically interconnected axles of equal weight.

Temperature Gradient—Variation of temperature of the concrete over the cross-section.

Tendon—A high-strength steel element used to prestress the concrete.

Tensile Strength—The maximum tensile stress that a material is capable of sustaining.

Tied Arch—An arch in which the horizontal thrust of the arch rib is resisted by a horizontal tie.

Transfer—The operation of imparting the force in a pretensioning anchoring device to the concrete.

Transient Loads—Loads and forces that can vary over a short time interval relative to the lifetime of the structure.

U

Unbraced Length—Distance between brace points resisting the mode of buckling or distortion under consideration; generally, the distance between panel points or brace locations.

V

V-Load Method—An approximate method for the analysis of curved I-girder bridges in which the curved girders are represented by equivalent straight girders and the effects of curvature are represented by vertical and lateral forces applied at cross-frame locations. Lateral flange bending at brace points due to curvature is estimated.

W

Waterway—Any stream, river, pond, lake, or ocean.

Wheel Load—One-half of a specified design axle load.

X

Y

Yield Strength—The stress at which a material exhibits a specified limiting deviation from the proportionality of stress to strain.

Z